

NASA Technical Memorandum 106035

1N-82
203568
P - 440

Bibliography of Lewis Research Center Technical Publications Announced in 1992

November 1993

(NASA-TM-106035) BIBLIOGRAPHY OF
LEWIS RESEARCH CENTER TECHNICAL
PUBLICATIONS ANNOUNCED IN 1992
(NASA) 440 p

N94-23562

Unclas

G3/82 0203568





NASA Technical Memorandum 106035

Bibliography of Lewis Research Center Technical Publications Announced in 1992

November 1993

NASA
National Aeronautics and
Space Administration

Lewis Research Center
Cleveland, Ohio 44135



PREFACE

Making the results of our research available to others has always been a vital part of Lewis' mission. In 1992, Lewis Research Center's 1911 research authors (1394 civil servants and 517 on-site contractor and university staff) published 655 technical publications that were announced to and reached the worldwide scientific community. Included in this total are 145 high-numbered Technical Memorandums—the most published in a single year. In addition to this total, 13 technical videos and 133 contractor-authored research reports were produced at NASA Lewis in 1992.

In 1992, Lewis authors published approximately 56 percent of their research contributions in outside publications and the remainder as NASA research reports. Seventy-seven percent of Lewis-authored society presentations and journal articles were addressed to members of the following 10 organizations—AIAA, ASME, SAE, American Society of Engineering Education (ASEE), American Nuclear Society (ANS), American Chemical Society (ACS), AIChE, NASA, Materials Research Society (MRS), and IEEE.

This year Lewis scientists and engineers wrote or edited the following books and manuals that are of lasting reference value:

- NASA RP-1280, Three-Dimensional Laser Window Formation by Vincent G. Verhoff
- NASA RP-1271, Computer Program for Calculating and Fitting Thermodynamic Functions by Bonnie J. McBride and Sanford Gordon
- NASA RP-1253, Reliability Training, edited by Vincent R. Lalli and Henry A. Malec

Lewis hosted or sponsored nine research conferences and workshops in 1992. Five of these resulted in the following NASA Conference Publications:

- NASA CP-10090, Rocket-Based Combined-Cycle (RBCC) Propulsion Technology Workshop, March 23-27
- NASA CP-10106, Fourth Annual Thermal and Fluids Analysis Workshop, August 17-21
- NASA CP-10113, Second International Microgravity Combustion Workshop, September 15
- NASA CP-3210, Proceedings of the XII Space Photovoltaic Research and Technology Conference—SPRAT XII, October 20-22
- NASA CP-10104, HITEMP Review—1992: Advanced High Temperature Engine Materials Technology Program, October 27-28

Other conferences and workshops hosted or sponsored by Lewis in 1992 included

- National Technology Initiative Conference, April 23
- Second International Microgravity Combustion Workshop, September 15-17
- NASA Space Communications Symposium, October 20-21
- Workshop on the Thermophysical Properties of Molten Materials, October 22

In 1992, 28 patents were applied for and 12 patents were issued. Items patented include an oxidation resistance coating, methods of producing heat flux gauges and thermal barrier coatings, selective emitters, a solar thermal energy receiver, a monolithic MM-wave phase shifter, a thermal energy transport/storage system, and a removable hand hold.

Several Lewis researchers received awards for their publications. The 1992 Lewis Distinguished Publication Award was presented to Michael D. Hathaway, Randall M. Chriss, Jerry R. Wood, and Anthony J. Strazisar for their paper entitled "Experimental and Computational Investigation of the NASA Low-Speed Centrifugal Compressor Flow Field."

For their paper "Relationship Between Voids and Interlaminar Shear Strength of Polymer Matrix Composites," Kenneth J. Bowles and Stephen Frimpong received the Frye-Perry Award for the best paper presented at the 36th International Society for the Advancement of Materials and Process Engineering (SAMPE) Symposium and Exhibition. Renee M. Kent received first prize from the American Ceramics Society for her research paper "Tensile Strain Measurements of Ceramic Fibers Using Scanning Laser Acoustic Microscopy." Kim K. de Groh and Joyce A. Dever received the best paper award from the American Society of Mechanical Engineers, Solar Energy Division, Solar Space Power Committee for their paper "Low Earth Orbit Durability Evaluation of Solar Concentrator Materials." Mark A. Richard received first place for his paper "Performance of a K-Band Superconducting Gap-Coupled Micro-Strip Antenna" in a student competition held at the 1992 meeting of the IEEE Antennas and Propagation Society, and Geoffrey A. Landis won a Hugo Award for his story, "A Walk in the Sun," considered to be the best science fiction story of 1992.

A few of the other awards received by Lewis scientists and engineers in 1992 follow. Twenty-one researchers received Silver Snoopy awards this year for their contributions to astronaut safety in the manned flight program—Robert L. Butcher, William K. Coho, Richard DeLombard, Paul S. Greenberg, John B. Haggard, Robert H. Knoll, Sheldon James Meyer, Angel M. Otero, Dennis W. Rohn, William K. Thompson, Joyce S. Wanhainen, and the Physical/Mechanical Calibration Group (James M. Vrtis, Frank A. Della Torre, Katharine Webster, Richard Abbott, Terry Wells, Harry James Gentry, Kenneth Monai, Peter Stiasny, Richard Hanzel, and Harland Kasa). Louis M. Russell received the Dr. A.T. Weathers Award from the National Technical Association (NTA) for his significant technical achievements and contributions, and Christos Chamis received the first Aircraft Engine Technology Award at the 1992 TURBO EXPO in Cologne, Germany, in recognition of his contributions in the fields of structures and dynamics.

All of the publications in this collection were announced in the 1992 issues of STAR (Scientific and Technical Aerospace Reports) and IAA (International Aerospace Abstracts). Some 1992 publications will be announced in the 1993 issues of STAR and IAA and will thus appear in the 1993 Lewis Bibliography. However, a few Lewis-authored publications are not included in this compilation because of FEDD (For Early Domestic Dissemination) and ITAR (International Traffic in Arms Regulations) considerations which limit their announcement and distribution.

The arrangement of the material is by NASA subject category, as noted in the Contents. In addition, the various indexes will help locate specific publications by subject, author, contractor organization, contract number, and report number.

Richard E. Texler
Chief, Technical Information Services Division

TABLE OF CONTENTS

AERONAUTICS For related information see also *Aeronautics*.

01 AERONAUTICS (GENERAL)	1
02 AERODYNAMICS	2
Includes aerodynamics of bodies, combinations, wings, rotors, and control surfaces; and internal flow in ducts and turbomachinery. For related information see also <i>34 Fluid Mechanics and Heat Transfer</i> .	
03 AIR TRANSPORTATION AND SAFETY	21
Includes passenger and cargo air transport operations; and aircraft accidents. For related information see also <i>16 Space Transportation</i> and <i>85 Urban Technology and Transportation</i> .	
04 AIRCRAFT COMMUNICATIONS AND NAVIGATION	22
Includes digital and voice communication with aircraft; air navigation systems (satellite and ground based); and air traffic control. For related information see also <i>17 Space Communications, Spacecraft Communications, Command and Tracking</i> and <i>32 Communications and Radar</i> .	
05 AIRCRAFT DESIGN, TESTING AND PERFORMANCE	22
Includes aircraft simulation technology. For related information see also <i>18 Spacecraft Design, Testing and Performance</i> and <i>39 Structural Mechanics</i> . For land transportation vehicles see <i>85 Urban Technology and Transportation</i> .	
06 AIRCRAFT INSTRUMENTATION	24
Includes cockpit and cabin display devices; and flight instruments. For related information see also <i>19 Spacecraft Instrumentation</i> and <i>35 Instrumentation and Photography</i> .	
07 AIRCRAFT PROPULSION AND POWER	24
Includes prime propulsion systems and systems components, e.g., gas turbine engines and compressors; and onboard auxiliary power plants for aircraft. For related information see also <i>20 Spacecraft Propulsion and Power</i> , <i>28 Propellants and Fuels</i> , and <i>44 Energy Production and Conversion</i> .	
08 AIRCRAFT STABILITY AND CONTROL	39
Includes aircraft handling qualities; piloting; flight controls; and autopilots. For related information see also <i>05 Aircraft Design, Testing and Performance</i> .	
09 RESEARCH AND SUPPORT FACILITIES (AIR)	40
Includes airports, hangars and runways; aircraft repair and overhaul facilities; wind tunnels; shock tubes; and aircraft engine test stands. For related information see also <i>14 Ground Support Systems and Facilities (Space)</i> .	

ASTRONAUTICS For related information see also *Aeronautics*.

12 ASTRONAUTICS (GENERAL)	43
For extraterrestrial exploration see <i>91 Lunar and Planetary Exploration</i> .	
13 ASTRODYNAMICS	44
Includes powered and free-flight trajectories; and orbital and launching dynamics.	
14 GROUND SUPPORT SYSTEMS AND FACILITIES (SPACE)	44
Includes launch complexes, research and production facilities; ground support equipment, e.g., mobile transporters; and simulators. For related information see also <i>09 Research and Support Facilities (Air)</i> .	
15 LAUNCH VEHICLES AND SPACE VEHICLES	47
Includes boosters; operating problems of launch/space vehicle systems; and reusable vehicles. For related information see also <i>20 Spacecraft Propulsion and Power</i> .	
16 SPACE TRANSPORTATION	49
Includes passenger and cargo space transportation, e.g., shuttle operations; and space rescue techniques. For related information see also <i>03 Air Transportation and Safety</i> and <i>18 Spacecraft Design, Testing and Performance</i> . For space suits see <i>54 Man/System Technology and Life Support</i> .	
17 SPACE COMMUNICATIONS, SPACECRAFT COMMUNICATIONS, COMMAND AND TRACKING ...	49
Includes telemetry; space communications networks; astronavigation and guidance; and radio blackout. For related information see also <i>04 Aircraft Communications and Navigation</i> and <i>32 Communications and Radar</i> .	

N.A.—no abstracts were assigned to this category for this issue.

18 SPACECRAFT DESIGN, TESTING AND PERFORMANCE 52
 Includes satellites; space platforms; space stations; spacecraft systems and components such as thermal and environmental controls; and attitude controls. For life support systems see *54 Man/System Technology and Life Support*. For related information see also *05 Aircraft Design, Testing and Performance*, *39 Structural Mechanics*, and *16 Space Transportation*.

19 SPACECRAFT INSTRUMENTATION 56
 For related information see also *06 Aircraft Instrumentation* and *35 Instrumentation and Photography*.

20 SPACECRAFT PROPULSION AND POWER 58
 Includes main propulsion systems and components, e.g., rocket engines; and spacecraft auxiliary power sources. For related information see also *07 Aircraft Propulsion and Power*, *28 Propellants and Fuels*, *44 Energy Production and Conversion*, and *15 Launch Vehicles and Space Vehicles*.

CHEMISTRY AND MATERIALS

23 CHEMISTRY AND MATERIALS (GENERAL) 93

24 COMPOSITE MATERIALS 98
 Includes physical, chemical, and mechanical properties of laminates and other composite materials. For ceramic materials see *27 Nonmetallic Materials*.

25 INORGANIC AND PHYSICAL CHEMISTRY 111
 Includes chemical analysis, e.g., chromatography; combustion theory; electrochemistry; and photochemistry. For related information see also *77 Thermodynamics and Statistical Physics*.

26 METALLIC MATERIALS 116
 Includes physical, chemical, and mechanical properties of metals, e.g., corrosion; and metallurgy.

27 NONMETALLIC MATERIALS 123
 Includes physical, chemical, and mechanical properties of plastics, elastomers, lubricants, polymers, textiles, adhesives, and ceramic materials. For composite materials see *24 Composite Materials*.

28 PROPELLANTS AND FUELS 133
 Includes rocket propellants, igniters and oxidizers; their storage and handling procedures; and aircraft fuels. For related information see also *07 Aircraft Propulsion and Power*, *20 Spacecraft Propulsion and Power*, and *44 Energy Production and Conversion*.

29 MATERIALS PROCESSING 136
 Includes space-based development of products and processes for commercial application. For biological materials see *55 Space Biology*.

ENGINEERING For related information see also *Physics*.

31 ENGINEERING (GENERAL) 140
 Includes vacuum technology; control engineering; display engineering; cryogenics; and fire prevention.

32 COMMUNICATIONS AND RADAR 142
 Includes radar; land and global communications; communications theory; and optical communications. For related information see also *04 Aircraft Communications and Navigation* and *17 Space Communications, Spacecraft Communications, Command and Tracking*. For search and rescue see *03 Air Transportation and Safety*, and *16 Space Transportation*.

33 ELECTRONICS AND ELECTRICAL ENGINEERING 153
 Includes test equipment and maintainability; components, e.g., tunnel diodes and transistors; microminiaturization; and integrated circuitry. For related information see also *60 Computer Operations and Hardware* and *76 Solid-State Physics*.

34 FLUID MECHANICS AND HEAT TRANSFER 164
 Includes boundary layers; hydrodynamics; fluidics; mass transfer; and ablation cooling. For related information see also *02 Aerodynamics* and *77 Thermodynamics and Statistical Physics*

35 INSTRUMENTATION AND PHOTOGRAPHY 197
 Includes remote sensors; measuring instruments and gauges; detectors; cameras and photographic supplies; and holography. For aerial photography see *43 Earth Resources and Remote Sensing*. For related information see also *06 Aircraft Instrumentation* and *19 Spacecraft Instrumentation*.

36 LASERS AND MASERS N.A.
 Includes parametric amplifiers. For related information see also *76 Solid-State Physics*.

N.A.—no abstracts were assigned to this category for this issue.

37 MECHANICAL ENGINEERING	203
Includes auxiliary systems (nonpower); machine elements and processes; and mechanical equipment.	
38 QUALITY ASSURANCE AND RELIABILITY	215
Includes product sampling procedures and techniques; and quality control.	
39 STRUCTURAL MECHANICS	216
Includes structural element design and weight analysis; fatigue; and thermal stress. For applications see <i>05 Aircraft Design, Testing and Performance</i> and <i>18 Spacecraft Design, Testing and Performance</i> .	

GEOSCIENCES For related information see also *Space Sciences*.

42 GEOSCIENCES (GENERAL)	N.A.
43 EARTH RESOURCES AND REMOTE SENSING	N.A.
Includes remote sensing of earth resources by aircraft and spacecraft; photogrammetry; and aerial photography. For instrumentation see <i>35 Instrumentation and Photography</i> .	
44 ENERGY PRODUCTION AND CONVERSION	231
Includes specific energy conversion systems, e.g., fuel cells; global sources of energy; geophysical conversion; and windpower. For related information see also <i>07 Aircraft Propulsion and Power</i> , <i>20 Spacecraft Propulsion and Power</i> , and <i>28 Propellants and Fuels</i> .	
45 ENVIRONMENT POLLUTION	239
Includes atmospheric, noise, thermal, and water pollution.	
46 GEOPHYSICS	239
Includes aeronomy; upper and lower atmosphere studies; ionospheric and magnetospheric physics; and geomagnetism. For space radiation see <i>93 Space Radiation</i> .	
47 METEOROLOGY AND CLIMATOLOGY	N.A.
Includes weather forecasting and modification.	
48 OCEANOGRAPHY	N.A.
Includes biological, dynamic, and physical oceanography; and marine resources. For related information see also <i>43 Earth Resources and Remote Sensing</i> .	

LIFE SCIENCES

51 LIFE SCIENCES (GENERAL)	240
52 AEROSPACE MEDICINE	N.A.
Includes physiological factors; biological effects of radiation; and effects of weightlessness on man and animals.	
53 BEHAVIORAL SCIENCES	N.A.
Includes psychological factors; individual and group behavior; crew training and evaluation; and psychiatric research.	
54 MAN/SYSTEM TECHNOLOGY AND LIFE SUPPORT	240
Includes human engineering; biotechnology; and space suits and protective clothing. For related information see also <i>16 Space Transportation</i> .	
55 SPACE BIOLOGY	N.A.
Includes exobiology; planetary biology; and extraterrestrial life.	

MATHEMATICAL AND COMPUTER SCIENCES

59 MATHEMATICAL AND COMPUTER SCIENCES (GENERAL)	240
60 COMPUTER OPERATIONS AND HARDWARE	241
Includes hardware for computer graphics, firmware, and data processing. For components see <i>33 Electronics and Electrical Engineering</i> .	
61 COMPUTER PROGRAMMING AND SOFTWARE	241
Includes computer programs, routines, algorithms, and specific applications, e.g., CAD/CAM.	
62 COMPUTER SYSTEMS	245
Includes computer networks and special application computer systems.	

N.A.—no abstracts were assigned to this category for this issue.

63 CYBERNETICS	245
Includes feedback and control theory, artificial intelligence, robotics and expert systems. For related information see also <i>54 Man/System Technology and Life Support</i> .	
64 NUMERICAL ANALYSIS	248
Includes iteration, difference equations, and numerical approximation.	
65 STATISTICS AND PROBABILITY	251
Includes data sampling and smoothing; Monte Carlo method; and stochastic processes.	
66 SYSTEMS ANALYSIS	251
Includes mathematical modeling; network analysis; and operations research.	
67 THEORETICAL MATHEMATICS	251
Includes topology and number theory.	
 PHYSICS For related information see also <i>Engineering</i> .	
70 PHYSICS (GENERAL)	252
For precision time and time interval (PTTI) see <i>35 Instrumentation and Photography</i> ; for geophysics, astrophysics or solar physics see <i>46 Geophysics</i> , <i>90 Astrophysics</i> , or <i>92 Solar Physics</i> .	
71 ACOUSTICS	252
Includes sound generation, transmission, and attenuation. For noise pollution see <i>45 Environment Pollution</i> .	
72 ATOMIC AND MOLECULAR PHYSICS	255
Includes atomic structure, electron properties, and molecular spectra.	
73 NUCLEAR AND HIGH-ENERGY PHYSICS	255
Includes elementary and nuclear particles; and reactor theory. For space radiation see <i>93 Space Radiation</i> .	
74 OPTICS	256
Includes light phenomena and optical devices. For lasers see <i>36 Lasers and Masers</i> .	
75 PLASMA PHYSICS	257
Includes magnetohydrodynamics and plasma fusion. For ionospheric plasmas see <i>46 Geophysics</i> . For space plasmas see <i>90 Astrophysics</i> .	
76 SOLID-STATE PHYSICS	259
Includes superconductivity. For related information see also <i>33 Electronics and Electrical Engineering</i> and <i>36 Lasers and Masers</i> .	
77 THERMODYNAMICS AND STATISTICAL PHYSICS	266
Includes quantum mechanics; theoretical physics; and Bose and Fermi statistics. For related information see also <i>25 Inorganic and Physical Chemistry</i> and <i>34 Fluid Mechanics and Heat Transfer</i> .	
 SOCIAL SCIENCES	
80 SOCIAL SCIENCES (GENERAL)	266
Includes educational matters.	
81 ADMINISTRATION AND MANAGEMENT	267
Includes management planning and research.	
82 DOCUMENTATION AND INFORMATION SCIENCE	267
Includes information management; information storage and retrieval technology; technical writing; graphic arts; and micrography. For computer documentation see <i>61 Computer Programming and Software</i> .	
83 ECONOMICS AND COST ANALYSIS	N.A.
Includes cost effectiveness studies.	
84 LAW, POLITICAL SCIENCE AND SPACE POLICY	N.A.
Includes NASA appropriation hearings; aviation law; space law and policy; international law; international cooperation; and patent policy.	
85 URBAN TECHNOLOGY AND TRANSPORTATION	267
Includes applications of space technology to urban problems; technology transfer; technology assessment; and surface and mass transportation. For related information see <i>03 Air Transportation and Safety</i> , <i>16 Space Transportation</i> , and <i>44 Energy Production and Conversion</i> .	
N.A.—no abstracts were assigned to this category for this issue.	

SPACE SCIENCES For related information see also *Geosciences*.

88 SPACE SCIENCES (GENERAL)	N.A.
89 ASTRONOMY	N.A.
Includes radio, gamma-ray, and infrared astronomy; and astrometry.	
90 ASTROPHYSICS	267
Includes cosmology; celestial mechanics; space plasmas; and interstellar and interplanetary gases and dust. For related information see also <i>75 Plasma Physics</i> .	
91 LUNAR AND PLANETARY EXPLORATION	269
Includes planetology; and manned and unmanned flights. For spacecraft design or space stations see <i>18 Spacecraft Design, Testing and Performance</i> .	
92 SOLAR PHYSICS	270
Includes solar activity, solar flares, solar radiation and sunspots. For related information see <i>93 Space Radiation</i> .	
93 SPACE RADIATION	N.A.
Includes cosmic radiation; and inner and outer Earth's radiation belts. For biological effects of radiation see <i>52 Aerospace Medicine</i> . For theory see <i>73 Nuclear and High-Energy Physics</i> .	

GENERAL

Includes aeronautical, astronomical, and space science related histories, biographies, and pertinent reports too broad for categorization; histories or broad overviews of NASA programs.

99 GENERAL	271
SUBJECT INDEX	A-1
PERSONAL AUTHOR INDEX	B-1
CORPORATE SOURCE INDEX	C-1
CONTRACT NUMBER INDEX	D-1
REPORT/ACCESSION NUMBER INDEX	E-1

N.A.—no abstracts were assigned to this category for this issue.

Bibliography of Lewis Research Center Technical Publications Announced in 1992

01

AERONAUTICS (GENERAL)

N92-10002*# National Aeronautics and Space Administration.
Lewis Research Center, Cleveland, OH.

TECHNICAL EVALUATION REPORT, AGARD FLUID DYNAMICS PANEL SYMPOSIUM ON EFFECTS OF ADVERSE WEATHER ON AERODYNAMICS

J. J. REINMANN Oct. 1991 19 p Meeting held in Toulouse,
France, 29 Apr. - 1 May 1991
(Contract RTOP 505-68-10)
(NASA-TM-105192; E-6460; NAS 1.15:105192) Avail: CASI HC
A03/MF A01

The purpose of the meeting on Effects of Adverse Weather on Aerodynamics was to provide an update of the state-of-the-art with respect to the prediction, simulation, and measurement of the effects of icing, anti-icing fluids, and various precipitation on the aerodynamic characteristics of flight vehicles. Sessions were devoted to introductory and survey papers and icing certification issues, to analytical and experimental simulation of ice frost contamination and its effects of aerodynamics, and to the effects of heavy rain and deicing/anti-icing fluids. Author

N92-17346*# National Aeronautics and Space Administration.
Lewis Research Center, Cleveland, OH.

VISCOUS THREE-DIMENSIONAL CALCULATIONS OF TRANSONIC FAN PERFORMANCE

RODRICK V. CHIMA 1991 19 p Presented at the 77th
Symposium of the Propulsion and Energetics Panel entitled CFD
Techniques for Propulsion Applications, San Antonio, TX, 27-31
May 1991; sponsored by AGARD Original contains color
illustrations
(Contract RTOP 505-62-20)
(NASA-TM-103800; E-6088; NAS 1.15:103800)

A 3-D flow analysis code was used to compute the design speed operating line of a transonic fan rotor, and the results were compared with experimental data. The code is an explicit finite difference code with an algebraic turbulence model. The transonic fan, called rotor 67, was tested experimentally at NASA-Lewis with conventional aerodynamic probes and with user anemometry and was included as one of the AGARD test cases for the computation of internal flows. The experimental data are described. Maps of total pressure ratio and adiabatic efficiency versus mass flow were computed and are compared with the experimental maps, with good agreement. Detailed comparisons between calculations and experiment are made at two operating points, one near peak efficiency and the other near stall. Blade-to-blade contour plots are used to show the shock structure. Comparisons of circumferentially integrated flow quantities downstream of the rotor show spanwise distributions of several aerodynamic parameters. Calculated Mach number distributions are compared with laser anemometer data within the blade row and the wake to quantify the accuracy of the calculations. Particle traces are used to show the nature of secondary flow. Author

N92-22659*# National Aeronautics and Space Administration.
Lewis Research Center, Cleveland, OH.

RESEARCH AND TECHNOLOGY, 1991

1991 169 p
(NASA-TM-105320; E-6677; NAS 1.15:105320) Avail: CASI HC
A08/MF A02

NASA Lewis' research and technology accomplishments are summarized for the fiscal year 1991. Approximately 150 articles are presented which were submitted by the technical directorates. There are six major sections: Aeronautics; Aerospace technology; Space flight systems; Space Station Freedom; Engineering and Computational support; and Lewis Research Academy. A table of contents by subject was developed to assist the reader in finding articles of special interest. For each article, a Lewis contact person is identified, and where possible, a reference document is listed so that additional information can be easily obtained. The diversity of topics attests to the breadth of research and technology being pursued and to the skill mix of the staff that makes it possible. Author

N92-23336*# National Aeronautics and Space Administration.
Lewis Research Center, Cleveland, OH.

CENTER FOR MODELING OF TURBULENCE AND TRANSITION (CMOTT). RESEARCH BRIEFS: 1990

LOUIS A. POVINELLI, comp., MENG-SING LIOU, comp., and
TSAN-HSING SHIH, comp. Oct. 1991 166 p
(Contract NASA ORDER C-99066-6; RTOP 505-62-21)
(NASA-TM-105243; ICOMP-91-17; CMOTT-91-07; E-6570; NAS
1.15:105243) Avail: CASI HC A08/MF A02

Brief progress reports of the Center for Modeling of Turbulence and Transition (CMOTT) research staff from May 1990 to May 1991 are given. The objectives of the CMOTT are to develop, validate, and implement the models for turbulence and boundary layer transition in the practical engineering flows. The flows of interest are three dimensional, incompressible, and compressible flows with chemistry. The schemes being studied include the two-equation and algebraic Reynolds stress models, the full Reynolds stress (or second moment closure) models, the probability density function models, the Renormalization Group Theory (RNG) and Interaction Approximation (DIA), the Large Eddy Simulation (LES) and Direct Numerical Simulation (DNS).

N92-31267*# National Aeronautics and Space Administration.
Lewis Research Center, Cleveland, OH.

PRELIMINARY EVALUATION OF ADHESION STRENGTH MEASUREMENT DEVICES FOR CERAMIC/TITANIUM MATRIX COMPOSITE BONDS

BOBBY POHLCHUCK (Kent State Univ., OH.) and MARY V.
ZELLER Aug. 1992 24 p
(Contract NCC3-189; RTOP 763-22-51)
(NASA-TM-105803; E-7233; NAS 1.15:105803) Avail: CASI HC
A03/MF A01

The adhesive bond between ceramic cement and a titanium matrix composite substrate to be used in the National Aerospace Plane program is evaluated. Two commercially available adhesion testers, the Sebastian Adherence Tester and the CSEM REVETEST Scratch Tester, are evaluated to determine their suitability for quantitatively measuring adhesion strength. Various thicknesses of cements are applied to several substrates, and bond strengths are determined with both testers. The Sebastian Adherence Tester

A
B
S
T
R
A
C
T
S

02 AERODYNAMICS

has provided limited data due to an interference from the sample mounting procedure, and has been shown to be incapable of distinguishing adhesion strength from tensile and shear properties of the cement itself. The data from the scratch tester has been found to be difficult to interpret due to the porosity and hardness of the cement. Recommendations are proposed for a more reliable adhesion test method. Author

02

AERODYNAMICS

Includes aerodynamics of bodies, combinations, wings, rotors, and control surfaces; and internal flow in ducts and turbomachinery.

A92-14407* National Aeronautics and Space Administration. Lewis Research Center, Cleveland, OH.

ONGOING DEVELOPMENT OF A COMPUTER JOBSTREAM TO PREDICT HELICOPTER MAIN ROTOR PERFORMANCE IN ICING CONDITIONS

RANDALL K. BRITTON (NASA, Lewis Research Center, Cleveland; Sverdrup Technology, Inc., Brook Park, OH) IN: AHS, Annual Forum, 47th, Phoenix, AZ, May 6-8, 1991, Proceedings. Vol. 2 1991 8 p refs
(Contract NAS3-25266)
Copyright

Work is currently underway at the NASA Lewis Research Center to develop an analytical method for predicting the performance degradation of a helicopter operating in icing conditions. A brief survey is performed of possibilities available to perform such a calculation along with the reasons for choosing the present approach. A complete description of the proposed jobstream is given as well as a discussion of the present state of the development. Author

A92-15539* National Aeronautics and Space Administration. Lewis Research Center, Cleveland, OH.

A VISCOUS FLOW STUDY OF SHOCK-BOUNDARY LAYER INTERACTION, RADIAL TRANSPORT, AND WAKE DEVELOPMENT IN A TRANSONIC COMPRESSOR

CHUNILL HAH and LONNIE REID (NASA, Lewis Research Center, Cleveland, OH) ASME, International Gas Turbine and Aeroengine Congress and Exposition, 36th, Orlando, FL, June 3-6, 1991. 14 p. Jun. 1991 14 p refs
(ASME PAPER 91-GT-69)

A numerical study based on the 3D Reynolds-averaged Navier-Stokes equation has been conducted to investigate the detailed flow physics inside a transonic compressor. 3D shock structure, shock-boundary layer interaction, flow separation, radial mixing, and wake development are all investigated at design and off-design conditions. Experimental data based on laser anemometer measurements are used to assess the overall quality of the numerical solution. An additional experimental study to investigate end-wall flow with a hot-film was conducted, and these results are compared with the numerical results. Detailed comparison with experimental data indicates that the overall features of the 3D shock structure, the shock-boundary layer interaction, and the wake development are all calculated very well in the numerical solution. The numerical results are further analyzed to examine the radial mixing phenomena in the transonic compressor. A thin sheet of particles is injected in the numerical solution upstream of the compressor. The movement of particles is traced with a 3D plotting package. This numerical survey of tracer concentration reveals the fundamental mechanisms of radial transport in this transonic compressor. Author

A92-15550* National Aeronautics and Space Administration. Lewis Research Center, Cleveland, OH.

THE ROLE OF TIP CLEARANCE IN HIGH-SPEED FAN STALL

J. J. ADAMCZYK (NASA, Lewis Research Center, Cleveland, OH),

M. L. CELESTINA (NASA, Lewis Research Center; Sverdrup Technology, Inc., Cleveland, OH), and E. M. GREITZER (MIT, Cambridge, MA) ASME, International Gas Turbine and Aeroengine Congress and Exposition, 36th, Orlando, FL, June 3-6, 1991. 14 p. Jun. 1991 14 p refs
(Contract NSG-3208)
(ASME PAPER 91-GT-83)

A numerical experiment has been carried out to define the near-stall casing endwall flowfield of a high-speed fan rotor. The experiment used a simulation code incorporating a simple clearance model, whose calibration is presented. The results of the simulation show that the interaction of the tip leakage vortex and the in-passage shock plays a major role in determining the fan flow range. More specifically, the computations imply that it is the area increase of this vortex as it passes through the in-passage shock, which is the source of the blockage associated with stall. In addition, for fans of this type, it is the clearance over the forward portion of the fan blade which controls the flow processes leading to stall. Author

A92-15574* National Aeronautics and Space Administration. Lewis Research Center, Cleveland, OH.

THE EFFECT OF STEADY AERODYNAMIC LOADING ON THE FLUTTER STABILITY OF TURBOMACHINERY BLADING

TODD E. SMITH (NASA, Lewis Research Center, Cleveland; Sverdrup Technology, Inc., Brook Park, OH) and JAIKRISHNAN R. KADAMBI (Case Western Reserve University, Cleveland, OH) ASME, International Gas Turbine and Aeroengine Congress and Exposition, 36th, Orlando, FL, June 3-6, 1991. 9 p. Previously announced in STAR as N91-19479. Jun. 1991 9 p refs
(Contract NAS3-25266)
(ASME PAPER 91-GT-130)

An aeroelastic analysis is presented which accounts for the effect of steady aerodynamic loading on the aeroelastic stability of a cascade of compressor blades. The aeroelastic model is a two degree of freedom model having bending and torsional displacements. A linearized unsteady potential flow theory is used to determine the unsteady aerodynamic response coefficients for the aeroelastic analysis. The steady aerodynamic loading was caused by the addition of airfoil thickness and camber and steady flow incidence. The importance of steady loading on the airfoil unsteady pressure distribution is demonstrated. Additionally, the effect of steady loading on the tuned flutter behavior and flutter boundaries indicates that neglecting either airfoil thickness, camber or incidence could result in nonconservative estimates of flutter behavior. Author

A92-15576* National Aeronautics and Space Administration. Lewis Research Center, Cleveland, OH.

WIND TUNNEL WALL EFFECTS IN A LINEAR OSCILLATING CASCADE

D. H. BUFFUM (NASA, Lewis Research Center, Cleveland, OH) and S. FLEETER (Purdue University, West Lafayette, IN) ASME, International Gas Turbine and Aeroengine Congress and Exposition, 36th, Orlando, FL, June 3-6, 1991. 12 p. Previously announced in STAR as N91-19098. Jun. 1991 12 p refs
(ASME PAPER 91-GT-133)

Experiments in a linear oscillating cascade reveal that the wind tunnel walls enclosing the airfoils have, in some cases, a detrimental effect on the oscillating cascade aerodynamics. In a subsonic flowfield, biconvex airfoils are driven simultaneously in harmonic, torsion-mode oscillations for a range of interblade phase angle values. It is found that the cascade dynamic periodicity - the airfoil to airfoil variation in unsteady surface pressure - is good for some values of interblade phase angle but poor for others. Correlation of the unsteady pressure data with oscillating flat plate cascade predictions is generally good for conditions where the periodicity is good and poor where the periodicity is poor. Calculations based upon linearized unsteady aerodynamic theory indicate that pressure waves reflected from the wind tunnel walls are responsible for the cases where there is poor periodicity and poor correlation with the predictions. Author

A92-15580* Army Aviation Systems Command, Cleveland, OH.
NASA LOW-SPEED CENTRIFUGAL COMPRESSOR FOR 3-D VISCIOUS CODE ASSESSMENT AND FUNDAMENTAL FLOW PHYSICS RESEARCH

M. D. HATHAWAY (U.S. Army, Propulsion Directorate, Cleveland, OH), J. R. WOOD (NASA, Lewis Research Center, Cleveland, OH), and C. A. WASSERBAUER (NASA, Lewis Research Center; Sverdrup Technology, Inc., Cleveland, OH) ASME, International Gas Turbine and Aeroengine Congress and Exposition, 36th, Orlando, FL, June 3-6, 1991. 13 p. Previously announced in STAR as N91-20044. Jun. 1991 13 p refs (ASME PAPER 91-GT-140)

A low speed centrifugal compressor facility recently built by the NASA Lewis Research Center is described. The purpose of this facility is to obtain detailed flow field measurements for computational fluid dynamic code assessment and flow physics modeling in support of Army and NASA efforts to advance small gas turbine engine technology. The facility is heavily instrumented with pressure and temperature probes, both in the stationary and rotating frames of reference, and has provisions for flow visualization and laser velocimetry. The facility will accommodate rotational speeds to 2400 rpm and is rated at pressures to 1.25 atm. The initial compressor stage being tested is geometrically and dynamically representative of modern high-performance centrifugal compressor stages with the exception of Mach number levels. Preliminary experimental investigations of inlet and exit flow uniformly and measurement repeatability are presented. These results demonstrate the high quality of the data which may be expected from this facility. The significance of synergism between computational fluid dynamic analysis and experimentation throughout the development of the low speed centrifugal compressor facility is demonstrated. Author

A92-15623* National Aeronautics and Space Administration. Lewis Research Center, Cleveland, OH.

EULER FLOW PREDICTIONS FOR AN OSCILLATING CASCADE USING A HIGH RESOLUTION WAVE-SPLIT SCHEME

DENNIS L. HUFF (NASA, Lewis Research Center, Cleveland, OH), TIMOTHY W. SWAFFORD (Mississippi State University, Mississippi State), and T. S. R. REDDY (Toledo, University, OH) ASME, International Gas Turbine and Aeroengine Congress and Exposition, 36th, Orlando, FL, June 3-6, 1991. 8 p. Previously announced in STAR as N91-24107. Jun. 1991 8 p refs (ASME PAPER 91-GT-198)

A compressible flow code that can predict the nonlinear unsteady aerodynamic associated with transonic flows over oscillating cascades is developed and validated. The code solves the two dimensional, unsteady Euler equations using a time-marching, flux-difference splitting scheme. The unsteady pressures and forces can be determined for arbitrary input motions, although only harmonic pitching and plunging motions are addressed. The code solves the flow equations on a H-grid which is allowed to deform with the airfoil motion. Predictions are presented for both flat plate cascades and loaded airfoil cascades. Results are compared to flat plate theory and experimental data. Predictions are also presented for several oscillating cascades with strong normal shocks where the pitching amplitudes, cascade geometry and interblade phase angles are varied to investigate nonlinear behavior. Author

A92-15669* National Aeronautics and Space Administration. Lewis Research Center, Cleveland, OH.

THE NUMERICAL SIMULATION OF A HIGH-SPEED AXIAL FLOW COMPRESSOR

RICHARD A. MULAC (NASA, Lewis Research Center; Sverdrup Technology, Inc., Cleveland, OH) and JOHN J. ADAMCZYK (NASA, Lewis Research Center, Cleveland, OH) ASME, International Gas Turbine and Aeroengine Congress and Exposition, 36th, Orlando, FL, June 3-6, 1991. 14 p. Jun. 1991 14 p refs (ASME PAPER 91-GT-272)

The advancement of high-speed axial-flow multistage compressors is impeded by a lack of detailed flow-field information.

Recent development in compressor flow modeling and numerical simulation have the potential to provide needed information in a timely manner. The development of a computer program is described to solve the viscous form of the average-passage equation system for multistage turbomachinery. Programming issues such as in-core versus out-of-core data storage and CPU utilization (parallelization, vectorization, and chaining) are addressed. Code performance is evaluated through the simulation of the first four stages of a five-stage, high-speed, axial-flow compressor. The second part addresses the flow physics which can be obtained from the numerical simulation. In particular, an examination of the endwall flow structure is made, and its impact on blockage distribution assessed. Author

A92-15670* Sverdrup Technology, Inc., Brook Park, OH.
DETERMINISTIC BLADE ROW INTERACTIONS IN A CENTRIFUGAL COMPRESSOR STAGE

K. R. KIRTLEY (Sverdrup Technology, Inc., Brook Park, OH) and T. A. BEACH (NASA, Lewis Research Center, Cleveland, OH) ASME, International Gas Turbine and Aeroengine Congress and Exposition, 36th, Orlando, FL, June 3-6, 1991. 12 p. Jun. 1991 12 p refs (Contract NAS3-25266) (ASME PAPER 91-GT-273)

The three-dimensional viscous flow in a low speed centrifugal compressor stage is simulated using an average passage Navier-Stokes analysis. The impeller discharge flow is of the jet/wake type with low momentum fluid in the shroud-pressure side corner coincident with the tip leakage vortex. This nonuniformity introduces periodic unsteadiness in the vane frame of reference. The effect of such deterministic unsteadiness on the time-mean is included in the analysis through the average passage stress, which allows the analysis of blade row interactions. The magnitude of the divergence of the deterministic unsteady stress is of the order of the divergence of the Reynolds stress over most of the span, from the impeller trailing edge to the vane throat. Although the potential effects on the blade trailing edge from the diffuser vane are small, strong secondary flows generated by the impeller degrade the performance of the diffuser vanes. Author

A92-17178* Sverdrup Technology, Inc., Brook Park, OH.

UNSTEADY BLADE-SURFACE PRESSURES ON A LARGE-SCALE ADVANCED PROPELLER - PREDICTION AND DATA

M. NALLASAMY (Sverdrup Technology, Inc., Brook Park, OH) and J. F. GROENEWEG (NASA, Lewis Research Center, Cleveland, OH) Dec. 1991 7 p refs Copyright

A92-17429* National Aeronautics and Space Administration. Lewis Research Center, Cleveland, OH.

EIGENVALUE CALCULATION PROCEDURE FOR AN EULER/NAVIER-STOKES SOLVER WITH APPLICATION TO FLOWS OVER AIRFOILS

APARAJIT J. MAHAJAN (NASA, Lewis Research Center, Cleveland; Toledo, University, OH; Duke University, Durham, NC), EARL H. DOWELL, and DONALD B. BLISS (Duke University, Durham, NC) Journal of Computational Physics (ISSN 0021-9991), vol. 97, Dec. 1991, p. 398-413. Dec. 1991 16 p refs (Contract NAG3-724) Copyright

A Lanczos procedure is presently applied to a Navier-Stokes (N-S) solver for eigenvalues and eigenvectors associated with the small-perturbation analysis of the N-S equations' finite-difference representation for airfoil flows; the matrix used is very large, sparse, real, and nonsymmetric. The Lanczos procedure is shown to furnish complete spectral information for the eigenvalues, as required for transient-stability analysis of N-S solvers. O.C.

A92-21070* Sverdrup Technology, Inc., Brook Park, OH.

UNSTEADY EULER ANALYSIS OF THE FLOWFIELD OF A PROPFAN AT AN ANGLE OF ATTACK

02 AERODYNAMICS

M. NALLASAMY (Sverdrup Technology, Inc., Brook Park, OH) and J. F. GROENEWEG (NASA, Lewis Research Center, Cleveland, OH) Feb. 1992 8 p refs
Copyright

A92-23762*# National Aeronautics and Space Administration. Lewis Research Center, Cleveland, OH.

AERODYNAMICS OF LOADED CASCADES IN SUBSONIC FLOWS SUBJECT TO UNSTEADY THREE-DIMENSIONAL VORTICAL DISTURBANCES

J. FANG and H. M. ATASSI (Notre Dame, University, IN) AIAA, Aerospace Sciences Meeting and Exhibit, 30th, Reno, NV, Jan. 6-9, 1992. 14 p. Jan. 1992 14 p refs
(Contract NAG3-732)
(AIAA PAPER 92-0146) Copyright

A highly efficient numerical method is developed for three-dimensional, periodic, vortical flows around a cascade of loaded airfoils. The method linearizes Euler's equations about the mean flow of the cascade and thus fully accounts for the effects of distortion of the vortical disturbances as they propagate and interact with the cascade mean flow. The numerical scheme is based on splitting the unsteady velocity into vortical and potential parts. The latter is governed by a non-constant coefficient inhomogeneous convective wave equation. A new and computationally suitable out-flow conditions are derived and avoid the difficulties associated with the singular velocity downstream. Solutions were obtained in the frequency domain by using a body-fitted coordinate system. Results are presented to demonstrate the effects of the out-flow boundary conditions, cascade spacing, mean blade loading and gust upstream conditions on the aerodynamics response and unsteady pressure field of a cascade. Author

A92-23764*# National Aeronautics and Space Administration. Lewis Research Center, Cleveland, OH.

THE BALDWIN-LOMAX MODEL FOR SEPARATED AND WAKE FLOWS USING THE ENTROPY ENVELOPE CONCEPT

J. S. BROCK and W. F. NG (Virginia Polytechnic Institute and State University, Blacksburg) AIAA, Aerospace Sciences Meeting and Exhibit, 30th, Reno, NV, Jan. 6-9, 1992. 10 p. Research supported by NASA. Jan. 1992 10 p refs
(AIAA PAPER 92-0148) Copyright

Implementation of the Baldwin-Lomax algebraic turbulence model is difficult and ambiguous within flows characterized by strong viscous-inviscid interactions and flow separations. A new method of implementation is proposed which uses an entropy envelope concept and is demonstrated to ensure the proper evaluation of modeling parameters. The method is simple, computationally fast, and applicable to both wake and boundary layer flows. The method is general, making it applicable to any turbulence model which requires the automated determination of the proper maxima of a vorticity-based function. The new method is evaluated within two test cases involving strong viscous-inviscid interaction. Author

A92-23767*# National Aeronautics and Space Administration. Lewis Research Center, Cleveland, OH.

A STUDY ON VORTEX FLOW CONTROL OF INLET DISTORTION IN THE RE-ENGINE 727-100 CENTER INLET DUCT USING COMPUTATIONAL FLUID DYNAMICS

BERNHARD H. ANDERSON (NASA, Lewis Research Center, Cleveland, OH), PAO S. HUANG, WILLIAM A. PASCHAL, and ENRICO CAVATORTA (Dee Howard Co., San Antonio, TX) AIAA, Aerospace Sciences Meeting and Exhibit, 30th, Reno, NV, Jan. 6-9, 1992. 12 p. Previously announced in STAR as N92-13998. Jan. 1992 12 p refs
(AIAA PAPER 92-0152) Copyright

Computational fluid dynamics was used to investigate the management of inlet distortion by the introduction of discrete vorticity sources at selected locations in the inlet for the purpose of controlling secondary flow. These sources of vorticity were introduced by means of vortex generators. A series of design observations were made concerning the importance of various

vortex generator design parameters in minimizing engine face circumferential distortion. The study showed that vortex strength, generator scale, and secondary flow field structure have a complicated and interrelated influence on the engine face distortion, over and above the initial geometry and arrangement of the generators. The installed vortex generator performance was found to be a function of three categories of variables: the inflow conditions, the aerodynamic characteristics associated with the inlet duct, and the design parameters related to the geometry, arrangement, and placement of the vortex generators within the outlet duct itself. Author

A92-24653* National Aeronautics and Space Administration. Lewis Research Center, Cleveland, OH.

IMPROVED NONEQUILIBRIUM VISCOUS SHOCK-LAYER SCHEME FOR HYPERSONIC BLUNT-BODY FLOWFIELDS

BILAL A. BHUTTA and CLARK H. LEWIS (VRA, Inc., Blacksburg, VA) Journal of Spacecraft and Rockets (ISSN 0022-4650), vol. 29, Jan.-Feb. 1992, p. 24-34. Feb. 1992 11 p refs
(Contract NAS3-25450)
Copyright

The nonequilibrium viscous shock-layer (VSL) solution scheme is revisited to improve its solution accuracy in the stagnation region and also to minimize and control errors in the conservation of elemental mass. The stagnation-point solution is improved by using a second-order expansion for the normal velocity, and the elemental mass conservation is improved by directly imposing the element conservation equations as solution constraints. These modifications are such that the general structure and computational efficiency of the nonequilibrium VSL scheme is not affected. This revised nonequilibrium VSL scheme is used to study the Mach 20 flow over a 7-deg sphere-cone vehicle under 0- and 20-deg angle-of-attack conditions. Comparisons are made with the corresponding predictions of Navier-Stokes and parabolized Navier-Stokes solution schemes. The results of these tests show that the nonequilibrium blunt-body VSL scheme is indeed an accurate, fast, and extremely efficient means for generating the blunt-body flowfield over spherical nose tips at zero-to-large angles of attack. Author

A92-25676*# National Aeronautics and Space Administration. Lewis Research Center, Cleveland, OH.

LEWICE/E - AN EULER BASED ICE ACCRETION CODE

MARK G. POTAPCZUK (NASA, Lewis Research Center, Cleveland, OH) AIAA, Aerospace Sciences Meeting and Exhibit, 30th, Reno, NV, Jan. 6-9, 1992. 24 p. Previously announced in STAR as N92-14001. Jan. 1992 24 p refs
(AIAA PAPER 92-0037) Copyright

A new version of the LEWICE ice accretion computer code was developed which calculates the ice growth on two dimensional surfaces, incorporating the effects of compressibility through the solution of the Euler equations. The code is modular and contains separate stand-alone program elements that create a grid, calculate the flow field parameters, calculate the droplet trajectory paths, determine the amount of ice growth, and plot results. This code increases the applicability of ice accretion predictions by allowing calculations at higher Mach numbers. The new elements of the code are described. Calculated results are compared to experiment for several cases, including a LEWICE example case and a thin airfoil section at a Mach number of 0.58. Author

A92-25677*# National Aeronautics and Space Administration. Lewis Research Center, Cleveland, OH.

PREDICTION OF ICE ACCRETION ON A SWEEPED NACA 0012 AIRFOIL AND COMPARISONS TO FLIGHT TEST RESULTS

ANDREW L. REEHORST (NASA, Lewis Research Center, Cleveland, OH) AIAA, Aerospace Sciences Meeting and Exhibit, 30th, Reno, NV, Jan. 6-9, 1992. 59 p. Previously announced in STAR as N92-15968. Jan. 1992 59 p refs
(AIAA PAPER 92-0043) Copyright

In the winter of 1989-90, an icing research flight project was conducted to obtain swept wing ice accretion data. Utilizing the NASA Lewis Research Center's DHC-6 DeHavilland Twin Otter

aircraft, research flights were made into known icing conditions in Northeastern Ohio. The icing cloud environment and aircraft flight data were measured and recorded by an onboard data acquisition system. Upon entry into the icing environment, a 24 inch span, 15 inch chord NACA 0012 airfoil was extended from the aircraft and set to the desired sweep angle. After the growth of a well defined ice shape, the airfoil was retracted into the aircraft cabin for ice shape documentation. The ice accretions were recorded by ice tracings and photographs. Ice accretions were mostly of the glaze type and exhibited scalloping. The ice was accreted at sweep angles of 0, 30, and 45 degrees. A 3-D ice accretion prediction code was used to predict ice profiles for five selected flight test runs, which include sweep angle of zero, 30, and 45 degrees. The code's roughness input parameter was adjusted for best agreement. A simple procedure was added to the code to account for 3-D ice scalloping effects. The predicted ice profiles are compared to their respective flight test counterparts. This is the first attempt to predict ice profiles on swept wings with significant scalloped ice formations. Author

A92-25682*# National Aeronautics and Space Administration. Lewis Research Center, Cleveland, OH.

PRESSURE WAVE PROPAGATION STUDIES FOR OSCILLATING CASCADES

DENNIS L. HUFF (NASA, Lewis Research Center, Cleveland, OH) AIAA, Aerospace Sciences Meeting and Exhibit, 30th, Reno, NV, Jan. 6-9, 1992. 20 p. Previously announced in STAR as N92-15977. Jan. 1992 20 p refs (AIAA PAPER 92-0145) Copyright

The unsteady flowfield around an oscillating cascade of flat plates is studied using a time marching Euler code. Exact solutions based on linear theory serve as model problems to study pressure wave propagation in the numerical solution. The importance of using proper unsteady boundary conditions, grid resolution, and time step is demonstrated. Results show that an approximate non-reflecting boundary condition based on linear theory does a good job of minimizing reflections from the inflow and outflow boundaries and allows the placement of the boundaries to be closer than cases using reflective boundary conditions. Stretching the boundary to dampen the unsteady waves is another way to minimize reflections. Grid clustering near the plates does a better job of capturing the unsteady flowfield than cases using uniform grids as long as the CFL number is less than one for a sufficient portion of the grid. Results for various stagger angles and oscillation frequencies show good agreement with linear theory as long as the grid is properly resolved. Author

A92-25728*# National Aeronautics and Space Administration. Lewis Research Center, Cleveland, OH.

ANALYSIS OF AN ADVANCED DUCTED PROPELLER SUBSONIC INLET

CHANTHY IEK, DONALD R. BOLDMAN (NASA, Lewis Research Center, Cleveland, OH), and MOUNIR IBRAHIM (Cleveland State University, OH) AIAA, Aerospace Sciences Meeting and Exhibit, 30th, Reno, NV, Jan. 6-9, 1992. 17 p. Previously announced in STAR as N92-14002. Jan. 1992 17 p refs (AIAA PAPER 92-0274) Copyright

It is shown that a time marching Navier-Stokes code called PARC can be utilized to provide a reasonable prediction of the flow field within an inlet for an advanced ducted propeller. The code validation was implemented for a nonseparated flow condition associated with the inlet functioning at angles-of-attack of zero and 25 deg. Comparison of the computational results with the test data shows that the PARC code with the propeller face fixed flow properties boundary conditions (BC) provided a better prediction of the inlet surface static pressures than the prediction when the mass flow BC was employed. R.E.P.

A92-25731*# National Aeronautics and Space Administration. Lewis Research Center, Cleveland, OH.

UNSTEADY WING SURFACE PRESSURES IN THE WAKE OF A PROPELLER

R. T. JOHNSTON and J. P. SULLIVAN (Purdue University, West

Lafayette, IN) AIAA, Aerospace Sciences Meeting and Exhibit, 30th, Reno, NV, Jan. 6-9, 1992. 12 p. Research supported by NASA. Jan. 1992 12 p refs (AIAA PAPER 92-0277) Copyright

The unsteady nature of the propeller slipstream interacting with a wing has been studied by flow visualization and unsteady wing surface pressure measurements. Flow visualization was performed by marking the propeller tip vortex with smoke. Unsteady wing surface pressures were measured by traversing a wing instrumented with a chordwise array of 16 microphones in a spanwise direction through the propeller wake. This work yielded information on the motion of the propeller wake as it passes over the wing. As the propeller wake passed over the wing: the propeller tip vortex experienced an inviscid interaction at the leading edge; viscous action at the leading edge severed the propeller tip vortex; the propeller tip vortex experienced significant spanwise and chordwise displacements and then deformed in order to reconnect at the trailing edge; axial velocity in the vortex core caused the helical vortex to thicken or stretch near the wing surface; and, the magnitude of the pressure fluctuations decreased in magnitude with distance traveled along the chord. Author

A92-26264*# National Aeronautics and Space Administration. Lewis Research Center, Cleveland, OH.

NUMERICAL INVESTIGATION OF PERFORMANCE DEGRADATION OF WINGS AND ROTORS DUE TO ICING

OH J. KWON and LAKSHMI N. SANKAR (Georgia Institute of Technology, Atlanta) AIAA, Aerospace Sciences Meeting and Exhibit, 30th, Reno, NV, Jan. 6-9, 1992. 14 p. Jan. 1992 14 p refs

(Contract NAG3-768)

(AIAA PAPER 92-0412) Copyright

The aerodynamic load characteristics and the performance degradation of moderate aspect ratio wings and rotors with simulated glaze leading-edge ice have been studied using a three-dimensional, compressible Navier-Stokes solver. The effect of a splitter plate at the wing root on both clean and iced wing configurations has been studied and the results are compared with the experiment. A significant difference has been observed with and without splitter plates in the magnitude of flow separation and aerodynamic loading at the inboard stations for the iced wing at 8-deg angle of attack. Inviscid calculations were performed and compared with viscous calculations to investigate whether the performance of iced swept wings can be inexpensively predicted using Euler methods. It is shown that inviscid calculations predict higher aerodynamic loading than viscous calculations, and cannot model separation effects. A typical nonlifting helicopter rotor in forward flight condition is also studied, and the penalty due to the leading-edge ice formation on the required torque is numerically demonstrated. Author

A92-26265*# National Aeronautics and Space Administration. Lewis Research Center, Cleveland, OH.

FINITE WING AERODYNAMICS WITH SIMULATED GLAZE ICE

A. KHODADOUST, M. B. BRAGG, M. KERHO, S. WELLS, and M. R. SOLTANI (Illinois, University, Urbana) AIAA, Aerospace Sciences Meeting and Exhibit, 30th, Reno, NV, Jan. 6-9, 1992. 18 p. Research supported by NASA. Jan. 1992 18 p refs (AIAA PAPER 92-0414) Copyright

The effect of a simulated glaze ice accretion on the aerodynamic performance of a three-dimensional wing is studied experimentally. The model used for these tests was a semi-span wing of effective aspect ratio five, mounted from the sidewall of the UIUC subsonic wind tunnel. The model has an NACA 0012 airfoil section on a rectangular, untwisted planform with interchangeable leading edges to allow for testing both the baseline and the iced wing geometry. A three-component sidewall balance was used to measure lift, drag and pitching moment on the clean and iced model. A four-beam two-color fiberoptic laser Doppler velocimeter (LDV) was used to map the flowfield along several spanwise cuts on the model. Preliminary results from LDV scans, which will be the bulk of this paper, are presented following the force balance

02 AERODYNAMICS

measurement results. Initial comparison of LDV surveys compare favorably with inviscid theory results and 2D split hot-film measurements near the model surface. Author

A92-26266*# National Aeronautics and Space Administration. Lewis Research Center, Cleveland, OH.

AUTOMATIC GRID GENERATION FOR ICED AIRFOIL FLOWFIELD PREDICTIONS

STEVEN C. CARUSO and MOHAMMAD FARSHCHI (Nielsen Engineering and Research, Inc., Mountain View, CA) AIAA, Aerospace Sciences Meeting and Exhibit, 30th, Reno, NV, Jan. 6-9, 1992. 13 p. Jan. 1992 13 p refs (Contract NAS3-26059) (AIAA PAPER 92-0415) Copyright

This paper describes a flowfield mesh generation procedure which has been developed specifically for dealing with geometrically complex and time-dependent leading edge ice accretions on airfoils. The method produces an unstructured mesh using an automatic node point generation scheme that requires minimal user input. Flowfield predictions are obtained by solving the Navier-Stokes equations on an unstructured, triangular mesh. Laminar and turbulent flowfield calculations are presented which demonstrate the new method's ability to produce suitable meshes for such computations. Author

A92-26267*# National Aeronautics and Space Administration. Lewis Research Center, Cleveland, OH.

A TURBULENCE MODEL FOR ICED AIRFOILS AND ITS VALIDATION

JAIWON SHIN (NASA, Lewis Research Center, Cleveland, OH), HSUN H. CHEN, and TUNCER CEBECI (California State University, Long Beach) AIAA, Aerospace Sciences Meeting and Exhibit, 30th, Reno, NV, Jan. 6-9, 1992. 16 p. Previously announced in STAR as N92-15052. Jan. 1992 16 p refs (AIAA PAPER 92-0417) Copyright

A turbulence model based on the extension of the algebraic eddy viscosity formulation of Cebeci and Smith developed for two-dimensional flows over smooth and rough surfaces is described for iced airfoils and validated for computed ice shapes obtained for a range of total temperatures varying from 28 to -15 F. The validation is made with an interactive boundary layer method which uses a panel method to compute the inviscid flow and an inverse finite difference boundary layer method to compute the viscous flow. The interaction between inviscid and viscous flows is established by the use of the Hilbert integral. The calculated drag coefficients compare well with recent experimental data taken at the NASA-Lewis Icing Research Tunnel (IRT) and show that, in general, the drag increase due to ice accretion can be predicted well and efficiently. Author

A92-26932*# National Aeronautics and Space Administration. Lewis Research Center, Cleveland, OH.

SCREECH NOISE SOURCE STRUCTURE OF A SUPERSONIC RECTANGULAR JET

E. J. RICE (NASA, Lewis Research Center, Cleveland, OH) and R. TAGHAVI (NASA, Lewis Research Center, Cleveland; Sverdrup Technology, Inc., Brook Park, OH) AIAA, Aerospace Sciences Meeting and Exhibit, 30th, Reno, NV, Jan. 6-9, 1992. 15 p. Previously announced in STAR as N92-14000. Jan. 1992 15 p refs (Contract NAS3-25266) (AIAA PAPER 92-0503) Copyright

The near-field of the screech noise source structure of an under-expanded supersonic rectangular jet was studied in detail. A miniature probe microphone was used along with a reference microphone to determine the amplitude and phase of the sound pressure near and in the high speed flow field. The transverse structure of the unsteady pressure field was investigated by moving the probe microphone sufficiently far into the jet so that pressure fall-off was observed. Five islands of high sound pressure level have been distinguished which may be associated with the actual local sources of sound production. These sources of screech noise are closely associated with the jet shock structure as would be

expected, with the peak region of noise level being found slightly downstream of each of the five observed shocks. The third and fourth noise sources have the highest levels and are about equal in strength. All of the apparent noise sources have their peak levels in the subsonic flow region. Strong cancellations in the acoustic field are observed in the downstream and sideline directions which may account for the predominant upstream propagation of the fundamental tone noise. Author

A92-26946*# National Aeronautics and Space Administration. Lewis Research Center, Cleveland, OH.

UNSTEADY FLOWFIELD SIMULATION OF DUCTED PROP-FAN CONFIGURATIONS

J. M. JANUS, HOWARD Z. HORSTMAN, and DAVID L. WHITFIELD (Mississippi State University, Mississippi State) AIAA, Aerospace Sciences Meeting and Exhibit, 30th, Reno, NV, Jan. 6-9, 1992. 19 p. Jan. 1992 19 p refs (Contract NAG3-767) (AIAA PAPER 92-0521) Copyright

A technique for the simulation of unsteady flows in and around complex rotating machinery is presented. Additional domain decomposition mechanisms are introduced which extend the range of applicability of software developed for the time-accurate simulation of rotating machinery flowfields. The flow models use the unsteady 3D Euler equations, discretized as a finite-volume method, utilizing a high-resolution approximate Riemann solver for cell interface flux definitions. Multiblock domain decomposition is used to partition the field radially, axially, as well as circumferentially into an ordered arrangement of blocks which exhibit varying degrees of similarity. A general high-order numerical scheme is applied to satisfy the geometric conservation law. Two configurations are presented - ducted single rotation prop-fan and a rotor-deswirl vane combination which form a single stage fan. Comparisons are made to other numerical solutions for these geometries and to available experimental data. C.A.B.

A92-26947*# National Aeronautics and Space Administration. Lewis Research Center, Cleveland, OH.

AN UNSTEADY EULER SCHEME FOR THE ANALYSIS OF DUCTED PROPELLERS

R. SRIVASTAVA (NASA, Lewis Research Center, Cleveland; Toledo, University, OH) AIAA, Aerospace Sciences Meeting and Exhibit, 30th, Reno, NV, Jan. 6-9, 1992. 8 p. Jan. 1992 8 p refs (Contract NAG3-730)

(AIAA PAPER 92-0522) Copyright

An efficient unsteady solution procedure has been developed for analyzing inviscid unsteady flow past ducted propeller configurations. This scheme is first order accurate in time and second order accurate in space. The solution procedure has been applied to a ducted propeller consisting of an 8-bladed SR7 propeller with a duct of NACA 0003 airfoil cross section around it, operating in a steady axisymmetric flowfield. The variation of elemental blade loading with radius, compares well with other published numerical results. Author

A92-27014# National Aeronautics and Space Administration. Ames Research Center, Moffett Field, CA.

CROSSING SHOCK WAVE TURBULENT BOUNDARY LAYER INTERACTIONS - VARIABLE ANGLE AND SHOCK GENERATOR LENGTH GEOMETRY EFFECTS AT MACH 3

S. M. BOGDONOFF and W. L. STOKES (Princeton University, NJ) AIAA, Aerospace Sciences Meeting and Exhibit, 30th, Reno, NV, Jan. 6-9, 1992. 21 p. Research supported by USAF. Jan. 1992 21 p refs (Contract NAG2-718) (AIAA PAPER 92-0636) Copyright

By comparing the detailed wall static pressure distributions for 9 inch and 11 inch long fins generating a crossing shock configuration at $M = 2.93$, the high resolution results of the 9 inch fins are shown to be free of exit effects. Analysis of the static pressure profiles have delineated the limited regions where the single fin results are valid. The characteristics of the complex

interaction, with varying shock wave strength, have been described. The data provide a critical test for computational fluid dynamics which, in its initial phase, has performed poorly in predicting the measured wall static pressure distributions. Author

A92-27021*# National Aeronautics and Space Administration. Lewis Research Center, Cleveland, OH.

RESULTS OF AN ICING TEST ON A NACA 0012 AIRFOIL IN THE NASA LEWIS ICING RESEARCH TUNNEL

JAIWON SHIN and THOMAS H. BOND (NASA, Lewis Research Center, Cleveland, OH) AIAA, Aerospace Sciences Meeting and Exhibit, 30th, Reno, NV, Jan. 6-9, 1992. 20 p. Previously announced in STAR as N92-15051. Jan. 1992 20 p refs (AIAA PAPER 92-0647) Copyright

Tests were conducted in the Icing Research Tunnel (IRT) at the NASA Lewis Research Center to document the current capability of the IRT, focused mainly on the repeatability of the ice shape over a range of icing conditions. Measurements of drag increase due to the ice accretion were also made to document the repeatability of drag. Surface temperatures of the model were obtained to show the effects of latent-heat release by the freezing droplets and heat transfer through the ice layer. The repeatability of the ice shape was very good at low temperatures, but only fair at near freezing temperatures. In general, drag data shows good repeatability. Author

A92-28043* National Aeronautics and Space Administration. Lewis Research Center, Cleveland, OH.

TRANSIENT BEHAVIOR OF SUPERSONIC FLOW THROUGH INLETS

H. S. PORDAL, P. K. KHOSLA, and S. G. RUBIN (Cincinnati, University, OH) Mar. 1992 7 p refs (Contract NAG3-1178; AF-AFOSR-90-0096) Copyright

A92-28186*# National Aeronautics and Space Administration. Lewis Research Center, Cleveland, OH.

UNSTEADY AERODYNAMIC INTERACTION EFFECTS ON TURBOMACHINERY BLADE LIFE AND PERFORMANCE

JOHN J. ADAMCZYK (NASA, Lewis Research Center, Cleveland, OH) AIAA, Aerospace Sciences Meeting and Exhibit, 30th, Reno, NV, Jan. 6-9, 1992. 21 p. Jan. 1992 21 p refs (AIAA PAPER 92-0149) Copyright

This paper is an attempt to address the impact of a class of unsteady flows on the life and performance of turbomachinery blading. These class of flows to be investigated are those whose characteristic frequency is an integral multiple of rotor shaft speed. Analysis of data recorded downstream of a compressor and turbine rotor will reveal that this class of flows can be highly three-dimensional and may lead to the generation of secondary flows within downstream blading. By explicitly accounting for these unsteady flows in the design of turbomachinery blading for multistage applications, it may be possible to bring about gains in performance and blade life. Author

A92-28192*# National Aeronautics and Space Administration. Lewis Research Center, Cleveland, OH.

HELIUM BUBBLE FLOW VISUALIZATION OF THE SPANWISE SEPARATION ON A NACA 0012 WITH SIMULATED GLAZE ICE

M. KERHO, M. BRAGG (Illinois, University, Urbana), and J. SHIN (NASA, Lewis Research Center, Cleveland, OH) AIAA, Aerospace Sciences Meeting and Exhibit, 30th, Reno, NV, Jan. 6-9, 1992. 16 p. Jan. 1992 16 p refs (Contract NAG3-1134) (AIAA PAPER 92-0413) Copyright

Research has been performed to experimentally visualize and document the flow separation due to simulated glaze ice accretion on a NACA 0012 semispan with 30-deg sweep using helium bubbles as flow tracers. Results are compared to Navier-Stokes computational simulations for different angles of attack. Prior to acquiring data for the semispan model, a two-dimensional

experiment was conducted to determine the accuracy of using the helium bubbles as flow tracers. Results from the 3D experiment compare well to the computational simulations. Author

A92-28193*# National Aeronautics and Space Administration. Lewis Research Center, Cleveland, OH.

NUMERICAL EXPERIMENTS ON A NEW CLASS OF NONOSCILLATORY SCHEMES

AMBADY SURESH (NASA, Lewis Research Center; Sverdrup Technology, Inc., Cleveland, OH) and HUNG T. HUYNH (NASA, Lewis Research Center, Cleveland, OH) AIAA, Aerospace Sciences Meeting and Exhibit, 30th, Reno, NV, Jan. 6-9, 1992. 10 p. Jan. 1992 10 p refs (Contract NAS3-25266) (AIAA PAPER 92-0421) Copyright

Numerical experiments for the SONIC schemes on 2D inviscid, compressible, steady, and unsteady problems are presented. These schemes belong to a new class of uniformly second-order accurate nonoscillatory schemes introduced by Huynh, with the well known UNO2 scheme of Harten and Osher being the most 'diffusive' in this class. The SONIC schemes can also be considered as uniformly second order accurate extensions of the popular TVD schemes. For simplicity, a MUSCL approach for spatial discretization and a Runge-Kutta method for time integration are used. Test problems include steady oblique shock reflection and the well known unsteady double Mach reflection problem. Results confirm that the SONIC schemes are more accurate than their TVD counterparts. Author

A92-28194*# National Aeronautics and Space Administration. Lewis Research Center, Cleveland, OH.

AEROELASTIC ANALYSIS OF ADVANCED PROPELLERS USING AN EFFICIENT EULER SOLVER

R. SRIVASTAVA (NASA, Lewis Research Center, Cleveland; Toledo, University, OH), T. S. R. REDDY (Toledo, University, OH), and O. MEHMED (NASA, Lewis Research Center, Cleveland, OH) AIAA, Aerospace Sciences Meeting and Exhibit, 30th, Reno, NV, Jan. 6-9, 1992. 14 p. Jan. 1992 14 p refs (Contract NAG3-730) (AIAA PAPER 92-0488)

A 3D Euler solver is coupled with a 3D structural dynamics model to investigate flutter of propfans. A hybrid scheme is used to reduce computational time for the Euler equations and a normal mode analysis is used for flutter calculations. Experimental and calculated flutter results are compared for an advanced propeller propfan which experienced flutter at transonic tip relative velocities. The predicted flutter calculations are in close agreement with the experimental data. A structural damping value of 0.5 percent was required to predict the behavior observed in the experiment. Computations show that the flutter behavior is dominated by the second mode, but coupling with the first mode is required. The addition of other modes to the calculations did not affect the flutter behavior. Author

A92-28204*# National Aeronautics and Space Administration. Lewis Research Center, Cleveland, OH.

THE STRUCTURE AND DEVELOPMENT OF STREAMWISE VORTEX ARRAYS EMBEDDED IN A TURBULENT BOUNDARY LAYER

BRUCE J. WENDT, ISAAC GREBER (Case Western Reserve University, Cleveland, OH), and WARREN R. HINGST (NASA, Lewis Research Center, Cleveland, OH) AIAA, Aerospace Sciences Meeting and Exhibit, 30th, Reno, NV, Jan. 6-9, 1992. 21 p. Jan. 1992 21 p refs (Contract NAG3-520) (AIAA PAPER 92-0551) Copyright

The results of an experimental investigation of the structure and development of streamwise vortices embedded in a turbulent boundary layer are presented. Measurements of secondary velocity in the crossplane are used to characterize the vortex array structure. Measurements in the crossplane at two streamwise locations characterize the influence of interactions among the vortices on the array structure when the initial spacing between vortices is

02 AERODYNAMICS

varied. Evidence of the merging of counter-rotating cores is found in embedded arrays of closely spaced vortices. A model of vortex interaction and development is constructed from the experimental results. This model is based on the structure of the two dimensional Ossen vortex. The decay of vortex circulation due to the merging of the cores is correlated with the crossplane gradient in streamwise vorticity occurring between an embedded vortex and its adjacent counter-rotating neighbors. Author

A92-28215*# National Aeronautics and Space Administration. Lewis Research Center, Cleveland, OH.

COMPARISON OF TWO-DIMENSIONAL AND THREE-DIMENSIONAL DROPLET TRAJECTORY CALCULATIONS IN THE VICINITY OF FINITE WINGS

STANLEY R. MOHLER, JR. (NASA, Lewis Research Center, Cleveland; Sverdrup Technology, Inc., Brook Park, OH) and COLIN S. BIDWELL (NASA, Lewis Research Center, Cleveland, OH) AIAA, Aerospace Sciences Meeting and Exhibit, 30th, Reno, NV, Jan. 6-9, 1992. 33 p. Jan. 1992 33 p refs (AIAA PAPER 92-0645) Copyright

Computational predictions of ice accretion on flying aircraft most commonly rely on modeling in 2D. These 2D methods treat an aircraft geometry either as wing-like with infinite span, or as an axisymmetric body. Recently, fully 3D methods have been introduced that model an aircraft's true 3D shape. Because 3D methods are more computationally expensive than 2D methods, 2D methods continue to be widely used. However, a 3D method allows investigation of whether it is valid to continue applying 2D methods to a finite wing. The extent of disagreement between LEWICE, a 2D method, and LEWICE3D, a 3D method, in calculating local collection efficiencies at the leading edge of finite wings is investigated. Author

A92-28523* National Aeronautics and Space Administration. Lewis Research Center, Cleveland, OH.

NAVIER-STOKES SOLUTION OF TRANSONIC CASCADE FLOWS USING NONPERIODIC C-TYPE GRIDS

ANDREA ARNONE (Firenze, Universita, Florence, Italy), MENG-SING LIU, and LOUIS A. POVINELLI (NASA, Lewis Research Center, Cleveland, OH) Journal of Propulsion and Power (ISSN 0748-4658), vol. 8, Mar.-Apr. 1992, p. 410-417. Previously announced in STAR as N91-11192. Apr. 1992 8 p refs

Copyright

A new kind of C-type grid is proposed, this grid is non-periodic on the wake and allows minimum skewness for cascades with high turning and large camber. Reynolds-averaged Navier-Stokes equations are solved on this type of grid using a finite volume discretization and a full multigrid method which uses Runge-Kutta stepping as the driving scheme. The Baldwin-Lomax eddy-viscosity model is used for turbulence closure. A detailed numerical study is proposed for a highly loaded transonic blade. A grid independence analysis is presented in terms of pressure distribution, exit flow angles, and loss coefficient. Comparison with experiments clearly demonstrates the capability of the proposed procedure. Author

A92-28526* National Aeronautics and Space Administration. Lewis Research Center, Cleveland, OH.

THREE-DIMENSIONAL VISCOUS ANALYSIS OF A MACH 5 INLET AND COMPARISON WITH EXPERIMENTAL DATA

D. R. REDDY (NASA, Lewis Research Center, Cleveland; Sverdrup Technology, Inc., Brook Park, OH) and L. J. WEIR (NASA, Lewis Research Center, Cleveland, OH) Apr. 1992 9 p refs (Contract NAS3-25266)

Copyright

A92-29972*# National Aeronautics and Space Administration. Lewis Research Center, Cleveland, OH.

ANALYSIS OF ICED WINGS

TUNCER CEBECI, H. H. CHEN, K. KAUPS, S. SCHIMKE (California State University, Long Beach), and JAIWON SHIN (NASA, Lewis Research Center, Cleveland, OH) AIAA, Aerospace Sciences

Meeting and Exhibit, 30th, Reno, NV, Jan. 6-9, 1992. 13 p. Jan. 1992 13 p refs (AIAA PAPER 92-0416) Copyright

A method for computing ice shapes along the leading edge of a wing and a method for predicting its aerodynamic performance degradation due to icing is described. Ice shapes are computed using an extension of the LEWICE code which was developed for airfoils. The aerodynamic properties of the iced wing are determined with an interactive scheme in which the solutions of the inviscid flow equations are obtained from a panel method and the solutions of the viscous flow equations are obtained from an inverse three-dimensional finite-difference boundary-layer method. A new interaction law is used to couple the inviscid and viscous flow solutions. The application of the LEWICE wing code to the calculation of ice shapes on a MS-317 swept wing show good agreement with measurements. The interactive boundary layer method is applied to a tapered iced wing in order to study the effect of icing on the aerodynamic properties of the wing at several angles of attack. Author

A92-31679*# National Aeronautics and Space Administration. Lewis Research Center, Cleveland, OH.

AN IMPROVED PNS SCHEME FOR PREDICTING COMPLEX THREE-DIMENSIONAL HYPERSONIC FLOWS

BILAL A. BHUTTA and CLARK H. LEWIS (VRA, Inc., Blacksburg, VA) AIAA, Aerospace Sciences Meeting and Exhibit, 30th, Reno, NV, Jan. 6-9, 1992. 25 p. Jan. 1992 25 p refs (Contract NAS3-25450) (AIAA PAPER 92-0753) Copyright

Upwinding is incorporated into a numerical technique for predicting hypersonic viscous flows over lifting configurations at moderate angles of attack. A general real-gas flux-vector-splitting technique based on Van Leer's (1982) approach is employed to model upwinding, and three techniques are examined for flux-vector differencing. The three methods are evaluated by applying them to an axisymmetric configuration with a 10-deg afterbody flare. The results indicate that an oscillation-free shock front can be described by using first-order full upwinding across the embedded shock and central-differencing for the other zones. This combined approach is found to be highly convergent for the near-wall region, and its performance is examined for predicting a Mach 15 flow over a finned missile. Attention is given to the effects of gas chemistry which can significantly affect the flows over the missile configurations. C.C.S.

A92-33320*# National Aeronautics and Space Administration. Lewis Research Center, Cleveland, OH.

DESIGN AND ANALYSIS OF REENGINE BOEING 727-100 CENTER INLET S DUCT BY A REDUCED NAVIER-STOKES CODE

PAO S. HUANG, ANTONIO PICCOLO, WILLIAM PASCHAL (Dee Howard Co., San Antonio, TX), and BERNHARD H. ANDERSON (NASA, Lewis Research Center, Cleveland, OH) AIAA, Aerospace Design Conference, Irvine, CA, Feb. 3-6, 1992. 8 p. Feb. 1992 8 p refs (AIAA PAPER 92-1221) Copyright

This paper describes the application of a three-dimensional reduced Navier-Stokes code to perform design and analysis of the reengine Boeing 727-100 center engine inlet S duct. This computer code is shown to be cost effective, accurate and easy to use to design the optimal S duct geometries, predict its aerodynamic performance and provide the detailed flowfield information. Author

A92-34499# National Aeronautics and Space Administration. Ames Research Center, Moffett Field, CA.

UNSTEADY TRANSONIC EULER SOLUTIONS USING FINITE ELEMENTS

GARY A. DAVIS and ODDVAR O. BENDIKSEN (California, University, Los Angeles) IN: AIAA/ASME/ASCE/AHS/ASC Structures, Structural Dynamics and Materials Conference, 33rd, Dallas, TX, Apr. 13-15, 1992, Technical Papers. Pt. 4 1992

11 p refs

(Contract NCC2-374; NAS3-25574)

(AIAA PAPER 92-2504) Copyright

A finite element solution of the unsteady Euler equations is presented and demonstrated for 2D airfoil configurations oscillating in transonic flows. Computations are performed by spatially discretizing the conservation equations using the Galerkin weighted residual method and then employing a multistage Runge-Kutta scheme to march forward in time. A mesh deformation scheme has been developed to efficiently move interior points in a smooth fashion as the airfoil undergoes rigid body pitch and plunge motion. Both steady and unsteady results are presented, and a comparison is made with solutions obtained using finite-volume techniques. The effects of using either a lumped or consistent mass matrix are presented; the finite element method provides an accurate solution for unsteady transonic flows about isolated airfoils.

Author

A92-35689*# National Aeronautics and Space Administration. Lewis Research Center, Cleveland, OH.

FINITE ELEMENT EULER CALCULATIONS OF UNSTEADY TRANSONIC CASCADE FLOWS

CHINGTENG HSIAO and ODDVAR O. BENDIKSEN (California, University, Los Angeles) IN: AIAA Dynamics Specialists Conference, Dallas, TX, Apr. 16, 17, 1992, Technical Papers 1992 12 p refs

(Contract NAS3-25574)

(AIAA PAPER 92-2120) Copyright

A Galerkin finite element procedure incorporating an explicit Runge-Kutta time-stepping scheme has been developed in this work to solve unsteady transonic flow in cascades. The computational domain is discretized by a globally unstructured but locally structured blade-fitted deformable mesh. The Galerkin approximation is applied to the unsteady Euler equations based on a mixed Eulerian-Lagrangian description. The semi-discretized equations are integrated forward in time using a multistage Runge-Kutta scheme. An artificial dissipation operator of the type proposed by Jameson is adapted in the current scheme to capture shocks and suppress nonphysical oscillations. Phase-shifted boundary conditions are used to reduce the computational domain to a single reference passage. Results for both steady and unsteady transonic flows through cascades are presented and compared to existing finite volume solutions.

Author

A92-40105* National Aeronautics and Space Administration. Lewis Research Center, Cleveland, OH.

A STUDY OF THREE DIMENSIONAL TURBULENT BOUNDARY LAYER SEPARATION AND VORTEX FLOW CONTROL USING THE REDUCED NAVIER STOKES EQUATIONS

BERNHARD H. ANDERSON (NASA, Lewis Research Center, Cleveland, OH) and SAEED FAROKHI (Kansas, University, Lawrence) IN: Symposium on Turbulent Shear Flows, 8th, Munich, Federal Republic of Germany, Sept. 9-11, 1991, Proceedings. Vol. 1 1991 6 p refs

A reduced Navier-Stokes (RNS) initial value space marching solution technique was applied to vortex generator and separated flow problems and demonstrated good predictions of the engine face flow field. This RNS solution technique using FLARE approximations can adequately describe the topological and topographical structure flow separation associated with vortex liftoff, and this conclusion led to the concept of a subclass of separations which can be called vorticity separations: separations dominated by the transport of vorticity. Adequate near wall resolution of vorticity separations appears necessary for good predictions of these flows.

Author

A92-41261* National Aeronautics and Space Administration. Lewis Research Center, Cleveland, OH.

DOMAIN-DECOMPOSITION ALGORITHM APPLIED TO MULTIELEMENT AIRFOIL GRIDS

MARK E. M. STEWART (NASA, Lewis Research Center, Cleveland, OH; Princeton University, NJ) Jun. 1992 5 p refs

Copyright

A92-41265* National Aeronautics and Space Administration. Lewis Research Center, Cleveland, OH.

MODERN DEVELOPMENTS IN SHEAR FLOW CONTROL WITH SWIRL

S. FAROKHI, R. TAGHAVI (Kansas, University, Lawrence), and E. J. RICE (NASA, Lewis Research Center, Cleveland, OH) (ICAS, Congress, 17th, Stockholm, Sweden, Sept. 9-14, 1990, Proceedings. Vol. 2, p. 2111-2122) AIAA Journal (ISSN 0001-1452), vol. 30, no. 6, June 1992, p. 1482, 1483. Abridged. Previously cited in issue 09, p. 1311, Accession no. A91-24519. Jun. 1992 2 p refs

Copyright

A92-41267* National Aeronautics and Space Administration. Lewis Research Center, Cleveland, OH.

EFFECT OF ACOUSTIC EXCITATION ON STALLED FLOWS OVER AN AIRFOIL

K. B. M. Q. ZAMAN (NASA, Lewis Research Center, Cleveland, OH) Jun. 1992 8 p refs

Copyright

A92-41268* National Aeronautics and Space Administration. Lewis Research Center, Cleveland, OH.

RENORMALIZATION GROUP BASED ALGEBRAIC TURBULENCE MODEL FOR THREE-DIMENSIONAL TURBOMACHINERY FLOWS

K. R. KIRTLEY (Sverdrup Technology, Inc., Brook Park, OH) Jun. 1992 7 p refs

(Contract NAS3-25266)

A92-44513* National Aeronautics and Space Administration. Lewis Research Center, Cleveland, OH.

NUMERICAL ANALYSIS OF FLOW THROUGH OSCILLATING CASCADE SECTIONS

DENNIS L. HUFF (NASA, Lewis Research Center, Cleveland, OH) Aug. 1992 8 p refs

A92-45494*# National Aeronautics and Space Administration. Lewis Research Center, Cleveland, OH.

EXPERIMENTAL INVESTIGATION OF THE FLOWFIELD OF AN OSCILLATING AIRFOIL

J. PANDA and K. B. M. Q. ZAMAN (NASA, Lewis Research Center, Cleveland, OH) IN: AIAA Applied Aerodynamics Conference, 10th, Palo Alto, CA, June 22-24, 1992, Technical Papers. Pt. 1 1992 18 p refs

(AIAA PAPER 92-2622) Copyright

The flow field of an airfoil oscillated periodically over a wide range of reduced frequencies, 0 less than k less than 1.6, is studied experimentally at chord Reynolds numbers of $R_{sub c} = 22,000$ and $44,000$. The NACA0012 airfoil is pitched sinusoidally about one quarter chord between α of 5 deg and 25 deg. Detailed flow visualization and phase averaged vorticity measurements are carried out for $k = 0.2$ to document the evolution and the shedding of the dynamic stall vortex (DSV). In addition to the DSV, an intense vortex of opposite sign originates from the trailing edge just when the DSV is shed. After being shed into the wake, the two together take the shape of a large 'mushroom' while being convected away from the airfoil. The unsteady circulation around the airfoil and, therefore, the time varying component of the lift is estimated in a novel way from the shed vorticity flux and is found to be in good agreement with the lift variation reported by others. The delay in the shedding of the DSV with increasing k , as observed by previous researchers, is documented for the full range of k . The DSV, for example, is shed nearly at the maximum α of 25 deg at $k = 0.2$, but is shed at the minimum α of 5 deg at $k = 0.8$. At low k , the flowfield appears quasi-steady and the bluff body shedding corresponding to the maximum α (25 deg) dominates the unsteady fluctuations in the wake.

Author

02 AERODYNAMICS

A92-45537*# National Aeronautics and Space Administration. Lewis Research Center, Cleveland, OH.

LDV MEASUREMENTS ON A RECTANGULAR WING WITH A SIMULATED GLAZE ICE ACCRETION

A. KHODADOUST, M. B. BRAGG, and M. KERHO (Illinois, University, Urbana) IN: AIAA Applied Aerodynamics Conference, 10th, Palo Alto, CA, June 22-24, 1992, Technical Papers. Pt. 2 1992 16 p refs

(AIAA PAPER 92-2690) Copyright

LDV measurement results are presented for the upper surface of a rectangular semispan wing with and without simulated glaze ice accretion. Inspection of the model centerline flow field indicates that a large region of reverse flow exists aft of the ice horn on the iced model. At $\alpha = 0$ deg, this region extends to 7 percent chord, while at $\alpha = 4$ deg the bubble grows to more than 12 percent chord. At $\alpha = 8$ deg, the time-averaged separation bubble is measured well beyond 50 percent chord. Experimental and computational flow visualization support these findings. The flow in the vicinity of the ice shape contains many of the features of flow over a backward-facing step. C.D.

A92-45541*# National Aeronautics and Space Administration. Lewis Research Center, Cleveland, OH.

NAVIER-STOKES ANALYSIS AND EXPERIMENTAL DATA COMPARISON OF COMPRESSIBLE FLOW IN A DIFFUSING S-DUCT

GARY J. HARLOFF (Sverdrup Technology, Inc., Brook Park, OH), BRUCE A. REICHERT (NASA, Lewis Research Center, Cleveland, OH), and STEVEN R. WELLBORN (Iowa State University of Science and Technology, Ames) IN: AIAA Applied Aerodynamics Conference, 10th, Palo Alto, CA, June 22-24, 1992, Technical Papers. Pt. 2 1992 9 p refs

(Contract NAS3-25266)

(AIAA PAPER 92-2699) Copyright

Full three-dimensional Navier-Stokes computational results are compared with new experimental measurements for the flowfield within a round diffusing S-duct. The present study extends previous computational and experimental results for a similar smaller scale S-duct. Predicted results are compared with the experimental static and total pressure fields, and velocity vectors. Additionally, wall pressures, velocity profiles in wall coordinates, and skin friction values are presented. The CFD results employ algebraic and k-epsilon turbulence models. The CFD computed and experimentally determined separated flowfield is carefully examined. Author

A92-45542*# National Aeronautics and Space Administration. Lewis Research Center, Cleveland, OH.

DESIGN AND ANALYSIS OF VORTEX GENERATORS ON REENGINEED BOEING 727-100QF CENTER INLET S-DUCT BY A REDUCED NAVIER-STOKES CODE

PAO S. HUANG, ANTONIO PICCOLO, ANDY SLATER (Dee Howard Co., San Antonio, TX), and BERNHARD H. ANDERSON (NASA, Lewis Research Center, Cleveland, OH) IN: AIAA Applied Aerodynamics Conference, 10th, Palo Alto, CA, June 22-24, 1992, Technical Papers. Pt. 2 1992 8 p refs

(AIAA PAPER 92-2700) Copyright

This paper describes the application of a three dimensional reduced Navier-Stokes code to perform design and analysis of vortex generators on a reengineed Boeing 727-100QF center engine inlet S duct. This computer code with vortex generators modeling is shown to be cost-effective, accurate and easy to use to design the optimal vortex generators installed on a S-duct, predict its aerodynamic performance and provide the detailed flow field information. Author

A92-45561*# National Aeronautics and Space Administration. Lewis Research Center, Cleveland, OH.

THE FLIP FLOP NOZZLE EXTENDED TO SUPERSONIC FLOWS

GANESH RAMAN (Sverdrup Technology, Inc., Brook Park, OH), MICHAEL HAILYE (Michigan, University, Ann Arbor), and EDWARD J. RICE (NASA, Lewis Research Center, Cleveland, OH) IN:

AIAA Applied Aerodynamics Conference, 10th, Palo Alto, CA, June 22-24, 1992, Technical Papers. Pt. 2 1992 24 p refs (AIAA PAPER 92-2724) Copyright

An experiment studying a fluidically oscillated rectangular jet flow was conducted. The Mach number was varied over a range from low subsonic to supersonic. Unsteady velocity and pressure measurements were made using hot wires and piezoresistive pressure transducers. In addition smoke flow visualization using high speed photography was used to document the oscillation of the jet. For the subsonic flip-flop jet it was found that the apparent time-mean widening of the jet was not accompanied by an increase in mass flux. It was found that it is possible to extend the operation of these devices to supersonic flows. Most of the measurements were made for a fixed nozzle geometry for which the oscillations ceased at a fully expanded Mach number of 1.58. By varying the nozzle geometry this limitation was overcome and operation was extended to Mach 1.8. The streamwise velocity perturbation levels produced by this device were much higher than the perturbation levels that could be produced using conventional excitation sources such as acoustic drivers. In view of this ability to produce high amplitudes, the potential for using small scale fluidically oscillated jet as an unsteady excitation source for the control of shear flows in full scale practical applications seems promising. Author

A92-45574*# National Aeronautics and Space Administration. Lewis Research Center, Cleveland, OH.

SURFACE AND FLOW FIELD MEASUREMENTS IN A SYMMETRIC CROSSING SHOCK WAVE/TURBULENT BOUNDARY LAYER FLOW

D. O. DAVIS and W. R. HINGST (NASA, Lewis Research Center, Cleveland, OH) AIAA, Applied Aerodynamics Conference, 10th, Palo Alto, CA, June 22-24, 1992. 19 p. Jun. 1992 19 p refs (AIAA PAPER 92-2634) Copyright

Results of an experimental investigation of a symmetric crossing shock/turbulent boundary layer interaction are presented for a Mach number of 3.44 and deflections angles of 2, 6, 8 and 9 deg. The interaction strengths vary from weak to strong enough to cause a large region of separated flow. Measured quantities include surface static pressure and flowfield Pitot pressures. Pitot profiles in the plane of symmetry through the interaction region are shown for various deflection angles. Oil flow visualization and the results of a trace gas streamline tracking technique are also presented. Author

A92-46791* National Aeronautics and Space Administration. Lewis Research Center, Cleveland, OH.

PREDICTED PRESSURE DISTRIBUTION ON A PROP-FAN BLADE THROUGH EULER ANALYSIS

MAKOTO KOBAYAKAWA (Kyoto University, Japan), RYOJI TAKAKI (National Aerospace Laboratory, Chofu, Japan), YOSHIFUMI KAWAKAMI (Sumitomo Precision Products, Ltd., Amagasaki, Japan), and FREDERICK B. METZGER (Hamilton Standard, Windsor Locks, CT) (ICAS, Congress, 17th, Stockholm, Sweden, Sept. 9-14, 1990, Proceedings. Vol. 2, p. 2073-2081) Journal of Aircraft (ISSN 0021-8669), vol. 29, no. 4, July-Aug. 1992, p. 627-631. Research supported by NASA. Previously cited in issue 09, p. 1311, Accession no. A91-24514. Aug. 1992 5 p refs

Copyright

A92-48723*# National Aeronautics and Space Administration. Lewis Research Center, Cleveland, OH.

DEVELOPMENT OF AN EFFICIENT ANALYSIS FOR HIGH REYNOLDS NUMBER INVISCID/VISCID INTERACTIONS IN CASCADES

M. BARNETT, J. M. VERDON, and T. C. AYER (United Technologies Research Center, East Hartford, CT) AIAA, SAE, ASME, and ASEE, Joint Propulsion Conference and Exhibit, 28th, Nashville, TN, July 6-8, 1992. 15 p. Jul. 1992 15 p refs (Contract NAS3-25425)

(AIAA PAPER 92-3073) Copyright

An efficient steady analysis for predicting strong inviscid/viscid interaction phenomena such as viscous-layer separation,

shock/boundary-layer interaction, and trailing-edge/near-wake interaction in turbomachinery blade passages is described. It uses an inviscid/viscid interaction approach, wherein the flow in the outer inviscid region is assumed to be potential, and that in the inner or viscous-layer region is governed by Prandtl's equations. The inviscid solution is determined using an implicit, least-squares, finite-difference approximation. The viscous-layer solution is obtained using an inverse, finite-difference, space-marching method which is applied along the blade surfaces and the wake streamline. A semiinverse global iteration procedure permits the prediction of boundary-layer separation and other strong-interaction phenomena. Results are presented for two cascades where a range of inlet flow conditions was considered for one of them including conditions leading to large-scale flow separation. Author

A92-48724*# National Aeronautics and Space Administration. Lewis Research Center, Cleveland, OH.

AIRFOIL WAKE AND LINEAR THEORY GUST RESPONSE INCLUDING SUB AND SUPERRESONANT FLOW CONDITIONS
GREGORY H. HENDERSON and SANFORD FLEETER (Purdue University, West Lafayette, IN) AIAA, SAE, ASME, and ASEE, Joint Propulsion Conference and Exhibit, 28th, Nashville, TN, July 6-8, 1992. 12 p. Research supported by NASA. Jul. 1992 12 p refs

(AIAA PAPER 92-3074) Copyright

The unsteady aerodynamic gust response of a high solidity stator vane row is examined in terms of the fundamental gust modeling assumptions with particular attention given to the effects near an acoustic resonance. A series of experiments was performed with gusts generated by rotors comprised of perforated plates and airfoils. It is concluded that, for both the perforated plate and airfoil wake generated gusts, the unsteady pressure responses do not agree with the linear-theory gust predictions near an acoustic resonance. The effects of the acoustic resonance phenomena are clearly evident on the airfoil surface unsteady pressure responses. The transition of the measured lift coefficients across the acoustic resonance from the subresonant regime to the superresonant regime occurs in a simple linear fashion. O.G.

A92-48729*# National Aeronautics and Space Administration. Lewis Research Center, Cleveland, OH.

A FAST, UNCOUPLED, COMPRESSIBLE, TWO-DIMENSIONAL, UNSTEADY BOUNDARY LAYER ALGORITHM WITH SEPARATION FOR ENGINE INLETS

ROBERT L. ROACH, CHRIS NELSON (Georgia Institute of Technology, Atlanta), BARBARA SAKOWSKI, DOUGLAS DARLING (NASA, Lewis Research Center, Cleveland, OH), and ALLAN G. VAN DE WALL (Case Western Reserve University, Cleveland, OH) AIAA, SAE, ASME, and ASEE, Joint Propulsion Conference and Exhibit, 28th, Nashville, TN, July 6-8, 1992. 8 p. Previously announced in STAR as N92-27653. Jul. 1992 8 p refs

(AIAA PAPER 92-3082) Copyright

A finite difference boundary layer algorithm was developed to model viscous effects when an inviscid core flow solution is given. This algorithm solved each boundary layer equation separately, then iterated to find a solution. Solving the boundary layer equations sequentially was 2.4 to 4.0 times faster than solving the boundary layer equations simultaneously. This algorithm used a modified Baldwin-Lomax turbulence model, a weighted average of forward and backward differencing of the pressure gradient, and a backward sweep of the pressure. With these modifications, the boundary layer algorithm was able to model flows with and without separation. The number of grid points used in the boundary layer algorithm affected the stability of the algorithm as well as the accuracy of the predictions of friction coefficients and momentum thicknesses. Results of this boundary layer algorithm compared well with experimental observations of friction coefficients and momentum thicknesses. In addition, when used interactively with an inviscid flow algorithm, this boundary layer algorithm corrected for viscous effects to give a good match with experimental observations for pressures in a supersonic inlet. Author

A92-48730*# National Aeronautics and Space Administration. Lewis Research Center, Cleveland, OH.

INTERFACE OF AN UNCOUPLED BOUNDARY LAYER ALGORITHM WITH AN INVISCID CORE FLOW ALGORITHM FOR UNSTEADY SUPERSONIC ENGINE INLETS

DOUGLAS DARLING and BARBARA SAKOWSKI (NASA, Lewis Research Center, Cleveland, OH) AIAA, SAE, ASME, and ASEE, Joint Propulsion Conference and Exhibit, 28th, Nashville, TN, July 6-8, 1992. 11 p. Previously announced in STAR as N92-27037. Jul. 1992 11 p refs

(AIAA PAPER 92-3083) Copyright

An uncoupled boundary layer algorithm was combined with an inviscid core flow algorithm to model flows within supersonic engine inlets. The inviscid flow algorithm that was used was the Large Perturbation INlet Code (LAPIN). The boundary layer and inviscid core flow algorithms were formulated in different manners. The boundary layer algorithm was two dimensional and solved in nonconservation form, while the core flow algorithm was one dimensional and solved in conservation form. In order to interface the two codes, the following modifications were important. The coordinate system was set up to maintain the parabolic nature of the boundary layer algorithm while approaching the one dimensional core flow solution far from a wall. The pressure gradient used in the boundary layer equation was calculated using the core flow values and the boundary layer equations, so the boundary layer solution smoothly approached the core flow values far from the wall. Flaring was used for the advection terms perpendicular to the core flow to maintain the stability of the algorithm. With these modifications, the combined viscous/inviscid algorithm matched well experimental observations of pressure distributions with a supersonic inlet. Author

A92-48740# National Aeronautics and Space Administration. Lewis Research Center, Cleveland, OH.

COMPARATIVE STUDY OF TURBULENCE MODELS IN PREDICTING HYPERSONIC INLET FLOWS

KAMLESH KAPOOR, BERNHARD H. ANDERSON, and ROBERT J. SHAW (NASA, Lewis Research Center, Cleveland, OH) AIAA, SAE, ASME, and ASEE, Joint Propulsion Conference and Exhibit, 28th, Nashville, TN, July 6-8, 1992. 17 p. Previously announced in STAR as N92-28102. Jul. 1992 17 p refs

(Contract RTOP 505-62-40)

(AIAA PAPER 92-3098) Copyright

A numerical study was conducted to analyze the performance of different turbulence models when applied to the hypersonic NASA P8 inlet. Computational results from the PARC2D code, which solves the full two-dimensional Reynolds-averaged Navier-Stokes equation, were compared with experimental data. The zero-equation models considered for the study were the Baldwin-Lomax model, the Thomas model, and a combination of the Baldwin-Lomax and Thomas models; the two-equation models considered were the Chien model, the Speziale model (both low Reynolds number), and the Launder and Spalding model (high Reynolds number). The Thomas model performed best among the zero-equation models, and predicted good pressure distributions. The Chien and Speziale models compared very well with the experimental data, and performed better than the Thomas model near the walls. Author

A92-48744*# National Aeronautics and Space Administration. Lewis Research Center, Cleveland, OH.

COMPUTATIONAL ANALYSIS OF RAMJET ENGINE INLET INTERACTION

BEVERLY DUNCAN (Sverdrup Technology, Inc., Brook Park, OH) and SCOTT THOMAS (NASA, Lewis Research Center, Cleveland, OH) AIAA, SAE, ASME, and ASEE, Joint Propulsion Conference and Exhibit, 28th, Nashville, TN, July 6-8, 1992. 12 p. Jul. 1992 12 p refs

(AIAA PAPER 92-3102) Copyright

A computational analysis of a ramjet engine at Mach 3.5 has been conducted and compared to results obtained experimentally. This study focuses on the behavior of the inlet both with and without combustor backpressure. Increased backpressure results

02 AERODYNAMICS

in separation of the body side boundary layer and a resultant static pressure rise in the inlet throat region. The computational results compare well with the experimental data for static pressure distribution through the engine, inlet throat flow profiles, and mass capture. The computational analysis slightly underpredicts the thickness of the engine body surface boundary layer and the extent of the interaction caused by backpressure; however, the interaction is observed at approximately the same level of backpressure both experimentally and computationally. This study demonstrates the ability of two different Navier-Stokes codes, namely RPLUS and PARC, to calculate the flow features of this ramjet engine and to provide more detailed information on the process of inlet interaction and unstart. Author

A92-48909*# National Aeronautics and Space Administration. Lewis Research Center, Cleveland, OH.

INVESTIGATION OF THREE-DIMENSIONAL FLOW FIELD IN A TURBINE INCLUDING ROTOR/STATOR INTERACTION. II - THREE-DIMENSIONAL FLOW FIELD AT THE EXIT OF THE NOZZLE

M. ZACCARIA and B. LAKSHMINARAYANA (Pennsylvania State University, University Park) AIAA, SAE, ASME, and ASEE, Joint Propulsion Conference and Exhibit, 28th, Nashville, TN, July 6-8, 1992. 13 p. Jul. 1992 13 p refs

(Contract NSG-3555)

(AIAA PAPER 92-3326) Copyright

The nozzle exit flowfield was measured at two axial locations with a miniature five-hole probe. Measurements were taken from hub-to-tip, blade-to-blade at 21 radial locations and at two axial locations downstream of the nozzle trailing edge to resolve the flowfield accurately including the nozzle wake, secondary flow region, horseshoe vortex and losses. All three components of the velocity, stagnation pressure, static pressure, and pitch and yaw angles have been resolved very accurately. The wake data seems to indicate that the decay of the wake is faster than the wake of an isolated nozzle row. The cause of this is attributed to the presence of the rotor downstream. A distinct vortex core has been observed near the tip. The indications are that the horseshoe vortex and the passage vortex have merged to produce a single loss core region. Roughly a third of the blade height passage near the tip and a third of the blade height near the hub is dominated by secondary flow, passage vortex and the horseshoe vortex phenomena. Only the middle third of the nozzle behaves as per design. These and other data are presented, interpreted and synthesized to understand the nozzle flowfield. Author

A92-49063*# National Aeronautics and Space Administration. Lewis Research Center, Cleveland, OH.

SUPERSONIC JET MIXING ENHANCEMENT BY 'DELTA-TABS'

K. B. M. Q. ZAMAN (NASA, Lewis Research Center, Cleveland, OH), M. F. REEDER, and M. SAMIMY (Ohio State University, Columbus) AIAA, SAE, ASME, and ASEE, Joint Propulsion Conference and Exhibit, 28th, Nashville, TN, July 6-8, 1992. 15 p. Previously announced in STAR as N92-24958. Jul. 1992 15 p refs

(AIAA PAPER 92-3548) Copyright

The results of a continuing investigation of the effect of vortex generators, in the form of small tabs at the nozzle exit, on the evolution of a jet are reported. Primarily, tabs of triangular shape are considered, and the effect is studied up to an equivalent jet Mach number of 1.8. By changing the orientation of the tab with respect to the nozzle exit plane, streamwise vortex pairs of opposite sign were generated. This resulted in either an outward selection of jet core fluid into the ambient or an inward indentation of the mixing layer into the core of the jet. A triangular shaped tab with its apex leaning downstream, referred to as a delta tab, was found to be the most effective in influencing the jet evolution. Two delta tabs, spaced 180 degrees apart, completely bifurcated the jet. Four delta tabs increased jet mixing substantially, more than by various other methods tried previously; the mass flux at fourteen jet diameters downstream from the nozzle increased by about 50 percent over that for the no tab case. The tabs were found to be

effective in jets with laminar or turbulent boundary layers as well as in jets with low or high core turbulence intensities. Author

A92-50473 National Aeronautics and Space Administration. Lewis Research Center, Cleveland, OH.

TIME DOMAIN NUMERICAL CALCULATIONS OF UNSTEADY VORTICAL FLOWS ABOUT A FLAT PLATE AIRFOIL

S. I. HARIHARAN, YU PING (Akron, University, OH), and J. R. SCOTT (NASA, Lewis Research Center, Cleveland, OH) Journal of Computational Physics (ISSN 0021-9991), vol. 101, no. 2, Aug. 1992, p. 419-430. Research supported by Ohio Supercomputer Center. Aug. 1992 12 p refs
(Contract RTOP 505-62-21)

Copyright

A time domain numerical scheme is developed to solve for the unsteady flow about a flat plate airfoil due to imposed upstream, small amplitude, transverse velocity perturbations. The governing equation for the resulting unsteady potential is a homogeneous, constant coefficient, convective wave equation. Accurate solution of the problem requires the development of approximate boundary conditions which correctly model the physics of the unsteady flow in the far field. A uniformly valid far field boundary condition is developed, and numerical results are presented using this condition. The stability of the scheme is discussed, and the stability restriction for the scheme is established as a function of the Mach number. Finally, comparisons are made with the frequency domain calculation by Scott and Atassi, and the relative strengths and weaknesses of each approach are assessed. Author

A92-52730* National Aeronautics and Space Administration. Lewis Research Center, Cleveland, OH.

KINETIC THEORY MODEL FOR THE FLOW OF A SIMPLE GAS FROM A THREE-DIMENSIONAL AXISYMMETRIC NOZZLE

B. R. RILEY (Evansville, University, IN) IN: Rarefied gas dynamics; Proceedings of the 17th International Symposium, Aachen, Germany, July 8-14, 1990 1991 8 p refs

(Contract NAG3-746)

Copyright

A system of nonlinear integral equations equivalent to the Krook kinetic equations for the steady state is the mathematical basis used to develop a computer code to model the flowfields for low-thrust three-dimensional axisymmetric nozzles. The method of characteristics is used to solve numerically by an iteration process the approximated Boltzmann equation for the number density, temperature, and velocity profiles of a simple gas as it expands into a vacuum. Results predict backscatter and show the effect of the nozzle wall boundary layer on the external flowfields. Author

A92-54003*# National Aeronautics and Space Administration. Lewis Research Center, Cleveland, OH.

THREE-DIMENSIONAL NAVIER-STOKES HEAT TRANSFER PREDICTIONS FOR TURBINE BLADE ROWS

R. J. BOYLE (NASA, Lewis Research Center, Cleveland, OH) and P. W. GIEL (Sverdrup Technology, Inc.; NASA, Lewis Research Center, Cleveland, OH) AIAA, SAE, ASME, and ASEE, Joint Propulsion Conference and Exhibit, 28th, Nashville, TN, July 6-8, 1992. 15 p. Jul. 1992 15 p refs
(AIAA PAPER 92-3068)

Results are shown for a three-dimensional Navier-Stokes analysis of both the flow and the surface heat transfer for turbine applications. Heat transfer comparisons are made with the experimental shock-tunnel data of Dunn and Kim, and with the data of Blair for the rotor of the large scale rotating turbine. The analysis was done using the steady-state, three-dimensional, thin-layer Navier-Stokes code developed by Chima, which uses a multistage Runge-Kutta scheme with implicit residual smoothing. An algebraic mixing length turbulence model is used to calculate turbulent eddy viscosity. The variation in heat transfer due to variations in grid parameters is examined. The effects of rotation, tip clearance, and inlet boundary layer thickness variation on the predicted blade and endwall heat transfer are examined. Author

A92-54004*# National Aeronautics and Space Administration. Lewis Research Center, Cleveland, OH.

A COMPARISON OF THE CALCULATED AND EXPERIMENTAL OFF-DESIGN PERFORMANCE OF A RADIAL FLOW TURBINE
LIZET TIRRES (Sverdrup Technology, Inc., Brook Park, OH) AIAA, SAE, ASME, and ASEE, Joint Propulsion Conference and Exhibit, 28th, Nashville, TN, July 6-8, 1992. 15 p. Previously announced in STAR as N92-29402. Jul. 1992 15 p refs
(Contract NAS3-25266)
(AIAA PAPER 92-3069)

Off design aerodynamic performance of the solid version of a cooled radial inflow turbine is analyzed. Rotor surface static pressure data and other performance parameters were obtained experimentally. Overall stage performance and turbine blade surface static to inlet total pressure ratios were calculated by using a quasi-three dimensional inviscid code. The off design prediction capability of this code for radial inflow turbines shows accurate static pressure prediction. Solutions show a difference of 3 to 5 points between the experimentally obtained efficiencies and the calculated values. Author

A92-54005*# National Aeronautics and Space Administration. Lewis Research Center, Cleveland, OH.

INCREASED HEAT TRANSFER TO ELLIPTICAL LEADING EDGES DUE TO SPANWISE VARIATIONS IN THE FREESTREAM MOMENTUM - NUMERICAL AND EXPERIMENTAL RESULTS

D. L. RIGBY (Sverdrup Technology, Inc., Brook Park, OH) and G. J. VAN FOSSEN (NASA, Lewis Research Center, Cleveland, OH) AIAA, SAE, ASME, and ASEE, Joint Propulsion Conference and Exhibit, 28th, Nashville, TN, July 6-8, 1992. 12 p. Jul. 1992 12 p refs
(AIAA PAPER 92-3070)

A study of the effect of spanwise variation on leading edge heat transfer is presented. Experimental and numerical results are given for a circular leading edge and for a 3:1 elliptical leading edge. It is demonstrated that increases in leading edge heat transfer due to spanwise variations in freestream momentum are comparable to those due to freestream turbulence. R.E.P.

A92-54012*# National Aeronautics and Space Administration. Lewis Research Center, Cleveland, OH.

FULL NAVIER-STOKES CALCULATIONS ON THE INSTALLED F/A-18 INLET AT A HIGH ANGLE OF ATTACK

JAMES E. BRUNS and C. F. SMITH (Sverdrup Technology, Inc., Brook Park, OH) AIAA, SAE, ASME, and ASEE, Joint Propulsion Conference and Exhibit, 28th, Nashville, TN, July 6-8, 1992. 24 p. Jul. 1992 24 p refs
(Contract NAS3-25266)
(AIAA PAPER 92-3175)

Major objectives of the NASA High-Alpha Technology Program are the accurate prediction of the internal (inlet) aerodynamics of an aircraft operating at attitudes of up to 60 deg pitch and 10 deg yaw and the calibration of CFD codes for predicting the internal performance of inlets. Numerical results are presented for the three cases of a full-scale model, a 20-percent scale model at design mass flow, and a scale model at reduced mass flow; attention is given to the effects of Reynolds number. All three cases are at 30 deg angle of attack and zero deg yaw. The results thus obtained are helpful to experimentalists in determining some of their instrumentation requirements. O.C.

A92-54013*# National Aeronautics and Space Administration. Lewis Research Center, Cleveland, OH.

APPLICATION OF COMPUTATIONAL FLUID DYNAMICS TO THE STUDY OF VORTEX FLOW CONTROL FOR THE MANAGEMENT OF INLET DISTORTION

BERNHARD H. ANDERSON (NASA, Lewis Research Center, Cleveland, OH) and JAMES GIBB (Defence Research Agency, Bedford, United Kingdom) AIAA, SAE, ASME, and ASEE, Joint Propulsion Conference and Exhibit, 28th, Nashville, TN, July 6-8, 1992. 11 p. Jul. 1992 11 p refs
(AIAA PAPER 92-3177) Copyright

A study is presented to demonstrate that the Reduced Navier-Stokes code RNS3D can be employed effectively to develop a vortex generator installation that minimizes engine face circumferential distortion by controlling the development of secondary flow. The necessary computing times are small enough to show that similar studies are feasible within an analysis-design environment with all its constraints of costs and time. This study establishes the nature of the performance enhancements that can be realized with vortex flow control, and indicates a set of aerodynamic properties that can be utilized to arrive at a successful vortex generator installation design. R.E.P.

A92-54016*# National Aeronautics and Space Administration. Lewis Research Center, Cleveland, OH.

NAVIER-STOKES ANALYSIS OF THREE-DIMENSIONAL UNSTEADY FLOWS INSIDE TURBINE STAGES

C. HAH (NASA, Lewis Research Center, Cleveland, OH) AIAA, SAE, ASME, and ASEE, Joint Propulsion Conference and Exhibit, 28th, Nashville, TN, July 6-8, 1992. 10 p. Jul. 1992 10 p refs
(AIAA PAPER 92-3211)

This study presents a numerical method for solving the 3D Navier-Stokes equations for unsteady, viscous flow through multiple turbomachinery blade rows. The method solves the fully 3D Navier-Stokes equations with an implicit scheme which is based on a control volume approach. A two-equation turbulence model with a low Reynolds number modification is employed. A third-order accurate upwinding scheme is used to approximate convection terms, while a second order accurate central difference scheme is used for the discretization of viscous terms. A second-order accurate scheme is employed for the temporal discretization. The numerical method is applied to study the unsteady flowfield of the High Pressure Fuel side Turbo-Pump (HPFTP) of the Space Shuttle Main Engine (SSME). The stage calculation is performed by coupling the stator and the rotor flowfields at each time step through an over-laid grid. Numerical results for the complete geometry with the vane trailing edge cutback are presented and compared with the available experimental data. Author

A92-54090*# National Aeronautics and Space Administration. Lewis Research Center, Cleveland, OH.

AN EXPERIMENTAL INVESTIGATION OF THE FLOW IN A DIFFUSING S-DUCT

S. R. WELLBORN (Iowa State University of Science and Technology, Ames), B. A. REICHERT (NASA, Lewis Research Center, Cleveland, OH), and T. H. OKIISHI (Iowa State University of Science and Technology, Ames) AIAA, SAE, ASME, and ASEE, Joint Propulsion Conference and Exhibit, 28th, Nashville, TN, July 6-8, 1992. 12 p. Jul. 1992 12 p refs
(Contract NAG3-1275)
(AIAA PAPER 92-3622) Copyright

Compressible, subsonic flow through a diffusing S-duct has been experimentally investigated. Benchmark aerodynamic data are presented for flow through a representative S-duct configuration. The collected data would be beneficial to aircraft inlet designers and is suitable for the validation of computational codes. Measurements of the 3D velocity field and total and static pressures were obtained at five cross-sectional planes. Surface static pressures and flow visualization also helped to reveal flowfield characteristics. All reported tests were conducted with an inlet centerline Mach number of 0.6 and a Reynolds number, based on the inlet centerline velocity and duct inlet diameter, of 2.6×10^6 . The results show that a large region of streamwise flow separation occurred within the duct. Transverse velocity components indicate that the duct curvature induces strong pressure driven secondary flows, which evolve into a large pair of counter-rotating vortices. These vortices convect the low momentum fluid of the boundary layer toward the center of the duct, degrading both the uniformity and magnitude of the total pressure profile. Author

02 AERODYNAMICS

A92-54161*# National Aeronautics and Space Administration. Lewis Research Center, Cleveland, OH.

UNSTEADY BLADE PRESSURES ON A PROPFAN - PREDICTED AND MEASURED COMPRESSIBILITY EFFECTS

M. NALLASAMY (Sverdrup Technology, Inc., Brook Park; NASA, Lewis Research Center, Cleveland, OH) AIAA, SAE, ASME, and ASEE, Joint Propulsion Conference and Exhibit, 28th, Nashville, TN, July 6-8, 1992. 15 p. Jul. 1992 15 p refs (Contract NAS3-25266) (AIAA PAPER 92-3774)

The effect of compressibility on unsteady blade pressures is studied by solving the 3D Euler equations. The operation of the eight-bladed SR7L propfan at 4.75 deg angle of attack was considered. Euler solutions were obtained for three Mach numbers, 0.6, 0.7, and 0.8 and the predicted blade pressure waveforms were compared with flight data. In general, the effect of Mach number on pressure waveforms are correctly predicted. The change in pressure waveforms are minimal when the Mach number is increased from 0.6 to 0.7. Increasing the Mach number from 0.7 to 0.8 produces significant changes in predicted pressure levels. The predicted amplitudes, however, differ from measurements at some transducer locations. Also the predicted appearance of a shock in the highly loaded portion of the blade revolution is not indicated by the measurements. At all the three Mach numbers, the measured (installed propfan) pressure waveforms show a relative phase lag compared to the computed (propfan alone) waveforms due to installation effects. Measured waveforms in the blade tip region show nonlinear variations which are not captured by the present numerical procedure. Author

A92-56857*# National Aeronautics and Space Administration. Lewis Research Center, Cleveland, OH.

EXPERIMENTAL UNSTEADY PRESSURES ON AN OSCILLATING CASCADE WITH SUPERSONIC LEADING EDGE LOCUS

DANIEL ERWIN, G. M. GREGOREK (Ohio State University, Columbus), and JOHN RAMSEY (NASA, Lewis Research Center, Cleveland, OH) AIAA, Aerospace Ground Testing Conference, 17th, Nashville, TN, July 6-8, 1992. 15 p. Jul. 1992 15 p refs (AIAA PAPER 92-4035) Copyright

The first experimental data for an oscillating cascade with a supersonic leading edge locus (SLEL) at zero stagger angle is presented which were obtained in the NASA/OSU supersonic oscillating cascade facility. Reduced frequencies from .093 to .146, based on half chord were investigated. An influence coefficient technique for a linear oscillating cascade with constant interblade phase angle has been extended to a cascade with a SLEL. O.G.

A92-56861*# National Aeronautics and Space Administration. Lewis Research Center, Cleveland, OH.

EFFECT OF A SIMULATED GLAZE ICE SHAPE ON THE AERODYNAMIC PERFORMANCE OF A RECTANGULAR WING

ABDI KHODADOUST (Illinois, University, Urbana) AIAA, Aerospace Ground Testing Conference, 17th, Nashville, TN, July 6-8, 1992. 17 p. Research supported by NASA. Jul. 1992 17 p refs (AIAA PAPER 92-4042) Copyright

The effect of a simulated glaze-ice accretion on the flowfield of a 3D wing is studied experimentally. The model used for these tests was a semispan wing of effective aspect ratio five, mounted from the sidewall of a subsonic wind tunnel. The model has a NACA 0012 airfoil section on a rectangular untwisted planform with interchangeable leading edges to allow for testing both the baseline and the iced-wing geometry. A four-beam two-color fiberoptic laser Doppler velocimeter (LDV) was used to map the flowfield along three spanwise cuts on the model. Measurements on the centerline of the clean model compared favorably with theory and centerline measurements on the iced model compared well with measurements on a similar 2D model. The flow has the largest separation bubble at the model midspan with the smallest separation bubble occurring near the root and the wing tip. Author

N92-10012*# National Aeronautics and Space Administration. Lewis Research Center, Cleveland, OH.

THE STRUCTURE AND DEVELOPMENT OF STREAMWISE VORTEX ARRAYS EMBEDDED IN A TURBULENT BOUNDARY LAYER Ph.D. Thesis - Case Western Reserve Univ.

BRUCE J. WENDT (Case Western Reserve Univ., Cleveland, OH.), ISAAC GREBER (Case Western Reserve Univ., Cleveland, OH.), and WARREN R. HINGST Sep. 1991 319 p (Contract NAG3-520; RTOP 505-62-52) (NASA-TM-105211; E-6523; NAS 1.15:105211) Avail: CASI HC A14/MF A03

An investigation of the structure and development of streamwise vortices embedded in a turbulent boundary layer was conducted. The vortices were generated by a single spanwise row of rectangular vortex generator blades. A single embedded vortex was examined, as well as arrays of embedded counter rotating vortices produced by equally spaced vortex generators. Measurements of the secondary velocity field in the crossplane provided the basis for characterization of vortex structure. Vortex structure was characterized by four descriptors. The center of each vortex core was located at the spanwise and normal position of peak streamwise vorticity. Vortex concentration was characterized by the magnitude of the peak streamwise vorticity, and the vortex strength by its circulation. Measurements of the secondary velocity field were conducted at two crossplane locations to examine the streamwise development of the vortex arrays. Large initial spacings of the vortex generators produced pairs of strong vortices which tended to move away from the wall region while smaller spacings produced tight arrays of weak vortices close to the wall. A model of vortex interaction and development is constructed using the experimental results. The model is based on the structure of the Oseen Vortex. Vortex trajectories are modelled by including the convective effects of neighbors. Author

N92-10976*# National Aeronautics and Space Administration. Lewis Research Center, Cleveland, OH.

RESULTS FROM COMPUTATIONAL ANALYSIS OF A MIXED COMPRESSION SUPERSONIC INLET

J. D. SAUNDERS and T. G. KEITH (Ohio Aerospace Inst., Brook Park.) 1991 18 p Presented at the 27th Joint Propulsion Conference, Sacramento, CA, 24-27 Jun. 1991; sponsored by AIAA, SAE, ASME, and ASEE Previously announced in IAA as A91-45818 Original contains color illustrations (Contract RTOP 537-02-23) (NASA-TM-104475; E-6322; NAS 1.15:104475; AIAA PAPER 91-2581) Copyright

A numerical study was performed to simulate the critical flow through a supersonic inlet. This flow field has many phenomena such as shock waves, strong viscous effects, turbulent boundary layer development, boundary layer separations, and mass flow suction through the walls, (bleed). The computational tools used were two full Navier-Stokes (FNS) codes. The supersonic inlet that was analyzed is the Variable Diameter Centerbody, (VDC), inlet. This inlet is a candidate concept for the next generation supersonic involved effort in generating an efficient grid geometry and specifying boundary conditions, particularly in the bleed region and at the outflow boundary. Results for a critical inlet operation compare favorably to Method of Characteristics predictions and experimental data. Author

N92-13998*# National Aeronautics and Space Administration. Lewis Research Center, Cleveland, OH.

A STUDY ON VORTEX FLOW CONTROL ON INLET DISTORTION IN THE RE-ENGINEED 727-100 CENTER INLET DUCT USING COMPUTATIONAL FLUID DYNAMICS

BERNHARD H. ANDERSON (Dee-Howard Co., San Antonio, TX.), PAO S. HUANG, WILLIAM A. PASCHAL, and ENRICO CAVATORTA (Dee-Howard Co., San Antonio, TX.) 1992 13 p Presented at the 30th Aerospace Sciences Meeting and Exhibit, Reno, NV, 6-9 Jan. 1992; sponsored by AIAA (Contract RTOP 505-62-52)

(NASA-TM-105321; E-6679; NAS 1.15:105321; AIAA PAPER 92-0152) Avail: CASI HC A03/MF A01

Computational fluid dynamics was used to investigate the management of inlet distortion by the introduction of discrete vorticity sources at selected locations in the inlet for the purpose of controlling secondary flow. These sources of vorticity were introduced by means of vortex generators. A series of design observations were made concerning the importance of various vortex generator design parameters in minimizing engine face circumferential distortion. The study showed that vortex strength, generator scale, and secondary flow field structure have a complicated and interrelated influence on the engine face distortion, over and above the initial geometry and arrangement of the generators. The installed vortex generator performance was found to be a function of three categories of variables: the inflow conditions, the aerodynamic characteristics associated with the inlet duct, and the design parameters related to the geometry, arrangement, and placement of the vortex generators within the outlet duct itself. Author

N92-14000*# National Aeronautics and Space Administration. Lewis Research Center, Cleveland, OH.

SCREECH NOISE SOURCE STRUCTURE OF A SUPERSONIC RECTANGULAR JET

E. J. RICE and R. TAGHAVI (Sverdrup Technology, Inc., Brook Park, OH.) 1992 16 p Presented at the 30th Aerospace Sciences Meeting and Exhibit, Reno, NV, 6-9 Jan. 1992; sponsored by AIAA

(Contract NAS3-25266; RTOP 505-62-21)

(NASA-TM-105384; E-6744; NAS 1.15:105384; AIAA PAPER 92-0503) Avail: CASI HC A03/MF A01

The near-field of the screech noise source structure of an under-expanded supersonic rectangular jet was studied in detail. A miniature probe microphone was used along with a reference microphone to determine the amplitude and phase of the sound pressure near and in the high speed flow field. The transverse structure of the unsteady pressure field was investigated by moving the probe microphone sufficiently far into the jet so that pressure fall-off was observed. Five islands of high sound pressure level have been distinguished which may be associated with the actual local sources of sound production. These sources of screech noise are closely associated with the jet shock structure as would be expected, with the peak region of noise level being found slightly downstream of each of the five observed shocks. The third and fourth noise sources have the highest levels and are about equal in strength. All of the apparent noise sources have their peak levels in the subsonic flow region. Strong cancellations in the acoustic field are observed in the downstream and sideline directions which may account for the predominant upstream propagation of the fundamental tone noise. Author

N92-14001*# National Aeronautics and Space Administration. Lewis Research Center, Cleveland, OH.

LEWICE/E: AN EULER BASED ICE ACCRETION CODE

MARK G. POTAPCZUK 1992 25 p Presented at the 30th Aerospace Sciences Meeting and Exhibit, Reno, NV, 6-9 Jan. 1992; sponsored by AIAA

(Contract RTOP 505-68-10)

(NASA-TM-105389; E-6778; NAS 1.15:105389; AIAA PAPER 92-0037) Avail: CASI HC A03/MF A01

A new version of the LEWICE ice accretion computer code was developed which calculates the ice growth on two dimensional surfaces, incorporating the effects of compressibility through the solution of the Euler equations. The code is modular and contains separate stand-alone program elements that create a grid, calculate the flow field parameters, calculate the droplet trajectory paths, determine the amount of ice growth, and plot results. This code increases the applicability of ice accretion predictions by allowing calculations at higher Mach numbers. The new elements of the code are described. Calculated results are compared to experiment for several cases, including a LEWICE example case and a thin airfoil section at a Mach number of 0.58. Author

N92-14002*# National Aeronautics and Space Administration. Lewis Research Center, Cleveland, OH.

ANALYSIS OF AN ADVANCED DUCTED PROPELLER SUBSONIC INLET

CHANTHY IEK, DONALD R. BOLDMAN, and MOUNIR IBRAHIM (Cleveland State Univ., OH.) 1992 18 p Proposed for presentation at the 30th Aerospace Sciences Meeting and Exhibit, Reno, NV, 6-9 Jan. 1992; sponsored by AIAA

(Contract RTOP 535-03-10)

(NASA-TM-105393; E-6784; NAS 1.15:105393; AIAA PAPER

92-0274) Avail: CASI HC A03/MF A01

A time marching Navier-Stokes code called PARC (PARC2D for 2-D/axisymmetric and PARC3D for 3-D flow simulations) was validated for an advanced ducted propeller (ADP) subsonic inlet. The code validation for an advanced ducted propeller (ADP) subsonic inlet. The code validation was implemented for a non-separated flow condition associated with the inlet operating at angles-of-attack of 0 and 25 degrees. The inlet test data were obtained in the 9 x 15 ft Low Speed Wind Tunnel at NASA Lewis Research Center as part of a cooperative study with Pratt and Whitney. The experimental study focused on the ADP inlet performance for take-off and approach conditions. The inlet was tested at a free stream Mach number of 0.2, at angles-of-attack between 0 and 35 degrees, and at a maximum propeller speed of 12,000 RPM which induced a corrected air flow rate of about 46 lb/sec based on standard day conditions. The computational grid and flow boundary conditions (BC) were based on the actual inlet geometry and the funnel flow conditions. At the propeller face, two types of BC's were applied: a mass flow BC and a fixed flow properties BC. The fixed flow properties BC was based on a combination of data obtained from the experiment and calculations using a potential flow code. Comparison of the computational results with the test data indicates that the PARC code with the propeller face fixed flow properties BC provided a better prediction of the inlet surface static pressures than the predictions when the mass flow BC was used. For an angle-of-attack of 0 degrees, the PARC2D code with the propeller face mass flow BC provided a good prediction of inlet static pressures except in the region of high pressure gradient. With the propeller face fixed flow properties BC, the PARC2D code provided a good prediction of the inlet static pressures. For an angle-of-attack of 25 degrees with the mass flow BC, the PARC3D code predicted static pressures which deviated significantly from the test data; however, with the fixed flow properties BC, a good comparison with the test data was obtained. Author

N92-14003*# National Aeronautics and Space Administration. Lewis Research Center, Cleveland, OH.

ON THE MECHANISM OF TURBULENCE SUPPRESSION IN FREE SHEAR FLOWS UNDER ACOUSTIC EXCITATION

K. B. M. Q. ZAMAN and E. J. RICE 1992 13 p Proposed for presentation at the 30th Aerospace Sciences Meeting and Exhibit, Reno, NV, 6-9 Jan. 1992; sponsored by AIAA

(Contract RTOP 505-62-52)

(NASA-TM-105360; E-6739; AIAA PAPER 92-0065) Avail: CASI HC A03/MF A01

Acoustic excitation at certain high frequencies has been known to suppress large amplitude fluctuations otherwise occurring naturally in various free shear flows. The phenomenon has been observed in flows with initially laminar or transitional boundary layers. An experimental investigation is conducted to consider two possibilities in regards to the mechanism of the effect. (1) The natural shear layer is self excited by the instability waves already developed in the upstream boundary layer. This is overridden when the shear layer is excited at its maximally unstable mode, causing the observed decrease in the intensities downstream. (2) The upstream boundary layer is in a transitional or buffeted laminar state, characterized by large amplitude unsteady fluctuations, which force the large fluctuations downstream. Excitation trips the upstream boundary layer to full turbulence, reduces the unsteady fluctuations, and thus causes the observed suppression of the intensities throughout the flowfield. The present experimental

02 AERODYNAMICS

results refute either of these possibilities to be the general mechanism of the effect. Author

N92-14968*# National Aeronautics and Space Administration. Lewis Research Center, Cleveland, OH.

WIND TUNNEL INVESTIGATION OF VORTEX FLOWS ON F/A-18 CONFIGURATION AT SUBSONIC THROUGH TRANSONIC SPEED

GARY E. ERICKSON Washington Dec. 1991 166 p
(Contract RTOP 505-68-30-03)
(NASA-TP-3111; L-16799; NAS 1.60:3111) Avail: CASI HC A08/MF A02

A wind tunnel experiment was conducted in the David Taylor Research Center 7- by 10-Foot Transonic Tunnel of the wing leading-edge extension (LEX) and forebody vortex flows at subsonic and transonic speeds about a 0.06-scale model of the F/A-18. The primary goal was to improve the understanding and control of the vortical flows, including the phenomena of vortex breakdown and vortex interactions with the vertical tails. Laser vapor screen flow visualizations, LEX, and forebody surface static pressures, and six-component forces and moments were obtained at angles of attack of 10 to 50 degrees, free-stream Mach numbers of 0.20 to 0.90, and Reynolds numbers based on the wing mean aerodynamic chord of 0.96×10^6 to 1.75×10^6 . The wind tunnel results were correlated with in-flight flow visualizations and handling qualities trends obtained by NASA using an F-18 High-Alpha Research Vehicle (HARV) and by the Navy and McDonnell Douglas on F-18 aircraft with LEX fences added to improve the vertical tail buffet environment. Key issues that were addressed include the sensitivity of the vortical flows to the Reynolds number and Mach number; the reduced vertical tail excitation, and the corresponding flow mechanism, in the presence of the LEX fence; the repeatability of data obtained during high angle-of-attack wind tunnel testing of F-18 models; the effects of particle seeding for flow visualization on the quantitative model measurements; and the interpretation of off-body flow visualizations obtained using different illumination and particle seeding techniques. Author

N92-15051*# National Aeronautics and Space Administration. Lewis Research Center, Cleveland, OH.

RESULTS OF AN ICING TEST ON A NACA 0012 AIRFOIL IN THE NASA LEWIS ICING RESEARCH TUNNEL

JAIWON SHIN and THOMAS H. BOND 1992 21 p Presented at the 30th Aerospace Sciences Meeting and Exhibit, Reno, NV, 6-9 Jan. 1992; sponsored by AIAA
(Contract RTOP 505-68-10)
(NASA-TM-105374; E-6761; NAS 1.15:105374; AIAA PAPER 92-0647) Avail: CASI HC A03/MF A01

Tests were conducted in the Icing Research Tunnel (IRT) at the NASA Lewis Research Center to document the current capability of the IRT, focused mainly on the repeatability of the ice shape over a range of icing conditions. Measurements of drag increase due to the ice accretion were also made to document the repeatability of drag. Surface temperatures of the model were obtained to show the effects of latent-heat release by the freezing droplets and heat transfer through the ice layer. The repeatability of the ice shape was very good at low temperatures, but only fair at near freezing temperatures. In general, drag data shows good repeatability. Author

N92-15052*# National Aeronautics and Space Administration. Lewis Research Center, Cleveland, OH.

A TURBULENCE MODEL FOR ICED AIRFOILS AND ITS VALIDATION

JAIWON SHIN (California State Univ., Long Beach.), HSUN H. CHEN, and TUNCER CEBECI (California State Univ., Long Beach.) 1992 17 p Presented at the 30th Aerospace Sciences Meeting and Exhibit, Reno, NV, 6-9 Jan. 1992; sponsored by AIAA
(Contract RTOP 505-68-10)
(NASA-TM-105373; E-6760; NAS 1.15:105373; AIAA PAPER 92-0417) Avail: CASI HC A03/MF A01

A turbulence model based on the extension of the algebraic eddy viscosity formulation of Cebeci and Smith developed for two dimensional flows over smooth and rough surfaces is described for iced airfoils and validated for computed ice shapes obtained for a range of total temperatures varying from 28 to -15 F. The validation is made with an interactive boundary layer method which uses a panel method to compute the inviscid flow and an inverse finite difference boundary layer method to compute the viscous flow. The interaction between inviscid and viscous flows is established by the use of the Hilbert integral. The calculated drag coefficients compare well with recent experimental data taken at the NASA-Lewis Icing Research Tunnel (IRT) and show that, in general, the drag increase due to ice accretion can be predicted well and efficiently. Author

N92-15968*# National Aeronautics and Space Administration. Lewis Research Center, Cleveland, OH.

PREDICTION OF ICE ACCRETION ON A SWEEP NACA 0012 AIRFOIL AND COMPARISONS TO FLIGHT TEST RESULTS

ANDREW L. REEHORST 1992 60 p Presented at the 30th Aerospace Sciences Meeting and Exhibit, Reno, NV, 6-9 Jan. 1992; sponsored by AIAA
(Contract RTOP 505-68-10)
(NASA-TM-105368; E-6746; NAS 1.15:105368; AIAA PAPER 92-0043) Avail: CASI HC A04/MF A01

In the winter of 1989-90, an icing research flight project was conducted to obtain swept wing ice accretion data. Utilizing the NASA Lewis Research Center's DHC-6 DeHavilland Twin Otter aircraft, research flights were made into known icing conditions in Northeastern Ohio. The icing cloud environment and aircraft flight data were measured and recorded by an onboard data acquisition system. Upon entry into the icing environment, a 24 inch span, 15 inch chord NACA 0012 airfoil was extended from the aircraft and set to the desired sweep angle. After the growth of a well defined ice shape, the airfoil was retracted into the aircraft cabin for ice shape documentation. The ice accretions were recorded by ice tracings and photographs. Ice accretions were mostly of the glaze type and exhibited scalloping. The ice was accreted at sweep angles of 0, 30, and 45 degrees. A 3-D ice accretion prediction code was used to predict ice profiles for five selected flight test runs, which include sweep angle of zero, 30, and 45 degrees. The code's roughness input parameter was adjusted for best agreement. A simple procedure was added to the code to account for 3-D ice scalloping effects. The predicted ice profiles are compared to their respective flight test counterparts. This is the first attempt to predict ice profiles on swept wings with significant scalloped ice formations. Author

N92-15977*# National Aeronautics and Space Administration. Lewis Research Center, Cleveland, OH.

PRESSURE WAVE PROPAGATION STUDIES FOR OSCILLATING CASCADES

DENNIS L. HUFF 1992 21 p Presented at the 30th Aerospace Sciences Meeting and Exhibit, Reno, NV, 6-9 Jan. 1992; sponsored by AIAA
(Contract RTOP 535-03-10)
(NASA-TM-105406; E-6811; NAS 1.15:105406; AIAA PAPER 92-0145) Copyright Avail: CASI HC A03/MF A01

The unsteady flow field around an oscillating cascade of flat plates is studied using a time marching Euler code. Exact solutions based on linear theory serve as model problems to study pressure wave propagation in the numerical solution. The importance of using proper unsteady boundary conditions, grid resolution, and time step is demonstrated. Results show that an approximate non-reflecting boundary condition based on linear theory does a good job of minimizing reflections from the inflow and outflow boundaries and allows the placement of the boundaries to be closer than cases using reflective boundary conditions. Stretching the boundary to dampen the unsteady waves is another way to minimize reflections. Grid clustering near the plates does a better job of capturing the unsteady flow field than cases using uniform grids as long as the CFL number is less than one for a sufficient

portion of the grid. Results for various stagger angles and oscillation frequencies show good agreement with linear theory as long as the grid is properly resolved. Author

N92-17347*# National Aeronautics and Space Administration. Lewis Research Center, Cleveland, OH.

EXPERIMENTAL ICE SHAPE AND PERFORMANCE CHARACTERISTICS FOR A MULTI-ELEMENT AIRFOIL IN THE NASA LEWIS ICING RESEARCH TUNNEL

BRIAN M. BERKOWITZ (Sverdrup Technology, Inc., Brook Park, OH.), MARK G. POTAPCZUK (Boeing Computer Services Co., Seattle, WA.), BAHMAN S. NAMDAR, and TAMMY J. LANGHALS (Sverdrup Technology, Inc., Brook Park, OH.) Dec. 1991 323 p

(Contract NAS3-25266; RTOP 505-68-10) (NASA-TM-105380; E-6767; NAS 1.15:105380) Avail: CASI HC A14/MF A03

A study of the ice accretion patterns and performance of characteristics of a multi-element airfoil was undertaken at the NASA-Lewis Icing Research Tunnel. Several configurations were examined to determine the ice shape and performance characteristics. The testing included glaze, rime, and mixed icing regimes. Tunnel cloud conditions were set to correspond to those typical of the operating environment for commercial transport aircraft. Measurements acquired included ice profile tracings and aerodynamic forces both during the accretion process and in a post-accretion evaluation over a range of angle of attack. Substantial ice accretions developed on the main wing, flaps, and slat surfaces. Force measurements indicate severe performance degradation, especially near CL max, for both light and heavy ice accretion. Frost was seen on the lower surface of the airfoil which was found to contribute significantly to the force components.

Author

N92-18760*# National Aeronautics and Space Administration. Lewis Research Center, Cleveland, OH.

SEMI-EMPIRICAL MODEL FOR PREDICTION OF UNSTEADY FORCES ON AN AIRFOIL WITH APPLICATION TO FLUTTER

APARAJIT J. MAHAJAN (Toledo Univ., OH.) and KRISHNA RAO V. KAZA Feb. 1992 28 p

(Contract RTOP 535-03-10) (NASA-TM-105414; E-6820; NAS 1.15:105414) Avail: CASI HC A03/MF A01

A semi-empirical model is described for predicting unsteady aerodynamic forces on arbitrary airfoils under mildly stalled and unstalled conditions. Aerodynamic forces are modeled using second order ordinary differential equations for lift and moment with airfoil motion as the input. This model is simultaneously integrated with structural dynamics equations to determine flutter characteristics for a two degrees-of-freedom system. Results for a number of cases are presented to demonstrate the suitability of this model to predict flutter. Comparison is made to the flutter characteristics determined by a Navier-Stokes solver and also the classical incompressible potential flow theory. Author

N92-19437*# National Aeronautics and Space Administration. Lewis Research Center, Cleveland, OH.

UNSTEADY-FLOW-FIELD PREDICTIONS FOR OSCILLATING CASCADES

DENNIS L. HUFF 1991 24 p Presented at the Sixth International Symposium on Unsteady Aerodynamics, Aeroacoustics, and Aeroelasticity of Turbomachines and Propellers, Notre Dame, IN, 15-19 Sep. 1991; sponsored by the International Union for Theoretical and Applied Mechanics

(Contract RTOP 535-03-10) (NASA-TM-105283; E-6613; NAS 1.15:105283) Avail: CASI HC A03/MF A01

The unsteady flow field around an oscillating cascade of flat plates with zero stagger was studied by using a time marching Euler code. This case had an exact solution based on linear theory and served as a model problem for studying pressure wave propagation in the numerical solution. The importance of using proper unsteady boundary conditions, grid resolution, and time

step size was shown for a moderate reduced frequency. Results show that an approximate nonreflecting boundary condition based on linear theory does a good job of minimizing reflections from the inflow and outflow boundaries and allows the placement of the boundaries to be closer to the airfoils than when reflective boundaries are used. Stretching the boundary to dampen the unsteady waves is another way to minimize reflections. Grid clustering near the plates captures the unsteady flow field better than when uniform grids are used as long as the 'Courant Friedrichs Levy' (CFL) number is less than 1 for a sufficient portion of the grid. Finally, a solution based on an optimization of grid, CFL number, and boundary conditions shows good agreement with linear theory. Author

N92-19993*# National Aeronautics and Space Administration. Lewis Research Center, Cleveland, OH.

CALCULATIONS OF HOT GAS INGESTION FOR A STOVL AIRCRAFT MODEL

DAVID M. FRICKER (National Aeronautics and Space Administration. Lewis Research Center, Cleveland, OH.), JAMES D. HOLDEMAN (National Aeronautics and Space Administration. Lewis Research Center, Cleveland, OH.), and SURYA P. VANKA (Illinois Univ., Urbana.) 1992 10 p Presented at the 30th Aerospace Sciences Meeting and Exhibit, Reno, NV, 6-9 Jan. 1992; sponsored by AIAA Original contains color illustrations (Contract RTOP 505-68-71)

(NASA-TM-105437; E-6808; NAS 1.15:105437; AVSCOM-TR-91-C-053; AIAA PAPER 92-0385)

Hot gas ingestion problems for Short Take-Off, Vertical Landing (STOVL) aircraft are typically approached with empirical methods and experience. In this study, the hot gas environment around a STOVL aircraft was modeled as multiple jets in crossflow with inlet suction. The flow field was calculated with a Navier-Stokes, Reynolds-averaged, turbulent, 3D computational fluid dynamics code using a multigrid technique. A simple model of a STOVL aircraft with four choked jets at 1000 K was studied at various heights, headwind speeds, and thrust splay angles in a modest parametric study. Scientific visualization of the computed flow field shows a pair of vortices in front of the inlet. This and other qualitative aspects of the flow field agree well with experimental data. Author

N92-20934*# National Aeronautics and Space Administration. Lewis Research Center, Cleveland, OH.

FLOW STUDIES IN CLOSE-COUPLED VENTRAL NOZZLES FOR STOVL AIRCRAFT

JACK G. MCARDLE and C. FREDERIC SMITH (Sverdrup Technology, Inc., Cleveland, OH.) 1990 23 p Presented at the Aerospace Atlantic Conference, Dayton, OH, 23-26 Apr. 1990; sponsored by SAE Previously announced in IAA as A91-21242 (Contract RTOP 505-62-71)

(NASA-TM-102554; E-5369; NAS 1.15:102554; SAE-901033) Avail: CASI HC A03/MF A01

Flow in a generic ventral nozzle system was studied experimentally and analytically with the PARC3D computational fluid dynamics program in order to evaluate the program's ability to predict system performance and internal flow patterns. A generic model of a tailpipe with a rectangular ventral nozzle, about 1/3 of full size, was tested with unheated air at steady state pressure ratios up to 4.0. The end of the tailpipe was closed to simulate a blocked exhaust nozzle. Flow behavior into and through the ventral duct is discussed and illustrated with paint streak flow visualization photographs. PARC3D graphic images are shown for comparison with the experimental photographs. The program successfully predicted internal flow patterns; it also computed thrust and discharge coefficients within 1 pct. of measured values. Author

N92-23105*# National Aeronautics and Space Administration. Lewis Research Center, Cleveland, OH.

NASA'S AIRCRAFT ICING TECHNOLOGY PROGRAM

JOHN J. REINMANN 1991 12 p Presented at the 1991 Winter Annual Meeting of the ASME, Atlanta, GA, 1-6 Dec. 1991 Previously announced as N91-20120

02 AERODYNAMICS

(Contract RTOP 505-68-11)
(NASA-TM-104518; E-6388; NAS 1.15:104518) Avail: CASI HC A03/MF A01

NASA' Aircraft Icing Technology program is aimed at developing innovative technologies for safe and efficient flight into forecasted icing. The program addresses the needs of all aircraft classes and supports both commercial and military applications. The program is guided by three key strategic objectives: (1) numerically simulate an aircraft's response to an in-flight icing encounter, (2) provide improved experimental icing simulation facilities and testing techniques, and (3) offer innovative approaches to ice protection. Our research focuses on topics that directly support stated industry needs, and we work closely with industry to assure a rapid and smooth transfer of technology. This paper presents selected results that illustrate progress towards the three strategic objectives, and it provides a comprehensive list of references on the NASA icing program. Author

N92-23269*# National Aeronautics and Space Administration. Lewis Research Center, Cleveland, OH.

THE FLIP-FLOP NOZZLE EXTENDED TO SUPERSONIC FLOWS

GANESH RAMAN (Sverdrup Technology, Inc., Brook Park, OH.), MICHAEL HAILYE (Michigan Univ., Ann Arbor.), and EDWARD J. RICE 1992 26 p Proposed for presentation at the Tenth Applied Aerodynamic Conference, Palo Alto, CA, 22-24 Jun. 1992; sponsored by AIAA
(Contract NAS3-25266; RTOP 505-62-52)
(NASA-TM-105570; E-6895; NAS 1.15:105570) Avail: CASI HC A03/MF A01

An experiment studying a fluidically oscillated rectangular jet flow was conducted. The Mach number was varied over a range from low subsonic to supersonic. Unsteady velocity and pressure measurements were made using hot wires and piezoresistive pressure transducers. In addition smoke flow visualization using high speed photography was used to document the oscillation of the jet. For the subsonic flip-flop jet it was found that the apparent time-mean widening of the jet was not accompanied by an increase in mass flux. It was found that it is possible to extend the operation of these devices to supersonic flows. Most of the measurements were made for a fixed nozzle geometry for which the oscillations ceased at a fully expanded Mach number of 1.58. By varying the nozzle geometry this limitation was overcome and operation was extended to Mach 1.8. The streamwise velocity perturbation levels produced by this device were much higher than the perturbation levels that could be produced using conventional excitation sources such as acoustic drivers. In view of this ability to produce high amplitudes, the potential for using small scale fluidically oscillated jet as an unsteady excitation source for the control of shear flows in full scale practical applications seems promising. Author

N92-23563*# National Aeronautics and Space Administration. Lewis Research Center, Cleveland, OH.

INTERACTIVE SOLUTION-ADAPTIVE GRID GENERATION PROCEDURE

TODD L. HENDERSON (Illinois Univ., Urbana.), YUNG K. CHOO, and KI D. LEE (Illinois Univ., Urbana.) Apr. 1992 28 p Original contains color illustrations
(Contract RTOP 505-62-52)
(NASA-TM-105432; E-6853; NAS 1.15:105432)

TURBO-AD is an interactive solution adaptive grid generation program under development. The program combines an interactive algebraic grid generation technique and a solution adaptive grid generation technique into a single interactive package. The control point form uses a sparse collection of control points to algebraically generate a field grid. This technique provides local grid control capability and is well suited to interactive work due to its speed and efficiency. A mapping from the physical domain to a parametric domain was used to improve difficulties encountered near outwardly concave boundaries in the control point technique. Therefore, all grid modifications are performed on the unit square in the parametric domain, and the new adapted grid is then mapped back to the physical domain. The grid adaption is achieved by

adapting the control points to a numerical solution in the parametric domain using control sources obtained from the flow properties. Then a new modified grid is generated from the adapted control net. This process is efficient because the number of control points is much less than the number of grid points and the generation of the grid is an efficient algebraic process. TURBO-AD provides the user with both local and global controls. Author

N92-24861*# National Aeronautics and Space Administration. Lewis Research Center, Cleveland, OH.

A TWO-DIMENSIONAL EULER SOLUTION FOR AN UNBLADED JET ENGINE CONFIGURATION

MARK E. M. STEWART In CASI, Proceedings of the 3rd Canadian Symposium on Aerodynamics p 186-193 1991 Previously announced as N92-11328

Avail: Canadian Aeronautics and Space Inst., 222 Somerset St. W., Suite 601, Ottawa, ON K2P 0J1 Canada

A two dimensional nonaxisymmetric Euler solution in a geometric representation of a jet engine configuration without blades is presented. The domain, including internal and external flow, is covered with a multiblock grid. To construct the grid, a domain decomposition technique is used to subdivide the domain and smooth grids are dimensioned and placed in each block. The grid contains 44 blocks which cover the external field, the inlet, bypass duct, core duct and nozzle of the nonaxisymmetric engine configuration. The geometry is symmetric about the meanline of the hub, but the grid is not since there is no symmetry condition applied to the grid between the two halves. With a symmetric grid at zero angle of attack, the measures of the solution would cancel exactly. With an asymmetric grid, the solution will not necessarily be symmetric and the lift coefficient will not necessarily be zero. Thus, grid asymmetry can be exploited to verify the resolution of the solution. The solution may be verified on the basis of five theoretical quantities: conservation of mass and energy, deviation of the lift coefficient from zero, deviation of the drag coefficient from zero, deviations from constant entropy, and deviations in the pressure distributions over the symmetric surfaces of the components. This technique is suitable for obtaining numerical solutions in complex geometries and provides a foundation for complete engine throughflow calculations. Author (CISTI)

N92-24958*# National Aeronautics and Space Administration. Lewis Research Center, Cleveland, OH.

SUPERSONIC JET MIXING ENHANCEMENT BY DELTA-TABS

K. B. M. Q. ZAMAN (Ohio State Univ., Columbus.), M. F. REEDER, and M. SAMIMY (Ohio State Univ., Columbus.) 1992 17 p Proposed for presentation at the 28th Joint Propulsion Conference and Exhibit, Nashville, TN, 6-8 Jul. 1992; sponsored by AIAA, SAE, ASME, and ASEE

(Contract RTOP 505-52-62)

(NASA-TM-105664; E-6993; NAS 1.15:105664; AIAA PAPER 92-3548) Avail: CASI HC A03/MF A01

The results of a continuing investigation of the effect of vortex generators, in the form of small tabs at the nozzle exit, on the evolution of a jet are reported. Primarily, tabs of triangular shape are considered, and the effect is studied up to an equivalent jet Mach number of 1.8. By changing the orientation of the tab with respect to the nozzle exit plane, streamwise vortex pairs of opposite sign were generated. This resulted in either an outward ejection of jet core fluid into the ambient or an inward indentation of the mixing layer into the core of the jet. A triangular shaped tab with its apex leaning downstream, referred to as a delta tab, was found to be the most effective in influencing the jet evolution. Two delta tabs, spaced 180 degrees apart, completely bifurcated the jet. Four delta tabs increased jet mixing substantially, more than by various other methods tried previously; the mass flux at fourteen jet diameters downstream from the nozzle increased by about 50 percent over that for the no tab case. The tabs were found to be effective in jets with laminar or turbulent boundary layers as well as in jets with low or high core turbulence intensities. Author

N92-25713*# National Aeronautics and Space Administration. Lewis Research Center, Cleveland, OH.

GRID MANAGEMENT

DANNY HWANG *In its* Workshop on Grid Generation and Related Areas p 3-15 Apr. 1992
Avail: CASI HC A03/MF A02

A computational environment that allows many Computational Fluid Dynamics (CFD) engineers to work on the same project exists in the Special Project Office (SPO). This environment enables several users to carry out the task of grid generation. The grid management system, used by the engineers, is described in a brief overview. The topics will include the grid file naming system, the grid-generation procedure, grid storage, and the grid format standard. Author

N92-25814*# National Aeronautics and Space Administration. Lewis Research Center, Cleveland, OH.

A NEW LAGRANGIAN METHOD FOR REAL GASES AT SUPERSONIC SPEED

C. Y. LOH and MENG-SING LIOU *In its* Computational Fluid Dynamics p 75-81 Feb. 1992

With the renewed interest in high speed flights, the real gas effect is of theoretical as well as practical importance. In the past decade, upwind splittings or Godunov-type Riemann solutions have received tremendous attention and as a result significant progress has been made both in the ideal and non-ideal gas. In this paper, we propose a new approach that is formulated using the Lagrangian description, for the calculation of supersonic/hypersonic real gas inviscid flows. This new formulation avoids the grid generation step which is automatically obtained as the solution procedure marches in the 'time-like' direction. As a result, no remapping is required and the accuracy is faithfully maintained in the Lagrangian level. In this paper, we give numerical results for a variety of real gas problems consisting of essential elements in high speed flows, such as shock waves, expansion waves, slip surfaces and their interactions. Finally, calculations for flows in a generic inlet and nozzle are presented. Author

N92-26104*# National Aeronautics and Space Administration. Lewis Research Center, Cleveland, OH.

A COMPARISON OF PREDICTED AND MEASURED INLET DISTORTION FLOWS IN A SUBSONIC AXIAL INLET FLOW COMPRESSOR ROTOR

ALBERT K. OWEN Mar. 1992 198 p Prepared in cooperation with Army Aviation Systems Command, Cleveland, OH (Contract DA PROJ. 1L1-61102-AH-45; RTOP 505-62-0K) (NASA-TM-105427; E-6843; AVSCOM-TR-92-C-001; NAS 1.15:105427) Avail: CASI HC A09/MF A03

Detailed flow measurements were taken inside an isolated axial compressor rotor operating subsonically near peak efficiency. These Laser Anemometer measurements were made with two inlet velocity profiles. One profile consisted of an unmodified baseline flow, and the second profile was distorted by placing axisymmetric screens on the hub and shroud well upstream of the rotor. A detailed comparison in the rotor relative reference frame between a Navier-Stokes solver and the measured experimental results showed good agreement between the predicted and measured flows. A primary flow is defined in the rotor and deviations and the computed predictions is made to assess the development of a passage vortex due to the distortion of the inlet flow. Computer predictions indicate that a distorted inlet profile has a minimal effect on the development of the flow in the rotor passage and the resulting passage vortex. Author

N92-26612*# National Aeronautics and Space Administration. Lewis Research Center, Cleveland, OH.

HELIUM BUBBLE FLOW VISUALIZATION OF THE SPANWISE SEPARATION ON A NACA 0012 WITH SIMULATED GLAZE ICE

M. KERHO (Illinois Univ., Urbana.), M. BRAGG (Illinois Univ., Urbana.), and J. SHIN Jan. 1992 17 p Presented at the 30th Aerospace Sciences Meeting and Exhibit, Reno, NV, 6-9 Jan. 1992; sponsored by AIAA Previously announced in IAA as A92-28192

(Contract RTOP 505-68-10)

(NASA-TM-105742; E-7147; NAS 1.15:105742; AIAA PAPER 92-0413) Copyright Avail: CASI HC A03/MF A01

Research was performed to experimentally visualize and document the flow separation due to simulated glaze ice accretion on a NACA 0012 semispan with 30 deg sweep using helium bubbles as flow tracers. Results are compared to Navier-Stokes computational simulations for different angles of attack. Prior to acquiring data for the semispan model, a two dimensional experiment was conducted to determine the accuracy of using the helium bubbles as flow tracers. Results from the three dimensional experiment compare well to the computational simulations. Author

N92-27377*# National Aeronautics and Space Administration. Lewis Research Center, Cleveland, OH.

TURBULENT HEAT FLUX MEASUREMENTS IN A TRANSITIONAL BOUNDARY LAYER

K. H. SOHN (Case Western Reserve Univ., Cleveland, OH.), K. B. M. Q. ZAMAN (Case Western Reserve Univ., Cleveland, OH.), and E. RESHOTKO (Case Western Reserve Univ., Cleveland, OH.) Apr. 1992 20 p

(Contract NCC3-124; RTOP 505-62-52)

(NASA-TM-105623; E-6962; NAS 1.15:105623) Avail: CASI HC A03/MF A01

During an experimental investigation of the transitional boundary layer over a heated flat plate, an unexpected result was encountered for the turbulent heat flux (\bar{q}''). This quantity, representing the correlation between the fluctuating normal velocity and the temperature, was measured to be negative near the wall under certain conditions. The result was unexpected as it implied a counter-gradient heat transfer by the turbulent fluctuations. Possible reasons for this anomalous result were further investigated. The possible causes considered for this negative \bar{q}'' were: (1) plausible measurement error and peculiarity of the flow facility, (2) large probe size effect, (3) 'streaky structure' in the near wall boundary layer, and (4) contributions from other terms usually assumed negligible in the energy equation including the Reynolds heat flux in the streamwise direction (\bar{u}''). Even though the energy balance has remained inconclusive, none of the items (1) to (3) appear to be contributing directly to the anomaly. Author

N92-28102*# National Aeronautics and Space Administration. Lewis Research Center, Cleveland, OH.

COMPARATIVE STUDY OF TURBULENCE MODELS IN PREDICTING HYPERSONIC INLET FLOWS

KAMLESH KAPOOR, BERNHARD H. ANDERSON, and ROBERT J. SHAW Jul. 1992 17 p Proposed for presentation at the 28th Joint Propulsion Conference and Exhibit, Nashville, TN, 6-8 Jul. 1992; sponsored by AIAA, SAE, ASME, and ASEE Original contains color illustrations

(Contract RTOP 505-62-40)

(NASA-TM-105720; E-7116; NAS 1.15:105720; AIAA PAPER

92-3098) Avail: CASI HC A03/MF A01; 1 functional color page

A numerical study was conducted to analyze the performance of different turbulence models when applied to the hypersonic NASA P8 inlet. Computational results from the PARC2D code, which solves the full two-dimensional Reynolds-averaged Navier-Stokes equation, were compared with experimental data. The zero-equation models considered for the study were the Baldwin-Lomax model, the Thomas model, and a combination of the Baldwin-Lomax and Thomas models; the two-equation models considered were the Chien model, the Speziale model (both low Reynolds number), and the Launder and Spalding model (high Reynolds number). The Thomas model performed best among the zero-equation models, and predicted good pressure distributions. The Chien and Speziale models compared very well with the experimental data, and performed better than the Thomas model near the walls. Author

02 AERODYNAMICS

N92-28674*# National Aeronautics and Space Administration. Lewis Research Center, Cleveland, OH.

EXPERIMENTAL AND COMPUTATIONAL ICE SHAPES AND RESULTING DRAG INCREASE FOR A NACA 0012 AIRFOIL

JAIWON SHIN and THOMAS H. BOND Jan. 1992 12 p Presented at the 5th Symposium on Numerical and Physical Aspects of Aerodynamic Flows, Long Beach, CA, 13-16 Jan. 1992; sponsored in part by California State Univ.

(Contract RTOP 505-68-10)

(NASA-TM-105743; E-7148; NAS 1.15:105743) Avail: CASI HC A03/MF A01

Tests were conducted in the Icing Research Tunnel (IRT) at LeRC to document the repeatability of the ice shape over the range of temperatures varying from -15 to 28 F. Measurements of drag increase due to the ice accretion were also made. The ice shape and drag coefficient data, with varying total temperatures at two different airspeeds, were compared with the computational predictions. The calculations were made with the 2D LEWICE/IBL code which is a combined code of LEWICE and the interactive boundary layer method developed for iced airfoils. Comparisons show good agreement with the experimental data in ice shapes. The calculations show the ability of the code to predict drag increases as the ice shape changes from a rime shape to a glaze shape. Author

N92-28696*# National Aeronautics and Space Administration. Lewis Research Center, Cleveland, OH.

RESULTS OF A LOW POWER ICE PROTECTION SYSTEM TEST AND A NEW METHOD OF IMAGING DATA ANALYSIS

JAIWON SHIN, THOMAS H. BOND, and GEERT A. MESANDER (Air Force Logistics Command, Tinker AFB, OK.) Jun. 1992 18 p Presented at the 48th Annual Forum and Technology Display, Washington, DC, 3-5 Jun. 1992; sponsored in part by the American Helicopter Society

(Contract RTOP 505-68-10)

(NASA-TM-105745; E-6930; NAS 1.15:105745) Avail: CASI HC A03/MF A01

Tests were conducted on a BF Goodrich De-Icing System's Pneumatic Impulse Ice Protection (PIIP) system in the NASA Lewis Icing Research Tunnel (IRT). Characterization studies were done on shed ice particle size by changing the input pressure and cycling time of the PIIP de-icer. The shed ice particle size was quantified using a newly developed image software package. The tests were conducted on a 1.83 m (6 ft) span, 0.53 m (221 in) chord NACA 0012 airfoil operated at a 4 degree angle of attack. The IRT test conditions were a -6.7 C (20 F) glaze ice, and a -20 C (-4 F) rime ice. The ice shedding events were recorded with a high speed video system. A detailed description of the image processing package and the results generated from this analytical tool are presented. Author

N92-28980*# National Aeronautics and Space Administration. Lewis Research Center, Cleveland, OH.

LASER ANEMOMETER MEASUREMENTS AND COMPUTATIONS IN AN ANNULAR CASCADE OF HIGH TURNING CORE TURBINE VANES

LOUIS J. GOLDMAN and RICHARD G. SEASHOLTZ Jul. 1992 38 p

(Contract RTOP 505-62-52)

(NASA-TP-3252; E-6354; NAS 1.60:3252) Avail: CASI HC A03/MF A01

An advanced laser anemometer (LA) was used to measure the axial and tangential velocity components in an annular cascade of turbine stator vanes designed for a high bypass ratio engine. These vanes were based on a redesign of the first-stage stator, of a two-stage turbine, that produced 75 degrees of flow turning. Tests were conducted on a 0.771 scale model of the engine size stator. The advanced LA fringe system was designed to employ thinner than usual laser beams resulting in a 50-micron-diameter probe volume. Window correction optics were used to ensure that the laser beams did not uncross in passing through the curved optical access port. Experimental LA measurements of velocity and turbulence were obtained both upstream, within, and

downstream of the stator vane row at the design exit critical velocity ratio of 0.896 at the hub. Static pressures were also measured on the vane surface. The measurements are compared, where possible with calculations from a 3-D inviscid flow analysis. The data are presented in both graphic and tabulated form so that they may be readily used to compare against other turbomachinery computations. Author

N92-30182*# National Aeronautics and Space Administration. Lewis Research Center, Cleveland, OH.

EXPERIMENTAL INVESTIGATION OF THE FLOWFIELD OF AN OSCILLATING AIRFOIL

J. PANDA and K. B. M. Q. ZAMAN Jun. 1992 20 p Presented at the 10th Applied Aerodynamics Conference, Palo Alto, CA, 22-24 Jun. 1992; sponsored by AIAA

(Contract RTOP 505-62-52)

(NASA-TM-105675; E-7046; NAS 1.15:105675; AIAA PAPER 92-2622-CP) Avail: CASI HC A03/MF A01

The flowfield of an airfoil oscillated periodically over a wide range of reduced frequencies, 0 less than or = k less than or = 1.6 is studied experimentally at chord Reynolds numbers of $R_{sub c} = 22,000$ and 44,000. The NACA0012 airfoil is pitched sinusoidally about one quarter chord between angles of attack (α) of 5 and 25 degrees. Detailed flow visualization and phase averaged vorticity measurements are carried out for $k = 0.2$ to document the evolution and the shedding of the dynamic stall vortex (DSV). In addition to the DSV, an intense vortex of opposite sign originates from the trailing edge just when the DSV is shed. After being shed into the wake, the two together take the shape of a large 'mushroom' while being convected away from the airfoil. The unsteady circulation around the airfoil and, therefore, the time varying component of the lift is estimated in a novel way from the shed vorticity flux and is found to be in good agreement with the lift variation reported by others. The delay in the shedding of the DSV with increasing k, as observed by previous researchers, is documented for the full range of k. The DSV, for example, is shed nearly at the maximum α of 25 degrees at $k = 0.2$, but is shed at the minimum α of 5 degrees at $k = 0.8$. At low k, the flowfield appears quasi-steady and the bluff body shedding corresponding to the maximum α (25 degrees) dominates the unsteady fluctuations in the wake. Author

N92-34144*# National Aeronautics and Space Administration. Lewis Research Center, Cleveland, OH.

ANALYSIS OF ICED WINGS

T. CEBECI (California State Univ., Long Beach.), H. H. CHEN (California State Univ., Long Beach.), K. KAUPS (California State Univ., Long Beach.), S. SCHIMKE (California State Univ., Long Beach.), and J. SHIN Jan. 1992 14 p Presented at the 30th Aerospace Sciences Meeting and Exhibit, Reno, NV, 6-9 Jan. 1992; sponsored in part by AIAA Previously announced in IAA as A92-29972

(Contract RTOP 505-68-10)

(NASA-TM-105773; E-7201; NAS 1.15:105773) Avail: CASI HC A03/MF A01

A method for computing ice shapes along the leading edge of a wing and a method for predicting its aerodynamic performance degradation due to icing is described. Ice shapes are computed using an extension of the LEWICE code which was developed for airfoils. The aerodynamic properties of the iced wing are determined with an interactive scheme in which the solutions of the inviscid flow equations are obtained from a panel method and the solutions of the viscous flow equations are obtained from an inverse three-dimensional finite-difference boundary-layer method. A new interaction law is used to couple the inviscid and viscous flow solutions. The application of the LEWICE wing code to the calculation of ice shapes on a MS-317 swept wing shows good agreement with measurements. The interactive boundary-layer method is applied to a tapered ice wing in order to study the effect of icing on the aerodynamic properties of the wing at several angles of attack. Author

N92-34243*# National Aeronautics and Space Administration. Lewis Research Center, Cleveland, OH.

**METHOD OF REDUCING DRAG IN AERODYNAMIC SYSTEMS
Patent Application**

FRANK HRACH, inventor (to NASA) 11 Sep. 1992 10 p
(NASA-CASE-LEW-14791-1; NAS 1.71:LEW-14791-1;
US-PATENT-APPL-SN-943659) Avail: CASI HC A02/MF A01

In the present method, boundary layer thickening is combined with laminar flow control to reduce drag. An aerodynamic body is accelerated enabling a ram turbine on the body to receive air at velocity V sub 0. The discharge air is directed over an aft portion of the aerodynamic body producing boundary layer thickening. The ram turbine also drives a compressor by applying torque to a shaft connected between the ram turbine and the compressor. The compressor sucks in lower boundary layer air through inlets in the shell of the aircraft producing laminar flow control and reducing drag. The discharge from the compressor is expanded in a nozzle to produce thrust. NASA

03

AIR TRANSPORTATION AND SAFETY

Includes passenger and cargo air transport operations; and aircraft accidents.

A92-25750*# National Aeronautics and Space Administration. Lewis Research Center, Cleveland, OH.

MECHANISMS RESULTING IN ACCRETED ICE ROUGHNESS

ALAN J. BILANIN and KIAT CHUA (Continuum Dynamics, Inc., Princeton, NJ) AIAA, Aerospace Sciences Meeting and Exhibit, 30th, Reno, NV, Jan. 6-9, 1992. 11 p. Research supported by NASA. Jan. 1992 11 p refs
(AIAA PAPER 92-0297) Copyright

Icing tests conducted on rotating cylinders in the BF Goodrich's Icing Research Facility indicate that a regular, deterministic, icing roughness pattern is typical. The roughness pattern is similar to kernels of corn on a cob for cylinders of diameter typical of a cob. An analysis is undertaken to determine the mechanisms which result in this roughness to ascertain surface scale and amplitude of roughness. Since roughness and the resulting augmentation of the convected heat transfer coefficient has been determined to most strongly control the accreted ice in ice prediction codes, the ability to predict a priori, location, amplitude and surface scale of roughness would greatly augment the capabilities of current ice accretion models. Author

A92-41262* National Aeronautics and Space Administration. Lewis Research Center, Cleveland, OH.

**MEASUREMENTS IN A LEADING-EDGE SEPARATION
BUBBLE DUE TO A SIMULATED AIRFOIL ICE ACCRETION**

M. B. BRAGG, A. KHODADOUST (Illinois University, Urbana), and S. A. SPRING (CFD Research Corp., Huntsville, AL) AIAA Journal (ISSN 0001-1452), vol. 30, no. 6, June 1992, p. 1462-1467. Jun. 1992 6 p refs
(Contract NAG3-28; NAG3-1134)

Copyright

The separation bubble formed on an airfoil at low Reynolds number behind a simulated leading-edge glaze ice accretion is studied experimentally. Surface pressure and split hot-film measurements as well as flow visualization studies of the bubble reattachment point are reported. The simulated ice generates an adverse pressure gradient that causes a laminar separation bubble of the long bubble type to form. The boundary layer separates at a location on the ice accretion that is independent of angle of attack and reattaches at a downstream location 5-40 percent chord behind the leading edge, depending on the angle of attack. Velocity profiles show a large region of reverse flow that extends up from the airfoil surface as much as 2.5 percent chord. After reattachment, a thick distorted turbulent boundary layer exists. The separation

bubble growth and reattachment are clearly seen in the plots of boundary-layer momentum thickness vs surface distance. Local minima and maxima in the boundary-layer momentum thickness development compare well with the shear layer transition point as indicated by the surface pressures and the reattachment point as measured from surface oil flow, respectively. Author

N92-21684*# National Aeronautics and Space Administration. Lewis Research Center, Cleveland, OH.

**ICING SIMULATION: A SURVEY OF COMPUTER MODELS
AND EXPERIMENTAL FACILITIES**

M. G. POTAPCZUK and J. J. REINMANN *In* AGARD, Effects of Adverse Weather on Aerodynamics 27 p Dec. 1991 Previously announced as N91-23087

Copyright Avail: CASI HC A03/MF A03

A survey of the current methods for simulation of the response of an aircraft or aircraft subsystem to an icing encounter is presented. The topics discussed include a computer code modeling of aircraft icing and performance degradation, an evaluation of experimental facility simulation capabilities, and ice protection system evaluation tests in simulated icing conditions. Current research focused on upgrading simulation fidelity of both experimental and computational methods is discussed. The need for the increased understanding of the physical processes governing ice accretion, ice shedding, and iced aerodynamics is examined. Author

N92-21686*# National Aeronautics and Space Administration. Lewis Research Center, Cleveland, OH.

SIMULATION OF ICED WING AERODYNAMICS

M. G. POTAPCZUK (Illinois Univ. at Urbana-Champaign, Savoy.), M. B. BRAGG (Georgia Inst. of Tech., Atlanta.), O. J. KWON, and L. N. SANKAR (Georgia Inst. of Tech., Atlanta.) *In* AGARD, Effects of Adverse Weather on Aerodynamics 15 p Dec. 1991 Previously announced as N91-23086

Copyright Avail: CASI HC A03/MF A03

The sectional and total aerodynamic load characteristics of moderate aspect ratio wings with and without simulated glaze leading edge ice were studied both computationally, using a three dimensional, compressible Navier-Stokes solver, and experimentally. The wing has an untwisted, untapered planform shape with NACA 0012 airfoil section. The wing has an unswept and swept configuration with aspect ratios of 4.06 and 5.0. Comparisons of computed surface pressures and sectional loads with experimental data for identical configurations are given. The abrupt decrease in stall angle of attack for the wing, as a result of the leading edge ice formation, was demonstrated numerically and experimentally. Author

N92-21688*# National Aeronautics and Space Administration. Lewis Research Center, Cleveland, OH.

**MODEL ROTOR ICING TESTS IN THE NASA. LEWIS ICING
RESEARCH TUNNEL**

ROBERT J. FLEMMING (Sikorsky Aircraft, Stratford, CT.), RANDALL K. BRITTON (Sverdrup Technology, Inc., Brook Park, OH.), and THOMAS H. BOND *In* AGARD, Effects of Adverse Weather on Aerodynamics 25 p Dec. 1991 Previously announced as N91-23184

Copyright Avail: CASI HC A03/MF A03

Tests of a lightly instrumented two bladed teetering rotor and a heavily instrumented subscale articulated main rotor were conducted in the NASA Lewis Icing Research Tunnel (IRT). The first was an OH-58 tail rotor which had a diameter of 1.575 m and a blade chord of 0.133 m, and was mounted on a NASA designed test rig. The second, a four bladed articulated rotor, had a diameter of 1.83 m with 0.124 m chord blades specifically fabricated for the experiment. This rotor was mounted on a Sikorsky Aircraft Powered Force Model, which enclosed a rotor balance and other measurement systems. The models were exposed to variations in temperature, liquid water content, and medium droplet diameter, and were operated over ranges of advance ratio, shaft angle, tip Mach number (rotor speed), and weight coefficient to determine the effect of these parameters on ice accretion. In

addition to strain gage and balance data, the test was documented with still, video, and high speed photography, ice profile tracing, and ice molds. The sensitivity is presented of the model rotors to the test parameter and a comparison of the results to theoretical predictions.

Author

N92-30395*# National Aeronautics and Space Administration. Lewis Research Center, Cleveland, OH.

LEWIS ICING RESEARCH TUNNEL TEST OF THE AERODYNAMIC EFFECTS OF AIRCRAFT GROUND DEICING/ANTI-ICING FLUIDS

L. JAMES RUNYAN (Boeing Commercial Airplane Co., Seattle, WA.), THOMAS A. ZIERTEN (Boeing Commercial Airplane Co., Seattle, WA.), EUGENE G. HILL (Boeing Commercial Airplane Co., Seattle, WA.), and HAROLD E. ADDY, JR. Aug. 1992 134 p (Contract RTOP 505-68-11)

(NASA-TP-3238; E-5808; NAS 1.15:3238) Avail: CASI HC A07/MF A02

A wind tunnel investigation of the effect of aircraft ground deicing/anti-icing fluids on the aerodynamic characteristics of a Boeing 737-200ADV airplane was conducted. The test was carried out in the NASA Lewis Icing Research Tunnel. Fluids tested include a Newtonian deicing fluid, three non-Newtonian anti-icing fluids commercially available during or before 1988, and eight new experimental non-Newtonian fluids developed by four fluid manufacturers. The results show that fluids remain on the wind after liftoff and cause a measurable lift loss and drag increase. These effects are dependent on the high-lift configuration and on the temperature. For a configuration with a high-lift leading-edge device, the fluid effect is largest at the maximum lift condition. The fluid aerodynamic effects are related to the magnitude of the fluid surface roughness, particularly in the first 30 percent chord. The experimental fluids show a significant reduction in aerodynamic effects.

Author

04

AIRCRAFT COMMUNICATIONS AND NAVIGATION

Includes digital and voice communication with aircraft; air navigation systems (satellite and ground based); and air traffic control.

A92-29889*# National Aeronautics and Space Administration. Lewis Research Center, Cleveland, OH.

CHARACTERISTICS OF A FUTURE AERONAUTICAL SATELLITE COMMUNICATIONS SYSTEM

PHILIP Y. SOHN (NASA, Lewis Research Center, Cleveland, OH), ALAN STERN (General Electric Co., Princeton, NJ), and FRED SCHMIDT (Ball Corp., Bloomfield, CO) IN: AIAA International Communication Satellite Systems Conference and Exhibit, 14th, Washington, DC, Mar. 22-26, 1992, Technical Papers. Pt. 2 1992 17 p refs

(AIAA PAPER 92-2058) Copyright

A possible operational system scenario for providing satellite communications services to the future aviation community was analyzed. The system concept relies on a Ka-band (20/30 GHz) satellite that utilizes multibeam antenna (MBA) technology. The aircraft terminal uses an extremely small aperture antenna as a result of using this higher spectrum at Ka-band. The satellite functions as a relay between the aircraft and the ground stations. The ground stations function as interfaces to the existing terrestrial networks such as the Public Service Telephone Network (PSTN). Various system tradeoffs are first examined to ensure optimized system parameters. High level performance specifications and design approaches are generated for the space, ground, and aeronautical elements in the system. Both technical and economical issues affecting the feasibility of the studied concept are addressed with the 1995 timeframe in mind.

Author

05

AIRCRAFT DESIGN, TESTING AND PERFORMANCE

Includes aircraft simulation technology.

A92-14406* National Aeronautics and Space Administration. Lewis Research Center, Cleveland, OH.

ADVANCED ICE PROTECTION SYSTEMS TEST IN THE NASA LEWIS ICING RESEARCH TUNNEL

THOMAS H. BOND, JAIWAN SHIN (NASA, Lewis Research Center, Cleveland, OH), and GEERT A. MESANDER (USAF, Air Logistics Center, Tinker AFB, OK) IN: AHS, Annual Forum, 47th, Phoenix, AZ, May 6-8, 1991, Proceedings. Vol. 2 1991 8 p refs

Copyright

Tests of eight different deicing systems based on variations of three different technologies were conducted in the NASA Lewis Research Center Icing Research Tunnel (IRT) in June and July 1990. The systems used pneumatic, eddy current repulsive, and electroexpulsive means to shed ice. The tests were conducted on a 1.83 m span, 0.53 m chord NACA 0012 airfoil operated at a 4 degree angle of attack. The models were tested at two temperatures: a glaze condition at minus 3.9 C and a rime condition at minus 17.2 C. The systems were tested through a range of icing spray times and cycling rates. Characterization of the deicers was accomplished by monitoring power consumption, ice shed particle size, and residual ice. High speed video motion analysis was performed to quantify ice particle size.

Author

A92-26950*# National Aeronautics and Space Administration. Lewis Research Center, Cleveland, OH.

NUMERICAL ANALYSIS OF A THERMAL DEICER

W. B. WRIGHT (Sverdrup Technology, Inc., Brook Park, OH), T. G. KEITH, JR., and K. J. DEWITT (Toledo, University, OH) AIAA, Aerospace Sciences Meeting and Exhibit, 30th, Reno, NV, Jan. 6-9, 1992. 13 p. Research supported by Ohio Aerospace Institute and NASA. Jan. 1992 13 p refs

(AIAA PAPER 92-0527)

An algorithm has been developed to numerically model the concurrent phenomena of two-dimensional transient heat transfer, ice accretion and ice shedding which arise from the use of an electrothermal pad. The Alternating Direction Implicit method is used to simultaneously solve the heat transfer and accretion equations occurring in a multilayered body covered with ice. In order to model the phase change between ice and water, a technique was used which assumes a phase for each node. This allows the equations to be linearized such that a direct solution is possible. This technique requires an iterative procedure to find the correct phase at each node. The computer program developed to find this solution has been integrated with the NASA/Lewis flow/trajectory code LEWICE.

Author

A92-31670*# National Aeronautics and Space Administration. Lewis Research Center, Cleveland, OH.

AN EFFICIENT FINITE ELEMENT METHOD FOR AIRCRAFT DE-ICING PROBLEMS

J. R. HUANG, THEO G. KEITH, JR., and KENNETH J. DE WITT (Toledo, University, OH) AIAA, Aerospace Sciences Meeting and Exhibit, 30th, Reno, NV, Jan. 6-9, 1992. 20 p. Research supported by NASA. Jan. 1992 20 p refs

(AIAA PAPER 92-0532) Copyright

In this paper, a finite element formulation based on an assumed states method is proposed for the solution of heat conduction problems with phase change at a fixed temperature. Attention is directed toward reduction of computer cost through the use of an efficient formulation, solver and algorithm. The procedure is applied to the analysis of an electrothermally deiced aircraft surface.

Author

A92-44547# National Aeronautics and Space Administration. Hugh L. Dryden Flight Research Facility, Edwards, CA.

THE F/A-18 EXTERNAL BURNING FLIGHT TEST

C. YUNGKURTH (Johns Hopkins University, Laurel, MD), F. DAWSON, S. HOUCK (U.S. Navy, Naval Air Test Center, Patuxent River, MD), S. CORDA (NASA, Flight Research Center, Edwards, CA), and C. TREFNY (NASA, Lewis Research Center, Cleveland, OH) AIAA, International Aerospace Planes Conference, 3rd, Orlando, FL, Dec. 3-5, 1991. 16 p. Dec. 1991 16 p refs (AIAA PAPER 91-5050) Copyright

A flight test program was undertaken to demonstrate the feasibility of obtaining external burning (EB) data in a flight environment, and to address the question of facility interference in ground test external burning data. Results showed that external burning was effective at reducing transonic base drag in a flight environment having dynamically changing conditions. The flight test program demonstrated that external burning is not just a laboratory phenomenon but is a viable technology for aerospace vehicles. Author

A92-52459*# National Aeronautics and Space Administration. Lewis Research Center, Cleveland, OH.

PILOTED EVALUATION OF AN INTEGRATED PROPULSION AND FLIGHT CONTROL SIMULATOR

MICHELLE M. BRIGHT (NASA, Lewis Research Center, Cleveland, OH) and DONALD L. SIMON (U.S. Army, Propulsion Directorate; NASA, Lewis Research Center, Cleveland, OH) IN: AIAA/AHS Flight Simulation Technologies Conference, Hilton Head Island, SC, Aug. 24-26, 1992, Technical Papers 1992 11 p refs (AIAA PAPER 92-4178) Copyright

This paper describes a piloted evaluation of the integrated flight and propulsion control simulator at NASA Lewis Research Center. The purpose of this evaluation is to demonstrate the suitability and effectiveness of this fixed based simulator for advanced integrated propulsion and airframe control design. The evaluation will cover control effector gains and deadbands, control effectiveness and control authority, and heads up display functionality. For this evaluation the flight simulator is configured for transition flight using an advanced Short Take-Off and vertical Landing fighter aircraft model, a simplified high-bypass turbofan engine model, fighter cockpit, displays, and pilot effectors. The paper describes the piloted tasks used for rating displays and control effector gains. Pilot comments and simulation results confirm that the display symbology and control gains are very adequate for the transition flight task. Additionally, it is demonstrated that this small-scale, fixed base flight simulator facility can adequately perform a real time, piloted control evaluation. Author

A92-54026*# National Aeronautics and Space Administration. Lewis Research Center, Cleveland, OH.

SUMMARY HIGHLIGHTS OF THE ADVANCED ROTORCRAFT TRANSMISSION (ART) PROGRAM

ROBERT C. BILL (U.S. Army, Vehicle Propulsion Directorate; NASA, Lewis Research Center, Cleveland, OH) AIAA, SAE, ASME, and ASEE, Joint Propulsion Conference and Exhibit, 28th, Nashville, TN, July 6-8, 1992. 25 p. Jul. 1992 25 p refs (AIAA PAPER 92-3362)

The NASA/U.S. Army Advanced Rotorcraft Transmission (ART) program is charged with the development and demonstration of lightweight, durable drivetrains for next-generation rotorcraft: (1) a Future Air Attack Vehicle for tactical ground-support and air-to-air missions, and (2) an Advanced Cargo Aircraft for heavy-lift field-support operations. Both tilt-rotor and more conventional helicopter configurations have been studied by the ART program. ART performance goals are sought through the use of advanced component materials and lubrication systems, transmission and geartrain configurations, and airframe/drivetrain integrations. O.C.

A92-55131* National Aeronautics and Space Administration. Lewis Research Center, Cleveland, OH.

TURNING UP THE HEAT ON AIRCRAFT STRUCTURES

ALAN DOBYNS (Sikorsky Aircraft, Stratford, CT), CHARLES SAFF (McDonnell Aircraft Co., Saint Louis, MO), and ROBERT JOHNS (NASA, Lewis Research Center, Cleveland, OH) Aerospace America (ISSN 0740-722X), vol. 30, no. 9, Sept. 1992, p. 34-37. Sep. 1992 4 p

Copyright

An overview is presented of the current effort in design and development of aircraft structures to achieve the lowest cost for best performance. Enhancements in this area are focused on integrated design, improved design analysis tools, low-cost fabrication techniques, and more sophisticated test methods. 3D CAD/CAM data are becoming the method through which design, manufacturing, and engineering communicate. R.E.P.

A92-55300*# National Aeronautics and Space Administration. Lewis Research Center, Cleveland, OH.

ANALYSIS OF AIRFRAME/ENGINE INTERACTIONS FOR A STOVL AIRCRAFT WITH INTEGRATED FLIGHT/PROPULSION CONTROL

JOHN D. SCHIERMAN and T. A. LOWELL (Arizona State University, Tempe) IN: AIAA Guidance, Navigation and Control Conference, Hilton Head Island, SC, Aug. 10-12, 1992, Technical Papers. Pt. 3 1992 11 p refs

(Contract NAG3-998)

(AIAA PAPER 92-4623) Copyright

A multivariable analysis technique is used to evaluate the effects of the dynamic cross coupling between the airframe and engine subsystems in an advanced STOVL configuration. A critical frequency range is identified along with potentially poor stability robustness due to the airframe/engine interactions. Within the critical frequency range, stability and performance are found to be sensitive to variations in the coupling between the airframe's flight path angle and the engine's fuel flow rate. A stability sensitivity study indicates that the interactions between the flight path angle and the fuel flow rate are potentially the most critical with respect to stability and performance robustness. V.L.

N92-13959*# National Aeronautics and Space Administration. Lewis Research Center, Cleveland, OH.

VORTEX GENERATOR DESIGN FOR AIRCRAFT INLET DISTORTION AS A NUMERICAL OPTIMIZATION PROBLEM

BERNHARD H. ANDERSON and RALPH LEVY (Scientific Research Associates, Inc., Glastonbury, CT.) /n Pennsylvania State Univ., Third International Conference on Inverse Design Concepts and Optimization in Engineering Sciences (ICIDES-3) p 419-431 1991

Avail: CASI HC A03/MF A06

Aerodynamic compatibility of aircraft/inlet/engine systems is a difficult design problem for aircraft that must operate in many different flight regimes. Takeoff, subsonic cruise, supersonic cruise, transonic maneuvering, and high altitude loiter each place different constraints on inlet design. Vortex generators, small wing like sections mounted on the inside surfaces of the inlet duct, are used to control flow separation and engine face distortion. The design of vortex generator installations in an inlet is defined as a problem addressable by numerical optimization techniques. A performance parameter is suggested to account for both inlet distortion and total pressure loss at a series of design flight conditions. The resulting optimization problem is difficult since some of the design parameters take on integer values. If numerical procedures could be used to reduce multimillion dollar development test programs to a small set of verification tests, numerical optimization could have a significant impact on both cost and elapsed time to design new aircraft. Author

N92-22534*# National Aeronautics and Space Administration. Lewis Research Center, Cleveland, OH.

THE NASA AIRCRAFT ICING RESEARCH PROGRAM

ROBERT J. SHAW and JOHN J. REINMANN /n its Aeropropulsion 1987 p 315-341 Feb. 1990

Avail: CASI HC A03/MF A04

The objective of the NASA aircraft icing research program is to develop and make available to industry icing technology to

06 AIRCRAFT INSTRUMENTATION

support the needs and requirements for all-weather aircraft designs. Research is being done for both fixed wing and rotary wing applications. The NASA program emphasizes technology development in two areas, advanced ice protection concepts and icing simulation. Reviewed here are the computer code development/validation, icing wind tunnel testing, and icing flight testing efforts. Author

06

AIRCRAFT INSTRUMENTATION

Includes cockpit and cabin display devices; and flight instruments.

A92-42602* National Aeronautics and Space Administration. Lewis Research Center, Cleveland, OH.

WAVELENGTH-MULTIPLEXED FIBER-OPTIC POSITION ENCODER FOR AIRCRAFT CONTROL SYSTEMS

GLENN BEHEIM, MICHAEL J. KRASOWSKI, JORGE L. SOTOMAYOR (NASA, Lewis Research Center, Cleveland, OH), KLAUS FRITSCH, JOSEPH M. FLATICO, RICHARD L. BATHURST, JOHN G. EUSTACE (John Carroll University, Cleveland, OH), and DONALD J. ANTHAN (Cleveland State University, OH) IN: Fiber optic systems for mobile platforms IV; Proceedings of the Meeting, San Jose, CA, Sept. 18, 1990 1991 10 p refs Copyright

NASA-Lewis has developed wavelength-multiplexed digital position fiber-optics transducers for use in aircraft control systems. A prototype LED-powered rotary encoder for a commercial aircraft turbofan engine is under construction which will have 8-bit resolution and an operational temperature in the 90 C range. A compact electrooptics module is also under development which will be able to withstand gas turbine environments. A second-generation device will incorporate integrated photonics technologies to increase optical power margin. O.C.

A92-46244* National Aeronautics and Space Administration. Lewis Research Center, Cleveland, OH.

FIBER OPTIC CONTROLS FOR AIRCRAFT ENGINES - ISSUES AND IMPLICATIONS

SAMHITA DASGUPTA, GARY L. POPPEL, and WILLIAM P. ANDERSON (GE Aircraft Engines, Cincinnati, OH) IN: Integrated optics and optoelectronics II; Proceedings of the Meeting, San Jose, CA, Sept. 17-19, 1990 1991 12 p refs (Contract NAS3-25344) Copyright

Some of the issues involved with the application of fiber-optic controls for aircraft engines in the harsh operating environment are addressed, with emphasis on fiber-optic temperature, pressure, position, and speed sensors. Criteria are established to evaluate the optical modulation technique, the sensor/control unit interconnection, and the electrooptic architecture. Single mode and polarization dependent sensor types, sensors which depend on the reflection and/or transmission of light through the engine environment, and intensity-based analog sensors are eliminated as a possible candidate for engine implementation. Fiber-optic harnesses tested for their optical integrity, temperature stability, and mechanical strength, exhibit a capacity to meet mechanical strength requirements and still gain a significant reduction in cable weight. C.A.B.

A92-46246* National Aeronautics and Space Administration. Lewis Research Center, Cleveland, OH.

POTENTIAL FOR INTEGRATED OPTICAL CIRCUITS IN ADVANCED AIRCRAFT WITH FIBER OPTIC CONTROL AND MONITORING SYSTEMS

ROBERT BAUMBICK (NASA, Lewis Research Center, Cleveland, OH) IN: Integrated optics and optoelectronics II; Proceedings of the Meeting, San Jose, CA, Sept. 17-19, 1990 1991 13 p

refs

Copyright

The current Fiber Optic Control System Integration (FOCSI) program is reviewed and the potential role of IOCs in FOCSI applications is described. The program is intended for building, environmentally testing, and demonstrating operation in piggyback flight tests (no active control with optical sensors) of a representative sensor system for propulsion and flight control. The optical sensor systems are to be designed to fit alongside the bill-of-materials sensors for comparison. The sensors are to be connected to electrooptic architecture cards which will contain the optical sources and detectors to recover and process the modulated optical signals. The FOCSI program is to collect data on the behavior of passive optical sensor systems in a flight environment and provide valuable information on installation and maintenance problems for this technology, as well as component survivability (light sources, connectors, optical fibers, etc.). C.A.B.

07

AIRCRAFT PROPULSION AND POWER

Includes prime propulsion systems and systems components, e.g., gas turbine engines and compressors; and onboard auxiliary power plants for aircraft.

A92-15591* National Aeronautics and Space Administration. Lewis Research Center, Cleveland, OH.

RELIABILITY ANALYSIS OF A STRUCTURAL CERAMIC COMBUSTION CHAMBER

JONATHAN A. SALEM, JANE M. MANDERSCHIED, MARC R. FREEDMAN, and JOHN P. GYEKENYESI (NASA, Lewis Research Center, Cleveland, OH) ASME, International Gas Turbine and Aeroengine Congress and Exposition, 36th, Orlando, FL, June 3-6, 1991. 8 p. Previously announced in STAR as N90-28112. Jun. 1991 8 p refs (ASME PAPER 91-GT-155)

The Weibull modulus, fracture toughness and thermal properties of a silicon nitride material used to make a gas turbine combustor were experimentally measured. The location and nature of failure origins resulting from bend tests were determined with fractographic analysis. The measured Weibull parameters were used along with thermal and stress analysis to determine failure probabilities of the combustor with the CARES design code. The effect of data censoring, FEM mesh refinement, and fracture criterion were considered in the analysis. Author

A92-15634* CFD Research Corp., Huntsville, AL.

CFD ANALYSIS OF JET MIXING IN LOW NO(X) FLAMETUBE COMBUSTORS

M. V. TALPALLIKAR, C. E. SMITH (CFD Research Corp., Huntsville, AL), M. C. LAI (Wayne State University, Detroit, MI), and J. D. HOLDEMAN (NASA, Lewis Research Center, Cleveland, OH) ASME, International Gas Turbine and Aeroengine Congress and Exposition, 36th, Orlando, FL, June 3-6, 1991. 10 p. Previously announced in STAR as N91-26146. Jun. 1991 10 p refs (Contract NAS3-25834) (ASME PAPER 91-GT-217)

The Rich-burn/Quick-mix/Lean-burn (RQL) combustor has been identified as a potential gas turbine combustor concept to reduce NO(x) emissions in High Speed Civil Transport (HSCT) aircraft. To demonstrate reduced NO(x) levels, cylindrical flametube versions of RQL combustors are being tested at NASA Lewis Research Center. A critical technology needed for the RQL combustor is a method of quickly mixing by-pass combustion air with rich-burn gases. Jet mixing in a cylindrical quick-mix section was numerically analyzed. The quick-mix configuration was five inches in diameter and employed twelve radial-inflow slots. The numerical analyses were performed with an advanced, validated

3D Computational Fluid Dynamics (CFD) code named REFLEQS. Parametric variation of jet-to-mainstream momentum flux ratio (J) and slot aspect ratio was investigated. Both non-reacting and reacting analyses were performed. Results showed mixing and NO(x) emissions to be highly sensitive to J and slot aspect ratio. Lowest NO(x) emissions occurred when the dilution jet penetrated to approximately mid-radius. The viability of using 3D CFD analyses for optimizing jet mixing was demonstrated. Author

A92-24403* National Aeronautics and Space Administration. Lewis Research Center, Cleveland, OH.

HOT GAS ENVIRONMENT AROUND STOVL AIRCRAFT IN GROUND PROXIMITY. II - NUMERICAL STUDY

D. K. TAFTI and S. P. VANKA (Illinois, University, Urbana) Feb. 1992 8 p refs
(Contract NAG3-1026)
Copyright

A92-25696*# National Aeronautics and Space Administration. Lewis Research Center, Cleveland, OH.

A NEW UNSTEADY MIXING MODEL TO PREDICT NO(X) PRODUCTION DURING RAPID MIXING IN A DUAL-STAGE COMBUSTOR

SURESH MENON (Quest Integrated, Inc., Kent, WA), PATRICK A. MCMURTRY (Utah, University, Salt Lake City), ALAN R. KERSTEIN (Sandia National Laboratories, Livermore, CA), and J.-Y. CHEN (California, University, Berkeley) AIAA, Aerospace Sciences Meeting and Exhibit, 30th, Reno, NV, Jan. 6-9, 1992. 13 p. Research supported by DOE and University of Utah. Jan. 1992 13 p refs

(Contract NAS3-26242)
(AIAA PAPER 92-0233) Copyright

An advanced gas turbine engine to power supersonic transport aircraft is currently under study. In addition to high combustion efficiency requirements, environmental concerns have placed stringent restrictions on the pollutant emissions from these engines. A dual-stage combustor with the potential for minimizing pollutants such as NO(x) emissions is undergoing experimental evaluation. A major technical issue in the design of this combustor is how to rapidly mix the hot, fuel-rich primary stage product with the secondary diluent air to obtain a fuel-lean mixture for combustion in the secondary stage. Numerical design studies using steady-state methods cannot account for the unsteady phenomena in the mixing region. Therefore, to evaluate the effect of unsteady mixing and combustion processes, a novel unsteady mixing model is demonstrated here. This model has been used in a stand-alone mode to study mixing and combustion in hydrogen-air nonpremixed jet flames. NO(x) production in these jet flames was also predicted. Comparison of the computed results with experimental data show good agreement thereby providing validation of the mixing model. Author

A92-26234*# National Aeronautics and Space Administration. Lewis Research Center, Cleveland, OH.

UNSTEADY BLADE PRESSURES ON A PROPFAN AT TAKEOFF - EULER ANALYSIS AND FLIGHT DATA

M. NALLASAMY (Sverdrup Technology, Inc., Brook Park, OH) AIAA, Aerospace Sciences Meeting and Exhibit, 30th, Reno, NV, Jan. 6-9, 1992. 11 p. Previously announced in STAR as N92-13071. Jan. 1992 11 p refs

(Contract NAS3-25266)
(AIAA PAPER 92-0376)

The unsteady blade pressures due to the operation of the propfan at an angle to the direction of the mean flow are obtained by solving the unsteady three dimensional Euler equations. The configurations considered is the eight bladed SR7L propfan at takeoff conditions and the inflow angles considered are 6.3 deg, 8.3 deg, 11.3 deg. The predicted blade pressure waveforms are compared with inflight measurements. At the inboard radial station ($r/R = 0.68$) the phase of the predicted waveforms show reasonable agreement with the measurements while the amplitudes are over predicted in the leading edge region of the blade. At the outboard radial station ($r/R = 0.95$), the predicted amplitudes of

the waveforms on the pressure surface are in good agreement with flight data for all inflow angles. The measured (installed propfan) waveforms show a relative phase lag compared to the computed (propfan alone) waveforms. The phase lag depends on the axial location of the transducer and the surface of the blade. On the suction surface, in addition to the relative phase lag, the measurements show distortion (widening and steepening) of the waveforms. The extend of distortion increases with increase in inflow angle. This distortion seems to be due to viscous separation effects which depend on the azimuthal location of the blade and the axial location of the transducer. Author

A92-28191*# National Aeronautics and Space Administration. Lewis Research Center, Cleveland, OH.

CALCULATIONS OF HOT GAS INGESTION FOR A STOVL AIRCRAFT MODEL

D. M. FRICKER (NASA, Lewis Research Center; U.S. Army, Propulsion Directorate, Cleveland, OH), J. D. HOLDEMAN (NASA, Lewis Research Center, Cleveland, OH), and S. P. VANKA (Illinois, University, Urbana) AIAA, Aerospace Sciences Meeting and Exhibit, 30th, Reno, NV, Jan. 6-9, 1992. 10 p. Jan. 1992 10 p refs

(AIAA PAPER 92-0385)

Hot gas ingestion problems for STOVL (Short Take-Off, Vertical Landing) aircraft are typically approached with empirical methods and experience. In this study, the hot gas environment around a STOVL aircraft was modeled as multiple jets in crossflow with inlet suction. The flow field was calculated with a Navier-Stokes, Reynolds-averaged, turbulent, 3D CFD code using a multigrid technique. A simple model of a STOVL aircraft with four choked jets at 1000 K was studied at various heights, headwind speeds, and thrust splay angles in a modest parametric study. Scientific visualization of the computed flow field shows a pair of vortices in front of the inlet. This and other qualitative aspects of the flow field agree well with experimental data. Author

A92-28538* National Aeronautics and Space Administration. Lewis Research Center, Cleveland, OH.

FLOW IN A VENTRAL NOZZLE FOR SHORT TAKEOFF AND VERTICAL LANDING AIRCRAFT

CRAWFORD F. SMITH (NASA, Lewis Research Center, Cleveland; Sverdrup Technology, Inc., Brook Park, OH) and JACK G. MCARDLE (NASA, Lewis Research Center, Cleveland, OH) Apr. 1992 7 p refs

(Contract NAS3-25266)
Copyright

A92-34408*# National Aeronautics and Space Administration. Lewis Research Center, Cleveland, OH.

AEROELASTIC STABILITY ANALYSES OF TWO COUNTER ROTATING PROPFAN DESIGNS FOR A CRUISE MISSILE MODEL

APARAJIT J. MAHAJAN, JOHN M. LUCERO, ORAL MEHMED, and GEORGE L. STEFKO (NASA, Lewis Research Center, Cleveland, OH) IN: AIAA/ASME/ASCE/AHS/ASC Structures, Structural Dynamics and Materials Conference, 33rd, Dallas, TX, Apr. 13-15, 1992, Technical Papers. Pt. 3 1992 11 p refs
(AIAA PAPER 92-2218) Copyright

A modal aeroelastic analysis combining structural and aerodynamic models is applied to counterrotating propfans to evaluate their structural integrity for wind-tunnel testing. The aeroelastic analysis code is an extension of the 2D analysis code called the Aeroelastic Stability and Response of Propulsion Systems. Rotational speed and freestream Mach number are the parameters for calculating the stability of the two blade designs with a modal method combining a finite-element structural model with 2D steady and unsteady cascade aerodynamic models. The model demonstrates convergence to the least stable aeroelastic mode, describes the effects of a nonuniform inflow, and permits the modification of geometry and rotation. The analysis shows that the propfan designs are suitable for the wind-tunnel test and confirms that the propfans should be flutter-free under the range of conditions of the testing. C.C.S.

07 AIRCRAFT PROPULSION AND POWER

A92-34598*# National Aeronautics and Space Administration. Lewis Research Center, Cleveland, OH.

ANALYSIS OF CASCADES USING A TWO DIMENSIONAL EULER AEROELASTIC SOLVER

T. S. R. REDDY, MILIND A. BAKHLE (Toledo, University, OH), DENNIS L. HUFF (NASA, Lewis Research Center, Cleveland, OH), and TIMOTHY W. SWAFFORD (Mississippi State University, Mississippi State) IN: AIAA/ASME/ASCE/AHS/ASC Structures, Structural Dynamics and Materials Conference, 33rd, Dallas, TX, Apr. 13-15, 1992, Technical Papers. Pt. 5 1992 15 p refs (Contract NAG3-3139; NAG3-1137; NAG3-983) (AIAA PAPER 92-2370)

A two-dimensional unsteady aerodynamic Euler solver based on a flux differencing scheme is being developed to analyze oscillating cascades. The cascades can have subsonic, transonic, or supersonic flow with either subsonic or supersonic axial velocity. The aerodynamic solver is coupled with a typical section structural model for each blade of the cascade. Flutter analysis methods both in time and frequency domains are then implemented into the resulting aeroelastic solver. Methods that reduce computational time for calculating the unsteady aerodynamic coefficients, namely the influence coefficient method and the pulse response method, are also implemented and validated. The present solver showed good correlation with published results for all the flow regimes. It is shown that grid coarsening improved the accuracy of the predictions. A representative flutter calculation showed that both the frequency domain and time domain methods are implemented correctly into the aeroelastic solver. Author

A92-35687*# National Aeronautics and Space Administration. Lewis Research Center, Cleveland, OH.

A NUMERICAL CLASSICAL FLUTTER ANALYSIS OF ADVANCED PROPELLERS

R. SRIVASTAVA, T. S. R. REDDY (Toledo, University, OH), and O. MEHMED (NASA, Lewis Research Center, Cleveland, OH) IN: AIAA Dynamics Specialists Conference, Dallas, TX, Apr. 16, 17, 1992, Technical Papers 1992 11 p refs (Contract NAG3-3139; NAG3-1230) (AIAA PAPER 92-2118)

A three-dimensional Euler solver is coupled with a three-dimensional structural dynamics model to investigate flutter of propfans. An implicit-explicit hybrid scheme is used to reduce computational time for the solution of Euler equations. The aeroelastic equations are formulated in normal modes and are solved for flutter in frequency domain. The required generalized forces are obtained using a pulse response method. Computations show that the instability is dominated by the second mode frequency as was observed in experiment. Author

A92-40151* National Aeronautics and Space Administration. Lewis Research Center, Cleveland, OH.

EFFECT OF TABS ON THE EVOLUTION OF AN AXISYMMETRIC JET

K. B. M. Q. ZAMAN (NASA, Lewis Research Center, Cleveland, OH), M. SAMIMY, and M. F. REEDER (Ohio State University, Columbus) IN: Symposium on Turbulent Shear Flows, 8th, Munich, Federal Republic of Germany, Sept. 9-11, 1991, Proceedings. Vol. 2 1991 6 p refs

The effect of vortex generators, in the form of small tabs at the nozzle exit, on the evolution of an axisymmetric jet was investigated experimentally over a jet Mach number range of 0.34 to 1.81. The effects of one, two, and four tabs were studied in comparison with the corresponding case without a tab. Each tab introduced an indentation in the shear layer, apparently through the action of streamwise vortices which appeared to be of the trailing vortex type originating from the tips of the tab rather than of the necklace vortex type originating from the base of the tab. The resultant effect of two tabs, placed at diametrically opposite locations, was to essentially bifurcate the jet. The influence of the tabs was essentially the same at subsonic and supersonic conditions indicating that compressibility has little to do with the effect. Author

A92-44514* National Aeronautics and Space Administration. Lewis Research Center, Cleveland, OH.

ROW-BY-ROW OFF-DESIGN PERFORMANCE CALCULATION METHOD FOR TURBINES

T. SCHOBIERI and M. ABOUELKHEIR (Texas A & M University, College Station) Aug. 1992 6 p refs Copyright

A92-45316* National Aeronautics and Space Administration. Lewis Research Center, Cleveland, OH.

HOT GAS INGESTION CHARACTERISTICS AND FLOW VISUALIZATION OF A VECTORED THRUST STOVL CONCEPT

ALBERT L. JOHNS, GEORGE H. NEINER, TIMOTHY J. BENCIC (NASA, Lewis Research Center, Cleveland, OH), JOSEPH D. FLOOD, KURT C. AMUEDO, THOMAS W. STROCK, and BEN R. WILLIAMS (McDonnell Aircraft Co., Saint Louis, MO) IN: International Powered Lift Conference, London, England, Aug. 29-31, 1990, Proceedings 1990 20 p refs Copyright

The study presents results obtained at the compressor face of a 9.2-percent scale vectored thrust model in ground effects from Phases I and II of a test program to evaluate the hot ingestion phenomena and control techniques, and to conduct flow visualization of the model flowfield in and out of ground effects, respectively. A description of the model, facility, a new model support system, and a sheet laser illumination system are provided. The findings contain the compressor face pressure and temperature distortions, compressor face temperature rise, and the environmental effects of the hot gas. The environmental effects include the ground plane temperature and pressure distributions, model airframe heating, and the location of the ground flow separation. Results from the sheet laser flow visualization test are also presented. C.A.B.

A92-45325* National Aeronautics and Space Administration. Lewis Research Center, Cleveland, OH.

EXPERIMENTAL AND ANALYTICAL STUDY OF CLOSE-COUPLED VENTRAL NOZZLES FOR ASTOVL AIRCRAFT

JACK G. MCARDLE (NASA, Lewis Research Center, Cleveland, OH) and C. F. SMITH (Sverdrup Technology, Inc., Cleveland, OH) IN: International Powered Lift Conference, London, England, Aug. 29-31, 1990, Proceedings 1990 14 p refs Copyright

Flow in a generic ventral nozzle system was studied experimentally and analytically with a block version of the PARC3D computational fluid dynamics program (a full Navier-Stokes equation solver) in order to evaluate the program's ability to predict system performance and internal flow patterns. Measurements showed about 5.5-percent flow-turning loss, reasonable nozzle performance coefficients, and a significant aftward axial component of thrust due to flow turning more than 90 deg. Flow behavior into and through the ventral duct is discussed and illustrated with paint streak flow visualization photographs. PARC3D flow visualization images are shown for comparison with the paint streak photographs. Modeling and computational issues encountered in the analytical work are discussed. Author

A92-49128*# National Aeronautics and Space Administration. Lewis Research Center, Cleveland, OH.

ANALYTICAL AND EXPERIMENTAL STUDIES OF HEAT PIPE RADIATION COOLING OF HYPERSONIC PROPULSION SYSTEMS

R. A. MARTIN, M. A. MERRIGAN, M. G. ELDER, J. T. SENA, E. S. KEDDY (Los Alamos National Laboratory, NM), and C. C. SILVERSTEIN (CCS Associates, Bethel Park, PA) AIAA, SAE, ASME, and ASEE, Joint Propulsion Conference and Exhibit, 28th, Nashville, TN, July 6-8, 1992. 8 p. Research sponsored by DOE. Jul. 1992 8 p refs (Contract NASA ORDER C-30002-M) (AIAA PAPER 92-3809)

Analytical and experimental studies were completed to assess the feasibility of using high-temperature heat pipes to cool

hypersonic engine components. This new approach involves using heat pipes to transport heat away from the combustor, nozzle, or inlet regions, and to reject it to the environment by thermal radiation from an external heat pipe nacelle. For propulsion systems using heat pipe radiation cooling (HPRC), it is possible to continue to use hydrocarbon fuels into the Mach 4 to Mach 6 speed range, thereby enhancing the economic attractiveness of commercial or military hypersonic flight. In the second-phase feasibility program recently completed, it is found that heat loads produced by considering both convection and radiation heat transfer from the combustion gas can be handled with HPRC design modifications. The application of thermal insulation to ramburner and nozzle walls was also found to reduce the heat load by about one-half and to reduce peak HPRC system temperatures to below 2700 F. In addition, the operation of HPRC at cruise conditions of around Mach 4.5 and at an altitude of 90,000 ft lowers the peak hot-section temperatures to around 2800 F. An HPRC heat pipe was successfully fabricated and tested at Mach 5 conditions of heat flux, heat load, and temperature. Author

A92-54011*# National Aeronautics and Space Administration. Lewis Research Center, Cleveland, OH.

DETONATION DUCT GAS GENERATOR DEMONSTRATION PROGRAM

A. WORTMAN (ISTAR, Inc., Santa Monica, CA), P. OTHMER (California State University, Fullerton), and W. ROSTAFINSKI (NASA, Lewis Research Center, Cleveland, OH) AIAA, SAE, ASME, and ASEE, Joint Propulsion Conference and Exhibit, 28th, Nashville, TN, July 6-8, 1992. 12 p. Jul. 1992 12 p refs (Contract NAS3-25453) (AIAA PAPER 92-3174) Copyright

An experimental demonstration is presented for the generation of detonation waves that move periodically across high speed channel flow; these waves can compress the outflow from a low pressure compressor, and thereby both reduce the compressor requirements associated with conventional gas turbines and enhance thermodynamic efficiency through isochoric energy addition. By generating transient transverse waves, rather than standing waves, shock-wave losses are reduced by an order of magnitude; the result is a Humphrey cycle augmenting the basic Brayton-cycle gas turbine. Attention is presently given to results from an experimental detonation duct. O.C.

A92-54020*# National Aeronautics and Space Administration. Lewis Research Center, Cleveland, OH.

PRELIMINARY DYNAMIC TESTS OF A FLIGHT-TYPE EJECTOR

COLIN K. DRUMMOND (NASA, Lewis Research Center, Cleveland, OH) AIAA, SAE, ASME, and ASEE, Joint Propulsion Conference and Exhibit, 28th, Nashville, TN, July 6-8, 1992. 21 p. Previously announced in STAR as N92-30998. Jul. 1992 21 p refs (AIAA PAPER 92-3261)

A thrust augmenting ejector was tested to provide experimental data to assist in the assessment of theoretical models to predict duct and ejector fluid-dynamic characteristics. Eleven full-scale thrust augmenting ejector tests were conducted in which a rapid increase in the ejector nozzle pressure ratio was effected through a unique bypass/burst-disk subsystem. The present work examines two cases representative of the test performance window. In the first case, the primary nozzle pressure ratio (NPR) increased 36 percent from one unchoked (NPR = 1.29) primary flow condition to another (NPR = 1.75) over a 0.15 second interval. The second case involves choked primary flow conditions, where a 17 percent increase in primary nozzle flowrate (from NPR = 2.35 to NPR = 2.77) occurred over approximately 0.1 seconds. Transient signal treatment of the present dataset is discussed and initial interpretations of the results are compared with theoretical predictions for a similar STOVLE ejector model. Author

A92-54025*# National Aeronautics and Space Administration. Lewis Research Center, Cleveland, OH.

APPLIED ANALYTICAL COMBUSTION/EMISSIONS RESEARCH AT THE NASA LEWIS RESEARCH CENTER - A PROGRESS REPORT

J. M. DEUR (Sverdrup Technology, Inc., Brook Park, OH), K. P. KUNDU, and H. L. NGUYEN (NASA, Lewis Research Center, Cleveland, OH) AIAA, SAE, ASME, and ASEE, Joint Propulsion Conference and Exhibit, 28th, Nashville, TN, July 6-8, 1992. 13 p. Previously announced in STAR as N92-29343. Jul. 1992 13 p refs (AIAA PAPER 92-3338) Copyright

Emissions of pollutants from future commercial transports are a significant concern. As a result, the Lewis Research Center (LeRC) is investigating various low emission combustor technologies. As part of this effort, a combustor analysis code development program was pursued to guide the combustor design process, to identify concepts having the greatest promise, and to optimize them at the lowest cost in the minimum time. Author

A92-54035*# National Aeronautics and Space Administration. Lewis Research Center, Cleveland, OH.

THE VRT GAS TURBINE COMBUSTOR - PHASE II

JERRY O. MELCONIAN (SOL-3 Resources, Inc., Reading, MA), HUKAM C. MONGIA (General Motors Corp., Allison Gas Turbine Div., Indianapolis, IN), and HUNG L. NGUYEN (NASA, Lewis Research Center, Cleveland, OH) AIAA, SAE, ASME, and ASEE, Joint Propulsion Conference and Exhibit, 28th, Nashville, TN, July 6-8, 1992. 14 p. Jul. 1992 14 p refs (AIAA PAPER 92-3471) Copyright

An innovative annular combustor configuration is being developed for aircraft and other gas turbine engines. This design has the potential of permitting higher turbine inlet temperatures by reducing the pattern factor and providing a major reduction in NO(x) emission. The design concept is based on a Variable Residence Time (VRT) technique which allows large fuel particles adequate time to completely burn in the circumferentially mixed primary zone. High durability of the combustor is achieved by dual-function use of the incoming air. In Phase I, the feasibility of the concept was demonstrated by water analogue tests and 3D computer modeling. The flow pattern within the combustor was as predicted. The VRT combustor uses only half the number of fuel nozzles of the conventional configuration. In Phase II, hardware was designed, procured, and tested under conditions simulating typical supersonic civil aircraft cruise conditions to the limits of the rig. The test results confirmed many of the superior performance predictions of the VRT concept. The Hastelloy X liner showed no signs of distress after nearly six hours of tests using JP5 fuel. Author

A92-54059*# National Aeronautics and Space Administration. Lewis Research Center, Cleveland, OH.

FULL NAVIER-STOKES ANALYSIS OF A TWO-DIMENSIONAL MIXER/EJECTOR NOZZLE FOR NOISE SUPPRESSION

JAMES R. DEBONIS (NASA, Lewis Research Center, Cleveland, OH) AIAA, SAE, ASME, and ASEE, Joint Propulsion Conference and Exhibit, 28th, Nashville, TN, July 6-8, 1992. 16 p. Previously announced in STAR as N92-28419. Jul. 1992 16 p refs (AIAA PAPER 92-3570) Copyright

A three-dimensional full Navier-Stokes (FNS) analysis was performed on a mixer/ejector nozzle designed to reduce the jet noise created at takeoff by a future supersonic transport. The PARC3D computational fluid dynamics (CFD) code was used to study the flow field of the nozzle. The grid that was used in the analysis consisted of approximately 900,000 node points contained in eight grid blocks. Two nozzle configurations were studied: a constant area mixing section and a diverging mixing section. Data are presented for predictions of pressure, velocity, and total temperature distributions and for evaluations of internal performance and mixing effectiveness. The analysis provided good insight into the behavior of the flow. Author

07 AIRCRAFT PROPULSION AND POWER

A92-54060*# National Aeronautics and Space Administration. Lewis Research Center, Cleveland, OH.

FLOW INDUCTION BY PRESSURE FORCES

C. A. GARRIS, K. H. TOH, and S. AMIN (George Washington University, Washington) AIAA, SAE, ASME, and ASEE, Joint Propulsion Conference and Exhibit, 28th, Nashville, TN, July 6-8, 1992. 7 p. Jul. 1992 7 p refs
(Contract NAG3-860)

(AIAA PAPER 92-3571) Copyright

A dual experimental/computational approach to the fluid mechanics of complex interactions that take place in a rotary-jet ejector is presented. The long-range goal is to perform both detailed flow mapping and finite element computational analysis. The described work represents an initial finding on the experimental mapping program. Test results on the hubless rotary-jet are discussed. O.G.

A92-54159*# National Aeronautics and Space Administration. Lewis Research Center, Cleveland, OH.

WIND TUNNEL PERFORMANCE RESULTS OF SWIRL

RECOVERY VANES AS TESTED WITH AN ADVANCED HIGH SPEED PROPELLER

JOHN A. GAZZANIGA (Sverdrup Technology Inc., Brook Park, OH) and GAYLE E. ROSE (NASA, Lewis Research Center, Cleveland, OH) AIAA, SAE, ASME, and ASEE, Joint Propulsion Conference and Exhibit, 28th, Nashville, TN, July 6-8, 1992. 42 p. Jul. 1992 42 p refs

(AIAA PAPER 92-3770)

Tests of swirl recovery vanes designed for use in conjunction with advanced high speed propellers were carried out at the NASA Lewis Research Center. The eight bladed 62.23 cm vanes were tested with a 62.23 cm SR = 7A high speed propeller in the NASA Lewis 2.44 x 1.83 m Supersonic Wind Tunnel for a Mach number range of 0.60 to 0.80. At the design operating condition for cruise of Mach 0.80 at an advance ratio of 3.26, the vane contribution to the total efficiency approached 2 percent. At lower off-design Mach numbers, the vane efficiency is even higher, approaching 4.5 percent for the Mach 0.60 condition. Use of the swirl recovery vanes essentially shifts the peak of the high speed propeller efficiency to a higher operating speed. This allows a greater degree of freedom in the selection of rpm over a wider operating range. Another unique result of the swirl recovery vane configuration is their essentially constant torque split between the propeller and the swirl vanes over a wide range of operating conditions for the design vane angle. Author

A92-54168*# National Aeronautics and Space Administration. Lewis Research Center, Cleveland, OH.

EXPERIMENTAL PERFORMANCE OF THREE DESIGN

FACTORS FOR VENTRAL NOZZLES FOR SSTOVL AIRCRAFT

BARBARA S. ESKER and GAIL P. PERUSEK (NASA, Lewis Research Center, Cleveland, OH) AIAA, SAE, ASME, and ASEE, Joint Propulsion Conference and Exhibit, 28th, Nashville, TN, July 6-8, 1992. 15 p. Previously announced in STAR as N92-27669. Jul. 1992 15 p refs

(AIAA PAPER 92-3789) Copyright

An experimental study of three variations of a ventral nozzle system for supersonic short-takeoff and vertical-landing (SSTOVL) aircraft was performed at the NASA LeRC Powered Lift Facility. These test results include the effects of an annular duct flow into the ventral duct, a blocked tailpipe, and a short ventral duct length. An analytical study was also performed on the short ventral duct configuration using the PARC3D computational dynamics code. Data presented include pressure losses, thrust and flow performance, internal flow visualization, and pressure distributions at the exit plane of the ventral nozzle. Author

A92-54169*# National Aeronautics and Space Administration. Lewis Research Center, Cleveland, OH.

INTERNAL REVERSING FLOW IN A TAILPIPE OFFTAKE CONFIGURATION FOR SSTOVL AIRCRAFT

JACK G. MCARDLE, BARBARA S. ESKER (NASA, Lewis Research Center, Cleveland, OH), and JAMES A. RHODES (McDonnell

Aircraft Co., Saint Louis, MO) AIAA, SAE, ASME, and ASEE, Joint Propulsion Conference and Exhibit, 28th, Nashville, TN, July 6-8, 1992. 22 p. Previously announced in STAR as N92-28418. Jul. 1992 22 p refs

(AIAA PAPER 92-3790) Copyright

A generic one-third scale model of a tailpipe offtake system for a supersonic short takeoff vertical landing (SSTOVL) aircraft was tested at LeRC Powered Lift Facility. The model consisted of a tailpipe with twin elbows, offtake ducts, and flow control nozzles, plus a small ventral nozzle and a blind flange to simulate a blocked cruise nozzle. The offtake flow turned through a total angle of 177 degrees relative to the tailpipe inlet axis. The flow split was 45 percent to each offtake and 10 percent to the ventral nozzle. The main test objective was to collect data for comparison to the performance of the same configuration predicted by a computational fluid dynamics (CFD) analysis. Only the experimental results are given - the analytical results are published in a separate paper. Performance tests were made with unheated air at tailpipe-to-ambient pressure ratios up to 5. The total pressure loss through the offtakes was as high as 15.5 percent. All test results are shown as graphs, contour plots, and wall pressure distributions. The complex flow patterns in the tailpipe and elbows at the offtake openings are described with traversing flow angle probe and paint streak flow visualization data. Author

A92-54171*# National Aeronautics and Space Administration. Lewis Research Center, Cleveland, OH.

USE OF AN APPROXIMATE SIMILARITY PRINCIPLE FOR THE THERMAL SCALING OF A FULL-SCALE THRUST AUGMENTING EJECTOR

WENDY BARANKIEWICZ, GAIL P. PERUSEK (NASA, Lewis Research Center, Cleveland, OH), and MOUNIR IBRAHIM (Cleveland State University, OH) AIAA, SAE, ASME, and ASEE, Joint Propulsion Conference and Exhibit, 28th, Nashville, TN, July 6-8, 1992. 12 p. Previously announced in STAR as N92-26613. Jul. 1992 12 p refs
(AIAA PAPER 92-3792) Copyright

Full temperature ejector model simulations are expensive, and difficult to implement experimentally. If an approximate similarity principle could be established, properly chosen performance parameters should be similar for both hot and cold flow tests if the initial Mach number and total pressures of the flow field are held constant. Existing ejector data is used to explore the utility of one particular similarity principle; the Munk and Prim similarity principle for isentropic flows. Static performance test data for a full-scale thrust augmenting ejector are analyzed for primary flow temperatures up to 1560 R. At different primary temperatures, exit pressure contours are compared for similarity. A nondimensional flow parameter is then used to eliminate primary nozzle temperature dependence and verify similarity between the hot and cold flow experiments. Author

A92-55281*# National Aeronautics and Space Administration. Lewis Research Center, Cleveland, OH.

PROPULSION SYSTEM PERFORMANCE RESULTING FROM AN INTEGRATED FLIGHT/PROPULSION CONTROL DESIGN

DUANE MATTERN (Sverdrup Technology, Inc., Brook Park, OH) and SANJAY GARG (NASA, Lewis Research Center, Cleveland, OH) IN: AIAA Guidance, Navigation and Control Conference, Hilton Head Island, SC, Aug. 10-12, 1992, Technical Papers. Pt. 3 1992 10 p refs
(AIAA PAPER 92-4602) Copyright

Propulsion system specific results are presented from the application of the Integrated Methodology for Propulsion and Airframe Control (IMPAC) design approach to Integrated Flight/Propulsion Control design for a STOVL aircraft in transition flight. The IMPAC method is briefly discussed and the propulsion system specifications for the integrated control design are examined. The structure of a linear engine controller that results from partitioning a linear centralized controller is discussed. The details of a nonlinear propulsion control system are presented, including a scheme to protect the engine operational limits: the fan surge margin and the acceleration/deceleration schedule which

limits the fuel flow. Also, a simple but effective multivariable integrator windup protection scheme is investigated. Nonlinear closed-loop simulation results are presented for two typical pilot commands for transition flight: acceleration while maintaining flight path angle and a change in flight path angle while maintaining airspeed. The simulation nonlinearities include the airframe/engine coupling, the actuator and sensor dynamics and limits, the protection scheme for the engine operational limits, and the integrator windup protection. Satisfactory performance of the total airframe plus engine system for transition flight, as defined by the specifications, is maintained during the limit operation of the closed-loop engine subsystem. Author

N92-11017*# National Aeronautics and Space Administration. Lewis Research Center, Cleveland, OH.

REAL-TIME FAULT DIAGNOSIS FOR PROPULSION SYSTEMS
WALTER C. MERRILL, TEN-HUEI GUO, JOHN C. DELAAT, and AHMET DUYAR (Florida Atlantic Univ., Boca Raton.) 1991 8 p Presented at the International Federation of Automatic Control Symposium on Fault Detection, Supervision and Safety for Technical Processes-SAFEPROCESS 1991, Baden-Baden, Germany, 10-13 Sep. 1991 (Contract RTOP 582-01-11) (NASA-TM-105303; E-6650; NAS 1.15:105303) Avail: CASI HC A02/MF A01

Current research toward real time fault diagnosis for propulsion systems at NASA-Lewis is described. The research is being applied to both air breathing and rocket propulsion systems. Topics include fault detection methods including neural networks, system modeling, and real time implementations. Author

N92-11995*# National Aeronautics and Space Administration. Lewis Research Center, Cleveland, OH.

THE DESIGN AND PERFORMANCE ESTIMATES FOR THE PROPULSION MODULE FOR THE BOOSTER OF A TSTO VEHICLE
CHRISTOPHER A. SNYDER and JAIME J. MALDONADO Oct. 1991 14 p Presented at the Aircraft Design Systems and Operations Meeting, Baltimore, MD, 23-25 Sep. 1991; sponsored by AIAA, AHS, and ASEE Previously announced in IAA as A91-54054 (Contract RTOP 505-69-40) (NASA-TM-105299; E-6642; NAS 1.15:105299; AIAA PAPER 91-3136) Copyright Avail: CASI HC A03/MF A01

A NASA study of the propulsion systems for possible low-risk replacements for the Space Shuttle is presented. Results of preliminary studies to define the USAF two-stage-to-orbit (TSTO) concept to deliver 10,000 pounds to low polar orbit are described. The booster engine module consists of an over/under turbine bypass engines/ramjet engine design for acceleration from takeoff to the staging point of Mach 6.5 and approximately 100,000 feet altitude. Propulsion system performance and weight are presented with preliminary mission study results of vehicle size. Author

N92-13070*# National Aeronautics and Space Administration. Lewis Research Center, Cleveland, OH.

DEVELOPMENT OF A COMPUTER ALGORITHM FOR THE ANALYSIS OF VARIABLE-FREQUENCY AC DRIVES: CASE STUDIES INCLUDED
M. DAVID KANKAM and OWEN BENJAMIN (Cornell Univ., Ithaca, NY.) Nov. 1991 34 p (Contract RTOP 946-02-2E) (NASA-TM-105327; E-6688; NAS 1.15:105327) Avail: CASI HC A03/MF A01

The development of computer software for performance prediction and analysis of voltage-fed, variable-frequency AC drives for space power applications is discussed. The AC drives discussed include the pulse width modulated inverter (PWMI), a six-step inverter and the pulse density modulated inverter (PDMI), each individually connected to a wound-rotor induction motor. Various d-q transformation models of the induction motor are incorporated for user-selection of the most applicable model for the intended purpose. Simulation results of selected AC drives correlate

satisfactorily with published results. Future additions to the algorithm are indicated. These improvements should enhance the applicability of the computer program to the design and analysis of space power systems. Author

N92-14061*# National Aeronautics and Space Administration. Lewis Research Center, Cleveland, OH.

PARTICLE-LADEN WEAKLY SWIRLING FREE JETS: MEASUREMENTS AND PREDICTIONS Ph.D. Thesis - Pennsylvania State Univ.

DANIEL L. BULZAN May 1988 240 p (Contract RTOP 505-62-21) (NASA-TM-100881; E-2913; NAS 1.15:100881) Avail: CASI HC A11/MF A03

A theoretical and experimental investigation of particle-laden, weakly swirling, turbulent free jets was conducted. Glass particles, having a Sauter mean diameter of 39 microns, with a standard deviation of 15 microns, were used. A single loading ratio (the mass flow rate of particles per unit mass flow rate of air) of 0.2 was used in the experiments. Measurements are reported for three swirl numbers, ranging from 0 to 0.33. The measurements included mean and fluctuating velocities of both phases, and particle mass flux distributions. Measurements were also completed for single-phase non-swirling and swirling jets, as baselines. Measurements were compared with predictions from three types of multiphase flow analysis, as follows: (1) locally homogeneous flow (LHF) where slip between the phases was neglected; (2) deterministic separated flow (DSF), where slip was considered but effects of turbulence/particle interactions were neglected; and (3) stochastic separated flow (SSF), where effects of both interphase slip and turbulence/particle interactions were considered using random sampling for turbulence properties in conjunction with random-walk computations for particle motion. Single-phase weakly swirling jets were considered first. Predictions using a standard k-epsilon turbulence model, as well as two versions modified to account for effects of streamline curvature, were compared with measurements. Predictions using a streamline curvature modification based on the flux Richardson number gave better agreement with measurements for the single-phase swirling jets than the standard k-epsilon model. For the particle-laden jets, the LHF and DSF models did not provide very satisfactory predictions. The LHF model generally overestimated the rate of decay of particle mean axial and angular velocities with streamwise distance, and predicted particle mass fluxes also showed poor agreement with measurements, due to the assumption of no-slip between phases. The DSF model also performed quite poorly for predictions of particle mass flux because turbulent dispersion of the particles was neglected. The SSF model, which accounts for both particle inertia and turbulent dispersion of the particles, yielded reasonably good predictions throughout the flow field for the particle-laden jets. Author

N92-14063*# National Aeronautics and Space Administration. Lewis Research Center, Cleveland, OH.

THE AERODYNAMIC EFFECT OF FILLET RADIUS IN A LOW SPEED COMPRESSOR CASCADE Thesis - Von Karman Inst. for Fluid Dynamics

BRIAN P. CURLETT Nov. 1991 49 p (Contract RTOP 505-69-10) (NASA-TM-105347; E-6717; NAS 1.15:105347) Avail: CASI HC A03/MF A01

The aerodynamic effects of fillet size in a low speed compressor cascade were experimentally studied. Two blade profiles were used during the experiment, namely a controlled diffusion blade and a double circular arc blade. Cascades were tested with three fillet radii and two boundary layer thicknesses over a large range of incidence angles. The cascade performance was determined by extensive downstream flow measurements using a two head, 5 hole pressure probe. Results differ significantly between the two types of blades tested. As fillet radius increases secondary flows and total pressure losses were found to increase for the controlled diffusion blades; whereas, for the double circular arc blades the losses decrease, particularly at high incidence angles. Author

07 AIRCRAFT PROPULSION AND POWER

N92-15993*# National Aeronautics and Space Administration. Lewis Research Center, Cleveland, OH.
SUPERSONIC PROPULSION SIMULATION BY INCORPORATING COMPONENT MODELS IN THE LARGE PERTURBATION INLET (LAPIN) COMPUTER CODE
GARY L. COLE and JACQUES C. RICHARD Dec. 1991 33 p
(Contract RTOP 509-10-03)
(NASA-TM-105193; E-6494; NAS 1.15:105193) Avail: CASI HC A03/MF A01

An approach to simulating the internal flows of supersonic propulsion systems is presented. The approach is based on a fairly simple modification of the Large Perturbation Inlet (LAPIN) computer code. LAPIN uses a quasi-one dimensional, inviscid, unsteady formulation of the continuity, momentum, and energy equations. The equations are solved using a shock capturing, finite difference algorithm. The original code, developed for simulating supersonic inlets, includes engineering models of unstart/restart, bleed, bypass, and variable duct geometry, by means of source terms in the equations. The source terms also provide a mechanism for incorporating, with the inlet, propulsion system components such as compressor stages, combustors, and turbine stages. This requires each component to be distributed axially over a number of grid points. Because of the distributed nature of such components, this representation should be more accurate than a lumped parameter model. Components can be modeled by performance map(s), which in turn are used to compute the source terms. The general approach is described. Then, simulation of a compressor/fan stage is discussed to show the approach in detail. Author

N92-15994*# National Aeronautics and Space Administration. Lewis Research Center, Cleveland, OH.
JET MIXING INTO A HEATED CROSS FLOW IN A CYLINDRICAL DUCT: INFLUENCE OF GEOMETRY AND FLOW VARIATIONS
M. S. HATCH (California Univ., Irvine.), W. A. SOWA (California Univ., Irvine.), G. S. SAMUELSEN (California Univ., Irvine.), and J. D. HOLDEMAN 1992 18 p Presented at the 30th Aerospace Sciences Meeting and Exhibit, Reno, NV, 6-9 Jan. 1992; sponsored by AIAA Original contains color illustrations
(Contract NAG3-1110; RTOP 537-02-20)
(NASA-TM-105390; E-6780; NAS 1.15:105390; AIAA PAPER 92-0773)

To examine the mixing characteristics of jets in an axi-symmetric can geometry, temperature measurements were obtained downstream of a row of cold jets injected into a heated cross stream. Parametric, non-reacting experiments were conducted to determine the influence of geometry and flow variations on mixing patterns in a cylindrical configuration. Results show that jet to mainstream momentum flux ratio and orifice geometry significantly impact the mixing characteristics of jets in a can geometry. For a fixed number of orifices, the coupling between momentum flux ratio and injector determines (1) the degree of jet penetration at the injection plane, and (2) the extent of circumferential mixing downstream of the injection plane. The results also show that, at a fixed momentum flux ratio, jet penetration decreases with (1) an increase in slanted slot aspect ratio, and (2) an increase in the angle of the slots with respect to the mainstream direction. Author

N92-17061*# National Aeronautics and Space Administration. Lewis Research Center, Cleveland, OH.
SAFETY CONSIDERATIONS IN TESTING A FUEL-RICH AEROPROPULSION GAS GENERATOR
R. JAMES ROLLBUHLER and DAVID D. HULLIGAN (Sverdrup Technology, Inc., Brook Park, OH.) 1991 9 p Presented at the Combustion Fundamentals and Applications Meeting, Nashville, TN, 21-24 Apr. 1991; sponsored by the Combustion Inst.
(Contract RTOP 537-02-20)
(NASA-TM-105258; E-5976; NAS 1.15:105258) Avail: CASI HC A02/MF A01

A catalyst containing reactor is being tested using a fuel-rich mixture of Jet A fuel and hot input air. The reactor product is a

gaseous fuel that can be utilized in aeropropulsion gas turbine engines. Because the catalyst material is susceptible to damage from high temperature conditions, fuel-rich operating conditions are attained by introducing the fuel first into an inert gas stream in the reactor and then displacing the inert gas with reaction air. Once a desired fuel-to-air ratio is attained, only limited time is allowed for a catalyst induced reaction to occur; otherwise the inert gas is substituted for the air and the fuel flow is terminated. Because there presently is not a gas turbine combustor in which to burn the reactor product gas, the gas is combusted at the outlet of the test facility flare stack. This technique in operations has worked successfully in over 200 tests. Author

N92-17546*# National Aeronautics and Space Administration. Lewis Research Center, Cleveland, OH.
EXPERIMENTS AND ANALYSIS CONCERNING THE USE OF EXTERNAL BURNING TO REDUCE AEROSPACE VEHICLE TRANSONIC DRAG Ph.D. Thesis - Maryland Univ., 1991
CHARLES J. TREFNY Jan. 1992 294 p
(Contract RTOP 763-01-21)
(NASA-TM-105397; E-6789; NAS 1.15:105397) Avail: CASI HC A13/MF A03

The external combustion of hydrogen to reduce transonic drag was investigated. A control volume analysis is developed and indicates that the specific impulse performance of external burning is competitive with other forms of airbreathing propulsion and depends on the fuel-air ratio, freestream Mach number, and the severity of the base drag. A method is presented for sizing fuel injectors for a desired fuel-air ratio in the unconfined stream. A two-dimensional Euler analysis is also presented which indicates that the total axial force generated by external burning depends on the total amount of energy input and is independent of the transverse and streamwise distribution of heat addition. Good agreement between the Euler and control volume analysis is demonstrated. Features of the inviscid external burning flowfield are discussed. Most notably, a strong compression forms at the sonic line within the burning stream which may induce separation of the plume and prevent realization of the full performance potential. An experimental program was conducted in a Mach 1.26 free-jet to demonstrate drag reduction on a simple expansion ramp geometry, and verify hydrogen-air stability limits at external burning conditions. Stable combustion appears feasible to Mach number of between 1.4 and 2 depending on the vehicle flight trajectory. Drag reduction is demonstrated on the expansion ramp at Mach 1.26; however, force levels showed little dependence on fuel pressure or altitude in contrast to control volume analysis predictions. Various facility interference mechanisms and scaling issues were studied and are discussed. Author

N92-20033*# National Aeronautics and Space Administration. Lewis Research Center, Cleveland, OH.
NASA'S ROTARY ENGINE TECHNOLOGY ENABLEMENT PROGRAM: 1983-1991
EDWARD A. WILLIS (Sverdrup Technology, Inc., Brook Park, OH.) and JOHN J. MCFADDEN 1992 13 p Presented at the International Congress and Exposition, Detroit, MI, 24-28 Feb. 1992; sponsored by SAE
(Contract RTOP 505-62-12)
(NASA-TM-105562; E-6868; NAS 1.15:105562) Avail: CASI HC A03/MF A01

A brief review is provided of NASA's Rotary Engine Technology Enablement Program from 1983 through 1991, with primary emphasis on the CFD approaches used since 1987. The main discussion includes both code development and applications to several particularly difficult internal air flow, fuel air mixing, and combustion related problems. A summary of the final status of the technology is given. Author

N92-20523*# National Aeronautics and Space Administration. Lewis Research Center, Cleveland, OH.
PERFORMANCE TESTS OF A CRYOGENIC HYBRID MAGNETIC BEARING FOR TURBOPUMPS
ELISEO DIRUSSO and GERALD V. BROWN 1992 14 p

Proposed for presentation at the Third International Symposium on Magnetic Bearings, Alexandria, VA, 29-31 Jul. 1992
(Contract RTOP 590-21-31)
(NASA-TM-105627; E-6775; NAS 1.15:105627) Avail: CASI HC A03/MF A01

Experiments were performed on a Hybrid Magnetic Bearing designed for cryogenic applications such as turbopumps. This bearing is considerably smaller and lighter than conventional magnetic bearings and is more efficient because it uses a permanent magnet to provide a bias flux. The tests were performed in a test rig that used liquid nitrogen to simulate cryogenic turbopump temperatures. The bearing was tested at room temperature and at liquid nitrogen temperature (-320 F). The maximum speed for the test rig was 14000 rpm. For a magnetic bearing stiffness of 20000 lb/in, the flexible rotor had two critical speeds. A static (nonrotating) bearing stiffness of 85000 lb/in was achieved. Magnetic bearing stiffness, permanent magnet stiffness, actuator gain, and actuator force interaction between two axes were evaluated, and controller/power amplifier characteristics were determined. The tests revealed that it is feasible to use this bearing in the cryogenic environment and to control the rotor dynamics of flexible rotors when passing through bending critical speeds. The tests also revealed that more effort should be placed on enhancing the controller to achieve higher bearing stiffness and on developing displacement sensors that reduce drift caused by temperature and reduce sensor electrical noise. Author

N92-20525*# National Aeronautics and Space Administration. Lewis Research Center, Cleveland, OH.

DEVELOPMENT OF A STEADY POTENTIAL SOLVER FOR USE WITH LINEARIZED, UNSTEADY AERODYNAMIC ANALYSES

DANIEL HOYNIK (ST Systems Corp., Lanham, MD.) and JOSEPH M. VERDON (United Technologies Research Center, East Hartford, CT.) 1991 14 p Presented at the Sixth International Symposium on Unsteady Aerodynamics, Aeroacoustics, and Aeroelasticity of Turbomachines and Propellers, Notre Dame, IN, 15-19 Sep. 1991; sponsored by the International Union for Theoretical and Applied Mechanics
(Contract RTOP 505-62-10)
(NASA-TM-105288; E-6620; NAS 1.15:105288) Avail: CASI HC A03/MF A01

A full potential steady flow solver (SFLOW) developed explicitly for use with an inviscid unsteady aerodynamic analysis (LINFLO) is described. The steady solver uses the nonconservative form of the nonlinear potential flow equations together with an implicit, least squares, finite difference approximation to solve for the steady flow field. The difference equations were developed on a composite mesh which consists of a C grid embedded in a rectilinear (H grid) cascade mesh. The composite mesh is capable of resolving blade to blade and far field phenomena on the H grid, while accurately resolving local phenomena on the C grid. The resulting system of algebraic equations is arranged in matrix form using a sparse matrix package and solved by Newton's method. Steady and unsteady results are presented for two cascade configurations: a high speed compressor and a turbine with high exit Mach number. Author

N92-21523*# National Aeronautics and Space Administration. Lewis Research Center, Cleveland, OH.

AIRBREATHING COMBINED CYCLE ENGINE SYSTEMS

JOHN ROHDE *In its* Rocket-Based Combined-Cycle (RBCC) Propulsion Technology Workshop. Tutorial Session 9 p 1992
Avail: CASI HC A02/MF A03

The Air Force and NASA share a common interest in developing advanced propulsion systems for commercial and military aerospace vehicles which require efficient acceleration and cruise operation in the Mach 4 to 6 flight regime. The principle engine of interest is the turboramjet; however, other combined cycles such as the turbosramjet, air turbojet, supercharged ejector ramjet, ejector ramjet, and air liquefaction based propulsion are also of interest. Over the past months careful planning and program implementation have resulted in a number of development efforts

that will lead to a broad technology base for those combined cycle propulsion systems. Individual development programs are underway in thermal management, controls materials, endothermic hydrocarbon fuels, air intake systems, nozzle exhaust systems, gas turbines and ramjet ramburners. Author

N92-22510*# National Aeronautics and Space Administration. Lewis Research Center, Cleveland, OH.

AEROPROPULSION 1987

Washington Feb. 1990 498 p Conference held in Cleveland, OH, 17-19 Nov. 1987 Previously announced as N88-16697, N88-15785, N88-15790, N88-15794, N88-15800 and N88-15807
(Contract RTOP 505-62-3B)
(NASA-CP-3049; E-3798; NAS 1.55:3049) Avail: CASI HC A21/MF A04

Papers from the Aeropropulsion '87 Conference, held at the NASA Lewis Research Center (LeRC), are presented. Unclassified presentations by LeRC and NASA Headquarters senior management and many LeRC technical authors covered the philosophy and major directions of the LeRC aeropropulsion program, and presented a broad spectrum of recent research results in materials, structures, internal fluid mechanics, instrumentation and controls, and both subsonic and high-speed propulsion technology.

N92-22511*# National Aeronautics and Space Administration. Lewis Research Center, Cleveland, OH.

IMPACT AND PROMISE OF NASA AEROPROPULSION TECHNOLOGY

NEAL T. SAUNDERS and DAVID N. BOWDITCH *In its* Aeropropulsion 1987 p 13-36 Feb. 1990
Avail: CASI HC A03/MF A04

The aeropropulsion industry in the U.S. has established an enviable record of leading the world in aeropropulsion for commercial and military aircraft. NASA's aeropropulsion program (primarily conducted through the Lewis Research Center) has significantly contributed to that success through research and technology advances and technology demonstration. Some past NASA contributions to engines in current aircraft are reviewed, and technologies emerging from current research programs for the aircraft of the 1990's are described. Finally, current program thrusts toward improving propulsion systems in the 2000's for subsonic commercial aircraft and higher speed aircraft such as the High-Speed Civil Transport and the National Aerospace Plane are discussed. D.R.D.

N92-22512*# National Aeronautics and Space Administration. Lewis Research Center, Cleveland, OH.

NASA. LEWIS RESEARCH CENTER MATERIALS RESEARCH AND TECHNOLOGY: AN OVERVIEW

SALVATORE J. GRISAFFE *In its* Aeropropulsion 1987 p 37-44 Feb. 1990
Avail: CASI HC A02/MF A04

The Materials Division at the Lewis Research Center has a long record of contributions to both materials and process technology as well as to the understanding of key high-temperature phenomena. This paper overviews the division staff, facilities, past history, recent progress, and future interests. D.R.D.

N92-22518*# National Aeronautics and Space Administration. Lewis Research Center, Cleveland, OH.

AEROPROPULSION STRUCTURES

LESTER D. NICHOLS *In its* Aeropropulsion 1987 p 105-111 Feb. 1990
Avail: CASI HC A02/MF A04

Aeropropulsion systems present unique problems to the structural engineer. The extremes in operating temperatures, rotational effects, and behaviors of advance material systems combine into complexities that require advances in many scientific disciplines involved in structural analysis and design procedures. This paper provides an overview of the complexities of aeropropulsion structures and the theoretical, computational, and

07 AIRCRAFT PROPULSION AND POWER

experimental research conducted to achieve the needed advances. D.R.D.

N92-22519*# National Aeronautics and Space Administration. Lewis Research Center, Cleveland, OH.

DETERMINING STRUCTURAL PERFORMANCE

MICHAEL A. ERNST, ed., GERALD BROWN, ELISEO DIRUSSO, DAVID FLEMING, DAVID JANETZKE, ALBERT KASCAK, KRISHNA KAZA, ROBERT KIELB, LOUIS J. KIRALY, CHARLES LAWRENCE et al. *In its* Aeropropulsion 1987 p 113-128 Feb. 1990

Avail: CASI HC A03/MF A04

An overview of the methods and concepts developed to enhance and predict structural dynamic characteristics of advanced aeropropulsion systems is presented. Aeroelasticity, vibration control, dynamic systems, and computational structural methods are four disciplines that make up the structural dynamic effort at LeRC. The aeroelasticity program develops analytical and experimental methods for minimizing flutter and forced vibration of aerospace propulsion systems. Both frequency domain and time domain methods were developed for applications on the turbofan, turbopump, and advanced turboprop. In order to improve life and performance, the vibration control program conceives, analyzes, develops, and demonstrates new methods for controlling vibrations in aerospace systems. Active and passive vibration control is accomplished with electromagnetic dampers, magnetic bearings, and piezoelectric crystals to control rotor vibrations. The dynamic systems program analyzes and verifies the dynamics of interacting systems, as well as develops concepts and methods for high-temperature dynamic seals. Work in this field involves the analysis and parametric identification of large, nonlinear, damped, stochastic systems. The computational structural methods program exploits modern computer science as an aid to the solutions of structural problems. Author

N92-22520*# National Aeronautics and Space Administration. Lewis Research Center, Cleveland, OH.

LIFE PREDICTION TECHNOLOGIES FOR AERONAUTICAL PROPULSION SYSTEMS

MICHAEL A. MCGAW *In its* Aeropropulsion 1987 p 129-139 Feb. 1990

Avail: CASI HC A03/MF A04

Fatigue and fracture problems continue to occur in aeronautical gas turbine engines. Components whose useful life is limited by these failure modes include turbine hot-section blades, vanes, and disks. Safety considerations dictate that catastrophic failures be avoided, while economic considerations dictate that catastrophic failures be avoided, while economic considerations dictate that noncatastrophic failures occur as infrequently as possible. Therefore, the decision in design is making the tradeoff between engine performance and durability. LeRC has contributed to the aeropropulsion industry in the area of life prediction technology for over 30 years, developing creep and fatigue life prediction methodologies for hot-section materials. At the present time, emphasis is being placed on the development of methods capable of handling both thermal and mechanical fatigue under severe environments. Recent accomplishments include the development of more accurate creep-fatigue life prediction methods such as the total strain version of LeRC's strain-range partitioning (SRP) and the HOST-developed cyclic damage accumulation (CDA) model. Other examples include the development of a more accurate cumulative fatigue damage rule - the double damage curve approach (DDCA), which provides greatly improved accuracy in comparison with usual cumulative fatigue design rules. Other accomplishments in the area of high-temperature fatigue crack growth may also be mentioned. Finally, we are looking to the future and are beginning to do research on the advanced methods which will be required for development of advanced materials and propulsion systems over the next 10-20 years. Author

N92-22521*# National Aeronautics and Space Administration. Lewis Research Center, Cleveland, OH.

INTEGRATED ANALYSIS AND APPLICATIONS

DALE A. HOPKINS *In its* Aeropropulsion 1987 p 141-153 Feb. 1990

Avail: CASI HC A03/MF A04

An overview is presented of current research activities which, in a broad context, are focused on the development and verification of integrated structural analysis and optimal design capabilities for advanced aerospace propulsion and power systems. The overview encompasses a variety of subject areas including: (1) composite materials; (2) advanced structural analysis; (3) constitutive modeling; (4) computational simulation; (5) probabilistic analysis; and (6) multidisciplinary optimization. Typical results are presented which illustrate the benefit and utility of the emerging technologies as applied to propulsion and power system structures. K.S.

N92-22524*# National Aeronautics and Space Administration. Lewis Research Center, Cleveland, OH.

TURBOMACHINERY

ROBERT J. SIMONEAU, ANTHONY J. STRAZISAR, PETER M. SOCKOL, LONNIE REID, and JOHN J. ADAMCZYK *In its* Aeropropulsion 1987 p 175-195 Feb. 1990

Avail: CASI HC A03/MF A04

The discipline research in turbomachinery, which is directed toward building the tools needed to understand such a complex flow phenomenon, is based on the fact that flow in turbomachinery is fundamentally unsteady or time dependent. Success in building a reliable inventory of analytic and experimental tools will depend on how we treat time and time-averages, as well as how we treat space and space-averages. The challenge is to develop a set of computational and experimental tools which genuinely increase our understanding of the fluid flow and heat transfer in a turbomachine. Examples of the types of computational and experimental tools under current development, with progress to date, are examined. The examples include work in both the time-resolved and time-averaged domains. K.S.

N92-22530*# National Aeronautics and Space Administration. Lewis Research Center, Cleveland, OH.

DIRECTIONS IN PROPULSION CONTROL

CARL F. LORENZO *In its* Aeropropulsion 1987 p 251-260 Feb. 1990

Avail: CASI HC A02/MF A04

Discussed here is research at NASA Lewis in the area of propulsion controls as driven by trends in advanced aircraft. The objective of the Lewis program is to develop the technology for advanced reliable propulsion control systems and to integrate the propulsion control with the flight control for optimal full-system control. Author

N92-22531*# National Aeronautics and Space Administration. Lewis Research Center, Cleveland, OH.

OVERVIEW OF THE SUBSONIC PROPULSION TECHNOLOGY SESSION

G. KEITH SIEVERS *In its* Aeropropulsion 1987 p 271-278 Feb. 1990

Avail: CASI HC A02/MF A04

NASA is conducting aeronautical research over a broad range of Mach numbers. In addition to the generic and high speed propulsion research, the Lewis Research Center is continuing its substantial efforts towards propulsion technology for a broad range of subsonic flight applications. Reviewed here are some of the elements of that program, including small engine technology, rotorcraft, icing research, hot section technology, and the Advanced Turboprop Project. Author

N92-22532*# National Aeronautics and Space Administration. Lewis Research Center, Cleveland, OH.

SMALL ENGINE TECHNOLOGY PROGRAMS

RICHARD W. NIEDZWIECKI *In its* Aeropropulsion 1987 p 279-302 Feb. 1990

Avail: CASI HC A03/MF A04

Described here is the small engine technology program being sponsored at the Lewis Research Center. Small gas turbine research is aimed at general aviation, commuter aircraft, rotorcraft,

and cruise missile applications. The Rotary Engine program is aimed at supplying fuel flexible, fuel efficient technology to the general aviation industry, but also has applications to other missions. The Automotive Gas Turbine (AGT) and Heavy-Duty Diesel Transport Technology (HDTT) programs are sponsored by DOE. The Compound Cycle Engine program is sponsored by the Army. All of the programs are aimed towards highly efficient engine cycles, very efficient components, and the use of high temperature structural ceramics. This research tends to be generic in nature and has broad applications. The HDTT, rotary technology, and the compound cycle programs are all examining approaches to minimum heat rejection, or 'adiabatic' systems employing advanced materials. The AGT program is also directed towards ceramics application to gas turbine hot section components. Turbomachinery advances in the gas turbine programs will benefit advanced turbochargers and turbocompounders for the intermittent combustion systems, and the fundamental understandings and analytical codes developed in the research and technology programs will be directly applicable to the system projects.

Author

N92-22533*# National Aeronautics and Space Administration. Lewis Research Center, Cleveland, OH.

ROTORCRAFT TRANSMISSIONS

JOHN J. COY *In its* Aeropropulsion 1987 p 303-313 Feb. 1990

Avail: CASI HC A03/MF A04

Highlighted here is that portion of the Lewis Research Center's helicopter propulsion systems program that deals with drive train technology and the related mechanical components. The major goals of the program are to increase life, reliability, and maintainability, to reduce weight, noise, and vibration, and to maintain the relatively high mechanical efficiency of the gear train. The current activity emphasizes noise reduction technology and analytical code development, followed by experimental verification. Selected significant advances in technology for transmissions are reviewed, including advanced configurations and new analytical tools. Finally, the plan for transmission research in the future is presented.

Author

N92-22535*# National Aeronautics and Space Administration. Lewis Research Center, Cleveland, OH.

AIRCRAFT ENGINE HOT SECTION TECHNOLOGY: AN OVERVIEW OF THE HOST PROJECT

DANIEL E. SOKOLOWSKI and MARVIN H. HIRSCHBERG *In its* Aeropropulsion 1987 p 343-361 Feb. 1990

Avail: CASI HC A03/MF A04

NASA sponsored the Turbine Engine Hot Section (HOST) project to address the need for improved durability in advanced aircraft engine combustors and turbines. Analytical and experimental activities aimed at more accurate prediction of the aerothermal environment, the thermomechanical loads, the material behavior and structural responses to loads, and life predictions for cyclic high temperature operation were conducted from 1980 to 1987. The project involved representatives from six engineering disciplines who are spread across three work disciplines - industry, academia, and NASA. The HOST project not only initiated and sponsored 70 major activities, but also was the keystone in joining the multiple disciplines and work sectors to focus on critical research needs. A broad overview of the project is given along with initial indications of the project's impact.

Author

N92-22536*# National Aeronautics and Space Administration. Lewis Research Center, Cleveland, OH.

OVERVIEW OF NASA PTA PROPFAN FLIGHT TEST PROGRAM

EDWIN J. GRABER *In its* Aeropropulsion 1987 p 363-382 Feb. 1990

Avail: CASI HC A03/MF A04

The progress is covered of the NASA sponsored Propfan Test Assessment (PTA) flight test program. In PTA, a 9 ft. diameter propfan was installed on the left wing of a Gulfstream GII executive jet and is undergoing extensive flight testing to evaluate propfan

structural integrity, near and far field noise, and cabin interior noise characteristics. This research testing includes variations in propeller tip speed and power loading, nacelle tilt angle, and aircraft Mach number and altitude. As a result, extensive parametric data will be obtained to verify and improve computer codes for predicting propfan aeroelastic, aerodynamic, and aeroacoustic characteristics. Over 600 measurements are being recorded for each of approx. 600 flight test conditions.

Author

N92-22537*# National Aeronautics and Space Administration. Lewis Research Center, Cleveland, OH.

ADVANCED PROPELLER RESEARCH

JOHN F. GROENEWEG and LAWRENCE J. BOBER *In its* Aeropropulsion 1987 p 383-406 Feb. 1990

Avail: CASI HC A03/MF A04

Recent results of aerodynamic and acoustic research on both single rotation and counterrotation propellers are reviewed. Data and analytical results are presented for three propellers: SR-7A, the single rotation design used in the NASA Propfan Test Assessment (PTA) flight program; CRP-X1, the initial 5+5 Hamilton Standard counterrotating design; and F7-A7, the 8+8 counterrotating G.E. design used in the proof of concept Unducted Fan (UDF) engine. In addition to propeller efficiencies, cruise and takeoff noise, and blade pressure data, off-design phenomena involving formation of leading edge vortices are described. Aerodynamic and acoustic computational results derived from 3-D Euler and acoustic radiation codes are presented. Research on unsteady flows which are particularly important for understanding counterrotation interaction noise, unsteady loading effects on acoustics, and flutter or forced response is described. The first results of 3-D unsteady Euler solutions are illustrated for a single rotation propeller at angle of attack and for a counterrotation propeller. Basic experimental and theoretical results from studies on the unsteady aerodynamics of oscillating cascades are outlined.

Author

N92-22538*# National Aeronautics and Space Administration. Lewis Research Center, Cleveland, OH.

NASA THRUSTS IN HIGH-SPEED AEROPROPULSION RESEARCH AND DEVELOPMENT: AN OVERVIEW

JOSEPH A. ZIEMIANSKI *In its* Aeropropulsion 1987 p 407-411 Feb. 1990

Avail: CASI HC A01/MF A04

NASA is conducting aeronautical research over a broad range of Mach numbers. In addition to the advanced conventional takeoff or landing (CTOL) propulsion research described elsewhere, NASA Lewis has intensified its efforts towards propulsion technology for selected high speed flight applications. In a companion program, NASA Langley has also accomplished significant research in supersonic combustion ramjet (SCRAM) propulsion. An unclassified review is presented of the propulsion research results that are applicable for supersonic to hypersonic vehicles. This overview not only provides a preview of the more detailed presentations which follow, it also presents a viewpoint on future research directions by calling attention to the unique cycles, components, and facilities involved in this expanding area of work.

Author

N92-22539*# National Aeronautics and Space Administration. Lewis Research Center, Cleveland, OH.

SUPERSONIC STOVL PROPULSION TECHNOLOGY PROGRAM: AN OVERVIEW

BERNARD J. BLAHA and PETER G. BATTERTON *In its* Aeropropulsion 1987 p 413-436 Feb. 1990

Avail: CASI HC A03/MF A04

Planning activities are continuing between NASA, the DoD, and two foreign governments to develop the technology and to show the design capability by the mid-1990's for advanced, supersonic, short takeoff and vertical landing (STOVL) aircraft. Propulsion technology is the key to achieving viable STOVL aircraft, and NASA Lewis will play a lead role in the development of these required propulsion technologies. The initial research programs are focused on technologies common to two or more of the possible STOVL propulsion system concepts. An overview is presented of

07 AIRCRAFT PROPULSION AND POWER

the NASA Lewis role in the overall program plan and recent results of the research program. The future research program will be focused on one or possibly two of the propulsion concepts seen as most likely to be successful in the post advanced tactical fighter time frame. Author

N92-22540*# National Aeronautics and Space Administration. Lewis Research Center, Cleveland, OH.
PROPULSION CHALLENGES AND OPPORTUNITIES FOR HIGH-SPEED TRANSPORT AIRCRAFT
WILLIAM C. STRACK *In its* Aeropropulsion 1987 p 437-452 Feb. 1990
Avail: CASI HC A03/MF A04

The major challenges confronting the propulsion community for supersonic transport applications are identified. Both past progress and future opportunities are discussed in relation to perceived technology shortfalls for an economically successful SST that satisfies environmental constraint. A very large improvement in propulsion system efficiency is needed both at supersonic cruise and subsonic cruise conditions. Toward this end, several advanced engine concepts are being considered that promise up to 25 pct. better efficiency than the Concorde engine. The quest for high productivity through higher speed is also thwarted by the lack of a conventional, low priced fuel that is thermally stable at the higher temperatures associated with faster flight. Extending Jet A type fuel to higher temperatures and the adoption of liquid natural gas or methane are two possibilities requiring further study. Airport noise remains a tough challenge because previously researched concepts fall short of achieving FAR 36 Stage III noise levels. Innovative solutions may be necessary to reach acceptably low noise. Author

N92-22541*# National Aeronautics and Space Administration. Lewis Research Center, Cleveland, OH.
SUPERSONIC THROUGHFLOW FANS FOR HIGH-SPEED AIRCRAFT
CALVIN L. BALL and ROYCE D. MOORE *In its* Aeropropulsion 1987 p 453-468 Feb. 1990
Avail: CASI HC A03/MF A04

A brief overview is provided of past supersonic throughflow fan activities; technology needs are discussed; the design is described of a supersonic throughflow fan stage, a facility inlet, and a downstream diffuser; and the results are presented from the analysis codes used in executing the design. Also presented is a unique engine concept intended to permit establishing supersonic throughflow within the fan on the runway and maintaining the supersonic throughflow condition within the fan throughout the flight envelope. Author

N92-22863*# National Aeronautics and Space Administration. Lewis Research Center, Cleveland, OH.
DESIGN AND PERFORMANCE OF CONTROLLED-DIFFUSION STATOR COMPARED WITH ORIGINAL DOUBLE-CIRCULAR-ARC STATOR
THOMAS F. GELDER, JAMES F. SCHMIDT, KENNETH L. SUDER, and MICHAEL D. HATHAWAY (Army Aviation Systems Command, Cleveland, OH.) Mar. 1989 80 p Presented at the 1987 Aerospace Technology Conference and Exposition, Long Beach, CA, 5-8 Oct. 1987; sponsored by SAE
(Contract DA PROJ. 1L1-61102-AH-45; RTOP 505-62-51)
(NASA-TP-2852; E-4195; NAS 1.60:2852; AVSCOM-TR-88-C-013; SAE-871783) Avail: CASI HC A05/MF A01

The performance of a fan stator blade row having Controlled Diffusion (CD) blade sections were compared with the performance of a fan stator blade row having Double Circular Arc (DCA) blade sections. A CD stator with the same chord length but half the blades of the DCA stator was designed and tested. The same fan rotor (tip speed, 429 m/sec; pressure ratio, 1.64) was used with each stator row. The design and analysis system for the CD stator is described. The overall stage and rotor performance with each stator are then compared along with selected stator blade element data. The CD stator efficiency drop (rotor minus stage efficiency

overall) was about one percentage point higher than for the DCA stator at or near design speed of high losses in the hub region. Author

N92-23225*# National Aeronautics and Space Administration. Lewis Research Center, Cleveland, OH.
DEPOSITION OF ADHERENT AG-TI DUPLEX FILMS ON CERAMICS IN A MULTIPLE-CATHODE SPUTTER DEPOSITION SYSTEM
FRANK S. HONEYCY Apr. 1992 10 p
(Contract RTOP 506-43-11)
(NASA-TM-105586; E-6914; NAS 1.15:105586) Avail: CASI HC A02/MF A01

The adhesion of Ag films deposited on oxide ceramics can be increased by first depositing intermediate films of active metals such as Ti. Such duplex coatings can be fabricated in a widely used three target sputter deposition system. It is shown here that the beneficial effect of the intermediate Ti film can be defeated by commonly used in situ target and substrate sputter cleaning procedures which result in Ag under the Ti. Auger electron spectroscopy and wear testing of the coatings are used to develop a cleaning strategy resulting in an adherent film system. Author

N92-23254*# National Aeronautics and Space Administration. Lewis Research Center, Cleveland, OH.
EFFECTS OF CHEMICAL EQUILIBRIUM ON TURBINE ENGINE PERFORMANCE FOR VARIOUS FUELS AND COMBUSTOR TEMPERATURES
DONALD H. TRAN and CHRISTOPHER A. SNYDER Apr. 1992 22 p
(Contract RTOP 505-69-40)
(NASA-TM-105399; E-6795; NAS 1.15:105399) Avail: CASI HC A03/MF A01

A study was performed to quantify the differences in turbine engine performance with and without the chemical dissociation effects for various fuel types over a range of combustor temperatures. Both turbojet and turbofan engines were studied with hydrocarbon fuels and cryogenic, nonhydrocarbon fuels. Results of the study indicate that accuracy of engine performance decreases when nonhydrocarbon fuels are used, especially at high temperatures where chemical dissociation becomes more significant. For instance, the deviation in net thrust for liquid hydrogen fuel can become as high as 20 percent at 4160 R. This study reveals that computer central processing unit (CPU) time increases significantly when dissociation effects are included in the cycle analysis. Author

N92-23537*# National Aeronautics and Space Administration. Lewis Research Center, Cleveland, OH.
EFFECTS OF TURBINE COOLING ASSUMPTIONS ON PERFORMANCE AND SIZING OF HIGH-SPEED CIVIL TRANSPORT
PAUL F. SENICK May 1992 11 p
(Contract RTOP 537-01-22)
(NASA-TM-105610; E-6948; NAS 1.15:105610) Avail: CASI HC A03/MF A01

The analytical study presented examines the effects of varying turbine cooling assumptions on the performance of a high speed civil transport propulsion system as well as the sizing sensitivity of this aircraft to these performance variations. The propulsion concept employed in this study was a two spool, variable cycle engine with a sea level thrust of 55,000 lbf. The aircraft used for this study was a 250 passenger vehicle with a cruise Mach number of 2.4 and 5000 nautical mile range. The differences in turbine cooling assumptions were represented by varying the amount of high pressure compressor bleed air used to cool the turbines. It was found that as this cooling amount increased, engine size and weight increased, but specific fuel consumption (SFC) decreased at takeoff and climb only. Because most time is spent at cruise, the SFC advantage of the higher bleed engines seen during subsonic flight was minimized and the lower bleed, lighter engines led to the lowest takeoff gross weight vehicles. Finally, the change

in aircraft takeoff gross weight versus turbine cooling level is presented. Author

N92-25164*# National Aeronautics and Space Administration. Lewis Research Center, Cleveland, OH.

THE FUTURE CHALLENGE FOR AEROPROPULSION

ROBERT ROSEN (National Aeronautics and Space Administration, Washington, DC.) and DAVID N. BOWDITCH 1992 14 p Presented at the Aeroengine 1992, Moscow, USSR, 6-12 Apr. 1992

(Contract RTOP 505-62-00)

(NASA-TM-105613; E-6943; NAS 1.15:105613) Avail: CASI HC A03/MF A01

NASA's research in aeropropulsion is focused on improving the efficiency, capability, and environmental compatibility for all classes of future aircraft. The development of innovative concepts, and theoretical, experimental, and computational tools provide the knowledge base for continued propulsion system advances. Key enabling technologies include advances in internal fluid mechanics, structures, light-weight high-strength composite materials, and advanced sensors and controls. Recent emphasis has been on the development of advanced computational tools in internal fluid mechanics, structural mechanics, reacting flows, and computational chemistry. For subsonic transport applications, very high bypass ratio turbofans with increased engine pressure ratio are being investigated to increase fuel efficiency and reduce airport noise levels. In a joint supersonic cruise propulsion program with industry, the critical environmental concerns of emissions and community noise are being addressed. NASA is also providing key technologies for the National Aerospaceplane, and is studying propulsion systems that provide the capability for aircraft to accelerate to and cruise in the Mach 4-6 speed range. The combination of fundamental, component, and focused technology development underway at NASA will make possible dramatic advances in aeropropulsion efficiency and environmental compatibility for future aeronautical vehicles. Author

N92-25712*# National Aeronautics and Space Administration. Lewis Research Center, Cleveland, OH.

WORKSHOP ON GRID GENERATION AND RELATED AREAS

Apr. 1992 160 p Workshop held in Cleveland, OH, 14-15 Nov. 1991

(Contract RTOP 505-62-52)

(NASA-CP-10089; E-6823; NAS 1.55:10089) Avail: CASI HC A08/MF A02

A collection of papers given at the Workshop on Grid Generation and Related Areas is presented. The purpose of this workshop was to assemble engineers and scientists who are currently working on grid generation for computational fluid dynamics (CFD), surface modeling, and related areas. The objectives were to provide an informal forum on grid generation and related topics, to assess user experience, to identify needs, and to help promote synergy among engineers and scientists working in this area. The workshop consisted of four sessions representative of grid generation and surface modeling research and application within NASA LeRC. Each session contained presentations and an open discussion period.

N92-25716*# National Aeronautics and Space Administration. Lewis Research Center, Cleveland, OH.

TCGRID: A THREE DIMENSIONAL C-GRID GENERATOR FOR TURBOMACHINERY

RODRICK V. CHIMA *In its* Workshop on Grid Generation and Related Areas p 39-53 Apr. 1992

Avail: CASI HC A03/MF A02

A fast 3-D grid code for turbomachinery was developed. The code, TCGRID (Turbomachinery C-GRID), can generate either C or H type grids for fairly arbitrary axial or radial turbomachinery geometries. The code also has limited blocked grid capability and can generate an axisymmetric H type grid upstream of the blade row or an O type grid within the tip clearance region. Hub and tip geometries are input as a simple list of pairs. All geometric data is handled using parametric splines so that geometries that turn

90 degrees can be handled without difficulty. Blade input is in standard MERIDL or Lewis compressor design code format. TCGRID adds leading and trailing edge circles to MERIDL geometries and intersects the blade with the hub and tip if necessary using a novel intersection algorithm. The procedure used to generate the grid is given. Output is in PLOT3D format, which can also be read by the RVC3D (Rotor Viscous Code 3-D) Navier-Stokes code for turbomachinery. Intermediate 2-D or 3-D grids useful for debug and other purposes can also be output using a convenient output flag. A grid generated figure is given. Author

N92-25719*# National Aeronautics and Space Administration. Lewis Research Center, Cleveland, OH.

TIGGERC: TURBOMACHINERY INTERACTIVE GRID GENERATOR ENERGY DISTRIBUTOR AND RESTART CODE

DAVID P. MILLER *In its* Workshop on Grid Generation and Related Areas p 65-73 Apr. 1992

Avail: CASI HC A02/MF A02

A two dimensional multi-block grid generator was developed for a new design and analysis system for studying multi-blade row turbomachinery problems with an axisymmetric viscous/inviscid 'average passage' through flow code. TIGGERC is a mouse driven, fully interactive grid generation program which can be used to modify boundary coordinates and grid packing. TIGGERC generates grids using a hyperbolic tangent or algebraic distribution of grid points on the block boundaries and the interior points of each block grid are distributed using a transfinite interpolation approach. TIGGERC generates a blocked axisymmetric H grid, C grid, I grid, or O grid for studying turbomachinery flow problems. TIGGERC was developed for operation on small high speed graphic workstations. Author

N92-25720*# National Aeronautics and Space Administration. Lewis Research Center, Cleveland, OH.

MULTIBLOCK GRID GENERATION FOR JET ENGINE CONFIGURATIONS

MARK E. M. STEWART *In its* Workshop on Grid Generation and Related Areas p 79-84 Apr. 1992

Avail: CASI HC A02/MF A02

The goal was to create methods for generating grids with minimal human intervention that are applicable to a wide range of problems and compatible with existing numerical methods and with existing and proposed computers. The following topics that are related to multiblock grid generation are briefly covered in viewgraph form: finding a domain decomposition, dimensioning grids, grid smoothing, manipulating grids and decompositions, and some specializations for jet engine configurations. Author

N92-25808*# National Aeronautics and Space Administration. Lewis Research Center, Cleveland, OH.

COMPUTATIONAL FLUID DYNAMICS

Feb. 1992 219 p Conference held at Moffett Field, CA, 12-14 Mar. 1991; sponsored by NASA. Ames Research Center Original contains color illustrations

(Contract RTOP 505-62-52)

(NASA-CP-10078; E-6374; NAS 1.55:10078)

This collection of papers was presented at the Computational Fluid Dynamics (CFD) Conference held at Ames Research Center in California on March 12 through 14, 1991. It is an overview of CFD activities at NASA Lewis Research Center. The main thrust of computational work at Lewis is aimed at propulsion systems. Specific issues related to propulsion CFD and associated modeling will also be presented. Examples of results obtained with the most recent algorithm development will also be presented.

N92-26553*# National Aeronautics and Space Administration. Lewis Research Center, Cleveland, OH.

A PARAMETRIC NUMERICAL STUDY OF MIXING IN A CYLINDRICAL DUCT

V. L. OECHSLE (General Motors Corp., Indianapolis, IN.), H. C. MONGIA (General Motors Corp., Indianapolis, IN.), and J. D. HOLDEMAN Jul. 1992 22 p Proposed for presentation at

07 AIRCRAFT PROPULSION AND POWER

the 28th Joint Propulsion Conference and Exhibit, Nashville, TN, 6-8 Jul. 1992; sponsored by AIAA, SAE, ASME, and ASEE Original contains color illustrations
(Contract RTOP 537-02-02)
(NASA-TM-105695; E-7083; NAS 1.15:105695) Copyright

The interaction is described of some of the important parameters affecting the mixing process in a quick mixing region of a rich burn/quick mix/lean burn (RQL) combustor. The performance of the quick mixing region is significantly affected by the geometric designs of both the mixing domain and the jet inlet orifices. Several of the important geometric parameters and operating conditions affecting the mixing process were analytically studied. Parameters such as jet-to-mainstream momentum flux ratio (J), mass flow ratio (MR), orifice geometry, orifice orientation, and number of orifices/row (equally spaced) around the circumferential direction were analyzed. Three different sets of orifice shapes were studied: (1) square, (2) elongated slots, and (3) equilateral triangles. Based on the analytical results, the best mixing configuration depends significantly on the penetration depth of the jet to prevent the hot mainstream flow from being entrained behind the orifice. The structure in a circular mixing section is highly weighted toward the outer wall and any mixing structure affecting this area significantly affects the overall results. The increase in the number of orifices per row increases the mixing at higher J conditions. Higher slot slant angles and aspect ratios are generally the best mixing configurations at higher momentum flux ratio (J) conditions. However, the square and triangular shaped orifices were more effective mixing configurations at lower J conditions. Author

N92-26561*# National Aeronautics and Space Administration. Lewis Research Center, Cleveland, OH.

CFD MIXING ANALYSIS OF JETS INJECTED FROM STRAIGHT AND SLANTED SLOTS INTO CONFINED CROSSFLOW IN RECTANGULAR DUCTS

D. B. BAIN (CFD Research Corp., Huntsville, AL.), C. E. SMITH (CFD Research Corp., Huntsville, AL.), and J. D. HOLDEMAN Jul. 1992 24 p Proposed for presentation at the 28th Joint Propulsion Conference and Exhibit, Nashville, TN, 6-8 Jul. 1992; sponsored by AIAA, SAE, ASME, and ASEE Original contains color illustrations

(Contract RTOP 537-02-20)
(NASA-TM-105699; E-7087; NAS 1.15:105699; AIAA PAPER 92-3087) Copyright

A CFD study was performed to analyze the mixing potential of opposed rows of staggered jets injected into confined crossflow in a rectangular duct. Three jet configurations were numerically tested: (1) straight (0 deg) slots; (2) perpendicular slanted (45 deg) slots angled in opposite directions on top and bottom walls; and (3) parallel slanted (45 deg) slots angled in the same direction on top and bottom walls. All three configurations were tested at slot spacing-to-duct height ratios (S/H) of 0.5, 0.75, and 1.0; a jet-to-mainstream momentum flux ratio (J) of 100; and a jet-to-mainstream mass flow ratio of 0.383. Each configuration had its best mixing performance at S/H of 0.75. Asymmetric flow patterns were expected and predicted for all slanted slot configurations. The parallel slanted slot configuration was the best overall configuration at x/H of 1.0 for S/H of 0.75. Author

N92-26613*# National Aeronautics and Space Administration. Lewis Research Center, Cleveland, OH.

USE OF AN APPROXIMATE SIMILARITY PRINCIPLE FOR THE THERMAL SCALING OF A FULL-SCALE THRUST AUGMENTING EJECTOR

WENDY S. BARANKIEWICZ, GAIL P. PERUSEK, and MOUNIR B. IBRAHIM (Cleveland State Univ., OH.) Jul. 1992 14 p Proposed for presentation at the 28th Joint Propulsion Conference, Nashville, TN, 6-8 Jul. 1992; sponsored by AIAA, ASME, SAE, and ASEE

(Contract RTOP 505-62-71)
(NASA-TM-105724; E-7124; NAS 1.15:105724; AIAA PAPER 92-3792) Avail: CASI HC A03/MF A01

Full temperature ejector model simulations are expensive, and

difficult to implement experimentally. If an approximate similarity principle could be established, properly chosen performance parameters should be similar for both hot and cold flow tests if the initial Mach number and total pressures of the flow field are held constant. Existing ejector data is used to explore the utility of one particular similarity principle; the Munk and Prim similarity principle for isentropic flows. Static performance test data for a full-scale thrust augmenting ejector are analyzed for primary flow temperatures up to 1560 R. At different primary temperatures, exit pressure contours are compared for similarity. A nondimensional flow parameter is then used to eliminate primary nozzle temperature dependence and verify similarity between the hot and cold flow experiments. Author

N92-27037*# National Aeronautics and Space Administration. Lewis Research Center, Cleveland, OH.

INTERFACE OF AN UNCOUPLED BOUNDARY LAYER ALGORITHM WITH AN INVISCID CORE FLOW ALGORITHM FOR UNSTEADY SUPERSONIC ENGINE INLETS

DOUGLAS DARLING and BARBARA SAKOWSKI Jul. 1992 12 p Proposed for presentation at the 28th Joint Propulsion Conference and Exhibit, Nashville, TN, 6-8 Jul. 1992; sponsored by AIAA, SAE, ASME, and ASEE

(Contract RTOP 505-62-20)
(NASA-TM-105684; E-7063; NAS 1.15:105684; AIAA PAPER 92-3083) Avail: CASI HC A03/MF A01

An uncoupled boundary layer algorithm was combined with an inviscid core flow algorithm to model flows within supersonic engine inlets. The inviscid flow algorithm that was used was the LARge Perturbation INlet Code (LAPIN). The boundary layer and inviscid core flow algorithms were formulated in different manners. The boundary layer algorithm was two dimensional and solved in nonconservation form, while the core flow algorithm was one dimensional and solved in conservation form. In order to interface the two codes, the following modifications were important. The coordinate system was set up to maintain the parabolic nature of the boundary layer algorithm while approaching the one dimensional core flow solution far from a wall. The pressure gradient used in the boundary layer equation was calculated using the core flow values and the boundary layer equations, so the boundary layer solution smoothly approached the core flow values far from the wall. Flaring was used for the advection terms perpendicular to the core flow to maintain the stability of the algorithm. With these modifications, the combined viscous/inviscid algorithm matched well with experimental observations of pressure distributions with a supersonic inlet. Author

N92-27652*# National Aeronautics and Space Administration. Lewis Research Center, Cleveland, OH.

EXPERIMENTAL STUDY OF CROSS-STREAM MIXING IN A RECTANGULAR DUCT

D. S. LISCINSKY (United Technologies Research Center, East Hartford, CT.), B. TRUE (AB Research Associates, South Windsor, CT.), A. VRANOS (AB Research Associates, South Windsor, CT.), and J. D. HOLDEMAN 1992 13 p Proposed for presentation at the 28th Joint Propulsion Conference and Exhibit, Nashville, TN, 6-8 Jul. 1992; sponsored by AIAA, SAE, ASME, and ASEE Original contains color illustrations

(Contract RTOP 537-02-20)
(NASA-TM-105694; E-7082; NAS 1.15:105694; AIAA PAPER 92-3090) Copyright

An experimental investigation of non-reacting cross-stream jet injection and mixing in a rectangular duct was conducted for application in a low emissions combustor. Planar digital imaging was used to measure concentration distributions in planes perpendicular to the duct axis. Mixing rate was measured for 45 deg slanted slot and round orifice injectors. Five areas of inquiry are discussed: (1) mixing improves continuously with increasing momentum-flux ratio; (2) given a momentum-flux ratio, there is an optimum, orifice spacing; (3) mixing is more dependent on injector geometry than mass flow ratio; (4) mixing is influenced by relative slot orientation; and (5) jet structure is different for round holes

and slanted slots injectors. The utility of acquiring multipoint fluctuating properties of the flow field is also demonstrated.

Author

N92-27669*# National Aeronautics and Space Administration. Lewis Research Center, Cleveland, OH.

EXPERIMENTAL PERFORMANCE OF THREE DESIGN FACTORS FOR VENTRAL NOZZLES FOR SSTOVL AIRCRAFT
BARBARA S. ESKER and GAIL P. PERUSEK Jul. 1992 16 p
Presented at the 28th Joint Propulsion Conference and Exhibit; sponsored by AIAA, SAE, ASME, and ASEE
(Contract RTOP 505-68-32)
(NASA-TM-105697; E-7085; NAS 1.15:105697; AIAA PAPER 92-3789) Avail: CASI HC A03/MF A01

An experimental study of three variations of a ventral nozzle system for supersonic short-takeoff and vertical-landing (SSTOVL) aircraft was performed at the NASA LeRC Powered Lift Facility. These test results include the effects of an annular duct flow into the ventral duct, a blocked tailpipe, and a short ventral duct length. An analytical study was also performed on the short ventral duct configuration using the PARC3D computational dynamics code. Data presented include pressure losses, thrust and flow performance, internal flow visualization, and pressure distributions at the exit plane of the ventral nozzle.

Author

N92-28418*# National Aeronautics and Space Administration. Lewis Research Center, Cleveland, OH.

INTERNAL REVERSING FLOW IN A TAILPIPE OFFTAKE CONFIGURATION FOR SSTOVL AIRCRAFT
JACK G. MCARDLE, BARBARA S. ESKER, and JAMES A. RHODES (McDonnell Aircraft Co., Saint Louis, MO.) Jul. 1992 23 p
Proposed for presentation at the 28th Joint Propulsion Conference and Exhibit, Nashville, TN, 6-8 Jul. 1992; sponsored by AIAA, SAE, ASME, and ASEE
(Contract RTOP 505-68-32)
(NASA-TM-105698; E-7086; NAS 1.15:105698; AIAA PAPER 92-3790) Avail: CASI HC A03/MF A01

A generic one-third scale model of a tailpipe offtake system for a supersonic short takeoff vertical landing (SSTOVL) aircraft was tested at LeRC Powered Lift Facility. The model consisted of a tailpipe with twin elbows, offtake ducts, and flow control nozzles, plus a small ventral nozzle and a blind flange to simulate a blocked cruise nozzle. The offtake flow turned through a total angle of 177 degrees relative to the tailpipe inlet axis. The flow split was 45 percent to each offtake and 10 percent to the ventral nozzle. The main test objective was to collect data for comparison to the performance of the same configuration predicted by a computational fluid dynamics (CFD) analysis. Only the experimental results are given - the analytical results are published in a separate paper. Performance tests were made with unheated air at tailpipe-to-ambient pressure ratios up to 5. The total pressure loss through the offtakes was as high as 15.5 percent. All test results are shown as graphs, contour plots, and wall pressure distributions. The complex flow patterns in the tailpipe and elbows at the offtake openings are described with traversing flow angle probe and paint streak flow visualization data.

Author

N92-28419*# National Aeronautics and Space Administration. Lewis Research Center, Cleveland, OH.

FULL NAVIER-STOKES ANALYSIS OF A TWO-DIMENSIONAL MIXER/EJECTOR NOZZLE FOR NOISE SUPPRESSION
JAMES R. DEBONIS Jul. 1992 17 p
Proposed for presentation at the 28th Joint Propulsion Conference and Exhibit, Nashville, TN, 6-8 Jul. 1992; sponsored by AIAA, SAE, ASME, and ASEE
(Contract RTOP 537-02-23)
(NASA-TM-105715; E-7109; NAS 1.15:105715; AIAA PAPER 92-3570) Avail: CASI HC A03/MF A01

A three-dimensional full Navier-Stokes (FNS) analysis was performed on a mixer/ejector nozzle designed to reduce the jet noise created at takeoff by a future supersonic transport. The PARC3D computational fluid dynamics (CFD) code was used to study the flow field of the nozzle. The grid that was used in the analysis consisted of approximately 900,000 node points contained

in eight grid blocks. Two nozzle configurations were studied: a constant area mixing section and a diverging mixing section. Data are presented for predictions of pressure, velocity, and total temperature distributions and for evaluations of internal performance and mixing effectiveness. The analysis provided good insight into the behavior of the flow.

Author

N92-28985*# National Aeronautics and Space Administration. Lewis Research Center, Cleveland, OH.

ELECTROMECHANICAL SYSTEMS WITH TRANSIENT HIGH POWER RESPONSE OPERATING FROM A RESONANT AC LINK
LINDA M. BURROWS and IRVING G. HANSEN 1992 6 p
Proposed for presentation at the 27th Intersociety Energy Conversion Engineering Conference, San Diego, CA, 3-7 Aug. 1992; sponsored by SAE, ACS, AIAA, ASME, IEEE, AIChE, and ANS
(Contract RTOP 906-11-03)
(NASA-TM-105716; E-7113; NAS 1.15:105716) Avail: CASI HC A02/MF A01

The combination of an inherently robust asynchronous (induction) electrical machine with the rapid control of energy provided by a high frequency resonant AC link enables the efficient management of higher power levels with greater versatility. This could have a variety of applications from launch vehicles to all-electric automobiles. These types of systems utilize a machine which is operated by independent control of both the voltage and frequency. This is made possible by using an indirect field-oriented control method which allows instantaneous torque control in all four operating quadrants. Incorporating the AC link allows the converter in these systems to switch at the zero crossing of every half cycle of the AC waveform. This zero loss switching of the link allows rapid energy variations to be achieved without the usual frequency proportional switching loss. Several field-oriented control systems were developed by LeRC and General Dynamics Space Systems Division under contract to NASA. A description of a single motor, electromechanical actuation system is presented. Then, focus is on a conceptual design for an AC electric vehicle. This design incorporates an induction motor/generator together with a flywheel for peak energy storage. System operation and implications along with the associated circuitry are addressed. Such a system would greatly improve all-electric vehicle ranges over the Federal Urban Driving Cycle (FUD).

Author

N92-29661*# National Aeronautics and Space Administration. Lewis Research Center, Cleveland, OH.

CONTINGENCY POWER FOR A SMALL TURBOSHAFT ENGINE BY USING WATER INJECTION INTO TURBINE COOLING AIR
THOMAS J. BIESIADNY and GARY A. KLANN (Army Aviation Systems Command, Cleveland, OH.) 1992 10 p
Prepared for presentation at the 80th Symposium on Heat Transfer and Cooling in Gas Turbines, Antalya, Turkey, 12-16 Oct. 1992; sponsored in part by AGARD Propulsion and Energetics Panel
(Contract RTOP 505-68-32)
(NASA-TM-105680; AVSCOM-TR-92-C-019; E-7058; NAS 1.15:105680) Avail: CASI HC A02/MF A01

Because of one-engine-inoperative (OEI) requirements, together with hot-gas reingestion and hot-day, high-altitude take-off situations, power augmentation for multiengine rotorcraft has always been of critical interest. However, power augmentation by using overtemperature at the turbine inlet will shorten turbine life unless a method of limiting thermal and mechanical stress is found. A possible solution involves allowing the turbine inlet temperature to rise to augment power while injecting water into the turbine cooling air to limit hot-section metal temperatures. An experimental water injection device was installed in an engine and successfully tested. Although concern for unprotected subcomponents in the engine hot section prevented demonstration of the technique's maximum potential, it was still possible to demonstrate increases in power while maintaining nearly constant turbine rotor blade temperature.

Author

07 AIRCRAFT PROPULSION AND POWER

N92-30972*# National Aeronautics and Space Administration. Lewis Research Center, Cleveland, OH.

NAVIER-STOKES ANALYSIS AND EXPERIMENTAL DATA COMPARISON OF COMPRESSIBLE FLOW WITHIN DUCTS

G. J. HARLOFF (Sverdrup Technology, Inc., Brook Park, OH.), B. A. REICHERT, J. R. SIRBAUGH (Sverdrup Technology, Inc., Brook Park, OH.), and S. R. WELLBORN (Iowa State Univ. of Science and Technology, Ames.) Jul. 1992 7 p Presented at the 13th International Conference on Numerical Methods in Fluid Dynamics, Rome (Italy), 6-10 Jul. 1992

(Contract NAS3-25266; RTOP 505-62-52)

(NASA-TM-105796; E-7226; NAS 1.15:105796) Avail: CASI HC A02/MF A01

Many aircraft employ ducts with centerline curvature or changing cross-sectional shape to join the engine with inlet and exhaust components. S-ducts convey air to the engine compressor from the intake and often decelerate the flow to achieve an acceptable Mach number at the engine compressor by increasing the cross-sectional area downstream. Circular-to-rectangular transition ducts are used on aircraft with rectangular exhaust nozzles to connect the engine and nozzle. To achieve maximum engine performance, the ducts should minimize flow total pressure loss and total pressure distortion at the duct exit. Changes in the curvature of the duct centerline or the duct cross-sectional shape give rise to streamline curvature which causes cross stream pressure gradients. Secondary flows can be caused by deflection of the transverse vorticity component of the boundary layer. This vortex tilting results in counter-rotating vortices. Additionally, the adverse streamwise pressure gradient caused by increasing cross-sectional area can lead to flow separation. Vortex pairs have been observed in the exit planes of both duct types. These vortices are due to secondary flows induced by pressure gradients resulting from streamline curvature. Regions of low total pressure are produced when the vortices convect boundary layer fluid into the main flow. The purpose of the present study is to predict the measured flow field in a diffusing S-duct and a circular-to-rectangular transition duct with a full Navier-Stokes computer program, PARC3D, and to compare the numerical predictions with new detailed experimental measurements. The work was undertaken to extend previous studies and to provide additional CFD validation data needed to help model flows with strong secondary flow and boundary layer separation. The S-duct computation extends the study of Smith et al, and Harloff et al, which concluded that the computation might be improved by using a finer grid and more advanced turbulence models. The present study compares results for both the Baldwin-Lomas and k-epsilon turbulence models and is conducted with a refined grid. For the transition duct, two inlet conditions were considered, the first with straight flow and the second with swirling flow. The first case permits examination of the effects of the geometric transition on the flow field, while the second case includes the rotational flow effect characteristic of a gas turbine engine. Author

N92-30998*# National Aeronautics and Space Administration. Lewis Research Center, Cleveland, OH.

PRELIMINARY DYNAMIC TESTS OF A FLIGHT-TYPE EJECTOR

COLIN K. DRUMMOND Jul. 1992 22 p Presented at the 28th Joint Propulsion Conference, Nashville, TN, 6-9 Jul. 1992; sponsored by AIAA, SAE, ASME, and ASEE (Contract RTOP 505-62-30)

(NASA-TM-105814; E-7245; NAS 1.15:105814) Copyright Avail: CASI HC A03/MF A01

A thrust augmenting ejector was tested to provide experimental data to assist in the assessment of theoretical models to predict duct and ejector fluid-dynamic characteristics. Eleven full-scale thrust augmenting ejector tests were conducted in which a rapid increase in the ejector nozzle pressure ratio was effected through a unique facility, bypass/burst-disk subsystem. The present work examines two cases representative of the test performance window. In the first case, the primary nozzle pressure ratio (NPR) increased 36 percent from one unchoked (NPR = 1.29) primary flow condition to another (NPR = 1.75) over a 0.15 second interval. The second

case involves choked primary flow conditions, where a 17 percent increase in primary nozzle flowrate (from NPR = 2.35 to NPR = 2.77) occurred over approximately 0.1 seconds. Although the real-time signal measurements support qualitative remarks on ejector performance, extracting quantitative ejector dynamic response was impeded by excessive aerodynamic noise and thrust stand dynamic (resonance) characteristics. It does appear, however, that a quasi-steady performance assumption is valid for this model with primary nozzle pressure increased on the order of 50 lb(sub f)/s. Transient signal treatment of the present dataset is discussed and initial interpretations of the results are compared with theoretical predictions for a similar Short Takeoff and Vertical Landing (STOVL) ejector model. Author

N92-31172*# National Aeronautics and Space Administration. Lewis Research Center, Cleveland, OH.

TRENDS IN AEROPROPULSION RESEARCH AND THEIR IMPACT ON ENGINEERING EDUCATION

LOUIS A. POVINELLI, BRUCE A. REICHERT, and ARTHUR J. GLASSMAN (Toledo Univ., OH.) Jun. 1992 7 p Presented at the ASEE 1992 Annual Conference, Toledo, OH, 21-25 Jun. 1992 (Contract RTOP 505-62-52)

(NASA-TM-105682; E-7061; NAS 1.15:105682) Avail: CASI HC A02/MF A01

This presentation is concerned with the trends in aeropropulsion both in the U.S. and abroad and the impact of these trends on the educational process in our universities. In this paper, we shall outline the new directions for research which may be of interest to educators in the aeropropulsion field. Awareness of new emphases, such as emission reductions, noise control, maneuverability, speed, etc., will have a great impact on engineering educators responsible for restructuring courses in propulsion. The information presented herein will also provide some background material for possible consideration in the future development of propulsion courses. In describing aeropropulsion, we are concerned primarily with air-breathing propulsion; however many observations apply equally as well to rocket engine systems. Aeropropulsion research needs are primarily motivated by technologies required for advanced vehicle systems and frequently driven by external requirements such as economic competitiveness, environmental concern and national security. In this presentation, vehicle based research is first described, followed by a discussion of discipline and multidiscipline research necessary to implement the vehicle-focused programs. The importance of collaboration in research and the training of future researchers concludes this presentation. Author

N92-33746*# National Aeronautics and Space Administration. Lewis Research Center, Cleveland, OH.

NAVIER-STOKES ANALYSIS AND EXPERIMENTAL DATA COMPARISON OF COMPRESSIBLE FLOW IN A DIFFUSING S-DUCT

GARY J. HARLOFF (Sverdrup Technology, Inc., Brook Park, OH.), BRUCE A. REICHERT, and STEVEN R. WELLBORN (Iowa State Univ. of Science and Technology, Ames.) Jul. 1992 11 p Presented at the 10th Applied Aerodynamics Conference Exhibit, Palo Alto, CA, 22-24 Jun. 1992; sponsored by AIAA Previously announced in IAA as A92-45541

(Contract NAS3-25266; RTOP 505-62-52)

(NASA-TM-105683; E-7062; NAS 1.15:105683; AIAA PAPER 92-2699) Avail: CASI HC A03/MF A01

Full three-dimensional Navier-Stokes computational results are compared with new experimental measurements for the flowfield within a round diffusing S-duct. The present study extends previous computational and experimental results for a similar smaller scale S-duct. Predicted results are compared with the experimental static and total pressure fields, and velocity vectors. Additionally, wall pressures, velocity profiles in wall coordinates, and skin friction values are presented. The CFD results employ algebraic and k-epsilon turbulence models. The CFD computed and experimentally determined separated flowfield is carefully examined. Author

AIRCRAFT STABILITY AND CONTROL

Includes aircraft handling qualities; piloting; flight controls; and autopilots.

A92-29093* National Aeronautics and Space Administration. Lewis Research Center, Cleveland, OH.

INTEGRATED FLIGHT/PROPULSION CONTROL DESIGN FOR A STOVL AIRCRAFT USING H-INFINITY CONTROL DESIGN TECHNIQUES

SANJAY GARG and PETER J. OUZTS (NASA, Lewis Research Center, Cleveland, OH) IN: 1991 American Control Conference, 10th, Boston, MA, June 26-28, 1991, Proceedings. Vol. 1 1991 9 p refs

Copyright

Results are presented from an application of H(infinity) control design methodology to a centralized integrated flight/propulsion control (IFPC) system design for a supersonic short take-off and vertical landing (STOVL) fighter aircraft in transition flight. The emphasis is on formulating the H(infinity) control design problem such that the resulting controller provides robustness to modeling uncertainties and model parameter variations with flight condition. Experience gained from a preliminary H(infinity)-based IFPC design study performed earlier is used as the base to formulate the robust H(infinity) control design problem and improve the previous design. Detailed evaluation results are presented for a reduced-order controller obtained from the improved H(infinity) control design showing that the control design meets the specified nominal performance objectives as well as provides stability robustness for variations in plant system dynamics with changes in aircraft trim speed within the transition flight envelope. Author

A92-29117* National Aeronautics and Space Administration. Lewis Research Center, Cleveland, OH.

INTEGRATED FLIGHT/PROPULSION CONTROL SPECIFICATIONS FOR SYSTEMS WITH TWO-WAY COUPLING

STEPHEN M. ROCK (Stanford University, CA) IN: 1991 American Control Conference, 10th, Boston, MA, June 26-28, 1991, Proceedings. Vol. 1 1991 6 p refs

(Contract NAG3-1177)

Copyright

A general technique for generating specifications for integrated flight propulsion control is extended to include systems with significant two-way coupling between the flight and propulsion systems. These specifications define how the subsystems must perform within an integrated control system in order to assure that performance goals (specifically stability) are met when the subsystems are combined to form a closed-loop integrated system. Such specifications are useful for a large class of integrated control problems that are best approached in a partitioned or decentralized manner. An example demonstrating the application of these techniques to a simple helicopter problem is provided. I.E.

A92-29118* National Aeronautics and Space Administration. Lewis Research Center, Cleveland, OH.

IMPAC - AN INTEGRATED METHODOLOGY FOR PROPULSION AND AIRFRAME CONTROL

SANJAY GARG, PETER J. OUZTS, CARL F. LORENZO, and DUANE L. MATTERN (NASA, Lewis Research Center, Cleveland, OH) IN: 1991 American Control Conference, 10th, Boston, MA, June 26-28, 1991, Proceedings. Vol. 1 1991 8 p refs

Copyright

The NASA Lewis Research Center approach to developing integrated flight propulsion control (IFPC) technologies is an in-house research program referred to as IMPAC-Integrated Methodology for Propulsion and Airframe Control. The goals of IMPAC are to develop a viable alternative to the existing integrated control design methodologies that will allow for improved system performance and simplicity of control law synthesis and

implementation, and to demonstrate the applicability of the methodology to a supersonic STOVL fighter aircraft. An overview of IMPAC is presented, including a detailed discussion of the various important design and evaluation steps in the methodology. I.E.

A92-29119* National Aeronautics and Space Administration. Lewis Research Center, Cleveland, OH.

DECENTRALIZED HIERARCHICAL PARTITIONING OF CENTRALIZED INTEGRATED CONTROLLERS

PHILLIP SCHMIDT (Akron, University, OH) and SANJAY GARG (NASA, Lewis Research Center, Cleveland, OH) IN: 1991 American Control Conference, 10th, Boston, MA, June 26-28, 1991, Proceedings. Vol. 1 1991 6 p refs

Copyright

A framework for a decentralized hierarchical controller partitioning structure is developed. This structure allows for the design of separate airframe and propulsion controllers which, when assembled, will meet the overall design criterion for the integrated airframe/propulsion system. An algorithm based on parameter optimization of the state-space representation for the subsystem controllers is described. The algorithm is currently being applied to an integrated flight propulsion control design example. I.E.

A92-29120* National Aeronautics and Space Administration. Lewis Research Center, Cleveland, OH.

A FRAMEWORK FOR THE ANALYSIS OF AIRFRAME/ENGINE INTERACTIONS AND INTEGRATED FLIGHT/PROPULSION CONTROL

DAVID K. SCHMIDT and JOHN D. SCHIERMAN (Arizona State University, Tempe) IN: 1991 American Control Conference, 10th, Boston, MA, June 26-28, 1991, Proceedings. Vol. 1 1991 6 p refs

(Contract NAG3-998)

Copyright

Potential sources of airframe/engine interactions are explored for aircraft subject to the study of integrated flight/propulsion control. A quasi-linear framework for the analysis of these dynamical interactions between the airframe and engine systems is presented. This analysis can be used to quantify, in a meaningful way, the magnitude of the interactions between the airframe and engine systems, determine if these interactions are significant to warrant further consideration in the control law synthesis, and if so, what are the critical frequency ranges where problems may occur due to these interactions. Justification for the use of this method, along with the assumptions, conditions, and restrictions that apply are discussed. I.E.

A92-45320 National Aeronautics and Space Administration. Ames Research Center, Moffett Field, CA.

INTEGRATED FLIGHT/PROPULSION CONTROL FOR SUPERSONIC STOVL AIRCRAFT

JAMES A. FRANKLIN, MICHAEL W. STORTZ (NASA, Ames Research Center, Moffett Field, CA), and JAMES R. MIHALOEWSKI (NASA, Lewis Research Center, Cleveland, OH) IN: International Powered Lift Conference, London, England, Aug. 29-31, 1990, Proceedings 1990 12 p refs

Copyright

A technology program to investigate integrated flight/propulsion control-system design for STOVL fighter aircraft is described. Integrated control systems being developed by U.S. industry for specific STOVL concepts are discussed. Attention is given to NASA involvement in the definition of control concepts, design-methods and flying-qualities criteria, and the evaluation of these concepts and criteria in analytical design studies, in ground-based experiments, and in flight on the Harrier V/STOL research aircraft. Initial fixed-base simulation experiments conducted for two STOVL fighter concepts are discussed. These simulations defined acceptable transition flight envelopes, determined control power used during transition and hover, and provided evaluations of the integration of the flight and propulsion controls to achieve good flying qualities throughout the low-speed flight envelope. C.A.B.

08 AIRCRAFT STABILITY AND CONTROL

N92-20586*# National Aeronautics and Space Administration. Lewis Research Center, Cleveland, OH.

DESIGN AND EVALUATION OF A ROBUST DYNAMIC NEUROCONTROLLER FOR A MULTIVARIABLE AIRCRAFT CONTROL PROBLEM

T. TROUDET (Sverdrup Technology, Inc., Brook Park, OH.), S. GARG, and W. MERRILL 1992 9 p Proposed for presentation at the International Joint Conference on Neural Networks, Baltimore, MD, 7 Jun. 1992

(Contract RTOP 505-62-50)

(NASA-TM-105579; E-6905; NAS 1.15:105579) Avail: CASI HC A02/MF A01

The design of a dynamic neurocontroller with good robustness properties is presented for a multivariable aircraft control problem. The internal dynamics of the neurocontroller are synthesized by a state estimator feedback loop. The neurocontrol is generated by a multilayer feedforward neural network which is trained through backpropagation to minimize an objective function that is a weighted sum of tracking errors, and control input commands and rates. The neurocontroller exhibits good robustness through stability margins in phase and vehicle output gains. By maintaining performance and stability in the presence of sensor failures in the error loops, the structure of the neurocontroller is also consistent with the classical approach of flight control design. Author

N92-22529*# National Aeronautics and Space Administration. Lewis Research Center, Cleveland, OH.

FIBER OPTICS FOR CONTROLS

GARY T. SENG *In its* Aeropropulsion 1987 p 243-249 Feb. 1990

Avail: CASI HC A02/MF A04

The design, development, and testing of a fiber optic integrated propulsion/flight control system for an advanced supersonic dash aircraft (flies at supersonic speeds for short periods of time) is the goal of the joint NASA/DOD Fiber Optic Control System Integration (FOCSI) program. Phase 1 provided a comparison of electronic and optical control systems, identified the status of current optical sensor technology, defined the aircraft sensor/actuator environment, proposed architectures for fully optical control systems, and provided schedules for development. Overall, it was determined that there are sufficient continued efforts to develop such a system. It was also determined that it is feasible to build a fiber optic control system for the development of a data base for this technology, but that further work is necessary in sensors, actuators, and components to develop an optimum design, fully fiber optic integrated control system compatible with advanced aircraft environments. Phase 2 is to design, construct, and ground test a fly by light control system. Its first task is to provide a detailed design of the electro-optic architecture. Author

N92-32241*# National Aeronautics and Space Administration. Lewis Research Center, Cleveland, OH.

A PARAMETER OPTIMIZATION APPROACH TO CONTROLLER PARTITIONING FOR INTEGRATED FLIGHT/PROPULSION CONTROL APPLICATION

PHILLIP SCHMIDT (Akron Univ., OH.), SANJAY GARG, and BRIAN HOLOWECKY (Akron Univ., OH.) Aug. 1992 30 p

(Contract RTOP 505-62-50)

(NASA-TM-105826; E-7260; NAS 1.15:105826) Avail: CASI HC A03/MF A01

A parameter optimization framework is presented to solve the problem of partitioning a centralized controller into a decentralized hierarchical structure suitable for integrated flight/propulsion control implementation. The controller partitioning problem is briefly discussed and a cost function to be minimized is formulated, such that the resulting 'optimal' partitioned subsystem controllers will closely match the performance (including robustness) properties of the closed-loop system with the centralized controller while maintaining the desired controller partitioning structure. The cost function is written in terms of parameters in a state-space representation of the partitioned sub-controllers. Analytical expressions are obtained for the gradient of this cost function

with respect to parameters, and an optimization algorithm is developed using modern computer-aided control design and analysis software. The capabilities of the algorithm are demonstrated by application to partitioned integrated flight/propulsion control design for a modern fighter aircraft in the short approach to landing task. The partitioning optimization is shown to lead to reduced-order subcontrollers that match the closed-loop command tracking and decoupling performance achieved by a high-order centralized controller. Author

N92-34107*# National Aeronautics and Space Administration. Lewis Research Center, Cleveland, OH.

PILOTED EVALUATION OF AN INTEGRATED PROPULSION AND FLIGHT CONTROL SIMULATOR

MICHELLE M. BRIGHT and DONALD L. SIMON (Army Aviation Systems Command, Cleveland, OH.) Aug. 1992 13 p Proposed for presentation at the Flight Simulation Technologies Conference and Exhibit, Hilton Head, SC, 24-26 Aug. 1992; sponsored by AIAA

(Contract RTOP 505-62-50)

(NASA-TM-105797; E-7227; NAS 1.15:105797;

AVSCOM-TR-92-C-028; AD-A254805) Copyright Avail: CASI HC A03/MF A01

A piloted evaluation of the integrated flight and propulsion control simulator for advanced integrated propulsion and airframe control design is described. The evaluation will cover control effector gains and deadbands, control effectiveness and control authority, and heads up display functionality. For this evaluation the flight simulator is configured for transition flight using an advanced Short Take-Off and Vertical Landing fighter aircraft model, a simplified high-bypass turbofan engine model, fighter cockpit displays, and pilot effectors. The piloted tasks used for rating displays and control effector gains are described. Pilot comments and simulation results confirm that the display symbology and control gains are very adequate for the transition flight task. Additionally, it is demonstrated that this small-scale, fixed base flight simulator facility can adequately perform a real time, piloted control evaluation. Author

09

RESEARCH AND SUPPORT FACILITIES (AIR)

Includes airports, hangars and runways; aircraft repair and overhaul facilities; wind tunnels; shock tubes; and aircraft engine test stands.

A92-24406* National Aeronautics and Space Administration. Lewis Research Center, Cleveland, OH.

INVESTIGATION OF THE DIFFUSER FLOW QUALITY IN AN ICING RESEARCH WIND TUNNEL

HAROLD E. ADDY, JR. (NASA, Lewis Research Center, Cleveland, OH) and THEO G. KEITH, JR. (Toledo, University, OH) Feb. 1992 5 p refs

Copyright

A92-48908*# National Aeronautics and Space Administration. Lewis Research Center, Cleveland, OH.

INVESTIGATION OF THREE-DIMENSIONAL FLOW FIELD IN A TURBINE INCLUDING ROTOR/STATOR INTERACTION. I - DESIGN DEVELOPMENT AND PERFORMANCE OF THE RESEARCH FACILITY

B. LAKSHMINARAYANA, C. CAMCI (Pennsylvania State University, University Park), I. HALLIWELL (GE Aircraft Engines, Cincinnati, OH), and M. ZACCARIA (Pennsylvania State University, University Park) AIAA, SAE, ASME, and ASEE, Joint Propulsion Conference and Exhibit, 28th, Nashville, TN, July 6-8, 1992. 13 p. Research supported by Pennsylvania State University. Jul. 1992 13 p refs

09 RESEARCH AND SUPPORT FACILITIES (AIR)

(Contract DAAL03-86-G-0013; NSG-3555)
(AIAA PAPER 92-3325) Copyright

A description of the Axial Flow Turbine Research Facility (AFTRF) installed at the Turbomachinery Laboratory of the Pennsylvania State University is presented in this paper. The facility diameter is 91.66 cm (3 feet) and the hub-to-tip ratio of the blading is 0.73. The flow path consists of turbulence generating grid, 23 nozzle vane and 29 rotor blades followed by outlet guide vanes. The blading design, carried out by General Electric Company personnel, embody modern HP turbine design philosophy, loading and flow coefficient, reaction, aspect ratio, and blade turning angles; all within the current aircraft engine design turbine practice. State-of-the-art quasi-3D blade design techniques were used to design the vane and the blade shapes. The vanes and blades are heavily instrumented with fast response pressure, shear stress, and velocity probes and have provision for flow visualization and laser Doppler anemometer measurement. Furthermore, provision has been made for detailed nozzle wake, rotor wake and boundary layer surveys. A 150 channel slip ring unit is used for transmitting the rotor data to a stationary instrumentation system. All the design objectives have been met. Author

A92-54058*# National Aeronautics and Space Administration, Lewis Research Center, Cleveland, OH.

EXPERIMENTAL INVESTIGATION OF AN EJECTOR-POWERED FREE-JET FACILITY

MARY J. LONG (NASA, Lewis Research Center, Cleveland, OH) AIAA, SAE, ASME, and ASEE, Joint Propulsion Conference and Exhibit, 28th, Nashville, TN, July 6-8, 1992. 13 p. Jul. 1992 13 p refs
(AIAA PAPER 92-3569) Copyright

The Nozzle Acoustic Test Rig (NATR) is a large free-jet test facility powered by an ejector system. Prior to the operation of the actual facility a 1/5-scale model of the NATR was built and tested to assess the pumping performance of the ejector concept as well as its sensitivity to various design parameters. The 1/5 scale model and full-scale facility are described as well as the design parameters which were investigated. The results of the scale model tests are discussed and compared with the findings of the full-scale tests. A.O.

A92-56748*# National Aeronautics and Space Administration, Lewis Research Center, Cleveland, OH.

FLOW QUALITY STUDIES OF THE NASA LEWIS RESEARCH CENTER 8- BY 6-FOOT SUPERSONIC/9- BY 15-FOOT LOW SPEED WIND TUNNEL

E. A. ARRINGTON (Sverdrup Technology, Inc., Lewis Research Center Group, Brook Park, OH) and MARK T. PICKETT (NASA, Lewis Research Center, Cleveland, OH) AIAA, Aerospace Ground Testing Conference, 17th, Nashville, TN, July 6-8, 1992. 46 p. Previously announced in STAR as N92-28673. Jul. 1992 46 p refs
(AIAA PAPER 92-3916) Copyright

A series of studies were conducted to determine the existing flow quality in the NASA Lewis 8 by 6 Foot Supersonic/9 by 15 Foot Low Speed Wind Tunnel. The information gathered from these studies was used to determine the types and designs of flow manipulators which can be installed to improve overall tunnel flow quality and efficiency. Such manipulators include honeycomb flow straighteners, turbulence reduction screens, corner turning vanes, and acoustic treatments. The types of measurements, instrumentation, and results obtained from experiments conducted at several locations throughout the tunnel loop are described. Author

A92-56753*# National Aeronautics and Space Administration, Lewis Research Center, Cleveland, OH.

LASER-DRIVEN HYPERSONIC AIR-BREATHING PROPULSION SIMULATOR

PRAKASH B. JOSHI, EDMOND Y. LO, and EVAN R. PUGH (Physical Sciences, Inc., Andover, MA) AIAA, Aerospace Ground Testing Conference, 17th, Nashville, TN, July 6-8, 1992. 19 p.

Jul. 1992 19 p refs
(Contract NAS3-26146)
(AIAA PAPER 92-3922) Copyright

A feasibility study is presented of simulating airbreathing propulsion on small scale hypersonic models using laser energy. The laser heat addition scheme allows simultaneous inlet and exhaust flows during wind tunnel testing of models with scramjet models. The proposed propulsion simulation concept has extended the Kantrowitz (1974) idea to propulsive wind tunnel models of hypersonic aircraft. Critical issues in aeropropulsive testing of models based on a ramjet power plant are addressed which include transfer of the correct amount of energy to the flowing gas, efficient absorption of laser energy into the gas, and test performance under tunnel reservoir conditions and at reasonable Reynolds numbers. O.G.

A92-56806# National Aeronautics and Space Administration, Lewis Research Center, Cleveland, OH.

SMALL ENGINE COMPONENTS TEST FACILITY COMPRESSOR TESTING CELL AT NASA LEWIS RESEARCH CENTER

RICHARD A. BROKOPP (NASA, Lewis Research Center, Cleveland, OH) and ROBERT S. GRONSKI (Sverdrup Technology, Inc., Brook Park; NASA, Lewis Research Center, Cleveland, OH) AIAA, Aerospace Ground Testing Conference, 17th, Nashville, TN, July 6-8, 1992. 12 p. Previously announced in STAR as N92-30508. Jul. 1992 12 p
(Contract RTOP 505-62-84)
(AIAA PAPER 92-3980) Copyright

LeRC has designed and constructed a new test facility. This facility, called the Small Engine Components Facility (SECTF) is used to test gas turbines and compressors at conditions similar to actual engine conditions. The SECTF is comprised of a compressor testing cell and a turbine testing cell. Only the compressor testing cell is described. The capability of the facility, the overall facility design, the instrumentation used in the facility, and the data acquisition system are discussed in detail. Author

A92-56816# National Aeronautics and Space Administration, Lewis Research Center, Cleveland, OH.

ADVANCED NOZZLE AND ENGINE COMPONENTS TEST FACILITY

LUIS R. BELTRAN, RICHARD L. DEL ROSO, and RUBEN DEL ROSARIO (NASA, Lewis Research Center, Cleveland, OH) AIAA, Aerospace Ground Testing Conference, 17th, Nashville, TN, July 6-8, 1992. 17 p. Previously announced in STAR as N92-17059. Jul. 1992 17 p
(Contract RTOP 505-62-84)
(AIAA PAPER 92-3993) Copyright

A test facility for conducting scaled advanced nozzle and engine component research is described. The CE-22 test facility, located in the Engine Research Building of the NASA Lewis Research Center, contains many systems for the economical testing of advanced scale-model nozzles and engine components. The combustion air and altitude exhaust systems are described. Combustion air can be supplied to a model up to 40 psig for primary air flow, and 40, 125, and 450 psig for secondary air flow. Altitude exhaust can be simulated up to 48,000 ft, or the exhaust can be atmospheric. Descriptions of the multi-axis thrust stand, a color schlieren flow visualization system used for qualitative flow analysis, a labyrinth flow measurement system, a data acquisition system, and auxiliary systems are discussed. Model recommended design information and temperature and pressure instrumentation recommendations are included. Author

A92-56818# National Aeronautics and Space Administration, Lewis Research Center, Cleveland, OH.

ENGINE COMPONENT INSTRUMENTATION DEVELOPMENT FACILITY AT NASA LEWIS RESEARCH CENTER

ROBERT J. BRUCKNER, ALVIN E. BUGGELE (NASA, Lewis Research Center, Cleveland, OH), and JAN LEPICOVSKY (Sverdrup Technology, Inc., Brook Park; NASA, Lewis Research Center, Cleveland, OH) AIAA, Aerospace Ground Testing

09 RESEARCH AND SUPPORT FACILITIES (AIR)

Conference, 17th, Nashville, TN, July 6-8, 1992. 9 p. Previously announced in STAR as N92-25449. Jul. 1992 9 p (Contract RTOP 505-62-84) (AIAA PAPER 92-3995) Copyright

The Engine Components Instrumentation Development Facility at NASA Lewis is a unique aeronautics facility dedicated to the development of innovative instrumentation for turbine engine component testing. Containing two separate wind tunnels, the facility is capable of simulating many flow conditions found in most turbine engine components. This facility's broad range of capabilities as well as its versatility provide an excellent location for the development of novel testing techniques. These capabilities thus allow a more efficient use of larger and more complex engine component test facilities. Author

A92-56856*# National Aeronautics and Space Administration. Lewis Research Center, Cleveland, OH.

TRANSONIC TURBINE BLADE CASCADE TESTING FACILITY
VINCENT G. VERHOFF, WILLIAM P. CAMPERCHIOLI (NASA, Lewis Research Center, Cleveland, OH), and ISAAC LOPEZ (USAF, Propulsion Directorate; NASA, Lewis Research Center, Cleveland, OH) AIAA, Aerospace Ground Testing Conference, 17th, Nashville, TN, July 6-8, 1992. 12 p. Previously announced in STAR as N92-26129. Jul. 1992 12 p (AIAA PAPER 92-4034) Copyright

NASA LeRC has designed and constructed a new state-of-the-art test facility. This facility, the Transonic Turbine Blade Cascade, is used to evaluate the aerodynamics and heat transfer characteristics of blade geometries for future turbine applications. The facility's capabilities make it unique: no other facility of its kind can combine the high degree of airflow turning, infinitely adjustable incidence angle, and high transonic flow rates. The facility air supply and exhaust pressures are controllable to 16.5 psia and 2 psia, respectively. The inlet air temperatures are at ambient conditions. The facility is equipped with a programmable logic controller with a capacity of 128 input/output channels. The data acquisition system is capable of scanning up to 1750 channels per sec. This paper discusses in detail the capabilities of the facility, overall facility design, instrumentation used in the facility, and the data acquisition system. Actual research data is not discussed. Author

N92-17059*# National Aeronautics and Space Administration. Lewis Research Center, Cleveland, OH.

ADVANCED NOZZLE AND ENGINE COMPONENTS TEST FACILITY

LUIS R. BELTRAN, RICHARD L. DELROSO, and RUBEN DELROSARIO Jan. 1992 21 p (Contract RTOP 505-62-84) (NASA-TM-103684; E-5902; NAS 1.15:103684) Avail: CASI HC A03/MF A01

A test facility for conducting scaled advanced nozzle and engine component research is described. The CE-22 test facility, located in the Engine Research Building of the NASA Lewis Research Center, contains many systems for the economical testing of advanced scale-model nozzles and engine components. The combustion air and altitude exhaust systems are described. Combustion air can be supplied to a model up to 40 psig for primary air flow, and 40, 125, and 450 psig for secondary air flow. Altitude exhaust can be simulated up to 48,000 ft, or the exhaust can be atmospheric. Descriptions of the multiaxis thrust stand, a color schlieren flow visualization system used for qualitative flow analysis, a labyrinth flow measurement system, a data acquisition system, and auxiliary systems are discussed. Model recommended design information and temperature and pressure instrumentation recommendations are included. Author

N92-25449*# National Aeronautics and Space Administration. Lewis Research Center, Cleveland, OH.

ENGINE COMPONENT INSTRUMENTATION DEVELOPMENT FACILITY AT NASA LEWIS RESEARCH CENTER

ROBERT J. BRUCKNER, ALVIN E. BUGGELE, and JAN LEPICOVSKY (Sverdrup Technology, Inc., Brook Park, OH.)

1992 10 p Proposed for presentation at the 17th Aerospace Ground Testing Conference, Nashville, TN, 6-8 Jul. 1992; sponsored by AIAA (Contract RTOP 505-62-84) (NASA-TM-105644; E-6999; NAS 1.15:105644; AIAA PAPER 92-3995) Avail: CASI HC A02/MF A01

The Engine Components Instrumentation Development Facility at NASA Lewis is a unique aeronautics facility dedicated to the development of innovative instrumentation for turbine engine component testing. Containing two separate wind tunnels, the facility is capable of simulating many flow conditions found in most turbine engine components. This facility's broad range of capabilities as well as its versatility provide an excellent location for the development of novel testing techniques. These capabilities thus allow a more efficient use of larger and more complex engine component test facilities. Author

N92-28673*# National Aeronautics and Space Administration. Lewis Research Center, Cleveland, OH.

FLOW QUALITY STUDIES OF THE NASA LEWIS RESEARCH CENTER 8- BY 6-FOOT SUPERSONIC/9- BY 15-FOOT LOW SPEED WIND TUNNEL

E. ALLEN ARRINGTON and MARK T. PICKETT Jul. 1992 47 p Presented at the 17th Aerospace Ground Testing Conference, Nashville, TN, 6-8 Jul. 1992; sponsored in part by AIAA

(Contract NAS3-25266; RTOP 505-62-84) (NASA-TM-105417; E-6827; NAS 1.15:105417; AIAA PAPER 92-3916) Avail: CASI HC A03/MF A01

A series of studies were conducted to determine the existing flow quality in the NASA Lewis 8 by 6 Foot Supersonic/9 by 15 Foot Low Speed Wind Tunnel. The information gathered from these studies was used to determine the types and designs of flow manipulators which can be installed to improve overall tunnel flow quality and efficiency. Such manipulators include honeycomb flow straighteners, turbulence reduction screens, corner turning vanes, and acoustic treatments. The types of measurements, instrumentation, and results obtained from experiments conducted at several locations throughout the tunnel loop are described. Author

N92-30508*# National Aeronautics and Space Administration. Lewis Research Center, Cleveland, OH.

SMALL ENGINE COMPONENTS TEST FACILITY COMPRESSOR TESTING CELL AT NASA LEWIS RESEARCH CENTER

RICHARD A. BROKOPP and ROBERT S. GRONSKI (Sverdrup Technology, Inc., Brook Park, OH.) Jul. 1992 13 p Proposed for presentation at the 17th AIAA Aerospace Ground Testing Conference, Nashville, TN, 6-8 Jul. 1992 (Contract RTOP 505-62-84)

(NASA-TM-105685; E-7064; NAS 1.15:105685; AIAA PAPER 92-3980) Avail: CASI HC A03/MF A01

LeRC has designed and constructed a new test facility. This facility, called the Small Engine Components Tests Facility (SECTF), is used to test gas turbines and compressors at conditions similar to actual engine conditions. The SECTF is comprised of a compressor testing cell and a turbine testing cell. Only the compressor testing cell is described. The capability of the facility, the overall facility design, the instrumentation used in the facility, and the data acquisition system are discussed in detail. Author

ASTRONAUTICS (GENERAL)

A92-23850* National Aeronautics and Space Administration. Lewis Research Center, Cleveland, OH.

CONE - AN STS-BASED CRYOGENIC FLUID MANAGEMENT EXPERIMENT

R. S. BELL (Ball Aerospace Systems Group, Electro-Optics/Cryogenics Div., Boulder, CO), D. M. VENTO (NASA, Lewis Research Center, Cleveland, OH), and G. J. HANNA (Hanna Technology Resources, Boulder, CO) (Space Cryogenics Workshop, 10th, Cleveland, OH, June 18-20, 1991, Proceedings. A92-23826 08-31) Cryogenics (ISSN 0011-2275), vol. 32, no. 2, 1992, p. 215-220. 1992 6 p
(Contract NAS3-25054)

Copyright

An overview of the CONE program is presented which includes a definition of the technology addressed by CONE and a baseline experiment set, a description of the experimental and support subsystems, interface requirements between the STS and the experiment carrier (Hitchhiker M), and the reusability and expansion capacity for additional experiment flights. CONE evaluates three primary technologies: the active thermodynamic vent system, the passive thermodynamic vent system, and liquid acquisition device performance. The cryogenic fluid management technology database that the system offers will allow for efficient subcritical cryogenic system designs for operation in a low-gravity environment. This system maximizes the balance between existing component technology and the need for the development of a cryogenic-fluid-management (CFM) test bed to investigate and demonstrate methods of storage and handling arenas. P.D.

A92-23851* National Aeronautics and Space Administration. Lewis Research Center, Cleveland, OH.

CRYOGENIC FLUID MANAGEMENT INVESTIGATIONS USING THE CONE FLIGHT EXPERIMENT

W. J. BAILEY (Martin Marietta Astronautics Group, Denver, CO) and H. ARIF (NASA, Lewis Research Center, Cleveland, OH) (Space Cryogenics Workshop, 10th, Cleveland, OH, June 18-20, 1991, Proceedings. A92-23826 08-31) Cryogenics (ISSN 0011-2275), vol. 32, no. 2, 1992, p. 221-229. 1992 9 p
(Contract NAS3-25063)

Copyright

The Cryogenic Orbital Nitrogen Experiment (CONE) is a liquid nitrogen cryogenic storage and supply system demonstration placed in orbit by the National Space Transportation System (NSTS) Orbiter and operated as an in-bay payload whose objective is to demonstrate needed critical components and technologies. A conceptual approach has been developed by Martin Marietta under contract with the NASA Lewis Research Center and an overview of the CONE program is described which includes a definition of the background and scope of the technology objectives being investigated, a description of the payload design and operation, major features and rationale for the experiments being conducted and the justification for CONE relating to potential near-term benefits and risk mitigation for future systems. Author

A92-38634*# National Aeronautics and Space Administration. Lewis Research Center, Cleveland, OH.

REPAIR-LEVEL ANALYSIS FOR SPACE STATION FREEDOM

M. CHADWICK (Rockwell International Corp., Rocketdyne Div., Canoga Park, CA) and J. YANIEC (NASA, Lewis Research Center, Cleveland, OH) AIAA, Space Programs and Technologies Conference, Huntsville, AL, Mar. 24-27, 1992. 11 p. Mar. 1992 11 p
(AIAA PAPER 92-1537) Copyright

Copyright

To assign repair or discard-at-failure designations for orbital replacement units (ORUs) used on Space Station Freedom Electric

Power System (SSFEPS), new algorithms and methods were required. Unique parameters, such as upmass costs, extravehicular activity costs and intravehicular activity (IVA) costs specific to Space Station Freedom's maintenance concept were incorporated into the Repair-Level Analysis (RLA). Additional outputs were also required of the SSFEPS RLA that were not required of previous RLAs. These outputs included recommendations for the number of launches that an ORU should be capable of attaining and an economic basis for condemnation rate. These unique parameters were not addressable using existing RLA models; therefore, a new approach was developed. In addition, it was found that preemptive analysis could be performed using spreadsheet-based Boolean expressions to represent the logical condition of the items under analysis. Author

A92-57053* National Aeronautics and Space Administration. Lewis Research Center, Cleveland, OH.

AN ACCELERATED DEVELOPMENT, REDUCED COST APPROACH TO LUNAR/MARS EXPLORATION USING A MODULAR NTR-BASED SPACE TRANSPORTATION SYSTEM

S. BOROWSKI, J. CLARK, R. SEFCIK, R. CORBAN, and S. ALEXANDER (NASA, Lewis Research Center, Cleveland, OH) IAF, International Astronautical Congress, 43rd, Washington, Aug. 28-Sept. 5, 1992. 28 p. Aug. 1992 28 p refs
(IAF PAPER 92-0574)

Benefits and rationale for developing a common, modular lunar/Mars space transportation system (STS) based on nuclear thermal rocket (NTR) are presented. The modular NTR is based on three key components including a 50 klbf NERVA-derived engine used in clusters of 2 or 3, two standardized tank sizes developed for the First Lunar Outpost and Mars cargo vehicle applications, and a preintegrated truss/propellant feed system used for transferring LH2 from the drop tanks into the 'in-line' tank. It is concluded that, by using these components in a 'building block' fashion, a variety of single and multi-engine lunar and Mars vehicles can be configured to satisfy particular mission requirements. O.G.

N92-20925*# National Aeronautics and Space Administration. Langley Research Center, Hampton, VA.

REPORT OF THE NUCLEAR PROPULSION MISSION

ANALYSIS, FIGURES OF MERIT SUBPANEL: QUANTIFIABLE FIGURES OF MERIT FOR NUCLEAR THERMAL PROPULSION

DAVY A. HAYNES Nov. 1991 11 p Prepared in cooperation with NASA, Washington; NASA Johnson Space Center, Houston, TX; NASA Lewis Research Center, Cleveland, OH; Idaho National Engineering Lab., Idaho Falls; PNL, Richland, WA; Phillips Lab., Edwards AFB, CA; and Sandia National Labs., Albuquerque, NM (Contract RTOP 594-81-12-11)
(NASA-TM-104179; NAS 1.15:104179) Avail: CASI HC A03/MF A01

The results of an inquiry by the Nuclear Propulsion Mission Analysis, Figures of Merit subpanel are given. The subpanel was tasked to consider the question of what are the appropriate and quantifiable parameters to be used in the definition of an overall figure of merit (FoM) for Mars transportation system (MTS) nuclear thermal rocket engines (NTR). Such a characterization is needed to resolve the NTR engine design trades by a logical and orderly means, and to provide a meaningful method for comparison of the various NTR engine concepts. The subpanel was specifically tasked to identify the quantifiable engine parameters which would be the most significant engine factors affecting an overall FoM for a MTS and was not tasked with determining 'acceptable' or 'recommended' values for the identified parameters. In addition, the subpanel was asked not to define an overall FoM for a MTS. Thus, the selection of a specific approach, applicable weighting factors, to any interrelationships, for establishing an overall numerical FoM were considered beyond the scope of the subpanel inquiry. Author

13 ASTRODYNAMICS

13

ASTRODYNAMICS

Includes powered and free-flight trajectories; and orbital and launching dynamics.

A92-17797* National Aeronautics and Space Administration. Lewis Research Center, Cleveland, OH.

TETHER METHODS FOR REACTIONLESS ORBITAL PROPULSION

GEOFFREY A. LANDIS (NASA, Lewis Research Center; Sverdrup Technology, Inc., Cleveland, OH) IN: Space manufacturing 8 - Energy and materials from space; Proceedings of the 10th Princeton/AIAA/SSI Conference, Princeton, NJ, May 15-18, 1991 1991 5 p refs

Copyright

In space, limits on transportation effectiveness are set by requirements for reaction mass, since reaction mass must be carried on board and often comprises the majority of the launch mass of a space system. Thus, applications where a tether can be used for propulsion with no requirement of reaction mass are extremely attractive for space development. It is a remarkable fact that tethers can be used to increase orbital energy with no requirement for reaction mass. Author

A92-43339* National Aeronautics and Space Administration. Lewis Research Center, Cleveland, OH.

MINIMUM IMPULSE TRAJECTORIES FOR MARS ROUND TRIP MISSIONS

GLEN M. HORVAT and STEPHEN W. ALEXANDER (NASA, Lewis Research Center, Cleveland, OH) IN: Astrodynamics 1991; Proceedings of the AAS/AIAA Astrodynamics Conference, Durango, CO, Aug. 19-22, 1991. Pt. 2 1992 18 p refs (AAS PAPER 91-500) Copyright

Data are presented for minimum-impulse earth-Mars round-trip trajectories for the 2010 to 2027 Mars launch opportunities. Round-trip mission times from 120 to 600 days, including a 30-day rendezvous at Mars, for direct trajectories and trajectories utilizing a Venus gravitational assist are considered. Optimal planetary launch and arrival dates and total impulse requirements are based on all maneuvers being performed propulsively with no finite burn or other losses. Direct trajectories have the lowest impulse requirements for shorter mission times and Venus gravitational assist trajectories have the lowest impulse requirements for longer mission times. It is shown that one can depart on trajectories to Mars, beginning with lower energy trajectories to the moon. The fuel savings varies, depending on the final energy level required and on the swingby procedure used. Procedures discussed include single lunar swingbys, double-powered or unpowered lunar swingbys, third lunar flybys a year later, and gravity assists by Venus and earth after the final lunar swingby. S.A.V.

A92-46753* National Aeronautics and Space Administration. Lewis Research Center, Cleveland, OH.

DISCRETE APPROXIMATIONS TO OPTIMAL TRAJECTORIES USING DIRECT TRANSCRIPTION AND NONLINEAR PROGRAMMING

PAUL J. ENRIGHT and BRUCE A. CONWAY (Illinois, University, Urbana) Aug. 1992 9 p refs (Contract NAG3-805; NAG3-1138)

Copyright

A92-46760* National Aeronautics and Space Administration. Lewis Research Center, Cleveland, OH.

SIMPLE PROOF OF THE GLOBAL OPTIMALITY OF THE HOHMANN TRANSFER

JOHN E. PRUSSING (Illinois, University, Urbana) Journal of Guidance, Control, and Dynamics (ISSN 0731-5090), vol. 15, no. 4, July-Aug. 1992, p. 1037, 1038. Aug. 1992 2 p refs (Contract NAG3-1138)

Copyright

The case of two-impulse transfer between coplanar circular orbits is considered. The global optimality of the Hohmann transfer among the class of two-impulse transfers is proved via ordinary calculus by using the familiar orbital elements, eccentricity e and parameter (semilatus rectum) p . It is noted that this proof is simpler than existing proofs in the literature. L.M.

A92-52079*# National Aeronautics and Space Administration. Lewis Research Center, Cleveland, OH.

CANONICAL TRANSFORMATIONS FOR SPACE TRAJECTORY OPTIMIZATION

CHRISTINE M. HAISSIG, KENNETH D. MEASE (Princeton University, NJ), and NGUYEN X. VINH (Michigan, University, Ann Arbor) IN: 1992 AIAA/AAS Astrodynamics Conference, Hilton Head Island, SC, Aug. 10-12, 1992, Technical Papers 1992 9 p refs

(Contract NAG3-915)

(AIAA PAPER 92-4509) Copyright

Canonical transformations are developed between the Cartesian coordinates, equinoctial elements, trajectory variables, and orbital elements for coplanar space trajectory optimization problems. The canonical transformations permit the state and adjoint or their solution, transversality conditions, the optimal control, and integrals of the motion, to be transformed between any of the common sets of coordinates for planar space trajectory optimization problems. Variations on the canonical transformations shown are straightforward to develop given the group properties of the canonical transformations. R.E.P.

14

GROUND SUPPORT SYSTEMS AND FACILITIES (SPACE)

Includes launch complexes, research and production facilities; ground support equipment, e.g., mobile transporters; and simulators.

A92-21086* National Aeronautics and Space Administration. Lewis Research Center, Cleveland, OH.

MOONBASE NIGHT POWER BY LASER ILLUMINATION

GEOFFREY A. LANDIS (NASA, Lewis Research Center, Cleveland; Sverdrup Technology, Inc., Brook Park, OH) Journal of Propulsion and Power (ISSN 0748-4658), vol. 8, Jan.-Feb. 1992, p. 251-254. Feb. 1992 4 p refs

Copyright

Moonbase solar-power concepts must somehow address the energy storage problem posed by the 354-hour lunar night. Attention is presently given to the feasibility of laser-array illumination of a lunar base, using technology that is projected to be available in the near term. Beam-spreading due to atmospheric distortions could be reduced through the use of adaptive optics to compensate for atmospheric turbulence. O.C.

A92-23842* National Aeronautics and Space Administration. Lewis Research Center, Cleveland, OH.

DESCRIPTION OF LIQUID NITROGEN EXPERIMENTAL TEST FACILITY

J. M. JURNS (NASA, Lewis Research Center; Sverdrup Technology, Inc., Cleveland, OH), R. E. JACOBS (NASA, Lewis Research Center; Analex Corp., Cleveland, OH), and N. H. SAIYED (NASA, Lewis Research Center, Cleveland, OH) (Space Cryogenics Workshop, 10th, Cleveland, OH, June 18-20, 1991, Proceedings. A92-23826 08-31) Cryogenics (ISSN 0011-2275), vol. 32, no. 2, 1992, p. 173-178. Previously announced in STAR as N92-11208. 1992 6 p

Copyright

The Liquid Nitrogen Test Facility is a unique test facility for ground-based liquid nitrogen experimentation. The test rig consists of an insulated tank of approximately 12.5 cubic ft in volume,

which is supplied with liquid nitrogen from a 300 gal dewar via a vacuum jacketed piping system. The test tank is fitted with pressure and temperature measuring instrumentation, and with two view ports which allow visual observation of test conditions. To demonstrate the capabilities of the facility, the initial test program is briefly described. The objective of the test program is to measure the condensation rate by injecting liquid nitrogen as a subcooled spray into the ullage of a tank 50 percent full of liquid nitrogen at saturated conditions. The condensation rate of the nitrogen vapor on the subcooled spray can be analytically modeled, and results validated and corrected by experimentally measuring the vapor condensation on liquid sprays. Author

A92-23847* National Aeronautics and Space Administration. Lewis Research Center, Cleveland, OH.

ON-ORBIT CRYOGENIC FLUID TRANSFER RESEARCH AT NASA LEWIS RESEARCH CENTER

W. J. TAYLOR, D. J. CHATO, M. M. MORAN, and T. W. NYLAND (NASA, Lewis Research Center, Cleveland, OH) (Space Cryogenics Workshop, 10th, Cleveland, OH, June 18-20, 1991, Proceedings. A92-23826 08-31) Cryogenics (ISSN 0011-2275), vol. 32, no. 2, 1992, p. 199-204. 1992 6 p refs

A summary of research into on-orbit cryogenic fluid transfer at the NASA Lewis Research Center (LRC) is presented. Variable test parameters and liquid injection configurations elucidated the conditions necessary for a successful transfer of liquid hydrogen by the no-vent fill method. The model is based on conservation of mass and a first-law energy balance for a control volume. The ullage, the bulk liquid, and the tank wall are each represented by a single node. The magnitude of the maximum receiver tank pressure was found to be dependent on the liquid inlet temperature, the inlet mass flow rate, and the initial temperature. A comparison of the test data and the analytical results for a no-vent fill test with a small receiver tank is presented. P.D.

A92-29888*# National Aeronautics and Space Administration. Lewis Research Center, Cleveland, OH.

THE ACTS NASA GROUND STATION/MASTER CONTROL STATION

DAVID N. MEADOWS (COMSAT Laboratories, Clarksburg, MD) IN: AIAA International Communication Satellite Systems Conference and Exhibit, 14th, Washington, DC, Mar. 22-26, 1992, Technical Papers. Pt. 2 1992 11 p refs (Contract NAS3-25084) (AIAA PAPER 92-1965) Copyright

Two of the major components of the ACTS Ground Segment are the NASA Ground Station (NGS) and the Master Control Station (MCS), collocated at the NASA Lewis Research Center. Essentially, the NGS provides the communications links by which the MCS performs its various network control and monitoring functions. The NGS also provides telecommunications links capable of transmission/reception of up to approximately 70 Mbit/s of digital telephonic traffic. Operating as a system, the entire complex of equipment is referred to as the NGS/MCS. This paper provides an 'as-built' description of the NGS/MCS as a system. Author

A92-49052*# National Aeronautics and Space Administration. Lewis Research Center, Cleveland, OH.

SIMULATING THE ARCJET THRUSTER USING A NONLINEAR ACTIVE LOAD

GENE P. ALTENBURGER (Devilbiss-Ransburg Industrial Liquid Systems, Toledo, OH) and ROGER J. KING (Toledo, University, OH) AIAA, SAE, ASME, and ASEE, Joint Propulsion Conference and Exhibit, 28th, Nashville, TN, July 6-8, 1992. 10 p. Jul. 1992 10 p refs (Contract NAG3-1102) (AIAA PAPER 92-3528) Copyright

Arcjet thrusters are known to have distinctly nonlinear electrical characteristics with negative incremental resistance throughout their normal operating region. The 1-kW arcjet simulator proposed here accurately mimics these characteristics statically, and dynamically up to 40 kHz. Testing with a power-processing unit (PPU) and the simulator, a 1-kW arcjet, and a resistive load bank established

that the simulator accurately predicted the transient behavior of the PPU-arcjet combination, while the resistive load bank did not. The simulator uses resistors and insulated-gate bipolar transistors to dissipate the PPU output power; a nonlinear feedback is applied to produce the desired v-i characteristics. This feedback is analyzed dynamically. The arcjet simulator allows development of a PPU to a higher level of confidence before beginning testing at an arcjet facility. Author

A92-50573* National Aeronautics and Space Administration. Lewis Research Center, Cleveland, OH.

EFFECTS OF WINDBLOWN DUST ON PHOTOVOLTAIC SURFACES ON MARS

JAMES R. GAIER, MARLA E. PEREZ-DAVIS (NASA, Lewis Research Center, Cleveland, OH), and ALIA M. MOINUDDIN (Case Western Reserve University, Cleveland, OH) IN: IECEC '91; Proceedings of the 26th Intersociety Energy Conversion Engineering Conference, Boston, MA, Aug. 4-9, 1991. Vol. 1 1991 6 p refs Copyright

Photovoltaic (PV) coverslip material was subjected to Martian dust storm conditions using basaltic dust flowing through the Martian Surface Wind Tunnel at NASA Ames. Initially dusted and clear coverslips were held at angles from 0 to 90 deg., and the dust laden wind velocity was varied from 20 to 97 m/s. Blowing dust was found to adhere more to the coverslips as the angle was increased. However, dust was partially cleared from surfaces that were initially dusted at substantially lower velocities in dust laden wind than in clear wind. Thus, an equilibrium amount of dust accumulated which was dependent only upon angle and wind velocity and not upon initial concentration of dust. Abrasion was also evident in the coverslips. It increased with wind velocity and angle of attack. It appears that an initial dust layer may help to protect PV surfaces from abrasion. Author

A92-50574* National Aeronautics and Space Administration. Lewis Research Center, Cleveland, OH.

SEI ROVER SOLAR-ELECTROCHEMICAL POWER SYSTEM OPTIONS

COLLEEN A. WITHROW, LISA L. KOHOUT, DAVID J. BENTS (NASA, Lewis Research Center, Cleveland, OH), and ANTHONY J. COLOZZA (Sverdrup Technology, Inc., Brook Park, OH) IN: IECEC '91; Proceedings of the 26th Intersociety Energy Conversion Engineering Conference, Boston, MA, Aug. 4-9, 1991. Vol. 1 1991 7 p refs Copyright

A trade study of power system technology for proposed lunar vehicles and services is presented. A variety of solar-based power systems were selected and analyzed for each. The analysis determined the power system mass, volume, and deployed area. A comparison was made between periodic refueling/recharging systems and onboard power systems to determine the most practical system. The trade study concluded that the power system significantly impacts the physical characteristics of the vehicle. The refueling/recharging systems were lighter and more compact, but dependent on availability of established lunar base infrastructure. Onboard power systems pay a mass penalty for being fully developed systems. Author

A92-50654 National Aeronautics and Space Administration. Lewis Research Center, Cleveland, OH.

DESCRIPTION OF THE CONTROL SYSTEM DESIGN FOR THE SSF PMAD DC TESTBED

ANASTACIO N. BAEZ and GREG L. KIMNACH (NASA, Lewis Research Center, Cleveland, OH) IN: IECEC '91; Proceedings of the 26th Intersociety Energy Conversion Engineering Conference, Boston, MA, Aug. 4-9, 1991. Vol. 2 1991 6 p refs (Contract RTOP 474-42-10) Copyright

The Power Management and Distribution (PMAD) DC Testbed Control System for Space Station Freedom was developed using a top down approach based on classical control system and conventional terrestrial power utilities design techniques. The

14 GROUND SUPPORT SYSTEMS AND FACILITIES (SPACE)

design methodology includes the development of a testbed operating concept. This operating concept describes the operation of the testbed under all possible scenarios. A unique set of operating states was identified and a description of each state, along with state transitions, was generated. Each state is represented by a unique set of attributes and constraints, and its description reflects the degree of system security within which the power system is operating. Using the testbed operating states description, a functional design for the control system was developed. This functional design consists of a functional outline, a text description, and a logical flowchart for all the major control system functions. Described here are the control system design techniques, various control system functions, and the status of the design and implementation. Author

A92-50655 National Aeronautics and Space Administration. Lewis Research Center, Cleveland, OH.

DESCRIPTION OF THE PMAD DC TEST BED ARCHITECTURE AND INTEGRATION SEQUENCE

R. F. BEACH, L. TRASH, D. FONG (NASA, Lewis Research Center, Cleveland, OH), and B. BOLERJACK (Rockwell International Corp., Rocketdyne Div., Canoga Park, CA) IN: IECEC '91; Proceedings of the 26th Intersociety Energy Conversion Engineering Conference, Boston, MA, Aug. 4-9, 1991. Vol. 2 1991 6 p refs

(Contract RTOP 474-42-10)

Copyright

NASA-LEWIS is responsible for the development, fabrication, and assembly of the electric power system (EPS) for the Space Station Freedom (SSF). The SSF power system is radically different from previous spacecraft power systems in both the size and complexity of the system. Unlike past spacecraft power systems, the SSF EPS will grow and be maintained on orbit and must be flexible to meet challenging user power needs. The SSF power system is also unique in comparison with terrestrial power systems because it is dominated by power electronic converters which regulate and control the power. A description is provided of the Power Management and Distribution DC Testbed which was assembled to support the design and early evaluation of the SSF EPS. A description of the integration process used in the assembly sequence is also given along with a description of the support facility. Author

A92-50656 National Aeronautics and Space Administration. Lewis Research Center, Cleveland, OH.

THE DEVELOPMENT OF TEST BEDS TO SUPPORT THE DEFINITION AND EVOLUTION OF THE SPACE STATION FREEDOM POWER SYSTEM

JAMES F. SOEDER, ROBERT J. FRYE (NASA, Lewis Research Center, Cleveland, OH), and RUDY L. PHILLIPS (Rockwell International Corp., Rocketdyne Div., Canoga Park, CA) IN: IECEC '91; Proceedings of the 26th Intersociety Energy Conversion Engineering Conference, Boston, MA, Aug. 4-9, 1991. Vol. 2 1991 6 p refs

(Contract RTOP 474-42-10)

Copyright

Since the beginning of the Space Station Freedom Program (SSFP), the NASA Lewis Research Center (LeRC) and the Rocketdyne Division of Rockwell International have had extensive efforts underway to develop testbeds to support the definition of the detailed electrical power system design. Because of the extensive redirections that have taken place in the Space Station Freedom Program in the past several years, the test bed effort was forced to accommodate a large number of changes. A short history of these program changes and their impact on the LeRC test beds is presented to understand how the current test bed configuration has evolved. The current test objectives and the development approach for the current DC test bed are discussed. A description of the test bed configuration, along with its power and controller hardware and its software components, is presented. Next, the uses of the test bed during the mature design and verification phase of SSFP are examined. Finally, the uses of the

test bed in the operation and evolution of the SSF are addressed. Author

A92-50657 National Aeronautics and Space Administration. Lewis Research Center, Cleveland, OH.

AN EMTP SYSTEM LEVEL MODEL OF THE PMAD DC TEST BED

NARAYAN V. DRAVID (NASA, Lewis Research Center, Cleveland, OH), THOMAS J. KACPURA (Sverdrup Technology, Inc., Brook Park, OH), and KWA-SUR TAM (Virginia Polytechnic Institute and State University, Blacksburg) IN: IECEC '91; Proceedings of the 26th Intersociety Energy Conversion Engineering Conference, Boston, MA, Aug. 4-9, 1991. Vol. 2 1991 6 p refs

(Contract RTOP 474-42-10)

Copyright

A power management and distribution direct current (PMAD DC) test bed was set up at the NASA Lewis Research Center to investigate Space Station Freedom Electric Power Systems issues. Efficiency of test bed operation significantly improves with a computer simulation model of the test bed as an adjunct tool of investigation. Such a model is developed using the Electromagnetic Transients Program (EMTP) and is available to the test bed developers and experimenters. The computer model is assembled on a modular basis. Device models of different types can be incorporated into the system model with only a few lines of code. A library of the various model types is created for this purpose. Simulation results and corresponding test bed results are presented to demonstrate model validity. Author

A92-50659 National Aeronautics and Space Administration. Lewis Research Center, Cleveland, OH.

DEVELOPMENT AND TESTING OF A SOURCE SUBSYSTEM FOR THE SUPPORTING DEVELOPMENT PMAD DC TEST BED

ROBERT M. BUTTON (NASA, Lewis Research Center, Cleveland, OH) IN: IECEC '91; Proceedings of the 26th Intersociety Energy Conversion Engineering Conference, Boston, MA, Aug. 4-9, 1991. Vol. 2 1991 6 p refs

(Contract RTOP 474-42-10)

Copyright

The supporting Development Power Management and Distribution (PMAD) DC test bed is described. Its benefits to the Space Station Freedom Electrical Power System design are discussed along with a short description of how the PMAD DC test bed was systematically integrated. The source subsystem of the PMAD DC test bed, consisting of a Sequential Shunt Unit (SSU) and a Battery Charge/Discharge Unit (BCDU), is introduced. The SSU is described in detail and component-level test data is presented. Next, the BCDU's operation and design are given along with component-level test data. The Source Subsystem is then presented and early data given to demonstrate an effective subsystem design. Author

A92-50660 National Aeronautics and Space Administration. Lewis Research Center, Cleveland, OH.

DEVELOPMENT OF A NINETY STRING SOLAR ARRAY SIMULATOR

THOMAS E. VASEK and ARTHUR G. BIRCHENOUGH (NASA, Lewis Research Center, Cleveland, OH) IN: IECEC '91; Proceedings of the 26th Intersociety Energy Conversion Engineering Conference, Boston, MA, Aug. 4-9, 1991. Vol. 2 1991 6 p refs

(Contract RTOP 474-74-10)

Copyright

A power source was developed to support testing for the Space Station Freedom Power Management and Distribution (PMAD) DC Testbed. The intent was to simulate as closely as possible the steady-state and transient responses of a solar array. Several breadboards and one thermal prototype were built and tested. Responses were successfully verified and improved upon during successive breadboards. The completed 90-string simulator consists of four power MOSFETs, four 25-watt source resistors, and four 250-watt drain source bypass resistors per string, in addition to the control circuitry. Author

15 LAUNCH VEHICLES AND SPACE VEHICLES

A92-56800# National Aeronautics and Space Administration. Lyndon B. Johnson Space Center, Houston, TX.

FAST OXYGEN ATOM FACILITY FOR STUDIES RELATED TO LOW EARTH ORBIT ACTIVITIES

G. E. CALEDONIA, R. H. KRECH, B. L. UPSCHULTE, D. M. SONNENFROH, D. OAKES, and K. W. HOLTZCLAW (Physical Sciences, Inc., Andover, MA) AIAA, Aerospace Ground Testing Conference, 17th, Nashville, TN, July 6-8, 1992. 9 p. Research supported by NASA, USAF, SDIO, et al. Jul. 1992 9 p refs (AIAA PAPER 92-3974) Copyright

The operating principles and characteristics of an 8 km/s oxygen atom beam source are described. The source has been used for many applications relevant to low earth orbit (LEO) including both gas/surface and gas/gas interactions. Representative data from these activities are provided. Author

N92-26129*# National Aeronautics and Space Administration. Lewis Research Center, Cleveland, OH.

TRANSONIC TURBINE BLADE CASCADE TESTING FACILITY

VINCENT G. VERHOFF, WILLIAM P. CAMPERCHIOLI, and ISAAC LOPEZ 1992 13 p Presented at the 17th Aerospace Ground Testing Conference, Nashville, TN, 6-8 Jul. 1992; sponsored in part by AIAA

(Contract DA PROJ. 1L1-61102-AH-45; RTOP 505-62-84)

(NASA-TM-105646; E-7002; NAS 1.15:105646;

AVSCOM-TR-C-016; AIAA PAPER 92-4034; AD-A253127) Avail: CASI HC A03/MF A01

NASA LeRC has designed and constructed a new state-of-the-art test facility. This facility, the Transonic Turbine Blade Cascade, is used to evaluate the aerodynamics and heat transfer characteristics of blade geometries for future turbine applications. The facility's capabilities make it unique: no other facility of its kind can combine the high degree of airflow turning, infinitely adjustable incidence angle, and high transonic flow rates. The facility air supply and exhaust pressures are controllable to 16.5 psia and 2 psia, respectively. The inlet air temperatures are at ambient conditions. The facility is equipped with a programmable logic controller with a capacity of 128 input/output channels. The data acquisition system is capable of scanning up to 1750 channels per sec. This paper discusses in detail the capabilities of the facility, overall facility design, instrumentation used in the facility, and the data acquisition system. Actual research data is not discussed. Author

N92-30307*# National Aeronautics and Space Administration. Lewis Research Center, Cleveland, OH.

THREE-DIMENSIONAL LASER WINDOW FORMATION

VINCENT G. VERHOFF Jul. 1992 12 p

(Contract RTOP 505-62-84)

(NASA-RP-1280; E-6096; NAS 1.61:1280) Avail: CASI HC A03/MF A01

The NASA Lewis Research Center has developed and implemented a unique process for forming flawless three-dimensional laser windows. These windows represent a major part of specialized, nonintrusive laser data acquisition systems used in a variety of compressor and turbine research test facilities. This report discusses in detail the aspects of three-dimensional laser window formation. It focuses on the unique methodology and the peculiarities associated with the formation of these windows. Included in this discussion are the design criteria, bonding mediums, and evaluation testing for three-dimensional laser windows. Author

N92-34114*# National Aeronautics and Space Administration. Lewis Research Center, Cleveland, OH.

LOW POWER ARCJET TEST FACILITY IMPACTS

W. EARL MORREN and PAUL J. LICHON (Rocket Research Corp., Redmond, WA.) Sep. 1992 22 p Presented at the 28th Joint Propulsion Conference and Exhibit, Nashville, TN, 6-8 Jul. 1992; sponsored by AIAA, SAE, ASME, and ASEE

(Contract RTOP 506-42-31)

(NASA-TM-105876; E-7341; NAS 1.15:105876; AIAA PAPER 92-3532) Copyright Avail: CASI HC A03/MF A01

Performance characterization of a flight-type 1.4 kW arcjet system were conducted at the Rocket Research Company (RRC) in Redmond, WA, and at the NASA LeRC in Cleveland, OH. The objectives of these tests were as follows: to compare low-power arcjet performance at two different test facilities; to compare arcjet performance obtained with a 2:1 mixture of gaseous hydrogen and nitrogen and hydrazine; and to quantify the effects of test cell pressure on thruster operating characteristics. Performance and thruster temperature distributions were measured at thruster input power levels and propellant mass flow rates ranging from 1274 to 1370 W and from 3.2×10^{-5} to 5.1×10^{-5} kg/s, respectively. Specific impulses measured at the two facilities, at comparable test cell pressures, using gaseous hydrogen-nitrogen propellant mixtures agreed to within 1 percent over the range of operating conditions tested. The specific impulses measured using hydrazine propellant were higher than that for the cold hydrogen-nitrogen mixtures. Agreement between by hydrazine and gas mixture data was good, however, when the differences in propellant enthalpies at the thruster inlet were considered. Specific impulse showed a strong dependence on test facility pressure, and was 3 to 4 percent higher below 0.1 Pa than for test cell pressures above 5 Pa. Author

15

LAUNCH VEHICLES AND SPACE VEHICLES

Includes boosters; operating problems of launch/space vehicle systems; and reusable vehicles.

A92-28512* National Aeronautics and Space Administration. Lewis Research Center, Cleveland, OH.

EVALUATION OF SUPERCRITICAL CRYOGEN STORAGE AND TRANSFER SYSTEMS FOR FUTURE NASA MISSIONS

HUGH ARIF, JOHN C. AYDELOTT, and DAVID J. CHATO (NASA, Lewis Research Center, Cleveland, OH) Apr. 1992 7 p refs

Copyright

A92-35868*# National Aeronautics and Space Administration. Lewis Research Center, Cleveland, OH.

MISSION AND SIZING ANALYSIS FOR THE BETA II TWO-STAGE-TO-ORBIT VEHICLE

SHARI-BETH NADELL, WILLIAM J. BAUMGARTEN, and STEPHEN W. ALEXANDER (NASA, Lewis Research Center, Cleveland, OH) AIAA, Aerospace Design Conference, Irvine, CA, Feb. 3-6, 1992. 14 p. Previously announced in STAR as N92-21547. Feb. 1992 14 p refs

(AIAA PAPER 92-1264) Copyright

NASA Lewis Research Center studied a horizontal takeoff and landing, fully reusable, two-stage-to-orbit (TSTO) vehicle capable of launching and returning a 10,000 pound payload to low earth orbit using low-risk technology. The vehicle, called Beta 2, was derived from the USAF/Boeing Beta vehicle, a TSTO study vehicle capable of launching a 50,000 pound payload to low earth orbit. Development of the Beta 2 from the USAF/Boeing Beta vehicle occurred in a series of iterations during which the size of the vehicle was decreased to accommodate the smaller payload, the staging Mach number was decreased from 8.0 to 6.5, and the rocket propulsion system was removed from the booster. The final Beta 2 vehicle consisted of a rocket powered orbiter and an all airbreathing booster. The gross takeoff weight of the Beta 2 vehicle was approximately 1.1 million pounds. In addition to its baseline mission, the Beta 2 was capable of delivering approximately 17,500 pounds to the Space Station with the same takeoff gross weight. The mission and sizing analysis performed to arrive at the Beta 2 vehicle is discussed. Author

15 LAUNCH VEHICLES AND SPACE VEHICLES

N92-11034*# National Aeronautics and Space Administration. Lewis Research Center, Cleveland, OH.

OVERVIEW OF THE BETA II TWO-STAGE-TO-ORBIT VEHICLE DESIGN

ROBERT M. PLENCNER Oct. 1991 12 p Presented at the Aircraft Design Systems and Operations Meeting, Baltimore, MD, 23-25 Sep. 1991; sponsored by AIAA, AHS, and ASEE Previously announced in IAA as A91-54088

(Contract RTOP 505-69-40)

(NASA-TM-105298; E-6641; NAS 1.15:105298; AIAA PAPER 91-3175) Copyright Avail: CASI HC A03/MF A01

A study of a near-term, low risk two-stage-to-orbit (TSTO) vehicle was undertaken. The goal of the study was to assess a fully reusable TSTO vehicle with horizontal takeoff and landing capability that could deliver 10,000 pounds to a 120 nm polar orbit. The configuration analysis was based on the Beta vehicle design. A cooperative study was performed to redesign and refine the Beta concept to meet the mission requirements. The vehicle resulting from this study was named Beta II. It has an all-airbreathing first stage and a staging Mach number of 6.5. The second stage is a conventional wing-body configuration with a single SSME.

Author

N92-21547*# National Aeronautics and Space Administration. Lewis Research Center, Cleveland, OH.

MISSION AND SIZING ANALYSIS FOR THE BETA 2 TWO-STAGE-TO-ORBIT VEHICLE

SHARI-BETH NADELL, WILLIAM J. BAUMGARTEN, and STEPHEN W. ALEXANDER 1992 15 p Presented at the 1992 Aerospace Design Conference, Irvine, CA, 3-6 Feb. 1992; sponsored by AIAA

(Contract RTOP 505-69-40)

(NASA-TM-105559; E-6883; NAS 1.15:105559; AIAA PAPER 92-1264) Avail: CASI HC A03/MF A01

NASA Lewis Research Center studied a horizontal takeoff and landing, fully reusable, two-stage-to-orbit (TSTO) vehicle capable of launching and returning a 10,000 pound payload to low Earth polar orbit using low-risk technology. The vehicle, called Beta 2, was derived from the USAF/Boeing Beta vehicle, a TSTO study vehicle capable of launching a 50,000 pound payload to low Earth polar orbit. Development of the Beta 2 from the USAF/Boeing Beta vehicle occurred in a series of iterations during which the size of the vehicle was decreased to accommodate the smaller payload, the staging Mach number was decreased from 8.0 to 6.5, and the rocket propulsion system was removed from the booster. The final Beta 2 vehicle consisted of a rocket powered orbiter and an all airbreathing booster. The gross takeoff weight of the Beta 2 vehicle was approximately 1.1 million pounds. In addition to its baseline mission, the Beta 2 was capable of delivering approximately 17,500 pounds to the Space Station with the same takeoff gross weight. The mission and sizing analysis performed to arrive at the Beta 2 vehicle is discussed.

Author

N92-25092*# National Aeronautics and Space Administration. Lewis Research Center, Cleveland, OH.

RESONANT MODE CONTROLLERS FOR LAUNCH VEHICLE APPLICATIONS

KEN E. SCHREINER (General Dynamics Corp., San Diego, CA.) and MARY ELLEN ROTH 1992 8 p Presented at the Applied Power Electronics Conference and Exposition, Boston, MA, 23-27 Feb. 1992; sponsored by IEEE

(Contract RTOP 946-02-2E)

(NASA-TM-105563; E-6887; NAS 1.15:105563) Avail: CASI HC A02/MF A01

Electro-mechanical actuator (EMA) systems are currently being investigated for the National Launch System (NLS) as a replacement for hydraulic actuators due to the large amount of manpower and support hardware required to maintain the hydraulic systems. EMA systems in weight sensitive applications, such as launch vehicles, have been limited to around 5 hp due to system size, controller efficiency, thermal management, and battery size. Presented here are design and test data for an EMA system that competes favorably in weight and is superior in maintainability to

the hydraulic system. An EMA system uses dc power provided by a high energy density bipolar lithium thionyl chloride battery, with power conversion performed by low loss resonant topologies, and a high efficiency induction motor controlled with a high performance field oriented controller to drive a linear actuator.

Author

N92-25958*# National Aeronautics and Space Administration. Lewis Research Center, Cleveland, OH.

AN EXPERIMENTAL INVESTIGATION OF HIGH-ASPECT-RATIO COOLING PASSAGES

JULIE A. CARLILE and RICHARD J. QUENTMEYER (Sverdrup Technology, Inc., Brook Park, OH.) 1992 13 p Proposed for presentation at the 28th Joint Propulsion Conference, Nashville, TN, 6-8 Jul. 1992; sponsored by AIAA, SAE, ASME, and ASEE

(Contract RTOP 590-21-11)

(NASA-TM-105679; E-6991; NAS 1.15:105679; AIAA PAPER 92-3154) Avail: CASI HC A03/MF A01

An experimental investigation was conducted to evaluate the effectiveness of using high-aspect-ratio cooling passages to improve the life and reduce the coolant pressure drop in high-pressure rocket thrust chambers. A plug-nozzle rocket-engine test apparatus was used to test two cylindrical chambers with low-aspect-ratio cooling passages and one with high-aspect-ratio cooling passages. The chambers were cyclically tested and data were taken over a wide range of coolant mass flows. The results showed that for the same coolant pressure drop, the hot-gas-side wall temperature of the high-aspect-ratio chamber was 30 percent lower than the baseline low-aspect-ratio chamber, resulting in no fatigue damage to the wall. The coolant pressure drop for the high-aspect-ratio chamber was reduced in increments to one-half that of the baseline chamber, by reducing the coolant mass flow, and still resulted in a reduction in the hot-gas-side wall temperature when compared to the low-aspect-ratio chambers.

Author

N92-30310*# National Aeronautics and Space Administration. Lewis Research Center, Cleveland, OH.

AN ELECTROMECHANICAL ACTUATION SYSTEM FOR AN EXPENDABLE LAUNCH VEHICLE

LINDA M. BURROWS and MARY ELLEN ROTH Aug. 1992 7 p Presented at the 27th Intersociety Energy Conversion Engineering Conference, San Diego, CA, 3-7 Aug. 1992; sponsored by SAE, ACS, AIAA, ASME, IEEE, AICHE, and ANS

(Contract RTOP 506-41-41)

(NASA-TM-105774; E-7202; NAS 1.15:105774) Avail: CASI HC A02/MF A01

A major effort at the NASA Lewis Research Center in recent years has been to develop electro-mechanical actuators (EMA's) to replace the hydraulic systems used for thrust vector control (TVC) on launch vehicles. This is an attempt to overcome the inherent inefficiencies and costs associated with the existing hydraulic structures. General Dynamics Space Systems Division, under contract to NASA Lewis, is developing 18.6 kW (25 hp), 29.8 kW (40 hp), and 52.2 kW (70 hp) peak EMA systems to meet the power demands for TVC on a family of vehicles developed for the National Launch System. These systems utilize a pulse population modulated converter and field-oriented control scheme to obtain independent control of both the voltage and frequency. These techniques allow an induction motor to be operated at its maximum torque at all times. At NASA Lewis, we are building on this technology to develop our own in-house system capable of meeting the peak power requirements for an expendable launch vehicle (ELV) such as the Atlas. Our EMA will be capable of delivering 22.4 kW (30 hp) peak power with a nominal of 6.0 kW (8 hp). This system differs from the previous ones in two areas: (1) the use of advanced control methods, and (2) the incorporation of built-in-test. The advanced controls are essential for minimizing the controller size, while the built-in-test is necessary to enhance the system reliability and vehicle health monitoring. The ultimate goal of this program is to demonstrate an EMA which will be capable of self-test and easy integration into other projects. This paper will describe the effort underway at NASA Lewis to develop an EMA for an Atlas class ELV. An explanation will be given for

each major technology block, and the status of each major technology block and the status of the overall program will be reported. Author

N92-31251*# National Aeronautics and Space Administration. Lewis Research Center, Cleveland, OH.

GRAPHITE/EPOXY COMPOSITE ADAPTERS FOR THE SPACE SHUTTLE/CENTAUR VEHICLE

HAROLD J. KASPER and DARRYL S. RING (General Dynamics Corp., San Diego, CA.) Sep. 1990 34 p (Contract NAS3-2290)

(NASA-TP-3014; E-4969; NAS 1.60:3014) Avail: CASI HC A03/MF A01

The decision to launch various NASA satellite and Air Force spacecraft from the Space Shuttle created the need for a high-energy upper stage capable of being deployed from the cargo bay. Two redesigned versions of the Centaur vehicle which employed a graphite/epoxy composite material for the forward and aft adapters were selected. Since this was the first time a graphite/epoxy material was used for Centaur major structural components, the development of the adapters was a major effort. An overview of the composite adapter designs, subcomponent design evaluation test results, and composite adapter test results from a full-scale vehicle structural test is presented. Author

N92-32456*# National Aeronautics and Space Administration. Lewis Research Center, Cleveland, OH.

RELIABILITY TRAINING

VINCENT R. LALLI, ed., HENRY A. MALEC, ed. (Siemens Stromberg-Carlson, Albuquerque, NM.), RICHARD B. DILLARD (Martin Marietta Corp., Orlando, FL.), KAM L. WONG (Hughes Aircraft Co., El Segundo, CA.), FRANK J. BARBER, and FRANK J. BARINA Jun. 1992 225 p A reliability/probability device as supplement (Contract RTOP 572-10-00)

(NASA-RP-1253; E-5456; NAS 1.61:1253) Avail: CASI HC A10/MF A03

Discussed here is failure physics, the study of how products, hardware, software, and systems fail and what can be done about it. The intent is to impart useful information, to extend the limits of production capability, and to assist in achieving low cost reliable products. A review of reliability for the years 1940 to 2000 is given. Next, a review of mathematics is given as well as a description of what elements contribute to product failures. Basic reliability theory and the disciplines that allow us to control and eliminate failures are elucidated. Author

16

SPACE TRANSPORTATION

Includes passenger and cargo space transportation, e.g., shuttle operations; and space rescue techniques.

N92-15082*# National Aeronautics and Space Administration. Lewis Research Center, Cleveland, OH.

SEALS FLOW CODE DEVELOPMENT

Mar. 1991 172 p Workshop held in Cleveland, OH, 26 Mar. 1991

(Contract RTOP 506-42-72)

(NASA-CP-10070; E-6219; NAS 1.55:10070) Avail: CASI HC A08/MF A02

In recognition of a deficiency in the current modeling capability for seals, an effort was established by NASA to develop verified computational fluid dynamic concepts, codes, and analyses for seals. The objectives were to develop advanced concepts for the design and analysis of seals, to effectively disseminate the information to potential users by way of annual workshops, and to provide experimental verification for the models and codes under a wide range of operating conditions.

17

SPACE COMMUNICATIONS, SPACECRAFT COMMUNICATIONS, COMMAND AND TRACKING

Includes telemetry; space communications networks; astronavigation and guidance; and radio blackout.

A92-10465* Toledo Univ., OH.

MULTICARRIER DEMODULATOR ARCHITECTURE FOR ONBOARD PROCESSING SATELLITES

L. P. EUGENE, P. J. FERNANDES, M. M. JAMALI, S. C. KWATRA (Toledo, University, OH), and J. BUDINGERS (NASA, Lewis Research Center, Cleveland, OH) Oct. 1991 7 p refs (Contract NAG3-799; NAG3-865)

Copyright

A92-29924*# National Aeronautics and Space Administration. Lewis Research Center, Cleveland, OH.

CIRCUIT-SWITCH ARCHITECTURE FOR A 30/20-GHZ FDMA/TDM GEOSTATIONARY SATELLITE COMMUNICATIONS NETWORK

WILLIAM D. IVANCIC (NASA, Lewis Research Center, Cleveland, OH) IN: AIAA International Communication Satellite Systems Conference and Exhibit, 14th, Washington, DC, Mar. 22-26, 1992, Technical Papers. Pt. 3 1992 11 p refs (AIAA PAPER 92-2005) Copyright

A circuit-switching architecture is described for a 30/20-GHz frequency-division, multiple-access uplink/time-division-multiplexed downlink (FDMA/TDM) geostationary satellite communications network. Critical subsystems and problem areas are identified and addressed. Work was concentrated primarily on the space segment; however, the ground segment was considered concurrently to ensure cost efficiency and realistic operational constraints.

Author

A92-29933# National Aeronautics and Space Administration. Lewis Research Center, Cleveland, OH.

EXPERIMENTAL CODE VERIFICATION RESULTS FOR REFLECTOR ANTENNA DISTORTION COMPENSATION BY ARRAY FEEDS

A. J. ZAMAN (NASA, Lewis Research Center, Cleveland, OH), Y. RAHMAT-SAMII, and K. WOO (JPL, Pasadena, CA) IN: AIAA International Communication Satellite Systems Conference and Exhibit, 14th, Washington, DC, Mar. 22-26, 1992, Technical Papers. Pt. 3 1992 6 p refs (AIAA PAPER 92-2014) Copyright

Electronic compensation of reflector surface distortion using array feed with individual amplitude and phase control of the array elements is becoming increasingly attractive because of the recent advances in monolithic microwave integrated circuit (MMIC) technology. An algorithm has been developed previously using the concept of focal plane conjugate field matching in the receive mode and a computer code has been generated that predicts the proper excitation coefficients for the elements of the reflector feed array to compensate the effects of reflector surface distortion. This paper presents the results of an experimental study to verify the above compensation algorithm and in general to demonstrate the effectiveness of the array feed compensation technique.

Author

A92-29954*# National Aeronautics and Space Administration. Lewis Research Center, Cleveland, OH.

THE LINK EVALUATION TERMINAL FOR THE ADVANCED COMMUNICATIONS TECHNOLOGY SATELLITE EXPERIMENTS PROGRAM

BRIAN D. MAY (NASA, Lewis Research Center, Cleveland, OH) IN: AIAA International Communication Satellite Systems Conference and Exhibit, 14th, Washington, DC, Mar. 22-26, 1992, Technical Papers. Pt. 3 1992 9 p refs (AIAA PAPER 92-2040) Copyright

17 SPACE COMMUNICATIONS, SPACECRAFT COMMUNICATIONS, COMMAND AND TRACKING

The experimental NASA satellite, Advanced Communications Technology Satellite (ACTS), introduces new technology for high throughput 30 to 20 GHz satellite services. Contained in a single communication payload is both a regenerative TDMA system and multiple 800 MHz 'bent pipe' channels routed to spot beams by a switch matrix. While only one mode of operation is typical during any experiment, both modes can operate simultaneously with reduced capability due to sharing of the transponder. NASA-Lewis instituted a ground terminal development program in anticipation of the satellite launch to verify the performance of the switch matrix mode of operations. Specific functions are built into the ground terminal to evaluate rain fade compensation with uplink power control and to monitor satellite transponder performance with bit error rate measurements. These functions were the genesis of the ground terminal's name, Link Evaluation Terminal, often referred to as LET. Connectors are included in LET that allow independent experimenters to run unique modulation or network experiments through ACTS using only the RF transmit and receive portions of LET. Test data indicate that LET will be able to verify important parts of ACTS technology and provide independent experimenters with a useful ground terminal. Lab measurements of major subsystems integrated into LET are presented. Bit error rate is measured with LET in an internal loopback mode. Author

A92-29956# Jet Propulsion Lab., California Inst. of Tech., Pasadena.

ACTS AERONAUTICAL EXPERIMENTS

TIEN M. NGUYEN, POLLY ESTABROOK, BRIAN ABBE, MILES K. SUE (JPL, Pasadena, CA), and CHARLES A. RAQUET (NASA, Lewis Research Center, Cleveland, OH) IN: AIAA International Communication Satellite Systems Conference and Exhibit, 14th, Washington, DC, Mar. 22-26, 1992, Technical Papers. Pt. 3 1992 13 p refs

(AIAA PAPER 92-2042) Copyright

A description of the two aeronautical mobile satellite experiments utilizing NASA's Advanced Communications Technology Satellite (ACTS) is presented. The low bit rate experiment is principally a Ka-band technology demonstration of a prototype 4.8 Kbps aeronautic mobile terminal employing three experimental active electronically steered arrays. The high bit rate experiment can demonstrate a 64 Kbps to 384 Kbps satellite link between a ground terminal and an aircraft. R.E.P.

A92-38164* National Aeronautics and Space Administration. Lewis Research Center, Cleveland, OH.

ADVANCED COMMUNICATIONS TECHNOLOGY SATELLITE (ACTS)

RICHARD T. GEDNEY and RONALD J. SCHERTLER (NASA, Lewis Research Center, Cleveland, OH) IEEE, International Conference on Communications, Boston, MA, June 11-14, 1989, Paper. 12 p. Jun. 1989 12 p refs

Copyright

The NASA Advanced Communications Technology Satellite (ACTS) was conceived to help maintain U.S. leadership in the world's communications-satellite market. This experimental satellite is expected to be launched by NASA in 1992 and to furnish the technology necessary for establishing very small aperture terminal digital networks which provide on-demand full-mesh connectivity, and 1.544-MBPS services with only a single hop. Utilizing on-board switching and processing, each individual voice or data circuit can be separately routed to any location in the network. This paper provides an overview of the ACTS and discusses the value of the technology for future communications systems. Author

A92-53693* National Aeronautics and Space Administration. Lewis Research Center, Cleveland, OH.

ADVANCED COMMUNICATION TECHNOLOGY SATELLITE (ACTS) BASEBAND PROCESSOR DEVELOPMENT

LARRY BROWN and DICK MOAT (Motorola, Inc., Strategic Electronics Div., Chandler, AZ) IN: International Symposium on Space Technology and Science, 17th, Tokyo, Japan, May 20-25, 1990, Proceedings. Vol. 2 1990 7 p

(Contract NAS3-23790)

Copyright

NASA-Lewis' ACTS spacecraft uses a baseband processor (BBP) to furnish the flexible message routing/switching capability required for this satellite's TDMA burst communications; its functions encompass the dynamic reconfiguration of message routing to accommodate traffic changes and to individually apply forward error-correction coding. In addition to describing key technologies for the ACTS BBP, the present work functionally describes the BBP to indicate how its hardware is partitioned into subassemblies. O.C.

A92-55788* National Aeronautics and Space Administration. Lewis Research Center, Cleveland, OH.

ADVANCED COMMUNICATIONS TECHNOLOGY SATELLITE (ACTS)

RONALD J. SCHERTLER and RICHARD T. GEDNEY (NASA, Lewis Research Center, Cleveland, OH) IAF, International Astronautical Congress, 43rd, Washington, Aug. 28-Sept. 5, 1992. 19 p. Aug. 1992 19 p refs

(IAF PAPER 92-0407) Copyright

An overview of the NASA ACTS program is presented. The key technologies of ACTS include spot beams, on-board baseband processing and routing, wide bandwidth (900 MHz), and Ka-band transponders. The discussion covers system description, current status of the spacecraft development, ACTS earth stations, NGS traffic terminal, USAT, land and aeronautical mobiles, high data rate and propagation receive only terminals, and ACTS experiments program. V.L.

A92-55790 National Aeronautics and Space Administration. Lyndon B. Johnson Space Center, Houston, TX.

A HIGH TEMPERATURE SUPERCONDUCTIVITY COMMUNICATIONS FLIGHT EXPERIMENT

P. NGO, K. KRISHEN, D. ARNDT (NASA, Johnson Space Center, Houston, TX), G. RAFFOUL, V. KARASACK (Lockheed Engineering & Sciences Co., Houston, TX), K. BHASIN, and R. LEONARD (NASA, Lewis Research Center, Cleveland, OH) IAF, International Astronautical Congress, 43rd, Washington, Aug. 28-Sept. 5, 1992. 10 p. Aug. 1992 10 p refs

(IAF PAPER 92-0410)

The proposed high temperature superconductivity (HTSC) millimeter-wave communications flight experiment from the payload bay of the Space Shuttle Orbiter to the Advanced Communications Technology Satellite (ACTS) in geosynchronous orbit is described. The experiment will use a Ka-band HTSC phased array antenna and front-end electronics to receive a downlink communications signal from the ACTS. The discussion covers the system configuration, a description of the ground equipment, the spacecraft receiver, link performance, thermal loading, and the superconducting antenna array. V.L.

A92-55793* National Aeronautics and Space Administration. Lewis Research Center, Cleveland, OH.

DESTINATION DIRECTED PACKET SWITCH ARCHITECTURE FOR A GEOSTATIONARY COMMUNICATION SATELLITE NETWORK

W. D. IVANCIC, M. J. SHALKHAUSER, E. A. BOBINSKY, N. J. SONI, J. A. QUINTANA, H. KIM (NASA, Lewis Research Center, Cleveland, OH), P. WAGNER, and M. VANDERAAR (Sverdrup Technology, Inc., Cleveland, OH) IAF, International Astronautical Congress, 43rd, Washington, Aug. 28-Sept. 5, 1992. 22 p. Aug. 1992 22 p refs

(IAF PAPER 92-0413) Copyright

A major effort at NASA/Lewis is to identify and develop critical digital technologies and components that enable new commercial missions or significantly improve the performance, cost efficiency, and/or reliability of existing and planned space communications systems. NASA envisions the need for low data rate, direct to the user communications services, for data, facsimile, voice, and video conferencing. A report that focuses on destination directed packet switching architectures for geostationary communication satellites is presented. R.E.P.

17 SPACE COMMUNICATIONS, SPACECRAFT COMMUNICATIONS, COMMAND AND TRACKING

N92-15109*# National Aeronautics and Space Administration. Lewis Research Center, Cleveland, OH.

CIRCUIT-SWITCH ARCHITECTURE FOR A 30/20-GHZ FDMA/TDM GEOSTATIONARY SATELLITE COMMUNICATIONS NETWORK

WILLIAM D. IVANCIC 1992 13 p Proposed for presentation at the 14th International Communications Satellite Systems Conference, Washington, DC, 22-26 Mar. 1992; sponsored by AIAA

(Contract RTOP 650-60-21)

(NASA-TM-105302; E-6649; NAS 1.15:105302; AIAA PAPER

92-122) Avail: CASI HC A03/MF A01

A circuit switching architecture is described for a 30/20 GHz frequency division, multiple access uplink/time division multiplexed downlink (FDMA/TDM) geostationary satellite communications network. Critical subsystems and problem areas are identified and addressed. Work was concentrated primarily on the space segment; however, the ground segment was considered concurrently to ensure cost efficiency and realistic operational constraints.

Author

N92-16008*# National Aeronautics and Space Administration. Lewis Research Center, Cleveland, OH.

THE LINK EVALUATION TERMINAL FOR THE ADVANCED COMMUNICATIONS TECHNOLOGY SATELLITE EXPERIMENTS PROGRAM

BRIAN D. MAY 1992 11 p Presented at the 14th International Communications Satellite Systems Conference, Washington, DC, 22-26 Mar. 1992; sponsored in part by AIAA

(Contract RTOP 649-40-00)

(NASA-TM-105367; E-6735; NAS 1.15:105367; AIAA PAPER

92-2040) Avail: CASI HC A03/MF A01

The experimental NASA satellite, Advanced Communications Technology Satellite (ACTS), introduces new technology for high throughput 30 to 20 GHz satellite services. Contained in a single communication payload is both a regenerative TDMA system and multiple 800 MHz 'bent pipe' channels routed to spot beams by a switch matrix. While only one mode of operation is typical during any experiment, both modes can operate simultaneously with reduced capability due to sharing of the transponder. NASA-Lewis instituted a ground terminal development program in anticipation of the satellite launch to verify the performance of the switch matrix mode of operations. Specific functions are built into the ground terminal to evaluate rain fade compensation with uplink power control and to monitor satellite transponder performance with bit error rate measurements. These functions were the genesis of the ground terminal's name, Link Evaluation Terminal, often referred to as LET. Connectors are included in LET that allow independent experimenters to run unique modulation or network experiments through ACTS using only the RF transmit and receive portions of LET. Test data indicate that LET will be able to verify important parts of ACTS technology and provide independent experimenters with a useful ground terminal. Lab measurements of major subsystems integrated into LET are presented. Bit error rate is measured with LET in an internal loopback mode. Author

N92-18342*# National Aeronautics and Space Administration. Lewis Research Center, Cleveland, OH.

MULTICHANNEL DEMULTIPLEXER/DEMODULATOR TECHNOLOGIES FOR FUTURE SATELLITE COMMUNICATION SYSTEMS

WILLIAM D. IVANCIC (Amerasia Technology, Inc., Westlake Village, CA.), JAMES M. BUDINGER (Westinghouse Electric Corp., Baltimore, MD.), EDWARD J. STAPLES, IRWIN ABRAMOVITZ, and HECTOR A. COURTOIS (TRW Electronic Systems Group, Redondo Beach, CA.) 1992 9 p Proposed for presentation at the Ninth International Conference on Digital Satellite Communications, Copenhagen, Denmark, 18-22 May 1992; sponsored by Intelsat and Telecom Denmark

(Contract RTOP 506-72-21)

(NASA-TM-105377; E-6765; NAS 1.15:105377) Avail: CASI HC

A02/MF A01

NASA-Lewis' Space Electronics Div. supports ongoing research

in advanced satellite communication architectures, onboard processing, and technology development. Recent studies indicate that meshed VSAT (very small aperture terminal) satellite communication networks using FDMA (frequency division multiple access) uplinks and TDMA (time division multiplexed) downlinks are required to meet future communication needs. One of the critical advancements in such a satellite communication network is the multichannel demultiplexer/demodulator (MCDD). The progress is described which was made in MCDD development using either acousto-optical, optical, or digital technologies.

Author

N92-19762*# National Aeronautics and Space Administration. Lewis Research Center, Cleveland, OH.

DESTINATION-DIRECTED, PACKET-SWITCHING ARCHITECTURE FOR 30/20-GHZ FDMA/TDM GEOSTATIONARY COMMUNICATIONS SATELLITE NETWORK

WILLIAM D. IVANCIC and MARY JO SHALKHAUSER Feb. 1992 14 p Previously announced as N92-14204

(Contract RTOP 650-60-21)

(NASA-TP-3201; E-6539; NAS 1.60:3201) Avail: CASI HC

A03/MF A01

A destination-directed packet switching architecture for a 30/20-GHz frequency division multiple access/time division multiplexed (FDMA/TDM) geostationary satellite communications network is discussed. Critical subsystems and problem areas are identified and addressed. Efforts have concentrated heavily on the space segment; however, the ground segment has been considered concurrently to ensure cost efficiency and realistic operational constraints.

Author

N92-22001*# National Aeronautics and Space Administration. Lewis Research Center, Cleveland, OH.

ADVANCED MODULATION AND CODING TECHNOLOGY CONFERENCE

Feb. 1992 324 p Conference held in Cleveland, OH, 21-22 Jun. 1989

(Contract RTOP 650-60-21)

(NASA-CP-10053; E-5535; NAS 1.55:10053) Avail: CASI HC

A14/MF A03

The objectives, approach, and status of all current LeRC-sponsored industry contracts and university grants are presented. The following topics are covered: (1) the LeRC Space Communications Program, and Advanced Modulation and Coding Projects; (2) the status of four contracts for development of proof-of-concept modems; (3) modulation and coding work done under three university grants, two small business innovation research contracts, and two demonstration model hardware development contracts; and (4) technology needs and opportunities for future missions.

N92-22002*# National Aeronautics and Space Administration. Lewis Research Center, Cleveland, OH.

NASA. LEWIS RESEARCH CENTER ADVANCED MODULATION AND CODING PROJECT: INTRODUCTION AND OVERVIEW

JAMES M. BUDINGER *In its* Advanced Modulation and Coding Technology Conference p 7-30 Feb. 1992

Avail: CASI HC A03/MF A03

The Advanced Modulation and Coding Project at LeRC is sponsored by the Office of Space Science and Applications, Communications Division, Code EC, at NASA Headquarters and conducted by the Digital Systems Technology Branch of the Space Electronics Division. Advanced Modulation and Coding is one of three focused technology development projects within the branch's overall Processing and Switching Program. The program consists of industry contracts for developing proof-of-concept (POC) and demonstration model hardware, university grants for analyzing advanced techniques, and in-house integration and testing of performance verification and systems evaluation. The Advanced Modulation and Coding Project is broken into five elements: (1) bandwidth- and power-efficient modems; (2) high-speed codecs;

17 SPACE COMMUNICATIONS, SPACECRAFT COMMUNICATIONS, COMMAND AND TRACKING

(3) digital modems; (4) multichannel demodulators; and (5) very high-data-rate modems. At least one contract and one grant were awarded for each element. Author

N92-22019*# National Aeronautics and Space Administration. Lewis Research Center, Cleveland, OH.

FUTURE COMMUNICATIONS SATELLITE APPLICATIONS

JAMES W. BAGWELL *In its* Advanced Modulation and Coding Technology Conference p 295-306 Feb. 1992

Avail: CASI HC A03/MF A03

The point of view of the research is made through the use of viewgraphs. It is suggested that future communications satellite applications will be made through switched point to point narrowband communications. Some characteristics of which are as follows: small/low cost terminals; single hop communications; voice compatible; full mesh networking; ISDN compatible; and possible limited use of full motion video. Some target applications are as follows: voice/data networks between plants and offices in a corporation; data base networking for commercial and science users; and cellular radio internodal voice/data networking.

Author

N92-22319*# National Aeronautics and Space Administration. Lewis Research Center, Cleveland, OH.

OPERATING AND SERVICE MANUAL FOR THE NASA LEWIS AUTOMATED FAR-FIELD ANTENNA RANGE

JOHN D. TERRY Jan. 1992 28 p

(Contract RTOP 506-72-1C)

(NASA-TM-105343; E-6712; NAS 1.15:105343) Avail: CASI HC A03/MF A01

This NASA Lewis far-field antenna range was recently upgraded and automated to meet the growing and demanding needs of the satellite communications program. Here, assistance is offered in the operation and service of this range. The procedures for configuring the test hardware and for operating the Far-Field Antenna Measurement Program (FAMP) are given. Included are the steps for getting started and for installing the proper microwave equipment. Author

N92-23187*# National Aeronautics and Space Administration. Lewis Research Center, Cleveland, OH.

ACHIEVING SPECTRUM CONSERVATION FOR THE MINIMUM-SPAN AND MINIMUM-ORDER FREQUENCY ASSIGNMENT PROBLEMS

ANN O. HEYWARD 1992 28 p Presented at the 14th International Communications Satellite Systems Conference, Washington, DC, 22-26 Mar. 1992; sponsored by AIAA Previously announced in IAA as A92-29883

(Contract RTOP 643-10-01)

(NASA-TM-105649; E-7010; NAS 1.15:105649; AIAA PAPER

92-1960) Avail: CASI HC A03/MF A01

Effective and efficient solutions of frequency assignment problems assumes increasing importance as the radiofrequency spectrum experiences ever increasing utilization by diverse communications services, requiring that the most efficient use of this resource be achieved. The research presented explores a general approach to the frequency assignment problem, in which such problems are categorized by the appropriate spectrum conserving objective function, and are each treated as an N-job, M-machine scheduling problem appropriate for the objective. Results obtained and presented illustrate that such an approach presents an effective means of achieving spectrum conserving frequency assignments for communications systems in a variety of environments. Author

N92-30383*# National Aeronautics and Space Administration. Lewis Research Center, Cleveland, OH.

THE ACTS MULTIBEAM ANTENNA

FRANK A. REGIER Apr. 1992 12 p

(Contract RTOP 679-40-00)

(NASA-TM-105645; E-7000; NAS 1.15:105645) Avail: CASI HC A03/MF A01

The Advanced Communications Technology Satellite (ACTS)

to be launched in 1993 introduces several new technologies including a multibeam antenna (MBA) operating at Ka-band. The satellite is introduced briefly, and then the MBA, consisting of electrically similar 30 GHz received and 20 GHz transmit offset Cassegrain systems utilizing orthogonal linear polarizations, is described. Dual polarization is achieved by using one feed assembly for each polarization in conjunction with nested front and back subreflectors, the gridded front subreflector acting as a window for one polarization and a reflector for the other. The antennas produce spot beams with approximately 0.3 deg beamwidth and gains of approximately 50 dbi. High surface accuracy and high edge taper produce low sidelobe levels and high cross-polarization isolation. A brief description is given of several Ka-band components fabricated for ACTS. These include multifeed antenna feedhorns, beam-forming networks utilizing latching ferrite waveguide switches, a 30 GHz high mobility electron transmitter (HEMT) low-noise amplifier and a 20 GHz TWT power amplifier. Author

Author

18

SPACECRAFT DESIGN, TESTING AND PERFORMANCE

Includes satellites; space platforms; space stations; spacecraft systems and components such as thermal and environmental controls; and attitude controls.

A92-13425* National Aeronautics and Space Administration. Lewis Research Center, Cleveland, OH.

COLD-SAT - A TECHNOLOGY SATELLITE FOR CRYOGENIC EXPERIMENTATION

H. ARIF and E. W. KROEGER (NASA, Lewis Research Center, Cleveland, OH) IN: Advances in cryogenic engineering. Vol. 35B - Proceedings of the 1989 Cryogenic Engineering Conference, Los Angeles, CA, July 24-28, 1989 1990 12 p refs Copyright

NASA-Lewis (LeRC) is involved in the development and validation of analytical models which describe the fluid dynamic and thermodynamic processes associated with the storage, acquisition and transfer of subcritical cryogenic fluids in low gravity. Four concurrent studies, including one in-house at LeRC, are underway to determine the feasibility of performing model validation experiments aboard a free-flying spacecraft (S/C) called Cryogenic On-Orbit Liquid Depot-Storage, Acquisition and Transfer (COLD-SAT), using liquid hydrogen as the cryogen. The technology requirements for the experiments are described along with the initial LeRC concepts for the S/C and an experiment subsystem comprising of cryogenic tankage (a supply dewar and three receiver tanks), gas pressurization bottles (both helium and autogenous hydrogen), their associated plumbing, and instrumentation for data collection. Experiments were categorized into enabling/high priority Class 1 technologies and component/system Class 2 demonstrations. As initially envisioned by LeRC, COLD-SAT would have had a 1997 launch aboard a Delta-2 for a 6 month active lifetime in a 925 km orbit with a pseudo-inertial attitude. Author

A92-14734* National Aeronautics and Space Administration. Lewis Research Center, Cleveland, OH.

DYNAMICS AND CONTROL OF THE SPACE STATION FREEDOM DOCKING/ARRAY FEATHERING MANEUVER

RONALD E. GRAHAM (NASA, Lewis Research Center, Cleveland, OH) IAF, International Astronautical Congress, 42nd, Montreal, Canada, Oct. 5-11, 1991. 9 p. Oct. 1991 9 p refs (IAF PAPER 91-321) Copyright

Analysis performed at Lewis Research Center has indicated that it is possible to fail a photovoltaic array of the Space Station Freedom during a Shuttle approach, due to impingements by Shuttle attitude jet firing plumes. A solution to this potential problem is the feathering of the arrays. This study deals with fine adjustments

in feathered position for extra plume load relief. A mathematical model for fine feathering is described. The Shuttle is treated as a single rigid body, with prescribed jet firings. Freedom is treated as a system of rigid bodies, with high-fidelity gimbal dynamics. Uncertainty is found in disturbances, plume dynamic pressure, gimbal friction and misalignments. Assumptions, model structure and analysis test plan are presented. Author

A92-16318* Texas Univ., Austin.
EFFECT OF AN ARCJET PLUME ON SATELLITE REFLECTOR PERFORMANCE

HAO LING, HYEONGDONG KIM, GARY A. HALLOCK, BJORN W. BIRKNER (Texas, University, Austin), and AFROZ J. M. ZAMAN (NASA, Lewis Research Center, Cleveland, OH) IEEE Transactions on Antennas and Propagation (ISSN 0018-926X), vol. 39, Sept. 1991, p. 1412-1420. Sep. 1991 9 p refs (Contract NCC3-127; NSF ECS-86-57524) Copyright

The effect of an arcjet plume on the performance of satellite reflector antennas is studied. The arcjet plume is modeled as a weakly ionized plasma. The spatial permittivity distribution of the plume is approximated using the measured electron density profile and a cold plasma model. Geometrical optics is applied to determine the ray paths as well as the transmitted fields through the inhomogeneous plume. The ray optics results are compared against several exact solutions for scattering from inhomogeneous dielectrics, and good agreement is observed for sufficiently large scatterer size. The far-field antenna patterns of the reflector in the presence of the plume are calculated from the transmitted ray fields using a ray-tube integration scheme. For arcjet prototypes in the 1-kW class, the plume effect on the antenna performance is small. As the electron density increases, the main beam and sidelobe level gradually degrade. The main beam also tends to squint away from the plume region. I.E.

A92-17780 National Aeronautics and Space Administration. Lewis Research Center, Cleveland, OH.

ADVANCED COMMUNICATIONS TECHNOLOGY SATELLITE (ACTS)

MARK S. PLECITY (NASA, Lewis Research Center, Cleveland, OH) and MARK E. NALL (NASA, Office of Commercial Programs, Washington, DC) IN: Space manufacturing 8 - Energy and materials from space; Proceedings of the 10th Princeton/AIAA/SSI Conference, Princeton, NJ, May 15-18, 1991 1991 8 p refs Copyright

The NASA Advanced Communications Technology Satellite (ACTS) provides high risk technologies having the potential to dramatically enhance the capabilities of the satellite communications industry. This experimental satellite, which will be launched by NASA in 1993, will furnish the technology necessary for providing a range of services. Utilizing the ACTS very-high-gain-hopping spot-beam antennas with on-board routing and processing, Very Small Aperture Terminal (VSAT) digital networks which provide on-demand, full-mesh-connectivity 1.544-MBPS services with only a single hop can be established. The high-gain spot-beam antenna at Ka-band permits wide area, flexible networks providing high data rate services between modest-size earth terminals. Author

A92-17796* National Aeronautics and Space Administration. Lewis Research Center, Cleveland, OH.

MAGNETIC RADIATION SHIELDING - AN IDEA WHOSE TIME HAS RETURNED?

GEOFFREY A. LANDIS (NASA, Lewis Research Center; Sverdrup Technology, Inc., Cleveland, OH) IN: Space manufacturing 8 - Energy and materials from space; Proceedings of the 10th Princeton/AIAA/SSI Conference, Princeton, NJ, May 15-18, 1991 1991 4 p refs Copyright

One solution to the problem of shielding crew from particulate radiation in space is to use active electromagnetic shielding. Practical types of shield include the magnetic shield, in which a strong magnetic field diverts charged particles from the crew region,

and the magnetic/electrostatic plasma shield, in which an electrostatic field shields the crew from positively charged particles, while a magnetic field confines electrons from the space plasma to provide charge neutrality. Advances in technology include high-strength composite materials, high-temperature superconductors, numerical computational solutions to particle transport in electromagnetic fields, and a technology base for construction and operation of large superconducting magnets. These advances make electromagnetic shielding a practical alternative for near-term future missions. Author

A92-24369*# National Aeronautics and Space Administration. Lewis Research Center, Cleveland, OH.

MAINTENANCE AND RESUPPLY IN THE UNPRESSURIZED ENVIRONMENT - DESIGN AND OPERATIONAL CONCEPTS FOR THE SPACE STATION FREEDOM LOGISTICS CARRIERS

GARY M. CREPS, STEVEN A. ERNST (Rockwell International Corp., Rocketdyne Div., Canoga Park, CA), and ROBERT D. CRAWFORD (NASA, Lewis Research Center, Cleveland, OH) IN: AIAA/SOLE Space Logistics Symposium, 4th, Cocoa Beach, FL, Nov. 4-6, 1991, Technical Papers 1991 11 p refs (AIAA PAPER 91-4116) Copyright

A significant percentage of the maintenance tasks for Space Station Freedom are anticipated to be conducted in the unpresurized environment. The maintenance concept for this environment essentially involves the removal and replacement of relatively large orbital replacement units (ORUs). Major constraints will be the on-orbit availability of both crew time and spare ORUs. The challenge presented to the program will be the performance of unpresurized cargo resupply that provides maximum cargo-carrying capability (mass and volume) and flexibility (type and quantity), while minimizing the impact to maintenance task times. The design of the logistics carriers is a critical component for successful resupply and maintenance operations, and to the success of Space Station Freedom. Author

A92-26983*# National Aeronautics and Space Administration. Lewis Research Center, Cleveland, OH.

THE ARCING RATE FOR A HIGH VOLTAGE SOLAR ARRAY - THEORY, EXPERIMENT AND PREDICTIONS

DANIEL E. HASTINGS, MENGU CHO (MIT, Cambridge, MA), and HITOSHI KUNINAKA (Institute of Space and Astronautical Science, Sagami-hara, Japan) AIAA, Aerospace Sciences Meeting and Exhibit, 30th, Reno, NV, Jan. 6-9, 1992. 28 p. Research supported by NASA, NSF, USAF, et al. Jan. 1992 28 p refs (AIAA PAPER 92-0576) Copyright

All solar arrays have biased surfaces which can be exposed to the space environment. It has been observed that when the array bias is less than a few hundred volts negative then the exposed conductive surfaces may undergo arcing in the space plasma. A theory for arcing is developed on these high voltage solar arrays which ascribes the arcing to electric field runaway at the interface of the plasma, conductor and solar cell dielectric. Experiments were conducted in the laboratory for the High Voltage Solar Array (HVSA) experiment which will fly on the Japanese Space Flyer Unit (SFU) in 1994. The theory was compared in detail to the experiment and shown to give a reasonable explanation for the data. The combined theory and ground experiments were then used to develop predictions for the SFU flight. Author

A92-29614*# National Aeronautics and Space Administration. Lewis Research Center, Cleveland, OH.

APPLICABILITY OF LONG DURATION EXPOSURE FACILITY ENVIRONMENTAL EFFECTS DATA TO THE DESIGN OF SPACE STATION FREEDOM ELECTRICAL POWER SYSTEM

ROBERT J. CHRISTIE, CHENG-YI LU, and IRENE ARONOFF (Rockwell International Corp., Rocketdyne Div., Canoga Park, CA) AIAA, Aerospace Sciences Meeting and Exhibit, 30th, Reno, NV, Jan. 6-9, 1992. 14 p. Jan. 1992 14 p refs (Contract NAS3-25082) (AIAA PAPER 92-0848) Copyright

Data defining space environmental effects on the Long Duration Exposure Facility (LDEF) are examined in terms of the design of

the electrical power system (EPS) of the Space Station Freedom (SSF). The significant effects of long-term exposure to space are identified with respect to the performance of the LDEF's materials, components, and systems. A total of 57 experiments were conducted on the LDEF yielding information regarding coatings, thermal systems, electronics, optics, and power systems. The resulting database is analyzed in terms of the specifications of the SSF EPS materials and subsystems and is found to be valuable in the design of control and protection features. Specific applications are listed for findings regarding the thermal environment, atomic oxygen, UV and ionizing radiation, debris, and contamination. The LDEF data are shown to have a considerable number of applications to the design and planning of the SSF and its EPS. C.C.S.

A92-34325*# National Aeronautics and Space Administration. Lewis Research Center, Cleveland, OH.
NONUNIFORM THERMAL ENVIRONMENTAL EFFECTS ON SPACE TRUSS STRUCTURAL RELIABILITY
 SHANTARAM S. PAI and CHRISTOS C. CHAMIS (NASA, Lewis Research Center, Cleveland, OH) IN: AIAA/ASME/ASCE/AHS/ASC Structures, Structural Dynamics and Materials Conference, 33rd, Dallas, TX, Apr. 13-15, 1992, Technical Papers. Pt. 1 1992 8 p refs (AIAA PAPER 92-2352) Copyright

A three-bay, space, cantilever truss is probabilistically evaluated to quantify the range of uncertainties of buckling loads and member forces due to nonuniform thermal loads, applied loads and moments (mechanical loads), and combination of both. The truss members are assumed to be made from (1) aluminum tubes or (2) high modulus graphite-fiber/intermediate modulus epoxy-matrix composite tubes. Cumulative distribution function results show that certain combinations of thermal loads with mechanical loads reduce the probabilistic buckling loads and increase the magnitude of the member axial forces for aluminum truss. However, the reverse is true for composite truss due to very low coefficient of thermal expansion and higher stiffness of the composite. Finally, the sensitivities associated with the uncertainties in the structural, material, and load variables (primitive variables) are investigated. They show that buckling loads and member axial forces are most sensitive to the uncertainties in spacial (geometry) variables. Author

A92-34380*# National Aeronautics and Space Administration. Lewis Research Center, Cleveland, OH.
STRUCTURAL DESIGN CONCEPTS FOR A MULTIMEGAWATT SOLAR ELECTRIC PROPULSION (SEP) SPACECRAFT
 CHARLES LAWRENCE and J. M. HICKMAN (NASA, Lewis Research Center, Cleveland, OH) IN: AIAA/ASME/ASCE/AHS/ASC Structures, Structural Dynamics and Materials Conference, 33rd, Dallas, TX, Apr. 13-15, 1992, Technical Papers. Pt. 2 1992 9 p refs (AIAA PAPER 92-2536) Copyright

As a part of the Space Exploratory Initiative (SEI), NASA-Lewis is studying Solar Electric Propulsion (SEP) spacecraft to be used as a cargo transport vehicle to Mars. Two preliminary structural design concepts are offered for SEP spacecraft: a split blanket array configuration, and a ring structure. The split blanket configuration is an expansion of the photovoltaic solar array design proposed for Space Station Freedom and consists of eight independent solar blankets stretched and supported from a central mast. The ring structural concept is a circular design with the solar blanket stretched inside a ring. This concept uses a central mast with guy wires to provide additional support to the ring. The two design concepts are presented, then compared by performing stability, normal modes, and forced response analyses for varying levels of blanket and guy wire preloads. The ring structure configuration is shown to be advantageous because it is much stiffer, more stable, and deflects less under loading than the split blanket concept. Author

A92-43284* National Aeronautics and Space Administration. Lewis Research Center, Cleveland, OH.

POINTING AND TRACKING CONTROL FOR FREEDOM'S SOLAR DYNAMIC MODULES AND VIBRATION CONTROL OF FREEDOM

ROGER D. QUINN and JIUNN-LIANG CHEN (Case Western Reserve University, Cleveland, OH) IN: Astrodynamics 1991; Proceedings of the AAS/AIAA Astrodynamics Conference, Durango, CO, Aug. 19-22, 1991. Pt. 1 1992 20 p refs (Contract NAG3-1099) (AAS PAPER 91-459) Copyright

A control strategy is presented for pointing particular modules of flexible multibody space structures while simultaneously attenuating structural vibrations. The application that is addressed is the planned Space Station Freedom in a growth configuration with Solar Dynamic (SD) module. A NASTRAN model of Freedom is used to demonstrate the control strategy. Two cases of SD concentrator fine-pointing controller bandwidths are studied with examples. The effect of limiting the controller motor torques to realistic baseline values is examined. SD pointing and station vibration control is accomplished during realistic disturbances due to aerodynamic drag, Shuttle docking, and Shuttle reaction control system plume impingement on SD. Gravity gradient induced torques on SD are relatively small and pseudo-steady. Author

A92-47495* National Aeronautics and Space Administration. Lewis Research Center, Cleveland, OH.

OPTIMAL MICROGRAVITY VIBRATION ISOLATION - AN ALGEBRAIC INTRODUCTION

R. D. HAMPTON (Virginia, University, Charlottesville), C. M. GRODSINSKY (NASA, Lewis Research Center, Cleveland, OH), P. E. ALLAIRE, D. W. LEWIS, and C. R. KNOSPE (Virginia, University, Charlottesville) Journal of the Astronautical Sciences (ISSN 0021-9142), vol. 40, no. 2, Apr.-June 1992, p. 241-259. Previously announced in STAR as N92-11217. Jun. 1992 19 p refs

Copyright

Certain experiments contemplated for space platforms must be isolated from the accelerations of the platforms. An optimal active control is developed for microgravity vibration isolation, using constant state feedback gains (identical to those obtained from the Linear Quadratic Regulator (LQR) approach) along with constant feedforward (preview) gains. The quadratic cost function for this control algorithm effectively weights external accelerations of the platform disturbances by a factor proportional to $(1/\omega)^4$ (exp 4). Low frequency accelerations (less than 50 Hz) are attenuated by greater than two orders of magnitude. The control relies on the absolute position and velocity feedback of the experiment and the absolute position and velocity feedforward of the platform, and generally derives the stability robustness characteristics guaranteed by the LQR approach to optimality. The method as derived is extendable to the case in which only the relative positions and velocities and the absolute accelerations of the experiment and space platform are available. Author

A92-50578* National Aeronautics and Space Administration. Lewis Research Center, Cleveland, OH.

CONTAMINATION EFFECTS ON SPACE STATION FREEDOM ELECTRIC POWER SYSTEM PERFORMANCE

CHENG-YI LU and IRENE ARONOFF (Rockwell International Corp., Rocketdyne Div., Canoga Park, CA) IN: IECEC '91; Proceedings of the 26th Intersociety Energy Conversion Engineering Conference, Boston, MA, Aug. 4-9, 1991. Vol. 1 1991 6 p refs

(Contract NAS3-25082)

Copyright

One design issue for Space Station Freedom (SSF) is the potential performance decrease of the electric power system (EPS) solar arrays and radiators as a result of contamination on sensitive surfaces. The authors discuss SSF potential contamination sources and contamination effects on the solar array and radiator performance due to these sources. With these contamination consideration, the SSF EPS is designed for the induced

contamination environment at an optimal cost. The efforts on contamination protection and control are undergoing continual update because of the changes in the SSF configuration and in the contamination requirements, and observations from recent flight and laboratory test data are continuously being incorporated into the design. I.E.

A92-50581* National Aeronautics and Space Administration. Lewis Research Center, Cleveland, OH.

ASSESSMENT OF ENVIRONMENTAL EFFECTS ON SPACE STATION FREEDOM ELECTRICAL POWER SYSTEM

CHENG-YI LU (Rockwell International Corp., Rocketdyne Div., Canoga Park, CA) and HENRY K. NAHRA (NASA, Lewis Research Center, Cleveland, OH) IN: IECEC '91; Proceedings of the 26th Intersociety Energy Conversion Engineering Conference, Boston, MA, Aug. 4-9, 1991. Vol. 1 1991 6 p refs
Copyright

Analyses of EPS (electrical power system) interactions with the LEO (low earth orbit) environment are described. The results of these analyses will support EPS design so as to be compatible with the natural and induced environments and to meet power, lifetime, and performance requirements. The environmental impacts to the Space Station Freedom EPS include aerodynamic drag, atomic oxygen erosion, ultraviolet degradation, VXB effect, ionizing radiation dose and single event effects, electromagnetic interference, electrostatic discharge, plasma interactions (ion sputtering, arcing, and leakage current), meteoroid and orbital debris threats, thermal cycling effects, induced current and voltage potential differences in the SSF due to induced electric field, and contamination degradation. I.E.

A92-50661 National Aeronautics and Space Administration. Lewis Research Center, Cleveland, OH.

LARGE TRANSIENT FAULT CURRENT TEST OF AN ELECTRICAL ROLL RING

EDWARD J. YENNI (Rockwell International Corp., Rocketdyne Div., Cleveland, OH) and ARTHUR G. BIRCHENOUGH (NASA, Lewis Research Center, Cleveland, OH) IN: IECEC '91; Proceedings of the 26th Intersociety Energy Conversion Engineering Conference, Boston, MA, Aug. 4-9, 1991. Vol. 2 1991 5 p refs
(Contract RTOP 474-42-10)
Copyright

The Space Station Freedom uses precision rotary gimbals to provide for sun tracking of its photoelectric arrays. Electrical power, command signals, and data are transferred across the gimbals by roll rings. Roll rings have been shown to be capable of highly efficient electrical transmission and long life, through tests conducted at the NASA Lewis Research Center and Honeywell's Satellite and Space Systems Division in Phoenix, AZ. Large potential fault currents inherent to the power system's DC distribution architecture have brought about the need to evaluate the effects of large transient fault currents on roll rings. A test recently conducted at Lewis subjected a roll ring to a simulated worst case space station electrical fault. The system model used to obtain the fault profile is described, along with details of the reduced order circuit that was used to simulate the fault. Test results comparing roll ring performance before and after the fault are also presented. Author

N92-11086*# National Aeronautics and Space Administration. Lewis Research Center, Cleveland, OH.

DEVELOPMENT OF A NINETY STRING SOLAR ARRAY SIMULATOR

THOMAS E. VASEK and ARTHUR G. BIRCHENOUGH Oct. 1991 11 p
(Contract RTOP 474-74-10)
(NASA-TM-105278; E-6601; NAS 1.15:105278) Avail: CASI HC A03/MF A01

A power source was developed to support testing for the Space Station Freedom Power Management and Distribution (PMAD) DC Testbed. The intent was to simulate as closely as possible the steady-state and transient responses of a solar array. Several breadboards and one thermal prototype were built and tested.

Responses were successfully verified and improved upon during successive breadboards. The completed 90-string simulator consists of four power MOSFETs, four 25 watt source resistors, and four 250 watt drain source bypass resistors per string, in addition to the control circuitry. Author

N92-13143*# National Aeronautics and Space Administration. Lewis Research Center, Cleveland, OH.

PARAMETRIC STUDIES OF PHASE CHANGE THERMAL ENERGY STORAGE CANISTERS FOR SPACE STATION FREEDOM

THOMAS W. KERSLAKE 1991 9 p Presented at the International Solar Energy Conference, Maui, HI, 4-8 Apr. 1991; sponsored by the American Society of Mechanical Engineers (Contract RTOP 474-52-10)
(NASA-TM-105350; E-6724; NAS 1.15:105350) Avail: CASI HC A02/MF A01

Phase Change Materials (PCM) canister parametric studies are discussed wherein the thermal-structural effects of changing various canister dimensions and contained PCM mass values are examined. With the aim of improving performance, 11 modified canister designs are analyzed and judged relative to a baseline design using five quantitative performance indicators. Consideration is also given to qualitative factors such as fabrication/inspection, canister mass production, and PCM containment redundancy. Canister thermal analyses are performed using the finite-difference based computer program NUCAM-2DV. Thermal-stresses are calculated using closed-form solutions and simplifying assumptions. Canister wall thickness, outer radius, length, and contained PCM mass are the parameters considered for this study. Results show that singular canister design modifications can offer improvements on one or two performance indicators. Yet, improvement in one indicator is often realized at the expense of another. This confirms that the baseline canister is well designed. However, two alternative canister designs, which incorporate multiple modifications, are presented that offer modest improvements in mass or thermal performance, respectively. Author

N92-17416*# National Aeronautics and Space Administration. Lewis Research Center, Cleveland, OH.

SPACE STATION FREEDOM/LUNAR TRANSFER VEHICLE PROPELLANT OPERATION HAZARD ANALYSIS

SAM DOMINICK (Martin Marietta Corp., Vandenberg AFB, CA.), STEVEN M. STEVENSON, and HARVEY FEINGOLD (Science Applications International Corp., Schaumburg, IL.) In NASA, Washington, Beyond the Baseline 1991: Proceedings of the Space Station Evolution Symposium. Volume 1: Space Station Freedom, Part 2 p 533-564 Sep. 1991
Avail: CASI HC A03/MF A03

Space Station Freedom (SSF), as a transportation node for Space Exploration Initiative missions, would involve the assembly and refurbishing of lunar and Mars transfer vehicles. This includes operations involving cryogenic propellants (LH2 7 LO2) such as storing and handling of loaded propellant tanks, assembly onto the vehicle, and propellant transfer. Cryogenic propellants dictate rigorous safety precautions and impose unique requirements to ensure flight safety to both personnel and SSF elements. The objective of this study is to identify potential hazards and risks associated with cryogenic propellants. This involves identification of pertinent system design features and operational procedures. Criticality of identified risks/hazards shall be assessed and those that fall in the catastrophic and critical categories shall include mitigating solutions. Author

N92-22361*# National Aeronautics and Space Administration. Lewis Research Center, Cleveland, OH.

NASCAP/LEO SIMULATIONS OF SHUTTLE ORBITER CHARGING DURING THE SAMPI EXPERIMENT

RICARTE CHOCK In NASA. Johnson Space Center, 5th Annual Workshop on Space Operations Applications and Research (SOAR 1991), Volume 2 p 655-661 Feb. 1992
Avail: CASI HC A02/MF A04

The electrostatic charging of the Space Shuttle Orbiter during

18 SPACECRAFT DESIGN, TESTING AND PERFORMANCE

the operation of the Solar Array Module Plasma Interaction Experiment (SAMPIE) was modeled using the NASA Charging Analyzer Program/ low Earth orbit (NASCAP/LEO) computer code. The SAMPIE experiment consists of an array of various solar cells representing the present technologies. The objectives of the experiment are to investigate the arcing and current collection characteristics of these cells when biased to high potentials in a LEO plasma. NASCAP/LEO is a 3-D code designed to simulate the electrostatic charging of a spacecraft exposed to a plasma at LEO or ground test conditions. At its most extreme configuration, with the largest array segment of the SAMPIE experiment biased + 600 V with respect to the orbiter and facing the ram direction, the computer simulations predict that the orbiter's potential will be approximately -20 V with respect to the plasma. Author

N92-23824*# National Aeronautics and Space Administration. Lewis Research Center, Cleveland, OH.

SIMULATION OF SPACE STATION LOADS WITH ACTIVE CONTROL SYSTEMS

P. A. BLELLOCH (SDRC Engineering Services Ltd., Herts (England).), N. R. BEAGLEY (SDRC Engineering Services Ltd., Herts, England), D. R. LUDWICZAK, and I. YUNIS *in* ESA, *Spacecraft Structures and Mechanical Testing*, Volume 1 p 309-315 Oct. 1991

Copyright Avail: CASI HC A02/MF A04

A methodology for calculating dynamic loads for the Space Station Freedom is presented. The methodology minimizes the repeated calculation of duplicate structural elements, while analyzing a large number of different Space Station configurations with different alpha and beta joint angles. Particular attention is paid to the issue of model reduction using a combination of component mode synthesis (superelements) and component mode selection to generate accurate system level models with a minimum of modal degrees of freedom. The modeling of the control systems during simulation of the structural response is discussed. ESA

N92-24349*# National Aeronautics and Space Administration. Lewis Research Center, Cleveland, OH.

APPLICATIONS OF HIGH THERMAL CONDUCTIVITY COMPOSITES TO ELECTRONICS AND SPACECRAFT THERMAL DESIGN

G. RICHARD SHARP and TIMOTHY A. LOFTIN (DWA Composite Specialities, Inc., Chatsworth, CA.) 1990 8 p Presentd at the 13th International Communication Satellite Systems Conference, Los Angeles, CA, 11-15 Mar. 1990; sponsored by AIAA Previously announced in IAA as A90-25609

(Contract NAS3-24896; RTOP 324-02-00) (NASA-TM-102434; E-5175; NAS 1.15:102434; AIAA PAPER 90-0783) Avail: CASI HC A02/MF A01

Recently, high thermal conductivity continuous graphite fiber reinforced metal matrix composites (MMC's) have become available that can save much weight over present methods of heat conduction. These materials have two or three times higher thermal conductivity in the fiber direction than the pure metals when compared on a thermal conductivity to weight basis. Use of these materials for heat conduction purposes can result in weight savings of from 50 to 70 percent over structural aluminum. Another significant advantage is that these materials can be used without the plumbing and testing complexities that accompany the use of liquid heat pipes. A spinoff of this research was the development of other MMC's as electronic device heat sinks. These use particulates rather than fibers and are formulated to match the coefficient of thermal expansion of electronic substrates in order to alleviate thermally induced stresses. The development of both types of these materials as viable weight saving substitutes for traditional methods of thermal control for electronics packaging and also for spacecraft thermal control applications are the subject of this report. Author

N92-28683*# National Aeronautics and Space Administration. Lewis Research Center, Cleveland, OH.

SOLAR ARRAY MODULE PLASMA INTERACTION EXPERIMENT (SAMPIE): TECHNICAL REQUIREMENTS DOCUMENT

G. BARRY HILLARD (Sverdrup Technology, Inc., Brook Park, OH.) and DALE C. FERGUSON May 1992 25 p (Contract RTOP 589-01-1B) (NASA-TM-105660; E-7033; NAS 1.15:105660) Avail: CASI HC A03/MF A01

The Solar Array Module Plasma Interactions Experiment (SAMPIE) is a NASA shuttle space flight experiment scheduled for launch in early 1994. The SAMPIE experiment will investigate plasma interactions of high voltage space power systems in low earth orbit. Solar cell modules, representing several technologies, will be biased to high voltages to characterize both arcing and plasma current collection. Other solar modules, specially modified in accordance with current theories of arcing and breakdown, will demonstrate the possibility of arc suppression. Finally, several test modules will be included to study the basic nature of these interactions. The science and technology goals for the project are defined in the Technical Requirements Document (TRD) which is presented here. Author

19

SPACECRAFT INSTRUMENTATION

A92-27119*# National Aeronautics and Space Administration. Lewis Research Center, Cleveland, OH.

A FULL FIELD, 3-D VELOCIMETER FOR NASA'S MICROGRAVITY SCIENCE PROGRAM

MARYJO B. MEYER and MARK D. BETHEA (NASA, Lewis Research Center, Cleveland, OH) AIAA, Aerospace Sciences Meeting and Exhibit, 30th, Reno, NV, Jan. 6-9, 1992. 8 p. Jan. 1992 8 p refs (AIAA PAPER 92-0784) Copyright

One of NASA's new Advanced Technology Development projects is stereo imaging velocimetry. Using multiple CCD cameras, the velocimeter will digitize and store images of microscopic seed particles suspended in flowing transparent fluid systems. The data will be processed to obtain full-field, three-dimensional, quantitative velocity data. With successful evolution of the technology, the velocimeter will become part of NASA's flight hardware arsenal, available to both established experiments and new proposals. Author

A92-28189# National Aeronautics and Space Administration. Lewis Research Center, Cleveland, OH.

DEVELOPMENT OF AND FLIGHT RESULTS FROM THE SPACE ACCELERATION MEASUREMENT SYSTEM (SAMS)

RICHARD DELOMBARD (NASA, Lewis Research Center, Cleveland, OH), BRIAN D. FINLEY (Sverdrup Technology, Inc., Brook Park, OH), and CHARLES R. BAUGHER (NASA, Marshall Space Flight Center, Huntsville, AL) AIAA, Aerospace Sciences Meeting and Exhibit, 30th, Reno, NV, Jan. 6-9, 1992. 11 p. Jan. 1992 11 p refs (AIAA PAPER 92-0354) Copyright

This paper describes the development of and flight results from the Space Acceleration Measurement System (SAMS) flight units used in the Orbiter middeck, Spacelab module and the Orbiter cargo bay. The SAMS units are general purpose microgravity accelerometers designed to support a variety of science experiments with microgravity acceleration measurements. A total of six flight units have been fabricated; four for use in the Orbiter middeck and Spacelab module, and two for use in the Orbiter cargo bay. The design of the units is briefly described. The initial two flights of SAMS units on STS-40 (June 1991) and STS-43

(August 1991) resulted in 371 megabytes and 2.6 gigabytes of data, respectively. Analytical techniques developed to examine this quantity of acceleration data are described and sample plots of analyzed data are illustrated. Future missions for the SAMS units are listed.

Author

A92-54165*# National Aeronautics and Space Administration. Lewis Research Center, Cleveland, OH.

DEMONSTRATION OF A FLIGHT CAPABLE SYSTEM FOR PLUME SPECTROSCOPY

R. L. BICKFORD (Aerojet, Propulsion Div., Sacramento, CA), D. B. DUNCAN (Duncan Technologies, Auburn, CA), and G. MADZSAR (NASA, Lewis Research Center, Cleveland, OH) AIAA, SAE, ASME, and ASEE, Joint Propulsion Conference and Exhibit, 28th, Nashville, TN, July 6-8, 1992. 8 p. Jul. 1992 8 p refs (AIAA PAPER 92-3786) Copyright

A small, rugged, high-speed/resolution Fabry-Perot interferometer (FPI) based spectrometer has been developed for detecting the spectral signatures of eroding rocket engine components during ground tests and/or flight operations, with a view to use in future rocket engine health-management systems (HMSs). A flight-capable HMS will furnish prognoses and responses to incipient engine failures, as well as diagnoses of wear and degradation during maintenance. Attention is given to the development of a prototype FPI spectrometer for demonstration and validation testing at NASA-Marshall.

O.C.

A92-55314*# National Aeronautics and Space Administration. Lewis Research Center, Cleveland, OH.

CLASSICAL AND ADAPTIVE CONTROL ALGORITHMS FOR THE SOLAR ARRAY POINTING SYSTEM OF THE SPACE STATION FREEDOM

G. D. IANCULESCU and J. J. KLOP (Rockwell International Corp., Rocketdyne Div., Canoga Park, CA) IN: AIAA Guidance, Navigation and Control Conference, Hilton Head Island, SC, Aug. 10-12, 1992, Technical Papers. Pt. 3 1992 14 p refs (Contract NAS3-25082) (AIAA PAPER 92-4484) Copyright

Classical and adaptive control algorithms for the solar array pointing system of the Space Station Freedom are designed using a continuous rigid body model of the solar array gimbal assembly containing both linear and nonlinear dynamics due to various friction components. The robustness of the design solution is examined by performing a series of sensitivity analysis studies. Adaptive control strategies are examined in order to compensate for the unfavorable effect of static nonlinearities, such as dead-zone uncertainties.

V.L.

N92-13151*# National Aeronautics and Space Administration. Lewis Research Center, Cleveland, OH.

SPACE ACCELERATION MEASUREMENT SYSTEM DESCRIPTION AND OPERATIONS ON THE FIRST SPACELAB LIFE SCIENCES MISSION

RICHARD DELOMBARD and BRIAN D. FINLEY (Sverdrup Technology, Inc., Brook Park, OH.) Nov. 1991 28 p (Contract NAS3-25266; RTOP 694-03-OH) (NASA-TM-105301; E-6648; NAS 1.15:105301) Avail: CASI HC A03/MF A01

The Space Acceleration Measurement System (SAMS) project and flight units are briefly described. The SAMS operations during the STS-40 mission are summarized, and a preliminary look at some of the acceleration data from that mission are provided. The background and rationale for the SAMS project is described to better illustrate its goals. The functions and capabilities of each SAMS flight unit are first explained, then the STS-40 mission, the SAMS's function for that mission, and the preparation of the SAMS are described. Observations about the SAMS operations during the first SAMS mission are then discussed. Some sample data are presented illustrating several aspects of the mission's microgravity environment.

Author

N92-25134*# National Aeronautics and Space Administration. Lewis Research Center, Cleveland, OH.

SPACE ACCELERATION MEASUREMENT SYSTEM TRIAXIAL SENSOR HEAD ERROR BUDGET

JOHN E. THOMAS, REX B. PETERS, and BRIAN D. FINLEY (Sverdrup Technology, Inc., Brook Park, OH.) Jan. 1992 28 p (Contract NAS3-24816; NAS3-25266; RTOP 694-03-OH) (NASA-TM-105300; E-6647; NAS 1.15:105300) Avail: CASI HC A03/MF A01

The objective of the Space Acceleration Measurement System (SAMS) is to measure and record the microgravity environment for a given experiment aboard the Space Shuttle. To accomplish this, SAMS uses remote triaxial sensor heads (TSH) that can be mounted directly on or near an experiment. The errors of the TSH are reduced by calibrating it before and after each flight. The associated error budget for the calibration procedure is discussed here.

Author

N92-28451*# National Aeronautics and Space Administration. Lewis Research Center, Cleveland, OH.

EARLY MISSION SCIENCE SUPPORT: SPACE ACCELERATION MEASUREMENT SYSTEM (SAMS)

RICHARD DELOMBARD *In its* International Workshop on Vibration Isolation Technology for Microgravity Science Applications p 345-355 May 1992 Avail: CASI HC A03/MF A04

The Space Acceleration Measurement System (SAMS) is discussed in viewgraph form. Applications of the SAMS are as follows: (1) measurement of low-g accelerations; (2) monitoring of low-g environment; (3) monitoring of experiment-induced vibrations; and (4) validation of vibration isolation techniques. Additionally, typical locations for the SAMS are given.

Author

N92-30301*# National Aeronautics and Space Administration. Lewis Research Center, Cleveland, OH.

DEVELOPMENT OF AND FLIGHT RESULTS FROM THE SPACE ACCELERATION MEASUREMENT SYSTEM (SAMS)

RICHARD DELOMBARD, BRIAN D. FINLEY (Sverdrup Technology, Inc., Brook Park, OH.), and CHARLES R. BAUGHER (National Aeronautics and Space Administration, Marshall Space Flight Center, Huntsville, AL.) Jan. 1992 12 p Presented at the 30th Aerospace Science Meeting and Exhibit, Reno, NV, 6-9 Jan. 1992; sponsored in part by AIAA Previously announced in IAA as A92-28189 (Contract RTOP 694-03-OH) (NASA-TM-105652; E-7018; NAS 1.15:105652; AIAA PAPER 92-0354) Avail: CASI HC A03/MF A01

Described here is the development of and the flight results from the Space Acceleration Measurement System (SAMS) flight units used in the Orbiter middeck, Spacelab module, and the Orbiter cargo bay. The SAMS units are general purpose microgravity accelerometers designed to support a variety of science experiments with microgravity acceleration measurements. A total of six flight units have been fabricated; four for use in the Orbiter middeck and Spacelab module, and two for use in the Orbiter cargo bay. The design of the units is briefly described. The initial two flights of SAMS units on STS-40 (June 1991) and STS-43 (August 1991) resulted in 371 megabytes and 2.6 gigabytes of data respectively. Analytical techniques developed to examine this quantity of acceleration data are described and sample plots of analyzed data are illustrated. Future missions for the SAMS units are listed.

Author

SPACECRAFT PROPULSION AND POWER

Includes main propulsion systems and components, e.g., rocket engines; and spacecraft auxiliary power sources.

A92-11474* Florida Atlantic Univ., Boca Raton.
A FAILURE DIAGNOSIS SYSTEM BASED ON A NEURAL NETWORK CLASSIFIER FOR THE SPACE SHUTTLE MAIN ENGINE

AHMET DUYAR (Florida Atlantic University, Boca Raton) and WALTER MERRILL (NASA, Lewis Research Center, Cleveland, OH) IN: IEEE Conference on Decision and Control, 29th, Honolulu, HI, Dec. 5-7, 1990, Proceedings. Vol. 4 1990 10 p refs
 Copyright

A conceptual design of a model based failure detection and diagnosis system is developed for the Space Shuttle Main Engine. This design relies on the accurate and reliable identification of the parameters of the highly nonlinear and very complex engine. The design approach is presented in some detail and results for a failed valve are presented. These preliminary results verify that the developed parameter identification technique, together with a neural network classifier, can be used for this purpose. Author

A92-13154 National Aeronautics and Space Administration, Washington, DC.

STATUS OF NASA'S EARTH-TO-ORBIT PROPULSION TECHNOLOGY PROGRAM

W. J. D. ESCHER (NASA, Washington, DC), J. L. MOSES (NASA, Marshall Space Flight Center, Huntsville, AL), S. H. GORLAND (NASA, Lewis Research Center, Cleveland, OH), and F. W. STEPHENSON (W.J. Schafer Associates, Inc., Chelmsford, MA) IAF, International Astronautical Congress, 42nd, Montreal, Canada, Oct. 5-11, 1991. 10 p. Oct. 1991 10 p refs
 (IAF PAPER 91-258) Copyright

Earth-to-Orbit Propulsion Technology program is considered. The program's three major technical areas include combustion devices, turbomachinery, and controls and monitoring. Directed toward reducing acquisition and operations risk and cost the ETO program is conducted in two serially-performed categories: technology acquisition and technology validation. The former is constituted of studies, tool building, and bench-scale experimentation. The latter involves next-step verification of the acquisition results and findings, usually leading to a test-bed validated technology 'product'. O.G.

A92-13155* National Aeronautics and Space Administration, Lewis Research Center, Cleveland, OH.

HIGH TEMPERATURE THRUSTER TECHNOLOGY FOR SPACECRAFT PROPULSION

STEVEN J. SCHNEIDER (NASA, Lewis Research Center, Cleveland, OH) IAF, International Astronautical Congress, 42nd, Montreal, Canada, Oct. 5-11, 1991. 15 p. Oct. 1991 15 p refs
 (IAF PAPER 91-254) Copyright

A technology program intended to develop high-temperature oxidation-resistant thrusters for spacecraft applications is considered. The program will provide the requisite material characterizations and fabrication to incorporate iridium coated rhenium material into small rockets for spacecraft propulsion. This material increases the operating temperature of thrusters to 2200 C, a significant increase over the 1400 C of the silicide-coated niobium chambers currently used. Stationkeeping class 22 N engines fabricated from iridium-coated rhenium have demonstrated steady state specific impulses 20-25 seconds higher than niobium chambers. These improved performances are obtained by reducing or eliminating the fuel film cooling requirements in the combustion chamber while operating at the same overall mixture ratio as conventional engines. O.G.

A92-13158* National Aeronautics and Space Administration, Lewis Research Center, Cleveland, OH.

ELECTRIC PROPULSION - AN EVOLUTIONARY TECHNOLOGY

FRANCIS M. CURRAN, JAMES S. SOVEY (NASA, Lewis Research Center, Cleveland, OH), and ROGER M. MYERS (NASA, Lewis Research Center, Cleveland; Sverdrup Technology, Inc., Brookpark, OH) IAF, International Astronautical Congress, 42nd, Montreal, Canada, Oct. 5-11, 1991. 25 p. Oct. 1991 25 p refs
 (IAF PAPER 91-241) Copyright

The NASA Lewis Research Center conducts and directs an electric propulsion research and technology program aimed at providing high-performance electric propulsion system options for a broad range of near- and far-term missions. This evolutionary program emphasizes the development of propulsion systems for three classes of missions: (1) near-term auxiliary propulsion applications such as North-South Stationkeeping for next generation communications satellites and orbit maintenance for orbiting platforms such as Space Station Freedom; (2) advanced solar electric propulsion and SP-100-class nuclear electric propulsion (NEP) for earth-space orbit transfer and robotic planetary missions; and (3) very high power systems to support major space missions including the Space Exploration Initiative. To cover widely disparate mission requirements, the program includes research on electrothermal, electrostatic, and electromagnetic systems. This paper provides an overview of the program with a focus on recent progress. Author

A92-13159* National Aeronautics and Space Administration, Lewis Research Center, Cleveland, OH.

NUCLEAR ROCKET PROPULSION TECHNOLOGY - A JOINT NASA/DOE PROJECT

JOHN S. CLARK (NASA, Lewis Research Center, Cleveland, OH) IAF, International Astronautical Congress, 42nd, Montreal, Canada, Oct. 5-11, 1991. 11 p. Oct. 1991 11 p refs
 (IAF PAPER 91-236) Copyright

NASA and the DOE have initiated critical technology development for nuclear rocket propulsion systems for SEI human and robotic missions to the moon and to Mars. The activities and project plan of the interagency project planning team in FY 1990 and 1991 are summarized. The project plan includes evolutionary technology development for both nuclear thermal and nuclear electric propulsion systems. R.E.P.

A92-13160* Los Alamos National Lab., NM.

INNOVATIVE NUCLEAR THERMAL PROPULSION TECHNOLOGY EVALUATION - RESULTS OF THE NASA/DOE TASK TEAM STUDY

STEVEN D. HOWE (Los Alamos National Laboratory, NM), STANLEY BOROWSKI (NASA, Lewis Research Center, Cleveland, OH), CHET MOTLOCH (Idaho National Engineering Laboratory, Idaho Falls), IRA HELMS (Nuclear Utility Services, Damascus, MD), NILS DIAZ, SAMIM ANGHAI (Florida, University, Gainesville), and THOMAS LATHAM (United Technologies Research Center, East Hartford, CT) IAF, International Astronautical Congress, 42nd, Montreal, Canada, Oct. 5-11, 1991. 13 p. Oct. 1991 13 p refs
 (IAF PAPER 91-235)

In response to findings from two NASA/DOE nuclear propulsion workshops, six task teams were created to continue evaluation of various propulsion concepts, from which evolved an innovative concepts subpanel to evaluate thermal propulsion concepts which did not utilize solid fuel. This subpanel endeavored to evaluate each concept on a level technology basis, and to identify critical issues, technologies, and early proof-of-concept experiments. Results of the concept studies including the liquid core fission, the gas core fission, the fission foil reactors, explosively driven systems, fusion, and antimatter are presented. R.E.P.

A92-15355* # National Aeronautics and Space Administration, Lewis Research Center, Cleveland, OH.

MEDIUM POWER HYDROGEN ARCJET PERFORMANCE

FRANCIS M. CURRAN, S. R. BULLOCK, THOMAS W. HAAG,

CHARLES J. SARMIENTO, and JOHN M. SANKOVIC (NASA, Lewis Research Center, Cleveland, OH) AIAA, SAE, ASME, and ASEE, Joint Propulsion Conference, 27th, Sacramento, CA, June 24-27, 1991. 21 p. Previously announced in STAR as N91-31216. Jun. 1991 21 p refs
 (AIAA PAPER 91-2227) Copyright

An experimental investigation was performed to evaluate hydrogen arcjet operating characteristics in the range of 1 to 4 kW. A series of nozzles were operated in modular laboratory thrusters to examine the effects of geometric parameters such as constrictor diameter and nozzle divergence angle. Each nozzle was tested over a range of current and mass flow rates to explore stability and performance. In the range of mass flow rates and power levels tested, specific impulse values between 650 and 1250 sec were obtained at efficiencies between 30 and 40 percent. The performance of the two larger half angle (20, 15 deg) nozzles was similar for each of the two constrictor diameters tested. The nozzles with the smallest half angle (10 deg) were difficult to operate. A restrike mode of operation was identified and described. Damage in the form of melting was observed in the constrictor region of all the nozzle inserts tested. Arcjet ignition was also difficult in many tests and a glow discharge mode that prevents starting was identified. Author

A92-17187* Washington Univ., Saint Louis, MO.
MODELING OF IMPULSIVE PROPELLANT REORIENTATION
 JOHN I. HOCHSTEIN, T. P. KORAKIANITIS, ALFREDO E. PATAG (Washington University, Saint Louis, MO), and DAVID J. CHATO (NASA, Lewis Research Center, Cleveland, OH) Dec. 1991 8 p refs
 Copyright

A92-18401* National Aeronautics and Space Administration. Lewis Research Center, Cleveland, OH.
SPACE POWER BY GROUND-BASED LASER ILLUMINATION
 GEOFFREY A. LANDIS (NASA, Lewis Research Center; Sverdrup Technology, Inc., Cleveland, OH) IEEE Aerospace and Electronic Systems Magazine (ISSN 0885-8985), vol. 6, Nov. 1991, p. 3-7. Nov. 1991 5 p refs
 Copyright

Reducing energy storage requirements of space power systems by illuminating the photovoltaic arrays with a remotely located laser system is addressed. It is proposed that large lasers be located on cloud-free sites at one or more ground locations and that large lenses or mirrors with adaptive optical correction be used to reduce the beam spread due to diffraction or atmospheric turbulence. During the eclipse periods or lunar night, the lasers illuminate the solar arrays to a level sufficient to provide operating power. Two applications are discussed: illumination of geosynchronous orbit satellites and illumination of a moonbase power system. Issues for photovoltaic receivers for such a system are discussed. I.E.

A92-19607* Florida Atlantic Univ., Boca Raton.
STATE SPACE REPRESENTATION OF THE OPEN-LOOP DYNAMICS OF THE SPACE SHUTTLE MAIN ENGINE
 AHMET DUYAR, VASFI ELDEM (Florida Atlantic University, Boca Raton), WALTER C. MERRILL, and TEN-HUEI GUO (NASA, Lewis Research Center, Cleveland, OH) ASME, Transactions, Journal of Dynamic Systems, Measurement, and Control (ISSN 0022-0434), vol. 113, Dec. 1991, p. 684-690. Dec. 1991 7 p refs
 Copyright

A parameter and structure estimation technique for multivariable systems is used to obtain state space representation of open loop dynamics of the Space Shuttle Main Engine (SSME). The parameterization being used is both minimal and unique. The simplified linear models may be used for fault detection studies and control system design and development. Author

A92-20194* National Aeronautics and Space Administration. Lewis Research Center, Cleveland, OH.
NUMERICAL PROPULSION SYSTEM SIMULATION
 R. W. CLAUS, A. L. EVANS, J. K. LYLTE, and L. D. NICHOLS

(NASA, Lewis Research Center, Cleveland, OH) Computing Systems in Engineering (ISSN 0956-0521), vol. 2, no. 4, 1991, p. 357-364. 1991 8 p refs
 Copyright

The approach currently being developed at the NASA Lewis Research Center to address the issues of high-fidelity propulsion systems computational simulations is discussed. The approach focuses on interdisciplinary analysis, system simulation, simulation environment, and parallel computing. The Numerical Propulsion System Simulation is a long range program with the ultimate goal of developing the capability to reduce the cost and time of developing advanced technology propulsion systems. V.L.

A92-21062* Aerojet TechSystems Co., Sacramento, CA.
DESIGN AND TEST OF AN OXYGEN TURBOPUMP FOR A DUAL EXPANDER CYCLE ROCKET ENGINE
 P. S. BUCKMANN, N. R. SHRIMP, F. VITERI (Aerojet TechSystems, Sacramento, CA), and M. PROCTOR (NASA, Lewis Research Center, Cleveland, OH) Feb. 1992 7 p refs
 (Contract NAS3-23772)
 Copyright

A92-21087* National Aeronautics and Space Administration. Lewis Research Center, Cleveland, OH.
TECHNIQUES FOR SPECTROSCOPIC MEASUREMENTS IN AN ARCJET NOZZLE
 DIETER M. ZUBE and ROGER M. MYERS (NASA, Lewis Research Center, Cleveland, OH) Journal of Propulsion and Power (ISSN 0748-4658), vol. 8, Jan.-Feb. 1992, p. 254-256. Feb. 1992 3 p refs
 Copyright

A successful attempt has been made to gain optical access to the inside of an arcjet nozzle without changing internal thruster design or affecting performance characteristics. Both fiber optics and small open holes have been used for emission spectroscopy of a small, confined, high-temperature plasma source. The plasma was found to be in a highly nonequilibrium state, with electron excitation temperatures more than double the rotational or vibrational temperatures. O.C.

A92-23695* National Aeronautics and Space Administration. Lewis Research Center, Cleveland, OH.
LDEXPT, AN INTELLIGENT DATABASE SYSTEM FOR THE COMPOSITE LOAD SPECTRA PROJECT
 H. HO, J. F. NEWELL (Rockwell International Corp., Rocketdyne Div., Canoga Park, CA), D. HOPKINS, and C. C. CHAMIS (NASA, Lewis Research Center, Cleveland, OH) IN: i-SAIRAS '90; Proceedings of the International Symposium on Artificial Intelligence, Robotics and Automation in Space, Kobe, Japan, Nov. 18-20, 1990 4 p refs

The Composite Load Spectra project develops probabilistic models to simulate the probabilistic loads for selected components of a generic space propulsion system. Tremendous information such as engine load variables and their distributions is needed by the simulation program. An intelligent data base system was constructed and integrated with the probabilistic load simulation program to manage and maintain the knowledge base of the Composite Load Spectra project. The intelligent data base system takes care of the data retrieval and storage functions and has expert knowledge on engine load models and associated engine variables. The integration of the intelligent data base into the load simulation program achieves a smooth coupling between the numeric processing (load simulation calculation) and the symbolic processing (intelligent load information management). Author

A92-26985*# National Aeronautics and Space Administration. Lewis Research Center, Cleveland, OH.
ARCING OF NEGATIVELY BIASED SOLAR CELLS IN LOW EARTH ORBIT
 B. L. UPSCHULTE, G. M. WEYL, W. J. MARINELLI (Physical Sciences, Inc., Andover, MA), E. AIFER (Boston University, MA), and D. HASTINGS (MIT, Cambridge, MA) AIAA, Aerospace

20 SPACECRAFT PROPULSION AND POWER

Sciences Meeting and Exhibit, 30th, Reno, NV, Jan. 6-9, 1992. 8 p. Research supported by NASA. Jan. 1992 8 p refs (AIAA PAPER 92-0578) Copyright

A set of experiments is described in which the arcing of negatively biased solar cells is examined and characterized in terms of the primary factors that cause such behavior. The experiments are conducted in an ultrahigh vacuum chamber, and an image-intensified CCD camera is employed to monitor UV emission from arc events at the interfacial edge between the cover slip and the solar cell. A bead of encapsulant along the interfacial edge is noted which can be removed to reduce arc frequency, and water contamination is found to further enhance arcing. Frequency of arcing is found to vary indirectly with temperature and directly with exposure to H₂O, but no other significant correlations are noted. The sensitivity to H₂O vapor is eliminated by simply removing the adhesive/encapsulant, and the corresponding arc-rate performance is low. C.C.S.

A92-27045*# National Aeronautics and Space Administration. Lewis Research Center, Cleveland, OH.

LASER-INDUCED FLUORESCENCE OF ATOMIC HYDROGEN IN AN ARC-JET THRUSTER

JOHN G. LIEBESKIND, RONALD K. HANSON, and MARK A. CAPPELLI (Stanford University, CA) AIAA, Aerospace Sciences Meeting and Exhibit, 30th, Reno, NV, Jan. 6-9, 1992. 11 p. Research supported by NASA and SDIO. Jan. 1992 11 p refs (AIAA PAPER 92-0678) Copyright

A diagnostic has been developed to measure gas kinetic temperature and velocity in a 1 kW hydrogen fueled arcjet thruster. The technique is based on laser-induced fluorescence of the Balmer alpha transition (656 nm) in atomic hydrogen. A narrowband CW ring dye laser scans the excitation spectrum, permitting accurate determination of the atomic line shape and position. The velocity is inferred from the Doppler shift of the transition while the temperature is obtained from the shape. Near the exit plane, measured axial velocity varies between 4 and 14 km/s; measured radial velocity varies from 0 to 4 km/s. Temperatures were measured in the range from 1000 K near the edge of the plume to 5000 K at the centerline. Relevant broadening mechanisms are discussed. Author

A92-28137* National Aeronautics and Space Administration. Lewis Research Center, Cleveland, OH.

FAULT DIAGNOSIS FOR THE SPACE SHUTTLE MAIN ENGINE
AHMET DUYAR (Florida Atlantic University, Boca Raton) and WALTER MERRILL (NASA, Lewis Research Center, Cleveland, OH) Journal of Guidance, Control, and Dynamics (ISSN 0731-5090), vol. 15, Mar.-Apr. 1992, p. 384-389. Apr. 1992 6 p refs
Copyright

A conceptual design of a model-based fault detection and diagnosis system is developed for the Space Shuttle main engine. The design approach consists of process modeling, residual generation, and fault detection and diagnosis. The engine is modeled using a discrete time, quasilinear state-space representation. Model parameters are determined by identification. Residuals generated from the model are used by a neural network to detect and diagnose engine component faults. Fault diagnosis is accomplished by training the neural network to recognize the pattern of the respective fault signatures. Preliminary results for a failed valve, generated using a full, nonlinear simulation of the engine, are presented. These results indicate that the developed approach can be used for fault detection and diagnosis. The results also show that the developed model is an accurate and reliable predictor of the highly nonlinear and very complex engine. Author

A92-29289* National Aeronautics and Space Administration. Lewis Research Center, Cleveland, OH.

A SIMPLIFIED DYNAMIC MODEL OF SPACE SHUTTLE MAIN ENGINE

AHMET DUYAR, VASFI ELDEM (Florida Atlantic University, Boca Raton), WALTER MERRILL, and TEN-HUEI GUO (NASA, Lewis

Research Center, Cleveland, OH) IN: 1991 American Control Conference, 10th, Boston, MA, June 26-28, 1991, Proceedings. Vol. 2 1991 6 p refs

Copyright

A simplified dynamic model is presented of the Space Shuttle Main Engine (SSME) dynamics valid within the range of operation of the engine. This model is obtained by linking the linearized point models obtained at 25 different operating points of SSME. The simplified model was developed for use with a model-based diagnostic scheme for failure detection and diagnostics studies, as well as control design purposes. Author

A92-29591*# National Aeronautics and Space Administration. Lewis Research Center, Cleveland, OH.

SELF-PRESSURIZATION OF A FLIGHTWEIGHT LIQUID HYDROGEN TANK - EFFECTS OF FILL LEVEL AT LOW WALL HEAT FLUX

N. T. VAN DRESAR (NASA, Lewis Research Center, Cleveland, OH), C. S. LIN (Analex Corp., Brook Park, OH), and M. M. HASAN (NASA, Lewis Research Center, Cleveland, OH) AIAA, Aerospace Sciences Meeting and Exhibit, 30th, Reno, NV, Jan. 6-9, 1992. 10 p. Previously announced in STAR as N92-18442. Jan. 1992 10 p refs (AIAA PAPER 92-0818) Copyright

Experimental results are presented for the self pressurization and thermal stratification of a 4.89 cu m liquid hydrogen storage tank subjected to low heat flux (2.0 and 3.5 W/sq m) in normal gravity. The test tank was representative of future spacecraft tankage, having a low mass to volume ratio and high performance multilayer thermal insulation. Tests were performed at fill levels of 29 and 49 pcts. (by volume) and complement previous tests at 83 pct. fill. As the heat flux increases, the pressure rise rate at each fill level exceeds the homogeneous rate by an increasing ratio. Herein, this ratio did not exceed a value of 2. The slowest pressure rise rate was observed for the 49 pct. fill level at both heat fluxes. This result is attributed to the oblate spheroidal tank geometry which introduces the variables of wetted wall area, liquid-vapor interfacial area, and ratio of side wall to bottom heating as a function of fill level or liquid depth. Initial tank thermal conditions were found to affect the initial pressure rise rate. Quasi steady pressure rise rates are independent of starting conditions. Author

A92-33299*# National Aeronautics and Space Administration. Lewis Research Center, Cleveland, OH.

DESIGN ISSUES FOR LUNAR IN SITU ALUMINUM/OXYGEN PROPELLANT ROCKET ENGINES

MICHAEL L. MEYER (NASA, Lewis Research Center, Cleveland, OH) AIAA, Aerospace Design Conference, Irvine, CA, Feb. 3-6, 1992. 20 p. Previously announced in STAR as N92-16023. Feb. 1992 20 p refs (AIAA PAPER 92-1185) Copyright

Design issues for lunar ascent and lunar descent rocket engines fueled by aluminum/oxygen propellant produced in situ at the lunar surface were evaluated. Key issues are discussed which impact the design of these rockets: aluminum combustion, throat erosion, and thrust chamber cooling. Four engine concepts are presented, and the impact of combustion performance, throat erosion and thrust chamber cooling on overall engine design are discussed. The advantages and disadvantages of each engine concept are presented. Author

A92-34343*# National Aeronautics and Space Administration. Lewis Research Center, Cleveland, OH.

A PROBABILISTIC APPROACH TO THE EVALUATION OF FATIGUE DAMAGE IN A SPACE PROPULSION SYSTEM INJECTOR ELEMENT

K. R. RAJAGOPAL, J. KEREMES, H. HO, and G. ORIENT (Rockwell International Corp., Rocketdyne Div., Canoga Park, CA) IN: AIAA/ASME/ASCE/AHS/ASC Structures, Structural Dynamics and Materials Conference, 33rd, Dallas, TX, Apr. 13-15, 1992, Technical Papers. Pt. 2 1992 15 p refs (AIAA PAPER 92-2413) Copyright

The fatigue damage of a space propulsion system component is computed using probabilistic structural analysis methods. The analysis takes into account the variations in static and dynamic loads, the uncertainty in structural damping, and the scatter in material fatigue resistance. The key elements of the probabilistic approach include: (1) a numerical engine model for describing the global component interface loads consistent with engine balance, (2) models for computing the local mode boundary conditions on the component, (3) a static structural analysis model that captures the strains at a damage critical location as a function of engine performance variables, (4) a finite element model for assessment of the random amplitude stress response due to random base and pressure excitations with uncertain power and correlation length, and (5) advanced first order reliability methods for computing the probabilities associated with the fatigue damage. O.G.

A92-38597# National Aeronautics and Space Administration, Washington, DC.

THE NASA-OAST EARTH-TO-ORBIT PROPULSION TECHNOLOGY PROGRAM - THE ACTION PLAN

W. J. D. ESCHER (NASA, Washington, DC), J. L. MOSES (NASA, Marshall Space Flight Center, Huntsville, AL), A. D. LIANG (NASA, Lewis Research Center, Cleveland, OH), and F. W. STEPHENSON (W.J. Schafer Associates, Inc., Chelmsford, MA) AIAA, Space Programs and Technologies Conference, Huntsville, AL, Mar. 24-27, 1992. 8 p. Mar. 1992 8 p refs (AIAA PAPER 92-1478) Copyright

The paper discusses the primary objective of the NASA-OAST earth-to-orbit (ETO) propulsion technology program, namely, to completely overhaul the nation's liquid rocket design and analysis capabilities which were found to be severely limited when used for the design and development of the Space Shuttle Main Engine (SSME). Meeting this objective is to provide a much sounder, very comprehensive technology base that will enable the cost-effective low-risk development, acquisition, and operation of high-performance, expendable, or reusable ETO propulsion systems. This in turn will enable the future development of space transportation system launch vehicles with greatly reduced life-cycle costs. Work is carried out in three major areas: combustion devices, turbomachinery, and controls and health management. P.D.

A92-38605# National Aeronautics and Space Administration, Lewis Research Center, Cleveland, OH.

A DYNAMIC ISOTOPE POWER SYSTEM FOR SPACE EXPLORATION INITIATIVE SURFACE TRANSPORT SYSTEMS

MARIBETH E. HUNT, RICHARD B. HARTY (Rockwell International Corp., Rocketdyne Div., Canoga Park, CA), and ROBERT CATALDO (NASA, Lewis Research Center, Cleveland, OH) AIAA, Space Programs and Technologies Conference, Huntsville, AL, Mar. 24-27, 1992. 9 p. Research sponsored by DOE and NASA. Mar. 1992 9 p refs (AIAA PAPER 92-1489) Copyright

The Dynamic Isotope Power System (DIPS) Demonstration Program, sponsored by the U.S. Department of Energy with support funding from NASA, is currently focused on the development of a standardized 2.5-kWe portable generator for multiple applications on the lunar or Martian surface. A variety of remote and mobile potential applications have been identified by NASA, including surface rovers for both short- and extended-duration missions, remote power to science packages, and backup to central base power. Recent work focused on refining the 2.5-kWe design and emphasizing the compatibility of the system with potential surface transport systems. Work included an evaluation of the design to ensure compatibility with the Martian atmosphere while imposing only a minor mass penalty on lunar operations. Additional work included a study performed to compare the DIPS with regenerative fuel cell systems for lunar mobile and remote power systems. Power requirements were reviewed and a modular system chosen for the comparison. Author

A92-38650*# National Aeronautics and Space Administration, Lewis Research Center, Cleveland, OH.

THE EVOLUTIONARY DEVELOPMENT OF HIGH SPECIFIC IMPULSE ELECTRIC THRUSTER TECHNOLOGY

JAMES S. SOVEY, JOHN A. HAMLEY, MICHAEL J. PATTERSON, VINCENT K. RAWLIN (NASA, Lewis Research Center, Cleveland, OH), and ROGER M. MYERS (Sverdrup Technology, Inc., Brook Park, OH) AIAA, Space Programs and Technologies Conference, Huntsville, AL, Mar. 24-27, 1992. 31 p. Mar. 1992 31 p refs (AIAA PAPER 92-1556) Copyright

Electric propulsion flight and technology demonstrations conducted in the USA, Europe, Japan, China, and USSR are reviewed with reference to the major flight qualified electric propulsion systems. These include resistojets, ion thrusters, ablative pulsed plasma thrusters, stationary plasma thrusters, pulsed magnetoplasmic thrusters, and arcjets. Evolutionary mission applications are presented for high specific impulse electric thruster systems. The current status of arcjet, ion, and magnetoplasmadynamic thrusters and their associated power processor technologies are summarized. V.L.

A92-38651# National Aeronautics and Space Administration, Washington, DC.

NASA PROGRAM PLANNING ON NUCLEAR ELECTRIC PROPULSION

GARY L. BENNETT (NASA, Washington, DC) and THOMAS J. MILLER (NASA, Lewis Research Center, Cleveland, OH) AIAA, Space Programs and Technologies Conference, Huntsville, AL, Mar. 24-27, 1992. 18 p. Mar. 1992 18 p refs (AIAA PAPER 92-1557) Copyright

As part of the focused technology planning for future NASA space science and exploration missions, NASA has initiated a focused technology program to develop the technologies for nuclear electric propulsion and nuclear thermal propulsion. Beginning in 1990, NASA began a series of interagency planning workshops and meetings to identify key technologies and program priorities for nuclear propulsion. The high-priority, near-term technologies that must be developed to make NEP operational for space exploration include scaling thrusters to higher power, developing high-temperature power processing units, and developing high power, low-mass, long-lived nuclear reactors. Author

A92-38652*# National Aeronautics and Space Administration, Lewis Research Center, Cleveland, OH.

SPACE REACTOR POWER SYSTEM PROGRAMS OVERVIEW

HARVEY S. BLOOMFIELD (NASA, Lewis Research Center, Cleveland, OH) AIAA, Space Programs and Technologies Conference, Huntsville, AL, Mar. 24-27, 1992. 11 p. Mar. 1992 11 p refs (AIAA PAPER 92-1558) Copyright

The present development history and current development status evaluation of space reactor power system technologies gives attention to subsystem and component readiness and performance, and assesses the technology data base available in each case. This data base characterization gives attention to the most compatible reactor-power conversion system combinations for prospective DOD and commercial missions, as well as NASA missions. Candidate systems for near, middle, and far term application are selected and prioritized on the basis of technical risk. The programs covered encompass SNAPs 1, 2, 8, and 10A, SNAP 50, and SP-100. O.C.

A92-40429* National Aeronautics and Space Administration, Lewis Research Center, Cleveland, OH.

BEAM POWER OPTIONS FOR THE MOON

E. H. FAY, M. STAVNES (Sverdrup Technology, Inc., Brook Park, OH), and R. C. CULL (NASA, Lewis Research Center, Cleveland, OH) IN: SPS 91 - Power from space; Proceedings of the 2nd International Symposium, Gif-sur-Yvette, France, Aug. 27-30, 1991 1991 10 p refs (Contract NAS3-25266)

A study to determine the feasibility of providing long-term

20 SPACECRAFT PROPULSION AND POWER

electrical power to the moon's surface by beaming power from satellites is reported. The model used to develop the reference designs are described, and the major system tradeoffs and reference design characteristics are discussed. The beam power masses and the lunar surface power system masses are compared. In some cases, the beam power system have a quarter of the mass of surface power systems, but the beam power satellites have large space structures that may present complex transportation, deployment, pointing, and control problems. C.D.

A92-41550* National Aeronautics and Space Administration. Lewis Research Center, Cleveland, OH.

SYSTEMS ANALYSIS OF ELECTRODYNAMIC TETHERS

R. I. SAMANTHA ROY, D. E. HASTINGS, and E. AHEDO (MIT, Cambridge, MA) *Journal of Spacecraft and Rockets* (ISSN 0022-4650), vol. 29, no. 3, May-June 1992, p. 415-424. Jun. 1992 10 p refs

(Contract NAG3-681)

Copyright

A dynamic simulation model is developed and employed in a new system study to investigate the performance of electrodynamic tethers, both as power generators and thrusters. The electron collection performance of a contactor and a bare wire tether, both separately and in combination, are compared and contrasted. The power and thrust generated by a bare wire tether is found to have a higher dependence on the geomagnetic and ionospheric fluctuations. However, depending on the performance of the contactor, the combination of a bare tether and contactor can substantially boost performance for power generation. As a pure thruster, the contactor tether is examined at constant current, voltage, thrust, and power. It is found that the best mode of operation is with constant power, with resulting power/thrust ratios better than those for ion or magnetoplasmadynamic engines. It is concluded that tethers offer greater potential than previously envisioned. Author

A92-42610* National Aeronautics and Space Administration. Lewis Research Center, Cleveland, OH.

FIBER OPTICS IN LIQUID PROPELLANT ROCKET ENGINE ENVIRONMENTS

R. DELCHER, D. DINNSEN, and S. BARKHOUDARIAN (Rockwell International Corp., Rocketdyne Div., Canoga Park, CA) IN: *Fiber optic systems for mobile platforms IV; Proceedings of the Meeting, San Jose, CA, Sept. 18, 1990* 1991 7 p refs

(Contract NAS3-25346)

Copyright

Fiber optics have recently been seen to offer several major benefits in liquid-fuel rocket engine applications. Fiber-optic sensors can provide measurements that cannot be made with conventional techniques. Fiber optics also can reduce harness weight, provide lightning immunity, and increase frequency response. This paper discusses the results of feasibility testing optical fibers in simulated liquid-fuel rocket engine environments. The environments included cryogenic and high temperatures, and high vibration levels. Author

A92-44507* National Aeronautics and Space Administration. Lewis Research Center, Cleveland, OH.

PULSED THRUST PROPELLANT REORIENTATION - CONCEPT AND MODELING

JOHN I. HOCHSTEIN (Memphis State University, TN), ALFREDO E. PATAG, T. P. KORAKIANITIS (Washington University, Saint Louis, MO), and DAVID J. CHATO (NASA, Lewis Research Center, Cleveland, OH) *Journal of Propulsion and Power* (ISSN 0748-4658), vol. 8, no. 4, July-Aug. 1992, p. 770-777. Aug. 1992 8 p refs

(Contract NAG3-578)

Copyright

The use of pulsed thrust to optimize the propellant reorientation process is proposed. The ECLIPSE code is used to study the performance of pulsed reorientation in small-scale and full-scale propellant tanks. A dimensional analysis of the process is performed and the resulting dimensionless groups are used to present and

correlate the computational predictions of reorientation performance. Based on the results obtained from this study, it is concluded that pulsed thrust reorientation seems to be a feasible technique for optimizing the propellant reorientation process across a wide range of spacecraft, for a variety of missions, for the entire duration of a mission, and with a minimum of hardware design and qualification. Author

A92-44509* National Aeronautics and Space Administration. Lewis Research Center, Cleveland, OH.

ADVANCED TUBE-BUNDLE ROCKET THRUST CHAMBERS

JOHN M. KAZAROFF (NASA, Lewis Research Center, Cleveland, OH) and ALBERT J. PAVLI (Sverdrup Technology, Inc., Brook Park, OH) Aug. 1992 6 p refs

Copyright

A92-45446* National Aeronautics and Space Administration. Lewis Research Center, Cleveland, OH.

ENERGY REQUIREMENTS FOR THE SPACE FRONTIER

HENRY W. BRANDHORST, JR. (NASA, Lewis Research Center, Cleveland, OH) IN: *International Pacific Air and Space Technology Conference and Aircraft Symposium, 29th, Gifu, Japan, Oct. 7-11, 1991, Proceedings 1991* 6 p refs

(SAE PAPER 912064) Copyright

The cost of delivering payloads to Mars orbital locations from LEO is determined and future launch cost reductions are projected. The performance necessary for future solar and nuclear space power options is predicted, categorizing the needs as survival, self-sufficiency, and industrialization. The cost of present space power systems is determined and projections are made for future systems. C.D.

A92-45447* National Aeronautics and Space Administration. Lewis Research Center, Cleveland, OH.

ELECTRICAL SYSTEM OPTIONS FOR SPACE EXPLORATION

ROBERT W. BERCAW and RONALD C. CULL (NASA, Lewis Research Center, Cleveland, OH) IN: *International Pacific Air and Space Technology Conference and Aircraft Symposium, 29th, Gifu, Japan, Oct. 7-11, 1991, Proceedings 1991* 10 p refs

(SAE PAPER 912065) Copyright

The need for a space power utility concept is discussed and the impact of this concept on the engineering of space power systems is examined. Experiences gained from Space Station Freedom and SEI systems studies are used to discuss the factors that may affect the choice of frequency standards on which to build such a space power utility. Emphasis is given to electrical power control, conditioning, and distribution subsystems. C.D.

A92-45448* National Aeronautics and Space Administration. Lewis Research Center, Cleveland, OH.

SMALL STIRLING DYNAMIC ISOTOPE POWER SYSTEM FOR MULTIHUNDRED-WATT ROBOTIC MISSIONS

DAVID J. BENTS (NASA, Lewis Research Center, Cleveland, OH) IN: *International Pacific Air and Space Technology Conference and Aircraft Symposium, 29th, Gifu, Japan, Oct. 7-11, 1991, Proceedings 1991* 14 p refs

(SAE PAPER 912066) Copyright

Free Piston Stirling Engine (FPSE) and linear alternator (LA) technology is combined with radioisotope heat sources to produce a compact dynamic isotope power system (DIPS) suitable for multihundred watt space application which appears competitive with advanced radioisotope thermoelectric generators (RTGs). The small Stirling DIPS is scalable to multihundred watt power levels or lower. The FPSE/LA is a high efficiency convertor in sizes ranging from tens of kilowatts down to only a few watts. At multihundred watt unit size, the FPSE can be directly integrated with the General Purpose Heat Source (GPHS) via radiative coupling; the resulting dynamic isotope power system has a size and weight that compares favorably with the advanced modular (Mod) RTG, but requires less than a third the amount of isotope fuel. Thus the FPSE extends the high efficiency advantage of dynamic systems into a power range never previously considered

competitive for DIPS. This results in lower fuel cost and reduced radiological hazard per delivered electrical watt. Author

A92-46049* National Aeronautics and Space Administration. Lewis Research Center, Cleveland, OH.

MICROWAVE ELECTROTHERMAL PROPULSION FOR SPACE
JOHN L. POWER (NASA, Lewis Research Center, Cleveland, OH) IEEE Transactions on Microwave Theory and Techniques (ISSN 0018-9480), vol. 40, no. 6, June 1992, p. 1179-1191. Jun. 1992 13 p refs

Copyright

The microwave electrothermal thruster (MET) concept for medium or high-power spacecraft propulsion is described. The MET employs continuous wave microwave energy to create and maintain a plasma discharge in a flowing propellant gas. The discharge then acts to absorb the applied microwave energy and transform it into thermal and internal energy of the propellant. Expansion and expulsion of the hot propellant through a throat and nozzle finally converts the energy of the gas into thrust. The MET concept is electrodeless, synergistically combines high pressure and high power capability, provides external control over the energy-conversion discharge, and operates on hydrogen propellant. The potential performance of the MET on hydrogen propellant has been modeled with a two-dimensional kinetics computer code. The MET concept is particularly suitable for use with a magnetic nozzle. Apparatus is described for testing the resonant-cavity MET to power levels of 30 kW at 915 MHz on nitrogen, helium, and hydrogen. The low-ripple operation of the microwave generator has been verified, as has a procedure for starting the microwave discharge and raising the power applied to the cavity via a phase shifter-tuner. S.A.V.

A92-47000* # National Aeronautics and Space Administration. Lewis Research Center, Cleveland, OH.

ARCING OF NEGATIVELY BIASED SOLAR CELLS IN A PLASMA ENVIRONMENT. I - EXPERIMENTAL OBSERVATIONS
B. L. UPSCHULTE, W. J. MARINELLI, G. WEYL, K. L. CARLETON (Physical Sciences, Inc., Andover, MA), and E. AIFER (Boston University, MA) AIAA, Plasmadynamics and Lasers Conference, 23rd, Nashville, TN, July 6-8, 1992. 16 p. Jul. 1992 16 p refs (Contract NAS3-25797) (AIAA PAPER 92-2990) Copyright

A variety of experiments have been performed which identify key factors contributing to the arcing of negatively biased high voltage solar cells operating in a low earth orbit plasma environment. These efforts have led to a reduction of greater than a factor of 100 in the arc frequency of a single cells following proper remediation procedures. Experiments naturally led to and focused on the adhesive/encapsulating that is used to bond the protective cover slip to the solar cell. An image-intensified CCD camera system recorded UV emission from arc events which occurred exclusively along the interfacial edge between the cover slip and the solar cell. Microscopic inspection of this interfacial region showed a bead of encapsulant along this entire edge. Elimination of this encapsulant bead reduced the arc frequency by two orders of magnitude. Author

A92-47027* # National Aeronautics and Space Administration. Lewis Research Center, Cleveland, OH.

SPACE POWER BY GROUND-BASED LASER TRANSMISSION
GEOFFREY A. LANDIS (Sverdrup Technology, Inc.; NASA, Lewis Research Center, Cleveland, OH) AIAA, Plasmadynamics and Lasers Conference, 23rd, Nashville, TN, July 6-8, 1992. 8 p. Jul. 1992 8 p refs (Contract NAS3-25266) (AIAA PAPER 92-3024) Copyright

A new method for providing power to space vehicles consists of using high-power CW lasers on the ground to beam power to photovoltaic receivers in space. Such large lasers could be located at cloud-free sites at one or more ground locations, and use large mirrors with adaptive optical correction to reduce the beam spread due to diffraction or atmospheric turbulence. This can result in lower requirements for battery storage, due to continuous

illumination of arrays even during periods of shadow by the earth, and higher power output, due to the higher efficiency of photovoltaic arrays under laser illumination compared to solar and the ability to achieve higher intensities of illumination. Applications include providing power for satellites during eclipse, providing power to resurrect satellites which are failing due to solar array degradation, powering orbital transfer vehicles or lunar transfer shuttles, and providing night power to a solar array on the moon. Author

A92-48385* National Aeronautics and Space Administration. Lewis Research Center, Cleveland, OH.

NUCLEAR THERMAL ROCKETS - KEY TO MOON-MARS EXPLORATION

STANLEY K. BOROWSKI, JOHN S. CLARK (NASA, Lewis Research Center, Cleveland, OH), MELVIN C. MCILWAIN (Aerojet, Propulsion Div., Sacramento, CA), and DENNIS G. PELACCIO (Science Applications International Corp., Torrance, CA) Aerospace America (ISSN 0740-722X), vol. 30, no. 7, July 1992, p. 34-37, 48. Jul. 1992 5 p

Copyright

The Space Exploration Initiative (SEI) calls for lunar and Martian exploration missions for which solid-core nuclear thermal rockets (NTRs), in virtue of their single-stage, fully-reusable nature, are ideally suited. NTRs promise double the specific impulse of chemical propulsion. A lunar mission employing a reusable NTR is currently being conducted by NASA. The NTR would be assembled in LEO in such a way that it remained 'radioactively cold' during earth-to-orbit deployment by a heavy-lift chemical booster, and therefore presented no radioactive hazard. Also under consideration is a particle-bed reactor in which the hydrogen propulsive fluid directly cools coated-particle fuel spheres. O.C.

A92-48386 National Aeronautics and Space Administration, Washington, DC.

ELECTRIC PROPULSION - THE FUTURE IS NOW

PETER J. TURCHI (Ohio State University, Columbus), FRANCIS M. CURRAN (NASA, Washington, DC), J. C. ANDREWS (USAF, Phillips Laboratory, Edwards AFB, CA), JOHN R. BEATTLE (Hughes Research Laboratories, Malibu, CA), and JAMES GILLAND (Sverdrup Technology, Inc.; NASA, Lewis Research Center, Cleveland, OH) Aerospace America (ISSN 0740-722X), vol. 30, no. 7, July 1992, p. 38-41, 49. Jul. 1992 5 p

Copyright

A comprehensive development status evaluation is presented for the field of electric propulsion. Specific impulses range from 500-800 sec for satellite stationkeeping and 800-1500 sec for earth-earth orbit-raising maneuvers to 2000-5000 sec for trajectories to Mars and as much as 5000-100,000 sec for trajectories to more distant destinations. The successful deployment of low-power arcjet systems for auxiliary propulsion has been critical to the development of designs for higher-performance devices. O.C.

A92-48719* # National Aeronautics and Space Administration. Lewis Research Center, Cleveland, OH.

HYDROGEN NO-VENT TESTING IN A 5 CUBIC FOOT (142 LITER) TANK USING SPRAY NOZZLE AND SPRAY BAR LIQUID INJECTION

MATTHEW E. MORAN and TED W. NYLAND (NASA, Lewis Research Center, Cleveland, OH) AIAA, SAE, ASME, and ASEE, Joint Propulsion Conference and Exhibit, 28th, Nashville, TN, July 6-8, 1992. 10 p. Previously announced in STAR as N92-28433. Jul. 1992 10 p refs (AIAA PAPER 92-3063) Copyright

A total of 38 hydrogen no-vent fill tests were performed in this test series using various size spray nozzles and a spray bar with different hole sizes in a 5 cubic foot receiver tank. Fill levels of 90 percent by volume or greater were achieved in 26 of the tests while maintaining a receiver tank pressure below 30 psia. Spray nozzles were mounted at the top of the tank, whereas, the spray bar was centered in the tank axially. The spray nozzle no-vent fills demonstrated tank pressure and temperature responses comparable to previous test series. Receiver tank pressure

20 SPACECRAFT PROPULSION AND POWER

responses for the spray bar configuration were similar to the spray nozzle tests with the pressure initially rising rapidly, then leveling off as vapor condenses onto the discharging liquid streams, and finally ramping up near the end of the test due to ullage compression. Both liquid injection techniques tested were capable of filling the receiver tank to 90 percent under variable test conditions. Comparisons between the spray nozzle and spray bar configurations for well matched test conditions indicate the spray nozzle injection technique is more effective in minimizing the receiving tank pressure throughout a no-vent fill compared to the spray bar under normal gravity conditions. Author

A92-48748# National Aeronautics and Space Administration. Lewis Research Center, Cleveland, OH.

MEASUREMENT AND ANALYSIS OF A SMALL NOZZLE PLUME IN VACUUM

PAUL F. PENKO (NASA, Lewis Research Center, Cleveland, OH), I. D. BOYD (Eloret Institute; NASA, Ames Research Center, Moffett Field, CA), D. L. MEISSNER, and KENNETH J. DE WITT (Toledo, University, OH) AIAA, SAE, ASME, and ASEE, Joint Propulsion Conference and Exhibit, 28th, Nashville, TN, July 6-8, 1992. 17 p. Jul. 1992 17 p refs (AIAA PAPER 92-3108) Copyright

Measurements of Pitot pressure and flow angle were made in the plume of a nozzle flowing nitrogen and exhausting to a vacuum. The measurements were compared to results from a numerical simulation of the flow that was based on kinetic theory and used the direct-simulation Monte Carlo (DSMC) method. Numerical results were compared with measurements made in the plume at various axial and radial stations. Total pressure measurements were made with Pitot tubes sized for specific regions of the plume. Flow angle measurements were made with a conical probe. The measurement area for flow angle extended to 160 mm (5 exit diameters) downstream of the nozzle exit plane and radially to 60 mm (1.9 exit diameters) from the plume axis. The total pressure measurements extended 480 mm (16 exit diameters) downstream and radially to 60 mm. Comparisons of computed results from the DSMC method with measurements of flow angle displayed improved agreement with increasing distance from the exit plane. Pitot pressures computed from the DSMC method were in reasonably good agreement with experimental results over the entire measurement area. Author

A92-48750*# National Aeronautics and Space Administration. Lewis Research Center, Cleveland, OH.

THEORETICAL NOZZLE PERFORMANCE OF A MICROWAVE ELECTROTHERMAL THRUSTER USING EXPERIMENTAL DATA

SCOTT S. HARABURDA (U.S. Military Academy, West Point, NY) and MARTIN C. HAWLEY (Michigan State University, East Lansing) AIAA, SAE, ASME, and ASEE, Joint Propulsion Conference and Exhibit, 28th, Nashville, TN, July 6-8, 1992. 11 p. Jul. 1992 11 p refs (Contract NSG-3299) (AIAA PAPER 92-3110)

Research aimed at developing a fundamental understanding of the plasma processes as applied to spacecraft propulsion is presented. Calorimetric, photographic, and spectrophotometric measurements based on the TM011 and TM012 modes in the resonance cavity have been performed. The efficiency of a thruster has been calculated using a theoretical model for predicting temperature, velocity, and species density within the propellant. It is concluded that the microwave electrothermal thruster is a viable alternative to electrode thrusters. O.G.

A92-48752*# National Aeronautics and Space Administration. Lewis Research Center, Cleveland, OH.

PRELIMINARY INVESTIGATION OF A LOW POWER PULSED ARCJET THRUSTER

RUSSELL D. TAYLOR, RODNEY L. BURTON, and KYLE K. WETZEL (Illinois, University, Urbana) AIAA, SAE, ASME, and ASEE, Joint Propulsion Conference and Exhibit, 28th, Nashville,

TN, July 6-8, 1992. 16 p. Research supported by University of Illinois and NASA. Jul. 1992 16 p refs (AIAA PAPER 92-3113) Copyright

A type of pulsed arcjet is examined which operates with gaseous helium propellant at powers from 100 to 1500 W and pulse rates from 360 to 6000 pulses per second. During the pulse, peak power is 50 to 250 kW generating chamber pressures of 10 to 50 atmospheres. The high operating pressure substantially reduces ionization in the 2.5 mm diameter x 12.5 mm long capillary and lowers frozen flow losses in the nozzle. The thruster thermal efficiency, measured calorimetrically, is 43 percent at 440 W and 8 mg/sec helium mass flow rate. Thruster performance trends are predicted by a time-dependent lumped-parameter model which includes heat exchange between the propellant and the wall. The model substantially underpredicts the experimental thermal efficiency values. Alternative thruster configurations yielding significant improvements in thrust efficiency and specific impulse are discussed. Author

A92-48772*# National Aeronautics and Space Administration. Lewis Research Center, Cleveland, OH.

KRYPTON ION THRUSTER PERFORMANCE

MICHAEL J. PATTERSON (NASA, Lewis Research Center, Cleveland, OH) and GEORGE J. WILLIAMS, JR. (Auburn University, AL) AIAA, SAE, ASME, and ASEE, Joint Propulsion Conference and Exhibit, 28th, Nashville, TN, July 6-8, 1992. 12 p. Jul. 1992 12 p refs (AIAA PAPER 92-3144) Copyright

Preliminary data were obtained from a 30 cm ion thruster operating on krypton propellant over the input power range of 0.4-5.5 kW. The data are presented, and compared and contrasted to those obtained with xenon propellant over the same input power envelope. Typical krypton thruster efficiency was 70 percent at a specific impulse of approximately 5000 s, with a maximum demonstrated thrust-to-power ratio of approximately 42 mN/kW at 2090 s specific impulse and 1580 watts input power. Critical thruster performance and component lifetime issues were evaluated. Order-of-magnitude power throttling was demonstrated using a simplified power-throttling strategy. Author

A92-48776*# National Aeronautics and Space Administration. Lewis Research Center, Cleveland, OH.

PRELIMINARY TESTS OF ANNULAR ION OPTICS

GRAEME ASTON, MARTHA B. ASTON, and JAMES B. KOLTS (Electric Propulsion Laboratory, Inc., Tehachapi, CA) AIAA, SAE, ASME, and ASEE, Joint Propulsion Conference and Exhibit, 28th, Nashville, TN, July 6-8, 1992. 7 p. Research sponsored by SDIO. Jul. 1992 7 p refs (Contract NAS3-25623) (AIAA PAPER 92-3148) Copyright

The analyses and fabrication techniques used to develop a prototype 50-cm annular ion engine optics are described. Based on a finite element analysis of several different electrode geometries, the prototype ion optics was fabricated in the shape of a half torus dished into the annular discharge chamber. Results of thermal/mechanical characterization during extensive thermal cycle testing of the prototype ion optics are presented, together with results of initial beam extraction tests performed using Xe propellant. I.S.

A92-48780*# National Aeronautics and Space Administration. Lewis Research Center, Cleveland, OH.

AN EXPERIMENTAL INVESTIGATION OF HIGH-ASPECT-RATIO COOLING PASSAGES

JULIE A. CARLILE (NASA, Lewis Research Center, Cleveland, OH) and RICHARD J. QUENTMEYER (Sverdrup Technology, Inc., Brook Park; NASA, Lewis Research Center, Cleveland, OH) AIAA, SAE, ASME, and ASEE, Joint Propulsion Conference and Exhibit, 28th, Nashville, TN, July 6-8, 1992. 12 p. Previously announced in STAR as N92-25958. Jul. 1992 12 p refs (AIAA PAPER 92-3154) Copyright

An experimental investigation was conducted to evaluate the effectiveness of using high-aspect-ratio cooling passages to

improve the life and reduce the coolant pressure drop in high-pressure rocket thrust chambers. A plug-nozzle rocket-engine test apparatus was used to test two cylindrical chambers with low-aspect-ratio cooling passages and one with high-aspect-ratio cooling passages. The chambers were cyclically tested and data were taken over a wide range of coolant mass flows. The results showed that for the same coolant pressure drop, the hot-gas-side wall temperature of the high-aspect-ratio chamber was 30 percent lower than the baseline low-aspect-ratio chamber, resulting in no fatigue damage to the wall. The coolant pressure drop for the high-aspect-ratio chamber was reduced in increments to one-half that of the baseline chamber, by reducing the coolant mass flow, and still resulted in a reduction in the hot-gas-side wall temperature when compared to the low-aspect-ratio chambers. Author

A92-48784*# National Aeronautics and Space Administration. Lewis Research Center, Cleveland, OH.

QUALITATIVE SPECTROSCOPIC STUDY OF MAGNETIC NOZZLE FLOW

T. UMEKI and P. J. TURCHI (Ohio State University, Columbus) AIAA, SAE, ASME, and ASEE, Joint Propulsion Conference and Exhibit, 28th, Nashville, TN, July 6-8, 1992. 8 p. Jul. 1992 8 p refs

(Contract NAS3-843) (AIAA PAPER 92-3161) Copyright

The physics of the magnetic nozzle flow for a 100-kW-level quasi-steady MPD thruster was studied by photographic spectroscopy focusing on the plasma model in the flow and the acceleration mechanism. Spectroscopic visualization for the flow-species analysis indicates that the plasma-exhaust flow dominated by NII species were confined by the magnetic nozzle effect to collimate the flow for the better thruster performance. Inside the nozzle, the plasma flow was found to be in nonhomogeneous collisional-radiative condition. There appears to be a substantial flow acceleration from the magnetic nozzle inlet to the outlet with slight expansion. This suggests that the flow resembles that of constant area supersonic duct flow with cooling. Author

A92-48785*# National Aeronautics and Space Administration. Lewis Research Center, Cleveland, OH.

AN ADVANCED INTELLIGENT CONTROL SYSTEM FRAMEWORK

ED NEMETH, RONALD R. ANDERSON, JON MARAM, ARNIE NORMAN (Rockwell International Corp., Rocketdyne Div., Los Angeles, CA), and WALT MERRILL (NASA, Lewis Research Center, Cleveland, OH) AIAA, SAE, ASME, and ASEE, Joint Propulsion Conference and Exhibit, 28th, Nashville, TN, July 6-8, 1992. 13 p. Jul. 1992 13 p refs

(AIAA PAPER 92-3162) Copyright

A reusable rocket-engine intelligent control system (RREICS) framework was developed to a define a control framework for rocket-engine systems that reduces the required engine maintenance, extends the useful operating life, and maximizes the probability of mission success. The RREICS framework defines a controller that handles a rocket engine cluster as a single system rather than as a collection of individual engines. This enables the controller to alter individual engine operations in response to engine performance or integrity degradations while maintaining the propulsion subsystem external parameters at the levels required for mission success. A simplified model of a three engine cluster and the associated propulsion subsystem controller is also described. Author

A92-48787*# National Aeronautics and Space Administration. Lewis Research Center, Cleveland, OH.

ROCKET ENGINE DIAGNOSTICS USING QUALITATIVE MODELING TECHNIQUES

MICHAEL BINDER, WILLIAM MAUL, CLAUDIA MEYER (Sverdrup Technology, Inc., Brook Park; NASA, Lewis Research Center, Cleveland, OH), and AMY SOVIE (NASA, Lewis Research Center, Cleveland, OH) AIAA, SAE, ASME, and ASEE, Joint Propulsion Conference and Exhibit, 28th, Nashville, TN, July 6-8, 1992. 15 p.

Previously announced in STAR as N92-27033. Jul. 1992 15 p refs

(Contract NAS3-25266) (AIAA PAPER 92-3164) Copyright

Researchers at NASA Lewis Research Center are presently developing qualitative modeling techniques for automated rocket engine diagnostics. A qualitative model of a turbopump interpellant seal system has been created. The qualitative model describes the effects of seal failures on the system steady-state behavior. This model is able to diagnose the failure of particular seals in the system based on anomalous temperature and pressure values. The anomalous values input to the qualitative model are generated using numerical simulations. Diagnostic test cases include both single and multiple seal failures. Author

A92-48808*# National Aeronautics and Space Administration. Lewis Research Center, Cleveland, OH.

EARLY TRACK NEP SYSTEM OPTIONS FOR SEI MISSIONS

J. H. GILLAND (Sverdrup Technology, Inc., Brook Park; NASA, Lewis Research Center, Cleveland, OH) and J. A. GEORGE (NASA, Lewis Research Center, Cleveland, OH) AIAA, SAE, ASME, and ASEE, Joint Propulsion Conference and Exhibit, 28th, Nashville, TN, July 6-8, 1992. 10 p. Jul. 1992 10 p refs

(AIAA PAPER 92-3200) Copyright

A development option for nuclear electric propulsion, the 'Early Track' option, is considered from system and mission application viewpoints. The intent of this development option is to address demanding missions of the future, such as robotic outer planet exploration or the Space Exploration Initiative. The 'Early Track' scheme utilizes existing technologies, such as the SP-100 space reactor and radiator components, as well as subsystems scalable from existing programs, such as 50 to 100 kWe ion thrusters. Up to 1.5 MWe of powder can be generated by the existing 2.4 MWt SP-100 reactor through the use of dynamic Rankine or Brayton power conversion. The performance characteristics of these systems are projected, and assessed for SEI missions currently under consideration. Author

A92-48811*# National Aeronautics and Space Administration. Lewis Research Center, Cleveland, OH.

EXTENDED TESTING OF XENON ION THRUSTER HOLLOW CATHODES

TIMOTHY R. SARVER-VERHEY (Sverdrup Technology, Inc., Brook Park; NASA, Lewis Research Center, Cleveland, OH) AIAA, SAE, ASME, and ASEE, Joint Propulsion Conference and Exhibit, 28th, Nashville, TN, July 6-8, 1992. 25 p. Jul. 1992 25 p refs

(AIAA PAPER 92-3204)

A hollow cathode wear-test of 508 hours was successfully completed at an emission current of 23.0 A and a xenon flow rate of 10 Pa-L/s. This test was the continuation of a hollow cathode contamination investigation. Discharge voltage was stable at 16.7 V. The cathode temperature averaged 1050 C with a 7 percent drop during the wear-test. Discharge ignition voltage was found to be approximately 20 V and was repeatable over four starts. Post-test analyses of the hollow cathode found a much improved internal cathode condition with respect to earlier wear-test cathodes. Negligible tungsten movement occurred and no formation of mono-barium tungstate was observed. These results correlated with an order-of-magnitude reduction in propellant feed-system leakage rate. Ba₂CaWO₆ and extensive calcium crystal formation occurred on the upstream end of the insert. Ba-Ca compound depositions were found on the Mo insert collar, on the Re electrical leads, and in the gap between the insert and cathode wall. This wear-test cathode was found to be in the best internal condition and had the most stable operating performance of any hollow cathode tested during this contamination investigation. Author

A92-48827*# National Aeronautics and Space Administration. Lewis Research Center, Cleveland, OH.

EFFECT OF MODEL SELECTION ON COMBUSTOR PERFORMANCE AND STABILITY USING ROCCID

JAMES E. GIULIANI (Ohio Aerospace Institute, Brook Park) and MARK D. KLEM (NASA, Lewis Research Center, Cleveland, OH)

20 SPACECRAFT PROPULSION AND POWER

AIAA, SAE, ASME, and ASEE, Joint Propulsion Conference and Exhibit, 28th, Nashville, TN, July 6-8, 1992. 15 p. Previously announced in STAR as N92-27036. Jul. 1992 15 p refs (AIAA PAPER 92-3226) Copyright

The ROCKET Combustor Interactive Design (ROCCID) methodology is an interactive computer program that combines previously developed combustion analysis models to calculate the combustion performance and stability of liquid rocket engines. Test data from a 213 kN (48,000 lbf) Liquid Oxygen (LOX)/RP-1 combustor with a O-F-O (oxidizer-fuel-oxidizer) triplet injector were used to characterize the predictive capabilities of the ROCCID analysis models for this injector/propellant configuration. Thirteen combustion performance and stability models have been incorporated into ROCCID, and ten of them, which have options for triplet injectors, were examined in this study. Calculations using different combinations of analysis models, with little or no anchoring, were carried out on a test matrix of operating conditions matching those of the test program. Results of the computer analyses were compared to test data, and the ability of the model combinations to correctly predict combustion stability or instability was determined. For the best model combination(s), sensitivity of the calculations to fuel drop size and mixing efficiency was examined. Error in the stability calculations due to uncertainty in the pressure interaction index (N) was examined. The recommended model combinations for this O-F-O triplet LOX/RP-1 configuration are proposed. Author

A92-48829*# National Aeronautics and Space Administration. Lewis Research Center, Cleveland, OH.

3D ROCKET COMBUSTOR ACOUSTICS MODEL

RICHARD J. PRIEM (Priem Consultants, Inc., Cleveland, OH) and KEVIN J. BREISACHER (NASA, Lewis Research Center, Cleveland, OH) AIAA, SAE, ASME, and ASEE, Joint Propulsion Conference and Exhibit, 28th, Nashville, TN, July 6-8, 1992. 12 p. Previously announced in STAR as N92-27035. Jul. 1992 12 p refs (AIAA PAPER 92-3228) Copyright

The theory and procedures for determining the characteristics of pressure oscillations in rocket engines with prescribed burning rate oscillations are presented. Analyses including radial and hub baffles and absorbers can be performed in one, two, or three dimensions. Pressure and velocity oscillations calculated using this procedure are presented for the SSME to show the influence of baffles and absorbers on the burning rate oscillations required to achieve neutral stability. Comparisons are made between the results obtained utilizing 1D, 2D, and 3D assumption with regards to capturing the physical phenomena of interest and computational requirements. Author

A92-48928*# National Aeronautics and Space Administration. Lewis Research Center, Cleveland, OH.

ROCKET PLUME FLOWFIELD CHARACTERIZATION USING LASER RAYLEIGH SCATTERING

FRANK J. ZUPANC (NASA, Lewis Research Center, Cleveland, OH) and JONATHAN M. WEISS (Pennsylvania State University, University Park) AIAA, SAE, ASME, and ASEE, Joint Propulsion Conference and Exhibit, 28th, Nashville, TN, July 6-8, 1992. 19 p. Previously announced in STAR as N92-28475. Jul. 1992 19 p refs

(AIAA PAPER 92-3351) Copyright

A Doppler-resolved laser Rayleigh scattering diagnostic was applied to a 111 N thrust, regenerative and fuel-film cooled, gaseous hydrogen/gaseous oxygen rocket engine. The axial and radial mean gas velocities were measured from the net Doppler shifts observed for two different scattering angles. Translational temperatures and number densities were estimated from the Doppler widths and scattered intensities, respectively, by assuming that water was the dominant scattering species in the exhaust. The experimental results are compared with theoretical predictions from a full Navier-Stokes code (RD/RPLUS) and the JANNAF Two-Dimensional Kinetics (TDK) and Standardized Plume Flowfield (SPF-II) codes. Discrepancies between the measured and predicted axial velocities, temperatures, and number densities are evident. Radial velocity measurements, however, show excellent agreement

with predictions. The discrepancies are attributed primarily to inefficient mixing and combustion caused by the injection of excessive oxidizer along one side of the thrust chamber. Thrust and mass flow rate estimates obtained from the Rayleigh measurements show excellent agreement with the globally measured values. Author

A92-48980*# National Aeronautics and Space Administration. Lewis Research Center, Cleveland, OH.

ROCKET ENGINE PROPULSION 'SYSTEM RELIABILITY'

K. J. O'HARA AIAA, SAE, ASME, and ASEE, Joint Propulsion Conference and Exhibit, 28th, Nashville, TN, July 6-8, 1992. 11 p. Research supported by NASA. Jul. 1992 11 p refs (AIAA PAPER 92-3421) Copyright

A system reliability approach is discussed which is based on a quantitative assessment of both the engine system and hardware reliability during the design process. The approach makes it possible to evaluate design trades as the design matures. It is concluded that the system reliability assessment approach offers the following benefits. The uncertainty of each design variable is explicitly considered in the analysis process. The most significant design variables are ranked in order of their effect on reliability. Design trades can be assessed for reliability impact. It is concluded that the approach facilitates communication between disciplines and thus aids in concurrent engineering. O.G.

A92-49001*# National Aeronautics and Space Administration. Lewis Research Center, Cleveland, OH.

PROPULSION SYSTEMS USING IN SITU PROPELLANTS FOR A MARS ASCENT VEHICLE

MARY F. WADEL and ELIZABETH A. RONCACE (NASA, Lewis Research Center, Cleveland, OH) AIAA, SAE, ASME, and ASEE, Joint Propulsion Conference and Exhibit, 28th, Nashville, TN, July 6-8, 1992. 11 p. Previously announced in STAR as N92-27654. Jul. 1992 11 p refs (AIAA PAPER 92-3445) Copyright

The indigenous propellants of oxygen and carbon monoxide were studied for use in a Mars Ascent Vehicle (MAV). Both the oxygen and carbon monoxide were evaluated as turbine working fluids for a full expander engine cycle used in the MAV. Two oxygen working fluid engines and four carbon monoxide engines were investigated. The maximum hot-gas-side wall temperature was limited to either 445 K (800R) or 556 K (1000 R) over a range of working fluid mass flows. An engine thrust of 44.5 kN (1,000 lb(sub f)) was assumed. The engine characteristics of coolant inlet pressure, total engine length, specific impulse, pump efficiencies, and turbine power required were optimized. Of the six engines evaluated, the study showed that either type of working fluid was feasible for a MAV engine. Using carbon monoxide as the working fluid resulted in the best engine characteristics. Author

A92-49069*# National Aeronautics and Space Administration. Lewis Research Center, Cleveland, OH.

DESIGN CONSIDERATIONS IN CLUSTERING NUCLEAR ROCKET ENGINES

PAUL H. SAGER (General Dynamics Corp., Space Systems Div., San Diego, CA) AIAA, SAE, ASME, and ASEE, Joint Propulsion Conference and Exhibit, 28th, Nashville, TN, July 6-8, 1992. 8 p. Jul. 1992 8 p refs (Contract NAS3-25972) (AIAA PAPER 92-3587) Copyright

An initial investigation of the design considerations in clustering nuclear rocket engines for space transfer vehicles has been made. The clustering of both propulsion modules (which include start tanks) and nuclear rocket engines installed directly to a vehicle core tank appears to be feasible. Special provisions to shield opposite run tanks and the opposite side of a core tank - in the case of the boost pump concept - are required; the installation of a circumferential reactor side shield sector appears to provide an effective solution to this problem. While the time response to an engine-out event does not appear to be critical, the gimbal displacement required appears to be important. Since an installation

of three engines offers a substantial reduction in gimbal requirements for engine-out and it may be possible to further enhance mission reliability with the greater number of engines, it is recommended that a cluster of four engines be considered.

Author

A92-49127# National Aeronautics and Space Administration. Lewis Research Center, Cleveland, OH.

TEST EXPERIENCE, 490 N HIGH PERFORMANCE (321 SEC ISP) ENGINE

L. SCHOENMAN, S. D. ROSENBERG, and D. M. JASSOWSKI (Aerojet, Propulsion Div., Sacramento, CA) AIAA, SAE, ASME, and ASEE, Joint Propulsion Conference and Exhibit, 28th, Nashville, TN, July 6-8, 1992. 8 p. Jul. 1992 8 p refs (Contract NAS3-24643; NAS3-25646; JPL-957882) (AIAA PAPER 92-3800) Copyright

Engines with area ratios of 44:1 and 286:1 are tested by means of hot fire tests using the NTO/MMH bipropellant to maximize the performance of the combined technologies. The low-thrust engine systems are designed with oxidation resistant materials that can operate at temperatures of more than 2204 C for tens of hours. The chamber is attached to the injector in a configuration that prevents overheating of the injector, valve, and the spacecraft interface. Three injectors with 44:1 area ratios are capable of nominal specific impulse values of 309 sec, and a performance of 321 lbf-sec/lbm is noted for an all-welded engine assembly with area ratio of 286:1. The all-welded engine is shown to have an acceptable design margin for thermal characteristics. High-performance liquid apogee engines are shown to perform optimally when based on iridium/rhenium chamber technology, use of a special platelet injector, and the minimization of losses due to fuel-film cooling.

C.C.S.

A92-49129*# National Aeronautics and Space Administration. Lewis Research Center, Cleveland, OH.

RADIATION ENHANCED DISSOCIATION OF HYDROGEN IN NUCLEAR ROCKETS

YOICHI WATANABE (Florida, University, Gainesville) AIAA, SAE, ASME, and ASEE, Joint Propulsion Conference and Exhibit, 28th, Nashville, TN, July 6-8, 1992. 8 p. Research supported by SDIO and NASA. Jul. 1992 8 p refs (AIAA PAPER 92-3817) Copyright

The effect of radiation-induced dissociation of hydrogen gas in nuclear rockets is studied. The dissociation degree is obtained by solving rate equations, which include the fast-ion induced dissociation and ionization of atomic and molecular hydrogens. Analytical formulas are used to estimate a change in the viscosity and the specific impulse. It was found that the fast-ion induced dissociation plays an important role in enhancing the specific impulse for nuclear rocket concepts using hydrogen gas at low pressures (less than 0.1 MPa) and low temperatures (less than 3000 K). It is also shown that the specific impulse is enhanced by mixing helium-3, lithium-6, boron-10, or uranium-235 with hydrogen.

Author

A92-50253* National Aeronautics and Space Administration. Lewis Research Center, Cleveland, OH.

SPECTRALLY RESOLVED RAYLEIGH SCATTERING DIAGNOSTIC FOR HYDROGEN-OXYGEN ROCKET PLUME STUDIES

R. G. SEASHOLTZ, F. J. ZUPANC, and S. J. SCHNEIDER (NASA, Lewis Research Center, Cleveland, OH) Oct. 1992 8 p refs Copyright

A92-50264* National Aeronautics and Space Administration. Lewis Research Center, Cleveland, OH.

NUMERICAL STUDY OF LOW-CURRENT STEADY ARCS

S. C. KIM (Sverdrup Technology, Inc., Brook Park; NASA, Lewis Research Center, Cleveland, OH) and H. T. NAGAMATSU (Rensselaer Polytechnic Institute, Troy, NY) Journal of Propulsion and Power (ISSN 0748-4658), vol. 8, no. 5, Sept.-Oct. 1992, p.

1012-1016. Research supported by EPRI. Oct. 1992 5 p refs Copyright

The development of a high-efficiency CW YLF laser doped with Er,Tm,Ho: and featuring a strongly focusing resonator that collects a high density of pump power on the active crystal is described. The emission is investigated at 2.06 microns and a tuning range both at liquid-nitrogen (77 K) and at dry-ice (210 K) temperature. The noise characteristics and the long-term power stability of the laser is studied with an eye to employing this source for high-resolution spectroscopy in the 2-micron wavelength region. The detection of several absorption lines of NH3 at low pressure is described. The output power of the laser as a function of the power impinging on the crystal for different transmission of the output mirror is illustrated. The best result obtained is 1.46 W output for 3.2 W of argon pump. The minimum threshold achieved is 3.5 mW with a 1-percent transmission mirror. It is concluded that it is possible to develop a highly efficient Ho:YLF laser featuring low noise and sufficient tunability for high-resolution spectroscopy in the 2-micron region.

P.D.

A92-50266* National Aeronautics and Space Administration. Lewis Research Center, Cleveland, OH.

PLASMA FLOW PROCESSES WITHIN MAGNETIC NOZZLE CONFIGURATIONS

THOMAS M. YORK (Ohio State University, Columbus), BARRY A. JACOBY (Lawrence Livermore National Laboratory, Livermore, CA), and PAVLOS MIKELLIDES (Ohio State University, Columbus) Oct. 1992 8 p refs (Contract NAG3-843; DE-AC02-76ET-53018) Copyright

A92-50274* National Aeronautics and Space Administration. Lewis Research Center, Cleveland, OH.

MAGNESIUM FLUORIDE AS ENERGY STORAGE MEDIUM FOR SPACECRAFT SOLAR THERMAL POWER SYSTEMS

CHARLES A. LURIO (Aerodyne Research, Inc., Billerica, MA) Journal of Propulsion and Power (ISSN 0748-4658), vol. 8, no. 5, Sept.-Oct. 1992, p. 1087-1092. Research supported by NASA. Oct. 1992 6 p refs Copyright

MgF2 was investigated as a phase-change energy-storage material for LEO power systems using solar heat to run thermal cycles. It provides a high heat of fusion per unit mass at a high melting point (1536 K). Theoretical evaluation showed the basic chemical compatibility of liquid MgF2 with refractory metals at 1600 K, though transient high pressures of H2 can occur in a closed container due to reaction with residual moisture. The compatibility was tested in two refractory metal containers for over 2000 h. Some showed no deterioration, while there was evidence that the fluoride reacted with hafnium in others. Corollary tests showed that the MgF2 supercooled by 10-30 K and 50-90 K.

Author

A92-50495* National Aeronautics and Space Administration. Lewis Research Center, Cleveland, OH.

LINEAR QUADRATIC SERVO CONTROL OF A REUSABLE ROCKET ENGINE

JEFFREY L. MUSGRAVE (NASA, Lewis Research Center, Cleveland, OH) Oct. 1992 6 p refs Copyright

A92-50529* National Aeronautics and Space Administration. Lewis Research Center, Cleveland, OH.

DEVELOPMENT OF AN ANALYTICAL TOOL TO STUDY POWER QUALITY OF AC POWER SYSTEMS FOR LARGE SPACECRAFT

L. A. KRAFT (Valparaiso University, IN) and M. D. KANKAM (NASA, Lewis Research Center, Cleveland, OH) IN: IECEC '91; Proceedings of the 26th Intersociety Energy Conversion Engineering Conference, Boston, MA, Aug. 4-9, 1991. Vol. 1 1991 5 p refs Copyright

A harmonic power flow program applicable to space power

20 SPACECRAFT PROPULSION AND POWER

systems with sources of harmonic distortion is described. The algorithm is a modification of Electric Power Research Institute's HARMFLO program which assumes a three-phase, balanced, ac system with loads of harmonic distortion. The modified power flow program can be used with single phase, ac systems. Early results indicate that the required modifications and the models developed are quite adequate for the analysis of a 20-kHz testbed built by General Dynamics Corporation. This is demonstrated by the acceptable correlation of the present results with published data. Although the results are not exact, the discrepancies are relatively small. Author

A92-50541* National Aeronautics and Space Administration. Lewis Research Center, Cleveland, OH.

MULTIKILOWATT POWER ELECTRONICS DEVELOPMENT FOR SPACECRAFT

D. K. DECKER, L. Y. INOUE, and D. L. ROLANDELLI (TRW Space and Technology Group, Redondo Beach, CA) IN: IECEC '91; Proceedings of the 26th Intersociety Energy Conversion Engineering Conference, Boston, MA, Aug. 4-9, 1991. Vol. 1 1991 6 p
(Contract NAS3-25093)
Copyright

Attention is given to several multikilowatt power electronic components developed by TRW for the Space Station Power Management and Distribution test bed at NASA Lewis Research Center. These components include a 12.5-kW DC-DC converter, a 6.25-kW battery charge/discharge regulator, an 82-channel sequential shunt unit, a 10-A remote power controllers, and three different types of 1-kW load converters. TRW is also monitoring the development of 120-V fuses for space applications. The authors discuss these developments and provide steady-state and dynamic performance parameters. I.E.

A92-50559* National Aeronautics and Space Administration. Lewis Research Center, Cleveland, OH.

MODELING OF SPACE STATION POWER SYSTEM COMPONENTS AND THEIR INTERACTIONS

KWA-SUR TAM, LIFENG YANG (Virginia Polytechnic Institute and State University, Blacksburg), and NARAYAN DRAVID (NASA, Lewis Research Center, Cleveland, OH) IN: IECEC '91; Proceedings of the 26th Intersociety Energy Conversion Engineering Conference, Boston, MA, Aug. 4-9, 1991. Vol. 1 1991 6 p refs
(Contract NAG3-1120)
Copyright

The authors demonstrate that the functional modeling approach is feasible in modeling large-scale spacecraft power systems such as the Space Station electric power system (EPS). The functional models for the solar array sequential shunt unit and the battery charging/discharging unit are presented. The functional modeling approach has also been applied to simulate other major EPS components. The usefulness of this approach in system-level studies has been demonstrated by incorporating these models into a power system model and simulating the system behavior under various conditions. The simulation results are consistent with those obtained experimentally. With larger time step size and reduced model complexity, the computation time required by the functional modeling approach is short. Functional models are effective in simulation studies of system-level issues, especially for large-scale power systems including many power electronic components. I.E.

A92-50565* National Aeronautics and Space Administration. Lewis Research Center, Cleveland, OH.

FULL-SIZE SOLAR DYNAMIC HEAT RECEIVER THERMAL-VACUUM TESTS

L. M. SEDGWICK, K. J. KAUFMANN (Boeing Aerospace and Electronics, Seattle, WA), K. L. MCLALLIN, and T. W. KERSLAKE (NASA, Lewis Research Center, Cleveland OH) IN: IECEC '91; Proceedings of the 26th Intersociety Energy Conversion Engineering Conference, Boston, MA, Aug. 4-9, 1991. Vol. 1

1991 6 p refs

Copyright

The testing of a full-size, 102 kW, solar dynamic heat receiver utilizing high-temperature thermal energy storage is described. The purpose of the test program was to quantify receiver thermodynamic performance, operating temperatures, and thermal response to changes in environmental and power module interface boundary conditions. The heat receiver was tested in a vacuum chamber with liquid nitrogen cold shrouds and an aperture cold plate to partly simulate a low-Earth-orbit environment. The cavity of the receiver was heated by an infrared quartz lamp heater with 30 independently controllable zones to allow axially and circumferentially varied flux distributions. A closed-Brayton cycle engine simulator conditioned a helium-xenon gas mixture to specific interface conditions to simulate the various operational modes of the solar dynamic power module on the Space Station Freedom. Inlet gas temperature, pressure, and flow rate were independently varied. A total of 58 simulated orbital cycles, each 94 minutes in duration, was completed during the test period. Author

A92-50566* National Aeronautics and Space Administration. Lewis Research Center, Cleveland, OH.

GROUND TEST PROGRAM FOR A FULL-SIZE SOLAR DYNAMIC HEAT RECEIVER

L. M. SEDGWICK, K. J. KAUFMANN (Boeing Aerospace and Electronics, Seattle, WA), K. L. MCLALLIN, and T. W. KERSLAKE (NASA, Lewis Research Center, Cleveland, OH) IN: IECEC '91; Proceedings of the 26th Intersociety Energy Conversion Engineering Conference, Boston, MA, Aug. 4-9, 1991. Vol. 1 1991 6 p refs
Copyright

Test hardware, facilities, and procedures were developed to conduct ground testing of a full-size, solar dynamic heat receiver in a partially simulated, low earth orbit environment. The heat receiver was designed to supply 102 kW of thermal energy to a helium and xenon gas mixture continuously over a 94 minute orbit, including up to 36 minutes of eclipse. The purpose of the test program was to quantify the receiver thermodynamic performance, its operating temperatures, and thermal response to changes in environmental and power module interface boundary conditions. The heat receiver was tested in a vacuum chamber using liquid nitrogen cold shrouds and an aperture cold plate. Special test equipment was designed to provide the required ranges in interface boundary conditions that typify those expected or required for operation as part of the solar dynamic power module on the Space Station Freedom. The support hardware includes an infrared quartz lamp heater with 30 independently controllable zones and a closed-Brayton cycle engine simulator to circulate and condition the helium-xenon gas mixture. The test article, test support hardware, facilities, and instrumentation developed to conduct the ground test program are all described. Author

A92-50567* National Aeronautics and Space Administration. Lewis Research Center, Cleveland, OH.

SOLAR DYNAMIC POWER FOR EARTH ORBITAL AND LUNAR APPLICATIONS

JAMES E. CALOGERAS, MILES O. DUSTIN, and RICHARD R. SECUNDE (NASA, Lewis Research Center, Cleveland, OH) IN: IECEC '91; Proceedings of the 26th Intersociety Energy Conversion Engineering Conference, Boston, MA, Aug. 4-9, 1991. Vol. 1 1991 10 p refs
Copyright

Development of solar dynamic (SD) technologies for space over the past 25 years by NASA Lewis Research Center brought SD power to the point where it was selected in the design phase of Space Station Freedom Program as the power source for evolutionary growth. More recent studies showed that large cost savings are possible in establishing manufacturing processes at Lunar Base if SD is considered as a power source. Technology efforts over the past 5 years has made possible lighter, more durable, SD components for these applications. A review of these efforts and respective benefits is presented. Author

A92-50583* National Aeronautics and Space Administration. Lewis Research Center, Cleveland, OH.

THE SOLAR ARRAY MODULE PLASMA INTERACTIONS EXPERIMENT (SAMPIE) - A SHUTTLE-BASED PLASMA INTERACTIONS EXPERIMENT

LAWRENCE W. WALD and G. B. HILLARD (NASA, Lewis Research Center, Cleveland, OH) IN: IECEC '91; Proceedings of the 26th Intersociety Energy Conversion Engineering Conference, Boston, MA, Aug. 4-9, 1991. Vol. 1 1991 6 p refs
Copyright

The Solar Array Module Plasma Interactions Experiment (SAMPIE), an approved Shuttle space flight experiment with a tentative launch date in July 1993, is intended to investigate plasma interactions of high-voltage space power systems. Solar cell modules, representing several technologies, will be biased to high voltages to characterize both arcing (negative potential) and current collection (positive potential). Other solar modules, specially modified in accordance with current theories of arcing and breakdown, will demonstrate the possibility of arc suppression. Finally, several additional test specimens will be included to study the basic nature of these interactions. The authors describe the rationale for the space flight experiment, the measurements to be made, the significance of the expected results, and the current design status of the flight hardware.
I.E.

A92-50584* National Aeronautics and Space Administration. Lewis Research Center, Cleveland, OH.

NUCLEAR ROCKET PROPULSION: NASA PLANS AND PROGRESS - FY 1991

JOHN S. CLARK and THOMAS J. MILLER (NASA, Lewis Research Center, Cleveland, OH) IN: IECEC '91; Proceedings of the 26th Intersociety Energy Conversion Engineering Conference, Boston, MA, Aug. 4-9, 1991. Vol. 1 1991 6 p refs
Copyright

NASA has initiated planning for a technology development project for nuclear rocket propulsion systems for space exploration initiative (SEI) human and robotic missions to the Moon and to Mars. An interagency project is underway that includes the Department of Energy National Laboratories for nuclear technology development. The activities of the project planning team in FY 1990 and 1991 are summarized. The progress to date is discussed, and the project plan is reviewed. Critical technology issues were identified and include: (1) nuclear fuel temperature, life, and reliability; (2) nuclear system ground test; (3) safety; (4) autonomous system operation and health monitoring; and (5) minimum mass and high specific impulse.
Author

A92-50608* National Aeronautics and Space Administration. Lewis Research Center, Cleveland, OH.

STATUS OF NASA'S STIRLING SPACE POWER CONVERTER PROGRAM

JAMES E. DUDENHOEFER and JERRY M. WINTER (NASA, Lewis Research Center, Cleveland, OH) IN: IECEC '91; Proceedings of the 26th Intersociety Energy Conversion Engineering Conference, Boston, MA, Aug. 4-9, 1991. Vol. 2 1991 6 p refs
Copyright

An overview is presented of the NASA free-piston Stirling space power converter technology program. The authors discuss Stirling experience in space and progress toward 1050 K and 1300 K Stirling space power converters. Fabrication is nearly completed for the 1050 K component test power converter (CTPC); results of motoring tests of the cold end (525 K), are presented. The success of these and future designs is dependent upon supporting research and technology efforts including heat pipes, bearings, superalloy joining technologies, high efficiency alternators, life and reliability testing and predictive methodologies. The authors provide an update of progress in some of these technologies.
I.E.

A92-50615 National Aeronautics and Space Administration. Lewis Research Center, Cleveland, OH.

CONCENTRATOR TESTING USING PROJECTED IMAGES

KENT S. JEFFERIES (NASA, Lewis Research Center, Cleveland, OH) IN: IECEC '91; Proceedings of the 26th Intersociety Energy

Conversion Engineering Conference, Boston, MA, Aug. 4-9, 1991. Vol. 2 1991 6 p

(Contract RTOP 474-12-10)

Copyright

The projected image system can be used to evaluate concentrator optical properties by comparing images reflected onto the ceiling of the test facility to theoretical facet outlines. This system was tested by comparing ceiling images to facet outlines computed using facet characteristics measured by the digital-image-radiometer (DIR) optical measuring system. The agreement was good, confirming the accuracy of both optical systems. Six facets were mounted in the centers of the pie sectors of one hexagonal panel. Differences between the facets and facet nonsymmetries were observed in photographs of the ceiling images of the facets.
Author

A92-50633* National Aeronautics and Space Administration. Lewis Research Center, Cleveland, OH.

DESIGN OF MULTIHUNDRED-WATT DYNAMIC ISOTOPE POWER SYSTEM FOR ROBOTIC SPACE MISSIONS

D. J. BENTS, S. M. GENG, J. G. SCHREIBER, C. A. WITHROW (NASA, Lewis Research Center, Cleveland, OH), P. C. SCHMITZ (Sverdrup Technology, Inc., Brook Park; NASA, Lewis Research Center, Cleveland, OH), and T. J. MCCOMAS (Florida, University, Gainesville) IN: IECEC '91; Proceedings of the 26th Intersociety Energy Conversion Engineering Conference, Boston, MA, Aug. 4-9, 1991. Vol. 2 1991 6 p refs
Copyright

The design of a multihundred-watt dynamic isotope power system (DIPS) based on the US Department of Energy (DOE) general-purpose heat source (GPHS) and small (multihundred-watt) free-piston Stirling engine (FPSE) is described as a potential lower cost alternative to radioisotope thermoelectric generators (RTGs). The design is targeted at the power needs of future unmanned deep space and planetary surface exploration missions. Since the competitive potential of FPSE as an isotope converter was first identified, work has focused on the feasibility of directly integrating GPHS with the Stirling heater head. Thermal modeling of various radiatively coupled heat source/heater head geometries has been performed using data furnished by the developers of FPSE and GPHS. The analysis indicates that, for the 1050 K heater head configurations considered, GPHS fuel clad temperatures remain safe operating limits under all conditions including shutdown of one engine on a twin engine unit. Based on these results, preliminary characterizations of multihundred-watt units have been established. They indicate that, per electrical watt, the GPHS/small Stirling DIPS will be roughly equivalent to MOD RTG in size and mass but will require about a third the amount of isotope fuel.
I.E.

A92-50637* National Aeronautics and Space Administration. Lewis Research Center, Cleveland, OH.

THERMAL ANALYSIS OF A CONCEPTUAL DESIGN FOR A 250 WE GPHS/FPSE SPACE POWER SYSTEM

THOMAS J. MCCOMAS and EDWARD T. DUGAN (Florida, University, Gainesville) IN: IECEC '91; Proceedings of the 26th Intersociety Energy Conversion Engineering Conference, Boston, MA, Aug. 4-9, 1991. Vol. 2 1991 6 p refs
(Contract NAG3-1123)
Copyright

A thermal analysis has been performed for a 250-We space nuclear power system which combines the US Department of Energy's general purpose heat source (GPHS) modules with a state-of-the-art free-piston Stirling engine (FPSE). The focus of the analysis is on the temperature of the indium fuel clad within the GPHS modules. The thermal analysis results indicate fuel clad temperatures slightly higher than the design goal temperature of 1573 K. The results are considered favorable due to numerous conservative assumptions used. To demonstrate the effects of the conservatism, a brief sensitivity analysis is performed in which a few of the key system parameters are varied to determine their effect on the fuel clad temperatures. It is shown that thermal

20 SPACECRAFT PROPULSION AND POWER

analysis of a more detailed thermal mode should yield fuel clad temperatures below 1573 K. I.E.

A92-50640 National Aeronautics and Space Administration. Lewis Research Center, Cleveland, OH.

ADVANCED POWER SYSTEMS FOR EOS

SHEILA G. BAILEY, IRVING WEINBERG, and DENNIS J. FLOOD (NASA, Lewis Research Center, Cleveland, OH) IN: IECEC '91; Proceedings of the 26th Intersociety Energy Conversion Engineering Conference, Boston, MA, Aug. 4-9, 1991. Vol. 2 1991 6 p refs (Contract RTOP 506-41-11)

Copyright

The Earth Observing System (EOS), which is part of the International Mission to Planet Earth, is NASA's main contribution to the Global Change Research Program. Five large platforms are to be launched into polar orbit: two by NASA, two by the European Space Agency, and one by the Japanese. In such an orbit the radiation resistance of indium phosphide solar cells combined with the potential of utilizing 5-micron cell structures yields an increase of 10 percent in the payload capability. If further combined with the Advanced Photovoltaic Solar Array, the total additional payload capability approaches 12 percent. Author

A92-50641* National Aeronautics and Space Administration. Lewis Research Center, Cleveland, OH.

APPLICATIONS OF THIN-FILM PHOTOVOLTAICS FOR SPACE
GEOFFREY A. LANDIS (Sverdrup Technology, Inc.; NASA, Lewis Research Center, Cleveland, OH) and ALOYSIUS F. HEPP (NASA, Lewis Research Center, Cleveland, OH) IN: IECEC '91; Proceedings of the 26th Intersociety Energy Conversion Engineering Conference, Boston, MA, Aug. 4-9, 1991. Vol. 2 1991 6 p refs

Copyright

The authors discuss the potential applications of thin-film polycrystalline and amorphous cells for space. There have been great advances in thin-film solar cells for terrestrial applications. Transfer of this technology to space applications could result in ultra low-weight solar arrays with potentially large gains in specific power. Recent advances in thin-film solar cells are reviewed, including polycrystalline copper indium selenide and related I-III-VI₂ compounds, polycrystalline cadmium telluride and related II-VI compounds, and amorphous silicon arrays. The possibility of using thin-film multi-bandgap cascade solar cells is discussed. I.E.

A92-50648* National Aeronautics and Space Administration. Lewis Research Center, Cleveland, OH.

THE MINI-DOME FRESNEL LENS PHOTOVOLTAIC CONCENTRATOR ARRAY - CURRENT PROGRAM STATUS

MICHAEL F. PISZCZOR (NASA, Lewis Research Center, Cleveland, OH), MARK J. O'NEILL (ENTECH, Inc., Dallas, TX), and LEWIS FRAAS (Boeing High Technology Center, Seattle, WA) IN: IECEC '91; Proceedings of the 26th Intersociety Energy Conversion Engineering Conference, Boston, MA, Aug. 4-9, 1991. Vol. 2 1991 6 p refs

Copyright

Over the last seven years, NASA Lewis, ENTECH, and Boeing have been developing a high-efficiency, lightweight space photovoltaic concentrator array. The authors report the current status of the mini-dome Fresnel lens concentrator program, emphasizing the latest results on the fabrication and testing of a space-qualifiable version of the concentrator lens and panel structure. Calculations indicated that such an array can achieve 300 W/sq m at a specific power of 100 W/kg. The authors describe the current status of component and prototype panel testing and the preliminary development of a flight panel for the Photovoltaic Array Space Power Plus Diagnostics (PASP Plus) flight experiment. I.E.

A92-50700 National Aeronautics and Space Administration. Lewis Research Center, Cleveland, OH.

NICKEL-HYDROGEN CELL LOW-EARTH-ORBIT LIFE TEST UPDATE

DAVID T. FRATE (NASA, Lewis Research Center, Cleveland, OH) IN: IECEC '91; Proceedings of the 26th Intersociety Energy Conversion Engineering Conference, Boston, MA, Aug. 4-9, 1991. Vol. 3 1991 6 p refs (Contract RTOP 474-46-10)

Copyright

When individual pressure vessel (IPV) nickel-hydrogen (Ni/H₂) cells were selected as the energy storage system for Space Station Freedom in March of 1986, a limited database existed on life and performance characteristics of these cells in a low earth orbit (LEO) regime. Therefore, NASA LeRC initiated a Ni/H₂ cell test program with the primary objectives of building a test facility, procuring cells from existing NASA contracts, and screening several cell designs by life testing in a LEO 35 percent depth of discharge (DOD) scenario. A total of 40 cells incorporating 13 designs were purchased from Yardney, Hughes, and Eagle-Picher. Thirty-two of the cells purchased were 65 A-hr nameplate capacity and eight cells were 50 A-hr. Yardney and Eagle-Picher cells were built with both the Air Force recirculating and the advanced back-to-back electrode stack configurations and incorporated 31 and 26 percent KOH. Acceptance testing of the first delivered cells began in March of 1988, with life testing following in September of that year. Performance comparisons of these cells are made here while specifically addressing life test data relative to the design differences. Author

A92-50702* National Aeronautics and Space Administration. Lewis Research Center, Cleveland, OH.

EFFECT OF KOH CONCENTRATION ON LEO CYCLE LIFE OF IPV NICKEL-HYDROGEN FLIGHT CELLS - AN UPDATE

JOHN J. SMITHRICK (NASA, Lewis Research Center, Cleveland, OH) and STEPHEN W. HALL (U.S. Navy, Naval Weapons Support Center, Crane, IN) IN: IECEC '91; Proceedings of the 26th Intersociety Energy Conversion Engineering Conference, Boston, MA, Aug. 4-9, 1991. Vol. 3 1991 6 p refs

Copyright

An update of validation test results confirming the breakthrough in LEO cycle life of nickel-hydrogen cells containing 26 percent potassium hydroxide (KOH) electrolyte is presented. A breakthrough in the LEO cycle life of individual pressure vessel nickel-hydrogen cells is reported. The cycle life of boiler plate cells containing 26 percent KOH electrolyte was about 40,000 LEO cycles compared to 3500 cycles for cells containing 31 percent KOH. Author

A92-50707 National Aeronautics and Space Administration. Lewis Research Center, Cleveland, OH.

DESTRUCTIVE PHYSICAL ANALYSIS RESULTS OF NI/H₂ CELLS CYCLED IN LEO REGIME

HONG S. LIM, GABRIELA R. ZELTER (Hughes Aircraft Co., Torrance, CA), JOHN J. SMITHRICK (NASA, Lewis Research Center, Cleveland, OH), and STEPHEN W. HALL (U.S. Navy, Naval Weapons Support Center, Crane, IN) IN: IECEC '91; Proceedings of the 26th Intersociety Energy Conversion Engineering Conference, Boston, MA, Aug. 4-9, 1991. Vol. 3 1991 7 p refs

(Contract NAS3-22238; RTOP 506-41-21)

Copyright

Six 48-Ah individual pressure vessel (IPV) Ni/H₂ cells containing 26 and 31 percent KOH electrolyte were life cycle tested in low earth orbit. All three cells containing 31 percent KOH failed (3729, 4165, and 11,355 cycles), while those with 26 percent KOH were cycled over 14,000 times in the continuing test. Destructive physical analysis (DPA) of the failed cells included visual inspections, measurements of electrode thickness, scanning electron microscopy, chemical analysis, and measurements of nickel electrode capacity in an electrolyte flooded cell. The cycling failure was due to a decrease of nickel electrode capacity. As possible causes of the capacity decrease, researchers observed electrode expansion, rupture, and corrosion of the nickel electrode substrate active material redistribution, and accumulation of electrochemically undischARGEABLE active material with cycling. Author

A92-50708 National Aeronautics and Space Administration. Lewis Research Center, Cleveland, OH.

EFFECT OF LEO CYCLING ON 125 AH ADVANCED DESIGN IPV NICKEL-HYDROGEN FLIGHT CELLS - AN UPDATE

JOHN J. SMITHRICK (NASA, Lewis Research Center, Cleveland, OH) and STEPHEN W. HALL (U.S. Navy, Naval Weapons Support Center, Crane, IN) IN: IECEC '91; Proceedings of the 26th Intersociety Energy Conversion Engineering Conference, Boston, MA, Aug. 4-9, 1991. Vol. 3 1991 7 p refs (Contract RTOP 506-41-21)

Copyright

An update of validation test results confirming the breakthrough in LEO cycle life of nickel-hydrogen cells containing 26 percent potassium hydroxide (KOH) electrolyte is presented. A breakthrough in the LEO cycle life of individual pressure vessel nickel-hydrogen cells is reported. The cycle life of boiler plate cells containing 26 percent KOH electrolyte was about 40,000 LEO cycles compared to 3500 cycles for cells containing 31 percent KOH. Author

A92-50712* National Aeronautics and Space Administration. Lewis Research Center, Cleveland, OH.

THERMAL MODELING OF NICKEL-HYDROGEN BATTERY CELLS OPERATING UNDER TRANSIENT ORBITAL CONDITIONS

DEAN S. SCHRAGE (Sverdrup Technology, Inc., Brook Park, OH) IN: IECEC '91; Proceedings of the 26th Intersociety Energy Conversion Engineering Conference, Boston, MA, Aug. 4-9, 1991. Vol. 3 1991 6 p refs (Contract NAS3-25266)

Copyright

An analytical study of the thermal operating characteristics of nickel-hydrogen battery cells is presented. Combined finite-element and finite-difference techniques are employed to arrive at a computationally efficient composite thermal model representing a series-cell arrangement operating in conjunction with a radiately coupled baseplate and coldplate thermal bus. An aggressive, low-mass design approach indicates that thermal considerations can and should direct the design of the thermal bus arrangement. Special consideration is given to the potential for mixed conductive and convective processes across the hydrogen gap. Results of a compressible flow model are presented and indicate the transfer process is suitably represented by molecular conduction. A high-fidelity thermal model of the cell stack (and related components) indicates the presence of axial and radial temperature gradients. A detailed model of the thermal bus reveals the thermal interaction of individual cells and is imperative for assessing the intercell temperature gradients. I.E.

A92-50780* National Aeronautics and Space Administration. Lewis Research Center, Cleveland, OH.

UPDATE ON RESULTS OF SPRE TESTING AT NASA LEWIS

JAMES E. CAIRELLI, DIANE M. SWEC, WAYNE A. WONG, THOMAS J. DOEBERLING (NASA, Lewis Research Center, Cleveland, OH), and FRANK J. MADY (Sverdrup Technology, Inc., Brook Park, OH) IN: IECEC '91; Proceedings of the 26th Intersociety Energy Conversion Engineering Conference, Boston, MA, Aug. 4-9, 1991. Vol. 5 1991 6 p refs

Copyright

The Space Power Research Engine (SPRE), a free-piston Stirling engine with a linear alternator, is being tested at NASA Lewis Research Center as part of the Civilian Space Technology Initiative (CSTI) as a candidate for high capacity space power. Results are presented from recent SPRE tests designed to investigate the effects of variation in the displacer seal clearance and piston centering port area on engine performance and dynamics. The effects of these variations on PV power and efficiency are presented. Comparisons of the displacer seal clearance test results with HFAST code predictions show good agreement for PV power but poor agreement for PV efficiency. Correlations are presented relating the piston mid-stroke position to the dynamic Delta P across the piston and the centering port area. Test results indicate that a modest improvement in PV power

and efficiency may be realized with a reduction in piston centering port area. I.E.

A92-50829* National Aeronautics and Space Administration. Lewis Research Center, Cleveland, OH.

ALKALI METAL COMPATIBILITY TESTING OF CANDIDATE HEATER HEAD MATERIALS FOR A STIRLING ENGINE HEAT TRANSPORT SYSTEM

JACK E. NOBLE, GARY L. HICKMAN (Stirling Technology Co., Richland, WA), and TONI GROBSTEIN (NASA, Lewis Research Center, Cleveland, OH) IN: IECEC '91; Proceedings of the 26th Intersociety Energy Conversion Engineering Conference, Boston, MA, Aug. 4-9, 1991. Vol. 6 1991 5 p refs (Contract DEN3-377)

Copyright

The authors describe work performed as part of the 25-kWe advanced Stirling conversion system project. Liquid alkali metal compatibility is being assessed in an ongoing test program to evaluate candidate heater head materials and fabrication processes at the temperatures and operating conditions required for Stirling engines. Specific materials under evaluation are alloy 713LC, alloy 713LC coated with nickel aluminide, and Udimet 720, each in combination with Waspaloy. The tests were run at a constant 700 C. A eutectic alloy of sodium and potassium (NaK) was the working fluid. Titanium sheet in the system was shown to be an effective oxygen getter. Metallographic and microchemical examination of material surfaces, joints, and their interfaces revealed little or no corrosion after 1000 h. Tests are in progress, with up to 10,000 h exposure. I.E.

A92-53190* National Aeronautics and Space Administration. Lewis Research Center, Cleveland, OH.

LDEF SPACECRAFT, GROUND LABORATORY, AND COMPUTATIONAL MODELING IMPLICATIONS ON SPACE STATION FREEDOM'S SOLAR ARRAY MATERIALS AND SURFACES DURABILITY

BRUCE A. BANKS, SHARON K. RUTLEDGE, KIM K. DE GROH, BRUCE M. AUER, MICHAEL J. MIRTICH (NASA, Lewis Research Center, Cleveland, OH), LINDA GEBAUER (Cleveland State University, OH), CAROL M. HILL, and RICHARD F. LEBED (California, University, Berkeley) IN: IEEE Photovoltaic Specialists Conference, 22nd, Las Vegas, NV, Oct. 7-11, 1991, Conference Record. Vol. 2 1991 6 p refs

Copyright

The low earth orbital (LEO) durability of Space Station Freedom (SSF) solar array materials and surfaces is evaluated using results from the Long Duration Exposure Facility (LDEF), ground laboratory simulation tests, and Monte Carlo modeling. These results indicate that thin-film SiO_x protective coatings are adequately durable to atomic oxygen, ultraviolet (UV) radiation, thermal cycling, and micrometeoroid or debris impact. I.E.

A92-53197* National Aeronautics and Space Administration. Lewis Research Center, Cleveland, OH.

PILOT PRODUCTION OF 4 SQ CM ITO/INP PHOTOVOLTAIC SOLAR CELLS

T. A. GESSERT, X. LI, T. J. COUTTS (National Renewable Energy Laboratory, Golden, CO), and N. TZAFARAS (AT&T Microelectronics, Reading, PA) IN: IEEE Photovoltaic Specialists Conference, 22nd, Las Vegas, NV, Oct. 7-11, 1991, Conference Record. Vol. 2 1991 6 p refs (Contract NASA ORDER C-3000-K; DE-AC02-83CH-10093)

Copyright

Experimental results of a pilot production of 32 4-sq cm indium tin oxide (ITO)/InP space solar cells are presented. The discussion includes analysis of the device performance of the best cells produced as well as the performance range of all production cells. The experience gained from the production is discussed, indicating other issues that may be encountered when large-scale productions are initiated. Available data on a 4-sq cm ITO/InP cell that was flown on the UoSAT-5 satellite is reported. I.E.

20 SPACECRAFT PROPULSION AND POWER

A92-53199* National Aeronautics and Space Administration. Lewis Research Center, Cleveland, OH.

A HIGH-PERFORMANCE PHOTOVOLTAIC CONCENTRATOR ARRAY - THE MINI-DOME FRESNEL LENS CONCENTRATOR WITH 30 PERCENT EFFICIENT GAAS/GASB TANDEM CELLS
M. F. PISZCZOR, D. J. BRINKER, D. J. FLOOD (NASA, Lewis Research Center, Cleveland, OH), J. E. AVERY, L. M. FRAAS, E. S. FAIRBANKS, J. W. YERKES (Boeing High Technology Center, Seattle, WA), and M. J. O'NEILL (Entech, Inc., Dallas, TX) IN: IEEE Photovoltaic Specialists Conference, 22nd, Las Vegas, NV, Oct. 7-11, 1991, Conference Record. Vol. 2 1991 6 p refs
Copyright

A high-efficiency, lightweight space photovoltaic concentrator array is described. Previous work on the minidome Fresnel lens concentrator concept is being integrated with Boeing's 30 percent efficient tandem GaAs/GaSb concentrator cells into a high-performance photovoltaic array. Calculations indicate that, in the near term, such an array can achieve 300 W/sq m at a specific power of 100 W/kg. Emphasis of the program has now shifted to integrating the concentrator lens, tandem cell, and supporting panel structure into a space-qualifiable array. A description is presented of the current status of component and prototype panel testing and the development of a flight panel for the Photovoltaic Array Space Power Plus Diagnostics (PASP PLUS) flight experiment. I.E.

A92-53201* National Aeronautics and Space Administration. Lewis Research Center, Cleveland, OH.

PHOTOVOLTAIC RECEIVERS FOR LASER BEAMED POWER IN SPACE

GEOFFREY A. LANDIS (Sverdrup Technology, Inc.; NASA, Lewis Research Center, Cleveland, OH) IN: IEEE Photovoltaic Specialists Conference, 22nd, Las Vegas, NV, Oct. 7-11, 1991, Conference Record. Vol. 2 1991 9 p refs
(Contract NAS3-25266)

Copyright

There has recently been a resurgence of interest in the use of beamed power to support space exploration activities. One of the most promising beamed power concepts uses a laser beam to transmit power to a remote photovoltaic array. Large lasers can be located on cloud-free sites at one or more ground locations and illuminate solar arrays to a level sufficient to provide operating power. Issues involved in providing photovoltaic receivers for such applications are discussed. Author

A92-53209* National Aeronautics and Space Administration. Lewis Research Center, Cleveland, OH.

EVALUATION OF KAPTON PYROLYSIS, ARC TRACKING, AND ARC PROPAGATION ON THE SPACE STATION FREEDOM (SSF) SOLAR ARRAY FLEXIBLE CURRENT CARRIER (FCC)

THOMAS J. STUEBER (Sverdrup Technology, Inc.; NASA, Lewis Research Center, Cleveland, OH) IN: IEEE Photovoltaic Specialists Conference, 22nd, Las Vegas, NV, Oct. 7-11, 1991, Conference Record. Vol. 2 1991 5 p refs
(Contract NAS3-25266)

Copyright

Recent studies involving the use of polyimide Kapton coated wires indicate that if a momentary electrical short circuit occurs between two wires, sufficient heating of the Kapton can occur to thermally char (pyrolyze) the Kapton. Such charred Kapton has sufficient electrical conductivity to create an arc which tracks down the wires and possibly propagates to adjoining wires. These studies prompted an investigation to ascertain the likelihood of Kapton pyrolysis, arc tracking and propagation phenomena, and the magnitude of destruction conceivably inflicted on Space Station Freedom's (SSF's) Flexible Current Carrier (FCC) for the photovoltaic array. The geometric layout of the FCC, having a planar-type orientation as opposed to bundles, may reduce the probability of sustaining an arc. An experimental investigation was conducted to simulate conditions under which an arc can occur on the FCC of the SSF, and the consequences of arc initiation. Author

A92-53211* National Aeronautics and Space Administration. Lewis Research Center, Cleveland, OH.

ATOMIC OXYGEN EFFECTS ON SiO(X) COATED KAPTON FOR PHOTOVOLTAIC ARRAYS IN LOW EARTH ORBIT

SHARON K. RUTLEDGE (NASA, Lewis Research Center, Cleveland OH), RAYMOND M. OLLE, and JILL M. COOPER (Cleveland, State University, OH) IN: IEEE Photovoltaic Specialists Conference, 22nd, Las Vegas, NV, Oct. 7-11, 1991, Conference Record. Vol. 2 1991 4 p refs
Copyright

Commercially applied SiO_x was evaluated as a protective coating for the polyimide Kapton solar array blankets for Space Station Freedom. Three different rolls of coated material were tested in a plasma asher to determine their durability to attack by atomic oxygen. Mass loss data indicated that all of the coatings tested would structurally survive for 15 years in LEO (low earth orbit), except for one which had several uncoated lines across the sample which were caused by ridgelanes in the Kapton. It appears that the size rather than number of defects alone effects the mass loss the most. Careful handling of the material after coating and during processing may be critical for array survival. I.E.

A92-54002*# National Aeronautics and Space Administration. Lewis Research Center, Cleveland, OH.

PRESSURIZATION OF CRYOGENS - A REVIEW OF CURRENT TECHNOLOGY AND ITS APPLICABILITY TO LOW-GRAVITY CONDITIONS

N. T. VAN DRESAR (NASA, Lewis Research Center, Cleveland, OH) AIAA, SAE, ASME, and ASEE, Joint Propulsion Conference and Exhibit, 28th, Nashville, TN, July 6-8, 1992. 9 p. Previously announced in STAR as N92-29669. Jul. 1992 9 p refs
(AIAA PAPER 92-3061)

A review of technology, history, and current status for pressurized expulsion of cryogenic tankage is presented. Use of tank pressurization to expel cryogenic fluid will continue to be studied for future spacecraft applications over a range of operating conditions in the low-gravity environment. The review examines experimental test results and analytical model development for quiescent and agitated conditions in normal-gravity followed by a discussion of pressurization and expulsion in low-gravity. Validated, 1-D, finite difference codes exist for the prediction of pressurant mass requirements within the range of quiescent normal-gravity test data. To date, the effects of liquid sloshing have been characterized by tests in normal-gravity, but analytical models capable of predicting pressurant gas requirements remain unavailable. Efforts to develop multidimensional modeling capabilities in both normal and low-gravity have recently occurred. Low-gravity cryogenic fluid transfer experiments are needed to obtain low-gravity pressurized expulsion data. This data is required to guide analytical model development and to verify code performance. Author

A92-54007*# National Aeronautics and Space Administration. Lewis Research Center, Cleveland, OH.

COMPARING THE RESULTS OF AN ANALYTICAL MODEL OF THE NO-VENT FILL PROCESS WITH NO-VENT FILL TEST RESULTS FOR A 4.96 CU M (175 CU FT) TANK

WILLIAM J. TAYLOR and DAVID J. CHATO (NASA, Lewis Research Center, Cleveland, OH) AIAA, SAE, ASME, and ASEE, Joint Propulsion Conference and Exhibit, 28th, Nashville, TN, July 6-8, 1992. 24 p. Jul. 1992 24 p refs
(AIAA PAPER 92-3078) Copyright

NASA-Lewis has been investigating a no-vent fill method for refilling cryogenic storage tanks in low gravity. Analytical modeling based on analyzing the heat transfer of a droplet has successfully represented the process in 0.034 and 0.142 sq m commercial dewars using liquid nitrogen and hydrogen. Recently a large tank (4.96 sq m) was tested with hydrogen. This lightweight tank is representative of spacecraft construction. This paper presents efforts to model the large tank test data. The droplet heat transfer model is found to overpredict the tank pressure level when compared to the large tank data. A new model based on equilibrium

thermodynamics has been formulated. This new model is compared to the published large scale tank's test results as well as some additional test runs with the same equipment. The results are shown to match the test results within the measurement uncertainty of the test data except for the initial transient wall cooldown where it is conservative (i.e., overpredicts the initial pressure spike found in this time frame).
Author

A92-54017*# National Aeronautics and Space Administration, Lewis Research Center, Cleveland, OH.

SPACE TRANSFER WITH GROUND-BASED LASER/ELECTRIC PROPULSION

GEOFFREY A. LANDIS, MARK STAVNES, STEVE OLESON (Sverdrup Technology, Inc.; NASA, Lewis Research Center, Cleveland, OH), and JOHN BOZEK (NASA, Lewis Research Center, Cleveland, OH) AIAA, SAE, ASME, and ASEE, Joint Propulsion Conference and Exhibit, 28th, Nashville, TN, July 6-8, 1992. 13 p. Jul. 1992 13 p refs

(Contract NAS3-25266)

(AIAA PAPER 92-3213) Copyright

Ground-based high-power CW lasers can be used to beam power to photovoltaic receivers in space that furnish electricity to space vehicles; this energy can also be used to power electric-propulsion orbital transfer vehicles. An account is presently given of the anticipated requirements for the pulsed FEL lasers, large adaptive optics, photovoltaic receivers, and high specific impulse electrical propulsion. Preliminary system analysis results are presented.
O.C.

A92-54018# National Aeronautics and Space Administration, Washington, DC.

AN OVERVIEW OF THE NASA ADVANCED PROPULSION CONCEPTS PROGRAM

FRANCIS M. CURRAN, GARY L. BENNETT (NASA, Washington), ROBERT H. FRISBEE, JOEL C. SERCEL (JPL, Pasadena, CA), and MICHAEL R. LAPOINTE (Sverdrup Technology, Inc., Brook Park; NASA, Lewis Research Center, Cleveland, OH) AIAA, SAE, ASME, and ASEE, Joint Propulsion Conference and Exhibit, 28th, Nashville, TN, July 6-8, 1992. 21 p. Jul. 1992 21 p refs

(AIAA PAPER 92-3216) Copyright

NASA Advanced Propulsion Concepts (APC) program for the development of long-term space propulsion system schemes is managed by both NASA-Lewis and the JPL and is tasked with the identification and conceptual development of high-risk/high-payoff configurations. Both theoretical and experimental investigations have been undertaken in technology areas deemed essential to the implementation of candidate concepts. These APC candidates encompass very high energy density chemical propulsion systems, advanced electric propulsion systems, and an antiproton-catalyzed nuclear propulsion concept. A development status evaluation is presented for these systems.
O.C.

A92-54022*# National Aeronautics and Space Administration, Lewis Research Center, Cleveland, OH.

IDENTIFICATION OF THE SPACE SHUTTLE MAIN ENGINE DYNAMIC MODELS FROM FIRING DATA

N. SARAVANAN, A. DUYAR (Florida Atlantic University, Boca Raton), W. C. MERRILL, and T.-H. GUO (NASA, Lewis Research Center, Cleveland, OH) AIAA, SAE, ASME, and ASEE, Joint Propulsion Conference and Exhibit, 28th, Nashville, TN, July 6-8, 1992. 11 p. Jul. 1992 11 p refs

(Contract NAG3-1006)

(AIAA PAPER 92-3317) Copyright

A multi-input multi-output system identification technique is used to obtain linearized point models of the Space Shuttle Main Engine (SSME) at five different operating conditions (power levels) from the engine firing data. This study demonstrates that the open-loop dynamics of the SSME can be successfully modeled from the engine firing data. The identified linear models may be used for fault detection studies and control system design and development.
Author

A92-54027*# National Aeronautics and Space Administration, Lewis Research Center, Cleveland, OH.

PERFORMANCE COMPARISON OF AXISYMMETRIC AND THREE-DIMENSIONAL HYDROGEN FILM COOLANT INJECTION IN A 110 N HYDROGEN/OXYGEN ROCKET

LYNN A. ARRINGTON (Sverdrup Technology, Inc., Brook Park, OH) and BRIAN D. REED (NASA, Lewis Research Center, Cleveland, OH) AIAA, SAE, ASME, and ASEE, Joint Propulsion Conference and Exhibit, 28th, Nashville, TN, July 6-8, 1992. 21 p. Jul. 1992 21 p refs

(AIAA PAPER 92-3390)

An experimental performance comparison of two geometrically different fuel film coolant injection sleeves was conducted on a 110 N gaseous hydrogen/oxygen rocket. One sleeve had slots milled axially down the walls and the other had a smooth surface to give axisymmetric flow. The comparison was made to investigate a conclusion in an earlier study that attributed a performance underprediction to a simplifying modeling assumption of axisymmetric fuel film flow. The smooth sleeve had higher overall performance at one film coolant percentage and approximately the same or slightly better at another. The study showed that the lack of modeling of three-dimensional effects was not the cause of the performance underprediction as speculated in earlier analytical studies.
Author

A92-54030*# National Aeronautics and Space Administration, Lewis Research Center, Cleveland, OH.

ENGINE SYSTEM ASSESSMENT STUDY USING MARTIAN PROPELLANTS

D. PELACCIO, M. JACOBS, J. COLLINS, C. SCHEIL (Science Applications International Corp., Torrance, CA), and M. MEYER (NASA, Lewis Research Center, Cleveland, OH) AIAA, SAE, ASME, and ASEE, Joint Propulsion Conference and Exhibit, 28th, Nashville, TN, July 6-8, 1992. 34 p. Jul. 1992 34 p refs

(Contract NAS3-25809)

(AIAA PAPER 92-3446) Copyright

A feasibility study was performed that identified and characterized promising chemical propulsion system designs that utilize two or more of the propellant combinations: LOX/H₂, LOX/CH₄ and LOX/CO. The engine systems examined focused on the usage of common subsystem/component hardware where feasible. From the evaluation baseline employed, tripropellant MTV LOX cooled and bipropellant LEV and MEV engine systems are identified.
R.E.P.

A92-54031*# National Aeronautics and Space Administration, Lewis Research Center, Cleveland, OH.

EFFECT OF INERT PROPELLANT INJECTION ON MARS ASCENT VEHICLE PERFORMANCE

JAMES E. COLVIN and GEOFFREY A. LANDIS (NASA, Lewis Research Center, Cleveland, OH) AIAA, SAE, ASME, and ASEE, Joint Propulsion Conference and Exhibit, 28th, Nashville, TN, July 6-8, 1992. 23 p. Jul. 1992 23 p refs

(AIAA PAPER 92-3447) Copyright

A Mars ascent vehicle is limited in performance by the amount of propellant which can be brought from earth. In some cases the vehicle performance can be improved by injecting inert gas into the engine, if the inert gas is available as an in situ resource. CO₂, N₂ and Ar are constituents of the Martian atmosphere which are available at every point on the Martian surface and could be produced by a very simple processing technique, consisting essentially of compressing the atmosphere. The effect of inert gas injection on rocket engine performance was analyzed with a numerical code calculating chemical equilibrium in the engine, for engines of varying combustion chamber pressure, expansion ratio, oxidizer/fuel ratio, and inert injection fraction. Results of this analysis were applied to several candidate missions to determine how the required mass of return propellant needed in LEO could be decreased using inert propellant injection.
Author

20 SPACECRAFT PROPULSION AND POWER

A92-54033*# National Aeronautics and Space Administration. Lewis Research Center, Cleveland, OH.

SCALING OF 100 KW CLASS APPLIED-FIELD MPD THRUSTERS

ROGER M. MYERS (Sverdrup Technology, Inc., Brook Park; NASA, Lewis Research Center, Cleveland, OH) AIAA, SAE, ASME, and ASEE, Joint Propulsion Conference and Exhibit, 28th, Nashville, TN, July 6-8, 1992. 29 p. Jul. 1992 29 p refs (AIAA PAPER 92-3462)

Three cylindrical applied-field magnetoplasmadynamic thrusters were tested with argon propellant over a broad range of operating conditions to establish empirical scaling laws for thruster performance. Argon flow rates, discharge currents, and applied-field strengths were varied between 0.025 and 0.14 g/s, 750 to 2000 A, and 0.034 to 0.20 T, respectively. The results showed that the thrust reached over five times the self-field value, and that thrust increased linearly with the product of discharge current and applied-field strength, and quadratically with the anode radius. While increasing the propellant flow rate increased the thrust, it did not affect the rate of thrust increase with applied-field strength, and, at low propellant flow rates, the self-field thrust approached 30 percent of the measured thrust. The voltage increased linearly with applied-field strength but was insensitive to the discharge current. The rate of voltage increase with applied-field strength was strongly dependent on anode radius. Thruster efficiency increased monotonically with applied-field strength and propellant flow rate. Author

A92-54034*# National Aeronautics and Space Administration. Lewis Research Center, Cleveland, OH.

ANODE POWER DEPOSITION IN APPLIED-FIELD MPD THRUSTERS

ROGER M. MYERS (Sverdrup Technology, Inc., Brook Park; NASA, Lewis Research Center, Cleveland, OH) and GEORGE C. SOULAS (Ohio State University, Columbus) AIAA, SAE, ASME, and ASEE, Joint Propulsion Conference and Exhibit, 28th, Nashville, TN, July 6-8, 1992. 24 p. Jul. 1992 24 p refs (AIAA PAPER 92-3463)

Anode power deposition is the principle performance limiter of magnetoplasmadynamic (MPD) thrusters. Current thrusters lose between 50 and 70 percent of the input power to the anode. In this work, anode power deposition was studied for three cylindrical applied magnetic field thrusters for a range of argon propellant flow rates, discharge currents, and applied-field strengths. Between 60 and 95 percent of the anode power deposition resulted from electron current conduction into the anode, with cathode radiation depositing between 5 and 35 percent of the anode power, and convective heat transfer from the hot plasma accounting for less than 5 percent. While the fractional anode power loss decreased with increasing applied-field strength and anode size, the magnitude of the anode power increased. The rise in anode power resulted from a linear rise in the anode fall voltage with applied-field strength and anode radius. The anode fall voltage also rose with decreasing propellant flow rate. The trends indicate that the anode fall region is magnetized, and suggest techniques for reducing the anode power loss in MPD thrusters. Author

A92-54038*# National Aeronautics and Space Administration. Lewis Research Center, Cleveland, OH.

DEVELOPMENT AND FLIGHT HISTORY OF SERT 2 SPACECRAFT

WILLIAM R. KERSLAKE (Sverdrup Technology, Inc., Brook Park; NASA, Lewis Research Center, Cleveland, OH) and LOUIS R. IGNACZAK (NASA, Lewis Research Center, Cleveland, OH) AIAA, SAE, ASME, and ASEE, Joint Propulsion Conference and Exhibit, 28th, Nashville, TN, July 6-8, 1992. 52 p. Previously announced in STAR as N92-28983. Jul. 1992 52 p refs (AIAA PAPER 92-3516) Copyright

A 25-year historical review of the Space Electric Rocket Test 2 (SERT 2) mission is presented. The Agena launch vehicle; the SERT 2 spacecraft; and mission-peculiar spacecraft hardware, including two ion thruster systems are described. The 3 1/2-year development period, from 1966 to 1970, that was needed to design,

fabricate, and qualify the ion thruster system and the supporting spacecraft components, is documented. Major testing of two ion thruster systems and related auxiliary experiments that were conducted in space after the 3 Feb. 1970, launch are reviewed. Extended ion thruster restarts from 1973 to 1981 are reported, in addition to cross-neutralization tests. Tests of a reflector erosion experiment were continued in 1989 to 1991. The continuing performance of spacecraft subsystems, including the solar arrays, over the 1970-1991 period is summarized. Finally, the knowledge of thruster-spacecraft interactions learned from SERT 2 is listed. Author

A92-54039*# National Aeronautics and Space Administration. Lewis Research Center, Cleveland, OH.

DEPENDENCE OF HYDROGEN ARCJET OPERATION ON ELECTRODE GEOMETRY

ERIC J. PENCIL, JOHN M. SANKOVIC, CHARLES J. SARMIENTO, and JOHN A. HAMLEY (NASA, Lewis Research Center, Cleveland, OH) AIAA, SAE, ASME, and ASEE, Joint Propulsion Conference and Exhibit, 28th, Nashville, TN, July 6-8, 1992. 21 p. Jul. 1992 21 p refs (AIAA PAPER 92-3530) Copyright

The dependence of 2kW hydrogen arcjet performance on cathode to anode electrode spacing was evaluated at specific impulses of 900 and 1000 s. Less than 2 absolute percent change in efficiency was measured for the spacings tested which did not repeat the 14 absolute percent variation reported in earlier work with similar electrode designs. A different nozzle configuration was used to quantify the variation in hydrogen arcjet performance over an extended range of electrode spacing. Electrode gap variation resulted in less than 3 absolute percent change in efficiency. These null results suggested that electrode spacing is decoupled from hydrogen arcjet ignition. The dependence of breakdown voltage on mass flow rate and electrode agreed with Paschen curves for hydrogen. Preliminary characterization of the dependence of hydrogen arcjet ignition on rates of pulse repetition and pulse voltage rise were also included for comparison with previous results obtained using simulated hydrazine. Author

A92-54040*# National Aeronautics and Space Administration. Lewis Research Center, Cleveland, OH.

LOW-POWER ARCJET TEST FACILITY IMPACTS

W. E. MORREN (NASA, Lewis Research Center, Cleveland, OH) and PAUL J. LICHON (Rocket Research Co., Redmond, WA) AIAA, SAE, ASME, and ASEE, Joint Propulsion Conference and Exhibit, 28th, Nashville, TN, July 6-8, 1992. 21 p. Jul. 1992 21 p refs (AIAA PAPER 92-3532) Copyright

Performance characterizations of a flight-type 1.4 kW arcjet system were conducted. Performance and thruster temperature distributions were measured at thruster input power levels and propellant mass flow rates ranging from 1274 to 1370 W and from 3.2×10^{-5} to 5.1×10^{-5} kg/s, respectively. Specific impulses measured at the two facilities, at comparable test cell pressures, using gaseous hydrogen-nitrogen propellant mixtures agreed to within 1 percent over the range of operating conditions tested. The specific impulses measured using hydrazine propellant were higher than that for the cold hydrogen/nitrogen mixtures. Agreement between the hydrazine and gas mixture data was good, however, when the differences in propellant enthalpies at the thruster inlet were considered. Specific impulse showed a strong dependence on test facility pressure, and was 3 to 4 percent higher below 0.1 Pa than for test cell pressures above 5 Pa. Author

A92-54041*# National Aeronautics and Space Administration. Lewis Research Center, Cleveland, OH.

PRELIMINARY CHARACTERIZATIONS OF A WATER VAPORIZER FOR RESISTOJET APPLICATIONS

W. E. MORREN (NASA, Lewis Research Center, Cleveland, OH) AIAA, SAE, ASME, and ASEE, Joint Propulsion Conference and Exhibit, 28th, Nashville, TN, July 6-8, 1992. 16 p. Jul. 1992

16 p refs

(AIAA PAPER 92-3533) Copyright

A series of tests were conducted to explore the characteristics of a water vaporizer intended for application to resistojet propulsion systems. A laboratory model of a forced-flow, once-through water vaporizer employing a porous heat exchange medium was built and characterized over a range of flow rates and power levels of interest for application to water resistojets. In a test during which the vaporizer was rotated about a horizontal axis normal to its own axis, the outlet temperature and mass flow rate through the vaporizer remained steady. Throttability to 30 percent of the maximum flow rate tested was demonstrated. The measured thermal efficiency of the vaporizer was near 0.9 for all tests. The water vaporizer was integrated with an engineering model multipropellant resistojet. Performance of the vaporizer/thruster assembly was measured over a narrow range of operating conditions. The maximum specific impulse measured was 234 s at a mass flow rate and specific power level (vaporizer and thruster combined) of $154 \times 10 \text{ exp } -6 \text{ kg/s}$ and 6.8 MJ/kg , respectively.

Author

A92-54062*# National Aeronautics and Space Administration. Lewis Research Center, Cleveland, OH.

NASA'S NUCLEAR THERMAL PROPULSION TECHNOLOGY PROJECT

KEITH M. PEECOOK and JAMES R. STONE (NASA, Lewis Research Center, Cleveland, OH) AIAA, SAE, ASME, and ASEE, Joint Propulsion Conference and Exhibit, 28th, Nashville, TN, July 6-8, 1992. 8 p. Jul. 1992 8 p refs
(AIAA PAPER 92-3581) Copyright

The nonnuclear subsystem technologies required for incorporating nuclear thermal propulsion (NTP) into space-exploration missions are discussed. Of particular interest to planned missions are such technologies as materials, instrumentation and controls, turbomachinery, CFD modeling, nozzle extension designs and models, and analyses of exhaust plumes. NASA studies are described and/or proposed for refractory metals and alloys, robotic NTP controls, and turbopump materials candidates. Alternative nozzle concepts such as aerospikes and truncated plugs are proposed, and numerical simulations are set forth for studying heavy molecules and the backstreaming of highly reactive free-radical hydrogen in the exhaust plume. The critical technologies described in the paper are central to the development of NTP, and NTP has the potential to facilitate a range of space exploration activities.

C.C.S.

A92-54063*# National Aeronautics and Space Administration. Lewis Research Center, Cleveland, OH.

AN IMPROVED HEAT TRANSFER CONFIGURATION FOR A SOLID-CORE NUCLEAR THERMAL ROCKET ENGINE

JOHN S. CLARK, JAMES T. WALTON (NASA, Lewis Research Center, Cleveland, OH), and MELISSA L. MCGUIRE (Cincinnati, University, OH) AIAA, SAE, ASME, and ASEE, Joint Propulsion Conference and Exhibit, 28th, Nashville, TN, July 6-8, 1992. 11 p. Jul. 1992 11 p refs
(AIAA PAPER 92-3583) Copyright

Interrupted flow, impingement cooling, and axial power distribution are employed to enhance the heat-transfer configuration of a solid-core nuclear thermal rocket engine. Impingement cooling is introduced to increase the local heat-transfer coefficients between the reactor material and the coolants. Increased fuel loading is used at the inlet end of the reactor to enhance heat-transfer capability where the temperature differences are the greatest. A thermal-hydraulics computer program for an unfueled NERVA reactor core is employed to analyze the proposed configuration with attention given to uniform fuel loading, number of channels through the impingement wafers, fuel-element length, mass-flow rate, and wafer gap. The impingement wafer concept (IWC) is shown to have heat-transfer characteristics that are better than those of the NERVA-derived reactor at 2500 K. The IWC concept is argued to be an effective heat-transfer configuration for solid-core nuclear thermal rocket engines.

C.C.S.

A92-54144*# National Aeronautics and Space Administration. Lewis Research Center, Cleveland, OH.

PRELIMINARY INVESTIGATION OF POWER FLOW AND ELECTRODE PHENOMENA IN A MULTI-MEGAWATT COAXIAL PLASMA THRUSTER

KURT F. SCHOENBERG, RICHARD A. GERWIN, IVARS HENINS (Los Alamos National Laboratory, NM), ROBERT MAYO (North Carolina State University, Raleigh), JAY SCHEUER, and GLEN WURDEN (Los Alamos National Laboratory, NM) AIAA, SAE, ASME, and ASEE, Joint Propulsion Conference and Exhibit, 28th, Nashville, TN, July 6-8, 1992. 47 p. Research supported by NASA and DOE. Jul. 1992 47 p refs
(AIAA PAPER 92-3741) Copyright

The present report on preliminary results of theoretical and experimental investigations of power flow in a large, unoptimized, multimegawatt coaxial thruster evaluates the significance of these data for the development of efficient, megawatt-class magnetoplasmadynamic (MPD) thrusters. The good agreement obtained between thruster operational performance and model predictions suggests that ideal MHD processes, including those of a magnetic nozzle, play an important role in coaxial plasma thruster dynamics at power levels relevant to advanced space propulsion. An optimized magnetic nozzle design would aid the development of efficient, multimegawatt MPD thrusters.

O.C.

A92-54164*# National Aeronautics and Space Administration. Lewis Research Center, Cleveland, OH.

AN OVERVIEW OF IN-FLIGHT PLUME DIAGNOSTICS FOR ROCKET ENGINES

G. C. MADZSAR (NASA, Lewis Research Center, Cleveland, OH), R. L. BICKFORD (Aerojet, Propulsion Div., Sacramento, CA), and D. B. DUNCAN (Duncan Technologies, Auburn, CA) AIAA, SAE, ASME, and ASEE, Joint Propulsion Conference and Exhibit, 28th, Nashville, TN, July 6-8, 1992. 25 p. Previously announced in STAR as N92-28417. Jul. 1992 25 p refs
(AIAA PAPER 92-3785) Copyright

An overview and progress report of the work performed or sponsored by LeRC toward the development of in-flight plume spectroscopy technology for health and performance monitoring of liquid propellant rocket engines are presented. The primary objective of this effort is to develop technology that can be utilized on any flight engine. This technology will be validated by a hardware demonstration of a system capable of being retrofitted onto the Space Shuttle Main Engines for spectroscopic measurements during flight. The philosophy on system definition and status on the development of instrumentation, optics, and signal processing with respect to implementation on a flight engine are discussed.

Author

A92-54182*# National Aeronautics and Space Administration. Lewis Research Center, Cleveland, OH.

NUMERICAL STUDY OF LOW PRESSURE NUCLEAR THERMAL ROCKETS

SUK C. KIM (Sverdrup Technology, Inc.; NASA, Lewis Research Center, Cleveland, OH) and ROBERT M. STUBBS (NASA, Lewis Research Center, Cleveland, OH) AIAA, SAE, ASME, and ASEE, Joint Propulsion Conference and Exhibit, 28th, Nashville, TN, July 6-8, 1992. 12 p. Jul. 1992 12 p refs
(Contract NAS3-25266)
(AIAA PAPER 92-3815)

The flowfields and performance of low pressure nuclear thermal rockets, which use hydrogen as a propellant, are studied by solving the Navier-Stokes equations and the species equations. A finite-rate chemistry model is used in the species equations, and the turbulence is simulated by the Baldwin-Lomax turbulence model with a modified van Driest's damping constant. The calculated results for the chamber temperatures of 3200 K and 4000 K with a chamber pressure range of 0.1 atm to 6 atm are presented as contours, centerline variations, and exit profiles. The performance values from the present calculations, such as the vacuum specific impulse and thrust, are compared with those from the 1D, inviscid equilibrium and frozen flow code.

Author

20 SPACECRAFT PROPULSION AND POWER

A92-54190*# National Aeronautics and Space Administration. Lewis Research Center, Cleveland, OH.

AN EXPERIMENTAL STUDY OF IMPINGEMENT-ION-PRODUCTION MECHANISMS

JEFF M. MONHEISER and PAUL J. WILBUR (Colorado State University, Fort Collins) AIAA, SAE, ASME, and ASEE, Joint Propulsion Conference and Exhibit, 28th, Nashville, TN, July 6-8, 1992. 11 p. Jul. 1992 11 p refs
(Contract NAG3-1206)
(AIAA PAPER 92-3826) Copyright

A simple model for the production of ions that impinge on and sputter erode the accelerator grid of an ion thruster is presented. Charge-exchange and electron-impact ion production processes are considered, but experimental results show the charge-exchange process dominates. Additional experimental results show the effects of changes in thruster operating conditions on the length of the region from which these ions are drawn upstream into the grid. Results which show erosion patterns and indicate molybdenum accelerator grids erode more rapidly than graphite ones are also presented. Author

A92-54191*# National Aeronautics and Space Administration. Lewis Research Center, Cleveland, OH.

CHARACTERIZATION OF ION ACCELERATING SYSTEMS ON NASA LERC'S ION THRUSTERS

VINCENT K. RAWLIN (NASA, Lewis Research Center, Cleveland, OH) AIAA, SAE, ASME, and ASEE, Joint Propulsion Conference and Exhibit, 28th, Nashville, TN, July 6-8, 1992. 33 p. Jul. 1992 33 p refs
(AIAA PAPER 92-3827) Copyright

An investigation is conducted regarding ion-accelerating systems for two NASA thrusters to study the limits of ion-extraction capability or perveance. A total of nine two-grid ion-accelerating systems are tested with the 30- and 50-cm-diam ring-cusp inert-gas ion thrusters emphasizing the extension of ion-extraction. The vacuum-tank testing is described using xenon, krypton, and argon propellants, and thruster performance is computed with attention given to theoretical design considerations. Reductions in perveance are noted with decreasing accelerator-hole-to-screen-hole diameter ratios. Perveance values vary indirectly with the ratio of discharge voltage to total accelerating voltage, and screen/accelerator electrode hole-pair alignment is also found to contribute to perveance values. C.C.S.

A92-54192*# National Aeronautics and Space Administration. Lewis Research Center, Cleveland, OH.

FURTHER STUDY OF THE EFFECT OF THE DOWNSTREAM PLASMA CONDITION ON ACCELERATOR GRID EROSION IN AN ION THRUSTER

XIAOHANG PENG, WILHELMUS M. RUYTEN (Tennessee, University; Calspan Center for Space Transportation and Applied Research, Tullahoma), and DENNIS KEEFER (Tennessee, University, Tullahoma) AIAA, SAE, ASME, and ASEE, Joint Propulsion Conference and Exhibit, 28th, Nashville, TN, July 6-8, 1992. 5 p. Research supported by Boeing Defense & Space Group. Jul. 1992 5 p refs
(Contract NAG3-1315)
(AIAA PAPER 92-3829) Copyright

Further numerical results are presented of earlier particle-in-cell/Monte Carlo calculations of accelerator grid erosion in an ion thruster. A comparison between numerical and experimental results suggests that the accelerator grid impingement is primarily due to ions created far downstream from the accelerator grid. In particular, for the same experimental conditions as those of Monheiser and Wilbur at Colorado State University, it is found that a downstream plasma density of $2 \times 10^{14}/\text{cu m}$ is required to give the same ratio of accelerator grid impingement current to beam current (5 percent). For this condition, a potential hill is found in the downstream region of 2.5 V. Author

A92-57033*# National Aeronautics and Space Administration. Lewis Research Center, Cleveland, OH.

NASA'S NUCLEAR ELECTRIC PROPULSION TECHNOLOGY PROJECT

JAMES R. STONE and JAMES S. SOVEY (NASA, Lewis Research Center, Cleveland, OH) AIAA, SAE, ASME, and ASEE, Joint Propulsion Conference and Exhibit, 28th, Nashville, TN, July 6-8, 1992. 17 p. Previously announced in STAR as N92-32463. Jul. 1992 17 p refs
(AIAA PAPER 92-3705) Copyright

The National Aeronautics and Space Administration (NASA) has initiated a program to establish the readiness of nuclear electric propulsion (NEP) technology for relatively near-term applications to outer planet robotic science missions with potential future evolution to system for piloted Mars vehicles. This program was initiated in 1991 with a very modest effort identified with nuclear thermal propulsion (NTP); however, NEP is also an integral part of this program and builds upon NASA's Base Research and Technology Program in power and electric propulsion as well as the SP-100 space nuclear power program. The NEP Program will establish the feasibility and practicality of electric propulsion for robotic and piloted solar system exploration. The performance objectives are high specific impulse (200 greater than $I(\text{sub sp})$ greater than 10000 s), high efficiency (over 0.50), and low specific mass. The planning for this program was initially focussed on piloted Mars missions, but has since been redirected to first focus on 100-kW class systems for relatively near-term robotic missions, with possible future evolution to megawatt-and multi-megawatt-class systems applicable to cargo vehicles supporting human missions as well as to the piloted vehicles. This paper reviews current plans and recent progress for the overall nuclear electric propulsion project and closely related activities. Author

A92-57054 National Aeronautics and Space Administration. Lewis Research Center, Cleveland, OH.

NUCLEAR PROPULSION FOR SPACE EXPLORATION

THOMAS J. MILLER (NASA, Lewis Research Center, Cleveland, OH) and GARY L. BENNETT (NASA, Washington) IAF, International Astronautical Congress, 43rd, Washington, Aug. 28-Sept. 5, 1992. 8 p. Aug. 1992 8 p refs
(IAF PAPER 92-0575) Copyright

The results of some recent studies of the application of both nuclear electric and nuclear thermal propulsion systems in space exploration are presented. Issues that require further study and which have a significant effect on the propulsion system design and selection are identified. Attention is given to robotic missions, lunar piloted and cargo missions, and Mars missions. R.E.P.

A92-57056* National Aeronautics and Space Administration. Lewis Research Center, Cleveland, OH.

LASER BEAMED POWER - SATELLITE DEMONSTRATION APPLICATIONS

GEOFFREY A. LANDIS (Sverdrup Technology, Inc.; NASA, Lewis Research Center, Cleveland, OH) and LARRY H. WESTERLUND (Satellite Communications Consultants, Rockville, MD) IAF, International Astronautical Congress, 43rd, Washington, Aug. 28-Sept. 5, 1992. 11 p. Aug. 1992 11 p refs
(IAF PAPER 92-0600) Copyright

Feasibility of using a ground-based laser to beam light to the solar arrays of orbiting satellites to a level sufficient to provide the operating power required is discussed. An example case of a GEO communications satellite near the end of life due to radiation damage of the solar arrays or battery failure is considered. It is concluded that the commercial satellite industry should be able to reap significant economic benefits through the use of power beaming which is capable of providing supplemental power for satellites with failing arrays, or primary power for failed batteries. O.G.

A92-57058* National Aeronautics and Space Administration. Lewis Research Center, Cleveland, OH.

DEVELOPMENT OF ARCJET AND ION PROPULSION FOR SPACECRAFT STATIONKEEPING

JAMES S. SOVEY, FRANCIS M. CURRAN, THOMAS W. HAAG, MICHAEL J. PATTERSON, ERIC J. PENCIL, VINCENT K. RAWLIN, and JOHN M. SANKOVIC (NASA, Lewis Research Center, Cleveland, OH) IAF, International Astronautical Congress, 43rd, Washington, Aug. 28-Sept. 5, 1992. 16 p. Aug. 1992 16 p refs

(IAF PAPER 92-0607) Copyright

Near term flight applications of arcjet and ion thruster satellite station-keeping systems as well as development activities in Europe, Japan, and the United States are reviewed. At least two arcjet and three ion propulsion flights are scheduled during the 1992 - 1995 period. Ground demonstration technology programs are focusing on the development of kW-class hydrazine and ammonia arcjets and xenon ion thrusters. Recent work at NASA Lewis Research Center on electric thruster and system integration technologies relating to satellite stationkeeping and repositioning will also be summarized. Author

A92-57089 National Aeronautics and Space Administration. Marshall Space Flight Center, Huntsville, AL.

HEALTH MANAGEMENT AND CONTROLS FOR EARTH TO ORBIT PROPULSION SYSTEMS

R. L. BICKFORD (Aerojet, Propulsion Div., Sacramento, CA) IAF, International Astronautical Congress, 43rd, Washington, Aug. 28-Sept. 5, 1992. 8 p. Research supported by NASA. Aug. 1992 8 p refs

(Contract NAS8-38074; NAS3-25624; NAS3-25883)

(IAF PAPER 92-0646) Copyright

Fault detection and isolation for advanced rocket engine controllers are discussed focusing on advanced sensing systems and software which significantly improve component failure detection for engine safety and health management. Aerojet's Space Transportation Main Engine controller for the National Launch System is the state of the art in fault tolerant engine avionics. Health management systems provide high levels of automated fault coverage and significantly improve vehicle delivered reliability and lower preflight operations costs. Key technologies, including the sensor data validation algorithms and flight capable spectrometers, have been demonstrated in ground applications and are found to be suitable for bridging programs into flight applications. O.G.

A92-57105* National Aeronautics and Space Administration. Lewis Research Center, Cleveland, OH.

LOW THRUST CHEMICAL ROCKET TECHNOLOGY

STEVEN J. SCHNEIDER (NASA, Lewis Research Center, Cleveland, OH) IAF, International Astronautical Congress, 43rd, Washington, Aug. 28-Sept. 5, 1992. 31 p. Aug. 1992 31 p refs

(IAF PAPER 92-0669)

A technology program aimed at improving the performance of low thrust chemical rockets for spacecraft onboard applications is reviewed. Navier-Stokes analyses of low Reynolds number rocket flows have been compared with local flow property measurements obtained using Rayleigh and Raman diagnostics in a 100 N gaseous hydrogen/gaseous oxygen rocket. It is indicated that computational domain should include the near injector flow and that the shear layer combustion model needs improvement. The system analyses and technical efforts intended to develop a technology base for higher performance propellants are presented. A LOX/hydrazine engine is demonstrated to have a 95 percent theoretical c-star which translates into a projected vacuum specific impulse of 345 seconds at an area ratio of 204:1. O.G.

N92-10044*# National Aeronautics and Space Administration. Lewis Research Center, Cleveland, OH.

MAGNETOPLASMA DYNAMIC THRUSTER WORKSHOP

1991 178 p Workshop held in Washington, DC, 16 May 1991; sponsored in part by NASA, Washington

(Contract RTOP 506-42-31)

(NASA-CP-10084; E-6518; NAS 1.55:10084) Avail: CASI HC A09/MF A02

On May 16, 1991, the NASA Headquarters Propulsion, Power, and Energy Division and the NASA Lewis Research Center Low Thrust Propulsion Branch hosted a workshop attended by key experts in magnetoplasmadynamic (MPD) thrusters and associated sciences. The scope was limited to high power MPD thrusters suitable for major NASA space exploration missions, and its purpose was to initiate the process of increasing the expectations and prospects for MPD research, primarily by increasing the level of cooperation, interaction, and communication between parties within the MPD community.

N92-10054* National Aeronautics and Space Administration. Lewis Research Center, Cleveland, OH.

EXTENDED TEMPERATURE RANGE ROCKET INJECTOR Patent

STEVEN J. SCHNEIDER, inventor (to NASA) 8 Oct. 1991 5 p Filed 30 Nov. 1989 Supersedes N90-15130 (28 - 7 p 887)

(NASA-CASE-LEW-14846-1; US-PATENT-5,054,287;

US-PATENT-APPL-SN-443523; US-PATENT-CLASS-60-240;

US-PATENT-CLASS-60-258; US-PATENT-CLASS-60-39.281;

INT-PATENT-CLASS-F02R-9/52) Avail: US Patent and Trademark Office

A rocket injector is provided with multiple sets of manifolds for supplying propellants to injector elements. Sensors transmit the temperatures of the propellants to a suitable controller which is operably connected to valves between these manifolds and propellant storage tanks. When cryogenic propellant temperatures are sensed, only a portion of the valves are opened to furnish propellants to some of the manifolds. When lower temperatures are sensed, additional valves are opened to furnish propellants to more of the manifolds.

Official Gazette of the U.S. Patent and Trademark Office

N92-10055*# National Aeronautics and Space Administration. Lewis Research Center, Cleveland, OH.

DESCRIPTION OF THE PMAD DC TEST BED ARCHITECTURE AND INTEGRATION SEQUENCE

R. F. BEACH, L. TRASH, D. FONG, and B. BOLERJACK (Rockwell International Corp., Canoga Park, CA.) 1991 10 p Presented at the 26th Intersociety Energy Conversion Engineering Conference, Boston, MA, 4-9 Aug. 1991; sponsored by ANS, SAE, ACS, AIAA, ASME, IEEE, and AIChE

(Contract RTOP 474-42-10)

(NASA-TM-105284; E-6614; NAS 1.15:105284) Avail: CASI HC A02/MF A01

NASA-Lewis is responsible for the development, fabrication, and assembly of the electric power system (EPS) for the Space Station Freedom (SSF). The SSF power system is radically different from previous spacecraft power systems in both the size and complexity of the system. Unlike past spacecraft power system the SSF EPS will grow and be maintained on orbit and must be flexible to meet changing user power needs. The SSF power system is also unique in comparison with terrestrial power systems because it is dominated by power electronic converters which regulate and control the power. Although spacecraft historically have used power converters for regulation they typically involved only a single series regulating element. The SSF EPS involves multiple regulating elements, two or more in series, prior to the load. These unique system features required the construction of a testbed which would allow the development of spacecraft power system technology. A description is provided of the Power Management and Distribution (PMAD) DC Testbed which was assembled to support the design and early evaluation of the SSF EPS. A description of the integration process used in the assembly sequence is also given along with a description of the support facility. Author

N92-10057*# National Aeronautics and Space Administration. Lewis Research Center, Cleveland, OH.

MULTI-REACTOR POWER SYSTEM CONFIGURATIONS FOR MULTIMEGAWATT NUCLEAR ELECTRIC PROPULSION

20 SPACECRAFT PROPULSION AND POWER

JEFFREY A. GEORGE Sep. 1991 9 p
(Contract RTOP 920-00-00)
(NASA-TM-105212; E-6607; NAS 1.15:105212) Avail: CASI HC
A02/MF A01

A modular, multi-reactor power system and vehicle configuration for piloted nuclear electric propulsion (NEP) missions to Mars is presented. Such a design could provide enhanced system and mission reliability, allowing a comfortable safety margin for early manned flights, and would allow a range of piloted and cargo missions to be performed with a single power system design. Early use of common power modules for cargo missions would also provide progressive flight experience and validation of standardized systems for use in later piloted applications. System and mission analysis are presented to compare single and multi-reactor configurations for piloted Mars missions. A conceptual design for the Hydra modular multi-reactor NEP vehicle is presented. Author

N92-11088*# National Aeronautics and Space Administration. Lewis Research Center, Cleveland, OH.

NUCLEAR THERMAL PROPULSION: A JOINT NASA/DOE/DOD WORKSHOP

JOHN S. CLARK, ed. 1991 500 p Workshop held in Cleveland, OH, 10-12 Jul. 1990
(Contract RTOP 593-71-00)
(NASA-CP-10079; E-6456; NAS 1.55:10079) Avail: CASI HC
A21/MF A04

Papers presented at the joint NASA/DOE/DOD workshop on nuclear thermal propulsion are compiled. The following subject areas are covered: nuclear thermal propulsion programs; Rover/NERVA and NERVA systems; Low Pressure Nuclear Thermal Rocket (LPNTR); particle bed reactor nuclear rocket; hybrid propulsion systems; wire core reactor; pellet bed reactor; foil reactor; Droplet Core Nuclear Rocket (DCNR); open cycle gas core nuclear rockets; vapor core propulsion reactors; nuclear light bulb; Nuclear rocket using Indigenous Martian Fuel (NIMF); mission analysis; propulsion and reactor technology; development plans; and safety issues.

N92-11090*# National Aeronautics and Space Administration. Lewis Research Center, Cleveland, OH.

NUCLEAR THERMAL PROPULSION WORKSHOP OVERVIEW

JOHN S. CLARK *In its* Nuclear Thermal Propulsion: A Joint NASA/DOE/DOD Workshop p 37-52 1991
Avail: CASI HC A03/MF A04

NASA is planning an Exploration Technology Program as part of the Space Exploration Initiative to return U.S. astronauts to the moon, conduct intensive robotic exploration of the moon and Mars, and to conduct a piloted mission to Mars by 2019. Nuclear Propulsion is one of the key technology thrust for the human mission to Mars. The workshop addresses NTP (Nuclear Thermal Rocket) technologies with purpose to: assess the state-of-the-art of nuclear propulsion concepts; assess the potential benefits of the concepts for the mission to Mars; identify critical, enabling technologies; lay-out (first order) technology development plans including facility requirements; and estimate the cost of developing these technologies to flight-ready status. The output from the workshop will serve as a data base for nuclear propulsion project planning. Author

N92-11091*# National Aeronautics and Space Administration. Lewis Research Center, Cleveland, OH.

NUCLEAR THERMAL ROCKET WORKSHOP REFERENCE SYSTEM ROVER/NERVA

STANLEY K. BOROWSKI *In its* Nuclear Thermal Propulsion: A Joint NASA/DOE/DOD Workshop p 53-92 1991
Avail: CASI HC A03/MF A04

The Rover/NERVA engine system is to be used as a reference, against which each of the other concepts presented in the workshop will be compared. The following topics are reviewed: the operational characteristics of the nuclear thermal rocket (NTR); the accomplishments of the Rover/NERVA programs; and performance characteristics of the NERVA-type systems for both

Mars and lunar mission applications. Also, the issues of ground testing, NTR safety, NASA's nuclear propulsion project plans, and NTR development cost estimates are briefly discussed. Author

N92-11115*# National Aeronautics and Space Administration. Lewis Research Center, Cleveland, OH.

SAFETY ISSUES

R. ROHAL *In its* Nuclear Thermal Propulsion: A Joint NASA/DOE/DOD Workshop p 441-444 1991
Avail: CASI HC A01/MF A04

The purpose of the NASA safety review process is to make sure that any system hazards that can endanger the manned flight system are precluded. The systems that address manned flight in a payload safety review process are discussed. The types of basic hazards that are normally addressed on any of the payloads are: contamination, electrical shock, explosions, radiation, and temperature extremes. Author

N92-11120*# National Aeronautics and Space Administration. Lewis Research Center, Cleveland, OH.

DEVELOPMENTS IN REDES: THE ROCKET ENGINE DESIGN EXPERT SYSTEM

KENNETH O. DAVIDIAN *In* JHU, The 27th JANNAF Combustion Subcommittee Meeting, Volume 3 p 185-193 Nov. 1990
Previously announced as N91-10119
Avail: CASI HC A02/MF A06

The Rocket Engine Design Expert System (REDES) was developed at NASA-Lewis to collect, automate, and perpetuate the existing expertise of performing a comprehensive rocket engine analysis and design. Currently, REDES uses the rigorous JANNAF methodology to analyze the performance of the thrust chamber and perform computational studies of liquid rocket engine problems. The following computer codes were included in REDES: a gas properties program named GASP; a nozzle design program named RAO; a regenerative cooling channel performance evaluation code named RTE; and the JANNAF standard liquid rocket engine performance prediction code TDK (including performance evaluation modules ODE, ODK, TDE, TDK, and BLM). Computational analyses are being conducted by REDES to provide solutions to liquid rocket engine thrust chamber problems. REDES was built in the Knowledge Engineering Environment (KEE) expert system shell and runs on a Sun 4/110 computer. Author

N92-11126*# National Aeronautics and Space Administration. Lewis Research Center, Cleveland, OH.

ANALYTICAL STUDY OF NOZZLE PERFORMANCE FOR NUCLEAR THERMAL ROCKETS

KENNETH O. DAVIDIAN and KENNETH J. KACYNSKI 1991
29 p Presented at the Conference on Advanced Space Exploration Initiative Technologies, Cleveland, OH, 4-6 Sep. 1991; sponsored in part by NASA, AIAA, and OAI Previously announced in IAA as A91-52451
(Contract RTOP 506-42-72)
(NASA-TM-105251; E-6580; NAS 1.15:105251; AIAA PAPER 91-3578) Avail: CASI HC A03/MF A01

Nuclear propulsion has been identified as one of the key technologies needed for human exploration of the Moon and Mars. The Nuclear Thermal Rocket (NTR) uses a nuclear reactor to heat hydrogen to a high temperature followed by expansion through a conventional convergent-divergent nozzle. A parametric study of NTR nozzles was performed using the Rocket Engine Design Expert System (REDES) at the NASA Lewis Research Center. The REDES used the JANNAF standard rigorous methodology to determine nozzle performance over a range of chamber temperatures, chamber pressures, thrust levels, and different nozzle configurations. A design condition was set by fixing the propulsion system exit radius at five meters and throat radius was varied to achieve a target thrust level. An adiabatic wall was assumed for the nozzle, and its length was assumed to be 80 percent of a 15 degree cone. The results conclude that although the performance of the NTR, based on infinite reaction rates, looks promising at low chamber pressures, finite rate chemical reactions will cause the actual performance to be considerably lower. Parameters which

have a major influence on the delivered specific impulse value include the chamber temperature and the chamber pressures in the high thrust domain. Other parameters, such as 2-D and boundary layer effects, kinetic rates, and number of nozzles, affect the deliverable performance of an NTR nozzle to a lesser degree. For a single nozzle, maximum performance of 930 seconds and 1030 seconds occur at chamber temperatures of 2700 and 3100 K, respectively. Dissert. Abstr.

N92-11128*# National Aeronautics and Space Administration, Lewis Research Center, Cleveland, OH.

LINEAR QUADRATIC SERVO CONTROL OF A REUSABLE ROCKET ENGINE

JEFFREY L. MUSGRAVE 1991 12 p Presented at the 27th Joint Propulsion Conference, Sacramento, CA, 24-27 Jun. 1991; cosponsored by AIAA, SAE, ASME, and ASEE (Contract RTOP 582-01-11) (NASA-TM-105291; E-6628; NAS 1.15:105291; AIAA PAPER 91-1999) Avail: CASI HC A03/MF A01

A design method for a servo compensator is developed in the frequency domain using singular values. The method is applied to a reusable rocket engine. An intelligent control system for reusable rocket engines was proposed which includes a diagnostic system, a control system, and an intelligent coordinator which determines engine control strategies based on the identified failure modes. The method provides a means of generating various linear multivariable controllers capable of meeting performance and robustness specifications and accommodating failure modes identified by the diagnostic system. Command following with set point control is necessary for engine operation. A Kalman filter reconstructs the state while loop transfer recovery recovers the required degree of robustness while maintaining satisfactory rejection of sensor noise from the command error. The approach is applied to the design of a controller for a rocket engine satisfying performance constraints in the frequency domain. Simulation results demonstrate the performance of the linear design on a nonlinear engine model over all power levels during mainstage operation.

Author

N92-11129*# National Aeronautics and Space Administration, Lewis Research Center, Cleveland, OH.

IMPROVED THERMODYNAMIC MODELING OF THE NO-VENT FILL PROCESS AND CORRELATION WITH EXPERIMENTAL DATA

WILLIAM J. TAYLOR and DAVID J. CHATO 1991 18 p Presented at the 26th Thermophysics Conference, Honolulu, HI, 24-26 Jun. 1991; sponsored by AIAA Previously announced in IAA as A91-43444

(Contract RTOP 506-48-00) (NASA-TM-104492; E-6350; NAS 1.15:104492; AIAA PAPER 91-1379) Avail: CASI HC A03/MF A01

The United States' plans to establish a permanent manned presence in space and to explore the Solar System created the need to efficiently handle large quantities of subcritical cryogenic fluids, particularly propellants such as liquid hydrogen and liquid oxygen, in low- to zero-gravity environments. One of the key technologies to be developed for fluid handling is the ability to transfer the cryogens between storage and spacecraft tanks. The no-vent fill method was identified as one way to perform this transfer. In order to understand how to apply this method, a model of the no-vent fill process is being developed and correlated with experimental data. The verified models then can be used to design and analyze configurations for tankage and subcritical fluid depots. The development of an improved macroscopic thermodynamic model is discussed of the no-vent fill process and the analytical results from the computer program implementation of the model are correlated with experimental results for two different test tanks. Author

N92-11130*# National Aeronautics and Space Administration, Lewis Research Center, Cleveland, OH.

TECHNOLOGY READINESS ASSESSMENT OF ADVANCED SPACE ENGINE INTEGRATED CONTROLS AND HEALTH MONITORING

MARC G. MILLIS 1991 17 p Presented at the Conference on Advanced Space Exploration Initiative Technologies, Cleveland, OH, 4-6 Sep. 1991; cosponsored by AIAA, NASA, and OAI Previously announced in IAA as A91-52467

(Contract RTOP 593-12-11) (NASA-TM-105255; E-6584; NAS 1.15:105255; AIAA PAPER 91-3601) Copyright Avail: CASI HC A03/MF A01

An evaluation is given for an integrated control and health monitoring system (ICHM) system that is designed to be used with hydrogen-oxygen rocket engines. The minimum required ICHM functions, system elements, technology readiness, and system cost are assessed for a system which permits the operation of H-O engines that are space-based, reusable, and descent throttleable. Based on the evaluation of the H-O ICHM, it is estimated that the minimum system requirements for demonstration on an engine system testbed will require an investment of 30 to 45 million dollars over six years. Author

N92-11133*# National Aeronautics and Space Administration, Lewis Research Center, Cleveland, OH.

EFFECT OF PARTICLE SIZE OF MARTIAN DUST ON THE DEGRADATION OF PHOTOVOLTAIC CELL PERFORMANCE

JAMES R. GAIER and MARLA E. PEREZ-DAVIS 1991 17 p Proposed for presentation at the International Solar Energy Conference, Maui, HI, 4-8 Apr. 1992; sponsored by ASME (Contract RTOP 506-41-41)

(NASA-TM-105232; E-6556; NAS 1.15:105232) Avail: CASI HC A03/MF A01

Glass coverglass and SiO₂ covered and uncovered silicon photovoltaic (PV) cells were subjected to conditions simulating a Mars dust storm, using the Martian Surface Wind Tunnel, to assess the effect of particle size on the performance of PV cells in the Martian environment. The dust used was an artificial mineral of the approximate elemental composition of Martian soil, which was sorted into four different size ranges. Samples were tested both initially clean and initially dusted. The samples were exposed to clear and dust laden winds, wind velocities varying from 23 to 116 m/s, and attack angles from 0 to 90 deg. It was found that transmittance through the coverglass approximates the power produced by a dusty PV cell. Occultation by the dust was found to dominate the performance degradation for wind velocities below 50 m/s, whereas abrasion dominates the degradation at wind velocities above 85 m/s. Occultation is most severe at 0 deg (parallel to the wind), is less pronounced from 22.5 to 67.5 deg, and is somewhat larger at 90 deg (perpendicular to the wind). Abrasion is negligible at 0 deg, and increases to a maximum at 90 deg. Occultation is more of a problem with small particles, whereas large particles (unless they are agglomerates) cause more abrasion. Author

N92-11135*# National Aeronautics and Space Administration, Lewis Research Center, Cleveland, OH.

PLANS FOR THE DEVELOPMENT OF CRYOGENIC ENGINES FOR SPACE EXPLORATION

JAMES R. STONE (Sverdrup Technology, Inc., Brook Park, OH.), LORETTA M. SHAW, and CARL A. AUKERMAN (Sverdrup Technology, Inc., Brook Park, OH.) Sep. 1991 21 p Presented at the Conference on Advanced Space Exploration Initiative Technologies, Cleveland, OH, 4-6 Sep. 1991; cosponsored by AIAA, NASA, and OAI Previously announced in IAA as A91-52351 (Contract RTOP 591-41-41)

(NASA-TM-105250; E-6579; NAS 1.15:105250; AIAA PAPER 91-3438) Copyright Avail: CASI HC A03/MF A01

The NASA Lewis Research Center (LeRC) is conducting a broad range of basic research and focused technology development activities in both aeronautical and space propulsion. By virtue of the successful conduct of these programs, LeRC is strongly qualified to lead Advanced Development and subsequent

20 SPACECRAFT PROPULSION AND POWER

development programs on cryogenic space propulsion systems on support of the Space Exploration Initiative. A review is provided of technology status, including recent progress in the ongoing activities, and a top level description of the proposed program.

Author

N92-11136*# National Aeronautics and Space Administration. Lewis Research Center, Cleveland, OH.

TEST FACILITIES FOR HIGH POWER ELECTRIC PROPULSION

JAMES S. SOVEY (Sverdrup Technology, Inc., Brook Park, OH.), ROBERT H. VETRONE, STANLEY P. GRISNIK, ROGER M. MYERS, and JAMES E. PARKES (Sverdrup Technology, Inc., Brook Park, OH.) 1991 23 p Presented at the Conference on Advanced Space Exploration Initiative Technologies, Cleveland, OH, 4-6 Sep. 1991; cosponsored by AIAA, NASA, and OAI Previously announced in IAA as A91-52396

(Contract RTOP 506-42-31)
(NASA-TM-105247; E-6576; NAS 1.15:105247; AIAA PAPER 91-3499) Avail: CASI HC A03/MF A01

Electric propulsion has applications for orbit raising, maneuvering of large space systems, and interplanetary missions. These missions involve propulsion power levels from tenths to tens of megawatts, depending upon the application. General facility requirements for testing high power electric propulsion at the component and thrust systems level are defined. The characteristics and pumping capabilities of many large vacuum chambers in the United States are reviewed and compared with the requirements for high power electric propulsion testing.

Author

N92-11137*# National Aeronautics and Space Administration. Lewis Research Center, Cleveland, OH.

AN OVERVIEW OF TESTED AND ANALYZED NTP CONCEPTS

JAMES T. WALTON 1991 25 p Presented at the Conference on Advanced Space Exploration Initiative Technologies, Cleveland, OH, 4-6 Sep. 1991; cosponsored by AIAA, NASA, and OAI Previously announced in IAA as A91-52400

(Contract RTOP 593-71-11)
(NASA-TM-105252; E-6581; NAS 1.15:105252; AIAA PAPER 91-3503) Copyright Avail: CASI HC A03/MF A01

If we buy into the goals of the Space Exploration Initiative (SEI) and accept that they are worthy of the hefty investment of our tax dollars, then we must begin to evaluate the technologies which enable their attainment. The main driving technology is the propulsion systems; for interplanetary missions, the safest and most affordable is a Nuclear Thermal Propulsion (NTP) system. An overview is presented of the NTP systems which received detailed conceptual design and, for several, testing.

Author

N92-11138*# National Aeronautics and Space Administration. Lewis Research Center, Cleveland, OH.

EFFECTS OF ANISOTROPIC CONDUCTION AND HEAT PIPE INTERACTION ON MINIMUM MASS SPACE RADIATORS

KARL W. BAKER and KURT O. LUND (California Univ., San Diego.) 1991 10 p Proposed for presentation at the International Solar Energy Conference, Maui, HI, 4-8 Apr. 1992; sponsored by ASME

(Contract RTOP 590-13-21)
(NASA-TM-105297; E-6636; NAS 1.15:105297) Avail: CASI HC A02/MF A01

Equations are formulated for the two dimensional, anisotropic conduction of heat in space radiator fins. The transverse temperature field was obtained by the integral method, and the axial field by numerical integration. A shape factor, defined for the axial boundary condition, simplifies the analysis and renders the results applicable to general heat pipe/conduction fin interface designs. The thermal results are summarized in terms of the fin efficiency, a radiation/axial conductance number, and a transverse conductance surface Biot number. These relations, together with those for mass distribution between fins and heat pipes, were used in predicting the minimum radiator mass for fixed thermal properties and fin efficiency. This mass is found to decrease

monotonically with increasing fin conductivity. Sensitivities of the minimum mass designs to the problem parameters are determined.

Author

N92-13205*# National Aeronautics and Space Administration. Lewis Research Center, Cleveland, OH.

POWER SUPPLY FOR A MANNED INTERNATIONAL ASTEROID MISSION

STEFAN WEINGARTNER, HENRY K. NAHRA, LISA L. KOHOUT, and MAX LARIN (Moscow Inst. of Aviation Technology, USSR) *In* ESA, European Space Power Conference. Volume 1: Power Systems, Power Electronics, Batteries and Fuel Cells p 359-364 Aug. 1991

Copyright Avail: CASI HC A02/MF A04; ESA, EPD, Noordwijk, Netherlands, HC 120 Dutch guilders (2 vols)

A feasibility study considering the exploitation of a near Earth asteroid was performed. The power requirements and proposed power systems for the crew vehicle, cargo vehicles, mining and processing equipment are described. A photovoltaic power system was selected to meet the 52.1 kWe and the 3.9 kWe power requirements of the crew and cargo vehicles, respectively. A nuclear power plant using a thermodynamic Rankine cycle with a total mass of 62.1 tons was chosen to provide the 7.225 MWe and the 5.5 MWth required for the mining and processing activities at the asteroid.

ESA

N92-13206*# National Aeronautics and Space Administration. Lewis Research Center, Cleveland, OH.

SEI POWER SOURCE ALTERNATIVES FOR ROVERS AND OTHER MULTI-KWE DISTRIBUTED SURFACE APPLICATIONS

D. J. BENTS, LISA L. KOHOUT, B. I. MCKISSOCK, C. D. RODRIGUEZ, C. A. WITHROW, A. COLOZZA, J. C. HANLON, and P. C. SCHMITZ (Sverdrup Technology, Inc., Brook Park, OH.) *In* ESA, European Space Power Conference. Volume 1: Power Systems, Power Electronics, Batteries and Fuel Cells p 365-374 Aug. 1991 Previously announced as N91-28277

Copyright Avail: CASI HC A02/MF A04; ESA, EPD, Noordwijk, Netherlands, HC 120 Dutch guilders (2 vols)

Results of the study performed to support the Space Exploration Initiative (SEI) which investigated power system alternatives for the rover vehicles and servicers that would be used for construction and operation of a lunar base is described. Using the mission requirements and power profiles that were subsequently generated for each of these rovers and servicers, candidate power sources incorporating various power generation and energy storage technologies were identified. The technologies were those believed most appropriate to the SEI missions, and included solar, electrochemical, and isotope systems. The candidates were characterized with respect to system mass, deployed area and volume. For each of the missions a preliminary selection was made. Results of this study depict the available power sources in light of the mission requirements as they are currently defined.

ESA

N92-13207*# National Aeronautics and Space Administration. Lewis Research Center, Cleveland, OH.

ISSUES AND STATUS OF POWER DISTRIBUTION OPTIONS FOR SPACE EXPLORATION

ROBERT W. BERCAW, RONALD C. CULL, and BARBARA H. KENNY *In* ESA, European Space Power Conference. Volume 1: Power Systems, Power Electronics, Batteries and Fuel Cells p 375-380 Aug. 1991

Copyright Avail: CASI HC A02/MF A04; ESA, EPD, Noordwijk, Netherlands, HC 120 Dutch guilders (2 vols)

The Space Exploration Initiative (SEI) will need a wide variety of manned systems with requirements significantly different than those for existing systems. The concept of a space power utility is discussed and the impact of this concept on the engineering of space power systems is examined. Almost all existing space power systems use low voltage direct current. Although they have been very successful, increasing power system requirements in recent years have exposed their inherent limitations and led to the proposal of a number of alternatives including high voltage DC

and AC at various frequencies. Drawing on the experience gained from Space Station Freedom and SEI systems studies, factors that may affect the choice of frequency standards on which to build such a space power utility are discussed. ESA

N92-13228*# National Aeronautics and Space Administration. Lewis Research Center, Cleveland, OH.

THIN-FILM PHOTOVOLTAICS: STATUS AND APPLICATIONS TO SPACE POWER

GEOFFREY A. LANDIS (Sverdrup Technology, Inc., Brook Park, OH.) and ALOYSIUS F. HEPP /in ESA, European Space Power Conference. Volume 2: Photovoltaic Generators p 517-522 Aug. 1991

Copyright Avail: CASI HC A02/MF A03; ESA, EPD, Noordwijk, Netherlands, HC 150 Dutch guilders (2 vols)

The potential applications of thin film polycrystalline and amorphous cells for space are discussed. There have been great advances in thin film solar cells for terrestrial applications; transfer of this technology to space applications could result in ultra low weight solar arrays with potentially large gains in specific power. Recent advances in thin film solar cells are reviewed, including polycrystalline copper iridium selenide and related I-III-VI₂ compounds, polycrystalline cadmium telluride and related II-VI compounds, and amorphous silicon alloys. The possibility of thin film multi bandgap cascade solar cells is discussed. ESA

N92-13230*# National Aeronautics and Space Administration. Lewis Research Center, Cleveland, OH.

THIN FILM, CONCENTRATOR, AND MULTI-JUNCTION SPACE SOLAR CELLS: STATUS AND POTENTIAL

DENNIS J. FLOOD /in ESA, European Space Power Conference. Volume 2: Photovoltaic Generators p 531-536 Aug. 1991 Previously announced as N91-31218

Copyright Avail: CASI HC A02/MF A03; ESA, EPD, Noordwijk, Netherlands, HC 150 Dutch guilders (2 vols)

Recent, rapid advances in a variety of solar cell technologies offer the potential for significantly enhancing, or enabling entirely new, mission capabilities. Thin film solar cells are of particular interest. A review is provided of the status of those thin film cell technologies of interest for space applications, and the issues to be resolved before mission planners can consider them. A short summary of recent developments in concentrator and multijunction space solar cell and array technology is given. ESA

N92-13248*# National Aeronautics and Space Administration. Lewis Research Center, Cleveland, OH.

ENHANCED EOS PHOTOVOLTAIC POWER SYSTEM CAPABILITY WITH INP SOLAR CELLS

SHEILA G. BAILEY, IRVING WEINBERG, and DENNIS J. FLOOD /in ESA, European Space Power Conference. Volume 2: Photovoltaic Generators p 641-645 Aug. 1991

Copyright Avail: CASI HC A01/MF A03; ESA, EPD, Noordwijk, Netherlands, HC 150 Dutch guilders (2 vols)

The Earth Observing System (EOS), which is part of the International Mission to Planet Earth, is NASA's main contribution to the Global Change Research Program which opens a new era in international cooperation to study the Earth's environment. Five large platforms are to be launched into polar orbit, two by NASA, two by ESA, and one by the Japanese. In such an orbit the radiation resistance of indium phosphide solar cells combined with the potential of utilizing five micron cell structures yields an increase of 10 percent in the payload capability. If further combined with the advanced photovoltaic solar array the payload savings approaches 12 percent. ESA

N92-13255*# National Aeronautics and Space Administration. Lewis Research Center, Cleveland, OH.

ENVIRONMENTAL INTERACTIONS OF THE SPACE STATION FREEDOM ELECTRIC POWER SYSTEM

HENRY K. NAHRA and C. Y. LU (Rockwell International Corp., Canoga Park, CA.) /in ESA, European Space Power Conference. Volume 2: Photovoltaic Generators p 683-688 Aug. 1991

Copyright Avail: CASI HC A02/MF A03; ESA, EPD, Noordwijk, Netherlands, HC 150 Dutch guilders (2 vols)

The Space Station Freedom will be operating in the Low Earth Orbit (LEO) environment. LEO environment operation results in different potential interactions with the Space Station systems including the Electric Power Systems (EPS). These potential interactions result in environmental effects which include neutral species effects such as atomic oxygen erosion, effects of micrometeoroid and orbital debris impacts, plasma effects, ionizing radiation effects, and induced contamination degradation effects. The EPS design and its interactions with the LEO environment are described. The results of analyses and testing programs planned and performed thus far to resolve the environmental concerns related to the EPS and its function in the LEO environment are discussed. ESA

N92-13259*# National Aeronautics and Space Administration. Lewis Research Center, Cleveland, OH.

SOLAR RADIATION FOR MARS POWER SYSTEMS

JOSEPH APPELBAUM and GEOFFREY A. LANDIS (Sverdrup Technology, Inc., Brook Park, OH.) /in ESA, European Space Power Conference. Volume 2: Photovoltaic Generators p 707-712 Aug. 1991

(Contract NAGW-2022)

Copyright Avail: CASI HC A02/MF A03; ESA, EPD, Noordwijk, Netherlands, HC 150 Dutch guilders (2 vols)

Detailed information about the solar radiation characteristics on Mars are necessary for effective design of future planned solar energy systems operating on the surface of Mars. A procedure and solar radiation related data from which the diurnally and daily variation of the global, direct (or beam), and diffuse insolation on Mars are calculated, are presented. The radiation data are based on measured optical depth of the Martian atmosphere derived from images taken of the Sun with a special diode on the Viking Lander cameras; and computation based on multiple wavelength and multiple scattering of the solar radiation. ESA

N92-13274*# National Aeronautics and Space Administration. Lewis Research Center, Cleveland, OH.

OVERVIEW OF ROCKET ENGINE CONTROL

CARL F. LORENZO and JEFFREY L. MUSGRAVE 1991 13 p Proposed for presentation at the Ninth Symposium on Space Nuclear Power Systems, Albuquerque, NM, 12-16 Jan. 1991; sponsored by the Univ. of New Mexico

(Contract RTOP 505-62-50)

(NASA-TM-105318; E-6673; NAS 1.15:105318) Avail: CASI HC A03/MF A01

The issues of Chemical Rocket Engine Control are broadly covered. The basic feedback information and control variables used in expendable and reusable rocket engines, such as Space Shuttle Main Engine, are discussed. The deficiencies of current approaches are considered and a brief introduction to Intelligent Control Systems for rocket engines (and vehicles) is presented.

Author

N92-13275*# National Aeronautics and Space Administration. Lewis Research Center, Cleveland, OH.

DEVELOPMENT OF A SINGLE-PHASE HARMONIC POWER FLOW PROGRAM TO STUDY THE 20 KHZ AC POWER SYSTEM FOR LARGE SPACECRAFT

L. ALAN KRAFT (Valparaiso Univ., IN.) and M. DAVID KANKAM Nov. 1991 37 p

(Contract RTOP 506-41-41)

(NASA-TM-105326; E-6687; NAS 1.15:105326) Avail: CASI HC A03/MF A01

The development of software is described to aid in design and analysis of AC power systems for large spacecraft. The algorithm is an important version of harmonic power flow program, HARMFLO, used for the study of AC power quality. The new program is applicable to three-phase systems typified by terrestrial power systems, and single-phase systems characteristic of space power systems. The modified HARMFLO accommodates system operating frequencies ranging from terrestrial 60 Hz to and beyond

20 SPACECRAFT PROPULSION AND POWER

aerospace 20 kHz, and can handle both source and load-end harmonic distortions. Comparison of simulation and test results of a representative spacecraft power system shows a satisfactory correlation. Recommendations are made for the direction of future improvements to the software, to enhance its usefulness to power system designer and analysts. Author

N92-14109*# National Aeronautics and Space Administration. Lewis Research Center, Cleveland, OH.

HIGH-POWER HYDROGEN ARCJET PERFORMANCE

THOMAS W. HAAG and FRANCIS M. CURRAN 1991 23 p Presented at the 27th Joint Propulsion Conference, Sacramento, CA, 24-27 Jun. 1991; cosponsored by AIAA, SAE, ASME, and ASEE Previously announced in IAA as A91-45795 (Contract RTOP 506-42-31) (NASA-TM-105143; E-6418; NAS 1.15:105143; AIAA PAPER 91-2226) Avail: CASI HC A03/MF A01

A hydrogen arcjet was operated at power levels ranging from 5 to 30 kW with three different nozzle geometries. Test results using all three nozzle geometries are reported and include variations of specific impulse with flow rate, and thrust with power. Geometric variables investigated included constrictor diameter, length, and diverging exit angle. The nozzle with a constrictor diameter of 1.78 mm and divergence angle of 20 degrees was found to give the highest performance. A specific impulse of 1460 s was attained with this nozzle at a thrust efficiency of 29.8 percent. The best efficiency measured was 34.4 percent at a specific impulse of 1045 s. Post test examination of the cathode showed erosion after 28 hours of operation to be small, and limited to the conical tip where steady state arc attachment occurred. Each nozzle was tested to destruction. Author

N92-14111*# National Aeronautics and Space Administration. Lewis Research Center, Cleveland, OH.

ENHANCING OPTICAL ABSORPTION IN INP AND GAAS UTILIZING PROFILE ETCHING

SHEILA G. BAILEY, NAVID S. FATEMI, and GEOFFREY A. LANDIS (Sverdrup Technology, Inc., Brook Park, OH.) 1991 7 p Presented at the 22nd Photovoltaic Specialists Conference, Las Vegas, NV, 8-11 Oct. 1991; sponsored by IEEE (Contract RTOP 506-41-11) (NASA-TM-105325; E-6683; NAS 1.15:105325) Avail: CASI HC A02/MF A01

The current state of profile etching in GaAs and InP is summarized, including data on novel geometries attainable as a function of etchant temperature, composition, and rate; substrate orientation; carrier concentration; and oxide thickness between substrate and photoresist. V-grooved solar cells were manufactured with both GaAs and InP, and the improved optical absorption was demonstrated. Preferred parameters for various applications are listed and discussed. Author

N92-14112*# National Aeronautics and Space Administration. Lewis Research Center, Cleveland, OH.

COAXIAL INJECTOR SPRAY CHARACTERIZATION USING WATER/AIR AS SIMULANTS

MICHELLE M. ZALLER (Sverdrup Technology, Inc., Brook Park, OH.) and MARK D. KLEM 1991 10 p Presented at the 28th JANNAF Combustion Meeting, San Antonio, TX, 28 Oct. - 1 Nov. 1991 (Contract NAS3-25266; RTOP 506-42-72) (NASA-TM-105322; E-6681; NAS 1.15:105322) Avail: CASI HC A02/MF A01

Quantitative information about the atomization of injector sprays is required to improve the accuracy of computational models that predict the performance and stability of liquid propellant rocket engines. An experimental program is being conducted at NASA-Lewis to measure the drop size and velocity distributions in shear coaxial injector sprays. A phase/Doppler interferometer is used to obtain drop size data in water air shear coaxial injector sprays. Droplet sizes and axial component of droplet velocities are measured at different radii for various combinations of water flow rate, air flow rate, injector liquid jet diameter, injector annular

gap, and liquid post recess. Sauter mean diameters measured in the spray center 51 mm downstream of the liquid post tip range from 28 to 68 microns, and mean axial drop velocities at the same location range from 37 to 120 m/s. The shear coaxial injector sprays show a high degree of symmetry; the mean drop size and velocity profiles vary with liquid flow rate, post recess, and distance from the injector face. The drop size data can be used to estimate liquid oxygen/hydrogen spray drop sizes by correcting property differences between water-air and liquid oxygen/hydrogen. Author

N92-15119*# National Aeronautics and Space Administration. Lewis Research Center, Cleveland, OH.

HYDROGEN ARCJET TECHNOLOGY

JOHN M. SANKOVIC, JOHN A. HAMLEY, THOMAS W. HAAG, CHARLES J. SARMIENTO, and FRANCIS M. CURRAN 1991 26 p Presented at the 22nd International Electric Propulsion Conference, Viareggio, Italy, 14-17 Oct. 1991; sponsored by AIDAA, AIAA, DGLR, and JSASS (Contract RTOP 506-42-31) (NASA-TM-105340; E-6707; NAS 1.15:105340; IEPC-91-018) Avail: CASI HC A03/MF A01

During the 1960's, a substantial research effort was centered on the development of arcjets for space propulsion applications. The majority of the work was at the 30 kW power level with some work at 1-2 kW. At the end of the research effort, the hydrogen arcjet had demonstrated over 700 hours of life in a continuous endurance test at 30 kW, at a specific impulse over 1000 s, and at an efficiency of 0.41. Another high power design demonstrated 500 h life with an efficiency of over 0.50 at the same specific impulse and power levels. At lower power levels, a life of 150 hours was demonstrated at 2 kW with an efficiency of 0.31 and a specific impulse of 935 s. Lack of a space power source hindered arcjet acceptance and research ceased. Over three decades after the first research began, renewed interest exists for hydrogen arcjets. The new approach includes concurrent development of the power processing technology with the arcjet thruster. Performance data were recently obtained over a power range of 0.3-30 kW. The 2 kW performance has been repeated; however, the present high power performance is lower than that obtained in the 1960's at 30 kW, and lifetimes of present thrusters have not yet been demonstrated. Laboratory power processing units have been developed and operated with hydrogen arcjets for the 0.1 kW to 5 kW power range. A 10 kW power processing unit is under development and has been operated at design power into a resistive load. Author

N92-15125*# National Aeronautics and Space Administration. Lewis Research Center, Cleveland, OH.

HIGH TEMPERATURE THRUSTER TECHNOLOGY FOR SPACECRAFT PROPULSION

STEVEN J. SCHNEIDER 1991 16 p Presented at the 42nd Congress of the International Astronautical Federation, Montreal, Quebec, 5-11 Oct. 1991 Previously announced in IAA as A92-13155 (Contract RTOP 506-42-31) (NASA-TM-105348; E-6718; NAS 1.15:105348; IAF-91-254) Avail: CASI HC A03/MF A01

A technology program intended to develop high-temperature oxidation-resistant thrusters for spacecraft applications is considered. The program will provide the requisite material characterizations and fabrication to incorporate iridium coated rhenium material into small rockets for spacecraft propulsion. This material increases the operating temperature of thrusters to 2200 C, a significant increase over the 1400 C of the silicide-coated niobium chambers currently used. Stationkeeping class 22 N engines fabricated from iridium-coated rhenium have demonstrated steady state specific impulses 20-25 seconds higher than niobium chambers. These improved performances are obtained by reducing or eliminating the fuel film cooling requirements in the combustion chamber while operating at the same overall mixture ratio as conventional engines. Author

N92-16019*# National Aeronautics and Space Administration. Lewis Research Center, Cleveland, OH.

NUCLEAR ELECTRIC PROPULSION: AN INTEGRAL PART OF NASA'S NUCLEAR PROPULSION PROJECT

JAMES R. STONE 1992 8 p Presented at the 9th Symposium on Space Nuclear Power Systems, Albuquerque, NM, 12-16 Jan. 1992; sponsored by New Mexico Univ. (Contract RTOP 593-71-11)

(NASA-TM-105309; E-6662; NAS 1.15:105309) Avail: CASI HC A02/MF A01

NASA has initiated a technology program to establish the readiness of nuclear propulsion technology for the Space Exploration Initiative (SEI). This program was initiated with a very modest effort identified with nuclear thermal propulsion (NTP); however, nuclear electric propulsion (NEP) is also an integral part of this program and builds upon NASA's Base Research and Technology Program in power and electric propulsion as well as the SP-100 space nuclear power program. Although the Synthesis Group On America's SEI has identified NEP only as an option for cargo missions, recent studies conducted by NASA-Lewis show that NEP offers the potential for early manned Mars missions as well. Lower power NEP is also of current interest for outer planetary robotic missions. Current plans are reviewed for the overall nuclear propulsion project, with emphasis on NEP and those elements of NTP program which have synergism with NEP. Author

N92-16022*# National Aeronautics and Space Administration. Lewis Research Center, Cleveland, OH.

ARCJET NOZZLE AREA RATIO EFFECTS

FRANCIS M. CURRAN (Texas Univ., Austin.), CHARLES J. SARMIENTO, BJORN W. BIRKNER, and JAMES KWASNY (Air Force Academy, CO.) 1990 13 p Presented at the 1990 JANNAF Propulsion Meeting, Anaheim, CA, 2-4 Oct. 1990 Previously announced as N91-24271

(Contract RTOP 506-42-31) (NASA-TM-104477; E-6397; NAS 1.15:104477) Avail: CASI HC A03/MF A01

An experimental investigation was conducted to determine the effect of nozzle area ratio on the operating characteristics and performance of a low power dc arcjet thruster. Conical thoriated tungsten nozzle inserts were tested in a modular laboratory arcjet thruster run on hydrogen/nitrogen mixtures simulating the decomposition products of hydrazine. The converging and diverging sides of the inserts had half angles of 30 and 20 degrees, respectively, similar to a flight type unit currently under development. The length of the diverging side was varied to change the area ratio. The nozzle inserts were run over a wide range of specific power. Current, voltage, mass flow rate, and thrust were monitored to provide accurate comparisons between tests. While small differences in performance were observed between the two nozzle inserts, it was determined that for each nozzle insert, arcjet performance improved with increasing nozzle area ratio to the highest area ratio tested and that the losses become very pronounced for area ratios below 50. These trends are somewhat different than those obtained in previous experimental and analytical studies of low Re number nozzles. It appears that arcjet performance can be enhanced via area ratio optimization. Author

N92-16023*# National Aeronautics and Space Administration. Lewis Research Center, Cleveland, OH.

DESIGN ISSUES FOR LUNAR IN SITU ALUMINUM/OXYGEN PROPELLANT ROCKET ENGINES

MICHAEL L. MEYER 1992 21 p Proposed for presentation at the 1992 Aerospace Design Conference, Irvine, CA, 3-6 Feb. 1992; sponsored by AIAA

(Contract RTOP 506-42-00) (NASA-TM-105433; E-6855; NAS 1.15:105433; AIAA PAPER 92-1185) Avail: CASI HC A03/MF A01

Design issues for lunar ascent and lunar descent rocket engines fueled by aluminum/oxygen propellant produced in situ at the lunar surface were evaluated. Key issues are discussed which impact the design of these rockets: aluminum combustion, throat erosion,

and thrust chamber cooling. Four engine concepts are presented, and the impact of combustion performance, throat erosion and thrust chamber cooling on overall engine design are discussed. The advantages and disadvantages of each engine concept are presented. Author

N92-16024*# National Aeronautics and Space Administration. Lewis Research Center, Cleveland, OH.

MULTIMEGAWATT MPD THRUSTER DESIGN CONSIDERATIONS

ROGER M. MYERS (Sverdrup Technology, Inc., Brook Park, OH.), JAMES E. PARKES (Sverdrup Technology, Inc., Brook Park, OH.), and MARIS A. MANTENIEKS 1992 11 p Presented at the Ninth Symposium on Space Nuclear Power Systems, Albuquerque, NM, 12-16 Jan. 1992; sponsored by New Mexico Univ. (Contract RTOP 506-42-31)

(NASA-TM-105405; E-6807; NAS 1.15:105405) Avail: CASI HC A03/MF A01

Performance and lifetime requirements for multimegawatt magnetoplasmadynamic (MPD) thrusters were used to establish a baseline 2.5 MW thruster design. The chamber surface power deposition resulting from current conduction, plasma and surface radiation, and conduction from the hot plasma was then evaluated to establish the feasibility of thruster operation. It was determined that state of the art lithium heat pipes were adequate to cool the anode electrode, and that the liquid hydrogen propellant could be used to cool the applied field magnet, cathode, and backplate. Unresolved issues having an impact of thruster design are discussed to help focus future research. Author

N92-17151*# National Aeronautics and Space Administration. Lewis Research Center, Cleveland, OH.

UPPER STAGES USING LIQUID PROPULSION AND METALLIZED PROPELLANTS

BRYAN A. PALASZEWSKI Washington Feb. 1992 22 p (Contract RTOP 506-42-72)

(NASA-TP-3191; E-6105; NAS 1.60:3191) Avail: CASI HC A03/MF A01

Metallized propellants are liquid propellants with a metal additive suspended in a gelled fuel. Typically, aluminum particles are the metal additive. These propellants increase the density and/or the specific impulse of the propulsion system. Using metallized propellants for volume- and mass-constrained upper stages can deliver modest increases in performance for low Earth orbit to geosynchronous Earth orbit (LEO-GEO) and other Earth-orbital transfer missions. However, using metallized propellants for planetary missions can deliver great reductions in flight time with a single-stage, upper-stage system. Tradeoff studies comparing metallized propellant stage performance with nonmetallized upper stages and the Inertial Upper Stage (IUS) are presented. These upper stages, launched from the STS and STS-C, are both one- and two-stage vehicles that provide the added energy to send payloads to high altitude orbits and onto interplanetary trajectories that are unattainable with only the Space Transportation System (STS) and the Space Transportation System-Cargo (STS-C). The stage designs are controlled by the volume and the mass constraints of the STS and STS-C launch vehicles. The influences of the density and specific impulse increases enabled by metallized propellants are examined for a variety of different stage and propellant combinations. Author

N92-17770*# National Aeronautics and Space Administration. Lewis Research Center, Cleveland, OH.

SOLAR DYNAMIC TECHNOLOGY STATUS FOR SPACE STATION FREEDOM APPLICATION

MICHAEL J. ZERNIC /n NASA, Washington, Beyond the Baseline 1991: Proceedings of the Space Station Evolution Symposium. Volume 2: Space Station Freedom, Part 1 p 765-811 Sep. 1991 Avail: CASI HC A03/MF A03

The objectives of this presentation is to emphasize the (1) rationale to incorporate solar dynamic (SD) systems onto Space Station Freedom (SSF) as the power demand increases onboard SSF, (2) SD technical progress made through the SSF Program,

20 SPACECRAFT PROPULSION AND POWER

(3) areas of further technology development, and (4) future plans for SD system development. The SD status summary is presented in graph form. Author

N92-17771*# National Aeronautics and Space Administration. Lewis Research Center, Cleveland, OH.

SPACE STATION FREEDOM ELECTRIC POWER SYSTEM EVOLUTION ANALYSIS STATUS

MICHAEL J. ZERNIC *in* NASA, Washington, Beyond the Baseline 1991: Proceedings of the Space Station Evolution Symposium. Volume 2: Space Station Freedom, Part 1 p 813-833 Sep. 1991 Avail: CASI HC A03/MF A03

The ability is examined of the SSF baselined EPS to transition to operate at a greater system capacity beyond the SSF Permanent Manned Capability (PMC) milestone. Specifically, a status of a current analysis is discussed concerning additions, modifications, changeout, or combination thereof of baseline EPS hardware and/or software needed to accomplish the power generation, distribution, operation, and use needed to meet evolving SSF mission objectives. This discussion results in several EPS architectural options that facilitate the addition or substitution of new technologies. Author

N92-17773*# National Aeronautics and Space Administration. Lewis Research Center, Cleveland, OH.

AUTOMATED POWER MANAGEMENT AND CONTROL

JAMES L. DOLCE *in* NASA, Washington, Beyond the Baseline 1991: Proceedings of the Space Station Evolution Symposium. Volume 2: Space Station Freedom, Part 1 p 853-883 Sep. 1991 Avail: CASI HC A03/MF A03

A comprehensive automation design is being developed for Space Station Freedom's electric power system. A joint effort between NASA's Office of Aeronautics and Exploration Technology and NASA's Office of Space Station Freedom, it strives to increase station productivity by applying expert systems and conventional algorithms to automate power system operation. The initial station operation will use ground-based dispatches to perform the necessary command and control tasks. These tasks constitute planning and decision-making activities that strive to eliminate unplanned outages. We perceive an opportunity to help these dispatchers make fast and consistent on-line decisions by automating three key tasks: failure detection and diagnosis, resource scheduling, and security analysis. Expert systems will be used for the diagnostics and for the security analysis; conventional algorithms will be used for the resource scheduling. Author

N92-18280*# National Aeronautics and Space Administration. Lewis Research Center, Cleveland, OH.

A SURVEY OF INSTABILITIES WITHIN CENTRIFUGAL PUMPS AND CONCEPTS FOR IMPROVING THE FLOW RANGE OF PUMPS IN ROCKET ENGINES

JOSEPH P. VERES Feb. 1992 17 p Proposed for presentation at the 1992 JANNAF Propulsion Meeting, Indianapolis, IN, 24-28 1992

(Contract RTOP 506-42-72)
(NASA-TM-105439; E-6859; NAS 1.15:105439) Avail: CASI HC A03/MF A01

Design features and concepts that have primary influence on the stable operating flow range of propellant-fed centrifugal turbopumps in a rocket engine are discussed. One of the throttling limitations of a pump-fed rocket engine is the stable operating range of the pump. Several varieties of pump hydraulic instabilities are mentioned. Some pump design criteria are summarized and a qualitative correlation of key parameters to pump stall and surge are referenced. Some of the design criteria were taken from the literature on high pressure ratio centrifugal compressors. Therefore, these have yet to be validated for extending the stable operating flow range of high-head pumps. Casing treatment devices, dynamic fluid-damping plenums, backflow-stabilizing vanes and flow-reinjection techniques are summarized. A planned program was undertaken at LeRC to validate these concepts. Technologies developed by this program will be available for the design of

turbopumps for advanced space rocket engines for use by NASA in future space missions where throttling is essential. Author

N92-18474*# National Aeronautics and Space Administration. Lewis Research Center, Cleveland, OH.

PRELIMINARY TEST RESULTS OF A HOLLOW CATHODE MPD THRUSTER

MARIS A. MANTENIEKS and ROGER M. MYERS (Sverdrup Technology, Inc., Brook Park, OH.) 1991 16 p Presented at the 22d International Electric Propulsion Conference, Viareggio, Italy, 14-17 Oct. 1991; sponsored by AIDAA, AIAA, DGLR, and JSASS

(Contract RTOP 506-42-31)
(NASA-TM-105324; E-6608; NAS 1.15:105324; IEPC-91-076)
Avail: CASI HC A03/MF A01

Performance of four hollow cathode configurations with low work function inserts was evaluated in a steady-state 100 kW class applied magnetic field magnetoplasmadynamic (MPD) thruster. Two of the configurations exhibited stable discharge current attachment to the low work function inserts of the hollow cathodes. A maximum discharge current of 2250 A was attained. While the applied-field increased the performance of the thruster, at high applied fields the discharge current attachment moved from the insert to the cathode body. The first successful hollow cathode performed well in comparison with a conventional rod cathode MPD thruster, attaining a thrust efficiency with argon of close to 20 percent at a specific impulse of about 2000 s. The second successful configuration had significantly lower performance. Author

N92-19780*# National Aeronautics and Space Administration. Lewis Research Center, Cleveland, OH.

SOLAR DYNAMIC MODULES FOR SPACE STATION FREEDOM: THE RELATIONSHIP BETWEEN FINE-POINTING CONTROL AND THERMAL LOADING OF THE APERTURE PLATE

ROGER D. QUINN (Case Western Reserve Univ., Cleveland, OH.) and THOMAS W. KERSLAKE 1992 20 p Proposed for presentation at the International Solar Energy Conference, Lahaina, HI, 5-9 Apr. 1992; sponsored by ASME
(Contract RTOP 474-52-10)

(NASA-TM-104498; E-6109; NAS 1.15:104498) Avail: CASI HC A03/MF A01

Dynamic simulations of Space Station Freedom (SSF) configured with solar dynamic (SD) power modules were performed. The structure was subjected to Space Shuttle docking disturbances, while being controlled with a 'natural' vibration and tracking control approach. Three control cases were investigated for the purpose of investigating the relationship between actuator effort, SD pointing, and thermal loading on the receiver aperture plate. Transient, one-dimensional heat transfer analyses were performed to conservatively predict temperatures of the multi-layered receiver aperture plate assembly and thermal stresses in its shield layer. Results indicate that the proposed aperture plate is tolerant of concentrated flux impingement during short-lived structural disturbances. Pointing requirements may be loosened and the requirement control torques lessened from that previously specified. Downsizing and simplifying the joint drive system should result in a considerable savings mass. Author

N92-20043*# National Aeronautics and Space Administration. Lewis Research Center, Cleveland, OH.

COMBUSTION-WAVE IGNITION FOR ROCKET ENGINES

LARRY C. LIOU 1992 19 p Presented at the 1992 JANNAF Propulsion Meeting, Indianapolis, IN, 24-26 Feb. 1992
(Contract RTOP 506-21-11)

(NASA-TM-105545; E-6809; NAS 1.15:105545) Avail: CASI HC A03/MF A01

The combustion wave ignition concept was experimentally studied in order to verify its suitability for application in baffled sections of a large booster engine combustion chamber. Gaseous oxygen/gaseous methane (GOX/GH4) and gaseous oxygen/gaseous hydrogen (GOX/GH2) propellant combinations

were evaluated in a subscale combustion wave ignition system. The system included four element tubes capable of carrying ignition energy simultaneously to four locations, simulating four baffled sections. Also, direct ignition of a simulated Main Combustion Chamber (MCC) was performed. Tests were conducted over a range of mixture ratios and tube geometries. Ignition was consistently attained over a wide range of mixture ratios. And at every ignition, the flame propagated through all four element tubes. For GOX/GH4, the ignition system ignited the MCC flow at mixture ratios from 2 to 10 and for GOX/GH2 the ratios is from 2 to 13. The ignition timing was found to be rapid and uniform. The total ignition delay when using the MCC was under 11 ms, with the tube-to-tube, as well as the run-to-run, variation under 1 ms. Tube geometries were found to have negligible effect on the ignition outcome and timing.

Author

N92-20065*# National Aeronautics and Space Administration. Lewis Research Center, Cleveland, OH.

ATOMIC OXYGEN DURABILITY OF SOLAR CONCENTRATOR MATERIALS FOR SPACE STATION FREEDOM

KIM K. DEGROH (National Aeronautics and Space Administration. Lewis Research Center, Cleveland, OH.), JUDITH A. TERLEP (Case Western Reserve Univ., Cleveland, OH.), and THERESA M. DEVER (Cleveland State Univ., OH.) 1990 13 p Presented at the 5th Annual Air Force Workshop on Surface Reactions in the Space Environment, Evanston, IL, 24-25 Sep. 1990; sponsored by Northwestern Univ.

(Contract NCC3-19; RTOP 474-52-10)

(NASA-TM-105378; E-6745; NAS 1.15:105378) Avail: CASI HC A03/MF A01

The findings are reviewed of atomic oxygen exposure testing of candidate solar concentrator materials containing SiO₂ and Al₂O₃ protective coatings for use on Space Station Freedom solar dynamic power modules. Both continuous and iterative atomic oxygen exposure tests were conducted. Iterative air plasma ashing resulted in larger specular reflectance decreases and solar absorptance increases than continuous ashing to the same fluence, and appears to provide a more severe environment than the continuous atomic oxygen exposure that would occur in the low Earth orbit environment. First generation concentrator fabrication techniques produced surface defects including scratches, macroscopic bumps, dendritic regions, porosity, haziness, and pin hole defects. Several of these defects appear to be preferential sites for atomic oxygen attack leading to erosive undercutting. Extensive undercutting and flaking of reflective and protective coatings were found to be promoted through an undercutting tearing propagation process. Atomic oxygen erosion processes and effects on optical performance is presented.

Author

N92-20355*# National Aeronautics and Space Administration. Lewis Research Center, Cleveland, OH.

NUCLEAR ELECTRIC PROPULSION TECHNOLOGY PANEL FINDINGS AND RECOMMENDATIONS

MICHAEL P. DOHERTY 1992 11 p Presented at the 9th Symposium on Space Nuclear Power Systems, Albuquerque, NM, 12-16 Jan. 1992

(Contract RTOP 593-72-00)

(NASA-TM-105547; E-6870; NAS 1.15:105547) Avail: CASI HC A03/MF A01

Summarized are the findings and recommendations of a triagency (NASA/DOE/DOD) panel on Nuclear Electric Propulsion (NEP) Technology. NEP has been identified as a candidate nuclear propulsion technology for exploration of the Moon and Mars as part of the Space Exploration Initiative (SEI). The findings are stated in areas of system and subsystem considerations, technology readiness, and ground test facilities. Recommendations made by the panel are summarized concerning: (1) existing space nuclear power and propulsion programs, and (2) the proposed multiagency NEP technology development program.

Author

N92-20522*# National Aeronautics and Space Administration. Lewis Research Center, Cleveland, OH.

HYDROGEN/OXYGEN AUXILIARY PROPULSION TECHNOLOGY

BRIAN D. REED and STEVEN J. SCHNEIDER 1991 23 p Presented at the Conference on Advanced Space Exploration Initiative Technologies, Cleveland, OH, 4-6 Sep. 1991; cosponsored by AIAA, NASA, and OAI

(Contract RTOP 506-42-31)

(NASA-TM-105249; E-6578; NAS 1.15:105249; AIAA PAPER 91-3440) Avail: CASI HC A03/MF A01

A survey is provided of hydrogen/oxygen (H/O) auxiliary propulsion system (APS) concepts and low thrust H/O rocket technology. A review of H/O APS studies performed for the Space Shuttle, Space Tug, Space Station Freedom, and Advanced Manned Launch System programs is given. The survey also includes a review of low thrust H/O rocket technology programs, covering liquid H/O and gaseous H/O thrusters, ranging from 6600 N (1500 lbf) to 440 mN (0.1 lbf) thrust. Ignition concepts for H/O thrusters and high temperature, oxidation resistant chamber materials are also reviewed.

Author

N92-20585*# National Aeronautics and Space Administration. Lewis Research Center, Cleveland, OH.

A STUDY OF Na(X)PT3O4 AS AN O2 ELECTRODE BIFUNCTIONAL ELECTROCATALYST

WILLIAM L. FIELDER and JOSEPH SINGER Dec. 1991 25 p (Contract RTOP 506-42-21)

(NASA-TM-105311; E-6664; NAS 1.15:105311) Avail: CASI HC A03/MF A01

The present study suggests that polytetrafluoroethylene (PTFE) bonded Na(X)Pt3O4 gas porous diffusion electrodes may be a viable candidate for bifunctional O₂ reduction and evolution activity. The electrodes exhibited Tafel slopes of about 0.06 V/decade for both O₂ reduction and evolution. For O₂ reduction, the 0.06 slope doubled to 0.12 V/decade at larger current densities. Preliminary stability testing at 24 C suggest that the Na(x)Pt3O4 electrodes were relatively stable at reducing and oxidizing potentials typically encountered at the O₂ electrodes in a regenerative fuel cell.

Author

N92-21187*# National Aeronautics and Space Administration. Lewis Research Center, Cleveland, OH.

FUELS AND MATERIALS DEVELOPMENT FOR SPACE NUCLEAR PROPULSION

S. K. BHATTACHARYYA (Argonne National Lab., IL.), R. B. MATTHEWS (Los Alamos National Lab., NM.), and R. H. TITRAN 1992 12 p Presented at the 9th Symposium on Space Nuclear Power Systems, Albuquerque, NM, 13-16 Jan. 1992

(Contract W-31-109-ENG-38)

(NASA-TM-107806; NAS 1.15:107806; DE92-007378;

ANL/CP-75370; CONF-920104-31) Avail: CASI HC A03/MF A01

Nuclear propulsion has been identified as an enabling technology in meeting the mission of the Space Exploration Initiative (SEI). Both Nuclear Thermal Propulsion (NTP) and Nuclear Electric Propulsion (NEP) have roles to play in the initiative. Of the numerous specific development items that need to be undertaken for these technologies, nuclear fuels and materials are considered by experts as the most challenging and therefore require early attention. One of the six panels organized by the NASA/DOE/DoD Steering Committee to help plan the nuclear propulsion development tasks was dedicated to nuclear fuels, materials and related technologies. Considering only the solid core concepts presented in the 1990 workshops on NTP and NEP, the panel concluded that there were classes of fuels and materials that had the potential to meet the demanding temperature and lifetime requirements for SEI in the timeframe of interest. Plans for the development of fuels and materials were prepared. A full development plan is going to involve the construction of several major new facilities and the modification of many existing ones. For the fuels, areas of commonality have been explored to allow for effective early activity while the downselection process to focus the development takes place. For materials, the lack of definition

20 SPACECRAFT PROPULSION AND POWER

of candidate selection by the concept proposers makes this somewhat more difficult. Careful coordination of the work will be essential to keep the development and characterization of fuels and materials on schedule and costs within bounds. DOE

N92-21216*# National Aeronautics and Space Administration. Lewis Research Center, Cleveland, OH.

EXPERIMENTS WITH PHASE CHANGE THERMAL ENERGY STORAGE CANISTERS FOR SPACE STATION FREEDOM
THOMAS W. KERSLAKE 1991 17 p Presented at the 26th Intersociety Energy Conversion Engineering Conference, Boston, MA, 4-9 Aug. 1991; cosponsored by ANS, SAE, ACS, AIAA, ASME, IEEE, and AICHE
(Contract RTOP 474-52-10)
(NASA-TM-104427; E-6102; NAS 1.15:104427) Avail: CASI HC A03/MF A01

The solar dynamic power module proposed for the Space Station Freedom (SSF) uses the heat of fusion of a phase change material (PCM) to efficiently store thermal energy for use during eclipse periods. The PCM, a LiF-20CaF₂ salt, is contained in annular, metal canisters located in a heat receiver at the focus of a solar concentrator. PCM canister ground-based experiments and analytical heat transfer studies are discussed. The hardware, test procedures, and test results from these experiments are discussed. After more than 900 simulated SSF orbital cycles, no canister cracks or leaks were observed and all data were successfully collected. The effect of 1-g test orientation on canister wall temperatures was generally small while void position was strongly dependent on test orientation and canister cooling. In one test orientation, alternating wall temperature data were measured that supports an earlier theory of oscillating vortex flow in the PCM melt. Analytical canister wall temperatures compared very favorably with experimental temperature data. This illustrates that ground-based canister thermal performance can be predicted well by analyses that employ straight-forward, engineering models of void behavior and liquid PCM free convection. Because of the accuracy of analytical models and the relative insensitivity of 1-g performance to test orientation, canister performance in micro-g should be predictable with a high degree of confidence by removing gravity effects from the analytical modeling. Author

N92-21517*# National Aeronautics and Space Administration. Lewis Research Center, Cleveland, OH.

ROCKET-BASED COMBINED-CYCLE (RBCC) PROPULSION TECHNOLOGY WORKSHOP. TUTORIAL SESSION
1992 259 p Workshop held in Huntsville, AL, 23-27 Mar. 1992; sponsored by NASA, Washington
(Contract RTOP 590-21-11)
(NASA-CP-10090; E-6929; NAS 1.55:10090) Avail: CASI HC A12/MF A03

The goal of this workshop was to illuminate the nation's space transportation and propulsion engineering community on the potential of hypersonic combined cycle (airbreathing/rocket) propulsion systems for future space transportation applications. Four general topics were examined: (1) selections from the expansive advanced propulsion archival resource; (2) related propulsion systems technical backgrounds; (3) RBCC engine multimode operations related subsystem background; and (4) focused review of propulsion aspects of current related programs.

N92-21536*# National Aeronautics and Space Administration. Lewis Research Center, Cleveland, OH.

BETA 2: A NEAR TERM, FULLY REUSABLE, HORIZONTAL TAKEOFF AND LANDING TWO-STAGE-TO-ORBIT LAUNCH VEHICLE CONCEPT

LEO A. BURKARDT *In its* Rocket-Based Combined-Cycle (RBCC) Propulsion Technology Workshop. Tutorial Session 7 p 1992
Avail: CASI HC A02/MF A03

A recent study has confirmed the feasibility of a near term, fully reusable, horizontal takeoff and landing two-stage-to-orbit (TSTO) launch vehicle concept. The vehicle stages at Mach 6.5. The first stage is powered by a turboramjet propulsion system with the turbojets being fueled by JP and the ramjet by LH₂. The

second stage is powered by a space shuttle main engine (SSME) rocket engine. For about the same gross weight as growth versions of the 747, the vehicle can place 10,000 lbm. in low polar orbit or 16,000 lbm. to Space Station Freedom. D.R.D.

N92-21976*# National Aeronautics and Space Administration. Lewis Research Center, Cleveland, OH.

NEUTRALIZER OPTIMIZATION
MICHAEL J. PATTERSON and KAYHAN MOHAJERI (Purdue Univ., West Lafayette, IN.) Oct. 1991 20 p Presented at the 22nd International Electric Propulsion Conference, Viareggio, Italy, 14-17 Oct. 1991; sponsored in part by AIDAA, AIAA, DGLR, and JSASS (Contract RTOP 506-42-31)
(NASA-TM-105578; E-6903; NAS 1.15:105578) Avail: CASI HC A03/MF A01

The preliminary results of a test program to optimize a neutralizer design for 30 cm xenon ion thrusters are discussed. The impact of neutralizer geometry, neutralizer axial location, and local magnetic fields on neutralizer performance is discussed. The effect of neutralizer performance on overall thruster performance is quantified, for thruster operation in the 0.5-3.2 kW power range. Additionally, these data are compared to data published for other north-south stationkeeping (NSSK) and primary propulsion xenon ion thruster neutralizers. Author

N92-22360*# National Aeronautics and Space Administration. Lewis Research Center, Cleveland, OH.

THE SOLAR ARRAY MODULE PLASMA INTERACTIONS EXPERIMENT (SAMPIE): SCIENCE AND TECHNOLOGY OBJECTIVES

G. BARRY HILLARD *In* NASA. Johnson Space Center, 5th Annual Workshop on Space Operations Applications and Research (SOAR 1991), Volume 2 p 650-654 Feb. 1992
Avail: CASI HC A01/MF A04

The Solar Array Module Plasma Interactions Experiment (SAMPIE) is an approved NASA Space Shuttle space flight experiment to be launched in Jul. 1993. The SAMPIE experiment is designed to investigate the interaction of high voltage space power systems with ionospheric plasma. To study the behavior of solar cells, a number of cell coupons, representing technologies of current interest, will be biased to high voltages to characterize both negative potential arcing and positive potential current collection. Additionally, various theories of arc suppression will be tested by including several specially modified cell coupons. Finally, SAMPIE will include experiments to study the basic nature of these interactions. The rationale for a space flight experiment, the measurements to be made, the significance of the expected results, and the current design status of the flight hardware are described. Author

N92-23252*# National Aeronautics and Space Administration. Lewis Research Center, Cleveland, OH.

BLAZING THE TRAILWAY: NUCLEAR ELECTRIC PROPULSION AND ITS TECHNOLOGY PROGRAM PLANS

MICHAEL P. DOHERTY 1992 18 p Presented at the Conference on Advanced Space Exploration Initiative Technologies, Cleveland, OH, 4-6 Sep. 1991; sponsored by AIAA, and OAI Previously announced in IAA as A91-52353
(Contract RTOP 593-72-00)
(NASA-TM-105605; E-6941; NAS 1.15:105605; AIAA PAPER 91-3441) Avail: CASI HC A03/MF A01

An overview is given of the plans for a program in nuclear electric propulsion (NEP) technology for space applications being considered by NASA, DOE, and DOD. Possible missions using NEP are examined, and NEP technology plans are addressed regarding concept development, systems engineering, nuclear fuels, power conversion, thermal management, power management and distribution, electric thrusters, facilities, and issues related to safety and environment. The programmatic characteristics are considered. Author

20 SPACECRAFT PROPULSION AND POWER

N92-23534*# National Aeronautics and Space Administration. Lewis Research Center, Cleveland, OH.

DERATED ION THRUSTER DESIGN ISSUES

MICHAEL J. PATTERSON and VINCENT K. RAWLIN Oct. 1991 16 p Presented at the 22nd International Electric Propulsion Conference, Viareggio, Italy, 14-17 Oct. 1991; sponsored by AIDAA, AIAA, DGLR, and JSASS (Contract RTOP 506-42-31) (NASA-TM-105576; E-6902; NAS 1.15:105576) Avail: CASI HC A03/MF A01

Preliminary activities to develop and refine a lightweight 30 cm engineering model ion thruster are discussed. The approach is to develop a 'derated' ion thruster capable of performing both auxiliary and primary propulsion roles over an input power range of at least 0.5 to 5.0 kilo-W. Design modifications to a baseline thruster to reduce mass and volume are discussed. Performance data over an order of magnitude input power range are presented, with emphasis on the performance impact of engine throttling. Thruster design modifications to optimize performance over specific power envelopes are discussed. Additionally, lifetime estimates based on wear test measurements are made for the operation envelope of the engine. Author

N92-24201*# National Aeronautics and Space Administration. Lewis Research Center, Cleveland, OH.

LARGE TRANSIENT FAULT CURRENT TEST OF AN ELECTRICAL ROLL RING

EDWARD J. YENNI (Rockwell International Corp., Cleveland, OH.) and ARTHUR G. BIRCHENOUGH 1992 7 p Presented at the 26th Intersociety Energy Conversion Engineering Conference, Boston, MA, 4-9 Aug. 1991; sponsored by ANS, SAE, ACS, AIAA, ASME, IEEE, and AIChE (Contract RTOP 474-42-10) (NASA-TM-105667; E-7029; NAS 1.15:105667) Avail: CASI HC A02/MF A01

The space station uses precision rotary gimbals to provide for sun tracking of its photoelectric arrays. Electrical power, command signals and data are transferred across the gimbals by roll rings. Roll rings have been shown to be capable of highly efficient electrical transmission and long life, through tests conducted at the NASA Lewis Research Center and Honeywell's Satellite and Space Systems Division in Phoenix, AZ. Large potential fault currents inherent to the power system's DC distribution architecture, have brought about the need to evaluate the effects of large transient fault currents on roll rings. A test recently conducted at Lewis subjected a roll ring to a simulated worst case space station electrical fault. The system model used to obtain the fault profile is described, along with details of the reduced order circuit that was used to simulate the fault. Test results comparing roll ring performance before and after the fault are also presented. Author

N92-24557*# National Aeronautics and Space Administration. Lewis Research Center, Cleveland, OH.

METALLIZED GELLED MONOPROPELLANTS

ERIN G. NIEDER (Atlantic Research Corp., Gainesville, VA.), CHARLES E. HARROD (Atlantic Research Corp., Gainesville, VA.), FREDERICK C. RODGERS (Atlantic Research Corp., Gainesville, VA.), DOUGLAS C. RAPP (Sverdrup Technology, Inc., Brook Park, OH.), and BRYAN A. PALASZEWSKI Apr. 1992 22 p (Contract NAS3-25831; NAS3-25266; RTOP 506-42-72) (NASA-TM-105418; E-6829; NAS 1.15:105418) Avail: CASI HC A03/MF A01

Thermochemical calculations of seven metallized monopropellants were conducted to quantify theoretical specific impulse and density specific impulse performance. On the basis of theoretical performance, commercial availability of formulation constituents, and anticipated viscometric behavior, two metallized monopropellants were selected for formulation characterization: triethylene glycol dinitrate, ammonium perchlorate, aluminum and hydrogen peroxide, aluminum. Formulation goals were established, and monopropellant formulation compatibility and hazard sensitivity were experimentally determined. These experimental results

indicate that the friction sensitivity, detonation susceptibility, and material handling difficulties of the elevated monopropellant formulations and their constituents pose formidable barriers to their future application as metallized monopropellants. Author

N92-24560*# National Aeronautics and Space Administration. Lewis Research Center, Cleveland, OH.

ADVANCED LIQUID ROCKETS

STEVEN J. SCHNEIDER 1992 16 p Presented at the JANNAF Propulsion Meeting, Indianapolis, IN, 24-27 Feb. 1992 (Contract RTOP 506-42-31) (NASA-TM-105633; E-6976; NAS 1.15:105633) Avail: CASI HC A03/MF A01

A program to substitute iridium coated rhenium for silicide coated niobium in thrust chamber fabrications is reviewed. The life limiting phenomena in each of these material systems is also reviewed. Coating cracking and spalling is not a problem with iridium-coated rhenium as in silicide-coated niobium. Use of the new material system enables an 800 K increase in thruster operating temperature from around 1700 K for niobium to 2500 K for rhenium. Specific impulse iridium-coated rhenium rockets is nominally 20 seconds higher than comparable niobium rockets in the 22 N class and nominally 10 seconds higher in the 440 N class. Author

N92-24957*# National Aeronautics and Space Administration. Lewis Research Center, Cleveland, OH.

DEVELOPMENT OF ADVANCED SEALS FOR SPACE PROPULSION TURBOMACHINERY

R. C. HENDRICKS (Texas A&M Univ., College Station.), A. D. LIANG, D. W. CHILDS (Texas A&M Univ., College Station.), and M. P. PROCTOR Apr. 1992 15 p Presented at the 1992 Aerospace Atlantic International Conference and Exposition, Dayton, OH, 6-10 Apr. 1992; sponsored by the Society of Automatic Engineers (Contract RTOP 590-21-11) (NASA-TM-105659; E-7024; NAS 1.15:105659) Avail: CASI HC A03/MF A01

Current activities in seals for space propulsion turbomachinery that the NASA Lewis Research Center sponsors are surveyed. The overall objective is to provide the designer and researcher with the concepts and the data to control seal dynamics and leakage. Included in the program are low-leakage seals, such as the brush seal, the 'ceramic rope' seal, low-leakage seals for liquid oxygen turbopumps, face seals for two phase flow, and swirl brakes for stability. Two major efforts are summarized: a seal dynamics in rotating machinery and an effort in seal code development. Author

N92-25343*# National Aeronautics and Space Administration. Lewis Research Center, Cleveland, OH.

NASA PROGRAMS IN SPACE PHOTOVOLTAICS

DENNIS J. FLOOD 1992 14 p Presented at the 6th International Photovoltaic Science and Engineering Conference, New Delhi, India, 10-14 Feb. 1992; sponsored by Dept. of Non-Conventional Energy Sources, Government of India, Solar Energy Society of India and National Physical Lab (Contract RTOP 506-41-11) (NASA-TM-105428; E-6844; NAS 1.15:105428) Avail: CASI HC A03/MF A01

Highlighted here are some of the current programs in advanced space solar cell and array development conducted by NASA in support of its future mission requirements. Recent developments are presented for a variety of solar cell types, including both single crystal and thin film cells. A brief description of an advanced concentrator array capable of AM0 efficiencies approaching 25 percent is also provided. Author

N92-25616*# National Aeronautics and Space Administration. Lewis Research Center, Cleveland, OH.

THERMAL STRATIFICATION POTENTIAL IN ROCKET ENGINE COOLANT CHANNELS

KENNETH J. KACYNSKI May 1992 14 p

20 SPACECRAFT PROPULSION AND POWER

(Contract RTOP 506-42-41)
(NASA-TM-4378; E-6135; NAS 1.15:4378) Avail: CASI HC
A03/MF A01

The potential for rocket engine coolant channel flow stratification was computationally studied. A conjugate, 3-D, conduction/advection analysis code (SINDA/FLUINT) was used. Core fluid temperatures were predicted to vary by over 360 K across the coolant channel, at the throat section, indicating that the conventional assumption of a fully mixed fluid may be extremely inaccurate. Because of the thermal stratification of the fluid, the walls exposed to the rocket engine exhaust gases will be hotter than an assumption of full mixing would imply. In this analysis, wall temperatures were 160 K hotter in the turbulent mixing case than in the full mixing case. The discrepancy between the full mixing and turbulent mixing analyses increased with increasing heat transfer. Both analysis methods predicted identical channel resistances at the coolant inlet, but in the stratified analysis the thermal resistance was negligible. The implications are significant. Neglect of thermal stratification could lead to underpredictions in nozzle wall temperatures. Even worse, testing at subscale conditions may be inadequate for modeling conditions that would exist in a full scale engine. Author

N92-26654*# National Aeronautics and Space Administration.
Lewis Research Center, Cleveland, OH.

HEAT TRANSFER IN OSCILLATING FLOWS WITH SUDDEN CHANGE IN CROSS SECTION

MOUNIR IBRAHIM (Cleveland State Univ., OH.), WAQAR HASHIM (Cleveland State Univ., OH.), ROY C. TEW, and JAMES E. DUDENHOEFER 1992 8 p Proposed for presentation at the 27th Intersociety Energy Conversion Engineering Conference, San Diego, CA, 3-7 Aug. 1992; sponsored by SAE, ACS, AIAA, ASME, IEEE, AIChE, and ANS
(Contract RTOP 590-13-11)
(NASA-TM-105692; E-7077; NAS 1.15:105692) Avail: CASI HC
A02/MF A01

Oscillating fluid flow (zero mean) with heat transfer, between two parallel plates with a sudden change in cross section, was examined computationally. The flow was assumed to be laminar and incompressible with inflow velocity uniform over the channel cross section but varying sinusoidally with time. Over 30 different cases were examined; these cases cover wide ranges of Re_{sub} max (187.5 to 30000), Va (1 to 350), expansion ratio (1:2, 1:4, 1:8, and 1:12) and A_{sub} (0.68 to 4). Three different geometric cases were considered (asymmetric expansion and/or contraction, symmetric expansion/contraction, and symmetric blunt body). The heat transfer cases were based on constant wall temperature at higher (heating) or lower (cooling) value than the inflow fluid temperature. As a result of the oscillating flow, the fluid undergoes sudden expansion in one half of the cycle and sudden contraction in the other half. One heating case is examined in detail, and conclusions are drawn from all the cases (documented in detail elsewhere). Instantaneous friction factors and heat transfer coefficients, for some ranges of Re_{sub} max and Va , deviated substantially from those predicted with steady state correlations. Author

N92-26792*# National Aeronautics and Space Administration.
Lewis Research Center, Cleveland, OH.

NASA/DOE/DOD NUCLEAR PROPULSION TECHNOLOGY PLANNING: SUMMARY OF FY 1991 INTERAGENCY PANEL RESULTS

JOHN S. CLARK (Sandia National Labs., Albuquerque, NM.), TIMOTHY J. WICKENHEISER (Argonne National Lab., IL.), MICHAEL P. DOHERTY, ALBERT MARSHALL, SAMIT K. BHATTACHARYYA, and JOHN WARREN (Department of Energy, Germantown, MD.) 1992 12 p Proposed for presentation at the Nuclear Technologies for Space Exploration, Jackson Hole, WY, 16-19 Aug. 1992
(Contract RTOP 593-71-00)
(NASA-TM-105703; E-7092; NAS 1.15:105703) Avail: CASI HC
A03/MF A01
Interagency (NASA/DOE/DOD) technical panels worked in

1991 to evaluate critical nuclear propulsion issues, compare nuclear propulsion concepts for a manned Mars mission on a consistent basis, and to continue planning a technology development project for the Space Exploration Initiative (SEI). Panels were formed to address mission analysis, nuclear facilities, safety policy, nuclear fuels and materials, nuclear electric propulsion technology, and nuclear thermal propulsion technology. A summary of the results and recommendations of the panels is presented. Author

N92-27033*# National Aeronautics and Space Administration.
Lewis Research Center, Cleveland, OH.

ROCKET ENGINE DIAGNOSTICS USING QUALITATIVE MODELING TECHNIQUES

MICHAEL BINDER (Sverdrup Technology, Inc., Brook Park, OH.), WILLIAM MAUL (Sverdrup Technology, Inc., Brook Park, OH.), CLAUDIA MEYER (Sverdrup Technology, Inc., Brook Park, OH.), and AMY SOVIE 1992 15 p Proposed for presentation at the 28th Joint Propulsion Conference, Nashville, TN, 6-8 Jul. 1992; sponsored by AIAA, SAE, ASME, and ASEE
(Contract NAS3-25266; RTOP 593-12-21)
(NASA-TM-105714; E-7108; NAS 1.15:105714; AIAA PAPER 92-3164) Avail: CASI HC A03/MF A01

Researchers at NASA Lewis Research Center are presently developing qualitative modeling techniques for automated rocket engine diagnostics. A qualitative model of a turbopump interpellant seal system was created. The qualitative model describes the effects of seal failures on the system steady state behavior. This model is able to diagnose the failure of particular seals in the system based on anomalous temperature and pressure values. The anomalous values input to the qualitative model are generated using numerical simulations. Diagnostic test cases include both single and multiple seal failures. Author

N92-27034*# National Aeronautics and Space Administration.
Lewis Research Center, Cleveland, OH.

OVERVIEW OF NASA SUPPORTED STIRLING THERMODYNAMIC LOSS RESEARCH

ROY C. TEW and STEVEN M. GENG 1992 8 p Proposed for presentation at the 27th Intersociety Energy Conversion Engineering Conference, San Diego, CA, 3-7 Aug. 1992; sponsored by SAE
(Contract RTOP 590-13-11)
(NASA-TM-105690; E-7071; NAS 1.15:105690) Avail: CASI HC
A02/MF A01

NASA is funding research to characterize Stirling machine thermodynamic losses. NASA's primary goal is to improve Stirling design codes to support engine development for space and terrestrial power. However, much of the fundamental data is applicable to Stirling cooling and heat pump applications. The research results are reviewed. Much was learned about oscillating flow hydrodynamics, including laminar/turbulent transition, and tabulated data was documented for further analysis. Now, with a better understanding of the oscillating flow field, it is time to begin measuring the effects of oscillating flow and oscillating pressure level on heat transfer in heat exchanger flow passages and in cylinders. Author

N92-27035*# National Aeronautics and Space Administration.
Lewis Research Center, Cleveland, OH.

THE 3D ROCKET COMBUSTOR ACOUSTICS MODEL

RICHARD J. PRIEM (Priem Consultants, Inc., Cleveland, OH.) and KEVIN J. BREISACHER Jul. 1992 13 p Proposed for presentation at the 28th Joint Propulsion Conference and Exhibit, Nashville, TN, 6-8 Jul. 1992; sponsored by AIAA, SAE, ASME, and ASEE
(Contract RTOP 590-21-21)
(NASA-TM-105734; E-7137; NAS 1.15:105734; AIAA PAPER 92-3228) Avail: CASI HC A03/MF A01

The theory and procedures for determining the characteristics of pressure oscillations in rocket engines with prescribed burning rate oscillations are presented. Analyses including radial and hub baffles and absorbers can be performed in one, two, and three dimensions. Pressure and velocity oscillations calculated using this

procedure are presented for the SSME to show the influence of baffles and absorbers on the burning rate oscillations required to achieve neutral stability. Comparisons are made between the results obtained utilizing 1-D, 2-D, and 3-D assumptions with regards to capturing the physical phenomena of interest and computational requirements.

Author

N92-27036*# National Aeronautics and Space Administration. Lewis Research Center, Cleveland, OH.

EFFECT OF MODEL SELECTION ON COMBUSTOR PERFORMANCE AND STABILITY PREDICTIONS USING ROCCID

JAMES E. GIULIANI (Ohio Aerospace Inst., Brook Park.) and MARK D. KLEM Jul. 1992 16 p Proposed for presentation at the 28th Joint Propulsion Conference and Exhibit, Nashville, TN, 6-8 Jul. 1992; sponsored by AIAA, SAE, ASME, and ASEE (Contract RTOP 590-21-21) (NASA-TM-105750; E-7154; NAS 1.15:105750; AIAA PAPER 92-3226) Avail: CASI HC A03/MF A01

The ROCKET Combustor Interactive Design (ROCCID) methodology is an interactive computer program that combines previously developed combustion analysis models to calculate the combustion performance and stability of liquid rocket engines. Test data from 213 kN (48,000 lbf) Liquid Oxygen (LOX)/RP-1 combustor with an O-F-O (oxidizer-fuel-oxidizer) triplet injector were used to characterize the predictive capabilities of the ROCCID analysis models for this injector/propellant configuration. Thirteen combustion performance and stability models were incorporated into ROCCID, and ten of them, which have options for triplet injectors, were examined. Calculations using different combinations of analysis models, with little or no anchoring, were carried out on a test matrix of operating combinations matching those of the test program. Results of the computer analyses were compared to test data, and the ability of the model combinations to correctly predict combustion stability or instability was determined. For the best model combination(s), sensitivity of the calculations to fuel drop size and mixing efficiency was examined. Error in the stability calculations due to uncertainty in the pressure interaction index (N) was examined. The recommended model combinations for this O-F-O triplet LOX/RP-1 configuration are proposed.

Author

N92-27161*# National Aeronautics and Space Administration. Lewis Research Center, Cleveland, OH.

THE EVALUATION OF LAYERED SEPARATORS FOR NICKEL-HYDROGEN CELLS

RANDALL F. GAHN *in* NASA. Marshall Space Flight Center, The 1990 NASA Aerospace Battery Workshop p 653-676 May 1991

Avail: CASI HC A03/MF A10

The concept of using layered separators to achieve the required electrolyte retention and bubble pressure for nickel-hydrogen cells was evaluated in a boilerplate cell test. Zircar cloth, polyethylene paper and polypropylene felt were combined with a layer of radiation-grafted polyethylene film to achieve the required properties. Three cells of each layered separator were built and tested by characterization cycling and by low earth orbit cycling for 5000 cycles at 80 percent DOD. Three cells containing asbestos separators were used as the reference.

Author

N92-27167*# National Aeronautics and Space Administration. Lewis Research Center, Cleveland, OH.

RESULTS OF A TECHNICAL ANALYSIS OF THE HUBBLE SPACE TELESCOPE NICKEL-CADMIUM AND NICKEL-HYDROGEN BATTERIES

MICHELLE A. MANZO et al. *in* NASA. Marshall Space Flight Center, The 1990 NASA Aerospace Battery Workshop p 789-860 May 1991

Avail: CASI HC A04/MF A10

The Hubble Space Telescope (HST) Program Office requested the expertise of the NASA Aerospace Flight Battery Systems Steering Committee (NAFBSSC) in the conduct of an independent assessment of the HST's battery system to assist in their decision of whether to fly nickel-cadmium or nickel-hydrogen batteries on

the telescope. In response, a subcommittee to the NAFBSSC was organized with membership comprised of experts with background in the nickel-cadmium/nickel-hydrogen secondary battery/power systems areas. The work and recommendations of that subcommittee are presented.

Author

N92-27654*# National Aeronautics and Space Administration. Lewis Research Center, Cleveland, OH.

PROPULSION SYSTEMS USING IN SITU PROPELLANTS FOR A MARS ASCENT VEHICLE

MARY F. WADEL and ELIZABETH A. RONCACE Jul. 1992 12 p Proposed for presentation at the 28th Joint Propulsion Conference and Exhibit, Nashville, TN, 6-8 Jul. 1992; sponsored by AIAA, SAE, ASME, and ASEE (Contract RTOP 506-42-72)

(NASA-TM-105741; E-7146; NAS 1.15:105741; AIAA PAPER 92-3445) Copyright Avail: CASI HC A03/MF A01

The indigenous propellants of oxygen and carbon monoxide were studied for use in a Mars Ascent Vehicle (MAV). Both the oxygen and carbon monoxide were evaluated as turbine working fluids for a full expander engine cycle used in the MAV. Two oxygen working fluid engines and four carbon monoxide engines were investigated. The maximum hot-gas-side wall temperature was limited to either 445 K (800 R) or 556 K (1000 R) over a range of working fluid mass flows. An engine thrust of 44.5 kN (1,000 lb(sub f)) was assumed. The engine characteristics of coolant inlet pressure, total engine length, specific impulse, pump efficiencies, and turbine power required were optimized. Of the six engines evaluated, the study showed that either type of working fluid was feasible for a MAV engine. Using carbon monoxide as the working fluid resulted in the best engine characteristics.

Author

N92-27878*# National Aeronautics and Space Administration. Lewis Research Center, Cleveland, OH.

VALIDATION TEST OF ADVANCED TECHNOLOGY FOR IPV NICKEL-HYDROGEN FLIGHT CELLS: UPDATE

JOHN J. SMITHRICK and STEPHEN W. HALL (Naval Weapons Support Center, Crane, IN.) 1992 13 p Presented at the 27th Intersociety Energy Conversion Engineering Conference; sponsored by SAE, ACS, AIAA, ASME, IEEE, AIChE, and ANS (Contract RTOP 506-41-21)

(NASA-TM-105689; E-7069; NAS 1.15:105689) Avail: CASI HC A03/MF A01

Individual pressure vessel (IPV) nickel-hydrogen technology was advanced at NASA Lewis and under Lewis contracts with the intention of improving cycle life and performance. One advancement was to use 26 percent potassium hydroxide (KOH) electrolyte to improve cycle life. Another advancement was to modify the state-of-the-art cell design to eliminate identified failure modes. The modified design is referred to as the advanced design. A breakthrough in the low-earth-orbit (LEO) cycle life of IPV nickel-hydrogen cells has been previously reported. The cycle life of boiler plate cells containing 26 percent KOH electrolyte was about 40,000 LEO cycles compared to 3,500 cycles for cells containing 31 percent KOH. The boiler plate test results are in the process of being validated using flight hardware and real time LEO testing at the Naval Weapons Support Center (NWSC), Crane, Indiana under a NASA Lewis Contract. An advanced 125 Ah IPV nickel-hydrogen cell was designed. The primary function of the advanced cell is to store and deliver energy for long-term, LEO spacecraft missions. The new features of this design are: (1) use of 26 percent rather than 31 percent KOH electrolyte; (2) use of a patented catalyzed wall wick; (3) use of serrated-edge separators to facilitate gaseous oxygen and hydrogen flow within the cell, while still maintaining physical contact with the wall wick for electrolyte management; and (4) use of a floating rather than a fixed stack (state-of-the-art) to accommodate nickel electrode expansion due to charge/discharge cycling. The significant improvements resulting from these innovations are: extended cycle life; enhanced thermal, electrolyte, and oxygen management; and accommodation of nickel electrode expansion. The advanced cell

20 SPACECRAFT PROPULSION AND POWER

design is in the process of being validated using real time LEO cycle life testing of NWSC, Crane, Indiana. An update of validation test results confirming this technology is presented. Author

N92-28417*# National Aeronautics and Space Administration. Lewis Research Center, Cleveland, OH.

AN OVERVIEW OF IN-FLIGHT PLUME DIAGNOSTICS FOR ROCKET ENGINES

G. C. MADZSAR (Aerojet Tactical Propulsion Co., Sacramento, CA.), R. L. BICKFORD (Aerojet Solid Propulsion Co., Sacramento, CA.), and D. B. DUNCAN (Duncan Technologies, Auburn, CA.) Jul. 1992 25 p Proposed for presentation at the 28th Joint Propulsion Conference and Exhibit, Nashville, TN, 6-8 Jul. 1992; sponsored by AIAA, SAE, ASME, and ASEE (Contract RTOP 590-21-41) (NASA-TM-105727; E-7130; NAS 1.15:105727; AIAA PAPER 92-3785) Avail: CASI HC A03/MF A01

An overview and progress report of the work performed or sponsored by LeRC toward the development of in-flight plume spectroscopy technology for health and performance monitoring of liquid propellant rocket engines are presented. The primary objective of this effort is to develop technology that can be utilized on any flight engine. This technology will be validated by a hardware demonstration of a system capable of being retrofitted onto the Space Shuttle Main Engines for spectroscopic measurements during flight. The philosophy on system definition and status on the development of instrumentation, optics, and signal processing with respect to implementation on a flight engine are discussed. Author

N92-28682*# National Aeronautics and Space Administration. Lewis Research Center, Cleveland, OH.

NASA LEWIS STEADY-STATE HEAT PIPE CODE USERS MANUAL

LEONARD K. TOWER (Sverdrup Technology, Inc., Brook Park, OH.), KARL W. BAKER, and TIMOTHY S. MARKS (Oregon State Univ., Corvallis.) Jun. 1992 45 p (Contract RTOP 590-13-21) (NASA-TM-105161; E-6450; NAS 1.15:105161) Avail: CASI HC A03/MF A01

The NASA Lewis heat pipe code was developed to predict the performance of heat pipes in the steady state. The code can be used as a design tool on a personal computer or with a suitable calling routine, as a subroutine for a mainframe radiator code. A variety of wick structures, including a user input option, can be used. Heat pipes with multiple evaporators, condensers, and adiabatic sections in series and with wick structures that differ among sections can be modeled. Several working fluids can be chosen, including potassium, sodium, and lithium, for which monomer-dimer equilibrium is considered. The code incorporates a vapor flow algorithm that treats compressibility and axially varying heat input. This code facilitates the determination of heat pipe operating temperatures and heat pipe limits that may be encountered at the specified heat input and environment temperature. Data are input to the computer through a user-interactive input subroutine. Output, such as liquid and vapor pressures and temperatures, is printed at equally spaced axial positions along the pipe as determined by the user. Author

N92-28693*# National Aeronautics and Space Administration. Lewis Research Center, Cleveland, OH.

INTEGRATED HEALTH MONITORING AND CONTROLS FOR ROCKET ENGINES

W. C. MERRILL, J. L. MUSGRAVE, and T. H. GUO Apr. 1992 7 p Presented at the SAE Aerospace Atlantic, Dayton, OH, 7-10 Apr. 1992; sponsored in part by the Engineering Society for Advancing Mobility Land, Sea, Air, and Space (Contract RTOP 506-42-72) (NASA-TM-105763; E-7180; NAS 1.15:105763) Avail: CASI HC A02/MF A01

Current research in intelligent control systems at the Lewis Research Center is described in the context of a functional framework. The framework is applicable to a variety of reusable

space propulsion systems for existing and future launch vehicles. It provides a 'road map' technology development to enable enhanced engine performance with increased reliability, durability, and maintainability. The framework hierarchy consists of a mission coordination level, a propulsion system coordination level, and an engine control level. Each level is described in the context of the Space Shuttle Main Engine. The concept of integrating diagnostics with control is discussed within the context of the functional framework. A distributed real time simulation testbed is used to realize and evaluate the functionalities in closed loop. Author

N92-28983*# National Aeronautics and Space Administration. Lewis Research Center, Cleveland, OH.

DEVELOPMENT AND FLIGHT HISTORY OF SERT 2 SPACECRAFT

WILLIAM R. KERSLAKE (Sverdrup Technology, Inc., Brook Park, OH.) and LOUIS R. IGNACZAK 1992 53 p Proposed for presentation at the 28th Joint Propulsion Conference and Exhibit, Nashville, TN, 6-8 Jul. 1992; sponsored by AIAA, SAE, ASME, and ASEE (Contract RTOP 506-42-31) (NASA-TM-105636; E-6839; NAS 1.15:105636; AIAA PAPER 92-3516) Avail: CASI HC A04/MF A01

A 25-year historical review of the Space Electric Rocket Test 2 (SERT 2) mission is presented. The Agena launch vehicle; the SERT 2 spacecraft; and mission-peculiar spacecraft hardware, including two ion thruster systems, are described. The 3 1/2-year development period, from 1966 to 1970, that was needed to design, fabricate, and qualify the ion thruster system and the supporting spacecraft components, is documented. Major testing of two ion thruster systems and related auxiliary experiments that were conducted in space after the 3 Feb. 1970, launch are reviewed. Extended ion thruster restarts from 1973 to 1981 are reported, in addition to cross-neutralization tests. Tests of a reflector erosion experiment were continued in 1989 to 1991. The continuing performance of spacecraft subsystems, including the solar arrays, over the 1970-1991 period is summarized. Finally, the knowledge of thruster-spacecraft interactions learned from SERT 2 is listed. Author

N92-29343*# National Aeronautics and Space Administration. Lewis Research Center, Cleveland, OH.

APPLIED ANALYTICAL COMBUSTION/EMISSIONS RESEARCH AT THE NASA LEWIS RESEARCH CENTER Progress Report

J. M. DEUR (Sverdrup Technology, Inc., Brook Park, OH.), K. P. KUNDU, and H. L. NGUYEN Jul. 1992 14 p Presented at the 28th Joint Propulsion Conference and Exhibit, Nashville, TN, 6-8 Jul. 1992 (Contract RTOP 537-02-20) (NASA-TM-105731; E-7135; AIAA PAPER 92-3338; NAS 1.15:105731) Avail: CASI HC A03/MF A01; 3 functional color pages

Emissions of pollutants from future commercial transports are a significant concern. As a result, the Lewis Research Center (LeRC) is investigating various low emission combustor technologies. As part of this effort, a combustor analysis code development program was pursued to guide the combustor design process, to identify concepts having the greatest promise, and to optimize them at the lowest cost in the minimum time. Author

N92-29667*# National Aeronautics and Space Administration. Lewis Research Center, Cleveland, OH.

THE O2 REDUCTION AT THE IFC MODIFIED O2 FUEL CELL ELECTRODE

WILLIAM L. FIELDER, JOSEPH SINGER, RICHARD S. BALDWIN, and RICHARD E. JOHNSON (LeTourneau Coll., Longview, TX.) Jul. 1992 13 p (Contract RTOP 506-41-21) (NASA-TM-105691; E-7073; NAS 1.15:105691) Avail: CASI HC A03/MF A01

The International Fuel Corporation (IFC) state of the art (SOA) O2 electrode (Au-10 percent Pt electrocatalyst by weight) is

currently being used in the alkaline H₂-O₂ fuel cell in the NASA Space Shuttle. Recently, IFC modified O₂ electrode, as a possible replacement for the SOA electrode. In the present study, O₂ reduction data were obtained for the modified electrode at temperatures between 23.3 and 91.7 C. BET measurements gave an electrode BET surface area of about 2070 sq. cm/sq. cm of geometric surface area. The Tafel data could be fitted to two straight line regions. The slope for the lower region, designated as the 0.04 V/decade region, was temperature dependent, and the transfer coefficient was about 1.5. The 'apparent' energy of activation for this region was about 19 kcal/mol. An O₂ reduction mechanism for this 0.04 region is presented. In the upper region, designated as the 0.08 V/decade region, diffusion may be the controlling process. Tafel data are presented to illustrate the increase in performance with increasing temperature. Author

N92-30187*# National Aeronautics and Space Administration. Lewis Research Center, Cleveland, OH.

OPTIMIZATION OF ARMORED SPHERICAL TANKS FOR STORAGE ON THE LUNAR SURFACE

D. J. BENTS and D. A. KNIGHT 1992 10 p Presented at the 27th Intersociety Energy Conversion Engineering Conference, San Diego, CA, 3-7 Aug. 1992; sponsored in part by SAE, ACS, AIAA, ASME, IEEE, AIChE and ANS (Contract RTOP 326-81-10) (NASA-TM-105700; E-7088; NAS 1.15:105700) Avail: CASI HC A02/MF A01

A redundancy strategy for reducing micrometeoroid armoring mass is investigated, with application to cryogenic reactant storage for a regenerative fuel cell (RFC) on the lunar surface. In that micrometeoroid environment, the cryogenic fuel must be protected from loss due to tank puncture. The tankage must have a sufficiently high probability of survival over the length of the mission so that the probability of system failure due to tank puncture is low compared to the other mission risk factors. Assuming that a single meteoroid penetration can cause a storage tank to lose its contents, two means are available to raise the probability of surviving micrometeoroid attack to the desired level. One can armor the tanks to a thickness sufficient to reduce probability of penetration of any tank to the desired level or add extra capacity in the form of spare tanks that results in survival of a given number out of the ensemble at the desired level. A combination of these strategies (armoring and redundancy) is investigated. The objective is to find the optimum combination which yields the lowest shielding mass per cubic meter of surviving fuel out of the original ensemble. The investigation found that, for the volumes of fuel associated with multikilowatt class cryo storage RFC's, and the armoring methodology and meteoroid models used, storage should be fragmented into small individual tanks. Larger installations (more fuel) pay less of a shielding penalty than small installations. For the same survival probability over the same time period, larger volumes will require less armoring mass per unit volume protected. Author

N92-30308*# National Aeronautics and Space Administration. Lewis Research Center, Cleveland, OH.

NEP SYSTEMS ENGINEERING EFFORTS IN FY-92: PLANS AND STATUS

MICHAEL P. DOHERTY and JAMES H. GILLAND (Sverdrup Technology, Inc., Brook Park, OH.) Aug. 1992 10 p Presented at the Nuclear Technologies for Space Exploration Conference, Jackson Hole, WY, 16-19 Aug. 1992; sponsored in part by American Nuclear Society (Contract NAS3-25266; RTOP 593-72-00) (NASA-TM-105775; E-7203; NAS 1.15:105775) Avail: CASI HC A02/MF A01

A system engineering effort has been initiated by NASA in FY-92 to define, address, and resolve issues associated with the use of Nuclear Electric Propulsion (NEP) for megawatt (MW) space propulsion applications associated with the Space Exploration Initiative (SEI). It is intended that key technical issues will be addressed by activities conducted in the early years of a project in NEP, with the objective of resolving such issues. Also, in

response to more recent programmatic direction, a concept definition activity for 100 kilowatt NEP is being initiated. This paper will present key issues associated with megawatt NEP, and the plans and status for their resolution, and present the scope and rationale for the 100 kilowatt concept definition activity. Author

N92-30818*# National Aeronautics and Space Administration. Lewis Research Center, Cleveland, OH.

NUCLEAR ELECTRIC PROPULSION DEVELOPMENT AND QUALIFICATION FACILITIES

D. S. DUTT (Westinghouse Hanford Co., Richland, WA.), K. THOMASSEN (Lawrence Livermore National Lab., CA.), J. SOVEY, and MARIO FONTANA (Oak Ridge National Lab., TN.) Nov. 1991 11 p Presented at the 9th Symposium on Space Nuclear Power Systems, Albuquerque, NM, 13-16 Jan. 1992 (Contract DE-AC06-87RL-10930) (NASA-TM-105521; NAS 1.15:105521; DE92-004262; WHC-SA-1402; CONF-920104-23) Avail: CASI HC A03/MF A01

This paper summarizes the findings of a Tri-Agency panel consisting of members from the National Aeronautics and Space Administration (NASA), U.S. Department of Energy (DOE), and U.S. Department of Defense (DOD) that were charged with reviewing the status and availability of facilities to test components and subsystems for megawatt-class nuclear electric propulsion (NEP) systems. The facilities required to support development of NEP are available in NASA centers, DOE laboratories, and industry. However, several key facilities require significant and near-term modification in order to perform the testing required to meet a 2014 launch date. For the higher powered Mars cargo and piloted missions, the priority established for facility preparation is: (1) a thruster developmental testing facility, (2) a thruster lifetime testing facility, (3) a dynamic energy conversion development and demonstration facility, and (4) an advanced reactor testing facility (if required to demonstrate an advanced multiwatt power system). Facilities to support development of the power conditioning and heat rejection subsystems are available in industry, federal laboratories, and universities. In addition to the development facilities, a new preflight qualifications and acceptance testing facility will be required to support the deployment of NEP systems for precursor, cargo, or piloted Mars missions. Because the deployment strategy for NEP involves early demonstration missions, the demonstration of the SP-100 power system is needed by the early 2000's. Author

N92-31249*# National Aeronautics and Space Administration. Lewis Research Center, Cleveland, OH.

CYCLIC HOT FIRING RESULTS OF TUNGSTEN-WIRE-REINFORCED, COPPER-LINED THRUST CHAMBERS

JOHN M. KAZAROFF and ROBERT S. JANKOVSKY Sep. 1990 16 p (Contract RTOP 505-01-11) (NASA-TM-4214; E-5337; NAS 1.15:4214) Avail: CASI HC A03/MF A01

An advanced thrust liner material for potential long life reusable rocket engines is described. This liner material was produced with the intent of improving the reusable life of high pressure thrust chambers by strengthening the chamber in the hoop direction, thus avoiding the longitudinal cracking due to low cycle fatigue that is observed in conventional homogeneous copper chambers, but yet not reducing the high thermal conductivity that is essential when operating with high heat fluxes. The liner material produced was a tungsten wire reinforced copper composite. Incorporating this composite into two hydrogen-oxygen test rocket chambers was done so that its performance as a reusable liner material could be evaluated. Testing results showed that both chambers failed prematurely, but the crack sites were perpendicular to the normal direction of cracking indicating a degree of success in containing the tremendous thermal strain associated with high temperature rocket engines. The failures, in all cases, were associated with drilled instrumentation ports and no other damages or deformations were found elsewhere in the composite liners. Author

20 SPACECRAFT PROPULSION AND POWER

N92-31342*# National Aeronautics and Space Administration. Lewis Research Center, Cleveland, OH.

THE EVOLUTIONARY DEVELOPMENT OF HIGH SPECIFIC IMPULSE ELECTRIC THRUSTER TECHNOLOGY

JAMES S. SOVEY, JOHN A. HAMLEY, MICHAEL J. PATTERSON, VINCENT K. RAWLIN, and ROGER M. MYERS (Sverdrup Technology, Inc., Brook Park, OH.) 1992 28 p Presented at the Space Programs and Technologies Conference, Huntsville, AL, 24-27 Mar. 1992; sponsored by AIAA Previously announced in IAA as A92-38650

(Contract NAS3-25266; RTOP 506-42-31)
(NASA-TM-105712; E-7104; NAS 1.15:105712; AIAA PAPER 92-1556) Avail: CASI HC A03/MF A01

Electric propulsion flight and technology demonstrations conducted primarily by Europe, Japan, China, the U.S., and the USSR are reviewed. Evolutionary mission applications for high specific impulse electric thruster systems are discussed, and the status of arcjet, ion, and magnetoplasmadynamic thrusters and associated power processor technologies are summarized.

Author

N92-31507*# National Aeronautics and Space Administration. Lewis Research Center, Cleveland, OH.

A DEMONSTRATION OF AN INTELLIGENT CONTROL SYSTEM FOR A REUSABLE ROCKET ENGINE

JEFFREY L. MUSGRAVE, DANIEL E. PAXSON, JONATHAN S. LITT, and WALTER C. MERRILL Jun. 1992 11 p Submitted for publication Prepared in cooperation with Army Aviation Systems Command, Cleveland, OH

(Contract RTOP 582-01-11)
(NASA-TM-105794; E-7224; NAS 1.15:105794; AD-A255720)
Avail: CASI HC A03/MF A01

An Intelligent Control System for reusable rocket engines is under development at NASA Lewis Research Center. The primary objective is to extend the useful life of a reusable rocket propulsion system while minimizing between flight maintenance and maximizing engine life and performance through improved control and monitoring algorithms and additional sensing and actuation. This paper describes current progress towards proof-of-concept of an Intelligent Control System for the Space Shuttle Main Engine. A subset of identifiable and accommodatable engine failure modes is selected for preliminary demonstration. Failure models are developed retaining only first order effects and included in a simplified nonlinear simulation of the rocket engine for analysis under closed loop control. The engine level coordinator acts as an interface between the diagnostic and control systems, and translates thrust and mixture ratio commands dictated by mission requirements, and engine status (health) into engine operational strategies carried out by a multivariable control. Control reconfiguration achieves fault tolerance if the nominal (healthy engine) control cannot. Each of the aforementioned functionalities is discussed in the context of an example to illustrate the operation of the system in the context of a representative failure. A graphical user interface allows the researcher to monitor the Intelligent Control System and engine performance under various failure modes selected for demonstration.

Author

N92-31901*# National Aeronautics and Space Administration. Lewis Research Center, Cleveland, OH.

KRYPTON ION THRUSTER PERFORMANCE

MICHAEL J. PATTERSON and GEORGE J. WILLIAMS Aug. 1992 13 p Presented at the 28th Joint Propulsion Conference and Exhibit, Nashville, TN, 6-8 Jul. 1992; sponsored by AIAA, SAE, ASME, and ASEE

(Contract RTOP 506-42-31)
(NASA-TM-105818; E-7249; JPC-92-3144; NAS 1.15:105818)
Copyright Avail: CASI HC A03/MF A01

Preliminary data were obtained from a 30 cm ion thruster operating on krypton propellant over the input power range of 0.4 to 5.5 kW. The data presented are compared and contrasted to the data obtained with xenon propellant over the same input power envelope. Typical krypton thruster efficiency was 70 percent at a specific impulse of approximately 5000 s, with a maximum

demonstrated thrust to power ratio of approximately 42 mN/kW at 2090 s specific impulse and 1580 watts input power. Critical thruster performance and component lifetime issues were evaluated. Order of magnitude power throttling was demonstrated using a simplified power-throttling strategy.

Author

N92-31916*# National Aeronautics and Space Administration. Lewis Research Center, Cleveland, OH.

AN OVERVIEW OF THE LEWIS RESEARCH CENTER CSTI THERMAL MANAGEMENT PROGRAM

ALBERT J. JUHASZ 1991 13 p Presented at the Conference on Advanced Space Exploration Initiative Technologies, Cleveland, OH, 4-6 Sep. 1991; sponsored in part by NASA, AIAA, and OAI Previously announced in IAA as A91-52422

(Contract RTOP 590-13-21)
(NASA-TM-105310; E-6542; NAS 1.15:105310; AIAA PAPER 91-3528) Avail: CASI HC A03/MF A01

An integrated multi-element project effort, currently being carried out at NASA LeRC, for the development of space heat rejection subsystems, with special emphasis on lightweight radiators, in support of SEI power system technology, and in particular the SP-100 program, is reported. Principal project elements include both contracted and in-house efforts. Included in the first category are two contracts aimed at the development of advanced radiator concepts, and demonstration of a flexible fabric heat pipe radiator concept. In-house work is designed to guide and support the overall program by system integration studies, heat pipe testing and analytical code development, radiator surface morphology alteration for emissivity enhancement, and composite materials research focused on the development of lightweight high conductivity fins.

Author

N92-32108*# National Aeronautics and Space Administration. Lewis Research Center, Cleveland, OH.

SP-100 REACTOR WITH BRAYTON CONVERSION FOR LUNAR SURFACE APPLICATIONS

LEE S. MASON, CARLOS D. RODRIGUEZ, BARBARA I. MCKISSOCK, JAMES C. HANLON (Sverdrup Technology, Inc., Brook Park, OH.), and BRIAN C. MANSFIELD (Dayton Univ., OH.) 1992 18 p Presented at the Ninth Symposium on Space Nuclear Power Systems, Albuquerque, NM, 12-16 Jan. 1992

(Contract RTOP 506-49-11)
(NASA-TM-105637; E-6983; NAS 1.15:105637) Avail: CASI HC A03/MF A01

Examined here is the potential for integrating Brayton-cycle power conversion with the SP-100 reactor for lunar surface power system applications. Two designs were characterized and modeled. The first design integrates a 100-kWe SP-100 Brayton power system with a lunar lander. This system is intended to meet early lunar mission power needs while minimizing on-site installation requirements. Man-rated radiation protection is provided by an integral multilayer, cylindrical lithium hydride/tungsten (LiH/W) shield encircling the reactor vessel. Design emphasis is on ease of deployment, safety, and reliability, while utilizing relatively near-term technology. The second design combines Brayton conversion with the SP-100 reactor in an erectable 550-kWe powerplant concept intended to satisfy later-phase lunar base power requirements. This system capitalizes on experience gained from operating the initial 100-kWe module and incorporates some technology improvements. For this system, the reactor is emplaced in a lunar regolith excavation to provide man-rated shielding, and the Brayton engines and radiators are mounted on the lunar surface and extend radially from the central reactor. Design emphasis is on performance, safety, long life, and operational flexibility.

Author

N92-32237*# National Aeronautics and Space Administration. Lewis Research Center, Cleveland, OH.

LOW-ISP DERATED ION THRUSTER OPERATION

MICHAEL J. PATTERSON Aug. 1992 18 p Presented at the 28th Joint Propulsion Conference and Exhibit, Nashville, TN, 6-8 Jul. 1992; sponsored by AIAA, SAE, ASME, and ASEE

23 CHEMISTRY AND MATERIALS (GENERAL)

(Contract RTOP 506-42-31)
(NASA-TM-105787; E-7217; JPC-92-3203; NAS 1.15:105787)
Copyright Avail: CASI HC A03/MF A01

The performance and lifetime expectations of 30 cm xenon ion thruster technology at low values of specific impulse were evaluated, with emphasis on 1000-2500 s operation. Power levels of up to 2.0 kW, appropriate for auxiliary and orbit maneuvering propulsion, were processed at thrust-to-power ratios up to 57 mN/kW. These tests were conducted using a derated 30 cm ion thruster with high-perveance design two-grid ion optics with xenon propellant. Lifetime projections were made based on a simple analysis of critical component erosion rates, and it was found that a strong correlation exists with the ratio of the specific impulse-to-input power. Under all operating conditions for which the projected thruster lifetime is less than 10,000 hrs, the life-limiting component of this technology is erosion of the accelerator grid due to charge-exchange ions. The use of alternative grid materials such as carbon is estimated to increase useful thruster lifetimes by as much as an order of magnitude and may enable long-life high thrust-density, sub-2500 s Isp operation. The performance and life of the derated thruster appears similar to that of the Russian SPT-100 thruster in the 1.0-2.0 kW, 1600-2000 s operational envelope.

Author

N92-32463*# National Aeronautics and Space Administration, Lewis Research Center, Cleveland, OH.

NASA'S NUCLEAR ELECTRIC PROPULSION TECHNOLOGY PROJECT

JAMES R. STONE and JAMES S. SOVEY Jul. 1992 18 p Presented at the 28th Joint Propulsion Conference and Exhibit, Nashville, TN, 6-8 Jul. 1992; sponsored by AIAA, SAE, ASME, and ASEE

(Contract RTOP 593-72-41)
(NASA-TM-105811; E-7242; NAS 1.15:105811) Copyright Avail: CASI HC A03/MF A01

The National Aeronautics and Space Administration (NASA) has initiated a program to establish the readiness of nuclear electric propulsion (NEP) technology for relatively near-term applications to outer planet robotic science missions with potential future evolution to system for piloted Mars vehicles. This program was initiated in 1991 with a very modest effort identified with nuclear thermal propulsion (NTP); however, NEP is also an integral part of this program and builds upon NASA's Base Research and Technology Program in power and electric propulsion as well as the SP-100 space nuclear power program. The NEP Program will establish the feasibility and practicality of electric propulsion for robotic and piloted solar system exploration. The performance objectives are high specific impulse (200 greater than I(sub sp) greater than 10000 s), high efficiency (over 0.50), and low specific mass. The planning for this program was initially focussed on piloted Mars missions, but has since been redirected to first focus on 100-kW class systems for relatively near-term robotic missions, with possible future evolution to megawatt- and multi-megawatt-class systems applicable to cargo vehicles supporting human missions as well as to the piloted vehicles. This paper reviews current plans and recent progress for the overall nuclear electric propulsion project and closely related activities.

Author

N92-33064*# National Aeronautics and Space Administration, Lewis Research Center, Cleveland, OH.

THE EVOLUTIONARY DEVELOPMENT OF HIGH SPECIFIC IMPULSE ELECTRIC THRUSTER TECHNOLOGY

JAMES S. SOVEY, JOHN A. HAMLEY, MICHAEL J. PATTERSON, VINCENT K. RAWLIN, and ROGER M. MEYERS (Sverdrup Technology, Inc., Brook Park, OH.) Mar. 1992 33 p Presented at the Space Programs and Technologies Conference; sponsored by AIAA

(Contract RTOP 506-42-31)
(NASA-TM-105758; E-7170; NAS 1.15:105758) Avail: CASI HC A03/MF A01

Electric propulsion flight and technology demonstrations conducted primarily by Europe, Japan, Peoples Republic of China,

USA, and USSR are reviewed. Evolutionary mission applications for high specific impulse electric thruster systems are discussed, and the status of arcjet, ion, and magnetoplasmadynamic thruster and associated power processor technologies are summarized.

Author

N92-34113*# National Aeronautics and Space Administration, Lewis Research Center, Cleveland, OH.

DEPENDENCE OF HYDROGEN ARCJET OPERATION ON ELECTRODE GEOMETRY

ERIC J. PENCIL, JOHN M. SANKOVIC, CHARLES J. SARMIENTO, and JOHN A. HAMLEY Sep. 1992 22 p Presented at the 28th Joint Propulsion Conference and Exhibit, Nashville, TN, 6-8 Jul. 1992; sponsored by AIAA, SAE, ASME, and ASEE (Contract RTOP 506-42-31)

(NASA-TM-105855; E-7311; NAS 1.15:105855; AIAA PAPER 92-3530) Copyright Avail: CASI HC A03/MF A01

The dependence of 2 kW hydrogen arcjet performance on cathode to anode electrode spacing was evaluated at specific impulses of 900 and 1000 s. Less than 2 absolute percent change in efficiency was measured for the spacings tested which did not repeat the 14 absolute percent variation reported in earlier work with similar electrode designs. A different nozzle configuration was used to quantify the variation in hydrogen arcjet performance over an extended range of electrode spacing. Electrode gap variation resulted in less than 3 absolute percent change in efficiency. These null results suggested that electrode spacing is decoupled from hydrogen arcjet performance considerations over the ranges tested. Initial studies were conducted on hydrogen arcjet ignition. The dependence of breakdown voltage on mass flow rate and hydrogen arcjet ignition on rates of pulse repetition and pulse voltage rise were also included for comparison with previous results obtained using simulated hydrazine.

Author

23

CHEMISTRY AND MATERIALS (GENERAL)

A92-11823* National Aeronautics and Space Administration, Lewis Research Center, Cleveland, OH.

THE APPLICATION OF A COMPUTER DATA ACQUISITION SYSTEM TO A NEW HIGH TEMPERATURE TRIBOMETER

CHARLES D. BONHAM (NASA, Lewis Research Center; Sverdrup Technology, Inc., Cleveland, OH) and CHRISTOPHER DELLACORTE (NASA, Lewis Research Center, Cleveland, OH) (STLE, Annual Meeting, 45th, Denver, CO, May 7-10, 1990) Lubrication Engineering (ISSN 0024-7154), vol. 47, Nov. 1991, p. 907-923. Previously announced in STAR as N90-17811. Nov. 1991 17 p refs

Copyright

The two data acquisition computer programs are described which were developed for a high temperature friction and wear test apparatus, a tribometer. The raw data produced by the tribometer and the methods used to sample that data are explained. In addition, the instrumentation and computer hardware and software are presented. Also shown is how computer data acquisition was applied to increase convenience and productivity on a high temperature tribometer.

Author

A92-27125*# National Aeronautics and Space Administration, Lewis Research Center, Cleveland, OH.

SYNERGISTIC EFFECTS OF ULTRAVIOLET RADIATION, THERMAL CYCLING AND ATOMIC OXYGEN ON ALTERED AND COATED KAPTON SURFACES

JOYCE A. DEVER (NASA, Lewis Research Center, Cleveland, OH), ERIC J. BRUCKNER, and ELVIN RODRIGUEZ (Cleveland State University, OH) AIAA, Aerospace Sciences Meeting and Exhibit,

23 CHEMISTRY AND MATERIALS (GENERAL)

30th, Reno, NV, Jan. 6-9, 1992. 10 p. Previously announced in STAR as N92-14114. Jan. 1992 10 p refs
(AIAA PAPER 92-0794) Copyright

The photovoltaic (PV) power system for Space Station Freedom (SSF) uses solar array blankets which provide structural support for the solar cells and house the electrical interconnections. In the low earth orbital (LEO) environment where SSF will be located, surfaces will be exposed to potentially damaging environmental conditions including solar ultraviolet (UV) radiation, thermal cycling, and atomic oxygen. It is necessary to use ground based tests to determine how these environmental conditions would affect the mass loss and optical properties of candidate SSF blanket materials. Silicone containing, silicone coated, and SiO(x) coated polyimide film materials were exposed to simulated LEO environmental conditions to determine their durability and whether the environmental conditions of UV, thermal cycling and oxygen atoms act synergistically on these materials. A candidate PV blanket material called AOR Kapton, a polysiloxane polyimide cast from a solution mixture, shows an improvement in durability to oxygen atoms erosion after exposure to UV radiation or thermal cycling combined with UV radiation. This may indicate that the environmental conditions react synergistically with this material, and the damage predicted by exposure to atomic oxygen alone is more severe than that which would occur in LEO where atomic oxygen, thermal cycling and UV radiation are present together.

Author

A92-29644*# National Aeronautics and Space Administration. Lewis Research Center, Cleveland, OH.

TENSILE PROPERTIES OF IMPACT ICES

M. L. CHU, R. J. SCAVUZZO, and C. J. KELLACKEY (Akron, University, OH) AIAA, Aerospace Sciences Meeting and Exhibit, 30th, Reno, NV, Jan. 6-9, 1992. 7 p. Research supported by NASA. Jan. 1992 7 p refs

(AIAA PAPER 92-0883) Copyright

A special test apparatus was developed to measure the tensile strength of impact ices perpendicular to the direction of growth. The apparatus consists of a split tube carefully machined to minimize the effect of the joint on impact ice strength. The tube is supported in the wind tunnel by two carefully aligned bearings. During accretion the tube is turned slowly in the icing cloud to form a uniform coating of ice on the split tube specimen. The two halves of the split tube are secured firmly by a longitudinal bolt to prevent relative motion between the two halves during ice accretion and handling. Tensile test strength results for a variety of icing conditions were obtained. Both glaze and rime ice conditions were investigated. In general, the tensile strength of impact ice was significantly less than refrigerator ice. Based on the limited data taken, the median strength of rime ice was less than glaze ice. However, the mean values were similar.

Author

A92-31286*# National Aeronautics and Space Administration. Lewis Research Center, Cleveland, OH.

SiO(X) COATINGS FOR ATOMIC OXYGEN PROTECTION OF POLYIMIDE KAPTON IN LOW EARTH ORBIT

BRUCE A. BANKS, SHARON K. RUTLEDGE (NASA, Lewis Research Center, Cleveland, OH), LINDA GEBAUER, and CINDY LAMOREAUX (Cleveland State University, OH) IN: AIAA Materials Specialist Conference - Coating Technology for Aerospace Systems, Dallas, TX, Apr. 16, 17, 1992, Technical Papers 1992 10 p refs

(AIAA PAPER 92-2151) Copyright

Sputter-deposited SiO(X) (where X between 1.9 and 2.0) thin film coatings have been found to be durable to atomic oxygen. Such coatings will be used to protect polyimide Kapton photovoltaic array blankets from atomic oxygen attack in low earth orbit (LEO) on the Space Station Freedom (SSF). Monte Carlo modeling of atomic oxygen attack at defect sites in protected Kapton exposed in laboratory RF plasma ashers and on solar tracking photovoltaic arrays in space has been conducted to enable understanding of degradation processes relevant to the durability of the SSF solar array blanket. SiO(X) protective coating performance data from RF plasma asher tests will be presented, along with Monte Carlo

modeling considerations, to enable the projection of in-space durability of the SSF solar array blankets based on ground laboratory test results.

Author

A92-31300*# National Aeronautics and Space Administration. Lewis Research Center, Cleveland, OH.

ATOMIC OXYGEN EFFECTS ON THIN FILM SPACE COATINGS STUDIED BY SPECTROSCOPIC ELLIPSOMETRY, ATOMIC FORCE MICROSCOPY, AND LASER LIGHT SCATTERING

R. A. SYNOWICKI, JEFFREY S. HALE, and JOHN A. WOOLLAM (Nebraska, University, Lincoln) IN: AIAA Materials Specialist Conference - Coating Technology for Aerospace Systems, Dallas, TX, Apr. 16, 17, 1992, Technical Papers 1992 5 p refs
(Contract NAG3-95)

(AIAA PAPER 92-2172) Copyright

The University of Nebraska is currently evaluating Low Earth Orbit (LEO) simulation techniques as well as a variety of thin film protective coatings to withstand atomic oxygen (AO) degradation. Both oxygen plasma ashers and an electron cyclotron resonance (ECR) source are being used for LEO simulation. Thin film coatings are characterized by optical techniques including Variable Angle Spectroscopic Ellipsometry, Optical spectrophotometry, and laser light scatterometry. Atomic Force Microscopy (AFM) is also used to characterize surface morphology. Results on diamondlike carbon (DLC) films show that DLC degrades with simulated AO exposure at a rate comparable to Kapton polyimide. Since DLC is not as susceptible to environmental factors such as moisture absorption, it could potentially provide more accurate measurements of AO fluence on short space flights.

Author

A92-34474*# National Aeronautics and Space Administration. Lewis Research Center, Cleveland, OH.

CERAMICS AND CERAMIC MATRIX COMPOSITES - AEROSPACE POTENTIAL AND STATUS

STANLEY R. LEVINE (NASA, Lewis Research Center, Cleveland, OH) IN: AIAA/ASME/ASCE/AHS/ASC Structures, Structural Dynamics and Materials Conference, 33rd, Dallas, TX, Apr. 13-15, 1992, Technical Papers. Pt. 4 1992 6 p refs
(AIAA PAPER 92-2445) Copyright

Thermostuctural ceramics and ceramic-matrix composites are attractive in numerous aerospace applications; the noncatastrophic fracture behavior and flaw-insensitivity of continuous fiber-reinforced CMCs renders them especially desirable. The present development status evaluation notes that, for most highly-loaded high-temperature applications, the requisite fiber-technology base is at present insufficient. In addition to materials processing techniques, the life prediction and NDE methods are immature and require a projection of 15-20 years for the maturity of CMC turbine rotors. More lightly loaded, moderate temperature aircraft engine applications are approaching maturity.

O.C.

A92-39852* National Aeronautics and Space Administration. Lewis Research Center, Cleveland, OH.

FLIGHT-VEHICLE MATERIALS, STRUCTURES, AND DYNAMICS - ASSESSMENT AND FUTURE DIRECTIONS. VOL. 3 - CERAMICS AND CERAMIC-MATRIX COMPOSITES

STANLEY R. LEVINE, ED. (NASA, Lewis Research Center, Cleveland, OH) New York, American Society of Mechanical Engineers, 1992, 372 p. For individual items see A92-39853 to A92-39867. 1992 372 p
(ISBN 0-7918-0661-8) Copyright

The present volume discusses ceramics and ceramic-matrix composites in prospective aerospace systems, monolithic ceramics, transformation-toughened and whisker-reinforced ceramic composites, glass-ceramic matrix composites, reaction-bonded Si₃N₄ and SiC composites, and chemical vapor-infiltrated composites. Also discussed are the sol-gel-processing of ceramic composites, the fabrication and properties of fiber-reinforced ceramic composites with directed metal oxidation, the fracture behavior of ceramic-matrix composites (CMCs), the fatigue of

fiber-reinforced CMCs, creep and rupture of CMCs, structural design methodologies for ceramic-based materials systems, the joining of ceramics and CMCs, and carbon-carbon composites. O.C.

A92-39853* National Aeronautics and Space Administration. Lewis Research Center, Cleveland, OH.

CERAMICS AND CERAMIC COMPOSITES IN FUTURE AERONAUTICAL AND SPACE SYSTEMS

STANLEY R. LEVINE (NASA, Lewis Research Center, Cleveland, OH) IN: Flight-vehicle materials, structures, and dynamics - Assessment and future directions. Vol. 3 - Ceramics and ceramic-matrix composites 1992 17 p refs Copyright

An account is given of the advantages of ceramics-based materials systems in thermostructural applications in aircraft propulsion, spacecraft propulsion and power systems, aerospace (transatmospheric) vehicles, and space structures. Prototype component applications are evaluated with a view to further technical requirements entailed by the implementation of such ceramic components. Typical near-term applications are the Space Shuttle's thermal protection system and high temperature aircraft thermal insulators; a major long-term development goal is that of integrally bladed turbine rotors in aircraft gas turbines. The fiber technology required for highly loaded/high temperature operations is not yet mature; use temperatures are restricted to 1100-1300 C. O.C.

A92-39862* National Aeronautics and Space Administration. Lewis Research Center, Cleveland, OH.

ENVIRONMENTAL DURABILITY OF CERAMICS AND CERAMIC COMPOSITES

DENNIS S. FOX (NASA, Lewis Research Center, Cleveland, OH) IN: Flight-vehicle materials, structures, and dynamics - Assessment and future directions. Vol. 3 - Ceramics and ceramic-matrix composites 1992 11 p refs Copyright

An account is given of the current understanding of the environmental durability of both monolithic ceramics and ceramic-matrix composites, with a view to the prospective development of methods for the characterization, prediction, and improvement of ceramics' environmental durability. Attention is given to the environmental degradation behaviors of SiC, Si₃N₄, Al₂O₃, and glass-ceramic matrix compositions. The focus of corrosion prevention in Si-based ceramics such as SiC and Si₃N₄ is on the high and low sulfur fuel combustion-product effects encountered in heat engine applications of these ceramics; sintering additives and raw material impurities are noted to play a decisive role in ceramics' high temperature environmental response. O.C.

A92-41117* National Aeronautics and Space Administration. Lewis Research Center, Cleveland, OH.

NASA'S HIGH-TEMPERATURE ENGINE MATERIALS PROGRAM FOR CIVIL AERONAUTICS

HUGH R. GRAY and CAROL A. GINTY (NASA, Lewis Research Center, Cleveland, OH) JOM (ISSN 1047-4838), vol. 44, no. 5, May 1992, p. 12. May 1992 1 p Copyright

The Advanced High-Temperature Engine Materials Technology Program is described in terms of its research initiatives and its goal of developing propulsion systems for civil aeronautics with low levels of noise, pollution, and fuel consumption. The program emphasizes the analysis and implementation of structural materials such as polymer-matrix composites in fans, casings, and engine-control systems. Also investigated in the program are intermetallic- and metal-matrix composites for uses in compressors and turbine disks as well as ceramic-matrix composites for extremely high-temperature applications such as turbine vanes. C.C.S.

A92-50868* National Aeronautics and Space Administration. Lewis Research Center, Cleveland, OH.

ON THE DRAG OF MODEL DENDRITE FRAGMENTS AT LOW REYNOLDS NUMBER

R. ZAKHEM, P. D. WEIDMAN (Colorado, University, Boulder), and H. C. DE GROH, III (NASA, Lewis Research Center, Cleveland, OH) Metallurgical Transactions A - Physical Metallurgy and Materials Science (ISSN 0360-2133), vol. 23A, no. 8, Aug. 1992, p. 2169-2181. Aug. 1992 13 p refs Copyright

An experimental study of low Reynolds number drag on laboratory models of dendrite fragments has been conducted. The terminal velocities of the dendrites undergoing free fall along their axis of symmetry were measured in a large Stokes flow facility. Corrections for wall interference give nearly linear drag vs Reynolds number curves. Corrections for both wall interference and inertia effects show that the dendrite Stokes settling velocities are always less than that of a sphere of equal mass and volume. In the Stokes limit, the settling speed ratio is found to correlate well with the primary dendrite arm aspect ratio and a second dimensionless shape parameter which serves as a measure of the fractal-like nature of the dendrite models. These results can be used to estimate equiaxed grain velocities and distance of travel in metal castings. The drag measurements may be used in numerical codes to calculate the movement of grains in a convecting melt in an effort to determine macrosegregation patterns caused by the sink/float mechanism. Author

N92-10064*# National Aeronautics and Space Administration. Lewis Research Center, Cleveland, OH.

RELATIVE SLIDING DURABILITY OF TWO CANDIDATE HIGH TEMPERATURE OXIDE FIBER SEAL MATERIALS

CHRISTOPHER DELLACORTE and BRUCE M. STEINETZ Sep. 1991 18 p (Contract RTOP 505-63-1A) (NASA-TM-105199; E-6502; NAS 1.15:105199) Avail: CASI HC A03/MF A01

A test program to determine the relative sliding durability of two candidate ceramic fibers for high temperature sliding seal applications is described. Pin on disk tests were used to evaluate potential seal materials. Friction during the tests and fiber wear, indicated by the extent of fibers broken in a test bundle or yarn, was measured at the end of a test. In general, friction and wear increase with test temperature. This may be due to a reduction in fiber strength, a change in the surface chemistry at the fiber/counterface interface due to oxidation, adsorption and/or desorption of surface species and, to a lesser extent, an increase in counterface surface roughness due to oxidation at elevated temperatures. The relative fiber durability correlates with tensile strength indicating that tensile data, which is more readily available than sliding durability data, may be useful in predicting fiber wear behavior under various conditions. A simple model developed using dimensional analysis shows that the fiber durability is related to a dimensionless parameter which represents the ratio of the fiber strength to the fiber stresses imposed by sliding. Author

N92-13281*# National Aeronautics and Space Administration. Lewis Research Center, Cleveland, OH.

NEW ADDITION CURING POLYIMIDES

ARYEH A. FRIMER and PAUL CAVANO (Case Western Reserve Univ., Cleveland, OH.) 1991 7 p Presented at the Fourth International Conference on Polyimides, Ellenville, NY, 30 Oct. - 1 Nov. 1991; sponsored by the Society of Plastic Engineers (Contract RTOP 510-01-50) (NASA-TM-105335; E-6702; NAS 1.15:105335) Avail: CASI HC A02/MF A01

In an attempt to improve the thermal-oxidative stability (TOS) of PMR-type polymers, the use of 1,4-phenylenebis (phenylmaleic anhydride) PPMA, was evaluated. Two series of nadic end-capped addition curing polyimides were prepared by imidizing PPMA with either 4,4'-methylene dianiline or p-phenylenediamine. The first resulted in improved solubility and increased resin flow while the latter yielded a compression molded neat resin sample with a T(sub g) of 408 C, close to 70 C higher than PME-15. The performance of these materials in long term weight loss studies was below that of PMR-15, independent of post-cure conditions. These results can be rationalized in terms of the thermal lability

23 CHEMISTRY AND MATERIALS (GENERAL)

of the pendant phenyl groups and the incomplete imidization of the sterically congested PPMA. The preparation of model compounds as well as future research directions are discussed.

Author

N92-14114*# National Aeronautics and Space Administration. Lewis Research Center, Cleveland, OH.

SYNERGISTIC EFFECTS OF ULTRAVIOLET RADIATION, THERMAL CYCLING, AND ATOMIC OXYGEN ON ALTERED AND COATED KAPTON SURFACES

JOYCE A. DEVER (Cleveland State Univ., OH.), ERIC J. BRUCKNER, and ELVIN RODRIGUEZ (Cleveland State Univ., OH.) 1992 11 p Presented at the 30th Aerospace Sciences Meeting and Exhibit, Reno, NV, 6-9 Jan. 1992; sponsored by AIAA

(Contract RTOP 474-46-10)

(NASA-TM-105363; E-6741; NAS 1.15:105363; AIAA PAPER 92-0794) Avail: CASI HC A03/MF A01

The photovoltaic (PV) power system for Space Station Freedom (SSF) uses solar array blankets which provide structural support for the solar cells and house the electrical interconnections. In the low Earth orbital (LEO) environment where SSF will be located, surfaces will be exposed to potentially damaging environmental conditions including solar ultraviolet (UV) radiation, thermal cycling, and atomic oxygen. It is necessary to use ground based tests to determine how these environmental conditions would affect the mass loss and optical properties of candidate SSF blanket materials. Silicone containing, silicone coated, and SiO(x) coated polyimide film materials were exposed to simulated LEO environmental conditions to determine their durability and whether the environmental conditions of UV, thermal cycling and oxygen atoms act synergistically on these materials. A candidate PV blanket material called AOR Kapton, a polysiloxane polyimide cast from a solution mixture, shows an improvement in durability to oxygen atoms erosion after exposure to UV radiation or thermal cycling combined with UV radiation. This may indicate that the environmental conditions react synergistically with this material, and the damage predicted by exposure to atomic oxygen alone is more severe than that which would occur in LEO where atomic oxygen, thermal cycling and UV radiation are present together.

Author

N92-15128*# National Aeronautics and Space Administration. Lewis Research Center, Cleveland, OH.

TRIBOLOGICAL AND MECHANICAL COMPARISON OF SINTERED AND HIPPED PM212: HIGH TEMPERATURE SELF-LUBRICATING COMPOSITES

CHRISTOPHER DELLACORTE, HAROLD E. SLINEY, and MICHAEL S. BOGDANSKI (Case Western Reserve Univ., Cleveland, OH.) 1992 27 p Proposed for presentation at the Annual Meeting of the Society of Tribologists and Lubrication Engineers, Philadelphia, PA, 4-7 May 1992

(Contract RTOP 505-63-1A)

(NASA-TM-105379; E-6592; NAS 1.15:105379) Avail: CASI HC A03/MF A01

Selected tribological, mechanical and thermophysical properties of two versions of PM212 (sintered and hot isostatically pressed, HIPped) are compared. PM212, a high temperature self-lubricating composite, contains 70 wt percent metal bonded chromium carbide, 15 wt percent CaF₂/BaF₂ eutectic and 15 wt percent silver. PM212 in the sintered form is about 80 percent dense and has previously been shown to have good tribological properties from room temperature to 850 C. Tribological results of a fully densified, HIPped version of PM212 are given. They are compared to sintered PM212. In addition, selected mechanical and thermophysical properties of both types of PM212 are discussed and related to the tribological similarities and differences between the two PM212 composites. In general, both composites display similar friction and wear properties. However, the fully dense PM212 HIPped composite exhibits slight lower friction and wear than sintered PM212. This may be attributed to its generally higher strength properties. The sintered version displays stable wear properties over a wide load range indicating its promise for use in a variety

of applications. Based upon their properties, both the sintered and HIPped PM212 have potential as bearing and seal materials for advanced high temperature applications.

Author

N92-17882*# National Aeronautics and Space Administration. Lewis Research Center, Cleveland, OH.

SUBSTITUTED 1,1,1-TRIARYL-2,2,2-TRIFLUOROETHANES AND PROCESSES FOR THEIR SYNTHESIS Patent Application

WILLIAM B. ALSTON, inventor (to NASA) (Army Aviation Systems Command, Cleveland, OH.) and ROY F. GRATZ, inventor (to NASA) (Mary Washington Coll., Fredricksburg, VA.) 17 Jan. 1992 24 p

(NASA-CASE-LEW-14345-6; NAS 1.71:LEW-14345-6;

US-PATENT-APPL-SN-822240) Avail: CASI HC A03/MF A01

Synthetic procedures are given for tetraalkyl, tetraacid and dianhydrides substituted 1,1,1-triaryl-2,2,2-trifluoroethanes which comprises: (1) 1,1-bis (dialkylaryl) 1-aryl-2,2,2 trifluoroethane; (2) 1,1-bis (dicarboxyaryl) 1-aryl-2,2,2 trifluoroethane; or (3) cyclic dianhydride or diamine of 1,1-bis (dialkylaryl) 1-aryl-2,2,2 trifluoroethanes. The synthesis of (1) is accomplished by the condensation reaction of an aryl(trifluoromethyl) ketone with a dialkylaryl compound. The synthesis of (2) is accomplished by oxidation of (1). The synthesis dianhydride of (3) is accomplished by the conversion of (2) to its corresponding cyclic dianhydride. The synthesis of the diamine is accomplished by the similar reaction of an aryl(trifluoromethyl) ketone with aniline or alkyl substituted or disubstituted anilines. Also, other derivatives of the above are formed by nucleophilic displacement reactions.

NASA

N92-18457*# National Aeronautics and Space Administration. Lewis Research Center, Cleveland, OH.

CHEMICAL VAPOR DEPOSITION MODELING FOR HIGH TEMPERATURE MATERIALS

SUELEYMAN GOEKOGLU 1992 14 p Presented at the 1991 Fall Meeting of the Materials Research Society, Boston, MA, 2-6 Dec. 1991

(Contract RTOP 510-01-50)

(NASA-TM-105386; E-6772; NAS 1.15:105386) Avail: CASI HC A03/MF A01

The formalism for the accurate modeling of chemical vapor deposition (CVD) processes has matured based on the well established principles of transport phenomena and chemical kinetics in the gas phase and on surfaces. The utility and limitations of such models are discussed in practical applications for high temperature structural materials. Attention is drawn to the complexities and uncertainties in chemical kinetics. Traditional approaches based on only equilibrium thermochemistry and/or transport phenomena are defended as useful tools, within their validity, for engineering purposes. The role of modeling is discussed within the context of establishing the link between CVD process parameters and material microstructures/properties. It is argued that CVD modeling is an essential part of designing CVD equipment and controlling/optimizing CVD processes for the production and/or coating of high performance structural materials.

Author

N92-18970*# National Aeronautics and Space Administration. Lewis Research Center, Cleveland, OH.

FLUORESCENCE MICROSCOPY FOR THE CHARACTERIZATION OF STRUCTURAL INTEGRITY

KENNETH W. STREET and TODD A. LEONHARDT (Sverdrup Technology, Inc., Brook Park, OH.) 1991 14 p Presented at the 24th Annual International Metallographic Society Technical Meeting, Monterey, CA, 29 Jul. - 1 Aug. 1991 Original contains color illustrations

(Contract NAS3-25266; RTOP 505-63-5A)

(NASA-TM-105253; E-6582; NAS 1.15:105253)

The absorption characteristics of light and the optical technique of fluorescence microscopy for enhancing metallographic interpretation are presented. Characterization of thermally sprayed coatings by optical microscopy suffers because of the tendency for misidentification of the microstructure produced by metallographic preparation. Gray scale, in bright field microscopy, is frequently the only means of differentiating the actual structural

details of porosity, cracking, and debonding of coatings. Fluorescence microscopy is a technique that helps to distinguish the artifacts of metallographic preparation (pullout, cracking, debonding) from the microstructure of the specimen by color contrasting structural differences. Alternative instrumentation and the use of other dye systems are also discussed. The combination of epoxy vacuum infiltration with fluorescence microscopy to verify microstructural defects is an effective means to characterize advanced materials and to assess structural integrity. Author

N92-21175*# National Aeronautics and Space Administration, Lewis Research Center, Cleveland, OH.

SLIDING DURABILITY OF TWO CARBIDE-OXIDE CANDIDATE HIGH TEMPERATURE FIBER SEAL MATERIALS IN AIR TO 900 C

CHRISTOPHER DELLACORTE and BRUCE M. STEINETZ 1992 15 p Proposed for presentation at the Ninth International Conference of Wear of Materials, San Francisco, CA, 13-17 Apr. 1993

(Contract RTOP 505-63-1A)

(NASA-TM-105554; E-6877; NAS 1.15:105554) Avail: CASI HC A03/MF A01

A test program to determine the friction and wear properties of two complex carbide oxide ceramic fibers for high temperature sliding seal applications is described. The fibers are based on Si, C, O, and Ti or Si, C, N, and O ceramic systems. Pin on disk tests using ceramic fiber covered pins and Inconel 718 disks, were conducted in air from 25 to 900 C to evaluate potential seal materials. This testing procedure was used in a previous study of oxide ceramic fibers which were found to exhibit wear behavior based predominantly on their mechanical properties. Like the oxide fibers tested previously, these carbide oxide ceramic fibers, show an increase in friction and wear with increased test temperature. At room temperature, the wear behavior seems to be based upon mechanical properties, namely tensile strength. At 500 and especially 900 C, the fibers wear by both mechanical fracture and by oxidative type wear. Based upon post test microscopic and x ray analyses, interaction between the fiber constituents and elements transferred from the counterface, namely Ni and Cr, may have occurred enhancing the tribochemical wear process. These results are interpreted. Author

N92-21548*# National Aeronautics and Space Administration, Lewis Research Center, Cleveland, OH.

ION BEAM TREATMENT OF POTENTIAL SPACE MATERIALS AT THE NASA LEWIS RESEARCH CENTER

MICHAEL KUSSMAUL (Sverdrup Technology, Inc., Brook Park, OH.), MICHAEL J. MIRTICH, and ARTHUR CURREN 1992 17 p Presented at the Surface Modification of Metals by Ion Beams, Washington, DC, 15-19 Jul. 1991; sponsored by the Naval Research Lab.

(Contract RTOP 506-41-41)

(NASA-TM-105398; E-6794; NAS 1.15:105398) Avail: CASI HC A03/MF A01

Ion source systems in different configurations, have been used to generate unique morphologies for several NASA space applications. The discharge chamber of a 30 cm ion source was successfully used to texture potential space radiator materials for the purpose of obtaining values of thermal emittance greater than 0.85 at 700 and 900 K. High absorptance surfaces were obtained using ion beam seed texturing, for space radiator materials that were flown on the Long Duration Exposure Facility (LDEF) for 5.8 years in space. An ion source discharge chamber was also used to develop electrode surfaces with suppressed secondary electron emission characteristics for use in collectors in microwave amplifier traveling wave tubes. This was accomplished by sputtering textured carbon onto copper as well as texturing copper using tantalum and molybdenum as sacrificial texture inducing seeding materials. In a third configuration, a dual ion beam system was used to generate high transmittance diamondlike carbon (DLC) films. Author

N92-23190*# National Aeronautics and Space Administration, Lewis Research Center, Cleveland, OH.

TRIBOLOGICAL EVALUATION OF AN AL₂O₃-SiO₂ CERAMIC FIBER CANDIDATE FOR HIGH TEMPERATURE SLIDING SEALS

CHRISTOPHER DELLACORTE and BRUCE STEINETZ Apr. 1992 19 p

(Contract RTOP 505-63-5A)

(NASA-TM-105611; E-6949; NAS 1.15:105611) Avail: CASI HC A03/MF A01

A test program to determine the relative sliding durability of an alumina-silica candidate ceramic fiber for high temperature sliding seal applications as described. This work represents the first reporting of the sliding durability of this material system. Pin-on-disk tests were used to evaluate the potential seal material by sliding a tow or bundle of the candidate ceramic fiber against a superalloy test disk. Friction was measured during the tests and fiber wear, indicated by the extent of fibers broken in the tow or bundle, was measured at the end of each test. Test variables studied included ambient temperatures from 25 C to 900 C, loads from 1.3 to 21.2 Newtons, and sliding velocities from 0.025 to 0.25 m/sec. In addition, the effects of fiber diameter, elastic modulus, and a pretest fiber heat treatment on friction and wear were measured. In most cases, wear increased with temperature. Friction ranged from about 0.36 at 500 C and low velocity (0.025 m/s) to over 1.1 at 900 C and high velocity (0.25 m/s). The pretest fiber heat treatment, which caused significant durability reductions for alumina-boria-silica ceramic fibers tested previously, had little effect on the alumina-silica fibers tested here. These results indicate that the alumina-silica (Al₂O₃-SiO₂) fiber is a good candidate material system for high temperature sliding seal applications. Author

N92-25203*# National Aeronautics and Space Administration, Lewis Research Center, Cleveland, OH.

GRAPHITE INTERCALATION COMPOUND WITH IODINE AS THE MAJOR INTERCALANT

CHING-CHEH HUNG and DONALD KUCERA (Cleveland State Univ., OH.) 1992 20 p Presented at the 20th Biennial Conference on Carbon, Santa Barbara, CA, 23-28 Jun. 1991; sponsored by the American Carbon Society

(Contract RTOP 506-41-41)

(NASA-TM-105375; E-6762; NAS 1.15:105375) Avail: CASI HC A03/MF A01

Halogenated CBr(sub x)(sub y) (1 less than y/x less than 10) was made by exposing graphite materials with interplanar spacing in the 3.35 to 3.41 A range to either pure Br₂ or an I₂-Br₂ mixture, and then to iodine vapor containing a small amount of Br₂. The electrical resistivity of this product is from 3 to 6.5 times the pristine value. The presence of a small amount of isoprene rubber in the reaction significantly increased the iodine to bromine ratio in the product. In this reaction, rubber is known to generate HBr and to slowly remove bromine from the vapor. The halogenation generally caused a 22 to 25 percent weight increase. The halogens were found uniformly distributed in the product interior. However, although the surface contains very little iodine, it has high concentrations of bromine and oxygen. It is believed that the high concentrations of bromine and oxygen in this surface cause the halogenated fiber to be more resistant to fluorine attack during subsequent fluorination to fabricate graphite fluoride fibers. Author

N92-26142*# National Aeronautics and Space Administration, Lewis Research Center, Cleveland, OH.

TRIBOLOGICAL AND MICROSTRUCTURAL COMPARISON OF HIPPED PM212 AND PM212/AU SELF-LUBRICATING COMPOSITES

MICHAEL S. BOGDANSKI, HAROLD E. SLINEY, and CHRISTOPHER DELLACORTE Apr. 1992 19 p Prepared for presentation at the STLE-ASME Joint Tribology Conference, San Diego, CA, 18-21 Oct. 1992

(Contract DE-AI01-91CR-50306; RTOP 505-63-5A)

24 COMPOSITE MATERIALS

(NASA-TM-105615; E-6952; NAS 1.15:105615; DOE/NASA/50306-1) Avail: CASI HC A03/MF A01

The feasibility of replacing the silver with the volumetric equivalent of gold in the chromium carbide-based self-lubricating composite PM212 (70 wt. percent NiCo-Cr₃C₂, 15 percent BaF₂/CaF₂ eutectic) was studied. The new composite, PM212/Au has the following composition: 62 wt. percent NiCo-Cr₃C₂, 25 percent Au, 13 percent BaF₂/CaF₂ eutectic. The silver was replaced with gold to minimize the potential reactivity of the composite with possible environmental contaminants such as sulfur. The composites were fabricated by hot isostatic pressing (HIPping) and machined into pin specimens. The pins were slid against nickel-based superalloy disks. Sliding velocities ranged from 0.27 to 10.0 m/s and temperatures from 25 to 900 C. Friction coefficients ranged from 0.25 to 0.40 and wear factors for the pin and disk were typically low 10(exp -5) cu mm/N-m. HIPped PM212 measured fully dense, whereas PM212/Au had 15 percent residual porosity. Examination of the microstructures with optical and scanning electron microscopy revealed the presence of pores in PM212/Au that were not present in PM212. Though the exact reason for the residual porosity in PM212/Au was not determined, it may be due to particle morphology differences between the gold and silver and their effect on powder metallurgy processing. Author

24

COMPOSITE MATERIALS

Includes physical, chemical, and mechanical properties of laminates and other composite materials.

A92-10241* National Aeronautics and Space Administration. Lewis Research Center, Cleveland, OH.
RELATIONSHIP BETWEEN VOIDS AND INTERLAMINAR SHEAR STRENGTH OF POLYMER MATRIX COMPOSITES
KENNETH J. BOWLES and STEPHEN FRIMPONG (NASA, Lewis Research Center, Cleveland, OH) IN: International SAMPE Symposium and Exhibition, 36th, San Diego, CA, Apr. 15-18, 1991, Proceedings. Book 2 1991 18 p refs
Copyright

The effect of voids on the interlaminar shear strength of a polyimide matrix composite system is described. The AS4 graphite/PMR-15 composite was chosen for study because this system can be readily processed by using the standard specified cure cycle to produce void-free composites and because preliminary work in this study had shown that the processing parameters of this resin matrix system can be altered to produce cured composites of varying void contents. Thirty-eight 12-ply unidirectional composite panels were fabricated for this study. A significant range of void contents (0 to 10 percent) was produced. The panels were mapped, ultrasonically inspected, and sectioned into interlaminar shear, flexure, and fiber content specimens. The density of each specimen was measured and interlaminar shear and flexure strength measurements were then made. The fiber content was measured last. The results of these tests were evaluated by using ultrasonic results, photomicrographs, statistical methods, theoretical relationships derived by other investigations, and comparison of the test data with the Integrated Composite Analyzer (ICAN) computer program developed at the Lewis Research Center for predicting composite ply properties. The testing is described in as much detail as possible in order to help others make realistic comparisons. Author

A92-10262* National Aeronautics and Space Administration. Lewis Research Center, Cleveland, OH.
INTERPHASE LAYER OPTIMIZATION FOR METAL MATRIX COMPOSITES WITH FABRICATION CONSIDERATIONS
MICHAEL MOREL, DIMITRIS A. SARAVANOS, and C. C. CHAMIS (NASA, Lewis Research Center, Cleveland, OH) IN: International

SAMPE Symposium and Exhibition, 36th, San Diego, CA, Apr. 15-18, 1991, Proceedings. Book 2 1991 13 p refs
Copyright

A methodology is presented to reduce the final matrix microstresses for metal matrix composites by concurrently optimizing the interphase characteristics and fabrication process. Application cases include interphase tailoring with and without fabrication considerations for two material systems, graphite/copper and silicon carbide/titanium. Results indicate that concurrent interphase/fabrication optimization produces significant reductions in the matrix residual stresses and strong coupling between interphase and fabrication tailoring. The interphase coefficient of thermal expansion and the fabrication consolidation pressure are the most important design parameters and must be concurrently optimized to further reduce the microstresses to more desirable magnitudes. Author

A92-10263* National Aeronautics and Space Administration. Lewis Research Center, Cleveland, OH.
COMPUTATIONAL SIMULATION OF MICROFRACTURE IN HIGH TEMPERATURE METAL MATRIX COMPOSITES
SUBODH K. MITAL and CHRISTOS C. CHAMIS (NASA, Lewis Research Center, Cleveland, OH) IN: International SAMPE Symposium and Exhibition, 36th, San Diego, CA, Apr. 15-18, 1991, Proceedings. Book 2 1991 15 p refs
Copyright

A computational simulation procedure, using three-dimensional finite element method and global strain energy release rates, is described to predict the microfracture process and identify/quantify the hierarchy of respective fracture modes in metal matrix composites. The procedure is used to predict the microfracture in unidirectional composites under longitudinal loads and accounts for the interphase strength in the in situ state. A novel procedure to computationally simulate the fiber pushthrough process is also described. In this simulation, the interface material is replaced by an anisotropic material with greatly reduced shear modulus in order to simulate the fiber pushthrough process using a linear analysis. Such a procedure is easily implemented and is computationally very effective. Author

A92-10264* National Aeronautics and Space Administration. Lewis Research Center, Cleveland, OH.
METCAN UPDATES FOR HIGH TEMPERATURE COMPOSITE BEHAVIOR - SIMULATION/VERIFICATION
H.-J. LEE, P. L. N. MURTHY, and C. C. CHAMIS (NASA, Lewis Research Center, Cleveland, OH) IN: International SAMPE Symposium and Exhibition, 36th, San Diego, CA, Apr. 15-18, 1991, Proceedings. Book 2 1991 13 p refs
Copyright

The continued verification (comparisons with experimental data) of the METCAN (Metal Matrix Composite Analyzer) computer code is updated. Verification includes comparisons at room and high temperatures for two composites, SiC/Ti-15-3 and SiC/Ti-6-4. Specifically, verification of the SiC/Ti-15-3 composite includes comparisons of strength, modulus, and Poisson's ratio as well as stress-strain curves for four laminates at room temperatures. High temperature verification includes comparisons of strength and stress-strain curves for two laminates. Verification of SiC/Ti-6-4 is for a transverse room temperature stress-strain curve and comparisons for transverse strength at three temperatures. Results of the verification indicates that METCAN can be used with confidence to simulate the high temperature nonlinear behavior of metal matrix composites. Author

A92-10282* National Aeronautics and Space Administration. Lewis Research Center, Cleveland, OH.
MICROMECHANICS FOR CERAMIC MATRIX COMPOSITES
P. L. N. MURTHY and C. C. CHAMIS (NASA, Lewis Research Center, Cleveland, OH) IN: International SAMPE Symposium and Exhibition, 36th, San Diego, CA, Apr. 15-18, 1991, Proceedings. Book 2 1991 15 p refs
Copyright

The fiber substructuring concepts and the micromechanics

equations that are embedded in the Ceramic Matrix Composite Analyzer (CEMCAN) computer code are described as well as the code itself, its current features and capabilities, and some examples to demonstrate the code's versatility. The methodology is equally applicable to metal matrix and polymer matrix composites. The prediction of ply mechanical and thermal properties agree very well with the existing models in the Integrated Composite Analyzer and the Ceramic Matrix Composite Analyzer, lending credence to the fiber substructuring approach. Fiber substructuring can capture greater local detail than conventional unit-cell-based micromechanical theories. It offers promise in simulating complex aspects of micromechanics in ceramic matrix composites. P.D.

A92-15128* National Aeronautics and Space Administration. Lewis Research Center, Cleveland, OH.

INTERMETALLIC AND CERAMIC MATRIX COMPOSITES FOR 815 TO 1370 C (1500 TO 2500 F) GAS TURBINE ENGINE APPLICATIONS

JOSEPH R. STEPHENS (NASA, Lewis Research Center, Cleveland, OH) IN: Metal and ceramic matrix composites: Processing, modeling and mechanical behavior; Proceedings of the International Conference, Anaheim, CA, Feb. 19-22, 1990 1990 9 p refs Copyright

Revolutionary improvements in gas turbine engine specific fuel consumption and specific thrust are expected to be gained through incorporation of CMCs and of MMCs (whose intermetallic matrices are reinforced by highly refractory ceramic fibers). A status development evaluation is presented for NASA's Advanced High Temperature Engine Materials Technology Program, with a view to projections of early-21st century transport aircraft performance levels obtainable through the use of MMCs and CMCs in ultrahigh bypass turbofan engines. O.C.

A92-15145* National Aeronautics and Space Administration. Lewis Research Center, Cleveland, OH.

INFLUENCE OF INTERFACIAL SHEAR STRENGTH ON THE MECHANICAL PROPERTIES OF SiC FIBER REINFORCED REACTION-BONDED SILICON NITRIDE MATRIX COMPOSITES

RAMAKRISHNA T. BHATT (NASA, Lewis Research Center; U.S. Army, Propulsion Laboratory, Cleveland, OH) IN: Metal and ceramic matrix composites: Processing, modeling and mechanical behavior; Proceedings of the International Conference, Anaheim, CA, Feb. 19-22, 1990 1990 14 p refs Copyright

An evaluation is made of the influence of interfacial microstructure and shear strength on the mechanical properties of a 30 vol pct uniaxially-aligned SiC fiber-reinforced reaction-bonded Si₃N₄-matrix composite whose interface microstructure was varied through control of fabrication conditions and by heat-treatment in an oxidizing environment. The carbon-rich coating of the as-produced SiC fibers was stable in composites fabricated at 1200 C in an N or N + 4-percent H mixture for 40 hrs. This coating was degraded in composites fabricated at 1350 C in N + 4 percent H for 40 and 72 hrs, as well as after heat-treatment in an oxidizing environment at 600 C for 100 hrs even after fabrication at 1200 C in N. This degradation occurred via carbon removal. O.C.

A92-15629* National Aeronautics and Space Administration. Lewis Research Center, Cleveland, OH.

MECHANICAL BEHAVIOR OF FIBER REINFORCED SiC/RBSN CERAMIC MATRIX COMPOSITES - THEORY AND EXPERIMENT

ABHISAK CHULYA (NASA, Lewis Research Center; Cleveland State University, OH), JOHN P. GYEKENYESI (NASA, Lewis Research Center, Cleveland, OH), and RAMAKRISHNA T. BHATT (NASA, Lewis Research Center; U.S. Army, Propulsion Directorate, Cleveland, OH) ASME, International Gas Turbine and Aeroengine Congress and Exposition, 36th, Orlando, FL, June 3-6, 1991. 17 p. Previously announced in STAR as N91-21243. Jun. 1991 17 p refs

(Contract NCC3-81)
(ASME PAPER 91-GT-209)

The mechanical behavior of continuous fiber reinforced SiC/RBSN (Reaction Bonded Silicon Nitride) composites with various fiber contents is evaluated. Both catastrophic and noncatastrophic failures are observed in tensile specimens. Damage and failure mechanisms are identified via in-situ monitoring using NDE (nondestructive evaluation) techniques throughout the loading history. Effects of fiber/matrix interface debonding (splitting) parallel to fibers are discussed. Statistical failure behavior of fibers is also observed, especially when the interface is weak. Micromechanical models incorporating residual stresses to calculate the critical matrix cracking strength, ultimate strength, and work of pull-out are reviewed and used to predict composite response. For selected test problems, experimental measurements are compared to analytical predictions. Author

A92-15630* National Aeronautics and Space Administration. Lewis Research Center, Cleveland, OH.

STRUCTURAL RELIABILITY ANALYSIS OF LAMINATED CMC COMPONENTS

STEPHEN F. DUFFY, JOSEPH L. PALKO (NASA, Lewis Research Center; Cleveland State University, OH), and JOHN P. GYEKENYESI (NASA, Lewis Research Center, Cleveland, OH) ASME, International Gas Turbine and Aeroengine Congress and Exposition, 36th, Orlando, FL, June 3-6, 1991. 8 p. Previously announced in STAR as N91-19292. Jun. 1991 8 p refs (ASME PAPER 91-GT-210)

For laminated ceramic matrix composite (CMC) materials to realize their full potential in aerospace applications, design methods and protocols are a necessity. The time independent failure response of these materials is focussed on and a reliability analysis is presented associated with the initiation of matrix cracking. A public domain computer algorithm is highlighted that was coupled with the laminate analysis of a finite element code and which serves as a design aid to analyze structural components made from laminated CMC materials. Issues relevant to the effect of the size of the component are discussed, and a parameter estimation procedure is presented. The estimation procedure allows three parameters to be calculated from a failure population that has an underlying Weibull distribution. Author

A92-16220* National Aeronautics and Space Administration. Lewis Research Center, Cleveland, OH.

THE EFFECT OF MATRIX MECHANICAL PROPERTIES ON (0)8 UNIDIRECTIONAL SiC/Ti COMPOSITE FATIGUE RESISTANCE

T. P. GABB, J. GAYDA, B. A. LERCH, and G. R. HALFORD (NASA, Lewis Research Center, Cleveland, OH) Scripta Metallurgica et Materialia (ISSN 0956-716X), vol. 25, Dec. 1991, p. 2879-2884. Dec. 1991 6 p refs

Copyright

The relationship between constituent and MMC properties in fatigue loading is investigated with low-cycle fatigue-resistance testing of an alloy Ti-15-3 matrix reinforced with SiC SCS-6 fibers. The fabrication of the composite is described, and specimens are generated that are weak and ductile (WD), strong and moderately ductile (SM), or strong and brittle (SB). Strain is measured during MMC fatigue tests at a constant load amplitude with a load-controlled waveform and during matrix-alloy fatigue tests at a constant strain amplitude using a strain-controlled waveform. The fatigue resistance of the (0)8 SiC/Ti-15-3 composite is found to be slightly influenced by matrix mechanical properties, and the composite- and matrix-alloy fatigue lives are not correlated. This finding is suggested to relate to the different crack-initiation and -growth processes in MMCs and matrix alloys. C.C.S.

A92-19734* National Aeronautics and Space Administration. Lewis Research Center, Cleveland, OH.

FATIGUE CRACK GROWTH IN UNIDIRECTIONAL METAL MATRIX COMPOSITE

L. J. GHOSN (NASA, Lewis Research Center; Sverdrup Technology, Inc., Cleveland, OH), J. TELESMA, and P. KANTZOS (NASA, Lewis Research Center, Cleveland, OH) IN: Fatigue 90; Proceedings of the 4th International Conference on Fatigue and

24 COMPOSITE MATERIALS

Fatigue Thresholds, Honolulu, HI, July 15-20, 1990. Vol. 2 1990
6 p refs
Copyright

The weight function method was used to determine the effective stress intensity factor and the crack opening profile for a fatigue tested composite which exhibited fiber bridging. The bridging mechanism was modeled using two approaches; the crack closure approach and the shear lag approach. The numerically determined stress intensity factor values from both methods were compared and correlated with the experimentally obtained crack growth rates for SiC/Ti-15-3 (0) (sub 8) oriented composites. The near crack tip opening profile was also determined for both methods and compared with the experimentally obtained measurements.

Author

A92-23104* National Aeronautics and Space Administration. Lewis Research Center, Cleveland, OH.

MECHANICAL BEHAVIORS OF CERAMIC MATRIX COMPOSITES WITH MATRIX CRACKING AND FIBER DEBONDING

WEN-SHYONG KUO and TSU-WEI CHOU (Delaware, University, Newark) IN: Achievement in composites in Japan and the United States; Proceedings of the 5th Japan-U.S. Conference on Composite Materials, Tokyo, Japan, June 24-27, 1990 1990
8 p refs
Copyright

The purpose of this paper is to summarize the current research of the authors on the mechanical behaviors of ceramic matrix composites, including (1) the stress distributions in a composite with matrix cracking and interfacial debonding, (2) the critical strain for matrix cracking, and (3) the effects of fiber/matrix debonding and thermal residual stresses on the critical strain. The stress fields in both bonded and debonded regions are evaluated by taking into account thermal effects. An energy balance approach is followed to determine the critical strain for matrix cracking. From the general equation of the critical strain for matrix cracking, close form solutions have been obtained for two limiting cases: perfect bonding and complete debonding. Numerical solutions are given for the cases of partial fiber debonding and nonzero debonding energy. It is found that thermal residual stresses and the debonding energy have significant effects on the critical strain.

Author

A92-23313* National Aeronautics and Space Administration. Lewis Research Center, Cleveland, OH.

ISOTHERMAL FATIGUE BEHAVIOUR OF A (90 DEG)8 SIC/TI-15-3 COMPOSITE AT 426 C

J. GAYDA and T. P. GABB (NASA, Lewis Research Center, Cleveland, OH) International Journal of Fatigue (ISSN 0142-1123), vol. 14, Jan. 1992, p. 14-20. Jan. 1992 7 p refs
Copyright

The transverse fatigue behavior of a unidirectional SiC/Ti-15-3 composite is characterized at 426 C. The fatigue behavior of this composite along the (0 deg)8 fiber direction and that of unreinforced Ti-15-3 alloy is compared. It is found that the (90 deg)8 composite fatigue life is much shorter than that of the (0 deg)8 composite. The (90 deg)8 fatigue life is much lower than that of the unreinforced Ti-15-3 alloy. Results from 1D model and fractographic evidence for the (90 deg)8 fatigue behavior indicate that the short life of the composite in this orientation is caused by weak fiber-matrix bond strength.

O.G.

A92-25443* National Aeronautics and Space Administration. Lewis Research Center, Cleveland, OH.

ROLE OF INTERFACIAL CARBON LAYER IN THE THERMAL DIFFUSIVITY/CONDUCTIVITY OF SILICON CARBIDE FIBER-REINFORCED REACTION-BONDED SILICON NITRIDE MATRIX COMPOSITES

HEMANSHU BHATT, KIMBERLY Y. DONALDSON, D. P. H. HASSELMAN (Virginia Polytechnic Institute and State University, Blacksburg), and RAMAKRISHNA T. BHATT (NASA, Lewis Research Center, Cleveland, OH) American Ceramic Society, Journal (ISSN 0002-7820), vol. 75, Feb. 1992, p. 334-340. Research

supported by Virginia Polytechnic Institute and State University. Feb. 1992 7 p refs

Copyright

Experiments were carried out on samples of reaction-bonded silicon nitride uniaxially reinforced by SiC monofilaments with and without a 3-micron-thick carbon-rich coating. It is found that a combination of a carbon coatings on the fibers and an interfacial gap due to the thermal expansion mismatch in the composite can significantly (by a factor of 2) lower the effective thermal diffusivity in the direction transverse to the fiber. At atmospheric pressure, gaseous conduction across the interfacial gap makes a significant contribution to the heat transfer across the interface, indicated by significantly lower values of the effective thermal diffusivity under vacuum than in nitrogen or helium at atmospheric pressure. V.L.

A92-25445* National Aeronautics and Space Administration. Lewis Research Center, Cleveland, OH.

OXIDATION EFFECTS ON THE MECHANICAL PROPERTIES OF A SIC-FIBER-REINFORCED REACTION-BONDED Si3N4 MATRIX COMPOSITE

RAMAKRISHNA T. BHATT (NASA, Lewis Research Center; U.S. Army, Propulsion Laboratory, Cleveland, OH) American Ceramic Society, Journal (ISSN 0002-7820), vol. 75, Feb. 1992, p. 406-412. Previously announced in STAR as N90-14287. Feb. 1992 7 p refs

Copyright

The room-temperature mechanical properties of SiC fiber reinforced reaction bonded silicon nitride composites were measured after 100 hrs exposure at temperatures to 1400 C in nitrogen and oxygen environments. The composites consisted of approx. 30 vol percent uniaxially aligned 142 micron diameter SiC fibers in a reaction bonded Si3N4 matrix. The results indicate that composites heat treated in a nitrogen environment at temperatures to 1400 C showed deformation and fracture behavior equivalent to that of the as-fabricated composites. Also, the composites heat treated in an oxidizing environment beyond 400 C yielded significantly lower tensile strength values. Specifically in the temperature range from 600 to 1000 C, composites retained approx. 40 percent of their as-fabricated strength, and those heat treated in the temperatures from 1200 to 1400 C retained 70 percent. Nonetheless, for all oxygen heat treatment conditions, composite specimens displayed strain capability beyond the matrix fracture stress; a typical behavior of a tough composite.

Author

A92-25627* National Aeronautics and Space Administration. Lewis Research Center, Cleveland, OH.

EFFECT OF HEAT TREATMENT ON STIFFNESS AND DAMPING OF SIC/TI-15-3

JOSEPH E. GRADY and BRADLEY A. LERCH (NASA, Lewis Research Center, Cleveland, OH) SAMPE Quarterly (ISSN 0036-0821), vol. 23, Jan. 1992, p. 11-16. Jan. 1992 6 p refs
Copyright

The effect of heat treatment on material properties of SiC/Ti-15-3 was measured by vibration tests. Heat treatment changes the microstructure, which stiffens the matrix and reduces its damping capacity. Test results illustrate how the changes in matrix material affect the stiffness and damping properties of the composite. Damping was found to be more sensitive than stiffness to microstructural changes in the matrix. Effects of heat treatment temperature and exposure time are presented.

Author

A92-32727* National Aeronautics and Space Administration. Lewis Research Center, Cleveland, OH.

TENSION, COMPRESSION, AND BEND PROPERTIES FOR SIC/RBSN COMPOSITES

RAMAKRISHNA T. BHATT (NASA, Lewis Research Center, Cleveland, OH) IN: Composites; Proceedings of the 8th International Conference on Composite Materials (ICCM/8), Honolulu, HI, July 15-19, 1991. Section 22-29 1991 13 p refs

The room-temperature tension, compression, and bend properties of unidirectional SiC fiber-reinforced reaction-bonded silicon nitride composites (SiC/RBSN) have been investigated. The

effects of fiber content on the modulus, first matrix cracking strength, and ultimate strength properties were determined. In tension, composites with greater than 8-percent fiber content showed strain capability beyond matrix fracture and fiber-dominated ultimate strength. In compression, the composites displayed essentially elastic behavior, and matrix-dominated ultimate strength. For both deformation modes, most mechanical properties increased with fiber content. In bend, the modulus, strength properties, and failure modes of the composites were influenced by span-to-thickness ratio.

Author

A92-32753* National Aeronautics and Space Administration, Lewis Research Center, Cleveland, OH.

COMPUTATIONAL SIMULATION OF HIGH TEMPERATURE METAL MATRIX COMPOSITE BEHAVIOR

P. L. N. MURTHY and C. C. CHAMIS (NASA, Lewis Research Center, Cleveland, OH) IN: Composites; Proceedings of the 8th International Conference on Composite Materials (ICCM/8), Honolulu, HI, July 15-19, 1991. Section 22-29 1991 13 p refs

Computational procedures were developed for simulating the thermal and mechanical behaviors of high-temperature metal-matrix composites (HT-MMCs) in the following application areas: (1) the behavior of HT-MMCs from micromechanics to laminate, (2) the structural response of HT-MMCs' simple and complex structural components, (3) the HT-MMC microfracture, and (4) the tailoring of HT-MMCs' behavior for optimum specific performances. Representative results are presented from each area of application, illustrating the effectiveness of the computational procedures.

I.S.

A92-33587* National Aeronautics and Space Administration, Lewis Research Center, Cleveland, OH.

EFFECT OF FIBER REINFORCEMENT ON THERMO-OXIDATIVE STABILITY AND MECHANICAL PROPERTIES OF POLYMER MATRIX COMPOSITES

K. J. BOWLES (NASA, Lewis Research Center, Cleveland, OH) SAMPE Quarterly (ISSN 0036-0821), vol. 23, April 1992, p. 2-12. Previously announced in STAR as N91-19234. Apr. 1992 11 p refs

Copyright

A number of studies have investigated the thermooxidative behavior of polymer matrix composites. Two significant observations have been made from these research efforts: (1) fiber reinforcement has a significant effect on composite thermal stability; and (2) geometric effects must be considered when evaluating thermal aging data. The polyimide PMR-15 was the matrix material used in these studies. The control composite material was reinforced with Celion 6000 graphite fiber. T-4OR graphite fibers, along with some very stable ceramic fibers were selected as reinforcing fibers because of their high thermal stability. The ceramic fibers were Nicalon (silicon carbide) and Nextel 312 (alumina-silica-boron oxide). The mechanical properties of the two graphite fiber composites were significantly different, probably owing to variations in interfacial bonding between the fibers and the polyimide matrix. Three oxidation mechanisms were observed: (1) the preferential oxidation of the Celion 6000 fiber ends at cut surfaces, leaving a surface of matrix material with holes where the fiber ends were originally situated; (2) preferential oxidation of the composite matrix; and (3) interfacial degradation by oxidation. The latter two mechanisms were also observed on fiber end cut surfaces. The fiber and interface attacks appeared to initiate interfiber cracking along these surfaces.

Author

A92-34202* National Aeronautics and Space Administration, Lewis Research Center, Cleveland, OH.

STRENGTH, TOUGHNESS AND R-CURVE BEHAVIOUR OF SiC WHISKER-REINFORCED COMPOSITE Si3N4 WITH REFERENCE TO MONOLITHIC Si3N4

S. R. CHOI (Cleveland State University, OH) and J. A. SALEM (NASA, Lewis Research Center, Cleveland, OH) Journal of Materials Science (ISSN 0022-2461), vol. 27, March 15, 1992, p.

1491-1498. 15 Mar. 1992 8 p refs
Copyright

The flexural strength and fracture toughness of 30 vol pct SiC whisker-reinforced Si₃N₄ material were determined as a function of temperature from 25 to 1400 C in an air environment. It was found that both strength and toughness of the composite material were almost the same as those of the monolithic counterpart. The room-temperature strength was retained up to 1100 C; however, appreciable strength degradation started at 1200 C and reached a maximum at 1400 C due to stable crack growth. In contrast, the fracture toughness of the two materials was independent of temperature with an average value of 5.66 MPa sq rt m. It was also observed that the composite material exhibited no rising R-curve behavior at room temperature, as was the case for the monolithic material. These results indicate that SiC whisker addition to the Si₃N₄ matrix did not provide any favorable effects on strength, toughness and R-curve behavior.

Author

A92-34584*# National Aeronautics and Space Administration, Lewis Research Center, Cleveland, OH.

DAMAGE MECHANISMS IN THREE-DIMENSIONAL WOVEN REINFORCED CERAMIC MATRIX COMPOSITES UNDER TENSILE AND FLEXURAL LOADING AT ROOM AND ELEVATED TEMPERATURES

ABHISAK CHULYA, JOHN Z. GYEKENYESI (NASA, Lewis Research Center, Cleveland State University, OH), and JOHN P. GYEKENYESI (NASA, Lewis Research Center, Cleveland, OH) IN: AIAA/ASME/ASCE/AHS/ASC Structures, Structural Dynamics and Materials Conference, 33rd, Dallas, TX, Apr. 13-15, 1992, Technical Papers, Pt. 5 1992 18 p refs
(AIAA PAPER 92-2492) Copyright

Three-dimensional Nicalon SiC/SiC matrix composites made through a chemical vapor infiltration process were studied under tensile and flexural loading at 23, 1200, and 1550 C in air. In situ damage accumulation monitoring NDE techniques were utilized to identify failure mechanisms in these materials. The effectiveness and durability of a chemical vapor deposition SiC surface coating were also evaluated in severe oxidizing environment. Results show that the failure response was very similar for the 23 and 1200 C specimens, while at 1550 C there were significant changes in both the composite mechanical behavior and the matrix microstructure. Extensive fiber pull-out was observed only in the 1550 C specimen. It is also found that the SiC surface coating can protect the composite up to the critical matrix cracking strength.

Author

A92-36273* National Aeronautics and Space Administration, Lewis Research Center, Cleveland, OH.

MECHANICAL PROPERTIES OF MONOLITHIC AND PARTICULATE COMPOSITES OF L12 FORMS OF Al3Ti

J. D. WHITTENBERGER (NASA, Lewis Research Center, Cleveland, OH), K. S. KUMAR, S. BROWN, M. S. DIPIETRO (Martin Marietta Laboratories, Baltimore, MD), and S. C. FARMER (NASA, Lewis Research Center, Cleveland, OH) IN: Light-weight alloys for aerospace applications II; Proceedings of the 2nd Symposium, New Orleans, LA, Feb. 17-21, 1991 1991 23 p refs
Copyright

Preliminary studies of simple compressive properties of particulate composites with L1(2)-modified Al₃Ti's as the matrices were performed as functions of matrix composition, amount of TiB₂, processing technique, temperature, and strain rate. At and below about 900 K the introduction of TiB₂ particles overwhelms minor chemical effects, and extremely high-yield strengths (about 2000 MPa at the 20 vol pct TiB₂ level) were obtained. As L1(2)-modified Al₃Ti has about half the density of the Ni-base superalloys, such values translate to strength/density ratios approximately four times those for superalloys. This advantage is not maintained by the Al₃Ti-based composites above about 1000 K, particularly under slow strain rate plastic flow conditions, and it is proposed that this behavior could be due to the dissolution of intermetallic second phases as well as grain boundary creep mechanisms.

C.A.B.

24 COMPOSITE MATERIALS

A92-36389* National Aeronautics and Space Administration. Lewis Research Center, Cleveland, OH.

EFFECT OF FIBER STRENGTH ON THE ROOM TEMPERATURE TENSILE PROPERTIES OF SiC/Ti-24Al-11Nb
S. L. DRAPER, P. K. BRINDLEY, and M. V. NATHAL (NASA, Lewis Research Center, Cleveland, OH) IN: Developments in ceramic and metal-matrix composites; Proceedings of the Symposium, TMS Annual Meeting, San Diego, CA, Mar. 1-5, 1992 1991 14 p refs

Copyright

SCA-6 SiC fibers of known strength were incorporated into SiC/Ti-24Al-11Nb (at. percent) composites and the effect of fiber strength variability on room temperature composite strength was investigated. Fiber was etched out of a composite fabricated by the powder cloth technique and the effect of the fabrication process on fiber strength was assessed. The strength of the composite was directly correlated with the strength of the as-received fiber. The strength of composite plates containing mixed fiber strengths was dominated by the lower strength fiber. Fabrication by the powder cloth technique resulted in only a slight degradation of fiber strength. The strength of the composite was found to be overestimated by the rule of mixtures strength calculation. Examination of failed tensile specimens revealed periodic fiber cracks and the failure mode was concluded to be cumulative. With the variation in fiber strength eliminated, the composite UTS was found to have a positive correlation with volume fraction of fiber. Author

A92-36391* National Aeronautics and Space Administration. Lewis Research Center, Cleveland, OH.

COMBUSTION SYNTHESIS OF TiB₂-Al₂O₃-Al COMPOSITE MATERIALS

H. J. FENG, J. J. MOORE (Colorado School of Mines, Golden), and D. G. WIRTH (Coors Ceramics Co., Golden, CO) IN: Developments in ceramic and metal-matrix composites; Proceedings of the Symposium, TMS Annual Meeting, San Diego, CA, Mar. 1-5, 1992 1991 21 p refs

Copyright

The oxide-aluminum exothermic reduction reaction is presently used in the combustion-synthesis of ceramic/metal composites. An excess of Al is used in the reacting materials, which rapidly generate enough heat to exceed Al's melting point. The molten Al thus evolved is allowed to infiltrate the porous ceramic matrix as the exothermic reaction proceeds; this feature of the process turns the disadvantage of high porosity levels in combustion-synthesized materials into an advantage. Attention is given to the system obtained with $3\text{TiO}_2 + 3\text{B}_2\text{O}_3 + (10-x)\text{Al}$ starting materials. O.C.

A92-38125* National Aeronautics and Space Administration. Lewis Research Center, Cleveland, OH.

1200 AND 1300 K SLOW PLASTIC COMPRESSION PROPERTIES OF Ni-50Al COMPOSITES

J. D. WHITTENBERGER (NASA, Lewis Research Center, Cleveland, OH), K. S. KUMAR (Martin Marietta Laboratories, Baltimore, MD), and S. K. MANNAN (Inco Alloys International, Inc., Huntington, WV) Materials at High Temperatures (ISSN 0960-3409), vol. 9, no. 1, 1991, p. 3-12. 1991 10 p refs

Copyright

XD synthesis, powder blending, and hot pressing techniques have been utilized to produce NiAl composites containing 4, 7.5, 15, and 25 vol pct alumina whiskers and hybrid composite materials with 15 vol pct Al₂O₃ + 10 or 20 vol pct, nominally 1 micron TiB₂ particles. The resistance to slow plastic flow was determined at 1200 and 1300 K via compression testing in air under constant velocity conditions. The stress-strain behavior of the intermetallic composites depended on the fraction of second phases where the 4 and 7.5 percent Al₂O₃ materials flowed at a nominally constant stress after about 2 percent deformation, while all the other composites exhibited diffuse yielding followed by strain softening. The flow stress-strain rate properties increased with volume fraction of Al₂O₃ whiskers except for the 4 and 7.5 percent materials, which had similar strengths. The hybrid composite NiAl

+ 15Al₂O₃ + 10TiB₂ was substantially stronger than the materials simply containing alumina. Deformation in these composites can be described by the Kelly and Street model of creep in perfectly bonded, rigid, discontinuous fiber materials. Author

A92-39036* National Aeronautics and Space Administration. Lewis Research Center, Cleveland, OH.

FATIGUE CRACK GROWTH IN A UNIDIRECTIONAL SCS-6/Ti-15-3 COMPOSITE

PETER KANTZOS, JACK TELESMA (NASA, Lewis Research Center, Cleveland, OH), and LOUIS GHOSN (Sverdrup Technology, Inc.; NASA, Lewis Research Center, Cleveland, OH) IN: Composite materials: Fatigue and fracture. Vol. 3 1991 21 p refs

Copyright

An investigation was conducted to characterize and model the fatigue crack growth (FCG) behavior of an SCS-6/Ti-15-3 metal matrix composite. Part of the study was conducted using a fatigue loading stage mounted inside a scanning electron microscope (SEM). The results of the study reveal that the fatigue crack growth behavior of the composite is a function of specimen geometry, fiber orientation, and interaction of local stress fields with the highly anisotropic composite. In the case of (0)8 oriented single edge notch specimens and (90)8 oriented compact tension (CT) specimens, the crack growth was normal to the loading direction. However, for the (0)8 CT specimens, the crack grew mostly parallel to the loading and the fiber direction. The unusual fatigue behavior of the (0)8 CT specimens is attributed to the specimen geometry and the associated high tensile bending stresses perpendicular to the fiber direction. Author

A92-39604* National Aeronautics and Space Administration. Lewis Research Center, Cleveland, OH.

FIBER COATING/MATRIX REACTIONS IN SILICON-BASE CERAMIC MATRIX COMPOSITES

K. N. LEE and N. S. JACOBSON (NASA, Lewis Research Center, Cleveland, OH) Aug. 1992 8 p refs

Copyright

The Knudsen cell technique and coupons of carbon coated Si₃N₄ and BN coated SiC were employed to study the possible reactions at the SiC/C/Si₃N₄ and SiC/BN/SiC interface. Carbon reacts with Si₃N₄ to form gaseous N₂ and solid SiC. Solid SiC acts as a physical barrier to the reaction, which prevents the generation of high N₂ pressure predicted from thermochemical calculations. Thus, deleterious effects of the reaction to the composite are limited. Limited reactions between BN and C-rich SiC was observed. However, the vapor pressure was so low that it is not likely to cause any interfacial instability. The predicted formation of a BN-C solid solution was not observed. Author

A92-39605* National Aeronautics and Space Administration. Lewis Research Center, Cleveland, OH.

ROLE OF INTERFACIAL THERMAL BARRIER IN THE TRANSVERSE THERMAL CONDUCTIVITY OF UNIAXIAL SiC FIBER-REINFORCED REACTION BONDED SILICON NITRIDE

H. BHATT, K. Y. DONALDSON, D. P. H. HASSELMAN (Virginia Polytechnic Institute and State University, Blacksburg), and R. T. BHATT (NASA, Lewis Research Center, Cleveland, OH) Aug. 1992 8 p refs

Copyright

The transverse thermal conductivity of reaction-bonded Si₃N₄ is significantly affected by an interfacial barrier at the interface formed with SiC reinforcing fibers. A comparative study of composites with and without reinforcing-fiber carbon coatings found the coating to reduce effective thermal conductivity by a factor of about 2; this, however, is partially due to a thermal expansion-mismatch gap between fiber and matrix. HIPing of composites with coated fibers led to an enhancement of thermal conductivity via improved interfacial thermal contact and greater grain size and crystallinity of the fibers. O.C.

A92-39642* National Aeronautics and Space Administration. Lewis Research Center, Cleveland, OH.

FAILURE MECHANISMS OF 3-D WOVEN SiC/SiC COMPOSITES UNDER TENSILE AND FLEXURAL LOADING AT ROOM AND ELEVATED TEMPERATURES

ABHISAK CHULYA, JOHN Z. GYEKENYESI (Cleveland State University, OH), and JOHN P. GYEKENYESI (NASA, Lewis Research Center, Cleveland, OH) Aug. 1992 13 p refs Copyright

Nicalon silicon carbide 3D yarn with silicon carbide matrix composites made through a chemical vapor infiltration (CVI) process were investigated under tensile and flexural loading at 23, 1200 and 1550 C in air. The effectiveness of a chemical vapor deposition (CVD) SiC surface coating was also evaluated in severe oxidizing environment. Acoustic emission sensors and in situ optical microscopy were used at room temperature to monitor the failure mechanisms. It is shown that the level of tensile stress at which nonlinear behavior begins is not drastically reduced at 1200 and 1550 C when composites were protected by a SiC surface coating. Extensive fiber pull-out was observed only in the 1550 C specimen. Similar behaviors were also found in flexural specimens. Author

A92-39858* National Aeronautics and Space Administration. Lewis Research Center, Cleveland, OH.

REACTION-BONDED Si₃N₄ AND SiC MATRIX COMPOSITES

RAMAKRISHNA T. BHATT (U.S. Army, Propulsion Directorate, Cleveland, OH) and DONALD R. BEHRENDT (NASA, Lewis Research Center, Cleveland, OH) IN: Flight-vehicle materials, structures, and dynamics - Assessment and future directions. Vol. 3 - Ceramics and ceramic-matrix composites 1992 11 p refs Copyright

A development status evaluation is presented for the reaction-bonded SiC- and Si₃N₄-matrix types of fiber-reinforced ceramic-matrix composite (FRCMC). A variety of reaction-bonding methods are being pursued for FRCMC fabrication: CVI, CVD, directed metal oxidation, and self-propagating high-temperature synthesis. Due to their high specific modulus and strength, toughness, and fabricability, reaction-bonded FRCMC are important candidate materials for such heat-engine components as combustor liners, nozzles, and turbine and stator blading. The improvement of long-term oxidative stability in these composites is a major goal of current research. O.C.

A92-39866* National Aeronautics and Space Administration. Lewis Research Center, Cleveland, OH.

STRUCTURAL DESIGN METHODOLOGIES FOR CERAMIC-BASED MATERIAL SYSTEMS

STEPHEN F. DUFFY, ABHISAK CHULYA (Cleveland State University, OH), and JOHN P. GYEKENYESI (NASA, Lewis Research Center, Cleveland, OH) IN: Flight-vehicle materials, structures, and dynamics - Assessment and future directions. Vol. 3 - Ceramics and ceramic-matrix composites 1992 21 p refs Copyright

One of the primary pacing items for realizing the full potential of ceramic-based structural components is the development of new design methods and protocols. The focus here is on low temperature, fast-fracture analysis of monolithic, whisker-toughened, laminated, and woven ceramic composites. A number of design models and criteria are highlighted. Public domain computer algorithms, which aid engineers in predicting the fast-fracture reliability of structural components, are mentioned. Emphasis is not placed on evaluating the models, but instead is focused on the issues relevant to the current state of the art. Author

A92-41575* National Aeronautics and Space Administration. Lewis Research Center, Cleveland, OH.

1400 AND 1500 K COMPRESSIVE CREEP PROPERTIES OF AN NiAl-ALN COMPOSITE

J. D. WHITTENBERGER (NASA, Lewis Research Center, Cleveland, OH), EDUARD ARZT (Max-Planck-Institut fuer Metallforschung, Stuttgart, Federal Republic of Germany), and

MICHAEL J. LUTON (Exxon Research and Engineering Co., Annandale, NJ) Scripta Metallurgica et Materialia (ISSN 0956-716X), vol. 26, no. 12, June 15, 1992, p. 1925-1930. 15 Jun. 1992 6 p refs Copyright

Compressive creep properties of an NiAl/AlN(p) composite produced by a reaction milling process were investigated at 1400 and 1500 K and at slow strain rates, to investigate the relative strength of this composite at high temperatures, and to determine if the consolidation technique affects the 1400 K creep properties. Results indicate that the stress exponent of the NiAl/AlN(p) composite was similar to that for unreinforced NiAl. However, the activation energy for the composite was found to be more than twice that measured in the unreinforced matrix. Oxidation did not affect the composite at 1400 K, but a significant attack was observed in a sample subjected to fast deformation at 1500 K. I.S.

A92-41841* National Aeronautics and Space Administration. Lewis Research Center, Cleveland, OH.

EFFECT OF FIBER ORIENTATION ON THE FRACTURE TOUGHNESS OF BRITTLE MATRIX COMPOSITES

L. K. JAIN and R. C. WETHERHOLD (New York, State University, Buffalo) Acta Metallurgica et Materialia (ISSN 0956-7151), vol. 40, no. 6, June 1992, p. 1135-1143. Jun. 1992 9 p refs (Contract NAG3-862) Copyright

The effective fracture toughness of brittle matrix materials can be increased through the addition of short, poorly bonded fibers which bridge the growing crack. The orientation distribution of the fibers is likely to be biased, and not in an ideal random or aligned state. A micromechanical model is formulated for the postcracking behavior using the force-displacement relation for an arbitrary fiber bridging a crack, the fiber orientation density function, and the fiber location density function. This model is then used to determine an effective traction law for the bridging fibers, as well as the steady state bridging toughness increment. In most cases, the results may be placed in the form of a product of the aligned fiber results times a modifying integrated orientation factor. The frictional shear stress on fiber pull-out is allowed to vary during pull-out, modeling the effects of matrix breakdown, fiber surface smoothing or wear debris accumulation. Results are presented for a variety of representative planar and three-dimensional fiber orientation states. Author

A92-41867* National Aeronautics and Space Administration. Lewis Research Center, Cleveland, OH.

DISCONTINUOUSLY REINFORCED INTERMETALLIC MATRIX COMPOSITES VIA XD SYNTHESIS

K. S. KUMAR (Martin Marietta Laboratories, Baltimore, MD) and J. D. WHITTENBERGER (NASA, Lewis Research Center, Cleveland, OH) (Institute of Metals, Conference on High Temperature Intermetallics, London, England, Apr. 30-May 1, 1991) Materials Science and Technology (ISSN 0267-0836), vol. 8, no. 4, April 1992, p. 317-330. Research supported by SDIO. Apr. 1992 14 p refs (Contract N00014-85-C-0639; N00014-86-C-2277; NAS3-25787; MDA972-88-C-0047) Copyright

A review is given of recent results obtained for discontinuously reinforced intermetallic matrix composites produced using the XD process. Intermetallic matrices investigated include NiAl, multiphase NiAl + Ni₂AlTi, CoAl, near-gamma titanium aluminides, and Li₂ trialuminides containing minor amounts of second phase. Such mechanical properties as low and high temperature strength, compressive and tensile creep, elastic modulus, ambient ductility, and fracture toughness are discussed as functions of reinforcement size, shape, and volume fraction. Microstructures before and after deformation are examined and correlated with measured properties. An observation of interest in many of the systems examined is 'dispersion weakening' at high temperatures and high strain rates. This behavior is not specific to the XD process; rather similar

24 COMPOSITE MATERIALS

observations have been reported in other discontinuous composites. Proposed mechanisms for this behavior are presented. Author

A92-43085* National Aeronautics and Space Administration. Lewis Research Center, Cleveland, OH.

MODELING OF CRACK BRIDGING IN A UNIDIRECTIONAL METAL MATRIX COMPOSITE

LOUIS J. GHOSN (Sverdrup Technology, Inc.; NASA, Lewis Research Center, Brook Park, OH), PETE KANTZOS, and JACK TELESMAN (NASA, Lewis Research Center, Cleveland, OH) International Journal of Fracture (ISSN 0376-9429), vol. 54, no. 4, April 15, 1992, p. 345-357. Previously announced in STAR as N91-24660. 15 Apr. 1992 13 p refs
Copyright

The effective fatigue crack driving force and crack opening profiles were determined analytically for fatigue tested unidirectional composite specimens exhibiting fiber bridging. The crack closure pressure due to bridging was modeled using two approaches: the fiber pressure model and the shear lag model. For both closure models, the Bueckner weight function method and the finite element method were used to calculate crack opening displacements and the crack driving force. The predicted near crack tip opening profile agreed well with the experimentally measured profiles for single edge notch SCS-6/Ti-15-3 metal matrix composite specimens. The numerically determined effective crack driving force, $\Delta K(\text{eff})$, was calculated using both models to correlate the measure crack growth rate in the composite. The calculated $\Delta K(\text{eff})$ from both models accounted for the crack bridging by showing a good agreement between the measured fatigue crack growth rates of the bridged composite and that of unreinforced, unbridged titanium matrix alloy specimens. Author

A92-43682* National Aeronautics and Space Administration. Lewis Research Center, Cleveland, OH.

METAL- AND INTERMETALLIC-MATRIX COMPOSITES FOR AEROSPACE PROPULSION AND POWER SYSTEMS

J. DOYCHAK (NASA, Lewis Research Center, Cleveland, OH) JOM (ISSN 1047-4838), vol. 44, no. 6, June 1992, p. 46-51. Jun. 1992 6 p refs
Copyright

The requirements for high specific strength refractory materials of prospective military, civil, and space propulsion systems are presently addressed in the context of emerging capabilities in metal- and intermetallic-matrix composites. The candidate systems encompass composite matrix compositions of superalloy, Nb-Zr refractory alloy, Cu-base, and Ti-base alloy types, as well as such intermetallics as TiAl, Ti₃Al, NiAl, and MoSi₂. The brittleness of intermetallic matrices remains a major consideration, as does their general difficulty of fabrication. O.C.

A92-44606* National Aeronautics and Space Administration. Lewis Research Center, Cleveland, OH.

THERMOMECHANICAL TESTING OF HIGH-TEMPERATURE COMPOSITES - THERMOMECHANICAL FATIGUE (TMF) BEHAVIOR OF SiC(SCS-6)/Ti-15-3

MICHAEL G. CASTELLI (Sverdrup Technology, Inc., Brook Park, OH), PAUL BAROLOTTA, and JOHN R. ELLIS (NASA, Lewis Research Center, Cleveland, OH) IN: Composite materials: Testing and design. Vol. 10; Proceedings of the 10th Conference, San Francisco, CA, Apr. 24, 25, 1990 1992 17 p refs
Copyright

Thermomechanical testing techniques recently developed for monolithic structural alloys were successfully extended to continuous fiber reinforced composite materials in plate form. The success of this adaptation was verified on a model metal matrix composite (MMC) material, namely SiC(SCS-6)/Ti-15V-3Cr-3Al-3Sn. Effects of heating system type and specimen preparation are also addressed. Cyclic lives determined under full thermomechanical conditions were shown to be significantly reduced from those obtained under comparable isothermal and in-phase bi-thermal conditions. Fractography and metallography from specimens subjected to isothermal,

out-of-phase and in-phase conditions reveal distinct differences in damage-failure modes. Isothermal metallography revealed extensive matrix cracking associated with fiber damage throughout the entire cross-section of the specimen. Out-of-phase metallography revealed extensive matrix damage associated with minimal (if any) fiber cracking. However, the damage was located exclusively at surface and near-surface locations. In-phase conditions produced extensive fiber cracking throughout the entire cross-section, associated with minimal (if any) matrix damage. Author

A92-44613* National Aeronautics and Space Administration. Lewis Research Center, Cleveland, OH.

HIGH-TEMPERATURE FATIGUE BEHAVIOR OF A SiC/Ti-24Al-11Nb COMPOSITE

PAUL A. BAROLOTTA and PAMELA K. BRINDLEY (NASA, Lewis Research Center, Cleveland, OH) IN: Composite materials: Testing and design. Vol. 10; Proceedings of the 10th Conference, San Francisco, CA, Apr. 24, 25, 1990 1992 12 p refs
Copyright

A series of tension-tension strain- and load-controlled tests were conducted on unidirectional SiC/Ti-24Al-11Nb (at. percent) composites at 425 and 815 C. Several regimes of damage were identified using Talreja's concept of fatigue life diagrams. Issues of test technique, test control mode, and definition of failure were also addressed. Author

A92-46826* National Aeronautics and Space Administration. Lewis Research Center, Cleveland, OH.

INTERMETALLIC MATRIX COMPOSITES; PROCEEDINGS OF THE MRS SYMPOSIUM, SAN FRANCISCO, CA, APR. 18-20, 1990

D. L. ANTON, ED. (United Technologies Research Center, East Hartford, CT), P. L. MARTIN, ED. (Rockwell International Science Center, Thousand Oaks, CA), D. B. MIRACLE, ED. (USAF, Wright Research and Development Center, Wright-Patterson AFB, OH), and R. MCMEEKING, ED. (California, University, Santa Barbara) Symposium sponsored by GE Aircraft Engines, Los Alamos National Laboratory, NASA, Martin Marietta Corp., United Technologies Corp., Rockwell International Corp., and U.S. Navy., Pittsburgh, PA, Materials Research Society (MRS Symposium Proceedings. Vol. 194), (ISSN 0272-9172), 1990, 460 p. For individual items see A92-46827 to A92-46881. 1990 460 p
(Contract N00014-90-J-1672)
(ISBN 1-55899-083-6) Copyright

The present volume on intermetallic matrix composites discusses the modeling, processing, microstructure/property relationships, and compatibility of intermetallic matrix composites. Attention is given to models for the strength of ductile matrix composites, innovative processing techniques for intermetallic matrix composites, ductile phase toughening of brittle intermetallics, and reactive synthesis of NbAl₃ matrix composites. Topics addressed include solidification processing of NbCr₂ alloys, Ta and Nb reinforced MoSi₂, the microstructure and mechanical behavior of Ni₃Al-matrix composites, and ductile-phase toughening of Cr₃Si with chromium. Also discussed are dislocation morphologies in TiB₂/NiAl, the development of highly impact resistant NiAl matrix composites, the effect of notches on the fatigue life of the SCS-6Ti₃Al composite, and the chemical stability of fiber-metal matrix composites. P.D.

A92-46867* National Aeronautics and Space Administration. Lewis Research Center, Cleveland, OH.

INITIAL EVALUATION OF CONTINUOUS FIBER REINFORCED NiAl COMPOSITES

R. D. NOEBE, R. R. BOWMAN (NASA, Lewis Research Center, Cleveland, OH), and J. I. ELDRIDGE (Sverdrup Technology, Inc.; NASA, Lewis Research Center, Cleveland, OH) IN: Intermetallic matrix composites; Proceedings of the MRS Symposium, San Francisco, CA, Apr. 18-20, 1990 1990 9 p refs
Copyright

NiAl is being evaluated as a potential matrix material as part of an overall program to develop and understand high-temperature

structural composites. Currently, continuous fiber composites have been fabricated by the powder cloth technique incorporating either W(218) or single crystal Al₂O₃ fibers as reinforcements in both binary NiAl and a solute strengthened NiAl(.05 at. pct Zr) matrix. Initial evaluation of these composite systems have included: fiber push-out testing to measure matrix/fiber bond strengths, bend testing to determine strength as a function of temperature and composite structure, and thermal cycling to establish the effect of matrix and fiber properties on composite life. The effect of matrix/fiber bond strength and matrix strength on several composite properties will be discussed.

Author

A92-46871* National Aeronautics and Space Administration. Lewis Research Center, Cleveland, OH.

CYCLIC OXIDATION RESISTANCE OF A REACTION MILLED NiAl-ALN COMPOSITE

CARL E. LOWELL, CHARLES A. BARRETT, and J. D. WHITTENBERGER (NASA, Lewis Research Center, Cleveland, OH) IN: Intermetallic matrix composites; Proceedings of the MRS Symposium, San Francisco, CA, Apr. 18-20, 1990 1990 6 p refs

Copyright

Based upon recent mechanical property tests a NiAl-AlN composite produced by cryomilling has very attractive high temperature strength. This paper focuses on the oxidation resistance of the NiAl-AlN composite at 1473 and 1573 K as compared to that of Ni-47Al-0.15Zr, one of the most oxidation resistant intermetallics. The results of cyclic oxidation tests show that the NiAl-AlN composite has excellent properties although not quite as good as those of Ni-47Al-0.15Zr. The onset of failure of the NiAl-AlN was unique in that it was not accompanied by a change in scale composition from alumina to less protective oxides. Failure in the composite appears to be related to the entrapment of AlN particles within the alumina scale.

Author

A92-46874* National Aeronautics and Space Administration. Lewis Research Center, Cleveland, OH.

COMPATIBILITY OF POTENTIAL REINFORCING CERAMICS WITH Ni AND Fe ALUMINIDES

J. A. MOSER, M. AINDOW, W. A. T. CLARK (Ohio State University, Columbus), S. DRAPER (NASA, Lewis Research Center, Cleveland, OH), and H. L. FRASER (Ohio State University, Columbus) IN: Intermetallic matrix composites; Proceedings of the MRS Symposium, San Francisco, CA, Apr. 18-20, 1990 1990 6 p refs

(Contract NAG3-942)

Copyright

The compatibility of candidate ceramic reinforcement materials with intermetallic matrices for high temperature composite systems has been evaluated. Powders of FeAl and NiAl were mixed with ceramic powders and consolidated by hot isostatic pressing and subsequent heat treatment. The microstructures of these composites and the nature of the ceramic/matrix interfaces were assessed using a wide variety of electron-beam techniques. The system FeAl/TiB₂ was found to be particularly promising. The matrix appears to be bonded to the ceramic particles, which may be the result of diffusion of Fe into the ceramic. The particles stabilized in a previously unreported monoclinic crystal structure, rather than the equilibrium hexagonal form exhibited by the binary compound.

Author

A92-47106* National Aeronautics and Space Administration. Lewis Research Center, Cleveland, OH.

REDUCTION OF THERMAL RESIDUAL STRESSES IN ADVANCED METALLIC COMPOSITES BASED UPON A COMPENSATING/COMPLIANT LAYER CONCEPT

S. M. ARNOLD (NASA, Lewis Research Center, Cleveland, OH), V. K. ARYA (Toledo, University, OH), and M. E. MELIS (NASA, Lewis Research Center, Cleveland, OH) Journal of Composite Materials (ISSN 0021-9983), vol. 26, no. 9, 1992, p. 1287-1309. 1992 23 p refs

Copyright

A detailed parametric study is carried out to investigate the

viability of the recently proposed compensating/compliant layer concept (i.e., the insertion of an interface material between SiC fiber and metal matrix to reduce or eliminate the residual stress buildup during cooling of the composite). The study uses a finite-element concentric cylinder model with generalized plane strain end conditions and free boundary conditions, assuming the SiC fiber to be isotropic and linear elastic and the compliant layer cylinder and matrix (Ti₃Al + Nb) cylinder to be isotropic and bilinear elastic-plastic. Results show that a compensating/compliant layer acts to reduce in-plane residual stresses within the fiber and the matrix and, therefore, reduces radial cracking. However, this decrease in in-plane stresses is accompanied by an increase of longitudinal stress, which may initiate longitudinal cracking. I.S.

A92-49819* National Aeronautics and Space Administration. Lewis Research Center, Cleveland, OH.

HIGH MOLECULAR WEIGHT FIRST GENERATION PMR POLYIMIDES FOR 343 C APPLICATIONS

D. C. MALARIK and R. D. VANNUCCI (NASA, Lewis Research Center, Cleveland, OH) SAMPE Quarterly (ISSN 0036-0821), vol. 23, no. 4, July 1992, p. 3-8. Previously announced in STAR as N92-19498. Jul. 1992 6 p refs

Copyright

The effect of molecular weight on 343 C thermo-oxidative stability (TOS), mechanical properties, and processability, of the first generation PMR polyimides was studied. Graphite fiber reinforced PMR-15, PMR-30, PMR-50, and PMR-75 composites (corresponding to formulated molecular weights of 1500, 3000, 5000, and 7500, respectively) were fabricated using a simulated autoclave process. The data reveal that while alternate autoclave cure schedules are required for the high molecular weight resins, low void laminates can be fabricated which have significantly improved TDS over PMR-15, with only a small sacrifice in mechanical properties.

Author

A92-50347* National Aeronautics and Space Administration. Lewis Research Center, Cleveland, OH.

REDUCTION OF THERMAL STRESSES IN CONTINUOUS FIBER REINFORCED METAL MATRIX COMPOSITES WITH INTERFACE LAYERS

S. JANSSON and F. A. LECKIE (California, University, Santa Barbara) Journal of Composite Materials (ISSN 0021-9983), vol. 26, no. 10, 1992, p. 1474-1486. Research supported by NASA. 1992 13 p refs

Copyright

The potential of using interface layer to reduce thermal stresses in the matrix of composites with a mismatch in coefficients of thermal expansion of fiber and matrix has been investigated. It was found that compliant layers, with properties of readily available materials, do not have the potential to reduce thermal stresses significantly. However, interface layers with high coefficient of thermal expansion can compensate for the mismatch and reduce thermal stresses in the matrix significantly.

Author

A92-50348* National Aeronautics and Space Administration. Lewis Research Center, Cleveland, OH.

VOID EFFECTS ON THE INTERLAMINAR SHEAR STRENGTH OF UNIDIRECTIONAL GRAPHITE-FIBER-REINFORCED COMPOSITES

KENNETH J. BOWLES and STEPHEN FRIMPONG (NASA, Lewis Research Center, Cleveland, OH) Journal of Composite Materials (ISSN 0021-9983), vol. 26, no. 10, 1992, p. 1487-1509. 1992 23 p refs

Copyright

A study was conducted to evaluate the effect of voids on the interlaminar shear strength (ILSS) of a polyimide matrix composite system. The graphite/PMR-15 composite was chosen for study because of the extensive amount of experience that has been amassed in the processing of this material. Void contents were calculated and the void geometry and distribution were noted using microscope techniques such as those used in metallography. A good empirical correlation between ILSS and composite density was found. The most acceptable relationship between the ILSS

24 COMPOSITE MATERIALS

and density was found to be a power equation that closely resembles theoretically derived expressions. It was found that void-free composites could be processed in matched metal die molds at pressures greater than 1.4 MPa and less than 6.9 MPa.
Author

A92-55143* National Aeronautics and Space Administration. Lewis Research Center, Cleveland, OH.

THE EFFECT OF TEMPERATURE ON THE DEFORMATION AND FRACTURE OF SiC/Ti-24Al-11Nb

P. K. BRINDLEY, S. L. DRAPER, J. I. ELDRIDGE, M. V. NATHAL, and S. M. ARNOLD (NASA, Lewis Research Center, Cleveland, OH) Metallurgical Transactions A - Physical Metallurgy and Materials Science (ISSN 0360-2133), vol. 23A, no. 9, Sept. 1992, p. 2527-2540. Sep. 1992 14 p refs

Copyright

The effect of temperature on the stress-strain behavior in air and the failure mechanisms of Ti-24Al-11Nb alloy and of a SiC/Ti-24Al-11Nb composite with continuous SiC fibers oriented parallel to the loading direction was investigated over temperature range 23-815 C. It was found that the tensile failure process of SiC/Ti-24Al-11Nb was controlled at all temperatures by fiber fracture. Composite failure occurred at 0.8 percent strain at all temperatures. Debond and frictional stresses at the fiber-matrix interface decreased with increased temperature. I.S.

A92-57029* National Aeronautics and Space Administration. Lewis Research Center, Cleveland, OH.

OXIDATION OF Al₂O₃ CONTINUOUS FIBER-REINFORCED/NiAl COMPOSITES

J. DOYCHAK, J. A. NESBITT, R. D. NOEBE, and R. R. BOWMAN (NASA, Lewis Research Center, Cleveland, OH) Oxidation of Metals (ISSN 0030-770X), vol. 38, no. 1-2, Aug. 1992, p. 45-72. Aug. 1992 28 p refs

Copyright

The 1200 C and 1300 C isothermal and cyclic oxidation behavior of Al₂O₃ continuous fiber-reinforced/NiAl composites were studied. Oxidation resulted in formation of Al₂O₃ external scales in a similar manner as scales formed on monolithic NiAl. The isothermal oxidation of an Al₂O₃/NiAl composite resulted in oxidation of the matrix along the fiber/matrix interface near the fiber ends. This oxide acted as a wedge between the fiber and the matrix, and, under cyclic oxidation conditions, led to further oxidation along the fiber lengths and eventual cracking of the composite. The oxidation behavior of composites in which the Al₂O₃ fibers were sputter coated with nickel prior to processing was much more severe. This was attributed to open channels around the fibers which formed during processing, most likely as a result of the diffusion of the nickel coating into the matrix. Author

N92-13284*# National Aeronautics and Space Administration. Lewis Research Center, Cleveland, OH.

DAMAGE AND FRACTURE IN COMPOSITE THIN SHELLS

LEVON MINNETYAN (Clarkson Univ., Potsdam, NY.), CHRISTOS C. CHAMIS, and PAPPU L. N. MURTHY 1991 26 p Presented at the 23rd International SAMPE Technical Conference, Lake Kiamesha, NY, 22-24 Oct. 1991 (Contract RTOP 505-63-5B) (NASA-TM-105289; E-6624; NAS 1.15:105289) Avail: CASI HC A03/MF A01

The effect of fiber fracture on the load carrying capability and structural behavior of a composite cylindrical shell under internal pressure is investigated. An integrated computer code is utilized for the simulation of composite structural degradation under loading. Damage initiation, damage growth, fracture progression, and global structural fracture are included in the simulation. Results demonstrate the significance of local damage on the structural durability of pressurized composite cylindrical shells. Author

N92-14118*# National Aeronautics and Space Administration. Lewis Research Center, Cleveland, OH.

COMPUTATIONAL SIMULATION OF SURFACE WAVINESS IN GRAPHITE/EPOXY WOVEN COMPOSITES DUE TO INITIAL CURING

JOSE G. SANFELIZ, PAPPU L. N. MURTHY, and CHRISTOS C. CHAMIS 1992 21 p Proposed for presentation at the 37th International Symposium and Exhibit, Anaheim, CA, 9-12 Mar. 1992; sponsored by the Society for the Advancement of Material and Process Engineering (Contract RTOP 505-63-5B) (NASA-TM-105313; E-6666; NAS 1.15:105313) Avail: CASI HC A03/MF A01

Several models simulating plain weave, graphite/epoxy woven composites are presented, along with the effects that the simultaneous application of pressure and thermal loads have on their surfaces. The surface effects created by moisture absorption are also examined. The computational simulation consisted of using a two-dimensional finite element model for the composite. The properties of the finite element (FE) model are calculated by using the in-house composite mechanics computer code ICAN (Integrated Composite ANalyzer). MSC/NASTRAN is used for the FE analysis which yields the composite's top surface normalized displacements. These results demonstrate the importance of parameters such as the cure temperature (T_{sub o}) and the resin content in the curing process of polymer-matrix composites. The modification of these parameters will help tailor the composite system to the desired requirements and applications. Author

N92-14120*# National Aeronautics and Space Administration. Lewis Research Center, Cleveland, OH.

THERMAL CONDUCTIVITY AND THERMAL EXPANSION OF GRAPHITE FIBER/COPPER MATRIX COMPOSITES

DAVID L. ELLIS (Case Western Reserve Univ., Cleveland, OH.) and DAVID L. MCDANELS 1991 19 p Presented at the Annual Meeting of The Metallurgical Society, New Orleans, LA, 17-21 Feb. 1991 (Contract NCC3-94; RTOP 590-13-11) (NASA-TM-105233; E-6557; NAS 1.15:105233) Avail: CASI HC A03/MF A01

The high specific conductivity of graphite fiber/copper matrix (Gr/Cu) composites offers great potential for high heat flux structures operating at elevated temperatures. To determine the feasibility of applying Gr/Cu composites to high heat flux structures, composite plates were fabricated using unidirectional and cross-plyed pitch-based P100 graphite fibers in a pure copper matrix. Thermal conductivity of the composites was measured from room temperature to 1073 K, and thermal expansion was measured from room temperature to 1050 K. The longitudinal thermal conductivity, parallel to the fiber direction, was comparable to pure copper. The transverse thermal conductivity, normal to the fiber direction, was less than that of pure copper and decreased with increasing fiber content. The longitudinal thermal expansion decreased with increasing fiber content. The transverse thermal expansion was greater than pure copper and nearly independent of fiber content. Author

N92-14122*# National Aeronautics and Space Administration. Lewis Research Center, Cleveland, OH.

MICROFRACTURE IN HIGH TEMPERATURE METAL MATRIX LAMINATES

SUBODH K. MITAL (Toledo Univ., OH.), CHRISTOS C. CHAMIS, and PASCAL K. GOTSIS 1991 26 p Presented at the 32nd Structures, Structural Dynamics, and Materials Conference, Baltimore, MD, 8-10 Apr. 1991; cosponsored by AIAA, ASME, ASCE, AHS, and ASC (Contract NAG3-1264; RTOP 505-63-5B) (NASA-TM-105189; E-6491; NAS 1.15:105189) Avail: CASI HC A03/MF A01

Computational simulation procedures are described to evaluate the composite microfracture behavior, establish the hierarchy/sequence of fracture modes, and the influence of compliant layers and partial debonding on composite properties

and microfracture initiation. These procedures are based upon three-dimensional finite element analysis and composite micromechanics equations. Typical results for the effects of compliant layers and partial debonding, microfracture initiation, and propagation and the thermomechanical cyclic loading on a SiC/Ti15 composite system are presented and discussed. The results show that interfacial debonding follows fiber or matrix fracture, and the thermomechanical cyclic loading severely degrades the composite integrity. Author

N92-15136*# National Aeronautics and Space Administration. Lewis Research Center, Cleveland, OH.

THERMALLY-DRIVEN MICROFRACTURE IN HIGH TEMPERATURE METAL MATRIX COMPOSITES

SUBODH K. MITAL (Toledo Univ., OH.) and CHRISTOS C. CHAMIS 1991 13 p Presented at the Symposium on the Mechanics of Composites at Elevated and Cryogenic Temperatures, ASME Applied Mechanics and Biomechanics Summer Conference, Columbus, OH, 16-19 Jun. 1991 (Contract RTOP 510-01-0A) (NASA-TM-105305; E-6657; NAS 1.15:105305) Avail: CASI HC A03/MF A01

Microfracture (fiber/matrix fracture, interphase debonding and interply delamination) in high temperature metal matrix composites (HTMMC), subjected to thermal loading, is computationally simulated. Both unidirectional and crossply SiC/Ti15 composites are evaluated for microfracture driven by thermal loads, using multicell finite element models. Results indicate that under thermal loads alone, microfracture propagation is not as sensitive as it is under mechanical loads. Author

N92-15137*# National Aeronautics and Space Administration. Lewis Research Center, Cleveland, OH.

EFFECTS OF A NONCOPLANAR BIPHENYLDIAMINE ON THE PROCESSING AND PROPERTIES OF ADDITION POLYIMIDES

KATHY C. CHUANG, RAYMOND D. VANNUCCI, and BRAD W. MOORE (Akron Univ., OH.) 1992 4 p Proposed for presentation at the 203rd National Meeting of the American Chemical Society Symposium on Advances in Polymer Matrix Composites, San Francisco, CA, 5-10 Apr. 1992 (Contract RTOP 510-01-50) (NASA-TM-105383; E-6720; NAS 1.15:105383) Avail: CASI HC A01/MF A01

Addition curing polyimides, prepared from noncoplanar 2,2'-bis(trifluoromethyl) 4,4' diaminobiphenyl (BTDB) with various dianhydrides were evaluated as high temperature polymer matrix materials. T sub g of these polymers were measured by mechanical methods as well as by thermal mechanical analysis. Physical and mechanical properties as well as the thermo-oxidative stability of neat resins and the corresponding G40-600 graphite fiber reinforced composites were compared to that of PMR-II-50 and V-CAP-75. Author

N92-16025* National Aeronautics and Space Administration. Lewis Research Center, Cleveland, OH.

METHOD OF INTERCALATING LARGE QUANTITIES OF FIBROUS STRUCTURES Patent

JAMES R. GAIER, inventor (to NASA) 17 Dec. 1991 7 p Filed 2 Nov. 1990 (NASA-CASE-LEW-15077-1; US-PATENT-5,073,412; US-PATENT-APPL-SN-608493; US-PATENT-CLASS-427-294; US-PATENT-CLASS-118-416; US-PATENT-CLASS-252-502; US-PATENT-CLASS-423-447.2; US-PATENT-CLASS-423-448; US-PATENT-CLASS-423-460; US-PATENT-CLASS-427-443.2) Avail: US Patent and Trademark Office

A method of intercalating large quantities of fibrous structures uses a rotatable reaction chamber containing a liquid phase intercalate. The intercalate liquid phase is controlled by appropriately heating, cooling, or pressurizing the reaction. Rotation of the chamber containing the fiber sample enables total submergence of the fiber during intercalation. Intercalated graphite fibers having metal-like resistivities are achieved and are

conceivably useful as electrical conductors.

Official Gazette of the U.S. Patent and Trademark Office

N92-16036*# National Aeronautics and Space Administration. Lewis Research Center, Cleveland, OH.

DESKTOP FIBER PUSH-OUT APPARATUS

JEFFREY I. ELDRIDGE Dec. 1991 12 p (Contract RTOP 510-01-04) (NASA-TM-105341; E-6709; NAS 1.15:105341) Avail: CASI HC A03/MF A01

A desktop fiber push-out was developed which offers the advantage of being compact, easy to operate, and inexpensive. A description of the design and operation of this apparatus is given. Author

N92-16037*# National Aeronautics and Space Administration. Lewis Research Center, Cleveland, OH.

HIGH TEMPERATURE STRUCTURAL FIBERS: STATUS AND NEEDS

JAMES A. DICARLO Sep. 1991 12 p Presented at the Fiber Producer Conference, Greenville, SC, 6-9 May 1991; sponsored by Clemson Univ. (Contract RTOP 510-01-50) (NASA-TM-105174; E-6511; NAS 1.15:105174) Avail: CASI HC A03/MF A01

The key to high temperature structural composites is the selection and incorporation of continuous fiber reinforcement with optimum mechanical, physical, and chemical properties. Critical fiber property needs are high strength, high stiffness, and retention of these properties during composite fabrication and use. However, unlike polymeric composites where all three requirements are easily achieved with a variety of commercially available carbon-based fibers, structural fibers with sufficient stiffness and strength retention for high temperature metal, intermetallic, and ceramic composites are not available. The objective here is to discuss in a general manner the thermomechanical stability problem for current high performance fibers which are based on silicon and alumina compositions. This is accomplished by presenting relevant fiber property data with a brief discussion of potential underlying mechanisms. From this general overview, some possible materials engineering approaches are suggested which may lead to minimization and/or elimination of this critical stability problem for current high temperature fibers. Author

N92-17861*# National Aeronautics and Space Administration. Lewis Research Center, Cleveland, OH.

INTERCALATED HYBRID GRAPHITE FIBER COMPOSITE Patent Application

JAMES R. GAIER, inventor (to NASA) 25 Nov. 1991 13 p (NASA-CASE-LEW-15241-1; NAS 1.71:LEW-15241-1; US-PATENT-APPL-SN-798464) Avail: CASI HC A03/MF A01

The invention is directed to a highly conductive lightweight hybrid material and methods of producing the same. The hybrid composite is obtained by weaving strands of a high strength carbon or graphite fiber into a fabric-like structure, depositing a layer of carbon onto the structure, heat treating the structure to graphitize the carbon layer, and intercalating the graphitic carbon layer structure. A laminate composite material useful for protection against lightning strikes comprises at least one layer of the hybrid material over at least one layer of high strength carbon or graphite fibers. The composite material of the present invention is compatible with matrix compounds, has a coefficient of thermal expansion which is the same as underlying fiber layers, and is resistant to galvanic corrosion in addition to being highly conductive. These materials are useful in the aerospace industry, in particular as lightning strike protection for airplanes. NASA

N92-18439*# National Aeronautics and Space Administration. Lewis Research Center, Cleveland, OH.

CVD OF SILICON CARBIDE ON STRUCTURAL FIBERS: MICROSTRUCTURE AND COMPOSITION

LISA C. VEITCH, FRANCIS M. TEREPA, and SULEYMAN A. GOKOGLU 1992 7 p Presented at the 1991 Fall Meeting of

24 COMPOSITE MATERIALS

the Materials Research Society, Boston, MA, 2-6 Dec. 1991
(Contract RTOP 510-01-01)
(NASA-TM-105385; E-6770; NAS 1.15:105385) Avail: CASI HC
A02/MF A01

Structural fibers are currently being considered as reinforcements for intermetallic and ceramic materials. Some of these fibers, however, are easily degraded in a high temperature oxidative environment. Therefore, coatings are needed to protect the fibers from environmental attack. Silicon carbide (SiC) was chemically vapor deposited (CVD) on Textron's SCS6 fibers. Fiber temperatures ranging from 1350 to 1500 C were studied. Silane (SiH₄) and propane (C₂H₆) were used for the source gases and different concentrations of these source gases were studied. Deposition rates were determined for each group of fibers at different temperatures. Less variation in deposition rates were observed for the dilute source gas experiments than the concentrated source gas experiments. A careful analysis was performed on the stoichiometry of the CVD SiC coating using electron microprobe. Microstructures for the different conditions were compared. At 1350 C, the microstructures were similar; however, at higher temperatures, the microstructure for the more concentrated source gas group were porous and columnar in comparison to the cross sections taken from the same area for the dilute source gas group. Author

N92-19595*# National Aeronautics and Space Administration. Lewis Research Center, Cleveland, OH.

TOWARDS THE DEVELOPMENT OF MICROMECHANICS EQUATIONS FOR CERAMIC MATRIX COMPOSITES VIA FIBER SUBSTRUCTURING

P. L. N. MURTHY and C. C. CHAMIS Feb. 1992 21 p
(Contract RTOP 510-10-50)
(NASA-TM-105246; E-6574; NAS 1.15:105246) Avail: CASI HC
A03/MF A01

A generic unit cell model which includes a unique fiber substructuring concept is proposed for the development of micromechanics equations for continuous fiber reinforcement ceramic composites. The unit cell consists of three constituents: fiber, matrix, and an interphase. In the present approach, the unit cell is further subdivided into several slices and the equations of micromechanics are derived for each slice. These are subsequently integrated to obtain ply level properties. A stand alone computer code containing the micromechanics model as a module is currently being developed specifically for the analysis of ceramic matrix composites. Towards this development, equivalent ply property results for a SiC/Ti-15-3 composite with 0.5 fiber volume ratio are presented and compared with those obtained from customary micromechanics models to illustrate the concept. Also, comparisons with limited experimental data for the ceramic matrix composite, SiC/RBSN (Reaction Bonded Silicon Nitride) with a 0.3 fiber volume ratio are given to validate the concepts. Author

N92-20039*# National Aeronautics and Space Administration. Lewis Research Center, Cleveland, OH.

STRUCTURE-TO-PROPERTY RELATIONSHIPS IN ADDITION CURED POLYMERS. 4: CORRELATIONS BETWEEN THERMO-OXIDATIVE WEIGHT LOSSES OF NORBORNENYL CURED POLYIMIDE RESINS AND THEIR COMPOSITES

WILLIAM B. ALSTON 1992 12 p Proposed for presentation at the 203rd National Meeting of the American Chemical Society, Symposium on Advances in Polymer Matrix Composites, San Francisco, CA, 5-10 Apr. 1992
(Contract DA PROJ. 1L1-61102-AH-45; RTOP 510-01-50)
(NASA-TM-105553; E-6876; NAS 1.15:105553;
AVSCOM-TR-92-C-002; AD-A253050) Avail: CASI HC A03/MF
A01

Relationships are identified between the thermo-oxidative stability (TOS) at 316 C of a wide variety of PMR (polymerization of monomeric reactants) addition cured polyimide resins and their corresponding graphite fiber composites. Weight loss results at 316 C confirmed the expected relationship of increasing aliphatic endcap content with decreasing TOS. Moreover, the resin TOS study also showed an unexpected linear correlation of decreasing

weight loss to increasing ratio of benzylic diamine to aliphatic endcap in the range of the stoichiometries studied. Only after long term 316 C aging does the dianhydride used with the benzylic diamines become an additional factor in influencing the amount of PMR resin and composite weight losses. Also, the benzylic systems consistently showed much lower resin and composite weight losses at 316 C than the corresponding nonbenzylic norbornenyl resins and composites, except when the nonbenzylic diamine monomer does not contain a connecting group. Instead, this diamine resulted in a 316 C resin and composite weight loss that was only competitive with benzylic type diamines. Results show excellent correlation between TOS of all graphite fiber PMR composites and resins. Author

N92-20841*# National Aeronautics and Space Administration. Lewis Research Center, Cleveland, OH.

EFFECT OF HEAT TREATMENT ON STIFFNESS AND DAMPING OF SiC/TI-15-3

JOSEPH E. GRADY and BRADLEY A. LERCH 1992 10 p
Proposed for presentation at the 1992 Winter Annual Meeting of the ASME, Anaheim, CA, 8-13 Nov. 1992
(Contract RTOP 505-63-00)
(NASA-TM-105564; E-6888; NAS 1.15:105564) Avail: CASI HC
A02/MF A01

The effect of heat treatment on material properties of SiC/Ti-15-3 was measured by vibration tests. Heat treatment changes the microstructure, which was found to stiffen the matrix and reduce its damping capacity. Test results indicate how these changes in the matrix affect the corresponding properties of the composite. Measurements show that heat treatment affects damping properties of the composite to a greater extent than stiffness properties. The extent of change in mechanical properties is shown to depend on heat treatment temperature and exposure time. Author

N92-21725* National Aeronautics and Space Administration. Lewis Research Center, Cleveland, OH.

COMPOSITE THERMAL BARRIER COATING Patent
ISIDOR ZAPLATYNSKY, inventor (to NASA) 14 Jan. 1992 4 p
Filed 31 Jul. 1990 Supersedes N91-13500 (29 - 5, p 632)
(NASA-CASE-LEW-14999-1; US-PATENT-5,080,977;
US-PATENT-APPL-SN-560926; US-PATENT-CLASS-428-432;
US-PATENT-CLASS-428-212; US-PATENT-CLASS-428-213;
US-PATENT-CLASS-428-426; US-PATENT-CLASS-428-433;
US-PATENT-CLASS-428-469; US-PATENT-CLASS-428-472.2)
Avail: US Patent and Trademark Office

A composite thermal barrier coating for a substrate is presented. The coating is comprised of a first layer that includes a ceramic material and a second layer that includes a ceramic material impregnated with glass. The glass is a ternary eutectic. The glass consists of about 14.6 weight percent Al₂O₃, about 23.3 weight percent CaO, and about 62.1 weight percent SiO₂. The ceramic materials may include yttria-stabilized zirconia.
Official Gazette of the U.S. Patent and Trademark Office

N92-22513*# National Aeronautics and Space Administration. Lewis Research Center, Cleveland, OH.

HIGH-TEMPERATURE POLYMER MATRIX COMPOSITES
MICHAEL A. MEADOR *in its* Aeropropulsion 1987 p 45-54 Feb. 1990
Avail: CASI HC A02/MF A04

Polymers research at the NASA Lewis Research Center has produced high-temperature, easily processable resin systems, such as PMR-15. In addition, the Polymers Branch has investigated ways to improve the mechanical properties of polymers and the microcracking resistance of polymer matrix composites in response to industry need for new and improved aeropropulsion materials. Current and future research in the Polymers Branch is aimed at advancing the upper use temperature of polymer matrix composites to 700 F and beyond by developing new resins, by examining the use of fiber reinforcements other than graphite, and by developing coatings for polymer matrix composites to increase their oxidation resistance. D.R.D.

N92-22515*# National Aeronautics and Space Administration. Lewis Research Center, Cleveland, OH.

DEVELOPMENT OF A NEW GENERATION OF HIGH-TEMPERATURE COMPOSITE MATERIALS

P. K. BRINDLEY *In its* Aeropropulsion 1987 p 65-78 Feb. 1990

Avail: CASI HC A03/MF A04

Intermetallic matrix composites proposed to meet advanced aeropropulsion requirements are discussed. The powder metallurgy fabrication process currently being used to produce these intermetallic matrix composites will be presented, as will properties of one such composite, SiC/Ti3Al+Nb. In addition, the direction of future research will be outlined, including plans for enhanced fabrication of intermetallic composites by the arc-spray technique and fiber development by the floating-zone process. D.R.D.

N92-22762*# National Aeronautics and Space Administration. Lewis Research Center, Cleveland, OH.

COMPOSITE OVERWRAPPED NICKEL-HYDROGEN PRESSURE VESSELS

JOHN REAGAN and JOE LEWIS (TRW, Inc., Redondo Beach, CA.) *In* NASA. Marshall Space Flight Center, The 1991 NASA Aerospace Battery Workshop p 471-484 Feb. 1992

Avail: CASI HC A03/MF A10

The presentation is made in viewgraph format, the first of which states the purpose, which is to stimulate interest in composite overwrapped pressure vessel technology as applied to nickel hydrogen battery pressure vessels. The next viewgraph presents the history of nickel hydrogen pressure vessels over the last 15 years including materials, operating conditions, and market expansion to internationals. Basic materials properties are itemized such as thermal conductivity, corrosion resistance, and strength to weight ratio. The monolithic and composite overwrapped construction approaches are compared. A detailed description is presented of the advantages of composite overwrapped pressure vessels showing weight savings, manufacturing schedule reductions, and improved fatigue life. A discussion is also presented of B-1 application, the wide range of usable materials, and a sketch of a possible optimized design. E.R.

N92-23194*# National Aeronautics and Space Administration. Lewis Research Center, Cleveland, OH.

PROGRESSIVE FRACTURE OF POLYMER MATRIX COMPOSITE STRUCTURES: A NEW APPROACH

C. C. CHAMIS, P. L. N. MURTHY, and L. MINNETYAN (Clarkson Univ., Potsdam, NY.) 1992 22 p Presented at the 14th Annual Energy-Sources Technology Conference and Exhibition, Houston, TX, 26-29 Jan. 1992; sponsored by ASME (Contract RTOP 505-63-53)

(NASA-TM-105574; E-6900; NAS 1.15:105574) Avail: CASI HC A03/MF A01

A new approach independent of stress intensity factors and fracture toughness parameters has been developed and is described for the computational simulation of progressive fracture of polymer matrix composite structures. The damage stages are quantified based on physics via composite mechanics while the degradation of the structural behavior is quantified via the finite element method. The approach account for all types of composite behavior, structures, load conditions, and fracture processes starting from damage initiation, to unstable propagation and to global structural collapse. Results of structural fracture in composite beams, panels, plates, and shells are presented to demonstrate the effectiveness and versatility of this new approach. Parameters and guidelines are identified which can be used as criteria for structural fracture, inspection intervals, and retirement for cause. Generalization to structures made of monolithic metallic materials are outlined and lessons learned in undertaking the development of new approaches, in general, are summarized. Author

N92-23195*# National Aeronautics and Space Administration. Lewis Research Center, Cleveland, OH.

INFLUENCE OF ENGINEERED INTERFACES ON RESIDUAL STRESSES AND MECHANICAL RESPONSE IN METAL MATRIX COMPOSITES

STEVEN M. ARNOLD and THOMAS E. WILT (Toledo Univ., OH.) Mar. 1992 27 p Proposed for presentation at the Fourth International Conference on Composite Interfaces, Cleveland, OH, 26-29 May 1992; sponsored by Case Western Reserve Univ. (Contract RTOP 510-01-50)

(NASA-TM-105438; E-6866; NAS 1.15:105438) Avail: CASI HC A03/MF A01

Because of the inherent coefficient of thermal expansion (CTE) mismatch between fiber and matrix within metal and intermetallic matrix composite systems, high residual stresses can develop under various thermal loading conditions. These conditions include cooling from processing temperature to room temperature as well as subsequent thermal cycling. As a result of these stresses, within certain composite systems, radial, circumferential, and/or longitudinal cracks have been observed to form at the fiber matrix interface region. A number of potential solutions for reducing this thermally induced residual stress field have been proposed recently. Examples of some potential solutions are high CTE fibers, fiber preheating, thermal anneal treatments, and an engineered interface. Here the focus is on designing an interface (by using a compensating/compliant layer concept) to reduce or eliminate the thermal residual stress field and, therefore, the initiation and propagation of cracks developed during thermal loading. Furthermore, the impact of the engineered interface on the composite's mechanical response when subjected to isothermal mechanical load histories is examined. Author

N92-25346*# National Aeronautics and Space Administration. Lewis Research Center, Cleveland, OH.

COMPOSITES OF LOW-DENSITY TRIALUMINIDES: PARTICULATE AND LONG FIBER REINFORCEMENTS

K. S. KUMAR (Martin Marietta Labs., Baltimore, MD.), M. S. DIPIETRO (Martin Marietta Labs., Baltimore, MD.), S. A. BROWN (Martin Marietta Labs., Baltimore, MD.), and J. D. WHITTENBERGER Apr. 1992 99 p

(Contract NAS3-26069; RTOP 510-01-50) (NASA-TM-105628; E-6970; NAS 1.15:105628) Avail: CASI HC A05/MF A02

An examination of the ternary L1(sub 2) trialuminides, Al66Ti25Mn9, Al67Ti25Cr8, and Al22Ti8Fe3 in compression, bending, and tension revealed that none of these compounds exhibited a desirable balance of strength, ductility, and oxidation resistance. Subsequently, specific quaternary and quinary compositions were cast, homogenized, and isothermally forged. Both, the monolithic material and its particulate reinforced counterparts were examined in compression, three point bend, and tension as a function of temperature, and at high temperatures as a function of strain rate. An alternate approach that was examined in this program to enhance the low temperature damage tolerance of these materials was to incorporate long refractory metal wires in the matrix. In summary, it appears that of the various matrix compositions examined, ternary Al66Ti25Mn9 exhibits the best balance in strength, ductility, and oxidation resistance. Although the idea of refractory metal wire reinforcement is an attractive one, a successful combination remains to be identified. Author

N92-25754*# National Aeronautics and Space Administration. Lewis Research Center, Cleveland, OH.

FREE VIBRATIONS OF DELAMINATED BEAMS

M.-H. H. SHEN (Ohio State Univ., Columbus.) and J. E. GRADY Apr. 1992 27 p

(Contract RTOP 505-63-00) (NASA-TM-105582; E-6909; NAS 1.15:105582) Avail: CASI HC A03/MF A01

Free vibration of laminated composite beams is studied. The effect of interply delaminations on natural frequencies and mode shapes is evaluated both analytically and experimentally. A

24 COMPOSITE MATERIALS

generalized vibrational principle is used to formulate the equation of motion and associated boundary conditions for the free vibration of a composite beam with a delamination of arbitrary size and location. The effect of coupling between longitudinal vibration and bending vibration is considered. This coupling effect is shown to significantly affect the calculated natural frequencies and mode shapes of the delaminated beam. Author

N92-25996*# National Aeronautics and Space Administration. Lewis Research Center, Cleveland, OH.

X RAY ATTENUATION MEASUREMENTS FOR HIGH-TEMPERATURE MATERIALS CHARACTERIZATION AND IN-SITU MONITORING OF DAMAGE ACCUMULATION Ph.D. Thesis - Cleveland State Univ., 1991

GEORGE Y. BAAKLINI Mar. 1992 221 p Original contains color illustrations

(Contract RTOP 510-01-50)

(NASA-TM-105577; E-6652; NAS 1.15:105577)

The scope of this dissertation is to develop and apply x ray attenuation measurement systems that are capable of: (1) characterizing density variations in high-temperature materials, e.g., monolithic ceramics, ceramic and intermetallic matrix composites, and (2) noninvasively monitoring damage accumulation and failure sequences in ceramic matrix composites under room temperature tensile testing. This dissertation results in the development of: (1) a point scan digital radiography system, and (2) an in-situ x ray material testing system. Radiographic evaluation before, during, and after loading shows the effect of preexisting volume flaws on the fracture behavior of composites. Results show that x ray film radiography can monitor damage accumulation during tensile loading. Matrix cracking, fiber matrix debonding, fiber bridging, and fiber pullout are imaged throughout the tensile loading of the specimens. Further in-situ radiography is found to be a practical technique for estimating interfacial shear strength between the silicon carbide fibers and the reaction bonded silicon nitride matrix. It is concluded that pretest, in-situ, and post test x ray imaging can provide for greater understanding of ceramic matrix composite mechanical behavior. Author

N92-29660*# National Aeronautics and Space Administration. Lewis Research Center, Cleveland, OH.

APPROACHES TO POLYMER-DERIVED CMC MATRICES

FRANCES I. HURWITZ 1992 9 p Presented at the Society for the Advancement of Materials and Process Engineering, Toronto, Ontario, 20-22 Oct. 1992

(Contract RTOP 505-63-40)

(NASA-TM-105754; E-7165; NAS 1.15:105754) Avail: CASI HC A02/MF A01

The use of polymeric precursors to ceramics permits the fabrication of large, complex-shaped ceramic matrix composites (CMC's) at temperatures which do not degrade the fiber. Processing equipment and techniques readily available in the resin matrix composite industry can be adapted for CMC fabrication using this approach. Criteria which influence the choice of candidate precursor polymers, the use of fillers, and the role of fiber architecture and ply layup are discussed. Three polymer systems, polycarbosilanes, polysilazanes, and polysilsesquioxanes, are compared as candidate ceramic matrix precursors. Author

N92-30779*# National Aeronautics and Space Administration. Lewis Research Center, Cleveland, OH.

METAL MATRIX COMPOSITE ANALYZER (METCAN) USER'S MANUAL, VERSION 4.0

H.-J. LEE, P. K. GOTSIS, P. L. N. MURTHY, and D. A. HOPKINS Mar. 1992 176 p

(Contract RTOP 510-01-50)

(NASA-TM-105244; E-6571; NAS 1.15:105244) Avail: CASI HC A09/MF A02

The Metal Matrix Composite Analyzer (METCAN) is a computer code developed at Lewis Research Center to simulate the high temperature nonlinear behavior of metal matrix composites. An updated version of the METCAN User's Manual is presented. The manual provides the user with a step by step outline of the

procedure necessary to run METCAN. The preparation of the input file is demonstrated, and the output files are explained. The sample problems are presented to highlight various features of METCAN. An overview of the geometric conventions, micromechanical unit cell, and the nonlinear constitutive relationships is also provided. Author

N92-30986*# National Aeronautics and Space Administration. Lewis Research Center, Cleveland, OH.

ISOTHERMAL AGING EFFECTS ON PMR-15 RESIN

KENNETH J. BOWLES, DOUGLAS JAYNE (Case Western Reserve Univ., Cleveland, OH.), and TODD A. LEONHARDT (Sverdrup Technology, Inc., Brook Park, OH.) Jul. 1992 22 p

(Contract RTOP 510-01-50)

(NASA-TM-105648; E-7007; NAS 1.15:105648) Avail: CASI HC A03/MF A01

Specimens of PMR-15 polyimide neat resin were aged in air at temperatures of 288, 316, and 343 C. Weight losses and dimensional changes were monitored during the course of the exposure time. Physical changes were also observed by optical and electron microscopy. It was found that polyimide polymer degradation occurred within a thin surface layer that developed and grew during thermal aging. The cores of the polymer specimens were protected from oxidative degradation, and they were relatively unchanged by the thermal treatment. Surface cracking was observed at 343 C and was probably due to an interaction between voids and stresses that developed in the surface layer. Author

N92-31506*# National Aeronautics and Space Administration. Lewis Research Center, Cleveland, OH.

COMPUTATIONAL SIMULATION OF INTERMINGLED-FIBER HYBRID COMPOSITE BEHAVIOR

SUBODH K. MITAL (Toledo Univ., OH.) and CHRISTOS C. CHAMIS Mar. 1992 11 p Presented at the 37th International SAMPE Symposium and Exhibition, Anaheim, CA, 9-12 Mar. 1992

(Contract RTOP 510-01-50)

(NASA-TM-105666; E-7028; NAS 1.15:105666) Avail: CASI HC A03/MF A01

Three-dimensional finite-element analysis and a micro-mechanics based computer code ICAN (Integrated Composite Analyzer) are used to predict the composite properties and microstresses of a unidirectional graphite/epoxy primary composite with varying percentages of S-glass fibers used as hybridizing fibers at a total fiber volume of 0.54. The three-dimensional finite-element model used in the analyses consists of a group of nine fibers, all unidirectional, in a three-by-three unit cell array. There is generally good agreement between the composite properties and microstresses obtained from both methods. The results indicate that the finite-element methods and the micromechanics equations embedded in the ICAN computer code can be used to obtain the properties of intermingled fiber hybrid composites needed for the analysis/design of hybrid composite structures. However, the finite-element model should be big enough to be able to simulate the conditions assumed in the micromechanics equations. Author

N92-32234*# National Aeronautics and Space Administration. Lewis Research Center, Cleveland, OH.

EFFECTS OF FIBER AND INTERFACIAL LAYER ARCHITECTURES ON THE THERMOPLASTIC RESPONSE OF METAL MATRIX COMPOSITES

MAREK-JERZY PINDERA (Virginia Univ., Charlottesville.), ALAN D. FREED, and STEVEN M. ARNOLD Aug. 1992 38 p

(Contract RTOP 519-01-50)

(NASA-TM-105802; E-7232; NAS 1.15:105802) Avail: CASI HC A03/MF A01

Examined here is the effect of fiber and interfacial layer morphologies on thermal fields in metal matrix composites (MMCs). A micromechanics model based on an arbitrarily layered concentric cylinder configuration is used to calculate thermal stress fields in MMCs subjected to spatially uniform temperature changes. The fiber is modelled as a layered material with isotropic or orthotropic elastic layers, whereas the surrounding matrix, including interfacial

layers, is treated as a strain-hardening, elastoplastic, von Mises solid with temperature-dependent parameters. The solution to the boundary-value problem of an arbitrarily layered concentric cylinder under the prescribed thermal loading is obtained using the local/global stiffness matrix formulation originally developed for stress analysis of multilayered elastic media. Examples are provided that illustrate how the morphology of the SCS6 silicon carbide fiber and the use of multiple compliant layers at the fiber/matrix interface affect the evolution of residual stresses in SiC/Ti composites during fabrication cool-down. Author

N92-32466*# National Aeronautics and Space Administration. Lewis Research Center, Cleveland, OH.

COMPUTATIONAL SIMULATION OF MATRIX MICRO-SLIP BANDS IN SiC/TI-15 COMPOSITE

S. K. MITAL (Toledo Univ., OH.), H.-J. LEE, P. L. N. MURTHY, and C. C. CHAMIS 1992 9 p Proposed for presentation at the 1992 Winter Annual Meeting of ASME, Anaheim, CA, 8-13 Nov. 1992

(Contract RTOP 505-63-5B)

(NASA-TM-105762; E-7179; NAS 1.15:105762) Avail: CASI HC A02/MF A01

Computational simulation procedures are used to identify the key deformation mechanisms for (0)(sub 8) and (90)(sub 8) SiC/Ti-15 metal matrix composites. The computational simulation procedures employed consist of a three-dimensional finite-element analysis and a micromechanics based computer code METCAN. The interphase properties used in the analysis have been calibrated using the METCAN computer code with the (90)(sub 8) experimental stress-strain curve. Results of simulation show that although shear stresses are sufficiently high to cause the formation of some slip bands in the matrix concentrated mostly near the fibers, the nonlinearity in the composite stress-strain curve in the case of (90)(sub 8) composite is dominated by interfacial damage, such as microcracks and debonding rather than microplasticity. The stress-strain curve for (0)(sub 8) composite is largely controlled by the fibers and shows only slight nonlinearity at higher strain levels that could be the result of matrix microplasticity. Author

N92-32531*# National Aeronautics and Space Administration. Lewis Research Center, Cleveland, OH.

COMPUTATIONAL SIMULATION OF STRUCTURAL FRACTURE IN FIBER COMPOSITES

C. C. CHAMIS and P. L. N. MURTHY *In* NASA. Langley Research Center, Eighth DOD/NASA/FAA Conference on Fibrous Composites in Structural Design, Part 1 p 355-371 Sep. 1990 Avail: CASI HC A03/MF A03

A methodology was developed for the computational simulation of structural fracture in fiber composites. This methodology consists of step-by-step procedures for mixed mode fracture in generic components and of an integrated computer code, Composite Durability Structural Analysis (CODSTRAN). The generic types of composite structural fracture include single and combined mode fracture in beams, laminate free-edge delamination fracture, and laminate center flaw progressive fracture. Structural fracture is assessed in one or all of the following: (1) the displacements increase very rapidly; (2) the frequencies decrease very rapidly; (3) the buckling loads decrease very rapidly; or (4) the strain energy release rate increases very rapidly. These rapid changes are herein assumed to denote imminent structural fracture. Based on these rapid changes, parameters/guidelines are identified which can be used as criteria for structural fracture, inspection intervals, and retirement for cause. Author

N92-34208*# National Aeronautics and Space Administration. Lewis Research Center, Cleveland, OH.

HEAT TRANSFER DEVICE Patent Application

BRUCE A. BANKS, inventor (to NASA) and JAMES R. GAIER, inventor (to NASA) 11 May 1992 11 p (NASA-CASE-LEW-14162-3; NAS 1.71:LEW-14162-3; US-PATENT-APPL-SN-880851) Avail: CASI HC A03/MF A01

Gas derived graphite fibers generated by the decomposition of an organic gas are joined with a suitable binder. This produces a

high thermal conductivity composite material which passively conducts heat from a source, such as a semiconductor, to a heat sink. The fibers may be intercalated. The intercalate can be halogen or halide salt, alkaline metal, or any other species which contributes to the electrical conductivity improvement of the graphite fiber. The fibers are bundled and joined with a suitable binder to form a high thermal conductivity composite material device. The heat transfer device may also be made of intercalated highly oriented pyrolytic graphite and machined, rather than made of fibers. NASA

25

INORGANIC AND PHYSICAL CHEMISTRY

Includes chemical analysis, e.g., chromatography; combustion theory; electrochemistry; and photochemistry.

A92-12897* Princeton Univ., NJ.

SOME FURTHER OBSERVATIONS ON DROPLET COMBUSTION CHARACTERISTICS - NASA LERC-PRINCETON RESULTS

MUN Y. CHOI, SEOG Y. CHO, FREDERICK L. DRYER (Princeton University, NJ), and JOHN B. HAGGARD, JR. (NASA, Lewis Research Center, Cleveland, OH) *In*: AIAA/IKI Microgravity Science Symposium, 1st, Moscow, USSR, May 13-17, 1991, Proceedings 1991 11 p refs (Contract NAS3-24640)

Copyright

Experimental and numerical studies are reviewed which are designed to examine the effects of droplet/gas motion, product-intermediate absorption, extinction, and sooting on droplet combustion. The experimental work at the NASA-Lewis Research Center involves a 2.2-s droptower for investigating microgravitational effects of droplet combustion over a relatively extended range. The droplet-gas velocities are very low because the spherically symmetrical nature of the major combustion processes produces a quiescent environment. The refined experimental results are combined with numerical modeling based on a technique that is fully transient, comprehensive, and has few empirical simplifications. The combination of techniques improves the present understanding of convection-induced effects, reducing soot formation, and promoting quiescent droplet combustion. C.C.S.

A92-12898* Mississippi State Univ., Mississippi State.

OPPOSED FLOW FLAME SPREAD IN NORMAL, ENHANCED AND REDUCED GRAVITY

ROBERT A. ALTENKIRCH, SUBRATA BHATTACHARJEE, JEFF WEST (Mississippi State University, Mississippi State), and SANDRA L. OLSON (NASA, Lewis Research Center, Cleveland, OH) *In*: AIAA/IKI Microgravity Science Symposium, 1st, Moscow, USSR, May 13-17, 1991, Proceedings 1991 9 p refs (Contract NAS3-23901)

Copyright

Experimental and theoretical aspects of opposed-flow flame spread over solid fuels are presented with emphasis on the microgravity environments of spacecraft. For high opposing flow velocities, spread rate decreases with increasing velocity eventually leading to flame blowoff due to kinetic effects. At low opposing flow velocities, where diffusional effects are slowed and radiation becomes important, flame spread rate increases with increasing flow velocity. Extinction at low velocities is due to radiative effects. Modeling efforts that include radiation, both solid surface radiation and gas-phase radiation, predict qualitatively the experimental trends observed. Computationally, gas-phase radiation is conveniently included in solution of the conservation equations by employing a Plank mean absorption coefficient, a fraction of radiation that is fed back to the surface, and a shape function that describes the radiative flux distribution along the surface. Author

Author

25 INORGANIC AND PHYSICAL CHEMISTRY

A92-16601* National Aeronautics and Space Administration. Lewis Research Center, Cleveland, OH.

THE IMPLICATIONS OF EXPERIMENTALLY CONTROLLED GRAVITATIONAL ACCELERATIONS FOR COMBUSTION SCIENCE

KURT R. SACKSTEDER (NASA, Lewis Research Center, Cleveland, OH) IN: Symposium (International) on Combustion, 23rd, Orleans, France, July 22-27, 1990, Proceedings 1991 8 p refs

Copyright

An overview of basic combustion problems which have been investigated under the condition of reduced gravity is presented to identify promising research directions. Attention is given to the broad categories of gas-jet diffusion flames, droplet combustions, particle clouds, flame spreading over liquid pools, smoldering, and flame spreading over solid fuels. Fire safety in spacecraft is the primary application that is addressed by the studies of combustion under microgravity. The need for more complete testing of the issues discussed in orbiting spacecraft is identified in the light of limited earth-based testing. Attention is also directed toward the need for advanced diagnostic methods for in-flight and other combustion investigations. C.C.S.

A92-16602* Princeton Univ., NJ.

OBSERVATIONS ON A SLOW BURNING REGIME FOR HYDROCARBON DROPLETS - N-HEPTANE/AIR RESULTS

MUN Y. CHOI, FREDERICK L. DRYER (Princeton University, NJ), and JOHN B. HAGGARD, JR. (NASA, Lewis Research Center, Cleveland, OH) IN: Symposium (International) on Combustion, 23rd, Orleans, France, July 22-27, 1990, Proceedings 1991 8 p refs

(Contract NAS3-24640)

Copyright

Experiments on n-heptane/air droplet combustion under reduced gravity have served as a benchmark for much of the existing theoretical efforts on the modeling of spherically-symmetric droplet burning. New experiments conducted in the NASA-Lewis Research Center 2.2 second droptower (at less than 10×10^{-5} g) which emphasize the production of spherically-symmetry and low relative droplet/gas convection produce burning rates in air (for about 1 mm droplets) as much as 40-percent lower than the classical result (0.78 sq mm/s). The burning rate is proportional to the measured droplet/gas relative velocity, and the observed functional dependence is much larger than predicted by published convective correlations. New results clearly indicate that the droplet/laboratory velocity does not correspond to the relative droplet/gas velocity. Thus, the convective effects on droplet combustion is not properly characterized by droplet motion alone. Differences in the burning rates are speculated to result from the effects of the accumulated soot as well as the asymmetry (caused by convection) in the temperature and species distributions surrounding the droplet. Author

A92-16609* National Aeronautics and Space Administration. Lewis Research Center, Cleveland, OH.

AN INVESTIGATION OF FLAME SPREAD OVER SHALLOW LIQUID POOLS IN MICROGRAVITY AND NONAIR ENVIRONMENTS

HOWARD D. ROSS and RAYMOND G. SOTOS (NASA, Lewis Research Center, Cleveland, OH) IN: Symposium (International) on Combustion, 23rd, Orleans, France, July 22-27, 1990, Proceedings 1991 7 p refs

Copyright

Experiments of interest to combustion fundamentals and spacecraft fire safety investigated flame spread of alcohol fuels over shallow, 15 cm diameter pools in a 5.2 sec free-fall, microgravity facility. Results showed that, independent O₂ concentrations, alcohol fuel, and diluent types, microgravity flame spread rates were nearly identical to those corresponding normal-gravity flames for conditions where the normal gravity flames spread uniformly. This similarity indicated buoyancy-related convection in either phase does not affect flame spread, at least for the physical scale of the experiments. However, microgravity

extinction coincided with the onset conditions for pulsating spread in normal gravity, implicating gas phase, buoyant flow as a requirement for pulsating spread. When the atmospheric nitrogen was replaced with argon, the conditions for the onset of normal-gravity pulsating flame spread and microgravity flame extinction were changed, in agreement with the expected lowering of the flash point through the thermal properties of the diluent. Helium-diluted flames, however, showed unexpected results with a shift to apparently higher flash-point temperatures and high normal gravity pulsation amplitudes. Author

A92-16981* National Aeronautics and Space Administration. Lewis Research Center, Cleveland, OH.

COMBUSTION KINETICS AND SENSITIVITY ANALYSIS COMPUTATIONS

K. RADHAKRISHNAN (NASA, Lewis Research Center, Cleveland, OH) IN: Numerical approaches to combustion modeling 1991 46 p refs

(Contract NAG3-147; NAG3-294; NAS3-24105; NAS3-25266)

The stiff ordinary differential equation solution methods more commonly used for chemical kinetics problems are examined, and the efficiency and accuracy of several of the methods are compared by applying them to two combustion kinetics problems. The local sensitivity analysis methods developed to date are outlined, and their advantages and difficulties are briefly discussed. Examples are used to make comparisons among the different techniques. C.D.

A92-17296* Illinois Univ., Chicago.

OXIDATION-CHLORINATION OF BINARY NI-CR ALLOYS IN FLOWING AR-O₂-CL₂ GAS MIXTURES AT 1200 K

M. J. MCNALLAN, Y. Y. LEE, Y. W. CHANG (Illinois, University, Chicago), N. S. JACOBSON, and J. DOYCHAK (NASA, Lewis Research Center, Cleveland, OH) (Electrochemical Society, Meeting, Seattle, WA, Oct. 14-19, 1990) Electrochemical Society, Journal (ISSN 0013-4651), vol. 138, Dec. 1991, p. 3692-3696. Research supported by Illinois Dept. of Energy and Natural Resources. Dec. 1991 5 p refs

(Contract DE-FG02-85ER-45178)

Copyright

Nickel-chromium alloys are resistant to oxidation because of the selective oxidation of chromium to form a protective Cr₂O₃ scale. In chlorine-containing environments, volatile corrosion products can also be formed. The mixed oxidation-chlorination of Ni-4.5Cr, Ni-13.8Cr, and Ni-26.5Cr (by weight) alloys in Ar-O₂-Cl₂ gas mixtures is investigated using thermogravimetric analysis and atmospheric-pressure-sampling mass spectrometry, followed by examination of the corrosion products using scanning electron microscopy and X-ray diffraction analysis. The overall kinetics of the corrosion are affected by the relative amounts of oxides and chlorides formed and the composition of the oxide corrosion products. Author

A92-18484* National Aeronautics and Space Administration. Lewis Research Center, Cleveland, OH.

THE NASA MICROGRAVITY COMBUSTION SPACE EXPERIMENT PROGRAM

KURT SACKSTEDER (NASA, Lewis Research Center, Cleveland, OH) IAF, International Astronautical Congress, 42nd, Montreal, Canada, Oct. 5-11, 1991. 6 p. Oct. 1991 6 p refs

(IAF PAPER 91-398) Copyright

This paper summarizes the scientific objectives of the expanded microgravity combustion science program including efforts in laminar and turbulent premixed-gas flames, laminar and turbulent gas-jet diffusion flames, droplet combustion, smoldering, flame spreading, pool fires, and metals combustion. Secondly, the paper will summarize the flight hardware that is currently flying and new hardware being proposed to carry out this extensive program of microgravity combustion experiments. Author

A92-19300* Pennsylvania State Univ., University Park.
**OPTIMIZATION AND ANALYSIS OF LARGE CHEMICAL
 KINETIC MECHANISMS USING THE SOLUTION MAPPING
 METHOD - COMBUSTION OF METHANE**

MICHAEL FRENKLACH, HAI WANG (Pennsylvania State University, University Park), and MARTIN J. RABINOWITZ (NASA, Lewis Research Center, Cleveland, OH) Progress in Energy and Combustion Science (ISSN 0360-1285), vol. 18, no. 1, 1992, p. 47-73. Research supported by Gas Research Institute. 1992 27 p refs

Copyright

A method of systematic optimization, solution mapping, as applied to a large-scale dynamic model is presented. The basis of the technique is parameterization of model responses in terms of model parameters by simple algebraic expressions. These expressions are obtained by computer experiments arranged in a factorial design. The developed parameterized responses are then used in a joint multiparameter multidata-set optimization. A brief review of the mathematical background of the technique is given. The concept of active parameters is discussed. The technique is applied to determine an optimum set of parameters for a methane combustion mechanism. Five independent responses - comprising ignition delay times, pre-ignition methyl radical concentration profiles, and laminar premixed flame velocities - were optimized with respect to thirteen reaction rate parameters. The numerical predictions of the optimized model are compared to those computed with several recent literature mechanisms. The utility of the solution mapping technique in situations where the optimum is not unique is also demonstrated. Author

A92-25781*# National Aeronautics and Space Administration. Lewis Research Center, Cleveland, OH.

**GRAVITATIONAL INFLUENCES ON THE BEHAVIOR OF
 CONFINED DIFFUSION FLAMES**

U. HEGDE (NASA, Lewis Research Center, Cleveland; Sverdrup Technology, Inc., Brook Park, OH) and M. Y. BAHADORI (Science Applications International Corp., Thermal Sciences Div., Torrance, CA) AIAA, Aerospace Sciences Meeting and Exhibit, 30th, Reno, NV, Jan. 6-9, 1992. 9 p. Jan. 1992 9 p refs

(Contract NAS3-25266; NAS3-22822)

(AIAA PAPER 92-0334)

Closed form, mathematical representations for the shapes of laminar diffusion flames stabilized on two-dimensional slot burners are derived for arbitrary gravitational levels. The solution technique employs the Schvab-Zeldovich conserved species variable. Effects of gravity on the velocity field are incorporated through the momentum equation; these effects, in turn, influence the species field. The results reduce smoothly to the classical Burke-Schumann solution as gravity approaches zero. It is shown that both flame height and width increase with decreasing gravity levels. Several interesting cases are considered explicitly; these include effects of negative and extremely high values of gravity. In the latter case, it is shown that the flame collapses onto the burner surface. The analysis finds application in the modeling of steady and unsteady gas and solid propellant diffusion flames. Author

A92-26927*# National Aeronautics and Space Administration. Lewis Research Center, Cleveland, OH.

**MICROGRAVITY COMBUSTION OF ISOLATED N-DECANE
 AND N-HEPTANE DROPLETS**

MUN Y. CHOI, FREDERICK L. DRYER (Princeton University, NJ), JOHN M. CARD, FORMAN A. WILLIAMS (California, University, La Jolla), JOHN B. HAGGARD, and BRIAN A. BOROWSKI (NASA, Lewis Research Center, Cleveland, OH) AIAA, Aerospace Sciences Meeting and Exhibit, 30th, Reno, NV, Jan. 6-9, 1992. 10 p. Jan. 1992 10 p refs

(Contract NAG3-1231; NAG3-1081)

(AIAA PAPER 92-0242) Copyright

This paper presents recent experimental results on n-heptane droplet combustion from a 5.0 second Zero-Gravity Facility. For these experiments, droplet sizes from 1 mm to 1.75 mm were studied, oxygen mole fractions in nitrogen ranged from 12 to 21 percent, and the pressure was varied from 0.25 to 1 atm. Disruptive

burning mechanisms were observed in some of the experiments conducted in air environments. However, this behavior was inhibited by reducing the oxygen concentration and/or the system pressure. The above results suggest that combinations of lower oxygen indices and reduced ambient pressures are important to reducing the effects of sooting on droplet vaporization-rates. Author

A92-26928*# National Aeronautics and Space Administration. Lewis Research Center, Cleveland, OH.

**EFFECTS OF OXYGEN CONCENTRATION ON RADIATIVE
 LOSS FROM NORMAL-GRAVITY AND MICROGRAVITY
 METHANE DIFFUSION FLAMES**

M. Y. BAHADORI (Science Applications International Corp., Torrance, CA), RAYMOND B. EDELMAN (Rockwell International Corp., Rocketdyne Div., Canoga Park, CA), DENNIS P. STOCKER, RAYMOND G. SOTOS, and DAVID F. VAUGHAN (NASA, Lewis Research Center, Cleveland, OH) AIAA, Aerospace Sciences Meeting and Exhibit, 30th, Reno, NV, Jan. 6-9, 1992. 7 p. Jan. 1992 7 p refs

(Contract NAS3-22822; NCC3-157)

(AIAA PAPER 92-0243)

Laminar diffusion flames of methane, burning in quiescent oxidizing environments at atmospheric pressure, have been studied under both normal-gravity and microgravity conditions. Radiation from these flames is measured using a wide-view-angle, thermopile detector radiometer. The oxidizer was 18, 21, and 30 percent oxygen in nitrogen. Author

A92-29488* National Aeronautics and Space Administration. Lewis Research Center, Cleveland, OH.

**GLOBAL KINETIC CONSTANTS FOR THERMAL OXIDATIVE
 DEGRADATION OF A CELLULOSIC PAPER**

TAKASHI KASHIWAGI and HIDESABURO NAMBU (NIST, Building and Fire Research Laboratory, Gaithersburg, MD) Combustion and Flame (ISSN 0010-2180), vol. 88, March 1992, p. 345-368. Mar. 1992 24 p refs

(Contract NASA ORDER C-32000-K)

Copyright

Values of global kinetic constants for pyrolysis, thermal oxidative degradation, and char oxidation of a cellulosic paper were determined by a derivative thermal gravimetric study. The study was conducted at heating rates of 0.5, 1, 1.5, 3, and 5 C/min in ambient atmospheres of nitrogen, 0.28, 1.08, 5.2 percent oxygen concentrations, and air. Sample weight loss rate, concentrations of CO, CO₂, and H₂O in the degradation products, and oxygen consumption were continuously measured during the experiment. Values of activation energy, preexponential factor, orders of reaction, and yields of CO, CO₂, H₂O, total hydrocarbons, and char for each degradation reaction were derived from the results. Heat of reaction for each reaction was determined by differential scanning calorimetry. A comparison of the calculated CO, CO₂, H₂O, total hydrocarbons, sample weight loss rate, and oxygen consumption was made with the measured results using the derived kinetic constants, and the accuracy of the values of kinetic constants was discussed. Author

A92-30978* National Aeronautics and Space Administration. Lewis Research Center, Cleveland, OH.

**ELECTROCHEMICAL IMPREGNATION AND CYCLE LIFE OF
 LIGHTWEIGHT NICKEL ELECTRODES FOR
 NICKEL-HYDROGEN CELLS**

DORIS L. BRITTON (NASA, Lewis Research Center, Cleveland, OH) IN: International Power Sources Symposium, 34th, Cherry Hill, NJ, June 25-28, 1990, Proceedings 1990 4 p refs

Copyright

Development of a high specific energy nickel electrode is the main goal of the lightweight nickel electrode program at NASA-Lewis. The approach was to improve the nickel electrode by continuing combined in-house and contract efforts to develop a more efficient and lighter weight electrode for the nickel-hydrogen cell. Lightweight plaques are used as conductive supports for the nickel hydroxide active material. These plaques are commercial products that are fabricated into nickel electrodes by

25 INORGANIC AND PHYSICAL CHEMISTRY

electrochemically impregnating them with active material. The electrodes are life cycle tested in a low earth orbit regime at 40 and 80 percent depths-of-discharge. I.E.

A92-31849* National Aeronautics and Space Administration. Lewis Research Center, Cleveland, OH.

COSP - A COMPUTER MODEL OF CYCLIC OXIDATION

CARL E. LOWELL, CHARLES A. BARRETT, RAYMOND W. PALMER, JUDITH V. AUPING, and HUBERT B. PROBST (NASA, Lewis Research Center, Cleveland, OH) Oxidation of Metals (ISSN 0030-770X), vol. 36, Aug. 1991, p. 81-112. Aug. 1991 32 p refs

Copyright

A computer model useful in predicting the cyclic oxidation behavior of alloys is presented. The model considers the oxygen uptake due to scale formation during the heating cycle and the loss of oxide due to spalling during the cooling cycle. The balance between scale formation and scale loss is modeled and used to predict weight change and metal loss kinetics. A simple uniform spalling model is compared to a more complex random spall site model. In nearly all cases, the simpler uniform spall model gave predictions as accurate as the more complex model. The model has been applied to several nickel-base alloys which, depending upon composition, form Al₂O₃ or Cr₂O₃ during oxidation. The model has been validated by several experimental approaches. Versions of the model that run on a personal computer are available. Author

A92-33924 National Aeronautics and Space Administration. Marshall Space Flight Center, Huntsville, AL.

ELECTROPHORESIS OF SMALL PARTICLES AND FLUID GLOBULES IN WEAK ELECTROLYTES

J. C. BAYGENTS (NASA, Marshall Space Flight Center, Huntsville, AL; Princeton University, NJ) and D. A. SAVILLE (Princeton University, NJ) Journal of Colloid and Interface Science (ISSN 0021-9797), vol. 146, Oct. 1, 1991, p. 9-37. Research supported by Universities Space Research Association. 1 Oct. 1991 29 p refs

(Contract NAG3-259)

Copyright

An examination is conducted of the influence of partial ionization on the electrophoresis of small particles and fluid globules, with a view to the nature of conditions under which dissociation-association (D-A) alters electrokinetics. It is found that, since D-A processes are important in cases where double-layer polarization and relaxation would otherwise prevail, the predicted effect on electrophoretic mobility is greatest for the drops and bubbles whose surfaces are fluid and convection within the interface is significant. While the computation scheme used applies only to situations where forcing-field magnitude is small, the results obtained indicate that D-A processes involving ionogenic solutes may be significant in apolar liquids where electrokinetic phenomena are driven by strong forcing fields. O.C.

A92-43778 National Aeronautics and Space Administration. Lewis Research Center, Cleveland, OH.

COMBUSTION OF LIQUID-FUEL DROPLETS IN SUPERCRITICAL CONDITIONS

J. S. SHUEN (NASA, Lewis Research Center; Sverdrup Technology, Inc., Cleveland, OH), VIGOR YANG, and C. C. HSAIO (Pennsylvania State University, University Park) Combustion and Flame (ISSN 0010-2180), vol. 89, no. 3-4, June 1992, p. 299-319. Research supported by NASA and Pennsylvania State University. Jun. 1992 21 p refs

Copyright

A comprehensive analysis of liquid-fuel droplet combustion in both subcritical and supercritical environments has been conducted. The formulation is based on the complete conservation equations for both gas and liquid phases, and accommodates variable thermophysical properties, finite-rate chemical kinetics, and a full treatment of liquid-vapor phase equilibrium at the drop surface. The governing equations and associated interfacial boundary conditions are solved numerically using a fully coupled, implicit

scheme with the dual time-stepping integration technique. The model is capable of treating the entire droplet history, including the transition from the subcritical to supercritical state. As a specific example, the combustion of n-pentane fuel droplets in air is studied for pressures in the range of 5-140 atm. Results indicate that the ambient gas pressure exerts significant control of droplet gasification and burning processes through its influence on fluid transport, gas-liquid interfacial thermodynamics, and chemical reactions. The droplet gasification rate increases progressively with pressure. However, the data for the overall burnout time exhibit a considerable change in the combustion mechanism at the critical pressure, mainly as a result of reduced mass diffusivity and latent heat of vaporization with increased pressure. Author

A92-43779* National Aeronautics and Space Administration. Lewis Research Center, Cleveland, OH.

THE STRUCTURE OF PREMIXED PARTICLE-CLOUD FLAMES

K. SESHADRI, A. L. BERLAD, and V. TANGIRALA (California, University, La Jolla) Combustion and Flame (ISSN 0010-2180), vol. 89, no. 3-4, June 1992, p. 333-342. Jun. 1992 10 p refs (Contract NAG3-925)

Copyright

The structure of premixed flames propagating in combustible systems, containing uniformly distributed volatile fuel particles, in an oxidizing gas mixture, is analyzed. It is presumed that the fuel particles vaporize first to yield a gaseous fuel of known chemical structure, which is subsequently oxidized in the gas phase. The analysis is performed in the asymptotic limit, where the value of the characteristic Zeldovich number, based on the gas-phase oxidation of the gaseous fuel is large, and for values of $\phi(u)$ greater than or equal to 1.0, where $\phi(u)$ is the equivalence ratio based on the fuel available in the fuel particles. The structure of the flame is presumed to consist of a preheat vaporization zone where the rate of the gas-phase chemical reaction is small, a reaction zone where convection and the rate of vaporization of the fuel particles are small and a convection zone where diffusive terms in the conservation equations are small. For given values $\phi(u)$ the analysis yields results for the burning velocity and $\phi(g)$ where $\phi(g)$ is the effective equivalence ratio in the reaction zone. The analysis shows that even though $\phi(u)$ greater than or equal to 1.0, for certain cases the calculated value of $\phi(g)$ is less than unity. This prediction is in agreement with experimental observations. Author

A92-46976*# National Aeronautics and Space Administration. Lewis Research Center, Cleveland, OH.

QUANTITATIVE FLUORESCENCE MEASUREMENTS OF THE OH RADICAL IN HIGH PRESSURE METHANE FLAMES

B. E. BATTLES and R. K. HANSON (Stanford University, CA) AIAA, Plasmadynamics and Lasers Conference, 23rd, Nashville, TN, July 6-8, 1992. 15 p. Research supported by NASA. Jul. 1992 15 p refs

(AIAA PAPER 92-2960) Copyright

A method for quantifying laser-induced fluorescence signals from the OH radical in high-pressure flames is presented. The fluorescence signal per unit OH mole fraction is modeled as a function of temperature, pressure, and overall flame stoichiometry. Known values of the collisional quenching cross sections as a function of temperature are used to model the electronic quench rate. The reverse A - X (1.0) Q15 transition is used with broadband collection to measure single-point fluorescence produced by a pulsed Nd:YAG-pumped, frequency-doubled dye laser. Laser absorption and thermocouples are used to measure absolute OH concentration and temperature, respectively, which are used to confirm the validity of the model. Measurements are made in CH₄/O₂/N₂ flames up to 10 atm. Author

A92-48919*# National Aeronautics and Space Administration. Lewis Research Center, Cleveland, OH.

A SIMPLIFIED REACTION MECHANISM FOR PREDICTION OF NO(X) EMISSIONS IN THE COMBUSTION OF HYDROCARBONS

K. P. KUNDU (NASA, Lewis Research Center, Cleveland, OH)

and J. M. DEUR (Sverdrup Technology, Inc., Brookpark, OH) AIAA, SAE, ASME, and ASEE, Joint Propulsion Conference and Exhibit, 28th, Nashville, TN, July 6-8, 1992. 10 p. Jul. 1992 10 p refs (AIAA PAPER 92-3340) Copyright

A simplified reaction mechanism is developed for the prediction of NO(x) in hydrocarbon combustion. The mechanism uses fewer reacting species and reaction steps than the detailed mechanisms available in the literature and therefore takes less computer time when used in CFD calculations. The mechanism has been used to calculate NO(x) emissions in the combustion of propane. With slight modifications, the same mechanism can be used to calculate NO(x) in the combustion of other hydrocarbons. Results obtained with the simplified reaction are compared with experimental results and results obtained with a detailed kinetic mechanism. V.L.

A92-50447 National Aeronautics and Space Administration. Lewis Research Center, Cleveland, OH.

OBSERVATIONS OF SOOT DURING DROPLET COMBUSTION AT LOW GRAVITY - HEPTANE AND HEPTANE/MONOCHLOROALKANE MIXTURES

G. S. JACKSON, C. T. AVEDISIAN, and J. C. YANG (Cornell University, Ithaca, NY) International Journal of Heat and Mass Transfer (ISSN 0017-9310), vol. 35, no. 8, Aug. 1992, p. 2017-2033. Research supported by New York State Center for Hazardous Waste Management and NASA. Aug. 1992 17 p refs (Contract NAG3-987; NSF CBT-84-51075) Copyright

Experimental observations of the combustion of sooting fuel droplets, performed in a drop tower to create a low gravity environment, are reported. Free n-heptane droplets and suspended droplets of heptane, monochloroalkanes, and mixtures of monochloro-octane and heptane were studied. Initial droplet diameters ranged from 0.4 to 1.1 mm. The results suggest that soot may influence droplet vaporization rates. Spherical symmetry of the flame allowed for extended observation of soot agglomerates inside the droplet flame. Effects of slight convective flows were also observed, both through variations of natural convection around the suspended droplets and through variations in the drift velocities of the unsupported droplets. Slight convective flows around the suspended droplets reduced flame luminosity as well as soot accumulation inside the flame and increased droplet vaporization rates. Mixing monochloro-octane with n-heptane demonstrated the effectiveness of n-heptane in reducing soot emissions from the flames of the chlorinated fuels. Finally, trends of initial droplet diameter with burning rate were observed and may be linked to the effect of droplet size upon soot formation inside the flame.

Author

A92-50729* National Aeronautics and Space Administration. Lewis Research Center, Cleveland, OH.

BIFUNCTIONAL ALKALINE OXYGEN ELECTRODES

L. SWETTE, N. KACKLEY, and S. A. MCCATTY (Giner, Inc., Waltham, MA) IN: IECEC '91; Proceedings of the 26th Intersociety Energy Conversion Engineering Conference, Boston, MA, Aug. 4-9, 1991. Vol. 3 1991 6 p refs

(Contract NAS3-24635)

Copyright

The authors describe the identification and testing of electrocatalysts and supports for the positive electrode of moderate-temperature, single-unit, rechargeable alkaline fuel cells. Recent work on Na(x)Pt₃O₄, a potential bifunctional catalyst, is described, as well as the application of novel approaches to the development of more efficient bifunctional electrode structures. The three dual-character electrodes considered here showed similar superior performance; the Pt/RhO₂ and Rh/RhO₂ electrodes showed slightly better performance than the Pt/IrO₂ electrode. It is concluded that Na(x)Pt₃O₄ continues to be a promising bifunctional oxygen electrode catalyst but requires further investigation and development. I.E.

A92-55139* National Aeronautics and Space Administration. Lewis Research Center, Cleveland, OH.

COMBUSTION SYNTHESIS OF CERAMIC-METAL COMPOSITE MATERIALS - THE TiC-AL₂O₃-AL SYSTEM

H. J. FENG, JOHN J. MOORE (Colorado School of Mines, Golden), and D. G. WIRTH (Coors Ceramics Co., Golden, CO) Metallurgical Transactions A - Physical Metallurgy and Materials Science (ISSN 0360-2133), vol. 23A, no. 9, Sept. 1992, p. 2373-2379. Research supported by NASA. Sep. 1992 7 p refs Copyright

Combustion synthesis was applied for producing ceramic-metal composites with reduced levels of porosity, by allowing an excess amount of liquid metal, generated by the exothermic reaction during synthesis, to infiltrate the pores. It is shown that this method, when applied to TiC-Al₂O₃ system, led to a decreased level of porosity in the resulting TiC-Al₂O₃-Al product, as compared with that of TiC-Al₂O₃ system. This in situ procedure is more efficient than the two-stage conventional processes (i.e., sintering followed by liquid metal infiltration), although there are limitations with respect to total penetration of the liquid metal and maintaining a stable propagation of the combustion reaction. I.S.

A92-56950 National Aeronautics and Space Administration. Lyndon B. Johnson Space Center, Houston, TX.

TEMPERATURE DEPENDENCE OF THE ELECTRODE KINETICS OF OXYGEN REDUCTION AT THE PLATINUM/NAFION INTERFACE - A MICROELECTRODE INVESTIGATION

ARVIND PARTHASARATHY, SUPRAMANIAN SRINIVASAN, A. J. APPLEBY (Texas A & M University, College Station), and CHARLES R. MARTIN (Colorado State University, Fort Collins) Electrochemical Society, Journal (ISSN 0013-4651), vol. 139, no. 9, Sept. 1992, p. 2530-2537. Sep. 1992 8 p refs (Contract NAG9-342; NAG3-1255) Copyright

Results of a study of the temperature dependence of the oxygen reduction kinetics at the Pt/Nafion interface are presented. This study was carried out in the temperature range of 30-80 C and at 5 atm of oxygen pressure. The results showed a linear increase of the Tafel slope with temperature in the low current density region, but the Tafel slope was found to be independent of temperature in the high current density region. The values of the activation energy for oxygen reduction at the platinum/Nafion interface are nearly the same as those obtained at the platinum/trifluoromethane sulfonic acid interface but less than values obtained at the Pt/H₃PO₄ and Pt/HClO₄ interfaces. The diffusion coefficient of oxygen in Nafion increases with temperature while its solubility decreases with temperature. These temperatures also depend on the water content of the membrane. P.D.

N92-11124*# National Aeronautics and Space Administration. Lewis Research Center, Cleveland, OH.

JANNAF LIQUID ROCKET COMBUSTION INSTABILITY PANEL RESEARCH RECOMMENDATIONS

MARK D. KLEM *in* JHU, The 27th JANNAF Combustion Subcommittee Meeting, Volume 3 p 345-351 Nov. 1990 Previously announced as N91-13491 Avail: CASI HC A02/MF A06

The Joint Army, Navy, NASA, Air Force (JANNAF) Liquid Rocket Combustion Instability Panel was formed in 1988, drawing its members from industry, academia, and government experts. The panel was chartered to address the needs of near-term engine development programs and to make recommendations whose implementation would provide not only sufficient data but also the analysis capabilities to design stable and efficient engines. The panel was also chartered to make long-term recommendations toward developing mechanistic analysis models that would not be limited by design geometry or operating regime. These models would accurately predict stability and thereby minimize the amount of subscale testing for anchoring. The panel has held workshops on acoustic absorbing devices and combustion instability computational methods. At these workshops, research projects that would meet the panel's charter were suggested. The panel's

conclusions about the work that needs to be done and recommendations on how to approach it, based on evaluation of the suggested research projects, are presented. Author

N92-25816*# National Aeronautics and Space Administration. Lewis Research Center, Cleveland, OH.

STUDY OF SHOCK-INDUCED COMBUSTION USING AN IMPLICIT TVD SCHEME

SHAYNE YUNGSTER *In its* Computational Fluid Dynamics p 93-101 Feb. 1992 Original contains color illustrations

The supersonic combustion flowfields associated with various hypersonic propulsion systems, such as the ram accelerator, the oblique detonation wave engine, and the scramjet, are being investigated using a new computational fluid dynamics (CFD) code. The code solves the fully coupled Reynolds-averaged Navier-Stokes equations and species continuity equations in an efficient manner. It employs an iterative method and a second order differencing scheme to improve computational efficiency. The code is currently being applied to study shock wave/boundary layer interactions in premixed combustible gases, and to investigate the ram accelerator concept. Results obtained for a ram accelerator configuration indicate a new combustion mechanism in which a shock wave induces combustion in the boundary layer, which then propagates outward and downstream. The combustion process creates a high pressure region over the back of the projectile resulting in a net positive thrust forward. H.A.

N92-26670*# National Aeronautics and Space Administration. Lewis Research Center, Cleveland, OH.

PROGRESS IN THE DEVELOPMENT OF LIGHTWEIGHT NICKEL ELECTRODE

DORIS L. BRITTON Jun. 1992 8 p Proposed for presentation at the 35th International Power Sources Symposium, Cherry Hill, NJ, 22-25 Jun. 1992; sponsored by IEEE, Industry Application Society

(Contract RTOP 506-41-21)
(NASA-TM-105638; E-6984; NAS 1.15:105638) Avail: CASI HC A02/MF A01

The use of the lightweight nickel electrode, in place of the heavy-sintered state-of-the-art nickel electrode, will lead to improvements in specific energy and performance of the nickel-hydrogen cell. Preliminary testing indicates that a nickel fiber mat is a promising support candidate for the nickel hydroxide active material. Nickel electrodes made from fiber mats, with nickel and cobalt powder added to the fiber, were tested at LeRC. To date, over 8000 cycles have been accumulated, at 40 percent depth-of-discharge, using the lightweight fiber electrode, in a boiler plate nickel-hydrogen cell. Author

N92-34206*# National Aeronautics and Space Administration. Lewis Research Center, Cleveland, OH.

GRAPHITE FLUORIDE FROM IODINE INTERCALATED GRAPHITIZED CARBON Patent Application

CHING-CHEH HUNG, inventor (to NASA) 15 May 1992 14 p (NASA-CASE-LEW-15360-1; NAS 1.71:LEW-15360-1; US-PATENT-APPL-SN-884097) Avail: CASI HC A03/MF A01

Graphite fluoride is produced from graphitized carbon. A bromine iodine mixture reacts with graphitized carbon to produce iodine intercalated graphitized carbon that is then exposed to fluorine. NASA

METALLIC MATERIALS

Includes physical, chemical, and mechanical properties of metals, e.g., corrosion; and metallurgy.

A92-12046* National Aeronautics and Space Administration. Lewis Research Center, Cleveland, OH.

THE EFFECT OF POROSITY AND GAMMA-GAMMA-PRIME EUTECTIC CONTENT ON THE FATIGUE BEHAVIOR OF HYDROGEN CHARGED PWA 1480

J. GAYDA, R. L. DRESHFIELD, and T. P. GABB (NASA, Lewis Research Center, Cleveland, OH) Scripta Metallurgica et Materialia (ISSN 0956-716X), vol. 25, Nov. 1991, p. 2589-2594. Nov. 1991 6 p refs

Copyright

The study addresses the effect of systematically varying gamma-gamma-prime eutectic content and porosity level on the fatigue life of a hydrogen-charged single crystal PWA 1480 superalloy. Four microstructural variants are produced, and differences in gamma-gamma-prime eutectic morphology among the four processing variants are analyzed. Single valued tensile test data indicate that the tensile and yield strength of the PWA 1480 are degraded by hydrogen charging, with the exception of the material given a eutectic solution treatment. It is shown that the reduction of the fatigue life can be minimized by a duplex thermomechanical treatment consisting of a eutectic solution followed by hot isostatic pressing. V.T.

A92-17977* National Aeronautics and Space Administration. Lewis Research Center, Cleveland, OH.

SLOW STRAIN RATE 1200-1400 K COMPRESSIVE PROPERTIES OF NiAl-1Hf

J. D. WHITTENBERGER, M. V. NATHAL, S. V. RAJ (NASA, Lewis Research Center, Cleveland, OH), and V. M. PATHARE (CPS Superconductor Corp., Milford, MA) Materials Letters (ISSN 0167-577X), vol. 11, July 1991, p. 267-272. Jul. 1991 6 p refs

Copyright

Compression tests are conducted on NiAl-1Hf to assess the elevated-temperature creep behavior of this precipitation-hardened aluminide. While the strength is high under fast strain rates (more than 10 exp -5/s), under slower conditions the alloy is weak. Thus, it is unlikely that effective creep resistance can be obtained in NiAl through small Hf additions. Author

A92-24832* National Aeronautics and Space Administration. Lewis Research Center, Cleveland, OH.

HARDENING MECHANISMS IN A DYNAMIC STRAIN AGING ALLOY, HASTELLOY X, DURING ISOTHERMAL AND THERMOMECHANICAL CYCLIC DEFORMATION

R. V. MINER (NASA, Lewis Research Center, Cleveland, OH) and M. G. CASTELLI (NASA, Lewis Research Center; Sverdrup Technology, Inc., Cleveland, OH) Metallurgical Transactions A - Physical Metallurgy and Materials Science (ISSN 0360-2133), vol. 23A, Feb. 1992, p. 551-561. Feb. 1992 11 p refs

Copyright

The relative contributions of the hardening mechanisms in Hastelloy X during cyclic deformation were investigated by conducting isothermal cyclic deformation tests within a total strain range of +/-0.3 pct and at several temperatures and strain rates, and thermomechanical tests within several different temperature limits. The results of the TEM examinations and special constant structure tests showed that the precipitation on dislocations of Cr23C6 contributed to hardening, but only after sufficient time above 500 C. Solute drag alone produced very considerable cyclic hardening. Heat dislocation densities, peaking around 10 exp 11 per sq cm, were found to develop at temperatures producing the greatest cyclic hardening. I.S.

A92-26526* National Aeronautics and Space Administration, Lewis Research Center, Cleveland, OH.

GROWTH-SPEED DEPENDENCE OF PRIMARY ARM SPACINGS IN DIRECTIONALLY SOLIDIFIED PB-10 WT PCT SN

M. A. CHOPRA (IBM Corp., Austin, TX) and S. N. TEWARI (Cleveland State University, OH) Metallurgical Transactions A - Physical Metallurgy and Materials Science (ISSN 0360-2133), vol. 22A, Oct. 1991, p. 2467-2474. Oct. 1991 8 p refs (Contract NCC3-95)

Copyright

The dependence of primary arm spacings on growth speed has been investigated for cellular and dendritic arrays in directionally solidified Pb-10 wt pct Sn. The spatial arrangements of cells and dendrites, as given by their coordination number, are not very different from each other. The primary arm spacing maxima and the cell-to-dendrite transition appear to be strongly influenced by the magnitude of the solute partition coefficient (k). The planar-to-cellular transition in Pb-Sn ($k = 0.50$) is supercritical as compared to the subcritical behavior reported in Al-Cu ($k = 0.14$) and succinonitrile-acetone ($k = 0.1$).

Author

A92-27422* National Aeronautics and Space Administration, Lewis Research Center, Cleveland, OH.

FRACTURE TOUGHNESS AND THE EFFECTS OF STRESS STATE ON FRACTURE OF NICKEL ALUMINIDES

JOHN J. LEWANDOWSKI, GARY M. MICHAL, IVAN LOCCI, and JOSEPH D. RIGNEY (Case Western Reserve University, Cleveland, OH) IN: Alloy phase stability and design; Proceedings of the Symposium, San Francisco, CA, Apr. 18-20, 1990 1991 7 p refs

Copyright

The effects of stress state on the fracture behavior of Ni₃Al, Ni₃Al + B, and NiAl were determined using either notched or fatigue-precracked bend bars tested to failure at room temperature, in addition to testing specimens in tension under superposed hydrostatic pressure. Although Ni₃Al is observed to fail in a macroscopically brittle intergranular manner in tension tests conducted at room temperature, the fracture toughnesses presently obtained on Ni₃Al exceeded 20 MPam, and R-curve behavior was exhibited. In situ monitoring of the fracture experiments was utilized to aid in interpreting the source(s) of the high toughness in Ni₃Al, while SEM fractography was utilized to determine the operative fracture modes. The superposition by hydrostatic pressure during tensile testing of NiAl specimens was observed to produce increased ductility without changing the fracture mode.

Author

A92-28017* National Aeronautics and Space Administration, Lewis Research Center, Cleveland, OH.

DIFFUSION MECHANISMS IN CHEMICAL VAPOR-DEPOSITED IRIIDIUM COATED ON CHEMICAL VAPOR-DEPOSITED RHENIUM

J. C. HAMILTON, N. Y. C. YANG, W. M. CLIFT, D. R. BOEHME, K. F. MCCARTY (Sandia National Laboratories, Livermore, CA), and J. E. FRANKLIN (Aerojet, Propulsion Div., Sacramento, CA) Metallurgical Transactions A - Physical Metallurgy and Materials Science (ISSN 0360-2133), vol. 23A, March 1992, p. 851-855. Mar. 1992 5 p refs (Contract NAS3-25646)

Copyright

Radiation-cooled rocket thruster chambers have been developed which use CVD Re coated with CVD Ir on the interior surface that is exposed to hot combustion gases. The Ir serves as an oxidation barrier which protects the structural integrity-maintaining Re at elevated temperatures. The diffusion kinetics of CVD materials at elevated temperatures is presently studied with a view to the prediction and extension of these thrusters' performance limits. Line scans for Ir and Re were fit on the basis of a diffusion model, in order to extract relevant diffusion constants; the fastest diffusion process is grain-boundary diffusion, where Re diffuses down grain boundaries in the Ir overlayer.

O.C.

A92-28113* National Aeronautics and Space Administration, Lewis Research Center, Cleveland, OH.

THE EFFECT OF STRAIN RATE AND TEMPERATURE ON THE TENSILE PROPERTIES OF NIAL

R. D. NOEBE, C. L. CULLERS, and R. R. BOWMAN (NASA, Lewis Research Center, Cleveland, OH) Journal of Materials Research (ISSN 0884-2914), vol. 7, March 1992, p. 605-612. Mar. 1992 8 p refs

Copyright

Tensile testing of cast and extruded binary NiAl was performed from 300 to 900 K at strain rates of 0.00014 to 0.14/s. The brittle-to-ductile transition temperature (BDTT) was dependent on strain rate, with a three-order-of-magnitude increase in strain rate resulting in approximately a 200-K increase in transition temperature. Regardless of strain rate, at temperatures just above the BDTT the fracture strength increased significantly and the fracture morphology changed from mostly intergranular to predominantly transgranular. It was also determined that the mechanism responsible for the brittle-to-ductile transition in NiAl had an apparent activation energy of approximately 118 kJ/mol. These results support the argument that the mechanism for the brittle-to-ductile transition in NiAl is associated with the onset of thermally activated deformation process. This process is probably dislocation climb controlled by short circuit diffusion.

Author

A92-28240* National Aeronautics and Space Administration, Lewis Research Center, Cleveland, OH.

A NEW APPROXIMATE SUM RULE FOR BULK ALLOY PROPERTIES

GUILLERMO BOZZOLO (NASA, Lewis Research Center, Cleveland; Analex Corp., Brook Park, OH) and JOHN FERRANTE (NASA, Lewis Research Center, Cleveland, OH) Scripta Metallurgica et Materialia (ISSN 0956-716X), vol. 26, March 15, 1992, p. 907-912. Previously announced in STAR as N91-32204. 15 Mar. 1992 6 p refs

Copyright

A new, approximate sum rule is introduced for determining bulk properties of multicomponent systems, in terms of the pure components properties. This expression is applied for the study of lattice parameters, cohesive energies, and bulk moduli of binary alloys. The correct experimental trends (i.e., departure from average values) are predicted in all cases.

Author

A92-28248* National Aeronautics and Space Administration, Lewis Research Center, Cleveland, OH.

COMPRESSIVE STRENGTH OF DIRECTIONALLY SOLIDIFIED NIAL-NIALNB INTERMETALLICS AT 1200 AND 1300 K

J. D. WHITTENBERGER (NASA, Lewis Research Center, Cleveland, OH), R. REVIERE (Tennessee, University, Knoxville), R. D. NOEBE (NASA, Lewis Research Center, Cleveland, OH), and B. F. OLIVER (Tennessee, University, Knoxville) Scripta Metallurgica et Materialia (ISSN 0956-716X), vol. 26, March 15, 1992, p. 987-992. 15 Mar. 1992 6 p refs

Copyright

Results are presented from measurements of 1200 K and 1300 K compressive properties of two directionally solidified NiAl-NiAlNb compositions (in at. pct): Ni-41.75Al-16.5Nb (eutectic composition) and Ni-47.5Al-8.9Nb-1.3C (Al-rich composition). Results showed that the strength of the eutectic was a factor of 2 greater than that of the Al-rich composition. However, the analysis of the compressive stress-strain data indicated that the deformation mechanism was the same in both materials.

I.S.

A92-29616* National Aeronautics and Space Administration, Lewis Research Center, Cleveland, OH.

LOW EARTH ORBIT DURABILITY EVALUATION OF HAYNES 188 SOLAR RECEIVER MATERIAL

KIM K. DE GROH, SHARON K. RUTLEDGE (NASA, Lewis Research Center, Cleveland, OH), CHRISTOPHER A. BURKE, THERESE M. DEVER, RAYMOND M. OLLE (Cleveland State University, OH), and JUDITH A. TERLEP (Ohio Aerospace Institute, Cleveland) AIAA, Aerospace Sciences Meeting and Exhibit, 30th,

26 METALLIC MATERIALS

Reno, NV, Jan. 6-9, 1992. 9 p. Jan. 1992 9 p refs
(AIAA PAPER 92-0850) Copyright

The effects of elevated-temperature vacuum and elevated-temperature atomic oxygen exposure on the mass, surface chemistry, surface morphology, and optical properties of Haynes 188, a possible heat receiver material for space-based solar dynamic power systems, have been studied. Pristine and surface modified Haynes 188 were exposed to vacuum less than or equal to $10 \text{ exp } -6 \text{ torr}$ at 820 C for 5215.5 h , and to atomic oxygen in an air plasma asher at 34 and 827 C for fluences up to $5.6 \times 10 \text{ exp } 21 \text{ atoms/sq cm}$. Results obtained indicate that vacuum heat treatment caused surface morphology and chemistry changes with corresponding optical property changes. Atomic oxygen exposure caused optical property changes which diminished with time. Mass changes are considered to be negligible for both exposures.

O.G.

A92-30766* National Aeronautics and Space Administration. Lewis Research Center, Cleveland, OH.

COMPRESSION, BEND, AND TENSION STUDIES ON FORGED AL67Ti25Cr8 AND AL66Ti25Mn(G) L1(2) COMPOUNDS

K. S. KUMAR, S. A. BROWN (Martin Marietta Laboratories, Baltimore, MD), and J. D. WHITTENBERGER (NASA, Lewis Research Center, Cleveland, OH) IN: High-temperature ordered intermetallic alloys IV; Proceedings of the 4th MRS Symposium, Boston, MA, Nov. 27-30, 1990 1991 6 p refs
(Contract NAS3-25787)

Copyright

Cast, homogenized, and isothermally forged aluminum-rich L1(2) compounds Al67Ti25Cr8 and Al66Ti25Mn(g) were tested in compression as a function of temperature and as a function of strain rate at elevated temperatures (1000 K and 1100 K). Three-point bend specimens were tested as a function of temperature in the range 300 K to 873 K . Strain gages glued on the tensile side of the ambient and 473 K specimens enabled direct strain measurements. A number of 'buttonhead' tensile specimens were electro-discharge machined, fine polished, and tested between ambient and 1073 K for yield strength and ductility as a function of temperature. Scanning electron microscope (SEM) examination of fracture surfaces from both the bend and tensile specimens revealed a gradual transition from transgranular cleavage to intergranular failure with increasing temperature.

Author

A92-30780* National Aeronautics and Space Administration. Lewis Research Center, Cleveland, OH.

DOES A THRESHOLD STRESS FOR CREEP EXIST IN HfC-DISPERSED NiAl?

J. D. WHITTENBERGER (NASA, Lewis Research Center, Cleveland, OH), RANJAN RAY (Marko Materials, Inc., Billerica, MA), and SUNIL C. JHA (Texas Instruments, Inc., Attleboro, MA) IN: High-temperature ordered intermetallic alloys IV; Proceedings of the 4th MRS Symposium, Boston, MA, Nov. 27-30, 1990 1991 7 p refs

Copyright

Recently it was proposed (Jha et al., 1989; Whittenberger et al., 1990) on the basis of constant velocity testing at 1300 K that dispersion strengthened NiAl composites containing about 4 wt pct HfC possess threshold stresses for creep. Further, 1300 K compression testing has been conducted on NiAl+4HfC, and diametrically opposite behavior has been found: for constant load creep tests a normal power law behavior was observed. However, additional constant velocity testing still indicates that the flow stress is essentially independent of strain rate below $10 \text{ exp } -6/\text{s}$. Examination of NiAl+4.3HfC specimens deformed under constant velocity conditions revealed that the original hot extruded small grain structure could be converted to large, elongated grains during testing. Such a transformation appears to be responsible for the apparent threshold stress behavior in HfC dispersed NiAl.

Author

A92-30781* National Aeronautics and Space Administration. Lewis Research Center, Cleveland, OH.

FLOW AND FRACTURE BEHAVIOR OF NiAl IN RELATION TO THE BRITTLE-TO-DUCTILE TRANSITION TEMPERATURE

R. D. NOEBE, R. R. BOWMAN, C. L. CULLERS, and S. V. RAJ (NASA, Lewis Research Center, Cleveland, OH) IN: High-temperature ordered intermetallic alloys IV; Proceedings of the 4th MRS Symposium, Boston, MA, Nov. 27-30, 1990 1991 8 p refs

Copyright

NiAl has only three independent slip systems operating at low and intermediate temperatures whereas five independent deformation mechanisms are required to satisfy the von Mises criterion for general plasticity in polycrystalline materials. Yet, it is generally recognized that polycrystalline NiAl can be deformed extensively in compression at room temperature and that limited tensile ductility can be obtained in extruded materials. In order to determine whether these results are in conflict with the von Mises criterion, tension and compression tests were conducted on powder-extruded, binary NiAl between 300 and 1300 K . The results indicate that below the brittle-to-ductile transition temperature (BDTT) the failure mechanism in NiAl involves the initiation and propagation of cracks at the grain boundaries which is consistent with the von Mises analysis. Furthermore, evaluation of the flow behavior of NiAl indicates that the transition from brittle to ductile behavior with increasing temperature coincides with the onset of recovery mechanisms such as dislocation climb. The increase in ductility above the BDTT is therefore attributed to the climb of the 001 line type dislocations which in combination with dislocation glide enable grain boundary compatibility to be maintained at the higher temperatures.

Author

A92-30793* National Aeronautics and Space Administration. Lewis Research Center, Cleveland, OH.

THE MECHANICAL PROPERTIES OF A Ni-30Al-20Fe-0.05Zr INTERMETALLIC ALLOY IN THE TEMPERATURE RANGE 300-1200 K

S. V. RAJ, R. D. NOEBE, and I. E. LOCCI (NASA, Lewis Research Center, Cleveland, OH) IN: High-temperature ordered intermetallic alloys IV; Proceedings of the 4th MRS Symposium, Boston, MA, Nov. 27-30, 1990 1991 6 p refs

Copyright

Tensile tests were conducted on an extruded Ni-30(at. pct)Al-20Fe-0.05Zr intermetallic alloy in the temperature range 300 - 1200 K , and the microstructures were characterized by optical, scanning, and transmission electron microscopy. The alloy did not exhibit any room temperature ductility and failed by transgranular cleavage at a stress of about 710 MPa . This mode of fracture was observed at and below 873 K with the total ductility being less than 2.5 percent. However, the failure mode changed to dimpled fracture, triple point cracking, and rupture above 873 K . Scanning electron microscopy of the fracture surfaces revealed that transgranular cleavage failure had always originated at preexisting defects. In these cases, the fracture stress exhibited a good correlation with the defect size, in accordance with linear elastic fracture mechanics, where the critical stress intensity factor was estimated to be about 4 MPa sq rt m .

Author

A92-30794* National Aeronautics and Space Administration. Lewis Research Center, Cleveland, OH.

ON IMPROVING THE FRACTURE TOUGHNESS OF A NiAl-BASED ALLOY BY MECHANICAL ALLOYING

J. KOSTRUBANIC, D. A. KOSS (Pennsylvania State University, University Park), I. E. LOCCI, and M. NATHAL (NASA, Lewis Research Center, Cleveland, OH) IN: High-temperature ordered intermetallic alloys IV; Proceedings of the 4th MRS Symposium, Boston, MA, Nov. 27-30, 1990 1991 6 p refs

Copyright

Mechanical alloying (MA) has been used to process the NiAl-based alloy Ni-35Al-20Fe, such that a fine-grain (about 2 microns) microstructure is obtained through the addition of 2 vol pct Y₂O₃ particles. When compared to a conventionally processed, coarse-grained (about 28 microns) Ni-35-20 alloy without the Y₂O₃

particles, the MA alloy exhibits two to three times higher fracture toughness values, despite a 50-percent increase in yield strength. Room-temperature K_{IC} values as high as 34 MPa sq rt m are observed, accompanied by a yield strength in excess of 1100 MPa. Fractography confirms a change in fracture characteristics of the fine-grained MA alloy. Author

A92-30841* National Aeronautics and Space Administration, Lewis Research Center, Cleveland, OH.

MICROSTRUCTURE AND MECHANICAL PROPERTIES OF A SINGLE CRYSTAL NiAl ALLOY WITH Zr OR Hf RICH G-PHASE PRECIPITATES

I. E. LOCCI, R. D. NOEBE, R. R. BOWMAN, R. V. MINER, M. V. NATHAL (NASA, Lewis Research Center, Cleveland, OH), and R. DAROLIA (GE Aircraft Engines, Cincinnati, OH) IN: High-temperature ordered intermetallic alloys IV; Proceedings of the 4th MRS Symposium, Boston, MA, Nov. 27-30, 1990 1991 6 p refs

Copyright

The possibility of producing NiAl reinforced with the G-phase ($Ni_{16}X_6Si_7$), where X is Zr or Hf, has been investigated. The microstructure of these NiAl alloys has been characterized in the as-cast and annealed conditions. The G-phases are present as fine cuboidal precipitates (10 to 40 nm) and have lattice parameters almost four times that of NiAl. They are coherent with the matrix and fairly resistant to coarsening during annealing heat treatments. Segregation and nonuniform precipitate distribution observed in as-cast materials were eliminated by homogenization at temperatures near 1600 K. Slow cooling from these temperatures resulted in large plate shaped precipitates, denuded zones, and a loss of coherency in some of the large particles. Faster cooling produced a homogeneous fine distribution of cuboidal G-phase particles in the matrix. Preliminary mechanical properties for the Zr-doped alloy are presented and compared to binary single crystal NiAl. The presence of these precipitates appears to have an important strengthening effect at temperatures not less than 1000 K compared to binary NiAl single crystals. Author

A92-30844* National Aeronautics and Space Administration, Lewis Research Center, Cleveland, OH.

MICROSTRUCTURE AND MECHANICAL PROPERTIES OF NEAR EUTECTIC BETA-NiAl PLUS ALPHA-RE ALLOYS PRODUCED BY RAPID SOLIDIFICATION AND EXTRUSION

D. P. MASON, D. C. VAN AKEN (Michigan, University, Ann Arbor), R. D. NOEBE, I. E. LOCCI, and K. L. KING (NASA, Lewis Research Center, Cleveland, OH) IN: High-temperature ordered intermetallic alloys IV; Proceedings of the 4th MRS Symposium, Boston, MA, Nov. 27-30, 1990 1991 6 p refs

Copyright

A92-30845* National Aeronautics and Space Administration, Lewis Research Center, Cleveland, OH.

COMPRESSION STUDIES ON PARTICULATE COMPOSITES OF TERNARY AL-TI-FE, AND QUATERNARY AL-TI-FE-NB AND AL-TI-FE-MN L1(2) COMPOUNDS

K. S. KUMAR, M. S. DIPIETRO (Martin Marietta Laboratories, Baltimore, MD), and J. D. WHITTENBERGER (NASA, Lewis Research Center, Cleveland, OH) IN: High-temperature ordered intermetallic alloys IV; Proceedings of the 4th MRS Symposium, Boston, MA, Nov. 27-30, 1990 1991 6 p refs (Contract NAS3-25787)

Copyright

Compression studies were conducted on monolithic and TiB₂ particulate-reinforced composites of Al₂₂Fe₃Ti₈, both with and without minor quaternary alloying additions (2 at. pct Nb and 2 at. pct Mn) as a function of temperature and as a function of strain rate at high temperature. The volume fraction of reinforcement was varied between 0 and 20 percent. The particulate reinforcements were found to be effective in increasing ambient- and warm-temperature strength; at high temperatures, the monolithic material is stronger than the composites, although the composites are superior at slow strain rates. The microstructures

of the monolithic and composite specimens were examined before and after deformation to explain these observations. Author

A92-31850* National Aeronautics and Space Administration, Lewis Research Center, Cleveland, OH.

PROTECTIVE AL₂O₃ SCALE FORMATION ON NbAl₃-BASE ALLOYS

J. DOYCHAK (NASA, Lewis Research Center, Cleveland, OH) and M. G. HEBUR (NASA, Lewis Research Center, Cleveland; Sverdrup Technology, Inc., Brook Park, OH) Oxidation of Metals (ISSN 0030-770X), vol. 36, Aug. 1991, p. 113-141. Research supported by NASA. Aug. 1991 29 p refs

Copyright

The oxidation of NbAl₃ with additions of Cr and Y was studied to determine the mechanisms of the beneficial effects of these elements upon oxidation. Cr additions to the binary NbAl₃ alloy of up to 6.8 at. percent reduced the scale growth rates and promoted alpha-Al₂O₃ formation over much longer times relative to binary NbAl₃. A major effect of Cr is to form a layer of AlNbCr at the metal/scale interface, which is inherently more oxidation-resistant than the matrix alloy in the long term. Yttrium additions to a Cr-containing alloy improved the scale growth rate and adherence and changed the scale microstructure to mimic that of a typical protective Al₂O₃ scale. Author

A92-32398* National Aeronautics and Space Administration, Lewis Research Center, Cleveland, OH.

THERMAL BARRIER COATING LIFE AND ISOTHERMAL OXIDATION OF LOW-PRESSURE PLASMA-SPRAYED BOND COAT ALLOYS

W. J. BRINDLEY and R. A. MILLER (NASA, Lewis Research Center, Cleveland, OH) IN: Metallurgical coatings and thin films 1990; Proceedings of the 17th International Conference on Metallurgical Coatings and 8th International Conference on Thin Films, San Diego, CA, Apr. 2-6, 1990. Vol. 1 1990 12 p refs

Copyright

The paper investigates the isothermal oxidation kinetics of Ni-35Cr-6Al-0.95Y, Ni-18Cr-12Al-0.3Y, and Ni-16Cr-6Al-0.3Y low-pressure plasma-sprayed bond coat alloys and examines the effect of these alloys on the thermal barrier coating (TBC) cyclic life. TBC life was examined by cycling substrates coated with the different bond coats and a ZrO₂-7 wt pct Y₂O₃ TBC in an air-rich burner rig flame between 1150 C and room temperature. The oxidation kinetics of the three bond coat alloys was examined by isothermal oxidation of monolithic NiCrAlY coupons at 1083 C. The Ni-35Cr-6Al-0.95Y alloy exhibits comparatively high isothermal oxidation weight gains and provides the longest TBC life, whereas the Ni-16Cr-6Al-0.3Y alloy had the lowest weight gains and provided the shortest TBC life. The results show that, although bond coat oxidation is known to have a strong detrimental effect on TBC life, it is not the only bond coat factor that determines TBC life. P.D.

A92-32399* National Aeronautics and Space Administration, Lewis Research Center, Cleveland, OH.

THERMAL RESPONSE OF VARIOUS THERMAL BARRIER COATINGS IN A HIGH HEAT FLUX ROCKET ENGINE

J. A. NESBITT (NASA, Lewis Research Center, Cleveland, OH) IN: Metallurgical coatings and thin films 1990; Proceedings of the 17th International Conference on Metallurgical Coatings and 8th International Conference on Thin Films, San Diego, CA, Apr. 2-6, 1990. Vol. 1 1990 12 p refs

Copyright

Traditional APS ZrO₂-Y₂O₃ thermal barrier coatings (TBCs) formed by air plasma spraying and low pressure and air plasma sprayed ZrO₂-Y₂O₃/NiCrAlY cermet coatings were tested in an H₂-O₂ rocket engine. The test cycle was approximately 1.2 s at 1400 C in a hydrogen-rich environment. During testing, the maximum metal temperature without a coating was 1310 C. The traditional ZrO₂-Y₂O₃ TBCs with a 100-125 micron thick ceramic layer reduced the maximum metal temperature by approximately 350 C. Increasing the ceramic layer thickness to 200-225 microns resulted in an additional metal temperature reduction of 100 C.

However, the cermet coatings, consisting of a ceramic and metal mixture, exhibited a much lower thermal protection capability by reducing the maximum metal temperature by approximately 100 C. It was also found that the surface roughness of the traditional TBCs had little effect on the thermal response. Author

A92-32898* National Aeronautics and Space Administration. Lewis Research Center, Cleveland, OH.

LATTICE PARAMETERS OF FCC BINARY ALLOYS USING A NEW SEMIEMPIRICAL METHOD

GUILLERMO BOZZOLO (NASA, Lewis Research Center, Cleveland; Analex Corp., Brook Park, OH) and JOHN FERRANTE (NASA, Lewis Research Center, Cleveland, OH) Scripta Metallurgica et Materialia (ISSN 0956-716X), vol. 26, April 15, 1992, p. 1275-1280. 15 Apr. 1992 6 p refs

Copyright

A new semiempirical method has been developed to predict the concentration dependence of the heats of formation and lattice parameters of binary alloys consistent with equivalent crystal theory. This method accurately predicts the composition dependence of the lattice parameters both qualitatively and quantitatively. A simple formulation is provided of the algorithm for performing defect calculations. C.D.

A92-33866 National Aeronautics and Space Administration. Lewis Research Center, Cleveland, OH.

SOLIDIFICATION PROCESSING OF INTERMETALLIC Nb-AL ALLOYS

PRESTON P. SMITH, BEN F. OLIVER (Tennessee, University, Knoxville), and RONALD D. NOEBE (NASA, Lewis Research Center, Cleveland, OH) Scripta Metallurgica et Materialia (ISSN 0956-716X), vol. 26, May 1, 1992, p. 1365-1370. Research supported by NASA. 1 May 1992 6 p refs

Copyright

Several Nb-Al alloys, including single-phase NbAl₃ and the eutectic of Nb₂Al and NbAl₃, were prepared either by nonconsumable arc melting in Ar or by zone processing in He following initial induction melting and rod casting, and the effect of the solidification route on the microstructure and room-temperature mechanical properties of these alloys was investigated. Automated control procedures and melt conditions for directional solidification of NbAl₃ and the Nb₂Al/Nb₃Al eutectic were developed; high purity and stoichiometry were obtained. The effects of ternary additions of Ti and Ni are described. I.S.

A92-33947* National Aeronautics and Space Administration. Lewis Research Center, Cleveland, OH.

FATIGUE DAMAGE ACCUMULATION IN NICKEL PRIOR TO CRACK INITIATION

T. L. GROBSTEIN (NASA, Lewis Research Center; Case Western Reserve University, Cleveland, OH), S. SIVASHANKARAN, G. WELSCH, N. PANIGRAHI, J. D. MCGERVEY (Case Western Reserve University, Cleveland, OH), and J. W. BLUE (NASA, Lewis Research Center, Cleveland; Cleveland Clinic Foundation, OH) Materials Science and Engineering, Part A - Structural Materials: Properties, Microstructure and Processing (ISSN 0921-5093), vol. A138, 1991, p. 191-203. Research supported by NASA. 1991 13 p refs

Copyright

The accumulation of lattice defects during fatigue cycling of nickel was investigated by electrical resistivity measurements, positron annihilation lifetime spectroscopy and transmission electron microscopy. Dislocations and vacancy clusters were found to be the main defect types. During cycling of axial and flexural samples at constant load amplitude, the dislocations form a saturated structure early in the fatigue life. This saturated structure consists of a cellular dislocation matrix, in which persistent slip bands (PSBs) begin to operate after the saturation has been established. Vacancies and vacancy clusters are formed during fatigue as a consequence of repetitive dislocation glide in the PSB structure. When PSBs operate, the matrix is assumed to be dormant, allowing vacancies to accumulate preferentially in the PSBs. The increase in vacancy concentration then accounts for

the monotonic accumulation of fatigue damage, which points to the importance of vacancy accumulation as a precursor to crack nucleation. Author

A92-37088* National Aeronautics and Space Administration. Lewis Research Center, Cleveland, OH.

INTERDIFFUSION BETWEEN THE L1(2) TRIALUMINIDES AL66Ti25Mn9 AND AL67Ti25Cr8

K. S. KUMAR (Martin Marietta Laboratories, Baltimore, MD) and J. D. WHITTENBERGER (NASA, Lewis Research Center, Cleveland, OH) Journal of Materials Research (ISSN 0884-2914), vol. 7, no. 5, May 1992, p. 1043-1045. May 1992 3 p refs (Contract NAS3-26069)

Copyright

Concentration-distance profiles obtained from Al₆₆Ti₂₅Mn₉/Al₆₇Ti₂₅Cr₈ diffusion couples are used to determine the interdiffusion coefficients in the temperature range 1373-1073 K. The couples are treated as pseudobinaries, and the diffusion coefficients are determined using the Matano approach. The results are then used to compute the activation energies for diffusion, and a comparison is made with some existing data for the activation energy for creep of Al₂₂Ti₈Fe₃. V.L.

A92-38019* National Aeronautics and Space Administration. Lewis Research Center, Cleveland, OH.

CORRELATION OF DEFORMATION MECHANISMS WITH THE TENSILE AND COMPRESSIVE BEHAVIOR OF NiAl AND NiAl(Zr) INTERMETALLIC ALLOYS

R. R. BOWMAN, R. D. NOEBE, S. V. RAJ, and I. E. LOCCI (NASA, Lewis Research Center, Cleveland, OH) Metallurgical Transactions A - Physical Metallurgy and Materials Science (ISSN 0360-2133), vol. 23A, no. 5, May 1992, p. 1493-1508. May 1992 16 p refs

To identify the mechanisms controlling strength and ductility in powder-extruded NiAl and NiAl + 0.05 at. pct Zr, tensile and compressive testing was performed from 300 to 1300 K for several grain sizes. Grain size refinement significantly increased yield stress in both alloys and, in some cases, slightly lowered the ductile-to-brittle transition temperature (DBTT), although no room-temperature tensile ductility was observed even in the finest grain size specimens. The small Zr addition increased the DBTT and changed the low-temperature fracture mode from intergranular in NiAl to a combination of intergranular and transgranular in the Zr-doped alloy. Scanning electron microscopy of compression specimens deformed at room temperature revealed the presence of grain-boundary cracks in both alloys. These cracks were due to the incompatibility of strain in the polycrystalline material, owing to the lack of five independent slip systems. The tendency to form grain-boundary cracks, in addition to the low fracture stress of these alloys, contributed to the lack of tensile ductility at low temperatures. Author

A92-38990* National Aeronautics and Space Administration. Lewis Research Center, Cleveland, OH.

THE DECREASE IN YIELD STRENGTH IN NiAl DUE TO HYDROSTATIC PRESSURE

R. W. MARGEVICIUS, J. J. LEWANDOWSKI, and I. LOCCI (Case Western Reserve University, Cleveland, OH) Scripta Metallurgica et Materialia (ISSN 0956-716X), vol. 26, no. 11, June 1, 1992, p. 1733-1736. Research supported by NASA. 1 Jun. 1992 4 p refs

(Contract N00014-91-J-1370)

Copyright

The decrease in yield strength in NiAl due to hydrostatic pressure is examined via a comparison of the tensile flow behavior in the low strain regime at 0.1 MPa for NiAl which was cast, extruded, and annealed for 2 hr at 827 C in argon and very slowly cooled to room temperature. Pressurization to 1.4 GPa produces a subsequent reduction at 0.1 MPa in proportional limit by 40 percent as well as a 25-percent reduction in the 0.2-percent offset yield strength, while pressurization with lower pressures produces a similar reduction, although smaller in magnitude. P.D.

A92-38993* National Aeronautics and Space Administration. Lewis Research Center, Cleveland, OH.

OXIDATION KINETICS OF CAST TiAl₃

J. L. SMIALEK (NASA, Lewis Research Center, Cleveland, OH) and D. L. HUMPHREY (NASA, Lewis Research Center; Sverdrup Technology, Inc., Cleveland, OH) Scripta Metallurgica et Materialia (ISSN 0956-716X), vol. 26, no. 11, June 1, 1992, p. 1763-1768. 1 Jun. 1992 6 p refs

Copyright

The isothermal oxidation kinetics of the TiAl₃ compound over a wide temperature range is documented, and these rates are related to exclusive alpha-Al₂O₃ scale growth. The specific weight change vs time curves are shown. Two abnormalities are immediately apparent. One is that a rapid initial uptake of oxygen occurs at times less than 5 h, followed by a lower oxidation rate at longer times, for tests at 900 C and below. The other is that the final weight changes for the 700, 800, and 900 C tests are not in the sequence expected with respect to temperature. Isothermal oxidation of drop cast TiAl above 1000 C was found to exhibit parabolic oxidation controlled by protective alpha-Al₂O₃ scale formation. TiAl is the only phase in the binary Ti-Al system that forms exclusive scales of alpha-Al₂O₃ in isothermal oxidation. High anomalous rates at short times and at temperatures below 1000 C resulted from the internal oxidation of a second phase of aluminum. P.D.

A92-41667* National Aeronautics and Space Administration. Lewis Research Center, Cleveland, OH.

FRACTURE BEHAVIOR OF A B2 Ni-30Al-20Fe-0.05Zr INTERMETALLIC ALLOY IN THE TEMPERATURE RANGE 300 TO 1300 K

S. V. RAJ (NASA, Lewis Research Center, Cleveland, OH) Metallurgical Transactions A - Physical Metallurgy and Materials Science (ISSN 0360-2133), vol. 23A, no. 6, June 1992, p. 1691-1703. Jun. 1992 13 p refs

Copyright

The fracture behavior of a B2 Ni-30Al-20Fe-0.05Zr (at. pct) alloy was investigated using results of tensile tests conducted in the temperature range 300-1300 K under initial strain rates that varied between 10 exp -6 and 10 exp -3/sec, together with results of deformation measurements reported by Raj et al. (1992). Microstructural observations revealed that the alloy had failed by transgranular cleavage fracture below 873 K and by ductile fracture, power-law cavitation, triple point cracking, and rupture above this temperature. The fracture map constructed using fracture results is compared with those for other classes of materials, showing that the atomic bonding plays a significant role in the low-temperature ductility of NiAl-based alloys. I.S.

A92-41668* National Aeronautics and Space Administration. Lewis Research Center, Cleveland, OH.

DEFORMATION BEHAVIOR OF A Ni-30Al-20Fe-0.05Zr INTERMETALLIC ALLOY IN THE TEMPERATURE RANGE 300 TO 1300 K

S. V. RAJ (NASA, Lewis Research Center, Cleveland, OH), I. E. LOCCI (Case Western Reserve University, Cleveland, OH), and R. D. NOEBE (NASA, Lewis Research Center, Cleveland, OH) Metallurgical Transactions A - Physical Metallurgy and Materials Science (ISSN 0360-2133), vol. 23A, no. 6, June 1992, p. 1705-1718. Jun. 1992 14 p refs

Copyright

The deformation properties of an extruded Ni-30Al-20Fe-0.05Zr (at. pct) alloy in the temperature range 300-1300 K were investigated under initial tensile strain rates that varied between 10 exp -6 and 10 exp -3/sec and in constant load compression creep between 1073 and 1300 K. Three deformation regimes were observed: region I, occurring between 400 and 673 K, which consisted of an athermal regime of less than 0.3 percent tensile ductility; region II, between 673 and 1073, where exponential creep was dominant; and region III, between 1073 and 1300 K, where a significant improvement in tensile ductility was observed. I.S.

A92-44218* National Aeronautics and Space Administration. Lewis Research Center, Cleveland, OH.

THREE-DIMENSIONAL DEFORMATION ANALYSIS OF TWO-PHASE DISLOCATION SUBSTRUCTURES

ALAN D. FREED, S. V. RAJ (NASA, Lewis Research Center, Cleveland, OH), and KEVIN P. WALKER (Engineering Science Software, Inc., Smithfield, RI) Scripta Metallurgica et Materialia (ISSN 0956-716X), vol. 27, no. 2, July 15, 1992, p. 233-238. 15 Jul. 1992 6 p refs

(Contract DE-FG02-92ER-14247)

Copyright

Three-dimensional deformation analysis of two-phase dislocation substructures was carried out, extending the Qian and Fan (1991) approach to 3D stress-strain fields by using the Budiansky and Wu (1962) criterion for strain compatibility between the 'hard' and 'soft' regions. The result is a rate-dependent viscoplastic theory, named the dislocation substructure viscoplasticity (DSV), which incorporates a self-consistent effect of dislocation substructure on material response. An algorithm developed for numerical implementation of the DSV theory is presented. I.S.

A92-45231* National Aeronautics and Space Administration. Lewis Research Center, Cleveland, OH.

CUMULATIVE CREEP-FATIGUE DAMAGE EVOLUTION IN AN AUSTENITIC STAINLESS STEEL

MICHAEL A. MCGAW (NASA, Lewis Research Center, Cleveland, OH) IN: Advances in fatigue lifetime predictive techniques; Proceedings of the Symposium, San Francisco, CA, Apr. 24, 1990 1992 23 p refs

Copyright

A model of cumulative creep-fatigue damage has been developed which is based on the use of damage curve equations to describe the evolution of creep-fatigue damage for four basic creep-fatigue cycle types. These cycle types correspond to the four fundamental cycles of the Strain Range Partitioning Life Prediction approach of Manson, Halford, and Hirschberg. A concept referred to as Damage Coupling is introduced to analytically account for the differences in the nature of the damage introduced by each cycle type. For application of this model, the cumulative creep-fatigue damage behavior of type 316 stainless steel at 816 C has been experimentally established for the two-level loading cases involving fatigue and creep-fatigue, in various permutations. The tests were conducted such that the lower life (high strain) cycling was applied first, for a controlled number of cycles, and the higher life (lower strain) cycling was conducted at the second level, to failure. The proposed model correlated the majority of the observed cumulative creep-fatigue data. Author

A92-45232* National Aeronautics and Space Administration. Lewis Research Center, Cleveland, OH.

APPLICATION OF A THERMAL FATIGUE LIFE PREDICTION MODEL TO HIGH-TEMPERATURE AEROSPACE ALLOYS B1900 + HF AND HAYNES 188

G. R. HALFORD, J. F. SALISMAN, M. J. VERRILLI (NASA, Lewis Research Center, Cleveland, OH), and V. ARYA (Toledo, University, OH) IN: Advances in fatigue lifetime predictive techniques; Proceedings of the Symposium, San Francisco, CA, Apr. 24, 1990 1992 13 p refs

Copyright

The results of the application of a newly proposed thermomechanical fatigue (TMF) life prediction method to a series of laboratory TMF results on two high-temperature aerospace engine alloys are presented. The method, referred to as TMF/TS-SRP, is based on three relatively recent developments: the total strain version of the method of Strain Range Partitioning (TS-SRP), the bithermal testing technique for characterizing TMF behavior, and advanced viscoplastic constitutive models. The high-temperature data reported in a companion publication are used to evaluate the constants in the model and to provide the TMF verification data to check its accuracy. Predicted lives are in agreement with the experimental lives to within a factor of approximately 2. Author

26 METALLIC MATERIALS

A92-45233* National Aeronautics and Space Administration. Lewis Research Center, Cleveland, OH.
THERMOMECHANICAL AND BITHERMAL FATIGUE BEHAVIOR OF CAST B1900 + HF AND WROUGHT HAYNES 188

G. R. HALFORD, M. J. VERRILLI (NASA, Lewis Research Center, Cleveland, OH), S. KALLURI (NASA, Lewis Research Center, Sverdrup Technology, Inc., Cleveland, OH), F. J. RITZERT (NASA, Lewis Research Center, Cleveland, OH), R. E. DUCKERT (McDonnell Douglas Aircraft Co., Saint Louis, MO), and F. A. HOLLAND (NASA, Lewis Research Center, Cleveland, OH) IN: Advances in fatigue lifetime predictive techniques; Proceedings of the Symposium, San Francisco, CA, Apr. 24, 1990 1992 23 p refs

Copyright

A thermomechanical fatigue (TMF) high-temperature life prediction method has been evaluated using the experimental data. Bithermal fatigue (BTF), bithermal creep-fatigue (BTC-F), and TMF experiments were performed using two aerospace structural alloys, cast B1900 + Hf and wrought Haynes 188. The method which is based on the total strain version of strain range partitioning and unified cyclic constitutive modeling requires, as an input, information on the flow and failure behavior of the material of interest. Bithermal temperatures of 483 and 871 C were used for the cast B1900 + Hf nickel-base alloy and 316 and 760 C for the wrought Haynes 188 cobalt-base alloy. Maximum and minimum temperatures were also used in both TMF and BTF tests. Comparisons were made between the results of these tests and isothermal tensile and fatigue test data obtained previously. Qualitative correlations were observed between tensile and isothermal fatigue tests. O.G.

A92-46850* National Aeronautics and Space Administration. Lewis Research Center, Cleveland, OH.

DUCTILITY ENHANCEMENT FROM INTERFACE DISLOCATION SOURCES IN A DIRECTIONALLY SOLIDIFIED BETA + GAMMA + GAMMA-PRIME NI-FE-AL COMPOSITE ALLOY

M. LARSEN, A. MISRA, S. HARTFIELD-WUNSCH (Michigan, University, Ann Arbor), R. NOEBE (Michigan, University, Ann Arbor; NASA, Lewis Research Center, Cleveland, OH), and R. GIBALA (Michigan, University, Ann Arbor) IN: Intermetallic matrix composites; Proceedings of the MRS Symposium, San Francisco, CA, Apr. 18-20, 1990 1990 8 p refs (Contract NSF DMR-88-10058)

Copyright

A directionally solidified beta + gamma + gamma-prime Ni-Fe-Al in situ composite alloy of composition Ni₅₀Fe₃₀Al₂₀ has been used to investigate the effect of a plastically soft second phase on the mechanical behavior of a B2 ordered intermetallic alloy. This material exhibits extensive plasticity during compressive deformation at room temperature and fails in shear with extensive gamma + gamma-prime lamellar or rod pullout. The material also exhibits about 10 percent tensile elongation to fracture at room temperature, with final fracture that includes substantial necking of the gamma + gamma-prime lamellae or rods. Observation of slip lines and dislocation substructures discloses that the normally brittle beta matrix undergoes extensive plasticity in order to deform compatibly with the more ductile gamma phase. The plasticity of the beta matrix is accomplished by the generation of glissile dislocations into the beta matrix from the beta/gamma interface region and is enhanced because of a favorable beta-gamma orientation relationship for slip transfer. Ductility enhancement from interface-generated mobile dislocations generated from beta-gamma interfaces is compared to that observed in film-coated beta-NiAl single crystals and FeAl polycrystals. Author

A92-48152* National Aeronautics and Space Administration. Lewis Research Center, Cleveland, OH.

INFLUENCE OF PROCESSING ON THE MICROSTRUCTURE AND MECHANICAL PROPERTIES OF A NBAL3-BASE ALLOY

MOHAN G. HEB SUR (Sverdrup Technology, Inc., Brook Park, OH), IVAN E. LOCCI, S. V. RAJ, and MICHAEL V. NATHAL (NASA, Lewis Research Center, Cleveland, OH) Journal of Materials

Research (ISSN 0884-2914), vol. 7, no. 7, July 1992, p. 1696-1706. Jul. 1992 11 p refs

Copyright

Induction melting and rapid solidification processing, followed by grinding to 75-micron powder and P/M consolidation, have been used to produce a multiphase, NbAl₃-based, oxidation-resistant alloy of Nb-67Al-7Cr-0.5Y-0.25W composition whose strength and ductility are significantly higher than those of the induction-melted alloy at test temperatures of up to 1200 K. Attention is given to the beneficial role of microstructural refinement; the major second phase, AlNbCr, improves both oxidation resistance and mechanical properties. O.C.

A92-49694* National Aeronautics and Space Administration. Lewis Research Center, Cleveland, OH.

TENSILE BEHAVIOR OF THE L(1)2 COMPOUND AL67TI25CR8

K. S. KUMAR and S. A. BROWN (Martin Marietta Laboratories, Baltimore, MD) Acta Metallurgica et Materialia (ISSN 0956-7151), vol. 40, no. 8, Aug. 1992, p. 1923-1932. Aug. 1992 10 p refs (Contract NAS3-26069)

Copyright

Temperature-related variations in tensile yield strength and ductility were studied on cast, homogenized and isothermally forged Al₆₇Ti₂₅Cr₈. Yield strength dropped discontinuously between 623 K and 773 K and then decreased gradually with increasing temperature. Below 623 K, fracture occurred prior to macroscopic yielding. Ductility decreased from 0.2 percent at 623 K to zero at 773 K, but increased again at higher temperatures. At 1073 K, an elongation of 19 percent was obtainable, and ultimate tensile strength and localized necking were observed. Fracture surfaces and deformed microstructures were examined. The 1073 K tensile specimen that exhibited 19 percent elongation showed grain boundary serrations and some evidence of recrystallization (likely dynamic) although fracture occurred predominantly via an intergranular mode. Author

A92-57028* National Aeronautics and Space Administration. Lewis Research Center, Cleveland, OH.

VOLATILE SPECIES IN HALIDE-ACTIVATED-DIFFUSION COATING PACKS

ROBERT BIANCO, ROBERT A. RAPP (Ohio State University, Columbus), and NATHAN S. JACOBSON (NASA, Lewis Research Center, Cleveland, OH) Oxidation of Metals (ISSN 0030-770X), vol. 38, no. 1-2, Aug. 1992, p. 33-43. Aug. 1992 11 p refs (Contract N00014-87-K-0030; N00014-90-J-1765)

Copyright

An atmospheric pressure sampling mass spectrometer was used to identify the vapor species generated in a halide-activated cementation pack. Pack powder mixtures containing a Cr-Al binary masteralloy powder, an NH₄Cl activator salt, and either ZrO₂ or Y₂O₃ (or neither) were analyzed at 1000 C. Both the equilibrium calculations for the pack and mass spectrometer results indicated that volatile AlCl_x and CrCl_y species were generated by the pack powder mixture; in packs containing the reactive element oxide, volatile ZrCl_z and YCl_w species were formed by the conversion of their oxide sources. Author

N92-16086*# National Aeronautics and Space Administration. Lewis Research Center, Cleveland, OH.

HEATS OF FORMATION OF BCC BINARY ALLOYS

GUILLERMO BOZZOLO (Analex Corp., Brook Park, OH), JOHN FERRANTE, and JOHN R. SMITH (General Motors Research Labs., Warren, MI.) Dec. 1991 23 p (Contract RTOP 505-90-52) (NASA-TM-105281; E-6588; NAS 1.15:105281) Avail. CASI HC A03/MF A01

The method of Bozzolo, Ferrante and Smith is applied for the calculation of alloy energies for bcc elements. The heat of formation of several alloys is computed with the help of the Connolly-Williams method within the tetrahedron approximation. The dependence of the results on the choice of different sets of ordered structures is discussed. Author

N92-16111*# National Aeronautics and Space Administration. Lewis Research Center, Cleveland, OH.

LATTICE PARAMETERS OF FCC BINARY ALLOYS USING A NEW SEMIEMPIRICAL METHOD

GUILLERMO BOZZOLO (Analex Corp., Brook Park, OH.) and JOHN FERRANTE Jan. 1992 8 p
(Contract RTOP 505-90-54)
(NASA-TM-105304; E-6653; NAS 1.15:105304) Avail: CASI HC A02/MF A01

A new method is presented for the calculation of heats of formation, lattice parameters and cohesive energies of binary alloys. The method is applied to some fcc alloys and compared with experimental data, as well as other semiempirical results. Author

N92-22444*# National Aeronautics and Space Administration. Lewis Research Center, Cleveland, OH.

NOVEL APPLICATIONS FOR TAZ-8A

STEPHEN M. RIDDLEBAUGH and WILLIAM J. WATERS /n NASA, Washington, Technology 2001: The Second National Technology Transfer Conference and Exposition, Volume 1 p 171-182 Dec. 1991

Avail: CASI HC A03/MF A04

Recent needs in the non-aerospace industrial sector have revitalized interest in high performance alloys. TAZ-8A has a combination of properties that makes it unique: a high temperature strength, oxidation resistance, abrasion resistance, and exceptional thermal shock resistance. The major drawback for the utilization of this alloy is the relatively high cost compared with the more common iron base alloys. Reduced material consumption and lower costs are possible by using coatings of TAZ-8A on a low cost substrate. Coatings were applied using plasma spray techniques developed by NASA as well as modified plasma vapor deposition (PVD) techniques. Author

N92-24554*# National Aeronautics and Space Administration. Lewis Research Center, Cleveland, OH.

THE CYCLIC OXIDATION RESISTANCE AT 1200 C OF BETA-NIAL, FEAL, AND COAL ALLOYS WITH SELECTED THIRD ELEMENT ADDITIONS

C. A. BARRETT and R. H. TITRAN Apr. 1992 13 p
(Contract RTOP 505-63-01)
(NASA-TM-105620; E-5326; NAS 1.15:105620) Avail: CASI HC A03/MF A01

The intermetallic compounds Beta-NiAl, FeAl, and CoAl were tested in cyclic oxidation with selected third element alloy additions. Tests in static air for 200 1-hr cycles at 1200 C indicated by specific weight change/time data and x-ray diffraction analysis that the 5 at percent alloy additions did not significantly improve the oxidation resistance over the alumina forming baseline alloys without the additions. Many of the alloy additions were actually deleterious. Ta and Nb were the only alloy additions that actually altered the nature of the oxide(s) formed and still maintained the oxidation resistance of the protective alumina scale. Author

N92-27192*# National Aeronautics and Space Administration. Lewis Research Center, Cleveland, OH.

POST-TEST EXAMINATION OF A POOL BOILER RECEIVER

ROBERT L. DRESHFIELD, THOMAS J. MOORE, and PAUL A. BARTOLOTTA Apr. 1992 15 p
(Contract DE-AI04-85AL-33408; RTOP 590-13-11)
(NASA-TM-105635; E-6978; DOE/NASA/33408-6; NAS 1.15:105635) Avail: CASI HC A03/MF A01

A subscale pool boiler test apparatus to evaluate boiling stability developed a leak after being operated with boiling NaK for 791.4 hr at temperatures from 700 to 750 C. The boiler was constructed using Inconel 625 with a type 304L stainless steel wick for the boiler and type 316 stainless steel for the condenser. The boiler assembly was metallurgically evaluated to determine the cause of the leak and to assess the effects of the NaK on the materials. It was found that the leak was caused by insufficient (about 30 pct.) joint penetration in a butt joint. There was no general corrosion of the construction materials, but the room temperature ductility of the Inconel 625 was only about 6.5 pct. A crack in the heat

affected zone of the Inconel 625 near the Inconel 625 to type 316 stainless steel butt joint was probably caused by excessive heat input. The crack was observed to have a zone depleted of iron at the crack surface and porosity below that zone. The mechanism of the iron depletion was not conclusively determined. Author

27

NONMETALLIC MATERIALS

Includes physical, chemical, and mechanical properties of plastics, elastomers, lubricants, polymers, textiles, adhesives, and ceramic materials.

A92-21096* National Aeronautics and Space Administration. Lewis Research Center, Cleveland, OH.

A SIMPLE TEST FOR THERMOMECHANICAL EVALUATION OF CERAMIC FIBERS

GREGORY N. MORSCHER and JAMES A. DICARLO (NASA, Lewis Research Center, Cleveland, OH) American Ceramic Society, Journal (ISSN 0002-7820), vol. 75, Jan. 1992, p. 136-140. Previously announced in STAR as N91-21309. Jan. 1992 5 p refs

Copyright

A simple bend stress relaxation (BSR) test was developed to measure the creep related properties of ceramic fibers and whiskers. The test was applied to a variety of commercial and developmental Si based fibers to demonstrate capabilities and to evaluate the relative creep resistance of the fibers at 1200 to 1400 C. The implications of these results and the advantages of the BSR test over typical tensile creep tests are discussed. Author

A92-21099* National Aeronautics and Space Administration. Lewis Research Center, Cleveland, OH.

CONTROLLED CRACK GROWTH SPECIMEN FOR BRITTLE SYSTEMS

ANTHONY M. CALOMINO (NASA, Lewis Research Center, Cleveland, OH) and DAVID N. BREWER (NASA, Lewis Research Center; U.S. Army, Propulsion Directorate, Cleveland, OH) American Ceramic Society, Communications (ISSN 0002-7820), vol. 75, Jan. 1992, p. 206-208. Previously announced in STAR as N90-23543. Jan. 1992 3 p refs

Copyright

A pure Mode I fracture specimen and test procedure has been developed which provides extended, stable, through-thickness crack growth in ceramics and other brittle, nonmetallic materials. Fixed displacement loading, applied at the crack mouth, promotes stable crack extension by reducing the stored elastic strain energy. Extremely fine control of applied displacements is achieved by utilizing the Poisson's expansion of a compressively loaded cylindrical pin. Stable cracks were successfully grown in soda-lime glass and monolithic Al₂O₃ for lengths in excess of 20 mm without uncontrollable catastrophic failure. Author

A92-23225* National Aeronautics and Space Administration. Lewis Research Center, Cleveland, OH.

A COMBINED ANALYTICAL-EXPERIMENTAL TENSILE TEST TECHNIQUE FOR BRITTLE MATERIALS

M. L. CHU, R. J. SCAVUZZO, and T. S. SRIVATSAN (Akron, University, OH) Experimental Techniques (ISSN 0732-8818), vol. 16, Jan.-Feb. 1992, p. 46-50. Research supported by BF Goodrich Tire and Rubber Co. Feb. 1992 5 p refs
(Contract NAG3-479)

Copyright

A semiconventional tensile test technique is developed for impact ices and other brittle materials. Accurate results have been obtained on ultimate strength and modulus of elasticity in a

27 NONMETALLIC MATERIALS

refrigerated ice test. It is noted that the technique can be used to determine the physical properties of impact ices accreted inside icing wind tunnels or other brittle materials. O.G.

A92-31299* National Aeronautics and Space Administration. Lewis Research Center, Cleveland, OH.

THE EFFECTS OF RF PLASMA ASHING ON ZINC ORTHOTITANATE/POTASSIUM SILICATE THERMAL CONTROL COATINGS

JOYCE A. DEVER (NASA, Lewis Research Center, Cleveland, OH) and ERIC J. BRUCKNER (Cleveland State University, OH) IN: AIAA Materials Specialist Conference - Coating Technology for Aerospace Systems, Dallas, TX, Apr. 16, 17, 1992, Technical Papers 1992 10 p refs (AIAA PAPER 92-2171) Copyright

Samples of YB-71, a white thermal control coating composed of zinc orthotitanate pigment in a potassium silicate binder, were exposed in air plasma and in oxygen plasma to determine optical property and surface chemistry changes. Results show that YB-71 undergoes a significant reflectance decrease upon exposure to the simulated LEO atomic oxygen environment provided by an air plasma asher. YB-71 samples exposed to the same effective fluence in oxygen plasma, or in a UV screening Faraday cage in air or oxygen, do not undergo as severe reflectance decreases as the samples exposed in the air plasma asher environment. The UV and VUV radiation present in the plasma ashers affects the YB-71 degradation. It is noted that, when using plasma ashers to determine LEO degradation, it is necessary to take into account the sensitivity of the material to the synergistic effects of atomic oxygen and accelerated UV radiation. O.G.

A92-32407* National Aeronautics and Space Administration. Lewis Research Center, Cleveland, OH.

TRIBOLOGICAL PROPERTIES OF CERAMIC-(Ti3Al-Nb) SLIDING COUPLES FOR USE AS CANDIDATE SEAL MATERIALS TO 700 C

CHRISTOPHER DELLACORTE, BRUCE M. STEINETZ, and PAMELA K. BRINDLEY (NASA, Lewis Research Center, Cleveland, OH) IN: Metallurgical coatings and thin films 1990; Proceedings of the 17th International Conference on Metallurgical Coatings and 8th International Conference on Thin Films, San Diego, CA, Apr. 2-6, 1990. Vol. 1 1990 11 p refs Copyright

Tribological properties of Ti3Al-Nb intermetallic disks sliding against alumina-boria-silicate fabric were ascertained in air at temperatures from 25 to 700 C. These materials are candidates for sliding seal applications for the National AeroSpace Plane. The tests were done using a pin on disk tribometer. Sliding was unidirectional at 0.27 m/sec under a nominal contact stress of 340 kPa. Gold sputter or ion plating deposited films were used to reduce friction and wear. Rhodium and palladium films were used beneath the gold lubricating films to prevent diffusion of the substrate into the gold at high temperature. The friction and wear of the unlubricated specimens was unacceptable. Friction coefficients were generally greater than 1.0. The ion plated gold films, when used with a rhodium diffusion barrier reduced friction by almost a factor of 2. Wear was also substantially reduced. The sputter deposited films were not adherent unless the substrate was sputter cleaned immediately prior to film deposition. Palladium did not function as a diffusion barrier. Author

A92-32410* National Aeronautics and Space Administration. Lewis Research Center, Cleveland, OH.

STUDIES OF MECHANOCHEMICAL INTERACTIONS IN THE TRIBOLOGICAL BEHAVIOR OF MATERIALS

KAZUHISA MIYOSHI (NASA, Lewis Research Center, Cleveland, OH) IN: Metallurgical coatings and thin films 1990; Proceedings of the 17th International Conference on Metallurgical Coatings and 8th International Conference on Thin Films, San Diego, CA, Apr. 2-6, 1990. Vol. 1 1990 14 p refs Copyright

Mechanochemical interaction studies can contribute to the understanding of wear and friction of materials. Specific examples

of experimental results relative to the subject are discussed. There are two parts: one describes the synergistic effect of corrosion and wear of iron sliding on sapphire in sulfuric acid, and the other describes the effect of surface films on the wear and friction of plasma-deposited diamondlike carbon (amorphous hydrogenated carbon) films in sliding contact with silicon nitride. The concentration of acid (pH) is an important factor in controlling the iron loss caused by wear-corrosion processes in sulfuric acid. The mechanical action can cause chemical reactions to proceed much faster than they would otherwise. The diamondlike carbon (DLC) films are shown to behave tribologically much like bulk diamond. In a dry nitrogen environment, a mechanochemical reaction produces a substance which greatly decreases the coefficient of friction. In a moist air environment, mechanochemical interactions drastically reduce the wear life of DLC films and water vapor greatly increases friction. Author

A92-32632* National Aeronautics and Space Administration. Lewis Research Center, Cleveland, OH.

VISCOELASTIC PROPERTIES OF ADDITION-CURED POLYIMIDES USED IN HIGH TEMPERATURE POLYMER MATRIX COMPOSITES

GARY D. ROBERTS, DIANE C. MALARIK (NASA, Lewis Research Center, Cleveland, OH), and JERROLD O. ROBAIDEK (Case Western Reserve University, Cleveland, OH) IN: Composites; Proceedings of the 8th International Conference on Composite Materials (ICCM/8), Honolulu, HI, July 15-19, 1991. Section 12-21 1991 10 p refs

The viscoelastic properties of an addition-cured polyimide, PMR-15, were evaluated through dynamic mechanical and stress relaxation testing. Below the glass transition temperature, the dynamic mechanical properties of the composites are strongly affected by the absorbed moisture in the resin. At temperature 20 C and more above the glass transition temperature, the storage modulus increases continuously with time, indicating that additional crosslinking is occurring in the resin. For resin moisture contents less than 2 percent, stress relaxation curves measured at different temperatures can be superimposed using horizontal shifts along the log(time) axis with only small shifts along the vertical axis. V.L.

A92-32896* National Aeronautics and Space Administration. Lewis Research Center, Cleveland, OH.

CRACK HEALING BEHAVIOR OF HOT PRESSED SILICON NITRIDE DUE TO OXIDATION

S. R. CHOI (Cleveland State University, OH) and V. TIKARE (NASA, Lewis Research Center, Cleveland, OH) Scripta Metallurgica et Materialia (ISSN 0956-716X), vol. 26, April 1992, p. 1263-1268. 15 Apr. 1992 6 p refs (Contract DE-AI05-87OR-21749) Copyright

It is shown that limited oxidation of an MgO-containing, hot-pressed silicon nitride ceramic at 800 deg C and above results in increased strength due to crack healing. Slight oxidation of the surface produces enstatite and cristobalite which fills in cracks. More extensive oxidation leads to strength degradation due to the formation of new flaws by the evolution of N2 gas at the surface. The apparent fracture toughness also increased at 800 deg C and above due to oxidation. Bonds formed between the two surfaces of the crack during oxidation leads to a reduction in stress intensity at the crack tip, suggesting that valid high-temperature toughness values cannot be obtained in an air environment. The increase in strength due to crack healing by oxidation can be achieved without compromising the fatigue properties of the silicon nitride ceramic. C.D.

A92-33918* National Aeronautics and Space Administration. Lewis Research Center, Cleveland, OH.

ADDITION CURING THERMOSETS ENDCAPPED WITH 4-AMINO (2.2) PARACYCLOPHANE

JOHN F. WATERS (Case Western Reserve University, Cleveland, OH), JAMES K. SUTTER, MARY A. B. MEADOR, LARRY J. BALDWIN, and MICHAEL A. MEADOR (NASA, Lewis Research

Center, Cleveland, OH) Journal of Polymer Science, Part A - Polymer Chemistry (ISSN 0887-624X), vol. 29, 1991, p. 1917-1924. 1991 8 p refs

Copyright

A new family of addition curing polyimides were prepared that contained 4-amino (2.2)-paracyclophane as the endcap. An improved synthesis of the endcap 4-amino-(2.2) cyclophane was accomplished increasing the yield to 60 percent and simplifying the procedure. DSC and rheological analysis of endcapped polyimide oligomers confirmed that the onset for polymerization of the ethylene bridge was 250 C. C-13 CP/MAS NMR was used to determine the structural changes of the oligomers after thermal treatment. The cyclophane capped polyimides were successfully compression molded to form void free neat resin specimens. Tg's as high as 353 C were obtained by thermomechanical analysis for postcured samples. Preliminary thermal stability studies suggest that these resins have a high onset of decomposition ranging from 549 to 567 C.

Author

A92-33930* National Aeronautics and Space Administration. Lewis Research Center, Cleveland, OH.

PRECAUTIONS TOWARD XTEM OF Si3N4/SiO2

LINUS U. J. T. OGBUJI (NASA, Lewis Research Center, Cleveland, OH) IN: Electron Microscopy Society of America, Annual Meeting, 49th, San Jose, CA, Aug. 4-9, 1991, Proceedings. San Francisco, CA, San Francisco Press, Inc., 1991, p. 1120, 1121. 1991 2 p refs

Copyright

Severe difficulties are encountered in the preparation of oxidized Si3N4 specimens for XTEM transmission electromicroscopic inspection, in virtue of the extreme difference between Si3N4 and SiO2 mechanical properties. Attention is presently given to a preparation method in which an overlayer of the nitride is always occluded; this protects the oxide through most of the thinning that specimen preparation entails. An XTEM image of the oxide/nitride interface is presented.

O.C.

A92-36287* National Aeronautics and Space Administration. Lewis Research Center, Cleveland, OH.

DIELECTRIC BREAKDOWN STUDIES OF TEFLON PERFLUOROALKOXY AT HIGH TEMPERATURE

J. L. SUTHAR and J. R. LAGHARI (New York, State University, Buffalo) Journal of Materials Science (ISSN 0022-2461), vol. 27, no. 7, April 1, 1992, p. 1795-1800. Research supported by NASA. 1 Apr. 1992 6 p refs

Copyright

Teflon perfluoroalkoxy (PFA) was evaluated for use as a dielectric material in high-temperature high-voltage capacitors for space applications. The properties that were characterized included the dc dielectric strength at temperatures up to 250 C and the permittivity and dielectric loss as a function of frequency, temperature and voltage. To understand the breakdown mechanism taking place at high temperatures, the pre-breakdown discharge and conduction currents, and the dependence of dielectric strength on thickness of the film were determined. Confocal laser microscopy was performed to diagnose for microimperfections within the film structure. The results obtained show a significant decrease in the dielectric strength and an increase in dielectric loss with an increase in temperature, suggesting that impulsive thermal breakdown could be a responsible mechanism in PFA film at temperatures above 150 C.

Author

A92-39628* National Aeronautics and Space Administration. Lewis Research Center, Cleveland, OH.

BONDED CERAMIC FOAMS REINFORCED WITH FIBERS FOR HIGH TEMPERATURE USE

G. MCDONALD, R. C. HENDRICKS (NASA, Lewis Research Center, Cleveland, OH), and R. L. MULLEN (Case Western Reserve University, Cleveland, OH) Aug. 1992 4 p

Copyright

High quality SiC ceramic foams, which have only recently become available, have for the first time made possible the construction of low density ceramic fiber-ceramic foam sandwiches

for high temperature applications. This report describes the construction of some ceramic fiber-ceramic foam structures and the preliminary measurement of strength at elevated temperature.

Author

A92-39674* National Aeronautics and Space Administration. Lewis Research Center, Cleveland, OH.

OXIDATION KINETICS OF CVD SILICON CARBIDE AND SILICON NITRIDE

DENNIS S. FOX (NASA, Lewis Research Center, Cleveland, OH) Oct. 1992 16 p refs

Copyright

The long-term oxidation behavior of pure, monolithic CVD SiC and Si3N4 is studied, and the isothermal oxidation kinetics of these two materials are obtained for the case of 100 hrs at 1200-1500 C in flowing oxygen. Estimates are made of lifetimes at the various temperatures investigated. Parabolic rate constants for SiC are within an order of magnitude of shorter exposure time values reported in the literature. The resulting silica scales are in the form of cristobalite, with cracks visible after exposure. The oxidation protection afforded by silica for these materials is adequate for long service times under isothermal conditions in 1-atm dry oxygen.

O.C.

A92-39687* National Aeronautics and Space Administration. Lewis Research Center, Cleveland, OH.

RELATIONSHIPS BETWEEN TOUGHNESS AND MICROSTRUCTURE OF REACTION BONDED Si3N4

ANNAMARIE LIGHTFOOT, JULIA SIGALOVSKY, and JOHN S. HAGGERTY (MIT, Cambridge, MA) Oct. 1992 8 p refs (Contract DAAL03-88-K-0099; NAG3-845)

Copyright

Fracture toughnesses of nominally identical batches of reaction bonded silicon nitride (RBSN) differed significantly (about 2.0 and about 2.7 MPa sq rt m). Detailed fractographic and microstructural characterizations investigated underlying factors. Subtle differences between high and low toughness RBSN and between constituent Si powders have been revealed through SEM/FEG, TEM, BET, Hg-porosimetry, and XRD. The results illustrate the need for behavioral models to guide microstructural design and to interpret properties of brittle materials with intermediate levels of porosity.

Author

A92-39854* National Aeronautics and Space Administration. Lewis Research Center, Cleveland, OH.

MONOLITHIC CERAMICS

THOMAS P. HERBELL and WILLIAM A. SANDERS (NASA, Lewis Research Center, Cleveland, OH) IN: Flight-vehicle materials, structures, and dynamics - Assessment and future directions. Vol. 3 - Ceramics and ceramic-matrix composites 1992 23 p refs

Copyright

A development history and current development status evaluation are presented for SiC and Si3N4 monolithic ceramics. In the absence of widely sought improvements in these materials' toughness, and associated reliability in structural applications, uses will remain restricted to components in noncritical, nonman-rated aerospace applications such as cruise missile and drone gas turbine engine components. In such high temperature engine-section components, projected costs lie below those associated with superalloy-based short-life/expendable engines. Advancements are required in processing technology for the sake of fewer and smaller microstructural flaws.

O.C.

A92-39856* National Aeronautics and Space Administration. Lewis Research Center, Cleveland, OH.

POLYMERIC PRECURSORS FOR FIBERS AND MATRICES

FRANCES I. HURWITZ (NASA, Lewis Research Center, Cleveland, OH) IN: Flight-vehicle materials, structures, and dynamics - Assessment and future directions. Vol. 3 - Ceramics and ceramic-matrix composites 1992 19 p refs

Copyright

Candidate polymeric precursors for ceramic fiber and matrix processing are discussed, with a view to the advantages and

27 NONMETALLIC MATERIALS

disadvantages of this approach relative to existing alternatives. The properties of ceramic products thus derived are noted to strongly depend on the molecular weight and structure of the starting polymer; in particular, the ceramic's composition and morphology are dependent on the character and extent of crosslinking, as well as on the path of pyrolysis. While large and complex structural ceramic components may ultimately be obtainable by these means, the polymer-precursor method is still in its developmental infancy. O.C.

A92-43478* National Aeronautics and Space Administration. Lewis Research Center, Cleveland, OH.

ESTIMATION OF CRACK CLOSURE STRESSES FOR IN SITU TOUGHENED SILICON NITRIDE WITH 8 WT PCT SCANDIA

SUNG R. CHOI (NASA, Lewis Research Center; Cleveland State University, OH), JONATHAN A. SALEM (NASA, Lewis Research Center, Cleveland, OH), and WILLIAM A. SANDERS (Analex Corp., Brook Park, OH) American Ceramic Society, Journal (ISSN 0002-7820), vol. 75, no. 6, June 1992, p. 1508-1511. Jun. 1992 4 p refs

Copyright

An 8-wt pct-scandia silicon nitride with an elongated grain structure was fabricated. The material exhibited high fracture toughness and a rising R-curve as measured by the indentation strength technique. The 'toughening' exponent m was found to be m about 0.1. The high fracture toughness and R-curve behavior was attributed mainly to bridging of the crack faces by the elongated grains. The crack closure (bridging) stress distribution in the wake region of the crack tip was estimated as a function of crack size from the R-curve data, with an arbitrarily assumed distribution function. Author

A92-43483* National Aeronautics and Space Administration. Lewis Research Center, Cleveland, OH.

REACTIONS OF SILICON CARBIDE AND SILICON(IV) OXIDE AT ELEVATED TEMPERATURES

NATHAN S. JACOBSON, KANG N. LEE, and DENNIS S. FOX (NASA, Lewis Research Center, Cleveland, OH) American Ceramic Society, Journal (ISSN 0002-7820), vol. 75, no. 6, June 1992, p. 1603-1611. Jun. 1992 9 p refs

Copyright

The reaction between SiC and SiO₂ has been studied in the temperature range 1400-1600 K. A Knudsen cell in conjunction with a vacuum microbalance and a high-temperature mass spectrometer was used for this study. Two systems were studied - 1:1 SiC (2 wt pct excess carbon) and SiO₂; and 1:1:1 SiC, carbon, and SiO₂. In both cases the excess carbon forms additional SiC within the Knudsen cell and adjusts to the direct reaction of stoichiometric SiC and SiO₂ to form SiO(g) and CO(g) in approximately a 3:1 ratio. These results are interpreted in terms of the Si-C-O stability diagram. Author

A92-43761* National Aeronautics and Space Administration. Lewis Research Center, Cleveland, OH.

MECHANICAL PROPERTIES OF 3C SILICON CARBIDE

LIJUN TONG, MEHRAN MEHREGANY (Case Western Reserve University, Cleveland, OH), and LAWRENCE G. MATUS (NASA, Lewis Research Center, Cleveland, OH) Applied Physics Letters (ISSN 0003-6951), vol. 60, no. 24, June 15, 1992, p. 2992-2994. 15 Jun. 1992 3 p refs

Copyright

The residual stress and Young's modulus of 3C silicon carbide (SiC) epitaxial films deposited on silicon substrates were measured by load-deflection measurements using suspended SiC diaphragms fabricated with silicon micromachining techniques. The film's residual stress was tensile and averaged 274 MPa while the in-plane Young's modulus averaged 394 GPa. In addition, the bending moment due to the residual stress variation through the thickness of the film was determined by measuring the deflection of free-standing 3C-SiC cantilever beams. The bending moment was in the range of $2.6 \times 10 \exp -8$ - $4.2 \times 10 \exp -8$ N m. Author

A92-44479* National Aeronautics and Space Administration. Lewis Research Center, Cleveland, OH.

LOW TEMPERATURE SYNTHESIS OF CAO-SIO2 GLASSES HAVING STABLE LIQUID-LIQUID IMMISCIBILITY BY THE SOL-GEL PROCESS

N. P. BANSAL (NASA, Lewis Research Center, Cleveland, OH) Journal of Materials Science (ISSN 0022-2461), vol. 27, no. 11, June 1, 1992, p. 2922-2933. Previously announced in STAR as N91-11806. 1 Jun. 1992 12 p refs (Contract NCC3-133)

Copyright

Calcium silicate glass compositions lying within the liquid-liquid immiscibility dome of the phase diagram, which could not have been prepared by the conventional melting method, were synthesized by the sol-gel process. Hydrolysis and polycondensation of tetraethyl orthosilicate (TEOS) solutions containing up to 20 mol percent calcium nitrate resulted in the formation of clear and transparent gels. The gel formation time decreased with increase in water: TEOS mole ratio, calcium content, and the reaction temperature. Smaller values of gel times in the presence of calcium nitrate are probably caused by lowering of the ionic charge on the sol particles by the salt present. The gelation activation energy, $E(\text{sub gel})$, was evaluated from temperature dependence of the gel time. Presence of Ca(2+) ions or the water:TEOS mole ratio did not have an appreciable effect on the value of $E(\text{sub gel})$. Presence of glycerol in the solution helped in the formation of crack-free monolithic gel specimens. Chemical and structural changes occurring in the gels, as a function of the heat treatments, have been monitored using DTA, TGA, IR-spectroscopy, X-ray diffraction, surface area and pore size distribution measurements. Author

A92-49095*# National Aeronautics and Space Administration. Lewis Research Center, Cleveland, OH.

RELATIVE SLIDING DURABILITY OF TWO CANDIDATE HIGH TEMPERATURE OXIDE FIBER SEAL MATERIALS

CHRISTOPHER DELLACORTE and BRUCE M. STEINETZ (NASA, Lewis Research Center, Cleveland, OH) AIAA, SAE, ASME, and ASEE, Joint Propulsion Conference and Exhibit, 28th, Nashville, TN, July 6-8, 1992. 8 p. Previously announced in STAR as N92-10064. Jul. 1992 8 p refs (AIAA PAPER 92-3713) Copyright

A test program to determine the relative sliding durability of two candidate ceramic fibers for high temperature sliding seal applications is described. Pin on disk tests were used to evaluate potential seal materials. Friction during the tests and fiber wear, indicated by the extent of fibers broken in a test bundle or yarn, was measured at the end of a test. In general, friction and wear increase with test temperature. This may be due to a reduction in fiber strength, a change in the surface chemistry at the fiber/counterface interface due to oxidation, adsorption and/or desorption of surface species and, to a lesser extent, an increase in counterface surface roughness due to oxidation at elevated temperatures. The relative fiber durability correlates with tensile strength indicating that tensile data, which is more readily available than sliding durability data, may be useful in predicting fiber wear behavior under various conditions. A simple model developed using dimensional analysis shows that the fiber durability is related to a dimensionless parameter which represents the ratio of the fiber strength to the fiber stresses imposed by sliding. Author

A92-49814* National Aeronautics and Space Administration. Lewis Research Center, Cleveland, OH.

FRACTAL DIMENSION OF ALUMINA AGGREGATES GROWN IN TWO DIMENSIONS

JUDITH L. LAROSA and JAMES D. CAWLEY (Ohio State University, Columbus) American Ceramic Society, Communications (ISSN 0002-7820), vol. 75, no. 7, July 1992, p. 1981-1984. Research supported by IBM Corp. Jul. 1992 4 p refs (Contract NAG3-755)

Copyright

The concepts of fractal geometry are applied to the analysis of 0.4-micron alumina constrained to agglomerate in two

dimensions. Particles were trapped at the bottom surface of a drop of a dilute suspension, and the agglomeration process was directly observed, using an inverted optical microscope. Photographs were digitized and analyzed, using three distinct approaches. The results indicate that the agglomerates are fractal, having a dimension of approximately 1.5, which agrees well with the predictions of the diffusion-limited cluster-cluster aggregation model.

Author

A92-50191* National Aeronautics and Space Administration. Lewis Research Center, Cleveland, OH.

EXTREME VALUE STATISTICS ANALYSIS OF FRACTURE STRENGTHS OF A SINTERED SILICON NITRIDE FAILING FROM PORES

LUEN-YUAN CHAO and DINESH K. SHETTY (Utah, University, Salt Lake City) American Ceramic Society, Journal (ISSN 0002-7820), vol. 75, no. 8, Aug. 1992, p. 2116-2124. Aug. 1992 9 p refs

(Contract NAG3-789)

Copyright

A92-54504* National Aeronautics and Space Administration. Lewis Research Center, Cleveland, OH.

MECHANICAL BEHAVIOUR AND FAILURE PHENOMENON OF AN IN SITU TOUGHENED SILICON NITRIDE

J. A. SALEM, S. R. CHOI, M. R. FREEDMAN (NASA, Lewis Research Center, Cleveland, OH), and M. G. JENKINS (Oak Ridge National Laboratory, TN) Journal of Materials Science (ISSN 0022-2461), vol. 27, no. 16, Aug. 15, 1992, p. 4421-4428. Previously announced in STAR as N91-23311. 15 Aug. 1992 8 p refs

(Contract DE-AI05-87OR-21749)

Copyright

The Weibull modulus, fracture toughness and crack growth resistance of an in-situ toughened, silicon nitride material used to manufacture a turbine combustor were determined from room temperature to 1371 C. The material exhibited an elongated grain structure that resulted in improved fracture toughness, nonlinear crack growth resistance, and good elevated temperature strength. However, low temperature strength was limited by grains of excessive length (30 to 100 microns). These excessively long grains were surrounded by regions rich in sintering additives.

Author

A92-56585* National Aeronautics and Space Administration. Lewis Research Center, Cleveland, OH.

ASYMMETRIC TIP MORPHOLOGY OF CREEP MICROCRACKS GROWING ALONG BIMATERIAL INTERFACES

TZE-JER CHUANG (NIST, Ceramics Div., Gaithersburg, MD), JUNE-LIANG CHU, and SANBOH LEE (National Tsing Hua University, Hsinchu, Taiwan) Acta Metallurgica et Materialia (ISSN 0956-7151), vol. 40, no. 10, Oct. 1992, p. 2683-2691. Oct. 1992 9 p refs

(Contract NASA ORDER C-82000-R)

Copyright

The asymmetric tip morphology of a creep microcrack propagating along a bimaterial interface is presented based on the assumptions that the near-tip shapes are developed from surface diffusion controlled crack growth and that a steady state prevails. A single master curve still can adequately describe the near-tip shapes to within 6 percent accuracy, but four cases of crack-tip morphology emerge depending on the ratios of surface to interfacial free energy and diffusivity of the adjoining phases. For fixed ratios of the two surface diffusivities, crack tip morphology maps in the space of specific surface energies are constructed with which areas associated with each individual case are indicated. Predicted cases on a set of bimaterial systems are tabulated and discussed.

Author

A92-57027* National Aeronautics and Space Administration. Lewis Research Center, Cleveland, OH.

ANODIC ETCHING OF P-TYPE CUBIC SILICON CARBIDE

G. L. HARRIS, K. FEKADE, and K. WONGCHOTIGUL (Howard University, Washington) Journal of Materials Science: Materials in Electronics (ISSN 0957-4522), vol. 3, no. 3, Sept. 1992, p. 162,

163. Research supported by Howard University. Sep. 1992 2 p refs

(Contract NAG3-431; NSF RII-87-14676; NSF RII-84-13805) Copyright

p-Type cubic silicon carbide was anodically etched using an electrolyte of HF:HCl:H₂O. The etching depth was determined versus time with a fixed current density of 96.4 mA/sq cm. It was found that the etching was very smooth and very uniform. An etch rate of 22.7 nm/s was obtained in a 1:1:50 HF:HCl:H₂O electrolyte.

Author

N92-10090* National Aeronautics and Space Administration. Lewis Research Center, Cleveland, OH.

BROMINATED GRAPHITIZED CARBON FIBERS Patent

CHING-CHEH HUNG, inventor (to NASA) 22 Oct. 1991 83 p Filed 30 Nov. 1989 Supersedes N90-15262 (28 - 7, p 910) Continuation-in-part of abandoned US-Patent-Appl-SN-219016, filed 14 Jul. 1988

(NASA-CASE-LEW-14698-2; US-PATENT-5,059,409; US-PATENT-APPL-SN-443289; US-PATENT-APPL-SN-219016; US-PATENT-CLASS-423-448; US-PATENT-CLASS-423-439; US-PATENT-CLASS-423-460; US-PATENT-CLASS-252-502; INT-PATENT-CLASS-C01B-31/04) Avail: US Patent and Trademark Office

Low cost, high break elongation graphitized carbon fibers having low degree of graphitization are inert to bromine at room or higher temperatures, but are brominated at -7 to 20 C, and then debrominated at ambient. Repetition of this bromination-debromination process can bring the bromine content to 18 percent. Electrical conductivity of the brominated fibers is three times of the before-bromination value.

Official Gazette of the U.S. Patent and Trademark Office

N92-11186*# National Aeronautics and Space Administration. Lewis Research Center, Cleveland, OH.

SOLID LUBRICANTS ON PRETREATED SURFACES Patent Application

ROBERT L. FUSARO, inventor (to NASA) 16 Sep. 1991 12 p (NASA-CASE-LEW-14474-2; NAS 1.71:LEW-14474-2; US-PATENT-APPL-SN-760670) Avail: CASI HC A03/MF A01

A solid lubricant film on a pretreated surface is described. The surface topography of the material to be lubricated is first selectively altered. Photochemical etching is employed to selectively determine contact area and shape to maximize the proper ratio of reservoir area to sliding contact area. Cadmium oxide is then sputtered onto the altered surface. The cadmium oxide acts as an intermediate layer to more tightly bond the solid lubricant, such as graphite, onto the material surface.

NASA

N92-11188*# National Aeronautics and Space Administration. Lewis Research Center, Cleveland, OH.

HIGH-T SUB C FLUORINE-DOPED YBa₂Cu₃O_y FILMS ON CERAMIC SUBSTRATES BY SCREEN PRINTING

NAROTTAM P. BANSAL Oct. 1991 18 p (Contract RTOP 307-51-00)

(NASA-TM-105296; E-6635; NAS 1.15:105296) Avail: CASI HC A03/MF A01

Thick films of fluorine-doped YBa₂Cu₃O_y were screen printed on highly polished alumina, magnesia spinel, strontium titanate, and yttria-stabilized zirconia (YSZ) substrates. They were annealed at 1000 C and soaked in oxygen at 450 C, followed by slow cooling to room temperature. The films were characterized by electrical resistivity measurements as a function of temperature and x-ray diffraction. The film on YSZ showed the best characteristics with a T_{sub c} (onset) of 91 K, T_{sub c} (R equals 0) of 88.2 K, and a transition width, delta T_{sub c} (10-90 percent), of approximately 1.7 K. The film adhesion, probably controlled by interdiffusion of cations between the film and the substrate, was good in all cases except on strontium titanate where the film completely detached from the substrate.

Author

27 NONMETALLIC MATERIALS

N92-11202*# National Aeronautics and Space Administration.
Lewis Research Center, Cleveland, OH.

GLASS FORMATION, PROPERTIES, AND STRUCTURE OF SODA-YTTRIA-SILICATE GLASSES

PAUL W. ANGEL and RAIFORD E. HANN Oct. 1991 14 p
(Contract RTOP 505-62-00)
(NASA-TM-104488; E-6336; NAS 1.15:104488) Avail: CASI HC
A03/MF A01

The glass formation region of the soda yttria silicate system was determined. The glasses within this region were measured to have a density of 2.4 to 3.1 g/cu cm, a refractive index of 1.50 to 1.60, a coefficient of thermal expansion of $7 \times 10^{-6}/C$, softening temperatures between 500 and 780 C, and Vickers hardness values of 3.7 to 5.8 GPa. Aqueous chemical durability measurements were made on select glass compositions while infrared transmission spectra were used to study the glass structure and its effect on glass properties. A compositional region was identified which exhibited high thermal expansion, high softening temperatures, and good chemical durability. Author

N92-14170*# National Aeronautics and Space Administration.
Lewis Research Center, Cleveland, OH.

PROPERTIES OF NOVEL CVD GRAPHITE FIBERS AND THEIR BROMINE INTERCALATION COMPOUNDS

JAMES R. GAIER (Applied Sciences, Inc., Cedarville, OH.), MAX L. LAKE (Cleveland State Univ., OH.), ALIA MOINUDDIN, and MARK MARABITO (Cleveland State Univ., OH.) 1991 10 p
Presented at the 20th Biennial Conference on Carbon, Santa Barbara, CA, 23-28 Jun. 1991; sponsored by the American Carbon Society

(Contract RTOP 506-41-41)
(NASA-TM-105295; E-6595; NAS 1.15:105295) Avail: CASI HC
A02/MF A01

A hybrid fiber with a PAN core surrounded by a vapor grown carbon fiber (VGCF) sheath was fabricated using a proprietary process. The density, ultimate tensile strength, Young's modulus, and resistivity of pristine and bromine intercalated fibers made by this technique having diameters varying from 5 to 50 microns were compared with the values predicted from the rule of mixtures model. For both the pristine and intercalated fibers, the density, ultimate tensile strength, and Young's modulus of the fibers were lower than predicted, but the resistivity was measured to be consistent with predictions. The lower than theoretical mechanical properties may be evidence of a low density disordered interface between the core and the sheath which would lower the density and degrade the mechanical properties, but would leave the resistivity nearly unaffected. Intercalation had little if any effect on the ultimate tensile strength and Young's modulus, but raised the density by about 11 pct., and lowered the resistivity by an order of magnitude. The diameter dependence of the resistivity showed evidence of a depletion layer of the type found in VGCF. Author

N92-14179*# National Aeronautics and Space Administration.
Lewis Research Center, Cleveland, OH.

THE CHEMISTRY OF SAUDI ARABIAN SAND: A DEPOSITION PROBLEM ON HELICOPTER TURBINE AIRFOILS

JAMES L. SMIALEK 1991 11 p Presented at the Gordon Conference on Corrosion, New London, NH, 14 Jul. 1991
(Contract RTOP 505-62-0K)

(NASA-TM-105234; E-6559; NAS 1.15:105234) Avail: CASI HC
A03/MF A01

Recent operations in the Persian Gulf have exposed military helicopter turbines to excessive amounts of ingested sand. Fine particles, less than 10 microns, are able to bypass the particle separators and enter the cooling and combustion systems. The initial sand chemistry varies by location, but is made up of a calcium aluminum silicate glass, SiO₂ low quartz (Ca,Mg) CO₃ dolomite, CaCO₃ calcite, and occasionally CaCl rocksalt. The sand reacts in the hot combustion gases and deposits onto the turbine vanes as CaSO₄, glass, and various crystalline silicates. Deposits up to 0.25 in. thick have been collected. Although cooling hole plugging is a considerable problem, excessive corrosion is not

commonly observed due to the high melting point of GaSO₄.

Author

N92-15191*# National Aeronautics and Space Administration.
Lewis Research Center, Cleveland, OH.

TRIBOLOGY NEEDS FOR FUTURE SPACE AND AERONAUTICAL SYSTEMS

ROBERT L. FUSARO Dec. 1991 40 p
(Contract RTOP 505-63-5B)
(NASA-TM-104525; E-6399; NAS 1.15:104525) Avail: CASI HC
A03/MF A01

Future aeronautical and space missions will push tribology technology beyond its current capability. The objective is to discuss the current state of the art of tribology as it is applied to advanced aircraft and spacecraft. Areas of discussion include materials lubrication mechanisms, factors affecting lubrication, current and future tribological problem areas, potential new lubrication techniques, and perceived technology requirements that need to be met in order to solve these tribology problems. Author

N92-15192*# National Aeronautics and Space Administration.
Lewis Research Center, Cleveland, OH.

ELEVATED TEMPERATURE MECHANICAL BEHAVIOR OF MONOLITHIC AND SiC WHISKER-REINFORCED SILICON NITRIDES

JONATHAN A. SALEM (Cleveland State Univ., OH.), SUNG R. CHOI (Analex Corp., Cleveland, OH.), WILLIAM A. SANDERS (Analex Corp., Brook Park, OH.), and DENNIS S. FOX Dec. 1991 22 p
(Contract RTOP 505-63-1M)
(NASA-TM-105245; E-6572; NAS 1.15:105245) Avail: CASI HC
A03/MF A01

The mechanical behavior of a 30 volume percent SiC whisker reinforced silicon nitride and a similar monolithic silicon nitride were measured at several temperatures. Measurements included strength, fracture toughness, crack growth resistance, dynamic fatigue susceptibility, post oxidation strength, and creep rate. Strength controlling defects were determined with fractographic analysis. The addition of SiC whiskers to silicon nitride did not substantially improve the strength, fracture toughness, or crack growth resistance. However, the fatigue resistance, post oxidation strength, and creep resistance were diminished by the whisker addition. Author

N92-16122*# National Aeronautics and Space Administration.
Lewis Research Center, Cleveland, OH.

METHOD OF MAKING CONTAMINATION-FREE CERAMIC BODIES Patent

WARREN H. PHILIPP, inventor (to NASA) 19 Nov. 1991 5 p
Filed 9 Nov. 1990 Supersedes N91-16152 (29 - 8, p 1120)
(NASA-CASE-LEW-14984-1; US-PATENT-5,066,625;
US-PATENT-APPL-SN-610883; US-PATENT-CLASS-501-127;
US-PATENT-CLASS-501-123; US-PATENT-CLASS-423-630;
US-PATENT-CLASS-264-63; INT-PATENT-CLASS-C04B-35/10)
Avail: US Patent and Trademark Office

Ceramic structures having high strength at temperatures above 1000 C after sintering are made by mixing ceramic powders with binder deflocculants such as guanidine salts of polymeric acids, guanidine salts of aliphatic organic carboxylic acids or guanidine alkylsulfates with the foregoing guanidine salts. The novelty of the invention appears to lie in the substitution of guanidine salts for the alkali metal salt components or organic fatty acids of the prior art binder-deflocculant, ceramic processing aids whereby no undesirable metal contaminants are present in the final ceramic structure. Guanidine alkylsulfates also replace the Na or K alkylsulfates commonly used with binder-deflocculants in making high temperature ceramic structures.

Official Gazette of the U.S. Patent and Trademark Office

N92-16129*# National Aeronautics and Space Administration, Lewis Research Center, Cleveland, OH.

A VACUUM (10(EXP -9) TORR) FRICTION APPARATUS FOR DETERMINING FRICTION AND ENDURANCE LIFE OF MOSX FILMS

KAZUHISA MIYOSHI, FRANK S. HONEY, PHILLIP B. ABEL, STEPHEN V. PEPPER, TALIVALDIS SPALVINS, and DONALD R. WHEELER Jan. 1992 15 p

(Contract RTOP 506-43-11)

(NASA-TM-104478; E-6324; NAS 1.15:104478) Avail: CASI HC A03/MF A01

The first part of this paper describes an ultrahigh vacuum friction apparatus (tribometer). The tribometer can be used in a ball-on-disk configuration and is specifically designed to measure the friction and endurance life of solid lubricating films such as MoS(x) in vacuum at a pressure of $10 \text{ exp } -7 \text{ Pa}$. The sliding mode is typically unidirectional at a constant rotating speed. The second part of this paper presents some representative friction and endurance life data for magnetron sputtered MoS(x) films (110 nm thick) deposited on sputter-cleaned 440 C stainless-steel disk substrates, which were slid against a 6-mm-diameter 440 C stainless-steel bearing ball. All experiments were conducted with loads of 0.49 to 3.6 N (average Hertzian contact pressure, 0.33 to 0.69 GPa), at a constant rotating speed of 120 rpm (sliding velocity ranging from 31 to 107 mm/s due to the range of wear track radii involved in the experiments), in a vacuum of $7 \times 10 \text{ exp } -7 \text{ Pa}$ and at room temperature. The results indicate that there are similarities in friction behavior of MoS(x) films over their life cycles regardless of load applied. The coefficient of friction (μ) decreases as load W increases according to $\mu = kW \text{ exp } -1/3$. The endurance life E of MoS(x) films decreases as the load W increases according to $E = KW \text{ exp } -1.4$ for the load range. The load- (or contact-pressure-) dependent endurance life allows us to reduce the time for wear experiments and to accelerate endurance life testing of MoS(x) films. For the magnetron-sputtered MoS(x) films deposited on 440 C stainless-steel disks: the specific wear rate normalized to the load and the number of revolutions was $3 \times 10 \text{ exp } -8 \text{ mm exp } 3/N\text{-revolution}$; the specific wear rate normalized to the load and the total sliding distance was $8 \times 10 \text{ exp } -7 \text{ mm exp } 3/N\text{-m}$; and the nondimensional wear coefficient of was approximately $5 \times 10 \text{ exp } -6$. The values are almost independent of load in the range 0.49 to 3.6 N (average Hertzian contact pressures of 0.33 to 0.69 GPa). Author

N92-17060*# National Aeronautics and Space Administration, Lewis Research Center, Cleveland, OH.

RELIABILITY ANALYSIS OF STRUCTURAL CERAMIC COMPONENTS USING A THREE-PARAMETER WEIBULL DISTRIBUTION

STEPHEN F. DUFFY, LYNN M. POWERS (Cleveland State Univ., OH.), and ALOIS STARLINGER 1992 12 p Proposed for presentation at the 37th International Gas Turbine and Aeroengine Congress and Exposition, Cologne, Germany, 1-4 Jun. 1992; sponsored by ASME

(Contract NCC3-81; RTOP 778-32-11)

(NASA-TM-105370; E-6749; NAS 1.15:105370) Avail: CASI HC A03/MF A01

Described here are nonlinear regression estimators for the three-Weibull distribution. Issues relating to the bias and invariance associated with these estimators are examined numerically using Monte Carlo simulation methods. The estimators were used to extract parameters from sintered silicon nitride failure data. A reliability analysis was performed on a turbopump blade utilizing the three-parameter Weibull distribution and the estimates from the sintered silicon nitride data. Author

N92-17070*# National Aeronautics and Space Administration, Lewis Research Center, Cleveland, OH.

HIGH-TEMPERATURE DURABILITY CONSIDERATIONS FOR HSCT COMBUSTOR

NATHAN S. JACOBSON Washington Jan. 1992 19 p

(Contract RTOP 505-63-20)

(NASA-TP-3162; E-6343; NAS 1.60:3162) Avail: CASI HC A03/MF A01

The novel combustor designs for the High Speed Civil Transport will require high temperature materials with long term environmental stability. Higher liner temperatures than in conventional combustors and the need for reduced weight necessitates the use of advanced ceramic matrix composites. The combustor environment is defined at the current state of design, the major degradation routes are discussed for each candidate ceramic material, and where possible, the maximum use temperatures are defined for these candidate ceramics. Author

N92-19450*# National Aeronautics and Space Administration, Lewis Research Center, Cleveland, OH.

THE EFFECT OF ION PLATED SILVER AND SLIDING FRICTION ON TENSILE STRESS-INDUCED CRACKING IN ALUMINUM OXIDE

HAROLD E. SLINEY and TALIVALDIS SPALVINS 1991 17 p Proposed for presentation at the Annual Meeting of the Society of Tribologists and Lubrication Engineers, Philadelphia, PA, 4-7 May 1992

(Contract RTOP 505-63-5A)

(NASA-TM-105366; E-6651; NAS 1.15:105366) Avail: CASI HC A03/MF A01

A Hertzian analysis of the effect of sliding friction on contact stresses in alumina is used to predict the critical load for crack generation. The results for uncoated alumina and alumina coated with ion plated silver are compared. Friction coefficient inputs to the analysis are determined experimentally with a scratch test instrument employing an 0.2 mm radius diamond stylus. A series of scratches were made at constant load increments on coated and uncoated flat alumina surfaces. Critical loads for cracking are detected by microscopic examination of cross sections of scratches made at various loads and friction coefficients. Acoustic emission (AE) and friction trends were also evaluated as experimental techniques for determining critical loads for cracking. Analytical predictions correlate well with micrographic evidence and with the lowest load at which AE is detected in multiple scratch tests. Friction/load trends are not good indicators of early crack formation. Lubrication with silver films reduced friction and thereby increased the critical load for crack initiation in agreement with analytical predictions. Author

N92-19498*# National Aeronautics and Space Administration, Lewis Research Center, Cleveland, OH.

HIGH MOLECULAR WEIGHT FIRST GENERATION PMR POLYIMIDES FOR 343 C APPLICATIONS

DIANE C. MALARIK and RAYMOND D. VANNUCCI Dec. 1991 17 p

(Contract RTOP 510-01-50)

(NASA-TM-105364; E-6742; NAS 1.15:105364) Avail: CASI HC A03/MF A01

The effect of molecular weight on 343 C thermo-oxidative stability (TOS), mechanical properties, and processability, of the first generation PMR polyimides was studied. Graphite fiber reinforced PMR-15, PMR-30, PMR-50, and PMR-75 composites (corresponding to formulated molecular weights of 1500, 3000, 5000, and 7500, respectively) were fabricated using a simulated autoclave process. The data reveals that while alternate autoclave cure schedules are required for the high molecular weight resins, low void laminates can be fabricated which have significantly improved TOS over PMR-15, with only a small sacrifice in mechanical properties. Author

N92-20380*# National Aeronautics and Space Administration, Lewis Research Center, Cleveland, OH.

RELIABILITY ANALYSIS OF LAMINATED CMC COMPONENTS THROUGH SHELL SUBELEMENT TECHNIQUES

ALOIS STARLINGER (Cleveland State Univ., OH.), STEPHEN F. DUFFY (Cleveland State Univ., OH.), and JOHN P. GYKENYESI 1992 12 p Proposed for presentation at the 33rd Structures, Structural Dynamics and Materials Conference, Dallas, TX, 13-15 Apr. 1992; sponsored by AIAA

27 NONMETALLIC MATERIALS

(Contract RTOP 505-63-5B)
(NASA-TM-105413; E-6819; NAS 1.15:105413; AIAA PAPER 92-2348) Avail: CASI HC A03/MF A01

An updated version of the integrated design program Composite Ceramics Analysis and Reliability Evaluation of Structures (C/CARES) was developed for the reliability evaluation of ceramic matrix composites (CMC) laminated shell components. The algorithm is now split into two modules: a finite-element data interface program and a reliability evaluation algorithm. More flexibility is achieved, allowing for easy implementation with various finite-element programs. The interface program creates a neutral data base which is then read by the reliability module. This neutral data base concept allows easy data transfer between different computer systems. The new interface program from the finite-element code Matrix Automated Reduction and Coupling (MARC) also includes the option of using hybrid laminates (a combination of plies of different materials or different layups) and allows for variations in temperature fields throughout the component. In the current version of C/CARES, a subelement technique was implemented, enabling stress gradients within an element to be taken into account. The noninteractive reliability function is now evaluated at each Gaussian integration point instead of using averaging techniques. As a result of the increased number of stress evaluation points, considerable improvements in the accuracy of reliability analyses were realized. Author

N92-20660*# National Aeronautics and Space Administration. Lewis Research Center, Cleveland, OH.
PROPERTIES DATA FOR OPENING THE GALILEO'S PARTIALLY UNFURLED MAIN ANTENNA
KAZUHISA MIYOSHI and STEPHEN V. PEPPER Feb. 1992
25 p
(Contract RTOP 506-43-11)
(NASA-TM-105355; E-6729; NAS 1.15:105355) Avail: CASI HC A03/MF A01

An investigation was conducted into the friction and wear behavior of both unlubricated and dry-film-lubricated (Tiolube 460) titanium alloy (Ti-6Al-4V) in contact with an uncoated high-nickel-content superalloy (Inconel 718) both in vacuum and in air. The acquisition of friction and wear data for this sliding couple was motivated by the need for input data for the 'antenna stuck ribs model' effort to free Galileo's High Gain Antenna. The results of the investigation indicate that galling occurred in the unlubricated system in vacuum and that the coefficient of friction increased to 1.2. The abnormally high friction (1.45) was observed when relatively large wear debris clogged at the sliding interface. The coefficient of friction for the dry-film-lubricated system in vacuum is 0.04, while the value in air is 0.13. The endurance life of the dry-film lubricant is about three orders of magnitude greater in vacuum than in air. The worn surfaces of the dry-film-lubricated Ti-6Al-4V pin and Inconel 718 disk first run in humid air and then rerun in vacuum was completely different from that of the pin and disk run only in vacuum. When galling occurred in the humid-air and vacuum contact, coefficient of friction rose to 0.32 when sliding in humid air and to 1.4 when sliding in vacuum. The galling was accompanied by severe surface damage and extensive transfer of the Ti-6Al-4V to the Inconel 718, or vice versa. When spalling occurred in the dry-film-lubricated Ti-6Al-4V pin run only in vacuum, the coefficient of friction rose to 0.36 or greater. The wear damage caused by spalling can self-heal when rerun in vacuum - the coefficient of friction decreased to 0.05. The friction and wear data obtained can be used for the 'antenna stuck ribs model' effort to free Galileo's high gain antenna. Author

N92-21579*# National Aeronautics and Space Administration. Lewis Research Center, Cleveland, OH.
LUBRICATION OF SPACE SYSTEMS: CHALLENGES AND POTENTIAL SOLUTIONS
ROBERT L. FUSARO 1992 23 p Presented at the International Conference on Metallurgical Coatings and Thin Films, San Diego, CA, 6-10 Apr. 1991; sponsored by the American Vacuum Society (Contract RTOP 506-43-41)

(NASA-TM-105560; E-6864; NAS 1.15:105560) Avail: CASI HC A03/MF A01

Future space missions will all require advanced mechanical moving components which will require wear protection and lubrication. The tribology practices used today are primarily based upon a technology base that is more than 20 years old. This paper will discuss NASA's future space missions and some of the mechanism tribology challenges that will be encountered. Potential solutions to these challenges using coatings technology will be assessed. Author

N92-22278*# National Aeronautics and Space Administration. Lewis Research Center, Cleveland, OH.
SCREEN CAGE ION PLATING (SCIP) AND SCRATCH TESTING OF POLYCRYSTALLINE ALUMINUM OXIDE
TALIVALDIS SPALVINS, HAROLD E. SLINEY, and DANIEL L. DEADMORE Feb. 1992 16 p
(Contract RTOP 505-63-5A)
(NASA-TM-105404; E-6391; NAS 1.15:105404) Avail: CASI HC A03/MF A01

A screen cage ion plating (SCIP) technique was developed to apply silver films on electrically nonconducting aluminum oxide. It is shown that SCIP has remarkable throwing power; surfaces to be coated need not be in direct line of sight with the evaporation source. Scratch tests, employing a diamond stylus with a 200 micro m radius tip, were performed on uncoated and on silver coated alumina. Subsequent surface analysis show that a significant amount of silver remains on the scratched surfaces, even in areas where high stylus load produced severe crack patterns in the ceramic. Friction coefficients were lowered during the scratch tests on the coated alumina indicating that this modification of the ion plating process should be useful for applying lubricating films of soft metals to electrical insulating materials. The very good throwing power of SCIP also strongly suggests general applicability of this process in other areas of technology, e.g., electronics, in addition to tribology. Author

N92-22305*# National Aeronautics and Space Administration. Lewis Research Center, Cleveland, OH.
PLASMA ETCHING A CERAMIC COMPOSITE
DAVID R. HULL (Sverdrup Technology, Inc., Brook Park, OH.), TODD A. LEONHARDT, and WILLIAM A. SANDERS (Analex Corp., Brook Park, OH.) 1992 12 p Presented at the 24th Annual Convention of the International Metallographic Society, Monterey, CA, 29 Jul. - 1 Aug. 1991
(Contract RTOP 505-63-5A)
(NASA-TM-105430; E-6846; NAS 1.15:105430) Avail: CASI HC A03/MF A01

Plasma etching is found to be a superior metallographic technique for evaluating the microstructure of a ceramic matrix composite. The ceramic composite studied is composed of silicon carbide whiskers (SiC(sub W)) in a matrix of silicon nitride (Si3N4), glass, and pores. All four constituents are important in evaluating the microstructure of the composite. Conventionally prepared samples, both as-polished or polished and etched with molten salt, do not allow all four constituents to be observed in one specimen. As-polished specimens allow examination of the glass phase and porosity, while molten salt etching reveals the Si3N4 grain size by removing the glass phase. However, the latter obscures the porosity. Neither technique allows the SiC(sub W) to be distinguished from the Si3N4. Plasma etching with CF4 + 4 percent O2 selectively attacks the Si3N4 grains, leaving SiC(sub W) and glass in relief, while not disturbing the pores. An artifact of the plasma etching reaction is the deposition of a thin layer of carbon on Si3N4, allowing Si3N4 grains to be distinguished from SiC(sub W) by back scattered electron imaging. Author

N92-22516*# National Aeronautics and Space Administration. Lewis Research Center, Cleveland, OH.
SELF-LUBRICATING COATINGS FOR HIGH-TEMPERATURE APPLICATIONS
HAROLD E. SLINEY *In its* Aeropropulsion 1987 p 79-90 Feb.

1990

Avail: CASI HC A03/MF A04

Solid lubricants with maximum temperature capabilities of about 1100 C are known. Unfortunately, none of the solid lubricants with the highest temperature capabilities are effective below 400 C. However, research at NASA's Lewis Research Center shows that silver and stable fluorides such as calcium and barium fluorides act synergistically to provide lubrication from below room temperature to about 900 C. This paper describes plasma-sprayed composite coatings that contain these solid lubricants in combination with a metal-bonded chromium carbide. The lubricants control friction, and the carbide matrix provides wear resistance. Successful tests of these coatings as backup lubricants for compliant gas bearings in turbomachinery and as self-lubricating liners in a four-cylinder Stirling engine are discussed. D.R.D.

N92-22517*# National Aeronautics and Space Administration. Lewis Research Center, Cleveland, OH.

CERAMICS FOR ENGINES

JAMES D. KISER, STANLEY R. LEVINE, and JAMES A. DICARLO *In its* Aeropropulsion 1987 p 91-103 Feb. 1990

Avail: CASI HC A03/MF A04

The NASA Lewis Research Center's Ceramic Technology Program is focused on aerospace propulsion and power needs. Thus, emphasis is on high-temperature ceramics and their structural and environmental durability and reliability. The program is interdisciplinary in nature with major emphasis on materials and processing, but with significant efforts in design methodology and life prediction. D.R.D.

N92-23185*# National Aeronautics and Space Administration. Lewis Research Center, Cleveland, OH.

AN XPS STUDY OF THE STABILITY OF FOMBLIN Z25 ON THE NATIVE OXIDE OF ALUMINUM

PILAR HERRERA-FIERRO, STEPHEN V. PEPPER, and WILLIAM R. JONES Nov. 1991 12 p Presented at the 38th National Symposium of the American Vacuum Society, Seattle WA, 11-15 Nov. 1991

(Contract RTOP 505-33-13)

(NASA-TM-105594; E-6926; NAS 1.15:105594) Avail: CASI HC A03/MF A01

Thin films of Fomblin Z25, a perfluoropolyalkylether lubricant, were vapor deposited onto clean, oxidized aluminum and sapphire surfaces, and their behavior at different temperatures was studied using x ray photoelectron spectroscopy (XPS) and thermal desorption spectroscopy (TDS). It was found that the interfacial fluid molecules decompose on the native oxide at room temperature, and continue to decompose at elevated temperatures, as previous studies had shown to occur on clean metal. TDS indicated that different degradation mechanisms were operative for clean and oxidized aluminum. On sapphire substrates, no reaction was observed at room temperature. Our conclusion is that the native oxide of aluminum is neither passive nor protective towards Fomblin Z25. At high temperatures (150 C) degradation of the polymer on sapphire produced a debris layer at the interface with a chemical composition similar to the one formed on aluminum oxide. Rubbing a Fomblin film on a single crystal sapphire also induced the decomposition of the lubricant in contact with the interface and the formulation of a debris layer. Author

N92-23192*# National Aeronautics and Space Administration. Lewis Research Center, Cleveland, OH.

ENVIRONMENTAL EFFECTS ON FRICTION AND WEAR OF DIAMOND AND DIAMONDLIKE CARBON COATINGS

KAZUHISA MIYOSHI, RICHARD L. C. WU, and ALAN GARSCADDEN (Wright Lab., Wright-Patterson AFB, OH.) 1992 22 p Presented at the International Conference on Metallurgical Coatings and Thin Films, San Diego, CA, 6-10 Apr. 1992; sponsored by American Vacuum Society

(Contract RTOP 506-43-11)

(NASA-TM-105634; E-6977; NAS 1.15:105634) Avail: CASI HC A03/MF A01

Reciprocating sliding friction experiments were conducted with

a natural diamond flat, diamond film, and low and high density diamondlike carbon (DLC) films in contact with pin specimens of natural diamond and silicon nitride (Si₃N₄) both in humid air and dry air nitrogen. The results indicated that for natural diamond pin contacts the diamond films and the natural diamond flat were not susceptible to moisture but that moisture could increase both the coefficient of friction and the wear factors of the DLC films. The coefficients of friction and wear factors of the diamond films were generally similar to those of the natural diamond flat both in humid air and dry air nitrogen. In dry nitrogen the coefficients of friction of the high density DLC films in contact with pin specimens of both diamond and Si₃N₄ were generally low (about 0.02) and similar to those of the natural diamond flat and the diamond films. The wear factors of the materials in contact with both natural diamond and Si₃N₄ were generally in the ascending order of natural diamond flat, diamond film, high density DLC film, and low density DLC film. The moisture in the environment increased the coefficients of friction for Si₃N₄ pins in contact with all the materials. This increase in friction is due to the silicon oxide film produced on the surface of Si₃N₄ pins in humid air. Author

N92-23461*# National Aeronautics and Space Administration. Lewis Research Center, Cleveland, OH.

GUANIDINE BASED VEHICLE/BINDERS FOR USE WITH OXIDES, METALS, AND CERAMICS Patent Application

WARREN H. PHILIPP, inventor (to NASA), LISA C. VEITCH, inventor (to NASA), and MARTHA H. JASKOWIAK, inventor (to NASA) 13 Mar. 1992 14 p

(NASA-CASE-LEW-15314-1; NAS 1.71:LEW-15314-1; US-PATENT-APPL-SN-842313) Avail: CASI HC A03/MF A01

The use of guanidine salts of organic fatty acids (guanidine soaps) as vehicles and binders for coating substrate surfaces is disclosed. Being completely organic, the guanidine soaps can be burned off leaving no undesirable residue. Of special interest is the use of guanidine 2-ethyl hexanoate as the vehicle and binder for coating problematic surfaces such as in coating alumina fibers with platinum or zirconia. For this application, the guanidine soap is used as a melt. For applications, the guanidine soap may be used in a solution with a variety of solvents, the solution containing chlorometalates or powdered metals, refractories, or ceramics. NASA

N92-24053*# National Aeronautics and Space Administration. Lewis Research Center, Cleveland, OH.

VINYL CAPPED ADDITION POLYIMIDES Patent Application

RAYMOND D. VANNUCCI, inventor (to NASA), DIANE C. MALARIK, inventor (to NASA), and PETER DELVIGS, inventor (to NASA) 24 Dec. 1991 15 p

(NASA-CASE-LEW-15027-2; NAS 1.71:LEW-15027-2; US-PATENT-APPL-SN-824858) Avail: CASI HC A03/MF A01

Polyimide resins (PMR) are generally useful where high strength and temperature capabilities are required (at temperatures up to about 700 F). Polyimide resins are particularly useful in applications such as jet engine compressor components, for example, blades, vanes, air seals, air splitters, and engine casing parts. Aromatic vinyl capped addition polyimides are obtained by reacting a diamine, an ester of tetracarboxylic acid, and an aromatic vinyl compound. Low void materials with improved oxidative stability when exposed to 700 F air may be fabricated as fiber reinforced high molecular weight capped polyimide composites. The aromatic vinyl capped polyimides are provided with a more aromatic nature and are more thermally stable than highly aliphatic, norbornenyl-type end-capped polyimides employed in PMR resins. The substitution of aromatic vinyl end-caps for norbornenyl end-caps in addition polyimides results in polymers with improved oxidative stability. NASA

N92-24715*# National Aeronautics and Space Administration. Lewis Research Center, Cleveland, OH.

COMPOSITION DEPENDENCE OF SUPERCONDUCTIVITY IN YBA₂(Cu(3-X)Al(X))O_Y

NAROTTAM P. BANSAL Dec. 1991 17 p

(Contract RTOP 307-51-00)

27 NONMETALLIC MATERIALS

(NASA-TM-105358; E-6737; NAS 1.15:105358) Avail: CASI HC A03/MF A01

Eleven different compositions in the system $YBa_2(Cu_{3-x}Al(x))O(y)$ ($x = 0$ to 0.3) have been synthesized and characterized by electrical resistivity measurements, powder x-ray diffraction, and scanning electron microscopy. The superconducting transition temperature $T_{sub c}$ (onset) was almost unaffected by the presence of alumina due to its limited solubility in $YBa_2Cu_3O(7-x)$. However, $T_{sub c}(R = 0)$ gradually decreased, and the resistive tails became longer with increasing Al_2O_3 concentration. This was probably due to formation of $BaAl_2O_4$ and other impurity phases from chemical decomposition of the superconducting phase by reaction with Al_2O_3 . Author

N92-24820*# National Aeronautics and Space Administration. Lewis Research Center, Cleveland, OH.

ATOMIC OXYGEN INTERACTIONS WITH FEP TEFLON AND SILICONES ON LDEF

BRUCE A. BANKS (Cleveland State Univ., OH.), JOYCE A. DEVER, LINDA GEBAUER, and CAROL M. HILL (Akron Univ., OH.) *In* NASA. Langley Research Center, LDEF: 69 Months in Space. First Post-Retrieval Symposium, Part 2 p 801-815 Jan. 1992

The Long Duration Exposure Facility (LDEF) spacecraft has enabled the measurement of the effects of fixed orientation exposure of high fluence atomic oxygen on fluorinated ethylene propylene (FEP Teflon) and silicones. The atomic oxygen erosion yield for the FEP Teflon was found to be $3.64 \times 10^{(exp -25)} \text{ cm}(exp 3)/\text{atom}$. This erosion yield is significantly higher than that measured from previous low fluence orbital data. The FEP Teflon erosion yield was found to have the same dependence on oxygen arrival angle as Kapton and Mylar. Atomic oxygen interaction with silicon polymers results in the crazing of silicon. Released silicone contaminants were found to darken upon further atomic oxygen exposure. Author

N92-24832*# National Aeronautics and Space Administration. Lewis Research Center, Cleveland, OH.

ION BEAM TEXTURED AND COATED SURFACES EXPERIMENT (IBEX)

MICHAEL J. MIRTICH (Ohio State Univ., Columbus.), SHARON K. RUTLEDGE (Cleveland State Univ., OH.), NICHOLAS STEVENS, RAYMOND OLLE, and JAMES MERROW (Cleveland State Univ., OH.) *In* NASA. Langley Research Center, LDEF: 69 Months in Space. First Post-Retrieval Symposium, Part 2 p 989-1004 Jan. 1992

Ion beam textured and commercial materials suitable for use in space power systems were flown in low Earth orbit on the Long Duration Exposure Facility (LDEF) for 5.8 years. Because of their location on LDEF (98 deg from the ram direction), the 36 materials were primarily exposed to vacuum ultraviolet radiation, thermal cycling, the vacuum of space, the micrometeoroid environment, and grazing incidence atomic oxygen. Measurements of solar absorptance and thermal emittance (pre- and post-flight) showed no changes for almost all of the materials, except for the S-13G and Kapton and coated Kapton samples. The optical property stability of ion beam textured surfaces and most other surfaces indicates that they are functionally durable to the synergistic rigors of the space environment. D.R.D.

N92-25348*# National Aeronautics and Space Administration. Lewis Research Center, Cleveland, OH.

CYCLOPENTADIENE EVOLUTION DURING PYROLYSIS-GAS CHROMATOGRAPHY OF PMR POLYIMIDES

WILLIAM B. ALSTON, RICHARD E. GLUYAS, and WILLIAM J. SNYDER (Bucknell Univ., Lewisburg, PA.) 1992 23 p Presented at the 4th International Conference on Polyimides, Ellenville, NY, 30 Oct. - 1 Nov. 1991; sponsored in part by Society of Plastic Engineers

(Contract DA PROJ. 1L1-61102-AH-45; RTOP 510-01-50)

(NASA-TM-105629; E-6971; NAS 1.15:105629;

AVSCOM-TR-91-C-023) Avail: CASI HC A03/MF A01

The effect of formulated molecular weight (FMW), extent of cure, and cumulative aging on the amount of cyclopentadiene

(CPD) evolved from Polymerization of Monomeric Reactants (PMR) polyimides were investigated by pyrolysis-gas chromatography (PY-GC). The PMR polyimides are additional crosslinked resins formed from an aromatic diamine, a diester of an aromatic tetracarboxylic acid and a monoester of 5-norbornene-2,3-dicarboxylic acid. The PY-GC results were related to the degree of crosslinking and to the thermo-oxidative stability (weight loss) of PMR polyimides. Thus, PY-GC has shown to be a valid technique for the characterization of PMR polyimide resins and composites via correlation of the CPD evolved versus the thermal history of the PMR sample. Author

N92-27100*# National Aeronautics and Space Administration. Lewis Research Center, Cleveland, OH.

DURABILITY EVALUATION OF PHOTOVOLTAIC BLANKET MATERIALS EXPOSED ON LDEF TRAY S1003

SHARON K. RUTLEDGE and RAYMOND M. OLLE (Cleveland State Univ., OH.) *In* NASA. Langley Research Center, LDEF: 69 Months in Space. First Post-Retrieval Symposium, Part 3 p 1379-1394 Jan. 1992

Avail: CASI HC A03/MF A04; 1 functional color page

Several candidate protective coatings on Kapton and uncoated Kapton were exposed to the low Earth orbital (LEO) environment on the Long Duration Exposure Facility (LDEF) to determine if the coatings could be used to protect polymeric substrates from degradation in the LEO environment. The coatings that were evaluated were 700 Å of aluminum oxide, 650 Å of silicon dioxide, and 650 Å of a 4 percent polytetrafluoroethylene-96 percent silicon dioxide mixed coating. All of the coatings evaluated were ion beam sputter deposited. These materials were exposed to a very low atomic oxygen fluence ($4.8 \times 10^{(exp 19)} \text{ atoms/sq. cm}$) as a result of the experiment tray being located 98 degrees from the ram direction. As a result of the low atomic oxygen fluence, determination of a change in mass was not possible for any of the samples including the uncoated Kapton. There was no evidence of spalling of any of the coatings after the approximately 33,600 thermal cycles recorded for LDEF. The surface of the uncoated Kapton, however, did show evidence of grazing incidence texturing. There was a 7-8 percent increase in solar absorptance for the silicon dioxide and aluminum oxide coated Kapton and only a 4 percent increase for the mixed coating. It appears that the addition of a small amount of fluoropolymer may reduce the magnitude of absorptance increase due to environmental exposure. Thermal emittance did not change significantly for any of the exposed samples. Scanning electron microscopy revealed few micrometeoroid or debris impacts, but the impact sites found indicated that the extent of damage or cracking of the coating around the defect site did not extend beyond a factor of three of the impact crater diameter. This limiting of impact damage is of great significance for the durability of thin film coatings used for protection against the LEO environment. Author

N92-27281*# National Aeronautics and Space Administration. Lewis Research Center, Cleveland, OH.

MONTE CARLO MODELING OF ATOMIC OXYGEN ATTACK OF POLYMERS WITH PROTECTIVE COATINGS ON LDEF

Abstract Only

BRUCE A. BANKS, KIM K. DEGROH, and EDWARD A. SECHKAR (Cleveland State Univ., OH.) *In* NASA. Langley Research Center, Second LDEF Post-Retrieval Symposium Abstracts p 75 Jun. 1992

Avail: CASI HC A01/MF A02

Characterization of the behavior of atomic oxygen interaction with materials on the Long Duration Exposure Facility (LDEF) will assist in understanding the mechanisms involved, and will lead to improved reliability in predicting in-space durability of materials based on ground laboratory testing. A computational simulation of atomic oxygen interaction with protected polymers was developed using Monte Carlo techniques. Through the use of assumed mechanistic behavior of atomic oxygen and results of both ground laboratory and LDEF data, a predictive Monte Carlo model was developed which simulates the oxidation processes that occur on polymers with applied protective coatings that have defects. The

use of high atomic oxygen fluence-directed ram LDEF results has enabled mechanistic implications to be made by adjusting Monte Carlo modeling assumptions to match observed results based on scanning electron microscopy. Modeling assumptions, implications, and predictions are presented, along with comparison of observed ground laboratory and LDEF results. Author

N92-27378* # National Aeronautics and Space Administration. Lewis Research Center, Cleveland, OH.

CERAMIC COMPOSITES: ENABLING AEROSPACE MATERIALS

S. R. LEVINE Jun. 1992 12 p Presented at the 37th International Gas Turbine and Aeroengine Congress and Exposition, Cologne, Germany, 1-4 Jun. 1992; sponsored by the 1992 Turbo Expo-Land, Sea and Air

(Contract RTOP 505-63-5A)

(NASA-TM-105599; E-6935; NAS 1.15:105599) Avail: CASI HC A03/MF A01

Ceramics and ceramic matrix composites (CMC) have the potential for significant impact on the performance of aerospace propulsion and power systems. In this paper, the potential benefits are discussed in broad qualitative terms and are illustrated by some specific application case studies. The key issues in need of resolution for the potential of ceramics to be realized are discussed. Author

N92-29090* National Aeronautics and Space Administration. Lewis Research Center, Cleveland, OH.

OXIDATION RESISTANT COATING FOR TITANIUM ALLOYS AND TITANIUM ALLOY MATRIX COMPOSITES Patent

WILLIAM J. BRINDLEY, inventor (to NASA), JAMES L. SMIALEK, inventor (to NASA), and CARL J. ROUGE, inventor (to NASA) 26 May 1992 5 p Filed 1 Apr. 1991 Supersedes N91-26375 (29 - 18, p 2966)

(NASA-CASE-LEW-15155-1; US-PATENT-5,116,690; US-PATENT-APPL-SN-682160; US-PATENT-CLASS-428-614; US-PATENT-CLASS-428-660; US-PATENT-CLASS-428-661; INT-PATENT-CLASS-B32B-5/02; INT-PATENT-CLASS-B32B-15/01; INT-PATENT-CLASS-B32B-15/20) Avail: US Patent and Trademark Office

An oxidation resistant coating for titanium alloys and titanium alloy matrix composites comprises an MCrAlX material. M is a metal selected from nickel, cobalt, and iron. X is an active element selected from Y, Yb, Zr, and Hf.

Official Gazette of the U.S. Patent and Trademark Office

N92-31840* # National Aeronautics and Space Administration. Lewis Research Center, Cleveland, OH.

LIQUID LUBRICATION FOR SPACE APPLICATIONS

ROBERT L. FUSARO and MICHAEL M. KHONSARI (Pittsburgh Univ., PA.) Jul. 1992 34 p

(Contract RTOP 505-63-5B)

(NASA-TM-105198; E-6500; NAS 1.15:105198) Avail: CASI HC A03/MF A01

Reviewed here is the state of the art of liquid lubrication for space applications. The areas discussed are types of liquid lubrication mechanisms, space environmental effects on lubrication, classification of lubricants, liquid lubricant additives, grease lubrication, mechanism materials, bearing anomalies and failures, lubricant supply techniques, and application types and lubricant needs for those applications. Author

N92-32863* # National Aeronautics and Space Administration. Lewis Research Center, Cleveland, OH.

LIQUID LUBRICANTS FOR ADVANCED AIRCRAFT ENGINES

WILLIAM R. LOOMIS and ROBERT L. FUSARO Aug. 1992 28 p

(Contract RTOP 505-63-5A)

(NASA-TM-104531; E-6407; NAS 1.15:104531) Avail: CASI HC A03/MF A01

An overview of liquid lubricants for use in current and projected high performance turbojet engines is discussed. Chemical and

physical properties are reviewed with special emphasis placed on the oxidation and thermal stability requirements imposed upon the lubrication system. A brief history is given of the development of turbine engine lubricants which led to the present day synthetic oils with their inherent modification advantages. The status and state of development of some eleven candidate classes of fluids for use in advanced turbine engines are discussed. Published examples of fundamental studies to obtain a better understanding of the chemistry involved in fluid degradation are reviewed. Alternatives to high temperature fluid development are described. The importance of continuing work on improving current high temperature lubricant candidates and encouraging development of new and improved fluid base stocks are discussed. Author

PROPELLANTS AND FUELS

Includes rocket propellants, igniters, and oxidizers; their storage and handling procedures; and aircraft fuels.

A92-20612* National Aeronautics and Space Administration. Lewis Research Center, Cleveland, OH.

TECHNICAL PROSPECTS FOR UTILIZING EXTRATERRESTRIAL PROPELLANTS FOR SPACE EXPLORATION

DIANE L. LINNE and MICHAEL L. MEYER (NASA, Lewis Research Center, Cleveland, OH) IAF, International Astronautical Congress, 42nd, Montreal, Canada, Oct. 5-11, 1991. 19 p. Previously announced in STAR as N91-31318. Oct. 1991 19 p refs (IAF PAPER 91-669) Copyright

NASA's LeRC has supported several efforts to understand how lunar and Martian produced propellants can be used to their best advantage for space exploration propulsion. A discussion of these efforts and their results is presented. A Manned Mars Mission Analysis Study identified that a more thorough technology base for propellant production is required before the net economic benefits of in situ propellants can be determined. Evaluation of the materials available on the moon indicated metal/oxygen combinations are the most promising lunar propellants. A hazard analysis determined that several lunar metal/LOX monopropellants could be safely worked with in small quantities, and a characterization study was initiated to determine the physical and chemical properties of potential lunar monopropellant formulations. A bipropellant metal/oxygen subscale test engine which utilizes pneumatic injection of powdered metal is being pursued as an alternative to the monopropellant systems. The technology for utilizing carbon monoxide/oxygen, a potential Martian propellant, was studied in subscale ignition and rocket performance experiments. Author

A92-32199* National Aeronautics and Space Administration. Lewis Research Center, Cleveland, OH.

ACETYLENE FUEL FROM ATMOSPHERIC CO₂ ON MARS

GEOFFREY A. LANDIS and DIANE L. LINNE (NASA, Lewis Research Center, Cleveland, OH) Journal of Spacecraft and Rockets (ISSN 0022-4650), vol. 29, Mar.-Apr. 1992, p. 294-296. Apr. 1992 3 p refs

Copyright

The Mars mission scenario proposed by Baker and Zubrin (1990) intended for an unmanned preliminary mission is extended to maximize the total impulse of fuel produced with a minimum mass of hydrogen from Earth. The hydrogen along with atmospheric carbon dioxide is processed into methane and oxygen by the exothermic reaction in an atmospheric processing module. Use of simple chemical reactions to produce acetylene/oxygen rocket fuel on Mars from hydrogen makes it possible to produce an amount of fuel that is nearly 100 times the mass of hydrogen brought from earth. If such a process produces the return propellant for a

28 PROPELLANTS AND FUELS

manned Mars mission, the required mission mass in LEO is significantly reduced over a system using all earth-derived propellants. O.G.

A92-48727*# National Aeronautics and Space Administration. Lewis Research Center, Cleveland, OH.

TECHNOLOGY ISSUES ASSOCIATED WITH USING DENSIFIED HYDROGEN FOR SPACE VEHICLES

TERRY L. HARDY and MARGARET V. WHALEN (NASA, Lewis Research Center, Cleveland, OH) AIAA, SAE, ASME, and ASEE, Joint Propulsion Conference and Exhibit, 28th, Nashville, TN, July 6-8, 1992. 14 p. Previously announced in STAR as N92-25277. Jul. 1992 14 p refs

(AIAA PAPER 92-3079) Copyright

Slush hydrogen and triple-point hydrogen offer the potential for reducing the size and weight of future space vehicles because these fluids have greater densities than normal-boiling-point liquid hydrogen. In addition, these fluids have greater heat capacities, which make them attractive fuels for such applications as the National Aerospace Plane and cryogenic depots. Some of the benefits of using slush hydrogen and triple-point hydrogen for space missions are quantified. Some of the major issues associated with using these densified cryogenic fuels for space applications are examined, and the technology efforts that have been made to address many of these issues are summarized. Author

A92-49004*# National Aeronautics and Space Administration. Lewis Research Center, Cleveland, OH.

GELLED LIQUID OXYGEN/METAL POWDER MONOPROPELLANTS

JOHN H. WICKMAN and ERIC JAMES (Wickman Spacecraft and Propulsion Co., Citrus Heights, CA) AIAA, SAE, ASME, and ASEE, Joint Propulsion Conference and Exhibit, 28th, Nashville, TN, July 6-8, 1992. 16 p. Jul. 1992 16 p refs

(Contract NAS3-26056)

(AIAA PAPER 92-3450) Copyright

Al, Al-80/Mg-20 wt pct, Si, and Fe powders were mixed with LOX and gelled with 2-3 wt pct Cab-o-Sil to viscosities of 100 to 900 cps, at shear rates of up to 300/sec. These monopropellants were burned in a cylinder that was submerged in a liquid nitrogen bath. Ambient pressure data have shown that the monopropellants were extinguished when the flame front reached regions that had been submerged under the liquid nitrogen. Burning occurred in a pulsed fashion, and was most nearly steady in the case of the Al-Mg mixture. No sparking or energetic burning occurred in any of the cases tested. O.C.

A92-50613* National Aeronautics and Space Administration. Lewis Research Center, Cleveland, OH.

IN-SITU CARBON DIOXIDE FIXATION ON MARS

ALOYSIUS F. HEPP (NASA, Langley Research Center, Cleveland, OH), GEOFFREY A. LANDIS (Sverdrup Technology, Inc.; NASA, Lewis Research Center, Cleveland, OH), and CLIFFORD P. KUBIAK (Purdue University, West Lafayette, IN) IN: IECEC '91; Proceedings of the 26th Intersociety Energy Conversion Engineering Conference, Boston, MA, Aug. 4-9, 1991. Vol. 2 1991 6 p refs

Copyright

The authors examine several novel proposals for CO₂ fixation through chemical, photochemical, and photoelectrochemical means. For example, the reduction of CO₂ to hydrocarbons such as acetylene (C₂H₂) can be accomplished with hydrogen. Acetylene has a theoretical vacuum specific impulse of about 375 s. The authors also examine potential uses of CO, as obtained or further reduced to carbon, as a reducing agent in metal oxide processing to form metals or metal carbides for use as structural or power materials. The CO₂ can be recycled to generate O₂ and CO. In this study, the authors examine reaction schemes for processing in situ resources. The authors highlight chemistry with hydrogen and carbon monoxide to produce propellants and other necessities of manned exploration. I.E.

N92-11208*# National Aeronautics and Space Administration. Lewis Research Center, Cleveland, OH.

DESCRIPTION OF LIQUID NITROGEN EXPERIMENTAL TEST FACILITY

JOHN M. JURNS (Sverdrup Technology, Inc., Brook Park, OH.), RICHARD E. JACOBS (Analex Corp., Brook Park, OH.), and NASEEM H. SAIYED Sep. 1991 14 p

(Contract RTOP 591-23-00)

(NASA-TM-105215; E-6530; NAS 1.15:105215) Avail: CASI HC A03/MF A01

The Liquid Nitrogen Test Facility is a unique test facility for ground-based liquid nitrogen experimentation. The test rig consists of an insulated tank of approximately 12.5 cubic ft in volume, which is supplied with liquid nitrogen from a 300 gal dewar via a vacuum jacketed piping system. The test tank is fitted with pressure and temperature measuring instrumentation, and with two view ports which allow visual observation of test conditions. To demonstrate the capabilities of the facility, the initial test program is briefly described. The objective of the test program is to measure the condensation rate by injecting liquid nitrogen as a subcooled spray into the ullage of a tank 50 percent full of liquid nitrogen at saturated conditions. The condensation rate of the nitrogen vapor on the subcooled spray can be analytically modeled, and results validated and corrected by experimentally measuring the vapor condensation on liquid sprays. Author

N92-11214*# National Aeronautics and Space Administration. Lewis Research Center, Cleveland, OH.

BENEFITS OF SLUSH HYDROGEN FOR SPACE MISSIONS

ALAN FRIEDLANDER (Science Applications International Corp., Schaumburg, IL.), ROBERT ZUBRIN (Martin Marietta Corp., Littleton, CO.), and TERRY L. HARDY Oct. 1991 18 p

(Contract RTOP 763-01-21)

(NASA-TM-104503; E-6364; NAS 1.15:104503) Avail: CASI HC A03/MF A01

A study was performed to quantify the benefits of using slush hydrogen instead of normal boiling point liquid hydrogen as a fuel for several space missions. Vehicles considered in the study included the Space Shuttle/Shuttle-C, LEO to GEO transfer vehicles, Lunar and Mars transfer vehicles, and cryogenic depots in low Earth orbit. The advantages of using slush hydrogen were expressed in terms of initial mass differences at a constant payload, payload differences at a constant tank volume, and increases in fuel storage time for cryogenic depots. Both chemical oxygen/hydrogen and hydrogen nuclear thermal rocket propulsion were considered in the study. The results indicated that slush hydrogen offers the potential for significant decreases in initial mass and increases in payload for most missions studied. These advantages increase as the mission difficulty, or energy, increases. Author

N92-13336*# National Aeronautics and Space Administration. Lewis Research Center, Cleveland, OH.

A REVIEW OF CANDIDATE MULTILAYER INSULATION SYSTEMS FOR POTENTIAL USE ON WET-LAUNCHED LH2 TANKAGE FOR THE SPACE EXPLORATION INITIATIVE LUNAR MISSIONS

RICHARD H. KNOLL, ROBERT J. STOCHL, and RAFAEL SANABRIA 1991 21 p Presented at the 27th Joint Propulsion Conference, Sacramento, CA, 24-27 Jun. 1991; sponsored by AIAA, SAE, ASME, and ASEE Previously announced in IAA as A91-45793

(Contract RTOP 506-48-00)

(NASA-TM-104493; E-6351; NAS 1.15:104493; AIAA PAPER 91-2176) Avail: CASI HC A03/MF A01

The storage of cryogenic propellants such as liquid hydrogen (LH₂) and liquid oxygen (LO₂) for the future Space Exploration Initiative (SEI) will require lightweight, high performance thermal protection systems (TPS's). For the near-term lunar missions, the major weight element for most of the TPS's will be multilayer insulation (MLI) and/or the special structures/systems required to accommodate the MLI. Methods of applying MLI to LH₂ tankage to avoid condensation or freezing of condensable gases such as

nitrogen or oxygen while in the atmosphere are discussed. Because relatively thick layers of MLI will be required for storage times of a month or more, the transient performance from ground-hold to space-hold of the systems will become important in optimizing the TPS's for many of the missions. The ground-hold performance of several candidate systems are given as well as a qualitative assessment of the transient performance effects. Author

N92-18442*# National Aeronautics and Space Administration. Lewis Research Center, Cleveland, OH.

SELF-PRESSURIZATION OF A FLIGHTWEIGHT LIQUID HYDROGEN TANK: EFFECTS OF FILL LEVEL AT LOW WALL HEAT FLUX

N. T. VANDRESAR, M. M. HASAN, and C.-S. LIN (Analex Corp., Brook Park, OH.) 1991 11 p Presented at the 30th Aerospace Sciences Meeting and Exhibit, Reno, NV, 6-9 Jan. 1992; sponsored by AIAA

(Contract RTOP 593-21-00)
(NASA-TM-105411; E-6813; NAS 1.15:105411; AIAA PAPER 92-0818) Avail: CASI HC A03/MF A01

Experimental results are presented for the self pressurization and thermal stratification of a 4.89 cu m liquid hydrogen storage tank subjected to low heat flux (2.0 and 3.5 W/sq m) in normal gravity. The test tank was representative of future spacecraft tankage, having a low mass to volume ratio and high performance multilayer thermal insulation. Tests were performed at fill levels of 29 and 49 pct. (by volume) and complement previous tests at 83 pct. fill. As the heat flux increases, the pressure rise rate at each fill level exceeds the homogeneous rate by an increasing ratio. Herein, this ratio did not exceed a value of 2. The slowest pressure rise rate was observed for the 49 pct. fill level at both heat fluxes. This result is attributed to the oblate spheroidal tank geometry which introduces the variables of wetted wall area, liquid-vapor interfacial area, and ratio of side wall to bottom heating as a function of fill level or liquid depth. Initial tank thermal conditions were found to affect the initial pressure rise rate. Quasi steady pressure rise rates are independent of starting conditions. Author

N92-19837*# National Aeronautics and Space Administration. Lewis Research Center, Cleveland, OH.

A COMPILATION OF LUNAR AND MARS EXPLORATION STRATEGIES UTILIZING INDIGENOUS PROPELLANTS

DIANE L. LINNE and MICHAEL L. MEYER Jan. 1992 23 p
(Contract RTOP 506-42-72)

(NASA-TM-105262; E-6790; NAS 1.15:105262) Avail: CASI HC A03/MF A01

The use of propellants manufactured from indigenous space materials has the potential to significantly reduce the amount of mass required to be launched from the Earth's surface. The extent of the leverage, however, along with the cost for developing the infrastructure necessary to support such a process, is unclear. Many mission analyses have been performed that have attempted to quantify the potential benefits of in situ propellant utilization. Because the planning of future space missions includes many unknowns, the presentation of any single study on the use of in situ propellants is often met with critics' claims of the inaccuracy of assumptions or omission of infrastructure requirements. The results of many such mission analyses are presented in one format. Each summarized mission analysis used different assumptions and baseline mission scenarios. The conclusion from the studies is that the use of in situ produced propellants will provide significant reductions in Earth launch requirements. This result is consistent among all of the analyses regardless of the assumptions used to obtain the quantitative results. The determination of the best propellant combination and the amount of savings will become clearer and more apparent as the technology work progresses. Author

N92-25277*# National Aeronautics and Space Administration. Lewis Research Center, Cleveland, OH.

TECHNOLOGY ISSUES ASSOCIATED WITH USING DENSIFIED HYDROGEN FOR SPACE VEHICLES

TERRY L. HARDY and MARGARET V. WHALEN 1992 15 p
Proposed for presentation at the 28th Joint Propulsion Conference and Exhibit, Nashville, TN, 6-8 Jul. 1992; sponsored by AIAA, SAE, ASME, and ASEE

(Contract RTOP 763-22-21)
(NASA-TM-105642; E-6988; NAS 1.15:105642; AIAA PAPER 92-3079) Avail: CASI HC A03/MF A01

Slush hydrogen and triple-point hydrogen offer the potential for reducing the size and weight of future space vehicles because these fluids have greater densities than normal-boiling-point liquid hydrogen. In addition, these fluids have greater heat capacities, which make them attractive fuels for such applications as the National Aerospace Plane and cryogenic depots. Some of the benefits of using slush hydrogen and triple-point hydrogen for space missions are quantified. Some of the major issues associated with using these densified cryogenic fuels for space applications are examined, and the technology efforts that have been made to address many of these issues are summarized. Author

N92-25957*# National Aeronautics and Space Administration. Lewis Research Center, Cleveland, OH.

SLUSH HYDROGEN TRANSFER STUDIES AT THE NASA K-SITE TEST FACILITY

TERRY L. HARDY and MARGARET V. WHALEN 1992 10 p
Proposed for presentation at the 28th Joint Propulsion Conference and Exhibit, Nashville, TN, 6-8 Jul. 1992; sponsored by AIAA, SAE, ASME, and ASEE

(Contract RTOP 763-22-21)
(NASA-TM-105596; E-6932; NAS 1.15:105596; AIAA PAPER 92-3384) Avail: CASI HC A02/MF A01

An experimental study was performed as part of the National Aerospace Plane (NASP) effort to determine slush hydrogen production and transfer characteristics. Flow rate and pressure drop characteristics were determined for slush hydrogen flow through a vacuum-jacketed transfer system. These characteristics were compared to similar tests using normal boiling point and triple point hydrogen. In addition, experimental flow characteristic data was compared with predictions from the FLUSH analytical model. Slush hydrogen density loss during the transfer process was also examined. Author

N92-26131*# National Aeronautics and Space Administration. Lewis Research Center, Cleveland, OH.

SLUSH HYDROGEN PRESSURIZED EXPULSION STUDIES AT THE NASA K-SITE FACILITY

MARGARET V. WHALEN and TERRY L. HARDY 1992 10 p
Presented at the 28th Joint Propulsion Conference and Exhibit, Nashville, TN, 6-8 Jul. 1992; sponsored in part by AIAA, SAE, ASME, and ASEE

(Contract RTOP 763-22-21)
(NASA-TM-105597; E-6933; NAS 1.15:105597; AIAA PAPER 92-3385) Avail: CASI HC A02/MF A01

An experiment test series of the slush hydrogen (SLH2) project at the NASA LeRC Plum Brook K-Site Facility was completed. This testing was done as part of the characterization and technology database development on slush hydrogen required for the National Aero-Space Plane (NASP) Program. The primary objective of these experiments was to investigate tank thermodynamic parameters during the pressurized expulsion of slush hydrogen. To accomplish this, maintenance of tank pressure control was investigated during pressurized expulsion of slush hydrogen using gaseous hydrogen and gaseous helium pressurant. In addition, expulsion tests were performed using gaseous helium for initial pressurization, then gaseous hydrogen during expulsion. These tests were conducted with and without mixing of the slush hydrogen. Results from the testing included an evaluation of tank pressure control, pressurant requirements, SLH2 density change, and system mass and energy balances. Author

N92-28433*# National Aeronautics and Space Administration. Lewis Research Center, Cleveland, OH.

HYDROGEN NO-VENT FILL TESTING IN A 5 CUBIC FOOT (142 LITER) TANK USING SPRAY NOZZLE AND SPRAY BAR LIQUID INJECTION

MATTHEW E. MORAN and TED W. NYLAND Jul. 1992 10 p Proposed for presentation at the 28th Joint Propulsion Conference and Exhibit, Nashville, TN, 6-8 Jul. 1992; sponsored by AIAA, SAE, ASME, and ASEE (Contract RTOP 506-42-73) (NASA-TM-105759; E-7173; NAS 1.15:105759; AIAA PAPER 92-3063) Avail: CASI HC A02/MF A01

A total of 38 hydrogen no-vent fill tests were performed in this test series using various size spray nozzles and a spray bar with different hole sizes in a 5 cubic foot receiver tank. Fill levels of 90 percent by volume or greater were achieved in 26 of the tests while maintaining a receiver tank pressure below 30 psia. Spray nozzles were mounted at the top of the tank, whereas, the spray bar was centered in the tank axially. The spray nozzle no-vent fills demonstrated tank pressure and temperature responses comparable to previous test series. Receiver tank pressure responses for the spray bar configuration were similar to the spray nozzle tests with the pressure initially rising rapidly, then leveling off as vapor condenses onto the discharging liquid streams, and finally ramping up near the end of the test due to ullage compression. Both liquid injection techniques tested were capable of filling the receiver tank to 90 percent under variable test conditions. Comparisons between the spray nozzle and spray bar configurations for well matched test conditions indicate the spray nozzle injection technique is more effective in minimizing the receiving tank pressure throughout a no-vent fill compared to the spray bar under normal gravity conditions. Author

N92-29669*# National Aeronautics and Space Administration. Lewis Research Center, Cleveland, OH.

PRESSURIZATION OF CRYOGENS: A REVIEW OF CURRENT TECHNOLOGY AND ITS APPLICABILITY TO LOW-GRAVITY CONDITIONS

N. T. VANDRESAR Jul. 1992 10 p Presented at the 28th Joint Propulsion Conference and Exhibit, Nashville, TN, 6-8 Jul. 1992; sponsored in part by AIAA, SAE, ASME, and ASEE (Contract RTOP 506-42-73) (NASA-TM-105746; E-7150; AIAA PAPER 92-3061; NAS 1.15:105746) Avail: CASI HC A02/MF A01

A review of technology, history, and current status for pressurized expulsion of cryogenic tankage is presented. Use of tank pressurization to expel cryogenic fluids will continue to be studied for future spacecraft applications over a range of operating conditions in the low-gravity environment. The review examines experimental test results and analytical model development for quiescent and agitated conditions in normal-gravity, followed by a discussion of pressurization and expulsion in low-gravity. Validated, 1-D, finite difference codes exist for the prediction of pressurant mass requirements within the range of quiescent normal-gravity test data. To date, the effects of liquid sloshing have been characterized by tests in normal-gravity, but analytical models capable of predicting pressurant gas requirements remain unavailable. Efforts to develop multidimensional modeling capabilities in both normal and low-gravity have recently occurred. Low-gravity cryogenic fluid transfer experiments are needed to obtain low-gravity pressurized expulsion data. This data is required to guide analytical model development and to verify code performance. Author

N92-32230*# National Aeronautics and Space Administration. Lewis Research Center, Cleveland, OH.

DEMONSTRATED SURVIVABILITY OF A HIGH TEMPERATURE OPTICAL FIBER CABLE ON A 1500 POUND THRUST ROCKET CHAMBER

AMY L. SOVIE Sep. 1992 11 p Proposed for presentation at the SPIE's International Symposium OE/Fibers 1992, Boston, MA, 8-11 Sep. 1992; sponsored by the International Society for Optical Engineering

(Contract RTOP 590-21-41) (NASA-TM-105835; E-7270; NAS 1.15:105835) Avail: CASI HC A03/MF A01

A demonstration of the ability of an existing optical fiber cable to survive the harsh environment of a rocket engine was performed at the NASA Lewis Research Center. The intent of this demonstration was to prove the feasibility of applying fiber optic technology to rocket engine instrumentation systems. Extreme thermal transient tests were achieved by wrapping a high temperature optical fiber, which was cablized for mechanical robustness, around the combustion chamber outside wall of a 1500 lb Hydrogen-Oxygen rocket engine. Additionally, the fiber was wrapped around coolant inlet pipes which were subject to near liquid hydrogen temperatures. Light from an LED was sent through the multimode fiber, and output power was monitored as a function of time while the engine was fired. The fiber showed no mechanical damage after 419 firings during which it was subject to transients from 30 K to 350 K, and total exposure time to near liquid hydrogen temperatures in excess of 990 seconds. These extreme temperatures did cause attenuation greater than 3 dB, but the signal was fully recovered at room temperature. This experiment demonstrates that commercially available optical fiber cables can survive the environment seen by a typical rocket engine instrumentation system, and disclose a temperature-dependent attenuation observed during exposure to near liquid hydrogen temperatures. Author

N92-33343*# National Aeronautics and Space Administration. Lewis Research Center, Cleveland, OH.

BENEFITS AND TECHNOLOGY READINESS FOR USING CRYOGENIC INSTEAD OF STORABLE PROPELLANTS FOR RETURN MISSION FROM MOON

DAVID W. PLACHTA /n NASA. Lyndon B. Johnson Space Center, Third SEI Technical Interchange: Proceedings p 522-539 1992 Avail: CASI HC A03/MF A05

Cryogenic requirements are examined for new missions to the moon. A comparison is made with previous moon landings and a technology assessment investigates the new requirements for such missions. All of the material is presented in viewgraph format. H.A.

MATERIALS PROCESSING

Includes space-based development of products and processes for commercial applications.

A92-12863* National Aeronautics and Space Administration. Lewis Research Center, Cleveland, OH.

NUMERICAL SIMULATIONS OF SPACE PROCESSING - THE REALITY, THE MYTH, AND THE FUTURE

A. CHAIT (NASA, Lewis Research Center, Cleveland, OH) IN: AIAA/IKI Microgravity Science Symposium, 1st, Moscow, USSR, May 13-17, 1991, Proceedings 1991 7 p refs Copyright

The present capabilities offered by the combination of advanced special and general purpose numerical codes and supercomputers are discussed. Emphasis is placed on unique demands placed by the space environment on the computation of realistic space experiments and recommendations for improving the scientific return on the space investment. It is concluded that numerical simulations can provide timely and relevant answers which can guide and improve future space experiments. O.G.

A92-12880 Westinghouse Electric Corp., Pittsburgh, PA. **FLIGHT EXPERIMENT ON ACOUSTO-OPTIC CRYSTAL GROWTH**

N. B. SINGH (Westinghouse Science and Technology Center, Pittsburgh, PA) and WALTER M. B. DUVAL (NASA, Lewis Research

Center, Cleveland, OH; Westinghouse Science and Technology Center, Pittsburgh, PA) IN: AIAA/IKI Microgravity Science Symposium, 1st, Moscow, USSR, May 13-17, 1991, Proceedings 1991 4 p refs
Copyright

The physical vapor transport method was used for growing mercurous chloride crystals in different convective conditions. Optical homogeneity is found to be extremely dependent on convection levels. Results of numerical studies indicate that for a gravity level of 0.001 g or less the Stefan wind drives the flow and no recirculating cells are observed. O.G.

A92-17056* Akron Univ., OH.

STEADY-STATE THERMAL-SOLUTAL CONVECTION AND DIFFUSION IN A SIMULATED FLOAT ZONE

G. W. YOUNG (Akron, University, OH) and A. CHAIT (NASA, Lewis Research Center, Cleveland, OH) IN: Low-gravity fluid dynamics and transport phenomena 1990 39 p refs
(Contract NCC3-104)
Copyright

Models describing the steady-state thermal diffusion in a pure system, the thermal-solutal diffusion in a binary system, and heat and momentum transverse in a pure system are presented. The geometry of the model is described by a 2D Cartesian coordinate system that is applicable for crystal sheets. The melting, solidifying, and melt/gas interfacial shapes as well as the thermal, flow, and solutal profiles are analytically evaluated as functions of the heat and ambient temperature profiles and material properties. The solution procedure involves a coupled asymptotic/numerical approach which reduces the coupled set of partial differential equations to ordinary type. The results should be applicable in situations where melt flows are not intense enough to change the thermal field in pure systems, or where the physical properties of the melt are such that the convective field is decoupled from the thermal field, the latter being established primarily by diffusion. C.D.

A92-25702*# National Aeronautics and Space Administration, Lewis Research Center, Cleveland, OH.

INTENSIFIED ARRAY CAMERA IMAGING OF SOLID SURFACE COMBUSTION ABOARD THE NASA LEARJET

KAREN J. WEILAND (NASA, Lewis Research Center, Cleveland, OH) AIAA, Aerospace Sciences Meeting and Exhibit, 30th, Reno, NV, Jan. 6-9, 1992. 12 p. Previously announced in STAR as N92-16156. Jan. 1992 12 p refs
(AIAA PAPER 92-0240) Copyright

An intensified array camera has been used to image weakly luminous flames spreading over thermally thin paper samples in a low-gravity environment aboard the NASA-Lewis Learjet. The aircraft offers 10 to 20 sec of reduced gravity during execution of a Keplerian trajectory and allows the use of instrumentation that is delicate or requires higher electrical power than is available in drop towers. The intensified array camera is a charge intensified device type that responds to light between 400 and 900 nm and has a minimum sensitivity of 10(exp 6) footcandles. The paper sample, either ashless filter paper or a lab wiper, burns inside a sealed chamber which is filled with 21, 18, or 15 pct. oxygen in nitrogen at one atmosphere. The camera views the edge of the paper and its output is recorded on videotape. Flame positions are measured every 0.1 sec to calculate flame spread rates. Comparisons with drop tower data indicate that the flame shapes and spread rates are affected by the residual g level in the aircraft. Author

A92-27002*# National Aeronautics and Space Administration, Lewis Research Center, Cleveland, OH.

STABILITY ANALYSIS OF SURFACE TENSION EFFECTS ON A DOUBLE-DIFFUSIVE LAYER

C. F. CHEN and T. F. SU (Arizona, University, Tucson) AIAA, Aerospace Sciences Meeting and Exhibit, 30th, Reno, NV, Jan. 6-9, 1992. 9 p. Jan. 1992 9 p refs
(Contract NAG3-1268)
(AIAA PAPER 92-0605) Copyright

The linear stability characteristics of a fluid layer with simultaneous temperature and concentration gradients in a reduced gravity field are examined. The surface tension of the fluid is assumed to be a linear function of temperature and concentration. It is concluded that a small amount of gravity may damp out oscillatory instability or may alter its dynamics so that instability appears as steady convection. The onset of salt-finger instability may be in the overstable mode due to the surface tension method. The Lewis and Prandtl numbers of the material have a strong influence on the stability boundaries and onset characteristics of the system. O.G.

A92-27122*# National Aeronautics and Space Administration, Lewis Research Center, Cleveland, OH.

A VERSATILE GET AWAY SPECIAL FURNACE FOR MATERIALS PROCESSING IN SPACE

A. H. BELLOWES, D. H. MATTHIESEN, G. A. DUCHENE, and G. C. CHEN (GTE Laboratories, Inc., Waltham, MA) AIAA, Aerospace Sciences Meeting and Exhibit, 30th, Reno, NV, Jan. 6-9, 1992. 7 p. Jan. 1992 7 p
(Contract NAS3-25058)
(AIAA PAPER 92-0787) Copyright

A furnace suitable for performing a variety of high-temperature materials science experiments, including crystal growth in the microgravity of Shuttle orbit, has been developed by GTE Laboratories under the sponsorship of NASA Lewis Research Center. It has been designed for use in NASA's Get Away Special (GAS), small self-contained payload program. A prototype has been designed, built, installed in a simulated GAS container, purged with argon, and used for a series of characterization tests. Also, it was outfitted twice with high-temperature GaAs crystal growth charges and used to successfully grow both. Two different GAS payload configurations have been outlined; one is entirely self-contained and includes one furnace; the other requires external power but incorporates 3 furnaces and their control systems. Author

A92-28188*# National Aeronautics and Space Administration, Lewis Research Center, Cleveland, OH.

THE ISOTHERMAL DENDRITIC GROWTH EXPERIMENT - A USMP-2 SPACE FLIGHT EXPERIMENT

M. E. GLICKSMAN, M. B. KOSS, K.-K. KOO, R. C. HAHN, A. ROJAS (Rensselaer Polytechnic Institute, Troy, NY), and E. WINSKA (NASA, Lewis Research Center, Cleveland, OH) AIAA, Aerospace Sciences Meeting and Exhibit, 30th, Reno, NV, Jan. 6-9, 1992. 8 p. Jan. 1992 8 p refs
(Contract NAS3-25368)
(AIAA PAPER 92-0350) Copyright

The NASA Isothermal Dendritic Growth Experiment (IDGE), which is to be performed on three of the U.S. Microgravity Payload flights, is discussed. IDGE is designed to investigate dendritic growth under microgravity. The theory of dendritic growth and the effects of gravity on it are reviewed, and the IDGE experimental apparatus, design, and ground-based tests are discussed. C.D.

A92-29243* National Aeronautics and Space Administration, Lewis Research Center, Cleveland, OH.

ADAPTIVE TEMPERATURE PROFILE CONTROL OF A MULTIZONE CRYSTAL GROWTH FURNACE

C. BATUR, R. B. SHARPLESS (Akron, University, OH), W. M. B. DUVAL, and B. N. ROSENTHAL (NASA, Lewis Research Center, Cleveland, OH) IN: 1991 American Control Conference, 10th, Boston, MA, June 26-28, 1991, Proceedings. Vol. 2 1991 6 p refs
Copyright

An intelligent measurement system is described which is used to assess the shape of a crystal while it is growing inside a multizone transparent furnace. A color video imaging system observes the crystal in real time, and determines the position and the shape of the interface. This information is used to evaluate the crystal growth rate, and to analyze the effects of translational velocity and temperature profiles on the shape of the interface.

29 MATERIALS PROCESSING

Creation of this knowledge base is the first step to incorporate image processing into furnace control. I.E.

A92-29611*# National Aeronautics and Space Administration. Lewis Research Center, Cleveland, OH.

AN INITIAL STUDY OF VOID FORMATION DURING SOLIDIFICATION OF ALUMINUM IN NORMAL AND REDUCED-GRAVITY

FRANCIS P. CHIARAMONTE, GEORGE FOERSTER, DANIEL J. GOTTI, ERIC S. NEUMANN, J. C. JOHNSTON (NASA, Lewis Research Center, Cleveland, OH), and KENNETH J. DE WITT (Toledo, University, OH) AIAA, Aerospace Sciences Meeting and Exhibit, 30th, Reno, NV, Jan. 6-9, 1992. 10 p. Research supported by NASA. Jan. 1992 10 p refs (AIAA PAPER 92-0845)

Void formation due to volumetric shrinkage during aluminum solidification was observed in real time using a radiographic viewing system in normal and reduced gravity. An end chill directional solidification furnace with water quench was developed to solidify aluminum samples during the approximately 16 seconds of reduced gravity (+/- 0.02g) achieved by flying an aircraft through a parabolic trajectory. Void formation was recorded for two cases: first a nonwetting system; and second, a wetting system where wetting occurs between the aluminum and crucible lid. The void formation in the nonwetting case is similar in normal and reduced gravity, with a single vapor cavity forming at the top of the crucible. In the wetting case in reduced gravity, surface tension causes two voids to form in the top corners of the crucible, but in normal gravity only one large voids forms across the top. Author

A92-33835 National Aeronautics and Space Administration. Lewis Research Center, Cleveland, OH.

TRANSPORT MODES DURING CRYSTAL GROWTH IN A CENTRIFUGE

WILLIAM A. ARNOLD, WILLIAM R. WILCOX, FREDERICK CARLSON (Clarkson University, Potsdam, NY), ARNON CHAIT (NASA, Lewis Research Center, Cleveland, OH), and LIIA L. REGEL' (Russian Academy of Sciences, Space Research Institute, Moscow, Russia) (Material processing in high gravity; Proceedings of the 1st International Workshop, Dubna, Russia, May 20-25, 1991. A92-33832 13-29) Journal of Crystal Growth (ISSN 0022-0248), vol. 119, no. 1-2, April 1992, p. 24-40. Apr. 1992 17 p refs (Contract NAGW-976)

Copyright

Flow modes arising under average acceleration in centrifugal crystal growth, the gradient of acceleration, and the Coriolis force are investigated using a fully nonlinear three-dimensional numerical model for a centrifugal crystal growth experiment. The analysis focuses on an examination of the quasi-steady state flow modes. The importance of the gradient acceleration is determined by the value of a new nondimensional number, Ad. V.L.

A92-56956 National Aeronautics and Space Administration. Lewis Research Center, Cleveland, OH.

GROWTH AND CHARACTERIZATION OF LEAD BROMIDE CRYSTALS

N. B. SINGH, M. GOTTLIEB, T. HENNINGSEN, R. H. HOPKINS, R. MAZELSKY (Westinghouse Science and Technology Center, Pittsburgh, PA), M. E. GLICKSMAN (Rensselaer Polytechnic Institute, Troy, NY), S. R. CORIELL (NIST, Gaithersburg, MD), G. J. SANTORO, and W. M. B. DUVAL (NASA, Lewis Research Center, Cleveland, OH) Journal of Crystal Growth (ISSN 0022-0248), vol. 123, no. 1-2, Sept. 1992, p. 221-226. Research supported by NASA. Sep. 1992 6 p refs

Copyright

Lead(II) bromide was purified by a combination of directional freezing and zone-refining methods. Differential thermal analysis of the lead bromide showed that a destructive phase transformation occurs below the melting temperature. This transformation causes extensive cracking, making it very difficult to grow a large single crystal. Energy of phase transformation for pure lead bromide was determined to be 24.67 cal/g. To circumvent this limitation, crystals

were doped by silver bromide which decreased the energy of phase transformation. The addition of silver helped in achieving the size, but enhanced the inhomogeneity in the crystal. The acoustic attenuation constant was almost identical for the pure and doped (below 3000 ppm) crystals. Author

A92-56957 National Aeronautics and Space Administration. Lewis Research Center, Cleveland, OH.

EFFECT OF GROWTH CONDITIONS ON THE QUALITY OF LEAD BROMIDE CRYSTALS

N. B. SINGH, M. GOTTLIEB, T. HENNINGSEN, R. H. HOPKINS, R. MAZELSKY (Westinghouse Science and Technology Center, Pittsburgh, PA), M. E. GLICKSMAN (Rensselaer Polytechnic Institute, Troy, NY), S. R. CORIELL (NIST, Gaithersburg, MD), W. M. B. DUVAL, and G. J. SANTORO (NASA, Lewis Research Center, Cleveland, OH) Journal of Crystal Growth (ISSN 0022-0248), vol. 123, no. 1-2, Sept. 1992, p. 227-235. Research supported by NASA. Sep. 1992 9 p refs

Copyright

Single crystals of pure and doped lead bromide were grown by the Bridgman method in different convective conditions. The convection level was varied by changing the thermal and solutal Rayleigh number. The homogeneity in refractive index, and hence the optical quality, was estimated by examining the optical distortion, birefringence interferograms, and laser scattering through the crystal. The optical quality of the crystal varied significantly with the variation of convection level during the crystal growth. The critical concentration of the solute was estimated for several values of growth velocity by numerical analysis at the thermal gradient of 20 K/cm. Author

A92-57131 National Aeronautics and Space Administration. Washington, DC.

EARLY USE OF SPACE STATION FREEDOM FOR NASA'S MICROGRAVITY SCIENCE AND APPLICATIONS PROGRAM

ROBERT C. RHOME (NASA, Microgravity Science and Applications Div., Washington) and TERENCE F. O'MALLEY (NASA, Microgravity Science and Applications Div., Washington; NASA, Lewis Research Center, Cleveland, OH) IAF, International Astronautical Congress, 43rd, Washington, Aug. 28-Sept. 5, 1992. 8 p. Aug. 1992 8 p (IAF PAPER 92-0702) Copyright

The paper describes microgravity science opportunities inherent to the restructured Space Station and presents a synopsis of the scientific utilization plan for the first two years of ground-tended operations. In the ground-tended utilization mode the Space Station is a large free-flyer providing a continuous microgravity environment unmatched by any other platform within any existing U.S. program. It is pointed out that the importance of this period of early Space Station mixed-mode utilization between crew-tended and ground-tended approaches is of such magnitude that Station-based microgravity science experiments many become benchmarks to the disciplines involved. The traffic model that is currently being pursued is designed to maximize this opportunity for the U.S. microgravity science community. L.M.

N92-16156*# National Aeronautics and Space Administration. Lewis Research Center, Cleveland, OH.

INTENSIFIED ARRAY CAMERA IMAGING OF SOLID SURFACE COMBUSTION ABOARD THE NASA LEARJET

KAREN J. WEILAND 1992 13 p Presented at the 30th Aerospace Sciences Meeting and Exhibit, Reno, NV, 6-9 Jan. 1992; sponsored by AIAA (Contract RTOP 694-03-0C) (NASA-TM-105361; E-6740; NAS 1.15:105361; AIAA PAPER 92-0240) Avail: CASI HC A03/MF A01

An intensified array camera was used to image weakly luminous flames spreading over thermally thin paper samples in a low gravity environment aboard the NASA-Lewis Learjet. The aircraft offers 10 to 20 sec of reduced gravity during execution of a Keplerian trajectory and allows the use of instrumentation that is delicate or requires higher electrical power than is available in drop towers. The intensified array camera is a charge intensified device type

that responds to light between 400 and 900 nm and has a minimum sensitivity of 10(exp 6) footcandles. The paper sample, either ashless filter paper or a lab wiper, burns inside a sealed chamber which is filled with 21, 18, or 15 pct. oxygen in nitrogen at one atmosphere. The camera views the edge of the paper and its output is recorded on videotape. Flame positions are measured every 0.1 sec to calculate flame spread rates. Comparisons with drop tower data indicate that the flame shapes and spread rates are affected by the residual g level in the aircraft. Author

N92-16158*# National Aeronautics and Space Administration. Lewis Research Center, Cleveland, OH.

VAPOR CRYSTAL GROWTH TECHNOLOGY DEVELOPMENT: APPLICATION TO CADMIUM TELLURIDE

FRANZ ROSENBERGER (Alabama Univ., Huntsville.), MICHAEL BANISH (Alabama Univ., Huntsville.), and WALTER M. B. DUVAL Dec. 1991 55 p

(Contract NAS3-25361; RTOP 674-21-05)

(NASA-TM-103786; E-6062; NAS 1.15:103786) Avail: CASI HC A04/MF A01

Growth of bulk crystals by physical vapor transport was developed and applied to cadmium telluride. The technology makes use of effusive ampoules, in which part of the vapor contents escapes to a vacuum shroud through defined leaks during the growth process. This approach has the advantage over traditional sealed ampoule techniques that impurity vapors and excess vapor constituents are continuously removed from the vicinity of the growing crystal. Thus, growth rates are obtained routinely at magnitudes that are rather difficult to achieve in closed ampoules. Other advantages of this effusive ampoule physical vapor transport (EAPVT) technique include the predetermination of transport rates based on simple fluid dynamics and engineering considerations, and the growth of the crystal from close to congruent vapors, which largely alleviates the compositional nonuniformities resulting from buoyancy driven convective transport. After concisely reviewing earlier work on improving transport rates, nucleation control, and minimization of crystal wall interactions in vapor crystal growth, a detail account is given of the largely computer controlled EAPVT experimentation. Author

N92-23640*# National Aeronautics and Space Administration. Lewis Research Center, Cleveland, OH.

CRITICAL FLUID THERMAL EQUILIBRATION EXPERIMENT (19-IML-1)

R. ALLEN WILKINSON *In* NASA. Marshall Space Flight Center, First International Microgravity Laboratory Experiment Descriptions p 261-263 Feb. 1992

Avail: CASI HC A01/MF A03

Gravity sometimes blocks all experimental techniques of making a desired measurement. Any pure fluid possesses a liquid-vapor critical point. It is defined by a temperature, pressure, and density state in thermodynamics. The critical issue that this experiment attempts to understand is the time it takes for a sample to reach temperature and density equilibrium as the critical point is approached; is it infinity due to mass and thermal diffusion, or do pressure waves speed up energy transport while mass is still under diffusion control. The objectives are to observe: (1) large phase domain homogenization without and with stirring; (2) time evolution of heat and mass after temperature step is applied to a one phase equilibrium sample; (3) phase evolution and configuration upon going two phase from a one phase equilibrium state; (4) effects of stirring on a low g two phase configuration; (5) two phase to one phase healing dynamics starting from a two phase low g configuration; and (6) effects of shuttle acceleration events on spatially and temporally varying compressible critical fluid dynamics. Author

N92-23642*# National Aeronautics and Space Administration. Lewis Research Center, Cleveland, OH.

MICROGRAVITY ACCELERATION MEASUREMENT AND ENVIRONMENT CHARACTERIZATION SCIENCE (17-IML-1)

In NASA. Marshall Space Flight Center, First International

Microgravity Laboratory Experiment Descriptions p 271-275 Feb. 1992

Avail: CASI HC A01/MF A03

The Space Acceleration Measurement System (SAMS) is a general purpose instrumentation system designed to measure the accelerations onboard the Shuttle Orbiter and Shuttle/Spacelab vehicles. These measurements are used to support microgravity experiments and investigation into the microgravity environment of the vehicle. Acceleration measurements can be made at locations remote from the SAMS main instrumentation unit by the use of up to three remote triaxial sensor heads. The prime objective for SAMS on the International Microgravity Lab (IML-1) mission will be to measure the accelerations experienced by the Fluid Experiment System (FES). The SAMS acceleration measurements for FES will be complemented by low level, low frequency acceleration measurements made by the Orbital Acceleration Research Experiment (OARE) installed on the shuttle. Secondary objectives for SAMS will be to measure accelerations at several specific locations to enable the acceleration transfer function of the Spacelab module to be analyzed. This analysis effort will be in conjunction with similar measurements analyses on other Spacelab missions. Author

N92-26611*# National Aeronautics and Space Administration. Lewis Research Center, Cleveland, OH.

COLOR IMAGE PROCESSING AND OBJECT TRACKING WORKSTATION

ROBERT B. KLIMEK and MICHAEL J. PAULICK (Baldwin-Wallace Coll., Berea, OH.) Apr. 1992 23 p Original contains color illustrations

(Contract NCC3-206; RTOP 694-03-00)

(NASA-TM-105561; E-6885; NAS 1.15:105561)

A system is described for automatic and semiautomatic tracking of objects on film or video tape which was developed to meet the needs of the microgravity combustion and fluid science experiments at NASA Lewis. The system consists of individual hardware parts working under computer control to achieve a high degree of automation. The most important hardware parts include 16 mm film projector, a lens system, a video camera, an S-VHS tape deck, a frame grabber, and some storage and output devices. Both the projector and tape deck have a computer interface enabling remote control. Tracking software was developed to control the overall operation. In the automatic mode, the main tracking program controls the projector or the tape deck frame incrementation, grabs a frame, processes it, locates the edge of the objects being tracked, and stores the coordinates in a file. This process is performed repeatedly until the last frame is reached. Three representative applications are described. These applications represent typical uses and include tracking the propagation of a flame front, tracking the movement of a liquid-gas interface with extremely poor visibility, and characterizing a diffusion flame according to color and shape. Author

N92-27197*# National Aeronautics and Space Administration. Lewis Research Center, Cleveland, OH.

MICROGRAVITY COMBUSTION SCIENCE: PROGRESS, PLANS, AND OPPORTUNITIES

Apr. 1992 49 p Original contains color illustrations

(Contract RTOP 674-22-05)

(NASA-TM-105410; E-6816; NAS 1.15:105410)

An earlier overview is updated which introduced the promise of microgravity combustion research and provided a brief survey of results and then current research participants, the available set of reduced gravity facilities, and plans for experimental capabilities in the space station era. Since that time, several research studies have been completed in drop towers and aircraft, and the first space based combustion experiments since Skylab have been conducted on the Shuttle. The microgravity environment enables a new range of experiments to be performed since buoyancy induced flows are nearly eliminated, normally obscured forces and flows may be isolated, gravitational settling or sedimentation is nearly eliminated, and larger time or length scales in experiments

29 MATERIALS PROCESSING

are feasible. In addition to new examinations of classical problems, (e.g., droplet burning), current areas of interest include soot formation and weak turbulence, as influenced by gravity. Author

N92-28438* National Aeronautics and Space Administration. Lewis Research Center, Cleveland, OH.

AN EXAMINATION OF ANTICIPATED G-JITTER ON SPACE STATION AND ITS EFFECTS ON MATERIALS PROCESSES

EMILY NELSON *In its* International Workshop on Vibration Isolation Technology for Microgravity Science Applications p 115-131 May 1992

Avail: CASI HC A03/MF A04

Information on anticipated g-jitter on Space Station Freedom and the effect of the jitter on materials processes is given in viewgraph form. It was concluded that g-jitter will dominate the acceleration environment; that it is a 3D multifrequency phenomenon; and that it varies dramatically in orientation. Information is given on calculated or measured sources of residual acceleration, aerodynamic drag, Shuttle acceleration measurements, the Space Station environment, tolerable g-levels as a function of frequency, directional solidification, vapor crystal growth, protein crystal growth, float zones, and liquid bridges.

Author

N92-28442* National Aeronautics and Space Administration. Lewis Research Center, Cleveland, OH.

VIBRATION ISOLATION TECHNOLOGY DEVELOPMENT TO DEMONSTRATION

CARLOS GRODSINSKY *In its* International Workshop on Vibration Isolation Technology for Microgravity Science Applications p 193-207 May 1992

Avail: CASI HC A03/MF A04

The main thrust of these studies has resulted in an active inertial feedforward/feedback isolation system. This prototype magnetic suspension system has been demonstrated in a laboratory setting in six degrees-of-freedom and has been preliminarily characterized in its isolation performance with favorable results. This isolation system consists of a closed loop digital control system referencing a platform around six relative and six inertial sensors. These sensors control the isolated mass through nine attractive electromagnetic actuators with a system capability of \pm three-tenths of an inch travel in three dimensions. The development of a prototype system from design to fabrication leads directly into the demonstration phase of the project which will attempt a low gravity environmental demonstration of engineering hardware for the isolation of a scientific payload. The demonstration phase of the project will use an aircraft low gravity maneuver to establish a research testbed for the study of isolation hardware and control strategies in an off-loaded environment. In developing this demonstration capability the Lewis Learjet aircraft has been characterized through its parabolic flight maneuvers and a trunnioned experimental volume has been designed for the test of both active and passive isolation packages. This vibration isolation testbed is operational and has two data acquisition systems available for both autonomous and interactive operation, with a combined input capability of 32 channels.

Author

31

ENGINEERING (GENERAL)

Includes vacuum technology; control engineering; display engineering; cryogenics; and fire prevention.

A92-13413* Lockheed Missiles and Space Co., Huntsville, AL. **INVESTIGATION OF TWO AND THREE PARAMETER EQUATIONS OF STATE FOR CRYOGENIC FLUIDS**

SUSAN L. JENKINS (Lockheed Missiles and Space Co., Inc., Huntsville, AL), ALOK K. MAJUMDAR (Sverdrup Technology, Inc., Huntsville, AL), and ROBERT C. HENDRICKS (NASA, Lewis

Research Center, Cleveland, OH) *IN: Advances in cryogenic engineering. Vol. 35B - Proceedings of the 1989 Cryogenic Engineering Conference, Los Angeles, CA, July 24-28, 1989* 1990 8 p refs

Copyright

Two-phase flows are a common occurrence in cryogenic engines and an accurate evaluation of the heat-transfer coefficient in two-phase flow is of significant importance in their analysis and design. The thermodynamic equation of state plays a key role in calculating the heat transfer coefficient which is a function of thermodynamic and thermophysical properties. An investigation has been performed to study the performance of two- and three-parameter equations of state to calculate the compressibility factor of cryogenic fluids along the saturation loci. The two-parameter equations considered here are van der Waals and Redlich-Kwong equations of state. The three-parameter equation represented here is the generalized Benedict-Webb-Rubin (BWR) equation of Lee and Kesler. Results have been compared with the modified BWR equation of Bender and the extended BWR equations of Stewart. Seven cryogenic fluids have been tested; oxygen, hydrogen, helium, nitrogen, argon, neon, and air. The performance of the generalized BWR equation is poor for hydrogen and helium. The van der Waals equation is found to be inaccurate for air near the critical point. For helium, all three equations of state become inaccurate near the critical point.

Author

A92-13432* National Aeronautics and Space Administration. Lewis Research Center, Cleveland, OH.

SLUSH HYDROGEN (SLH2) TECHNOLOGY DEVELOPMENT FOR APPLICATION TO THE NATIONAL AEROSPACE PLANE (NASP)

RICHARD L. DEWITT, TERRY L. HARDY, MARGARET V. WHALEN, and G. P. RICHTER (NASA, Lewis Research Center, Cleveland, OH) *IN: Advances in cryogenic engineering. Vol. 35B - Proceedings of the 1989 Cryogenic Engineering Conference, Los Angeles, CA, July 24-28, 1989* 1990 14 p refs

Copyright

The National Aerospace Plane (NASP) program is giving us the opportunity to reach new unique answers in a number of engineering categories. The answers are considered enhancing technology or enabling technology. Airframe materials and densified propellants are examples of enabling technology. The National Aeronautics and Space Administration's Lewis Research Center has the task of providing the technology data which will be used as the basis to decide if slush hydrogen (SLH2) will be the fuel of choice for the NASP. The objectives of this NASA Lewis program are: (1) to provide, where possible, verified numerical models of fluid production, storage, transfer, and feed systems, and (2) to provide verified design criteria for other engineered aspects of SLH2 systems germane to an NASP. This program is a multiyear multimillion dollar effort. The present pursuit of the above listed objectives is multidimensional, covers a range of problem areas, works these to different levels of depth, and takes advantage of the resources available in private industry, academia, and the U.S. Government. The NASA Lewis overall program plan is summarized. The initial implementation of the plan will be unfolded and the present level of efforts in each of the resource areas will be discussed. Results already in hand will be pointed out. A description of additionally planned near-term experimental and analytical work is described.

Author

A92-23845* National Aeronautics and Space Administration. Lewis Research Center, Cleveland, OH.

EFFECT OF GAS MASS FLUX ON CRYOGENIC LIQUID JET BREAKUP

R. D. INGEBO (NASA, Lewis Research Center, Cleveland, OH) (Space Cryogenics Workshop, 10th, Cleveland, OH, June 18-20, 1991, Proceedings. A92-23826 08-31) *Cryogenics* (ISSN 0011-2275), vol. 32, no. 2, 1992, p. 191-193. 1992 3 p refs

Copyright

A scattered-light scanning instrument developed at NASA Lewis Research Center was used to measure the characteristic drop size of clouds of liquid nitrogen droplets. The instrument was

calibrated with suspensions of monosized polystyrene spheres. In this investigation of the mechanism of liquid nitrogen jet disintegration in a high-velocity gas flow, the Sauter mean diameter, D_{32} , was found to vary inversely with the nitrogen gas mass flux raised to the power 1.33. Values of D_{32} varied from 5 to 25 microns and the mass flux exponent of 1.33 agrees well with theory for liquid jet breakup in high-velocity gas flows. The loss of very small droplets due to the high vaporization rate of liquid nitrogen was avoided by sampling the spray very close to the atomizer, i.e., 1.3 cm downstream of the nozzle orifice. The presence of high velocity and thermal gradients in the gas phase also made sampling of the particles difficult. As a result, it was necessary to correct the measurements for background noise produced by both highly turbulent gas flows and thermally induced density gradients in the gas phase.

Author

A92-48951# National Aeronautics and Space Administration. Lewis Research Center, Cleveland, OH.

SLUSH HYDROGEN PRESSURIZED EXPULSION STUDIES AT THE NASA K-SITE FACILITY

MARGARET V. WHALEN and TERRY L. HARDY (NASA, Lewis Research Center, Cleveland, OH) AIAA, SAE, ASME, and ASEE, Joint Propulsion Conference and Exhibit, 28th, Nashville, TN, July 6-8, 1992. 8 p. Previously announced in STAR as N92-26131. Jul. 1992 8 p refs

(Contract RTOP 763-22-21)

(AIAA PAPER 92-3385)

An experiment test series of the slush hydrogen (SLH2) project at the NASA LeRC Plum Brook K-Site Facility was completed. This testing was done as part of the characterization and technology database development on slush hydrogen required for the National Aero-Space Plane (NASP) Program. The primary objective of these experiments was to investigate tank thermodynamic parameters during the pressurized expulsion of slush hydrogen. To accomplish this, maintenance of tank pressure control was investigated during pressurized expulsion of slush hydrogen using gaseous hydrogen and gaseous helium pressurant. In addition, expulsion tests were performed using gaseous helium for initial pressurization, then gaseous hydrogen during expulsion. These tests were conducted with and without mixing of the slush hydrogen. Results from the testing included an evaluation of tank pressure control, pressurant requirements, SLH2 density change, and system mass and energy balances.

Author

A92-52205* National Aeronautics and Space Administration. Lewis Research Center, Cleveland, OH.

SOLUTIONS OF THE HEAT CONDUCTION EQUATION IN MULTILAYERS FOR PHOTOTHERMAL DEFLECTION EXPERIMENTS

WILLIAM A. MCGAHAN and K. D. COLE (Nebraska, University, Lincoln) Journal of Applied Physics (ISSN 0021-8979), vol. 72, no. 4, Aug. 15, 1992, p. 1362-1373. 15 Aug. 1992 12 p refs (Contract NAG3-95; NAG3-154; NSF DMR-89-18889) Copyright

Analytical expressions for temperature and laser beam deflection in multilayer medium is derived using Green function techniques. The approach is based on calculation of the normal component of heat fluxes across the boundaries, from which either the beam deflections or the temperature anywhere in space can be found. A general expression for the measured signals for the case of four-quadrant detection is also presented and compared with previous calculations of detector response for finite probe beams.

V.L.

N92-11217*# National Aeronautics and Space Administration. Lewis Research Center, Cleveland, OH.

MICROGRAVITY VIBRATION ISOLATION: AN OPTIMAL CONTROL LAW FOR THE ONE-DIMENSIONAL CASE

R. D. HAMPTON (Virginia Univ., Charlottesville.), C. M. GRODSINSKY (Virginia Univ., Charlottesville.), P. E. ALLAIRE (Virginia Univ., Charlottesville.), D. W. LEWIS, and C. R. KNOSPE (Virginia Univ., Charlottesville.) Oct. 1991 23 p

(Contract RTOP 694-03-0C)

(NASA-TM-105146; E-6422; NAS 1.15:105146) Avail: CASI HC A03/MF A01

Certain experiments contemplated for space platforms must be isolated from the accelerations of the platforms. An optimal active control is developed for microgravity vibration isolation, using constant state feedback gains (identical to those obtained from the Linear Quadratic Regulator (LQR) approach) along with constant feedforward (preview) gains. The quadratic cost function for this control algorithm effectively weights external accelerations of the platform disturbances by a factor proportional to $(1/\omega)(\exp 4)$. Low frequency accelerations (less than 50 Hz) are attenuated by greater than two orders of magnitude. The control relies on the absolute position and velocity feedback of the experiment and the absolute position and velocity feedforward of the platform, and generally derives the stability robustness characteristics guaranteed by the LQR approach to optimality. The method as derived is extendable to the case in which only the relative positions and velocities and the absolute accelerations of the experiment and space platform are available.

Author

N92-11221*# National Aeronautics and Space Administration. Lewis Research Center, Cleveland, OH.

THERMAL VERIFICATION TESTING OF COMMERCIAL PRINTED-CIRCUIT BOARDS FOR SPACEFLIGHT

WILLIAM M. FOSTER, II 1991 9 p Proposed for presentation at the 1992 Annual Reliability and Maintainability Symposium, Las Vegas, NV, 21-23 Jan. 1991; sponsored by IEEE

(Contract RTOP 694-03-0H)

(NASA-TM-105261; E-6593; NAS 1.15:105261) Avail: CASI HC A02/MF A01

A method is discussed developed to verify commercial printed-circuit boards for a shuttle orbital flight. The Space Acceleration Measurement System Project used this method first with great success. The test sequence is based on early fault detection, desire to test the final assembly, and integration with other verification testing. A component thermal screening test is performed first to force flaws in design, workmanship, parts, processes, and materials into observable failures. Then temperature definition tests are performed that consist of infrared scanning, thermal vacuum testing, and preliminary thermal operational testing. Only the engineering unit is used for temperature definition testing, but the preliminary thermal operational testing is performed on the flight unit after the temperature range has been defined. In the sequence of testing, vibration testing is performed next, but most vibration failures cannot be detected without subsequent temperature cycling. Finally, final assembly testing is performed to simulate the shuttle flight. An abbreviated thermal screening test is performed as a check after the vibration test, and then a complete thermal operational test is performed. The final assembly test finishes up with a burn-in of 100 hours of trouble-free operation. Verification is successful when all components and final assemblies have passed each test satisfactory. This method was very successful in verifying that commercial printed-circuit boards will survive in the shuttle environment.

Author

N92-28436*# National Aeronautics and Space Administration. Lewis Research Center, Cleveland, OH.

INTERNATIONAL WORKSHOP ON VIBRATION ISOLATION TECHNOLOGY FOR MICROGRAVITY SCIENCE APPLICATIONS

JOSEPH F. LUBOMSKI, ed. May 1992 405 p Workshop held in Cleveland, OH, 23-25 Apr. 1991

(Contract RTOP 694-03-0C)

(NASA-CP-10094; E-7035; NAS 1.55:10094) Avail: CASI HC A18/MF A04

The International Workshop on Vibration Isolation Technology for Microgravity Science Applications was held on April 23-25, 1991 at the Holiday Inn in Middleburg Heights, Ohio. The main objective of the conference was to explore vibration isolation requirements of space experiments and what level of vibration isolation could be provided both by present and planned systems

on the Space Shuttle and Space Station Freedom and by state of the art vibration isolation technology.

N92-30692*# National Aeronautics and Space Administration. Lewis Research Center, Cleveland, OH.

MICROGRAVITY VIBRATION ISOLATION: OPTIMAL PREVIEW AND FEEDBACK CONTROL

R. D. HAMPTON (Virginia Univ., Charlottesville.), C. R. KNOSPE (Virginia Univ., Charlottesville.), C. M. GRODSINSKY, P. E. ALLAIRE (Virginia Univ., Charlottesville.), and D. W. LEWIS (Virginia Univ., Charlottesville.) May 1992 25 p (NASA-TM-105673; E-7042; NAS 1.15:105673) Avail: CASI HC A03/MF A01

In order to achieve adequate low-frequency vibration isolation for certain space experiments an active control is needed, due to inherent passive-isolator limitations. Proposed here are five possible state-space models for a one-dimensional vibration isolation system with a quadratic performance index. The five models are subsets of a general set of nonhomogeneous state space equations which includes disturbance terms. An optimal control is determined, using a differential equations approach, for this class of problems. This control is expressed in terms of constant, Linear Quadratic Regulator (LQR) feedback gains and constant feedforward (preview) gains. The gains can be easily determined numerically. They result in a robust controller and offers substantial improvements over a control that uses standard LQR feedback alone. Author

N92-31263*# National Aeronautics and Space Administration. Lewis Research Center, Cleveland, OH.

LIFE EXTENDING CONTROL FOR ROCKET ENGINES

C. F. LORENZO, J. R. SAUS, A. RAY (Pennsylvania State Univ., University Park.), M. CARPINO (Pennsylvania State Univ., University Park.), and M.-K. WU (Pennsylvania State Univ., University Park.) Aug. 1992 19 p (Contract RTOP 590-21-11) (NASA-TM-105789; E-7219; NAS 1.15:105789) Avail: CASI HC A03/MF A01

The concept of life extending control is defined. A brief discussion of current fatigue life prediction methods is given and the need for an alternative life prediction model based on a continuous functional relationship is established. Two approaches to life extending control are considered: (1) the implicit approach which uses cyclic fatigue life prediction as a basis for control design; and (2) the continuous life prediction approach which requires a continuous damage law. Progress on an initial formulation of a continuous (in time) fatigue model is presented. Finally, nonlinear programming is used to develop initial results for life extension for a simplified rocket engine (model). Author

N92-33334*# National Aeronautics and Space Administration. Lewis Research Center, Cleveland, OH.

FAST TRACK LUNAR NTR SYSTEMS ASSESSMENT FOR THE FIRST LUNAR OUTPOST AND ITS EVOLVABILITY TO MARS

STANLEY K. BOROWSKI and STEPHEN W. ALEXANDER /in NASA. Lyndon B. Johnson Space Center, Third SEI Technical Interchange: Proceedings p 421-436 1992 Avail: CASI HC A01/MF A05

The objectives of the 'fast track' lunar Nuclear Thermal Rocket (NTR) analysis are to quantify necessary engine/stage characteristics to perform NASA's 'First Lunar Outpost' scenario and to assess the potential for evolution to Mars mission applications. By developing NTR/stage technologies for use in NASA's 'First Lunar Outpost' scenario, NASA will make a major down payment on the key components needed for the follow-on Mars Space Transportation System. A faster, cheaper approach to overall lunar/Mars exploration is expected. Author

COMMUNICATIONS AND RADAR

Includes radar; land and global communications; communications theory; and optical communications.

A92-23964* National Aeronautics and Space Administration. Lewis Research Center, Cleveland, OH.

EFFECT OF SURFACE DEPOSITS ON ELECTROMAGNETIC PROPAGATION IN UNIFORM DUCTS

KENNETH J. BAUMEISTER (NASA, Lewis Research Center, Cleveland, OH) (IEEE Biennial Conference on Electromagnetic Field Computation, 4th, Toronto, Canada, Oct. 22-24, 1990) IEEE Transactions on Magnetics (ISSN 0018-9464), vol. 27, Sept. 1991, p. 4044-4047. Previously announced in STAR as N91-10208. Sep. 1991 4 p refs

Copyright

A finite-element Galerkin formulation has been used to study the effect of material surface deposits on the reflective characteristics of straight uniform ducts with PEC (perfectly electric conducting) walls. Over a wide frequency range, the effect of both single and multiple dielectric surface deposits on the duct reflection coefficient were examined. The power reflection coefficient was found to be significantly increased by the addition of deposits on the wall. Author

A92-29777*# National Aeronautics and Space Administration. Lewis Research Center, Cleveland, OH.

SATELLITE DELIVERY OF B-ISDN SERVICES

R. K. KWAN, K. M. PRICE (Space Systems/Loral, Palo Alto, CA), D. M. CHITRE, L. W. WHITE, and T. R. HENDERSON (COMSAT Laboratories, Clarksburg, MD) IN: AIAA International Communication Satellite Systems Conference and Exhibit, 14th, Washington, DC, Mar. 22-26, 1992, Technical Papers. Pt. 1 1992 12 p refs (Contract NAS3-25092) (AIAA PAPER 92-1831) Copyright

This paper will address the role of technology in the satellite delivery of B-ISDN services. Satellites excel in serving remote users and in providing multicast and broadcast services. Benefits to potential users employing these satellite broadband services will be examined together with their respective network architecture. Two application requirements are then proposed. The critical technologies needed in the realization of these architectures will be identified. Author

A92-29807*# National Aeronautics and Space Administration. Lewis Research Center, Cleveland, OH.

LEAST RELIABLE BITS CODING (LRBC) FOR HIGH DATA RATE SATELLITE COMMUNICATIONS

MARK VANDERAAR (Sverdrup Technology, Inc., Brook Park, OH), JAMES BUDINGER (NASA, Lewis Research Center, Cleveland, OH), and PAUL WAGNER (Sverdrup Technology, Inc., Brook Park, OH) IN: AIAA International Communication Satellite Systems Conference and Exhibit, 14th, Washington, DC, Mar. 22-26, 1992, Technical Papers. Pt. 1 1992 8 p refs (Contract NAS3-25266) (AIAA PAPER 92-1868) Copyright

LRBC, a bandwidth efficient multilevel/multistage block-coded modulation technique, is analyzed. LRBC uses simple multilevel component codes that provide increased error protection on increasingly unreliable modulated bits in order to maintain an overall high code rate that increases spectral efficiency. Soft-decision multistage decoding is used to make decisions on unprotected bits through corrections made on more protected bits. Analytical expressions and tight performance bounds are used to show that LRBC can achieve increased spectral efficiency and maintain equivalent or better power efficiency compared to that of BPSK. The relative simplicity of Galois field algebra vs the Viterbi algorithm

and the availability of high-speed commercial VLSI for block codes indicates that LRBC using block codes is a desirable method for high data rate implementations.
C.A.B.

A92-29821*# National Aeronautics and Space Administration. Lewis Research Center, Cleveland, OH.

DISTRIBUTION OF SPACE-GATHERED DATA

KENT M. PRICE and RONALD E. JORASCH (Space Systems/Loral, Palo Alto, CA) IN: AIAA International Communication Satellite Systems Conference and Exhibit, 14th, Washington, DC, Mar. 22-26, 1992, Technical Papers. Pt. 1 1992 9 p
(Contract NAS3-25092)

(AIAA PAPER 92-1888) Copyright

A Data Distribution Satellite (DDS) concept for directly distributing space-gathered data to users on the ground and allowing users access to their experiments for real-time control is described. The DDS would operate in conjunction with the Tracking and Data Relay Satellite System; high-capacity, optical intersatellite links would be used to establish connectivity with other satellites for international data relay or data gathering. The requirements, scenarios, and satellite communications payload are examined along with the benefits of the concept and the payload technologies that must be developed.
C.D.

A92-29833*# National Aeronautics and Space Administration. Lewis Research Center, Cleveland, OH.

KA-BAND DUAL FREQUENCY ARRAY FEED FOR A LOW COST ACTS GROUND TERMINAL

RICHARD Q. LEE, RAINEE N. SIMONS, and AJIT K. SIL (NASA, Lewis Research Center, Cleveland, OH) IN: AIAA International Communication Satellite Systems Conference and Exhibit, 14th, Washington, DC, Mar. 22-26, 1992, Technical Papers. Pt. 2 1992 6 p refs
(AIAA PAPER 92-1902) Copyright

Because of low cost and ease of fabrication, microstrip arrays are attractive as feeds for reflector antenna systems. This paper describes the development of a 4x4 microstrip array which will be used as a feed for a low cost ACTS ground terminal. The array feed consisting of four 2x2 subarrays is fed with coplanar waveguide power dividing networks. The patch radiator is designed to excite two orthogonal, linearly polarized waves at Ka-band frequencies (around 20 and 30 GHz). Test results for the developed array are presented.
Author

A92-29839*# National Aeronautics and Space Administration. Lewis Research Center, Cleveland, OH.

20/30 GHZ SATELLITE PERSONAL COMMUNICATIONS NETWORKS

L. C. PALMER (Hughes Network Systems, Germantown, MD), A. STERN (General Electric Co., Astro Space Div., Princeton, NJ), and P. Y. SOHN (NASA, Lewis Research Center, Cleveland, OH) IN: AIAA International Communication Satellite Systems Conference and Exhibit, 14th, Washington, DC, Mar. 22-26, 1992, Technical Papers. Pt. 2 1992 6 p refs
(AIAA PAPER 92-1908) Copyright

The feasibility of personal communications networks that can provide 4.8-kbps voice communications between portable terminals and a hub station via a Ka-band geosynchronous satellite has been investigated. Tradeoffs are examined so that the combined system of hub and gateway earth stations, the satellite, and the personal terminals can provide a competitive service in terms of cost, availability, and quality. A baseline system is described using a spacecraft with approximately 140 spot beams that cover CONUS with 5-watt power amplifiers in each beam. Satellite access in both the forward and return directions uses frequency division multiple access/code division multiple access with a chip rate of 2.5 Mchip/sec.
Author

A92-29848*# National Aeronautics and Space Administration. Lewis Research Center, Cleveland, OH.

FLEXIBLE HIGH SPEED CODEC (FHSC)

G. P. SEGALLIS and J. V. WERNLUND (Harris Corp., Melbourne,

FL) IN: AIAA International Communication Satellite Systems Conference and Exhibit, 14th, Washington, DC, Mar. 22-26, 1992, Technical Papers. Pt. 2 1992 6 p refs
(Contract NAS3-25087)
(AIAA PAPER 92-1919) Copyright

This paper describes the on going NASA/Harris FHSC CODEC program. The program objectives are to design and build an encoder decoder that allows operation in either burst or continuous modes at data rates of up to 300 megabits per second. The decoder handles both hard and soft decision decoding and can switch between modes on a burst by burst basis. Bandspeaking is low since the code rate is greater than or equal to 7/8. The encoder and a hard decision decoder fit on a single application specific integrated circuit (ASIC) chip. A soft decision applique is implemented using 300 K ECL logic which can be easily translated to an ECL gate array.
Author

A92-29861*# National Aeronautics and Space Administration. Lewis Research Center, Cleveland, OH.

FREQUENCY ALLOCATIONS FOR A NEW SATELLITE SERVICE - DIGITAL AUDIO BROADCASTING

EDWARD E. REINHART IN: AIAA International Communication Satellite Systems Conference and Exhibit, 14th, Washington, DC, Mar. 22-26, 1992, Technical Papers. Pt. 2 1992 10 p
(AIAA PAPER 92-1957) Copyright

The allocation in the range 500-3000 MHz for digital audio broadcasting (DAB) is described in terms of key issues such as the transmission-system architectures. Attention is given to the optimal amount of spectrum for allocation and the technological considerations relevant to downlink bands for satellite and terrestrial transmissions. Proposals for DAB allocations are compared, and reference is made to factors impinging on the provision of ground/satellite feeder links. The allocation proposals describe the implementation of 50-60-MHz bandwidths for broadcasting in the ranges near 800 MHz, below 1525 MHz, near 2350 MHz, and near 2600 MHz. Three specific proposals are examined in terms of characteristics such as service areas, coverage/beam, channels/satellite beam, and FCC license status. Several existing problems are identified including existing services crowded with systems, the need for new bands in the 1000-3000-MHz range, and variations in the nature and intensity of implementations of existing allocations that vary from country to country.
C.C.S.

A92-29883*# National Aeronautics and Space Administration. Lewis Research Center, Cleveland, OH.

ACHIEVING SPECTRUM CONSERVATION FOR THE MINIMUM SPAN AND MINIMUM-ORDER FREQUENCY ASSIGNMENT PROBLEMS

ANN O. HEYWARD (NASA, Lewis Research Center, Cleveland, OH) IN: AIAA International Communication Satellite Systems Conference and Exhibit, 14th, Washington, DC, Mar. 22-26, 1992, Technical Papers. Pt. 2 1992 26 p refs
(AIAA PAPER 92-1960) Copyright

Effective and efficient solution of frequency assignment problems assumes increasing importance as the radiofrequency spectrum experiences ever-increasing utilization by diverse communications services, requiring that the most efficient use of this resource be achieved. The research presented explores a general approach to the frequency assignment problem, in which such problems are categorized by the appropriate spectrum-conserving objective function, and are each treated as an N-job, M-machine scheduling problem appropriate for the objective. Results obtained and presented illustrate that such an approach presents an effective means of achieving spectrum-conserving frequency assignments for communications systems in a variety of environments.
Author

A92-29884*# National Aeronautics and Space Administration. Lewis Research Center, Cleveland, OH.

ACTS SYSTEM CAPABILITY AND PERFORMANCE

DAVID L. WRIGHT and JOSEPH R. BALOMBIN (NASA, Lewis Research Center, Cleveland, OH) IN: AIAA International Communication Satellite Systems Conference and Exhibit, 14th,

Washington, DC, Mar. 22-26, 1992, Technical Papers. Pt. 2
1992 11 p
(AIAA PAPER 92-1961) Copyright

The potential and actual performance of NASA's ACTS Flight and Ground Hardware are reviewed for the final assembly/integrate/test phase. ACTS communications capability is assessed for the two operational modes which include the baseband-processor and switched-repeater communications modes. Key technologies are evaluated with measured performance data relating to the Ka-band equipment at 30 and 20 GHz, the hopping-antenna spot beams, and the satellite on-board processing. Ground stations under development for ACTS operations capability and support are also described including the ACTS Mobile Terminal and the NASA Ground Station. Two link budgets are given to demonstrate the expected performance of the ACTS processor mode and the ACTS microwave switch matrix. The baseband processor and the multibeam antenna are shown to function adequately with good characteristics for typical traffic patterns and accuracies. C.C.S.

A92-29887*# National Aeronautics and Space Administration.
Lewis Research Center, Cleveland, OH.

OPERATIONAL USES OF ACTS TECHNOLOGY

RICHARD T. GEDNEY, DAVID L. WRIGHT, JOSEPH L. BALOMBIN, PHILIP Y. SOHN (NASA, Lewis Research Center, Cleveland, OH), WILLIAM F. CASHMAN, ALAN L. STERN (General Electric Co., Astro-Space Div., Princeton, NJ), LEN GOLDING, and LARRY PALMER (Hughes Network Systems, Germantown, MD) IN: AIAA International Communication Satellite Systems Conference and Exhibit, 14th, Washington, DC, Mar. 22-26, 1992, Technical Papers. Pt. 2 1992 10 p refs
(AIAA PAPER 92-1964) Copyright

The NASA Advanced Communications Technology Satellite (ACTS) provides the technologies for very high gain hopping spot beam antennas, on-board baseband routing and processing, and wideband (1 GHz) Ka-band transponders. A number of studies have recently been completed using the experience gained in developing the actual ACTS system hardware to quantify how well the ACTS technology can be used in future operational systems. This paper provides a summary of these study results including the spacecraft (S/C) weight per unit circuit for providing services by ACTS technologies as compared to present-day satellites. The uses of the ACTS technology discussed are for providing T1 VSAT mesh networks, aeronautical mobile communications, supervisory control and data acquisition (SCADA) services, and high data rate networks for supercomputer and other applications. Author

A92-29892*# National Aeronautics and Space Administration.
Lewis Research Center, Cleveland, OH.

FAULT TOLERANCE IN ONBOARD PROCESSORS - PROTECTING EFFICIENT FDM DEMULTIPLEXERS

ROBERT REDINBO (California, University, Davis) IN: AIAA International Communication Satellite Systems Conference and Exhibit, 14th, Washington, DC, Mar. 22-26, 1992, Technical Papers. Pt. 2 1992 11 p refs
(Contract NAG3-1166; NSF MIP-90-02664)
(AIAA PAPER 92-1969) Copyright

The application of convolutional codes to protect demultiplexer filter banks is demonstrated analytically for efficient implementations. An overview is given of the parameters for the efficient implementations of filter banks, and real convolutional codes are discussed in terms of DSP operations. Methods for composite filtering and parity generation are outlined, and attention is given to the protection of polyphase filter demultiplexing systems. Real convolutional codes can be applied to protect demultiplexer filter banks by employing two forms of low-rate parity calculation to each filter bank. The parity values are computed either by the output with an FIR parity filter or in parallel with the normal processing by a composite filter. Hardware similarities between the filter bank and the main demultiplexer bank permit efficient redeployment of the processing resources to the main processing function in any configuration. C.C.S.

A92-29895*# National Aeronautics and Space Administration.
Lewis Research Center, Cleveland, OH.

A MULTI-CHANNEL DEMULTIPLEXER/DEMODULATOR ARCHITECTURE, SIMULATION AND IMPLEMENTATION

P. CANGIANE, H. A. COURTOIS, D. D. LEE, M. A. SHERRY, and M. E. SPENCER (TRW Electronic Systems Group, Redondo Beach, CA) IN: AIAA International Communication Satellite Systems Conference and Exhibit, 14th, Washington, DC, Mar. 22-26, 1992, Technical Papers. Pt. 2 1992 11 p refs
(Contract NAS3-25866)
(AIAA PAPER 92-1972) Copyright

The development of multichannel demultiplexer/demodulator is described in which the aim is to optimize bandwidth and hardware efficiency. Attention is given to the simulation and performance analysis of the proposed architectures for the demultiplexer and the demodulator. The project is presently in the test phase, and it is suggested that the present results demonstrate the feasibility and efficiency of incorporating on-board processing in commercial communications satellites. C.C.S.

A92-29902*# National Aeronautics and Space Administration.
Lewis Research Center, Cleveland, OH.

TECHNOLOGY REQUIREMENTS FOR MESH VSAT APPLICATIONS

R. K. KWAN, K. M. PRICE (Space Systems/Loral, Palo Alto, CA), T. INUKAI, and F. FARDIS (COMSAT Laboratories, Clarksburg, MD) IN: AIAA International Communication Satellite Systems Conference and Exhibit, 14th, Washington, DC, Mar. 22-26, 1992, Technical Papers. Pt. 3 1992 11 p
(Contract NAS3-25092)
(AIAA PAPER 92-1982) Copyright

This paper first examines the trends and the roles of VSAT services in the year 2010 time frame based on an overall network and service model for that period. An estimate of the VSAT traffic is then made and the service and general network requirements are identified. In order to accommodate these traffic needs, four satellite VSAT architectures based on the use of fixed or scanning multibeam antennas in conjunction with IF switching or onboard regeneration and baseband processing are suggested. The performance of each of these architectures is assessed and the key enabling technologies are identified. Author

A92-29923*# National Aeronautics and Space Administration.
Lewis Research Center, Cleveland, OH.

PREDICTIVE ONBOARD FLOW CONTROL IN PACKET SWITCHING SATELLITES

E. A. BOBINSKY (NASA, Lewis Research Center, Cleveland, OH) IN: AIAA International Communication Satellite Systems Conference and Exhibit, 14th, Washington, DC, Mar. 22-26, 1992, Technical Papers. Pt. 3 1992 8 p refs
(AIAA PAPER 92-2004) Copyright

We outline two alternate approaches to predicting the onset of congestion in a packet switching satellite, and argue that predictive, rather than reactive, flow control is necessary for the efficient operation of such a system. The first method discussed is based on standard, statistical techniques which are used to periodically calculate a probability of near-term congestion based on arrival rate statistics. If this probability exceeds a present threshold, the satellite would transmit a rate-reduction signal to all active ground stations. The second method discussed would utilize a neural network to periodically predict the occurrence of buffer overflow based on input data which would include, in addition to arrival rates, the distributions of packet lengths, source addresses, and destination addresses. Author

A92-29936*# National Aeronautics and Space Administration.
Lewis Research Center, Cleveland, OH.

INTERFERENCE SUSCEPTIBILITY MEASUREMENTS FOR AN MSK SATELLITE COMMUNICATION LINK

ROBERT J. KERCZEWSKI and GENE FUJIKAWA (NASA, Lewis Research Center, Cleveland, OH) IN: AIAA International Communication Satellite Systems Conference and Exhibit, 14th,

Washington, DC, Mar. 22-26, 1992, Technical Papers. Pt. 3
1992 9 p refs

(AIAA PAPER 92-2018) Copyright

The results are presented of measurements of the degradation of an MSK satellite link due to modulated and CW (unmodulated) interference. These measurements were made using a hardware based satellite communication link simulator at NASA-Lewis. The results indicate the amount of bit error rate degradation caused by CW interference as a function of frequency and power level, and the degradation caused by adjacent channel and cochannel modulated interference as a function of interference power level. Results were obtained for both the uplink case (including satellite nonlinearity) and the downlink case (linear channel). Author

A92-29951# National Aeronautics and Space Administration, Washington, DC.

ADVANCED COMMUNICATIONS TECHNOLOGY SATELLITE (ACTS) EXPERIMENTS PROGRAM - A MARKET-DRIVEN APPROACH TO GOVERNMENT/INDUSTRY COOPERATION

DEAN A. OLMSTEAD (NASA, Office of Commercial Programs, Washington, DC), RONALD J. SCHERTLER (NASA, Lewis Research Center, Cleveland, OH), and LAURA A. RANDALL (Public Service Satellite Consortium, Washington, DC) IN: AIAA International Communication Satellite Systems Conference and Exhibit, 14th, Washington, DC, Mar. 22-26, 1992, Technical Papers. Pt. 3 1992 8 p refs

(AIAA PAPER 92-2036) Copyright

The Advanced Communications Technology Satellite (ACTS), now under development and scheduled for launch in early 1993, is the current focus of NASA's commercial communications satellite program. The full power of the key technologies on ACTS can only be realized if industry assumes an active role in the conduct of experiments and demonstrations. This paper discusses the current market-driven rationale behind the ACTS Experiments Program activities aimed at getting industry involved - a rationale that addresses industry concerns and responds to industry inputs. Author

A92-29952*# National Aeronautics and Space Administration, Lewis Research Center, Cleveland, OH.

ACTS T1-VSAT - THE INTELLIGENT EARTH STATION

JOHN R. MANNING, JEFFREY D. SPIGLER (Sverdrup Technology, Inc., Brook Park, OH), and PETER A. LOWRY (NASA, Lewis Research Center, Cleveland, OH) IN: AIAA International Communication Satellite Systems Conference and Exhibit, 14th, Washington, DC, Mar. 22-26, 1992, Technical Papers. Pt. 3 1992 8 p

(AIAA PAPER 92-2037) Copyright

The functional design of the software for NASA's Advanced Communication Technology Satellite (ACTS) T1-VSAT (Very Small Aperture Terminal) is described. The design provides a flexible interface to allow customized control of a satellite network and to provide external processes with access to network capabilities without requiring modification to the network hardware or software. Some of the envisioned features are: automatic number location; dynamic reconfiguration of the number plan tables; security features of call priority, call preemption, and remote verification; automatic reconfiguration of least cost routing tables; circuit availability verification prior to call setup; audio and video conferencing; on demand broadband dial-up service; on demand dial-up broadband broadcast service; and ISDN. A brief review is also given of the ACTS satellite and network, the network management, and the ACTS T1-VSAT earth station. C.D.

A92-29953*# National Aeronautics and Space Administration, Lewis Research Center, Cleveland, OH.

NETWORK ARCHITECTURES AND PROTOCOLS FOR THE INTEGRATION OF ACTS AND ISDN

D. M. CHITRE (COMSAT Laboratories, Clarksburg, MD) and P. A. LOWRY (NASA, Lewis Research Center, Cleveland, OH) IN: AIAA International Communication Satellite Systems Conference and Exhibit, 14th, Washington, DC, Mar. 22-26, 1992, Technical

Papers. Pt. 3 1992 11 p

(AIAA PAPER 92-2039) Copyright

A close integration of satellite networks and the integrated services digital network (ISDN) is essential for satellite networks to carry ISDN traffic effectively. This also shows how a given (pre-ISDN) satellite network architecture can be enhanced to handle ISDN signaling and provide ISDN services. It also describes the functional architecture and high-level protocols that could be implemented in the NASA Advanced Communications Technology Satellite (ACTS) low burst rate communications system to provide ISDN services. Author

A92-29966*# National Aeronautics and Space Administration, Lewis Research Center, Cleveland, OH.

TECHNICAL AND ECONOMIC FEASIBILITY OF INTEGRATED VIDEO SERVICE BY SATELLITE

K. M. PRICE, R. K. KWAN (Space Systems/Loral, Palo Alto, CA), L. W. WHITE, R. K. GARLOW, and T. R. HENDERSON (COMSAT Laboratories, Clarksburg, MD) IN: AIAA International Communication Satellite Systems Conference and Exhibit, 14th, Washington, DC, Mar. 22-26, 1992, Technical Papers. Pt. 3 1992 8 p refs

(Contract NAS3-25092)

(AIAA PAPER 92-2054) Copyright

A feasibility study is presented of utilizing modern satellite technology, or more advanced technology, to create a cost-effective, user-friendly, integrated video service, which can provide videophone, video conference, or other equivalent wideband service on demand. A system is described that permits a user to select a desired audience and establish the required links similar to arranging a teleconference by phone. Attention is given to video standards, video traffic scenarios, satellite system architecture, and user costs. R.E.P.

A92-31711*# National Aeronautics and Space Administration, Lewis Research Center, Cleveland, OH.

DYNAMIC RAIN FADE COMPENSATION TECHNIQUES FOR THE ADVANCED COMMUNICATIONS TECHNOLOGY SATELLITE

ROBERT M. MANNING (NASA, Lewis Research Center, Cleveland, OH) AIAA, International Communication Satellite Systems Conference and Exhibit, 14th, Washington, DC, Mar. 22-26, 1992. 12 p. Mar. 1992 12 p refs

(AIAA PAPER 92-2038) Copyright

The dynamic and composite nature of propagation impairments that are incurred on earth-space communications links at frequencies in and above the 30/20 GHz Ka band necessitate the use of dynamic statistical identification and prediction processing of the fading signal in order to optimally estimate and predict the levels of each of the deleterious attenuation components. Such requirements are being met in NASA's Advanced Communications Technology Satellite (ACTS) project by the implementation of optimal processing schemes derived through the use of the ACTS Rain Attenuation Prediction Model and nonlinear Markov filtering theory. The ACTS Rain Attenuation Prediction Model discerns climatological variations on the order of 0.5 deg in latitude and longitude in the continental U.S. The time-dependent portion of the model gives precise availability predictions for the 'spot beam' links of ACTS. However, the structure of the dynamic portion of the model, which yields performance parameters such as fade duration probabilities, is isomorphic to the state-variable approach of stochastic control theory and is amenable to the design of such statistical fade processing schemes which can be made specific to the particular climatological location at which they are employed. Author

A92-31780* National Aeronautics and Space Administration, Lewis Research Center, Cleveland, OH.

A PERSONAL COMMUNICATIONS NETWORK USING A KA-BAND SATELLITE

LARRY C. PALMER, ENRIQUE LABORDE (Hughes Network Systems, Inc., Germantown, MD), ALAN STERN (GE Astro Space, Princeton, NJ), and PHILIP Y. SOHN (NASA, Lewis Research

Center, Cleveland, OH) IEEE Journal on Selected Areas in Communications (ISSN 0733-8716), vol. 10, Feb. 1992, p. 401-417. Research supported by Analex Corp. Feb. 1992 17 p refs Copyright

The feasibility of a personal communications network using portable terminals that can provide 4.8-kb/s voice communications to a hub station via a Ka-band geosynchronous satellite has been investigated. Tradeoffs are examined so that the combined system of hub and gateway earth stations, the satellite, and the personal terminals can provide a competitive service in terms of cost, availability, and quality. A baseline system that uses a spacecraft with approximately 140 spot beams to cover the contiguous US (CONUS) and 5-W power amplifiers in each beam is described. Satellite access in both the forward and return directions uses frequency-division multiple-access/code-division multiple-access (FDMA/CDMA) with a chip rate of 2.5 Mchip/s. I.E.

A92-37067* National Aeronautics and Space Administration. Lewis Research Center, Cleveland, OH.

PERFORMANCE OF A K-BAND SUPERCONDUCTING ANNULAR RING ANTENNA

M. A. RICHARD (Case Western Reserve University, Cleveland, OH), K. B. BHASIN, R. Q. LEE (NASA, Lewis Research Center, Cleveland, OH), and P. C. CLASPY (Case Western Reserve University, Cleveland, OH) Microwave and Optical Technology Letters (ISSN 0895-2477), vol. 5, no. 6, June 1992, p. 257-259. Jun. 1992 3 p refs

Copyright

Superconducting annular ring antennas operating in the TM₁₂ mode at 21 GHz are designed and fabricated on a lanthanum aluminate substrate using a YBCO high-temperature superconducting thin film. The efficiencies and far-field antenna patterns are measured and compared with an identical antenna patterned with silver. The resonant frequencies and experimental far-field patterns agree well with published models, and efficiency measurements show a maximum improvement of 6 percent at 20 K in the efficiency of the HTS antenna when compared to the silver ring at the same temperature. Author

A92-37222* National Aeronautics and Space Administration. Lewis Research Center, Cleveland, OH.

COPLANAR WAVEGUIDE APERTURE-COUPLED MICROSTRIP PATCH ANTENNA

RICHARD Q. LEE and RAINEE N. SIMONS (NASA, Lewis Research Center, Cleveland, OH) IEEE Microwave and Guided Wave Letters (ISSN 1051-8207), vol. 2, no. 4, April 1992, p. 138, 139. Apr. 1992 2 p refs

Copyright

The performance characteristics of a coplanar waveguide (CPW) aperture-coupled microstrip patch antenna was investigated experimentally. A grounded CPW with a series gap in the center strip conductor was used to couple microwave power to the antenna through an aperture in the common ground plane. Results indicate good coupling efficiency and confirms the feasibility of this feeding technique. Author

A92-37224* National Aeronautics and Space Administration. Lewis Research Center, Cleveland, OH.

PERFORMANCE OF A FOUR-ELEMENT KA-BAND HIGH-TEMPERATURE SUPERCONDUCTING MICROSTRIP ANTENNA

M. A. RICHARD (Case Western Reserve University, Cleveland, OH), K. B. BHASIN (NASA, Lewis Research Center, Cleveland, OH), C. GILBERT, S. METZLER, G. KOEPEF (Ball Aerospace Systems Group, Broomfield, CO), and P. C. CLASPY (Case Western Reserve University, Cleveland, OH) IEEE Microwave and Guided Wave Letters (ISSN 1051-8207), vol. 2, no. 4, April 1992, p. 143-145. Apr. 1992 3 p refs

Copyright

Superconducting four-element microstrip array antennas operating at 30 GHz have been designed and fabricated on a lanthanum aluminate (LaAlO₃) substrates. The experimental performance of these thin film Y-Ba-Cu-O superconducting

antennas is compared with that of identical antenna patterned with evaporated gold. Efficiency measurements of these antennas show an improvement of 2 dB at 70 K and as much as 3.5 dB at 40 K in the superconducting antenna over the gold antenna. Author

A92-44233* National Aeronautics and Space Administration. Lewis Research Center, Cleveland, OH.

ROTATIVE QUADRATURE PHASE-SHIFT KEYING

J. LIU, J. KIM, S. C. KWATRA (Toledo, University, OH), and G. H. STEVENS (NASA, Lewis Research Center, Cleveland, OH) Electronics Letters (ISSN 0013-5194), vol. 28, no. 12, June 4, 1992, p. 1095-1097. 4 Jun. 1992 3 p (Contract NAG3-157)

Copyright

A rotative quadrature phase-shift keying (RQPSK) modulation scheme is proposed. By rotating the QPSK signal constellation by $\pi/2$, either clockwise or anticlockwise, during a symbol duration, the conventional QPSK scheme can be modified to transmit 3 bits per symbol to achieve both power and bandwidth efficiency. Author

A92-46046* National Aeronautics and Space Administration. Lewis Research Center, Cleveland, OH.

THE ACTS MULTIBEAM ANTENNA

FRANK A. REGIER (NASA, Lewis Research Center, Cleveland, OH) IEEE Transactions on Microwave Theory and Techniques (ISSN 0018-9480), vol. 40, no. 6, June 1992, p. 1159-1164. Jun. 1992 6 p refs

Copyright

The Advanced Communications Technology Satellite (ACTS) to be launched in 1993 is briefly introduced. Its multibeam antenna, consisting of electrically similar 30 GHz receive and 20 GHz transmit offset Cassegrain systems, both utilizing orthogonal polarizations, is described. Dual polarization is achieved by using one feed assembly for each polarization in conjunction with nested front and back subreflectors, the gridded front subreflector acting as a window for one polarization and a reflector for the other. The antennas produce spot beams with approximately 0.3 degree beamwidth and gains of approximately 50 dbi. High surface accuracy and high edge taper produce low sidelobe levels and high cross-polarization isolation. A brief description is given of several Ka-band components fabricated for ACTS. These include multiflare antenna feedhorns, beam-forming networks utilizing latching ferrite waveguide switches, a 30 GHz HEMT low-noise amplifier and a 20 GHz TWT power amplifier. S.A.V.

A92-48224* National Aeronautics and Space Administration. Lewis Research Center, Cleveland, OH.

DATA DISTRIBUTION SATELLITE

GRADY H. STEVENS (NASA, Lewis Research Center, Cleveland, OH) International Space Year Conference on Information Systems, Pasadena, CA, Feb. 10-13, 1992, Paper. 15 p. Feb. 1992 15 p refs

The Data Distribution Satellite (DDS) is described in terms of its role in providing space-data and communication services for the National Research and Education Network. The DDS is envisioned as a processing link in the microwave network that would connect academic, industrial, and government institutions to a high-data-rate service of space data. The general need for science communications is assessed, and it is shown that the data potential exceeds the available spectrum. The DDS could act as a bridge between terrestrial facilities the space network, and other space platforms to provide efficient access to space science data. Government demand for this type of data is high suggesting that the DDS could make use of hopping beams to provide more data at reduced costs. C.C.S.

A92-51092* National Aeronautics and Space Administration. Lewis Research Center, Cleveland, OH.

ELECTROMAGNETIC SCATTERING FROM AN INHOMOGENEOUS OBJECT BY RAY TRACING

HYEONGDONG KIM and HAO LING (Texas, University, Austin)

IEEE Transactions on Antennas and Propagation (ISSN 0018-926X), vol. 40, no. 5, May 1992, p. 517-525. May 1992
9 p refs
(Contract NSF ECS-86-57524; NCCC-127)
Copyright

A 'shooting and bouncing ray' (SBR) formulation is presented for treating the electromagnetic scattering from electrically large, inhomogeneous objects. A dense grid of rays representing the incident plane wave is shot toward the inhomogeneous object. At the scatterer boundary, reflected rays and refracted rays are generated due to discontinuity of the medium parameters. The trajectory, amplitude, phase and polarization of the rays inside the inhomogeneous object are traced based on geometrical optics. Whenever the rays cross the scatterer surface, additional reflected/refracted rays are generated and are tracked. This process is repeated until the intensities of the refracted/reflected rays become negligible. The contributions of the exiting rays to the total scattered field are calculated by using the equivalence principle in conjunction with a ray-tube integration scheme. The ray formulation is applied to calculate the backscattering from cylinders and spheres and good agreement with the exact series solutions is observed in the high frequency range. In addition, the backscattering mechanisms in penetrable objects are interpreted in terms of simple ray pictures. Author

A92-54763* National Aeronautics and Space Administration, Lewis Research Center, Cleveland, OH.

COMPARATIVE STUDY ON THE PERFORMANCE OF POWER AND BANDWIDTH EFFICIENT MODULATIONS IN LMSS UNDER FADING AND INTERFERENCE

JIAN LIU, JUNGHWAN KIM, S. C. KWATRA (Toledo, University, OH), and GRADY H. STEVENS (NASA, Lewis Research Center, Cleveland, OH) IN: MILCOM '91 - IEEE Military Communications Conference, McLean, VA, Nov. 4-7, 1991, Conference Record. Vol. 1 1991 5 p refs
(Contract NAG3-157)
Copyright

Aspects of error performance of various power and bandwidth efficient modulations for the land mobile satellite systems (LMSS) were investigated under multipath fading and interferences by using Monte-Carlo simulation. A differential detection for 16QAM (quadrature amplitude modulation) was proposed to cope with Ricean fading and Doppler shift. Computer simulation results show that the performance of 16QAM with differential detection is as good as that of 16PSK with coherent detection and 3 dB better than that of 16PSK with differential detection, although it degrades by about 4.5 dB as compared to 16QAM with coherent detection under an additive white Gaussian noise (AWGN) channel. For the nonlinear channels, 16QAM with modified signal constellations is introduced and analyzed. The simulation results show that the modified 16QAM exhibits a gain of 2.5 dB over 16PSK under traveling-wave tube nonlinearity, and about 4 dB gain over 16PSK at the bit error rate of 10×10^{-5} under AWGN. Computer simulation results for modified 16 QAM under cochannel interference and adjacent-channel interference are also presented. I.E.

A92-55792* National Aeronautics and Space Administration, Lewis Research Center, Cleveland, OH.

SATCOM SYSTEMS AND TECHNOLOGIES INTO THE 21ST CENTURY

ROBERT K. KWAN (Space Systems/Loral, Palo Alto, CA) and GRADY STEVENS (NASA, Lewis Research Center, Cleveland, OH) IAF, International Astronautical Congress, 43rd, Washington, Aug. 28-Sept. 5, 1992. 7 p. Aug. 1992 7 p refs
(IAF PAPER 92-0412) Copyright

The role of communications satellites in the domestic U.S. telecommunications market for the next 25 years is examined, the focus being on the new satellite communications systems concepts and their enabling technologies. A simple procedure for the identification of critical satellite technologies in the years 2000-2015 is described. Study results indicate that by the year 2015, satellites will find commercial applications in the distribution

of space-gathered data, supercomputer network, scientific visualization to remote areas, mobile services, VSAT, broadband ISDN, and data services. L.M.

N92-10128* National Aeronautics and Space Administration, Lewis Research Center, Cleveland, OH.

REAL-TIME DATA COMPRESSION OF BROADCAST VIDEO SIGNALS Patent

MARY JO W. SHALKAUSER, inventor (to NASA), WAYNE A. WHYTE, JR., inventor (to NASA), and SCOTT P. BARNES, inventor (to NASA) 15 Oct. 1991 30 p Filed 9 Nov. 1990 Supersedes N91-15469 (29 - 7, p 996) Continuation-in-part of US-Patent-Appl-SN-540976, filed 20 Jun. 1990
(NASA-CASE-LEW-14945-2; US-PATENT-5,057,917; US-PATENT-APPL-SN-611214; US-PATENT-APPL-SN-540976; US-PATENT-CLASS-358-135; US-PATENT-CLASS-358-133; INT-PATENT-CLASS-H04N-7/13) Avail: US Patent and Trademark Office

A non-adaptive predictor, a nonuniform quantizer, and a multi-level Huffman coder are incorporated into a differential pulse code modulation system for coding and decoding broadcast video signals in real time.

Official Gazette of the U.S. Patent and Trademark Office

N92-12151*# National Aeronautics and Space Administration, Lewis Research Center, Cleveland, OH.

EVALUATION OF COMPONENTS, SUBSYSTEMS, AND NETWORKS FOR HIGH RATE, HIGH FREQUENCY SPACE COMMUNICATIONS

ROBERT J. KERCZEWSKI, WILLIAM D. IVANCIC, and JOHN E. ZUZEK 1991 13 p Presented at the Conference on Advanced Space Exploration Initiative Technologies, Cleveland, OH, 4-6 Sep. 1991; cosponsored by AIAA, NASA, and OAI Previously announced in IAA as A91-52343
(Contract RTOP 316-30-19)
(NASA-TM-105274; E-6597; NAS 1.15:105274; AIAA PAPER 91-3423) Avail: CASI HC A03/MF A01

The development of new space communications technologies by NASA has included both commercial applications and space science requirements. NASA's Systems Integration, Test and Evaluation (SITE) Space Communication System Simulator is a hardware based laboratory simulator for evaluating space communications technologies at the component, subsystem, system, and network level, geared toward high frequency, high data rate systems. The SITE facility is well-suited for evaluation of the new technologies required for the Space Exploration Initiative (SEI) and advanced commercial systems. Described here are the technology developments and evaluation requirements for current and planned commercial and space science programs. Also examined are the capabilities of SITE, the past, present and planned future configurations of the SITE facility, and applications of SITE to evaluation of SEI technology. Author

N92-14202*# National Aeronautics and Space Administration, Lewis Research Center, Cleveland, OH.

SPACE COMMUNICATIONS TECHNOLOGY CONFERENCE: ONBOARD PROCESSING AND SWITCHING

Washington Nov. 1991 288 p Conference held in Cleveland, OH, 12-14 Nov. 1991
(Contract RTOP 650-60-21)
(NASA-CP-3132; E-6548; NAS 1.55:3132) Avail: CASI HC A13/MF A03

Papers and presentations from the conference are presented. The topics covered include the following: satellite network architecture, network control and protocols, fault tolerance and autonomy, multichannel demultiplexing and demodulation, information switching and routing, modulation and coding, and planned satellite communications systems.

N92-14204*# National Aeronautics and Space Administration. Lewis Research Center, Cleveland, OH.

DESTINATION DIRECTED PACKET SWITCH ARCHITECTURE FOR A 30/20 GHZ FDMA/TDM GEOSTATIONARY COMMUNICATION SATELLITE NETWORK

WILLIAM D. IVANCIC and MARY JO SHALKHAUSER *In its Space Communications Technology Conference: Onboard Processing and Switching p 9-24 Nov. 1991*
 Avail: CASI HC A03/MF A03

Emphasis is on a destination directed packet switching architecture for a 30/20 GHz frequency division multiplex access/time division multiplex (FDMA/TDM) geostationary satellite communication network. Critical subsystems and problem areas are identified and addressed. Efforts have concentrated heavily on the space segment; however, the ground segment was considered concurrently to ensure cost efficiency and realistic operational constraints. Author

N92-14212*# National Aeronautics and Space Administration. Lewis Research Center, Cleveland, OH.

AN OVERVIEW OF SPACE COMMUNICATION ARTIFICIAL INTELLIGENCE FOR LINK EVALUATION TERMINAL (SCAILET) PROJECT

ANOOSH K. SHAHIDI (Sverdrup Technology, Inc., Brook Park, OH.), RICHARD F. SCHLEGELMILCH (Akron Univ., OH.), EDWARD J. PETRIK, and JERRY L. WALTERS *In its Space Communications Technology Conference: Onboard Processing and Switching p 83-86 Nov. 1991*
 Avail: CASI HC A01/MF A03

A software application to assist end-users of the link evaluation terminal (LET) for satellite communications is being developed. This software application incorporates artificial intelligence (AI) techniques and will be deployed as an interface to LET. The high burst rate (HBR) LET provides 30 GHz transmitting/20 GHz receiving (220/110 Mbps) capability for wideband communications technology experiments with the Advanced Communications Technology Satellite (ACTS). The HBR LET can monitor and evaluate the integrity of the HBR communications uplink and downlink to the ACTS satellite. The uplink HBR transmission is performed by bursting the bit-pattern as a modulated signal to the satellite. The HBR LET can determine the bit error rate (BER) under various atmospheric conditions by comparing the transmitted bit pattern with the received bit pattern. An algorithm for power augmentation will be applied to enhance the system's BER performance at reduced signal strength caused by adverse conditions. Author

N92-14215*# National Aeronautics and Space Administration. Lewis Research Center, Cleveland, OH.

GTEX: AN EXPERT SYSTEM FOR DIAGNOSING FAULTS IN SATELLITE GROUND STATIONS

RICHARD F. SCHLEGELMILCH (Akron Univ., OH.), JOHN DURKIN (Akron Univ., OH.), and EDWARD J. PETRIK *In its Space Communications Technology Conference: Onboard Processing and Switching p 103-112 Nov. 1991*
 Avail: CASI HC A02/MF A03

A proof of concept expert system called Ground Terminal Expert (GTEX) was developed at The University of Akron in collaboration with NASA Lewis Research Center. The objective of GTEX is to aid in diagnosing data faults occurring with a digital ground terminal. This strategy can also be applied to the Very Small Aperture Terminal (VSAT) technology. An expert system which detects and diagnoses faults would enhance the performance of the VSAT by improving reliability and reducing maintenance time. GTEX is capable of detecting faults, isolating the cause and recommending appropriate actions. Isolation of faults is completed to board-level modules. A graphical user interface provides control and a medium where data can be requested and cryptic information logically displayed. Interaction with GTEX consists of user responses and input from data files. The use of data files provides a method of simulating dynamic interaction between the digital ground terminal and the expert system. GTEX as described is

capable of both improving reliability and reducing the time required for necessary maintenance. Author

N92-14218*# National Aeronautics and Space Administration. Lewis Research Center, Cleveland, OH.

FIDEX: AN EXPERT SYSTEM FOR SATELLITE DIAGNOSTICS

JOHN DURKIN (Akron Univ., OH.), DONALD TALLO (Akron Univ., OH.), and EDWARD J. PETRIK *In its Space Communications Technology Conference: Onboard Processing and Switching p 143-152 Nov. 1991*
 Avail: CASI HC A02/MF A03

A Fault Isolation and Diagnostic Expert system (FIDEX) was developed for communication satellite diagnostics. It was designed specifically for the 30/20 GHz satellite transponder. The expert system was designed with a generic structure and features that make it applicable to other types of space systems. FIDEX is a frame based system that enjoys many of the inherent frame base features, such as hierarchy that describes the transponder's components, with other hierarchies that provide structural and fault information about the transponder. This architecture provides a flexible diagnostic structure and enhances maintenance of the system. FIDEX also includes an inexact reasoning technique and a primitive learning ability. Inexact reasoning was an important feature for this system due to the sparse number of sensors available to provide information on the transponder's performance. FIDEX can determine the most likely faulted component under the constraint of limited information. FIDEX learns about the most likely faults in the transponder by keeping a record of past established faults. FIDEX also has the ability to detect anomalies in the sensors that provide information on the transponders performance. Author

N92-14228*# National Aeronautics and Space Administration. Lewis Research Center, Cleveland, OH.

ON-BOARD CONGESTION CONTROL FOR SATELLITE PACKET SWITCHING NETWORKS

PONG P. CHU (Cleveland State Univ., OH.) *In its Space Communications Technology Conference: Onboard Processing and Switching p 239-245 Nov. 1991*
 Avail: CASI HC A02/MF A03

It is desirable to incorporate packet switching capability on-board for future communication satellites. Because of the statistical nature of packet communication, incoming traffic fluctuates and may cause congestion. Thus, it is necessary to incorporate a congestion control mechanism as part of the on-board processing to smooth and regulate the bursty traffic. Although there are extensive studies on congestion control for both baseband and broadband terrestrial networks, these schemes are not feasible for space based switching networks because of the unique characteristics of satellite link. Here, we propose a new congestion control method for on-board satellite packet switching. This scheme takes into consideration the long propagation delay in satellite link and takes advantage of the the satellite's broadcasting capability. It divides the control between the ground terminals and satellite, but distributes the primary responsibility to ground terminals and only requires minimal hardware resource on-board satellite. Author

N92-14235*# National Aeronautics and Space Administration. Lewis Research Center, Cleveland, OH.

FLEXIBLE DIGITAL MODULATION AND CODING SYNTHESIS FOR SATELLITE COMMUNICATIONS

MARK VANDERAAR (Sverdrup Technology, Inc., Brook Park, OH.), JAMES BUDINGER (Ohio Univ., Athens.), CRAIG HOERIG, and JOHN TAGUE (Ohio Univ., Athens.) *In its Space Communications Technology Conference: Onboard Processing and Switching p 295-303 Nov. 1991*
 (Contract NAS3-25266; NAG3-1183)
 Avail: CASI HC A02/MF A03

An architecture and a hardware prototype of a flexible trellis modem/codec (FTMC) transmitter are presented. The theory of operation is built upon a pragmatic approach to trellis-coded modulation that emphasizes power and spectral efficiency. The system incorporates programmable modulation formats, variations

of trellis-coding, digital baseband pulse-shaping, and digital channel precompensation. The modulation formats examined include (uncoded and coded) binary phase shift keying (BPSK), quaternary phase shift keying (QPSK), octal phase shift keying (8PSK), 16-ary quadrature amplitude modulation (16-QAM), and quadrature phase shift keying (Q squared PSK) at programmable rates up to 20 megabits per second (Mbps). The FTMC is part of the developing test bed to quantify modulation and coding concepts. Author

N92-15306*# National Aeronautics and Space Administration. Lewis Research Center, Cleveland, OH.

INTERFERENCE SUSCEPTIBILITY MEASUREMENTS FOR AN MSK SATELLITE COMMUNICATION LINK

ROBERT J. KERCZEWSKI and GENE FUJIKAWA 1992 10 p Proposed for presentation at the 14th International Communications Satellite Systems Conference, Washington, DC, 22-26 Mar. 1992; sponsored by AIAA

(Contract RTOP 650-60-23)

(NASA-TM-105395; E-6786; NAS 1.15:105395; AIAA PAPER

92-2018) Avail: CASI HC A02/MF A01

The results are presented of measurements of the degradation of an MSK satellite link due to modulated and CW (unmodulated) interference. These measurements were made using a hardware based satellite communication link simulator at NASA-Lewis. The results indicate the amount of bit error rate degradation caused by CW interference as a function of frequency and power level, and the degradation caused by adjacent channel and cochannel modulated interference as a function of interference power level. Results were obtained for both the uplink case (including satellite nonlinearity) and the downlink case (linear channel). Author

N92-16191*# National Aeronautics and Space Administration. Lewis Research Center, Cleveland, OH.

ADVANCED COMMUNICATION TECHNOLOGY SATELLITE (ACTS) MULTIBEAM ANTENNA TECHNOLOGY VERIFICATION EXPERIMENTS

ROBERTO J. ACOSTA, JEFFREY M. LARKO, and ALAN R. LAGIN (Analex Corp., Brook Park, OH.) 1992 6 p Proposed for presentation at the 1992 AP-S International Symposium, Chicago, IL, 18-25 Jul. 1992; sponsored by IEEE

(Contract RTOP 679-40-00)

(NASA-TM-105421; E-6836; NAS 1.15:105421) Avail: CASI HC A02/MF A01

The Advanced Communication Technology Satellite (ACTS) is a key to reaching NASA's goal of developing high-risk, advanced communications technology using multiple frequency bands to support the nation's future communication needs. Using the multiple, dynamic hopping spot beams, and advanced on board switching and processing systems, ACTS will open a new era in communications satellite technology. One of the key technologies to be validated as part of the ACTS program is the multibeam antenna with rapidly reconfigurable hopping and fixed spot beam to serve users equipped with small-aperture terminals within the coverage areas. The proposed antenna technology experiments are designed to evaluate in-orbit ACTS multibeam antenna performance (radiation pattern, gain, cross pol levels, etc.). Author

N92-17047*# National Aeronautics and Space Administration. Lewis Research Center, Cleveland, OH.

ADVANCED COMMUNICATION TECHNOLOGY SATELLITE (ACTS) MULTIBEAM ANTENNA ANALYSIS AND EXPERIMENT

ROBERTO J. ACOSTA (Analex Corp., Brook Park, OH.), ALAN R. LAGIN (Analex Corp., Brook Park, OH.), JEFFREY M. LARKO, and ADABELLE NARVAEZ 1992 5 p Proposed for presentation at the 1992 AP-S International Symposium, Chicago, IL, 18-25 Jul. 1992; sponsored by IEEE

(Contract RTOP 679-40-00)

(NASA-TM-105420; E-6835; NAS 1.15:105420) Avail: CASI HC A01/MF A01

One of the most important aspects of a satellite communication system design is the accurate estimation of antenna performance

degradation. Pointing error, end coverage gain, peak gain degradation, etc. are the main concerns. The thermal or dynamic distortions of a reflector antenna structural system can affect the far-field antenna power distribution in a least four ways. (1) The antenna gain is reduced; (2) the main lobe of the antenna can be mispointed thus shifting the destination of the delivered power away from the desired locations; (3) the main lobe of the antenna pattern can be broadened, thus spreading the RF power over a larger area than desired; and (4) the antenna pattern sidelobes can increase, thus increasing the chances of interference among adjacent beams of multiple beam antenna system or with antenna beams of other satellites. The in-house developed NASA Lewis Research Center thermal/structural/RF analysis program was designed to accurately simulate the ACTS in-orbit thermal environment and predict the RF antenna performance. The program combines well established computer programs (TRASYS, SINDA and NASTAN) with a dual reflector-physical optics RF analysis program. The ACTS multibeam antenna configuration is analyzed and several thermal cases are presented and compared with measurements (pre-flight). Author

N92-17062*# National Aeronautics and Space Administration. Lewis Research Center, Cleveland, OH.

MULTIPLE-ACCESS PHASED ARRAY ANTENNA SIMULATOR FOR A DIGITAL BEAM FORMING SYSTEM INVESTIGATION

ROBERT J. KERCZEWSKI, JOHN YU, JOANNE C. WALTON, THOMAS D. PERL, MONTY ANDRO, and ROBERT E. ALEXOVICH (Analex Corp., Brook Park, OH.) 1992 8 p Proposed for presentation at the Ninth International Conference on Digital Satellite Communications, Copenhagen, Denmark, 18-22 May 1992; sponsored by Intelsat and Telecom

(Contract RTOP 650-60-23)

(NASA-TM-105422; E-6838; NAS 1.15:105422) Avail: CASI HC A02/MF A01

Future versions of data relay satellite systems are currently being planned by NASA. Being given consideration for implementation are on-board digital beamforming techniques which will allow multiple users to simultaneously access a single S-band phased array antenna system. To investigate the potential performance of such a system, a laboratory simulator has been developed at NASA's Lewis Research Center. This paper describes the system simulator, and in particular, the requirements, design, and performance of a key subsystem, the phased array antenna simulator, which provides realistic inputs to the digital processor including multiple signals, noise, and nonlinearities. Author

N92-18281*# National Aeronautics and Space Administration. Lewis Research Center, Cleveland, OH.

ANALYSIS OF A GENERALIZED DUAL REFLECTOR ANTENNA SYSTEM USING PHYSICAL OPTICS

ROBERTO J. ACOSTA and ALAN R. LAGIN Feb. 1992 47 p (Contract RTOP 679-40-00)

(NASA-TM-105425; E-6842; NAS 1.15:105425) Avail: CASI HC A03/MF A01

Reflector antennas are widely used in communication satellite systems because they provide high gain at low cost. Offset-fed single paraboloids and dual reflector offset Cassegrain and Gregorian antennas with multiple focal region feeds provide a simple, blockage-free means of forming multiple, shaped, and isolated beams with low sidelobes. Such antennas are applicable to communications satellite frequency reuse systems and earth stations requiring access to several satellites. While the single offset paraboloid has been the most extensively used configuration for the satellite multiple-beam antenna, the trend toward large apertures requiring minimum scanned beam degradation over the field of view 18 degrees for full earth coverage from geostationary orbit may lead to impractically long focal length and large feed arrays. Dual reflector antennas offer packaging advantages and more degrees of design freedom to improve beam scanning and cross-polarization properties. The Cassegrain and Gregorian antennas are the most commonly used dual reflector antennas. A computer program for calculating the secondary pattern and directivity of a generalized dual reflector antenna system was

developed and implemented at LeRC. The theoretical foundation for this program is based on the use of physical optics methodology for describing the induced currents on the sub-reflector and main reflector. The resulting induced currents on the main reflector are integrated to obtain the antenna far-zone electric fields. The computer program is verified with other physical optics programs and with measured antenna patterns. The comparison shows good agreement in far-field sidelobe reproduction and directivity.

Author

N92-18921*# National Aeronautics and Space Administration. Lewis Research Center, Cleveland, OH.

LEAST RELIABLE BITS CODING (LRBC) FOR HIGH DATA RATE SATELLITE COMMUNICATIONS

MARK VANDERAAR (Sverdrup Technology, Inc., Brook Park, OH.), PAUL WAGNER (Sverdrup Technology, Inc., Brook Park, OH.), and JAMES BUDINGER 1992 10 p Proposed for presentation at the 14th International Communications Satellite Systems Conference, Washington, DC, 22-26 Mar. 1992; sponsored by AIAA

(Contract NAS3-25266; RTOP 506-72-00)
(NASA-TM-105431; E-6848; NAS 1.15:105431) Avail: CASI HC A03/MF A01

An analysis and discussion of a bandwidth efficient multi-level/multi-stage block coded modulation technique called Least Reliable Bits Coding (LRBC) is presented. LRBC uses simple multi-level component codes that provide increased error protection on increasingly unreliable modulated bits in order to maintain an overall high code rate that increases spectral efficiency. Further, soft-decision multi-stage decoding is used to make decisions on unprotected bits through corrections made on more protected bits. Using analytical expressions and tight performance bounds it is shown that LRBC can achieve increased spectral efficiency and maintain equivalent or better power efficiency compared to that of Binary Phase Shift Keying (BPSK). Bit error rates (BER) vs. channel bit energy with Additive White Gaussian Noise (AWGN) are given for a set of LRB Reed-Solomon (RS) encoded 8PSK modulation formats with an ensemble rate of 8/9. All formats exhibit a spectral efficiency of $2.67 = (\log_2(8)) / (8/9)$ information bps/Hz. Bit by bit coded and uncoded error probabilities with soft-decision information are determined. These are traded with code rate to determine parameters that achieve good performance. The relative simplicity of Galois field algebra vs. the Viterbi algorithm and the availability of high speed commercial Very Large Scale Integration (VLSI) for block codes indicates that LRBC using block codes is a desirable method for high data rate implementations.

Author

N92-19379*# National Aeronautics and Space Administration. Lewis Research Center, Cleveland, OH.

PREDICTIVE ONBOARD FLOW CONTROL FOR PACKET SWITCHING SATELLITES

ERIC A. BOBINSKY Mar. 1992 10 p Proposed for presentation at the 14th International Communications Satellite Systems Conference, Washington, DC, 22 Mar. 1992; sponsored by AIAA (Contract RTOP 506-72-21)
(NASA-TM-105566; E-6890; NAS 1.15:105566) Avail: CASI HC A02/MF A01

We outline two alternate approaches to predicting the onset of congestion in a packet switching satellite, and argue that predictive, rather than reactive, flow control is necessary for the efficient operation of such a system. The first method discussed is based on standard, statistical techniques which are used to periodically calculate a probability of near-term congestion based on arrival rate statistics. If this probability exceeds a present threshold, the satellite would transmit a rate-reduction signal to all active ground stations. The second method discussed would utilize a neural network to periodically predict the occurrence of buffer overflow based on input data which would include, in addition to arrival rates, the distributions of packet lengths, source addresses, and destination addresses.

Author

N92-19700*# National Aeronautics and Space Administration. Lewis Research Center, Cleveland, OH.

REAL-TIME DEMONSTRATION HARDWARE FOR ENHANCED DPCM VIDEO COMPRESSION ALGORITHM

THOMAS P. BIZON, WAYNE A. WHYTE, JR., and VINCENT R. MARCOPOLI (Case Western Reserve Univ., Cleveland, OH.) 1992 17 p Proposed for presentation at the Data Compression Conference (DCC 1992), Snowbird, UT, 24-26 Mar. 1992; sponsored by IEEE

(Contract RTOP 144-10-10)
(NASA-TM-105616; E-6954; NAS 1.15:105616) Avail: CASI HC A03/MF A01

The lack of available wideband digital links as well as the complexity of implementation of bandwidth efficient digital video CODECs (encoder/decoder) has worked to keep the cost of digital television transmission too high to compete with analog methods. Terrestrial and satellite video service providers, however, are now recognizing the potential gains that digital video compression offers and are proposing to incorporate compression systems to increase the number of available program channels. NASA is similarly recognizing the benefits of and trend toward digital video compression techniques for transmission of high quality video from space and therefore, has developed a digital television bandwidth compression algorithm to process standard National Television Systems Committee (NTSC) composite color television signals. The algorithm is based on differential pulse code modulation (DPCM), but additionally utilizes a non-adaptive predictor, non-uniform quantizer and multilevel Huffman coder to reduce the data rate substantially below that achievable with straight DPCM. The non-adaptive predictor and multilevel Huffman coder combine to set this technique apart from other DPCM encoding algorithms. All processing is done on an intra-field basis to prevent motion degradation and minimize hardware complexity. Computer simulations have shown the algorithm will produce broadcast quality reconstructed video at an average transmission rate of 1.8 bits/pixel. Hardware implementation of the DPCM circuit, non-adaptive predictor and non-uniform quantizer has been completed, providing realtime demonstration of the image quality at full video rates. Video sampling/reconstruction circuits have also been constructed to accomplish the analog video processing necessary for the real-time demonstration. Performance results for the completed hardware compare favorably with simulation results. Hardware implementation of the multilevel Huffman encoder/decoder is currently under development along with implementation of a buffer control algorithm to accommodate the variable data rate output of the multilevel Huffman encoder. A video CODEC of this type could be used to compress NTSC color television signals where high quality reconstruction is desirable (e.g., Space Station video transmission, transmission direct-to-the-home via direct broadcast satellite systems or cable television distribution to system headends and direct-to-the-home).

Author

N92-19992*# National Aeronautics and Space Administration. Lewis Research Center, Cleveland, OH.

MICROWAVE BEAM POWER TRANSMISSION AT AN ARBITRARY RANGE

L. R. PINERO, J. L. CHRISTIAN, JR., and R. J. ACOSTA Feb. 1992 18 p
(Contract RTOP 679-40-00)
(NASA-TM-105424; E-6841; NAS 1.15:105424) Avail: CASI HC A03/MF A01

The power transfer efficiency between two circular apertures at an arbitrary range is obtained numerically. The apertures can have generally different sizes and arbitrary taper illuminations. The effects of distance and taper illumination on the transmission efficiency are investigated for equal size apertures. The result shows that microwave beam power is more effective at close ranges, namely distances less than $2D(\exp 2)/\lambda$. Also shown was the power transfer efficiency increase with taper illumination for close range distances. A computer program was developed for calculating the power transfer efficiency at an arbitrary range.

Author

N92-20032*# National Aeronautics and Space Administration. Lewis Research Center, Cleveland, OH.

SUBBAND CODING FOR IMAGE DATA ARCHIVING

D. GLOVER (National Aeronautics and Space Administration, Ames Research Center, Moffett Field, CA.) and S. C. KWATRA (Toledo Univ., OH.) 1992 15 p Proposed for presentation at the Data Compression Conference, Snowbird, UT, 24-27 Mar. 1992; sponsored by IEEE

(Contract RTOP 144-10-10)

(NASA-TM-105407; E-6722; NAS 1.15:105407) Avail: CASI HC A03/MF A01

The use of subband coding on image data is discussed. An overview of subband coding is given. Advantages of subbanding for browsing and progressive resolution are presented. Implementations for lossless and lossy coding are discussed. Algorithm considerations and simple implementations of subband are given.

Author

N92-23412*# National Aeronautics and Space Administration. Lewis Research Center, Cleveland, OH.

SOLID STATE TECHNOLOGY BRANCH OF NASA LEWIS RESEARCH CENTER Third Annual Digest, Jun. 1990 - Jun. 1991

1991 153 p

(Contract RTOP 506-59-4C)

(NASA-TM-105159; E-6447; NAS 1.15:105159) Avail: CASI HC A08/MF A02

Reprints of one year's production of research publications (June 1990 to June 1991) are presented. These are organized into three major sections: microwave circuits, both hybrid and monolithic microwave integrated circuits (MMICs); materials and device work; and superconductivity. The included papers also cover more specific topics involving waveguides, phase array antennas, dielectrics, and high temperature superconductors.

N92-30932*# National Aeronautics and Space Administration. Lewis Research Center, Cleveland, OH.

CHARACTERISTICS OF A FUTURE AERONAUTICAL SATELLITE COMMUNICATIONS SYSTEM

PHILIP Y. SOHN, ALAN STERN (General Electric Co., Princeton, NJ.), and FRED SCHMIDT (Ball Corp., Bloomfield, CO.) *In* JPL, Proceedings of the Workshop on Advanced Network and Technology Concepts for Mobile, Micro, and Personal Communications p 125-152 15 Sep. 1991 Previously announced as N91-23102

Avail: CASI HC A03/MF A03

A possible operational system scenario for providing satellite communications services to the future aviation community was analyzed. The system concept relies on a Ka-band (20/30 GHz) satellite that utilizes Multibeam Antenna (MBA) technology. The aircraft terminal uses an extremely small aperture antenna as a result of using this higher spectrum at Ka-band. The satellite functions as a relay between the aircraft and the ground stations. The ground stations function as interfaces to the existing terrestrial networks such as the Public Service Telephone Network (PSTN). Various system tradeoffs are first examined to ensure optimized system parameters. High level performance specifications and design approaches are generated for the space, ground, and aeronautical elements in the system. Both technical and economical issues affecting the feasibility of the studied concept are addressed with the 1995 timeframe in mind.

Author

N92-30934*# National Aeronautics and Space Administration. Lewis Research Center, Cleveland, OH.

A PERSONAL COMMUNICATIONS NETWORK USING A KA-BAND SATELLITE

L. C. PALMER (Hughes Network Systems, Inc., Germantown, MD.), A. STERN (General Electric Co., Princeton, NJ.), and P. Y. SOHN *In* JPL, Proceedings of the Workshop on Advanced Network and Technology Concepts for Mobile, Micro, and Personal Communications p 165-176 15 Sep. 1991

(Contract AC-90-695)

Avail: CASI HC A03/MF A03

The feasibility of portable communications terminals that can provide 4.8-kbps voice communications to a hub station via a Ka-band geosynchronous satellite was investigated. Tradeoffs are examined so that the combined system of the hub and gateway earth stations, the satellite, and the personal terminals can provide a competitive service in terms of cost, availability, and quality. A baseline system is described using a spacecraft with approximately 140 spot beams that cover CONUS with 5-watt power amplifiers in each beam. Satellite access in both the forward and return directions uses Frequency Division Multiple Access/Code Division Multiple Access (FDMA/CDMA) with a chip rate of 2.5 Mchip/sec. An experiment is recommended using the Advanced Communications Technology Satellite (ACTS) to demonstrate some of the features of the portable terminal concept.

Author

N92-31855*# National Aeronautics and Space Administration. Lewis Research Center, Cleveland, OH.

HIGH-PERFORMANCE PACKAGING FOR MONOLITHIC MICROWAVE AND MILLIMETER-WAVE INTEGRATED CIRCUITS

K. A. SHALKHAUSER, K. LI (Hughes Aircraft Co., Torrance, CA.), and Y. C. SHIH (Hughes Aircraft Co., Torrance, CA.) 1992 11 p Presented at the 14th International Communications Satellite Systems Conference, Washington, DC, 22-26 Mar. 1992; sponsored by AIAA Previously announced in IAA as A92-31706

(Contract NAS3-25870; RTOP 506-72-1C)

(NASA-TM-105744; E-7149; NAS 1.15:105744) Copyright

Avail: CASI HC A03/MF A01

Packaging schemes were developed that provide low-loss, hermetic enclosure for advanced monolithic microwave and millimeter-wave integrated circuits (MMICs). The package designs are based on a fused quartz substrate material that offers improved radio frequency (RF) performance through 44 gigahertz (GHz). The small size and weight of the packages make them appropriate for a variety of applications, including phased array antenna systems. Packages were designed in two forms; one for housing a single MMIC chip, the second in the form of a multi-chip phased array module. The single chip array module was developed in three separate sizes, for chips of different geometry and frequency requirements. The phased array module was developed to address packaging directly for antenna applications, and includes transmission line and interconnect structures to support multi-element operation. All packages are fabricated using fused quartz substrate materials. As part of the packaging effort, a test fixture was developed to interface the single chip packages to conventional laboratory instrumentation for characterization of the packaged devices. The package and test fixture designs were both developed in a generic sense, optimizing performance for a wide range of possible applications and devices.

Author

N92-32965*# National Aeronautics and Space Administration. Lewis Research Center, Cleveland, OH.

SOLID STATE TECHNOLOGY BRANCH OF NASA LEWIS RESEARCH CENTER Fourth Annual Digest, Jun. 1991 - Jun. 1992

Aug. 1992 214 p

(Contract RTOP 506-72-1B)

(NASA-TM-105752; E-7160; NAS 1.15:105752) Avail: CASI HC A10/MF A03

A collection of papers written by the members of the Solid State Technology Branch of NASA LeRC from Jun. 1991 - Jun. 1992 is presented. A range of topics relating to superconductivity, Monolithic Microwave Circuits (MMIC's), coplanar waveguides, and material characterization is covered.

N92-32966*# National Aeronautics and Space Administration. Lewis Research Center, Cleveland, OH.

V-BAND PSEUDOMORPHIC HEMT MMIC PHASED ARRAY COMPONENTS FOR SPACE COMMUNICATIONS

G. L. LAN (Hughes Aircraft Co., Torrance, CA.), C. K. PAO (Hughes Aircraft Co., Torrance, CA.), C. S. WU (Hughes Aircraft Co., Torrance, CA.), M. HU (Hughes Aircraft Co., Torrance, CA.), and ALAN N. DOWNEY *In* its Solid State Technology Branch of

NASA Lewis Research Center p 15-20 Aug. 1992
(Contract NAS3-25088)
Avail: CASI HC A02/MF A03

Recent advances in pseudomorphic high-electron-mobility transistor (PMHEMT) monolithic microwave integrated circuit (MMIC) technology have made it the preferred candidate for high performance millimeter-wave components for phased array applications. The development of V-band PMHEMT/MMIC components including power amplifiers and phase shifters is described. For the single-stage MMIC power amplifier employing a 200 micron PMHEMT, we achieved 151.4 mW output power (757.0 mW/mm) with 1.8 dB associated gain and 26.4 percent power-added efficiency at 60 GHz. A two-stage MMIC amplifier utilizing the same devices demonstrated small-signal gain as high as 15 dB at 58 GHz. And, for the phase shifter, a four-bit phase shifter with less than 8 dB insertion loss from 61 to 63 GHz was measured. Author

N92-32967*# National Aeronautics and Space Administration. Lewis Research Center, Cleveland, OH.

PLANAR DIELECTRIC RESONATOR STABILIZED HEMT OSCILLATOR INTEGRATED WITH CPW/APERTURE COUPLED PATCH ANTENNA

RAINEE N. SIMONS and RICHARD Q. LEE *In its* Solid State Technology Branch of NASA Lewis Research Center p 21-23 Aug. 1992 Previously announced as N92-18473
Avail: CASI HC A01/MF A03

A design of an active antenna with a dielectric resonator stabilized high-electron-mobility transistor (HEMT) oscillator (DRO) and an aperture-coupled patch antenna is reported. The circuit is fabricated using coplanar waveguide (CPW) with the oscillator and the antenna on opposite sides of the substrate. The active antenna was demonstrated at 7.6 GHz; however, the design can be scaled to higher frequencies. Excellent oscillator characteristics and radiation patterns were obtained. Author

N92-32968*# National Aeronautics and Space Administration. Lewis Research Center, Cleveland, OH.

AN OPTICALLY CONTROLLED KA-BAND PHASED ARRAY ANTENNA

R. R. KUNATH, RICHARD Q. LEE, K. S. MARTZAKLIS, K. A. SHALKHAUSER, ALAN N. DOWNEY, and RAINEE N. SIMONS (Sverdrup Technology, Inc., Middleburg Heights, OH.) *In its* Solid State Technology Branch of NASA Lewis Research Center p 35-44 Aug. 1992
Avail: CASI HC A02/MF A03

The design and development of a small, optically controlled phased array antenna suitable for communication satellite applications are discussed. A vertical integration architecture is used which minimizes the size of the array with its associated beamforming network (BFN). The antenna features a four-element linear microstrip array that uses aperture coupling of the antenna elements to the BFN; a modified Wilkinson power divider BFN; and 32 GHz, four-bit monolithic microwave integrated circuit (MMIC) phase shifters in customized quartz packages with corresponding optoelectronic interface circuits (OEIC's) for control signal reception. Author

N92-32969*# National Aeronautics and Space Administration. Lewis Research Center, Cleveland, OH.

KA-BAND DUAL FREQUENCY ARRAY FEED FOR A LOW COST ACTS GROUND TERMINAL

RICHARD Q. LEE, RAINEE N. SIMONS, and AJIT K. SIL *In its* Solid State Technology Branch of NASA Lewis Research Center p 55-60 Aug. 1992 Previously announced in IAA as A92-29833
Avail: CASI HC A02/MF A03

Because of low cost and ease of fabrication, microstrip arrays are attractive as feeds for reflector antenna systems. The development of a 4 x 4 microstrip array which will be used as a feed for a low cost Advanced Communications Technology Satellite (ACTS) ground terminal is described. The array feed consisting of four 2 x 2 subarrays is fed with coplanar waveguide power dividing

networks. The patch radiator is designed to excite two orthogonal, linearly polarized waves at Ka-band frequencies (around 20 and 30 GHz). Test results for the developed array are presented. Author

N92-32970*# National Aeronautics and Space Administration. Lewis Research Center, Cleveland, OH.

COPLANAR WAVEGUIDE FEEDS FOR PHASED ARRAY ANTENNAS

RAINEE N. SIMONS (Sverdrup Technology, Inc., Brook Park, OH.) and RICHARD Q. LEE *In its* Solid State Technology Branch of NASA Lewis Research Center p 61-67 Aug. 1992
Avail: CASI HC A02/MF A03

The design and performance of the following coplanar waveguide (CPW) microwave distribution networks for linear as well as circularly polarized microstrip patches and printed dipole arrays is presented: (1) CPW/microstrip line feed; (2) CPW/balanced stripline feed; (3) CPW/slotline feed; (4) grounded CPW (GCPW)/balanced coplanar stripline feed; and (5) CPW/slot coupled feed. Typical measured radiation patterns are presented, and their relative advantages and disadvantages are compared. Author

N92-32971*# National Aeronautics and Space Administration. Lewis Research Center, Cleveland, OH.

ANALYSIS OF SHIELDED CPW DISCONTINUITIES WITH AIR-BRIDGES

N. I. DIB (Michigan Univ., Ann Arbor.), P. B. KATEHI (Michigan Univ., Ann Arbor.), and GEORGE E. PONCHAK *In its* Solid State Technology Branch of NASA Lewis Research Center p 71-74 Aug. 1992 Repr. from MTT-S Digest (IEEE), Apr. 1991 p 469-472
(Contract NSF ECS-86-57951)
Avail: CASI HC A01/MF A03

The effect of air-bridges on the performance of various coplanar waveguides (CPW) discontinuities is studied. Specifically, the coupled open-end CPW's and the short-end shunt CPW stub discontinuities are considered. The high frequency effect of the air-bridge is evaluated using a hybrid technique. At first, the frequency dependent equivalent circuit of the planar discontinuity without the air-bridge is derived using the Space Domain Integral Equation (SDIE) method. Then, the circuit is modified by incorporating the air-bridge's parasitic inductance and capacitance which are evaluated using a simple quasi-static model. The frequency response of each discontinuity with and without the air-bridge is studied and the scattering parameters are plotted in the frequency range 30-50 GHz for typical CPW dimensions. Author

N92-32972*# National Aeronautics and Space Administration. Lewis Research Center, Cleveland, OH.

A FLEXIBLE CPW PACKAGE FOR A 30 GHZ MMIC AMPLIFIER

RAINEE N. SIMONS and SUSAN R. TAUB *In its* Solid State Technology Branch of NASA Lewis Research Center p 75-78 Aug. 1992 Previously announced as N92-23193
Avail: CASI HC A01/MF A03

A package, which consists of a carrier and housing, was developed for monolithic-millimeter wave integrated circuit amplifiers which operate at 30 GHz. The carrier has coplanar waveguide (CPW) interconnects and provides heat-sinking, tuning, and cascading capabilities. The housing provides electrical isolation, mechanical protection, and a feed-through for biasing. Author

N92-32973*# National Aeronautics and Space Administration. Lewis Research Center, Cleveland, OH.

A 1-W, 30-GHZ, CPW AMPLIFIER FOR ACTS SMALL TERMINAL UPLINK

SUSAN R. TAUB and RAINEE N. SIMONS (Sverdrup Technology, Inc., Brook Park, OH.) *In its* Solid State Technology Branch of NASA Lewis Research Center p 79-82 Aug. 1992 Previously

announced as N92-26096
 Avail: CASI HC A01/MF A03

The progress to date of the development of a 1-W, 30-GHz, coplanar waveguide (CPW) amplifier for the Advanced Communication Technology Satellite (ACTS) Small Terminal Uplink is described. The amplifier is based on Texas Instruments' monolithic microwave integrated circuit (MMIC) amplifiers; a three-stage, low-power amplifier and a single stage, high-power amplifier. The amplifiers have a power output of 190 mW and 0.710 W, gain of 23 and 4.2 dB, and efficiencies of 30.2 and 24 percent for the three-stage and one-stage amplifiers, respectively. The chips are to be combined via a CPW power divider/combiner circuit to yield the desired 1 W of output power. Author

N92-32974*# National Aeronautics and Space Administration, Lewis Research Center, Cleveland, OH.

COMPARATIVE EVALUATION OF OPTICAL WAVEGUIDES AS ALTERNATIVE INTERCONNECTIONS FOR HIGH PERFORMANCE PACKAGING

S. E. SCHACHAM, HENRI MERKELO, L.-T. HWANG, BRADLEY D. MCCREDIE, MARK S. VEATCH, and I. TURLIK *In its* Solid State Technology Branch of NASA Lewis Research Center p 83-92 Aug. 1992 Repr. from Transactions on Components, Hybrids, and Manufacturing Technology (IEEE), v. 15, no. 1, Feb. 1992 p 63-72

Avail: CASI HC A02/MF A03

A detailed comparison between optical and electrical interconnections is presented, with emphasis on advantages and drawbacks of optical link utilization. The impact of attenuation, dispersive degradation, and fan out on signal integrity is discussed. Reflections from discontinuities are taken into account in the section on fan out. According to our results, there is no obvious advantage of using optical interconnections for the distribution of digital signals containing significant frequency components in excess of 10 GHz, unless substantial distances are involved, for which low dispersion optical waveguides could provide a solution. The implementation of a polyimide optical waveguide in the MCNC package is discussed. Author

N92-32981*# National Aeronautics and Space Administration, Lewis Research Center, Cleveland, OH.

MEASUREMENT TECHNIQUES FOR CRYOGENIC KA-BAND MICROSTRIP ANTENNAS

M. A. RICHARD (Case Western Reserve Univ., Cleveland, OH.), KUL B. BHASIN, C. GILBERT (Ball Communication Systems Div., Broomfield, CO.), S. METZLER (Ball Communication Systems Div., Broomfield, CO.), and P. C. CLASPY (Case Western Reserve Univ., Cleveland, OH.) *In its* Solid State Technology Branch of NASA Lewis Research Center p 151-157 Aug. 1992 Previously announced as N91-30426

Avail: CASI HC A02/MF A03

The measurement of cryogenic antennas poses unique logistical problems since the antenna under test must be embedded in the cooling chamber. A method for measuring the performance of cryogenic microstrip antennas using a closed cycle gas-cooled refrigerator in a far field range is described. Antenna patterns showing the performance of gold and superconducting Ka-band microstrip antennas at various temperatures are presented. Author

ELECTRONICS AND ELECTRICAL ENGINEERING

Includes test equipment and maintainability; components, e.g., tunnel diodes and transistors; microminiaturization; and integrated circuitry.

A92-12272* National Aeronautics and Space Administration, Lewis Research Center, Cleveland, OH.

SIGNIFICANT LONG-TERM REDUCTION IN N-CHANNEL MESFET SUBTHRESHOLD LEAKAGE USING AMMONIUM-SULFIDE SURFACE TREATED GATES

P. G. NEUDECK (NASA, Lewis Research Center, Cleveland, OH), M. S. CARPENTER (Cypress Semiconductor, San Jose, CA), MICHAEL R. MELLOCH, and JAMES A. COOPER, JR. (Purdue University, West Lafayette, IN) *IEEE Electron Device Letters* (ISSN 0741-3106), vol. 12, Oct. 1991, p. 553-555. Research supported by SDIO and SERI. Oct. 1991 3 p refs (Contract N00014-88-K-0527; N00014-89-J-1864) Copyright

Ammonium-sulfide (NH₄)₂S treated gates have been employed in the fabrication of GaAs MESFETs that exhibit a remarkable reduction in subthreshold leakage current. A greater than 100-fold reduction in drain current minimum is observed due to a decrease in Schottky gate leakage. The electrical characteristics have remained stable for over a year during undecicated storage at room temperature, despite the absence of passivation layers. I.E.

A92-13266* National Aeronautics and Space Administration, Lewis Research Center, Cleveland, OH.

CALCULATED PERFORMANCE OF P(+)N INP SOLAR CELLS WITH IN(0.52)AL(0.48)AS WINDOW LAYERS

R. K. JAIN (NASA, Lewis Research Center, Cleveland, OH) and G. A. LANDIS (Sverdrup Technology, Inc., Brook Park, OH) *Applied Physics Letters* (ISSN 0003-6951), vol. 59, Nov. 11, 1991, p. 2555-2557. 11 Nov. 1991 3 p refs (Contract NAS3-25266) Copyright

The performance of indium phosphide solar cells with lattice matched wide band-gap In(0.52)Al(0.48)As window layers was calculated using the PC-1D computer code. The conversion efficiency of p(+)n InP solar cells is improved significantly by the window layer. No improvement is seen for n(+)p structures. The improvement in InP cell efficiency was studied as a function of In(0.52)Al(0.48)As layer thickness. The use of the window layer improves both the open circuit voltage and short circuit current. For a typical In(0.52)Al(0.48)As window layer thickness of 20 nm, the cell efficiency improves in excess of 27 percent to a value of 18.74 percent. Author

A92-14938* National Aeronautics and Space Administration, Lewis Research Center, Cleveland, OH.

MICROWAVE PROPERTIES OF YBA2CU3O(7-DELTA) HIGH-TRANSITION-TEMPERATURE SUPERCONDUCTING THIN FILMS MEASURED BY THE POWER TRANSMISSION METHOD

F. A. MIRANDA (NASA, Lewis Research Center, Case Western Reserve University, Cleveland, OH), W. L. GORDON (Case Western Reserve University, Cleveland, OH), K. B. BHASIN, V. O. HEINEN, and J. D. WARNER (NASA, Lewis Research Center, Cleveland, OH) *Journal of Applied Physics* (ISSN 0021-8979), vol. 70, pt. 1, Nov. 15, 1991, p. 5450-5462. 15 Nov. 1991 13 p refs Copyright

The microwave response of YBa₂Cu₃O(7-delta) superconducting thin films deposited on LaAlO₃, MgO, YSZ, and LaGaO₃ substrates are studied. It is found that the microwave transmission properties are very weakly dependent on temperature in the normal state but change drastically upon transition to the superconducting state. In particular, the transmission decreases

and there is a negative phase shift with respect to the phase at room temperature when the sample is cooled through its transition temperature. The magnetic penetration depth for all the films was determined from the surface reactance of the films. The microwave complex conductivity is determined in both the normal and the superconducting state. It is observed that both σ_1 and σ_2 increase in transition to the superconducting state. The surface resistivity is calculated for all the films. C.D.

A92-18455* National Aeronautics and Space Administration. Lewis Research Center, Cleveland, OH.

COAXIAL LINE CONFIGURATION FOR MICROWAVE POWER TRANSMISSION STUDY OF YBA₂CU₃O₇(δ) THIN FILMS

C. M. CHOREY (NASA, Lewis Research Center, Cleveland; Sverdrup Technology, Inc., Brook Park, OH), F. A. MIRANDA, and K. B. BHASIN (NASA, Lewis Research Center, Cleveland, OH) IEEE Transactions on Applied Superconductivity (ISSN 1051-8223), vol. 1, Dec. 1991, p. 178-180. Dec. 1991 3 p refs Copyright

Microwave transmission measurements through YBa₂Cu₃O₇(δ) (YBCO) high-transition-temperature superconducting thin films on lanthanum aluminate (LaAlO₃) have been performed in a coaxial line at 10 GHz. LaAlO₃ substrates were ultrasonically machined into washer-shaped discs, polished, and coated with laser-ablated YBCO. These samples were mounted in a 50-ohm coaxial air line to form a short circuit. The power transmitted through the films as a function of temperature was used to calculate the normal state conductivity and the magnetic penetration depth for the films. I.E.

A92-21292* National Aeronautics and Space Administration. Lewis Research Center, Cleveland, OH.

ELECTROMAGNETIC COUPLING BETWEEN COPLANAR WAVEGUIDE AND MICROSTRIP ANTENNAS

RAINEE N. SIMONS, RICHARD Q. LEE, and GLENN R. LINDAMOOD (NASA, Lewis Research Center, Cleveland, OH) Microwave and Optical Technology Letters (ISSN 0895-2477), vol. 5, Feb. 1992, p. 60-62. Feb. 1992 3 p refs Copyright

Electromagnetic coupling between coplanar waveguides (CPW) and microstrip patch antennas has been investigated for two feed configurations: (1) direct aperture-coupled feeding of a patch antenna by a CPW feed, and (2) proximity-coupled feeding of a patch antenna by a microstrip line which is aperture-coupled to a CPW feed. Results indicate that both feeding approaches are feasible and yield high coupling efficiency. Author

A92-23959* National Aeronautics and Space Administration. Lewis Research Center, Cleveland, OH.

A COMBINED VECTOR POTENTIAL-SCALAR POTENTIAL METHOD FOR FE COMPUTATION OF 3D MAGNETIC FIELDS IN ELECTRICAL DEVICES WITH IRON CORES

R. WANG and N. A. DEMERDASH (Clarkson University, Potsdam, NY) (IEEE Biennial Conference on Electromagnetic Field Computation, 4th, Toronto, Canada, Oct. 22-24, 1990) IEEE Transactions on Magnetics (ISSN 0018-9464), vol. 27, Sept. 1991, p. 3971-3977. Sep. 1991 7 p refs (Contract NAG3-818) Copyright

A method of combined use of magnetic vector potential based finite-element (FE) formulations and magnetic scalar potential (MSP) based formulations for computation of three-dimensional magnetostatic fields is introduced. In this method, the curl-component of the magnetic field intensity is computed by a reduced magnetic vector potential. This field intensity forms the basis of a forcing function for a global magnetic scalar potential solution over the entire volume of the region. This method allows one to include iron portions sandwiched in between conductors within partitioned current-carrying subregions. The method is most suited for large-scale global-type 3-D magnetostatic field computations in electrical devices, and in particular rotating electric machinery. I.E.

A92-24488* National Aeronautics and Space Administration. Lewis Research Center, Cleveland, OH.

COPLANAR WAVEGUIDE APERTURE COUPLED PATCH ANTENNAS WITH GROUND PLANE/SUBSTRATE OF FINITE EXTENT

R. N. SIMONS and R. Q. LEE (NASA, Lewis Research Center, Cleveland, OH) Electronics Letters (ISSN 0013-5194), vol. 28, Jan. 2, 1992, p. 75, 76. 2 Jan. 1992 2 p refs Copyright

Coplanar waveguide (CPW)/aperture coupled microstrip patch antennas constructed with ground coplanar waveguide (GCPW), finite coplanar waveguide (FCPW) and channelized coplanar waveguide (CCPW) are demonstrated. The measured characteristics show that the CCPW/aperture coupled microstrip patch antenna has the largest bandwidth, whereas the GCPW/aperture coupled microstrip patch antenna has the best front-to-back ratio. Author

A92-29769# National Aeronautics and Space Administration. Lewis Research Center, Cleveland, OH.

A LOW-POWER, HIGH-EFFICIENCY KA-BAND TWT

ARTHUR N. CURREN, JAMES A. DAYTON, JR., RAYMOND W. PALMER, DALE A. FORCE (NASA, Lewis Research Center, Cleveland, OH), RODNEY N. TAMASHIRO, JOHN F. WILSON, LOUIS DOMBRO (Hughes Aircraft Co., Electron Dynamics Div., Torrance, CA), and WAYNE L. HARVEY (JPL, Pasadena, CA) IN: AIAA International Communication Satellite Systems Conference and Exhibit, 14th, Washington, DC, Mar. 22-26, 1992, Technical Papers. Pt. 1 1992 6 p refs (AIAA PAPER 92-1822) Copyright

NASA has developed a new class of Ka-band TWT amplifiers (TWTAs) which achieve their high efficiency/low power performance goals by means of an advanced dynamic velocity taper (DVT). The DVT is characterized by a continuous, nonlinear reduction in helix pitch from its initial synchronous value in the output section of the TWT to near the end of the helix. Another efficiency-maximizing feature is the inclusion of a multistage depressed collector employing oxygen-free, high-conductivity Cu electrodes treated for secondary electron emission suppression by means of ion bombardment. An efficiency of 43 percent is expected to be reached. O.C.

A92-29771*# National Aeronautics and Space Administration. Lewis Research Center, Cleveland, OH.

A THREE-DIMENSIONAL FINITE-ELEMENT THERMAL/MECHANICAL ANALYTICAL TECHNIQUE FOR HIGH-PERFORMANCE TRAVELING WAVE TUBES

KURT A. SHALKHAUSER, KAREN F. BARTOS, E. B. FITE, and G. R. SHARP (NASA, Lewis Research Center, Cleveland, OH) IN: AIAA International Communication Satellite Systems Conference and Exhibit, 14th, Washington, DC, Mar. 22-26, 1992, Technical Papers. Pt. 1 1992 12 p refs (AIAA PAPER 92-1824) Copyright

Current research in high-efficiency, high-performance traveling wave tubes (TWT's) has led to the development of novel thermal/mechanical computer models for use with helical slow-wave structures. A three-dimensional, finite element computer model and analytical technique used to study the structural integrity and thermal operation of a high-efficiency, diamond-rod, K-band TWT designed for use in advanced space communications systems. This analysis focused on the slow-wave circuit in the radiofrequency section of the TWT, where an inherent localized heating problem existed and where failures were observed during earlier cold compression, or 'coining' fabrication technique that shows great potential for future TWT development efforts. For this analysis, a three-dimensional, finite element model was used along with MARC, a commercially available finite element code, to simulate the fabrication of a diamond-rod TWT. This analysis was conducted by using component and material specifications consistent with actual TWT fabrication and was verified against empirical data. The analysis is nonlinear owing to material plasticity introduced by the forming process and also to geometric nonlinearities presented by the component assembly configuration. The computer

model was developed by using the high efficiency, K-band TWT design but is general enough to permit similar analyses to be performed on a wide variety of TWT designs and styles. The results of the TWT operating condition and structural failure mode analysis, as well as a comparison of analytical results to test data are presented.
Author

A92-29801*# National Aeronautics and Space Administration, Lewis Research Center, Cleveland, OH.

ADVANCED LARGE SCALE GAAS MONOLITHIC IF SWITCH MATRIX SUBSYSTEM

D. R. CH'EN, W. C. PETERSEN, and W. M. KIBA (Microwave Monolithics, Inc., Simi Valley, CA) IN: AIAA International Communication Satellite Systems Conference and Exhibit, 14th, Washington, DC, Mar. 22-26, 1992, Technical Papers. Pt. 1 1992 9 p refs

(Contract NAS3-25713)

(AIAA PAPER 92-1861) Copyright

Attention is given to a novel chip design and packaging technique to overcome the limitations due to the high signal isolation requirements of advanced communications systems. A hermetically sealed 6 x 6 monolithic GaAs switch matrix subsystem with integral control electronics based on this technique is presented. An 0-dB insertion loss and 60-dB crosspoint isolation over a 3.5-to-6-GHz band were achieved. The internal controller portion of the switching subsystem provides crosspoint control via a standard RS-232 computer interface and can be synchronized with an external systems control computer. The measured performance of this advanced switching subsystem is fully compatible with relatively static 'switchboard' as well as dynamic TDMA modes of operation.
C.A.B.

A92-29803*# National Aeronautics and Space Administration, Lewis Research Center, Cleveland, OH.

KA-BAND ACTIVE MMIC SUBARRAY DEVELOPMENT

RICHARD LEE and CHARLES RAQUET (NASA, Lewis Research Center, Cleveland, OH) IN: AIAA International Communication Satellite Systems Conference and Exhibit, 14th, Washington, DC, Mar. 22-26, 1992, Technical Papers. Pt. 1 1992 7 p refs

(AIAA PAPER 92-1863) Copyright

A 4 x 8 array consisting of two adjacent 4 x 4 MMIC subarray modules under development as part of a MMIC insertion program for the ACTS communication experiments is presented. The subarray features a high-density 'tile' configuration integrating 16 MMIC power amplifiers and 16 MMIC phase shifters. The radiating elements are cavity-backed, aperture coupled, linearly polarized microstrip patches arranged on a 4 x 4 square grid. Each module also incorporates a MMIC controller to set the phase shifts and to turn individual amplifiers 'on' or 'off'. The novel module construction technique is expected to establish a benchmark in Ka-band and higher-frequency array architectures. The hybrid integration approach used for the module can be replaced by multifunctional chips and multilayer distribution boards. The higher level of integration is to permit the dense grid spacing required for wide-angle scanning and reduced size, weight, and cost for the array.
C.A.B.

A92-29830*# National Aeronautics and Space Administration, Lewis Research Center, Cleveland, OH.

ADVANCES IN MMIC TECHNOLOGY FOR COMMUNICATIONS SATELLITES

REGIS F. LEONARD (NASA, Lewis Research Center, Cleveland, OH) IN: AIAA International Communication Satellite Systems Conference and Exhibit, 14th, Washington, DC, Mar. 22-26, 1992, Technical Papers. Pt. 1 1992 5 p refs

(AIAA PAPER 92-1899) Copyright

This paper discusses NASA Lewis Research Center's program for development of monolithic microwave integrated circuits (MMIC) for application in space communications. Emphasis will be on the improved performance in power amplifiers and low noise receivers which has been made possible by the development of new semiconductor materials and devices. Possible applications of high

temperature superconductivity for space communications will also be presented.
Author

A92-31631* National Aeronautics and Space Administration, Lewis Research Center, Cleveland, OH.

LASER ABLATED YBA₂CU₃O(7-X) HIGH TEMPERATURE SUPERCONDUCTOR COPLANAR WAVEGUIDE RESONATOR

G. J. VALCO, A. R. BLEMKER (Ohio State University, Columbus), and K. B. BHASIN (NASA, Lewis Research Center, Cleveland, OH) Microwave and Optical Technology Letters (ISSN 0895-2477), vol. 5, May 1992, p. 234-236. May 1992 3 p refs

(Contract NCC3-197)

Copyright

Several 8.8-GHz coplanar waveguide resonators are fabricated and tested that are made from laser ablated YBa₂Cu₃O(7-x) thin films on LaAlO₃ substrates. A quality factor of 1250 at 77 K was measured. A correlation between the microwave performance of the resonators and the critical temperature and morphology of the films was observed.
Author

A92-31706*# National Aeronautics and Space Administration, Lewis Research Center, Cleveland, OH.

HIGH-PERFORMANCE PACKAGING FOR MONOLITHIC MICROWAVE AND MILLIMETER-WAVE INTEGRATED CIRCUITS

K. A. SHALKHAUSER (NASA, Lewis Research Center, Cleveland, OH), K. LI, and Y. C. SHIH (Hughes Aircraft Co., Microelectronic Circuits Div., Torrance, CA) AIAA, International Communication Satellite Systems Conference and Exhibit, 14th, Washington, DC, Mar. 22-26, 1992. 10 p. Mar. 1992 10 p

(Contract NAS3-25870)

(AIAA PAPER 92-1935) Copyright

Packaging schemes are developed that provide low-loss, hermetic enclosure for enhanced monolithic microwave and millimeter-wave integrated circuits. These package schemes are based on a fused quartz substrate material offering improved RF performance through 44 GHz. The small size and weight of the packages make them useful for a number of applications, including phased array antenna systems. As part of the packaging effort, a test fixture was developed to interface the single chip packages to conventional laboratory instrumentation for characterization of the packaged devices.
R.E.P.

A92-34844* National Aeronautics and Space Administration, Lewis Research Center, Cleveland, OH.

NEW TECHNIQUES FOR EXCITING LINEARLY TAPERED SLOT ANTENNAS WITH COPLANAR WAVEGUIDE

R. N. SIMONS, R. Q. LEE, and T. D. PERL (NASA, Lewis Research Center, Cleveland, OH) Electronics Letters (ISSN 0013-5194), vol. 28, no. 7, March 26, 1992, p. 620, 621. 26 Mar. 1992 2 p refs

Copyright

Two new techniques for exciting a linearly tapered slot antenna (L TSA) with coplanar waveguide (CPW) are introduced. In the first approach, an air bridge is used to couple power from a CPW to an L TSA. In the second approach, power is electromagnetically coupled from a finite CPW (FCPW) to an L TSA. Measured results at 18 GHz show excellent return loss and radiation patterns.
Author

A92-35054* National Aeronautics and Space Administration, Lewis Research Center, Cleveland, OH.

SUBMILLIMETER BACKWARD-WAVE OSCILLATORS

N. STANKIEWICZ and J. A. DAYTON, JR. (NASA, Lewis Research Center, Cleveland, OH) IN: IGARSS '91; Proceedings of the 11th Annual International Geoscience and Remote Sensing Symposium, Espoo, Finland, June 3-6, 1991. Vol. 2 1991 2 p refs

Copyright

A novel submillimeter wave backward-wave oscillator (BWO) that can provide tens of mW of power over a voltage tunable frequency range of more than an octave could serve as the local oscillator for a new class of array sensors in the range from 200

to 2000 GHz. The BWO appears to be the best device available for supporting a wide variety of heterodyne detection systems. It is voltage tunable, able to be phase locked, and can provide sufficient power for all envisioned systems including the arrays of detectors needed for fast data recovery in monitoring upper atmospheric conditions. I.E.

A92-37953* National Aeronautics and Space Administration. Lewis Research Center, Cleveland, OH.

PERFORMANCE OF A WIDEBAND GAAS LOW-NOISE AMPLIFIER AT CRYOGENIC TEMPERATURES

S. S. TONCICH, K. B. BHASIN (NASA, Lewis Research Center, Cleveland, OH), T. K. CHEN, and P. C. CLASPY (Case Western Reserve University, Cleveland, OH) *Microwave and Optical Technology Letters* (ISSN 0895-2477), vol. 5, no. 8, July 1992, p. 372-374. Jul. 1992 3 p refs

Copyright

The gain and noise figure performance of a GaAs amplifier at cryogenic temperatures has been studied. Results obtained indicate that a lower noise figure and a higher gain are induced by decreasing the temperature, while no significant change in the input 1-dB compression point is observed. Repeated temperature cycling had no adverse effect on the amplifier performance. O.G.

A92-38140*# National Aeronautics and Space Administration. Lewis Research Center, Cleveland, OH.

A VERTICALLY INTEGRATED KA-BAND PHASED ARRAY ANTENNA

R. R. KUNATH, R. Q. LEE, K. S. MARTZAKLIS, K. A. SHALKHAUSER, A. N. DOWNEY (NASA, Lewis Research Center, Cleveland, OH), and R. SIMONS (Sverdrup Technology, Inc., Middleburg Heights, OH) *AIAA, International Communication Satellite Systems Conference and Exhibit, 14th, Washington, DC, Mar. 22-26, 1992*. 9 p. Mar. 1992 9 p refs (AIAA PAPER 92-1976) Copyright

The design, development, and experimental demonstration of a small phased array antenna suitable for applications on communications satellites are discussed. Each of the vertical layers was optimized for performance, and MMICs on custom carriers were characterized prior to insertion. A vertical integration architecture is used which minimizes the size of the array with its associated beamforming network (BFN). The antenna features a four-element linear microstrip array that uses aperture coupling of the antenna elements to the BFN; a modified Wilkinson power divider BFN; and 32 GHz, 4-bit MMIC phase shifters on customized alumina carriers. Performance data are presented for all components, and far-field antenna radiation patterns are given. P.D.

A92-38163 National Aeronautics and Space Administration. Lewis Research Center, Cleveland, OH.

A LOW-POWER, HIGH-EFFICIENCY KA-BAND TWTA

A. N. CURREN, J. A. DAYTON, JR., R. W. PALMER, D. A. FORCE (NASA, Lewis Research Center, Cleveland, OH), R. N. TAMASHIRO, J. F. WILSON, L. DOMBRO (Hughes Aircraft Co., Torrance, CA), and W. L. HARVEY (JPL, Pasadena, CA) *IN: 1991 International Electron Devices Meeting, Washington, DC, Dec. 8-11, 1991, Proceedings*. New York, Institute of Electrical and Electronics Engineers, Inc., 1991, p. 581-584. 1991 4 p refs Copyright

A NASA-sponsored program is described for developing a high-efficiency low-power TWTA operating at 32 GHz and meeting the requirements for the Cassini Mission to study Saturn. The required RF output power of the helix TWT is 10 watts, while the dc power from the spacecraft is limited to about 30 watts. The performance level permits the transmission to earth of all mission data. Several novel technologies are incorporated into the TWT to achieve this efficiency including an advanced dynamic velocity taper characterized by a nonlinear reduction in pitch in the output helix section and a multistage depressed collector employing copper electrodes treated for secondary electron-emission suppression. Preliminary program results are encouraging: RF

output power of 10.6 watts is obtained at 14-mA beam current and 5.2-kV helix voltage with overall TWT efficiency exceeding 40 percent. Author

A92-43891* National Aeronautics and Space Administration. Lewis Research Center, Cleveland, OH.

DC AND MICROWAVE PERFORMANCE OF A 0.1-MICRON GATE INAS/IN(0.52)AL(0.48)AS MODFET

D. YANG, Y. C. CHEN, T. BROCK, and PALLAB K. BHATTACHARYA (Michigan, University, Ann Arbor) *IEEE Electron Device Letters* (ISSN 0741-3106), vol. 13, no. 6, June 1992, p. 350-352. Jun. 1992 3 p refs (Contract NAG3-988; DAAL03-87-K-0007; N00019-89-J-1519) Copyright

The performance characteristics of 0.1-micron gate InAs/In(0.52)Al(0.48)As MODFETs grown by molecular beam epitaxy are measured and analyzed. The transistors are characterized by measured $g_{sub m} (max) = 840$ mS/mm, $f_{sub T} = 128$ GHz, and a very high current carrying capability, e.g., $I_{sub dss} = 934$ mA/mm at $V_{sub gs} = 0.4$ V and $V_{sub ds} = 2.7$ V. The value of $f_{sub T}$ is estimated from extrapolation of the current gain (H21) at a -6-dB/octave rolloff. This is the first report on the microwave characteristics of an InAs-channel MODFET and establishes the superiority of this heterostructure system. Author

A92-44243* National Aeronautics and Space Administration. Lewis Research Center, Cleveland, OH.

NEW COPLANAR WAVEGUIDE TO RECTANGULAR WAVEGUIDE END LAUNCHER

R. N. SIMONS and S. R. TAUB (NASA, Lewis Research Center, Cleveland, OH) *Electronics Letters* (ISSN 0013-5194), vol. 28, no. 12, June 4, 1992, p. 1138, 1139. 4 Jun. 1992 2 p refs Copyright

A new coplanar waveguide to rectangular waveguide end launcher is experimentally demonstrated. The end launcher operates over the Ka-band frequencies that are designated for the NASA Advanced Communication Technology Satellite uplink. The measured insertion loss and return loss are better than 0.5 and -10 dB, respectively. Author

A92-45619* National Aeronautics and Space Administration. Lewis Research Center, Cleveland, OH.

NEW COPLANAR WAVEGUIDE FEED NETWORK FOR 2 X 2 LINEARLY TAPERED SLOT ANTENNA SUBARRAY

RAINEE N. SIMONS, THOMAS D. PERL, and RICHARD Q. LEE (NASA, Lewis Research Center, Cleveland, OH) *Microwave and Optical Technology Letters* (ISSN 0895-2477), vol. 5, no. 9, Aug. 1992, p. 420-423. Aug. 1992 4 p refs Copyright

A novel feed method is presently demonstrated for a 2 x 2 linearly tapered slot antenna (LTSA) on the basis of a coplanar-waveguide (CPW)-to-slotline transition and a coax-to-CPW in-phase, four-way power divider. The LTSA subarray exhibits excellent radiation patterns and return-loss characteristics at 18 GHz, and has symmetric beamwidth; its compactness renders it applicable as either a feed for a reflector antenna or as a building-block for large arrays. O.C.

A92-46007* National Aeronautics and Space Administration. Lewis Research Center, Cleveland, OH.

A MODEL FOR THE TRAP-ASSISTED TUNNELING MECHANISM IN DIFFUSED N-P AND IMPLANTED N(+)-P HgCdTe PHOTODIODES

DAVID ROSENFELD (NASA, Lewis Research Center, Cleveland, OH) and GAD BAHIR (Technion - Israel Institute of Technology, Haifa) *IEEE Transactions on Electron Devices* (ISSN 0018-9383), vol. 39, no. 7, July 1992, p. 1638-1645. Jul. 1992 8 p refs Copyright

This paper presents a theoretical model for the trap-assisted tunneling process in diffused n-on-p and implanted n(+)-on-p HgCdTe photodiodes. The model describes the connection between the leakage current associated with the traps and the

trap characteristics: concentration, energy level, and capture cross sections. It is observed that the above two types of diodes differ the voltage dependence of the trap-assisted tunneling current and dynamic resistance. The model takes this difference into account and offers an explanation of the phenomenon. The good fit between measured and calculated dc characteristics of the photodiodes supports the validity of the model. Author

A92-46080* National Aeronautics and Space Administration, Lewis Research Center, Cleveland, OH.

A THEORETICAL AND EXPERIMENTAL STUDY OF THE NOISE BEHAVIOR OF SUBHARMONICALLY INJECTION LOCKED LOCAL OSCILLATORS

XIANGDONG ZHANG, XUESONG ZHOU, and AFSHIN S. DARYOUSH (Drexel University, Philadelphia, PA) IEEE Transactions on Microwave Theory and Techniques (ISSN 0018-9480), vol. 40, no. 5, May 1992, p. 895-902. Research supported by NASA and General Electric Corp. May 1992 8 p refs

Copyright

A method for the noise characterization of optically controlled subharmonically injection-locked oscillators is presented. Based on a nonlinear model of synchronized oscillators, this method is used to formulate a general expression for phase noise calculation, so that FM noise degradation of a subharmonically synchronized LO at large-signal levels can be predicted easily and accurately. Experimental results of FM noise measurement of an oscillator confirmed the accuracy of the analysis. Author

A92-49596* National Aeronautics and Space Administration, Lewis Research Center, Cleveland, OH.

TEMPERATURE INDEPENDENT QUANTUM WELL FET WITH DELTA CHANNEL DOPING

P. G. YOUNG, R. A. MENA, S. A. ALTEROVITZ, S. E. SCHACHAM, and E. J. HAUGLAND (NASA, Lewis Research Center, Cleveland, OH) Electronics Letters (ISSN 0013-5194), vol. 28, no. 14, July 2, 1992, p. 1352-1354. 2 Jul. 1992 3 p refs

Copyright

A temperature independent device is presented which uses a quantum well structure and delta doping within the channel. The device requires a high delta doping concentration within the channel to achieve a constant Hall mobility and carrier concentration across the temperature range 300-1.4 K. Transistors were RF tested using on-wafer probing and a constant G_{sub} max and F_{sub} max were measured over the temperature range 300-70 K. Author

A92-50530* National Aeronautics and Space Administration, Lewis Research Center, Cleveland, OH.

LOAD FLOWS AND FAULTS CONSIDERING DC CURRENT INJECTIONS

G. L. KUSIC (Pittsburgh, University, PA) and R. F. BEACH (NASA, Lewis Research Center, Cleveland, OH) IN: IECEC '91; Proceedings of the 26th Intersociety Energy Conversion Engineering Conference, Boston, MA, Aug. 4-9, 1991. Vol. 1 1991 6 p refs

Copyright

The authors present novel methods for incorporating current injection sources into dc power flow computations and determining network fault currents when electronic devices limit fault currents. Combinations of current and voltage sources into a single network are considered in a general formulation. An example of relay coordination is presented. The present study is pertinent to the development of the Space Station Freedom electrical generation, transmission, and distribution system. I.E.

A92-50537* National Aeronautics and Space Administration, Lewis Research Center, Cleveland, OH.

A 1 MW, 100 KV, LESS THAN 100 KG SPACE BASED DC-DC POWER CONVERTER

J. R. COOPER and C. W. WHITE (Maxwell Laboratories, Inc., San Diego, CA) IN: IECEC '91; Proceedings of the 26th Intersociety Energy Conversion Engineering Conference, Boston,

MA, Aug. 4-9, 1991. Vol. 1 1991 6 p

(Contract NAS3-25800)

Copyright

A 1 MW dc-dc power converter has been designed which has an input voltage of 5 kV +/- 3 percent, an output voltage of 100 kV +/- 0.25 percent, and a run time of 1000 s at full power. The estimated system mass is 83.8 kg, giving a power density of 11.9 kW/kg. The system exceeded the weight goal of 10 kW/kg through the use of innovative components and system concepts. The system volume is approximately 0.1 cu m, and the overall system efficiency is estimated to be 87 percent. Some of the unique system features include a 50-kHz H-bridge inverter using MOS-controlled thyristors as the switching devices, a resonance transformer to step up the voltage, open-cycle cryogenic hydrogen gas cooling, and a nonrigid, inflatable housing which provides on-demand pressurization of the power converter local environment. This system scales very well to higher output powers. The weight of the 10-MW system with the same input and output voltage requirements and overall system configuration is estimated to be 575.3 kg. This gives a power density of 17.4 kW/kg, significantly higher than the 11.9 kW/kg estimated at 1 MW. I.E.

A92-50539* National Aeronautics and Space Administration, Lewis Research Center, Cleveland, OH.

ANALOG SYNTHESIZED FAST-VARIABLE LINEAR LOAD

JANIS M. NIEDRA (Sverdrup Technology, Inc.; NASA, Lewis Research Center, Cleveland, OH) IN: IECEC '91; Proceedings of the 26th Intersociety Energy Conversion Engineering Conference, Boston, MA, Aug. 4-9, 1991. Vol. 1 1991 5 p refs

(Contract NAS3-25266)

Copyright

A several-kilowatt power level, fast-variable linear resistor has been synthesized by using analog components to control the conductance of power MOSFETs. Risetimes observed have been as short as 500 ns with respect to the control signal and 1 to 2 microsec with respect to the power source voltage. A variant configuration of this load that dissipates a constant power set by a control signal is indicated. Replacement of the MOSFETs by static induction transistors to increase power handling, speed, and radiation hardness is discussed. I.E.

A92-50551* National Aeronautics and Space Administration, Lewis Research Center, Cleveland, OH.

COMPARISON OF HIGH TEMPERATURE, HIGH FREQUENCY CORE LOSS AND DYNAMIC B-H LOOPS OF TWO 50 NI-FE CRYSTALLINE ALLOYS AND AN IRON-BASED AMORPHOUS ALLOY

W. R. WIESERMAN (Pittsburgh, University, Johnstown, PA), G. E. SCHWARZE (NASA, Lewis Research Center, Cleveland, OH), and J. M. NIEDRA (Sverdrup Technology, Inc.; NASA, Lewis Research Center, Cleveland, OH) IN: IECEC '91; Proceedings of the 26th Intersociety Energy Conversion Engineering Conference, Boston, MA, Aug. 4-9, 1991. Vol. 1 1991 6 p refs

Copyright

The availability of experimental data that characterize the performance of soft magnetic materials for the combined conditions of high temperature and high frequency is almost nonexistent. An experimental investigation was conducted over the temperature range of 23 to 300 C and frequency range of 1 to 50 kHz to determine the effects of temperature and frequency on the core loss and dynamic B-H loops of three different soft magnetic materials: an oriented-grain 50Ni-50Fe alloy, a nonoriented-grain 50Ni-50Fe alloy, and an iron-based amorphous material (Metglas 2605SC). A comparison of these materials shows that the nonoriented-grain 50Ni-50Fe alloy tends to have either the lowest or the next lowest core loss for all temperatures and frequencies investigated. Author

A92-50558* National Aeronautics and Space Administration, Lewis Research Center, Cleveland, OH.

FUNCTIONAL MODELS OF POWER ELECTRONIC COMPONENTS FOR SYSTEM STUDIES

KWA-SUR TAM, LIFENG YANG (Virginia Polytechnic Institute and

State University, Blacksburg), and NARAYAN DRAVID (NASA, Lewis Research Center, Cleveland, OH) IN: IECEC '91; Proceedings of the 26th Intersociety Energy Conversion Engineering Conference, Boston, MA, Aug. 4-9, 1991. Vol. 1 1991 6 p refs
(Contract NAG3-1120)
Copyright

A novel approach to model power electronic circuits has been developed to facilitate simulation studies of system-level issues. The underlying concept for this approach is to develop an equivalent circuit, the functional model, that performs the same functions as the actual circuit but whose operation can be simulated by using larger time step size and the reduction in model complexity, the computation time required by a functional model is significantly shorter than that required by alternative approaches. The authors present this novel modeling approach and discuss the functional models of two major power electronic components, the DC/DC converter unit and the load converter, that are being considered by NASA for use in the Space Station Freedom electric power system. The validity of these models is established by comparing the simulation results with available experimental data and other simulation results obtained by using a more established modeling approach. The usefulness of this approach is demonstrated by incorporating these models into a power system model and simulating the system responses and interactions between components under various conditions. I.E.

A92-50580* National Aeronautics and Space Administration. Lewis Research Center, Cleveland, OH.
USING EPSAT TO ANALYZE HIGH POWER SYSTEMS IN THE SPACE ENVIRONMENT

ROBERT A. KUHARSKI, GARY A. JONGEWARD, KATHERINE G. WILCOX, TOM R. RANKIN (Maxwell Laboratories, Inc., S-Cubed Div., La Jolla, CA), and JAMES C. ROCHE (NASA, Lewis Research Center, Cleveland, OH) IN: IECEC '91; Proceedings of the 26th Intersociety Energy Conversion Engineering Conference, Boston, MA, Aug. 4-9, 1991. Vol. 1 1991 6 p refs
(Contract NAS3-25347)
Copyright

The authors review the Environment Power System Analysis Tool (EPSAT) design and demonstrate its capabilities by using it to address some questions that arose in designing the SPEAR III experiment. It is shown that the rocket body cannot be driven to large positive voltages under the constraints of this experiment. Hence, attempts to measure the effects of a highly positive rocket body in the plasma environment should not be made in this experiment. It is determined that a hollow cathode will need to draw only about 50 mA to ground the rocket body. It is shown that a relatively small amount of gas needs to be released to induce a bulk breakdown near the rocket body, and this gas release should not discharge the sphere. Therefore, the experiment provides an excellent opportunity to study the neutralization of a differential charge. I.E.

A92-50653 National Aeronautics and Space Administration. Lewis Research Center, Cleveland, OH.

RECENT PROGRESS IN INP SOLAR CELL RESEARCH
I. WEINBERG, D. J. BRINKER, R. K. JAIN, and C. K. SWARTZ (NASA, Lewis Research Center, Cleveland, OH) IN: IECEC '91; Proceedings of the 26th Intersociety Energy Conversion Engineering Conference, Boston, MA, Aug. 4-9, 1991. Vol. 2 1991 7 p refs
(Contract RTOP 506-41-11)
Copyright

Significant new developments in InP solar cell research are reviewed. Recent accomplishments include monolithic multibandgap two junction cells (three and two terminal) using InP as the top cell and lattice matched GaInAs and GaInAsP as the bottom, low bandgap, component. Concentrator cells include the three terminal multibandgap cell and an n + p cell using an InP substrate. The review also includes small scale production of ITO/InP cells and results for n+p InP and ITO/InP cells in space on board the LIPS 3 satellite. Author

A92-50658* National Aeronautics and Space Administration. Lewis Research Center, Cleveland, OH.

DEVELOPMENT AND TESTING OF A 180-VOLT DC ELECTRONIC CIRCUIT BREAKER WITH A 335-AMPERE CARRY AND 1200-AMPERE INTERRUPT RATING

A. S. BRUSH (Sverdrup Technology, Inc., Brook Park; NASA, Lewis Research Center, Cleveland, OH) and R. L. PHILLIPS (Rockwell International Corp., Rocketdyne Div., Canoga Park, CA) IN: IECEC '91; Proceedings of the 26th Intersociety Energy Conversion Engineering Conference, Boston, MA, Aug. 4-9, 1991. Vol. 2 1991 6 p refs
(Contract NAS3-25266; NAS3-25711)
Copyright

NASA Lewis Research Center and associated contractors have conducted a program to assess the potential requirements for a high-current switch to conceptually design a switch using the best existing technology, and to build and demonstrate a breadboard which meets the requirements. The result is the high current remote bus isolator (HRBI). The HRBI is rated at 180 V dc, 335 A continuous with a 1200 A interrupt rating. It also incorporates remote-control and protective features called for by the Space Station Freedom PMAD dc test bed design. Two breadboard 335 A circuit breakers were built and tested that demonstrate a promising concept of paralleled current-limiting modules. The units incorporated all control and protective features required by advanced aerospace power systems. Component stresses in each unit were determined by design, and are consistent with a life of many thousands of fault operations. I.E.

A92-50662 National Aeronautics and Space Administration. Lewis Research Center, Cleveland, OH.

TEST AND EVALUATION OF LOAD CONVERTER TOPOLOGIES USED IN THE SPACE STATION FREEDOM POWER MANAGEMENT AND DISTRIBUTION DC TEST BED

RAMON C. LEBRON, ANGELA C. OLIVER (NASA, Lewis Research Center, Cleveland, OH), and ROBERT F. BODI (Analytical Engineering Corp., North Olmsted, OH) IN: IECEC '91; Proceedings of the 26th Intersociety Energy Conversion Engineering Conference, Boston, MA, Aug. 4-9, 1991. Vol. 2 1991 6 p refs
(Contract RTOP 474-42-10)
Copyright

Power components hardware in support of the Space Station freedom dc Electric Power System were tested. One type of breadboard hardware tested is the dc Load Converter Unit, which constitutes the power interface between the electric power system and the actual load. These units are dc to dc converters that provide the final system regulation before power is delivered to the load. Three load converters were tested: a series resonant converter, a series inductor switch-mode converter, and a switching full-bridge forward converter. The topology, operation principles, and test results are described, in general. A comparative analysis of the three units is given with respect to efficiency, regulation, short circuit behavior (protection), and transient characteristics. Author

A92-51042* National Aeronautics and Space Administration. Lewis Research Center, Cleveland, OH.

CONDUCTOR-BACKED COPLANAR WAVEGUIDE RESONATORS OF YBa2Cu3O(7-DELTA) ON LAAlO3

FELIX A. MIRANDA, KUL B. BHASIN (NASA, Lewis Research Center, Cleveland, OH), KEON-SHIK KONG (Texas, University, Austin), TATSUO ITOH (California, University, Los Angeles), and MARK A. STAN (Kent State University, OH) IEEE Microwave and Guided Wave Letters (ISSN 1051-8207), vol. 2, no. 7, July 1992, p. 287, 288. Jul. 1992 2 p refs
Copyright

Conductor-backed coplanar waveguide (CBCPW) resonators operating at 10.8 GHz have been fabricated from laser ablated and off-axis magnetron sputtered YBa2Cu3O(7-delta) (YBCO) high-temperature superconducting (HTS) thin films on LaAlO3. These resonators were tested in the temperature range from 14 to 92 K. The unloaded quality factor at 77 K of the HTS CBCPW

resonators was 3 to 4 times that of a similar gold resonator. To the authors' knowledge, these results represent the first reported measurements of HTS-based CBCPW resonators. Author

A92-52423* National Aeronautics and Space Administration. Lewis Research Center, Cleveland, OH.

MUTUAL COUPLING BETWEEN RECTANGULAR MICROSTRIP PATCH ANTENNAS

TAN HUYNH (Decibel Products, Dallas, TX), KAI-FONG LEE, SIVA R. CHEBOLU (Toledo, University, OH), and R. Q. LEE (NASA, Lewis Research Center, Cleveland, OH) Microwave and Optical Technology Letters (ISSN 0895-2477), vol. 5, no. 11, Oct. 1992, p. 572-576. Research supported by Ohio Supercomputer Center. Oct. 1992 5 p refs

Copyright

The paper presents a comprehensive study of the mutual coupling between two rectangular microstrip patch antennas. The cavity model is employed to give numerical results for both mutual impedance and mutual coupling parameters for the E-plane, H-plane, diagonal, and perpendicular orientations. The effects of substrate thickness, substrate permittivity, and feed positions are discussed.

C.A.B.

A92-53157* National Aeronautics and Space Administration. Lewis Research Center, Cleveland, OH.

MOLECULAR DYNAMICS INVESTIGATION OF RADIATION DAMAGE IN SEMICONDUCTORS

BRIAN S. GOOD (NASA, Lewis Research Center, Cleveland, OH) IN: IEEE Photovoltaic Specialists Conference, 22nd, Las Vegas, NV, Oct. 7-11, 1991, Conference Record. Vol. 1 1991 6 p refs

Results of a molecular dynamics investigation of the effects of radiation damage on the crystallographic structure of semiconductors are reported. Particular consideration is given to the formation of point defects and small defect complexes in silicon at the end of a radiation-damage cascade. The calculations described make use of the equivalent crystal theory of Smith and Banerjee (1988). Results on the existence of an atomic displacement threshold, the defect formation energy, and some crystallographic information on the defects observed are reported.

I.E.

A92-53192* National Aeronautics and Space Administration. Lewis Research Center, Cleveland, OH.

RADIATION AND TEMPERATURE EFFECTS IN HETEROEPITAXIAL AND HOMOEPITAXIAL INP CELLS

I. WEINBERG, H. B. CURTIS, C. K. SWARTZ, D. J. BRINKER (NASA, Lewis Research Center, Cleveland, OH), P. P. JENKINS, and M. FAUR (Cleveland State University, OH) IN: IEEE Photovoltaic Specialists Conference, 22nd, Las Vegas, NV, Oct. 7-11, 1991, Conference Record. Vol. 2 1991 7 p refs

Copyright

Heteroepitaxial (InP/GaAs) and homo-epitaxial (InP/InP) cells were irradiated by 1-MeV electrons and their performance, temperature dependencies and carrier removal rates determined. The radiation resistances of the InP/GaAs cells were significantly higher than that of the InP/InP cells. This was attributed to the high dislocation density present in the heteroepitaxial cells. In addition, the effects of dislocations in these latter cells were dominant in determining the temperature dependence of open-circuit voltage.

I.E.

A92-53193 National Aeronautics and Space Administration. Lewis Research Center, Cleveland, OH.

RADIATION PERFORMANCE OF GAAS CONCENTRATOR CELLS FOR 0.4 TO 12 MEV ELECTRONS AND 0.1 TO 37 MEV PROTONS

HENRY B. CURTIS (NASA, Lewis Research Center, Cleveland, OH) and BRUCE ANSPAUGH (JPL, Pasadena, CA) IN: IEEE Photovoltaic Specialists Conference, 22nd, Las Vegas, NV, Oct. 7-11, 1991, Conference Record. Vol. 2 1991 5 p refs

Copyright

Gallium arsenide concentrator cells have been irradiated with

both electrons and protons with a wide variety of energies. The cells are made using OM-VPE growth process with a junction depth of a half micron. All data are taken with bare cells without coverglasses or shielding. Performance data are given at the designed concentration level of 100X AMO. Results are presented in a number of ways, including performance of electrical parameters (Pmax, Isc, and Voc) as a function of fluence for different electron and proton energies. Critical fluences (defined at a degradation of 25 percent in Pmax) are calculated for each energy level and presented for both electron and proton irradiations. I.E.

A92-55785* National Aeronautics and Space Administration. Lewis Research Center, Cleveland, OH.

KA-BAND MMIC ARRAYS FOR ACTS AERO TERMINAL EXPERIMENT

C. RAQUET, R. ZAKRAJSEK, R. LEE (NASA, Lewis Research Center, Cleveland, OH), and J. TURTLE (USAF, Rome Laboratory, Hanscom AFB, MA) IAF, International Astronautical Congress, 43rd, Washington, Aug. 28-Sept. 5, 1992. 9 p. Aug. 1992 9 p refs

(IAF PAPER 92-0398) Copyright

An antenna system consisting of three experimental Ka-band active arrays using GaAs MMIC devices at each radiating element for electronic beam steering and distributed power amplification is presented. The MMIC arrays are to be demonstrated in the ACTS Aeronautical Terminal Experiment, planned for early 1994. The experiment is outlined, with emphasis on a description of the antenna system. Attention is given to the way in which proof-of-concept MMIC arrays featuring three different state-of-the-art approaches to Ka-band MMIC insertion are being incorporated into an experimental aircraft terminal for the demonstration of an aircraft-to-satellite link, providing a basis for follow-on MMIC array development.

P.D.

N92-11252*# National Aeronautics and Space Administration. Lewis Research Center, Cleveland, OH.

THE 23 TO 300 C DEMAGNETIZATION RESISTANCE OF SAMARIUM-COBALT PERMANENT MAGNETS

JANIS M. NIEDRA (Sverdrup Technology, Inc., Brook Park, OH.) and ERIC OVERTON Washington Nov. 1991 11 p (Contract RTOP 590-13-11)

(NASA-TP-3119; E-6123; NAS 1.60:3119) Avail: CASI HC A03/MF A01

The influence of temperature on knee point and squareness of the M-H demagnetization characteristic of permanent magnets is important information for the full utilization of the capabilities of samarium-cobalt magnets at high temperature in demagnetization resistant permanent magnet devices. Composite plots of the knee field and the demagnetizing field required to produce a given magnetic induction swing below remanence were obtained for several commercial Sm₂Co₁₇ type magnet samples in the temperature range of 23 to 300 C. Using the knee point to define the limits of operation safe against irreversible demagnetization, such plots are shown to provide an effective overview of the useable regions in the space of temperature-induction swing parameters. The observed second quadrant M-H characteristic squareness is shown, by two measures, to increase gradually with temperature, reaching a peak in the interval 200 to 300 C.

Author

N92-14294*# National Aeronautics and Space Administration. Lewis Research Center, Cleveland, OH.

MULTI-MEGAWATT INVERTER/CONVERTER TECHNOLOGY FOR SPACE POWER APPLICATIONS

IRA T. MYERS (Schafer (W. J.) Associates, Inc., Arlington, VA.), ERIC D. BAUMANN, ROBERT KRAUS, and AHMAD N. HAMMOUD (Sverdrup Technology, Inc., Brook Park, OH.) 1992 11 p Proposed for presentation at the Ninth Symposium on Space Nuclear Power Systems, Albuquerque, NM, 12-16 Jan. 1992; sponsored by the Institute for Space Nuclear Power Studies (Contract NAS3-25266; RTOP 506-41-41)

(NASA-TM-105307; E-6543; NAS 1.15:105307) Avail: CASI HC A03/MF A01

Large power conditioning mass reductions will be required to enable megawatt power systems envisioned by the Strategic Defense Initiative, the Air Force, and NASA. Phase 1 of a proposed two phase interagency program has been completed to develop an 0.1 kg/kW DC/DC converter technology base for these future space applications. Three contractors, Hughes, General Electric (GE), and Maxwell were Phase 1 contractors in a competitive program to develop a megawatt lightweight DC/DC converter. Researchers at NASA Lewis Research Center and the University of Wisconsin also investigated technology in topology and control. All three contractors, as well as the University of Wisconsin, concluded at the end of the Phase 1 study, which included some critical laboratory work, that 0.1-kg/kW megawatt DC/DC converters can be built. This is an order of magnitude lower specific weight than is presently available. A brief description of each of the concepts used to meet the ambitious goals of this program are presented. Author

N92-18473*# National Aeronautics and Space Administration. Lewis Research Center, Cleveland, OH.

PLANAR DIELECTRIC RESONATOR STABILIZED HEMT OSCILLATOR INTEGRATED WITH CPW/APERTURE COUPLED PATCH ANTENNA

RAINEE N. SIMONS (Sverdrup Technology, Inc., Brook Park, OH.) and RICHARD Q. LEE 1992 6 p Proposed for presentation at the 1992 IEEE MTT-S International Microwave Symposium, Albuquerque, NM, 2-4 Jun. 1992 (Contract NAS3-25266; RTOP 506-44-2C) (NASA-TM-105544; E-6860; NAS 1.15:105544) Avail: CASI HC A02/MF A01

A new design of an active antenna with a dielectric resonator stabilized high electron mobility transistor (HEMT) oscillator (DRO) and an aperture-coupled patch antenna is reported. The circuit is fabricated using coplanar waveguide (CPW) with the oscillator and the antenna on opposite sides of the substrate. The active antenna was demonstrated at 7.6 GHz; however, the design can be scaled to higher frequencies. Excellent oscillator characteristics and radiation patterns were obtained. Author

N92-18920*# National Aeronautics and Space Administration. Lewis Research Center, Cleveland, OH.

STATUS AND FUTURE DIRECTIONS OF INP SOLAR CELL RESEARCH

R. K. JAIN and I. WEINBERG 1992 8 p Presented at the 6th International Photovoltaic Science and Engineering Conference, New Delhi, India, 10-14 Feb. 1992; sponsored by Dept. of Non-Conventional Energy Sources, Government of India, Solar Energy Society of India, and Nat'l. Physical Lab. (Contract RTOP 506-41-11) (NASA-TM-105426; E-6738; NAS 1.15:105426) Avail: CASI HC A02/MF A01

An overview of the current status and future directions of InP space solar cell research is provided. The scope of the paper does not allow us to discuss other recent major developments in InP cell modeling, contacts, and characterization, or developments in other solar cell materials. Solar cells made from InP and related materials are not expected to be used in the near future for terrestrial applications, but significant Air-Mass1.5 (AM1.5) cell efficiencies are given for comparison. This paper deals with the developments in single-junction cells, multijunction tandem cells, and space flight testing, including radiation effects. Concentrator InP solar cells are also discussed, since they offer the possibility of simultaneous thermal and current injection annealing. These cells also promise cost effectiveness and the concentrator elements may provide cells with extra protection from space radiation. The concluding section addresses the steps to be taken in the future and provides guidelines for further research and development. Author

N92-20040*# National Aeronautics and Space Administration. Lewis Research Center, Cleveland, OH.

ELECTRICAL PROPERTIES OF TEFLON AND CERAMIC CAPACITORS AT HIGH TEMPERATURES

A. N. HAMMOUD (Sverdrup Technology, Inc., Brook Park, OH.), E. D. BAUMANN, I. T. MYERS, and E. OVERTON 1992 6 p Proposed for presentation at the 1992 International Symposium on Electrical Insulation, Baltimore, MD, 7-9 Jun. 1992; sponsored by IEEE Dielectrics and Electrical Insulation Society (Contract RTOP 506-41-41) (NASA-TM-105569; E-6894; NAS 1.15:105569) Avail: CASI HC A02/MF A01

Space power systems and components are often required to operate efficiently and reliably in harsh environments where stresses, such as high temperature, are encountered. These systems must, therefore, withstand exposure to high temperature while still providing good electrical and other functional properties. Experiments were carried out to evaluate Teflon and ceramic capacitors for potential use in high temperature applications. The capacitors were characterized in terms of their capacitance and dielectric loss as a function of temperature, up to 200 C. At a given temperature, these properties were obtained in a frequency range of 50 Hz to 100 kHz. DC leakage current measurements were also performed in a temperature range from 25 to 200 C. The results obtained are discussed and conclusions are made concerning the suitability of the capacitors studied for high temperature applications. Author

N92-21370*# National Aeronautics and Space Administration. Lewis Research Center, Cleveland, OH.

PERFORMANCE OF A Y-BA-CU-O SUPERCONDUCTING FILTER/GAAS LOW NOISE AMPLIFIER HYBRID CIRCUIT

K. B. BHASIN (Sverdrup Technology, Inc., Brook Park, OH.), S. S. TONCICH (Communications Satellite Corp., Clarksburg, MD.), C. M. CHOREY, R. R. BONETTI, and A. E. WILLIAMS (Communications Satellite Corp., Clarksburg, MD.) 1992 5 p Proposed for presentation at the 1992 IEEE MTT-S International Microwave Symposium, Albuquerque, NM, 2-4 Jun. 1992 (Contract NAS3-25266; RTOP 506-72-1B) (NASA-TM-105546; E-6869; NAS 1.26:105546) Avail: CASI HC A01/MF A01

A superconducting 7.3 GHz two-pole microstrip bandpass filter and a GaAs low noise amplifier (LNA) were combined into an active circuit and characterized at liquid nitrogen temperatures. This superconducting/semiconducting circuit's performance was compared to a gold filter/GaAs LNA hybrid circuit. The superconducting filter/GaAs LNA hybrid circuit showed higher gain and lower noise figure than its gold counterpart. Author

N92-22453*# National Aeronautics and Space Administration. Lewis Research Center, Cleveland, OH.

A VIDEO EVENT TRIGGER FOR HIGH FRAME RATE, HIGH RESOLUTION VIDEO TECHNOLOGY

GLENN L. WILLIAMS In NASA, Washington, Technology 2001: The Second National Technology Transfer Conference and Exposition, Volume 1 p 254-260 Dec. 1991 Avail: CASI HC A02/MF A04

When video replaces film the digitized video data accumulates very rapidly, leading to a difficult and costly data storage problem. One solution exists for cases when the video images represent continuously repetitive 'static scenes' containing negligible activity, occasionally interrupted by short events of interest. Minutes or hours of redundant video frames can be ignored, and not stored, until activity begins. A new, highly parallel digital state machine generates a digital trigger signal at the onset of a video event. High capacity random access memory storage coupled with newly available fuzzy logic devices permits the monitoring of a video image stream for long term or short term changes caused by spatial translation, dilation, appearance, disappearance, or color change in a video object. Pretrigger and post-trigger storage techniques are then adaptable for archiving the digital stream from only the significant video images. Author

N92-22528*# National Aeronautics and Space Administration. Lewis Research Center, Cleveland, OH.

HIGH-TEMPERATURE ELECTRONICS

LAWRENCE G. MATUS and GARY T. SENG *In its* Aeropropulsion
1987 p 233-241 Feb. 1990
Avail: CASI HC A02/MF A04

To meet the needs of the aerospace propulsion and space power communities, the high temperature electronics program at the Lewis Research Center is developing silicon carbide (SiC) as a high temperature semiconductor material. This program supports a major element of the Center's mission - to perform basic and developmental research aimed at improving aerospace propulsion systems. Research is focused on developing the crystal growth, characterization, and device fabrication technologies necessary to produce a family of SiC devices. Author

N92-23193*# National Aeronautics and Space Administration.
Lewis Research Center, Cleveland, OH.

A FLEXIBLE CPW PACKAGE FOR A 30 GHZ MMIC AMPLIFIER

RAINEE N. SIMONS (Sverdrup Technology, Inc., Brook Park, OH.) and SUSAN R. TAUB 1992 6 p Presented at the Topical Meeting on Electrical Performance of Electronic Packaging, Tucson, AZ, 22-24 Apr. 1992; sponsored by IEEE, MTT, and CHMT (Contract NAS3-25266; RTOP 506-44-2C) (NASA-TM-105630; E-6973; NAS 1.15:105630) Avail: CASI HC A02/MF A01

A novel package, which consists of a carrier housing, has been developed for monolithic-millimeter wave Integrated Circuit amplifiers which operate at 30 giga-Hz. The carrier has coplanar waveguide (CPW) interconnects and provides heat-sinking, tuning, and cascading capabilities. The housing provides electrical isolation, mechanical protection and a feed-thru for biasing. Author

Author

N92-23535*# National Aeronautics and Space Administration.
Lewis Research Center, Cleveland, OH.

NONPLANAR LINEARLY TAPERED SLOT ANTENNA WITH BALANCED MICROSTRIP FEED

RAINEE N. SIMONS (Sverdrup Technology, Inc., Brook Park, OH.), RICHARD Q. LEE, and THOMAS D. PERL (Akron Univ., OH.) 1992 6 p Proposed for presentation at the IEEE-APS International Symposium, Chicago, IL, 18-25 Jul. 1992 (Contract NAS3-25266; RTOP 506-44-2C) (NASA-TM-105647; E-6754; NAS 1.15:105647) Avail: CASI HC A02/MF A01

A nonplanar linearly tapered slot antenna (LTSA) has been fabricated and tested at frequencies from 8 to 32 giga-Hz. The LTSA is excited by a broadband balanced microstrip transformer. The measured results include the input term return loss as well as the radiation pattern of the antenna. Author

Author

N92-23561*# National Aeronautics and Space Administration.
Lewis Research Center, Cleveland, OH.

EVALUATION OF HIGH TEMPERATURE CAPACITOR DIELECTRICS

AHMAD N. HAMMOUD (Sverdrup Technology, Inc., Brook Park, OH.) and IRA T. MYERS 1992 8 p Presented at the Conference on Electrical Insulation and Dielectric Phenomena, Leesburg, VA, 29 Oct. - 2 Nov. 1989; sponsored by IEEE (Contract RTOP 506-41-41) (NASA-TM-105622; E-6960; NAS 1.15:105622) Avail: CASI HC A02/MF A01

Experiments were carried out to evaluate four candidate materials for high temperature capacitor dielectric applications. The materials investigated were polybenzimidazole polymer and three aramid papers: Voltex 450, Nomex 410, and Nomex M 418, an aramid paper containing 50 percent mica. The samples were heat treated for six hours at 60 C and the direct current and 60 Hz alternating current breakdown voltages of both dry and impregnated samples were obtained in a temperature range of 20 to 250 C. The samples were also characterized in terms of their dielectric constant, dielectric loss, and conductivity over this temperature range with an electrical stress of 60 Hz, 50 V/mil present. Additional measurements are underway to determine the volume resistivity, thermal shrinkage, and weight loss of the materials. Preliminary

data indicate that the heat treatment of the films slightly improves the dielectric properties with no influence on their breakdown behavior. Impregnation of the samples leads to significant increases in both alternating and direct current breakdown strength. The results are discussed and conclusions made concerning their suitability as high temperature capacitor dielectrics. Author

Author

N92-23562*# National Aeronautics and Space Administration.
Lewis Research Center, Cleveland, OH.

DEFECT BEHAVIOR, CARRIER REMOVAL AND PREDICTED IN-SPACE INJECTION ANNEALING OF INP SOLAR CELLS

I. WEINBERG, C. K. SWARTZ, and P. J. DREVINSKY (Phillips Lab., Hanscom AFB, MA.) 1992 6 p Presented at the Fourth International Conference on Indium Phosphide and Related Materials, Newport, RI, 20-24 Apr. 1992; sponsored by IEE and LEOS

(Contract RTOP 506-41-11)

(NASA-TM-105624; E-6963; NAS 1.15:105624) Avail: CASI HC A02/MF A01

Defect behavior, observed by deep level transient spectroscopy (DLTS), is used to predict carrier removal and the effects of simultaneous electron irradiation and injection annealing of the performance of InP solar cells. For carrier removal, the number of holes trapped per defect is obtained from measurements of both carrier concentrations and defect concentrations during an isochronal anneal. In addition, from kinetic considerations, the behavior of the dominant defect during injection annealing is used to estimate the degradation expected from exposure to the ambient electron environment in geostationary orbit. Author

Author

N92-25176*# National Aeronautics and Space Administration.
Lewis Research Center, Cleveland, OH.

EFFECT OF INALAS WINDOW LAYER ON EFFICIENCY OF INDIUM PHOSPHIDE SOLAR CELLS

RAJ K. JAIN and GEOFFREY A. LANDIS (Sverdrup Technology, Inc., Brook Park, OH.) 1992 8 p Presented at the 22d Photovoltaic Specialists Conference, Las Vegas, NV, 7-11 Oct. 1991; sponsored by IEEE

(Contract RTOP 506-41-11)

(NASA-TM-105354; E-6728; NAS 1.15:105354) Avail: CASI HC A02/MF A01

Indium phosphide (InP) solar cell efficiencies are limited by surface recombination. The effect of a wide bandgap, lattice-matched indium aluminum arsenide (In_{0.52}Al_{0.48}As) window layer on the performance of InP solar cells was investigated by using the numerical code PC-1D. The p(+)-n InP solar cell performance improved significantly with the use of the window layer. No improvement was seen for the n(+)-p InP cells. The cell results were explained by the band diagram of the heterostructure and the conduction band energy discontinuity. The calculated current voltage and internal quantum efficiency results clearly demonstrated that In_{0.52}Al_{0.48}As is a very promising candidate for a window layer material for p(+)-n InP solar cells. Author

Author

N92-26096*# National Aeronautics and Space Administration.
Lewis Research Center, Cleveland, OH.

A 1-W, 30-GHZ, CPW AMPLIFIER FOR ACTS SMALL TERMINAL UPLINK

SUSAN R. TAUB and RAINEE N. SIMONS (Sverdrup Technology, Inc., Brook Park, OH.) 1992 6 p Presented at the Monolithic Microwave Integrated Circuit Space and Ground Applications Symposium, Pasadena, CA, 28-29 Apr. 1992; sponsored by JPL (Contract NAS3-25266; RTOP 506-72-1E) (NASA-TM-105671; E-7037; NAS 1.15:105671) Avail: CASI HC A02/MF A01

The progress is described of the development of a 1 W, 30 GHz, coplanar waveguide (CPW) amplifier for the Advanced Communication Technology Satellite (ACTS) Small Terminal Uplink. The amplifier is based on Texas Instruments' monolithic microwave integrated circuit (MMIC) amplifiers; a three stage, low power amplifier, and a single stage, high power amplifier. The amplifiers have a power output of 190 mW and 0.710 W, gain of 23 and 4.2 dB, and efficiencies of 30.2 and 24 percent for the three stage

and one stage amplifiers, respectively. The chips are to be combined via a CPW power divider/combiner circuit to yield the desired 1 W of output power. Author

N92-28432*# National Aeronautics and Space Administration. Lewis Research Center, Cleveland, OH.

NEUTRON, GAMMA RAY, AND TEMPERATURE EFFECTS ON THE ELECTRICAL CHARACTERISTICS OF THYRISTORS

A. J. FRASCA (Wittenberg Univ., Springfield, OH.) and G. E. SCHWARZE 1992 9 p Proposed for presentation at the 27th Intersociety Energy Conversion Engineering Conference, San Diego, CA, 3-7 Aug. 1992; sponsored by SAE, ACS, AIAA, ASME, IEEE, AIChE, and ANS

(Contract RTOP 590-13-31)
(NASA-TM-105728; E-7131; NAS 1.15:105728) Avail: CASI HC A02/MF A01

Experimental data showing the effects of neutrons, gamma rays, and temperature on the electrical and switching characteristics of phase-control and inverter-type SCR's are presented. The special test fixture built for mounting, heating, and instrumenting the test devices is described. Four SCR's were neutron irradiated at 300 K and four at 365 K for fluences up to 3.2×10^{13} n/sq. cm, and eight were gamma irradiated at 300 K only for gamma doses up to 5.1 Mrads. The electrical measurements were made during irradiation and the switching measurements were made only before and after irradiation. Radiation induced crystal defects, resulting primarily from fast neutrons, caused the reduction of minority carrier lifetime through the generation of R-G centers. The reduction in lifetime caused increases in the on-state voltage drop and in the reverse and forward leakage currents, and decreases in the turn-off time. Author

N92-28675*# National Aeronautics and Space Administration. Lewis Research Center, Cleveland, OH.

HIGH TEMPERATURE DIELECTRIC PROPERTIES OF APICAL, KAPTON, PEEK, TEFLON AF, AND UPILEX POLYMERS

A. N. HAMMOUD (Sverdrup Technology, Inc., Brook Park, OH.), E. D. BAUMANN (State Univ. of New York, Buffalo.), E. OVERTON (State Univ. of New York, Buffalo.), I. T. MYERS, J. L. SUTHAR (State Univ. of New York, Buffalo.), W. KHACHEN (State Univ. of New York, Buffalo.), and J. R. LAGHARI (State Univ. of New York, Buffalo.) 1992 8 p Prepared for presentation at the 1992 Conference on Electrical Insulation and Dielectric Phenomena, Victoria, British Columbia, 18-21 Oct. 1992; sponsored by IEEE

(Contract RTOP 506-41-41)
(NASA-TM-105753; E-7161; NAS 1.15:105753) Avail: CASI HC A02/MF A01

Reliable lightweight systems capable of providing electrical power at the megawatt level are a requirement for future manned space exploration missions. This can be achieved by the development of high temperature insulating materials which are not only capable of surviving the hostile space environment but can contribute to reducing the mass and weight of the heat rejection system. In this work, Apical, Uplex, Kapton, Teflon AF, and Peek polymers are characterized for AC and DC dielectric breakdown in air and in silicone oil at temperatures up to 250 C. The materials are also tested in terms of their dielectric constant and dissipation factor at high temperatures with an electrical stress of 60 Hz, 200 V/mil present. The effects of thermal aging on the properties of the films are determined after 15 hours of exposure to 200 and 250 C, each. The results obtained are discussed and conclusions are made concerning the suitability of these dielectrics for use in capacitors and cable insulations in high temperature environments. Author

N92-30397*# National Aeronautics and Space Administration. Lewis Research Center, Cleveland, OH.

COMPARISON OF HIGH TEMPERATURE, HIGH FREQUENCY CORE LOSS AND DYNAMIC B-H LOOPS OF A 2V-49FE-49CO AND A GRAIN ORIENTED 3SI-FE ALLOY

W. R. WIESERMAN (Pittsburgh Univ., Johnstown, PA.), G. E. SCHWARZE, and J. M. NIEDRA (Sverdrup Technology, Inc.,

Cleveland, OH.) Aug. 1992 9 p Presented at the 27th Intersociety Energy Conversion Engineering Conference, San Diego, CA, 3-7 Aug. 1992; sponsored by SAE, ACS, AIAA, ASME, IEEE, AIChE, and ANS

(Contract RTOP 590-13-31)
(NASA-TM-105791; E-7221; NAS 1.15:105791) Avail: CASI HC A02/MF A01

The design of power magnetic components such as transformers, inductors, motors, and generators, requires specific knowledge about the magnetic and electrical characteristics of the magnetic materials used in these components. Limited experimental data exists that characterizes the performance of soft magnetic materials for the combined conditions of high temperature and high frequency over a wide flux density range. An experimental investigation of a 2V-49-Fe-49Co (Supermendur) and a grain oriented 3 Si-Fe (Magnesil) alloy was conducted over the temperature range of 23 to 300 C and frequency range of 0.1 to 10 kHz. The effects of temperature, frequency, and maximum flux density on the core loss and dynamic B-H loops for sinusoidal voltage excitation conditions are examined for each of these materials. A comparison of the core loss of these two materials is also made over the temperature and frequency range investigated. Author

N92-30427*# National Aeronautics and Space Administration. Lewis Research Center, Cleveland, OH.

WIRING FOR AEROSPACE APPLICATIONS

J. L. CHRISTIAN, JR., J. E. DICKMAN, R. W. BERCAW, I. T. MYERS, A. N. HAMMOUD (Sverdrup Technology, Inc., Brook Park, OH.), M. STAVNES (Sverdrup Technology, Inc., Brook Park, OH.), and J. EVANS (National Aeronautics and Space Administration, Washington, DC.) Jul. 1992 9 p Presented at the 1992 Power Electronics Specialist Conference, Toledo (Spain), 29 Jun. - 3 Jul. 1992; sponsored by IEEE

(Contract RTOP 323-57-4A)
(NASA-TM-105777; E-7204; NAS 1.15:105777) Avail: CASI HC A02/MF A01

In this paper, the authors summarize the current state of knowledge of arc propagation in aerospace power wiring and efforts by the National Aeronautics and Space Administration (NASA) towards the understanding of the arc tracking phenomena in space environments. Recommendations will be made for additional testing. A database of the performance of commonly used insulating materials will be developed to support the design of advanced high power missions, such as Space Station Freedom and Lunar/Mars Exploration. Author

N92-31282*# National Aeronautics and Space Administration. Lewis Research Center, Cleveland, OH.

STABILITY TESTING AND ANALYSIS OF A PMAD DC TEST BED FOR THE SPACE STATION FREEDOM

ROBERT M. BUTTON and ANDREW S. BRUSH (Sverdrup Technology, Inc., Brook Park, OH.) Aug. 1992 8 p Presented at the 27th Intersociety Energy Conversion Engineering Conference, San Diego, CA, 3-7 Aug. 1992; sponsored by ANS, SAE, ACS, AIAA, ASME, and IEEE

(Contract RTOP 474-42-10)
(NASA-TM-105846; E-7289; NAS 1.15:105846) Avail: CASI HC A02/MF A01

The Power Management and Distribution (PMAD) DC Test Bed at the NASA Lewis Research Center is introduced. Its usefulness to the Space Station Freedom Electrical Power (EPS) development and design are discussed in context of verifying system stability. Stability criteria developed by Middlebrook and Cuk are discussed as they apply to constant power DC to DC converters exhibiting negative input impedance at low frequencies. The utility-type Secondary Subsystem is presented and each component is described. The instrumentation used to measure input and output impedance under load is defined. Test results obtained from input and output impedance measurements of test bed components are presented. It is shown that the PMAD DC Test Bed Secondary Subsystem meets the Middlebrook stability criterion for certain loading conditions. Author

N92-32233*# National Aeronautics and Space Administration.
Lewis Research Center, Cleveland, OH.

MONOLITHIC AND MECHANICAL MULTI-JUNCTION SPACE SOLAR CELLS

RAJ K. JAIN and DENNIS J. FLOOD Aug. 1992 13 p
(Contract RTOP 506-41-11)
(NASA-TM-105832; E-7009-1; NAS 1.15:105832) Avail: CASI
HC A03/MF A01

High-efficiency, lightweight, radiation-resistant solar cells are essential to meet the large power requirements of future space missions. Single-junction cells are limited in efficiency. Higher cell efficiencies could be realized by developing multijunction, multibandgap solar cells. Monolithic and mechanically stacked tandem solar cells surpassing single-junction cell efficiencies have been fabricated. This article surveys the current status of monolithic and mechanically stacked multibandgap space solar cells, and outlines problems yet to be resolved. The monolithic and mechanically stacked cells each have their own problems related to size, processing, current and voltage matching, weight, and other factors. More information is needed on the effect of temperature and radiation on the cell performance. Proper reference cells and full-spectrum range simulators are also needed to measure efficiencies correctly. Cost issues are not addressed, since the two approaches are still in the developmental stage.

Author

N92-32243*# National Aeronautics and Space Administration.
Lewis Research Center, Cleveland, OH.

SOLAR RADIATION ON A CATENARY COLLECTOR

M. CRUTCHIK (Tel-Aviv Univ., Israel) and J. APPELBAUM Jul. 1992 32 p

(Contract NAGW-2022; RTOP 506-41-11)
(NASA-TM-105751; E-7156; NAS 1.15:105751) Avail: CASI HC
A03/MF A01

A tent-shaped structure with a flexible photovoltaic blanket acting as a catenary collector is presented. The shadow cast by one side of the collector produces a shadow on the other side of the collector. This self-shading effect is analyzed. The direct beam, the diffuse, and the albedo radiation on the collector are determined. An example is given for the insolation on the collector operating on Viking Lander 1 (VL1).

Author

N92-32867*# National Aeronautics and Space Administration.
Lewis Research Center, Cleveland, OH.

OVERVIEW AND EVOLUTION OF THE LERC PMAD DC TESTBED

JAMES F. SOEDER and ROBERT J. FRYE Aug. 1992 10 p
Presented at the 27th Intersociety Energy Conversion Engineering Conference, San Diego, CA, 3-7 Aug. 1992; sponsored by ANS, SAE, ACS, AIAA, ASME, and IEEE
(Contract RTOP 474-42-10)

(NASA-TM-105842; E-7285; NAS 1.15:105842) Avail: CASI HC
A02/MF A01

Since the beginning of the Space Station Freedom Program (SSFP), the Lewis Research Center (LeRC) has been developed electrical power system test beds to support the overall design effort. Through this time, the SSFP has changed the design baseline numerous times, however, the test bed effort has endeavored to track these changes. Beginning in August 1989 with the baseline and an all DC system, a test bed was developed to support the design baseline. The LeRC power measurement and distribution (PMAD) DC test bed and the changes in the restructure are described. The changes included the size reduction of primary power channel and various power processing elements. A substantial reduction was also made in the amount of flight software with the subsequent migration of these functions to ground control centers. The impact of these changes on the design of the power hardware, the controller algorithms, the control software, and a description of their current status is presented. An overview of the testing using the test bed is described, which includes investigation of stability and source impedance, primary and secondary fault protection, and performance of a rotary utility

transfer device. Finally, information is presented on the evolution of the test bed to support the verification and operational phases of the SSFP in light of these restructure scrubs.

Author

N92-32975*# National Aeronautics and Space Administration.
Lewis Research Center, Cleveland, OH.

INTERMODULATION IN THE OSCILLATORY MAGNETORESISTANCE OF A TWO-DIMENSIONAL ELECTRON GAS

S. E. SCHACHAM, E. J. HAUGLAND, and S. A. ALTEROVITZ
In its Solid State Technology Branch of NASA Lewis Research Center p 105-110 Aug. 1992 Sponsored in part by NAS-NRC Repr. from Physical Review B (American Physical Society), v. 45, no. 23, Jun. 1992 p 45-50

Avail: CASI HC A02/MF A03

The oscillatory magnetoresistance wave form of a 2-D electron gas shows multiple structures when two subbands are populated. In addition to high-field oscillations at a frequency equal to the sum of the two frequencies corresponding to the concentrations of the subbands, and to a superposition at intermediate fields, we observed oscillations at the difference frequency at low fields and higher temperatures. The field range at which the frequency difference is observed increases with increasing temperature. The crossover from superposition to frequency difference is accompanied by a beat. Similar beats, whose field location shows identical temperature dependence, can be observed in data obtained by other groups on different structures. The various components of the wave form can be attributed to different phase relations between the diagonal and off-diagonal elements of the conductivity tensor. It is shown how the intermodulation term, when inserted into the extended oscillatory equation, can give rise to all three structures.

Author

N92-32982*# National Aeronautics and Space Administration.
Lewis Research Center, Cleveland, OH.

PERFORMANCE OF A Y-Ba-Cu-O SUPERCONDUCTING FILTER/GAAS LOW NOISE AMPLIFIER HYBRID CIRCUIT

KUL B. BHASIN, S. S. TONCICH, C. M. CHOREY (Sverdrup Technology, Inc., Brook Park, OH.), R. R. BONETTI (Communications Satellite Corp., Clarksburg, MD.), and A. E. WILLIAMS (Communications Satellite Corp., Clarksburg, MD.) *In its Solid State Technology Branch of NASA Lewis Research Center p 163-165 Aug. 1992* Previously announced as N92-21370

Avail: CASI HC A01/MF A03

A superconducting 7.3 GHz two-pole microstrip bandpass filter and a GaAs low noise amplifier (LNA) were combined into a hybrid circuit and characterized at liquid nitrogen temperatures. This superconducting/seismology circuit's performance was compared to a gold filter/GaAs LNA hybrid circuit. The superconducting filter/GaAs LNA hybrid circuit showed higher gain and lower noise figure than its gold counterpart.

Author

N92-34204*# National Aeronautics and Space Administration.
Lewis Research Center, Cleveland, OH.

C-BAND SUPERCONDUCTOR/SEMICONDUCTOR HYBRID FIELD-EFFECT TRANSISTOR AMPLIFIER ON A LAALO3 SUBSTRATE

J. J. NAHRA (Cincinnati Univ., OH.), K. B. BHASIN, S. S. TONCICH, G. SUBRAMANYAM (Cincinnati Univ., OH.), and V. J. KAPOOR (Cincinnati Univ., OH.) Sep. 1992 6 p Presented at the 1992 Applied Superconductivity Conference, Chicago, IL, 23-26 Aug. 1992; sponsored by IEEE

(Contract NCC3-33; RTOP 506-72-1B)

(NASA-TM-105828; E-7263; NAS 1.15:105828) Avail: CASI HC
A02/MF A01

A single-stage C-band superconductor/semiconductor hybrid field-effect transistor amplifier was designed, fabricated, and tested at 77 K. The large area (1 inch x 0.5 inches) high temperature superconducting Ti-Ba-Ca-Cu-O (TBCCO) thin film was rf magnetron sputtered onto a LaAlO3 substrate. The film had a transition temperature of about 92 K after it was patterned and etched. The amplifier showed a gain of 6 dB and a 3 dB bandwidth

33 ELECTRONICS AND ELECTRICAL ENGINEERING

of 100 MHz centered at 7.9 GHz. An identical gold amplifier circuit was tested at 77 K, and these results are compared with those from the hybrid amplifier. Author

N92-34219*# National Aeronautics and Space Administration. Lewis Research Center, Cleveland, OH.

LOAD CONVERTER INTERACTIONS WITH THE SECONDARY SYSTEM IN THE SPACE STATION FREEDOM POWER MANAGEMENT AND DISTRIBUTION DC TEST BED

RAMON C. LEBRON Aug. 1992 9 p Presented at the 27th Intersociety Energy Conversion Engineering Conference, San Diego, CA, 3-7 Aug. 1992; sponsored by ANS, SAE, ACS, AIAA, ASME, and IEEE (Contract RTOP 474-42-10) (NASA-TM-105844; E-7287; NAS 1.15:105844) Avail: CASI HC A02/MF A01

The NASA LeRC in Cleveland, Ohio, is responsible for the design, development, and assembly of the Space Station Freedom (SSF) Electrical Power System (EPS). In order to identify and understand system level issues during the SSF Program design and development phases, a system Power Management and Distribution (PMAD) DC test bed was assembled. Some of the objectives of this test bed facility are the evaluation of, system efficiency, power quality, system stability, and system protection and reconfiguration schemes. In order to provide a realistic operating scenario, dc Load Converter Units are used in the PMAD dc test bed to characterize the user interface with the power system. These units are dc to dc converters that provide the final system regulation before power is delivered to the load. This final regulation is required on the actual space station because the majority of user loads will require voltage levels different from the secondary bus voltage. This paper describes the testing of load converters in an end to end system environment (from solar array to loads) where their interactions and compatibility with other system components are considered. Some of the system effects of interest that are presented include load converters transient behavior interactions with protective current limiting switchgear, load converters ripple effects, and the effects of load converter constant power behavior with protective features such as foldback. Author

34

FLUID MECHANICS AND HEAT TRANSFER

Includes boundary layers; hydrodynamics; fluidics; mass transfer; and ablation cooling.

A92-10432* National Aeronautics and Space Administration. Lewis Research Center, Cleveland, OH.

TRANSIENT COOLING OF A SQUARE REGION OF RADIATING MEDIUM

ROBERT SIEGEL (NASA, Lewis Research Center, Cleveland, OH) Journal of Thermophysics and Heat Transfer (ISSN 0887-8722), vol. 5, Oct.-Dec. 1991, p. 495-501. Dec. 1991 7 p refs Copyright

A time-accurate numerical solution was carried out for transient radiative cooling of a gray emitting and absorbing medium in a square two-dimensional region. The integro-differential energy equation for transient temperature distributions was solved in two stages. At each time increment, the local radiative source term was obtained by numerical integration of the temperature field using two-dimensional Gaussian integration over rectangular subregions. Then the differential portion of the equation was integrated forward in time by use of the local first and second time derivatives. The results were compared with available limiting case, and excellent agreement was obtained. Transient results are given for a wide range of optical thicknesses of the region.

Optimum transient cooling is obtained when the optical side length is about 4. Author

A92-10446* National Aeronautics and Space Administration. Lewis Research Center, Cleveland, OH.

VAPOR CONDENSATION ON LIQUID SURFACE DUE TO LAMINAR JET-INDUCED MIXING

C. S. LIN (NASA, Lewis Research Center; Analex Corp., Cleveland, OH) and M. M. HASAN (NASA, Lewis Research Center, Cleveland, OH) Dec. 1991 6 p refs Copyright

A92-12865* National Aeronautics and Space Administration. Lewis Research Center, Cleveland, OH.

NUMERICAL INVESTIGATION ON BENARD INSTABILITY IN A FINITE LIQUID LAYER

J. C. DUH (NASA, Lewis Research Center; Sverdrup Technology, Inc., Cleveland, OH) IN: AIAA/IKI Microgravity Science Symposium, 1st, Moscow, USSR, May 13-17, 1991, Proceedings 1991 7 p refs

A numerical procedure for directly simulating the Benard-Marangoni instabilities (B-M-I) in a bounded liquid layer is presented in this paper. The procedure consists of applying a finite amplitude disturbance to the basic static state, and then integrating the Navier-Stokes equations to determine whether the disturbance will die down or will reach a state of finite-strength steady convection. The critical Marangoni number (Mac) for the onset of B-M-I can thus be determined and can be correlated as a function of the aspect ratio (Ar), Prandtl number (Pr), and Rayleigh number (Ra). The Biot number (B) between the liquid and the air is analyzed to approximate the heat transfer condition along the free surface. A 2D calculation is performed to investigate the effect of various initial disturbances, and the Mac is determined for $Ar = 2$, $Ra = 0$, and $Pr = 0.7$. Current results show that disturbances of different nature and amplitude have little effect on Mac . The Mac determined in this study also clearly demonstrates the dominant effect of the sidewalls. Author

A92-13360* National Aeronautics and Space Administration. Lewis Research Center, Cleveland, OH.

QUALITATIVE INVESTIGATION OF CRYOGENIC FLUID INJECTION INTO A SUPERSONIC FLOW FIELD

R. C. HENDRICKS, D. R. BOLDMAN, H. E. NEUMANN, and B. L. VLCEK (NASA, Lewis Research Center, Cleveland, OH) IN: Advances in cryogenic engineering. Vol. 35A - Proceedings of the 1989 Cryogenic Engineering Conference, Los Angeles, CA, July 24-28, 1989 1990 8 p refs Copyright

The behavior of liquid nitrogen injected into a supersonic nitrogen flow field was investigated using an experimental apparatus in which a Mach 2.7 2D gas nitrogen tunnel is coupled with a high-pressure cryogenic source. Observations were monitored and recorded via a video camera and a motion picture camera. It was found that the penetration of a supersonic flow field by injection of liquid nitrogen is strongly dependent on the flow Mach number, the cryogen injection pressure (Pi/Pc), the injector configuration, and the cryogen temperature. For a 2D gaseous N_2 , Mach 2.7 tunnel, with cryogen injection Pi/Pc approaching 2, the injected fluid penetration for the 1/8-in. injection port approached one half of the tunnel width at 90-deg injection, and one fourth of the tunnel width at 20-deg injection. I.S.

A92-15593* Texas A&M Univ., College Station. **AERODYNAMICS AND HEAT TRANSFER INVESTIGATIONS ON A HIGH REYNOLDS NUMBER TURBINE CASCADE**

TAHER SCHOBELI (Texas A & M University, College Station), ERIC MCFARLAND, and FREDERICK YEH (NASA, Lewis Research Center, Cleveland, OH) ASME, International Gas Turbine and Aeroengine Congress and Exposition, 36th, Orlando, FL, June 3-6, 1991. 11 p. Previously announced in STAR as N91-15134. Jun. 1991 11 p refs (ASME PAPER 91-GT-157)

The results of aerodynamic and heat transfer experimental

investigations performed in a high Reynolds number turbine cascade test facility are analyzed. The experimental facility simulates the high Reynolds number flow conditions similar to those encountered in the Space Shuttle Main Engine. In order to determine the influence of Reynolds number on aerodynamic and thermal behavior of the blades, heat transfer coefficients were measured at various Reynolds numbers using liquid crystal temperature measurement technique. Potential flow calculation methods were used to predict the cascade pressure distributions. Boundary layer and heat transfer calculation methods were used with these pressure distributions to verify the experimental results.

Author

A92-15663* United Technologies Research Center, East Hartford, CT.

HEAT TRANSFER IN ROTATING SERPENTINE PASSAGES WITH TRIPS NORMAL TO THE FLOW

J. H. WAGNER, B. V. JOHNSON (United Technologies Research Center, East Hartford, CT), R. A. GRAZIANI (Pratt and Whitney Group, East Hartford, CT), and F. C. YEH (NASA, Lewis Research Center, Cleveland, OH) ASME, International Gas Turbine and Aeroengine Congress and Exposition, 36th, Orlando, FL, June 3-6, 1991. 13 p. Research supported by United Technology Corp. Previously announced in STAR as N91-19443. Jun. 1991 13 p refs

(Contract NAS3-23691)

(ASME PAPER 91-GT-265)

Experiments were conducted to determine the effects of buoyancy and Coriolis forces on heat transfer in turbine blade internal coolant passages. The experiments were conducted with a large scale, multipass, heat transfer model with both radially inward and outward flow. Trip strips on the leading and trailing surfaces of the radial coolant passages were used to produce the rough walls. An analysis of the governing flow equations showed that four parameters influence the heat transfer in rotating passages: coolant-to-wall temperature ratio, Rossby number, Reynolds number, and radius-to-passage hydraulic diameter ratio. The first three of these four parameters were varied over ranges which are typical of advanced gas turbine engine operating conditions. Results were correlated and compared to previous results from stationary and rotating similar models with trip strips. The heat transfer coefficients on surfaces, where the heat increased with rotation and buoyancy, varied by as much as a factor of four. Maximum values of the heat transfer coefficients with high rotation were only slightly above the highest levels obtained with the smooth wall model. The heat transfer coefficients on surfaces, where the heat transfer decreased with rotation, varied by as much as a factor of three due to rotation and buoyancy. It was concluded that both Coriolis and buoyancy effects must be considered in turbine blade cooling designs with trip strips and that the effects of rotation were markedly different depending upon the flow direction.

Author

A92-15665* National Aeronautics and Space Administration, Lewis Research Center, Cleveland, OH.

PREDICTION OF UNSTEADY ROTOR-SURFACE PRESSURE AND HEAT TRANSFER FROM WAKE PASSINGS

LE T. TRAN (NASA, Lewis Research Center; Sverdrup Technology, Inc., Cleveland, OH) and DALE B. TAULBEE (New York, State University, Buffalo) ASME, International Gas Turbine and Aeroengine Congress and Exposition, 36th, Orlando, FL, June 3-6, 1991. 13 p. Jun. 1991 13 p refs

(Contract NAG3-581)

(ASME PAPER 91-GT-267)

The research described in this paper is a numerical investigation of the effects of unsteady flow on gas turbine heat transfer, particularly on a rotor blade surface. The unsteady flow in a rotor blade passage and the unsteady heat transfer on the blade surface as a result of wake/blade interaction are modeled by the inviscid flow/boundary layer approach. The Euler equations which govern the inviscid flow are solved using a time-accurate marching scheme. The unsteady flow in the blade passage is induced by periodically moving a wake model across the passage inlet. Unsteady flow

solutions in the passage provide pressure gradients and boundary conditions for the boundary-layer equations which govern the viscous flow adjacent to the blade surface. Numerical solutions of the unsteady turbulent boundary layer yield surface heat flow values which can then be compared to experimental data. Comparisons with experimental data show that unsteady heat flux on the blade suction surface is well predicted, but the predictions of unsteady heat flux on the blade pressure surface do not agree.

Author

A92-17193* National Aeronautics and Space Administration, Lewis Research Center, Cleveland, OH.

NAVIER-STOKES ANALYSIS OF FLOW AND HEAT TRANSFER INSIDE HIGH-PRESSURE-RATIO TRANSONIC TURBINE BLADE ROWS

C. HAH (NASA, Lewis Research Center, Cleveland, OH) and R. J. SELVA (Cray Research, Inc., Mendota Heights, MN) Dec. 1991 7 p refs

Copyright

A92-19959* National Aeronautics and Space Administration, Lewis Research Center, Cleveland, OH.

NONLINEAR DYNAMICS NEAR THE STABILITY MARGIN IN ROTATING PIPE FLOW

Z. YANG (NASA, Lewis Research Center, Cleveland, OH; Cornell University, Ithaca, NY) and S. LEIBOVICH (Cornell University, Ithaca, NY) Journal of Fluid Mechanics (ISSN 0022-1120), vol. 233, Dec. 1991, p. 329-347. Dec. 1991 19 p refs

(Contract AF-AFOSR-89-0346)

Copyright

The nonlinear evolution of marginally unstable wave packets in rotating pipe flow is studied. These flows depend on two control parameters, which may be taken to be the axial Reynolds number R and a Rossby number, q . Marginal stability is realized on a curve in the (R, q) -plane, and the entire marginal stability boundary is explored. As the flow passes through any point on the marginal stability curve, it undergoes a supercritical Hopf bifurcation and the steady base flow is replaced by a traveling wave. The envelope of the wave system is governed by a complex Ginzburg-Landau equation. The Ginzburg-Landau equation admits Stokes waves, which correspond to standing modulations of the linear traveling wavetrain, as well as traveling wave modulations of the linear wavetrain. Bands of wavenumbers are identified in which the nonlinear modulated waves are subject to a sideband instability.

Author

A92-20215* National Aeronautics and Space Administration, Lewis Research Center, Cleveland, OH.

HEAT TRANSFER MEASUREMENTS FROM A SMOOTH NACA 0012 AIRFOIL

PHILIP E. POINSATTE, G. J. VAN FOSSEN, JAMES E. NEWTON (NASA, Lewis Research Center, Cleveland, OH), and KENNETH J. DE WITT (Toledo, University, OH) Journal of Aircraft (ISSN 0021-8669), vol. 28, Dec. 1991, p. 892-898. Dec. 1991 7 p refs

(Contract NAG3-72)

Copyright

Local convective heat transfer coefficients were measured from a smooth NACA 0012 airfoil having a chord length of 0.533 m. Flight data were taken for the smooth airfoil at Reynolds numbers based on chord in the range 1.24 to 2.50 million and at various angles of attack up to 4 deg. During these flight tests, the freestream velocity turbulence intensity was found to be very low. Wind tunnel data were acquired in the Reynolds number range 1.20 to 4.52 million and at angles of attack from -4 to +8 deg. The turbulence intensity in the IRT was 0.5-0.7 percent with the cloud-generating sprays off. A direct comparison between the results obtained in flight and in the IRT showed that the higher level of turbulence intensity in the IRT had little effect on the heat transfer for the lower Reynolds numbers but caused a moderate increase in heat transfer at the higher Reynolds numbers. Turning on the cloud-generating spray nozzle atomizing air in the IRT did not alter the heat transfer. The present data were compared

34 FLUID MECHANICS AND HEAT TRANSFER

with leading-edge cylinder and flat plate heat transfer correlations that are often used to estimate airfoil heat transfer in computer codes. Author

A92-20217* National Aeronautics and Space Administration. Lewis Research Center, Cleveland, OH.

ROUGHNESS EFFECTS ON HEAT TRANSFER FROM A NACA 0012 AIRFOIL

PHILIP E. POINSATTE, G. J. VAN FOSSEN (NASA, Lewis Research Center, Cleveland, OH), and KENNETH J. DE WITT (Toledo, University, OH) Dec. 1991 4 p refs (Contract NAG3-72) Copyright

A92-20310* National Aeronautics and Space Administration. Lewis Research Center, Cleveland, OH.

FINITE DIFFERENCE SOLUTION FOR TRANSIENT COOLING OF A RADIATING-CONDUCTING SEMITRANSSPARENT LAYER

ROBERT SIEGEL (NASA, Lewis Research Center, Cleveland, OH) Journal of Thermophysics and Heat Transfer (ISSN 0887-8722), vol. 6, Jan.-Mar. 1992, p. 77-83. Mar. 1992 7 p refs Copyright

Transient solutions were obtained for cooling a semitransparent material by radiation and conduction. The layer is in a vacuum environment so the only means for heat dissipation is by radiation from within the medium leaving through the boundaries. Heat conduction serves only to partially equalize temperatures across the layer. As the optical thickness is increased, steep temperature gradients exist near the boundaries when conduction is relatively small. A solution procedure is required that will provide accurate temperature distributions adjacent to the boundaries, or radiative heat losses will be in error. The approach utilized numerical Gaussian integration to obtain the local radiative source term, and a finite difference procedure with variable space and time increments to solve the transient energy equation. Author

A92-20743* California Univ., Berkeley.

DROP-TOWER EXPERIMENTS FOR CAPILLARY SURFACES IN AN EXOTIC CONTAINER

PAUL CONCUS (California, University, Berkeley), ROBERT FINN (Stanford University, CA), and MARK WEISLOGEL (NASA, Lewis Research Center, Cleveland, OH) Jan. 1992 4 p refs (Contract NAG3-1143; NSF DMS-89-02831; DE-AC03-76SF-00098) Copyright

A92-21079* National Aeronautics and Space Administration. Lewis Research Center, Cleveland, OH.

STUDIES OF THE EFFECTS OF CURVATURE ON DILUTION JET MIXING

JAMES D. HOLDEMAN (NASA, Lewis Research Center, Cleveland, OH), RAM SRINIVASAN, ROBERT S. REYNOLDS, and CRAIG D. WHITE (Allied-Signal Aerospace Co., Phoenix, AZ) Journal of Propulsion and Power (ISSN 0748-4658), vol. 8, Jan.-Feb. 1992, p. 209-218. Feb. 1992 10 p refs Copyright

An analytical program was conducted using both three-dimensional numerical and empirical models to investigate the effects of transition liner curvature on the mixing of jets injected into a confined crossflow. The numerical code is of the TEACH type with hybrid numerics; it uses the power-law and SIMPLER algorithms, an orthogonal curvilinear coordinate system, and an algebraic Reynolds stress turbulence model. From the results of the numerical calculations, an existing empirical model for the temperature field downstream of single and multiple rows of jets injected into a straight rectangular duct was extended to model the effects of curvature. Temperature distributions, calculated with both the numerical and empirical models, are presented to show the effects of radius of curvature and inner and outer wall injection for single and opposed rows of cool dilution jets injected into a hot mainstream flow. Author

A92-22168# National Aeronautics and Space Administration. Lewis Research Center, Cleveland, OH.

CENTRAL DIFFERENCE TVD AND TVB SCHEMES FOR TIME DEPENDENT AND STEADY STATE PROBLEMS

P. JORGENSON (NASA, Lewis Research Center, Cleveland, OH) and E. TURKEL (NASA, Lewis Research Center, Cleveland, OH; Tel Aviv University, Israel) AIAA, Aerospace Sciences Meeting and Exhibit, 30th, Reno, NV, Jan. 6-9, 1992. 11 p. Previously announced in STAR as N92-15663. Jan. 1992 11 p refs (AIAA PAPER 92-0053) Copyright

We use central differences to solve the time dependent Euler equations. The schemes are all advanced using a Runge-Kutta formula in time. Near shocks, a second difference is added as an artificial viscosity. This reduces the scheme to a first order upwind scheme at shocks. The switch that is used guarantees that the scheme is locally total variation diminishing (TVD). For steady state problems it is usually advantageous to relax this condition. Then small oscillations do not activate the switches and the convergence to a steady state is improved. To sharpen the shocks, different coefficients are needed for different equations and so a matrix valued dissipation is introduced and compared with the scalar viscosity. The connection between this artificial viscosity and flux limiters is shown. Any flux limiter can be used as the basis of a shock detector for an artificial viscosity. We compare the use of the van Leer, van Albada, mimmod, superbee, and the 'average' flux limiters for this central difference scheme. For time dependent problems, we need to use a small enough time step so that the CFL was less than one even though the scheme was linearly stable for larger time steps. Using a total variation bounded (TVB) Runge-Kutta scheme yields minor improvements in the accuracy. Author

A92-23300* National Aeronautics and Space Administration. Lewis Research Center, Cleveland, OH.

FACTORS INFLUENCING THE EFFECTIVE SPRAY CONE ANGLE OF PRESSURE-SWIRL ATOMIZERS

S. K. CHEN, A. H. LEFEBVRE (Purdue University, West Lafayette, IN), and J. ROLLBUHLER (NASA, Lewis Research Center, Cleveland, OH) ASME, Transactions, Journal of Engineering for Gas Turbines and Power (ISSN 0742-4795), vol. 114, Jan. 1992, p. 97-103. Jan. 1992 7 p refs Copyright

The spray cone angles produced by several simplex pressure-swirl nozzles are examined using three liquids whose viscosities range from 0.001 to 0.012 kg/ms (1 to 12 cp). Measurements of both the visible spray cone angle and the effective spray cone angle are carried out over wide ranges of injection pressure and for five different values of the discharge orifice length/diameter ratio. The influence of the number of swirl chamber feed slots on spray cone angle is also examined. The results show that the spray cone angle widens with increase in injection pressure but is reduced by increases in liquid viscosity and/or discharge orifice length/diameter ratio. Variation in the number of swirl chamber feed slots between one and three has little effect on the effective spray cone angle. Author

A92-24415 National Aeronautics and Space Administration. Lewis Research Center, Cleveland, OH.

HEAT TRANSFER ON ACCRETING ICE SURFACES

KEIKO YAMAGUCHI and R. J. HANSMAN, JR. (MIT, Cambridge, MA) Feb. 1992 6 p refs (Contract NAG3-666; NGL-22-009-640) Copyright

A92-24654* National Aeronautics and Space Administration. Lewis Research Center, Cleveland, OH.

NEW TECHNIQUE FOR LOW-TO-HIGH ALTITUDE PREDICTIONS OF ABLATIVE HYPERSONIC FLOWFIELDS

BILAL A. BHUTTA and CLARK H. LEWIS (VRA, Inc., Blacksburg, VA) Feb. 1992 16 p refs (Contract NAS3-25450) Copyright

A92-24752* National Aeronautics and Space Administration. Lewis Research Center, Cleveland, OH.

CONVECTION IN SUPERPOSED FLUID AND POROUS LAYERS
 FALIN CHEN (National Taiwan University, Taipei, Republic of China) and C. F. CHEN (Arizona, University, Tucson) *Journal of Fluid Mechanics* (ISSN 0022-1120), vol. 234, Jan. 1992, p. 97-119. Jan. 1992 23 p refs

(Contract NAG3-723; NSF MSM-87-02732)
 Copyright

Thermal convection due to heating from below in a porous layer underlying a fluid layer has been analyzed using the Navier-Stokes equations for the fluid layers and the extended Darcy equation (including Brinkman and Forchheimer terms) for the porous layer. The flow is assumed to be two-dimensional and periodic in the horizontal direction. The numerical scheme used is a combined Galerkin and finite-difference method, and appropriate boundary conditions are applied at the interface. Results have been obtained for depth ratios of 0, 0.1, 0.2, 0.5, and 1.0, where this ratio is defined as the ratio of the thickness of the fluid layer to that of the porous layer. For the depth ratio of 0.1, the convection is dominated by the porous layer, similar to the situation at onset, even though the Rayleigh number for the fluid layer is well into the supercritical regime.

O.G.

A92-24757* National Aeronautics and Space Administration. Lewis Research Center, Cleveland, OH.

THE THREE-DIMENSIONAL TURBULENT BOUNDARY LAYER NEAR A PLANE OF SYMMETRY
 A. T. DEGANI (Lehigh University, Bethlehem, PA), F. T. SMITH (University College, London, England), and J. D. A. WALKER (Lehigh University, Bethlehem, PA) *Journal of Fluid Mechanics* (ISSN 0022-1120), vol. 234, Jan. 1992, p. 329-360. Jan. 1992 32 p refs

(Contract NAG3-771; AF-AFOSR-89-0487)
 Copyright

The asymptotic structure of the three-dimensional turbulent boundary layer near a plane of symmetry is considered in the limit of large Reynolds number. A self-consistent two-layer structure is shown to exist wherein the streamwise velocity is brought to rest through an outer defect layer and an inner wall layer in a manner similar to that in two-dimensional boundary layers. The cross-stream velocity distribution is more complex and two terms in the asymptotic expansion are required to yield a complete profile which is shown to exhibit a logarithmic region. The flow in the inner wall layer is demonstrated to be collateral to leading order; pressure-gradient effects are formally of higher order but can cause the velocity profile to skew substantially near the wall at the large but finite Reynolds numbers encountered in practice. The governing set of ordinary differential equations describing a self-similar flow is derived. The calculated numerical solutions of these equations are matched asymptotically to an inner wall-layer solution and the results show trends that are consistent with experimental observations.

Author

A92-25704*# National Aeronautics and Space Administration. Lewis Research Center, Cleveland, OH.

EFFECTIVE DIFFUSION EQUATION IN A RANDOM VELOCITY FIELD

JORGE VINALS (Florida State University, Tallahassee) and ROBERT F. SEKERKA (Carnegie Mellon University, Pittsburgh, PA) *AIAA, Aerospace Sciences Meeting and Exhibit, 30th, Reno, NV, Jan. 6-9, 1992, 5 p. Jan. 1992 5 p refs*
 (Contract NAG3-1284; DE-FC05-85ER-25000)
 (AIAA PAPER 92-0245) Copyright

The effects are studied of assumed random velocity fields on diffusion in a binary fluid. Random velocity fields can result, for example, from the high-frequency components of residual accelerations onboard spacecraft (often called g-jitter). An effective diffusion equation is derived for an average concentration which includes spatial and temporal correlations induced by the fluctuating velocity fields assumed to be Gaussianly distributed. The resulting equation becomes nonlocal, and if correlations between different components of the velocity field exist, it is also anisotropic. The

simple limiting case of short correlation times is discussed and an effective diffusivity is obtained which reflects the enhanced mixing caused by the velocity fields. The results obtained in the limit of short correlation times are valid even if the probability distribution of the velocity field is not Gaussian.

Author

A92-25705*# National Aeronautics and Space Administration. Lewis Research Center, Cleveland, OH.

EFFECTS OF G-JITTER AND CROSS-DIFFUSION ON THE ONSET OF CONVECTION IN DOUBLY DIFFUSIVE SYSTEMS
 GUILLERMO TERRONES (Battelle Pacific Northwest Laboratories, Richland, WA) and C. F. CHEN (Arizona, University, Tucson) *AIAA, Aerospace Sciences Meeting and Exhibit, 30th, Reno, NV, Jan. 6-9, 1992, 13 p. Jan. 1992 13 p refs*
 (Contract NAG3-1268)

(AIAA PAPER 92-0246) Copyright

The effects of a modulated gravity field in doubly diffusive layers with and without cross-diffusion are studied. Attention is focused on the determination of linear stability criteria for such systems. Floquet theory is used to establish the stability criteria by a systematic analysis of the topology of the neutral curves from which stability boundaries can be constructed. Convective stability boundaries for gravity-modulated doubly cross-diffusive systems are presented for the cases of dynamically free and rigid boundaries. Two physically different forms of layer stratification are considered: (1) imposed independent gradients of two components and (2) a solute gradient induced by a fixed temperature gradient.

C.D.

A92-25715# National Aeronautics and Space Administration. Langley Research Center, Hampton, VA.

MODEL FREE SIMULATIONS OF A HIGH SPEED REACTING MIXING LAYER

CRAIG J. STEINBERGER (New York, State University, Buffalo) *AIAA, Aerospace Sciences Meeting and Exhibit, 30th, Reno, NV, Jan. 6-9, 1992, 9 p. Jan. 1992 9 p refs*
 (Contract NAG1-1122; NAG3-1011)

(AIAA PAPER 92-0257) Copyright

The effects of compressibility, chemical reaction exothermicity and non-equilibrium chemical modeling in a combustor plane mixing layer were investigated by means of two-dimensional model free numerical simulations. It was shown that increased compressibility generally had a stabilizing effect, resulting in reduced mixing and chemical reaction conversion rate. The appearance of 'eddy shocklets' in the flow was observed at high convective Mach numbers. Reaction exothermicity was found to enhance mixing at the initial stages of the layer's growth, but had a stabilizing effect at later times. Calculations were performed for a constant rate chemical rate kinetics model and an Arrhenius type kinetics prototype. The Arrhenius model was found to cause a greater temperature increase due to reaction than the constant kinetics model. This had the same stabilizing effect as increasing the exothermicity of the reaction. Localized flame quenching was also observed when the Zeldovich number was relatively large.

Author

A92-25792*# National Aeronautics and Space Administration. Lewis Research Center, Cleveland, OH.

CONICAL DETONATION WAVES - A COMPARISON OF THEORETICAL AND NUMERICAL RESULTS

JAMES A. FORT (Battelle Pacific Northwest Laboratory, Richland, WA) and DAVID T. PRATT (Washington, University, Seattle) *AIAA, Aerospace Sciences Meeting and Exhibit, 30th, Reno, NV, Jan. 6-9, 1992, 15 p. Research supported by Marquardt Corp., USAF, NASA, et al. Jan. 1992 15 p refs*
 (AIAA PAPER 92-0348) Copyright

A predictive capability for conical oblique detonation waves (ODWs) is discussed with particular attention given to the special case of an axisymmetric conical projectile, which yields necessary conditions for attached waves. A multidimensional numerical model was used to study the influence of a finite Damkoehler number (Da) and viscosity on the formation of a conical ODW. The ODW is predicted for Da on the order of 10, and is found to be important

34 FLUID MECHANICS AND HEAT TRANSFER

in the ODW formation. For a Da of 1, shock induced combustion is predicted. Simulations of the experimental geometry showed general agreement with experimental flow features, but underpredicted the shock angle. It is suggested that this difference may be caused by inadequate boundary layer resolution, lack of grid orthogonality at the cone surface, and an inappropriate chemical mechanism. O.G.

A92-25798* # National Aeronautics and Space Administration. Lewis Research Center, Cleveland, OH.

SELF-PRESSURIZATION OF A SPHERICAL LIQUID HYDROGEN STORAGE TANK IN A MICROGRAVITY ENVIRONMENT

C. S. LIN (Analex Corp., Brook Park, OH) and M. M. HASAN (NASA, Lewis Research Center, Cleveland, OH) AIAA, Aerospace Sciences Meeting and Exhibit, 30th, Reno, NV, Jan. 6-9, 1992. 10 p. Previously announced in STAR as N92-14323. Jan. 1992 10 p refs (AIAA PAPER 92-0363) Copyright

Thermal stratification and self-pressurization of partially filled liquid hydrogen (LH2) storage tanks under microgravity condition is studied theoretically. A spherical tank is subjected to a uniform and constant wall heat flux. It is assumed that a vapor bubble is located in the tank center such that the liquid-vapor interface and tank wall form two concentric spheres. This vapor bubble represents an idealized configuration of a wetting fluid in microgravity conditions. Dimensionless mass and energy conservation equations for both vapor and liquid regions are numerically solved. Coordinate transformation is used to capture the interface location which changes due to liquid thermal expansion, vapor compression, and mass transfer at liquid-vapor interface. The effects of tank size, liquid fill level, and wall heat flux on the pressure rise and thermal stratification are studied. Liquid thermal expansion tends to cause vapor condensation and wall heat flux tends to cause liquid evaporation at the interface. The combined effects determine the direction of mass transfer at the interface. Liquid superheat increases with increasing wall heat flux and liquid fill level and approaches an asymptotic value. Author

A92-26227* # National Aeronautics and Space Administration. Lewis Research Center, Cleveland, OH.

LOW-TO-HIGH ALTITUDE PREDICTIONS OF THREE-DIMENSIONAL ABLATIVE REENTRY FLOWFIELDS

BILAL A. BHUTTA and CLARK H. LEWIS (VRA, Inc., Blacksburg, VA) AIAA, Aerospace Sciences Meeting and Exhibit, 30th, Reno, NV, Jan. 6-9, 1992. 23 p. Jan. 1992 23 p refs (Contract NAS3-25450) (AIAA PAPER 92-0366) Copyright

A new coupled-chemistry PNS scheme has been developed to study 3D hypersonic reentry flows over sphere cones at small angles of attack. A new quasi-steady ablation model for Teflon was used to predict ablative reentry flow fields under laminar, transitional, and turbulent conditions. This solution scheme uses a new two-step solution scheme for solving the species conservation equations under low-altitude conditions. As an example, the scheme is used to study hypersonic flow over a 6-deg sphere-cone configuration at 50 and 125 kft conditions under zero and nonzero angle of attack conditions. C.D.

A92-26270* # National Aeronautics and Space Administration. Lewis Research Center, Cleveland, OH.

VORTICITY DYNAMICS OF INVISCID SHEAR LAYERS

JEFFREY W. YOKOTA (Sverdrup Technology, Inc., Cleveland, OH) AIAA, Aerospace Sciences Meeting and Exhibit, 30th, Reno, NV, Jan. 6-9, 1992. 12 p. Previously announced in STAR as N92-12212. Jan. 1992 12 p refs (Contract NAS3-25266) (AIAA PAPER 92-0420) Copyright

The inviscid evolution of a two-dimensional shear layer is simulated numerically by a scheme based on a kinematic decomposition of the unsteady flow. Lagrangian and Weber transformations of the incompressible Euler equations result in a

Clebsch representation that separates the flowfield into rotational and irrotational components. These transformations produce the initial construction of the flowfield and define its subsequent evolution. Author

A92-26412* National Aeronautics and Space Administration. Lewis Research Center, Cleveland, OH.

EXPERIMENTAL INVESTIGATION OF TURBULENT FLOW THROUGH A CIRCULAR-TO-RECTANGULAR TRANSITION DUCT

D. O. DAVIS (NASA, Lewis Research Center, Cleveland, OH; Washington, University, Seattle) and F. B. GESSNER (Washington, University, Seattle) Feb. 1992 9 p refs (Contract NAG3-376) Copyright

A92-27058* # National Aeronautics and Space Administration. Lewis Research Center, Cleveland, OH.

EFFECT OF RADIATION ON CONVECTION AT MODERATE TEMPERATURES

H. C. DE GROH, III and M. KASSEMI (NASA, Lewis Research Center, Cleveland, OH) AIAA, Aerospace Sciences Meeting and Exhibit, 30th, Reno, NV, Jan. 6-9, 1992. 10 p. Jan. 1992 10 p refs (AIAA PAPER 92-0691) Copyright

A combined numerical and experimental investigation of radiation-induced convection is presented to show that the convective stability of the top-heated enclosure is disrupted by heat transfer conditions at the wall. When the enclosure is not insulated the thermal stratification of the fluid is modified by convective and radiative losses to the surrounding environment. This results in a double annular cell flow which, when cut by the laser sheet, shows a four-vortex pattern with a weak annular cell at the bottom and a large counter-rotating annular cell at the top. When the enclosure is insulated the convective stability of the fluid is again disrupted - this time as a result of radiative heat transfer between the enclosing surfaces which drives two annular flow cells of relatively equal size. Comparison between model and experiment shows that radiation effects are important even at temperature levels as low as 300 C and, if these effects are not included, numerical predictions can be highly erroneous. P.D.

A92-27072* # National Aeronautics and Space Administration. Lewis Research Center, Cleveland, OH.

DETERMINATION OF THE NATURAL CONVECTION COEFFICIENT IN LOW-GRAVITY

J. GOLDMEER (Case Western Reserve University, Cleveland, OH), V. MOTEVALLI, M. HAGHDoust (Worcester Polytechnic Institute, MA), and G. JUMPER (Systems Integration Engineering, Inc., Lexington, MA) AIAA, Aerospace Sciences Meeting and Exhibit, 30th, Reno, NV, Jan. 6-9, 1992. 7 p. Research supported by NASA. Jan. 1992 7 p refs (AIAA PAPER 92-0712) Copyright

Fire safety is an important issue in the current space program; ignition in low-g needs to be studied. The reduction in the gravitational acceleration causes changes in the ignition process. This paper examines the effect of gravity on natural convection, which is one of the important parameters in the ignition process. The NASA-Lewis 2.2 Second Drop Tower provided the low-gravity environment for the experiments. A series of experiments was conducted to measure the temperature of a small copper plate which was heated by a high intensity lamp. These experiments verified that in low-gravity the plate temperature increased faster than in the corresponding 1-g cases, and that the natural convection coefficient rapidly decreased in the low-gravity environment. Author

A92-27110* # National Aeronautics and Space Administration. Lewis Research Center, Cleveland, OH.

JET MIXING INTO A HEATED CROSS FLOW IN A CYLINDRICAL DUCT - INFLUENCE OF GEOMETRY AND FLOW VARIATIONS

M. S. HATCH, W. A. SOWA, G. S. SAMUELSON (California,

University, Irvine), and J. D. HOLDEMAN (NASA, Lewis Research Center, Cleveland, OH) AIAA, Aerospace Sciences Meeting and Exhibit, 30th, Reno, NV, Jan. 6-9, 1992. 17 p. Previously announced in STAR as N92-15994. Jan. 1992 17 p refs (Contract NAG3-1110)

(AIAA PAPER 92-0773) Copyright

To examine the mixing characteristics of jets in an axis-symmetric can geometry, temperature measurements were obtained downstream of a row of cold jets injected into a heated cross stream. Parametric, non-reacting experiments were conducted to determine the influence of geometry and flow variations on mixing patterns in a cylindrical configuration. Results show that jet to mainstream momentum flux ratio and orifice geometry significantly impact the mixing characteristics of jets in a can geometry. For a fixed number of orifices, the coupling between momentum flux ratio and injector determines (1) the degree of jet penetration at the injection plane, and (2) the extent of circumferential mixing downstream of the injection plane. The results also show that, at a fixed momentum flux ratio, jet penetration decreases with (1) an increase in slanted slot aspect ratio, and (2) an increase in the angle of the slots with respect to the mainstream direction.

Author

A92-27774* National Aeronautics and Space Administration, Lewis Research Center, Cleveland, OH.

UNSTEADY THERMOCAPILLARY MIGRATION OF ISOLATED DROPS IN CREEPING FLOW

LOREN H. DILL (NASA, Lewis Research Center, Cleveland, OH) and R. BALASUBRAMANIAM (Case Western Reserve University, Cleveland, OH) International Journal of Heat and Fluid Flow (ISSN 0142-727X), vol. 13, March 1992, p. 78-85. Mar. 1992 8 p refs

Copyright

The problem of an isolated immiscible drop that slowly migrates due to unsteady thermocapillary stresses is considered. All physical properties except for interfacial tension are assumed constant for the two Newtonian fluids. Explicit expressions are found for the migration rate and stream functions in the Laplace domain. The resulting microgravity theory is useful, e.g., in predicting the distance a drop will migrate due to an impulsive interfacial temperature gradient as well as the time required to attain steady flow conditions from an initially resting state.

Author

A92-28187# National Aeronautics and Space Administration, Lewis Research Center, Cleveland, OH.

ANALYSIS OF SURFACE ROUGHNESS GENERATION IN AIRCRAFT ICE ACCRETION

R. J. HANSMAN, JR. (MIT, Cambridge, MA), ANDREW REEHORST (NASA, Lewis Research Center, Cleveland, OH), and JAMES SIMS (Cortez III Service Corp., Cleveland, OH) AIAA, Aerospace Sciences Meeting and Exhibit, 30th, Reno, NV, Jan. 6-9, 1992. 12 p. Research supported by FAA. Jan. 1992 12 p refs (Contract NAG3-666; NGL-22-069-640)

(AIAA PAPER 92-0298) Copyright

Patterns of roughness evolution have been studied analysis of high magnification video observations of accreting ice surfaces provided by the NASA Lewis Research Center. Three distinct patterns of surface roughness generation have been identified within the parametric regions studied. They include: Rime, Multi-Zone Glaze, and Uniform Glaze. Under most icing conditions, a brief period of transient rime ice growth was observed caused by heat conduction into the body. The resulting thin rime layer explains previously observed insensitivity of some ice accretions to substrate insensitivity of some ice accretions to substrate surface chemistry and may provide justification for simplifying assumptions in ice accretion sailing and modeling effects.

Author

A92-28195*# National Aeronautics and Space Administration, Lewis Research Center, Cleveland, OH.

INTERNAL STRUCTURE OF SHOCK WAVES IN DISPARATE MASS MIXTURES

CHAN-HONG CHUNG (NASA, Lewis Research Center, Cleveland, OH), KENNETH J. DE WITT, DUEN-REN JENG (Toledo, University,

OH), and PAUL F. PENKO (NASA, Lewis Research Center, Cleveland, OH) AIAA, Aerospace Sciences Meeting and Exhibit, 30th, Reno, NV, Jan. 6-9, 1992. 8 p. Jan. 1992 8 p refs (Contract NCC3-171)

(AIAA PAPER 92-0496)

The detailed flow structure of a normal shock wave for a gas mixture is investigated using the direct-simulation Monte Carlo method. A variable diameter hard-sphere (VDHS) model is employed to investigate the effect of different viscosity temperature exponents (VTE) for each species in a gas mixture. Special attention is paid to the irregular behavior in the density profiles which was previously observed in a helium-xenon experiment. It is shown that the VTE can have substantial effects in the prediction of the structure of shock waves. The variable hard-sphere model of Bird shows good agreement, but with some limitations, with the experimental data if a common VTE is chosen properly for each case. The VDHS model shows better agreement with the experimental data without adjusting the VTE. The irregular behavior of the light-gas component in shock waves of disparate mass mixtures is observed not only in the density profile, but also in the parallel temperature profile. The strength of the shock wave, the type of molecular interactions, and the mole fraction of heavy species have substantial effects on the existence and structure of the irregularities.

Author

A92-28198*# National Aeronautics and Space Administration, Lewis Research Center, Cleveland, OH.

FLUID-FLOW OF A ROW OF JETS IN CROSSFLOW - A NUMERICAL STUDY

S.-W. KIM and T. J. BENSON (NASA, Lewis Research Center, Cleveland, OH) AIAA, Aerospace Sciences Meeting and Exhibit, 30th, Reno, NV, Jan. 6-9, 1992. 10 p. Jan. 1992 10 p refs (Contract NCC3-229)

(AIAA PAPER 92-0534) Copyright

A detailed computer-visualized flow field of a row of jets in a confined crossflow is presented. The Reynolds averaged Navier-Stokes equations are solved using a finite volume method that incorporates a partial differential equation for incremental pressure to obtain a divergence-free flow field. The turbulence is described by a multiple-time-scale turbulence model. The computational domain includes the upstream region of the circular jet so that the interaction between the jet and the crossflow is simulated accurately. It is shown that the row of jets in the crossflow is characterized by a highly complex flow field that includes a horse-shoe vortex and two helical vortices whose secondary velocity components are co-rotating in space. It is also shown that the horse-shoe vortex is a ring of reversed flows located along the circumference of the jet exit.

Author

A92-28201*# National Aeronautics and Space Administration, Lewis Research Center, Cleveland, OH.

EULER SOLUTIONS FOR AN UNBLADED JET ENGINE CONFIGURATION

MARK E. M. STEWART (NASA, Lewis Research Center, Cleveland, OH) AIAA, Aerospace Sciences Meeting and Exhibit, 30th, Reno, NV, Jan. 6-9, 1992. 8 p. Previously announced in STAR as N92-11328. Jan. 1992 8 p refs (AIAA PAPER 92-0544)

An Euler solution for an axisymmetric jet engine configuration without blade effects is presented. The Euler equations are solved on a multiblock grid which covers a domain including the inlet, bypass duct, core passage, nozzle, and the far field surrounding the engine. The simulation is verified by considering five theoretical properties of the solution. The solution demonstrates both multiblock grid generation techniques and a foundation for a full jet engine throughflow calculation.

Author

A92-28211*# National Aeronautics and Space Administration, Lewis Research Center, Cleveland, OH.

LINEAR-STABILITY THEORY OF THERMOCAPILLARY CONVECTION IN A MODEL OF FLOAT-ZONE CRYSTAL GROWTH

G. P. NEITZEL (Georgia Institute of Technology, Atlanta), K.-T.

34 FLUID MECHANICS AND HEAT TRANSFER

CHANG, D. F. JANKOWSKI, and H. D. MITTELMANN (Arizona State University, Tempe) AIAA, Aerospace Sciences Meeting and Exhibit, 30th, Reno, NV, Jan. 6-9, 1992. 11 p. Jan. 1992 11 p refs

(Contract NAG3-1221; AF-AFOSR-90-0080) (AIAA PAPER 92-0604) Copyright

Linear-stability theory has been applied to a basic state of thermocapillary convection in a model half-zone to determine values of the Marangoni number above which instability is guaranteed. The basic state must be determined numerically since the half-zone is of finite, $O(1)$ aspect ratio with two-dimensional flow and temperature fields. This, in turn, means that the governing equations for disturbance quantities will remain partial differential equations. The disturbance equations are treated by a staggered-grid discretization scheme. Results are presented for a variety of parameters of interest in the problem, including both terrestrial and microgravity cases. Author

A92-28222* National Aeronautics and Space Administration. Lewis Research Center, Cleveland, OH.

ON THE NONLINEAR DEVELOPMENT OF THREE-DIMENSIONAL INSTABILITY WAVES IN NATURAL TRANSITION

REDA R. MANKBADI (NASA, Lewis Research Center, Cleveland, OH) AIAA, Aerospace Sciences Meeting and Exhibit, 30th, Reno, NV, Jan. 6-9, 1992. 9 p. Jan. 1992 9 p refs (AIAA PAPER 92-0741) Copyright

The nonlinear development of a pair of symmetrical three-dimensional oblique instability waves in transitioning boundary layers is investigated based on critical-layer nonlinearity (CLN). Particular emphasis is placed on understanding the mechanisms leading to the naturally occurring transition in which the amplitudes of the plane and oblique modes can be of the same order. Results indicate that the self-interaction of the oblique waves reduces their growth rate. A relatively large oblique mode can either suppress or enhance the growth of the plane mode, depending on the initial phase difference. If the plane mode amplitude is not negligible with respect to that of the oblique modes, it causes a strong amplification of the oblique mode at the subharmonic frequency. The comparison with observations are quite encouraging and several novel features of the natural transition process are revealed. Author

A92-28518* National Aeronautics and Space Administration. Lewis Research Center, Cleveland, OH.

NAVIER-STOKES ANALYSIS OF TURBOMACHINERY BLADE EXTERNAL HEAT TRANSFER

A. A. AMERI (Cleveland State University, OH), P. M. SOCKOL (NASA, Lewis Research Center, Cleveland, OH), and R. S. R. GORLA (Cleveland State University, OH) Journal of Propulsion and Power (ISSN 0748-4658), vol. 8, Mar.-Apr. 1992, p. 374-381. Apr. 1992 8 p refs (Contract NAG3-548)

The two-dimensional, compressible, thin-layer Navier-Stokes and energy equations were solved numerically to obtain heat transfer rates on turbomachinery blades. The Baldwin-Lomax algebraic model and the $q - \omega$ low Reynolds number, two-equation model were used for modeling of turbulence. For the numerical solution of the governing equations a four-stage Runge-Kutta solver was employed. The turbulence model equations were solved using an implicit scheme. Numerical solutions are presented for two-dimensional flow within two vane cascades. The heat transfer results and the pressure distributions were compared with published experimental data. The agreement between the numerical calculations and the experimental values were found to be generally favorable. The position of transition from laminar to turbulent flow was also predicted accurately. Author

A92-28525* National Aeronautics and Space Administration. Lewis Research Center, Cleveland, OH.

MULTIGRID CALCULATIONS OF A JET IN CROSSFLOW

R. W. CLAUS (NASA, Lewis Research Center, Cleveland, OH)

and S. P. VANKA (Illinois, University, Urbana) Apr. 1992 7 p refs Copyright

A92-29553* National Aeronautics and Space Administration. Lewis Research Center, Cleveland, OH.

UPWIND RELAXATION METHODS FOR THE NAVIER-STOKES EQUATIONS USING INNER ITERATIONS

ARTHUR C. TAYLOR, III (Old Dominion University, Norfolk, VA), WING-FAI NG, and ROBERT W. WALTERS (Virginia Polytechnic Institute and State University, Blacksburg) Journal of Computational Physics (ISSN 0021-9991), vol. 99, March 1992, p. 68-78. Research supported by NASA. Mar. 1992 11 p refs Copyright

A subsonic and a supersonic problem are respectively treated by an upwind line-relaxation algorithm for the Navier-Stokes equations using inner iterations to accelerate steady-state solution convergence and thereby minimize CPU time. While the ability of the inner iterative procedure to mimic the quadratic convergence of the direct solver method is attested to in both test problems, some of the nonquadratic inner iterative results are noted to have been more efficient than the quadratic. In the more successful, supersonic test case, inner iteration required only about 65 percent of the line-relaxation method-entailed CPU time. O.C.

A92-29597* National Aeronautics and Space Administration. Lewis Research Center, Cleveland, OH.

A NUMERICAL AND EXPERIMENTAL STUDY OF THREE-DIMENSIONAL LIQUID SLOSHING IN A ROTATING SPHERICAL CONTAINER

KUO-HUEY CHEN (NASA, Lewis Research Center, Cleveland; Toledo, University, OH), FRANKLYN J. KELECY, and RICHARD H. PLETCHER (Iowa State University of Science and Technology, Ames) AIAA, Aerospace Sciences Meeting and Exhibit, 30th, Reno, NV, Jan. 6-9, 1992. 11 p. Jan. 1992 11 p refs (Contract AF-AFOSR-89-0403) (AIAA PAPER 92-0829) Copyright

A numerical and experimental study of three dimensional liquid sloshing inside a partially-filled spherical container undergoing an orbital rotating motion is described. Solutions of the unsteady, three-dimensional Navier-Stokes equations for the case of a gradual spin-up from rest are compared with experimental data obtained using a rotating test rig fitted with two liquid-filled spherical tanks. Data gathered from several experiments are reduced in terms of a dimensionless free surface height for comparison with transient results from the numerical simulations. The numerical solutions are found to compare favorably with the experimental data. Author

A92-30494* National Aeronautics and Space Administration. Lewis Research Center, Cleveland, OH.

TRANSIENT POOL BOILING IN MICROGRAVITY

J. S. ERVIN (Dayton, University, OH), H. MERTE, JR., R. B. KELLER, and K. KIRK (Michigan, University, Ann Arbor) International Journal of Heat and Mass Transfer (ISSN 0017-9310), vol. 35, March 1992, p. 659-674. Mar. 1992 16 p refs (Contract NAG3-663) Copyright

Transient nucleate pool boiling experiments using R113 are conducted for short times in microgravity and in earth gravity with different heater surface orientations and subcoolings. The heating surface is a transparent gold film sputtered on a quartz substrate, which simultaneously provides surface temperature measurements and permits viewing of the boiling process from beneath. For the microgravity experiments, which have uniform initial temperatures and no fluid motion, the temperature distribution in the R 113 at the moment of boiling inception is known. High speed cameras with views both across and through the heating surface record the boiling spread across the heater surface, which is classified into six distinct categories. Author

A92-31469* National Aeronautics and Space Administration. Lewis Research Center, Cleveland, OH.

NONLINEAR SPATIAL EQUILIBRATION OF AN EXTERNALLY EXCITED INSTABILITY WAVE IN A FREE SHEAR LAYER
LENNART S. HULTGREN (NASA, Lewis Research Center, Cleveland, OH) *Journal of Fluid Mechanics* (ISSN 0022-1120), vol. 236, March 1992, p. 635-664. Mar. 1992 30 p refs
Copyright

A two-dimensional disturbance evolving from a strictly linear, finite-growth-rate instability wave, with nonlinear effects first becoming important in the critical layer is considered. The analysis is carried out for a general weakly nonparallel mean flow using matched asymptotic expansions. The flow in the critical layer is governed by a nonlinear vorticity equation which includes a spatial-evolution term. As in Goldstein and Hultgren (1988), the critical layer ages into a quasi-equilibrium one and the initial exponential growth of the instability wave is converted into a weak algebraic growth during the roll-up process. This leads to a next stage of evolution where the instability-wave growth is simultaneously affected by mean-flow divergence and nonlinear critical-layer effects and is eventually converted to decay. Expansions for the various streamwise regions of the flow are combined into a single composite formula accounting for both shear-layer spreading and nonlinear critical-layer effects and good agreement with the experimental results of Thomas and Chu (1989) and Freymuth (1966) is demonstrated.
Author

A92-31638* National Aeronautics and Space Administration. Lewis Research Center, Cleveland, OH.

FEATURES OF WAVY VORTICES IN A CURVED CHANNEL FROM EXPERIMENTAL AND NUMERICAL STUDIES
P. M. LIGRANI (U.S. Naval Postgraduate School, Monterey, CA), W. H. FINLAY (Alberta, University, Edmonton, Canada), W. A. FIELDS, S. J. FUQUA, and C. S. SUBRAMANIAN (U.S. Naval Postgraduate School, Monterey, CA) *Physics of Fluids A* (ISSN 0899-8213), vol. 4, April 1992, p. 695-709. Research supported by NSERC and U.S. Army. Apr. 1992 15 p refs
(Contract NASA ORDER C-80019-F; NASA ORDER C-30030-P)
Copyright

Results are reported from an experimental study obtaining evidence of time-dependent, wavy vortex motions associated with undulating and twisting Dean vortices in a curved channel with 40-to-1 aspect ratio, and mild curvature (radius ratio = 0.979). The results are compared with direct numerical simulations of time-dependent 3D Navier-Stokes equations using boundary conditions in the spanwise and streamwise directions. When viewed in cross section, experimental visualizations of undulating and twisting vortex flows show rocking motion and changes in the direction of the flow between vortices that are like those observed in the simulations. Experimental spectra show that undulating vortices are replaced by the higher-frequency, shorter streamwise wavelength twisting vortices at higher Reynolds numbers. When undulating vortices are present, experimental power spectra and visualizations give frequencies that are somewhat lower than the most unstable frequencies predicted by linear stability analysis.
P.D.

A92-32258* National Aeronautics and Space Administration. Lewis Research Center, Cleveland, OH.

EFFECTS OF G-JITTER ON A THERMALLY BUOYANT FLOW
F. TSAU, S. ELGHOBASHI, and W. A. SIRIGNANO (California, University, Irvine) Jun. 1992 9 p refs
(Contract NAG3-627)
Copyright

A92-32277* National Aeronautics and Space Administration. Lewis Research Center, Cleveland, OH.

CONVECTIVE FLOWS IN ENCLOSURES WITH VERTICAL TEMPERATURE OR CONCENTRATION GRADIENTS
L. W. WANG (Yuan-Ze Institute of Technology, Chung-Li, Republic of China), A. T. CHAI (NASA, Lewis Research Center, Cleveland, OH), and D. J. SUN (National Cheng Kung University, Tainan,

Republic of China) Jun. 1992 3 p refs
Copyright

A92-32940* National Aeronautics and Space Administration. Lewis Research Center, Cleveland, OH.

ON TURBULENT FLOWS DOMINATED BY CURVATURE EFFECTS

G. C. CHENG (Seca, Inc., Huntsville, AL) and S. FAROKHI (Kansas, University, Lawrence) *ASME, Transactions, Journal of Fluids Engineering* (ISSN 0098-2202), vol. 114, March 1992, p. 52-57. Mar. 1992 6 p refs
(Contract NAG3-841)
Copyright

A technique for improving the numerical predictions of turbulent flows with the effect of streamline curvature is developed. Separated flows and the flow in a curved duct are examples of flowfields where streamline curvature plays a dominant role. New algebraic formulations for the eddy viscosity incorporating the k-epsilon turbulence model are proposed to account for various effects of streamline curvature. The loci of flow reversal of the separated flows over various backward-facing steps are employed to test the capability of the proposed turbulence model in capturing the effect of local curvature.
Author

A92-33829* National Aeronautics and Space Administration. Lewis Research Center, Cleveland, OH.

UPWIND DIFFERENCING AND LU FACTORIZATION FOR CHEMICAL NON-EQUILIBRIUM NAVIER-STOKES EQUATIONS
JIAN-SHUN SHUEN (NASA, Lewis Research Center; Sverdrup Technology, Inc., Cleveland, OH) *Journal of Computational Physics* (ISSN 0021-9991), vol. 99, April 1992, p. 233-250. Apr. 1992 18 p refs
Copyright

By means of either the Roe or the Van Leer flux-splittings for inviscid terms, in conjunction with central differencing for viscous terms in the explicit operator and the Steger-Warming splitting and lower-upper approximate factorization for the implicit operator, the present, robust upwind method for solving the chemical nonequilibrium Navier-Stokes equations yields formulas for finite-volume discretization in general coordinates. Numerical tests in the illustrative cases of a hypersonic blunt body, a ramped duct, divergent nozzle flows, and shock wave/boundary layer interactions, establish the method's efficiency.
O.C.

A92-33912* National Aeronautics and Space Administration. Lewis Research Center, Cleveland, OH.

PRESSURE DEPENDENCE OF THE MELTING TEMPERATURE OF SOLIDS - RARE-GAS SOLIDS

HERBERT SCHLOSSER (Cleveland State University, OH) and JOHN FERRANTE (NASA, Lewis Research Center, Cleveland, OH) *Physical Review B - Condensed Matter, 3rd Series* (ISSN 0163-1829), vol. 43, June 1, 1991, p. 13305-13308. Research supported by Ohio Aerospace Institute and NASA. 1 Jun. 1991 4 p refs
Copyright

A method presented by Schlosser et al. (1989) for analyzing the pressure dependence of experimental melting-temperature data is applied to rare-gas solids. The plots of the logarithm of the reduced melting temperature vs that of the reduced pressure are straight lines in the absence of phase transitions. The plots of the reduced melting temperatures for Ar, Kr, and Xe are shown to be approximately straight lines.
C.C.S.

A92-35978* National Aeronautics and Space Administration. Lewis Research Center, Cleveland, OH.

EFFECT OF THERMAL CONVECTION ON THE SHAPE OF A SOLID-LIQUID INTERFACE

C. MENNETRIER, M. A. CHOPRA, and H. C. DE GROH, III (NASA, Lewis Research Center, Cleveland, OH) *IN: Forum on Microgravity Flows - 1991; ASME and JSME Joint Fluids Engineering Conference, 1st, Portland, OR, June 23-27, 1991, Proceedings 1991* 6 p refs
Copyright

34 FLUID MECHANICS AND HEAT TRANSFER

The effect of thermal convection on the shape of solid-liquid interface was investigated in experiments conducted in a transparent Bridgman-type directional solidification furnace. The relationship was numerically modeled using a standard 2D finite-difference approach, with the solid-liquid deformable interface approximated by a blocking-off technique. The directional solidification furnace was used with pure succinonitrile (which is also transparent) contained in a long square ampoule made of borosilicate glass. With the furnace in the vertical configuration, a flat interface was observed, in agreement with the model. On the other hand, a highly distorted interface was obtained in the horizontal configuration; the numerical results showed a strong recirculating cell in front of the interface due to natural thermal convection. The results indicate that thermal convection is responsible for the interface distortion. I.S.

A92-35979* National Aeronautics and Space Administration. Lewis Research Center, Cleveland, OH.

STABILITY OF CAPILLARY SURFACES

MARK WEISLOGEL (NASA, Lewis Research Center, Cleveland, OH) IN: Forum on Microgravity Flows - 1991; ASME and JSME Joint Fluids Engineering Conference, 1st, Portland, OR, June 23-27, 1991, Proceedings 1991 3 p refs
Copyright

An extensive data set quantifying the stability limits of capillary surfaces for a wide range of fluid properties, container geometry, and input disturbance and orientation does not currently exist. To begin to provide such a data set an experimental apparatus has been designed for which the dynamics and stability of fluid interfaces will be investigated. The apparatus consists primarily of a programmable shaker table and a high speed motion picture and video camera for viewing the fluid surface as drop tower tests will be performed to note the stability of a variety of surface/vessel configurations. Author

A92-35994* National Aeronautics and Space Administration. Lewis Research Center, Cleveland, OH.

SUBHARMONIC ROUTE TO BOUNDARY-LAYER TRANSITION - CRITICAL LAYER NONLINEARITY

REDA R. MANKBADI (NASA, Lewis Research Center, Cleveland, OH) IN: Forum on Turbulent Flows - 1991; ASME and JSME Joint Fluids Engineering Conference, 1st, Portland, OR, June 23-27, 1991, Proceedings 1991 7 p refs
Copyright

The linear and nonlinear dynamics of a triad of initially linear stability waves comprising a single plane wave at fundamental frequency and two symmetric oblique waves with half the frequency and streamwise wave number of the plane wave are presented. Analysis is performed for the initial nonlinear development of the waves where the order of the oblique waves' amplitude is equal to or less than that of the plane wave. Results show that the fundamental basically follows the linear theory, while the subharmonic follows an exponential-of-an-exponential growth. R.E.P.

A92-35998* National Aeronautics and Space Administration. Lewis Research Center, Cleveland, OH.

NATURALLY OCCURRING AND FORCED AZIMUTHAL MODES IN A TURBULENT JET

GANESH RAMAN (NASA, Lewis Research Center; Sverdrup Technology, Inc., Brook Park, OH), EDWARD J. RICE (NASA, Lewis Research Center, Cleveland, OH), and ELI RESHOTKO (Case Western Reserve University, Cleveland, OH) IN: Forum on Turbulent Flows - 1991; ASME and JSME Joint Fluids Engineering Conference, 1st, Portland, OR, June 23-27, 1991, Proceedings 1991 8 p refs
Copyright

Naturally occurring instability modes in an axisymmetric jet are studied utilizing the modal frequency spectrum method. In the early evolution of the jet the axisymmetric mode was predominant, with the azimuthal modes growing quickly but dominating only after the end of the potential core. The growth of the azimuthal modes is seen nearer to the nozzle exit for the jet in the laminar

boundary layer case than for the turbulent. Based on the results from these naturally occurring jet instability mode tests, target modes for efficient excitation were determined and two cases of excitation were examined. R.E.P.

A92-36001* National Aeronautics and Space Administration. Lewis Research Center, Cleveland, OH.

A 2-D OSCILLATING FLOW ANALYSIS IN STIRLING ENGINE HEAT EXCHANGERS

KYUNG H. AHN (NASA, Lewis Research Center, Cleveland, OH) and MOUNIR B. IBRAHIM (Cleveland State University, OH) IN: Forum on Turbulent Flows - 1991; ASME and JSME Joint Fluids Engineering Conference, 1st, Portland, OR, June 23-27, 1991, Proceedings 1991 6 p refs
Copyright

A two-dimensional oscillating flow analysis was conducted, simulating the gas flow inside Stirling heat exchangers. Both laminar and turbulent oscillating pipe flow were investigated numerically for $Re(\max) = 1920$ ($Va = 80$), 10800 ($Va = 272$), 19300 ($Va = 272$), and 60800 ($Va = 126$). The results are compared with experimental results of previous investigators. Also, predictions of the flow regime on present oscillating flow conditions were checked by comparing velocity amplitudes and phase differences with those from laminar theory and quasi-steady profile. A high Reynolds number k -epsilon turbulence model was used for turbulent oscillating pipe flow. Finally, performance evaluation of the K -epsilon model was made to explore the applicability of quasi-steady turbulent models to unsteady oscillating flow analysis. Author

A92-36022* National Aeronautics and Space Administration. Lewis Research Center, Cleveland, OH.

EXPERIMENTAL STUDY OF BOUNDARY LAYER TRANSITION ON A HEATED FLAT PLATE

K. H. SOHN, E. RESHOTKO (Case Western Reserve University, Cleveland, OH), and K. B. M. Q. ZAMAN (NASA, Lewis Research Center, Cleveland, OH) IN: Boundary layer stability and transition to turbulence; Proceedings of the Symposium, ASME and JSME Joint Fluids Engineering Conference, 1st, Portland, OR, June 23-27, 1991 1991 10 p refs
Copyright

A detailed investigation to the document momentum and thermal development of boundary layers undergoing natural transition on a heated flat plate was performed. Experimental results of both overall and conditionally sampled characteristics of laminar, transitional, and low Reynolds number turbulent boundary layers are presented. Measurements were done in a low-speed, closed-loop wind tunnel with a freestream velocity of 100 ft/s and zero pressure gradient over a range of freestream turbulence intensities from 0.4 to 6 percent. The distributions of skin friction, heat transfer rate, and Reynolds shear stress were all consistent with previously published data. Reynolds analogy factors for momentum thickness Reynolds number, $Re(\text{sub } \theta)$ less than 2300 were found to be well predicted by laminar and turbulent correlations which accounted for an unheated starting length and uniform heat flux. A small dependence of turbulence results on the freestream turbulence intensity was observed. Author

A92-36184* National Aeronautics and Space Administration. Lewis Research Center, Cleveland, OH.

AN EXPERIMENTAL STUDY OF OSCILLATORY THERMOCAPILLARY CONVECTION IN CYLINDRICAL CONTAINERS

Y. KAMOTANI, J. H. LEE, S. OSTRACH (Case Western Reserve University, Cleveland, OH), and A. PLINE (NASA, Lewis Research Center, Cleveland, OH) Physics of Fluids A (ISSN 0899-8213), vol. 4, no. 5, May 1992, p. 955-962. May 1992 8 p refs (Contract NAG3-570)
Copyright

An experimental study of oscillatory thermocapillary in small cylindrical containers with a heating wire placed along the center axis is performed by investigating the flow structures and temperature distributions under various conditions. To supplement

the flow visualization the surface is scanned using an infrared imager. Here, 2 cS viscosity ($Pr = 27$) silicone oil is used as the test fluid. It is observed that beyond a certain temperature difference between the container wall and the heating wire, a distinctive unsteady flow pattern appears. This unsteady phenomenon is identified as oscillatory thermocapillary. After the onset of oscillations the flow structure becomes nonaxisymmetric and wave motion is observed at the free surface. It is shown that the critical temperature difference is independent of container dimensions if the aspect ratio is fixed. Author

A92-36187* National Aeronautics and Space Administration. Lewis Research Center, Cleveland, OH.

LINEAR STABILITY OF COMPRESSIBLE TAYLOR-COUETTE FLOW

KAI-HSIUNG KAO and CHUEN-YEN CHOW (Colorado, University, Boulder) Physics of Fluids A (ISSN 0899-8213), vol. 4, no. 5, May 1992, p. 984-996. May 1992 13 p refs (Contract NCC3-168)

Copyright

A temporal stability analysis of compressible Taylor-Couette flow is presented. The viscous flow studied in this paper is contained between two concentric cylinders of infinite length, which are rotating with different angular velocities and are kept at different surface temperatures. The effects of differential rotation and temperature difference on the stability of Taylor-Couette flow are contrasted for a range of Mach numbers ranging from incompressible to Mach 3.0. The relative motion of the cylinders dramatically affects the characteristics of the Couette flow at the onset of instability. The flow is stabilized or destabilized depending upon the temperature ratio and speeds of the two cylinders. Independent of Mach number and temperature ratio, increasing Reynolds number generally promotes a destabilizing effect, indicating the inviscid nature of the Taylor-Couette flow. Author

A92-36343* National Aeronautics and Space Administration. Lewis Research Center, Cleveland, OH.

DISTORTION OF A FLAT-PLATE BOUNDARY LAYER BY FREE-STREAM VORTICITY NORMAL TO THE PLATE

M. E. GOLDSTEIN (NASA, Lewis Research Center, Cleveland, OH), S. J. LEIB (NASA, Lewis Research Center, Cleveland; Sverdrup Technology, Inc., Brook Park, OH), and S. J. COWLEY (Cambridge, University, England) Journal of Fluid Mechanics (ISSN 0022-1120), vol. 237, April 1992, p. 231-260. Apr. 1992 30 p refs

Copyright

A nominally uniform flow over a semiinfinite flat plate is considered. The analysis shows how a small streamwise disturbance in the otherwise uniform flow ahead of the plate is amplified by leading-edge bluntness effects and eventually leads to a small-amplitude but nonlinear spanwise motion far downstream from the leading edge of the plate. This spanwise motion is then imposed on the viscous boundary-layer flow at the surface of the plate - causing an order-one change in its profile shape. This ultimately reduces the wall shear stress to zero, causing the boundary layer to undergo a localized separation, which may be characterized as a kind of bursting phenomenon that could be related to the turbulent bursts observed in some flat-plate boundary-layer experiments. Author

A92-37387* National Aeronautics and Space Administration. Lewis Research Center, Cleveland, OH.

A LEAST-SQUARES FINITE ELEMENT METHOD FOR INCOMPRESSIBLE NAVIER-STOKES PROBLEMS

BO-NAN JIANG (NASA, Lewis Research Center, Cleveland, OH) International Journal for Numerical Methods in Fluids (ISSN 0271-2091), vol. 14, no. 7, April 15, 1992, p. 843-859. Previously announced in STAR as N90-12231. 15 Apr. 1992 17 p refs Copyright

A least-squares finite element method, based on the velocity-pressure-vorticity formulation, is developed for solving steady incompressible Navier-Stokes problems. This method leads to a minimization problem rather than to a saddle-point problem

by the classic mixed method and can thus accommodate equal-order interpolations. This method has no parameter to tune. The associated algebraic system is symmetric, and positive definite. Numerical results for the cavity flow at Reynolds number up to 10,000 and the backward-facing step flow at Reynolds number up to 900 are presented. Author

A92-37489* National Aeronautics and Space Administration. Lewis Research Center, Cleveland, OH.

STABLE LOCALIZED PATTERNS IN THIN LIQUID FILMS

ROBERT J. DEISSLER (NASA, Lewis Research Center, Cleveland, OH) and ALEXANDER ORON (Technion - Israel Institute of Technology, Haifa) Physical Review Letters (ISSN 0031-9007), vol. 68, no. 19, May 11, 1992, p. 2948-2951. Research supported by Technion Israel - Mexico Energy Research Fund. 11 May 1992 4 p refs

Copyright

A two-dimensional nonlinear evolution equation is studied which describes the three-dimensional spatiotemporal behavior of the air-liquid interface of a thin liquid film lying on the underside of a cooled horizontal plate. It is shown that the equation has a Liapunov functional, and this fact is exploited to demonstrate that the Marangoni effect can stabilize the destabilizing effect of gravity (the Rayleigh-Taylor instability), allowing for the existence of stable localized axisymmetric solutions for a wide range of parameter values. Various properties of these structures are discussed. Author

A92-37506* National Aeronautics and Space Administration. Lewis Research Center, Cleveland, OH.

AN ERROR ANALYSIS OF LEAST-SQUARES FINITE ELEMENT METHOD OF VELOCITY-PRESSURE-VORTICITY FORMULATION FOR STOKES PROBLEM

CHING L. CHANG (Cleveland State University, OH) and BO-NAN JIANG (NASA, Lewis Research Center, Cleveland, OH) Computer Methods in Applied Mechanics and Engineering (ISSN 0045-7825), vol. 84, no. 3, Dec. 1990, p. 247-255. Dec. 1990 9 p refs Copyright

A theoretical proof of the optimal rate of convergence for the least-squares method is developed for the Stokes problem based on the velocity-pressure-vorticity formula. The 2D Stokes problem is analyzed to define the product space and its inner product, and the a priori estimates are derived to give the finite-element approximation. The least-squares method is found to converge at the optimal rate for equal-order interpolation. C.C.S.

A92-37518* National Aeronautics and Space Administration. Lewis Research Center, Cleveland, OH.

A VARIABLE MULTI-STEP METHOD FOR TRANSIENT HEAT CONDUCTION

PATRICK SMOLINSKI (Pittsburgh, University, PA) Computer Methods in Applied Mechanics and Engineering (ISSN 0045-7825), vol. 86, no. 1, March 1991, p. 61-71. Research supported by NASA and Pittsburgh Supercomputing Center. Mar. 1991 11 p refs

Copyright

A variable explicit time integration algorithm is developed for unsteady diffusion problems. The algorithm uses nodal partitioning and allows the nodal groups to be updated with different time steps. The stability of the algorithm is analyzed using energy methods and critical time steps are found in terms of element eigenvalues with no restrictions on element types. Several numerical examples are given to illustrate the accuracy of the method. Author

A92-39337* National Aeronautics and Space Administration. Lewis Research Center, Cleveland, OH.

COMPRESSIBILITY EFFECTS ON LARGE STRUCTURES IN FREE SHEAR FLOWS

M. SAMIMY, M. F. REEDER, and G. S. ELLIOTT (Ohio State University, Columbus) Physics of Fluids A (ISSN 0899-8213), vol. 4, no. 6, June 1992, p. 1251-1258. Research supported by

34 FLUID MECHANICS AND HEAT TRANSFER

U.S. Navy and NASA. Jun. 1992 8 p refs
Copyright

Space-time correlations were used to study compressibility effects on large structures in mixing layers. Two high-Reynolds number mixing layers with $M(c) = 0.51$ (case 1) and 0.86 (case 2) were studied. The results indicate that the structures in case 1 are similar to those in the incompressible case, but less organized. The structures in case 2 are highly three-dimensional, with a good spatial but a poor temporal organization. The streamwise correlations showed a decay rate four to five times greater for case 2 relative to case 1. While the spanwise correlations for case 1 showed trends similar to incompressible mixing layers, the behavior of case 2 was very different. The pressure fluctuations in the fully developed region of case 2 displayed significant rms variation in the spanwise direction with a well-defined pattern. Based on these measurements, the structures in case 2 seem to be of a horseshoe type, transversely spanning the mixing layer with the head in the low-speed side and the legs inclined in both the x-y and the x-z planes. Author

A92-40071* National Aeronautics and Space Administration. Lewis Research Center, Cleveland, OH.

CONTROL OF AN AXISYMMETRIC TURBULENT JET BY MULTI-MODAL EXCITATION

GANESH RAMAN (Sverdrup Technology, Inc.; NASA, Lewis Research Center, Brook Park, OH), EDWARD J. RICE (NASA, Lewis Research Center, Cleveland, OH), and ELI RESHOTKO (Case Western Reserve University, Cleveland, OH) IN: Symposium on Turbulent Shear Flows, 8th, Munich, Federal Republic of Germany, Sept. 9-11, 1991, Proceedings. Vol. 1 1991 6 p refs
(Contract NAS3-25266)

Experimental measurements of naturally occurring instability modes in the axisymmetric shear layer of high Reynolds number turbulent jet are presented. The region up to the end of the potential core was dominated by the axisymmetric mode. The azimuthal modes dominated only downstream of the potential core region. The energy content of the higher order modes (m is greater than 1) was significantly lower than that of the axisymmetric and $m = +$ or -1 modes. Under optimum conditions, two-frequency excitation (both at $m = 0$) was more effective than single frequency excitation (at $m = 0$) for jet spreading enhancement. An extended region of the jet was controlled by forcing combinations of both axisymmetric ($m = 0$) and helical modes ($m = +$ or -1). Higher spreading rates were obtained when multi-modal forcing was applied. Author

A92-40139* National Aeronautics and Space Administration. Lewis Research Center, Cleveland, OH.

A CONTINUOUS MIXING MODEL FOR PDF SIMULATIONS AND ITS APPLICATIONS TO COMBUSTING SHEAR FLOWS

A. T. HSU (Sverdrup Technology, Inc.; NASA, Lewis Research Center, Cleveland, OH) and J.-Y. CHEN (Sandia National Laboratories, Livermore, CA) IN: Symposium on Turbulent Shear Flows, 8th, Munich, Federal Republic of Germany, Sept. 9-11, 1991, Proceedings. Vol. 2 1991 5 p refs
(Contract NAS3-25266)

The problem of time discontinuity (or jump condition) in the coalescence/dispersion (C/D) mixing model is addressed in this work. A C/D mixing model continuous in time is introduced. With the continuous mixing model, the process of chemical reaction can be fully coupled with mixing. In the case of homogeneous turbulence decay, the new model predicts a pdf very close to a Gaussian distribution, with finite higher moments also close to that of a Gaussian distribution. Results from the continuous mixing model are compared with both experimental data and numerical results from conventional C/D models. Author

A92-40153* National Aeronautics and Space Administration. Lewis Research Center, Cleveland, OH.

EXPERIMENTAL BALANCES FOR THE SECOND MOMENTS FOR A BUOYANT PLUME AND THEIR IMPLICATION ON TURBULENCE MODELING

AAMIR SHABBIR (NASA, Lewis Research Center, Cleveland, OH) IN: Symposium on Turbulent Shear Flows, 8th, Munich, Federal Republic of Germany, Sept. 9-11, 1991, Proceedings. Vol. 2 1991 6 p refs

The heat flux and Reynolds stress budgets are presented for a buoyant plume. The terms involving pressure correlations are obtained as the closing terms in these budgets. Despite certain measurement errors, these budgets provide useful information about how various phenomena contribute to the transport of second moments. These experimental results are used to assess the local equilibrium assumption and to investigate why the mechanical to thermal time scale ratio for a buoyant plume is different than the commonly recommended value. Analysis shows that this departure is a consequence of the local equilibrium assumption being not satisfied in the present experiment. Author

A92-41274* National Aeronautics and Space Administration. Lewis Research Center, Cleveland, OH.

SPATIAL INSTABILITY OF A SWIRLING JET - THEORY AND EXPERIMENT

C. WU, S. FAROKHI (Kansas, University, Lawrence), and R. TAGHAVI (Sverdrup Technology, Inc., Brook Park, OH) Jun. 1992 8 p refs
(Contract NAG3-1098)
Copyright

A92-41275 National Aeronautics and Space Administration. Lewis Research Center, Cleveland, OH.

SECOND ORDER MODELING OF BOUNDARY-FREE TURBULENT SHEAR FLOWS

T.-H. SHIH (NASA, Lewis Research Center, Cleveland, OH), J.-Y. CHEN (California, University, Berkeley), and J. L. LUMLEY (Cornell University, Ithaca, NY) Jun. 1992 8 p refs
(Contract AF-AFOSR-89-0226; NAG1-954; NSF DMS-88-14553; NSF MSM-86-11164)
Copyright

A92-41652* National Aeronautics and Space Administration. Lewis Research Center, Cleveland, OH.

NEAR-WALL RESPONSE IN TURBULENT SHEAR FLOWS SUBJECTED TO IMPOSED UNSTEADINESS

REDA R. MANKBADI (NASA, Lewis Research Center, Cleveland, OH) and JOSEPH T. C. LIU (Brown University, Providence, RI) Journal of Fluid Mechanics (ISSN 0022-1120), vol. 238, May 1992, p. 55-71. Research supported by NSF and DARPA. May 1992 17 p refs
(Contract NAG3-1016)
Copyright

Rapid-distortion theory is adapted to introduce a truly unsteady closure into a simple phenomenological turbulence model in order to describe the unsteady response of a turbulent wall layer exposed to a temporarily oscillating pressure gradient. The closure model is built by taking the ratio of turbulent shear stress to turbulent kinetic energy to be a function of the effective strain. The latter accounts for the history of the flow. The computed unsteady velocity fluctuations and modulated turbulent stresses compare favorably in the 'non-quasi-steady' frequency range, where quasi-steady assumptions would fail. This suggests that the concept of rapid distortion is especially appropriate for unsteady flows. This paper forms the basis for acoustical studies of the problem to be reported elsewhere. Author

A92-41810* National Aeronautics and Space Administration. Lewis Research Center, Cleveland, OH.

HEAT AND MASS TRANSPORT FROM THERMALLY DEGRADING THIN CELLULOSIC MATERIALS IN A MICROGRAVITY ENVIRONMENT

G. KUSHIDA, H. R. BAUM, T. KASHIWAGI (NIST, Center for Fire Research, Gaithersburg, MD), and C. DI BLASI (Naples, University, Italy) May 1992 9 p refs
(Contract NASA ORDER C-32000-K)
Copyright

Attention is given to a theoretical model describing the behavior

of a thermally thin cellulosic sheet heated by external thermal radiation in a quiescent microgravity environment. This model describes thermal and oxidative degradation of the sheet and the heat and mass transfer of evolved degradation products from the heated cellulosic surface into the gas phase. Two calculations are carried out: heating without thermal degradation, and heating with thermal degradation of the sheet with endothermic pyrolysis, exothermic thermal oxidative degradation, and highly exothermic char oxidation. It is shown that pyrolysis is the main degradation reaction. Self-sustained smoldering is controlled and severely limited by the reduced oxygen supply. P.D.

A92-44388* National Aeronautics and Space Administration. Lewis Research Center, Cleveland, OH.

BOUNDARY HEAT FLUXES FOR SPECTRAL RADIATION FROM A UNIFORM TEMPERATURE RECTANGULAR MEDIUM
ROBERT SIEGEL (NASA, Lewis Research Center, Cleveland, OH) *Journal of Thermophysics and Heat Transfer* (ISSN 0887-8722), vol. 6, no. 3, July-Sept. 1992, p. 543-545. Sep. 1992 3 p refs
Copyright

The effect of spectral behavior is analytically shown for radiation in a 2D rectangular geometry. The solution provides exact boundary heat flux values that can be used for comparison with values obtained from general computer programs. The spectral solution presented can be easily evaluated by numerical integration for complex variations of the spectral absorption coefficient with wavelength. C.D.

A92-44390* National Aeronautics and Space Administration. Lewis Research Center, Cleveland, OH.

COMBINED CONJUGATED HEAT TRANSFER FROM A SCATTERING MEDIUM
M. KASSEMI (NASA, Lewis Research Center, Cleveland, OH) and B. T. F. CHUNG (Akron, University, OH) *Journal of Thermophysics and Heat Transfer* (ISSN 0887-8722), vol. 6, no. 3, July-Sept. 1992, p. 548-551. Sep. 1992 4 p refs
Copyright

Combined heat transfer from a radiating and convecting flow of an absorbing, emitting, and scattering medium in a reflecting channel with conducting wall was numerically investigated. The results clearly indicate that in any high-temperature applications, if the effects of scattering and wall reflection are ignored, the position and magnitude of the maximum wall temperature and the behavior of the convective Nusselt number can be grossly misrepresented. C.D.

A92-45707* National Aeronautics and Space Administration. Lewis Research Center, Cleveland, OH.

A CONTINUUM METHOD FOR MODELING SURFACE TENSION
J. U. BRACKBILL, D. B. KOTHE, and C. ZEMACH (Los Alamos National Laboratory, NM) *Journal of Computational Physics* (ISSN 0021-9991), vol. 100, no. 2, June 1992, p. 335-354. Jun. 1992 20 p refs
(Contract NASA ORDER C-32008-K; W-7405-ENG-36)
Copyright

In the novel method presented for modeling the effects of surface tension on fluid motion, the interfaces between fluids with different, color-represented properties are finite-thickness transition regions across which the color varies continuously. A force density proportional to the surface curvature of constant color is defined at each point in the transition region; this force-density is normalized in such a way that the conventional description of surface tension on an interface is recovered when the ratio of local transition-region thickness to local curvature radius approaches zero. The properties of the method are illustrated by computational results for 2D flows. O.C.

A92-45716* National Aeronautics and Space Administration. Lewis Research Center, Cleveland, OH.

EFFECT OF SPATIAL RESOLUTION ON APPARENT SENSITIVITY TO INITIAL CONDITIONS OF A DECAYING FLOW AS IT BECOMES TURBULENT

ROBERT G. DEISSLER and FRANK B. MOLLS (NASA, Lewis Research Center, Cleveland, OH) *Journal of Computational Physics* (ISSN 0021-9991), vol. 100, no. 2, June 1992, p. 430-432. Jun. 1992 3 p refs
Copyright

In order to check for spurious chaos and obtain superior solutions for decaying Navier-Stokes flows, an investigation is conducted of the effect of spatial resolution on numerical results. The fourth-order finite difference method results obtained with grids of 32-cubed and 64-cubed points, and those of a pseudospectral method for 128-cubed points, indicate that the sensitivity of initially neighboring solutions to small changes in initial conditions increases with improving spatial resolution. O.C.

A92-45844* National Aeronautics and Space Administration. Lewis Research Center, Cleveland, OH.

NATURE OF BUOYANCY-DRIVEN FLOWS IN A REDUCED-GRAVITY ENVIRONMENT
SIAVASH A. KASSEMI (NASA, Lewis Research Center, Cleveland, OH) and SIMON OSTRACH (Case Western Reserve University, Cleveland, OH) *AIAA Journal* (ISSN 0001-1452), vol. 30, no. 7, July 1992, p. 1815-1818. Jul. 1992 4 p refs
Copyright

The role of buoyancy-driven convection in reduced-gravity environments has been emphasized. It is shown that for some materials-processing experiments the values of the fundamental dimensionless parameters such as Gr or Ra are shifted from the very large (ground-based values) to moderately large (space-based values). As a consequence, in cases where approximate analytical solutions are desired, the accuracy of the usual asymptotic (boundary-layer) analysis in which infinitely large parametric ranges are assumed is reduced. Approximate analytical techniques for refinement of the asymptotic solutions are identified that will extend the accuracy to the moderately large parametric ranges associated with space-based processing. Author

A92-46251 Jet Propulsion Lab., California Inst. of Tech., Pasadena.

THE INFLUENCE OF HIGHER HARMONICS ON VORTEX PAIRING IN AN AXISYMMETRIC MIXING LAYER
R. A. PETERSEN (Arizona, University, Tucson; JPL, Pasadena, CA) and R. C. CLOUGH (Arizona, University, Tucson) *Journal of Fluid Mechanics* (ISSN 0022-1120), vol. 239, June 1992, p. 81-98. Jun. 1992 18 p refs
(Contract NAG3-460; NSF MSM-88-00086)
Copyright

Strong forcing was used to produce vortex pairing in a submerged axisymmetric water jet. Phase-averaged hot-wire measurements were combined with phase-averaged flow visualization to identify the relevant nonlinear interactions. The leading resonant interaction was not a subharmonic resonance. Instead, it was a triad resonance involving the subharmonic, the fundamental and the 3/2 harmonic. The profound influence of higher harmonics on the amplification of the fundamental and subharmonic was demonstrated in a systematic way by successive truncation of the Fourier series representation of the excitation waveform. Author

A92-47158 National Aeronautics and Space Administration. Lewis Research Center, Cleveland, OH.

COMPARISON OF THE SMAC, PISO, AND ITERATIVE TIME-ADVANCING SCHEMES FOR UNSTEADY FLOWS
S.-W. KIM and T. J. BENSON (NASA, Lewis Research Center, Cleveland, OH) (*International Symposium on Computational Fluid Dynamics*, 4th, Davis, CA, Sept. 9-12, 1991) *Computers & Fluids* (ISSN 0045-7930), vol. 21, no. 3, July 1992, p. 435-454. Previously announced in STAR as N91-24550. Jul. 1992 20 p refs
(Contract RTOP 505-62-52; NCC3-180)
Copyright

Calculations of unsteady flows using a simplified marker and cell (SMAC), a pressure implicit splitting of operators (PISO), and an iterative time advancing scheme (ITA) are presented. A partial differential equation for incremental pressure is used in each time

34 FLUID MECHANICS AND HEAT TRANSFER

advancing scheme. Example flows considered are a polar cavity flow starting from rest and self-sustained oscillating flows over a circular and a square cylinder. For a large time step size, the SMAC and ITA are more strongly convergent and yield more accurate results than PISO. The SMAC is the most efficient computationally. For a small time step size, the three time advancing schemes yield equally accurate Strouhal numbers. The capability of each time advancing scheme to accurately resolve unsteady flows is attributed to the use of new pressure correction algorithm that can strongly enforce the conservation of mass. The numerical results show that the low frequency of the vortex shedding is caused by the growth time of each vortex shed into the wake region. Author

A92-47269* National Aeronautics and Space Administration. Lewis Research Center, Cleveland, OH.

THREE-DIMENSIONAL BOUNDARY ELEMENT THERMAL SHAPE SENSITIVITY ANALYSIS

K. G. PRASAD and J. H. KANE (Clarkson University, Potsdam, NY) International Journal of Heat and Mass Transfer (ISSN 0017-9310), vol. 35, no. 6, June 1992, p. 1427-1439. Jun. 1992 13 p refs
(Contract NAG3-1089; NSF DDM-89-96171)
Copyright

A computationally efficient and accurate shape design sensitivity analysis approach for the thermal response of 3D solid objects is presented which utilizes a direct, singular, boundary element analysis formulation. The theoretical formulation for the primary response (the surface temperature and normal heat flux) sensitivities and the secondary response (tangential components of the heat flux, vector, interior point temperature and heat flux vector components) sensitivities are presented. A number of computational issues related to the overall efficiency of implementation of these formulations are discussed. Numerical results are presented to demonstrate the accuracy and efficiency of this approach. Author

A92-47271* National Aeronautics and Space Administration. Lewis Research Center, Cleveland, OH.

SCALING OF LOW-PRANDTL-NUMBER THERMOCAPILLARY FLOWS

DAMIAN RIVAS (Escuela Tecnica Superior de Ingenieros Aeronauticos, Madrid, Spain) and SIMON OSTRACH (Case Western Reserve University, Cleveland, OH) International Journal of Heat and Mass Transfer (ISSN 0017-9310), vol. 35, no. 6, June 1992, p. 1469-1479. Jun. 1992 11 p refs
(Contract NAG3-570)
Copyright

Scaling analysis was used to study thermocapillary flows of low-Prandtl-number fluids in shallow rectangular enclosures under an imposed-heat-flux configuration. Different regimes that appear in the thermo-fluid problem are identified and the proper parameters and reference quantities that define them are obtained. Assuming that the flow is driven by thermocapillary effects and it is concluded that the extent of the region where the thermocapillary driving force is important defines the region of applicability of the scaling results. O.G.

A92-47841*# National Aeronautics and Space Administration. Lewis Research Center, Cleveland, OH.

FDDO AND DSMC ANALYSES OF RAREFIED GAS FLOW THROUGH 2D NOZZLES

CHAN-HONG CHUNG (NASA, Lewis Research Center, Cleveland, OH), KENNETH J. DE WITT, DUEN-REN JENG (Toledo, University, OH), and PAUL F. PENKO (NASA, Lewis Research Center, Cleveland, OH) AIAA, Thermophysics Conference, 27th, Nashville, TN, July 6-8, 1992. 12 p. Jul. 1992 12 p refs
(Contract NAG3-171)
(AIAA PAPER 92-2858)

Two different approaches, the finite-difference method coupled with the discrete-ordinate method (FDDO), and the direct-simulation Monte Carlo (DSMC) method, are used in the analysis of the flow of a rarefied gas expanding through a two-dimensional nozzle

and into a surrounding low-density environment. In the FDDO analysis, by employing the discrete-ordinate method, the Boltzmann equation simplified by a model collision integral is transformed to a set of partial differential equations which are continuous in physical space but are point functions in molecular velocity space. The set of partial differential equations are solved by means of a finite-difference approximation. In the DSMC analysis, the variable hard sphere model is used as a molecular model and the no time counter method is employed as a collision sampling technique. The results of both the FDDO and the DSMC methods show good agreement. The FDDO method requires less computational effort than the DSMC method by factors of 10 to 40 in CPU time, depending on the degree of rarefaction. Author

A92-47842*# National Aeronautics and Space Administration. Lewis Research Center, Cleveland, OH.

DSMC ANALYSIS OF SPECIES SEPARATION IN RAREFIED NOZZLE FLOWS

CHAN-HONG CHUNG (NASA, Lewis Research Center, Cleveland, OH), KENNETH J. DE WITT, DUEN-REN JENG (Toledo, University, OH), and PAUL F. PENKO (NASA, Lewis Research Center, Cleveland, OH) AIAA, Thermophysics Conference, 27th, Nashville, TN, July 6-8, 1992. 10 p. Jul. 1992 10 p refs
(Contract NAG3-171)
(AIAA PAPER 92-2859)

The direct-simulation Monte Carlo method has been used to investigate the behavior of a small amount of a harmful species in the plume and the backflow region of nuclear thermal propulsion rockets. Species separation due to pressure diffusion and nonequilibrium effects due to rapid expansion into a surrounding low-density environment are the most important factors in this type of flow. It is shown that a relatively large amount of the lighter species is scattered into the backflow region and the heavier species becomes negligible in this region due to the extreme separation between species. It is also shown that the type of molecular interaction between the species can have a substantial effect on separation of the species. Author

A92-47862*# National Aeronautics and Space Administration. Lewis Research Center, Cleveland, OH.

LIQUID HYDROGEN MASS FLOW THROUGH A MULTIPLE ORIFICE JOULE-THOMSON DEVICE

S. S. PAPELL (Analex Corp., Brook Park, OH), TED W. NYLAND, and NASEEM H. SAIYED (NASA, Lewis Research Center, Cleveland, OH) AIAA, Thermophysics Conference, 27th, Nashville, TN, July 6-8, 1992. 12 p. Previously announced in STAR as N92-23268. Jul. 1992 12 p refs
(AIAA PAPER 92-2881) Copyright

Liquid hydrogen mass flow rate, pressure drop, and temperature drop data were obtained for a number of multiple orifice Joule-Thomson devices known as visco jets. The present investigation continues a study to develop an equation for predicting two phase flow of cryogens through these devices. The test apparatus design allowed isenthalpic expansion of the cryogen through the visco jets. The data covered a range of inlet and outlet operating conditions. The mass flow rate range single phase or two phase was 0.015 to 0.98 lbm/hr. The manufacturer's equation was found to overpredict the single phase hydrogen data by 10 percent and the two phase data by as much as 27 percent. Two modifications of the equation resulted in a data correlation that predicts both the single and two phase flow across the visco jet. The first modification was of a theoretical nature, and the second strictly empirical. The former reduced the spread in the two phase data. It was a multiplication factor of 1-X applied to the manufacturer's equation. The parameter X is the flow quality downstream of the visco jet based on isenthalpic expansion across the device. The latter modification was a 10 percent correction term that correlated 90 percent of the single and two phase data to within +/- 10 percent scatter band. Author

A92-48149* National Aeronautics and Space Administration. Lewis Research Center, Cleveland, OH.

THE OSHER SCHEME FOR NON-EQUILIBRIUM REACTING FLOWS

AMBADY SURESH (Sverdrup Technology, Inc.; NASA, Lewis Research Center, Cleveland, OH) and MENG-SING LIOU (NASA, Lewis Research Center, Cleveland, OH) International Journal for Numerical Methods in Fluids (ISSN 0271-2091), vol. 15, no. 2, July 30, 1992, p. 219-232. 30 Jul. 1992 14 p refs (Contract NAS3-25266)

Copyright

An extension of the Osher upwind scheme to nonequilibrium reacting flows is presented. Owing to the presence of source terms, the Riemann problem is no longer self-similar and therefore its approximate solution becomes tedious. With simplicity in mind, a linearized approach which avoids an iterative solution is used to define the intermediate states and sonic points. The source terms are treated explicitly. Numerical computations are presented to demonstrate the feasibility, efficiency and accuracy of the proposed method. The test problems include a ZND (Zeldovich-Neumann-Doring) detonation problem for which spurious numerical solutions which propagate at mesh speed have been observed on coarse grids. With the present method, a change of limiter causes the solution to change from the physically correct CJ detonation solution to the spurious weak detonation solution.

Author

A92-48204* National Aeronautics and Space Administration. Lewis Research Center, Cleveland, OH.

QUASI-STEADY TURBULENCE MODELING OF UNSTEADY FLOWS

REDA R. MANKBADI (NASA, Lewis Research Center, Cleveland, OH; Cairo, University, Egypt) and AMIN MOBARK (Cairo, University, Egypt) International Journal of Heat and Fluid Flow (ISSN 0142-727X), vol. 12, no. 2, June 1991, p. 122-129. Jun. 1991 8 p refs

Copyright

This article describes the results of numerical simulations of oscillating wall-bounded developing flows. The full phase-averaged Navier-Stokes equations are solved. The application of quasi-steady turbulence modeling to unsteady flows is demonstrated using an unsteady version of the k-epsilon model. The effects of unsteadiness on the mean flow and turbulence are studied. Critical evaluation of the applicability of the quasi-steady approach to turbulence modeling is presented. Suggestions are given for the future efforts in turbulence modeling of unsteady flows.

Author

A92-48721*# National Aeronautics and Space Administration. Lewis Research Center, Cleveland, OH.

NAVIER-STOKES TURBINE HEAT TRANSFER PREDICTIONS USING TWO-EQUATION TURBULENCE CLOSURES

ALI A. AMERI (University of Kansas Center for Research, Inc., Lawrence) and ANDREA ARNONE (Firenze, Universita, Florence, Italy) AIAA, SAE, ASME, and ASEE, Joint Propulsion Conference and Exhibit, 28th, Nashville, TN, July 6-8, 1992. 11 p. Jul. 1992 11 p refs

(Contract NAG3-548)

(AIAA PAPER 92-3067)

Navier-Stokes calculations were carried out in order to predict the heat-transfer rates on turbine blades. The calculations were performed using TRAF2D which is a k-epsilon, explicit, finite volume mass-averaged Navier-Stokes solver. Turbulence was modeled using Coakley's q-omega and Chien's k-epsilon two-equation models and the Baldwin-Lomax algebraic model. The model equations along with the flow equations were solved explicitly on a nonperiodic C grid. Implicit residual smoothing (IRS) or a combination of multigrid technique and IRS was applied to enhance convergence rates. Calculations were performed to predict the Stanton number distributions on the first stage vane and blade row as well as the second stage vane row of the SSME high-pressure fuel turbine. The comparison serves to highlight the weaknesses of the turbulence models for use in turbomachinery heat-transfer calculations.

Author

A92-48732*# National Aeronautics and Space Administration. Lewis Research Center, Cleveland, OH.

CFD MIXING ANALYSIS OF JETS INJECTED FROM STRAIGHT AND SLANTED SLOTS INTO CONFINED CROSSFLOW IN RECTANGULAR DUCTS

D. B. BAIN, C. E. SMITH (CFD Research Corp., Huntsville, AL), and J. D. HOLDEMAN (NASA, Lewis Research Center, Cleveland, OH) AIAA, SAE, ASME, and ASEE, Joint Propulsion Conference and Exhibit, 28th, Nashville, TN, July 6-8, 1992. 24 p. Previously announced in STAR as N92-26561. Jul. 1992 24 p refs (Contract NAS3-25967)

(AIAA PAPER 92-3087) Copyright

A CFD study was performed to analyze the mixing potential of opposed rows of staggered jets injected into confined crossflow in a rectangular duct. Three jet configurations were numerically tested: (1) straight (0 deg) slots; (2) perpendicular slanted (45 deg) slots angled in opposite directions on top and bottom walls; and (3) parallel slanted (45 deg) slots angled in the same direction on top and bottom walls. All three configurations were tested at slot spacing-to-duct height ratios (S/H) of 0.5, 0.75, and 1.0; a jet-to-mainstream momentum flux ratio (J) of 100; and a jet-to-mainstream mass flow ratio of 0.383. Each configuration had its best mixing performance at S/H of 0.75. Asymmetric flow patterns were expected and predicted for all slanted slot configurations. The parallel slanted slot configuration was the best overall configuration at x/H of 1.0 for S/H of 0.75.

Author

A92-48733*# National Aeronautics and Space Administration. Lewis Research Center, Cleveland, OH.

A PARAMETRIC NUMERICAL STUDY OF MIXING IN A CYLINDRICAL DUCT

V. L. OECHSLE, H. C. MONGIA (General Motors Corp., Allison Gas Turbine Div., Indianapolis, IN), and J. D. HOLDERMAN (NASA, Lewis Research Center, Cleveland, OH) AIAA, SAE, ASME, and ASEE, Joint Propulsion Conference and Exhibit, 28th, Nashville, TN, July 6-8, 1992. 22 p. Jul. 1992 22 p refs (AIAA PAPER 92-3088) Copyright

The interaction is described of some of the important parameters affecting the mixing process in a quick mixing region of a rich burn/quick mix/lean burn (RQL) combustor. The performance of the quick mixing region is significantly affected by the geometric designs of both the mixing domain and the jet inlet orifices. Several of the important geometric parameters and operating conditions affecting the mixing process were analytically studied. Parameters such as jet-to-mainstream momentum flux ratio (J), mass flow ratio (MR), orifice geometry, orifice orientation, and number of orifices/row (equally spaced around the circumferential direction) were analyzed. Three different sets of orifice shapes were studied: (1) square, (2) elongated slots, and (3) equilateral triangles. Based on the analytical results, the best mixing configuration depends significantly on the penetration depth of the jet to prevent the hot mainstream flow from being entrained behind the orifice. The structure in a circular mixing section is highly weighted toward the outer wall and any mixing structure affecting this area significantly affects the overall results. The increase in the number of orifices per row increases the mixing at higher J conditions. Higher slot slant angles and aspect ratios are generally the best mixing configurations at higher momentum flux ratio (J) conditions. However, the square and triangular shaped orifices were more effective mixing configurations at lower J conditions.

Author

A92-48734*# National Aeronautics and Space Administration. Lewis Research Center, Cleveland, OH.

MIXING IN THE DOME REGION OF A STAGED GAS TURBINE COMBUSTOR

W. A. SOWA, R. A. BRADY, and G. S. SAMUELSEN (California, University, Irvine) AIAA, SAE, ASME, and ASEE, Joint Propulsion Conference and Exhibit, 28th, Nashville, TN, July 6-8, 1992. 10 p. Jul. 1992 10 p refs (Contract NAG3-1124)

(AIAA PAPER 92-3089) Copyright

To lower NO(x) emissions from gas-turbine engines the effect

of dome design and operational changes on the mixing quality in the fuel-rich region is studied. A statistical analysis is employed to establish the parametric sensitivity in this complex flow. A mixing-effectiveness index is defined and used to optimize the gas-species uniformity and the extent of reaction at the exit plane of the dome. Mixing effectiveness is tied to the fuel and air injection locations, the macroscale structure of the dome aerodynamics, and the level of turbulence. Increases in nozzle/air to fuel ratio, reference velocities, and the dome expansion angle increased the level of turbulence. The optimum configuration featured counter-swirling fuel and air streams and produced a strong toroidal recirculation zone, an effective spray angle of 45 degrees, and azimuthal velocities that decayed to zero inside of two duct diameters. The results underscore the system specific nature of mixing optimization. Author

A92-48735*# National Aeronautics and Space Administration. Lewis Research Center, Cleveland, OH.
EXPERIMENTAL STUDY OF CROSS-STREAM MIXING IN A RECTANGULAR DUCT

D. S. LISCINSKY, B. TRUE (United Technologies Research Center, East Hartford, CT), A. VRANOS (AB Research Associates, South Windsor, CT), and J. D. HOLDEMAN (NASA, Lewis Research Center, Cleveland, OH) AIAA, SAE, ASME, and ASEE, Joint Propulsion Conference and Exhibit, 28th, Nashville, TN, July 6-8, 1992. 13 p. Previously announced in STAR as N92-27652. Jul. 1992 13 p refs (Contract NAS3-25952) (AIAA PAPER 92-3090) Copyright

An experimental investigation of non-reacting cross-stream jet injection and mixing in a rectangular duct was conducted for application in a low emissions combustor. Planar digital imaging was used to measure concentration distributions in planes perpendicular to the duct axis. Mixing rate was measured for 45 deg slanted slot and round orifice injectors. Five areas of inquiry are discussed: (1) mixing improves continuously with increasing momentum-flux ratio; (2) given a momentum-flux ratio, there is an optimum, orifice spacing; (3) mixing is more dependent on injector geometry than mass flow ratio; (4) mixing is influenced by relative slot orientation; and (5) jet structure is different for round holes and slanted slots injectors. The utility of acquiring multipoint fluctuating properties of the flow field is also demonstrated. Author

A92-48795*# National Aeronautics and Space Administration. Lewis Research Center, Cleveland, OH.
PERTURBATION OF A NORMAL SHOCK - A TEST CASE FOR UNSTEADY EULER CODES

AMBADY SURESH and JACK WILSON (Sverdrup Technology, Inc.; NASA, Lewis Research Center, Cleveland, OH) AIAA, SAE, ASME, and ASEE, Joint Propulsion Conference and Exhibit, 28th, Nashville, TN, July 6-8, 1992. 14 p. Jul. 1992 14 p refs (Contract NAS3-25266) (AIAA PAPER 92-3180)

Shock tracking capabilities of modern nonoscillatory schemes for solving the Euler equations are studied by comparing their solutions to solutions obtained using the method of characteristics on two test problems. Both test problems involve accelerating and decelerating shock motions. The schemes tested include first order upwind, second order SONIC-A, third order ENO, and third order TONIC-A. Results show that the second and higher order schemes give nearly identical shock trajectories that are closer to the characteristic solution than the first order upwind scheme. All schemes approach the characteristic solution upon mesh refinement. Author

A92-48930*# National Aeronautics and Space Administration. Lewis Research Center, Cleveland, OH.
SPECIES AND TEMPERATURE MEASUREMENT IN H₂/O₂ ROCKET FLOW FIELDS BY MEANS OF RAMAN SCATTERING DIAGNOSTICS

WIM A. DE GROOT (Sverdrup Technology, Inc., Brook Park; NASA, Lewis Research Center, Cleveland, OH) and JONATHAN M. WEISS

(Pennsylvania State University, University Park) AIAA, SAE, ASME, and ASEE, Joint Propulsion Conference and Exhibit, 28th, Nashville, TN, July 6-8, 1992. 19 p. Jul. 1992 19 p refs (AIAA PAPER 92-3353)

Validation of CFD codes developed for prediction and evaluation of rocket performance is hampered by a lack of experimental data. Nonintrusive laser based diagnostics are needed to provide spatially and temporally resolved gas dynamic and fluid dynamic measurements. This paper reports the first nonintrusive temperature and species measurements in the plume of a 110 N gaseous hydrogen/oxygen thruster at and below ambient pressures, obtained with spontaneous Raman spectroscopy. Measurements at 10 mm downstream of the exit plane are compared with predictions from a numerical solution of the axisymmetric Navier-Stokes and species transport equations with chemical kinetics, which fully model the combustor-nozzle-plume flowfield. The experimentally determined oxygen number density at the centerline at 10 mm downstream of the exit plane is four times that predicted by the model. The experimental number density data fall between those numerically predicted for the exit and 10 mm downstream planes in both magnitude and radial gradient. The predicted temperature levels are within 10 to 15 percent of measured values. Author

A92-48994# National Aeronautics and Space Administration. Lewis Research Center, Cleveland, OH.

PROPULSION-RELATED FLOWFIELDS USING THE PRECONDITIONED NAVIER-STOKES EQUATIONS

S. VENKATESWARAN, J. M. WEISS, C. L. MERKLE (Pennsylvania State University, University Park), and Y.-H. CHOI (Sverdrup Technology, Inc., Brook Park; NASA, Lewis Research Center, Cleveland, OH) AIAA, SAE, ASME, and ASEE, Joint Propulsion Conference and Exhibit, 28th, Nashville, TN, July 6-8, 1992. 16 p. Jul. 1992 16 p refs (Contract NAS8-38861; NAG3-1020; NAGW-1356) (AIAA PAPER 92-3437) Copyright

A previous time-derivative preconditioning procedure for solving the Navier-Stokes is extended to the chemical species equations. The scheme is implemented using both the implicit ADI and explicit Runge-Kutta algorithms. A new definition for time-step is proposed to enable grid-independent convergence. Several examples of both reacting and non-reacting propulsion-related flowfields are considered. In all cases, convergence that is superior to conventional methods is demonstrated. Accuracy is verified using the example of a backward facing step. These results demonstrate that preconditioning can enhance the capability of density-based methods over a wide range of Mach and Reynolds numbers. Author

A92-49068*# National Aeronautics and Space Administration. Lewis Research Center, Cleveland, OH.

INITIAL DEVELOPMENT OF THE AXISYMMETRIC EJECTOR SHEAR LAYER

M. DUFFLOCQ, M. A. BENJAMIN, V. P. ROAN, and W. E. LEAR (Florida University, Gainesville) AIAA, SAE, ASME, and ASEE, Joint Propulsion Conference and Exhibit, 28th, Nashville, TN, July 6-8, 1992. 13 p. Jul. 1992 13 p refs (Contract NAG3-1187) (AIAA PAPER 92-3567) Copyright

An experimental investigation designed to study the development of shear layers in an axisymmetric single-nozzle ejector has been completed. In this study, combinations of air/air, argon/air and helium/air were used as the supersonic primary and subsonic secondary, respectively. Mixing of the gases occurred in a constant-area tube, where the inlet pressure was maintained at 5 psia. The cases studied resulted in convective Mach numbers between 0.3 and 1.9. The resulting data shows dramatic differences in the shear-layer development for the various combinations of independent variables utilized in the investigation. Further, in the region immediately after the inlet to the mixing tube, the axisymmetric shear layers seem to behave in a manner similar to that of two-dimensional mixing layers. The results have enhanced

the ability to analyze and design ejector systems as well as providing a better understanding of the physics. Author

A92-49126*# National Aeronautics and Space Administration, Lewis Research Center, Cleveland, OH.

A COMPUTATIONAL STUDY OF ADVANCED EXHAUST SYSTEM TRANSITION DUCTS WITH EXPERIMENTAL VALIDATION

C. WU, S. FAROKHI, and R. TAGHAVI (Kansas, University, Lawrence) AIAA, SAE, ASME, and ASEE, Joint Propulsion Conference and Exhibit, 28th, Nashville, TN, July 6-8, 1992. 12 p. Research supported by GE Aircraft Engines. Jul. 1992 12 p refs

(Contract NAG3-841)

(AIAA PAPER 92-3794) Copyright

The current study is an application of CFD to a 'real' design and analysis environment. A subsonic, three-dimensional parabolized Navier-Stokes (PNS) code is used to construct stall margin design charts for optimum-length advanced exhaust systems' circular-to-rectangular transition ducts. Computer code validation has been conducted to examine the capability of wall static pressure predictions. The comparison of measured and computed wall static pressures indicates a reasonable accuracy of the PNS computer code results. Computations have also been conducted on 15 transition ducts, three area ratios, and five aspect ratios. The three area ratios investigated are constant area ratio of unity, moderate contracting area ratio of 0.8, and highly contracting area ratio of 0.5. The degree of mean flow acceleration is identified as a dominant parameter in establishing the minimum duct length requirement. The effect of increasing aspect ratio in the minimum length transition duct is to increase the length requirement, as well as to increase the mass-averaged total pressure losses. The design guidelines constructed from this investigation may aid in the design and manufacture of advanced exhaust systems for modern fighter aircraft. Author

A92-49493* National Aeronautics and Space Administration, Lewis Research Center, Cleveland, OH.

RENORMALIZATION GROUP ANALYSIS OF THE REYNOLDS STRESS TRANSPORT EQUATION

R. RUBINSTEIN and J. M. BARTON (Sverdrup Technology, Inc.; NASA, Lewis Research Center, Cleveland, OH) Physics of Fluids A (ISSN 0899-8213), vol. 4, no. 8, Aug. 1992, p. 1759-1766. Previously announced in STAR as N92-23542. Aug. 1992 8 p refs

(Contract NAS3-25266; NCC3-233)

Copyright

A92-49847* National Aeronautics and Space Administration, Lewis Research Center, Cleveland, OH.

FROZEN START-UP BEHAVIOR OF LOW-TEMPERATURE HEAT PIPES

AMIR FAGHRI (Wright State University, Dayton, OH) International Journal of Heat and Mass Transfer (ISSN 0017-9310), vol. 35, no. 7, July 1992, p. 1681-1694. Research supported by NASA and USAF. Jul. 1992 14 p refs

Copyright

Start-up and subsequent operation of a low-temperature heat pipe requires the liquid phase of the operating fluid to be continuously pumped back to the evaporator by the capillary action of the wick. If the pipe has been in an environment where ambient temperatures are below the freezing point of the working fluid prior to start-up, the frozen fluid in the condenser and adiabatic region can prevent initial flow to the evaporator, causing dryout of the evaporator before all of the working fluid is in the liquid phase. This paper examines the time-dependent wall and vapor temperature profiles along the axial length of a low-temperature heat pipe during start-up from the frozen state, and freeze-out during a normal operation by applying a subfreezing temperature fluid through the condenser. In addition, the experimental transient frozen start-up wall temperature profile is compared with a two-dimensional numerical phase-change model. A successful start-up method using a pulsed power input is presented. Author

A92-50445* National Aeronautics and Space Administration, Lewis Research Center, Cleveland, OH.

NATURAL CONVECTION BETWEEN CONCENTRIC SPHERES

VIJAY K. GARG (Pittsburgh, University, PA; NASA, Lewis Research Center, Cleveland, OH) International Journal of Heat and Mass Transfer (ISSN 0017-9310), vol. 35, no. 8, Aug. 1992, p. 1935-1945. Research supported by Pittsburgh Supercomputing Center. Aug. 1992 11 p refs

Copyright

A finite-difference solution for steady natural convective flow in a concentric spherical annulus with isothermal walls has been obtained. The stream function-vorticity formulation of the equations of motion for the unsteady axisymmetric flow is used; interest lying in the final steady solution. Forward differences are used for the time derivatives and second-order central differences for the space derivatives. The alternating direction implicit method is used for solution of the discretization equations. Local one-dimensional grid adaptation is used to resolve the steep gradients in some regions of the flow at large Rayleigh numbers. The break-up into multi-cellular flow is found at high Rayleigh numbers for air and water, and at significantly low Rayleigh numbers for liquid metals. Excellent agreement with previous experimental and numerical data is obtained. Author

A92-50465* National Aeronautics and Space Administration, Lewis Research Center, Cleveland, OH.

THREE-DIMENSIONAL CALCULATIONS OF SUPERSONIC REACTING FLOWS USING AN LU SCHEME

SHENG-TAO YU, Y.-L. P. TSAI, and JIAN-SHUN SHUEN (Sverdrup Technology, Inc.; NASA, Lewis Research Center, Cleveland, OH) Journal of Computational Physics (ISSN 0021-9991), vol. 101, no. 2, Aug. 1992, p. 276-286. Aug. 1992 11 p refs

Copyright

An implicit finite volume lower-upper time-marching method which efficiently solves the complete Navier-Stokes and species equations in a fully coupled fashion is the basis of the present 3D numerical program for simulating the supersonic reacting flows of H₂ in air. The chemistry model incorporated has nine species and 18 reaction steps. Calculations are presented for flowfields of underexpanded hydrogen jets that are transversely injected into the supersonic airstream within scramjet combustors; the shock structure, separated flow regions around the injector, and combustion-product distributions are clearly represented. O.C.

A92-50564* National Aeronautics and Space Administration, Lewis Research Center, Cleveland, OH.

EXPERIMENTS WITH PHASE CHANGE THERMAL ENERGY STORAGE CANISTERS FOR SPACE STATION FREEDOM

THOMAS W. KERSLAKE (NASA, Lewis Research Center, Cleveland, OH) IN: IECEC '91; Proceedings of the 26th Intersociety Energy Conversion Engineering Conference, Boston, MA, Aug. 4-9, 1991. Vol. 1 1991 14 p refs

Copyright

The solar dynamic power module proposed for the Space Station Freedom (SSF) uses the heat of fusion of a phase change material (PCM) to efficiently store thermal energy for use during eclipse periods. The PCM, a LiF-20CaF₂ salt, is contained in annular, metal canisters located in a heat receiver at the focus of a solar concentrator. PCM canister ground-based experiments and analytical heat transfer studies are discussed. The hardware, test procedures, and test results from these experiments are discussed. After more than 900 simulated SSF orbital cycles, no canister cracks or leaks were observed and all data were successfully collected. The effect of 1-g test orientation on canister wall temperatures was generally small while void position was strongly dependent on test orientation and canister cooling. In one test orientation, alternating wall temperature data were measured that supports an earlier theory of oscillating vortex flow in the PCM melt. Analytical canister wall temperatures compared very favorably with experimental temperature data. This illustrates that ground-based canister thermal performance can be predicted well by analyses that employ straight-forward, engineering models of void behavior and liquid PCM free convection. Author

34 FLUID MECHANICS AND HEAT TRANSFER

A92-50568* National Aeronautics and Space Administration. Lewis Research Center, Cleveland, OH.

CRITICAL TECHNOLOGY EXPERIMENT RESULTS FOR LIGHTWEIGHT SPACE HEAT RECEIVER

MICHAEL G. SCHNEIDER, MARK A. BREGE, and GARY R. HEIDENREICH (Sundstrand Corp., Rockford, IL) IN: IECEC '91; Proceedings of the 26th Intersociety Energy Conversion Engineering Conference, Boston, MA, Aug. 4-9, 1991. Vol. 1 1991 7 p refs
(Contract NAS3-25554)

Copyright

Critical technology experiments have been performed on thermal energy storage modules in support of the NASA Advanced Solar Dynamic Brayton Heat Receiver Program. The modules, wedge-shaped canisters containing lithium fluoride (LiF), were designed to minimize the mechanical stresses that occur during the phase change of the LiF. Nickel foam inserts were placed in two of the test canisters to provide thermal conductivity enhancement and to distribute the void volume throughout the canister. A procedure was developed for reducing the nickel oxides on the nickel foam to enhance the wicking ability of the foam. The canisters were filled with LiF and closure-welded at the NASA Lewis Research Center. Two canisters, one with a nickel foam insert, the other without an insert, were thermally cycled in various orientations in a fluidized bed furnace. Computer-aided tomography was successfully used to nondestructively determine void locations in the canisters. Finally, canister dimensional stability was measured after thermal cycling with an inspection fixture. I.E.

A92-50570* National Aeronautics and Space Administration. Lewis Research Center, Cleveland, OH.

SENSIBLE HEAT RECEIVER FOR SOLAR DYNAMIC SPACE POWER SYSTEM

MARLA E. PEREZ-DAVIS, JAMES R. GAIER (NASA, Lewis Research Center, Cleveland, OH), and CHRIS PETREFSKI (Cleveland State University, OH) IN: IECEC '91; Proceedings of the 26th Intersociety Energy Conversion Engineering Conference, Boston, MA, Aug. 4-9, 1991. Vol. 1 1991 4 p refs

Copyright

A sensible heat receiver is considered which uses a vapor grown carbon fiber-carbon (VGCF/C) composite as the thermal storage medium and which was designed for a 7-kW Brayton engine. This heat receiver stores the required energy to power the system during eclipse in the VGCF/C composite. The heat receiver thermal analysis was conducted through the Systems Improved Numerical Differencing Analyzer and Fluid Integrator (SINDA) software package. The sensible heat receiver compares well with other latent and advanced sensible heat receivers analyzed in other studies, while avoiding the problems associated with latent heat storage salts and liquid metal heat pipes. The concept also satisfies the design requirements for a 7-kW Brayton engine system. The weight and size of the system can be optimized by changes in geometry and technology advances for this new material. I.E.

A92-50591* National Aeronautics and Space Administration. Lewis Research Center, Cleveland, OH.

HEAT TRANSFER AND CORE NEUTRONICS CONSIDERATIONS OF THE HEAT PIPE COOLED THERMIONIC REACTOR

W. R. DETERMAN (Rockwell International Corp., Rocketdyne Div., Canoga Park, CA) and BRIAN LEWIS (General Atomics, San Diego, CA) IN: IECEC '91; Proceedings of the 26th Intersociety Energy Conversion Engineering Conference, Boston, MA, Aug. 4-9, 1991. Vol. 1 1991 5 p refs
(Contract NAS3-25209)

Copyright

The authors summarize the results of detailed neutronic and thermal-hydraulic evaluations of the heat pipe cooled thermionic (HPTI) reactor design, identify its key design attributes, and quantify its performance characteristics. The HPTI core uses modular, liquid-metal core heat transfer assemblies to replace the liquid-metal heat transport loop employed by in-core thermionic

reactor designs of the past. The nuclear fuel, power conversion, heat transport, and heat rejection functions are all combined into a single modular unit. The reactor/converter assembly uses UN fuel pins to obtain a critical core configuration with in-core safety rods and reflector controls added to complete the subassembly. By thermally bonding the core heat transfer assemblies during the reactor core is coupled neutronically, thermally, and electrically into a modular assembly of individual power sources with cross-tied architecture. A forward-facing heat pipe radiator assembly extends from the reactor head in the shape of a frustum of a cone on the opposite side of the power system from the payload. Important virtues of the concept are the absence of any single-point failures and the ability of the core to effectively transfer the TFE waste heat load laterally to other in-core heat transfer assemblies in the event of multiple failures in either in-core and radiator heat pipes. I.E.

A92-50596* National Aeronautics and Space Administration. Lewis Research Center, Cleveland, OH.

SHRINKAGE VOID FORMATION AND ITS EFFECT ON FREEZE AND THAW PROCESSES OF LITHIUM AND LITHIUM-FLUORIDE FOR SPACE APPLICATIONS

JAE Y. YANG and MOHAMED S. EL-GENK (New Mexico, University, Albuquerque) IN: IECEC '91; Proceedings of the 26th Intersociety Energy Conversion Engineering Conference, Boston, MA, Aug. 4-9, 1991. Vol. 1 1991 5 p refs
(Contract NAG3-1045)

Copyright

The effects of shrinkage void forming during freezing of lithium and lithium fluoride on subsequent thaw processes are investigated using a numerical scheme that is based on a single (solid/liquid) cell approach. Results show that a void forming at the wall appreciably reduces the solid-liquid interface velocity, during both freeze and thaw, and causes a substantial rise in the wall temperature during thaw. However, in the case of Li, the maximum wall temperature was much lower than the melting temperature of PWC-11, which is used as the structure material in the SP-100 system. Hence, it is concluded that a formation of hot spots is unlikely during the startup or restart of the SP-100 system. I.E.

A92-50738* National Aeronautics and Space Administration. Lewis Research Center, Cleveland, OH.

MEASUREMENTS OF THE EFFECTS OF THERMAL CONTACT RESISTANCE ON STEADY STATE HEAT TRANSFER IN PHOSPHORIC-ACID FUEL CELL STACK

ALI ABDUL-AZIZ (Sverdrup Technology, Inc.; NASA, Lewis Research Center, Cleveland, OH) and KALIL A. ALKASAB (Cleveland State University, OH) IN: IECEC '91; Proceedings of the 26th Intersociety Energy Conversion Engineering Conference, Boston, MA, Aug. 4-9, 1991. Vol. 3 1991 6 p refs

Copyright

The influence of the thermal contact resistance on the heat transfer between the electrode plates, and the cooling system plate in a phosphoric-acid fuel-cell stack was experimentally investigated. The investigation was conducted using a set-up that simulates the operating conditions prevailing in a phosphoric acid fuel-cell stack. The fuel-cell cooling system utilized three types of coolants, water, engine oil, and air, to remove excess heat generated in the cell electrode and to maintain a reasonably uniform temperature distribution in the electrode plate. The thermal contact resistance was measured as a function of pressure at the interface between the electrode plate and the cooling system plate. The interface pressure range was from 0 kPa to 3448 kPa, while the Reynolds number for the cooling limits varied from 15 to 79 for oil, 1165 to 6165 for water, and 700 to 6864 for air. Results showed that increasing the interface pressure resulted in a higher heat transfer coefficient. I.E.

A92-50751* National Aeronautics and Space Administration. Lewis Research Center, Cleveland, OH.

OBSERVATIONS OF THE FREEZE/THAW PERFORMANCE OF LITHIUM FLUORIDE BY MOTION PICTURE PHOTOGRAPHY

D. A. JAWORSKE (NASA, Lewis Research Center, Cleveland, OH)

and W. D. PERRY (Auburn University, AL) IN: IECEC '91; Proceedings of the 26th Intersociety Energy Conversion Engineering Conference, Boston, MA, Aug. 4-9, 1991. Vol. 4 1991 4 p refs
Copyright

To gain direct observation of the molten salt phase change, a novel containerless technique was developed where the high surface tension of lithium fluoride was used to suspend a bead of the molten salt inside a specially designed wire cage. By varying the current passing through the wire, the cage also served as a variable heat source. In this way, the freeze/thaw performance of the lithium fluoride could be photographed by motion picture photography without the influence of container walls. The motion picture photography of the lithium fluoride sample revealed several zones during the phase change, a solid zone and a liquid zone, as expected, and a slush zone that was predicted by thermal analysis modeling. I.E.

A92-50802* National Aeronautics and Space Administration. Lewis Research Center, Cleveland, OH.

DESIGN OF A POOL BOILER HEAT TRANSPORT SYSTEM FOR A 25 KWE ADVANCED STIRLING CONVERSION SYSTEM

W. G. ANDERSON, J. H. ROSENFELD (Thermacore, Inc., Lancaster, PA), J. NOBLE (Stirling Technologies Co., Richland, WA), and J. KESSELI (Kesseli Associates, Mount Vernon, NH) IN: IECEC '91; Proceedings of the 26th Intersociety Energy Conversion Engineering Conference, Boston, MA, Aug. 4-9, 1991. Vol. 5 1991 6 p refs

(Contract DEN3-377)

Copyright

The overall operating temperature and efficiency of solar-powered Stirling engines can be improved by adding a heat transport system to more uniformly supply heat to the heater head tubes. One heat transport system with favorable characteristics is an alkali metal pool boiler. An alkali metal pool boiler heat transport system was designed for a 25-kW advanced Stirling conversion system (ASCS). Solar energy concentrated on the absorber dome boils a eutectic mixture of sodium and potassium. The alkali metal vapors condense on the heater head tubes, supplying the Stirling engine with a uniform heat flux at a constant temperature. Boiling stability is achieved with the use of an enhanced boiling surface and noncondensable gas. I.E.

A92-50821* National Aeronautics and Space Administration. Lewis Research Center, Cleveland, OH.

DESIGN CONSIDERATIONS FOR SPACE RADIATORS BASED ON THE LIQUID SHEET (LSR) CONCEPT

ALBERT J. JUHASZ and DONALD L. CHUBB (NASA, Lewis Research Center, Cleveland, OH) IN: IECEC '91; Proceedings of the 26th Intersociety Energy Conversion Engineering Conference, Boston, MA, Aug. 4-9, 1991. Vol. 6 1991 6 p refs

Copyright

This study is directed at performing a comparative examination of LSR characteristics as they affect the basic design of low earth orbit solar dynamic conversion systems. The power systems considered were based on the closed Brayton (CBC) and the free piston Stirling (FPS) cycles, each with a power output of 2 kW and using previously tested silicone oil (Dow-Corning Me2) as the radiator working fluid. Conclusions indicate that, due to its ability for direct cold end cooling, an LSR based heat rejection subsystem is far more compatible with a Stirling space power system than with a CBC, which requires LSR coupling by means of an intermediate gas/liquid heat exchanger and adjustment of cycle operating conditions. Author

A92-50827* National Aeronautics and Space Administration. Lewis Research Center, Cleveland, OH.

INSTANTANEOUS HEAT TRANSFER COEFFICIENT BASED UPON TWO-DIMENSIONAL ANALYSES OF STIRLING SPACE ENGINE COMPONENTS

MOUNIR IBRAHIM, MOHAN KANNAPAREDDY (Cleveland State University, OH), ROY C. TEW, and JAMES E. DUDENHOEFER (NASA, Lewis Research Center, Cleveland, OH) IN: IECEC '91;

Proceedings of the 26th Intersociety Energy Conversion Engineering Conference, Boston, MA, Aug. 4-9, 1991. Vol. 6 1991 11 p refs

Copyright

Twelve different cases of multidimensional models of Stirling engine components for space applications have been numerically investigated for oscillating, incompressible laminar flow with heat transfer. The cases studied covered wide ranges of Valensi number (from 44 to 700), Re(max) number (from 8250 to 60,000), and relative amplitude of fluid motion of 0.686 and 1.32. The Nusselt numbers obtained from the present study indicate a very complex shape with respect to time and axial location in the channel. The results indicate that three parameters can be used to define the local Nusselt number variation, namely: time average, amplitude, and phase angle. These parameters could be correlated respectively using: Re(max), Va and Re(max), and the relative amplitude of fluid motion. I.E.

A92-50968* National Aeronautics and Space Administration. Lewis Research Center, Cleveland, OH.

PROPAGATING CONFINED STATES IN PHASE DYNAMICS

HELMUT R. BRAND (Los Alamos National Laboratory, NM; Universitaet Essen-Gesamthochschule, Federal Republic of Germany) and ROBERT J. DEISSLER (Los Alamos National Laboratory, NM; NASA, Lewis Research Center, Cleveland, OH) Physical Review A (ISSN 1050-2947), vol. 46, no. 2, July 15, 1992, p. 888-892. Research supported by DOE and DFG. 15 Jul. 1992 5 p refs

Copyright

Theoretical treatment is given to the possibility of the existence of propagating confined states in the nonlinear phase equation by generalizing stationary confined states. The nonlinear phase equation is set forth for the case of propagating patterns with long wavelengths and low-frequency modulation. A large range of parameter values is shown to exist for propagating confined states which have spatially localized regions which travel on a background with unique wavelengths. The theoretical phenomena are shown to correspond to such physical systems as spirals in Taylor instabilities, traveling waves in convective systems, and slot-convection phenomena for binary fluid mixtures. C.C.S.

A92-52406* National Aeronautics and Space Administration. Lewis Research Center, Cleveland, OH.

A COMPUTER MODEL FOR ONE-DIMENSIONAL MASS AND ENERGY TRANSPORT IN AND AROUND CHEMICALLY REACTING PARTICLES, INCLUDING COMPLEX GAS-PHASE CHEMISTRY, MULTICOMPONENT MOLECULAR DIFFUSION, SURFACE EVAPORATION, AND HETEROGENEOUS REACTION

S. Y. CHO, R. A. YETTER, and F. L. DRYER (Princeton University, NJ) Journal of Computational Physics (ISSN 0021-9991), vol. 102, no. 1, Sept. 1992, p. 160-179. Research supported by EPRI. Sep. 1992 20 p refs

(Contract NAS3-24640; F49670-86-C-0087)

Copyright

Various chemically reacting flow problems highlighting chemical and physical fundamentals rather than flow geometry are presently investigated by means of a comprehensive mathematical model that incorporates multicomponent molecular diffusion, complex chemistry, and heterogeneous processes, in the interest of obtaining sensitivity-related information. The sensitivity equations were decoupled from those of the model, and then integrated one time-step behind the integration of the model equations, and analytical Jacobian matrices were applied to improve the accuracy of sensitivity coefficients that are calculated together with model solutions. O.C.

A92-53031* National Aeronautics and Space Administration. Lewis Research Center, Cleveland, OH.

EFFECT OF INDEX OF REFRACTION ON RADIATION CHARACTERISTICS IN A HEATED ABSORBING, EMITTING, AND SCATTERING LAYER

R. SIEGEL and C. M. SPUCKLER (NASA, Lewis Research Center,

Cleveland, OH) ASME, Transactions, Journal of Heat Transfer (ISSN 0022-1481), vol. 114, no. 3, Aug. 1992, p. 781-784. Aug. 1992 4 p refs

Copyright

The effect of the index of refraction on the temperature distribution and radiative heat flux in semitransparent materials, such as some ceramics, is investigated analytically. In the case considered here, a plane layer of a ceramic material is subjected to external radiative heating incident on each of its surfaces; the material emits, absorbs, and isotropically scatters radiation. It is shown that, for radiative equilibrium in a gray layer with diffuse interfaces, the temperature distribution and radiative heat flux for any index of refraction can be obtained in a simple manner from the results for an index of refraction of unity. V.L.

A92-54001*# National Aeronautics and Space Administration. Lewis Research Center, Cleveland, OH.

JET MIXING IN LOW GRAVITY - RESULTS OF THE TANK PRESSURE CONTROL EXPERIMENT

M. D. BENTZ, J. S. MESEROLE (Boeing Defense & Space Group, Seattle, WA), and R. H. KNOLL (NASA, Lewis Research Center, Cleveland, OH) AIAA, SAE, ASME, and ASEE, Joint Propulsion Conference and Exhibit, 28th, Nashville, TN, July 6-8, 1992. 10 p. Jul. 1992 10 p refs (AIAA PAPER 92-3060) Copyright

The Tank Pressure Control Experiment (TPCE) is discussed with attention given to the results for controlling storage-tank pressures by forced-convective mixing in microgravitational environments. The fluid dynamics of cryogenic fluids in space is simulated with freon-113 during axial-jet-induced mixing. The experimental flow-pattern data are found to confirm previous data as well as existing mixing correlations. Thermal nonuniformities and tank pressure can be reduced by employing low-energy mixing jets which are useful for enhancing heat/mass transfer between phases. It is found that space cryogenic systems based on the principle of active mixing can be more reliable and predictable than other methods, and continuous or periodic mixing can be accomplished with only minor energy addition to the fluid. C.C.S.

A92-54008*# National Aeronautics and Space Administration. Lewis Research Center, Cleveland, OH.

AN INVESTIGATION OF SHOCK/TURBULENT BOUNDARY LAYER BLEED INTERACTIONS

A. HAMED, S. H. SHIH, and J. J. YEUN (Cincinnati, University, OH) AIAA, SAE, ASME, and ASEE, Joint Propulsion Conference and Exhibit, 28th, Nashville, TN, July 6-8, 1992. 11 p. Jul. 1992 11 p refs (Contract AF-AFOSR-91-0101; NAG3-1213) (AIAA PAPER 92-3085) Copyright

A numerical investigation was conducted to determine the effect of bleed on oblique shock wave/turbulent boundary layer interactions. The numerical solution to the compressible Navier-Stokes equations reveal the flow details throughout the interaction zone and inside the normal bleed slot. Results are presented for an incident oblique shock of sufficient strength to cause boundary layer separation in the absence of bleed. Bleed is applied across the shock impingement location over a range of bleed mass flow rates corresponding to different values of plenum pressures. The results indicate a complex flow structure with large variations in both normal and tangential flow velocities across the bleed slot. The flow entrainment into the slot is accompanied by an expansion-compression wave system with a bow shock originating inside the bleed slot. Increasing the bleed mass flow by decreasing the plenum pressure caused an initial decrease then a later increase in the boundary layer momentum and displacement thickness downstream of the interaction. Author

A92-54015*# National Aeronautics and Space Administration. Lewis Research Center, Cleveland, OH.

RUNGE-KUTTA METHODS COMBINED WITH COMPACT DIFFERENCE SCHEMES FOR THE UNSTEADY EULER EQUATIONS

S. T. YU, Y.-L. P. TSAI, and K. C. HSIEH (Sverdrup Technology,

Inc., Brook Park; NASA, Lewis Research Center, Cleveland, OH) AIAA, SAE, ASME, and ASEE, Joint Propulsion Conference and Exhibit, 28th, Nashville, TN, July 6-8, 1992. 28 p. Jul. 1992 28 p refs

(AIAA PAPER 92-3210) Copyright

An investigation of the Runge-Kutta time-stepping, combined with compact difference schemes to solve the unsteady Euler equations, is presented. Initially, a generalized form of a N-step Runge-Kutta technique is derived. By comparing this generalized form with its Taylor's series counterpart, the criteria for the three-step and four-step schemes to be of third- and fourth-order accurate are obtained. R.E.P.

A92-54043*# National Aeronautics and Space Administration. Lewis Research Center, Cleveland, OH.

FILTERED RAYLEIGH SCATTERING BASED MEASUREMENTS IN COMPRESSIBLE MIXING LAYERS

G. S. ELLIOTT, M. SAMIMY, and S. A. ARNETTE (Ohio State University, Columbus) AIAA, SAE, ASME, and ASEE, Joint Propulsion Conference and Exhibit, 28th, Nashville, TN, July 6-8, 1992. 24 p. Jul. 1992 24 p refs (Contract NAG3-764; NSF CTS-90-06879) (AIAA PAPER 92-3543) Copyright

Results are presented of experiments in which a Rayleigh-scattering-based technique was used to make quantitative planar measurements in the compressible free shear layers. To this end, the absorption characteristics of the iodine molecular filter were investigated, and initial planar density measurements in $M(c) = 0.51$ shear layer were performed. The preliminary results presented here demonstrate the validity of the measurement technique. I.S.

A92-54112*# National Aeronautics and Space Administration. Lewis Research Center, Cleveland, OH.

A TIME-ACCURATE ALGORITHM FOR CHEMICAL NON-EQUILIBRIUM VISCOUS FLOWS AT ALL SPEEDS

J.-S. SHUEN (Sverdrup Technology, Inc.; NASA, Lewis Research Center, Cleveland, OH), K.-H. CHEN (Toledo, University; NASA, Lewis Research Center, Cleveland, OH), and Y. CHOI (Sverdrup Technology, Inc.; NASA, Lewis Research Center, Cleveland, OH) AIAA, SAE, ASME, and ASEE, Joint Propulsion Conference and Exhibit, 28th, Nashville, TN, July 6-8, 1992. 27 p. Jul. 1992 27 p refs (AIAA PAPER 92-3639) Copyright

A time-accurate, coupled solution procedure is described for the chemical nonequilibrium Navier-Stokes equations over a wide range of Mach numbers. This method employs the strong conservation form of the governing equations, but uses primitive variables as unknowns. Real gas properties and equilibrium chemistry are considered. Numerical tests include steady convergent-divergent nozzle flows with air dissociation/recombination chemistry, dump combustor flows with n-pentane-air chemistry, nonreacting flow in a model double annular combustor, and nonreacting unsteady driven cavity flows. Numerical results for both the steady and unsteady flows demonstrate the efficiency and robustness of the present algorithm for Mach numbers ranging from the incompressible limit to supersonic speeds. Author

A92-54115*# National Aeronautics and Space Administration. Lewis Research Center, Cleveland, OH.

COMPUTATION OF H2/AIR REACTING FLOWFIELDS IN DRAG-REDUCTION EXTERNAL COMBUSTION

H. T. LAI (Sverdrup Technology, Inc.; NASA, Lewis Research Center, Cleveland, OH) AIAA, SAE, ASME, and ASEE, Joint Propulsion Conference and Exhibit, 28th, Nashville, TN, July 6-8, 1992. 17 p. Jul. 1992 17 p refs (Contract NAS3-24105; NAS3-25266) (AIAA PAPER 92-3672)

Numerical simulation and analysis of the solution are presented for a laminar reacting flowfield of air and hydrogen in the case of an external combustion employed to reduce base drag in hypersonic vehicles operating at transonic speeds. The flowfield

consists of a transonic air stream at a Mach number of 1.26, and a sonic transverse hydrogen injection along a row of 26 orifices. Self-sustained combustion is computed over an expansion ramp downstream of the injection and a flameholder, using the recently developed RPLUS code. Measured data is available only for surface pressure distributions, and is used for validation of the code in practical 3D reacting flowfields. Pressure comparison shows generally good agreements and the main effects of combustion are also qualitatively consistent with experiment. Author

A92-54132*# National Aeronautics and Space Administration. Lewis Research Center, Cleveland, OH.

A FINITE-VOLUME NUMERICAL METHOD TO CALCULATE FLUID FORCES AND ROTORDYNAMIC COEFFICIENTS IN SEALS

M. M. ATHAVALE, A. J. PRZEKAWAS (CFD Research Corp., Huntsville, AL), and R. C. HENDRICKS (NASA, Lewis Research Center, Cleveland, OH) AIAA, SAE, ASME, and ASEE, Joint Propulsion Conference and Exhibit, 28th, Nashville, TN, July 6-8, 1992. 12 p. Jul. 1992 12 p refs (Contract NAS3-25644)

(AIAA PAPER 92-3712) Copyright

A numerical method to calculate rotordynamic coefficients of seals is presented. The flow in a seal is solved by using a finite-volume formulation of the full Navier-Stokes equations with appropriate turbulence models. The seal rotor is perturbed along a diameter such that the position of the rotor is a sinusoidal function of time. The resulting flow domain changes with time, and the time-dependent flow in the seal is solved using a space conserving moving grid formulation. The time-varying fluid pressure reaction forces are then linked with the rotor center displacement, velocity and acceleration to yield the rotordynamic coefficients. Results for an annular seal are presented, and compared with experimental data and other more simplified numerical methods.

Author

A92-54170*# National Aeronautics and Space Administration. Lewis Research Center, Cleveland, OH.

COMPUTATIONAL AND EXPERIMENTAL INVESTIGATION OF SUBSONIC INTERNAL REVERSING FLOWS

JAMES A. RHODES (McDonnell Aircraft Co., Saint Louis, MO), BARBARA S. ESKER (NASA, Lewis Research Center, Cleveland, OH), and C. F. SMITH (Sverdrup Technology Inc., Brook Park, OH) AIAA, SAE, ASME, and ASEE, Joint Propulsion Conference and Exhibit, 28th, Nashville, TN, July 6-8, 1992. 12 p. Jul. 1992 12 p refs

(AIAA PAPER 92-3791) Copyright

The flow inside a model exhaust configuration was studied using both experimental and computational techniques. The hardware was tested at the NASA Lewis Research Center's Powered Lift Facility at tailpipe total pressure to ambient static pressure ratios ranging from 1.0 to 5.0. The flow simulations were obtained using the two 3-D Navier-Stokes CFD codes run on the Lewis Cray Y-MP computer. Both codes produced oscillatory solutions due to the inflow boundary condition reflecting acoustic waves. The CFD solutions correctly predicted the flow separation along the inside elbow of the takeoff and also along the walls of the ventral duct. Mass flow rates were overpredicted due to underprediction of the turbulent energy dissipation and subsequent total pressure loss.

Author

A92-54209*# National Aeronautics and Space Administration. Lewis Research Center, Cleveland, OH.

DEVELOPMENT OF AN ALGEBRAIC TURBULENCE MODEL FOR ANALYSIS OF PROPULSION FLOWS

N. J. GEORGIADIS (NASA, Lewis Research Center, Cleveland, OH), J. E. DRUMMOND, and B. P. LEONARD (Akron, University, OH) AIAA, SAE, ASME, and ASEE, Joint Propulsion Conference and Exhibit, 28th, Nashville, TN, July 6-8, 1992. 13 p. Previously announced in STAR as N92-27517. Jul. 1992 13 p refs (AIAA PAPER 92-3861) Copyright

A simple turbulence model that will be applicable to propulsion flows having both wall bounded and unbounded regions was

developed and installed within the PARC Navier-Stokes code by linking two existing algebraic turbulence models. The first is the Modified Mixing Length (MML) model which is optimized for wall bounded flows. The second is the Thomas model, the standard algebraic turbulence model in PARC which has been used to calculate both bounded and unbounded turbulent flows but was optimized for the latter. This paper discusses both models and the method employed to link them into one model (referred to as the MMLT model). The PARC code with the MMLT model was applied to two dimensional turbulent flows over a flat plate and over a backward facing step to validate and optimize the model and to compare its predictions to those obtained with the three turbulence models already available in PARC. Author

A92-54907* National Aeronautics and Space Administration. Lewis Research Center, Cleveland, OH.

NUMERICAL STUDY OF SHOCK-WAVE/BOUNDARY-LAYER INTERACTIONS IN PREMIXED COMBUSTIBLE GASES

SHAYE YUNGSTER (NASA, Lewis Research Center, Cleveland, OH) Oct. 1992 9 p refs

Copyright

A92-54917 National Aeronautics and Space Administration. Lewis Research Center, Cleveland, OH.

EXPERIMENTAL AND NUMERICAL INVESTIGATIONS OF LOW-DENSITY NOZZLE AND PLUME FLOWS OF NITROGEN

IAIN D. BOYD (Eloret Institute, Palo Alto, CA), PAUL F. PENKO (NASA, Lewis Research Center, Cleveland, OH), DANA L. MEISSNER, and KENNETH J. DEWITT (Toledo, University, OH) AIAA Journal (ISSN 0001-1452), vol. 30, no. 10, Oct. 1992, p. 2453-2461. Oct. 1992 9 p refs (Contract NCC2-582)

Copyright

New experimental data are used to show that the direct simulation Monte Carlo (DSMC) method provides an accurate description of a low-density flow in the nozzle and the near-field expansion of a small rocket for two slightly different experimental configurations. These results verify the DSMC method in an expansion flow for the first time. From a number of different gas/surface interaction models, it is found that fully diffuse reflection gives the best agreement with experiment. C.D.

A92-54937* National Aeronautics and Space Administration. Lewis Research Center, Cleveland, OH.

STUDY OF COMPRESSIBLE MIXING LAYERS USING FILTERED RAYLEIGH SCATTERING BASED VISUALIZATIONS

GREGORY S. ELLIOTT, MO SAMIMY, and STEPHEN A. ARNETTE (Ohio State University, Columbus) AIAA Journal (ISSN 0001-1452), vol. 30, no. 10, Oct. 1992, p. 2567-2569. Oct. 1992 3 p refs (Contract NAG3-764; NSF CTS-90-06879; N00014-90-J-1730)

Copyright

Filtered Rayleigh scattering-based flow visualizations of compressible mixing layers are reported. The lower compressibility case ($Mc = 0.51$) displays well-defined roller-type spanwise structures and streamwise streaks. The structures of the high compressibility case ($Mc = 0.86$) are more 3D and oblique. C.D.

A92-56371* National Aeronautics and Space Administration. Lewis Research Center, Cleveland, OH.

SURFACE HEAT TRANSFER AND FLOW PROPERTIES OF VORTEX ARRAYS INDUCED ARTIFICIALLY AND FROM CENTRIFUGAL INSTABILITIES

C. S. SUBRAMANIAN (Florida Institute of Technology, Melbourne), P. M. LIGRANI (Utah, University, Salt Lake City), and M. F. TUZZOLO (U.S. Naval Postgraduate School, Monterey, CA) International Journal of Heat and Fluid Flow (ISSN 0142-727X), vol. 13, no. 3, Sept. 1992, p. 210-223. Research sponsored by U.S. Navy and U.S. Army. Sep. 1992 14 p refs (Contract NASA ORDER C-30030-P)

Copyright

The paper presents and compares fluid-flow and heat transfer properties from artificially induced vortices in a flat-plate turbulent boundary layer and naturally occurring vortices due to centrifugal

instabilities in a curved-channel laminar flow. Pairs and arrays of vortices are artificially induced by placing half-delta wings on the plate surface. With both arrays and pairs of vortices, streamwise velocities and total pressures are high, and surface heat transfer is locally augmented in vortex downwash regions. In contrast to vortices in the arrays vortices in the pairs tend to move in the streamwise direction with significant divergence (when the common flow between pair is toward the wall) or convergence (when the common flow between pair is away from the wall). The vortices in the arrays cause maximum peak-to-peak heat transfer variations of up to 12 percent of local spanwise-averaged values for initial vortex spacings between 1 to 2.5 generator heights. C.A.B.

A92-56941* National Aeronautics and Space Administration. Lewis Research Center, Cleveland, OH.

SCALAR RATE CORRELATION AT A TURBULENT LIQUID FREE SURFACE - A TWO-REGIME CORRELATION FOR HIGH SCHMIDT NUMBERS

BOO-CHEONG KHOO and AIN A. SONIN (MIT, Cambridge, MA) International Journal of Heat and Mass Transfer (ISSN 0017-9310), vol. 35, no. 9, Sept. 1992, p. 2233-2244. Sep. 1992 12 p refs

(Contract NAG3-731) Copyright

An experimental correlation is derived for gas absorption at a turbulent, shear-free liquid interface. The correlation is expressed in terms of the liquid-side turbulence intensity, liquid-side macroscale, and the properties of the diffusing gas and solvent. The transfer coefficient increases linearly with rms velocity up to a point where the eddy Reynolds number reaches a critical (Schmidt number dependent) value. At higher velocities, there is a more rapid linear rise. The slope of the lower Reynolds number region is proportional to the square root of the diffusivity; at Reynolds numbers much higher than that of the break point, the slope becomes independent of diffusivity. Author

A92-57286* National Aeronautics and Space Administration. Lewis Research Center, Cleveland, OH.

INTERFACIAL AND GRAVITATIONAL CONVECTION IN IMMISCIBLE LIQUID LAYERS

A. PRAKASH and J. N. KOSTER (Colorado, University, Boulder) IAF, International Astronautical Congress, 43rd, Washington, Aug. 28-Sept. 5, 1992. 8 p. Aug. 1992 8 p refs

(Contract NAG3-1094) (IAF PAPER 92-0907) Copyright

Liquid encapsulation of electronic melts is currently being investigated by several materials science research groups. Pertinent fluid dynamics of immiscible liquid layers is the objective of this investigation. First results on convective flow in double liquid layers, in preparation for a spacelift experiment aboard the International Microgravity Laboratory, IML-2, are discussed. Author

N92-11299*# National Aeronautics and Space Administration. Lewis Research Center, Cleveland, OH.

MODELING OF THE HEAT TRANSFER IN BYPASS TRANSITIONAL BOUNDARY-LAYER FLOWS

FREDERICK F. SIMON and CRAIG A. STEPHENS (PRC Kentron, Inc., Edwards, CA.) Washington Oct. 1991 15 p

(Contract RTOP 505-62-52) (NASA-TP-3170; E-6046; NAS 1.60:3170) Avail: CASI HC A03/MF A01

A low Reynolds number k-epsilon turbulence model and conditioned momentum, energy and turbulence equations were used to predict bypass transition heat transfer on a flat plate in a high-disturbance environment with zero pressure gradient. The use of conditioned equations was demonstrated to be an improvement over the use of the global-time-averaged equations for the calculation of velocity profiles and turbulence intensity profiles in the transition region of a boundary layer. The approach of conditioned equations is extended to include heat transfer and a modeling of transition events is used to predict transition onset and the extent of transition on a flat plate. The events, which describe the boundary layer at the leading edge, result in

boundary-layer regions consisting of: (1) the laminar, (2) pseudolaminar, (3) transitional, and (4) turbulent boundary layers. The modeled transition events were incorporated into the TEXSTAN 2-D boundary-layer code which is used to numerically predict the heat transfer. The numerical predictions in general compared well with the experimental data and revealed areas where additional experimental information is needed. Author

N92-11302*# National Aeronautics and Space Administration. Lewis Research Center, Cleveland, OH.

ON THE BASIC EQUATIONS FOR THE SECOND-ORDER MODELING OF COMPRESSIBLE TURBULENCE

W. W. LIOU and T.-H. SHIH Oct. 1991 28 p (Contract NASA ORDER C-99066-G; RTOP 505-62-21) (NASA-TM-105277; ICOMP-91-19; CMOTT-91-08; E-6600; NAS 1.15:105277) Avail: CASI HC A03/MF A01

Equations for the mean and turbulent quantities for compressible turbulent flows are derived. Both the conventional Reynolds average and the mass-weighted, Favre average were employed to decompose the flow variable into a mean and a turbulent quality. These equations are to be used later in developing second order Reynolds stress models for high speed compressible flows. A few recent advances in modeling some of the terms in the equations due to compressibility effects are also summarized. Author

N92-11317*# National Aeronautics and Space Administration. Lewis Research Center, Cleveland, OH.

TURBULENT FLUID MOTION 3: BASIC CONTINUUM EQUATIONS

ROBERT G. DEISSLER Oct. 1991 20 p (Contract RTOP 505-90-01)

(NASA-TM-104386; E-6196; NAS 1.15:104386) Avail: CASI HC A03/MF A01

A derivation of the continuum equations used for the analysis of turbulence is given. These equations include the continuity equation, the Navier-Stokes equations, and the heat transfer or energy equation. An experimental justification for using a continuum approach for the study of turbulence is given. Author

N92-11320*# National Aeronautics and Space Administration. Lewis Research Center, Cleveland, OH.

AN EFFICIENT AND ROBUST ALGORITHM FOR TWO DIMENSIONAL TIME DEPENDENT INCOMPRESSIBLE NAVIER-STOKES EQUATIONS: HIGH REYNOLDS NUMBER FLOWS

JOHN W. GOODRICH 1991 17 p Presented at the Seventh International Conference on Numerical Methods in Laminar and Turbulent Flow, Stanford, CA, 15-19 Jul. 1991; sponsored by LMSC, Stanford Univ., International Journal for Numerical Methods in Fluids, and International Journal for Computational Methods in Heat and Fluid Flow

(Contract RTOP 505-62-21) (NASA-TM-104424; E-6257; NAS 1.15:104424) Avail: CASI HC A03/MF A01

An algorithm is presented for unsteady two-dimensional incompressible Navier-Stokes calculations. This algorithm is based on the fourth order partial differential equation for incompressible fluid flow which uses the streamfunction as the only dependent variable. The algorithm is second order accurate in both time and space. It uses a multigrid solver at each time step. It is extremely efficient with respect to the use of both CPU time and physical memory. It is extremely robust with respect to Reynolds number. Author

N92-11328*# National Aeronautics and Space Administration. Lewis Research Center, Cleveland, OH.

EULER SOLUTIONS FOR AN UNBLADED JET ENGINE CONFIGURATION

MARK E. M. STEWART 1991 9 p Proposed for presentation at the 30th Aerospace Sciences Meeting and Exhibit, Reno, NV, 6-9 Jan. 1991; sponsored by AIAA (Contract NASA ORDER C-99066-G; RTOP 505-62-21)

(NASA-TM-105332; ICOMP-91-23; E-6695; NAS 1.15:105332)
 Avail: CASI HC A02/MF A01

A Euler solution for an axisymmetric jet engine configuration without blade effects is presented. The Euler equations are solved on a multiblock grid which covers a domain including the inlet, bypass duct, core passage, nozzle, and the far field surrounding the engine. The simulation is verified by considering five theoretical properties of the solution. The solution demonstrates both multiblock grid generation techniques and a foundation for a full jet engine throughflow calculation.
 Author

N92-13401*# National Aeronautics and Space Administration.
 Lewis Research Center, Cleveland, OH.

HYDROGEN NO-VENT FILL TESTING IN A 1.2 CUBIC FOOT (34 LITER) TANK

MATTHEW E. MORAN, TED W. NYLAND, and SUSAN L. DRISCOLL (National Aeronautics and Space Administration, Marshall Space Flight Center, Huntsville, AL.) Oct. 1991 43 p (Contract RTOP 593-21-41)
 (NASA-TM-105273; E-6596; NAS 1.15:105273) Avail: CASI HC A03/MF A01

Experimental results of no-vent fill testing with liquid hydrogen in a 1.2 cubic foot (34 liter) stainless steel tank are presented. More than 40 tests were performed with various liquid inlet temperatures, inlet flowrates, initial tank wall temperatures, and liquid injection techniques. Fill levels equal to or exceeding 90 percent by volume were achieved in 40 percent of the tests with the tank pressure limited to a maximum of 30 psia. Three liquid injection techniques were employed; top spray, upward pipe discharge, and bottom diffuser. Effects of each of the varied parameters on the tank pressure history and final fill level are evaluated. The final fill level is found to be indirectly proportional to the initial wall and inlet liquid temperatures and directly proportional to the inlet liquid flowrate. Furthermore, the top spray is the most efficient no-vent fill method of the three configurations examined. The success of this injection method is primarily due to condensation of the ullage vapor onto the incoming liquid droplets. Ullage condensation counteracts the tank pressure rise resulting from energy exchange between the fluid and the warmer tank walls, and ullage compression. Upward pipe discharge from the tank bottom is the next most efficient method. Fluid circulation induced by this fill configuration tends to diminish thermal stratification in the bulk liquid, thus enhancing condensation at the liquid gas interface.
 Author

N92-13402*# National Aeronautics and Space Administration.
 Lewis Research Center, Cleveland, OH.

THERMAL MODELING WITH SOLID/LIQUID PHASE CHANGE OF THE THERMAL ENERGY STORAGE EXPERIMENT

J. RAYMOND LEE SKARDA Nov. 1991 49 p Original contains color illustrations
 (Contract RTOP 506-41-31)
 (NASA-TM-103770; E-6032; NAS 1.15:103770)

A thermal model which simulates combined conduction and phase change characteristics of thermal energy storage (TES) materials is presented. Both the model and results are presented for the purpose of benchmarking the conduction and phase change capabilities of recently developed and unvalidated microgravity TES computer programs. Specifically, operation of TES-1 is simulated. A two-dimensional SINDA85 model of the TES experiment in cylindrical coordinates was constructed. The phase change model accounts for latent heat stored in, or released from, a node undergoing melting and freezing.
 Author

N92-14322*# National Aeronautics and Space Administration.
 Lewis Research Center, Cleveland, OH.

STABLE LOCALIZED PATTERNS IN THIN LIQUID FILMS

ROBERT J. DEISSLER and ALEXANDER ORON (Technion - Israel Inst. of Tech., Haifa.) Nov. 1991 14 p
 (Contract NASA ORDER C-99066-G; RTOP 505-62-21)
 (NASA-TM-105352; ICOMP-91-26; E-6726; NAS 1.15:105352)
 Avail: CASI HC A03/MF A01

We study a 2-D nonlinear evolution equation which describes

the 3-D spatiotemporal behavior of the air-liquid interface of a thin liquid film lying on the underside of a cooled horizontal plate. We show that the Marangoni effect can stabilize the destabilizing effect of gravity (the Rayleigh-Taylor instability) allowing for the existence of stable localized axisymmetric solutions for a wide range of parameter values. Various properties of these structures are discussed.
 Author

N92-14323*# National Aeronautics and Space Administration.
 Lewis Research Center, Cleveland, OH.

SELF-PRESSURIZATION OF A SPHERICAL LIQUID HYDROGEN STORAGE TANK IN A MICROGRAVITY ENVIRONMENT

C. S. LIN (Analex Corp., Brook Park, OH.) and M. M. HASAN 1992 11 p Presented at the 30th Aerospace Sciences Meeting and Exhibit, Reno, NV, 6-9 Jan. 1992; sponsored by AIAA (Contract RTOP 593-21-00)
 (NASA-TM-105372; E-6759; NAS 1.15:105372; AIAA PAPER 92-0363) Avail: CASI HC A03/MF A01

Thermal stratification and self-pressurization of partially filled liquid hydrogen (LH2) storage tanks under microgravity condition is studied theoretically. A spherical tank is subjected to a uniform and constant wall heat flux. It is assumed that a vapor bubble is located in the tank center such that the liquid-vapor interface and tank wall form two concentric spheres. This vapor bubble represents an idealized configuration of a wetting fluid in microgravity conditions. Dimensionless mass and energy conservation equations for both vapor and liquid regions are numerically solved. Coordinate transformation is used to capture the interface location which changes due to liquid thermal expansion, vapor compression, and mass transfer at liquid-vapor interface. The effects of tank size, liquid fill level, and wall heat flux on the pressure rise and thermal stratification are studied. Liquid thermal expansion tends to cause vapor condensation and wall heat flux tends to cause liquid evaporation at the interface. The combined effects determine the direction of mass transfer at the interface. Liquid superheat increases with increasing wall heat flux and liquid fill level and approaches an asymptotic value.
 Author

N92-15336*# National Aeronautics and Space Administration.
 Lewis Research Center, Cleveland, OH.

THE ECKHAUS AND THE BENJAMIN-FEIR INSTABILITY NEAR A WEAKLY INVERTED BIFURCATION

HELMUT R. BRAND (Essen Univ. (Germany, F.R.)) and ROBERT J. DEISSLER (Los Alamos National Lab., NM.) Nov. 1991 16 p Submitted for publication
 (Contract NASA ORDER C-99066-G; RTOP 505-62-21)
 (NASA-TM-105334; E-6701; NAS 1.15:105334; ICOMP-91-24)
 Avail: CASI HC A03/MF A01

We investigate how the criteria for two prototype instabilities in one dimensional pattern forming systems, namely for the Eckhaus instability and for the Benjamin-Feir instability, change as one goes from a continuous bifurcation, to a spatially periodic or spatially and/or time periodic state, to the corresponding weakly inverted, i.e., hysteretic, cases. We also give the generalization to two dimensional patterns in systems with anisotropy as they arise from hydrodynamic instabilities in nematic liquid crystals.
 Author

N92-15357*# National Aeronautics and Space Administration.
 Lewis Research Center, Cleveland, OH.

A CRITICAL COMPARISON OF SECOND ORDER CLOSURES WITH DIRECT NUMERICAL SIMULATION OF HOMOGENEOUS TURBULENCE

TSAN-HSING SHIH and JOHN L. LUMLEY (Cornell Univ., Ithaca, NY.) Nov. 1991 63 p
 (Contract NASA ORDER C-99066-G; RTOP 505-62-21)
 (NASA-TM-105351; ICOMP-91-25; CMOTT-91-10; E-6725; NAS 1.15:105351) Avail: CASI HC A04/MF A01

Recently, several second order closure models have been proposed for closing the second moment equations, in which the velocity-pressure gradient (and scalar-pressure gradient) tensor and the dissipation rate tensor are two of the most important terms.

34 FLUID MECHANICS AND HEAT TRANSFER

In the literature, these correlation tensors are usually decomposed into a so called rapid term and a return-to-isotropy term. Models of these terms have been used in global flow calculations together with other modeled terms. However, their individual behavior in different flows have not been fully examined because they are un-measurable in the laboratory. Recently, the development of direct numerical simulation (DNS) of turbulence has given us the opportunity to do this kind of study. With the direct numerical simulation, we may use the solution to exactly calculate the values of these correlation terms and then directly compare them with the values from their modeled formulations (models). Here, we make direct comparisons of five representative rapid models and eight return-to-isotropy models using the DNS data of forty five homogeneous flows which were done by Rogers et al. (1986) and Lee et al. (1985). The purpose of these direct comparisons is to explore the performance of these models in different flows and identify the ones which give the best performance. The modeling procedure, model constraints, and the various evaluated models are described. The detailed results of the direct comparisons are discussed, and a few concluding remarks on turbulence models are given. Author

N92-15358* # National Aeronautics and Space Administration. Lewis Research Center, Cleveland, OH.

THERMAL AND SOLUTAL CONVECTION WITH CONDUCTION EFFECTS INSIDE A RECTANGULAR ENCLOSURE

CHRISTOPHE MENNETRIER (Ecole Nationale Supérieure des Mines, Paris, France) and WALTER M. B. DUVAL Dec. 1991
25 p Sponsored in part by USRA
(Contract RTOP 674-21-05)
(NASA-TM-105371; E-5521; NAS 1.15:105371) Avail: CASI HC A03/MF A01

We numerically investigate the effects of various boundary conditions on the flow field characteristics of the physical vapor transport process. We use a prescribed temperature profile as boundary condition on the enclosure walls, and we consider parametric variations applicable to ground-based and space microgravity conditions. For ground-based applications, density gradients in the fluid phase generate buoyancy-driven convection which in turn disrupts the uniformity of the mass flux at the interface depending on the orientation. Heat conduction in the crystal can affect the fluid flow near the interface of the crystal. When considering isothermal source and sink at the interfaces, we observe a diffusive mode and three modes (i.e., thermal, solutal, and thermo-solutal). The convective modes show opposing flow field trends between thermal and solutal convection; theoretically, these trends can be used to achieve a uniform mass flux near the crystal. However, under the physical conditions chosen, the mathematical condition necessary for uniform mass flux cannot be satisfied because of thermodynamic restrictions. When a longitudinal thermal gradient is prescribed on the boundary of the crystal, a non-uniform interface temperature results, which induces a symmetrical fluid flow near the interface for the vertical case. For space microgravity applications, we show that the flow field is dominated by the Stefan wind and a uniform mass flux results at the interface. Author

N92-16265* # National Aeronautics and Space Administration. Lewis Research Center, Cleveland, OH.

BRUSH SEAL LEAKAGE PERFORMANCE WITH GASEOUS WORKING FLUIDS AT STATIC AND LOW ROTOR SPEED CONDITIONS

JULIE A. CARLILE, ROBERT C. HENDRICKS, and DENNIS A. YODER 1992 9 p Proposed for presentation at the 37th International Gas Turbine and Aeroengine Congress and Exposition, Cologne, Germany, 1-4 Jun. 1992; sponsored by the American Inst. of Mechanical Engineers
(Contract RTOP 506-42-72)
(NASA-TM-105400; E-6796; NAS 1.15:105400) Avail: CASI HC A02/MF A01

The leakage performance of a brush seal with gaseous working fluids at static and low rotor speed conditions was studied. The leakage results are included for air, helium, and carbon dioxide at

several bristle/rotor interferences. Also, the effects of packing a lubricant into the bristles and also of reversing the pressure drop across the seal were studied. Results were compared to that of an annular seal at similar operating conditions. In order to generalize the results, they were correlated using corresponding state theory. The brush seal tested had a bore diameter of 3.792 cm (1.4930 in), a fence height of 0.0635 cm (0.025 in), and 1800 bristles/cm circumference (4500 bristles/in circumference). Various bristle/rotor radial interferences were achieved by using a tapered rotor. The brush seal reduced the leakage in comparison to the annular seal, up to 9.5 times. Reversing the pressure drop across the brush seal produced leakage rates approx. the same as that of the annular seal. Addition of a lubricant reduced the leakage by 2.5 times. The air and carbon dioxide data were successfully correlated using corresponding state theory. However, the helium data followed a different curve than the air and carbon dioxide data. Author

N92-18775* # National Aeronautics and Space Administration. Lewis Research Center, Cleveland, OH.

MULTIGRID ACCELERATION AND TURBULENCE MODELS FOR COMPUTATIONS OF 3D TURBULENT JETS IN CROSSFLOW

A. O. DEMUREN (Old Dominion Univ., Norfolk, VA.) Nov. 1991
23 p
(Contract NASA ORDER C-99066-G; RTOP 505-62-21)
(NASA-TM-105306; ICOMP-91-20; E-6658; NAS 1.15:105306; CMOTT-91-09) Avail: CASI HC A03/MF A01

A multigrid method is presented for the calculation of three-dimensional turbulent jets in crossflow. Turbulence closure is achieved with either the standard k-epsilon model or a Reynolds Stress Model (RSM). Multigrid acceleration enables convergence rates which are far superior to that for a single grid method. With the k-epsilon model the rate approaches that for laminar flow, but with RSM it is somewhat slower. The increased stiffness of the system of equations in the latter may be responsible. Computed results with both turbulence models are compared with experimental data for a pair of opposed jets in crossflow. Both models yield reasonable agreement with mean flow velocity but RSM yields better prediction of the Reynolds stresses. Author

N92-18809* # National Aeronautics and Space Administration. Lewis Research Center, Cleveland, OH.

FREQUENCY EFFECTS ON THE STABILITY OF A JOURNAL BEARING FOR PERIODIC LOADING

D. VIJAYARAGHAVAN and D. E. BREWE 1991 21 p Presented at the STLE-ASME Joint Tribology Conference, St. Louis, MO, 13-16 Oct. 1991
(Contract DA PROJ. 1L1-61102-AH-45; RTOP 505-63-5A)
(NASA-TM-105226; E-6242; NAS 1.15:105226; AVSCOM-TR-91-C-040; AD-A247566) Avail: CASI HC A03/MF A01

The stability of a journal bearing is numerically predicted when a unidirectional periodic external load is applied. The analysis is performed using a cavitation algorithm, which mimics the Jakobsson-Floberg and Olsson (JFO) theory by accounting for the mass balance through the complete bearing. Hence, the history of the film is taken into consideration. The loading pattern is taken to be sinusoidal and the frequency of the load cycle is varied. The results are compared with the predictions using Reynolds boundary conditions for both film rupture and reformation. With such comparisons, the need for accurately predicting the cavitation regions for complex loading patterns is clearly demonstrated. For a particular frequency of loading, the effects of mass, amplitude of load variation and frequency of journal speed are also investigated. The journal trajectories, transient variations in fluid film forces, net surface velocity and minimum film thickness, and pressure profiles are also presented. Author

N92-20235* # National Aeronautics and Space Administration. Lewis Research Center, Cleveland, OH.

HEAT TRANSFER IN ROTATING SERPENTINE PASSAGES WITH TRIPS SKEWED TO THE FLOW

B. V. JOHNSON (United Technologies Corp., East Hartford, CT.), J. H. WAGNER (United Technologies Corp., East Hartford, CT.), G. D. STEUBER (Pratt and Whitney Aircraft, East Hartford, CT.), and F. C. YEH 1992 13 p Proposed for presentation at the 37th ASME International Gas Turbine and Aeroengine Congress and Exposition, Cologne, Germany, 1-4 Jun. 1992; sponsored by the 1992 AMSE Turbo Expo-Land, Sea and Air (Contract RTOP 505-62-52) (NASA-TM-105581; E-6908; NAS 1.15:105581) Avail: CASI HC A03/MF A01

Experiments were conducted to determine the effects of buoyancy and Coriolis forces on heat transfer in turbine blade internal coolant passages. The experiments were conducted with a large scale, multi-pass, heat transfer model with both radially inward and outward flow. Trip strips, skewed at 45 deg to the flow direction, were machined on the leading and trailing surfaces of the radial coolant passages. An analysis of the governing flow equations showed that four parameters influence the heat transfer in rotating passages: coolant-to-wall temperature, rotation number, Reynolds number, and radius-to-passage hydraulic diameter ratio. The first three of these four parameters were varied over ranges which are typical of advanced gas turbine engine operating conditions. Results were correlated and compared to previous results from similar stationary and rotating models with smooth walls and with trip strips normal to the flow direction. The heat transfer coefficients on surfaces, where the heat transfer decreased with rotation and buoyancy, decreased to as low as 40 percent of the value without rotation. However, the maximum values of the heat transfer coefficients with high rotation were only slightly above the highest levels previously obtained with the smooth wall models. It was concluded that (1) both Coriolis and buoyancy effects must be considered in turbine blade cooling designs with trip strips, (2) the effects of rotation are markedly different depending upon the flow direction, and (3) the heat transfer with skewed trip strips is less sensitive to buoyancy than the heat transfer in models with either smooth or normal trips. Therefore, skewed trip strips rather than normal trip strips are recommended and geometry-specific tests are required for accurate design information. Author

N92-20520*# National Aeronautics and Space Administration, Lewis Research Center, Cleveland, OH.

IMPLEMENTATION/VALIDATION OF A LOW REYNOLDS NUMBER TWO-EQUATION TURBULENCE MODEL IN THE PROTEUS NAVIER-STOKES CODE: TWO-DIMENSIONAL/AXISYMMETRIC

TRONG T. BUI Apr. 1992 21 p

(Contract RTOP 505-62-52) (NASA-TM-105619; E-6955; NAS 1.15:105619) Avail: CASI HC A03/MF A01

The implementation and validation of the Chien low Reynolds number k-epsilon turbulence model in the two dimensional axisymmetric version Proteus, a compressible Navier-Stokes computer code, are presented. The set of k-epsilon equations are solved by marching in time using a coupled alternating direction implicit (ADI) solution procedure with generalized first or second order time differencing. To validate Proteus and the k-epsilon turbulence model, laminar and turbulent computations were done for several benchmark test cases: incompressible fully developed 2-D channel flow; fully developed axisymmetric pipe flow; boundary layer flow over a flat plate; and turbulent Sajben subsonic transonic diffuser flows. Proteus results from these test cases showed good agreement with analytical results and experimental data. Detailed comparisons of both mean flow and turbulent quantities showed that the Chien k-epsilon turbulence model given good results over a wider range of turbulent flow than the Baldwin-Lomax turbulence model in the Proteus code with no significant CPU time penalty for more complicated flow cases. Author

N92-21498*# National Aeronautics and Space Administration, Lewis Research Center, Cleveland, OH.

EFFECT OF LIQUID SURFACE TURBULENT MOTION ON THE VAPOR CONDENSATION IN A MIXING TANK

C. S. LIN (Analex Corp., Brook Park, OH.) and M. M. HASAN

Jul. 1991 14 p Presented at the Fourth International Symposium on Transport Phenomena in Heat and Mass Transfer, Sydney, Australia, 14-19 Jul. 1991; sponsored by Univ. of New South Wales

(Contract NAS3-25726; RTOP 506-48-00) (NASA-TM-105555; E-6152; NAS 1.15:105555) Avail: CASI HC A03/MF A01

The effect of liquid surface motion on the vapor condensation in a tank mixed by an axial turbulent jet is numerically investigated. The average value (over the interface area) of the root-mean-squared (rms) turbulent velocity at the interface is shown to be linearly increasing with decreasing liquid height and increasing jet diameter for a given tank size. The average rms turbulent velocity is incorporated in Brown et al. (1990) condensation correlation to predict the condensation of vapor on a liquid surface. The results are in good agreement with available condensation data. Author

N92-22226*# National Aeronautics and Space Administration, Lewis Research Center, Cleveland, OH.

ULTRA-SHARP SOLUTION OF THE SMITH-HUTTON PROBLEM

B. P. LEONARD and SIMIN MOKHTARI (Akron Univ., OH.) Feb. 1992 40 p

(Contract NASA ORDER C-99066-G; RTOP 505-62-21) (NASA-TM-105435; ICOMP-92-03; E-6393; NAS 1.15:105435) Avail: CASI HC A03/MF A01

Highly convective scalar transport involving near-discontinuities and strong streamline curvature was addressed in a paper by Smith and Hutton in 1982, comparing several different convection schemes applied to a specially devised test problem. First order methods showed significant artificial diffusion, whereas higher order methods gave less smearing but had a tendency to overshoot and oscillate. Perhaps because unphysical oscillations are more obvious than unphysical smearing, the intervening period has seen a rise in popularity of low order artificially diffusive schemes, especially in the numerical heat transfer industry. The present paper describes an alternate strategy of using non-artificially diffusive high order methods, while maintaining strictly monotonic transitions through the use of simple flux limited constraints. Limited third order upwinding is usually found to be the most cost effective basic convection scheme. Tighter resolution of discontinuities can be obtained at little additional cost by using automatic adaptive stencil expansion to higher order in local regions, as needed. Author

N92-22398*# National Aeronautics and Space Administration, Lewis Research Center, Cleveland, OH.

A KAPPA-EPSILON CALCULATION OF TRANSITIONAL BOUNDARY LAYERS

Z. YANG and T. H. SHIH Mar. 1992 12 p

(Contract NASA ORDER C-99066-G; RTOP 505-62-21) (NASA-TM-105604; ICOMP-92-08; CMOTT-92-05; E-6939; NAS 1.15:105604) Avail: CASI HC A03/MF A01

A recently proposed kappa-epsilon model for low Reynolds number turbulent flows was modified by introducing a new damping function $f(\text{sub } \mu)$. The modified model is used to calculate the transitional boundary layer over a flat plate with different freestream turbulence levels. It is found that the model could mimic the transitional flow. However, the predicted transition is found to be sensitive to the initial conditions. Author

N92-22487*# National Aeronautics and Space Administration, Lewis Research Center, Cleveland, OH.

A PRELIMINARY CHARACTERIZATION OF THE TENSILE AND FATIGUE BEHAVIOR OF

TUNGSTEN-FIBER/WASPALLOY-MATRIX COMPOSITE

RALPH E. CORNER and BRAD A. LERCH Jan. 1992 17 p

(Contract RTOP 510-01-50) (NASA-TM-105346; E-6716; NAS 1.15:105346) Avail: CASI HC A03/MF A01

A microstructural study and a preliminary characterization of the room temperature tensile and fatigue behavior of a continuous,

tungsten fiber, Waspaloy-matrix composite was conducted. A heat treatment was chosen that would allow visibility of planar slip if it occurred during deformation, but would not allow growth of the reaction zone. Tensile and fatigue tests showed that the failed specimens contained transverse cracks in the fibers. The cracks that occurred in the tensile specimen were observed at the fracture surface and up to approximately 4.0 mm below the fracture surface. The crack spacing remained constant along the entire length of the cracked fibers. Conversely, the cracks that occurred in the fatigue specimen were only observed in the vicinity of the fracture surface. In instances where two fiber cracks occurred in the same plane, the matrix often necked between the two cracked fibers. Large groups of slip bands were generated in the matrix near the fiber cracks. Slip bands in the matrix of the tensile specimen were also observed in areas where there were no fiber cracks, at distances greater than 4 mm from the fracture surface. This suggests that the matrix plastically flows before fiber cracking occurs. Author

N92-22522*# National Aeronautics and Space Administration. Lewis Research Center, Cleveland, OH.

INTRODUCTION TO THE INTERNAL FLUID MECHANICS RESEARCH SESSION Abstract Only

BRENT A. MILLER and LOUIS A. POVINELLI *In its* Aeropropulsion 1987 p 155 Feb. 1990
Avail: CASI HC A01/MF A04

Internal fluid mechanics research at LeRC is directed toward an improved understanding of the important flow physics affecting aerospace propulsion systems, and applying this improved understanding to formulate accurate predictive codes. To this end, research is conducted involving detailed experimentation and analysis. The following three papers summarize ongoing work and indicate future emphasis in three major research thrusts: inlets, ducts, and nozzles; turbomachinery; and chemical reacting flows. The underlying goal of the research in each of these areas is to bring internal computational fluid mechanic to a state of practical application for aerospace propulsion systems. Achievement of this goal requires that carefully planned and executed experiments be conducted in order to develop and validate useful codes. It is critical that numerical code development work and experimental work be closely coupled. The insights gained are represented by mathematical models that form the basis for code development. The resultant codes are then tested by comparing them with appropriate experiments in order to ensure their validity and determine their applicable range. The ultimate user community must be a part of this process to assure relevancy of the work and to hasten its practical application. Propulsion systems are characterized by highly complex and dynamic internal flows. Many complex, 3-D flow phenomena may be present, including unsteadiness, shocks, and chemical reactions. By focusing on specific portions of a propulsion system, it is often possible to identify the dominant phenomena that must be understood and modeled for obtaining accurate predictive capability. The three major research thrusts serve as a focus leading to greater understanding of the relevant physics and to an improvement in analytic tools. This in turn will hasten continued advancements in propulsion system performance and capability. Author

N92-22523*# National Aeronautics and Space Administration. Lewis Research Center, Cleveland, OH.

INLETS, DUCTS, AND NOZZLES

JOHN M. ABBOTT, BERNHARD H. ANDERSON, and EDWARD J. RICE *In its* Aeropropulsion 1987 p 157-174 Feb. 1990
Avail: CASI HC A03/MF A04

The internal fluid mechanics research program in inlets, ducts, and nozzles consists of a balanced effort between the development of computational tools (both parabolized Navier-Stokes and full Navier-Stokes) and the conduct of experimental research. The experiments are designed to better understand the fluid flow physics, to develop new or improved flow models, and to provide benchmark quality data sets for validation of the computational methods. The inlet, duct, and nozzle research program is described according to three major classifications of flow phenomena: (1)

highly 3-D flow fields; (2) shock-boundary-layer interactions; and (3) shear layer control. Specific examples of current and future elements of the research program are described for each of these phenomenon. In particular, the highly 3-D flow field phenomenon is highlighted by describing the computational and experimental research program in transition ducts having a round-to-rectangular area variation. In the case of shock-boundary-layer interactions, the specific details of research for normal shock-boundary-layer interactions are described. For shear layer control, research in vortex generators and the use of aerodynamic excitation for enhancement of the jet mixing process are described. Author

N92-22525*# National Aeronautics and Space Administration. Lewis Research Center, Cleveland, OH.

CHEMICAL REACTING FLOWS

EDWARD J. MULARZ (Army Aviation Systems Command, Cleveland, OH.) and PETER M. SOCKOL *In its* Aeropropulsion 1987 p 197-208 Feb. 1990
Avail: CASI HC A03/MF A04

Future aerospace propulsion concepts involve the combustion of liquid or gaseous fuels in a highly turbulent internal airstream. Accurate predictive computer codes which can simulate the fluid mechanics, chemistry, and turbulence-combustion interaction of these chemical reacting flows will be a new tool that is needed in the design of these future propulsion concepts. Experimental and code development research is being performed at LeRC to better understand chemical reacting flows with the long-term goal of establishing these reliable computer codes. Our approach to understand chemical reacting flows is to look at separate, more simple parts of this complex phenomenon as well as to study the full turbulent reacting flow process. As a result, we are engaged in research on the fluid mechanics associated with chemical reacting flows. We are also studying the chemistry of fuel-air combustion. Finally, we are investigating the phenomenon of turbulence-combustion interaction. Research, both experimental and analytical, is highlighted in each of these three major areas. Author

N92-22542*# National Aeronautics and Space Administration. Lewis Research Center, Cleveland, OH.

HIGH-SPEED INLET RESEARCH PROGRAM AND SUPPORTING ANALYSIS

ROBERT E. COLTRIN *In its* Aeropropulsion 1987 p 469-486 Feb. 1990
Avail: CASI HC A03/MF A04

The technology challenges faced by the high speed inlet designer are discussed by describing the considerations that went into the design of the Mach 5 research inlet. It is shown that the emerging three dimensional viscous computational fluid dynamics (CFD) flow codes, together with small scale experiments, can be used to guide larger scale full inlet systems research. Then, in turn, the results of the large scale research, if properly instrumented, can be used to validate or at least to calibrate the CFD codes. Author

N92-23154*# National Aeronautics and Space Administration. Lewis Research Center, Cleveland, OH.

COMPARISON OF TWO-DIMENSIONAL AND THREE-DIMENSIONAL DROPLET TRAJECTORY CALCULATIONS IN THE VICINITY OF FINITE WINGS

STANLEY R. MOHLER, JR. (Sverdrup Technology, Inc., Brook Park, OH.) and COLIN S. BIDWELL 1992 34 p Presented at the 30th Aerospace Sciences Meeting, Reno, NV, 6-9 Jan. 1992; sponsored by AIAA Previously announced in IAA as A92-28215 (Contract RTOP 505-68-10) (NASA-TM-105617; E-6806; NAS 1.15:105617; AIAA PAPER 92-0645) Avail: CASI HC A03/MF A01

Computational predictions of ice accretion on flying aircraft most commonly rely on modeling in two dimensions (2D). These 2D methods treat an aircraft geometry either as wing-like with infinite span, or as an axisymmetric body. Recently, fully three dimensional (3D) methods have been introduced that model an aircrafts true 3D shape. Because 3D methods are more computationally

expensive than 2D methods, 2D methods continue to be widely used. However, a 3D method allows us to investigate whether it is valid to continue applying 2D methods to a finite wing. The extent of disagreement between LEWICE, a 2D method, and LEWICE3D, a 3D method, in calculating local collection efficiencies at the leading edge of finite wings is investigated in this paper.

Author

N92-23224*# National Aeronautics and Space Administration, Lewis Research Center, Cleveland, OH.

MODELLING AND EXPERIMENTAL VERIFICATION OF A WATER ALLEVIATION SYSTEM FOR THE NASP

G. JAMES VANFOSSEN 1992 13 p Proposed for presentation at the 92nd National Heat Transfer Conference, San Diego, CA, 9-12 Aug. 1992; sponsored by ASME (Contract RTOP 763-22-00)

(NASA-TM-105661; E-7026; NAS 1.15:105661) Avail: CASI HC A03/MF A01

One possible low speed propulsion system for the National Aerospace Plane is a liquid air cycle engine (LACE). The LACE system uses the heat sink in the liquid hydrogen propellant to liquefy air in a heat exchanger which is then pumped up to high pressure and used as the oxidizer in a hydrogen liquid air rocket. The inlet airstream must be dehumidified or moisture could freeze on the cryogenic heat exchangers and block them. The main objective of this research has been to develop a computer simulation of the cold tube/antifreeze-spray water alleviation system and to verify the model with experimental data. An experimental facility has been built and humid air tests were conducted on a generic heat exchanger to obtain condensing data for code development. The paper describes the experimental setup, outlines the method of calculation used in the code, and presents comparisons of the calculations and measurements. Cause of discrepancies between the model and data are explained.

Author

N92-23268*# National Aeronautics and Space Administration, Lewis Research Center, Cleveland, OH.

LIQUID HYDROGEN MASS FLOW THROUGH A MULTIPLE ORIFICE JOULE-THOMSON DEVICE

S. STEPHEN PAPELL (Analex Corp., Brook Park, OH.), TED W. NYLAND, and NASEEM H. SAIYED 1992 13 p Proposed for presentation at the 27th Thermophysics Conference, Nashville, TN, 6-8 Jul. 1992; sponsored by AIAA (Contract RTOP 506-42-73)

(NASA-TM-105583; E-6910; NAS 1.15:105583; AIAA PAPER 92-2881) Avail: CASI HC A03/MF A01

Liquid hydrogen mass flow rate, pressure drop, and temperature drop data were obtained for a number of multiple orifice Joule-Thomson devices known as visco jets. The present investigation continues a study to develop an equation for predicting two phase flow of cryogenics through these devices. The test apparatus design allowed isenthalpic expansion of the cryogen through the visco jets. The data covered a range of inlet and outlet operating conditions. The mass flow rate range single phase or two phase was 0.015 to 0.98 lbm/hr. The manufacturer's equation was found to overpredict the single phase hydrogen data by 10 percent and the two phase data by as much as 27 percent. Two modifications of the equation resulted in a data correlation that predicts both the single and two phase flow across the visco jet. The first modification was of a theoretical nature, and the second strictly empirical. The former reduced the spread in the two phase data. It was a multiplication factor of $1 - X$ applied to the manufacturer's equation. The parameter X is the flow quality downstream of the visco jet based on isenthalpic expansion across the device. The latter modification was a 10 percent correction term that correlated 90 percent of the single and two phase data to within ± 10 percent scatter band.

Author

N92-23338*# National Aeronautics and Space Administration, Lewis Research Center, Cleveland, OH.

TURBULENCE MODELING

TSAN-HSING SHIH *In its* Center for Modeling of Turbulence

and Transition (CMOTT). Research Briefs: 1990 p 4-8 Oct 1991 Prepared in cooperation with Stanford Univ., CA Avail: CASI HC A01/MF A02

The performance of existing two-equation eddy viscosity models was examined. An effort was made to develop better models for near-wall turbulence using direct numerical simulations of plane channel and boundary layer flows. The asymptotic near-wall behavior of turbulence was used to examine the problems of current second order closure models and develop new models with the correct near-wall behavior. Rapid Distortion Theory was used to analytically study the effects of mean deformation on turbulence, obtain analytical solutions for the spectrum tensor, Reynolds stress tensor, anisotropy tensor and its invariants, which can be used in the turbulence model development. The potential of the renormalization group theory in turbulence modeling was studied, as well as compressible turbulent flows, and modeling of bypass transition.

Author

N92-23340*# National Aeronautics and Space Administration, Lewis Research Center, Cleveland, OH.

MODELING OF COMPRESSIBLE TURBULENT SHEAR FLOWS

WILLIAM W. LIOU *In its* Center for Modeling of Turbulence and Transition (CMOTT). Research Briefs: 1990 p 13-15 Oct. 1991 Avail: CASI HC A01/MF A02

Despite all the recent developments in computer technologies and numerical algorithms, full numerical simulations of turbulent flows are feasible only at moderate Reynolds numbers and for flows with relatively simple geometries. The main goal of this research is to develop new second order moment closures for compressible turbulence. It has been shown that the models based on the extension of those developed originally for incompressible flows fail to adequately predict turbulent flows at high Mach numbers. In this attempt, the compressibility effects are explicitly considered. A successful development of these models that directly takes into account the compressibility effects may have a range of technological implications in the design of supersonic and hypersonic vehicles.

Author

N92-23343*# National Aeronautics and Space Administration, Lewis Research Center, Cleveland, OH.

DEVELOPMENT OF NEW FLUX SPLITTING SCHEMES

MENG-S. LIOU and CHRISTOPHER J. STEFFEN, JR. *In its* Center for Modeling of Turbulence and Transition (CMOTT). Research Briefs: 1990 p 22-23 Oct. 1991 Avail: CASI HC A01/MF A02

Maximizing both accuracy and efficiency has been the primary objective in designing a numerical algorithm for CFD. This is especially important for solution of complex three-dimensional systems of Navier-Stokes equations which often include turbulence modeling and chemistry effects. Recently, upwind schemes have been well received for both their capability of resolving discontinuities and their sound theoretical basis in characteristic theory for hyperbolic systems. With this in mind, two new flux splitting techniques are presented for upwind differencing.

Author

N92-23350*# National Aeronautics and Space Administration, Lewis Research Center, Cleveland, OH.

ADVANCEMENTS IN ENGINEERING TURBULENCE MODELING

T.-H. SHIH *In its* Center for Modeling of Turbulence and Transition (CMOTT). Research Briefs: 1990 p 108-125 Oct. 1991 Presented at the 9th National Aero-Space Plane Technology Symposium, 1-2 Nov. 1990

(PAPER-105) Avail: CASI HC A03/MF A02

Some new developments in two-equation models and second order closure models are presented. Two-equation models (k -epsilon models) have been widely used in computational fluid dynamics (CFD) for engineering problems. Most of low-Reynolds number two-equation models contain some wall-distance damping functions to account for the effect of wall on turbulence. However, this often causes the confusion and difficulties in computing flows with complex geometry and also needs an ad hoc treatment near the separation and reattachment points. A set of modified

two-equation models is proposed to remove the aforementioned shortcomings. The calculations using various two-equation models are compared with direct numerical simulations of channel flow and flat boundary layers. Development of a second order closure model is also discussed with emphasis on the modeling of pressure related correlation terms and dissipation rates in the second moment equations. All the existing models poorly predict the normal stresses near the wall and fail to predict the 3-D effect of mean flow on the turbulence (e.g. decrease in the shear stress caused by the cross flow in the boundary layer). The newly developed second order near-wall turbulence model is described and is capable of capturing the near-wall behavior of turbulence as well as the effect of 3-D mean flow on the turbulence. Author

N92-23351*# National Aeronautics and Space Administration. Lewis Research Center, Cleveland, OH.

ON THE BASIC EQUATIONS FOR THE SECOND-ORDER MODELING OF COMPRESSIBLE TURBULENCE

WILLIAM W. LIOU and T.-H. SHIH *In its* Center for Modeling of Turbulence and Transition (CMOTT). Research Briefs: 1990 p 134 Oct. 1991

Avail: CASI HC A01/MF A02

Equations for the mean and the turbulence quantities of compressible turbulent flows are derived in this report. Both the conventional Reynolds average and the mass-weighted Favre average were employed to decompose the flow variable into mean and turbulent quantities. These equations are to be used later in developing second-order Reynolds stress models for high-speed compressible flows. A few recent advances in modeling some of the terms in the equation due to compressibility effects are also summarized. Author

N92-23352*# National Aeronautics and Space Administration. Lewis Research Center, Cleveland, OH.

DEVELOPMENT OF A NEW FLUX SPLITTING SCHEME

MENG-SING LIOU and CHRISTOPHER J. STEFFEN, JR. *In its* Center for Modeling of Turbulence and Transition (CMOTT). Research Briefs: 1990 p 144-145 Oct. 1991 Previously announced in IAA as A91-40793

Avail: CASI HC A01/MF A02

The use of a new splitting scheme, the advection upstream splitting method, for model aerodynamic problems where Van Leer and Roe schemes had failed previously is discussed. The present scheme is based on splitting in which the convective and pressure terms are separated and treated differently depending on the underlying physical conditions. The present method is found to be both simple and accurate. Author

N92-23353*# National Aeronautics and Space Administration. Lewis Research Center, Cleveland, OH.

HIGH-ORDER POLYNOMIAL EXPANSIONS (HOPE) FOR FLUX-VECTOR SPLITTING

MENG-SING LIOU and CHRIS J. STEFFEN, JR. *In its* Center for Modeling of Turbulence and Transition (CMOTT). Research Briefs: 1990 p 146-150 Oct. 1991 Previously announced as N91-25739

Avail: CASI HC A01/MF A02

The Van Leer flux splitting is known to produce excessive numerical dissipation for Navier-Stokes calculations. Researchers attempt to remedy this deficiency by introducing a higher order polynomial expansion (HOPE) for the mass flux. In addition to Van Leer's splitting, a term is introduced so that the mass diffusion error vanishes at $M = 0$. Several splittings for pressure are proposed and examined. The effectiveness of the HOPE scheme is illustrated for 1-D hypersonic conical viscous flow and 2-D supersonic shock-wave boundary layer interactions. Author

N92-23355*# National Aeronautics and Space Administration. Lewis Research Center, Cleveland, OH.

SIMULATIONS OF FREE SHEAR LAYERS USING A COMPRESSIBLE KAPPA-EPSILON MODEL

S. T. YU (Sverdrup Technology, Inc., Cleveland, OH.), C. T. CHANG, and C. J. MAREK *In its* Center for Modeling of Turbulence and

Transition (CMOTT). Research Briefs: 1990 p 152-160 Oct. 1991 Previously announced in IAA as A91-45778
Avail: CASI HC A02/MF A02

A two-dimensional, compressible Navier-Stokes equation with a k-epsilon turbulence model is solved numerically to simulate the flow of a compressible free shear layer. The appropriate form of k and epsilon equations for compressible flow is discussed. Sarkar's modeling is adopted to simulate the compressibility effects in the k and epsilon equations. The numerical results show that the spreading rate of the shear layers decreases with increasing convective Mach number. In addition, favorable comparison was found between the calculated results and experimental data. Author

N92-23542*# National Aeronautics and Space Administration. Lewis Research Center, Cleveland, OH.

RENORMALIZATION GROUP ANALYSIS OF THE REYNOLDS STRESS TRANSPORT EQUATION

R. RUBINSTEIN (Sverdrup Technology, Inc., Brook Park, OH.) and J. M. BARTON (Sverdrup Technology, Inc., Brook Park, OH.) Mar. 1992 27 p

(Contract NCC3-233; RTOP 505-62-21)

(NASA-TM-105588; ICOMP-92-06; E-6917; NAS 1.15:105588; CMOTT-92-03) Avail: CASI HC A03/MF A01

The pressure velocity correlation and return to isotropy term in the Reynolds stress transport equation are analyzed using the Yakhot-Orszag renormalization group. The perturbation series for the relevant correlations, evaluated to lowest order in the epsilon-expansion of the Yakhot-Orszag theory, are infinite series in tensor product powers of the mean velocity gradient and its transpose. Formal lowest order Padé approximations to the sums of these series produce a fast pressure strain model of the form proposed by Launder, Reece, and Rodi, and a return to isotropy model of the form proposed by Rotta. In both cases, the model constant are computed theoretically. The predicted Reynolds stress ratios in simple shear flows are evaluated and compared with experimental data. The possibility is discussed of driving higher order nonlinear models by approximating the sums more accurately. Author

N92-23560*# National Aeronautics and Space Administration. Lewis Research Center, Cleveland, OH.

A TWO-DIMENSIONAL EULER SOLUTION FOR AN UNBLADED JET ENGINE CONFIGURATION

MARK E. M. STEWART Apr. 1992 10 p Presented at the Third Canadian Symposium on Aerodynamics, Toronto (Ontario), 20-21 Nov. 1991; sponsored by the Canadian Aeronautics and Space Inst.

(Contract NASA ORDER C-99066-G; RTOP 505-62-21)

(NASA-TM-105329; ICOMP-91-22; E-6691; NAS 1.15:105329)
Avail: CASI HC A02/MF A01

A two dimensional, nonaxisymmetric Euler solution in a geometry representative of a jet engine configuration without blades is presented. The domain, including internal and external flow, is covered with a multiblock grid. In order to construct this grid, a domain decomposition technique is used to subdivide the domain, and smooth grids are dimensioned and placed in each block. The Euler solution is verified by examining five theoretical properties. The result demonstrates techniques for performing numerical solutions in complex geometries and provides a foundation for complete engine throughflow calculations. Author

N92-23565*# National Aeronautics and Space Administration. Lewis Research Center, Cleveland, OH.

LONG TIME BEHAVIOR OF UNSTEADY FLOW COMPUTATIONS

S. I. HARIHARAN (Akron Univ., OH.) Mar. 1992 24 p

(Contract NCC3-233; NSF DMS-89-21189; RTOP 505-62-21)
(NASA-TM-105584; ICOMP-92-04; E-6912; NAS 1.15:105584)

Avail: CASI HC A03/MF A01

This paper addresses a specific issue of time accuracy in the calculation of external aerodynamic problems. The class of problems discussed consists of inviscid compressible subsonic

flows. These problems are governed by a convective equation. A key issue that is not understood is the long time behavior of the solution. This is important if one desires transient calculations of problems governed by the Euler equations or its derivatives such as the small disturbance equations or the potential formulations for the gust problem. Difficulties arise for two dimensional problems where the time rate decay solutions of the wave equation is slow. In concert with the above mentioned problem, exterior flows require proper modeling of the boundary conditions. In particular, this requires the truncation of infinite regions into finite regions with the aid of artificial boundaries. These boundary conditions must be consistent with the physics of the unbounded problem as well as consistent in time and space. Our treatment of the problem is discussed in detail and examples are given to verify the results.

Author

N92-24050*# National Aeronautics and Space Administration, Lewis Research Center, Cleveland, OH.

KOLMOGOROV BEHAVIOR OF NEAR-WALL TURBULENCE AND ITS APPLICATION IN TURBULENCE MODELING

TSAN-HSING SHIH and JOHN L. LUMLEY (Cornell Univ., Ithaca, NY.) 1992 17 p

(Contract NCC3-233; RTOP 505-62-21)

(NASA-TM-105663; ICOMP-92-10; NAS 1.15:105663;

CMOTT-92-06) Avail: CASI HC A03/MF A01

The near-wall behavior of turbulence is re-examined in a way different from that proposed by Hanjalic and Launder and followers. It is shown that at a certain distance from the wall, all energetic large eddies will reduce to Kolmogorov eddies (the smallest eddies in turbulence). All the important wall parameters, such as friction velocity, viscous length scale, and mean strain rate at the wall, are characterized by Kolmogorov microscales. According to this Kolmogorov behavior of near-wall turbulence, the turbulence quantities, such as turbulent kinetic energy, dissipation rate, etc. at the location where the large eddies become Kolmogorov eddies, can be estimated by using both direct numerical simulation (DNS) data and asymptotic analysis of near-wall turbulence. This information will provide useful boundary conditions for the turbulent transport equations. As an example, the concept is incorporated in the standard k-epsilon model which is then applied to channel and boundary flows. Using appropriate boundary conditions (based on Kolmogorov behavior of near-wall turbulence), there is no need for any wall-modification to the k-epsilon equations (including model constants). Results compare very well with the DNS and experimental data.

Author

N92-24514*# National Aeronautics and Space Administration, Lewis Research Center, Cleveland, OH.

WORKSHOP ON ENGINEERING TURBULENCE MODELING

LOUIS A. POVINELLI, ed., W. W. LIOU, ed., A. SHABBIR, ed., and T.-H. SHIH, ed. Mar. 1992 510 p Workshop held in Cleveland, OH, 21-22 Aug. 1991

(Contract NASA ORDER C-99066-G; RTOP 505-62-21)

(NASA-CP-10088; E-6830; ICOMP-92-02; CMOTT-92-02; NAS

1.55:10088) Avail: CASI HC A22/MF A04

Discussed here is the future direction of various levels of engineering turbulence modeling related to computational fluid dynamics (CFD) computations for propulsion. For each level of computation, there are a few turbulence models which represent the state-of-the-art for that level. However, it is important to know their capabilities as well as their deficiencies in order to help engineers select and implement the appropriate models in their real world engineering calculations. This will also help turbulence modelers perceive the future directions for improving turbulence models. The focus is on one-point closure models (i.e., from algebraic models to higher order moment closure schemes and partial differential equation methods) which can be applied to CFD computations. However, other schemes helpful in developing one-point closure models, are also discussed.

N92-24520*# National Aeronautics and Space Administration, Lewis Research Center, Cleveland, OH.

COMMENT ON TWO-EQUATION MODELS

N. LANG and T. CHITSOMBOON *In its Workshop on Engineering Turbulence Modeling* p 87-99 Mar. 1992

Avail: CASI HC A03/MF A04

Several turbulence models are studied and evaluated. All models are compared to each other and experimental values for flat plate boundary layer flow and channel flow. Among the models examined are: K-epsilon, k-omega, q-omega, and k-tau turbulence models. All results are presented in viewgraph format. H.A.

N92-24523*# National Aeronautics and Space Administration, Lewis Research Center, Cleveland, OH.

THE PRESENT STATUS AND THE FUTURE DIRECTION OF SECOND ORDER CLOSURE MODELS FOR INCOMPRESSIBLE FLOWS

T.-H. SHIH *In its Workshop on Engineering Turbulence Modeling* p 163-217 Mar. 1992

Avail: CASI HC A04/MF A04

The topics are covered in viewgraph form and include: (1) basic equations and model terms; (2) model constraints and assumptions; (3) the present state of various closure models; and (4) future directions. K.S.

N92-24535*# National Aeronautics and Space Administration, Lewis Research Center, Cleveland, OH.

THE PRESENT STATE OF USING RDT IN TURBULENCE MODELLING OF UNSTEADY FLOWS

REDA R. MANKBADI *In its Workshop on Engineering Turbulence Modeling* p 435-461 Mar. 1992

Avail: CASI HC A03/MF A04

The dissipation transport equation should not be based upon the local-equilibrium hypothesis, but should instead be based upon the rapid-distortion hypothesis. A differential equation to describe this situation is not currently available. An investigation of this topic is presented in viewgraph form. Author

N92-25196*# National Aeronautics and Space Administration, Lewis Research Center, Cleveland, OH.

CONSERVATIVE-VARIABLE AVERAGE STATES FOR EQUILIBRIUM GAS MULTI-DIMENSIONAL FLUXES

G. S. IANNELLI (Tennessee Univ., Knoxville.) Mar. 1992 46 p

(Contract NASA ORDER C-99066-G; RTOP 505-12-21)

(NASA-TM-105585; ICOMP-92-05; E-6913; NAS 1.15:105585)

Avail: CASI HC A03/MF A01

Modern split component evaluations of the flux vector Jacobians are thoroughly analyzed for equilibrium-gas average-state determinations. It is shown that all such derivations satisfy a fundamental eigenvalue consistency theorem. A conservative-variable average state is then developed for arbitrary equilibrium-gas equations of state and curvilinear-coordinate fluxes. Original expressions for eigenvalues, sound speed, Mach number, and eigenvectors are then determined for a general average Jacobian, and it is shown that the average eigenvalues, Mach number, and eigenvectors may not coincide with their classical pointwise counterparts. A general equilibrium-gas equation of state is then discussed for conservative-variable computational fluid dynamics (CFD) Euler formulations. The associated derivations lead to unique compatibility relations that constrain the pressure Jacobian derivatives. Thereafter, alternative forms for the pressure variation and average sound speed are developed in terms of two average pressure Jacobian derivatives. Significantly, no additional degree of freedom exists in the determination of these two average partial derivatives of pressure. Therefore, they are simultaneously computed exactly without any auxiliary relation, hence without any geometric solution projection or arbitrary scale factors. Several alternative formulations are then compared and key differences highlighted with emphasis on the determination of the pressure variation and average sound speed. The relevant underlying assumptions are identified, including some subtle approximations that are inherently employed in published average-state procedures. Finally, a representative test case is discussed for which an intrinsically exact average state is determined. This exact state is then compared with the predictions of recent methods, and their inherent approximations are appropriately quantified. Author

34 FLUID MECHANICS AND HEAT TRANSFER

N92-25296* National Aeronautics and Space Administration. Lewis Research Center, Cleveland, OH.

EFFECT OF RADIATION ON CONVECTION AT MODERATE TEMPERATURES

HENRY C. DEGROH, III and MOHAMMAD KASSEMI (Ohio Aerospace Inst., Brook Park.) 1992 11 p Presented at the 30th Aerospace Sciences Meeting and Exhibit, Reno, NV, 6-9 Jan. 1992; sponsored by AIAA Previously announced in IAA as A92-27058

(Contract RTOP 674-21-05)

(NASA-TM-105632; E-6975; NAS 1.15:105632; AIAA PAPER 92-0691) Copyright Avail: CASI HC A03/MF A01

A combined numerical and experimental investigation of radiation-induced convection is presented to show that the convective stability of the top-heated enclosure is disrupted by heat transfer conditions at the wall. When the enclosure is not insulated the thermal stratification of the fluid is modified by convective and radiative losses to the surrounding environment. This results in a double annular cell flow which, when cut by the laser sheet, shows a four-vortex pattern with a weak annular cell at the bottom and a large counter-rotating annular cell at the top. When the enclosure is insulated the convective stability of the fluid is again disrupted - this time as a result of radiative heat transfer between the enclosing surfaces which drives two annular flow cells of relatively equal size. Comparison between model and experiment shows that radiation effects are important even at temperature levels as low as 300 C and, if these effects are not included, numerical predictions can be highly erroneous. Author

N92-25721*# National Aeronautics and Space Administration. Lewis Research Center, Cleveland, OH.

TWO-DIMENSIONAL UNSTRUCTURED TRIANGULAR GRID GENERATION

PHILIP C. E. JORGENSON *In its Workshop on Grid Generation and Related Areas* p 85-106 Apr. 1992
Avail: CASI HC A03/MF A02

The capability of generating 2-D unstructured triangular meshes about arbitrary geometries is demonstrated. This work uses a distribution of boundary points and triangulates the computational domain using a Delaunay triangulation algorithm. Typically, initial cells are added based on cell aspect ratios or cell areas. A resulting mesh can then be used along with the connectivity of the cells to solve either a Euler or Navier-Stokes flow problem. Author

N92-25722*# National Aeronautics and Space Administration. Lewis Research Center, Cleveland, OH.

CARTESIAN BASED GRID GENERATION/ADAPTIVE MESH REFINEMENT

WILLIAM J. COIRIER *In its Workshop on Grid Generation and Related Areas* p 107-120 Apr. 1992
Avail: CASI HC A03/MF A02

Grid adaptation has recently received attention in the computational fluid dynamics (CFD) community as a means to capture the salient features of a flowfield by either moving grid points of a structured or by adding cells in an unstructured manner. An approach based on a background cartesian mesh is investigated from which the geometry is 'cut' out of the mesh. Once the mesh is obtained, a solution on this coarse grid is found, that indicates which cells need to be refined. This process of refining/solving continues until the flow is grid refined in terms of a user specified global parameter (such as drag coefficient etc.). The advantages of this approach are twofold: the generation of the base grid is independent of the topology of the bodies or surfaces around/through which the flow is to be computed, and the resulting grid (in uncut regions) is highly isotropic, so that the truncation error is low. The flow solver (which, along with the grid generation is still under development) uses a completely unstructured data base, and is a finite volume, upwinding scheme. Current and future work will address generating Navier-Stokes suitable grids by using locally aligned and normal face/cell refining. The attached plot shows a simple grid about two turbine blades. Author

N92-25727*# National Aeronautics and Space Administration. Lewis Research Center, Cleveland, OH.

INTEGRATING AERODYNAMIC SURFACE MODELING FOR COMPUTATIONAL FLUID DYNAMICS WITH COMPUTER AIDED STRUCTURAL ANALYSIS, DESIGN, AND MANUFACTURING

SCOTT A. THORP *In its Workshop on Grid Generation and Related Areas* p 159-168 Apr. 1992
Avail: CASI HC A02/MF A02

This presentation will discuss the development of a NASA Geometry Exchange Specification for transferring aerodynamic surface geometry between LeRC systems and grid generation software used for computational fluid dynamics research. The proposed specification is based on a subset of the Initial Graphics Exchange Specification (IGES). The presentation will include discussion of how the NASA-IGES standard will accommodate improved computer aided design inspection methods and reverse engineering techniques currently being developed. The presentation is in viewgraph format. Author

N92-25809*# National Aeronautics and Space Administration. Lewis Research Center, Cleveland, OH.

DEVELOPMENT OF NEW FLUX SPLITTING SCHEMES

MENG-SING LIOU and CHRISTOPHER J. STEFFEN, JR. *In its Computational Fluid Dynamics* p 19-28 Feb. 1992

Maximizing both accuracy and efficiency has been the primary objective in designing a numerical algorithm for computational fluid dynamics (CFD). This is especially important for solutions of complex three dimensional systems of Navier-Stokes equations which often include turbulence modeling and chemistry effects. Recently, upwind schemes have been well received for their capability in resolving discontinuities. With this in mind, presented are two new flux splitting techniques for upwind differencing. The first method is based on High-Order Polynomial Expansions (HOPE) of the mass flux vector. The second new flux splitting is based on the Advection Upwind Splitting Method (AUSM). The calculation of the hypersonic conical flow demonstrates the accuracy of the splitting in resolving the flow in the presence of strong gradients. A second series of tests involving the two dimensional inviscid flow over a NACA 0012 airfoil demonstrates the ability of the AUSM to resolve the shock discontinuity at transonic speed. A third case calculates a series of supersonic flows over a circular cylinder. Finally, the fourth case deals with tests of a two dimensional shock wave/boundary layer interaction. H.A.

N92-25810*# National Aeronautics and Space Administration. Lewis Research Center, Cleveland, OH.

AN ITERATIVE IMPLICIT DDADI ALGORITHM FOR SOLVING THE NAVIER-STOKES EQUATION

S. C. CHEN, N. S. LIU, and H. D. KIM *In its Computational Fluid Dynamics* p 29-46 Feb. 1992

An algorithm utilizing a first order upwind split flux technique and the diagonally dominant treatment is proposed to be the temporal operator for solving the Navier-Stokes equations. Given the limit of a five point stencil, the right hand side flux derivatives are formulated by several commonly used central and upwind schemes. Their performances are studied through a test case of free vortex convection in a uniform stream. From these results, a superior treatment for evaluating the flux term is proposed and compared with the rest. The application of the proposed algorithm to the full Navier-Stokes equations is demonstrated through a calculation of flow over a backward facing step. Results are compared against the calculation done by using the fourth order central differencing scheme with artificial damping. H.A.

N92-25811*# National Aeronautics and Space Administration. Lewis Research Center, Cleveland, OH.

THE PROTEUS NAVIER-STOKES CODE

CHARLES E. TOWNE and JOHN R. SCHWAB *In its Computational Fluid Dynamics* p 47-56 Feb. 1992

An effort is currently underway at NASA Lewis to develop two and three dimensional Navier-Stokes codes, called Proteus, for aerospace propulsion applications. Proteus solves the

Reynolds-averaged, unsteady, compressible Navier-Stokes equations in strong conservation law form. Turbulence is modeled using a Baldwin-Lomax based algebraic eddy viscosity model. In addition, options are available to solve thin layer or Euler equations, and to eliminate the energy equation by assuming constant stagnation enthalpy. An extensive series of validation cases have been run, primarily using the two dimensional planar/axisymmetric version of the code. Several flows were computed that have exact solution such as: fully developed channel and pipe flow; Couette flow with and without pressure gradients; unsteady Couette flow formation; flow near a suddenly accelerated flat plate; flow between concentric rotating cylinders; and flow near a rotating disk. The two dimensional version of the Proteus code has been released, and the three dimensional code is scheduled for release in late 1991. H.A.

N92-25812*# National Aeronautics and Space Administration, Lewis Research Center, Cleveland, OH.

ACCURATE UPWIND-MONOTONE (NONOSCILLATORY) METHODS FOR CONSERVATION LAWS

HUNG T. HUYNH *In its* Computational Fluid Dynamics p 57-64 Feb. 1992

The well known MUSCL scheme of Van Leer is constructed using a piecewise linear approximation. The MUSCL scheme is second order accurate at the smooth part of the solution except at extrema where the accuracy degenerates to first order due to the monotonicity constraint. To construct accurate schemes which are free from oscillations, the author introduces the concept of upwind monotonicity. Several classes of schemes, which are upwind monotone and of uniform second or third order accuracy are then presented. Results for advection with constant speed are shown. It is also shown that the new scheme compares favorably with state of the art methods. H.A.

N92-25813*# National Aeronautics and Space Administration, Lewis Research Center, Cleveland, OH.

NUMERICAL SIMULATION OF CONSERVATION LAWS

CHUNG-CHANG SIN and MING TO WAI (Sverdrup Technology, Inc., Cleveland, OH.) *In its* Computational Fluid Dynamics p 65-74 Feb. 1992

A new numerical framework for solving conservation laws is being developed. This new approach differs substantially from the well established methods, i.e., finite difference, finite volume, finite element and spectral methods, in both concept and methodology. The key features of the current scheme include: (1) direct discretization of the integral forms of conservation laws, (2) treating space and time on the same footing, (3) flux conservation in space and time, and (4) unified treatment of the convection and diffusion fluxes. The model equation considered in the initial study is the standard one dimensional unsteady constant-coefficient convection-diffusion equation. In a stability study, it is shown that the principal and spurious amplification factors of the current scheme, respectively, are structurally similar to those of the leapfrog/DuFort-Frankel scheme. As a result, the current scheme has no numerical diffusion in the special case of pure convection and is unconditionally stable in the special case of pure diffusion. Assuming smooth initial data, it will be shown theoretically and numerically that, by using an easily determined optimal time step, the accuracy of the current scheme may reach a level which is several orders of magnitude higher than that of the MacCormack scheme, with virtually identical operation count. Author

N92-25817*# National Aeronautics and Space Administration, Lewis Research Center, Cleveland, OH.

UPWIND SCHEMES AND BIFURCATING SOLUTIONS IN REAL GAS COMPUTATIONS

AMBADY SURESH (Sverdrup Technology, Inc., Cleveland, OH.) and MENG-SING LIU *In its* Computational Fluid Dynamics p 103-114 Feb. 1992

The area of high speed flow is seeing a renewed interest due to advanced propulsion concepts such as the National Aerospace Plane (NASP), Space Shuttle, and future civil transport concepts. Upwind schemes to solve such flows have become increasingly

popular in the last decade due to their excellent shock capturing properties. In the first part of this paper the authors present the extension of the Osher scheme to equilibrium and non-equilibrium gases. For simplicity, the source terms are treated explicitly. Computations based on the above scheme are presented to demonstrate the feasibility, accuracy and efficiency of the proposed scheme. One of the test problems is a Chapman-Jouguet detonation problem for which numerical solutions have been known to bifurcate into spurious weak detonation solutions on coarse grids. Results indicate that the numerical solution obtained depends both on the upwinding scheme used and the limiter employed to obtain second order accuracy. For example, the Osher scheme gives the correct CJ solution when the super-bee limiter is used, but gives the spurious solution when the Van Leer limiter is used. With the Roe scheme the spurious solution is obtained for all limiters. H.A.

N92-25818*# National Aeronautics and Space Administration, Lewis Research Center, Cleveland, OH.

HIGH ORDER PARALLEL NUMERICAL SCHEMES FOR SOLVING INCOMPRESSIBLE FLOWS

AVI LIN (Pennsylvania Univ., Philadelphia.), EDWARD J. MILNER, MAY-FUN LIOU, and RICHARD A. BELCH *In its* Computational Fluid Dynamics p 115-131 Feb. 1992 Original contains color illustrations

The use of parallel computers for numerically solving flow fields has gained much importance in recent years. This paper introduces a new high order numerical scheme for computational fluid dynamics (CFD) specifically designed for parallel computational environments. A distributed MIMD system gives the flexibility of treating different elements of the governing equations with totally different numerical schemes in different regions of the flow field. The parallel decomposition of the governing operator to be solved is the primary parallel split. The primary parallel split was studied using a hypercube like architecture having clusters of shared memory processors at each node. The approach is demonstrated using examples of simple steady state incompressible flows. Future studies should investigate the secondary split because, depending on the numerical scheme that each of the processors applies and the nature of the flow in the specific subdomain, it may be possible for a processor to seek better, or higher order, schemes for its particular subcase. H.A.

N92-25819*# National Aeronautics and Space Administration, Lewis Research Center, Cleveland, OH.

AN EFFICIENT AND ROBUST ALGORITHM FOR TIME DEPENDENT VISCOUS INCOMPRESSIBLE NAVIER-STOKES EQUATIONS

JOHN W. GOODRICH *In its* Computational Fluid Dynamics p 133-141 Feb. 1992

A recently developed finite difference algorithm is presented for steady incompressible Navier-Stokes calculations. The algorithm is extremely robust with respect to Reynolds number, and has been used to directly compute incompressible flows with smoothly resolved streamfunction, kinetic energy and vorticity contours for Reynolds numbers as high as $Re = 100,000$ without requiring any subscale modelling. The algorithm is second order accurate in both time and space, with Crank-Nicolson differencing for the diffusion terms, with a lagged second order Adams-Basforth differencing for the convection terms, and with central differencing for all space derivatives. The algorithm is extremely efficient with respect to both computing time and physical memory. Solutions are shown for cavity and channel flows at various Reynolds numbers. H.A.

N92-25820*# National Aeronautics and Space Administration, Lewis Research Center, Cleveland, OH.

ADVANCES IN ENGINEERING TURBULENCE MODELING

T.-H. SHIH *In its* Computational Fluid Dynamics p 143-161 Feb. 1992

Some new developments in two equation models and second order closure models are presented. In this paper, modified two equation models are proposed to remove shortcomings such as

34 FLUID MECHANICS AND HEAT TRANSFER

computing flows over complex geometries and the ad hoc treatment near the separation and reattachment points. The calculations using various two equation models are compared with direct numerical solutions of channel flows and flat plate boundary layers. Development of second order closure models will also be discussed with emphasis on the modeling of pressure related correlation terms and dissipation rates in the second moment equations. All existing models poorly predict the normal stresses near the wall and fail to predict the three dimensional effect of mean flow on the turbulence. The newly developed second order near-wall turbulence model to be described in this paper is capable of capturing the near-wall behavior of turbulence as well as the effect of three dimension mean flow on the turbulence. Author

N92-25822* # National Aeronautics and Space Administration. Lewis Research Center, Cleveland, OH.

IMPLEMENTATION OF A KAPPA-EPSILON TURBULENCE MODEL TO RPLUS3D CODE

TAWIT CHITSOMBOON *In its* Computational Fluid Dynamics p 175-180 Feb. 1992

The RPLUS3D code has been developed at the NASA Lewis Research Center to support the National Aerospace Plane (NASP) project. The code has the ability to solve three dimensional flowfields with finite rate combustion of hydrogen and air. The combustion process of the hydrogen-air system are simulated by an 18 reaction path, 8 species chemical kinetic mechanism. The code uses a Lower-Upper (LU) decomposition numerical algorithm as its basis, making it a very efficient and robust code. Except for the Jacobian matrix for the implicit chemistry source terms, there is no inversion of a matrix even though a fully implicit numerical algorithm is used. A k-epsilon turbulence model has recently been incorporated into the code. Initial validations have been conducted for a flow over a flat plate. Results of the validation studies are shown. Some difficulties in implementing the k-epsilon equations to the code are also discussed. Author

N92-25823* # National Aeronautics and Space Administration. Lewis Research Center, Cleveland, OH.

TURBULENCE AND DETERMINISTIC CHAOS

ROBERT G. DEISSLER *In its* Computational Fluid Dynamics p 181-192 Feb. 1992

Several turbulent and nonturbulent solutions of the Navier-Stokes equations are obtained. The unaveraged equations are used numerically in conjunction with tools and concepts from nonlinear dynamics, including time series, phase portraits, Poincare sections, largest Liapunov exponents, power spectra, and strange attractors. Initially neighboring solutions for a low Reynolds number fully developed turbulence are compared. Several flows are noted: fully chaotic, complex periodic, weakly chaotic, simple periodic, and fixed-point. Of these, only fully chaotic is classified as turbulent. Besides the sustained flows, a flow which decays as it becomes turbulent is examined. For the finest grid, 128(exp 3) points, the spatial resolution appears to be quite good. As a final note, the variation of the velocity derivatives skewness of a Navier-Stokes flow as the Reynolds number goes to zero is calculated numerically. The value of the skewness is shown to become small at low Reynolds numbers, in agreement with intuitive arguments that nonlinear terms should be negligible. Author

N92-25825* # National Aeronautics and Space Administration. Lewis Research Center, Cleveland, OH.

TECHNIQUES FOR ANIMATION OF CFD RESULTS

JAY HOROWITZ and JEFFERY C. HANSON (Sverdrup Technology, Inc., Cleveland, OH.) *In its* Computational Fluid Dynamics p 205-217 Feb. 1992 Original contains color illustrations

Video animation is becoming increasingly vital to the computational fluid dynamics researcher, not just for presentation, but for recording and comparing dynamic visualizations that are beyond the current capabilities of even the most powerful graphic workstation. To meet these needs, Lewis Research Center has recently established a facility to provide users with easy access to advanced video animation capabilities. However, producing animation that is both visually effective and scientifically accurate

involves various technological and aesthetic considerations that must be understood both by the researcher and those supporting the visualization process. These considerations include: scan conversion, color conversion, and spatial ambiguities. Author

N92-25826* # National Aeronautics and Space Administration. Lewis Research Center, Cleveland, OH.

DISTRIBUTED VISUALIZATION FOR COMPUTATIONAL FLUID DYNAMICS

DON J. SOSOKA and ANTHONY A. FACCA *In its* Computational Fluid Dynamics p 219-223 Feb. 1992 Original contains color illustrations

Distributed concurrent visualization and computation in computational fluid dynamics (CFD) is not a new concept. Specialized applications such as Realtime Interactive Particle-tracer (RIP) and vendor specific tools like Distributed Graphics Language (DGL) have been in use for some time. This paper describes a current project underway at NASA Lewis Research Center to provide the CFD researcher with an easy method for incorporating distributed processing concepts into program development. Details on the FORTRAN capable interface to a set of network and visualization functions are presented along with some results from initial CFD case studies that employ these techniques. H.A.

N92-25827* # National Aeronautics and Space Administration. Lewis Research Center, Cleveland, OH.

TECHNIQUES FOR GRID MANIPULATION AND ADAPTATION

YUNG K. CHOO, PETER R. EISEMANN, and KI D. LEE (Illinois Univ., Urbana.) *In its* Computational Fluid Dynamics p 225-234 Feb. 1992

Two approaches have been taken to provide systematic grid manipulation for improved grid quality. One is the control point form (CPF) of algebraic grid generation. It provides explicit control of the physical grid shape and grid spacing through the movement of the control points. It works well in the interactive computer graphics environment and hence can be a good candidate for integration with other emerging technologies. The other approach is grid adaptation using a numerical mapping between the physical space and a parametric space. Grid adaptation is achieved by modifying the mapping functions through the effects of grid control sources. The adaptation process can be repeated in a cyclic manner if satisfactory results are not achieved after a single application. Author

N92-26690* # National Aeronautics and Space Administration. Lewis Research Center, Cleveland, OH.

PROGRESS TOWARDS UNDERSTANDING AND PREDICTING CONVECTION HEAT TRANSFER IN THE TURBINE GAS PATH

ROBERT J. SIMONEAU and FREDERICK F. SIMON 1992 32 p Proposed for presentation at the International Symposium on Heat Transfer in Turbomachinery, Athens, Greece, 24-28 Aug. 1992; sponsored by the International Centre for Heat and Mass Transfer (Contract RTOP 505-62-52) (NASA-TM-105674; E-7043; NAS 1.15:105674) Avail: CASI HC A03/MF A01

A new era is drawing in the ability to predict convection heat transfer in the turbine gas path. We feel that the technical community now has the capability to mount a major assault on this problem, which has eluded significant progress for a long time. We hope to make a case for this bold statement by reviewing the state of the art in three major heat transfer, configuration-specific experiments, whose data have provided the big picture and guided both the fundamental modeling research and the code development. Following that, we review progress and directions in the development of computer codes to predict turbine gas path heat transfer. Finally, we cite examples and make observations on the more recent efforts to do all this work in a simultaneous, interactive, and more synergistic manner. We conclude with an assessment of progress, suggestions for how to use the current state of the art, and recommendations for the future. Author

N92-27458*# National Aeronautics and Space Administration, Lewis Research Center, Cleveland, OH.

A MATHEMATICAL CONSTRAINT PLACED UPON INTER-BLADE ROW BOUNDARY CONDITIONS USED IN THE SIMULATION OF MULTISTAGE TURBOMACHINERY FLOWS
J. J. ADAMCZYK *In* AGARD, CFD Techniques for Propulsion Applications 8 p Feb. 1992

Copyright Avail: CASI HC A02/MF A06

A number of researchers have suggested using an inter-blade row boundary condition to extend isolated blade row flow solvers to multiple blade row configurations. This suggestion is worth consideration for it appears to result in codes that are computationally more efficient than those based on other schemes that were suggested to accomplish the same task. The work is concerned with the development of a mathematical constraint which this boundary condition must satisfy to insure the proper transfer of momentum and vorticity across the plane. Using experimental data, the work quantifies the error in the time-averaged vorticity field which results from simply requiring continuity across the boundary plane of the momentum based on the time-averaged velocity fields associated with a multiple blade row configuration.

Author

N92-27459*# National Aeronautics and Space Administration, Lewis Research Center, Cleveland, OH.

A CRITICAL EVALUATION OF A THREE-DIMENSIONAL NAVIER-STOKES METHOD AS A TOOL TO CALCULATE TRANSONIC FLOWS INSIDE A LOW-ASPECT-RATIO COMPRESSOR

CHUNILL HAH and STEVEN L. PUTERBAUGH (Air Force Systems Command, Wright-Patterson AFB, OH.) *In* AGARD, CFD Techniques for Propulsion Applications 14 p Feb. 1992 Original contains color illustrations

Copyright Avail: CASI HC A03/MF A06

A numerical study to evaluate a three-dimensional Navier-Stokes method as a tool to predict the detailed flow field inside a low-aspect-ratio compressor at various operating conditions was conducted. The details of the flow structure inside a low aspect ratio compressor (three-dimensional shock structure, shock-boundary layer interaction, and tip leakage vortex) and the overall aerodynamic performance at design and off-design conditions are numerically analyzed and the results are compared with the available experimental data. The flow field inside a state-of-the-art transonic compressor is used for the purpose of the evaluation.

D.R.D.

N92-27467*# National Aeronautics and Space Administration, Lewis Research Center, Cleveland, OH.

VISCOUS THREE-DIMENSIONAL CALCULATIONS OF TRANSONIC FAN PERFORMANCE

RODRICK V. CHIMA *In* AGARD, CFD Techniques for Propulsion Applications 19 p Feb. 1992 Previously announced as N92-17346

Copyright Avail: CASI HC A03/MF A06

A 3-D flow analysis code was used to compute the design speed operating line of a transonic fan rotor, and the results were compared with experimental data. The code is an explicit finite difference code with an algebraic turbulence model. The transonic fan, called Rotor 67, was tested experimentally at NASA Lewis conventional aerodynamic probes and with user anemometry and was included as one of the AGARD test cases for the computation of internal flows. The experimental data are described. Maps of total pressure ratio and adiabatic efficiency vs mass flow were computed and are compared with the experimental maps, with good agreement. Detailed comparisons between calculations and experiment are made at two operating points, one near peak efficiency and the other near stall. Blade-to-blade contour plots are used to show the shock structure. Comparisons of circumferentially integrated flow quantities downstream of the rotor show spanwise distributions of several aerodynamic parameters. Calculated Mach number distributions are compared with laser anemometer data within the blade row and the wake to quantify

the accuracy of the calculations. Particle traces are used to show the nature of secondary flow.

Author

N92-27653*# National Aeronautics and Space Administration, Lewis Research Center, Cleveland, OH.

A FAST, UNCOUPLED, COMPRESSIBLE, TWO-DIMENSIONAL, UNSTEADY BOUNDARY LAYER ALGORITHM WITH SEPARATION FOR ENGINE INLETS

ROBERT L. ROACH (Georgia Tech Research Inst., Atlanta.), CHRIS NELSON (Georgia Tech Research Inst., Atlanta.), BARBARA SAKOWSKI, DOUGLAS DARLING, and ALLAN G. VANDEWALL (Case Western Reserve Univ., Cleveland, OH.) Jul. 1992 9 p Proposed for presentation at the 28th Joint Propulsion Conference and Exhibit, Nashville, TN, 6-8 Jul. 1992; sponsored by AIAA, SAE, ASME, and ASEE (Contract RTOP 505-62-20)

(NASA-TM-105686; E-7065; NAS 1.15:105686; AIAA PAPER 92-3082) Avail: CASI HC A02/MF A01

A finite difference boundary layer algorithm was developed to model viscous effects when an inviscid core flow solution is given. This algorithm solved each boundary layer equation separately, then iterated to find a solution. Solving the boundary layer equations sequentially was 2.4 to 4.0 times faster than solving the boundary layer equations simultaneously. This algorithm used a modified Baldwin-Lomax turbulence model, a weighted average of forward and backward differencing of the pressure gradient, and a backward sweep of the pressure. With these modifications, the boundary layer algorithm was able to model flows with and without separation. The number of grid points used in the boundary layer algorithm affected the stability of the algorithm as well as the accuracy of the predictions of friction coefficients and momentum thicknesses. Results of this boundary layer algorithm compared well with experimental observations of friction coefficients and momentum thicknesses. In addition, when used interactively with an inviscid flow algorithm, this boundary layer algorithm corrected for viscous effects to give a good match with experimental observations for pressures in a supersonic inlet.

Author

N92-29125* National Aeronautics and Space Administration, Lewis Research Center, Cleveland, OH.

PULSE THERMAL ENERGY TRANSPORT/STORAGE SYSTEM Patent

MARK W. WEISLOGEL, inventor (to NASA) 7 Jul. 1992 11 p Filed 26 Jul. 1991 Supersedes N92-10167 (30 - 1, p 32) (NASA-CASE-LEW-15235-1; US-PATENT-5,127,471; US-PATENT-APPL-SN-736145; US-PATENT-CLASS-165-104.22; US-PATENT-CLASS-165-41; US-PATENT-CLASS-165-104.14; US-PATENT-CLASS-417-209; INT-PATENT-CLASS-F28D-15/02) Avail: US Patent and Trademark Office

A pulse-thermal pump is described. The pump has a novel fluid flow wherein heat admitted to a closed system raises the pressure in a closed evaporator chamber, while another interconnected evaporator chamber remains open. This creates a pressure differential, and at a predetermined pressure, the closed evaporator is opened and the opened evaporator is closed. The difference in pressure initiates fluid flow in the system.

Official Gazette of the U.S. Patent and Trademark Office

N92-30297*# National Aeronautics and Space Administration, Lewis Research Center, Cleveland, OH.

NUMERICAL SOLUTION OF A THREE-DIMENSIONAL CUBIC CAVITY FLOW BY USING THE BOLTZMANN EQUATION

DANNY P. HWANG Jul. 1992 17 p Presented at the 18th International Symposium on Rarefied Gas Dynamics, Vancouver, British Columbia, 26-31 Jul. 1992; sponsored in part by British Columbia Univ. Original contains color illustrations (Contract RTOP 505-62-20)

(NASA-TM-105693; E-7080; NAS 1.15:105693) Avail: CASI HC A03/MF A01; 2 functional color pages

A three-dimensional cubic cavity flow has been analyzed for diatomic gases by using the Boltzmann equation with the Bhatnagar-Gross-Krook (B-G-K) model. The method of discrete ordinate was applied, and the diffuse reflection boundary condition

34 FLUID MECHANICS AND HEAT TRANSFER

was assumed. The results, which show a consistent trend toward the Navier-Stokes solution as the Knudson number is reduced, give us confidence to apply the method to a three-dimensional geometry for practical predictions of rarefied-flow characteristics. The CPU time and the main memory required for a three-dimensional geometry using this method seem reasonable.

Author

N92-31484*# National Aeronautics and Space Administration. Lewis Research Center, Cleveland, OH.

A GENERAL NUMERICAL MODEL FOR WAVE ROTOR ANALYSIS

DANIEL W. PAXSON Jul. 1992 38 p
(Contract RTOP 505-62-10)
(NASA-TM-105740; E-7141; NAS 1.15:105740) Avail: CASI HC A03/MF A01

Wave rotors represent one of the promising technologies for achieving very high core temperatures and pressures in future gas turbine engines. Their operation depends upon unsteady gas dynamics and as such, their analysis is quite difficult. This report describes a numerical model which has been developed to perform such an analysis. Following a brief introduction, a summary of the wave rotor concept is given. The governing equations are then presented, along with a summary of the assumptions used to obtain them. Next, the numerical integration technique is described. This is an explicit finite volume technique based on the method of Roe. The discussion then focuses on the implementation of appropriate boundary conditions. Following this, some results are presented which first compare the numerical approximation to the governing differential equations and then compare the overall model to an actual wave rotor experiment. Finally, some concluding remarks are presented concerning the limitations of the simplifying assumptions and areas where the model may be improved. I.I.C.

N92-32268*# National Aeronautics and Space Administration. Lewis Research Center, Cleveland, OH.

A CRITICAL EVALUATION OF A THREE-DIMENSIONAL NAVIER-STOKES CFD AS A TOOL TO DESIGN SUPERSONIC TURBINE STAGES

C. HAH, O. KWON, and M. SHOEMAKER *In* NASA. Goddard Space Flight Center, Tenth Workshop for Computational Fluid Dynamic Applications in Rocket Propulsion, Part 2 p 1227-1241 Jul. 1992
Avail: CASI HC A03/MF A05

Three-dimensional flow phenomena in a supersonic turbine blade row were studied numerically to evaluate CFD as a tool to design supersonic turbine stages. The details of the three-dimensional flow structure inside the supersonic turbine blade row and the overall aerodynamic performance at design and off-design conditions are analyzed and the results are compared between the experimental data and the numerical results.

Author

N92-32291*# National Aeronautics and Space Administration. Lewis Research Center, Cleveland, OH.

THREE-DIMENSIONAL FLOW FIELDS INSIDE A SHROUDED INDUCER AT DESIGN AND OFF-DESIGN CONDITIONS (CFD STUDY)

C. HAH, O. KWON, D. A. GREENWALD, and R. GARCIA (National Aeronautics and Space Administration, Marshall Space Flight Center, Huntsville, AL.) *In* NASA. Goddard Space Flight Center, Tenth Workshop for Computational Fluid Dynamic Applications in Rocket Propulsion, Part 1 p 289-314 Jul. 1992
Avail: CASI HC A03/MF A05

Three-dimensional flow phenomena in a shrouded inducer were studied with a three-dimensional Navier-Stokes method. The details of the three-dimensional flow structure inside the inducer at design and off-design conditions are analyzed and the results are compared with some flow visualization results obtained at the California Institute of Technology.

Author

N92-32472*# National Aeronautics and Space Administration. Lewis Research Center, Cleveland, OH.

BREAKDOWN OF THE KARMAN VORTEX STREET DUE TO FORCED CONVECTION AND FLOW COMPRESSIBILITY

SHU-CHENG CHEN Jul. 1992 41 p
(Contract RTOP 505-62-52)
(NASA-TM-105853; E-7212; NAS 1.15:105853) Avail: CASI HC A03/MF A01

Low speed compressible flow around a heated/cooled circular cylinder was investigated. The phenomenon of sudden disappearing of the Karman vortex street was numerically simulated and studied. The vortex street at $Re(\text{sub } d) = 100$ and $M(\text{sub } \infty) = 0.3$ is primarily an effect of forced convection. The contribution of natural convection to the current event is inconsequential. The reason for the breakdown of vortex street is believed to be due to a high temperature zone in the wake generated by a high level of wall heating. This produces an effectively lower Reynolds number flow in the near wall region when a compressible gaseous media is used. Vortex shedding stops for a reason similar when flow Reynolds number is reduced globally below its minimum value. Periodic vortex sheddings were observed when the wall heating ratio was less than 0.6. In that region, the coefficient of lift decreased sharply to zero, drag increased slowly, and the Strouhal number reduced monotonically with respect to the wall heating. When the heating ratio was greater than or equal to 0.6, vortex shedding stopped, and steady flows with symmetric twin trailing vortices were observed. In this region, both lift and Strouhal number remained zero, the drag increased sharply, and the Nusselt number maintained the same decreasing slope as the one obtained from the previous region. In this paper quantitative results such as Strouhal number, lift, drag, and Nusselt number, as well as qualitative results such as streamline, isothermal, and vorticity contours obtained at various flow conditions are presented and compared with the results of Noto et al. and Chang et al. Contrast between the two are discussed.

Author

N92-32868*# National Aeronautics and Space Administration. Lewis Research Center, Cleveland, OH.

A NEW TIME SCALE BASED K-EPSILON MODEL FOR NEAR WALL TURBULENCE

Z. YANG and T. H. SHIH Sep. 1992 23 p
(Contract NASA ORDER C-99066-6; RTOP 505-62-21)
(NASA-TM-105768; ICOMP-92-11; CMOTT-92-07; E-7194; NAS 1.15:105768) Avail: CASI HC A03/MF A01

A k-epsilon model is proposed for wall bonded turbulent flows. In this model, the eddy viscosity is characterized by a turbulent velocity scale and a turbulent time scale. The time scale is bounded from below by the Kolmogorov time scale. The dissipation equation is reformulated using this time scale and no singularity exists at the wall. The damping function used in the eddy viscosity is chosen to be a function of $R(\text{sub } y) = (k(\text{sup } 1/2)y)/\nu$ instead of $y(+)$. Hence, the model could be used for flows with separation. The model constants used are the same as in the high Reynolds number standard k-epsilon model. Thus, the proposed model will be also suitable for flows far from the wall. Turbulent channel flows at different Reynolds numbers and turbulent boundary layer flows with and without pressure gradient are calculated. Results show that the model predictions are in good agreement with direct numerical simulation and experimental data.

Author

INSTRUMENTATION AND PHOTOGRAPHY

Includes remote sensors; measuring instruments and gauges; detectors; cameras and photographic supplies; and holography.

A92-13416* Case Western Reserve Univ., Cleveland, OH.

MEASUREMENTS OF COMPLEX PERMITTIVITY OF MICROWAVE SUBSTRATES IN THE 20 TO 300 K TEMPERATURE RANGE FROM 26.5 TO 40.0 GHZ

FELIX A. MIRANDA, WILLIAM L. GORDON (Case Western Reserve University, Cleveland, OH), VERNON O. HEINEN, BEN T. EBIHARA, and KUL B. BHASIN (NASA, Lewis Research Center, Cleveland, OH) IN: Advances in cryogenic engineering. Vol. 35B - Proceedings of the 1989 Cryogenic Engineering Conference, Los Angeles, CA, July 24-28, 1989 1990 7 p refs
Copyright

A knowledge of the dielectric properties of microwave substrates at low temperatures is useful in the design of superconducting microwave circuits. Results are reported for a study of the complex permittivity of sapphire (Al₂O₃), magnesium oxide (MgO), silicon oxide (SiO₂), lanthanum aluminate (LaAlO₃), and zirconium oxide (ZrO₂), in the 20 to 300 Kelvin temperature range, at frequencies from 26.5 to 40.0 GHz. The values of the real and imaginary parts of the complex permittivity were obtained from the scattering parameters, which were measured using an HP-8510 automatic network analyzer. For these measurements, the samples were mounted on the cold head of a helium gas closed cycle refrigerator, in a specially designated vacuum chamber. An arrangement of wave guides, with mica windows, was used to connect the cooling system to the network analyzer. A decrease in the value of the real part of the complex permittivity of these substrates, with decreasing temperature, was observed. For MgO and Al₂O₃, the decrease from room temperature to 20 K was of 7 and 15 percent, respectively. For LaAlO₃, it decreased by 14 percent, for ZrO₂ by 15 percent, and for SiO₂ by 2 percent, in the above mentioned temperature range.
Author

A92-15510* National Aeronautics and Space Administration, Lewis Research Center, Cleveland, OH.

OPTICAL MEASUREMENTS OF INDUCED FAN FLUTTER

ANATOLE P. KURKOV and ORAL MEHMED (NASA, Lewis Research Center, Cleveland, OH) ASME, International Gas Turbine and Aeroengine Congress and Exposition, 36th, Orlando, FL, June 3-6, 1991. 9 p. Previously announced in STAR as N91-15174. Jun. 1991 9 p refs
(ASME PAPER 91-GT-19)

A nonintrusive optical method is described for flutter vibrations in unducted fan or propeller rotors and provides detailed spectral results for two flutter modes of a scaled unducted fan. The measurements were obtained in a high-speed wind tunnel. A single-rotor and a dual-rotor counterrotating configuration of the model were tested; however, only the forward rotor of the counterrotating configuration fluttered. Conventional strain gages were used to obtain flutter frequency; optical data provided complete phase results and an indication of the flutter mode shape through the ratio of the leading- to trailing-edge flutter amplitudes near the blade tip. The transonic regime exhibited some features that are usually associated with nonlinear vibrations. Experimental mode shape and frequencies were compared with calculated values that included centrifugal effects.
Author

A92-21241* Missouri Univ., Rolla.

EXTRAPOLATION PROCEDURES IN MOTT ELECTRON POLARIMETRY

T. J. GAY, M. A. KHAKOO, J. A. BRAND, J. E. FURST, W. M. K. P. WIJAYARATNA (Missouri-Rolla, University, Rolla), W. V. MEYER (NASA, Lewis Research Center, Cleveland, OH; Missouri-Rolla, University, Rolla), and F. B. DUNNING (Rice University, Houston, TX) Review of Scientific Instruments (ISSN 0034-6748), vol. 63,

Jan. 1992, p. 114-130. Jan. 1992 17 p refs
(Contract NSF PHY-90-0772)
Copyright

In standard Mott electron polarimetry using thin gold film targets, extrapolation procedures must be used to reduce the experimentally measured asymmetries A to the values they would have for scattering from single atoms. These extrapolations involve the dependent of A on either the gold film thickness or the maximum detected electron energy loss in the target. A concentric cylindrical-electrode Mott polarimeter, has been used to study and compare these two types of extrapolations over the electron energy range 20-100 keV. The potential systematic errors which can result from such procedures are analyzed in detail, particularly with regard to the use of various fitting functions in thickness extrapolations, and the failure of perfect energy-loss discrimination to yield accurate polarizations when thick foils are used.
Author

A92-21244* National Aeronautics and Space Administration, Lewis Research Center, Cleveland, OH.

THE INTRODUCTION OF SPURIOUS MODES IN A HOLE-COUPLED FABRY-PEROT OPEN RESONATOR

JERRY D. COOK (Eastern Kentucky University, Richmond, KY), KENWYN J. LONG, VERNON O. HEINEN, and NORBERT STANKIEWICZ (NASA, Lewis Research Center, Cleveland, OH) Review of Scientific Instruments (ISSN 0034-6748), vol. 63, Jan. 1992, p. 267, 268. Research supported by American Society for Engineering Education. Jan. 1992 2 p refs
Copyright

A hemispherical open resonator has previously been used to make relative comparisons of the surface resistivity of metallic thin-film samples in the submillimeter wavelength region. This resonator is fed from a far-infrared laser via a small coupling hole in the center of the concave spherical mirror. The experimental arrangement, while desirable as a coupling geometry for monitoring weak emissions from the cavity, can lead to the introduction of spurious modes into the cavity. Sources of these modes are identified, and a simple alteration of the experimental apparatus to eliminate such modes is suggested.
Author

A92-21371 State Univ. of New York, Stony Brook.

A FIBER-OPTIC PROBE FOR PARTICLE SIZING IN CONCENTRATED SUSPENSIONS

HARBANS S. DHADWAL (New York, State University, Stony Brook), RAFAT R. ANSARI, and WILLIAM V. MEYER (NASA, Lewis Research Center, Cleveland, OH) Review of Scientific Instruments (ISSN 0034-6748), vol. 62, Dec. 1991, p. 2963-2968. Research supported by NASA. Dec. 1991 6 p refs
(Contract NCC3-172)
Copyright

A fiber-optic probe employing two monomode optical fibers, one for transmitting a Gaussian laser beam to the scattering volume and the second, positioned at some backscatter angle, for receiving the scattered light is described. Performance and suitability of the system for a process control environment is assessed by studying a suspension of polystyrene latex particles over a wide range of sizes and concentrations. The results show that the probe is ideal for a process control environment in industrial and laboratory applications. Particle size is recovered, without any additional corrections for multiple light scattering, in concentrations containing up to 10 percent solids of 39-nm polystyrene latex spheres.
Author

A92-23852* National Aeronautics and Space Administration, Lewis Research Center, Cleveland, OH.

LIQUID-VAPOUR SURFACE SENSORS FOR LIQUID NITROGEN AND HYDROGEN

J. D. SIEGWARTH, R. O. VOTH, and S. M. SNYDER (NIST, Boulder, CO) (Space Cryogenics Workshop, 10th, Cleveland, OH, June 18-20, 1991, Proceedings. A92-23826 08-31) Cryogenics (ISSN 0011-2275), vol. 32, no. 2, 1992, p. 236-242. 1992 7 p refs
(Contract NASA ORDER C-32009-K)

The present paper identifies devices to serve as liquid-vapor detectors in zero gravity. The testing in LH2 was done in a sealed

glass Dewar system to eliminate any chance of mixing H₂ and air. Most of the tests were performed with the leads to the sensor horizontal. Some results of rapid cycle testing of LVVG in LH₂ are presented. Findings of rapid-cycle testing of LVVG in LH₂ are discussed. The sensor crossed the liquid surface when the position sensor registered 1.9 V, which occurred at about 0.4075 s. The delay time was about 1.5 ms. From the estimated slope of the position sensor curve at 1.9 V, the velocity of the sensor through the liquid surface is over 3 m/s. Results of tests of optical sensors are presented as well. P.D.

A92-26926* National Aeronautics and Space Administration, Lewis Research Center, Cleveland, OH.

PERFORMANCE OF THE PHASE DOPPLER PARTICLE ANALYZER ICING CLOUD DROPLET SIZING PROBE IN THE NASA LEWIS ICING RESEARCH TUNNEL

R. C. RUDOFF, E. J. BACHALO, W. D. BACHALO (Aerometrics, Inc., Sunnyvale, CA), and J. R. OLDENBURG (NASA, Lewis Research Center, Cleveland, OH) AIAA, Aerospace Sciences Meeting and Exhibit, 30th, Reno, NV, Jan. 6-9, 1992. 15 p. Jan. 1992 15 p refs

(Contract NAS3-25653)

(AIAA PAPER 92-0162) Copyright

The design, development, and testing of an icing cloud droplet sizing probe based upon the Phase Doppler Particle Analyzer (PDPA) are discussed. This probe is an in-situ laser interferometry based single particle measuring device capable of determining size distributions. The probe is designed for use in harsh environments such as icing tunnels and natural icing clouds. From the measured size distribution, Median Volume Diameter (MVD) and Liquid Water Content (LWC) may be determined. Both the theory of measurement and the mechanical aspects of the probe design and development are discussed. The MVD results from the probe are compared to an existing calibration based upon different instruments in a series of tests in the NASA Lewis Icing Research Tunnel. Agreement between the PDPA probe and the existing calibration is close for MVDs between 15 to 30 microns, but the PDPA results are considerably smaller for MVDs under 15 microns. Author

A92-33987* National Aeronautics and Space Administration, Lewis Research Center, Cleveland, OH.

SATURATED FLUORESCENCE MEASUREMENTS OF THE HYDROXYL RADICAL IN LAMINAR HIGH-PRESSURE C₂H₆/O₂/N₂ FLAMES

CAMPBELL D. CARTER, GALEN B. KING, and NORMAND M. LAURENDEAU (Purdue University, West Lafayette, IN) Applied Optics (ISSN 0003-6935), vol. 31, April 1, 1992, p. 1511-1522. Research supported by NASA and USAF. 1 Apr. 1992 12 p refs

Copyright

Saturation of a transition of the OH molecule in high-pressure flames is demonstrated by obtaining saturation curves in C₂H₆/O₂/N₂ laminar flames at 1, 6.1, 9.2, and 12.3 atm. Quantitative fluorescence measurements of OH number density at pressures to 12.3 atm are presented. To assess the efficacy of the balanced cross-rate model for high-pressure flames, laser-saturated fluorescence measurements, which were calibrated in an atmospheric-pressure flame, are compared with absorption measurements at 3.1 and 6.1 atm. At 3.1 atm the absorption and fluorescence measurements compare well. At 6.1 atm, however, the concentrations given by laser-saturated fluorescence are about 25 percent lower than the absorption values, indicating some depletion of the laser-coupled levels beyond that at atmospheric pressure. By using a reasonable estimate for the finite sensitivity to quenching, it is anticipated that fluorescence measurements that are calibrated at 1 atm can be applied to flames at about 10 atm with absolute errors within +/- 50 percent. Author

A92-34831* National Aeronautics and Space Administration, Lewis Research Center, Cleveland, OH.

A FIBER OPTIC SENSOR FOR OPHTHALMIC REFRACTIVE DIAGNOSTICS

RAFAT R. ANSARI, HARBANS S. DHADWAL, MELANIE C. W. CAMPBELL, and MICHAEL A. DELLAVECCHIA (NASA, Lewis Research Center, Cleveland, OH) IN: Fiber optic medical and fluorescent sensors and applications; Proceedings of the Meeting, Los Angeles, CA, Jan. 23, 24, 1992 1992 23 p refs
Copyright

This paper demonstrates the application of a lensless fiber optic spectrometer (sensor) to study the onset of cataracts. This new miniaturized and rugged fiber optic probe is based upon dynamic light scattering (DLS) principles. It has no moving parts, no apertures, and requires no optical alignment. It is flexible and easy to use. Results are presented for cold-induced cataract in excised bovine eye lenses, and aging effects in excised human eye lenses. The device can be easily incorporated into a slit-lamp apparatus (ophthalmoscope) for complete eye diagnostics. Author

A92-36738* National Aeronautics and Space Administration, Lewis Research Center, Cleveland, OH.

PLASMA EROSION RATE DIAGNOSTICS USING LASER-INDUCED FLUORESCENCE

C. J. GAETA, R. S. TURLEY, J. N. MATOSSIAN, J. R. BEATTIE, and W. S. WILLIAMSON (Hughes Research Laboratories, Malibu, CA) Review of Scientific Instruments (ISSN 0034-6748), vol. 63, no. 5, May 1992, p. 3090-3095. May 1992 6 p refs
(Contract NAS3-25553)

Copyright

An optical technique for measuring the sputtering rate of a molybdenum surface immersed in a xenon plasma has been developed and demonstrated. This approach, which may be useful in real-time wear diagnostics for ion thrusters, relies on laser-induced fluorescence to determine the density of sputtered molybdenum atoms. Author

A92-38067* National Aeronautics and Space Administration, Lewis Research Center, Cleveland, OH.

RAYLEIGH-BRILLOUIN SCATTERING TO DETERMINE ONE-DIMENSIONAL TEMPERATURE AND NUMBER DENSITY PROFILES OF A GAS FLOW FIELD

JAMES A. LOCK (Cleveland State University, OH), RICHARD G. SEASHOLTZ (NASA, Lewis Research Center, Cleveland, Ohio), and W. T. JOHN (NASA, Lewis Research Center; Calspan Corp., Cleveland, OH) Applied Optics (ISSN 0003-6935), vol. 31, no. 15, May 20, 1992, p. 2839-2848. 20 May 1992 10 p refs
Copyright

Rayleigh-Brillouin spectra for heated nitrogen gas were measured by imaging the output of a Fabry-Perot interferometer onto a CCD array. The spectra were compared with the theoretical 6-moment model of Rayleigh-Brillouin scattering convolved with the Fabry-Perot instrument function. Estimates of the temperature and a dimensionless parameter proportional to the number density of the gas as functions of position in the laser beam were calculated by least-squares deviation fits between theory and experiment. Author

A92-39629* National Aeronautics and Space Administration, Lewis Research Center, Cleveland, OH.

TENSILE STRAIN MEASUREMENTS OF CERAMIC FIBERS USING SCANNING LASER ACOUSTIC MICROSCOPY

RENEE M. KENT (Dayton, University, OH) and ALEX VARY (NASA, Lewis Research Center, Cleveland, OH) Aug. 1992 8 p refs

Copyright

A noncontacting technique using scanning laser acoustic microscopy for making in situ tensile strain measurements of small diameter fibers was implemented for the tensile strain analysis of individual Nicalon SiC fibers (nominal diameter 15 microns). Stress vs strain curves for the fibers were plotted from the experimental data. The mean elastic modulus of the fibers was determined to be 185.3 GPa. Similar measurements were made for Carborundum SiC fibers (nominal diameter 28 microns) and Saphikon sapphire fibers (nominal diameter 140 microns). Author

A92-39699* National Aeronautics and Space Administration. Lewis Research Center, Cleveland, OH.

IDENTIFICATION AND CONTROL OF A MULTIZONE CRYSTAL GROWTH FURNACE

C. BATUR, R. B. SHARPLESS (Akron, University, OH), W. M. B. DUVAL, B. N. ROSENTHAL (NASA, Lewis Research Center, Cleveland, OH), and N. B. SINGH (Westinghouse Science and Technology Center, Pittsburgh, PA) *Journal of Crystal Growth* (ISSN 0022-0248), vol. 119, no. 3-4, May 1992, p. 371-380. May 1992 10 p refs

Copyright

This paper presents an intelligent adaptive control system for the control of a solid-liquid interface of a crystal while it is growing via directional solidification inside a multizone transparent furnace. The task of the process controller is to establish a user-specified axial temperature profile and to maintain a desirable interface shape. Both single-input-single-output and multi-input-multi-output adaptive pole placement algorithms have been used to control the temperature. Also described is an intelligent measurement system to assess the shape of the crystal while it is growing. A color video imaging system observes the crystal in real time and determines the position and the shape of the interface. This information is used to evaluate the crystal growth rate, and to analyze the effects of translational velocity and temperature profiles on the shape of the interface. Creation of this knowledge base is the first step to incorporate image processing into furnace control.

Author

A92-39994 National Aeronautics and Space Administration. Lewis Research Center, Cleveland, OH.

ADVANCED OPTICAL CONDITION MONITORING

G. CROSS and S. BARKHOUDARIAN (Rockwell International Corp., Rocketdyne Div., Canoga Park, CA) *SAE, Aerospace Technology Conference and Exposition, Long Beach, CA, Sept. 23-26, 1991*. 7 p. Research supported by NASA and USAF. Sep. 1991 7 p refs

(SAE PAPER 912164) Copyright

The application of Advanced Optical Condition Monitoring to optical leak detection and plume spectrometry is discussed. The development of these selected sensors for propulsion system monitoring is addressed.

C.D.

A92-46497* National Aeronautics and Space Administration. Lewis Research Center, Cleveland, OH.

AN EVALUATION OF STRAIN MEASURING DEVICES FOR CERAMIC COMPOSITES

JOHN Z. GYEKENYESI (Cleveland State University; NASA, Lewis Research Center, OH) and PAUL A. BARTOLOTTA (NASA, Lewis Research Center, Cleveland, OH) *Journal of Testing and Evaluation* (ISSN 0090-3973), vol. 20, no. 4, July 1992, p. 285-295. Jul. 1992 11 p refs

Copyright

A series of tensile tests were conducted on SiC/RBSN composites using different methods of strain measurement. The tests were used to find the optimum strain sensing device for use with continuous fiber reinforced ceramic matrix composites in ambient and high temperature environments. Bonded resistance strain gages were found to offer excellent performance for room temperature tests. The clip-on gage offers the same performance but significantly less time is required for mounting it to the specimen. Low contact force extensometers track the strain with acceptable results at high specimen temperatures. Silicon carbide rods with knife edges are preferred. The edges must be kept sharp. The strain measuring devices should be mounted on the flat side of the specimen. This is in contrast to mounting on the rough thickness side.

Author

A92-46979*# National Aeronautics and Space Administration. Lewis Research Center, Cleveland, OH.

DOPPLER-SHIFTED FLUORESCENCE IMAGING OF VELOCITY FIELDS IN SUPERSONIC REACTING FLOWS

M. G. ALLEN, S. J. DAVIS, W. J. KESSLER, and D. M. SONNENFROH (Physical Sciences, Inc., Andover, MA) *AIAA,*

Plasmadynamics and Lasers Conference, 23rd, Nashville, TN, July 6-8, 1992. 11 p. Jul. 1992 11 p refs

(Contract NAS3-26254)

(AIAA PAPER 92-2964) Copyright

The application of Doppler-shifted fluorescence imaging of velocity fields in supersonic reacting flows is analyzed. Focussing on fluorescence of the OH molecule in typical H₂-air Scramjet flows, the effects of uncharacterized variations in temperature, pressure, and collisional partner composition across the measurement plane are examined. Detailed measurements of the (1,0) band OH lineshape variations in H₂-air combustions are used, along with single-pulse and time-averaged measurements of an excimer-pumped dye laser, to predict the performance of a model velocimeter with typical Scramjet flow properties. The analysis demonstrates the need for modification and control of the laser bandsape in order to permit accurate velocity measurements in the presence of multivariant flow properties.

Author

A92-48843*# National Aeronautics and Space Administration. Lewis Research Center, Cleveland, OH.

FLOW DIAGNOSTICS OF AN ARCJET USING LASER-INDUCED FLUORESCENCE

JOHN G. LIEBESKIND, RONALD K. HANSON, and MARK A. CAPPELLI (Stanford University, CA) *AIAA, SAE, ASME, and ASEE, Joint Propulsion Conference and Exhibit, 28th, Nashville, TN, July 6-8, 1992*. 12 p. Research supported by NASA and SDIO. Jul. 1992 12 p refs

(AIAA PAPER 92-3243) Copyright

A diagnostic has been developed to measure velocity and translational temperature in the plume of an arcjet thruster. Laser induced fluorescence with a narrowband CW laser is used to probe the Balmer alpha transition of excited atomic hydrogen. The velocity is determined from the Doppler shift of the fluorescence excitation spectrum while temperature is inferred from its shape. Analysis shows that while Doppler broadening is the only significant broadening mechanism, the fine structure of the transition must be accounted for. Near the exit plane, axial velocities vary from 4 to 14 km/s; radial velocities vary from 0 to 4 km/s; and swirl velocities are shown to be relatively small. Temperatures from 1000 to 5000 K indicate high dissociation fractions.

Author

A92-50040* National Aeronautics and Space Administration. Lewis Research Center, Cleveland, OH.

FULL FIELD FLOW VISUALIZATION AND COMPUTER-AIDED VELOCITY MEASUREMENTS IN A BANK OF CYLINDERS IN A WIND TUNNEL

M. J. BRAUN, V. A. CANACCI (Akron, University, OH), and L. M. RUSSELL (NASA, Lewis Research Center, Cleveland, OH) *Experiments in Fluids* (ISSN 0723-4864), vol. 13, no. 2-3, 1992, p. 117-127. 1992 11 p refs

(Contract NCC3-165)

Copyright

The full field flow tracking (FFFT) method that is presented in this paper uses a laser-generated, mechanically strobed planar sheet of light, a low luminosity TV camera coupled with a long distance microscope, and a computer-controlled video recorder to study nonintrusively and qualitatively the flow structures in a bank of cylinders that are placed in a wind tunnel. This setup simulates an upscale version of the geometry of internal cooling passageways characteristic of small air-cooled radial turbines. The qualitative images supplied by the FFFT system are processed by means of a computer-integrated image quantification (CIQ) method into quantitative information, trajectories and velocities, that describe the flow upstream of and within the bank of cylinders. The tracking method is Lagrangian in concept, and permits identification and tracking of the same particle, thus facilitating construction of time dependent trajectories and the calculation of true velocities and accelerations. The error analysis evaluates the accuracy with which the seed particles follow the flow and the errors incurred during the quantitative processing of the raw data derived from the FFFT/CIQ method.

Author

A92-50630 National Aeronautics and Space Administration. Lewis Research Center, Cleveland, OH.

FIBER-OPTIC SENSORS FOR AEROSPACE ELECTRICAL MEASUREMENTS - AN UPDATE

RICHARD L. PATTERSON (NASA, Lewis Research Center, Cleveland, OH), A. H. ROSE, D. TANG, and G. W. DAY (NIST, Boulder, CO) IN: IECEC '91; Proceedings of the 26th Intersociety Energy Conversion Engineering Conference, Boston, MA, Aug. 4-9, 1991. Vol. 2 1991 4 p refs

The authors report the progress made on the development of aerospace current and voltage sensors which use fiber-optic and optical sensing heads. These sensors are presently designed to cover ac frequencies from 60 Hz to 20 kHz. The current sensor, based on the Faraday effect in optical fiber, is in advanced development after some initial testing. The emphasis is on packaging methods and ways to maintain consistent sensitivity with changes in temperature. The voltage sensor, utilizing the Pockels effect in a crystal, has excelled in temperature tests. The authors report on the development of these sensors. The authors also relate the technology used in the sensors, the results of evaluation, improvements being made, and the future direction of the work. I.E.

A92-54106*# National Aeronautics and Space Administration. Lewis Research Center, Cleveland, OH.

DESIGN OF A SELF-DIAGNOSTIC BEAM-MODE PIEZOELECTRIC ACCELEROMETER

PATRICK M. FLANAGAN (Cleveland State University, OH) AIAA, SAE, ASME, and ASEE, Joint Propulsion Conference and Exhibit, 28th, Nashville, TN, July 6-8, 1992. 8 p. Jul. 1992 8 p refs (Contract NAG3-1151) (AIAA PAPER 92-3656) Copyright

A technique was developed for detecting in situ real-time soft failures in a beam-mode piezoelectric accelerometer. The new technique can be used to detect changes in the piezoelectric capacitance, the equivalent mechanical stiffness of the piezoelectric element and the surface mounting impedance, and the piezoelectric efficiency. I.S.

A92-54318* National Aeronautics and Space Administration. Lewis Research Center, Cleveland, OH.

A LASER-INDUCED HEAT FLUX TECHNIQUE FOR CONVECTIVE HEAT TRANSFER MEASUREMENTS IN HIGH SPEED FLOWS

A. R. PORRO (NASA, Lewis Research Center, Cleveland, OH), T. G. KEITH, JR. (Toledo, University, OH), and W. R. HINGST (NASA, Lewis Research Center, Cleveland, OH) IN: ICIASF '91 - International Congress on Instrumentation in Aerospace Simulation Facilities, 14th, Rockville, MD, Oct. 27-31, 1991, Record 1991 10 p refs Copyright

A technique is developed to measure the local convective heat transfer coefficient on a model surface in a supersonic flow field. The technique uses a laser to apply a discrete local heat flux at the model test surface, and an infrared camera system determines the local temperature distribution due to the heating. From this temperature distribution and an analysis of the heating process, a local convective heat transfer coefficient is determined. The technique was used to measure the local surface convective heat transfer coefficient distribution on a flat plate at nominal Mach numbers of 2.5, 3.0, 3.5, and 4.0. The flat plate boundary layer initially was laminar and became transitional in the measurement region. The experimentally determined convective heat transfer coefficients were generally higher than the theoretical predictions for flat plate laminar boundary layers. However, the results indicate that this nonintrusive optical measurement technique has the potential to measure surface convective heat transfer coefficients in high-speed flowfields. Author

A92-56733# National Aeronautics and Space Administration. Langley Research Center, Hampton, VA.
FILTERED RAYLEIGH SCATTERING MEASUREMENTS IN SUPERSONIC/HYPERSONIC FACILITIES

RICHARD B. MILES, JOSEPH N. FORKEY, and WALTER R. LEMPERT (Princeton University, NJ) AIAA, Aerospace Ground Testing Conference, 17th, Nashville, TN, July 6-8, 1992. 11 p. Research supported by NASA, USAF, U.S. Army, et al. Jul. 1992 11 p refs (AIAA PAPER 92-3894) Copyright

Preliminary measurements are presented of flow field properties in Mach 3 and Mach 5 flows using filtered Rayleigh scattering. Filter properties have been characterized by high resolution spectroscopy in order to optimize the selection of laser frequency and filter operating conditions, as well as for the development of an accurate filter modeling program. An optimized filter is used the background suppression feature of this technique to image the boundary layer structure in a Mach 3 high Reynolds number facility and the shock structure in a Mach 5 overexpanded jet. This had been achieved using a visible laser source. By frequency scanning the laser, time-averaged velocity measurements in the Mach 3 and Mach 5 flows are made. Data acquisition at 10 torr and below indicates that this approach can be extrapolated for use in hypersonic flow facilities and is applicable as an in-flight optical air data device for hypersonic vehicles. Author

A92-56828*# National Aeronautics and Space Administration. Lewis Research Center, Cleveland, OH.

CALIBRATION OF HEMISPHERICAL-HEAD FLOW ANGULARITY PROBES

EDWARD L. CLARK, JOHN F. HENFLING, and DANIEL P. AESCHLIMAN (Sandia National Laboratories, Albuquerque, NM) AIAA, Aerospace Ground Testing Conference, 17th, Nashville, TN, July 6-8, 1992. 10 p. Jul. 1992 10 p refs (Contract DE-AC04-76DP-00789; NASA ORDER C-22955-P) (AIAA PAPER 92-4005)

The hemisphere-cylinder flow angularity probes were calibrated over a Mach number range of 0.5 to 2.0 at pitch and yaw angles of -5 to +5 deg. Each probe had five pressure orifices in the hemispherical head - one on the axis and four located 45 deg from the axis and equally spaced circumferentially. The probes were identical within fabrication tolerances. Details of probe design, test procedures and data analysis are described and selected test results are presented. Author

A92-56829# National Aeronautics and Space Administration. Lewis Research Center, Cleveland, OH.

DESCRIPTION OF A PRESSURE MEASUREMENT TECHNIQUE FOR OBTAINING SURFACE STATIC PRESSURES OF A RADIAL TURBINE

L. D. DICICCO, BRENT C. NOWLIN (NASA, Lewis Research Center, Cleveland, OH), and LIZET TIRRES (Sverdrup Technology, Inc., Brook Park) AIAA, Aerospace Ground Testing Conference, 17th, Nashville, TN, July 6-8, 1992. 10 p. Previously announced in STAR as N92-24959. Jul. 1992 10 p refs (Contract RTOP 535-05-10) (AIAA PAPER 92-4006)

The aerodynamic performance of a solid uncooled version of a cooled radial turbine was evaluated in the Small Engine Components Test Facility Turbine rig at the NASA Lewis Research Center. Specifically, an experiment was conducted to rotor surface static pressures. This was the first time surface static pressures had been measured on a radial turbine at NASA Lewis. These pressures were measured by a modified Rotating Data Package (RDP), a standard product manufactured by Scanivalve, Inc. Described here are the RDP, and the modifications that were made, as well as the checkout, installation, and testing procedures. The data presented are compared to analytical results obtained from NASA's MERIDL TSONIC BLAYER (MTSB) code. Author

N92-15366*# National Aeronautics and Space Administration. Lewis Research Center, Cleveland, OH.

AN OPTICAL METHOD FOR DETERMINING LEVEL IN TWO-PHASE CRYOGENIC FLUIDS

LAWRENCE G. OBERLE and DONALD H. WEIKLE Jan. 1992 12 p Original contains color illustrations

(Contract RTOP 590-21-11)

(NASA-TM-104524; E-6398; NAS 1.15:104524)

A method was evaluated to measure the liquid-gas and the liquid-slush interfaces in two-phase cryogen systems using optical means. This method makes use of the attenuation of a directed light beam caused by the difference in the index of refraction between the solid particles and the surrounding liquid. Preliminary experimental results obtained in slush nitrogen are shown. The possibility of extending this technique to include a measure of solid fraction is also discussed.

Author

N92-18456*# National Aeronautics and Space Administration. Lewis Research Center, Cleveland, OH.

USING SILICON DIODES FOR DETECTING THE LIQUID-VAPOR INTERFACE IN HYDROGEN

PAULA J. DEMPSEY and RICHARD H. FABIK 1992 15 p

Proposed for presentation at the 38th International Instrumentation Symposium, Las Vegas, NV, 26-30 Apr. 1992; sponsored by the Instrument Society of America

(Contract RTOP 593-21-00)

(NASA-TM-105541; E-6851; NAS 1.15:105541) Avail: CASI HC A03/MF A01

Tests were performed using commercially available silicon diode temperature sensors to detect the location of the liquid-vapor interface in hydrogen during ground test programs. Results show that by increasing the current into the sensor, silicon diodes can be used as liquid level point sensors. After cycling the sensors from liquid to vapor several times, it was found that with a 30 mA (milliamps) input current, the sensors respond within 2 seconds by measuring a large voltage difference when transitioning from liquid to vapor across the interface. Nearly instantaneous response resulted during a transition from vapor to liquid. Detailed here are test procedures, experimental results, and guidelines for applying this information to other test facilities.

Author

N92-18759*# National Aeronautics and Space Administration. Lewis Research Center, Cleveland, OH.

MINIATURE HIGH TEMPERATURE PLUG-TYPE HEAT FLUX GAUGES

CURT H. LIEBERT 1992 11 p Proposed for presentation at the 38th International Instrumentation Symposium, Las Vegas, NV,

26-30 Apr. 1992; sponsored by the Instrument Society of America (Contract RTOP 553-13-00)

(NASA-TM-105403; E-6805; NAS 1.15:105403) Avail: CASI HC A03/MF A01

The objective is to describe continuing efforts to develop methods for measuring surface heat flux, gauge active surface temperature, and heat transfer coefficient quantities. The methodology involves inventing a procedure for fabricating improved plug-type heat flux gauges and also for formulating inverse heat conduction models and calculation procedures. These models and procedures are required for making indirect measurements of these quantities from direct temperature measurements at gauge interior locations. Measurements of these quantities were made in a turbine blade thermal cycling tester (TBT) located at MSFC. The TBT partially simulates the turbopump turbine environment in the Space Shuttle Main Engine. After the TBT test, experiments were performed in an arc lamp to analyze gauge quality.

Author

N92-19107*# National Aeronautics and Space Administration. Lewis Research Center, Cleveland, OH.

MULTIWAVELENGTH PYROMETRY FOR NONGRAY SURFACES IN THE PRESENCE OF INTERFERING RADIATION

DANIEL NG Feb. 1992 10 p

(Contract RTOP 510-01-50)

(NASA-TM-105286; E-6617; NAS 1.15:105286) Avail: CASI HC A02/MF A01

A NASA developed multiwavelength pyrometry technique for nongray surfaces was extended to also measure surface temperature in the presence of interfering radiation. This radiation is produced by heat lamps used to raise the temperature of the surface. The necessary instruments are a spectral radiometer, an

auxiliary radiation source, and a computer. Four radiation spectra are recorded: (1) the unobstructed spectrum characterizing an auxiliary radiation source; (2) the unobstructed spectrum characterizing the interfering radiation; (3) the radiation spectrum consisting of surface emission plus the interfering radiation; and (4) a spectrum consisting of the radiations of (3) plus the reflected radiation due to the incidence of the auxiliary radiation source on this surface. With these spectra, application of two variable, nonlinear, least squares, curve fitting computer software determines the surface temperature and the spectral emissivity. Use of the method to measure the surface temperature of silicon carbide under a simulated interference condition is shown at a low temperature just above ambient. The instrumentation necessary to extend the method to elevated temperatures is discussed.

Author

N92-19263*# National Aeronautics and Space Administration. Lewis Research Center, Cleveland, OH.

TEMPERATURE-DEPENDENT REFLECTIVITY OF SILICON CARBIDE

DANIEL NG Feb. 1992 11 p

(Contract RTOP 510-01-50)

(NASA-TM-105287; E-6618; NAS 1.15:105287) Avail: CASI HC A03/MF A01

The spectral reflectivity of a commercial silicon carbide (SiC) ceramic surface was measured at wavelengths from 2.5 to 14.5 microns and at temperatures ranging from 358 to 520 K using a NASA-developed multiwavelength pyrometer. The SiC surface reflectivity was low at the short wavelengths, decreasing to almost zero at 10 microns, then increasing rapidly to a maximum at approximately 12.5 microns, and decreasing gradually thereafter. The reflectivity maximum increased in magnitude with increasing surface temperature. The wavelength and temperature dependence can be explained in terms of the classical dispersion theory of crystals and the Lorentz electron theory. Electronic transitions between the donor state and the conduction band states were responsible for the dispersion. The concentration of the donor state in SiC was determined to be approximately 4×10^{18} and its ionization energy was determined to be approximately 71 meV.

Author

N92-21723*# National Aeronautics and Space Administration. Lewis Research Center, Cleveland, OH.

ADJUSTABLE DEPTH GAGE Patent

ROGER C. FORSGREN, inventor (to NASA) 17 Mar. 1992 6 p Filed 7 Jul. 1989 Supersedes N90-10415 (28 - 1, p 72)

(NASA-CASE-LEW-14880-1; US-PATENT-5,096,340;

US-PATENT-APPL-SN-376738; US-PATENT-CLASS-408-14;

US-PATENT-CLASS-408-16; US-PATENT-CLASS-408-241S;

INT-PATENT-CLASS-B23B-39/00) Avail: US Patent and Trademark Office

A quick adjust depth gage includes a handle-clamp assembly wherein the clamp includes an opening in which a cylindrical shaft with suitable depth measurement markings thereon is reviewed. Turning the handle on the clamp enables the gage to be set to the desired depth.

Official Gazette of the U.S. Patent and Trademark Office

N92-22038*# National Aeronautics and Space Administration. Lewis Research Center, Cleveland, OH.

METHOD OF PRODUCING A PLUG-TYPE HEAT FLUX GAUGE Patent

CURT H. LIEBERT, inventor (to NASA) and JOHN KOCH, JR., inventor (to NASA) 4 Feb. 1992 6 p Filed 8 Apr. 1991

Supersedes N91-23460 (29 - 15, p 2430) Division of

(NASA-CASE-LEW-14967-2; US-PATENT-5,086,204;

US-PATENT-APPL-SN-685062; US-PATENT-APPL-SN-531433;

US-PATENT-CLASS-219-69.17; US-PATENT-CLASS-374-29;

US-PATENT-CLASS-40-703; INT-PATENT-CLASS-B23H-9/00)

Avail: US Patent and Trademark Office

A method of making a plug-type heat flux gauge in a material specimen in which a thermoplug is integrally formed in the specimen

35 INSTRUMENTATION AND PHOTOGRAPHY

is disclosed. The thermoplug and concentric annulus are formed in the material specimen by electrical discharge machining and trepanning procedures. The thermoplug is surrounded by a concentric annulus through which thermocouple wires are routed. The end of each thermocouple wire is welded to the thermoplug, with each thermocouple wire welded at a different location along the length of the thermoplug.

Official Gazette of the U.S. Patent and Trademark Office

N92-22526*# National Aeronautics and Space Administration. Lewis Research Center, Cleveland, OH.

RESEARCH SENSORS

DAVID R. ENGLUND *In its* Aeropropulsion 1987 p 217-224 Feb. 1990

Avail: CASI HC A02/MF A04

The LeRC program in research sensors is directed at development of sensors and sensing techniques for research applications on turbine engines and propulsion systems. In general, the sensors are used either to measure to response of an engine component to the imposed environment. Locations of concern are generally within the gas path and, for the most part, are within the hot section of the engine. Since these sensors are used for research testing as opposed to operational use, a sensor lifetime of the order of 50 hr is considered sufficient. The following discussion presents a sample of this work, describing programs to develop a dynamic gas temperature measuring system, total heat flux sensors, a variety of thin-film sensors, and high-temperature strain measuring systems. Author

N92-22527*# National Aeronautics and Space Administration. Lewis Research Center, Cleveland, OH.

OPTICAL MEASUREMENT SYSTEMS

DANIEL J. LESCO *In its* Aeropropulsion 1987 p 225-232 Feb. 1990

Avail: CASI HC A02/MF A04

Some of the areas of research conducted at the LeRC on optical measurement techniques for propulsion systems research are described. Most of the optical techniques used to measure gas parameters depend on very inefficient light scattering principles and, therefore, require the high light intensities provided by lasers. Significant advances in laser technology, together with the availability of sensitive photodetection systems, provide much of the impetus for research in optical diagnostics techniques. The goal of the research is to enhance the capabilities of nonintrusive research instrumentation to meet the special needs of aeropropulsion research. Optical techniques are being used to validate analytical codes and to verify the performance of aeropropulsion components and systems. Author

N92-23155*# National Aeronautics and Space Administration. Lewis Research Center, Cleveland, OH.

X RAY BASED DISPLACEMENT MEASUREMENT FOR HOSTILE ENVIRONMENTS

HOWARD A. CANISTRARO (Connecticut Univ., Storrs.), ERIC H. JORDON (Connecticut Univ., Storrs.), DOUGLAS M. PEASE (Connecticut Univ., Storrs.), and GUSTAVE C. FRALICK Mar. 1992 17 p

(Contract NAG3-1004; RTOP 505-90-01)

(NASA-TM-105551; E-6872; NAS 1.15:105551) Avail: CASI HC A03/MF A01

A new method on noncontacting, high temperature extensometry based on the focus and scanning of x rays is currently under development and shows great promise of overcoming limitations associated with available techniques. The chief advantage is the ability to make undisturbed measurements through stratified or flowing gases, smoke, and flame. The system is based on the ability to focus and scan low energy, hard x rays such as those emanating from copper or molybdenum sources. The x rays are focused into a narrow and intense line image which can be scanned onto targets that fluoresce secondary x ray radiation. The final goal of the system is the ability to conduct macroscopic strain measurements in hostile environments by utilizing two or more fluorescing targets. Current work is limited to displacement

measurement of a single target with a resolution of 1.25 micro-m and a target temperature of 1200 C, directly through an open flame. The main advantage of the technique lies in the penetrating nature of x rays which are not affected by the presence of refracting gas layers, smoke, flame, or intense thermal radiation, all of which could render conventional extensometry methods inoperative or greatly compromise their performance. Author

N92-24681*# National Aeronautics and Space Administration. Lewis Research Center, Cleveland, OH.

MULTIWAVELENGTH PYROMETRY FOR NONGRAY BODIES

DANIEL NG Feb. 1992 11 p

(Contract RTOP 510-01-50)

(NASA-TM-105285; E-6616; NAS 1.15:105285) Avail: CASI HC A03/MF A01

A multiwavelength technique was developed and applied to measure the temperatures of nongray surfaces. The instruments required are a spectral radiometer, a dedicated auxiliary radiation source, and a computer. In general, three radiation spectra are recorded: (1) spectrum S sub 0 of the auxiliary radiation source; (2) spectrum S sub 1 of the surface-emitted radiation; and (3) spectrum S sub 2, the sum of the radiation of S sub 1 plus the reflected radiation due to the incidence of the auxiliary radiation source on the surface. Subtracting spectrum S sub 1 from spectrum S sub 2 yields the reflection spectrum resulting from the incidence radiation. From these spectra, a quantity $z(\lambda)$ is derived and is related to the reflectivity $r(\lambda)$ by $r(\lambda) = z(\lambda)/f$, where f is a constant. Spectrum S sub 1 is represented mathematically as the product of a wavelength-dependent emissivity obtained from Kirchhoff's law and a Planck function of temperature T . Application of two-variable (λ and z), nonlinear, least-squares curve-fitting computer software to fit spectrum S sub 1 to this mathematical expression yielded the surface temperature. This technique also measured the spectral reflectivity and emissivity of the surface. Instrumentation necessary to extend measurement to elevated temperatures and in the presence of reflective interference is discussed. Author

N92-24959*# National Aeronautics and Space Administration. Lewis Research Center, Cleveland, OH.

DESCRIPTION OF A PRESSURE MEASUREMENT TECHNIQUE FOR OBTAINING SURFACE STATIC PRESSURES OF A RADIAL TURBINE

L. DANIELLE DICICCO, BRENT C. NOWLIN, and LIZET TIRRES (Sverdrup Technology, Inc., Brook Park, OH.) 1992 11 p

Proposed for presentation at the 17th Aerospace Ground Testing Conference, Nashville, TN, 6-8 Jul. 1992; sponsored by AIAA (Contract RTOP 535-05-10)

(NASA-TM-105643; E-6989; NAS 1.15:105643; AIAA PAPER 92-4006) Avail: CASI HC A03/MF A01

The aerodynamic performance of a solid uncooled version of a cooled radial turbine was evaluated in the Small Engine Components Test Facility Turbine rig at the NASA Lewis Research Center. Specifically, an experiment was conducted to rotor surface static pressures. This was the first time surface static pressures had been measured on a radial turbine at NASA Lewis. These pressures were measured by a modified Rotating Data Package (RDP), a standard product manufactured by Scanivalve, Inc. Described here are the RDP, and the modifications that were made, as well as the checkout, installation, and testing procedures. The data presented are compared to analytical results obtained from NASA's MERIDL TSONIC BLAYER (MTSB) code. Author

N92-29105*# National Aeronautics and Space Administration. Lewis Research Center, Cleveland, OH.

A 4-SPOT TIME-OF-FLIGHT ANEMOMETER FOR SMALL CENTRIFUGAL COMPRESSOR VELOCITY MEASUREMENTS

MARK P. WERNET and GARY J. SKOCH Jul. 1992 8 p

Presented at the Sixth International Symposium on the Application of Laser Techniques to Fluid Mechanics, Lisbon, Portugal, 20-23 Jul. 1992; sponsored by the Instituto Superior Tecnico (Contract DA PROJ. 1L1-62211-A-47-A; RTOP 505-62-50)

(NASA-TM-105717; E-7112; NAS 1.15:105717; AVSCOM-TR-92-C-026) Avail: CASI HC A02/MF A01

The application of laser anemometry techniques in turbomachinery facilities is a challenging dilemma requiring an anemometer system with special qualities. Here, we describe the use of a novel laser anemometry technique applied to a small 4.5 kg/s, 4:1 pressure ratio centrifugal compressor. Sample velocity profiles across the blade pitch are presented for a single location along the rotor. The results of the intra-blade passage velocity measurements will ultimately be used to verify CFD 3-D viscous code predictions.

Author

37

MECHANICAL ENGINEERING

Includes auxiliary systems (nonpower); machine elements and processes; and mechanical equipment.

A92-15650* Texas A&M Univ., College Station.
ELECTROMECHANICAL SIMULATION AND TESTING OF ACTIVELY CONTROLLED ROTORDYNAMIC SYSTEMS WITH PIEZOELECTRIC ACTUATORS

RENG RONG LIN, A. B. PALAZZOLO (Texas A & M University, College Station), A. F. KASCAK (NASA, Lewis Research Center; U.S. Army, Cleveland, OH), and G. T. MONTAGUE (NASA, Lewis Research Center; Sverdrup Technology, Inc., Cleveland, OH) ASME, International Gas Turbine and Aeroengine Congress and Exposition, 36th, Orlando, FL, June 3-6, 1991. 16 p. Research supported by NASA, Texas A & M Turbomachinery Research Consortium, and U.S. Army. Jun. 1991 16 p refs (ASME PAPER 91-GT-245)

A method is presented for simulating the coupled 'electromechanical' system to predict rotordynamic stability and unbalance response along with control system stability. The piezoelectric actuators and their amplifiers are represented as equivalent linear electrical circuits. The electromechanical system modeling approach is utilized to correlate test results from a double overhung rotor rig. The test results also show the effectiveness of the control system for suppressing the unbalance response of two modes using active stiffness and active damping.

Author

A92-15651* Cleveland State Univ., OH.
DESIGN OF A HYDRAULIC ACTUATOR FOR ACTIVE CONTROL OF ROTATING MACHINERY

MAJID RASHIDI (Cleveland State University, OH) and ELISEO DIRUSSO (NASA, Lewis Research Center, Cleveland, OH) ASME, International Gas Turbine and Aeroengine Congress and Exposition, 36th, Orlando, FL, June 3-6, 1991. 8 p. Jun. 1991 8 p refs (ASME PAPER 91-GT-246)

A hydraulic actuator is described which consists of a pump, a hydraulic servo-valve, and a thin elastic plate which transduces the generated pressure variations into forces acting on a mass which simulates the bearing of a rotor system. An actuator characteristic number is defined to provide a base for an optimum design of force actuators with combined weight, frequency, and force considerations. This characteristic number may also be used to compare hydraulic and electromagnetic force actuators. In tests, this actuator generated 182.3 Newton force at a frequency of 100 Hz and a displacement amplitude of 5.8×10^{-5} meter.

Author

A92-15696* National Aeronautics and Space Administration.
 Lewis Research Center, Cleveland, OH.

A BULK FLOW MODEL OF A BRUSH SEAL SYSTEM

R. C. HENDRICKS, S. SCHLUMBERGER (NASA, Lewis Research Center, Cleveland, OH), M. J. BRAUN, F. CHOY (Akron, University, OH), and R. L. MULLEN (Case Western Reserve University, Cleveland, OH) ASME, International Gas Turbine and Aeroengine

Congress and Exposition, 36th, Orlando, FL, June 3-6, 1991. 10 p. Jun. 1991 10 p refs (ASME PAPER 91-GT-325)

Fibers can be readily fabricated into a variety of seal configurations that are compliant and responsive to high speed or lightly loaded systems. A linear, circular, or contoured brush seal system is a contact seal consisting of the bristle pattern and hardened interface. When compared to a labyrinth seal, the brush seal system is superior and features low leakage, dynamic stability, and permits compliant structures. But in turn, the system usually requires a hardened smooth interface and permits only limited pressure drops. Wear life and wear debris for operations with static or dynamic excitation are largely undetermined. A seal system involves control of fluid within specific boundaries. The brush and rub ring (or rub surface) form a seal system. Design similitudes, a bulk flow model, and rub ring (interface) coatings are discussed. The bulk flow model calculations are based on flows in porous media and filters. The coatings work is based on experience and expanded to include current practice.

Author

A92-21333* National Aeronautics and Space Administration.
 Lewis Research Center, Cleveland, OH.

EFFECT OF TYPE AND LOCATION OF OIL GROOVE ON THE PERFORMANCE OF JOURNAL BEARINGS

D. VIJAYARAGHAVAN (NASA, Lewis Research Center, Cleveland, OH) and T. G. KEITH, JR. (Toledo, University, OH) (STLE, Annual Meeting, 45th, Denver, CO, May 7-10, 1990) STLE Tribology Transactions (ISSN 0569-8197), vol. 35, Jan. 1992, p. 98-106. Jan. 1992 9 p refs

Copyright

A numerical study is performed of oil groove type (circumferential and axial), groove number (single and double) and groove location on journal bearing performance. The analysis involves the use of a cavitation algorithm. The interaction between cavitation phenomena and grooving is determined. Quantitative information is provided which will aid designers to better locate oil feed grooves.

Author

A92-22665* National Aeronautics and Space Administration.
 Lewis Research Center, Cleveland, OH.

FREQUENCY EFFECTS ON THE STABILITY OF A JOURNAL BEARING FOR PERIODIC LOADING

D. VIJAYARAGHAVAN (NASA, Lewis Research Center, Cleveland, OH) and D. E. BREWE (NASA, Lewis Research Center; U.S. Army, Propulsion Directorate, Cleveland, OH) (STLE and ASME, Tribology Conference, Saint Louis, MO, Oct. 13-16, 1991) ASME, Transactions, Journal of Tribology (ISSN 0742-4787), vol. 114, Jan. 1992, p. 107-115. Jan. 1992 9 p refs

Copyright

The stability of a journal bearing is numerically predicted when an unidirectional periodic external load is applied. The analysis is performed using a cavitation algorithm, which mimics the JFO theory by accounting for the mass balance through the complete bearing. Hence, the history of the film is taken into consideration. The loading pattern is taken to be sinusoidal and the frequency of the load cycle is varied. The results are compared with the predictions using Reynolds boundary conditions for both film rupture and reformation. With such comparisons, the need for accurately predicting the cavitation regions for complex loading patterns is clearly demonstrated. For a particular frequency of loading, the effects of mass, amplitude of load vibration and frequency of journal speed are also investigated.

Author

A92-23719* National Aeronautics and Space Administration.
 Lewis Research Center, Cleveland, OH.

REACTION-COMPENSATION TECHNOLOGY FOR MICROGRAVITY LABORATORY ROBOTS

DOUGLAS A. ROHN, CHARLES LAWRENCE (NASA, Lewis Research Center, Cleveland, OH), and JEFFREY H. MILLER (Sverdrup Technology, Inc., Brookpark, OH) IN: i-SAIRAS '90; Proceedings of the International Symposium on Artificial Intelligence, Robotics and Automation in Space, Kobe, Japan, Nov. 18-20, 1990 1990 4 p refs

37 MECHANICAL ENGINEERING

Robots operating in the microgravity environment of an orbiting laboratory should be capable of manipulating payloads such that the motion of the robot does not disturb adjacent experiments. The current results of a NASA Lewis Research Center technology program to develop smooth, reaction-compensated manipulation based on both mechanism technology and trajectory planning strategies are present. Experimental validation of methods to reduce robot base reactions through the use of redundant degrees of freedom is discussed. Merits of smooth operation roller-driven robot joints for microgravity manipulators are also reviewed. Author

A92-35421* National Aeronautics and Space Administration. Lewis Research Center, Cleveland, OH.

A SYSTEM-APPROACH TO THE ELASTOHYDRODYNAMIC LUBRICATION POINT-CONTACT PROBLEM

SANG G. LIM and DAVID E. BREWE (NASA, Lewis Research Center, Cleveland, OH) (STLE, Annual Meeting, 46th, Montreal, Canada, Apr. 29-May-2, 1991) STLE Tribology Transactions (ISSN 0569-8197), vol. 35, no. 2, April 1992, p. 367-373. Previously announced in STAR as N91-23439. Apr. 1992 7 p refs Copyright

The classical EHL (elastohydrodynamic lubrication) point contact problem is solved using a new system-approach, similar to that introduced by Houpert and Hamrock for the line-contact problem. Introducing a body-fitted coordinate system, the troublesome free-boundary is transformed to a fixed domain. The Newton-Raphson method can then be used to determine the pressure distribution and the cavitation boundary subject to the Reynolds boundary condition. This method provides an efficient and rigorous way of solving the EHL point contact problem with the aid of a supercomputer and a promising method to deal with the transient EHL point contact problem. A typical pressure distribution and film thickness profile are presented and the minimum film thicknesses are compared with the solution of Hamrock and Dowson. The details of the cavitation boundaries for various operating parameters are discussed. Author

A92-36976* National Aeronautics and Space Administration. Lewis Research Center, Cleveland, OH.

FLOW VISUALIZATION AND MOTION ANALYSIS FOR A SERIES OF FOUR SEQUENTIAL BRUSH SEALS

M. J. BRAUN, V. A. CANACCI (Akron, University, OH), and R. C. HENDRICKS (NASA, Lewis Research Center, Cleveland, OH) Jun. 1992 6 p refs (Contract NAG3-969) Copyright

A92-39227* National Aeronautics and Space Administration. Lewis Research Center, Cleveland, OH.

STATISTICAL ENERGY ANALYSIS OF A GEARED ROTOR SYSTEM

TEIK C. LIM (Structural Dynamics Research Corp., Milford, OH) and RAJENDRA SINGH (Ohio State University, Columbus) IN: NOISE-CON 90; Proceedings of the 10th National Conference on Noise Control Engineering, Austin, TX, Oct. 15-17, 1990 1990 6 p refs Copyright

The vibroacoustic response of a generic geared rotor system is analyzed on an order of magnitude basis utilizing an approximate statistical energy analysis method. This model includes a theoretical coupling loss factor for a generic bearing component, which properly accounts for the vibration transmission through rolling element bearing. A simplified model of a NASA test stand that assumes vibratory energy flow from the gear mesh source to the casing through shafts and bearings is given as an example. Effects of dissipation loss factor and gearbox radiation efficiency models are studied by comparing predictions with NASA test results. R.E.P.

A92-39258* National Aeronautics and Space Administration. Lewis Research Center, Cleveland, OH.

ELECTROMECHANICAL SIMULATION AND TESTING OF ACTIVELY CONTROLLED ROTORDYNAMIC SYSTEMS WITH PIEZOELECTRIC ACTUATORS

RENG R. LIN, A. B. PALAZZOLO (Texas A & M University, College Station), A. F. KASCAK (U.S. Army; NASA, Lewis Research Center, Cleveland, OH), and G. T. MONTAGUE (Sverdrup Technology, Inc.; NASA, Lewis Research Center, Cleveland, OH) IN: Joint U.S./Japan Conference on Adaptive Structures, 1st, Maui, HI, Nov. 13-15, 1990, Proceedings 1991 21 p refs Copyright

Theoretical developments for the simulation of an actively controlled rotorbearing system with piezoelectric type actuators are summarized. Two simulation models were derived; the first assumes that the actuators and other electrical components in the feedback system operate at all frequencies without phase lag or rolloff, while the second model includes the nonideal behavior of these components which are modeled with linear electric circuits. The two models predict identical unbalance response at low frequencies, and the nonideal model also predicts instability-onset feedback gains. The agreement between the measured and predicted results for unbalance response and instability onset gain is very good. The predicted instability-onset feedback gain for active damping was found to be very sensitive to the tare (uncontrolled) damping in the unstable mode. P.D.

A92-40024* National Aeronautics and Space Administration. Lewis Research Center, Cleveland, OH.

RECENT MANUFACTURING ADVANCES FOR SPIRAL BEVEL GEARS

ROBERT F. HANDSCHUH and ROBERT C. BILL (NASA, Lewis Research Center; U.S. Army, Propulsion Directorate, Cleveland, OH) SAE, Aerospace Technology Conference and Exposition, Long Beach, CA, Sept. 23-26, 1991. 14 p. Previously announced in STAR as N91-31654. Sep. 1991 14 p refs (SAE PAPER 912229) Copyright

The U.S. Army Aviation Systems Command (AVSCOM), through the Propulsion Directorate at NASA Lewis Research Center, has recently sponsored projects to advance the manufacturing process for spiral bevel gears. This type of gear is a critical component in rotary-wing propulsion systems. Two successfully completed contracted projects are described. The first project addresses the automated inspection of spiral bevel gears through the use of coordinate measuring machines. The second project entails the computer-numerical-control (CNC) conversion of a spiral bevel gear grinding machine that is used for all aerospace spiral bevel gears. The results of these projects are described with regard to the savings effected in manufacturing time. Author

A92-47173* National Aeronautics and Space Administration. Lewis Research Center, Cleveland, OH.

TWO REFERENCE TIME SCALES FOR STUDYING THE DYNAMIC CAVITATION OF LIQUID FILMS

D. C. SUN (New York, State University, Binghamton) and D. E. BREWE (NASA, Lewis Research Center; U.S. Army, Propulsion Directorate, Cleveland, OH) ASME, Transactions, Journal of Tribology (ISSN 0742-4787), vol. 114, no. 3, July 1992, p. 612-615. Jul. 1992 4 p refs Copyright

Two formulas, one for the characteristic time of filling a void with the vapor of the surrounding liquid, and one of filling the void by diffusion of the dissolved gas in the liquid, are derived. By comparing these time scales with that of the dynamic operation of oil film bearings, it is concluded that the evaporation process is usually fast enough to fill the cavitation bubble with oil vapor; whereas the diffusion process is much too slow for the dissolved air to liberate itself and enter the cavitation bubble. These results imply that the formation of a two phase fluid in dynamically loaded bearings, as often reported in the literature, is caused by air entrainment. They further indicate a way to simplify the treatment of the dynamic problem of bubble evolution. Author

A92-48936*# National Aeronautics and Space Administration. Lewis Research Center, Cleveland, OH.

ADVANCED ROTORCRAFT TRANSMISSION PROGRAM SUMMARY

ROBERT B. BOSSLER, JR. (Lucas Western, Inc., Applied Technology Div., City of Industry, CA) and GREGORY F. HEATH (McDonnell Douglas Helicopter Co., Mesa, AZ) AIAA, SAE, ASME, and ASEE, Joint Propulsion Conference and Exhibit, 28th, Nashville, TN, July 6-8, 1992. 12 p. Research supported by U.S. Army. Jul. 1992 12 p refs

(Contract NAS3-25454)

(AIAA PAPER 92-3363) Copyright

The current status of the Advanced Rotorcraft Transmission (ART) program is reviewed. The discussion includes a general configuration and face gear description, weight analysis, stress analysis, reliability analysis, acoustic analysis, face gear testing, and planned torque split testing. Design descriptions include the face gear webs sized for equal stiffness, a positive engagement clutch, the lubrication system, and a high contact ratio planetary. Test results for five gear materials and three housing materials are presented.

V.L.

A92-48937*# National Aeronautics and Space Administration. Lewis Research Center, Cleveland, OH.

BOEING HELICOPTERS ADVANCED ROTORCRAFT TRANSMISSION (ART) PROGRAM SUMMARY OF COMPONENT TESTS

JOSEPH W. LENSKI, JR. (Boeing Defense and Space Group, Helicopters Div., Philadelphia, PA) and MARK J. VALCO (U.S. Army, Propulsion Directorate; NASA, Lewis Research Center, Cleveland, OH) AIAA, SAE, ASME, and ASEE, Joint Propulsion Conference and Exhibit, 28th, Nashville, TN, July 6-8, 1992. 28 p. Research supported by U.S. Army. Jul. 1992 28 p

(Contract NAS3-25421)

(AIAA PAPER 92-3364) Copyright

The principal objectives of the ART program are briefly reviewed, and the results of advanced technology component tests are summarized. The tests discussed include noise reduction by active cancellation, hybrid bidirectional tapered roller bearings, improved bearing life theory and friction tests, transmission lube study with hybrid bearings, and precision near-net-shape forged spur gears. Attention is also given to the study of high profile contact ratio noninvolute tooth form spur gears, parallel axis gear noise study, and surface modified titanium accessory spur gears.

V.L.

A92-48938# National Aeronautics and Space Administration. Lewis Research Center, Cleveland, OH.

ADVANCED ROTORCRAFT TRANSMISSION (ART) PROGRAM SUMMARY

T. L. KRANTZ (U.S. Army, Propulsion Directorate; NASA, Lewis Research Center, Cleveland, OH) and J. G. KISH (Sikorsky Aircraft, Stratford, CT) AIAA, SAE, ASME, and ASEE, Joint Propulsion Conference and Exhibit, 28th, Nashville, TN, July 6-8, 1992. 13 p. Previously announced in STAR as N92-24984. Jul. 1992 13 p refs

(Contract RTOP 505-63-36)

(AIAA PAPER 92-3365) Copyright

The Advanced Rotorcraft Transmission (ART) Program was initiated to advance the state of the art for rotorcraft transmissions. The goal of the ART Program was to develop and demonstrate the technologies needed to reduce transmission weight by 25 pct and reduce noise by 10 dB while obtaining a 5000 hr 'mean time between failure'. The research done under the ART Program is summarized. A split path design was selected as best able to meet the program goals. Key part technologies needed for this design were identified, studied, and developed. Two of these technologies are discussed in detail: the load sharing of split path designs including the use of a compliant elastomeric torque splitter and the application of a high ratio, low pitch line velocity gear mesh. Development of an angular contact spherical roller bearing, transmission error analysis, and fretting fatigue testing are discussed. The technologies for a light weight, quiet, and reliable rotorcraft transmission were demonstrated.

Author

A92-48939*# National Aeronautics and Space Administration. Lewis Research Center, Cleveland, OH.

ADVANCED ROTORCRAFT TRANSMISSION (ART) - COMPONENT TEST RESULTS

Z. S. HENRY (Bell Helicopter Textron, Inc., Fort Worth, TX) AIAA, SAE, ASME, and ASEE, Joint Propulsion Conference and Exhibit, 28th, Nashville, TN, July 6-8, 1992. 13 p. Research supported by U.S. Army. Jul. 1992 13 p

(Contract NAS3-25455)

(AIAA PAPER 92-3366) Copyright

The preliminary design of the ART and some of the component test results are presented. The goals for the future rotorcraft transmissions include a 25-percent weight reduction in comparison with current state-of-the-art transmissions, a 10-dB reduction in the transmitted noise level, and a system reliability of 5,000 hr mean-time-between-removal for the transmission. The ART tests completed to date support the attainment of the three major goals of the program.

V.L.

A92-49027*# National Aeronautics and Space Administration. Lewis Research Center, Cleveland, OH.

SEPARATION DISTANCE AND STATIC TRANSMISSION ERROR OF INVOLUTE SPUR GEARS

DAVID K. TSE and HSIANG H. LIN (Memphis State University, TN) AIAA, SAE, ASME, and ASEE, Joint Propulsion Conference and Exhibit, 28th, Nashville, TN, July 6-8, 1992. 9 p. Jul. 1992 9 p refs

(Contract NAG3-961)

(AIAA PAPER 92-3490) Copyright

The effects of separation distance and deflection of gear teeth on the static transmission error of involute spur gears are investigated. In this paper, only low-contact-ratio gears with true involute profile are studied. Gear ratio and tooth addendum are varied to examine their effects on the separation distance and static transmission error. Results obtained from the investigation shows that the contact ratio and static transmission error are affected significantly if considering the separation distance. In general, the magnitude of contact ratio has been increased and the variation of static transmission error has been smoothed. The most significant change occurs for a gear pair with a theoretical contact ratio close to 1.95.

Author

A92-49030*# National Aeronautics and Space Administration. Lewis Research Center, Cleveland, OH.

MAXIMUM LIFE SPIRAL BEVEL REDUCTION DESIGN

M. SAVAGE, M. G. PRASANNA (Akron, University, OH), and H. H. COE (NASA, Lewis Research Center, Cleveland, OH) AIAA, SAE, ASME, and ASEE, Joint Propulsion Conference and Exhibit, 28th, Nashville, TN, July 6-8, 1992. 9 p. Jul. 1992 9 p refs

(AIAA PAPER 92-3493) Copyright

Optimization is applied to the design of a spiral bevel gear reduction for maximum life at a given size. A modified feasible directions search algorithm permits a wide variety of inequality constraints and exact design requirements to be met with low sensitivity to initial values. Gear tooth bending strength and minimum contact ratio under load are included in the active constraints. The optimal design of the spiral bevel gear reduction includes the selection of bearing and shaft proportions in addition to gear mesh parameters. System life is maximized subject to a fixed backcone distance of the spiral bevel gear set for a specified speed reduction, shaft angle, input torque, and power. Design examples show the influence of the bearing lives on the gear parameters in the optimal configurations. For a fixed back-cone distance, optimal designs with larger shaft angles have larger service lives.

Author

A92-50271* National Aeronautics and Space Administration. Lewis Research Center, Cleveland, OH.

EXPERIMENTAL VERIFICATION OF A SECONDARY RECIRCULATION ZONE IN A LABYRINTH SEAL

G. L. MORRISON (Texas A & M University, College Station), M. C. JOHNSON (Allied-Signal Corp., Phoenix, AZ), and G. B. TATTERSON (North Carolina Agricultural and Technical State

37 MECHANICAL ENGINEERING

University, Greensboro) Oct. 1992 7 p refs
(Contract NAG3-181)
Copyright

A92-50781* National Aeronautics and Space Administration. Lewis Research Center, Cleveland, OH.

COMPONENT TECHNOLOGY FOR STIRLING POWER CONVERTERS

LANNY G. THIEME (NASA, Lewis Research Center, Cleveland, OH) IN: IECEC '91; Proceedings of the 26th Intersociety Energy Conversion Engineering Conference, Boston, MA, Aug. 4-9, 1991. Vol. 5 1991 6 p refs

Copyright

NASA Lewis Research Center has organized a component technology program as part of the efforts to develop Stirling converter technology for space power applications. The Stirling Space Power Program is part of the NASA High Capacity Power Project of the Civil Space Technology Initiative (CSTI). NASA Lewis is also providing technical management for the DOE/Sandia program to develop Stirling converters for solar terrestrial power producing electricity for the utility grid. The primary contractors for the space power and solar terrestrial programs develop component technologies directly related to their goals. This Lewis component technology effort, while coordinated with the main programs, aims at longer term issues, advanced technologies, and independent assessments. An overview of work on linear alternators, engine/alternator/load interactions and controls, heat exchangers, materials, life and reliability, and bearings is presented. Author

A92-50784* National Aeronautics and Space Administration. Lewis Research Center, Cleveland, OH.

FREE-PISTON STIRLING COMPONENT TEST POWER CONVERTER

GEORGE DOCHAT and MANMOHAN DHAR (Mechanical Technology, Inc., Latham, NY) IN: IECEC '91; Proceedings of the 26th Intersociety Energy Conversion Engineering Conference, Boston, MA, Aug. 4-9, 1991. Vol. 5 1991 6 p refs

Copyright

The National Aeronautics and Space Administration (NASA) has been evaluating free-piston Stirling power converters (FPSPCs) for use on a wide variety of space missions. They provide high reliability, long life, and efficient operation and can be coupled with all potential heat sources, various heat input and heat rejection systems, and various power management and distribution systems. FPSPCs can compete favorably with alternative power conversion systems over a range of hundreds of watts to megawatts. Mechanical Technology Incorporated (MTI) is developing FPSPC technology under contract to NASA Lewis Research Center and will demonstrate this technology in two full-scale power converters operating at space temperature conditions. The testing of the first of these, the component test power converter (CTPC), was initiated in Spring 1991 to evaluate mechanical operation at space operating temperatures. The CTPC design, hardware fabrication, and initial test results are reviewed. I.E.

A92-50788 National Aeronautics and Space Administration. Lewis Research Center, Cleveland, OH.

STIRLING MACHINE OPERATING EXPERIENCE

BRAD A. ROSS (Stirling Technology Co., Richland, WA) and JAMES E. DUDENHOEFER (NASA, Lewis Research Center, Cleveland, OH) IN: IECEC '91; Proceedings of the 26th Intersociety Energy Conversion Engineering Conference, Boston, MA, Aug. 4-9, 1991. Vol. 5 1991 6 p refs

(Contract RTOP 590-13-11)

Copyright

Numerous Stirling machines have been built and operated, but the operating experience of these machines is not well known. It is important to examine this operating experience in detail, because it largely substantiates the claim that Stirling machines are capable of reliable and lengthy lives. The amount of data that exists is impressive, considering that many of the machines that have been built are developmental machines intended to show proof of concept, and were not expected to operate for any lengthy period

of time. Some Stirling machines (typically free-piston machines) achieve long life through non-contact bearings, while other Stirling machines (typically kinematic) have achieved long operating lives through regular seal and bearing replacements. In addition to engine and system testing, life testing of critical components is also considered. Author

A92-50793 National Aeronautics and Space Administration. Lewis Research Center, Cleveland, OH.

COMPARATIVE SURVEY OF DYNAMIC ANALYSES OF FREE-PISTON STIRLING ENGINES

M. D. KANKAM (NASA, Lewis Research Center, Cleveland, OH) and J. S. RAUCH (Sverdrup Technologies, Inc., Cleveland, OH) IN: IECEC '91; Proceedings of the 26th Intersociety Energy Conversion Engineering Conference, Boston, MA, Aug. 4-9, 1991. Vol. 5 1991 6 p refs

(Contract RTOP 590-13-11)

Copyright

Reported dynamics analyses for evaluating the steady-state response and stability of free-piston Stirling engine (FPSE) systems are compared. Various analytical approaches are discussed to provide guidance on their salient features. Recommendations are made in the recommendations remarks for an approach which captures most of the inherent properties of the engine. Such an approach has the potential for yielding results which will closely match practical FPSE-load systems. Author

A92-50797* National Aeronautics and Space Administration. Lewis Research Center, Cleveland, OH.

ALKALI METAL POOL BOILER LIFE TESTS FOR A 25 KWE ADVANCED STIRLING CONVERSION SYSTEM

W. G. ANDERSON, J. H. ROSENFELD (Thermacore, Inc., Lancaster, PA), and J. NOBLE (Stirling Technologies, Co., Richland, WA) IN: IECEC '91; Proceedings of the 26th Intersociety Energy Conversion Engineering Conference, Boston, MA, Aug. 4-9, 1991. Vol. 5 1991 6 p refs

(Contract DEN3-377)

Copyright

The overall operating temperature and efficiency of solar-powered Stirling engines can be improved by adding an alkali metal pool boiler heat transport system to supply heat more uniformly to the heater head tubes. One issue with liquid metal pool boilers is unstable boiling. Stable boiling is obtained with an enhanced boiling surface containing nucleation sites that promote continuous boiling. Over longer time periods, it is possible that the boiling behavior of the system will change. An 800-h life test was conducted to verify that pool boiling with the chosen fluid/surface combination remains stable as the system ages. The apparatus uses NaK boiling on a - 100 + 140 stainless steel sintered porous layer, with the addition of a small amount of xenon. Pool boiling remained stable to the end of life test. The pool boiler life test included a total of 82 cold starts, to simulate startup each morning, and 60 warm restarts, to simulate cloud cover transients. The behavior of the cold and warm starts showed no significant changes during the life test. In the experiments, the fluid/surface combination provided stable, high-performance boiling at the operating temperature of 700 C. Based on these experiments, a pool boiler was designed for a full-scale 25-kWe Stirling system. I.E.

A92-50798* National Aeronautics and Space Administration. Lewis Research Center, Cleveland, OH.

FINAL DESIGN OF A FREE-PISTON HYDRAULIC ADVANCED STIRLING CONVERSION SYSTEM

D. A. WALLACE, J. E. NOBLE, S. G. EMIGH, B. A. ROSS, and G. A. LEHMANN (Stirling Technology Co., Richland, WA) IN: IECEC '91; Proceedings of the 26th Intersociety Energy Conversion Engineering Conference, Boston, MA, Aug. 4-9, 1991. Vol. 5 1991 6 p refs

(Contract DEN3-377)

Copyright

Under the US Department of Energy's (DOEs) Solar Thermal Technology Program, Sandia National Laboratories is evaluating

heat engines for solar distributed receiver systems. The final design is described of an engineering prototype advanced Stirling conversion system (ASCS) with a free-piston hydraulic engine output capable of delivering about 25 kW of electric power to a utility grid. The free-piston Stirling engine has the potential for a highly reliable engine with long life because it has only a few moving parts, has noncontacting bearings, and can be hermetically sealed. The ASCS is designed to deliver maximum power per year over a range of solar input with a design life of 30 years (60,000 h). The system includes a liquid NaK pool boiler heat transport system and a free-piston Stirling engine with high-pressure hydraulic output, coupled with a bent axis variable displacement hydraulic motor and a rotary induction generator. I.E.

A92-50804* National Aeronautics and Space Administration, Lewis Research Center, Cleveland, OH.

STATUS OF THE ADVANCED STIRLING CONVERSION SYSTEM PROJECT FOR 25 KW DISH STIRLING APPLICATIONS

RICHARD K. SHALTENS and JEFFREY G. SCHREIBER (NASA, Lewis Research Center, Cleveland, OH) IN: IECEC '91; Proceedings of the 26th Intersociety Energy Conversion Engineering Conference, Boston, MA, Aug. 4-9, 1991. Vol. 5 1991 7 p refs
Copyright

Technology development for Stirling convertors directed toward a dynamic power source for space applications is discussed. Space power requirements include high reliability with very long life, low vibration, and high system efficiency. The free-piston Stirling engine has the potential for future high power space conversion systems, either nuclear or solar powered. Although these applications appear to be quite different, their requirements complement each other. The advanced Stirling conversion system (ASCS) project at NASA Lewis Research Center is described. Each system design features a solar receiver/liquid metal heat transport system and a free-piston Stirling convertor with a means to provide nominally 25 kW of electric power to utility grid while meeting the US Department of Energy (DOE) performance and long term cost goals. The design is compared with other ASCS designs. I.E.

A92-54036*# National Aeronautics and Space Administration, Lewis Research Center, Cleveland, OH.

MODAL SIMULATION OF GEARBOX VIBRATION WITH EXPERIMENTAL CORRELATION

FRED K. CHOY, YEEFENG F. RUAN (Akron, University, OH), JAMES J. ZAKRAJSEK, and FRED B. OSWALD (NASA, Lewis Research Center, Cleveland, OH) AIAA, SAE, ASME, and ASEE, Joint Propulsion Conference and Exhibit, 28th, Nashville, TN, July 6-8, 1992. 16 p. Previously announced in STAR as N92-31485. Jul. 1992 16 p refs
(AIAA PAPER 92-3494) Copyright

A newly developed global dynamic model was used to simulate the dynamics of a gear noise rig at NASA Lewis Research Center. Experimental results from the test rig were used to verify the analytical model. In this global dynamic model, the number of degrees of freedom of the system are reduced by transforming the system equations of motion into modal coordinates. The vibration of the individual gear-shaft system are coupled through the gear mesh forces. A three-dimensional, axial-lateral coupled, bearing model was used to couple the casing structural vibration to the gear-rotor dynamics. The coupled system of modal equations is solved to predict the resulting vibration at several locations on the test rig. Experimental vibration data was compared to the predictions of the global dynamic model. There is excellent agreement between the vibration results from analysis and experiment. Author

N92-10195*# National Aeronautics and Space Administration, Lewis Research Center, Cleveland, OH.

A METHOD FOR DETERMINING SPIRAL-BEVEL GEAR TOOTH GEOMETRY FOR FINITE ELEMENT ANALYSIS

ROBERT F. HANDSCHUH and FAYDOR L. LITVIN (Illinois Univ., Chicago.) Aug. 1991 16 p Original contains color illustrations

(Contract DA PROJ. 1L1-62211-A-47-A; RTOP 505-63-51) (NASA-TP-3096; E-5837; NAS 1.60:3096; AVSCOM-TR-91-C-020; AD-A242332) Avail: CASI HC A03/MF A01; 1 functional color page

An analytical method was developed to determine gear tooth surface coordinates of face-milled spiral bevel gears. The method uses the basic gear design parameters in conjunction with the kinematical aspects of spiral bevel gear manufacturing machinery. A computer program, SURFACE, was developed. The computer program calculates the surface coordinates and outputs 3-D model data that can be used for finite element analysis. Development of the modeling method and an example case are presented. This analysis method could also find application for gear inspection and near-net-shape gear forging die design. Author

N92-14346*# National Aeronautics and Space Administration, Lewis Research Center, Cleveland, OH.

ROTORDYNAMIC INSTABILITY PROBLEMS IN HIGH-PERFORMANCE TURBOMACHINERY, 1990

Washington Oct. 1991 458 p Workshop held in College Station, TX, 21-23 May 1990; sponsored by Texas A and M Univ. and NASA, Lewis Research Center
(Contract RTOP 553-13-00) (NASA-CP-3122; E-5628; NAS 1.55:3122) Avail: CASI HC A20/MF A04

The present workshop continues to report field experience and experimental results, and it expands the use of computational and control techniques with the integration of damper, bearing, and eccentric seal operation results. The intent of the workshop was to provide a continuing impetus for an understanding and resolution of these problems.

N92-15087*# National Aeronautics and Space Administration, Lewis Research Center, Cleveland, OH.

SEALS RELATED RESEARCH AT NASA. LEWIS RESEARCH CENTER

ROBERT C. HENDRICKS *In its* Seals Flow Code Development p 53-65 Mar. 1991
Avail: CASI HC A03/MF A02

Some current efforts in seal research at the Lewis Research Center include self-sealing linear segmented ceramic configurations, the T700 brush seal engine test, flow and duration characteristics of brush seals and other configurations, cryogenic hydrogen brush seal tests, and a brush seal tester. Information is given in diagram and graphs for a labyrinth seal and a straight cylindrical seal. Author

N92-15103*# National Aeronautics and Space Administration, Lewis Research Center, Cleveland, OH.

NATIONAL AEROSPACE PLANE ENGINE SEALS: HIGH TEMPERATURE SEAL PERFORMANCE EVALUATION

BRUCE M. STEINETZ *In its* Seals Flow Code Development p 165-170 Mar. 1991
Avail: CASI HC A02/MF A02

The key to the successful development of the single stage to orbit National Aerospace Plane (NASP) is the successful development of combined cycle ramjet/scramjet engines that can propel the vehicle to 17,000 mph to reach low Earth orbit. To achieve engine performance over this speed range, movable engine panels are used to tailor engine flow that require low leakage, high temperature seals around their perimeter. NASA-Lewis is developing a family of new high temperature seals to form effective barriers against leakage of extremely hot (greater than 2000 F), high pressure (up to 100 psi) flow path gases containing hydrogen and oxygen. Preventing backside leakage of these explosive gas mixtures is paramount in preventing the potential loss of the engine or the entire vehicle. Seal technology development accomplishments are described in the three main areas of concept development, test, and evaluation and analytical development. Author

37 MECHANICAL ENGINEERING

N92-16318* National Aeronautics and Space Administration.
Lewis Research Center, Cleveland, OH.

HIGH TEMPERATURE, FLEXIBLE PRESSURE-ACTUATED, BRUSH SEAL Patent

BRUCE M. STEINETZ, inventor (to NASA) and PAUL J. SIROCKY,
inventor (to NASA) 31 Dec. 1991 8 p Filed 26 Nov. 1990
(NASA-CASE-LEW-15086-1; US-PATENT-5,076,590;
US-PATENT-APPL-SN-617752; US-PATENT-CLASS-277-53;
US-PATENT-CLASS-277-27; US-PATENT-CLASS-239-127.1;
US-PATENT-CLASS-239-127.3; INT-PATENT-CLASS-F16J-15/32)
Avail: US Patent and Trademark Office

A high temperature, flexible brush seal comprises a bundle of fibers or bristles held tightly together and secured at one end with a backing plate. The assembly includes a secondary spring-clip having one end anchored to the brush seal backing plate. An alternate embodiment of the seal utilizes a metal bellows containing coolant holes. Another embodiment of the seal uses non-circular cross-sectional fibers which may be square, rectangular or hexagonal in cross section.

Official Gazette of the U.S. Patent and Trademark Office

N92-16336*# National Aeronautics and Space Administration.
Lewis Research Center, Cleveland, OH.

ENGINE PANEL SEALS FOR HYPERSONIC ENGINE APPLICATIONS: HIGH TEMPERATURE LEAKAGE ASSESSMENTS AND FLOW MODELLING

BRUCE M. STEINETZ (Drexel Univ., Philadelphia, PA.),
RAJAKANNU MUTHARASAN (Drexel Univ., Philadelphia, PA.),
GUANG-WU DU (Sverdrup Technology, Inc., Brook Park, OH.),
JEFFREY H. MILLER, and FRANK KO (Drexel Univ., Philadelphia,
PA.) 1992 14 p Proposed for presentation at the Fourth
International Symposium on Transport Phenomena and Dynamics
of Rotating Machinery, Honolulu, HI, 5-8 Apr. 1992; sponsored by
the Pacific Center of Thermal-Fluids Engineering
(Contract NAS3-25266; RTOP 505-63-5B)
(NASA-TM-105260; E-6545; NAS 1.15:105260) Avail: CASI HC
A03/MF A01

A critical mechanical system in advanced hypersonic engines is the panel-edge seal system that seals gaps between the articulating horizontal engine panels and the adjacent engine splitter walls. Significant advancements in seal technology are required to meet the extreme demands placed on the seals, including the simultaneous requirements of low leakage, conformable, high temperature, high pressure, sliding operation. In this investigation, the seal concept design and development of two new seal classes that show promise of meeting these demands will be presented. These seals include the ceramic wafer seal and the braided ceramic rope seal. Presented are key elements of leakage flow models for each of these seal types. Flow models such as these help designers to predict performance-robbing parasitic losses past the seals, and estimate purge coolant flow rates. Comparisons are made between measured and predicted leakage rates over a wide range of engine simulated temperatures and pressures, showing good agreement. Author

N92-17678*# National Aeronautics and Space Administration.
Lewis Research Center, Cleveland, OH.

THREE POINT LEAD SCREW POSITIONING APPARATUS Patent Application

FRANK S. CALCO, inventor (to NASA) 27 Jan. 1992 16 p
(NASA-CASE-LEW-15216-1; NAS 1.71:LEW-15216-1;
US-PATENT-APPL-SN-826547) Avail: CASI HC A03/MF A01

Three lead screws are provided for adjusting the position of a traversing plate. Each of the three lead screws is threaded through a collar that is press fitted through the center of one of three pinion gears. A sun gear meshes with all three pinion gears and transversely moves the three lead screws upon actuation of a drive gear. The drive gear meshes with the sun gear and is driven by a handle or servomotor. When the handle or servomotor rotates the drive gear, the sun gear rotates causing the three pinion gears to rotate, thus, causing transverse movement of the three lead screws and, accordingly, transverse movement of the transversing plate. When the drive gear rotates, the traversing plate is driven

in and out of a microwave cavity. Thus, the length or size of the cavity can be tuned while maintaining the traversing plate in an exact parallel relationship with an opposing plate on another end of the cavity. NASA

N92-20815*# National Aeronautics and Space Administration.
Lewis Research Center, Cleveland, OH.

EVALUATION OF AN INNOVATIVE HIGH TEMPERATURE CERAMIC WAFER SEAL FOR HYPERSONIC ENGINE APPLICATIONS Ph.D. Thesis, 1991

BRUCE M. STEINETZ Feb. 1992 195 p
(Contract RTOP 505-63-5B)
(NASA-TM-105556; E-6048; NAS 1.15:105556) Avail: CASI HC
A09/MF A03

A critical mechanical system in advanced hypersonic engines is the panel-edge seal system that seals gaps between the articulating engine panels and the adjacent engine splitter walls. Significant advancements in seal technology are required to meet the extreme demands placed on the seals, including the simultaneous requirements of low leakage, conformable, high temperature, high pressure, sliding operation. In this investigation, the design, development, analytical and experimental evaluation of a new ceramic wafer seal that shows promise of meeting these demands will be addressed. A high temperature seal test fixture was designed and fabricated to measure static seal leakage performance under engine simulated conditions. Ceramic wafer seal leakage rates are presented for engine-simulated air pressure differentials (up to 100 psi), and temperature (up to 1350 F), sealing both flat and distorted wall conditions, where distortions can be as large as 0.15 inches in only an 18 inch span. Seal leakage rates are low, meeting an industry-established tentative leakage limit for all combinations of temperature, pressure and wall conditions considered. A seal leakage model developed from externally-pressurized gas film bearing theory is also presented. Predicted leakage rates agree favorably with the measured data for nearly all conditions of temperature and pressure. Discrepancies noted at high engine pressure and temperature are attributed to thermally-induced, non-uniform changes in the size and shape of the leakage gap condition. The challenging thermal environment the seal must operate in places considerable demands on the seal concept and material selection. Of the many high temperature materials considered in the design, ceramics were the only materials that met the many challenging seal material design requirements. Of the aluminum oxide, silicon carbide, and silicon nitride ceramics considered in the material ranking scheme developed herein, the silicon nitride class of ceramics ranked the highest because of their high temperature strength; resistance to the intense heating rates; resistance to hydrogen damage; and good structural properties. Baseline seal feasibility has been established through the research conducted in this investigation. Recommendations for future work are also discussed. Author

N92-22043* National Aeronautics and Space Administration.
Lewis Research Center, Cleveland, OH.

HIGH TEMPERATURE, FLEXIBLE, FIBER-PREFORM SEAL Patent

BRUCE M. STEINETZ, inventor (to NASA) and PAUL J. STROCKY,
inventor (to NASA) 21 Jan. 1992 8 p Filed 9 Nov. 1990
(NASA-CASE-LEW-15085-1; US-PATENT-5,082,293;
US-PATENT-APPL-SN-610879; US-PATENT-CLASS-277-3;
US-PATENT-CLASS-239-265.11; US-PATENT-CLASS-277-34;
US-PATENT-CLASS-277-76; US-PATENT-CLASS-277-229;
US-PATENT-CLASS-277-234; INT-PATENT-CLASS-F16J-15/46)
Avail: US Patent and Trademark Office

A seal is mounted in a rectangular groove in a movable structural panel. The seal comprises a fiber preform constructed of multiple layers of fiber having a uniaxial core. Helical fibers are wound over the core. The fibers are of materials capable of withstanding high temperatures and are both left-hand and right-hand wound. An outer layer wrapped over said helical fibers prevents abrasion damage.

Official Gazette of the U.S. Patent and Trademark Office

N92-22692*# National Aeronautics and Space Administration. Lewis Research Center, Cleveland, OH.

INFLATABLE TRAVERSING PROBE SEAL

PAUL A. TRIMARCHI /in NASA, Washington, Technology 2001: The Second National Technology Transfer Conference and Exposition, Volume 2 p 140-145 Dec. 1991
Avail: CASI HC A02/MF A04

An inflatable seal acts as a pressure-tight zipper to provide traversing capability for instrumentation rakes and probes. A specially designed probe segment with a teardrop cross-section in the vicinity of the inflatable seal minimizes leakage at the interface. The probe is able to travel through a lengthwise slot in a pressure vessel or wind tunnel section, while still maintaining pressure integrity. The design uses two commercially available inflatable seals, opposing each other, to cover the probe slot in a wind tunnel wall. Proof-of-concept tests were conducted at vessel pressures up to 30 psig, with seals inflated to 50 psig, showing no measurable leakage along the seal's length or around the probe teardrop cross-section. This seal concept can replace the existing technology of sliding face plate/O-ring systems in applications where lengthwise space is limited. Author

N92-23226*# National Aeronautics and Space Administration. Lewis Research Center, Cleveland, OH.

NUMERICAL EXPERIMENTS WITH FLOWS OF ELONGATED GRANULES

HAROLD G. ELROD (Elrod, Harold G., Old Saybrook, CT) and DAVID E. BREWE 1992 10 p Presented at the Leeds-Lyon Symposium, Lyon, France, 3-6 Sep. 1991
(Contract DA PROJ. 1L1-61102-AH-45; RTOP 505-62-OK)
(NASA-TM-105567; E-6891; NAS 1.15:105567;
AVSCOM-TR-91-C-006) Avail: CASI HC A02/MF A01

Theory and numerical results are given for a program simulating two dimensional granular flow (1) between two infinite, counter-moving, parallel, roughened walls, and (2) for an infinitely wide slider. Each granule is simulated by a central repulsive force field ratcheted with force restitution factor to introduce dissipation. Transmission of angular momentum between particles occurs via Coulomb friction. The effect of granular hardness is explored. Gaps from 7 to 28 particle diameters are investigated, with solid fractions ranging from 0.2 to 0.9. Among features observed are: slip flow at boundaries, coagulation at high densities, and gross fluctuation in surface stress. A videotape has been prepared to demonstrate the foregoing effects. Author

N92-23435*# National Aeronautics and Space Administration. Lewis Research Center, Cleveland, OH.

HIGH TEMPERATURE DYNAMIC ENGINE SEAL TECHNOLOGY DEVELOPMENT

BRUCE M. STEINETZ (Pratt and Whitney Aircraft, West Palm Beach, FL.), CHRISTOPHER DELLACORTE (Drexel Univ., Philadelphia, PA.), MICHAEL MACHINCHICK (Drexel Univ., Philadelphia, PA.), RAJAKKANNU MUTHARASAN (Drexel Univ., Philadelphia, PA.), GUANG-WU DU (Sverdrup Technology, Inc., Brook Park, OH.), FRANK KO, PAUL J. SIROCKY, and JEFFREY H. MILLER (Sverdrup Technology, Inc., Brook Park, OH.) 1992 24 p Presented at the National Aerospace Plane Mid-Term Technology Review, Monterey, CA, 20-24 Apr. 1992
(Contract RTOP 763-22-41)
(NASA-TM-105641; E-6945; NAS 1.15:105641) Avail: CASI HC A03/MF A01

Combined cycle ramjet/scramjet engines being designed for advanced hypersonic vehicles, including the National Aerospace Plane (NASP), require innovative high temperature dynamic seals to seal the sliding interfaces of the articulated engine panels. New seals are required that will operate hot (1200 to 2000 F), seal pressures ranging from 0 to 100 psi, remain flexible to accommodate significant sidewall distortions, and resist abrasion over the engine's operational life. This report reviews the recent high temperature durability screening assessments of a new braided rope seal concept, braided of emerging high temperature materials, that shows promise of meeting many of the seal demands of hypersonic engines. The paper presents durability data for: (1)

the fundamental seal building blocks, a range of candidate ceramic fiber tows; and for (2) braided rope seal subelements scrubbed under engine simulated sliding, temperature, and preload conditions. Seal material/architecture attributes and limitations are identified through the investigations performed. The paper summarizes the current seal technology development status and presents areas in which future work will be performed. Author

N92-23536*# National Aeronautics and Space Administration. Lewis Research Center, Cleveland, OH.

CONTACT STRESSES IN MESHING SPUR GEAR TEETH: USE OF AN INCREMENTAL FINITE ELEMENT PROCEDURE

CHIH-MING HSIEH (Cincinnati Univ., OH.), RONALD L. HUSTON (Cincinnati Univ., OH.), and FRED B. OSWALD Mar. 1992 22 p
(Contract NSG-3188; DA PROJ. 1L1-62211-A-47A)
(NASA-TM-105388; E-6776; NAS 1.15:105388;
AVSCOM-TR-90-C-029) Avail: CASI HC A03/MF A01

Contact stresses in meshing spur gear teeth are examined. The analysis is based upon an incremental finite element procedure that simultaneously determines the stresses in the contact region between the meshing teeth. The teeth themselves are modeled by two dimensional plain strain elements. Friction effects are included, with the friction forces assumed to obey Coulomb's law. The analysis assumes that the displacements are small and that the tooth materials are linearly elastic. The analysis procedure is validated by comparing its results with those for the classical two contacting semicylinders obtained from the Hertz method. Agreement is excellent. Author

N92-23564*# National Aeronautics and Space Administration. Lewis Research Center, Cleveland, OH.

NIST TORSION OSCILLATOR VISCOMETER RESPONSE: PERFORMANCE ON THE LERC ACTIVE VIBRATION ISOLATION PLATFORM

ROBERT F. BERG (National Inst. of Standards and Technology, Gaithersburg, MD.) and CARLOS M. GRODSINSKY Mar. 1992 20 p
(Contract RTOP 694-03-0K)
(NASA-TM-105571; E-6896; NAS 1.15:105571) Avail: CASI HC A03/MF A01

Critical point viscosity measurements are limited to their reduced temperature approach to $T_{(sub\ c)}$ in an Earth bound system, because of density gradients imposed by gravity. Therefore, these classes of experiments have been proposed as good candidates for 'microgravity' science experiments where this limitation is not present. The nature of these viscosity measurements dictate hardware that is sensitive to low frequency excitations. Because of the vibratory acceleration sensitivity of a torsion oscillator viscometer, used to acquire such measurements, a vibration isolation sensitivity test was performed on candidate 'microgravity' hardware to study the possibility of meeting the stringent oscillatory sensitivity requirements of a National Institute of Standards and Technology (NIST) torsion oscillator viscometer. A prototype six degree of freedom active magnetic isolation system, developed at NASA Lewis Research Center, was used as the isolation system. The ambient acceleration levels of the platform were reduced to the noise floor levels of its control sensors, about one microgravity in the 0.1 to 10 Hz bandwidth. Author

N92-24202*# National Aeronautics and Space Administration. Lewis Research Center, Cleveland, OH.

A BASIS FOR SOLID MODELING OF GEAR TEETH WITH APPLICATION IN DESIGN AND MANUFACTURE

RONALD L. HUSTON (Cincinnati Univ., OH.), DIMITRIOS MAVRIPLIS (Miles Labs., Elkhart, IN.), FRED B. OSWALD, and YUNG SHENG LIU (Cincinnati Univ., OH.) Apr. 1992 17 p
(Contract NSG-3188; DA PROJ. 1L1-62211-A-47-A; RTOP 505-62-36)
(NASA-TM-105392; E-6782; NAS 1.15:105392;
AVSCOM-TR-91-C-044; AD-A250302) Avail: CASI HC A03/MF A01

A new approach to modeling gear tooth surfaces is discussed.

37 MECHANICAL ENGINEERING

A computer graphics solid modeling procedure is used to simulate the tooth fabrication process. This procedure is based on the principles of differential geometry that pertain to envelopes of curves and surfaces. The procedure is illustrated with the modeling of spur, helical, bevel, spiral bevel, and hypoid gear teeth. Applications in design and manufacturing are discussed. Extensions to nonstandard tooth forms, to cams, and to rolling element bearings are proposed. Author

N92-24984*# National Aeronautics and Space Administration. Lewis Research Center, Cleveland, OH.

ADVANCED ROTORCRAFT TRANSMISSION (ART) PROGRAM SUMMARY

T. L. KRANTZ and J. G. KISH (Sikorsky Aircraft, Stratford, CT.) 1992 14 p Presented at the 28th Joint Propulsion Conference, Nashville, TN, 6-8 Jul. 1992; sponsored in part by AIAA, SAE, ASME, and ASEE
(Contract DA PROJ. 1L1-62211-A-47-A; RTOP 505-63-36)
(NASA-TM-105665; E-7027; AVSCOM-TR-92-C-011; NAS 1.15:105665; AIAA PAPER 92-3365; AD-A252379) Avail: CASI HC A03/MF A01

The Advanced Rotorcraft Transmission (ART) Program was initiated to advance the state of the art for rotorcraft transmissions. The goal of the ART Program was to develop and demonstrate the technologies needed to reduce transmission weight by 25 pct. and reduce noise by 10 dB while obtaining a 5000 hr 'mean time between failure'. The research done under the ART Program is summarized. A split path design was selected as best able to meet the program goals. Key part technologies needed for this design were identified, studied, and developed. Two of these technologies are discussed in detail: the load sharing of split path designs including the use of a compliant elastomeric torque splitter and the application of a high ratio, low pitch line velocity gear mesh. Development of an angular contact spherical roller bearing, transmission error analysis, and fretting fatigue testing are discussed. The technologies for a light weight, quiet, and reliable rotorcraft transmission were demonstrated. Author

N92-25085*# National Aeronautics and Space Administration. Lewis Research Center, Cleveland, OH.

A 23.2:1 RATIO, 300-WATT, 26 N-M OUTPUT TORQUE, PLANETARY ROLLER-GEAR ROBOTIC TRANSMISSION: DESIGN AND EVALUATION

WYATT S. NEWMAN (Case Western Reserve Univ., Cleveland, OH.), WILLIAM J. ANDERSON (NASTEC, Inc., Cleveland, OH.), WILLIAM SHIPITALO (NASTEC, Inc., Cleveland, OH.), and DOUGLAS ROHN *in* NASA. Goddard Space Flight Center, The 26th Aerospace Mechanisms Symposium p 263-279 May 1992
Avail: CASI HC A03/MF A04

The design philosophy and measurements performed on a new roller-gear transmission prototype for a robotic manipulator are described. The design incorporates smooth rollers in a planetary configuration integrated with conventional toothed gears. The rollers were designed to handle low torque with low backlash and friction while the complementary gears support higher torques and prevent accumulated creep or slip of the rollers. The introduction of gears with finite numbers of teeth to function in parallel with the rollers imposes severe limits on available designs. Solutions for two-planet row designs are discussed. A two-planet row, four-planet design was conceived, fabricated, and tested. Detailed calculations of cluster geometry, gear stresses, and gear geometry are given. Measurement data reported here include transmission linearity, static and dynamic friction, inertia, backlash, stiffness, and forward and reverse efficiency. Initial test results are reported describing performance of the transmission in a servomechanism with torque feedback. Author

N92-25347*# National Aeronautics and Space Administration. Lewis Research Center, Cleveland, OH.

A COMPARISON BETWEEN THEORETICAL PREDICTION AND EXPERIMENTAL MEASUREMENT OF THE DYNAMIC BEHAVIOR OF SPUR GEARS

BRIAN REBBECHI, B. DAVID FORRESTER (Materials Research

Labs., Melbourne, Australia), FRED B. OSWALD, and DENNIS P. TOWNSEND 1992 10 p Proposed for presentation at the Sixth International Power Transmission and Gear Conference, Phoenix, AZ, 13-16 Sep. 1992; sponsored by ASME (Contract RTOP 505-63-36)
(NASA-TM-105362; E-6953; NAS 1.15:105362; AVSCOM-TR-91-C-009) Avail: CASI HC A02/MF A01

A comparison was made between computer model predictions of gear dynamics behavior and experimental results. The experimental data were derived from the NASA gear noise rig, which was used to record dynamic tooth loads and vibration. The experimental results were compared with predictions from the DSTO Aeronautical Research Laboratory's gear dynamics code for a matrix of 28 load speed points. At high torque the peak dynamic load predictions agree with the experimental results with an average error of 5 percent in the speed range 800 to 6000 rpm. Tooth separation (or bounce), which was observed in the experimental data for light torque, high speed conditions, was simulated by the computer model. The model was also successful in simulating the degree of load sharing between gear teeth in the multiple tooth contact region. Author

N92-25396*# National Aeronautics and Space Administration. Lewis Research Center, Cleveland, OH.

COMPARISON OF ANALYSIS AND EXPERIMENT FOR GEARBOX NOISE

FRED B. OSWALD (Kentucky Univ., Lexington.), A. F. SEYBERT (Kentucky Univ., Lexington.), T. W. WU, and WILLIAM ATHERTON (Cleveland State Univ., OH.) 1992 7 p Proposed for presentation at the Sixth International Power Transmission and Gearing Conference, Phoenix, AZ, 13-16 Sep. 1992; sponsored by ASME and Journal of Mechanical Design
(Contract RTOP 505-63-36)
(NASA-TM-105330; E-6696; NAS 1.15:105330; AVSCOM-TR-91-C-030) Avail: CASI HC A02/MF A01

Low contact ratio spur gears were tested in the NASA gear-noise rig to study the noise radiated from the top of the gearbox. Experimental results were compared with a NASA acoustics code to validate the code for predicting transmission noise. The analytical code is based on the boundary element method (BEM) which models the gearbox top as a plate in an infinite baffle. Narrow band vibration spectra measured at 63 nodes on the gearbox top were used to produce input data for the BEM model. The BEM code predicted the total sound power based on the measured vibration. The measured sound power was obtained from an acoustic intensity scan taken near the surface of the gearbox at the same 63 nodes used for vibration measurement. Analytical and experimental results were compared at four different speeds for sound power at each of the narrow band frequencies over the range of 400 to 3200 Hz. Results are also compared for the sound power level at meshing frequency plus three sideband pairs and at selected gearbox resonant frequencies. The difference between predicted and measure sound power is typically less than 3 dB with the predicted value generally less than the measured value. Author

N92-25447*# National Aeronautics and Space Administration. Lewis Research Center, Cleveland, OH.

EFFECT OF CONTACT RATIO ON SPUR GEAR DYNAMIC LOAD

CHUEN-HUEI LIOU, HSIANG HSI LIN, FRED B. OSWALD, and DENNIS P. TOWNSEND 1992 7 p Proposed for presentation at the Sixth International Power Transmission and Gearing Conference, Phoenix, AZ, 13-16 Sep. 1992; sponsored by ASME (Contract DA PROJ. 1L1-62211-A-47-A; RTOP 505-63-36)
(NASA-TM-105606; E-6942; NAS 1.15:105606; AVSCOM-TR-91-C-025) Avail: CASI HC A02/MF A01

A computer simulation is presented which shows how the gear contact ratio affects the dynamic load on a spur gear transmission. The contact ratio can be affected by the tooth addendum, the pressure angle, the tooth size (diametral pitch), and the center distance. The analysis presented was performed using the NASA gear dynamics code, DANST. In the analysis, the contact ratio

was varied over the range 1.20 to 2.40 by changing the length of the tooth addendum. In order to simplify the analysis, other parameters related to contact ratio were held constant. The contact ratio was found to have a significant influence on gear dynamics. Over a wide range of operating speeds, a contact ratio close to 2.0 minimized dynamic load. For low contact ratio gears (contact ratio less than 2.0), increasing the contact ratio reduced the gear dynamic load. For high contact ratio gears (contact ratio = or greater than 2.0), the selection of contact ratio should take into consideration the intended operating speeds. In general, high contact ratio gears minimized dynamic load better than low contact ratio gears.

Author

N92-25448* # National Aeronautics and Space Administration, Lewis Research Center, Cleveland, OH.

MINIMIZATION OF THE VIBRATION ENERGY OF THIN-PLATE STRUCTURE

KATSUMI INOUE, DENNIS P. TOWNSEND, and JOHN J. COY 1992 10 p Proposed for presentation at the 1992 Design Automation Conference, Phoenix, AZ, 13-16 Sep. 1992; sponsored by ASME

(Contract DA PROJ. 1L1-62211-A-47-A; RTOP 505-63-36) (NASA-TM-105654; E-6623; NAS 1.15:105654;

AVSCOM-TR-91-C-028) Avail: CASI HC A02/MF A01

An optimization method is proposed to reduce the vibration of thin plate structures. The method is based on a finite element shell analysis, a modal analysis, and a structural optimization method. In the finite element analysis, a triangular shell element with 18 dof is used. In the optimization, the overall vibration energy of the structure is adopted as the objective function, and it is minimized at the given exciting frequency by varying the thickness of the elements. The technique of modal analysis is used to derive the sensitivity of the vibration energy with respect to the design variables. The sensitivity is represented by the sensitivities of both eigenvalues and eigenvectors. The optimum value is computed by the gradient projection method and a unidimensional search procedure under the constraint condition of constant weight. A computer code, based on the proposed method, is developed and is applied to design problems using a beam and a plate as test cases. It is confirmed that the vibration energy is reduced at the given exciting frequency. For the beam excited by a frequency slightly less than the fundamental natural frequency, the optimized shape is close to the beam of uniform strength.

Author

N92-26106* # National Aeronautics and Space Administration, Lewis Research Center, Cleveland, OH.

EFFECT OF LUBRICANT JET LOCATION ON SPIRAL BEVEL GEAR OPERATING TEMPERATURES

ROBERT F. HANDSCHUH 1992 10 p Proposed for presentation at the Sixth International Power Transmission and Gearing Conference, Phoenix, AZ, 13-16 Sep. 1992; sponsored by ASME (Contract DA PROJ. 1L1-62211-A-47-A; RTOP 505-63-36)

(NASA-TM-105656; E-7020; NAS 1.15:105656; AVSCOM-TR-91-C-033) Avail: CASI HC A02/MF A01

An experimental study was conducted to determine the effect of lubricant jet location on spiral bevel gear bulk temperatures. Transient surface temperatures were also measured. Tests were conducted on aircraft quality spiral bevel gears in a closed loop test facility. Thermocoupled pinions and an infrared microscope were used to collect the pertinent data. A single fan jet lubricated the test gears. Lubricant flow rate (lubricant jet pressure) and applied torque were also varied. The results showed that jet placement had a significant effect on the gear bulk temperatures.

Author

N92-26107* # National Aeronautics and Space Administration, Lewis Research Center, Cleveland, OH.

EFFECT OF OPERATING CONDITIONS ON GEARBOX NOISE

FRED B. OSWALD (Cleveland State Univ., OH.), JAMES J. ZAKRAJSEK, DENNIS P. TOWNSEND, WILLIAM ATHERTON, and HSIANG HSI LIN (Memphis State Univ., TN.) 1992 8 p Proposed for presentation at the Sixth International Power Transmission and Gearing Conference, Phoenix, AZ, 13-16 Sep. 1992; sponsored

by ASME

(Contract DA PROJ. 1L1-62211-A-47-A; RTOP 505-63-36) (NASA-TM-105331; E-6732; NAS 1.15:105331;

AVSCOM-TR-91-C-031) Avail: CASI HC A02/MF A01

Low contact ratio spur gears were tested in the NASA gear noise rig to study the noise radiated from the top of the gearbox. The measured sound power from the gearbox top was obtained from a near field acoustic intensity scan taken at 63 nodes just above the surface. The sound power was measured at a matrix of 45 operating speeds and torque levels. Results are presented in the form of a spectral speed map and as a plot of sound power versus torque (at constant speed) and as sound power versus speed (at constant torque). Because of the presence of vibration modes, operating speed was found to have more impact on noise generation than torque level. A NASA gear dynamics code was used to compute the gear tooth dynamic overload at the same 45 operating conditions used for the experiment. Similar trends were found between the analytical results for dynamic tooth overload and experimental results for sound power. Dynamic analysis may be used to design high quality gears with profile relief optimized for minimum dynamic load and noise.

Author

N92-26108* # National Aeronautics and Space Administration, Lewis Research Center, Cleveland, OH.

IMPROVEMENT IN SURFACE FATIGUE LIFE OF HARDENED GEARS BY HIGH-INTENSITY SHOT PEENING

DENNIS P. TOWNSEND 1992 9 p Proposed for presentation at the Sixth International Power Transmission and Gearing Conference, Scottsdale, AZ, 13-16 Sep. 1992; sponsored by ASME

(Contract DA PROJ. 1L1-62211-A-47-A; RTOP 505-63-36) (NASA-TM-105678; E-6986; NAS 1.15:105678;

AVSCOM-TR-91-C-042) Avail: CASI HC A02/MF A01

Two groups of carburized, hardened, and ground spur gears that were manufactured from the same heat vacuum induction melted vacuum arc melted (VIM VAR) AISI 9310 steel were endurance tested for surface fatigue. Both groups were manufactured with a standard ground 16 rms surface finish. One group was subjected to a shot peening (SP) intensity of 7 to 9A, and the second group was subjected to a SP intensity of 15 to 17A. All gears were honed after SP to a surface finish of 16 rms. The gear pitch diameter was 8.89 cm. Test conditions were a maximum Hertz stress of 1.71 GPa, a gear temperature of 350 K, and a speed of 10000 rpm. The lubricant used for the tests was a synthetic paraffinic oil with an additive package. The following results were obtained: The 10 pct. surface fatigue (pitting) life of the high intensity (15 to 17A) SPed gears was 2.15 times that of the medium intensity (7 to 9A) SPed gears, the same as that calculated from measured residual stress at a depth of 127 microns. The measured residual stress for the high intensity SPed gears was 57 pct. higher than that for the medium intensity SPed gears at a depth of 127 microns and 540 pct. higher at a depth of 51 microns.

Author

N92-26555* # National Aeronautics and Space Administration, Lewis Research Center, Cleveland, OH.

GEAR TOOTH STRESS MEASUREMENTS OF TWO HELICOPTER PLANETARY STAGES

TIMOTHY L. KRANTZ 1992 10 p Proposed for presentation at the Sixth International Power Transmission and Gearing Conference, Phoenix, AZ, 13-16 Sep. 1992; sponsored by ASME (Contract RTOP 505-63-36; DA PROJ. 1L1-62211-A-47-A)

(NASA-TM-105651; E-7015; NAS 1.15:105651; AVSCOM-TR-91-C-038; AD-A252378) Avail: CASI HC A02/MF A01

Two versions of the planetary reduction stages from U.S. Army OH-58 helicopter main rotor transmissions were tested at NASA Lewis. One sequential and one nonsequential planetary were tested. Sun gear and ring gear teeth strains were measured, and stresses were calculated from the strains. The alternating stress at the fillet of both the loaded and unloaded sides of the teeth and at the root of the sun gear teeth are reported. Typical stress variations as the gear tooth moves through mesh are illustrated.

37 MECHANICAL ENGINEERING

At the tooth root location of the thin rimmed sun gear, a significant stress was produced by a phenomenon other than the passing of a planet gear. The load variation among the planets was studied. Each planet produced its own distinctive load distribution on the ring and sun gears. The load variation was less for a three planet, nonsequential design as compared to that of a four planet, sequential design. The reported results enhance the data base for gear stress levels and provide data for the validation of analytical methods. Author

N92-26560*# National Aeronautics and Space Administration. Lewis Research Center, Cleveland, OH.

FULL-SCALE TRANSMISSION TESTING TO EVALUATE ADVANCED LUBRICANTS

DAVID G. LEWICKI, HARRY J. DECKER, and JOHN T. SHIMSKI (Naval Air Propulsion Test Center, Trenton, NJ.) 1992 9 p Proposed for presentation at the Sixth International Power Transmission and Gearing Conference, Phoenix, AZ, 13-16 Sep. 1992; sponsored by ASME (Contract RTOP 505-63-36; DA PROJ. 1L1-62211-A-47-A) (NASA-TM-105668; E-7032; NAS 1.15:105668; AVSCOM-TR-91-C-035; AD-A252382) Avail: CASI HC A02/MF A01

Experimental tests were performed on the OH-58A helicopter main rotor transmission in the NASA Lewis 500 hp helicopter transmission test stand. The testing was part of a lubrication program. The objectives are to develop and show a separate lubricant for gearboxes with improved performance in life and load carrying capacity. The goal was to develop a testing procedure to fail certain transmission components using a MIL-L-23699 based reference oil and then to run identical tests with improved lubricants and show improved performance. The tests were directed at parts that failed due to marginal lubrication from Navy field experience. These failures included mast shaft bearing micropitting, sun gear and planet bearing fatigue, and spiral bevel gear scoring. A variety of tests were performed and over 900 hrs of total run time accumulated for these tests. Some success was achieved in developing a testing procedure to produce sun gear and planet bearing fatigue failures. Only marginal success was achieved in producing mast shaft bearing micropitting and spiral bevel gear scoring. Author

N92-27795*# National Aeronautics and Space Administration. Lewis Research Center, Cleveland, OH.

FORCE ANALYSIS OF MAGNETIC BEARINGS WITH POWER-SAVING CONTROLS

DEXTER JOHNSON (State Univ. Coll. of New York, Buffalo.), GERALD V. BROWN, and DANIEL J. INMAN (State Univ. of New York, Buffalo.) In NASA. Langley Research Center, International Symposium on Magnetic Suspension Technology, Part 2 p 595-613 May 1992
Avail: CASI HC A03/MF A04

Most magnetic bearing control schemes use a bias current with a superimposed control current to linearize the relationship between the control current and the force it delivers. For most operating conditions, the existence of the bias current requires more power than alternative methods that do not use conventional bias. Two such methods are examined which diminish or eliminate bias current. In the typical bias control scheme it is found that for a harmonic control force command into a voltage limited transconductance amplifier, the desired force output is obtained only up to certain combinations of force amplitude and frequency. Above these values, the force amplitude is reduced and a phase lag occurs. The power saving alternative control schemes typically exhibit such deficiencies at even lower command frequencies and amplitudes. To assess the severity of these effects, a time history analysis of the force output is performed for the bias method and the alternative methods. Results of the analysis show that the alternative approaches may be viable. The various control methods examined were mathematically modeled using nondimensionalized variables to facilitate comparison of the various methods. Author

N92-27879*# National Aeronautics and Space Administration. Lewis Research Center, Cleveland, OH.

ANALYSIS AND MODIFICATION OF A SINGLE-MESH GEAR FATIGUE RIG FOR USE IN DIAGNOSTIC STUDIES

JAMES J. ZAKRAJSEK, DENNIS P. TOWNSEND, FRED B. OSWALD, and HARRY J. DECKER May 1992 20 p (Contract RTOP 505-63-36; DA PROJ. 1L1-62211-A-47-A) (NASA-TM-105416; E-6826; NAS 1.15:105416; AVSCOM-TR-91-C-049; AD-A252381) Avail: CASI HC A03/MF A01

A single-mesh gear fatigue rig was analyzed and modified for use in gear mesh diagnostic research. The fatigue rig allowed unwanted vibration to mask the test-gear vibration signal, making it difficult to perform diagnostic studies. Several possible sources and factors contributing to the unwanted components of the vibration signal were investigated. Sensor mounting location was found to have a major effect on the content of the vibration signal. In the presence of unwanted vibration sources, modal amplification made unwanted components strong. A sensor location was found that provided a flatter frequency response. This resulted in a more useful vibration signal. A major network was performed on the fatigue rig to reduce the influence of the most probable sources of the noise in the vibration signal. The slave gears were machined to reduce weight and increase tooth loading. The housing and the shafts were modified to reduce imbalance, looseness, and misalignment in the rotating components. These changes resulted in an improved vibration signal, with the test-gear mesh frequency now the dominant component in the signal. Also, with the unwanted sources eliminated, the sensor mounting location giving the most robust representation of the test-gear meshing energy was found to be at a point close to the test gears in the load zone of the bearings. Author

N92-28434*# National Aeronautics and Space Administration. Lewis Research Center, Cleveland, OH.

APPLICATION OF FACE-GEAR DRIVES IN HELICOPTER TRANSMISSIONS

F. L. LITVIN (Illinois Univ., Chicago.), J.-C. WANG (Illinois Univ., Chicago.), R. B. BOSSLER, JR. (Lucas Western, Inc., City of Industry, CA.), Y.-J. D. CHEN (McDonnell-Douglas Helicopter Co., Mesa, AZ.), G. HEATH (McDonnell-Douglas Helicopter Co., Mesa, AZ.), and D. G. LEWICKI 1992 10 p Proposed for presentation at the Sixth International Power Transmission and Gearing Conference, Scottsdale, AZ, 13-16 Sep. 1992; sponsored by ASME (Contract RTOP 505-63-36; DA PROJ. 1L1-62211-A-47-A) (NASA-TM-105655; E-7019; NAS 1.15:105655; AVSCOM-TR-91-C-036) Avail: CASI HC A02/MF A01

The use of face gears in helicopter transmissions was explored. A light-weight, split torque transmission design utilizing face gears was described. Face-gear design and geometry were investigated. Topics included tooth generation, limiting inner and outer radii, tooth contact analysis, contact ratio, gear eccentricity, and structural stiffness. Design charts were developed to determine minimum and maximum face-gear inner and outer radii. Analytical study of transmission error showed face-gear drives were relatively insensitive to gear misalignment, but tooth contact was affected by misalignment. A method of localizing bearing contact to compensate for misalignment was explored. The proper choice of shaft support stiffness enabled good load sharing in the split torque transmission design. Face-gear experimental studies were also included and the feasibility of face gears in high-speed, high-load applications such as helicopter transmissions was demonstrated. Author

N92-28476*# National Aeronautics and Space Administration. Lewis Research Center, Cleveland, OH.

OPTIMUM DESIGN OF A GEARBOX FOR LOW VIBRATION

KATSUMI INOUE, DENNIS P. TOWNSEND, and JOHN J. COY 1992 10 p Proposed for presentation at the Sixth International Power Transmission and Gearing Conference, Scottsdale, AZ, 13-16 Sep. 1992; sponsored by ASME (Contract RTOP 505-63-36; DA PROJ. 1L1-62211-A-47-A)

(NASA-TM-105653; E-6622; NAS 1.15:105653; AVSCOM-TR-91-C-027; AD-A252380) Avail: CASI HC A02/MF A01

A computer program was developed for designing a low vibration gearbox. The code is based on a finite element shell analysis, a modal analysis, and a structural optimization method. In the finite element analysis, a triangular shell element with 18 degrees-of-freedom is used. In the optimization method, the overall vibration energy of the gearbox is used as the objective function and is minimized at the exciting frequency by varying the finite element thickness. Modal analysis is used to derive the sensitivity of the vibration energy with respect to the design variable. The sensitivity is representative of both eigenvalues and eigenvectors. The optimum value is computed by the gradient projection method and a unidimensional search procedure under the constraint condition of constant weight. The computer code is applied to a design problem derived from an experimental gearbox in use at the NASA Lewis Research Center. The top plate and two side plates of the gearbox are redesigned and the contribution of each surface to the total vibration is determined. Results show that optimization of the top plate alone is effective in reducing total gearbox vibration. Author

N92-29092* National Aeronautics and Space Administration. Lewis Research Center, Cleveland, OH.

REMOVABLE HAND HOLD Patent

ROBERT D. CORRIGAN, inventor (to NASA) and ROBERT L. HAUER, inventor (to NASA) 30 Jun. 1992 9 p Filed 15 Apr. 1991 Supersedes N91-26543 (29 - 18, p 2995) (NASA-CASE-LEW-15196-1; US-PATENT-5,126,131; US-PATENT-APPL-SN-687606; US-PATENT-CLASS-16-114R; US-PATENT-CLASS-248-222.1; US-PATENT-CLASS-248-251; US-PATENT-CLASS-256-59; US-PATENT-CLASS-16-111R; INT-PATENT-CLASS-A47H-1/144) Avail: US Patent and Trademark Office

A hand hold utilizes joining means which comprises two different mounting brackets that are permanently fastened to a supporting structure. An alignment/capture bracket is disposed at one end of the hand rail or hand hold which mates with one of the mounting brackets. A securing bracket is disposed at the opposite end of the hand rail/hand hold which connects with the other mounting bracket by means of a locking device. The alignment/capture bracket has a central tapered tongue with two matching slots disposed on each side.

Official Gazette of the U.S. Patent and Trademark Office

N92-29136* National Aeronautics and Space Administration. Lewis Research Center, Cleveland, OH.

DYNAMICS OF A SPLIT TORQUE HELICOPTER TRANSMISSION

MAJID RASHIDI (Cleveland State Univ., OH.) and TIMOTHY KRANTZ (Army Aviation Systems Command, Cleveland, OH.) 1992 14 p Prepared for presentation of the 6th International Power Transmission and Gearing Conference, Scottsdale, AZ, 13-16 Sep. 1992; sponsored in part by ASME (Contract DA PROJ. 1L1-62211-A-47-A; RTOP 505-63-36) (NASA-TM-105681; E-7060; AVSCOM-TR-91-C-043; NAS 1.15:105681; AD-A257375) Avail: CASI HC A03/MF A01

A high reduction ratio split torque gear train has been proposed as an alternative to a planetary configuration for the final stage of a helicopter transmission. A split torque design allows a high ratio of power-to-weight for the transmission. The design studied in this work includes a pivoting beam that acts to balance thrust loads produced by the helical gear meshes in each of two parallel power paths. When the thrust loads are balanced, the torque is split evenly. A mathematical model was developed to study the dynamics of the system. The effects of time varying gear mesh stiffness, static transmission errors, and flexible bearing supports are included in the model. The model was demonstrated with a test case. Results show that although the gearbox has a symmetric configuration, the simulated dynamic behavior of the first and second compound gears are not the same. Also, results show

that shaft location and mesh stiffness tuning are significant design parameters that influence the motions of the system. Author

N92-29351* National Aeronautics and Space Administration. Lewis Research Center, Cleveland, OH.

OPTIMAL DESIGN OF COMPACT SPUR GEAR REDUCTIONS

M. SAVAGE (Akron Univ., OH.), S. B. LATTIME (Akron Univ., OH.), J. A. KIMMEL (Akron Univ., OH.), and H. H. COE 1992 10 p Proposed for presentation at the Sixth International Power Transmission and Gearing Conference, Scottsdale, AZ, 13-16 Sep. 1992; sponsored by ASME

(Contract NAG3-1047; DA PROJ. 1L1-62211-A-47-A; RTOP 505-63-36)

(NASA-TM-105676; E-7048; NAS 1.15:105676; AVSCOM-TR-91-C-041; AD-A254358) Avail: CASI HC A02/MF A01

The optimal design of compact spur gear reductions includes the selection of bearing and shaft proportions in addition to gear mesh parameters. Designs for single mesh spur gear reductions are based on optimization of system life, system volume, and system weight including gears, support shafts, and the four bearings. The overall optimization allows component properties to interact, yielding the best composite design. A modified feasible directions search algorithm directs the optimization through a continuous design space. Interpolated polynomials expand the discrete bearing properties and proportions into continuous variables for optimization. After finding the continuous optimum, the designer can analyze near optimal designs for comparison and selection. Design examples show the influence of the bearings on the optimal configurations. Author

N92-29697* National Aeronautics and Space Administration. Lewis Research Center, Cleveland, OH.

VALIDATION OF FINITE ELEMENT AND BOUNDARY ELEMENT METHODS FOR PREDICTING STRUCTURAL VIBRATION AND RADIATED NOISE

A. F. SEYBERT (Kentucky Univ., Lexington.), X. F. WU (Kentucky Univ., Lexington.), and FRED B. OSWALD 1992 9 p Prepared for presentation at the Winter Annual Meeting of the ASME, Anaheim, CA, 8-13 Nov. 1992

(Contract RTOP 505-63-39)

(NASA-TM-105359; AVSCOM-TR-92-C-050; E-7127; NAS 1.15:105359) Avail: CASI HC A02/MF A01

Analytical and experimental validation of methods to predict structural vibration and radiated noise are presented. A rectangular box excited by a mechanical shaker was used as a vibrating structure. Combined finite element method (FEM) and boundary element method (BEM) models of the apparatus were used to predict the noise radiated from the box. The FEM was used to predict the vibration, and the surface vibration was used as input to the BEM to predict the sound intensity and sound power. Vibration predicted by the FEM model was validated by experimental modal analysis. Noise predicted by the BEM was validated by sound intensity measurements. Three types of results are presented for the total radiated sound power: (1) sound power predicted by the BEM modeling using vibration data measured on the surface of the box; (2) sound power predicted by the FEM/BEM model; and (3) sound power measured by a sound intensity scan. The sound power predicted from the BEM model using measured vibration data yields an excellent prediction of radiated noise. The sound power predicted by the combined FEM/BEM model also gives a good prediction of radiated noise except for a shift of the natural frequencies that are due to limitations in the FEM model. Author

N92-30396* National Aeronautics and Space Administration. Lewis Research Center, Cleveland, OH.

DEVELOPMENT OF A FULL-SCALE TRANSMISSION TESTING PROCEDURE TO EVALUATE ADVANCED LUBRICANTS

DAVID G. LEWICKI, HARRY J. DECKER, and JOHN T. SHIMSKI (Naval Air Propulsion Test Center, Trenton, NJ.) Aug. 1992 25 p

37 MECHANICAL ENGINEERING

(Contract DA PROJ. 1L1-62211-A-47-A; RTOP 505-63-36)
(NASA-TP-3265; E-6531; NAS 1.60:3265; AVSCOM-TR-91-C-026;
AD-A257204) Avail: CASI HC A03/MF A01

Experimental tests were performed on the OH-58A helicopter main rotor transmission in the NASA Lewis 500-hp Helicopter Transmission Test Stand. The testing was part of a joint Navy/NASA/Army lubrication program. The objective of the program was to develop a separate lubricant for gearboxes and demonstrate an improved performance in life and load-carrying capacity. The goal of the experiments was to develop a testing procedure to fail certain transmission components using a MIL-L-23699 base reference oil, then run identical tests with improved lubricants and demonstrate performance. The tests were directed at failing components that the Navy has had problems with due to marginal lubrication. These failures included mast shaft bearing micropitting, sun gear and planet bearing fatigue, and spiral bevel gear scoring. A variety of tests were performed and over 900 hours of total run time accumulated for these tests. Some success was achieved in developing a testing procedure to produce sun gear and planet bearing fatigue failures. Only marginal success was achieved in producing mast shaft bearing micropitting and spiral bevel gear scoring. Author

N92-30571*# National Aeronautics and Space Administration.
Lewis Research Center, Cleveland, OH.

DESIGN FEASIBILITY STUDY OF A SPACE STATION FREEDOM TRUSS

SASAN C. ARMAND and CAROLINE A. DOHOGNE (Michigan Univ., Ann Arbor.) Apr. 1992 15 p Original contains color illustrations

(Contract RTOP 474-46-10)
(NASA-TM-105558; E-6882; NAS 1.15:105558) Avail: CASI HC
A03/MF A01; 1 functional color page

Here, the focus is on the design and configuration feasibility of the short spacer for the Space Station Program in its launch configuration. The product of this study is being used by Rockwell International (Rocketdyne Division) as they continue their design concept of the current short spacer configuration. It is anticipated that the launch loads will dominate the on-orbit loads and dictate the design configuration of the short spacer. At the present time, the on-orbit loads have not been generated. The structural analysis discussed herein is based on the transient events derived from the Space Transportation System (STS) Interface Control Document (ICD). The transient loading events consist of liftoff loads, landing loads, and emergency landing loads. The quasi-static loading events have been neglected, since the magnitude of the acceleration factors are lower than the transient acceleration factors. The normal mode analyses presented herein are based on the most feasible configurations with acceptable stress ranges. Author

N92-30722*# National Aeronautics and Space Administration.
Lewis Research Center, Cleveland, OH.

FAST METHODS TO NUMERICALLY INTEGRATE THE REYNOLDS EQUATION FOR GAS FLUID FILMS

FLORIN DIMOFTE 1992 26 p Presented at the STLE-ASME
Joint Tribology Conference, St. Louis, MO, 13-16 Oct. 1991

(Contract RTOP 590-21-11)
(NASA-TM-105415; E-6824; NAS 1.15:105415) Avail: CASI HC
A03/MF A01

The alternating direction implicit (ADI) method is adopted, modified, and applied to the Reynolds equation for thin, gas fluid films. An efficient code is developed to predict both the steady-state and dynamic performance of an aerodynamic journal bearing. An alternative approach is shown for hybrid journal gas bearings by using Liebmann's iterative solution (LIS) for elliptic partial differential equations. The results are compared with known design criteria from experimental data. The developed methods show good accuracy and very short computer running time in comparison with methods based on an inverting of a matrix. The computer codes need a small amount of memory and can be run on either personal computers or on mainframe systems. Author

N92-30734*# National Aeronautics and Space Administration.
Lewis Research Center, Cleveland, OH.

MAGNETIC BEARINGS FOR FREE-PISTON STIRLING ENGINES

P. W. CURWEN (Mechanical Technology, Inc., Latham, NY.), D. P. FLEMING, D. K. RAO (Mechanical Technology, Inc., Latham, NY.), and D. S. WILSON (Mechanical Technology, Inc., Latham, NY.) Aug. 1992 8 p Proposed for presentation at the 27th Intersociety Energy Conversion Engineering Conference, San Diego, CA, 3-7 Aug. 1992; sponsored by SAE, ACS, AIAA, ASME, IEEE, AIChE, and ANS

(Contract NAS3-26061; RTOP 590-13-11)
(NASA-TM-105730; E-7091; NAS 1.15:105730) Avail: CASI HC
A02/MF A01

The feasibility and efficacy of applying magnetic bearings to free-piston Stirling-cycle power conversion machinery currently being developed for long-term space missions are assessed. The study was performed for a 50-kWe Reference Stirling Space Power Converter (RSSPC) which currently uses hydrostatic gas bearings to support the reciprocating displacer and power piston assemblies. Active magnetic bearings of the attractive electromagnetic type are feasible for the RSSPC power piston. Magnetic support of the displacer assembly would require unacceptable changes to the design of the current RSSPC. However, magnetic suspension of both displacer and power piston is feasible for a relative-displacer version of the RSSPC. Magnetic suspension of the RSSPC power piston can potentially increase overall efficiency by 0.5 to 1 percent (0.1 to 0.3 efficiency points). Magnetic bearings will also overcome several operational concerns associated with hydrostatic gas bearing systems. These advantages, however, are accompanied by a 5 percent increase in specific mass of the RSSPC. Author

N92-30948*# National Aeronautics and Space Administration.
Lewis Research Center, Cleveland, OH.

MINIMIZATION OF DEVIATIONS OF GEAR REAL TOOTH SURFACES DETERMINED BY COORDINATE MEASUREMENTS

F. L. LITVIN (Illinois Univ., Chicago.), C. KUAN (Illinois Univ., Chicago.), J.-C. WANG (Illinois Univ., Chicago.), R. F. HANDSCHUH, J. MASSETH (Dana Corp., Fort Wayne, IN.), and N. MARUYAMA (Nissan Motor Co. Ltd., Yokosuka, Japan) 1992 10 p Proposed for presentation at the 1992 Power Transmission and Gearing Conference, Phoenix, AZ, 13-16 Sep. 1992

(Contract DA PROJ. 1L1-62211-A-47A; RTOP 505-63-36)
(NASA-TM-105718; E-7115; NAS 1.15:105718;
AVSCOM-TR-92-C-003; AD-A257176) Avail: CASI HC A02/MF
A01

The deviations of a gear's real tooth surface from the theoretical surface are determined by coordinate measurements at the grid of the surface. A method was developed to transform the deviations from Cartesian coordinates to those along the normal at the measurement locations. Equations are derived that relate the first order deviations with the adjustment to the manufacturing machine-tool settings. The deviations of the entire surface are minimized. The minimization is achieved by application of the least-square method for an overdetermined system of linear equations. The proposed method is illustrated with a numerical example for hypoid gear and pinion. Author

N92-31349*# National Aeronautics and Space Administration.
Lewis Research Center, Cleveland, OH.

EXPERIMENTAL TESTING OF PROTOTYPE FACE GEARS FOR HELICOPTER TRANSMISSIONS

R. HANDSCHUH, D. LEWICKI, and R. BOSSLER (Lucas Western, Inc., City of Industry, CA.) 1992 15 p Proposed for presentation at the Gearbox Configurations of the 1990's, Solihull, England, 28 Oct. 1992; sponsored by Inst. of Mechanical Engineers Prepared in cooperation with Army Aviation Systems Command, Cleveland, OH

(Contract RTOP 505-63-36; DA PROJ. 1L1-62211-A-47-A)
(NASA-TM-105434; E-7084; NAS 1.15:105434;
AVSCOM-TR-92-C-008; AD-A257175) Avail: CASI HC A03/MF
A01

An experimental program to test the feasibility of using face gears in a high-speed and high-power environment was conducted. Four face gear sets were tested, two sets at a time, in a closed-loop test stand at pinion rotational speeds to 19,100 rpm and to 271 kW. The test gear sets were one-half scale of the helicopter design gear set. Testing the gears at one-eighth power, the test gear set had slightly increased bending and compressive stresses when compared to the full scale design. The tests were performed in the LeRC spiral bevel gear test facility. All four sets of gears successfully ran at 100 percent of design torque and speed for 30 million pinion cycles, and two sets successfully ran at 200 percent of torque for an additional 30 million pinion cycles. The results, although limited, demonstrated the feasibility of using face gears for high-speed, high-load applications.

Author

92-31485*# National Aeronautics and Space Administration, Lewis Research Center, Cleveland, OH.

MODAL SIMULATION OF GEARBOX VIBRATION WITH EXPERIMENTAL CORRELATION

FRED K. CHOY (Akron Univ., OH.), YEEFENG F. RUAN (Akron Univ., OH.), JAMES J. ZAKRAJSEK, and FRED B. OSWALD 1992 17 p Presented at the 28th Joint Propulsion Conference and Exhibit, Nashville, TN, 6-8 Jul. 1992; sponsored by AIAA, SAE, ASME, and ASEE

(Contract DA PROJ. 1L1-62211-A-47-A; RTOP 505-63-36)

(NASA-TM-105702; E-7090; NAS 1.15:105702;

AVSCOM-TR-92-C-018; AIAA PAPER 92-3494) Avail: CASI HC A03/MF A01

A newly developed global dynamic model was used to simulate the dynamics of a gear noise rig at NASA Lewis Research Center. Experimental results from the test rig were used to verify the analytical model. In this global dynamic model, the number of degrees of freedom of the system are reduced by transforming the system equations of motion into modal coordinates. The vibration of the individual gear-shaft system are coupled through the gear mesh forces. A three-dimensional, axial-lateral coupled, bearing model was used to couple the casing structural vibration to the gear-rotor dynamics. The coupled system of modal equations is solved to predict the resulting vibration at several locations on the test rig. Experimental vibration data was compared to the predictions of the global dynamic model. There is excellent agreement between the vibration results from analysis and experiment.

Author

92-31536*# National Aeronautics and Space Administration, Lewis Research Center, Cleveland, OH.

EFFECT OF OUT-OF-ROUNDNESS ON THE PERFORMANCE OF A DIESEL ENGINE CONNECTING-ROD BEARING

D. VIJAYARAGHAVAN, D. E. BREWE, and T. G. KEITH, JR. (Ohio Aerospace Inst., Brook Park.) Oct. 1991 19 p Presented at the STLE/ASME Tribology Conference, St. Louis, MO, 17-19 Oct. 1991; sponsored by the ASME Journal of Tribology

(Contract RTOP 505-63-5A)

(NASA-TM-105600; E-6863; NAS 1.15:105600;

AVSCOM-TR-92-C-029; AD-A257220) Avail: CASI HC A03/MF A01

In this paper, the dynamic performance of the Ruston and Hornsby VEB diesel engine connecting-rod bearing with circular and out-of-round profiles is analyzed. The effect of cavitation is considered by using a cavitation algorithm, which mimics JFO boundary conditions. The effect of mass inertia is accounted for by solving coupled nonlinear equations of motion. The journal profiles considered are circular, elliptical, semi-elliptical, and three lobe epicycloid. The predicted journal trajectory and other performance parameters for one complete load cycle are presented for all of the out-of-round profiles and are also compared with the predictions for the circular bearing.

Author

QUALITY ASSURANCE AND RELIABILITY

Includes product sampling procedures and techniques; and quality control.

A92-15681* National Aeronautics and Space Administration, Lewis Research Center, Cleveland, OH.

NDE OF ADVANCED TURBINE ENGINE COMPONENTS AND MATERIALS BY COMPUTED TOMOGRAPHY

R. N. YANCEY (Advanced Research and Applications Corp., Fairborn, OH), GEORGE Y. BAAKLINI, and STANLEY J. KLIMA (NASA, Lewis Research Center, Cleveland, OH) ASME, International Gas Turbine and Aeroengine Congress and Exposition, 36th, Orlando, FL, June 3-6, 1991. 4 p. Research supported by DNA and DARPA. Jun. 1991 4 p refs

(Contract F33615-89-C-5618; F33615-88-C-2823)

(ASME PAPER 91-GT-287)

Computed tomography (CT) is an X-ray technique that provides quantitative 3D density information of materials and components and can accurately detail spatial distributions of cracks, voids, and density variations. CT scans of ceramic materials, composites, and engine components were taken and the resulting images will be discussed. Scans were taken with two CT systems with different spatial resolution capabilities. The scans showed internal damage, density variations, and geometrical arrangement of various features in the materials and components. It was concluded that CT can play an important role in the characterization of advanced turbine engine materials and components. Future applications of this technology will be outlined.

Author

A92-17201* Akron Univ., OH.

TRANSMISSION OVERHAUL AND COMPONENT REPLACEMENT PREDICTIONS USING WEIBULL AND RENEWAL THEORY

M. SAVAGE (Akron, University, OH) and D. G. LEWICKI (NASA, Lewis Research Center, Cleveland, OH) Dec. 1991 6 p refs

A92-28722* National Aeronautics and Space Administration, Lewis Research Center, Cleveland, OH.

REVIEW AND STATISTICAL ANALYSIS OF THE USE OF ULTRASONIC VELOCITY FOR ESTIMATING THE POROSITY FRACTION IN POLYCRYSTALLINE MATERIALS

D. J. ROTH, S. M. SWICKARD (NASA, Lewis Research Center, Cleveland, OH), D. B. STANG (NASA, Lewis Research Center; Sverdrup Technology, Inc., Cleveland, OH), and M. R. DEGUIRE (Case Western Reserve University, Cleveland, OH) IN: Review of progress in quantitative nondestructive evaluation; Proceedings of the 17th Annual Review, La Jolla, CA, July 15-20, 1990. Vol. 10B 1991 8 p refs

Copyright

A review and statistical analysis of the ultrasonic velocity method for estimating the porosity fraction in polycrystalline materials is presented. Initially, a semiempirical model is developed showing the origin of the linear relationship between ultrasonic velocity and porosity fraction. Then, from a compilation of data produced by many researchers, scatter plots of velocity versus percent porosity data are shown for Al₂O₃, MgO, porcelain-based ceramics, PZT, SiC, Si₃N₄, steel, tungsten, UO₂(U_{0.30}Pu_{0.70})C, and YBa₂Cu₃O(7-x). Linear regression analysis produces predicted slope, intercept, correlation coefficient, level of significance, and confidence interval statistics for the data. Velocity values predicted from regression analysis of fully-dense materials are in good agreement with those calculated from elastic properties. Author

A92-48789*# National Aeronautics and Space Administration, Lewis Research Center, Cleveland, OH.

ALGORITHMS FOR REAL-TIME FAULT DETECTION OF THE SPACE SHUTTLE MAIN ENGINE

C. A. RUIZ, M. W. HAWMAN, and W. S. GALINAITIS (United

Technologies Research Center, East Hartford, CT) AIAA, SAE, ASME, and ASEE, Joint Propulsion Conference and Exhibit, 28th, Nashville, TN, July 6-8, 1992. 10 p. Jul. 1992 10 p refs (Contract NAS3-25626) (AIAA PAPER 92-3167) Copyright

This paper reports on the results of a program to develop and demonstrate concepts related to a realtime health management system (HMS) for the Space Shuttle Main Engine (SSME). An HMS framework was developed on the basis of a top-down analysis of the current rocket engine failure modes and the engine monitoring requirements. One result of Phase I of this program was the identification of algorithmic approaches for detecting failures of the SSME. Three different analytical techniques were developed which demonstrated the capability to detect failures significantly earlier than the existing redlines. Based on promising initial results, Phase II of the program was initiated to further validate and refine the fault detection strategy on a large data base of 140 SSME test firings, and implement the resultant algorithms in real time. The paper begins with an overview of the refined algorithms used to detect failures during SSME start-up and main-stage operation. Results of testing these algorithms on a data base of nominal and off-nominal SSME test firings is discussed. The paper concludes with a discussion of the performance of the algorithms operating on a real-time computer system. Author

A92-50625* National Aeronautics and Space Administration. Lewis Research Center, Cleveland, OH.

BALANCING RELIABILITY AND COST TO CHOOSE THE BEST POWER SUBSYSTEM

RONALD C. SUICH (California State University, Fullerton) and RICHARD L. PATTERSON (NASA, Lewis Research Center, Cleveland, OH) IN: IECEC '91; Proceedings of the 26th Intersociety Energy Conversion Engineering Conference, Boston, MA, Aug. 4-9, 1991. Vol. 2 1991 5 p refs (Contract NAG3-1100) Copyright

The justification of the increased cost of a more reliable power subsystem is discussed. A mathematical model is presented for computing total spacecraft subsystem cost including both the basic subsystem cost and the expected cost due to the failure of the subsystem. This is then used to determine the power subsystem cost as a function of reliability and redundancy. Minimum cost and maximum reliability and/or redundancy are not generally equivalent. Two example cases are presented. One is a small satellite, and the other is an interplanetary spacecraft. I.E.

A92-56217* National Aeronautics and Space Administration. Lewis Research Center, Cleveland, OH.

THERMAL VERIFICATION TESTING OF COMMERCIAL PRINTED-CIRCUIT BOARDS FOR SPACEFLIGHT

WILLIAM M. FOSTER, II (NASA, Lewis Research Center, Cleveland, OH) IN: Annual Reliability and Maintainability Symposium, Las Vegas, NV, Jan. 21-23, 1992, Proceedings 1992 7 p refs

A method developed to verify commercial printed-circuit boards for a Shuttle orbital flight is discussed. The test sequence is based on early fault detection, desire to test the final assembly, and integration with other verification testing. A component thermal screening test is performed first to force flaws in design, workmanship, parts, processes, and materials into observable failures. Temperature definition and vibration tests are performed next. Final assembly testing is performed to simulate the Shuttle flight. An abbreviated thermal screening test is performed as a check after the vibration test, and then a complete thermal operational test is performed. The final assembly test finishes up with a burn-in of 100 h of trouble-free operation. Verification is successful when all components and final assemblies have passed each test. This method was very successful in verifying that commercial printed-circuit boards will survive in the Shuttle environment. I.E.

N92-23189*# National Aeronautics and Space Administration. Lewis Research Center, Cleveland, OH.

DETECTING LAMB WAVES WITH BROAD-BAND ACOUSTO-ULTRASONIC SIGNALS IN COMPOSITE STRUCTURES

HAROLD E. KAUTZ Mar. 1992 23 p (Contract RTOP 510-01-50) (NASA-TM-105557; E-6881; NAS 1.15:105557) Avail: CASI HC A03/MF A01

Lamb waves can be produced and detected in ceramic matrix composites (CMC) and metal matrix composites (MMC) plates using the acousto-ultrasonic configuration employing broadband transducers. Experimental dispersion curves of lowest symmetric and antisymmetric modes behave in a manner analogous to the graphite/polymer theoretical curves. In this study a basis has been established for analyzing Lamb wave velocities for characterizing composite plates. Lamb wave dispersion curves and group velocities were correlated with variations in axial stiffness and shear stiffness in MMC and CMC. For CMC, interfacial shear strength was also correlated with the first antisymmetric Lamb mode. Author

N92-24986*# National Aeronautics and Space Administration. Lewis Research Center, Cleveland, OH.

TENSILE STRAIN MEASUREMENTS OF CERAMIC FIBERS USING SCANNING LASER ACOUSTIC MICROSCOPY

RENEE M. KENT (Dayton Univ., OH.) and ALEX VARY 1992 8 p Presented at the 16th Annual Conference on Composites and Advanced Ceramics, Cocoa Beach, FL, 7-10 Jan. 1992; sponsored in part by American Ceramic Society (Contract RTOP 510-01-50) (NASA-TM-105589; E-6919; NAS 1.15:105589) Avail: CASI HC A02/MF A01

A noncontacting technique using scanning laser acoustic microscopy for making in situ tensile strain measurements of small diameter fibers was implemented for the tensile strain analysis of individual Nicalon SiC fibers (nominal diameter 15 microns). Stress versus strain curves for the fibers were plotted from the experimental data. The mean elastic modulus of the fibers was determined to be 185.3 GPa. Similar measurements were made for Carborundum SiC fibers (nominal diameter 28 microns) and Saphikon sapphire fibers (nominal diameter 140 microns), yielding and elastic modulus of 401 and 466.8 GPa, respectively. Author

STRUCTURAL MECHANICS

Includes structural element design and weight analysis; fatigue; and thermal stress.

A92-14546* Oak Ridge National Lab., TN. DETERMINATION OF THE STRESS DISTRIBUTIONS IN A CERAMIC, TENSILE SPECIMEN USING NUMERICAL TECHNIQUES

M. E. JENKINS, M. K. FERBER (Oak Ridge National Laboratory, TN), and J. A. SALEM (NASA, Lewis Research Center, Cleveland, OH) IN: Computers in engineering 1990; Proceedings of the ASME International Computers in Engineering Conference and Exposition, Boston, MA, Aug. 5-9, 1990. Vol. 2 1990 8 p refs Copyright

Finite element analyses (FEA) were used to determine the stress distributions in a ceramic, tensile specimen with two types of button-head gripping systems. The FEA revealed stress raisers at both the button-head and the transition from the gage section to the shank. However, the stress field within the bulk of the gage section is uniform and uniaxial. The stress ratio, σ/σ_{max} , between the button-head and gage section stresses varied from 0.35 to 0.72 for the tapered collet or the straight collet systems, respectively. Previous empirical tests confirm these results whereby

the tapered collet system, compared to the straight collet system, sustained over twice the average load before failure at the button-head.

Author

A92-15972* Toledo Univ., OH.

CASCADE FLUTTER ANALYSIS WITH TRANSIENT RESPONSE AERODYNAMICS

M. A. BAKHLE, A. J. MAHAJAN, T. G. KEITH, JR. (Toledo University, OH), and G. L. STEFKO (NASA, Lewis Research Center, Cleveland, OH) *Computers and Structures* (ISSN 0045-7949), vol. 41, no. 5, 1991, p. 1073-1085. Previously announced in STAR as N91-19475. 1991 13 p refs

Copyright

Two methods for calculating linear frequency domain aerodynamic coefficients from a time marching Full Potential cascade solver are developed and verified. In the first method, the Influence Coefficient, solutions to elemental problems are superposed to obtain the solutions for a cascade in which all blades are vibrating with a constant interblade phase angle. The elemental problem consists of a single blade in the cascade oscillating while the other blades remain stationary. In the second method, the Pulse Response, the response to the transient motion of a blade is used to calculate influence coefficients. This is done by calculating the Fourier Transforms of the blade motion and the response. Both methods are validated by comparison with the Harmonic Oscillation method and give accurate results. The aerodynamic coefficients obtained from these methods are used for frequency domain flutter calculations involving a typical section blade structural model. An eigenvalue problem is solved for each interblade phase angle mode and the eigenvalues are used to determine aeroelastic stability. Flutter calculations are performed for two examples over a range of subsonic Mach numbers.

Author

A92-21081* Texas Univ., San Antonio.

PROBABILISTIC CONSTITUTIVE RELATIONSHIPS FOR CYCLIC MATERIAL STRENGTH MODELS

L. BOYCE (Texas University, San Antonio) and C. C. CHAMIS (NASA, Lewis Research Center, Cleveland, OH) (*Structures, Structural Dynamics and Materials Conference*, 29th, Williamsburg, VA, Apr. 18-20, 1988, Technical Papers. Pt. 3, p. 1299-1306) *Journal of Propulsion and Power* (ISSN 0748-4658), vol. 8, Jan.-Feb. 1992, p. 227-232. Previously cited in issue 12, p. 1908. Accession no. A88-32313. Feb. 1992 6 p refs

Copyright

A92-24717* National Aeronautics and Space Administration. Lewis Research Center, Cleveland, OH.

A VISCOPLASTIC MODEL FOR SINGLE CRYSTALS

E. H. JORDAN (Connecticut, University, Storrs) and K. P. WALKER (Engineering Science Software, Inc., Smithfield, RI) *ASME, Transactions, Journal of Engineering Materials and Technology* (ISSN 0094-4289), vol. 114, Jan. 1992, p. 19-26. Jan. 1992 8 p refs

(Contract NAG3-512; DE-AC02-88ER-13895)

Copyright

A viscoplastic constitutive model is described in which deformation behavior is postulated on representative slip systems and the behavior of the entire crystal is determined by summing the slip on the active slip systems. By building in the slip geometry known from the metallurgical literature, it is possible to predict the anisotropic deformation behavior and to model in a straightforward manner other phenomena which have been described by metallurgists in crystallographic terms. Elevated temperature tension-torsion tests were run and used to verify the model's predictive abilities. Ratchetting behavior under thermomechanical loading conditions is specifically addressed.

Author

A92-24719* National Aeronautics and Space Administration. Lewis Research Center, Cleveland, OH.

STRESS VERSUS TEMPERATURE DEPENDENCE OF ACTIVATION ENERGIES FOR CREEP

A. D. FREED, S. V. RAJ (NASA, Lewis Research Center, Cleveland, OH), and K. P. WALKER (Engineering Science Software, Inc., Smithfield, RI) *ASME, Transactions, Journal of Engineering Materials and Technology* (ISSN 0094-4289), vol. 114, Jan. 1992, p. 46-50. Jan. 1992 5 p refs

Copyright

The activation energy for creep at low stresses and elevated temperatures is associated with lattice diffusion, where the rate controlling mechanism for deformation is dislocation climb. At higher stresses and intermediate temperatures, the rate controlling mechanism changes from dislocation climb to obstacle-controlled dislocation glide. Along with this change in deformation mechanism occurs a change in the activation energy. When the rate controlling mechanism for deformation is obstacle-controlled dislocation glide, it is shown that a temperature-dependent Gibbs free energy does better than a stress-dependent Gibbs free energy in correlating steady-state creep data for both copper and LiF-22mol percent CaF₂ hypereutectic salt.

Author

A92-24721* National Aeronautics and Space Administration. Lewis Research Center, Cleveland, OH.

A VISCOPLASTIC THEORY FOR ANISOTROPIC MATERIALS

D. NOUAILHAS (ONERA, Chatillon, France) and A. D. FREED (NASA, Lewis Research Center, Cleveland, OH) *ASME, Transactions, Journal of Engineering Materials and Technology* (ISSN 0094-4289), vol. 114, Jan. 1992, p. 97-104. Jan. 1992 8 p refs

(ONERA, TP NO. 1992-90) Copyright

The purpose of this work is the development of a unified, cyclic, viscoplastic model for anisotropic materials. The first part of the paper presents the foundations of the model in the framework of thermodynamics with internal variables. The second part considers the particular case of cubic symmetry, and addresses the cyclic behavior of a nickel-base single-crystal superalloy, CMSX-2, at high temperature (950 C).

Author

A92-25403* National Aeronautics and Space Administration. Lewis Research Center, Cleveland, OH.

BOUNDARY FORMULATIONS FOR SHAPE SENSITIVITY OF TEMPERATURE DEPENDENT CONDUCTIVITY PROBLEMS

JAMES H. KANE and HUA WANG (Clarkson University, Potsdam, NY) *International Journal for Numerical Methods in Engineering* (ISSN 0029-5981), vol. 33, Feb. 28, 1992, p. 667-693. 28 Feb. 1992 27 p refs

(Contract NAG3-1089; NSF DDM-89-96171)

Copyright

Used in concert with the Kirchhoff transformation, implicit differentiation of the discretized boundary integral equations governing the conduction of heat in solids with temperature dependent thermal conductivity is shown to generate an accurate and economical approach for computation of shape sensitivities. For problems with specified temperature and heat flux boundary conditions, a linear problem results for both the analysis and sensitivity analysis. In problems with either convection or radiation boundary conditions, a nonlinear problem is generated. Several iterative strategies are presented for the solution of the resulting sets of nonlinear equations and the computational performances examined in detail. Multizone analysis and zone condensation strategies are demonstrated to provide substantive computational economies in this process for models with either localized nonlinear boundary conditions or regions of geometric insensitivity to design variables. A series of nonlinear example problems is presented that have closed form solutions. Exact analytical expressions for the shape sensitivities associated with these problems are developed and these are compared with the sensitivities computed using the boundary element formulation.

Author

A92-26372* National Aeronautics and Space Administration. Lewis Research Center, Cleveland, OH.

A VISCOPLASTIC THEORY WITH THERMODYNAMIC CONSIDERATIONS

A. D. FREED (NASA, Lewis Research Center, Cleveland, OH), K. P. WALKER (Engineering Science Software, Inc., Smithfield, RI),

39 STRUCTURAL MECHANICS

and J.-L. CHABOCHE (ONERA, Chatillon, France) 1991
21 p refs
(ONERA, TP NO. 1991-220) Copyright

A thermodynamic foundation using the concept of internal state variables is given for a general theory of viscoplasticity for initially isotropic materials. Three fundamental, internal, state variables are admitted; they are: a tensorial back stress for kinematic effects, and scalar drag and yield strengths for isotropic effects. All three are considered to evolve phenomenologically according to competitive processes between strain hardening, deformation-induced dynamic recovery, and thermally induced static recovery. Within this phenomenological framework, a thermodynamically admissible set of evolution equations is proposed. The theory allows each of the three internal variables to be composed as a sum of independently evolving constituents. The evolution of internal state can also include terms that vary linearly with the external variable rates, whose presence affects the energy dissipation properties of a material. Author

A92-28052* National Aeronautics and Space Administration. Lewis Research Center, Cleveland, OH.

VISCOPLASTIC ANALYSIS OF AN EXPERIMENTAL CYLINDRICAL THRUST CHAMBER LINER

VINOD K. ARYA (Toledo, University, OH) and STEVEN M. ARNOLD (NASA, Lewis Research Center, Cleveland, OH) AIAA Journal (ISSN 0001-1452), vol. 30, March 1992, p. 781-789. Previously announced in STAR as N91-28622. Mar. 1992 9 p refs
Copyright

A viscoplastic stress-strain analysis of an experimental cylindrical thrust chamber is presented. A viscoelastic constitutive model incorporating a single internal state variable that represents kinematic hardening was employed to investigate whether such a viscoplastic model could predict the experimentally observed behavior of the thrust chamber. Two types of loading cycles were considered: a short cycle of 3.5-s duration that corresponded to the experiments, and an extended loading cycle of 485.1 s duration that is typical of the Space Shuttle Main Engine (SSME) operating cycle. The analysis qualitatively replicated the deformation behavior of the component as observed in experiments designed to simulate SSME operating conditions. The analysis also showed that the mode and location of failure in the component may depend on the loading cycle. The results indicate that using viscoplastic models for structural analysis can lead to a more realistic life assessment of thrust chambers. Author

A92-28055* National Aeronautics and Space Administration. Lewis Research Center, Cleveland, OH.

MULTIOBJECTIVE SHAPE AND MATERIAL OPTIMIZATION OF COMPOSITE STRUCTURES INCLUDING DAMPING

D. A. SARAVANOS and C. C. CHAMIS (NASA, Lewis Research Center, Cleveland, OH) Mar. 1992 9 p refs
Copyright

A92-28756* National Aeronautics and Space Administration. Lewis Research Center, Cleveland, OH.

VIBRATION TRANSMISSION THROUGH ROLLING ELEMENT BEARINGS. IV - STATISTICAL ENERGY ANALYSIS

T. C. LIM and R. SINGH (Ohio State University, Columbus) Journal of Sound and Vibration (ISSN 0022-460X), vol. 153, Feb. 22, 1992, p. 37-50. Research supported by NASA. 22 Feb. 1992 14 p refs
Copyright

A theoretical broadband coupling-loss factor is developed analytically for use in the statistical energy analysis (SEA) of a shaft-bearing-plate system. The procedure is based on the solution of the boundary-value problem at the plate-bearing interface and incorporates a bearing-stiffness matrix developed by the authors. Three examples are utilized to illustrate the SEA incorporating the coupling-loss factor including: (1) a shaft-bearing-plate system; (2) a plate-cantilevered beam; and (3) a circular-shaft-bearing plate. The coupling-loss factor in the case of the thin plate-cantilevered beam is found to be more accurate than that developed by Lyon and Eichler (1964). The coupling-loss factor is described for the

bearing system and extended to describe the mean-square vibratory response of a rectangular plate. The proposed techniques are of interest to the study of vibration and noise in rotating machinery such as gearboxes. C.C.S.

A92-29464* National Aeronautics and Space Administration. Lewis Research Center, Cleveland, OH.

MIXED-MODE FRACTURE IN UNIDIRECTIONAL GRAPHITE EPOXY COMPOSITE LAMINATES WITH CENTRAL NOTCH

WIESLAW K. BINIENDA (Akron, University, OH) and E. S. REDDY (NASA, Lewis Research Center, Cleveland; Sverdrup Technology, Inc., Brook Park, OH) Journal of Reinforced Plastics and Composites (ISSN 0731-6844), vol. 11, March 1992, p. 324-338. Mar. 1992 15 p refs
Copyright

Mixed-mode matrix fracture in central notched off-axis unidirectional composite laminates was investigated. A limited number of unidirectional tensile type specimens with a central, horizontal, notch were tested. Crack initiation and propagation were examined under various local stress fields that were controlled by fiber orientations. The tested specimens were simulated using a two dimensional finite element method with constant strain loading. The strain energy release rates along the crack were evaluated via crack closure technique. The variation of critical strain energy rates with off-axis angle was studied. The results from single (one-sided) and double (two-sided) crack simulations were presented and compared. Author

A92-30673* National Aeronautics and Space Administration. Lewis Research Center, Cleveland, OH.

MICROSTRESS ANALYSIS OF PERIODIC COMPOSITES

KEVIN P. WALKER (Engineering Science Software, Inc., Smithfield, RI), ALAN D. FREED (NASA, Lewis Research Center, Cleveland, OH), and ERIC H. JORDAN (Connecticut, University, Storrs) Composites Engineering (ISSN 0961-9526), vol. 1, no. 1, 1991, p. 29-40. 1991 12 p refs
(Contract NAG3-882; DE-AC02-88ER-13895)
Copyright

Local elastic fields in the unit cell of a periodic composite are examined numerically with an integral equation approach. Techniques of Fourier series and Green's functions are used to construct the integral equations. Numerical solutions are obtained using the Fourier series approach with rectangular subvolume elements. Specific results are given for a tungsten/copper metal matrix composite. Author

A92-33127* National Aeronautics and Space Administration. Lewis Research Center, Cleveland, OH.

PREDICTIONS OF THE CRITICAL STRAIN FOR MATRIX CRACKING OF CERAMIC MATRIX COMPOSITES

WEN-SHYONG KUO and TSU-WEI CHOU (Delaware, University, Newark) IN: Inelastic deformation of composite materials; Proceedings of the IUTAM Symposium, Troy, NY, May 29-June 1, 1990 1991 12 p refs
(Contract NAS3-25971)
Copyright

The critical strain for matrix cracking of ceramic matrix composites has been studied; emphasis is placed on the effects of the fiber/matrix debonding length and interfacial debonding energy. Based on a modified shear-lag model, stresses in the fiber and matrix have been found for both the bonded and debonded regions. An energy-balance approach, based upon the stress field, is then adopted to evaluate the critical strain for matrix cracking. From the general equation for the critical strain, close form solutions have been deduced for two limiting cases: complete debonding and perfect bonding. Numerical solutions are given for the cases of nonzero debonding energy and partial fiber debonding. The results show that the interfacial debonding energy, which has been ignored by most of the investigators, is an important factor in determining both the critical strain and the debonding length. Author

A92-33589* National Aeronautics and Space Administration. Lewis Research Center, Cleveland, OH.

EFFECT OF CONTACT STRESSES IN FOUR-POINT BEND TESTING OF GRAPHITE/EPOXY AND GRAPHITE/PMR-15 COMPOSITE BEAMS

W. K. BINIENDA (Akron, University, OH), G. D. ROBERTS (NASA, Lewis Research Center, Cleveland, OH), and D. S. PAPADOPOULOS (Case Western Reserve University, Cleveland, OH) SAMPE Quarterly (ISSN 0036-0821), vol. 23, April 1992, p. 20-28. Apr. 1992 9 p refs

Copyright

The results of in-plane four-point bend experiments on unidirectionally reinforced composite beams are presented for graphite/epoxy (T300/934) and graphite/polyimide (G30-500/PMR-15) composites. The maximum load and the location of cracks formed during failure were measured for testpieces with fibers oriented at various angles to the beam axis. Since most of the beams failed near one or more of the load points, the strength of the beams was evaluated in terms of a proposed model for the local stress distribution. In this model, an exact solution to the problem of a localized contact force acting on a unidirectionally reinforced half plane is used to describe the local stress field. The stress singularity at the load points is treated in a manner similar to the stress singularity at a crack tip in fracture mechanics problems. Using this approach, the effect of fiber angle and elastic material properties on the strength of the beam is described in terms of a load intensity factor. For fiber angles less than 45 deg from the beam axis, a single crack is initiated near one of the load points at a critical value of the load intensity factor. The critical load intensity factor decreases with increasing fiber angle. For larger fiber angles, multiple cracks occur at locations both near and away from the load points, and the load intensity factor at failure increases sharply with increasing fiber angle.

Author

A92-33903* National Aeronautics and Space Administration. Lewis Research Center, Cleveland, OH.

A VISCOPLASTIC THEORY WITH THERMODYNAMIC CONSIDERATIONS

A. D. FREED (NASA, Lewis Research Center, Cleveland, OH), J.-L. CHABOCHE (ONERA, Chatillon, France), and K. P. WALKER (Engineering Science Software, Inc., Smithfield, RI) Acta Mechanica (ISSN 0001-5970), vol. 90, 1991, p. 155-174. 1991 20 p refs

Copyright

A thermodynamic foundation using the concept of internal state variables is given for a general theory of viscoplasticity for initially isotropic materials. Three, fundamental, internal, state variables are admitted; they are: a tensorial back stress for kinematic effects, and scalar drag and yield strengths for isotropic effects. All three are considered to evolve phenomenologically according to competitive processes between strain hardening, deformation induced dynamic recovery, and thermally induced static recovery. Within this phenomenological framework, a thermodynamically admissible set of evolution equations is proposed. The theory allows each of the three internal variables to be composed as a sum of independently evolving constituents. The evolution of internal state can also include terms that vary linearly with the external variable rates, whose presence affects the energy dissipation properties of a material.

Author

A92-34321*# National Aeronautics and Space Administration. Lewis Research Center, Cleveland, OH.

MAPPING METHODS FOR COMPUTATIONALLY EFFICIENT AND ACCURATE STRUCTURAL RELIABILITY

MICHAEL C. SHIAO (NASA, Lewis Research Center; Sverdrup Technology, Inc., Cleveland, OH) and CHRISTOS C. CHAMIS (NASA, Lewis Research Center, Cleveland, OH) IN: AIAA/ASME/ASCE/AHS/ASC Structures, Structural Dynamics and Materials Conference, 33rd, Dallas, TX, Apr. 13-15, 1992, Technical Papers. Pt. 1 1992 11 p refs

(AIAA PAPER 92-2347) Copyright

Mapping methods are developed to improve the accuracy and

efficiency of probabilistic structural analyses with coarse finite element meshes. The mapping methods consist of: (1) deterministic structural analyses with fine (convergent) finite element meshes, (2) probabilistic structural analyses with coarse finite element meshes, (3) the relationship between the probabilistic structural responses from the coarse and fine finite element meshes, and (4) a probabilistic mapping. The results show that the scatter of the probabilistic structural responses and structural reliability can be accurately predicted using a coarse finite element model with proper mapping methods. Therefore, large structures can be analyzed probabilistically using finite element methods. Author

A92-34322*# National Aeronautics and Space Administration. Lewis Research Center, Cleveland, OH.

RELIABILITY ANALYSIS OF LAMINATED CMC COMPONENTS THROUGH SHELL SUBELEMENT TECHNIQUES

A. STARLINGER (NASA, Lewis Research Center, Cleveland, OH), S. F. DUFFY (Cleveland State University, OH), and J. P. GYEKENYESI (NASA, Lewis Research Center, Cleveland, OH) IN: AIAA/ASME/ASCE/AHS/ASC Structures, Structural Dynamics and Materials Conference, 33rd, Dallas, TX, Apr. 13-15, 1992, Technical Papers. Pt. 1 1992 10 p refs

(AIAA PAPER 92-2348)

An updated version of the integrated design program C/CARES (composite ceramic analysis and reliability evaluation of structures) was developed for the reliability evaluation of CMC laminated shell components. The algorithm is now split in two modules: a finite-element data interface program and a reliability evaluation algorithm. More flexibility is achieved, allowing for easy implementation with various finite-element programs. The new interface program from the finite-element code MARC also includes the option of using hybrid laminates and allows for variations in temperature fields throughout the component. Author

A92-34339*# National Aeronautics and Space Administration. Lewis Research Center, Cleveland, OH.

A NEW RESPONSE SURFACE APPROACH FOR STRUCTURAL RELIABILITY ANALYSIS

B. H. THACKER and X.-T. WU (Southwest Research Institute, San Antonio, TX) IN: AIAA/ASME/ASCE/AHS/ASC Structures, Structural Dynamics and Materials Conference, 33rd, Dallas, TX, Apr. 13-15, 1992, Technical Papers. Pt. 2 1992 8 p refs

(Contract NAS3-24389)

(AIAA PAPER 92-2408) Copyright

This paper describes a new approach for computing structural reliability by post-processing previously computed probabilistic results for stress and strength. The objective is to provide an accurate method whereby independent probabilistic analyses for stress and strength functions can be performed independently and combined at a later time to compute probability of failure. The method provides a capability for testing different strength measures without the need for re-computing the probabilistic stress response. The proposed approach takes full account of the basic random variables effecting both stress and strength, and the failure region in the variable space identified during separate stress/strength probabilistic analyses. A simple closed-form example and a more complex analysis of a turbine blade subject to creep rupture is used to illustrate the method. Author

A92-34360*# National Aeronautics and Space Administration. Lewis Research Center, Cleveland, OH.

STRUCTURAL TAILORING/ANALYSIS FOR HYPERSONIC COMPONENTS - EXECUTIVE SYSTEM DEVELOPMENT

G. V. NARAYANAN, JANE R. KRAMER (Sverdrup Technology, Inc., Brook Park, OH), DALE A. HOPKINS, and CHRISTOS C. CHAMIS (NASA, Lewis Research Center, Cleveland, OH) IN: AIAA/ASME/ASCE/AHS/ASC Structures, Structural Dynamics and Materials Conference, 33rd, Dallas, TX, Apr. 13-15, 1992, Technical Papers. Pt. 2 1992 9 p refs

(Contract NAS3-25266)

(AIAA PAPER 92-2471)

No direct analytical or integrated numerical tool exists today for the optimal design of a generic class of built-up actively cooled

composite structure for applications in hypersonic propulsion ducts. The need exists for a numerical tool to perform the comprehensive design/analysis of a panel on the inlet wall under hypersonic flight conditions. Such a tool requires relatively complex multi-disciplinary analysis. One such numerical tool controlled by an executive system has been developed and is named as STAHYC (Structural Tailoring/Analysis for HYPersonic Components). A detailed account of the executive system development of STAHYC along with the results of one example inlet panel design problem is given in this paper. Author

A92-34368*# National Aeronautics and Space Administration. Lewis Research Center, Cleveland, OH.

MATERIAL NONLINEAR ANALYSIS VIA MIXED-ITERATIVE FINITE ELEMENT METHOD

EDHI SUTJAHJO (Sverdrup Technology, Inc., Brook Park, OH) and CHRISTOS C. CHAMIS (NASA, Lewis Research Center, Cleveland, OH) IN: AIAA/ASME/ASCE/AHS/ASC Structures, Structural Dynamics and Materials Conference, 33rd, Dallas, TX, Apr. 13-15, 1992, Technical Papers. Pt. 2 1992 8 p refs (AIAA PAPER 92-2479) Copyright

The performance of elastic-plastic mixed-iterative analysis is examined through a set of convergence studies. Membrane and bending behaviors are tested using 4-node quadrilateral finite elements. The membrane result is excellent, which indicates the implementation of elastic-plastic mixed-iterative analysis is appropriate. On the other hand, further research to improve bending performance of the method seems to be warranted. Author

A92-34523*# National Aeronautics and Space Administration. Lewis Research Center, Cleveland, OH.

MINIMIZING DISTORTION IN TRUSS STRUCTURES - A HOPFIELD NETWORK SOLUTION

B. FU and P. HAJELA (Rensselaer Polytechnic Institute, Troy, NY) IN: AIAA/ASME/ASCE/AHS/ASC Structures, Structural Dynamics and Materials Conference, 33rd, Dallas, TX, Apr. 13-15, 1992, Technical Papers. Pt. 5 1992 9 p refs (Contract NAG3-1196) (AIAA PAPER 92-2302) Copyright

Distortions in truss structures can result from random errors in element lengths that are typical of a manufacturing process. These distortions may be minimized by an optimal selection of elements from those available for placement between the prescribed nodes - a combinatorial optimization problem requiring significant investment of computational resource for all but the smallest problems. The present paper describes a formulation in which near-optimal element assignments are obtained as minimum-energy stable states, of an analogous Hopfield neural network. This requires mapping of the optimization problem into an energy function of the appropriate Liapunov form. The computational architecture is ideally suited to a parallel processor implementation and offers significant savings in computational effort. A numerical implementation of the approach is discussed with reference to planar truss problems. Author

A92-34555*# National Aeronautics and Space Administration. Lewis Research Center, Cleveland, OH.

APPLICATION OF NEWTON MODIFIED BARRIER METHOD (NMBM) TO STRUCTURAL OPTIMIZATION

N. S. KHOT (USAF, Flight Dynamics Directorate, Wright-Patterson AFB, OH), R. POLYAK, R. SCHNEUR (IBM Thomas J. Watson Research Center, Yorktown Heights, NY), and L. BERKE (NASA, Lewis Research Center, Cleveland, OH) IN: AIAA/ASME/ASCE/AHS/ASC Structures, Structural Dynamics and Materials Conference, 33rd, Dallas, TX, Apr. 13-15, 1992, Technical Papers. Pt. 5 1992 8 p refs (AIAA PAPER 92-2498) Copyright

This paper presents the application of the NMBM to obtain a minimum weight structure with constraints on displacements and minimum sizes. The solution to the problem is obtained via minimizing the Modified Barrier Function (MBF) at each step by using the Newton Method and updating Lagrange multipliers. The Lagrange multipliers are updated by using the value of the

constraints at the minimum of the MBF. Three truss problems with a different number of design variables are solved. The convergence to the minimum weight design was found to be monotonic and the algorithm is potentially robust for solving problems with a large number of design variables. Author

A92-34564*# National Aeronautics and Space Administration. Lewis Research Center, Cleveland, OH.

MULTIDISCIPLINARY TAILORING OF HOT COMPOSITE STRUCTURES

SURENDRA N. SINGHAL (Sverdrup Technology, Inc., Cleveland, OH) and CHRISTOS C. CHAMIS (NASA, Lewis Research Center, Cleveland, OH) IN: AIAA/ASME/ASCE/AHS/ASC Structures, Structural Dynamics and Materials Conference, 33rd, Dallas, TX, Apr. 13-15, 1992, Technical Papers. Pt. 5 1992 11 p refs (AIAA PAPER 92-2563) Copyright

A computational simulation procedure is described for multidisciplinary analysis and tailoring of multilayered multimaterial hot composite engine structural components subjected to simultaneous multiple discipline-specific thermal, structural, vibration, and acoustic loadings including the effect of aggressive environments. The simulation is based on a 3D finite element analysis technique in conjunction with structural mechanics codes, thermal/acoustic analysis methods, and tailoring procedures. The integrated multidisciplinary simulation procedure is general-purpose including the coupled effects of nonlinearities in structure geometry, material, loading, and environmental complexities. The composite material behavior is assessed at all composite scales, i.e., the laminate/ply/constituents (fiber/matrix), via a nonlinear material characterization hygro-thermomechanical model. Sample tailoring cases exhibiting nonlinear material/loading/environmental behavior of aircraft engine fan blades, are presented. The various multidisciplinary loadings lead to different tailored designs, even those opposite of each other, as in the case of minimum material cost versus minimum structure weight and in the case of minimum vibration frequency versus minimum acoustic noise. Author

A92-34569*# National Aeronautics and Space Administration. Lewis Research Center, Cleveland, OH.

STRUCTURAL DURABILITY OF STIFFENED COMPOSITE SHELLS

LEVON MINNETYAN, JAMES M. RIVERA (Clarkson University, Potsdam, NY), PAPPU L. N. MURTHY, and CHRISTOS C. CHAMIS (NASA, Lewis Research Center, Cleveland, OH) IN: AIAA/ASME/ASCE/AHS/ASC Structures, Structural Dynamics and Materials Conference, 33rd, Dallas, TX, Apr. 13-15, 1992, Technical Papers. Pt. 5 1992 8 p refs (Contract NAG3-1101) (AIAA PAPER 92-2244) Copyright

The durability of a stiffened composite cylindrical shell panel is investigated under several loading conditions. An integrated computer code is utilized for the simulation of load induced structural degradation. Damage initiation, growth, and accumulation up to the stage of propagation to fracture and included in the computational simulation. Results indicate significant differences in the degradation paths for different loading cases. Effects of combined loading on structural durability and ultimate structural strength of a stiffened shell are assessed. Author

A92-34580*# National Aeronautics and Space Administration. Lewis Research Center, Cleveland, OH.

DIFFUSIVE CRACK GROWTH AT A BIMATERIAL INTERFACE

TZE-JER CHUANG (NIST, Ceramics Div., Gaithersburg, MD), JUNE-LIANG CHU, and SANBOH LEE (National Tsing Hua University, Hsinchu, Republic of China) IN: AIAA/ASME/ASCE/AHS/ASC Structures, Structural Dynamics and Materials Conference, 33rd, Dallas, TX, Apr. 13-15, 1992, Technical Papers. Pt. 5 1992 6 p refs (Contract NASA ORDER C-82000-R) (AIAA PAPER 92-2432)

The diffusional microcrack growth behavior in a bimaterial system is investigated with an aim at estimating service life of advanced ceramic composites under creep-rupture conditions. The

crack is assumed to grow via a coupled surface and grain-boundary diffusion under steady state conditions. The tensile stress distribution along the interface ahead of the moving crack tip is solved, and it is found that a new length parameter exists as a scaling factor for which the solution becomes identical to the single phase case when plotted on the nondimensional physical plane. In contrast to the elastic stress solution which shows singularity at the tip, together with oscillatory character away from the tip, the creep stresses have a peak value away from the tip due to a wedging effect and interfacial sliding eliminates stress oscillation resulting in a decoupling between mode I and mode II loading. This solution ties the far-field loading parameter to the crack tip conditions in terms of the unknown crack velocity to give a specific V-K(1) relationship. It is shown that an exponent of 12 in the conventional crack growth power law emerges at the higher applied stress range.

Author

A92-34582*# National Aeronautics and Space Administration, Lewis Research Center, Cleveland, OH.

ANALYSIS OF WHISKER-TOUGHENED CMC STRUCTURAL COMPONENTS USING AN INTERACTIVE RELIABILITY MODEL
STEPHEN F. DUFFY and JOSEPH L. PALKO (NASA, Lewis Research Center, Cleveland State University, OH) IN: AIAA/ASME/ASCE/AHS/ASC Structures, Structural Dynamics and Materials Conference, 33rd, Dallas, TX, Apr. 13-15, 1992, Technical Papers, Pt. 5 1992 11 p refs (AIAA PAPER 92-2490) Copyright

Realizing wider utilization of ceramic matrix composites (CMC) requires the development of advanced structural analysis technologies. This article focuses on the use of interactive reliability models to predict component probability of failure. The deterministic William-Warner failure criterion serves as theoretical basis for the reliability model presented here. The model has been implemented into a test-bed software program. This computer program has been coupled to a general-purpose finite element program. A simple structural problem is presented to illustrate the reliability model and the computer algorithm.

Author

A92-34583*# National Aeronautics and Space Administration, Lewis Research Center, Cleveland, OH.

NEAR-TIP DUAL-LENGTH SCALE MECHANICS OF MODE-I CRACKING IN LAMINATE BRITTLE MATRIX COMPOSITES
R. BALLARINI, S. ISLAM (Case Western Reserve University, Cleveland, OH), and P. G. CHARALAMBIDES (Michigan Technological University, Houghton) IN: AIAA/ASME/ASCE/AHS/ASC Structures, Structural Dynamics and Materials Conference, 33rd, Dallas, TX, Apr. 13-15, 1992, Technical Papers, Pt. 5 1992 10 p refs (Contract NAG3-856; NSF MSS-91-57090) (AIAA PAPER 92-2491) Copyright

This paper presents the preliminary results of an on-going study of the near-tip mechanics of mode-I cracking in brittle matrix composite laminates. A finite element model is developed within the context of two competing characteristic lengths present in the composite: the microstructural length (the thickness of the layers) and a macro-length (crack-length, uncracked ligament size, etc.). For various values of the parameters which describe the ratio of these lengths and the constituent properties, the stresses ahead of a crack perpendicular to the laminates are compared with those predicted by assuming the composite is homogeneous orthotropic. The results can be used to determine the conditions for which homogenization can provide a sufficiently accurate description of the stresses in the vicinity of the crack-tip.

Author

A92-34585*# National Aeronautics and Space Administration, Lewis Research Center, Cleveland, OH.

FRACTURE RESISTANCE DEVELOPMENT IN CERAMIC COMPOSITES WITH NONLINEAR FIBER PULLOUT RELATIONSHIP

ASHER A. RUBINSTEIN (Tulane University, New Orleans, LA) IN: AIAA/ASME/ASCE/AHS/ASC Structures, Structural Dynamics and Materials Conference, 33rd, Dallas, TX, Apr. 13-15, 1992, Technical

Papers, Pt. 5 1992 5 p refs

(Contract NAG3-967)

(AIAA PAPER 92-2493) Copyright

This paper addresses the fracture resistance mechanism in fiber reinforced ceramics, and focuses attention on the specific effects associated with nonlinear nature of the fiber pullout mechanism. The model is based on a consideration of the representative boundary value problem typical for the bridging process. The theoretical solution includes an accurate account of the nonlinear fiber matrix friction. The developed approach allows consideration of several types of nonlinear fiber pullout-force dependence. The distinct features of the nonlinear process demonstrate that, contrary to the linear case, the universal fracture resistance curves cannot be developed in cases with significant nonlinear contribution in the fiber friction law. The resulting resistance curves depend strongly on the absolute values of the matrix fracture toughness. On the other hand, these distinct patterns may be used for identification of the particular friction law and determination of the friction parameters.

Author

A92-34586*# National Aeronautics and Space Administration, Lewis Research Center, Cleveland, OH.

LOAD REDISTRIBUTION CONSIDERATIONS IN THE FRACTURE OF CERAMIC MATRIX COMPOSITES

DAVID J. THOMAS and ROBERT C. WETHERHOLD (New York State University, Buffalo) IN: AIAA/ASME/ASCE/AHS/ASC Structures, Structural Dynamics and Materials Conference, 33rd, Dallas, TX, Apr. 13-15, 1992, Technical Papers, Pt. 5 1992 9 p refs

(Contract NAG3-862)

(AIAA PAPER 92-2494) Copyright

Using a macroscopic viewpoint, composite laminae are homogeneous orthotropic solids whose directional strengths are random variables. Incorporation of these random variable strengths into failure models, either interactive or noninteractive, allows for the evaluation of the lamina reliability under a given stress state. Using a noninteractive criterion for demonstration purposes, laminate reliabilities are calculated assuming previously established load sharing rules for the redistribution of load as the failure of laminae occur. The matrix cracking predicted by ACK theory is modeled to allow a loss of stiffness in the fiber direction. The subsequent failure in the fiber direction is controlled by a modified bundle theory. Results are compared with previous models which did not permit separate consideration of matrix cracking, as well as to results obtained from experimental data. The effects of variations from the ideal physical geometry which is normally used to depict the matrix cracking are also studied.

Author

A92-36245* National Aeronautics and Space Administration, Lewis Research Center, Cleveland, OH.

ON THE DEVELOPMENT OF EXPLICIT ROBUST SCHEMES FOR IMPLEMENTATION OF A CLASS OF HYPERELASTIC MODELS IN LARGE-STRAIN ANALYSIS OF RUBBERS

A. F. SALEEB, T. Y. P. CHANG (Akron, University, OH), and S. M. ARNOLD (NASA, Lewis Research Center, Cleveland, OH) International Journal for Numerical Methods in Engineering (ISSN 0029-5981), vol. 33, no. 6, April 30, 1992, p. 1237-1249. 30 Apr. 1992 13 p refs

(Contract NSF EET-87-14628)

Copyright

The issue of developing effective and robust schemes to implement a class of the Ogden-type hyperelastic constitutive models, for large-strain analysis of rubber-like materials, is addressed. To this end, explicit forms for the corresponding material tangent-stiffness tensors are developed, and these are valid for the entire deformation range; i.e., with both distinct as well as repeated principal-stretch values. Throughout the analysis the various implications of the underlying property of separability of the strain-energy functions are exploited, thus leading to compact final forms of the tensor expressions. In particular, this facilitated the treatment of the complex cases of uncoupled volumetric/deviatoric formulations for incompressible materials,

39 STRUCTURAL MECHANICS

which are becoming increasingly popular in recent years. The forms derived are also amenable for use with symbolic-manipulation packages for systematic code generation. Author

A92-36853* National Aeronautics and Space Administration, Lewis Research Center, Cleveland, OH.

FREE VIBRATIONS OF DELAMINATED BEAMS

M.-H. H. SHEN (Ohio State University, Columbus) and J. E. GRADY (NASA, Lewis Research Center, Cleveland, OH) May 1992

10 p refs
Copyright

A92-36896* National Aeronautics and Space Administration, Lewis Research Center, Cleveland, OH.

HITCAN FOR ACTIVELY COOLED HOT-COMPOSITE THERMOSTRUCTURAL ANALYSIS

C. C. CHAMIS, P. L. N. MURTHY (NASA, Lewis Research Center, Cleveland, OH), S. N. SINGHAL, and J. J. LACKNEY (Sverdrup Technology, Inc., Cleveland, OH) Apr. 1992 6 p refs (ASME PAPER 91-GT-116) Copyright

A computer code, high temperature composite analyzer (HITCAN), was developed to analyze/design hot metal matrix composite structures. HITCAN is a general purpose code for predicting the global structural and local stress-strain response of multilayered (arbitrarily oriented) metal matrix structures both at the constituent (fiber, matrix, and interphase) and the structural level, including the fabrication process effects. The thermomechanical properties of the constituents are considered to be nonlinearly dependent on several parameters, including temperature, stress, and stress rate. The computational procedure employs an incremental iterative nonlinear approach utilizing a multifactor-interaction material behavior model, i.e., the material properties are expressed in terms of a product of several factors that affect the properties. HITCAN structural analysis capabilities (static, load stepping - a multistep static analysis with material properties updated at each step, modal, and buckling) for cooled hot structures are demonstrated through a specific example problem. Author

A92-37510* National Aeronautics and Space Administration, Lewis Research Center, Cleveland, OH.

A VARIATIONALLY COUPLED FE-BE METHOD FOR ELASTICITY AND FRACTURE MECHANICS

Y. Y. LU, T. BELYTSCSKO, and W. K. LIU (Northwestern University, Evanston, IL) Computer Methods in Applied Mechanics and Engineering (ISSN 0045-7825), vol. 85, no. 1, Jan. 1991, p. 21-37. Jan. 1991 17 p refs (Contract DAAL03-87-K-0035; NAG3-822)

Copyright

A new method for coupling finite element and boundary element subdomains in elasticity and fracture mechanics problems is described. The essential feature of this new method is that a single variational statement is obtained for the entire domain, and in this process the terms associated with tractions on the interfaces between the subdomains are eliminated. This provides the additional advantage that the ambiguities associated with the matching of discontinuous tractions are circumvented. The method leads to a direct procedure for obtaining the discrete equations for the coupled problem without any intermediate steps. In order to evaluate this method and compare it with previous methods, a patch test for coupled procedures has been devised. Evaluation of this variationally coupled method and other methods, such as stiffness coupling and constraint traction matching coupling, shows that this method is substantially superior. Solutions for a series of fracture mechanics problems are also reported to illustrate the effectiveness of this method. Author

A92-37517 National Aeronautics and Space Administration, Washington, DC.

AN UNCONDITIONALLY STABLE STAGGERED ALGORITHM FOR TRANSIENT FINITE ELEMENT ANALYSIS OF COUPLED THERMOELASTIC PROBLEMS

CHARBEL FARHAT, K. C. PARK (Colorado, University, Boulder),

and YVES DUBOIS-PELERIN (Lausanne, Ecole Polytechnique Federale, Switzerland) Computer Methods in Applied Mechanics and Engineering (ISSN 0045-7825), vol. 85, no. 3, Feb. 1991, p. 349-365. Previously announced in STAR as N92-13457. Feb. 1991 17 p refs

(Contract NAGW-1388; NAG3-934)
Copyright

An unconditionally stable second order accurate implicit-implicit staggered procedure for the finite element solution of fully coupled thermoelasticity transient problems is proposed. The procedure is stabilized with a semi-algebraic augmentation technique. A comparative cost analysis reveals the superiority of the proposed computational strategy to other conventional staggered procedures. Numerical examples of one- and two-dimensional thermomechanical coupled problems demonstrate the accuracy of the proposed numerical solution algorithm. Author

A92-37524* National Aeronautics and Space Administration, Lewis Research Center, Cleveland, OH.

FATIGUE CRACK GROWTH RELIABILITY BY PROBABILISTIC FINITE ELEMENTS

GLEN H. BESTERFIELD (South Florida, University, Tampa, FL), WING K. LIU, MARK A. LAWRENCE, and TED BELYTSCSKO (Northwestern University, Evanston, IL) Computer Methods in Applied Mechanics and Engineering (ISSN 0045-7825), vol. 86, no. 3, April 1991, p. 297-320. Research supported by University of South Florida. Apr. 1991 24 p refs (Contract NAG3-822)

Copyright

Fusion of the probabilistic finite-element method and reliability analysis for probabilistic fatigue-crack growth is presented. A comprehensive method for determining the probability of fatigue failure for mixed-mode cyclic loading is also presented. The loading is mixed-mode with randomness in the initial and final crack lengths, initial crack angle and position, material properties, crack-growth law, crack-direction law, and loading. The methodology consists of calculating the reliability index via an optimization procedure which is used to calculate the probability of fatigue failure. Performance of the methodology presented is demonstrated on a classical mode-I fatigue problem. Author

A92-38097* National Aeronautics and Space Administration, Lewis Research Center, Cleveland, OH.

THERMAL STRESS ANALYSIS OF A SILICON CARBIDE/ALUMINUM COMPOSITE

E. E. GDOUTOS (Thrace, University, Xanthi, Greece), D. KARALEKAS (European Centre of Advanced Technology, Athens, Greece), and I. M. DANIEL (Northwestern University, Evanston, IL) Experimental Mechanics (ISSN 0014-4851), vol. 31, no. 3, Sept. 1991, p. 202-208. Research sponsored by NASA. Sep. 1991 7 p refs

Copyright

Thermal deformations and stresses were studied in a silicon-carbide/aluminum filamentary composite at temperatures up to 370 C (700 F). Longitudinal and transverse thermal strains were measured with strain gages and a dilatometer. An elastoplastic micromechanical analysis based on a one-dimensional rule-of-mixtures model and an axisymmetric two-material composite cylinder model was performed. It was established that beyond a critical temperature thermal strains become nonlinear with decreasing longitudinal and increasing transverse thermal-expansion coefficients. This behavior was attributed to the plastic stresses in the aluminum matrix above the critical temperature. An elastoplastic analysis of both micromechanical models was performed to determine the stress distributions and thermal deformation in the fiber and matrix of the composite. While only axial stresses can be determined by the rule-of-mixtures model, the complete triaxial state of stress is established by the composite cylinder model. Theoretical predictions for the two thermal-expansion coefficients were in satisfactory agreement with experimental results. Author

A92-38142*# National Aeronautics and Space Administration. Lewis Research Center, Cleveland, OH.

PROBABILISTIC PROGRESSIVE BUCKLING OF TRUSSES

SHANTARAM S. PAI and CHRISTOS C. CHAMIS (NASA, Lewis Research Center, Cleveland, OH) AIAA, ASME, ASCE, AHS, and ASC, Structures, Structural Dynamics, and Materials Conference, 32nd, Baltimore, MD, Apr. 8-10, 1991. 15 p. Previously announced in STAR as N92-15403. Apr. 1991 15 p refs (AIAA PAPER 91-0916) Copyright

A three-bay, space, cantilever truss is probabilistically evaluated to describe progressive buckling and truss collapse in view of the numerous uncertainties associated with the structural, material, and load variables (primitive variables) that describe the truss. Initially, the truss is deterministically analyzed for member forces, and member(s) in which the axial force exceeds the Euler buckling load are identified. These member(s) are then discretized with several intermediate nodes and a probabilistic buckling analysis is performed on the truss to obtain its probabilistic buckling loads and respective mode shapes. Furthermore, sensitivities associated with the uncertainties in the primitive variables are investigated, margin of safety values for the truss are determined, and truss end node displacements are noted. These steps are repeated by sequentially removing the buckled member(s) until onset of truss collapse is reached. Results show that this procedure yields an optimum truss configuration for a given loading and for a specified reliability.

Author

A92-43494* National Aeronautics and Space Administration. Lewis Research Center, Cleveland, OH.

COMBINED BENDING AND THERMAL FATIGUE OF HIGH-TEMPERATURE METAL-MATRIX COMPOSITES - COMPUTATIONAL SIMULATION

PASCAL K. GOTSIS and CHRISTOS C. CHAMIS (NASA, Lewis Research Center, Cleveland, OH) International Journal of Damage Mechanics (ISSN 1056-7895), vol. 1, no. 3, July 1992, p. 290-319. Previously announced in STAR as N91-23247. Jul. 1992 30 p refs

Copyright

The nonlinear behavior of a high-temperature metal-matrix composite (HT-MMC) was simulated by using the metal matrix composite analyzer (METCAN) computer code. The simulation started with the fabrication process, proceeded to thermomechanical cyclic loading, and ended with the application of a monotonic load. Classical laminate theory and composite micromechanics and macromechanics are used in METCAN, along with a multifactor interaction model for the constituents behavior. The simulation of the stress-strain behavior from the macromechanical and the micromechanical points of view, as well as the initiation and final failure of the constituents and the plies in the composite, were examined in detail. It was shown that, when the fibers and the matrix were perfectly bonded, the fracture started in the matrix and then propagated with increasing load to the fibers. After the fibers fractured, the composite lost its capacity to carry additional load and fractured.

Author

A92-44681* National Aeronautics and Space Administration. Lewis Research Center, Cleveland, OH.

STOCHASTIC MODELING OF CRACK INITIATION AND SHORT-CRACK GROWTH UNDER CREEP AND CREEP-FATIGUE CONDITIONS

TAKAYUKI KITAMURA (NASA, Lewis Research Center, Cleveland, OH), LOUIS J. GHOSN (Sverdrup Technology, Inc., Brook Park, OH), and RYUICHI OHTANI (Kyoto University, Japan) Jun. 1992 8 p refs

(ASME PAPER 92-APM-5) Copyright

A simplified stochastic model is proposed for crack initiation and short-crack growth under creep and creep-fatigue conditions. Material inhomogeneity provides the random nature of crack initiation and early growth. In the model, the influence of microstructure is introduced by the variability of: (1) damage accumulation along grain boundaries, (2) critical damage required for crack initiation or growth, and (3) the grain-boundary length. The probabilities of crack initiation and growth are derived by

using convolution integrals. The model is calibrated and used to predict the crack density and crack-growth rate of short cracks of 304 stainless steel under creep and creep-fatigue conditions. The mean-crack initiation lives are predicted to be within an average deviation of about 10 percent from the experimental results. The predicted cumulative distributions of crack-growth rate follow the experimental data closely. The applicability of the simplified stochastic model is discussed and the future research direction is outlined.

Author

A92-46829* National Aeronautics and Space Administration. Lewis Research Center, Cleveland, OH.

MICROMECHANICAL MODEL OF CRACK GROWTH IN FIBER REINFORCED BRITTLE MATERIALS

ASHER A. RUBINSTEIN and KANG XU (Tulane University, New Orleans, LA) IN: Intermetallic matrix composites; Proceedings of the MRS Symposium, San Francisco, CA, Apr. 18-20, 1990 1990 6 p refs

(Contract NAG3-967)

Copyright

A model based on the micromechanical mechanism of crack growth resistance in fiber reinforced ceramics is presented. The formulation of the model is based on a small scale geometry of a macrocrack with a bridging zone, the process zone, which governs the resistance mechanism. The effect of high toughness of the fibers in retardation of the crack advance, and the significance of the fiber pullout mechanism on the crack growth resistance, are reflected in this model. The model allows one to address issues such as influence of fiber spacing, fiber flexibility, and fiber matrix friction. Two approaches were used. One represents the fracture initiation and concentrated on the development of the first microcracks between fibers. An exact closed form solution was obtained for this case. The second case deals with the development of an array of microcracks between fibers forming the bridging zone. An implicit exact solution is formed for this case. In both cases, a discrete fiber distribution is incorporated into the solution.

Author

A92-47283* National Aeronautics and Space Administration. Lewis Research Center, Cleveland, OH.

APPLICATIONS OF ARTIFICIAL NEURAL NETS IN STRUCTURAL MECHANICS

L. BERKE (NASA, Lewis Research Center, Cleveland, OH) and P. HAJELA (Rensselaer Polytechnic Institute, Troy, NY) (CISM, Course on Shape and Layout Optimization in Structural Design, Udine, Italy, July 16-20, 1990) Structural Optimization (ISSN 0934-4373), vol. 4, no. 2, June 1992, p. 90-98. Previously announced in STAR as N91-21559. Jun. 1992 9 p refs

Copyright

A brief introduction to the fundamental of Neural Nets is given, followed by two applications in structural optimization. In the first case, the feasibility of simulating with neural nets the many structural analyses performed during optimization iterations was studied. In the second case, the concept of using neural nets to capture design expertise was studied.

Author

A92-48976*# National Aeronautics and Space Administration. Lewis Research Center, Cleveland, OH.

STRUCTURAL RELIABILITY ASSESSMENT CAPABILITY IN NESSUS

H. MILLWATER and Y.-T. WU (Southwest Research Institute, San Antonio, TX) AIAA, SAE, ASME, and ASEE, Joint Propulsion Conference and Exhibit, 28th, Nashville, TN, July 6-8, 1992. 9 p. Jul. 1992 9 p refs

(Contract NAS3-24389)

(AIAA PAPER 92-3417) Copyright

The principal capabilities of NESSUS (Numerical Evaluation of Stochastic Structures Under Stress), an advanced computer code developed for probabilistic structural response analysis, are reviewed, and its structural reliability assessed. The code combines flexible structural modeling tools with advanced probabilistic algorithms in order to compute probabilistic structural response

and resistance, component reliability and risk, and system reliability and risk. An illustrative numerical example is presented. V.L.

A92-48978* National Aeronautics and Space Administration. Lewis Research Center, Cleveland, OH.

PROBABILISTIC MATERIAL DEGRADATION MODEL FOR AEROSPACE MATERIALS SUBJECTED TO HIGH TEMPERATURE, MECHANICAL AND THERMAL FATIGUE, AND CREEP

L. BOYCE (Texas, University, San Antonio) AIAA, SAE, ASME, and ASEE, Joint Propulsion Conference and Exhibit, 28th, Nashville, TN, July 6-8, 1992. 11 p. Research supported by NASA. Jul. 1992 11 p refs
(AIAA PAPER 92-3419) Copyright

A probabilistic general material strength degradation model has been developed for structural components of aerospace propulsion systems subjected to diverse random effects. The model has been implemented in two FORTRAN programs, PROMISS (Probabilistic Material Strength Simulator) and PROMISC (Probabilistic Material Strength Calibrator). PROMISS calculates the random lifetime strength of an aerospace propulsion component due to as many as eighteen diverse random effects. Results are presented in the form of probability density functions and cumulative distribution functions of lifetime strength. PROMISC calibrates the model by calculating the values of empirical material constants. V.L.

A92-49777* National Aeronautics and Space Administration. Lewis Research Center, Cleveland, OH.

AN ENERGY ANALYSIS OF CRACK-INITIATION AND ARREST IN EPOXY

A. CHUDNOVSKY, A. KIM (Illinois, University, Chicago), and C. P. BOSNYAK (Dow Chemical Co., Freeport, TX) International Journal of Fracture (ISSN 0376-9429), vol. 55, no. 3, June 1, 1992, p. 209-222. Research supported by U.S. Navy. 1 Jun. 1992 14 p refs
(Contract NAG3-1034) Copyright

The objective of this work is to study fracture processes such as crack initiation and arrest in epoxy. A compact tension specimen with displacement-controlled loading is employed to observe multiple crack initiations and arrests. The energy release rate at crack initiation is significantly higher than that at crack arrest, as has been observed elsewhere. In this study, the difference between these energy release rates is found to depend on specimen size (scale effect), and is quantitatively related to the fracture surface morphology. The scale effect, similar to that in strength theory, is conventionally attributed to the statistics of defects which control the fracture process. Triangular shaped ripples, deltsoids, are formed on the fracture surface of the epoxy during the slow sub-critical crack growth, prior to the smooth mirrorlike surface characteristic of fast cracks. The deltsoids are complimentary on the two crack faces which excludes any inelastic deformation from consideration. The deltsoids are analogous to the ripples created on a river surface downstream from a small obstacle. However, in spite of the expectation based on this analogy and the observed scale effect, there are no 'defects' at the apex of the deltsoids detectable down to the 0.1 micron level. This suggests that the formation of deltsoids during the slow process of subcritical crack growth is an intrinsic feature of the fracture process itself, triggered by inhomogeneity of material on a submicron scale. This inhomogeneity may be related to a fluctuation in the cross-link density of the epoxy.

Author

A92-49784* National Aeronautics and Space Administration. Lewis Research Center, Cleveland, OH.

A STOCHASTIC DAMAGE MODEL FOR THE RUPTURE PREDICTION OF A MULTI-PHASE SOLID. I - PARAMETRIC STUDIES. II - STATISTICAL APPROACH

YUAN J. LUA, WING K. LIU, and TED BELYTSCHKO (Northwestern University, Evanston, IL) International Journal of Fracture (ISSN 0376-9429), vol. 55, no. 4, June 15, 1992, p. 321-361. 15 Jun. 1992 41 p refs

(Contract NAG3-822)

Copyright

A stochastic damage model for predicting the rupture of a brittle multiphase material is developed, based on the microcrack-macrocrack interaction. The model, which incorporates uncertainties in locations, orientations, and numbers of microcracks, characterizes damage by microcracking and fracture by macrocracking. A parametric study is carried out to investigate the change of the stress intensity at the macrocrack tip by the configuration of microcracks. The inherent statistical distribution of the fracture toughness arising from the intrinsic random nature of microcracks is explored using a statistical approach. For this purpose, a computer simulation model is introduced, which incorporates a statistical characterization of geometrical parameters of a random microcrack array. I.S.

A92-50511* National Aeronautics and Space Administration. Lewis Research Center, Cleveland, OH.

MINIMIZATION OF VIBRATION IN ELASTIC BEAMS WITH TIME-VARIANT BOUNDARY CONDITIONS

F. M. L. AMIROUCHE and MINGJUN XIE (Illinois, University, Chicago) Journal of Guidance, Control, and Dynamics (ISSN 0731-5090), vol. 15, no. 5, Sept.-Oct. 1992, p. 1265-1271. Oct. 1992 7 p refs
(Contract NAG3-1092) Copyright

This paper presents an innovative method for minimizing the vibration of structures with time-variant boundary conditions (supports). The elastic body is modeled in two ways: (1) the first model is a letter seven type beam with a movable mass not to exceed the lower tip; (2) the second model has an arm that is a hollow beam with an inside mass with adjustable position. The complete solutions to both problems are carried out where the body is undergoing large rotation. The quasi-static procedure is used for the time-variant boundary conditions. The method developed employs partial differential equations governing the motion of the beam, including the effects of rigid-body motion, time-variant boundary conditions, and calculus of variations. The analytical solution is developed using Laplace and Fourier transforms. Examples of elastic robotic arms are given to illustrate the effectiveness of the methods developed. Author

A92-50883* National Aeronautics and Space Administration. Lewis Research Center, Cleveland, OH.

BOUNDARY FORMULATIONS FOR SENSITIVITIES OF THREE-DIMENSIONAL STRESS INVARIANTS

K. GURU PRASAD and J. H. KANE (Clarkson University, Potsdam, NY) Computers and Structures (ISSN 0045-7949), vol. 43, no. 6, June 17, 1992, p. 1165-1174. 17 Jun. 1992 10 p refs
(Contract NAG3-1089; NSF DDM-89-96171) Copyright

The direct, singular, boundary element analysis (BEA) formulation has been shown to provide a basis for a computationally efficient and accurate shape structural design sensitivity analysis (DSA) approach for three-dimensional solid objects. Within the boundary element analysis context, the theoretical formulation for sensitivities of important stress-related quantities including principal and deviatoric stresses, von Mises, maximum shear, and other stress invariants are presented, both for the surface as well as the interior of a continuum structure. Numerical results are given to demonstrate the accuracy of this approach. Author

A92-51550* National Aeronautics and Space Administration. Lewis Research Center, Cleveland, OH.

DAMAGE AND FRACTURE IN COMPOSITE THIN SHELLS

LEVON MINNETYAN (Clarkson University, Potsdam, NY), CHRISTOS C. CHAMIS, and PAPPU L. N. MURTHY (NASA, Lewis Research Center, Cleveland, OH) IN: International SAMPE Technical Conference, 23rd, Kiamesha Lake, NY, Oct. 21-24, 1991, Proceedings 1991 15 p refs
(Contract NAG3-1101)

The effect of fiber fracture on the load carrying capability and structural behavior of a composite cylindrical shell under internal

pressure is investigated. An integrated computer code is utilized for the simulation of composite structural degradation under loading. Damage initiation, damage growth, fracture progression, and global structural fracture are included in the simulation. Results demonstrate the significance of local damage on the structural durability of pressurized composite cylindrical shells. Author

A92-52005* National Aeronautics and Space Administration. Lewis Research Center, Cleveland, OH.

MODELING OF THE FLEXURAL BEHAVIOR OF CERAMIC-MATRIX COMPOSITES

WEN-SHYONG KUO and TSU-WEI CHOU (Delaware, University, Newark) IN: Microcracking-induced damage in composites; Proceedings of the Symposium, ASME Winter Annual Meeting, Dallas, TX, Nov. 25-30, 1990 1990 5 p refs Copyright

This paper examines the effects of matrix cracking and fiber breakage on the flexural behavior of ceramic composite beams. A model has been proposed to represent the damage evolution of the beam, of which the matrix fracture strain is smaller than that of the fibers. Close form solutions of the critical loads for the initiation of matrix cracking and fiber breakage in the tension side of the beam have been found. The effects of thermal residual stresses and fiber/matrix debonding have been taken into account. The initial deviation of the load-deflection curve from linearity is due to matrix cracking, while fiber breakages are responsible for the drop in the load carrying capacity of the beam. The proportional limit as well as the nonlinear behavior of the beam deflection have been identified. The growth of the damaged zone has also been predicted. A three-point bending case is given as a numerical example. Author

A92-54921* National Aeronautics and Space Administration. Lewis Research Center, Cleveland, OH.

AEROELASTIC MODAL CHARACTERISTICS OF MISTUNED BLADE ASSEMBLIES - MODE LOCALIZATION AND LOSS OF EIGENSTRUCTURE

CHRISTOPHE PIERRE (Michigan, University, Ann Arbor) and DURBHA V. MURTHY (NASA, Lewis Research Center, Cleveland, OH) Oct. 1992 14 p refs (Contract NAG3-1163) Copyright

N92-11373*# National Aeronautics and Space Administration. Lewis Research Center, Cleveland, OH.

FIRST-PASSAGE PROBLEMS: A PROBABILISTIC DYNAMIC ANALYSIS FOR DEGRADED STRUCTURES

MICHAEL C. SHIAO (Sverdrup Technology, Inc., Brook Park, OH.) and CHRISTOS C. CHAMIS 1990 17 p Presented at the 2nd International Conference on Stochastic Structural Dynamics, Boca Raton, FL, 9-11 May 1990 (Contract RTOP 553-13-00) (NASA-TM-103755; E-6011; NAS 1.15:103755) Avail: CASI HC A03/MF A01

Structures subjected to random excitations with uncertain system parameters degraded by surrounding environments (a random time history) are studied. Methods are developed to determine the statistics of dynamic responses, such as the time-varying mean, the standard deviation, the autocorrelation functions, and the joint probability density function of any response and its derivative. Moreover, the first-passage problems with deterministic and stationary/evolutionary random barriers are evaluated. The time-varying (joint) mean crossing rate and the probability density function of the first-passage time for various random barriers are derived. Author

N92-12316*# National Aeronautics and Space Administration. Lewis Research Center, Cleveland, OH.

MODAL INTERACTION IN LINEAR DYNAMIC SYSTEMS NEAR DEGENERATE MODES

D. AFOLABI (Purdue Univ., Indianapolis, IN.) Nov. 1991 47 p (Contract NASA ORDER C-99066-G; RTOP 505-62-21)

(NASA-TM-105315; ICOMP-91-21; E-6668; NAS 1.15:105315) Avail: CASI HC A03/MF A01

In various problems in structural dynamics, the eigenvalues of a linear system depend on a characteristic parameter of the system. Under certain conditions, two eigenvalues of the system approach each other as the characteristic parameter is varied, leading to modal interaction. In a system with conservative coupling, the two eigenvalues eventually repel each other, leading to the curve veering effect. In a system with nonconservative coupling, the eigenvalues continue to attract each other, eventually colliding, leading to eigenvalue degeneracy. Modal interaction is studied in linear systems with conservative and nonconservative coupling using singularity theory, sometimes known as catastrophe theory. The main result is this: eigenvalue degeneracy is a cause of instability; in systems with conservative coupling, it induces only geometric instability, whereas in systems with nonconservative coupling, eigenvalue degeneracy induces both geometric and elastic instability. Illustrative examples of mechanical systems are given. Author

N92-14433*# National Aeronautics and Space Administration. Lewis Research Center, Cleveland, OH.

AN EVALUATION OF STRAIN MEASURING DEVICES FOR CERAMIC COMPOSITES

JOHN Z. GYEKENYESI (Cleveland State Univ., OH.) and PAUL A. BARTOLOTTA Nov. 1991 24 p (Contract RTOP 510-01-50) (NASA-TM-105337; E-6704; NAS 1.15:105337) Avail: CASI HC A03/MF A01

A series of tensile tests was conducted on SiC/reaction bonded silicon nitrides (RBSN) composites using different methods of strain measurement. The tests were used to find the optimum strain sensing device for use with continuous fiber reinforced ceramic matrix composites in ambient and high temperature environments. Bonded resistance gages were found to offer excellent performance for room temperature tests. The clip-on gage offers the same performance, but less time is required for mounting it to the specimen. Low contact force extensometers track the strain with acceptable results at high specimen temperatures. Silicon carbide rods with knife edges are preferred. The edges must be kept sharp. The strain measuring devices should be mounted on the flat side of the specimen. This is in contrast to mounting on the rough thickness side. Author

N92-14434*# National Aeronautics and Space Administration. Lewis Research Center, Cleveland, OH.

ON THE THERMODYNAMIC FRAMEWORK OF GENERALIZED COUPLED THERMOELASTIC-VISCOPLASTIC-DAMAGE MODELING

S. M. ARNOLD and A. F. SALEEB (Akron Univ., OH.) Nov. 1991 22 p (Contract RTOP 510-01-50) (NASA-TM-105349; E-6723; NAS 1.15:105349) Avail: CASI HC A03/MF A01

A complete potential based framework using internal state variables is put forth for the derivation of reversible and irreversible constitutive equations. In this framework, the existence of the total (integrated) form of either the (Helmholtz) free energy or the (Gibbs) complementary free energy are assumed a priori. Two options for describing the flow and evolutionary equations are described, wherein option one (the fully coupled form) is shown to be over restrictive while the second option (the decoupled form) provides significant flexibility. As a consequence of the decoupled form, a new operator, i.e., the Compliance operator, is defined which provides a link between the assumed Gibb's and complementary dissipation potential and ensures a number of desirable numerical features, for example the symmetry of the resulting consistent tangent stiffness matrix. An important conclusion reached, is that although many theories in the literature do not conform to the general potential framework outlined, it is still possible in some cases, by slight modifications of the used forms, to restore the complete potential structure. Author

39 STRUCTURAL MECHANICS

N92-15402*# National Aeronautics and Space Administration.
Lewis Research Center, Cleveland, OH.

ANALYSIS OF AIRCRAFT ENGINE BLADE SUBJECT TO ICE IMPACT

E. S. REDDY (Sverdrup Technology, Inc., Brook Park, OH.), G. H. ABUMERI (Sverdrup Technology, Inc., Brook Park, OH.), CHRISTOS C. CHAMIS, and P. L. N. MURTHY 1991 24 p
Presented at the Ninth Conference on Fibrous Composites in Structural Design, Lake Tahoe, NV, 4-7 Nov. 1991; cosponsored by DOD, NASA, and FAA
(Contract RTOP 505-68-1C)
(NASA-TM-105336; E-6703; NAS 1.15:105336) Avail: CASI HC A03/MF A01

The ice impact on the engine blade made of layered composite is simulated. The ice piece is modeled as an equivalent spherical object and has the velocity opposite to that of the aircraft with direction parallel to the engine axis. Near the impact region and along the leading edge, the blade is assumed to be fully stressed and undergoes large deflection. A specified portion of the blade around the impact region is modeled. The effect of ice size and velocity on the average leading edge strain are investigated for a modified SR-2 model unswept composite propfan blade. Parametric studies are performed to study the response due to ice impact at various locations along the span. Also, the effects of engine speed on the strain and impact displacements are discussed. It is found that for a given engine speed, a critical ice speed exists that corresponds to the maximum strain and this critical speed increases with increase in the engine speed. Author

N92-15403*# National Aeronautics and Space Administration.
Lewis Research Center, Cleveland, OH.

PROBABILISTIC PROGRESSIVE BUCKLING OF TRUSSES

SHANTARAM S. PAI and CHRISTOS C. CHAMIS 1991 16 p
Presented at the 32d Structures, Structural Dynamics, and Materials Conference, Baltimore, MD, 8-10 Apr. 1991; sponsored by AIAA, ASME, ASCE, AHS, and ASC
(Contract RTOP 553-13-00)
(NASA-TM-105162; E-6451; NAS 1.15:105162) Avail: CASI HC A03/MF A01

A three-bay, space, cantilever truss is probabilistically evaluated to describe progressive buckling and truss collapse in view of the numerous uncertainties associated with the structural, material, and load variables (primitive variables) that describe the truss. Initially, the truss is deterministically analyzed for member forces, and member(s) in which the axial force exceeds the Euler buckling load are identified. These member(s) are then discretized with several intermediate nodes and a probabilistic buckling analysis is performed on the truss to obtain its probabilistic buckling loads and respective mode shapes. Furthermore, sensitivities associated with the uncertainties in the primitive variables are investigated, margin of safety values for the truss are determined, and truss end node displacements are noted. These steps are repeated by sequentially removing the buckled member(s) until onset of truss collapse is reached. Results show that this procedure yields an optimum truss configuration for a given loading and for a specified reliability. Author

N92-15405*# National Aeronautics and Space Administration.
Lewis Research Center, Cleveland, OH.

SPACE STATION FREEDOM SOLAR DYNAMIC MODULES STRUCTURAL MODELLING AND ANALYSIS

CHARLES LAWRENCE and RON MORRIS (Sverdrup Technology, Inc., Brook Park, OH.) Dec. 1991 25 p
(Contract RTOP 505-63-1B)
(NASA-TM-104506; E-6367; NAS 1.15:104506) Avail: CASI HC A03/MF A01

In support of the Space Station Freedom (SSF) Solar Dynamic Power Module effort, structural design studies were performed to investigate issues related to the design of the power module, its pointing capabilities, and the integration of the module into the SSF infrastructure. Of particular concern from a structural viewpoint are the dynamics of the power module, the impact of the power module on the Space Station dynamics and controls, and the

required control effort for obtaining the specified Solar Dynamic Power Module pointing accuracy. Structural analyses were performed to determine the structural dynamics attributes of both the existing and the proposed structural dynamics module designs. The objectives of these analyses were to generate validated Solar Dynamic Power Module NASTRAN finite element models, combine Space Station and power module models into integrated system models, perform finite element modal analyses to assess the effect of the relocations of the power module center of mass, and provide modal data to controls designers for control systems design. Author

N92-15406*# National Aeronautics and Space Administration.
Lewis Research Center, Cleveland, OH.

STRUCTURAL DYNAMICS BRANCH RESEARCH AND ACCOMPLISHMENTS FOR FY 1990

Nov. 1991 43 p
(Contract RTOP 505-63-5B)
(NASA-TM-103747; E-5993; NAS 1.15:103747) Avail: CASI HC A03/MF A01

Presented here is a collection of FY 1990 research highlights from the Structural Dynamics Branch at the NASA Lewis Research Center. Highlights are from the branch's major work areas: aeroelasticity, vibration control, dynamic systems, and computational structural methods. A listing is given of FY 1990 branch publications. Author

N92-16371*# National Aeronautics and Space Administration.
Lewis Research Center, Cleveland, OH.

DIFFERENTIAL CONTINUUM DAMAGE MECHANICS MODELS FOR CREEP AND FATIGUE OF UNIDIRECTIONAL METAL MATRIX COMPOSITES

S. M. ARNOLD and S. KRUCH (Office National d'Etudes et de Recherches Aérospatiales, Paris, France) Nov. 1991 54 p
(Contract RTOP 510-01-50)
(NASA-TM-105213; E-6629; NAS 1.15:105213) Avail: CASI HC A04/MF A01

Three multiaxial isothermal continuum damage mechanics models for creep, fatigue, and creep/fatigue interaction of a unidirectional metal matrix composite volume element are presented, only one of which will be discussed in depth. Each model is phenomenological and stress based, with varying degrees of complexity to accurately predict the initiation and propagation of intergranular and transgranular defects over a wide range of loading conditions. The development of these models is founded on the definition of an initially transversely isotropic fatigue limit surface, static fracture surface, normalized stress amplitude function and isochronous creep damage failure surface, from which both fatigue and creep damage evolutionary laws can be obtained. The anisotropy of each model is defined through physically meaningful invariants reflecting the local stress and material orientation. All three transversely isotropic models have been shown, when taken to their isotropic limit, to directly simplify to previously developed and validated creep and fatigue continuum damage theories. Results of a nondimensional parametric study illustrate (1) the flexibility of the present formulation when attempting to characterize a large class of composite materials, and (2) its ability to predict anticipated qualitative trends in the fatigue behavior of unidirectional metal matrix composites. Additionally, the potential for the inclusion of various micromechanical effects (e.g., fiber/matrix bond strength, fiber volume fraction, etc.), into the phenomenological anisotropic parameters is noted, as well as a detailed discussion regarding the necessary exploratory and characterization experiments needed to utilize the featured damage theories. Author

N92-19779*# National Aeronautics and Space Administration.
Lewis Research Center, Cleveland, OH.

COMGEN-BEM: BOUNDARY ELEMENT MODEL GENERATION FOR COMPOSITE MATERIALS MICROMECHANICAL ANALYSIS

ROBERT K. GOLDBERG Mar. 1992 22 p

(Contract RTOP 510-01-50)
(NASA-TM-105548; E-6871; NAS 1.15:105548) Avail: CASI HC
A03/MF A01

Composite Model Generation-Boundary Element Method (COMGEN-BEM) is a program developed in PATRAN command language (PCL) which generates boundary element models of continuous fiber composites at the micromechanical (constituent) scale. Based on the entry of a few simple parameters such as fiber volume fraction and fiber diameter, the model geometry and boundary element model are generated. In addition, various mesh densities, material properties, fiber orientation angles, loads, and boundary conditions can be specified. The generated model can then be translated to a format consistent with a boundary element analysis code such as BEST-CMS.

Author

N92-20045*# National Aeronautics and Space Administration.
Lewis Research Center, Cleveland, OH.

COLLAPSE ANALYSIS OF A WAFFLE PLATE STRONGBACK FOR SPACE STATION FREEDOM

FRANK F. MONASA (Michigan Technological Univ., Houghton.)
and JOSEPH M. ROCHE Mar. 1992 36 p

(Contract RTOP 474-46-10)
(NASA-TM-105412; E-6817; NAS 1.15:105412) Avail: CASI HC
A03/MF A01

The structural integrity was studied of the Integrated Equipment Assembly (IEA) Strongback of the SSF for the launch environment. The strongback structure supports the electrical power system for SSF. To achieve minimum launch mass, it is essential that flight structures are designed as light as possible. A nonlinear structural analysis was conducted to determine the collapse load of the structure and the associated factor of safety against the service loads. A modeling technique is provided for simulating the load conditions and the buckling and post buckling (collapse) load is evaluated of the IEA Strongback structure, using the finite element computer code MARC. Two of four strongback panels were modeled and analyzed. The effects were examined of the following factors on the global behavior of the strongback panels: (1) load simplification and simulation; (2) type of support boundary conditions; and (3) the possibility of weight reduction of the original structure. For this purpose, several models of the two panels of the strongback were considered. The stress level and distribution in the panels for launch condition, the Eigenvalue critical buckling load and/or the collapse load were determined.

Author

N92-20212*# National Aeronautics and Space Administration.
Lewis Research Center, Cleveland, OH.

EXPLICIT ROBUST SCHEMES FOR IMPLEMENTATION OF A CLASS OF PRINCIPAL VALUE-BASED CONSTITUTIVE MODELS: THEORETICAL DEVELOPMENT

A. F. SALEEB (Akron Univ., OH.) and S. M. ARNOLD Nov. 1991 21 p

(Contract RTOP 510-01-50)
(NASA-TM-105345; E-6714; NAS 1.15:105345) Avail: CASI HC
A03/MF A01

The issue of developing effective and robust schemes to implement a class of the Ogden-type hyperelastic constitutive models is addressed. To this end, explicit forms for the corresponding material tangent stiffness tensors are developed, and these are valid for the entire deformation range; i.e., with both distinct as well as repeated principal-stretch values. Throughout the analysis the various implications of the underlying property of separability of the strain-energy functions are exploited, thus leading to compact final forms of the tensor expressions. In particular, this facilitated the treatment of complex cases of uncoupled volumetric/deviatoric formulations for incompressible materials. The forms derived are also amenable for use with symbolic-manipulation packages for systematic code generation.

Author

N92-22227*# National Aeronautics and Space Administration.
Lewis Research Center, Cleveland, OH.

IMPROVED ACCURACY FOR FINITE ELEMENT STRUCTURAL ANALYSIS VIA A NEW INTEGRATED FORCE METHOD

SURYA N. PATNAIK (Ohio Aerospace Inst., Brook Park.), DALE A. HOPKINS, ROBERT A. AIELLO, and LASZLO BERKE Apr. 1992 28 p

(Contract RTOP 505-63-5B)
(NASA-TP-3204; E-5638; NAS 1.60:3204) Avail: CASI HC
A03/MF A01

A comparative study was carried out to determine the accuracy of finite element analyses based on the stiffness method, a mixed method, and the new integrated force and dual integrated force methods. The numerical results were obtained with the following software: MSC/NASTRAN and ASKA for the stiffness method; an MHOST implementation method for the mixed method; and GIFT for the integrated force methods. The results indicate that on an overall basis, the stiffness and mixed methods present some limitations. The stiffness method generally requires a large number of elements in the model to achieve acceptable accuracy. The MHOST method tends to achieve a higher degree of accuracy for coarse models than does the stiffness method implemented by MSC/NASTRAN and ASKA. The two integrated force methods, which bestow simultaneous emphasis on stress equilibrium and strain compatibility, yield accurate solutions with fewer elements in a model. The full potential of these new integrated force methods remains largely unexploited, and they hold the promise of spawning new finite element structural analysis tools.

Author

N92-22267*# National Aeronautics and Space Administration.
Lewis Research Center, Cleveland, OH.

PROBABILISTIC STRUCTURAL ANALYSIS OF ADAPTIVE/SMART/INTELLIGENT SPACE STRUCTURES

SHANTARAM S. PAI and CHRISTOS C. CHAMIS 1991 20 p

(Contract RTOP 533-13-00)
(NASA-TM-105408; E-6637; NAS 1.15:105408) Avail: CASI HC
A03/MF A01

A three-bay, space, cantilever truss is probabilistically evaluated for adaptive/smart/intelligent behavior. For each behavior, the scatter (ranges) in buckling loads, vibration frequencies, and member axial forces are probabilistically determined. Sensitivities associated with uncertainties in the structure, material and load variables that describe the truss are determined for different probabilities. The relative magnitude for these sensitivities are used to identify significant truss variables that control/classify its behavior to respond as an adaptive/smart/intelligent structure. Results show that the probabilistic buckling loads and vibration frequencies increase for each truss classification, with a substantial increase for intelligent trusses. Similarly, the probabilistic member axial forces reduce for adaptive and intelligent trusses and increase for smart trusses.

Author

N92-22514*# National Aeronautics and Space Administration.
Lewis Research Center, Cleveland, OH.

CREEP AND FATIGUE RESEARCH EFFORTS ON ADVANCED MATERIALS

JOHN GAYDA *In its* Aeropropulsion 1987 p 55-63 Feb. 1990
Avail: CASI HC A02/MF A04

Two of the more important materials problems encountered in turbine blades of aircraft engines are creep and fatigue. To withstand these high-temperature phenomena, modern engines utilize single-crystal, nickel-base superalloys as the material of choice in critical applications. This paper will present recent research activities at NASA's Lewis Research Center on single-crystal blading material, related to creep and fatigue. The goal of these research efforts is to improve the understanding of microstructure-property relationships and thereby guide material development.

D.R.D.

N92-23191*# National Aeronautics and Space Administration.
Lewis Research Center, Cleveland, OH.

AEROELASTIC STABILITY ANALYSES OF TWO COUNTER ROTATING PROPFAN DESIGNS FOR A CRUISE MISSILE MODEL

APARAJIT J. MAHAJAN (Toledo Univ., OH.), JOHN M. LUCERO, ORAL MEHMED, and GEORGE L. STEFKO Apr. 1992 13 p

39 STRUCTURAL MECHANICS

(Contract RTOP 535-03-0B)
(NASA-TM-105268; E-7001; NAS 1.15:105268) Avail: CASI HC
A03/MF A01

Aeroelastic stability analyses were performed to insure structural integrity of two counterrotating propfan blade designs for a NAVY/Air Force/NASA cruise missile model wind tunnel test. This analysis predicted if the propfan designs would be flutter free at the operating conditions of the wind tunnel test. Calculated stability results are presented for the two blade designs with rotational speed and Mach number as the parameters. A aeroelastic analysis code ASTROP2 (Aeroelastic Stability and Response of Propulsion Systems - 2 Dimensional Analysis), developed at LeRC, was used in this project. The aeroelastic analysis is a modal method and uses the combination of a finite element structural model and two dimensional steady and unsteady cascade aerodynamic models. This code was developed to analyze single rotation propfans but was modified and applied to counterrotating propfans for the present work. Modifications were made to transform the geometry and rotation of the aft rotor to the same reference frame as the forward rotor, to input a non-uniform inflow into the rotor being analyzed, and to automatically converge to the least stable aeroelastic mode. Author

N92-23196* # National Aeronautics and Space Administration.
Lewis Research Center, Cleveland, OH.

EVALUATION OF MHOST ANALYSIS CAPABILITIES FOR A PLATE ELEMENT

HO-JUN LEE (Sverdrup Technology, Inc., Saint Louis, MO.), GALIB H. ABUMERI, and HELEN C. BROWN (Sverdrup Technology, Inc., Brook Park, OH.) Feb. 1992 23 p
(Contract RTOP 510-10-50)
(NASA-TM-105387; E-6773; NAS 1.15:105387) Avail: CASI HC
A03/MF A01

Results of the evaluation of the static, buckling, and free vibration analyses capabilities of MHOST for the plate elements are presented. Two large scale, general purpose finite element codes (MARC and MSC/NASTRAN) are used to validate MHOST. Comparisons of MHOST results with those from MARC and MSC/NASTRAN show good agreement and indicate that MHOST can be used with confidence to perform the aforementioned analyses using the plate element. Author

N92-23267* # National Aeronautics and Space Administration.
Lewis Research Center, Cleveland, OH.

COUPLED MULTI-DISCIPLINARY SIMULATION OF COMPOSITE ENGINE STRUCTURES IN PROPULSION ENVIRONMENT

CHRISTOS C. CHAMIS and SURENDRA N. SINGHAL (Sverdrup Technology, Inc., Brook Park, OH.) 1992 24 p Proposed for presentation at the International Gas Turbine and Aeroengine Congress and Exposition, Cologne, Fed. Republic of Germany, 1-4 Jun. 1991
(Contract NAS3-25266; RTOP 505-63-53)
(NASA-TM-105575; E-6901; NAS 1.15:105575) Avail: CASI HC
A03/MF A01

A computational simulation procedure is described for the coupled response of multi-layered multi-material composite engine structural components which are subjected to simultaneous multi-disciplinary thermal, structural, vibration, and acoustic loadings including the effect of hostile environments. The simulation is based on a three dimensional finite element analysis technique in conjunction with structural mechanics codes and with acoustic analysis methods. The composite material behavior is assessed at the various composite scales, i.e., the laminate/ply/constituents (fiber/matrix), via a nonlinear material characterization model. Sample cases exhibiting nonlinear geometrical, material, loading, and environmental behavior of aircraft engine fan blades, are presented. Results for deformed shape, vibration frequency, mode shapes, and acoustic noise emitted from the fan blade, are discussed for their coupled effect in hot and humid environments. Results such as acoustic noise for coupled composite-mechanics/heat transfer/structural/vibration/acoustic analyses

demonstrate the effectiveness of coupled multi-disciplinary computational simulation and the various advantages of composite materials compared to metals. Author

N92-23527* # National Aeronautics and Space Administration.
Lewis Research Center, Cleveland, OH.

SINGULARITIES IN OPTIMAL STRUCTURAL DESIGN

S. N. PATNAIK, J. D. GUPTILL, and L. BERKE Mar. 1992
12 p

(Contract RTOP 307-50-00)
(NASA-TM-4365; E-6686; NAS 1.15:4365) Avail: CASI HC
A03/MF A01

Singularity conditions that arise during structural optimization can seriously degrade the performance of the optimizer. The singularities are intrinsic to the formulation of the structural optimization problem and are not associated with the method of analysis. Certain conditions that give rise to singularities have been identified in earlier papers, encompassing the entire structure. Further examination revealed more complex sets of conditions in which singularities occur. Some of these singularities are local in nature, being associated with only a segment of the structure. Moreover, the likelihood that one of these local singularities may arise during an optimization procedure can be much greater than that of the global singularity identified earlier. Examples are provided of these additional forms of singularities. A framework is also given in which these singularities can be recognized. In particular, the singularities can be identified by examination of the stress displacement relations along with the compatibility conditions and/or the displacement stress relations derived in the integrated force method of structural analysis. Author

N92-24985* # National Aeronautics and Space Administration.
Lewis Research Center, Cleveland, OH.

DAMAGE MECHANISMS IN BITHERMAL AND THERMOMECHANICAL FATIGUE OF HAYNES 188

SREERAMESH KALLURI (Sverdrup Technology, Inc., Brook Park, OH.) and GARY R. HALFORD 1992 19 p Presented at the Symposium on Thermo-Mechanical Fatigue Behavior of Materials, San Diego, CA, 16 Oct. 1991; sponsored in part by American Society for Testing and Materials
(Contract RTOP 553-13-00)
(NASA-TM-105381; E-6768; NAS 1.15:105381) Avail: CASI HC
A03/MF A01

Post failure fractographic and metallographic studies were conducted on Haynes 188 specimens fatigued under bithermal and thermomechanical loading conditions between 316 and 760 C. Bithermal fatigue specimens examined included those tested under high strain rate in-phase and out-phase, tensile creep in-phase, and compressive creep out-of-phase loading conditions. Specimens tested under in-phase and out-of-phase thermomechanical fatigue were also examined. The nature of failure mode (transgranular versus intergranular), the topography of the fracture surface, and the roles of oxidation and metallurgical changes were studied for each type of bithermal and thermomechanical test. Author

N92-25179* # National Aeronautics and Space Administration.
Lewis Research Center, Cleveland, OH.

THERMOMECHANICAL DEFORMATION BEHAVIOR OF A DYNAMIC STRAIN AGING ALLOY, HASTELLOY X

MICHAEL G. CASTELLI (Sverdrup Technology, Inc., Brook Park, OH.), ROBERT V. MINER, and DAVID N. ROBINSON (Akron Univ., OH.) Apr. 1992 27 p Presented at the Symposium on Thermomechanical Fatigue Behavior of Materials, San Diego, CA, 16 Oct. 1991; sponsored by the American Society for Testing and Materials
(Contract NAS3-25266; RTOP 505-63-40)
(NASA-TM-105316; E-6899; NAS 1.15:105316) Avail: CASI HC
A03/MF A01

An experimental study was performed to identify the effects of dynamic strain aging (solute drag) and metallurgical instabilities under thermomechanical loading conditions. The study involved a series of closely controlled thermomechanical deformation tests

on the solid-solution-strengthened nickel-base superalloy, Hastelloy X. This alloy exhibits a strong isothermal strain aging peak at approximately 600 C, promoted by the effects of solute drag and precipitation hardening. Macroscopic thermomechanical hardening trends are correlated with microstructural characteristics through the use of transmission electron microscopy. These observations are compared and contrasted with isothermal conditions. Thermomechanical behavior unique to the isothermal database is identified and discussed. The microstructural characteristics are shown to be dominated by effects associated with the highest temperature of the thermomechanical cycle. Results indicate that the deformation behavior of Hastelloy X is thermomechanically path dependent. In addition, guidance is given pertaining to deformation modeling in the context of macroscopic unified theory. An internal state variable is formulated to qualitatively reflect the isotropic hardening trends identified in the TMD experiments.

Author

N92-25446*# National Aeronautics and Space Administration, Lewis Research Center, Cleveland, OH.

STRUCTURAL OPTIMIZATION OF LARGE STRUCTURAL SYSTEMS BY OPTIMALITY CRITERIA METHODS

LASZLO BERKE 1992 23 p Presented at the Lecture Series on Shape and Layout Optimization of Structural Systems, Udine, Italy, 16-20 Jul. 1990

(Contract RTOP 307-50-00)

(NASA-TM-105423; E-5506; NAS 1.15:105423) Avail: CASI HC A03/MF A01

The fundamental concepts of the optimality criteria method of structural optimization are presented. The effect of the separability properties of the objective and constraint functions on the optimality criteria expressions is emphasized. The single constraint case is treated first, followed by the multiple constraint case with a more complex evaluation of the Lagrange multipliers. Examples illustrate the efficiency of the method.

Author

N92-25753*# National Aeronautics and Space Administration, Lewis Research Center, Cleveland, OH.

STRUCTURAL ANALYSIS OF LOW-SPEED COMPOSITE PROPFAN BLADES FOR THE LRCSW WIND TUNNEL MODEL

MICHAEL A. ERNST Jan. 1992 27 p Original contains color illustrations

(Contract RTOP 535-03-0B)

(NASA-TM-105266; E-6291; NAS 1.15:105266) Avail: CASI HC A03/MF A01; 1 functional color page

The Naval Weapons Center at China Lake, CA, is currently in the process of evaluating propulsion systems for the Long Range Conventional Standoff Weapons (LRCSW). At present, the Advanced Counter-Rotating Propfan system is being considered. The methodologies are documented which were used to structurally analyze the 0.55 scale CM1 composite propfan blades for the LRCSW with COBSTRAN and MSC/NASTRAN. Significant results are also reported.

Author

N92-25915*# National Aeronautics and Space Administration, Lewis Research Center, Cleveland, OH.

A BRIEF OVERVIEW OF COMPUTATIONAL STRUCTURES TECHNOLOGY RELATED ACTIVITIES AT NASA LEWIS RESEARCH CENTER

DALE A. HOPKINS In NASA, Langley Research Center, Computational Structures Technology for Airframes and Propulsion Systems p 81-89 May 1992

Avail: CASI HC A02/MF A04

The presentation gives a partial overview of research and development underway in the Structures Division of LeRC, which collectively is referred to as the Computational Structures Technology Program. The activities in the program are diverse and encompass four major categories: (1) composite materials and structures; (2) probabilistic analysis and reliability; (3) design optimization and expert systems; and (4) computational methods and simulation. The approach of the program is comprehensive and entails exploration of fundamental theories of structural mechanics to accurately represent the complex physics governing

engine structural performance, formulation, and implementation of computational techniques and integrated simulation strategies to provide accurate and efficient solutions of the governing theoretical models by exploiting the emerging advances in computer technology, and validation and verification through numerical and experimental tests to establish confidence and define the qualities and limitations of the resulting theoretical models and computational solutions. The program comprises both in-house and sponsored research activities. The remainder of the presentation provides a sample of activities to illustrate the breadth and depth of the program and to demonstrate the accomplishments and benefits that have resulted.

Author

N92-28701*# National Aeronautics and Space Administration, Lewis Research Center, Cleveland, OH.

ELEVATED TEMPERATURE AXIAL AND TORSIONAL FATIGUE BEHAVIOR OF HAYNES 188

PETER J. BONACUSE (Army Aviation Systems Command, Cleveland, OH.) and SREERAMESH KALLURI (Sverdrup Technology, Inc., Brook Park, OH.) Jun. 1992 23 p (Contract RTOP 553-13-00)

(NASA-TM-105396; E-6788; NAS 1.15:105396;

AVSCOM-TR-91-C-045) Avail: CASI HC A03/MF A01

The results of high-temperature axial and torsional low-cycle fatigue experiments performed on Haynes 188, a wrought cobalt-base superalloy, are reported. Fatigue tests were performed at 760 C in air on thin-walled tubular specimens at various ranges under strain control. Data are also presented for coefficient of thermal expansion, elastic modulus, and shear modulus at various temperatures from room to 1000 C, and monotonic and cyclic stress-strain curves in tension and in shear at 760 C. The data set is used to evaluate several multiaxial fatigue life models (most were originally developed for room temperature multiaxial life prediction) including von Mises equivalent strain range (ASME boiler and pressure vessel code), Manson-Halford, Modified Multiaxiality Factor (proposed here), Modified Smith-Watson-Topper, and Fatemi-Socie-Kurath. At von Mises equivalent strain ranges (the torsional strain range divided by the square root of 3, taking the Poisson's ratio to be 0.5), torsionally strained specimens lasted, on average, factors of 2 to 3 times longer than axially strained specimens. The Modified Multiaxiality Factor approach shows promise as a useful method of estimating torsional fatigue life from axial fatigue data at high temperatures. Several difficulties arose with the specimen geometry and extensometry used in these experiments. Cracking at extensometer probe indentations was a problem at smaller strain ranges. Also, as the largest axial and torsional strain range fatigue tests neared completion, a small amount of specimen buckling was observed.

Author

N92-29342*# National Aeronautics and Space Administration, Lewis Research Center, Cleveland, OH.

STRUCTURAL DURABILITY OF STIFFENED COMPOSITE SHELLS

LEVON MINNETYAN (Clarkson Univ., Potsdam, NY.), JAMES M. RIVERS (Clarkson Univ., Potsdam, NY.), PAPPU L. N. MURTHY, and CHRISTOS C. CHAMIS 1992 33 p Presented at the 33rd Structures, Structural Dynamics and Materials Conference, Dallas, TX, 13-15 Apr. 1992; sponsored in part by AIAA, ASME, ASCE, AHS, and ASC

(Contract NAG3-1101)

(NASA-CR-190588; NAS 1.26:190588) Avail: CASI HC A03/MF A01

The durability of a stiffened composite cylindrical shell panel is investigated under several loading conditions. An integrated computer code is utilized for the simulation of load induced structural degradation. Damage initiation, growth, and accumulation up to the stage of propagation to fracture are included in the computational simulation. Results indicate significant differences in the degradation paths for different loading cases. The effects of combined loading on structural durability and ultimate structural strength of a stiffened shell are assessed.

Author

N92-31505*# National Aeronautics and Space Administration. Lewis Research Center, Cleveland, OH.

A DIFFERENTIAL CDM MODEL FOR FATIGUE OF UNIDIRECTIONAL METAL MATRIX COMPOSITES

S. M. ARNOLD and S. KRUCH (Office National d'Etudes et de Recherches Aérospatiales, Paris, France) 1992 22 p Proposed for presentation at the ASME, Anaheim, CA, 8-13 Nov. 1992 (Contract RTOP 510-01-50)

(NASA-TM-105726; E-7128; NAS 1.15:105726) Avail: CASI HC A03/MF A01

A multiaxial, isothermal, continuum damage mechanics (CDM) model for fatigue of a unidirectional metal matrix composite volume element is presented. The model is phenomenological, stress based, and assumes a single scalar internal damage variable, the evolution of which is anisotropic. The development of the fatigue damage model, (i.e., evolutionary law) is based on the definition of an initially transversely isotropic fatigue limit surface, a static fracture surface, and a normalized stress amplitude function. The anisotropy of these surfaces and function, and therefore the model, is defined through physically meaningful invariants reflecting the local stress and material orientation. This transversely isotropic model is shown, when taken to its isotropic limit, to directly simplify to a previously developed and validated isotropic fatigue continuum damage model. Results of a nondimensional parametric study illustrate (1) the flexibility of the present formulation in attempting to characterize a class of composite materials, and (2) the capability of the formulation in predicting anticipated qualitative trends in the fatigue behavior of unidirectional metal matrix composites. Also, specific material parameters representing an initial characterization of the composite system SiC/Ti 15-3 and the matrix material (Ti 15-3) are reported. Author

N92-33476*# National Aeronautics and Space Administration. Lewis Research Center, Cleveland, OH.

INFLUENCE OF MASS MOMENT OF INERTIA ON NORMAL MODES OF PRELOADED SOLAR ARRAY MAST

SASAN C. ARMAND and PAUL LIN (Cleveland State Univ., OH.) Aug. 1992 12 p (Contract RTOP 474-46-10)

(NASA-TP-3273; E-6847; NAS 1.60:3273) Avail: CASI HC A03/MF A01

Earth-orbiting spacecraft often contain solar arrays or antennas supported by a preloaded mast. Because of weight and cost considerations, the structures supporting the spacecraft appendages are extremely light and flexible; therefore, it is vital to investigate the influence of all physical and structural parameters that may influence the dynamic behavior of the overall structure. The study primarily focuses on the mast for the space station solar arrays, but the formulations and the techniques developed in this study apply to any large and flexible mast in zero gravity. Furthermore, to determine the influence on the circular frequencies, the mass moment of inertia of the mast was incorporated into the governing equation of motion for bending. A finite element technique (MSC/NASTRAN) was used to verify the formulation. Results indicate that when the mast is relatively flexible and long, the mass moment inertia influences the circular frequencies. Author

N92-33935*# National Aeronautics and Space Administration. Lewis Research Center, Cleveland, OH.

PROBABILISTIC ASSESSMENT OF SPACE TRUSSES SUBJECTED TO COMBINED MECHANICAL AND THERMAL LOADS

SHANTARAM S. PAI and CHRISTOS C. CHAMIS 1992 10 p Presented at the 33rd Structures, Structural Dynamics and Materials Conference, Dallas TX, 13-15 Apr. 1992; cosponsored by AIAA, ASME, ASCE, AHS, and ASC Previously announced in IAA as A92-34325

(Contract RTOP 553-13-00) (NASA-TM-105429; E-6845; NAS 1.15:105429; AIAA PAPER 92-2352) Avail: CASI HC A02/MF A01

A three-bay, space, cantilever truss is probabilistically evaluated to quantify the range of uncertainties of buckling loads and member

forces due to nonuniform thermal loads, applied loads and moments (mechanical loads), and combination of both. The truss members are assumed to be made from Aluminum tubes or high modulus graphite-fiber/intermediate modulus epoxy-matrix composite tubes. Cumulative distribution function results show that certain combinations of thermal loads with mechanical loads reduce the probabilistic buckling loads and increase the magnitude of the member axial forces for the aluminum truss. The same trend is observed for the composite truss as well, as however, the thermal effects on the probabilistic buckling loads and member axial forces are not as substantial as that for an aluminum truss. This can be attributed to the large differences in the values of coefficient of thermal expansion. Finally, the sensitivities associated with the uncertainties in the structural, material, and load variables (primitive variables) are investigated. They show that buckling loads and member axial forces are most sensitive to the uncertainties in spatial (geometry) variables. Author

N92-34112*# National Aeronautics and Space Administration. Lewis Research Center, Cleveland, OH.

APPLICATION OF COMPUTATIONAL FLUID DYNAMICS TO THE STUDY OF VORTEX FLOW CONTROL FOR THE MANAGEMENT OF INLET DISTORTION

BERNHARD H. ANDERSON and JAMES GIBB (Defence Research Agency, Bedford, England) Jul. 1992 12 p Presented at the 28th Joint Propulsion Conference and Exhibit, Nashville, TN, 6-8 Jul. 1992; sponsored by AIAA, SAE, ASME, and ASEE (Contract RTOP 505-62-52)

(NASA-TM-105672; E-7039; NAS 1.15:105672; AIAA PAPER 92-3177) Copyright Avail: CASI HC A03/MF A01

The present study demonstrates that the Reduced Navier-Stokes code RNS3D can be used very effectively to develop a vortex generator installation for the purpose of minimizing the engine face circumferential distortion by controlling the development of secondary flow. The computing times required are small enough that studies such as this are feasible within an analysis-design environment with all its constraints of time and costs. This research study also established the nature of the performance improvements that can be realized with vortex flow control, and suggests a set of aerodynamic properties (called observations) that can be used to arrive at a successful vortex generator installation design. The ultimate aim of this research is to manage inlet distortion by controlling secondary flow through an arrangements of vortex generators configurations tailored to the specific aerodynamic characteristics of the inlet duct. This study also indicated that scaling between flight and typical wind tunnel test conditions is possible only within a very narrow range of generator configurations close to an optimum installation. This paper also suggests a possible law that can be used to scale generator blade height for experimental testing, but further research in this area is needed before it can be effectively applied to practical problems. Lastly, this study indicated that vortex generator installation design for inlet ducts is more complex than simply satisfying the requirement of attached flow, it must satisfy the requirement of minimum engine face distortion. Author

N92-34221*# National Aeronautics and Space Administration. Lewis Research Center, Cleveland, OH.

MODAL TEST/ANALYSIS CORRELATION OF SPACE STATION STRUCTURES USING NONLINEAR SENSITIVITY

VINEY K. GUPTA (Rockwell International Corp., Canoga Park, CA.), JAMES F. NEWELL (Rockwell International Corp., Canoga Park, CA.), LASZLO BERKE, and SASAN ARMAND Sep. 1992 10 p Presented at the Fourth Symposium on Multidisciplinary Analysis and Optimization, Cleveland, OH, 21-23 Sep. 1992; sponsored by AIAA/USAF, NASA, and OAI (Contract RTOP 474-46-10)

(NASA-TM-105850; E-7297; NAS 1.15:105850) Copyright Avail: CASI HC A02/MF A01

The modal correlation problem is formulated as a constrained optimization problem for validation of finite element models (FEM's). For large-scale structural applications, a pragmatic procedure for substructuring, model verification, and system integration is

described to achieve effective modal correlation. The space station substructure FEM's are reduced using Lanczos vectors and integrated into a system FEM using Craig-Bampton component modal synthesis. The optimization code is interfaced with MSC/NASTRAN to solve the problem of modal test/analysis correlation; that is, the problem of validating FEM's for launch and on-orbit coupled loads analysis against experimentally observed frequencies and mode shapes. An iterative perturbation algorithm is derived and implemented to update nonlinear sensitivity (derivatives of eigenvalues and eigenvectors) during optimizer iterations, which reduced the number of finite element analyses.

Author

44

ENERGY PRODUCTION AND CONVERSION

Includes specific energy conversion systems, e.g., fuel cells; global sources of energy; geophysical conversion; and windpower.

A92-17769* National Aeronautics and Space Administration, Lewis Research Center, Cleveland, OH.

MATERIAL PROCESSING WITH HYDROGEN AND CARBON MONOXIDE ON MARS

ALOYSIUS F. HEPP, DIANE L. LINNE (NASA, Lewis Research Center, Cleveland, OH), and GEOFFREY A. LANDIS (NASA, Lewis Research Center; Sverdrup Technology, Inc., Cleveland, OH) IN: Space manufacturing 8 - Energy and materials from space; Proceedings of the 10th Princeton/AIAA/SSI Conference, Princeton, NJ, May 15-18, 1991 1991 9 p refs

Copyright

Several novel proposals are examined for propellant production from carbon dioxide and monoxide and hydrogen. Potential uses were also examined of CO as a fuel or as a reducing agent in metal oxide processing as obtained or further reduced to carbon. Hydrogen can be reacted with CO to produce a wide variety of hydrocarbons, alcohols, and other organic compounds. Methanol, produced by Fischer-Tropsch chemistry may be useful as a fuel; it is easy to store and handle because it is a liquid at Mars temperatures. The reduction of CO₂ to hydrocarbons such as methane or acetylene can be accomplished with hydrocarbons. Carbon monoxide and hydrogen require cryogenic temperatures for storage as liquid. Noncryogenic storage of hydrogen may be accomplished using hydrocarbons, inorganic hydrides, or metal hydrides. Noncryogenic storage of CO may be accomplished in the form of iron carbonyl (Fe(CO)₅) or other metal carbonyls. Low hydrogen content fuels such as acetylene (C₂H₂) may be effective propellants with low requirements for earth derived resources. The impact on manned Mars missions of alternative propellant production and utilization is discussed.

Author

A92-18936* National Aeronautics and Space Administration, Lewis Research Center, Cleveland, OH.

SPACE ELECTROCHEMICAL RESEARCH AND TECHNOLOGY CONFERENCE, 3RD, NASA LEWIS RESEARCH CENTER, CLEVELAND, OH, APR. 9, 10, 1991, PROCEEDINGS

MARVIN WARSHAY, ED. (NASA, Lewis Research Center, Cleveland, OH) Conference supported by NASA. Journal of Power Sources (ISSN 0378-7753), vol. 36, Dec. 1, 1991, 202 p. Previously announced in STAR as N91-32549; No individual items are abstracted in this volume. 1 Dec. 1991 202 p

Copyright

The proceedings of NASA's third Space Electrochemical Research and Technology (SERT) conference are presented. The objective of the conference was to assess the present status and general thrust of research and development in those areas of electrochemical technology required to enable NASA missions in the next century. The conference provided a forum for the exchange of ideas and opinions of those actively involved in the field, in order to define new opportunities for the application of

electrochemical processes in future NASA missions. Papers were presented in three technical areas: the electrochemical interface, the next generation in aerospace batteries and fuel cells, and electrochemistry for nonenergy storage applications.

Author

A92-20366 Sverdrup Technology, Inc., Brook Park, OH.

PHOTOVOLTAIC POWER OPTIONS FOR MARS

GEOFFREY A. LANDIS (Sverdrup Technology, Inc., Brookpark, OH) and JOSEPH APPELBAUM (NASA, Lewis Research Center, Cleveland, OH; Tel Aviv University, Israel) Space Power - Resources, Manufacturing and Development (ISSN 0883-6272), vol. 10, no. 2, 1991, p. 225-237. 1991 13 p refs (Contract NAS3-25266; NAGW-2022)

Copyright

The performance of a photovoltaic array is considered in terms of the properties of the Martian surface. Attention is given to the low solar intensity and high temperatures of Mars and to the performance of different chemical structures for the cells such as GaAs and silicon cells. A sample case is examined and it is shown that certain variables are still not understood with respect to photovoltaic performance on other planets.

C.C.S.

A92-29679* National Aeronautics and Space Administration, Lewis Research Center, Cleveland, OH.

SPACE BATTERIES FOR MOBILE BATTLEFIELD POWER APPLICATIONS

PATRICIA M. O'DONNELL (NASA, Lewis Research Center, Cleveland, OH) IEEE Aerospace and Electronic Systems Magazine (ISSN 0885-8985), vol. 6, Dec. 1991, p. 45-48. Dec. 1991 4 p refs

Copyright

A review of space power systems was undertaken to identify advanced space batteries for mobile applications. State-of-the-art systems are described. The technology issues that need to be addressed in order to bring these systems along and meet the needs of the user are discussed. Future research directions are examined.

I.E.

A92-40427* National Aeronautics and Space Administration, Lewis Research Center, Cleveland, OH.

INTEGRATED SOLAR POWER SATELLITES - AN APPROACH TO LOW-MASS SPACE POWER

G. A. LANDIS and R. C. CULL (NASA, Lewis Research Center, Cleveland, OH) IN: SPS 91 - Power from space; Proceedings of the 2nd International Symposium, Gif-sur-Yvette, France, Aug. 27-30, 1991 1991 8 p refs

Previous concepts for solar power satellites have used conventional-technology photovoltaic arrays feeding a power collection and transmission system connected to microwave tubes used in a phased array antenna. This paper proposes using thin-film photovoltaics with an integrated solid-state phased-array to design an ultra-lightweight solar power satellite. The enabling technologies, conceptual designs, possible applications, and development steps are discussed. As these technologies evolve, their use results in a potential reduction in weight by a factor of ten to a hundred over conventional concepts for solar power satellites, and increases the utility by allowing service to smaller receivers at multiple receiving sites.

Author

A92-40935* National Aeronautics and Space Administration, Lewis Research Center, Cleveland, OH.

STRUCTURAL SCALING APPROXIMATIONS FOR SOLAR ARRAYS

GEOFFREY A. LANDIS (NASA, Lewis Research Center; Sverdrup Technology, Inc., Cleveland, OH) Space Power - Resources, Manufacturing and Development (ISSN 0883-6272), vol. 10, no. 3-4, 1991, p. 401-409. Previously announced in STAR as N92-13265. 1991 9 p refs (Contract NAS3-25266)

Copyright

General scaling rules for a photovoltaic array structure are required in order to compare the effectiveness of different cell technologies. Important evaluation criteria for an array are moment

44 ENERGY PRODUCTION AND CONVERSION

of inertia, resonant frequency of vibrational modes, stiffness against acceleration, and resistance losses in the wiring. Approximate scaling relationships for these parameters for a generic solar array structure are presented. Author

A92-44548* National Aeronautics and Space Administration, Lewis Research Center, Cleveland, OH.

INCREASED EFFICIENCY WITH SURFACE TEXTURING IN ITO/INP SOLAR CELLS

PHILLIP JENKINS, GEOFFREY A. LANDIS, NAVID FATEMI (Sverdrup Technology, Inc., Brook Park, OH), XIAONAN LI (National Renewable Laboratory, Golden, CO), DAVID SCHEIMAN (Sverdrup Technology, Inc., Brook Park, OH), and SHEILA BAILEY (NASA, Lewis Research Center, Cleveland, OH) International Conference on Indium Phosphide and Related Materials, 4th, Newport, RI, Apr. 20-24, 1992, Paper. 4 p. Apr. 1992 4 p refs (Contract NAS3-25266)

Copyright
Optimization of an InP solar cell with a V-grooved surface is discussed. Total internal reflection in the coverglass reduces surface reflection and can recover light reflected from the front metallization. Results from the first ITO/InP solar cells on low-angle V-grooved substrates are presented, showing a 5.8 percent increase in current. Author

A92-48091* National Aeronautics and Space Administration, Lewis Research Center, Cleveland, OH.

SURFACE ETCHING FOR LIGHT TRAPPING IN ENCAPSULATED INP SOLAR CELLS

PHILLIP JENKINS (Cleveland State University, OH) and GEOFFREY A. LANDIS (Sverdrup Technology, Inc., Brook Park, OH) IEEE, International Conference on InP and Related Materials, 3rd, Cardiff, Wales, Apr. 1991, Paper. 4 p. Apr. 1991 4 p refs (Contract NAG3-658; NAS3-25266)

Copyright
Reducing the reflection from the surface of InP is important for increasing the efficiency of solar cells and photodetectors. In this paper a new technique for reducing reflectance of glass-encapsulated InP is reported. Low-angle grooves are produced on the surface by a maskless anisotropic etch. Light reflected from the low angle grooves is trapped by total internal reflection at the glass/air interface and directed back to the InP surface. A significant decrease in surface reflection is measured. Author

A92-48212* National Aeronautics and Space Administration, Lewis Research Center, Cleveland, OH.

EFFECT OF KOH CONCENTRATION ON LEO CYCLE LIFE OF IPV NICKEL-HYDROGEN FLIGHT CELL - UPDATE II

JOHN J. SMITHRICK (NASA, Lewis Research Center, Cleveland, OH) and STEPHEN W. HALL (U.S. Navy, Naval Weapons Support Center, Crane, IN) (California State University, Annual Battery Conference on Applications and Advances, 7th, Long Beach, CA, Jan. 21-23, 1992) IEEE Aerospace and Electronic Systems Magazine (ISSN 0885-8985), vol. 7, no. 4, April 1992, p. 9-13. Previously announced in STAR as N92-13483. Apr. 1992 5 p refs

Copyright
An update of validation test results confirming the breakthrough in LEO cycle life of nickel-hydrogen cells containing 26 percent KOH electrolyte is presented. A breakthrough in the LEO cycle life of individual pressure vessel (IPV) nickel-hydrogen cells has been previously reported. The cycle life of boiler plate cells containing 26 percent potassium hydroxide (KOH) electrolyte was about 40,000 LEO cycles, compared to 3500 cycles for cells containing 31 percent KOH. The cycle regime was a stressful accelerated LEO, which consisted of a 27.5 min charge followed by a 17.5 min discharge (2X normal rate). The depth-of-discharge was 80 percent. Six 48-Ah Hughes recirculation design IPV nickel-hydrogen flight battery cells are being evaluated. Three of the cells contain 26 percent KOH (test cells), and three contain 31 percent KOH (control cells). They are undergoing real time

LEO cycle life testing. The cycle regime is a 90-min LEO orbit consisting of a 54-min charge followed by a 36-min discharge. The depth-of-discharge is 80 percent. The cell temperature is maintained at 10 C. The three 31 percent KOH cells failed (cycles 3729, 4165, and 11355). One of the 26 percent KOH cells failed at cycle 15314. The other two 26 percent KOH cells were cycled for over 16,000 cycles during the continuing test. Author

A92-50571* National Aeronautics and Space Administration, Lewis Research Center, Cleveland, OH.

TECHNOLOGY DEVELOPMENT OF FABRICATION TECHNIQUES FOR ADVANCED SOLAR DYNAMIC CONCENTRATORS

SCOTT W. RICHTER (Sverdrup Technology, Inc.; NASA, Lewis Research Center, Cleveland, OH) IN: IECEC '91; Proceedings of the 26th Intersociety Energy Conversion Engineering Conference, Boston, MA, Aug. 4-9, 1991. Vol. 1 1991 7 p refs
Copyright

The objective of the advanced concentrator program is to develop the technology that will lead to lightweight, highly reflective, accurate, scaleable, and long lived space solar dynamic concentrators. The advanced concentrator program encompasses new and innovative concepts, fabrication techniques, materials selection, and simulated space environmental testing. Fabrication techniques include methods of fabricating the substrates and coating substrate surfaces to produce high-quality optical surfaces, acceptable for further coating with vapor deposited optical films. The selected materials to obtain a high quality optical surface include microsheet glass and Eccocoat EP-3 epoxy, with DC-93-500 selected as a candidate silicone adhesive and leveling layer. The following procedures are defined: cutting, cleaning, forming, and bonding microsheet glass. Procedures are also defined for surface cleaning, and EP-3 epoxy application. The results and analyses from atomic oxygen and thermal cycling tests are used to determine the effects of orbital conditions in a space environment. Author

A92-50619* National Aeronautics and Space Administration, Lewis Research Center, Cleveland, OH.

A MASS SENSITIVITY ANALYSIS OF LUNAR ORBITING BEAM POWER SYSTEMS

MARK W. STAVNES (Sverdrup Technology, Inc.; NASA, Lewis Research Center, Cleveland, OH) and RONALD C. CULL (NASA, Lewis Research Center, Cleveland, OH) IN: IECEC '91; Proceedings of the 26th Intersociety Energy Conversion Engineering Conference, Boston, MA, Aug. 4-9, 1991. Vol. 2 1991 8 p refs (Contract NAS3-25266)

Copyright
At NASA Lewis Research Center, the feasibility of beaming power from orbiting satellites to the surface of the moon was studied. Reference microwave and laser beam power concepts were found to be 1/3 to 1/6 the mass of surface solar systems. Further analysis was performed to determine the sensitivity of the reference concepts to technology performance levels and mission architecture scenarios, such as beaming to multiple surface sites and lunar rovers. Previous studies concluded that frequencies above 35 GHz for the microwave systems were not critical for reducing the main base mass; however, when multiple sites and rovers are considered, this may become necessary. In addition, for the laser system, the pointing accuracy of the satellites becomes a critical factor for rover applications. These issues and other important results of the parametric studies, are discussed. I.E.

A92-50634* National Aeronautics and Space Administration, Lewis Research Center, Cleveland, OH.

A DYNAMIC ISOTOPE POWER SYSTEM PORTABLE GENERATOR FOR THE MOON OR MARS

RICHARD A. JOHNSON, MARIBETH E. HUNT (Rockwell International Corp., Rocketdyne Div., Canoga Park, CA), RICHARD E. PEPPING (Sandia National Laboratories, NM), and LEE S. MASON (NASA, Lewis Research Center, Cleveland, OH) IN: IECEC '91; Proceedings of the 26th Intersociety Energy Conversion

Engineering Conference, Boston, MA, Aug. 4-9, 1991. Vol. 2
1991 6 p refs
Copyright

The dynamic isotope power systems (DIPS) demonstration program is focused on a standardized 2.5 kWe portable generator for multiple uses on the lunar or Martian surface. A variety of potential remote or mobile applications has been identified by NASA. These applications include remote power to science packages, surface rovers for both short and extended duration missions, and backup to central base power. Reviews conducted on alternative power sources for these applications are described. These include the comparison of DIPS to regenerative fuel cells (RFCs). Recent work is presented refining the 2.5 kWe design to assure compatibility with the Martian environment while imposing only a minor mass penalty on lunar operations. This was accomplished by limiting temperatures, except in the heat source unit (HSU), to the nonrefractory materials regime and protecting the necessary refractories in the HSU from the environment. Design changes to the HSU are described. Work related to recent concerns regarding astronaut radiation doses is described. This work includes the bases for the calculations to determine the necessary shielding or operational limitations.

I.E.

A92-50635 National Aeronautics and Space Administration. Lewis Research Center, Cleveland, OH.

PRELIMINARY DESIGN OF A MOBILE LUNAR POWER SUPPLY

PAUL C. SCHMITZ (Sverdrup Technology, Inc., Cleveland, OH), BARBARA H. KENNY (NASA, Lewis Research Center, Cleveland, OH), and CHRISTOPHER FULMER (General Dynamics Corp., San Diego, CA) IN: IECEC '91; Proceedings of the 26th Intersociety Energy Conversion Engineering Conference, Boston, MA, Aug. 4-9, 1991. Vol. 2 1991 7 p refs
(Contract RTOP 590-13-11)

Copyright

A preliminary design for a Stirling isotope power system for use as a mobile lunar power supply is presented. Performance and mass of the components required for the system are estimated. These estimates are based on power requirements and the operating environment. Optimization routines are used to determine minimum mass operational points. Shielding for the isotope system is given as a function of the allowed dose, distance from the source, and the time spent near the source. The technologies used in the power conversion and radiator systems are taken from research in the Civil Space Technology Initiative (CSTI) program.

Author

A92-50642* National Aeronautics and Space Administration. Lewis Research Center, Cleveland, OH.

DESIGN AND OPTIMIZATION OF A SELF-DEPLOYING PV TENT ARRAY

ANTHONY J. COLOZZA (Sverdrup Technology, Inc.; NASA, Lewis Research Center, Cleveland, OH) IN: IECEC '91; Proceedings of the 26th Intersociety Energy Conversion Engineering Conference, Boston, MA, Aug. 4-9, 1991. Vol. 2 1991 7 p refs
Copyright

A study was performed to design a self-deploying tent shaped PV (photovoltaic) array and optimize the design for maximum specific power. Each structural component of the design was analyzed to determine the size necessary to withstand the various forces it would be subjected to. Through this analysis the component weights were determined. An optimization was performed to determine the array dimensions and blanket geometry which produce the maximum specific power for a given PV blanket. This optimization was performed for both Lunar and Martian environmental conditions. The performance specifications for the array at both locations and with various PV blankets were determined.

I.E.

A92-50737* National Aeronautics and Space Administration. Lewis Research Center, Cleveland, OH.

EFFECTS OF COOLANT PARAMETERS ON STEADY STATE TEMPERATURE DISTRIBUTION IN PHOSPHORIC-ACID FUEL CELL ELECTRODE

K. A. ALKASAB (Cleveland State University, OH) and A. ABDUL-AZIZ (Sverdrup Technology, Inc., Cleveland, OH) IN: IECEC '91; Proceedings of the 26th Intersociety Energy Conversion Engineering Conference, Boston, MA, Aug. 4-9, 1991. Vol. 3 1991 6 p refs

Copyright

The influence of thermophysical properties and flow rate on the steady-state temperature distribution in a phosphoric-acid fuel cell electrode plate was experimentally investigated. An experimental setup that simulates the operating conditions prevailing in a phosphoric-acid fuel cell stack was used. The fuel cell cooling system utilized three types of coolants to remove excess heat generated in the cell electrode and to maintain a reasonably uniform temperature distribution in the electrode plate. The coolants used were water, engine oil, and air. These coolants were circulated at Reynolds number ranging from 1165 to 6165 for water; 3070 to 6864 for air; and 15 to 79 for oil. Experimental results are presented.

I.E.

A92-50758* National Aeronautics and Space Administration. Lewis Research Center, Cleveland, OH.

FLYWHEEL ENERGY STORAGE FOR ELECTROMECHANICAL ACTUATION SYSTEMS

RICHARD L. HOCKNEY, JAMES H. GOLDIE (SatCon Technology Corp., Cambridge, MA), and JAMES L. KIRTLEY (MIT, Cambridge, MA) IN: IECEC '91; Proceedings of the 26th Intersociety Energy Conversion Engineering Conference, Boston, MA, Aug. 4-9, 1991. Vol. 4 1991 6 p refs
(Contract NAS3-26232)

Copyright

The authors describe a flywheel energy storage system designed specifically to provide load-leveling for a thrust vector control (TVC) system using electromechanical actuators (EMAs). One of the major advantages of an EMA system over a hydraulic system is the significant reduction in total energy consumed during the launch profile. Realization of this energy reduction will, however, require localized energy storage capable of delivering the peak power required by the EMAs. A combined flywheel-motor/generator unit which interfaces directly to the 20-kHz power bus represents an ideal candidate for this load leveling. The overall objective is the definition of a flywheel energy storage system for this application. The authors discuss progress on four technical objectives: (1) definition of the specifications for the flywheel-motor/generator system, including system-level trade-off analysis; (2) design of the flywheel rotor; (3) design of the motor/generator; and (4) determination of the configuration for the power management system.

I.E.

A92-53146* National Aeronautics and Space Administration. Lewis Research Center, Cleveland, OH.

A VERY LOW RESISTANCE, NON-SINTERED CONTACT SYSTEM FOR USE ON INDIUM PHOSPHIDE CONCENTRATOR/SHALLOW JUNCTION SOLAR CELLS

VICTOR G. WEIZER (NASA, Lewis Research Center, Cleveland, OH) and NAVID S. FATEMI (Sverdrup Technology, Inc., Cleveland, OH) IN: IEEE Photovoltaic Specialists Conference, 22nd, Las Vegas, NV, Oct. 7-11, 1991, Conference Record. Vol. 1 1991 6 p refs
(Contract NAS3-25266)

Copyright

An investigation is made into the possibility of providing low resistance contacts to shallow junction InP solar cells which do not require sintering and which do not cause device degradation even when subjected to extended annealing at elevated temperatures. We show that the addition of In to Au contacts in amounts that exceed the solid solubility limit lowers the as-fabricated (unsintered) contact resistivity ($R_{sub c}$) to the $10(\exp -5)$ ohm cm($\exp 2$) range. We next consider the contact system

44 ENERGY PRODUCTION AND CONVERSION

Au/Au₂P₃ which has been shown to exhibit as-fabricated R sub c values in the 10(exp -6) ohm cm(exp 2) range, but which fails quickly when heated. We show that the substitution of a refractory metal (W, Ta) for Au preserves the low R sub c values while preventing the destructive reactions that would normally take place in this system at high temperatures. We show, finally, that R sub c values in the 10(exp -7) ohm cm(exp 2) range can be achieved without sintering by combining the effects of In or Ga additions to Au contacts with the effects of introducing a thin Au₂P₃ layer at the metal-InP interface. Author

A92-53152* National Aeronautics and Space Administration. Lewis Research Center, Cleveland, OH.

THEORETICAL MODELING, NEAR-OPTIMUM DESIGN AND PREDICTED PERFORMANCE OF N(+)PP(+) AND P(+)NN(+) INDIUM PHOSPHIDE HOMOJUNCTION SOLAR CELLS

CHANDRA GORADIA, WILLIAM THESLING (Cleveland State University, OH), and IRVING WEINBERG (NASA, Lewis Research Center, Cleveland, OH) IN: IEEE Photovoltaic Specialists Conference, 22nd, Las Vegas, NV, Oct. 7-11, 1991, Conference Record. Vol. 1 1991 7 p refs

Copyright

Using a detailed simulation model of p(+)nn(+) and n(+)pp(+) indium phosphide (InP) homojunction solar cells, extensive parametric variation computer simulation runs are conducted to help arrive at near-optimum designs of these two solar cell configurations. Values of all the geometrical and material parameters corresponding to the near-optimal designs of both these configurations are presented. For each configuration, results are given for parametric variation runs showing how the performance parameters JSC, VOC, and eta vary with each of the cell parameters for the near-optimally designed cell. I.E.

A92-53153* National Aeronautics and Space Administration. Lewis Research Center, Cleveland, OH.

MODELED PERFORMANCE OF MONOLITHIC, 3-TERMINAL INP/GA(0.47)IN(0.53)AS CONCENTRATOR SOLAR CELLS AS A FUNCTION OF TEMPERATURE AND CONCENTRATION RATIO

C. R. OSTERWALD, M. W. WANLASS, J. S. WARD, B. M. KEYES, K. A. EMERY, and T. J. COUTTS (National Renewable Energy Laboratory, Golden, CO) IN: IEEE Photovoltaic Specialists Conference, 22nd, Las Vegas, NV, Oct. 7-11, 1991, Conference Record. Vol. 1 1991 4 p refs
(Contract DE-AC02-83HC-10093; NASA ORDER C-300005-K)

Copyright

Using measured device parameters from a monolithic three-terminal In/GaInAs (0.75 eV) tandem concentrator solar cell, a numerical model is constructed that calculates efficiency as a function of temperature and concentration ratio. The device measurements indicate that the series resistance in the InP top cell severely limits the maximum efficiency at high concentration ratios. Results from the model in which a single-junction InP concentrator solar cell that has a lower resistance by a factor of six was substituted for the top cell show that peak 20 C air-mass-zero (AM0) efficiencies should approach 30 percent at concentration ratios greater than 100. At 80 C, this tandem cell should exceed 24 percent AM0 efficiency. I.E.

A92-53156* National Aeronautics and Space Administration. Lewis Research Center, Cleveland, OH.

INFLUENCE OF THE DISLOCATION DENSITY ON THE PERFORMANCE OF HETEROEPITAXIAL INDIUM PHOSPHIDE SOLAR CELLS

R. K. JAIN and D. J. FLOOD (NASA, Lewis Research Center, Cleveland, OH) IN: IEEE Photovoltaic Specialists Conference, 22nd, Las Vegas, NV, Oct. 7-11, 1991, Conference Record. Vol. 1 1991 6 p refs

Copyright

Calculations are made to study the dependence of heteroepitaxial InP solar-cell efficiency on dislocation density. Effects of surface recombination velocity and cell emitter thickness are considered. Calculated results are compared with the available

experimental results on representative InP solar cells. It is shown that heteroepitaxial InP cells with over 20 percent AM0 efficiency could be fabricated if dislocations are reduced to less than 100,000/sq cm. I.E.

A92-53162* National Aeronautics and Space Administration. Lewis Research Center, Cleveland, OH.

EVALUATION OF THE MINORITY CARRIER DIFFUSION LENGTH AND SURFACE-RECOMBINATION VELOCITY IN GAAS P/N SOLAR CELLS

ROSHANAK HAKIMZADEH (Sverdrup Technology, Inc., Brook Park; Case Western Reserve University, Cleveland, OH), HANS J. MOELLER (Case Western Reserve University, Cleveland, OH), and SHEILA BAILEY (NASA, Lewis Research Center, Cleveland, OH) IN: IEEE Photovoltaic Specialists Conference, 22nd, Las Vegas, NV, Oct. 7-11, 1991, Conference Record. Vol. 1 1991 6 p refs

Copyright

The minority carrier diffusion length (Lp) and the surface recombination velocity (Vs) were measured as a function of distance (x) from the p-n junction in GaAs p/n concentrator solar cells. The measured Vs values were used in a theoretical expression for the normalized electron-beam-induced current. A fitting procedure was then used to fit this expression with experimental values to obtain Lp. The results show that both Vs and Lp vary with x. Lp measured in irradiated cells showed a marked reduction. These values were compared to those measured previously which did not account for Vs. I.E.

A92-53163* National Aeronautics and Space Administration. Lewis Research Center, Cleveland, OH.

EFFECT OF INALAS WINDOW LAYER ON THE EFFICIENCY OF INDIUM PHOSPHIDE SOLAR CELLS

R. K. JAIN (NASA, Lewis Research Center, Cleveland, OH) and G. A. LANDIS (Sverdrup Technology, Inc., Brook Park, OH) IN: IEEE Photovoltaic Specialists Conference, 22nd, Las Vegas, NV, Oct. 7-11, 1991, Conference Record. Vol. 1 1991 6 p refs
(Contract NAS3-25266)

Copyright

Indium phosphide (InP) solar cell efficiencies are limited by surface recombination. The effect of a wide-bandgap lattice-matched indium aluminum arsenide (In_{0.52}Al_{0.48}As) window layer on the performance of InP solar cells was investigated using a numerical code PC-1D. The p(+)n InP solar cell performance improves significantly with the use of a window layer. No improvement is seen for n(+)p InP cells. Cell results are explained by the band diagram of the heterostructure and the conduction-band energy discontinuity. The calculated I-V and internal quantum efficiency results clearly demonstrate that In_{0.52}Al_{0.48}As is a promising candidate as a window layer material for p(+)n InP solar cells. Author

A92-53166* National Aeronautics and Space Administration. Lewis Research Center, Cleveland, OH.

INP CONCENTRATOR SOLAR CELLS

J. S. WARD, M. W. WANLASS, T. J. COUTTS, K. A. EMERY, and C. R. OSTERWALD (National Renewable Energy Laboratory, Golden, CO) IN: IEEE Photovoltaic Specialists Conference, 22nd, Las Vegas, NV, Oct. 7-11, 1991, Conference Record. Vol. 1 1991 6 p refs
(Contract DE-AC02-83HC-10093; NASA ORDER C-300005-K)

Copyright

The design, fabrication, and characterization of high-performance, n(+)/p InP shallow-homojunction (SHJ) concentrator solar cells are described. The InP device structures were grown by atmospheric-pressure metalorganic vapor phase epitaxy. A preliminary assessment of the effects of grid-collection distance and emitter-sheet resistance on cell performance is presented. At concentration ratios of around 100, cells with efficiencies of 21.4 percent AM0 (24.3 percent direct) at 25 C are fabricated. These are the highest efficiencies yet reported for single-junction InP solar cells. The performance of these cells as

a function of temperature is discussed, and areas for future improvement are outlined. Application of these results to other InP-based photovoltaic devices is discussed. I.E.

A92-53172* National Aeronautics and Space Administration, Lewis Research Center, Cleveland, OH.

HIGH VOLTAGE THERMALLY DIFFUSED P(+)N SOLAR CELLS

M. FAUR, M. FAUR (Cleveland State University, OH), D. J. FLOOD, D. J. BRINKER, I. WEINBERG (NASA, Lewis Research Center, Cleveland, OH), C. GORADIA, N. FATEMI, M. GORADIA, and W. THESLING (Cleveland State University, OH) IN: IEEE Photovoltaic Specialists Conference, 22nd, Las Vegas, NV, Oct. 7-11, 1991, Conference Record. Vol. 1 1991 6 p refs
Copyright

The possibility of fabricating thermally diffused p(+)n InP solar-cells with high open-circuit voltage without sacrificing the short circuit current is discussed. The p(+)n InP junctions were formed by Cd and Zn diffusion through a 3-5-nm-thick anodic or chemical phosphorus-rich oxide cap layer grown on n:InP:S (with ND-NA = 3.5×10^{16} and 4.5×10^{17} /cu cm) Czochralski LEC-grown substrates. After thinning the emitter from its initial thickness of 1 to 2.5 micron down to 0.06-0.15 micron, the maximum efficiency was found when the emitter was 0.2 to 0.3 micron thick. Typical AM0, 25 C values of 854-860 mV were achieved for Voc, Jsc values were from 25.9 to 29.1 mA/sq cm using only the P-rich passivating layer left after the thinning process as an antireflection coating. I.E.

A92-57055* National Aeronautics and Space Administration, Lewis Research Center, Cleveland, OH.

ADVANCES IN PHOTOVOLTAIC TECHNOLOGY

G. A. LANDIS and S. G. BAILEY (NASA, Lewis Research Center, Cleveland, OH) IAF, International Astronautical Congress, 43rd, Washington, Aug. 28-Sept. 5, 1992. 14 p. Aug. 1992 14 p refs
(IAF PAPER 92-0599) Copyright

The advances in solar cell efficiency, radiation tolerance, and cost in the last 10 years are presented. The potential performance of thin-film solar cells in space is examined, and the cost and the historical trends in production capability of the photovoltaics industry are considered with respect to the needs of satellite solar power systems. Attention is given to single-crystal cells, concentrator and cascade cells, and thin-film solar cells. R.E.P.

N92-10221* National Aeronautics and Space Administration, Lewis Research Center, Cleveland, OH.

TRADE STUDIES FOR NUCLEAR SPACE POWER SYSTEMS

JOHN M. SMITH, DAVID J. BENTS, and HARVEY S. BLOOMFIELD 1991 12 p Presented at the Conference on Advanced Space Exploration Initiative Technologies, Cleveland, OH, 4-6 Sep. 1991; cosponsored by AIAA, NASA, and OAI Previously announced in IAA as A91-52413
(Contract RTOP 590-13-00)

(NASA-TM-105231; E-6554; NAS 1.15:105231; AIAA PAPER 91-3518) Avail: CASI HC A03/MF A01

As human visions of space applications expand and as we probe further out into the universe, our needs for power will also expand, and missions will evolve which are enabled by nuclear power. A broad spectrum of missions which are enhanced or enabled by nuclear power sources have been defined. These include Earth orbital platforms, deep space platforms, planetary exploration, and terrestrial resource exploration. The recently proposed Space Exploration Initiative (SEI) to the Moon and Mars has more clearly defined these missions and their power requirements. Presented here are results of recent studies of radioisotope and nuclear reactor energy sources, combined with various energy conversion devices for Earth orbital applications, SEI lunar/Mars rovers, surface power, and planetary exploration.

Author

N92-10222* National Aeronautics and Space Administration, Lewis Research Center, Cleveland, OH.

ALKALI METAL CARBON DIOXIDE ELECTROCHEMICAL SYSTEM FOR ENERGY STORAGE AND/OR CONVERSION OF CARBON DIOXIDE TO OXYGEN Patent Application

NORMAN H. HAGEDORN, inventor (to NASA) 26 Sep. 1991 15 p
(NASA-CASE-LEW-14973-1; NAS 1.71:LEW-14973-1; US-PATENT-APPL-SN-766593) Avail: CASI HC A03/MF A01

An alkali metal, such as lithium, is the anodic reactant, carbon dioxide or a mixture of carbon dioxide and carbon monoxide is the cathodic reactant, and carbonate of the alkali metal is the electrolyte in an electrochemical cell for the storage and delivery of electrical energy. Additionally, alkali metal-carbon dioxide battery systems include a plurality of such electrochemical cells. Gold is a preferred catalyst for reducing the carbon dioxide at the cathode. The fuel cell of the invention produces electrochemical energy through the use of an anodic reactant which is extremely energetic and light, and a cathodic reactant which can be extracted from its environment and therefore exacts no transportation penalty. The invention is therefore especially useful in extraterrestrial environments. NASA

N92-13482* National Aeronautics and Space Administration, Lewis Research Center, Cleveland, OH.

A VERY LOW RESISTANCE, NON-SINTERED CONTACT SYSTEM FOR USE ON INDIUM PHOSPHIDE CONCENTRATOR/SHALLOW JUNCTION SOLAR CELLS

VICTOR G. WEIZER and NAVID S. FATEMI (Sverdrup Technology, Inc., Brook Park, OH.) Oct. 1991 9 p Presented at the 22nd Photovoltaic Specialists Conference, Las Vegas, NV, 7-11 Oct. 1991; sponsored by IEEE
(Contract RTOP 506-41-11)

(NASA-TM-105279; E-6604; NAS 1.15:105279) Avail: CASI HC A02/MF A01

An investigation is made into the possibility of providing low resistance contacts to shallow junction InP solar cells which do not require sintering and which do not cause device degradation even when subjected to extended annealing at elevated temperatures. We show that the addition of In to Au contacts in amounts that exceed the solid solubility limit lowers the as-fabricated (unsintered) contact resistivity ($R_{sub c}$) to the $10(\exp -5)$ ohm cm($\exp 2$) range. We next consider the contact system Au/Au2P3, which has been shown to exhibit as-fabricated $R_{sub c}$ values in the $10(\exp -6)$ ohm cm($\exp 2$) range, but which fails quickly when heated. We show that the substitution of a refractory metal (W, Ta) for Au preserves the low $R_{sub c}$ values while preventing the destructive reactions that would normally take place in this system at high temperatures. We show, finally, that $R_{sub c}$ values in the $10(\exp -7)$ ohm cm($\exp 2$) range can be achieved without sintering by combining the effects of In or Ga additions to Au contacts with the effects of introducing a thin Au2P3 layer at the metal-InP interface. Author

N92-13483* National Aeronautics and Space Administration, Lewis Research Center, Cleveland, OH.

EFFECT OF KOH CONCENTRATION ON LEO CYCLE LIFE OF IPV NICKEL-HYDROGEN FLIGHT CELLS-UPDATE 2

JOHN J. SMITHRICK and STEPHEN W. HALL (Naval Weapons Support Center, Crane, IN.) 1991 11 p Proposed for presentation at the Seventh Annual Battery Conference on Applications and Advances, Long Beach, CA, 21-23 Jan. 1992; sponsored by California State Univ.
(Contract RTOP 506-41-21)

(NASA-TM-105314; E-6667; NAS 1.15:105314) Avail: CASI HC A03/MF A01

An update of validation test results confirming the breakthrough in low earth orbit (LEO) cycle life of nickel-hydrogen cells containing 26 percent KOH electrolyte is presented. A breakthrough in the LEO cycle life of individual pressure vessel (IPV) nickel-hydrogen cells has been previously reported. The cycle life of boiler plate cells containing 26 percent potassium hydroxide (KOH) electrolyte was about 40 000 LEO cycles compared to 3500 cycles for cells

44 ENERGY PRODUCTION AND CONVERSION

containing 31 percent KOH. This test was conducted at Hughes Aircraft Company under a NASA Lewis contract. The purpose was to investigate the effect of KOH concentration on cycle life. The cycle regime was a stressful accelerated LEO, which consisted of a 27.5 min charge followed by a 17.5 min discharge (2x normal rate). The depth of discharge (DOD) was 80 percent. The cell temperature was maintained at 23 C. The boiler plate test results are in the process of being validated using flight hardware and real time LEO test at the Naval Weapons Support Center (NWSC), Crane, Indiana under a NASA Lewis Contract. Six 48 Ah Hughes recirculation design IPV nickel-hydrogen flight battery cells are being evaluated. Three of the cells contain 26 percent KOH (test cells), and three contain 31 percent KOH (control cells). They are undergoing real time LEO cycle life testing. The cycle regime is a 90-min LEO orbit consisting of a 54-min charge followed by a 36-min discharge. The depth-of-discharge is 80 percent. The cell temperature is maintained at 10 C. The three 31 percent KOH cells failed (cycles 3729, 4165, and 11355). One of the 26 percent KOH cells failed at cycle 15314. The other two 26 percent KOH cells were cycled for over 16600 cycles during the continuing test. Author

N92-13484*# National Aeronautics and Space Administration. Lewis Research Center, Cleveland, OH.

IMPEDANCES OF LI/SO₂ CELLS RETRIEVED FROM THE LONG DURATION EXPOSURE FACILITY (LDEF SATELLITE) AND COMPARISON WITH CELLS STORED TERRESTRIALLY

MARGARET A. REID Nov. 1991 9 p
(Contract RTOP 506-41-21)
(NASA-TM-104526; E-6400; NAS 1.15:104526) Avail: CASI HC A02/MF A01

Impedances were measured on several Li/SO₂ cells retrieved from the Long Duration Exposure Facility (LDEF) satellite. These cells were used to power instruments and recorders and had all been partially or fully discharged. Impedances were also measured on several cells that were stored in cold storage since manufacture. Unfortunately, none of the cells stored terrestrially had undergone any discharge, whereas all of the cells on the satellite were at least partially discharged early in the mission and then remained on orbit for about 5 years further. It has been observed by others that storage of an Li/SO₂ cell after partial discharge, increases the resistance and thickness of the passive film on the Li electrode, as indicated by an increase in the time for recovery of voltage when a load is applied (voltage lag), or in some cases by an inability of a cell to sustain a normal current after such storage. Since the cells stored terrestrially were not discharged in the same manner as the LDEF cells, a direct comparison cannot be made. Thus, the effects of the space environment cannot be separated from the effects of storage after partial discharge. It is believed that the increases in impedance in the LDEF cells are largely due to the storage upon partial discharge rather than the effects of the space environment. Author

N92-14485*# National Aeronautics and Space Administration. Lewis Research Center, Cleveland, OH.

THERMOCHEMICAL ENERGY STORAGE FOR A LUNAR BASE

MARLA E. PEREZ-DAVIS, BARBARA I. MCKISSOCK, and FRANK DIFILIPPO (Case Western Reserve Univ., Cleveland, OH.) 1992 7 p Proposed for presentation at the International Solar Energy Conference, Lahaina, Maui, HI, 4-8 Apr. 1992; sponsored by ASME
(Contract RTOP 506-41-41)
(NASA-TM-105333; E-6700; NAS 1.15:105333) Avail: CASI HC A02/MF A01

A thermochemical solar energy storage concept involving the reversible reaction $\text{CaO} + \text{H}_2\text{O}$ yields Ca(OH)_2 is proposed as a power system element for a lunar base. The operation and components of such a system are described. The $\text{CaO}/\text{H}_2\text{O}$ system is capable of generating electric power during both the day and night. Mass of the required amount of CaO is neglected since it is obtained from lunar soil. Potential technical problems, such as reactor design and lunar soil processing, are reviewed. Author

N92-16481*# National Aeronautics and Space Administration. Lewis Research Center, Cleveland, OH.

THE NASA CSTI HIGH CAPACITY POWER PROGRAM

JERRY M. WINTER Sep. 1991 18 p Presented at the Conference on Advanced Space Exploration Initiative Technologies, Cleveland, OH, 4-6 Sep. 1991; sponsored by AIAA, and OAI Previously announced in IAA as A91-52493
(Contract RTOP 590-13-11)
(NASA-TM-105240; E-6567; NAS 1.15:105240; AIAA PAPER 91-3629) Avail: CASI HC A03/MF A01

The SP-100 program was established in 1983 by DOD, DOE, and NASA as a joint program to develop the technology necessary for space nuclear power systems for military and civil applications. During 1986 and 1987, the NASA Advanced Technology Program was responsible for maintaining the momentum of promising technology advancement efforts started during Phase 1 of SP-100 and to strengthen, in key areas, the chances for successful development and growth capability of space nuclear reactor power systems for future space applications. In 1988, the NASA Advanced Technology Program was incorporated into NASA's new Civil Space Technology Initiative (CSTI). The CSTI program was established to provide the foundation for technology development in automation and robotics, information, propulsion, and power. The CSTI High Capacity Power Program builds on the technology efforts of the SP-100 program, incorporates the previous NASA advanced technology project, and provides a bridge to the NASA exploration technology programs. The elements of CSTI high capacity power development include conversion systems: Stirling and thermoelectric, thermal management, power management, system diagnostics, and environmental interactions. Technology advancement in all areas, including materials, is required to provide the growth capability, high reliability, and 7 to 10 year lifetime demanded for future space nuclear power systems. The overall program will develop and demonstrate the technology base required to provide a wide range of modular power systems while minimizing the impact of day/night operations as well as attitudes and distance from the Sun. Significant accomplishments in all of the program elements will be discussed, along with revised goals and project timelines recently developed. Author

N92-20493*# National Aeronautics and Space Administration. Lewis Research Center, Cleveland, OH.

PROGRESS IN THE DEVELOPMENT OF LIGHTWEIGHT NICKEL ELECTRODE FOR AEROSPACE APPLICATIONS

DORIS L. BRITTON Mar. 1992 19 p Presented at the 3rd International Rechargeable Battery Seminar, Deerfield Beach, FL, 2-4 Mar. 1992; sponsored in part by Ansum Enterprises, Inc.
(Contract RTOP 506-41-21)
(NASA-TM-105591; E-6922; NAS 1.15:105591) Avail: CASI HC A03/MF A01

The NASA Lewis Research Center is currently developing nickel electrodes for nickel-hydrogen (Ni-H₂) cells and batteries. These electrodes are lighter in weight and have higher specific energy than the heavy sintered state of the art nickel electrodes. In the present approach, lightweight materials or plaques are used as conductive supports for the nickel hydroxide active material. These plaques (fiber, felt, and nickel plated plastic) are fabricated into nickel electrodes by electrochemically impregnating them with active material. Initial performance tests include capacity measurements at five discharge levels, C/2, 1.0C, 1.37C, 2.0C, and 2.74C. The electrodes that pass the initial tests are life cycle tested at 40 and 80 percent depths of discharge (DOD). Different formulations of nickel fiber materials obtained from several manufacturers are currently being tested as possible candidates for nickel electrodes. Over 7,000 cycles of life cycle testing have been accumulated at 40 percent DOD, using the lightweight fiber electrode in a boiler plate Ni-H₂ cell with stable voltage. Author

N92-22037*# National Aeronautics and Space Administration. Lewis Research Center, Cleveland, OH.

SELECTIVE EMITTERS Patent

DONALD L. CHUBB, inventor (to NASA) 14 Jan. 1992 8 p
Filed 30 Mar. 1990 Supersedes N91-13802 (29 - 5, p 684)

(NASA-CASE-LEW-14731-1; US-PATENT-5,080,724; US-PATENT-APPL-SN-503486; US-PATENT-CLASS-136-253; INT-PATENT-CLASS-H01C-31/58) Avail: US Patent and Trademark Office

This invention relates to a small particle selective emitter for converting thermal energy into narrow band radiation with high efficiency. The small particle selective emitter is used in combination with a photovoltaic array to provide a thermal to electrical energy conversion device. An energy conversion apparatus of this type is called a thermo-photovoltaic device. In the first embodiment, small diameter particles of a rare earth oxide are suspended in an inert gas enclosed between concentric cylinders. The rare earth oxides are used because they have the desired property of large emittance in a narrow wavelength band and small emittance outside the band. However, it should be emphasized that it is the smallness of the particles that enhances the radiation property. The small particle selective emitter is surrounded by a photovoltaic array. In an alternate embodiment, the small particle gas mixture is circulated through a thermal energy source. This thermal energy source can be a nuclear reactor, solar receiver, or combustor of a fossil fuel.

Official Gazette of the U.S. Patent and Trademark Office

N92-22741*# National Aeronautics and Space Administration. Lewis Research Center, Cleveland, OH.

NASA AEROSPACE FLIGHT BATTERY SYSTEMS PROGRAM: AN UPDATE

MICHELLE A. MANZO *In* NASA. Marshall Space Flight Center, The 1991 NASA Aerospace Battery Workshop p 7-18 Feb. 1992

Avail: CASI HC A03/MF A10

The major objective of the NASA Aerospace Flight Battery Systems Program is to provide NASA with the policy and posture to increase and ensure the safety, performance, and reliability of batteries for space power systems. The program was initiated in 1985 to address battery problems experienced by NASA and other space battery users over the previous ten years. The original program plan was approved in May 1986 and modified in 1990 to reflect changes in the agency's approach to battery related problems that are affecting flight programs. The NASA Battery Workshop is supported by the NASA Aerospace Flight Battery Systems Program. The main objective of the discussions is to aid in defining the direction which the agency should head with respect to aerospace battery issues. Presently, primary attention in the Battery Program is being devoted to issues revolving around the future availability of nickel-cadmium batteries as a result of the proposed OSHA standards with respect to allowable cadmium levels in the workplace. The decision of whether or not to pursue the development of an advanced nickel-cadmium cell design and the qualification of vendors to produce cells for flight programs hinges on the impact of the OSHA ruling. As part of a unified Battery Program, the evaluation of a nickel-hydrogen cell design options and primary cell issues are also being pursued to provide high performance NASA Standards and space qualified state-of-the-art cells. The resolution of issues is being addressed with the full participation of the aerospace battery community.

Author

N92-24057*# National Aeronautics and Space Administration. Lewis Research Center, Cleveland, OH.

SELF-DEPLOYING PHOTOVOLTAIC POWER SYSTEM Patent Application

ANTHONY J. COLOZZA, inventor (to NASA) 2 Apr. 1992 19 p (NASA-CASE-LEW-15308-1; NAS 1.71:LEW-15308-1; US-PATENT-APPL-SN-862113) Avail: CASI HC A03/MF A01

A lightweight flexible photovoltaic (PV) blanket is attached to a support structure of initially stowed telescoping members. The deployment mechanism comprises a series of extendable and rotatable columns. As these columns are extended the PV blanket is deployed to its proper configuration. NASA

N92-24802*# National Aeronautics and Space Administration. Lewis Research Center, Cleveland, OH.

SINTERLESS CONTACTS TO SHALLOW JUNCTION INP SOLAR CELLS

V. G. WEIZER (Sverdrup Technology, Inc., Brook Park, OH.), N. S. FATEMI, and A. L. KORENYI-BOTH (Calspan Corp., Cleveland, OH.) 1992 7 p Presented at the Fourth International Conference on Indium Phosphide and Related Materials, Newport, RI, 21-24 Apr. 1992; sponsored by IEEE

(Contract NAS3-25266; NAS3-30759; RTOP 506-41-11) (NASA-TM-105670; E-7036; NAS 1.15:105670) Avail: CASI HC A02/MF A01

In the past, the achievement of good electrical contact to InP has inevitably been accompanied by mechanical degradation of the InP itself. Most contact systems require heat treatment after metal deposition that results in the dissolution of substantial amounts of InP into the metallization. Devices such as the solar cell, where shallow junctions are the rule, can be severely degraded if the damage to the semiconductor substrate is not precisely controlled. Two contact systems are described that provide low contact resistance to InP solar cells that do not require subjecting the current carrying metallization to a post deposition sintering process. It is shown that these two systems, one nickel based and the other silver based, provide contact resistivity values in the low $10(\exp -6)$ ohm sq cm range, as fabricated, without the need for sintering. Author

N92-27101*# National Aeronautics and Space Administration. Lewis Research Center, Cleveland, OH.

ADVANCED PHOTOVOLTAIC EXPERIMENT, S0014: PRELIMINARY FLIGHT RESULTS AND POST-FLIGHT FINDINGS

DAVID J. BRINKER (Eppley Lab., Inc., Newport, RI.), JOHN R. HICKEY (Eppley Lab., Inc., Newport, RI.), and DAVID A. SCHEIMAN *In* NASA. Langley Research Center, LDEF: 69 Months in Space. First Post-Retrieval Symposium, Part 3 p 1395-1404 Jan. 1992

Avail: CASI HC A02/MF A04; 1 functional color page

The Advanced Photovoltaic Experiment is a Long Duration Exposure Facility (LDEF) experiment originally designed to provide reference solar cell standards for laboratory measurements as well as to investigate the solar spectrum and the effects of long term exposure of space solar cells to the low earth orbit (LEO) environment. The experiment functioned on-orbit as designed, successfully measuring and recording cell performance and solar insolation data over the first 325 days. The objectives and design of the experiment are presented as well as the preliminary flight results and postflight findings. Author

N92-27320*# National Aeronautics and Space Administration. Lewis Research Center, Cleveland, OH.

THE EFFECT OF THE LOW EARTH ORBIT ENVIRONMENT ON SPACE SOLAR CELLS: RESULTS OF THE ADVANCED PHOTOVOLTAIC EXPERIMENT (S0014) Abstract Only

DAVID J. BRINKER (Martin Marietta Labs., Baltimore, MD.) and JOHN R. HICKEY (Eppley Lab., Inc., Newport, RI.) *In* NASA. Langley Research Center, Second LDEF Post-Retrieval Symposium Abstracts p 117 Jun. 1992

Avail: CASI HC A01/MF A02

The Advanced Photovoltaic Experiment (APEX), containing over 150 solar cells and sensors, was designed to generate laboratory reference standards as well as to explore the durability of a wide variety of space solar cells. Located on the leading edge of the Long Duration Exposure Facility (LDEF), APEX received the maximum possible dosage of atomic oxygen and ultraviolet radiation, as well as enormous numbers of impacts from micrometeoroids and debris. The effect of the low earth orbital (LEO) environment on the solar cells and materials of APEX will be discussed in this paper. The on-orbit performance of the solar cells, as well as a comparison of pre- and postflight laboratory performance measurements, will be presented. Author

44 ENERGY PRODUCTION AND CONVERSION

N92-28837*# National Aeronautics and Space Administration. Lewis Research Center, Cleveland, OH.

NASA LEWIS STIRLING SPRE TESTING AND ANALYSIS WITH REDUCED NUMBER OF COOLER TUBES

WAYNE A. WONG, JAMES E. CAIRELLI, DIANE M. SWEC, THOMAS J. DOEBERLING, THOMAS F. LAKATOS, and FRANK J. MADI (Sverdrup Technology, Inc., Brook Park, OH.) Aug. 1992 9 p Proposed for presentation at the 27th Intersociety Conversion Engineering Conference, San Diego, CA, 3-7 Aug. 1992; sponsored by SAE, AIAA, ASME, IEEE, ACS, AIChE, and ANS (Contract RTOP 590-13-11) (NASA-TM-105767; E-7184; NAS 1.15:105767) Avail: CASI HC A02/MF A01

Free-piston Stirling power converters are candidates for high capacity space power applications. The Space Power Research Engine (SPRE), a free-piston Stirling engine coupled with a linear alternator, is being tested at the NASA Lewis Research Center in support of the Civil Space Technology Initiative. The SPRE is used as a test bed for evaluating converter modifications which have the potential to improve the converter performance and for validating computer code predictions. Reducing the number of cooler tubes on the SPRE has been identified as a modification with the potential to significantly improve power and efficiency. Experimental tests designed to investigate the effects of reducing the number of cooler tubes on converter power, efficiency and dynamics are described. Presented are test results from the converter operating with a reduced number of cooler tubes and comparisons between this data and both baseline test data and computer code predictions. Author

N92-29143* National Aeronautics and Space Administration. Lewis Research Center, Cleveland, OH.

SOLAR THERMAL ENERGY RECEIVER Patent

KARL W. BAKER, inventor (to NASA) and MILES O. DUSTIN, inventor (to NASA) 19 May 1992 9 p Filed 27 Mar. 1991 Supersedes N91-23617 (29 - 15, p 2457) (NASA-CASE-LEW-14949-1; US-PATENT-5,113,659; US-PATENT-APPL-SN-676910; US-PATENT-CLASS-60-641.8; US-PATENT-CLASS-60-659; US-PATENT-CLASS-126-433; US-PATENT-CLASS-126-436; INT-PATENT-CLASS-F03G-6/00) Avail: US Patent and Trademark Office

A plurality of heat pipes in a shell receive concentrated solar energy and transfer the energy to a heat activated system. To provide for even distribution of the energy despite uneven impingement of solar energy on the heat pipes, absence of solar energy at times, or failure of one or more of the heat pipes, energy storage means are disposed on the heat pipes which extend through a heat pipe thermal coupling means into the heat activated device. To enhance energy transfer to the heat activated device, the heat pipe coupling cavity means may be provided with extensions into the device. For use with a Stirling engine having passages for working gas, heat transfer members may be positioned to contact the gas and the heat pipes. The shell may be divided into sections by transverse walls. To prevent cavity working fluid from collecting in the extensions, a porous body is positioned in the cavity.

Official Gazette of the U.S. Patent and Trademark Office

N92-29662*# National Aeronautics and Space Administration. Lewis Research Center, Cleveland, OH.

DESIGN CHARACTERISTICS OF A HEAT PIPE TEST CHAMBER

KARL W. BAKER, J. HOON JANG (Sverdrup Technology, Inc., Brook Park, OH.), and JUIN S. YU (West Virginia Inst. of Tech., Montgomery.) Jul. 1992 26 p Proposed for presentation at the First International Conference on Aerospace Heat Exchanger Technology, Palo Alto, CA, 15-17 Feb. 1993; sponsored by ASME and IAA (Contract RTOP 506-41-51) (NASA-TM-105737; E-7142; NAS 1.15:105737) Avail: CASI HC A03/MF A01

LeRC has designed a heat pipe test facility which will be used to provide data for validating heat pipe computer codes. A heat

pipe test chamber that uses helium gas for enhancing heat transfer was investigated. The conceptual design employs the technique of guarded heating and guarded cooling to facilitate accurate measurements of heat transfer rates to the evaporator and from the condenser. The design parameters are selected for a baseline heat pipe made of stainless steel with an inner diameter of 38.10 mm and a wall thickness of 1.016 mm. The heat pipe operates at a design temperature of 1000 K with an evaporator radial heat flux of 53 W/sq. cm. Author

N92-30426*# National Aeronautics and Space Administration. Lewis Research Center, Cleveland, OH.

HIGH EFFICIENCY THERMAL TO ELECTRIC ENERGY CONVERSION USING SELECTIVE EMITTERS AND SPECTRALLY TUNED SOLAR CELLS

DONALD L. CHUBB, DENNIS J. FLOOD, and ROLAND A. LOWE (Cleveland State Univ., OH.) Aug. 1992 12 p Proposed for presentation at the Nuclear Technologies for Space Exploration Conference, Jackson Hole, WY, 16-19 Aug. 1992; sponsored by ANS (Contract RTOP 506-41-11) (NASA-TM-105755; E-7166; NAS 1.15:105755) Avail: CASI HC A03/MF A01

Thermophotovoltaic (TPV) systems are attractive possibilities for direct thermal-to-electric energy conversion, but have typically required the use of black body radiators operating at high temperatures. Recent advances in both the understanding and performance of solid rare-earth oxide selective emitters make possible the use of TPV at temperatures as low as 1500 K. Depending on the nature of parasitic losses, overall thermal-to-electric conversion efficiencies greater than 20 percent are feasible. Author

N92-31262*# National Aeronautics and Space Administration. Lewis Research Center, Cleveland, OH.

A FREE-PISTON STIRLING ENGINE/LINEAR ALTERNATOR CONTROLS AND LOAD INTERACTION TEST FACILITY

JEFFREY S. RAUCH (Sverdrup Technology, Inc., Brook Park, OH.), M. DAVID KANKAM, WALTER SANTIAGO, and FRANK J. MADI (Sverdrup Technology, Inc., Brook Park, OH.) Aug. 1992 8 p Presented at the 27th Intersociety Energy Conversion Conference, San Diego, CA, 3-7 Aug. 1992; sponsored by SAE (Contract NAS3-25266; RTOP 590-13-11) (NASA-TM-105825; E-7259; NAS 1.15:105825) Avail: CASI HC A02/MF A01

A test facility at LeRC was assembled for evaluating free-piston Stirling engine/linear alternator control options, and interaction with various electrical loads. This facility is based on a 'SPIKE' engine/alternator. The engine/alternator, a multi-purpose load system, a digital computer based load and facility control, and a data acquisition system with both steady-periodic and transient capability are described. Preliminary steady-periodic results are included for several operating modes of a digital AC parasitic load control. Preliminary results on the transient response to switching a resistive AC user load are discussed. Author

N92-33895*# National Aeronautics and Space Administration. Lewis Research Center, Cleveland, OH.

THE ACHIEVEMENT OF LOW CONTACT RESISTANCE TO INDIUM PHOSPHIDE: THE ROLES OF NI, AU, GE, AND COMBINATIONS THEREOF

NAVID S. FATEMI (Sverdrup Technology, Inc., Brook Park, OH.) and VICTOR G. WEIZER Apr. 1992 8 p Presented at the 1992 Semi-Annual Meeting, San Francisco, CA, 27 Apr. - 1 May 1992; sponsored by the Materials Research Society (Contract NAS3-25266; RTOP 506-41-11) (NASA-TM-105770; E-7195; NAS 1.15:105770) Avail: CASI HC A02/MF A01

We have investigated the electrical and metallurgical behavior of Ni, Au-Ni, and Au-Ge-Ni contacts on n-InP. We have found that very low values of contact resistivity $\rho_{(sub\ c)}$ in the E-7 omega-sq cm range are obtained with Ni-only contacts. We show that the addition of Au to Ni contact metallization effects an

additional order of magnitude reduction in ρ (sub c). Ultra-low contact resistivities in the E-8 $\Omega\text{-cm}$ range are obtained with both the Au-Ni and the Au-Ge-Ni systems, effectively eliminating the need for the presence of Ge in the Au-Ge-Ni system. The formation of various nickel phosphides at the metal-InP interface is shown to be responsible for the observed ρ (sub c) values in the Ni and Au-Ni systems. We show, finally, that the order in which the constituents of Au-Ni and Au-Ge-Ni contacts are deposited has a significant bearing on the composition of the reaction products formed at the metal-InP interface and therefore on the contact resistivity at that interface.

Author

N92-33898* # National Aeronautics and Space Administration, Lewis Research Center, Cleveland, OH.

PROGRESS UPDATE OF NASA'S FREE-PISTON STIRLING SPACE POWER CONVERTER TECHNOLOGY PROJECT

JAMES E. DUDENHOEFER, JERRY M. WINTER, and DONALD ALGER (Sverdrup Technology, Inc., Brook Park, OH.) Aug. 1992 12 p Proposed for presentation at the Nuclear Technologies for Space Exploration Conference, Jackson Hole, WY, 16-19 Aug. 1992; sponsored by ANS

(Contract RTOP 590-13-11)

(NASA-TM-105748; E-7153; NAS 1.15:105748) Avail: CASI HC A03/MF A01

A progress update is presented of the NASA LeRC Free-Piston Stirling Space Power Converter Technology Project. This work is being conducted under NASA's Civil Space Technology Initiative (CSTI). The goal of the CSTI High Capacity Power Element is to develop the technology base needed to meet the long duration, high capacity power requirements for future NASA space initiatives. Efforts are focused upon increasing system power output and system thermal and electric energy conversion efficiency at least five fold over current SP-100 technology, and on achieving systems that are compatible with space nuclear reactors. This paper will discuss progress toward 1050 K Stirling Space Power Converters. Fabrication is nearly completed for the 1050 K Component Test Power Converter (CTPC); results of motoring tests of the cold end (525 K), are presented. The success of these and future designs is dependent upon supporting research and technology efforts including heat pipes, bearings, superalloy joining technologies, high efficiency alternators, life and reliability testing, and predictive methodologies. This paper will compare progress in significant areas of component development from the start of the program with the Space Power Development Engine (SPDE) to the present work on CTPC.

Author

45

ENVIRONMENT POLLUTION

Includes atmospheric, noise, thermal, and water pollution.

N92-22382* # National Aeronautics and Space Administration, Lewis Research Center, Cleveland, OH.

ENVIRONMENTAL INTERACTIONS IN SPACE EXPLORATION: ENVIRONMENTAL INTERACTIONS WORKING GROUP

JOSEPH C. KOLECKI and G. BARRY HILLARD *In* NASA, Johnson Space Center, 5th Annual Workshop on Space Operations Applications and Research (SOAR 1991), Volume 2 p 785-787 Feb. 1992 Previously announced as N92-17069

Avail: CASI HC A01/MF A04

With the advent of the Space Exploration Initiative, the possibility of designing and using systems on scales heretofore unattempted presents exciting new challenges in systems design and space science. The environments addressed by the Space Exploration Initiative include the surfaces of the Moon and Mars, as well as the varied plasma and field environments which will be encountered by humans and cargo enroute to these destinations. Systems designers will need to understand environmental interactions and be able to model these mechanisms from the

earliest conceptual design stages through design completion. To the end of understanding environmental interactions and establishing robotic precursor mission requirements, an Environmental Interactions Working Group was established as part of the Robotic Missions Working Group. The working group is described, and its current activities are updated.

Author

46

GEOPHYSICS

Includes aeronomy; upper and lower atmosphere studies; ionospheric and magnetospheric physics; and geomagnetism.

A92-26984* # Jet Propulsion Lab., California Inst. of Tech., Pasadena.

THE FORMATION AND STRUCTURE OF PLASMA WAKES BEHIND LARGE HIGH-VOLTAGE SPACE PLATFORMS IN IONOSPHERE

J. WANG (JPL, Pasadena, CA) and DANIEL E. HASTINGS (MIT, Cambridge, MA) AIAA, Aerospace Sciences Meeting and Exhibit, 30th, Reno, NV, Jan. 6-9, 1992. 18 p. Jan. 1992 18 p refs (Contract NAG3-695)

(AIAA PAPER 92-0577) Copyright

Theory and particle simulation results are presented for ionospheric plasma flow over space platforms in the large-dimension and high-voltage range. Both the transient formation of the space-charge wake and its steady state structure are studied. The wake-side ion impact and current collection are obtained. It is found that the wake behind a high-voltage plate is characterized by two ion-rich sheaths embedded in a quasi-neutral background wake. The embedded sheath is formed by the ions passing through the sheath around the plate edge and serves as their trajectory path. Depending on the surface potential, the plate dimension, and the angle of attack, the embedded sheath may either extend downstream or curve back to the plate causing a high, localized ion flux density at the location it strikes.

Author

N92-14500* # National Aeronautics and Space Administration, Lewis Research Center, Cleveland, OH.

MEASUREMENT OF TRACE STRATOSPHERIC CONSTITUENTS WITH A BALLOON BORNE LASER RADAR

WILLIAM S. HEAPS and THOMAS J. MCGEE *In* NASA, Washington, NASA Upper Atmosphere Research Program: Research Summaries 1988-1989 p 11 Jan. 1990

Avail: CASI HC A01/MF A03

The objective of this research was to measure the concentration of the stratospheric hydroxyl radical and related chemical species as a function of altitude, season, and time of day. Although hydroxyl plays a very important role in the chemistry controlling stratospheric ozone, little is known about its behavior because it has been a difficult species to measure. The instrument employed in this program was a laser radar, employing the technique of remote laser induced fluorescence. This instrument offers a number of attractive features including extreme specificity and sensitivity, a straightforward relationship between observed quantity and the desired concentration, and immunity to self-contamination.

Author

LIFE SCIENCES (GENERAL)

A92-44385* National Aeronautics and Space Administration. Lewis Research Center, Cleveland, OH.

THERMOPHYSICAL PROPERTIES OF LYSOZYME (PROTEIN) SOLUTIONS

JIACHING LIU and WEN-JEI YANG (Michigan, University, Ann Arbor) Journal of Thermophysics and Heat Transfer (ISSN 0887-8722), vol. 6, no. 3, July-Sept. 1992, p. 531-536. Sep. 1992 6 p refs
(Contract NAG3-903)
Copyright

Thermophysical properties of protein solutions composed of the lysozyme crystals with a 0.1 M sodium acetate and 5 percent NaCl solution as the buffer (pH = 4.0) are determined. The properties being measured include specific heat, thermal conductivity, dynamic viscosity, and surface tension. The protein concentrations are varied. Thermal diffusivity is calculated using the measured results. The purpose of the research is to measure thermophysical properties of lysozyme solutions which would serve as the data bank for controlling and modeling the crystal growth process on earth as well as in space. Author

MAN/SYSTEM TECHNOLOGY AND LIFE SUPPORT

Includes human engineering; biotechnology; and space suits and protective clothing.

A92-12447* Rensselaer Polytechnic Inst., Troy, NY.
DETERMINATION OF THE CRITICAL PARAMETERS FOR REMOTE MICROSCOPE CONTROL

R. C. HAHN, B. A. HERBACH (Rensselaer Polytechnic Institute, Troy, NY), J. C. JOHNSTON, and M. BETHEA (NASA, Lewis Research Center, Cleveland, OH) IAF, International Astronautical Congress, 42nd, Montreal, Canada, Oct. 5-11, 1991. 6 p. Oct. 1991 6 p
(Contract NAG3-1065)
(IAF PAPER 91-026) Copyright

A remote-controlled microscope has been designed as part of a program to determine the capacities of telescience as applied to microgravity materials science. The hardware involves a microscope with positioning device, motors on the zoom and focus controls, a mounted standard TV camera, and computer control of the devices and output. Tests show that the focus setting can be established well within the resolution limit of the TV system, that each motion takes about 50 sec, and that about 12 min are required to reach 'best' focus. C.D.

N92-13581*# National Aeronautics and Space Administration. Lewis Research Center, Cleveland, OH.
RISKS, DESIGNS, AND RESEARCH FOR FIRE SAFETY IN SPACECRAFT

ROBERT FRIEDMAN (National Aeronautics and Space Administration, Lewis Research Center, Cleveland, OH.), KURT R. SACKSTEDER, and DAVID URBAN (Sverdrup Technology, Inc., Brook Park, OH.) 1991 22 p Presented at the Fall Meeting of the National Fire Protection Association, Inc., Montreal, Quebec, 19 Nov. 1991
(Contract NAS3-25266; RTOP 323-53-62)
(NASA-TM-105317; E-6672; NAS 1.15:105317) Avail: CASI HC A03/MF A01

Current fire protection for spacecraft relies mainly on fire prevention through the use of nonflammable materials and strict storage controls of other materials. The Shuttle also has smoke detectors and fire extinguishers, using technology similar to aircraft practices. While experience has shown that the current fire protection is adequate, future improvements in fire safety technology to meet the challenges of long duration space missions, such as the Space Station Freedom, are essential. All spacecraft fire protection systems, however, must deal with the unusual combustion characteristics and operational problems in the low gravity environment. The features of low gravity combustion that affect spacecraft fire safety, and the issues in fire protection for Freedom that must be addressed eventually to provide effective and conservative fire protection systems are discussed. Author

MATHEMATICAL AND COMPUTER SCIENCES (GENERAL)

A92-26968# National Aeronautics and Space Administration. Ames Research Center, Moffett Field, CA.
THE NASA COMPUTATIONAL AEROSCIENCES PROGRAM - TOWARD TERAFLOPS COMPUTING

TERRY L. HOLST (NASA, Ames Research Center, Moffett Field, CA), MANUEL D. SALAS (NASA, Langley Research Center, Hampton, VA), and RUSSELL W. CLAUS (NASA, Lewis Research Center, Cleveland, OH) AIAA, Aerospace Sciences Meeting and Exhibit, 30th, Reno, NV, Jan. 6-9, 1992. 25 p. Jan. 1992 25 p refs
(AIAA PAPER 92-0558) Copyright

The Computational Aerosciences (CAS) project of the High Performance Computing and Communications program is presented and discussed. The main emphasis of this presentation is on the applications portion of the CAS program, which includes a High-Speed Civil Transport element, a High Performance Aircraft element, a NASP-Derived Vehicle element, and an Aerobraking element. Two major thrusts of this program are the enhancement of simulation capabilities using multidiscipline formulations and the improvement in processing efficiency via massive parallel computer hardware. Current activities in these two areas at Ames, Langley and Lewis, are presented and discussed. Author

N92-10289*# National Aeronautics and Space Administration. Lewis Research Center, Cleveland, OH.
ON THE MOST GENERAL TENSOR B(SUB IJ) WHICH IS ZERO FOR I DOES NOT EQUAL J, AND THE MOST GENERAL ISOTROPIC TENSOR I(SUB IJ)

ROBERT G. DEISSLER Oct. 1991 8 p
(Contract RTOP 505-90-52)
(NASA-TM-105236; E-6561; NAS 1.15:105236) Avail: CASI HC A02/MF A01

It is shown that the most general second order tensor B sub ij which is zero for i not = j is proportional to the Kronecker delta (Delta sub ij). By a slight modification of that argument, the known result was obtained that the most general second order isotropic tensor is also proportional to Delta sub ij. These results are useful for instance in obtaining the stress tensor for a viscous fluid. Author

COMPUTER OPERATIONS AND HARDWARE

Includes hardware for computer graphics, firmware, and data processing.

N92-11642*# National Aeronautics and Space Administration. Lewis Research Center, Cleveland, OH.

COMPUTERS IN AERONAUTICS AND SPACE RESEARCH AT THE LEWIS RESEARCH CENTER

1991 12 p Prepared in cooperation with Sverdrup Technology, Inc., Cleveland, OH

(NASA-TM-105096; NAS 1.15:105096)

This brochure presents a general discussion of the role of computers in aerospace research at NASA's Lewis Research Center (LeRC). Four particular areas of computer applications are addressed: computer modeling and simulation, computer assisted engineering, data acquisition and analysis, and computer controlled testing.

M.G.

N92-33897*# National Aeronautics and Space Administration. Lewis Research Center, Cleveland, OH.

IMPLEMENTATION OF AN INTELLIGENT CONTROL SYSTEM

D. L. SIMON (Army Aviation Systems Command, Cleveland, OH.), E. WONG, and J. L. MUSGRAVE May 1992 12 p Presented at the 1992 Advanced Earth-to-Orbit Propulsion Technology Conference, Huntsville, AL, 19-21 May 1992; sponsored by NASA. Marshall Space Flight Center

(NASA-TM-105795; E-7225; NAS 1.15:105795;

AVSCOM-TR-92-C-014; AD-A255413) Avail: CASI HC A03/MF A01

A laboratory testbed facility which was constructed at NASA LeRC for the development of an Intelligent Control System (ICS) for reusable rocket engines is described. The framework of the ICS consists of a hierarchy of various control and diagnostic functions. The traditional high speed, closed-loop controller resides at the lowest level of the ICS hierarchy. Above this level resides the diagnostic functions which identify engine faults. The ICS top level consists of the coordination function which manages the interaction between an expert system and a traditional control system. The purpose of the testbed is to demonstrate the feasibility of the OCS concept by implementing the ICS as the primary controller in a simulation of the Space Shuttle Main Engine (SSME). The functions of the ICS which are implemented in the testbed are as follows: an SSME dynamic simulation with selected fault mode models, a reconfigurable controller, a neural network for sensor validation, a model-based failure detection algorithm, a rule based failure detection algorithm, a diagnostic expert system, an intelligent coordinator, and a user interface which provides a graphical representation of the event occurring within the testbed. The diverse nature of the ICS has led to the development of a distributed architecture consisting of specialized hardware and software for the implementation of the various functions. This testbed is made up of five different computer systems. These individual computers are discussed along with the schemes used to implement the various ICS components. The communication between computers and the timing and synchronization between components are also addressed.

Author

COMPUTER PROGRAMMING AND SOFTWARE

Includes computer programs, routines, algorithms, and specific applications, e.g., CAD/CAM.

A92-12367* National Aeronautics and Space Administration. Lewis Research Center, Cleveland, OH.

PARALLEL COMPUTATION OF AERODYNAMIC INFLUENCE COEFFICIENTS FOR AEROELASTIC ANALYSIS ON A TRANSPUTER NETWORK

D. C. JANETZKE (NASA, Lewis Research Center, Cleveland, OH) and D. V. MURTHY (Toledo, University, OH) (Parallel methods on large-scale structural analysis and physics applications; Symposium, Hampton, VA, Feb. 5, 6, 1991, Selected Papers. A92-12351 02-61) Computing Systems in Engineering (ISSN 0956-0521), vol. 2, no. 2-3, 1991, p. 289-297. 1991 9 p refs Copyright

Aeroelastic analysis is multi-disciplinary and computationally expensive. Hence, it can greatly benefit from parallel processing. As part of an effort to develop an aeroelastic analysis capability on a distributed-memory transputer network, a parallel algorithm for the computation of aerodynamic influence coefficients is implemented on a network of 32 transputers. The aerodynamic influence coefficients are calculated using a three-dimensional unsteady aerodynamic model and a panel discretization. Efficiencies up to 85 percent are demonstrated using 32 processors. The effects of subtask ordering, problem size and network topology are presented. A comparison to results on a shared-memory computer indicates that higher speedup is achieved on the distributed-memory system.

Author

A92-23849* National Aeronautics and Space Administration. Lewis Research Center, Cleveland, OH.

COMPUTER PROGRAM FOR COMPUTING THE PROPERTIES OF SEVENTEEN FLUIDS

J. A. BRENNAN, D. G. FRIEND, V. D. ARP, and R. D. MCCARTY (NIST, Boulder, CO) (Space Cryogenics Workshop, 10th, Cleveland, OH, June 18-20, 1991, Proceedings. A92-23826 08-31) Cryogenics (ISSN 0011-2275), vol. 32, no. 2, 1992, p. 212-214. 1992 3 p refs

(Contract NASA ORDER C-32009-K)

The present study describes modifications and additions to the MIPROPS computer program for calculating the thermophysical properties of 17 fluids. These changes include adding new fluids, new properties, and a new interface to the program. The new program allows the user to select the input and output parameters and the units to be displayed for each parameter. Fluids added to the MIPROPS program are carbon dioxide, carbon monoxide, deuterium, helium, normal hydrogen, and xenon. The most recent modifications to the MIPROPS program are the addition of viscosity and thermal conductivity correlations for parahydrogen and the addition of the fluids normal hydrogen and xenon. The recently added interface considerably increases the program's utility.

P.D.

A92-33285*# National Aeronautics and Space Administration. Lewis Research Center, Cleveland, OH.

COMPUTATIONAL SIMULATION OF CONCURRENT ENGINEERING FOR AEROSPACE PROPULSION SYSTEMS

C. C. CHAMIS (NASA, Lewis Research Center, Cleveland, OH) and S. N. SINGHAL (Sverdrup Technology, Inc., Cleveland, OH) AIAA, Aerospace Design Conference, Irvine, CA, Feb. 3-6, 1992. 12 p. Feb. 1992 12 p refs

(AIAA PAPER 92-1144) Copyright

Results are summarized of an investigation to assess the infrastructure available and the technology readiness in order to develop computational simulation methods/software for concurrent engineering. These results demonstrate that development of computational simulations methods for concurrent engineering is

61 COMPUTER PROGRAMMING AND SOFTWARE

timely. Extensive infrastructure, in terms of multi-discipline simulation, component-specific simulation, system simulators, fabrication process simulation, and simulation of uncertainties - fundamental in developing such methods, is available. An approach is recommended which can be used to develop computational simulation methods for concurrent engineering for propulsion systems and systems in general. Benefits and facets needing early attention in the development are outlined. Author

A92-34342* # National Aeronautics and Space Administration. Lewis Research Center, Cleveland, OH.

RECENT DEVELOPMENTS OF THE NESSUS PROBABILISTIC STRUCTURAL ANALYSIS COMPUTER PROGRAM

H. MILLWATER, Y.-T. WU, T. TORNG, B. THACKER, D. RIHA, and C. P. LEUNG (Southwest Research Institute, San Antonio, TX) IN: AIAA/ASME/ASCE/AHS/ASC Structures, Structural Dynamics and Materials Conference, 33rd, Dallas, TX, Apr. 13-15, 1992, Technical Papers. Pt. 2 1992 11 p refs (Contract NAS3-24389)

(AIAA PAPER 92-2411) Copyright

The NESSUS probabilistic structural analysis computer program combines state-of-the-art probabilistic algorithms with general purpose structural analysis methods to compute the probabilistic response and the reliability of engineering structures. Uncertainty in loading, material properties, geometry, boundary conditions and initial conditions can be simulated. The structural analysis methods include nonlinear finite element and boundary element methods. Several probabilistic algorithms are available such as the advanced mean value method and the adaptive importance sampling method. The scope of the code has recently been expanded to include probabilistic life and fatigue prediction of structures in terms of component and system reliability and risk analysis of structures considering cost of failure. The code is currently being extended to structural reliability considering progressive crack propagation. Several examples are presented to demonstrate the new capabilities. Author

A92-34367* # National Aeronautics and Space Administration. Lewis Research Center, Cleveland, OH.

A STUDY OF EQUATION SOLVERS FOR LINEAR AND NON-LINEAR FINITE ELEMENT ANALYSIS ON PARALLEL PROCESSING COMPUTERS

BRIAN C. WATSON and MANOHAR P. KAMAT (Georgia Institute of Technology, Atlanta) IN: AIAA/ASME/ASCE/AHS/ASC Structures, Structural Dynamics and Materials Conference, 33rd, Dallas, TX, Apr. 13-15, 1992, Technical Papers. Pt. 2 1992 8 p refs

(Contract NAG3-895)

(AIAA PAPER 92-2478) Copyright

Concurrent computing environments provide the means to achieve very high performance for finite element analysis of systems, provided the algorithms take advantage of multiple processors. The authors have examined several algorithms for both linear and nonlinear finite element analysis. The performance of these algorithms on an Alliant FX/80 parallel supercomputer has been studied. For single load case linear analysis, the optimal solution algorithm is strongly problem dependent. For multiple load cases or nonlinear analysis through a modified Newton-Raphson method, decomposition algorithms are shown to have a decided advantage over element-by-element preconditioned conjugate gradient algorithms. Author

A92-38490* # National Aeronautics and Space Administration. Lewis Research Center, Cleveland, OH.

MISTEC - A SOFTWARE APPLICATION FOR SUPPORTING SPACE EXPLORATION SCENARIO OPTIONS AND TECHNOLOGY DEVELOPMENT ANALYSIS AND PLANNING

GARY A. P. HORSHAM (NASA, Lewis Research Center, Cleveland, OH) AIAA, Space Programs and Technologies Conference, Huntsville, AL, Mar. 24-27, 1992. 14 p. Previously announced in STAR as N92-14649. Mar. 1992 14 p

(Contract NAS3-25266)

(AIAA PAPER 92-1293) Copyright

This structure and composition of a new, emerging software application, which models and analyzes space exploration scenario options for feasibility based on technology development projections is presented. The software application consists of four main components: a scenario generator for designing and inputting scenario options and constraints; a processor which performs algorithmic coupling and options analyses of mission activity requirements and technology capabilities; a results display which graphically and textually shows coupling and options analysis on a variety of mission activities and (power and propulsion) technology system capabilities. The general long-range study process used by NASA to support recent studies is briefly introduced to provide the primary basis for comparison for discussing the potential advantages to be gained from developing and applying this kind of application. A hypothetical example of a scenario option to facilitate the best conceptual understanding of what the application is, how it works, or the operating methodology, and when it might be applied is presented. Author

A92-50533* # National Aeronautics and Space Administration. Lewis Research Center, Cleveland, OH.

DESCRIPTION OF REAL-TIME ADA SOFTWARE IMPLEMENTATION OF A POWER SYSTEM MONITOR FOR THE SPACE STATION FREEDOM PMAD DC TESTBED

KIMBERLY LUDWIG (Sverdrup Technology, Inc., Brook Park, OH), MICHAEL MACKIN, and THEODORE WRIGHT (NASA, Lewis Research Center, Cleveland, OH) IN: IECEC '91; Proceedings of the 26th Intersociety Energy Conversion Engineering Conference, Boston, MA, Aug. 4-9, 1991. Vol. 1 1991 5 p refs

Copyright

The authors describe the Ada language software developed to perform the electrical power system monitoring functions for the NASA Lewis Research Center's Power Management and Distribution (PMAD) DC testbed. The results of the effort to implement this monitor are presented. The PMAD DC testbed is a reduced-scale prototype of the electric power system to be used in Space Station Freedom. The power is controlled by smart switches known as power control components (or switchgear). The power control components are currently coordinated by five Compaq 386/20e computers connected through an 802.4 local area network. The power system monitor algorithm comprises several functions, including periodic data acquisition, data smoothing, system performance analysis, and status reporting. Data are collected from the switchgear sensors every 100 ms, then passed through a 2-Hz digital filter. System performance analysis includes power interruption and overcurrent detection. The system monitor required a hardware timer interrupt to activate the data acquisition function. The execution time of the code was optimized by using an assembly language routine. The routine allows direct vectoring of the processor to Ada language procedures that perform periodic control activities. I.E.

A92-54006* # National Aeronautics and Space Administration. Lewis Research Center, Cleveland, OH.

FREPS - A FORCED RESPONSE PREDICTION SYSTEM FOR TURBOMACHINERY BLADE ROWS

DURBHA V. MURTHY (Toledo, University, OH) and GEORGE L. STEFKO (NASA, Lewis Research Center, Cleveland, OH) AIAA, SAE, ASME, and ASEE, Joint Propulsion Conference and Exhibit, 28th, Nashville, TN, July 6-8, 1992. 9 p. Jul. 1992 9 p refs (AIAA PAPER 92-3072)

FREPS (Forced REsponse Prediction System) is a software system that integrates structural dynamic, steady and unsteady aerodynamic analyses to efficiently predict the forced dynamic stresses of turbomachinery blades to aerodynamic and mechanical excitations. The program performs flutter analysis also. The FREPS system uses a modal approach for aeroelastic analysis. The structural dynamic analysis is based on MSC/NASTRAN, the steady aerodynamic analysis is based on potential theory and the unsteady aerodynamic analysis is based on a linearization of the non-uniform potential mean flow. The capabilities of the program are described

61 COMPUTER PROGRAMMING AND SOFTWARE

and illustrated by application to the High Pressure Oxygen Turbopump turbine of the Space Shuttle Main Engine. Author

A92-54114*# National Aeronautics and Space Administration, Lewis Research Center, Cleveland, OH.

GRID GENERATION FOR 3D TURBOMACHINERY CONFIGURATIONS

MING-HSIN SHIH and BHARAT K. SONI (Mississippi State University, Mississippi State) AIAA, SAE, ASME, and ASEE, Joint Propulsion Conference and Exhibit, 28th, Nashville, TN, July 6-8, 1992. 8 p. Research supported by NASA. Jul. 1992 8 p refs

(AIAA PAPER 92-3671) Copyright

A numerical grid generation algorithm associated with the flow field about turbomachinery geometries is presented. Graphical user interface is developed with the FORMS Library to create an interactive, user-friendly working environment. This customized algorithm reduces the man-hours required to generate a grid associated with turbomachinery geometry, as compared to those required by general-purpose grid generation softwares. Bezier curves are utilized both interactively and automatically to accomplish grid line smoothness and orthogonality. Graphical user interactions are provided in the algorithm and allow the user to design and manipulate the grid lines with a mouse. Author

N92-11691*# National Aeronautics and Space Administration, Lewis Research Center, Cleveland, OH.

COMPUTER PROGRAM FOR BESSEL AND HANKEL FUNCTIONS

KEVIN L. KREIDER (Akron Univ., OH.), ARTHUR V. SAULE, EDWARD J. RICE, and BRUCE J. CLARK Oct. 1991 66 p

(Contract RTOP 505-62-21)
(NASA-TM-105154; E-6439; NAS 1.15:105154) Avail: CASI HC A04/MF A01

A set of FORTRAN subroutines for calculating Bessel and Hankel functions is presented. The routines calculate Bessel and Hankel functions of the first and second kinds, as well as their derivatives, for wide ranges of integer order and real or complex argument in single or double precision. Depending on the order and argument, one of three evaluation methods is used: the power series definition, an Airy function expansion, or an asymptotic expansion. Routines to calculate Airy functions and their derivatives are also included. Author

N92-14649*# National Aeronautics and Space Administration, Lewis Research Center, Cleveland, OH.

MISTEC: A SOFTWARE APPLICATION FOR SUPPORTING SPACE EXPLORATION SCENARIO OPTIONS AND TECHNOLOGY DEVELOPMENT ANALYSIS AND PLANNING

GARY A. P. HORSHAM Nov. 1991 15 p Proposed for presentation at the Space Programs and Technologies Conference, Huntsville, AL, 24-27 Mar. 1992; sponsored by AIAA (Contract RTOP 594-81-21)

(NASA-TM-105214; E-6529; NAS 1.15:105214; AIAA PAPER 92-1293) Avail: CASI HC A03/MF A01

The structure and composition of a new, emerging software application, which models and analyzes space exploration scenario options for feasibility based on technology development projections is presented. The software application consists of four main components: a scenario generator for designing and inputting scenario options and constraints; a processor which performs algorithmic coupling and options analyses of mission activity requirements and technology capabilities; a results display which graphically and textually shows coupling and options analysis results; and a data/knowledge base which contains information on a variety of mission activities and (power and propulsion) technology system capabilities. The general long-range study process used by NASA to support recent studies is briefly introduced to provide the primary basis for comparison for discussing the potential advantages to be gained from developing and applying this kind of application. A hypothetical example of a scenario option to facilitate the best conceptual understanding of

what the application is, how it works, or the operating methodology, and when it might be applied is presented. Author

N92-16628*# National Aeronautics and Space Administration, Lewis Research Center, Cleveland, OH.

A SOFTWARE CONTROL SYSTEM FOR THE ACTS HIGH-BURST-RATE LINK EVALUATION TERMINAL

RICHARD C. REINHART (Analex Corp., Brook Park, OH.) and ELAINE S. DAUGHERTY Dec. 1991 12 p

(Contract RTOP 650-60-23)
(NASA-TM-105207; E-6520; NAS 1.15:105207) Avail: CASI HC A03/MF A01

Control and performance monitoring of NASA's High Burst Rate Link Evaluation Terminal (HBR-LET) is accomplished by using several software control modules. Different software modules are responsible for controlling remote radio frequency (RF) instrumentation, supporting communication between a host and a remote computer, controlling the output power of the Link Evaluation Terminal and data display. Remote commanding of microwave RF instrumentation and the LET digital ground terminal allows computer control of various experiments, including bit error rate measurements. Computer communication allows system operators to transmit and receive from the Advanced Communications Technology Satellite (ACTS). Finally, the output power control software dynamically controls the uplink output power of the terminal to compensate for signal loss due to rain fade. Included is a discussion of each software module and its applications. Author

N92-24420*# National Aeronautics and Space Administration, Lewis Research Center, Cleveland, OH.

INTERACTIVE SOLUTION-ADAPTIVE GRID GENERATION

YUNG K. CHOO and TODD L. HENDERSON (Illinois Univ., Urbana.) *In* NASA. Langley Research Center, Software Surface Modeling and Grid Generation Steering Committee p 347-361 Apr. 1992

Avail: CASI HC A03/MF A04

TURBO-AD is an interactive solution-adaptive grid generation program under development. The program combines an interactive algebraic grid generation technique and a solution-adaptive grid generation technique into a single interactive solution-adaptive grid generation package. The control point form uses a sparse collection of control points to algebraically generate a field grid. This technique provides local grid control capability and is well suited to interactive work due to its speed and efficiency. A mapping from the physical domain to a parametric domain was used to improve difficulties that had been encountered near outwardly concave boundaries in the control point technique. Therefore, all grid modifications are performed on a unit square in the parametric domain, and the new adapted grid in the parametric domain is then mapped back to the physical domain. The grid adaptation is achieved by first adapting the control points to a numerical solution in the parametric domain using control sources obtained from flow properties. Then a new modified grid is generated from the adapted control net. This solution-adaptive grid generation process is efficient because the number of control points is much less than the number of grid points and the generation of a new grid from the adapted control net is an efficient algebraic process. TURBO-AD provides the user with both local and global grid controls. Author

N92-24421*# National Aeronautics and Space Administration, Lewis Research Center, Cleveland, OH.

MAG3D AND ITS APPLICATION TO INTERNAL FLOWFIELD ANALYSIS

K. D. LEE (Illinois Univ. at Urbana-Champaign, Savoy.), T. L. HENDERSON (Illinois Univ., Urbana.), and Y. K. CHOO *In* NASA. Langley Research Center, Software Surface Modeling and Grid Generation Steering Committee p 363-377 Apr. 1992

Avail: CASI HC A03/MF A04

MAG3D (multiblock adaptive grid, 3D) is a 3D solution-adaptive grid generation code which redistributes grid points to improve the accuracy of a flow solution without increasing the number of grid points. The code is applicable to structured grids with a

multiblock topology. It is independent of the original grid generator and the flow solver. The code uses the coordinates of an initial grid and the flow solution interpolated onto the new grid. MAG3D uses a numerical mapping and potential theory to modify the grid distribution based on properties of the flow solution on the initial grid. The adaptation technique is discussed, and the capability of MAG3D is demonstrated with several internal flow examples. Advantages of using solution-adaptive grids are also shown by comparing flow solutions on adaptive grids with those on initial grids. Author

N92-24428*# National Aeronautics and Space Administration. Lewis Research Center, Cleveland, OH.

A MULTIBLOCK GRID GENERATION TECHNIQUE APPLIED TO A JET ENGINE CONFIGURATION

MARK E. M. STEWART *In* NASA. Langley Research Center, Software Surface Modeling and Grid Generation Steering Committee p 477-485 Apr. 1992
 Avail: CASI HC A02/MF A04

Techniques are presented for quickly finding a multiblock grid for a 2D geometrically complex domain from geometrical boundary data. An automated technique for determining a block decomposition of the domain is explained. Techniques for representing this domain decomposition and transforming it are also presented. Further, a linear optimization method may be used to solve the equations which determine grid dimensions within the block decomposition. These algorithms automate many stages in the domain decomposition and grid formation process and limit the need for human intervention and inputs. They are demonstrated for the meridional or throughflow geometry of a bladed jet engine configuration. D.R.D.

N92-25715*# National Aeronautics and Space Administration. Lewis Research Center, Cleveland, OH.

QX MAN: Q AND X FILE MANIPULATION

MARK A. KREIN *In its* Workshop on Grid Generation and Related Areas p 29-33 Apr. 1992
 Avail: CASI HC A01/MF A02

QX MAN is a grid and solution file manipulation program written primarily for the PARC code and the GRIDGEN family of grid generation codes. QX MAN combines many of the features frequently encountered in grid generation, grid refinement, the setting-up of initial conditions, and post processing. QX MAN allows the user to manipulate single block and multi-block grids (and their accompanying solution files) by splitting, concatenating, rotating, translating, re-scaling, and stripping or adding points. In addition, QX MAN can be used to generate an initial solution file for the PARC code. The code was written to provide several formats for input and output in order for it to be useful in a broad spectrum of applications. Author

N92-25724*# National Aeronautics and Space Administration. Lewis Research Center, Cleveland, OH.

INTERACTIVE SOLUTION-ADAPTIVE GRID GENERATION PROCEDURE

YUNG K. CHOO and TODD HENDERSON *In its* Workshop on Grid Generation and Related Areas p 123-138 Apr. 1992
 Avail: CASI HC A03/MF A02

TURBO-AD is a two dimensional interactive solution adaptive grid generation program. The code uniquely combines a grid adaptation technique that uses parametric mapping with control sources and an algebraic grid generation that uses control points into a single software package. The grid adaptation is achieved by first adapting the control points to a numerical solution in the parametric domain using the control sources obtained from flow properties. Then a new grid is generated from the adapted control net using the control point formulation. The new adapted grid in the parametric domain is then mapped back to the physical domain. This solution adaptive grid generation process is efficient because the number of control points is much less than the number of grid points and the grid generation from the adapted control net is an efficient algebraic process. Author

N92-25726*# National Aeronautics and Space Administration. Lewis Research Center, Cleveland, OH.

ACTIVITIES FOR NUMERICAL PROPULSION SYSTEMS SIMULATION PROGRAM

AUSTIN L. EVANS *In its* Workshop on Grid Generation and Related Areas p 151-157 Apr. 1992
 Avail: CASI HC A02/MF A02

The Interdisciplinary Technology Office (ITO) has been tasked with the responsibility of coordinating interdisciplinary research and technology programs; establish and maintain interface with the various disciplines at LeRC, industry, government, and academic organizations; and facilitating the exploitation of advances in the individual disciplinary efforts that have multidisciplinary implications. H.A.

N92-25913*# National Aeronautics and Space Administration. Lewis Research Center, Cleveland, OH.

COMPUTER CODES DEVELOPED AND UNDER DEVELOPMENT AT LEWIS

CHRISTOS C. CHAMIS *In* NASA. Langley Research Center, Computational Structures Technology for Airframes and Propulsion Systems p 43-57 May 1992
 Avail: CASI HC A03/MF A04

The objective of this summary is to provide a brief description of: (1) codes developed or under development at LeRC; and (2) the development status of IPACS with some typical early results. The computer codes that have been developed and/or are under development at LeRC are listed in the accompanying charts. This list includes: (1) the code acronym; (2) select physics descriptors; (3) current enhancements; and (4) present (9/91) code status with respect to its availability and documentation. The computer codes list is grouped by related functions such as: (1) composite mechanics; (2) composite structures; (3) integrated and 3-D analysis; (4) structural tailoring; and (5) probabilistic structural analysis. These codes provide a broad computational simulation infrastructure (technology base-readiness) for assessing the structural integrity/durability/reliability of propulsion systems. These codes serve two other very important functions: they provide an effective means of technology transfer; and they constitute a depository of corporate memory. Author

N92-28684*# National Aeronautics and Space Administration. Lewis Research Center, Cleveland, OH.

PC GRAPHICS GENERATION AND MANAGEMENT TOOL FOR REAL-TIME APPLICATIONS

LONG V. TRUONG Jul. 1992 10 p Presented at the 23rd Conference on Modeling and Simulation, Pittsburgh, PA, 30 Apr. - 1 May 1992
 (Contract RTOP 506-41-41)
 (NASA-TM-105749; E-7053; NAS 1.15:105749) Avail: CASI HC A02/MF A01

A graphics tool was designed and developed for easy generation and management of personal computer graphics. It also provides methods and 'run-time' software for many common artificial intelligence (AI) or expert system (ES) applications. Author

N92-33894*# National Aeronautics and Space Administration. Lewis Research Center, Cleveland, OH.

A GRAPHICAL USER-INTERFACE FOR PROPULSION SYSTEM ANALYSIS

BRIAN P. CURLETT and KATHLEEN RYALL (Harvard Univ., Cambridge, MA.) Aug. 1992 28 p
 (Contract RTOP 505-69-50)
 (NASA-TM-105696; E-7158; NAS 1.15:105696) Avail: CASI HC A03/MF A01

NASA LeRC uses a series of computer codes to calculate installed propulsion system performance and weight. The need to evaluate more advanced engine concepts with a greater degree of accuracy has resulted in an increase in complexity of this analysis system. Therefore, a graphical user interface was developed to allow the analyst to more quickly and easily apply these codes. The development of this interface and the rationale for the approach taken are described. The interface consists of a method of

pictorially representing and editing the propulsion system configuration, forms for entering numerical data, on-line help and documentation, post processing of data, and a menu system to control execution.

Author

62

COMPUTER SYSTEMS

Includes computer networks and special application computer systems.

A92-13595* National Aeronautics and Space Administration, Lewis Research Center, Cleveland, OH.

INTERFACING LABORATORY INSTRUMENTS TO MULTIUSER, VIRTUAL MEMORY COMPUTERS

EDWARD R. GENERAZIO, DON J. ROTH (NASA, Lewis Research Center, Cleveland, OH), and DAVID B. STANG (NASA, Lewis Research Center; Sverdrup Technology, Inc., Cleveland, OH) IN: Review of progress in quantitative nondestructive evaluation. Vol. 9A 1990 7 p refs

Copyright

Incentives, problems and solutions associated with interfacing laboratory equipment with multiuser, virtual memory computers are presented. The major difficulty concerns how to utilize these computers effectively in a medium sized research group. This entails optimization of hardware interconnections and software to facilitate multiple instrument control, data acquisition and processing. The architecture of the system that was devised, and associated programming and subroutines are described. An example program involving computer controlled hardware for ultrasonic scan imaging is provided to illustrate the operational features.

Author

A92-50535* National Aeronautics and Space Administration, Lewis Research Center, Cleveland, OH.

MODEL-BASED DIAGNOSTICS FOR SPACE STATION FREEDOM

LORRAINE M. FESQ, AMY STEPHAN, ERIC R. MARTIN, and MARCEL G. LERUTTE (TRW Space and Technology Group, Redondo Beach, CA) IN: IECEC '91; Proceedings of the 26th Intersociety Energy Conversion Engineering Conference, Boston, MA, Aug. 4-9, 1991. Vol. 1 1991 6 p refs

Copyright

An innovative approach to fault management was recently demonstrated for the NASA LeRC Space Station Freedom (SSF) power system testbed. This project capitalized on research in model-based reasoning, which uses knowledge of a system's behavior to monitor its health. The fault management system (FMS) can isolate failures online, or in a post analysis mode, and requires no knowledge of failure symptoms to perform its diagnostics. An in-house tool called MARPLE was used to develop and run the FMS. MARPLE's capabilities are similar to those available from commercial expert system shells, although MARPLE is designed to build model-based as opposed to rule-based systems. These capabilities include functions for capturing behavioral knowledge, a reasoning engine that implements a model-based technique known as constraint suspension, and a tool for quickly generating new user interfaces. The prototype produced by applying MARPLE to SSF not only demonstrated that model-based reasoning is a valuable diagnostic approach, but it also suggested several new applications of MARPLE, including an integration and testing aid, and a complement to state estimation.

I.E.

A92-55855* National Aeronautics and Space Administration, Lewis Research Center, Cleveland, OH.

SCAILET - AN INTELLIGENT ASSISTANT FOR SATELLITE GROUND TERMINAL OPERATIONS

A. K. SHAHIDI, J. A. CRAPO, R. F. SCHLEGELMILCH (Sverdrup Technology, Inc., Tullahoma, TN), R. C. REINHART (Analex Corp.,

Brook Park, OH), E. J. PETRIK, J. L. WALTERS, and R. E. JONES (NASA, Lewis Research Center, Cleveland, OH) IAF, International Astronautical Congress, 43rd, Washington, Aug. 28-Sept. 5, 1992. 8 p. Aug. 1992 8 p refs (IAF PAPER 92-0552)

Space communication artificial intelligence for the link evaluation terminal (SCAILET) is an experimenter interface to the link evaluation terminal (LET) developed by NASA through the application of artificial intelligence to an advanced ground terminal. The high-burst-rate (HBR) LET provides the required capabilities for wideband communications experiments with the advanced communications technology satellite (ACTS). The HBR-LET terminal consists of seven major subsystems and is controlled and monitored by a minicomputer through an IEEE-488 or RS-232 interface. Programming scripts configure HBR-LET and allow data acquisition but are difficult to use and therefore the full capabilities of the system are not utilized. An intelligent assistant module was developed as part of the SCAILET module and solves problems encountered during configuration of the HBR-LET system. This assistant is a graphical interface with an expert system running in the background and allows users to configure instrumentation, program sequences and reference documentation. The simplicity of use makes SCAILET a superior interface to the ASCII terminal and continuous monitoring allows nearly flawless configuration and execution of HBR-LET experiments.

A.O.

63

CYBERNETICS

Includes feedback and control theory, artificial intelligence, robotics and expert systems.

A92-14509* Rensselaer Polytechnic Inst., Troy, NY. **NEUROBIOLOGICAL COMPUTATIONAL MODELS IN STRUCTURAL ANALYSIS AND DESIGN**

P. HAJELA (Rensselaer Polytechnic Institute, Troy, NY) and L. BERKE (NASA, Lewis Research Center, Cleveland, OH) Computers and Structures (ISSN 0045-7949), vol. 41, no. 4, 1991, p. 657-667. 1991 11 p refs (Contract NAG3-1086)

Copyright

This paper examines the role of neural computing strategies in structural analysis and design. A principal focus of the work resides in the use of neural networks to represent the force-displacement relationship in static structural analysis. Such models provide computationally efficient capabilities for reanalysis, and appear to be well suited for application in numerical optimum design. The paper presents an overview of the neural computing approach, with special emphasis on supervised learning techniques adopted in the present work. Special features of such learning strategies which have a direct bearing on numerical accuracy and efficiency, are examined in the context of representative structural optimization problems.

Author

A92-21694* National Aeronautics and Space Administration, Lewis Research Center, Cleveland, OH.

A REAL TIME NEURAL NET ESTIMATOR OF FATIGUE LIFE

T. TROUDET (NASA, Lewis Research Center; Sverdrup Technology, Inc., Cleveland, OH) and W. MERRILL (NASA, Lewis Research Center, Cleveland, OH) IN: IJCNN - International Joint Conference on Neural Networks, San Diego, CA, June 17-21, 1990, Proceedings. Vol. 2 1990 6 p refs

Copyright

A neural network architecture is proposed to estimate, in real-time, the fatigue life of mechanical components, as part of the intelligent Control System for Reusable Rocket Engines. Arbitrary component loading values were used as input to train a two hidden-layer feedforward neural net to estimate component fatigue damage. The ability of the net to learn, based on a local

strain approach, the mapping between load sequence and fatigue damage has been demonstrated for a uniaxial specimen. Because of its demonstrated performance, the neural computation may be extended to complex cases where the loads are biaxial or triaxial, and the geometry of the component is complex (e.g., turbopumps blades). The generality of the approach is such that load/damage mappings can be directly extracted from experimental data without requiring any knowledge of the stress/strain profile of the component. In addition, the parallel network architecture allows real-time life calculations even for high-frequency vibrations. Owing to its distributed nature, the neural implementation will be robust and reliable, enabling its use in hostile environments such as rocket engines. Author

A92-25878* National Aeronautics and Space Administration. Lewis Research Center, Cleveland, OH.

STOCHASTIC STABILITY PROPERTIES OF JUMP LINEAR SYSTEMS

XIANGBO FENG, KENNETH A. LOPARO, YUANDONG JI, and HOWARD J. CHIZECK (Case Western Reserve University, Cleveland, OH) IEEE Transactions on Automatic Control (ISSN 0018-9286), vol. 37, Jan. 1992, p. 38-53. Jan. 1992 16 p refs

(Contract NSF ECS-88-16733; NAG3-788)
Copyright

Jump linear systems are defined as a family of linear systems with randomly jumping parameters (usually governed by a Markov jump process) and are used to model systems subject to failures or changes in structure. The authors study stochastic stability properties in jump linear systems and the relationship among various moment and sample path stability properties. It is shown that all second moment stability properties are equivalent and are sufficient for almost sure sample path stability, and a testable necessary and sufficient condition for second moment stability is derived. The Lyapunov exponent method for the study of almost sure sample stability is discussed, and a theorem which characterizes the Lyapunov exponents of jump linear systems is presented. I.E.

A92-29030* National Aeronautics and Space Administration. Lewis Research Center, Cleveland, OH.

DESIGN OF MULTI-LAYER NEURAL NETWORKS FOR ACCURATE IDENTIFICATION OF NONLINEAR MAPPINGS

EDILBERTO TEIXEIRA, KENNETH LOPARO (Case Western Reserve University, Cleveland, OH), and FERNANDO A. C. GOMIDE (Campinas, Universidade Estadual, Brazil) IN: 1991 American Control Conference, 10th, Boston, MA, June 26-28, 1991, Proceedings. Vol. 1 1991 2 p refs

(Contract NAG3-788; CNPQ-300729/86-3)
Copyright

Guidelines for the design of multilayer neural networks for the identification of nonlinear mappings are considered. Since nonlinear mappings can be approximated by a one-hidden-layer neural network, an approach to determine the sufficient number of hidden layer nodes to achieve a global minima of the identification error function is considered. I.E.

A92-29162* National Aeronautics and Space Administration. Lewis Research Center, Cleveland, OH.

TEMPERATURE CONTROL IN CONTINUOUS FURNACE BY STRUCTURAL DIAGRAM METHOD

LEI XIA and TOM T. HARTLEY (Akron, University, OH) IN: 1991 American Control Conference, 10th, Boston, MA, June 26-28, 1991, Proceedings. Vol. 1 1991 3 p refs

(Contract NAG3-904)
Copyright

The fundamentals of the structural diagram method for distributed parameter systems (DPSs) are presented and reviewed. An example is given to illustrate the application of this method for control design. I.E.

A92-29166* National Aeronautics and Space Administration. Lewis Research Center, Cleveland, OH.

LIFE EXTENDING CONTROL

CARL F. LORENZO and WALTER C. MERRILL (NASA, Lewis Research Center, Cleveland, OH) IN: 1991 American Control Conference, 10th, Boston, MA, June 26-28, 1991, Proceedings. Vol. 2 1991 15 p refs

Copyright

The concept of Life Extending Control is defined. Life is defined in terms of mechanical fatigue life. A brief description is given of the current approach to life prediction using a local, cyclic, stress-strain approach for a critical system component. An alternative approach to life prediction based on a continuous functional relationship to component performance is proposed. Based on cyclic life prediction, an approach to life extending control, called the Life Management Approach, is proposed. A second approach, also based on cyclic life prediction, called the implicit approach, is presented. Assuming the existence of the alternative functional life prediction approach, two additional concepts for Life Extending Control are presented. Author

A92-29316* National Aeronautics and Space Administration. Lewis Research Center, Cleveland, OH.

A LYAPUNOV BASED NONLINEAR CONTROL SCHEME FOR STABILIZING A BASIC COMPRESSION SYSTEM USING A CLOSE-COUPLED CONTROL VALVE

J. S. SIMON and L. VALAVANI (MIT, Cambridge, MA) IN: 1991 American Control Conference, 10th, Boston, MA, June 26-28, 1991, Proceedings. Vol. 3 1991 9 p refs

(Contract NAG3-770)
Copyright

The use of a closed-loop control to allow surge-free operation of a compression system beyond its uncontrolled surge line is addressed. In contrast to previous analyses which used a linearized model, the approach described directly addresses the nonlinear nature of the compressor characteristic using a Lyapunov-based control law design formulation. The proposed approach is fairly generic and should be of interest for gas turbine engines as well as other applications. I.E.

A92-40375* National Aeronautics and Space Administration. Lewis Research Center, Cleveland, OH.

AN IIR MEDIAN HYBRID FILTER

PETER H. BAUER, MICHAEL A. SARTORI (Notre Dame, University, IN), and TIMOTHY M. BRYDEN (IBM Corp., Poughkeepsie, NY) IEEE Transactions on Signal Processing (ISSN 1053-587X), vol. 40, no. 5, May 1992, p. 1068-1078. May 1992 11 p refs

(Contract NAG3-1186)
Copyright

A new class of nonlinear filters, the so-called class of multidirectional infinite impulse response median hybrid filters, is presented and analyzed. The input signal is processed twice using a linear shift-invariant infinite impulse response filtering module: once with normal causality and a second time with inverted causality. The final output of the MIMH filter is the median of the two-directional outputs and the original input signal. Thus, the MIMH filter is a concatenation of linear filtering and nonlinear filtering (a median filtering module). Because of this unique scheme, the MIMH filter possesses many desirable properties which are both proven and analyzed (including impulse removal, step preservation, and noise suppression). A comparison to other existing median type filters is also provided. Author

A92-41165* National Aeronautics and Space Administration. Lewis Research Center, Cleveland, OH.

A FUNDAMENTAL THEOREM FOR THE MODEL REDUCTION OF NONLINEAR SYSTEMS

FARAMARZ MOSSAYEBI, TOM T. HARTLEY, and J. A. DE ABREU-GARCIA (Akron, University, OH) Franklin Institute, Journal (ISSN 0016-0032), vol. 329, no. 1, Jan. 1992, p. 145-153. Jan. 1992 9 p refs

(Contract NAG3-904)
Copyright

A simple, but fundamental, theorem is given on the extent to which a nonlinear system model can have its order reduced. Essentially, the result is that the order, or the dimension of the state space representation, cannot be reduced to, or below, the dimension of the system's attractor. Several examples are given to illustrate this point. The result is especially applicable to higher order systems such as the infinite dimensional systems arising from the modeling of distributed parameter systems. Author

A92-41895* National Aeronautics and Space Administration. Lewis Research Center, Cleveland, OH.

NEURAL NETWORK BASED DECOMPOSITION IN OPTIMAL STRUCTURAL SYNTHESIS

P. HAJELA (Rensselaer Polytechnic Institute, Troy, NY) and L. BERKE (NASA, Lewis Research Center, Cleveland, OH) (International Conference on Computational Structures Technology, 1st, Edinburgh, Scotland, Aug. 20-22, 1991) Computing Systems in Engineering (ISSN 0956-0521), vol. 2, no. 5-6, 1992, p. 473-481. 1992 9 p refs

(Contract NAG3-1196)

Copyright

The present paper describes potential applications of neural networks in the multilevel decomposition based optimal design of structural systems. The generic structural optimization problem of interest, if handled as a single problem, results in a large dimensionality problem. Decomposition strategies allow for this problem to be represented by a set of smaller, decoupled problems, for which solutions may either be obtained with greater ease or may be obtained in parallel. Neural network models derived through supervised training, are used in two distinct modes in this work. The first uses neural networks to make available efficient analysis models for use in repetitive function evaluations as required by the optimization algorithm. In the second mode, neural networks are used to represent the coupling that exists between the decomposed subproblems. The approach is illustrated by application to the multilevel decomposition-based synthesis of representative truss and frame structures. Author

A92-50387* National Aeronautics and Space Administration. Lewis Research Center, Cleveland, OH.

SELF-ALIGNING OPTICAL MEASUREMENT SYSTEMS

ARTHUR J. DECKER (NASA, Lewis Research Center, Cleveland, OH) Applied Optics (ISSN 0003-6935), vol. 31, no. 22, Aug. 1, 1992, p. 4339, 4340. 1 Aug. 1992 2 p refs

Copyright

The paper discusses how to teach a system of neural networks to respond to the alignment clues used by a human operator in performing routine, initial alignments. A paradigm is proposed for automating the alignment of the components of optical measurement systems. The paradigm which was tested on a spatial filter has proved to be successful for optical alignment. O.G.

A92-50532* National Aeronautics and Space Administration. Lewis Research Center, Cleveland, OH.

AUTONOMOUS POWER SYSTEM INTELLIGENT DIAGNOSIS AND CONTROL

MARK J. RINGER, TODD M. QUINN, and ANTHONY MEROLLA (Sverdrup Technology, Inc., Brook Park; NASA, Lewis Research Center, Cleveland, OH) IN: IECEC '91; Proceedings of the 26th Intersociety Energy Conversion Engineering Conference, Boston, MA, Aug. 4-9, 1991. Vol. 1 1991 6 p refs

Copyright

The Autonomous Power System (APS) project at NASA Lewis Research Center is designed to demonstrate the abilities of integrated intelligent diagnosis, control, and scheduling techniques to space power distribution hardware. Knowledge-based software provides a robust method of control for highly complex space-based power systems that conventional methods do not allow. The project consists of three elements: the Autonomous Power Expert System (APEX) for fault diagnosis and control, the Autonomous Intelligent Power Scheduler (AIPS) to determine system configuration, and power hardware (Brassboard) to simulate a space based power system. The operation of the Autonomous Power System as a

whole is described and the responsibilities of the three elements - APEX, AIPS, and Brassboard - are characterized. A discussion of the methodologies used in each element is provided. Future plans are discussed for the growth of the Autonomous Power System. Author

A92-55930* National Aeronautics and Space Administration. Lewis Research Center, Cleveland, OH.

DISCRETE-TIME ENTROPY FORMULATION OF OPTIMAL AND ADAPTIVE CONTROL PROBLEMS

YWETING A. TSAI, FRANCISCO A. CASIELLO, and KENNETH A. LOPARO (Case Western Reserve University, Cleveland, OH) IEEE Transactions on Automatic Control (ISSN 0018-9286), vol. 37, no. 7, July 1992, p. 1083-1088. Jul. 1992 6 p refs

(Contract NAG3-788)

Copyright

The discrete-time version of the entropy formulation of optimal control of problems developed by G. N. Saridis (1988) is discussed. Given a dynamical system, the uncertainty in the selection of the control is characterized by the probability distribution (density) function which maximizes the total entropy. The equivalence between the optimal control problem and the optimal entropy problem is established, and the total entropy is decomposed into a term associated with the certainty equivalent control law, the entropy of estimation, and the so-called equivocation of the active transmission of information from the controller to the estimator. This provides a useful framework for studying the certainty equivalent and adaptive control laws. I.E.

A92-57327* National Aeronautics and Space Administration. Lewis Research Center, Cleveland, OH.

CONTROLLER DESIGN FOR MICROGRAVITY VIBRATION ISOLATION SYSTEMS

R. D. HAMPTON, C. R. KNOSPE (Virginia, University, Charlottesville), and C. M. GRODSINSKY (NASA, Lewis Research Center, Cleveland, OH) IAF, International Astronautical Congress, 43rd, Washington, Aug. 28-Sept. 5, 1992. 11 p. Aug. 1992 11 p refs

(IAF PAPER 92-0969) Copyright

Control aspects of the vibration isolation problem of manned orbiters are investigated, and a viable robust control is proposed. The application of modern control theory to this problem, incorporating frequency-weighting and disturbance accommodation techniques, is investigated. The resulting controller achieves excellent performance for plants within a reasonable range of variations from the nominal. Robust stability and performance guarantees are measured by singular value and structured singular value checks, yielding guarantees on allowable real plant parameter uncertainties and on acceptable controller and sensor phase and gain variations. The problem of unmodeled HG modes is eliminated by using frequency weighting to reduce controller bandwidth. The method is applied successfully to the single-degree-of-freedom isolation problem. P.D.

N92-13717*# National Aeronautics and Space Administration. Lewis Research Center, Cleveland, OH.

AN SSME HIGH PRESSURE OXIDIZER TURBOPUMP DIAGNOSTIC SYSTEM USING G2(TM) REAL-TIME EXPERT SYSTEM

TEN-HUEI GUO Nov. 1991 14 p Presented at the Third Annual Health Monitoring Conference for Space Propulsion Systems, Cincinnati, OH, 13-14 Nov. 1991; sponsored by the Univ. of Cincinnati

(Contract RTOP 582-01-41)

(NASA-TM-105328; E-6689; NAS 1.15:105328) Avail: CASI HC A03/MF A01

An expert system which diagnoses various seal leakage faults in the High Pressure Oxidizer Turbopump of the SSME was developed using G2(TM) real-time expert system. Three major functions of the software were implemented: model-based data generation, real-time expert system reasoning, and real-time input/output communication. This system is proposed as one module of a complete diagnostic system for Space Shuttle Main

Engine. Diagnosis of a fault is defined as the determination of its type, severity, and likelihood. Since fault diagnosis is often accomplished through the use of heuristic human knowledge, an expert system based approach was adopted as a paradigm to develop this diagnostic system. To implement this approach, a software shell which can be easily programmed to emulate the human decision process, the G2 Real-Time Expert System, was selected. Lessons learned from this implementation are discussed. Author

N92-23365* National Aeronautics and Space Administration. Lewis Research Center, Cleveland, OH.

INTELLIGENT FAULT ISOLATION AND DIAGNOSIS FOR COMMUNICATION SATELLITE SYSTEMS

DONALD P. TALLO (Akron Univ., OH.), JOHN DURKIN (Akron Univ., OH.), and EDWARD J. PETRIK *In* NASA. Goddard Space Flight Center, The 1992 Goddard Conference on Space Applications of Artificial Intelligence p 105-120 1992
Avail: CASI HC A03/MF A03

Discussed here is a prototype diagnosis expert system to provide the Advanced Communication Technology Satellite (ACTS) System with autonomous diagnosis capability. The system, the Fault Isolation and Diagnosis Expert (FIDEX) system, is a frame-based system that uses hierarchical structures to represent such items as the satellite's subsystems, components, sensors, and fault states. This overall frame architecture integrates the hierarchical structures into a lattice that provides a flexible representation scheme and facilitates system maintenance. FIDEX uses an inexact reasoning technique based on the incrementally acquired evidence approach developed by Shortliffe. The system is designed with a primitive learning ability through which it maintains a record of past diagnosis studies. Author

64

NUMERICAL ANALYSIS

Includes iteration, difference equations, and numerical approximation.

A92-47058* National Aeronautics and Space Administration. Lewis Research Center, Cleveland, OH.

IMPLEMENTATION OF CONTROL POINT FORM OF ALGEBRAIC GRID-GENERATION TECHNIQUE

YUNG K. CHOO, DAVID P. MILLER (NASA, Lewis Research Center, Cleveland, OH), and CHARLES J. RENO (Cleveland State University, OH) *In*: Numerical grid generation in computational fluid dynamics and related fields; Proceedings of the 3rd International Conference, Barcelona, Spain, June 3-7, 1991 1991 11 p refs
(Contract NCC3-153)
Copyright

The control point form (CPF) provides explicit control of physical grid shape and grid spacing through the movement of the control points. The control point array, called a control net, is a space grid type arrangement of locations in physical space with an index for each direction. As an algebraic method CPF is efficient and works well with interactive computer graphics. A family of menu-driven, interactive grid-generation computer codes (TURBO) is being developed by using CPF. Key features of Turbol (a TURBO member) are discussed and typical results are presented. Turbol runs on any IRIS 4D series workstation. Author

A92-47059* National Aeronautics and Space Administration. Lewis Research Center, Cleveland, OH.

A CONFORMAL BLOCK STRUCTURED GRID FOR TURBOMACHINERY CASCADES IN TWO DIMENSIONS

ZHU WANG and PETER R. EISEMAN (Program Development Corp., White Plains, NY) *In*: Numerical grid generation in computational fluid dynamics and related fields; Proceedings of

the 3rd International Conference, Barcelona, Spain, June 3-7, 1991 1991 11 p refs
(Contract NAS3-25880)

Copyright

A block structured conformal transformation is presented for application to turbomachinery cascades. In comparison with the traditional single block cases that are, at best, supplemented with branch cuts, there is a richer variety of choices for the grid topology. The choice presented leads to a substantial improvement in the grid quality. This is reflected in a relatively uniform covering of the cascade region. While grid clustering is not intended or supplied with the block conformal structure, it can be injected afterwards. When viewed as a controlled experiment, the present study provides a significant example of the effect of grid topology upon the grid quality. In a larger sense, this puts some focus upon the effects of grid topology in more general situations. Author

A92-47072* National Aeronautics and Space Administration. Lewis Research Center, Cleveland, OH.

GRID QUALITY IMPROVEMENT BY A GRID ADAPTATION TECHNIQUE

K. D. LEE, T. L. HENDERSON (Illinois, University, Urbana), and Y. K. CHOO (NASA, Lewis Research Center, Cleveland, OH) *In*: Numerical grid generation in computational fluid dynamics and related fields; Proceedings of the 3rd International Conference, Barcelona, Spain, June 3-7, 1991 1991 10 p refs
Copyright

A grid adaptation technique is presented which improves grid quality. The method begins with an assessment of grid quality by defining an appropriate grid quality measure. Then, undesirable grid properties are eliminated by a grid-quality-adaptive grid generation procedure. The same concept has been used for geometry-adaptive and solution-adaptive grid generation. The difference lies in the definition of the grid control sources; here, they are extracted from the distribution of a particular grid property. Several examples are presented to demonstrate the versatility and effectiveness of the method. Author

A92-50469* National Aeronautics and Space Administration. Lewis Research Center, Cleveland, OH.

MAPPINGS AND ACCURACY FOR CHEBYSHEV PSEUDO-SPECTRAL APPROXIMATIONS

ALVIN BAYLISS (Northwestern University, Evanston, IL) and ELI TURKEL (Tel Aviv University, Israel) *Journal of Computational Physics* (ISSN 0021-9991), vol. 101, no. 2, Aug. 1992, p. 349-359. Research supported by NASA. Previously announced in STAR as N91-14781. Aug. 1992 11 p refs
(Contract NSF ASC-87-19573; NSF MSS-91-02981)
Copyright

The effect of mappings on the approximation, by Chebyshev collocation, of functions which exhibit localized regions of rapid variation is studied. A general strategy is introduced whereby mappings are adaptively constructed which map specified classes of rapidly varying functions into low order polynomials which can be accurately approximated by Chebyshev polynomial expansions. A particular family of mappings constructed in this way is tested on a variety of rapidly varying functions similar to those occurring in approximations. It is shown that the mapped function can be approximated much more accurately by Chebyshev polynomial approximations than in physical space or where mappings constructed from other strategies are employed. Author

A92-52552* National Aeronautics and Space Administration. Lewis Research Center, Cleveland, OH.

ENHANCING CONTROL OF GRID DISTRIBUTION IN ALGEBRAIC GRID GENERATION

E. STEINTHORSSON, T. I.-P. SHIH (Carnegie Mellon University, Pittsburgh, PA), and R. J. ROELKE (NASA, Lewis Research Center, Cleveland, OH) *International Journal for Numerical Methods in Fluids* (ISSN 0271-2091), vol. 15, no. 3, Aug. 15, 1992, p. 297-311. 15 Aug. 1992 15 p refs
(Contract NAG3-929)
Copyright

Three techniques are presented to enhance the control of grid-point distribution for a class of algebraic grid generation methods known as the two-, four- and six-boundary methods. First, multidimensional stretching functions are presented, and a technique is devised to construct them based on the desired distribution of grid points along certain boundaries. Second, a normalization procedure is proposed which allows more effective control over orthogonality of grid lines at boundaries and curvature of grid lines near boundaries. And third, interpolating functions based on tension splines are introduced to control curvature of grid lines in the interior of the spatial domain. In addition to these three techniques, consistency conditions are derived which must be satisfied by all user-specified data employed in the grid generation process to control grid-point distribution. The usefulness of the techniques developed in this study was demonstrated by using them in conjunction with the two- and four-boundary methods to generate several grid systems, including a three-dimensional grid system in the coolant passage of a radial turbine blade with serpentine channels and pin fins.

Author

N92-10345*# National Aeronautics and Space Administration, Lewis Research Center, Cleveland, OH.

MULTIGRID CALCULATION OF THREE-DIMENSIONAL VISCOUS CASCADE FLOWS

A. ARNONE (Florence Univ., Italy), M.-S. LIQU, and L. A. POVINELLI Oct. 1991 25 p Previously announced in IAA as A91-53754

(Contract NASA ORDER C-99066-G; RTOP 505-62-21)
(NASA-TM-105257; ICOMP-91-18; E-6587; NAS 1.15:105257)
Avail: CASI HC A03/MF A01

A 3-D code for viscous cascade flow prediction was developed. The space discretization uses a cell-centered scheme with eigenvalue scaling to weigh the artificial dissipation terms. Computational efficiency of a four stage Runge-Kutta scheme is enhanced by using variable coefficients, implicit residual smoothing, and a full multigrid method. The Baldwin-Lomax eddy viscosity model is used for turbulence closure. A zonal, nonperiodic grid is used to minimize mesh distortion in and downstream of the throat region. Applications are presented for an annular vane with and without end wall contouring, and for a large scale linear cascade. The calculation is validated by comparing with experiments and by studying grid dependency.

Author

N92-15662*# National Aeronautics and Space Administration, Lewis Research Center, Cleveland, OH.

OPTIMAL LEAST-SQUARES FINITE ELEMENT METHOD FOR ELLIPTIC PROBLEMS

BO-NAN JIANG and LOUIS A. POVINELLI Dec. 1991 18 p
(Contract NASA ORDER C-99066-G; RTOP 505-62-21)
(NASA-TM-105382; ICOMP-91-29; E-6769; NAS 1.15:105382)
Avail: CASI HC A03/MF A01

An optimal least squares finite element method is proposed for two dimensional and three dimensional elliptic problems and its advantages are discussed over the mixed Galerkin method and the usual least squares finite element method. In the usual least squares finite element method, the second order equation $(-\Delta x (\Delta u) + u = f)$ is recast as a first order system $(-\Delta x p + u = f, \Delta u - p = 0)$. The error analysis and numerical experiment show that, in this usual least squares finite element method, the rate of convergence for flux p is one order lower than optimal. In order to get an optimal least squares method, the irrotationality $\Delta x p = 0$ should be included in the first order system.

Author

N92-15663*# National Aeronautics and Space Administration, Lewis Research Center, Cleveland, OH.

CENTRAL DIFFERENCE TVD AND TVB SCHEMES FOR TIME DEPENDENT AND STEADY STATE PROBLEMS

P. JORGENSON and E. TURKEL (Tel-Aviv Univ., Israel) 1992 12 p Presented at the 30th Aerospace Sciences Meeting and Exhibit, Reno, NV, 6-9 Jan. 1992; sponsored by AIAA (Contract NASA ORDER C-99066-G; RTOP 505-62-21)

(NASA-TM-105357; ICOMP-91-27; E-6734; NAS 1.15:105357; AIAA PAPER 92-0053) Avail: CASI HC A03/MF A01

We use central differences to solve the time dependent Euler equations. The schemes are all advanced using a Runge-Kutta formula in time. Near shocks, a second difference is added as an artificial viscosity. This reduces the scheme to a first order upwind scheme at shocks. The switch that is used guarantees that the scheme is locally total variation diminishing (TVD). For steady state problems it is usually advantageous to relax this condition. Then small oscillations do not activate the switches and the convergence to a steady state is improved. To sharpen the shocks, different coefficients are needed for different equations and so a matrix valued dissipation is introduced and compared with the scalar viscosity. The connection between this artificial viscosity and flux limiters is shown. Any flux limiter can be used as the basis of a shock detector for an artificial viscosity. We compare the use of the van Leer, van Albada, mimmod, superbee, and the 'average' flux limiters for this central difference scheme. For time dependent problems, we need to use a small enough time step so that the CFL was less than one even though the scheme was linearly stable for larger time steps. Using a total variation bounded (TVB) Runge-Kutta scheme yields minor improvements in the accuracy.

Author

N92-16663*# National Aeronautics and Space Administration, Lewis Research Center, Cleveland, OH.

AN ITERATIVE IMPLICIT DIAGONALLY-DOMINANT FACTORIZATION ALGORITHM FOR SOLVING THE NAVIER-STOKES EQUATIONS

SHU-CHENG CHEN, NAN-SUEY LIU, and HYUN DAE KIM Oct. 1991 30 p Submitted for publication
(Contract RTOP 505-62-52)
(NASA-TM-105259; E-6589; NAS 1.15:105259) Avail: CASI HC A03/MF A01

Presented here is an algorithm for solving the multidimensional unsteady Navier-Stokes equations for compressible flows. It is based on a diagonally-dominant approximate factorization procedure. The factorization error and the timewise linearization error associated with this procedure are reduced by performing Newton-type inner iterations at each time step. The inviscid fluxes are evaluated by the fourth-order central differencing scheme amended with a numerical dissipation directly proportional to the entire dissipative part of the truncation error intrinsic to the third order biased upwind scheme. The important features of the proposed solution are elucidated by the numerical results of the convection of a vortex and the backward-facing step flows.

Author

N92-22230*# National Aeronautics and Space Administration, Lewis Research Center, Cleveland, OH.

AN INVESTIGATION OF DTNS2D FOR USE AS AN INCOMPRESSIBLE TURBULENCE MODELLING TEST-BED

CHRISTOPHER J. STEFFEN, JR. Mar. 1992 18 p
(Contract RTOP 505-62-21)
(NASA-TM-105593; ICOMP-92-07; CMOTT-92-04; E-6924; NAS 1.15:105593) Avail: CASI HC A03/MF A01

This paper documents an investigation of a two dimensional, incompressible Navier-Stokes solver for use as a test-bed for turbulence modelling. DTNS2D is the code under consideration for use at the Center for Modelling of Turbulence and Transition (CMOTT). This code was created by Gorski at the David Taylor Research Center and incorporates the pseudo compressibility method. Two laminar benchmark flows are used to measure the performance and implementation of the method. The classical solution of the Blasius boundary layer is used for validating the flat plate flow, while experimental data is incorporated in the validation of backward facing step flow. Velocity profiles, convergence histories, and reattachment lengths are used to quantify these calculations. The organization and adaptability of the code are also examined in light of the role as a numerical test-bed.

Author

N92-24974*# National Aeronautics and Space Administration. Lewis Research Center, Cleveland, OH.

ASYMPTOTIC INTEGRATION ALGORITHMS FOR FIRST-ORDER ODES WITH APPLICATION TO VISCOPLASTICITY

ALAN D. FREED (Ohio Aerospace Inst., Brook Park.), MINWU YAO, and KEVIN P. WALKER (Engineering Science Software, Inc., Smithfield, RI.) Apr. 1992 18 p Proposed for presentation at the Conference Recent Advances in Damage Mechanics and Plasticity, Tempe, AZ, 28 Apr. - 1 May 1992; sponsored by the 1992 ASME Summer Mechanics and Materials Conference (Contract RTOP 505-63-5A) (NASA-TM-105587; E-6916; NAS 1.15:105587) Avail: CASI HC A03/MF A01

When constructing an algorithm for the numerical integration of a differential equation, one must first convert the known ordinary differential equation (ODE), which is defined at a point, into an ordinary difference equation (O(delta)E), which is defined over an interval. Asymptotic, generalized, midpoint, and trapezoidal, O(delta)E algorithms are derived for a nonlinear first order ODE written in the form of a linear ODE. The asymptotic forward (typically underdamped) and backward (typically overdamped) integrators bound these midpoint and trapezoidal integrators, which tend to cancel out unwanted numerical damping by averaging, in some sense, the forward and backward integrations. Viscoplasticity presents itself as a system of nonlinear, coupled first-ordered ODE's that are mathematically stiff, and therefore, difficult to numerically integrate. They are an excellent application for the asymptotic integrators. Considering a general viscoplastic structure, it is demonstrated that one can either integrate the viscoplastic stresses or their associated eigenstrains. Author

N92-27196*# National Aeronautics and Space Administration. Lewis Research Center, Cleveland, OH.

INSTITUTE FOR COMPUTATIONAL MECHANICS IN PROPULSION (ICOMP) Annual Report No. 6, 1991

CHARLES E. FEILER, ed. May 1992 50 p (Contract NCC3-233; RTOP 505-62-21) (NASA-TM-105612; ICOMP-92-01; E-6950; NAS 1.15:105612) Avail: CASI HC A03/MF A01

The Institute for Computational Mechanics in Propulsion (ICOMP) is a combined activity of Case Western Reserve University, Ohio Aerospace Institute (OAI) and NASA Lewis. The purpose of ICOMP is to develop techniques to improve problem solving capabilities in all aspects of computational mechanics related to propulsion. The activities at ICOMP during 1991 are described. Author

N92-27517*# National Aeronautics and Space Administration. Lewis Research Center, Cleveland, OH.

DEVELOPMENT OF AN ALGEBRAIC TURBULENCE MODEL FOR ANALYSIS OF PROPULSION FLOWS

N. J. GEORGIADIS (Akron Univ., OH.), J. E. DRUMMOND, and B. P. LEONARD (Akron Univ., OH.) Jul. 1992 14 p Proposed for presentation at the 28th Joint Propulsion Conference and Exhibit, Nashville, TN, 6-8 Jul. 1992; sponsored by AIAA, SAE, ASME, and ASEE (Contract RTOP 537-02-23) (NASA-TM-105701; E-7089; NAS 1.15:105701; AIAA PAPER 92-3861) Avail: CASI HC A03/MF A01

A simple turbulence model that will be applicable to propulsion flows having both wall bounded and unbounded regions was developed and installed within the PARC Navier-Stokes code by linking two existing algebraic turbulence models. The first is the Modified Mixing Length (MML) model which is optimized for wall bounded flows. The second is the Thomas model, the standard algebraic turbulence model in PARC which has been used to calculate both bounded and unbounded turbulent flows but was optimized for the latter. This paper discusses both models and the method employed to link them into one model (referred to as the MMLT model). The PARC code with the MMLT model was applied to two dimensional turbulent flows over a flat plate and

over a backward facing step to validate and optimize the model and to compare its predictions to those obtained with the three turbulence models already available in PARC. Author

N92-33571*# National Aeronautics and Space Administration. Lewis Research Center, Cleveland, OH.

APPLICATION OF VECTOR-VALUED RATIONAL APPROXIMATIONS TO THE MATRIX EIGENVALUE PROBLEM AND CONNECTIONS WITH KRYLOV SUBSPACE METHODS

AVRAM SIDI (Technion - Israel Inst. of Tech., Haifa.) Sep. 1992 35 p Presented at the International Meeting on Approximation, Interpolation, and Summability, Tel-Aviv, Israel, Jun. 1990 and the International Congress on Extrapolation and Rational Approximation, Tenerife, Spain, Jan. 1992 (Contract NASA ORDER C-99066-G; RTOP 505-62-21) (NASA-TM-105858; ICOMP-92-18; E-7317; NAS 1.15:105858) Avail: CASI HC A03/MF A01

Let $F(z)$ be a vector-valued function $F: C \rightarrow C^N$ which is analytic at $z=0$ and meromorphic in a neighborhood of $z=0$, and let its Maclaurin series be given. We use vector-valued rational approximation procedures for $F(z)$ that are based on its Maclaurin series in conjunction with power iterations to develop bona fide generalizations of the power method for an arbitrary $N \times N$ matrix that may be diagonalizable or not. These generalizations can be used to obtain simultaneously several of the largest distinct eigenvalues and the corresponding invariant subspaces, and present a detailed convergence theory for them. In addition, it is shown that the generalized power methods of this work are equivalent to some Krylov subspace methods, among them the methods of Arnoldi and Lanczos. Thus, the theory provides a set of completely new results and constructions for these Krylov subspace methods. This theory suggests at the same time a new mode of usage for these Krylov subspace methods that were observed to possess computational advantages over their common mode of usage. Author

N92-33742*# National Aeronautics and Space Administration. Lewis Research Center, Cleveland, OH.

UPPER BOUNDS FOR CONVERGENCE RATES OF VECTOR EXTRAPOLATION METHODS ON LINEAR SYSTEMS WITH INITIAL ITERATIONS Ph.D. Thesis

AVRAM SIDI (Technion - Israel Inst. of Tech., Haifa.) and YAIR SHAPIRA (Technion - Israel Inst. of Tech., Haifa.) Jul. 1992 58 p (Contract RTOP 505-62-21) (NASA-TM-105608; E-6946; NAS 1.15:105608; ICOMP-92-09) Avail: CASI HC A04/MF A01

The application of the minimal polynomial extrapolation (MPE) and the reduced rank extrapolation (RRE) to a vector sequence obtained by the linear iterative technique $x^{(j)} + 1 = Ax^{(j)} + b$, $j = 1, 2, \dots$, is considered. Both methods produce a two dimensional array of approximations $s^{(n,k)}$ to the solution of the system $(I - A)x = b$. Here, $s^{(n,k)}$ is obtained from the vectors $x^{(j)}$, n is less than or equal to j is less than or equal to $n + k + 1$. It was observed in an earlier publication by the first author that the sequence $s^{(n,k)}$, $k = 1, 2, \dots$, for n greater than 0, but fixed, possesses better convergence properties than the sequence $s^{(0,k)}$, $k = 1, 2, \dots$. A detailed theoretical explanation for this phenomenon is provided in the present work. This explanation is heavily based on approximations by incomplete polynomials. It is demonstrated by numerical examples when the matrix A is sparse that cycling with $s^{(n,k)}$ for n greater than 0, but fixed, produces better convergence rates and costs less computationally than cycling with $s^{(0,k)}$. It is also illustrated numerically with a convection-diffusion problem that the former may produce excellent results where the latter may fail completely. As has been shown in an earlier publication, the results produced by $s^{(n,k)}$ are identical to the corresponding results obtained by applying the Arnoldi method or generalized minimal residual scheme (GMRES) to the system $(I - A)x = b$. Author

STATISTICS AND PROBABILITY

Includes data sampling and smoothing; Monte Carlo method; and stochastic processes.

A92-34341*# National Aeronautics and Space Administration, Lewis Research Center, Cleveland, OH.

STRUCTURAL SYSTEM RELIABILITY CALCULATION USING A PROBABILISTIC FAULT TREE ANALYSIS METHOD

T. Y. TORNG, Y.-T. WU, and H. R. MILLWATER (Southwest Research Institute, San Antonio, TX) IN: AIAA/ASME/ASCE/AHS/ASC Structures, Structural Dynamics and Materials Conference, 33rd, Dallas, TX, Apr. 13-15, 1992, Technical Papers. Pt. 2 1992 11 p refs

(Contract NAS3-24389)

(AIAA PAPER 92-2410) Copyright

The development of a new probabilistic fault tree analysis (PFTA) method for calculating structural system reliability is summarized. The proposed PFTA procedure includes: developing a fault tree to represent the complex structural system, constructing an approximation function for each bottom event, determining a dominant sampling sequence for all bottom events, and calculating the system reliability using an adaptive importance sampling method. PFTA is suitable for complicated structural problems that require computer-intensive computer calculations. A computer program has been developed to implement the PFTA. Author

N92-30898*# National Aeronautics and Space Administration, Lewis Research Center, Cleveland, OH.

A SIMPLIFIED DYNAMIC MODEL OF THE T700 TURBOSHAFT ENGINE

AHMET DUYAR (Florida Atlantic Univ., Boca Raton.), ZHEN GU (Florida Atlantic Univ., Boca Raton.), and JONATHAN S. LITT Jun. 1992 22 p Presented at the 48th American Helicopter Society Annual Forum, Washington, DC, 3-5 Jun. 1992; sponsored by the American Helicopter Society

(Contract NAG3-1198; DA PROJ. 1L1-61102-AH-45)

(NASA-TM-105805; E-7235; NAS 1.15:105805;

AVSCOM-TR-92-C-024; RTOP 505-62-0K; AD-A254804) Avail: CASI HC A03/MF A01

A simplified open-loop dynamic model of the T700 turboshaft engine, valid within the normal operating range of the engine, is developed. This model is obtained by linking linear state space models obtained at different engine operating points. Each linear model is developed from a detailed nonlinear engine simulation using a multivariable system identification and realization method. The simplified model may be used with a model-based real time diagnostic scheme for fault detection and diagnostics, as well as for open loop engine dynamics studies and closed loop control analysis utilizing a user generated control law. Author

THEORETICAL MATHEMATICS

Includes topology and number theory.

SYSTEMS ANALYSIS

Includes mathematical modeling; network analysis; and operations research.

A92-50609* National Aeronautics and Space Administration, Lewis Research Center, Cleveland, OH.

APPLICATION OF ENHANCED MODERN STRUCTURED ANALYSIS TECHNIQUES TO SPACE STATION FREEDOM ELECTRIC POWER SYSTEM REQUIREMENTS

JOHN BIERNACKI, JOHN JUHASZ, and GERALD SADLER (NASA, Lewis Research Center, Cleveland, OH) IN: IECEC '91; Proceedings of the 26th Intersociety Energy Conversion Engineering Conference, Boston, MA, Aug. 4-9, 1991. Vol. 2 1991 6 p refs

Copyright

A team of Space Station Freedom (SSF) system engineers are in the process of extensive analysis of the SSF requirements, particularly those pertaining to the electrical power system (EPS). The objective of this analysis is the development of a comprehensive, computer-based requirements model, using an enhanced modern structured analysis methodology (EMSA). Such a model provides a detailed and consistent representation of the system's requirements. The process outlined in the EMSA methodology is unique in that it allows the graphical modeling of real-time system state transitions, as well as functional requirements and data relationships, to be implemented using modern computer-based tools. These tools permit flexible updating and continuous maintenance of the models. Initial findings resulting from the application of EMSA to the EPS have benefited the space station program by linking requirements to design, providing traceability of requirements, identifying discrepancies, and fostering an understanding of the EPS. I.E.

N92-33942*# National Aeronautics and Space Administration, Lewis Research Center, Cleveland, OH.

RATIONAL APPROXIMATIONS FROM POWER SERIES OF VECTOR-VALUED MEROMORPHIC FUNCTIONS

AVRAM SIDI (Technion - Israel Inst. of Tech., Haifa.) Sep. 1992 25 p Presented at the International Meeting on Approximation, Interpolation, and Summability, Tel-Aviv, Israel, Jun. 1990, and at the International Congress on Extrapolation and Rational Approximation, Tenerife, Spain, Jan. 1992

(Contract NASA ORDER C-99066-G; RTOP 505-62-21)

(NASA-TM-105859; ICOMP-92-17; E-7318; NAS 1.15:105859)

Avail: CASI HC A03/MF A01

Let $F(z)$ be a vector-valued function, $F: C$ yields $C(\sup N)$, which is analytic at $z = 0$ and meromorphic in a neighborhood of $z = 0$, and let its Maclaurin series be given. In this work we developed vector-valued rational approximation procedures for $F(z)$ by applying vector extrapolation methods to the sequence of partial sums of its Maclaurin series. We analyzed some of the algebraic and analytic properties of the rational approximations thus obtained, and showed that they were akin to Pade approximations. In particular, we proved a Koenig type theorem concerning their poles and a de Montessus type theorem concerning their uniform convergence. We showed how optical approximations to multiple poles and to Laurent expansions about these poles can be constructed. Extensions of the procedures above and the accompanying theoretical results to functions defined in arbitrary linear spaces was also considered. One of the most interesting and immediate applications of the results of this work is to the matrix eigenvalue problem. In a forthcoming paper we exploited the developments of the present work to devise bona fide generalizations of the classical power method that are especially suitable for very large and sparse matrices. These generalizations can be used to approximate simultaneously several of the largest distinct eigenvalues and corresponding eigenvectors and invariant subspaces of arbitrary matrices which may or may not be diagonalizable, and are very closely related with known Krylov subspace methods. Author

PHYSICS (GENERAL)

N92-26671*# National Aeronautics and Space Administration. Lewis Research Center, Cleveland, OH.

COMPUTATIONAL TECHNIQUES IN TRIBOLOGY AND MATERIAL SCIENCE AT THE ATOMIC LEVEL

J. FERRANTE and G. H. BOZZOLO (Analex Corp., Brook Park, OH.) 1992 30 p Presented at the NATO Research Inst. Workshop on Fundamentals of Friction, Braunlage, Germany, 5-19 Aug. 1991; sponsored by the North Atlantic Treaty Organization (Contract RTOP 505-90-53) (NASA-TM-105573; E-6777; NAS 1.15:105573) Avail: CASI HC A03/MF A01

Computations in tribology and material science at the atomic level present considerable difficulties. Computational techniques ranging from first-principles to semi-empirical and their limitations are discussed. Example calculations of metallic surface energies using semi-empirical techniques are presented. Finally, application of the methods to calculation of adhesion and friction are presented. Author

ACOUSTICS

Includes sound generation, transmission, and attenuation.

A92-25678*# National Aeronautics and Space Administration. Lewis Research Center, Cleveland, OH.

ON THE MECHANISM OF TURBULENCE SUPPRESSION IN FREE SHEAR FLOWS UNDER ACOUSTIC EXCITATION

K. B. M. Q. ZAMAN and E. J. RICE (NASA, Lewis Research Center, Cleveland, OH) AIAA, Aerospace Sciences Meeting and Exhibit, 30th, Reno, NV, Jan. 6-9, 1992. 12 p. Previously announced in STAR as N92-14003. Jan. 1992 12 p refs (AIAA PAPER 92-0065) Copyright

Acoustic excitation at certain high frequencies has been known to suppress large amplitude fluctuations otherwise occurring naturally in various free shear flows. The phenomenon has been observed in flows with initially laminar or transitional boundary layers. An experimental investigation is conducted to consider two possibilities in regards to the mechanism of the effect. (1) The natural shear layer is self excited by the instability waves already developed in the upstream boundary layer. This is overridden when the shear layer is excited at its maximally unstable mode, causing the observed decrease in the intensities downstream. (2) The upstream boundary layer is in a transitional or buffeted laminar state, characterized by large amplitude unsteady fluctuations, which force the large fluctuations downstream. Excitation trips the upstream boundary layer to full turbulence, reduces the unsteady fluctuations, and thus causes the observed suppression of the intensities throughout the flowfield. The present experimental results refute either of these possibilities to be the general mechanism of the effect. Author

A92-26230*# National Aeronautics and Space Administration. Lewis Research Center, Cleveland, OH.

FAR-FIELD NOISE AND INTERNAL MODES FROM A DUCTED PROPELLER AT SIMULATED AIRCRAFT TAKEOFF CONDITIONS

RICHARD P. WOODWARD (NASA, Lewis Research Center, Cleveland, OH), LAWRENCE A. BOCK (Pratt and Whitney Group, East Hartford, CT), LAURENCE J. HEIDELBERG (NASA, Lewis Research Center, Cleveland, OH), and DAVID G. HALL (NASA,

Lewis Research Center, Cleveland; Sverdrup Technology, Inc., Brook Park, OH) AIAA, Aerospace Sciences Meeting and Exhibit, 30th, Reno, NV, Jan. 6-9, 1992. 16 p. Previously announced in STAR as N92-16702. Jan. 1992 16 p refs (AIAA PAPER 92-0371) Copyright

The ducted propeller offers structural and acoustic benefits typical of conventional turbofan engines while retaining much of the aeroacoustic benefits of the unducted propeller. A model Advanced Ducted Propeller (ADP) was tested in the NASA Lewis Low-Speed Anechoic Wind Tunnel at a simulated takeoff velocity of Mach 0.2. The ADP model was designed and manufactured by the Pratt and Whitney Division of United Technologies. The 16-blade rotor ADP was tested with 22- and 40-vane stators to achieve cut-on and cut-off criterion with respect to propagation of the fundamental rotor-stator interaction tone. Additional test parameters included three inlet lengths, three nozzle sizes, two spinner configurations, and two rotor rub strip configurations. The model was tested over a range of rotor blade setting angles and propeller axis angles-of-attack. Acoustic data were taken with a sideline translating microphone probe and with a unique inlet microphone probe which identified inlet rotating acoustic modes. The beneficial acoustic effects of cut-off were clearly demonstrated. A 5 dB fundamental tone reduction was associated with the long inlet and 40-vane sector, which may relate to inlet propeller axis angle-of-attack at rotor speeds of at least 96 percent design. Author

A92-26328*# National Aeronautics and Space Administration. Lewis Research Center, Cleveland, OH.

COMPUTATION OF SUPERSONIC JET MIXING NOISE FOR AN AXISYMMETRIC CD NOZZLE USING K-EPSILON TURBULENCE MODEL

A. KHAVARAN (NASA, Lewis Research Center; Sverdrup Technology, Inc., Cleveland, OH), E. A. KREJSA, and C. M. KIM (NASA, Lewis Research Center, Cleveland, OH) AIAA, Aerospace Sciences Meeting and Exhibit, 30th, Reno, NV, Jan. 6-9, 1992. 15 p. Previously announced in STAR as N92-14795. Jan. 1992 15 p refs (AIAA PAPER 92-0500)

The turbulent mixing noise of a supersonic jet is calculated for a round convergent-divergent nozzle at the design pressure ratio. Aerodynamic computations are performed using the PARC code with a k-epsilon turbulence model. Lighthill's acoustic analogy combined with Ribner's assumption is adopted. The acoustics solution is based upon the methodology followed by GE in the MGB code. The source correlation function is expressed as a linear combination of second-order tensors. Assuming separable second-order correlations and incorporating Batchelor's isotropic turbulence model, the source term was calculated from the kinetic energy of turbulence. A Gaussian distribution for the time-delay of correlation was introduced. The computational fluid dynamics (CFD) solution was used to obtain the source strength as well as the characteristic time-delay of correlation. The effect of sound/flow interaction was incorporated using the high frequency asymptotic solution to Lilley's equation for axisymmetric geometries. Acoustic results include sound pressure level directivity and spectra at different polar angles. The aerodynamic and acoustic results demonstrate favorable agreement with experimental data. Author

A92-26930*# National Aeronautics and Space Administration. Lewis Research Center, Cleveland, OH.

A SURVEY OF THE BROADBAND SHOCK ASSOCIATED NOISE PREDICTION METHODS

CHAN M. KIM, EUGENE A. KREJSA (NASA, Lewis Research Center, Cleveland, OH), and ABBAS KHAVARAN (NASA, Lewis Research Center, Cleveland; Sverdrup Technology, Inc., Brook Park, OH) AIAA, Aerospace Sciences Meeting and Exhibit, 30th, Reno, NV, Jan. 6-9, 1992. 25 p. Previously announced in STAR as N92-14797. Jan. 1992 25 p refs (AIAA PAPER 92-0501) Copyright

Several different prediction methods to estimate the broadband shock associated noise of a supersonic jet are introduced and

compared with experimental data at various test conditions. The nozzle geometries considered for comparison include a convergent and a convergent-divergent nozzle, both axisymmetric. Capabilities and limitations of prediction methods in incorporating the two nozzle geometries, flight effect, and temperature effect are discussed. Predicted noise field shows the best agreement for a convergent nozzle geometry under static conditions. Predicted results for nozzles in flight show larger discrepancies from data and more dependable flight data are required for further comparison. Qualitative effects of jet temperature, as observed in experiment, are reproduced in predicted results.

Author

6 p refs
(Contract NAG3-354)
Copyright

A number of studies in the area of propeller design and advanced configuration performance/acoustics are reviewed. Various designs are analyzed in the area of propeller efficiency, lift-to-drag ratio, and differential thrust and power coefficients. Predictions are compared to experiment and the numerical analyses are examined for restrictions and potential enhancements.

R.E.P.

A92-26934*# National Aeronautics and Space Administration. Lewis Research Center, Cleveland, OH.

ACOUSTIC ANALYSIS USING NUMERICAL SOLUTIONS OF THE NAVIER-STOKES EQUATIONS

JAMES N. SCOTT (Ohio State University, Columbus) AIAA, Aerospace Sciences Meeting and Exhibit, 30th, Reno, NV, Jan. 6-9, 1992. 11 p. Jan. 1992 11 p refs
(Contract NAG3-1058)

(AIAA PAPER 92-0506) Copyright

Numerical solutions of the time-dependent compressible Navier-Stokes equations are employed to analyze the unsteady features of jet flows which contribute to jet noise. The turbulent-mass flux spectra are examined in detail in the numerical analysis, and MacCormack's explicit finite difference algorithm is used to solve the governing equations. The computational grid is based on an axisymmetric jet with simple exponential stretching used to optimize the resolution of critical unsteady flow features. The time-varying numerical data are analyzed, and the time averages of the velocity and turbulence-intensity profiles are shown to agree with experimental data. Grid refinement and longer run times improved the prediction of the experimental mass-flux spectra. The numerical procedure can be extended to 3D jet-flow configurations to study the related 3D unsteady flow features.

C.C.S.

A92-28190# National Aeronautics and Space Administration. Langley Research Center, Hampton, VA.

ACOUSTIC CHARACTERISTICS AND DYNAMIC STRUCTURAL LOADING OF AN ASTOVL AIRCRAFT IN HOVER

L. K. MITCHELL, THOMAS D. NORUM (NASA, Langley Research Center, Hampton, VA), and ALBERT L. JOHNS (NASA, Lewis Research Center, Cleveland, OH) AIAA, Aerospace Sciences Meeting and Exhibit, 30th, Reno, NV, Jan. 6-9, 1992. 9 p. Jan. 1992 9 p refs

(AIAA PAPER 92-0370) Copyright

Measurements of surface dynamic loading and freestream acoustics were made for an ASTOVL model in hover, to quantify the effects of elevated temperature on the acoustic field and surface loading. Data were acquired for a many combinations of operating parameters: model height above the ground plane, nozzle pressure ratio, and jet exit stagnation temperature. For many conditions, strong tones were observed, with amplitudes up to 150 dB. The frequencies of the strongest tones were well predicted by a model assuming feedback between the nozzle exit and the ground plane. The model also accounts for many of the variations in frequency observed with changes in model height, nozzle pressure ratio, and jet temperature. Broadband sound pressure levels up to 170 dB were also recorded. The maximum levels occurred at approximately 3 equivalent jet diameters above the ground plane. For the majority of the cases, the increase in noise due to temperature was less than expected based on free jet correlations.

Author

A92-39241* National Aeronautics and Space Administration. Lewis Research Center, Cleveland, OH.

A REVIEW OF COMPUTATIONAL/EXPERIMENTAL METHODOLOGY DEVELOPMENTS IN AEROACOUSTICS

L. A. EAGLESON (Texas A & M University, College Station) IN: NOISE-CON 90; Proceedings of the 10th National Conference on Noise Control Engineering, Austin, TX, Oct. 15-17, 1990 1990

A92-44512* National Aeronautics and Space Administration. Lewis Research Center, Cleveland, OH.

UNSTEADY AIRLOADING PANEL METHOD FOR PROPFANS

D. B. HANSON (United Technologies Corp., Windsor Locks, CT) Aug. 1992 9 p refs
(Contract NAS3-23720)

Copyright

A92-46799* National Aeronautics and Space Administration. Lewis Research Center, Cleveland, OH.

NOISE OF TWO HIGH-SPEED MODEL COUNTER-ROTATION PROPELLERS AT TAKEOFF/APPROACH CONDITIONS

RICHARD P. WOODWARD (NASA, Lewis Research Center, Cleveland, OH) Journal of Aircraft (ISSN 0021-8669), vol. 29, no. 4, July-Aug. 1992, p. 679-685. Aug. 1992 7 p refs

Copyright

This paper presents acoustic results for two model counter-rotation propellers which were tested in the NASA Lewis 9- x 15-ft Anechoic Wind Tunnel. The propellers had a common forward rotor, but the diameter of the aft rotor of the second propeller was reduced in an effort to reduce its interaction with the forward rotor tip vortex. The propellers were tested at Mach 0.20, which is representative of takeoff/approach operation. Acoustic results are presented for these propellers which show the effect of rotor spacing, reduced aft rotor diameter, operation at angle-of-attack, blade loading, and blade number. Limited aerodynamic results are also presented to establish the propeller operating conditions.

Author

A92-50296* National Aeronautics and Space Administration. Lewis Research Center, Cleveland, OH.

DIRECT EVALUATION OF AEROACOUSTIC THEORY IN A JET

JAMES BRIDGES (Sverdrup Technology, Inc.; NASA, Lewis Research Center, Cleveland, OH; Houston, University, TX) and FAZLE HUSSAIN (Houston, University, TX) Journal of Fluid Mechanics (ISSN 0022-1120), vol. 240, July 1992, p. 469-501. Jul. 1992 33 p refs

(Contract NAG3-639; N00014-89-J-1361)

Copyright

Aeroacoustic theory is applied to low-Mach ($M = 0.08$) cold jets, focusing on motion at scales which allow the assumption that the entire jet diameter is acoustically compact. The primary result is that the measured sound field directivity of vortex ring pairing in circular jets is similar to that predicted by the theory: a stationary axisymmetric lateral quadrupole. It is also shown that pairing of purely axisymmetric coherent structures is not the dominant sound source in low-Mach-number jets and that vortex asymmetry must be an essential aspect of the vortex motions which produce noise in such jets.

V.L.

N92-10601*# National Aeronautics and Space Administration. Lewis Research Center, Cleveland, OH.

TURBOMACHINERY NOISE

JOHN F. GROENEWEG (United Technologies Corp., Windsor Locks, CT.), THOMAS G. SOFRIN, EDWARD J. RICE, and PHILLIP R. GLIEBE (General Electric Co., Cincinnati, OH.) IN: NASA. Langley Research Center, Aeroacoustics of Flight Vehicles: Theory and Practice. Volume 1: Noise Sources p 151-209 Aug. 1991
Avail: CASI HC A04/MF A06

Summarized here are key advances in experimental techniques and theoretical applications which point the way to a broad understanding and control of turbomachinery noise. On the

experimental side, the development of effective inflow control techniques makes it possible to conduct, in ground based facilities, definitive experiments in internally controlled blade row interactions. Results can now be valid indicators of flight behavior and can provide a firm base for comparison with analytical results. Inflow control coupled with detailed diagnostic tools such as blade pressure measurements can be used to uncover the more subtle mechanisms such as rotor strut interaction, which can set tone levels for some engine configurations. Initial mappings of rotor wake-vortex flow fields have provided a data base for a first generation semiempirical flow disturbance model. Laser velocimetry offers a nonintrusive method for validating and improving the model. Digital data systems and signal processing algorithms are bringing mode measurement closer to a working tool that can be frequently applied to a real machine such as a turbofan engine. On the analytical side, models of most of the links in the chain from turbomachine blade source to far field observation point have been formulated. Three dimensional lifting surface theory for blade rows, including source noncompactness and cascade effects, blade row transmission models incorporating mode and frequency scattering, and modal radiation calculations, including hybrid numerical-analytical approaches, are tools which await further application. Author

N92-10603*# National Aeronautics and Space Administration. Lewis Research Center, Cleveland, OH.

NOISE FROM TURBULENT SHEAR FLOWS

M. E. GOLDSTEIN *In* NASA. Langley Research Center, Aeroacoustics of Flight Vehicles: Theory and Practice. Volume 1: Noise Sources p 291-310 Aug. 1991
Avail: CASI HC A03/MF A06

The generation of sound in turbulent shear flows with high Reynolds numbers is discussed. Solid surface effects, representation of incident turbulence, sound generation and the role of instability waves, sound generation by turbulence interacting with itself (the jet noise problem), compressible Rayleigh equations, sound generation from streamwise variations in mean flow, complex turbulent flows, and supersonic flows are among the topics discussed. Author

N92-10607*# National Aeronautics and Space Administration. Lewis Research Center, Cleveland, OH.

COMBUSTION AND CORE NOISE

J. ROBERT MAHAN (Virginia Polytechnic Inst. and State Univ., Blacksburg.) and ALLEN KARCHMER *In* NASA. Langley Research Center, Aeroacoustics of Flight Vehicles: Theory and Practice. Volume 1: Noise Sources p 483-517 Aug. 1991
Avail: CASI HC A03/MF A06

Two types of aircraft power plant are considered: the gas turbine and the reciprocating engine. The engine types considered are: the reciprocating engine, the turbojet engine, the turboprop engine, and the turbofan engine. Combustion noise in gas turbine engines is discussed, and reciprocating-engine combustion noise is also briefly described. The following subject areas are covered: configuration variables, operational variables, characteristics of combustion and core noise, sources of combustion noise, combustion noise theory and comparison with experiment, available prediction methods, diagnostic techniques, measurement techniques, data interpretation, and example applications. Author

N92-14795*# National Aeronautics and Space Administration. Lewis Research Center, Cleveland, OH.

COMPUTATION OF SUPERSONIC JET MIXING NOISE FOR AN AXISYMMETRIC CD NOZZLE USING K-EPSILON TURBULENCE MODEL

ABBAS KHAVARAN (Sverdrup Technology, Inc., Brook Park, OH.), EUGENE A. KREJSA, and CHAN M. KIM 1991 16 p Proposed for presentation at the 30th Aerospace Sciences Meeting and Exhibit, Reno, NV, 6-9 Jan. 1992; sponsored by AIAA (Contract RTOP 537-02-23)
(NASA-TM-105338; E-6705; NAS 1.15:105338; AIAA PAPER 92-0500) Avail: CASI HC A03/MF A01

The turbulent mixing noise of a supersonic jet is calculated for

a round convergent-divergent nozzle at the design pressure ratio. Aerodynamic computations are performed using the PARC code with a k-epsilon turbulence model. Lighthill's acoustic analogy combined with Ribner's assumption is adopted. The acoustics solution is based upon the methodology followed by GE in the MGB code. The source correlation function is expressed as a linear combination of second-order tensors. Assuming separable second-order correlations and incorporating Batchelor's isotropic turbulence model, the source term was calculated from the kinetic energy of turbulence. A Gaussian distribution for the time-delay of correlation was introduced. The computational fluid dynamics (CFD) solution was used to obtain the source strength as well as the characteristic time-delay of correlation. The effect of sound/flow interaction was incorporated using the high frequency asymptotic solution to Lilley's equation for axisymmetric geometries. Acoustic results include sound pressure level directivity and spectra at different polar angles. The aerodynamic and acoustic results demonstrate favorable agreement with experimental data. Author

N92-14797*# National Aeronautics and Space Administration. Lewis Research Center, Cleveland, OH.

A SURVEY OF THE BROADBAND SHOCK ASSOCIATED NOISE PREDICTION METHODS

CHAN M. KIM, EUGENE A. KREJSA, and ABBAS KHAVARAN (Sverdrup Technology, Inc., Brook Park, OH.) 1992 26 p Proposed for presentation at the 30th Aerospace Sciences Meeting and Exhibit, Reno, NV, 6-9 Jan. 1992; sponsored by AIAA (Contract NAS3-25266; RTOP 537-02-23)
(NASA-TM-105365; E-6743; NAS 1.15:105365; AIAA PAPER 92-0501) Avail: CASI HC A03/MF A01

Several different prediction methods to estimate the broadband shock associated noise of a supersonic jet are introduced and compared with experimental data at various test conditions. The nozzle geometries considered for comparison include a convergent and a convergent-divergent nozzle, both axisymmetric. Capabilities and limitations of prediction methods in incorporating the two nozzle geometries, flight effect, and temperature effect are discussed. Predicted noise field shows the best agreement for a convergent nozzle geometry under static conditions. Predicted results for nozzles in flight show larger discrepancies from data and more dependable flight data are required for further comparison. Qualitative effects of jet temperature, as observed in experiment, are reproduced in predicted results. Author

N92-16702*# National Aeronautics and Space Administration. Lewis Research Center, Cleveland, OH.

FAR-FIELD NOISE AND INTERNAL MODES FROM A DUCTED PROPELLER AT SIMULATED AIRCRAFT TAKEOFF CONDITIONS

RICHARD P. WOODWARD (Pratt and Whitney Aircraft, East Hartford, CT.), LAWRENCE A. BOCK, LAURENCE J. HEIDELBERG, and DAVID G. HALL (Sverdrup Technology, Inc., Brook Park, OH.) 1992 17 p Presented at the 30th Aerospace Sciences Meeting and Exhibit, Reno, NV, 6-9 Jan. 1992; sponsored by AIAA
(Contract RTOP 535-03-10)
(NASA-TM-105369; E-6747; NAS 1.15:105369; AIAA PAPER 92-0371) Avail: CASI HC A03/MF A01

The ducted propeller offers structural and acoustic benefits typical of conventional turbofan engines while retaining much of the aeroacoustic benefits of the unducted propeller. A model Advanced Ducted Propeller (ADP) was tested in the NASA Lewis Low-Speed Anechoic Wind Tunnel at a simulated takeoff velocity of Mach 0.2. The ADP model was designed and manufactured by the Pratt and Whitney Division of United Technologies. The 16-blade rotor ADP was tested with 22- and 40-vane stators to achieve cut-on and cut-off criterion with respect to propagation of the fundamental rotor-stator interaction tone. Additional test parameters included three inlet lengths, three nozzle sizes, two spinner configurations, and two rotor rub strip configurations. The model was tested over a range of rotor blade setting angles and propeller axis angles-of-attack. Acoustic data were taken with a

sideline translating microphone probe and with a unique inlet microphone probe which identified inlet rotating acoustic modes. The beneficial acoustic effects of cut-off were clearly demonstrated. A 5 dB fundamental tone reduction was associated with the long inlet and 40-vane sector, which may relate to inlet duct geometry. The fundamental tone level was essentially unaffected by propeller axis angle-of-attack at rotor speeds of at least 96 percent design.
Author

N92-16705*# National Aeronautics and Space Administration. Lewis Research Center, Cleveland, OH.

DETAILED NOISE MEASUREMENTS ON THE SR-7A PROPELLER: TONE BEHAVIOR WITH HELICAL TIP MACH NUMBER

JAMES H. DITTMAR and DAVID G. HALL (Sverdrup Technology, Inc., Brook Park, OH.) Dec. 1991 31 p
(Contract RTOP 535-03-10)
(NASA-TM-105206; E-6519; NAS 1.15:105206) Avail: CASI HC A03/MF A01

Detailed noise measurements were taken on the SR-7A propeller to investigate the behavior of the noise with helical tip Mach number and then to level off as Mach number was increased further. This behavior was further investigated by obtaining detailed pressure-time histories of data. The pressure-time histories indicate that a portion of the primary pressure pulse is progressively cancelled by a secondary pulse which results in the noise leveling off as the helical tip Mach number is increased. This second pulse appears to originate on the same blade as the primary pulse and is in some way connected to the blade itself. This leaves open the possibility of redesigning the blade to improve the cancellation; thereby, the propeller noise is reduced. Author

N92-18282*# National Aeronautics and Space Administration. Lewis Research Center, Cleveland, OH.

AN EVALUATION OF SOME ALTERNATIVE APPROACHES FOR REDUCING FAN TONE NOISE

JAMES H. DITTMAR and RICHARD P. WOODWARD Feb. 1992 21 p
(Contract RTOP 535-03-10)
(NASA-TM-105356; E-6730; NAS 1.15:105356) Avail: CASI HC A03/MF A01

The potential of two alternative approaches for reducing fan ton noise was investigated in this study. One of these approaches increases the number of rotor blades to shift the tone noise to higher frequencies that are not rated as strongly by the perceived noise scale. This alternative fan also would have a small number of long chord stator vanes which would reduce the stator response and lower rotor-stator interaction noise. Comparison of the conventional and alternative fan concepts showed that this alternative approach has as large or larger a perceived tone noise reduction potential as the conventional approach. The other alternative, a high Mach number inlet, is evaluated both for its noise attenuation and for its change in noise directivity. Author

N92-28984*# National Aeronautics and Space Administration. Lewis Research Center, Cleveland, OH.

MODAL ELEMENT METHOD FOR SCATTERING OF SOUND BY ABSORBING BODIES

KENNETH J. BAUMEISTER and KEVIN L. KREIDER (Akron Univ., OH.) 1992 14 p Proposed for presentation at the ASME Winter Annual Meeting, Anaheim, CA, 8-13 Nov. 1992
(Contract RTOP 505-62-52)
(NASA-TM-105722; E-7126; NAS 1.15:105722) Avail: CASI HC A03/MF A01

The modal element method for acoustic scattering from 2-D body is presented. The body may be acoustically soft (absorbing) or hard (reflecting). The infinite computational region is divided into two subdomains - the bounded finite element domain, which is characterized by complicated geometry and/or variable material properties, and the surrounding unbounded homogeneous domain. The acoustic pressure field is represented approximately in the finite element domain by a finite element solution, and is represented analytically by an eigenfunction expansion in the

homogeneous domain. The two solutions are coupled by the continuity of pressure and velocity across the interface between the two subdomains. Also, for hard bodies, a compact modal ring grid system is introduced for which computing requirements are drastically reduced. Analysis for 2-D scattering from solid and coated (acoustically treated) bodies is presented, and several simple numerical examples are discussed. In addition, criteria are presented for determining the number of modes to accurately resolve the scattered pressure field from a solid cylinder as a function of the frequency of the incoming wave and the radius of the cylinder.
Author

72

ATOMIC AND MOLECULAR PHYSICS

Includes atomic structure, electron properties, and molecular spectra.

N92-24818*# National Aeronautics and Space Administration. Lewis Research Center, Cleveland, OH.

ATOMIC OXYGEN UNDERCUTTING OF LDEF ALUMINIZED-KAPTON MULTILAYER INSULATION

KIM K. DEGROH and BRUCE A. BANKS *In* NASA. Langley Research Center, LDEF: 69 Months in Space. First Post-Retrieval Symposium, Part 2 p 781-795 Jan. 1992

Atomic oxygen undercutting is a potential threat to vulnerable spacecraft materials which have atomic oxygen protective coatings. Such undercutting is due to atomic oxygen attack of oxidizable materials at microscopic defects in the protective coatings. These defects occur during fabrication and handling, or from micrometeoroid and debris bombardment in space. An aluminized-polyimide Kapton multilayer insulation sample that was located on the leading edge of the Long Duration Exposure Facility (LDEF) was used to study low Earth orbit directed ram atomic oxygen undercutting. Cracks in the aluminized coatings located around vent holes provided excellent defect sites for evaluation of atomic oxygen undercutting. The experimentally observed undercutting profiles were compared to predictions from Monte Carlo models for normal incident ram atomic oxygen attack. The shape of the undercut profile was found to vary with crack width, which is proportional to the number of oxygen atoms entering the crack. The resulting profiles of atomic oxygen which occurred on LDEF indicated wide undercut cavities in spite of the fixed ram orientation. Potential causes of the observed undercutting are presented. Implications of the undercutting profiles relevant to the Space Station Freedom are also discussed.
Author

73

NUCLEAR AND HIGH-ENERGY PHYSICS

Includes elementary and nuclear particles; and reactor theory.

A92-36249 National Aeronautics and Space Administration. Lewis Research Center, Cleveland, OH.

CONSTRAINTS TO THE DECAYS OF DIRAC NEUTRINOS FROM SN 1987A

SCOTT DODELSON (NASA/Fermilab Astrophysics Center, Batavia, IL), JOSHUA A. FRIEMAN, and MICHAEL S. TURNER (NASA/Fermilab Astrophysics Center, Batavia; Chicago, University, IL) *Physical Review Letters* (ISSN 0031-9007), vol. 68, no. 17, April 27, 1992, p. 2572-2575. Research supported by DOE. 27 Apr. 1992 4 p refs
(Contract NAGW-2381)
Copyright

The decay mode of a keV-mass Dirac neutrino is addressed

with reference to the nineteen neutrino events associated with SN 1987A that were detected by the Kamiokande II and Irvine-Brookhaven-Michigan detectors. A complementary constraint is presented which is based upon a distinctive signal associated with the decay of wrong-helicity neutrinos that was not seen: high-energy (50 MeV and higher) neutrino events. The absence of such events excludes the decay of wrong-helicity neutrinos into proper-helicity neutrinos for a Dirac neutrino of mass between 1 and 300 keV. The constraint also rules out models of the 17-keV neutrino. V.L.

74

OPTICS

Includes light phenomena; and optical devices.

A92-20288* National Aeronautics and Space Administration. Lewis Research Center, Cleveland, OH.

CALCULATION OF FAR-FIELD SCATTERING FROM NONSPHERICAL PARTICLES USING A GEOMETRICAL OPTICS APPROACH

EDWARD A. HOVENAC (NASA, Lewis Research Center; Sverdrup Technology, Inc., Cleveland, OH) Applied Optics (ISSN 0003-6935), vol. 30, Nov. 20, 1991, p. 4739-4746. 20 Nov. 1991 8 p refs
Copyright

A numerical method was developed using geometrical optics to predict far-field optical scattering from particles that are symmetric about the optic axis. The diffractive component of scattering is calculated and combined with the reflective and refractive components to give the total scattering pattern. The phase terms of the scattered light are calculated as well. Verification of the method was achieved by assuming a spherical particle and comparing the results to Mie scattering theory. Agreement with the Mie theory was excellent in the forward-scattering direction. However, small-amplitude oscillations near the rainbow regions were not observed using the numerical method. Numerical data from spheroidal particles and hemispherical particles are also presented. The use of hemispherical particles as a calibration standard for intensity-type optical particle-sizing instruments is discussed. Author

A92-24002* National Aeronautics and Space Administration. Lewis Research Center, Cleveland, OH.

INTERFACES FOR HIGH-SPEED FIBER-OPTIC LINKS - ANALYSIS AND EXPERIMENT

AFSHIN S. DARYOUSH (Drexel University, Philadelphia, PA), EDWARD ACKERMAN (GE Electronics Laboratory, Syracuse, NY), NIRANJAN R. SAMANT (Drexel University, Philadelphia, PA), STEPHEN WANUGA, and DUMRONG KASEMSET (GE Electronics Laboratory, Syracuse, NY) (1991 IEEE MTT-S International Microwave Symposium and Microwave and Millimeter-Wave Monolithic Circuits Symposium, Boston, MA, June 10-14, 1991, Proceedings. A92-23988 08-33) IEEE Transactions on Microwave Theory and Techniques (ISSN 0018-9480), vol. 39, Dec. 1991, p. 2031-2044. Research supported by General Electric Co., NASA, and Ben Franklin Partnership of the State of Pennsylvania. Dec. 1991 14 p refs
Copyright

An analysis of directly and externally modulated fiberoptic links is presented. The theoretical analysis is based on the signal flow diagram of the interface circuits to the laser diode, Mach-Zehnder electro-optic modulator, and p-i-n photodiode. System parameters such as gain, noise figure, two-tone intermodulation distortion, and spurious free and compression dynamic range are expressed as a function of frequency and operating point of the laser and external modulator. Two directly and externally modulated fiber-optic links were designed and fabricated to verify the analytical models. The direct modulation FO link was developed at the Ku-band (11.6-12.4

GHz), whereas the external modulation link was at L-band (875-925 MHz). Spurious-free dynamic ranges of 95.8 dB-Hz exp 2/3 and 113 dB-Hz exp 2/3, respectively, were achieved. The predictions based on the analytical models match the measured results. I.E.

A92-37448 National Aeronautics and Space Administration. Lewis Research Center, Cleveland, OH.

RECONFIGURABLE OPTICAL INTERCONNECTION NETWORK FOR MULTIMODE OPTICAL FIBER SENSOR ARRAYS

R. T. CHEN, D. ROBINSON, H. LU, M. R. WANG, T. JANNSON (Physical Optics Corp., Torrance, CA), and R. BAUMBICK (NASA, Lewis Research Center, Cleveland, OH) Optical Engineering (ISSN 0091-3286), vol. 31, no. 5, May 1992, p. 1098-1106. Research sponsored by USAF and NASA. May 1992 9 p refs
Copyright

A single-source, single-detector architecture has been developed to implement a reconfigurable optical interconnection network multimode optical fiber sensor arrays. The network was realized by integrating LiNbO₃ electrooptic (EO) gratings working at the Raman Na regime and a massive fan-out waveguide hologram (WH) working at the Bragg regime onto a multimode glass waveguide. The glass waveguide utilized the whole substrate as a guiding medium. A 1-to-59 massive waveguide fan-out was demonstrated using a WH operating at 514 nm. Measured diffraction efficiency of 59 percent was experimentally confirmed. Reconfigurability of the interconnection was carried out by generating an EO grating through an externally applied electric field. Unlike conventional single-mode integrated optical devices, the guided mode demonstrated has an azimuthal symmetry in mode profile which is the same as that of a fiber mode. Author

A92-46240 National Aeronautics and Space Administration. Lewis Research Center, Cleveland, OH.

LENGTH MINIMIZATION DESIGN CONSIDERATIONS IN PHOTONIC INTEGRATED CIRCUITS INCORPORATING DIRECTIONAL COUPLERS

JOSEPH T. BOYD, CARL J. RADENS, and MICHAEL T. KAUFFMAN (Cincinnati, University, OH) IN: Integrated optics and optoelectronics II; Proceedings of the Meeting, San Jose, CA, Sept. 17-19, 1990 1991 6 p refs
(Contract NAG3-852; NAGW-1407)
Copyright

Because directional couplers involve channel waveguides which are very close to one another, transition regions to regions where channel waveguides are widely separated are utilized. The total length of a directional coupler and transition regions can be minimized for a particular degree of field confinement. Calculations presented for LiNbO₃-, GaAlAs-, and SiO₂/Si-based optical channel waveguides demonstrate the presence of a minimum total length corresponding to a particular degree of field confinement. The overall length at the minimum is shown to be significantly lower than for other values of field confinement allowing single-mode operation. This implies that either more devices can be integrated on a substrate or that less material is needed for an integrated optical circuit. Author

A92-46245* National Aeronautics and Space Administration. Lewis Research Center, Cleveland, OH.

MULTIPLE-MODE RECONFIGURABLE ELECTRO-OPTIC SWITCHING NETWORK FOR OPTICAL FIBER SENSOR ARRAY

RAY T. CHEN, MICHAEL R. WANG, TOMASZ JANNSON (Physical Optics Corp., Torrance, CA), and ROBERT BAUMBICK (NASA, Lewis Research Center, Cleveland, OH) IN: Integrated optics and optoelectronics II; Proceedings of the Meeting, San Jose, CA, Sept. 17-19, 1990 1991 14 p refs
Copyright

This paper reports the first switching network compatible with multimode fibers. A one-to-many cascaded reconfigurable interconnection was built. A thin glass substrate was used as the guiding medium which provides not only higher coupling efficiency from multimode fiber to waveguide but also better tolerance of phase-matching conditions. Involvement of a total-internal-reflection

hologram and multimode waveguide eliminates interface problems between fibers and waveguides. The DCG polymer graft has proven to be reliable from -180 C to +200 C. Survivability of such an electrooptic system in harsh environments is further ensured. LiNbO₃ was chosen as the E-O material because of its stability at high temperatures (phase-transition temperature of more than 1000 C) and maturity of E-O device technology. Further theoretical calculation was conducted to provide the optimal interaction length and device capacitance.

Author

N92-13783*# National Aeronautics and Space Administration. Lewis Research Center, Cleveland, OH.

A NEW TECHNIQUE FOR OIL BACKSTREAMING CONTAMINATION MEASUREMENTS

S. A. ALTEROVITZ (Cleveland State Univ., OH.), H. J. SPEIER (Cleveland State Univ., OH.), R. M. SIEG, M. N. DROTOS, and J. E. DUNNING (Michigan State Univ., East Lansing.) 1991 13 p Presented at the 38th Annual American Vacuum Society Symposium, Seattle, WA, 11-15 Nov. 1991 (Contract RTOP 506-44-21)

(NASA-TM-105312; E-6665; NAS 1.15:105312) Avail: CASI HC A03/MF A01

Due to the large size and the number of diffusion pumps, space simulation chambers cannot be easily calibrated by the usual test dome method for measuring backstreaming from oil diffusion pumps. In addition, location dependent contamination may be an important parameter of the test. The backstreaming contamination was measured in the Space Power Facility (SPF) near Sandusky, OH, the largest space simulation vacuum test chamber in the U.S.. Small clean silicon wafers placed at all desired measurement sites were used as contamination sensors. The facility used diffusion pumps with DC 705 oil. The thickness of the contamination oil film was measured using ellipsometry. Since the oil did not wet the silicon substrate uniformly, two analysis models were developed to measure the oil film: (1) continuous, homogeneous film; and (2) islands of oil with the islands varying in coverage fraction and height. In both cases, the contamination film refractive index was assumed to be that of DC 705. The second model improved the ellipsometric analysis quality parameter by up to two orders of magnitude, especially for the low coverage cases. Comparison of the two models shows that the continuous film model overestimates the oil volume by less than 50 percent. Absolute numbers for backstreaming are in good agreement with published results for diffusion pumps. Good agreement was also found between the ellipsometric results and measurements done by x-ray photoelectron spectroscopy (XPS) and by scanning electron microscopy (SEM) on examples exposed to the same vacuum runs.

Author

N92-28475*# National Aeronautics and Space Administration. Lewis Research Center, Cleveland, OH.

ROCKET PLUME FLOWFIELD CHARACTERIZATION USING LASER RAYLEIGH SCATTERING

FRANK J. ZUPANC and JONATHAN M. WEISS (Pennsylvania State Univ., University Park.) Jul. 1992 20 p Proposed for presentation at the 28th Joint Propulsion Conference and Exhibit, Nashville, TN, 6-8 Jul. 1992; sponsored by AIAA, SAE, ASME, and ASEE

(Contract RTOP 506-42-31)

(NASA-TM-105739; E-7145; NAS 1.15:105739; AIAA PAPER 92-3351) Copyright Avail: CASI HC A03/MF A01

A Doppler-resolved laser Rayleigh scattering diagnostic was applied to a 111 N thrust, regenerative and fuel-film cooled, gaseous hydrogen/gaseous oxygen rocket engine. The axial and radial mean gas velocities were measured from the net Doppler shifts observed for two different scattering angles. Translational temperatures and number densities were estimated from the Doppler widths and scattered intensities, respectively, by assuming that water was the dominant scattering species in the exhaust. The experimental results are compared with theoretical predictions from a full Navier-Stokes code (RD/RPLUS) and the JANNAF Two-Dimensional Kinetics (TDK) and Standardized Plume Flowfield (SPF-II) codes. Discrepancies between the measured and predicted

axial velocities, temperatures, and number densities are evident. Radial velocity measurements, however, show excellent agreement with predictions. The discrepancies are attributed primarily to inefficient mixing and combustion caused by the injection of excessive oxidizer along one side of the thrust chamber. Thrust and mass flow rate estimates obtained from the Rayleigh measurements show excellent agreement with the globally measured values.

Author

N92-28571* National Aeronautics and Space Administration. Lewis Research Center, Cleveland, OH.

MONOLITHIC MM-WAVE PHASE SHIFTER USING OPTICALLY ACTIVATED SUPERCONDUCTING SWITCHES Patent

ROBERT R. ROMANOFKY, inventor (to NASA) and KUL B. BHASIN, inventor (to NASA) 26 May 1992 6 p Filed 25 Sep. 1990 Supersedes N91-13996 (29 - 5, p 716)

(NASA-CASE-LEW-14878-1; US-PATENT-5,116,807; US-PATENT-APPL-SN-587921; US-PATENT-CLASS-505-1; US-PATENT-CLASS-505-703; US-PATENT-CLASS-505-848; US-PATENT-CLASS-505-866; US-PATENT-CLASS-333-161; US-PATENT-CLASS-333-995; INT-PATENT-CLASS-H01P-1/18) Avail: US Patent and Trademark Office

A phase shifter is disclosed having a reference path and a delay path, light sources, and superconductive switches. Each of the superconductive switches is terminated in a virtual short circuit, which may be a radial stub. Switching between the reference path and delayed path is accomplished by illuminating the superconductive switches connected to the desired path, while not illuminating the superconductive switches connected to the other path.

Official Gazette of the U.S. Patent and Trademark Office

N92-33896*# National Aeronautics and Space Administration. Lewis Research Center, Cleveland, OH.

RF MODULATED FIBER OPTIC SENSING SYSTEMS AND THEIR APPLICATIONS

GRIGORY ADAMOVSKY and JOHN G. EUSTACE (John Carroll Univ., Cleveland, OH.) 1992 7 p Proposed for presentation at the SPIE's International Symposium OE/Fibers 1992, Boston, MA, 8-11 Sep. 1992; sponsored by the International Society for Optical Engineering

(Contract NAG3-984; RTOP 505-62-50)

(NASA-TM-105801; E-7231; NAS 1.15:105801) Avail: CASI HC A02/MF A01

A fiber optic sensing system with an intensity sensor and a Radio Frequency (RF) modulated source was shown to have sensitivity and resolution much higher than a comparable system employing low modulating frequencies or DC mode of operation. Also the RF modulation with an appropriate configuration of the sensing system provides compensation for the unwanted intensity losses. The basic principles and applications of a fiber optic sensing system employing an RF modulated source are described. In addition the paper discusses various configurations of the system itself, its components, and modulation and detection schemes. Experimental data are also presented.

Author

75

PLASMA PHYSICS

Includes magnetohydrodynamics and plasma fusion.

A92-22693 National Aeronautics and Space Administration. Lewis Research Center, Cleveland, OH.

REACTIVE COLLISION TERMS FOR FLUID TRANSPORT THEORY

J. V. ECCLES (Mission Research Corp., Atmospheric and Space Sciences Div., Nashua, NH) and W. J. RAITT (Utah State University, Logan) Planetary and Space Science (ISSN 0032-0633), vol. 40,

Jan. 1992, p. 47-62. Jan. 1992 16 p refs
(Contract NAG3-792; NAGW-235)

Copyright

A modified Bhatnagar-Gross-Krook (BGK) collision method is used for the derivation of reactive collision terms to allow for complete higher-moment approximations in fluid transport theory. The general reactive collision terms for the 8-, 10- and 13-moment approximation for binary reactions are derived. Then, reactive collision terms for specific chemistry are derived with the assumptions: (1) all reactants and products have 13-moment distribution functions; (2) simple, classical assumptions provide sufficient models for reaction dynamics; and (3) the reaction rate is energy-independent. The derived specific formulas reflect two extremes in reactive collision dynamics: direct and indirect reaction mechanisms. Finally, considerations for correct use of the reactive collision terms are discussed in the context of space plasma environments. Author

A92-33667* National Aeronautics and Space Administration. Lewis Research Center, Cleveland, OH.

STUDY OF A CESIUM PLASMA AS A SELECTIVE EMITTER FOR THERMOPHOTOVOLTAIC APPLICATIONS

R. LOWE, C. GORADIA, M. GORADIA (Cleveland State University, OH), and DONALD L. CHUBB (NASA, Lewis Research Center, Cleveland, OH) Journal of Applied Physics (ISSN 0021-8979), vol. 68, Nov. 15, 1990, p. 5033-5035. 15 Nov. 1990 3 p refs
Copyright

This experimental study evaluates the potential of a cesium plasma as an emitter for a thermophotovoltaic (TPV) energy conversion system. A cesium plasma, as a result of the ground-state transitions of its single outer-shell electron, produces large amounts of radiation in the 850-890-nm wavelength region. This would provide excellent coupling to silicon, gallium arsenide, and indium phosphide photovoltaic cells. Measurements of the radiative efficiency, the sum of the power at the 852 and 894 nm wavelengths relative to the total emitted power, were made and correlated to the plasma operating variables. It was determined that, for atomic density in the range $(3-6) \times 10^{21}/\text{cm}^3$ and electron temperature in the range 2000-3000 K, radiative efficiencies in excess of 70 percent are attainable. This would indicate that a cesium plasma with its selective emission characteristics and low electron operating temperatures of 2000-3000 K would be an excellent candidate as an emitter in a TPV system. Author

A92-41359 Jet Propulsion Lab., California Inst. of Tech., Pasadena.

IONOSPHERIC PLASMA FLOW OVER LARGE HIGH-VOLTAGE SPACE PLATFORMS. I - ION-PLASMA-TIME SCALE INTERACTIONS OF A PLATE AT ZERO ANGLE OF ATTACK. II - THE FORMATION AND STRUCTURE OF PLASMA WAKE

J. WANG (JPL, Pasadena, CA; MIT, Cambridge, MA) and D. E. HASTINGS (MIT, Cambridge, MA) Physics of Fluids B (ISSN 0899-8221), vol. 4, no. 6, June 1992, p. 1597-1629. Jun. 1992 33 p refs

(Contract NAG3-695)

Copyright

The paper presents the theory and particle simulation results for the ionospheric plasma flow over a large high-voltage space platform at a zero angle of attack and at a large angle of attack. Emphasis is placed on the structures in the large, high-voltage regime and the transient plasma response on the ion-plasma time scale. Special consideration is given to the transient formation of the space-charge wake and its steady-state structure. I.S.

A92-41549* National Aeronautics and Space Administration. Lewis Research Center, Cleveland, OH.

THEORY OF PLASMA CONTACTOR NEUTRAL GAS EMISSIONS FOR ELECTRODYNAMIC TETHERS

R. I. SAMANTA ROY and D. E. HASTINGS (MIT, Cambridge, MA) Jun. 1992 10 p refs

(Contract NAG3-681)

Copyright

A92-47936 National Aeronautics and Space Administration. Lewis Research Center, Cleveland, OH.

HIGH VOLTAGE SPHERES IN AN UNMAGNETIZED PLASMA - FLUID AND PIC SIMULATIONS

H. THIEMANN (Thiemann & Noack, Freiburg im Breisgau, Federal Republic of Germany), T.-Z. MA, and R. W. SCHUNK (Utah State University, Logan) Dec. 1992 4 p refs

(Contract NAG3-792; NAG5-1484; AF-AFOSR-90-0026)

Copyright

The basic physics involving the interaction of a high voltage sphere with a LEO-Plasma was investigated via computer experiments. Two approaches were used: the fluid description and the more general particle pushing method. Both techniques displayed qualitatively similar features. Thus, the initial time-dependent response of the plasma predicted by the fluid model, including the initial current surge and sheath formation, the formation of ion and electron density shells about the sphere with a double layer potential structure, and the subsequent propagation of the density shells away from the sphere. The PIC results also displayed an oscillatory character and slightly different time constants for the growth and decay mechanisms involved. Author

A92-48747*# National Aeronautics and Space Administration. Lewis Research Center, Cleveland, OH.

NUMERICAL MODELING OF FLUID AND ELECTROMAGNETIC PHENOMENA IN AN ARCJET

ANITA C. FLOWE, KENNETH J. DEWITT, THEO G. KEITH, JR., GARY E. PAWLAS (Toledo, University, OH), and PAUL F. PENKO (NASA, Lewis Research Center, Cleveland, OH) AIAA, SAE, ASME, and ASEE, Joint Propulsion Conference and Exhibit, 28th, Nashville, TN, July 6-8, 1992. 6 p. Jul. 1992 6 p refs
(AIAA PAPER 92-3106) Copyright

An explicit numerical technique is used to solve the axisymmetric reduced electromagnetic field equation. The effect of an electrical arc on a viscous, axisymmetric flow is approximated using an implicit thin layer Navier-Stokes solver with additional electromagnetic source terms in conjunction with the explicit finite difference code. O.G.

A92-48749*# National Aeronautics and Space Administration. Lewis Research Center, Cleveland, OH.

MODELING OF THE NEAR-ELECTRODE REGIONS OF ARCJETS. I - COUPLING OF THE FLOWFIELD TO THE NON-EQUILIBRIUM BOUNDARY LAYERS

MARK A. CAPPELLI (Stanford University, CA) AIAA, SAE, ASME, and ASEE, Joint Propulsion Conference and Exhibit, 28th, Nashville, TN, July 6-8, 1992. 11 p. Research supported by NASA and Rocket Research Co. Jul. 1992 11 p refs
(AIAA PAPER 92-3109) Copyright

A model for arc attachment at an anode in contact with a flowing thermal plasma is described. Current limitations are identified which arise when the convective transport of ions into the electrical, thermal and hydrodynamic boundary layers is incapable of supplying the loss of ions through three-body recombination in the volume, and catalytic recombination on the electrode surface. It is shown that the anode current where this condition is achieved can be exceeded provided there is a significant Joule heating in the boundary layer. The saturation current (current density above which the anode must emit ions) is found to substantially increase with increasing free stream velocity and anode temperature. O.G.

A92-48885*# National Aeronautics and Space Administration. Lewis Research Center, Cleveland, OH.

NUMERICAL SIMULATION OF GEOMETRIC SCALE EFFECTS IN CYLINDRICAL SELF-FIELD MPD THRUSTERS

M. LAPOINTE (Sverdrup Technology, Inc., Brook Park; NASA, Lewis Research Center, Cleveland, OH) AIAA, SAE, ASME, and ASEE, Joint Propulsion Conference and Exhibit, 28th, Nashville, TN, July 6-8, 1992. 27 p. Jul. 1992 27 p refs
(AIAA PAPER 92-3297)

A 2D, two-temperature, single fluid MHD code which

incorporates classical plasma transport coefficients and Hall effects has been developed to predict steady-state, self-field MPD thruster performance. The governing equations and numerical methods of solution are outlined and discussed. Experimental comparisons are used to validate model predictions. The model accurately predicts thrust and reproduces trends in the discharge voltage for discharge currents below experimentally measured onset values. However, because the model does not include electrode effects the calculated voltage drops are significantly lower than experimentally measured values. Predictions of thrust and flow efficiency are made for a matrix of fifteen cylindrical thruster geometries assuming a fully ionized argon propellant. Author

A92-54055*# National Aeronautics and Space Administration, Lewis Research Center, Cleveland, OH.

VACUUM ULTRAVIOLET ABSORPTION IN A HYDROGEN ARCJET

DAVID H. MANZELLA and MARK A. CAPPELLI (Stanford University, CA) AIAA, SAE, ASME, and ASEE, Joint Propulsion Conference and Exhibit, 28th, Nashville, TN, July 6-8, 1992. 9 p. Research supported by NASA. Jul. 1992 9 p refs (AIAA PAPER 92-3564) Copyright

Atomic absorption spectroscopy was utilized to measure the ground state atomic hydrogen number density in the plasma produced in a low power hydrogen arcjet. A microwave driven hydrogen plasma was used as the source of radiation resonant with the vacuum ultraviolet Lyman alpha transition. The suitability of this radiation source is discussed. The optical depth of this transition prevented measurements at locations where the ground state atomic hydrogen number density was larger than $3 \times 10^{19}/\text{cu m}$. These results indicate that other single-photon optical diagnostic techniques are equally ineffective in locations of higher hydrogen number density unless the spectral line shape of the atomic hydrogen absorbers is known. Author

A92-54145*# National Aeronautics and Space Administration, Lewis Research Center, Cleveland, OH.

A FIRST-PRINCIPLES MODEL FOR ORIFICED HOLLOW CATHODE OPERATION

A. SALHI and P. J. TURCHI (Ohio State University, Columbus) AIAA, SAE, ASME, and ASEE, Joint Propulsion Conference and Exhibit, 28th, Nashville, TN, July 6-8, 1992. 11 p. Research supported by NASA and Ohio State University. Jul. 1992 11 p refs (AIAA PAPER 92-3742) Copyright

A theoretical model describing orificed hollow cathode discharge is presented. The approach adopted is based on a purely analytical formulation founded on first principles. The present model predicts the emission surface temperature and plasma properties such as electron temperature, number densities and plasma potential. In general, good agreements between theory and experiment are obtained. Comparison of the results with the available related experimental data shows a maximum difference of 10 percent in emission surface temperature, 20 percent in electron temperature and 35 percent in plasma potential. In case of the variation of the electron number density with the discharge current a maximum discrepancy of 36 percent is obtained. However, in the case of the variation with the cathode internal pressure, the predicted electron number density is higher than the experimental data by a maximum factor of 2. Author

N92-22368*# National Aeronautics and Space Administration, Lewis Research Center, Cleveland, OH.

ION COLLECTION FROM A PLASMA BY A PINHOLE

DAVID B. SNYDER and JOEL L. HERR (Sverdrup Technology, Inc., Cleveland, OH.) In NASA, Johnson Space Center, 5th Annual Workshop on Space Operations Applications and Research (SOAR 1991), Volume 2 p 694-702 Feb. 1992 Avail: CASI HC A02/MF A04

Ion focusing by a biased pinhole is studied numerically. Laplace's equation is solved in 3-D for cylindrical symmetry on a constant grid to determine the potential field produced by a biased pinhole in a dielectric material. Focusing factors are studied for

ions of uniform incident velocity with a 3-D Maxwellian distribution superimposed. Ion currents to the pinhole are found by particle tracking. The focusing factor of positive ions as a function of initial velocity, temperature, injection radius, and hole size is reported. For a typical Space Station Freedom environment (oxygen ions having a 4.5 eV ram energy, 0.1 eV temperature, and a -140 V biased pinhole), a focusing factor of 13.35 is found for a 1.5 mm radius pinhole. Author

N92-22369*# National Aeronautics and Space Administration, Lewis Research Center, Cleveland, OH.

EXPERIMENTAL BREAKDOWN OF SELECTED ANODIZED ALUMINUM SAMPLES IN DILUTE PLASMAS

NORMAN T. GRIER and STANLEY DOMITZ In NASA, Johnson Space Center, 5th Annual Workshop on Space Operations Applications and Research (SOAR 1991), Volume 2 p 703-709 Feb. 1992

Avail: CASI HC A02/MF A04

Anodized aluminum samples representative of Space Station Freedom structural material were tested for electrical breakdown under space plasma conditions. In space, this potential arises across the insulating anodized coating when the spacecraft structure is driven to a negative bias relative to the external plasma potential due to plasma-surface interaction phenomena. For anodized materials used in the tests, it was found that breakdown voltage varied from 100 to 2000 volts depending on the sample. The current in the arcs depended on the sample, the capacitor, and the voltage. The level of the arc currents varied from 60 to 1000 amperes. The plasma number density varied from 3×10^{19} to 10^{20} ions per cc. The time between arcs increased as the number density was lowered. Corona testing of anodized samples revealed that samples with higher corona inception voltage had higher arcing inception voltages. From this it is concluded that corona testing may provide a method of screening the samples. Author

SOLID-STATE PHYSICS

Includes superconductivity.

A92-14724 National Aeronautics and Space Administration, Lewis Research Center, Cleveland, OH.

SPACE APPLICATIONS OF HIGH TEMPERATURE SUPERCONDUCTIVITY TECHNOLOGY

D. J. CONNOLLY, P. R. ARON, R. F. LEONARD (NASA, Lewis Research Center, Cleveland, OH), and E. G. WINTUCKY (NASA, Washington, DC) IAF, International Astronautical Congress, 42nd, Montreal, Canada, Oct. 5-11, 1991. 9 p. Oct. 1991 9 p refs (IAF PAPER 91-307) Copyright

A review is presented of the present status of high temperature superconductivity (HTS) technology and related areas of potential space application. Attention is given to areas of application that include microwave communications, cryogenic systems, remote sensing, and space propulsion and power. Consideration is given to HTS phase shifters, miniaturization of microwave filters, far-IR bolometers, and magnetic refrigeration using flux compression. R.E.P.

A92-14950* Brookhaven National Lab., Upton, NY.

NEAR-EDGE STUDY OF GOLD-SUBSTITUTED YBA₂CU₃O(7-DELTA)

MARK W. RUCKMAN (Brookhaven National Laboratory, Upton, NY) and ALOYSIUS F. HEPP (NASA, Lewis Research Center, Cleveland, OH) Journal of Applied Physics (ISSN 0021-8979), vol. 70, pt. 1, Nov. 15, 1991, p. 5713-5715. Previously announced in STAR as N91-31977. 15 Nov. 1991 3 p refs (Contract DE-AC05-80ER-10742; DE-AC02-76CH-00016) Copyright

The valence of Cu and Au in YBa₂Au_{0.3}Cu_{2.7}O_{7- δ} was investigated using X-ray absorption near edge structure (XANES). X-ray and neutron diffraction studies indicate that Au goes on the Cu(1) site and Cu K-edge XANES shows that this has little effect on the oxidation state of the remaining copper. The Au L₃ edge develops a white line feature whose position lies between that of trivalent gold oxide and monovalent potassium gold cyanide, and whose height relative to the edge step is smaller than in the two reference compounds. The appearance of the Au L₃ edge suggests that fewer Au 3d states are involved in forming the Au-O bond in YBa₂Au_{0.3}Cu_{2.7}O_{7- δ} than in trivalent gold oxide. Author

A92-17979* National Aeronautics and Space Administration. Lewis Research Center, Cleveland, OH.

UNIVERSAL ASPECTS OF ADHESION AND ATOMIC FORCE MICROSCOPY

AMITAVA BANERJEA (NASA, Lewis Research Center, Cleveland; Kent State University, OH), JOHN R. SMITH (GM Research Laboratories, Warren, MI), and JOHN FERRANTE (NASA, Lewis Research Center, Cleveland, OH) *Journal of Physics: Condensed Matter* (ISSN 0953-8984), vol. 2, 1990, p. 8841-8846. 1990 6 p refs

Copyright

Adhesive energies are computed for flat and atomically sharp tips as a function of the normal distance to the substrate. The dependence of binding energies on tip shape is investigated. The magnitudes of the binding energies for the atomic force microscope are found to depend sensitively on tip material, tip shape and the sample site being probed. The form of the energy-distance curve, however, is universal and independent of these variables, including tip shape. Author

A92-25444* National Aeronautics and Space Administration. Lewis Research Center, Cleveland, OH.

EFFECT OF TEMPERATURE ON THE FORMATION OF CREEP SUBSTRUCTURE IN SODIUM CHLORIDE SINGLE CRYSTALS

SAI V. RAJ (NASA, Lewis Research Center, Cleveland, OH) and GEORGE M. PHARR (Rice University, Houston, TX) *American Ceramic Society, Journal* (ISSN 0002-7820), vol. 75, Feb. 1992, p. 347-352. Research supported by IBM Corp. Feb. 1992 6 p refs

Copyright

The effect of temperature on the substructure morphology and the cell and subgrain size was investigated experimentally in NaCl single crystals under creep in the temperature range 573-873 K. It is found that the effect of temperature on the cell and subgrain sizes is weak in comparison with the effect of stress. However, there was a qualitative change in the substructure morphology with temperature, with the cells and subgrains better defined at higher temperatures. The volume fraction of the cell boundaries decreased with increasing temperature, thereby indicating a refinement of the microstructure at higher temperatures. V.L.

A92-27297* National Aeronautics and Space Administration. Lewis Research Center, Cleveland, OH.

'WRONG' BOND INTERACTIONS AT INVERSION DOMAIN BOUNDARIES IN GAAS

W. R. L. LAMBRECHT, C. AMADOR, and B. SEGALL (Case Western Reserve University, Cleveland, OH) *Physical Review Letters* (ISSN 0031-9007), vol. 68, March 2, 1992, p. 1363-1366. Research supported by DARPA and Universidad Nacional Autonoma de Mexico. 2 Mar. 1992 4 p refs (Contract NAG3-25; NAG3-698; NSF PHY-87-0036P; N00013-86-K-0773)

Copyright

Electronic structure calculations of GaAs inversion-domain boundaries (IDBs) on different planes are reported. The resulting interface energies are analyzed in terms of the number of 'wrong' bonds (Ga-Ga and As-As) and their mutual compensation. The compensation energy varies roughly inversely proportionally to the distance between the wrong bonds. This favors local compensation in stoichiometric material. This automatically occurs for 110-plane

planes or by chemical reconstruction for other planes. Ga-rich IDBs are predicted to have low energy in either Ga-rich or n-type material. Author

A92-28075* National Aeronautics and Space Administration. Lewis Research Center, Cleveland, OH.

MELTING OF THE ABRIKOSOV FLUX LATTICE IN ANISOTROPIC SUPERCONDUCTORS

R. G. BECK, D. E. FARRELL (Case Western Reserve University, Cleveland, OH), J. P. RICE, D. M. GINSBERG (Illinois, University, Urbana), and V. G. KOGAN (DOE, Ames Laboratory; Iowa State University of Science and Technology, Ames) *Physical Review Letters* (ISSN 0031-9007), vol. 68, March 9, 1992, p. 1594-1596. 9 Mar. 1992 3 p refs

(Contract NAG3-814; NSF DMR-89-13651; NSF DMR-90-17371; DE-FG02-90ER-45427)

Copyright

It has been proposed that the Abrikosov flux lattice in high-T_c superconductors is melted over a significant fraction of the phase diagram. A thermodynamic argument is provided which establishes that the angular dependence of the melting temperature is controlled by the superconducting mass anisotropy. Using a low-frequency torsional-oscillator technique, this relationship has been tested in untwinned single-crystal YBa₂Cu₃O_{7- δ} . The results offer decisive support for the melting proposal. Author

A92-32414* National Aeronautics and Space Administration. Lewis Research Center, Cleveland, OH.

STUDY OF TEMPERATURE-DEPENDENT ULTRATHIN OXIDE GROWTH ON SI(111) USING VARIABLE-ANGLE SPECTROSCOPIC ELLIPSOMETRY

BHOLA N. DE and JOHN A. WOOLLAM (Nebraska, University, Lincoln) IN: *Metallurgical coatings and thin films 1990; Proceedings of the 17th International Conference on Metallurgical Coatings and 8th International Conference on Thin Films, San Diego, CA, Apr. 2-6, 1990. Vol. 2 1990 6 p refs* (Contract NAG3-95)

Copyright

The monolayer-sensitive variable-angle spectroscopic ellipsometry technique was used to study the temperature-dependent growth mechanisms of an ultrathin oxide layer on top of silicon. The oxidation was done in atomic oxygen produced in a pure oxygen plasma and driven by an RF power source. The results have been compared with the recently proposed model of Murali and Murarka for ultrathin oxide growth on top of silicon. The activation energies of different growth parameters associated with the oxide growth have also been determined. Author

A92-33911* National Aeronautics and Space Administration. Lewis Research Center, Cleveland, OH.

PROPERTIES OF LARGE AREA ERBA₂CU₃O(7-X) THIN FILMS DEPOSITED BY IONIZED CLUSTER BEAMS

L. L. LEVENSON (Colorado, University, Colorado Springs), M. STAN, and K. B. BHASIN (NASA, Lewis Research Center, Cleveland, OH) *Journal of Vacuum Science and Technology A* (ISSN 0734-2101), vol. 9, May-June 1991, p. 405-408. Jun. 1991 4 p refs

Copyright

Ionized cluster beam (ICB) deposition is employed to produce ErBa₂Cu₃O(7-x) films on different substrates without post-annealing. Films with diameters of up to 70 mm are grown on SrTiO₃ 100 plane and exhibit T_c values of 84-87 K, J_c of about 10 exp 6 A/sq m at 77 K. These films are epitaxial with the c-axis perpendicular to the plane of the substrate surface, and they can be routinely produced by ICB with good J_c and T_c. C.C.S.

A92-33946* National Aeronautics and Space Administration. Lewis Research Center, Cleveland, OH.

COMMENTS ON THE PAPER 'DOES THE SUBGRAIN SIZE INFLUENCE THE RATE OF CREEP?'

S. V. RAJ, J. D. WHITTENBERGER (NASA, Lewis Research Center,

Cleveland, OH), and G. M. PHARR (Rice University, Houston, TX) Materials Science and Engineering, Part A - Structural Materials: Properties, Microstructure and Processing (ISSN 0921-5093), vol. A145, 1991, p. L13-L17. 1991 5 p refs
Copyright

A reply is given to a recent paper which questioned the validity of experimental observations and conclusions on the importance of cells in determining the creep behavior of materials. The reply clarifies experimental procedures and observations on NaCl single crystals and examines the importance of cells in determining creep behavior. It is concluded that cells are not spurious microstructural features and that they should be included along with subgrains and 'free' dislocations in developing creep models. C.D.

A92-35349* National Aeronautics and Space Administration, Lewis Research Center, Cleveland, OH.

HALL VOLTAGE SIGN REVERSAL IN THIN SUPERCONDUCTING FILMS

RICHARD A. FERRELL (California, University, Santa Barbara; Maryland, University, College Park) Physical Review Letters (ISSN 0031-9007), vol. 68, no. 16, April 20, 1992, p. 2524-2527. 20 Apr. 1992 4 p refs
(Contract NSF DMR-89-01723; NSF PHY-89-04035; NAG3-1180)
Copyright

A novel approach to the superconducting Hall effect is developed, based on the opposing drift of the thermally excited quasi-particles. These collide quasi-elastically with the hydrodynamics superfluid velocity field circulating for outside the core of a vortex, thereby transferring momentum to the latter. The predicted Hall angle, by BCS theory, is of the order of kB_Tc divided by the Fermi energy, has sign opposite to that in the normal state because of the backflow, and disappears at low temperature. Author

A92-37562* National Aeronautics and Space Administration, Lewis Research Center, Cleveland, OH.

VERTICAL SOLIDIFICATION OF DENDRITIC BINARY ALLOYS

J. C. HEINRICH, S. FELICELLI, and D. R. POIRIER (Arizona, University, Tucson) (World Congress on Computational Mechanics, 2nd, Stuttgart, Federal Republic of Germany, Aug. 27-31, 1990, Selected Papers. A92-37547 15-31) Computer Methods in Applied Mechanics and Engineering (ISSN 0045-7825), vol. 89, no. 1-3, Aug. 1991, p. 435-461. Research supported by San Diego Supercomputer Center. Aug. 1991 27 p refs
(Contract NAG3-723; NAG3-1060)
Copyright

Three numerical techniques are employed to analyze the influence of thermosolutal convection on defect formation in directionally solidified (DS) alloys. The finite-element models are based on the Boussinesq approximation and include the plane-front model and two plane-front models incorporating special dendritic regions. In the second model the dendritic region has a time-independent volume fraction of liquid, and in the last model the dendritic region evolves as local conditions dictate. The finite-element models permit the description of nonlinear thermosolutal convection by treating the dendritic regions as porous media with variable porosities. The models are applied to lead-tin alloys including DS alloys, and severe segregation phenomena such as freckles and channels are found to develop in the DS alloys. The present calculations and the permeability functions selected are shown to predict behavior in the dendritic regions that qualitatively matches that observed experimentally. C.C.S.

A92-38418* National Aeronautics and Space Administration, Lewis Research Center, Cleveland, OH.

ULTRASONIC EVALUATION OF OXYGEN CONTENT, MODULUS, AND MICROSTRUCTURE CHANGES IN YBA₂CU₃O(7-x) OCCURRING DURING OXIDATION AND REDUCTION

DON J. ROTH (NASA, Lewis Research Center, Cleveland, OH), MARK R. DEGUIRE (Case Western Reserve University, Cleveland, OH), and LEONARD E. DOLHERT (W.R. Grace and Co., Research Div., Columbia, MD) American Ceramic Society, Journal (ISSN

0002-7820), vol. 75, no. 5, May 1992, p. 1182-1190. Previously announced in STAR as N91-27575. May 1992 9 p refs
Copyright

Ultrasonic velocity measurement techniques were used to evaluate the effects of oxidation and reduction on the elastic properties, global microstructure and oxygen content of the YBa₂Cu₃O(7-x) ceramic superconductor for samples ranging from 70 to 90 pct of theoretical density. Bulk density, velocity, and elastic modulus generally increased with increasing oxygen content upon oxidation, and this behavior was reversible. Velocity image patterns were similar after oxidation and reduction treatments for a 90 pct. dense sample, although the velocity value at any given point on the sample was changed following the treatments. The unchanging pattern correlated with destructive measurements showing that the spatial pore distribution (fraction and size) was not measurably altered after the treatments. Changes in superconducting behavior, crystal structure, and grain structure were observed consistent with changes in oxygen content.

Author

A92-41637* National Aeronautics and Space Administration, Lewis Research Center, Cleveland, OH.

CRYSTALLINE ORIENTATIONS OF TL₂BA₂CA₂CU₃O(x) GRAINS ON MGO, SR₂TIO₃, AND LAAL₃ SUBSTRATES

S. H. LIOU and C. Y. WU (Nebraska, University, Lincoln) Applied Physics Letters (ISSN 0003-6951), vol. 60, no. 22, June 1, 1992, p. 2803-2805. Research supported by Nebraska Energy Office. 1 Jun. 1992 3 p refs
(Contract NAG3-886)
Copyright

Crystalline orientations of Tl₂Ba₂Ca₂Cu₃O(x) grains in magnetron sputtered films on MgO (001), SrTiO₃ (001), and LaAlO₃ (001) substrates were investigated by scanning electron microscopy. In contrast to the nearly single crystalline films on the lattice matched substrates SrTiO₃ and LaAlO₃, films on the MgO (001) substrate, being polycrystalline in nature, exhibit several preferred in-plane grain orientations. These orientations agree well with a simplified theory of near-coincidence site lattices between Tl₂Ba₂Ca₂Cu₃O(x) and MgO. Author

A92-42858* National Aeronautics and Space Administration, Lewis Research Center, Cleveland, OH.

SURFACE MORPHOLOGIES AND PHOTOLUMINESCENCE OF DIAMOND FILMS DEPOSITED IN A HOT FILAMENT REACTOR

T. SRIVINYUNON, R. PHILLIPS, C. CUTSHAW, A. J. JOSEPH, and Y. TZENG (Auburn University, AL) IN: New diamond science and technology; Proceedings of the 2nd International Conference, Washington, DC, Sept. 23-27, 1990 1991 6 p refs
(Contract DASG60-88-C-0115; N60921-86-C-A226; N00014-90-J-1921)
Copyright

A diamond film made of (100)-oriented diamond crystallites has relatively flat surfaces in parallel with the silicon surface. This is desirable because it provides a smoother surface of the diamond film. The difficulty in retaining the (100)-oriented diamond crystallites is strongly influenced by the growth temperature. This paper reports the results from a study on the surface morphologies of diamond films deposited in a hot filament reactor at reduced substrate temperature compared to that deposited at higher temperature. Author

A92-44273* National Aeronautics and Space Administration, Lewis Research Center, Cleveland, OH.

EVALUATION OF HIGH TEMPERATURE DIELECTRIC FILMS FOR HIGH VOLTAGE POWER ELECTRONIC APPLICATIONS

J. L. SUTHAR and J. R. LAGHARI (New York, State University, Buffalo) Journal of Materials Science: Materials in Electronics (ISSN 0957-4522), vol. 3, no. 2, June 1992, p. 77-81. Jun. 1992 5 p refs
(Contract NAG3-1039)
Copyright

Three high temperature films, polyimide, Teflon perfluoroalkoxy and poly-P-xylyene, were evaluated for possible use in high voltage

power electronic applications, such as in high energy density capacitors, cables and microelectronic circuits. The dielectric properties, including permittivity and dielectric loss, were obtained in the frequency range of 50 Hz to 100 kHz at temperatures up to 200 C. The dielectric strengths at 60 Hz were determined as a function of temperature to 250 C. Confocal laser microscopy was performed to diagnose for voids and microimperfections within the film structure. The results obtained indicate that all films evaluated are capable of maintaining their high voltage properties, with minimal degradation, at temperatures up to 200 C. However, above 200 C, they lose some of their electrical properties. These films may therefore become viable candidates for high voltage power electronic applications at high temperatures. Author

A92-44533* National Aeronautics and Space Administration. Lewis Research Center, Cleveland, OH.

OPTICAL DISPERSION RELATIONS FOR 'DIAMONDLIKE' CARBON FILMS

SAMUEL A. ALTEROVITZ (NASA, Lewis Research Center, Cleveland, OH), ROBERT M. SIEG (NASA, Lewis Research Center; Cleveland State University, OH), NEIL S. SHOEMAKER (NASA, Lewis Research Center; Case Western Reserve University, Cleveland, OH), and JOHN J. POUCH (NASA, Lewis Research Center, Cleveland, OH) IN: Optical materials: Processing and science. Pittsburgh, PA, Materials Research Society (MRS Symposia Proceedings. Vol. 152), 1989, p. 21-26. Previously announced in STAR as N90-10738. 1989 6 p refs
Copyright

Ellipsometric measurements on plasma deposited diamondlike amorphous carbon (a-C:H) films were taken in the visible, ($E = 1.75$ to 3.5 eV). The films were deposited on Si and their properties were varied using high temperature (up to 750 C) anneals. The real (n) and imaginary (k) parts of the complex index of refraction N were obtained simultaneously. Following the theory of Forouhi and Bloomer, a least squares fit was used to find the dispersion relations $n(E)$ and $k(E)$. Reasonably good fits were obtained, showing that the theory can be used for a-C:H films. Moreover, the value of the energy gap (E_g) obtained in this way was compared to the E_g value using conventional Tauc plots and reasonably good agreement was obtained. Author

A92-46330* National Aeronautics and Space Administration. Lewis Research Center, Cleveland, OH.

SYNTHESIS AND CHARACTERIZATION OF FINE GRAIN DIAMOND FILMS

RICHARD L. C. WU, A. K. RAI (UES, Inc., Dayton, OH), ALAN GARCADDEN, PATRICK KEE (USAF, Wright Laboratory, Wright-Patterson AFB, OH), HEMANT D. DESAI (CVD, Inc., Woburn, MA), and KAZUHISA MIYOSHI (NASA, Lewis Research Center, Cleveland, OH) Journal of Applied Physics (ISSN 0021-8979), vol. 72, no. 1, July 1, 1992, p. 110-116. Research supported by SDIO. 1 Jul. 1992 7 p refs
(Contract F33615-89-C-2950)
Copyright

A fine grain diamond film has been developed by microwave plasma assisted chemical vapor deposition. Various analytical techniques, including Rutherford backscattering, proton recoil analysis, Raman spectroscopy, and X-ray diffraction, were utilized to characterize the diamond films. The grain size of the film was determined from bright and dark field electron micrographs, and found to be 200-1000 Å. The films exhibited good optical transmission between 2.5 and 10 microns, with a calculated absorption coefficient of 490/cm. The friction coefficients of this film were found to be 0.035 and 0.030 at dry nitrogen and humid air environments, respectively, and the films had low wear rates. Author

A92-46331* National Aeronautics and Space Administration. Lewis Research Center, Cleveland, OH.
HIGH-FIELD TRANSPORT PROPERTIES OF INAS(X)P(1-X)/INP (X = 0.3-1.0) MODULATION DOPED HETEROSTRUCTURES AT 300 AND 77 K
D. YANG, P. K. BHATTACHARYA (Michigan, University, Ann Arbor),

W. P. HONG, R. BHAT, and J. R. HAYES (Bell Communications Research, Inc., Red Bank, NJ) Journal of Applied Physics (ISSN 0021-8979), vol. 72, no. 1, July 1, 1992, p. 174-178. 1 Jul. 1992 5 p refs
(Contract NAG3-988)
Copyright

Detailed measurements at 300 and 77 K have been made of the high-field transport properties of pseudomorphic InAsP/InP modulation-doped heterostructures grown by low-pressure organometallic CVD. The high-field channel velocities are comparable to or better than that of InGaAs/InAlAs heterostructures, and the transport properties of InAs/InP heterostructure suggest that carriers remain confined in the channel even at high fields. C.D.

A92-48092* National Aeronautics and Space Administration. Lewis Research Center, Cleveland, OH.

PHOTOLUMINESCENCE LIFETIME MEASUREMENTS IN INP WAFERS

GEOFFREY A. LANDIS, PHILLIP JENKINS, and IRVING WEINBERG (NASA, Lewis Research Center, Cleveland, OH) IEEE, International Conference on InP and Related Materials, 3rd, Cardiff, Wales, Apr. 1991, Paper. 4 p. Apr. 1991 4 p refs
(Contract NAS3-25266)
Copyright

A simple apparatus to measure the minority carrier lifetime in InP has been developed. The technique stimulates the sample with a short pulse of light from a diode laser and measures the photoluminescence decay to extract the minority carrier lifetime. The photoluminescence lifetime in InP as a function of doping on both n- and p-type material is examined. The results also show a marked difference in the lifetime of n-type InP and p-type InP of similar doping levels. N-type InP shows a lifetime considerably longer than the expected radiative limited lifetime. Author

A92-50911* National Aeronautics and Space Administration. Lewis Research Center, Cleveland, OH.

ENHANCEMENT OF SHUBNIKOV-DE HAAS OSCILLATIONS BY CARRIER MODULATION

S. E. SCHACHAM, E. J. HAUGLAND, and S. A. ALTEROVITZ (NASA, Lewis Research Center, Cleveland, OH) Applied Physics Letters (ISSN 0003-6951), vol. 61, no. 5, Aug. 3, 1992, p. 551-553. 3 Aug. 1992 3 p refs
Copyright

A novel technique for drastically enhancing the Shubnikov-de Haas (SdH) pattern of oscillatory magnetoresistance is presented. The technique is based on measuring the change in the magnetoresistance due to a carrier generated by a modulated light source. The technique also has the important property of selectively increasing the amplitude of the slower oscillations due to carriers in the second subband much more than oscillations generated by the ground subband electrons. Very clear oscillations generated by a carrier concentration well below 5×10^{10} exp 10^{10} /sq cm were recorded using the technique. C.D.

A92-53148* National Aeronautics and Space Administration. Lewis Research Center, Cleveland, OH.

MINORITY CARRIER LIFETIME IN INDIUM PHOSPHIDE

PHILLIP JENKINS, GEOFFREY A. LANDIS (Sverdrup Technology, Inc., Brook Park, OH), IRVING WEINBERG (NASA, Lewis Research Center, Cleveland, OH), and KEITH KNEISEL (Northern Michigan University, Marquette, MI) IN: IEEE Photovoltaic Specialists Conference, 22nd, Las Vegas, NV, Oct. 7-11, 1991, Conference Record. Vol. 1 1991 5 p refs
(Contract NAG3-658; NAS3-25266)
Copyright

Transient photoluminescence is used to measure the minority carrier lifetime on n-type and p-type InP wafers. The measurements show that unprocessed InP wafers have very high minority carrier lifetimes. Lifetimes of 200 ns and 700 ns were observed for lightly-doped p- and n-type material respectively. Lifetimes over 5 ns were found in heavily doped n-type material. I.E.

A92-53154* National Aeronautics and Space Administration, Lewis Research Center, Cleveland, OH.

ENHANCING OPTICAL ABSORPTION IN INP AND GAAS UTILIZING PROFILE ETCHING

SHEILA G. BAILEY (NASA, Lewis Research Center, Cleveland, OH), NAVID S. FATEMI, and GEOFFREY A. LANDIS (Sverdrup Technology, Inc., Brook Park; NASA, Lewis Research Center, Cleveland, OH) IN: IEEE Photovoltaic Specialists Conference, 22nd, Las Vegas, NV, Oct. 7-11, 1991, Conference Record. Vol. 1 1991 6 p refs

The current state of profile etching in GaAs and InP is summarized, including data on novel geometries attainable as a function of etchant temperature, composition, and rate; substrate orientation; carrier concentration; and oxide thickness between substrate and photoresist. V-grooved solar cells have been manufactured with both GaAs and InP, and the improved optical absorption demonstrated. Preferred parameters for various applications are listed and discussed. Author

A92-53155* National Aeronautics and Space Administration, Lewis Research Center, Cleveland, OH.

HIGH PERFORMANCE ETCHANT FOR THINNING P(+)-INP AND ITS APPLICATION TO P(+)-N INP SOLAR CELL FABRICATION

MARIA FAUR, MIRCEA FAUR (Cleveland State University, OH), SHEILA BAILEY, DAVID BRINKER (NASA, Lewis Research Center, Cleveland, OH), MANJU GORADIA (Cleveland State University, OH), IRVING WEINBERG (NASA, Lewis Research Center, Cleveland, OH), and NAVID FATEMI IN: IEEE Photovoltaic Specialists Conference, 22nd, Las Vegas, NV, Oct. 7-11, 1991, Conference Record. Vol. 1 1991 5 p refs

Copyright

An etchant, namely (o-H3PO4)u: (HNO3)v: (H2O2)t: (H2O)1-(u+v+t) is developed for thinning, after contacting, the p(+) emitter layer of p(+)n InP structures made by thermal diffusion. Varying u, v, and t, reproducible etch rates of 5 to 110 nm/min are obtained. After thinning the 0.6- to 2.5-micron thick p(+) InP layer down to 60-250 nm, specular surfaces are obtained at up to 80 nm/min etch rate. Due to its intrinsic qualities the residual P-rich oxide after thinning the emitter layer provides surface passivation of p(+) InP surfaces and can also serve as a first-layer AR coating. I.E.

A92-56599* National Aeronautics and Space Administration, Lewis Research Center, Cleveland, OH.

ELECTRICAL-TRANSPORT PROPERTIES AND MICROWAVE DEVICE PERFORMANCE OF SPUTTERED TlCaBaCuO SUPERCONDUCTING THIN FILMS

G. SUBRAMANYAM, V. J. KAPOOR (Cincinnati, University, OH), C. M. CHOREY (Sverdrup Technology, Inc., Cleveland, OH), and K. B. BHASIN (NASA, Lewis Research Center, Cleveland, OH) Journal of Applied Physics (ISSN 0021-8979), vol. 72, no. 6, Sept. 15, 1992, p. 2396-2403. Research supported by NASA. 15 Sep. 1992 8 p refs

Copyright

The paper describes the processing and electrical transport measurements for achieving reproducible high-T_c and high-J_c sputtered TlCaBaCuO thin films on LaAlO₃ substrates, for microelectronic applications. The microwave properties of TlCaBaCuO thin films were investigated by designing, fabricating, and characterizing microstrip ring resonators with a fundamental resonance frequency of 12 GHz on 10-mil-thick LaAlO₃ substrates. Typical unloaded quality factors for a ring resonator with a superconducting ground plane of 0.3 micron-thickness and a gold ground plane of 1-micron-thickness were above 1500 at 65 K. Typical values of penetration depth at 0 K in the TlCaBaCuO thin films were between 7000 and 8000 Å. I.S.

N92-15815*# National Aeronautics and Space Administration, Lewis Research Center, Cleveland, OH.

AN OVERVIEW OF SILICON CARBIDE DEVICE TECHNOLOGY

PHILIP G. NEUDECK (Ohio Aerospace Inst., Brook Park.) and LAWRENCE G. MATUS 1992 9 p Presented at the Ninth

Symposium on Space Nuclear Power Systems, Albuquerque, NM, 12-16 Jan. 1992; sponsored by New Mexico Univ.

(Contract RTOP 505-62-50)

(NASA-TM-105402; E-6803; NAS 1.15:105402) Avail: CASI HC A02/MF A01

Recent progress in the development of silicon carbide (SiC) as a semiconductor is briefly reviewed. This material shows great promise towards providing electronic devices that can operate under the high-temperature, high-radiation, and/or high-power conditions where current semiconductor technologies fail. High quality single crystal wafers have become available, and techniques for growing high quality epilayers have been refined to the point where experimental SiC devices and circuits can be developed. The prototype diodes and transistors that have been produced to date show encouraging characteristics, but by the same token they also exhibit some device-related problems that are not unlike those faced in the early days of silicon technology development. Although these problems will not prevent the implementation of some useful circuits, the performance and operating regime of SiC electronics will be limited until these device-related issues are solved. Author

N92-19398*# National Aeronautics and Space Administration, Lewis Research Center, Cleveland, OH.

CHEMICAL STABILITY OF HIGH-TEMPERATURE SUPERCONDUCTORS

NAROTTAM P. BANSAL Feb. 1992 23 p

(Contract RTOP 307-51-00)

(NASA-TM-105391; E-6781; NAS 1.15:105391) Avail: CASI HC A03/MF A01

A review of the available studies on the chemical stability of the high temperature superconductors (HTS) in various environments was made. The La(1.8)Ba(0.2)CuO₄ HTS is unstable in the presence of H₂O, CO₂, and CO. The YBa₂Cu₃O(7-x) superconductor is highly susceptible to degradation in different environments, especially water. The La(2-x)Ba(x)CuO₄ and Bi-Sr-Ca-Cu-O HTS are relatively less reactive than the YBa₂Cu₃O(7-x). Processing of YBa₂Cu₃O(7-x) HTS in purified oxygen, rather than in air, using high purity noncarbon containing starting materials is recommended. Exposure of this HTS to the ambient atmosphere should also be avoided at all stages during processing and storage. Devices and components made out of these oxide superconductors would have to be protected with an impermeable coating of a polymer, glass, or metal to avoid deterioration during use. Author

N92-20519*# National Aeronautics and Space Administration, Lewis Research Center, Cleveland, OH.

GLASS PRECURSOR APPROACH TO HIGH-TEMPERATURE SUPERCONDUCTORS

NAROTTAM P. BANSAL Mar. 1992 51 p

(Contract RTOP 307-51-00)

(NASA-TM-105590; E-6852; NAS 1.15:105590) Avail: CASI HC A04/MF A01

The available studies on the synthesis of high T_{sub c} superconductors (HTS) via the glass precursor approach were reviewed. Melts of the Bi-Sr-Ca-Cu-O system as well as those doped with oxides of some other elements (Pb, Al, V, Te, Nb, etc.) could be quenched into glasses which, on further heat treatments under appropriate conditions, crystallized into the superconducting phase(s). The nature of the HTS phase(s) formed depends on the annealing temperature, time, atmosphere, and the cooling rate and also on the glass composition. Long term annealing was needed to obtain a large fraction of the 110 K phase. The high T_{sub c} phase did not crystallize out directly from the glass matrix, but was preceded by the precipitation of other phases. The 110 K HTS was produced at high temperatures by reaction between the phases formed at lower temperatures resulting in multiphase material. The presence of a glass former such as B₂O₃ was necessary for the Y-Ba-Cu-O melt to form a glass on fast cooling. A discontinuous YBa₂Cu₃O(7-δ) HTS phase crystallized out on heat treatment of this glass. Attempts

to prepare Ti-Ba-Ca-Cu-O system in the glassy state were not successful. Author

N92-21639*# National Aeronautics and Space Administration. Lewis Research Center, Cleveland, OH.

MICROWAVE CONDUCTIVITY OF LASER ABLATED YBa2Cu3O(7-DELTA) SUPERCONDUCTING FILMS AND ITS RELATION TO MICROSTRIP TRANSMISSION LINE PERFORMANCE

K. B. BHASIN (Sverdrup Technology, Inc., Cleveland, OH.), J. D. WARNER (Case Western Reserve Univ., Cleveland, OH.), C. M. CHOREY, B. T. EBIHARA, R. R. ROMANOFSKY, V. O. HEINEN, F. A. MIRANDA, and W. L. GORDON (Case Western Reserve Univ., Cleveland, OH.) *In* NASA. Goddard Space Flight Center, AMSAHTS 1990: Advances in Materials Science and Applications of High Temperature Superconductors p 261-269 Jan. 1991
Avail: CASI HC A02/MF A04

The discovery of high temperature superconductor oxides has raised the possibility of a new class of millimeter and microwave devices operating at temperatures considerably higher than liquid helium temperatures. Therefore, materials properties such as conductivity, current density, and sheet resistance as a function of temperature and frequency, possible anisotropies, moisture absorption, thermal expansion, and others, have to be well characterized and understood. The millimeter wave response of laser ablated YBa2Cu3O(7-delta)/LaAlO3 thin films was studied as a function of temperature and frequency. In particular, the evaluation of their microwave conductivity was emphasized, since knowledge of this parameter provides a basis for the derivation of other relevant properties of these superconducting oxides, and for using them in the fabrication of actual passive circuits. The microwave conductivity for these films was measured at frequencies from 26.5 to 40.0 GHz, in the temperature range from 20 to 300 K. The values of the conductivity are obtained from the millimeter wave power transmitted through the films, using a two fluid model. Author

N92-23413*# National Aeronautics and Space Administration. Lewis Research Center, Cleveland, OH.

MICROWAVE RESPONSE OF HIGH TRANSITION TEMPERATURE SUPERCONDUCTING THIN FILMS Abstract Only

FELIX ANTONIO MIRANDA *In its* Solid State Technology Branch of NASA Lewis Research Center p 121-122 1991
Avail: CASI HC A01/MF A02

We have studied the microwave response of YBa2Cu3O(7 - delta), Bi-Sr-Ca-Cu-O, and Ti-Ba-Ca-Cu-O high transition temperature superconducting (HTS) thin films by performing power transmission measurements. These measurements were carried out in the temperature range of 300 K to 20 K and at frequencies within the range of 30 to 40 GHz. Through these measurements we have determined the magnetic penetration depth (λ), the complex conductivity ($\sigma(\text{sup } *) = \sigma(\text{sub } 1) - j \sigma(\text{sub } 2)$) and the surface resistance ($R(\text{sub } s)$). An estimate of the intrinsic penetration depth (λ approx. 121 nm) for the YBa2Cu3O(7 - delta) HTS has been obtained from the film thickness dependence of λ . This value compares favorably with the best values reported so far (approx. 140 nm) in single crystals and high quality c-axis oriented thin films. Furthermore, it was observed that our technique is sensitive to the intrinsic anisotropy of λ in this superconductor. Values of λ are also reported for Bi-based and Ti-based thin films. We observed that for the three types of superconductors, both $\sigma(\text{sub } 1)$ and $\sigma(\text{sub } 2)$ increased when cooling the films below their transition temperature. The measured $R(\text{sub } s)$ are in good agreement with other $R(\text{sub } S)$ values obtained using resonant activity techniques if we assume a quadratic frequency dependence. Our analysis shows that, of the three types of HTS films studied, the YBa2Cu3O(7 - delta) thin film, deposited by laser ablation and off-axis magnetron sputtering are the most promising for microwave applications. Author

N92-23414*# National Aeronautics and Space Administration. Lewis Research Center, Cleveland, OH.

PROPERTIES OF LARGE AREA ERBa2Cu3O(7-X) THIN FILMS DEPOSITED BY IONIZED CLUSTER BEAMS

L. L. LEVENSON (Colorado Univ., Colorado Springs.), MARK A. STAN, and KUL B. BHASIN *In its* Solid State Technology Branch of NASA Lewis Research Center p 127-130 1991 Revised Repr. from Journal of Vacuum Society Science Technology (American Vacuum Society), v. 9, no. 3, May/June. 1991
Avail: CASI HC A01/MF A02

ErBa2Cu3O(7-x) films have been produced by simultaneous deposition of Er, Ba, and Cu from three ionized cluster beam (ICB) sources at acceleration voltages of 0.3 to 0.5 kV. Combining ozone oxidation with ICB deposition at 650 C eliminated any need of post annealing processing. The substrates were rotated at 10 rotations per minute during the deposition which took place at a rate of about 3 to 4 nm. Films with areas up to 70 mm in diameter have been made by ICB deposition. These films, 100 nm thick, were deposited on SrTiO3 (100) substrates at 650 C in a mixture of six percent O3 in O2 at a total pressure of 4 x 10(exp -4) Torr. They had T(sub c) ranging from 84.3 K to 86.8 K over a 70 mm diameter and J(sub c) above 10(exp 6) A/sq cm at 77 K. X ray diffraction measurements of the three samples showed preferential c-axis orientation normal to the substrate surface. Scanning electron micrographs (SEM) of the three samples also show some texture dependence on sample position. For the three samples, there is a correlation between SEM texture, full width at half-maximum of rocking curves and J(sub c) versus temperature curves. Author

N92-23415*# National Aeronautics and Space Administration. Lewis Research Center, Cleveland, OH.

DEPENDENCE OF THE CRITICAL TEMPERATURE OF LASER-ABLATED YBa2Cu3O(7-DELTA) THIN FILMS ON LaAlO3 SUBSTRATE GROWTH TECHNIQUE

JOSEPH D. WARNER, KUL B. BHASIN, and FELIX A. MIRANDA (Case Western Reserve Univ., Cleveland, OH.) *In its* Solid State Technology Branch of NASA Lewis Research Center p 135-137 1991 Repr. from Supercond. Sci. Technol. (England), v. 3, 1990 p 437-439
Avail: CASI HC A01/MF A02

Samples of LaAlO3 made by flame fusion and Czochralski method were subjected to the same temperature conditions that they have to undergo during the laser ablation deposition of YBa2Cu3O(7 - delta) thin films. After oxygen annealing at 750 C, the LaAlO3 substrate made by two methods experienced surface roughening. The degree of roughening on the substrate made by Czochralski method was three times greater than that on the substrate made by flame fusion. This excessive surface roughening may be the origin of the experimentally observed lowering of the critical temperature of a film deposited by laser ablation on a LaAlO3 substrate made by Czochralski method with respect to its counterpart deposited on LaAlO3 substrates made by flame fusion. Author

N92-23890*# National Aeronautics and Space Administration. Lewis Research Center, Cleveland, OH.

PHASE TRANSFORMATIONS IN SrAl2Si2O8 GLASS

CHARLES H. DRUMMOND, III (Ohio State Univ., Columbus.) and NAROTTAM P. BANSAL 1992 12 p Proposed for presentation at the 16th International Congress on Glass, Madrid, Spain, 4-9 Oct. 1992
(Contract RTOP 510-01-50)
(NASA-TM-105657; E-7021; NAS 1.15:105657) Avail: CASI HC A03/MF A01

Bulk glass of SrAl2Si2O8 composition crystallized at temperatures below 1000 C into hexacelsian, a hexagonal phase which undergoes a reversible, rapid transformation to an orthorhombic phase at 758 C, and at higher temperatures crystallized as celsian, a monoclinic phase. The glass transition temperature and crystallization onset temperature were determined to be 883 C and 1086 C, respectively, from DSC at a heating rate of 20 C/min. Thermal expansion of the various phases and

density and bend strengths of cold isostatically pressed glass powder bars, sintered at various temperatures, were measured. The kinetics of the hexacelsian-to-celsian transformation for $\text{SrAl}_2\text{Si}_2\text{O}_8$ were studied. Hexacelsian flakes were isothermally heat treated at temperatures from 1025-1200 C for various times. Avrami plots were determined by quantitatively measuring the amount of monoclinic celsian formed at various times using x ray diffraction. The Avrami constant was determined to be 1.1, suggesting a diffusionless, one dimensional transformation mechanism. The activation energy was determined from an Arrhenius plot of $\ln k$ vs. $1/T$ to be 125 kilocal/mole. This value is consistent with a mechanism which transforms the layered hexacelsian structure to a three dimensional framework celsian structure and involves the breaking of Si-O bonds. Author

N92-32976*# National Aeronautics and Space Administration, Lewis Research Center, Cleveland, OH.

REDUCED MOBILITY AND PPC IN $\text{In}_{(20)}\text{Ga}_{(80)}\text{As}$ / $\text{Al}_{(23)}\text{Ga}_{(77)}\text{As}$ HEMT STRUCTURE

S. E. SCHACHAM (Technion - Israel Inst. of Tech., Haifa.), RAFAEL A. MENA, EDWARD J. HAUGLAND, and SAMUEL A. ALTEROVITZ *In its* Solid State Technology Branch of NASA Lewis Research Center p 111-116 Aug. 1992 Submitted for publication

Avail: CASI HC A02/MF A03

Transport properties of a pseudomorphic $\text{In}_{(20)}\text{Ga}_{(80)}\text{As}/\text{Al}_{(23)}\text{Ga}_{(77)}\text{As}$ High Electron Mobility Transistor (HEMT) structure were measured by Hall and SdH techniques. Two samples of identical structures but with different doping levels were compared. Low temperature mobility measurements as a function of concentration coincides with the onset of second subband occupancy, indicating that the decrease in mobility is due to intersubband scattering. In spite of the low Al content (23 percent), large persistent photoconductivity (PPC) was observed in the highly doped sample only, showing a direct correlation between the PPC and doping concentration of the barrier layer. Author

N92-32977*# National Aeronautics and Space Administration, Lewis Research Center, Cleveland, OH.

STUDY OF INGAAS-BASED MODULATION DOPED FIELD EFFECT TRANSISTOR STRUCTURES USING VARIABLE-ANGLE SPECTROSCOPIC ELLIPSOMETRY

SAMUEL A. ALTEROVITZ, R. M. SIEG (Cleveland State Univ., OH.), H. D. YAO (Nebraska Univ., Lincoln.), P. G. SNYDER (Nebraska Univ., Lincoln.), J. A. WOOLLAM (Nebraska Univ., Lincoln.), J. PAMULAPATI (Michigan Univ., Ann Arbor.), P. K. BHATTACHARYA (Michigan Univ., Ann Arbor.), and P. A. SEKULA-MOISE (Spire Corp., Bedford, MA.) *In its* Solid State Technology Branch of NASA Lewis Research Center p 117-122 Aug. 1992 Repr. from Journal of Thin Solid Films (Lausanne, Switzerland, Elsevier Sequoia), no. 206, 1991 p 288-293

Avail: CASI HC A02/MF A03

Variable-angle spectroscopic ellipsometry was used to estimate the thicknesses of all layers within the optical penetration depth of InGaAs-based modulation doped field effect transistor structures. Strained and unstrained InGaAs channels were made by molecular beam epitaxy (MBE) on InP substrates and by metal organic chemical vapor deposition on GaAs substrates. In most cases, ellipsometrically determined thicknesses were within 10 percent of the growth-calibration results. The MBE-made InGaAs strained layers showed large strain effects, indicating a probable shift in the critical point of their dielectric function toward the InP lattice-matched concentration. Author

N92-32978*# National Aeronautics and Space Administration, Lewis Research Center, Cleveland, OH.

MICROWAVE PROPERTIES OF PEELED HEMT DEVICES SAPPHERE SUBSTRATES

PAUL G. YOUNG (Toledo Univ., OH.), SAMUEL A. ALTEROVITZ, RAFAEL A. MENA, and EDWYN D. SMITH (Toledo Univ., OH.) *In its* Solid State Technology Branch of NASA Lewis Research

Center p 123-126 Aug. 1992

Avail: CASI HC A01/MF A03

The focus of this research is to demonstrate the first full radio frequency characterization of high electron mobility transistor (HEMT) device parameters. The results of this research are used in the design of circuits with peeled HEMT devices, e.g. 10 GHz amplifiers. Devices were fabricated using two HEMT structures grown by molecular beam epitaxy methods. A 500 Å AlAs release layer for 'peel off' was included under the active layers of the structure. The structures are a homogeneously doped $\text{Al}_{(0.3)}\text{Ga}_{(0.7)}\text{As}/\text{GaAs}$ and a delta doped square well $\text{Al}_{(23)}\text{Ga}_{(77)}\text{As}/\text{GaAs}$ HEMT structure. Devices were fabricated using a mesa isolation process. Contacts were done by sequentially evaporating Au/Ge/Au/Ni/Au followed by rapid thermal anneal at 400 C for 15 seconds. Gates were wet etch recessed and 1 to 1.4 micron Ti/Au gate metal was deposited. Devices were peeled off the GaAs substrate using Apiezon wax to support the active layer and a HF:DI (1:10) solution to remove the AlAs separation layer. Devices were then attached to sapphire substrates using van der Waals bonding. Author

N92-32980*# National Aeronautics and Space Administration, Lewis Research Center, Cleveland, OH.

NASA SPACE APPLICATIONS OF HIGH-TEMPERATURE SUPERCONDUCTORS

VERNON O. HEINEN, MARTIN M. SOKOLOSKI (National Aeronautics and Space Administration, Washington, DC.), PAUL R. ARON, and KUL B. BHASIN *In its* Solid State Technology Branch of NASA Lewis Research Center p 143-149 Aug. 1992

Avail: CASI HC A02/MF A03

The application of superconducting technology in space has been limited by the requirement of cooling to near liquid helium temperatures. The only means of attaining these temperatures has been with cryogenic fluids which severely limits mission lifetime. The development of materials with superconducting transition temperatures ($T_{sub c}$) above 77 K has made superconducting technology more attractive and feasible for employment in aerospace systems. Potential applications of high-temperature superconducting technology in cryocoolers and remote sensing, communications, and power systems are discussed. Author

N92-32983*# National Aeronautics and Space Administration, Lewis Research Center, Cleveland, OH.

MAGNETIC PENETRATION DEPTH OF $\text{YBa}_2\text{Cu}_3\text{O}_{7-\delta}$ THIN FILMS DETERMINED BY THE POWER TRANSMISSION METHOD

VERNON O. HEINEN, FELIX A. MIRANDA, and KUL B. BHASIN *In its* Solid State Technology Branch of NASA Lewis Research Center p 201-204 Aug. 1992

Avail: CASI HC A01/MF A03

A power transmission measurement technique was used to determine the magnetic penetration depth (λ) of $\text{YBa}_2\text{Cu}_3\text{O}_{7-\delta}$ superconducting thin films on LaAlO_3 within the 26.5 to 40.0 GHz frequency range, and at temperatures from 20 to 300 K. Values of λ ranging from 1100 to 2500 Å were obtained at low temperatures. The anisotropy of λ was determined from measurements of c-axis and a-axis oriented films. An estimate of the intrinsic value of λ of 90 ± 30 nm was obtained from the dependence of λ on film thickness. The advantage of this technique is that it allows λ to be determined nondestructively. Author

N92-32984*# National Aeronautics and Space Administration, Lewis Research Center, Cleveland, OH.

MAGNETIC FLUX RELAXATION IN $\text{YBa}_2\text{Cu}_3\text{O}_{7-x}$ THIN FILM: THERMAL OR ATERNAL

SATISH VITTA, M. A. STAN (Kent State Univ., OH.), JOSEPH D. WARNER, and SAMUEL A. ALTEROVITZ *In its* Solid State Technology Branch of NASA Lewis Research Center p 205-210 Aug. 1992 Repr. from Journal of Thin Solid Films (Lausanne, Switzerland, Elsevier Sequoia), no. 206, 1991 p 137-142 (Contract NAG3-440751)

Avail: CASI HC A02/MF A03

77 THERMODYNAMICS AND STATISTICAL PHYSICS

The magnetic flux relaxation behavior of $\text{YBa}_2\text{Cu}_3\text{O}_{(7-x)}$ thin film on LaAlO_3 for H parallel c was studied in the range of 4.2-40 k and 0.2-1.0 T. Both the normalized flux relaxation rate (S) and the net flux pinning energy (U) increase continuously from $1.3 \times 10 \exp^{-2}$ to $3.0 \times 10 \exp^{-2}$ and from 70-240 meV respectively, as the temperature (T) increases from 10 to 40 K. This behavior is consistent with the thermally activated flux motion model. At low temperatures, however, S is found to decrease much more slowly as compared with kT , in contradiction to the thermal activation model. This behavior is discussed in terms of the athermal quantum tunneling of flux lines. The magnetic field dependence of U , however, is not completely understood.

Author

77

THERMODYNAMICS AND STATISTICAL PHYSICS

Includes quantum mechanics; theoretical physics; and Bose and Fermi statistics.

A92-15443* Minnesota Univ., Minneapolis. NONGRAY RADIATIVE GAS ANALYSES USING THE S-N DISCRETE ORDINATES METHOD

T. K. KIM (Korea Institute of Energy and Resources, Taejon, Republic of Korea), J. A. MENART (Minnesota, University, Minneapolis), and H. S. LEE (NASA, Lewis Research Center, Cleveland, OH; Minnesota, University, Minneapolis) Nov. 1991 7 p refs

(Contract NSF CBT-84-51076)

Copyright

The S-N discrete ordinates method is applied to analyze radiative heat transfer in nongray gases. Spectral correlation between the terms in the equation of transfer is considered for black or nearly nonreflecting walls. Formulations to apply the S-N method using a narrow-band or the exponential wide-band model are presented. The net radiative wall heat fluxes and the radiative source distributions are obtained for uniform, parabolic, and boundary layer-type temperature profiles, as well as for a parabolic concentration profile. The narrow- and wide-band nongray solutions are compared with gray-band approximations using the same band models. The computational speed of the gray-band approximation is obtained at the expense of accuracy in the internal fluxes and radiative source distributions. The wall radiative flux predictions by the gray-band approximation are satisfactory.

Author

A92-16101* Cleveland State Univ., OH. THE ANALYSIS OF HIGH PRESSURE EXPERIMENTAL DATA HERBERT SCHLOSSER (Cleveland State University, OH) and JOHN FERRANTE (NASA, Lewis Research Center, Cleveland, OH) Journal of Physics and Chemistry of Solids (ISSN 0022-3697), vol. 52, no. 4, 1991, p. 635-637. Research supported by Ohio Board of Regents. 1991 3 p refs

Copyright

This letter is concerned with the analysis of high pressure experimental data. It is demonstrated that $\ln H$ plots based on the Vinet et al. (1988) universal equation of state are a simple sensitive means for identifying anomalous P-V data in high pressure experiments and for detecting structural and phase transitions in solids subjected to high pressure.

Author

A92-28185*# National Aeronautics and Space Administration. Lewis Research Center, Cleveland, OH. RADIATIVE TRANSFER SOLUTIONS FOR CYLINDRICAL COORDINATES WITH EMITTING, ABSORBING, AND ANISOTROPIC SCATTERING MEDIUM SLAH JENDOUBI (Minnesota, University, Minneapolis), HAEOK LEE, S. (NASA, Lewis Research Center, Cleveland, OH), and TAE-KUK KIM (Korea Institute of Energy and Resources, Taejon, Republic of Korea) AIAA, Aerospace Sciences Meeting and

Exhibit, 30th, Reno, NV, Jan. 6-9, 1992. 11 p. Research supported by Minnesota Supercomputer Institute. Jan. 1992 11 p refs (Contract NSF CBT-84-51076) (AIAA PAPER 92-0123) Copyright

The radiative transfer equation is solved by the S-N discrete ordinates method in one-dimensional radial and two-dimensional r-z coordinates systems. The walls of the enclosures are diffuse, and the participating medium absorbs, emits and anisotropically scatters the radiative energy. Diffuse wall incidence, isothermal medium emission and collimated incidence problems are considered. Effects of the scattering phase functions on average incident radiation and net radiative heat fluxes are studied. In addition, the effects of scattering albedo, optical thickness and the wall emissivity are briefly discussed.

Author

A92-54287*# National Aeronautics and Space Administration. Lewis Research Center, Cleveland, OH. COMPARISONS OF CYLINDRICAL AND RECTANGULAR MEDIA RADIATIVE TRANSFER SOLUTIONS USING THE S-N DISCRETE ORDINATES METHOD

SLAH JENDOUBI (Minnesota, University, Minneapolis) and HAEOK S. LEE (NASA, Lewis Research Center, Cleveland, OH) AIAA, Thermophysics Conference, 27th, Nashville, TN, July 6-8, 1992. 9 p. Research supported by University of Minnesota. Jul. 1992 9 p refs

(Contract NSF CTS-84-51076)

(AIAA PAPER 92-2894) Copyright

The application of the S-N discrete ordinates method is compared for r-z and x-y problems with similar boundary conditions. The complexities of the r-z solution come from the additional angular derivative, which makes this into a virtual three-dimensional problem. Effects of spatial differencing schemes, phase functions, and grid spacing are considered and compared for these x-y and r-z problems.

Author

80

SOCIAL SCIENCES (GENERAL)

Includes educational matters.

N92-30908*# Winthrop Group, Inc., Cambridge, MA. ROCKET PROPULSION RESEARCH AT LEWIS RESEARCH CENTER Final Report

VIRGINIA P. DAWSON Jul. 1992 8 p Presented at the 28th Joint Propulsion Conference and Exhibit, Nashville, TN, 6-8 Jul. 1992; sponsored by AIAA, SAE, ASME, and ASEE Prepared for NASA Lewis Research Center (Contract NASW-3920; RTOP 506-42-00) (NASA-CR-189187; E-7119; NAS 1.26:189187; AIAA PAPER 92-3123) Avail: CASI HC A02/MF A01

A small contingent of engineers at NASA LeRC pioneered the basic research on liquid propellants for rockets shortly after World War 2. Carried on through the 1950s, this work influenced the important early decisions made by Abe Silverstein when he took charge of the Office of Space Flight Programs for NASA. He strongly supported the development of liquid hydrogen as a propulsion fuel in the face of resistance from Wernher von Braun. Members of the LeRC staff played an important role in bringing liquid hydrogen technology to the point of reliability through their management of the Centaur Program. This paper demonstrates how the personality and engineering intuition of Abe Silverstein shaped the Centaur program and left a lasting imprint on the laboratory research tradition. Many of the current leaders of LeRC received their first hands-on engineering experience when they worked on the Centaur program in the 1960s.

Author

81

ADMINISTRATION AND MANAGEMENT

Includes management planning and research.

N92-25725*# National Aeronautics and Space Administration. Lewis Research Center, Cleveland, OH.

NASA SURFACE-MODELING AND GRID-GENERATION (SM/GG) ACTIVITIES

YUNG K. CHOO *In its Workshop on Grid Generation and Related Areas* p 143-149 Apr. 1992
Avail: CASI HC A02/MF A02

A NASA Steering Committee was formed to carry out the recommendations from the NASA Workshop on Future Directions in Surface Modeling and Grid Generation. Its function is to communicate and coordinate within NASA the acquisition and distribution of geometry/grid generation software/data, establish geometry data exchange standards, and interface with other government, university, and industry efforts. Two speakers present the committee's activities in viewgraph format. H.A.

82

DOCUMENTATION AND INFORMATION SCIENCE

Includes information management; information storage and retrieval technology; technical writing; graphic arts; and micrography.

N92-12786*# National Aeronautics and Space Administration. Lewis Research Center, Cleveland, OH.

BIBLIOGRAPHY OF LEWIS RESEARCH CENTER TECHNICAL PUBLICATIONS ANNOUNCED IN 1990

Aug. 1991 437 p
(NASA-TM-103753; E-6007; NAS 1.15:103753) Avail: CASI HC A19/MF A04

This compilation of abstracts describes and indexes the technical reporting that resulted from the scientific and engineering work performed and managed by the Lewis Research Center in 1990. All the publications were announced in the 1990 issues of STAR (Scientific and Technical Aerospace Reports) and/or IAA (International Aerospace Abstracts). Included are research reports, journal articles, conference presentations, patents and patent applications, and theses. Author

85

URBAN TECHNOLOGY AND TRANSPORTATION

Includes applications of space technology to urban problems; technology transfer; technology assessment; and surface and mass transportation.

N92-25395*# National Aeronautics and Space Administration. Lewis Research Center, Cleveland, OH.

COMPARISON OF GLIMPS AND HFAST STIRLING ENGINE CODE PREDICTIONS WITH EXPERIMENTAL DATA

STEVEN M. GENG and ROY C. TEW 1992 8 p Proposed for presentation at the 27th Intersociety Energy Conversion Engineering Conference, San Diego, CA, 3-7 Aug. 1992; sponsored by SAE, ACS, AIAA, ASME, IEEE, AIChE, and ANS (Contract RTOP 590-13-11)

(NASA-TM-105549; E-7078; NAS 1.15:105549) Avail: CASI HC A02/MF A01

Predictions from GLIMPS and HFAST design codes are

compared with experimental data for the RE-1000 and SPRE free piston Stirling engines. Engine performance and available power loss predictions are compared. Differences exist between GLIMPS and HFAST loss predictions. Both codes require engine specific calibration to bring predictions and experimental data into agreement. Author

90

ASTROPHYSICS

Includes cosmology; celestial mechanics; space plasmas; and interstellar and interplanetary gases and dust.

A92-14477 National Aeronautics and Space Administration. Lewis Research Center, Cleveland, OH.

DARK MATTER AND THE EQUIVALENCE PRINCIPLE

JOSHUA A. FRIEMAN and BEN-AMI GRADWOHL (NASA/Fermilab National Accelerator Laboratory, Batavia, IL) *Physical Review Letters* (ISSN 0031-9007), vol. 67, Nov. 18, 1991, p. 2926-2929. Research supported by DOE. 18 Nov. 1991 4 p refs (Contract NAGW-1340)
Copyright

If the dark matter in galaxies and clusters is nonbaryonic, it can interact with additional long-range fields that are invisible to experimental tests of the equivalence principle. The astrophysical and cosmological implications of a long-range force coupled only to the dark matter are discussed and rather tight constraints on its strength are found. If the force is repulsive (attractive), the masses of galaxy groups and clusters (and the mean density of the universe inferred from them) have been systematically underestimated (overestimated). Such an interaction also has unusual implications for the growth of large-scale structure. Author

A92-24456 National Aeronautics and Space Administration. Lewis Research Center, Cleveland, OH.

VOID PROBABILITY AS A FUNCTION OF THE VOID'S SHAPE AND SCALE-INVARIANT MODELS

E. ELIZALDE (Barcelona, Universidad, Spain) and E. GAZTANAGA (NASA/Fermilab Astrophysics Center, Batavia, IL) *Royal Astronomical Society, Monthly Notices* (ISSN 0035-8711), vol. 254, Jan. 15, 1992, p. 247-256. Research supported by CICYT and DOE. Previously announced in STAR as N91-29113. 15 Jan. 1992 10 p refs (Contract NAGW-1340)
Copyright

The dependence of counts in cells on the shape of the cell for the large scale galaxy distribution is studied. A very concrete prediction can be done concerning the void distribution for scale invariant models. The prediction is tested on a sample of the CfA catalog, and good agreement is found. It is observed that the probability of a cell to be occupied is bigger for some elongated cells. A phenomenological scale invariant model for the observed distribution of the counts in cells, an extension of the negative binomial distribution, is presented in order to illustrate how this dependence can be quantitatively determined. An original, intuitive derivation of this model is presented. Author

A92-26397 National Aeronautics and Space Administration. Lewis Research Center, Cleveland, OH.

A CLASSICAL INSTABILITY OF REISSNER-NORDSTROM SOLUTIONS AND THE FATE OF MAGNETICALLY CHARGED BLACK HOLES

KIMYEONG LEE, V. P. NAIR (Columbia University, New York), and ERICK J. WEINBERG (NASA/Fermilab Astrophysics Center, Batavia, IL; Columbia University, New York) *Physical Review Letters* (ISSN 0031-9007), vol. 68, Feb. 24, 1992, p. 1100-1103. Research supported by DOE. 24 Feb. 1992 4 p refs

(Contract NAGW-2381)

Copyright

Working in the context of spontaneously broken gauge theories, it is shown that the magnetically charged Reissner-Nordstrom solution develops a classical instability if the horizon is sufficiently small. This instability has significant implications for the evolution of a magnetically charged black hole. In particular, it leads to the possibility that such a hole could evaporate completely, leaving in its place a nonsingular magnetic monopole. Author

A92-33069 National Aeronautics and Space Administration. Lewis Research Center, Cleveland, OH.

POSSIBLE SOURCES OF THE POPULATION I LITHIUM ABUNDANCE AND LIGHT-ELEMENT EVOLUTION

LAWRENCE E. BROWN (NASA/Fermilab Astrophysics Center, Batavia; Chicago, University, IL) *Astrophysical Journal*, Part 1 (ISSN 0004-637X), vol. 389, April 10, 1992, p. 251-268. Research supported by DOE. 10 Apr. 1992 18 p refs (Contract NAGW-1321; NAGW-1340)

Copyright

One-zone numerical models of Galactic chemical evolution of the light elements (lithium, beryllium, boron, and deuterium) with a broad sample of possible stellar lithium production sites and star formation histories, including the multiple merger model of Mathews and Schramm (1992), are examined. Models with high primordial lithium are constrained by observations of lithium and potassium in the interstellar medium of the LMC to have Li abundances close to the Population I value of about $10 \exp^{-9}$. Li-7 production in intermediate- or high-mass stars (greater than 4 solar masses) is found to fit observations somewhat better than production in low-mass (1-5 solar masses) stars. Since elevated levels of lithium are commonly observed in intermediate-mass stars in the LMC, it is argued that this is indeed the major source of the Population I Li-7 abundance. P.D.

A92-33353 National Aeronautics and Space Administration. Lewis Research Center, Cleveland, OH.

PERTURBATIONS FROM COSMIC STRINGS IN COLD DARK MATTER

ANDREAS ALBRECHT and ALBERT STEBBINS (NASA/Fermilab Astrophysics Center, Batavia, IL) *Physical Review Letters* (ISSN 0031-9007), vol. 68, April 6, 1992, p. 2121-2124. Research supported by DOE. Previously announced in STAR as N91-31043. 6 Apr. 1992 4 p refs (Contract NAGW-2381)

Copyright

A systematic linear analysis of the perturbations induced by cosmic strings in cold dark matter is presented. The power spectrum is calculated and it is found that the strings produce a great deal of power on small scales. It is shown that the perturbations on interesting scales are the result of many uncorrelated string motions, which indicates a much more Gaussian distribution than was previously supposed. Author

A92-37413 National Aeronautics and Space Administration. Lewis Research Center, Cleveland, OH.

FRACTALS AND COSMOLOGICAL LARGE-SCALE STRUCTURE

XIAOCHUN LUO (Chicago, University, IL) and DAVID N. SCHRAMM (NASA/Fermilab Astrophysics Center, Batavia, IL) *Science* (ISSN 0036-8075), vol. 256, no. 5056, April 24, 1992, p. 513-515. Research supported by DOE and NSF. 24 Apr. 1992 3 p refs (Contract NAGW-1321; NAGW-2381)

Copyright

Observations of galaxy-galaxy and cluster-cluster correlations as well as other large-scale structure can be fit with a 'limited' fractal with dimension D of about 1.2. This is not a 'pure' fractal out to the horizon: the distribution shifts from power law to random behavior at some large scale. If the observed patterns and structures are formed through an aggregation growth process, the fractal dimension D can serve as an interesting constraint on the properties of the stochastic motion responsible for limiting the

fractal structure. In particular, it is found that the observed fractal should have grown from two-dimensional sheetlike objects such as pancakes, domain walls, or string wakes. This result is generic and does not depend on the details of the growth process. Author

A92-43837 National Aeronautics and Space Administration. Lewis Research Center, Cleveland, OH.

THE DIFFUSE GAMMA-RAY BACKGROUND, LIGHT ELEMENT ABUNDANCES, AND SIGNATURES OF EARLY MASSIVE STAR FORMATION

JOSEPH SILK (California, University, Berkeley) and DAVID N. SCHRAMM (California, University, Berkeley; Chicago, University; NASA/Fermilab Astrophysics Center, Batavia, IL) *Astrophysical Journal*, Part 2 - Letters (ISSN 0004-637X), vol. 393, no. 1, July 1, 1992, p. L9-L11. Research supported by DOE, NASA, and NSF. 1 Jul. 1992 3 p refs

Copyright

Attention is drawn to a potentially observable flux of diffuse extragalactic gamma rays produced by inelastic cosmic-ray interactions that is inevitably a by-product of spallation-synthesized Be. The epoch of cosmic ray-induced Population II light element nucleosynthesis is constrained to be at redshift greater than 0.5. A spectral feature in the diffuse extragalactic gamma-ray background with amplitude 0.1 above 10 MeV is predicted if the Be is synthesized at z less than 10. The possibility is discussed that the cosmic-ray flux responsible for Population II Be and B synthesis may be associated with a precursor hypothesized Population III. C.D.

A92-45808 National Aeronautics and Space Administration. Lewis Research Center, Cleveland, OH.

MASSIVE DIRAC NEUTRINOS AND SN 1987A

ADAM BURROWS, RAJ GANDHI (Arizona, University, Tucson), and MICHAEL S. TURNER (NASA/Fermilab Astrophysics Center; Fermi National Accelerator Laboratory, Batavia; Chicago, University, IL) *Physical Review Letters* (ISSN 0031-9007), vol. 68, no. 26, June 29, 1992, p. 3834-3837. Research supported by DOE. 29 Jun. 1992 4 p refs (Contract NAGW-2381; NAGW-2145; NSF AST-89-14346)

Copyright

The wrong-helicity states of a Dirac neutrino can provide an important cooling mechanism for young neutron stars. Based on numerical models of the early cooling of the neutron star associated with SN 1987A which self-consistently incorporate wrong-helicity neutrino emission, it is argued that a Dirac neutrino of mass greater than 30 keV (25 keV if it is degenerate) leads to shortening of the neutrino burst that is inconsistent with the Irvine-Michigan-Brookhaven and Kamiokande II data. If pions are as abundant as nucleons in the cores of neutron stars, the present limit improves to 15 keV. Author

A92-48103 National Aeronautics and Space Administration. Lewis Research Center, Cleveland, OH.

THICK STRINGS, THE LIQUID CRYSTAL BLUE PHASE, AND COSMOLOGICAL LARGE-SCALE STRUCTURE

XIAOCHUN LUO and DAVID N. SCHRAMM (Chicago, University; NASA/Fermilab Astrophysics Center, Batavia, IL) *Astrophysical Journal*, Part 1 (ISSN 0004-637X), vol. 394, no. 1, July 20, 1992, p. 12-18. Research supported by DOE. 20 Jul. 1992 7 p refs (Contract NSF AST-88-22595; NAGW-1321; NAGW-1340)

Copyright

A phenomenological model based on the liquid crystal blue phase is proposed as a model for a late-time cosmological phase transition. Topological defects, in particular thick strings and/or domain walls, are presented as seeds for structure formation. It is shown that the observed large-scale structure, including quasi-periodic wall structure, can be well fitted in the model without violating the microwave background isotropy bound or the limits from induced gravitational waves and the millisecond pulsar timing. Furthermore, such late-time transitions can produce objects such as quasars at high redshifts. The model appears to work with either cold or hot dark matter. Author

A92-54464 National Aeronautics and Space Administration. Lewis Research Center, Cleveland, OH.

FLUCTUATION-DRIVEN ELECTROWEAK PHASE TRANSITION
MARCELO GLEISER (Dartmouth College, Hanover, NH) and EDWARD W. KOLB (NASA/Fermilab Astrophysics Center, Batavia; Chicago, University, IL) *Physical Review Letters* (ISSN 0031-9007), vol. 69, no. 9, Aug. 31, 1992, p. 1304-1307. Research supported by DOE. Previously announced in STAR as N92-17647. 31 Aug. 1992 4 p refs

(Contract NAGW-2381)

Copyright

We examine the dynamics of the electroweak phase transition in the early Universe. For Higgs masses in the range 46 less than or = $M_{sub H}$ less than or = 150 GeV and top quark masses less than 200 GeV, regions of symmetric and asymmetric vacuum coexist to below the critical temperature, with thermal equilibrium between the two phases maintained by fluctuations of both phases. We propose that the transition to the asymmetric vacuum is completed by percolation of these subcritical fluctuations. Our results are relevant to scenarios of baryogenesis that invoke a weakly first-order phase transition at the electroweak scale.

Author

A92-56914 National Aeronautics and Space Administration. Lewis Research Center, Cleveland, OH.

LARGE-SCALE MICROWAVE ANISOTROPY FROM GRAVITATING SEEDS

SHOBA VEERARAGHAVAN (Massachusetts, University, Amherst) and ALBERT STEBBINS (NASA/Fermilab Astrophysics Center, Batavia, IL) *Astrophysical Journal, Part 2 - Letters* (ISSN 0004-637X), vol. 395, no. 2, Aug. 20, 1992, p. L55-L58. Research supported by NSF and DOE. 20 Aug. 1992 4 p refs

(Contract NAGW-2381)

Copyright

Topological defects could have seeded primordial inhomogeneities in cosmological matter. We examine the horizon-scale matter and geometry perturbations generated by such seeds in an expanding homogeneous and isotropic universe. Evolving particle horizons generally lead to perturbations around motionless seeds, even when there are compensating initial underdensities in the matter. We describe the pattern of the resulting large angular scale microwave anisotropy.

Author

N92-27252*# National Aeronautics and Space Administration. Lewis Research Center, Cleveland, OH.

CHARACTERISTICS OF HYPERVELOCITY IMPACT CRATERS ON LDEF EXPERIMENT S1003 AND IMPLICATIONS OF SMALL PARTICLE IMPACTS ON REFLECTIVE SURFACES

Abstract Only

MICHAEL J. MIRTICH and JAMES E. MERROW (Cleveland State Univ., OH.) *In* NASA. Langley Research Center, Second LDEF Post-Retrieval Symposium Abstracts p 41 Jun. 1992
Avail: CASI HC A01/MF A02

The Ion Beam Textured and Coated Surfaces Experiment (IBEX) was designated S1003 on the Long Duration Exposure Facility (LDEF) at a location of 98 degrees relative to the ram direction. Thirty-six diverse materials were exposed to the micrometeoroid (and some debris) environment for 5.8 years. Optical property measurements indicated no changes for almost all of the materials except S-13G, Kapton, and Kapton-coated surfaces, and these changes can be explained by other environmental effects. From the predicted micrometeoroid flux of NASA SP-8013, no changes in optical properties of the surfaces due to micrometeoroids were expected. However, there were hypervelocity impacts on the various diverse materials flown on IBEX. The characteristics of these craters were documented using scanning electron microscopy (SEM) and are presented. Interest in placing large solar concentrator/solar dynamic systems in space for power generation has again brought up a concern for maintaining the integrity of the optical properties of highly specular reflecting surfaces in the near-Earth space environment. It has been shown that highly reflective polished metals and thin film coatings degrade when exposed to simulated micrometeoroids in

the laboratory. At LeRC, a shock tube was used to simulate the phenomenon of micrometeoroid optical properties of surfaces exposed to this impact were then evaluated. A calibrated sensor, 2000 A Al/stainless steel, was developed to not only detect the small size micrometeoroid environment, but also to evaluate the degradation of the optical properties of thin aluminum films in space. This sensor was flown on LDEF experiment S1003 and also on the OSO 3 and SERT 2 satellites that were launched in 1967 and 1970, respectively. No changes in the optical properties of the highly reflective surface sensor on SERT 2 were measured during 20 years in space. The results, as determined by the accuracy of the sensor, indicate that a highly reflective surface should lose less than 1 percent of its specular reflectance in near-Earth orbit during 20 years.

Author

91

LUNAR AND PLANETARY EXPLORATION

Includes planetology; and manned and unmanned flights.

N92-13910*# National Aeronautics and Space Administration. Lewis Research Center, Cleveland, OH.

POWER MANAGEMENT AND DISTRIBUTION CONSIDERATIONS FOR A LUNAR BASE

BARBARA H. KENNY and ANTHONY S. COLEMAN (Sverdrup Technology, Inc., Brook Park, OH.) 1991 9 p Proposed for presentation at the Ninth Symposium on Space Nuclear Power Systems, Albuquerque, NM, 12-16 Jan. 1992, sponsored by the Univ. of New Mexico

(Contract RTOP 506-41-41)

(NASA-TM-105342; E-6710; NAS 1.15:105342) Avail: CASI HC A02/MF A01

Design philosophies and technology needs for the power management and distribution (PMAD) portion of a lunar base power system are discussed. A process is described whereby mission planners may proceed from a knowledge of the PMAD functions and mission performance requirements to a definition of design options and technology needs. Current research efforts at the NASA LRC to meet the PMAD system needs for a Lunar base are described. Based on the requirements, the lunar base PMAD is seen as best being accomplished by a utility like system, although with some additional demands including autonomous operation and scheduling and accurate, predictive modeling during the design process.

Author

N92-14953*# National Aeronautics and Space Administration. Lewis Research Center, Cleveland, OH.

OVERVIEW OF KA-BAND COMMUNICATIONS TECHNOLOGY REQUIREMENTS FOR THE SPACE EXPLORATION INITIATIVE

EDWARD F. MILLER 1991 11 p Presented at the Conference on Advanced Space Exploration Initiative Technologies, Cleveland, OH, 4-6 Sep. 1991; cosponsored by AIAA, NASA, and OAI Previously announced in IAA as A91-52344

(Contract RTOP 316-30-19)

(NASA-TM-105308; E-6661; NAS 1.15:105308; AIAA PAPER 91-3424) Avail: CASI HC A03/MF A01

In the Space Exploration Initiative, Ka-band frequencies are likely to carry the bulk of the communications traffic both in the vicinity of and on the return links from the moon and Mars. The four exploration architectures identified by the Synthesis Group are examined and Ka-band technology requirements to meet the data traffic needs and schedule are identified. Specific Ka-band technology requirements identified are: transmitters - 0.5 to 200 W with high efficiency; antennas - 5m and 9m diameter, with multiple beams and/or scanning beams; and spacecraft receivers - noise figure of 2 dB. For each component, the current state of technology is assessed and needed technology development programs are identified. It is concluded that to meet the schedules of lunar and Mars precursor missions beginning in approximately

the year 2000, aggressive technology development and advanced development programs are required immediately for Ka-band communications systems components. Additionally, the greater data transmission rates for the cargo and piloted phases of the exploration program require further Ka-band communications technology developments targeted for operations beginning in about 2010. Author

N92-17069*# National Aeronautics and Space Administration. Lewis Research Center, Cleveland, OH.
ENVIRONMENTAL INTERACTIONS IN SPACE EXPLORATION: ANNOUNCEMENT OF THE FORMATION OF AN ENVIRONMENTAL INTERACTIONS WORKING GROUP
 JOSEPH C. KOLECKI and G. BARRY HILLARD Nov. 1991
 10 p
 (Contract RTOP 506-41-41)
 (NASA-TM-105294; E-6633; NAS 1.15:105294) Avail: CASI HC A02/MF A01

With the advent of the Space Exploration Initiative, the possibility of designing and using systems on scales not heretofore attempted presents exciting new challenges in systems design and space science. The environments addressed by the Space Exploration Initiative include the surfaces of the Moon and Mars, as well as the varied plasma and field environments which will be encountered by humans and cargo enroute to these destinations. Systems designers will need to understand environmental interactions and be able to model these mechanisms from the earliest conceptual design stages through design completion. To the end of understanding environmental interactions and establishing robotic precursor mission requirements, an Environmental Interactions Working Group has been established as part of the Robotic Missions Working Group. The current paper describes the working group and gives an update of its current activities. Working group charter and operation are reviewed, background information on the environmental interactions and their characteristics is offered, and the current status of the group's activities is presented along with anticipations for the future. Author

N92-30302*# National Aeronautics and Space Administration. Lewis Research Center, Cleveland, OH.
ELECTRICAL AND CHEMICAL INTERACTIONS AT MARS WORKSHOP, PART 1 Final Report
 1992 31 p Workshop held in Cleveland, OH, 19-20 Nov. 1991
 (Contract RTOP 506-41-41)
 (NASA-CP-10093; E-7016-1; NAS 1.55:10093) Avail: CASI HC A03/MF A01

The Electrical and Chemical Interactions at Mars Workshop, hosted by NASA Lewis Research Center on November 19 and 20, 1991, was held with the following objectives in mind: (1) to identify issues related to electrical and chemical interactions between systems and their local environments on Mars, and (2) to recommend means of addressing those issues, including the dispatch of robotic spacecraft to Mars to acquire necessary information. The workshop began with presentations about Mars' surface and orbital environments, Space Exploration Initiative (SEI) systems, environmental interactions, modeling and analysis, and plans for exploration. Participants were then divided into two working groups: one to examine the surface of Mars; and the other, the orbit of Mars. The working groups were to identify issues relating to environmental interactions; to state for each issue what is known and what new knowledge is needed; and to recommend ways to fulfill the need. Issues were prioritized within each working group using the relative severity of effects as a criterion. Described here are the two working groups' contributions. A bibliography of materials used during the workshop and suggested reference materials is included. Author

SOLAR PHYSICS

Includes solar activity, solar flares, solar radiation and sunspots.

A92-50927* National Aeronautics and Space Administration. Lewis Research Center, Cleveland, OH.
MONTE CARLO EXPLORATION OF MIKHEYEV-SMIRNOV-WOLFENSTEIN SOLUTIONS TO THE SOLAR NEUTRINO PROBLEM
 X. SHI (Chicago, University, IL), D. N. SCHRAMM (Chicago, University; NASA/Fermilab Astrophysics Center, Batavia, IL), and J. N. BAHCALL (Institute for Advanced Study, Princeton, NJ) Physical Review Letters (ISSN 0031-9007), vol. 69, no. 5, Aug. 3, 1992, p. 717-720. Research supported by DOE, NSF, and NASA. 3 Aug. 1992 4 p refs
 Copyright

The paper explores the impact of astrophysical uncertainties on the Mikheyev-Smirnov-Wolfenstein (MSW) solution by calculating the allowed MSW solutions for 1000 different solar models with a Monte Carlo selection of solar model input parameters, assuming a full three-family MSW mixing. Applications are made to the chlorine, gallium, Kamiokande, and Borexino experiments. The initial GALLEX result limits the mixing parameters to the upper diagonal and the vertical regions of the MSW triangle. The expected event rates in the Borexino experiment are also calculated, assuming the MSW solutions implied by GALLEX. Author

N92-33899*# National Aeronautics and Space Administration. Lewis Research Center, Cleveland, OH.
PHOTOVOLTAIC ARRAY FOR MARTIAN SURFACE POWER
 J. APPELBAUM (Tel-Aviv Univ., Israel) and G. A. LANDIS (Sverdrup Technology, Inc., Brook Park, OH.) Aug. 1992 23 p Proposed for presentation at the 43rd Congress of the International Astronautical Federation, Washington, DC, 28 Aug. - 5 Sep. 1992; sponsored by AIAA, NASA, and NAS
 (Contract NAS3-25266; NAGW-2022; RTOP 506-41-11)
 (NASA-TM-105827; E-7262; NAS 1.15:105827) Avail: CASI HC A03/MF A01

Missions to Mars will require electric power. A leading candidate for providing power is solar power produced by photovoltaic arrays. To design such a power system, detailed information on solar-radiation availability on the Martian surface is necessary. The variation of the solar radiation on the Martian surface is governed by three factors: (1) variation in Mars-Sun distance; (2) variation in solar zenith angle due to Martian season and time of day; and (3) dust in the Martian atmosphere. A major concern is the dust storms, which occur on both local and global scales. However, there is still appreciable diffuse sunlight available even at high opacity, so that solar array operation is still possible. Typical results for tracking solar collectors are also shown and compared to the fixed collectors. During the Northern Hemisphere spring and summer the isolation is relatively high, 2-5 kW-hr/sq m-day, due to the low optical depth of the Martian atmosphere. These seasons, totalling a full terrestrial year, are the likely ones during which manned mission will be carried out. Author

GENERAL

Includes aeronautical, astronautical, and space science related histories, biographies, and pertinent reports too broad for categorization; histories or broad overviews of NASA programs.

N92-18455*# National Aeronautics and Space Administration. Lewis Research Center, Cleveland, OH.

NASA SPACE APPLICATIONS OF HIGH-TEMPERATURE SUPERCONDUCTORS

VERNON O. HEINEN, MARTIN M. SOKOLOSKI (National Aeronautics and Space Administration, Washington, DC.), PAUL R. ARON, KUL B. BHASIN, EDWIN G. WINTUCKY, and DENIS J. CONNOLLY 1992 9 p Presented at the Fourth International Symposium on Superconductivity, Tokyo, Japan, 14-17 Oct. 1991; sponsored by the International Superconductivity Technology Center

(Contract RTOP 506-59-40)

(NASA-TM-105401; E-6801; NAS 1.15:105401) Avail: CASI HC A02/MF A01

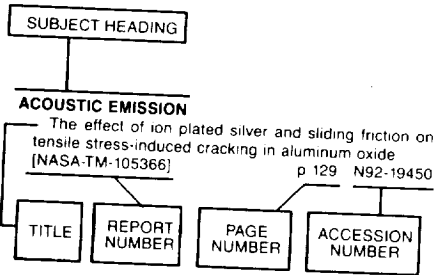
The application of superconducting technology in space has been limited by the requirement of cooling to near liquid helium temperatures. The only means of obtaining these temperatures has been with cryogenic fluids which severely limit mission lifetime. The development of materials with superconducting transition temperatures above 77 K has made superconducting technology more attractive and feasible for employment in aerospace systems. Here, potential applications of high temperature superconducting technology in cryocoolers, remote sensing, communications, and power systems are discussed.

Author



SUBJECT INDEX

Typical Subject Index Listing



The subject heading is a key to the subject content of the document. Titles, report numbers, and accession numbers of pertinent documents are provided under each subject heading. When the title is insufficiently descriptive of document content, a title extension is added, separated from the title by three hyphens. The report number helps to indicate the type of document cited (e.g., NASA report, NASA translation, NASA contractor report). The accession number is the number by which the document abstracts are arranged in this journal and by which the document is sold or requested. The titles, with title extensions if present, are arranged under each subject heading in ascending accession number order. The subject headings have been selected from the latest revision of the *NASA Thesaurus*.

A

ABLATION

- New technique for low-to-high altitude predictions of ablative hypersonic flowfields p 166 A92-24654 [AIAA PAPER 92-0366]
- Low-to-high altitude predictions of three-dimensional ablative reentry flowfields p 168 A92-26227 [AIAA PAPER 92-0366]

ABRASION

- High temperature, flexible, fiber-preform seal [NASA-CASE-LEW-15085-1] p 208 N92-22043

ABRASION RESISTANCE

- Novel applications for TAZ-8A p 123 N92-22444

ABRIKOSOV THEORY

- Melting of the Abrikosov flux lattice in anisotropic superconductors p 260 A92-28075

ABSORBERS (MATERIALS)

- Modal element method for scattering of sound by absorbing bodies [NASA-TM-105722] p 255 N92-28984

ABUNDANCE

- Possible sources of the Population I lithium abundance and light-element evolution p 268 A92-33069

AC GENERATORS

- Development of an analytical tool to study power quality of ac power systems for large spacecraft p 67 A92-50529
- Update on results of SPRE testing at NASA Lewis p 71 A92-50780
- Component technology for Stirling power converters p 206 A92-50781

ACCELERATED LIFE TESTS

- Effect of KOH concentration on LEO cycle life of IPV nickel-hydrogen flight cell - Update II p 232 A92-48212 [NASA-TM-105314]
- Effect of KOH concentration on LEO cycle life of IPV nickel-hydrogen flight cells-update 2 [NASA-TM-105314] p 235 N92-13483
- Ceramics for engines p 131 N92-22517

ACCELERATION (PHYSICS)

- Effective diffusion equation in a random velocity field [AIAA PAPER 92-0245] p 167 A92-25704
- Microgravity acceleration measurement and environment characterization science (17-IML-1) p 139 N92-23642
- Space acceleration measurement system triaxial sensor head error budget [NASA-TM-105300] p 57 N92-25134
- Early mission science support: Space Acceleration Measurement System (SAMS) p 57 N92-28451

ACCELEROMETERS

- Development of and flight results from the Space Acceleration Measurement System (SAMS) [AIAA PAPER 92-0354] p 56 A92-28189
- Design of a self-diagnostic beam-mode piezoelectric accelerometer [AIAA PAPER 92-3656] p 200 A92-54106
- Space acceleration measurement system description and operations on the First Spacelab Life Sciences Mission [NASA-TM-105301] p 57 N92-13151
- Space acceleration measurement system triaxial sensor head error budget [NASA-TM-105300] p 57 N92-25134
- Early mission science support: Space Acceleration Measurement System (SAMS) p 57 N92-28451
- Development of and flight results from the Space Acceleration Measurement System (SAMS) [NASA-TM-105652] p 57 N92-30301

ACCURACY

- Accurate upwind-monotone (nonoscillatory) methods for conservation laws p 193 N92-25812
- Numerical simulation of conservation laws p 193 N92-25813

ACETYLENE

- Acetylene fuel from atmospheric CO₂ on Mars p 133 A92-32199

ACOUSTIC EMISSION

- The effect of ion plated silver and sliding friction on tensile stress-induced cracking in aluminum oxide [NASA-TM-105366] p 129 N92-19450

ACOUSTIC EXCITATION

- On the mechanism of turbulence suppression in free shear flows under acoustic excitation [AIAA PAPER 92-0065] p 252 A92-25678
- Effect of acoustic excitation on stalled flows over an airfoil p 9 A92-41267
- On the mechanism of turbulence suppression in free shear flows under acoustic excitation [NASA-TM-105360] p 15 N92-14003

ACOUSTIC MEASUREMENT

- A survey of the broadband shock associated noise prediction methods [AIAA PAPER 92-0501] p 252 A92-26930
- A survey of the broadband shock associated noise prediction methods [NASA-TM-105365] p 254 N92-14797

ACOUSTIC MICROSCOPES

- Tensile strain measurements of ceramic fibers using scanning laser acoustic microscopy p 198 A92-39629

ACOUSTIC SCATTERING

- Modal element method for scattering of sound by absorbing bodies [NASA-TM-105722] p 255 N92-28984

ACOUSTIC VELOCITY

- Effect of operating conditions on gearbox noise [NASA-TM-105331] p 211 N92-26107

ACOUSTICS

- Screech noise source structure of a supersonic rectangular jet [AIAA PAPER 92-0503] p 6 A92-26932
- Control of an axisymmetric turbulent jet by multi-modal excitation p 174 A92-40071
- 3D rocket combustor acoustics model [AIAA PAPER 92-3228] p 66 A92-48829
- Screech noise source structure of a supersonic rectangular jet [NASA-TM-105384] p 15 N92-14000
- The 3D rocket combustor acoustics model [NASA-TM-105734] p 88 N92-27035

ACOUSTO-OPTICS

- Flight experiment on acousto-optic crystal growth p 136 A92-12880

ACTIVATION ENERGY

- Stress versus temperature dependence of activation energies for creep p 217 A92-24719
- Temperature-dependent reflectivity of silicon carbide [NASA-TM-105287] p 201 N92-19263
- Phase transformations in SrAl₂Si₂O₈ glass [NASA-TM-105657] p 264 N92-23890

ACTIVE CONTROL

- Electromechanical simulation and testing of actively controlled rotordynamic systems with piezoelectric actuators [ASME PAPER 91-GT-245] p 203 A92-15650
- Design of a hydraulic actuator for active control of rotating machinery [ASME PAPER 91-GT-246] p 203 A92-15651
- Electromechanical simulation and testing of actively controlled rotordynamic systems with piezoelectric actuators p 204 A92-39258
- Modern developments in shear flow control with swirl p 9 A92-41265
- Optimal microgravity vibration isolation - An algebraic introduction p 54 A92-47495
- Microgravity vibration isolation: An optimal control law for the one-dimensional case [NASA-TM-105146] p 141 N92-11217
- Performance tests of a cryogenic hybrid magnetic bearing for turbopumps [NASA-TM-105627] p 30 N92-20523
- Simulation of Space Station loads with active control systems p 56 N92-23824

ACTS

- Advanced Communications Technology Satellite (ACTS) p 53 A92-17780
- Ka-band active MMIC subarray development [AIAA PAPER 92-1863] p 155 A92-29803
- Ka-band dual frequency array feed for a low cost ACTS ground terminal p 143 A92-29833
- ACTS system capability and performance [AIAA PAPER 92-1961] p 143 A92-29884
- Operational uses of ACTS technology [AIAA PAPER 92-1964] p 144 A92-29887
- The ACTS NASA Ground Station/Master Control Station [AIAA PAPER 92-1965] p 45 A92-29888
- Advanced Communications Technology Satellite (ACTS) Experiments Program - A market-driven approach to government/industry cooperation [AIAA PAPER 92-2036] p 145 A92-29951
- ACTS T1-VSAT - The intelligent earth station [AIAA PAPER 92-2037] p 145 A92-29952
- Network architectures and protocols for the integration of ACTS and ISDN [AIAA PAPER 92-2039] p 145 A92-29953
- The Link Evaluation Terminal for the Advanced Communications Technology Satellite Experiments Program [AIAA PAPER 92-2040] p 49 A92-29954
- ACTS aeronautical experiments [AIAA PAPER 92-2042] p 50 A92-29956
- Dynamic rain fade compensation techniques for the advanced communications technology satellite [AIAA PAPER 92-2038] p 145 A92-31711
- Advanced Communications Technology Satellite (ACTS) p 50 A92-38164
- New coplanar waveguide to rectangular waveguide end launcher p 156 A92-44243
- The ACTS multibeam antenna p 146 A92-46046
- Advanced Communication Technology Satellite (ACTS) baseband processor development p 50 A92-53693
- Ka-band MMIC arrays for ACTS Aero Terminal Experiment [IAF PAPER 92-0398] p 159 A92-55785
- Advanced Communications Technology Satellite (ACTS) [IAF PAPER 92-0407] p 50 A92-55788
- A high temperature superconductivity communications flight experiment [IAF PAPER 92-0410] p 50 A92-55790

SUBJECT

ACTUATORS

The link evaluation terminal for the advanced communications technology satellite experiments program
[NASA-TM-105367] p 51 N92-16008

Advanced Communication Technology Satellite (ACTS) multibeam antenna technology verification experiments
[NASA-TM-105421] p 149 N92-16191

A software control system for the ACTS high-burst-rate link evaluation terminal
[NASA-TM-105207] p 243 N92-16628

Advanced Communication Technology Satellite (ACTS) multibeam antenna analysis and experiment
[NASA-TM-105420] p 149 N92-17047

Intelligent fault isolation and diagnosis for communication satellite systems
[NASA-TM-105645] p 248 N92-23365

The ACTS multibeam antenna
[NASA-TM-105645] p 52 N92-30383

A personal communications network using a Ka-band satellite
[NASA-TM-105420] p 151 N92-30934

Ka-band dual frequency array feed for a low cost ACTS ground terminal
[NASA-TM-105420] p 152 N92-32969

A 1-W, 30-GHz, CPW amplifier for ACTS small terminal uplink
[NASA-TM-105420] p 152 N92-32973

ACTUATORS

Electromechanical simulation and testing of actively controlled rotordynamic systems with piezoelectric actuators
[ASME PAPER 91-GT-245] p 203 A92-15650

Design of a hydraulic actuator for active control of rotating machinery
[ASME PAPER 91-GT-246] p 203 A92-15651

Potential for integrated optical circuits in advanced aircraft with fiber optic control and monitoring systems
[ASME PAPER 91-GT-246] p 24 A92-46246

Flywheel energy storage for electromechanical actuation systems
[ASME PAPER 91-GT-246] p 233 A92-50758

High temperature, flexible pressure-actuated, brush seal
[NASA-CASE-LEW-15086-1] p 208 N92-16318

A video event trigger for high frame rate, high resolution video technology
[NASA-TM-105774] p 160 N92-22453

Resonant mode controllers for launch vehicle applications
[NASA-TM-105563] p 48 N92-25092

Electromechanical systems with transient high power response operating from a resonant AC link
[NASA-TM-105716] p 37 N92-28985

An electromechanical actuation system for an expendable launch vehicle
[NASA-TM-105774] p 48 N92-30310

ADA (PROGRAMMING LANGUAGE)
Description of real-time Ada software implementation of a power system monitor for the Space Station Freedom PMAD DC testbed
[NASA-TM-105774] p 242 A92-50533

ADAPTERS
Graphite/epoxy composite adapters for the Space Shuttle/Centaur vehicle
[NASA-TP-3014] p 49 N92-31251

ADAPTIVE CONTROL
Adaptive temperature profile control of a multizone crystal growth furnace
[NASA-TM-105774] p 137 A92-29243

Identification and control of a multizone crystal growth furnace
[NASA-TM-105774] p 199 A92-39699

Classical and adaptive control algorithms for the solar array pointing system of the Space Station Freedom
[AIAA PAPER 92-4484] p 57 A92-55314

Discrete-time entropy formulation of optimal and adaptive control problems
[AIAA PAPER 92-4484] p 247 A92-55930

Probabilistic structural analysis of adaptive/smart/intelligent space structures
[NASA-TM-105408] p 227 N92-22267

Interactive solution-adaptive grid generation
[NASA-TM-105408] p 243 N92-24420

MAG3D and its application to internal flowfield analysis
[NASA-TM-105408] p 243 N92-24421

ADAPTIVE OPTICS
Space power by ground-based laser transmission
[AIAA PAPER 92-3024] p 63 A92-47027

Self-aligning optical measurement systems
[AIAA PAPER 92-3024] p 247 A92-50387

ADDITION RESINS
New addition curing polyimides
[NASA-TM-105335] p 95 N92-13281

Effects of a noncoplanar biphenyldiamine on the processing and properties of addition polyimides
[NASA-TM-105335] p 107 N92-15137

Structure-to-property relationships in addition cured polymers. 4. Correlations between thermo-oxidative weight losses of norbornenyl cured polyimide resins and their composites
[NASA-TM-105553] p 108 N92-20039

Vinyl capped addition polyimides
[NASA-CASE-LEW-15027-2] p 131 N92-24053

ADDITIVES

High-T sub c fluorine-doped YBa₂Cu₃O_(y) films on ceramic substrates by screen printing
[NASA-TM-105296] p 127 N92-11188

The cyclic oxidation resistance at 1200 C of beta-NiAl, FeAl, and CoAl alloys with selected third element additions
[NASA-TM-105620] p 123 N92-24554

Reduced mobility and PPC in In₂(Ga₂(80)As / Al₂(23)Ga(77)As HEMT structure
[NASA-TM-105620] p 265 N92-32976

ADHESION
Deposition of adherent Ag-Ti duplex films on ceramics in a multiple-cathode sputter deposition system
[NASA-TM-105586] p 34 N92-23225

Computational techniques in tribology and material science at the atomic level
[NASA-TM-105573] p 252 N92-26671

Preliminary evaluation of adhesion strength measurement devices for ceramic/titanium matrix composite bonds
[NASA-TM-105803] p 1 N92-31267

ADHESION TESTS
Preliminary evaluation of adhesion strength measurement devices for ceramic/titanium matrix composite bonds
[NASA-TM-105803] p 1 N92-31267

ADHESIVE BONDING
Preliminary evaluation of adhesion strength measurement devices for ceramic/titanium matrix composite bonds
[NASA-TM-105803] p 1 N92-31267

ADHESIVES
Preliminary evaluation of adhesion strength measurement devices for ceramic/titanium matrix composite bonds
[NASA-TM-105803] p 1 N92-31267

ADVECTION
Development of a new flux splitting scheme
[AIAA PAPER 92-0500] p 190 N92-23352

Development of new flux splitting schemes --- computational fluid dynamics algorithms
[AIAA PAPER 92-0500] p 192 N92-25809

Accurate upwind-monotone (nonoscillatory) methods for conservation laws
[AIAA PAPER 92-0500] p 193 N92-25812

AEROACOUSTICS
Far-field noise and internal modes from a ducted propeller at simulated aircraft takeoff conditions
[AIAA PAPER 92-0371] p 252 A92-26230

Computation of supersonic jet mixing noise for an axisymmetric CD nozzle using k-epsilon turbulence model
[AIAA PAPER 92-0500] p 252 A92-26328

A survey of the broadband shock associated noise prediction methods
[AIAA PAPER 92-0501] p 252 A92-26930

Acoustic analysis using numerical solutions of the Navier-Stokes equations
[AIAA PAPER 92-0506] p 253 A92-26934

Acoustic characteristics and dynamic structural loading of an ASTOVL aircraft in hover
[AIAA PAPER 92-0370] p 253 A92-28190

A review of computational/experimental methodology developments in aeroacoustics
[AIAA PAPER 92-0370] p 253 A92-39241

Direct evaluation of aeroacoustic theory in a jet
[AIAA PAPER 92-0370] p 253 A92-50296

Computation of supersonic jet mixing noise for an axisymmetric CD nozzle using k-epsilon turbulence model
[NASA-TM-105338] p 254 N92-14795

A survey of the broadband shock associated noise prediction methods
[NASA-TM-105365] p 254 N92-14797

Far-field noise and internal modes from a ducted propeller at simulated aircraft takeoff conditions
[NASA-TM-105369] p 254 N92-16702

AEROACOUSTICS
Model rotor icing tests in the NASA Lewis Icing Research Tunnel
[NASA-TM-105380] p 21 N92-21688

AEROACOUSTIC CHARACTERISTICS
Finite wing aerodynamics with simulated glaze ice
[AIAA PAPER 92-0414] p 5 A92-26265

A comparison of the calculated and experimental off-design performance of a radial flow turbine
[AIAA PAPER 92-3069] p 13 A92-54004

An experimental investigation of the flow in a diffusing S-duct
[AIAA PAPER 92-3622] p 13 A92-54090

Description of a pressure measurement technique for obtaining surface static pressures of a radial turbine
[AIAA PAPER 92-4006] p 200 A92-56829

Effect of a simulated glaze ice shape on the aerodynamic performance of a rectangular wing
[AIAA PAPER 92-4042] p 14 A92-56861

Technical evaluation report, AGARD Fluid Dynamics Panel Symposium on Effects of Adverse Weather on Aerodynamics
[NASA-TM-105192] p 1 N92-10002

Development of a steady potential solver for use with linearized, unsteady aerodynamic analyses
[NASA-TM-105288] p 31 N92-20525

Description of a pressure measurement technique for obtaining surface static pressures of a radial turbine
[NASA-TM-105643] p 202 N92-24959

Experimental and computational ice shapes and resulting drag increase for a NACA 0012 airfoil
[NASA-TM-105743] p 20 N92-28674

Lewis icing research tunnel test of the aerodynamic effects of aircraft ground deicing/anti-icing fluids
[NASA-TP-3238] p 22 N92-30395

A critical evaluation of a three-dimensional Navier-Stokes CFD as a tool to design supersonic turbine stages
[NASA-TM-105743] p 196 N92-32268

Analysis of iced wings
[NASA-TM-105773] p 20 N92-34144

AERODYNAMIC COEFFICIENTS
Parallel computation of aerodynamic influence coefficients for aeroelastic analysis on a transputer network
[NASA-TM-105773] p 241 A92-12367

Cascade flutter analysis with transient response aerodynamics
[NASA-TM-105773] p 217 A92-15972

Time domain numerical calculations of unsteady vortical flows about a flat plate airfoil
[NASA-TM-105773] p 12 A92-50473

Experimental and computational ice shapes and resulting drag increase for a NACA 0012 airfoil
[NASA-TM-105743] p 20 N92-28674

AERODYNAMIC CONFIGURATIONS
An improved PNS scheme for predicting complex three-dimensional hypersonic flows
[AIAA PAPER 92-0753] p 8 A92-31679

Predicted pressure distribution on a prop-fan blade through Euler analysis
[AIAA PAPER 92-0753] p 10 A92-46791

AERODYNAMIC DRAG
A turbulence model for iced airfoils and its validation
[AIAA PAPER 92-0417] p 6 A92-26267

A turbulence model for iced airfoils and its validation
[NASA-TM-105373] p 16 N92-15052

Experiments and analysis concerning the use of external burning to reduce aerospace vehicle transonic drag
[NASA-TM-105397] p 30 N92-17546

Experimental and computational ice shapes and resulting drag increase for a NACA 0012 airfoil
[NASA-TM-105743] p 20 N92-28674

Method of reducing drag in aerodynamic systems
[NASA-CASE-LEW-14791-1] p 21 N92-34243

AERODYNAMIC FORCES
Experimental ice shape and performance characteristics for a multi-element airfoil in the NASA Lewis Icing Research Tunnel
[NASA-TM-105380] p 17 N92-17347

AERODYNAMIC HEATING
Structural tailoring/analysis for hypersonic components - Executive system development
[AIAA PAPER 92-2471] p 219 A92-34360

AERODYNAMIC LOADS
The effect of steady aerodynamic loading on the flutter stability of turbomachinery blading
[ASME PAPER 91-GT-130] p 2 A92-15574

Unsteady Euler analysis of the flowfield of a propfan at an angle of attack
[AIAA PAPER 92-0370] p 3 A92-21070

Numerical investigation of performance degradation of wings and rotors due to icing
[AIAA PAPER 92-0412] p 5 A92-26264

An unsteady Euler scheme for the analysis of ducted propellers
[AIAA PAPER 92-0522] p 6 A92-26947

Acoustic characteristics and dynamic structural loading of an ASTOVL aircraft in hover
[AIAA PAPER 92-0370] p 253 A92-28190

Unsteady airloading panel method for propfans
[AIAA PAPER 92-0370] p 253 A92-44512

Simulation of iced wing aerodynamics
[NASA-TM-105380] p 21 N92-21686

AERODYNAMIC NOISE
Computation of supersonic jet mixing noise for an axisymmetric CD nozzle using k-epsilon turbulence model
[AIAA PAPER 92-0500] p 252 A92-26328

Direct evaluation of aeroacoustic theory in a jet
[AIAA PAPER 92-0370] p 253 A92-50296

Computation of supersonic jet mixing noise for an axisymmetric CD nozzle using k-epsilon turbulence model
[NASA-TM-105338] p 254 N92-14795

An evaluation of some alternative approaches for reducing fan tone noise
[NASA-TM-105356] p 255 N92-18282

AERODYNAMIC STABILITY

Aeroelastic stability analyses of two counter rotating proplan designs for a cruise missile model
[NASA-TM-105268] p 227 N92-23191

AERODYNAMIC STALLING

The role of tip clearance in high-speed fan stall
[ASME PAPER 91-GT-83] p 2 A92-15550
Effect of acoustic excitation on stalled flows over an airfoil p 9 A92-41267

AERODYNAMICS

Aerodynamics and heat transfer investigations on a high Reynolds number turbine cascade
[ASME PAPER 91-GT-157] p 164 A92-15593
Flight-vehicle materials, structures, and dynamics - Assessment and future directions. Vol. 3 - Ceramics and ceramic-matrix composites --- Book
[ISBN 0-7918-0661-8] p 94 A92-39852
Transonic turbine blade cascade testing facility
[AIAA PAPER 92-4034] p 42 A92-56856
Overview of the subsonic propulsion technology session p 32 N92-22531
Transonic turbine blade cascade testing facility
[NASA-TM-105646] p 47 N92-26129

AEROELASTICITY

Parallel computation of aerodynamic influence coefficients for aeroelastic analysis on a transputer network p 241 A92-12367
Optical measurements of unducted fan flutter
[ASME PAPER 91-GT-19] p 197 A92-15510
The effect of steady aerodynamic loading on the flutter stability of turbomachinery blading
[ASME PAPER 91-GT-130] p 2 A92-15574
Aeroelastic analysis of advanced propellers using an efficient Euler solver
[AIAA PAPER 92-0488] p 7 A92-28194
Aeroelastic stability analyses of two counter rotating proplan designs for a cruise missile model
[AIAA PAPER 92-2218] p 25 A92-34408
Analysis of cascades using a two dimensional Euler aeroelastic solver
[AIAA PAPER 92-2370] p 26 A92-34598
A numerical classical flutter analysis of advanced propellers
[AIAA PAPER 92-2118] p 26 A92-35687
FREPS - A forced response prediction system for turbomachinery blade rows
[AIAA PAPER 92-3072] p 242 A92-54006
Aeroelastic modal characteristics of mistuned blade assemblies - Mode localization and loss of eigenstructure p 225 A92-54921
Semi-empirical model for prediction of unsteady forces on an airfoil with application to flutter
[NASA-TM-105414] p 17 N92-18760
Determining structural performance p 32 N92-22519
Aeroelastic stability analyses of two counter rotating proplan designs for a cruise missile model
[NASA-TM-105268] p 227 N92-23191

AERONAUTICAL ENGINEERING

Bibliography of Lewis Research Center technical publications announced in 1990
[NASA-TM-103753] p 267 N92-12786

AERONAUTICAL SATELLITES

Characteristics of a future aeronautical satellite communications system
[AIAA PAPER 92-2058] p 22 A92-29889
ACTS aeronautical experiments
[AIAA PAPER 92-2042] p 50 A92-29956
Characteristics of a future aeronautical satellite communications system p 151 N92-30932

AERONAUTICS

Research and technology, 1991
[NASA-TM-105320] p 1 N92-22659

AEROSPACE ENGINEERING

Metal- and intermetallic-matrix composites for aerospace propulsion and power systems p 104 A92-43682
Computers in aeronautics and space research at the Lewis Research Center
[NASA-TM-105096] p 241 N92-11642
Bibliography of Lewis Research Center technical publications announced in 1990
[NASA-TM-103753] p 267 N92-12786
Research and technology, 1991
[NASA-TM-105320] p 1 N92-22659
Writing for aerospace applications
[NASA-TM-105777] p 162 N92-30427
Trends in aer propulsion research and their impact on engineering education
[NASA-TM-105682] p 38 N92-31172

AEROSPACE ENVIRONMENTS

Environmental durability of ceramics and ceramic composites p 95 A92-39862

Probabilistic material degradation model for aerospace materials subjected to high temperature, mechanical and thermal fatigue, and creep
[AIAA PAPER 92-3419] p 224 A92-48978
Technology development of fabrication techniques for advanced solar dynamic concentrators p 232 A92-50571

Using EPSAT to analyze high power systems in the space environment --- Environment Power System Analysis Tool p 158 A92-50580
The NASA CSTI High Capacity Power Program
[NASA-TM-105240] p 236 N92-16481
Electrical and chemical interactions at Mars Workshop, part 1
[NASA-CP-10093] p 270 N92-30302
Liquid lubrication for space applications
[NASA-TM-105198] p 133 N92-31840

AEROSPACE INDUSTRY

Impact and promise of NASA aer propulsion technology p 31 N92-22511

AEROSPACE PLANES

Slush hydrogen (SLH2) technology development for application to the National Aerospace Plane (NASP)
p 140 A92-13432
Technology issues associated with using densified hydrogen for space vehicles
[AIAA PAPER 92-3079] p 134 A92-48727
Overview of the Beta II Two-Stage-To-Orbit vehicle design
[NASA-TM-105298] p 48 N92-11034
Rocket-Based Combined-Cycle (RBCC) Propulsion Technology Workshop. Tutorial session
[NASA-CP-10090] p 86 N92-21517
The future challenge for aer propulsion
[NASA-TM-105613] p 35 N92-25164
Technology issues associated with using densified hydrogen for space vehicles
[NASA-TM-105642] p 135 N92-25277
Slush hydrogen transfer studies at the NASA K-Site Test Facility
[NASA-TM-105596] p 135 N92-25957

AEROSPACE SAFETY

Safety issues p 78 N92-11115
Risks, designs, and research for fire safety in spacecraft
[NASA-TM-105317] p 240 N92-13581
NASA Aerospace Flight Battery Systems Program: An update p 237 N92-22741

AEROSPACE SCIENCES

Bibliography of Lewis Research Center technical publications announced in 1990
[NASA-TM-103753] p 267 N92-12786

AEROSPACE SYSTEMS

NASA Space applications of high-temperature superconductors
[NASA-TM-105401] p 271 N92-18455
Lubrication of space systems: Challenges and potential solutions
[NASA-TM-105560] p 130 N92-21579
NASA Aerospace Flight Battery Systems Program: An update p 237 N92-22741
Integrated health monitoring and controls for rocket engines
[NASA-TM-105763] p 90 N92-28693
NASA space applications of high-temperature superconductors p 265 N92-32980

AEROSPACE VEHICLES

Mission and sizing analysis for the Beta II two-stage-to-orbit vehicle
[AIAA PAPER 92-1264] p 47 A92-35868
Development of a single-phase harmonic power flow program to study the 20 kHz AC power system for large spacecraft
[NASA-TM-105326] p 81 N92-13275
Experiments and analysis concerning the use of external burning to reduce aerospace vehicle transonic drag
[NASA-TM-105397] p 30 N92-17546
Mission and sizing analysis for the Beta 2 two-stage-to-orbit vehicle
[NASA-TM-105559] p 48 N92-21547

AEROTHERMOCHEMISTRY

New technique for low-to-high altitude predictions of ablative hypersonic flowfields p 166 A92-24654

AEROTHERMODYNAMICS

An improved PNS scheme for predicting complex three-dimensional hypersonic flows
[AIAA PAPER 92-0753] p 8 A92-31679

AGENA ROCKET VEHICLES

Development and flight history of SERT 2 spacecraft
[AIAA PAPER 92-3516] p 74 A92-54038
Development and flight history of SERT 2 spacecraft
[NASA-TM-105636] p 90 N92-28983

AGING (MATERIALS)

Effect of fiber reinforcement on thermo-oxidative stability and mechanical properties of polymer matrix composites p 101 A92-33587

Thermomechanical deformation behavior of a dynamic strain aging alloy, Hastelloy X
[NASA-TM-105316] p 228 N92-25179
Isothermal aging effects on PMR-15 resin
[NASA-TM-105648] p 110 N92-30986

AGING (METALLURGY)

Hardening mechanisms in a dynamic strain aging alloy, Hastelloy X, during isothermal and thermomechanical cyclic deformation p 116 A92-24832

AIR

Numerical study of shock-wave/boundary-layer interactions in premixed combustible gases p 183 A92-54907
Brush seal leakage performance with gaseous working fluids at static and low rotor speed conditions
[NASA-TM-105400] p 186 N92-16265

AIR BREATHING BOOSTERS

Mission and sizing analysis for the Beta II two-stage-to-orbit vehicle
[AIAA PAPER 92-1264] p 47 A92-35868
Mission and sizing analysis for the Beta 2 two-stage-to-orbit vehicle
[NASA-TM-105559] p 48 N92-21547

AIR BREATHING ENGINES

Laser-driven hypersonic air-breathing propulsion simulator
[AIAA PAPER 92-3922] p 41 A92-56753
Overview of the Beta II Two-Stage-To-Orbit vehicle design
[NASA-TM-105298] p 48 N92-11034
Experiments and analysis concerning the use of external burning to reduce aerospace vehicle transonic drag
[NASA-TM-105397] p 30 N92-17546
Airbreathing combined cycle engine systems p 31 N92-21523
Trends in aer propulsion research and their impact on engineering education
[NASA-TM-105682] p 38 N92-31172

AIR FLOW

Time domain numerical calculations of unsteady vortical flows about a flat plate airfoil p 12 A92-50473
NASA's rotary engine technology enablement program: 1983-1991
[NASA-TM-105562] p 30 N92-20033
Chemical reacting flows p 188 N92-22525

AIR INTAKES

Analysis of an advanced ducted propeller subsonic inlet
[AIAA PAPER 92-0274] p 5 A92-25728
Analysis of an advanced ducted propeller subsonic inlet
[NASA-TM-105393] p 15 N92-14002

AIR JETS

The influence of higher harmonics on vortex pairing in an axisymmetric mixing layer p 175 A92-46251

AIRCRAFT COMMUNICATION

ACTS aeronautical experiments
[AIAA PAPER 92-2042] p 50 A92-29956

AIRCRAFT CONFIGURATIONS

The NASA Computational Aerosciences Program - Toward IeraFLOPS computing
[AIAA PAPER 92-0558] p 240 A92-26968
Multiblock grid generation for jet engine configurations p 35 N92-25720

AIRCRAFT CONSTRUCTION MATERIALS

Flight-vehicle materials, structures, and dynamics - Assessment and future directions. Vol 3 - Ceramics and ceramic-matrix composites --- Book
[ISBN 0-7918-0661-8] p 94 A92-39852
Ceramic composites: Enabling aerospace materials
[NASA-TM-105599] p 133 N92-27378

AIRCRAFT CONTROL

Wavelength-multiplexed fiber-optic position encoder for aircraft control systems p 24 A92-46260
Hot gas ingestion characteristics and flow visualization of a vectored thrust STOVL concept p 26 A92-45316
Fiber optic controls for aircraft engines - Issues and implications p 24 A92-46244
Potential for integrated optical circuits in advanced aircraft with fiber optic control and monitoring systems p 24 A92-46246
Design and evaluation of a robust dynamic neurocontroller for a multivariable aircraft control problem
[NASA-TM-105579] p 40 N92-20586
Fiber optics for controls p 40 N92-22529
Piloted evaluation of an integrated propulsion and flight control simulator
[NASA-TM-105797] p 40 N92-34107

AIRCRAFT DESIGN

Mission and sizing analysis for the Beta II two-stage-to-orbit vehicle
[AIAA PAPER 92-1264] p 47 A92-35868
An experimental investigation of the flow in a diffusing S-duct
[AIAA PAPER 92-3622] p 13 A92-54090

AIRCRAFT ENGINES

Turning up the heat on aircraft structures --- design and analysis for high-temperature conditions p 23 A92-55131
 Vortex generator design for aircraft inlet distortion as a numerical optimization problem p 23 N92-13959
 Mission and sizing analysis for the Beta 2 two-stage-to-orbit vehicle p 48 N92-21547
 [NASA-TM-105559]
 The NASA aircraft icing research program p 23 N92-22534
 Supersonic throughflow fans for high-speed aircraft p 34 N92-22541
 Computer codes developed and under development at Lewis p 244 N92-25913

AIRCRAFT ENGINES

Intermetallic and ceramic matrix composites for B15 to 1370 C (1500 to 2500 F) gas turbine engine applications p 99 A92-15128
 Transient behavior of supersonic flow through inlets p 7 A92-28043
 Ceramics and ceramic matrix composites - Aerospace potential and status p 94 A92-34474
 [AIAA PAPER 92-2445]
 Monolithic ceramics p 125 A92-39854
 Fiber optic controls for aircraft engines - Issues and implications p 24 A92-46244
 Analytical and experimental studies of heat pipe radiation cooling of hypersonic propulsion systems p 26 A92-49128
 [AIAA PAPER 92-3809]
 The VRT gas turbine combustor - Phase II p 27 A92-54035
 [AIAA PAPER 92-3471]
 Analysis of aircraft engine blade subject to ice impact [NASA-TM-105336] p 226 N92-15402
 Safety considerations in testing a fuel-rich aeropropulsion gas generator [NASA-TM-105258] p 30 N92-17061
 Aeropropulsion 1987 p 31 N92-22510
 [NASA-CP-3049]
 Impact and promise of NASA aeropropulsion technology p 31 N92-22511
 High-temperature polymer matrix composites p 108 N92-22513
 Development of a new generation of high-temperature composite materials p 109 N92-22515
 Aeropropulsion structures p 31 N92-22518
 Determining structural performance p 32 N92-22519
 Life prediction technologies for aeronautical propulsion systems p 32 N92-22520
 Optical measurement systems p 202 N92-22527
 Overview of the subsonic propulsion technology session p 32 N92-22531
 Aircraft engine hot section technology: An overview of the HOST Project p 33 N92-22535
 NASA thrusts in high-speed aeropropulsion research and development: An overview p 33 N92-22538
 Coupled multi-disciplinary simulation of composite engine structures in propulsion environment [NASA-TM-105575] p 228 N92-23267
 The future challenge for aeropropulsion [NASA-TM-105613] p 35 N92-25164
 Multiblock grid generation for jet engine configurations p 35 N92-25720
 Trends in aeropropulsion research and their impact on engineering education [NASA-TM-105682] p 38 N92-31172
 Liquid lubricants for advanced aircraft engines [NASA-TM-104531] p 133 N92-32863

AIRCRAFT EQUIPMENT
 Method of reducing drag in aerodynamic systems [NASA-CASE-LEW-14791-1] p 21 N92-34243

AIRCRAFT HAZARDS
 LEWICE/E - An Euler based ice accretion code [AIAA PAPER 92-0037] p 4 A92-25676
 LEWICE/E: An Euler based ice accretion code p 15 N92-14001
 [NASA-TM-105389]
 NASA's aircraft icing technology program [NASA-TM-104518] p 17 N92-23105

AIRCRAFT ICING
 Heat transfer measurements from a smooth NACA 0012 airfoil p 165 A92-20215
 Roughness effects on heat transfer from a NACA 0012 airfoil p 166 A92-20217
 Investigation of the diffuser flow quality in an icing research wind tunnel p 40 A92-24406
 Heat transfer on accreting ice surfaces p 166 A92-24415
 Analysis of surface roughness generation in aircraft ice accretion [AIAA PAPER 92-0298] p 169 A92-28187
 Helium bubble flow visualization of the spanwise separation on a NACA 0012 with simulated glaze ice [AIAA PAPER 92-0413] p 7 A92-28192

Comparison of two-dimensional and three-dimensional droplet trajectory calculations in the vicinity of finite wings p 8 A92-28215
 [AIAA PAPER 92-0645]
 Analysis of iced wings p 8 A92-29972
 [AIAA PAPER 92-0416]
 Measurements in a leading-edge separation bubble due to a simulated airfoil ice accretion p 21 A92-41262
 Experimental ice shape and performance characteristics for a multi-element airfoil in the NASA Lewis Icing Research Tunnel p 17 N92-17347
 [NASA-TM-105380]
 Icing simulation: A survey of computer models and experimental facilities p 21 N92-21684
 The NASA aircraft icing research program p 23 N92-22534

NASA's aircraft icing technology program p 17 N92-23105
 [NASA-TM-104518]
 Comparison of two-dimensional and three-dimensional droplet trajectory calculations in the vicinity of finite wings p 188 N92-23154
 [NASA-TM-105617]

AIRCRAFT MODELS

Calculations of hot gas ingestion for a STOVL aircraft model p 25 A92-28191
 [AIAA PAPER 92-0385]
 Calculations of hot gas ingestion for a STOVL aircraft model [NASA-TM-105437] p 17 N92-19993

AIRCRAFT NOISE

An evaluation of some alternative approaches for reducing fan tone noise p 255 N92-18282
 [NASA-TM-105356]
 Overview of NASA PTA proptan flight test program p 33 N92-22536
 Propulsion challenges and opportunities for high-speed transport aircraft p 34 N92-22540
 The future challenge for aeropropulsion [NASA-TM-105613] p 35 N92-25164

AIRCRAFT PARTS

Tribology needs for future space and aeronautical systems p 128 N92-15191
 [NASA-TM-104525]

AIRCRAFT STRUCTURES

Computer codes developed and under development at Lewis p 244 N92-25913
 A brief overview of computational structures technology related activities at NASA Lewis Research Center p 229 N92-25915

AIRFOIL OSCILLATIONS

Unsteady transonic Euler solutions using finite elements p 8 A92-34499
 [AIAA PAPER 92-2504]
 Experimental investigation of the flowfield of an oscillating airfoil p 9 A92-45494
 [AIAA PAPER 92-2622]

AIRFOIL PROFILES

Eigenvalue calculation procedure for an Euler/Navier-Stokes solver with application to flows over airfoils p 3 A92-17429
 Heat transfer measurements from a smooth NACA 0012 airfoil p 165 A92-20215
 Roughness effects on heat transfer from a NACA 0012 airfoil p 166 A92-20217
 Automatic grid generation for iced airfoil flowfield predictions p 6 A92-26266
 [AIAA PAPER 92-0415]
 A turbulence model for iced airfoils and its validation p 6 A92-26267
 [AIAA PAPER 92-0417]
 Unsteady transonic Euler solutions using finite elements p 8 A92-34499
 [AIAA PAPER 92-2504]
 Domain-decomposition algorithm applied to multielement airfoil grids p 9 A92-41261
 Measurements in a leading-edge separation bubble due to a simulated airfoil ice accretion p 21 A92-41262
 Effect of acoustic excitation on stalled flows over an airfoil p 9 A92-41267
 A turbulence model for iced airfoils and its validation [NASA-TM-105373] p 16 N92-15052
 Unsteady-flow-field predictions for oscillating cascades [NASA-TM-105283] p 17 N92-19437

AIRFOILS

Advanced ice protection systems test in the NASA Lewis Icing Research Tunnel p 22 A92-14406
 Wind tunnel wall effects in a linear oscillating cascade [ASME PAPER 91-GT-133] p 2 A92-15576
 Results of an icing test on a NACA 0012 airfoil in the NASA Lewis Icing Research Tunnel p 7 A92-27021
 [AIAA PAPER 92-0647]
 Airfoil wake and linear theory gust response including sub and superresonant flow conditions p 11 A92-48724
 [AIAA PAPER 92-3074]
 The chemistry of Saudi Arabian sand: A deposition problem on helicopter turbine airfoils [NASA-TM-105234] p 128 N92-14179

Results of an icing test on a NACA 0012 airfoil in the NASA Lewis Icing Research Tunnel p 16 N92-15051
 [NASA-TM-105374]
 Experimental ice shape and performance characteristics for a multi-element airfoil in the NASA Lewis Icing Research Tunnel p 17 N92-17347
 [NASA-TM-105380]
 Semi-empirical model for prediction of unsteady forces on an airfoil with application to flutter p 17 N92-18760
 [NASA-TM-105414]
 Experimental and computational ice shapes and resulting drag increase for a NACA 0012 airfoil p 20 N92-28674
 [NASA-TM-105743]
 Results of a low power ice protection system test and a new method of imaging data analysis p 20 N92-28696
 [NASA-TM-105745]
 Experimental investigation of the flowfield of an oscillating airfoil p 20 N92-30182
 [NASA-TM-105675]
 Analysis of iced wings p 20 N92-34144
 [NASA-TM-105773]

AIRFRAMES

IMPAC - An integrated methodology for propulsion and airframe control p 39 A92-29118

AIRY FUNCTION

Computer program for Bessel and Hankel functions [NASA-TM-105154] p 243 N92-11691

ALCOHOLS

An investigation of flame spread over shallow liquid pools in microgravity and nonair environments p 112 A92-16609

ALGEBRA

Development of an algebraic turbulence model for analysis of propulsion flows p 183 A92-54209
 [AIAA PAPER 92-3861]
 Development of an algebraic turbulence model for analysis of propulsion flows p 250 N92-27517
 [NASA-TM-105701]
 Upper bounds for convergence rates of vector extrapolation methods on linear systems with initial iterations p 250 N92-33742
 [NASA-TM-105608]

ALGORITHMS

An unconditionally stable staggered algorithm for transient finite element analysis of coupled thermoelastic problems p 222 A92-37517
 MisTec - A software application for supporting space exploration scenario options and technology development analysis and planning p 242 A92-38490
 [AIAA PAPER 92-1293]
 A fast, uncoupled, compressible, two-dimensional, unsteady boundary layer algorithm with separation for engine inlets p 11 A92-48729
 [AIAA PAPER 92-3082]
 Interface of an uncoupled boundary layer algorithm with an inviscid core flow algorithm for unsteady supersonic engine inlets p 11 A92-48730
 [AIAA PAPER 92-3083]
 Rocket engine diagnostics using qualitative modeling techniques p 65 A92-48787
 [AIAA PAPER 92-3164]
 Algorithms for real-time fault detection of the Space Shuttle Main Engine p 215 A92-48789
 [AIAA PAPER 92-3167]
 Real-time fault diagnosis for propulsion systems [NASA-TM-105303] p 29 N92-11017
 An efficient and robust algorithm for two dimensional time dependent incompressible Navier-Stokes equations: High Reynolds number flows p 184 N92-11320
 [NASA-TM-104424]
 MisTec: A software application for supporting space exploration scenario options and technology development analysis and planning p 243 N92-14649
 [NASA-TM-105214]
 Supersonic propulsion simulation by incorporating component models in the large perturbation inlet (LAPIN) computer code p 30 N92-15993
 [NASA-TM-105193]
 Lattice parameters of fcc binary alloys using a new semiempirical method p 123 N92-16111
 [NASA-TM-105304]
 An iterative implicit diagonally-dominant factorization algorithm for solving the Navier-Stokes equations p 249 N92-16663
 [NASA-TM-105259]
 Frequency effects on the stability of a journal bearing for periodic loading p 186 N92-18809
 [NASA-TM-105226]
 Real-time demonstration hardware for enhanced DPCM video compression algorithm p 150 N92-19700
 [NASA-TM-105616]
 Subband coding for image data archiving p 151 N92-20032
 [NASA-TM-105407]
 Development of new flux splitting schemes p 189 N92-23343

- Asymptotic integration algorithms for first-order ODEs with application to viscoplasticity [NASA-TM-105587] p 250 N92-24974
- TCGRID: A three dimensional C-grid generator for turbomachinery p 35 N92-25716
- Computational Fluid Dynamics --- numerical methods and algorithm development [NASA-CP-10078] p 35 N92-25808
- Development of new flux splitting schemes --- computational fluid dynamics algorithms p 192 N92-25809
- An iterative implicit DDAD algorithm for solving the Navier-Stokes equation --- upwind split flux technique p 192 N92-25810
- The Proteus Navier-Stokes code --- two and three dimensional computational fluid dynamics p 192 N92-25811
- Numerical simulation of conservation laws p 193 N92-25813
- Upwind schemes and bifurcating solutions in real gas computations p 193 N92-25817
- High order parallel numerical schemes for solving incompressible flows p 193 N92-25818
- An efficient and robust algorithm for time dependent viscous incompressible Navier-Stokes equations p 193 N92-25819
- Implementation of a kappa-epsilon turbulence model to RPLUS3D code p 194 N92-25822
- Techniques for grid manipulation and adaptation --- computational fluid dynamics p 194 N92-25827
- Rocket engine diagnostics using qualitative modeling techniques [NASA-TM-105714] p 88 N92-27033
- Interface of an uncoupled boundary layer algorithm with an inviscid core flow algorithm for unsteady supersonic engine inlets [NASA-TM-105684] p 36 N92-27037
- A fast, uncoupled, compressible, two-dimensional, unsteady boundary layer algorithm with separation for engine inlets [NASA-TM-105686] p 195 N92-27653
- A parameter optimization approach to controller partitioning for integrated flight/propulsion control application [NASA-TM-105826] p 40 N92-32241
- ALKALI METALS**
- Alkali metal pool boiler life tests for a 25 kWe advanced Stirling conversion system p 206 A92-50797
- Final design of a free-piston hydraulic advanced Stirling conversion system p 206 A92-50798
- Design of a pool boiler heat transport system for a 25 kWe advanced Stirling conversion system p 181 A92-50802
- Alkali metal compatibility testing of candidate heater head materials for a Stirling engine heat transport system p 71 A92-50829
- ALKALINE BATTERIES**
- Bifunctional alkaline oxygen electrodes p 115 A92-50729
- Validation test of advanced technology for IPV nickel-hydrogen flight cells: Update [NASA-TM-105689] p 89 N92-27878
- The O₂ reduction at the IFC modified O₂ fuel cell electrode [NASA-TM-105691] p 90 N92-29667
- ALLOYING**
- On improving the fracture toughness of a NiAl-based alloy by mechanical alloying p 118 A92-30794
- ALTERNATING CURRENT**
- Development of a computer algorithm for the analysis of variable-frequency AC drives: Case studies included [NASA-TM-105327] p 29 N92-13070
- Development of a single-phase harmonic power flow program to study the 20 kHz AC power system for large spacecraft [NASA-TM-105326] p 81 N92-13275
- Electromechanical systems with transient high power response operating from a resonant AC link [NASA-TM-105716] p 37 N92-28985
- ALTERNATING DIRECTION IMPLICIT METHODS**
- Numerical analysis of a thermal deicer [AIAA PAPER 92-0527] p 22 A92-26950
- Implementation/validation of a low Reynolds number two-equation turbulence model in the Proteus Navier-Stokes code: Two-dimensional/axisymmetric [NASA-TM-105619] p 187 N92-20520
- Fast methods to numerically integrate the Reynolds equation for gas fluid films [NASA-TM-105415] p 214 N92-30722
- ALUMINIDES**
- Fracture toughness and the effects of stress state on fracture of nickel aluminides p 117 A92-27422
- The effect of strain rate and temperature on the tensile properties of NiAl p 117 A92-28113
- Compressive strength of directionally solidified NiAl-NiAlNb intermetallics at 1200 and 1300 K p 117 A92-28248
- Does a threshold stress for creep exist in HfC-dispersed NiAl? p 118 A92-30780
- Flow and fracture behavior of NiAl in relation to the brittle-to-ductile transition temperature p 118 A92-30781
- Compression studies on particulate composites of ternary Al-Ti-Fe, and quaternary Al-Ti-Fe-Nb and Al-Ti-Fe-Mn L1(2) compounds p 119 A92-30845
- Protective Al₂O₃ scale formation on NbAl₃-base alloys p 119 A92-31850
- Solidification processing of intermetallic Nb-Al alloys p 120 A92-33866
- Interdiffusion between the L1(2) trialuminides Al₆₆Ti₂₅Mn₉ and Al₆₇Ti₂₅Cr₈ p 120 A92-37088
- 1200 and 1300 K slow plastic compression properties of Ni-50Al composites p 102 A92-38125
- 1400 and 1500 K compressive creep properties of an NiAl-AlN composite p 103 A92-41575
- Discontinuously reinforced intermetallic matrix composites via XD synthesis --- exothermal dispersion p 103 A92-41867
- Initial evaluation of continuous fiber reinforced NiAl composites p 104 A92-46867
- Cyclic oxidation resistance of a reaction milled NiAl-AlN composite p 105 A92-46871
- Compatibility of potential reinforcing ceramics with Ni and Fe aluminides p 105 A92-46874
- Influence of processing on the microstructure and mechanical properties of a NbAl₃-base alloy p 122 A92-48152
- ALUMINUM**
- An initial study of void formation during solidification of aluminum in normal and reduced-gravity [AIAA PAPER 92-0845] p 138 A92-29611
- Tribological properties of ceramic-(Ti₃Al-Nb) sliding couples for use as candidate seal materials to 700 C p 124 A92-32407
- Design issues for lunar in situ aluminum/oxygen propellant rocket engines [AIAA PAPER 92-1185] p 60 A92-33299
- Design issues for lunar in situ aluminum/oxygen propellant rocket engines [NASA-TM-105433] p 83 N92-16023
- Experimental breakdown of selected anodized aluminum samples in dilute plasmas p 259 N92-22369
- An XPS study of the stability of Fomblin Z25 on the native oxide of aluminum --- x ray photoelectron spectroscopy [NASA-TM-105594] p 131 N92-23185
- Atomic oxygen undercutting of LDEF aluminized-Kapton multilayer insulation p 255 N92-24818
- ALUMINUM ALLOYS**
- Slow strain rate 1200-1400 K compressive properties of NiAl-1Hf p 116 A92-17977
- Compression, bend, and tension studies on forged Al₆₇Ti₂₅Cr₈ and Al₆₆Ti₂₅Mn₉(L) L1(2) compounds p 118 A92-30766
- The mechanical properties of a Ni-30Al-20Fe-0.05Zr intermetallic alloy in the temperature range 300-1200 K p 118 A92-30793
- On improving the fracture toughness of a NiAl-based alloy by mechanical alloying p 118 A92-30794
- Microstructure and mechanical properties of a single crystal NiAl alloy with Zr or Hf rich G-phase precipitates p 119 A92-30841
- Microstructure and mechanical properties of near eutectic beta-NiAl plus alpha-Fe alloys produced by rapid solidification and extrusion p 119 A92-30844
- Correlation of deformation mechanisms with the tensile and compressive behavior of NiAl and NiAl(Zr) intermetallic alloys p 120 A92-38019
- Thermal stress analysis of a silicon carbide/aluminum composite p 222 A92-38097
- The decrease in yield strength in NiAl due to hydrostatic pressure p 120 A92-38990
- Fracture behavior of a B2 Ni-30Al-20Fe-0.05Zr intermetallic alloy in the temperature range 300 to 1300 K p 121 A92-41667
- Deformation behavior of a Ni-30Al-20Fe-0.05Zr intermetallic alloy in the temperature range 300 to 1300 K p 121 A92-41668
- Gelled liquid oxygen/metal powder monopropellants [AIAA PAPER 92-3450] p 134 A92-49004
- Tensile behavior of the L1(2) compound Al₆₇Ti₂₅Cr₈ p 122 A92-49694
- Volatile species in halide-activated-diffusion coating packs p 122 A92-57028
- ALUMINUM ARSENIDES**
- Calculated performance of p(In)-InP solar cells with In(0.52)Al(0.48)As window layers p 153 A92-13266
- dc and microwave performance of a 0.1-micron gate InAs/In(0.52)Al(0.48)As MODFET p 156 A92-43891
- Effect of InAlAs window layer on the efficiency of indium phosphide solar cells p 234 A92-53163
- Effect of InAlAs window layer on efficiency of indium phosphide solar cells [NASA-TM-105354] p 161 N92-25176
- ALUMINUM COMPOUNDS**
- Mechanical properties of monolithic and particulate composites of L12 forms of Al₃Ti p 101 A92-36273
- Oxidation kinetics of cast TiAl₃ p 121 A92-38993
- Oxidation of Al₂O₃ continuous fiber-reinforced/NiAl composites p 106 A92-57029
- ALUMINUM GALLIUM ARSENIDES**
- Temperature independent quantum well FET with delta channel doping p 157 A92-49596
- Intermodulation in the oscillatory magnetoresistance of a two-dimensional electron gas p 163 N92-32975
- Reduced mobility and PPC in In(20)Ga(80)As / Al(23)Ga(77)As HEMT structure p 265 N92-32976
- ALUMINUM NITRIDES**
- 1400 and 1500 K compressive creep properties of an NiAl-AlN composite p 103 A92-41575
- Cyclic oxidation resistance of a reaction milled NiAl-AlN composite p 105 A92-46871
- ALUMINUM OXIDES**
- Protective Al₂O₃ scale formation on NbAl₃-base alloys p 119 A92-31850
- Combustion synthesis of TiB₂-Al₂O₃-Al composite materials p 102 A92-36391
- Oxidation kinetics of cast TiAl₃ p 121 A92-38993
- Fractal dimension of alumina aggregates grown in two dimensions p 126 A92-49814
- Combustion synthesis of ceramic-metal composite materials - The TiC-Al₂O₃-Al system p 115 A92-55139
- Oxidation of Al₂O₃ continuous fiber-reinforced/NiAl composites p 106 A92-57029
- High temperature structural fibers: Status and needs [NASA-TM-105174] p 107 N92-16037
- The effect of ion plated silver and sliding friction on tensile stress-induced cracking in aluminum oxide [NASA-TM-105366] p 129 N92-19450
- Atomic oxygen durability of solar concentrator materials for Space Station Freedom [NASA-TM-105378] p 85 N92-20065
- Screen Cage Ion Plating (SCIP) and scratch testing of polycrystalline aluminum oxide [NASA-TM-105404] p 130 N92-22278
- Tribological evaluation of an Al₂O₃-SiO₂ ceramic fiber candidate for high temperature sliding seals [NASA-TM-105611] p 97 N92-23190
- Guanidine based vehicle/binders for use with oxides, metals, and ceramics [NASA-CASE-LEW-15314-1] p 131 N92-23461
- The cyclic oxidation resistance at 1200 C of beta-NiAl, FeAl, and CoAl alloys with selected third element additions [NASA-TM-105620] p 123 N92-24554
- Composition dependence of superconductivity in YBa₂(Cu_{3-x}Al_x)O_y [NASA-TM-105358] p 131 N92-24715
- AMORPHOUS MATERIALS**
- Optical dispersion relations for 'diamondlike' carbon films p 262 A92-44533
- Method of intercalating large quantities of fibrous structures [NASA-CASE-LEW-15077-1] p 107 N92-16025
- AMORPHOUS SILICON**
- Thin-film photovoltaics: Status and applications to space power p 81 N92-13228
- AMPLIFIER DESIGN**
- Performance of a wideband GaAs low-noise amplifier at cryogenic temperatures p 156 A92-37953
- AMPLIFIERS**
- Performance of a Y-Ba-Cu-O superconducting filter/GaAs low noise amplifier hybrid circuit [NASA-TM-105546] p 160 N92-21370
- A flexible CPW package for a 30 GHz MMIC amplifier --- coplanar waveguide [NASA-TM-105630] p 161 N92-23193
- A flexible CPW package for a 30 GHz MMIC amplifier p 152 N92-32972
- Performance of a Y-Ba-Cu-O superconducting filter/GaAs low noise amplifier hybrid circuit p 163 N92-32982
- ANALOG CIRCUITS**
- Analog synthesized fast-variable linear load p 157 A92-50539
- ANGLE OF ATTACK**
- Unsteady Euler analysis of the flowfield of a propan at an angle of attack p 3 A92-21070
- The formation and structure of plasma wakes behind large high-voltage space platforms in ionosphere [AIAA PAPER 92-0577] p 239 A92-26984
- Experimental investigation of the flowfield of an oscillating airfoil [AIAA PAPER 92-2622] p 9 A92-45494

ANHYDRIDES

Full Navier-Stokes calculations on the installed F/A-18 inlet at a high angle of attack p 13 A92-54012
 [AIAA PAPER 92-3175]
 Unsteady blade pressures on a propfan - Predicted and measured compressibility effects p 14 A92-54161
 [AIAA PAPER 92-3774]

ANHYDRIDES

Substituted 1,1,1-triaryl-2,2,2-trifluoroethanes and processes for their synthesis p 96 N92-17882
 [NASA-CASE-LEW-14345-6]

ANIMATION

Techniques for animation of CFD results --- computational fluid dynamics p 194 N92-25825

ANISOTROPIC MEDIA

A viscoplastic theory for anisotropic materials [ONERA, TP NO. 1992-90] p 217 A92-24721
 Melting of the Abrikosov flux lattice in anisotropic superconductors p 260 A92-28075
 Radiative transfer solutions for cylindrical coordinates with emitting, absorbing, and anisotropic scattering medium p 266 A92-28185
 [AIAA PAPER 92-0123]
 Effects of anisotropic conduction and heat pipe interaction on minimum mass space radiators [NASA-TM-105297] p 80 N92-11138
 The Eckhaus and the Benjamin-Feir instability near a weakly inverted bifurcation p 185 N92-15336
 [NASA-TM-105334]

ANISOTROPY

Differential continuum damage mechanics models for creep and fatigue of unidirectional metal matrix composites p 226 N92-16371
 [NASA-TM-105213]

ANNEALING

Correlation of deformation mechanisms with the tensile and compressive behavior of NiAl and NiAl(Zr) intermetallic alloys p 120 A92-38019
 A very low resistance, non-sintered contact system for use on indium phosphide concentrator/shallow junction solar cells p 233 A92-53146
 High-T sub c fluorine-doped YBa₂Cu₃O(y) films on ceramic substrates by screen printing p 127 N92-11188
 [NASA-TM-105296]
 A very low resistance, non-sintered contact system for use on indium phosphide concentrator/shallow junction solar cells p 235 N92-13482
 [NASA-TM-105279]
 Dependence of the critical temperature of laser-ablated YBa₂Cu₃O(7-delta) thin films on LaAlO₃ substrate growth technique p 264 N92-23415
 Defect behavior, carrier removal and predicted in-space injection annealing of InP solar cells p 161 N92-23562
 [NASA-TM-105624]

ANNULAR DUCTS

Experimental performance of three design factors for ventral nozzles for SSTOVL aircraft p 28 A92-54168
 [AIAA PAPER 92-3789]
 Experimental performance of three design factors for ventral nozzles for SSTOVL aircraft p 37 N92-27669
 [NASA-TM-105697]

ANNULAR FLOW

Laser anemometer measurements and computations in an annular cascade of high turning core turbine vanes [NASA-TP-3252] p 20 N92-28980

ANODES

Modeling of the near-electrode regions of arcjets. I - Coupling of the flowfield to the non-equilibrium boundary layers p 258 A92-48749
 [AIAA PAPER 92-3109]
 Anode power deposition in applied-field MPD thrusters [AIAA PAPER 92-3463] p 74 A92-54034
 Alkali metal carbon dioxide electrochemical system for energy storage and/or conversion of carbon dioxide to oxygen [NASA-CASE-LEW-14973-1] p 235 N92-10222

ANODIZING

Experimental breakdown of selected anodized aluminum samples in dilute plasmas p 259 N92-22369

ANTENNA ARRAYS

Experimental code verification results for reflector antenna distortion compensation by array feeds [AIAA PAPER 92-2014] p 49 A92-29933
 A vertically integrated Ka-band phased array antenna [AIAA PAPER 92-1976] p 156 A92-38140
 New coplanar waveguide feed network for 2 x 2 linearly tapered slot antenna subarray p 156 A92-45619
 A high temperature superconductivity communications flight experiment p 50 A92-55790
 [IAF PAPER 92-0410]
 Multiple-access phased array antenna simulator for a digital beam forming system investigation p 149 N92-17062
 [NASA-TM-105422]
 Solid State Technology Branch of NASA Lewis Research Center p 151 N92-23412
 [NASA-TM-105159]

High-performance packaging for monolithic microwave and millimeter-wave integrated circuits [NASA-TM-105744] p 151 N92-31855
 V-band pseudomorphic HEMT MMIC phased array components for space communications p 151 N92-32966
 An optically controlled Ka-band phased array antenna p 152 N92-32968
 Ka-band dual frequency array feed for a low cost ACTS ground terminal p 152 N92-32969
 Coplanar waveguide feeds for phased array antennas p 152 N92-32970

ANTENNA DESIGN

Coplanar waveguide aperture coupled patch antennas with ground plane/substrate of finite extent p 154 A92-24488
 Ka-band dual frequency array feed for a low cost ACTS ground terminal p 143 A92-29833
 [AIAA PAPER 92-1902]
 Characteristics of a future aeronautical satellite communications system p 22 A92-29889
 [AIAA PAPER 92-2058]
 Laser ablated YBa₂Cu₃O(7-x) high temperature superconductor coplanar waveguide resonator p 155 A92-31631
 Coplanar waveguide aperture-coupled microstrip patch antenna p 146 A92-37222
 A vertically integrated Ka-band phased array antenna [AIAA PAPER 92-1976] p 156 A92-38140
 Advanced Communication Technology Satellite (ACTS) multibeam antenna technology verification experiments [NASA-TM-105421] p 149 N92-16191
 Advanced Communication Technology Satellite (ACTS) multibeam antenna analysis and experiment [NASA-TM-105420] p 149 N92-17047
 Multiple-access phased array antenna simulator for a digital beam forming system investigation [NASA-TM-105422] p 149 N92-17062
 Analysis of a generalized dual reflector antenna system using physical optics p 149 N92-18281
 [NASA-TM-105425]
 Nonplanar linearly tapered slot antenna with balanced microstrip feed p 161 N92-23535
 [NASA-TM-105647]
 High-performance packaging for monolithic microwave and millimeter-wave integrated circuits [NASA-TM-105744] p 151 N92-31855
 Ka-band dual frequency array feed for a low cost ACTS ground terminal p 152 N92-32969

ANTENNA FEEDS

Electromagnetic coupling between coplanar waveguide and microstrip antennas p 154 A92-21292
 Ka-band dual frequency array feed for a low cost ACTS ground terminal p 143 A92-29833
 [AIAA PAPER 92-1902]
 Experimental code verification results for reflector antenna distortion compensation by array feeds p 49 A92-29933
 [AIAA PAPER 92-2014]
 New techniques for exciting linearly tapered slot antennas with coplanar waveguide p 155 A92-34844
 Coplanar waveguide aperture-coupled microstrip patch antenna p 146 A92-37222
 New coplanar waveguide feed network for 2 x 2 linearly tapered slot antenna subarray p 156 A92-45619
 Ka-band dual frequency array feed for a low cost ACTS ground terminal p 152 N92-32969
 Coplanar waveguide feeds for phased array antennas p 152 N92-32970

ANTENNA RADIATION PATTERNS

New techniques for exciting linearly tapered slot antennas with coplanar waveguide p 155 A92-34844
 Performance of a K-band superconducting annular ring antenna p 146 A92-37067
 Performance of a four-element Ka-band high-temperature superconducting microstrip antenna p 146 A92-37224
 Advanced Communication Technology Satellite (ACTS) multibeam antenna technology verification experiments [NASA-TM-105421] p 149 N92-16191
 Advanced Communication Technology Satellite (ACTS) multibeam antenna analysis and experiment p 149 N92-17047
 [NASA-TM-105420]
 Planar dielectric resonator stabilized HEMT oscillator integrated with CPW/aperture coupled patch antenna [NASA-TM-105544] p 160 N92-18473
 Planar dielectric resonator stabilized HEMT oscillator integrated with CPW/aperture coupled patch antenna p 152 N92-32967
 Measurement techniques for cryogenic Ka-band microstrip antennas p 153 N92-32981

ANTENNAS

Operating and service manual for the NASA Lewis automated far-field antenna range [NASA-TM-105343] p 52 N92-22319

ANTICING ADDITIVES

Technical evaluation report, AGARD Fluid Dynamics Panel Symposium on Effects of Adverse Weather on Aerodynamics [NASA-TM-105192] p 1 N92-10002

APERTURES

Microwave beam power transmission at an arbitrary range [NASA-TM-105424] p 150 N92-19992

APPLICATION SPECIFIC INTEGRATED CIRCUITS

Flexible high speed CODEC (FHSC) [AIAA PAPER 92-1919] p 143 A92-29848

APPLICATIONS PROGRAMS (COMPUTERS)

Micromechanics for ceramic matrix composites p 98 A92-10282
 Development of an analytical tool to study power quality of ac power systems for large spacecraft p 67 A92-50529

A method for determining spiral-bevel gear tooth geometry for finite element analysis [NASA-TP-3096] p 207 N92-10195
 Turbomachinery p 32 N92-22524
 OX MAN: Q and X file manipulation p 244 N92-25715

Fast methods to numerically integrate the Reynolds equation for gas fluid films [NASA-TM-105415] p 214 N92-30722
 Metal matrix composite analyzer (METCAN) user's manual, version 4.0 p 110 N92-30779
 [NASA-TM-105244]
 Computational simulation of matrix micro-slip bands in SiC/Ti-15 composite [NASA-TM-105762] p 111 N92-32466

APPROXIMATION

Application of vector-valued rational approximations to the matrix eigenvalue problem and connections with Krylov subspace methods p 250 N92-33571
 [NASA-TM-105858]
 Upper bounds for convergence rates of vector extrapolation methods on linear systems with initial iterations [NASA-TM-105608] p 250 N92-33742

AQUEOUS SOLUTIONS

A fiber-optic probe for particle sizing in concentrated suspensions p 197 A92-21371
 Electrophoresis of small particles and fluid globules in weak electrolytes p 114 A92-33924

ARC JET ENGINES

Medium power hydrogen arcjet performance [AIAA PAPER 91-2227] p 58 A92-15355
 Effect of an arcjet plume on satellite reflector performance p 53 A92-16318
 Techniques for spectroscopic measurements in an arcjet nozzle p 59 A92-21087
 Laser-induced fluorescence of atomic hydrogen in an arcjet thruster p 60 A92-27045
 [AIAA PAPER 92-0678]
 Electric propulsion - The future is now p 63 A92-48386

Numerical modeling of fluid and electromagnetic phenomena in an arcjet [AIAA PAPER 92-3106] p 258 A92-48747

Modeling of the near-electrode regions of arcjets. I - Coupling of the flowfield to the non-equilibrium boundary layers p 258 A92-48749
 [AIAA PAPER 92-3109]

Preliminary investigation of a low power pulsed arcjet thruster p 64 A92-48752
 [AIAA PAPER 92-3113]

Flow diagnostics of an arcjet using laser-induced fluorescence [AIAA PAPER 92-3243] p 199 A92-48843

Simulating the arcjet thruster using a nonlinear active load [AIAA PAPER 92-3528] p 45 A92-49052

Dependence of hydrogen arcjet operation on electrode geometry [AIAA PAPER 92-3530] p 74 A92-54039

Low-power arcjet test facility impacts [AIAA PAPER 92-3532] p 74 A92-54040

Development of arcjet and ion propulsion for spacecraft stationkeeping [IAF PAPER 92-0607] p 77 A92-57058

High-power hydrogen arcjet performance [NASA-TM-105143] p 82 N92-14109

Hydrogen arcjet technology [NASA-TM-105340] p 82 N92-15119

Arcjet nozzle area ratio effects [NASA-TM-104477] p 83 N92-16022

The evolutionary development of high specific impulse electric thruster technology [NASA-TM-105712] p 92 N92-31342

The evolutionary development of high specific impulse electric thruster technology [NASA-TM-105758] p 93 N92-33064

- Dependence of hydrogen arcjet operation on electrode geometry
[NASA-TM-105855] p 93 N92-34113
- Low power arcjet test facility impacts
[NASA-TM-105876] p 47 N92-34114
- ARC SPRAYING**
Development of a new generation of high-temperature composite materials p 109 N92-22515
- ARCHITECTURE (COMPUTERS)**
Destination directed packet switch architecture for a 30/20 GHz FDMA/TDM geostationary communication satellite network p 148 N92-14204
Destination-directed, packet-switching architecture for 30/20-GHz FDMA/TDM geostationary communications satellite network
[NASA-TP-3201] p 51 N92-19762
- ARMOR**
Optimization of armored spherical tanks for storage on the lunar surface
[NASA-TM-105700] p 91 N92-30187
- ARTIFICIAL INTELLIGENCE**
LDEXPT, an intelligent database system for the Composite Load Spectra project p 59 A92-23695
Applications of artificial neural nets in structural mechanics p 223 A92-47283
An advanced intelligent control system framework
[AIAA PAPER 92-3162] p 65 A92-48785
Autonomous Power System intelligent diagnosis and control p 247 A92-50532
SCAILET - An intelligent assistant for satellite ground terminal operations
[IAF PAPER 92-0552] p 245 A92-55855
An overview of Space Communication Artificial Intelligence for Link Evaluation Terminal (SCAILET) Project p 148 N92-14212
- ASPECT RATIO**
Simulation of iced wing aerodynamics p 21 N92-21686
- ASPHERICITY**
Calculation of far-field scattering from nonspherical particles using a geometrical optics approach p 256 A92-20288
- ASTEROIDS**
Power supply for a manned international asteroid mission p 80 N92-13205
- ASYMMETRY**
Fluctuation-driven electroweak phase transition ... in early universe p 269 A92-54464
- ASYMPTOTIC METHODS**
Combustion kinetics and sensitivity analysis computations p 112 A92-16981
Turbulence modeling p 189 N92-23338
Asymptotic integration algorithms for first-order ODEs with application to viscoplasticity
[NASA-TM-105587] p 250 N92-24974
- ASYMPTOTIC PROPERTIES**
Stochastic stability properties of jump linear systems p 246 A92-25878
- ATMOSPHERIC ATTENUATION**
Dynamic rain fade compensation techniques for the advanced communications technology satellite
[AIAA PAPER 92-2038] p 145 A92-31711
- ATMOSPHERIC COMPOSITION**
Measurement of trace stratospheric constituents with a balloon borne laser radar p 239 N92-14500
- ATMOSPHERIC ENERGY SOURCES**
Acetylene fuel from atmospheric CO₂ on Mars p 133 A92-32199
- ATMOSPHERIC ENTRY**
New technique for low-to-high altitude predictions of ablative hypersonic flowfields p 166 A92-24654
- ATMOSPHERIC SOUNDING**
Submillimeter backward-wave oscillators p 155 A92-35054
- ATOMIC BEAMS**
Fast oxygen atom facility for studies related to low earth orbit activities
[AIAA PAPER 92-3974] p 47 A92-56800
- ATOMIC INTERACTIONS**
Universal aspects of adhesion and atomic force microscopy p 260 A92-17979
- ATOMIC STRUCTURE**
"Wrong" bond interactions at inversion domain boundaries in GaAs p 260 A92-27297
Computational techniques in tribology and material science at the atomic level
[NASA-TM-105573] p 252 N92-26671
- ATTENUATION**
X ray attenuation measurements for high-temperature materials characterization and in-situ monitoring of damage accumulation
[NASA-TM-105577] p 110 N92-25996
- AUDIO SIGNALS**
Frequency allocations for a new satellite service - Digital audio broadcasting
[AIAA PAPER 92-1957] p 143 A92-29881
- AUGER SPECTROSCOPY**
Deposition of adherent Ag-Ti duplex films on ceramics in a multiple-cathode sputter deposition system
[NASA-TM-105586] p 34 N92-23225
- AUGMENTATION**
Control of an axisymmetric turbulent jet by multi-modal excitation p 174 A92-40071
- AUSTENITIC STAINLESS STEELS**
Cumulative creep-fatigue damage evolution in an austenitic stainless steel p 121 A92-45231
- AUTOCORRELATION**
First-passage problems: A probabilistic dynamic analysis for degraded structures
[NASA-TM-103751] p 225 N92-11373
- AUTOMATIC CONTROL**
Power management and distribution considerations for a lunar base
[NASA-TM-105342] p 269 N92-13910
Automated power management and control p 84 N92-17773
- AUTOMATIC TEST EQUIPMENT**
Recent manufacturing advances for spiral bevel gears
[SAE PAPER 912229] p 204 A92-40024
- AUTONOMY**
Autonomous Power System intelligent diagnosis and control p 247 A92-50532
- AUXILIARY PROPULSION**
Hydrogen/oxygen auxiliary propulsion technology
[NASA-TM-105249] p 85 N92-20522
Derated ion thruster design issues
[NASA-TM-105576] p 87 N92-23534
Low-Isp derated ion thruster operation
[NASA-TM-105787] p 92 N92-32237
Dependence of hydrogen arcjet operation on electrode geometry
[NASA-TM-105855] p 93 N92-34113
- AXIAL FLOW**
The numerical simulation of a high-speed axial flow compressor
[ASME PAPER 91-GT-272] p 3 A92-15669
A comparison of predicted and measured inlet distortion flows in a subsonic axial inlet flow compressor rotor
[NASA-TM-105427] p 19 N92-26104
- AXIAL FLOW TURBINES**
Investigation of three-dimensional flow field in a turbine including rotor/stator interaction. I - Design development and performance of the research facility
[AIAA PAPER 92-3325] p 40 A92-48908
Investigation of three-dimensional flow field in a turbine including rotor/stator interaction. II - Three-dimensional flow field at the exit of the nozzle
[AIAA PAPER 92-3326] p 12 A92-48909
- AXIAL LOADS**
Probabilistic assessment of space trusses subjected to combined mechanical and thermal loads
[NASA-TM-105429] p 230 N92-33935
- AXISYMMETRIC BODIES**
Comparison of two-dimensional and three-dimensional droplet trajectory calculations in the vicinity of finite wings
[NASA-TM-105617] p 188 N92-23154
- AXISYMMETRIC FLOW**
Effect of tabs on the evolution of an axisymmetric jet p 26 A92-40151
Initial development of the axisymmetric ejector shear layer
[AIAA PAPER 92-3567] p 178 A92-49068
Performance comparison of axisymmetric and three-dimensional hydrogen film coolant injection in a 110 N hydrogen/oxygen rocket
[AIAA PAPER 92-3390] p 73 A92-54027

B

BACKGROUND RADIATION

The diffuse gamma-ray background, light element abundances, and signatures of early massive star formation p 268 A92-43837

BACKSCATTERING

Plasma etching a ceramic composite ... evaluating microstructure
[NASA-TM-105430] p 130 N92-22305

BACKWARD FACING STEPS

An iterative implicit diagonally-dominant factorization algorithm for solving the Navier-Stokes equations
[NASA-TM-105259] p 249 N92-16663

BAFFLES

3D rocket combustor acoustics model
[AIAA PAPER 92-3228] p 66 A92-48829
The 3D rocket combustor acoustics model
[NASA-TM-105734] p 88 N92-27035

BALMER SERIES

Flow diagnostics of an arcjet using laser-induced fluorescence
[AIAA PAPER 92-3243] p 199 A92-48843

BANDPASS FILTERS

Performance of a Y-Ba-Cu-O superconducting filter/GaAs low noise amplifier hybrid circuit
[NASA-TM-105546] p 160 N92-21370
Performance of a Y-Ba-Cu-O superconducting filter/GaAs low noise amplifier hybrid circuit p 163 N92-32982

BARIUM

High-T sub c fluorine-doped YBa₂Cu₃O_y films on ceramic substrates by screen printing
[NASA-TM-105296] p 127 N92-11188

BARIUM FLUORIDES

Self-lubricating coatings for high-temperature applications p 130 N92-22516

BARIUM OXIDES

Near-edge study of gold-substituted YBa₂Cu₃O_{7-δ} p 259 A92-14950
Composition dependence of superconductivity in YBa₂(Cu_{3-x}Al_x)O_y
[NASA-TM-105358] p 131 N92-24715

BARYONS

Fluctuation-driven electroweak phase transition ... in early universe p 269 A92-54464

BAYS (STRUCTURAL UNITS)

Development of and flight results from the Space Acceleration Measurement System (SAMS)
[NASA-TM-105652] p 57 N92-30301

BCS THEORY

Hall voltage sign reversal in thin superconducting films p 261 A92-35349

BEAMS (SUPPORTS)

Effect of contact stresses in four-point bend testing of graphite/epoxy and graphite/PMR-15 composite beams p 219 A92-33589

Minimization of vibration in elastic beams with time-variant boundary conditions p 224 A92-50511
Free vibrations of delaminated beams
[NASA-TM-105582] p 109 N92-25754

Influence of mass moment of inertia on normal modes of preloaded solar array mast
[NASA-TP-3273] p 230 N92-33476

BEARINGS

Full-scale transmission testing to evaluate advanced lubricants
[NASA-TM-105668] p 212 N92-26560

Dynamics of a split torque helicopter transmission
[NASA-TM-105681] p 213 N92-29136

Effect of out-of-roundness on the performance of a diesel engine connecting-rod bearing
[NASA-TM-105600] p 215 N92-31536

BEND TESTS

A simple test for thermomechanical evaluation of ceramic fibers p 123 A92-21096
Compression, bend, and tension studies on forged Al67Ti25Cr8 and Al66Ti25Mn(g) L1(2) compounds p 118 A92-30766

Effect of contact stresses in four-point bend testing of graphite/epoxy and graphite/PMR-15 composite beams p 219 A92-33589

BENDING

Influence of mass moment of inertia on normal modes of preloaded solar array mast
[NASA-TP-3273] p 230 N92-33476

BENDING FATIGUE

Combined bending and thermal fatigue of high-temperature metal-matrix composites - Computational simulation p 223 A92-43494

BENDING MOMENTS

Tension, compression, and bend properties for SiC/RBSN composites p 100 A92-32727
Material nonlinear analysis via mixed-iterative finite element method

[AIAA PAPER 92-2479] p 220 A92-34368
Modeling of the flexural behavior of ceramic-matrix composites p 225 A92-52005

BESSEL FUNCTIONS

Computer program for Bessel and Hankel functions
[NASA-TM-105154] p 243 N92-11691

BIAS

Arcing of negatively biased solar cells in low earth orbit
[AIAA PAPER 92-0578] p 59 A92-26985

BIBLIOGRAPHIES

Bibliography of Lewis Research Center technical publications announced in 1990
[NASA-TM-103753] p 267 N92-12786

Research and technology, 1991
[NASA-TM-105320] p 1 N92-22659

BIG BANG COSMOLOGY

Possible sources of the Population I lithium abundance and light-element evolution p 268 A92-33069

BINARY ALLOYS

A new approximate sum rule for bulk alloy properties p 117 A92-28240
Lattice parameters of fcc binary alloys using a new semiempirical method p 120 A92-32898

BINARY CODES

- Vertical solidification of dendritic binary alloys
p 261 A92-37562
- Heats of formation of bcc binary alloys
[NASA-TM-105281] p 122 N92-16086
- Lattice parameters of fcc binary alloys using a new semiempirical method
[NASA-TM-105304] p 123 N92-16111
- BINARY CODES**
- Frequency allocations for a new satellite service - Digital audio broadcasting
[AIAA PAPER 92-1957] p 143 A92-29881
- BINARY FLUIDS**
- Effective diffusion equation in a random velocity field
[AIAA PAPER 92-0245] p 167 A92-25704
- The Eckhaus and the Benjamin-Fear instability near a weakly inverted bifurcation
[NASA-TM-105334] p 185 N92-15336
- BINARY PHASE SHIFT KEYING**
- Least reliable bits coding (LRBC) for high data rate satellite communications
[AIAA PAPER 92-1868] p 142 A92-29807
- BINARY SYSTEMS (MATERIALS)**
- Asymmetric tip morphology of creep microcracks growing along bimaterial interfaces p 127 A92-56585
- An optical method for determining level in two-phase cryogenic fluids
[NASA-TM-104524] p 200 N92-15366
- BINDERS (MATERIALS)**
- Method of making contamination-free ceramic bodies
[NASA-CASE-LEW-14984-1] p 128 N92-16122
- Guanidine based vehicle/binders for use with oxides, metals, and ceramics
[NASA-CASE-LEW-15314-1] p 131 N92-23461
- Heat transfer device
[NASA-CASE-LEW-14162-3] p 111 N92-34208
- BIT ERROR RATE**
- Least reliable bits coding (LRBC) for high data rate satellite communications
[AIAA PAPER 92-1868] p 142 A92-29807
- Flexible high speed CODEC (FHSC)
[AIAA PAPER 92-1919] p 143 A92-29848
- An overview of Space Communication Artificial Intelligence for Link Evaluation Terminal (SCAILET) Project
p 148 N92-14212
- Least Reliable Bits Coding (LRBC) for high data rate satellite communications
[NASA-TM-105431] p 150 N92-18921
- BLACK HOLES (ASTRONOMY)**
- A classical instability of Reissner-Nordstrom solutions and the fate of magnetically charged black holes
p 267 A92-26397
- BLADE SLAP NOISE**
- Noise of two high-speed model counter-rotation propellers at takeoff/approach conditions
p 253 A92-46799
- BLADE TIPS**
- Optical measurements of unducted fan flutter
[ASME PAPER 91-GT-19] p 197 A92-15510
- The role of tip clearance in high-speed fan stall
[ASME PAPER 91-GT-83] p 2 A92-15550
- Detailed noise measurements on the SR-7A propeller: Tone behavior with helical tip Mach number
[NASA-TM-105206] p 255 N92-16705
- TCGRID: A three dimensional C-grid generator for turbomachinery
p 35 N92-25716
- BLADE-VORTEX INTERACTION**
- A viscous flow study of shock-boundary layer interaction, radial transport, and wake development in a transonic compressor
[ASME PAPER 91-GT-69] p 2 A92-15539
- The role of tip clearance in high-speed fan stall
[ASME PAPER 91-GT-83] p 2 A92-15550
- BLASIUS FLOW**
- An investigation of DTNS2D for use as an incompressible turbulence modelling test-bed
[NASA-TM-105593] p 249 N92-22230
- BLUNT LEADING EDGES**
- Improved nonequilibrium viscous shock-layer scheme for hypersonic blunt-body flowfields
p 4 A92-24653
- BODY CENTERED CUBIC LATTICES**
- Heats of formation of bcc binary alloys
[NASA-TM-105281] p 122 N92-16086
- BOEING AIRCRAFT**
- Boeing Helicopters Advanced Rotorcraft Transmission (ART) Program summary of component tests
[AIAA PAPER 92-3364] p 205 A92-48937
- Lewis icing research tunnel test of the aerodynamic effects of aircraft ground deicing/anti-icing fluids
[NASA-TP-3238] p 22 N92-30395
- BOEING 727 AIRCRAFT**
- Design and analysis of reengine Boeing 727-100 center inlet S duct by a reduced Navier-Stokes code
[AIAA PAPER 92-1221] p 8 A92-33320
- Design and analysis of vortex generators on reengine Boeing 727-100QF center inlet S-duct by a reduced Navier-Stokes code
[AIAA PAPER 92-2700] p 10 A92-45542
- BOILER PLATE**
- Progress in the development of lightweight nickel electrode
[NASA-TM-105638] p 116 N92-26670
- BOILERS**
- Alkali metal pool boiler life tests for a 25 kWe advanced Stirling conversion system
p 206 A92-50797
- Final design of a free-piston hydraulic advanced Stirling conversion system
p 206 A92-50798
- Design of a pool boiler heat transport system for a 25 kWe advanced Stirling conversion system
p 181 A92-50802
- Post-test examination of a pool boiler receiver
[NASA-TM-105635] p 123 N92-27192
- Elevated temperature axial and torsional fatigue behavior of Haynes 188
[NASA-TM-105396] p 229 N92-28701
- BOOSTER ROCKET ENGINES**
- The design and performance estimates for the propulsion module for the booster of a TSTO vehicle
[NASA-TM-105299] p 29 N92-11995
- Combustion-wave ignition for rocket engines
[NASA-TM-105545] p 84 A92-29043
- BORON NITRIDES**
- Fiber coating/matrix reactions in silicon-base ceramic matrix composites
p 102 A92-39604
- BOUNDARY CONDITIONS**
- A system-approach to the elasto-hydrodynamic lubrication point-contact problem
p 204 A92-35421
- Minimization of vibration in elastic beams with time-variant boundary conditions
p 224 A92-50511
- Full-size solar dynamic heat receiver thermal-vacuum tests
p 68 A92-50565
- Enhancing control of grid distribution in algebraic grid generation
p 248 A92-52552
- Thermal and solutal convection with conduction effects inside a rectangular enclosure
[NASA-TM-105371] p 186 N92-15358
- Long time behavior of unsteady flow computations
[NASA-TM-105584] p 190 N92-23565
- A mathematical constraint placed upon inter-blade row boundary conditions used in the simulation of multistage turbomachinery flows
p 195 N92-27458
- BOUNDARY ELEMENT METHOD**
- A variationally coupled FE-BE method for elasticity and fracture mechanics
p 222 A92-37510
- Three-dimensional boundary element thermal shape sensitivity analysis
p 176 A92-47269
- Boundary formulations for sensitivities of three-dimensional stress invariants
p 224 A92-50883
- COMGEN-BEM: Boundary element model generation for composite materials micromechanical analysis
[NASA-TM-105548] p 226 N92-19779
- Validation of finite element and boundary element methods for predicting structural vibration and radiated noise
[NASA-TM-105359] p 213 N92-29697
- BOUNDARY INTEGRAL METHOD**
- Boundary formulations for shape sensitivity of temperature dependent conductivity problems
p 217 A92-25403
- BOUNDARY LAYER CONTROL**
- A study of three dimensional turbulent boundary layer separation and vortex flow control using the reduced Navier Stokes equations
p 9 A92-40105
- Results from computational analysis of a mixed compression supersonic inlet
[NASA-TM-104475] p 14 N92-10976
- Method of reducing drag in aerodynamic systems
[NASA-CASE-LEW-14791-1] p 21 N92-34243
- BOUNDARY LAYER FLOW**
- The three-dimensional turbulent boundary layer near a plane of symmetry
p 167 A92-24757
- Naturally occurring and forced azimuthal modes in a turbulent jet
p 172 A92-35998
- Distortion of a flat-plate boundary layer by free-stream vorticity normal to the plate
p 173 A92-36343
- Surface and flow field measurements in a symmetric crossing shock wave/turbulent boundary layer flow
[AIAA PAPER 92-2634] p 10 A92-45574
- Interface of an uncoupled boundary layer algorithm with an inviscid core flow algorithm for unsteady supersonic engine inlets
[AIAA PAPER 92-3083] p 11 A92-48730
- A laser-induced heat flux technique for convective heat transfer measurements in high speed flows
p 200 A92-54318
- Modeling of the heat transfer in bypass transitional boundary-layer flows
[NASA-TP-3170] p 184 N92-11299
- Implementation/validation of a low Reynolds number two-equation turbulence model in the Proteus Navier-Stokes code: Two-dimensional/axisymmetric
[NASA-TM-105619] p 187 N92-20520
- Turbulence modeling
p 189 N92-23338
- Development of new flux splitting schemes
p 189 N92-23343
- Comment on two-equation models --- turbulence models
p 191 N92-24520
- Interface of an uncoupled boundary layer algorithm with an inviscid core flow algorithm for unsteady supersonic engine inlets
[NASA-TM-105684] p 36 N92-27037
- BOUNDARY LAYER SEPARATION**
- A study of three dimensional turbulent boundary layer separation and vortex flow control using the reduced Navier Stokes equations
p 9 A92-40105
- Measurements in a leading-edge separation bubble due to a simulated airfoil ice accretion
p 21 A92-41262
- An investigation of shock/turbulent boundary layer bleed interactions
[AIAA PAPER 92-3085] p 182 A92-54008
- Vortex generator design for aircraft inlet distortion as a numerical optimization problem
p 23 N92-13959
- BOUNDARY LAYER TRANSITION**
- Heat transfer on accreting ice surfaces
p 166 A92-24415
- On the nonlinear development of three-dimensional instability waves in natural transition
[AIAA PAPER 92-0741] p 170 A92-28222
- Subharmonic route to boundary-layer transition - Critical layer nonlinearity
p 172 A92-35994
- Experimental study of boundary layer transition on a heated flat plate
p 172 A92-36022
- Modeling of the heat transfer in bypass transitional boundary-layer flows
[NASA-TP-3170] p 184 N92-11299
- A kappa-epsilon calculation of transitional boundary layers
[NASA-TM-105604] p 187 N92-22398
- Center for Modeling of Turbulence and Transition (CMOTT). Research briefs: 1990
[NASA-TM-105243] p 1 N92-23336
- Turbulent heat flux measurements in a transitional boundary layer
[NASA-TM-105623] p 19 N92-27377
- BOUNDARY LAYERS**
- Analysis of an advanced ducted propeller subsonic inlet
[AIAA PAPER 92-0274] p 5 A92-25728
- Numerical study of shock-wave/boundary-layer interactions in premixed combustible gases
p 183 A92-54907
- Analysis of an advanced ducted propeller subsonic inlet
[NASA-TM-105393] p 15 N92-14002
- The aerodynamic effect of fillet radius in a low speed compressor cascade
[NASA-TM-105347] p 29 N92-14063
- An investigation of DTNS2D for use as an incompressible turbulence modelling test-bed
[NASA-TM-105593] p 249 N92-22230
- A kappa-epsilon calculation of transitional boundary layers
[NASA-TM-105604] p 187 N92-22398
- Inlets, ducts, and nozzles
p 188 N92-22523
- BOUNDARY LUBRICATION**
- A system-approach to the elasto-hydrodynamic lubrication point-contact problem
p 204 A92-35421
- BOUNDARY VALUE PROBLEMS**
- Numerical analysis of flow through oscillating cascade sections
p 9 A92-44513
- A kappa-epsilon calculation of transitional boundary layers
[NASA-TM-105604] p 187 N92-22398
- BRACKETS**
- Removable hand hold
[NASA-CASE-LEW-15196-1] p 213 N92-29092
- BRAYTON CYCLE**
- Full-size solar dynamic heat receiver thermal-vacuum tests
p 68 A92-50565
- Critical technology experiment results for lightweight space heat receiver
p 180 A92-50568
- Design considerations for space radiators based on the liquid sheet (LSR) concept
p 181 A92-50821
- Detonation duct gas generator demonstration program
[AIAA PAPER 92-3174] p 27 A92-54011
- SP-100 reactor with Brayton conversion for lunar surface applications
[NASA-TM-105637] p 92 N92-32108
- BREADBOARD MODELS**
- Autonomous Power System intelligent diagnosis and control
p 247 A92-50532
- Development of a ninety string solar array simulator
p 46 A92-50660

- Test and evaluation of load converter topologies used in the Space Station Freedom power management and distribution dc test bed p 158 A92-50662
- Development of a ninety string solar array simulator [NASA-TM-105278] p 55 N92-11086
- BRIDGMAN METHOD**
- Effect of thermal convection on the shape of a solid-liquid interface p 171 A92-35978
- Effect of growth conditions on the quality of lead bromide crystals p 138 A92-56957
- BRILLOUIN EFFECT**
- Rayleigh-Brillouin scattering to determine one-dimensional temperature and number density profiles of a gas flow field p 198 A92-38067
- BRITTLE MATERIALS**
- Controlled crack growth specimen for brittle systems p 123 A92-21099
- A combined analytical-experimental tensile test technique for brittle materials p 123 A92-23225
- Effect of fiber orientation on the fracture toughness of brittle matrix composites p 103 A92-41841
- A stochastic damage model for the rupture prediction of a multi-phase solid. I - Parametric studies. II - Statistical approach p 224 A92-49784
- BRITTLENESS**
- Controlled crack growth specimen for brittle systems p 123 A92-21099
- Flow and fracture behavior of NiAl in relation to the brittle-to-ductile transition temperature p 118 A92-30781
- Near-tip dual-length scale mechanics of mode-I cracking in laminate brittle matrix composites [AIAA PAPER 92-2491] p 221 A92-34583
- BROADBAND**
- A survey of the broadband shock associated noise prediction methods [AIAA PAPER 92-0501] p 252 A92-26930
- Satellite delivery of B-ISDN services [AIAA PAPER 92-1831] p 142 A92-29777
- A survey of the broadband shock associated noise prediction methods [NASA-TM-105365] p 254 N92-14797
- Detecting Lamb waves with broad-band acousto-ultrasonic signals in composite structures [NASA-TM-105557] p 216 N92-23189
- BROADBAND AMPLIFIERS**
- Performance of a wideband GaAs low-noise amplifier at cryogenic temperatures p 156 A92-37953
- BROADCASTING**
- Frequency allocations for a new satellite service - Digital audio broadcasting [AIAA PAPER 92-1957] p 143 A92-29881
- Real-time data compression of broadcast video signals [NASA-CASE-LEW-14945-2] p 147 N92-10128
- On-board congestion control for satellite packet switching networks p 148 N92-14228
- Real-time demonstration hardware for enhanced DPCM video compression algorithm [NASA-TM-105616] p 150 N92-19700
- BROMIDES**
- Growth and characterization of lead bromide crystals p 138 A92-56956
- Effect of growth conditions on the quality of lead bromide crystals p 138 A92-56957
- BROMINATION**
- Brominated graphitized carbon fibers [NASA-CASE-LEW-14698-2] p 127 N92-10090
- BROMINE**
- Brominated graphitized carbon fibers [NASA-CASE-LEW-14698-2] p 127 N92-10090
- Properties of novel CVD graphite fibers and their bromine intercalation compounds [NASA-TM-105295] p 128 N92-14170
- BROMINE COMPOUNDS**
- Properties of novel CVD graphite fibers and their bromine intercalation compounds [NASA-TM-105295] p 128 N92-14170
- BRUSH SEALS**
- A bulk flow model of a brush seal system [ASME PAPER 91-GT-325] p 203 A92-15696
- Seals related research at NASA. Lewis Research Center p 207 N92-15087
- Brush seal leakage performance with gaseous working fluids at static and low rotor speed conditions [NASA-TM-105400] p 186 N92-16265
- High temperature, flexible pressure-actuated, brush seal [NASA-CASE-LEW-15086-1] p 208 N92-16318
- Development of advanced seals for space propulsion turbomachinery [NASA-TM-105659] p 87 N92-24957
- BRUSHES (ELECTRICAL CONTACTS)**
- Flow visualization and motion analysis for a series of four sequential brush seals p 204 A92-36976
- BUBBLES**
- Helium bubble flow visualization of the spanwise separation on a NACA 0012 with simulated glaze ice [AIAA PAPER 92-0413] p 7 A92-28192
- Measurements in a leading-edge separation bubble due to a simulated airfoil ice accretion p 21 A92-41262
- Helium bubble flow visualization of the spanwise separation on a NACA 0012 with simulated glaze ice [NASA-TM-105742] p 19 N92-26612
- BUCKLING**
- Collapse analysis of a waffle plate strongback for Space Station Freedom [NASA-TM-105412] p 227 N92-20045
- Evaluation of MHOST analysis capabilities for a plate element --- finite element modeling [NASA-TM-105387] p 228 N92-23196
- Probabilistic assessment of space trusses subjected to combined mechanical and thermal loads [NASA-TM-105429] p 230 N92-33935
- BULK MODULUS**
- Pressure dependence of the melting temperature of solids - Flare-gas solids p 171 A92-33912
- BUOYANCY**
- Heat transfer in rotating serpentine passages with trips normal to the flow [ASME PAPER 91-GT-265] p 165 A92-15663
- Transient pool boiling in microgravity p 170 A92-30494
- Nature of buoyancy-driven flows in a reduced-gravity environment p 175 A92-45844
- Heat transfer in rotating serpentine passages with trips skewed to the flow [NASA-TM-105581] p 186 N92-20235
- BURNING RATE**
- Observations on a slow burning regime for hydrocarbon droplets - n-heptane/air results p 112 A92-16602
- 3D rocket combustor acoustics model [AIAA PAPER 92-3228] p 66 A92-48829
- The 3D rocket combustor acoustics model [NASA-TM-105734] p 88 N92-27035
- BUTT JOINTS**
- Post-test examination of a pool boiler receiver [NASA-TM-105635] p 123 N92-27192
- BYPASSES**
- Modeling of the heat transfer in bypass transitional boundary-layer flows [NASA-TP-3170] p 184 N92-11299
- Turbulence modeling p 189 N92-23338
- C**
- C BAND**
- C-band superconductor/semiconductor hybrid field-effect transistor amplifier on a LaAlO₃ substrate [NASA-TM-105828] p 163 N92-34204
- CADMIUM COMPOUNDS**
- Solid lubricants on pretreated surfaces [NASA-CASE-LEW-14474-2] p 127 N92-11186
- CADMIUM TELLURIDES**
- Vapor crystal growth technology development: Application to cadmium telluride [NASA-TM-103786] p 139 N92-16158
- CALCIUM FLUORIDES**
- Self-lubricating coatings for high-temperature applications p 130 N92-22516
- CALCIUM SILICATES**
- Low temperature synthesis of CaO-SiO₂ glasses having stable liquid-liquid immiscibility by the sol-gel process p 126 A92-44479
- CALIBRATING**
- Design of a self-diagnostic beam-mode piezoelectric accelerometer [AIAA PAPER 92-3656] p 200 A92-54106
- Space acceleration measurement system triaxial sensor head error budget [NASA-TM-105300] p 57 N92-25134
- CANONICAL FORMS**
- Functional models of power electronic components for system studies p 157 A92-50558
- Modeling of Space Station power system components and their interactions p 68 A92-50559
- Canonical transformations for space trajectory optimization [AIAA PAPER 92-4509] p 44 A92-52079
- CANS**
- Experiments with phase change thermal energy storage canisters for Space Station Freedom p 179 A92-50564
- Parametric studies of phase change thermal energy storage canisters for Space Station Freedom [NASA-TM-105350] p 55 N92-13143
- Experiments with phase change thermal energy storage canisters for Space Station Freedom [NASA-TM-104427] p 86 N92-21216
- CANTILEVER BEAMS**
- Vibration transmission through rolling element bearings. IV - Statistical energy analysis p 218 A92-28756
- Free vibrations of delaminated beams p 222 A92-36853
- CAPACITORS**
- Electrical properties of teflon and ceramic capacitors at high temperatures [NASA-TM-105569] p 160 N92-20040
- Evaluation of high temperature capacitor dielectrics [NASA-TM-105622] p 161 N92-23561
- CAPILLARY FLOW**
- Drop-tower experiments for capillary surfaces in an exotic container p 166 A92-20743
- Unsteady thermocapillary migration of isolated drops in creeping flow p 169 A92-27774
- Linear-stability theory of thermocapillary convection in a model of float-zone crystal growth [AIAA PAPER 92-0604] p 169 A92-28211
- Stability of capillary surfaces p 172 A92-35979
- An experimental study of oscillatory thermocapillary convection in cylindrical containers p 172 A92-36184
- Scaling of low-Prandtl-number thermocapillary flows p 176 A92-47271
- CARBIDES**
- Sliding durability of two carbide-oxide candidate high temperature fiber seal materials in air to 900 C [NASA-TM-105554] p 97 N92-21175
- CARBON**
- Optical dispersion relations for 'diamondlike' carbon films p 262 A92-44533
- Environmental effects on friction and wear of diamond and diamondlike carbon coatings [NASA-TM-105634] p 131 N92-23192
- Graphite fluoride from iodine intercalated graphitized carbon [NASA-CASE-LEW-15360-1] p 116 N92-34206
- CARBON COMPOUNDS**
- Graphite fluoride from iodine intercalated graphitized carbon [NASA-CASE-LEW-15360-1] p 116 N92-34206
- CARBON DIOXIDE**
- Material processing with hydrogen and carbon monoxide on Mars p 231 A92-17769
- Acetylene fuel from atmospheric CO₂ on Mars p 133 A92-32199
- In-situ carbon dioxide fixation on Mars p 134 A92-50613
- Alkali metal carbon dioxide electrochemical system for energy storage and/or conversion of carbon dioxide to oxygen [NASA-CASE-LEW-14973-1] p 235 N92-10222
- Brush seal leakage performance with gaseous working fluids at static and low rotor speed conditions [NASA-TM-105400] p 186 N92-16265
- CARBON FIBER REINFORCED PLASTICS**
- Effect of fiber reinforcement on thermo-oxidative stability and mechanical properties of polymer matrix composites p 101 A92-33587
- Void effects on the interlaminar shear strength of unidirectional graphite-fiber-reinforced composites p 105 A92-50348
- CARBON FIBERS**
- Brominated graphitized carbon fibers [NASA-CASE-LEW-14698-2] p 127 N92-10090
- Thermal conductivity and thermal expansion of graphite fiber/copper matrix composites [NASA-TM-105233] p 106 N92-14120
- Properties of novel CVD graphite fibers and their bromine intercalation compounds [NASA-TM-105295] p 128 N92-14170
- Intercalated hybrid graphite fiber composite [NASA-CASE-LEW-15241-1] p 107 N92-17861
- CARBON MONOXIDE**
- Material processing with hydrogen and carbon monoxide on Mars p 231 A92-17769
- Propulsion systems using in situ propellants for a Mars Ascent Vehicle [AIAA PAPER 92-3445] p 66 A92-49001
- Propulsion systems using in situ propellants for a Mars ascent vehicle [NASA-TM-105741] p 89 N92-27654
- CARBURIZING**
- Improvement in surface fatigue life of hardened gears by high-intensity shot peening [NASA-TM-105678] p 211 N92-26108
- CARRIER DENSITY (SOLID STATE)**
- Enhancement of Shubnikov-de Haas oscillations by carrier modulation p 262 A92-50911
- Defect behavior, carrier removal and predicted in-space injection annealing of InP solar cells [NASA-TM-105624] p 161 N92-23562
- CARRIER LIFETIME**
- Photoluminescence lifetime measurements in InP wafers p 262 A92-48092

CARRIER MOBILITY

Minority carrier lifetime in indium phosphide
p 262 A92-53148

CARRIER MOBILITY

Radiation and temperature effects in heteroepitaxial and homoepitaxial InP cells p 159 A92-53192
Reduced mobility and PPC in In₂₀Ga₈₀As / Al₂₃Ga₇₇As HEMT structure p 265 N92-32976

CARRIER TRANSPORT (SOLID STATE)

Evaluation of the minority carrier diffusion length and surface-recombination velocity in GaAs p/n solar cells p 234 A92-53162

CARTESIAN COORDINATES

On the most general tensor B(sub ij) which is zero for i does not equal j, and the most general isotropic tensor l(sub ij) p 240 N92-10289
[NASA-TM-105236]
Cartesian based grid generation/adaptive mesh refinement p 192 N92-25722
Minimization of deviations of gear real tooth surfaces determined by coordinate measurements p 214 N92-30948
[NASA-TM-105718]

CASCADE FLOW

The effect of steady aerodynamic loading on the flutter stability of turbomachinery blading p 2 A92-15574
[ASME PAPER 91-GT-130]
Aerodynamics and heat transfer investigations on a high Reynolds number turbine cascade p 164 A92-15593
[ASME PAPER 91-GT-157]
Cascade flutter analysis with transient response aerodynamics p 217 A92-15972
Navier-Stokes analysis of flow and heat transfer inside high-pressure-ratio transonic turbine blade rows p 165 A92-17193
Aerodynamics of loaded cascades in subsonic flows subject to unsteady three-dimensional vortical disturbances p 4 A92-23762
[AIAA PAPER 92-0146]
Pressure wave propagation studies for oscillating cascades p 5 A92-25682
[AIAA PAPER 92-0145]
Navier-Stokes solution of transonic cascade flows using nonperiodic C-type grids p 8 A92-28523
Analysis of cascades using a two dimensional Euler aeroelastic solver p 26 A92-34598
[AIAA PAPER 92-2370]
Finite element Euler calculations of unsteady transonic cascade flows p 9 A92-35689
[AIAA PAPER 92-2120]
Renormalization group based algebraic turbulence model for three-dimensional turbomachinery flows p 9 A92-41268
Numerical analysis of flow through oscillating cascade sections p 9 A92-44513
Row-by-row off-design performance calculation method for turbines p 26 A92-44514
A conformal block structured grid for turbomachinery cascades in two dimensions p 248 A92-47059
Development of an efficient analysis for high Reynolds number inviscid/viscid interactions in cascades p 10 A92-48723
[AIAA PAPER 92-3073]
Full field flow visualization and computer-aided velocity measurements in a bank of cylinders in a wind tunnel p 199 A92-50040
Transonic turbine blade cascade testing facility p 42 A92-56856
[AIAA PAPER 92-4034]
Experimental unsteady pressures on an oscillating cascade with supersonic leading edge locus p 14 A92-56857
[AIAA PAPER 92-4035]
Multigrid calculation of three-dimensional viscous cascade flows p 249 N92-10345
[NASA-TM-105257]
The aerodynamic effect of fillet radius in a low speed compressor cascade p 29 N92-14063
[NASA-TM-105347]
Pressure wave propagation studies for oscillating cascades p 16 N92-15977
[NASA-TM-105406]
Unsteady-flow-field predictions for oscillating cascades p 17 N92-19437
[NASA-TM-105283]
Transonic turbine blade cascade testing facility p 47 N92-26129
[NASA-TM-105646]
Laser anemometer measurements and computations in an annular cascade of high turning core turbine vanes p 20 N92-28980
[NASA-TP-3252]

CASSEGRAIN ANTENNAS
Analysis of a generalized dual reflector antenna system using physical optics p 149 N92-18281
[NASA-TM-105425]

CASSINI MISSION
A low-power, high-efficiency Ka-band TWTA p 154 A92-29769
[AIAA PAPER 92-1822]
A low-power, high-efficiency Ka-band TWTA p 156 A92-38163

CAST ALLOYS
Oxidation kinetics of cast TiAl₃ p 121 A92-38993

Thermomechanical and bithermal fatigue behavior of cast B1900 + Hf and wrought Haynes 188 p 122 A92-45233

CATALYSIS

Validation test of advanced technology for IPV nickel-hydrogen flight cells: Update p 89 N92-27878
[NASA-TM-105689]

CATALYSTS

Safety considerations in testing a fuel-rich aeropropulsion gas generator p 30 N92-17061
[NASA-TM-105258]

CATARACTS

A fiber optic sensor for ophthalmic refractive diagnostics p 198 A92-34831

CATASTROPHE THEORY

Modal interaction in linear dynamic systems near degenerate modes p 225 N92-12316
[NASA-TM-105315]

CATENARIES

Solar radiation on a catenary collector p 163 N92-32243
[NASA-TM-105751]

CATHODES

Alkali metal carbon dioxide electrochemical system for energy storage and/or conversion of carbon dioxide to oxygen p 235 N92-10222
[NASA-CASE-LEW-14973-1]

CATIONS

High-T sub c fluorine-doped YBa₂Cu₃O_(y) films on ceramic substrates by screen printing p 127 N92-11188
[NASA-TM-105296]

CAVITATION FLOW

Effect of type and location of oil groove on the performance of journal bearings p 203 A92-21333
Helium bubble flow visualization of the spanwise separation on a NACA 0012 with simulated glaze ice p 7 A92-28192
[AIAA PAPER 92-0413]
Two reference time scales for studying the dynamic cavitation of liquid films p 204 A92-47173
Helium bubble flow visualization of the spanwise separation on a NACA 0012 with simulated glaze ice p 19 N92-26612
[NASA-TM-105742]
Effect of out-of-roundness on the performance of a diesel engine connecting-rod bearing p 215 N92-31536
[NASA-TM-105600]
Three-dimensional flow fields inside a shrouded inducer at design and off-design conditions (CFD study) p 196 N92-32291

CAVITIES

Atomic oxygen undercutting of LDEF aluminized-Kapton multilayer insulation p 255 N92-24818

CAVITY FLOW

Numerical solution of a three-dimensional cubic cavity flow by using the Boltzmann equation p 195 N92-30297
[NASA-TM-105693]

CAVITY RESONATORS

The introduction of spurious modes in a hole-coupled Fabry-Perot open resonator p 197 A92-21244
Three point lead screw positioning apparatus p 208 N92-17678
[NASA-CASE-LEW-15216-1]

CELL ANODES

Anodic etching of p-type cubic silicon carbide p 127 A92-57027

CELLULOSE

Global kinetic constants for thermal oxidative degradation of a cellulose paper p 113 A92-29488
Heat and mass transport from thermally degrading thin cellulosic materials in a microgravity environment p 174 A92-41810

CEMENTATION

Volatile species in halide-activated-diffusion coating packs p 122 A92-57028

CEMENTS

Preliminary evaluation of adhesion strength measurement devices for ceramic/titanium matrix composite bonds p 1 N92-31267
[NASA-TM-105803]

CENTAUR LAUNCH VEHICLE

Rocket propulsion research at Lewis Research Center p 266 N92-30908
[NASA-CR-189187]
Graphite/epoxy composite adapters for the Space Shuttle/Centaur vehicle p 49 N92-31251
[NASA-TP-3014]

CENTRIFUGAL COMPRESSORS

NASA low-speed centrifugal compressor for 3-D viscous code assessment and fundamental flow physics research p 3 A92-15580
[ASME PAPER 91-GT-140]
Deterministic blade row interactions in a centrifugal compressor stage p 3 A92-15670
[ASME PAPER 91-GT-273]
A survey of instabilities within centrifugal pumps and concepts for improving the flow range of pumps in rocket engines p 84 N92-18280
[NASA-TM-105439]

A 4-spot time-of-flight anemometer for small centrifugal compressor velocity measurements p 202 N92-29105
[NASA-TM-105717]

CENTRIFUGAL FORCE

Optical measurements of unducted fan flutter p 197 A92-15510
[ASME PAPER 91-GT-19]
Transport modes during crystal growth in a centrifuge p 138 A92-33835
Surface heat transfer and flow properties of vortex arrays induced artificially and from centrifugal instabilities p 183 A92-56371

CENTRIFUGAL PUMPS

A survey of instabilities within centrifugal pumps and concepts for improving the flow range of pumps in rocket engines p 84 N92-18280
[NASA-TM-105439]

CERAMIC BONDING

Bonded ceramic foams reinforced with fibers for high temperature use p 125 A92-39628

CERAMIC COATINGS

SiC(X) coatings for atomic oxygen protection of polyimide Kapton in low earth orbit p 94 A92-31286
[AIAA PAPER 92-2151]

CERAMIC FIBERS

A simple test for thermomechanical evaluation of ceramic fibers p 123 A92-21096
Thermal stress analysis of a silicon carbide/aluminum composite p 222 A92-38097
Fatigue crack growth in a unidirectional SCS-6/Ti-15-3 composite p 102 A92-39036
Bonded ceramic foams reinforced with fibers for high temperature use p 125 A92-39628
Tensile strain measurements of ceramic fibers using scanning laser acoustic microscopy p 198 A92-39629
Failure mechanisms of 3-D woven SiC/SiC composites under tensile and flexural loading at room and elevated temperatures p 103 A92-39642
Polymeric precursors for fibers and matrices p 125 A92-39856
Reaction-bonded Si₃N₄ and SiC matrix composites p 103 A92-39858
High-temperature fatigue behavior of a SiC/Ti-24Al-11Nb composite p 104 A92-44613
Compatibility of potential reinforcing ceramics with Ni and Fe aluminides p 105 A92-46874
Relative sliding durability of two candidate high temperature oxide fiber seal materials p 126 A92-49095
[AIAA PAPER 92-3713]
The effect of temperature on the deformation and fracture of SiC/Ti-24Al-11Nb p 106 A92-55143
Oxidation of Al₂O₃ continuous fiber-reinforced/NiAl composites p 106 A92-57029
Relative sliding durability of two candidate high temperature oxide fiber seal materials p 95 N92-10064
[NASA-TM-105199]
Sliding durability of two carbide-oxide candidate high temperature fiber seal materials in air to 900 C p 97 N92-21175
[NASA-TM-105554]
Plasma etching a ceramic composite ... evaluating microstructure p 130 N92-22305
[NASA-TM-105430]
Tribological evaluation of an Al₂O₃-SiO₂ ceramic fiber candidate for high temperature sliding seals p 97 N92-23190
[NASA-TM-105611]
High temperature dynamic engine seal technology development p 209 N92-23435
[NASA-TM-105641]
Tensile strain measurements of ceramic fibers using scanning laser acoustic microscopy p 216 N92-24986
[NASA-TM-105589]
Ceramic composites: Enabling aerospace materials p 133 N92-27378
[NASA-TM-105599]

CERAMIC MATRIX COMPOSITES
Micromechanics for ceramic matrix composites p 98 A92-10282
Intermetallic and ceramic matrix composites for B15 to 1370 C (1500 to 2500 F) gas turbine engine applications p 99 A92-15128
Influence of interfacial shear strength on the mechanical properties of SiC fiber reinforced reaction-bonded silicon nitride matrix composites p 99 A92-15145
Mechanical behavior of fiber reinforced SiC/RBSN ceramic matrix composites - Theory and experiment ... Reaction Bonded Silicon Nitride p 99 A92-15629
[ASME PAPER 91-GT-209]
Structural reliability analysis of laminated CMC components p 99 A92-15630
[ASME PAPER 91-GT-210]
Mechanical behaviors of ceramic matrix composites with matrix cracking and fiber debonding p 100 A92-23104
Role of interfacial carbon layer in the thermal diffusivity/conductivity of silicon carbide fiber-reinforced reaction-bonded silicon nitride matrix composites p 100 A92-25443

- Oxidation effects on the mechanical properties of a SiC-fiber-reinforced reaction-bonded Si₃N₄ matrix composite p 100 A92-25445
- Tension, compression, and bend properties for SiC/RBSN composites p 100 A92-32727
- Predictions of the critical strain for matrix cracking of ceramic matrix composites p 218 A92-33127
- Strength, toughness and R-curve behaviour of SiC whisker-reinforced composite Si₃N₄ with reference to monolithic Si₃N₄ p 101 A92-34202
- Reliability analysis of laminated CMC components through shell subelement techniques [AIAA PAPER 92-2348] p 219 A92-34322
- Ceramics and ceramic matrix composites - Aerospace potential and status [AIAA PAPER 92-2445] p 94 A92-34474
- Analysis of whisker-toughened CMC structural components using an interactive reliability model [AIAA PAPER 92-2490] p 221 A92-34582
- Damage mechanisms in three-dimensional woven reinforced ceramic matrix composites under tensile and flexural loading at room and elevated temperatures [AIAA PAPER 92-2492] p 101 A92-34584
- Fracture resistance development in ceramic composites with nonlinear fiber pullout relationship [AIAA PAPER 92-2493] p 221 A92-34585
- Load redistribution considerations in the fracture of ceramic matrix composites [AIAA PAPER 92-2494] p 221 A92-34586
- Combustion synthesis of TiB₂-Al₂O₃-Al composite materials p 102 A92-36391
- Fiber coating/matrix reactions in silicon-base ceramic matrix composites p 102 A92-39604
- Role of interfacial thermal barrier in the transverse thermal conductivity of uniaxial SiC fiber-reinforced reaction bonded silicon nitride p 102 A92-39605
- Tensile strain measurements of ceramic fibers using scanning laser acoustic microscopy p 198 A92-39629
- Failure mechanisms of 3-D woven SiC/SiC composites under tensile and flexural loading at room and elevated temperatures p 103 A92-39642
- Flight-vehicle materials, structures, and dynamics - Assessment and future directions. Vol. 3 - Ceramics and ceramic-matrix composites --- Book [ISBN 0-7918-0661-8] p 94 A92-39852
- Ceramics and ceramic composites in future aeronautical and space systems p 95 A92-39853
- Polymeric precursors for fibers and matrices p 125 A92-39856
- Reaction-bonded Si₃N₄ and SiC matrix composites p 103 A92-39858
- Environmental durability of ceramics and ceramic composites p 95 A92-39862
- NASA's high-temperature engine materials program for civil aeronautics p 95 A92-41117
- An evaluation of strain measuring devices for ceramic composites p 199 A92-46497
- Modeling of the flexural behavior of ceramic-matrix composites p 225 A92-52005
- An evaluation of strain measuring devices for ceramic composites [NASA-TM-105337] p 225 A92-14433
- High-temperature durability considerations for HSCT combustor [NASA-TP-3162] p 129 A92-17070
- Towards the development of micromechanics equations for ceramic matrix composites via fiber substructuring [NASA-TM-105246] p 108 A92-19595
- Reliability analysis of laminated CMC components through shell subelement techniques [NASA-TM-105413] p 129 A92-20380
- Plasma etching a ceramic composite --- evaluating microstructure [NASA-TM-105430] p 130 A92-22305
- NASA Lewis Research Center materials research and technology: An overview p 31 A92-22512
- Detecting Lamb waves with broad-band acousto-ultrasonic signals in composite structures [NASA-TM-105557] p 216 A92-23189
- X ray attenuation measurements for high-temperature materials characterization and in-situ monitoring of damage accumulation [NASA-TM-105577] p 110 A92-25996
- Ceramic composites: Enabling aerospace materials [NASA-TM-105599] p 133 A92-27378
- Approaches to polymer-derived CMC matrices [NASA-TM-105754] p 110 A92-29660
- CERAMICS**
- Determination of the stress distributions in a ceramic, tensile specimen using numerical techniques p 216 A92-14546
- Controlled crack growth specimen for brittle systems p 123 A92-21099
- Tribological properties of ceramic-(Ti₃Al-Nb) sliding couples for use as candidate seal materials to 700 C p 124 A92-32407
- Reliability analysis of laminated CMC components through shell subelement techniques [AIAA PAPER 92-2348] p 219 A92-34322
- Ceramics and ceramic matrix composites - Aerospace potential and status [AIAA PAPER 92-2445] p 94 A92-34474
- Flight-vehicle materials, structures, and dynamics - Assessment and future directions. Vol. 3 - Ceramics and ceramic-matrix composites --- Book [ISBN 0-7918-0661-8] p 94 A92-39852
- Ceramics and ceramic composites in future aeronautical and space systems p 95 A92-39853
- Monolithic ceramics p 125 A92-39854
- Environmental durability of ceramics and ceramic composites p 95 A92-39862
- Structural design methodologies for ceramic-based material systems p 103 A92-39866
- Micromechanical model of crack growth in fiber reinforced brittle materials p 223 A92-46829
- Fractal dimension of alumina aggregates grown in two dimensions p 126 A92-49814
- Effect of index of refraction on radiation characteristics in a heated absorbing, emitting, and scattering layer p 181 A92-53031
- High-T sub c fluorine-doped YBa₂Cu₃O₇(y) films on ceramic substrates by screen printing [NASA-TM-105296] p 127 A92-11188
- An evaluation of strain measuring devices for ceramic composites [NASA-TM-105337] p 225 A92-14433
- National Aerospace Plane engine seals: High temperature seal performance evaluation p 207 A92-15103
- Method of making contamination-free ceramic bodies [NASA-CASE-LEW-14984-1] p 128 A92-16122
- Reliability analysis of structural ceramic components using a three-parameter Weibull distribution [NASA-TM-105370] p 129 A92-17060
- CVD of silicon carbide on structural fibers: Microstructure and composition [NASA-TM-105385] p 107 A92-18439
- Multiwavelength pyrometry for nongray surfaces in the presence of interfering radiation [NASA-TM-105286] p 201 A92-19107
- Temperature-dependent reflectivity of silicon carbide [NASA-TM-105287] p 201 A92-19263
- Electrical properties of teflon and ceramic capacitors at high temperatures [NASA-TM-105569] p 160 A92-20040
- Reliability analysis of laminated CMC components through shell subelement techniques [NASA-TM-105413] p 129 A92-20380
- Evaluation of an innovative high temperature ceramic water seal for hypersonic engine applications [NASA-TM-105556] p 208 A92-20815
- Composite thermal barrier coating [NASA-CASE-LEW-14999-1] p 108 A92-21725
- Screen Cage Ion Plating (SCIP) and scratch testing of polycrystalline aluminum oxide [NASA-TM-105404] p 130 A92-22278
- Ceramics for engines p 131 A92-22517
- Small engine technology programs p 32 A92-22532
- Deposition of adherent Ag-Ti duplex films on ceramics in a multiple-cathode sputter deposition system [NASA-TM-105586] p 34 A92-23225
- Guanidine based vehicle/binders for use with oxides, metals, and ceramics [NASA-CASE-LEW-15314-1] p 131 A92-23461
- Development of advanced seals for space propulsion turbomachinery [NASA-TM-105659] p 87 A92-24957
- Preliminary evaluation of adhesion strength measurement devices for ceramic/titanium matrix composite bonds [NASA-TM-105803] p 1 A92-31267
- CERMETS**
- Combustion synthesis of TiB₂-Al₂O₃-Al composite materials p 102 A92-36391
- Combustion synthesis of ceramic-metal composite materials - The TiC-Al₂O₃-Al system p 115 A92-55139
- CESIUM PLASMA**
- Study of a cesium plasma as a selective emitter for thermophotovoltaic applications p 258 A92-33667
- CHANGE DETECTION**
- Design of a self-diagnostic beam-mode piezoelectric accelerometer [AIAA PAPER 92-3656] p 200 A92-54106
- CHANNEL FLOW**
- Features of wavy vortices in a curved channel from experimental and numerical studies p 171 A92-31638
- Detonation duct gas generator demonstration program [AIAA PAPER 92-3174] p 27 A92-54011
- Turbulence modeling p 189 A92-23338
- Advancements in engineering turbulence modeling [PAPER-105] p 189 A92-23350
- Comment on two-equation models --- turbulence models p 191 A92-24520
- Thermal stratification potential in rocket engine coolant channels [NASA-TM-4378] p 87 A92-25616
- Heat transfer in oscillating flows with sudden change in cross section [NASA-TM-105692] p 88 A92-26654
- A new time scale based k-epsilon model for near wall turbulence [NASA-TM-105768] p 196 A92-32868
- CHAOS**
- Turbulence and deterministic chaos --- computational fluid dynamics p 194 A92-25823
- CHARGE COUPLED DEVICES**
- A full field, 3-D velocimeter for NASA's microgravity science program [AIAA PAPER 92-0784] p 56 A92-27119
- CHARGE EXCHANGE**
- An experimental study of impingement-ion-production mechanisms [AIAA PAPER 92-3826] p 76 A92-54190
- CHARGED PARTICLES**
- Magnetic radiation shielding - An idea whose time has returned? p 53 A92-17796
- CHARRING**
- Evaluation of Kapton pyrolysis, arc tracking, and arc propagation on the Space Station Freedom (SSF) solar array flexible current carrier (FCC) p 72 A92-53209
- CHEBYSHEV APPROXIMATION**
- Mappings and accuracy for Chebyshev pseudo-spectral approximations p 248 A92-50469
- CHECKOUT**
- Technology readiness assessment of advanced space engine integrated controls and health monitoring [NASA-TM-105255] p 79 A92-11130
- CHEMICAL ATTACK**
- Chemical stability of high-temperature superconductors [NASA-TM-105391] p 263 A92-19398
- CHEMICAL BONDS**
- 'Wrong' bond interactions at inversion domain boundaries in GaAs p 260 A92-27297
- CHEMICAL COMPOSITION**
- Brominated graphitized carbon fibers [NASA-CASE-LEW-14698-2] p 127 A92-10090
- Glass formation, properties, and structure of soda-yttria-silicate glasses [NASA-TM-104488] p 128 A92-11202
- CVD of silicon carbide on structural fibers: Microstructure and composition [NASA-TM-105385] p 107 A92-18439
- Electrical and chemical interactions at Mars Workshop, part 1 [NASA-CP-10093] p 270 A92-30302
- CHEMICAL EQUILIBRIUM**
- A new approximate sum rule for bulk alloy properties p 117 A92-28240
- Effects of chemical equilibrium on turbine engine performance for various fuels and combustor temperatures [NASA-TM-105399] p 34 A92-23254
- CHEMICAL PROPERTIES**
- Low earth orbit durability evaluation of Haynes 188 solar receiver material [AIAA PAPER 92-0850] p 117 A92-29616
- CHEMICAL PROPULSION**
- An overview of the NASA Advanced Propulsion Concepts program [AIAA PAPER 92-3216] p 73 A92-54018
- Engine system assessment study using Martian propellants [AIAA PAPER 92-3446] p 73 A92-54030
- Overview of rocket engine control [NASA-TM-105318] p 81 A92-13274
- CHEMICAL REACTIONS**
- Fiber coating/matrix reactions in silicon-base ceramic matrix composites p 102 A92-39604
- Reactions of silicon carbide and silicon(IV) oxide at elevated temperatures p 126 A92-43483
- Radiation enhanced dissociation of hydrogen in nuclear rockets [AIAA PAPER 92-3817] p 67 A92-49129
- Substituted 1,1,1-triary-2,2,2-trifluoroethanes and processes for their synthesis [NASA-CASE-LEW-14345-6] p 96 A92-17882
- Chemical stability of high-temperature superconductors [NASA-TM-105391] p 263 A92-19398
- CHEMICAL REACTORS**
- Thermochemical energy storage for a lunar base [NASA-TM-105333] p 236 A92-14485
- CHIPS (ELECTRONICS)**
- Flexible high speed CODEC (FHSC) [AIAA PAPER 92-1919] p 143 A92-29848

CHLORIDES

- High-performance packaging for monolithic microwave and millimeter-wave integrated circuits
[NASA-TM-105744] p 151 N92-31855

CHLORIDES

- Flight experiment on acousto-optic crystal growth
p 136 A92-12880

CHLORINATION

- Oxidation-chlorination of binary Ni-Cr alloys in flowing Ar-O₂-Cl₂ gas mixtures at 1200 K p 112 A92-17296

CHROMATOGRAPHY

- Cyclopentadiene evolution during pyrolysis-gas chromatography of PMR polyimides
[NASA-TM-105629] p 132 N92-25348

CHROMIUM ALLOYS

- Oxidation-chlorination of binary Ni-Cr alloys in flowing Ar-O₂-Cl₂ gas mixtures at 1200 K p 112 A92-17296
Tensile behavior of the L(1)₂ compound Al67Ti25Cr8 p 122 A92-49694

- Volatile species in halide-activated-diffusion coating packs p 122 A92-57028

CIRCUIT BREAKERS

- Numerical study of low-current steady arcs p 67 A92-50264

- Development and testing of a 180-volt dc electronic circuit breaker with a 335-ampere carry and 1200-ampere interrupt rating p 158 A92-50658

CIRCUITS

- Large transient fault current test of an electrical roll ring --- for Space Station Freedom p 55 A92-50661

- An overview of silicon carbide device technology
[NASA-TM-105402] p 263 N92-15815

- Microwave conductivity of laser ablated YBa₂Cu₃O(7- δ) superconducting films and its relation to microstrip transmission line performance p 264 N92-21639

- Large transient fault current test of an electrical roll ring
[NASA-TM-105667] p 87 N92-24201

CIRCULAR CYLINDERS

- Breakdown of the Karman vortex street due to forced convection and flow compressibility
[NASA-TM-105853] p 196 N92-32472

CIRCULAR TUBES

- Tensile properties of impact ices p 94 A92-29644
[AIAA PAPER 92-0883]

CIVIL AVIATION

- NASA's high-temperature engine materials program for civil aeronautics p 95 A92-41117

CLASSIFIERS

- A failure diagnosis system based on a neural network classifier for the Space Shuttle Main Engine p 58 A92-11474

CLOSURE LAW

- The present status and the future direction of second order closure models for incompressible flows p 191 N92-24523

- Advances in engineering turbulence modeling --- computational fluid dynamics p 193 N92-25820

CLOSURES

- A critical comparison of second order closures with direct numerical simulation of homogeneous turbulence
[NASA-TM-105351] p 185 N92-15357

COATING

- Chemical vapor deposition modeling for high temperature materials p 96 N92-18457
[NASA-TM-105386]

- Advanced liquid rockets p 87 N92-24560
[NASA-TM-105633]

COATINGS

- Synergistic effects of ultraviolet radiation, thermal cycling and atomic oxygen on altered and coated Kapton surfaces p 93 A92-27125
[AIAA PAPER 92-0794]

- Evaluation of Kapton pyrolysis, arc tracking, and arc propagation on the Space Station Freedom (SSF) solar array flexible current carrier (FCC) p 72 A92-53209

- Synergistic effects of ultraviolet radiation, thermal cycling, and atomic oxygen on altered and coated Kapton surfaces p 96 N92-14114
[NASA-TM-105363]

- The effect of ion plated silver and sliding friction on tensile stress-induced cracking in aluminum oxide p 129 N92-19450
[NASA-TM-105366]

- Screen Cage Ion Plating (SCIP) and scratch testing of polycrystalline aluminum oxide p 130 N92-22278
[NASA-TM-105404]

- Advanced liquid rockets p 87 N92-24560
[NASA-TM-105633]

COAXIAL CABLES

- Coaxial line configuration for microwave power transmission study of YBa₂Cu₃O(7- δ) thin films p 154 A92-18455

COAXIAL NOZZLES

- Coaxial injector spray characterization using water/air as simulants p 82 N92-14112
[NASA-TM-105322]

COAXIAL PLASMA ACCELERATORS

- Preliminary investigation of power flow and electrode phenomena in a multi-megawatt coaxial plasma thruster [AIAA PAPER 92-3741] p 75 A92-54144

COBALT

- The 23 to 300 C demagnetization resistance of samarium-cobalt permanent magnets p 159 N92-11252
[NASA-TP-3119]

- Elevated temperature axial and torsional fatigue behavior of Haynes 188 p 229 N92-26701
[NASA-TM-105396]

COBALT COMPOUNDS

- Method of intercalating large quantities of fibrous structures p 107 N92-16025
[NASA-CASE-LEW-15077-1]

CODE DIVISION MULTIPLE ACCESS

- A personal communications network using a Ka-band satellite p 151 N92-30934

CODERS

- Real-time demonstration hardware for enhanced DPCM video compression algorithm p 150 N92-19700
[NASA-TM-105616]

CODING

- Real-time data compression of broadcast video signals p 147 N92-10128
[NASA-CASE-LEW-14945-2]

- Least Reliable Bits Coding (LRBC) for high data rate satellite communications p 150 N92-18921
[NASA-TM-105431]

- Subband coding for image data archiving p 151 N92-20032
[NASA-TM-105407]

- Advanced Modulation and Coding Technology Conference p 51 N92-22001
[NASA-CP-10053]

- NASA, Lewis Research Center Advanced Modulation and Coding Project: Introduction and overview p 51 N92-22002

COEFFICIENT OF FRICTION

- Studies of mechanochemical interactions in the tribological behavior of materials p 124 A92-32410

- Properties data for opening the Galileo's partially unfurled main antenna p 130 N92-20660
[NASA-TM-105355]

COLLAPSE

- Collapse analysis of a waffle plate strongback for Space Station Freedom p 227 N92-20045
[NASA-TM-105412]

COLLIMATION

- Multiple-access phased array antenna simulator for a digital beam forming system investigation p 149 N92-17062
[NASA-TM-105422]

- The ACTS multibeam antenna p 52 N92-30383
[NASA-TM-105645]

COLLISIONAL PLASMAS

- Reactive collision terms for fluid transport theory p 257 A92-22693

COLLOCATION

- Mappings and accuracy for Chebyshev pseudo-spectral approximations p 248 A92-50469

COLOR

- Color image processing and object tracking workstation p 139 N92-26611
[NASA-TM-105561]

COLOR TELEVISION

- Real-time demonstration hardware for enhanced DPCM video compression algorithm p 150 N92-19700
[NASA-TM-105616]

- A video event trigger for high frame rate, high resolution video technology p 160 N92-22453

COMBINED STRESS

- Nonuniform thermal environmental effects on space truss structural reliability p 54 A92-34325
[AIAA PAPER 92-2352]

COMBUSTIBLE FLOW

- Model free simulations of a high speed reacting mixing layer p 167 A92-25715
[AIAA PAPER 92-0257]

- A continuous mixing model for pdf simulations and its applications to combustor shear flows p 174 A92-40139

- Computation of H₂/air reacting flowfields in drag-reduction external combustion p 182 A92-54115
[AIAA PAPER 92-3672]

- Chemical reacting flows p 188 N92-22525

COMBUSTION

- Advanced nozzle and engine components test facility [AIAA PAPER 92-3993] p 41 A92-56816

- Risks, designs, and research for fire safety in spacecraft p 240 N92-13581
[NASA-TM-105317]

- Advanced nozzle and engine components test facility [NASA-TM-103684] p 42 N92-17059

- Microgravity combustion science: Progress, plans, and opportunities p 139 N92-27197
[NASA-TM-105410]

COMBUSTION CHAMBERS

- Reliability analysis of a structural ceramic combustion chamber p 24 A92-15591
[ASME PAPER 91-GT-155]

- CFD analysis of jet mixing in low NO(x) flametube combustors p 24 A92-15634
[ASME PAPER 91-GT-217]

- A new unsteady mixing model to predict NO(x) production during rapid mixing in a dual-stage combustor [AIAA PAPER 92-0233] p 25 A92-25696

- A simplified dynamic model of Space Shuttle Main Engine p 60 A92-29289

- A parametric numerical study of mixing in a cylindrical duct p 177 A92-48733
[AIAA PAPER 92-3088]

- Mixing in the dome region of a staged gas turbine combustor p 177 A92-48734
[AIAA PAPER 92-3089]

- Experimental study of cross-stream mixing in a rectangular duct p 178 A92-48735
[AIAA PAPER 92-3090]

- An experimental investigation of high-aspect-ratio cooling passages p 64 A92-48780
[AIAA PAPER 92-3154]

- 3D rocket combustor acoustics model p 66 A92-48829
[AIAA PAPER 92-3228]

- Applied analytical combustion/emissions research at the NASA Lewis Research Center - A progress report [AIAA PAPER 92-3338] p 27 A92-54025

- The VRT gas turbine combustor - Phase II p 27 A92-54035
[AIAA PAPER 92-3471]

- Mechanical behaviour and failure phenomenon of an in situ toughened silicon nitride p 127 A92-54504
Combustion and core noise p 254 N92-10607

- High temperature thruster technology for spacecraft propulsion p 82 N92-15125
[NASA-TM-105348]

- Safety considerations in testing a fuel-rich aeroproulsion gas generator p 30 N92-17061
[NASA-TM-105258]

- High-temperature durability considerations for HSCST combustor p 129 N92-17070
[NASA-TP-3162]

- Combustion-wave ignition for rocket engines p 84 N92-20043
[NASA-TM-105545]

- Aircraft engine hot section technology: An overview of the HOST Project p 33 N92-22535

- Effects of chemical equilibrium on turbine engine performance for various fuels and combustor temperatures p 34 N92-23254
[NASA-TM-105399]

- An experimental investigation of high-aspect-ratio cooling passages p 48 N92-25958
[NASA-TM-105679]

- A parametric numerical study of mixing in a cylindrical duct p 35 N92-26553
[NASA-TM-105695]

- The 3D rocket combustor acoustics model p 88 N92-27035
[NASA-TM-105734]

- Experimental study of cross-stream mixing in a rectangular duct p 36 N92-27652
[NASA-TM-105694]

- Applied analytical combustion/emissions research at the NASA Lewis Research Center p 90 N92-29343
[NASA-TM-105731]

COMBUSTION CHEMISTRY

- Combustion kinetics and sensitivity analysis computations p 112 A92-16981
[NASA-TM-105730]

- Combustion synthesis of TiB₂-Al₂O₃-Al composite materials p 102 A92-36391
[NASA-TM-105750]

- The structure of premixed particle-cloud flames p 114 A92-43779

- Combustion synthesis of ceramic-metal composite materials - The TiC-Al₂O₃-Al system p 115 A92-55139

COMBUSTION EFFICIENCY

- A new unsteady mixing model to predict NO(x) production during rapid mixing in a dual-stage combustor [AIAA PAPER 92-0233] p 25 A92-25696

- Effect of model selection on combustor performance and stability using ROCCID --- Rocket Combustor Interactive Design p 65 A92-48827
[AIAA PAPER 92-3226]

- Effect of model selection on combustor performance and stability predictions using ROCCID p 89 N92-27036
[NASA-TM-105750]

COMBUSTION PHYSICS

- Some further observations on droplet combustion characteristics - NASA LeRC-Princeton results p 111 A92-12897

- The implications of experimentally controlled gravitational accelerations for combustion science p 112 A92-16601
[AIAA PAPER 91-398]

- The NASA microgravity combustion space experiment program p 112 A92-18484

- Intensified array camera imaging of solid surface combustion aboard the NASA Learjet [AIAA PAPER 92-0240] p 137 A92-25702
- Conical detonation waves - A comparison of theoretical and numerical results [AIAA PAPER 92-0348] p 167 A92-25792
- Combustion of liquid-fuel droplets in supercritical conditions p 114 A92-43778
- Observations of soot during droplet combustion at low gravity - Heptane and heptane/monochloroalkane mixtures p 115 A92-50447
- Numerical study of shock-wave/boundary-layer interactions in premixed combustible gases p 183 A92-54907
- Combustion and core noise p 254 N92-10607
- Intensified array camera imaging of solid surface combustion aboard the NASA Learjet [NASA-TM-105361] p 138 N92-16156
- Aircraft engine hot section technology: An overview of the HOST Project p 33 N92-22535
- Implementation of a kappa-epsilon turbulence model to RPLUS3D code p 194 N92-25822
- COMBUSTION STABILITY**
- Effect of model selection on combustor performance and stability using ROCCID --- Rocket Combustor Interactive Design [AIAA PAPER 92-3226] p 65 A92-48827
- 3D rocket combustor acoustics model [AIAA PAPER 92-3228] p 66 A92-48829
- JANNAF Liquid Rocket Combustion Instability Panel research recommendations p 115 N92-11124
- The 3D rocket combustor acoustics model [NASA-TM-105734] p 88 N92-27035
- Effect of model selection on combustor performance and stability predictions using ROCCID [NASA-TM-105750] p 89 N92-27036
- COMMERCIAL AIRCRAFT**
- Effects of turbine cooling assumptions on performance and sizing of high-speed civil transport [NASA-TM-105610] p 34 N92-23537
- COMMERCIAL SPACECRAFT**
- Laser beamed power - Satellite demonstration applications [IAF PAPER 92-0600] p 76 A92-57056
- COMMUNICATION EQUIPMENT**
- Overview of Ka-band communications technology requirements for the space exploration initiative [NASA-TM-105308] p 269 N92-14953
- COMMUNICATION NETWORKS**
- 20/30 GHz satellite personal communications networks [AIAA PAPER 92-1908] p 143 A92-29839
- Achieving spectrum conservation for the minimum span and minimum-order frequency assignment problems [AIAA PAPER 92-1960] p 143 A92-29883
- Technology requirements for mesh VSAT applications [AIAA PAPER 92-1982] p 144 A92-29902
- Predictive onboard flow control in packet switching satellites [AIAA PAPER 92-2004] p 144 A92-29923
- Circuit-switch architecture for a 30/20-GHz FDMA/TDM geostationary satellite communications network [AIAA PAPER 92-2005] p 49 A92-29924
- Interference susceptibility measurements for an MSK satellite communication link [AIAA PAPER 92-2018] p 144 A92-29936
- A personal communications network using a Ka-band satellite [AIAA PAPER 92-1982] p 144 A92-29902
- Data Distribution Satellite p 146 A92-48224
- Evaluation of components, subsystems, and networks for high rate, high frequency space communications [NASA-TM-105274] p 147 N92-12151
- Space Communications Technology Conference: Onboard Processing and Switching [NASA-CP-3132] p 147 N92-14202
- Destination directed packet switch architecture for a 30/20 GHz FDMA/TDM geostationary communication satellite network p 148 N92-14204
- An overview of Space Communication Artificial Intelligence for Link Evaluation Terminal (SCAILET) Project p 148 N92-14212
- Circuit-switch architecture for a 30/20-GHz FDMA/TDM geostationary satellite communications network [NASA-TM-105302] p 51 N92-15109
- Interference susceptibility measurements for an MSK satellite communication link [NASA-TM-105395] p 149 N92-15306
- Predictive onboard flow control for packet switching satellites [NASA-TM-105566] p 150 N92-19379
- Achieving spectrum conservation for the minimum-span and minimum-order frequency assignment problems [NASA-TM-105649] p 52 N92-23187
- The ACTS multibeam antenna [NASA-TM-105645] p 52 N92-30383
- A personal communications network using a Ka-band satellite p 151 N92-30934
- COMMUNICATION SATELLITES**
- Advances in MMIC technology for communications satellites [AIAA PAPER 92-1899] p 155 A92-29830
- Technology requirements for mesh VSAT applications [AIAA PAPER 92-1982] p 144 A92-29902
- A personal communications network using a Ka-band satellite p 145 A92-31780
- Data Distribution Satellite p 146 A92-48224
- Satcom systems and technologies into the 21st century [IAF PAPER 92-0412] p 147 A92-55792
- Destination directed packet switch architecture for a geostationary communication satellite network [IAF PAPER 92-0413] p 50 A92-55793
- Space Communications Technology Conference: Onboard Processing and Switching [NASA-CP-3132] p 147 N92-14202
- Destination directed packet switch architecture for a 30/20 GHz FDMA/TDM geostationary communication satellite network p 148 N92-14204
- On-board congestion control for satellite packet switching networks p 148 N92-14228
- Destination-directed, packet-switching architecture for 30/20-GHz FDMA/TDM geostationary communications satellite network [NASA-TP-3201] p 51 N92-19762
- Future communications satellite applications p 52 N92-22019
- COMPARISON**
- Structural scaling approximations for solar arrays p 231 A92-40935
- COMPENSATORS**
- Linear quadractic servo control of a reusable rocket engine [NASA-TM-105291] p 79 N92-11128
- COMPONENT RELIABILITY**
- Transmission overhaul and component replacement predictions using Weibull and renewal theory p 215 A92-17201
- Fault diagnosis for the Space Shuttle main engine p 60 A92-28137
- Advanced Rotorcraft Transmission program summary [AIAA PAPER 92-3363] p 205 A92-48936
- FIDEX: An expert system for satellite diagnostics p 148 N92-14218
- COMPOSITE MATERIALS**
- Combustion synthesis of ceramic-metal composite materials - The TiC-Al₂O₃-Al system p 115 A92-55139
- Asymmetric tip morphology of creep microcracks growing along bimaterial interfaces p 127 A92-56585
- Phase transformations in SrAl₂Si₂O₈ glass [NASA-TM-105657] p 264 N92-23890
- Heat transfer device [NASA-CASE-LEW-14162-3] p 111 N92-34208
- COMPOSITE STRUCTURES**
- Relationship between voids and interlaminar shear strength of polymer matrix composites p 98 A92-10241
- Multiojective shape and material optimization of composite structures including damping p 218 A92-28055
- Effect of contact stresses in four-point bend testing of graphite/epoxy and graphite/PMR-15 composite beams p 219 A92-33589
- Structural tailoring/analysis for hypersonic components - Executive system development [AIAA PAPER 92-2471] p 219 A92-34360
- Multidisciplinary tailoring of hot composite structures [AIAA PAPER 92-2563] p 220 A92-34564
- Structural durability of stiffened composite shells [AIAA PAPER 92-2244] p 220 A92-34569
- Free vibrations of delaminated beams p 222 A92-36853
- HITCAN for actively cooled hot-composite thermostructural analysis [ASME PAPER 91-GT-116] p 222 A92-36896
- Damage and fracture in composite thin shells p 224 A92-51550
- Damage and fracture in composite thin shells [NASA-TM-105289] p 106 N92-13284
- High temperature structural fibers: Status and needs [NASA-TM-105174] p 107 N92-16037
- Probabilistic structural analysis of adaptive/smart/intelligent space structures [NASA-TM-105408] p 227 N92-22267
- Composite overwrapped nickel-hydrogen pressure vessels p 109 N92-22762
- Detecting Lamb waves with broad-band acousto-ultrasonic signals in composite structures [NASA-TM-105557] p 216 N92-23189
- Progressive fracture of polymer matrix composite structures: A new approach [NASA-TM-105574] p 109 N92-23194
- Coupled multi-disciplinary simulation of composite engine structures in propulsion environment [NASA-TM-105575] p 228 N92-23267
- Free vibrations of delaminated beams [NASA-TM-105582] p 109 N92-25754
- Computer codes developed and under development at Lewis p 244 N92-25913
- A brief overview of computational structures technology related activities at NASA Lewis Research Center p 229 N92-25915
- Structural durability of stiffened composite shells [NASA-CR-190588] p 229 N92-29342
- Graphite/epoxy composite adapters for the Space Shuttle/Centaur vehicle [NASA-TP-3014] p 49 N92-31251
- Probabilistic assessment of space trusses subjected to combined mechanical and thermal loads [NASA-TM-105429] p 230 N92-33935
- COMPRESSIBILITY**
- Breakdown of the Karman vortex street due to forced convection and flow compressibility [NASA-TM-105853] p 196 N92-32472
- COMPRESSIBILITY EFFECTS**
- Compressibility effects on large structures in free shear flows p 173 A92-39337
- Unsteady blade pressures on a propfan - Predicted and measured compressibility effects [AIAA PAPER 92-3774] p 14 A92-54161
- On the basic equations for the second-order modeling of compressible turbulence [NASA-TM-105277] p 184 N92-11302
- Modeling of compressible turbulent shear flows p 189 N92-23340
- On the basic equations for the second-order modeling of compressible turbulence p 190 N92-23351
- COMPRESSIBLE BOUNDARY LAYER**
- A fast, uncoupled, compressible, two-dimensional, unsteady boundary layer algorithm with separation for engine inlets [AIAA PAPER 92-3082] p 11 A92-48729
- A fast, uncoupled, compressible, two-dimensional, unsteady boundary layer algorithm with separation for engine inlets [NASA-TM-105686] p 195 N92-27653
- COMPRESSIBLE FLOW**
- Euler flow predictions for an oscillating cascade using a high resolution wave-split scheme [ASME PAPER 91-GT-198] p 3 A92-15623
- Acoustic analysis using numerical solutions of the Navier-Stokes equations [AIAA PAPER 92-0506] p 253 A92-26934
- Numerical experiments on a new class of nonoscillatory schemes [AIAA PAPER 92-0421] p 7 A92-28193
- Navier-Stokes analysis of turbomachinery blade external heat transfer p 170 A92-28518
- Linear stability of compressible Taylor-Couette flow p 173 A92-36187
- Navier-Stokes analysis and experimental data comparison of compressible flow in a diffusing S-duct [AIAA PAPER 92-2699] p 10 A92-45541
- Interface of an uncoupled boundary layer algorithm with an inviscid core flow algorithm for unsteady supersonic engine inlets [AIAA PAPER 92-3083] p 11 A92-48730
- An investigation of shock/turbulent boundary layer bleed interactions [AIAA PAPER 92-3085] p 182 A92-54008
- Filtered Rayleigh scattering based measurements in compressible mixing layers [AIAA PAPER 92-3543] p 182 A92-54043
- An experimental investigation of the flow in a diffusing S-duct [AIAA PAPER 92-3622] p 13 A92-54090
- Study of compressible mixing layers using filtered Rayleigh scattering based visualizations p 183 A92-54937
- Center for Modeling of Turbulence and Transition (CMOTT). Research briefs. 1990 [NASA-TM-105243] p 1 N92-23336
- On the basic equations for the second-order modeling of compressible turbulence p 190 N92-23351
- Simulations of free shear layers using a compressible kappa-epsilon model p 190 N92-23355
- Long time behavior of unsteady flow computations [NASA-TM-105584] p 190 N92-23565
- Interface of an uncoupled boundary layer algorithm with an inviscid core flow algorithm for unsteady supersonic engine inlets [NASA-TM-105684] p 36 N92-27037
- Navier-Stokes analysis and experimental data comparison of compressible flow within ducts [NASA-TM-105796] p 38 N92-30972

COMPRESSIBLE FLUIDS

- Breakdown of the Karman vortex street due to forced convection and flow compressibility [NASA-TM-105853] p 196 N92-32472
- Navier-Stokes analysis and experimental data comparison of compressible flow in a diffusing S-duct [NASA-TM-105683] p 38 N92-33746
- COMPRESSIBLE FLUIDS**
- Investigation of two and three parameter equations of state for cryogenic fluids p 140 A92-13413
- Critical fluid thermal equilibration experiment (19-IML-1) p 139 N92-23640
- COMPRESSION LOADS**
- 1200 and 1300 K slow plastic compression properties of Ni-50Al composites p 102 A92-38125
- Damage mechanisms in bithermal and thermomechanical fatigue of Haynes 188 [NASA-TM-105381] p 228 N92-24985
- COMPRESSION TESTS**
- Slow strain rate 1200-1400 K compressive properties of NiAl-1Hf p 116 A92-17977
- COMPRESSIVE STRENGTH**
- Compressive strength of directionally solidified NiAl-NiAlNb intermetallics at 1200 and 1300 K p 117 A92-28248
- Compression, bend, and tension studies on forged Al67Ti25Cr8 and Al66Ti25Mn(g) L1(2) compounds p 118 A92-30766
- Compression studies on particulate composites of ternary Al-Ti-Fe, and quaternary Al-Ti-Fe-Nb and Al-Ti-Fe-Mn L1(2) compounds p 119 A92-30845
- Tension, compression, and bend properties for SiC/RBSN composites p 100 A92-32727
- Correlation of deformation mechanisms with the tensile and compressive behavior of NiAl and NiAl(Zr) intermetallic alloys p 120 A92-38019
- 1400 and 1500 K compressive creep properties of an NiAl-AlN composite p 103 A92-41575
- COMPRESSOR BLADES**
- The effect of steady aerodynamic loading on the flutter stability of turbomachinery blading [ASME PAPER 91-GT-130] p 2 A92-15574
- COMPRESSOR EFFICIENCY**
- A viscous flow study of shock-boundary layer interaction, radial transport, and wake development in a transonic compressor [ASME PAPER 91-GT-69] p 2 A92-15539
- COMPRESSORS**
- Small engine components test facility compressor testing cell at NASA Lewis Research Center [AIAA PAPER 92-3980] p 41 A92-56806
- The aerodynamic effect of fillet radius in a low speed compressor cascade [NASA-TM-105347] p 29 N92-14063
- Small engine components test facility compressor testing cell at NASA Lewis Research Center [NASA-TM-105685] p 42 N92-30508
- Navier-Stokes analysis and experimental data comparison of compressible flow within ducts [NASA-TM-105796] p 38 N92-30972
- Method of reducing drag in aerodynamic systems [NASA-CASE-LEW-14791-1] p 21 N92-34243
- COMPUTATIONAL ASTROPHYSICS**
- Dark matter and the equivalence principle p 267 A92-14477
- Monte Carlo exploration of Mikheyev-Smirnov-Wolfenstein solutions to the solar neutrino problem p 270 A92-50927
- COMPUTATIONAL FLUID DYNAMICS**
- NASA low-speed centrifugal compressor for 3-D viscous code assessment and fundamental flow physics research [ASME PAPER 91-GT-140] p 3 A92-15580
- CFD analysis of jet mixing in low NO(x) flametube combustors [ASME PAPER 91-GT-217] p 24 A92-15634
- The numerical simulation of a high-speed axial flow compressor [ASME PAPER 91-GT-272] p 3 A92-15669
- Unsteady blade-surface pressures on a large-scale advanced propeller - Prediction and data p 3 A92-17178
- Navier-Stokes analysis of flow and heat transfer inside high-pressure-ratio transonic turbine blade rows p 165 A92-17193
- Eigenvalue calculation procedure for an Euler/Navier-Stokes solver with application to flows over airfoils p 3 A92-17429
- Nonlinear dynamics near the stability margin in rotating pipe flow p 165 A92-19959
- A study on vortex flow control of inlet distortion in the re-engined 727-100 center inlet duct using computational fluid dynamics [AIAA PAPER 92-0152] p 4 A92-23767
- Hot gas environment around STOVL aircraft in ground proximity. II - Numerical study p 25 A92-24403
- Convection in superposed fluid and porous layers p 166 A92-24752
- Model free simulations of a high speed reacting mixing layer [AIAA PAPER 92-0257] p 167 A92-25715
- Low-to-high altitude predictions of three-dimensional ablative reentry flowfields [AIAA PAPER 92-0366] p 168 A92-26227
- Numerical investigation of performance degradation of wings and rotors due to icing [AIAA PAPER 92-0412] p 5 A92-26264
- Automatic grid generation for iced airfoil flowfield predictions [AIAA PAPER 92-0415] p 6 A92-26266
- Acoustic analysis using numerical solutions of the Navier-Stokes equations [AIAA PAPER 92-0506] p 253 A92-26934
- Unsteady flowfield simulation of ducted prop-fan configurations [AIAA PAPER 92-0521] p 6 A92-26946
- An unsteady Euler scheme for the analysis of ducted propellers [AIAA PAPER 92-0522] p 6 A92-26947
- The NASA Computational Aerosciences Program - Toward teraFLOPS computing [AIAA PAPER 92-0558] p 240 A92-26968
- Calculations of hot gas ingestion for a STOVL aircraft model [AIAA PAPER 92-0385] p 25 A92-28191
- Aeroelastic analysis of advanced propellers using an efficient Euler solver [AIAA PAPER 92-0488] p 7 A92-28194
- Navier-Stokes solution of transonic cascade flows using nonperiodic C-type grids p 8 A92-28523
- Three-dimensional viscous analysis of a Mach 5 inlet and comparison with experimental data p 8 A92-28526
- Upwind relaxation methods for the Navier-Stokes equations using inner iterations p 170 A92-29553
- A numerical and experimental study of three-dimensional liquid sloshing in a rotating spherical container [AIAA PAPER 92-0829] p 170 A92-29597
- Nonlinear spatial equilibration of an externally excited instability wave in a free shear layer p 170 A92-31469
- Analysis of cascades using a two dimensional Euler aeroelastic solver [AIAA PAPER 92-2370] p 26 A92-34598
- An error analysis of least-squares finite element method of velocity-pressure-vorticity formulation for Stokes problem p 173 A92-37506
- A continuous mixing model for pdf simulations and its applications to combusting shear flows p 174 A92-40139
- Numerical analysis of flow through oscillating cascade sections p 9 A92-44513
- Experimental and analytical study of close-coupled ventral nozzles for ASTOVL aircraft p 26 A92-45325
- Navier-Stokes analysis and experimental data comparison of compressible flow in a diffusing S-duct [AIAA PAPER 92-2699] p 10 A92-45541
- Predicted pressure distribution on a prop-fan blade through Euler analysis p 10 A92-46791
- Implementation of control point form of algebraic grid-generation technique p 248 A92-47058
- DSMC analysis of species separation in rarefied nozzle flows [AIAA PAPER 92-2859] p 176 A92-47842
- The Osher scheme for non-equilibrium reacting flows p 176 A92-48149
- Quasi-steady turbulence modeling of unsteady flows p 177 A92-48204
- Computational analysis of ramjet engine inlet interaction [AIAA PAPER 92-3102] p 11 A92-48744
- Perturbation of a normal shock - A test case for unsteady Euler codes [AIAA PAPER 92-3180] p 178 A92-48795
- Numerical simulation of geometric scale effects in cylindrical self-field MPD thrusters [AIAA PAPER 92-3297] p 258 A92-48885
- Rocket plume flowfield characterization using laser Rayleigh scattering [AIAA PAPER 92-3351] p 66 A92-48928
- Propulsion-related flowfields using the preconditioned Navier-Stokes equations [AIAA PAPER 92-3437] p 178 A92-48994
- A computational study of advanced exhaust system transition ducts with experimental validation [AIAA PAPER 92-3794] p 179 A92-49126
- Kinetic theory model for the flow of a simple gas from a three-dimensional axisymmetric nozzle p 12 A92-52730
- A comparison of the calculated and experimental off-design performance of a radial flow turbine [AIAA PAPER 92-3069] p 13 A92-54004
- Full Navier-Stokes calculations on the installed F/A-18 inlet at a high angle of attack [AIAA PAPER 92-3175] p 13 A92-54012
- Application of computational fluid dynamics to the study of vortex flow control for the management of inlet distortion [AIAA PAPER 92-3177] p 13 A92-54013
- Flunge-Kutta methods combined with compact difference schemes for the unsteady Euler equations [AIAA PAPER 92-3210] p 182 A92-54015
- Applied analytical combustion/emissions research at the NASA Lewis Research Center - A progress report [AIAA PAPER 92-3338] p 27 A92-54025
- A time-accurate algorithm for chemical non-equilibrium viscous flows at all speeds [AIAA PAPER 92-3639] p 182 A92-54112
- Grid generation for 3D turbomachinery configurations [AIAA PAPER 92-3671] p 243 A92-54114
- Computation of H2/air reacting flowfields in drag-reduction external combustion [AIAA PAPER 92-3672] p 182 A92-54115
- Computational and experimental investigation of subsonic internal reversing flows [AIAA PAPER 92-3791] p 183 A92-54170
- A study on vortex flow control on inlet distortion in the re-engined 727-100 center inlet duct using computational fluid dynamics [NASA-TM-105321] p 14 N92-13998
- Seals Flow Code Development [NASA-CP-10070] p 49 N92-15082
- ULTRA-SHARP solution of the Smith-Hutton problem [NASA-TM-105435] p 187 N92-22226
- An investigation of DTNS2D for use as an incompressible turbulence modelling test-bed [NASA-TM-105593] p 249 N92-22230
- Turbomachinery p 32 N92-22524
- High-speed inlet research program and supporting analysis p 188 N92-22542
- Center for Modeling of Turbulence and Transition (CMOTT). Research briefs: 1990 [NASA-TM-105243] p 1 N92-23336
- Turbulence modeling p 189 N92-23338
- Modeling of compressible turbulent shear flows p 189 N92-23340
- Advancements in engineering turbulence modeling [PAPER-105] p 189 N92-23350
- A two-dimensional Euler solution for an unbladed jet engine configuration [NASA-TM-105329] p 190 N92-23560
- Interactive solution-adaptive grid generation procedure [NASA-TM-105432] p 18 N92-23563
- Interactive solution-adaptive grid generation p 243 N92-24420
- MAG3D and its application to internal flowfield analysis p 243 N92-24421
- Workshop on Engineering Turbulence Modeling [NASA-CP-10088] p 191 N92-24514
- A two-dimensional Euler solution for an unbladed jet engine configuration p 18 N92-24861
- Conservative-variable average states for equilibrium gas multi-dimensional fluxes [NASA-TM-105585] p 191 N92-25196
- Two-dimensional unstructured triangular grid generation p 192 N92-25721
- Cartesian based grid generation/adaptive mesh refinement p 192 N92-25722
- Computational Fluid Dynamics --- numerical methods and algorithm development p 35 N92-25808
- [NASA-CP-10078] p 35 N92-25808
- Development of new flux splitting schemes --- computational fluid dynamics algorithms p 192 N92-25809
- An iterative implicit DDADI algorithm for solving the Navier-Stokes equation --- upwind split flux technique p 192 N92-25810
- The Proteus Navier-Stokes code --- two and three dimensional computational fluid dynamics p 192 N92-25811
- Accurate upwind-monotone (nonoscillatory) methods for conservation laws p 193 N92-25812
- Numerical simulation of conservation laws p 193 N92-25813
- A new Lagrangian method for real gases at supersonic speed p 19 N92-25814
- Study of shock-induced combustion using an implicit TVD scheme p 116 N92-25816
- Upwind schemes and bifurcating solutions in real gas computations p 193 N92-25817
- High order parallel numerical schemes for solving incompressible flows p 193 N92-25818
- Advances in engineering turbulence modeling --- computational fluid dynamics p 193 N92-25820
- Implementation of a kappa-epsilon turbulence model to RPLUS3D code p 194 N92-25822
- Turbulence and deterministic chaos --- computational fluid dynamics p 194 N92-25823

- Techniques for animation of CFD results ...
 computational fluid dynamics p 194 N92-25825
- Distributed visualization for computational fluid
 dynamics p 194 N92-25826
- Rocket plume flowfield characterization using laser
 Rayleigh scattering
 [NASA-TM-105739] p 257 N92-28475
- Applied analytical combustion/emissions research at the
 NASA Lewis Research Center
 [NASA-TM-105731] p 90 N92-29343
- Navier-Stokes analysis and experimental data
 comparison of compressible flow within ducts
 [NASA-TM-105796] p 38 N92-30972
- A general numerical model for wave rotor analysis
 [NASA-TM-105740] p 196 N92-31484
- Three-dimensional flow fields inside a shrouded inducer
 at design and off-design conditions (CFD study)
 p 196 N92-32291
- Breakdown of the Karman vortex street due to forced
 convection and flow compressibility
 [NASA-TM-105853] p 196 N92-32472
- A new time scale based k-epsilon model for near wall
 turbulence
 [NASA-TM-105768] p 196 N92-32868
- Navier-Stokes analysis and experimental data
 comparison of compressible flow in a diffusing S-duct
 [NASA-TM-105683] p 38 N92-33746
- Application of computational fluid dynamics to the study
 of vortex flow control for the management of inlet
 distortion
 [NASA-TM-105672] p 230 N92-34112
- COMPUTATIONAL GRIDS**
- Analysis of an advanced ducted propeller subsonic
 inlet
 [AIAA PAPER 92-0274] p 5 A92-25728
- Navier-Stokes solution of transonic cascade flows using
 nonperiodic C-type grids p 8 A92-28523
- Multigrd calculations of a jet in crossflow
 p 170 A92-28525
- Domain-decomposition algorithm applied to
 multielement airfoil grids p 9 A92-41261
- Effect of spatial resolution on apparent sensitivity to
 initial conditions of a decaying flow as it becomes
 turbulent p 175 A92-45716
- Implementation of control point form of algebraic
 grid-generation technique p 248 A92-47058
- A conformal block structured grid for turbomachinery
 cascades in two dimensions p 248 A92-47059
- Grid quality improvement by a grid adaptation
 technique p 248 A92-47072
- Comparisons of cylindrical and rectangular media
 radiative transfer solutions using the S-N discrete ordinates
 method
 [AIAA PAPER 92-2894] p 266 A92-54287
- Multigrd calculation of three-dimensional viscous
 cascade flows
 [NASA-TM-105257] p 249 N92-10345
- Analysis of an advanced ducted propeller subsonic
 inlet
 [NASA-TM-105393] p 15 N92-14002
- ULTRA-SHARP solution of the Smith-Hutton problem
 [NASA-TM-105435] p 187 N92-22226
- Interactive solution-adaptive grid generation procedure
 [NASA-TM-105432] p 18 N92-23563
- Interactive solution-adaptive grid generation
 p 243 N92-24420
- MAG3D and its application to internal flowfield
 analysis p 243 N92-24421
- A multiblock grid generation technique applied to a jet
 engine configuration p 244 N92-24428
- A two-dimensional Euler solution for an unbladed jet
 engine configuration p 18 N92-24861
- Workshop on Grid Generation and Related Areas
 [NASA-CP-10089] p 35 N92-25712
- Grid management p 19 N92-25713
- QX MAN: O and X file manipulation p 244 N92-25715
- TIGGERC: Turbomachinery interactive grid generator
 energy distributor and restart code p 35 N92-25719
- Multiblock grid generation for jet engine configurations
 p 35 N92-25720
- Two-dimensional unstructured triangular grid
 generation p 192 N92-25721
- Cartesian based grid generation/adaptive mesh
 refinement p 192 N92-25722
- Interactive solution-adaptive grid generation procedure
 p 244 N92-25724
- Integrating aerodynamic surface modeling for
 computational fluid dynamics with computer aided
 structural analysis, design, and manufacturing
 p 192 N92-25727
- Turbulence and deterministic chaos ... computational
 fluid dynamics p 194 N92-25823
- Techniques for grid manipulation and adaptation ...
 computational fluid dynamics p 194 N92-25827
- Minimization of deviations of gear real tooth surfaces
 determined by coordinate measurements
 [NASA-TM-105718] p 214 N92-30948
- COMPUTER AIDED DESIGN**
- Neurobiological computational models in structural
 analysis and design p 245 A92-14509
- Structural reliability analysis of laminated CMC
 components
 [ASME PAPER 91-GT-210] p 99 A92-15630
- The NASA Computational Aerosciences Program -
 Toward teraFLOPS computing
 [AIAA PAPER 92-0558] p 240 A92-26968
- Computational simulation of concurrent engineering for
 aerospace propulsion systems
 [AIAA PAPER 92-1144] p 241 A92-33285
- HITCAN for actively cooled hot-composite
 thermostructural analysis
 [ASME PAPER 91-GT-116] p 222 A92-36896
- A method for determining spiral-bevel gear tooth
 geometry for finite element analysis
 [NASA-TP-3096] p 207 N92-10195
- Developments in REDES: The Rocket Engine Design
 Expert System p 78 N92-11120
- Computers in aeronautics and space research at the
 Lewis Research Center
 [NASA-TM-105096] p 241 N92-11642
- Integrating aerodynamic surface modeling for
 computational fluid dynamics with computer aided
 structural analysis, design, and manufacturing
 p 192 N92-25727
- Computer codes developed and under development at
 Lewis
 NASA Lewis steady-state heat pipe code users
 manual
 [NASA-TM-105161] p 90 N92-28682
- A parameter optimization approach to controller
 partitioning for integrated flight/propulsion control
 application
 [NASA-TM-105826] p 40 N92-32241
- COMPUTER AIDED MANUFACTURING**
- Recent manufacturing advances for spiral bevel gears
 [SAE PAPER 912229] p 204 A92-40024
- COMPUTER AIDED TOMOGRAPHY**
- NDE of advanced turbine engine components and
 materials by computed tomography
 [ASME PAPER 91-GT-287] p 215 A92-15681
- COMPUTER GRAPHICS**
- Implementation of control point form of algebraic
 grid-generation technique p 248 A92-47058
- A basis for solid modeling of gear teeth with application
 in design and manufacture
 [NASA-TM-105392] p 209 N92-24202
- Techniques for animation of CFD results ...
 computational fluid dynamics p 194 N92-25825
- Distributed visualization for computational fluid
 dynamics p 194 N92-25826
- Techniques for grid manipulation and adaptation ...
 computational fluid dynamics p 194 N92-25827
- PC graphics generation and management tool for
 real-time applications
 [NASA-TM-105749] p 244 N92-28684
- A graphical user-interface for propulsion system
 analysis
 [NASA-TM-105696] p 244 N92-33894
- COMPUTER NETWORKS**
- Interfacing laboratory instruments to multiuser, virtual
 memory computers p 245 A92-13595
- Predictive onboard flow control in packet switching
 satellites
 [AIAA PAPER 92-2004] p 144 A92-29923
- Predictive onboard flow control for packet switching
 satellites
 [NASA-TM-105566] p 150 N92-19379
- COMPUTER PROGRAMMING**
- Recent developments of the NESSUS probabilistic
 structural analysis computer program
 [AIAA PAPER 92-2411] p 242 A92-34342
- COMPUTER PROGRAMS**
- Relationship between voids and interlaminar shear
 strength of polymer matrix composites
 p 98 A92-10241
- METCAN updates for high temperature composite
 behavior - Simulation/verification p 98 A92-10264
- The application of a computer data acquisition system
 to a new high temperature tribometer
 p 93 A92-11823
- Interfacing laboratory instruments to multiuser, virtual
 memory computers p 245 A92-13595
- Euler flow predictions for an oscillating cascade using
 a high resolution wave-split scheme
 [ASME PAPER 91-GT-198] p 3 A92-15623
- Modeling of impulsive propellant reorientation
 p 59 A92-17187
- Computer program for computing the properties of
 seventeen fluids ... cryogenic liquids
 p 241 A92-23849
- LEWICE/E - An Euler based ice accretion code
 [AIAA PAPER 92-0037] p 4 A92-25676
- Prediction of ice accretion on a swept NACA 0012 airfoil
 and comparisons to flight test results
 [AIAA PAPER 92-0043] p 4 A92-25677
- Analysis of an advanced ducted propeller subsonic
 inlet
 [AIAA PAPER 92-0274] p 5 A92-25728
- A three-dimensional finite-element thermal/mechanical
 analytical technique for high-performance traveling wave
 tubes
 [AIAA PAPER 92-1824] p 154 A92-29771
- MisTec - A software application for supporting space
 exploration scenario options and technology development
 analysis and planning
 [AIAA PAPER 92-1293] p 242 A92-38490
- Implementation of control point form of algebraic
 grid-generation technique p 248 A92-47058
- Effect of model selection on combustor performance
 and stability using ROCCID ... Rocket Combustor
 Interactive Design
 [AIAA PAPER 92-3226] p 65 A92-48827
- 3D rocket combustor acoustics model
 [AIAA PAPER 92-3228] p 66 A92-48829
- Structural reliability assessment capability in NESSUS
 [AIAA PAPER 92-3417] p 223 A92-48976
- Three-dimensional calculations of supersonic reacting
 flows using an LU scheme p 179 A92-50465
- The development of test beds to support the definition
 and evolution of the Space Station Freedom power
 system p 46 A92-50656
- Damage and fracture in composite thin shells
 p 224 A92-51550
- Developments in REDES: The Rocket Engine Design
 Expert System p 78 N92-11120
- Computer program for Bessel and Hankel functions
 [NASA-TM-105154] p 243 N92-11691
- Development of a computer algorithm for the analysis
 of variable-frequency AC drives: Case studies included
 [NASA-TM-105327] p 29 N92-13070
- Parametric studies of phase change thermal energy
 storage canisters for Space Station Freedom
 [NASA-TM-105350] p 55 N92-13143
- Development of a single-phase harmonic power flow
 program to study the 20 kHz AC power system for large
 spacecraft
 [NASA-TM-105326] p 81 N92-13275
- Damage and fracture in composite thin shells
 [NASA-TM-105289] p 106 N92-13284
- Thermal modeling with solid/liquid phase change of the
 thermal energy storage experiment
 [NASA-TM-103770] p 185 N92-13402
- LEWICE/E: An Euler based ice accretion code
 [NASA-TM-105389] p 15 N92-14001
- Analysis of an advanced ducted propeller subsonic
 inlet
 [NASA-TM-105393] p 15 N92-14002
- MisTec: A software application for supporting space
 exploration scenario options and technology development
 analysis and planning
 [NASA-TM-105214] p 243 N92-14649
- Prediction of ice accretion on a swept NACA 0012 airfoil
 and comparisons to flight test results
 [NASA-TM-105368] p 16 N92-15968
- Supersonic propulsion simulation by incorporating
 component models in the large perturbation inlet (LAPIN)
 computer code
 [NASA-TM-105193] p 30 N92-15993
- A software control system for the ACTS high-burst-rate
 link evaluation terminal
 [NASA-TM-105207] p 243 N92-16628
- Viscous three-dimensional calculations of transonic fan
 performance
 [NASA-TM-103800] p 1 N92-17346
- Multiwavelength pyrometry for nongray surfaces in the
 presence of interfering radiation
 [NASA-TM-105286] p 201 N92-19107
- Towards the development of micromechanics equations
 for ceramic matrix composites via fiber substructuring
 [NASA-TM-105246] p 108 N92-19595
- Collapse analysis of a waffle plate strongback for Space
 Station Freedom
 [NASA-TM-105412] p 227 N92-20045
- Flow studies in close-coupled ventral nozzles for STOVL
 aircraft
 [NASA-TM-102554] p 17 N92-20934
- Icing simulation: A survey of computer models and
 experimental facilities p 21 N92-21684
- ULTRA-SHARP solution of the Smith-Hutton problem
 [NASA-TM-105435] p 187 N92-22226
- Improved accuracy for finite element structural analysis
 via a new integrated force method
 [NASA-TP-3204] p 227 N92-22227
- Overview of NASA PTA propan flight test program
 p 33 N92-22536

COMPUTER SYSTEMS DESIGN

- High-speed inlet research program and supporting analysis p 168 A92-22542
- Evaluation of MHOST analysis capabilities for a plate element --- finite element modeling [NASA-TM-105387] p 228 A92-23196
- Effects of chemical equilibrium on turbine engine performance for various fuels and combustor temperatures [NASA-TM-105399] p 34 A92-23254
- Minimization of the vibration energy of thin-plate structure [NASA-TM-105654] p 211 A92-25448
- TCGRID: A three dimensional C-grid generator for turbomachinery p 35 A92-25716
- The Proteus Navier-Stokes code --- two and three dimensional computational fluid dynamics p 192 A92-25811
- Techniques for grid manipulation and adaptation --- computational fluid dynamics p 194 A92-25827
- Computer codes developed and under development at Lewis p 244 A92-25913
- Progress towards understanding and predicting convection heat transfer in the turbine gas path [NASA-TM-105674] p 194 A92-26690
- Overview of NASA supported Stirling thermodynamic loss research [NASA-TM-105690] p 88 A92-27034
- The 3D rocket combustor acoustics model [NASA-TM-105734] p 88 A92-27035
- Effect of model selection on combustor performance and stability predictions using ROCCID [NASA-TM-105750] p 89 A92-27036
- Viscous three-dimensional calculations of transonic fan performance p 195 A92-27467
- Design characteristics of a heat pipe test chamber [NASA-TM-105737] p 238 A92-29662
- COMPUTER SYSTEMS DESIGN**
- A brief overview of computational structures technology related activities at NASA Lewis Research Center p 229 A92-25915
- COMPUTER TECHNIQUES**
- Computers in aeronautics and space research at the Lewis Research Center [NASA-TM-105096] p 241 A92-11642
- Development of a computer algorithm for the analysis of variable-frequency AC drives: Case studies included [NASA-TM-105327] p 29 A92-13070
- Integrating aerodynamic surface modeling for computational fluid dynamics with computer aided structural analysis, design, and manufacturing p 192 A92-25727
- Techniques for animation of CFD results --- computational fluid dynamics p 194 A92-25825
- Distributed visualization for computational fluid dynamics p 194 A92-25826
- COMPUTERIZED SIMULATION**
- Computational simulation of microfracture in high temperature metal matrix composites p 98 A92-10263
- Numerical simulations of space processing - The reality, the myth, and the future p 136 A92-12863
- Numerical investigation on Benard instability in a finite liquid layer p 164 A92-12865
- Numerical propulsion system simulation p 59 A92-20194
- Probabilistic constitutive relationships for cyclic material strength models p 217 A92-21081
- LDEXPT, an intelligent database system for the Composite Load Spectra project p 59 A92-23695
- Vorticity dynamics of inviscid shear layers [AIAA PAPER 92-0420] p 168 A92-26270
- Internal structure of shock waves in disparate mass mixtures [AIAA PAPER 92-0496] p 169 A92-28195
- A simplified dynamic model of Space Shuttle Main Engine p 60 A92-29289
- COSP - A computer model of cyclic oxidation p 114 A92-31849
- Computational simulation of high temperature metal matrix composite behavior p 101 A92-32753
- Computational simulation of concurrent engineering for aerospace propulsion systems [AIAA PAPER 92-1144] p 241 A92-33285
- Multidisciplinary tailoring of hot composite structures [AIAA PAPER 92-2563] p 220 A92-34564
- A review of computational/experimental methodology developments in aeroacoustics p 253 A92-39241
- DSMC analysis of species separation in rarefied nozzle flows [AIAA PAPER 92-2859] p 176 A92-47842
- Numerical modeling of fluid and electromagnetic phenomena in an arcjet [AIAA PAPER 92-3106] p 258 A92-48747
- Theoretical nozzle performance of a microwave electrothermal thruster using experimental data [AIAA PAPER 92-3110] p 64 A92-48750

- An EMTP system level model of the PMAD DC test bed p 46 A92-50657
- Damage and fracture in composite thin shells p 224 A92-51550
- Identification of the Space Shuttle Main Engine dynamic models from firing data [AIAA PAPER 92-3317] p 73 A92-54022
- Results from computational analysis of a mixed compression supersonic inlet [NASA-TM-104475] p 14 A92-10976
- Modeling of the heat transfer in bypass transitional boundary-layer flows [NASA-TP-3170] p 184 A92-11299
- Computers in aeronautics and space research at the Lewis Research Center [NASA-TM-105096] p 241 A92-11642
- Development of a single-phase harmonic power flow program to study the 20 kHz AC power system for large spacecraft [NASA-TM-105326] p 81 A92-13275
- Damage and fracture in composite thin shells [NASA-TM-105289] p 106 A92-13284
- A critical comparison of second order closures with direct numerical simulation of homogeneous turbulence [NASA-TM-105351] p 185 A92-15357
- Supersonic propulsion simulation by incorporating component models in the large perturbation inlet (LAPIN) computer code [NASA-TM-105193] p 30 A92-15993
- Icing simulation: A survey of computer models and experimental facilities p 21 A92-21684
- Simulation of iced wing aerodynamics p 21 A92-21686
- NASCAP/LEO simulations of Shuttle Orbiter charging during the SAMPIE experiment p 55 A92-22361
- NASA's aircraft icing technology program [NASA-TM-104518] p 17 A92-23105
- Numerical experiments with flows of elongated granules [NASA-TM-105567] p 209 A92-23226
- Coupled multi-disciplinary simulation of composite engine structures in propulsion environment [NASA-TM-105575] p 228 A92-23267
- A comparison between theoretical prediction and experimental measurement of the dynamic behavior of spur gears [NASA-TM-105362] p 210 A92-25347
- Effect of contact ratio on spur gear dynamic load [NASA-TM-105606] p 210 A92-25447
- Interactive solution-adaptive grid generation procedure p 244 A92-25724
- Techniques for animation of CFD results --- computational fluid dynamics p 194 A92-25825
- A mathematical constraint placed upon inter-blade row boundary conditions used in the simulation of multistage turbomachinery flows p 195 A92-27458
- Structural durability of stiffened composite shells [NASA-CR-190588] p 229 A92-29342
- Computational simulation of intermingled-fiber hybrid composite behavior [NASA-TM-105666] p 110 A92-31506
- Computational simulation of structural fracture in fiber composites p 111 A92-32531
- CONCENTRATION (COMPOSITION)**
- Effect of KOH concentration on LEO cycle life of IPV nickel-hydrogen flight cell - Update II p 232 A92-48212
- Effect of KOH concentration on LEO cycle life of IPV nickel-hydrogen flight cells-update 2 [NASA-TM-105314] p 235 A92-13483
- Composition dependence of superconductivity in YBa₂(Cu_{3-x})Al_xO_y [NASA-TM-105358] p 131 A92-24715
- CONCENTRATORS**
- Technology development of fabrication techniques for advanced solar dynamic concentrators p 232 A92-50571
- Concentrator testing using projected images p 69 A92-50615
- Thin film, concentrator, and multijunction space solar cells: Status and potential p 81 A92-13230
- Status and future directions of InP solar cell research [NASA-TM-105426] p 160 A92-18920
- CONCENTRIC CYLINDERS**
- Effects of fiber and interfacial layer architectures on the thermoplastic response of metal matrix composites [NASA-TM-105802] p 110 A92-32234
- CONCENTRIC SPHERES**
- Natural convection between concentric spheres p 179 A92-50445
- CONDENSATION**
- Effect of liquid surface turbulent motion on the vapor condensation in a mixing tank [NASA-TM-105555] p 187 A92-21498

CONDENSING

- Vapor condensation on liquid surface due to laminar jet-induced mixing p 164 A92-10446
- Modelling and experimental verification of a water alleviation system for the NASP --- National Aerospace Plane p 189 A92-23224

CONDUCTIVE HEAT TRANSFER

- Finite difference solution for transient cooling of a radiating-conducting semitransparent layer p 166 A92-20310
- An efficient finite element method for aircraft de-icing problems [AIAA PAPER 92-0532] p 22 A92-31670
- A variable multi-step method for transient heat conduction p 173 A92-37518
- Solutions of the heat conduction equation in multilayers for photothermal deflection experiments p 141 A92-52205
- Effects of anisotropic conduction and heat pipe interaction on minimum mass space radiators [NASA-TM-105297] p 80 A92-11138
- Thermal and solutal convection with conduction effects inside a rectangular enclosure [NASA-TM-105371] p 186 A92-15358
- Applications of high thermal conductivity composites to electronics and spacecraft thermal design [NASA-TM-102434] p 56 A92-24349

CONFERENCES

- Space Electrochemical Research and Technology Conference, 3rd, NASA Lewis Research Center, Cleveland, OH, Apr. 9, 10, 1991, Proceedings p 231 A92-18936
- Intermetallic matrix composites; Proceedings of the MRS Symposium, San Francisco, CA, Apr. 18-20, 1990 [ISBN 1-55899-083-6] p 104 A92-46826
- Magnetoplasmadynamic Thruster Workshop [NASA-CP-10084] p 77 A92-10044
- Space Communications Technology Conference: Onboard Processing and Switching [NASA-CP-3132] p 147 A92-14202
- Rotordynamic Instability Problems in High-Performance Turbomachinery, 1990 [NASA-CP-3122] p 207 A92-14346
- Advanced Modulation and Coding Technology Conference [NASA-CP-10053] p 51 A92-22001
- Aeropropulsion 1987 [NASA-CP-3049] p 31 A92-22510
- Workshop on Engineering Turbulence Modeling [NASA-CP-10088] p 191 A92-24514
- Workshop on Grid Generation and Related Areas [NASA-CP-10089] p 35 A92-25712
- International Workshop on Vibration Isolation Technology for Microgravity Science Applications [NASA-CP-10094] p 141 A92-28436
- Electrical and chemical interactions at Mars Workshop, part 1 [NASA-CP-10093] p 270 A92-30302

CONFORMAL MAPPING

- Mapping methods for computationally efficient and accurate structural reliability [AIAA PAPER 92-2347] p 219 A92-34321
- A conformal block structured grid for turbomachinery cascades in two dimensions p 248 A92-47059

CONGESTION

- On-board congestion control for satellite packet switching networks p 148 A92-14228

CONICAL BODIES

- Improved nonequilibrium viscous shock-layer scheme for hypersonic blunt-body flowfields p 4 A92-24653

CONICAL FLOW

- Conical detonation waves - A comparison of theoretical and numerical results [AIAA PAPER 92-0348] p 167 A92-25792
- High-Order Polynomial Expansions (HOPE) for flux-vector splitting p 190 A92-23353

CONICAL NOZZLES

- Arcjet nozzle area ratio effects [NASA-TM-104477] p 83 A92-16022

CONJUGATE GRADIENT METHOD

- A study of equation solvers for linear and non-linear finite element analysis on parallel processing computers [AIAA PAPER 92-2478] p 242 A92-34367

CONSERVATION

- Achieving spectrum conservation for the minimum-span and minimum-order frequency assignment problems [NASA-TM-105649] p 52 A92-18187

CONSERVATION LAWS

- Accurate upwind-monotone (nonoscillatory) methods for conservation laws p 193 A92-25812
- Numerical simulation of conservation laws p 193 A92-25813

CONSTITUTIVE EQUATIONS

- Probabilistic constitutive relationships for cyclic material strength models p 217 A92-21081

- A viscoplastic model for single crystals p 217 A92-24717
- A viscoplastic theory with thermodynamic considerations p 217 A92-26372 [ONERA, TP NO. 1991-220]
- On the development of explicit robust schemes for implementation of a class of hyperelastic models in large-strain analysis of rubbers p 221 A92-36245
- On the thermodynamic framework of generalized coupled thermoelastic-viscoplastic-damage modeling [NASA-TM-105349] p 225 N92-14434
- CONTACT LOADS**
- Effect of contact stresses in four-point bend testing of graphite/epoxy and graphite/PMR-15 composite beams p 219 A92-33589
- A system-approach to the elastohydrodynamic lubrication point-contact problem p 204 A92-35421
- Contact stresses in meshing spur gear teeth: Use of an incremental finite element procedure [NASA-TM-105388] p 209 N92-23536
- Effect of contact ratio on spur gear dynamic load [NASA-TM-105606] p 210 N92-25447
- Effect of operating conditions on gearbox noise [NASA-TM-105331] p 211 N92-26107
- CONTACT RESISTANCE**
- Sinterless contacts to shallow junction InP solar cells [NASA-TM-105670] p 237 N92-24802
- The achievement of low contact resistance to indium phosphide: The roles of Ni, Au, Ge, and combinations thereof [NASA-TM-105770] p 238 N92-33895
- CONTAINERLESS MELTS**
- Interfacial and gravitational convection in immiscible liquid layers [IAF PAPER 92-0907] p 184 A92-57286
- CONTAINERS**
- Drop-tower experiments for capillary surfaces in an exotic container p 166 A92-20743
- An experimental study of oscillatory thermocapillary convection in cylindrical containers p 172 A92-36184
- CONTAMINANTS**
- Applied analytical combustion/emissions research at the NASA Lewis Research Center - A progress report [AIAA PAPER 92-3338] p 27 A92-54025
- Method of making contamination-free ceramic bodies [NASA-CASE-LEW-14984-1] p 128 N92-16122
- Applied analytical combustion/emissions research at the NASA Lewis Research Center [NASA-TM-105731] p 90 N92-29343
- CONTAMINATION**
- A new technique for oil backstreaming contamination measurements [NASA-TM-105312] p 257 N92-13783
- CONTINUITY EQUATION**
- Turbulent fluid motion 3: Basic continuum equations [NASA-TM-104386] p 184 N92-11317
- CONTINUOUS WAVE LASERS**
- Space power by ground-based laser transmission [AIAA PAPER 92-3024] p 63 A92-47027
- Flow diagnostics of an arcjet using laser-induced fluorescence [AIAA PAPER 92-3243] p 199 A92-48843
- Space transfer with ground-based laser/electric propulsion [AIAA PAPER 92-3213] p 73 A92-54017
- CONTINUUM MECHANICS**
- Differential continuum damage mechanics models for creep and fatigue of unidirectional metal matrix composites [NASA-TM-105213] p 226 N92-16371
- A differential CDM model for fatigue of unidirectional metal matrix composites [NASA-TM-105726] p 230 N92-31505
- CONTINUUM MODELING**
- A continuum method for modeling surface tension p 175 A92-45707
- A differential CDM model for fatigue of unidirectional metal matrix composites [NASA-TM-105726] p 230 N92-31505
- CONTRAROTATING PROPELLERS**
- Noise of two high-speed model counter-rotation propellers at takeoff/approach conditions p 253 A92-46799
- Advanced propeller research p 33 N92-22537
- CONTROL**
- Preliminary dynamic tests of a flight-type ejector [AIAA PAPER 92-3261] p 27 A92-54020
- Preliminary dynamic tests of a flight-type ejector [NASA-TM-105814] p 38 N92-30998
- CONTROL EQUIPMENT**
- An electromechanical actuation system for an expendable launch vehicle [NASA-TM-105774] p 48 N92-30310
- Piloted evaluation of an integrated propulsion and flight control simulator [NASA-TM-105797] p 40 N92-34107

CONTROL SIMULATION

- Piloted evaluation of an integrated propulsion and flight control simulator [NASA-TM-105797] p 40 N92-34107

CONTROL STABILITY

- Integrated flight/propulsion control design for a STOVL aircraft using H-infinity control design techniques p 39 A92-29093
- Design and evaluation of a robust dynamic neurocontroller for a multivariable aircraft control problem [NASA-TM-105579] p 40 N92-20586

CONTROL SYSTEMS DESIGN

- State space representation of the open-loop dynamics of the Space Shuttle Main Engine p 59 A92-19607
- Integrated flight/propulsion control design for a STOVL aircraft using H-infinity control design techniques p 39 A92-29093
- Decentralized hierarchical partitioning of centralized integrated controllers ... for flight propulsion in STOVLs p 39 A92-29119

- Temperature control in continuous furnace by structural diagram method p 246 A92-29162
- Life Extending Control ... mechanical fatigue in reusable rocket engines p 246 A92-29166
- Adaptive temperature profile control of a multizone crystal growth furnace p 137 A92-29243
- Control of an axisymmetric turbulent jet by multi-modal excitation p 174 A92-40071
- A fundamental theorem for the model reduction of nonlinear systems p 246 A92-41165
- Integrated flight/propulsion control for superersonic STOVL aircraft p 39 A92-45320
- Fiber optic controls for aircraft engines - Issues and implications p 24 A92-46244
- Potential for integrated optical circuits in advanced aircraft with fiber optic control and monitoring systems p 24 A92-46246

- An advanced intelligent control system framework [AIAA PAPER 92-3162] p 65 A92-48785
- Description of the control system design for the SSF PMAD DC testbed p 45 A92-50654
- The development of test beds to support the definition and evolution of the Space Station Freedom power system p 46 A92-50656
- Development and testing of a source subsystem for the supporting development PMAD DC test bed p 46 A92-50659

- Piloted evaluation of an integrated propulsion and flight control simulator [AIAA PAPER 92-4178] p 23 A92-52459
- Propulsion system performance resulting from an Integrated Flight/Propulsion Control design [AIAA PAPER 92-4602] p 28 A92-55281

- Health management and controls for earth to orbit propulsion systems [IAF PAPER 92-0646] p 77 A92-57089
- Controller design for microgravity vibration isolation systems [IAF PAPER 92-0969] p 247 A92-57327

- Turbomachinery noise p 253 N92-10601
- Linear quadratic servo control of a reusable rocket engine [NASA-TM-105291] p 79 N92-11128

- Overview of rocket engine control [NASA-TM-105318] p 81 N92-13274
- Space Station Freedom solar dynamic modules structural modelling and analysis [NASA-TM-104506] p 226 N92-15405

- Design and evaluation of a robust dynamic neurocontroller for a multivariable aircraft control problem [NASA-TM-105579] p 40 N92-20586
- Directions in propulsion control p 32 N92-22530

- Simulation of Space Station loads with active control systems p 56 N92-23824
- Electromechanical systems with transient high power response operating from a resonant AC link [NASA-TM-105716] p 37 N92-28985

- A free-piston Stirling engine/linear alternator controls and load interaction test facility [NASA-TM-105825] p 238 N92-31262
- A parameter optimization approach to controller partitioning for integrated flight/propulsion control application [NASA-TM-105826] p 40 N92-32241

- An optically controlled Ka-band phased array antenna p 152 N92-32968

CONTROL THEORY

- IMPAC - An integrated methodology for propulsion and airframe control p 39 A92-29118
- A framework for the analysis of airframe/engine interactions and integrated flight/propulsion control p 39 A92-29120

- Implementation of control point form of algebraic grid-generation technique p 248 A92-47058

CONVECTIVE HEAT TRANSFER

- Optimal microgravity vibration isolation - An algebraic introduction p 54 A92-47495
- Controller design for microgravity vibration isolation systems [IAF PAPER 92-0969] p 247 A92-57327

- Microgravity vibration isolation: An optimal control law for the one-dimensional case [NASA-TM-105146] p 141 N92-11217

- A simplified dynamic model of the T700 turboshaft engine [NASA-TM-105805] p 251 N92-30898

CONTROLLERS

- An advanced intelligent control system framework [AIAA PAPER 92-3162] p 65 A92-48785
- Description of the control system design for the SSF PMAD DC testbed p 45 A92-50654

- Propulsion system performance resulting from an Integrated Flight/Propulsion Control design [AIAA PAPER 92-4602] p 28 A92-55281
- Controller design for microgravity vibration isolation systems [IAF PAPER 92-0969] p 247 A92-57327

- On-board congestion control for satellite packet switching networks p 148 N92-14228
- A software control system for the ACTS high-burst-rate link evaluation terminal [NASA-TM-105207] p 243 N92-16628

- Design and evaluation of a robust dynamic neurocontroller for a multivariable aircraft control problem [NASA-TM-105579] p 40 N92-20586

- Resonant mode controllers for launch vehicle applications [NASA-TM-105563] p 48 N92-25092
- International Workshop on Vibration Isolation Technology for Microgravity Science Applications [NASA-CP-10094] p 141 N92-28436

- Microgravity vibration isolation: Optimal preview and feedback control [NASA-TM-105673] p 142 N92-30692

- Stability testing and analysis of a PMAD DC test bed for the Space Station Freedom [NASA-TM-105846] p 162 N92-31282

- A parameter optimization approach to controller partitioning for integrated flight/propulsion control application [NASA-TM-105826] p 40 N92-32241

- Implementation of an intelligent control system [NASA-TM-105795] p 241 N92-33897

CONVECTION

- Steady-state thermal-solutal convection and diffusion in a simulated float zone p 137 A92-17056
- Effects of g-jitter and cross-diffusion on the onset of convection in doubly diffusive systems [AIAA PAPER 92-0246] p 167 A92-25705

- An iterative implicit diagonally-dominant factorization algorithm for solving the Navier-Stokes equations [NASA-TM-105259] p 249 N92-16663
- ULTRA-SHARP solution of the Smith-Hutton problem [NASA-TM-105435] p 187 N92-22226

CONVECTION-DIFFUSION EQUATION

- ULTRA-SHARP solution of the Smith-Hutton problem [NASA-TM-105435] p 187 N92-22226

CONVECTIVE FLOW

- Convective flows in enclosures with vertical temperature or concentration gradients p 171 A92-32277
- Nature of buoyancy-driven flows in a reduced-gravity environment p 175 A92-45844
- Natural convection between concentric spheres p 179 A92-50445

- Interfacial and gravitational convection in immiscible liquid layers [IAF PAPER 92-0907] p 184 A92-57286
- Development of a new flux spitting scheme p 190 N92-23352

- Breakdown of the Karman vortex street due to forced convection and flow compressibility [NASA-TM-105853] p 196 N92-32472

CONVECTIVE HEAT TRANSFER

- Heat transfer in rotating serpentine passages with trips normal to the flow [ASME PAPER 91-GT-265] p 165 A92-15663
- Roughness effects on heat transfer from a NACA 0012 airfoil p 166 A92-20217

- Determination of the natural convection coefficient in low-gravity [AIAA PAPER 92-0712] p 168 A92-27072
- Combined conjugated heat transfer from a scattering medium p 175 A92-44390

- Analytical and experimental studies of heat pipe radiation cooling of hypersonic propulsion systems [AIAA PAPER 92-3809] p 26 A92-49128
- Thermal modeling of nickel-hydrogen battery cells operating under transient orbital conditions p 71 A92-50712

CONVERGENCE

A laser-induced heat flux technique for convective heat transfer measurements in high speed flows p 200 A92-54318

Effect of radiation on convection at moderate temperatures [NASA-TM-105632] p 192 N92-25296

Progress towards understanding and predicting convection heat transfer in the turbine gas path [NASA-TM-105674] p 194 N92-26690

CONVERGENCE

Comparison of the SMAC, PISO, and iterative time-advancing schemes for unsteady flows p 175 A92-47158

Optimal least-squares finite element method for elliptic problems [NASA-TM-105382] p 249 N92-15662

Upper bounds for convergence rates of vector extrapolation methods on linear systems with initial iterations [NASA-TM-105608] p 250 N92-33742

CONVERGENT-DIVERGENT NOZZLES

Computation of supersonic jet mixing noise for an axisymmetric CD nozzle using k-epsilon turbulence model [AIAA PAPER 92-0500] p 252 A92-26328

Analytical study of nozzle performance for nuclear thermal rockets [NASA-TM-105251] p 78 N92-11126

Computation of supersonic jet mixing noise for an axisymmetric CD nozzle using k-epsilon turbulence model [NASA-TM-105338] p 254 N92-14795

Arcjet nozzle area ratio effects [NASA-TM-104477] p 83 N92-16022

COOLANTS

Effects of coolant parameters on steady state temperature distribution in phosphoric-acid fuel cell electrode p 233 A92-50737

COOLERS

NASA Lewis Stirling SPRE testing and analysis with reduced number of cooler tubes [NASA-TM-105767] p 238 N92-28837

COOLING

NASA Space applications of high-temperature superconductors [NASA-TM-105401] p 271 N92-18455

Effects of turbine cooling assumptions on performance and sizing of high-speed civil transport [NASA-TM-105610] p 34 N92-23537

COOLING FINS

Effects of anisotropic conduction and heat pipe interaction on minimum mass space radiators [NASA-TM-105297] p 80 N92-11138

COOLING SYSTEMS

Heat transfer in rotating serpentine passages with trips normal to the flow [ASME PAPER 91-GT-265] p 165 A92-15663

Structural tailoring/analysis for hypersonic components - Executive system development [AIAA PAPER 92-2471] p 219 A92-34360

An experimental investigation of high-aspect-ratio cooling passages [AIAA PAPER 92-3154] p 64 A92-48780

Heat transfer and core neutronics considerations of the heat pipe cooled thermionic reactor p 180 A92-50591

Measurements of the effects of thermal contact resistance on steady state heat transfer in phosphoric-acid fuel cell stack p 180 A92-50738

Heat transfer in rotating serpentine passages with trips skewed to the flow [NASA-TM-105581] p 186 N92-20235

An experimental investigation of high-aspect-ratio cooling passages [NASA-TM-105679] p 48 N92-25958

Contingency power for a small turboshaft engine by using water injection into turbine cooling air [NASA-TM-105680] p 37 N92-29661

COORDINATE TRANSFORMATIONS

Canonical transformations for space trajectory optimization [AIAA PAPER 92-4509] p 44 A92-52079

COPPER

Near-edge study of gold-substituted YBa₂Cu₃O₇(δ) p 259 A92-14950

High-T sub c fluorine-doped YBa₂Cu₃O_y films on ceramic substrates by screen printing [NASA-TM-105296] p 127 N92-11188

Thermal conductivity and thermal expansion of graphite fiber/copper matrix composites [NASA-TM-105233] p 106 N92-14120

COPPER OXIDES

Microwave properties of YBa₂Cu₃O₇(δ) high-transition-temperature superconducting thin films measured by the power transmission method p 153 A92-14938

Near-edge study of gold-substituted YBa₂Cu₃O₇(δ) p 259 A92-14950

Laser ablated YBa₂Cu₃O₇(δ) high temperature superconductor coplanar waveguide resonator p 155 A92-31631

Crystalline orientations of Ti₂Ba₂Ca₂Cu₃O_x grains on MgO, SrTiO₃, and LaAlO₃ substrates p 261 A92-41637

Glass precursor approach to high-temperature superconductors [NASA-TM-105590] p 263 N92-20519

CORE FLOW

A fast, uncoupled, compressible, two-dimensional, unsteady boundary layer algorithm with separation for engine inlets [AIAA PAPER 92-3082] p 11 A92-48729

Interface of an uncoupled boundary layer algorithm with an inviscid core flow algorithm for unsteady supersonic engine inlets [AIAA PAPER 92-3083] p 11 A92-48730

Interface of an uncoupled boundary layer algorithm with an inviscid core flow algorithm for unsteady supersonic engine inlets [NASA-TM-105684] p 36 N92-27037

A fast, uncoupled, compressible, two-dimensional, unsteady boundary layer algorithm with separation for engine inlets [NASA-TM-105686] p 195 N92-27653

CORIOLIS EFFECT

Heat transfer in rotating serpentine passages with trips normal to the flow [ASME PAPER 91-GT-265] p 165 A92-15663

Transport modes during crystal growth in a centrifuge p 138 A92-33835

Heat transfer in rotating serpentine passages with trips skewed to the flow [NASA-TM-105581] p 186 N92-20235

CORRELATION COEFFICIENTS

Review and statistical analysis of the use of ultrasonic velocity for estimating the porosity fraction in polycrystalline materials p 215 A92-28722

CORROSION

The chemistry of Saudi Arabian sand: A deposition problem on helicopter turbine airfoils [NASA-TM-105234] p 128 N92-14179

Post-test examination of a pool boiler receiver [NASA-TM-105635] p 123 N92-27192

CORROSION PREVENTION

Chemical stability of high-temperature superconductors [NASA-TM-105391] p 263 N92-19398

CORROSION RESISTANCE

The effect of matrix mechanical properties on (0)8 unidirectional SiC/Ti composite fatigue resistance p 99 A92-16220

Composite overwrapped nickel-hydrogen pressure vessels p 109 N92-22762

COSMOCHEMISTRY

Possible sources of the Population I lithium abundance and light-element evolution p 268 A92-33069

COSMOLOGY

Perturbations from cosmic strings in cold dark matter p 268 A92-33353

Fractals and cosmological large-scale structure p 268 A92-37413

Thick strings, the liquid crystal blue phase, and cosmological large-scale structure p 268 A92-48103

Fluctuation-driven electroweak phase transition --- in early universe p 269 A92-54464

COST ANALYSIS

Repair-level analysis for Space Station Freedom [AIAA PAPER 92-1537] p 43 A92-38634

Balancing reliability and cost to choose the best power subsystem p 216 A92-50625

COST EFFECTIVENESS

Technical and economic feasibility of integrated video service by satellite p 145 A92-29966

Design and analysis of vortex generators on reengineered Boeing 727-100QF center inlet S-duct by a reduced Navier-Stokes code [AIAA PAPER 92-2700] p 10 A92-45542

COST REDUCTION

Energy requirements for the space frontier [SAE PAPER 912064] p 62 A92-45446

COUETTE FLOW

Linear stability of compressible Taylor-Couette flow p 173 A92-36187

COUNTER ROTATION

Optical measurements of unducted fan flutter [ASME PAPER 91-GT-19] p 197 A92-15510

Aeroelastic stability analyses of two counter rotating propfan designs for a cruise missile model [NASA-TM-105268] p 227 N92-23191

Effect of radiation on convection at moderate temperatures [NASA-TM-105632] p 192 N92-25296

COUNTERS

Real-time data compression of broadcast video signals [NASA-CASE-LEW-14945-2] p 147 N92-10128

CRACK ARREST

Crack healing behavior of hot pressed silicon nitride due to oxidation p 124 A92-32896

Fatigue crack growth in a unidirectional SCS-6/Ti-15-3 composite p 102 A92-39036

An energy analysis of crack-initiation and arrest in epoxy p 224 A92-49777

CRACK CLOSURE

Estimation of crack closure stresses for in situ toughened silicon nitride with 8 wt pct scandia p 126 A92-43478

CRACK INITIATION

Mixed-mode fracture in unidirectional graphite epoxy composite laminates with central notch p 218 A92-29464

Stochastic modeling of crack initiation and short-crack growth under creep and creep-fatigue conditions [ASME PAPER 92-APM-5] p 223 A92-44681

Thermomechanical and bithermal fatigue behavior of cast B1900 + Hf and wrought Haynes 188 p 122 A92-45233

An energy analysis of crack-initiation and arrest in epoxy p 224 A92-49777

Modeling of the flexural behavior of ceramic-matrix composites p 225 A92-52005

The effect of ion plated silver and sliding friction on tensile stress-induced cracking in aluminum oxide [NASA-TM-105366] p 129 N92-19450

A preliminary characterization of the tensile and fatigue behavior of tungsten-fiber/Waspaloy-matrix composite [NASA-TM-105346] p 187 N92-22487

Structural durability of stiffened composite shells [NASA-CR-190588] p 229 N92-29342

CRACK OPENING DISPLACEMENT

Fracture toughness and the effects of stress state on fracture of nickel aluminides p 117 A92-27422

CRACK PROPAGATION

Fatigue crack growth in unidirectional metal matrix composite p 99 A92-19734

Controlled crack growth specimen for brittle systems p 123 A92-21099

Mixed-mode fracture in unidirectional graphite epoxy composite laminates with central notch p 218 A92-29464

Diffusive crack growth at a bimaterial interface [AIAA PAPER 92-2432] p 220 A92-34580

Fatigue crack growth reliability by probabilistic finite elements p 222 A92-37524

Fatigue crack growth in a unidirectional SCS-6/Ti-15-3 composite p 102 A92-39036

Modeling of crack bridging in a unidirectional metal matrix composite p 104 A92-43085

Stochastic modeling of crack initiation and short-crack growth under creep and creep-fatigue conditions [ASME PAPER 92-APM-5] p 223 A92-44681

Micromechanical model of crack growth in fiber reinforced brittle materials p 223 A92-46829

Mechanical behaviour and failure phenomenon of an in situ toughened silicon nitride p 127 A92-54504

Asymmetric tip morphology of creep microcracks growing along bimaterial interfaces p 127 A92-56585

Microfracture in high temperature metal matrix laminates [NASA-TM-105189] p 106 N92-14122

Elevated temperature mechanical behavior of monolithic and SiC whisker-reinforced silicon nitrides [NASA-TM-105245] p 128 N92-15192

Structural durability of stiffened composite shells [NASA-CR-190588] p 229 N92-29342

CRACK TIPS

Near-tip dual-length scale mechanics of mode-I cracking in laminate brittle matrix composites [AIAA PAPER 92-2491] p 221 A92-34583

Estimation of crack closure stresses for in situ toughened silicon nitride with 8 wt pct scandia p 126 A92-43478

CRACKING (FRACTURING)

Computational simulation of microfracture in high temperature metal matrix composites p 98 A92-10263

Mechanical behaviors of ceramic matrix composites with matrix cracking and fiber debonding p 100 A92-23104

Predictions of the critical strain for matrix cracking of ceramic matrix composites p 218 A92-33127

Cyclic hot firing results of tungsten-wire-reinforced, copper-lined thrust chambers [NASA-TM-4214] p 91 N92-31249

CRACKS

Modeling of crack bridging in a unidirectional metal matrix composite p 104 A92-43085

- The effect of ion plated silver and sliding friction on tensile stress-induced cracking in aluminum oxide
[NASA-TM-105366] p 129 N92-19450
- CRATERS**
Characteristics of hypervelocity impact craters on LDEF experiment S1003 and implications of small particle impacts on reflective surfaces p 269 N92-27252
- CREEP ANALYSIS**
Stochastic modeling of crack initiation and short-crack growth under creep and creep-fatigue conditions
[ASME PAPER 92-APM-5] p 223 A92-44681
- CREEP PROPERTIES**
Comments on the paper 'Does the subgrain size influence the rate of creep?' p 260 A92-33946
Cumulative creep-fatigue damage evolution in an austenitic stainless steel p 121 A92-45231
Asymmetric tip morphology of creep microcracks growing along bimaterial interfaces p 127 A92-56585
Elevated temperature mechanical behavior of monolithic and SiC whisker-reinforced silicon nitrides
[NASA-TM-105245] p 128 N92-15192
Differential continuum damage mechanics models for creep and fatigue of unidirectional metal matrix composites
[NASA-TM-105213] p 226 N92-16371
Creep and fatigue research efforts on advanced materials p 227 N92-22514
Aeropropulsion structures p 31 N92-22518
- CREEP RUPTURE STRENGTH**
A new response surface approach for structural reliability analysis
[AIAA PAPER 92-2408] p 219 A92-34339
Diffusive crack growth at a bimaterial interface
[AIAA PAPER 92-2432] p 220 A92-34580
- CREEP STRENGTH**
A simple test for thermomechanical evaluation of ceramic fibers p 123 A92-21096
Does a threshold stress for creep exist in HfC-dispersed NiAl? p 118 A92-30780
Stochastic modeling of crack initiation and short-crack growth under creep and creep-fatigue conditions
[ASME PAPER 92-APM-5] p 223 A92-44681
- CREEP TESTS**
Effect of temperature on the formation of creep substructure in sodium chloride single crystals p 260 A92-25444
Does a threshold stress for creep exist in HfC-dispersed NiAl? p 118 A92-30780
1400 and 1500 K compressive creep properties of an NiAl-AlN composite p 103 A92-41575
- CRITICAL FLOW**
Results from computational analysis of a mixed compression supersonic inlet
[NASA-TM-104475] p 14 N92-10976
- CRITICAL LOADING**
The effect of ion plated silver and sliding friction on tensile stress-induced cracking in aluminum oxide
[NASA-TM-105366] p 129 N92-19450
Collapse analysis of a waffle plate strongback for Space Station Freedom
[NASA-TM-105412] p 227 N92-20045
- CRITICAL POINT**
Critical fluid thermal equilibration experiment (19-IML-1) p 139 N92-23640
- CRITICAL TEMPERATURE**
Investigation of two and three parameter equations of state for cryogenic fluids p 140 A92-13413
Glass precursor approach to high-temperature superconductors
[NASA-TM-105590] p 263 N92-20519
Dependence of the critical temperature of laser-ablated YBa₂Cu₃O₇(δ) thin films on LaAlO₃ substrate growth technique p 264 N92-23415
- CRITICAL VELOCITY**
Laser anemometer measurements and computations in an annular cascade of high turning core turbine vanes
[NASA-TP-3252] p 20 N92-28980
- CROSS FLOW**
The three-dimensional turbulent boundary layer near a plane of symmetry p 167 A92-24757
Jet mixing into a heated cross flow in a cylindrical duct - Influence of geometry and flow variations
[AIAA PAPER 92-0773] p 168 A92-27110
Fluid-flow of a row of jets in crossflow - A numerical study
[AIAA PAPER 92-0534] p 169 A92-28198
The structure and development of streamwise vortex arrays embedded in a turbulent boundary layer
[AIAA PAPER 92-0551] p 7 A92-28204
Multigrad calculations of a jet in crossflow p 170 A92-28525
Flow visualization and motion analysis for a series of four sequential brush seals p 204 A92-36976
CFD mixing analysis of jets injected from straight and slanted slots into confined crossflow in rectangular ducts
[AIAA PAPER 92-3087] p 177 A92-48732
- Jet mixing into a heated cross flow in a cylindrical duct: Influence of geometry and flow variations
[NASA-TM-105390] p 30 N92-15994
Multigrad acceleration and turbulence models for computations of 3D turbulent jets in crossflow
[NASA-TM-105306] p 186 N92-18775
Calculations of hot gas ingestion for a STOV aircraft model
[NASA-TM-105437] p 17 N92-19993
CFD mixing analysis of jets injected from straight and slanted slots into confined crossflow in rectangular ducts
[NASA-TM-105699] p 36 N92-26561
- CROSSLINKING**
Cyclopentadiene evolution during pyrolysis-gas chromatography of PMR polyimides
[NASA-TM-105629] p 132 N92-25348
- CRUISE MISSILES**
Aeroelastic stability analyses of two counter rotating propan designs for a cruise missile model
[AIAA PAPER 92-2218] p 25 A92-34408
Small engine technology programs p 32 N92-22532
Aeroelastic stability analyses of two counter rotating propan designs for a cruise missile model
[NASA-TM-105268] p 227 N92-23191
- CRYOGENIC COMPUTER STORAGE**
Pressurization of cryogens - A review of current technology and its applicability to low-gravity conditions
[AIAA PAPER 92-3061] p 72 A92-54002
Pressurization of cryogens: A review of current technology and its applicability to low-gravity conditions
[NASA-TM-105746] p 136 N92-29669
- CRYOGENIC COOLING**
NASA space applications of high-temperature superconductors p 265 N92-32980
- CRYOGENIC EQUIPMENT**
Description of liquid nitrogen experimental test facility p 44 A92-23842
Status of NASA's Stirling space power converter program p 69 A92-50608
Description of Liquid Nitrogen Experimental Test Facility
[NASA-TM-105215] p 134 N92-11208
NASA space applications of high-temperature superconductors p 265 N92-32980
Measurement techniques for cryogenic Ka-band microstrip antennas p 153 N92-32981
- CRYOGENIC FLUID STORAGE**
COLD-SAT - A technology satellite for cryogenic experimentation p 52 A92-13425
Cryogenic fluid management investigations using the CONE flight experiment p 43 A92-23851
Evaluation of supercritical cryogen storage and transfer systems for future NASA missions p 47 A92-28512
Self-pressurization of a lightweight liquid hydrogen tank - Effects of fill level at low wall heat flux
[AIAA PAPER 92-0818] p 60 A92-29591
Slush hydrogen pressurized expulsion studies at the NASA K-Site Facility
[AIAA PAPER 92-3385] p 141 A92-48951
Jet mixing in low gravity - Results of the Tank Pressure Control Experiment
[AIAA PAPER 92-3060] p 182 A92-54001
Comparing the results of an analytical model of the no-vent fill process with no-vent fill test results for a 4.96 cu m (175 cu ft) tank
[AIAA PAPER 92-3078] p 72 A92-54007
Improved thermodynamic modeling of the no-vent fill process and correlation with experimental data
[NASA-TM-104492] p 79 N92-11129
A review of candidate multilayer insulation systems for potential use on wet-launched LH2 tankage for the space exploration initiative lunar missions
[NASA-TM-104493] p 134 N92-13336
Hydrogen no-vent fill testing in a 1.2 cubic foot (34 liter) tank
[NASA-TM-105273] p 185 N92-13401
Self-pressurization of a lightweight liquid hydrogen tank: Effects of fill level at low wall heat flux
[NASA-TM-105411] p 135 N92-18442
Slush hydrogen transfer studies at the NASA K-Site Facility
[NASA-TM-105596] p 135 N92-25957
Slush hydrogen pressurized expulsion studies at the NASA K-Site Facility
[NASA-TM-105597] p 135 N92-26131
- CRYOGENIC FLUIDS**
Qualitative investigation of cryogenic fluid injection into a supersonic flow field p 164 A92-13360
Investigation of two and three parameter equations of state for cryogenic fluids p 140 A92-13413
On-orbit cryogenic fluid transfer research at NASA Lewis Research Center p 45 A92-23847
Computer program for computing the properties of seventeen fluids --- cryogenic liquids p 241 A92-23849
- Liquid hydrogen mass flow through a multiple orifice Joule-Thomson device
[AIAA PAPER 92-2881] p 176 A92-47862
Pressurization of cryogens - A review of current technology and its applicability to low-gravity conditions
[AIAA PAPER 92-3061] p 72 A92-54002
An optical method for determining level in two-phase cryogenic fluids
[NASA-TM-104524] p 200 N92-15366
NASA Space applications of high-temperature superconductors p 271 N92-18455
Liquid hydrogen mass flow through a multiple orifice Joule-Thomson device
[NASA-TM-105583] p 189 N92-23268
Pressurization of cryogens: A review of current technology and its applicability to low-gravity conditions
[NASA-TM-105746] p 136 N92-29669
NASA space applications of high-temperature superconductors p 265 N92-32980
- CRYOGENIC ROCKET PROPELLANTS**
A review of candidate multilayer insulation systems for potential use on wet-launched LH2 tankage for the space exploration initiative lunar missions
[NASA-TM-104493] p 134 N92-13336
Space Station Freedom/lunar transfer vehicle propellant operation hazard analysis p 55 N92-17416
Benefits and technology readiness for using cryogenic instead of storable propellants for return mission from Moon p 136 N92-33343
- CRYOGENIC STORAGE**
Optimization of armored spherical tanks for storage on the lunar surface
[NASA-TM-105700] p 91 N92-30187
- CRYOGENIC TEMPERATURE**
Performance of a wideband GaAs low-noise amplifier at cryogenic temperatures p 156 A92-37953
Fiber optics in liquid propellant rocket engine environments p 62 A92-42610
Performance tests of a cryogenic hybrid magnetic bearing for turbopumps
[NASA-TM-105627] p 30 N92-20523
- CRYOGENICS**
Liquid-vapour surface sensors for liquid nitrogen and hydrogen p 197 A92-23852
Technology issues associated with using densified hydrogen for space vehicles
[AIAA PAPER 92-3079] p 134 A92-48727
Benefits of slush hydrogen for space missions
[NASA-TM-104503] p 134 N92-11214
An optical method for determining level in two-phase cryogenic fluids
[NASA-TM-104524] p 200 N92-15366
Technology issues associated with using densified hydrogen for space vehicles
[NASA-TM-105642] p 135 N92-25277
- CRYOPUMPING**
Design and test of an oxygen turbopump for a dual expander cycle rocket engine p 59 A92-21062
On-orbit cryogenic fluid transfer research at NASA Lewis Research Center p 45 A92-23847
- CRYSTAL DEFECTS**
An initial study of void formation during solidification of aluminum in normal and reduced-gravity
[AIAA PAPER 92-0845] p 138 A92-29611
Vertical solidification of dendritic binary alloys p 261 A92-37562
Molecular dynamics investigation of radiation damage in semiconductors p 159 A92-53157
Heats of formation of bcc binary alloys
[NASA-TM-105281] p 122 N92-16086
Computational techniques in tribology and material science at the atomic level
[NASA-TM-105573] p 252 N92-26671
- CRYSTAL DISLOCATIONS**
Comments on the paper 'Does the subgrain size influence the rate of creep?' p 260 A92-33946
Fatigue damage accumulation in nickel prior to crack initiation p 120 A92-33947
Three-dimensional deformation analysis of two-phase dislocation substructures p 121 A92-44218
Influence of the dislocation density on the performance of heteroepitaxial indium phosphide solar cells p 234 A92-53156
- CRYSTAL GROWTH**
Numerical simulations of space processing - The reality, the myth, and the future p 136 A92-12863
Flight experiment on acousto-optic crystal growth p 136 A92-12880
A versatile get away special furnace for materials processing in space
[AIAA PAPER 92-0787] p 137 A92-27122
The isothermal dendritic growth experiment - A USMP-2 space flight experiment
[AIAA PAPER 92-0350] p 137 A92-28188

CRYSTAL LATTICES

- Linear-stability theory of thermocapillary convection in a model of float-zone crystal growth
[AIAA PAPER 92-0604] p 169 A92-28211
- Adaptive temperature profile control of a multizone crystal growth furnace p 137 A92-29243
- Convective flows in enclosures with vertical temperature or concentration gradients p 171 A92-32277
- Effect of thermal convection on the shape of a solid-liquid interface p 171 A92-35978
- Identification and control of a multizone crystal growth furnace p 199 A92-39699
- Surface morphologies and photoluminescence of diamond films deposited in a hot filament reactor p 261 A92-42858
- Fractal dimension of alumina aggregates grown in two dimensions p 126 A92-49814
- Growth and characterization of lead boride crystals p 138 A92-56956
- Thermal and solutal convection with conduction effects inside a rectangular enclosure [NASA-TM-105371] p 186 A92-15358
- Vapor crystal growth technology development: Application to cadmium telluride p 139 A92-16158 [NASA-TM-103786]
- High-temperature electronics p 160 A92-22528
- CRYSTAL LATTICES**
- Melting of the Abrikosov flux lattice in anisotropic superconductors p 260 A92-28075
- CRYSTAL STRUCTURE**
- Molecular dynamics investigation of radiation damage in semiconductors p 159 A92-53157
- Heats of formation of bcc binary alloys [NASA-TM-105281] p 122 A92-16086
- Computational techniques in tribology and material science at the atomic level [NASA-TM-105573] p 252 A92-26671
- CRYSTAL SURFACES**
- Evaluation of the minority carrier diffusion length and surface-recombination velocity in GaAs p/n solar cells p 234 A92-53162
- CRYSTALLINITY**
- Crystalline orientations of Ti₂Ba₂Cu₂O₃(x) grains on MgO, SrTiO₃, and LaAlO₃ substrates p 261 A92-41637
- CRYSTALLITES**
- Surface morphologies and photoluminescence of diamond films deposited in a hot filament reactor p 261 A92-42858
- CRYSTALLIZATION**
- Glass precursor approach to high-temperature superconductors [NASA-TM-105590] p 263 A92-20519
- Phase transformations in SrAl₂Si₂O₈ glass [NASA-TM-105657] p 264 A92-23890
- CRYSTALLOGRAPHY**
- Molecular dynamics investigation of radiation damage in semiconductors p 159 A92-53157
- CUBIC LATTICES**
- Anodic etching of p-type cubic silicon carbide p 127 A92-57027
- CUMULATIVE DAMAGE**
- Fatigue damage accumulation in nickel prior to crack initiation p 120 A92-33947
- Cumulative creep-fatigue damage evolution in an austenitic stainless steel p 121 A92-45231
- Progressive fracture of polymer matrix composite structures: A new approach [NASA-TM-105574] p 109 A92-23194
- CURING**
- Viscoelastic properties of addition-cured polyimides used in high temperature polymer matrix composites p 124 A92-32632
- Addition curing thermosets endcapped with 4-amino (2,2) paracyclophane p 124 A92-33918
- New addition curing polyimides [NASA-TM-105335] p 95 A92-13281
- Computational simulation of surface waviness in graphite/epoxy woven composites due to initial curing [NASA-TM-105313] p 106 A92-14118
- CURRENT DENSITY**
- Modeling of the near-electrode regions of arcs. I - Coupling of the flowfield to the non-equilibrium boundary layers [AIAA PAPER 92-3109] p 258 A92-48749
- Microwave conductivity of laser ablated YBa₂Cu₃O_{7-δ} superconducting films and its relation to microstrip transmission line performance p 264 A92-21639
- CURVE FITTING**
- Multiwavelength pyrometry for nongray bodies [NASA-TM-105285] p 202 A92-24881
- CYCLIC LOADS**
- Probabilistic constitutive relationships for cyclic material strength models p 217 A92-21081
- Frequency effects on the stability of a journal bearing for periodic loading p 203 A92-22665

- Fatigue damage accumulation in nickel prior to crack initiation p 120 A92-33947
- Microfracture in high temperature metal matrix laminates p 106 A92-14122 [NASA-TM-105189]
- Frequency effects on the stability of a journal bearing for periodic loading [NASA-TM-105226] p 186 A92-18809
- CYLINDRICAL BODIES**
- Controlled crack growth specimen for brittle systems p 123 A92-21099
- Jet mixing into a heated cross flow in a cylindrical duct - Influence of geometry and flow variations [AIAA PAPER 92-0773] p 168 A92-27110
- An experimental study of oscillatory thermocapillary convection in cylindrical containers p 172 A92-36184
- Seals related research at NASA, Lewis Research Center p 207 A92-15087
- Jet mixing into a heated cross flow in a cylindrical duct: Influence of geometry and flow variations [NASA-TM-105390] p 30 A92-15994
- CYLINDRICAL CHAMBERS**
- Viscoplastic analysis of an experimental cylindrical thrust chamber liner p 218 A92-28052
- CYLINDRICAL COORDINATES**
- Radiative transfer solutions for cylindrical coordinates with emitting, absorbing, and anisotropic scattering medium [AIAA PAPER 92-0123] p 266 A92-28185
- Thermal modeling with solid/liquid phase change of the thermal energy storage experiment [NASA-TM-103770] p 185 A92-13402
- CYLINDRICAL SHELLS**
- Structural durability of stiffened composite shells [AIAA PAPER 92-2244] p 220 A92-34569
- Damage and fracture in composite thin shells p 224 A92-51550
- Damage and fracture in composite thin shells [NASA-TM-105289] p 106 A92-13284
- Structural durability of stiffened composite shells [NASA-CR-190588] p 229 A92-29342
- CYLINDRICAL TANKS**
- Description of liquid nitrogen experimental test facility p 44 A92-23842
- Effects of g-jitter on a thermally buoyant flow p 171 A92-32258
- Description of Liquid Nitrogen Experimental Test Facility [NASA-TM-105215] p 134 A92-11208
- D**
- DAMAGE**
- A stochastic damage model for the rupture prediction of a multi-phase solid. I - Parametric studies. II - Statistical approach p 224 A92-49784
- Differential continuum damage mechanics models for creep and fatigue of unidirectional metal matrix composites [NASA-TM-105213] p 226 A92-16371
- High temperature, flexible, fiber-prefrom seal [NASA-CASE-LEW-15085-1] p 208 A92-22043
- A differential CDM model for fatigue of unidirectional metal matrix composites [NASA-TM-105726] p 230 A92-31505
- Demonstrated survivability of a high temperature optical fiber cable on a 1500 pound thrust rocket chamber [NASA-TM-105835] p 136 A92-32230
- Computational simulation of matrix micro-slip bands in SiC/Ti-15 composite [NASA-TM-105762] p 111 A92-32466
- DAMAGE ASSESSMENT**
- Damage mechanisms in three-dimensional woven reinforced ceramic matrix composites under tensile and flexural loading at room and elevated temperatures [AIAA PAPER 92-2492] p 101 A92-34584
- Cumulative creep-fatigue damage evolution in an austenitic stainless steel p 121 A92-45231
- Damage and fracture in composite thin shells p 224 A92-51550
- Damage and fracture in composite thin shells [NASA-TM-105289] p 106 A92-13284
- DARK MATTER**
- Dark matter and the equivalence principle p 267 A92-14477
- Perturbations from cosmic strings in cold dark matter p 268 A92-33353
- DATA ACQUISITION**
- The application of a computer data acquisition system to a new high temperature tribometer p 93 A92-11823
- Advanced nozzle and engine components test facility [AIAA PAPER 92-3993] p 41 A92-56816
- Advanced nozzle and engine components test facility [NASA-TM-103684] p 42 A92-17059
- Three-dimensional laser window formation [NASA-RP-1280] p 47 A92-30307
- A free-piston Stirling engine/linear alternator controls and load interaction test facility [NASA-TM-105825] p 238 A92-31262
- DATA BASE MANAGEMENT SYSTEMS**
- Grid management p 19 A92-25713
- DATA BASES**
- LDEXPT, an intelligent database system for the Composite Load Spectra project p 59 A92-23695
- Wiring for aerospace applications [NASA-TM-105777] p 162 A92-30427
- DATA COMPRESSION**
- Real-time data compression of broadcast video signals [NASA-CASE-LEW-14945-2] p 147 A92-10128
- DATA FLOW ANALYSIS**
- The analysis of high pressure experimental data p 266 A92-16101
- Predictive onboard flow control in packet switching satellites [AIAA PAPER 92-2004] p 144 A92-29923
- Predictive onboard flow control for packet switching satellites [NASA-TM-105566] p 150 A92-19379
- DATA LINKS**
- Distribution of space-gathered data [AIAA PAPER 92-1888] p 143 A92-29821
- Flexible high speed CODEC (FHSC) [AIAA PAPER 92-1919] p 143 A92-29848
- Data Distribution Satellite p 146 A92-48224
- A software control system for the ACTS high-burst-rate link evaluation terminal [NASA-TM-105207] p 243 A92-16628
- Multiple-access phased array antenna simulator for a digital beam forming system investigation [NASA-TM-105422] p 149 A92-17062
- DATA MANAGEMENT**
- QX MAN: Q and X file manipulation p 244 A92-25715
- DATA PROCESSING**
- Development of and flight results from the Space Acceleration Measurement System (SAMS) [NASA-TM-105652] p 57 A92-30301
- DATA REDUCTION**
- Real-time demonstration hardware for enhanced DPCM video compression algorithm [NASA-TM-105616] p 150 A92-19700
- DATA STORAGE**
- Subband coding for image data archiving [NASA-TM-105407] p 151 A92-20032
- A video event trigger for high frame rate, high resolution video technology p 160 A92-22453
- DATA TRANSFER (COMPUTERS)**
- Data Distribution Satellite p 146 A92-48224
- DC GENERATORS**
- Overview and evolution of the LeRC PMAD DC Testbed [NASA-TM-105842] p 163 A92-32867
- DE HAVILLAND AIRCRAFT**
- Prediction of ice accretion on a swept NACA 0012 airfoil and comparisons to flight test results [AIAA PAPER 92-0043] p 4 A92-25677
- Prediction of ice accretion on a swept NACA 0012 airfoil and comparisons to flight test results [NASA-TM-105358] p 16 A92-15968
- DEBONDING (MATERIALS)**
- Computational simulation of matrix micro-slip bands in SiC/Ti-15 composite [NASA-TM-105762] p 111 A92-32466
- DECISION MAKING**
- Automated power management and control p 84 A92-17773
- DECOMPOSITION**
- On the basic equations for the second-order modeling of compressible turbulence p 190 A92-23351
- A multiblock grid generation technique applied to a jet engine configuration p 244 A92-24428
- Composition dependence of superconductivity in YBa₂(Cu_{3-x}Al_x)O_y [NASA-TM-105358] p 131 A92-24715
- Heat transfer device [NASA-CASE-LEW-14162-3] p 111 A92-34208
- DEFECTS**
- Differential continuum damage mechanics models for creep and fatigue of unidirectional metal matrix composites [NASA-TM-105213] p 226 A92-16371
- Fluorescence microscopy for the characterization of structural integrity [NASA-TM-105253] p 96 A92-18970
- Defect behavior, carrier removal and predicted in-space injection annealing of InP solar cells [NASA-TM-105624] p 161 A92-23562
- Atomic oxygen undercutting of LDEF aluminized-Kapton multilayer insulation p 255 A92-24818

DEFENSE PROGRAM

Nuclear rocket propulsion technology - A joint NASA/DOE project [IAF PAPER 91-236] p 58 A92-13159
 Early Track NEP system options for SEI missions [AIAA PAPER 92-3200] p 65 A92-48808

DEFORMATION

Three-dimensional deformation analysis of two-phase dislocation substructures p 121 A92-44218
 Thermomechanical deformation behavior of a dynamic strain aging alloy, Hastelloy X [NASA-TM-105316] p 228 N92-25179

DEGRADATION

Ongoing development of a computer jobstream to predict helicopter main rotor performance in icing conditions p 2 A92-14407
 A very low resistance, non-sintered contact system for use on indium phosphide concentrator/shallow junction solar cells p 233 A92-53146

Effect of particle size of Martian dust on the degradation of photovoltaic cell performance [NASA-TM-105232] p 79 N92-11133
 Environmental interactions of the Space Station Freedom electric power system p 81 N92-13255

A very low resistance, non-sintered contact system for use on indium phosphide concentrator/shallow junction solar cells [NASA-TM-105279] p 235 N92-13482
 Isothermal aging effects on PMR-15 resin [NASA-TM-105648] p 110 N92-30986

DEGREES OF FREEDOM

Reaction-compensation technology for microgravity laboratory robots p 203 A92-23719

DEICERS

Advanced ice protection systems test in the NASA Lewis Icing Research Tunnel p 22 A92-14406
 Numerical analysis of a thermal deicer [AIAA PAPER 92-0527] p 22 A92-26950

An efficient finite element method for aircraft de-icing problems [AIAA PAPER 92-0532] p 22 A92-31670
 Technical evaluation report, AGARD Fluid Dynamics Panel Symposium on Effects of Adverse Weather on Aerodynamics [NASA-TM-105192] p 1 N92-10002

Results of a low power ice protection system test and a new method of imaging data analysis [NASA-TM-105745] p 20 N92-28696

DEICING

Advanced ice protection systems test in the NASA Lewis Icing Research Tunnel p 22 A92-14406
 Numerical analysis of a thermal deicer [AIAA PAPER 92-0527] p 22 A92-26950

An efficient finite element method for aircraft de-icing problems [AIAA PAPER 92-0532] p 22 A92-31670
 Technical evaluation report, AGARD Fluid Dynamics Panel Symposium on Effects of Adverse Weather on Aerodynamics [NASA-TM-105192] p 1 N92-10002

Icing simulation: A survey of computer models and experimental facilities p 21 N92-21684
 The NASA aircraft icing research program p 23 N92-22534

NASA's aircraft icing technology program [NASA-TM-104518] p 17 N92-23105
 Results of a low power ice protection system test and a new method of imaging data analysis [NASA-TM-105745] p 20 N92-28696

Lewis icing research tunnel test of the aerodynamic effects of aircraft ground deicing/anti-icing fluids [NASA-TP-3238] p 22 N92-30395

DELAMINATING

Mechanical behaviors of ceramic matrix composites with matrix cracking and fiber debonding p 100 A92-23104
 Predictions of the critical strain for matrix cracking of ceramic matrix composites p 218 A92-33127

Free vibrations of delaminated beams p 222 A92-36853
 Thermally-driven microfracture in high temperature metal matrix composites [NASA-TM-105305] p 107 N92-15136

Progressive fracture of polymer matrix composite structures: A new approach [NASA-TM-105574] p 109 N92-23194
 Free vibrations of delaminated beams [NASA-TM-105582] p 109 N92-25754

Computational simulation of structural fracture in fiber composites p 111 N92-32531

DEMAGNETIZATION

The 23 to 300 C demagnetization resistance of samarium-cobalt permanent magnets [NASA-TP-3119] p 159 N92-11252

DEMAND ASSIGNMENT MULTIPLE ACCESS

Network architectures and protocols for the integration of ACTS and ISDN [AIAA PAPER 92-2039] p 145 A92-29953

DEMODULATORS

Multicarrier demodulator architecture for onboard processing satellites p 49 A92-10465
 A multi-channel demultiplexer/demodulator architecture, simulation and implementation [AIAA PAPER 92-1972] p 144 A92-29895

Multichannel demultiplexer/demodulator technologies for future satellite communication systems [NASA-TM-105377] p 51 N92-18342
 NASA Lewis Research Center Advanced Modulation and Coding Project: Introduction and overview p 51 N92-22002

DEMULPLEXING

Fault tolerance in onboard processors - Protecting efficient FDM demultiplexers [AIAA PAPER 92-1969] p 144 A92-29892
 A multi-channel demultiplexer/demodulator architecture, simulation and implementation [AIAA PAPER 92-1972] p 144 A92-29895

DENDRITIC CRYSTALS

Growth-speed dependence of primary arm spacings in directionally solidified Pb-10 wt pct Sn p 117 A92-26526
 The isothermal dendritic growth experiment - A USMP-2 space flight experiment [AIAA PAPER 92-0350] p 137 A92-28188

Vertical solidification of dendritic binary alloys p 261 A92-37562
 On the drag of model dendrite fragments at low Reynolds number p 95 A92-50868

DENSITY MEASUREMENT

Filtered Rayleigh scattering based measurements in compressible mixing layers [AIAA PAPER 92-3543] p 182 A92-54043

DEPLOYMENT

Self-deploying photovoltaic power system [NASA-CASE-LEW-15308-1] p 237 N92-24057

DEPOSITION

Study of temperature-dependent ultrathin oxide growth on Si(111) using variable-angle spectroscopic ellipsometry p 260 A92-32414
 The chemistry of Saudi Arabian sand: A deposition problem on helicopter turbine airfoils [NASA-TM-105234] p 128 N92-14179

Properties of large area ErBa₂Cu₃O_{7-x} thin films deposited by ionized cluster beams p 264 N92-23414

DEPOSITS

Effect of surface deposits on electromagnetic propagation in uniform ducts p 142 A92-23964
 The chemistry of Saudi Arabian sand: A deposition problem on helicopter turbine airfoils [NASA-TM-105234] p 128 N92-14179

DEPTH

Magnetic penetration depth of YBa₂Cu₃O₇(δ) thin films determined by the power transmission method p 265 N92-32983

DEPTH MEASUREMENT

Adjustable depth gage [NASA-CASE-LEW-14880-1] p 201 N92-21723

DESIGN ANALYSIS

Reliability analysis of laminated CMC components through shell subelement techniques [AIAA PAPER 92-2348] p 219 A92-34322
 HITCAN for actively cooled hot-composite thermostructural analysis [ASME PAPER 91-GT-116] p 222 A92-36896

Structural design methodologies for ceramic-based material systems p 103 A92-39866
 Rocket engine propulsion 'system reliability' [AIAA PAPER 92-3421] p 66 A92-48980

Turning up the heat on aircraft structures --- design and analysis for high-temperature conditions p 23 A92-55131
 Power management and distribution considerations for a lunar base [NASA-TM-105342] p 269 N92-13910

Reliability analysis of laminated CMC components through shell subelement techniques [NASA-TM-105413] p 129 N92-20380
 NASA Aerospace Flight Battery Systems Program: An update p 237 N92-22741

A flexible CPW package for a 30 GHz MMIC amplifier --- coplanar waveguide [NASA-TM-105630] p 161 N92-23193
 A brief overview of computational structures technology related activities at NASA Lewis Research Center p 229 N92-25915

Dynamics of a split torque helicopter transmission [NASA-TM-105681] p 213 N92-29136
 Optimal design of compact spur gear reductions [NASA-TM-105676] p 213 N92-29351

DIFFERENCE EQUATIONS

Design characteristics of a heat pipe test chamber [NASA-TM-105737] p 238 N92-29662
 A flexible CPW package for a 30 GHz MMIC amplifier p 152 N92-32972

Benefits and technology readiness for using cryogenic instead of storable propellants for return mission from Moon p 136 N92-33343

DESTRUCTION

Destructive physical analysis results of Ni/H₂ cells cycled in LEO regime p 70 A92-50707

DETECTION

Using silicon diodes for detecting the liquid-vapor interface in hydrogen [NASA-TM-105541] p 201 N92-18456
 A simplified dynamic model of the T700 turboshaft engine [NASA-TM-105805] p 251 N92-30898

DETONABLE GAS MIXTURES

National Aerospace Plane engine seals: High temperature seal performance evaluation p 207 N92-15103

DETONATION WAVES

Conical detonation waves - A comparison of theoretical and numerical results [AIAA PAPER 92-0348] p 167 A92-25792
 The Osher scheme for non-equilibrium reacting flows p 176 A92-48149
 Detonation duct gas generator demonstration program [AIAA PAPER 92-3174] p 27 A92-54011

DIAGNOSIS

Autonomous Power System intelligent diagnosis and control p 247 A92-50532
 Model-based diagnostics for Space Station Freedom p 245 A92-50535

DIAMINES

Substituted 1,1,1-triaryl-2,2,2-trifluoroethanes and processes for their synthesis [NASA-CASE-LEW-14345-6] p 96 N92-17882
 Vinyl capped addition polyimides [NASA-CASE-LEW-15027-2] p 131 N92-24053

DIAMOND FILMS

Surface morphologies and photoluminescence of diamond films deposited in a hot filament reactor p 261 A92-42858
 Synthesis and characterization of fine grain diamond films p 262 A92-46330

Environmental effects on friction and wear of diamond and diamondlike carbon coatings [NASA-TM-105634] p 131 N92-23192

DIAMONDS

Studies of mechanochemical interactions in the tribological behavior of materials p 124 A92-32410
 Environmental effects on friction and wear of diamond and diamondlike carbon coatings [NASA-TM-105634] p 131 N92-23192

DIATOMIC GASES

Numerical solution of a three-dimensional cubic cavity flow by using the Boltzmann equation [NASA-TM-105693] p 195 N92-30297

DIELECTRIC PROPERTIES

Evaluation of high temperature dielectric films for high voltage power electronic applications p 261 A92-44273
 Evaluation of high temperature capacitor dielectrics [NASA-TM-105622] p 161 N92-23561

High temperature dielectric properties of Apical, Kapton, Peek, Teflon AF, and Uplix polymers [NASA-TM-105753] p 162 N92-28675

DIELECTRICS

Measurements of complex permittivity of microwave substrates in the 20 to 300 K temperature range from 26.5 to 40.0 GHz p 197 A92-13416
 Dielectric breakdown studies of Teflon perfluoroalkoxy at high temperature p 125 A92-36287

Planar dielectric resonator stabilized HEMT oscillator integrated with CPW/aperture coupled patch antenna [NASA-TM-105544] p 160 N92-18473
 Ion collection from a plasma by a pinhole p 259 N92-22368

Evaluation of high temperature capacitor dielectrics [NASA-TM-105622] p 161 N92-23561
 High temperature dielectric properties of Apical, Kapton, Peek, Teflon AF, and Uplix polymers [NASA-TM-105753] p 162 N92-28675
 Planar dielectric resonator stabilized HEMT oscillator integrated with CPW/aperture coupled patch antenna p 152 N92-32967

DIESEL ENGINES

Effect of out-of-roundness on the performance of a diesel engine connecting-rod bearing [NASA-TM-105600] p 215 N92-31536

DIFFERENCE EQUATIONS

Central difference TVD and TVB schemes for time dependent and steady state problems [AIAA PAPER 92-0053] p 166 A92-22168

DIFFERENTIAL EQUATIONS

- Central difference TVD and TVB schemes for time dependent and steady state problems
[NASA-TM-105357] p 249 N92-15663
- Asymptotic integration algorithms for first-order ODEs with application to viscoplasticity
[NASA-TM-105587] p 250 N92-24974

DIFFERENTIAL EQUATIONS

- Combustion kinetics and sensitivity analysis computations
p 112 A92-16981
- Asymptotic integration algorithms for first-order ODEs with application to viscoplasticity
[NASA-TM-105587] p 250 N92-24974

DIFFERENTIAL PRESSURE

- Calibration of hemispherical-head flow angularity probes
[AIAA PAPER 92-4005] p 200 A92-56828

DIFFERENTIAL PULSE CODE MODULATION

- Real-time data compression of broadcast video signals
[NASA-CASE-LEW-14945-2] p 147 N92-10128
- Real-time demonstration hardware for enhanced DPCM video compression algorithm
[NASA-TM-105616] p 150 N92-19700

DIFFUSE RADIATION

- Photovoltaic array for Martian surface power
[NASA-TM-105827] p 270 N92-33899

DIFFUSERS

- Investigation of the diffuser flow quality in an icing research wind tunnel p 40 A92-24406

DIFFUSION

- Effective diffusion equation in a random velocity field
[AIAA PAPER 92-0245] p 167 A92-25704
- Effects of g-jitter and cross-diffusion on the onset of convection in doubly diffusive systems
[AIAA PAPER 92-0246] p 167 A92-25705
- A variable multi-step method for transient heat conduction p 173 A92-37518
- The aerodynamic effect of fillet radius in a low speed compressor cascade
[NASA-TM-105347] p 29 N92-14063
- Design and performance of controlled-diffusion stator compared with original double-circular-arc stator
[NASA-TP-2852] p 34 N92-22863

DIFFUSION COEFFICIENT

- Interdiffusion between the L1(2) trialuminides Al₆₆Ti₂₅Mn₉ and Al₆₇Ti₂₅Cr₈ p 120 A92-37088

DIFFUSION ELECTRODES

- A study of Na(x)P₃O₄ as an O₂ electrode bifunctional electrocatalyst
[NASA-TM-105311] p 85 N92-20585

DIFFUSION FLAMES

- Some further observations on droplet combustion characteristics - NASA LeRC-Princeton results
p 111 A92-12897
- The implications of experimentally controlled gravitational accelerations for combustion science
p 112 A92-16601
- Gravitational influences on the behavior of confined diffusion flames
[AIAA PAPER 92-0334] p 113 A92-25781
- Effects of oxygen concentration on radiative loss from normal-gravity and microgravity methane diffusion flames
[AIAA PAPER 92-0243] p 113 A92-26928
- Color image processing and object tracking workstation
[NASA-TM-105561] p 139 N92-26611

DIFFUSION LENGTH

- Evaluation of the minority carrier diffusion length and surface-recombination velocity in GaAs p/n solar cells
p 234 A92-53162

DIFFUSION PUMPS

- A new technique for oil backstreaming contamination measurements
[NASA-TM-105312] p 257 N92-13783

DIFFUSION WAVES

- Critical fluid thermal equilibration experiment (19-IML-1) p 139 N92-23640

DIGITAL SYSTEMS

- Multicarrier demodulator architecture for onboard processing satellites
p 49 A92-10465
- NASA Lewis Research Center Advanced Modulation and Coding Project: Introduction and overview
p 51 N92-22002
- A free-piston Stirling engine/linear alternator controls and load interaction test facility
[NASA-TM-105825] p 238 N92-31262
- Comparative evaluation of optical waveguides as alternative interconnections for high performance packaging
p 153 N92-32974

DIGITAL TECHNIQUES

- Frequency allocations for a new satellite service - Digital audio broadcasting
[AIAA PAPER 92-1957] p 143 A92-29881

DIGITAL TELEVISION

- Real-time demonstration hardware for enhanced DPCM video compression algorithm
[NASA-TM-105616] p 150 N92-19700

DIGITAL TRANSDUCERS

- Wavelength-multiplexed fiber-optic position encoder for aircraft control systems p 24 A92-42602

DILUTION

- CFD mixing analysis of jets injected from straight and slanted slots into confined crossflow in rectangular ducts
[AIAA PAPER 92-3087] p 177 A92-48732
- CFD mixing analysis of jets injected from straight and slanted slots into confined crossflow in rectangular ducts
[NASA-TM-105699] p 36 N92-26561

DIMENSIONAL MEASUREMENT

- Effect of gas mass flux on cryogenic liquid jet breakup
p 140 A92-23845

DIODES

- Using silicon diodes for detecting the liquid-vapor interface in hydrogen
[NASA-TM-105541] p 201 N92-18456

DIRECT BROADCAST SATELLITES

- Real-time demonstration hardware for enhanced DPCM video compression algorithm
[NASA-TM-105616] p 150 N92-19700

DIRECT CURRENT

- dc and microwave performance of a 0.1-micron gate InAs/In(0.52)Al(0.48)As MODFET p 156 A92-43891
- Load flows and faults considering dc current injections
p 157 A92-50530

- The development of test beds to support the definition and evolution of the Space Station Freedom power system
p 46 A92-50656
- An EMTF system level model of the PMAD DC test bed
p 46 A92-50657
- Development and testing of a 180-volt dc electronic circuit breaker with a 335-ampere carry and 1200-ampere interrupt rating p 158 A92-50658

DIRECTIONAL CONTROL

- Force analysis of magnetic bearings with power-saving controls p 212 N92-27795

DIRECTIONAL COUPLERS

- Length minimization design considerations in photonic integrated circuits incorporating directional couplers
p 256 A92-46240

DIRECTIONAL SOLIDIFICATION (CRYSTALS)

- Growth-speed dependence of primary arm spacings in directionally solidified Pb-10 wt pct Sn
p 117 A92-26526
- Compressive strength of directionally solidified NiAl-NiAlNb intermetallics at 1200 and 1300 K
p 117 A92-28248
- Adaptive temperature profile control of a multizone crystal growth furnace p 137 A92-29243
- An initial study of void formation during solidification of aluminum in normal and reduced-gravity
[AIAA PAPER 92-0845] p 138 A92-29611
- Solidification processing of intermetallic Nb-Al alloys
p 120 A92-33866
- Effect of thermal convection on the shape of a solid-liquid interface p 171 A92-35978
- Vertical solidification of dendritic binary alloys
p 261 A92-37562
- Identification and control of a multizone crystal growth furnace p 199 A92-39699
- Ductility enhancement from interface dislocation sources in a directionally solidified beta + gamma + gamma-prime Ni-Fe-Al composite alloy
p 122 A92-46850
- An examination of anticipated g-jitter on Space Station and its effects on materials processes
p 140 N92-28438

DISCONTINUITY

- Analysis of shielded CPW discontinuities with air-bridges p 152 N92-32971

DISCRETE FUNCTIONS

- Nongray radiative gas analyses using the S-N discrete ordinates method p 266 A92-15443

DISILICIDES

- Method of intercalating large quantities of fibrous structures
[NASA-CASE-LEW-15077-1] p 107 N92-16025

DISPLACEMENT MEASUREMENT

- X ray based displacement measurement for hostile environments
[NASA-TM-105551] p 202 N92-23155

DISSIPATION

- A new time scale based k-epsilon model for near wall turbulence
[NASA-TM-105768] p 196 N92-32868

DISTANCE MEASURING EQUIPMENT

- Adjustable depth gage
[NASA-CASE-LEW-14880-1] p 201 N92-21723

DISTORTION

- A study on vortex flow control of inlet distortion in the re-engine 727-100 center inlet duct using computational fluid dynamics
[AIAA PAPER 92-0152] p 4 A92-23767
- Vortex generator design for aircraft inlet distortion as a numerical optimization problem p 23 N92-13959
- A study on vortex flow control on inlet distortion in the re-engine 727-100 center inlet duct using computational fluid dynamics
[NASA-TM-105321] p 14 N92-13998

DISTRIBUTED PARAMETER SYSTEMS

- Temperature control in continuous furnace by structural diagram method p 246 A92-29162

DISTRIBUTED PROCESSING

- Parallel computation of aerodynamic influence coefficients for aeroelastic analysis on a transputer network p 241 A92-12367
- Distributed visualization for computational fluid dynamics p 194 N92-25826

DISTRIBUTION FUNCTIONS

- Enhancing control of grid distribution in algebraic grid generation p 248 A92-52552

DOMES (STRUCTURAL FORMS)

- Mixing in the dome region of a staged gas turbine combustor
[AIAA PAPER 92-3089] p 177 A92-48734

DOPED CRYSTALS

- Temperature independent quantum well FET with delta channel doping p 157 A92-49596
- Minority carrier lifetime in indium phosphide p 262 A92-53148
- Effect of growth conditions on the quality of lead bromide crystals p 138 A92-56957
- Intermodulation in the oscillatory magnetoresistance of a two-dimensional electron gas p 163 N92-32975
- Reduced mobility and PPC in In(20)Ga(80)As / Al(23)Ga(77)As HEMT structure p 265 N92-32976
- Study of InGaAs-based modulation doped field effect transistor structures using variable-angle spectroscopic ellipsometry p 265 N92-32977
- Microwave properties of peeled HEMT devices sapphire substrates p 265 N92-32978

DOPPLER EFFECT

- Doppler-shifted fluorescence imaging of velocity fields in supersonic reacting flows
[AIAA PAPER 92-2964] p 199 A92-46979
- Flow diagnostics of an arcjet using laser-induced fluorescence
[AIAA PAPER 92-3243] p 199 A92-48843

DOWNLINKING

- Interference susceptibility measurements for an MSK satellite communication link
[AIAA PAPER 92-2018] p 144 A92-29936
- Interference susceptibility measurements for an MSK satellite communication link
[NASA-TM-105395] p 149 N92-15306
- Multichannel demultiplexer/demodulator technologies for future satellite communication systems
[NASA-TM-105377] p 51 N92-18342

DRAG

- Results of an icing test on a NACA 0012 airfoil in the NASA Lewis Icing Research Tunnel
[AIAA PAPER 92-0647] p 7 A92-27021
- On the drag of model dendrite fragments at low Reynolds number p 95 A92-50868
- Results of an icing test on a NACA 0012 airfoil in the NASA Lewis Icing Research Tunnel
[NASA-TM-105374] p 16 N92-15051

DRAG REDUCTION

- The F/A-18 external burning flight test
[AIAA PAPER 91-5050] p 23 A92-44547
- Computation of H₂/air reacting flowfields in drag-reduction external combustion
[AIAA PAPER 92-3672] p 182 A92-54115
- Experiments and analysis concerning the use of external burning to reduce aerospace vehicle transonic drag
[NASA-TM-105397] p 30 N92-17546
- Method of reducing drag in aerodynamic systems
[NASA-CASE-LEW-14791-1] p 21 N92-34243

DRILLING

- Adjustable depth gage
[NASA-CASE-LEW-14880-1] p 201 N92-21723

DROP SIZE

- Observations of soot during droplet combustion at low gravity - Heptane and heptane/monochloroalkane mixtures p 115 A92-50447
- Coaxial injector spray characterization using water/air as simulants
[NASA-TM-105322] p 82 N92-14112

DROP TOWERS

- Observations on a slow burning regime for hydrocarbon droplets - n-heptane/air results p 112 A92-16602
- Drop-tower experiments for capillary surfaces in an exotic container p 166 A92-20743
- Stability of capillary surfaces p 172 A92-35979

DROPS (LIQUIDS)

Some further observations on droplet combustion characteristics - NASA LeRC-Princeton results p 111 A92-12897
 Effect of gas mass flux on cryogenic liquid jet breakup p 140 A92-23845
 Unsteady thermocapillary migration of isolated drops in creeping flow p 169 A92-27774
 Comparison of two-dimensional and three-dimensional droplet trajectory calculations in the vicinity of finite wings [AIAA PAPER 92-0645] p 8 A92-28215
 Combustion of liquid-fuel droplets in supercritical conditions p 114 A92-43778
 Comparison of two-dimensional and three-dimensional droplet trajectory calculations in the vicinity of finite wings [NASA-TM-105617] p 188 N92-23154

DUCT GEOMETRY

Far-field noise and internal modes from a ducted propeller at simulated aircraft takeoff conditions [AIAA PAPER 92-0371] p 252 A92-26230
 Experimental investigation of turbulent flow through a circular-to-rectangular transition duct p 168 A92-26412
 On turbulent flows dominated by curvature effects p 171 A92-32940
 Design and analysis of reengine Boeing 727-100 center inlet S duct by a reduced Navier-Stokes code [AIAA PAPER 92-1221] p 8 A92-33320
 CFD mixing analysis of jets injected from straight and slanted slots into confined crossflow in rectangular ducts [AIAA PAPER 92-3087] p 177 A92-48732
 A parametric numerical study of mixing in a cylindrical duct [AIAA PAPER 92-3088] p 177 A92-48733
 A computational study of advanced exhaust system transition ducts with experimental validation [AIAA PAPER 92-3794] p 179 A92-49126
 Far-field noise and internal modes from a ducted propeller at simulated aircraft takeoff conditions [NASA-TM-105369] p 254 N92-16702
 A parametric numerical study of mixing in a cylindrical duct [NASA-TM-105695] p 35 N92-26553
 CFD mixing analysis of jets injected from straight and slanted slots into confined crossflow in rectangular ducts [NASA-TM-105699] p 36 N92-26561

DUCTED FANS

Supersonic throughflow fans for high-speed aircraft p 34 N92-22541

DUCTED FLOW

A study on vortex flow control of inlet distortion in the re-engine 727-100 center inlet duct using computational fluid dynamics [AIAA PAPER 92-0152] p 4 A92-23767
 Experimental investigation of turbulent flow through a circular-to-rectangular transition duct p 168 A92-26412
 Unsteady flowfield simulation of ducted prop-fan configurations [AIAA PAPER 92-0521] p 6 A92-26946
 Flow in a ventral nozzle for short takeoff and vertical landing aircraft p 25 A92-28538
 On turbulent flows dominated by curvature effects p 171 A92-32940
 Navier-Stokes analysis and experimental data comparison of compressible flow in a diffusing S-duct [AIAA PAPER 92-2699] p 10 A92-45541
 Design and analysis of vortex generators on reengine Boeing 727-100QF center inlet S-duct by a reduced Navier-Stokes code [AIAA PAPER 92-2700] p 10 A92-45542
 CFD mixing analysis of jets injected from straight and slanted slots into confined crossflow in rectangular ducts [AIAA PAPER 92-3087] p 177 A92-48732
 An experimental investigation of the flow in a diffusing S-duct [AIAA PAPER 92-3622] p 13 A92-54090
 Computational and experimental investigation of subsonic internal reversing flows [AIAA PAPER 92-3791] p 183 A92-54170
 A study on vortex flow control on inlet distortion in the re-engine 727-100 center inlet duct using computational fluid dynamics [NASA-TM-105321] p 14 N92-13998
 CFD mixing analysis of jets injected from straight and slanted slots into confined crossflow in rectangular ducts [NASA-TM-105699] p 36 N92-26561
 Navier-Stokes analysis and experimental data comparison of compressible flow within ducts [NASA-TM-105796] p 38 N92-30972
 Navier-Stokes analysis and experimental data comparison of compressible flow in a diffusing S-duct [NASA-TM-105683] p 38 N92-33746

DUCTILITY

Flow and fracture behavior of NiAl in relation to the brittle-to-ductile transition temperature p 118 A92-30781
 Ductility enhancement from interface dislocation sources in a directionally solidified beta + gamma + gamma-prime Ni-Fe-Al composite alloy p 122 A92-46850

DUCTS

A study on vortex flow control of inlet distortion in the re-engine 727-100 center inlet duct using computational fluid dynamics [AIAA PAPER 92-0152] p 4 A92-23767
 Effect of surface deposits on electromagnetic propagation in uniform ducts p 142 A92-23964
 Jet mixing into a heated cross flow in a cylindrical duct - influence of geometry and flow variations [AIAA PAPER 92-0773] p 168 A92-27110
 Experimental and analytical study of close-coupled ventral nozzles for ASTOVL aircraft p 26 A92-45325
 A parametric numerical study of mixing in a cylindrical duct [AIAA PAPER 92-3088] p 177 A92-48733
 A study on vortex flow control on inlet distortion in the re-engine 727-100 center inlet duct using computational fluid dynamics [NASA-TM-105321] p 14 N92-13998
 Jet mixing into a heated cross flow in a cylindrical duct: influence of geometry and flow variations [NASA-TM-105390] p 30 N92-15994
 Introduction to the internal fluid mechanics research session p 188 N92-22522
 Inlets, ducts, and nozzles p 188 N92-22523
 A parametric numerical study of mixing in a cylindrical duct [NASA-TM-105695] p 35 N92-26553
 Navier-Stokes analysis and experimental data comparison of compressible flow within ducts [NASA-TM-105796] p 38 N92-30972

DURABILITY

Structural durability of stiffened composite shells [AIAA PAPER 92-2244] p 220 A92-34569
 Relative sliding durability of two candidate high temperature oxide fiber seal materials [AIAA PAPER 92-3713] p 126 A92-49095
 Relative sliding durability of two candidate high temperature oxide fiber seal materials [NASA-TM-105199] p 95 N92-10064
 Composite thermal barrier coating [NASA-CASE-LEW-14999-1] p 108 N92-21725
 High temperature dynamic engine seal technology development [NASA-TM-105641] p 209 N92-23435
 Durability evaluation of photovoltaic blanket materials exposed on LDEF tray S1003 p 132 N92-27100
 Structural durability of stiffened composite shells [NASA-CR-190588] p 229 N92-29342

DUST

Effects of windblown dust on photovoltaic surfaces on Mars p 45 A92-50573

DUST STORMS

Effect of particle size of Martian dust on the degradation of photovoltaic cell performance [NASA-TM-105232] p 79 N92-11133
 Photovoltaic array for Martian surface power [NASA-TM-105827] p 270 N92-33899

DYNAMIC CHARACTERISTICS

Influence of mass moment of inertia on normal modes of preloaded solar array mast [NASA-TP-3273] p 230 N92-33476

DYNAMIC LOADS

Acoustic characteristics and dynamic structural loading of an ASTOVL aircraft in hover [AIAA PAPER 92-0370] p 253 A92-28190
 Frequency effects on the stability of a journal bearing for periodic loading [NASA-TM-105226] p 186 N92-18809

Simulation of Space Station loads with active control systems p 56 N92-23824
 A comparison between theoretical prediction and experimental measurement of the dynamic behavior of spur gears [NASA-TM-105362] p 210 N92-25347

DYNAMIC MODELS

Optimization and analysis of large chemical kinetic mechanisms using the solution mapping method - Combustion of methane p 113 A92-19300
 Systems analysis of electrodynamic tethers p 62 A92-41550
 Identification of the Space Shuttle Main Engine dynamic models from firing data [AIAA PAPER 92-3317] p 73 A92-54022
 Modal simulation of gearbox vibration with experimental correlation [AIAA PAPER 92-3494] p 207 A92-54036

DYNAMICAL SYSTEMS

A simplified dynamic model of the T700 turboshaft engine [NASA-TM-105805] p 251 N92-30898
 Modal simulation of gearbox vibration with experimental correlation [NASA-TM-105702] p 215 N92-31485

DYNAMIC RESPONSE

First-passage problems: A probabilistic dynamic analysis for degraded structures [NASA-TM-103755] p 225 N92-11373
 Semi-empirical model for prediction of unsteady forces on an airfoil with application to flutter [NASA-TM-105414] p 17 N92-18760
 Simulation of Space Station loads with active control systems p 56 N92-23824

DYNAMIC STABILITY

A bulk flow model of a brush seal system [ASME PAPER 91-GT-325] p 203 A92-15696
 Frequency effects on the stability of a journal bearing for periodic loading [NASA-TM-105226] p 186 N92-18809

DYNAMIC STRUCTURAL ANALYSIS

Acoustic characteristics and dynamic structural loading of an ASTOVL aircraft in hover [AIAA PAPER 92-0370] p 253 A92-28190
 A numerical classical flutter analysis of advanced propellers [AIAA PAPER 92-2118] p 26 A92-35687
 Structural reliability assessment capability in NESSUS [AIAA PAPER 92-3417] p 223 A92-48976
 Minimization of vibration in elastic beams with time-variant boundary conditions p 224 A92-50511
 Boundary formulations for sensitivities of three-dimensional stress invariants p 224 A92-50883
 FREPS - A forced response prediction system for turbomachinery blade rows [AIAA PAPER 92-3072] p 242 A92-54006

First-passage problems: A probabilistic dynamic analysis for degraded structures

[NASA-TM-103755] p 225 N92-11373
 Modal interaction in linear dynamic systems near degenerate modes [NASA-TM-105315] p 225 N92-12316
 Space Station Freedom solar dynamic modules structural modelling and analysis [NASA-TM-104506] p 226 N92-15405

Structural Dynamics Branch research and accomplishments for FY 1990 [NASA-TM-103747] p 226 N92-15406
 Semi-empirical model for prediction of unsteady forces on an airfoil with application to flutter [NASA-TM-105414] p 17 N92-18760

Solar dynamic modules for Space Station Freedom: The relationship between fine-pointing control and thermal loading of the aperture plate [NASA-TM-104498] p 84 N92-19780
 Performance tests of a cryogenic hybrid magnetic bearing for turbopumps [NASA-TM-105627] p 30 N92-20523

Determining structural performance p 32 N92-22519
 Simulation of Space Station loads with active control systems p 56 N92-23824
 A comparison between theoretical prediction and experimental measurement of the dynamic behavior of spur gears [NASA-TM-105362] p 210 N92-25347

Influence of mass moment of inertia on normal modes of preloaded solar array mast [NASA-TP-3273] p 230 N92-33476
 Modal test/analysis correlation of Space Station structures using nonlinear sensitivity [NASA-TM-105850] p 230 N92-34221

DYNAMIC TESTS
 Viscoelastic properties of addition-cured polyimides used in high temperature polymer matrix composites p 124 A92-32632
 Preliminary dynamic tests of a flight-type ejector [AIAA PAPER 92-3261] p 27 A92-54020

A comparison between theoretical prediction and experimental measurement of the dynamic behavior of spur gears [NASA-TM-105362] p 210 N92-25347
 Preliminary dynamic tests of a flight-type ejector [NASA-TM-105814] p 38 N92-30998

DYNAMICAL SYSTEMS

A Lyapunov based nonlinear control scheme for stabilizing a basic compression system using a close-coupled control valve p 246 A92-29316
 Discrete-time entropy formulation of optimal and adaptive control problems p 247 A92-55930
 Structural Dynamics Branch research and accomplishments for FY 1990 [NASA-TM-103747] p 226 N92-15406

EARLY STARS

E

EARLY STARS

The diffuse gamma-ray background, light element abundances, and signatures of early massive star formation p 268 A92-43837

EARTH IONOSPHERE

The formation and structure of plasma wakes behind large high-voltage space platforms in ionosphere [AIAA PAPER 92-0577] p 239 A92-26984
 Ionospheric plasma flow over large high-voltage space platforms. I - Ion-plasma-time scale interactions of a plate at zero angle of attack. II - The formation and structure of plasma wake p 258 A92-41359

EARTH OBSERVATIONS (FROM SPACE)

Enhanced EOS photovoltaic power system capability with InP solar cells p 81 N92-13248

EARTH OBSERVING SYSTEM (EOS)

Advanced power systems for EOS p 70 A92-50640
 Enhanced EOS photovoltaic power system capability with InP solar cells p 81 N92-13248

EARTH ORBITAL ENVIRONMENTS

Tether methods for reactionless orbital propulsion p 44 A92-17797

Arcing of negatively biased solar cells in low earth orbit p 59 A92-26985

[AIAA PAPER 92-0578] p 59 A92-26985
 Synergistic effects of ultraviolet radiation, thermal cycling and atomic oxygen on altered and coated Kapton surfaces p 93 A92-27125

[AIAA PAPER 92-0794] p 93 A92-27125
 Applicability of Long Duration Exposure Facility environmental effects data to the design of Space Station Freedom electrical power system p 53 A92-29614

[AIAA PAPER 92-0848] p 53 A92-29614
 Low earth orbit durability evaluation of Haynes 188 solar receiver material p 117 A92-29616

[AIAA PAPER 92-0850] p 117 A92-29616
 SiO(x) coatings for atomic oxygen protection of polyimide Kapton in low earth orbit p 94 A92-31286

[AIAA PAPER 92-2151] p 94 A92-31286
 Atomic oxygen effects on thin film space coatings studied by spectroscopic ellipsometry, atomic force microscopy, and laser light scattering p 94 A92-31300

[AIAA PAPER 92-2172] p 94 A92-31300
 Nonuniform thermal environmental effects on space truss structural reliability p 54 A92-34325

[AIAA PAPER 92-2352] p 54 A92-34325
 Arcing of negatively biased solar cells in a plasma environment. I - Experimental observations p 63 A92-47000

[AIAA PAPER 92-2990] p 63 A92-47000
 High voltage spheres in an unmagnetized plasma - Fluid and PIC simulations p 258 A92-47936

Effect of KOH concentration on LEO cycle life of IPV nickel-hydrogen flight cell - Update II p 232 A92-48212

Nuclear thermal rockets - Key to moon-Mars exploration p 63 A92-48385

Full-size solar dynamic heat receiver thermal-vacuum tests p 68 A92-50565

Assessment of environmental effects on Space Station Freedom Electrical Power System p 55 A92-50581

The Solar Array Module Plasma Interactions Experiment (SAMPIE) - A Shuttle-based plasma interactions experiment p 69 A92-50583

Nickel-hydrogen cell low-earth-orbit life test update p 70 A92-50700

Atomic oxygen effects on SiO(x) coated Kapton for photovoltaic arrays in low earth orbit p 72 A92-53211

Effect of inert propellant injection on Mars ascent vehicle performance p 73 A92-54031

[AIAA PAPER 92-3447] p 73 A92-54031
 Fast oxygen atom facility for studies related to low earth orbit activities p 47 A92-56800

[AIAA PAPER 92-3974] p 47 A92-56800
 Environmental interactions of the Space Station Freedom electric power system p 81 N92-13255

Effect of KOH concentration on LEO cycle life of IPV nickel-hydrogen flight cells-update 2 p 235 N92-13483

[NASA-TM-105314] p 235 N92-13483
 A new technique for oil backstreaming contamination measurements p 257 N92-13783

[NASA-TM-105312] p 257 N92-13783
 Synergistic effects of ultraviolet radiation, thermal cycling, and atomic oxygen on altered and coated Kapton surfaces p 96 N92-14114

[NASA-TM-105363] p 96 N92-14114
 Durability evaluation of photovoltaic blanket materials exposed on LDEF tray S1003 p 132 N92-27100

Advanced photovoltaic experiment, S0014: Preliminary flight results and post-flight findings p 237 N92-27101

The evaluation of layered separators for nickel-hydrogen cells p 89 N92-27161

Characteristics of hypervelocity impact craters on LDEF experiment S1003 and implications of small particle impacts on reflective surfaces p 269 N92-27252

The effect of the low Earth orbit environment on space solar cells: Results of the advanced photovoltaic experiment (S0014) p 237 N92-27320

EARTH ORBITS

Destructive physical analysis results of Ni/H₂ cells cycled in LEO regime p 70 A92-50707
 Ion Beam Textured and Coated Surfaces Experiment (IBEX) p 132 N92-24832

EARTH TERMINALS

Advanced Communications Technology Satellite (ACTS) p 50 A92-55788

[IAF PAPER 92-0407] p 50 A92-55788
 SCAILET - An intelligent assistant for satellite ground terminal operations p 245 A92-55855

EARTH-MARS TRAJECTORIES

Minimum impulse trajectories for Mars round trip missions p 44 A92-43339

EARTH-VENUS TRAJECTORIES

Minimum impulse trajectories for Mars round trip missions p 44 A92-43339

ECONOMIC ANALYSIS

Repair-level analysis for Space Station Freedom [AIAA PAPER 92-1537] p 43 A92-38634

EDDY VISCOSITY

A turbulence model for iced airfoils and its validation [AIAA PAPER 92-0417] p 6 A92-26267

Navier-Stokes solution of transonic cascade flows using nonperiodic C-type grids p 8 A92-28523

Renormalization group based algebraic turbulence model for three-dimensional turbomachinery flows p 9 A92-41268

A turbulence model for iced airfoils and its validation [NASA-TM-105373] p 16 N92-15052

Turbulence modeling p 189 N92-23338
 A new time scale based k-epsilon model for near wall turbulence p 196 N92-32868

EDGE DETECTION

Color image processing and object tracking workstation p 139 N92-26611

EDGE DISLOCATIONS

Computational simulation of matrix micro-slip bands in SiC/Ti-15 composite p 111 N92-32466

EDUCATION

Trends in aer propulsion research and their impact on engineering education [NASA-TM-105682] p 38 N92-31172

EFFICIENCY

Effect of InAlAs window layer on the efficiency of indium phosphide solar cells p 234 A92-53163

Effect of InAlAs window layer on efficiency of indium phosphide solar cells [NASA-TM-105354] p 161 N92-25176

EIGENVALUES

Eigenvalue calculation procedure for an Euler/Navier-Stokes solver with application to flows over airfoils p 3 A92-17429

Aeroelastic modal characteristics of mistuned blade assemblies - Mode localization and loss of eigenstructure p 225 A92-54921

Modal interaction in linear dynamic systems near degenerate modes p 225 N92-12316

[NASA-TM-105315] p 225 N92-12316
 Explicit robust schemes for implementation of a class of principal value-based constitutive models: Theoretical development p 227 N92-20212

[NASA-TM-105345] p 227 N92-20212
 Conservative-variable average states for equilibrium gas multi-dimensional fluxes p 191 N92-25196

[NASA-TM-105585] p 191 N92-25196
 Application of vector-valued rational approximations to the matrix eigenvalue problem and connections with Krylov subspace methods p 250 N92-33571

EIGENVECTORS

Conservative-variable average states for equilibrium gas multi-dimensional fluxes p 191 N92-25196

[NASA-TM-105585] p 191 N92-25196
 Preliminary dynamic tests of a flight-type ejector [AIAA PAPER 92-3261] p 27 A92-54020

Experimental investigation of an ejector-powered free-jet facility p 41 A92-54058

[AIAA PAPER 92-3569] p 41 A92-54058
 Flow induction by pressure forces p 28 A92-54060

[AIAA PAPER 92-3571] p 28 A92-54060
 Use of an approximate similarity principle for the thermal scaling of a full-scale thrust augmenting ejector [AIAA PAPER 92-3792] p 28 A92-54171

EJECTORS

Use of an approximate similarity principle for the thermal scaling of a full-scale thrust augmenting ejector p 36 N92-26613

[NASA-TM-105724] p 36 N92-26613
 Preliminary dynamic tests of a flight-type ejector [NASA-TM-105814] p 38 N92-30998

ELASTIC BODIES

Minimization of vibration in elastic beams with time-variant boundary conditions p 224 A92-50511

ELASTIC DAMPING

Effect of heat treatment on stiffness and damping of SiC/Ti-15-3 p 108 N92-20841

ELASTIC DEFORMATION

On the development of explicit robust schemes for implementation of a class of hyperelastic models in large-strain analysis of rubbers p 221 A92-36245

Contact stresses in meshing spur gear teeth: Use of an incremental finite element procedure [NASA-TM-105388] p 209 N92-23536

ELASTIC PROPERTIES
 Review and statistical analysis of the use of ultrasonic velocity for estimating the porosity fraction in polycrystalline materials p 215 A92-28722

A variationally coupled FE-BE method for elasticity and fracture mechanics p 222 A92-37510

Microfracture in high temperature metal matrix laminates p 106 N92-14122

[NASA-TM-105189] p 106 N92-14122
 On the thermodynamic framework of generalized coupled thermoelastic-viscoplastic-damage modeling [NASA-TM-105349] p 225 N92-14434

ELASTIC WAVES
 Pressure wave propagation studies for oscillating cascades p 5 A92-25682

[AIAA PAPER 92-0145] p 5 A92-25682
 Pressure wave propagation studies for oscillating cascades p 16 N92-15977

[NASA-TM-105406] p 16 N92-15977
 ELASTOHYDRODYNAMICS
 A system-approach to the elasto hydrodynamic lubrication point-contact problem p 204 A92-35421

ELASTOPLASTICITY
 Material nonlinear analysis via mixed-iterative finite element method p 220 A92-34368

[AIAA PAPER 92-2479] p 220 A92-34368
 Effects of fiber and interfacial layer architectures on the thermoplastic response of metal matrix composites [NASA-TM-105802] p 110 N92-32234

ELECTRIC ARCS
 The arcing rate for a High Voltage Solar Array - Theory, experiment and predictions p 53 A92-26983

[AIAA PAPER 92-0576] p 53 A92-26983
 Arcing of negatively biased solar cells in a plasma environment. I - Experimental observations p 63 A92-47000

[AIAA PAPER 92-2990] p 63 A92-47000
 Numerical study of low-current steady arcs p 67 A92-50264

Evaluation of Kapton pyrolysis, arc tracking, and arc propagation on the Space Station Freedom (SSF) solar array flexible current carrier (FCC) p 72 A92-53209

Wiring for aerospace applications [NASA-TM-105777] p 162 N92-30427

ELECTRIC BATTERIES
 Space Electrochemical Research and Technology Conference, 3rd, NASA Lewis Research Center, Cleveland, OH, Apr. 9, 10, 1991, Proceedings p 231 A92-18936

Space batteries for mobile battlefield power applications p 231 A92-29679

Development and testing of a source subsystem for the supporting development PMAD DC test bed p 46 A92-50659

ELECTRIC CONNECTORS
 Comparative evaluation of optical waveguides as alternative interconnections for high performance packaging p 153 N92-32974

ELECTRIC CONTACTS
 A system-approach to the elasto hydrodynamic lubrication point-contact problem p 204 A92-35421

Sinterless contacts to shallow junction InP solar cells [NASA-TM-105670] p 237 N92-24802

The achievement of low contact resistance to indium phosphide: The roles of Ni, Au, Ge, and combinations thereof [NASA-TM-105770] p 238 N92-33895

ELECTRIC CURRENT
 Force analysis of magnetic bearings with power-saving controls p 212 N92-27797

ELECTRIC ENERGY STORAGE
 Alkali metal carbon dioxide electrochemical system for energy storage and/or conversion of carbon dioxide to oxygen [NASA-CASE-LEW-14973-1] p 235 N92-10222

- ELECTRIC EQUIPMENT**
A combined vector potential-scalar potential method for FE computation of 3D magnetic fields in electrical devices with iron cores p 154 A92-23959
- ELECTRIC FURNACES**
A versatile get away special furnace for materials processing in space [AIAA PAPER 92-0787] p 137 A92-27122
- ELECTRIC GENERATORS**
A dynamic isotope power system for Space Exploration Initiative surface transport systems [AIAA PAPER 92-1489] p 61 A92-38605
Electrical system options for space exploration [SAE PAPER 912065] p 62 A92-45447
A dynamic isotope power system portable generator for the moon or Mars p 232 A92-50634
SEI power source alternatives for rovers and other multi-kWe distributed surface applications p 80 N92-13206
Space Station Freedom electric power system evolution analysis status p 84 N92-17771
- ELECTRIC MOTOR VEHICLES**
Electromechanical systems with transient high power response operating from a resonant AC link [NASA-TM-105716] p 37 N92-28985
- ELECTRIC NETWORKS**
Load flows and faults considering dc current injections p 157 A92-50530
- ELECTRIC POTENTIAL**
Experimental breakdown of selected anodized aluminum samples in dilute plasmas p 259 N92-22369
Monolithic and mechanical multijunction space solar cells [NASA-TM-105832] p 163 N92-32233
- ELECTRIC POWER SUPPLIES**
A dynamic isotope power system for Space Exploration Initiative surface transport systems [AIAA PAPER 92-1489] p 61 A92-38605
Beam power options for the moon p 61 A92-40429
A dynamic isotope power system portable generator for the moon or Mars p 232 A92-50634
Design and optimization of a self-deploying PV tent array p 233 A92-50642
Power management and distribution considerations for a lunar base [NASA-TM-105342] p 269 N92-13910
Self-deploying photovoltaic power system [NASA-CASE-LEW-15308-1] p 237 N92-24057
Solar radiation on a catenary collector [NASA-TM-105751] p 163 N92-32243
- ELECTRIC POWER TRANSMISSION**
Development and testing of a 180-volt dc electronic circuit breaker with a 335-ampere carry and 1200-ampere interrupt rating p 158 A92-50658
Space Station Freedom electric power system evolution analysis status p 84 N92-17771
- ELECTRIC PROPULSION**
Electric propulsion - An evolutionary technology [IAF PAPER 91-241] p 58 A92-13158
The evolutionary development of high specific impulse electric thruster technology [AIAA PAPER 92-1556] p 61 A92-38650
Electric propulsion - The future is now p 63 A92-48386
Measurement and analysis of a small nozzle plume in vacuum [AIAA PAPER 92-3108] p 64 A92-48748
Space transfer with ground-based laser/electric propulsion [AIAA PAPER 92-3213] p 73 A92-54017
An overview of the NASA Advanced Propulsion Concepts program [AIAA PAPER 92-3216] p 73 A92-54018
Development and flight history of SERT 2 spacecraft [AIAA PAPER 92-3516] p 74 A92-54038
NASA's nuclear electric propulsion technology project [AIAA PAPER 92-3705] p 76 A92-57033
Test facilities for high power electric propulsion [NASA-TM-105247] p 80 N92-11136
Hydrogen arcjet technology [NASA-TM-105340] p 82 N92-15119
Preliminary test results of a hollow cathode MPD thruster [NASA-TM-105324] p 84 N92-18474
Development and flight history of SERT 2 spacecraft [NASA-TM-105636] p 90 N92-28983
The evolutionary development of high specific impulse electric thruster technology [NASA-TM-105712] p 92 N92-31342
NASA's nuclear electric propulsion technology project [NASA-TM-105811] p 93 N92-32463
Dependence of hydrogen arcjet operation on electrode geometry [NASA-TM-105855] p 93 N92-34113
Low power arcjet test facility impacts [NASA-TM-105876] p 47 N92-34114
- ELECTRIC ROCKET ENGINES**
Magnetoplasmadynamic Thruster Workshop [NASA-CP-10084] p 77 N92-10044
Hydrogen arcjet technology [NASA-TM-105340] p 82 N92-15119
Arcjet nozzle area ratio effects [NASA-TM-104477] p 83 N92-16022
Multimegawatt MPD thruster design considerations [NASA-TM-105405] p 83 N92-16024
- ELECTRIC SWITCHES**
Neutron, gamma ray, and temperature effects on the electrical characteristics of thyristors [NASA-TM-105728] p 162 N92-28432
- ELECTRICAL FAULTS**
Dielectric breakdown studies of Teflon perfluoroalkoxy at high temperature p 125 A92-36287
Load flows and faults considering dc current injections p 157 A92-50530
Model-based diagnostics for Space Station Freedom p 245 A92-50535
Large transient fault current test of an electrical roll ring --- for Space Station Freedom p 55 A92-50661
Experimental breakdown of selected anodized aluminum samples in dilute plasmas p 259 N92-22369
Large transient fault current test of an electrical roll ring [NASA-TM-105667] p 87 N92-24201
- ELECTRICAL IMPEDANCE**
Mutual coupling between rectangular microstrip patch antennas p 159 A92-52423
Impedances of Li/SO₂ cells retrieved from the Long Duration Exposure Facility (LDEF satellite) and comparison with cells stored terrestrially [NASA-TM-104526] p 236 N92-13484
- ELECTRICAL INSULATION**
Evaluation of high temperature capacitor dielectrics [NASA-TM-105622] p 161 N92-23561
Wiring for aerospace applications [NASA-TM-105777] p 162 N92-30427
- ELECTRICAL MEASUREMENT**
Fiber-optic sensors for aerospace electrical measurements - An update p 200 A92-50630
- ELECTRICAL PROPERTIES**
Electrical properties of teflon and ceramic capacitors at high temperatures [NASA-TM-105569] p 160 N92-20040
Neutron, gamma ray, and temperature effects on the electrical characteristics of thyristors [NASA-TM-105728] p 162 N92-28432
Electrical and chemical interactions at Mars Workshop, part 1 [NASA-CP-10093] p 270 N92-30302
- ELECTRICAL RESISTIVITY**
Analog synthesized fast-variable linear load p 157 A92-50539
Brominated graphitized carbon fibers [NASA-CASE-LEW-14698-2] p 127 N92-10090
Composition dependence of superconductivity in YBa₂(Cu(3-x)Al(x))O_y [NASA-TM-105358] p 131 N92-24715
The achievement of low contact resistance to indium phosphide: The roles of Ni, Au, Ge, and combinations thereof [NASA-TM-105770] p 238 N92-33895
- ELECTRICITY**
Selective emitters [NASA-CASE-LEW-14731-1] p 236 N92-22037
- ELECTRO-OPTICS**
Reconfigurable optical interconnection network for multimode optical fiber sensor arrays p 256 A92-37448
Multiple-mode reconfigurable electro-optic switching network for optical fiber sensor array p 256 A92-46245
Thermal and solutal convection with conduction effects inside a rectangular enclosure [NASA-TM-105371] p 186 N92-15358
Fiber optics for controls p 40 N92-22529
- ELECTROCATALYSTS**
A study of Na(x)Pt₃O₄ as an O₂ electrode bifunctional electrocatalyst [NASA-TM-105311] p 85 N92-20585
The O₂ reduction at the IFC modified O₂ fuel cell electrode [NASA-TM-105691] p 90 N92-29667
- ELECTROCHEMICAL CELLS**
Temperature dependence of the electrode kinetics of oxygen reduction at the platinum/Nafion interface - A microelectrode investigation p 115 A92-56950
Alkali metal carbon dioxide electrochemical system for energy storage and/or conversion of carbon dioxide to oxygen [NASA-CASE-LEW-14973-1] p 235 N92-10222
SEI power source alternatives for rovers and other multi-kWe distributed surface applications p 80 N92-13206
- ELECTROCHEMISTRY**
Space Electrochemical Research and Technology Conference, 3rd, NASA Lewis Research Center, Cleveland, OH, Apr. 9, 10, 1991, Proceedings p 231 A92-18936
Electrochemical impregnation and cycle life of lightweight nickel electrodes for nickel-hydrogen cells p 113 A92-30978
Convective flows in enclosures with vertical temperature or concentration gradients p 171 A92-32277
- ELECTRODE MATERIALS**
Bifunctional alkaline oxygen electrodes p 115 A92-50729
Effects of coolant parameters on steady state temperature distribution in phosphoric-acid fuel cell electrode p 233 A92-50737
- ELECTRODES**
Electrochemical impregnation and cycle life of lightweight nickel electrodes for nickel-hydrogen cells p 113 A92-30978
Destructive physical analysis results of Ni/H₂ cells cycled in LEO regime p 70 A92-50707
Dependence of hydrogen arcjet operation on electrode geometry [AIAA PAPER 92-3530] p 74 A92-54039
Progress in the development of lightweight nickel electrode for aerospace applications [NASA-TM-105591] p 236 N92-20493
Progress in the development of lightweight nickel electrode [NASA-TM-105638] p 116 N92-26670
The O₂ reduction at the IFC modified O₂ fuel cell electrode [NASA-TM-105691] p 90 N92-29667
Dependence of hydrogen arcjet operation on electrode geometry [NASA-TM-105855] p 93 N92-34113
- ELECTRODYNAMICS**
Theory of plasma contactor neutral gas emissions for electrodynamic tethers p 258 A92-41549
Systems analysis of electrodynamic tethers p 62 A92-41550
- ELECTROKINETICS**
Electrophoresis of small particles and fluid globules in weak electrolytes p 114 A92-33924
- ELECTROLYSIS**
A study of Na(x)Pt₃O₄ as an O₂ electrode bifunctional electrocatalyst [NASA-TM-105311] p 85 N92-20585
- ELECTROLYTES**
Electrophoresis of small particles and fluid globules in weak electrolytes p 114 A92-33924
Effect of KOH concentration on LEO cycle life of IPV nickel-hydrogen flight cells - An update p 70 A92-50702
Destructive physical analysis results of Ni/H₂ cells cycled in LEO regime p 70 A92-50707
Effect of LEO cycling on 125 Ah advanced design IPV nickel-hydrogen flight cells - An update p 71 A92-50708
- ELECTROMAGNETIC ABSORPTION**
Enhancing optical absorption in InP and GaAs utilizing profile etching p 263 A92-53154
Enhancing optical absorption in InP and GaAs utilizing profile etching [NASA-TM-105325] p 82 N92-14111
- ELECTROMAGNETIC COUPLING**
Electromagnetic coupling between coplanar waveguide and microstrip antennas p 154 A92-21292
New techniques for exciting linearly tapered slot antennas with coplanar waveguide p 155 A92-34844
- ELECTROMAGNETIC INTERFERENCE**
Interference susceptibility measurements for an MSK satellite communication link [AIAA PAPER 92-2018] p 144 A92-29936
Interference susceptibility measurements for an MSK satellite communication link [NASA-TM-105395] p 149 N92-15306
- ELECTROMAGNETIC RADIATION**
Effect of surface deposits on electromagnetic propagation in uniform ducts p 142 A92-23964
- ELECTROMAGNETIC SCATTERING**
Electromagnetic scattering from an inhomogeneous object by ray tracing p 146 A92-51092
- ELECTROMAGNETIC SHIELDING**
Magnetic radiation shielding - An idea whose time has returned? p 53 A92-17796
- ELECTROMECHANICAL DEVICES**
Electromechanical simulation and testing of actively controlled rotordynamic systems with piezoelectric actuators p 204 A92-39258
Flywheel energy storage for electromechanical actuation systems p 233 A92-50758
Resonant mode controllers for launch vehicle applications [NASA-TM-105563] p 48 N92-25092

ELECTROMECHANICS

Electromechanical systems with transient high power response operating from a resonant AC link
[NASA-TM-105716] p 37 N92-28985
An electromechanical actuation system for an expendable launch vehicle
[NASA-TM-105774] p 48 N92-30310

ELECTROMECHANICS

An electromechanical actuation system for an expendable launch vehicle
[NASA-TM-105774] p 48 N92-30310

ELECTRON DENSITY (CONCENTRATION)

High voltage spheres in an unmagnetized plasma - Fluid and PIC simulations p 258 A92-47936

ELECTRON GAS

Intermodulation in the oscillatory magnetoresistance of a two-dimensional electron gas p 163 N92-32975

ELECTRON IMPACT

An experimental study of impingement-ion-production mechanisms p 76 A92-54190
[AIAA PAPER 92-3826]

ELECTRON IRRADIATION

Defect behavior, carrier removal and predicted in-space injection annealing of InP solar cells
[NASA-TM-105624] p 161 N92-23562

ELECTRON MICROSCOPY

Precautions toward XTEM of Si3N4/SiO2 p 125 A92-33930

ELECTRON SPIN

Extrapolation procedures in Mott electron polarimetry p 197 A92-21241

ELECTRON TRANSITIONS

Study of a cesium plasma as a selective emitter for thermophotovoltaic applications p 258 A92-33667

ELECTRONIC CONTROL

Fiber optics for controls p 40 N92-22529

ELECTRONIC EQUIPMENT

Evaluation of high temperature dielectric films for high voltage power electronic applications p 261 A92-44273

ELECTRONIC PACKAGING

High-performance packaging for monolithic microwave and millimeter-wave integrated circuits
[AIAA PAPER 92-1935] p 155 A92-31706

High-performance packaging for monolithic microwave and millimeter-wave integrated circuits
[NASA-TM-105744] p 151 N92-31855

ELECTROPHORESIS

Electrophoresis of small particles and fluid globules in weak electrolytes p 114 A92-33924

ELECTROSTATIC CHARGE

NASCAP/LEO simulations of Shuttle Orbiter charging during the SAMPIE experiment p 55 N92-22361

ELECTROSTATIC WAVES

Study of a cesium plasma as a selective emitter for thermophotovoltaic applications p 258 A92-33667

ELECTROTHERMAL ENGINES

Microwave electrothermal propulsion for space p 63 A92-46049

Theoretical nozzle performance of a microwave electrothermal thruster using experimental data
[AIAA PAPER 92-3110] p 64 A92-48750

ELLIPSONOMETRY

Study of temperature-dependent ultrathin oxide growth on Si(111) using variable-angle spectroscopic ellipsometry p 260 A92-32414

A new technique for oil backstreaming contamination measurements
[NASA-TM-105312] p 257 N92-13783

Study of InGaAs-based modulation doped field effect transistor structures using variable-angle spectroscopic ellipsometry p 265 N92-32977

ELLIPTICAL ORBITS

Simple proof of the global optimality of the Hohmann transfer p 44 A92-46760

EMISSION

A parametric numerical study of mixing in a cylindrical duct
[AIAA PAPER 92-3088] p 177 A92-48733

A parametric numerical study of mixing in a cylindrical duct
[NASA-TM-105695] p 35 N92-26553

EMISSION SPECTRA

Techniques for spectroscopic measurements in an arcjet nozzle p 59 A92-21087

Temperature-dependent reflectivity of silicon carbide
[NASA-TM-105287] p 201 N92-19263

EMITTERS

Selective emitters
[NASA-CASE-LEW-14731-1] p 236 N92-22037

High efficiency thermal to electric energy conversion using selective emitters and spectrally tuned solar cells
[NASA-TM-105755] p 238 N92-30426

END EFFECTORS

Determination of the stress distributions in a ceramic, tensile specimen using numerical techniques p 216 A92-14546

ENERGY CONSERVATION

Self-pressurization of a spherical liquid hydrogen storage tank in a microgravity environment
[AIAA PAPER 92-0363] p 168 A92-25798

Self-pressurization of a spherical liquid hydrogen storage tank in a microgravity environment
[NASA-TM-105372] p 185 N92-14323

ENERGY CONSUMPTION

Force analysis of magnetic bearings with power-saving controls p 212 N92-27795

ENERGY CONVERSION

Selective emitters
[NASA-CASE-LEW-14731-1] p 236 N92-22037

High efficiency thermal to electric energy conversion using selective emitters and spectrally tuned solar cells
[NASA-TM-105755] p 238 N92-30426

Magnetic bearings for free-piston Stirling engines
[NASA-TM-105730] p 214 N92-30734

ENERGY CONVERSION EFFICIENCY

Calculated performance of p(+)-n InP solar cells with In(0.52)Al(0.48)As window layers p 153 A92-13266

Study of a cesium plasma as a selective emitter for thermophotovoltaic applications p 258 A92-33667

Increased efficiency with surface texturing in ITO/InP solar cells p 232 A92-44548

Modeled performance of monolithic, 3-terminal InP/Ga(0.47)In(0.53)As concentrator solar cells as a function of temperature and concentration ratio p 234 A92-53153

Influence of the dislocation density on the performance of heteroepitaxial indium phosphide solar cells p 234 A92-53156

A high-performance photovoltaic concentrator array - The mini-dome Fresnel lens concentrator with 30 percent efficient GaAs/GaSb tandem cells p 72 A92-53199

Advances in photovoltaic technology
[IAF PAPER 92-0599] p 235 A92-57055

Thin film, concentrator, and multijunction space solar cells: Status and potential p 81 N92-13230

Enhanced EOS photovoltaic power system capability with InP solar cells p 81 N92-13248

Status and future directions of InP solar cell research
[NASA-TM-105426] p 160 N92-18920

Design and performance of controlled-diffusion stator compared with original double-circular-arc stator
[NASA-TP-2852] p 34 N92-22863

High efficiency thermal to electric energy conversion using selective emitters and spectrally tuned solar cells
[NASA-TM-105755] p 238 N92-30426

Monolithic and mechanical multijunction space solar cells
[NASA-TM-105832] p 163 N92-32233

Solar radiation on a catenary collector p 163 N92-32243
[NASA-TM-105751]

Progress update of NASA's free-piston Stirling space power converter technology project
[NASA-TM-105748] p 239 N92-33898

ENERGY DISSIPATION

Finite difference solution for transient cooling of a radiating-conducting semitransparent layer p 166 A92-20310

ENERGY DISTRIBUTION

Issues and status of power distribution options for space exploration p 80 N92-13207

ENERGY GAPS (SOLID STATE)

Optical dispersion relations for 'diamondlike' carbon films p 262 A92-44533

Thin-film photovoltaics: Status and applications to space power p 81 N92-13228

ENERGY REQUIREMENTS

Energy requirements for the space frontier
[SAE PAPER 912064] p 62 A92-45446

ENERGY STORAGE

Space power by ground-based laser illumination p 59 A92-18401

Magnesium fluoride as energy storage medium for spacecraft solar thermal power systems p 67 A92-50274

SEI rover solar-electrochemical power system options p 45 A92-50574

Observations of the freeze/thaw performance of lithium fluoride by motion picture photography p 180 A92-50751

Flywheel energy storage for electromechanical actuation systems p 233 A92-50758

SEI power source alternatives for rovers and other multi-kWe distributed surface applications p 80 N92-13206

Thermochemical energy storage for a lunar base
[NASA-TM-105333] p 236 N92-14485

Validation test of advanced technology for IPV nickel-hydrogen flight cells: Update
[NASA-TM-105689] p 89 N92-27878

Solar thermal energy receiver
[NASA-CASE-LEW-14949-1] p 238 N92-29143

ENERGY TECHNOLOGY

Structural scaling approximations for solar arrays p 231 A92-40935

Energy requirements for the space frontier
[SAE PAPER 912064] p 62 A92-45446

Advances in photovoltaic technology
[IAF PAPER 92-0599] p 235 A92-57055

ENERGY TRANSFER

A computer model for one-dimensional mass and energy transport in and around chemically reacting particles, including complex gas-phase chemistry, multicomponent molecular diffusion, surface evaporation, and heterogeneous reaction p 181 A92-52406

Pulse thermal energy transport/storage system
[NASA-CASE-LEW-15235-1] p 195 N92-29125

Solar thermal energy receiver
[NASA-CASE-LEW-14949-1] p 238 N92-29143

ENGINE AIRFRAME INTEGRATION

Integrated flight/propulsion control specifications for systems with two-way coupling p 39 A92-29117

A framework for the analysis of airframe/engine interactions and integrated flight/propulsion control p 39 A92-29120

Propulsion system performance resulting from an Integrated Flight/Propulsion Control design
[AIAA PAPER 92-4602] p 28 A92-55281

Analysis of airframe/engine interactions for a STOVL aircraft with integrated flight/propulsion control
[AIAA PAPER 92-4623] p 23 A92-55300

Vortex generator design for aircraft inlet distortion as a numerical optimization problem p 23 N92-13959

Application of computational fluid dynamics to the study of vortex flow control for the management of inlet distortion
[NASA-TM-105672] p 230 N92-34112

ENGINE CONTROL

A framework for the analysis of airframe/engine interactions and integrated flight/propulsion control p 39 A92-29120

A simplified dynamic model of Space Shuttle Main Engine p 60 A92-29289

Integrated flight/propulsion control for supersonic STOVL aircraft p 39 A92-45320

Fiber optic controls for aircraft engines - Issues and implications p 24 A92-46244

Plotted evaluation of an integrated propulsion and flight control simulator
[AIAA PAPER 92-4178] p 23 A92-52459

Propulsion system performance resulting from an Integrated Flight/Propulsion Control design
[AIAA PAPER 92-4602] p 28 A92-55281

Technology readiness assessment of advanced space engine integrated controls and health monitoring
[NASA-TM-105255] p 79 N92-11130

Integrated health monitoring and controls for rocket engines
[NASA-TM-105763] p 90 N92-28693

A demonstration of an intelligent control system for a reusable rocket engine
[NASA-TM-105794] p 92 N92-31507

Plotted evaluation of an integrated propulsion and flight control simulator
[NASA-TM-105797] p 40 N92-34107

ENGINE COOLANTS

An experimental investigation of high-aspect-ratio cooling passages
[AIAA PAPER 92-3154] p 64 A92-48780

An improved heat transfer configuration for a solid-core nuclear thermal rocket engine
[AIAA PAPER 92-3583] p 75 A92-54063

Thermal stratification potential in rocket engine coolant channels p 87 N92-25616
[NASA-TM-4378]

An experimental investigation of high-aspect-ratio cooling passages
[NASA-TM-105679] p 48 N92-25958

ENGINE DESIGN

A failure diagnosis system based on a neural network classifier for the Space Shuttle Main Engine p 58 A92-11474

Status of NASA's Earth-to-Orbit Propulsion Technology program
[IAF PAPER 91-258] p 58 A92-13154

Medium power hydrogen arcjet performance
[AIAA PAPER 91-2227] p 58 A92-15355

Design and analysis of reengine Boeing 727-100 center inlet S duct by a reduced Navier-Stokes code
[AIAA PAPER 92-1221] p 8 A92-33320

NASA's high-temperature engine materials program for civil aeronautics p 95 A92-41117

Row-by-row off-design performance calculation method for turbines p 26 A92-44514

Investigation of three-dimensional flow field in a turbine including rotor/stator interaction. I - Design development and performance of the research facility
[AIAA PAPER 92-3325] p 40 A92-48908

Advanced Rotorcraft Transmission program summary [AIAA PAPER 92-3363] p 205 A92-48936
 Boeing Helicopters Advanced Rotorcraft Transmission (ART) Program summary of component tests [AIAA PAPER 92-3364] p 205 A92-48937
 Design considerations in clustering nuclear rocket engines [AIAA PAPER 92-3587] p 66 A92-49069
 Final design of a free-piston hydraulic advanced Stirling conversion system [AIAA PAPER 92-4006] p 206 A92-50798
 The VRT gas turbine combustor - Phase II [AIAA PAPER 92-3471] p 27 A92-54035
 Characterization of ion accelerating systems on NASA LeRC's ion thrusters [AIAA PAPER 92-3827] p 76 A92-54191
 Description of a pressure measurement technique for obtaining surface static pressures of a radial turbine [AIAA PAPER 92-4006] p 200 A92-56829
 JANNAF Liquid Rocket Combustion Instability Panel research recommendations p 115 N92-11124
 An overview of tested and analyzed NTP concepts [NASA-TM-105252] p 80 N92-11137
 Aeropropulsion 1987 [NASA-CP-3049] p 31 N92-22510
 Ceramics for engines p 131 N92-22517
 Overview of the subsonic propulsion technology session p 32 N92-22531
 Small engine technology programs p 32 N92-22532
 Propulsion challenges and opportunities for high-speed transport aircraft p 34 N92-22540
 Supersonic throughflow fans for high-speed aircraft p 34 N92-22541
 Effects of turbine cooling assumptions on performance and sizing of high-speed civil transport [NASA-TM-105610] p 34 N92-23537
 A multiblock grid generation technique applied to a jet engine configuration p 244 N92-24428
 Description of a pressure measurement technique for obtaining surface static pressures of a radial turbine [NASA-TM-105643] p 202 N92-24959
 Contingency power for a small turboshaft engine by using water injection into turbine cooling air [NASA-TM-105680] p 37 N92-29661
 A graphical user-interface for propulsion system analysis [NASA-TM-105696] p 244 N92-33894
ENGINE FAILURE
 A demonstration of an intelligent control system for a reusable rocket engine [NASA-TM-105794] p 92 N92-31507
ENGINE INLETS
 Analysis of an advanced ducted propeller subsonic inlet [AIAA PAPER 92-0274] p 5 A92-25728
 Structural tailoring/analysis for hypersonic components - Executive system development [AIAA PAPER 92-2471] p 219 A92-34360
 A study of three dimensional turbulent boundary layer separation and vortex flow control using the reduced Navier Stokes equations p 9 A92-40105
 Design and analysis of vortex generators on reengineered Boeing 727-100QF center inlet S-duct by a reduced Navier-Stokes code [AIAA PAPER 92-2700] p 10 A92-45542
 Interface of an uncoupled boundary layer algorithm with an inviscid core flow algorithm for unsteady supersonic engine inlets [AIAA PAPER 92-3083] p 11 A92-48730
 Computational analysis of ramjet engine inlet interaction [AIAA PAPER 92-3102] p 11 A92-48744
 Application of computational fluid dynamics to the study of vortex flow control for the management of inlet distortion [AIAA PAPER 92-3177] p 13 A92-54013
 Vortex generator design for aircraft inlet distortion as a numerical optimization problem p 23 N92-13959
 Analysis of an advanced ducted propeller subsonic inlet [NASA-TM-105393] p 15 N92-14002
 Introduction to the internal fluid mechanics research session p 188 N92-22522
 Inlets, ducts, and nozzles p 188 N92-22523
 Interface of an uncoupled boundary layer algorithm with an inviscid core flow algorithm for unsteady supersonic engine inlets [NASA-TM-105684] p 36 N92-27037
 Navier-Stokes analysis and experimental data comparison of compressible flow within ducts [NASA-TM-105796] p 38 N92-30972
 Application of computational fluid dynamics to the study of vortex flow control for the management of inlet distortion [NASA-TM-105672] p 230 N92-34112

ENGINE MONITORING INSTRUMENTS

State space representation of the open-loop dynamics of the Space Shuttle Main Engine p 59 A92-19607
 Advanced optical condition monitoring ... of rocket engines [SAE PAPER 912164] p 199 A92-39994
 Rocket engine diagnostics using qualitative modeling techniques [AIAA PAPER 92-3164] p 65 A92-48787
 Algorithms for real-time fault detection of the Space Shuttle Main Engine [AIAA PAPER 92-3167] p 215 A92-48789
 An overview of in-flight plume diagnostics for rocket engines [AIAA PAPER 92-3785] p 75 A92-54164
 Demonstration of a flight capable system for plume spectroscopy [AIAA PAPER 92-3786] p 57 A92-54165
 Technology readiness assessment of advanced space engine integrated controls and health monitoring [NASA-TM-105255] p 79 N92-11130
 An SSME high pressure oxidizer turbopump diagnostic system using G2(TM) real-time expert system [NASA-TM-105328] p 247 N92-13717
 Research sensors p 202 N92-22526
 Rocket engine diagnostics using qualitative modeling techniques [NASA-TM-105714] p 88 N92-27033
 An overview of in-flight plume diagnostics for rocket engines [NASA-TM-105727] p 90 N92-28417
ENGINE NOISE
 A survey of the broadband shock associated noise prediction methods [AIAA PAPER 92-0501] p 252 A92-26930
 Combustion and core noise p 254 N92-10607
 A survey of the broadband shock associated noise prediction methods [NASA-TM-105365] p 254 N92-14797
 An evaluation of some alternative approaches for reducing fan tone noise [NASA-TM-105356] p 255 N92-18282
ENGINE PARTS
 NDE of advanced turbine engine components and materials by computed tomography [ASME PAPER 91-GT-287] p 215 A92-15681
 A probabilistic approach to the evaluation of fatigue damage in a space propulsion system injector element [AIAA PAPER 92-2413] p 60 A92-34343
 Advanced nozzle and engine components test facility [AIAA PAPER 92-3993] p 41 A92-56816
 Engine component instrumentation development facility at NASA Lewis Research Center [AIAA PAPER 92-3995] p 41 A92-56818
 Description of a pressure measurement technique for obtaining surface static pressures of a radial turbine [AIAA PAPER 92-4006] p 200 A92-56829
 National Aerospace Plane engine seals: High temperature seal performance evaluation p 207 N92-15103
 Advanced nozzle and engine components test facility [NASA-TM-103684] p 42 N92-17059
 Rocket-Based Combined-Cycle (RBCC) Propulsion Technology Workshop. Tutorial session [NASA-CP-10090] p 86 N92-21517
 Life prediction technologies for aeronautical propulsion systems p 32 N92-22520
 Optical measurement systems p 202 N92-22527
 Small engine technology programs p 32 N92-22532
 Coupled multi-disciplinary simulation of composite engine structures in propulsion environment [NASA-TM-105575] p 228 N92-23267
 Description of a pressure measurement technique for obtaining surface static pressures of a radial turbine [NASA-TM-105643] p 202 N92-24959
 Engine component instrumentation development facility at NASA Lewis Research Center [NASA-TM-105644] p 42 N92-25449
 Ceramic composites: Enabling aerospace materials [NASA-TM-105599] p 133 N92-27378
ENGINE TESTING LABORATORIES
 Low power arcjet test facility impacts [NASA-TM-105876] p 47 N92-34114
ENGINE TESTS
 Medium power hydrogen arcjet performance [AIAA PAPER 91-2227] p 58 A92-15355
 NASA low-speed centrifugal compressor for 3-D viscous code assessment and fundamental flow physics research [ASME PAPER 91-GT-140] p 3 A92-15580
 An experimental investigation of high-aspect-ratio cooling passages [AIAA PAPER 92-3154] p 64 A92-48780
 Rocket plume flowfield characterization using laser Rayleigh scattering [AIAA PAPER 92-3351] p 66 A92-48928

Stirling machine operating experience p 206 A92-50788
 A comparison of the calculated and experimental off-design performance of a radial flow turbine [AIAA PAPER 92-3069] p 13 A92-54004
 Low-power arcjet test facility impacts [AIAA PAPER 92-3532] p 74 A92-54040
 An overview of in-flight plume diagnostics for rocket engines [AIAA PAPER 92-3785] p 75 A92-54164
 Demonstration of a flight capable system for plume spectroscopy [AIAA PAPER 92-3786] p 57 A92-54165
 Small engine components test facility compressor testing cell at NASA Lewis Research Center [AIAA PAPER 92-3980] p 41 A92-56806
 Engine component instrumentation development facility at NASA Lewis Research Center [AIAA PAPER 92-3995] p 41 A92-56818
 High-power hydrogen arcjet performance [NASA-TM-105143] p 82 N92-14109
 Evaluation of an innovative high temperature ceramic wafer seal for hypersonic engine applications [NASA-TM-105556] p 208 N92-20815
 Neutralizer optimization [NASA-TM-105578] p 86 N92-21976
 Comparison of GLIMPS and HFAST Stirling engine code predictions with experimental data [NASA-TM-105549] p 267 N92-25395
 Engine component instrumentation development facility at NASA Lewis Research Center [NASA-TM-105644] p 42 N92-25449
 An experimental investigation of high-aspect-ratio cooling passages [NASA-TM-105679] p 48 N92-25958
 An overview of in-flight plume diagnostics for rocket engines [NASA-TM-105727] p 90 N92-28417
 Rocket plume flowfield characterization using laser Rayleigh scattering [NASA-TM-105739] p 257 N92-28475
 Small engine components test facility compressor testing cell at NASA Lewis Research Center [NASA-TM-105685] p 42 N92-30508
 Low-isp derated ion thruster operation [NASA-TM-105787] p 92 N92-32237
 Low power arcjet test facility impacts [NASA-TM-105876] p 47 N92-34114
ENTHALPY
 Sensible heat receiver for solar dynamic space power system p 180 A92-50570
ENTROPY
 Discrete-time entropy formulation of optimal and adaptive control problems p 247 A92-55930
ENVIRONMENT EFFECTS
 Environmental interactions of the Space Station Freedom electric power system p 81 N92-13255
 Environmental effects on friction and wear of diamond and diamondlike carbon coatings [NASA-TM-105634] p 131 N92-23192
 The effect of the low Earth orbit environment on space solar cells: Results of the advanced photovoltaic experiment (S0014) p 237 N92-27320
ENVIRONMENT MODELS
 Electrical and chemical interactions at Mars Workshop, part 1 [NASA-CP-10093] p 270 N92-30302
ENVIRONMENT SIMULATION
 Effect of KOH concentration on LEO cycle life of IPV nickel-hydrogen flight cell - Update II p 232 A92-48212
 Effect of a simulated glaze ice shape on the aerodynamic performance of a rectangular wing [AIAA PAPER 92-4042] p 14 A92-56861
 Effect of KOH concentration on LEO cycle life of IPV nickel-hydrogen flight cells-update 2 [NASA-TM-105314] p 235 N92-13483
 A new technique for oil backstreaming contamination measurements [NASA-TM-105312] p 257 N92-13783
 The NASA CSTI High Capacity Power Program [NASA-TM-105240] p 236 N92-16481
ENVIRONMENTAL TESTS
 Environmental durability of ceramics and ceramic composites p 95 A92-39862
 Effect of KOH concentration on LEO cycle life of IPV nickel-hydrogen flight cell - Update II p 232 A92-48212
 Nickel-hydrogen cell low-earth-orbit life test update p 70 A92-50700
 Effect of KOH concentration on LEO cycle life of IPV nickel-hydrogen flight cells-update 2 [NASA-TM-105314] p 235 N92-13483
 Durability evaluation of photovoltaic blanket materials exposed on LDEF tray S1003 p 132 N92-27100

EPITAXY

- Advanced photovoltaic experiment, S0014: Preliminary flight results and post-flight findings p 237 N92-27101
The evaluation of layered separators for nickel-hydrogen cells p 89 N92-27161

EPITAXY

- Properties of large area ErBa₂Cu₃O_{7-x} thin films deposited by ionized cluster beams p 260 A92-33911
Influence of the dislocation density on the performance of heteroepitaxial indium phosphide solar cells p 234 A92-53156
Radiation and temperature effects in heteroepitaxial and homoepitaxial InP cells p 159 A92-53192

EPOXY MATRIX COMPOSITES

- Probabilistic assessment of space trusses subjected to combined mechanical and thermal loads [NASA-TM-105429] p 230 N92-33935

EPOXY RESINS

- An energy analysis of crack-initiation and arrest in epoxy p 224 A92-49777

EQUATIONS OF MOTION

- Modal simulation of gearbox vibration with experimental correlation [AIAA PAPER 92-3494] p 207 A92-54036
Modal simulation of gearbox vibration with experimental correlation [NASA-TM-105702] p 215 N92-31485

EQUATIONS OF STATE

- Investigation of two and three parameter equations of state for cryogenic fluids p 140 A92-13413
The analysis of high pressure experimental data p 266 A92-16101

- State space representation of the open-loop dynamics of the Space Shuttle Main Engine p 59 A92-19607
A viscoplastic theory with thermodynamic considerations p 219 A92-33903
Pressure dependence of the melting temperature of solids - Rare-gas solids p 171 A92-33912

EQUILIBRIUM FLOW

- Conservative-variable average states for equilibrium gas multi-dimensional fluxes [NASA-TM-105585] p 191 N92-25196

EQUIPMENT SPECIFICATIONS

- Overview of Ka-band communications technology requirements for the space exploration initiative [NASA-TM-105308] p 269 N92-14953

ERBIUM COMPOUNDS

- Properties of large area ErBa₂Cu₃O_{7-x} thin films deposited by ionized cluster beams p 260 A92-33911

EROSION

- Plasma erosion rate diagnostics using laser-induced fluorescence p 198 A92-36738
Further study of the effect of the downstream plasma condition on accelerator grid erosion in an ion thruster [AIAA PAPER 92-3829] p 76 A92-54192
Atomic oxygen interactions with FEP Teflon and silicones on LDEF p 132 N92-24820

ERROR ANALYSIS

- An error analysis of least-squares finite element method of velocity-pressure-vorticity formulation for Stokes problem p 173 A92-37506
GTEX: An expert system for diagnosing faults in satellite ground stations p 148 N92-14215
Least Reliable Bits Coding (LRBC) for high data rate satellite communications [NASA-TM-105431] p 150 N92-18921
Intelligent fault isolation and diagnosis for communication satellite systems p 248 N92-23365

ERROR CORRECTING CODES

- Least Reliable Bits Coding (LRBC) for high data rate satellite communications [NASA-TM-105431] p 150 N92-18921

ERROR FUNCTIONS

- Design of multi-layer neural networks for accurate identification of nonlinear mappings p 246 A92-29030

EROSION

- Advanced Communication Technology Satellite (ACTS) multibeam antenna analysis and experiment [NASA-TM-105420] p 149 N92-17047
A simplified dynamic model of the T700 turboshaft engine [NASA-TM-105805] p 251 N92-30898

ESSENTIALLY NON-OSCILLATORY SCHEMES

- Numerical experiments on a new class of nonoscillatory schemes [AIAA PAPER 92-0421] p 7 A92-28193

ESTERS

- Vinyl capped addition polyimides [NASA-CASE-LEW-15027-2] p 131 N92-24053

ETCHANTS

- Enhancing optical absorption in InP and GaAs utilizing profile etching p 263 A92-53154
High performance etchant for thinning p(+)-InP and its application to p(+)-n InP solar cell fabrication p 263 A92-53155

- Enhancing optical absorption in InP and GaAs utilizing profile etching [NASA-TM-105325] p 82 N92-14111

ETCHING

- Surface etching for light trapping in encapsulated InP solar cells p 232 A92-48091
Enhancing optical absorption in InP and GaAs utilizing profile etching p 263 A92-53154
Anodic etching of p-type cubic silicon carbide p 127 A92-57027

- Solid lubricants on pretreated surfaces [NASA-CASE-LEW-14474-2] p 127 N92-11186

- Enhancing optical absorption in InP and GaAs utilizing profile etching [NASA-TM-105325] p 82 N92-14111

ETHANE

- Saturated fluorescence measurements of the hydroxyl radical in laminar high-pressure C₂H₆/O₂/N₂ flames p 198 A92-33987

- Substituted 1,1,1-triaryl-2,2,2-trifluoroethanes and processes for their synthesis [NASA-CASE-LEW-14345-6] p 96 N92-17882

ETHYLENE

- Atomic oxygen interactions with FEP Teflon and silicones on LDEF p 132 N92-24820

EULER BUCKLING

- Probabilistic progressive buckling of trusses [AIAA PAPER 91-0916] p 223 A92-38142
Probabilistic progressive buckling of trusses [NASA-TM-105162] p 226 N92-15403

EULER EQUATIONS OF MOTION

- Euler flow predictions for an oscillating cascade using a high resolution wave-split scheme [ASME PAPER 91-GT-198] p 3 A92-15623
Unsteady Euler analysis of the flowfield of a propfan at an angle of attack p 3 A92-21070
Central difference TVD and TVB schemes for time dependent and steady state problems [AIAA PAPER 92-0053] p 166 A92-22168
LEWICE/E - An Euler based ice accretion code [AIAA PAPER 92-0037] p 4 A92-25676
Unsteady blade pressures on a propfan at takeoff - Euler analysis and flight data [AIAA PAPER 92-0376] p 25 A92-26234
Euler solutions for an unbladed jet engine configuration [AIAA PAPER 92-0544] p 169 A92-28201

- Unsteady transonic Euler solutions using finite elements [AIAA PAPER 92-2504] p 8 A92-34499
Finite element Euler calculations of unsteady transonic cascade flows [AIAA PAPER 92-2120] p 9 A92-35689

- Domain-decomposition algorithm applied to multielement airfoil grids p 9 A92-41261
Numerical analysis of flow through oscillating cascade sections p 9 A92-44513
Predicted pressure distribution on a prop-fan blade through Euler analysis p 10 A92-46791

- Perturbation of a normal shock - A test case for unsteady Euler codes p 178 A92-48795

- Runge-Kutta methods combined with compact difference schemes for the unsteady Euler equations [AIAA PAPER 92-3210] p 182 A92-54015
Unsteady blade pressures on a propfan - Predicted and measured compressibility effects [AIAA PAPER 92-3774] p 14 A92-54161

- Euler solutions for an unbladed jet engine configuration [NASA-TM-105332] p 184 N92-11328

- LEWICE/E: An Euler based ice accretion code [NASA-TM-105389] p 15 N92-14001

- Central difference TVD and TVB schemes for time dependent and steady state problems [NASA-TM-105357] p 249 N92-15663
A two-dimensional Euler solution for an unbladed jet engine configuration [NASA-TM-105329] p 190 N92-23560

- A two-dimensional Euler solution for an unbladed jet engine configuration p 18 N92-24861
Conservative-variable average states for equilibrium gas multi-dimensional fluxes [NASA-TM-105585] p 191 N92-25196

EULER-LAGRANGE EQUATION

- A new Lagrangian method for real gases at supersonic speed p 19 N92-25814

EUTECTIC ALLOYS

- The effect of porosity and gamma-gamma-prime eutectic content on the fatigue behavior of hydrogen charged PWA 1480 p 116 A92-12046
Microstructure and mechanical properties of near eutectic beta-NiAl plus alpha-Re alloys produced by rapid solidification and extrusion p 119 A92-30844
Solidification processing of intermetallic Nb-Al alloys p 120 A92-33866

EUTECTICS

- Tribological and microstructural comparison of HIPped PM212 and PM212/Au self-lubricating composites [NASA-TM-105615] p 97 N92-26142

EVAPORATORS

- Pulse thermal energy transport/storage system [NASA-CASE-LEW-15235-1] p 195 N92-29125
Design characteristics of a heat pipe test chamber [NASA-TM-105737] p 238 N92-29662

EVOLUTION (DEVELOPMENT)

- Vorticity dynamics of inviscid shear layers [AIAA PAPER 92-0420] p 168 A92-26270

EVOLUTION (LIBERATION)

- A study of Na(x)P₃O₄ as an O₂ electrode bifunctional electrocatalyst [NASA-TM-105311] p 85 N92-20585

EXCITATION

- Control of an axisymmetric turbulent jet by multi-modal excitation p 174 A92-40071
The flip flop nozzle extended to supersonic flows [AIAA PAPER 92-2724] p 10 A92-45561
The flip-flop nozzle extended to supersonic flows [NASA-TM-105570] p 18 N92-23269

EXHAUST EMISSION

- Species and temperature measurement in H₂/O₂ rocket flow fields by means of Raman scattering diagnostics [AIAA PAPER 92-3353] p 178 A92-48930
Applied analytical combustion/emissions research at the NASA Lewis Research Center - A progress report [AIAA PAPER 92-3338] p 27 A92-54025
Propulsion challenges and opportunities for high-speed transport aircraft p 34 N92-22540
Applied analytical combustion/emissions research at the NASA Lewis Research Center [NASA-TM-105731] p 90 N92-29343

EXHAUST FLOW SIMULATION

- Flow in a ventral nozzle for short takeoff and vertical landing aircraft p 25 A92-28538
Experimental balances for the second moments for a buoyant plume and their implication on turbulence modeling p 174 A92-40153
Measurement and analysis of a small nozzle plume in vacuum [AIAA PAPER 92-3108] p 64 A92-48748

EXHAUST GASES

- A simplified reaction mechanism for prediction of NO(x) emissions in the combustion of hydrocarbons [AIAA PAPER 92-3340] p 114 A92-48919

EXHAUST NOZZLES

- Hot gas ingestion characteristics and flow visualization of a vectored thrust STOVL concept p 26 A92-45316
Experimental and analytical study of close-coupled ventral nozzles for ASTOVL aircraft p 26 A92-45325
Preliminary dynamic tests of a flight-type ejector [AIAA PAPER 92-3261] p 27 A92-54020
Experimental performance of three design factors for ventral nozzles for SStOVL aircraft [AIAA PAPER 92-3789] p 28 A92-54168
Flow studies in close-coupled ventral nozzles for STOVL aircraft [NASA-TM-102554] p 17 N92-20934
Experimental performance of three design factors for ventral nozzles for SStOVL aircraft [NASA-TM-105697] p 37 N92-27669
Navier-Stokes analysis and experimental data comparison of compressible flow within ducts [NASA-TM-105796] p 38 N92-30972
Preliminary dynamic tests of a flight-type ejector [NASA-TM-105814] p 38 N92-30998

EXHAUST SYSTEMS

- A computational study of advanced exhaust system transition ducts with experimental validation [AIAA PAPER 92-3794] p 179 A92-49126
Internal reversing flow in a tailpipe offtake configuration for SStOVL aircraft [AIAA PAPER 92-3790] p 28 A92-54169
Computational and experimental investigation of subsonic internal reversing flows [AIAA PAPER 92-3791] p 183 A92-54170
Advanced nozzle and engine components test facility [AIAA PAPER 92-3993] p 41 A92-56816
Advanced nozzle and engine components test facility [NASA-TM-103684] p 42 N92-17059
Internal reversing flow in a tailpipe offtake configuration for SStOVL aircraft [NASA-TM-105698] p 37 N92-28418

EXPENDABLE STAGES (SPACECRAFT)

- An electromechanical actuation system for an expendable launch vehicle [NASA-TM-105774] p 48 N92-30310

EXPERIMENT DESIGN

- The NASA microgravity combustion space experiment program [IAF PAPER 91-398] p 112 A92-18484
Advanced photovoltaic experiment, S0014: Preliminary flight results and post-flight findings p 237 N92-27101

- EXPERT SYSTEMS**
 LDEXPT, an intelligent database system for the Composite Load Spectra project p 59 A92-23695
 Fault diagnosis for the Space Shuttle main engine p 60 A92-28137
 MisTec - A software application for supporting space exploration scenario options and technology development analysis and planning [AIAA PAPER 92-1293] p 242 A92-38490
 Developments in REDES: The Rocket Engine Design Expert System p 78 N92-11120
 An SSME high pressure oxidizer turbopump diagnostic system using G2(TM) real-time expert system [NASA-TM-105328] p 247 N92-13717
 GTX: An expert system for diagnosing faults in satellite ground stations p 148 N92-14215
 FIDEX: An expert system for satellite diagnostics p 148 N92-14218
 MisTec: A software application for supporting space exploration scenario options and technology development analysis and planning [NASA-TM-105214] p 243 N92-14649
 Automated power management and control p 84 N92-17773
 Intelligent fault isolation and diagnosis for communication satellite systems p 248 N92-23365
 PC graphics generation and management tool for real-time applications [NASA-TM-105749] p 244 N92-28684
 Implementation of an intelligent control system [NASA-TM-105795] p 241 N92-33897
- EXPOSURE**
 Isothermal aging effects on PMR-15 resin [NASA-TM-105648] p 110 N92-30986
 Demonstrated survivability of a high temperature optical fiber cable on a 1500 pound thrust rocket chamber [NASA-TM-105835] p 136 N92-32230
- EXPULSION**
 Slush hydrogen pressurized expulsion studies at the NASA K-Site Facility [AIAA PAPER 92-3385] p 141 A92-48951
 Slush hydrogen pressurized expulsion studies at the NASA K-Site Facility [NASA-TM-105597] p 135 N92-26131
- EXTENSOMETERS**
 An evaluation of strain measuring devices for ceramic composites [NASA-TM-105337] p 225 N92-14433
- EXTERNAL COMBUSTION ENGINES**
 The F/A-18 external burning flight test [AIAA PAPER 91-5050] p 23 A92-44547
 Experiments and analysis concerning the use of external burning to reduce aerospace vehicle transonic drag [NASA-TM-105397] p 30 N92-17546
- EXTINCTION**
 An investigation of flame spread over shallow liquid pools in microgravity and nonair environments p 112 A92-16609
- EXTRAPOLATION**
 Extrapolation procedures in Mott electron polarimetry p 197 A92-21241
 Upper bounds for convergence rates of vector extrapolation methods on linear systems with initial iterations [NASA-TM-105608] p 250 N92-33742
- EXTRATERRESTRIAL ENVIRONMENTS**
 A dynamic isotope power system portable generator for the moon or Mars p 232 A92-50634
- EXTRATERRESTRIAL RADIATION**
 Magnetic radiation shielding - An idea whose time has returned? p 53 A92-17796
- EXTRATERRESTRIAL RESOURCES**
 Material processing with hydrogen and carbon monoxide on Mars p 231 A92-17769
 Technical prospects for utilizing extraterrestrial propellants for space exploration [IAF PAPER 91-669] p 133 A92-20612
 Acetylene fuel from atmospheric CO₂ on Mars p 133 A92-32199
 In-situ carbon dioxide fixation on Mars p 134 A92-50613
 Engine system assessment study using Martian propellants [AIAA PAPER 92-3446] p 73 A92-54030
 A compilation of lunar and Mars exploration strategies utilizing indigenous propellants [NASA-TM-105262] p 135 N92-19837
- EXTRAVEHICULAR ACTIVITY**
 Removable hand hold [NASA-CASE-LEW-15196-1] p 213 N92-29092
- EXTREMELY HIGH FREQUENCIES**
 A low-power, high-efficiency Ka-band TWTA [AIAA PAPER 92-1822] p 154 A92-29769
 Ka-band active MMIC subarray development [AIAA PAPER 92-1863] p 155 A92-29803
- Ka-band dual frequency array feed for a low cost ACTS ground terminal [AIAA PAPER 92-1902] p 143 A92-29833
 20/30 GHz satellite personal communications networks [AIAA PAPER 92-1908] p 143 A92-29839
 Characteristics of a future aeronautical satellite communications system [AIAA PAPER 92-2058] p 22 A92-29889
 A personal communications network using a Ka-band satellite p 145 A92-31780
 Performance of a four-element Ka-band high-temperature superconducting microstrip antenna p 146 A92-37224
 A vertically integrated Ka-band phased array antenna [AIAA PAPER 92-1976] p 156 A92-38140
 A low-power, high-efficiency Ka-band TWTA p 156 A92-38163
 The ACTS multibeam antenna p 146 A92-46046
 Ka-band MMIC arrays for ACTS Aero Terminal Experiment [IAF PAPER 92-0398] p 159 A92-55785
 Advanced Communications Technology Satellite (ACTS) [IAF PAPER 92-0407] p 50 A92-55788
 Overview of Ka-band communications technology requirements for the space exploration initiative [NASA-TM-105308] p 269 N92-14953
 The ACTS multibeam antenna [NASA-TM-105645] p 52 N92-30383
 Characteristics of a future aeronautical satellite communications system p 151 N92-30932
 A personal communications network using a Ka-band satellite p 151 N92-30934
 V-band pseudomorphic HEMT MMIC phased array components for space communications p 151 N92-32966
 An optically controlled Ka-band phased array antenna p 152 N92-32968
 Ka-band dual frequency array feed for a low cost ACTS ground terminal p 152 N92-32969
- EXTRUDING**
 Microstructure and mechanical properties of near eutectic beta-NiAl plus alpha-Re alloys produced by rapid solidification and extrusion p 119 A92-30844
- F**
- F-18 AIRCRAFT**
 Full Navier-Stokes calculations on the installed F/A-18 inlet at a high angle of attack [AIAA PAPER 92-3175] p 13 A92-54012
 Wind tunnel investigation of vortex flows on F/A-18 configuration at subsonic through transonic speed [NASA-TP-3111] p 16 N92-14968
- FABRICATION**
 Relationship between voids and interlaminar shear strength of polymer matrix composites p 98 A92-10241
 Interphase layer optimization for metal matrix composites with fabrication considerations p 98 A92-10262
 Preliminary tests of annular ion optics [AIAA PAPER 92-3148] p 64 A92-48776
 Technology development of fabrication techniques for advanced solar dynamic concentrators p 232 A92-50571
 Pilot production of 4 sq cm ITO/InP photovoltaic solar cells p 71 A92-53197
 Progress in the development of lightweight nickel electrode for aerospace applications [NASA-TM-105591] p 236 N92-20493
 Graphite intercalation compound with iodine as the major intercalant [NASA-TM-105375] p 97 N92-25203
- FABRY-PEROT INTERFEROMETERS**
 The introduction of spurious modes in a hole-coupled Fabry-Perot open resonator p 197 A92-21244
 Rayleigh-Brillouin scattering to determine one-dimensional temperature and number density profiles of a gas flow field p 198 A92-38067
 Demonstration of a flight capable system for plume spectroscopy [AIAA PAPER 92-3786] p 57 A92-54165
- FACE CENTERED CUBIC LATTICES**
 The effect of porosity and gamma-gamma-prime eutectic content on the fatigue behavior of hydrogen charged PWA 1480 p 116 A92-12046
 Lattice parameters of fcc binary alloys using a new semiempirical method p 120 A92-32898
 Ductility enhancement from interface dislocation sources in a directionally solidified beta + gamma + gamma-prime Ni-Fe-Al composite alloy p 122 A92-46850
- Lattice parameters of fcc binary alloys using a new semiempirical method [NASA-TM-105304] p 123 N92-16111
- FACTORIZATION**
 Upwind differencing and LU factorization for chemical non-equilibrium Navier-Stokes equations p 171 A92-33829
 An iterative implicit diagonally-dominant factorization algorithm for solving the Navier-Stokes equations [NASA-TM-105259] p 249 N92-16663
- FAILURE**
 Destructive physical analysis results of Ni/H₂ cells cycled in LEO regime p 70 A92-50707
 Mechanical behaviour and failure phenomenon of an in situ toughened silicon nitride p 127 A92-54504
 Differential continuum damage mechanics models for creep and fatigue of unidirectional metal matrix composites [NASA-TM-105213] p 226 N92-16371
 Reliability training [NASA-RP-1253] p 49 N92-32456
- FAILURE ANALYSIS**
 Fault diagnosis for the Space Shuttle main engine p 60 A92-28137
 A simplified dynamic model of Space Shuttle Main Engine p 60 A92-29289
 A three-dimensional finite-element thermal/mechanical analytical technique for high-performance traveling wave tubes [AIAA PAPER 92-1824] p 154 A92-29771
 Analysis of whisker-toughened CMC structural components using an interactive reliability model [AIAA PAPER 92-2490] p 221 A92-34582
 Failure mechanisms of 3-D woven SiC/SiC composites under tensile and flexural loading at room and elevated temperatures p 103 A92-39642
 Combined bending and thermal fatigue of high-temperature metal-matrix composites - Computational simulation p 223 A92-43944
 Thermal verification testing of commercial printed-circuit boards for spaceflight p 216 A92-56217
 Thermal verification testing of commercial printed-circuit boards for spaceflight [NASA-TM-105261] p 141 N92-11221
 Desktop fiber push-out apparatus [NASA-TM-105341] p 107 N92-16036
 Life prediction technologies for aeronautical propulsion systems p 32 N92-22520
 Reliability training [NASA-RP-1253] p 49 N92-32456
- FAILURE MODES**
 Mixed-mode fracture in unidirectional graphite epoxy composite laminates with central notch p 218 A92-29464
 Algorithms for real-time fault detection of the Space Shuttle Main Engine [AIAA PAPER 92-3167] p 215 A92-48789
 Linear quadratic servo control of a reusable rocket engine p 67 A92-50495
 Life prediction technologies for aeronautical propulsion systems p 32 N92-22520
 Damage mechanisms in bithermal and thermomechanical fatigue of Haynes 188 [NASA-TM-105381] p 228 N92-24985
 A demonstration of an intelligent control system for a reusable rocket engine [NASA-TM-105794] p 92 N92-31507
 Reliability training [NASA-RP-1253] p 49 N92-32456
- FAN BLADES**
 The role of tip clearance in high-speed fan stall [ASME PAPER 91-GT-83] p 2 A92-15550
 Design and performance of controlled-diffusion stator compared with original double-circular-arc stator [NASA-TP-2852] p 34 N92-22863
 Coupled multi-disciplinary simulation of composite engine structures in propulsion environment [NASA-TM-105575] p 228 N92-23267
 Structural analysis of low-speed composite propfan blades for the LRCSW wind tunnel model [NASA-TM-105266] p 229 N92-25753
- FAR FIELDS**
 Calculation of far-field scattering from nonspherical particles using a geometrical optics approach p 256 A92-20288
 Far-field noise and internal modes from a ducted propeller at simulated aircraft takeoff conditions [AIAA PAPER 92-0371] p 252 A92-26230
 Far-field noise and internal modes from a ducted propeller at simulated aircraft takeoff conditions [NASA-TM-105369] p 254 N92-16702
 Advanced Communication Technology Satellite (ACTS) multibeam antenna analysis and experiment [NASA-TM-105420] p 149 N92-17047

FAR ULTRAVIOLET RADIATION

Operating and service manual for the NASA Lewis automated far-field antenna range
[NASA-TM-105343] p 52 N92-22319

FAR ULTRAVIOLET RADIATION

Vacuum ultraviolet absorption in a hydrogen arcjet
[AIAA PAPER 92-3564] p 259 A92-54055

FAST NEUTRONS

Neutron, gamma ray, and temperature effects on the electrical characteristics of thyristors
[NASA-TM-105728] p 162 N92-28432

FATIGUE (MATERIALS)

The effect of matrix mechanical properties on (0)8 unidirectional SiC/Ti composite fatigue resistance
p 99 A92-16220

Fatigue crack growth in unidirectional metal matrix composite
p 99 A92-19734
A real time neural net estimator of fatigue life
p 245 A92-21694

Fatigue crack growth in a unidirectional SCS-6/Ti-15-3 composite
p 102 A92-39036

Modeling of crack bridging in a unidirectional metal matrix composite
p 104 A92-43085

Life prediction technologies for aeronautical propulsion systems
p 32 N92-22520

Damage mechanisms in bithermal and thermomechanical fatigue of Haynes 188
[NASA-TM-105381] p 228 N92-24985

A differential CDM model for fatigue of unidirectional metal matrix composites
[NASA-TM-105726] p 230 N92-31505

FATIGUE LIFE

Probabilistic constitutive relationships for cyclic material strength models
p 217 A92-21081

A real time neural net estimator of fatigue life
p 245 A92-21694

Life Extending Control --- mechanical fatigue in reusable rocket engines
p 246 A92-29166

Fatigue damage accumulation in nickel prior to crack initiation
p 120 A92-33947

A probabilistic approach to the evaluation of fatigue damage in a space propulsion system injector element
[AIAA PAPER 92-2413] p 60 A92-34343

Fatigue crack growth reliability by probabilistic finite elements
p 222 A92-37524

High-temperature fatigue behavior of a SiC/Ti-24Al-11Nb composite
p 104 A92-44613

Stochastic modeling of crack initiation and short-crack growth under creep and creep-fatigue conditions
[ASME PAPER 92-APM-5] p 223 A92-44681

Cumulative creep-fatigue damage evolution in an austenitic stainless steel
p 121 A92-45231

Application of a thermal fatigue life prediction model to high-temperature aerospace alloys B1900 + Hf and Haynes 188
p 121 A92-45232

Improvement in surface fatigue life of hardened gears by high-intensity shot peening
p 211 N92-26108

Elevated temperature axial and torsional fatigue behavior of Haynes 188
[NASA-TM-105396] p 229 N92-28701

Optimal design of compact spur gear reductions
[NASA-TM-105676] p 213 N92-29351

Cyclic hot firing results of tungsten-wire-reinforced, copper-lined thrust chambers
[NASA-TM-4214] p 91 N92-31249

Life extending control for rocket engines
[NASA-TM-105789] p 142 N92-31263

FATIGUE TESTING MACHINES

Analysis and modification of a single-mesh gear fatigue rig for use in diagnostic studies
[NASA-TM-105416] p 212 N92-27879

FATIGUE TESTS

Modeling of crack bridging in a unidirectional metal matrix composite
p 104 A92-43085

Thermomechanical and bithermal fatigue behavior of cast B1900 + Hf and wrought Haynes 188
p 122 A92-45233

A preliminary characterization of the tensile and fatigue behavior of tungsten-fiber/Waspaloy-matrix composite
[NASA-TM-105346] p 187 N92-22487

High temperature dynamic engine seal technology development
[NASA-TM-105641] p 209 N92-23435

Elevated temperature axial and torsional fatigue behavior of Haynes 188
[NASA-TM-105396] p 229 N92-28701

FAULT TOLERANCE

Fault tolerance in onboard processors - Protecting efficient FDM demultiplexers
[AIAA PAPER 92-1969] p 144 A92-29892

Thermal verification testing of commercial printed-circuit boards for spaceflight
p 216 A92-56217

Health management and controls for earth to orbit propulsion systems
[IAF PAPER 92-0646] p 77 A92-57089

Real-time fault diagnosis for propulsion systems
[NASA-TM-105303] p 29 N92-11017

Thermal verification testing of commercial printed-circuit boards for spaceflight
[NASA-TM-105261] p 141 N92-11221

FIDEX: An expert system for satellite diagnostics
p 148 N92-14218

FAULT TREES

Structural system reliability calculation using a probabilistic fault tree analysis method
[AIAA PAPER 92-2410] p 251 A92-34341

FAULTS

Fault diagnosis for the Space Shuttle main engine
p 60 A92-28137

Intelligent fault isolation and diagnosis for communication satellite systems
p 248 N92-23365

FEASIBILITY ANALYSIS

MisTec - A software application for supporting space exploration scenario options and technology development analysis and planning
[AIAA PAPER 92-1293] p 242 A92-38490

MisTec: A software application for supporting space exploration scenario options and technology development analysis and planning
[NASA-TM-105214] p 243 N92-14649

Design feasibility study of a Space Station Freedom truss
[NASA-TM-105558] p 214 N92-30571

Experimental testing of prototype face gears for helicopter transmissions
[NASA-TM-105434] p 214 N92-31349

FEEDBACK CONTROL

Integrated flight/propulsion control specifications for systems with two-way coupling
p 39 A92-29117

A Lyapunov based nonlinear control scheme for stabilizing a basic compression system using a close-coupled control valve
p 246 A92-29316

Linear quadratic servo control of a reusable rocket engine
[NASA-TM-105291] p 79 N92-11128

Integrated health monitoring and controls for rocket engines
[NASA-TM-105763] p 90 N92-28693

Microgravity vibration isolation: Optimal preview and feedback control
[NASA-TM-105673] p 142 N92-30692

A simplified dynamic model of the T700 turboshaft engine
[NASA-TM-105805] p 251 N92-30898

A demonstration of an intelligent control system for a reusable rocket engine
[NASA-TM-105794] p 92 N92-31507

A parameter optimization approach to controller partitioning for integrated flight/propulsion control application
[NASA-TM-105826] p 40 N92-32241

Implementation of an intelligent control system
[NASA-TM-105795] p 241 N92-33897

FEEDFORWARD CONTROL

Microgravity vibration isolation: Optimal preview and feedback control
[NASA-TM-105673] p 142 N92-30692

FIBER COMPOSITES

Influence of interfacial shear strength on the mechanical properties of SiC fiber reinforced reaction-bonded silicon nitride matrix composites
p 99 A92-15145

Mechanical behavior of fiber reinforced SiC/RBSN ceramic matrix composites - Theory and experiment --- Reaction Bonded Silicon Nitride
[ASME PAPER 91-GT-209] p 99 A92-15629

Isothermal fatigue behaviour of a (90 deg)8 SiC/Ti-15-3 composite at 426 C
p 100 A92-23313

Oxidation effects on the mechanical properties of a SiC-fiber-reinforced reaction-bonded Si3N4 matrix composite
p 100 A92-25445

Multiobjective shape and material optimization of composite structures including damping
p 218 A92-28055

Microstress analysis of periodic composites
p 218 A92-30673

Effect of fiber reinforcement on thermo-oxidative stability and mechanical properties of polymer matrix composites
p 101 A92-33587

Ceramics and ceramic matrix composites - Aerospace potential and status
[AIAA PAPER 92-2445] p 94 A92-34474

Diffusive crack growth at a bimaterial interface
[AIAA PAPER 92-2432] p 220 A92-34580

Near-tip dual-length scale mechanics of mode-I cracking in laminate brittle matrix composites
[AIAA PAPER 92-2491] p 221 A92-34583

Fracture resistance development in ceramic composites with nonlinear fiber pullout relationship
[AIAA PAPER 92-2493] p 221 A92-34585

Effect of fiber strength on the room temperature tensile properties of SiC/Ti-24Al-11Nb
p 102 A92-36389

Fatigue crack growth in a unidirectional SCS-6/Ti-15-3 composite
p 102 A92-39036

Fiber coating/matrix reactions in silicon-base ceramic matrix composites
p 102 A92-39604

Role of interfacial thermal barrier in the transverse thermal conductivity of uniaxial SiC fiber-reinforced reaction bonded silicon nitride
p 102 A92-39605

Reaction-bonded Si3N4 and SiC matrix composites
p 103 A92-39858

Effect of fiber orientation on the fracture toughness of brittle matrix composites
p 103 A92-41841

Thermomechanical testing of high-temperature composites - Thermomechanical fatigue (TMF) behavior of SiC(SCS-6)/Ti-15-3
p 104 A92-44606

High-temperature fatigue behavior of a SiC/Ti-24Al-11Nb composite
p 104 A92-44613

Micromechanical model of crack growth in fiber reinforced brittle materials
p 223 A92-46829

Initial evaluation of continuous fiber reinforced NIAI composites
p 104 A92-46867

Reduction of thermal residual stresses in advanced metallic composites based upon a compensating/compliant layer concept
p 105 A92-47106

High molecular weight first generation PMR polyimides for 343 C applications
p 105 A92-49819

Reduction of thermal stresses in continuous fiber reinforced metal matrix composites with interface layers
p 105 A92-50347

Computational simulation of surface waviness in graphite/epoxy woven composites due to initial curing
[NASA-TM-105313] p 106 N92-14118

Thermal conductivity and thermal expansion of graphite fiber/copper matrix composites
p 106 N92-14120

An evaluation of strain measuring devices for ceramic composites
[NASA-TM-105337] p 225 N92-14433

Effects of a noncoplanar biphenyldiamine on the processing and properties of addition polyimides
[NASA-TM-105383] p 107 N92-15137

Analysis of aircraft engine blade subject to ice impact
[NASA-TM-105336] p 226 N92-15402

Desktop fiber push-out apparatus
[NASA-TM-105341] p 107 N92-16036

Intercalated hybrid graphite fiber composite
[NASA-CASE-LEW-15241-1] p 107 N92-17861

High molecular weight first generation PMR polyimides for 343 C applications
[NASA-TM-105364] p 129 N92-19498

COMGEN-BEM: Boundary element model generation for composite materials micromechanical analysis
[NASA-TM-105548] p 226 N92-19779

Structure-to-property relationships in addition cured polymers. 4: Correlations between thermo-oxidative weight losses of norbornenyl cured polyimide resins and their composites
[NASA-TM-105553] p 108 N92-20039

Vinyl capped addition polyimides
[NASA-CASE-LEW-15027-2] p 131 N92-24053

Applications of high thermal conductivity composites to electronics and spacecraft thermal design
[NASA-TM-102434] p 56 N92-24349

Cyclic hot firing results of tungsten-wire-reinforced, copper-lined thrust chambers
[NASA-TM-4214] p 91 N92-31249

Computational simulation of matrix micro-slip bands in SiC/Ti-15 composite
[NASA-TM-105762] p 111 N92-32466

Computational simulation of structural fracture in fiber composites
p 111 N92-32531

FIBER OPTICS

Interfaces for high-speed fiber-optic links - Analysis and experiment
p 256 A92-24002

A fiber optic sensor for ophthalmic refractive diagnostics
p 198 A92-34831

Advanced Communications Technology Satellite (ACTS)
p 50 A92-38164

Wavelength-multiplexed fiber-optic position encoder for aircraft control systems
p 24 A92-42602

Fiber optics in liquid propellant rocket engine environments
p 62 A92-42610

LDV measurements on a rectangular wing with a simulated glaze ice accretion
[AIAA PAPER 92-2690] p 10 A92-45537

Fiber optic controls for aircraft engines - Issues and implications
p 24 A92-46244

Multiple-mode reconfigurable electro-optic switching network for optical fiber sensor array
p 256 A92-46245

- Potential for integrated optical circuits in advanced aircraft with fiber optic control and monitoring systems p 24 A92-46246
- Fiber-optic sensors for aerospace electrical measurements - An update p 200 A92-50630
- Fiber optics for controls p 40 N92-22529
- Demonstrated survivability of a high temperature optical fiber cable on a 1500 pound thrust rocket chamber [NASA-TM-105835] p 136 N92-32230
- RF modulated fiber optic sensing systems and their applications [NASA-TM-105801] p 257 N92-33896
- FIBER ORIENTATION**
- Fatigue crack growth in unidirectional metal matrix composite p 99 A92-19734
- Effect of fiber orientation on the fracture toughness of brittle matrix composites p 103 A92-41841
- Applications of high thermal conductivity composites to electronics and spacecraft thermal design [NASA-TM-102434] p 56 N92-24349
- FIBER STRENGTH**
- Relative sliding durability of two candidate high temperature oxide fiber seal materials [AIAA PAPER 92-3713] p 126 A92-49095
- Relative sliding durability of two candidate high temperature oxide fiber seal materials [NASA-TM-105199] p 95 N92-10064
- FIBERS**
- Method of intercalating large quantities of fibrous structures [NASA-CASE-LEW-15077-1] p 107 N92-16025
- High temperature, flexible pressure-actuated, brush seal [NASA-CASE-LEW-15086-1] p 208 N92-16318
- High temperature, flexible, fiber-preform seal [NASA-CASE-LEW-15085-1] p 208 N92-22043
- FIELD EFFECT TRANSISTORS**
- Significant long-term reduction in n-channel MESFET subthreshold leakage using ammonium-sulfide surface treated gates p 153 A92-12272
- Temperature independent quantum well FET with delta channel doping p 157 A92-49596
- Analog synthesized fast-variable linear load p 157 A92-50539
- Microwave properties of peeled HEMT devices sapphire substrates p 265 N92-32978
- C-band superconductor/semiconductor hybrid field-effect transistor amplifier on a LaAlO₃ substrate [NASA-TM-105828] p 163 N92-34204
- FIGHTER AIRCRAFT**
- A computational study of advanced exhaust system transition ducts with experimental validation [AIAA PAPER 92-3794] p 179 A92-49126
- A parameter optimization approach to controller partitioning for integrated flight/propulsion control application [NASA-TM-105826] p 40 N92-32241
- FIGURE OF MERIT**
- Report of the Nuclear Propulsion Mission Analysis, Figures of Merit Subpanel: Quantifiable figures of merit for nuclear thermal propulsion [NASA-TM-104179] p 43 N92-20925
- FILLETS**
- The aerodynamic effect of fillet radius in a low speed compressor cascade [NASA-TM-105347] p 29 N92-14063
- FILLING**
- On-orbit cryogenic fluid transfer research at NASA Lewis Research Center p 45 A92-23847
- FILM COOLING**
- Performance comparison of axisymmetric and three-dimensional hydrogen film coolant injection in a 110 N hydrogen/oxygen rocket [AIAA PAPER 92-3390] p 73 A92-54027
- High temperature thruster technology for spacecraft propulsion [NASA-TM-105348] p 82 N92-15125
- FILM THICKNESS**
- Magnetic penetration depth of YBa₂Cu₃O_{7-δ} thin films determined by the power transmission method p 265 N92-32983
- FINITE DIFFERENCE THEORY**
- Finite difference solution for transient cooling of a radiating-conducting semitransparent layer p 166 A92-20310
- FDDO and DSMC analyses of rarefied gas flow through 2D nozzles [AIAA PAPER 92-2858] p 176 A92-47841
- Pressurization of cryogenics - A review of current technology and its applicability to low-gravity conditions [AIAA PAPER 92-3061] p 72 A92-54002
- Runge-Kutta methods combined with compact difference schemes for the unsteady Euler equations [AIAA PAPER 92-3210] p 182 A92-54015
- Comparisons of cylindrical and rectangular media radiative transfer solutions using the S-N discrete ordinates method [AIAA PAPER 92-2894] p 266 A92-54287
- Parametric studies of phase change thermal energy storage canisters for Space Station Freedom [NASA-TM-105350] p 55 N92-13143
- An iterative implicit diagonally-dominant factorization algorithm for solving the Navier-Stokes equations [NASA-TM-105259] p 249 N92-16663
- Pressurization of cryogenics: A review of current technology and its applicability to low-gravity conditions [NASA-TM-105746] p 136 N92-29669
- FINITE ELEMENT METHOD**
- Determination of the stress distributions in a ceramic, tensile specimen using numerical techniques p 216 A92-14546
- A combined vector potential-scalar potential method for FE computation of 3D magnetic fields in electrical devices with iron cores p 154 A92-23959
- Effect of surface deposits on electromagnetic propagation in uniform ducts p 142 A92-23964
- A three-dimensional finite-element thermal/mechanical analytical technique for high-performance traveling wave tubes [AIAA PAPER 92-1824] p 154 A92-29771
- An efficient finite element method for aircraft de-icing problems [AIAA PAPER 92-0532] p 22 A92-31670
- Mapping methods for computationally efficient and accurate structural reliability [AIAA PAPER 92-2347] p 219 A92-34321
- Recent developments of the NESSUS probabilistic structural analysis computer program [AIAA PAPER 92-2411] p 242 A92-34342
- A study of equation solvers for linear and non-linear finite element analysis on parallel processing computers [AIAA PAPER 92-2478] p 242 A92-34367
- Material nonlinear analysis via mixed-iterative finite element method [AIAA PAPER 92-2479] p 220 A92-34368
- Unsteady transonic Euler solutions using finite elements [AIAA PAPER 92-2504] p 8 A92-34499
- Multidisciplinary tailoring of hot composite structures [AIAA PAPER 92-2563] p 220 A92-34564
- Finite element Euler calculations of unsteady transonic cascade flows [AIAA PAPER 92-2120] p 9 A92-35689
- A least-squares finite element method for incompressible Navier-Stokes problems p 173 A92-37387
- An error analysis of least-squares finite element method of velocity-pressure-vorticity formulation for Stokes problem p 173 A92-37506
- A variationally coupled FE-BE method for elasticity and fracture mechanics p 222 A92-37510
- An unconditionally stable staggered algorithm for transient finite element analysis of coupled thermoelastic problems p 222 A92-37517
- Fatigue crack growth reliability by probabilistic finite elements p 222 A92-37524
- Probabilistic progressive buckling of trusses [AIAA PAPER 91-0916] p 223 A92-38142
- A method for determining spiral-bevel gear tooth geometry for finite element analysis [NASA-TP-3096] p 207 N92-10195
- Computational simulation of surface waviness in graphite/epoxy woven composites due to initial curing [NASA-TM-105313] p 106 N92-14118
- Analysis of aircraft engine blade subject to ice impact [NASA-TM-105336] p 226 N92-15402
- Probabilistic progressive buckling of trusses [NASA-TM-105162] p 226 N92-15403
- Space Station Freedom solar dynamic modules structural modelling and analysis [NASA-TM-104506] p 226 N92-15405
- Optimal least-squares finite element method for elliptic problems [NASA-TM-105382] p 249 N92-15662
- Improved accuracy for finite element structural analysis via a new integrated force method [NASA-TP-3204] p 227 N92-22227
- Evaluation of MHOST analysis capabilities for a plate element --- finite element modeling [NASA-TM-105387] p 228 N92-23196
- Contact stresses in meshing spur gear teeth: Use of an incremental finite element procedure [NASA-TM-105388] p 209 N92-23536
- Minimization of the vibration energy of thin-plate structure [NASA-TM-105654] p 211 N92-25448
- Modal element method for scattering of sound by absorbing bodies [NASA-TM-105722] p 255 N92-28984
- Validation of finite element and boundary element methods for predicting structural vibration and radiated noise [NASA-TM-105359] p 213 N92-29697
- Computational simulation of intermingled-fiber hybrid composite behavior [NASA-TM-105666] p 110 N92-31506
- Computational simulation of matrix micro-slip bands in SiC/Ti-15 composite [NASA-TM-105762] p 111 N92-32466
- Modal test/analysis correlation of Space Station structures using nonlinear sensitivity [NASA-TM-105850] p 230 N92-34221
- FINITE VOLUME METHOD**
- Upwind differencing and LU factorization for chemical non-equilibrium Navier-Stokes equations p 171 A92-33829
- Three-dimensional calculations of supersonic reacting flows using an LU scheme p 179 A92-50465
- A finite-volume numerical method to calculate fluid forces and rotorodynamic coefficients in seals [AIAA PAPER 92-3712] p 183 A92-54132
- A general numerical model for wave rotor analysis [NASA-TM-105740] p 196 N92-31484
- FIR FILTERS**
- An IIR median hybrid filter p 246 A92-40375
- FIRE PREVENTION**
- Determination of the natural convection coefficient in low-gravity [AIAA PAPER 92-0712] p 168 A92-27072
- Risks, designs, and research for fire safety in spacecraft [NASA-TM-105317] p 240 N92-13581
- Microgravity combustion science: Progress, plans, and opportunities [NASA-TM-105410] p 139 N92-27197
- FIRING (IGNITING)**
- Identification of the Space Shuttle Main Engine dynamic models from firing data [AIAA PAPER 92-3317] p 73 A92-54022
- FIXED WINGS**
- The NASA aircraft icing research program p 23 N92-22534
- FLAME PROPAGATION**
- Opposed flow flame spread in normal, enhanced and reduced gravity p 111 A92-12898
- The implications of experimentally controlled gravitational accelerations for combustion science p 112 A92-16601
- An investigation of flame spread over shallow liquid pools in microgravity and nonair environments p 112 A92-16609
- Intensified array camera imaging of solid surface combustion aboard the NASA Learjet [AIAA PAPER 92-0240] p 137 A92-25702
- The structure of premixed particle-cloud flames p 114 A92-43779
- Intensified array camera imaging of solid surface combustion aboard the NASA Learjet [NASA-TM-105361] p 138 N92-16156
- Combustion-wave ignition for rocket engines [NASA-TM-105545] p 84 N92-20043
- Color image processing and object tracking workstation [NASA-TM-105561] p 139 N92-26611
- FLAME STABILITY**
- Gravitational influences on the behavior of confined diffusion flames [AIAA PAPER 92-0334] p 113 A92-25781
- FLAME TEMPERATURE**
- Quantitative fluorescence measurements of the OH radical in high pressure methane flames [AIAA PAPER 92-2960] p 114 A92-46976
- FLAMES**
- Saturated fluorescence measurements of the hydroxyl radical in laminar high-pressure C₂H₆/O₂/N₂ flames p 198 A92-33987
- FLAMMABILITY**
- Microgravity combustion science: Progress, plans, and opportunities [NASA-TM-105410] p 139 N92-27197
- FLAT PLATES**
- Experimental study of boundary layer transition on a heated flat plate p 172 A92-36022
- Distortion of a flat-plate boundary layer by free-stream vorticity normal to the plate p 173 A92-36343
- Time domain numerical calculations of unsteady vortical flows about a flat plate airfoil p 12 A92-50473
- Comment on two-equation models --- turbulence models p 191 N92-24520
- FLEXING**
- Damage mechanisms in three-dimensional woven reinforced ceramic matrix composites under tensile and flexural loading at room and elevated temperatures [AIAA PAPER 92-2492] p 101 A92-34584

FLIGHT CONTROL

Modeling of the flexural behavior of ceramic-matrix composites p 225 A92-52005

FLIGHT CONTROL

Integrated flight/propulsion control design for a STOVL aircraft using H-infinity control design techniques p 39 A92-29093

Integrated flight/propulsion control specifications for systems with two-way coupling p 39 A92-29117
IMPAC - An integrated methodology for propulsion and airframe control p 39 A92-29118

A framework for the analysis of airframe/engine interactions and integrated flight/propulsion control p 39 A92-29120

Integrated flight/propulsion control for supersonic STOVL aircraft p 39 A92-45320

Piloted evaluation of an integrated propulsion and flight control simulator p 23 A92-52459

[AIAA PAPER 92-4178] p 23 A92-52459
Analysis of airframe/engine interactions for a STOVL aircraft with integrated flight/propulsion control [AIAA PAPER 92-4623] p 23 A92-55300

Design and evaluation of a robust dynamic neurocontroller for a multivariable aircraft control problem p 40 N92-20586

[NASA-TM-105579] p 40 N92-20586
Directions in propulsion control p 32 N92-22530

A parameter optimization approach to controller partitioning for integrated flight/propulsion control application p 40 N92-32241

[NASA-TM-105826] p 40 N92-32241
Piloted evaluation of an integrated propulsion and flight control simulator p 40 N92-34107

[NASA-TM-105797] p 40 N92-34107

FLIGHT CREWS

Magnetic radiation shielding - An idea whose time has returned? p 53 A92-17796

FLIGHT OPTIMIZATION

Simple proof of the global optimality of the Hohmann transfer p 44 A92-46760

FLIGHT SAFETY

Space Station Freedom/lunar transfer vehicle propellant operation hazard analysis p 55 N92-17416

FLIGHT SIMULATORS

Piloted evaluation of an integrated propulsion and flight control simulator p 23 A92-52459

[AIAA PAPER 92-4178] p 23 A92-52459
Piloted evaluation of an integrated propulsion and flight control simulator p 40 N92-34107

[NASA-TM-105797] p 40 N92-34107

FLIGHT TESTS

Heat transfer measurements from a smooth NACA 0012 airfoil p 165 A92-20215

Prediction of ice accretion on a swept NACA 0012 airfoil and comparisons to flight test results p 4 A92-25677

[AIAA PAPER 92-0043] p 4 A92-25677
Development of and flight results from the Space Acceleration Measurement System (SAMS) p 56 A92-28189

[AIAA PAPER 92-0354] p 56 A92-28189
The F/A-18 external burning flight test p 23 A92-44547

[AIAA PAPER 91-5050] p 23 A92-44547
Prediction of ice accretion on a swept NACA 0012 airfoil and comparisons to flight test results p 16 N92-15968

[NASA-TM-105368] p 16 N92-15968
Overview of NASA PTA propan flight test program p 33 N92-22536

[NASA-TM-105797] p 40 N92-34107

Piloted evaluation of an integrated propulsion and flight control simulator p 40 N92-34107

[NASA-TM-105797] p 40 N92-34107

FLIGHT VEHICLES

Flight-vehicle materials, structures, and dynamics - Assessment and future directions. Vol. 3 - Ceramics and ceramic-matrix composites --- Book p 94 A92-39852

[ISBN 0-7918-0661-8] p 94 A92-39852

FLOAT ZONES

Steady-state thermal-solutal convection and diffusion in a simulated float zone p 137 A92-17056

Linear-stability theory of thermocapillary convection in a model of float-zone crystal growth p 169 A92-28211

[AIAA PAPER 92-0604] p 169 A92-28211
Interfacial and gravitational convection in immiscible liquid layers p 184 A92-57286

[IAF PAPER 92-0907] p 184 A92-57286
Development of a new generation of high-temperature composite materials p 109 N92-22515

An examination of anticipated g-jitter on Space Station and its effects on materials processes p 140 N92-28438

[NASA-TM-105797] p 40 N92-34107

[NASA-TM-105797] p 40 N92-34107

FLOW CHARACTERISTICS

Surface heat transfer and flow properties of vortex arrays induced artificially and from centrifugal instabilities p 183 A92-56371

[NASA-TM-105797] p 40 N92-34107

FLOW DEFLECTION

Experimental and analytical study of close-coupled ventral nozzles for ASTOVL aircraft p 26 A92-45325

FLOW DISTORTION

Numerical investigation on Benard instability in a finite liquid layer p 164 A92-12865

Aerodynamics of loaded cascades in subsonic flows subject to unsteady three-dimensional vortical disturbances p 4 A92-23762

[AIAA PAPER 92-0146] p 4 A92-23762
Distortion of a flat-plate boundary layer by free-stream vorticity normal to the plate p 173 A92-36343

Near-wall response in turbulent shear flows subjected to imposed unsteadiness p 174 A92-41652

The present state of using RDT in turbulence modelling of unsteady flows p 191 N92-24535

Application of computational fluid dynamics to the study of vortex flow control for the management of inlet distortion p 230 N92-34112

[NASA-TM-105672] p 230 N92-34112

Use of an approximate similarity principle for the thermal scaling of a full-scale thrust augmenting ejector [AIAA PAPER 92-3792] p 28 A92-54171

A laser-induced heat flux technique for convective heat transfer measurements in high speed flows p 200 A92-54318

Filtered Rayleigh scattering measurements in supersonic/hypersonic facilities p 200 A92-56733

[AIAA PAPER 92-3894] p 200 A92-56733
Flow quality studies of the NASA Lewis Research Center 8- by 6-foot supersonic/9- by 15-foot Low Speed Wind Tunnel p 41 A92-56748

[AIAA PAPER 92-3916] p 41 A92-56748
Engine component instrumentation development facility at NASA Lewis Research Center p 41 A92-56818

[AIAA PAPER 92-3995] p 41 A92-56818
Turbomachinery noise p 253 N92-10601

Results from computational analysis of a mixed compression supersonic inlet p 14 N92-10976

[NASA-TM-104475] p 14 N92-10976
A study on vortex flow control on inlet distortion in the re-engined 727-100 center inlet duct using computational fluid dynamics p 14 N92-13998

[NASA-TM-105321] p 14 N92-13998
Screch noise source structure of a supersonic rectangular jet p 15 N92-14000

[NASA-TM-105384] p 15 N92-14000
The aerodynamic effect of fillet radius in a low speed compressor cascade p 29 N92-14063

[NASA-TM-105347] p 29 N92-14063
A critical comparison of second order closures with direct numerical simulation of homogeneous turbulence p 185 N92-15357

[NASA-TM-105351] p 185 N92-15357
Thermal and solutal convection with conduction effects inside a rectangular enclosure p 186 N92-15358

[NASA-TM-105371] p 186 N92-15358
Pressure wave propagation studies for oscillating cascades p 16 N92-15977

[NASA-TM-105406] p 16 N92-15977
Jet mixing into a heated cross flow in a cylindrical duct: Influence of geometry and flow variations p 30 N92-15994

[NASA-TM-105390] p 30 N92-15994
Viscous three-dimensional calculations of transonic fan performance p 1 N92-17346

[NASA-TM-103800] p 1 N92-17346
Unsteady-flow-field predictions for oscillating cascades p 17 N92-19437

[NASA-TM-105283] p 17 N92-19437
Implementation/validation of a low Reynolds number two-equation turbulence model in the Proteus Navier-Stokes code: Two-dimensional/axisymmetric p 187 N92-20520

[NASA-TM-105619] p 187 N92-20520
Development of a steady potential solver for use with linearized, unsteady aerodynamic analyses p 31 N92-20525

[NASA-TM-105288] p 31 N92-20525
Flow studies in close-coupled ventral nozzles for STOVL aircraft p 17 N92-20934

[NASA-TM-102554] p 17 N92-20934
Inlets, ducts, and nozzles p 188 N92-22523

High-speed inlet research program and supporting analysis p 188 N92-22542

The flip-flop nozzle extended to supersonic flows p 18 N92-23269

[NASA-TM-105570] p 18 N92-23269
Development of new flux splitting schemes p 189 N92-23343

[NASA-TM-105570] p 189 N92-23343
MAG3D and its application to internal flowfield analysis p 243 N92-24421

[NASA-TM-105570] p 243 N92-24421
Engine component instrumentation development facility at NASA Lewis Research Center p 42 N92-25449

[NASA-TM-105644] p 42 N92-25449
Computational Fluid Dynamics --- numerical methods and algorithm development p 35 N92-25808

[NASA-CP-10078] p 35 N92-25808
Study of shock-induced combustion using an implicit TVD scheme p 116 N92-25816

Upwind schemes and bifurcating solutions in real gas computations p 193 N92-25817

High order parallel numerical schemes for solving incompressible flows p 193 N92-25818

Advances in engineering turbulence modeling --- computational fluid dynamics p 193 N92-25820

Implementation of a kappa-epsilon turbulence model to RPLUS3D code p 194 N92-25822

A comparison of predicted and measured inlet distortion flows in a subsonic axial inlet flow compressor rotor p 19 N92-26104

[NASA-TM-105427] p 19 N92-26104
CFD mixing analysis of jets injected from straight and slanted slots into confined crossflow in rectangular ducts p 36 N92-26561

[NASA-TM-105699] p 36 N92-26561
Use of an approximate similarity principle for the thermal scaling of a full-scale thrust augmenting ejector p 36 N92-26613

[NASA-TM-105724] p 36 N92-26613
Overview of NASA supported Stirling thermodynamic loss research p 88 N92-27034

[NASA-TM-105690] p 88 N92-27034

- A mathematical constraint placed upon inter-blade row boundary conditions used in the simulation of multistage turbomachinery flows p 195 N92-27458
- Viscous three-dimensional calculations of transonic fan performance p 195 N92-27467
- Full Navier-Stokes analysis of a two-dimensional mixer/ejector nozzle for noise suppression [NASA-TM-105715] p 37 N92-28419
- Rocket plume flowfield characterization using laser Rayleigh scattering [NASA-TM-105739] p 257 N92-28475
- Flow quality studies of the NASA Lewis Research Center 8- by 6-foot supersonic/9- by 15-foot low speed wind tunnel [NASA-TM-105417] p 42 N92-28673
- Experimental investigation of the flowfield of an oscillating airfoil [NASA-TM-105675] p 20 N92-30182
- Navier-Stokes analysis and experimental data comparison of compressible flow within ducts [NASA-TM-105796] p 38 N92-30972
- FLOW EQUATIONS**
- Heat transfer in rotating serpentine passages with trips normal to the flow [ASME PAPER 91-GT-265] p 165 A92-15663
- Development of a steady potential solver for use with linearized, unsteady aerodynamic analyses [NASA-TM-105288] p 31 N92-20525
- FLOW GEOMETRY**
- Studies of the effects of curvature on dilution jet mixing p 166 A92-21079
- Internal structure of shock waves in disparate mass mixtures [AIAA PAPER 92-0496] p 169 A92-28195
- FLOW MEASUREMENT**
- NASA low-speed centrifugal compressor for 3-D viscous code assessment and fundamental flow physics research [ASME PAPER 91-GT-140] p 3 A92-15580
- Surface and flow field measurements in a symmetric crossing shock wave/turbulent boundary layer flow [AIAA PAPER 92-2634] p 10 A92-45574
- Measurement and analysis of a small nozzle plume in vacuum [AIAA PAPER 92-3108] p 64 A92-48748
- Flow quality studies of the NASA Lewis Research Center 8- by 6-foot supersonic/9- by 15-foot Low Speed Wind Tunnel [AIAA PAPER 92-3916] p 41 A92-56748
- Advanced nozzle and engine components test facility [AIAA PAPER 92-3993] p 41 A92-56816
- Particle-laden weakly swirling free jets: Measurements and predictions [NASA-TM-100881] p 29 N92-14061
- Advanced nozzle and engine components test facility [NASA-TM-103684] p 42 N92-17059
- Flow quality studies of the NASA Lewis Research Center 8- by 6-foot supersonic/9- by 15-foot low speed wind tunnel [NASA-TM-105417] p 42 N92-28673
- Three-dimensional laser window formation [NASA-RP-1280] p 47 N92-30307
- FLOW STABILITY**
- Numerical investigation on Benard instability in a finite liquid layer p 164 A92-12865
- Nonlinear dynamics near the stability margin in rotating pipe flow p 165 A92-19959
- Effects of g-jitter and cross-diffusion on the onset of convection in doubly diffusive systems [AIAA PAPER 92-0246] p 167 A92-25705
- Nonlinear spatial equilibration of an externally excited instability wave in a free shear layer p 170 A92-31469
- Stability of capillary surfaces p 172 A92-35979
- Naturally occurring and forced azimuthal modes in a turbulent jet p 172 A92-35998
- Linear stability of compressible Taylor-Couette flow p 173 A92-36187
- Modern developments in shear flow control with swirl p 9 A92-41265
- Spatial instability of a swirling jet - Theory and experiment p 174 A92-41274
- A continuum method for modeling surface tension p 175 A92-45707
- Effect of spatial resolution on apparent sensitivity to initial conditions of a decaying flow as it becomes turbulent
- The Eckhaus and the Benjamin-Feir instability near a weakly inverted bifurcation [NASA-TM-105334] p 185 N92-15336
- FLOW THEORY**
- The effect of steady aerodynamic loading on the flutter stability of turbomachinery blading [ASME PAPER 91-GT-130] p 2 A92-15574
- FLOW VELOCITY**
- Experimental investigation of turbulent flow through a circular-to-rectangular transition duct p 168 A92-26412
- High-power hydrogen arcjet performance [NASA-TM-105143] p 82 N92-14109
- Unsteady-flow-field predictions for oscillating cascades [NASA-TM-105283] p 17 N92-19437
- A comparison of predicted and measured inlet distortion flows in a subsonic axial inlet flow compressor rotor [NASA-TM-105427] p 19 N92-26104
- Effect of lubricant jet location on spiral bevel gear operating temperatures [NASA-TM-105656] p 211 N92-26106
- FLOW VISUALIZATION**
- Unsteady wing surface pressures in the wake of a propeller [AIAA PAPER 92-0277] p 5 A92-25731
- Helium bubble flow visualization of the spanwise separation on a NACA 0012 with simulated glaze ice [AIAA PAPER 92-0413] p 7 A92-28192
- Features of wavy vortices in a curved channel from experimental and numerical studies p 171 A92-31638
- Flow visualization and motion analysis for a series of four sequential brush seals p 204 A92-36976
- Hot gas ingestion characteristics and flow visualization of a vectored thrust STOVL concept p 26 A92-45316
- Experimental investigation of the flowfield of an oscillating airfoil [AIAA PAPER 92-2622] p 9 A92-45494
- The flip flop nozzle extended to supersonic flows [AIAA PAPER 92-2724] p 10 A92-45561
- Qualitative spectroscopic study of magnetic nozzle flow [AIAA PAPER 92-3161] p 65 A92-48784
- Full field flow visualization and computer-aided velocity measurements in a bank of cylinders in a wind tunnel p 199 A92-50040
- Experimental investigation of an ejector-powered free-jet facility [AIAA PAPER 92-3569] p 41 A92-54058
- Study of compressible mixing layers using filtered Rayleigh scattering based visualizations p 183 A92-54937
- Advanced nozzle and engine components test facility [AIAA PAPER 92-3993] p 41 A92-56816
- Advanced nozzle and engine components test facility [NASA-TM-103684] p 42 N92-17059
- Calculations of hot gas ingestion for a STOVL aircraft model [NASA-TM-105437] p 17 N92-19993
- Flow studies in close-coupled ventral nozzles for STOVL aircraft [NASA-TM-102554] p 17 N92-20934
- Numerical experiments with flows of elongated granules [NASA-TM-105567] p 209 N92-23226
- The flip-flop nozzle extended to supersonic flows [NASA-TM-105570] p 18 N92-23269
- Helium bubble flow visualization of the spanwise separation on a NACA 0012 with simulated glaze ice [NASA-TM-105742] p 19 N92-26612
- Three-dimensional flow fields inside a shrouded inducer at design and off-design conditions (CFD study) p 196 N92-32291
- FLOWMETERS**
- Doppler-shifted fluorescence imaging of velocity fields in supersonic reacting flows [AIAA PAPER 92-2964] p 199 A92-46979
- FLUID BOUNDARIES**
- Stability analysis of surface tension effects on a double-diffusive layer --- in reduced gravity conditions [AIAA PAPER 92-0605] p 137 A92-27002
- Stable localized patterns in thin liquid films p 173 A92-37489
- FLUID DYNAMICS**
- COLD-SAT - A technology satellite for cryogenic experimentation p 52 A92-13425
- Reactive collision terms for fluid transport theory p 257 A92-22693
- Stability analysis of surface tension effects on a double-diffusive layer --- in reduced gravity conditions [AIAA PAPER 92-0605] p 137 A92-27002
- Jet mixing into a heated cross flow in a cylindrical duct - Influence of geometry and flow variations [AIAA PAPER 92-0773] p 168 A92-27110
- A least-squares finite element method for incompressible Navier-Stokes problems p 173 A92-37387
- Technical evaluation report, AGARD Fluid Dynamics Panel Symposium on Effects of Adverse Weather on Aerodynamics [NASA-TM-105192] p 1 N92-10002
- Turbulent fluid motion 3: Basic continuum equations [NASA-TM-104386] p 184 N92-11317
- An efficient and robust algorithm for two dimensional time dependent incompressible Navier-Stokes equations: High Reynolds number flows [NASA-TM-104424] p 184 N92-11320
- A critical comparison of second order closures with direct numerical simulation of homogeneous turbulence [NASA-TM-105351] p 185 N92-15357
- Jet mixing into a heated cross flow in a cylindrical duct: Influence of geometry and flow variations [NASA-TM-105390] p 30 N92-15994
- A mathematical constraint placed upon inter-blade row boundary conditions used in the simulation of multistage turbomachinery flows p 195 N92-27458
- FLUID FILMS**
- Effect of type and location of oil groove on the performance of journal bearings p 203 A92-21333
- Frequency effects on the stability of a journal bearing for periodic loading p 203 A92-22665
- A system-approach to the elastohydrodynamic lubrication point-contact problem p 204 A92-35421
- Stable localized patterns in thin liquid films p 173 A92-37489
- Two reference time scales for studying the dynamic cavitation of liquid films p 204 A92-47173
- Stable localized patterns in thin liquid films [NASA-TM-105352] p 185 N92-14322
- Fast methods to numerically integrate the Reynolds equation for gas fluid films [NASA-TM-105415] p 214 N92-30722
- FLUID FLOW**
- An efficient and robust algorithm for two dimensional time dependent incompressible Navier-Stokes equations: High Reynolds number flows [NASA-TM-104424] p 184 N92-11320
- A critical comparison of second order closures with direct numerical simulation of homogeneous turbulence [NASA-TM-105351] p 185 N92-15357
- Engine panel seals for hypersonic engine applications: High temperature leakage assessments and flow modelling [NASA-TM-105260] p 208 N92-16336
- Inlets, ducts, and nozzles p 188 N92-22523
- Turbomachinery p 32 N92-22524
- Pulse thermal energy transport/storage system [NASA-CASE-LEW-15235-1] p 195 N92-29125
- FLUID INJECTION**
- Qualitative investigation of cryogenic fluid injection into a supersonic flow field p 164 A92-13360
- FLUID JETS**
- CFD analysis of jet mixing in low NO(x) flametube combustors [ASME PAPER 91-GT-217] p 24 A92-15634
- Effect of gas mass flux on cryogenic liquid jet breakup p 140 A92-23845
- Jet mixing into a heated cross flow in a cylindrical duct - Influence of geometry and flow variations [AIAA PAPER 92-0773] p 168 A92-27110
- Supersonic jet mixing enhancement by 'delta-tabs' [AIAA PAPER 92-3548] p 12 A92-49063
- Jet mixing into a heated cross flow in a cylindrical duct: Influence of geometry and flow variations [NASA-TM-105390] p 30 N92-15994
- Supersonic jet mixing enhancement by delta-tabs [NASA-TM-105664] p 18 N92-24958
- FLUID MANAGEMENT**
- Modeling of impulsive propellant reorientation p 59 A92-17187
- On-orbit cryogenic fluid transfer research at NASA Lewis Research Center p 45 A92-23847
- CONE - An STS-based cryogenic fluid management experiment p 43 A92-23850
- Cryogenic fluid management investigations using the CONE flight experiment p 43 A92-23851
- Improved thermodynamic modeling of the no-vent fill process and correlation with experimental data [NASA-TM-104492] p 79 N92-11129
- FLUID MECHANICS**
- Flow induction by pressure forces [AIAA PAPER 92-3571] p 28 A92-54060
- Introduction to the internal fluid mechanics research session p 188 N92-22522
- Chemical reacting flows p 188 N92-22525
- The future challenge for aeropropulsion [NASA-TM-105613] p 35 N92-25164
- FLUORESCENCE**
- Doppler-shifted fluorescence imaging of velocity fields in supersonic reacting flows [AIAA PAPER 92-2964] p 199 A92-46979
- Fluorescence microscopy for the characterization of structural integrity [NASA-TM-105253] p 96 N92-18970
- FLUORIDES**
- Graphite intercalation compound with iodine as the major intercalant [NASA-TM-105375] p 97 N92-25203

FLUORINATION

Graphite fluoride from iodine intercalated graphitized carbon
[NASA-CASE-LEW-15360-1] p 116 N92-34206

FLUORINATION

Graphite intercalation compound with iodine as the major intercalant
[NASA-TM-105375] p 97 N92-25203

FLUORINE

High-T sub c fluorine-doped YBa₂Cu₃O_y films on ceramic substrates by screen printing
[NASA-TM-105296] p 127 N92-11188

FLUORO COMPOUNDS

Substituted 1,1,1-triaryl-2,2,2-trifluoroethanes and processes for their synthesis
[NASA-CASE-LEW-14345-6] p 96 N92-17882

FLUTTER

Optical measurements of unducted fan flutter
[ASME PAPER 91-GT-19] p 197 A92-15510
The effect of steady aerodynamic loading on the flutter stability of turbomachinery blading
[ASME PAPER 91-GT-130] p 2 A92-15574
Determining structural performance p 32 N92-22519

FLUTTER ANALYSIS

Cascade flutter analysis with transient response aerodynamics p 217 A92-15972
Aeroelastic analysis of advanced propellers using an efficient Euler solver
[AIAA PAPER 92-0488] p 7 A92-28194
Analysis of cascades using a two dimensional Euler aeroelastic solver
[AIAA PAPER 92-2370] p 26 A92-34598
A numerical classical flutter analysis of advanced propellers
[AIAA PAPER 92-2118] p 26 A92-35687
FREPS - A forced response prediction system for turbomachinery blade rows
[AIAA PAPER 92-3072] p 242 A92-54006
Semi-empirical model for prediction of unsteady forces on an airfoil with application to flutter
[NASA-TM-105414] p 17 N92-18760
Aeroelastic stability analyses of two counter rotating propfan designs for a cruise missile model
[NASA-TM-105268] p 227 N92-23191

FLUX PINNING

Magnetic flux relaxation in YBa₂Cu₃O_{7-x} thin film: Thermal or athermal p 265 N92-32984

FLUX VECTOR SPLITTING

Transient behavior of supersonic flow through inlets p 7 A92-28043
An improved PNS scheme for predicting complex three-dimensional hypersonic flows
[AIAA PAPER 92-0753] p 8 A92-31679
Development of new flux splitting schemes p 189 N92-23343
Development of a new flux splitting scheme p 190 N92-23352
High-Order Polynomial Expansions (HOPE) for flux-vector splitting p 190 N92-23353
Conservative-variable average states for equilibrium gas multi-dimensional fluxes
[NASA-TM-105585] p 191 N92-25196
Development of new flux splitting schemes --- computational fluid dynamics algorithms p 192 N92-25809
An iterative implicit DDADI algorithm for solving the Navier-Stokes equation --- upwind split flux technique p 192 N92-25810

FLYWHEELS

Flywheel energy storage for electromechanical actuation systems p 233 A92-50758

FOAMS

Bonded ceramic foams reinforced with fibers for high temperature use p 125 A92-39628

FORCED CONVECTION

Breakdown of the Karman vortex street due to forced convection and flow compressibility
[NASA-TM-105853] p 196 N92-32472

FORCED VIBRATION

Euler flow predictions for an oscillating cascade using a high resolution wave-split scheme
[ASME PAPER 91-GT-198] p 3 A92-15623

FOREBODIES

Wind tunnel investigation of vortex flows on F/A-18 configuration at subsonic through transonic speed
[NASA-TP-3111] p 16 N92-14968

FORTRAN

Computer program for Bessel and Hankel functions
[NASA-TM-105154] p 243 N92-11691

FOURIER ANALYSIS

Runge-Kutta methods combined with compact difference schemes for the unsteady Euler equations
[AIAA PAPER 92-3210] p 182 A92-54015

FOURIER TRANSFORMATION

Solutions of the heat conduction equation in multilayers for photothermal deflection experiments p 141 A92-52205

FRACTALS

Fractals and cosmological large-scale structure p 268 A92-37413
Fractal dimension of alumina aggregates grown in two dimensions p 126 A92-49814

FRACTURE MECHANICS

Controlled crack growth specimen for brittle systems p 123 A92-21099
Fracture toughness and the effects of stress state on fracture of nickel aluminides p 117 A92-27422
Flow and fracture behavior of NiAl in relation to the brittle-to-ductile transition temperature p 118 A92-30781

Near-tip dual-length scale mechanics of mode-I cracking in laminate brittle matrix composites
[AIAA PAPER 92-2491] p 221 A92-34583

Load redistribution considerations in the fracture of ceramic matrix composites
[AIAA PAPER 92-2494] p 221 A92-34586

A variationally coupled FE-BE method for elasticity and fracture mechanics p 222 A92-37510
Structural design methodologies for ceramic-based material systems p 103 A92-39866

Fracture behavior of a B2 Ni-30Al-20Fe-0.05Zr intermetallic alloy in the temperature range 300 to 1300 K p 121 A92-41667

Deformation behavior of a Ni-30Al-20Fe-0.05Zr intermetallic alloy in the temperature range 300 to 1300 K p 121 A92-41668

Tensile behavior of the L(1)2 compound Al₆Ti₂₅Cr₈ epoxy p 122 A92-49694

An energy analysis of crack-initiation and arrest in epoxy p 224 A92-49777

A stochastic damage model for the rupture prediction of a multi-phase solid. I - Parametric studies. II - Statistical approach p 224 A92-49784

The effect of temperature on the deformation and fracture of SiC/Ti-24Al-11Nb p 106 A92-55143

Thermally-driven microfracture in high temperature metal matrix composites p 107 N92-15136
Cyclic hot firing results of tungsten-wire-reinforced, copper-lined thrust chambers
[NASA-TM-4214] p 91 N92-31249

FRACTURE STRENGTH

Effect of heat treatment on stiffness and damping of SiC/Ti-15-3 p 100 A92-25627
Fracture toughness and the effects of stress state on fracture of nickel aluminides p 117 A92-27422

On improving the fracture toughness of a NiAl-based alloy by mechanical alloying p 118 A92-30794
Strength, toughness and R-curve behaviour of SiC whisker-reinforced composite Si₃N₄ with reference to monolithic Si₃N₄ p 101 A92-34202

Fracture resistance development in ceramic composites with nonlinear fiber pullout relationship
[AIAA PAPER 92-2493] p 221 A92-34585

Effect of fiber strength on the room temperature tensile properties of SiC/Ti-24Al-11Nb p 102 A92-36389
Relationships between toughness and microstructure of reaction bonded Si₃N₄ p 125 A92-39687

Effect of fiber orientation on the fracture toughness of brittle matrix composites p 103 A92-41841
Estimation of crack closure stresses for in situ toughened silicon nitride with 8 wt pct scandia p 126 A92-43478

Micromechanical model of crack growth in fiber reinforced brittle materials p 223 A92-46829
Extreme value statistics analysis of fracture strengths of a sintered silicon nitride failing from pores p 127 A92-50191

Mechanical behaviour and failure phenomenon of an in situ toughened silicon nitride p 127 A92-54504
Elevated temperature mechanical behavior of monolithic and SiC whisker-reinforced silicon nitrides
[NASA-TM-105245] p 128 N92-15192

FRACTURES (MATERIALS)

Thermally-driven microfracture in high temperature metal matrix composites p 107 N92-15136
[NASA-TM-105305]

FRACTURING

Damage and fracture in composite thin shells p 224 A92-51550
Damage and fracture in composite thin shells
[NASA-TM-105289] p 106 N92-13284

Thermally-driven microfracture in high temperature metal matrix composites p 107 N92-15136
[NASA-TM-105305]

Differential continuum damage mechanics models for creep and fatigue of unidirectional metal matrix composites p 226 N92-16371
[NASA-TM-105213]

Progressive fracture of polymer matrix composite structures: A new approach p 109 N92-23194
[NASA-TM-105574]

Structural durability of stiffened composite shells
[NASA-CR-190588] p 229 N92-29342

A differential CDM model for fatigue of unidirectional metal matrix composites p 230 N92-31505
[NASA-TM-105726]

Computational simulation of structural fracture in fiber composites p 111 N92-32531

FREE BOUNDARIES

A system approach to the elastohydrodynamic lubrication point-contact problem p 204 A92-35421
Scalar rate correlation at a turbulent liquid free surface - A two-regime correlation for high Schmidt numbers p 184 A92-56941

FREE CONVECTION

Opposed flow flame spread in normal, enhanced and reduced gravity p 111 A92-12898
Convection in superposed fluid and porous layers p 166 A92-24752

Effect of radiation on convection at moderate temperatures
[AIAA PAPER 92-0691] p 168 A92-27058

Determination of the natural convection coefficient in low-gravity p 168 A92-27072
[AIAA PAPER 92-0712]

Effects of g-jitter on a thermally buoyant flow p 171 A92-32258
Effect of thermal convection on the shape of a solid-liquid interface p 171 A92-35878

An experimental study of oscillatory thermocapillary convection in cylindrical containers p 172 A92-36184
Vertical solidification of dendritic binary alloys p 261 A92-37562

Nature of buoyancy-driven flows in a reduced-gravity environment p 175 A92-45844
Natural convection between concentric spheres p 179 A92-50445

Thermal and solutal convection with conduction effects inside a rectangular enclosure
[NASA-TM-105371] p 186 N92-15358

Effect of radiation on convection at moderate temperatures
[NASA-TM-105632] p 192 N92-25296

FREE FLOW

Nonlinear spatial equilibration of an externally excited instability wave in a free shear layer p 170 A92-31469
Experimental study of boundary layer transition on a heated flat plate p 172 A92-36022

Compressibility effects on large structures in free shear flows p 173 A92-39337
Increased heat transfer to elliptical leading edges due to spanwise variations in the freestream momentum - Numerical and experimental results
[AIAA PAPER 92-3070] p 13 A92-54005

FREE JETS

Vapor condensation on liquid surface due to laminar jet-induced mixing p 164 A92-10446
Experimental investigation of an ejector-powered free-jet facility
[AIAA PAPER 92-3569] p 41 A92-54058

Particle-laden weakly swirling free jets: Measurements and predictions
[NASA-TM-100881] p 29 N92-14061

FREE VIBRATION

Free vibrations of delaminated beams p 222 A92-36853
Evaluation of MHOST analysis capabilities for a plate element --- finite element modeling
[NASA-TM-105387] p 228 N92-23196

Free vibrations of delaminated beams
[NASA-TM-105582] p 109 N92-25754

FREE-PISTON ENGINES

Small Stirling dynamic isotope power system for multihundred-watt robotic missions
[SAE PAPER 912066] p 62 A92-45448

Update on results of SPRE testing at NASA Lewis
Free-piston Stirling component test power converter p 206 A92-50784

Comparative survey of dynamic analyses of free-piston Stirling engines p 206 A92-50793
Final design of a free-piston hydraulic advanced Stirling conversion system p 206 A92-50798

Status of the advanced Stirling conversion system project for 25 kW dish Stirling applications p 207 A92-50804
Comparison of GLIMPS and HFAST Stirling engine code predictions with experimental data
[NASA-TM-105549] p 267 N92-25395

Magnetic bearings for free-piston Stirling engines
[NASA-TM-105730] p 214 N92-30734

FREEZING

Shrinkage void formation and its effect on freeze and thaw processes of lithium and lithium-fluoride for space applications p 180 A92-50596
Observations of the freeze/thaw performance of lithium fluoride by motion picture photography p 180 A92-50751

Thermal modeling with solid/liquid phase change of the thermal energy storage experiment [NASA-TM-103770] p 185 N92-13402

FREQUENCY ASSIGNMENT

Satellite delivery of B-ISDN services [AIAA PAPER 92-1831] p 142 A92-29777
Frequency allocations for a new satellite service - Digital audio broadcasting [AIAA PAPER 92-1957] p 143 A92-29881
Achieving spectrum conservation for the minimum span and minimum-order frequency assignment problems [AIAA PAPER 92-1960] p 143 A92-29883
Achieving spectrum conservation for the minimum-span and minimum-order frequency assignment problems [NASA-TM-105649] p 52 N92-23187

FREQUENCY DIVISION MULTIPLE ACCESS

Multicarrier demodulator architecture for onboard processing satellites p 49 A92-10465
Circuit-switch architecture for a 30/20-GHz FDMA/TDM geostationary satellite communications network [AIAA PAPER 92-2005] p 49 A92-29924
Circuit-switch architecture for a 30/20-GHz FDMA/TDM geostationary satellite communications network [NASA-TM-105302] p 51 N92-15109
A personal communications network using a Ka-band satellite p 151 N92-30934

FREQUENCY DIVISION MULTIPLEXING

Fault tolerance in onboard processors - Protecting efficient FDM demultiplexers [AIAA PAPER 92-1969] p 144 A92-29892
Destination directed packet switch architecture for a 30/20 GHz FDMA/TDM geostationary communication satellite network p 148 N92-14204
Multichannel demultiplexer/demodulator technologies for future satellite communication systems [NASA-TM-105377] p 51 N92-18342
Destination-directed, packet-switching architecture for 30/20-GHz FDMA/TDM geostationary communications satellite network [NASA-TP-3201] p 51 N92-19762

FREQUENCY MODULATION

RF modulated fiber optic sensing systems and their applications [NASA-TM-105801] p 257 N92-33896

FREQUENCY RANGES

Comparison of high temperature, high frequency core loss and dynamic B-H loops of two 50 Ni-Fe crystalline alloys and an iron-based amorphous alloy p 157 A92-50551

FREQUENCY RESPONSE

Frequency effects on the stability of a journal bearing for periodic loading [NASA-TM-105226] p 186 N92-18809
Analysis and modification of a single-mesh gear fatigue rig for use in diagnostic studies [NASA-TM-105416] p 212 N92-27879

FREQUENCY SHIFT KEYING

Interference susceptibility measurements for an MSK satellite communication link [AIAA PAPER 92-2018] p 144 A92-29936
Interference susceptibility measurements for an MSK satellite communication link [NASA-TM-105395] p 149 N92-15306
Advanced Modulation and Coding Technology Conference [NASA-CP-10053] p 51 N92-22001

FRESNEL LENSES

The mini-dome Fresnel lens photovoltaic concentrator array - Current program status p 70 A92-50648
A high-performance photovoltaic concentrator array - The mini-dome Fresnel lens concentrator with 30 percent efficient GaAs/GaSb tandem cells p 72 A92-53199

FRICTION

Tribological and mechanical comparison of sintered and hipped PM212. High temperature self-lubricating composites [NASA-TM-105379] p 96 N92-15128
Tribology needs for future space and aeronautical systems [NASA-TM-104525] p 128 N92-15191
A vacuum (10(exp -9) Torr) friction apparatus for determining friction and endurance life of MoSx films [NASA-TM-104478] p 129 N92-16129
Environmental effects on friction and wear of diamond and diamondlike carbon coatings [NASA-TM-105634] p 131 N92-23192
Computational techniques in tribology and material science at the atomic level [NASA-TM-105573] p 252 N92-26671

FUEL CELLS

Space Electrochemical Research and Technology Conference, 3rd, NASA Lewis Research Center, Cleveland, OH, Apr. 9, 10, 1991, Proceedings p 231 A92-18936

Bifunctional alkaline oxygen electrodes p 115 A92-50729
Temperature dependence of the electrode kinetics of oxygen reduction at the platinum/Nafion interface - A microelectrode investigation p 115 A92-56950
The O2 reduction at the IFC modified O2 fuel cell electrode [NASA-TM-105691] p 90 N92-29667

FUEL COMBUSTION

An investigation of flame spread over shallow liquid pools in microgravity and nonair environments p 112 A92-16609
The structure of premixed particle-cloud flames p 114 A92-43779
NASA's rotary engine technology enablement program: 1983-1991 [NASA-TM-105562] p 30 N92-20033
Chemical reacting flows p 188 N92-22525

FUEL CONSUMPTION

Propulsion challenges and opportunities for high-speed transport aircraft p 34 N92-22540

FUEL CONTROL

Modeling of impulsive propellant reorientation p 59 A92-17187

FUEL FLOW

Safety considerations in testing a fuel-rich aeropropulsion gas generator [NASA-TM-105258] p 30 N92-17061

FUEL INJECTION

Hydrogen no-vent testing in a 5 cubic foot (142 liter) tank using spray nozzle and spray bar liquid injection [AIAA PAPER 92-3063] p 63 A92-48719
Performance comparison of axisymmetric and three-dimensional hydrogen film coolant injection in a 110 N hydrogen/oxygen rocket [AIAA PAPER 92-3390] p 73 A92-54027
Extended temperature range rocket injector [NASA-CASE-LEW-14846-1] p 77 N92-10054
NASA's rotary engine technology enablement program: 1983-1991 [NASA-TM-105562] p 30 N92-20033
Hydrogen no-vent fill testing in a 5 cubic foot (142 liter) tank using spray nozzle and spray bar liquid injection [NASA-TM-105759] p 136 N92-28433

FUEL PRODUCTION

Technical prospects for utilizing extraterrestrial propellants for space exploration [IAF PAPER 91-669] p 133 A92-20612
Slush hydrogen transfer studies at the NASA K-Site Test Facility [NASA-TM-105596] p 135 N92-25957

FUEL SPRAYS

Microgravity combustion of isolated n-decane and n-heptane droplets [AIAA PAPER 92-0242] p 113 A92-26927

FUEL SYSTEMS

Extended temperature range rocket injector [NASA-CASE-LEW-14846-1] p 77 N92-10054

FUEL TANK PRESSURIZATION

Self-pressurization of a spherical liquid hydrogen storage tank in a microgravity environment [AIAA PAPER 92-0363] p 168 A92-25798
Self-pressurization of a lightweight liquid hydrogen tank - Effects of fill level at low wall heat flux [AIAA PAPER 92-0818] p 60 A92-29591
Pressurization of cryogenics - A review of current technology and its applicability to low-gravity conditions [AIAA PAPER 92-3061] p 72 A92-54002
Self-pressurization of a spherical liquid hydrogen storage tank in a microgravity environment [NASA-TM-105372] p 185 N92-14323
Self-pressurization of a lightweight liquid hydrogen tank: Effects of fill level at low wall heat flux [NASA-TM-105411] p 135 N92-18442
Pressurization of cryogenics: A review of current technology and its applicability to low-gravity conditions [NASA-TM-105746] p 136 N92-29669

FUEL TANKS

A review of candidate multilayer insulation systems for potential use on wet-launched LH2 tankage for the space exploration initiative lunar missions [NASA-TM-104493] p 134 N92-13336

FUEL TESTS

Effects of chemical equilibrium on turbine engine performance for various fuels and combustor temperatures [NASA-TM-105399] p 34 N92-23254

FUEL-AIR RATIO

Effects of oxygen concentration on radiative loss from normal-gravity and microgravity methane diffusion flames [AIAA PAPER 92-0243] p 113 A92-26928

Experiments and analysis concerning the use of external burning to reduce aerospace vehicle transonic drag [NASA-TM-105397] p 30 N92-17546

NASA's rotary engine technology enablement program: 1983-1991 [NASA-TM-105562] p 30 N92-20033

FULL SCALE TESTS

Experimental investigation of an ejector-powered free-jet facility [AIAA PAPER 92-3569] p 41 A92-54058

FUNCTIONAL DESIGN SPECIFICATIONS

Characteristics of a future aeronautical satellite communications system [AIAA PAPER 92-2058] p 22 A92-29889

FUNCTIONS (MATHEMATICS)

Mappings and accuracy for Chebyshev pseudo-spectral approximations p 248 A92-50469

FURNACES

Temperature control in continuous furnace by structural diagram method p 246 A92-29162
Adaptive temperature profile control of a multizone crystal growth furnace p 137 A92-29243
Identification and control of a multizone crystal growth furnace p 199 A92-39699

G**GALACTIC CLUSTERS**

Dark matter and the equivalence principle p 267 A92-14477
Void probability as a function of the void's shape and scale-invariant models ... in studies of spacial galactic distribution p 267 A92-24456
Fractals and cosmological large-scale structure p 268 A92-37413
Thick strings, the liquid crystal blue phase, and cosmological large-scale structure p 268 A92-48103

GALACTIC EVOLUTION

Possible sources of the Population I lithium abundance and light-element evolution p 268 A92-33069

GALERKIN METHOD

Effect of surface deposits on electromagnetic propagation in uniform ducts p 142 A92-23964
Optimal least-squares finite element method for elliptic problems [NASA-TM-105382] p 249 N92-15662

GALILEO SPACECRAFT

Properties data for opening the Galileo's partially unfurled main antenna [NASA-TM-105355] p 130 N92-20660

GALLIUM ANTIMONIDES

A high-performance photovoltaic concentrator array - The mini-dome Fresnel lens concentrator with 30 percent efficient GaAs/GaSb tandem cells p 72 A92-53199

GALLIUM ARSENIDES

Significant long-term reduction in n-channel MESFET subthreshold leakage using ammonium-sulfide surface treated gates p 153 A92-12272
'Wrong' bond interactions at inversion domain boundaries in GaAs p 260 A92-27297
Advanced large scale GaAs monolithic IF switch matrix subsystem [AIAA PAPER 92-1861] p 155 A92-29801

Performance of a wideband GaAs low-noise amplifier at cryogenic temperatures p 156 A92-37953
Recent progress in InP solar cell research p 158 A92-50653

Enhancing optical absorption in InP and GaAs utilizing profile etching p 263 A92-53154
Evaluation of the minority carrier diffusion length and surface-recombination velocity in GaAs p/n solar cells p 234 A92-53162

Radiation and temperature effects in heteroepitaxial and homoepitaxial InP cells p 159 A92-53192
Radiation performance of GaAs concentrator cells for 0.4 to 12 MeV electrons and 0.1 to 37 MeV protons p 159 A92-53193

A high-performance photovoltaic concentrator array - The mini-dome Fresnel lens concentrator with 30 percent efficient GaAs/GaSb tandem cells p 72 A92-53199
Enhancing optical absorption in InP and GaAs utilizing profile etching [NASA-TM-105325] p 82 N92-14111
Intermodulation in the oscillatory magnetoresistance of a two-dimensional electron gas p 163 N92-32975
Study of InGaAs-based modulation doped field effect transistor structures using variable-angle spectroscopic ellipsometry p 265 N92-32977

GAMMA RAY ASTRONOMY

The diffuse gamma-ray background, light element abundances, and signatures of early massive star formation p 268 A92-43837

GAMMA RAYS

GAMMA RAYS

Neutron, gamma ray, and temperature effects on the electrical characteristics of thyristors
[NASA-TM-105728] p 162 N92-28432

GAS ATOMIZATION

Factors influencing the effective spray cone angle of pressure-swirl atomizers p 166 A92-23300

GAS BEARINGS

Fast methods to numerically integrate the Reynolds equation for gas fluid films
[NASA-TM-105415] p 214 N92-30722
Magnetic bearings for free-piston Stirling engines
[NASA-TM-105730] p 214 N92-30734

GAS DENSITY

Rayleigh-Brillouin scattering to determine one-dimensional temperature and number density profiles of a gas flow field p 198 A92-38067

GAS DISSOCIATION

Radiation enhanced dissociation of hydrogen in nuclear rockets
[AIAA PAPER 92-3817] p 67 A92-49129

GAS DYNAMICS

Conservative-variable average states for equilibrium gas multi-dimensional fluxes
[NASA-TM-105585] p 191 N92-25196

GAS EVOLUTION

Theory of plasma contactor neutral gas emissions for electrodynamic tethers p 258 A92-41549

GAS FLOW

Some further observations on droplet combustion characteristics - NASA LeRC-Princeton results p 111 A92-12897

Rayleigh-Brillouin scattering to determine one-dimensional temperature and number density profiles of a gas flow field p 198 A92-38067
Kinetic theory model for the flow of a simple gas from a three-dimensional axisymmetric nozzle p 12 A92-52730

Experimental and numerical investigations of low-density nozzle and plume flows of nitrogen p 183 A92-54917

Conservative-variable average states for equilibrium gas multi-dimensional fluxes
[NASA-TM-105585] p 191 N92-25196

GAS GENERATORS

Detonation duct gas generator demonstration program
[AIAA PAPER 92-3174] p 27 A92-54011

Safety considerations in testing a fuel-rich aeropropulsion gas generator
[NASA-TM-105258] p 30 N92-17061

GAS INJECTION

Effect of inert propellant injection on Mars ascent vehicle performance
[AIAA PAPER 92-3447] p 73 A92-54031

GAS JETS

The implications of experimentally controlled gravitational accelerations for combustion science p 112 A92-16601

GAS MIXTURES

Observations on a slow burning regime for hydrocarbon droplets - n-heptane/air results p 112 A92-16602

Oxidation-chlorination of binary Ni-Cr alloys in flowing Ar-O₂-Cl₂ gas mixtures at 1200 K p 112 A92-17296

Internal structure of shock waves in disparate mass mixtures
[AIAA PAPER 92-0496] p 169 A92-28195

Ground test program for a full-size solar dynamic heat receiver p 68 A92-50566

Numerical study of shock-wave/boundary-layer interactions in premixed combustible gases p 183 A92-54907

GAS PATH ANALYSIS

Progress towards understanding and predicting convection heat transfer in the turbine gas path
[NASA-TM-105674] p 194 N92-26690

GAS PRESSURE

Composite overwrapped nickel-hydrogen pressure vessels p 109 N92-22762

GAS TEMPERATURE

Laser-induced fluorescence of atomic hydrogen in an arcjet thruster
[AIAA PAPER 92-0678] p 60 A92-27045

GAS TURBINE ENGINES

Intermetallic and ceramic matrix composites for B15 to 1370 C (1500 to 2500 F) gas turbine engine applications p 99 A92-15128

NASA low-speed centrifugal compressor for 3-D viscous code assessment and fundamental flow physics research
[ASME PAPER 91-GT-140] p 3 A92-15580

A bulk flow model of a brush seal system
[ASME PAPER 91-GT-325] p 203 A92-15696

A new unsteady mixing model to predict NO(x) production during rapid mixing in a dual-stage combustor
[AIAA PAPER 92-0233] p 25 A92-25696

A Lyapunov based nonlinear control scheme for stabilizing a basic compression system using a close-coupled control valve p 246 A92-29316

Flow-by-row off-design performance calculation method for turbines p 26 A92-44514

Mixing in the dome region of a staged gas turbine combustor p 177 A92-48734

[AIAA PAPER 92-3089] p 177 A92-48734
Experimental study of cross-stream mixing in a rectangular duct
[AIAA PAPER 92-3090] p 178 A92-48735

Applied analytical combustion/emissions research at the NASA Lewis Research Center - A progress report
[AIAA PAPER 92-3338] p 27 A92-54025

The VRT gas turbine combustor - Phase II
[AIAA PAPER 92-3471] p 27 A92-54035

Small engine components test facility compressor testing cell at NASA Lewis Research Center
[AIAA PAPER 92-3980] p 41 A92-56806

Combustion and core noise p 254 A92-10607
Safety considerations in testing a fuel-rich aeropropulsion gas generator
[NASA-TM-105258] p 30 N92-17061

Heat transfer in rotating serpentine passages with trips skewed to the flow p 186 N92-20235

[NASA-TM-105581] p 186 N92-20235
Ceramics for engines p 131 N92-22517

Aeropropulsion structures p 31 N92-22518
Life prediction technologies for aeronautical propulsion systems p 32 N92-22520

Overview of the subsonic propulsion technology session p 32 N92-22531

Small engine technology programs p 32 N92-22532
Experimental study of cross-stream mixing in a rectangular duct
[NASA-TM-105694] p 36 N92-27652

Applied analytical combustion/emissions research at the NASA Lewis Research Center p 90 N92-29343

[NASA-TM-105731] p 90 N92-29343
Small engine components test facility compressor testing cell at NASA Lewis Research Center
[NASA-TM-105685] p 42 N92-30508

A general numerical model for wave rotor analysis
[NASA-TM-105740] p 196 N92-31484

A graphical user-interface for propulsion system analysis
[NASA-TM-105696] p 244 N92-33894

GAS TURBINES

Reliability analysis of a structural ceramic combustion chamber
[ASME PAPER 91-GT-155] p 24 A92-15591

CFD analysis of jet mixing in low NO(x) flametube combustors
[ASME PAPER 91-GT-217] p 24 A92-15634

CFD mixing analysis of jets injected from straight and slanted slots into confined crossflow in rectangular ducts
[AIAA PAPER 92-3087] p 177 A92-48732

A parametric numerical study of mixing in a cylindrical duct
[AIAA PAPER 92-3088] p 177 A92-48733

Detonation duct gas generator demonstration program
[AIAA PAPER 92-3174] p 27 A92-54011

Combustion and core noise p 254 N92-10607
A parametric numerical study of mixing in a cylindrical duct
[NASA-TM-105695] p 35 N92-26553

CFD mixing analysis of jets injected from straight and slanted slots into confined crossflow in rectangular ducts
[NASA-TM-105699] p 36 N92-26561

Progress towards understanding and predicting convection heat transfer in the turbine gas path
[NASA-TM-105674] p 194 N92-26690

GAS-SOLID INTERACTIONS

A computer model for one-dimensional mass and energy transport in and around chemically reacting particles, including complex gas-phase chemistry, multicomponent molecular diffusion, surface evaporation, and heterogeneous reaction p 181 A92-52406

GASEOUS FUELS

Safety considerations in testing a fuel-rich aeropropulsion gas generator
[NASA-TM-105258] p 30 N92-17061

Chemical reacting flows p 188 N92-22525

GASEOUS ROCKET PROPELLANTS

Preliminary investigation of a low power pulsed arcjet thruster
[AIAA PAPER 92-3113] p 64 A92-48752

Species and temperature measurement in H₂/O₂ rocket flow fields by means of Raman scattering diagnostics
[AIAA PAPER 92-3353] p 178 A92-48930

Combustion-wave ignition for rocket engines
[NASA-TM-105545] p 84 N92-20043

Low power arcjet test facility impacts
[NASA-TM-105876] p 47 N92-34114

GATES (CIRCUITS)

Significant long-term reduction in n-channel MESFET subthreshold leakage using ammonium-sulfide surface treated gates p 153 A92-12272

dc and microwave performance of a 0.1-micron gate InAs/In(0.52)Al(0.48)As MODFET p 156 A92-43891

GEAR TEETH

A method for determining spiral-bevel gear tooth geometry for finite element analysis
[NASA-TP-3096] p 207 N92-10195

Contact stresses in meshing spur gear teeth: Use of an incremental finite element procedure
[NASA-TM-105388] p 209 N92-23536

A basis for solid modeling of gear teeth with application in design and manufacture
[NASA-TM-105392] p 209 N92-24202

A comparison between theoretical prediction and experimental measurement of the dynamic behavior of spur gears
[NASA-TM-105362] p 210 N92-25347

Effect of contact ratio on spur gear dynamic load
[NASA-TM-105606] p 210 N92-25447

Effect of operating conditions on gearbox noise
[NASA-TM-105331] p 211 N92-26107

Gear tooth stress measurements of two helicopter planetary stages
[NASA-TM-105551] p 211 N92-26555

Minimization of deviations of gear real tooth surfaces determined by coordinate measurements
[NASA-TM-105718] p 214 N92-30948

GEARS

Recent manufacturing advances for spiral bevel gears
[SAE PAPER 91-2229] p 204 A92-40024

Advanced Rotorcraft Transmission program summary
[AIAA PAPER 92-3363] p 205 A92-48936

Separation distance and static transmission error of involute spur gears
[AIAA PAPER 92-3490] p 205 A92-49027

Maximum life spiral bevel reduction design
[AIAA PAPER 92-3493] p 205 A92-49030

Modal simulation of gearbox vibration with experimental correlation
[AIAA PAPER 92-3494] p 207 A92-54036

A 23.2:1 ratio, 300-watt, 26 N-m output torque, planetary roller-gear robotic transmission: Design and evaluation
[NASA-TM-105362] p 210 N92-25085

A comparison between theoretical prediction and experimental measurement of the dynamic behavior of spur gears
[NASA-TM-105362] p 210 N92-25347

Comparison of analysis and experiment for gearbox noise
[NASA-TM-105330] p 210 N92-25396

Effect of lubricant jet location on spiral bevel gear operating temperatures
[NASA-TM-105656] p 211 N92-26106

Improvement in surface fatigue life of hardened gears by high-intensity shot peening
[NASA-TM-105678] p 211 N92-26108

Full-scale transmission testing to evaluate advanced lubricants
[NASA-TM-105668] p 212 N92-26560

Analysis and modification of a single-mesh gear fatigue rig for use in diagnostic studies
[NASA-TM-105416] p 212 N92-27879

Application of face-gear drives in helicopter transmissions
[NASA-TM-105655] p 212 N92-28434

Optimum design of a gearbox for low vibration
[NASA-TM-105653] p 212 N92-28476

Dynamics of a split torque helicopter transmission
[NASA-TM-105681] p 213 N92-29136

Optimal design of compact spur gear reductions
[NASA-TM-105676] p 213 N92-29351

Development of a full-scale transmission testing procedure to evaluate advanced lubricants
[NASA-TP-3265] p 213 N92-30396

Minimization of deviations of gear real tooth surfaces determined by coordinate measurements
[NASA-TM-105718] p 214 N92-30948

Experimental testing of prototype face gears for helicopter transmissions
[NASA-TM-105434] p 214 N92-31349

Modal simulation of gearbox vibration with experimental correlation
[NASA-TM-105702] p 215 N92-31485

GELATION

Low temperature synthesis of CaO-SiO₂ glasses having stable liquid-liquid immiscibility by the sol-gel process p 126 A92-44479

GELLED PROPELLANTS

Gelled liquid oxygen/metal powder monopropellants
[AIAA PAPER 92-3450] p 134 A92-49004

Upper stages using liquid propulsion and metallized propellants
[NASA-TP-3191] p 83 N92-17151

- GELS**
Metallized gelled monopropellants
[NASA-TM-105418] p 87 N92-24557
- GENERAL AVIATION AIRCRAFT**
Small engine technology programs p 32 N92-22532
- GEOMETRICAL OPTICS**
Effect of an arcjet plume on satellite reflector performance p 53 A92-16318
Calculation of far-field scattering from nonspherical particles using a geometrical optics approach p 256 A92-20288
Concentrator testing using projected images p 69 A92-50615
- GEOSYNCHRONOUS ORBITS**
20/30 GHz satellite personal communications networks
[AIAA PAPER 92-1908] p 143 A92-29839
Circuit-switch architecture for a 30/20-GHz FDMA/TDM geostationary satellite communications network
[AIAA PAPER 92-2005] p 49 A92-29924
Destination directed packet switch architecture for a geostationary communication satellite network
[IAF PAPER 92-0413] p 50 A92-55793
Circuit-switch architecture for a 30/20-GHz FDMA/TDM geostationary satellite communications network
[NASA-TM-105302] p 51 N92-15109
- GET AWAY SPECIALS (STS)**
Thermal modeling with solid/liquid phase change of the thermal energy storage experiment
[NASA-TM-103770] p 185 N92-13402
- GIBBS FREE ENERGY**
Stress versus temperature dependence of activation energies for creep p 217 A92-24719
On the thermodynamic framework of generalized coupled thermoelastic-viscoplastic damage modeling
[NASA-TM-105349] p 225 N92-14434
- GIMBALS**
Dynamics and control of the Space Station Freedom docking/array feathering maneuver
[IAF PAPER 91-321] p 52 A92-14734
Design considerations in clustering nuclear rocket engines
[AIAA PAPER 92-3587] p 66 A92-49069
Large transient fault current test of an electrical roll ring for Space Station Freedom p 55 A92-50661
Large transient fault current test of an electrical roll ring
[NASA-TM-105667] p 87 N92-24201
- GLASS**
Low temperature synthesis of CaO-SiO₂ glasses having stable liquid-liquid immiscibility by the sol-gel process p 126 A92-44479
Glass formation, properties, and structure of soda-yttria-silicate glasses
[NASA-TM-104488] p 128 N92-11202
Glass precursor approach to high-temperature superconductors
[NASA-TM-105590] p 263 N92-20519
Phase transformations in SrAl₂Si₂O₈ glass
[NASA-TM-105657] p 264 N92-23890
Three-dimensional laser window formation
[NASA-RP-1280] p 47 N92-30307
- GLASS COATINGS**
Effect of particle size of Martian dust on the degradation of photovoltaic cell performance
[NASA-TM-105232] p 79 N92-11133
- GLASS TRANSITION TEMPERATURE**
Addition curing thermosets endcapped with 4-amino (2,2) paracyclophane p 124 A92-33918
- GLAZES**
LDV measurements on a rectangular wing with a simulated glaze ice accretion
[AIAA PAPER 92-2690] p 10 A92-45537
Experimental ice shape and performance characteristics for a multi-element airfoil in the NASA Lewis Icing Research Tunnel
[NASA-TM-105380] p 17 N92-17347
Results of a low power ice protection system test and a new method of imaging data analysis
[NASA-TM-105745] p 20 N92-28696
- GOERTLER INSTABILITY**
Spatial instability of a swirling jet - Theory and experiment p 174 A92-41274
- GOLD**
Tribological and microstructural comparison of HIPped PM212 and PM212/Au self-lubricating composites
[NASA-TM-105615] p 97 N92-26142
- GOVERNMENT/INDUSTRY RELATIONS**
Advanced Communications Technology Satellite (ACTS) Experiments Program - A market-driven approach to government/industry cooperation
[AIAA PAPER 92-2036] p 145 A92-29951
- GRAIN BOUNDARIES**
"Wrong" bond interactions at inversion domain boundaries in GaAs p 260 A92-27297
- GRAIN SIZE**
Synthesis and characterization of fine grain diamond films p 262 A92-46330
- GRANULAR MATERIALS**
Numerical experiments with flows of elongated granules
[NASA-TM-105567] p 209 N92-23226
- GRAPHITE**
High molecular weight first generation PMR polyimides for 343 C applications p 105 A92-49819
Thermal conductivity and thermal expansion of graphite fiber/copper matrix composites p 106 N92-14120
Properties of novel CVD graphite fibers and their bromine intercalation compounds p 128 N92-14170
Effects of a noncoplanar biphenyldiamine on the processing and properties of addition polyimides
[NASA-TM-105383] p 107 N92-15137
Intercalated hybrid graphite fiber composite
[NASA-CASE-LEW-15241-1] p 107 N92-17861
High molecular weight first generation PMR polyimides for 343 C applications p 129 N92-19498
Structure-to-property relationships in addition cured polymers. 4: Correlations between thermo-oxidative weight losses of norbornenyl cured polyimide resins and their composites
[NASA-TM-105553] p 108 N92-20039
Applications of high thermal conductivity composites to electronics and spacecraft thermal design
[NASA-TM-102434] p 56 N92-24349
Graphite intercalation compound with iodine as the major intercalant p 97 N92-25203
Graphite fluoride from iodine intercalated graphitized carbon
[NASA-CASE-LEW-15360-1] p 116 N92-34206
- GRAPHITE-EPOXY COMPOSITES**
Mixed-mode fracture in unidirectional graphite epoxy composite laminates with central notch p 218 A92-29464
Effect of contact stresses in four-point bend testing of graphite/epoxy and graphite/PMR-15 composite beams p 219 A92-33589
Computational simulation of surface waviness in graphite/epoxy woven composites due to initial curing
[NASA-TM-105313] p 106 N92-14118
Graphite/epoxy composite adapters for the Space Shuttle/Centaur vehicle
[NASA-TP-3014] p 49 N92-31251
Computational simulation of intermingled-fiber hybrid composite behavior
[NASA-TM-105666] p 110 N92-31506
- GRAPHITIZATION**
Brominated graphitized carbon fibers
[NASA-CASE-LEW-14698-2] p 127 N92-10090
Graphite fluoride from iodine intercalated graphitized carbon
[NASA-CASE-LEW-15360-1] p 116 N92-34206
- GRAVITATION**
Critical fluid thermal equilibration experiment (19-IML-1) p 139 N92-23640
- GRAVITATIONAL EFFECTS**
The implications of experimentally controlled gravitational accelerations for combustion science p 112 A92-16601
Effects of g-jitter and cross-diffusion on the onset of convection in doubly diffusive systems
[AIAA PAPER 92-0246] p 167 A92-25705
Gravitational influences on the behavior of confined diffusion flames
[AIAA PAPER 92-0334] p 113 A92-25781
Effects of g-jitter on a thermally buoyant flow p 171 A92-32258
Experiments with phase change thermal energy storage canisters for Space Station Freedom p 179 A92-50564
Stable localized patterns in thin liquid films
[NASA-TM-105352] p 185 N92-14322
Experiments with phase change thermal energy storage canisters for Space Station Freedom
[NASA-TM-104427] p 86 N92-21216
Microgravity acceleration measurement and environment characterization science (17-IML-1) p 139 N92-23642
- GRAVITATIONAL FIELDS**
Large-scale microwave anisotropy from gravitating seeds p 269 A92-56914
- GREASES**
Liquid lubrication for space applications
[NASA-TM-105198] p 133 N92-31840
- GREEN'S FUNCTIONS**
Solutions of the heat conduction equation in multilayers for photothermal deflection experiments p 141 A92-52205
- GREGORIAN ANTENNAS**
Analysis of a generalized dual reflector antenna system using physical optics
[NASA-TM-105425] p 149 N92-18281
- GRID GENERATION (MATHEMATICS)**
Automatic grid generation for iced airfoil flowfield predictions
[AIAA PAPER 92-0415] p 6 A92-26266
The NASA Computational Aerosciences Program - Toward teraFLOPS computing
[AIAA PAPER 92-0558] p 240 A92-26968
Euler solutions for an unbladed jet engine configuration
[AIAA PAPER 92-0544] p 169 A92-28201
Implementation of control point form of algebraic grid-generation technique p 248 A92-47058
A conformal block structured grid for turbomachinery cascades in two dimensions p 248 A92-47059
Investigation of three-dimensional flow field in a turbine including rotor/stator interaction. I - Design development and performance of the research facility
[AIAA PAPER 92-3325] p 40 A92-48908
Enhancing control of grid distribution in algebraic grid generation p 248 A92-52552
Grid generation for 3D turbomachinery configurations
[AIAA PAPER 92-3671] p 243 A92-54114
Euler solutions for an unbladed jet engine configuration
[NASA-TM-105332] p 184 N92-11328
A two-dimensional Euler solution for an unbladed jet engine configuration
[NASA-TM-105329] p 190 N92-23560
Interactive solution-adaptive grid generation procedure
[NASA-TM-105432] p 18 N92-23563
Interactive solution-adaptive grid generation p 243 N92-24420
MAG3D and its application to internal flowfield analysis p 243 N92-24421
A multiblock grid generation technique applied to a jet engine configuration p 244 N92-24428
Workshop on Grid Generation and Related Areas
[NASA-CP-10089] p 35 N92-25712
Grid management p 19 N92-25713
QX MAN: Q and X file manipulation p 244 N92-25715
TCGRID: A three dimensional C-grid generator for turbomachinery p 35 N92-25716
TIGGERC: Turbomachinery interactive grid generator energy distributor and restart code p 35 N92-25719
Multiblock grid generation for jet engine configurations p 35 N92-25720
Two-dimensional unstructured triangular grid generation p 192 N92-25721
Cartesian based grid generation/adaptive mesh refinement p 192 N92-25722
Interactive solution-adaptive grid generation procedure p 244 N92-25724
NASA Surface-Modeling and Grid-Generation (SM/GG) activities p 267 N92-25725
Integrating aerodynamic surface modeling for computational fluid dynamics with computer aided structural analysis, design, and manufacturing p 192 N92-25727
Numerical simulation of conservation laws p 193 N92-25813
A new Lagrangian method for real gases at supersonic speed p 19 N92-25814
Techniques for grid manipulation and adaptation --- computational fluid dynamics p 194 N92-25827
- GRINDING MACHINES**
Recent manufacturing advances for spiral bevel gears
[SAE PAPER 912229] p 204 A92-40024
- GROOVES**
Effect of type and location of oil groove on the performance of journal bearings p 203 A92-21333
- GROUND STATE**
Vacuum ultraviolet absorption in a hydrogen arcjet
[AIAA PAPER 92-3564] p 259 A92-54055
- GROUND STATIONS**
The ACTS NASA Ground Station/Master Control Station
[AIAA PAPER 92-1965] p 45 A92-29888
GTEX: An expert system for diagnosing faults in satellite ground stations p 148 N92-14215
- GROUND SUPPORT EQUIPMENT**
GTEX: An expert system for diagnosing faults in satellite ground stations p 148 N92-14215
Ka-band dual frequency array feed for a low cost ACTS ground terminal p 152 N92-32969
- GROUND SUPPORT SYSTEMS**
The ACTS NASA Ground Station/Master Control Station
[AIAA PAPER 92-1965] p 45 A92-29888

GROUND TESTS

LDEF spacecraft, ground laboratory, and computational modeling implications on Space Station Freedom's solar array materials and surfaces durability p 71 A92-53190

GROUND TESTS

Ground test program for a full-size solar dynamic heat receiver p 68 A92-50566

GUANIDINES

Method of making contamination-free ceramic bodies [NASA-CASE-LEW-14984-1] p 128 A92-16122
Guanidine based vehicle/binders for use with oxides, metals, and ceramics [NASA-CASE-LEW-15314-1] p 131 A92-23461

GUSTS

Airfoil wake and linear theory gust response including sub and superresonant flow conditions [AIAA PAPER 92-3074] p 11 A92-48724

H

HAFNIUM ALLOYS

Slow strain rate 1200-1400 K compressive properties of NiAl-1Hf p 116 A92-17977

HAFNIUM CARBIDES

Does a threshold stress for creep exist in HfC-dispersed NiAl? p 118 A92-30780

HALL EFFECT

Hall voltage sign reversal in thin superconducting films p 261 A92-35349
Enhancement of Shubnikov-de Haas oscillations by carrier modulation p 262 A92-50911

HALOGENATION

Graphite intercalation compound with iodine as the major intercalant [NASA-TM-105375] p 97 A92-25203

HANKEL FUNCTIONS

Computer program for Bessel and Hankel functions [NASA-TM-105154] p 243 A92-11691

HARMONIC MOTION

Euler flow predictions for an oscillating cascade using a high resolution wave-split scheme [ASME PAPER 91-GT-198] p 3 A92-15623

HARMONIC OSCILLATION

Wind tunnel wall effects in a linear oscillating cascade [ASME PAPER 91-GT-133] p 2 A92-15576

HARMONIC OSCILLATORS

A theoretical and experimental study of the noise behavior of subharmonically injection locked local oscillators p 157 A92-46080

HARMONICS

On the nonlinear development of three-dimensional instability waves in natural transition [AIAA PAPER 92-0741] p 170 A92-28222

HASTELLOY (TRADEMARK)

Hardening mechanisms in a dynamic strain aging alloy, Hastelloy X, during isothermal and thermomechanical cyclic deformation p 116 A92-24832
Thermomechanical deformation behavior of a dynamic strain aging alloy, Hastelloy X [NASA-TM-105316] p 228 A92-25179

HAZARDS

Safety issues p 78 A92-11115

HEAT AFFECTED ZONE

Post-test examination of a pool boiler receiver [NASA-TM-105635] p 123 A92-27192

HEAT BUDGET

Experimental balances for the second moments for a buoyant plume and their implication on turbulence modeling p 174 A92-40153

HEAT EXCHANGERS

A 2-D oscillating flow analysis in Stirling engine heat exchangers p 172 A92-36001
Modelling and experimental verification of a water alleviation system for the NASP --- National Aerospace Plane [NASA-TM-105661] p 189 A92-23224
An overview of the Lewis Research Center CSTI thermal management program [NASA-TM-105310] p 92 A92-31916

HEAT FLUX

Transient cooling of a square region of radiating medium p 164 A92-10432
Self-pressurization of a spherical liquid hydrogen storage tank in a microgravity environment [AIAA PAPER 92-0363] p 168 A92-25798
Self-pressurization of a flightweight liquid hydrogen tank - Effects of fill level at low wall heat flux [AIAA PAPER 92-0818] p 60 A92-29591
Thermal response of various thermal barrier coatings in a high heat flux rocket engine p 119 A92-32399
Experimental balances for the second moments for a buoyant plume and their implication on turbulence modeling p 174 A92-40153

Boundary heat fluxes for spectral radiation from a uniform temperature rectangular medium p 175 A92-44388

Three-dimensional boundary element thermal shape sensitivity analysis p 176 A92-47269
Scaling of low-Prandtl-number thermocapillary flows p 176 A92-47271

A laser-induced heat flux technique for convective heat transfer measurements in high speed flows p 200 A92-54318

Self-pressurization of a spherical liquid hydrogen storage tank in a microgravity environment [NASA-TM-105372] p 185 A92-14323

Self-pressurization of a flightweight liquid hydrogen tank: Effects of fill level at low wall heat flux [NASA-TM-105411] p 135 A92-18442

Miniature high temperature plug-type heat flux gauges [NASA-TM-105403] p 201 A92-18759

Method of producing a plug-type heat flux gauge [NASA-CASE-LEW-14967-2] p 201 A92-22038

Research sensors p 202 A92-22526
Turbulent heat flux measurements in a transitional boundary layer [NASA-TM-105623] p 19 A92-27377

HEAT MEASUREMENT

Miniature high temperature plug-type heat flux gauges [NASA-TM-105403] p 201 A92-18759

Research sensors p 202 A92-22526

HEAT OF FORMATION

Lattice parameters of fcc binary alloys using a new semiempirical method p 120 A92-32898

Heats of formation of bcc binary alloys [NASA-TM-105281] p 122 A92-16086

Lattice parameters of fcc binary alloys using a new semiempirical method [NASA-TM-105304] p 123 A92-16111

HEAT PIPES

Analytical and experimental studies of heat pipe radiation cooling of hypersonic propulsion systems [AIAA PAPER 92-3809] p 26 A92-49128

Frozen start-up behavior of low-temperature heat pipes p 179 A92-49847

Heat transfer and core neutronics considerations of the heat pipe cooled thermionic reactor p 180 A92-50591

Status of the advanced Stirling conversion system project for 25 kW dish Stirling applications p 207 A92-50804

Effects of anisotropic conduction and heat pipe interaction on minimum mass space radiators [NASA-TM-105297] p 80 A92-11138

Multimegawatt MPD thruster design considerations [NASA-TM-105405] p 83 A92-16024

NASA Lewis steady-state heat pipe code users manual [NASA-TM-105161] p 90 A92-28682

Solar thermal energy receiver [NASA-CASE-LEW-14949-1] p 238 A92-29143

Design characteristics of a heat pipe test chamber [NASA-TM-105737] p 238 A92-29662

An overview of the Lewis Research Center CSTI thermal management program [NASA-TM-105310] p 92 A92-31916

HEAT RADIATORS

Contamination effects on Space Station Freedom electric power system performance p 54 A92-50578

HEAT RESISTANT ALLOYS

The effect of porosity and gamma-gamma-prime eutectic content on the fatigue behavior of hydrogen charged PWA 1480 p 116 A92-12046

A viscoplastic theory for anisotropic materials [ONERA, TP NO. 1992-90] p 217 A92-24721

Low earth orbit durability evaluation of Haynes 188 solar receiver material [AIAA PAPER 92-0850] p 117 A92-29616

COSP - A computer model of cyclic oxidation p 114 A92-31849

Computational simulation of high temperature metal matrix composite behavior p 101 A92-32753

Solidification processing of intermetallic Nb-Al alloys p 120 A92-33866

Application of a thermal fatigue life prediction model to high-temperature aerospace alloys B1900 + Hf and Haynes 188 p 121 A92-45232

Thermomechanical and bithermal fatigue behavior of cast B1900 + Hf and wrought Haynes 188 p 122 A92-45233

Alkali metal compatibility testing of candidate heater head materials for a Stirling engine heat transport system p 71 A92-50829

Thermomechanical deformation behavior of a dynamic strain aging alloy, Hastelloy X [NASA-TM-105316] p 228 A92-25179

Elevated temperature axial and torsional fatigue behavior of Haynes 188 [NASA-TM-105396] p 229 A92-28701

HEAT SHIELDING

Solar dynamic modules for Space Station Freedom: The relationship between fine-pointing control and thermal loading of the aperture plate [NASA-TM-104498] p 84 A92-19780

HEAT SINKS

Heat transfer device [NASA-CASE-LEW-14162-3] p 111 A92-34208

HEAT STORAGE

Experiments with phase change thermal energy storage canisters for Space Station Freedom p 179 A92-50564

Full-size solar dynamic heat receiver thermal-vacuum tests p 68 A92-50565

Ground test program for a full-size solar dynamic heat receiver p 68 A92-50566

Critical technology experiment results for lightweight space heat receiver p 180 A92-50568

Sensible heat receiver for solar dynamic space power system p 180 A92-50570

Parametric studies of phase change thermal energy storage canisters for Space Station Freedom [NASA-TM-105350] p 55 A92-13143

Thermal modeling with solid/liquid phase change of the thermal energy storage experiment [NASA-TM-103770] p 185 A92-13402

Experiments with phase change thermal energy storage canisters for Space Station Freedom [NASA-TM-104427] p 86 A92-21216

Pulse thermal energy transport/storage system [NASA-CASE-LEW-15235-1] p 195 A92-29125

HEAT TRANSFER

Aerodynamics and heat transfer investigations on a high Reynolds number turbine cascade [ASME PAPER 91-GT-157] p 164 A92-15593

Navier-Stokes analysis of flow and heat transfer inside high-pressure-ratio transonic turbine blade rows p 165 A92-17193

Numerical analysis of a thermal deicer [AIAA PAPER 92-0527] p 22 A92-26950

Effects of g-jitter on a thermally buoyant flow p 171 A92-32258

Heat and mass transport from thermally degrading thin cellulose materials in a microgravity environment p 174 A92-41810

Navier-Stokes turbine heat transfer predictions using two-equation turbulence closures [AIAA PAPER 92-3067] p 177 A92-48721

Frozen start-up behavior of low-temperature heat pipes p 179 A92-49847

Heat transfer and core neutronics considerations of the heat pipe cooled thermionic reactor p 180 A92-50591

Measurements of the effects of thermal contact resistance on steady state heat transfer in phosphoric-acid fuel cell stack p 180 A92-50738

Alkali metal pool boiler life tests for a 25 kW advanced Stirling conversion system p 206 A92-50797

Final design of a free-piston hydraulic advanced Stirling conversion system p 206 A92-50798

Design of a pool boiler heat transport system for a 25 kW advanced Stirling conversion system p 181 A92-50802

Status of the advanced Stirling conversion system project for 25 kW dish Stirling applications p 207 A92-50804

Instantaneous heat transfer coefficient based upon two-dimensional analyses of Stirling space engine components p 181 A92-50827

Alkali metal compatibility testing of candidate heater head materials for a Stirling engine heat transport system p 71 A92-50829

Three-dimensional Navier-Stokes heat transfer predictions for turbine blade rows [AIAA PAPER 92-3068] p 12 A92-54003

Increased heat transfer to elliptical leading edges due to spanwise variations in the freestream momentum - Numerical and experimental results [AIAA PAPER 92-3070] p 13 A92-54005

Surface heat transfer and flow properties of vortex arrays induced artificially and from centrifugal instabilities p 183 A92-56371

Transonic turbine blade cascade testing facility [AIAA PAPER 92-4034] p 42 A92-56856

Modeling of the heat transfer in bypass transitional boundary-layer flows [NASA-TP-3170] p 184 A92-11299

Turbulent fluid motion 3: Basic continuum equations [NASA-TM-104386] p 184 A92-11317

Heat transfer in rotating serpentine passages with trips skewed to the flow [NASA-TM-105581] p 186 A92-20235

ULTRA-SHARP solution of the Smith-Hutton problem [NASA-TM-105435] p 187 A92-22226

Turbomachinery p 32 A92-22524

- Modelling and experimental verification of a water alleviation system for the NASP --- National Aerospace Plane
[NASA-TM-105661] p 189 N92-23224
- Thermal stratification potential in rocket engine coolant channels
[NASA-TM-4378] p 87 N92-25616
- Transonic turbine blade cascade testing facility
[NASA-TM-105646] p 47 N92-26129
- Pulse thermal energy transport/storage system
[NASA-CASE-LEW-15235-1] p 195 N92-29125
- Solar thermal energy receiver
[NASA-CASE-LEW-14949-1] p 238 N92-29143
- Design characteristics of a heat pipe test chamber
[NASA-TM-105737] p 238 N92-29662
- Heat transfer device
[NASA-CASE-LEW-14162-3] p 111 N92-34208
- HEAT TRANSFER COEFFICIENTS**
- Heat transfer measurements from a smooth NACA 0012 airfoil
[NASA-TM-105403] p 165 A92-20215
- Roughness effects on heat transfer from a NACA 0012 airfoil
[NASA-TM-105692] p 166 A92-20217
- Heat transfer on accreting ice surfaces
[NASA-TM-105692] p 166 A92-24415
- Mechanisms resulting in accreted ice roughness
[AIAA PAPER 92-0297] p 21 A92-25750
- Navier-Stokes analysis of turbomachinery blade external heat transfer
[NASA-TM-105683] p 170 A92-28518
- An improved heat transfer configuration for a solid-core nuclear thermal rocket engine
[AIAA PAPER 92-3583] p 75 A92-54063
- A laser-induced heat flux technique for convective heat transfer measurements in high speed flows
[NASA-TM-105403] p 200 A92-54318
- Miniature high temperature plug-type heat flux gauges
[NASA-TM-105403] p 201 N92-18759
- Heat transfer in rotating serpentine passages with trips skewed to the flow
[NASA-TM-105581] p 186 N92-20235
- Heat transfer in oscillating flows with sudden change in cross section
[NASA-TM-105692] p 88 N92-26654
- HEAT TREATMENT**
- Effect of heat treatment on stiffness and damping of SiC/Ti-15-3
[NASA-TM-105564] p 100 A92-25627
- Low temperature synthesis of CaO-SiO₂ glasses having stable liquid-liquid immiscibility by the sol-gel process
[NASA-TM-105628] p 126 A92-44479
- Effect of heat treatment on stiffness and damping of SiC/Ti-15-3
[NASA-TM-105564] p 108 N92-20841
- Composites of low-density trialuminides: Particulate and long fiber reinforcements
[NASA-TM-105628] p 109 N92-25346
- HEATING**
- Thermomechanical testing of high-temperature composites - Thermomechanical fatigue (TMF) behavior of SiC(SCS-6)/Ti-15-3
[NASA-TM-105628] p 104 A92-44606
- HELICAL WINDINGS**
- High temperature, flexible, fiber-preform seal
[NASA-CASE-LEW-15085-1] p 208 N92-22043
- HELICOPTER DESIGN**
- Advanced Rotorcraft Transmission (ART) program summary
[AIAA PAPER 92-3363] p 205 A92-48936
- Boeing Helicopters Advanced Rotorcraft Transmission (ART) Program summary of component tests
[AIAA PAPER 92-3364] p 205 A92-48937
- Summary highlights of the Advanced Rotorcraft Transmission (ART) program
[AIAA PAPER 92-3362] p 23 A92-54026
- Application of face-gear drives in helicopter transmissions
[NASA-TM-105655] p 212 N92-28434
- Experimental testing of prototype face gears for helicopter transmissions
[NASA-TM-105434] p 214 N92-31349
- HELICOPTER ENGINES**
- Advanced Rotorcraft Transmission (ART) - Component test results
[AIAA PAPER 92-3366] p 205 A92-48939
- A simplified dynamic model of the T700 turboshaft engine
[NASA-TM-105805] p 251 N92-30898
- HELICOPTER PERFORMANCE**
- Advanced Rotorcraft Transmission (ART) Program summary
[AIAA PAPER 92-3365] p 205 A92-48938
- Advanced Rotorcraft Transmission (ART) - Component test results
[AIAA PAPER 92-3366] p 205 A92-48939
- Advanced Rotorcraft Transmission (ART) program summary
[NASA-TM-105665] p 210 N92-24984
- HELICOPTER PROPELLER DRIVE**
- Advanced Rotorcraft Transmission (ART) Program summary
[AIAA PAPER 92-3365] p 205 A92-48938
- Modal simulation of gearbox vibration with experimental correlation
[AIAA PAPER 92-3494] p 207 A92-54036
- Rotorcraft transmissions
[NASA-TM-105665] p 33 N92-22533
- Advanced Rotorcraft Transmission (ART) program summary
[NASA-TM-105665] p 210 N92-24984
- Full-scale transmission testing to evaluate advanced lubricants
[NASA-TM-105668] p 212 N92-26560
- Application of face-gear drives in helicopter transmissions
[NASA-TM-105655] p 212 N92-28434
- Dynamics of a split torque helicopter transmission
[NASA-TM-105681] p 213 N92-29136
- Development of a full-scale transmission testing procedure to evaluate advanced lubricants
[NASA-TP-3265] p 213 N92-30396
- Experimental testing of prototype face gears for helicopter transmissions
[NASA-TM-105434] p 214 N92-31349
- Modal simulation of gearbox vibration with experimental correlation
[NASA-TM-105702] p 215 N92-31485
- HELICOPTERS**
- Ongoing development of a computer jobstream to predict helicopter main rotor performance in icing conditions
[NASA-TM-105434] p 2 A92-14407
- Rotorcraft transmissions
[NASA-TM-105665] p 33 N92-22533
- HELIUM**
- Helium bubble flow visualization of the spanwise separation on a NACA 0012 with simulated glaze ice
[AIAA PAPER 92-0413] p 7 A92-28192
- Brush seal leakage performance with gaseous working fluids at static and low rotor speed conditions
[NASA-TM-105400] p 186 N92-16265
- Helium bubble flow visualization of the spanwise separation on a NACA 0012 with simulated glaze ice
[NASA-TM-105742] p 19 N92-26612
- HEPTANES**
- Observations on a slow burning regime for hydrocarbon droplets - n-heptane/air results
[AIAA PAPER 92-0242] p 112 A92-16602
- Microgravity combustion of isolated n-decane and n-heptane droplets
[AIAA PAPER 92-0242] p 113 A92-26927
- Observations of soot during droplet combustion at low gravity - Heptane and heptane/monochloroalkane mixtures
[AIAA PAPER 92-0242] p 115 A92-50447
- HETEROJUNCTIONS**
- High-field transport properties of InAs(x)P(1-x)/InP (x = 0.3-1.0) modulation doped heterostructures at 300 and 77 K
[NASA-TM-105628] p 262 A92-46331
- Thin film, concentrator, and multijunction space solar cells: Status and potential
[NASA-TM-105628] p 81 N92-13230
- Intermodulation in the oscillatory magneto-resistance of a two-dimensional electron gas
[NASA-TM-105628] p 163 N92-32975
- HIERARCHIES**
- Development and testing of a source subsystem for the supporting development PMAD DC test bed
[NASA-TM-105628] p 46 A92-50659
- FIDEX: An expert system for satellite diagnostics
[NASA-TM-105628] p 148 N92-14218
- HIGH ALTITUDE**
- New technique for low-to-high altitude predictions of ablative hypersonic flowfields
[NASA-TM-105628] p 166 A92-24654
- HIGH ASPECT RATIO**
- An experimental investigation of high-aspect-ratio cooling passages
[AIAA PAPER 92-3154] p 64 A92-48780
- An experimental investigation of high-aspect-ratio cooling passages
[NASA-TM-105679] p 48 N92-25958
- HIGH ELECTRON MOBILITY TRANSISTORS**
- Enhancement of Shubnikov-de Haas oscillations by carrier modulation
[NASA-TM-105544] p 262 A92-50911
- Planar dielectric resonator stabilized HEMT oscillator integrated with CPW/aperture coupled patch antenna
[NASA-TM-105544] p 160 N92-18473
- V-band pseudomorphic HEMT MMIC phased array components for space communications
[NASA-TM-105544] p 151 N92-32966
- Planar dielectric resonator stabilized HEMT oscillator integrated with CPW/aperture coupled patch antenna
[NASA-TM-105544] p 152 N92-32967
- Reduced mobility and PPC in In(20)Ga(80)As / Al(23)Ga(77)As HEMT structure
[NASA-TM-105544] p 265 N92-32976
- Microwave properties of peeled HEMT devices sapphire substrates
[NASA-TM-105544] p 265 N92-32978
- HIGH FREQUENCIES**
- Evaluation of components, subsystems, and networks for high rate, high frequency space communications
[NASA-TM-105274] p 147 N92-12151
- Comparison of high temperature, high frequency core loss and dynamic B-H loops of a 2V-49Fe-49Co and a grain oriented 3Si-Fe alloy
[NASA-TM-105791] p 162 N92-30397
- HIGH IMPULSE**
- The evolutionary development of high specific impulse electric thruster technology
[NASA-TM-105758] p 93 N92-33064
- HIGH POWER LASERS**
- Space transfer with ground-based laser/electric propulsion
[AIAA PAPER 92-3213] p 73 A92-54017
- HIGH PRESSURE**
- Screech noise source structure of a supersonic rectangular jet
[AIAA PAPER 92-0503] p 6 A92-26932
- An SSME high pressure oxidizer turbopump diagnostic system using G2(TM) real-time expert system
[NASA-TM-105328] p 247 N92-13717
- Screech noise source structure of a supersonic rectangular jet
[NASA-TM-105384] p 15 N92-14000
- National Aerospace Plane engine seals: High temperature seal performance evaluation
[NASA-TM-105384] p 207 N92-15103
- HIGH RESOLUTION**
- Euler flow predictions for an oscillating cascade using a high resolution wave-split scheme
[ASME PAPER 91-GT-198] p 3 A92-15623
- HIGH REYNOLDS NUMBER**
- Aerodynamics and heat transfer investigations on a high Reynolds number turbine cascade
[ASME PAPER 91-GT-157] p 164 A92-15593
- The three-dimensional turbulent boundary layer near a plane of symmetry
[NASA-TM-105328] p 167 A92-24757
- Compressibility effects on large structures in free shear flows
[NASA-TM-105328] p 173 A92-39337
- Effect of spatial resolution on apparent sensitivity to initial conditions of a decaying flow as it becomes turbulent
[NASA-TM-105328] p 175 A92-45716
- Development of an efficient analysis for high Reynolds number inviscid/viscid interactions in cascades
[AIAA PAPER 92-3073] p 10 A92-48723
- Natural convection between concentric spheres
[NASA-TM-105328] p 179 A92-50445
- HIGH SPEED**
- The numerical simulation of a high-speed axial flow compressor
[ASME PAPER 91-GT-272] p 3 A92-15669
- Upwind schemes and bifurcating solutions in real gas computations
[NASA-TM-105328] p 193 N92-25817
- HIGH STRENGTH**
- High temperature structural fibers: Status and needs
[NASA-TM-105174] p 107 N92-16037
- Method of making contamination-free ceramic bodies
[NASA-CASE-LEW-14984-1] p 128 N92-16122
- HIGH TEMPERATURE**
- The application of a computer data acquisition system to a new high temperature tribometer
[NASA-TM-105189] p 93 A92-11823
- Thermomechanical testing of high-temperature composites - Thermomechanical fatigue (TMF) behavior of SiC(SCS-6)/Ti-15-3
[NASA-TM-105628] p 104 A92-44606
- Microfracture in high temperature metal matrix laminates
[NASA-TM-105189] p 106 N92-14122
- High temperature thruster technology for spacecraft propulsion
[NASA-TM-105348] p 82 N92-15125
- Tribological and mechanical comparison of sintered and HIPped PM212: High temperature self-lubricating composites
[NASA-TM-105379] p 96 N92-15128
- Thermally-driven microfracture in high temperature metal matrix composites
[NASA-TM-105305] p 107 N92-15136
- Elevated temperature mechanical behavior of monolithic and SiC whisker-reinforced silicon nitrides
[NASA-TM-105245] p 128 N92-15192
- High temperature structural fibers: Status and needs
[NASA-TM-105174] p 107 N92-16037
- High temperature, flexible pressure-actuated, brush seal
[NASA-CASE-LEW-15086-1] p 208 N92-16318
- Miniature high temperature plug-type heat flux gauges
[NASA-TM-105403] p 201 N92-18759
- Novel applications for TAZ-8A
[NASA-TM-105403] p 123 N92-22444
- High-temperature polymer matrix composites
[NASA-TM-105403] p 108 N92-22513
- Creep and fatigue research efforts on advanced materials
[NASA-TM-105403] p 227 N92-22514
- High-temperature electronics
[NASA-TM-105403] p 160 N92-22528
- Small engine technology programs
[NASA-TM-105403] p 32 N92-22532
- Aircraft engine hot section technology: An overview of the HOST Project
[NASA-TM-105403] p 33 N92-22535

HIGH TEMPERATURE ENVIRONMENTS

Effects of chemical equilibrium on turbine engine performance for various fuels and combustor temperatures

[NASA-TM-105399] p 34 N92-23254
High temperature dynamic engine seal technology development

[NASA-TM-105641] p 209 N92-23435

Evaluation of high temperature capacitor dielectrics

[NASA-TM-105622] p 161 N92-23561

Cyclopentadiene evolution during pyrolysis-gas chromatography of PMR polyimides

[NASA-TM-105629] p 132 N92-25348

High temperature dielectric properties of Apical, Kapton, Peek, Teflon AF, and Upilex polymers

[NASA-TM-105753] p 162 N92-28675

Comparison of high temperature, high frequency core loss and dynamic B-H loops of a 2V-49Fe-49Co and a grain oriented 3Si-Fe alloy

[NASA-TM-105791] p 162 N92-30397

Metal matrix composite analyzer (METCAN) user's manual, version 4.0

[NASA-TM-105244] p 110 N92-30779

HIGH TEMPERATURE ENVIRONMENTS

Finite difference solution for transient cooling of a radiating-conducting semitransparent layer

p 166 A92-20310

Multidisciplinary tailoring of hot composite structures

[AIAA PAPER 92-2563] p 220 A92-34564

Monolithic ceramics

p 125 A92-39854

Fracture behavior of a B2 Ni-30Al-20Fe-0.05Zr intermetallic alloy in the temperature range 300 to 1300 K

p 121 A92-41667

Deformation behavior of a Ni-30Al-20Fe-0.05Zr intermetallic alloy in the temperature range 300 to 1300 K

p 121 A92-41668

Fiber optics in liquid propellant rocket engine environments

p 62 A92-42610

Reactions of silicon carbide and silicon(IV) oxide at elevated temperatures

p 126 A92-43483

Evaluation of high temperature dielectric films for high voltage power electronic applications

p 261 A92-44273

An evaluation of strain measuring devices for ceramic composites

[NASA-TM-105337] p 225 N92-14433

Demonstrated survivability of a high temperature optical fiber cable on a 1500 pound thrust rocket chamber

[NASA-TM-105835] p 136 N92-32230

HIGH TEMPERATURE GASES

Hot gas environment around STOVL aircraft in ground proximity. II - Numerical study

p 25 A92-24403

Hot gas ingestion characteristics and flow visualization of a vectored thrust STOVL concept

p 26 A92-45316

Calculations of hot gas ingestion for a STOVL aircraft model

[NASA-TM-105437] p 17 N92-19993

Contingency power for a small turboshaft engine by using water injection into turbine cooling air

[NASA-TM-105680] p 37 N92-29661

HIGH TEMPERATURE LUBRICANTS

Liquid lubricants for advanced aircraft engines

[NASA-TM-104531] p 133 N92-32863

HIGH TEMPERATURE RESEARCH

Transient cooling of a square region of radiating medium

p 164 A92-10432

HIGH TEMPERATURE SUPERCONDUCTORS

Measurements of complex permittivity of microwave substrates in the 20 to 300 K temperature range from 26.5 to 40.0 GHz

p 197 A92-13416

Space applications of high temperature superconductivity technology

[IAF PAPER 91-307] p 259 A92-14724

Microwave properties of YBa₂Cu₃O(7- δ) high-transition-temperature superconducting thin films measured by the power transmission method

p 153 A92-14938

Coaxial line configuration for microwave power transmission study of YBa₂Cu₃O(7- δ) thin films

p 154 A92-18455

Melting of the Abrikosov flux lattice in anisotropic superconductors

p 260 A92-28075

Laser ablated YBa₂Cu₃O(7-x) high temperature superconductor coplanar waveguide resonator

p 155 A92-31631

Properties of large area ErBa₂Cu₃O(7-x) thin films deposited by ionized cluster beams

p 260 A92-33911

Performance of a K-band superconducting annular ring antenna

p 146 A92-37067

Performance of a four-element Ka-band high-temperature superconducting microstrip antenna

p 146 A92-37224

Ultrasonic evaluation of oxygen content, modulus, and microstructure changes in YBa₂Cu₃O(7-x) occurring during oxidation and reduction

p 261 A92-38418

Crystalline orientations of Ti₂Ba₂Ca₂Cu₃O(x) grains on MgO, SrTiO₃, and LaAlO₃ substrates

p 261 A92-41637

Conductor-backed coplanar waveguide resonators of YBa₂Cu₃O(7- δ) on LaAlO₃

p 158 A92-51042

A high temperature superconductivity communications flight experiment

[IAF PAPER 92-0410] p 50 A92-55790

Electrical-transport properties and microwave device performance of sputtered TiCaBaCuO superconducting thin films

p 263 A92-56599

NASA Space applications of high-temperature superconductors

[NASA-TM-105401] p 271 N92-18455

Chemical stability of high-temperature superconductors

[NASA-TM-105391] p 263 N92-19398

Glass precursor approach to high-temperature superconductors

[NASA-TM-105590] p 263 N92-20519

Microwave conductivity of laser ablated YBa₂Cu₃O(7- δ) superconducting films and its relation to microstrip transmission line performance

p 264 N92-21639

Solid State Technology Branch of NASA Lewis Research Center

[NASA-TM-105159] p 151 N92-23412

Microwave response of high transition temperature superconducting thin films

p 264 N92-23413

Properties of large area ErBa₂Cu₃O(7-x) thin films deposited by ionized cluster beams

p 264 N92-23414

Dependence of the critical temperature of laser-ablated YBa₂Cu₃O(7- δ) thin films on LaAlO₃ substrate growth technique

p 264 N92-23415

NASA space applications of high-temperature superconductors

p 265 N92-32980

Magnetic penetration depth of YBa₂Cu₃O(7- δ) thin films determined by the power transmission method

p 265 N92-32983

Magnetic flux relaxation in YBa₂Cu₃O(7-x) thin film: Thermal or athermal

p 265 N92-32984

C-band superconductor/semiconductor hybrid field-effect transistor amplifier on a LaAlO₃ substrate

[NASA-TM-105828] p 163 N92-34204

HIGH TEMPERATURE TESTS

Slow strain rate 1200-1400 K compressive properties of NiAl-1Hf

p 116 A92-17977

Stress versus temperature dependence of activation energies for creep

p 217 A92-24719

A viscoplastic theory for anisotropic materials

[ONERA, TP NO. 1992-90] p 217 A92-24721

The mechanical properties of a Ni-30Al-20Fe-0.05Zr intermetallic alloy in the temperature range 300-1200 K

p 118 A92-30793

Damage mechanisms in three-dimensional woven reinforced ceramic matrix composites under tensile and flexural loading at room and elevated temperatures

[AIAA PAPER 92-2492] p 101 A92-34584

Dielectric breakdown studies of Teflon perfluoroalkoxy at high temperature

p 125 A92-36287

An evaluation of strain measuring devices for ceramic composites

p 199 A92-46497

High-temperature durability considerations for HST combustor

[NASA-TP-3162] p 129 N92-17070

Evaluation of an innovative high temperature ceramic water seal for hypersonic engine applications

[NASA-TM-105556] p 208 N92-20815

X ray based displacement measurement for hostile environments

[NASA-TM-105551] p 202 N92-23155

Tribological evaluation of an Al₂O₃-SiO₂ ceramic fiber candidate for high temperature sliding seals

[NASA-TM-105611] p 97 N92-23190

Phase transformations in SrAl₂Si₂O₈ glass

[NASA-TM-105657] p 264 N92-23890

HIGH VOLTAGES

The arcing rate for a High Voltage Solar Array - Theory, experiment and predictions

[AIAA PAPER 92-0576] p 53 A92-26983

The formation and structure of plasma wakes behind large high-voltage space platforms in ionosphere

[AIAA PAPER 92-0577] p 239 A92-26984

Solar Array Module Plasma Interaction Experiment (SAMPIE): Technical requirements document

[NASA-TM-105660] p 56 N92-28683

HISTORIES

Rocket propulsion research at Lewis Research Center

[NASA-CR-189187] p 266 N92-30908

HOLDERS

Removable hand hold

[NASA-CASE-LEW-15196-1] p 213 N92-29092

HOLES (ELECTRON DEFICIENCIES)

Defect behavior, carrier removal and predicted in-space injection annealing of InP solar cells

[NASA-TM-105624] p 161 N92-23562

HOLLOW CATHODES

Extended testing of xenon ion thruster hollow cathodes

[AIAA PAPER 92-3204] p 65 A92-48811

A first-principles model for orificed hollow cathode operation

[AIAA PAPER 92-3742] p 259 A92-54145

Preliminary test results of a hollow cathode MPD thruster

[NASA-TM-105324] p 84 N92-18474

HOLOGRAPHY

Reconfigurable optical interconnection network for multimode optical fiber sensor arrays

p 256 A92-37448

HOMOGENEOUS TURBULENCE

A critical comparison of second order closures with direct numerical simulation of homogeneous turbulence

[NASA-TM-105351] p 185 N92-15357

HONEYCOMB STRUCTURES

Flow quality studies of the NASA Lewis Research Center 8- by 6-foot supersonic/9- by 15-foot Low Speed Wind Tunnel

[AIAA PAPER 92-3916] p 41 A92-56748

Flow quality studies of the NASA Lewis Research Center 8- by 6-foot supersonic/9- by 15-foot low speed wind tunnel

[NASA-TM-105417] p 42 N92-28673

HORSESHOE VORTICES

Investigation of three-dimensional flow field in a turbine including rotor/stator interaction. II - Three-dimensional flow field at the exit of the nozzle

[AIAA PAPER 92-3326] p 12 A92-48909

HOT PRESSING

Crack healing behavior of hot pressed silicon nitride due to oxidation

p 124 A92-32896

HOUSINGS

A flexible CPW package for a 30 GHz MMIC amplifier --- coplanar waveguide

[NASA-TM-105630] p 161 N92-23193

A flexible CPW package for a 30 GHz MMIC amplifier

p 152 N92-32972

HOVERING

Acoustic characteristics and dynamic structural loading of an ASTOVL aircraft in hover

[AIAA PAPER 92-0370] p 253 A92-28190

HUBBLE SPACE TELESCOPE

Results of a technical analysis of the Hubble Space Telescope nickel-cadmium and nickel-hydrogen batteries

p 89 N92-27167

HUMAN FACTORS ENGINEERING

Safety issues

p 78 N92-11115

HUMAN RESOURCES

NASA Lewis Research Center materials research and technology: An overview

p 31 N92-22512

HYBRID CIRCUITS

Performance of a Y-Ba-Cu-O superconducting filter/GaAs low noise amplifier hybrid circuit

[NASA-TM-105546] p 160 N92-21370

Performance of a Y-Ba-Cu-O superconducting filter/GaAs low noise amplifier hybrid circuit

p 163 N92-32982

HYBRID COMPOSITES

Computational simulation of intermingled-fiber hybrid composite behavior

[NASA-TM-105666] p 110 N92-31506

HYDRAULIC CONTROL

Design of a hydraulic actuator for active control of rotating machinery

[ASME PAPER 91-GT-246] p 203 A92-15651

HYDRAULIC EQUIPMENT

Final design of a free-piston hydraulic advanced Stirling conversion system

p 206 A92-50798

A survey of instabilities within centrifugal pumps and concepts for improving the flow range of pumps in rocket engines

[NASA-TM-105439] p 84 N92-18280

Resonant mode controllers for launch vehicle applications

[NASA-TM-105563] p 48 N92-25092

HYDRAZINES

Test experience, 490 N high performance (321 sec lsp) engine

[AIAA PAPER 92-3800] p 67 A92-49127

HYDROCARBON COMBUSTION

Observations on a slow burning regime for hydrocarbon droplets - n-heptane/air results

p 112 A92-16602

Optimization and analysis of large chemical kinetic mechanisms using the solution mapping method - Combustion of methane

p 113 A92-19300

Microgravity combustion of isolated n-decane and n-heptane droplets

[AIAA PAPER 92-0242] p 113 A92-26927

A simplified reaction mechanism for prediction of NO(x) emissions in the combustion of hydrocarbons

[AIAA PAPER 92-3340] p 114 A92-48919

- HYDROCARBON FUEL PRODUCTION**
Acetylene fuel from atmospheric CO₂ on Mars p 133 A92-32199
- HYDRODYNAMICS**
Effect of radiation on convection at moderate temperatures [AIAA PAPER 92-0691] p 168 A92-27058
Propagating confined states in phase dynamics p 181 A92-50968
The Eckhaus and the Benjamin-Feir instability near a weakly inverted bifurcation [NASA-TM-105334] p 185 N92-15336
- HYDROGEN**
Material processing with hydrogen and carbon monoxide on Mars p 231 A92-17769
Hydrogen no-vent testing in a 5 cubic foot (142 liter) tank using spray nozzle and spray bar liquid injection [AIAA PAPER 92-3063] p 63 A92-48719
Technology issues associated with using densified hydrogen for space vehicles [AIAA PAPER 92-3079] p 134 A92-48727
Numerical study of shock-wave/boundary-layer interactions in premixed combustible gases p 183 A92-54907
High-power hydrogen arcjet performance [NASA-TM-105143] p 82 N92-14109
Experiments and analysis concerning the use of external burning to reduce aerospace vehicle transonic drag [NASA-TM-105397] p 30 N92-17546
Technology issues associated with using densified hydrogen for space vehicles [NASA-TM-105642] p 135 N92-25277
Hydrogen no-vent fill testing in a 5 cubic foot (142 liter) tank using spray nozzle and spray bar liquid injection [NASA-TM-105759] p 136 N92-28433
- HYDROGEN ATOMS**
Laser-induced fluorescence of atomic hydrogen in an arcjet thruster [AIAA PAPER 92-0678] p 60 A92-27045
Vacuum ultraviolet absorption in a hydrogen arcjet [AIAA PAPER 92-3564] p 259 A92-54055
- HYDROGEN ENGINES**
Medium power hydrogen arcjet performance [AIAA PAPER 91-2227] p 58 A92-15355
Dependence of hydrogen arcjet operation on electrode geometry [AIAA PAPER 92-3530] p 74 A92-54039
Hydrogen arcjet technology [NASA-TM-105340] p 82 N92-15119
- HYDROGEN FUELS**
Slush hydrogen (SLH₂) technology development for application to the National Aerospace Plane (NASP) p 140 A92-13432
Material processing with hydrogen and carbon monoxide on Mars p 231 A92-17769
Hydrogen no-vent testing in a 5 cubic foot (142 liter) tank using spray nozzle and spray bar liquid injection [AIAA PAPER 92-3063] p 63 A92-48719
Technology issues associated with using densified hydrogen for space vehicles [AIAA PAPER 92-3079] p 134 A92-48727
Slush hydrogen pressurized expulsion studies at the NASA K-Site Facility [AIAA PAPER 92-3385] p 141 A92-48951
Benefits of slush hydrogen for space missions [NASA-TM-104503] p 134 N92-11214
Technology issues associated with using densified hydrogen for space vehicles [NASA-TM-105642] p 135 N92-25277
Slush hydrogen transfer studies at the NASA K-Site Test Facility [NASA-TM-105596] p 135 N92-25957
Slush hydrogen pressurized expulsion studies at the NASA K-Site Facility [NASA-TM-105597] p 135 N92-26131
Hydrogen no-vent fill testing in a 5 cubic foot (142 liter) tank using spray nozzle and spray bar liquid injection [NASA-TM-105759] p 136 N92-28433
- HYDROGEN OXYGEN ENGINES**
Thermal response of various thermal barrier coatings in a high heat flux rocket engine p 119 A92-32399
Rocket plume flowfield characterization using laser Rayleigh scattering [AIAA PAPER 92-3351] p 66 A92-48928
Species and temperature measurement in H₂/O₂ rocket flow fields by means of Raman scattering diagnostics [AIAA PAPER 92-3353] p 178 A92-48930
Spectrally resolved Rayleigh scattering diagnostic for hydrogen-oxygen rocket plume studies p 67 A92-50253
Performance comparison of axisymmetric and three-dimensional hydrogen film coolant injection in a 110 N hydrogen/oxygen rocket [AIAA PAPER 92-3390] p 73 A92-54027
- Computation of H₂/air reacting flowfields in drag-reduction external combustion [AIAA PAPER 92-3672] p 182 A92-54115
Technology readiness assessment of advanced space engine integrated controls and health monitoring [NASA-TM-105255] p 79 N92-11130
Hydrogen/oxygen auxiliary propulsion technology [NASA-TM-105249] p 85 N92-20522
Rocket plume flowfield characterization using laser Rayleigh scattering [NASA-TM-105739] p 257 N92-28475
Demonstrated survivability of a high temperature optical fiber cable on a 1500 pound thrust rocket chamber [NASA-TM-105835] p 136 N92-32230
- HYDROGEN OXYGEN FUEL CELLS**
SEI rover solar-electrochemical power system options p 45 A92-50574
A study of Na(x)Pt₃O₄ as an O₂ electrode bifunctional electrocatalyst [NASA-TM-105311] p 85 N92-20585
- HYDROGEN-BASED ENERGY**
Radiation enhanced dissociation of hydrogen in nuclear rockets [AIAA PAPER 92-3817] p 67 A92-49129
- HYDROLYSIS**
Low temperature synthesis of CaO-SiO₂ glasses having stable liquid-liquid immiscibility by the sol-gel process p 126 A92-44479
- HYDROSTATIC PRESSURE**
The decrease in yield strength in NiAl due to hydrostatic pressure p 120 A92-38990
- HYDROXYL RADICALS**
Saturated fluorescence measurements of the hydroxyl radical in laminar high-pressure C₂H₆/O₂/N₂ flames p 198 A92-33987
Quantitative fluorescence measurements of the OH radical in high pressure methane flames [AIAA PAPER 92-2960] p 114 A92-46976
Measurement of trace stratospheric constituents with a balloon borne laser radar p 239 N92-14500
- HYPERCUBE MULTIPROCESSORS**
High order parallel numerical schemes for solving incompressible flows p 193 N92-25818
- HYPERSONIC COMBUSTION**
Implementation of a kappa-epsilon turbulence model to RPLUS3D code p 194 N92-25822
- HYPERSONIC FLIGHT**
Structural tailoring/analysis for hypersonic components - Executive system development [AIAA PAPER 92-2471] p 219 A92-34360
Analytical and experimental studies of heat pipe radiation cooling of hypersonic propulsion systems [AIAA PAPER 92-3809] p 26 A92-49128
Rocket-Based Combined-Cycle (RBCC) Propulsion Technology Workshop. Tutorial session [NASA-CP-10090] p 86 N92-21517
Study of shock-induced combustion using an implicit TVD scheme p 116 N92-25816
- HYPERSONIC FLOW**
New technique for low-to-high altitude predictions of ablative hypersonic flowfields p 166 A92-24654
An improved PNS scheme for predicting complex three-dimensional hypersonic flows [AIAA PAPER 92-0753] p 8 A92-31679
Structural tailoring/analysis for hypersonic components - Executive system development [AIAA PAPER 92-2471] p 219 A92-34360
Numerical study of shock-wave/boundary-layer interactions in premixed combustible gases p 183 A92-54907
Filtered Rayleigh scattering measurements in supersonic/hypersonic facilities [AIAA PAPER 92-3894] p 200 A92-56733
Evaluation of an innovative high temperature ceramic wafer seal for hypersonic engine applications [NASA-TM-105556] p 208 N92-20815
Development of a new flux splitting scheme p 190 N92-23352
High-Order Polynomial Expansions (HOPE) for flux-vector splitting p 190 N92-23353
Development of new flux splitting schemes ... computational fluid dynamics algorithms p 192 N92-25809
- HYPERSONIC INLETS**
Three-dimensional viscous analysis of a Mach 5 inlet and comparison with experimental data p 8 A92-28526
Comparative study of turbulence models in predicting hypersonic inlet flows [AIAA PAPER 92-3098] p 11 A92-48740
Comparative study of turbulence models in predicting hypersonic inlet flows [NASA-TM-105720] p 19 N92-28102
- HYPERSONIC REENTRY**
Low-to-high altitude predictions of three-dimensional ablative reentry flowfields [AIAA PAPER 92-0366] p 168 A92-26227
- HYPERSONIC SPEED**
High-speed inlet research program and supporting analysis p 188 N92-22542
- HYPERSONIC TEST APPARATUS**
Laser-driven hypersonic air-breathing propulsion simulator [AIAA PAPER 92-3922] p 41 A92-56753
- HYPERSONIC VEHICLES**
Modeling of compressible turbulent shear flows p 189 N92-23340
- HYPERVELOCITY FLOW**
Improved nonequilibrium viscous shock-layer scheme for hypersonic blunt-body flowfields p 4 A92-24653
- HYPERVELOCITY IMPACT**
Characteristics of hypervelocity impact craters on LDEF experiment S1003 and implications of small particle impacts on reflective surfaces p 269 N92-27252
- HYSTERESIS**
The Eckhaus and the Benjamin-Feir instability near a weakly inverted bifurcation [NASA-TM-105334] p 185 N92-15336
- ICE**
A combined analytical-experimental tensile test technique for brittle materials p 123 A92-23225
LEWICE/E - An Euler based ice accretion code [AIAA PAPER 92-0037] p 4 A92-25676
Prediction of ice accretion on a swept NACA 0012 airfoil and comparisons to flight test results [AIAA PAPER 92-0043] p 4 A92-25677
A turbulence model for iced airfoils and its validation [AIAA PAPER 92-0417] p 6 A92-26267
Results of an icing test on a NACA 0012 airfoil in the NASA Lewis Icing Research Tunnel [AIAA PAPER 92-0647] p 7 A92-27021
LEWICE/E: An Euler based ice accretion code [NASA-TM-105389] p 15 N92-14001
Results of an icing test on a NACA 0012 airfoil in the NASA Lewis Icing Research Tunnel [NASA-TM-105374] p 16 N92-15051
A turbulence model for iced airfoils and its validation [NASA-TM-105373] p 16 N92-15052
Analysis of aircraft engine blade subject to ice impact [NASA-TM-105336] p 226 N92-15402
Prediction of ice accretion on a swept NACA 0012 airfoil and comparisons to flight test results [NASA-TM-105368] p 16 N92-15968
Experimental ice shape and performance characteristics for a multi-element airfoil in the NASA Lewis Icing Research Tunnel [NASA-TM-105380] p 17 N92-17347
Simulation of iced wing aerodynamics p 21 N92-21686
Experimental and computational ice shapes and resulting drag increase for a NACA 0012 airfoil [NASA-TM-105743] p 20 N92-28674
Analysis of iced wings [NASA-TM-105773] p 20 N92-34144
- ICE CLOUDS**
Performance of the Phase Doppler Particle Analyzer icing cloud droplet sizing probe in the NASA Lewis Icing Research Tunnel [AIAA PAPER 92-0162] p 198 A92-26926
- ICE FORMATION**
Advanced ice protection systems test in the NASA Lewis Icing Research Tunnel p 22 A92-14406
Ongoing development of a computer jobstream to predict helicopter main rotor performance in icing conditions p 2 A92-14407
LEWICE/E - An Euler based ice accretion code [AIAA PAPER 92-0037] p 4 A92-25676
Prediction of ice accretion on a swept NACA 0012 airfoil and comparisons to flight test results [AIAA PAPER 92-0043] p 4 A92-25677
Mechanisms resulting in accreted ice roughness [AIAA PAPER 92-0297] p 21 A92-25750
Numerical investigation of performance degradation of wings and rotors due to icing [AIAA PAPER 92-0412] p 5 A92-26264
Finite wing aerodynamics with simulated glaze ice [AIAA PAPER 92-0414] p 5 A92-26265
Automatic grid generation for iced airfoil flowfield predictions [AIAA PAPER 92-0415] p 6 A92-26266
Performance of the Phase Doppler Particle Analyzer icing cloud droplet sizing probe in the NASA Lewis Icing Research Tunnel [AIAA PAPER 92-0162] p 198 A92-26926

ICE PREVENTION

- Numerical analysis of a thermal deicer
[AIAA PAPER 92-0527] p 22 A92-26950
Results of an icing test on a NACA 0012 airfoil in the
NASA Lewis Icing Research Tunnel
[AIAA PAPER 92-0647] p 7 A92-27021
Analysis of surface roughness generation in aircraft ice
accretion p 169 A92-28187
[AIAA PAPER 92-0298]
Comparison of two-dimensional and three dimensional
droplet trajectory calculations in the vicinity of finite
wings p 8 A92-28215
[AIAA PAPER 92-0645]
Tensile properties of impact ices p 94 A92-29644
[AIAA PAPER 92-0883]
Analysis of iced wings p 8 A92-29972
[AIAA PAPER 92-0416]
LDV measurements on a rectangular wing with a
simulated glaze ice accretion p 10 A92-45537
[AIAA PAPER 92-2690]
Effect of a simulated glaze ice shape on the aerodynamic
performance of a rectangular wing p 14 A92-56861
[AIAA PAPER 92-4042]
Technical evaluation report, AGARD Fluid Dynamics
Panel Symposium on Effects of Adverse Weather on
Aerodynamics p 1 N92-10002
[NASA-TM-105192]
LEWICE/E: An Euler based ice accretion code p 15 N92-14001
[NASA-TM-105389]
Results of an icing test on a NACA 0012 airfoil in the
NASA Lewis Icing Research Tunnel p 16 N92-15051
[NASA-TM-105374]
Prediction of ice accretion on a swept NACA 0012 airfoil
and comparisons to flight test results p 16 N92-15968
[NASA-TM-105368]
Icing simulation: A survey of computer models and
experimental facilities p 21 N92-21684
Model rotor icing tests in the NASA, Lewis Icing
Research Tunnel p 21 N92-21688
The NASA aircraft icing research program p 23 N92-22534
Comparison of two-dimensional and three-dimensional
droplet trajectory calculations in the vicinity of finite
wings p 188 N92-23154
[NASA-TM-105617]
Helium bubble flow visualization of the spanwise
separation on a NACA 0012 with simulated glaze ice
[NASA-TM-105742] p 19 N92-26612
Experimental and computational ice shapes and
resulting drag increase for a NACA 0012 airfoil
[NASA-TM-105743] p 20 N92-28674
Results of a low power ice protection system test and
a new method of imaging data analysis p 20 N92-28696
[NASA-TM-105745]
Lewis icing research tunnel test of the aerodynamic
effects of aircraft ground deicing/anti-icing fluids
[NASA-TP-3238] p 22 N92-30395
Analysis of iced wings p 20 N92-34144
[NASA-TM-105773]
- ICE PREVENTION**
Advanced ice protection systems test in the NASA Lewis
Icing Research Tunnel p 22 A92-14406
Heat transfer measurements from a smooth NACA 0012
airfoil p 165 A92-20215
Technical evaluation report, AGARD Fluid Dynamics
Panel Symposium on Effects of Adverse Weather on
Aerodynamics p 1 N92-10002
[NASA-TM-105192]
Icing simulation: A survey of computer models and
experimental facilities p 21 N92-21684
The NASA aircraft icing research program p 23 N92-22534
NASA's aircraft icing technology program
[NASA-TM-104518] p 17 N92-23105
Results of a low power ice protection system test and
a new method of imaging data analysis p 20 N92-28696
[NASA-TM-105745]
- IDEAL GAS**
A new Lagrangian method for real gases at supersonic
speed p 19 N92-25814
- IGNITION**
Determination of the natural convection coefficient in
low-gravity p 168 A92-27072
[AIAA PAPER 92-0712]
Combustion-wave ignition for rocket engines
[NASA-TM-105545] p 84 N92-20043
Hydrogen/oxygen auxiliary propulsion technology
[NASA-TM-105249] p 85 N92-20522
- ILLUMINATING**
Moonbase night power by laser illumination p 44 A92-21086
- IMAGE ANALYSIS**
Concentrator testing using projected images p 69 A92-50615

IMAGE PROCESSING

- Color image processing and object tracking
workstation p 139 N92-26611
[NASA-TM-105561]
Results of a low power ice protection system test and
a new method of imaging data analysis p 20 N92-28696
[NASA-TM-105745]
- IMAGING TECHNIQUES**
Full field flow visualization and computer-aided velocity
measurements in a bank of cylinders in a wind tunnel p 199 A92-50040
Plasma etching a ceramic composite --- evaluating
microstructure p 130 N92-22305
[NASA-TM-105430]
X ray attenuation measurements for high-temperature
materials characterization and in-situ monitoring of damage
accumulation p 110 N92-25996
[NASA-TM-105577]
Results of a low power ice protection system test and
a new method of imaging data analysis p 20 N92-28696
[NASA-TM-105745]
- IMPACT DAMAGE**
Assessment of environmental effects on Space Station
Freedom Electrical Power System p 55 A92-50581
Analysis of aircraft engine blade subject to ice impact
[NASA-TM-105336] p 226 N92-15402
- IMPACT LOADS**
Analysis of aircraft engine blade subject to ice impact
[NASA-TM-105336] p 226 N92-15402
- IMPEDANCE MEASUREMENT**
Stability testing and analysis of a PMAD DC test bed
for the Space Station Freedom p 162 N92-31282
[NASA-TM-105846]
- IMPINGEMENT**
An experimental study of impingement-ion-production
mechanisms p 76 A92-54190
[AIAA PAPER 92-3826]
- IMPREGNATING**
Progress in the development of lightweight nickel
electrode for aerospace applications p 236 N92-20493
[NASA-TM-105591]
- IMPURITIES**
Composition dependence of superconductivity in
YBa₂(Cu_{3-x}Al_x)O_y p 131 N92-24715
[NASA-TM-105358]
- IN-FLIGHT MONITORING**
An overview of in-flight plume diagnostics for rocket
engines p 75 A92-54164
[AIAA PAPER 92-3785]
An overview of in-flight plume diagnostics for rocket
engines p 90 N92-28417
[NASA-TM-105727]
- INCOMPRESSIBLE FLOW**
A least-squares finite element method for
incompressible Navier-Stokes problems p 173 A92-37387
Instantaneous heat transfer coefficient based upon
two-dimensional analyses of Stirling space engine
components p 181 A92-50827
[NASA-TM-104424]
An efficient and robust algorithm for two dimensional
time dependent incompressible Navier-Stokes equations:
High Reynolds number flows p 184 N92-11320
[NASA-TM-105424]
Semi-empirical model for prediction of unsteady forces
on an airfoil with application to flutter p 17 N92-18760
[NASA-TM-105414]
An investigation of OTNS2D for use as an incompressible
turbulence modelling test-bed p 249 N92-22230
[NASA-TM-105593]
Center for Modeling of Turbulence and Transition
(CMOTT). Research briefs: 1990 p 1 N92-23336
[NASA-TM-105243]
The present status and the future direction of second
order closure models for incompressible flows p 191 N92-24523
High order parallel numerical schemes for solving
incompressible flows p 193 N92-25818
An efficient and robust algorithm for time dependent
viscous incompressible Navier-Stokes equations p 193 N92-25819
A new time scale based k-epsilon model for near wall
turbulence p 196 N92-32688
[NASA-TM-105768]
- INCOMPRESSIBLE FLUIDS**
An efficient and robust algorithm for two dimensional
time dependent incompressible Navier-Stokes equations:
High Reynolds number flows p 184 N92-11320
[NASA-TM-104424]
- INDEXES (DOCUMENTATION)**
Bibliography of Lewis Research Center technical
publications announced in 1990 p 267 N92-12786
[NASA-TM-103753]
- INDIUM ARSENIDES**
dc and microwave performance of a 0.1-micron gate
InAs/In(0.52)Al(0.48)As MODFET p 156 A92-43891

- High-field transport properties of InAs(x)P(1-x)/InP (x =
0.3-1.0) modulation doped heterostructures at 300 and 77
K p 262 A92-46331
Recent progress in InP solar cell research p 158 A92-50653
Effect of InAlAs window layer on the efficiency of indium
phosphide solar cells p 234 A92-53163
Effect of InAlAs window layer on efficiency of indium
phosphide solar cells p 161 N92-25176
[NASA-TM-105354]
- INDIUM GALLIUM ARSENIDES**
Modeled performance of monolithic, 3-terminal
InP/Ga(0.47)In(0.53)As concentrator solar cells as a
function of temperature and concentration ratio p 234 A92-53153
Reduced mobility and PPC in In(20)Ga(80)As /
Al(23)Ga(77)As HEMT structure p 265 N92-32976
Study of InGaAs-based modulation doped field effect
transistor structures using variable-angle spectroscopic
ellipsometry p 265 N92-32977
- INDIUM PHOSPHIDES**
Calculated performance of p(+)-n InP solar cells with
In(0.52)Al(0.48)As window layers p 153 A92-13266
Increased efficiency with surface texturing in ITO/InP
solar cells p 232 A92-44548
High-field transport properties of InAs(x)P(1-x)/InP (x =
0.3-1.0) modulation doped heterostructures at 300 and 77
K p 262 A92-46331
Surface etching for light trapping in encapsulated InP
solar cells p 232 A92-48091
Photoluminescence lifetime measurements in InP
wafers p 262 A92-48092
Advanced power systems for EOS p 70 A92-50640
Recent progress in InP solar cell research p 158 A92-50653
A very low resistance, non-sintered contact system for
use on indium phosphide concentrator/shallow junction
solar cells p 233 A92-53146
Minority carrier lifetime in indium phosphide p 262 A92-53148
Theoretical modeling, near-optimum design and
predicted performance of n(+)-pp(+) and p(+)-nn(+)
indium phosphide homojunction solar cells p 234 A92-53152
Modeled performance of monolithic, 3-terminal
InP/Ga(0.47)In(0.53)As concentrator solar cells as a
function of temperature and concentration ratio p 234 A92-53153
Enhancing optical absorption in InP and GaAs utilizing
profile etching p 263 A92-53154
High performance etchant for thinning p(+)-InP and its
application to p(+)-n InP solar cell fabrication p 263 A92-53155
Influence of the dislocation density on the performance
of heteroepitaxial indium phosphide solar cells p 234 A92-53156
Effect of InAlAs window layer on the efficiency of indium
phosphide solar cells p 234 A92-53163
InP concentrator solar cells p 234 A92-53166
High voltage thermally diffused p(+) solar cells p 235 A92-53172
Radiation and temperature effects in heteroepitaxial and
homoepitaxial InP cells p 159 A92-53192
Pilot production of 4 sq cm ITO/InP photovoltaic solar
cells p 71 A92-53197
Enhanced EOS photovoltaic power system capability
with InP solar cells p 81 N92-13248
A very low resistance, non-sintered contact system for
use on indium phosphide concentrator/shallow junction
solar cells p 235 N92-13482
[NASA-TM-105279]
Enhancing optical absorption in InP and GaAs utilizing
profile etching p 82 N92-14111
[NASA-TM-105325]
Status and future directions of InP solar cell research
[NASA-TM-105426] p 160 N92-18920
Defect behavior, carrier removal and predicted in-space
injection annealing of InP solar cells p 161 N92-23562
[NASA-TM-105624]
Sinterless contacts to shallow junction InP solar cells
[NASA-TM-105670] p 237 N92-24802
Effect of InAlAs window layer on efficiency of indium
phosphide solar cells p 161 N92-25176
[NASA-TM-105354]
The achievement of low contact resistance to indium
phosphide: The roles of Ni, Au, Ge, and combinations
thereof p 238 N92-33895
[NASA-TM-105770]
- INDUCTION MOTORS**
Development of a computer algorithm for the analysis
of variable-frequency AC drives: Case studies included
[NASA-TM-105327] p 29 N92-13070
Electromechanical systems with transient high power
response operating from a resonant AC link p 37 N92-28985
[NASA-TM-105716]

- INDUCTORS**
Comparison of high temperature, high frequency core loss and dynamic B-H loops of a 2V-49Fe-49Co and a grain oriented 3Si-Fe alloy
[NASA-TM-105791] p 162 N92-30397
- INERTIAL UPPER STAGE**
Upper stages using liquid propulsion and metallized propellants
[NASA-TP-3191] p 83 N92-17151
- INFLATABLE STRUCTURES**
Inflatable traversing probe seal p 209 N92-22692
- INFLUENCE COEFFICIENT**
Cascade flutter analysis with transient response aerodynamics p 217 A92-15972
- INFRARED SCANNERS**
Thermal verification testing of commercial printed-circuit boards for spaceflight p 216 A92-56217
Thermal verification testing of commercial printed-circuit boards for spaceflight
[NASA-TM-105261] p 141 N92-11221
- INFRARED SPECTRA**
Temperature-dependent reflectivity of silicon carbide
[NASA-TM-105287] p 201 N92-19263
- INGESTION (ENGINES)**
Calculations of hot gas ingestion for a STOVL aircraft model
[AIAA PAPER 92-0385] p 25 A92-28191
Hot gas ingestion characteristics and flow visualization of a vectored thrust STOVL concept p 26 A92-45316
- INJECTION**
Jet mixing into a heated cross flow in a cylindrical duct - Influence of geometry and flow variations
[AIAA PAPER 92-0773] p 168 A92-27110
Jet mixing into a heated cross flow in a cylindrical duct: Influence of geometry and flow variations
[NASA-TM-105390] p 30 N92-15994
- INJECTION LOCKING**
A theoretical and experimental study of the noise behavior of subharmonically injection locked local oscillators p 157 A92-46080
- INJECTORS**
Jet mixing into a heated cross flow in a cylindrical duct - Influence of geometry and flow variations
[AIAA PAPER 92-0773] p 168 A92-27110
Extended temperature range rocket injector
[NASA-CASE-LEW-14846-1] p 77 N92-10054
Coaxial injector spray characterization using water/air as simulants
[NASA-TM-105322] p 82 N92-14112
Jet mixing into a heated cross flow in a cylindrical duct: Influence of geometry and flow variations
[NASA-TM-105390] p 30 N92-15994
- INLET FLOW**
Transient behavior of supersonic flow through inlets p 7 A92-28043
Three-dimensional viscous analysis of a Mach 5 inlet and comparison with experimental data p 8 A92-28526
A study of three dimensional turbulent boundary layer separation and vortex flow control using the reduced Navier Stokes equations p 9 A92-40105
Comparative study of turbulence models in predicting hypersonic inlet flows
[AIAA PAPER 92-3098] p 11 A92-48740
Computational analysis of ramjet engine inlet interaction
[AIAA PAPER 92-3102] p 11 A92-48744
Full Navier-Stokes calculations on the installed F/A-18 inlet at a high angle of attack
[AIAA PAPER 92-3175] p 13 A92-54012
A comparison of predicted and measured inlet distortion flows in a subsonic axial inlet flow compressor rotor
[NASA-TM-105427] p 19 N92-26104
Comparative study of turbulence models in predicting hypersonic inlet flows
[NASA-TM-105720] p 19 N92-28102
Application of computational fluid dynamics to the study of vortex flow control for the management of inlet distortion
[NASA-TM-105672] p 230 N92-34112
- INLET NOZZLES**
Far-field noise and internal modes from a ducted propeller at simulated aircraft takeoff conditions
[AIAA PAPER 92-0371] p 252 A92-26230
Design and analysis of reengine Boeing 727-100 center inlet S duct by a reduced Navier-Stokes code
[AIAA PAPER 92-1221] p 8 A92-33320
Far-field noise and internal modes from a ducted propeller at simulated aircraft takeoff conditions
[NASA-TM-105369] p 254 N92-16702
- INLET TEMPERATURE**
Hydrogen no-vent fill testing in a 1.2 cubic foot (34 liter) tank
[NASA-TM-105273] p 185 N92-13401
- INSOLATION**
Solar radiation for Mars power systems p 81 N92-13259
- INSULATION**
Experimental breakdown of selected anodized aluminum samples in dilute plasmas p 259 N92-22369
High temperature dielectric properties of Apical, Kapton, Peek, Teflon AF, and Uplite polymers
[NASA-TM-105753] p 162 N92-28675
- INTAKE SYSTEMS**
A study on vortex flow control of inlet distortion in the re-engined 727-100 center inlet duct using computational fluid dynamics
[AIAA PAPER 92-0152] p 4 A92-23767
A study on vortex flow control on inlet distortion in the re-engined 727-100 center inlet duct using computational fluid dynamics
[NASA-TM-105321] p 14 N92-13998
High-speed inlet research program and supporting analysis p 188 N92-22542
- INTEGRAL EQUATIONS**
Analysis of shielded CPW discontinuities with air-bridges p 152 N92-32971
- INTEGRATED CIRCUITS**
Advanced large scale GaAs monolithic IF switch matrix subsystem
[AIAA PAPER 92-1861] p 155 A92-29801
Ka-band active MMIC subarray development
[AIAA PAPER 92-1863] p 155 A92-29803
Advances in MMIC technology for communications satellites
[AIAA PAPER 92-1899] p 155 A92-29830
High-performance packaging for monolithic microwave and millimeter-wave integrated circuits
[AIAA PAPER 92-1935] p 155 A92-31706
Length minimization design considerations in photonic integrated circuits incorporating directional couplers p 256 A92-46240
Ka-band MMIC arrays for ACTS Aero Terminal Experiment
[IAF PAPER 92-0398] p 159 A92-55785
A flexible CPW package for a 30 GHz MMIC amplifier --- coplanar waveguide
[NASA-TM-105630] p 161 N92-23193
Solid State Technology Branch of NASA Lewis Research Center
[NASA-TM-105159] p 151 N92-23412
A 1-W, 30-GHz, CPW amplifier for ACTS small terminal uplink
[NASA-TM-105671] p 161 N92-26096
High-performance packaging for monolithic microwave and millimeter-wave integrated circuits
[NASA-TM-105744] p 151 N92-31855
V-band pseudomorphic HEMT MMIC phased array components for space communications p 151 N92-32966
An optically controlled Ka-band phased array antenna p 152 N92-32968
A flexible CPW package for a 30 GHz MMIC amplifier p 152 N92-32972
A 1-W, 30-GHz, CPW amplifier for ACTS small terminal uplink p 152 N92-32973
- INTEGRATED OPTICS**
Potential for integrated optical circuits in advanced aircraft with fiber optic control and monitoring systems p 24 A92-46246
- INTEGRATORS**
Asymptotic integration algorithms for first-order ODEs with application to viscoplasticity
[NASA-TM-105587] p 250 N92-24974
- INTERACTIONAL AERODYNAMICS**
The Baldwin-Lomax model for separated and wake flows using the entropy envelope concept
[AIAA PAPER 92-0148] p 4 A92-23764
Crossing shock wave turbulent boundary layer interactions - Variable angle and shock generator length geometry effects at Mach 3
[AIAA PAPER 92-0636] p 6 A92-27014
Unsteady aerodynamic interaction effects on turbomachinery blade life and performance
[AIAA PAPER 92-0149] p 7 A92-28186
Computational analysis of ramjet engine inlet interaction
[AIAA PAPER 92-3102] p 11 A92-48744
Wind tunnel investigation of vortex flows on F/A-18 configuration at subsonic through transonic speed
[NASA-TP-3111] p 16 N92-14968
Inlets, ducts, and nozzles p 188 N92-22523
Advanced propeller research p 33 N92-22537
- INTERACTIONS**
Electrical and chemical interactions at Mars Workshop, part 1
[NASA-CP-10093] p 270 N92-30302
- INTERACTIVE CONTROL**
Interactive solution-adaptive grid generation p 243 N92-24420
- INTERMETALLICS**
INTERCALATION
Properties of novel CVD graphite fibers and their bromine intercalation compounds
[NASA-TM-105295] p 128 N92-14170
Method of intercalating large quantities of fibrous structures
[NASA-CASE-LEW-15077-1] p 107 N92-16025
Graphite intercalation compound with iodine as the major intercalant
[NASA-TM-105375] p 97 N92-25203
Heat transfer device
[NASA-CASE-LEW-14162-3] p 111 N92-34208
- INTERFACE STABILITY**
Interphase layer optimization for metal matrix composites with fabrication considerations p 98 A92-10262
Mechanical behaviors of ceramic matrix composites with matrix cracking and fiber debonding p 100 A92-23104
Stability analysis of surface tension effects on a double-diffusive layer --- in reduced gravity conditions
[AIAA PAPER 92-0605] p 137 A92-27002
Predictions of the critical strain for matrix cracking of ceramic matrix composites p 218 A92-33127
Stable localized patterns in thin liquid films p 173 A92-37489
Reduction of thermal stresses in continuous fiber reinforced metal matrix composites with interface layers p 105 A92-50347
Asymmetric tip morphology of creep microcracks growing along bimaterial interfaces p 127 A92-56585
- INTERFACES**
Interfacing laboratory instruments to multiuser, virtual memory computers p 245 A92-13595
Influence of engineered interfaces on residual stresses and mechanical response in metal matrix composites
[NASA-TM-105438] p 109 N92-23195
- INTERFACIAL ENERGY**
'Wrong' bond interactions at inversion domain boundaries in GaAs p 260 A92-27297
- INTERFACIAL TENSION**
Stability analysis of surface tension effects on a double-diffusive layer --- in reduced gravity conditions
[AIAA PAPER 92-0605] p 137 A92-27002
Unsteady thermocapillary migration of isolated drops in creeping flow p 169 A92-27774
A continuum method for modeling surface tension p 175 A92-45707
Flow induction by pressure forces
[AIAA PAPER 92-3571] p 28 A92-54060
- INTERLAMINAR STRESS**
Void effects on the interlaminar shear strength of unidirectional graphite-fiber-reinforced composites p 105 A92-50348
- INTERMETALLICS**
Intermetallic and ceramic matrix composites for 815 to 1370 C (1500 to 2500 F) gas turbine engine applications p 99 A92-15128
Fracture toughness and the effects of stress state on fracture of nickel aluminides p 117 A92-27422
The effect of strain rate and temperature on the tensile properties of NiAl p 117 A92-28113
Compressive strength of directionally solidified NiAl-NiAlNb intermetallics at 1200 and 1300 K p 117 A92-28248
Compression, bend, and tension studies on forged Al67Ti25Cr8 and Al66Ti25Mn(g) L1(2) compounds p 118 A92-30766
Does a threshold stress for creep exist in HfC-dispersed NiAl? p 118 A92-30780
The mechanical properties of a Ni-30Al-20Fe-0.05Zr intermetallic alloy in the temperature range 300-1200 K p 118 A92-30793
On improving the fracture toughness of a NiAl-based alloy by mechanical alloying p 118 A92-30794
Protective Al2O3 scale formation on NbAl3-base alloys p 119 A92-31850
Solidification processing of intermetallic Nb-Al alloys p 120 A92-33866
Mechanical properties of monolithic and particulate composites of L12 forms of Al3Ti: p 101 A92-36273
Interdiffusion between the L1(2) trialuminides Al66Ti25Mn9 and Al67Ti25Cr8 p 120 A92-37088
Correlation of deformation mechanisms with the tensile and compressive behavior of NiAl and NiAl(Zr) intermetallic alloys p 120 A92-38019
Oxidation kinetics of cast TiAl3 p 121 A92-38993
Fracture behavior of a B2 Ni-30Al-20Fe-0.05Zr intermetallic alloy in the temperature range 300 to 1300 K p 121 A92-41667
Deformation behavior of a Ni-30Al-20Fe-0.05Zr intermetallic alloy in the temperature range 300 to 1300 K p 121 A92-41668
Discontinuously reinforced intermetallic matrix composites via XD synthesis --- exothermal dispersion p 103 A92-41867

INTERMODULATION

- Metal- and intermetallic-matrix composites for aerospace propulsion and power systems p 104 A92-43682
- High-temperature fatigue behavior of a SiC/Ti-24Al-11Nb composite p 104 A92-44613
- Intermetallic matrix composites; Proceedings of the MRS Symposium, San Francisco, CA, Apr. 18-20, 1990 [ISBN 1-55899-083-6] p 104 A92-46826
- Ductility enhancement from interface dislocation sources in a directionally solidified beta + gamma + gamma-prime Ni-Fe-Al composite alloy p 122 A92-46850
- Initial evaluation of continuous fiber reinforced NiAl composites p 104 A92-46867
- Compatibility of potential reinforcing ceramics with Ni and Fe aluminides p 105 A92-46874
- Reduction of thermal residual stresses in advanced metallic composites based upon a compensating/compliant layer concept p 105 A92-47106
- Influence of processing on the microstructure and mechanical properties of a NbAl₃-base alloy p 122 A92-48152
- Oxidation of Al₂O₃ continuous fiber-reinforced/NiAl composites p 106 A92-57029
- Development of a new generation of high-temperature composite materials p 109 N92-22515
- The cyclic oxidation resistance at 1200 C of beta-NiAl, FeAl, and CoAl alloys with selected third element additions p 123 N92-24554 [NASA-TM-105620]
- INTERMODULATION**
Intermodulation in the oscillatory magnetoresistance of a two-dimensional electron gas p 163 N92-32975
- INTERPLANETARY FLIGHT**
An overview of the NASA Advanced Propulsion Concepts program [AIAA PAPER 92-3216] p 73 A92-54018
- INTERPLANETARY SPACECRAFT**
An accelerated development, reduced cost approach to lunar/Mars exploration using a modular NTR-based space transportation system [IAF PAPER 92-0574] p 43 A92-57053
- INTERPROCESSOR COMMUNICATION**
A software control system for the ACTS high-burst-rate link evaluation terminal [NASA-TM-105207] p 243 N92-16628
- INVERTERS**
Development of a computer algorithm for the analysis of variable-frequency AC drives: Case studies included [NASA-TM-105327] p 29 N92-13070
- INVISCID FLOW**
Prediction of unsteady rotor-surface pressure and heat transfer from wake passings [ASME PAPER 91-GT-267] p 165 A92-15665
- A turbulence model for iced airfoils and its validation [AIAA PAPER 92-0417] p 6 A92-26267
- Vorticity dynamics of inviscid shear layers [AIAA PAPER 92-0420] p 168 A92-26270
- An unsteady Euler scheme for the analysis of ducted propellers [AIAA PAPER 92-0522] p 6 A92-26947
- Numerical experiments on a new class of nonoscillatory schemes [AIAA PAPER 92-0421] p 7 A92-28193
- Development of an efficient analysis for high Reynolds number inviscid/viscid interactions in cascades [AIAA PAPER 92-3073] p 10 A92-48723
- A fast, uncoupled, compressible, two-dimensional, unsteady boundary layer algorithm with separation for engine inlets [AIAA PAPER 92-3082] p 11 A92-48729
- Interface of an uncoupled boundary layer algorithm with an inviscid core flow algorithm for unsteady supersonic engine inlets [AIAA PAPER 92-3083] p 11 A92-48730
- A comparison of the calculated and experimental off-design performance of a radial flow turbine [AIAA PAPER 92-3069] p 13 A92-54004
- A turbulence model for iced airfoils and its validation [NASA-TM-105373] p 16 N92-15052
- Supersonic propulsion simulation by incorporating component models in the large perturbation inlet (LAPIN) computer code [NASA-TM-105193] p 30 N92-15993
- An iterative implicit diagonally-dominant factorization algorithm for solving the Navier-Stokes equations [NASA-TM-105259] p 249 N92-16663
- Development of a steady potential solver for use with linearized, unsteady aerodynamic analyses [NASA-TM-105288] p 31 N92-20525
- Long time behavior of unsteady flow computations [NASA-TM-105584] p 190 N92-23565

- Interface of an uncoupled boundary layer algorithm with an inviscid core flow algorithm for unsteady supersonic engine inlets [NASA-TM-105684] p 36 N92-27037
- A fast, uncoupled, compressible, two-dimensional, unsteady boundary layer algorithm with separation for engine inlets [NASA-TM-105686] p 195 N92-27653
- Analysis of iced wings [NASA-TM-105773] p 20 N92-34144
- IODINE**
Graphite intercalation compound with iodine as the major intercalant [NASA-TM-105375] p 97 N92-25203
- Graphite fluoride from iodine intercalated graphitized carbon [NASA-CASE-LEW-15360-1] p 116 N92-34206
- ION ACCELERATORS**
An experimental study of impingement-ion-production mechanisms [AIAA PAPER 92-3826] p 76 A92-54190
- Characterization of ion accelerating systems on NASA LeRC's ion thrusters [AIAA PAPER 92-3827] p 76 A92-54191
- ION BEAMS**
Preliminary tests of annular ion optics [AIAA PAPER 92-3148] p 64 A92-48776
- Ion beam treatment of potential space materials at the NASA Lewis Research Center [NASA-TM-105398] p 97 N92-21548
- Ion Beam Textured and Coated Surfaces Experiment (IBEX) p 132 N92-24832
- Characteristics of hypervelocity impact craters on LDEF experiment S1003 and implications of small particle impacts on reflective surfaces p 269 N92-27252
- ION CURRENTS**
Ionospheric plasma flow over large high-voltage space platforms. I - Ion-plasma-time scale interactions of a plate at zero angle of attack. II - The formation and structure of plasma wake [AIAA PAPER 92-41359] p 259 N92-22368
- Ion collection from a plasma by a pinhole p 259 N92-22368
- ION DENSITY (CONCENTRATION)**
High voltage spheres in an unmagnetized plasma - Fluid and PIC simulations p 258 A92-47936
- ION ENGINES**
The evolutionary development of high specific impulse electric thruster technology [AIAA PAPER 92-1556] p 61 A92-38650
- Krypton ion thruster performance [AIAA PAPER 92-3144] p 64 A92-48772
- Preliminary tests of annular ion optics [AIAA PAPER 92-3148] p 64 A92-48776
- Extended testing of xenon ion thruster hollow cathodes [AIAA PAPER 92-3204] p 65 A92-48811
- Further study of the effect of the downstream plasma condition on accelerator grid erosion in an ion thruster [AIAA PAPER 92-3829] p 76 A92-54192
- Neutralizer optimization [NASA-TM-105578] p 86 N92-21976
- Derated ion thruster design issues [NASA-TM-105576] p 87 N92-23534
- The evolutionary development of high specific impulse electric thruster technology [NASA-TM-105712] p 92 N92-31342
- Krypton ion thruster performance [NASA-TM-105818] p 92 N92-31901
- ION EXTRACTION**
Characterization of ion accelerating systems on NASA LeRC's ion thrusters [AIAA PAPER 92-3827] p 76 A92-54191
- ION IMPACT**
The formation and structure of plasma wakes behind large high-voltage space platforms in ionosphere [AIAA PAPER 92-0577] p 239 A92-26984
- ION PLATING**
Screen Cage Ion Plating (SCIP) and scratch testing of polycrystalline aluminum oxide [NASA-TM-105404] p 130 N92-22278
- ION PRODUCTION RATES**
An experimental study of impingement-ion-production mechanisms [AIAA PAPER 92-3826] p 76 A92-54190
- ION PROPULSION**
Early Track NEP system options for SEI missions [AIAA PAPER 92-3200] p 65 A92-48808
- Development and flight history of SERT 2 spacecraft [AIAA PAPER 92-3516] p 74 A92-54038
- Characterization of ion accelerating systems on NASA LeRC's ion thrusters [AIAA PAPER 92-3827] p 76 A92-54191
- Development of arcjet and ion propulsion for spacecraft stationkeeping [IAF PAPER 92-0607] p 77 A92-57058

- Nuclear Electric Propulsion Technology Panel findings and recommendations [NASA-TM-105547] p 85 N92-20355
- Neutralizer optimization [NASA-TM-105578] p 86 N92-21976
- Derated ion thruster design issues [NASA-TM-105576] p 87 N92-23534
- Development and flight history of SERT 2 spacecraft [NASA-TM-105636] p 90 N92-28983
- Krypton ion thruster performance [NASA-TM-105818] p 92 N92-31901
- Low-Isp derated ion thruster operation [NASA-TM-105787] p 92 N92-32237
- The evolutionary development of high specific impulse electric thruster technology [NASA-TM-105758] p 93 N92-33064
- ION SOURCES**
Ion beam treatment of potential space materials at the NASA Lewis Research Center [NASA-TM-105398] p 97 N92-21548
- IRIDIUM**
Diffusion mechanisms in chemical vapor-deposited iridium coated on chemical vapor-deposited rhenium p 117 A92-28017
- Advanced liquid rockets [NASA-TM-105633] p 87 N92-24560
- IRON**
Studies of mechanochemical interactions in the tribological behavior of materials p 124 A92-32410
- IRON ALLOYS**
Compression studies on particulate composites of ternary Al-Ti-Fe, and quaternary Al-Ti-Fe-Nb and Al-Ti-Fe-Mn L1(2) compounds p 119 A92-30845
- Comparison of high temperature, high frequency core loss and dynamic B-H loops of two 50 Ni-Fe crystalline alloys and an iron-based amorphous alloy p 157 A92-50551
- ISOTHERMAL PROCESSES**
Hardening mechanisms in a dynamic strain aging alloy, Hastelloy X, during isothermal and thermomechanical cyclic deformation p 116 A92-24832
- The isothermal dendritic growth experiment - A USMP-2 space flight experiment [AIAA PAPER 92-0350] p 137 A92-28188
- Thermal barrier coating life and isothermal oxidation of low-pressure plasma-sprayed bond coat alloys p 119 A92-32398
- Thermomechanical deformation behavior of a dynamic strain aging alloy, Hastelloy X [NASA-TM-105316] p 228 N92-25179
- Isothermal aging effects on PMR-15 resin [NASA-TM-105648] p 110 N92-30986
- ISOTOPIES**
Preliminary design of a mobile lunar power supply p 233 A92-50635
- ISOTROPIC MEDIA**
A viscoplastic theory with thermodynamic considerations [ONERA, TP NO. 1991-220] p 217 A92-26372
- ITERATION**
An iterative implicit diagonally-dominant factorization algorithm for solving the Navier-Stokes equations [NASA-TM-105259] p 249 N92-16663
- Upper bounds for convergence rates of vector extrapolation methods on linear systems with initial iterations [NASA-TM-105608] p 250 N92-33742
- ITERATIVE SOLUTION**
Material nonlinear analysis via mixed-iterative finite element method [AIAA PAPER 92-2479] p 220 A92-34368
- Upper bounds for convergence rates of vector extrapolation methods on linear systems with initial iterations [NASA-TM-105608] p 250 N92-33742
- ITO (SEMICONDUCTORS)**
Increased efficiency with surface texturing in ITO/InP solar cells p 232 A92-44548
- Recent progress in InP solar cell research p 158 A92-50653
- Pilot production of 4 sq cm ITO/InP photovoltaic solar cells p 71 A92-53197

J

- JACOBI MATRIX METHOD**
Conservative-variable average states for equilibrium gas multi-dimensional fluxes [NASA-TM-105585] p 191 N92-25196
- JET AIRCRAFT NOISE**
Full Navier-Stokes analysis of a two-dimensional mixer/ejector nozzle for noise suppression [AIAA PAPER 92-3570] p 27 A92-54059
- Noise from turbulent shear flows p 254 N92-10603

- Full Navier-Stokes analysis of a two-dimensional mixer/ejector nozzle for noise suppression
[NASA-TM-105715] p 37 N92-28419
- JET ENGINE FUELS**
Safety considerations in testing a fuel-rich aeropropulsion gas generator
[NASA-TM-105258] p 30 N92-17061
- JET ENGINES**
A study on vortex flow control of inlet distortion in the re-engine 727-100 center inlet duct using computational fluid dynamics
[AIAA PAPER 92-0152] p 4 A92-23767
Euler solutions for an unbladed jet engine configuration
[AIAA PAPER 92-0544] p 169 A92-28201
Euler solutions for an unbladed jet engine configuration
[NASA-TM-105332] p 184 N92-11328
A study on vortex flow control of inlet distortion in the re-engine 727-100 center inlet duct using computational fluid dynamics
[NASA-TM-105321] p 14 N92-13998
Directions in propulsion control p 32 N92-22530
A two-dimensional Euler solution for an unbladed jet engine configuration
[NASA-TM-105329] p 190 N92-23560
A multiblock grid generation technique applied to a jet engine configuration p 244 N92-24428
A two-dimensional Euler solution for an unbladed jet engine configuration p 18 N92-24861
Multiblock grid generation for jet engine configurations p 35 N92-25720
- JET FLOW**
Acoustic analysis using numerical solutions of the Navier-Stokes equations
[AIAA PAPER 92-0506] p 253 A92-26934
Fluid-flow of a row of jets in crossflow - A numerical study
[AIAA PAPER 92-0534] p 169 A92-28198
Flow visualization and motion analysis for a series of four sequential brush seals p 204 A92-36976
Effect of tabs on the evolution of an axisymmetric jet p 26 A92-40151
Spatial instability of a swirling jet - Theory and experiment p 174 A92-41274
Second order modeling of boundary-free turbulent shear flows p 174 A92-41275
The influence of higher harmonics on vortex pairing in an axisymmetric mixing layer p 175 A92-46251
Direct evaluation of aeroacoustic theory in a jet p 253 A92-50296
Particle-laden weakly swirling free jets: Measurements and predictions
[NASA-TM-100881] p 29 N92-14061
Effect of lubricant jet location on spiral bevel gear operating temperatures
[NASA-TM-105656] p 211 N92-26106
- JET MIXING FLOW**
Vapor condensation on liquid surface due to laminar jet-induced mixing p 164 A92-10446
CFD analysis of jet mixing in low NO(x) flametube combustors
[ASME PAPER 91-GT-217] p 24 A92-15634
Studies of the effects of curvature on dilution jet mixing p 166 A92-21079
Computation of supersonic jet mixing noise for an axisymmetric CD nozzle using k-epsilon turbulence model
[AIAA PAPER 92-0500] p 252 A92-26328
Jet mixing into a heated cross flow in a cylindrical duct - Influence of geometry and flow variations
[AIAA PAPER 92-0773] p 168 A92-27110
Effect of tabs on the evolution of an axisymmetric jet p 26 A92-40151
CFD mixing analysis of jets injected from straight and slanted slots into confined crossflow in rectangular ducts
[AIAA PAPER 92-3087] p 177 A92-48732
A parametric numerical study of mixing in a cylindrical duct
[AIAA PAPER 92-3088] p 177 A92-48733
Experimental study of cross-stream mixing in a rectangular duct
[AIAA PAPER 92-3090] p 178 A92-48735
Supersonic jet mixing enhancement by 'delta-tabs'
[AIAA PAPER 92-3548] p 12 A92-49063
Jet mixing in low gravity - Results of the Tank Pressure Control Experiment
[AIAA PAPER 92-3060] p 182 A92-54001
Computation of supersonic jet mixing noise for an axisymmetric CD nozzle using k-epsilon turbulence model
[NASA-TM-105338] p 254 N92-14795
Jet mixing into a heated cross flow in a cylindrical duct: Influence of geometry and flow variations
[NASA-TM-105390] p 30 N92-15994
- Supersonic jet mixing enhancement by delta-tabs
[NASA-TM-105664] p 18 N92-24958
A parametric numerical study of mixing in a cylindrical duct
[NASA-TM-105695] p 35 N92-26553
CFD mixing analysis of jets injected from straight and slanted slots into confined crossflow in rectangular ducts
[NASA-TM-105699] p 36 N92-26561
Experimental study of cross-stream mixing in a rectangular duct
[NASA-TM-105694] p 36 N92-27652
- JET NOZZLES**
Full Navier-Stokes analysis of a two-dimensional mixer/ejector nozzle for noise suppression
[AIAA PAPER 92-3570] p 27 A92-54059
Full Navier-Stokes analysis of a two-dimensional mixer/ejector nozzle for noise suppression
[NASA-TM-105715] p 37 N92-28419
- JET PROPELLSION**
Flow induction by pressure forces
[AIAA PAPER 92-3571] p 28 A92-54060
- JETS**
Liquid hydrogen mass flow through a multiple orifice Joule-Thomson device
[AIAA PAPER 92-2881] p 176 A92-47862
Liquid hydrogen mass flow through a multiple orifice Joule-Thomson device
[NASA-TM-105583] p 189 N92-23268
- JOINTS (JUNCTIONS)**
Differential continuum damage mechanics models for creep and fatigue of unidirectional metal matrix composites
[NASA-TM-105213] p 226 N92-16371
Preliminary evaluation of adhesion strength measurement devices for ceramic/titanium matrix composite bonds
[NASA-TM-105803] p 1 N92-31267
- JOULE-THOMSON EFFECT**
Liquid hydrogen mass flow through a multiple orifice Joule-Thomson device
[AIAA PAPER 92-2881] p 176 A92-47862
Liquid hydrogen mass flow through a multiple orifice Joule-Thomson device
[NASA-TM-105583] p 189 N92-23268
- JOURNAL BEARINGS**
Effect of type and location of oil groove on the performance of journal bearings p 203 A92-21333
Frequency effects on the stability of a journal bearing for periodic loading p 203 A92-22665
Frequency effects on the stability of a journal bearing for periodic loading
[NASA-TM-105226] p 186 N92-18809
Fast methods to numerically integrate the Reynolds equation for gas fluid films
[NASA-TM-105415] p 214 N92-30722
- JP-5 JET FUEL**
The VRT gas turbine combustor - Phase II
[AIAA PAPER 92-3471] p 27 A92-54035
- K**
- K-EPSILON TURBULENCE MODEL**
Computation of supersonic jet mixing noise for an axisymmetric CD nozzle using k-epsilon turbulence model
[AIAA PAPER 92-0500] p 252 A92-26328
On turbulent flows dominated by curvature effects p 171 A92-32940
A 2-D oscillating flow analysis in Stirling engine heat exchangers p 172 A92-36001
Navier-Stokes analysis and experimental data comparison of compressible flow in a diffusing S-duct
[AIAA PAPER 92-2699] p 10 A92-45541
Quasi-steady turbulence modeling of unsteady flows p 177 A92-48204
Navier-Stokes turbine heat transfer predictions using two-equation turbulence closures
[AIAA PAPER 92-3067] p 177 A92-48721
Renormalization group analysis of the Reynolds stress transport equation p 179 A92-49493
Modeling of the heat transfer in bypass transitional boundary-layer flows
[NASA-TP-3170] p 184 N92-11299
Particle-laden weakly swirling free jets: Measurements and predictions
[NASA-TM-100881] p 29 N92-14061
Computation of supersonic jet mixing noise for an axisymmetric CD nozzle using k-epsilon turbulence model
[NASA-TM-105338] p 254 N92-14795
Multigrad acceleration and turbulence models for computations of 3D turbulent jets in crossflow
[NASA-TM-105306] p 186 N92-18775
- Implementation/validation of a low Reynolds number two-equation turbulence model in the Proteus Navier-Stokes code: Two-dimensional/axisymmetric
[NASA-TM-105619] p 187 N92-20520
A kappa-epsilon calculation of transitional boundary layers
[NASA-TM-105604] p 187 N92-22398
Advancements in engineering turbulence modeling
[PAPER-105] p 189 N92-23350
Simulations of free shear layers using a compressible kappa-epsilon model p 190 N92-23355
Renormalization group analysis of the Reynolds stress transport equation
[NASA-TM-105588] p 190 N92-23542
Kolmogorov behavior of near-wall turbulence and its application in turbulence modeling
[NASA-TM-105663] p 191 N92-24050
Advances in engineering turbulence modeling --- computational fluid dynamics p 193 N92-25820
Implementation of a kappa-epsilon turbulence model to RPLUS3D code p 194 N92-25822
A new time scale based k-epsilon model for near wall turbulence
[NASA-TM-105768] p 196 N92-32868
Navier-Stokes analysis and experimental data comparison of compressible flow in a diffusing S-duct
[NASA-TM-105683] p 38 N92-33746
- KAPTON (TRADEMARK)**
Synergistic effects of ultraviolet radiation, thermal cycling and atomic oxygen on altered and coated Kapton surfaces
[AIAA PAPER 92-0794] p 93 A92-27125
Evaluation of Kapton pyrolysis, arc tracking, and arc propagation on the Space Station Freedom (SSF) solar array flexible current carrier (FCC) p 72 A92-53209
Atomic oxygen effects on SiO(x) coated Kapton for photovoltaic arrays in low earth orbit p 72 A92-53211
Synergistic effects of ultraviolet radiation, thermal cycling, and atomic oxygen on altered and coated Kapton surfaces
[NASA-TM-105363] p 96 N92-14114
Atomic oxygen undercutting of LDEF aluminized-Kapton multilayer insulation p 255 N92-24818
Atomic oxygen interactions with FEP Teflon and silicones on LDEF p 132 N92-24820
Durability evaluation of photovoltaic blanket materials exposed on LDEF tray S1003 p 132 N92-27100
High temperature dielectric properties of Apical, Kapton, Peek, Teflon AF, and Uplix polymers
[NASA-TM-105753] p 162 N92-28675
- KARMAN VORTEX STREET**
Breakdown of the Karman vortex street due to forced convection and flow compressibility
[NASA-TM-105853] p 196 N92-32472
- KINEMATICS**
Vorticity dynamics of inviscid shear layers
[AIAA PAPER 92-0420] p 168 A92-26270
Viscoplastic analysis of an experimental cylindrical thrust chamber liner p 218 A92-28052
- KINETIC EQUATIONS**
Numerical experiments with flows of elongated granules
[NASA-TM-105567] p 209 N92-23226
- KINETIC THEORY**
Kinetic theory model for the flow of a simple gas from a three-dimensional axisymmetric nozzle p 12 A92-52730
- KNOWLEDGE BASES (ARTIFICIAL INTELLIGENCE)**
GTEX: An expert system for diagnosing faults in satellite ground stations p 148 N92-14215
- KNUDSEN GAGES**
Reactions of silicon carbide and silicon(IV) oxide at elevated temperatures p 126 A92-43483
- KOLMOGOROFF THEORY**
Kolmogorov behavior of near-wall turbulence and its application in turbulence modeling
[NASA-TM-105663] p 191 N92-24050
- KRYPTON**
Krypton ion thruster performance
[AIAA PAPER 92-3144] p 64 A92-48772
Krypton ion thruster performance
[NASA-TM-105818] p 92 N92-31901
- L**
- LABORATORIES**
Nuclear electric propulsion development and qualification facilities
[NASA-TM-105521] p 91 N92-30818
- LABYRINTH SEALS**
Experimental verification of a secondary recirculation zone in a labyrinth seal p 205 A92-50271
Seals related research at NASA, Lewis Research Center p 207 N92-15087

LAGRANGE MULTIPLIERS

LAGRANGE MULTIPLIERS

- Application of Newton modified barrier method (NMBM) to structural optimization p 220 A92-34555
[AIAA PAPER 92-2498]
Structural optimization of large structural systems by optimality criteria methods p 229 N92-25446
[NASA-TM-105423]

LAMB WAVES

- Detecting Lamb waves with broad-band acousto-ultrasonic signals in composite structures p 216 N92-23189
[NASA-TM-105557]

LAMINAR BOUNDARY LAYER

- Method of reducing drag in aerodynamic systems p 21 N92-34243
[NASA-CASE-LEW-14791-1]

LAMINAR FLOW

- Gravitational influences on the behavior of confined diffusion flames p 113 A92-25781
[AIAA PAPER 92-0334]
Saturated fluorescence measurements of the hydroxyl radical in laminar high-pressure C₂H₆/O₂/N₂ flames p 198 A92-33987
Instantaneous heat transfer coefficient based upon two-dimensional analyses of Stirling space engine components p 181 A92-50827
Multigrad acceleration and turbulence models for computations of 3D turbulent jets in crossflow p 186 N92-18775
[NASA-TM-105306]
Heat transfer in oscillating flows with sudden change in cross section p 88 N92-26654
[NASA-TM-105692]
Overview of NASA supported Stirling thermodynamic loss research p 88 N92-27034
[NASA-TM-105690]

LAMINAR HEAT TRANSFER

- Heat transfer in oscillating flows with sudden change in cross section p 88 N92-26654
[NASA-TM-105692]

LAMINAR MIXING

- Vapor condensation on liquid surface due to laminar jet-induced mixing p 164 A92-10446

LAMINATES

- METCAN updates for high temperature composite behavior - Simulation/verification p 98 A92-10264
Structural reliability analysis of laminated CMC components p 99 A92-15630
[ASME PAPER 91-GT-210]
Mixed-mode fracture in unidirectional graphite epoxy composite laminates with central notch p 218 A92-29464
Reliability analysis of laminated CMC components through shell subelement techniques p 219 A92-34322
[AIAA PAPER 92-2348]
Multidisciplinary tailoring of hot composite structures for 343 C applications p 220 A92-34564
[AIAA PAPER 92-2563]
Near-tip dual-length scale mechanics of mode-I cracking in laminate brittle matrix composites p 221 A92-34583
[AIAA PAPER 92-2491]
Load redistribution considerations in the fracture of ceramic matrix composites p 221 A92-34586
[AIAA PAPER 92-2494]
Free vibrations of delaminated beams p 222 A92-36853
Structural design methodologies for ceramic-based material systems p 103 A92-39866
High molecular weight first generation PMR polyimides for 343 C applications p 105 A92-49819
Void effects on the interlaminar shear strength of unidirectional graphite-fiber-reinforced composites p 105 A92-50348
Microfracture in high temperature metal matrix laminates p 106 N92-14122
[NASA-TM-105189]
Analysis of aircraft engine blade subject to ice impact p 226 N92-15402
[NASA-TM-105336]
Intercalated hybrid graphite fiber composite p 107 N92-17861
[NASA-CASE-LEW-15241-1]
High molecular weight first generation PMR polyimides for 343 C applications p 129 N92-19498
[NASA-TM-105364]
Reliability analysis of laminated CMC components through shell subelement techniques p 129 N92-20380
[NASA-TM-105413]
Free vibrations of delaminated beams p 109 N92-25754
[NASA-TM-105582]
Computational simulation of structural fracture in fiber composites p 111 N92-32531

LAND MOBILE SATELLITE SERVICE

- Comparative study on the performance of power and bandwidth efficient modulations in LMSS under fading and interference p 147 A92-54763

LANDAU-GINZBURG EQUATIONS

- Propagating confined states in phase dynamics p 181 A92-50968

LANTHANUM OXIDES

- Conductor-backed coplanar waveguide resonators of YBa₂Cu₃O₇(δ) on LaAlO₃ p 158 A92-51042

LARGE SPACE STRUCTURES

- Nonuniform thermal environmental effects on space truss structural reliability p 54 A92-34325
[AIAA PAPER 92-2352]
Beam power options for the moon p 61 A92-40429
Neural network based decomposition in optimal structural synthesis p 247 A92-41895
Advanced power systems for EOS p 70 A92-50640
Probabilistic structural analysis of adaptive/smart/intelligent space structures p 227 N92-22267
[NASA-TM-105408]

LASER ABLATION

- Laser ablated YBa₂Cu₃O₇(δ) high temperature superconductor coplanar waveguide resonator p 155 A92-31631

LASER ANEMOMETERS

- Laser anemometer measurements and computations in an annular cascade of high turning core turbine vanes p 20 N92-28980
[NASA-TP-3252]
A 4-spot time-of-flight anemometer for small centrifugal compressor velocity measurements p 202 N92-29105
[NASA-TM-105717]

LASER APPLICATIONS

- Species and temperature measurement in H₂/O₂ rocket flow fields by means of Raman scattering diagnostics p 178 A92-48930
[AIAA PAPER 92-3353]
Space transfer with ground-based laser/electric propulsion p 73 A92-54017
[AIAA PAPER 92-3213]
Optical measurement systems p 202 N92-22527
Three-dimensional laser window formation p 47 N92-30307
[NASA-RP-1280]

LASER ARRAYS

- Moonbase night power by laser illumination p 44 A92-21086

LASER BEAMS

- A fiber-optic probe for particle sizing in concentrated suspensions p 197 A92-21371
Space power by ground-based laser transmission p 5 A92-47027
[AIAA PAPER 92-3024]
Solutions of the heat conduction equation in multilayers for photothermal deflection experiments p 141 A92-52205
Photovoltaic receivers for laser beamed power in space p 72 A92-53201

LASER DOPPLER VELOCIMETERS

- Finite wing aerodynamics with simulated glaze ice p 5 A92-26265
[AIAA PAPER 92-0414]
LDV measurements on a rectangular wing with a simulated glaze ice accretion p 10 A92-45537
[AIAA PAPER 92-2690]
Experimental verification of a secondary recirculation zone in a labyrinth seal p 205 A92-50271

LASER HEATING

- Solutions of the heat conduction equation in multilayers for photothermal deflection experiments p 141 A92-52205
A laser-induced heat flux technique for convective heat transfer measurements in high speed flows p 200 A92-54318
Laser-driven hypersonic air-breathing propulsion simulator p 41 A92-56753
[AIAA PAPER 92-3922]

LASER INDUCED FLUORESCENCE

- Laser-induced fluorescence of atomic hydrogen in an arcjet thruster p 60 A92-27045
[AIAA PAPER 92-0678]
Saturated fluorescence measurements of the hydroxyl radical in laminar high-pressure C₂H₆/O₂/N₂ flames p 198 A92-33987
Plasma erosion rate diagnostics using laser-induced fluorescence p 198 A92-36738
Quantitative fluorescence measurements of the OH radical in high pressure methane flames p 114 A92-46976
[AIAA PAPER 92-2960]
Flow diagnostics of an arcjet using laser-induced fluorescence p 199 A92-48843
[AIAA PAPER 92-3243]
Measurement of trace stratospheric constituents with a balloon borne laser radar p 239 N92-14500

LASER INTERFEROMETRY

- Performance of the Phase Doppler Particle Analyzer icing cloud droplet sizing probe in the NASA Lewis Icing Research Tunnel p 198 A92-26926
[AIAA PAPER 92-0162]

LASER MICROSCOPY

- Tensile strain measurements of ceramic fibers using scanning laser acoustic microscopy p 198 A92-39629
Tensile strain measurements of ceramic fibers using scanning laser acoustic microscopy p 216 N92-24986
[NASA-TM-105589]

LASER POWER BEAMING

- Space power by ground-based laser illumination p 59 A92-18401
Moonbase night power by laser illumination p 44 A92-21086

- Space power by ground-based laser transmission p 63 A92-47027
[AIAA PAPER 92-3024]
A mass sensitivity analysis of lunar orbiting beam power systems p 232 A92-50619
Photovoltaic receivers for laser beamed power in space p 72 A92-53201
Space transfer with ground-based laser/electric propulsion p 73 A92-54017
[AIAA PAPER 92-3213]
Laser beamed power - Satellite demonstration applications p 76 A92-57056
[IAF PAPER 92-0600]

LASER WINDOWS

- Three-dimensional laser window formation p 47 N92-30307
[NASA-RP-1280]

LATENT HEAT

- Thermal modeling with solid/liquid phase change of the thermal energy storage experiment p 185 N92-13402
[NASA-TM-103770]

LATTICE PARAMETERS

- A new approximate sum rule for bulk alloy properties p 117 A92-28240
Lattice parameters of fcc binary alloys using a new semiempirical method p 120 A92-32898
Lattice parameters of fcc binary alloys using a new semiempirical method p 123 N92-16111
[NASA-TM-105304]

LAUNCH VEHICLE CONFIGURATIONS

- Mission and sizing analysis for the Beta II two-stage-to-orbit vehicle p 47 A92-35868
[AIAA PAPER 92-1264]
Overview of the Beta II Two-Stage-To-Orbit vehicle design p 48 N92-11034
[NASA-TM-105298]
Mission and sizing analysis for the Beta 2 two-stage-to-orbit vehicle p 48 N92-21547
[NASA-TM-105559]
Graphite/epoxy composite adapters for the Space Shuttle/Centaur vehicle p 49 N92-31251
[NASA-TP-3014]

LAUNCH VEHICLES

- The design and performance estimates for the propulsion module for the booster of a TSTO vehicle p 29 N92-11995
[NASA-TM-105299]
Upper stages using liquid propulsion and metallized propellants p 83 N92-17151
[NASA-TP-3191]
Beta 2: A near term, fully reusable, horizontal takeoff and landing two-stage-to-orbit launch vehicle concept p 86 N92-21536
Resonant mode controllers for launch vehicle applications p 48 N92-25092
[NASA-TM-105563]
Integrated health monitoring and controls for rocket engines p 90 N92-28693
[NASA-TM-105763]
An electromechanical actuation system for an expendable launch vehicle p 48 N92-30310
[NASA-TM-105774]

LAUNCHING

- Resonant mode controllers for launch vehicle applications p 48 N92-25092
[NASA-TM-105563]
LEAD ALLOYS
Growth-speed dependence of primary arm spacings in directionally solidified Pb-10 wt pct Sn p 117 A92-26526

LEAD COMPOUNDS

- Growth and characterization of lead bromide crystals p 138 A92-56956
Effect of growth conditions on the quality of lead bromide crystals p 138 A92-56957

LEADING EDGES

- Unsteady wing surface pressures in the wake of a propeller p 5 A92-25731
[AIAA PAPER 92-0277]
Analysis of iced wings p 8 A92-29972
[AIAA PAPER 92-0416]
Distortion of a flat-plate boundary layer by free-stream vorticity normal to the plate p 173 A92-36343
Measurements in a leading-edge separation bubble due to a simulated airfoil ice accretion p 21 A92-41262
Increased heat transfer to elliptical leading edges due to spanwise variations in the freestream momentum - Numerical and experimental results p 13 A92-54005
[AIAA PAPER 92-3070]
Experimental unsteady pressures on an oscillating cascade with supersonic leading edge locus p 14 A92-56857
[AIAA PAPER 92-4035]
Modeling of the heat transfer in bypass transitional boundary-layer flows p 184 N92-11299
[NASA-TP-3170]
Wind tunnel investigation of vortex flows on F/A-18 configuration at subsonic through transonic speed p 16 N92-14968
[NASA-TP-3111]

Atomic oxygen undercutting of LDEF aluminized-Kapton multilayer insulation p 255 N92-24818

LEAKAGE

National Aerospace Plane engine seals: High temperature seal performance evaluation p 207 N92-15103

Brush seal leakage performance with gaseous working fluids at static and low rotor speed conditions [NASA-TM-105400] p 186 N92-16265

Engine panel seals for hypersonic engine applications: High temperature leakage assessments and flow modelling [NASA-TM-105260] p 208 N92-16336

Evaluation of an innovative high temperature ceramic wafer seal for hypersonic engine applications [NASA-TM-105556] p 208 N92-20815

Inflatable traversing probe seal p 209 N92-22692

Development of advanced seals for space propulsion turbomachinery [NASA-TM-105659] p 87 N92-24957

Post-test examination of a pool boiler receiver [NASA-TM-105635] p 123 N92-27192

LEAST SQUARES METHOD

A least-squares finite element method for incompressible Navier-Stokes problems p 173 A92-37387

An error analysis of least-squares finite element method of velocity-pressure-vorticity formulation for Stokes problem p 173 A92-37506

Optimal least-squares finite element method for elliptic problems [NASA-TM-105382] p 249 N92-15662

LIAPUNOV FUNCTIONS

A Lyapunov based nonlinear control scheme for stabilizing a basic compression system using a close-coupled control valve p 246 A92-29316

LIFE (DURABILITY)

Life Extending Control --- mechanical fatigue in reusable rocket engines p 246 A92-29166

Electrochemical impregnation and cycle life of lightweight nickel electrodes for nickel-hydrogen cells p 113 A92-30978

Environmental durability of ceramics and ceramic composites p 95 A92-39862

Advanced tube-bundle rocket thrust chambers p 62 A92-44509

Application of a thermal fatigue life prediction model to high-temperature aerospace alloys B1900 + Hf and Haynes 188 p 121 A92-45232

Effect of KOH concentration on LEO cycle life of IPV nickel-hydrogen flight cell - Update II p 232 A92-48212

Nickel-hydrogen cell low-earth-orbit life test update p 70 A92-50700

Effect of KOH concentration on LEO cycle life of IPV nickel-hydrogen flight cells - An update p 70 A92-50702

Destructive physical analysis results of Ni/H₂ cells cycled in LEO regime p 70 A92-50707

Effect of LEO cycling on 125 Ah advanced design IPV nickel-hydrogen flight cells - An update p 71 A92-50708

Stirling machine operating experience p 206 A92-50788

Alkali metal pool boiler life tests for a 25 kWe advanced Stirling conversion system p 206 A92-50797

Effect of KOH concentration on LEO cycle life of IPV nickel-hydrogen flight cells-update 2 [NASA-TM-105314] p 235 N92-13483

A vacuum (10⁻⁹ Torr) friction apparatus for determining friction and endurance life of MoS₂ films [NASA-TM-104478] p 129 N92-16129

Progress in the development of lightweight nickel electrode for aerospace applications [NASA-TM-105591] p 236 N92-20493

Life prediction technologies for aeronautical propulsion systems p 32 N92-22520

Validation test of advanced technology for IPV nickel-hydrogen flight cells: Update [NASA-TM-105689] p 89 N92-27878

Low-Isp derated ion thruster operation [NASA-TM-105787] p 92 N92-32237

LIFT

Use of an approximate similarity principle for the thermal scaling of a full-scale thrust augmenting ejector [AIAA PAPER 92-3792] p 28 A92-54171

Use of an approximate similarity principle for the thermal scaling of a full-scale thrust augmenting ejector [NASA-TM-105724] p 36 N92-26613

Experimental investigation of the flowfield of an oscillating airfoil [NASA-TM-105675] p 20 N92-30182

LIFTING BODIES

An improved PNS scheme for predicting complex three-dimensional hypersonic flows [AIAA PAPER 92-0753] p 8 A92-31679

LIGHT ELEMENTS

Possible sources of the Population I lithium abundance and light-element evolution p 268 A92-33069

LIGHT SCATTERING

Calculation of far-field scattering from nonspherical particles using a geometrical optics approach p 256 A92-20288

A fiber-optic probe for particle sizing in concentrated suspensions p 197 A92-21371

Atomic oxygen effects on thin film space coatings studied by spectroscopic ellipsometry, atomic force microscopy, and laser light scattering [AIAA PAPER 92-2172] p 94 A92-31300

A fiber optic sensor for ophthalmic refractive diagnostics p 198 A92-34831

Rocket plume flowfield characterization using laser Rayleigh scattering [AIAA PAPER 92-3351] p 66 A92-48928

Optical measurement systems p 202 N92-22527

Rocket plume flowfield characterization using laser Rayleigh scattering [NASA-TM-105739] p 257 N92-28475

LINEAR ARRAYS

New coplanar waveguide feed network for 2 x 2 linearly tapered slot antenna subarray p 156 A92-45619

LINEAR EQUATIONS

Minimization of deviations of gear real tooth surfaces determined by coordinate measurements [NASA-TM-105718] p 214 N92-30948

LINEAR POLARIZATION

Mutual coupling between rectangular microstrip patch antennas p 159 A92-52423

LINEAR QUADRATIC GAUSSIAN CONTROL

Linear quadratic servo control of a reusable rocket engine p 67 A92-50495

LINEAR QUADRATIC REGULATOR

Optimal microgravity vibration isolation - An algebraic introduction p 54 A92-47495

Linear quadratic servo control of a reusable rocket engine [NASA-TM-105291] p 79 N92-11128

Microgravity vibration isolation: An optimal control law for the one-dimensional case [NASA-TM-105146] p 141 N92-11217

Microgravity vibration isolation: Optimal preview and feedback control [NASA-TM-105673] p 142 N92-30692

LINEAR SYSTEMS

Stochastic stability properties of jump linear systems p 246 A92-25878

Modal interaction in linear dynamic systems near degenerate modes [NASA-TM-105315] p 225 N92-12316

Upper bounds for convergence rates of vector extrapolation methods on linear systems with initial iterations [NASA-TM-105608] p 250 N92-33742

LINEARIZATION

An iterative implicit diagonally-dominant factorization algorithm for solving the Navier-Stokes equations [NASA-TM-105259] p 249 N92-16663

LININGS

High-temperature durability considerations for HSCT combustor [NASA-TP-3162] p 129 N92-17070

LIQUID ATOMIZATION

Coaxial injector spray characterization using water/air as simulants [NASA-TM-105322] p 82 N92-14112

LIQUID BEARINGS

Two reference time scales for studying the dynamic cavitation of liquid films p 204 A92-47173

LIQUID CRYSTALS

Thick strings, the liquid crystal blue phase, and cosmological large-scale structure p 268 A92-48103

The Eckhaus and the Benjamin-Feir instability near a weakly inverted bifurcation [NASA-TM-105334] p 185 N92-15336

LIQUID FILLED SHELLS

Comparing the results of an analytical model of the no-vent fill process with no-vent fill test results for a 4.96 cu m (175 cu ft) tank [AIAA PAPER 92-3078] p 72 A92-54007

LIQUID FLOW

Interfacial and gravitational convection in immiscible liquid layers [IAF PAPER 92-0907] p 184 A92-57286

LIQUID FUELS

Some further observations on droplet combustion characteristics - NASA LeRC-Princeton results p 111 A92-12897

Combustion of liquid-fuel droplets in supercritical conditions p 114 A92-43778

Chemical reacting flows p 188 N92-22525

LIQUID HYDROGEN

COLD-SAT - A technology satellite for cryogenic experimentation p 52 A92-13425

Liquid-vapour surface sensors for liquid nitrogen and hydrogen p 197 A92-23852

Self-pressurization of a spherical liquid hydrogen storage tank in a microgravity environment [AIAA PAPER 92-0363] p 168 A92-25798

Self-pressurization of a lightweight liquid hydrogen tank - Effects of fill level at low wall heat flux [AIAA PAPER 92-0818] p 60 A92-29591

Liquid hydrogen mass flow through a multiple orifice Joule-Thomson device [AIAA PAPER 92-2881] p 176 A92-47862

Technology issues associated with using densified hydrogen for space vehicles [AIAA PAPER 92-3079] p 134 A92-48727

Comparing the results of an analytical model of the no-vent fill process with no-vent fill test results for a 4.96 cu m (175 cu ft) tank [AIAA PAPER 92-3078] p 72 A92-54007

Improved thermodynamic modeling of the no-vent fill process and correlation with experimental data [NASA-TM-104492] p 79 N92-11129

A review of candidate multilayer insulation systems for potential use on wet-launched LH₂ tankage for the space exploration initiative lunar missions [NASA-TM-104493] p 134 N92-13336

Hydrogen no-vent fill testing in a 1.2 cubic foot (34 liter) tank [NASA-TM-105273] p 185 N92-13401

Self-pressurization of a spherical liquid hydrogen storage tank in a microgravity environment [NASA-TM-105372] p 185 N92-14323

Multimegawatt MPD thruster design considerations [NASA-TM-105405] p 83 N92-16024

Self-pressurization of a lightweight liquid hydrogen tank: Effects of fill level at low wall heat flux [NASA-TM-105411] p 135 N92-18442

Liquid hydrogen mass flow through a multiple orifice Joule-Thomson device [NASA-TM-105583] p 189 N92-23268

Technology issues associated with using densified hydrogen for space vehicles [NASA-TM-105642] p 135 N92-25277

Slush hydrogen transfer studies at the NASA K-Site Test Facility [NASA-TM-105596] p 135 N92-25957

LIQUID INJECTION

Factors influencing the effective spray cone angle of pressure-swirl atomizers p 166 A92-23300

Hydrogen no-vent testing in a 5 cubic foot (142 liter) tank using spray nozzle and spray bar liquid injection [AIAA PAPER 92-3063] p 63 A92-48719

Hydrogen no-vent fill testing in a 1.2 cubic foot (34 liter) tank [NASA-TM-105273] p 185 N92-13401

Hydrogen no-vent fill testing in a 5 cubic foot (142 liter) tank using spray nozzle and spray bar liquid injection [NASA-TM-105759] p 136 N92-28433

LIQUID METALS

Design of a pool boiler heat transport system for a 25 kWe advanced Stirling conversion system p 181 A92-50802

Alkali metal compatibility testing of candidate heater head materials for a Stirling engine heat transport system p 71 A92-50829

LIQUID NITROGEN

Qualitative investigation of cryogenic fluid injection into a supersonic flow field p 164 A92-13360

Description of liquid nitrogen experimental test facility p 44 A92-23842

Effect of gas mass flux on cryogenic liquid jet breakup [AIAA PAPER 92-23845] p 140 A92-23845

CONE - An STS-based cryogenic fluid management experiment p 43 A92-23850

Cryogenic fluid management investigations using the CONE flight experiment p 43 A92-23851

Liquid-vapour surface sensors for liquid nitrogen and hydrogen p 197 A92-23852

Comparing the results of an analytical model of the no-vent fill process with no-vent fill test results for a 4.96 cu m (175 cu ft) tank [AIAA PAPER 92-3078] p 72 A92-54007

Description of Liquid Nitrogen Experimental Test Facility [NASA-TM-105215] p 134 N92-11208

LIQUID OXYGEN

Gelled liquid oxygen/metal powder monopropellants [AIAA PAPER 92-3450] p 134 A92-49004

Improved thermodynamic modeling of the no-vent fill process and correlation with experimental data [NASA-TM-104492] p 79 N92-11129

LIQUID PHASES

A review of candidate multilayer insulation systems for potential use on wet-launched LH2 tankage for the space exploration initiative lunar missions
[NASA-TM-104493] p 134 N92-13336

LIQUID PHASES

Convective flows in enclosures with vertical temperature or concentration gradients p 171 A92-32277

LIQUID PROPELLANT ROCKET ENGINES

Status of NASA's Earth-to-Orbit Propulsion Technology program - The action plan p 58 A92-13154
[IAF PAPER 91-258]

Thermal response of various thermal barrier coatings in a high heat flux rocket engine p 119 A92-32399

The NASA-OAST earth-to-orbit propulsion technology program - The action plan p 61 A92-38597
[AIAA PAPER 92-1478]

Advanced optical condition monitoring ... of rocket engines p 199 A92-39994
[SAE PAPER 912164]

Fiber optics in liquid propellant rocket engine environments p 62 A92-42610

Effect of model selection on combustor performance and stability using ROCCID ... Rocket Combustor Interactive Design p 65 A92-48827
[AIAA PAPER 92-3226]

Propulsion systems using in situ propellants for a Mars Ascent Vehicle p 66 A92-49001
[AIAA PAPER 92-3445]

An overview of in-flight plume diagnostics for rocket engines p 75 A92-54164
[AIAA PAPER 92-3785]

Low thrust chemical rocket technology p 77 A92-57105
[IAF PAPER 92-0669]

Developments in REDES: The Rocket Engine Design Expert System p 78 N92-11120

JANNAF Liquid Rocket Combustion Instability Panel research recommendations p 115 N92-11124

Coaxial injector spray characterization using water/air as simulants p 82 N92-14112
[NASA-TM-105322]

Effect of model selection on combustor performance and stability predictions using ROCCID p 89 N92-27036
[NASA-TM-105750]

Propulsion systems using in situ propellants for a Mars ascent vehicle p 89 N92-27654
[NASA-TM-105741]

An overview of in-flight plume diagnostics for rocket engines p 90 N92-28417
[NASA-TM-105727]

Rocket propulsion research at Lewis Research Center [NASA-CR-189187] p 266 N92-30908

LIQUID ROCKET PROPELLANTS

Modeling of impulsive propellant reorientation p 59 A92-17187

Propulsion systems using in situ propellants for a Mars Ascent Vehicle p 66 A92-49001
[AIAA PAPER 92-3445]

Test experience, 490 N high performance (321 sec lsp) engine p 67 A92-49127
[AIAA PAPER 92-3800]

Extended temperature range rocket injector [NASA-CASE-LEW-14846-1] p 77 N92-10054

Improved thermodynamic modeling of the no-vent fill process and correlation with experimental data [NASA-TM-104492] p 79 N92-11129

Propulsion systems using in situ propellants for a Mars ascent vehicle p 89 N92-27654
[NASA-TM-105741]

Rocket propulsion research at Lewis Research Center [NASA-CR-189187] p 266 N92-30908

LIQUID SLOSHING

A numerical and experimental study of three-dimensional liquid sloshing in a rotating spherical container [AIAA PAPER 92-0829] p 170 A92-29597

Effects of g-jitter on a thermally buoyant flow p 171 A92-32258

Pulsed thrust propellant reorientation - Concept and modeling p 62 A92-44507

Pressurization of cryogenics - A review of current technology and its applicability to low-gravity conditions [AIAA PAPER 92-3061] p 72 A92-54002

Effect of liquid surface turbulent motion on the vapor condensation in a mixing tank p 187 N92-21498
[NASA-TM-105555]

Pressurization of cryogenics: A review of current technology and its applicability to low-gravity conditions [NASA-TM-105746] p 136 N92-29669

LIQUID SURFACES

Drop-tower experiments for capillary surfaces in an exotic container p 166 A92-20743

Stability of capillary surfaces p 172 A92-35979

Two reference time scales for studying the dynamic cavitation of liquid films p 204 A92-47173

Effect of liquid surface turbulent motion on the vapor condensation in a mixing tank p 187 N92-21498
[NASA-TM-105555]

LIQUID-LIQUID INTERFACES

A continuum method for modeling surface tension p 175 A92-45707

LIQUID-SOLID INTERFACES

Growth-speed dependence of primary arm spacings in directionally solidified Pb-10 wt pct Sn p 117 A92-26526

Effect of thermal convection on the shape of a solid-liquid interface p 171 A92-35978

Stability of capillary surfaces p 172 A92-35979

Identification and control of a multizone crystal growth furnace p 199 A92-39699

LIQUID-VAPOR INTERFACES

Vapor condensation on liquid surface due to laminar jet-induced mixing p 164 A92-10446

Liquid-vapour surface sensors for liquid nitrogen and hydrogen p 197 A92-23852

Self-pressurization of a spherical liquid hydrogen storage tank in a microgravity environment p 168 A92-25798
[AIAA PAPER 92-0363]

Scalar rate correlation at a turbulent liquid free surface - A two-regime correlation for high Schmidt numbers p 184 A92-56941

Hydrogen no-vent fill testing in a 1.2 cubic foot (34 liter) tank p 185 N92-13401
[NASA-TM-105273]

Self-pressurization of a spherical liquid hydrogen storage tank in a microgravity environment p 185 N92-14323
[NASA-TM-105372]

An optical method for determining level in two-phase cryogenic fluids p 200 N92-15366
[NASA-TM-104524]

Using silicon diodes for detecting the liquid-vapor interface in hydrogen p 201 N92-18456
[NASA-TM-105541]

Effect of liquid surface turbulent motion on the vapor condensation in a mixing tank p 187 N92-21498
[NASA-TM-105555]

Color image processing and object tracking workstation p 139 N92-26611
[NASA-TM-105561]

LIQUIDS

Stable localized patterns in thin liquid films [NASA-TM-105352] p 185 N92-14322

LITHIUM

Possible sources of the Population I lithium abundance and light-element evolution p 268 A92-33069

Shrinkage void formation and its effect on freeze and thaw processes of lithium and lithium-fluoride for space applications p 180 A92-50596

Alkali metal carbon dioxide electrochemical system for energy storage and/or conversion of carbon dioxide to oxygen p 235 N92-10222
[NASA-CASE-LEW-14973-1]

LITHIUM FLUORIDES

Shrinkage void formation and its effect on freeze and thaw processes of lithium and lithium-fluoride for space applications p 180 A92-50596

Observations of the freeze/thaw performance of lithium fluoride by motion picture photography p 180 A92-50751

LITHIUM NIOBATES

Reconfigurable optical interconnection network for multimode optical fiber sensor arrays p 256 A92-37448

LITHIUM SULFUR BATTERIES

Impedances of Li/SO₂ cells retrieved from the Long Duration Exposure Facility (LDEF satellite) and comparison with cells stored terrestrially p 236 N92-13484
[NASA-TM-104526]

LOAD DISTRIBUTION (FORCES)

Load redistribution considerations in the fracture of ceramic matrix composites p 221 A92-34586
[AIAA PAPER 92-2494]

Effect of contact ratio on spur gear dynamic load [NASA-TM-105606] p 210 N92-25447

Gear tooth stress measurements of two helicopter planetary stages p 211 N92-26555
[NASA-TM-105651]

LOAD TESTS

Desktop fiber push-out apparatus p 107 N92-16036
[NASA-TM-105341]

Frequency effects on the stability of a journal bearing for periodic loading p 186 N92-18809
[NASA-TM-105226]

A free-piston Stirling engine/linear alternator controls and load interaction test facility p 238 N92-31262
[NASA-TM-105825]

LOADING RATE

Frequency effects on the stability of a journal bearing for periodic loading p 203 A92-22665

A viscoplastic model for single crystals p 217 A92-24717

Structural durability of stiffened composite shells [AIAA PAPER 92-2244] p 220 A92-34569

LOADS (FORCES)

Thermally-driven microfracture in high temperature metal matrix composites p 107 N92-15136
[NASA-TM-105305]

Aircraft engine hot section technology: An overview of the HOST Project p 33 N92-22535

Structural optimization of large structural systems by optimality criteria methods p 229 N92-25446
[NASA-TM-105423]

Design feasibility study of a Space Station Freedom truss p 214 N92-30571
[NASA-TM-105558]

A free-piston Stirling engine/linear alternator controls and load interaction test facility p 238 N92-31262
[NASA-TM-105825]

LOCKING

Removable hand hold p 213 N92-29092
[NASA-CASE-LEW-15196-1]

LONG DURATION EXPOSURE FACILITY

Applicability of Long Duration Exposure Facility environmental effects data to the design of Space Station Freedom electrical power system p 53 A92-29614
[AIAA PAPER 92-0848]

LDEF spacecraft, ground laboratory, and computational modeling implications on Space Station Freedom's solar array materials and surfaces durability p 71 A92-53190

Impedances of Li/SO₂ cells retrieved from the Long Duration Exposure Facility (LDEF satellite) and comparison with cells stored terrestrially p 236 N92-13484
[NASA-TM-104526]

Ion beam treatment of potential space materials at the NASA Lewis Research Center p 97 N92-21548
[NASA-TM-105398]

Atomic oxygen undercutting of LDEF aluminized-Kapton multilayer insulation p 255 N92-24818

Atomic oxygen interactions with FEP Teflon and silicones on LDEF p 132 N92-24820

Ion Beam Textured and Coated Surfaces Experiment (IBEX) p 132 N92-24832

Durability evaluation of photovoltaic blanket materials exposed on LDEF tray S1003 p 132 N92-27100

Advanced photovoltaic experiment, S0014: Preliminary flight results and post-flight findings p 237 N92-27101

Characteristics of hypervelocity impact craters on LDEF experiment S1003 and implications of small particle impacts on reflective surfaces p 269 N92-27252

Monte Carlo modeling of atomic oxygen attack of polymers with protective coatings on LDEF p 132 N92-27281

The effect of the low Earth orbit environment on space solar cells: Results of the advanced photovoltaic experiment (S0014) p 237 N92-27320

LONG DURATION SPACE FLIGHT

Energy requirements for the space frontier [SAE PAPER 912064] p 62 A92-45446

Risks, designs, and research for fire safety in spacecraft [NASA-TM-105317] p 240 N92-13581

LOSSES

Comparison of high temperature, high frequency core loss and dynamic B-H loops of two 50 Ni-Fe crystalline alloys and an iron-based amorphous alloy p 157 A92-50551

Overview of NASA supported Stirling thermodynamic loss research [NASA-TM-105690] p 88 N92-27034

LOW ALTITUDE

New technique for low-to-high altitude predictions of ablative hypersonic flowfields p 166 A92-24654

LOW ASPECT RATIO

A critical evaluation of a three-dimensional Navier-Stokes method as a tool to calculate transonic flows inside a low-aspect-ratio compressor p 195 N92-27459

LOW DENSITY MATERIALS

Composites of low-density trialuminides: Particulate and long fiber reinforcements p 109 N92-25346
[NASA-TM-105628]

LOW FREQUENCIES

Stability testing and analysis of a PMAD DC test bed for the Space Station Freedom p 162 N92-31282
[NASA-TM-105846]

RF modulated fiber optic sensing systems and their applications [NASA-TM-105801] p 257 N92-33896

LOW GRAVITY MANUFACTURING

An examination of anticipated g-jitter on Space Station and its effects on materials processes p 140 N92-28438

Vibration isolation technology development to demonstration p 140 N92-28442

LOW NOISE

Performance of a wideband GaAs low-noise amplifier at cryogenic temperatures p 156 A92-37953

- LOW PRESSURE**
 Numerical study of low pressure nuclear thermal rockets [AIAA PAPER 92-3815] p 75 A92-54182
- LOW REYNOLDS NUMBER**
 Experimental study of boundary layer transition on a heated flat plate p 172 A92-36022
 Implementation/validation of a low Reynolds number two-equation turbulence model in the Proteus Navier-Stokes code: Two-dimensional/axisymmetric [NASA-TM-105619] p 187 N92-20520
 A kappa-epsilon calculation of transitional boundary layers [NASA-TM-105604] p 187 N92-22398
 Advancements in engineering turbulence modeling [PAPER-105] p 189 N92-23350
 Turbulence and deterministic chaos --- computational fluid dynamics p 194 N92-25823
- LOW SPEED**
 NASA low-speed centrifugal compressor for 3-D viscous code assessment and fundamental flow physics research [ASME PAPER 91-GT-140] p 3 A92-15580
- LOW SPEED WIND TUNNELS**
 Flow quality studies of the NASA Lewis Research Center 8- by 6-foot supersonic/9- by 15-foot Low Speed Wind Tunnel [AIAA PAPER 92-3916] p 41 A92-56748
 Flow quality studies of the NASA Lewis Research Center 8- by 6-foot supersonic/9- by 15-foot low speed wind tunnel [NASA-TM-105417] p 42 N92-28673
- LOW TEMPERATURE**
 Low temperature synthesis of CaO-SiO₂ glasses having stable liquid-liquid immiscibility by the sol-gel process p 126 A92-44479
 Magnetic penetration depth of YBa₂Cu₃O(7-delta) thin films determined by the power transmission method p 265 N92-32983
- LOW TEMPERATURE TESTS**
 Composites of low-density traluminides: Particulate and long fiber reinforcements [NASA-TM-105628] p 109 N92-25346
 Measurement techniques for cryogenic Ka-band microstrip antennas p 153 N92-32981
- LOW THRUST**
 Test experience, 490 N high performance (321 sec Isp) engine [AIAA PAPER 92-3800] p 67 A92-49127
- LOW THRUST PROPULSION**
 Rocket plume flowfield characterization using laser Rayleigh scattering [AIAA PAPER 92-3351] p 66 A92-48928
 An overview of the NASA Advanced Propulsion Concepts program [AIAA PAPER 92-3216] p 73 A92-54018
 Low thrust chemical rocket technology [IAF PAPER 92-0669] p 77 A92-57105
 Magnetoplasmadynamic Thruster Workshop [NASA-CP-10084] p 77 N92-10044
 Rocket plume flowfield characterization using laser Rayleigh scattering [NASA-TM-105739] p 257 N92-28475
- LOW WEIGHT**
 Thin-film photovoltaics: Status and applications to space power p 81 N92-13228
- LUBRICANT TESTS**
 Development of a full-scale transmission testing procedure to evaluate advanced lubricants [NASA-TP-3265] p 213 N92-30396
 Liquid lubricants for advanced aircraft engines [NASA-TM-104531] p 133 N92-32863
- LUBRICANTS**
 Effect of lubricant jet location on spiral bevel gear operating temperatures [NASA-TM-105656] p 211 N92-26106
 Full-scale transmission testing to evaluate advanced lubricants [NASA-TM-105668] p 212 N92-26560
 Liquid lubrication for space applications [NASA-TM-105198] p 133 N92-31840
- LUBRICATING OILS**
 Effect of type and location of oil groove on the performance of journal bearings p 203 A92-21333
 Two reference time scales for studying the dynamic cavitation of liquid films p 204 A92-47173
 A new technique for oil backstreaming contamination measurements [NASA-TM-105312] p 257 N92-13783
 Full-scale transmission testing to evaluate advanced lubricants [NASA-TM-105668] p 212 N92-26560
 Development of a full-scale transmission testing procedure to evaluate advanced lubricants [NASA-TP-3265] p 213 N92-30396
- Liquid lubricants for advanced aircraft engines [NASA-TM-104531] p 133 N92-32863
- LUBRICATION**
 Tribological properties of ceramic-(Ti3Al-Nb) sliding couples for use as candidate seal materials to 700 C p 124 A92-32407
 Tribological and mechanical comparison of sintered and hipped PM212: High temperature self-lubricating composites [NASA-TM-105379] p 96 N92-15128
 Tribology needs for future space and aeronautical systems [NASA-TM-104525] p 128 N92-15191
 Self-lubricating coatings for high-temperature applications p 130 N92-22516
 Development of a full-scale transmission testing procedure to evaluate advanced lubricants [NASA-TP-3265] p 213 N92-30396
 Liquid lubrication for space applications [NASA-TM-105198] p 133 N92-31840
- LUBRICATION SYSTEMS**
 Lubrication of space systems: Challenges and potential solutions [NASA-TM-105560] p 130 N92-21579
 Liquid lubricants for advanced aircraft engines [NASA-TM-104531] p 133 N92-32863
- LUMPED PARAMETER SYSTEMS**
 Preliminary investigation of a low power pulsed arcjet thruster [AIAA PAPER 92-3113] p 64 A92-48752
- LUNAR BASED EQUIPMENT**
 Power management and distribution considerations for a lunar base [NASA-TM-105342] p 269 N92-13910
 Optimization of armored spherical tanks for storage on the lunar surface [NASA-TM-105700] p 91 N92-30187
- LUNAR BASES**
 Moonbase night power by laser illumination p 44 A92-21086
 Solar dynamic power for earth orbital and lunar applications p 68 A92-50567
 A mass sensitivity analysis of lunar orbiting beam power systems p 232 A92-50619
 Component technology for Stirling power converters p 206 A92-50781
- Power management and distribution considerations for a lunar base [NASA-TM-105342] p 269 N92-13910
 Thermochemical energy storage for a lunar base [NASA-TM-105333] p 236 N92-14485
 SP-100 reactor with Brayton conversion for lunar surface applications p 92 N92-32108
 Fast track lunar NTR systems assessment for the First Lunar Outpost and its evolvability to Mars p 142 N92-33334
- LUNAR ENVIRONMENT**
 Environmental interactions in Space Exploration: Announcement of the formation of an Environmental Interactions Working Group [NASA-TM-105294] p 270 N92-17069
 Environmental interactions in space exploration: Environmental interactions working group p 239 N92-22382
- LUNAR EXPLORATION**
 Technical prospects for utilizing extraterrestrial propellants for space exploration [IAF PAPER 91-669] p 133 A92-20612
 Nuclear thermal rockets - Key to moon-Mars exploration p 63 A92-48385
 An accelerated development, reduced cost approach to lunar/Mars exploration using a modular NTR-based space transportation system [IAF PAPER 92-0574] p 43 A92-57053
 A compilation of lunar and Mars exploration strategies utilizing indigenous propellants [NASA-TM-105262] p 135 N92-19837
- LUNAR LANDING**
 Benefits and technology readiness for using cryogenic instead of storable propellants for return mission from Moon p 136 N92-33343
- LUNAR RESOURCES**
 Technical prospects for utilizing extraterrestrial propellants for space exploration [IAF PAPER 91-669] p 133 A92-20612
- LUNAR ROVING VEHICLES**
 SEI rover solar-electrochemical power system options p 45 A92-50574
- LUNAR SOIL**
 Design issues for lunar in situ aluminum/oxygen propellant rocket engines [AIAA PAPER 92-1185] p 60 A92-33299
 Thermochemical energy storage for a lunar base [NASA-TM-105333] p 236 N92-14485
- Design issues for lunar in situ aluminum/oxygen propellant rocket engines [NASA-TM-105433] p 83 N92-16023
- LUNAR SURFACE**
 Design issues for lunar in situ aluminum/oxygen propellant rocket engines [AIAA PAPER 92-1185] p 60 A92-33299
 Beam power options for the moon p 61 A92-40429
 Preliminary design of a mobile lunar power supply p 233 A92-50635
 Design issues for lunar in situ aluminum/oxygen propellant rocket engines [NASA-TM-105433] p 83 N92-16023
 SP-100 reactor with Brayton conversion for lunar surface applications [NASA-TM-105637] p 92 N92-32108
- LUNAR SURFACE VEHICLES**
 A dynamic isotope power system for Space Exploration Initiative surface transport systems [AIAA PAPER 92-1489] p 61 A92-38605
- LYSOZYME**
 Thermophysical properties of lysozyme (protein) solutions p 240 A92-44385

M

- MACH NUMBER**
 Three-dimensional viscous analysis of a Mach 5 inlet and comparison with experimental data p 8 A92-28526
 Effect of tabs on the evolution of an axisymmetric jet p 26 A92-40151
 Grid quality improvement by a grid adaptation technique p 248 A92-47072
 Direct evaluation of aeroacoustic theory in a jet p 253 A92-50296
 Detailed noise measurements on the SR-7A propeller: Tone behavior with helical tip Mach number [NASA-TM-105206] p 255 N92-16705
 NASA thrusts in high-speed aeropropulsion research and development: An overview p 33 N92-22538
- MACLAURIN SERIES**
 Application of vector-valued rational approximations to the matrix eigenvalue problem and connections with Krylov subspace methods [NASA-TM-105858] p 250 N92-33571
 Rational approximations from power series of vector-valued meromorphic functions [NASA-TM-105859] p 251 N92-33942
- MAGNESIUM ALLOYS**
 Gelled liquid oxygen/metal powder monopropellants [AIAA PAPER 92-3450] p 134 A92-49004
- MAGNESIUM FLUORIDES**
 Magnesium fluoride as energy storage medium for spacecraft solar thermal power systems p 67 A92-50274
- MAGNESIUM OXIDES**
 Crack healing behavior of hot pressed silicon nitride due to oxidation p 124 A92-32896
- MAGNETIC BEARINGS**
 Space applications of high temperature superconductivity technology [IAF PAPER 91-307] p 259 A92-14724
 Performance tests of a cryogenic hybrid magnetic bearing for turbopumps [NASA-TM-105627] p 30 N92-20523
 Force analysis of magnetic bearings with power-saving controls p 212 N92-27995
 Magnetic bearings for free-piston Stirling engines [NASA-TM-105730] p 214 N92-30734
- MAGNETIC CHARGE DENSITY**
 A classical instability of Reissner-Nordstrom solutions and the fate of magnetically charged black holes p 267 A92-26397
- MAGNETIC CORES**
 A combined vector potential-scalar potential method for FE computation of 3D magnetic fields in electrical devices with iron cores p 154 A92-23959
 Comparison of high temperature, high frequency core loss and dynamic B-H loops of a 2V-49Fe-49Co and a grain oriented 3Si-Fe alloy [NASA-TM-105791] p 162 N92-30397
- MAGNETIC EFFECTS**
 Magnetic flux relaxation in YBa₂Cu₃O(7-x) thin film: Thermal or athermal p 265 N92-32984
- MAGNETIC FIELDS**
 Plasma flow processes within magnetic nozzle configurations p 67 A92-50266
- MAGNETIC FLUX**
 Magnetic flux relaxation in YBa₂Cu₃O(7-x) thin film: Thermal or athermal p 265 N92-32984

MAGNETIC MATERIALS

MAGNETIC MATERIALS

Comparison of high temperature, high frequency core loss and dynamic B-H loops of two 50 Ni-Fe crystalline alloys and an iron-based amorphous alloy

p 157 A92-50551

Comparison of high temperature, high frequency core loss and dynamic B-H loops of a 2V-49Fe-49Co and a grain oriented 3Si-Fe alloy

[NASA-TM-105791] p 162 A92-30397

MAGNETIC MONOPOLES

A classical instability of Reissner-Nordstrom solutions and the fate of magnetically charged black holes

p 267 A92-26397

MAGNETIC SUSPENSION

Force analysis of magnetic bearings with power-saving controls

p 212 A92-27795

Vibration isolation technology development to demonstration

p 140 A92-28442

Magnetic bearings for free-piston Stirling engines

[NASA-TM-105730] p 214 A92-30734

MAGNETOHYDRODYNAMIC FLOW

The formation and structure of plasma wakes behind large high-voltage space platforms in ionosphere

[AIAA PAPER 92-0577] p 239 A92-26984

Ionspheric plasma flow over large high-voltage space platforms. I - Ion-plasma-time scale interactions of a plate at zero angle of attack. II - The formation and structure of plasma wake

p 258 A92-41359

Modeling of the near-electrode regions of arcjets. I - Coupling of the flowfield to the non-equilibrium boundary layers

p 258 A92-48749

Qualitative spectroscopic study of magnetic nozzle flow

[AIAA PAPER 92-3161] p 65 A92-48784

Plasma flow processes within magnetic nozzle configurations

p 67 A92-50266

Preliminary investigation of power flow and electrode phenomena in a multi-megawatt coaxial plasma thruster

[AIAA PAPER 92-3741] p 75 A92-54144

MAGNETOPLASMA DYNAMICS

The evolutionary development of high specific impulse electric thruster technology

[AIAA PAPER 92-1556] p 61 A92-38650

Qualitative spectroscopic study of magnetic nozzle flow

[AIAA PAPER 92-3161] p 65 A92-48784

Early Track NEP system options for SEI missions

[AIAA PAPER 92-3200] p 65 A92-48808

Numerical simulation of geometric scale effects in cylindrical self-field MPD thrusters

[AIAA PAPER 92-3297] p 258 A92-48885

Scaling of 100 kW class applied-field MPD thrusters

[AIAA PAPER 92-3462] p 74 A92-54033

Anode power deposition in applied-field MPD thrusters

[AIAA PAPER 92-3463] p 74 A92-54034

Preliminary investigation of power flow and electrode phenomena in a multi-megawatt coaxial plasma thruster

[AIAA PAPER 92-3741] p 75 A92-54144

Magnetoplasma dynamic Thruster Workshop

[NASA-CP-10084] p 77 A92-10044

Multimegawatt MPD thruster design considerations

[NASA-TM-105405] p 83 A92-16024

Preliminary test results of a hollow cathode MPD thruster

[NASA-TM-105324] p 84 A92-18474

MAGNETORESISTIVITY

Enhancement of Shubnikov-de Haas oscillations by carrier modulation

p 262 A92-50911

Intermodulation in the oscillatory magnetoresistance of a two-dimensional electron gas

p 163 A92-32975

MAGNETOSTATIC FIELDS

A combined vector potential-scalar potential method for FE computation of 3D magnetic fields in electrical devices with iron cores

p 154 A92-23959

MAGNETRON SPUTTERING

Crystalline orientations of Ti2Ba2Ca2Cu3O(x) grains on MgO, SrTiO3, and LaAlO3 substrates

p 261 A92-41637

C-band superconductor/semiconductor hybrid field-effect transistor amplifier on a LaAlO3 substrate

[NASA-TM-105828] p 163 A92-34204

MAINTAINABILITY

Resonant mode controllers for launch vehicle applications

[NASA-TM-105563] p 48 A92-25092

MAINTENANCE

Transmission overhaul and component replacement predictions using Weibull and renewal theory

p 215 A92-17201

Reliability training

[NASA-RP-1253] p 49 A92-32456

MAN-COMPUTER INTERFACE

SCAILET - An intelligent assistant for satellite ground terminal operations

[IAF PAPER 92-0552] p 245 A92-55855

A graphical user-interface for propulsion system analysis

[NASA-TM-105696] p 244 A92-33894

MANAGEMENT INFORMATION SYSTEMS

MisTec - A software application for supporting space exploration scenario options and technology development analysis and planning

[AIAA PAPER 92-1293] p 242 A92-38490

MisTec: A software application for supporting space exploration scenario options and technology development analysis and planning

[NASA-TM-105214] p 243 A92-14649

MANAGEMENT SYSTEMS

Power management and distribution considerations for a lunar base

[NASA-TM-105342] p 269 A92-13910

Automated power management and control

p 84 A92-17773

MANGANESE OXIDES

The analysis of high pressure experimental data

p 266 A92-16101

MANIFOLDS

Extended temperature range rocket injector

[NASA-CASE-LEW-14846-1] p 77 A92-10054

MANIPULATORS

Reaction-compensation technology for microgravity laboratory robots

p 203 A92-23719

Flow quality studies of the NASA Lewis Research Center 8- by 6-foot supersonic/9- by 15-foot Low Speed Wind Tunnel

[AIAA PAPER 92-3916] p 41 A92-56748

A 23.2:1 ratio, 300-watt, 26 N-m output torque, planetary roller-gear robotic transmission: Design and evaluation

p 210 A92-25085

Flow quality studies of the NASA Lewis Research Center 8- by 6-foot supersonic/9- by 15-foot low speed wind tunnel

[NASA-TM-105417] p 42 A92-28673

MANNED MARS MISSIONS

Technical prospects for utilizing extraterrestrial propellants for space exploration

[IAF PAPER 91-669] p 133 A92-20612

Effect of inert propellant injection on Mars ascent vehicle performance

[AIAA PAPER 92-3447] p 73 A92-54031

Multi-reactor power system configurations for multimegawatt nuclear electric propulsion

[NASA-TM-105212] p 77 A92-10057

A compilation of lunar and Mars exploration strategies utilizing indigenous propellants

[NASA-TM-105262] p 135 A92-19837

Fast track lunar NTR systems assessment for the First Lunar Outpost and its evolvability to Mars

p 142 A92-33334

MANNED SPACE FLIGHT

Safety issues

p 78 A92-11115

MANNED SPACECRAFT

Power supply for a manned international asteroid mission

p 80 A92-13205

MANUALS

Operating and service manual for the NASA Lewis automated far-field antenna range

[NASA-TM-105343] p 52 A92-22319

MANUFACTURING

A basis for solid modeling of gear teeth with application in design and manufacture

[NASA-TM-105392] p 209 A92-24202

MAPPING

Mappings and accuracy for Chebyshev pseudo-spectral approximations

p 248 A92-50469

Interactive solution-adaptive grid generation procedure

p 244 A92-25724

MARANGONI CONVECTION

Numerical investigation on Benard instability in a finite liquid layer

p 164 A92-12865

Linear-stability theory of thermocapillary convection in a model of float-zone crystal growth

[AIAA PAPER 92-0604] p 169 A92-28211

Stable localized patterns in thin liquid films

[NASA-TM-105352] p 185 A92-14322

MARS (PLANET)

Material processing with hydrogen and carbon monoxide on Mars

p 231 A92-17769

Nuclear thermal rockets - Key to moon-Mars exploration

p 63 A92-48385

In-situ carbon dioxide fixation on Mars

p 134 A92-50613

Engine system assessment study using Martian propellants

[AIAA PAPER 92-3446] p 73 A92-54030

Solar radiation for Mars power systems

p 81 A92-13259

Report of the Nuclear Propulsion Mission Analysis. Figures of Merit Subpanel: Quantifiable figures of merit for nuclear thermal propulsion

[NASA-TM-104179] p 43 A92-20925

MARS ATMOSPHERE

Acetylene fuel from atmospheric CO2 on Mars

p 133 A92-32199

Effect of inert propellant injection on Mars ascent vehicle performance

[AIAA PAPER 92-3447] p 73 A92-54031

Environmental interactions in Space Exploration: Announcement of the formation of an Environmental Interactions Working Group

[NASA-TM-105294] p 270 A92-17069

Environmental interactions in space exploration: Environmental interactions working group

p 239 A92-22382

Photovoltaic array for Martian surface power

[NASA-TM-105827] p 270 A92-33899

MARS ENVIRONMENT

Effect of particle size of Martian dust on the degradation of photovoltaic cell performance

[NASA-TM-105232] p 79 A92-11133

MARS PROBES

An accelerated development, reduced cost approach to lunar/Mars exploration using a modular NTR-based space transportation system

[IAF PAPER 92-0574] p 43 A92-57053

MARS SURFACE

Photovoltaic power options for Mars

p 231 A92-20366

A dynamic isotope power system for Space Exploration Initiative surface transport systems

[AIAA PAPER 92-1489] p 61 A92-38605

Effects of windblown dust on photovoltaic surfaces on Mars

p 45 A92-50573

Effect of particle size of Martian dust on the degradation of photovoltaic cell performance

[NASA-TM-105232] p 79 A92-11133

Electrical and chemical interactions at Mars Workshop, part 1

[NASA-CP-10093] p 270 A92-30302

Photovoltaic array for Martian surface power

[NASA-TM-105827] p 270 A92-33899

MASS FLOW

Liquid hydrogen mass flow through a multiple orifice Joule-Thomson device

[AIAA PAPER 92-2881] p 176 A92-47862

A parametric numerical study of mixing in a cylindrical duct

[AIAA PAPER 92-3088] p 177 A92-48733

Experimental study of cross-stream mixing in a rectangular duct

[AIAA PAPER 92-3090] p 178 A92-48735

Preliminary characterizations of a water vaporizer for resistorjet applications

[AIAA PAPER 92-3533] p 74 A92-54041

Liquid hydrogen mass flow through a multiple orifice Joule-Thomson device

[NASA-TM-105583] p 189 A92-23268

A parametric numerical study of mixing in a cylindrical duct

[NASA-TM-105695] p 35 A92-26553

Experimental study of cross-stream mixing in a rectangular duct

[NASA-TM-105694] p 36 A92-27652

MASS FLOW RATE

Dependence of hydrogen arcjet operation on electrode geometry

[AIAA PAPER 92-3530] p 74 A92-54039

Computational and experimental investigation of subsonic internal reversing flows

[AIAA PAPER 92-3791] p 183 A92-54170

MASS RATIOS

Enhanced EOS photovoltaic power system capability with InP solar cells

p 81 A92-13248

MASS TO LIGHT RATIOS

Dark matter and the equivalence principle

p 267 A92-14477

MASS TRANSFER

Self-pressurization of a spherical liquid hydrogen storage tank in a microgravity environment

[AIAA PAPER 92-0363] p 168 A92-25798

Heat and mass transport from thermally degrading thin cellulosic materials in a microgravity environment

p 174 A92-41810

A computer model for one-dimensional mass and energy transport in and around chemically reacting particles, including complex gas-phase chemistry, multicomponent molecular diffusion, surface evaporation, and heterogeneous reaction

p 181 A92-52406

Scalar rate correlation at a turbulent liquid free surface - A two-regime correlation for high Schmidt numbers

p 184 A92-56941

Self-pressurization of a spherical liquid hydrogen storage tank in a microgravity environment

[NASA-TM-105372] p 185 A92-14323

- Modelling and experimental verification of a water alleviation system for the NASP --- National Aerospace Plane
[NASA-TM-105661] p 189 N92-23224
- MASSIVE STARS**
The diffuse gamma-ray background, light element abundances, and signatures of early massive star formation p 268 A92-43837
- MATERIALS SCIENCE**
Determination of the critical parameters for remote microscope control
[IAF PAPER 91-026] p 240 A92-12447
- MATERIALS TESTS**
Screen Cage Ion Plating (SCIP) and scratch testing of polycrystalline aluminum oxide
[NASA-TM-105404] p 130 N92-22278
Composites of low-density trialuminides. Particulate and long fiber reinforcements
[NASA-TM-105628] p 109 N92-25346
- MATHEMATICAL MODELS**
Slush hydrogen (SLH2) technology development for application to the National Aerospace Plane (NASP)
p 140 A92-13432
Dynamics and control of the Space Station Freedom docking/array feathering maneuver
[IAF PAPER 91-321] p 52 A92-14734
Modeling of impulsive propellant reorientation
p 59 A92-17187
Viscoplastic analysis of an experimental cylindrical thrust chamber liner p 218 A92-28052
A simplified dynamic model of Space Shuttle Main Engine p 60 A92-29289
Modeling of crack bridging in a unidirectional metal matrix composite p 104 A92-43085
Three-dimensional deformation analysis of two-phase dislocation substructures p 121 A92-44218
Pulsed thrust propellant reorientation - Concept and modeling p 62 A92-44507
Application of a thermal fatigue life prediction model to high-temperature aerospace alloys B1900 + Hf and Haynes 188 p 121 A92-45232
Micromechanical model of crack growth in fiber reinforced brittle materials p 223 A92-46829
Liquid hydrogen mass flow through a multiple orifice Joule-Thomson device
[AIAA PAPER 92-2881] p 176 A92-47862
Development of an analytical tool to study power quality of ac power systems for large spacecraft p 67 A92-50529
Functional models of power electronic components for system studies p 157 A92-50558
Modeling of Space Station power system components and their interactions p 68 A92-50559
Comparative survey of dynamic analyses of free-piston Stirling engines p 206 A92-50793
Pressurization of cryogenics - A review of current technology and its applicability to low-gravity conditions
[AIAA PAPER 92-3061] p 72 A92-54002
Modal simulation of gearbox vibration with experimental correlation
[AIAA PAPER 92-3494] p 207 A92-54036
A first-principles model for orificed hollow cathode operation
[AIAA PAPER 92-3742] p 259 A92-54145
A method for determining spiral-bevel gear tooth geometry for finite element analysis
[NASA-TP-3096] p 207 N92-10195
Improved thermodynamic modeling of the no-vent fill process and correlation with experimental data
[NASA-TM-104492] p 79 N92-11129
Seals Flow Code Development
[NASA-CP-10070] p 49 N92-15082
Thermal and solutal convection with conduction effects inside a rectangular enclosure
[NASA-TM-105371] p 186 N92-15358
COMGEN-BEM: Boundary element model generation for composite materials micromechanical analysis
[NASA-TM-105548] p 226 N92-19779
Explicit robust schemes for implementation of a class of principal value-based constitutive models: Theoretical development
[NASA-TM-105345] p 227 N92-20212
Evaluation of an innovative high temperature ceramic wafer seal for hypersonic engine applications
[NASA-TM-105556] p 208 N92-20815
Effect of liquid surface turbulent motion on the vapor condensation in a mixing tank
[NASA-TM-105555] p 187 N92-21498
ULTRA-SHARP solution of the Smith-Hutton problem
[NASA-TM-105435] p 187 N92-22226
Improved accuracy for finite element structural analysis via a new integrated force method
[NASA-TP-3204] p 227 N92-22227
Probabilistic structural analysis of adaptive/smart/intelligent space structures
[NASA-TM-105408] p 227 N92-22267
- Ion collection from a plasma by a pinhole p 259 N92-22368
Turbomachinery p 32 N92-22524
Comparison of two-dimensional and three-dimensional droplet trajectory calculations in the vicinity of finite wings
[NASA-TM-105617] p 188 N92-23154
Achieving spectrum conservation for the minimum-span and minimum-order frequency assignment problems
[NASA-TM-105649] p 52 N92-23187
Aeroelastic stability analyses of two counter rotating propfan designs for a cruise missile model
[NASA-TM-105268] p 227 N92-23191
Progressive fracture of polymer matrix composite structures: A new approach
[NASA-TM-105574] p 109 N92-23194
Coupled multi-disciplinary simulation of composite engine structures in propulsion environment
[NASA-TM-105575] p 228 N92-23267
Liquid hydrogen mass flow through a multiple orifice Joule-Thomson device
[NASA-TM-105583] p 189 N92-23268
A two-dimensional Euler solution for an unbladed jet engine configuration
[NASA-TM-105329] p 190 N92-23560
Long time behavior of unsteady flow computations
[NASA-TM-105584] p 190 N92-23565
A two-dimensional Euler solution for an unbladed jet engine configuration p 18 N92-24861
Comparison of GLIMPS and HFAST Stirling engine code predictions with experimental data
[NASA-TM-105549] p 267 N92-25395
Comparison of analysis and experiment for gearbox noise
[NASA-TM-105330] p 210 N92-25396
Effect of contact ratio on spur gear dynamic load
[NASA-TM-105606] p 210 N92-25447
Interactive solution-adaptive grid generation procedure p 244 N92-25724
Activities for numerical propulsion systems simulation program p 244 N92-25726
Computational Fluid Dynamics --- numerical methods and algorithm development
[NASA-CP-10078] p 35 N92-25808
Accurate upwind-monotone (nonoscillatory) methods for conservation laws p 193 N92-25812
Numerical simulation of conservation laws p 193 N92-25813
Techniques for grid manipulation and adaptation --- computational fluid dynamics p 194 N92-25827
Computational techniques in tribology and material science at the atomic level
[NASA-TM-105573] p 252 N92-26671
A mathematical constraint placed upon inter-blade row boundary conditions used in the simulation of multistage turbomachinery flows p 195 N92-27458
Pressurization of cryogenics: A review of current technology and its applicability to low-gravity conditions
[NASA-TM-105746] p 136 N92-29669
Life extending control for rocket engines
[NASA-TM-105789] p 142 N92-31263
A general numerical model for wave rotor analysis
[NASA-TM-105740] p 196 N92-31484
Modal simulation of gearbox vibration with experimental correlation
[NASA-TM-105702] p 215 N92-31485
Effect of out-of-roundness on the performance of a diesel engine connecting-rod bearing
[NASA-TM-105600] p 215 N92-31536
Rational approximations from power series of vector-valued meromorphic functions
[NASA-TM-105859] p 251 N92-33942
- MATRICES (CIRCUITS)**
Advanced large scale GaAs monolithic IF switch matrix subsystem
[AIAA PAPER 92-1861] p 155 A92-29801
- MATRICES (MATHEMATICS)**
High order parallel numerical schemes for solving incompressible flows p 193 N92-25818
Application of vector-valued rational approximations to the matrix eigenvalue problem and connections with Krylov subspace methods
[NASA-TM-105858] p 250 N92-33571
Rational approximations from power series of vector-valued meromorphic functions
[NASA-TM-105859] p 251 N92-33942
- MATRIX MATERIALS**
Mechanical behavior of fiber reinforced SiC/RBSN ceramic matrix composites - Theory and experiment --- Reaction Bonded Silicon Nitride
[ASME PAPER 91-GT-209] p 99 A92-15629
Polymeric precursors for fibers and matrices p 125 A92-39856
Intermetallic matrix composites, Proceedings of the MRS Symposium, San Francisco, CA, Apr. 18-20, 1990
[ISBN 1-55899-083-6] p 104 A92-46826
- Effects of a noncoplanar biphenyldiamine on the processing and properties of addition polyimides
[NASA-TM-105383] p 107 N92-15137
Approaches to polymer-derived CMC matrices
[NASA-TM-105754] p 110 N92-29660
A differential CDM model for fatigue of unidirectional metal matrix composites
[NASA-TM-105726] p 230 N92-31505
- MAXIMUM ENTROPY METHOD**
The Baldwin-Lomax model for separated and wake flows using the entropy envelope concept
[AIAA PAPER 92-0148] p 4 A92-23764
- MEASURE AND INTEGRATION**
Improved accuracy for finite element structural analysis via a new integrated force method
[NASA-TP-3204] p 227 N92-22227
- MEASURING INSTRUMENTS**
Description of liquid nitrogen experimental test facility p 44 A92-23842
Flow quality studies of the NASA Lewis Research Center 8- by 6-foot supersonic/9- by 15-foot Low Speed Wind Tunnel
[AIAA PAPER 92-3916] p 41 A92-56748
Description of Liquid Nitrogen Experimental Test Facility
[NASA-TM-105215] p 134 N92-11208
Miniature high temperature plug-type heat flux gauges
[NASA-TM-105403] p 201 N92-18759
Method of producing a plug-type heat flux gauge
[NASA-CASE-LEW-14967-2] p 201 N92-22038
Research sensors p 202 N92-22526
Inflatable traversing probe seal p 209 N92-22692
X ray based displacement measurement for hostile environments p 202 N92-23155
Flow quality studies of the NASA Lewis Research Center 8- by 6-foot supersonic/9- by 15-foot low speed wind tunnel
[NASA-TM-105417] p 42 N92-28673
- MECHANICAL DRIVES**
A 23:2:1 ratio, 300-watt, 26 N-m output torque, planetary roller-gear robotic transmission: Design and evaluation p 210 N92-25085
- MECHANICAL PROPERTIES**
The effect of porosity and gamma-gamma-prime eutectic content on the fatigue behavior of hydrogen charged PWA 1480 p 116 A92-12046
The effect of matrix mechanical properties on (0)8 unidirectional SiC/Ti composite fatigue resistance p 99 A92-16220
Mechanical behaviors of ceramic matrix composites with matrix cracking and fiber debonding p 100 A92-23104
The mechanical properties of a Ni-30Al-20Fe-0.05Zr intermetallic alloy in the temperature range 300-1200 K p 118 A92-30793
Microstructure and mechanical properties of a single crystal NiAl alloy with Zr or Hf rich G-phase precipitates p 119 A92-30841
Microstructure and mechanical properties of near eutectic beta-NiAl plus alpha-Re alloys produced by rapid solidification and extrusion p 119 A92-30844
Computational simulation of high temperature metal matrix composite behavior p 101 A92-32753
Effect of fiber reinforcement on thermo-oxidative stability and mechanical properties of polymer matrix composites p 101 A92-33587
Analysis of whisker-toughened CMC structural components using an interactive reliability model
[AIAA PAPER 92-2490] p 221 A92-34582
Mechanical properties of monolithic and particulate composites of L12 forms of Al3Ti p 101 A92-36273
Monolithic ceramics p 125 A92-39854
Discontinuously reinforced intermetallic matrix composites via XD synthesis --- exothermal dispersion p 103 A92-41867
Mechanical properties of 3C silicon carbide p 126 A92-43761
Intermetallic matrix composites, Proceedings of the MRS Symposium, San Francisco, CA, Apr. 18-20, 1990
[ISBN 1-55899-083-6] p 104 A92-46826
Initial evaluation of continuous fiber reinforced NiAl composites p 104 A92-46867
Influence of processing on the microstructure and mechanical properties of a NbAl3-base alloy p 122 A92-48152
Probabilistic material degradation model for aerospace materials subjected to high temperature, mechanical and thermal fatigue, and creep
[AIAA PAPER 92-3419] p 224 A92-48978
Elevated temperature mechanical behavior of monolithic and SiC whisker-reinforced silicon nitrides
[NASA-TM-105245] p 128 N92-15192
A preliminary characterization of the tensile and fatigue behavior of tungsten-fiber/Waspaloy-matrix composite
[NASA-TM-105346] p 187 N92-22487

MELTING

Detecting Lamb waves with broad-band acousto-ultrasonic signals in composite structures [NASA-TM-105557] p 216 N92-23189

MELTING

Shrinkage void formation and its effect on freeze and thaw processes of lithium and lithium-fluoride for space applications p 180 A92-50596
Observations of the freeze/thaw performance of lithium fluoride by motion picture photography p 180 A92-50751

Thermal modeling with solid/liquid phase change of the thermal energy storage experiment [NASA-TM-103770] p 185 N92-13402

MELTING POINTS

Melting of the Abrikosov flux lattice in anisotropic superconductors p 260 A92-28075
Pressure dependence of the melting temperature of solids - Rare-gas solids p 171 A92-33912
Frozen start-up behavior of low-temperature heat pipes p 179 A92-49847
Growth and characterization of lead bromide crystals p 138 A92-56956

MELTS (CRYSTAL GROWTH)

Transport modes during crystal growth in a centrifuge p 138 A92-33835
Vertical solidification of dendritic binary alloys p 261 A92-37562

On the drag of model dendrite fragments at low Reynolds number p 95 A92-50868
Effect of growth conditions on the quality of lead bromide crystals p 138 A92-56957
Vapor crystal growth technology development: Application to cadmium telluride [NASA-TM-103786] p 139 N92-16158

MERCURY CADMIUM TELLURIDES

A model for the trap-assisted tunneling mechanism in diffused n-p and implanted n(+) - p HgCdTe photodiodes p 156 A92-46007

MERCURY COMPOUNDS

Flight experiment on acousto-optic crystal growth p 136 A92-12880

MERIDIONAL FLOW

A multiblock grid generation technique applied to a jet engine configuration p 244 N92-24428

MEROMORPHIC FUNCTIONS

Rational approximations from power series of vector-valued meromorphic functions [NASA-TM-105859] p 251 N92-33942

METAL COATINGS

Diffusion mechanisms in chemical vapor-deposited iridium coated on chemical vapor-deposited rhenium p 117 A92-28017

Thermal response of various thermal barrier coatings in a high heat flux rocket engine p 119 A92-32399
Plasma erosion rate diagnostics using laser-induced fluorescence p 198 A92-36738

Deposition of adherent Ag-Ti duplex films on ceramics in a multiple-cathode sputter deposition system [NASA-TM-105586] p 34 N92-23225

METAL COMBUSTION

Design issues for lunar in situ aluminum/oxygen propellant rocket engines p 60 A92-33299

Design issues for lunar in situ aluminum/oxygen propellant rocket engines [NASA-TM-105433] p 83 N92-16023

METAL FATIGUE

The effect of porosity and gamma-gamma-prime eutectic content on the fatigue behavior of hydrogen charged PWA 1480 p 116 A92-12046

Thermomechanical and bithermal fatigue behavior of cast B1900 + Hf and wrought Haynes 188 p 122 A92-45233

Differential continuum damage mechanics models for creep and fatigue of unidirectional metal matrix composites [NASA-TM-105213] p 226 N92-16371

A differential CDM model for fatigue of unidirectional metal matrix composites [NASA-TM-105726] p 230 N92-31505

METAL FIBERS

Microstress analysis of periodic composites p 218 A92-30673

A preliminary characterization of the tensile and fatigue behavior of tungsten-fiber/Waspaloy-matrix composite [NASA-TM-105346] p 187 N92-22487

METAL FILMS

Extrapolation procedures in Mott electron polarimetry p 197 A92-21241

Method of intercalating large quantities of fibrous structures [NASA-CASE-LEW-15077-1] p 107 N92-16025

The effect of ion plated silver and sliding friction on tensile stress-induced cracking in aluminum oxide [NASA-TM-105366] p 129 N92-19450

Screen Cage Ion Plating (SCIP) and scratch testing of polycrystalline aluminum oxide [NASA-TM-105404] p 130 N92-22278

METAL HALIDES

Volatile species in halide-activated-diffusion coating packs p 122 A92-57028

METAL MATRIX COMPOSITES

Interphase layer optimization for metal matrix composites with fabrication considerations p 98 A92-10262

Computational simulation of microfracture in high temperature metal matrix composites p 98 A92-10263

METCAN updates for high temperature composite behavior - Simulation/verification p 98 A92-10264

The effect of matrix mechanical properties on (0)8 unidirectional SiC/Ti composite fatigue resistance p 99 A92-16220

Fatigue crack growth in unidirectional metal matrix composite p 99 A92-19734

Isothermal fatigue behaviour of a (90 deg)8 SiC/Ti-15-3 composite at 426 C p 100 A92-23313

Effect of heat treatment on stiffness and damping of SiC/Ti-15-3 p 100 A92-25627
Microstress analysis of periodic composites p 218 A92-30673

Compression studies on particulate composites of ternary Al-Ti-Fe, and quaternary Al-Ti-Fe-Nb and Al-Ti-Fe-Mn L1(2) compounds p 119 A92-30845

Computational simulation of high temperature metal matrix composite behavior p 101 A92-32753

Mechanical properties of monolithic and particulate composites of L12 forms of Al3Ti p 101 A92-36273

Effect of fiber strength on the room temperature tensile properties of SiC/Ti-24Al-11Nb p 102 A92-36389

HITCAN for actively cooled hot-composite thermostructural analysis p 222 A92-36896

Thermal stress analysis of a silicon carbide/aluminum composite p 222 A92-38097

1200 and 1300 K slow plastic compression properties of Ni-50Al composites p 102 A92-38125

Fatigue crack growth in a unidirectional SCS-6/Ti-15-3 composite p 102 A92-39036

1400 and 1500 K compressive creep properties of an NiAl-AlN composite p 103 A92-41575

Discontinuously reinforced intermetallic matrix composites via XD synthesis --- exothermal dispersion p 103 A92-41867

Modeling of crack bridging in a unidirectional metal matrix composite p 104 A92-43085

Combined bending and thermal fatigue of high-temperature metal-matrix composites - Computational simulation p 223 A92-43494

Metal- and intermetallic-matrix composites for aerospace propulsion and power systems p 104 A92-43682

Thermomechanical testing of high-temperature composites - Thermomechanical fatigue (TMF) behavior of SiC(SCS-6)/Ti-15-3 p 104 A92-44606

High-temperature fatigue behavior of a SiC/Ti-24Al-11Nb composite p 104 A92-44613

Intermetallic matrix composites; Proceedings of the MRS Symposium, San Francisco, CA, Apr. 18-20, 1990 [ISBN 1-55899-083-6] p 104 A92-46826

Initial evaluation of continuous fiber reinforced NiAl composites p 104 A92-46867

Compatibility of potential reinforcing ceramics with Ni and Fe aluminides p 105 A92-46874

Reduction of thermal residual stresses in advanced metallic composites based upon a compensating/compliant layer concept p 105 A92-47106

Reduction of thermal stresses in continuous fiber reinforced metal matrix composites with interface layers p 105 A92-50347

The effect of temperature on the deformation and fracture of SiC/Ti-24Al-11Nb p 106 A92-55143

Oxidation of Al2O3 continuous fiber-reinforced/NiAl composites p 106 A92-57029

Effects of anisotropic conduction and heat pipe interaction on minimum mass space radiators [NASA-TM-105297] p 80 N92-11138

Thermal conductivity and thermal expansion of graphite fiber/copper matrix composites p 106 N92-14120

Microfracture in high temperature metal matrix laminates [NASA-TM-105189] p 106 N92-14122

Thermally-driven microfracture in high temperature metal matrix composites [NASA-TM-105305] p 107 N92-15136

Differential continuum damage mechanics models for creep and fatigue of unidirectional metal matrix composites [NASA-TM-105213] p 226 N92-16371

Effect of heat treatment on stiffness and damping of SiC/Ti-15-3 [NASA-TM-105564] p 108 N92-20841

A preliminary characterization of the tensile and fatigue behavior of tungsten-fiber/Waspaloy-matrix composite [NASA-TM-105346] p 187 N92-22487

NASA Lewis Research Center materials research and technology: An overview p 31 N92-22512

Detecting Lamb waves with broad-band acousto-ultrasonic signals in composite structures [NASA-TM-105557] p 216 N92-23189

Influence of engineered interfaces on residual stresses and mechanical response in metal matrix composites [NASA-TM-105438] p 109 N92-23195

Applications of high thermal conductivity composites to electronics and spacecraft thermal design [NASA-TM-102434] p 56 N92-24349

Composites of low-density trivalent oxides: Particulate and long fiber reinforcements [NASA-TM-105628] p 109 N92-25346

Oxidation resistant coating for titanium alloys and titanium alloy matrix composites [NASA-CASE-LEW-15155-1] p 133 N92-29090

Metal matrix composite analyzer (METCAN) user's manual, version 4.0 [NASA-TM-105244] p 110 N92-30779

Cyclic hot firing results of tungsten-wire-reinforced, copper-lined thrust chambers [NASA-TM-4214] p 91 N92-31249

Preliminary evaluation of adhesion strength measurement devices for ceramic/titanium matrix composite bonds [NASA-TM-105803] p 1 N92-31267

A differential CDM model for fatigue of unidirectional metal matrix composites [NASA-TM-105726] p 230 N92-31505

Effects of fiber and interfacial layer architectures on the thermoplastic response of metal matrix composites [NASA-TM-105802] p 110 N92-32234

Computational simulation of matrix micro-slip bands in SiC/Ti-15 composite [NASA-TM-105762] p 111 N92-32466

Design issues for lunar in situ aluminum/oxygen propellant rocket engines [AIAA PAPER 92-1185] p 60 A92-33299

Design issues for lunar in situ aluminum/oxygen propellant rocket engines [NASA-TM-105433] p 83 N92-16023

Gelled liquid oxygen/metal powder monopropellants [AIAA PAPER 92-3450] p 134 A92-49004

Upper stages using liquid propulsion and metallized propellants [NASA-TP-3191] p 83 N92-17151

Plasma erosion rate diagnostics using laser-induced fluorescence p 198 A92-36738

Computational techniques in tribology and material science at the atomic level [NASA-TM-105573] p 252 N92-26671

Alkali metal compatibility testing of candidate heater head materials for a Stirling engine heat transport system p 71 A92-50829

Metallized gelled monopropellants [NASA-TM-105418] p 87 N92-24557

Fluorescence microscopy for the characterization of structural integrity [NASA-TM-105253] p 96 N92-18970

Plasma etching a ceramic composite --- evaluating microstructure [NASA-TM-105430] p 130 N92-22305

Characteristics of hypervelocity impact craters on LDEF experiment S1003 and implications of small particle impacts on reflective surfaces p 269 N92-27252

Optimization of armored spherical tanks for storage on the lunar surface [NASA-TM-105700] p 91 N92-30187

Optimization and analysis of large chemical kinetic mechanisms using the solution mapping method - Combustion of methane p 113 A92-19300

Effects of oxygen concentration on radiative loss from normal-gravity and microgravity methane diffusion flames [AIAA PAPER 92-0243] p 113 A92-26928

Quantitative fluorescence measurements of the OH radical in high pressure methane flames [AIAA PAPER 92-2960] p 114 A92-46976

MICROCRACKS

- Computational simulation of microfracture in high temperature metal matrix composites p 98 A92-10263
- Asymmetric tip morphology of creep microcracks growing along bimaterial interfaces p 127 A92-56585
- Microfracture in high temperature metal matrix laminates
[NASA-TM-105189] p 106 N92-14122
- Thermally-driven microfracture in high temperature metal matrix composites
[NASA-TM-105305] p 107 N92-15136
- High-temperature polymer matrix composites
p 108 N92-22513
- Computational simulation of matrix micro-slip bands in SiC/Ti-15 composite
[NASA-TM-105762] p 111 N92-32466

MICROGRAVITY APPLICATIONS

- A full field, 3-D velocimeter for NASA's microgravity science program
[AIAA PAPER 92-0784] p 56 A92-27119
- Transient pool boiling in microgravity
p 170 A92-30494
- Optimal microgravity vibration isolation - An algebraic introduction p 54 A92-47495
- Microgravity vibration isolation: An optimal control law for the one-dimensional case
[NASA-TM-105146] p 141 N92-11217
- Space acceleration measurement system description and operations on the First Spacelab Life Sciences Mission
[NASA-TM-105301] p 57 N92-13151
- Thermal and solutal convection with conduction effects inside a rectangular enclosure
[NASA-TM-105371] p 186 N92-15358
- Microgravity combustion science: Progress, plans, and opportunities
[NASA-TM-105410] p 139 N92-27197

MICROMECHANICS

- Micromechanics for ceramic matrix composites
p 98 A92-10282
- Microstress analysis of periodic composites
p 218 A92-30673
- Combined bending and thermal fatigue of high-temperature metal-matrix composites - Computational simulation p 223 A92-43494
- Micromechanical model of crack growth in fiber reinforced brittle materials p 223 A92-46829
- Microfracture in high temperature metal matrix laminates
[NASA-TM-105189] p 106 N92-14122
- Differential continuum damage mechanics models for creep and fatigue of unidirectional metal matrix composites
[NASA-TM-105213] p 226 N92-16371
- Towards the development of micromechanics equations for ceramic matrix composites via fiber substructuring
[NASA-TM-105246] p 108 N92-19595
- COMGEN-BEM: Boundary element model generation for composite materials micromechanical analysis
[NASA-TM-105548] p 226 N92-19779
- Computational simulation of intermingled-fiber hybrid composite behavior
[NASA-TM-105666] p 110 N92-31506
- Effects of fiber and interfacial layer architectures on the thermoplastic response of metal matrix composites
[NASA-TM-105802] p 110 N92-32234
- Computational simulation of matrix micro-slip bands in SiC/Ti-15 composite
[NASA-TM-105762] p 111 N92-32466

MICROMETEORIODS

- Atomic oxygen undercutting of LDEF aluminized-Kapton multilayer insulation p 255 N92-24818
- Characteristics of hypervelocity impact craters on LDEF experiment S1003 and implications of small particle impacts on reflective surfaces p 269 N92-27252

MICROSCOPY

- Fluorescence microscopy for the characterization of structural integrity
[NASA-TM-105253] p 96 N92-18970

MICROSTRIP ANTENNAS

- Electromagnetic coupling between coplanar waveguide and microstrip antennas p 154 A92-21292
- Performance of a K-band superconducting annular ring antenna p 146 A92-37067
- Coplanar waveguide aperture-coupled microstrip patch antenna p 146 A92-37222
- Performance of a four-element Ka-band high-temperature superconducting microstrip antenna p 146 A92-37224
- Mutual coupling between rectangular microstrip patch antennas p 159 A92-52423
- Nonplanar linearly tapered slot antenna with balanced microstrip feed
[NASA-TM-105647] p 161 N92-23535
- An optically controlled Ka-band phased array antenna p 152 N92-32968

- Ka-band dual frequency array feed for a low cost ACTS ground terminal p 152 N92-32969
- Measurement techniques for cryogenic Ka-band microstrip antennas p 153 N92-32981

MICROSTRIP DEVICES

- Ka-band dual frequency array feed for a low cost ACTS ground terminal
[AIAA PAPER 92-1902] p 143 A92-29833

MICROSTRIP TRANSMISSION LINES

- Coplanar waveguide aperture coupled patch antennas with ground plane/substrate of finite extent
p 154 A92-24488
- Microwave conductivity of laser ablated YBa₂Cu₃O₇(δ) superconducting films and its relation to microstrip transmission line performance
p 264 N92-21639
- Coplanar waveguide feeds for phased array antennas p 152 N92-32970

MICROSTRUCTURE

- Microstructure and mechanical properties of a single crystal NiAl alloy with Zr or Hf rich G-phase precipitates p 119 A92-30841
- Microstructure and mechanical properties of near eutectic beta-NiAl plus alpha-Re alloys produced by rapid solidification and extrusion p 119 A92-30844
- Comments on the paper 'Does the subgrain size influence the rate of creep?' p 260 A92-33946
- Ultrasonic evaluation of oxygen content, modulus, and microstructure changes in YBa₂Cu₃O₇(δ) occurring during oxidation and reduction p 261 A92-38418
- Relationships between toughness and microstructure of reaction bonded Si₃N₄ p 125 A92-39687
- Three-dimensional deformation analysis of two-phase dislocation substructures p 121 A92-44218
- Influence of processing on the microstructure and mechanical properties of a NbAl₃-base alloy p 122 A92-48152
- CVD of silicon carbide on structural fibers: Microstructure and composition
[NASA-TM-105385] p 107 N92-18439
- Fluorescence microscopy for the characterization of structural integrity
[NASA-TM-105253] p 96 N92-18970
- Plasma etching a ceramic composite --- evaluating microstructure
[NASA-TM-105430] p 130 N92-22305
- A preliminary characterization of the tensile and fatigue behavior of tungsten-fiber/Waspaloy-matrix composite
[NASA-TM-105346] p 187 N92-22487
- Creep and fatigue research efforts on advanced materials p 227 N92-22514
- Aeropropulsion structures p 31 N92-22518
- Damage mechanisms in bithermal and thermomechanical fatigue of Haynes 188
[NASA-TM-105381] p 228 N92-24985
- Tribological and microstructural comparison of HIPped PM212 and PM212/Au self-lubricating composites
[NASA-TM-105615] p 97 N92-26142

MICROWAVE AMPLIFIERS

- Performance of a wideband GaAs low-noise amplifier at cryogenic temperatures p 156 A92-37953
- Operating and service manual for the NASA Lewis automated far-field antenna range
[NASA-TM-105343] p 52 N92-22319
- C-band superconductor/semiconductor hybrid field-effect transistor amplifier on a LaAlO₃ substrate
[NASA-TM-105828] p 163 N92-34204

MICROWAVE ANTENNAS

- Performance of a four-element Ka-band high-temperature superconducting microstrip antenna p 146 A92-37224
- Ka-band MMIC arrays for ACTS Aero Terminal Experiment
[IAF PAPER 92-0398] p 159 A92-55785
- Multiple-access phased array antenna simulator for a digital beam forming system investigation
[NASA-TM-105422] p 149 N92-17062
- Planar dielectric resonator stabilized HEMT oscillator integrated with CPW/aperture coupled patch antenna
[NASA-TM-105544] p 160 N92-18473
- Microwave beam power transmission at an arbitrary range
[NASA-TM-105424] p 150 N92-19992
- V-band pseudomorphic HEMT MMIC phased array components for space communications p 151 N92-32966
- Planar dielectric resonator stabilized HEMT oscillator integrated with CPW/aperture coupled patch antenna p 152 N92-32967
- An optically controlled Ka-band phased array antenna p 152 N92-32968
- Ka-band dual frequency array feed for a low cost ACTS ground terminal p 152 N92-32969
- Coplanar waveguide feeds for phased array antennas p 152 N92-32970

- Analysis of shielded CPW discontinuities with air-bridges p 152 N92-32971

MICROWAVE CIRCUITS

- Interfaces for high-speed fiber-optic links - Analysis and experiment p 256 A92-24002
- Advanced large scale GaAs monolithic IF switch matrix subsystem
[AIAA PAPER 92-1861] p 155 A92-29801
- Ka-band active MMIC subarray development
[AIAA PAPER 92-1863] p 155 A92-29803
- Advances in MMIC technology for communications satellites
[AIAA PAPER 92-1899] p 155 A92-29830
- High-performance packaging for monolithic microwave and millimeter-wave integrated circuits
[AIAA PAPER 92-1935] p 155 A92-31706
- New techniques for exciting linearly tapered slot antennas with coplanar waveguide p 155 A92-34844
- A vertically integrated Ka-band phased array antenna
[AIAA PAPER 92-1976] p 156 A92-38140
- Planar dielectric resonator stabilized HEMT oscillator integrated with CPW/aperture coupled patch antenna
[NASA-TM-105544] p 160 N92-18473
- Solid State Technology Branch of NASA Lewis Research Center
[NASA-TM-105159] p 151 N92-23412
- A 1-W, 30-GHz, CPW amplifier for ACTS small terminal uplink
[NASA-TM-105671] p 161 N92-26096
- High-performance packaging for monolithic microwave and millimeter-wave integrated circuits
[NASA-TM-105744] p 151 N92-31855
- V-band pseudomorphic HEMT MMIC phased array components for space communications p 151 N92-32966
- Planar dielectric resonator stabilized HEMT oscillator integrated with CPW/aperture coupled patch antenna p 152 N92-32967
- An optically controlled Ka-band phased array antenna p 152 N92-32968
- Coplanar waveguide feeds for phased array antennas p 152 N92-32970
- Analysis of shielded CPW discontinuities with air-bridges p 152 N92-32971
- A flexible CPW package for a 30 GHz MMIC amplifier p 152 N92-32972
- A 1-W, 30-GHz, CPW amplifier for ACTS small terminal uplink p 152 N92-32973
- Microwave properties of peeled HEMT devices sapphire substrates p 265 N92-32978
- C-band superconductor/semiconductor hybrid field-effect transistor amplifier on a LaAlO₃ substrate
[NASA-TM-105828] p 163 N92-34204

MICROWAVE COUPLING

- Coplanar waveguide aperture-coupled microstrip patch antenna p 146 A92-37222
- New coplanar waveguide to rectangular waveguide end launcher p 156 A92-44243
- Mutual coupling between rectangular microstrip patch antennas p 159 A92-52423

MICROWAVE EQUIPMENT

- Electrical-transport properties and microwave device performance of sputtered TiCaBaCuO superconducting thin films p 263 A92-56599
- Three point lead screw positioning apparatus
[NASA-CASE-LEW-15216-1] p 208 N92-17678

MICROWAVE FREQUENCIES

- dc and microwave performance of a 0.1-micron gate InAs/In(0.52)Al(0.48)As MODFET p 156 A92-43891
- Magnetic penetration depth of YBa₂Cu₃O₇(δ) thin films determined by the power transmission method p 265 N92-32983

MICROWAVE OSCILLATORS

- Submillimeter backward-wave oscillators p 155 A92-35054
- Planar dielectric resonator stabilized HEMT oscillator integrated with CPW/aperture coupled patch antenna
[NASA-TM-105544] p 160 N92-18473
- Planar dielectric resonator stabilized HEMT oscillator integrated with CPW/aperture coupled patch antenna p 152 N92-32967

MICROWAVE POWER BEAMING

- A mass sensitivity analysis of lunar orbiting beam power systems p 232 A92-50619
- Microwave beam power transmission at an arbitrary range
[NASA-TM-105424] p 150 N92-19992

MICROWAVE SWITCHING

- ACTS system capability and performance
[AIAA PAPER 92-1961] p 143 A92-29884

MICROWAVE TRANSMISSION

- Microwave properties of YBa₂Cu₃O₇(δ) high-transition-temperature superconducting thin films measured by the power transmission method p 153 A92-14938

MICROWAVES

- Coaxial line configuration for microwave power transmission study of $\text{YBa}_2\text{Cu}_3\text{O}(7-\delta)$ thin films p 154 A92-18455
- Interfaces for high-speed fiber-optic links - Analysis and experiment p 256 A92-24002
- 20/30 GHz satellite personal communications networks [AIAA PAPER 92-1908] p 143 A92-29839
- Dynamic rain fade compensation techniques for the advanced communications technology satellite [AIAA PAPER 92-2038] p 145 A92-31711

MICROWAVES

- Measurements of complex permittivity of microwave substrates in the 20 to 300 K temperature range from 26.5 to 40.0 GHz p 197 A92-13416
- Microwave electrothermal propulsion for space p 63 A92-46049
- Theoretical nozzle performance of a microwave electrothermal thruster using experimental data [AIAA PAPER 92-3110] p 64 A92-48750
- Large-scale microwave anisotropy from gravitating seeds p 269 A92-56914
- A software control system for the ACTS high-burst-rate link evaluation terminal [NASA-TM-105207] p 243 N92-16628
- Microwave conductivity of laser ablated $\text{YBa}_2\text{Cu}_3\text{O}(7-\delta)$ superconducting films and its relation to microstrip transmission line performance p 264 N92-21639
- Microwave response of high transition temperature superconducting thin films p 264 N92-23413
- Microwave properties of peeled HEMT devices sapphire substrates p 265 N92-32978

MIE SCATTERING

- Calculation of far-field scattering from nonspherical particles using a geometrical optics approach p 256 A92-20288

MILITARY HELICOPTERS

- Advanced Rotorcraft Transmission program summary [AIAA PAPER 92-3363] p 205 A92-48936
- Boeing Helicopters Advanced Rotorcraft Transmission (ART) Program summary of component tests [AIAA PAPER 92-3364] p 205 A92-48937
- Advanced Rotorcraft Transmission (ART) - Component test results [AIAA PAPER 92-3366] p 205 A92-48939
- The chemistry of Saudi Arabian sand: A deposition problem on helicopter turbine airfoils [NASA-TM-105234] p 128 N92-14179

MILLIMETER WAVES

- A low-power, high-efficiency Ka-band TWTA [AIAA PAPER 92-1822] p 154 A92-29769
- High-performance packaging for monolithic microwave and millimeter-wave integrated circuits [AIAA PAPER 92-1935] p 155 A92-31706
- A low-power, high-efficiency Ka-band TWTA p 156 A92-38163
- A high temperature superconductivity communications flight experiment [IAF PAPER 92-0410] p 50 A92-55790
- A flexible CPW package for a 30 GHz MMIC amplifier --- coplanar waveguide [NASA-TM-105630] p 161 N92-23193
- Monolithic mm-wave phase shifter using optically activated superconducting switches [NASA-CASE-LEW-14878-1] p 257 N92-28571
- High-performance packaging for monolithic microwave and millimeter-wave integrated circuits [NASA-TM-105744] p 151 N92-31855
- V-band pseudomorphic HEMT MMIC phased array components for space communications p 151 N92-32966
- A flexible CPW package for a 30 GHz MMIC amplifier p 152 N92-32972

MIMD (COMPUTERS)

- High order parallel numerical schemes for solving incompressible flows p 193 N92-25818

MIMO (CONTROL SYSTEMS)

- Identification of the Space Shuttle Main Engine dynamic models from firing data [AIAA PAPER 92-3317] p 73 A92-54022

MINIATURIZATION

- Miniature high temperature plug-type heat flux gauges [NASA-TM-105403] p 201 N92-18759

MINING

- Power supply for a manned international asteroid mission p 80 N92-13205

MINORITY CARRIERS

- Photoluminescence lifetime measurements in InP wafers p 262 A92-48092

MISALIGNMENT

- Analysis and modification of a single-mesh gear fatigue rig for use in diagnostic studies [NASA-TM-105416] p 212 N92-27879

MISSION PLANNING

- MisTec - A software application for supporting space exploration scenario options and technology development analysis and planning p 242 A92-38490
- [AIAA PAPER 92-1293]
- NASA program planning on nuclear electric propulsion [AIAA PAPER 92-1557] p 61 A92-38651
- Nuclear thermal propulsion workshop overview p 78 N92-11090

- Nuclear thermal rocket workshop reference system Rover/NERVA p 78 N92-11091

- Power management and distribution considerations for a lunar base [NASA-TM-105342] p 269 N92-13910

- MisTec: A software application for supporting space exploration scenario options and technology development analysis and planning p 243 N92-14649
- [NASA-TM-105214]

- Environmental interactions in Space Exploration: Announcement of the formation of an Environmental Interactions Working Group [NASA-TM-105294] p 270 N92-17069

- A compilation of lunar and Mars exploration strategies utilizing indigenous propellants [NASA-TM-105262] p 135 N92-19837

- Environmental interactions in space exploration: Environmental interactions working group p 239 N92-22382

- NASA programs in space photovoltaics [NASA-TM-105428] p 87 N92-25343

- A demonstration of an intelligent control system for a reusable rocket engine [NASA-TM-105794] p 92 N92-31507

MIXED OXIDES

- Microwave properties of $\text{YBa}_2\text{Cu}_3\text{O}(7-\delta)$ high-transition-temperature superconducting thin films measured by the power transmission method p 153 A92-14938
- Properties of large area $\text{ErBa}_2\text{Cu}_3\text{O}(7-x)$ thin films deposited by ionized cluster beams p 260 A92-33911
- Crystalline orientations of $\text{Ti}_2\text{Ba}_2\text{Ca}_2\text{Cu}_3\text{O}(x)$ grains on MgO , SrTiO_3 , and LaAlO_3 substrates p 261 A92-41637
- Electrical-transport properties and microwave device performance of sputtered TiCaBaCuO superconducting thin films p 263 A92-56599

MIXING LAYERS (FLUIDS)

- Model free simulations of a high speed reacting mixing layer [AIAA PAPER 92-0257] p 167 A92-25715
- Compressibility effects on large structures in free shear flows p 173 A92-39337
- Second order modeling of boundary-free turbulent shear flows p 174 A92-41275
- The influence of higher harmonics on vortex pairing in an axisymmetric mixing layer p 175 A92-46251
- Supersonic jet mixing enhancement by 'delta-tabs' [AIAA PAPER 92-3548] p 12 A92-49063
- Initial development of the axisymmetric ejector shear layer [AIAA PAPER 92-3567] p 178 A92-49068
- Filtered Rayleigh scattering based measurements in compressible mixing layers [AIAA PAPER 92-3543] p 182 A92-54043
- Study of compressible mixing layers using filtered Rayleigh scattering based visualizations p 183 A92-54937
- Supersonic jet mixing enhancement by delta-tabs [NASA-TM-105664] p 18 N92-24958

MIXING LENGTH FLOW THEORY

- Development of an algebraic turbulence model for analysis of propulsion flows p 183 A92-54209
- [AIAA PAPER 92-3861]
- Development of an algebraic turbulence model for analysis of propulsion flows [NASA-TM-105701] p 250 N92-27517

MODAL RESPONSE

- Aeroelastic modal characteristics of mistuned blade assemblies - Mode localization and loss of eigenstructure p 225 A92-54921
- Modal interaction in linear dynamic systems near degenerate modes [NASA-TM-105315] p 225 N92-12316
- Optimum design of a gearbox for low vibration [NASA-TM-105653] p 212 N92-28476

MODELS

- Stochastic modeling of crack initiation and short-crack growth under creep and creep-fatigue conditions [ASME PAPER 92-APM-5] p 223 A92-44681

MODEMS

- Flexible digital modulation and coding synthesis for satellite communications p 148 N92-14235
- NASA, Lewis Research Center Advanced Modulation and Coding Project: Introduction and overview p 51 N92-22002

MODFETS

- dc and microwave performance of a 0.1-micron gate $\text{InAs}/\text{In}(0.52)\text{Al}(0.48)\text{As}$ MODFET p 156 A92-43891
- Intermodulation in the oscillatory magnetoresistance of a two-dimensional electron gas p 163 N92-32975
- Study of InGaAs -based modulation doped field effect transistor structures using variable-angle spectroscopic ellipsometry p 265 N92-32977

MODULARITY

- Multi-reactor power system configurations for multimegawatt nuclear electric propulsion [NASA-TM-105212] p 77 N92-10057

MODULATION

- Enhancement of Shubnikov-de Haas oscillations by carrier modulation p 262 A92-50911
- Least Reliable Bits Coding (LRBC) for high data rate satellite communications [NASA-TM-105431] p 150 N92-18921
- Advanced Modulation and Coding Technology Conference [NASA-CP-10053] p 51 N92-22001
- NASA, Lewis Research Center Advanced Modulation and Coding Project: Introduction and overview p 51 N92-22002

MODULATION DOPING

- High-field transport properties of $\text{InAs}(\text{x})\text{P}(1-\text{x})/\text{InP}$ ($x = 0.3-1.0$) modulation doped heterostructures at 300 and 77 K p 262 A92-46331

MODULES

- Space Station Freedom solar dynamic modules structural modelling and analysis [NASA-TM-104506] p 226 N92-15405

MODULUS OF ELASTICITY

- Ultrasonic evaluation of oxygen content, modulus, and microstructure changes in $\text{YBa}_2\text{Cu}_3\text{O}(7-x)$ occurring during oxidation and reduction p 261 A92-38418

MOLECULAR BEAM EPITAXY

- Study of InGaAs -based modulation doped field effect transistor structures using variable-angle spectroscopic ellipsometry p 265 N92-32977

MOLECULAR DIFFUSION

- A computer model for one-dimensional mass and energy transport in and around chemically reacting particles, including complex gas-phase chemistry, multicomponent molecular diffusion, surface evaporation, and heterogeneous reaction p 181 A92-52406

MOLECULAR WEIGHT

- High molecular weight first generation PMR polyimides for 343 C applications p 105 A92-49819
- High molecular weight first generation PMR polyimides for 343 C applications [NASA-TM-105364] p 129 N92-19498
- Vinyl capped addition polyimides [NASA-CASE-LEW-15027-2] p 131 N92-24053
- Cyclopentadiene evolution during pyrolysis-gas chromatography of PMR polyimides [NASA-TM-105629] p 132 N92-25348

MOLTEN SALTS

- Observations of the freeze/thaw performance of lithium fluoride by motion picture photography p 180 A92-50751

MOLYBDENUM OXIDES

- A vacuum ($10(\text{exp } -9)$ Torr) friction apparatus for determining friction and endurance life of MoS_x films [NASA-TM-104478] p 129 N92-16129

MOMENTS OF INERTIA

- Influence of mass moment of inertia on normal modes of preloaded solar array mast [NASA-TP-3273] p 230 N92-33476

MOMENTUM

- Experimental study of boundary layer transition on a heated flat plate p 172 A92-36022

MOMENTUM TRANSFER

- Hall voltage sign reversal in thin superconducting films p 261 A92-35349

MONITORS

- Description of real-time Ada software implementation of a power system monitor for the Space Station Freedom PMAD DC testbed p 242 A92-50533
- Integrated health monitoring and controls for rocket engines [NASA-TM-105763] p 90 N92-28693

MONOMERS

- Cyclopentadiene evolution during pyrolysis-gas chromatography of PMR polyimides [NASA-TM-105629] p 132 N92-25348

MONOPROPELLANTS

- Gelled liquid oxygen/metal powder monopropellants [AIAA PAPER 92-3450] p 134 A92-49004
- Metallized gelled monopropellants [NASA-TM-105418] p 87 N92-24557

MONTE CARLO METHOD

- Internal structure of shock waves in disparate mass mixtures [AIAA PAPER 92-0496] p 169 A92-28195

- FDDO and DSMC analyses of rarefied gas flow through 2D nozzles
[AIAA PAPER 92-2858] p 176 A92-47841
- DSMC analysis of species separation in rarefied nozzle flows
[AIAA PAPER 92-2859] p 176 A92-47842
- Monte Carlo exploration of Mikheyev-Smirnov-Wolfenstein solutions to the solar neutrino problem p 270 A92-50927
- Further study of the effect of the downstream plasma condition on accelerator grid erosion in an ion thruster [AIAA PAPER 92-3829] p 76 A92-54192
- Monte Carlo modeling of atomic oxygen attack of polymers with protective coatings on LDEF p 132 N92-27281
- MOON**
Environmental interactions in Space Exploration: Announcement of the formation of an Environmental Interactions Working Group [NASA-TM-105294] p 270 N92-17069
- MORPHOLOGY**
Surface morphologies and photoluminescence of diamond films deposited in a hot filament reactor p 261 A92-42858
- MOUNTING**
Removable hand hold [NASA-CASE-LEW-15196-1] p 213 N92-29092
- MTBF**
Transmission overhaul and component replacement predictions using Weibull and renewal theory p 215 A92-17201
- MULTIBEAM ANTENNAS**
Technology requirements for mesh VSAT applications [AIAA PAPER 92-1982] p 144 A92-29902
- Advanced Communications Technology Satellite (ACTS) p 50 A92-38164
- The ACTS multibeam antenna p 146 A92-46046
- Advanced Communication Technology Satellite (ACTS) baseband processor development p 50 A92-53693
- Advanced Communication Technology Satellite (ACTS) multibeam antenna technology verification experiments [NASA-TM-105421] p 149 N92-16191
- Advanced Communication Technology Satellite (ACTS) multibeam antenna analysis and experiment [NASA-TM-105420] p 149 N92-17047
- Analysis of a generalized dual reflector antenna system using physical optics [NASA-TM-105425] p 149 N92-18281
- The ACTS multibeam antenna [NASA-TM-105645] p 52 N92-30383
- Characteristics of a future aeronautical satellite communications system p 151 N92-30932
- MULTICHANNEL COMMUNICATION**
A multi-channel demultiplexer/demodulator architecture, simulation and implementation [AIAA PAPER 92-1972] p 144 A92-29895
- MULTIENGINE VEHICLES**
Overview of the Beta II Two-Stage-To-Orbit vehicle design [NASA-TM-105298] p 48 N92-11034
- MULTIGRID METHODS**
Euler solutions for an unbladed jet engine configuration [AIAA PAPER 92-0544] p 169 A92-28201
- Multigrad calculations of a jet in crossflow p 170 A92-28525
- Multigrad calculation of three-dimensional viscous cascade flows [NASA-TM-105257] p 249 N92-10345
- Euler solutions for an unbladed jet engine configuration [NASA-TM-105332] p 184 N92-11328
- Multigrad acceleration and turbulence models for computations of 3D turbulent jets in crossflow [NASA-TM-105306] p 186 N92-18775
- MAG3D and its application to internal flowfield analysis p 243 N92-24421
- Workshop on Grid Generation and Related Areas [NASA-CP-10089] p 35 N92-25712
- QX MAN: Q and X file manipulation p 244 N92-25715
- Multiblock grid generation for jet engine configurations p 35 N92-25720
- MULTILAYER INSULATION**
A review of candidate multilayer insulation systems for potential use on wet-launched LH2 tankage for the space exploration initiative lunar missions [NASA-TM-104493] p 134 N92-13336
- Atomic oxygen undercutting of LDEF aluminized-Kapton multilayer insulation p 255 N92-24818
- MULTIPHASE FLOW**
Particle-laden weakly swirling free jets: Measurements and predictions [NASA-TM-100881] p 29 N92-14061
- MULTIPLE ACCESS**
Advanced large scale GaAs monolithic IF switch matrix subsystem [AIAA PAPER 92-1861] p 155 A92-29801
- Circuit-switch architecture for a 30/20-GHz FDMA/TDM geostationary satellite communications network [AIAA PAPER 92-2005] p 49 A92-29924
- Circuit-switch architecture for a 30/20-GHz FDMA/TDM geostationary satellite communications network [NASA-TM-105302] p 51 N92-15109
- Multiple-access phased array antenna simulator for a digital beam forming system investigation [NASA-TM-105422] p 149 N92-17062
- MULTIPLEXING**
Multichannel demultiplexer/demodulator technologies for future satellite communication systems [NASA-TM-105377] p 51 N92-18342
- MULTIPROCESSING (COMPUTERS)**
Interfacing laboratory instruments to multiuser, virtual memory computers p 245 A92-13595
- MULTISTAGE ROCKET VEHICLES**
Overview of the Beta II Two-Stage-To-Orbit vehicle design [NASA-TM-105298] p 48 N92-11034
- Beta 2: A near term, fully reusable, horizontal takeoff and landing two-stage-to-orbit launch vehicle concept p 86 N92-21536
- MULTIVARIABLE CONTROL**
State space representation of the open-loop dynamics of the Space Shuttle Main Engine p 59 A92-19607
- Design and evaluation of a robust dynamic neurocontroller for a multivariable aircraft control problem [NASA-TM-105579] p 40 N92-20586
- A demonstration of an intelligent control system for a reusable rocket engine [NASA-TM-105794] p 92 N92-31507
- MYLAR (TRADEMARK)**
Atomic oxygen interactions with FEP Teflon and silicones on LDEF p 132 N92-24820
- N**
- N-TYPE SEMICONDUCTORS**
"Wrong" bond interactions at inversion domain boundaries in GaAs p 260 A92-27297
- Minority carrier lifetime in indium phosphide p 262 A92-53148
- Anodic etching of p-type cubic silicon carbide p 127 A92-57027
- NARROWBAND**
Future communications satellite applications p 52 N92-22019
- Selective emitters [NASA-CASE-LEW-14731-1] p 236 N92-22037
- NASA PROGRAMS**
The NASA microgravity combustion space experiment program [IAF PAPER 91-398] p 112 A92-18484
- IMPAC - An integrated methodology for propulsion and airframe control p 39 A92-29118
- Advanced Communications Technology Satellite (ACTS) Experiments Program - A market-driven approach to government/industry cooperation [AIAA PAPER 92-2036] p 145 A92-29951
- Network architectures and protocols for the integration of ACTS and ISDN [AIAA PAPER 92-2039] p 145 A92-29953
- The NASA-OAST earth-to-orbit propulsion technology program - The action plan [AIAA PAPER 92-1478] p 61 A92-38597
- NASA's high-temperature engine materials program for civil aeronautics p 95 A92-41117
- NASA's nuclear electric propulsion technology project [AIAA PAPER 92-3705] p 76 A92-57033
- Early use of Space Station Freedom for NASA's Microgravity Science and Applications Program [IAF PAPER 92-0702] p 138 A92-57131
- Safety issues p 78 N92-11115
- Structural Dynamics Branch research and accomplishments for FY 1990 [NASA-TM-103747] p 226 N92-15406
- NASA's aircraft icing technology program [NASA-TM-104518] p 17 N92-23105
- The future challenge for aeropropulsion [NASA-TM-105613] p 35 N92-25164
- NASA programs in space photovoltaics [NASA-TM-105428] p 87 N92-25343
- NASA Surface-Modeling and Grid-Generation (SM/GG) activities p 267 N92-25725
- NASA's nuclear electric propulsion technology project [NASA-TM-105811] p 93 N92-32463
- Solid State Technology Branch of NASA Lewis Research Center [NASA-TM-105752] p 151 N92-32965
- NASA SPACE PROGRAMS**
Nuclear rocket propulsion technology - A joint NASA/DOE project [IAF PAPER 91-236] p 58 A92-13159
- Innovative nuclear thermal propulsion technology evaluation - Results of the NASA/DOE task team study [IAF PAPER 91-235] p 58 A92-13160
- A full field, 3-D velocimeter for NASA's microgravity science program [AIAA PAPER 92-0784] p 56 A92-27119
- NASA program planning on nuclear electric propulsion [AIAA PAPER 92-1557] p 61 A92-38651
- Nuclear thermal rockets - Key to moon-Mars exploration p 63 A92-48385
- Nuclear rocket propulsion: NASA plans and progress - FY 1991 p 69 A92-50584
- NASA's nuclear thermal propulsion technology project [AIAA PAPER 92-3581] p 75 A92-54062
- NASTRAN**
FREPS - A forced response prediction system for turbomachinery blade rows [AIAA PAPER 92-3072] p 242 A92-54006
- Computational simulation of surface waviness in graphite/epoxy woven composites due to initial curing [NASA-TM-105313] p 106 N92-14118
- Space Station Freedom solar dynamic modules structural modeling and analysis [NASA-TM-104506] p 226 N92-15405
- Structural analysis of low-speed composite propfan blades for the LRCSW wind tunnel model [NASA-TM-105266] p 229 N92-25753
- NATIONAL AEROSPACE PLANE PROGRAM**
Slush hydrogen (SLH2) technology development for application to the National Aerospace Plane (NASP) p 140 A92-13432
- The F/A-18 external burning flight test [AIAA PAPER 91-5050] p 23 A92-44547
- Slush hydrogen pressurized expulsion studies at the NASA K-Site Facility [AIAA PAPER 92-3385] p 141 A92-48951
- Modelling and experimental verification of a water alleviation system for the NASP --- National Aerospace Plane [NASA-TM-105661] p 189 N92-23224
- High temperature dynamic engine seal technology development [NASA-TM-105641] p 209 N92-23435
- Slush hydrogen transfer studies at the NASA K-Site Test Facility [NASA-TM-105596] p 135 N92-25957
- Slush hydrogen pressurized expulsion studies at the NASA K-Site Facility [NASA-TM-105597] p 135 N92-26131
- NAVIER-STOKES EQUATION**
Deterministic blade row interactions in a centrifugal compressor stage [ASME PAPER 91-GT-273] p 3 A92-15670
- Navier-Stokes analysis of flow and heat transfer inside high-pressure-ratio transonic turbine blade rows p 165 A92-17193
- Eigenvalue calculation procedure for an Euler/Navier-Stokes solver with application to flows over airfoils p 3 A92-17429
- Convection in superposed fluid and porous layers p 166 A92-24752
- Analysis of an advanced ducted propeller subsonic inlet [AIAA PAPER 92-0274] p 5 A92-25728
- Conical detonation waves - A comparison of theoretical and numerical results [AIAA PAPER 92-0348] p 167 A92-25792
- Navier-Stokes analysis of turbomachinery blade external heat transfer p 170 A92-28518
- Navier-Stokes solution of transonic cascade flows using nonperiodic C-type grids p 8 A92-28523
- Upwind relaxation methods for the Navier-Stokes equations using inner iterations p 170 A92-29553
- A numerical and experimental study of three-dimensional liquid sloshing in a rotating spherical container [AIAA PAPER 92-0829] p 170 A92-29597
- Features of wavy vortices in a curved channel from experimental and numerical studies p 171 A92-31638
- Design and analysis of reengine Boeing 727-100 center inlet S duct by a reduced Navier-Stokes code [AIAA PAPER 92-1221] p 8 A92-33320
- Upwind differencing and LU factorization for chemical non-equilibrium Navier-Stokes equations p 171 A92-33829
- A least-squares finite element method for incompressible Navier-Stokes problems p 173 A92-37387
- A study of three dimensional turbulent boundary layer separation and vortex flow control using the reduced Navier Stokes equations p 9 A92-40105
- Numerical analysis of flow through oscillating cascade sections p 9 A92-44513

NEAR FIELDS

Experimental and analytical study of close-coupled ventral nozzles for ASTOVL aircraft p 26 A92-45325

Navier-Stokes analysis and experimental data comparison of compressible flow in a diffusing S-duct [AIAA PAPER 92-2699] p 10 A92-45541

Design and analysis of vortex generators on reengineered Boeing 727-100QF center inlet S-duct by a reduced Navier-Stokes code p 10 A92-45542

Comparison of the SMAC, PISO, and iterative time-advancing schemes for unsteady flows p 175 A92-47158

Navier-Stokes turbine heat transfer predictions using two-equation turbulence closures [AIAA PAPER 92-3067] p 177 A92-48721

Computational analysis of ramjet engine inlet interaction [AIAA PAPER 92-3102] p 11 A92-48744

Propulsion-related flowfields using the preconditioned Navier-Stokes equations p 178 A92-48994

A computational study of advanced exhaust system transition ducts with experimental validation [AIAA PAPER 92-3794] p 179 A92-49126

Three-dimensional Navier-Stokes heat transfer predictions for turbine blade rows [AIAA PAPER 92-3068] p 12 A92-54003

Increased heat transfer to elliptical leading edges due to spanwise variations in the freestream momentum - Numerical and experimental results [AIAA PAPER 92-3070] p 13 A92-54005

An investigation of shock/turbulent boundary layer bleed interactions [AIAA PAPER 92-3085] p 182 A92-54008

Full Navier-Stokes calculations on the installed F/A-18 inlet at a high angle of attack [AIAA PAPER 92-3175] p 13 A92-54012

Application of computational fluid dynamics to the study of vortex flow control for the management of inlet distortion [AIAA PAPER 92-3177] p 13 A92-54013

Navier-Stokes analysis of three-dimensional unsteady flows inside turbine stages [AIAA PAPER 92-3211] p 13 A92-54016

Full Navier-Stokes analysis of a two-dimensional mixer/ejector nozzle for noise suppression [AIAA PAPER 92-3570] p 27 A92-54059

A time-accurate algorithm for chemical non-equilibrium viscous flows at all speeds [AIAA PAPER 92-3639] p 182 A92-54112

A finite-volume numerical method to calculate fluid forces and rotordynamic coefficients in seals [AIAA PAPER 92-3712] p 183 A92-54132

Numerical study of low pressure nuclear thermal rockets [AIAA PAPER 92-3815] p 75 A92-54182

An efficient and robust algorithm for two dimensional time dependent incompressible Navier-Stokes equations: High Reynolds number flows [NASA-TM-104424] p 184 A92-11320

Analysis of an advanced ducted propeller subsonic inlet [NASA-TM-105393] p 15 A92-14002

An iterative implicit diagonally-dominant factorization algorithm for solving the Navier-Stokes equations [NASA-TM-105259] p 249 A92-16663

Implementation/validation of a low Reynolds number two-equation turbulence model in the Proteus Navier-Stokes code: Two-dimensional/axisymmetric [NASA-TM-105619] p 187 A92-20520

ULTRA-SHARP solution of the Smith-Hutton problem [NASA-TM-105435] p 187 A92-22226

An investigation of DTNS2D for use as an incompressible turbulence modelling test-bed [NASA-TM-105593] p 249 A92-22230

Inlets, ducts, and nozzles p 188 A92-22523

Turbomachinery p 32 A92-22524

Development of new flux splitting schemes p 189 A92-23343

Two-dimensional unstructured triangular grid generation p 192 A92-25721

Cartesian based grid generation/adaptive mesh refinement p 192 A92-25722

An iterative implicit DDADI algorithm for solving the Navier-Stokes equation --- upwind split flux technique p 192 A92-25810

The Proteus Navier-Stokes code --- two and three dimensional computational fluid dynamics p 192 A92-25811

An efficient and robust algorithm for time dependent viscous incompressible Navier-Stokes equations p 193 A92-25819

Turbulence and deterministic chaos --- computational fluid dynamics p 194 A92-25823

A critical evaluation of a three-dimensional Navier-Stokes method as a tool to calculate transonic flows inside a low-aspect-ratio compressor p 195 A92-27459

Full Navier-Stokes analysis of a two-dimensional mixer/ejector nozzle for noise suppression [NASA-TM-105715] p 37 A92-28419

Navier-Stokes analysis and experimental data comparison of compressible flow within ducts [NASA-TM-105796] p 38 A92-30972

A critical evaluation of a three-dimensional Navier-Stokes CFD as a tool to design supersonic turbine stages p 196 A92-32268

Three-dimensional flow fields inside a shrouded inducer at design and off-design conditions (CFD study) p 196 A92-32291

Navier-Stokes analysis and experimental data comparison of compressible flow in a diffusing S-duct [NASA-TM-105683] p 38 A92-33746

NEAR FIELDS

Experimental and numerical investigations of low-density nozzle and plume flows of nitrogen p 183 A92-54917

NETWORK ANALYSIS

Modeled performance of monolithic, 3-terminal InP/Ga(0.47)In(0.53)As concentrator solar cells as a function of temperature and concentration ratio p 234 A92-53153

NETWORK CONTROL

Predictive onboard flow control in packet switching satellites [AIAA PAPER 92-2004] p 144 A92-29923

Space Communications Technology Conference: Onboard Processing and Switching [NASA-CP-3132] p 147 A92-14202

Predictive onboard flow control for packet switching satellites [NASA-TM-105566] p 150 A92-19379

NETWORK SYNTHESIS

High-performance packaging for monolithic microwave and millimeter-wave integrated circuits [AIAA PAPER 92-1935] p 155 A92-31706

Theoretical modeling, near-optimum design and predicted performance of n(+)/pp(+)- and p(+)/nn(+)- indium phosphide homojunction solar cells p 234 A92-53152

NEURAL NETS

A failure diagnosis system based on a neural network classifier for the Space Shuttle Main Engine p 245 A92-11474

Neurobiological computational models in structural analysis and design p 245 A92-14509

A real time neural net estimator of fatigue life p 245 A92-21694

Failure diagnosis for the Space Shuttle main engine p 60 A92-28137

Design of multi-layer neural networks for accurate identification of nonlinear mappings p 246 A92-29030

Predictive onboard flow control in packet switching satellites [AIAA PAPER 92-2004] p 144 A92-29923

Minimizing distortion in truss structures - A Hopfield network solution [AIAA PAPER 92-2302] p 220 A92-34523

Neural network based decomposition in optimal structural synthesis p 247 A92-41895

Applications of artificial neural nets in structural mechanics p 223 A92-47283

Self-aligning optical measurement systems p 247 A92-50387

Predictive onboard flow control for packet switching satellites [NASA-TM-105566] p 150 A92-19379

Design and evaluation of a robust dynamic neurocontroller for a multivariable aircraft control problem [NASA-TM-105579] p 40 A92-20586

Implementation of an intelligent control system [NASA-TM-105795] p 241 A92-33897

NEUTRAL GASES

Theory of plasma contactor neutral gas emissions for electrodynamic tethers p 258 A92-41549

NEUTRINOS

Constraints to the decays of Dirac neutrinos from SN 1987A p 255 A92-36249

Massive Dirac neutrinos and SN 1987A p 268 A92-45808

NEUTRON DIFFRACTION

Near-edge study of gold-substituted YBa₂Cu₃O(7-delta) p 259 A92-14950

NEUTRON STARS

Constraints to the decays of Dirac neutrinos from SN 1987A p 255 A92-36249

Massive Dirac neutrinos and SN 1987A p 268 A92-45808

NEWTON METHODS

Application of Newton modified barrier method (NMBM) to structural optimization [AIAA PAPER 92-2498] p 220 A92-34555

Development of a steady potential solver for use with linearized, unsteady aerodynamic analyses [NASA-TM-105288] p 31 A92-20525

NEWTON-RAPHSON METHOD

A study of equation solvers for linear and non-linear finite element analysis on parallel processing computers [AIAA PAPER 92-2478] p 242 A92-34367

NEWTONIAN FLUIDS

Lewis icing research tunnel test of the aerodynamic effects of aircraft ground deicing/anti-icing fluids [NASA-TP-3238] p 22 A92-30395

NICKEL

Fatigue damage accumulation in nickel prior to crack initiation p 120 A92-33947

Progress in the development of lightweight nickel electrode for aerospace applications [NASA-TM-105591] p 236 A92-20493

Sinterless contacts to shallow junction InP solar cells [NASA-TM-105670] p 237 A92-24802

Progress in the development of lightweight nickel electrode [NASA-TM-105638] p 116 A92-26670

NICKEL ALLOYS

Oxidation-chlorination of binary Ni-Cr alloys in flowing Ar-O₂-Cl₂ gas mixtures at 1200 K p 112 A92-17296

Slow strain rate 1200-1400 K compressive properties of NiAl-1Hf p 116 A92-17977

A viscoplastic theory for anisotropic materials [ONERA, TP NO. 1992-90] p 217 A92-24721

Compressive strength of directionally solidified NiAl-NiAlNb intermetallics at 1200 and 1300 K p 117 A92-28248

Does a threshold stress for creep exist in HfC-dispersed NiAl? p 118 A92-30780

Flow and fracture behavior of NiAl in relation to the brittle-to-ductile transition temperature p 118 A92-30781

The mechanical properties of a Ni-30Al-20Fe-0.05Zr intermetallic alloy in the temperature range 300-1200 K p 118 A92-30793

On improving the fracture toughness of a NiAl-based alloy by mechanical alloying p 118 A92-30794

Microstructure and mechanical properties of a single crystal NiAl alloy with Zr or Hf rich G-phase precipitates p 119 A92-30841

Microstructure and mechanical properties of near eutectic beta-NiAl plus alpha-Re alloys produced by rapid solidification and extrusion p 119 A92-30844

COSP - A computer model of cyclic oxidation p 114 A92-31849

Lattice parameters of fcc binary alloys using a new semiempirical method p 120 A92-32898

Correlation of deformation mechanisms with the tensile and compressive behavior of NiAl and NiAl(Zr) intermetallic alloys p 120 A92-38019

1200 and 1300 K slow plastic compression properties of Ni-50Al composites p 102 A92-38125

The decrease in yield strength in NiAl due to hydrostatic pressure p 120 A92-38990

1400 and 1500 K compressive creep properties of a NiAl-AlN composite p 103 A92-41575

Fracture behavior of a B2 Ni-30Al-20Fe-0.05Zr intermetallic alloy in the temperature range 300 to 1300 K p 121 A92-41667

Deformation behavior of a Ni-30Al-20Fe-0.05Zr intermetallic alloy in the temperature range 300 to 1300 K p 121 A92-41668

Ductility enhancement from interface dislocation sources in a directionally solidified beta + gamma + gamma-prime Ni-Fe-Al composite alloy p 122 A92-46850

Initial evaluation of continuous fiber reinforced NiAl composites p 104 A92-46867

Cyclic oxidation resistance of a reaction milled NiAl-AlN composite p 105 A92-46871

Compatibility of potential reinforcing ceramics with Ni and Fe aluminides p 105 A92-46874

Comparison of high temperature, high frequency core loss and dynamic B-H loops of two 50 Ni-Fe crystalline alloys and an iron-based amorphous alloy p 157 A92-50551

NICKEL CADMIUM BATTERIES

Space batteries for mobile battlefield power applications p 231 A92-29679

NASA Aerospace Flight Battery Systems Program: An update p 237 A92-22741

Results of a technical analysis of the Hubble Space Telescope nickel-cadmium and nickel-hydrogen batteries p 89 A92-27167

NICKEL COMPOUNDS

Fracture toughness and the effects of stress state on fracture of nickel aluminides p 117 A92-27422

- The effect of strain rate and temperature on the tensile properties of NiAl p 117 A92-28113
- Oxidation of Al₂O₃ continuous fiber-reinforced/NiAl composites p 106 A92-57029
- NICKEL HYDROGEN BATTERIES**
- Space batteries for mobile battlefield power applications p 231 A92-29679
- Electrochemical impregnation and cycle life of lightweight nickel electrodes for nickel-hydrogen cells p 113 A92-30978
- Effect of KOH concentration on LEO cycle life of IPV nickel-hydrogen flight cell - Update II p 232 A92-48212
- Nickel-hydrogen cell low-earth-orbit life test update p 70 A92-50700
- Effect of KOH concentration on LEO cycle life of IPV nickel-hydrogen flight cells - An update p 70 A92-50702
- Destructive physical analysis results of Ni/H₂ cells cycled in LEO regime p 70 A92-50707
- Effect of LEO cycling on 125 Ah advanced design IPV nickel-hydrogen flight cells - An update p 71 A92-50708
- Thermal modeling of nickel-hydrogen battery cells operating under transient orbital conditions p 71 A92-50712
- Effect of KOH concentration on LEO cycle life of IPV nickel-hydrogen flight cells-update 2 [NASA-TM-105314] p 235 N92-13483
- Progress in the development of lightweight nickel electrode for aerospace applications [NASA-TM-105591] p 236 N92-20493
- Composite overwrapped nickel-hydrogen pressure vessels p 109 N92-22762
- Progress in the development of lightweight nickel electrode [NASA-TM-105638] p 116 N92-26670
- Results of a technical analysis of the Hubble Space Telescope nickel-cadmium and nickel-hydrogen batteries p 89 N92-27167
- Validation test of advanced technology for IPV nickel-hydrogen flight cells. Update [NASA-TM-105689] p 89 N92-27878
- NIONIUM**
- Advanced liquid rockets [NASA-TM-105633] p 87 N92-24560
- NIONIUM ALLOYS**
- Solidification processing of intermetallic Nb-Al alloys p 120 A92-33866
- Effect of fiber strength on the room temperature tensile properties of SiC/Ti-24Al-11Nb p 102 A92-36389
- Influence of processing on the microstructure and mechanical properties of a NbAl₃-base alloy p 122 A92-48152
- NIONIUM COMPOUNDS**
- Protective Al₂O₃ scale formation on NbAl₃-base alloys p 119 A92-31850
- NITROGEN**
- Saturated fluorescence measurements of the hydroxyl radical in laminar high-pressure C₂H₆/O₂/N₂ flames p 198 A92-33987
- Experimental and numerical investigations of low-density nozzle and plume flows of nitrogen p 183 A92-54917
- An optical method for determining level in two-phase cryogenic fluids [NASA-TM-104524] p 200 N92-15366
- NITROGEN OXIDES**
- CFD analysis of jet mixing in low NO(x) flametube combustors [ASME PAPER 91-GT-217] p 24 A92-15634
- A simplified reaction mechanism for prediction of NO(x) emissions in the combustion of hydrocarbons [AIAA PAPER 92-3340] p 114 A92-48919
- NITROGEN TETROXIDE**
- Test experience, 490 N high performance (321 sec lsp) engine [AIAA PAPER 92-3800] p 67 A92-49127
- NOISE (SOUND)**
- Turbomachinery noise p 253 N92-10601
- Comparison of analysis and experiment for gearbox noise [NASA-TM-105330] p 210 N92-25396
- Effect of operating conditions on gearbox noise [NASA-TM-105331] p 211 N92-26107
- NOISE GENERATORS**
- Screech noise source structure of a supersonic rectangular jet [AIAA PAPER 92-0503] p 6 A92-26932
- Combustion and core noise p 254 N92-10607
- Screech noise source structure of a supersonic rectangular jet [NASA-TM-105384] p 15 N92-14000
- Effect of operating conditions on gearbox noise [NASA-TM-105331] p 211 N92-26107
- NOISE INTENSITY**
- Screech noise source structure of a supersonic rectangular jet [AIAA PAPER 92-0503] p 6 A92-26932
- Screech noise source structure of a supersonic rectangular jet [NASA-TM-105384] p 15 N92-14000
- NOISE MEASUREMENT**
- A theoretical and experimental study of the noise behavior of subharmonically injection locked local oscillators p 157 A92-46080
- Detailed noise measurements on the SR-7A propeller: Tone behavior with helical tip Mach number [NASA-TM-105206] p 255 N92-16705
- NOISE PREDICTION**
- Validation of finite element and boundary element methods for predicting structural vibration and radiated noise [NASA-TM-105359] p 213 N92-29697
- NOISE PREDICTION (AIRCRAFT)**
- A survey of the broadband shock associated noise prediction methods [AIAA PAPER 92-0501] p 252 A92-26930
- A review of computational/experimental methodology developments in aeroacoustics p 253 A92-39241
- Noise of two high-speed model counter-rotation propellers at takeoff/approach conditions p 253 A92-46799
- A survey of the broadband shock associated noise prediction methods [NASA-TM-105365] p 254 N92-14797
- NOISE PROPAGATION**
- Statistical energy analysis of a geared rotor system p 204 A92-39227
- NOISE REDUCTION**
- Advanced Rotorcraft Transmission (ART) Program summary [AIAA PAPER 92-3365] p 205 A92-48938
- Summary highlights of the Advanced Rotorcraft Transmission (ART) program [AIAA PAPER 92-3362] p 23 A92-54026
- Full Navier-Stokes analysis of a two-dimensional mixer/ejector nozzle for noise suppression [AIAA PAPER 92-3570] p 27 A92-54059
- An evaluation of some alternative approaches for reducing fan tone noise [NASA-TM-105356] p 255 N92-18282
- Performance of a Y-Ba-Cu-O superconducting filter/GaAs low noise amplifier hybrid circuit [NASA-TM-105546] p 160 N92-21370
- Advanced Rotorcraft Transmission (ART) program summary [NASA-TM-105665] p 210 N92-24984
- Full Navier-Stokes analysis of a two-dimensional mixer/ejector nozzle for noise suppression [NASA-TM-105715] p 37 N92-28419
- Performance of a Y-Ba-Cu-O superconducting filter/GaAs low noise amplifier hybrid circuit p 163 N92-32982
- NONDESTRUCTIVE TESTS**
- Mechanical behavior of fiber reinforced SiC/RBSN ceramic matrix composites - Theory and experiment --- Reaction Bonded Silicon Nitride [ASME PAPER 91-GT-209] p 99 A92-15629
- NDE of advanced turbine engine components and materials by computed tomography [ASME PAPER 91-GT-287] p 215 A92-15681
- Effect of heat treatment on stiffness and damping of SiC/Ti-15-3 p 100 A92-25627
- Effect of heat treatment on stiffness and damping of SiC/Ti-15-3 [NASA-TM-105564] p 108 N92-20841
- Detecting Lamb waves with broad-band acousto-ultrasonic signals in composite structures [NASA-TM-105557] p 216 N92-23189
- X ray attenuation measurements for high-temperature materials characterization and in-situ monitoring of damage accumulation [NASA-TM-105577] p 110 N92-25996
- NONEQUILIBRIUM FLOW**
- Improved nonequilibrium viscous shock-layer scheme for hypersonic blunt-body flowfields p 4 A92-24653
- Upwind differencing and LU factorization for chemical non-equilibrium Navier-Stokes equations p 171 A92-33829
- The Osher scheme for non-equilibrium reacting flows p 176 A92-48149
- A time-accurate algorithm for chemical non-equilibrium viscous flows at all speeds [AIAA PAPER 92-3639] p 182 A92-54112
- NONGRAY GAS**
- Nongray radiative gas analyses using the S-N discrete ordinates method p 266 A92-15443
- NONLINEAR EQUATIONS**
- Nonlinear dynamics near the stability margin in rotating pipe flow p 165 A92-19959
- A Lyapunov based nonlinear control scheme for stabilizing a basic compression system using a close-coupled control valve p 246 A92-29316
- NONLINEAR EVOLUTION EQUATIONS**
- Subharmonic route to boundary-layer transition - Critical layer nonlinearity p 172 A92-35994
- Stable localized patterns in thin liquid films p 173 A92-37489
- NONLINEAR FILTERS**
- An IIR median hybrid filter p 246 A92-40375
- NONLINEAR PROGRAMMING**
- Discrete approximations to optimal trajectories using direct transcription and nonlinear programming p 44 A92-46753
- Life extending control for rocket engines [NASA-TM-105789] p 142 N92-31263
- NONLINEAR SYSTEMS**
- Design of multi-layer neural networks for accurate identification of nonlinear mappings p 246 A92-29030
- A fundamental theorem for the model reduction of nonlinear systems p 246 A92-41165
- NONLINEARITY**
- Optical measurements of unducted fan flutter [ASME PAPER 91-GT-19] p 197 A92-15510
- On the nonlinear development of three-dimensional instability waves in natural transition [AIAA PAPER 92-0741] p 170 A92-28222
- NONOSCILLATORY ACTION**
- Accurate upwind-monotone (nonoscillatory) methods for conservation laws p 193 N92-25812
- NORMAL SHOCK WAVES**
- Perturbation of a normal shock - A test case for unsteady Euler codes [AIAA PAPER 92-3180] p 178 A92-48795
- NOTCH TESTS**
- Mixed-mode fracture in unidirectional graphite epoxy composite laminates with central notch p 218 A92-29464
- NOZZLE DESIGN**
- Computation of supersonic jet mixing noise for an axisymmetric CD nozzle using k-epsilon turbulence model [AIAA PAPER 92-0500] p 252 A92-26328
- Analytical study of nozzle performance for nuclear thermal rockets [NASA-TM-105251] p 78 N92-11126
- Computation of supersonic jet mixing noise for an axisymmetric CD nozzle using k-epsilon turbulence model [NASA-TM-105338] p 254 N92-14795
- NOZZLE EFFICIENCY**
- Experimental and analytical study of close-coupled ventral nozzles for ASTOVL aircraft p 26 A92-45325
- NOZZLE FLOW**
- Techniques for spectroscopic measurements in an arcjet nozzle p 59 A92-21087
- Flow in a ventral nozzle for short takeoff and vertical landing aircraft p 25 A92-28538
- Effect of tabs on the evolution of an axisymmetric jet p 26 A92-40151
- The flip flop nozzle extended to supersonic flows [AIAA PAPER 92-2724] p 10 A92-45561
- FD0 and DSMC analyses of rarefied gas flow through 2D nozzles [AIAA PAPER 92-2858] p 176 A92-47841
- DSMC analysis of species separation in rarefied nozzle flows [AIAA PAPER 92-2859] p 176 A92-47842
- Qualitative spectroscopic study of magnetic nozzle flow [AIAA PAPER 92-3161] p 65 A92-48784
- Investigation of three-dimensional flow field in a turbine including rotor/stator interaction. II - Three-dimensional flow field at the exit of the nozzle [AIAA PAPER 92-3326] p 12 A92-48909
- Propulsion-related flowfields using the preconditioned Navier-Stokes equations [AIAA PAPER 92-3437] p 178 A92-48994
- Numerical study of low-current steady arcs p 67 A92-50264
- Kinetic theory model for the flow of a simple gas from a three-dimensional axisymmetric nozzle p 12 A92-52730
- Preliminary dynamic tests of a flight-type ejector [AIAA PAPER 92-3261] p 27 A92-54020
- Experimental and numerical investigations of low-density nozzle and plume flows of nitrogen p 183 A92-54917
- The flip-flop nozzle extended to supersonic flows [NASA-TM-105570] p 18 N92-23269
- Preliminary dynamic tests of a flight-type ejector [NASA-TM-105814] p 38 N92-30998
- NOZZLE GEOMETRY**
- Medium power hydrogen arcjet performance [AIAA PAPER 91-2227] p 58 A92-15355
- The flip flop nozzle extended to supersonic flows [AIAA PAPER 92-2724] p 10 A92-45561

NOZZLE INSERTS

- Plasma flow processes within magnetic nozzle configurations p 67 A92-50266
 Preliminary investigation of power flow and electrode phenomena in a multi-megawatt coaxial plasma thruster [AIAA PAPER 92-3741] p 75 A92-54144
 High-power hydrogen arcjet performance [NASA-TM-105143] p 82 N92-14109
 Arcjet nozzle area ratio effects [NASA-TM-104477] p 83 N92-16022
 The flip-flop nozzle extended to supersonic flows [NASA-TM-105570] p 18 N92-23269

NOZZLE INSERTS

- Arcjet nozzle area ratio effects [NASA-TM-104477] p 83 N92-16022

NOZZLES

- Introduction to the internal fluid mechanics research session p 188 N92-22522
 Inlets, ducts, and nozzles p 188 N92-22523

NUCLEAR ELECTRIC POWER GENERATION

- Small Stirling dynamic isotope power system for multihundred-watt robotic missions [SAE PAPER 912066] p 62 A92-45448
 Multi-reactor power system configurations for multimegawatt nuclear electric propulsion [NASA-TM-105212] p 77 N92-10057

NUCLEAR ELECTRIC PROPULSION

- Electric propulsion - An evolutionary technology [IAF PAPER 91-241] p 58 A92-13158
 Nuclear rocket propulsion technology - A joint NASA/DOE project [IAF PAPER 91-236] p 58 A92-13159
 NASA program planning on nuclear electric propulsion [AIAA PAPER 92-1557] p 61 A92-38651
 Early Track NEP system options for SEI missions [AIAA PAPER 92-3200] p 65 A92-48808
 Nuclear rocket propulsion: NASA plans and progress - FY 1991 p 69 A92-50584
 NASA's nuclear electric propulsion technology project [AIAA PAPER 92-3705] p 76 A92-57033
 Multi-reactor power system configurations for multimegawatt nuclear electric propulsion [NASA-TM-105212] p 77 N92-10057
 Nuclear electric propulsion: An integral part of NASA's nuclear propulsion project [NASA-TM-105309] p 83 N92-16019
 Nuclear Electric Propulsion Technology Panel findings and recommendations [NASA-TM-105547] p 85 N92-20355
 Blazing the trailway: Nuclear electric propulsion and its technology program plans [NASA-TM-105605] p 86 N92-23252
 NASA/DOE/DOD nuclear propulsion technology planning: Summary of FY 1991 interagency panel results [NASA-TM-105703] p 88 N92-26792
 NEP systems engineering efforts in FY-92: Plans and status [NASA-TM-105775] p 91 N92-30308
 Nuclear electric propulsion development and qualification facilities [NASA-TM-105521] p 91 N92-30818
 NASA's nuclear electric propulsion technology project [NASA-TM-105811] p 93 N92-32463

NUCLEAR ENGINE FOR ROCKET VEHICLES

- Nuclear Thermal Propulsion: A Joint NASA/DOE/DOD Workshop [NASA-CP-10079] p 78 N92-11088
 Nuclear thermal rocket workshop reference system Rover/NERVA p 78 N92-11091
 An overview of tested and analyzed NTP concepts [NASA-TM-105252] p 80 N92-11137
 Overview of rocket engine control [NASA-TM-105318] p 81 N92-13274

NUCLEAR FUEL ELEMENTS

- An improved heat transfer configuration for a solid-core nuclear thermal rocket engine [AIAA PAPER 92-3583] p 75 A92-54063

NUCLEAR FUELS

- Fuels and materials development for space nuclear propulsion [NASA-TM-107806] p 85 N92-21187

NUCLEAR FUSION

- Possible sources of the Population I lithium abundance and light-element evolution p 268 A92-33069

NUCLEAR POWER PLANTS

- Power supply for a manned international asteroid mission p 80 N92-13205

NUCLEAR PROPULSION

- Innovative nuclear thermal propulsion technology evaluation - Results of the NASA/DOE task team study [IAF PAPER 91-235] p 58 A92-13160
 DSMC analysis of species separation in rarefied nozzle flows p 176 A92-47842 [AIAA PAPER 92-2859]
 Nuclear thermal rockets - Key to moon-Mars exploration p 63 A92-48385

- Nuclear rocket propulsion: NASA plans and progress - FY 1991 p 69 A92-50584

- NASA's nuclear thermal propulsion technology project [AIAA PAPER 92-3581] p 75 A92-54062

- Nuclear propulsion for space exploration [IAF PAPER 92-0575] p 76 A92-57054

- Trade studies for nuclear space power systems [NASA-TM-105231] p 235 N92-10221

- Nuclear Thermal Propulsion: A Joint NASA/DOE/DOD Workshop p 78 N92-11088

- [NASA-CP-10079] p 78 N92-11088
 Nuclear thermal propulsion workshop overview p 78 N92-11090

- Nuclear thermal rocket workshop reference system Rover/NERVA p 78 N92-11091

- Analytical study of nozzle performance for nuclear thermal rockets p 78 N92-11126

- [NASA-TM-105251] p 78 N92-11126
 An overview of tested and analyzed NTP concepts [NASA-TM-105252] p 80 N92-11137

- Report of the Nuclear Propulsion Mission Analysis, Figures of Merit Subpanel: Quantifiable figures of merit for nuclear thermal propulsion [NASA-TM-104179] p 43 N92-20925

- Fuels and materials development for space nuclear propulsion [NASA-TM-107806] p 85 N92-21187

- NASA/DOE/DOD nuclear propulsion technology planning: Summary of FY 1991 interagency panel results [IAF PAPER 91-236] p 88 N92-26792

- Fast track lunar NTR systems assessment for the First Lunar Outpost and its evolvability to Mars p 142 N92-33334

- Nuclear reactors Innovative nuclear thermal propulsion technology evaluation - Results of the NASA/DOE task team study [IAF PAPER 91-235] p 58 A92-13160

- The NASA CSTI High Capacity Power Program [NASA-TM-105240] p 236 N92-16481

- NEP systems engineering efforts in FY-92: Plans and status [NASA-TM-105775] p 91 N92-30308

NUCLEAR REACTORS

- Nuclear rocket propulsion technology - A joint NASA/DOE project [IAF PAPER 91-236] p 58 A92-13159

- Design considerations in clustering nuclear rocket engines [AIAA PAPER 92-3587] p 66 A92-49069

- Radiation enhanced dissociation of hydrogen in nuclear rockets [AIAA PAPER 92-3817] p 67 A92-49129

- Nuclear rocket propulsion: NASA plans and progress - FY 1991 p 69 A92-50584

- An improved heat transfer configuration for a solid-core nuclear thermal rocket engine [AIAA PAPER 92-3583] p 75 A92-54063

- Numerical study of low pressure nuclear thermal rockets [AIAA PAPER 92-3815] p 75 A92-54182

- An accelerated development, reduced cost approach to lunar/Mars exploration using a modular NTR-based space transportation system [IAF PAPER 92-0574] p 43 A92-57053

- Analytical study of nozzle performance for nuclear thermal rockets [NASA-TM-105251] p 78 N92-11126

- Report of the Nuclear Propulsion Mission Analysis, Figures of Merit Subpanel: Quantifiable figures of merit for nuclear thermal propulsion [NASA-TM-104179] p 43 N92-20925

- Fast track lunar NTR systems assessment for the First Lunar Outpost and its evolvability to Mars p 142 N92-33334

- NUCLEATE BOILING Transient pool boiling in microgravity p 170 A92-30494

- NUCLEONS Massive Dirac neutrinos and SN 1987A p 268 A92-45808

- NUMERICAL ANALYSIS Numerical analysis of flow through oscillating cascade sections p 9 A92-44513

- Numerical experiments with flows of elongated granules [NASA-TM-105567] p 209 N92-23226

- Computational Fluid Dynamics --- numerical methods and algorithm development [NASA-CP-10078] p 35 N92-25808

- Upper bounds for convergence rates of vector extrapolation methods on linear systems with initial iterations [NASA-TM-105608] p 250 N92-33742

NUMERICAL CONTROL

- A software control system for the ACTS high-burst-rate link evaluation terminal [NASA-TM-105207] p 243 N92-16628

NUMERICAL FLOW VISUALIZATION

- The numerical simulation of a high-speed axial flow compressor [ASME PAPER 91-GT-272] p 3 A92-15669

- Fluid-flow of a row of jets in crossflow - A numerical study [AIAA PAPER 92-0534] p 169 A92-28198

- Techniques for animation of CFD results --- computational fluid dynamics p 194 N92-25825

- Distributed visualization for computational fluid dynamics p 194 N92-25826

NUMERICAL INTEGRATION

- Asymptotic integration algorithms for first-order ODEs with application to viscoplasticity [NASA-TM-105587] p 250 N92-24974

- Fast methods to numerically integrate the Reynolds equation for gas fluid films [NASA-TM-105415] p 214 N92-30722

OBLIQUE SHOCK WAVES

- Conical detonation waves - A comparison of theoretical and numerical results [AIAA PAPER 92-0348] p 167 A92-25792

OH-58 HELICOPTER

- Gear tooth stress measurements of two helicopter planetary stages [NASA-TM-105651] p 211 N92-26555

OIL ADDITIVES

- Liquid lubrication for space applications [NASA-TM-105198] p 133 N92-31840

ON-LINE SYSTEMS

- Automated power management and control p 84 N92-17773

- TIGGERC: Turbomachinery interactive grid generator energy distributor and restart code p 35 N92-25719

ONBOARD DATA PROCESSING

- Fault tolerance in onboard processors - Protecting efficient FDM demultiplexers [AIAA PAPER 92-1969] p 144 A92-29892

- Technology requirements for mesh VSAT applications [AIAA PAPER 92-1982] p 144 A92-29902

- Predictive onboard flow control in packet switching satellites [AIAA PAPER 92-2004] p 144 A92-29923

- Advanced Communication Technology Satellite (ACTS) baseband processor development p 50 A92-53693

- Advanced Communications Technology Satellite (ACTS) [IAF PAPER 92-0407] p 50 A92-55788

- Space Communications Technology Conference: Onboard Processing and Switching [NASA-CP-3132] p 147 N92-14202

- On-board congestion control for satellite packet switching networks p 148 N92-14228

- Advanced Communication Technology Satellite (ACTS) multibeam antenna technology verification experiments [NASA-TM-105421] p 149 N92-16191

- Predictive onboard flow control for packet switching satellites [NASA-TM-105566] p 150 N92-19379

OPEN CIRCUIT VOLTAGE

- High voltage thermally diffused p(+)-n solar cells p 235 A92-53172

OPERATING TEMPERATURE

- High temperature thruster technology for spacecraft propulsion [NASA-TM-105348] p 82 N92-15125

- Effect of lubricant jet location on spiral bevel gear operating temperatures [NASA-TM-105656] p 211 N92-26106

OPHTHALMOLOGY

- A fiber optic sensor for ophthalmic refractive diagnostics p 198 A92-34831

OPTICAL ACTIVITY

- Monolithic mm-wave phase shifter using optically activated superconducting switches [NASA-CASE-LEW-14878-1] p 257 N92-28571

- OPTICAL COMMUNICATION Advanced Communications Technology Satellite (ACTS) p 50 A92-38164

- Fiber optic controls for aircraft engines - Issues and implications p 24 A92-46244

OPTICAL COUPLING

- Interfaces for high-speed fiber-optic links - Analysis and experiment p 256 A92-24002

- Reconfigurable optical interconnection network for multimode optical fiber sensor arrays p 256 A92-37448

- Length minimization design considerations in photonic integrated circuits incorporating directional couplers p 256 A92-46240
- OPTICAL DISKS**
Space acceleration measurement system description and operations on the First Spacelab Life Sciences Mission [NASA-TM-105301] p 57 N92-13151
- OPTICAL EQUIPMENT**
An optically controlled Ka-band phased array antenna p 152 N92-32968
- OPTICAL FIBERS**
A fiber-optic probe for particle sizing in concentrated suspensions p 197 A92-21371
Satellite delivery of B-ISDN services [AIAA PAPER 92-1831] p 142 A92-29777
Reconfigurable optical interconnection network for multimode optical fiber sensor arrays p 256 A92-37448
The NASA CSTI High Capacity Power Program [NASA-TM-105240] p 236 N92-16481
Demonstrated survivability of a high temperature optical fiber cable on a 1500 pound thrust rocket chamber [NASA-TM-105835] p 136 N92-32230
RF modulated fiber optic sensing systems and their applications [NASA-TM-105801] p 257 N92-33896
- OPTICAL MATERIALS**
Technology development of fabrication techniques for advanced solar dynamic concentrators p 232 A92-50571
Effect of InAlAs window layer on the efficiency of indium phosphide solar cells p 234 A92-53163
Effect of InAlAs window layer on efficiency of indium phosphide solar cells [NASA-TM-105354] p 161 N92-25176
- OPTICAL MEASUREMENT**
Optical measurements of unducted fan flutter [ASME PAPER 91-GT-19] p 197 A92-15510
Effect of gas mass flux on cryogenic liquid jet breakup p 140 A92-23845
An optical method for determining level in two-phase cryogenic fluids [NASA-TM-104524] p 200 N92-15366
Optical measurement systems p 202 N92-22527
Three-dimensional laser window formation [NASA-RP-1280] p 47 N92-30307
- OPTICAL MEASURING INSTRUMENTS**
Advanced optical condition monitoring ... of rocket engines [SAE PAPER 912164] p 199 A92-39994
Self-aligning optical measurement systems p 247 A92-50387
- OPTICAL MEMORY (DATA STORAGE)**
Space acceleration measurement system description and operations on the First Spacelab Life Sciences Mission [NASA-TM-105301] p 57 N92-13151
- OPTICAL MICROSCOPES**
Determination of the critical parameters for remote microscope control [IAF PAPER 91-026] p 240 A92-12447
- OPTICAL PROPERTIES**
Low earth orbit durability evaluation of Haynes 188 solar receiver material [AIAA PAPER 92-0850] p 117 A92-29616
Ion Beam Textured and Coated Surfaces Experiment (IBEX) p 132 N92-24832
- OPTICAL RADAR**
Measurement of trace stratospheric constituents with a balloon borne laser radar p 239 N92-14500
- OPTICAL REFLECTION**
Surface etching for light trapping in encapsulated InP solar cells p 232 A92-48091
- OPTICAL RESONATORS**
The introduction of spurious modes in a hole-coupled Fabry-Perot open resonator p 197 A92-21244
- OPTICAL SWITCHING**
Interfaces for high-speed fiber-optic links - Analysis and experiment p 256 A92-24002
Multiple-mode reconfigurable electro-optic switching network for optical fiber sensor array p 256 A92-46245
- OPTICAL THICKNESS**
Radiative transfer solutions for cylindrical coordinates with emitting, absorbing, and anisotropic scattering medium [AIAA PAPER 92-0123] p 266 A92-28185
Photovoltaic array for Martian surface power [NASA-TM-105827] p 270 N92-33899
- OPTICAL WAVEGUIDES**
Reconfigurable optical interconnection network for multimode optical fiber sensor arrays p 256 A92-37448
- Length minimization design considerations in photonic integrated circuits incorporating directional couplers p 256 A92-46240
- Comparative evaluation of optical waveguides as alternative interconnections for high performance packaging p 153 N92-32974
- OPTIMAL CONTROL**
Discrete approximations to optimal trajectories using direct transcription and nonlinear programming p 44 A92-46753
Optimal microgravity vibration isolation - An algebraic introduction p 54 A92-47495
Canonical transformations for space trajectory optimization [AIAA PAPER 92-4509] p 44 A92-52079
Discrete-time entropy formulation of optimal and adaptive control problems p 247 A92-55930
Microgravity vibration isolation: An optimal control law for the one-dimensional case [NASA-TM-105146] p 141 N92-11217
Directions in propulsion control p 32 N92-22530
Microgravity vibration isolation: Optimal preview and feedback control [NASA-TM-105673] p 142 N92-30692
- OPTIMIZATION**
Optimization and analysis of large chemical kinetic mechanisms using the solution mapping method - Combustion of methane p 113 A92-19300
Multiobjective shape and material optimization of composite structures including damping p 218 A92-28055
Minimizing distortion in truss structures - A Hopfield network solution [AIAA PAPER 92-2302] p 220 A92-34523
Application of Newton modified barrier method (NMBM) to structural optimization [AIAA PAPER 92-2498] p 220 A92-34555
Neural network based decomposition in optimal structural synthesis p 247 A92-41895
Applications of artificial neural nets in structural mechanics p 223 A92-47283
Maximum life spiral bevel reduction design [AIAA PAPER 92-3493] p 205 A92-49030
Minimization of vibration in elastic beams with time-variant boundary conditions p 224 A92-50511
Theoretical modeling, near-optimum design and predicted performance of n(+)/pp(+) and p(+)/nn(+) indium phosphide homojunction solar cells p 234 A92-53152
Dependence of hydrogen arcjet operation on electrode geometry [AIAA PAPER 92-3530] p 74 A92-54039
Vortex generator design for aircraft inlet distortion as a numerical optimization problem p 23 N92-13959
Singularities in optimal structural design [NASA-TM-4365] p 228 N92-23527
Structural optimization of large structural systems by optimality criteria methods [NASA-TM-105423] p 229 N92-25446
Minimization of the vibration energy of thin-plate structure [NASA-TM-105654] p 211 N92-25448
Optimum design of a gearbox for low vibration [NASA-TM-105653] p 212 N92-28476
Optimal design of compact spur gear reductions [NASA-TM-105676] p 213 N92-29351
- OPTOELECTRONIC DEVICES**
Interfaces for high-speed fiber-optic links - Analysis and experiment p 256 A92-24002
Multiple-mode reconfigurable electro-optic switching network for optical fiber sensor array p 256 A92-46245
Potential for integrated optical circuits in advanced aircraft with fiber optic control and monitoring systems p 24 A92-46246
- ORBIT TRANSFER VEHICLES**
Tether methods for reactionless orbital propulsion p 44 A92-17797
Design considerations in clustering nuclear rocket engines [AIAA PAPER 92-3587] p 66 A92-49069
Health management and controls for earth to orbit propulsion systems [IAF PAPER 92-0646] p 77 A92-57089
Space Station Freedom/lunar transfer vehicle propellant operation hazard analysis p 55 N92-17416
Krypton ion thruster performance [NASA-TM-105818] p 92 N92-31901
- ORBITAL MANEUVERS**
Dynamics and control of the Space Station Freedom docking/array feathering maneuver [IAF PAPER 91-321] p 52 A92-14734
Tether methods for reactionless orbital propulsion p 44 A92-17797
- ORBITAL SERVICING**
On-orbit cryogenic fluid transfer research at NASA Lewis Research Center p 45 A92-23847
Repair-level analysis for Space Station Freedom [AIAA PAPER 92-1537] p 43 A92-38634
- ORGANOMETALLIC COMPOUNDS**
Polymeric precursors for fibers and matrices p 125 A92-39856
- ORIFICES**
Jet mixing into a heated cross flow in a cylindrical duct - Influence of geometry and flow variations [AIAA PAPER 92-0773] p 168 A92-27110
A parametric numerical study of mixing in a cylindrical duct [AIAA PAPER 92-3088] p 177 A92-48733
Jet mixing into a heated cross flow in a cylindrical duct: Influence of geometry and flow variations [NASA-TM-105390] p 30 N92-15994
A parametric numerical study of mixing in a cylindrical duct [NASA-TM-105695] p 35 N92-26553
- OSCILLATING FLOW**
Pressure wave propagation studies for oscillating cascades [AIAA PAPER 92-0145] p 5 A92-25682
Effects of g-jitter on a thermally buoyant flow p 171 A92-32258
A 2-D oscillating flow analysis in Stirling engine heat exchangers p 172 A92-36001
An experimental study of oscillatory thermocapillary convection in cylindrical containers p 172 A92-36184
The flip flop nozzle extended to supersonic flows [AIAA PAPER 92-2724] p 10 A92-45561
Instantaneous heat transfer coefficient based upon two-dimensional analyses of Stirling space engine components p 181 A92-50827
Pressure wave propagation studies for oscillating cascades [NASA-TM-105406] p 16 N92-15977
Unsteady-flow-field predictions for oscillating cascades [NASA-TM-105283] p 17 N92-19437
The flip-flop nozzle extended to supersonic flows [NASA-TM-105570] p 18 N92-23269
Heat transfer in oscillating flows with sudden change in cross section [NASA-TM-105692] p 88 N92-26654
Overview of NASA supported Stirling thermodynamic loss research [NASA-TM-105690] p 88 N92-27034
Experimental investigation of the flowfield of an oscillating airfoil [NASA-TM-105675] p 20 N92-30182
- OSCILLATIONS**
Intermodulation in the oscillatory magnetoresistance of a two-dimensional electron gas p 163 N92-32975
- OSCILLATORS**
NIST torsion oscillator viscometer response: Performance on the LeRC active vibration isolation platform [NASA-TM-105571] p 209 N92-23564
- OSSEEN APPROXIMATION**
The structure and development of streamwise vortex arrays embedded in a turbulent boundary layer [NASA-TM-105211] p 14 N92-10012
- OXIDATION**
Near-edge study of gold-substituted YBa₂Cu₃O(7-delta) p 259 A92-14950
Effects of oxygen concentration on radiative loss from normal-gravity and microgravity methane diffusion flames [AIAA PAPER 92-0243] p 113 A92-26928
COSP - A computer model of cyclic oxidation p 114 A92-31849
Crack healing behavior of hot pressed silicon nitride due to oxidation p 124 A92-32896
Oxidation kinetics of cast TiAl₃ p 121 A92-38993
Oxidation kinetics of CVD silicon carbide and silicon nitride p 125 A92-39674
Substituted 1,1,1-triaryl-2,2,2-trifluoroethanes and processes for their synthesis [NASA-CASE-LEW-14345-6] p 96 N92-17882
Structure-to-property relationships in addition cured polymers. 4. Correlations between thermo-oxidative weight losses of norbornenyl cured polyimide resins and their composites [NASA-TM-105553] p 108 N92-20039
The cyclic oxidation resistance at 1200 C of beta-NiAl, FeAl, and CoAl alloys with selected third element additions [NASA-TM-105620] p 123 N92-24554
Damage mechanisms in bithermal and thermomechanical fatigue of Haynes 188 [NASA-TM-105381] p 228 N92-24985
Oxidation resistant coating for titanium alloys and titanium alloy matrix composites [NASA-CASE-LEW-15155-1] p 133 N92-29090

OXIDATION RESISTANCE

OXIDATION RESISTANCE

- Oxidation effects on the mechanical properties of a SiC-fiber-reinforced reaction-bonded Si₃N₄ matrix composite p 100 A92-25445
- Diffusion mechanisms in chemical vapor-deposited iridium coated on chemical vapor-deposited rhenium p 117 A92-28017
- SiO(X) coatings for atomic oxygen protection of polyimide Kapton in low earth orbit [AIAA PAPER 92-2151] p 94 A92-31286
- Atomic oxygen effects on thin film space coatings studied by spectroscopic ellipsometry, atomic force microscopy, and laser light scattering [AIAA PAPER 92-2172] p 94 A92-31300
- Protective Al₂O₃ scale formation on NbAl₃-base alloys p 119 A92-31850
- Thermal barrier coating life and isothermal oxidation of low-pressure plasma-sprayed bond coat alloys p 119 A92-32398
- Effect of fiber reinforcement on thermo-oxidative stability and mechanical properties of polymer matrix composites p 101 A92-33587
- Cyclic oxidation resistance of a reaction milled NiAl-AlN composite p 105 A92-46871
- Oxidation of Al₂O₃ continuous fiber-reinforced/NiAl composites p 106 A92-57029
- New addition curing polyimides [NASA-TM-105335] p 95 A92-13281
- Elevated temperature mechanical behavior of monolithic and SiC whisker-reinforced silicon nitrides [NASA-TM-105245] p 128 A92-15192
- Novel applications for TAZ-8A p 123 A92-22444
- The cyclic oxidation resistance at 1200 C of beta-NiAl, FeAl, and CoAl alloys with selected third element additions p 123 A92-24554
- [NASA-TM-105620] p 123 A92-24554
- Oxidation resistant coating for titanium alloys and titanium alloy matrix composites [NASA-CASE-LEW-15155-1] p 133 A92-29090
- Liquid lubricants for advanced aircraft engines [NASA-TM-104531] p 133 A92-32863
- OXIDATION-REDUCTION REACTIONS**
- Oxidation-chlorination of binary Ni-Cr alloys in flowing Ar-O₂-Cl₂ gas mixtures at 1200 K p 112 A92-17296
- Ultrasonic evaluation of oxygen content, modulus, and microstructure changes in YBa₂Cu₃O_{7-x} occurring during oxidation and reduction p 261 A92-38418
- A study of Na(x)Pt₃O₄ as an O₂ electrode bifunctional electrocatalyst [NASA-TM-105311] p 85 A92-20585
- OXIDE FILMS**
- Study of temperature-dependent ultrathin oxide growth on Si(111) using variable-angle spectroscopic ellipsometry p 260 A92-32414
- OXIDES**
- Solid lubricants on pretreated surfaces [NASA-CASE-LEW-14474-2] p 127 A92-11186
- Sliding durability of two carbide-oxide candidate high temperature fiber seal materials in air to 900 C [NASA-TM-105554] p 97 A92-21175
- An XPS study of the stability of Fomblin Z25 on the native oxide of aluminum --- x ray photoelectron spectroscopy [NASA-TM-105594] p 131 A92-23185
- OXIDIZERS**
- An SSME high pressure oxidizer turbopump diagnostic system using G2(TM) real-time expert system [NASA-TM-105328] p 247 A92-13717
- OXYGEN**
- Saturated fluorescence measurements of the hydroxyl radical in laminar high-pressure C₂H₆/O₂/N₂ flames p 198 A92-33987
- Propulsion systems using in situ propellants for a Mars Ascent Vehicle [AIAA PAPER 92-3445] p 66 A92-49001
- Bifunctional alkaline oxygen electrodes p 115 A92-50729
- Temperature dependence of the electrode kinetics of oxygen reduction at the platinum/Nafion interface - A microelectrode investigation p 115 A92-56950
- Propulsion systems using in situ propellants for a Mars ascent vehicle [NASA-TM-105741] p 89 A92-27654
- The O₂ reduction at the IFC modified O₂ fuel cell electrode [NASA-TM-105691] p 90 A92-29667
- OXYGEN ATOMS**
- Synergistic effects of ultraviolet radiation, thermal cycling and atomic oxygen on altered and coated Kapton surfaces [AIAA PAPER 92-0794] p 93 A92-27125
- Atomic oxygen effects on SiO(x) coated Kapton for photovoltaic arrays in low earth orbit p 72 A92-53211
- Fast oxygen atom facility for studies related to low earth orbit activities [AIAA PAPER 92-3974] p 47 A92-56800

- Synergistic effects of ultraviolet radiation, thermal cycling, and atomic oxygen on altered and coated Kapton surfaces [NASA-TM-105363] p 96 A92-14114
- Atomic oxygen durability of solar concentrator materials for Space Station Freedom [NASA-TM-105378] p 85 A92-20065
- Atomic oxygen undercutting of LDEF aluminized-Kapton multilayer insulation p 255 A92-24818
- Atomic oxygen interactions with FEP Teflon and silicones on LDEF p 132 A92-24820
- Monte Carlo modeling of atomic oxygen attack of polymers with protective coatings on LDEF p 132 A92-27281

OXYGEN IONS

- Ion collection from a plasma by a pinhole p 259 A92-22368

OXYGEN PRODUCTION

- Alkali metal carbon dioxide electrochemical system for energy storage and/or conversion of carbon dioxide to oxygen [NASA-CASE-LEW-14973-1] p 235 A92-10222

OZONE

- Measurement of trace stratospheric constituents with a balloon borne laser radar p 239 A92-14500

P

P-N JUNCTIONS

- A model for the trap-assisted tunneling mechanism in diffused n-p and implanted n(+)-p HgCdTe photodiodes p 156 A92-46007
- InP concentrator solar cells p 234 A92-53166

P-TYPE SEMICONDUCTORS

- Minority carrier lifetime in indium phosphide p 262 A92-53148
- High performance etchant for thinning p(+)-InP and its application to p(+)-n InP solar cell fabrication p 263 A92-53155

PACKAGES

- Comparative evaluation of optical waveguides as alternative interconnections for high performance packaging p 153 A92-32974

PACKAGING

- Comparative evaluation of optical waveguides as alternative interconnections for high performance packaging p 153 A92-32974

PACKET SWITCHING

- Predictive onboard flow control in packet switching satellites [AIAA PAPER 92-2004] p 144 A92-29923
- Destination directed packet switch architecture for a 30/20 GHz FDMA/TDM geostationary communication satellite network p 148 A92-14204
- On-board congestion control for satellite packet switching networks p 148 A92-14228
- Predictive onboard flow control for packet switching satellites [NASA-TM-105566] p 150 A92-19379
- Destination-directed, packet-switching architecture for 30/20-GHz FDMA/TDM geostationary communications satellite network [NASA-TP-3201] p 51 A92-19762

PACKETS (COMMUNICATION)

- On-board congestion control for satellite packet switching networks p 148 A92-14228

PANEL METHOD (FLUID DYNAMICS)

- A turbulence model for iced airfoils and its validation [AIAA PAPER 92-0417] p 6 A92-26267
- Unsteady airloading panel method for proflans p 253 A92-44512
- A turbulence model for iced airfoils and its validation [NASA-TM-105373] p 16 A92-15052

PANELS

- Relationship between voids and interlaminar shear strength of polymer matrix composites p 98 A92-10241
- Engine panel seals for hypersonic engine applications: High temperature leakage assessments and flow modelling [NASA-TM-105260] p 208 A92-16336
- Structural durability of stiffened composite shells [NASA-CR-190588] p 229 A92-29342

PAPER (MATERIAL)

- Intensified array camera imaging of solid surface combustion aboard the NASA Learjet [AIAA PAPER 92-0240] p 137 A92-25702
- Global kinetic constants for thermal oxidative degradation of a cellulosic paper p 113 A92-29488
- Intensified array camera imaging of solid surface combustion aboard the NASA Learjet [NASA-TM-105361] p 138 A92-16156

PARALLEL PLATES

- Heat transfer in oscillating flows with sudden change in cross section [NASA-TM-105692] p 88 A92-26654

PARALLEL PROCESSING (COMPUTERS)

- Parallel computation of aerodynamic influence coefficients for aeroelastic analysis on a transputer network p 241 A92-12367
- Numerical propulsion system simulation p 59 A92-20194

- A study of equation solvers for linear and non-linear finite element analysis on parallel processing computers [AIAA PAPER 92-2478] p 242 A92-34367

PARALLEL PROGRAMMING

- Multicarrier demodulator architecture for onboard processing satellites p 49 A92-10465

PARAMETER IDENTIFICATION

- A failure diagnosis system based on a neural network classifier for the Space Shuttle Main Engine p 58 A92-11474

PARTIAL DIFFERENTIAL EQUATIONS

- FDDO and DSMC analyses of rarefied gas flow through 2D nozzles [AIAA PAPER 92-2858] p 176 A92-47841
- Mappings and accuracy for Chebyshev pseudo-spectral approximations p 248 A92-50469
- An efficient and robust algorithm for two dimensional time dependent incompressible Navier-Stokes equations: High Reynolds number flows [NASA-TM-104424] p 184 A92-11320

PARTICLE ACCELERATORS

- Fast oxygen atom facility for studies related to low earth orbit activities [AIAA PAPER 92-3974] p 47 A92-56800

PARTICLE DIFFUSION

- Diffusion mechanisms in chemical vapor-deposited iridium coated on chemical vapor-deposited rhenium p 117 A92-28017

PARTICLE IN CELL TECHNIQUE

- High voltage spheres in an unmagnetized plasma - Fluid and PIC simulations p 258 A92-47936

PARTICLE LADEN JETS

- Particle-laden weakly swirling free jets: Measurements and predictions [NASA-TM-100881] p 29 A92-14061

PARTICLE PRODUCTION

- Fluctuation-driven electroweak phase transition --- in early universe p 269 A92-54464

PARTICLE SIZE DISTRIBUTION

- A fiber-optic probe for particle sizing in concentrated suspensions p 197 A92-21371
- Effect of gas mass flux on cryogenic liquid jet breakup p 140 A92-23845

PARTICLE TRACKS

- Ion collection from a plasma by a pinhole p 259 A92-22368

PARTICULATE REINFORCED COMPOSITES

- Compression studies on particulate composites of ternary Al-Ti-Fe, and quaternary Al-Ti-Fe-Nb and Al-Ti-Fe-Mn L1(2) compounds p 119 A92-30845
- Mechanical properties of monolithic and particulate composites of L12 forms of Al₃Ti p 101 A92-36273
- 1200 and 1300 K slow plastic compression properties of Ni-50Al composites p 102 A92-38125
- Discontinuously reinforced intermetallic matrix composites via XD synthesis --- exothermal dispersion p 103 A92-41867
- Cyclic oxidation resistance of a reaction milled NiAl-AlN composite p 105 A92-46871

PARTICULATES

- Numerical experiments with flows of elongated granules [NASA-TM-105567] p 209 A92-23226
- Composites of low-density trialuminides: Particulate and long fiber reinforcements [NASA-TM-105628] p 109 A92-25346

PARTITIONS (MATHEMATICS)

- Decentralized hierarchical partitioning of centralized integrated controllers --- for flight propulsion in STOVLS p 39 A92-29119

PAYLOADS

- Reaction-compensation technology for microgravity laboratory robots p 203 A92-23719
- Safety issues p 78 A92-11115
- Vibration isolation technology development to demonstration p 140 A92-28442

PEEK

- High temperature dielectric properties of Apical, Kapton, Peek, Teflon AF, and Uplix polymers [NASA-TM-105753] p 162 A92-28675

PENETRATION

- Magnetic penetration depth of YBa₂Cu₃O₇(δ) thin films determined by the power transmission method p 265 A92-32983

- PERCOLATION**
Fluctuation-driven electroweak phase transition --- in early universe p 269 A92-54464
- PERFLUORO COMPOUNDS**
An XPS study of the stability of Fomblin Z25 on the native oxide of aluminum --- x ray photoelectron spectroscopy [NASA-TM-105594] p 131 N92-23185
- PERFORMANCE PREDICTION**
Ongoing development of a computer jobstream to predict helicopter main rotor performance in icing conditions p 2 A92-14407
Row-by-row off-design performance calculation method for turbines p 26 A92-44514
Navier-Stokes turbine heat transfer predictions using two-equation turbulence closures [AIAA PAPER 92-3067] p 177 A92-48721
Contamination effects on Space Station Freedom electric power system performance p 54 A92-50578
Theoretical modeling, near-optimum design and predicted performance of n(+)/pp(+) and p(+)/nn(+) indium phosphide homojunction solar cells p 234 A92-53152
Performance comparison of axisymmetric and three-dimensional hydrogen film coolant injection in a 110 N hydrogen/oxygen rocket [AIAA PAPER 92-3390] p 73 A92-54027
Analytical study of nozzle performance for nuclear thermal rockets [NASA-TM-105251] p 78 N92-11126
Effect of particle size of Martian dust on the degradation of photovoltaic cell performance [NASA-TM-105232] p 79 N92-11133
Development of a computer algorithm for the analysis of variable-frequency AC drives: Case studies included [NASA-TM-105327] p 29 N92-13070
Effects of chemical equilibrium on turbine engine performance for various fuels and combustor temperatures [NASA-TM-105399] p 34 N92-23254
Derated ion thruster design issues [NASA-TM-105576] p 87 N92-23534
Nonplanar linearly tapered slot antenna with balanced microstrip feed [NASA-TM-105647] p 161 N92-23535
Comparison of GLIMPS and HFAST Stirling engine code predictions with experimental data [NASA-TM-105549] p 267 N92-25395
NASA Lewis steady-state heat pipe code users manual [NASA-TM-105161] p 90 N92-28682
NEP systems engineering efforts in FY-92: Plans and status [NASA-TM-105775] p 91 N92-30308
Effect of out-of-roundness on the performance of a diesel engine connecting-rod bearing [NASA-TM-105600] p 215 N92-31536
- PERFORMANCE TESTS**
Numerical investigation of performance degradation of wings and rotors due to icing [AIAA PAPER 92-0412] p 5 A92-26264
Performance of the Phase Doppler Particle Analyzer icing cloud droplet sizing probe in the NASA Lewis Icing Research Tunnel [AIAA PAPER 92-0162] p 198 A92-26926
Concentrator testing using projected images p 69 A92-50615
Test and evaluation of load converter topologies used in the Space Station Freedom power management and distribution dc test bed p 158 A92-50662
A comparison of the calculated and experimental off-design performance of a radial flow turbine [AIAA PAPER 92-3069] p 13 A92-54004
Internal reversing flow in a tailpipe offtake configuration for SSTOVL aircraft [AIAA PAPER 92-3790] p 28 A92-54169
Description of a pressure measurement technique for obtaining surface static pressures of a radial turbine [AIAA PAPER 92-4006] p 200 A92-56829
Effect of a simulated glaze ice shape on the aerodynamic performance of a rectangular wing [AIAA PAPER 92-4042] p 14 A92-56861
Test facilities for high power electric propulsion [NASA-TM-105247] p 80 N92-11136
Arcjet nozzle area ratio effects [NASA-TM-104477] p 83 N92-16022
Progress in the development of lightweight nickel electrode for aerospace applications [NASA-TM-105591] p 236 N92-20493
NASA Lewis Research Center Advanced Modulation and Coding Project: Introduction and overview p 51 N92-22002
Evaluation of MHOST analysis capabilities for a plate element --- finite element modeling [NASA-TM-105387] p 228 N92-23196
- Description of a pressure measurement technique for obtaining surface static pressures of a radial turbine [NASA-TM-105643] p 202 N92-24959
Comparison of GLIMPS and HFAST Stirling engine code predictions with experimental data [NASA-TM-105549] p 267 N92-25395
The evaluation of layered separators for nickel-hydrogen cells p 89 N92-27161
Validation test of advanced technology for IPV nickel-hydrogen flight cells: Update [NASA-TM-105689] p 89 N92-27878
Internal reversing flow in a tailpipe offtake configuration for SSTOVL aircraft [NASA-TM-105698] p 37 N92-28418
Experimental testing of prototype gear gears for helicopter transmissions [NASA-TM-105434] p 214 N92-31349
Overview and evolution of the LeRC PMAD DC Testbed [NASA-TM-105842] p 163 N92-32867
Load converter interactions with the secondary system in the Space Station Freedom power management and distribution DC test bed [NASA-TM-105844] p 164 N92-34219
- PERMANENT MAGNETS**
The 23 to 300 C demagnetization resistance of samarium-cobalt permanent magnets [NASA-TP-3119] p 159 N92-11252
Performance tests of a cryogenic hybrid magnetic bearing for turbopumps [NASA-TM-105627] p 30 N92-20523
- PERMITTIVITY**
Measurements of complex permittivity of microwave substrates in the 20 to 300 K temperature range from 26.5 to 40.0 GHz p 197 A92-13416
- PERSIAN GULF**
The chemistry of Saudi Arabian sand: A deposition problem on helicopter turbine airfoils [NASA-TM-105234] p 128 N92-14179
- PERSONAL COMPUTERS**
PC graphics generation and management tool for real-time applications [NASA-TM-105749] p 244 N92-28684
- PERTURBATION**
Perturbation of a normal shock - A test case for unsteady Euler codes [AIAA PAPER 92-3180] p 178 A92-48795
- PERTURBATION THEORY**
Perturbations from cosmic strings in cold dark matter p 268 A92-33353
Aeroelastic modal characteristics of mistuned blade assemblies - Mode localization and loss of eigenstructure p 225 A92-54921
- PERVEANCE**
Characterization of ion accelerating systems on NASA LeRC's ion thrusters [AIAA PAPER 92-3827] p 76 A92-54191
- PHASE CHANGE MATERIALS**
Experiments with phase change thermal energy storage canisters for Space Station Freedom p 179 A92-50564
Full-size solar dynamic heat receiver thermal-vacuum tests p 68 A92-50565
Ground test program for a full-size solar dynamic heat receiver p 68 A92-50566
Shrinkage void formation and its effect on freeze and thaw processes of lithium and lithium-fluoride for space applications p 180 A92-50596
Parametric studies of phase change thermal energy storage canisters for Space Station Freedom [NASA-TM-105350] p 55 N92-13143
Experiments with phase change thermal energy storage canisters for Space Station Freedom [NASA-TM-104427] p 86 N92-21216
- PHASE CONTROL**
Propagating confined states in phase dynamics p 181 A92-50968
- PHASE MODULATION**
Rotative quadrature phase-shift keying p 146 A92-44233
- PHASE SHIFT**
Monolithic mm-wave phase shifter using optically activated superconducting switches [NASA-CASE-LEW-14878-1] p 257 N92-28571
- PHASE SHIFT CIRCUITS**
Ka-band active MMIC subarray development [AIAA PAPER 92-1863] p 155 A92-29803
V-band pseudomorphic HEMT MMIC phased array components for space communications p 151 N92-32966
An optically controlled Ka-band phased array antenna p 152 N92-32968
- PHASE SHIFT KEYING**
Flexible high speed CODEC (FHSC) [AIAA PAPER 92-1919] p 143 A92-29848
- Comparative study on the performance of power and bandwidth efficient modulations in LMSS under fading and interference p 147 A92-54763
Flexible digital modulation and coding synthesis for satellite communications p 148 N92-14235
Advanced Modulation and Coding Technology Conference [NASA-CP-10053] p 51 N92-22001
- PHASE STABILITY (MATERIALS)**
Ductility enhancement from interface dislocation sources in a directionally solidified beta + gamma + gamma-prime Ni-Fe-Al composite alloy p 122 A92-46850
- PHASE TRANSFORMATIONS**
The analysis of high pressure experimental data p 266 A92-16101
Numerical analysis of a thermal deicer [AIAA PAPER 92-0527] p 22 A92-26950
An efficient finite element method for aircraft de-icing problems [AIAA PAPER 92-0532] p 22 A92-31670
Frozen start-up behavior of low-temperature heat pipes p 179 A92-49847
Fluctuation-driven electroweak phase transition --- in early universe p 269 A92-54464
Growth and characterization of lead bromide crystals p 138 A92-56956
Critical fluid thermal equilibration experiment (19-IML-1) p 139 N92-23640
Phase transformations in SrAl₂Si₂O₈ glass [NASA-TM-105657] p 264 N92-23890
- PHASED ARRAYS**
A vertically integrated Ka-band phased array antenna [AIAA PAPER 92-1976] p 156 A92-38140
Multiple-access phased array antenna simulator for a digital beam forming system investigation [NASA-TM-105422] p 149 N92-17062
High-performance packaging for monolithic microwave and millimeter-wave integrated circuits [NASA-TM-105744] p 151 N92-31855
V-band pseudomorphic HEMT MMIC phased array components for space communications p 151 N92-32966
An optically controlled Ka-band phased array antenna p 152 N92-32968
Coplanar waveguide feeds for phased array antennas p 152 N92-32970
- PHOSPHORIC ACID FUEL CELLS**
Effects of coolant parameters on steady state temperature distribution in phosphoric-acid fuel cell electrode p 233 A92-50737
Measurements of the effects of thermal contact resistance on steady state heat transfer in phosphoric-acid fuel cell stack p 180 A92-50738
- PHOTOCHEMICAL REACTIONS**
Solid lubricants on pretreated surfaces [NASA-CASE-LEW-14474-2] p 127 N92-11186
- PHOTOCONDUCTIVITY**
Reduced mobility and PPC in In₂₀Ga₈₀As / Al₂₃Ga₇₇As HEMT structure p 265 N92-32976
- PHOTODIODES**
A model for the trap-assisted tunneling mechanism in diffused n-p and implanted n(+)-p HgCdTe photodiodes p 156 A92-46007
- PHOTOELECTROCHEMISTRY**
Material processing with hydrogen and carbon monoxide on Mars p 231 A92-17769
- PHOTOELECTRON SPECTROSCOPY**
An XPS study of the stability of Fomblin Z25 on the native oxide of aluminum --- x ray photoelectron spectroscopy [NASA-TM-105594] p 131 N92-23185
- PHOTOLUMINESCENCE**
Surface morphologies and photoluminescence of diamond films deposited in a hot filament reactor p 261 A92-42858
Photoluminescence lifetime measurements in InP wafers p 262 A92-48092
- PHOTONICS**
Length minimization design considerations in photonic integrated circuits incorporating directional couplers p 256 A92-46240
- PHOTOVOLTAIC CELLS**
Moonbase night power by laser illumination p 44 A92-21086
Study of a cesium plasma as a selective emitter for thermophotovoltaic applications p 258 A92-33667
Effects of windblown dust on photovoltaic surfaces on Mars p 45 A92-50573
Applications of thin-film photovoltaics for space p 70 A92-50641
Design and optimization of a self-deploying PV tent array p 233 A92-50642
The mini-dome Fresnel lens photovoltaic concentrator array - Current program status p 70 A92-50648

PHOTOVOLTAIC CONVERSION

- A high-performance photovoltaic concentrator array - The mini-dome Fresnel lens concentrator with 30 percent efficient GaAs/GaSb tandem cells p 72 A92-53199
- Atomic oxygen effects on SiO(x) coated Kapton for photovoltaic arrays in low earth orbit p 72 A92-53211
- Advances in photovoltaic technology [IAF PAPER 92-0599] p 235 A92-57055
- Effect of particle size of Martian dust on the degradation of photovoltaic cell performance [NASA-TM-105232] p 79 N92-11133
- Power supply for a manned international asteroid mission p 80 N92-13205
- Selective emitters [NASA-CASE-LEW-14731-1] p 236 N92-22037
- Self-deploying photovoltaic power system [NASA-CASE-LEW-15308-1] p 237 N92-24057
- Solar radiation on a catenary collector [NASA-TM-105751] p 163 N92-32243
- Photovoltaic array for Martian surface power [NASA-TM-105827] p 270 N92-33899
- PHOTOVOLTAIC CONVERSION**
- Space power by ground-based laser illumination p 59 A92-18401
- Photovoltaic power options for Mars p 231 A92-20366
- Space power by ground-based laser transmission [AIAA PAPER 92-3024] p 63 A92-47027
- Space transfer with ground-based laser/electric propulsion [AIAA PAPER 92-3213] p 73 A92-54017
- Advances in photovoltaic technology [IAF PAPER 92-0599] p 235 A92-57055
- NASA programs in space photovoltaics [NASA-TM-105428] p 87 N92-25343
- PHYSICAL OPTICS**
- Analysis of a generalized dual reflector antenna system using physical optics [NASA-TM-105425] p 149 N92-18281
- PIEZOELECTRIC CERAMICS**
- Electromechanical simulation and testing of actively controlled rotordynamic systems with piezoelectric actuators p 204 A92-39258
- PIEZOELECTRIC TRANSDUCERS**
- Electromechanical simulation and testing of actively controlled rotordynamic systems with piezoelectric actuators [ASME PAPER 91-GT-245] p 203 A92-15650
- Design of a self-diagnostic beam-mode piezoelectric accelerometer [AIAA PAPER 92-3656] p 200 A92-54106
- PINHOLES**
- Ion collection from a plasma by a pinhole p 259 N92-22368
- PINS**
- Controlled crack growth specimen for brittle systems p 123 A92-21099
- PIONS**
- Massive Dirac neutrinos and SN 1987A p 268 A92-45808
- PIPE FLOW**
- Nonlinear dynamics near the stability margin in rotating pipe flow p 165 A92-19959
- PIPELINING (COMPUTERS)**
- Multicarrier demodulator architecture for onboard processing satellites p 49 A92-10465
- PIPES (TUBES)**
- NASA Lewis Stirling SPRE testing and analysis with reduced number of cooler tubes [NASA-TM-105767] p 238 N92-28837
- PISTON ENGINES**
- Stirling machine operating experience p 206 A92-50788
- Combustion and core noise p 254 N92-10607
- NASA Lewis Stirling SPRE testing and analysis with reduced number of cooler tubes [NASA-TM-105767] p 238 N92-28837
- A free-piston Stirling engine/linear alternator controls and load interaction test facility [NASA-TM-105825] p 238 N92-31262
- Progress update of NASA's free-piston Stirling space power converter technology project [NASA-TM-105748] p 239 N92-33898
- PITCH (INCLINATION)**
- Calibration of hemispherical-head flow angularity probes [AIAA PAPER 92-4005] p 200 A92-56828
- PITOT TUBES**
- Measurement and analysis of a small nozzle plume in vacuum [AIAA PAPER 92-3108] p 64 A92-48748
- PITTING**
- Full-scale transmission testing to evaluate advanced lubricants [NASA-TM-105668] p 212 N92-26560

PLANAR STRUCTURES

- Analysis of shielded CPW discontinuities with air-bridges p 152 N92-32971
- PLANT DESIGN**
- Small engine components test facility compressor testing cell at NASA Lewis Research Center [AIAA PAPER 92-3980] p 41 A92-56806
- Transonic turbine blade cascade testing facility [AIAA PAPER 92-4034] p 42 A92-56856
- Transonic turbine blade cascade testing facility [NASA-TM-105646] p 47 N92-26129
- Small engine components test facility compressor testing cell at NASA Lewis Research Center [NASA-TM-105685] p 42 N92-30508
- PLASMA ACCELERATION**
- Plasma flow processes within magnetic nozzle configurations p 67 A92-50266
- PLASMA ACCELERATORS**
- Further study of the effect of the downstream plasma condition on accelerator grid erosion in an ion thruster [AIAA PAPER 92-3829] p 76 A92-54192
- PLASMA CURRENTS**
- Solar Array Module Plasma Interaction Experiment (SAMPIE): Technical requirements document [NASA-TM-105660] p 56 N92-28683
- PLASMA DENSITY**
- Vacuum ultraviolet absorption in a hydrogen arcjet [AIAA PAPER 92-3564] p 259 A92-54055
- PLASMA DIAGNOSTICS**
- Plasma erosion rate diagnostics using laser-induced fluorescence p 198 A92-36738
- Anode power deposition in applied-field MPD thrusters [AIAA PAPER 92-3463] p 74 A92-54034
- PLASMA DYNAMICS**
- Reactive collision terms for fluid transport theory p 257 A92-22693
- PLASMA ELECTRODES**
- Theory of plasma contactor neutral gas emissions for electrodynamic tethers p 258 A92-41549
- PLASMA ENGINES**
- Preliminary investigation of power flow and electrode phenomena in a multi-megawatt coaxial plasma thruster [AIAA PAPER 92-3741] p 75 A92-54144
- The evolutionary development of high specific impulse electric thruster technology [NASA-TM-105712] p 92 N92-31342
- PLASMA ETCHING**
- Plasma etching a ceramic composite --- evaluating microstructure [NASA-TM-105430] p 130 N92-22305
- PLASMA INTERACTION EXPERIMENT**
- The Solar Array Module Plasma Interactions Experiment (SAMPIE): Science and technology objectives p 86 N92-22360
- NASCAP/LEO simulations of Shuttle Orbiter charging during the SAMPIE experiment p 55 N92-22361
- Solar Array Module Plasma Interaction Experiment (SAMPIE): Technical requirements document [NASA-TM-105660] p 56 N92-28683
- PLASMA INTERACTIONS**
- Assessment of environmental effects on Space Station Freedom Electrical Power System p 55 A92-50581
- The Solar Array Module Plasma Interactions Experiment (SAMPIE) - A Shuttle-based plasma interactions experiment p 69 A92-50583
- Environmental interactions in Space Exploration: Announcement of the formation of an Environmental Interactions Working Group [NASA-TM-105294] p 270 N92-17069
- The Solar Array Module Plasma Interactions Experiment (SAMPIE): Science and technology objectives p 86 N92-22360
- Experimental breakdown of selected anodized aluminum samples in dilute plasmas p 259 N92-22369
- Environmental interactions in space exploration: Environmental interactions working group p 239 N92-22382
- Solar Array Module Plasma Interaction Experiment (SAMPIE): Technical requirements document [NASA-TM-105660] p 56 N92-28683
- PLASMA JETS**
- Microwave electrothermal propulsion for space p 63 A92-46049
- Vacuum ultraviolet absorption in a hydrogen arcjet [AIAA PAPER 92-3564] p 259 A92-54055
- A first-principles model for orificed hollow cathode operation [AIAA PAPER 92-3742] p 259 A92-54145
- The Solar Array Module Plasma Interactions Experiment (SAMPIE): Science and technology objectives p 86 N92-22360
- PLASMA PROPULSION**
- Numerical simulation of geometric scale effects in cylindrical self-field MPD thrusters [AIAA PAPER 92-3297] p 258 A92-48885

- Anode power deposition in applied-field MPD thrusters [AIAA PAPER 92-3463] p 74 A92-54034
- Development and flight history of SERT 2 spacecraft [AIAA PAPER 92-3516] p 74 A92-54038
- Magnetoplasmadynamic Thruster Workshop [NASA-CP-10084] p 77 N92-10044
- Multimegawatt MPD thruster design considerations [NASA-TM-105405] p 83 N92-16024
- Preliminary test results of a hollow cathode MPD thruster [NASA-TM-105324] p 84 N92-18474
- Nuclear Electric Propulsion Technology Panel findings and recommendations p 85 N92-20355
- Development and flight history of SERT 2 spacecraft [NASA-TM-105636] p 90 N92-28983
- The evolutionary development of high specific impulse electric thruster technology [NASA-TM-105758] p 93 N92-33064
- PLASMA RADIATION**
- Multimegawatt MPD thruster design considerations [NASA-TM-105405] p 83 N92-16024
- PLASMA SHEATHS**
- High voltage spheres in an unmagnetized plasma - Fluid and PIC simulations p 258 A92-47936
- PLASMA SPRAYING**
- Thermal barrier coating life and isothermal oxidation of low-pressure plasma-sprayed bond coat alloys p 119 A92-32398
- Synthesis and characterization of fine grain diamond films p 262 A92-46330
- Composite thermal barrier coating [NASA-CASE-LEW-14999-1] p 108 N92-21725
- Novel applications for TAZ-8A p 123 N92-22444
- PLASMA-ELECTROMAGNETIC INTERACTION**
- Effect of an arcjet plume on satellite reflector performance p 53 A92-16318
- Arcing of negatively biased solar cells in a plasma environment. I - Experimental observations [AIAA PAPER 92-2990] p 63 A92-47000
- PLASMA-PARTICLE INTERACTIONS**
- Ionospheric plasma flow over large high-voltage space platforms. I - Ion-plasma-time scale interactions of a plate at zero angle of attack. II - The formation and structure of plasma wake p 258 A92-41359
- PLASMAS (PHYSICS)**
- Environmental interactions in Space Exploration: Announcement of the formation of an Environmental Interactions Working Group [NASA-TM-105294] p 270 N92-17069
- Environmental interactions in space exploration: Environmental interactions working group p 239 N92-22382
- PLASTIC DEFORMATION**
- The effect of temperature on the deformation and fracture of SiC/Ti-24Al-11Nb p 106 A92-55143
- Computational simulation of matrix micro-slip bands in SiC/Ti-15 composite [NASA-TM-105762] p 111 N92-32466
- PLASTIC PROPERTIES**
- 1200 and 1300 K slow plastic compression properties of Ni-50Al composites p 102 A92-38125
- Computational simulation of matrix micro-slip bands in SiC/Ti-15 composite [NASA-TM-105762] p 111 N92-32466
- PLATES (STRUCTURAL MEMBERS)**
- Three point lead screw positioning apparatus [NASA-CASE-LEW-15216-1] p 208 N92-17678
- PLATINUM**
- Temperature dependence of the electrode kinetics of oxygen reduction at the platinum/Nafion interface - A microelectrode investigation p 115 A92-56950
- Guanidine based vehicle/binders for use with oxides, metals, and ceramics [NASA-CASE-LEW-15314-1] p 131 N92-23461
- PLATINUM COMPOUNDS**
- A study of Na(x)P3O4 as an O2 electrode bifunctional electrocatalyst [NASA-TM-105311] p 85 N92-20585
- PLUGGING**
- The chemistry of Saudi Arabian sand: A deposition problem on helicopter turbine airfoils [NASA-TM-105234] p 128 N92-14179
- PLUGS**
- Method of producing a plug-type heat flux gauge [NASA-CASE-LEW-14967-2] p 201 N92-22038
- PLUMES**
- Experimental balances for the second moments for a buoyant plume and their implication on turbulence modeling p 174 A92-40153
- Measurement and analysis of a small nozzle plume in vacuum [AIAA PAPER 92-3108] p 64 A92-48748
- An overview of in-flight plume diagnostics for rocket engines [AIAA PAPER 92-3785] p 75 A92-54164

- Demonstration of a flight capable system for plume spectroscopy
[AIAA PAPER 92-3786] p 57 A92-54165
- Experimental and numerical investigations of low-density nozzle and plume flows of nitrogen p 183 A92-54917
- An overview of in-flight plume diagnostics for rocket engines
[NASA-TM-105727] p 90 N92-28417
- PNEUMATICS**
- Advanced ice protection systems test in the NASA Lewis Icing Research Tunnel p 22 A92-14406
- POINT TO POINT COMMUNICATION**
- Future communications satellite applications p 52 N92-22019
- POINTING CONTROL SYSTEMS**
- Pointing and tracking control for freedom's Solar Dynamic modules and vibration control of freedom
[AAS PAPER 91-459] p 54 A92-43284
- Classical and adaptive control algorithms for the solar array pointing system of the Space Station Freedom
[AIAA PAPER 92-4484] p 57 A92-55314
- Solar dynamic modules for Space Station Freedom: The relationship between fine-pointing control and thermal loading of the aperture plate
[NASA-TM-104498] p 84 N92-19780
- POLAR ORBITS**
- Overview of the Beta II Two-Stage-To-Orbit vehicle design
[NASA-TM-105298] p 48 N92-11034
- POLARIMETERS**
- Extrapolation procedures in Mott electron polarimetry p 197 A92-21241
- POLARIMETRY**
- Extrapolation procedures in Mott electron polarimetry p 197 A92-21241
- POLARIZATION (SPIN ALIGNMENT)**
- Extrapolation procedures in Mott electron polarimetry p 197 A92-21241
- POLICIES**
- NASA/DOE/DOD nuclear propulsion technology planning: Summary of FY 1991 interagency panel results
[NASA-TM-105703] p 88 N92-26792
- POLLUTION CONTROL**
- Applied analytical combustion/emissions research at the NASA Lewis Research Center - A progress report
[AIAA PAPER 92-3338] p 27 A92-54025
- Applied analytical combustion/emissions research at the NASA Lewis Research Center
[NASA-TM-105731] p 90 N92-29343
- POLYBENZIMIDAZOLE**
- Evaluation of high temperature capacitor dielectrics
[NASA-TM-105622] p 161 N92-23561
- POLYCRYSTALS**
- Review and statistical analysis of the use of ultrasonic velocity for estimating the porosity fraction in polycrystalline materials p 215 A92-28722
- Thin-film photovoltaics: Status and applications to space power p 81 N92-13228
- Screen Cage Ion Plating (SCIP) and scratch testing of polycrystalline aluminum oxide
[NASA-TM-105404] p 130 N92-22278
- POLYETHER RESINS**
- An XPS study of the stability of Fomblin Z25 on the native oxide of aluminum - x ray photoelectron spectroscopy
[NASA-TM-105594] p 131 N92-23185
- POLYIMIDE RESINS**
- SiO_x(X) coatings for atomic oxygen protection of polyimide Kapton in low earth orbit
[AIAA PAPER 92-2151] p 94 A92-31286
- Viscoelastic properties of addition-cured polyimides used in high temperature polymer matrix composites p 124 A92-32632
- Effect of contact stresses in four-point bend testing of graphite/epoxy and graphite/PMR-15 composite beams p 219 A92-33589
- Addition curing thermosets endcapped with 4-amino (2,2) paracyclophane p 124 A92-33918
- New addition curing polyimides p 95 N92-13281
- Effects of a noncoplanar biphenyldiamine on the processing and properties of addition polyimides
[NASA-TM-105383] p 107 N92-15137
- Structure-to-property relationships in addition cured polymers. 4: Correlations between thermo-oxidative weight losses of norbornenyl cured polyimide resins and their composites p 108 N92-20039
- Vinyl capped addition polyimides
[NASA-CASE-LEW-15027-2] p 131 N92-24053
- Cyclopentadiene evolution during pyrolysis-gas chromatography of PMR polyimides
[NASA-TM-105629] p 132 N92-25348
- Isothermal aging effects on PMR-15 resin
[NASA-TM-105648] p 110 N92-30986
- POLYIMIDES**
- High molecular weight first generation PMR polyimides for 343 C applications p 105 A92-49819
- Evaluation of Kapton pyrolysis, arc tracking, and arc propagation on the Space Station Freedom (SSF) solar array flexible current carrier (FCC) p 72 A92-53209
- New addition curing polyimides
[NASA-TM-105335] p 95 N92-13281
- High molecular weight first generation PMR polyimides for 343 C applications
[NASA-TM-105364] p 129 N92-19498
- Cyclopentadiene evolution during pyrolysis-gas chromatography of PMR polyimides
[NASA-TM-105629] p 132 N92-25348
- POLYMER CHEMISTRY**
- Substituted 1,1,1-triaryl-2,2,2-trifluoroethanes and processes for their synthesis
[NASA-CASE-LEW-14345-6] p 96 N92-17882
- POLYMER MATRIX COMPOSITES**
- Relationship between voids and interlaminar shear strength of polymer matrix composites p 98 A92-10241
- Viscoelastic properties of addition-cured polyimides used in high temperature polymer matrix composites p 124 A92-32632
- Effect of fiber reinforcement on thermo-oxidative stability and mechanical properties of polymer matrix composites p 101 A92-33587
- Addition curing thermosets endcapped with 4-amino (2,2) paracyclophane p 124 A92-33918
- Polymetric precursors for fibers and matrices p 125 A92-39856
- Void effects on the interlaminar shear strength of unidirectional graphite-fiber-reinforced composites p 105 A92-50348
- Computational simulation of surface waviness in graphite/epoxy woven composites due to initial curing
[NASA-TM-105313] p 106 N92-14118
- High-temperature polymer matrix composites p 108 N92-22513
- Progressive fracture of polymer matrix composite structures: A new approach
[NASA-TM-105574] p 109 N92-23194
- Approaches to polymer-derived CMC matrices
[NASA-TM-105754] p 110 N92-29660
- POLYMERIC FILMS**
- Dielectric breakdown studies of Teflon perfluoroalkoxy at high temperature p 125 A92-36287
- Evaluation of high temperature dielectric films for high voltage power electronic applications p 261 A92-44273
- POLYMERIZATION**
- Substituted 1,1,1-triaryl-2,2,2-trifluoroethanes and processes for their synthesis
[NASA-CASE-LEW-14345-6] p 96 N92-17882
- Structure-to-property relationships in addition cured polymers. 4: Correlations between thermo-oxidative weight losses of norbornenyl cured polyimide resins and their composites p 108 N92-20039
- Cyclopentadiene evolution during pyrolysis-gas chromatography of PMR polyimides
[NASA-TM-105629] p 132 N92-25348
- POLYNOMIALS**
- Mappings and accuracy for Chebyshev pseudo-spectral approximations p 248 A92-50469
- High-Order Polynomial Expansions (HOPE) for flux-vector splitting p 190 N92-23353
- Upper bounds for convergence rates of vector extrapolation methods on linear systems with initial iterations
[NASA-TM-105608] p 250 N92-33742
- POROSITY**
- The effect of porosity and gamma-gamma-prime eutectic content on the fatigue behavior of hydrogen charged PWA 1480 p 116 A92-12046
- Review and statistical analysis of the use of ultrasonic velocity for estimating the porosity fraction in polycrystalline materials p 215 A92-28722
- Extreme value statistics analysis of fracture strengths of a sintered silicon nitride failing from pores p 127 A92-50191
- POROUS BOUNDARY LAYER CONTROL**
- Convection in superposed fluid and porous layers p 166 A92-24752
- POSITION INDICATORS**
- Wavelength-multiplexed fiber-optic position encoder for aircraft control systems p 24 A92-42602
- POSITIONING DEVICES (MACHINERY)**
- Three point lead screw positioning apparatus
[NASA-CASE-LEW-15216-1] p 208 N92-17678
- POSTFLIGHT ANALYSIS**
- Advanced photovoltaic experiment, S0014: Preliminary flight results and post-flight findings p 237 N92-27101
- POTASSIUM HYDROXIDES**
- Effect of KOH concentration on LEO cycle life of IPV nickel-hydrogen flight cell - Update II p 232 A92-48212
- Effect of KOH concentration on LEO cycle life of IPV nickel-hydrogen flight cells - An update p 70 A92-50702
- Destructive physical analysis results of Ni/H₂ cells cycled in LEO regime p 70 A92-50707
- Effect of LEO cycling on 125 Ah advanced design IPV nickel-hydrogen flight cells - An update p 71 A92-50708
- Effect of KOH concentration on LEO cycle life of IPV nickel-hydrogen flight cells-update 2
[NASA-TM-105314] p 235 N92-13483
- POTASSIUM SILICATES**
- The effects of RF plasma ashing on zinc orthoitanate/potassium silicate thermal control coatings
[AIAA PAPER 92-2171] p 124 A92-31299
- POTENTIAL FIELDS**
- A combined vector potential-scalar potential method for FE computation of 3D magnetic fields in electrical devices with iron cores p 154 A92-23959
- Ion collection from a plasma by a pinhole p 259 N92-22368
- POTENTIAL FLOW**
- Development of a steady potential solver for use with linearized, unsteady aerodynamic analyses
[NASA-TM-105288] p 31 N92-20525
- POTENTIAL THEORY**
- Cascade flutter analysis with transient response aerodynamics p 217 A92-15972
- On the thermodynamic framework of generalized coupled thermoelastic-viscoplastic-damage modeling
[NASA-TM-105349] p 225 N92-14434
- POWDER (PARTICLES)**
- Method of making contamination-free ceramic bodies
[NASA-CASE-LEW-14984-1] p 128 N92-16122
- POWDER METALLURGY**
- Development of a new generation of high-temperature composite materials p 109 N92-22515
- Tribological and microstructural comparison of HIPped PM212 and PM212/Au self-lubricating composites
[NASA-TM-105615] p 97 N92-26142
- POWER AMPLIFIERS**
- Ka-band active MMIC subarray development
[AIAA PAPER 92-1863] p 155 A92-29803
- Advances in MMIC technology for communications satellites
[AIAA PAPER 92-1899] p 155 A92-29830
- A 1-W, 30-GHz, CPW amplifier for ACTS small terminal uplink
[NASA-TM-105671] p 161 N92-26096
- A 1-W, 30-GHz, CPW amplifier for ACTS small terminal uplink p 152 N92-32973
- POWER BEAMING**
- Beam power options for the moon p 61 A92-40429
- POWER CONDITIONING**
- Development of an analytical tool to study power quality of ac power systems for large spacecraft p 67 A92-50529
- Comparison of high temperature, high frequency core loss and dynamic B-H loops of two 50 Ni-Fe crystalline alloys and an iron-based amorphous alloy p 157 A92-50551
- Description of the PMAD DC test bed architecture and integration sequence p 46 A92-50655
- Description of the PMAD DC test bed architecture and integration sequence
[NASA-TM-105284] p 77 N92-10055
- Enhanced EOS photovoltaic power system capability with InP solar cells p 81 N92-13248
- Multi-megawatt inverter/converter technology for space power applications
[NASA-TM-105307] p 159 N92-14294
- Stability testing and analysis of a PMAD DC test bed for the Space Station Freedom
[NASA-TM-105846] p 162 N92-31282
- Load converter interactions with the secondary system in the Space Station Freedom power management and distribution DC test bed
[NASA-TM-105844] p 164 N92-34219
- POWER CONVERTERS**
- A 1 MW, 100 kV, less than 100 kg space based dc-dc power converter p 157 A92-50537
- Description of the PMAD DC test bed architecture and integration sequence p 46 A92-50655
- Component technology for Stirling power converters p 206 A92-50781
- Free-piston Stirling component test power converter p 206 A92-50784
- Description of the PMAD DC test bed architecture and integration sequence
[NASA-TM-105284] p 77 N92-10055

- NASA Lewis Stirling SPRE testing and analysis with reduced number of cooler tubes
[NASA-TM-105767] p 238 N92-28837
- Magnetic bearings for free-piston Stirling engines
[NASA-TM-105730] p 214 N92-30734
- Stability testing and analysis of a PMAD DC test bed for the Space Station Freedom
[NASA-TM-105846] p 162 N92-31282
- Progress update of NASA's free-piston Stirling space power converter technology project
[NASA-TM-105748] p 239 N92-33898
- Load converter interactions with the secondary system in the Space Station Freedom power management and distribution DC test bed
[NASA-TM-105844] p 164 N92-34219
- POWER EFFICIENCY**
- Microwave beam power transmission at an arbitrary range
[NASA-TM-105424] p 150 N92-19992
- POWER FACTOR CONTROLLERS**
- Development of an analytical tool to study power quality of ac power systems for large spacecraft p 67 A92-50529
- POWER SPECTRA**
- Rotative quadrature phase-shift keying p 146 A92-44233
- POWER SUPPLIES**
- Moonbase night power by laser illumination p 44 A92-21086
- Wiring for aerospace applications
[NASA-TM-105777] p 162 N92-30427
- POWER SUPPLY CIRCUITS**
- Functional models of power electronic components for system studies p 157 A92-50558
- POWER TRANSMISSION**
- Microwave properties of YBa₂Cu₃O₇(δ) high-transition-temperature superconducting thin films measured by the power transmission method p 153 A92-14938
- Microwave beam power transmission at an arbitrary range
[NASA-TM-105424] p 150 N92-19992
- Magnetic penetration depth of YBa₂Cu₃O₇(δ) thin films determined by the power transmission method p 265 N92-32983
- POWERED LIFT AIRCRAFT**
- Experimental performance of three design factors for ventral nozzles for SSTOVL aircraft
[AIAA PAPER 92-3789] p 28 A92-54168
- Internal reversing flow in a tailpipe offtake configuration for SSTOVL aircraft
[AIAA PAPER 92-3790] p 28 A92-54169
- Experimental performance of three design factors for ventral nozzles for SSTOVL aircraft
[NASA-TM-105697] p 37 N92-27669
- Internal reversing flow in a tailpipe offtake configuration for SSTOVL aircraft
[NASA-TM-105698] p 37 N92-28418
- PRANDTL NUMBER**
- Scaling of low-Prandtl-number thermocapillary flows p 176 A92-47271
- Scalar rate correlation at a turbulent liquid free surface - A two-regime correlation for high Schmidt numbers p 184 A92-56941
- PRECIPITATES**
- Microstructure and mechanical properties of a single crystal NiAl alloy with Zr or Hf rich G-phase precipitates p 119 A92-30841
- PRECIPITATION HARDENING**
- Thermomechanical deformation behavior of a dynamic strain aging alloy, Hastelloy X
[NASA-TM-105316] p 228 N92-25179
- PRECONDITIONING**
- Propulsion-related flowfields using the preconditioned Navier-Stokes equations
[AIAA PAPER 92-3437] p 178 A92-48994
- PREDICTION ANALYSIS TECHNIQUES**
- Mechanical behavior of fiber reinforced SiC/RBSN ceramic matrix composites - Theory and experiment --- Reaction Bonded Silicon Nitride
[ASME PAPER 91-GT-209] p 99 A92-15629
- A survey of the broadband shock associated noise prediction methods
[AIAA PAPER 92-0501] p 252 A92-26930
- Predictive onboard flow control in packet switching satellites
[AIAA PAPER 92-2004] p 144 A92-29923
- Application of a thermal fatigue life prediction model to high-temperature aerospace alloys B1900 + Hf and Haynes 188 p 121 A92-45232
- Three-dimensional Navier-Stokes heat transfer predictions for turbine blade rows
[AIAA PAPER 92-3068] p 12 A92-54003
- Modeling of the heat transfer in bypass transitional boundary-layer flows
[NASA-TP-3170] p 184 N92-11299
- Particle-laden weakly swirling free jets: Measurements and predictions
[NASA-TM-100881] p 29 N92-14061
- A survey of the broadband shock associated noise prediction methods
[NASA-TM-105365] p 254 N92-14797
- Predictive onboard flow control for packet switching satellites
[NASA-TM-105566] p 150 N92-19379
- The effect of ion plated silver and sliding friction on tensile stress-induced cracking in aluminum oxide
[NASA-TM-105366] p 129 N92-19450
- Life prediction technologies for aeronautical propulsion systems p 32 N92-22520
- Introduction to the internal fluid mechanics research session p 188 N92-22522
- Advancements in engineering turbulence modeling
[PAPER-105] p 189 N92-23350
- Progress towards understanding and predicting convection heat transfer in the turbine gas path
[NASA-TM-105674] p 194 N92-26690
- Experimental and computational ice shapes and resulting drag increase for a NACA 0012 airfoil
[NASA-TM-105743] p 20 N92-28674
- Validation of finite element and boundary element methods for predicting structural vibration and radiated noise
[NASA-TM-105359] p 213 N92-29697
- Life extending control for rocket engines
[NASA-TM-105789] p 142 N92-31263
- PREDICTIONS**
- Relationship between voids and interlaminar shear strength of polymer matrix composites p 98 A92-10241
- Prediction of ice accretion on a swept NACA 0012 airfoil and comparisons to flight test results
[AIAA PAPER 92-0043] p 4 A92-25677
- Life Extending Control --- mechanical fatigue in reusable rocket engines p 246 A92-29166
- Application of a thermal fatigue life prediction model to high-temperature aerospace alloys B1900 + Hf and Haynes 188 p 121 A92-45232
- Prediction of ice accretion on a swept NACA 0012 airfoil and comparisons to flight test results
[NASA-TM-105368] p 16 N92-15968
- Monte Carlo modeling of atomic oxygen attack of polymers with protective coatings on LDEF p 132 N92-27281
- PREFORMS**
- High temperature, flexible, fiber-preform seal
[NASA-CASE-LEW-15085-1] p 208 N92-22043
- PREMIXED FLAMES**
- The structure of premixed particle-cloud flames p 114 A92-43779
- PREMIXING**
- Numerical study of shock-wave/boundary-layer interactions in premixed combustible gases p 183 A92-54907
- PRESSURE**
- High temperature, flexible pressure-actuated, brush seal
[NASA-CASE-LEW-15086-1] p 208 N92-16318
- PRESSURE DEPENDENCE**
- Pressure dependence of the melting temperature of solids - Rare-gas solids p 171 A92-33912
- On the most general tensor B(sub ij) which is zero for i does not equal j, and the most general isotropic tensor l(sub ij)
[NASA-TM-105236] p 240 N92-10289
- PRESSURE DISTRIBUTION**
- Screech noise source structure of a supersonic rectangular jet p 6 A92-26932
- Renormalization group analysis of the Reynolds stress transport equation p 179 A92-49493
- Experimental performance of three design factors for ventral nozzles for SSTOVL aircraft
[AIAA PAPER 92-3789] p 28 A92-54168
- Use of an approximate similarity principle for the thermal scaling of a full-scale thrust augmenting ejector
[AIAA PAPER 92-3792] p 28 A92-54171
- Screech noise source structure of a supersonic rectangular jet
[NASA-TM-105384] p 15 N92-14000
- Renormalization group analysis of the Reynolds stress transport equation p 190 N92-23542
- Use of an approximate similarity principle for the thermal scaling of a full-scale thrust augmenting ejector
[NASA-TM-105724] p 36 N92-26613
- Experimental performance of three design factors for ventral nozzles for SSTOVL aircraft
[NASA-TM-105697] p 37 N92-27669
- PRESSURE DROP**
- A bulk flow model of a brush seal system
[ASME PAPER 91-GT-325] p 203 A92-15696
- Computational and experimental investigation of subsonic internal reversing flows
[AIAA PAPER 92-3791] p 183 A92-54170
- PRESSURE EFFECTS**
- Combustion of liquid-fuel droplets in supercritical conditions p 114 A92-43778
- Computational simulation of surface waviness in graphite/epoxy woven composites due to initial curing
[NASA-TM-105313] p 106 N92-14118
- Simulation of iced wing aerodynamics p 21 N92-21686
- Low power arcjet test facility impacts
[NASA-TM-105876] p 47 N92-34114
- PRESSURE GRADIENTS**
- Prediction of unsteady rotor-surface pressure and heat transfer from wake passages
[ASME PAPER 91-GT-267] p 165 A92-15665
- A new time scale based k-epsilon model for near wall turbulence
[NASA-TM-105768] p 196 N92-32868
- PRESSURE HEADS**
- The aerodynamic effect of fillet radius in a low speed compressor cascade
[NASA-TM-105347] p 29 N92-14063
- PRESSURE MEASUREMENT**
- Unsteady blade-surface pressures on a large-scale advanced propeller - Prediction and data p 3 A92-17178
- Unsteady wing surface pressures in the wake of a propeller
[AIAA PAPER 92-0277] p 5 A92-25731
- Measurement and analysis of a small nozzle plume in vacuum
[AIAA PAPER 92-3108] p 64 A92-48748
- Description of a pressure measurement technique for obtaining surface static pressures of a radial turbine
[AIAA PAPER 92-4006] p 200 A92-56829
- Description of a pressure measurement technique for obtaining surface static pressures of a radial turbine
[NASA-TM-105643] p 202 N92-24959
- PRESSURE OSCILLATIONS**
- Unsteady blade-surface pressures on a large-scale advanced propeller - Prediction and data p 3 A92-17178
- PRESSURE RATIO**
- Viscous three-dimensional calculations of transonic fan performance
[NASA-TM-103800] p 1 N92-17346
- Flow studies in close-coupled ventral nozzles for STOVL aircraft
[NASA-TM-102554] p 17 N92-20934
- PRESSURE REDUCTION**
- An experimental investigation of high-aspect-ratio cooling passages
[AIAA PAPER 92-3154] p 64 A92-48780
- Jet mixing in low gravity - Results of the Tank Pressure Control Experiment
[AIAA PAPER 92-3060] p 182 A92-54001
- Vortex generator design for aircraft inlet distortion as a numerical optimization problem p 23 N92-13959
- An experimental investigation of high-aspect-ratio cooling passages
[NASA-TM-105679] p 48 N92-25958
- PRESSURE SENSORS**
- Advanced nozzle and engine components test facility
[AIAA PAPER 92-3993] p 41 A92-56816
- Calibration of hemispherical-head flow angularity probes
[AIAA PAPER 92-4005] p 200 A92-56828
- Advanced nozzle and engine components test facility
[NASA-TM-103684] p 42 N92-17059
- PRESSURE VESSELS**
- Hydrogen no-vent testing in a 5 cubic foot (142 liter) tank using spray nozzle and spray bar liquid injection
[AIAA PAPER 92-3063] p 63 A92-48719
- Nickel-hydrogen cell low-earth-orbit life test update p 70 A92-50700
- Destructive physical analysis results of Ni/H₂ cells cycled in LEO regime p 70 A92-50707
- Inflatable traversing probe seal p 209 N92-22692
- Composite overwrapped nickel-hydrogen pressure vessels p 109 N92-22762
- Validation test of advanced technology for IPV nickel-hydrogen flight cells: Update
[NASA-TM-105689] p 89 N92-27878
- Hydrogen no-vent fill testing in a 5 cubic foot (142 liter) tank using spray nozzle and spray bar liquid injection
[NASA-TM-105759] p 136 N92-28433
- Elevated temperature axial and torsional fatigue behavior of Haynes 188
[NASA-TM-105396] p 229 N92-28701
- PRIMARY BATTERIES**
- NASA Aerospace Flight Battery Systems Program: An update p 237 N92-22741

- PRINTED CIRCUITS**
 New coplanar waveguide to rectangular waveguide end launcher p 156 A92-44243
 Thermal verification testing of commercial printed-circuit boards for spaceflight p 216 A92-56217
 Thermal verification testing of commercial printed-circuit boards for spaceflight [NASA-TM-105261] p 141 N92-11221
- PRINTING**
 High-T sub c fluorine-doped YBa₂Cu₃O₇(y) films on ceramic substrates by screen printing [NASA-TM-105296] p 127 N92-11188
- PROBABILITY DENSITY FUNCTIONS**
 A new response surface approach for structural reliability analysis [AIAA PAPER 92-2408] p 219 A92-34339
 Structural system reliability calculation using a probabilistic fault tree analysis method [AIAA PAPER 92-2410] p 251 A92-34341
 Recent developments of the NESSUS probabilistic structural analysis computer program [AIAA PAPER 92-2411] p 242 A92-34342
 A continuous mixing model for pdf simulations and its applications to combustor shear flows p 174 A92-40139
 Discrete-time entropy formulation of optimal and adaptive control problems p 247 A92-55930
- PROBABILITY DISTRIBUTION FUNCTIONS**
 Mapping methods for computationally efficient and accurate structural reliability [AIAA PAPER 92-2347] p 219 A92-34321
- PROBABILITY THEORY**
 Probabilistic constitutive relationships for cyclic material strength models p 217 A92-21081
 Void probability as a function of the void's shape and scale-invariant models --- in studies of spacial galactic distribution p 267 A92-24456
 A probabilistic approach to the evaluation of fatigue damage in a space propulsion system injector element [AIAA PAPER 92-2413] p 60 A92-34343
 Probabilistic progressive buckling of trusses [AIAA PAPER 91-0916] p 223 A92-38142
 Probabilistic progressive buckling of trusses [NASA-TM-105162] p 226 N92-15403
 Probabilistic assessment of space trusses subjected to combined mechanical and thermal loads [NASA-TM-105429] p 230 N92-33935
- PROBLEM SOLVING**
 Institute for Computational Mechanics in Propulsion (ICOMP) [NASA-TM-105612] p 250 N92-27196
- PROCESS CONTROL (INDUSTRY)**
 Identification and control of a multizone crystal growth furnace p 199 A92-39699
 Effects of a noncoplanar biphenyldiamine on the processing and properties of addition polyimides [NASA-TM-105383] p 107 N92-15137
 A basis for solid modeling of gear teeth with application in design and manufacture [NASA-TM-105392] p 209 N92-24202
- PRODUCT DEVELOPMENT**
 A multi-channel demultiplexer/demodulator architecture, simulation and implementation [AIAA PAPER 92-1972] p 144 A92-29895
 The NASA-OAST earth-to-orbit propulsion technology program - The action plan [AIAA PAPER 92-1478] p 61 A92-38597
 Turning up the heat on aircraft structures --- design and analysis for high-temperature conditions p 23 A92-55131
- PRODUCTIVITY**
 The application of a computer data acquisition system to a new high temperature tribometer p 93 A92-11823
- PROGRAM VERIFICATION (COMPUTERS)**
 Experimental code verification results for reflector antenna distortion compensation by array feeds [AIAA PAPER 92-2014] p 49 A92-29933
- PROJECT MANAGEMENT**
 Nuclear Thermal Propulsion: A Joint NASA/DOE/DOD Workshop [NASA-CP-10079] p 78 N92-11088
 Institute for Computational Mechanics in Propulsion (ICOMP) [NASA-TM-105612] p 250 N92-27196
- PROJECT PLANNING**
 Nuclear rocket propulsion: NASA plans and progress - FY 1991 p 69 A92-50584
 Nuclear Thermal Propulsion: A Joint NASA/DOE/DOD Workshop [NASA-CP-10079] p 78 N92-11088
 Nuclear thermal propulsion workshop overview p 78 N92-11090
 Nuclear thermal rocket workshop reference system Rover/NERVA p 78 N92-11091
- JANNAF Liquid Rocket Combustion Instability Panel research recommendations p 115 N92-11124
 NASA/DOE/DOD nuclear propulsion technology planning: Summary of FY 1991 interagency panel results [NASA-TM-105703] p 88 N92-26792
- PROP-FAN TECHNOLOGY**
 Unsteady Euler analysis of the flowfield of a propfan at an angle of attack p 3 A92-21070
 Unsteady blade pressures on a propfan at takeoff - Euler analysis and flight data [AIAA PAPER 92-0376] p 25 A92-26234
 Unsteady flowfield simulation of ducted prop-fan configurations [AIAA PAPER 92-0521] p 6 A92-26946
 Aeroelastic analysis of advanced propellers using an efficient Euler solver [AIAA PAPER 92-0488] p 7 A92-28194
 A numerical classical flutter analysis of advanced propellers [AIAA PAPER 92-2118] p 26 A92-35687
 Unsteady airloading panel method for propfans p 253 A92-44512
 Predicted pressure distribution on a prop-fan blade through Euler analysis p 10 A92-46791
 Wind tunnel performance results of swirl recovery vanes as tested with an advanced high speed propeller [AIAA PAPER 92-3770] p 28 A92-54159
 Unsteady blade pressures on a propfan - Predicted and measured compressibility effects [AIAA PAPER 92-3774] p 14 A92-54161
 Overview of NASA PTA propfan flight test program p 33 N92-22536
- PROPAGATION MODES**
 Naturally occurring and forced azimuthal modes in a turbulent jet p 172 A92-35998
- PROPELLANT ADDITIVES**
 Upper stages using liquid propulsion and metallized propellants [NASA-TP-3191] p 83 N92-17151
- PROPELLANT CHEMISTRY**
 Material processing with hydrogen and carbon monoxide on Mars p 231 A92-17769
- PROPELLANT COMBUSTION**
 Experiments and analysis concerning the use of external burning to reduce aerospace vehicle transonic drag [NASA-TM-105397] p 30 N92-17546
 Combustion-wave ignition for rocket engines [NASA-TM-105545] p 84 N92-20043
- PROPELLANT STORAGE**
 A review of candidate multilayer insulation systems for potential use on wet-launched LH₂ tankage for the space exploration initiative lunar missions [NASA-TM-104493] p 134 N92-13336
- PROPELLANT TANKS**
 Pulsed thrust propellant reorientation - Concept and modeling p 62 A92-44507
 Hydrogen no-vent testing in a 5 cubic foot (142 liter) tank using spray nozzle and spray bar liquid injection [AIAA PAPER 92-3063] p 63 A92-48719
 Hydrogen no-vent fill testing in a 5 cubic foot (142 liter) tank using spray nozzle and spray bar liquid injection [NASA-TM-105759] p 136 N92-28433
- PROPELLANT TRANSFER**
 Evaluation of supercritical cryogen storage and transfer systems for future NASA missions p 47 A92-28512
 Hydrogen no-vent testing in a 5 cubic foot (142 liter) tank using spray nozzle and spray bar liquid injection [AIAA PAPER 92-3063] p 63 A92-48719
 Improved thermodynamic modeling of the no-vent fill process and correlation with experimental data [NASA-TM-104492] p 79 N92-11129
 Space Station Freedom/lunar transfer vehicle propellant operation hazard analysis p 55 N92-17416
 Hydrogen no-vent fill testing in a 5 cubic foot (142 liter) tank using spray nozzle and spray bar liquid injection [NASA-TM-105759] p 136 N92-28433
- PROPELLANTS**
 Krypton ion thruster performance [NASA-TM-105818] p 92 N92-31901
- PROPELLER BLADES**
 Unsteady blade-surface pressures on a large-scale advanced propeller - Prediction and data p 3 A92-17178
 Analysis of aircraft engine blade subject to ice impact [NASA-TM-105336] p 226 N92-15402
 Detailed noise measurements on the SR-7A propeller: Tone behavior with helical tip Mach number [NASA-TM-105206] p 255 N92-16705
- PROPELLER DRIVE**
 A review of computational/experimental methodology developments in aeroacoustics p 253 A92-39241
- PROPELLER EFFICIENCY**
 A numerical classical flutter analysis of advanced propellers [AIAA PAPER 92-2118] p 26 A92-35687
- A review of computational/experimental methodology developments in aeroacoustics p 253 A92-39241
 Advanced propeller research p 33 N92-22537
- PROPELLER FANS**
 Unsteady blade pressures on a propfan at takeoff - Euler analysis and flight data [AIAA PAPER 92-0376] p 25 A92-26234
 Aeroelastic stability analyses of two counter rotating propfan designs for a cruise missile model [AIAA PAPER 92-2218] p 25 A92-34408
 Analysis of aircraft engine blade subject to ice impact [NASA-TM-105336] p 226 N92-15402
 Overview of NASA PTA propfan flight test program p 33 N92-22536
 Advanced propeller research p 33 N92-22537
 Aeroelastic stability analyses of two counter rotating propfan designs for a cruise missile model [NASA-TM-105268] p 227 N92-23191
 Structural analysis of low-speed composite propfan blades for the LRCSW wind tunnel model [NASA-TM-105266] p 229 N92-25753
- PROPELLER NOISE**
 Far-field noise and internal modes from a ducted propeller at simulated aircraft takeoff conditions [AIAA PAPER 92-0371] p 252 A92-26230
 Far-field noise and internal modes from a ducted propeller at simulated aircraft takeoff conditions [NASA-TM-105369] p 254 N92-16702
 Detailed noise measurements on the SR-7A propeller: Tone behavior with helical tip Mach number [NASA-TM-105206] p 255 N92-16705
- PROPELLER SLIPSTREAMS**
 Unsteady wing surface pressures in the wake of a propeller [AIAA PAPER 92-0277] p 5 A92-25731
- PROPELLERS**
 An unsteady Euler scheme for the analysis of ducted propellers [AIAA PAPER 92-0522] p 6 A92-26947
 Aeroelastic analysis of advanced propellers using an efficient Euler solver [AIAA PAPER 92-0488] p 7 A92-28194
 Wind tunnel performance results of swirl recovery vanes as tested with an advanced high speed propeller [AIAA PAPER 92-3770] p 28 A92-54159
- PUSPULSION**
 Development of an algebraic turbulence model for analysis of propulsion flows [AIAA PAPER 92-3861] p 183 A92-54209
 Directions in propulsion control p 32 N92-22530
 Overview of the subsonic propulsion technology session p 32 N92-22531
 Workshop on Engineering Turbulence Modeling [NASA-CP-10088] p 191 N92-24514
 The future challenge for aeropropulsion [NASA-TM-105613] p 35 N92-25164
 Development of an algebraic turbulence model for analysis of propulsion flows [NASA-TM-105701] p 250 N92-27517
 Trends in aeropropulsion research and their impact on engineering education [NASA-TM-105682] p 38 N92-31172
 A parameter optimization approach to controller partitioning for integrated flight/propulsion control application [NASA-TM-105826] p 40 N92-32241
- PROPULSION SYSTEM CONFIGURATIONS**
 Status of NASA's Earth-to-Orbit Propulsion Technology program [IAF PAPER 91-258] p 58 A92-13154
 Electric propulsion - An evolutionary technology [IAF PAPER 91-241] p 58 A92-13158
 Nuclear rocket propulsion technology - A joint NASA/DOE project [IAF PAPER 91-236] p 58 A92-13159
 Innovative nuclear thermal propulsion technology evaluation - Results of the NASA/DOE task team study [IAF PAPER 91-235] p 58 A92-13160
 Medium power hydrogen arcjet performance [AIAA PAPER 91-2227] p 58 A92-15355
 Numerical propulsion system simulation p 59 A92-20194
 Flow in a ventral nozzle for short takeoff and vertical landing aircraft p 25 A92-28538
 IMPAC - An integrated methodology for propulsion and airframe control p 39 A92-29118
 Computational simulation of concurrent engineering for aerospace propulsion systems [AIAA PAPER 92-1144] p 241 A92-33285
 The F/A-18 external burning flight test [AIAA PAPER 91-5050] p 23 A92-44547
 Fiber optic controls for aircraft engines - Issues and implications p 24 A92-46244
 Rocket engine propulsion 'system reliability' [AIAA PAPER 92-3421] p 66 A92-48980

PROPULSION SYSTEM PERFORMANCE

Propulsion systems using in situ propellants for a Mars Ascent Vehicle
[AIAA PAPER 92-3445] p 66 A92-49001
The VRT gas turbine combustor - Phase II
[AIAA PAPER 92-3471] p 27 A92-54035
Multi-reactor power system configurations for megawatt nuclear electric propulsion
[NASA-TM-105212] p 77 N92-10057
Nuclear Thermal Propulsion: A Joint NASA/DOE/DOD Workshop
[NASA-CP-10079] p 78 N92-11088
Nuclear thermal rocket workshop reference system
Rover/NERVA p 78 N92-11091
Plans for the development of cryogenic engines for space exploration
[NASA-TM-105250] p 79 N92-11135
An overview of tested and analyzed NTP concepts
[NASA-TM-105252] p 80 N92-11137
The design and performance estimates for the propulsion module for the booster of a TSTO vehicle
[NASA-TM-105299] p 29 N92-11995
Fuels and materials development for space nuclear propulsion
[NASA-TM-107806] p 85 N92-21187
Airbreathing combined cycle engine systems
Beta 2: A near term, fully reusable, horizontal takeoff and landing two-stage-to-orbit launch vehicle concept
p 86 N92-21536
Aeropropulsion 1987
[NASA-CP-3049] p 31 N92-22510
Impact and promise of NASA aeropropulsion technology
[NASA-TM-105251] p 31 N92-22511
Integrated analysis and applications
Rotorcraft transmissions p 32 N92-22521
NASA thrusts in high-speed aeropropulsion research and development: An overview p 33 N92-22538
Supersonic STOVL propulsion technology program: An overview p 33 N92-22539
Modelling and experimental verification of a water alleviation system for the NASP --- National Aerospace Plane
[NASA-TM-105661] p 189 N92-23224
The future challenge for aeropropulsion
[NASA-TM-105613] p 35 N92-25164
Activities for numerical propulsion systems simulation program p 244 N92-25726
Study of shock-induced combustion using an implicit TVD scheme p 116 N92-25816
Computer codes developed and under development at Lewis p 244 N92-25913
A brief overview of computational structures technology related activities at NASA Lewis Research Center p 229 N92-25915
Propulsion systems using in situ propellants for a Mars ascent vehicle
[NASA-TM-105741] p 89 N92-27654
Integrated health monitoring and controls for rocket engines
[NASA-TM-105763] p 90 N92-28693
NEP systems engineering efforts in FY-92: Plans and status
[NASA-TM-105775] p 91 N92-30308
Nuclear electric propulsion development and qualification facilities
[NASA-TM-105521] p 91 N92-30818
A graphical user-interface for propulsion system analysis
[NASA-TM-105696] p 244 N92-33894
PROPULSION SYSTEM PERFORMANCE
Medium power hydrogen arcjet performance
[AIAA PAPER 91-2227] p 58 A92-15355
Integrated flight/propulsion control specifications for systems with two-way coupling p 39 A92-29117
IMPAC - An integrated methodology for propulsion and airframe control p 39 A92-29118
Metal- and intermetallic-matrix composites for aerospace propulsion and power systems p 104 A92-43682
Electric propulsion - The future is now p 63 A92-48386
Preliminary investigation of a low power pulsed arcjet thruster
[AIAA PAPER 92-3113] p 64 A92-48752
Krypton ion thruster performance
[AIAA PAPER 92-3144] p 64 A92-48772
Qualitative spectroscopic study of magnetic nozzle flow
[AIAA PAPER 92-3161] p 65 A92-48784
An advanced intelligent control system framework
[AIAA PAPER 92-3162] p 65 A92-48785
Rocket engine diagnostics using qualitative modeling techniques
[AIAA PAPER 92-3164] p 65 A92-48787

Numerical simulation of geometric scale effects in cylindrical self-field MPD thrusters
[AIAA PAPER 92-3297] p 258 A92-48885
Propulsion systems using in situ propellants for a Mars Ascent Vehicle
[AIAA PAPER 92-3445] p 66 A92-49001
Test experience, 490 N high performance (321 sec isp) engine
[AIAA PAPER 92-3800] p 67 A92-49127
An overview of the NASA Advanced Propulsion Concepts program
[AIAA PAPER 92-3216] p 73 A92-54018
Effect of inert propellant injection on Mars ascent vehicle performance
[AIAA PAPER 92-3447] p 73 A92-54031
Scaling of 100 kW class applied-field MPD thrusters
[AIAA PAPER 92-3462] p 74 A92-54033
Numerical study of low pressure nuclear thermal rockets
[AIAA PAPER 92-3815] p 75 A92-54182
Further study of the effect of the downstream plasma condition on accelerator grid erosion in an ion thruster
[AIAA PAPER 92-3829] p 76 A92-54192
Propulsion system performance resulting from an Integrated Flight/Propulsion Control design
[AIAA PAPER 92-4602] p 28 A92-55281
Analysis of airframe/engine interactions for a STOVL aircraft with integrated flight/propulsion control
[AIAA PAPER 92-4623] p 23 A92-55300
Nuclear propulsion for space exploration
[IAF PAPER 92-0575] p 76 A92-57054
Low thrust chemical rocket technology
[IAF PAPER 92-0669] p 77 A92-57105
Real-time fault diagnosis for propulsion systems
[NASA-TM-105303] p 29 N92-11017
Nuclear Thermal Propulsion: A Joint NASA/DOE/DOD Workshop
[NASA-CP-10079] p 78 N92-11088
Nuclear thermal rocket workshop reference system
Rover/NERVA p 78 N92-11091
Plans for the development of cryogenic engines for space exploration
[NASA-TM-105250] p 79 N92-11135
An overview of tested and analyzed NTP concepts
[NASA-TM-105252] p 80 N92-11137
The design and performance estimates for the propulsion module for the booster of a TSTO vehicle
[NASA-TM-105299] p 29 N92-11995
Hydrogen/oxygen auxiliary propulsion technology
[NASA-TM-105249] p 85 N92-20522
Fuels and materials development for space nuclear propulsion
[NASA-TM-107806] p 85 N92-21187
Airbreathing combined cycle engine systems
p 31 N92-21523
Neutralizer optimization
[NASA-TM-105578] p 86 N92-21976
Aeropropulsion 1987
[NASA-CP-3049] p 31 N92-22510
Impact and promise of NASA aeropropulsion technology
[NASA-TM-105251] p 31 N92-22511
Determining structural performance p 32 N92-22519
Introduction to the internal fluid mechanics research session p 188 N92-22522
Optical measurement systems p 202 N92-22527
Directions in propulsion control p 32 N92-22530
NASA thrusts in high-speed aeropropulsion research and development: An overview p 33 N92-22538
Supersonic STOVL propulsion technology program: An overview p 33 N92-22539
The future challenge for aeropropulsion
[NASA-TM-105613] p 35 N92-25164
Activities for numerical propulsion systems simulation program p 244 N92-25726
Study of shock-induced combustion using an implicit TVD scheme p 116 N92-25816
Rocket engine diagnostics using qualitative modeling techniques
[NASA-TM-105714] p 88 N92-27033
Propulsion systems using in situ propellants for a Mars ascent vehicle
[NASA-TM-105741] p 89 N92-27654
Integrated health monitoring and controls for rocket engines
[NASA-TM-105763] p 90 N92-28693
Nuclear electric propulsion development and qualification facilities
[NASA-TM-105521] p 91 N92-30818
A graphical user-interface for propulsion system analysis
[NASA-TM-105696] p 244 N92-33894
PROPULSION EFFICIENCY
Techniques for spectroscopic measurements in an arcjet nozzle p 59 A92-21087

PROPYLENE

Atomic oxygen interactions with FEP Teflon and silicones on LDEF p 132 N92-24820

PROTECTIVE COATINGS

SiO(X) coatings for atomic oxygen protection of polyimide Kapton in low earth orbit
[AIAA PAPER 92-2151] p 94 A92-31286
Atomic oxygen effects on thin film space coatings studied by spectroscopic ellipsometry, atomic force microscopy, and laser light scattering
[AIAA PAPER 92-2172] p 94 A92-31300
Thermal barrier coating life and isothermal oxidation of low-pressure plasma-sprayed bond coat alloys p 119 A92-32398
Volatile species in halide-activated-diffusion coating packs p 122 A92-57028
Atomic oxygen durability of solar concentrator materials for Space Station Freedom
[NASA-TM-105378] p 85 N92-20065
Lubrication of space systems: Challenges and potential solutions p 130 N92-21579
Experimental breakdown of selected anodized aluminum samples in dilute plasmas p 259 N92-22369
Atomic oxygen undercutting of LDEF aluminized-Kapton multilayer insulation p 255 N92-24818
Ion Beam Textured and Coated Surfaces Experiment (IBEX) p 132 N92-24832
Durability evaluation of photovoltaic blanket materials exposed on LDEF tray S1003 p 132 N92-27100
Monte Carlo modeling of atomic oxygen attack of polymers with protective coatings on LDEF p 132 N92-27281
Oxidation resistant coating for titanium alloys and titanium alloy matrix composites
[NASA-CASE-LEW-15155-1] p 133 N92-29090
PROTEIN CRYSTAL GROWTH
Thermophysical properties of lysozyme (protein) solutions p 240 A92-44385
An examination of anticipated g-jitter on Space Station and its effects on materials processes p 140 N92-28438

PROTOCOL (COMPUTERS)

Network architectures and protocols for the integration of ACTS and ISDN
[AIAA PAPER 92-2039] p 145 A92-29953

PROTOTYPES

Development of a ninety string solar array simulator p 46 A92-50660
Development of a ninety string solar array simulator
[NASA-TM-105278] p 55 N92-11086
NIST torsion oscillator viscometer response: Performance on the LeRC active vibration isolation platform
[NASA-TM-105571] p 209 N92-23564

PROVING

NASA Lewis Research Center Advanced Modulation and Coding Project: Introduction and overview p 51 N92-22002

PULSE COMMUNICATION

Satellite delivery of B-ISDN services
[AIAA PAPER 92-1831] p 142 A92-29777

PULSE DURATION

Rotative quadrature phase-shift keying p 146 A92-44233

PULSED JET ENGINES

Preliminary investigation of a low power pulsed arcjet thruster
[AIAA PAPER 92-3113] p 64 A92-48752

PULSES

Pulsed thrust propellant reorientation - Concept and modeling p 62 A92-44507

PUMP SEALS

Seals Flow Code Development
[NASA-CP-10070] p 49 N92-15082

PYROLYSIS

Global kinetic constants for thermal oxidative degradation of a cellulosic paper p 113 A92-29488
Polymeric precursors for fibers and matrices p 125 A92-39856
Evaluation of Kapton pyrolysis, arc tracking, and arc propagation on the Space Station Freedom (SSF) solar array flexible current carrier (FCC) p 72 A92-53209

PYROLYTIC GRAPHITE

Heat transfer device
[NASA-CASE-LEW-14162-3] p 111 N92-34208

PYROMETERS

Multiwavelength pyrometry for nongray bodies
[NASA-TM-105285] p 202 N92-24881

Q

QUADRATURE AMPLITUDE MODULATION

Comparative study on the performance of power and bandwidth efficient modulations in LMSS under fading and interference p 147 A92-54763

Flexible digital modulation and coding synthesis for satellite communications p 148 N92-14235

QUADRATURE PHASE SHIFT KEYING

Flexible high speed CODEC (FHSC) [AIAA PAPER 92-1919] p 143 A92-29848

Rotative quadrature phase-shift keying p 146 A92-44233

Flexible digital modulation and coding synthesis for satellite communications p 148 N92-14235

QUALIFICATIONS

Nuclear electric propulsion development and qualification facilities [NASA-TM-105521] p 91 N92-30818

QUALITATIVE ANALYSIS

Advanced nozzle and engine components test facility [AIAA PAPER 92-3993] p 41 A92-56816

Advanced nozzle and engine components test facility [NASA-TM-103684] p 42 N92-17059

QUANTUM EFFICIENCY

Effect of InAlAs window layer on the efficiency of indium phosphide solar cells p 234 A92-53163

Effect of InAlAs window layer on efficiency of indium phosphide solar cells [NASA-TM-105354] p 161 N92-25176

QUANTUM WELLS

Temperature independent quantum well FET with delta channel doping p 157 A92-49596

R

RADIAL FLOW

A comparison of the calculated and experimental off-design performance of a radial flow turbine [AIAA PAPER 92-3069] p 13 A92-54004

RADIANT COOLING

Transient cooling of a square region of radiating medium p 164 A92-10432

Finite difference solution for transient cooling of a radiating-conducting semitransparent layer p 166 A92-20310

Analytical and experimental studies of heat pipe radiation cooling of hypersonic propulsion systems [AIAA PAPER 92-3809] p 26 A92-49128

RADIANT FLUX DENSITY

Effects of oxygen concentration on radiative loss from normal-gravity and microgravity methane diffusion flames [AIAA PAPER 92-0243] p 113 A92-26928

RADIATION ABSORPTION

Boundary heat fluxes for spectral radiation from a uniform temperature rectangular medium p 175 A92-44388

Effect of index of refraction on radiation characteristics in a heated absorbing, emitting, and scattering layer p 181 A92-53031

RADIATION DAMAGE

Assessment of environmental effects on Space Station Freedom Electrical Power System p 55 A92-50581

Molecular dynamics investigation of radiation damage in semiconductors p 159 A92-53157

Neutron, gamma ray, and temperature effects on the electrical characteristics of thyristors [NASA-TM-105728] p 162 N92-28432

RADIATION DOSAGE

The effect of the low Earth orbit environment on space solar cells. Results of the advanced photovoltaic experiment (S0014) p 237 N92-27320

RADIATION EFFECTS

Effect of radiation on convection at moderate temperatures [AIAA PAPER 92-0691] p 168 A92-27058

Synergistic effects of ultraviolet radiation, thermal cycling and atomic oxygen on altered and coated Kapton surfaces [AIAA PAPER 92-0794] p 93 A92-27125

Radiation and temperature effects in heteroepitaxial and homoepitaxial InP cells p 159 A92-53192

Radiation performance of GaAs concentrator cells for 0.4 to 12 MeV electrons and 0.1 to 37 MeV protons p 159 A92-53193

Synergistic effects of ultraviolet radiation, thermal cycling, and atomic oxygen on altered and coated Kapton surfaces [NASA-TM-105363] p 96 N92-14114

Status and future directions of InP solar cell research [NASA-TM-105426] p 160 N92-18920

Effect of radiation on convection at moderate temperatures [NASA-TM-105632] p 192 N92-25296

Neutron, gamma ray, and temperature effects on the electrical characteristics of thyristors [NASA-TM-105728] p 162 N92-28432

RADIATION SHIELDING

Magnetic radiation shielding - An idea whose time has returned? p 53 A92-17796

RADIATION SOURCES

Multiwavelength pyrometry for nongray bodies [NASA-TM-105285] p 202 N92-24881

RADIATION SPECTRA

Multiwavelength pyrometry for nongray surfaces in the presence of interfering radiation [NASA-TM-105286] p 201 N92-19107

Multiwavelength pyrometry for nongray bodies [NASA-TM-105285] p 202 N92-24881

RADIATION TOLERANCE

Advanced power systems for EOS p 70 A92-50640

RADIATIVE HEAT TRANSFER

Nongray radiative gas analyses using the S-N discrete ordinates method p 266 A92-15443

Effect of radiation on convection at moderate temperatures [AIAA PAPER 92-0691] p 168 A92-27058

Boundary heat fluxes for spectral radiation from a uniform temperature rectangular medium p 175 A92-44388

Combined conjugated heat transfer from a scattering medium p 175 A92-44390

Analytical and experimental studies of heat pipe radiation cooling of hypersonic propulsion systems [AIAA PAPER 92-3809] p 26 A92-49128

Effect of index of refraction on radiation characteristics in a heated absorbing, emitting, and scattering layer p 181 A92-53031

Effect of radiation on convection at moderate temperatures [NASA-TM-105632] p 192 N92-25296

RADIATIVE LIFETIME

Photoluminescence lifetime measurements in InP wafers p 262 A92-48092

RADIATIVE TRANSFER

Transient cooling of a square region of radiating medium p 164 A92-10432

Radiative transfer solutions for cylindrical coordinates with emitting, absorbing, and anisotropic scattering medium [AIAA PAPER 92-0123] p 266 A92-28185

Comparisons of cylindrical and rectangular media radiative transfer solutions using the S-N discrete ordinates method [AIAA PAPER 92-2894] p 266 A92-54287

RADIO COMMUNICATION

Overview of Ka-band communications technology requirements for the space exploration initiative [NASA-TM-105308] p 269 N92-14953

RADIO FREQUENCIES

The effects of RF plasma ashing on zinc orthotitanate/potassium silicate thermal control coatings [AIAA PAPER 92-2171] p 124 A92-31299

A software control system for the ACTS high-burst-rate link evaluation terminal [NASA-TM-105207] p 243 N92-16628

RF modulated fiber optic sensing systems and their applications [NASA-TM-105801] p 257 N92-33896

RADIO FREQUENCY DISCHARGE

Synthesis and characterization of fine grain diamond films p 262 A92-46330

Theoretical nozzle performance of a microwave electrothermal thruster using experimental data [AIAA PAPER 92-3110] p 64 A92-48750

RADIO FREQUENCY INTERFERENCE

Effect of an arcjet plume on satellite reflector performance p 53 A92-16318

RADIOACTIVE DECAY

Constraints to the decays of Dirac neutrinos from SN 1987A p 255 A92-36249

RADIOGRAPHY

X ray attenuation measurements for high-temperature materials characterization and in-situ monitoring of damage accumulation [NASA-TM-105577] p 110 N92-25996

RADIOISOTOPE BATTERIES

Small Stirling dynamic isotope power system for multihundred-watt robotic missions [SAE PAPER 912066] p 62 A92-45448

Design of multihundred-watt dynamic isotope power system for robotic space missions p 69 A92-50633

A dynamic isotope power system portable generator for the moon or Mars p 232 A92-50634

RADIOMETERS

Concentrator testing using projected images p 69 A92-50615

Multiwavelength pyrometry for nongray bodies [NASA-TM-105285] p 202 N92-24881

RAIN

Dynamic rain fade compensation techniques for the advanced communications technology satellite [AIAA PAPER 92-2038] p 145 A92-31711

RAMAN SPECTRA

Species and temperature measurement in H₂/O₂ rocket flow fields by means of Raman scattering diagnostics [AIAA PAPER 92-3353] p 178 A92-48930

RAMJET ENGINES

The design and performance estimates for the propulsion module for the booster of a TSTO vehicle [NASA-TM-105299] p 29 N92-11995

Engine panel seals for hypersonic engine applications: High temperature leakage assessments and flow modelling [NASA-TM-105260] p 208 N92-16336

NASA thrusts in high-speed aer propulsion research and development: An overview p 33 N92-22538

RANDOM ACCESS MEMORY

A video event trigger for high frame rate, high resolution video technology p 160 N92-22453

RANDOM PROCESSES

First-passage problems: A probabilistic dynamic analysis for degraded structures [NASA-TM-103755] p 225 N92-11373

RANDOM VIBRATION

Effective diffusion equation in a random velocity field [AIAA PAPER 92-0245] p 167 A92-25704

RANDOM WALK

Fractals and cosmological large-scale structure p 268 A92-37413

RANKINE CYCLE

Small engine technology programs p 32 N92-22532

RAPID QUENCHING (METALLURGY)

Microstructure and mechanical properties of near eutectic beta-NiAl plus alpha-Re alloys produced by rapid solidification and extrusion p 119 A92-30844

Influence of processing on the microstructure and mechanical properties of a NbAl₃-base alloy p 122 A92-48152

RARE GASES

Pressure dependence of the melting temperature of solids - Rare-gas solids p 171 A92-33912

RAREFIED GAS DYNAMICS

FDDO and DSMC analyses of rarefied gas flow through 2D nozzles [AIAA PAPER 92-2858] p 176 A92-47841

DSMC analysis of species separation in rarefied nozzle flows [AIAA PAPER 92-2859] p 176 A92-47842

Experimental and numerical investigations of low-density nozzle and plume flows of nitrogen p 183 A92-54917

Numerical solution of a three-dimensional cubic cavity flow by using the Boltzmann equation [NASA-TM-105693] p 195 N92-30297

RAREFIED GASES

Fast oxygen atom facility for studies related to low earth orbit activities [AIAA PAPER 92-3974] p 47 A92-56800

RAY TRACING

Electromagnetic scattering from an inhomogeneous object by ray tracing p 146 A92-51092

RAYLEIGH SCATTERING

Rayleigh-Brillouin scattering to determine one-dimensional temperature and number density profiles of a gas flow field p 198 A92-38067

Rocket plume flowfield characterization using laser Rayleigh scattering [AIAA PAPER 92-3351] p 66 A92-48928

Spectrally resolved Rayleigh scattering diagnostic for hydrogen-oxygen rocket plume studies p 67 A92-50253

Filtered Rayleigh scattering based measurements in compressible mixing layers [AIAA PAPER 92-3543] p 182 A92-54043

Study of compressible mixing layers using filtered Rayleigh scattering based visualizations p 183 A92-54937

Filtered Rayleigh scattering measurements in supersonic/hypersonic facilities [AIAA PAPER 92-3894] p 200 A92-56733

Rocket plume flowfield characterization using laser Rayleigh scattering [NASA-TM-105739] p 257 N92-28475

RAYLEIGH-BENARD CONVECTION

Numerical investigation on Benard instability in a finite liquid layer p 164 A92-12865

REACTING FLOW

Reactive collision terms for fluid transport theory p 257 A92-22693

Model free simulations of a high speed reacting mixing layer [AIAA PAPER 92-0257] p 167 A92-25715

Upwind differencing and LU factorization for chemical non-equilibrium Navier-Stokes equations p 171 A92-33829

REACTION BONDING

- A continuous mixing model for pdf simulations and its applications to combustor shear flows p 174 A92-40139
- Doppler-shifted fluorescence imaging of velocity fields in supersonic reacting flows [AIAA PAPER 92-2964] p 199 A92-46979
- The Osher scheme for non-equilibrium reacting flows p 176 A92-48149
- A simplified reaction mechanism for prediction of NO(x) emissions in the combustion of hydrocarbons [AIAA PAPER 92-3340] p 114 A92-48919
- Propulsion-related flowfields using the preconditioned Navier-Stokes equations [AIAA PAPER 92-3437] p 178 A92-48994
- Three-dimensional calculations of supersonic reacting flows using an LU scheme p 179 A92-50465
- A computer model for one-dimensional mass and energy transport in and around chemically reacting particles, including complex gas-phase chemistry, multicomponent molecular diffusion, surface evaporation, and heterogeneous reaction p 181 A92-52406
- A time-accurate algorithm for chemical non-equilibrium viscous flows at all speeds [AIAA PAPER 92-3639] p 182 A92-54112
- Computation of H₂/air reacting flowfields in drag-reduction external combustion [AIAA PAPER 92-3672] p 182 A92-54115
- Introduction to the internal fluid mechanics research session p 188 A92-22522
- REACTION BONDING**
- Role of interfacial carbon layer in the thermal diffusivity/conductivity of silicon carbide fiber-reinforced reaction-bonded silicon nitride matrix composites p 100 A92-25443
- Oxidation effects on the mechanical properties of a SiC-fiber-reinforced reaction-bonded Si₃N₄ matrix composite p 100 A92-25445
- Relationships between toughness and microstructure of reaction bonded Si₃N₄ p 125 A92-39687
- Reaction-bonded Si₃N₄ and SiC matrix composites p 103 A92-39858
- REACTION CONTROL**
- Hydrogen/oxygen auxiliary propulsion technology [NASA-TM-105249] p 85 A92-20522
- REACTION KINETICS**
- Combustion kinetics and sensitivity analysis computations p 112 A92-16981
- Optimization and analysis of large chemical kinetic mechanisms using the solution mapping method - Combustion of methane p 113 A92-19300
- Model free simulations of a high speed reacting mixing layer [AIAA PAPER 92-0257] p 167 A92-25715
- Global kinetic constants for thermal oxidative degradation of a cellulose paper p 113 A92-29488
- Oxidation kinetics of CVD silicon carbide and silicon nitride p 125 A92-39674
- The structure of premixed particle-cloud flames p 114 A92-43779
- A simplified reaction mechanism for prediction of NO(x) emissions in the combustion of hydrocarbons [AIAA PAPER 92-3340] p 114 A92-48919
- Temperature dependence of the electrode kinetics of oxygen reduction at the platinum/Nafion interface - A microelectrode investigation p 115 A92-56950
- Chemical vapor deposition modeling for high temperature materials p 96 A92-18457
- Phase transformations in SrAl₂Si₂O₈ glass [NASA-TM-105657] p 264 A92-23890
- Upwind schemes and bifurcating solutions in real gas computations p 193 A92-25817
- Implementation of a kappa-epsilon turbulence model to RPLUS3D code p 194 A92-25822
- REACTION PRODUCTS**
- Demonstration of a flight capable system for plume spectroscopy [AIAA PAPER 92-3786] p 57 A92-54165
- REACTOR CORES**
- Innovative nuclear thermal propulsion technology evaluation - Results of the NASA/DOE task team study [IAF PAPER 91-235] p 58 A92-13160
- Heat transfer and core neutronics considerations of the heat pipe cooled thermionic reactor p 180 A92-50591
- An improved heat transfer configuration for a solid-core nuclear thermal rocket engine [AIAA PAPER 92-3583] p 75 A92-54063
- REACTOR DESIGN**
- Heat transfer and core neutronics considerations of the heat pipe cooled thermionic reactor p 180 A92-50591
- Multi-reactor power system configurations for multimewatt nuclear electric propulsion [NASA-TM-105212] p 77 A92-10057
- Nuclear Thermal Propulsion: A Joint NASA/DOE/DOD Workshop [NASA-CP-10079] p 78 A92-11088

- Thermochemical energy storage for a lunar base [NASA-TM-105333] p 236 A92-14485
- REACTOR MATERIALS**
- Fuels and materials development for space nuclear propulsion [NASA-TM-107806] p 85 A92-21187
- REACTOR TECHNOLOGY**
- Nuclear Thermal Propulsion: A Joint NASA/DOE/DOD Workshop [NASA-CP-10079] p 78 A92-11088
- REAL GASES**
- Computational Fluid Dynamics --- numerical methods and algorithm development [NASA-CP-10078] p 35 A92-25808
- A new Lagrangian method for real gases at supersonic speed p 19 A92-25814
- Upwind schemes and bifurcating solutions in real gas computations p 193 A92-25817
- REAL TIME OPERATION**
- A real time neural net estimator of fatigue life p 245 A92-21694
- Algorithms for real-time fault detection of the Space Shuttle Main Engine [AIAA PAPER 92-3167] p 215 A92-48789
- Description of real-time Ada software implementation of a power system monitor for the Space Station Freedom PMAD DC testbed p 242 A92-50533
- Health management and controls for earth to orbit propulsion systems [IAF PAPER 92-0646] p 77 A92-57089
- Real-time data compression of broadcast video signals [NASA-CASE-LEW-14945-2] p 147 A92-10128
- Real-time fault diagnosis for propulsion systems [NASA-TM-105303] p 29 A92-11017
- An SSME high pressure oxidizer turbopump diagnostic system using G₂(TM) real-time expert system [NASA-TM-105328] p 247 A92-13717
- Real-time demonstration hardware for enhanced DPCM video compression algorithm [NASA-TM-105616] p 150 A92-19700
- PC graphics generation and management tool for real-time applications [NASA-TM-105749] p 244 A92-28684
- Piloted evaluation of an integrated propulsion and flight control simulator [NASA-TM-105797] p 40 A92-34107
- RECEIVERS**
- Photovoltaic receivers for laser beamed power in space p 72 A92-53201
- Post-test examination of a pool boiler receiver [NASA-TM-105635] p 123 A92-27192
- Solar thermal energy receiver [NASA-CASE-LEW-14949-1] p 238 A92-29143
- RECIRCULATIVE FLUID FLOW**
- Experimental verification of a secondary recirculation zone in a labyrinth seal p 205 A92-50271
- RECOMMENDATIONS**
- NASA Surface-Modeling and Grid-Generation (SM/GG) activities p 267 A92-25725
- RECTANGULAR WAVEGUIDES**
- New coplanar waveguide to rectangular waveguide end launcher p 156 A92-44243
- RECTANGULAR WINGS**
- LDV measurements on a rectangular wing with a simulated glaze ice accretion [AIAA PAPER 92-2690] p 10 A92-45537
- Effect of a simulated glaze ice shape on the aerodynamic performance of a rectangular wing [AIAA PAPER 92-4042] p 14 A92-56861
- REDUCED GRAVITY**
- Determination of the critical parameters for remote microscope control [IAF PAPER 91-026] p 240 A92-12447
- Flight experiment on acousto-optic crystal growth p 136 A92-12880
- Some further observations on droplet combustion characteristics - NASA LeRC-Princeton results p 111 A92-12897
- Opposed flow flame spread in normal, enhanced and reduced gravity p 111 A92-12898
- The implications of experimentally controlled gravitational accelerations for combustion science p 112 A92-16601
- Observations on a slow burning regime for hydrocarbon droplets - n-heptane/air results p 112 A92-16602
- An investigation of flame spread over shallow liquid pools in microgravity and nonair environments p 112 A92-16609
- Modeling of impulsive propellant reorientation p 59 A92-17187
- The NASA microgravity combustion space experiment program [IAF PAPER 91-398] p 112 A92-18484
- Drop-tower experiments for capillary surfaces in an exotic container p 166 A92-20743

- Reaction-compensation technology for microgravity laboratory robots p 203 A92-23719
- Intensified array camera imaging of solid surface combustion aboard the NASA Learjet [AIAA PAPER 92-0240] p 137 A92-25702
- Effective diffusion equation in a random velocity field [AIAA PAPER 92-0245] p 167 A92-25704
- Effects of g-jitter and cross-diffusion on the onset of convection in doubly diffusive systems [AIAA PAPER 92-0246] p 167 A92-25705
- Self-pressurization of a spherical liquid hydrogen storage tank in a microgravity environment [AIAA PAPER 92-0363] p 168 A92-25798
- Microgravity combustion of isolated n-decane and n-heptane droplets [AIAA PAPER 92-0242] p 113 A92-26927
- Effects of oxygen concentration on radiative loss from normal-gravity and microgravity methane diffusion flames [AIAA PAPER 92-0243] p 113 A92-26928
- Stability analysis of surface tension effects on a double-diffusive layer --- in reduced gravity conditions [AIAA PAPER 92-0605] p 137 A92-27002
- Determination of the natural convection coefficient in low-gravity [AIAA PAPER 92-0712] p 168 A92-27072
- The isothermal dendritic growth experiment - A USMP-2 space flight experiment [AIAA PAPER 92-0350] p 137 A92-28188
- Development of and flight results from the Space Acceleration Measurement System (SAMS) [AIAA PAPER 92-0354] p 56 A92-28189
- An initial study of void formation during solidification of aluminum in normal and reduced-gravity [AIAA PAPER 92-0845] p 138 A92-29611
- Heat and mass transport from thermally degrading thin cellulosic materials in a microgravity environment p 174 A92-41810
- Nature of buoyancy-driven flows in a reduced-gravity environment p 175 A92-45844
- Scaling of low-Prandtl-number thermocapillary flows p 176 A92-47271
- Hydrogen no-vent testing in a 5 cubic foot (142 liter) tank using spray nozzle and spray bar liquid injection [AIAA PAPER 92-3063] p 63 A92-48719
- Observations of soot during droplet combustion at low gravity - Heptane and heptane/monochloroalkane mixtures p 115 A92-50447
- Jet mixing in low gravity - Results of the Tank Pressure Control Experiment [AIAA PAPER 92-3060] p 182 A92-54001
- Pressurization of cryogens - A review of current technology and its applicability to low-gravity conditions [AIAA PAPER 92-3061] p 72 A92-54002
- Comparing the results of an analytical model of the no-vent fill process with no-vent fill test results for a 4.96 cu m (175 cu ft) tank [AIAA PAPER 92-3078] p 72 A92-54007
- Early use of Space Station Freedom for NASA's Microgravity Science and Applications Program [IAF PAPER 92-0702] p 138 A92-57131
- Interfacial and gravitational convection in immiscible liquid layers [IAF PAPER 92-0907] p 184 A92-57286
- Controller design for microgravity vibration isolation systems [IAF PAPER 92-0969] p 247 A92-57327
- Space acceleration measurement system description and operations on the First Spacelab Life Sciences Mission [NASA-TM-105301] p 57 A92-13151
- Risks, designs, and research for fire safety in spacecraft [NASA-TM-105317] p 240 A92-13581
- Self-pressurization of a spherical liquid hydrogen storage tank in a microgravity environment [NASA-TM-105372] p 185 A92-14323
- Intensified array camera imaging of solid surface combustion aboard the NASA Learjet [NASA-TM-105361] p 138 A92-16156
- NIST torsion oscillator viscometer response: Performance on the LeRC active vibration isolation platform [NASA-TM-105571] p 209 A92-23564
- Microgravity acceleration measurement and environment characterization science (17-IML-1) p 139 A92-23642
- Microgravity combustion science: Progress, plans, and opportunities [NASA-TM-105410] p 139 A92-27197
- Hydrogen no-vent fill testing in a 5 cubic foot (142 liter) tank using spray nozzle and spray bar liquid injection [NASA-TM-105759] p 136 A92-28433
- International Workshop on Vibration Isolation Technology for Microgravity Science Applications [NASA-CP-10094] p 141 A92-28436

- Vibration isolation technology development to demonstration p 140 N92-28442
- Early mission science support: Space Acceleration Measurement System (SAMS) p 57 N92-28451
- Pressurization of cryogen: A review of current technology and its applicability to low-gravity conditions [NASA-TM-105746] p 136 N92-29669
- Development of and flight results from the Space Acceleration Measurement System (SAMS) [NASA-TM-105652] p 57 N92-30301
- Microgravity vibration isolation: Optimal preview and feedback control [NASA-TM-105673] p 142 N92-30692
- REDUCED ORDER FILTERS**
A fundamental theorem for the model reduction of nonlinear systems p 246 A92-41165
- REDUCTION (CHEMISTRY)**
Temperature dependence of the electrode kinetics of oxygen reduction at the platinum/Nation interface - A microelectrode investigation p 115 A92-56950
- REDUNDANCY**
Real-time fault diagnosis for propulsion systems [NASA-TM-105303] p 29 N92-11017
- REFLECTANCE**
Surface etching for light trapping in encapsulated InP solar cells p 232 A92-48091
- Multiwavelength pyrometry for nongray surfaces in the presence of interfering radiation [NASA-TM-105286] p 201 N92-19107
- Temperature-dependent reflectivity of silicon carbide [NASA-TM-105287] p 201 N92-19263
- Atomic oxygen durability of solar concentrator materials for Space Station Freedom [NASA-TM-105378] p 85 N92-20065
- Multiwavelength pyrometry for nongray bodies [NASA-TM-105285] p 202 N92-24881
- REFLECTION**
Modal element method for scattering of sound by absorbing bodies [NASA-TM-105722] p 255 N92-28984
- REFLECTOR ANTENNAS**
Effect of an arcjet plume on satellite reflector performance p 53 A92-16318
- Ka-band dual frequency array feed for a low cost ACTS ground terminal [AIAA PAPER 92-1902] p 143 A92-29833
- Experimental code verification results for reflector antenna distortion compensation by array feeds [AIAA PAPER 92-2014] p 49 A92-29933
- Advanced Communication Technology Satellite (ACTS) multibeam antenna analysis and experiment [NASA-TM-105420] p 149 N92-17047
- Analysis of a generalized dual reflector antenna system using physical optics [NASA-TM-105425] p 149 N92-18281
- Ka-band dual frequency array feed for a low cost ACTS ground terminal p 152 N92-32969
- REFRACTIVITY**
A fiber optic sensor for ophthalmic refractive diagnostics p 198 A92-34831
- Effect of index of refraction on radiation characteristics in a heated absorbing, emitting, and scattering layer p 181 A92-53031
- REFRACTORY COATINGS**
High temperature thruster technology for spacecraft propulsion [IAF PAPER 91-254] p 58 A92-13155
- High temperature thruster technology for spacecraft propulsion [NASA-TM-105348] p 82 N92-15125
- REFRACTORY MATERIALS**
Intermetallic and ceramic matrix composites for 815 to 1370 C (1500 to 2500 F) gas turbine engine applications p 99 A92-15128
- A versatile get away special furnace for materials processing in space [AIAA PAPER 92-0787] p 137 A92-27122
- Tribological properties of ceramic-(Ti3Al-Nb) sliding couples for use as candidate seal materials to 700 C p 124 A92-32407
- NASA's high-temperature engine materials program for civil aeronautics p 95 A92-41117
- Combined bending and thermal fatigue of high-temperature metal-matrix composites - Computational simulation p 223 A92-43494
- Effects of a noncoplanar biphenyldiamine on the processing and properties of addition polyimides [NASA-TM-105383] p 107 N92-15137
- High-temperature durability considerations for HSCT combustor [NASA-TP-3162] p 129 N92-17070
- Chemical vapor deposition modeling for high temperature materials [NASA-TM-105386] p 96 N92-18457
- NASA Lewis Research Center materials research and technology: An overview p 31 N92-22512
- Development of a new generation of high-temperature composite materials p 109 N92-22515
- X ray attenuation measurements for high-temperature materials characterization and in-situ monitoring of damage accumulation [NASA-TM-105577] p 110 N92-25996
- High temperature dielectric properties of Apical, Kapton, Peek, Teflon AF, and Upilex polymers [NASA-TM-105753] p 162 N92-28675
- REFRACTORY METALS**
Composites of low-density trialuminides: Particulate and long fiber reinforcements [NASA-TM-105628] p 109 N92-25346
- REGENERATIVE FUEL CELLS**
SEI rover solar-electrochemical power system options [AIAA PAPER 91-0916] p 45 A92-50574
- A study of Na(x)Pt3O4 as an O2 electrode bifunctional electrocatalyst [NASA-TM-105311] p 85 N92-20585
- Optimization of armored spherical tanks for storage on the lunar surface [NASA-TM-105700] p 91 N92-30187
- REGRESSION ANALYSIS**
Review and statistical analysis of the use of ultrasonic velocity for estimating the porosity fraction in polycrystalline materials p 215 A92-28722
- REINFORCED SHELLS**
Structural durability of stiffened composite shells [AIAA PAPER 92-2244] p 220 A92-34569
- REINFORCING FIBERS**
Mechanical behavior of fiber reinforced SiC/RBSN ceramic matrix composites - Theory and experiment --- Reaction Bonded Silicon Nitride [ASME PAPER 91-GT-209] p 99 A92-15629
- Effect of fiber reinforcement on thermo-oxidative stability and mechanical properties of polymer matrix composites p 101 A92-33587
- Bonded ceramic foams reinforced with fibers for high temperature use p 125 A92-39628
- Modeling of crack bridging in a unidirectional metal matrix composite p 104 A92-43085
- Compatibility of potential reinforcing ceramics with Ni and Fe aluminides p 105 A92-46874
- Desktop fiber push-out apparatus [NASA-TM-105341] p 107 N92-16036
- High temperature structural fibers: Status and needs [NASA-TM-105174] p 107 N92-16037
- CVD of silicon carbide on structural fibers: Microstructure and composition [NASA-TM-105385] p 107 N92-18439
- Sliding durability of two carbide-oxide candidate high temperature fiber seal materials in air to 900 C [NASA-TM-105554] p 97 N92-21175
- Tensile strain measurements of ceramic fibers using scanning laser acoustic microscopy [NASA-TM-105589] p 216 N92-24986
- REINFORCING MATERIALS**
Composites of low-density trialuminides: Particulate and long fiber reinforcements [NASA-TM-105628] p 109 N92-25346
- REISSNER-NORDSTROM SOLUTION**
A classical instability of Reissner-Nordstrom solutions and the fate of magnetically charged black holes p 267 A92-26397
- RELAXATION (MECHANICS)**
Magnetic flux relaxation in YBa2Cu3O(7-x) thin film: Thermal or athermal p 265 N92-32984
- RELAXATION METHOD (MATHEMATICS)**
Upwind relaxation methods for the Navier-Stokes equations using inner iterations p 170 A92-29553
- RELAY SATELLITES**
Multiple-access phased array antenna simulator for a digital beam forming system investigation [NASA-TM-105422] p 149 N92-17062
- RELIABILITY**
Monte Carlo modeling of atomic oxygen attack of polymers with protective coatings on LDEF p 132 N92-27281
- NEP systems engineering efforts in FY-92: Plans and status [NASA-TM-105775] p 91 N92-30308
- Reliability training [NASA-RP-1253] p 49 N92-32456
- RELIABILITY ANALYSIS**
Reliability analysis of a structural ceramic combustion chamber [ASME PAPER 91-GT-155] p 24 A92-15591
- Transmission overhaul and component replacement predictions using Weibull and renewal theory p 215 A92-17201
- Reliability analysis of laminated CMC components through shell subelement techniques [AIAA PAPER 92-2348] p 219 A92-34322
- A new response surface approach for structural reliability analysis [AIAA PAPER 92-2408] p 219 A92-34339
- Structural system reliability calculation using a probabilistic fault tree analysis method [AIAA PAPER 92-2410] p 251 A92-34341
- A probabilistic approach to the evaluation of fatigue damage in a space propulsion system injector element [AIAA PAPER 92-2413] p 60 A92-34343
- Analysis of whisker-toughened CMC structural components using an interactive reliability model [AIAA PAPER 92-2490] p 221 A92-34582
- Fatigue crack growth reliability by probabilistic finite elements p 222 A92-37524
- Probabilistic progressive buckling of trusses [AIAA PAPER 91-0916] p 223 A92-38142
- Structural reliability assessment capability in NESSUS [AIAA PAPER 92-3417] p 223 A92-48976
- Balancing reliability and cost to choose the best power subsystem p 216 A92-50625
- Probabilistic progressive buckling of trusses [NASA-TM-105162] p 226 N92-15403
- Reliability analysis of structural ceramic components using a three-parameter Weibull distribution [NASA-TM-105370] p 129 N92-17060
- Reliability analysis of laminated CMC components through shell subelement techniques [NASA-TM-105413] p 129 N92-20380
- RELIABILITY ENGINEERING**
Recent developments of the NESSUS probabilistic structural analysis computer program [AIAA PAPER 92-2411] p 242 A92-34342
- Advanced Rotorcraft Transmission (ART) - Component test results [AIAA PAPER 92-3366] p 205 A92-48939
- Rocket engine propulsion 'system reliability' [AIAA PAPER 92-3421] p 66 A92-48980
- NASA Aerospace Flight Battery Systems Program: An update p 237 N92-22741
- RELIC RADIATION**
Large-scale microwave anisotropy from gravitating seeds p 269 A92-56914
- REMOTE CONTROL**
Determination of the critical parameters for remote microscope control [IAF PAPER 91-026] p 240 A92-12447
- REMOTE SENSING**
X ray based displacement measurement for hostile environments [NASA-TM-105551] p 202 N92-23155
- REMOTE SENSORS**
Microgravity acceleration measurement and environment characterization science (17-IML-1) p 139 N92-23642
- Space acceleration measurement system triaxial sensor head error budget [NASA-TM-105300] p 57 N92-25134
- RENORMALIZATION GROUP METHODS**
Renormalization group based algebraic turbulence model for three-dimensional turbomachinery flows p 9 A92-41268
- Renormalization group analysis of the Reynolds stress transport equation p 179 A92-49493
- Renormalization group analysis of the Reynolds stress transport equation [NASA-TM-105588] p 190 N92-23542
- REQUIREMENTS**
Test facilities for high power electric propulsion [NASA-TM-105247] p 80 N92-11136
- RESEARCH AND DEVELOPMENT**
Nuclear thermal rocket workshop reference system Rover/NERVA p 78 N92-11091
- JANNAF Liquid Rocket Combustion Instability Panel research recommendations p 115 N92-11124
- Plans for the development of cryogenic engines for space exploration [NASA-TM-105250] p 79 N92-11135
- Bibliography of Lewis Research Center technical publications announced in 1990 [NASA-TM-103753] p 267 N92-12786
- Impact and promise of NASA aer propulsion technology p 31 N92-22511
- NASA Lewis Research Center materials research and technology: An overview p 31 N92-22512
- NASA's aircraft icing technology program [NASA-TM-104518] p 17 N92-23105
- Computational Fluid Dynamics --- numerical methods and algorithm development [NASA-CP-10078] p 35 N92-25808
- Trends in aer propulsion research and their impact on engineering education [NASA-TM-105682] p 38 N92-31172
- RESEARCH FACILITIES**
Investigation of three-dimensional flow field in a turbine including rotor/stator interaction. I - Design development and performance of the research facility [AIAA PAPER 92-3325] p 40 A92-48908

RESEARCH MANAGEMENT

- Plans for the development of cryogenic engines for space exploration
[NASA-TM-105250] p 79 N92-11135
- Seals related research at NASA Lewis Research Center
Structural Dynamics Branch research and accomplishments for FY 1990
[NASA-TM-103747] p 226 N92-15406
- Icing simulation: A survey of computer models and experimental facilities
[NASA-TM-105795] p 21 N92-21684
- Implementation of an intelligent control system
[NASA-TM-105795] p 241 N92-33897

RESEARCH MANAGEMENT

- Nuclear thermal propulsion workshop overview
[NASA-CP-10079] p 78 N92-11090

RESEARCH PROJECTS

- Nuclear Thermal Propulsion: A Joint NASA/DOE/DOD Workshop
[NASA-CP-10079] p 78 N92-11088
- Nuclear thermal propulsion workshop overview
[NASA-CP-10079] p 78 N92-11090
- Nuclear thermal rocket workshop reference system
JANNAF Liquid Rocket Combustion Instability Panel research recommendations
[NASA-TM-105795] p 115 N92-11124

RESIDUAL STRESS

- Interphase layer optimization for metal matrix composites with fabrication considerations
[NASA-TM-105802] p 98 A92-10262
- Mechanical properties of 3C silicon carbide
[NASA-TM-105802] p 126 A92-43761
- Reduction of thermal residual stresses in advanced metallic composites based upon a compensating/compliant layer concept
[NASA-TM-105802] p 105 A92-47106
- Influence of engineered interfaces on residual stresses and mechanical response in metal matrix composites
[NASA-TM-105438] p 109 N92-23195
- Improvement in surface fatigue life of hardened gears by high-intensity shot peening
[NASA-TM-105678] p 211 N92-26108
- Effects of fiber and interfacial layer architectures on the thermoplastic response of metal matrix composites
[NASA-TM-105802] p 110 N92-32234

RESIN MATRIX COMPOSITES

- Approaches to polymer-derived CMC matrices
[NASA-TM-105754] p 110 N92-29660

RESINS

- High-temperature polymer matrix composites
[NASA-TM-105754] p 108 N92-22513

RESISTANCE HEATING

- An efficient finite element method for aircraft de-icing problems
[AIAA PAPER 92-0532] p 22 A92-31670

RESISTOJET ENGINES

- Preliminary characterizations of a water vaporizer for resistojet applications
[AIAA PAPER 92-3533] p 74 A92-54041
- The evolutionary development of high specific impulse electric thruster technology
[NASA-TM-105712] p 92 N92-31342

RESISTORS

- Analog synthesized fast-variable linear load
[NASA-TM-105330] p 157 A92-50539

RESOLUTION

- A two-dimensional Euler solution for an unbladed jet engine configuration
[NASA-TM-105330] p 18 N92-24861

RESONANT FREQUENCIES

- Performance of a K-band superconducting annular ring antenna
[NASA-TM-105330] p 146 A92-37067
- Comparison of analysis and experiment for gearbox noise
[NASA-TM-105330] p 210 N92-25396

RESONATORS

- Conductor-backed coplanar waveguide resonators of YBa₂Cu₃O_{7- δ} on LaAlO₃
[NASA-TM-105544] p 158 A92-51042
- Planar dielectric resonator stabilized HEMT oscillator integrated with CPW/aperture coupled patch antenna
[NASA-TM-105544] p 160 N92-18473
- Planar dielectric resonator stabilized HEMT oscillator integrated with CPW/aperture coupled patch antenna
[NASA-TM-105544] p 152 N92-32967

RETURN TO EARTH SPACE FLIGHT

- Minimum impulse trajectories for Mars round trip missions
[AAS PAPER 91-500] p 44 A92-43339

REUSABLE LAUNCH VEHICLES

- Mission and sizing analysis for the Beta II two-stage-to-orbit vehicle
[AIAA PAPER 92-1264] p 47 A92-35868
- Mission and sizing analysis for the Beta 2 two-stage-to-orbit vehicle
[NASA-TM-105559] p 48 N92-21547

REUSABLE ROCKET ENGINES

- A real time neural net estimator of fatigue life
[NASA-TM-105633] p 245 A92-21694

- An advanced intelligent control system framework
[AIAA PAPER 92-3162] p 65 A92-48785
- Linear quadratic servo control of a reusable rocket engine
[NASA-TM-105291] p 67 A92-50495
- Linear quadratic servo control of a reusable rocket engine
[NASA-TM-105291] p 79 N92-11128
- A demonstration of an intelligent control system for a reusable rocket engine
[NASA-TM-105794] p 92 N92-31507
- Implementation of an intelligent control system
[NASA-TM-105795] p 241 N92-33897

REUSABLE SPACECRAFT

- Mission and sizing analysis for the Beta II two-stage-to-orbit vehicle
[AIAA PAPER 92-1264] p 47 A92-35868
- Mission and sizing analysis for the Beta 2 two-stage-to-orbit vehicle
[NASA-TM-105559] p 48 N92-21547

REVERSE ENGINEERING

- Integrating aerodynamic surface modeling for computational fluid dynamics with computer aided structural analysis, design, and manufacturing
[NASA-TM-105559] p 192 N92-25727

REVERSED FLOW

- Internal reversing flow in a tailpipe offtake configuration for SSTOVL aircraft
[AIAA PAPER 92-3790] p 28 A92-54169
- Internal reversing flow in a tailpipe offtake configuration for SSTOVL aircraft
[NASA-TM-105698] p 37 N92-28418

REYNOLDS EQUATION

- A system-approach to the elasto-hydrodynamic lubrication point-contact problem
[AIAA PAPER 92-3098] p 204 A92-35421
- Comparative study of turbulence models in predicting hypersonic inlet flows
[AIAA PAPER 92-3098] p 11 A92-48740
- Comparative study of turbulence models in predicting hypersonic inlet flows
[NASA-TM-105720] p 19 N92-28102
- Fast methods to numerically integrate the Reynolds equation for gas fluid films
[NASA-TM-105415] p 214 N92-30722

REYNOLDS NUMBER

- Experimental verification of a secondary recirculation zone in a labyrinth seal
[NASA-TM-105720] p 205 A92-50271
- On the drag of model dendrite fragments at low Reynolds number
[NASA-TM-105853] p 95 A92-50868
- Increased heat transfer to elliptical leading edges due to spanwise variations in the freestream momentum - Numerical and experimental results
[AIAA PAPER 92-3070] p 13 A92-54005
- An efficient and robust algorithm for time dependent viscous incompressible Navier-Stokes equations
[NASA-TM-105579] p 193 N92-25819
- Breakdown of the Karman vortex street due to forced convection and flow compressibility
[NASA-TM-105853] p 196 N92-32472
- A new time scale based k-epsilon model for near wall turbulence
[NASA-TM-105768] p 196 N92-32868

REYNOLDS STRESS

- Deterministic blade row interactions in a centrifugal compressor stage
[ASME PAPER 91-GT-273] p 3 A92-15670
- Studies of the effects of curvature on dilution jet mixing
[NASA-TM-105853] p 166 A92-21079
- Experimental investigation of turbulent flow through a circular-to-rectangular transition duct
[NASA-TM-105768] p 168 A92-26412
- Experimental balances for the second moments for a buoyant plume and their implication on turbulence modeling
[NASA-TM-105768] p 174 A92-40153
- Second order modeling of boundary-free turbulent shear flows
[NASA-TM-105768] p 174 A92-41275
- Renormalization group analysis of the Reynolds stress transport equation
[NASA-TM-105588] p 179 A92-49493
- Experimental verification of a secondary recirculation zone in a labyrinth seal
[NASA-TM-105277] p 205 A92-50271
- On the basic equations for the second-order modeling of compressible turbulence
[NASA-TM-105277] p 184 N92-11302
- Multigrid acceleration and turbulence models for computations of 3D turbulent jets in crossflow
[NASA-TM-105306] p 186 N92-18775
- On the basic equations for the second-order modeling of compressible turbulence
[NASA-TM-105306] p 190 N92-23351
- Renormalization group analysis of the Reynolds stress transport equation
[NASA-TM-105588] p 190 N92-23542

RHENIUM

- Diffusion mechanisms in chemical vapor-deposited iridium coated on chemical vapor-deposited rhenium
[NASA-TM-105633] p 117 A92-28017
- Advanced liquid rockets
[NASA-TM-105633] p 87 N92-24560

RHENIUM ALLOYS

- Microstructure and mechanical properties of near eutectic beta-NiAl plus alpha-Re alloys produced by rapid solidification and extrusion
[NASA-TP-3238] p 119 A92-30844

RHEOLOGY

- Lewis icing research tunnel test of the aerodynamic effects of aircraft ground deicing/anti-icing fluids
[NASA-TP-3238] p 22 N92-30395

RING STRUCTURES

- Structural design concepts for a multimegawatt solar electric propulsion (SEP) spacecraft
[AIAA PAPER 92-2536] p 54 A92-34380
- Large transient fault current test of an electrical roll ring for Space Station Freedom
[NASA-TM-105667] p 55 A92-50661
- Large transient fault current test of an electrical roll ring
[NASA-TM-105667] p 87 N92-24201

RISK

- Risks, designs, and research for fire safety in spacecraft
[NASA-TM-105317] p 240 N92-13581

ROBOT ARMS

- Reaction-compensation technology for microgravity laboratory robots
[NASA-TM-105317] p 203 A92-23719
- A 23:2:1 ratio, 300-watt, 26 N-m output torque, planetary roller-gear robotic transmission: Design and evaluation
[NASA-TM-105317] p 210 N92-25085

ROBOT DYNAMICS

- Reaction-compensation technology for microgravity laboratory robots
[NASA-TM-105317] p 203 A92-23719

ROBOTICS

- NASA program planning on nuclear electric propulsion
[AIAA PAPER 92-1557] p 61 A92-38651
- Nuclear electric propulsion: An integral part of NASA's nuclear propulsion project
[NASA-TM-105309] p 83 N92-16019
- The NASA CSTI High Capacity Power Program
[NASA-TM-105240] p 236 N92-16481

ROBOTS

- Reaction-compensation technology for microgravity laboratory robots
[NASA-TM-105317] p 203 A92-23719

ROBUSTNESS (MATHEMATICS)

- Integrated flight/propulsion control design for a STOVL aircraft using H-infinity control design techniques
[NASA-TM-105240] p 39 A92-29093
- On the development of explicit robust schemes for implementation of a class of hyperelastic models in large-strain analysis of rubbers
[NASA-TM-105240] p 221 A92-36245
- Explicit robust schemes for implementation of a class of principal value-based constitutive models: Theoretical development
[NASA-TM-105345] p 227 N92-20212
- Design and evaluation of a robust dynamic neurocontroller for a multivariable aircraft control problem
[NASA-TM-105579] p 40 N92-20586
- An efficient and robust algorithm for time dependent viscous incompressible Navier-Stokes equations
[NASA-TM-105579] p 193 N92-25819

ROCKET ENGINE CONTROL

- An advanced intelligent control system framework
[AIAA PAPER 92-3162] p 65 A92-48785
- Linear quadratic servo control of a reusable rocket engine
[NASA-TM-105291] p 67 A92-50495
- Health management and controls for earth to orbit propulsion systems
[IAF PAPER 92-0646] p 77 A92-57089
- Real-time fault diagnosis for propulsion systems
[NASA-TM-105303] p 29 N92-11017
- Linear quadratic servo control of a reusable rocket engine
[NASA-TM-105291] p 79 N92-11128
- Overview of rocket engine control
[NASA-TM-105318] p 81 N92-13274

ROCKET ENGINE DESIGN

- High temperature thruster technology for spacecraft propulsion
[IAF PAPER 91-254] p 58 A92-13155
- Design and test of an oxygen turbopump for a dual expander cycle rocket engine
[AIAA PAPER 92-3421] p 59 A92-21062
- Preliminary tests of annular ion optics
[AIAA PAPER 92-3148] p 64 A92-48776
- Effect of model selection on combustor performance and stability using ROCCID --- Rocket Combustor Interactive Design
[AIAA PAPER 92-3226] p 65 A92-48827
- Rocket engine propulsion 'system reliability'
[AIAA PAPER 92-3421] p 66 A92-48980
- Development of arcjet and ion propulsion for spacecraft stationkeeping
[IAF PAPER 92-0607] p 77 A92-57058
- Nuclear Thermal Propulsion: A Joint NASA/DOE/DOD Workshop
[NASA-CP-10079] p 78 N92-11088
- Nuclear thermal rocket workshop reference system
[NASA-CP-10079] p 78 N92-11091

Developments in REDES: The Rocket Engine Design Expert System p 78 N92-11120

Analytical study of nozzle performance for nuclear thermal rockets
[NASA-TM-105251] p 78 N92-11126

High temperature thruster technology for spacecraft propulsion
[NASA-TM-105348] p 82 N92-15125

A survey of instabilities within centrifugal pumps and concepts for improving the flow range of pumps in rocket engines
[NASA-TM-105439] p 84 N92-18280

Rocket-Based Combined-Cycle (RBCC) Propulsion Technology Workshop. Tutorial session
[NASA-CP-10090] p 86 N92-21517

Blazing the trailway: Nuclear electric propulsion and its technology program plans
[NASA-TM-105605] p 86 N92-23252

Derated ion thruster design issues
[NASA-TM-105576] p 87 N92-23534

Effect of model selection on combustor performance and stability predictions using ROCCID
[NASA-TM-105750] p 89 N92-27036

Rocket propulsion research at Lewis Research Center
[NASA-CR-189187] p 266 N92-30908

Dependence of hydrogen arcjet operation on electrode geometry
[NASA-TM-105855] p 93 N92-34113

ROCKET ENGINES

Design issues for lunar in situ aluminum/oxygen propellant rocket engines
[AIAA PAPER 92-1185] p 60 A92-33299

Ceramics and ceramic matrix composites - Aerospace potential and status
[AIAA PAPER 92-2445] p 94 A92-34474

Monolithic ceramics
[NASA-TM-105605] p 125 A92-39854

An experimental investigation of high-aspect-ratio cooling passages
[AIAA PAPER 92-3154] p 64 A92-48780

Propulsion-related flowfields using the preconditioned Navier-Stokes equations
[AIAA PAPER 92-3437] p 178 A92-48994

An overview of in-flight plume diagnostics for rocket engines
[AIAA PAPER 92-3785] p 75 A92-54164

Demonstration of a flight capable system for plume spectroscopy
[AIAA PAPER 92-3786] p 57 A92-54165

Extended temperature range rocket injector
[NASA-CASE-LEW-14846-1] p 77 N92-10054

Overview of rocket engine control
[NASA-TM-105318] p 81 N92-13274

Design issues for lunar in situ aluminum/oxygen propellant rocket engines
[NASA-TM-105433] p 83 N92-16023

A survey of instabilities within centrifugal pumps and concepts for improving the flow range of pumps in rocket engines
[NASA-TM-105439] p 84 N92-18280

Rocket-Based Combined-Cycle (RBCC) Propulsion Technology Workshop. Tutorial session
[NASA-CP-10090] p 86 N92-21517

Beta 2: A near term, fully reusable, horizontal takeoff and landing two-stage-to-orbit launch vehicle concept
[NASA-TM-105633] p 87 N92-24560

Advanced liquid rockets
[NASA-TM-105633] p 87 N92-24560

Thermal stratification potential in rocket engine coolant channels
[NASA-TM-4378] p 87 N92-25616

An experimental investigation of high-aspect-ratio cooling passages
[NASA-TM-105679] p 48 N92-25958

An overview of in-flight plume diagnostics for rocket engines
[NASA-TM-105727] p 90 N92-28417

Integrated health monitoring and controls for rocket engines
[NASA-TM-105763] p 90 N92-28693

Life extending control for rocket engines
[NASA-TM-105789] p 142 N92-31263

Demonstrated survivability of a high temperature optical fiber cable on a 1500 pound thrust rocket chamber
[NASA-TM-105835] p 136 N92-32230

ROCKET EXHAUST

Effect of an arcjet plume on satellite reflector performance
[AIAA PAPER 92-3351] p 66 A92-48928

Rocket plume flowfield characterization using laser Rayleigh scattering
[AIAA PAPER 92-3351] p 66 A92-48928

Spectrally resolved Rayleigh scattering diagnostic for hydrogen-oxygen rocket plume studies
[NASA-TM-105739] p 67 A92-50253

Rocket plume flowfield characterization using laser Rayleigh scattering
[NASA-TM-105739] p 257 N92-28475

ROCKET LAUNCHING

Status of NASA's Earth-to-Orbit Propulsion Technology program
[IAF PAPER 91-258] p 58 A92-13154

ROCKET LININGS

Cyclic hot firing results of tungsten-wire-reinforced, copper-lined thrust chambers
[NASA-TM-4214] p 91 N92-31249

ROCKET NOZZLES

Analytical study of nozzle performance for nuclear thermal rockets
[NASA-TM-105251] p 78 N92-11126

Arcjet nozzle area ratio effects
[NASA-TM-104477] p 83 N92-16022

ROCKET PROPELLANTS

Technical prospects for utilizing extraterrestrial propellants for space exploration
[IAF PAPER 91-669] p 133 A92-20612

Design issues for lunar in situ aluminum/oxygen propellant rocket engines
[AIAA PAPER 92-1185] p 60 A92-33299

Design issues for lunar in situ aluminum/oxygen propellant rocket engines
[NASA-TM-105433] p 83 N92-16023

A compilation of lunar and Mars exploration strategies utilizing indigenous propellants
[NASA-TM-105262] p 135 N92-19837

ROCKET THRUST

Advanced tube-bundle rocket thrust chambers
[AIAA PAPER 92-44509] p 62 A92-44509

Theoretical nozzle performance of a microwave electrothermal thruster using experimental data
[AIAA PAPER 92-3110] p 64 A92-48750

Effect of model selection on combustor performance and stability using ROCCID - Rocket Combustor Interactive Design
[AIAA PAPER 92-3226] p 65 A92-48827

Effect of model selection on combustor performance and stability predictions using ROCCID
[NASA-TM-105750] p 89 N92-27036

ROCKET VEHICLES

Overview of rocket engine control
[NASA-TM-105318] p 81 N92-13274

RODS

Effect of out-of-roundness on the performance of a diesel engine connecting-rod bearing
[NASA-TM-105600] p 215 N92-31536

ROLL

Large transient fault current test of an electrical roll ring - for Space Station Freedom
[NASA-TM-105667] p 55 A92-50661

Large transient fault current test of an electrical roll ring
[NASA-TM-105667] p 87 N92-24201

ROLLER BEARINGS

Vibration transmission through rolling element bearings. IV - Statistical energy analysis
[AIAA PAPER 92-2218] p 218 A92-28756

ROLLERS

A 23:2:1 ratio, 300-watt, 26 N-m output torque, planetary roller-gear robotic transmission: Design and evaluation
[NASA-TM-105562] p 210 N92-25085

ROTARY ENGINES

NASA's rotary engine technology enablement program: 1983-1991
[NASA-TM-105562] p 30 N92-20033

Small engine technology programs
[AIAA PAPER 92-3365] p 32 N92-22532

ROTARY WING AIRCRAFT

Advanced Rotorcraft Transmission (ART) Program summary
[AIAA PAPER 92-3365] p 205 A92-48938

Summary highlights of the Advanced Rotorcraft Transmission (ART) program
[AIAA PAPER 92-3362] p 23 A92-54026

Small engine technology programs
[AIAA PAPER 92-3362] p 32 N92-22532

Rotorcraft transmissions
[AIAA PAPER 92-3362] p 33 N92-22533

Advanced Rotorcraft Transmission (ART) program summary
[NASA-TM-105665] p 210 N92-24984

Contingency power for a small turboshaft engine by using water injection into turbine cooling air
[NASA-TM-105680] p 37 N92-29661

ROTARY WINGS

Ongoing development of a computer jobstream to predict helicopter main rotor performance in icing conditions
[AIAA PAPER 92-0412] p 2 A92-14407

Numerical investigation of performance degradation of wings and rotors due to icing
[AIAA PAPER 92-0412] p 5 A92-26264

Recent manufacturing advances for spiral bevel gears
[SAE PAPER 911229] p 204 A92-40024

The NASA aircraft icing research program
[AIAA PAPER 92-3362] p 23 N92-22534

Development of a full-scale transmission testing procedure to evaluate advanced lubricants
[NASA-TP-3265] p 213 N92-30396

ROTATING FLUIDS

Nonlinear dynamics near the stability margin in rotating pipe flow
[AIAA PAPER 92-3571] p 165 A92-19959

Flow induction by pressure forces
[AIAA PAPER 92-3571] p 28 A92-54060

ROTATING SHAFTS

Design of a hydraulic actuator for active control of rotating machinery
[ASME PAPER 91-GT-246] p 203 A92-15651

ROTATING SPHERES

A numerical and experimental study of three-dimensional liquid sloshing in a rotating spherical container
[AIAA PAPER 92-0829] p 170 A92-29597

ROTATION

Advanced propeller research
[NASA-TM-105416] p 33 N92-22537

Analysis and modification of a single-mesh gear fatigue rig for use in diagnostic studies
[NASA-TM-105416] p 212 N92-27879

ROTOR AERODYNAMICS

A viscous flow study of shock-boundary layer interaction, radial transport, and wake development in a transonic compressor
[ASME PAPER 91-GT-69] p 2 A92-15539

The role of tip clearance in high-speed fan stall
[ASME PAPER 91-GT-83] p 2 A92-15550

Unsteady flowfield simulation of ducted prop-fan configurations
[AIAA PAPER 92-0521] p 6 A92-26946

A finite-volume numerical method to calculate fluid forces and rotordynamic coefficients in seals
[AIAA PAPER 92-3712] p 183 A92-54132

Model rotor icing tests in the NASA, Lewis Icing Research Tunnel
[NASA-TM-105740] p 21 N92-21688

A general numerical model for wave rotor analysis
[NASA-TM-105740] p 196 N92-31484

ROTOR BLADES

Numerical investigation of performance degradation of wings and rotors due to icing
[AIAA PAPER 92-0412] p 5 A92-26264

ROTOR BLADES (TURBOMACHINERY)

Prediction of unsteady rotor-surface pressure and heat transfer from wake passages
[ASME PAPER 91-GT-267] p 165 A92-15665

Heat transfer in rotating serpentine passages with trips skewed to the flow
[NASA-TM-105581] p 186 N92-20235

ROTOR DYNAMICS

Electromechanical simulation and testing of actively controlled rotordynamic systems with piezoelectric actuators
[ASME PAPER 91-GT-245] p 203 A92-15650

Aeroelastic stability analyses of two counter rotating propfan designs for a cruise missile model
[AIAA PAPER 92-2218] p 25 A92-34408

Statistical energy analysis of a geared rotor system
[AIAA PAPER 92-2218] p 204 A92-39227

Electromechanical simulation and testing of actively controlled rotordynamic systems with piezoelectric actuators
[ASME PAPER 91-GT-245] p 204 A92-39258

Rotordynamic Instability Problems in High-Performance Turbomachinery, 1990
[NASA-CP-3122] p 207 N92-14346

ROTOR SPEED

Brush seal leakage performance with gaseous working fluids at static and low rotor speed conditions
[NASA-TM-105400] p 186 N92-16265

Model rotor icing tests in the NASA, Lewis Icing Research Tunnel
[NASA-TM-105400] p 21 N92-21688

ROTORCRAFT AIRCRAFT

Summary highlights of the Advanced Rotorcraft Transmission (ART) program
[AIAA PAPER 92-3362] p 23 A92-54026

ROTORS

Optical measurements of unducted fan flutter
[ASME PAPER 91-GT-19] p 197 A92-15510

Description of a pressure measurement technique for obtaining surface static pressures of a radial turbine
[AIAA PAPER 92-4006] p 200 A92-56829

Viscous three-dimensional calculations of transonic fan performance
[NASA-TM-103800] p 1 N92-17346

Description of a pressure measurement technique for obtaining surface static pressures of a radial turbine
[NASA-TM-105643] p 202 N92-24959

Viscous three-dimensional calculations of transonic fan performance
[NASA-TM-105643] p 195 N92-27467

A general numerical model for wave rotor analysis
[NASA-TM-105740] p 196 N92-31484

ROVING VEHICLES

SEI power source alternatives for rovers and other multi-kWe distributed surface applications
[NASA-TM-105740] p 80 N92-13206

RUBBER

On the development of explicit robust schemes for implementation of a class of hyperelastic models in large-strain analysis of rubbers
[AIAA PAPER 92-3362] p 221 A92-36245

RUNGE-KUTTA METHOD

RUNGE-KUTTA METHOD

- Central difference TVD and TVB schemes for time dependent and steady state problems
[AIAA PAPER 92-0053] p 166 A92-22168
- Conical detonation waves - A comparison of theoretical and numerical results
[AIAA PAPER 92-0348] p 167 A92-25792
- Runge-Kutta methods combined with compact difference schemes for the unsteady Euler equations
[AIAA PAPER 92-3210] p 182 A92-54015
- Multigrid calculation of three-dimensional viscous cascade flows
[NASA-TM-105257] p 249 N92-10345
- Central difference TVD and TVB schemes for time dependent and steady state problems
[NASA-TM-105357] p 249 N92-15663

RUPTURING

- A stochastic damage model for the rupture prediction of a multi-phase solid. I - Parametric studies. II - Statistical approach p 224 A92-49784

S

S GLASS

- Computational simulation of intermingled-fiber hybrid composite behavior
[NASA-TM-105666] p 110 N92-31506

SAFETY DEVICES

- Risks, designs, and research for fire safety in spacecraft
[NASA-TM-105317] p 240 N92-13581

SAFETY FACTORS

- Probabilistic progressive buckling of trusses
[AIAA PAPER 91-0916] p 223 A92-38142
- Advanced optical condition monitoring --- of rocket engines
[SAE PAPER 912164] p 199 A92-39994
- Safety issues p 78 N92-11115
- Probabilistic progressive buckling of trusses
[NASA-TM-105162] p 226 N92-15403

SAFETY MANAGEMENT

- Safety issues p 78 N92-11115
- NASA Aerospace Flight Battery Systems Program: An update p 237 N92-22741

SAMARIUM

- The 23 to 300 C demagnetization resistance of samarium-cobalt permanent magnets
[NASA-TP-31119] p 159 N92-11252

SANDS

- The chemistry of Saudi Arabian sand: A deposition problem on helicopter turbine airfoils
[NASA-TM-105234] p 128 N92-14179

SAPPHIRE

- Microwave properties of peeled HEMT devices sapphire substrates p 265 N92-32978

SATELLITE ANTENNAS

- Advanced Communications Technology Satellite (ACTS) p 53 A92-17780
- A vertically integrated Ka-band phased array antenna
[AIAA PAPER 92-1976] p 156 A92-38140
- The ACTS multibeam antenna p 146 A92-46046
- Advanced Communication Technology Satellite (ACTS) multibeam antenna technology verification experiments
[NASA-TM-105421] p 149 N92-16191
- Advanced Communication Technology Satellite (ACTS) multibeam antenna analysis and experiment
[NASA-TM-105420] p 149 N92-17047
- Analysis of a generalized dual reflector antenna system using physical optics
[NASA-TM-105425] p 149 N92-18281
- The ACTS multibeam antenna p 52 N92-30383
- [NASA-TM-105645]
- Characteristics of a future aeronautical satellite communications system p 151 N92-30932

SATELLITE COMMUNICATION

- Multicarrier demodulator architecture for onboard processing satellites p 49 A92-10465
- Effect of an arcjet plume on satellite reflector performance p 53 A92-16318
- Advanced Communications Technology Satellite (ACTS) p 53 A92-17780
- Advanced large scale GaAs monolithic IF switch matrix subsystem
[AIAA PAPER 92-1861] p 155 A92-29801
- Least reliable bits coding (LRBC) for high data rate satellite communications
[AIAA PAPER 92-1868] p 142 A92-29807
- Distribution of space-gathered data
[AIAA PAPER 92-1888] p 143 A92-29821
- Advances in MMIC technology for communications satellites
[AIAA PAPER 92-1899] p 155 A92-29830
- 20/30 GHz satellite personal communications networks
[AIAA PAPER 92-1908] p 143 A92-29839

- ACTS system capability and performance
[AIAA PAPER 92-1961] p 143 A92-29884
- Operational uses of ACTS technology
[AIAA PAPER 92-1964] p 144 A92-29887
- The ACTS NASA Ground Station/Master Control Station
[AIAA PAPER 92-1965] p 45 A92-29888
- Characteristics of a future aeronautical satellite communications system
[AIAA PAPER 92-2058] p 22 A92-29889
- Fault tolerance in onboard processors - Protecting efficient FDM demultiplexers
[AIAA PAPER 92-1969] p 144 A92-29892
- A multi-channel demultiplexer/demodulator architecture, simulation and implementation
[AIAA PAPER 92-1972] p 144 A92-29895
- Predictive onboard flow control in packet switching satellites
[AIAA PAPER 92-2004] p 144 A92-29923
- Circuit-switch architecture for a 30/20-GHz FDMA/TDM geostationary satellite communications network
[AIAA PAPER 92-2005] p 49 A92-29924
- Experimental code verification results for reflector antenna distortion compensation by array feeds
[AIAA PAPER 92-2014] p 49 A92-29933
- Interference susceptibility measurements for an MSK satellite communication link
[AIAA PAPER 92-2018] p 144 A92-29936
- Advanced Communications Technology Satellite (ACTS) Experiments Program - A market-driven approach to government/industry cooperation
[AIAA PAPER 92-2036] p 145 A92-29951
- ACTS aeronautical experiments
[AIAA PAPER 92-2042] p 50 A92-29956
- Technical and economic feasibility of integrated video service by satellite
[AIAA PAPER 92-2054] p 145 A92-29966
- The ACTS multibeam antenna p 146 A92-46046
- Ka-band MMIC arrays for ACTS Aero Terminal Experiment
[IAF PAPER 92-0398] p 159 A92-55785
- Advanced Communications Technology Satellite (ACTS)
[IAF PAPER 92-0407] p 50 A92-55788
- A high temperature superconductivity communications flight experiment
[IAF PAPER 92-0410] p 50 A92-55790
- Satcom systems and technologies into the 21st century p 147 A92-55792
- [IAF PAPER 92-0412]
- SCAILET - An intelligent assistant for satellite ground terminal operations p 245 A92-55855
- [IAF PAPER 92-0552]
- Space Communications Technology Conference: Onboard Processing and Switching
[NASA-CP-3132] p 147 N92-14202
- Destination directed packet switch architecture for a 30/20 GHz FDMA/TDM geostationary communication satellite network p 148 N92-14204
- An overview of Space Communication Artificial Intelligence for Link Evaluation Terminal (SCAILET) Project p 148 N92-14212
- Flexible digital modulation and coding synthesis for satellite communications p 148 N92-14235
- Circuit-switch architecture for a 30/20-GHz FDMA/TDM geostationary satellite communications network
[NASA-TM-105302] p 51 N92-15109
- Interference susceptibility measurements for an MSK satellite communication link
[NASA-TM-105395] p 149 N92-15306
- Advanced Communication Technology Satellite (ACTS) multibeam antenna technology verification experiments
[NASA-TM-105421] p 149 N92-16191
- Advanced Communication Technology Satellite (ACTS) multibeam antenna analysis and experiment
[NASA-TM-105420] p 149 N92-17047
- Multichannel demultiplexer/demodulator technologies for future satellite communication systems
[NASA-TM-105377] p 51 N92-18342
- Least Reliable Bits Coding (LRBC) for high data rate satellite communications
[NASA-TM-105431] p 150 N92-18921
- Predictive onboard flow control for packet switching satellites
[NASA-TM-105566] p 150 N92-19379
- Destination-directed, packet-switching architecture for 30/20-GHz FDMA/TDM geostationary communications satellite network
[NASA-TP-3201] p 51 N92-19762
- Advanced Modulation and Coding Technology Conference
[NASA-CP-10053] p 51 N92-22001
- Operating and service manual for the NASA Lewis automated far-field antenna range
[NASA-TM-105343] p 52 N92-22319

- The ACTS multibeam antenna
[NASA-TM-105645] p 52 N92-30383
- Characteristics of a future aeronautical satellite communications system p 151 N92-30932
- A personal communications network using a Ka-band satellite p 151 N92-30934
- An optically controlled Ka-band phased array antenna p 152 N92-32968

SATELLITE DESIGN

- Integrated solar power satellites - An approach to low-mass space power p 231 A92-40427

SATELLITE INSTRUMENTS

- Advanced Modulation and Coding Technology Conference
[NASA-CP-10053] p 51 N92-22001

SATELLITE NETWORKS

- Satellite delivery of B-ISDN services
[AIAA PAPER 92-1831] p 142 A92-29777
- Distribution of space-gathered data
[AIAA PAPER 92-1888] p 143 A92-29821
- ACTS system capability and performance
[AIAA PAPER 92-1961] p 143 A92-29884
- The ACTS NASA Ground Station/Master Control Station
[AIAA PAPER 92-1965] p 45 A92-29888
- Network architectures and protocols for the integration of ACTS and ISDN
[AIAA PAPER 92-2039] p 145 A92-29953
- Advanced Communications Technology Satellite (ACTS) p 50 A92-38164
- Satcom systems and technologies into the 21st century p 147 A92-55792
- [IAF PAPER 92-0412]
- Destination directed packet switch architecture for a geostationary communication satellite network
[IAF PAPER 92-0413] p 50 A92-55793
- Space Communications Technology Conference: Onboard Processing and Switching
[NASA-CP-3132] p 147 N92-14202
- Destination directed packet switch architecture for a 30/20 GHz FDMA/TDM geostationary communication satellite network p 148 N92-14204
- Destination-directed, packet-switching architecture for 30/20-GHz FDMA/TDM geostationary communications satellite network
[NASA-TP-3201] p 51 N92-19762
- The ACTS multibeam antenna
[NASA-TM-105645] p 52 N92-30383

SATELLITE POWER TRANSMISSION

- Integrated solar power satellites - An approach to low-mass space power p 231 A92-40427
- Beam power options for the moon p 61 A92-40429

SATELLITE SOLAR ENERGY CONVERSION

- Design considerations for space radiators based on the liquid sheet (LSR) concept p 181 A92-50821

SATELLITE TRANSMISSION

- Frequency allocations for a new satellite service - Digital audio broadcasting
[AIAA PAPER 92-1957] p 143 A92-29881
- Advanced Communication Technology Satellite (ACTS) baseband processor development p 50 A92-53693
- GTEX: An expert system for diagnosing faults in satellite ground stations p 148 N92-14215
- FIDEX: An expert system for satellite diagnostics p 148 N92-14218

SCALE (CORROSION)

- Protective Al₂O₃ scale formation on NbAl₃-base alloys p 119 A92-31850

SCALE EFFECT

- Numerical simulation of geometric scale effects in cylindrical self-field MPD thrusters
[AIAA PAPER 92-3297] p 258 A92-48885

SCALE MODELS

- Experimental investigation of an ejector-powered free-jet facility
[AIAA PAPER 92-3569] p 41 A92-54058
- Aeroelastic stability analyses of two counter rotating propfan designs for a cruise missile model
[NASA-TM-105268] p 227 N92-23191

SCALING LAWS

- Scaling of 100 kW class applied-field MPD thrusters
[AIAA PAPER 92-3462] p 74 A92-54033

SCALLOPING

- Prediction of ice accretion on a swept NACA 0012 airfoil and comparisons to flight test results
[AIAA PAPER 92-0043] p 4 A92-25677
- Prediction of ice accretion on a swept NACA 0012 airfoil and comparisons to flight test results
[NASA-TM-105368] p 16 N92-15968

SCANDIUM

- Estimation of crack closure stresses for in situ toughened silicon nitride with 8 wt pct scandia p 126 A92-43478

SCANNING TUNNELING MICROSCOPY

- Universal aspects of adhesion and atomic force microscopy p 260 A92-17979

- SCATTERING**
Radiative transfer solutions for cylindrical coordinates with emitting, absorbing, and anisotropic scattering medium
[AIAA PAPER 92-0123] p 266 A92-28185
- SCATTERING FUNCTIONS**
Combined conjugated heat transfer from a scattering medium
p 175 A92-44390
- SCHMIDT NUMBER**
Scalar rate correlation at a turbulent liquid free surface
- A two-regime correlation for high Schmidt numbers
p 184 A92-56941
- SCHOTTKY DIODES**
Significant long-term reduction in n-channel MESFET subthreshold leakage using ammonium-sulfide surface treated gates
p 153 A92-12272
- SCREWS**
Three point lead screw positioning apparatus
[NASA-CASE-LEW-15216-1] p 208 N92-17678
- SEALING**
Evaluation of an innovative high temperature ceramic wafer seal for hypersonic engine applications
[NASA-TM-105556] p 208 N92-20815
- SEALS (STOPPERS)**
Flow visualization and motion analysis for a series of four sequential brush seals
p 204 A92-36976
Rocket engine diagnostics using qualitative modeling techniques
[AIAA PAPER 92-3164] p 65 A92-48787
Relative sliding durability of two candidate high temperature oxide fiber seal materials
[AIAA PAPER 92-3713] p 126 A92-49095
Update on results of SPRE testing at NASA Lewis
p 71 A92-50780
A finite-volume numerical method to calculate fluid forces and rotordynamic coefficients in seals
[AIAA PAPER 92-3712] p 183 A92-54132
Relative sliding durability of two candidate high temperature oxide fiber seal materials
[NASA-TM-105199] p 95 N92-10064
National Aerospace Plane engine seals: High temperature seal performance evaluation
p 207 N92-15103
Engine panel seals for hypersonic engine applications: High temperature leakage assessments and flow modelling
[NASA-TM-105260] p 208 N92-16336
Evaluation of an innovative high temperature ceramic wafer seal for hypersonic engine applications
[NASA-TM-105556] p 208 N92-20815
Sliding durability of two carbide-oxide candidate high temperature fiber seal materials in air to 900 C
[NASA-TM-105554] p 97 N92-21175
High temperature, flexible, fiber-preform seal
[NASA-CASE-LEW-15085-1] p 208 N92-22043
Inflatable traversing probe seal
p 209 N92-22692
Tribological evaluation of an Al₂O₃-SiO₂ ceramic fiber candidate for high temperature sliding seals
[NASA-TM-105611] p 97 N92-23190
High temperature dynamic engine seal technology development
[NASA-TM-105641] p 209 N92-23435
Rocket engine diagnostics using qualitative modeling techniques
[NASA-TM-105714] p 88 N92-27033
- SECONDARY FLOW**
Application of computational fluid dynamics to the study of vortex flow control for the management of inlet distortion
[AIAA PAPER 92-3177] p 13 A92-54013
Flow induction by pressure forces
[AIAA PAPER 92-3571] p 28 A92-54060
Viscous three-dimensional calculations of transonic fan performance
p 195 N92-27467
Application of computational fluid dynamics to the study of vortex flow control for the management of inlet distortion
[NASA-TM-105672] p 230 N92-34112
- SELF ALIGNMENT**
Self-aligning optical measurement systems
p 247 A92-50387
- SELF ERECTING DEVICES**
Self-deploying photovoltaic power system
[NASA-CASE-LEW-15308-1] p 237 N92-24057
- SELF SEALING**
Seals related research at NASA, Lewis Research Center
p 207 N92-15087
- SEMICONDUCTOR DEVICES**
Neutron, gamma ray, and temperature effects on the electrical characteristics of thyristors
[NASA-TM-105728] p 162 N92-28432
C-band superconductor/semiconductor hybrid field-effect transistor amplifier on a LaAlO₃ substrate
[NASA-TM-105828] p 163 N92-34204
- SEMICONDUCTOR JUNCTIONS**
Theoretical modeling, near-optimum design and predicted performance of n(+)-pp(+) and p(+)-nnn(+) indium phosphide homojunction solar cells
p 234 A92-53152
High voltage thermally diffused p(+)-n solar cells
p 235 A92-53172
Status and future directions of InP solar cell research
[NASA-TM-105426] p 160 N92-18920
- SEMICONDUCTORS (MATERIALS)**
Numerical simulations of space processing - The reality, the myth, and the future
p 136 A92-12863
Molecular dynamics investigation of radiation damage in semiconductors
p 159 A92-53157
An overview of silicon carbide device technology
[NASA-TM-105402] p 263 N92-15815
High-temperature electronics
p 160 N92-22528
Sinterless contacts to shallow junction InP solar cells
[NASA-TM-105670] p 237 N92-24802
Heat transfer device
[NASA-CASE-LEW-14162-3] p 111 N92-34208
- SEMIEMPIRICAL EQUATIONS**
Lattice parameters of fcc binary alloys using a new semiempirical method
p 120 A92-32898
- SENSITIVITY**
Boundary formulations for sensitivities of three-dimensional stress invariants
p 224 A92-50883
- SENSORS**
Research sensors
p 202 N92-22526
- SEPARATED FLOW**
The Baldwin-Lomax model for separated and wake flows using the entropy envelope concept
[AIAA PAPER 92-0148] p 4 A92-23764
On the mechanism of turbulence suppression in free shear flows under acoustic excitation
[AIAA PAPER 92-0065] p 252 A92-25678
Helium bubble flow visualization of the spanwise separation on a NACA 0012 with simulated glaze ice
[AIAA PAPER 92-0413] p 7 A92-28192
On turbulent flows dominated by curvature effects
p 171 A92-32940
Effect of acoustic excitation on stalled flows over an airfoil
p 9 A92-41267
An investigation of shock/turbulent boundary layer bleed interactions
[AIAA PAPER 92-3085] p 182 A92-54008
On the mechanism of turbulence suppression in free shear flows under acoustic excitation
[NASA-TM-105360] p 15 N92-14003
Advances in engineering turbulence modeling --- computational fluid dynamics
p 193 N92-25820
Helium bubble flow visualization of the spanwise separation on a NACA 0012 with simulated glaze ice
[NASA-TM-105742] p 19 N92-26612
A critical evaluation of a three-dimensional Navier-Stokes CFD as a tool to design supersonic turbine stages
p 196 N92-32268
- SEPARATION**
Separation distance and static transmission error of involute spur gears
[AIAA PAPER 92-3490] p 205 A92-49027
- SEPARATORS**
The evaluation of layered separators for nickel-hydrogen cells
p 89 N92-27161
- SERIES EXPANSION**
Rational approximations from power series of vector-valued meromorphic functions
[NASA-TM-105859] p 251 N92-33942
- SERT 2 SPACECRAFT**
Development and flight history of SERT 2 spacecraft
[AIAA PAPER 92-3516] p 74 A92-54038
Development and flight history of SERT 2 spacecraft
[NASA-TM-105636] p 90 N92-28983
- SERVICE LIFE**
Transmission overhaul and component replacement predictions using Weibull and renewal theory
p 215 A92-17201
Unsteady aerodynamic interaction effects on turbomachinery blade life and performance
[AIAA PAPER 92-0149] p 7 A92-28186
Thermal barrier coating life and isothermal oxidation of low-pressure plasma-sprayed bond coat alloys
p 119 A92-32398
Diffusive crack growth at a bimaterial interface
[AIAA PAPER 92-2432] p 220 A92-34580
Maximum life spiral bevel reduction design
[AIAA PAPER 92-3493] p 205 A92-49030
Reliability training
[NASA-RP-1253] p 49 N92-32456
- SERVOCONTROL**
Linear quadratic servo control of a reusable rocket engine
p 67 A92-50495
Linear quadratic servo control of a reusable rocket engine
[NASA-TM-105291] p 79 N92-11128
- SERVOMECHANISMS**
Linear quadratic servo control of a reusable rocket engine
[NASA-TM-105291] p 79 N92-11128
- SHAFTS (MACHINE ELEMENTS)**
Vibration transmission through rolling element bearings.
IV - Statistical energy analysis
p 218 A92-28756
Analysis and modification of a single-mesh gear fatigue rig for use in diagnostic studies
[NASA-TM-105416] p 212 N92-27879
Application of face-gear drives in helicopter transmissions
[NASA-TM-105655] p 212 N92-28434
Optimal design of compact spur gear reductions
[NASA-TM-105676] p 213 N92-29351
- SHAPE FUNCTIONS**
Three-dimensional boundary element thermal shape sensitivity analysis
p 176 A92-47269
- SHAPES**
Boundary formulations for shape sensitivity of temperature dependent conductivity problems
p 217 A92-25403
Results of an icing test on a NACA 0012 airfoil in the NASA Lewis Icing Research Tunnel
[AIAA PAPER 92-0647] p 7 A92-27021
Results of an icing test on a NACA 0012 airfoil in the NASA Lewis Icing Research Tunnel
[NASA-TM-105374] p 16 N92-15051
Experimental ice shape and performance characteristics for a multi-element airfoil in the NASA Lewis Icing Research Tunnel
[NASA-TM-105380] p 17 N92-17347
Experimental and computational ice shapes and resulting drag increase for a NACA 0012 airfoil
[NASA-TM-105743] p 20 N92-28674
- SHEAR FLOW**
Compressibility effects on large structures in free shear flows
p 173 A92-39337
A continuous mixing model for pdf simulations and its applications to combustor shear flows
p 174 A92-40139
Modern developments in shear flow control with swirl
p 9 A92-41265
Second order modeling of boundary-free turbulent shear flows
p 174 A92-41275
Near-wall response in turbulent shear flows subjected to imposed unsteadiness
p 174 A92-41652
Renormalization group analysis of the Reynolds stress transport equation
p 179 A92-49493
Noise from turbulent shear flows
p 254 N92-10603
Numerical experiments with flows of elongated granules
[NASA-TM-105567] p 209 N92-23226
Modeling of compressible turbulent shear flows
p 189 N92-23340
Renormalization group analysis of the Reynolds stress transport equation
[NASA-TM-105588] p 190 N92-23542
- SHEAR LAYERS**
On the mechanism of turbulence suppression in free shear flows under acoustic excitation
[AIAA PAPER 92-0065] p 252 A92-25678
Vorticity dynamics of inviscid shear layers
[AIAA PAPER 92-0420] p 168 A92-26270
Nonlinear spatial equilibration of an externally excited instability wave in a free shear layer
p 170 A92-31469
Control of an axisymmetric turbulent jet by multi-modal excitation
p 174 A92-40071
Initial development of the axisymmetric ejector shear layer
[AIAA PAPER 92-3567] p 178 A92-49068
Filtered Rayleigh scattering based measurements in compressible mixing layers
[AIAA PAPER 92-3543] p 182 A92-54043
On the mechanism of turbulence suppression in free shear flows under acoustic excitation
[NASA-TM-105360] p 15 N92-14003
Inlets, ducts, and nozzles
p 188 N92-22523
Simulations of free shear layers using a compressible kappa-epsilon model
p 190 N92-23355
- SHEAR STRENGTH**
Relationship between voids and interlaminar shear strength of polymer matrix composites
p 98 A92-10241
Influence of interfacial shear strength on the mechanical properties of SiC fiber reinforced reaction-bonded silicon nitride matrix composites
p 99 A92-15145
Void effects on the interlaminar shear strength of unidirectional graphite-fiber-reinforced composites
p 105 A92-50348
- SHEAR STRESS**
Micromechanics for ceramic matrix composites
p 98 A92-10282
Effect of fiber orientation on the fracture toughness of brittle matrix composites
p 103 A92-41841

SHELL STABILITY

- Boundary formulations for sensitivities of three-dimensional stress invariants p 224 A92-50883
- SHELL STABILITY**
Structural durability of stiffened composite shells [AIAA PAPER 92-2244] p 220 A92-34569
- SHELLS (STRUCTURAL FORMS)**
Optimum design of a gearbox for low vibration [NASA-TM-105653] p 212 N92-28476
- SHOCK DISCONTINUITY**
Development of new flux splitting schemes --- computational fluid dynamics algorithms p 192 N92-25809
- SHOCK LAYERS**
A viscous flow study of shock-boundary layer interaction, radial transport, and wake development in a transonic compressor [ASME PAPER 91-GT-69] p 2 A92-15539
Improved nonequilibrium viscous shock-layer scheme for hypersonic blunt-body flowfields p 4 A92-24653
Numerical study of shock-wave/boundary-layer interactions in premixed combustible gases p 183 A92-54907
Development of new flux splitting schemes --- computational fluid dynamics algorithms p 192 N92-25809
- SHOCK RESISTANCE**
Novel applications for TAZ-8A p 123 N92-22444
- SHOCK TUNNELS**
Three-dimensional Navier-Stokes heat transfer predictions for turbine blade rows [AIAA PAPER 92-3068] p 12 A92-54003
- SHOCK WAVE GENERATORS**
Crossing shock wave turbulent boundary layer interactions - Variable angle and shock generator length geometry effects at Mach 3 [AIAA PAPER 92-0636] p 6 A92-27014
- SHOCK WAVE INTERACTION**
Crossing shock wave turbulent boundary layer interactions - Variable angle and shock generator length geometry effects at Mach 3 [AIAA PAPER 92-0636] p 6 A92-27014
Surface and flow field measurements in a symmetric crossing shock wave/turbulent boundary layer flow [AIAA PAPER 92-2634] p 10 A92-45574
Numerical study of shock-wave/boundary-layer interactions in premixed combustible gases p 183 A92-54907
Inlets, ducts, and nozzles p 188 N92-22523
Development of a new flux splitting scheme p 190 N92-23352
- SHOCK WAVES**
Internal structure of shock waves in disparate mass mixtures [AIAA PAPER 92-0496] p 169 A92-28195
An investigation of shock/turbulent boundary layer bleed interactions [AIAA PAPER 92-3085] p 182 A92-54008
Numerical study of shock-wave/boundary-layer interactions in premixed combustible gases p 183 A92-54907
- SHORT CIRCUITS**
Evaluation of Kapton pyrolysis, arc tracking, and arc propagation on the Space Station Freedom (SSF) solar array flexible current carrier (FCC) p 72 A92-53209
- SHORT TAKEOFF AIRCRAFT**
Experimental performance of three design factors for ventral nozzles for SSTOVL aircraft [AIAA PAPER 92-3789] p 28 A92-54168
Internal reversing flow in a tailpipe offtake configuration for SSTOVL aircraft [AIAA PAPER 92-3790] p 28 A92-54169
Analysis of airframe/engine interactions for a STOVL aircraft with integrated flight/propulsion control [AIAA PAPER 92-4623] p 23 A92-55300
Experimental performance of three design factors for ventral nozzles for SSTOVL aircraft [NASA-TM-105697] p 37 N92-27669
Internal reversing flow in a tailpipe offtake configuration for SSTOVL aircraft [NASA-TM-105698] p 37 N92-28418
- SHOT PEENING**
Improvement in surface fatigue life of hardened gears by high-intensity shot peening [NASA-TM-105678] p 211 N92-26108
- SHRINKAGE**
Shrinkage void formation and its effect on freeze and thaw processes of lithium and lithium-fluoride for space applications p 180 A92-50596
- SHROUDED PROPELLERS**
Analysis of an advanced ducted propeller subsonic inlet [AIAA PAPER 92-0274] p 5 A92-25728
Far-field noise and internal modes from a ducted propeller at simulated aircraft takeoff conditions [AIAA PAPER 92-0371] p 252 A92-26230
Analysis of an advanced ducted propeller subsonic inlet [NASA-TM-105393] p 15 N92-14002
Far-field noise and internal modes from a ducted propeller at simulated aircraft takeoff conditions [NASA-TM-105369] p 254 N92-16702
- SIGNAL DISTORTION**
Experimental code verification results for reflector antenna distortion compensation by array feeds [AIAA PAPER 92-2014] p 49 A92-29933
- SIGNAL FADING**
Dynamic rain fade compensation techniques for the advanced communications technology satellite [NASA PAPER 92-2038] p 145 A92-31711
Comparative study on the performance of power and bandwidth efficient modulations in LMSS under fading and interference p 147 A92-54763
- SIGNAL PROCESSING**
An IIR median hybrid filter p 246 A92-40375
Rotative quadrature phase-shift keying p 146 A92-44233
Real-time data compression of broadcast video signals [NASA-CASE-LEW-14945-2] p 147 N92-10128
Subband coding for image data archiving [NASA-TM-105407] p 151 N92-20032
NASA, Lewis Research Center Advanced Modulation and Coding Project: Introduction and overview p 51 N92-22002
- SIKORSKY AIRCRAFT**
Model rotor icing tests in the NASA, Lewis Icing Research Tunnel p 21 N92-21688
- SILICATES**
Glass formation, properties, and structure of soda-yttria-silicate glasses [NASA-TM-104488] p 128 N92-11202
- SILICON**
High temperature structural fibers: Status and needs [NASA-TM-105174] p 107 N92-16037
Using silicon diodes for detecting the liquid-vapor interface in hydrogen p 201 N92-18456
[NASA-TM-105541] p 201 N92-18456
Intermodulation in the oscillatory magnetoresistance of a two-dimensional electron gas p 163 N92-32975
- SILICON CARBIDES**
METCAN updates for high temperature composite behavior - Simulation/verification p 98 A92-10264
Influence of interfacial shear strength on the mechanical properties of SiC fiber reinforced reaction-bonded silicon nitride matrix composites p 99 A92-15145
Mechanical behavior of fiber reinforced SiC/RBSN ceramic matrix composites - Theory and experiment --- Reaction Bonded Silicon Nitride [ASME PAPER 91-GT-209] p 99 A92-15629
The effect of matrix mechanical properties on (0)8 unidirectional SiC/Ti composite fatigue resistance p 99 A92-16220
Isothermal fatigue behaviour of a (90 deg)8 SiC/Ti-15-3 composite at 426 C p 100 A92-23313
Role of interfacial carbon layer in the thermal diffusivity/conductivity of silicon carbide fiber-reinforced reaction-bonded silicon nitride matrix composites p 100 A92-25443
Oxidation effects on the mechanical properties of a SiC-fiber-reinforced reaction-bonded Si3N4 matrix composite p 100 A92-25445
Effect of heat treatment on stiffness and damping of SiC/Ti-15-3 p 100 A92-25627
Tension, compression, and bend properties for SiC/RBSN composites p 100 A92-32727
Computational simulation of high temperature metal matrix composite behavior p 101 A92-32753
Strength, toughness and R-curve behaviour of SiC whisker-reinforced composite Si3N4 with reference to monolithic Si3N4 p 101 A92-34202
Effect of fiber strength on the room temperature tensile properties of SiC/Ti-24Al-11Nb p 102 A92-36389
Thermal stress analysis of a silicon carbide/aluminum composite p 222 A92-38097
Fiber coating/matrix reactions in silicon-base ceramic matrix composites p 102 A92-39604
Role of interfacial thermal barrier in the transverse thermal conductivity of uniaxial SiC fiber-reinforced reaction bonded silicon nitride p 102 A92-39605
Bonded ceramic foams reinforced with fibers for high temperature use p 125 A92-39628
Tensile strain measurements of ceramic fibers using scanning laser acoustic microscopy p 198 A92-39629
Failure mechanisms of 3-D woven SiC/SiC composites under tensile and flexural loading at room and elevated temperatures p 103 A92-39642
Oxidation kinetics of CVD silicon carbide and silicon nitride p 125 A92-39674
Reaction-bonded Si3N4 and SiC matrix composites p 103 A92-39858
- Reactions of silicon carbide and silicon(IV) oxide at elevated temperatures p 126 A92-43483
Mechanical properties of 3C silicon carbide p 126 A92-43761
Thermomechanical testing of high-temperature composites - Thermomechanical fatigue (TMF) behavior of SiC(SCS-6)/Ti-15-3 p 104 A92-44606
High-temperature fatigue behavior of a SiC/Ti-24Al-11Nb composite p 104 A92-44613
An evaluation of strain measuring devices for ceramic composites p 199 A92-46497
Anodic etching of p-type cubic silicon carbide p 127 A92-57027
An evaluation of strain measuring devices for ceramic composites [NASA-TM-105337] p 225 N92-14433
An overview of silicon carbide device technology [NASA-TM-105402] p 263 N92-15815
CVD of silicon carbide on structural fibers: Microstructure and composition p 107 N92-18439
Multiwavelength pyrometry for nongray surfaces in the presence of interfering radiation [NASA-TM-105286] p 201 N92-19107
Temperature-dependent reflectivity of silicon carbide [NASA-TM-105287] p 201 N92-19263
Development of a new generation of high-temperature composite materials p 109 N92-22515
High-temperature electronics p 160 N92-22528
Tensile strain measurements of ceramic fibers using scanning laser acoustic microscopy [NASA-TM-105589] p 216 N92-24986
Effects of fiber and interfacial layer architectures on the thermoplastic response of metal matrix composites [NASA-TM-105802] p 110 N92-32234
Computational simulation of matrix micro-slip bands in SiC/Ti-15 composite [NASA-TM-105762] p 111 N92-32466
- SILICON CONTROLLED RECTIFIERS**
Neutron, gamma ray, and temperature effects on the electrical characteristics of thyristors [NASA-TM-105728] p 162 N92-28432
- SILICON DIOXIDE**
Effect of particle size of Martian dust on the degradation of photovoltaic cell performance [NASA-TM-105232] p 79 N92-11133
Atomic oxygen durability of solar concentrator materials for Space Station Freedom [NASA-TM-105378] p 85 N92-20065
- SILICON NITRIDES**
Influence of interfacial shear strength on the mechanical properties of SiC fiber reinforced reaction-bonded silicon nitride matrix composites p 99 A92-15145
Reliability analysis of a structural ceramic combustion chamber [ASME PAPER 91-GT-155] p 24 A92-15591
Role of interfacial carbon layer in the thermal diffusivity/conductivity of silicon carbide fiber-reinforced reaction-bonded silicon nitride matrix composites p 100 A92-25443
Oxidation effects on the mechanical properties of a SiC-fiber-reinforced reaction-bonded Si3N4 matrix composite p 100 A92-25445
Tension, compression, and bend properties for SiC/RBSN composites p 100 A92-32727
Crack healing behavior of hot pressed silicon nitride due to oxidation p 124 A92-32896
Precautions toward XTEM of Si3N4/SiO2 p 125 A92-33930
Strength, toughness and R-curve behaviour of SiC whisker-reinforced composite Si3N4 with reference to monolithic Si3N4 p 101 A92-34202
Fiber coating/matrix reactions in silicon-base ceramic matrix composites p 102 A92-39604
Role of interfacial thermal barrier in the transverse thermal conductivity of uniaxial SiC fiber-reinforced reaction bonded silicon nitride p 102 A92-39605
Oxidation kinetics of CVD silicon carbide and silicon nitride p 125 A92-39674
Relationships between toughness and microstructure of reaction bonded Si3N4 p 125 A92-39687
Reaction-bonded Si3N4 and SiC matrix composites p 103 A92-39858
Estimation of crack closure stresses for in situ toughened silicon nitride with 8 wt pct scandia p 126 A92-43478
An evaluation of strain measuring devices for ceramic composites p 199 A92-46497
Extreme value statistics analysis of fracture strengths of a sintered silicon nitride failing from pores p 127 A92-50191
Mechanical behaviour and failure phenomenon of an in situ toughened silicon nitride p 127 A92-54504
An evaluation of strain measuring devices for ceramic composites [NASA-TM-105337] p 225 N92-14433

- Elevated temperature mechanical behavior of monolithic and SiC whisker-reinforced silicon nitrides
[NASA-TM-105245] p 128 N92-15192
- Reliability analysis of structural ceramic components using a three-parameter Weibull distribution
[NASA-TM-105370] p 129 N92-17060
- SILICON OXIDES**
- SiO(x) coatings for atomic oxygen protection of polyimide Kapton in low earth orbit
[AIAA PAPER 92-2151] p 94 A92-31286
- Precautions toward XTEM of Si3N4/SiO2
p 125 A92-33930
- Reactions of silicon carbide and silicon(IV) oxide at elevated temperatures
p 126 A92-43483
- Atomic oxygen effects on SiO(x) coated Kapton for photovoltaic arrays in low earth orbit
p 72 A92-53211
- Photobiological evaluation of an Al2O3-SiO2 ceramic fiber candidate for high temperature sliding seals
[NASA-TM-105611] p 97 N92-23190
- SILICON POLYMERS**
- Atomic oxygen interactions with FEP Teflon and silicones on LDEF
p 132 N92-24820
- SILICONES**
- Design considerations for space radiators based on the liquid sheet (LSF) concept
p 181 A92-50821
- SILVER**
- The effect of ion plated silver and sliding friction on tensile stress-induced cracking in aluminum oxide
[NASA-TM-105366] p 129 N92-19450
- Screen Cage Ion Plating (SCIP) and scratch testing of polycrystalline aluminum oxide
[NASA-TM-105404] p 130 N92-22278
- Self-lubricating coatings for high-temperature applications
p 130 N92-22516
- Sinterless contacts to shallow junction InP solar cells
[NASA-TM-105670] p 237 N92-24802
- SIMILARITY THEOREM**
- Use of an approximate similarity principle for the thermal scaling of a full-scale thrust augmenting ejector
[AIAA PAPER 92-3792] p 28 A92-54171
- Use of an approximate similarity principle for the thermal scaling of a full-scale thrust augmenting ejector
[NASA-TM-105724] p 36 N92-26613
- SIMULATION**
- Modal simulation of gearbox vibration with experimental correlation
[AIAA PAPER 92-3494] p 207 A92-54036
- Computational simulation of surface waviness in graphite/epoxy woven composites due to initial curing
[NASA-TM-105313] p 106 N92-14118
- Modal simulation of gearbox vibration with experimental correlation
[NASA-TM-105702] p 215 N92-31485
- SIMULATORS**
- Development of a ninety string solar array simulator
p 46 A92-50660
- Development of a ninety string solar array simulator
[NASA-TM-105278] p 55 N92-11086
- Multiple-access phased array antenna simulator for a digital beam forming system investigation
[NASA-TM-105422] p 149 N92-17062
- SINGLE CHANNEL PER CARRIER TRANSMISSION**
- Multicarrier demodulator architecture for onboard processing satellites
p 49 A92-10465
- SINGLE CRYSTALS**
- A viscoplastic model for single crystals
p 217 A92-24717
- A viscoplastic theory for anisotropic materials
[ONERA, TP NO. 1992-90] p 217 A92-24721
- Effect of temperature on the formation of creep substructure in sodium chloride single crystals
p 260 A92-25444
- Microstructure and mechanical properties of a single crystal NiAl alloy with Zr or Hf rich G-phase precipitates
p 119 A92-30841
- Comments on the paper 'Does the subgrain size influence the rate of creep?'
p 260 A92-33946
- Method of intercalating large quantities of fibrous structures
[NASA-CASE-LEW-15077-1] p 107 N92-16025
- Vapor crystal growth technology development: Application to cadmium telluride
[NASA-TM-103786] p 139 N92-16158
- Creep and fatigue research efforts on advanced materials
p 227 N92-22514
- Dependence of the critical temperature of laser-ablated YBa2Cu3O(7-delta) thin films on LaAlO3 substrate growth technique
p 264 N92-23415
- NASA programs in space photovoltaics
[NASA-TM-105428] p 87 N92-25343
- SINGLE-PHASE FLOW**
- Development of a single-phase harmonic power flow program to study the 20 kHz AC power system for large spacecraft
[NASA-TM-105326] p 81 N92-13275
- SINGULARITY (MATHEMATICS)**
- Singularities in optimal structural design
[NASA-TM-4365] p 228 N92-23527
- SINTERING**
- Discontinuously reinforced intermetallic matrix composites via XD synthesis --- exothermal dispersion
p 103 A92-41867
- Extreme value statistics analysis of fracture strengths of a sintered silicon nitride failing from pores
p 127 A92-50191
- A very low resistance, non-sintered contact system for use on indium phosphide concentrator/shallow junction solar cells
p 233 A92-53146
- Mechanical behaviour and failure phenomenon of an in situ toughened silicon nitride
p 127 A92-54504
- A very low resistance, non-sintered contact system for use on indium phosphide concentrator/shallow junction solar cells
[NASA-TM-105279] p 235 N92-13482
- Tribological and mechanical comparison of sintered and HIPped PM212: High temperature self-lubricating composites
[NASA-TM-105379] p 96 N92-15128
- Method of making contamination-free ceramic bodies
[NASA-CASE-LEW-14984-1] p 128 N92-16122
- Reliability analysis of structural ceramic components using a three-parameter Weibull distribution
[NASA-TM-105370] p 129 N92-17060
- Sinterless contacts to shallow junction InP solar cells
[NASA-TM-105670] p 237 N92-24802
- SLIDING FRICTION**
- Tribological properties of ceramic-(Ti3Al-Nb) sliding couples for use as candidate seal materials to 700 C
p 124 A92-32407
- Relative sliding durability of two candidate high temperature oxide fiber seal materials
[AIAA PAPER 92-3713] p 126 A92-49095
- Relative sliding durability of two candidate high temperature oxide fiber seal materials
[NASA-TM-105199] p 95 N92-10064
- A vacuum (10(expl-9) Torr) friction apparatus for determining friction and endurance life of MoSx films
[NASA-TM-104478] p 129 N92-16129
- The effect of ion plated silver and sliding friction on tensile stress-induced cracking in aluminum oxide
[NASA-TM-105366] p 129 N92-19450
- Properties data for opening the Galileo's partially unfurled main antenna
[NASA-TM-105355] p 130 N92-20660
- Sliding durability of two carbide-oxide candidate high temperature fiber seal materials in air to 900 C
[NASA-TM-105554] p 97 N92-21175
- Environmental effects on friction and wear of diamond and diamondlike carbon coatings
[NASA-TM-105634] p 131 N92-23192
- Tribological and microstructural comparison of HIPped PM212 and PM212/Au self-lubricating composites
[NASA-TM-105615] p 97 N92-26142
- SLOT ANTENNAS**
- New techniques for exciting linearly tapered slot antennas with coplanar waveguide
p 155 A92-34844
- New coplanar waveguide feed network for 2 x 2 linearly tapered slot antenna subarray
p 156 A92-45619
- Nonplanar linearly tapered slot antenna with balanced microstrip feed
[NASA-TM-105647] p 161 N92-23535
- SLOTS**
- CFD mixing analysis of jets injected from straight and slanted slots into confined crossflow in rectangular ducts
[AIAA PAPER 92-3087] p 177 A92-48732
- CFD mixing analysis of jets injected from straight and slanted slots into confined crossflow in rectangular ducts
[NASA-TM-105699] p 36 N92-26561
- SLUSH**
- Slush hydrogen (SLH2) technology development for application to the National Aerospace Plane (NASP)
p 140 A92-13432
- An optical method for determining level in two-phase cryogenic fluids
[NASA-TM-104524] p 200 N92-15366
- SLUSH HYDROGEN**
- Technology issues associated with using densified hydrogen for space vehicles
[AIAA PAPER 92-3079] p 134 A92-48727
- Slush hydrogen pressurized expulsion studies at the NASA K-Site Facility
[AIAA PAPER 92-3385] p 141 A92-48951
- Benefits of slush hydrogen for space missions
[NASA-TM-104503] p 134 N92-11214
- Technology issues associated with using densified hydrogen for space vehicles
[NASA-TM-105642] p 135 N92-25277
- Slush hydrogen transfer studies at the NASA K-Site Test Facility
[NASA-TM-105596] p 135 N92-25957
- Slush hydrogen pressurized expulsion studies at the NASA K-Site Facility
[NASA-TM-105597] p 135 N92-26131
- SMART STRUCTURES**
- Probabilistic structural analysis of adaptive/smart/intelligent space structures
[NASA-TM-105408] p 227 N92-22267
- SNAP**
- Space reactor power system programs overview
[AIAA PAPER 92-1558] p 61 A92-38652
- SOAPS**
- Guanidine based vehicle/binders for use with oxides, metals, and ceramics
[NASA-CASE-LEW-15314-1] p 131 N92-23461
- SODIUM CHLORIDES**
- Effect of temperature on the formation of creep substructure in sodium chloride single crystals
p 260 A92-25444
- Comments on the paper 'Does the subgrain size influence the rate of creep?'
p 260 A92-33946
- SODIUM PEROXIDES**
- Glass formation, properties, and structure of soda-yttria-silicate glasses
[NASA-TM-104488] p 128 N92-11202
- SODIUM SULFUR BATTERIES**
- SEI rover solar-electrochemical power system options
p 45 A92-50574
- SOFTWARE ENGINEERING**
- Description of real-time Ada software implementation of a power system monitor for the Space Station Freedom PMAD DC tested
p 242 A92-50533
- SOFTWARE TOOLS**
- The NASA Computational Aerosciences Program - Toward teraFLOPS computing
[AIAA PAPER 92-0558] p 240 A92-26968
- ACTS T1-VSAT - The intelligent earth station
[AIAA PAPER 92-2037] p 145 A92-29952
- FREPS - A forced response prediction system for turbomachinery blade rows
[AIAA PAPER 92-3072] p 242 A92-54006
- SOL-GEL PROCESSES**
- Low temperature synthesis of CaO-SiO2 glasses having stable liquid-liquid immiscibility by the sol-gel process
p 126 A92-44479
- SOLAR ARRAYS**
- Photovoltaic power options for Mars
p 231 A92-20366
- The arcing rate for a High Voltage Solar Array - Theory, experiment and predictions
[AIAA PAPER 92-0576] p 53 A92-26983
- Synergistic effects of ultraviolet radiation, thermal cycling and atomic oxygen on altered and coated Kapton surfaces
[AIAA PAPER 92-0794] p 93 A92-27125
- Applicability of Long Duration Exposure Facility environmental effects data to the design of Space Station Freedom electrical power system
[AIAA PAPER 92-0848] p 53 A92-29614
- Structural design concepts for a multimegawatt solar electric propulsion (SEP) spacecraft
[AIAA PAPER 92-2536] p 54 A92-34380
- Structural scaling approximations for solar arrays
p 231 A92-40935
- Space power by ground-based laser transmission
[AIAA PAPER 92-3024] p 63 A92-47027
- Contamination effects on Space Station Freedom electric power system performance
p 54 A92-50578
- The Solar Array Module Plasma Interactions Experiment (SAMPIE) - A Shuttle-based plasma interactions experiment
p 69 A92-50583
- Advanced power systems for EQS
p 70 A92-50640
- Applications of thin-film photovoltaics for space
p 70 A92-50641
- Design and optimization of a self-deploying PV tent array
p 233 A92-50642
- The mini-dome Fresnel lens photovoltaic concentrator array - Current program status
p 70 A92-50648
- Development of a ninety string solar array simulator
p 46 A92-50660
- LDEF spacecraft, ground laboratory, and computational modeling implications on Space Station Freedom's solar array materials and surfaces durability
p 71 A92-53190
- A high-performance photovoltaic concentrator array - The mini-dome Fresnel lens concentrator with 30 percent efficient GaAs/GaSe tandem cells
p 72 A92-53199
- Photovoltaic receivers for laser beamed power in space
p 72 A92-53201
- Atomic oxygen effects on SiO(x) coated Kapton for photovoltaic arrays in low earth orbit
p 72 A92-53211
- Classical and adaptive control algorithms for the solar array pointing system of the Space Station Freedom
[AIAA PAPER 92-4484] p 57 A92-55314
- Development of a ninety string solar array simulator
[NASA-TM-105278] p 55 N92-11086

SOLAR BLANKETS

- Synergistic effects of ultraviolet radiation, thermal cycling, and atomic oxygen on altered and coated Kapton surfaces
 [NASA-TM-105363] p 96 N92-14114
- Space Station Freedom solar dynamic modules structural modelling and analysis
 [NASA-TM-104506] p 226 N92-15405
- Selective emitters
 [NASA-CASE-LEW-14731-1] p 236 N92-22037
- The Solar Array Module Plasma Interactions Experiment (SAMPIE): Science and technology objectives
 p 86 N92-22360
- NASCAP/LEO simulations of Shuttle Orbiter charging during the SAMPIE experiment
 p 55 N92-22361
- Self-deploying photovoltaic power system
 [NASA-CASE-LEW-15308-1] p 237 N92-24057
- Solar Array Module Plasma Interaction Experiment (SAMPIE): Technical requirements document
 [NASA-TM-105660] p 56 N92-28683
- Influence of mass moment of inertia on normal modes of preloaded solar array mast
 [NASA-TP-3273] p 230 N92-33476
- Photovoltaic array for Martian surface power
 [NASA-TM-105827] p 270 N92-33899
- SOLAR BLANKETS**
- Structural design concepts for a multimewatt solar electric propulsion (SEP) spacecraft
 [AIAA PAPER 92-2536] p 54 A92-34380
- Self-deploying photovoltaic power system
 [NASA-CASE-LEW-15308-1] p 237 N92-24057
- Durability evaluation of photovoltaic blanket materials exposed on LDEF tray S1003
 p 132 N92-27100
- Solar radiation on a catenary collector
 [NASA-TM-105751] p 163 N92-32243
- SOLAR CELLS**
- Calculated performance of p(+)-n InP solar cells with In(0.52)Al(0.48)As window layers
 p 153 A92-13266
- Photovoltaic power options for Mars
 p 231 A92-20366
- Arcing of negatively biased solar cells in low earth orbit
 [AIAA PAPER 92-0578] p 59 A92-26985
- Structural scaling approximations for solar arrays
 p 231 A92-40935
- Increased efficiency with surface texturing in ITO/InP solar cells
 p 232 A92-44548
- Arcing of negatively biased solar cells in a plasma environment. I - Experimental observations
 [AIAA PAPER 92-2990] p 63 A92-47000
- Surface etching for light trapping in encapsulated InP solar cells
 p 232 A92-48091
- SEI rover solar-electrochemical power system options
 p 45 A92-50574
- Recent progress in InP solar cell research
 p 158 A92-50653
- Description of the control system design for the SSF PMAD DC testbed
 p 45 A92-50654
- Design considerations for space radiators based on the liquid sheet (LSR) concept
 p 181 A92-50821
- A very low resistance, non-sintered contact system for use on indium phosphide concentrator/shallow junction solar cells
 p 233 A92-53146
- Minority carrier lifetime in indium phosphide
 p 262 A92-53148
- Theoretical modeling, near-optimum design and predicted performance of n(+)-pp(+)- and p(+)-Inn(+)-indium phosphide homojunction solar cells
 p 234 A92-53152
- Modeled performance of monolithic, 3-terminal InP/Ga(0.47)In(0.53)As concentrator solar cells as a function of temperature and concentration ratio
 p 234 A92-53153
- Enhancing optical absorption in InP and GaAs utilizing profile etching
 p 263 A92-53154
- High performance etchant for thinning p(+)-InP and its application to p(+)-n InP solar cell fabrication
 p 263 A92-53155
- Influence of the dislocation density on the performance of heteroepitaxial indium phosphide solar cells
 p 234 A92-53156
- Evaluation of the minority carrier diffusion length and surface-recombination velocity in GaAs p/n solar cells
 p 234 A92-53162
- Effect of InAlAs window layer on the efficiency of indium phosphide solar cells
 p 234 A92-53163
- InP concentrator solar cells
 p 234 A92-53166
- High voltage thermally diffused p(+)-n solar cells
 p 235 A92-53172
- Radiation performance of GaAs concentrator cells for 0.4 to 12 MeV electrons and 0.1 to 37 MeV protons
 p 159 A92-53193
- Pilot production of 4 sq cm ITO/InP photovoltaic solar cells
 p 71 A92-53197
- Advances in photovoltaic technology
 [IAF PAPER 92-0599] p 235 A92-57055

- Effect of particle size of Martian dust on the degradation of photovoltaic cell performance
 [NASA-TM-105232] p 79 N92-11133
- Thin-film photovoltaics: Status and applications to space power
 p 81 N92-13228
- Thin film, concentrator, and multijunction space solar cells: Status and potential
 p 81 N92-13230
- Enhanced EOS photovoltaic power system capability with InP solar cells
 p 81 N92-13248
- Solar radiation for Mars power systems
 p 81 N92-13259
- A very low resistance, non-sintered contact system for use on indium phosphide concentrator/shallow junction solar cells
 [NASA-TM-105279] p 235 N92-13482
- Enhancing optical absorption in InP and GaAs utilizing profile etching
 [NASA-TM-105325] p 82 N92-14111
- Status and future directions of InP solar cell research
 [NASA-TM-105426] p 160 N92-18920
- The Solar Array Module Plasma Interactions Experiment (SAMPIE): Science and technology objectives
 p 86 N92-22360
- NASCAP/LEO simulations of Shuttle Orbiter charging during the SAMPIE experiment
 p 55 N92-22361
- Defect behavior, carrier removal and predicted in-space injection annealing of InP solar cells
 [NASA-TM-105624] p 161 N92-23562
- Sinterless contacts to shallow junction InP solar cells
 [NASA-TM-105670] p 237 N92-24802
- Effect of InAlAs window layer on efficiency of indium phosphide solar cells
 [NASA-TM-105354] p 161 N92-25176
- NASA programs in space photovoltaics
 [NASA-TM-105428] p 87 N92-25343
- Advanced photovoltaic experiment, S0014: Preliminary flight results and post-flight findings
 p 237 N92-27101
- The effect of the low Earth orbit environment on space solar cells: Results of the advanced photovoltaic experiment (S0014)
 p 237 N92-27320
- Solar Array Module Plasma Interaction Experiment (SAMPIE): Technical requirements document
 [NASA-TM-105660] p 56 N92-28683
- High efficiency thermal to electric energy conversion using selective emitters and spectrally tuned solar cells
 [NASA-TM-105755] p 238 N92-30426
- Monolithic and mechanical multijunction space solar cells
 [NASA-TM-105832] p 163 N92-32233
- SOLAR COLLECTORS**
- Low earth orbit durability evaluation of Haynes 188 solar receiver material
 [AIAA PAPER 92-0850] p 117 A92-29616
- Experiments with phase change thermal energy storage canisters for Space Station Freedom
 p 179 A92-50564
- Full-size solar dynamic heat receiver thermal-vacuum tests
 p 68 A92-50565
- Ground test program for a full-size solar dynamic heat receiver
 p 68 A92-50566
- Critical technology experiment results for lightweight space heat receiver
 p 180 A92-50568
- Sensible heat receiver for solar dynamic space power system
 p 180 A92-50570
- Technology development of fabrication techniques for advanced solar dynamic concentrators
 p 232 A92-50571
- Concentrator testing using projected images
 p 69 A92-50615
- Status of the advanced Stirling conversion system project for 25 kW dish Stirling applications
 p 207 A92-50804
- Modeled performance of monolithic, 3-terminal InP/Ga(0.47)In(0.53)As concentrator solar cells as a function of temperature and concentration ratio
 p 234 A92-53153
- InP concentrator solar cells
 p 234 A92-53166
- Atomic oxygen durability of solar concentrator materials for Space Station Freedom
 [NASA-TM-105378] p 85 N92-20065
- Experiments with phase change thermal energy storage canisters for Space Station Freedom
 [NASA-TM-104427] p 86 N92-21216
- Solar radiation on a catenary collector
 [NASA-TM-105751] p 163 N92-32243
- Photovoltaic array for Martian surface power
 [NASA-TM-105827] p 270 N92-33899
- SOLAR DYNAMIC POWER SYSTEMS**
- Low earth orbit durability evaluation of Haynes 188 solar receiver material
 [AIAA PAPER 92-0850] p 117 A92-29616
- Pointing and tracking control for freedom's Solar Dynamic modules and vibration control of freedom
 [AAS PAPER 91-459] p 54 A92-43284

- Experiments with phase change thermal energy storage canisters for Space Station Freedom
 p 179 A92-50564
- Full-size solar dynamic heat receiver thermal-vacuum tests
 p 68 A92-50565
- Ground test program for a full-size solar dynamic heat receiver
 p 68 A92-50566
- Solar dynamic power for earth orbital and lunar applications
 p 68 A92-50567
- Critical technology experiment results for lightweight space heat receiver
 p 180 A92-50568
- Sensible heat receiver for solar dynamic space power system
 p 180 A92-50570
- Technology development of fabrication techniques for advanced solar dynamic concentrators
 p 232 A92-50571
- Concentrator testing using projected images
 p 69 A92-50615
- Design considerations for space radiators based on the liquid sheet (LSR) concept
 p 181 A92-50821
- Parametric studies of phase change thermal energy storage canisters for Space Station Freedom
 [NASA-TM-105350] p 55 N92-13143
- Solar dynamic technology status for Space Station Freedom application
 p 83 N92-17770
- Solar dynamic modules for Space Station Freedom: The relationship between fine-pointing control and thermal loading of the aperture plate
 [NASA-TM-104498] p 84 N92-19780
- Experiments with phase change thermal energy storage canisters for Space Station Freedom
 [NASA-TM-104427] p 86 N92-21216
- SOLAR ELECTRIC PROPULSION**
- Structural design concepts for a multimewatt solar electric propulsion (SEP) spacecraft
 [AIAA PAPER 92-2536] p 54 A92-34380
- SOLAR ENERGY**
- Thermochemical energy storage for a lunar base
 [NASA-TM-105333] p 236 N92-14485
- Solar thermal energy receiver
 [NASA-CASE-LEW-14949-1] p 238 N92-29143
- SOLAR ENERGY ABSORBERS**
- Ion Beam Textured and Coated Surfaces Experiment (IBEX)
 p 132 N92-24832
- SOLAR ENERGY CONVERSION**
- Photovoltaic power options for Mars
 p 231 A92-20366
- Component technology for Stirling power converters
 p 206 A92-50781
- Trade studies for nuclear space power systems
 [NASA-TM-105231] p 235 N92-10221
- Solar radiation for Mars power systems
 p 81 N92-13259
- The effect of the low Earth orbit environment on space solar cells: Results of the advanced photovoltaic experiment (S0014)
 p 237 N92-27320
- Solar radiation on a catenary collector
 [NASA-TM-105751] p 163 N92-32243
- SOLAR GENERATORS**
- Observations of the freeze/thaw performance of lithium fluoride by motion picture photography
 p 180 A92-50751
- Alkali metal pool boiler life tests for a 25 kWe advanced Stirling conversion system
 p 206 A92-50797
- Design of a pool boiler heat transport system for a 25 kWe advanced Stirling conversion system
 p 181 A92-50802
- Status of the advanced Stirling conversion system project for 25 kW dish Stirling applications
 p 207 A92-50804
- Solar radiation for Mars power systems
 p 81 N92-13259
- Thermochemical energy storage for a lunar base
 [NASA-TM-105333] p 236 N92-14485
- SOLAR NEUTRINOS**
- Monte Carlo exploration of Mikheyev-Smirnov-Wolfenstein solutions to the solar neutrino problem
 p 270 A92-50927
- SOLAR POWER SATELLITES**
- Integrated solar power satellites - An approach to low-mass space power
 p 231 A92-40427
- Advances in photovoltaic technology
 [IAF PAPER 92-0599] p 235 A92-57055
- Laser beamed power - Satellite demonstration applications
 [IAF PAPER 92-0600] p 76 A92-57056
- SOLAR RADIATION**
- Solar radiation on a catenary collector
 [NASA-TM-105751] p 163 N92-32243
- Photovoltaic array for Martian surface power
 [NASA-TM-105827] p 270 N92-33899
- SOLAR SENSORS**
- The effect of the low Earth orbit environment on space solar cells: Results of the advanced photovoltaic experiment (S0014)
 p 237 N92-27320

- SOLAR THERMAL PROPULSION**
Magnesium fluoride as energy storage medium for spacecraft solar thermal power systems p 67 A92-50274
- SOLID LUBRICANTS**
Solid lubricants on pretreated surfaces [NASA-CASE-LEW-14474-2] p 127 N92-11186
A vacuum (10(exp -9) Torr) friction apparatus for determining friction and endurance life of MoSx films [NASA-TM-104478] p 129 N92-16129
Properties data for opening the Galileo's partially unfurled main antenna [NASA-TM-105355] p 130 N92-20660
Screen Cage Ion Plating (SCIP) and scratch testing of polycrystalline aluminum oxide [NASA-TM-105404] p 130 N92-22278
Self-lubricating coatings for high-temperature applications p 130 N92-22516
Tribological evaluation of an Al₂O₃-SiO₂ ceramic fiber candidate for high temperature sliding seals [NASA-TM-105611] p 97 N92-23190
- SOLID MECHANICS**
A stochastic damage model for the rupture prediction of a multi-phase solid. I - Parametric studies. II - Statistical approach p 224 A92-49784
Improved accuracy for finite element structural analysis via a new integrated force method [NASA-TP-3204] p 227 N92-22227
- SOLID PROPELLANTS**
Opposed flow flame spread in normal, enhanced and reduced gravity p 111 A92-12898
- SOLID STATE**
Solid State Technology Branch of NASA Lewis Research Center [NASA-TM-105159] p 151 N92-23412
Solid State Technology Branch of NASA Lewis Research Center [NASA-TM-105752] p 151 N92-32965
- SOLID STATE DEVICES**
Solid State Technology Branch of NASA Lewis Research Center [NASA-TM-105752] p 151 N92-32965
- SOLID SURFACES**
Universal aspects of adhesion and atomic force microscopy p 260 A92-17979
Intensified array camera imaging of solid surface combustion aboard the NASA Learjet [AIAA PAPER 92-0240] p 137 A92-25702
Intensified array camera imaging of solid surface combustion aboard the NASA Learjet [NASA-TM-105361] p 138 N92-16156
- SOLID SUSPENSIONS**
A fiber-optic probe for particle sizing in concentrated suspensions p 197 A92-21371
- SOLID-SOLID INTERFACES**
Interphase layer optimization for metal matrix composites with fabrication considerations p 98 A92-10262
Influence of interfacial shear strength on the mechanical properties of SiC fiber reinforced reaction-bonded silicon nitride matrix composites p 99 A92-15145
Diffusive crack growth at a bimaterial interface [AIAA PAPER 92-2432] p 220 A92-34580
Role of interfacial thermal barrier in the transverse thermal conductivity of uniaxial SiC fiber-reinforced reaction bonded silicon nitride p 102 A92-39605
- SOLIDIFICATION**
Microstructure and mechanical properties of near eutectic beta-NiAl plus alpha-Re alloys produced by rapid solidification and extrusion p 119 A92-30844
- SOLIDIFIED GASES**
Pressure dependence of the melting temperature of solids - Rare-gas solids p 171 A92-33912
- SOLUBILITY**
Low temperature synthesis of CaO-SiO₂ glasses having stable liquid-liquid immiscibility by the sol-gel process p 126 A92-44479
Composition dependence of superconductivity in YBa₂(Cu(3-x)Al(x))O_y [NASA-TM-105358] p 131 N92-24715
- SOLUTES**
Steady-state thermal-solutal convection and diffusion in a simulated float zone p 137 A92-17056
Thermomechanical deformation behavior of a dynamic strain aging alloy, Hastelloy X [NASA-TM-105316] p 228 N92-25179
- SOOT**
Observations of soot during droplet combustion at low gravity - Heptane and heptane/monochloroalkane mixtures p 115 A92-50447
- SOUND FIELDS**
Screech noise source structure of a supersonic rectangular jet [NASA-TM-105384] p 15 N92-14000
- SOUND GENERATORS**
Noise from turbulent shear flows p 254 N92-10603
- SOUND INTENSITY**
Validation of finite element and boundary element methods for predicting structural vibration and radiated noise [NASA-TM-105359] p 213 N92-29697
- SOUND PRESSURE**
Screech noise source structure of a supersonic rectangular jet [AIAA PAPER 92-0503] p 6 A92-26932
Screech noise source structure of a supersonic rectangular jet [NASA-TM-105384] p 15 N92-14000
Modal element method for scattering of sound by absorbing bodies [NASA-TM-105722] p 255 N92-28984
- SOUND WAVES**
Comparison of analysis and experiment for gearbox noise [NASA-TM-105330] p 210 N92-25396
- SPACE COMMERCIALIZATION**
Destination directed packet switch architecture for a geostationary communication satellite network [IAF PAPER 92-0413] p 50 A92-55793
- SPACE COMMUNICATION**
Dynamic rain fade compensation techniques for the advanced communications technology satellite [AIAA PAPER 92-2038] p 145 A92-31711
Evaluation of components, subsystems, and networks for high rate, high frequency space communications [NASA-TM-105274] p 147 N92-12151
Space Communications Technology Conference: Onboard Processing and Switching [NASA-CP-3132] p 147 N92-14202
An overview of Space Communication Artificial Intelligence for Link Evaluation Terminal (SCAILET) Project p 148 N92-14212
Overview of Ka-band communications technology requirements for the space exploration initiative [NASA-TM-105308] p 269 N92-14953
V-band pseudomorphic HEMT MMIC phased array components for space communications p 151 N92-32966
- SPACE DEBRIS**
Atomic oxygen undercutting of LDEF aluminized-Kapton multilayer insulation p 255 N92-24818
Characteristics of hypervelocity impact craters on LDEF experiment S1003 and implications of small particle impacts on reflective surfaces p 269 N92-27252
- SPACE ELECTRIC ROCKET TESTS**
Development and flight history of SERT 2 spacecraft [AIAA PAPER 92-3516] p 74 A92-54038
Development and flight history of SERT 2 spacecraft [NASA-TM-105636] p 90 N92-28983
- SPACE ENVIRONMENT SIMULATION**
Measurement and analysis of a small nozzle plume in vacuum [AIAA PAPER 92-3108] p 64 A92-48748
Full-size solar dynamic heat receiver thermal-vacuum tests p 68 A92-50565
- SPACE EXPLORATION**
MisTec - A software application for supporting space exploration scenario options and technology development analysis and planning [AIAA PAPER 92-1293] p 242 A92-38490
A dynamic isotope power system for Space Exploration Initiative surface transport systems [AIAA PAPER 92-1489] p 61 A92-38605
Electrical system options for space exploration [SAE PAPER 912065] p 62 A92-45447
An accelerated development, reduced cost approach to lunar/Mars exploration using a modular NTR-based space transportation system [IAF PAPER 92-0574] p 43 A92-57053
Nuclear propulsion for space exploration [IAF PAPER 92-0575] p 76 A92-57054
Trade studies for nuclear space power systems [NASA-TM-105231] p 235 N92-10221
Nuclear thermal propulsion workshop overview p 78 N92-11090
An overview of tested and analyzed NTP concepts [NASA-TM-105252] p 80 N92-11137
Issues and status of power distribution options for space exploration p 80 N92-13207
MisTec: A software application for supporting space exploration scenario options and technology development analysis and planning [NASA-TM-105214] p 243 N92-14649
Overview of Ka-band communications technology requirements for the space exploration initiative [NASA-TM-105308] p 269 N92-14953
- Screech noise source structure of a supersonic rectangular jet [NASA-TM-105384] p 15 N92-14000
- Nuclear electric propulsion: An integral part of NASA's nuclear propulsion project [NASA-TM-105309] p 83 N92-16019
Environmental interactions in Space Exploration: Announcement of the formation of an Environmental Interactions Working Group [NASA-TM-105294] p 270 N92-17069
Space Station Freedom/Lunar transfer vehicle propellant operation hazard analysis p 55 N92-17416
Nuclear Electric Propulsion Technology Panel findings and recommendations [NASA-TM-105547] p 85 N92-20355
Environmental interactions in space exploration: Environmental interactions working group p 239 N92-22382
NASA/DOE/DOD nuclear propulsion technology planning: Summary of FY 1991 interagency panel results [NASA-TM-105703] p 88 N92-26792
Electrical and chemical interactions at Mars Workshop, part 1 [NASA-CP-10093] p 270 N92-30302
- SPACE FLIGHT**
Thermal verification testing of commercial printed-circuit boards for spaceflight p 216 A92-56217
Thermal verification testing of commercial printed-circuit boards for spaceflight [NASA-TM-105261] p 141 N92-11221
Fuels and materials development for space nuclear propulsion [NASA-TM-107806] p 85 N92-21187
Research and technology, 1991 [NASA-TM-105320] p 1 N92-22659
- SPACE LOGISTICS**
Maintenance and resupply in the unpressurized environment - Design and operational concepts for the Space Station Freedom logistics carriers [AIAA PAPER 91-4116] p 53 A92-24369
- SPACE MAINTENANCE**
Maintenance and resupply in the unpressurized environment - Design and operational concepts for the Space Station Freedom logistics carriers [AIAA PAPER 91-4116] p 53 A92-24369
Repair-level analysis for Space Station Freedom [AIAA PAPER 92-1537] p 43 A92-38634
- SPACE MANUFACTURING**
International Workshop on Vibration Isolation Technology for Microgravity Science Applications [NASA-CP-10094] p 141 N92-28436
- SPACE MISSIONS**
Benefits of slush hydrogen for space missions [NASA-TM-104503] p 134 N92-11214
Upper stages using liquid propulsion and metallized propellants [NASA-TP-3191] p 83 N92-17151
Report of the Nuclear Propulsion Mission Analysis, Figures of Merit Subpanel: Quantifiable figures of merit for nuclear thermal propulsion [NASA-TM-104179] p 43 N92-20925
Monolithic and mechanical multijunction space solar cells [NASA-TM-105832] p 163 N92-32233
- SPACE PLASMAS**
The arcing rate for a High Voltage Solar Array - Theory, experiment and predictions [AIAA PAPER 92-0576] p 53 A92-26983
Arcing of negatively biased solar cells in low earth orbit [AIAA PAPER 92-0578] p 59 A92-26985
Arcing of negatively biased solar cells in a plasma environment. I - Experimental observations [AIAA PAPER 92-2990] p 63 A92-47000
High voltage spheres in an unmagnetized plasma - Fluid and PIC simulations p 258 A92-47936
The Solar Array Module Plasma Interactions Experiment (SAMPIE): Science and technology objectives p 86 N92-22360
NASCAP/LEO simulations of Shuttle Orbiter charging during the SAMPIE experiment p 55 N92-22361
Ion collection from a plasma by a pinhole p 259 N92-22368
Experimental breakdown of selected anodized aluminum samples in dilute plasmas p 259 N92-22369
- SPACE PLATFORMS**
The formation and structure of plasma wakes behind large high-voltage space platforms in ionosphere [AIAA PAPER 92-0577] p 239 A92-26984
Ionospheric plasma flow over large high-voltage space platforms. I - Ion-plasma-time scale interactions of a plate at zero angle of attack. II - The formation and structure of plasma wake p 258 A92-41359
Optimal microgravity vibration isolation - An algebraic introduction p 54 A92-47495
Advanced power systems for EOS p 70 A92-50640
Trade studies for nuclear space power systems [NASA-TM-105231] p 235 N92-10221

SPACE POWER REACTORS

Microgravity vibration isolation: An optimal control law for the one-dimensional case

[NASA-TM-105146] p 141 N92-11217
Vibration isolation technology development to demonstration p 140 N92-28442

SPACE POWER REACTORS

Innovative nuclear thermal propulsion technology evaluation - Results of the NASA/DOE task team study [IAF PAPER 91-235] p 58 A92-13160

Space reactor power system programs overview [AIAA PAPER 92-1558] p 61 A92-38652
Evaluation of high temperature dielectric films for high voltage power electronic applications p 261 A92-44273

Instantaneous heat transfer coefficient based upon two-dimensional analyses of Stirling space engine components p 181 A92-50827

NASA's nuclear electric propulsion technology project [AIAA PAPER 92-3705] p 76 A92-57033

Trade studies for nuclear space power systems [NASA-TM-105231] p 235 N92-10221

Analytical study of nozzle performance for nuclear thermal rockets

[NASA-TM-105251] p 78 N92-11126
Issues and status of power distribution options for space exploration p 80 N92-13207

Nuclear electric propulsion: An integral part of NASA's nuclear propulsion project

[NASA-TM-105309] p 83 N92-16019
The NASA CSTI High Capacity Power Program

[NASA-TM-105240] p 236 N92-16481
Nuclear Electric Propulsion Technology Panel findings and recommendations

[NASA-TM-105547] p 85 N92-20355
Fuels and materials development for space nuclear propulsion

[NASA-TM-107806] p 85 N92-21187
Nuclear electric propulsion development and qualification facilities

[NASA-TM-105521] p 91 N92-30818
An overview of the Lewis Research Center CSTI thermal management program

[NASA-TM-105310] p 92 N92-31916
SP-100 reactor with Brayton conversion for lunar surface applications

[NASA-TM-105637] p 92 N92-32108
NASA's nuclear electric propulsion technology project

[NASA-TM-105811] p 93 N92-32463
Progress update of NASA's free-piston Stirling space power converter technology project

[NASA-TM-105748] p 239 N92-33898

SPACE PROCESSING

Numerical simulations of space processing - The reality, the myth, and the future p 136 A92-12863

A versatile get away special furnace for materials processing in space

[AIAA PAPER 92-0787] p 137 A92-27122
Linear-stability theory of thermocapillary convection in a model of float-zone crystal growth

[AIAA PAPER 92-0604] p 169 A92-28211
Transport modes during crystal growth in a centrifuge

p 138 A92-33835
An examination of anticipated g-jitter on Space Station and its effects on materials processes

p 140 N92-28438

SPACE PROGRAMS

Evaluation of components, subsystems, and networks for high rate, high frequency space communications

[NASA-TM-105274] p 147 N92-12151

SPACE SHUTTLE MAIN ENGINE

A failure diagnosis system based on a neural network classifier for the Space Shuttle Main Engine

p 58 A92-11474
Aerodynamics and heat transfer investigations on a high Reynolds number turbine cascade

[ASME PAPER 91-GT-157] p 164 A92-15593
State space representation of the open-loop dynamics of the Space Shuttle Main Engine

p 59 A92-19607
Viscoplastic analysis of an experimental cylindrical thrust chamber liner

p 218 A92-28052
Fault diagnosis for the Space Shuttle main engine

p 60 A92-28137
A simplified dynamic model of Space Shuttle Main Engine

p 60 A92-29289
Advanced optical condition monitoring --- of rocket engines

[SAE PAPER 912164] p 199 A92-39994
Rocket engine diagnostics using qualitative modeling techniques

[AIAA PAPER 92-3164] p 65 A92-48787
Algorithms for real-time fault detection of the Space Shuttle Main Engine

[AIAA PAPER 92-3167] p 215 A92-48789
Identification of the Space Shuttle Main Engine dynamic models from firing data

[AIAA PAPER 92-3317] p 73 A92-54022

Overview of the Beta II Two-Stage-To-Orbit vehicle design

[NASA-TM-105298] p 48 N92-11034
An SSME high pressure oxidizer turbopump diagnostic system using G2(TM) real-time expert system

[NASA-TM-105328] p 247 N92-13717
Miniature high temperature plug-type heat flux gauges

[NASA-TM-105403] p 201 N92-18759
Rocket engine diagnostics using qualitative modeling techniques

[NASA-TM-105714] p 88 N92-27033
Integrated health monitoring and controls for rocket engines

[NASA-TM-105763] p 90 N92-28693
Implementation of an intelligent control system

[NASA-TM-105795] p 241 N92-33897

SPACE SHUTTLE ORBITERS

A high temperature superconductivity communications flight experiment

[IAF PAPER 92-0410] p 50 A92-55790
NASCAP/LEO simulations of Shuttle Orbiter charging during the SAMPE experiment

p 55 N92-22361
Development of and flight results from the Space Acceleration Measurement System (SAMS)

[NASA-TM-105652] p 57 N92-30301

SPACE SHUTTLE PAYLOADS

Graphite/epoxy composite adapters for the Space Shuttle/Centaur vehicle

[NASA-TP-3014] p 49 N92-31251

SPACE SHUTTLES

The design and performance estimates for the propulsion module for the booster of a TSTO vehicle

[NASA-TM-105299] p 29 N92-11995
Space acceleration measurement system triaxial sensor head error budget

[NASA-TM-105300] p 57 N92-25134
International Workshop on Vibration Isolation Technology for Microgravity Science Applications

[NASA-CP-10094] p 141 N92-28436
The O₂ reduction at the IFC modified O₂ fuel cell electrode

[NASA-TM-105691] p 90 N92-29667

SPACE STATION FREEDOM

Electric propulsion - An evolutionary technology [IAF PAPER 91-241] p 58 A92-13158

Dynamics and control of the Space Station Freedom docking/array feathering maneuver

[IAF PAPER 91-321] p 52 A92-14734
Maintenance and resupply in the unpressurized environment - Design and operational concepts for the Space Station Freedom logistics carriers

[AIAA PAPER 91-4116] p 53 A92-24369
The effects of RF plasma ashing on zinc orthotitanate/potassium silicate thermal control coatings

[AIAA PAPER 92-2171] p 124 A92-31299
Repair-level analysis for Space Station Freedom

[AIAA PAPER 92-1537] p 43 A92-38634
Pointing and tracking control for freedom's Solar Dynamic modules and vibration control of freedom

[AAS PAPER 91-459] p 54 A92-43284
Model-based diagnostics for Space Station Freedom

p 245 A92-50535
Multikilowatt power electronics development for spacecraft

p 68 A92-50541
Experiments with phase change thermal energy storage canisters for Space Station Freedom

p 179 A92-50564
Solar dynamic power for earth orbital and lunar applications

p 68 A92-50567
Contamination effects on Space Station Freedom electric power system performance

p 54 A92-50578
Assessment of environmental effects on Space Station Freedom Electrical Power System

p 55 A92-50581
Application of enhanced modern structured analysis techniques to Space Station Freedom electric power system requirements

p 251 A92-50609
Description of the PMAD DC test bed architecture and integration sequence

p 46 A92-50655
The development of test beds to support the definition and evolution of the Space Station Freedom power system

p 46 A92-50656
An EMTP system level model of the PMAD DC test bed

p 46 A92-50657
Development and testing of a 180-volt dc electronic circuit breaker with a 335-ampere carry and 1200-ampere interrupt rating

p 158 A92-50658
Development and testing of a source subsystem for the supporting development PMAD DC test bed

p 46 A92-50659
Development of a ninety string solar array simulator

p 46 A92-50660
Test and evaluation of load converter topologies used in the Space Station Freedom power management and distribution dc test bed

p 158 A92-50662
Nickel-hydrogen cell low-earth-orbit life test update

p 70 A92-50700

Thermal modeling of nickel-hydrogen battery cells operating under transient orbital conditions

[AIAA PAPER 92-3533] p 71 A92-50712
LDEF spacecraft, ground laboratory, and computational modeling implications on Space Station Freedom's solar array materials and surfaces durability

p 71 A92-53190
Evaluation of Kapton pyrolysis, arc tracking, and arc propagation on the Space Station Freedom (SSF) solar array flexible current carrier (FCC)

p 72 A92-53209
Preliminary characterizations of a water vaporizer for resistojet applications

[AIAA PAPER 92-3533] p 74 A92-54041
Classical and adaptive control algorithms for the solar array pointing system of the Space Station Freedom

[AIAA PAPER 92-4484] p 57 A92-55314
Early use of Space Station Freedom for NASA's Microgravity Science and Applications Program

[IAF PAPER 92-0702] p 138 A92-57131
Description of the PMAD DC test bed architecture and integration sequence

[NASA-TM-105284] p 77 N92-10055
Development of a ninety string solar array simulator [NASA-TM-105278] p 55 N92-11086

Parametric studies of phase change thermal energy storage canisters for Space Station Freedom

[NASA-TM-105350] p 55 N92-13143
Environmental interactions of the Space Station Freedom electric power system

p 81 N92-13255
Space Station Freedom solar dynamic modules structural modeling and analysis

[NASA-TM-104506] p 226 N92-15405
Solar dynamic technology status for Space Station Freedom application

p 83 N92-17770
Space Station Freedom electric power system evolution analysis status

p 84 N92-17771
Automated power management and control

p 84 N92-17773
Solar dynamic modules for Space Station Freedom: The relationship between fine-pointing control and thermal loading of the aperture plate

[NASA-TM-104498] p 84 N92-19780
Collapse analysis of a waffle plate strongback for Space Station Freedom

[NASA-TM-105412] p 227 N92-20045
Experiments with phase change thermal energy storage canisters for Space Station Freedom

[NASA-TM-104427] p 86 N92-21216
Ion collection from a plasma by a pinhole

p 259 N92-22368
Experimental breakdown of selected anodized aluminum samples in dilute plasmas

p 259 N92-22369
Atomic oxygen undercutting of LDEF aluminumized-Kapton multilayer insulation

p 255 N92-24818
International Workshop on Vibration Isolation Technology for Microgravity Science Applications

[NASA-CP-10094] p 141 N92-28436
An examination of anticipated g-jitter on Space Station and its effects on materials processes

p 140 N92-28438
Design feasibility study of a Space Station Freedom truss

[NASA-TM-105558] p 214 N92-30571
Stability testing and analysis of a PMAD DC test bed for the Space Station Freedom

[NASA-TM-105846] p 162 N92-31282
Overview and evolution of the LeRC PMAD DC Testbed

[NASA-TM-105842] p 163 N92-32867
Load converter interactions with the secondary system in the Space Station Freedom power management and distribution DC test bed

[NASA-TM-105844] p 164 N92-34219

SPACE STATION POWER SUPPLIES

Applicability of Long Duration Exposure Facility environmental effects data to the design of Space Station Freedom electrical power system

[AIAA PAPER 92-0848] p 53 A92-29614
Load flows and faults considering dc current injections

p 157 A92-50530
Description of real-time Ada software implementation of a power system monitor for the Space Station Freedom PMAD DC testbed

p 242 A92-50533
Model-based diagnostics for Space Station Freedom

p 245 A92-50535
A 1 MW, 100 kV, less than 100 kg space based dc-dc power converter

p 157 A92-50537
Multikilowatt power electronics development for spacecraft

p 68 A92-50541
Functional models of power electronic components for system studies

p 157 A92-50558
Modeling of Space Station power system components and their interactions

p 68 A92-50559
Solar dynamic power for earth orbital and lunar applications

p 68 A92-50567

- Critical technology experiment results for lightweight space heat receiver p 180 A92-50568
- Contamination effects on Space Station Freedom electric power system performance p 54 A92-50578
- Assessment of environmental effects on Space Station Freedom Electrical Power System p 55 A92-50581
- Application of enhanced modern structured analysis techniques to Space Station Freedom electric power system requirements p 251 A92-50609
- Concentrator testing using projected images p 69 A92-50615
- The development of test beds to support the definition and evolution of the Space Station Freedom power system p 46 A92-50656
- An EMTP system level model of the PMAD DC test bed p 46 A92-50657
- Development and testing of a source subsystem for the supporting development PMAD DC test bed p 46 A92-50659
- Test and evaluation of load converter topologies used in the Space Station Freedom power management and distribution dc test bed p 158 A92-50662
- Nickel-hydrogen cell low-earth-orbit life test update p 70 A92-50700
- Environmental interactions of the Space Station Freedom electric power system p 81 N92-13255
- Space Station Freedom solar dynamic modules structural modelling and analysis [NASA-TM-104506] p 226 N92-15405
- Solar dynamic technology status for Space Station Freedom application p 83 N92-17770
- Space Station Freedom electric power system evolution analysis status p 84 N92-17771
- Automated power management and control p 84 N92-17773
- Stability testing and analysis of a PMAD DC test bed for the Space Station Freedom [NASA-TM-105846] p 162 N92-31282
- Overview and evolution of the LeRC PMAD DC Testbed [NASA-TM-105842] p 163 N92-32867
- Load converter interactions with the secondary system in the Space Station Freedom power management and distribution DC test bed [NASA-TM-105844] p 164 N92-34219
- SPACE STATION STRUCTURES**
- Modal test/analysis correlation of Space Station structures using nonlinear sensitivity [NASA-TM-105850] p 230 N92-34221
- SPACE STATIONS**
- Full-size solar dynamic heat receiver thermal-vacuum tests p 68 A92-50565
- Ground test program for a full-size solar dynamic heat receiver p 68 A92-50566
- Description of the control system design for the SSF PMAD DC testbed p 45 A92-50654
- The development of test beds to support the definition and evolution of the Space Station Freedom power system p 46 A92-50656
- An EMTP system level model of the PMAD DC test bed p 46 A92-50657
- Development and testing of a source subsystem for the supporting development PMAD DC test bed p 46 A92-50659
- Large transient fault current test of an electrical roll ring --- for Space Station Freedom p 55 A92-50661
- Simulation of Space Station loads with active control systems p 56 N92-23824
- Large transient fault current test of an electrical roll ring [NASA-TM-105667] p 87 N92-24201
- SPACE TRANSPORTATION**
- Health management and controls for earth to orbit propulsion systems [IAF PAPER 92-0646] p 77 A92-57089
- Upper stages using liquid propulsion and metallized propellants [NASA-TP-3191] p 83 N92-17151
- Nuclear Electric Propulsion Technology Panel findings and recommendations [NASA-TM-105547] p 85 N92-20355
- SPACE TRANSPORTATION SYSTEM**
- CONE - An STS-based cryogenic fluid management experiment p 43 A92-23850
- Cryogenic fluid management investigations using the CONE flight experiment p 43 A92-23851
- Upper stages using liquid propulsion and metallized propellants [NASA-TP-3191] p 83 N92-17151
- Fast track lunar NTR systems assessment for the First Lunar Outpost and its evolvability to Mars p 142 N92-33334
- SPACEBORNE EXPERIMENTS**
- Numerical simulations of space processing - The reality, the myth, and the future p 136 A92-12863
- COLD-SAT - A technology satellite for cryogenic experimentation p 52 A92-13425
- The NASA microgravity combustion space experiment program [IAF PAPER 91-398] p 112 A92-18484
- A versatile get away special furnace for materials processing in space [AIAA PAPER 92-0787] p 137 A92-27122
- The isothermal dendritic growth experiment - A USMP-2 space flight experiment [AIAA PAPER 92-0350] p 137 A92-28188
- Development of and flight results from the Space Acceleration Measurement System (SAMS) [AIAA PAPER 92-0354] p 56 A92-28189
- ACTS aeronautical experiments [AIAA PAPER 92-2042] p 50 A92-29956
- The Solar Array Module Plasma Interactions Experiment (SAMPIE) - A Shuttle-based plasma interactions experiment p 69 A92-50583
- Pressurization of cryogenics - A review of current technology and its applicability to low-gravity conditions [AIAA PAPER 92-3061] p 72 A92-54002
- NIST torsion oscillator viscometer response: Performance on the LeRC active vibration isolation platform [NASA-TM-105571] p 209 N92-23564
- Durability evaluation of photovoltaic blanket materials exposed on LDEF tray S1003 p 132 N92-27100
- Advanced photovoltaic experiment, S0014: Preliminary flight results and post-flight findings p 237 N92-27101
- Characteristics of hypervelocity impact craters on LDEF experiment S1003 and implications of small particle impacts on reflective surfaces p 269 N92-27252
- Solar Array Module Plasma Interaction Experiment (SAMPIE): Technical requirements document [NASA-TM-105660] p 56 N92-28683
- Pressurization of cryogenics: A review of current technology and its applicability to low-gravity conditions [NASA-TM-105746] p 136 N92-29669
- Microgravity vibration isolation: Optimal preview and feedback control [NASA-TM-105673] p 142 N92-30692
- SPACECRAFT ANTENNAS**
- Properties data for opening the Galileo's partially unfurled main antenna [NASA-TM-105355] p 130 N92-20660
- Influence of mass moment of inertia on normal modes of preloaded solar array mast [NASA-TP-3273] p 230 N92-33476
- SPACECRAFT CHARGING**
- Ionospheric plasma flow over large high-voltage space platforms. I - Ion-plasma-time scale interactions of a plate at zero angle of attack. II - The formation and structure of plasma wake p 258 A92-41359
- Using EPSAT to analyze high power systems in the space environment --- Environment Power System Analysis Tool p 158 A92-50580
- NASCAP/LEO simulations of Shuttle Orbiter charging during the SAMPIE experiment p 55 N92-22361
- SPACECRAFT COMMUNICATION**
- Overview of Ka-band communications technology requirements for the space exploration initiative [NASA-TM-105308] p 269 N92-14953
- SPACECRAFT COMPONENTS**
- Tribology needs for future space and aeronautical systems [NASA-TM-104525] p 128 N92-15191
- SPACECRAFT CONFIGURATIONS**
- Multi-reactor power system configurations for multimegawatt nuclear electric propulsion [NASA-TM-105212] p 77 N92-10057
- SPACECRAFT CONSTRUCTION MATERIALS**
- Atomic oxygen effects on thin film space coatings studied by spectroscopic ellipsometry, atomic force microscopy, and laser light scattering [AIAA PAPER 92-2172] p 94 A92-31300
- Flight-vehicle materials, structures, and dynamics - Assessment and future directions. Vol. 3 - Ceramics and ceramic-matrix composites --- Book [ISBN 0-7918-0661-8] p 94 A92-39852
- Ceramics and ceramic composites in future aeronautical and space systems p 95 A92-39853
- Probabilistic material degradation model for aerospace materials subjected to high temperature, mechanical and thermal fatigue, and creep [AIAA PAPER 92-3419] p 224 A92-48978
- LDEF spacecraft, ground laboratory, and computational modeling implications on Space Station Freedom's solar array materials and surfaces durability p 71 A92-53190
- Ion beam treatment of potential space materials at the NASA Lewis Research Center [NASA-TM-105398] p 97 N92-21548
- Graphite/epoxy composite adapters for the Space Shuttle/Centaur vehicle [NASA-TP-3014] p 49 N92-31251
- SPACECRAFT CONTAMINATION**
- Contamination effects on Space Station Freedom electric power system performance p 54 A92-50578
- Assessment of environmental effects on Space Station Freedom Electrical Power System p 55 A92-50581
- SPACECRAFT CONTROL**
- Technology readiness assessment of advanced space engine integrated controls and health monitoring [NASA-TM-105255] p 79 N92-11130
- Solar dynamic modules for Space Station Freedom: The relationship between fine-pointing control and thermal loading of the aperture plate [NASA-TM-104498] p 84 N92-19780
- Simulation of Space Station loads with active control systems p 56 N92-23824
- SPACECRAFT DESIGN**
- Applicability of Long Duration Exposure Facility environmental effects data to the design of Space Station Freedom electrical power system [AIAA PAPER 92-0848] p 53 A92-29614
- Structural design concepts for a multimegawatt solar electric propulsion (SEP) spacecraft [AIAA PAPER 92-2536] p 54 A92-34380
- Mission and sizing analysis for the Beta II two-stage-to-orbit vehicle [AIAA PAPER 92-1264] p 47 A92-35868
- Electrical system options for space exploration [SAE PAPER 912065] p 62 A92-45447
- The development of test beds to support the definition and evolution of the Space Station Freedom power system p 46 A92-50656
- Risks, designs, and research for fire safety in spacecraft [NASA-TM-105317] p 240 N92-13581
- Mission and sizing analysis for the Beta 2 two-stage-to-orbit vehicle [NASA-TM-105559] p 48 N92-21547
- Integrated analysis and applications p 32 N92-22521
- Computer codes developed and under development at Lewis p 244 N92-25913
- Graphite/epoxy composite adapters for the Space Shuttle/Centaur vehicle [NASA-TP-3014] p 49 N92-31251
- SPACECRAFT DOCKING**
- Dynamics and control of the Space Station Freedom docking/array feathering maneuver [IAF PAPER 91-321] p 52 A92-14734
- Solar dynamic modules for Space Station Freedom: The relationship between fine-pointing control and thermal loading of the aperture plate [NASA-TM-104498] p 84 N92-19780
- SPACECRAFT EQUIPMENT**
- Space applications of high temperature superconductivity technology [IAF PAPER 91-307] p 259 A92-14724
- A versatile get away special furnace for materials processing in space [AIAA PAPER 92-0787] p 137 A92-27122
- SPACECRAFT INSTRUMENTS**
- Liquid-vapour surface sensors for liquid nitrogen and hydrogen p 197 A92-23852
- SPACECRAFT LAUNCHING**
- Mission and sizing analysis for the Beta II two-stage-to-orbit vehicle [AIAA PAPER 92-1264] p 47 A92-35868
- Mission and sizing analysis for the Beta 2 two-stage-to-orbit vehicle [NASA-TM-105559] p 48 N92-21547
- SPACECRAFT LUBRICATION**
- Lubrication of space systems: Challenges and potential solutions [NASA-TM-105560] p 130 N92-21579
- SPACECRAFT MAINTENANCE**
- Technology readiness assessment of advanced space engine integrated controls and health monitoring [NASA-TM-105255] p 79 N92-11130
- SPACECRAFT MANEUVERS**
- Electric propulsion - The future is now p 63 A92-48386
- SPACECRAFT PERFORMANCE**
- ACTS system capability and performance [AIAA PAPER 92-1961] p 143 A92-29884
- SPACECRAFT POWER SUPPLIES**
- Space power by ground-based laser illumination p 59 A92-18401
- Maintenance and resupply in the unpressurized environment - Design and operational concepts for the Space Station Freedom logistics carriers [AIAA PAPER 91-4116] p 53 A92-24369
- The arcing rate for a High Voltage Solar Array - Theory, experiment and predictions [AIAA PAPER 92-0576] p 53 A92-26983
- Space batteries for mobile battlefield power applications p 231 A92-29679

- Repair-level analysis for Space Station Freedom
[AIAA PAPER 92-1537] p 43 A92-38634
- Space reactor power system programs overview
[AIAA PAPER 92-1558] p 61 A92-38652
- Structural scaling approximations for solar arrays
p 231 A92-40935
- Systems analysis of electrodynamic tethers
p 62 A92-41550
- Energy requirements for the space frontier
[SAE PAPER 912064] p 62 A92-45446
- Electrical system options for space exploration
[SAE PAPER 912065] p 62 A92-45447
- Small Stirling dynamic isotope power system for multihundred-watt robotic missions
[SAE PAPER 912066] p 62 A92-45448
- Early Track NEP system options for SEI missions
[AIAA PAPER 92-3200] p 65 A92-48808
- Magnesium fluoride as energy storage medium for spacecraft solar thermal power systems
p 67 A92-50274
- Development of an analytical tool to study power quality of ac power systems for large spacecraft
p 67 A92-50529
- Autonomous Power System intelligent diagnosis and control
p 247 A92-50532
- Solar dynamic power for earth orbital and lunar applications
p 68 A92-50567
- Sensible heat receiver for solar dynamic space power system
p 180 A92-50570
- Using EPSAT to analyze high power systems in the space environment --- Environment Power System Analysis Tool
p 158 A92-50580
- Status of NASA's Stirling space power converter program
p 69 A92-50608
- A mass sensitivity analysis of lunar orbiting beam power systems
p 232 A92-50619
- Balancing reliability and cost to choose the best power subsystem
p 216 A92-50625
- Design of multihundred-watt dynamic isotope power system for robotic space missions
p 69 A92-50633
- Thermal analysis of a conceptual design for a 250 We GPHS/FPSE space power system
p 69 A92-50637
- Advanced power systems for EOS
p 70 A92-50640
- Applications of thin-film photovoltaics for space
p 70 A92-50641
- The mini-dome Fresnel lens photovoltaic concentrator array - Current program status
p 70 A92-50648
- Recent progress in InP solar cell research
p 158 A92-50653
- Description of the control system design for the SSF PMAD DC testbed
p 45 A92-50654
- Description of the PMAD DC test bed architecture and integration sequence
p 46 A92-50655
- Development and testing of a 180-volt dc electronic circuit breaker with a 335-ampere carry and 1200-ampere interrupt rating
p 158 A92-50658
- Update on results of SPRE testing at NASA Lewis
p 71 A92-50780
- Free-piston Stirling component test power converter
p 206 A92-50784
- Design considerations for space radiators based on the liquid sheet (LSR) concept
p 181 A92-50821
- Laser beamed power - Satellite demonstration applications
[IAF PAPER 92-0600] p 76 A92-57056
- Description of the PMAD DC test bed architecture and integration sequence
[NASA-TM-105284] p 77 A92-10055
- Trade studies for nuclear space power systems
[NASA-TM-105231] p 235 A92-10221
- Development of a computer algorithm for the analysis of variable-frequency AC drives: Case studies included
[NASA-TM-105327] p 29 A92-13070
- Power supply for a manned international asteroid mission
p 80 A92-13205
- SEI power source alternatives for rovers and other multi-kWe distributed surface applications
p 80 A92-13206
- Issues and status of power distribution options for space exploration
p 80 A92-13207
- Development of a single-phase harmonic power flow program to study the 20 kHz AC power system for large spacecraft
[NASA-TM-105326] p 81 A92-13275
- Impedances of Li/SO₂ cells retrieved from the Long Duration Exposure Facility (LDEF satellite) and comparison with cells stored terrestrially
[NASA-TM-104526] p 236 A92-13484
- Multi-megawatt inverter/converter technology for space power applications
[NASA-TM-105307] p 159 A92-14294
- Electrical properties of teflon and ceramic capacitors at high temperatures
[NASA-TM-105569] p 160 A92-20040
- The Solar Array Module Plasma Interactions Experiment (SAMPPIE): Science and technology objectives
p 86 A92-22360
- NASA Aerospace Flight Battery Systems Program: An update
p 237 A92-22741
- Ion Beam Textured and Coated Surfaces Experiment (IBEX)
p 132 A92-24832
- Validation test of advanced technology for IPV nickel-hydrogen flight cells: Update
[NASA-TM-105689] p 89 A92-27878
- High temperature dielectric properties of Apical, Kapton, Peek, Teflon AF, and Uplex polymers
[NASA-TM-105753] p 162 A92-28675
- Solar Array Module Plasma Interaction Experiment (SAMPPIE): Technical requirements document
[NASA-TM-105680] p 56 A92-28683
- NASA Lewis Stirling SPRE testing and analysis with reduced number of cooler tubes
[NASA-TM-105767] p 238 A92-28837
- The O₂ reduction at the IFC modified O₂ fuel cell electrode
[NASA-TM-105691] p 90 A92-29667
- Magnetic bearings for free-piston Stirling engines
[NASA-TM-105730] p 214 A92-30734
- Overview and evolution of the LeRC PMAD DC Testbed
[NASA-TM-105842] p 163 A92-32867
- SPACECRAFT PROPULSION**
- High temperature thruster technology for spacecraft propulsion
[IAF PAPER 91-254] p 58 A92-13155
- Numerical propulsion system simulation
p 59 A92-20194
- Technical prospects for utilizing extraterrestrial propellants for space exploration
[IAF PAPER 91-669] p 133 A92-20612
- Techniques for spectroscopic measurements in an arcjet nozzle
p 59 A92-21087
- LDEXPT, an intelligent database system for the Composite Load Spectra project
p 59 A92-23695
- A probabilistic approach to the evaluation of fatigue damage in a space propulsion system injector element
[AIAA PAPER 92-2413] p 60 A92-34343
- The NASA-OAST earth-to-orbit propulsion technology program - The action plan
[AIAA PAPER 92-1478] p 61 A92-38597
- The evolutionary development of high specific impulse electric thruster technology
[AIAA PAPER 92-1556] p 61 A92-38650
- Microwave electrothermal propulsion for space
p 63 A92-46049
- Arcing of negatively biased solar cells in a plasma environment. I - Experimental observations
[AIAA PAPER 92-2990] p 63 A92-47000
- Technology issues associated with using densified hydrogen for space vehicles
p 134 A92-48727
- Plasma flow processes within magnetic nozzle configurations
p 67 A92-50266
- Nuclear rocket propulsion: NASA plans and progress - FY 1991
p 69 A92-50584
- Engine system assessment study using Martian propellants
[AIAA PAPER 92-3446] p 73 A92-54030
- Development and flight history of SERT 2 spacecraft
[AIAA PAPER 92-3516] p 74 A92-54038
- Low-power arcjet test facility impacts
[AIAA PAPER 92-3532] p 74 A92-54040
- NASA's nuclear thermal propulsion technology project
[AIAA PAPER 92-3581] p 75 A92-54062
- Development of arcjet and ion propulsion for spacecraft stationkeeping
[IAF PAPER 92-0807] p 77 A92-57058
- Plans for the development of cryogenic engines for space exploration
[NASA-TM-105250] p 79 A92-11135
- Test facilities for high power electric propulsion
[NASA-TM-105247] p 80 A92-11136
- Hydrogen arcjet technology
[NASA-TM-105340] p 82 A92-15119
- High temperature thruster technology for spacecraft propulsion
[NASA-TM-105348] p 82 A92-15125
- Nuclear electric propulsion: An integral part of NASA's nuclear propulsion project
[NASA-TM-105309] p 83 A92-16019
- The NASA CSTI High Capacity Power Program
[NASA-TM-105240] p 236 A92-16481
- Upper stages using liquid propulsion and metallized propellants
[NASA-TP-3191] p 83 A92-17151
- A survey of instabilities within centrifugal pumps and concepts for improving the flow range of pumps in rocket engines
[NASA-TM-105439] p 84 A92-18280
- Preliminary test results of a hollow cathode MPD thruster
[NASA-TM-105324] p 84 A92-18474
- A compilation of lunar and Mars exploration strategies utilizing indigenous propellants
[NASA-TM-105262] p 135 A92-19837
- Nuclear Electric Propulsion Technology Panel findings and recommendations
[NASA-TM-105547] p 85 A92-20355
- Hydrogen/oxygen auxiliary propulsion technology
[NASA-TM-105249] p 85 A92-20522
- Report of the Nuclear Propulsion Mission Analysis, Figures of Merit Subpanel: Quantifiable figures of merit for nuclear thermal propulsion
[NASA-TM-104179] p 43 A92-20925
- Neutralizer optimization
[NASA-TM-105578] p 86 A92-21976
- Integrated analysis and applications
p 32 A92-22521
- Introduction to the internal fluid mechanics research session
p 188 A92-22522
- Chemical reacting flows
p 188 A92-22525
- High-temperature electronics
p 160 A92-22528
- Blazing the trailway: Nuclear electric propulsion and its technology program plans
[NASA-TM-105605] p 86 A92-23252
- Advanced liquid rockets
[NASA-TM-105633] p 87 A92-24560
- Development of advanced seals for space propulsion turbomachinery
[NASA-TM-105659] p 87 A92-24957
- Technology issues associated with using densified hydrogen for space vehicles
[NASA-TM-105642] p 135 A92-25277
- Development and flight history of SERT 2 spacecraft
[NASA-TM-105636] p 90 A92-28983
- NEP systems engineering efforts in FY-92: Plans and status
[NASA-TM-105775] p 91 A92-30308
- The evolutionary development of high specific impulse electric thruster technology
[NASA-TM-105712] p 92 A92-31342
- Fast track lunar NTR systems assessment for the First Lunar Outpost and its evolvability to Mars
p 142 A92-33334
- SPACECRAFT RADIATORS**
- Design considerations for space radiators based on the liquid sheet (LSR) concept
p 181 A92-50821
- Effects of anisotropic conduction and heat pipe interaction on minimum mass space radiators
[NASA-TM-105297] p 80 A92-11138
- The NASA CSTI High Capacity Power Program
[NASA-TM-105240] p 236 A92-16481
- An overview of the Lewis Research Center CSTI thermal management program
[NASA-TM-105310] p 92 A92-31916
- SPACECRAFT RELIABILITY**
- Technology readiness assessment of advanced space engine integrated controls and health monitoring
[NASA-TM-105255] p 79 A92-11130
- SPACECRAFT SHIELDING**
- Solar dynamic modules for Space Station Freedom: The relationship between fine-pointing control and thermal loading of the aperture plate
[NASA-TM-104498] p 84 A92-19780
- SPACECRAFT STRUCTURES**
- Probabilistic structural analysis of adaptive/smart/intelligent space structures
[NASA-TM-105408] p 227 A92-22267
- Ion collection from a plasma by a pinhole
p 259 A92-22368
- Experimental breakdown of selected anodized aluminum samples in dilute plasmas
p 259 A92-22369
- Computer codes developed and under development at Lewis
p 244 A92-25913
- A brief overview of computational structures technology related activities at NASA Lewis Research Center
p 229 A92-25915
- Graphite/epoxy composite adapters for the Space Shuttle/Centaur vehicle
[NASA-TP-3014] p 49 A92-31251
- Influence of mass moment of inertia on normal modes of preloaded solar array mast
[NASA-TP-3273] p 230 A92-33476
- SPACECRAFT TRAJECTORIES**
- Discrete approximations to optimal trajectories using direct transcription and nonlinear programming
p 44 A92-46753
- Canonical transformations for space trajectory optimization
[AIAA PAPER 92-4509] p 44 A92-52079
- SPACELAB**
- Space acceleration measurement system description and operations on the First Spacelab Life Sciences Mission
[NASA-TM-105301] p 57 A92-13151

- Microgravity acceleration measurement and environment characterization science (17-IML-1) p 139 N92-23642
- Development of and flight results from the Space Acceleration Measurement System (SAMS) [NASA-TM-105652] p 57 N92-30301
- SPACERS**
Design feasibility study of a Space Station Freedom truss [NASA-TM-105558] p 214 N92-30571
- SPACING**
Dependence of hydrogen arcjet operation on electrode geometry [AIAA PAPER 92-3530] p 74 A92-54039
- SPALLING**
Properties data for opening the Galileo's partially unfurled main antenna [NASA-TM-105355] p 130 N92-20660
- SPATIAL FILTERING**
Self-aligning optical measurement systems p 247 A92-50387
- SPATIAL RESOLUTION**
Effect of spatial resolution on apparent sensitivity to initial conditions of a decaying flow as it becomes turbulent p 175 A92-45716
Turbulence and deterministic chaos --- computational fluid dynamics p 194 N92-25823
- SPECIFIC IMPULSE**
The evolutionary development of high specific impulse electric thruster technology [AIAA PAPER 92-1556] p 61 A92-38650
Minimum impulse trajectories for Mars round trip missions [AAS PAPER 91-500] p 44 A92-43339
NASA's nuclear electric propulsion technology project [AIAA PAPER 92-3705] p 76 A92-57033
Development of arcjet and ion propulsion for spacecraft stationkeeping [IAF PAPER 92-0607] p 77 A92-57058
High temperature thruster technology for spacecraft propulsion [NASA-TM-105348] p 82 N92-15125
Experiments and analysis concerning the use of external burning to reduce aerospace vehicle transonic drag [NASA-TM-105397] p 30 N92-17546
The evolutionary development of high specific impulse electric thruster technology [NASA-TM-105712] p 92 N92-31342
NASA's nuclear electric propulsion technology project [NASA-TM-105811] p 93 N92-32463
The evolutionary development of high specific impulse electric thruster technology [NASA-TM-105758] p 93 N92-33064
Low power arcjet test facility impacts [NASA-TM-105876] p 47 N92-34114
- SPECTRA**
Achieving spectrum conservation for the minimum-span and minimum-order frequency assignment problems [NASA-TM-105649] p 52 N92-23187
- SPECTRAL CORRELATION**
Nongray radiative gas analyses using the S-N discrete ordinates method p 266 A92-15443
- SPECTRAL EMISSION**
Multiwavelength pyrometry for nongray surfaces in the presence of interfering radiation [NASA-TM-105286] p 201 N92-19107
- SPECTRAL METHODS**
Mappings and accuracy for Chebyshev pseudo-spectral approximations p 248 A92-50469
- SPECTRAL REFLECTANCE**
Temperature-dependent reflectivity of silicon carbide [NASA-TM-105287] p 201 N92-19263
- SPECTROMETERS**
A fiber optic sensor for ophthalmic refractive diagnostics p 198 A92-34831
- SPECTROSCOPIC ANALYSIS**
Qualitative spectroscopic study of magnetic nozzle flow [AIAA PAPER 92-3161] p 65 A92-48784
An overview of in-flight plume diagnostics for rocket engines [NASA-TM-105727] p 90 N92-28417
An overview of in-flight plume diagnostics for rocket engines [AIAA PAPER 92-3785] p 75 A92-54164
An overview of in-flight plume diagnostics for rocket engines [NASA-TM-105727] p 90 N92-28417
Study of InGaAs-based modulation doped field effect transistor structures using variable-angle spectroscopic ellipsometry p 265 N92-32977
- SPECTROSCOPY**
Techniques for spectroscopic measurements in an arcjet nozzle p 59 A92-21087
An overview of in-flight plume diagnostics for rocket engines [AIAA PAPER 92-3785] p 75 A92-54164
- An overview of in-flight plume diagnostics for rocket engines [NASA-TM-105727] p 90 N92-28417
- SPECTRUM ANALYSIS**
Multiwavelength pyrometry for nongray bodies [NASA-TM-105285] p 202 N92-24861
- SPHERICAL TANKS**
Optimization of armored spherical tanks for storage on the lunar surface [NASA-TM-105700] p 91 N92-30187
- SPIRALS**
Maximum life spiral bevel reduction design [AIAA PAPER 92-3493] p 205 A92-49030
- SPLINE FUNCTIONS**
Enhancing control of grid distribution in algebraic grid generation p 248 A92-52552
- SPRAY CHARACTERISTICS**
Factors influencing the effective spray cone angle of pressure-swirl atomizers p 166 A92-23300
Coaxial injector spray characterization using water/air as simulants [NASA-TM-105322] p 82 N92-14112
- SPRAY NOZZLES**
Hydrogen no-vent testing in a 5 cubic foot (142 liter) tank using spray nozzle and spray bar liquid injection [AIAA PAPER 92-3063] p 63 A92-48719
Hydrogen no-vent fill testing in a 5 cubic foot (142 liter) tank using spray nozzle and spray bar liquid injection [NASA-TM-105759] p 136 N92-28433
- SPRAYED COATINGS**
Fluorescence microscopy for the characterization of structural integrity [NASA-TM-105253] p 96 N92-18970
- SPRAYING**
Effect of gas mass flux on cryogenic liquid jet breakup p 140 A92-23845
- SPUTTERING**
Plasma erosion rate diagnostics using laser-induced fluorescence p 198 A92-36738
Ion beam treatment of potential space materials at the NASA Lewis Research Center [NASA-TM-105398] p 97 N92-21548
Deposition of adherent Ag-Ti duplex films on ceramics in a multiple-cathode sputter deposition system [NASA-TM-105586] p 34 N92-23225
- STABILITY**
Controlled crack growth specimen for brittle systems p 123 A92-21099
High temperature structural fibers: Status and needs [NASA-TM-105174] p 107 N92-16037
A study of Na(x)P₃O₄ as an O₂ electrode bifunctional electrocatalyst [NASA-TM-105311] p 85 N92-20585
An XPS study of the stability of Fomblin Z25 on the native oxide of aluminum --- x ray photoelectron spectroscopy [NASA-TM-105594] p 131 N92-23185
- STABILITY TESTS**
Frequency effects on the stability of a journal bearing for periodic loading [NASA-TM-105226] p 186 N92-18809
Overview and evolution of the LeRC PMAD DC Testbed [NASA-TM-105842] p 163 N92-32867
- STANDARD DEVIATION**
First-passage problems: A probabilistic dynamic analysis for degraded structures [NASA-TM-103755] p 225 N92-11373
- STAR DISTRIBUTION**
Void probability as a function of the void's shape and scale-invariant models --- in studies of spacial galactic distribution p 267 A92-24456
- STAR FORMATION**
The diffuse gamma-ray background, light element abundances, and signatures of early massive star formation p 268 A92-43837
- STATE ESTIMATION**
Propagating confined states in phase dynamics p 181 A92-50968
- STATIC PRESSURE**
Description of a pressure measurement technique for obtaining surface static pressures of a radial turbine [AIAA PAPER 92-4006] p 200 A92-56829
Description of a pressure measurement technique for obtaining surface static pressures of a radial turbine [NASA-TM-105643] p 202 N92-24959
- STATIONKEEPING**
Electric propulsion - An evolutionary technology [IAF PAPER 91-241] p 58 A92-13158
Electric propulsion - The future is now p 63 A92-48386
Development of arcjet and ion propulsion for spacecraft stationkeeping [IAF PAPER 92-0607] p 77 A92-57058
- STATISTICAL ANALYSIS**
Relationship between voids and interlaminar shear strength of polymer matrix composites p 98 A92-10241
Review and statistical analysis of the use of ultrasonic velocity for estimating the porosity fraction in polycrystalline materials p 215 A92-28722
Vibration transmission through rolling element bearings. IV - Statistical energy analysis p 218 A92-28756
Statistical energy analysis of a geared rotor system p 204 A92-39227
Extreme value statistics analysis of fracture strengths of a sintered silicon nitride failing from pores p 127 A92-50191
- STATISTICAL DISTRIBUTIONS**
Probabilistic progressive buckling of trusses [AIAA PAPER 91-0916] p 223 A92-38142
Probabilistic progressive buckling of trusses [NASA-TM-105162] p 226 N92-15403
- STATOR BLADES**
Design and performance of controlled-diffusion stator compared with original double-circular-arc stator [NASA-TP-2852] p 34 N92-22863
- STATORS**
Airfoil wake and linear theory gust response including sub and superresonant flow conditions [AIAA PAPER 92-3074] p 11 A92-48724
Design and performance of controlled-diffusion stator compared with original double-circular-arc stator [NASA-TP-2852] p 34 N92-22863
- STEADY FLOW**
Unsteady thermocapillary migration of isolated drops in creeping flow p 169 A92-27774
Numerical experiments on a new class of nonoscillatory schemes [AIAA PAPER 92-0421] p 7 A92-28193
Natural convection between concentric spheres p 179 A92-50445
Development of a steady potential solver for use with linearized, unsteady aerodynamic analyses [NASA-TM-105288] p 31 N92-20525
- STEADY STATE**
Steady-state thermal-solutal convection and diffusion in a simulated float zone p 137 A92-17056
Central difference TVD and TVB schemes for time dependent and steady state problems [AIAA PAPER 92-0053] p 166 A92-22168
Central difference TVD and TVB schemes for time dependent and steady state problems [NASA-TM-105357] p 249 N92-15663
High order parallel numerical schemes for solving incompressible flows p 193 N92-25818
NASA Lewis steady-state heat pipe code users manual [NASA-TM-105161] p 90 N92-28682
- STEADY STATE CREEP**
Stress versus temperature dependence of activation energies for creep p 217 A92-24719
- STEERABLE ANTENNAS**
Ka-band MMIC arrays for ACTS Aero Terminal Experiment [IAF PAPER 92-0398] p 159 A92-55785
- STELLAR CORES**
Constraints to the decays of Dirac neutrinos from SN 1987A p 255 A92-36249
- STELLAR MODELS**
Massive Dirac neutrinos and SN 1987A p 268 A92-45808
- STEREOTELEVISION**
A full field, 3-D velocimeter for NASA's microgravity science program [AIAA PAPER 92-0784] p 56 A92-27119
- STIFFNESS**
Performance tests of a cryogenic hybrid magnetic bearing for turbopumps [NASA-TM-105627] p 30 N92-20523
Effect of heat treatment on stiffness and damping of SiC/Ti-15-3 [NASA-TM-105564] p 108 N92-20841
- STIFFNESS MATRIX**
On the thermodynamic framework of generalized coupled thermoelastic-viscoplastic-damage modeling [NASA-TM-105349] p 225 N92-14434
- STIRLING CYCLE**
Small Stirling dynamic isotope power system for multihundred-watt robotic missions [SAE PAPER 912066] p 62 A92-45448
Status of NASA's Stirling space power converter program p 69 A92-50608
Preliminary design of a mobile lunar power supply p 233 A92-50635
Thermal analysis of a conceptual design for a 250 We GPHS/FPSE space power system p 69 A92-50637
Component technology for Stirling power converters p 206 A92-50781

STIRLING ENGINES

- Stirling machine operating experience p 206 A92-50788
- Design considerations for space radiators based on the liquid sheet (LSR) concept p 181 A92-50821
- Instantaneous heat transfer coefficient based upon two-dimensional analyses of Stirling space engine components p 181 A92-50827
- Overview of NASA supported Stirling thermodynamic loss research p 88 N92-27034 [NASA-TM-105690]
- NASA Lewis Stirling SPRE testing and analysis with reduced number of cooler tubes p 238 N92-28837 [NASA-TM-105767]
- A free-piston Stirling engine/linear alternator controls and load interaction test facility p 238 N92-31262 [NASA-TM-105825]
- Progress update of NASA's free-piston Stirling space power converter technology project p 239 N92-33898 [NASA-TM-105748]
- STIRLING ENGINES**
- A 2-D oscillating flow analysis in Stirling engine heat exchangers p 172 A92-36001
- Small Stirling dynamic isotope power system for multihundred-watt robotic missions [SAE PAPER 912066] p 62 A92-45448
- Update on results of SPRE testing at NASA Lewis p 71 A92-50780
- Free-piston Stirling component test power converter p 206 A92-50784
- Comparative survey of dynamic analyses of free-piston Stirling engines p 206 A92-50793
- Alkali metal pool boiler life tests for a 25 kWe advanced Stirling conversion system p 206 A92-50797
- Final design of a free-piston hydraulic advanced Stirling conversion system p 206 A92-50798
- Design of a pool boiler heat transport system for a 25 kWe advanced Stirling conversion system p 181 A92-50802
- Status of the advanced Stirling conversion system project for 25 kW dish Stirling applications p 207 A92-50804
- Alkali metal compatibility testing of candidate heater head materials for a Stirling engine heat transport system p 71 A92-50829
- The NASA CSTI High Capacity Power Program [NASA-TM-105240] p 236 N92-16481
- Comparison of GLIMPS and HFAST Stirling engine code predictions with experimental data p 267 N92-25395 [NASA-TM-105549]
- NASA Lewis Stirling SPRE testing and analysis with reduced number of cooler tubes p 238 N92-28837 [NASA-TM-105767]
- Solar thermal energy receiver [NASA-CASE-LEW-14949-1] p 238 N92-29143
- Magnetic bearings for free-piston Stirling engines [NASA-TM-105730] p 214 N92-30734
- STOCHASTIC PROCESSES**
- Stochastic stability properties of jump linear systems p 246 A92-25878
- Stochastic modeling of crack initiation and short-crack growth under creep and creep-fatigue conditions [ASME PAPER 92-APM-5] p 223 A92-44681
- A stochastic damage model for the rupture prediction of a multi-phase solid. I - Parametric studies. II - Statistical approach p 224 A92-49784
- STORABLE PROPELLANTS**
- Benefits and technology readiness for using cryogenic instead of storable propellants for return mission from Moon p 136 N92-33343
- STORAGE TANKS**
- Self-pressurization of a spherical liquid hydrogen storage tank in a microgravity environment [AIAA PAPER 92-0363] p 168 A92-25798
- Self-pressurization of a flightweight liquid hydrogen tank - Effects of fill level at low wall heat flux [AIAA PAPER 92-0818] p 60 A92-29591
- Design considerations in clustering nuclear rocket engines [AIAA PAPER 92-3587] p 66 A92-49069
- Jet mixing in low gravity - Results of the Tank Pressure Control Experiment [AIAA PAPER 92-3060] p 182 A92-54001
- Comparing the results of an analytical model of the no-vent fill process with no-vent fill test results for a 4.96 cu m (175 cu ft) tank [AIAA PAPER 92-3078] p 72 A92-54007
- Self-pressurization of a spherical liquid hydrogen storage tank in a microgravity environment [NASA-TM-105372] p 185 N92-14323
- Self-pressurization of a flightweight liquid hydrogen tank: Effects of fill level at low wall heat flux [NASA-TM-105411] p 135 N92-18442
- Optimization of armored spherical tanks for storage on the lunar surface [NASA-TM-105700] p 91 N92-30187

STOVL AIRCRAFT

- Hot gas environment around STOVL aircraft in ground proximity. II - Numerical study p 25 A92-24403
- Acoustic characteristics and dynamic structural loading of an ASTOVL aircraft in hover [AIAA PAPER 92-0370] p 253 A92-28190
- Calculations of hot gas ingestion for a STOVL aircraft model [AIAA PAPER 92-0385] p 25 A92-28191
- Integrated flight/propulsion control specifications for systems with two-way coupling p 39 A92-29117
- Decentralized hierarchical partitioning of centralized integrated controllers --- for flight propulsion in STOVLs p 39 A92-29119
- Hot gas ingestion characteristics and flow visualization of a vectored thrust STOVL concept p 26 A92-45316
- Integrated flight/propulsion control for supersonic STOVL aircraft p 39 A92-45320
- Preliminary dynamic tests of a flight-type ejector [AIAA PAPER 92-3261] p 27 A92-54020
- Computational and experimental investigation of subsonic internal reversing flows p 183 A92-54170 [AIAA PAPER 92-3791]
- Propulsion system performance resulting from an Integrated Flight/Propulsion Control design [AIAA PAPER 92-4602] p 28 A92-55281
- Calculations of hot gas ingestion for a STOVL aircraft model [NASA-TM-105437] p 17 N92-19993
- Supersonic STOVL propulsion technology program: An overview p 33 N92-22539
- Preliminary dynamic tests of a flight-type ejector [NASA-TM-105814] p 38 N92-30998
- STRAIN ENERGY METHODS**
- An energy analysis of crack-initiation and arrest in epoxy p 224 A92-49777
- STRAIN ENERGY RELEASE RATE**
- Computational simulation of microfracture in high temperature metal matrix composites p 98 A92-10263
- Computational simulation of high temperature metal matrix composite behavior p 101 A92-32753
- STRAIN GAGES**
- An evaluation of strain measuring devices for ceramic composites p 199 A92-46497
- STRAIN HARDENING**
- Effects of fiber and interfacial layer architectures on the thermoplastic response of metal matrix composites [NASA-TM-105802] p 110 N92-32234
- STRAIN MEASUREMENT**
- Tensile strain measurements of ceramic fibers using scanning laser acoustic microscopy p 198 A92-39629
- An evaluation of strain measuring devices for ceramic composites [NASA-TM-105337] p 225 N92-14433
- Research sensors p 202 N92-22526
- Tensile strain measurements of ceramic fibers using scanning laser acoustic microscopy [NASA-TM-105589] p 216 N92-24986
- STRAIN RATE**
- Slow strain rate 1200-1400 K compressive properties of NiAl-1H1 p 116 A92-17977
- Hardening mechanisms in a dynamic strain aging alloy, Hastelloy X, during isothermal and thermomechanical cyclic deformation p 116 A92-24832
- The effect of strain rate and temperature on the tensile properties of NiAl p 117 A92-28113
- Predictions of the critical strain for matrix cracking of ceramic matrix composites p 218 A92-33127
- Damage mechanisms in bithermal and thermomechanical fatigue of Haynes 188 [NASA-TM-105381] p 228 N92-24985
- STRATIFICATION**
- Self-pressurization of a spherical liquid hydrogen storage tank in a microgravity environment [AIAA PAPER 92-0363] p 168 A92-25798
- Self-pressurization of a flightweight liquid hydrogen tank - Effects of fill level at low wall heat flux [AIAA PAPER 92-0818] p 60 A92-29591
- Self-pressurization of a spherical liquid hydrogen storage tank in a microgravity environment [NASA-TM-105372] p 185 N92-14323
- Self-pressurization of a flightweight liquid hydrogen tank: Effects of fill level at low wall heat flux [NASA-TM-105411] p 135 N92-18442
- STRATIFIED FLOW**
- Thermal stratification potential in rocket engine coolant channels [NASA-TM-4378] p 87 N92-25616
- STRATOSPHERE**
- Measurement of trace stratospheric constituents with a balloon borne laser radar p 239 N92-14500
- STREAM FUNCTIONS (FLUIDS)**
- Unsteady thermocapillary migration of isolated drops in creeping flow p 169 A92-27774

The structure and development of streamwise vortex arrays embedded in a turbulent boundary layer [AIAA PAPER 92-0551] p 7 A92-28204

STREAMS

- Experimental study of cross-stream mixing in a rectangular duct [AIAA PAPER 92-3090] p 178 A92-48735
- Experimental study of cross-stream mixing in a rectangular duct [NASA-TM-105694] p 36 N92-27652

STRESS ANALYSIS

- Stress versus temperature dependence of activation energies for creep p 217 A92-24719
- Microstress analysis of periodic composites p 218 A92-30673
- On the development of explicit robust schemes for implementation of a class of hyperelastic models in large-strain analysis of rubbers p 221 A92-36245
- Thermal stress analysis of a silicon carbide/aluminum composite p 222 A92-38097
- Renormalization group analysis of the Reynolds stress transport equation p 179 A92-49493
- On the basic equations for the second-order modeling of compressible turbulence [NASA-TM-105277] p 184 N92-11302
- Towards the development of micromechanics equations for ceramic matrix composites via fiber substructuring [NASA-TM-105246] p 108 N92-19595
- Collapse analysis of a waffle plate strongback for Space Station Freedom [NASA-TM-105412] p 227 N92-20045
- Influence of engineered interfaces on residual stresses and mechanical response in metal matrix composites [NASA-TM-105438] p 109 N92-23195
- Contact stresses in meshing spur gear teeth: Use of an incremental finite element procedure [NASA-TM-105388] p 209 N92-23536
- Renormalization group analysis of the Reynolds stress transport equation [NASA-TM-105588] p 190 N92-23542
- Effects of fiber and interfacial layer architectures on the thermoplastic response of metal matrix composites [NASA-TM-105802] p 110 N92-32234
- STRESS CONCENTRATION**
- Gear tooth stress measurements of two helicopter planetary stages [NASA-TM-105651] p 211 N92-26555
- STRESS DISTRIBUTION**
- Determination of the stress distributions in a ceramic tensile specimen using numerical techniques p 216 A92-14546
- Reliability analysis of laminated CMC components through shell subelement techniques [AIAA PAPER 92-2348] p 219 A92-34322
- Estimation of crack closure stresses for in situ toughened silicon nitride with 8 wt pct scandia p 126 A92-43478
- Reliability analysis of laminated CMC components through shell subelement techniques [NASA-TM-105413] p 129 N92-20380
- Singularities in optimal structural design [NASA-TM-4365] p 228 N92-23527
- Effect of contact ratio on spur gear dynamic load [NASA-TM-105606] p 210 N92-25447
- Gear tooth stress measurements of two helicopter planetary stages [NASA-TM-105651] p 211 N92-26555
- Effects of fiber and interfacial layer architectures on the thermoplastic response of metal matrix composites [NASA-TM-105802] p 110 N92-32234
- STRESS FUNCTIONS**
- Boundary formulations for sensitivities of three-dimensional stress invariants p 224 A92-50883
- Differential continuum damage mechanics models for creep and fatigue of unidirectional metal matrix composites [NASA-TM-105213] p 226 N92-16371
- A differential CDM model for fatigue of unidirectional metal matrix composites [NASA-TM-105726] p 230 N92-31505
- STRESS INTENSITY FACTORS**
- Fatigue crack growth in unidirectional metal matrix composite p 99 A92-19734
- Boundary formulations for sensitivities of three-dimensional stress invariants p 224 A92-50883
- Improvement in surface fatigue life of hardened gears by high-intensity shot peening [NASA-TM-105678] p 211 N92-26108
- STRESS MEASUREMENT**
- Gear tooth stress measurements of two helicopter planetary stages [NASA-TM-105651] p 211 N92-26555
- STRESS RELAXATION**
- A simple test for thermomechanical evaluation of ceramic fibers p 123 A92-21096

- Viscoelastic properties of addition-cured polyimides used in high temperature polymer matrix composites p 124 A92-32632
- STRESS TENSORS**
 A viscoplastic theory with thermodynamic considerations
 [ONERA, TP NO. 1991-220] p 217 A92-26372
 On the most general tensor $B_{(sub\ ij)}$ which is zero for i does not equal j , and the most general isotropic tensor $I_{(sub\ ij)}$
 [NASA-TM-105236] p 240 N92-10289
- STRESS-STRAIN DIAGRAMS**
 METCAN updates for high temperature composite behavior - Simulation/verification p 98 A92-10264
 The decrease in yield strength in NiAl due to hydrostatic pressure p 120 A92-38990
- STRESS-STRAIN RELATIONSHIPS**
 Viscoplastic analysis of an experimental cylindrical thrust chamber liner p 218 A92-28052
 HITCAN for actively cooled hot-composite thermostructural analysis
 [ASME PAPER 91-GT-116] p 222 A92-36896
 Combined bending and thermal fatigue of high-temperature metal-matrix composites - Computational simulation p 223 A92-43494
 The effect of temperature on the deformation and fracture of SiC/Ti-24Al-11Nb p 106 A92-55143
 Improved accuracy for finite element structural analysis via a new integrated force method
 [NASA-TP-3204] p 227 N92-22227
 Tensile strain measurements of ceramic fibers using scanning laser acoustic microscopy
 [NASA-TM-105589] p 216 N92-24986
 Elevated temperature axial and torsional fatigue behavior of Haynes 188
 [NASA-TM-105396] p 229 N92-28701
 Computational simulation of matrix micro-slip bands in SiC/Ti-15 composite
 [NASA-TM-105762] p 111 N92-32466
- STRING THEORY**
 Perturbations from cosmic strings in cold dark matter p 268 A92-33353
 Thick strings, the liquid crystal blue phase, and cosmological large-scale structure p 268 A92-48103
- STRIP TRANSMISSION LINES**
 Nonplanar linearly tapered slot antenna with balanced microstrip feed
 [NASA-TM-105647] p 161 N92-23535
- STRUCTURAL NUMBER**
 Naturally occurring and forced azimuthal modes in a turbulent jet p 172 A92-35998
- STRUCTURAL ANALYSIS**
 Neurobiological computational models in structural analysis and design p 245 A92-14509
 Structural reliability analysis of laminated CMC components
 [ASME PAPER 91-GT-210] p 99 A92-15630
 LDEXPT, an intelligent database system for the Composite Load Spectra project p 59 A92-23695
 Viscoplastic analysis of an experimental cylindrical thrust chamber liner p 218 A92-28052
 Mapping methods for computationally efficient and accurate structural reliability
 [AIAA PAPER 92-2347] p 219 A92-34321
 A probabilistic approach to the evaluation of fatigue damage in a space propulsion system injector element
 [AIAA PAPER 92-2413] p 60 A92-34343
 A study of equation solvers for linear and non-linear finite element analysis on parallel processing computers
 [AIAA PAPER 92-2478] p 242 A92-34367
 Material nonlinear analysis via mixed-iterative finite element method
 [AIAA PAPER 92-2479] p 220 A92-34368
 HITCAN for actively cooled hot-composite thermostructural analysis
 [ASME PAPER 91-GT-116] p 222 A92-36896
 Applications of artificial neural nets in structural mechanics p 223 A92-47283
 Computational simulation of surface waviness in graphite/epoxy woven composites due to initial curing
 [NASA-TM-105313] p 106 N92-14118
 Collapse analysis of a waffle plate strongback for Space Station Freedom
 [NASA-TM-105412] p 227 N92-20045
 Improved accuracy for finite element structural analysis via a new integrated force method
 [NASA-TP-3204] p 227 N92-22227
 Probabilistic structural analysis of adaptive/smart/intelligent space structures
 [NASA-TM-105408] p 227 N92-22267
 Aeropropulsion structures
 Integrated analysis and applications p 31 N92-22518
 Research and technology, 1991
 [NASA-TM-105320] p 1 N92-22659
- Progressive fracture of polymer matrix composite structures: A new approach
 [NASA-TM-105574] p 109 N92-23194
 Evaluation of MHOST analysis capabilities for a plate element --- finite element modeling
 [NASA-TM-105387] p 228 N92-23196
 Coupled multi-disciplinary simulation of composite engine structures in propulsion environment
 [NASA-TM-105575] p 228 N92-23267
 Singularities in optimal structural design
 [NASA-TM-4365] p 228 N92-23527
 The future challenge for aeropropulsion
 [NASA-TM-105613] p 35 N92-25164
 Structural optimization of large structural systems by optimality criteria methods
 [NASA-TM-105423] p 229 N92-25446
 Minimization of the vibration energy of thin-plate structure
 [NASA-TM-105654] p 211 N92-25448
 Integrating aerodynamic surface modeling for computational fluid dynamics with computer aided structural analysis, design, and manufacturing p 192 N92-25727
 Structural analysis of low-speed composite propfan blades for the LRCSW wind tunnel model
 [NASA-TM-105266] p 229 N92-25753
 Computer codes developed and under development at Lewis p 244 N92-25913
 A brief overview of computational structures technology related activities at NASA Lewis Research Center p 229 N92-25915
 Design feasibility study of a Space Station Freedom truss
 [NASA-TM-105558] p 214 N92-30571
 Metal matrix composite analyzer (METCAN) user's manual, version 4.0
 [NASA-TM-105244] p 110 N92-30779
 Graphite/epoxy composite adapters for the Space Shuttle/Centaur vehicle
 [NASA-TP-3014] p 49 N92-31251
 Computational simulation of structural fracture in fiber composites p 111 N92-32531
- STRUCTURAL DESIGN**
 Neurobiological computational models in structural analysis and design p 245 A92-14509
 Structural reliability analysis of laminated CMC components
 [ASME PAPER 91-GT-210] p 99 A92-15630
 Multiobjective shape and material optimization of composite structures including damping p 218 A92-28055
 Nonuniform thermal environmental effects on space truss structural reliability
 [AIAA PAPER 92-2352] p 54 A92-34325
 Structural tailoring/analysis for hypersonic components - Executive system development
 [AIAA PAPER 92-2471] p 219 A92-34360
 Application of Newton modified barrier method (NMBM) to structural optimization
 [AIAA PAPER 92-2498] p 220 A92-34555
 Structural design methodologies for ceramic-based material systems p 103 A92-39866
 Neural network based decomposition in optimal structural synthesis p 247 A92-41895
 Turning up the heat on aircraft structures --- design and analysis for high-temperature conditions p 23 A92-55131
 Space Station Freedom solar dynamic modules structural modelling and analysis
 [NASA-TM-104506] p 226 N92-15405
 Reliability analysis of structural ceramic components using a three-parameter Weibull distribution
 [NASA-TM-105370] p 129 N92-17060
 Integrated analysis and applications p 32 N92-22521
 Singularities in optimal structural design
 [NASA-TM-4365] p 228 N92-23527
 Optimum design of a gearbox for low vibration
 [NASA-TM-105653] p 212 N92-28476
- STRUCTURAL ENGINEERING**
 A brief overview of computational structures technology related activities at NASA Lewis Research Center p 229 N92-25915
- STRUCTURAL FAILURE**
 Reliability analysis of a structural ceramic combustion chamber
 [ASME PAPER 91-GT-155] p 24 A92-15591
 A three-dimensional finite-element thermal/mechanical analytical technique for high-performance traveling wave tubes
 [AIAA PAPER 92-1824] p 154 A92-29771
 A new response surface approach for structural reliability analysis
 [AIAA PAPER 92-2408] p 219 A92-34339
- Structural system reliability calculation using a probabilistic fault tree analysis method
 [AIAA PAPER 92-2410] p 251 A92-34341
 Collapse analysis of a waffle plate strongback for Space Station Freedom
 [NASA-TM-105412] p 227 N92-20045
- STRUCTURAL RELIABILITY**
 Structural reliability analysis of laminated CMC components
 [ASME PAPER 91-GT-210] p 99 A92-15630
 Mapping methods for computationally efficient and accurate structural reliability
 [AIAA PAPER 92-2347] p 219 A92-34321
 Fatigue crack growth reliability by probabilistic finite elements p 222 A92-37524
 Probabilistic progressive buckling of trusses
 [AIAA PAPER 91-0916] p 223 A92-38142
 Structural reliability assessment capability in NESSUS
 [AIAA PAPER 92-3417] p 223 A92-48976
 First-passage problems: A probabilistic dynamic analysis for degraded structures
 [NASA-TM-103755] p 225 N92-11373
 Probabilistic progressive buckling of trusses
 [NASA-TM-105162] p 226 N92-15403
 Probabilistic structural analysis of adaptive/smart/intelligent space structures
 [NASA-TM-105408] p 227 N92-22267
- STRUCTURAL STABILITY**
 Frequency effects on the stability of a journal bearing for periodic loading p 203 A92-22665
 A new response surface approach for structural reliability analysis
 [AIAA PAPER 92-2408] p 219 A92-34339
 Structural system reliability calculation using a probabilistic fault tree analysis method
 [AIAA PAPER 92-2410] p 251 A92-34341
 Recent developments of the NESSUS probabilistic structural analysis computer program
 [AIAA PAPER 92-2411] p 242 A92-34342
 Structural design concepts for a multimegawatt solar electric propulsion (SEP) spacecraft
 [AIAA PAPER 92-2536] p 54 A92-34380
 Aeroelastic stability analyses of two counter rotating propfan designs for a cruise missile model
 [AIAA PAPER 92-2218] p 25 A92-34408
 Probabilistic material degradation model for aerospace materials subjected to high temperature, mechanical and thermal fatigue, and creep
 [AIAA PAPER 92-3419] p 224 A92-48978
 Frequency effects on the stability of a journal bearing for periodic loading
 [NASA-TM-105226] p 186 N92-18809
- STRUCTURAL VIBRATION**
 Vibration transmission through rolling element bearings. IV - Statistical energy analysis p 218 A92-28756
 Free vibrations of delaminated beams p 222 A92-36853
 Statistical energy analysis of a geared rotor system p 204 A92-39227
 Rotordynamic Instability Problems in High-Performance Turbomachinery, 1990
 [NASA-CP-3122] p 207 N92-14346
 Determining structural performance p 32 N92-22519
 An examination of anticipated g-jitter on Space Station and its effects on materials processes p 140 N92-28438
 Validation of finite element and boundary element methods for predicting structural vibration and radiated noise
 [NASA-TM-105359] p 213 N92-29697
 Modal test/analysis correlation of Space Station structures using nonlinear sensitivity
 [NASA-TM-105850] p 230 N92-34221
- STRUCTURAL WEIGHT**
 Electrochemical impregnation and cycle life of lightweight nickel electrodes for nickel-hydrogen cells p 113 A92-30978
 Application of Newton modified barrier method (NMBM) to structural optimization
 [AIAA PAPER 92-2498] p 220 A92-34555
- SUBMILLIMETER WAVES**
 Submillimeter backward-wave oscillators p 155 A92-35054
- SUBROUTINES**
 Computer program for Bessel and Hankel functions
 [NASA-TM-105154] p 243 N92-11691
- SUBSONIC FLOW**
 Wind tunnel wall effects in a linear oscillating cascade
 [ASME PAPER 91-GT-133] p 2 A92-15576
 Aerodynamics of loaded cascades in subsonic flows subject to unsteady three-dimensional vortical disturbances
 [AIAA PAPER 92-0146] p 4 A92-23762
 Upwind relaxation methods for the Navier-Stokes equations using inner iterations p 170 A92-29553

SUBSONIC SPEED

- An experimental investigation of the flow in a diffusing S-duct
[AIAA PAPER 92-3622] p 13 A92-54090
- Computational and experimental investigation of subsonic internal reversing flows
[AIAA PAPER 92-3791] p 183 A92-54170
- Long time behavior of unsteady flow computations
[NASA-TM-105584] p 190 N92-23565
- A comparison of predicted and measured inlet distortion flows in a subsonic axial inlet flow compressor rotor
[NASA-TM-105427] p 19 N92-26104
- SUBSONIC SPEED**
Overview of the subsonic propulsion technology session p 32 N92-22531
- SUBSTRATES**
Measurements of complex permittivity of microwave substrates in the 20 to 300 K temperature range from 26.5 to 40.0 GHz p 197 A92-13416
- High-T sub c fluorine-doped YBa₂Cu₃O_y films on ceramic substrates by screen printing
[NASA-TM-105296] p 127 N92-11188
- Properties of large area ErBa₂Cu₃O_{7-x} thin films deposited by ionized cluster beams p 264 N92-23414
- Dependence of the critical temperature of laser-etched YBa₂Cu₃O_{7-delta} thin films on LaAlO₃ substrate growth technique p 264 N92-23415
- Microwave properties of peeled HEMT devices sapphire substrates p 265 N92-32978
- SUCTION**
Calculations of hot gas ingestion for a STOVL aircraft model
[NASA-TM-105437] p 17 N92-19993
- SULFUR DIOXIDES**
Impedances of Li/SO₂ cells retrieved from the Long Duration Exposure Facility (LDEF satellite) and comparison with cells stored terrestrially
[NASA-TM-104526] p 236 N92-13484
- SUM RULES**
A new approximate sum rule for bulk alloy properties p 117 A92-28240
- SUPERCHARGERS**
Small engine technology programs p 32 N92-22532
- SUPERCONDUCTING FILMS**
Measurements of complex permittivity of microwave substrates in the 20 to 300 K temperature range from 26.5 to 40.0 GHz p 197 A92-13416
- Coaxial line configuration for microwave power transmission study of YBa₂Cu₃O_{7-delta} thin films p 154 A92-18455
- Laser ablated YBa₂Cu₃O_{7-x} high temperature superconductor coplanar waveguide resonator p 155 A92-31631
- Hall voltage sign reversal in thin superconducting films p 261 A92-35349
- Performance of a four-element Ka-band high-temperature superconducting microstrip antenna p 146 A92-37224
- Conductor-backed coplanar waveguide resonators of YBa₂Cu₃O_{7-delta} on LaAlO₃ p 158 A92-51042
- Electrical-transport properties and microwave device performance of sputtered TiCaBaCuO superconducting thin films p 263 A92-56599
- Microwave conductivity of laser ablated YBa₂Cu₃O_{7-delta} superconducting films and its relation to microstrip transmission line performance p 264 N92-21639
- Microwave response of high transition temperature superconducting thin films p 264 N92-23413
- Properties of large area ErBa₂Cu₃O_{7-x} thin films deposited by ionized cluster beams p 264 N92-23414
- Dependence of the critical temperature of laser-etched YBa₂Cu₃O_{7-delta} thin films on LaAlO₃ substrate growth technique p 264 N92-23415
- Magnetic penetration depth of YBa₂Cu₃O_{7-delta} thin films determined by the power transmission method p 265 N92-32983
- C-band superconductor/semiconductor hybrid field-effect transistor amplifier on a LaAlO₃ substrate
[NASA-TM-105828] p 163 N92-34204
- SUPERCONDUCTIVITY**
NASA Space applications of high-temperature superconductors
[NASA-TM-105401] p 271 N92-18455
- Performance of a Y-Ba-Cu-O superconducting filter/GaAs low noise amplifier hybrid circuit
[NASA-TM-105546] p 160 N92-21370
- Composition dependence of superconductivity in YBa₂(Cu_{3-x})Al_xO_y
[NASA-TM-105358] p 131 N92-24715
- Monolithic mm-wave phase shifter using optically activated superconducting switches
[NASA-CASE-LEW-14878-1] p 257 N92-28571
- NASA space applications of high-temperature superconductors p 265 N92-32980

- Performance of a Y-Ba-Cu-O superconducting filter/GaAs low noise amplifier hybrid circuit p 163 N92-32982
- SUPERCONDUCTORS**
Near-edge study of gold-substituted YBa₂Cu₃O_{7-delta} p 259 A92-14950
- Performance of a Y-Ba-Cu-O superconducting filter/GaAs low noise amplifier hybrid circuit
[NASA-TM-105546] p 160 N92-21370
- Microwave conductivity of laser ablated YBa₂Cu₃O_{7-delta} superconducting films and its relation to microstrip transmission line performance p 264 N92-21639
- Performance of a Y-Ba-Cu-O superconducting filter/GaAs low noise amplifier hybrid circuit p 163 N92-32982
- SUPERCritical FLUIDS**
Evaluation of supercritical cryogen storage and transfer systems for future NASA missions p 47 A92-28512
- SUPERCritical PRESSURES**
Qualitative investigation of cryogenic fluid injection into a supercritical flow field p 164 A92-13360
- Combustion of liquid-fuel droplets in supercritical conditions p 114 A92-43778
- SUPERFLUIDITY**
Hall voltage sign reversal in thin superconducting films p 261 A92-35349
- SUPERHIGH FREQUENCIES**
The Link Evaluation Terminal for the Advanced Communications Technology Satellite Experiments Program
[AIAA PAPER 92-2040] p 49 A92-29954
- The link evaluation terminal for the advanced communications technology satellite experiments program
[NASA-TM-105367] p 51 N92-16008
- The ACTS multibeam antenna
[NASA-TM-105645] p 52 N92-30383
- SUPERNOVA 1987A**
Constraints to the decays of Dirac neutrinos from SN 1987A p 255 A92-36249
- Massive Dirac neutrinos and SN 1987A p 268 A92-45808
- SUPERSONIC AIRCRAFT**
A review of computational/experimental methodology developments in aerodynamics p 253 A92-39241
- Integrated flight/propulsion control for supersonic STOVL aircraft p 39 A92-45320
- Fiber optics for controls p 40 N92-22529
- SUPERSONIC BOUNDARY LAYERS**
High-Order Polynomial Expansions (HOPE) for flux-vector splitting p 190 N92-23353
- SUPERSONIC COMBUSTION**
NASA thrusts in high-speed aeropropulsion research and development: An overview p 33 N92-22538
- Study of shock-induced combustion using an implicit TVD scheme p 116 N92-25816
- SUPERSONIC COMBUSTION RAMJET ENGINES**
Computational analysis of ramjet engine inlet interaction
[AIAA PAPER 92-3102] p 11 A92-48744
- High temperature dynamic engine seal technology development
[NASA-TM-105641] p 209 N92-23435
- Study of shock-induced combustion using an implicit TVD scheme p 116 N92-25816
- SUPERSONIC FLIGHT**
Supersonic propulsion simulation by incorporating component models in the large perturbation inlet (LAPIN) computer code
[NASA-TM-105193] p 30 N92-15993
- Supersonic STOVL propulsion technology program: An overview p 33 N92-22539
- Supersonic throughflow fans for high-speed aircraft p 34 N92-22541
- SUPERSONIC FLOW**
Qualitative investigation of cryogenic fluid injection into a supercritical flow field p 164 A92-13360
- The Baldwin-Lomax model for separated and wake flows using the entropy envelope concept
[AIAA PAPER 92-0148] p 4 A92-23764
- Acoustic analysis using numerical solutions of the Navier-Stokes equations
[AIAA PAPER 92-0506] p 253 A92-26934
- Crossing shock wave turbulent boundary layer interactions - Variable angle and shock generator length geometry effects at Mach 3
[AIAA PAPER 92-0636] p 6 A92-27014
- Upwind relaxation methods for the Navier-Stokes equations using inner iterations p 170 A92-29553
- Doppler-shifted fluorescence imaging of velocity fields in supersonic reacting flows
[AIAA PAPER 92-2964] p 199 A92-46979
- Grid quality improvement by a grid adaptation technique p 248 A92-47072

- Initial development of the axisymmetric ejector shear layer
[AIAA PAPER 92-3567] p 178 A92-49068
- Three-dimensional calculations of supersonic reacting flows using an LU scheme p 179 A92-50465
- A laser-induced heat flux technique for convective heat transfer measurements in high speed flows p 200 A92-54318
- Experimental unsteady pressures on an oscillating cascade with supersonic leading edge locus
[AIAA PAPER 92-4035] p 14 A92-56857
- Noise from turbulent shear flows p 254 N92-10603
- Supersonic throughflow fans for high-speed aircraft p 34 N92-22541
- Development of a new flux splitting scheme p 190 N92-23352
- Development of new flux splitting schemes --- computational fluid dynamics algorithms p 192 N92-25809
- SUPERSONIC INLETS**
Transient behavior of supersonic flow through inlets p 7 A92-28043
- A fast, uncoupled, compressible, two-dimensional, unsteady boundary layer algorithm with separation for engine inlets p 11 A92-48729
- Interface of an uncoupled boundary layer algorithm with an inviscid core flow algorithm for unsteady supersonic engine inlets p 11 A92-48730
- Results from computational analysis of a mixed compression supersonic inlet
[NASA-TM-104475] p 14 N92-10976
- Supersonic propulsion simulation by incorporating component models in the large perturbation inlet (LAPIN) computer code p 30 N92-15993
- Propulsion challenges and opportunities for high-speed transport aircraft p 34 N92-22540
- Interactive solution-adaptive grid generation procedure
[NASA-TM-105432] p 18 N92-23563
- Interface of an uncoupled boundary layer algorithm with an inviscid core flow algorithm for unsteady supersonic engine inlets p 36 N92-27037
- A fast, uncoupled, compressible, two-dimensional, unsteady boundary layer algorithm with separation for engine inlets p 195 N92-27653
- SUPERSONIC JET FLOW**
Computation of supersonic jet mixing noise for an axisymmetric CD nozzle using k-epsilon turbulence model
[AIAA PAPER 92-0500] p 252 A92-26328
- A survey of the broadband shock associated noise prediction methods
[AIAA PAPER 92-0501] p 252 A92-26930
- Screch noise source structure of a supersonic rectangular jet p 6 A92-26932
- The flip flop nozzle extended to supersonic flows
[AIAA PAPER 92-2724] p 10 A92-45561
- Supersonic jet mixing enhancement by 'delta-tabs'
[AIAA PAPER 92-3548] p 12 A92-49063
- Filtered Rayleigh scattering measurements in supersonic/hypersonic facilities
[AIAA PAPER 92-3894] p 200 A92-56733
- Screch noise source structure of a supersonic rectangular jet p 15 N92-14000
- Computation of supersonic jet mixing noise for an axisymmetric CD nozzle using k-epsilon turbulence model
[NASA-TM-105338] p 254 N92-14795
- A survey of the broadband shock associated noise prediction methods
[NASA-TM-105365] p 254 N92-14797
- The flip-flop nozzle extended to supersonic flows
[NASA-TM-105570] p 18 N92-23269
- Supersonic jet mixing enhancement by delta-tabs
[NASA-TM-105664] p 18 N92-24958
- SUPERSONIC SPEED**
The flip flop nozzle extended to supersonic flows
[AIAA PAPER 92-2724] p 10 A92-45561
- Detailed noise measurements on the SR-7A propeller: Tone behavior with helical tip Mach number
[NASA-TM-105206] p 255 N92-16705
- The flip-flop nozzle extended to supersonic flows
[NASA-TM-105570] p 18 N92-23269
- Effects of turbine cooling assumptions on performance and sizing of high-speed civil transport
[NASA-TM-105610] p 34 N92-23537
- A new Lagrangian method for real gases at supersonic speed p 19 N92-25814

- SUPERSONIC TRANSPORTS**
 A new unsteady mixing model to predict NO(x) production during rapid mixing in a dual-stage combustor [AIAA PAPER 92-0233] p 25 A92-25696
 Experimental investigation of an ejector-powered free-jet facility [AIAA PAPER 92-3569] p 41 A92-54058
 Full Navier-Stokes analysis of a two-dimensional mixer/ejector nozzle for noise suppression [AIAA PAPER 92-3570] p 27 A92-54059
 Propulsion challenges and opportunities for high-speed transport aircraft p 34 N92-22540
 Full Navier-Stokes analysis of a two-dimensional mixer/ejector nozzle for noise suppression [NASA-TM-105715] p 37 N92-28419
- SUPERSONIC TURBINES**
 A critical evaluation of a three-dimensional Navier-Stokes CFD as a tool to design supersonic turbine stages p 196 N92-32268
- SUPERSONIC WIND TUNNELS**
 Experimental unsteady pressures on an oscillating cascade with supersonic leading edge locus [AIAA PAPER 92-4035] p 14 A92-56857
- SURFACE DEFECTS**
 Atomic oxygen durability of solar concentrator materials for Space Station Freedom [NASA-TM-105378] p 85 N92-20065
- SURFACE DISTORTION**
 Minimizing distortion in truss structures - A Hopfield network solution [AIAA PAPER 92-2302] p 220 A92-34523
- SURFACE ENERGY**
 Computational techniques in tribology and material science at the atomic level [NASA-TM-105573] p 252 N92-26671
- SURFACE GEOMETRY**
 A method for determining spiral-bevel gear tooth geometry for finite element analysis [NASA-TP-3096] p 207 N92-10195
 NASA Surface-Modeling and Grid-Generation (SM/GG) activities p 267 N92-25725
- SURFACE IONIZATION**
 Ion beam treatment of potential space materials at the NASA Lewis Research Center [NASA-TM-105398] p 97 N92-21548
- SURFACE PROPERTIES**
 Increased efficiency with surface texturing in ITO/InP solar cells p 232 A92-44548
 Solid lubricants on pretreated surfaces [NASA-CASE-LEW-14474-2] p 127 N92-11186
 Ion beam treatment of potential space materials at the NASA Lewis Research Center [NASA-TM-105398] p 97 N92-21548
- SURFACE ROUGHNESS**
 Heat transfer on accreting ice surfaces p 166 A92-24415
 Prediction of ice accretion on a swept NACA 0012 airfoil and comparisons to flight test results [AIAA PAPER 92-0043] p 4 A92-25677
 Mechanisms resulting in accreted ice roughness [AIAA PAPER 92-0297] p 21 A92-25750
 Analysis of surface roughness generation in aircraft ice accretion [AIAA PAPER 92-0298] p 169 A92-28187
 Prediction of ice accretion on a swept NACA 0012 airfoil and comparisons to flight test results [NASA-TM-105368] p 16 N92-15968
- SURFACE ROUGHNESS EFFECTS**
 Roughness effects on heat transfer from a NACA 0012 airfoil p 166 A92-20217
- SURFACE TEMPERATURE**
 Miniature high temperature plug-type heat flux gauges [NASA-TM-105403] p 201 N92-18759
 Multiwavelength pyrometry for nongray surfaces in the presence of interfering radiation [NASA-TM-105286] p 201 N92-19107
 Temperature-dependent reflectivity of silicon carbide [NASA-TM-105287] p 201 N92-19263
- SURFACE TREATMENT**
 Significant long-term reduction in n-channel MESFET subthreshold leakage using ammonium-sulfide surface treated gates p 153 A92-12272
 Surface etching for light trapping in encapsulated InP solar cells p 232 A92-48091
 High performance etchant for thinning p(+)-InP and its application to p(+)-InP solar cell fabrication p 263 A92-53155
 Ion beam treatment of potential space materials at the NASA Lewis Research Center [NASA-TM-105398] p 97 N92-21548
- SURFACE VEHICLES**
 A dynamic isotope power system for Space Exploration Initiative surface transport systems [AIAA PAPER 92-1489] p 61 A92-38605
- SURFACES**
 Workshop on Grid Generation and Related Areas [NASA-CP-10089] p 35 N92-25712
- SURVEYS**
 Comparative survey of dynamic analyses of free-piston Stirling engines p 206 A92-50793
 Icing simulation: A survey of computer models and experimental facilities p 21 N92-21684
- SURVIVAL**
 Demonstrated survivability of a high temperature optical fiber cable on a 1500 pound thrust rocket chamber [NASA-TM-105835] p 136 N92-32230
- SWEPT WINGS**
 Prediction of ice accretion on a swept NACA 0012 airfoil and comparisons to flight test results [AIAA PAPER 92-0043] p 4 A92-25677
 Prediction of ice accretion on a swept NACA 0012 airfoil and comparisons to flight test results [NASA-TM-105368] p 16 N92-15968
 Analysis of iced wings [NASA-TM-105773] p 20 N92-34144
- SWINGBY TECHNIQUE**
 Minimum impulse trajectories for Mars round trip missions [AAS PAPER 91-500] p 44 A92-43339
- SWIRLING**
 Factors influencing the effective spray cone angle of pressure-swirl atomizers p 166 A92-23300
 Modern developments in shear flow control with swirl p 9 A92-41265
 Spatial instability of a swirling jet - Theory and experiment p 174 A92-41274
 Wind tunnel performance results of swirl recovery vanes as tested with an advanced high speed propeller [AIAA PAPER 92-3770] p 28 A92-54159
- SWITCHES**
 Monolithic mm-wave phase shifter using optically activated superconducting switches [NASA-CASE-LEW-14878-1] p 257 N92-28571
- SWITCHING**
 Circuit-switch architecture for a 30/20-GHz FDMA/TDM geostationary satellite communications network [AIAA PAPER 92-2005] p 49 A92-29924
 Space Communications Technology Conference: Onboard Processing and Switching [NASA-CP-3132] p 147 N92-14202
 Circuit-switch architecture for a 30/20-GHz FDMA/TDM geostationary satellite communications network [NASA-TM-105302] p 51 N92-15109
- SWITCHING CIRCUITS**
 Circuit-switch architecture for a 30/20-GHz FDMA/TDM geostationary satellite communications network [AIAA PAPER 92-2005] p 49 A92-29924
 The Link Evaluation Terminal for the Advanced Communications Technology Satellite Experiments Program [AIAA PAPER 92-2040] p 49 A92-29954
 Multiple-mode reconfigurable electro-optic switching network for optical fiber sensor array p 256 A92-46245
 Circuit-switch architecture for a 30/20-GHz FDMA/TDM geostationary satellite communications network [NASA-TM-105302] p 51 N92-15109
 The link evaluation terminal for the advanced communications technology satellite experiments program [NASA-TM-105367] p 51 N92-16008
- SYNCHRONIZED OSCILLATORS**
 A theoretical and experimental study of the noise behavior of subharmonically injection locked local oscillators p 157 A92-46080
- SYNCHRONOUS PLATFORMS**
 Destination directed packet switch architecture for a 30/20 GHz FDMA/TDM geostationary communication satellite network p 148 N92-14204
- SYNCHRONOUS SATELLITES**
 A personal communications network using a Ka-band satellite p 145 A92-31780
- SYNTHESIS (CHEMISTRY)**
 Addition curing thermosets endcapped with 4-amino (2,2) paracyclophane p 124 A92-33918
 Combustion synthesis of TiB₂-Al₂O₃-Al composite materials p 102 A92-36391
 Synthesis and characterization of fine grain diamond films p 262 A92-46330
 Combustion synthesis of ceramic-metal composite materials - The TiC-Al₂O₃-Al system p 115 A92-55139
 Graphite fluoride from iodine intercalated graphitized carbon [NASA-CASE-LEW-15360-1] p 116 N92-34206
- SYSTEM EFFECTIVENESS**
 Resonant mode controllers for launch vehicle applications [NASA-TM-105563] p 48 N92-25092
- SYSTEM FAILURES**
 Thermal verification testing of commercial printed-circuit boards for spaceflight p 216 A92-56217
 Thermal verification testing of commercial printed-circuit boards for spaceflight [NASA-TM-105261] p 141 N92-11221
- SYSTEM IDENTIFICATION**
 Design of multi-layer neural networks for accurate identification of nonlinear mappings p 246 A92-29030
 A simplified dynamic model of the T700 turboshaft engine [NASA-TM-105805] p 251 N92-30898
- SYSTEMS ANALYSIS**
 Using EPSAT to analyze high power systems in the space environment --- Environment Power System Analysis Tool p 158 A92-50580
 Application of enhanced modern structured analysis techniques to Space Station Freedom electric power system requirements p 251 A92-50609
 Comparative survey of dynamic analyses of free-piston Stirling engines p 206 A92-50793
 A graphical user-interface for propulsion system analysis [NASA-TM-105696] p 244 N92-33694
- SYSTEMS ENGINEERING**
 Computational simulation of concurrent engineering for aerospace propulsion systems [AIAA PAPER 92-1144] p 241 A92-33285
 Autonomous Power System intelligent diagnosis and control p 247 A92-50532
 A 1 MW, 100 kV, less than 100 kg space based dc-dc power converter p 157 A92-50537
 Application of enhanced modern structured analysis techniques to Space Station Freedom electric power system requirements p 251 A92-50609
 Multi-reactor power system configurations for multimegawatt nuclear electric propulsion [NASA-TM-105212] p 77 N92-10057
 Environmental interactions in Space Exploration: Announcement of the formation of an Environmental Interactions Working Group [NASA-TM-105294] p 270 N92-17069
 NEP systems engineering efforts in FY-92: Plans and status [NASA-TM-105775] p 91 N92-30308
- SYSTEMS INTEGRATION**
 IMPAC - An integrated methodology for propulsion and airframe control p 39 A92-29118
 Decentralized hierarchical partitioning of centralized integrated controllers --- for flight propulsion in STOLVs p 39 A92-29119
 Integrated flight/propulsion control for supersonic STOVL aircraft p 39 A92-45320
 Piloted evaluation of an integrated propulsion and flight control simulator [AIAA PAPER 92-4178] p 23 A92-52459
 Technology readiness assessment of advanced space engine integrated controls and health monitoring [NASA-TM-105255] p 79 N92-11130
 Evaluation of components, subsystems, and networks for high rate, high frequency space communications [NASA-TM-105274] p 147 N92-12151
 Integrated analysis and applications p 32 N92-22521
 Fiber optics for controls p 40 N92-22529
- SYSTEMS MANAGEMENT**
 Model-based diagnostics for Space Station Freedom p 245 A92-50535
 An EMTF system level model of the PMAD DC test bed p 46 A92-50657
- SYSTEMS SIMULATION**
 A multi-channel demultiplexer/demodulator architecture, simulation and implementation [AIAA PAPER 92-1972] p 144 A92-29895
 Simulating the arcjet thruster using a nonlinear active load [AIAA PAPER 92-3528] p 45 A92-49052
 Multikilowatt power electronics development for spacecraft p 68 A92-50541
 Functional models of power electronic components for system studies p 157 A92-50558
 Modeling of Space Station power system components and their interactions p 68 A92-50559
 Simulation of Space Station loads with active control systems p 56 N92-23824
 Activities for numerical propulsion systems simulation program p 244 N92-25726
- SYSTEMS STABILITY**
 Stochastic stability properties of jump linear systems p 246 A92-25878
 The Eckhaus and the Benjamin-Feir instability near a weakly inverted bifurcation [NASA-TM-105334] p 185 N92-15336

TABS (CONTROL SURFACES)

- A survey of instabilities within centrifugal pumps and concepts for improving the flow range of pumps in rocket engines
 [NASA-TM-105439] p 84 N92-18280
 Stability testing and analysis of a PMAD DC test bed for the Space Station Freedom
 [NASA-TM-105846] p 162 N92-31282

T

TABS (CONTROL SURFACES)

- Effect of tabs on the evolution of an axisymmetric jet
 p 26 A92-40151
 Supersonic jet mixing enhancement by 'delta-tabs'
 [AIAA PAPER 92-3548] p 12 A92-49063
 Supersonic jet mixing enhancement by delta-tabs
 [NASA-TM-105664] p 18 N92-24958

TAIL ROTORS

- Model rotor icing tests in the NASA Lewis Icing Research Tunnel p 21 N92-21688

TAKEOFF

- Far-field noise and internal modes from a ducted propeller at simulated aircraft takeoff conditions
 [AIAA PAPER 92-0371] p 252 A92-26230
 Unsteady blade pressures on a propfan at takeoff - Euler analysis and flight data
 [AIAA PAPER 92-0376] p 25 A92-26234
 Far-field noise and internal modes from a ducted propeller at simulated aircraft takeoff conditions
 [NASA-TM-105369] p 254 N92-16702

TANGENTS

- Explicit robust schemes for implementation of a class of principal value-based constitutive models: Theoretical development
 [NASA-TM-105345] p 227 N92-20212

TANTALUM ALLOYS

- Novel applications for TAZ-8A p 123 N92-22444

TAYLOR INSTABILITY

- Linear stability of compressible Taylor-Couette flow
 p 173 A92-36187
 Propagating confined states in phase dynamics
 p 181 A92-50968
 Stable localized patterns in thin liquid films
 [NASA-TM-105352] p 185 N92-14322

TDR SATELLITES

- Distribution of space-gathered data
 [AIAA PAPER 92-1888] p 143 A92-29821

TECHNOLOGICAL FORECASTING

- MisTec - A software application for supporting space exploration scenario options and technology development analysis and planning
 [AIAA PAPER 92-1293] p 242 A92-38490
 Ceramics and ceramic composites in future aeronautical and space systems p 95 A92-39853
 MisTec: A software application for supporting space exploration scenario options and technology development analysis and planning
 [NASA-TM-105214] p 243 N92-14649

TECHNOLOGY ASSESSMENT

- High temperature thruster technology for spacecraft propulsion
 [IAF PAPER 91-254] p 58 A92-13155
 Advances in MMIC technology for communications satellites
 [AIAA PAPER 92-1899] p 155 A92-29830
 Integrated solar power satellites - An approach to low-mass space power p 231 A92-40427
 Update on results of SPRE testing at NASA Lewis
 p 71 A92-50780
 NASA's nuclear thermal propulsion technology project
 [AIAA PAPER 92-3581] p 75 A92-54062
 Low thrust chemical rocket technology
 [IAF PAPER 92-0669] p 77 A92-57105
 Nuclear thermal propulsion workshop overview
 p 78 N92-11090

- Technology readiness assessment of advanced space engine integrated controls and health monitoring
 [NASA-TM-105255] p 79 N92-11130

- Plans for the development of cryogenic engines for space exploration
 [NASA-TM-105250] p 79 N92-11135

- Thin film, concentrator, and multijunction space solar cells: Status and potential p 81 N92-13230

- Overview of Ka-band communications technology requirements for the space exploration initiative
 [NASA-TM-105308] p 269 N92-14953

- An overview of silicon carbide device technology
 [NASA-TM-105402] p 263 N92-15815

- Nuclear Electric Propulsion Technology Panel findings and recommendations
 [NASA-TM-105547] p 85 N92-20355

- Lubrication of space systems: Challenges and potential solutions
 [NASA-TM-105560] p 130 N92-21579

- Blazing the trailway: Nuclear electric propulsion and its technology program plans
 [NASA-TM-105605] p 86 N92-23252

- High temperature dynamic engine seal technology development
 [NASA-TM-105641] p 209 N92-23435

- Ceramic composites: Enabling aerospace materials
 [NASA-TM-105599] p 133 N92-27378

- NEP systems engineering efforts in FY-92: Plans and status
 [NASA-TM-105775] p 91 N92-30308

- Wiring for aerospace applications
 [NASA-TM-105777] p 162 N92-30427

- Trends in aeropropulsion research and their impact on engineering education
 [NASA-TM-105682] p 38 N92-31172

- The evolutionary development of high specific impulse electric thruster technology
 [NASA-TM-105712] p 92 N92-31342

- Benefits and technology readiness for using cryogenic instead of storable propellants for return mission from Moon
 p 136 N92-33343

TECHNOLOGY UTILIZATION

- Operational uses of ACTS technology
 [AIAA PAPER 92-1964] p 144 A92-29887

- The NASA-OAST earth-to-orbit propulsion technology program - The action plan
 [AIAA PAPER 92-1478] p 61 A92-38597

- NASA program planning on nuclear electric propulsion
 [AIAA PAPER 92-1557] p 61 A92-38651

- Solar dynamic power for earth orbital and lunar applications
 p 68 A92-50567

- Nuclear thermal propulsion workshop overview
 p 78 N92-11090

- Future communications satellite applications
 p 52 N92-22019

- Ceramic composites: Enabling aerospace materials
 [NASA-TM-105599] p 133 N92-27378

- Solid State Technology Branch of NASA Lewis Research Center
 [NASA-TM-105752] p 151 N92-32965

- NASA space applications of high-temperature superconductors
 p 265 N92-32980

TEETERING

- Model rotor icing tests in the NASA Lewis Icing Research Tunnel p 21 N92-21688

TEFLON (TRADEMARK)

- Dielectric breakdown studies of Teflon perfluoroalkoxy at high temperature p 125 A92-36287

- Electrical properties of teflon and ceramic capacitors at high temperatures
 [NASA-TM-105569] p 160 N92-20040

- Atomic oxygen interactions with FEP Teflon and silicones on LDEF
 p 132 N92-24820

- High temperature dielectric properties of Apical, Kapton, Peek, Teflon AF, and Uplex polymers
 [NASA-TM-105753] p 162 N92-28675

TELECOMMUNICATION

- Technical and economic feasibility of integrated video service by satellite
 [AIAA PAPER 92-2054] p 145 A92-29966

TELECONFERENCING

- Technical and economic feasibility of integrated video service by satellite
 [AIAA PAPER 92-2054] p 145 A92-29966

TELEMETRY

- Determination of the critical parameters for remote microscopes control
 [IAF PAPER 91-026] p 240 A92-12447

TELEVISION CAMERAS

- A full field, 3-D velocimeter for NASA's microgravity science program
 [AIAA PAPER 92-0784] p 56 A92-27119

TELEVISION TRANSMISSION

- Real-time demonstration hardware for enhanced DPCM video compression algorithm
 [NASA-TM-105616] p 150 N92-19700

TEMPERATURE CONTROL

- Temperature control in continuous furnace by structural diagram method p 246 A92-29162

- Adaptive temperature profile control of a multizone crystal growth furnace p 137 A92-29243

- Applications of high thermal conductivity composites to electronics and spacecraft thermal design
 [NASA-TM-102434] p 56 N92-24349

- An overview of the Lewis Research Center CSTI thermal management program
 [NASA-TM-105310] p 92 N92-31916

TEMPERATURE DEPENDENCE

- Boundary formulations for shape sensitivity of temperature dependent conductivity problems
 p 217 A92-25403

- The effect of strain rate and temperature on the tensile properties of NiAl p 117 A92-28113

- Study of temperature-dependent ultrathin oxide growth on Si(111) using variable-angle spectroscopic ellipsometry p 260 A92-32414

- Relative sliding durability of two candidate high temperature oxide fiber seal materials
 [AIAA PAPER 92-3713] p 126 A92-49095

- Use of an approximate similarity principle for the thermal scaling of a full-scale thrust augmenting ejector
 [AIAA PAPER 92-3792] p 28 A92-54171

- Temperature dependence of the electrode kinetics of oxygen reduction at the platinum/Nafion interface - A microelectrode investigation p 115 A92-56950

- Relative sliding durability of two candidate high temperature oxide fiber seal materials
 [NASA-TM-105199] p 95 N92-10064

- Temperature-dependent reflectivity of silicon carbide
 [NASA-TM-105287] p 201 N92-19263

- Use of an approximate similarity principle for the thermal scaling of a full-scale thrust augmenting ejector
 [NASA-TM-105724] p 36 N92-28613

- Effects of fiber and interfacial layer architectures on the thermoplastic response of metal matrix composites
 [NASA-TM-105802] p 110 N92-32234

TEMPERATURE DISTRIBUTION

- Transient pool boiling in microgravity
 p 170 A92-30494

- Reliability analysis of laminated CMC components through shell subelement techniques
 [AIAA PAPER 92-2348] p 219 A92-34322

- Combined conjugated heat transfer from a scattering medium
 p 175 A92-44390

- Effects of coolant parameters on steady state temperature distribution in phosphoric-acid fuel cell electrode
 p 233 A92-50737

- Reliability analysis of laminated CMC components through shell subelement techniques
 [NASA-TM-105413] p 129 N92-20380

TEMPERATURE EFFECTS

- METCAN updates for high temperature composite behavior - Simulation/verification p 98 A92-10264

- HITCAN for actively cooled hot-composite thermostructural analysis
 [ASME PAPER 91-GT-116] p 222 A92-36896

- Radiation and temperature effects in heteroepitaxial and homoepitaxial InP cells
 p 159 A92-53192

- The effect of temperature on the deformation and fracture of SiC/Ti-24Al-11Nb p 106 A92-55143

- The 23 to 300 C demagnetization resistance of samarium-cobalt permanent magnets
 p 159 N92-11252

- Computational simulation of surface waviness in graphite/epoxy woven composites due to initial curing
 [NASA-TM-105313] p 106 N92-14118

- Thermal conductivity and thermal expansion of graphite fiber/copper matrix composites
 [NASA-TM-105233] p 106 N92-14120

- Thermally-driven microfracture in high temperature metal matrix composites
 [NASA-TM-105305] p 107 N92-15136

- Elevated temperature mechanical behavior of monolithic and SiC whisker-reinforced silicon nitrides
 [NASA-TM-105245] p 128 N92-15192

- CVD of silicon carbide on structural fibers: Microstructure and composition
 [NASA-TM-105385] p 107 N92-18439

- Towards the development of micromechanics equations for ceramic matrix composites via fiber substructuring
 [NASA-TM-105246] p 108 N92-19595

- Effect of heat treatment on stiffness and damping of SiC/Ti-15-3
 [NASA-TM-105564] p 108 N92-20841

- Sliding durability of two carbide-oxide candidate high temperature fiber seal materials in air to 900 C
 [NASA-TM-105554] p 97 N92-21175

- High temperature, flexible, fiber-preform seal
 [NASA-CASE-LEW-15085-1] p 208 N92-22043

- Influence of engineered interfaces on residual stresses and mechanical response in metal matrix composites
 [NASA-TM-105438] p 109 N92-23195

- Effect of lubricant jet location on spiral bevel gear operating temperatures
 [NASA-TM-105656] p 211 N92-26106

- Neutron, gamma ray, and temperature effects on the electrical characteristics of thyristors
 [NASA-TM-105728] p 162 N92-28432

- Experimental and computational ice shapes and resulting drag increase for a NACA 0012 airfoil
 [NASA-TM-105743] p 20 N92-28674

- Comparison of high temperature, high frequency core loss and dynamic B-H loops of a 2V-49Fe-49Co and a grain oriented 3Si-Fe alloy
 [NASA-TM-105791] p 162 N92-30397

- Metal matrix composite analyzer (METCAN) user's manual, version 4.0
 [NASA-TM-105244] p 110 N92-30779

- isothermal aging effects on PMR-15 resin [NASA-TM-105648] p 110 N92-30986
- Measurement techniques for cryogenic Ka-band microstrip antennas p 153 N92-32981
- Probabilistic assessment of space trusses subjected to combined mechanical and thermal loads [NASA-TM-105429] p 230 N92-33935
- TEMPERATURE GRADIENTS**
 - Convective flows in enclosures with vertical temperature or concentration gradients p 171 A92-32277
 - Low-power arcjet test facility impacts [AIAA PAPER 92-3532] p 74 A92-54040
 - Effect of growth conditions on the quality of lead bromide crystals p 138 A92-56957
 - Interfacial and gravitational convection in immiscible liquid layers [IAF PAPER 92-0907] p 184 A92-57286
- TEMPERATURE MEASUREMENT**
 - Species and temperature measurement in H₂/O₂ rocket flow fields by means of Raman scattering diagnostics [AIAA PAPER 92-3353] p 178 A92-48930
 - Miniature high temperature plug-type heat flux gauges [NASA-TM-105403] p 201 N92-18759
 - Multiwavelength pyrometry for nongray bodies [NASA-TM-105285] p 202 N92-24881
 - Reduced mobility and PPC in In₂₀Ga₈₀As / Al₂₃Ga₇₇As HEMT structure p 265 N92-32976
- TEMPERATURE PROFILES**
 - Nongray radiative gas analyses using the S-N discrete ordinates method p 266 A92-15443
 - Transport modes during crystal growth in a centrifuge p 138 A92-33835
 - Rayleigh-Brillouin scattering to determine one-dimensional temperature and number density profiles of a gas flow field p 198 A92-38067
- TEMPERATURE SENSORS**
 - Liquid-vapour surface sensors for liquid nitrogen and hydrogen p 197 A92-23852
 - Using silicon diodes for detecting the liquid-vapor interface in hydrogen [NASA-TM-105541] p 201 N92-18456
 - Research sensors p 202 N92-22526
- TENSILE CREEP**
 - Damage mechanisms in bithermal and thermomechanical fatigue of Haynes 188 [NASA-TM-105381] p 228 N92-24985
- TENSILE DEFORMATION**
 - Deformation behavior of a Ni-30Al-20Fe-0.05Zr intermetallic alloy in the temperature range 300 to 1300 K p 121 A92-41668
- TENSILE PROPERTIES**
 - Mechanical behavior of fiber reinforced SiC/RBSN ceramic matrix composites - Theory and experiment --- Reaction Bonded Silicon Nitride [AIAA PAPER 91-GT-209] p 99 A92-15629
 - The effect of strain rate and temperature on the tensile properties of NiAl p 117 A92-28113
 - Tensile properties of impact ices [AIAA PAPER 92-0883] p 94 A92-29644
 - Compression, bend, and tension studies on forged Al67Ti25Cr8 and Al66Ti25Mn(g) L1(2) compounds p 118 A92-30766
 - Tension, compression, and bend properties for SiC/RBSN composites p 100 A92-32727
 - Effect of fiber strength on the room temperature tensile properties of SiC/Ti-24Al-11Nb p 102 A92-36389
 - Correlation of deformation mechanisms with the tensile and compressive behavior of NiAl and NiAl(Zr) intermetallic alloys p 120 A92-38019
 - Tensile behavior of the L1(2) compound Al67Ti25Cr8 p 122 A92-49694
- TENSILE STRENGTH**
 - Tensile properties of impact ices [AIAA PAPER 92-0883] p 94 A92-29644
 - Sliding durability of two carbide-oxide candidate high temperature fiber seal materials in air to 900 C [NASA-TM-105554] p 97 N92-21175
 - Tensile strain measurements of ceramic fibers using scanning laser acoustic microscopy [NASA-TM-105589] p 216 N92-24986
- TENSILE STRESS**
 - Damage mechanisms in three-dimensional woven reinforced ceramic matrix composites under tensile and flexural loading at room and elevated temperatures [AIAA PAPER 92-2492] p 101 A92-34584
 - The decrease in yield strength in NiAl due to hydrostatic pressure p 120 A92-38990
 - Failure mechanisms of 3-D woven SiC/SiC composites under tensile and flexural loading at room and elevated temperatures p 103 A92-39642
- TENSILE TESTS**
 - Determination of the stress distributions in a ceramic, tensile specimen using numerical techniques p 216 A92-14546
 - A combined analytical-experimental tensile test technique for brittle materials p 123 A92-23225
- A viscoplastic model for single crystals p 217 A92-24717
- Fracture behavior of a B2 Ni-30Al-20Fe-0.05Zr intermetallic alloy in the temperature range 300 to 1300 K p 121 A92-41667
- An evaluation of strain measuring devices for ceramic composites p 199 A92-46497
- An evaluation of strain measuring devices for ceramic composites [NASA-TM-105337] p 225 N92-14433
- A preliminary characterization of the tensile and fatigue behavior of tungsten-fiber/Waspaloy-matrix composite [NASA-TM-105346] p 187 N92-22487
- X ray attenuation measurements for high-temperature materials characterization and in-situ monitoring of damage accumulation [NASA-TM-105577] p 110 N92-25996
- TENSORS**
 - A critical comparison of second order closures with direct numerical simulation of homogeneous turbulence [NASA-TM-105351] p 185 N92-15357
 - Explicit robust schemes for implementation of a class of principal value-based constitutive models: Theoretical development [NASA-TM-105345] p 227 N92-20212
- TERNARY ALLOYS**
 - Interdiffusion between the L1(2) trialuminides Al66Ti25Mn9 and Al67Ti25Cr8 p 120 A92-37088
- TEST CHAMBERS**
 - Description of liquid nitrogen experimental test facility p 44 A92-23842
 - Description of Liquid Nitrogen Experimental Test Facility [NASA-TM-105215] p 134 N92-11208
 - Design characteristics of a heat pipe test chamber [NASA-TM-105737] p 238 N92-29662
- TEST EQUIPMENT**
 - Desktop fiber push-out apparatus [NASA-TM-105341] p 107 N92-16036
- TEST FACILITIES**
 - NASA low-speed centrifugal compressor for 3-D viscous code assessment and fundamental flow physics research [ASME PAPER 91-GT-140] p 3 A92-15580
 - Description of liquid nitrogen experimental test facility p 44 A92-23842
 - Simulating the arcjet thruster using a nonlinear active load [AIAA PAPER 92-3528] p 45 A92-49052
 - Description of the PMAD DC test bed architecture and integration sequence p 46 A92-50655
 - Scaling of 100 kW class applied-field MPD thrusters [AIAA PAPER 92-3462] p 74 A92-54033
 - Low-power arcjet test facility impacts [AIAA PAPER 92-3532] p 74 A92-54040
 - Small engine components test facility compressor testing cell at NASA Lewis Research Center [AIAA PAPER 92-3980] p 41 A92-56806
 - Advanced nozzle and engine components test facility [AIAA PAPER 92-3993] p 41 A92-56816
 - Engine component instrumentation development facility at NASA Lewis Research Center [AIAA PAPER 92-3995] p 41 A92-56818
 - Calibration of hemispherical-head flow angularity probes [AIAA PAPER 92-4005] p 200 A92-56828
 - Transonic turbine blade cascade testing facility [AIAA PAPER 92-4034] p 42 A92-56856
 - Description of the PMAD DC test bed architecture and integration sequence [NASA-TM-105284] p 77 N92-10055
 - Test facilities for high power electric propulsion [NASA-TM-105247] p 80 N92-11136
 - Description of Liquid Nitrogen Experimental Test Facility [NASA-TM-105215] p 134 N92-11208
 - Advanced nozzle and engine components test facility [NASA-TM-103684] p 42 N92-17059
 - Safety considerations in testing a fuel-rich aeropropulsion gas generator [NASA-TM-105258] p 30 N92-17061
 - Using silicon diodes for detecting the liquid-vapor interface in hydrogen [NASA-TM-105541] p 201 N92-18456
 - Engine component instrumentation development facility at NASA Lewis Research Center [NASA-TM-105644] p 42 N92-25449
 - Transonic turbine blade cascade testing facility [NASA-TM-105646] p 47 N92-26129
 - Design characteristics of a heat pipe test chamber [NASA-TM-105737] p 238 N92-29662
 - Small engine components test facility compressor testing cell at NASA Lewis Research Center [NASA-TM-105685] p 42 N92-30508
- Nuclear electric propulsion development and qualification facilities [NASA-TM-105521] p 91 N92-30818
- A free-piston Stirling engine/linear alternator controls and load interaction test facility [NASA-TM-105825] p 238 N92-31262
- TEST FIRING**
 - Cyclic hot firing results of tungsten-wire-reinforced, copper-lined thrust chambers [NASA-TM-4214] p 91 N92-31249
- TEST STANDS**
 - The development of test beds to support the definition and evolution of the Space Station Freedom power system p 46 A92-50656
 - Development of a full-scale transmission testing procedure to evaluate advanced lubricants [NASA-TP-3265] p 213 N92-30396
 - Overview and evolution of the LeRC PMAD DC Testbed [NASA-TM-105842] p 163 N92-32867
- TEST VEHICLES**
 - Fast oxygen atom facility for studies related to low earth orbit activities [AIAA PAPER 92-3974] p 47 A92-56800
- TESTS**
 - Liquid hydrogen mass flow through a multiple orifice Joule-Thomson device [AIAA PAPER 92-2881] p 176 A92-47862
 - Modelling and experimental verification of a water alleviation system for the NASP --- National Aerospace Plane [NASA-TM-105661] p 189 N92-23224
 - Liquid hydrogen mass flow through a multiple orifice Joule-Thomson device [NASA-TM-105583] p 189 N92-23268
- TETHERED SATELLITES**
 - Tether methods for reactionless orbital propulsion Theory of plasma contactor neutral gas emissions for electrodynamic tethers p 258 A92-41549
- TETHERLINES**
 - Systems analysis of electrodynamic tethers p 62 A92-41550
- TEXTURES**
 - Increased efficiency with surface texturing in ITO/InP solar cells p 232 A92-44548
- THALLIUM COMPOUNDS**
 - Crystalline orientations of Ti2Ba2Ca2Cu3O(x) grains on MgO, SrTiO3, and LaAlO3 substrates p 261 A92-41637
 - Electrical-transport properties and microwave device performance of sputtered TiCaBaCuO superconducting thin films p 263 A92-56599
- THEOREM PROVING**
 - Rational approximations from power series of vector-valued meromorphic functions [NASA-TM-105859] p 251 N92-33942
- THERMAL ANALYSIS**
 - Boundary formulations for shape sensitivity of temperature dependent conductivity problems p 217 A92-25403
 - A three-dimensional finite-element thermal/mechanical analytical technique for high-performance traveling wave tubes [AIAA PAPER 92-1824] p 154 A92-29771
 - Three-dimensional boundary element thermal shape sensitivity analysis p 176 A92-47269
 - Thermal analysis of a conceptual design for a 250 We GPHS/FPSE space power system p 69 A92-50637
 - Growth and characterization of lead bromide crystals p 138 A92-56956
 - Thermal modeling with solid/liquid phase change of the thermal energy storage experiment [NASA-TM-103770] p 185 N92-13402
 - Effects of a noncoplanar biphenyldiamine on the processing and properties of addition polyimides [NASA-TM-105383] p 107 N92-15137
- THERMAL BOUNDARY LAYER**
 - Transient pool boiling in microgravity p 170 A92-30494
 - Experimental study of boundary layer transition on a heated flat plate p 172 A92-36022
 - Scaling of low-Prandtl-number thermocapillary flows p 176 A92-47271
 - Modeling of the near-electrode regions of arcjets. I - Coupling of the flowfield to the non-equilibrium boundary layers [AIAA PAPER 92-3109] p 258 A92-48749
- THERMAL CONDUCTIVITY**
 - Boundary formulations for shape sensitivity of temperature dependent conductivity problems p 217 A92-25403
 - Role of interfacial carbon layer in the thermal diffusivity/conductivity of silicon carbide fiber-reinforced reaction-bonded silicon nitride matrix composites p 100 A92-25443

THERMAL CONTROL COATINGS

Role of interfacial thermal barrier in the transverse thermal conductivity of uniaxial SiC fiber-reinforced reaction bonded silicon nitride p 102 A92-39605
Thermal modelling of nickel-hydrogen battery cells operating under transient orbital conditions p 71 A92-50712

Thermal conductivity and thermal expansion of graphite fiber/copper matrix composites p 106 N92-14120 [NASA-TM-105233]

Towards the development of micromechanics equations for ceramic matrix composites via fiber substructuring [NASA-TM-105246] p 108 N92-19595

Composite overwrapped nickel-hydrogen pressure vessels p 109 N92-22762

Applications of high thermal conductivity composites to electronics and spacecraft thermal design [NASA-TM-102434] p 56 N92-24349

An overview of the Lewis Research Center CSTI thermal management program [NASA-TM-105310] p 92 N92-31916

Heat transfer device [NASA-CASE-LEW-14162-3] p 111 N92-34208

THERMAL CONTROL COATINGS

The effects of RF plasma ashing on zinc orthotitanate/potassium silicate thermal control coatings [AIAA PAPER 92-2171] p 124 A92-31299

Thermal barrier coating life and isothermal oxidation of low-pressure plasma-sprayed bond coat alloys p 119 A92-32398

Thermal response of various thermal barrier coatings in a high heat flux rocket engine p 119 A92-32399

Composite thermal barrier coating [NASA-CASE-LEW-14999-1] p 108 N92-21725

THERMAL CYCLING TESTS

Synergistic effects of ultraviolet radiation, thermal cycling and atomic oxygen on altered and coated Kapton surfaces [AIAA PAPER 92-0794] p 93 A92-27125

COSP - A computer model of cyclic oxidation p 114 A92-31849

Cyclic oxidation resistance of a reaction milled NiAl-AIN composite p 105 A92-46871

Thermal verification testing of commercial printed-circuit boards for spaceflight p 216 A92-56217

Thermal verification testing of commercial printed-circuit boards for spaceflight [NASA-TM-105261] p 141 N92-11221

Synergistic effects of ultraviolet radiation, thermal cycling, and atomic oxygen on altered and coated Kapton surfaces [NASA-TM-105363] p 96 N92-14114

Ceramics for engines p 131 N92-22517

Cyclic hot firing results of tungsten-wire-reinforced, copper-lined thrust chambers [NASA-TM-4214] p 91 N92-31249

Thermal degradation of a cellulosic paper p 113 A92-29488

Heat and mass transport from thermally degrading thin cellulosic materials in a microgravity environment p 174 A92-41810

Global kinetic constants for thermal oxidative degradation of a cellulosic paper p 113 A92-29488

Heat and mass transport from thermally degrading thin cellulosic materials in a microgravity environment p 174 A92-41810

Heat and mass transport from thermally degrading thin cellulosic materials in a microgravity environment p 174 A92-41810

Heat and mass transport from thermally degrading thin cellulosic materials in a microgravity environment p 174 A92-41810

Heat and mass transport from thermally degrading thin cellulosic materials in a microgravity environment p 174 A92-41810

Heat and mass transport from thermally degrading thin cellulosic materials in a microgravity environment p 174 A92-41810

Heat and mass transport from thermally degrading thin cellulosic materials in a microgravity environment p 174 A92-41810

Heat and mass transport from thermally degrading thin cellulosic materials in a microgravity environment p 174 A92-41810

Heat and mass transport from thermally degrading thin cellulosic materials in a microgravity environment p 174 A92-41810

Heat and mass transport from thermally degrading thin cellulosic materials in a microgravity environment p 174 A92-41810

Heat and mass transport from thermally degrading thin cellulosic materials in a microgravity environment p 174 A92-41810

Heat and mass transport from thermally degrading thin cellulosic materials in a microgravity environment p 174 A92-41810

Heat and mass transport from thermally degrading thin cellulosic materials in a microgravity environment p 174 A92-41810

Heat and mass transport from thermally degrading thin cellulosic materials in a microgravity environment p 174 A92-41810

Heat and mass transport from thermally degrading thin cellulosic materials in a microgravity environment p 174 A92-41810

Heat and mass transport from thermally degrading thin cellulosic materials in a microgravity environment p 174 A92-41810

Heat and mass transport from thermally degrading thin cellulosic materials in a microgravity environment p 174 A92-41810

Heat and mass transport from thermally degrading thin cellulosic materials in a microgravity environment p 174 A92-41810

Heat and mass transport from thermally degrading thin cellulosic materials in a microgravity environment p 174 A92-41810

Heat and mass transport from thermally degrading thin cellulosic materials in a microgravity environment p 174 A92-41810

Heat and mass transport from thermally degrading thin cellulosic materials in a microgravity environment p 174 A92-41810

Heat and mass transport from thermally degrading thin cellulosic materials in a microgravity environment p 174 A92-41810

Heat and mass transport from thermally degrading thin cellulosic materials in a microgravity environment p 174 A92-41810

Heat and mass transport from thermally degrading thin cellulosic materials in a microgravity environment p 174 A92-41810

Heat and mass transport from thermally degrading thin cellulosic materials in a microgravity environment p 174 A92-41810

THERMAL ENVIRONMENTS

Evaluation of an innovative high temperature ceramic wafer seal for hypersonic engine applications [NASA-TM-105556] p 208 N92-20815

THERMAL EXPANSION

Reduction of thermal residual stresses in advanced metallic composites based upon a compensating/compliant layer concept p 105 A92-47106

Reduction of thermal stresses in continuous fiber reinforced metal matrix composites with interface layers p 105 A92-50347

Thermal conductivity and thermal expansion of graphite fiber/copper matrix composites [NASA-TM-105233] p 106 N92-14120

Influence of engineered interfaces on residual stresses and mechanical response in metal matrix composites [NASA-TM-105438] p 109 N92-23195

Probabilistic assessment of space trusses subjected to combined mechanical and thermal loads [NASA-TM-105429] p 230 N92-33935

THERMAL FATIGUE

Isothermal fatigue behaviour of a (90 deg)8 SiC/Ti-15-3 composite at 426 C p 100 A92-23313

Combined bending and thermal fatigue of high-temperature metal-matrix composites - Computational simulation p 223 A92-43494

High-temperature fatigue behavior of a SiC/Ti-24Al-11Nb composite p 104 A92-44613

Thermomechanical and bithermal fatigue behavior of cast B1900 + Hf and wrought Haynes 188 p 122 A92-45233

Elevated temperature axial and torsional fatigue behavior of Haynes 188 [NASA-TM-105396] p 229 N92-28701

Thermal insulation of a flightweight liquid hydrogen tank - Effects of fill level at low wall heat flux [AIAA PAPER 92-0818] p 60 A92-29591

Self-pressurization of a flightweight liquid hydrogen tank: Effects of fill level at low wall heat flux [NASA-TM-105411] p 135 N92-18442

Thermal plasmas Modeling of the near-electrode regions of arcjets. I - Coupling of the flowfield to the non-equilibrium boundary layers [AIAA PAPER 92-3109] p 258 A92-48749

Thermal protection A review of candidate multilayer insulation systems for potential use on wet-launched LH2 tankage for the space exploration initiative lunar missions [NASA-TM-104493] p 134 N92-13336

Applications of high thermal conductivity composites to electronics and spacecraft thermal design [NASA-TM-102434] p 56 N92-24349

Thermal radiation Transient cooling of a square region of radiating medium p 164 A92-10432

Thermal resistance Measurements of the effects of thermal contact resistance on steady state heat transfer in phosphoric-acid fuel cell stack p 180 A92-50738

Thermal shock Novel applications for TAZ-8A p 123 N92-22444

Thermal stability High temperature thruster technology for spacecraft propulsion [IAF PAPER 91-254] p 58 A92-13155

Effect of fiber reinforcement on thermo-oxidative stability and mechanical properties of polymer matrix composites p 101 A92-33587

Ceramics and ceramic matrix composites - Aerospace potential and status [AIAA PAPER 92-2445] p 94 A92-34474

High molecular weight first generation PMR polyimides for 343 C applications p 105 A92-49819

New addition curing polyimides [NASA-TM-105335] p 95 N92-13281

High temperature thruster technology for spacecraft propulsion [NASA-TM-105348] p 82 N92-15125

High-temperature durability considerations for HSC2 combustor [NASA-TP-3162] p 129 N92-17070

High molecular weight first generation PMR polyimides for 343 C applications p 105 A92-49819

Structure-to-property relationships in addition cured polymers. 4: Correlations between thermo-oxidative weight losses of norbornenyl cured polyimide resins and their composites [NASA-TM-105553] p 108 N92-20039

Vinyl capped addition polyimides [NASA-CASE-LEW-15027-2] p 131 N92-24053

Liquid lubricants for advanced aircraft engines [NASA-TM-104531] p 133 N92-32863

Liquid lubricants for advanced aircraft engines [NASA-TM-104531] p 133 N92-32863

Liquid lubricants for advanced aircraft engines [NASA-TM-104531] p 133 N92-32863

Liquid lubricants for advanced aircraft engines [NASA-TM-104531] p 133 N92-32863

Liquid lubricants for advanced aircraft engines [NASA-TM-104531] p 133 N92-32863

Liquid lubricants for advanced aircraft engines [NASA-TM-104531] p 133 N92-32863

Liquid lubricants for advanced aircraft engines [NASA-TM-104531] p 133 N92-32863

Liquid lubricants for advanced aircraft engines [NASA-TM-104531] p 133 N92-32863

Liquid lubricants for advanced aircraft engines [NASA-TM-104531] p 133 N92-32863

Liquid lubricants for advanced aircraft engines [NASA-TM-104531] p 133 N92-32863

Liquid lubricants for advanced aircraft engines [NASA-TM-104531] p 133 N92-32863

Liquid lubricants for advanced aircraft engines [NASA-TM-104531] p 133 N92-32863

Liquid lubricants for advanced aircraft engines [NASA-TM-104531] p 133 N92-32863

Liquid lubricants for advanced aircraft engines [NASA-TM-104531] p 133 N92-32863

Liquid lubricants for advanced aircraft engines [NASA-TM-104531] p 133 N92-32863

Liquid lubricants for advanced aircraft engines [NASA-TM-104531] p 133 N92-32863

Liquid lubricants for advanced aircraft engines [NASA-TM-104531] p 133 N92-32863

Liquid lubricants for advanced aircraft engines [NASA-TM-104531] p 133 N92-32863

Liquid lubricants for advanced aircraft engines [NASA-TM-104531] p 133 N92-32863

Liquid lubricants for advanced aircraft engines [NASA-TM-104531] p 133 N92-32863

THERMAL STRESSES

Compressive strength of directionally solidified NiAl-NiAlNb intermetallics at 1200 and 1300 K p 117 A92-28248

Nonuniform thermal environmental effects on space truss structural reliability [AIAA PAPER 92-2352] p 54 A92-34325

Thermal stress analysis of a silicon carbide/aluminum composite p 222 A92-38097

Reduction of thermal residual stresses in advanced metallic composites based upon a compensating/compliant layer concept p 105 A92-47106

Reduction of thermal stresses in continuous fiber reinforced metal matrix composites with interface layers p 105 A92-50347

Turning up the heat on aircraft structures --- design and analysis for high-temperature conditions p 23 A92-55131

Thermally-driven microfracture in high temperature metal matrix composites [NASA-TM-105305] p 107 N92-15136

Solar dynamic modules for Space Station Freedom: The relationship between fine-pointing control and thermal loading of the aperture plate [NASA-TM-104498] p 84 N92-19780

Aeropropulsion structures - Influence of engineered interfaces on residual stresses and mechanical response in metal matrix composites [NASA-TM-105438] p 109 N92-23195

Effects of fiber and interfacial layer architectures on the thermoplastic response of metal matrix composites [NASA-TM-105802] p 110 N92-32234

Thermal vacuum tests Full-size solar dynamic heat receiver thermal-vacuum tests p 68 A92-50565

Thermal verification testing of commercial printed-circuit boards for spaceflight p 216 A92-56217

Thermal verification testing of commercial printed-circuit boards for spaceflight [NASA-TM-105261] p 141 N92-11221

Thermionic converters Heat transfer and core neutronics considerations of the heat pipe cooled thermionic reactor p 180 A92-50591

Thermionic emitters Study of a cesium plasma as a selective emitter for thermophotovoltaic applications p 258 A92-33667

Thermochemistry Thermochemical energy storage for a lunar base [NASA-TM-105333] p 236 N92-14485

Chemical vapor deposition modeling for high temperature materials [NASA-TM-105386] p 96 N92-18457

Metallized gelled monopropellants [NASA-TM-105418] p 87 N92-24557

Thermocouples Method of producing a plug-type heat flux gauge [NASA-CASE-LEW-14967-2] p 201 N92-22038

Thermodynamic cycles Monolithic ceramics p 125 A92-39854

Small engine technology programs p 32 N92-22532

Thermodynamic efficiency Preliminary investigation of a low power pulsed arcjet thruster [AIAA PAPER 92-3113] p 64 A92-48752

Thermodynamic equilibrium Critical fluid thermal equilibration experiment (19-IML-1) p 139 N92-23640

Thermodynamic properties COLD-SAT - A technology satellite for cryogenic experimentation p 52 A92-13425

Computer program for computing the properties of seventeen fluids --- cryogenic liquids p 241 A92-23849

A viscoplastic theory with thermodynamic considerations [ONERA, TP NO. 1991-220] p 217 A92-26372

A viscoplastic theory with thermodynamic considerations p 219 A92-33903

Theoretical nozzle performance of a microwave electrothermal thruster using experimental data [AIAA PAPER 92-3110] p 64 A92-48750

Slush hydrogen pressurized expulsion studies at the NASA K-Site Facility [AIAA PAPER 92-3385] p 141 A92-48951

Improved thermodynamic modeling of the no-vent fill process and correlation with experimental data [NASA-TM-104492] p 79 N92-11129

Slush hydrogen pressurized expulsion studies at the NASA K-Site Facility [NASA-TM-105597] p 135 N92-26131

Thermodynamics Thermomechanical testing of high-temperature composites - Thermomechanical fatigue (TMF) behavior of SiC(SCS-6)/Ti-15-3 p 104 A92-44606

Thermomechanical testing of high-temperature composites - Thermomechanical fatigue (TMF) behavior of SiC(SCS-6)/Ti-15-3 p 104 A92-44606

Thermomechanical testing of high-temperature composites - Thermomechanical fatigue (TMF) behavior of SiC(SCS-6)/Ti-15-3 p 104 A92-44606

Thermomechanical testing of high-temperature composites - Thermomechanical fatigue (TMF) behavior of SiC(SCS-6)/Ti-15-3 p 104 A92-44606

Thermomechanical testing of high-temperature composites - Thermomechanical fatigue (TMF) behavior of SiC(SCS-6)/Ti-15-3 p 104 A92-44606

Thermomechanical testing of high-temperature composites - Thermomechanical fatigue (TMF) behavior of SiC(SCS-6)/Ti-15-3 p 104 A92-44606

Thermomechanical testing of high-temperature composites - Thermomechanical fatigue (TMF) behavior of SiC(SCS-6)/Ti-15-3 p 104 A92-44606

Thermomechanical testing of high-temperature composites - Thermomechanical fatigue (TMF) behavior of SiC(SCS-6)/Ti-15-3 p 104 A92-44606

Thermomechanical testing of high-temperature composites - Thermomechanical fatigue (TMF) behavior of SiC(SCS-6)/Ti-15-3 p 104 A92-44606

Thermomechanical testing of high-temperature composites - Thermomechanical fatigue (TMF) behavior of SiC(SCS-6)/Ti-15-3 p 104 A92-44606

Thermomechanical testing of high-temperature composites - Thermomechanical fatigue (TMF) behavior of SiC(SCS-6)/Ti-15-3 p 104 A92-44606

Thermomechanical testing of high-temperature composites - Thermomechanical fatigue (TMF) behavior of SiC(SCS-6)/Ti-15-3 p 104 A92-44606

Thermomechanical testing of high-temperature composites - Thermomechanical fatigue (TMF) behavior of SiC(SCS-6)/Ti-15-3 p 104 A92-44606

Thermomechanical testing of high-temperature composites - Thermomechanical fatigue (TMF) behavior of SiC(SCS-6)/Ti-15-3 p 104 A92-44606

Thermomechanical testing of high-temperature composites - Thermomechanical fatigue (TMF) behavior of SiC(SCS-6)/Ti-15-3 p 104 A92-44606

Thermomechanical testing of high-temperature composites - Thermomechanical fatigue (TMF) behavior of SiC(SCS-6)/Ti-15-3 p 104 A92-44606

Thermomechanical testing of high-temperature composites - Thermomechanical fatigue (TMF) behavior of SiC(SCS-6)/Ti-15-3 p 104 A92-44606

Thermomechanical testing of high-temperature composites - Thermomechanical fatigue (TMF) behavior of SiC(SCS-6)/Ti-15-3 p 104 A92-44606

Thermomechanical testing of high-temperature composites - Thermomechanical fatigue (TMF) behavior of SiC(SCS-6)/Ti-15-3 p 104 A92-44606

Thermomechanical testing of high-temperature composites - Thermomechanical fatigue (TMF) behavior of SiC(SCS-6)/Ti-15-3 p 104 A92-44606

- Application of a thermal fatigue life prediction model to high-temperature aerospace alloys B1900 + Hf and Haynes 188 p 121 A92-45232
- Thermal modeling with solid/liquid phase change of the thermal energy storage experiment [NASA-TM-103770] p 185 N92-13402
- On the thermodynamic framework of generalized coupled thermoelastic-viscoplastic-damage modeling [NASA-TM-105349] p 225 N92-14434
- High temperature structural fibers: Status and needs [NASA-TM-105174] p 107 N92-16037
- Aircraft engine hot section technology: An overview of the HOST Project p 33 N92-22535
- Thermomechanical deformation behavior of a dynamic strain aging alloy, Hastelloy X [NASA-TM-105316] p 228 N92-25179
- Overview of NASA supported Stirling thermodynamic loss research [NASA-TM-105690] p 88 N92-27034
- THERMOELASTICITY**
- An unconditionally stable staggered algorithm for transient finite element analysis of coupled thermoelastic problems p 222 A92-37517
- THERMOELECTRIC GENERATORS**
- Space reactor power system programs overview [AIAA PAPER 92-1558] p 61 A92-38652
- Small Stirling dynamic isotope power system for multihundred-watt robotic missions [SAE PAPER 912066] p 62 A92-45448
- Preliminary design of a mobile lunar power supply p 233 A92-50635
- THERMOELECTRIC MATERIALS**
- The NASA CSTI High Capacity Power Program [NASA-TM-105240] p 236 N92-16481
- THERMOELECTRIC POWER GENERATION**
- High efficiency thermal to electric energy conversion using selective emitters and spectrally tuned solar cells [NASA-TM-105755] p 238 N92-30426
- THERMOMECHANICAL TREATMENT**
- Hardening mechanisms in a dynamic strain aging alloy, Hastelloy X, during isothermal and thermomechanical cyclic deformation p 116 A92-24832
- THERMONUCLEAR POWER GENERATION**
- Numerical study of low pressure nuclear thermal rockets [AIAA PAPER 92-3815] p 75 A92-54182
- THERMOPHYSICAL PROPERTIES**
- Effect of temperature on the formation of creep substructure in sodium chloride single crystals p 260 A92-25444
- Effects of g-jitter and cross-diffusion on the onset of convection in doubly diffusive systems [AIAA PAPER 92-0246] p 167 A92-25705
- Thermophysical properties of lysozyme (protein) solutions p 240 A92-44385
- Effects of coolant parameters on steady state temperature distribution in phosphoric-acid fuel cell electrode p 233 A92-50737
- THERMOPLASTICITY**
- Effects of fiber and interfacial layer architectures on the thermoplastic response of metal matrix composites [NASA-TM-105802] p 110 N92-32234
- THERMOSETTING RESINS**
- Addition curing thermosets endcapped with 4-amino (2,2) paracyclophane p 124 A92-33918
- THICK FILMS**
- High-T sub c fluorine-doped YBa₂Cu₃O(y) films on ceramic substrates by screen printing [NASA-TM-105296] p 127 N92-11188
- THIN FILMS**
- Space applications of high temperature superconductivity technology [IAF PAPER 91-307] p 259 A92-14724
- Microwave properties of YBa₂Cu₃O(7-delta) high-transition-temperature superconducting thin films measured by the power transmission method p 153 A92-14938
- Atomic oxygen effects on thin film space coatings studied by spectroscopic ellipsometry, atomic force microscopy, and laser light scattering [AIAA PAPER 92-2172] p 94 A92-31300
- Study of temperature-dependent ultrathin oxide growth on Si(111) using variable-angle spectroscopic ellipsometry p 260 A92-32414
- Properties of large area ErBa₂Cu₃O(7-x) thin films deposited by ionized cluster beams p 260 A92-33911
- Performance of a K-band superconducting annular ring antenna p 146 A92-37067
- Structural scaling approximations for solar arrays p 231 A92-40935
- Mechanical properties of 3C silicon carbide p 126 A92-43761
- Optical dispersion relations for 'diamondlike' carbon films p 262 A92-44533
- Applications of thin-film photovoltaics for space p 70 A92-50641
- Solid lubricants on pretreated surfaces [NASA-CASE-LEW-14474-2] p 127 N92-11186
- Thin-film photovoltaics: Status and applications to space power p 81 N92-13228
- Thin film, concentrator, and multijunction space solar cells: Status and potential p 81 N92-13230
- Stable localized patterns in thin liquid films [NASA-TM-105352] p 185 N92-14322
- A vacuum (10(exp -9) Torr) friction apparatus for determining friction and endurance life of MoSx films [NASA-TM-104478] p 129 N92-16129
- Microwave conductivity of laser ablated YBa₂Cu₃O(7-delta) superconducting films and its relation to microstrip transmission line performance p 264 N92-21639
- Research sensors p 202 N92-22526
- An XPS study of the stability of Fomblin Z25 on the native oxide of aluminum --- x ray photoelectron spectroscopy [NASA-TM-105594] p 131 N92-23185
- Environmental effects on friction and wear of diamond and diamondlike carbon coatings [NASA-TM-105634] p 131 N92-23192
- Deposition of adherent Ag-Ti duplex films on ceramics in a multiple-cathode sputter deposition system [NASA-TM-105586] p 34 N92-23225
- Microwave response of high transition temperature superconducting thin films p 264 N92-23413
- Properties of large area ErBa₂Cu₃O(7-x) thin films deposited by ionized cluster beams p 264 N92-23414
- Dependence of the critical temperature of laser-ablated YBa₂Cu₃O(7-delta) thin films on LaAlO₃ substrate growth technique p 264 N92-23415
- NASA programs in space photovoltaics [NASA-TM-105428] p 87 N92-25343
- High efficiency thermal to electric energy conversion using selective emitters and spectrally tuned solar cells [NASA-TM-105755] p 238 N92-30426
- Fast methods to numerically integrate the Reynolds equation for gas fluid films [NASA-TM-105415] p 214 N92-30722
- Effect of out-of-roundness on the performance of a diesel engine connecting-rod bearing [NASA-TM-105600] p 215 N92-31536
- Magnetic penetration depth of YBa₂Cu₃O(7-delta) thin films determined by the power transmission method p 265 N92-32983
- Magnetic flux relaxation in YBa₂Cu₃O(7-x) thin film: Thermal or athermal p 265 N92-32984
- THIN PLATES**
- Vibration transmission through rolling element bearings. IV - Statistical energy analysis p 218 A92-28756
- Minimization of the vibration energy of thin-plate structure [NASA-TM-105654] p 211 N92-25448
- THIN WALLED SHELLS**
- Damage and fracture in composite thin shells p 224 A92-51550
- Damage and fracture in composite thin shells [NASA-TM-105289] p 106 N92-13284
- THREE DIMENSIONAL BODIES**
- Three-dimensional boundary element thermal shape sensitivity analysis p 176 A92-47269
- Three-dimensional laser window formation [NASA-RP-1280] p 47 N92-30307
- THREE DIMENSIONAL BOUNDARY LAYER**
- The three-dimensional turbulent boundary layer near a plane of symmetry p 167 A92-24757
- A study of three dimensional turbulent boundary layer separation and vortex flow control using the reduced Navier Stokes equations p 9 A92-40105
- THREE DIMENSIONAL COMPOSITES**
- Multidisciplinary tailoring of hot composite structures [AIAA PAPER 92-2563] p 220 A92-34564
- Damage mechanisms in three-dimensional woven reinforced ceramic matrix composites under tensile and flexural loading at room and elevated temperatures [AIAA PAPER 92-2492] p 101 A92-34584
- Failure mechanisms of 3-D woven SiC/SiC composites under tensile and flexural loading at room and elevated temperatures p 103 A92-39642
- THREE DIMENSIONAL FLOW**
- Deterministic blade row interactions in a centrifugal compressor stage [ASME PAPER 91-GT-273] p 3 A92-15670
- Studies of the effects of curvature on dilution jet mixing p 166 A92-21079
- Aerodynamics of loaded cascades in subsonic flows subject to unsteady three-dimensional vortical disturbances [AIAA PAPER 92-0146] p 4 A92-23762
- Low-to-high altitude predictions of three-dimensional ablative reentry flowfields [AIAA PAPER 92-0366] p 168 A92-26227
- An unsteady Euler scheme for the analysis of ducted propellers [AIAA PAPER 92-0522] p 6 A92-26947
- Aeroelastic analysis of advanced propellers using an efficient Euler solver [AIAA PAPER 92-0488] p 7 A92-28194
- On the nonlinear development of three-dimensional instability waves in natural transition [AIAA PAPER 92-0741] p 170 A92-28222
- Three-dimensional viscous analysis of a Mach 5 inlet and comparison with experimental data p 8 A92-28526
- A numerical and experimental study of three-dimensional liquid sloshing in a rotating spherical container [AIAA PAPER 92-0829] p 170 A92-29597
- An improved PNS scheme for predicting complex three-dimensional hypersonic flows [AIAA PAPER 92-0753] p 8 A92-31679
- Effects of g-jitter on a thermally buoyant flow p 171 A92-32258
- An experimental study of oscillatory thermocapillary convection in cylindrical containers p 172 A92-36184
- Renormalization group based algebraic turbulence model for three-dimensional turbomachinery flows p 9 A92-41268
- Investigation of three-dimensional flow field in a turbine including rotor/stator interaction. I - Design development and performance of the research facility [AIAA PAPER 92-3325] p 40 A92-48908
- Investigation of three-dimensional flow field in a turbine including rotor/stator interaction. II - Three-dimensional flow field at the exit of the nozzle [AIAA PAPER 92-3326] p 12 A92-48909
- Kinetic theory model for the flow of a simple gas from a three-dimensional axisymmetric nozzle p 12 A92-52730
- Navier-Stokes analysis of three-dimensional unsteady flows inside turbine stages [AIAA PAPER 92-3211] p 13 A92-54016
- Multigrad calculation of three-dimensional viscous cascade flows [NASA-TM-105257] p 249 N92-10345
- Viscous three-dimensional calculations of transonic fan performance [NASA-TM-103800] p 1 N92-17346
- High-speed inlet research program and supporting analysis p 188 N92-22542
- Advances in engineering turbulence modeling --- computational fluid dynamics p 193 N92-25820
- Implementation of a kappa-epsilon turbulence model to RPLUS3D code p 194 N92-25822
- A critical evaluation of a three-dimensional Navier-Stokes method as a tool to calculate transonic flows inside a low-aspect-ratio compressor p 195 N92-27459
- Viscous three-dimensional calculations of transonic fan performance p 195 N92-27467
- Numerical solution of a three-dimensional cubic cavity flow by using the Boltzmann equation [NASA-TM-105693] p 195 N92-30297
- A critical evaluation of a three-dimensional Navier-Stokes CFD as a tool to design supersonic turbine stages p 196 N92-32268
- Three-dimensional flow fields inside a shrouded inducer at design and off-design conditions (CFD study) p 196 N92-32291
- THREE DIMENSIONAL MODELS**
- Studies of the effects of curvature on dilution jet mixing p 166 A92-21079
- Comparison of two-dimensional and three-dimensional droplet trajectory calculations in the vicinity of finite wings [AIAA PAPER 92-0645] p 8 A92-28215
- A three-dimensional finite-element thermal/mechanical analytical technique for high-performance traveling wave tubes [AIAA PAPER 92-1824] p 154 A92-29771
- A numerical classical flutter analysis of advanced propellers [AIAA PAPER 92-2118] p 26 A92-35687
- Three-dimensional Navier-Stokes heat transfer predictions for turbine blade rows [AIAA PAPER 92-3068] p 12 A92-54003
- Performance comparison of axisymmetric and three-dimensional hydrogen film coolant injection in a 110 N hydrogen/oxygen rocket [AIAA PAPER 92-3390] p 73 A92-54027
- Modal simulation of gearbox vibration with experimental correlation [AIAA PAPER 92-3494] p 207 A92-54036
- Grid generation for 3D turbomachinery configurations [AIAA PAPER 92-3671] p 243 A92-54114
- Comparisons of cylindrical and rectangular media radiative transfer solutions using the S-N discrete ordinates method [AIAA PAPER 92-2894] p 266 A92-54287

THRUST

- A method for determining spiral-bevel gear tooth geometry for finite element analysis
[NASA-TP-3096] p 207 N92-10195
- Comparison of two-dimensional and three-dimensional droplet trajectory calculations in the vicinity of finite wings
[NASA-TM-105617] p 188 N92-23154
- Coupled multi-disciplinary simulation of composite engine structures in propulsion environment
[NASA-TM-105575] p 228 N92-23267
- TCGRID: A three dimensional C-grid generator for turbomachinery p 35 N92-25716
- The Proteus Navier-Stokes code --- two and three dimensional computational fluid dynamics p 192 N92-25811
- A critical evaluation of a three-dimensional Navier-Stokes method as a tool to calculate transonic flows inside a low-aspect-ratio compressor p 195 N92-27459
- Modal simulation of gearbox vibration with experimental correlation
[NASA-TM-105702] p 215 N92-31485
- THRUST**
- Preliminary dynamic tests of a flight-type ejector
[AIAA PAPER 92-3261] p 27 A92-54020
- Anode power deposition in applied-field MPD thrusters
[AIAA PAPER 92-3463] p 74 A92-54034
- Introduction to the internal fluid mechanics research session p 188 N92-22522
- Preliminary dynamic tests of a flight-type ejector
[NASA-TM-105814] p 38 N92-30998
- Krypton ion thruster performance
[NASA-TM-105818] p 92 N92-31901
- THRUST AUGMENTATION**
- Use of an approximate similarity principle for the thermal scaling of a full-scale thrust augmenting ejector
[AIAA PAPER 92-3792] p 28 A92-54171
- Use of an approximate similarity principle for the thermal scaling of a full-scale thrust augmenting ejector
[NASA-TM-105724] p 36 N92-26613
- THRUST CHAMBER PRESSURE**
- An experimental investigation of high-aspect-ratio cooling passages p 64 A92-48780
- [AIAA PAPER 92-3154]
- An experimental investigation of high-aspect-ratio cooling passages p 48 N92-25958
- [NASA-TM-105679]
- THRUST CHAMBERS**
- Diffusion mechanisms in chemical vapor-deposited iridium coated on chemical vapor-deposited rhenium p 117 A92-28017
- Viscoplastic analysis of an experimental cylindrical thrust chamber liner p 218 A92-28052
- Advanced tube-bundle rocket thrust chambers p 62 A92-44509
- An experimental investigation of high-aspect-ratio cooling passages p 64 A92-48780
- [AIAA PAPER 92-3154]
- Advanced liquid rockets p 87 N92-24560
- [NASA-TM-105633]
- An experimental investigation of high-aspect-ratio cooling passages p 48 N92-25958
- [NASA-TM-105679]
- Cyclic hot firing results of tungsten-wire-reinforced, copper-lined thrust chambers p 91 N92-31249
- [NASA-TM-4214]
- Demonstrated survivability of a high temperature optical fiber cable on a 1500 pound thrust rocket chamber
[NASA-TM-105835] p 136 N92-32230
- THRUST CONTROL**
- Pulsed thrust propellant reorientation - Concept and modeling p 62 A92-44507
- THRUST VECTOR CONTROL**
- Flywheel energy storage for electromechanical actuation systems p 233 A92-50758
- An electromechanical actuation system for an expendable launch vehicle
[NASA-TM-105774] p 48 N92-30310
- THRUST-WEIGHT RATIO**
- An improved heat transfer configuration for a solid-core nuclear thermal rocket engine
[AIAA PAPER 92-3583] p 75 A92-54063
- THRUSTORS**
- High temperature thruster technology for spacecraft propulsion p 58 A92-13155
- [IAF PAPER 91-254]
- Laser-induced fluorescence of atomic hydrogen in an arcjet thruster p 60 A92-27045
- [AIAA PAPER 92-0678]
- The evolutionary development of high specific impulse electric thruster technology p 61 A92-38650
- [AIAA PAPER 92-1556]
- Systems analysis of electrodynamic tethers p 62 A92-41550
- Scaling of 100 kW class applied-field MPD thrusters
[AIAA PAPER 92-3462] p 74 A92-54033

- Preliminary investigation of power flow and electrode phenomena in a multi-megawatt coaxial plasma thruster
[AIAA PAPER 92-3741] p 75 A92-54144
- An experimental study of impingement-ion-production mechanisms p 76 A92-54190
- [AIAA PAPER 92-3826]
- High temperature thruster technology for spacecraft propulsion p 82 N92-15125
- [NASA-TM-105348]
- Preliminary test results of a hollow cathode MPD thruster p 84 N92-18474
- [NASA-TM-105324]
- The evolutionary development of high specific impulse electric thruster technology p 92 N92-31342
- [NASA-TM-105712]
- THYRISTORS**
- Neutron, gamma ray, and temperature effects on the electrical characteristics of thyristors p 162 N92-28432
- [NASA-TM-105728]
- TILT ROTOR AIRCRAFT**
- Summary highlights of the Advanced Rotorcraft Transmission (ART) program p 23 A92-54026
- [AIAA PAPER 92-3362]
- TIME DEPENDENCE**
- Central difference TVD and TVB schemes for time dependent and steady state problems p 166 A92-22168
- [AIAA PAPER 92-0053]
- First-passage problems: A probabilistic dynamic analysis for degraded structures p 225 N92-11373
- [NASA-TM-103755]
- Central difference TVD and TVB schemes for time dependent and steady state problems p 249 N92-15663
- [NASA-TM-105357]
- Turbomachinery p 32 N92-22524
- An efficient and robust algorithm for time dependent viscous incompressible Navier-Stokes equations p 193 N92-25819
- TIME DIVISION MULTIPLE ACCESS**
- ACTS T1-VSAT - The intelligent earth station p 145 A92-29952
- [AIAA PAPER 92-2037]
- Network architectures and protocols for the integration of ACTS and ISDN p 145 A92-29953
- [AIAA PAPER 92-2039]
- The Link Evaluation Terminal for the Advanced Communications Technology Satellite Experiments Program p 49 A92-29954
- [AIAA PAPER 92-2040]
- Advanced Communication Technology Satellite (ACTS) baseband processor development p 50 A92-53693
- The link evaluation terminal for the advanced communications technology satellite experiments program p 51 N92-16008
- [NASA-TM-105367]
- TIME DIVISION MULTIPLEXING**
- Destination directed packet switch architecture for a 30/20 GHz FDMA/TDM geostationary communication satellite network p 148 N92-14204
- Multichannel demultiplexer/demodulator technologies for future satellite communication systems p 51 N92-18342
- [NASA-TM-105377]
- Destination-directed, packet-switching architecture for 30/20-GHz FDMA/TDM geostationary communications satellite network p 51 N92-19762
- [NASA-TP-3201]
- TIME MARCHING**
- Cascade flutter analysis with transient response aerodynamics p 217 A92-15972
- Analysis of an advanced ducted propeller subsonic inlet p 5 A92-25728
- [AIAA PAPER 92-0274]
- Three-dimensional calculations of supersonic reacting flows using an LU scheme p 179 A92-50465
- Analysis of an advanced ducted propeller subsonic inlet p 15 N92-14002
- [NASA-TM-105393]
- ULTRA-SHARP solution of the Smith-Hutton problem p 187 N92-22226
- [NASA-TM-105435]
- TIN ALLOYS**
- Growth-speed dependence of primary arm spacings in directionally solidified Pb-10 wt pct Sn p 117 A92-26526
- TIP SPEED**
- Detailed noise measurements on the SR-7A propeller: Tone behavior with helical tip Mach number p 255 N92-16705
- [NASA-TM-105206]
- Model rotor icing tests in the NASA, Lewis Icing Research Tunnel p 21 N92-21688
- Overview of NASA PTA proplan flight test program p 33 N92-22536
- TITANATES**
- The effects of RF plasma ashing on zinc orthotitanate/potassium silicate thermal control coatings
[AIAA PAPER 92-2171] p 124 A92-31299

TITANIUM

- Preliminary evaluation of adhesion strength measurement devices for ceramic/titanium matrix composite bonds p 1 N92-31267
- [NASA-TM-105803]
- TITANIUM ALLOYS**
- The effect of matrix mechanical properties on (0)8 unidirectional SiC/Ti composite fatigue resistance p 99 A92-16220
- Isothermal fatigue behaviour of a (90 deg)8 SiC/Ti-15-3 composite at 426 C p 100 A92-23313
- Compression, bend, and tension studies on forged Al67Ti25Cr8 and Al66Ti25Mn9(L)2 compounds p 118 A92-30766
- Compression studies on particulate composites of ternary Al-Ti-Fe, and quaternary Al-Ti-Fe-Nb and Al-Ti-Fe-Mn L1(2) compounds p 119 A92-30845
- Tribological properties of ceramic-(Ti3Al-Nb) sliding couples for use as candidate seal materials to 700 C p 124 A92-32407
- Computational simulation of high temperature metal matrix composite behavior p 101 A92-32753
- Effect of fiber strength on the room temperature tensile properties of SiC/Ti-24Al-11Nb p 102 A92-36389
- Interdiffusion between the L1(2) trialuminides Al66Ti25Mn9 and Al67Ti25Cr8 p 120 A92-37088
- Tensile behavior of the L1(2) compound Al67Ti25Cr8 p 122 A92-49694
- Oxidation resistant coating for titanium alloys and titanium alloy matrix composites p 133 N92-29090
- [NASA-CASE-LEW-15155-1]
- Computational simulation of matrix micro-slip bands in SiC/Ti-15 composite p 111 N92-32466
- [NASA-TM-105762]
- TITANIUM BORIDES**
- Compression studies on particulate composites of ternary Al-Ti-Fe, and quaternary Al-Ti-Fe-Nb and Al-Ti-Fe-Mn L1(2) compounds p 119 A92-30845
- Combustion synthesis of TiB2-Al2O3-Al composite materials p 102 A92-36391
- TITANIUM CARBIDES**
- Combustion synthesis of ceramic-metal composite materials - The TiC-Al2O3-Al system p 115 A92-55139
- TITANIUM COMPOUNDS**
- METCAN updates for high temperature composite behavior - Simulation/verification p 98 A92-10264
- Mechanical properties of monolithic and particulate composites of L12 forms of Al3Ti p 101 A92-36273
- Oxidation kinetics of cast TiAl3 p 121 A92-38993
- TOLLIEN-SCHLICHTING WAVES**
- On the nonlinear development of three-dimensional instability waves in natural transition p 170 A92-28222
- [AIAA PAPER 92-0741]
- TOOLS**
- Adjustable depth gage p 201 N92-21723
- [NASA-CASE-LEW-14880-1]
- TOPOGRAPHY**
- Universal aspects of adhesion and atomic force microscopy p 260 A92-17979
- TORQUE**
- Dynamics of a split torque helicopter transmission
[NASA-TM-105681] p 213 N92-29136
- TORQUE MOTORS**
- A 23:2:1 ratio, 300-watt, 26 N-m output torque, planetary roller-gear robotic transmission: Design and evaluation p 210 N92-25085
- TORSION**
- NIST torsion oscillator viscometer response: Performance on the LeRC active vibration isolation platform p 209 N92-23564
- [NASA-TM-105571]
- Elevated temperature axial and torsional fatigue behavior of Haynes 188 p 229 N92-28701
- [NASA-TM-105396]
- TRACE ELEMENTS**
- Measurement of trace stratospheric constituents with a balloon borne laser radar p 239 N92-14500
- TRACKING (POSITION)**
- Pointing and tracking control for freedom's Solar Dynamic modules and vibration control of freedom
[AAS PAPER 91-459] p 54 A92-43284
- Color image processing and object tracking workstation p 139 N92-26611
- [NASA-TM-105561]
- TRADEOFFS**
- Characteristics of a future aeronautical satellite communications system p 22 A92-29889
- [AIAA PAPER 92-2058]
- Benefits and technology readiness for using cryogenic instead of storable propellants for return mission from Moon p 136 N92-33343
- TRAINING EVALUATION**
- Plotted evaluation of an integrated propulsion and flight control simulator p 23 A92-52459
- [AIAA PAPER 92-4178]

- TRAJECTORY CONTROL**
Reaction-compensation technology for microgravity laboratory robots p 203 A92-23719
- TRAJECTORY MEASUREMENT**
Comparison of two-dimensional and three-dimensional droplet trajectory calculations in the vicinity of finite wings [AIAA PAPER 92-0645] p 8 A92-28215
Comparison of two-dimensional and three-dimensional droplet trajectory calculations in the vicinity of finite wings [NASA-TM-105617] p 188 N92-23154
- TRAJECTORY OPTIMIZATION**
Discrete approximations to optimal trajectories using direct transcription and nonlinear programming p 44 A92-46753
Canonical transformations for space trajectory optimization [AIAA PAPER 92-4509] p 44 A92-52079
- TRANSFER FUNCTIONS**
Microgravity acceleration measurement and environment characterization science (I7-IML-1) p 139 N92-23642
- TRANSFER ORBITS**
Simple proof of the global optimality of the Hohmann transfer p 44 A92-46760
- TRANSFERRING**
Slush hydrogen transfer studies at the NASA K-Site Test Facility [NASA-TM-105596] p 135 N92-25957
- TRANSFORMATIONS (MATHEMATICS)**
Design of multi-layer neural networks for accurate identification of nonlinear mappings p 246 A92-29030
- TRANSFORMERS**
Comparison of high temperature, high frequency core loss and dynamic B-H loops of a 2V-49Fe-49Co and a grain oriented 3Si-Fe alloy [NASA-TM-105791] p 162 N92-30397
- TRANSIENT HEATING**
Finite difference solution for transient cooling of a radiating-conducting semitransparent layer p 166 A92-20310
Transient pool boiling in microgravity p 170 A92-30494
A variable multi-step method for transient heat conduction p 173 A92-37518
- TRANSIENT RESPONSE**
An unconditionally stable staggered algorithm for transient finite element analysis of coupled thermoelastic problems p 222 A92-37517
Preliminary dynamic tests of a flight-type ejector [AIAA PAPER 92-3261] p 27 A92-54020
Electromechanical systems with transient high power response operating from a resonant AC link [NASA-TM-105716] p 37 N92-28985
Preliminary dynamic tests of a flight-type ejector [NASA-TM-105814] p 38 N92-30998
A free-piston Stirling engine/linear alternator controls and load interaction test facility [NASA-TM-105825] p 238 N92-31262
- TRANSISTOR AMPLIFIERS**
C-band superconductor/semiconductor hybrid field-effect transistor amplifier on a LaAlO₃ substrate [NASA-TM-105828] p 163 N92-34204
- TRANSITION FLOW**
Modeling of the heat transfer in bypass transitional boundary-layer flows [NASA-TP-3170] p 184 N92-11299
A kappa-epsilon calculation of transitional boundary layers [NASA-TM-105604] p 187 N92-22398
- TRANSITION TEMPERATURE**
The effect of strain rate and temperature on the tensile properties of NiAl p 117 A92-28113
Flow and fracture behavior of NiAl in relation to the brittle-to-ductile transition temperature p 118 A92-30781
Microwave response of high transition temperature superconducting thin films p 264 N92-23413
Properties of large area ErBa₂Cu₃O_{7-x} thin films deposited by ionized cluster beams p 264 N92-23414
- TRANSMISSION EFFICIENCY**
Least Reliable Bits Coding (LRBC) for high data rate satellite communications [NASA-TM-105431] p 150 N92-18921
Microwave beam power transmission at an arbitrary range [NASA-TM-105424] p 150 N92-19992
- TRANSMISSION LINES**
Coaxial line configuration for microwave power transmission study of YBa₂Cu₃O_{7-delta} thin films p 154 A92-18455
Mutual coupling between rectangular microstrip patch antennas p 159 A92-52423
- TRANSMISSIONS (MACHINE ELEMENTS)**
Transmission overhaul and component replacement predictions using Weibull and renewal theory p 215 A92-17201
Recent manufacturing advances for spiral bevel gears [SAE PAPER 912229] p 204 A92-40024
Advanced Rotorcraft Transmission program summary [AIAA PAPER 92-3363] p 205 A92-48936
Boeing Helicopters Advanced Rotorcraft Transmission (ART) Program summary of component tests [AIAA PAPER 92-3364] p 205 A92-48937
Advanced Rotorcraft Transmission (ART) Program summary [AIAA PAPER 92-3365] p 205 A92-48938
Advanced Rotorcraft Transmission (ART) - Component test results [AIAA PAPER 92-3366] p 205 A92-48939
Separation distance and static transmission error of involute spur gears [AIAA PAPER 92-3490] p 205 A92-49027
Maximum life spiral bevel reduction design [AIAA PAPER 92-3493] p 205 A92-49030
Summary highlights of the Advanced Rotorcraft Transmission (ART) program [AIAA PAPER 92-3362] p 23 A92-54026
Modal simulation of gearbox vibration with experimental correlation [AIAA PAPER 92-3494] p 207 A92-54036
Rotorcraft transmissions p 33 N92-22533
Advanced Rotorcraft Transmission (ART) program summary [NASA-TM-105665] p 210 N92-24984
A 23.2:1 ratio, 300-watt, 26 N-m output torque, planetary roller-gear robotic transmission: Design and evaluation p 210 N92-25085
Comparison of analysis and experiment for gearbox noise [NASA-TM-105330] p 210 N92-25396
Gear tooth stress measurements of two helicopter planetary stages [NASA-TM-105651] p 211 N92-26555
Full-scale transmission testing to evaluate advanced lubricants [NASA-TM-105668] p 212 N92-26560
Analysis and modification of a single-mesh gear fatigue rig for use in diagnostic studies [NASA-TM-105416] p 212 N92-27879
Application of face-gear drives in helicopter transmissions [NASA-TM-105655] p 212 N92-28434
Dynamics of a split torque helicopter transmission [NASA-TM-105681] p 213 N92-29136
Development of a full-scale transmission testing procedure to evaluate advanced lubricants [NASA-TP-3265] p 213 N92-30396
Experimental testing of prototype face gears for helicopter transmissions [NASA-TM-105434] p 214 N92-31349
Modal simulation of gearbox vibration with experimental correlation [NASA-TM-105702] p 215 N92-31485
- TRANSMITTER RECEIVERS**
GTEX: An expert system for diagnosing faults in satellite ground stations p 148 N92-14215
FIDEX: An expert system for satellite diagnostics p 148 N92-14218
- TRANSMITTERS**
Flexible digital modulation and coding synthesis for satellite communications p 148 N92-14235
- TRANSONIC COMPRESSORS**
A viscous flow study of shock-boundary layer interaction, radial transport, and wake development in a transonic compressor [ASME PAPER 91-GT-69] p 2 A92-15539
A critical evaluation of a three-dimensional Navier-Stokes method as a tool to calculate transonic flows inside a low-aspect-ratio compressor p 195 N92-27459
- TRANSONIC FLOW**
Euler flow predictions for an oscillating cascade using a high resolution wave-split scheme [ASME PAPER 91-GT-198] p 3 A92-15623
The Baldwin-Lomax model for separated and wake flows using the entropy envelope concept [AIAA PAPER 92-0148] p 4 A92-23764
Navier-Stokes solution of transonic cascade flows using nonperiodic C-type grids p 8 A92-28523
Unsteady transonic Euler solutions using finite elements [AIAA PAPER 92-2504] p 8 A92-34499
Finite element Euler calculations of unsteady transonic cascade flows [AIAA PAPER 92-2120] p 9 A92-35689
Experiments and analysis concerning the use of external burning to reduce aerospace vehicle transonic drag [NASA-TM-105397] p 30 N92-17546
- Development of new flux splitting schemes ... computational fluid dynamics algorithms p 192 N92-25809
A critical evaluation of a three-dimensional Navier-Stokes method as a tool to calculate transonic flows inside a low-aspect-ratio compressor p 195 N92-27459
- TRANSONIC FLUTTER**
Finite element Euler calculations of unsteady transonic cascade flows [AIAA PAPER 92-2120] p 9 A92-35689
- TRANSONIC WIND TUNNELS**
Transonic turbine blade cascade testing facility [AIAA PAPER 92-4034] p 42 A92-56856
Transonic turbine blade cascade testing facility [NASA-TM-105646] p 47 N92-26129
- TRANSPARENCE**
Effect of index of refraction on radiation characteristics in a heated absorbing, emitting, and scattering layer p 181 A92-53031
- TRANSPONDERS**
FIDEX: An expert system for satellite diagnostics p 148 N92-14218
- TRANSPORT AIRCRAFT**
Applied analytical combustion/emissions research at the NASA Lewis Research Center - A progress report [AIAA PAPER 92-3338] p 27 A92-54025
Effects of turbine cooling assumptions on performance and sizing of high-speed civil transport [NASA-TM-105610] p 34 N92-23537
Applied analytical combustion/emissions research at the NASA Lewis Research Center [NASA-TM-105731] p 90 N92-29343
- TRANSPORT PROPERTIES**
High-field transport properties of InAs(x)P(1-x)/InP (x = 0.3-1.0) modulation doped heterostructures at 300 and 77 K p 262 A92-46331
Electrical-transport properties and microwave device performance of sputtered TiCaBaCuO superconducting thin films p 263 A92-56599
Thermal and solutal convection with conduction effects inside a rectangular enclosure [NASA-TM-105371] p 186 N92-15358
Reduced mobility and PPC in In_{0.20}Ga_{0.80}As / Al_{0.23}Ga_{0.77}As HEMT structure p 265 N92-32976
- TRANSPORT THEORY**
Reactive collision terms for fluid transport theory p 257 A92-22693
- TRANSPUTERS**
Parallel computation of aerodynamic influence coefficients for aeroelastic analysis on a transputer network p 241 A92-12367
- TRANSVERSE WAVES**
Detonation duct gas generator demonstration program [AIAA PAPER 92-3174] p 27 A92-54011
- TRAVELING WAVE AMPLIFIERS**
A low-power, high-efficiency Ka-band TWTA p 156 A92-38163
- TRAVELING WAVE TUBES**
A low-power, high-efficiency Ka-band TWTA [AIAA PAPER 92-1822] p 154 A92-29769
A three-dimensional finite-element thermal/mechanical analytical technique for high-performance traveling wave tubes [AIAA PAPER 92-1824] p 154 A92-29771
A low-power, high-efficiency Ka-band TWTA p 156 A92-38163
- TRAVELING WAVES**
Propagating confined states in phase dynamics p 181 A92-50968
- TRELLIS CODING**
Flexible digital modulation and coding synthesis for satellite communications p 148 N92-14235
- TRIANGULATION**
Two-dimensional unstructured triangular grid generation p 192 N92-25721
- TRIBOLOGY**
The application of a computer data acquisition system to a new high temperature tribometer p 93 A92-11823
Tribological properties of ceramic-(Ti₃Al-Nb) sliding couples for use as candidate seal materials to 700 C p 124 A92-32407
Studies of mechanochemical interactions in the tribological behavior of materials p 124 A92-32410
Tribological and mechanical comparison of sintered and HIPped PM212: High temperature self-lubricating composites [NASA-TM-105379] p 96 N92-15128
Tribology needs for future space and aeronautical systems [NASA-TM-104525] p 128 N92-15191
A vacuum (10(exp -9) Torr) friction apparatus for determining friction and endurance life of MoSx films [NASA-TM-104478] p 129 N92-16129

TRUSSES

- Lubrication of space systems: Challenges and potential solutions
[NASA-TM-105560] p 130 N92-21579
- Tribological evaluation of an Al₂O₃-SiO₂ ceramic fiber candidate for high temperature sliding seals
[NASA-TM-105611] p 97 N92-23190
- Tribological and microstructural comparison of HIPped PM212 and PM212/Au self-lubricating composites
[NASA-TM-105615] p 97 N92-26142
- Computational techniques in tribology and material science at the atomic level
[NASA-TM-105573] p 252 N92-26671
- TRUSSES**
- Nonuniform thermal environmental effects on space truss structural reliability
[AIAA PAPER 92-2352] p 54 A92-34325
- Minimizing distortion in truss structures - A Hopfield network solution
[AIAA PAPER 92-2302] p 220 A92-34523
- Probabilistic progressive buckling of trusses
[AIAA PAPER 91-0916] p 223 A92-38142
- Probabilistic progressive buckling of trusses
[NASA-TM-105162] p 226 N92-15403
- Probabilistic structural analysis of adaptive/smart/intelligent space structures
[NASA-TM-105408] p 227 N92-22267
- Design feasibility study of a Space Station Freedom truss
[NASA-TM-105558] p 214 N92-30571
- Probabilistic assessment of space trusses subjected to combined mechanical and thermal loads
[NASA-TM-105429] p 230 N92-33935
- TUNNEL DIODES**
- A model for the trap-assisted tunneling mechanism in diffused n-p and implanted n(+)-p HgCdTe photodiodes
p 156 A92-46007
- TURBINE BLADES**
- Heat transfer in rotating serpentine passages with trips normal to the flow
[ASME PAPER 91-GT-265] p 165 A92-15663
- Navier-Stokes analysis of flow and heat transfer inside high-pressure-ratio transonic turbine blade rows
p 165 A92-17193
- A new response surface approach for structural reliability analysis
[AIAA PAPER 92-2408] p 219 A92-34339
- Navier-Stokes turbine heat transfer predictions using two-equation turbulence closures
[AIAA PAPER 92-3067] p 177 A92-48721
- Three-dimensional Navier-Stokes heat transfer predictions for turbine blade rows
[AIAA PAPER 92-3068] p 12 A92-54003
- FREPS - A forced response prediction system for turbomachinery blade rows
[AIAA PAPER 92-3072] p 242 A92-54006
- Unsteady blade pressures on a propfan - Predicted and measured compressibility effects
[AIAA PAPER 92-3774] p 14 A92-54161
- Transonic turbine blade cascade testing facility
[AIAA PAPER 92-4034] p 42 A92-56856
- Creep and fatigue research efforts on advanced materials
p 227 N92-22514
- Transonic turbine blade cascade testing facility
[NASA-TM-105646] p 47 N92-26129
- Laser anemometer measurements and computations in an annular cascade of high turning core turbine vanes
[NASA-TP-3252] p 20 N92-28980
- A critical evaluation of a three-dimensional Navier-Stokes CFD as a tool to design supersonic turbine stages
p 196 N92-32268
- TURBINE ENGINES**
- NDE of advanced turbine engine components and materials by computed tomography
[ASME PAPER 91-GT-287] p 215 A92-15681
- Engine component instrumentation development facility at NASA Lewis Research Center
[AIAA PAPER 92-3995] p 41 A92-56818
- The chemistry of Saudi Arabian sand: A deposition problem on helicopter turbine airfoils
[NASA-TM-105234] p 128 N92-14179
- Research sensors
p 202 N92-22526
- Aircraft engine hot section technology: An overview of the HOST Project
p 33 N92-22535
- Engine component instrumentation development facility at NASA Lewis Research Center
[NASA-TM-105644] p 42 N92-25449
- Ceramic composites: Enabling aerospace materials
[NASA-TM-105599] p 133 N92-27378
- Contingency power for a small turboshaft engine by using water injection into turbine cooling air
[NASA-TM-105680] p 37 N92-29661
- A simplified dynamic model of the T700 turboshaft engine
[NASA-TM-105805] p 251 N92-30898

TURBINE PUMPS

- Design and test of an oxygen turbopump for a dual expander cycle rocket engine
p 59 A92-21062
- Rocket engine diagnostics using qualitative modeling techniques
[AIAA PAPER 92-3164] p 65 A92-48787
- Investigation of three-dimensional flow field in a turbine including rotor/stator interaction. II - Three-dimensional flow field at the exit of the nozzle
[AIAA PAPER 92-3326] p 12 A92-48909
- An SSME high pressure oxidizer turbopump diagnostic system using G2(TM) real-time expert system
[NASA-TM-105328] p 247 N92-13717
- Reliability analysis of structural ceramic components using a three-parameter Weibull distribution
[NASA-TM-105370] p 129 N92-17060
- A survey of instabilities within centrifugal pumps and concepts for improving the flow range of pumps in rocket engines
[NASA-TM-105439] p 84 N92-18280
- Miniature high temperature plug-type heat flux gauges
[NASA-TM-105403] p 201 N92-18753
- Determining structural performance
p 32 N92-22519
- Development of advanced seals for space propulsion turbomachinery
[NASA-TM-105659] p 87 N92-24957
- Rocket engine diagnostics using qualitative modeling techniques
[NASA-TM-105714] p 88 N92-27033
- TURBINE WHEELS**
- Aeroelastic modal characteristics of mistuned blade assemblies - Mode localization and loss of eigenstructure
p 225 A92-54921
- TURBINES**
- Aerodynamics and heat transfer investigations on a high Reynolds number turbine cascade
[ASME PAPER 91-GT-157] p 164 A92-15593
- Full field flow visualization and computer-aided velocity measurements in a bank of cylinders in a wind tunnel
p 199 A92-50040
- A comparison of the calculated and experimental off-design performance of a radial flow turbine
[AIAA PAPER 92-3069] p 13 A92-54004
- Mechanical behaviour and failure phenomenon of an in situ toughened silicon nitride
p 127 A92-54504
- Description of a pressure measurement technique for obtaining surface static pressures of a radial turbine
[AIAA PAPER 92-4006] p 200 A92-56829
- Effects of turbine cooling assumptions on performance and sizing of high-speed civil transport
[NASA-TM-105610] p 34 N92-23537
- Description of a pressure measurement technique for obtaining surface static pressures of a radial turbine
[NASA-TM-105643] p 202 N92-24959
- Method of reducing drag in aerodynamic systems
[NASA-CASE-LEW-14791-1] p 21 N92-34243
- TURBOCOMPRESSORS**
- The numerical simulation of a high-speed axial flow compressor
[ASME PAPER 91-GT-272] p 3 A92-15669
- A comparison of predicted and measured inlet distortion flows in a subsonic axial inlet flow compressor rotor
[NASA-TM-105427] p 19 N92-26104
- TURBOFAN ENGINES**
- Turbomachinery noise
p 253 N92-10601
- An evaluation of some alternative approaches for reducing fan tone noise
[NASA-TM-105356] p 255 N92-18282
- Effects of chemical equilibrium on turbine engine performance for various fuels and combustor temperatures
[NASA-TM-105399] p 34 N92-23254
- TURBOFANS**
- An evaluation of some alternative approaches for reducing fan tone noise
[NASA-TM-105356] p 255 N92-18282
- Determining structural performance
p 32 N92-22519
- The future challenge for aeropropulsion
[NASA-TM-105613] p 35 N92-25164
- TURBOJET ENGINES**
- Liquid lubricants for advanced aircraft engines
[NASA-TM-104531] p 133 N92-32863
- TURBOMACHINE BLADES**
- Unsteady aerodynamic interaction effects on turbomachinery blade life and performance
[AIAA PAPER 92-0149] p 7 A92-28186
- Navier-Stokes analysis of turbomachinery blade external heat transfer
p 170 A92-28518
- Navier-Stokes analysis of three-dimensional unsteady flows inside turbine stages
[AIAA PAPER 92-3211] p 13 A92-54016
- Turbomachinery noise
p 253 N92-10601

TURBOMACHINERY

- The effect of steady aerodynamic loading on the flutter stability of turbomachinery blading
[ASME PAPER 91-GT-130] p 2 A92-15574
- A conformal block structured grid for turbomachinery cascades in two dimensions
p 248 A92-47059
- Development of an efficient analysis for high Reynolds number inviscid/viscid interactions in cascades
[AIAA PAPER 92-3073] p 10 A92-48723
- Grid generation for 3D turbomachinery configurations
[AIAA PAPER 92-3671] p 243 A92-54114
- Turbomachinery noise
p 253 N92-10601
- Rotordynamic Instability Problems in High-Performance Turbomachinery, 1990
[NASA-CP-3122] p 207 N92-14346
- Introduction to the internal fluid mechanics research session
p 188 N92-22522
- Turbomachinery
Development of advanced seals for space propulsion turbomachinery
p 87 N92-24957
- [NASA-TM-105659] p 87 N92-24957
- TCGRID: A three dimensional C-grid generator for turbomachinery
p 35 N92-25716
- TIGGERC: Turbomachinery interactive grid generator energy distributor and restart code
p 35 N92-25719
- A mathematical constraint placed upon inter-blade row boundary conditions used in the simulation of multistage turbomachinery flows
p 195 N92-27458
- Laser anemometer measurements and computations in an annular cascade of high turning core turbine vanes
[NASA-TP-3252] p 20 N92-28980
- TURBOPROP AIRCRAFT**
- Noise of two high-speed model counter-rotation propellers at takeoff/approach conditions
p 253 A92-46799
- TURBOPROP ENGINES**
- Determining structural performance
p 32 N92-22519
- TURBORAMJET ENGINES**
- Airbreathing combined cycle engine systems
p 31 N92-21523
- Beta 2: A near term, fully reusable, horizontal takeoff and landing two-stage-to-orbit launch vehicle concept
p 86 N92-21536
- TURBOROCKET ENGINES**
- Airbreathing combined cycle engine systems
p 31 N92-21523
- TURBOSHAFTS**
- Contingency power for a small turboshaft engine by using water injection into turbine cooling air
[NASA-TM-105680] p 37 N92-29661
- A simplified dynamic model of the T700 turboshaft engine
[NASA-TM-105805] p 251 N92-30898
- TURBULENCE**
- Scalar rate correlation at a turbulent liquid free surface - A two-regime correlation for high Schmidt numbers
p 184 A92-56941
- Effect of liquid surface turbulent motion on the vapor condensation in a mixing tank
[NASA-TM-105555] p 187 N92-21498
- Center for Modeling of Turbulence and Transition (CMOTT). Research briefs: 1990
p 1 N92-23336
- [NASA-TM-105243] p 189 N92-23338
- Turbulence modeling
p 189 N92-23340
- Modeling of compressible turbulent shear flows
p 189 N92-23340
- Advancements in engineering turbulence modeling (PAPER-105)
p 189 N92-23350
- On the basic equations for the second-order modeling of compressible turbulence
p 190 N92-23351
- Kolmogorov behavior of near-wall turbulence and its application in turbulence modeling
[NASA-TM-105663] p 191 N92-24050
- Workshop on Engineering Turbulence Modeling
[NASA-CP-10088] p 191 N92-24514
- Turbulence and deterministic chaos --- computational fluid dynamics
p 194 N92-25823
- Laser anemometer measurements and computations in an annular cascade of high turning core turbine vanes
[NASA-TP-3252] p 20 N92-28980
- A new time scale based k-epsilon model for near wall turbulence
[NASA-TM-105768] p 196 N92-32868
- TURBULENCE EFFECTS**
- Noise from turbulent shear flows
p 254 N92-10603
- Advances in engineering turbulence modeling --- computational fluid dynamics
p 193 N92-25820
- TURBULENCE MODELS**
- Studies of the effects of curvature on dilution jet mixing
p 166 A92-21079
- The Baldwin-Lomax model for separated and wake flows using the entropy envelope concept
[AIAA PAPER 92-0148] p 4 A92-23764
- A turbulence model for iced airfoils and its validation
[AIAA PAPER 92-0417] p 6 A92-26267

- Navier-Stokes solution of transonic cascade flows using nonperiodic C-type grids p 8 A92-28523
- Experimental balances for the second moments for a buoyant plume and their implication on turbulence modeling p 174 A92-40153
- Renormalization group based algebraic turbulence model for three-dimensional turbomachinery flows p 9 A92-41268
- Near-wall response in turbulent shear flows subjected to imposed unsteadiness p 174 A92-41652
- Comparative study of turbulence models in predicting hypersonic inlet flows [AIAA PAPER 92-3098] p 11 A92-48740
- Numerical study of low pressure nuclear thermal rockets [AIAA PAPER 92-3815] p 75 A92-54182
- Development of an algebraic turbulence model for analysis of propulsion flows [AIAA PAPER 92-3861] p 183 A92-54209
- A turbulence model for iced airfoils and its validation [NASA-TM-105373] p 16 N92-15052
- Viscous three-dimensional calculations of transonic fan performance [NASA-TM-103800] p 1 N92-17346
- An investigation of DTNS2D for use as an incompressible turbulence modelling test-bed [NASA-TM-105593] p 249 N92-22320
- Turbulence modeling p 189 N92-23338
- Development of new flux splitting schemes p 189 N92-23343
- Workshop on Engineering Turbulence Modeling [NASA-CP-10088] p 191 N92-24514
- Comment on two-equation models --- turbulence models p 191 N92-24520
- The present status and the future direction of second order closure models for incompressible flows p 191 N92-24523
- The present state of using RDT in turbulence modelling of unsteady flows p 191 N92-24535
- Viscous three-dimensional calculations of transonic fan performance p 195 N92-27467
- Development of an algebraic turbulence model for analysis of propulsion flows [NASA-TM-105701] p 250 N92-27517
- Comparative study of turbulence models in predicting hypersonic inlet flows [NASA-TM-105720] p 19 N92-28102
- TURBULENT BOUNDARY LAYER**
- The three-dimensional turbulent boundary layer near a plane of symmetry p 167 A92-24757
- On the mechanism of turbulence suppression in free shear flows under acoustic excitation [AIAA PAPER 92-0065] p 252 A92-25678
- Crossing shock wave turbulent boundary layer interactions - Variable angle and shock generator length geometry effects at Mach 3 [AIAA PAPER 92-0636] p 6 A92-27014
- The structure and development of streamwise vortex arrays embedded in a turbulent boundary layer [AIAA PAPER 92-0551] p 7 A92-28204
- Experimental study of boundary layer transition on a heated flat plate p 172 A92-36022
- A study of three dimensional turbulent boundary layer separation and vortex flow control using the reduced Navier Stokes equations p 9 A92-40105
- Surface and flow field measurements in a symmetric crossing shock wave/turbulent boundary layer flow [AIAA PAPER 92-2634] p 10 A92-45574
- Quasi-steady turbulence modeling of unsteady flows p 177 A92-48204
- Supersonic jet mixing enhancement by 'delta-tabs' [AIAA PAPER 92-3548] p 12 A92-49063
- An investigation of shock/turbulent boundary layer bleed interactions [AIAA PAPER 92-3085] p 182 A92-54008
- Surface heat transfer and flow properties of vortex arrays induced artificially and from centrifugal instabilities p 183 A92-56371
- The structure and development of streamwise vortex arrays embedded in a turbulent boundary layer [NASA-TM-105211] p 14 N92-10012
- Results from computational analysis of a mixed compression supersonic inlet [NASA-TM-104475] p 14 N92-10976
- On the mechanism of turbulence suppression in free shear flows under acoustic excitation [NASA-TM-105360] p 15 N92-14003
- The present state of using RDT in turbulence modelling of unsteady flows p 191 N92-24535
- Supersonic jet mixing enhancement by delta-tabs [NASA-TM-105664] p 18 N92-24958
- Turbulent heat flux measurements in a transitional boundary layer [NASA-TM-105623] p 19 N92-27377
- A new time scale based k-epsilon model for near wall turbulence [NASA-TM-105768] p 196 N92-32868
- TURBULENT DIFFUSION**
- An experimental investigation of the flow in a diffusing S-duct [AIAA PAPER 92-3622] p 13 A92-54090
- TURBULENT FLOW**
- On the mechanism of turbulence suppression in free shear flows under acoustic excitation [AIAA PAPER 92-0065] p 252 A92-25678
- Experimental investigation of turbulent flow through a circular-to-rectangular transition duct p 168 A92-26412
- On turbulent flows dominated by curvature effects p 171 A92-32940
- A 2-D oscillating flow analysis in Stirling engine heat exchangers p 172 A92-36001
- Second order modeling of boundary-free turbulent shear flows p 174 A92-41275
- Near-wall response in turbulent shear flows subjected to imposed unsteadiness p 174 A92-41652
- Effect of spatial resolution on apparent sensitivity to initial conditions of a decaying flow as it becomes turbulent p 175 A92-45716
- The influence of higher harmonics on vortex pairing in an axisymmetric mixing layer p 175 A92-46251
- Experimental verification of a secondary recirculation zone in a labyrinth seal p 205 A92-50271
- Development of an algebraic turbulence model for analysis of propulsion flows [AIAA PAPER 92-3861] p 183 A92-54209
- On the most general tensor B(sub ij) which is zero for i does not equal j, and the most general isotropic tensor I(sub ij) p 240 N92-10289
- Noise from turbulent shear flows p 254 N92-10603
- On the basic equations for the second-order modeling of compressible turbulence [NASA-TM-105277] p 184 N92-11302
- Turbulent fluid motion 3: Basic continuum equations [NASA-TM-104386] p 184 N92-11317
- On the mechanism of turbulence suppression in free shear flows under acoustic excitation [NASA-TM-105360] p 15 N92-14003
- Particle-laden weakly swirling free jets: Measurements and predictions [NASA-TM-100881] p 29 N92-14061
- Calculations of hot gas ingestion for a STOVL aircraft model [NASA-TM-105437] p 17 N92-19993
- Implementation/validation of a low Reynolds number two-equation turbulence model in the Proteus Navier-Stokes code: Two-dimensional/axisymmetric [NASA-TM-105619] p 187 N92-20520
- A kappa-epsilon calculation of transitional boundary layers [NASA-TM-105604] p 187 N92-22398
- Chemical reacting flows p 188 N92-22525
- Turbulence modeling p 189 N92-23338
- Modeling of compressible turbulent shear flows p 189 N92-23340
- Advancements in engineering turbulence modeling [PAPER-105] p 189 N92-23350
- On the basic equations for the second-order modeling of compressible turbulence p 190 N92-23351
- Simulations of free shear layers using a compressible kappa-epsilon model p 190 N92-23355
- Kolmogorov behavior of near-wall turbulence and its application in turbulence modeling [NASA-TM-105663] p 191 N92-24050
- The present state of using RDT in turbulence modelling of unsteady flows p 191 N92-24535
- Turbulence and deterministic chaos --- computational fluid dynamics p 194 N92-25823
- Turbulent heat flux measurements in a transitional boundary layer [NASA-TM-105623] p 19 N92-27377
- Development of an algebraic turbulence model for analysis of propulsion flows [NASA-TM-105701] p 250 N92-27517
- Laser anemometer measurements and computations in an annular cascade of high turning core turbine vanes [NASA-TP-3252] p 20 N92-28980
- A new time scale based k-epsilon model for near wall turbulence [NASA-TM-105768] p 196 N92-32868
- TURBULENT HEAT TRANSFER**
- Prediction of unsteady rotor-surface pressure and heat transfer from wake passages [ASME PAPER 91-GT-267] p 165 A92-15665
- Heat transfer on accreting ice surfaces p 166 A92-24415
- Navier-Stokes analysis of turbomachinery blade external heat transfer p 170 A92-28518
- Turbulent heat flux measurements in a transitional boundary layer [NASA-TM-105623] p 19 N92-27377
- Turbulent heat flux measurements in a transitional boundary layer [NASA-TM-105623] p 19 N92-27377
- Particle-laden weakly swirling free jets: Measurements and predictions [NASA-TM-100881] p 29 N92-14061
- Multigrid acceleration and turbulence models for computations of 3D turbulent jets in crossflow [NASA-TM-105306] p 186 N92-18775
- TURBULENT MIXING**
- A new unsteady mixing model to predict NO(x) production during rapid mixing in a dual-stage combustor [AIAA PAPER 92-0233] p 25 A92-25696
- Computation of supersonic jet mixing noise for an axisymmetric CD nozzle using k-epsilon turbulence model [AIAA PAPER 92-0500] p 252 A92-26328
- A continuous mixing model for pdf simulations and its applications to combustor shear flows p 174 A92-40139
- Mixing in the dome region of a staged gas turbine combustor [AIAA PAPER 92-3089] p 177 A92-48734
- Computation of supersonic jet mixing noise for an axisymmetric CD nozzle using k-epsilon turbulence model [NASA-TM-105338] p 254 N92-14795
- TURBULENT WAKES**
- A viscous flow study of shock-boundary layer interaction, radial transport, and wake development in a transonic compressor [ASME PAPER 91-GT-69] p 2 A92-15539
- TVD SCHEMES**
- Central difference TVD and TVB schemes for time dependent and steady state problems [AIAA PAPER 92-0053] p 166 A92-22168
- Predicted pressure distribution on a prop-fan blade through Euler analysis p 10 A92-46791
- Numerical study of shock-wave/boundary-layer interactions in premixed combustible gases p 183 A92-54907
- Central difference TVD and TVB schemes for time dependent and steady state problems [NASA-TM-105357] p 249 N92-15663
- Study of shock-induced combustion using an implicit TVD scheme p 116 N92-25816
- TWO DIMENSIONAL BOUNDARY LAYER**
- A fast, uncoupled, compressible, two-dimensional, unsteady boundary layer algorithm with separation for engine inlets [AIAA PAPER 92-3082] p 11 A92-48729
- A fast, uncoupled, compressible, two-dimensional, unsteady boundary layer algorithm with separation for engine inlets [NASA-TM-105686] p 195 N92-27653
- TWO DIMENSIONAL FLOW**
- Convection in superposed fluid and porous layers p 166 A92-24752
- Numerical experiments on a new class of nonoscillatory schemes [AIAA PAPER 92-0421] p 7 A92-28193
- Navier-Stokes analysis of turbomachinery blade external heat transfer p 170 A92-28518
- Analysis of cascades using a two dimensional Euler aeroelastic solver [AIAA PAPER 92-2370] p 26 A92-34598
- A 2-D oscillating flow analysis in Stirling engine heat exchangers p 172 A92-36001
- Development of an algebraic turbulence model for analysis of propulsion flows [AIAA PAPER 92-3861] p 183 A92-54209
- An investigation of DTNS2D for use as an incompressible turbulence modelling test-bed [NASA-TM-105593] p 249 N92-22230
- Numerical experiments with flows of elongated granules [NASA-TM-105567] p 209 N92-23226
- Simulations of free shear layers using a compressible kappa-epsilon model p 190 N92-23355
- Development of an algebraic turbulence model for analysis of propulsion flows [NASA-TM-105701] p 250 N92-27517

TWO DIMENSIONAL MODELS

TWO DIMENSIONAL MODELS

- Comparison of two-dimensional and three-dimensional droplet trajectory calculations in the vicinity of finite wings
[AIAA PAPER 92-0645] p 8 A92-28215
- On the development of explicit robust schemes for implementation of a class of hyperelastic models in large-strain analysis of rubbers p 221 A92-36245
- Boundary heat fluxes for spectral radiation from a uniform temperature rectangular medium p 175 A92-44388
- Thermal modeling with solid/liquid phase change of the thermal energy storage experiment
[NASA-TM-103770] p 185 N92-13402
- An investigation of DTNS2D for use as an incompressible turbulence modelling test-bed
[NASA-TM-105593] p 249 N92-22230
- Aeroelastic stability analyses of two counter rotating propfan designs for a cruise missile model
[NASA-TM-105268] p 227 N92-23191
- Contact stresses in meshing spur gear teeth: Use of an incremental finite element procedure
[NASA-TM-105388] p 209 N92-23536
- A two-dimensional Euler solution for an unbladed jet engine configuration
[NASA-TM-105329] p 190 N92-23560
- Interactive solution-adaptive grid generation procedure
[NASA-TM-105432] p 18 N92-23563
- The Proteus Navier-Stokes code --- two and three dimensional computational fluid dynamics p 192 N92-25811

TWO FLUID MODELS

- Initial development of the axisymmetric ejector shear layer
[AIAA PAPER 92-3567] p 178 A92-49068

TWO PHASE FLOW

- Liquid hydrogen mass flow through a multiple orifice Joule-Thomson device
[AIAA PAPER 92-2881] p 176 A92-47862
- Liquid hydrogen mass flow through a multiple orifice Joule-Thomson device
[NASA-TM-105583] p 189 N92-23268
- Critical fluid thermal equilibration experiment (19-IML-1) p 139 N92-23640

U

ULLAGE

- Hydrogen no-vent fill testing in a 1.2 cubic foot (34 liter) tank
[NASA-TM-105273] p 185 N92-13401

ULTRAHIGH VACUUM

- A vacuum (10(exp -9) Torr) friction apparatus for determining friction and endurance life of MoSx films
[NASA-TM-104478] p 129 N92-16129

ULTRASONIC TESTS

- Ultrasonic evaluation of oxygen content, modulus, and microstructure changes in YBa₂Cu₃O_{7-x} occurring during oxidation and reduction p 261 A92-38418
- Detecting Lamb waves with broad-band acousto-ultrasonic signals in composite structures
[NASA-TM-105557] p 216 N92-23189

ULTRAVIOLET ABSORPTION

- Vacuum ultraviolet absorption in a hydrogen arcjet
[AIAA PAPER 92-3564] p 259 A92-54055

ULTRAVIOLET RADIATION

- Synergistic effects of ultraviolet radiation, thermal cycling and atomic oxygen on altered and coated Kapton surfaces
[AIAA PAPER 92-0794] p 93 A92-27125
- Synergistic effects of ultraviolet radiation, thermal cycling, and atomic oxygen on altered and coated Kapton surfaces
[NASA-TM-105363] p 96 N92-14114

UNIFORM FLOW

- Distortion of a flat-plate boundary layer by free-stream vorticity normal to the plate p 173 A92-36343

UNIVERSE

- Void probability as a function of the void's shape and scale-invariant models --- in studies of spatial galactic distribution p 267 A92-24456
- Fluctuation-driven electroweak phase transition --- in early universe p 269 A92-54464
- Large-scale microwave anisotropy from gravitating seeds p 269 A92-56914

UNMANNED SPACECRAFT

- Design of multihundred-watt dynamic isotope power system for robotic space missions p 69 A92-50633

UNSTEADY AERODYNAMICS

- The effect of steady aerodynamic loading on the flutter stability of turbomachinery blading
[ASME PAPER 91-GT-130] p 2 A92-15574
- Wind tunnel wall effects in a linear oscillating cascade
[ASME PAPER 91-GT-133] p 2 A92-15576

- Unsteady blade-surface pressures on a large-scale advanced propeller - Prediction and data p 3 A92-17178

- Aerodynamics of loaded cascades in subsonic flows subject to unsteady three-dimensional vortical disturbances
[AIAA PAPER 92-0146] p 4 A92-23762

- Pressure wave propagation studies for oscillating cascades
[AIAA PAPER 92-0145] p 5 A92-25682
- A new unsteady mixing model to predict NO(x) production during rapid mixing in a dual-stage combustor
[AIAA PAPER 92-0233] p 25 A92-25696

- Transient behavior of supersonic flow through inlets
[AIAA PAPER 92-0233] p 7 A92-28043

- Unsteady aerodynamic interaction effects on turbomachinery blade life and performance
[AIAA PAPER 92-0149] p 7 A92-28186

- Analysis of cascades using a two dimensional Euler aeroelastic solver
[AIAA PAPER 92-2370] p 26 A92-34598

- Finite element Euler calculations of unsteady transonic cascade flows
[AIAA PAPER 92-2120] p 9 A92-35689

- Unsteady airloading panel method for propfans
[AIAA PAPER 92-2120] p 253 A92-44512
- Numerical analysis of flow through oscillating cascade sections p 9 A92-44513

- Airfoil wake and linear theory gust response including sub and superresonant flow conditions
[AIAA PAPER 92-3074] p 11 A92-48724

- Navier-Stokes analysis of three-dimensional unsteady flows inside turbine stages
[AIAA PAPER 92-3211] p 13 A92-54016

- Unsteady blade pressures on a propfan - Predicted and measured compressibility effects
[AIAA PAPER 92-3774] p 14 A92-54161

- Experimental unsteady pressures on an oscillating cascade with supersonic leading edge locus
[AIAA PAPER 92-4035] p 14 A92-56857

- Pressure wave propagation studies for oscillating cascades
[NASA-TM-105406] p 16 N92-15977

- Semi-empirical model for prediction of unsteady forces on an airfoil with application to flutter
[NASA-TM-105414] p 17 N92-18760

- Unsteady-flow-field predictions for oscillating cascades
[NASA-TM-105283] p 17 N92-19437
- Development of a steady potential solver for use with linearized, unsteady aerodynamic solvers
[NASA-TM-105288] p 31 N92-20525

- Experimental investigation of the flowfield of an oscillating airfoil
[NASA-TM-105675] p 20 N92-30182

UNSTEADY FLOW

- Euler flow predictions for an oscillating cascade using a high resolution wave-split scheme
[ASME PAPER 91-GT-198] p 3 A92-15623

- Prediction of unsteady rotor-surface pressure and heat transfer from wake passings
[ASME PAPER 91-GT-267] p 165 A92-15665

- Unsteady Euler analysis of the flowfield of a propfan at an angle of attack p 3 A92-21070
- Pressure wave propagation studies for oscillating cascades p 5 A92-25682

- Unsteady blade pressures on a propfan at takeoff - Euler analysis and flight data
[AIAA PAPER 92-0376] p 25 A92-26234

- Vorticity dynamics of inviscid shear layers
[AIAA PAPER 92-0420] p 168 A92-26270

- Acoustic analysis using numerical solutions of the Navier-Stokes equations
[AIAA PAPER 92-0506] p 253 A92-26934

- Unsteady flowfield simulation of ducted propfan configurations
[AIAA PAPER 92-0521] p 6 A92-26946

- An unsteady Euler scheme for the analysis of ducted propellers
[AIAA PAPER 92-0522] p 6 A92-26947

- Numerical experiments on a new class of nonoscillatory schemes
[AIAA PAPER 92-0421] p 7 A92-28193

- Unsteady transonic Euler solutions using finite elements
[AIAA PAPER 92-2504] p 8 A92-34499

- A variable multi-step method for transient heat conduction p 173 A92-37518
- Near-wall response in turbulent shear flows subjected to imposed unsteadiness p 174 A92-41652

- Comparison of the SMAC, PISO, and iterative time-advancing schemes for unsteady flows p 175 A92-47158
- Quasi-steady turbulence modeling of unsteady flows p 177 A92-48204

- Perturbation of a normal shock - A test case for unsteady Euler codes p 178 A92-48795

- [AIAA PAPER 92-3180] p 178 A92-48795
- Time domain numerical calculations of unsteady vortical flows about a flat plate airfoil p 12 A92-50473

- Navier-Stokes analysis of three-dimensional unsteady flows inside turbine stages
[AIAA PAPER 92-3211] p 13 A92-54016

- Experimental unsteady pressures on an oscillating cascade with supersonic leading edge locus
[AIAA PAPER 92-4035] p 14 A92-56857

- Pressure wave propagation studies for oscillating cascades p 16 N92-15977
- Unsteady-flow-field predictions for oscillating cascades
[NASA-TM-105283] p 17 N92-19437

- Turbomachinery
Advanced propeller research p 33 N92-22537
- Long time behavior of unsteady flow computations
[NASA-TM-105584] p 190 N92-23565

- The present state of using RDT in turbulence modelling of unsteady flows p 191 N92-24535

UPLINKING

- Interference susceptibility measurements for an MSK satellite communication link
[AIAA PAPER 92-2018] p 144 A92-29936

- The Link Evaluation Terminal for the Advanced Communications Technology Satellite Experiments Program p 49 A92-29954

- [AIAA PAPER 92-2040] p 49 A92-29954
- Interference susceptibility measurements for an MSK satellite communication link p 149 N92-15306

- [NASA-TM-105395] p 149 N92-15306
- The link evaluation terminal for the advanced communications technology satellite experiments program p 51 N92-16008

- [NASA-TM-105367] p 51 N92-16008
- A software control system for the ACTS high-burst-rate link evaluation terminal p 243 N92-16628

- [NASA-TM-105207] p 243 N92-16628
- Multichannel demultiplexer/demodulator technologies for future satellite communication systems p 51 N92-18342

- [NASA-TM-105377] p 51 N92-18342
- A 1-W, 30-GHz, CPW amplifier for ACTS small terminal uplink p 161 N92-26096

- [NASA-TM-105671] p 161 N92-26096
- A 1-W, 30-GHz, CPW amplifier for ACTS small terminal uplink p 152 N92-32973

UPPER STAGE ROCKET ENGINES

- Graphite/epoxy composite adapters for the Space Shuttle/Centaur vehicle
[NASA-TP-3014] p 49 N92-31251

UPSTREAM

- On the mechanism of turbulence suppression in free shear flows under acoustic excitation p 252 A92-25678

- [AIAA PAPER 92-0065] p 252 A92-25678
- On the mechanism of turbulence suppression in free shear flows under acoustic excitation p 15 N92-14003

UPWIND SCHEMES (MATHEMATICS)

- The Osher scheme for non-equilibrium reacting flows p 176 A92-48149

USER MANUALS (COMPUTER PROGRAMS)

- NASA Lewis steady-state heat pipe code users manual
[NASA-TM-105161] p 90 N92-28682

- [NASA-TM-105161] p 90 N92-28682
- Metal matrix composite analyzer (METCAN) user's manual, version 4.0 p 110 N92-30779

V

V/STOL AIRCRAFT

- Flow in a ventral nozzle for short takeoff and vertical landing aircraft p 25 A92-28538

- Integrated flight/propulsion control design for a STOVL aircraft using H-infinity control design techniques p 39 A92-29093

- [AIAA PAPER 92-0376] p 25 A92-26234
- IMPAC - An integrated methodology for propulsion and airframe control p 39 A92-29118

- Experimental and analytical study of close-coupled ventral nozzles for ASTOVL aircraft p 26 A92-45325
- Directions in propulsion control p 32 N92-22530

- Supersonic STOVL propulsion technology program: An overview p 33 N92-22539

VACUUM

- Fluctuation-driven electroweak phase transition --- in early universe p 269 A92-54464

- Properties data for opening the Galileo's partially unfurled main antenna
[NASA-TM-105355] p 130 N92-20660

VACUUM APPARATUS

- A vacuum (10(exp -9) Torr) friction apparatus for determining friction and endurance life of MoSx films
[NASA-TM-104478] p 129 N92-16129

VACUUM CHAMBERS

- Full-size solar dynamic heat receiver thermal-vacuum tests p 68 A92-50565
- Preliminary characterizations of a water vaporizer for resistojel applications [AIAA PAPER 92-3533] p 74 A92-54041
- Test facilities for high power electric propulsion [NASA-TM-105247] p 80 N92-11136
- A new technique for oil backstreaming contamination measurements [NASA-TM-105312] p 257 N92-13783

VACUUM TESTS

- A new technique for oil backstreaming contamination measurements [NASA-TM-105312] p 257 N92-13783

VALENCE

- Near-edge study of gold-substituted YBa₂Cu₃O_{7-δ} p 259 A92-14950

VAN DER WAALS FORCES

- Investigation of two and three parameter equations of state for cryogenic fluids p 140 A92-13413

VANES

- Airfoil wake and linear theory gust response including sub and superresonant flow conditions [AIAA PAPER 92-3074] p 11 A92-48724
- Wind tunnel performance results of swirl recovery vanes as tested with an advanced high speed propeller [AIAA PAPER 92-3770] p 28 A92-54159
- The chemistry of Saudi Arabian sand: A deposition problem on helicopter turbine airfoils [NASA-TM-105234] p 128 N92-14179
- Laser anemometer measurements and computations in an annular cascade of high turning core turbine vanes [NASA-TP-3252] p 20 N92-28980

VAPOR DEPOSITION

- Diffusion mechanisms in chemical vapor-deposited indium coated on chemical vapor-deposited rhenium p 117 A92-28017
- Properties of large area ErBa₂Cu₃O_{7-x} thin films deposited by ionized cluster beams p 260 A92-33911
- Oxidation kinetics of CVD silicon carbide and silicon nitride p 125 A92-39674
- Synthesis and characterization of fine grain diamond films p 262 A92-46330
- Properties of novel CVD graphite fibers and their bromine intercalation compounds [NASA-TM-105295] p 128 N92-14170
- Vapor crystal growth technology development: Application to cadmium telluride [NASA-TM-103786] p 139 N92-16158
- CVD of silicon carbide on structural fibers: Microstructure and composition [NASA-TM-105385] p 107 N92-18439
- Chemical vapor deposition modeling for high temperature materials [NASA-TM-105386] p 96 N92-18457
- Novel applications for TAZ-8A p 123 N92-22444
- An XPS study of the stability of Fomblin Z25 on the native oxide of aluminum --- x ray photoelectron spectroscopy [NASA-TM-105594] p 131 N92-23185
- Deposition of adherent Ag-Ti duplex films on ceramics in a multiple-cathode sputter deposition system [NASA-TM-105586] p 34 N92-23225

VAPOR PHASE EPITAXY

- InP concentrator solar cells p 234 A92-53166

VAPOR PHASES

- Vapor condensation on liquid surface due to laminar jet-induced mixing p 164 A92-10446

VAPORIZING

- Microgravity combustion of isolated n-decane and n-heptane droplets [AIAA PAPER 92-0242] p 113 A92-26927

VAPORS

- Vapor crystal growth technology development: Application to cadmium telluride [NASA-TM-103786] p 139 N92-16158
- Effect of liquid surface turbulent motion on the vapor condensation in a mixing tank [NASA-TM-105555] p 187 N92-21498

VARIABLE CYCLE ENGINES

- Effects of turbine cooling assumptions on performance and sizing of high-speed civil transport [NASA-TM-105610] p 34 N92-23537

VARIATIONAL PRINCIPLES

- A variationally coupled FE-BE method for elasticity and fracture mechanics p 222 A92-37510

VECTOR SPACES

- Application of vector-valued rational approximations to the matrix eigenvalue problem and connections with Krylov subspace methods [NASA-TM-105858] p 250 N92-33571

VECTORS (MATHEMATICS)

- Application of vector-valued rational approximations to the matrix eigenvalue problem and connections with Krylov subspace methods [NASA-TM-105858] p 250 N92-33571
- Upper bounds for convergence rates of vector extrapolation methods on linear systems with initial iterations [NASA-TM-105608] p 250 N92-33742
- Rational approximations from power series of vector-valued meromorphic functions [NASA-TM-105859] p 251 N92-33942

VELOCITY DISTRIBUTION

- Comparison of the SMAC, PISO, and iterative time-advancing schemes for unsteady flows p 175 A92-47158
- Renormalization group analysis of the Reynolds stress transport equation p 179 A92-49493
- Time domain numerical calculations of unsteady vortical flows about a flat plate airfoil p 12 A92-50473
- The structure and development of streamwise vortex arrays embedded in a turbulent boundary layer [NASA-TM-105211] p 14 N92-10012
- Coaxial injector spray characterization using water/air as simulants [NASA-TM-105322] p 82 N92-14112
- Renormalization group analysis of the Reynolds stress transport equation [NASA-TM-105588] p 190 N92-23542
- A comparison of predicted and measured inlet distortion flows in a subsonic axial inlet flow compressor rotor [NASA-TM-105427] p 19 N92-26104

VELOCITY MEASUREMENT

- Performance of the Phase Doppler Particle Analyzer icing cloud droplet sizing probe in the NASA Lewis Icing Research Tunnel [AIAA PAPER 92-0162] p 198 A92-26926
- Laser-induced fluorescence of atomic hydrogen in an arcjet thruster [AIAA PAPER 92-0678] p 60 A92-27045
- A full field, 3-D velocimeter for NASA's microgravity science program [AIAA PAPER 92-0784] p 56 A92-27119
- Doppler-shifted fluorescence imaging of velocity fields in supersonic reacting flows [AIAA PAPER 92-2964] p 199 A92-46979
- Full field flow visualization and computer-aided velocity measurements in a bank of cylinders in a wind tunnel p 199 A92-50040
- Filtered Rayleigh scattering based measurements in compressible mixing layers [AIAA PAPER 92-3543] p 182 A92-54043
- Viscous three-dimensional calculations of transonic fan performance [NASA-TM-103800] p 1 N92-17346
- A 4-spot time-of-flight anemometer for small centrifugal compressor velocity measurements [NASA-TM-105717] p 202 N92-29105

VERTICAL LANDING

- Experimental performance of three design factors for ventral nozzles for SSTOVL aircraft [AIAA PAPER 92-3789] p 28 A92-54168
- Internal reversing flow in a tailpipe offtake configuration for SSTOVL aircraft [AIAA PAPER 92-3790] p 28 A92-54169
- Analysis of airframe/engine interactions for a STOVL aircraft with integrated flight/propulsion control [AIAA PAPER 92-4623] p 23 A92-55300
- Experimental performance of three design factors for ventral nozzles for SSTOVL aircraft [NASA-TM-105697] p 37 N92-27669
- Internal reversing flow in a tailpipe offtake configuration for SSTOVL aircraft [NASA-TM-105698] p 37 N92-28418

VIBRATION

- Modal simulation of gearbox vibration with experimental correlation [AIAA PAPER 92-3494] p 207 A92-54036
- Modal interaction in linear dynamic systems near degenerate modes [NASA-TM-105315] p 225 N92-12316
- A comparison between theoretical prediction and experimental measurement of the dynamic behavior of spur gears [NASA-TM-105362] p 210 N92-25347
- Minimization of the vibration energy of thin-plate structure [NASA-TM-105654] p 211 N92-25448
- Optimum design of a gearbox for low vibration [NASA-TM-105653] p 212 N92-28476
- Modal simulation of gearbox vibration with experimental correlation [NASA-TM-105702] p 215 N92-31485

VIBRATION DAMPING

- Reaction-compensation technology for microgravity laboratory robots p 203 A92-23719

- Multiobjective shape and material optimization of composite structures including damping p 218 A92-28055

- Aeroelastic stability analyses of two counter rotating propfan designs for a cruise missile model [AIAA PAPER 92-2218] p 25 A92-34408

- Electromechanical simulation and testing of actively controlled rotordynamic systems with piezoelectric actuators p 204 A92-39258

- Pointing and tracking control for freedom's Solar Dynamic modules and vibration control of freedom [AAS PAPER 91-459] p 54 A92-43284

- Optimal microgravity vibration isolation - An algebraic introduction p 54 A92-47495
- Minimization of vibration in elastic beams with time-variant boundary conditions p 224 A92-50511
- Controller design for microgravity vibration isolation systems [IAF PAPER 92-0969] p 247 A92-57327

- Microgravity vibration isolation: An optimal control law for the one-dimensional case [NASA-TM-105146] p 141 N92-11217
- Rotordynamic Instability Problems in High-Performance Turbomachinery, 1990 [NASA-CP-3122] p 207 N92-14346

- Performance tests of a cryogenic hybrid magnetic bearing for turbopumps [NASA-TM-105627] p 30 N92-20523
- Effect of heat treatment on stiffness and damping of SiC/Ti-15-3 [NASA-TM-105564] p 108 N92-20841
- Determining structural performance p 32 N92-22519

- Analysis and modification of a single-mesh gear fatigue rig for use in diagnostic studies [NASA-TM-105416] p 212 N92-27879
- Optimum design of a gearbox for low vibration [NASA-TM-105653] p 212 N92-28476

- Free vibrations of delaminated beams [NASA-TM-105582] p 109 N92-25754

- Free vibrations of delaminated beams [NASA-TM-105582] p 109 N92-25754

- Optimal microgravity vibration isolation - An algebraic introduction p 54 A92-47495
- Microgravity vibration isolation: An optimal control law for the one-dimensional case [NASA-TM-105146] p 141 N92-11217

- International Workshop on Vibration Isolation Technology for Microgravity Science Applications [NASA-CP-10094] p 141 N92-28436
- Vibration isolation technology development to demonstration p 140 N92-28442

- Early mission science support: Space Acceleration Measurement System (SAMS) p 57 N92-28451
- Microgravity vibration isolation: Optimal preview and feedback control [NASA-TM-105673] p 142 N92-30692

- Comparison of analysis and experiment for gearbox noise [NASA-TM-105330] p 210 N92-25396

- Space acceleration measurement system description and operations on the First Spacelab Life Sciences Mission [NASA-TM-105301] p 57 N92-13151

- Optical measurements of unducted fan flutter [ASME PAPER 91-GT-19] p 197 A92-15510
- Modal simulation of gearbox vibration with experimental correlation [AIAA PAPER 92-3494] p 207 A92-54036

- Modal simulation of gearbox vibration with experimental correlation [NASA-TM-105702] p 215 N92-31485
- Influence of mass moment of inertia on normal modes of preloaded solar array mast [NASA-TP-3273] p 230 N92-33476

- Modal test/analysis correlation of Space Station structures using nonlinear sensitivity [NASA-TM-105850] p 230 N92-34221

- Effect of heat treatment on stiffness and damping of SiC/Ti-15-3 p 100 A92-25627
- Effect of heat treatment on stiffness and damping of SiC/Ti-15-3 [NASA-TM-105564] p 108 N92-20841

- NIST torsion oscillator viscometer response: Performance on the LeRC active vibration isolation platform [NASA-TM-105571] p 209 N92-23564
- Comparison of analysis and experiment for gearbox noise [NASA-TM-105330] p 210 N92-25396

- Comparison of analysis and experiment for gearbox noise [NASA-TM-105330] p 210 N92-25396

- Comparison of analysis and experiment for gearbox noise [NASA-TM-105330] p 210 N92-25396

- Comparison of analysis and experiment for gearbox noise [NASA-TM-105330] p 210 N92-25396

- Comparison of analysis and experiment for gearbox noise [NASA-TM-105330] p 210 N92-25396

- Comparison of analysis and experiment for gearbox noise [NASA-TM-105330] p 210 N92-25396

- Comparison of analysis and experiment for gearbox noise [NASA-TM-105330] p 210 N92-25396

- Comparison of analysis and experiment for gearbox noise [NASA-TM-105330] p 210 N92-25396

- Comparison of analysis and experiment for gearbox noise [NASA-TM-105330] p 210 N92-25396

- Comparison of analysis and experiment for gearbox noise [NASA-TM-105330] p 210 N92-25396

- Comparison of analysis and experiment for gearbox noise [NASA-TM-105330] p 210 N92-25396

VIDEO COMMUNICATION

VIDEO COMMUNICATION

- Technical and economic feasibility of integrated video service by satellite
[AIAA PAPER 92-2054] p 145 A92-29966
- VIDEO DATA**
A video event trigger for high frame rate, high resolution video technology p 160 N92-22453
- VIDEO SIGNALS**
Real-time data compression of broadcast video signals
[NASA-CASE-LEW-14945-2] p 147 N92-10128
- VIRTUAL MEMORY SYSTEMS**
Interfacing laboratory instruments to multiuser, virtual memory computers p 245 A92-13595
- VISCOELASTICITY**
Viscoplastic analysis of an experimental cylindrical thrust chamber liner p 218 A92-28052
Viscoelastic properties of addition-cured polyimides used in high temperature polymer matrix composites p 124 A92-32632
- VISCOMETERS**
NIST torsion oscillator viscometer response: Performance on the LeRC active vibration isolation platform
[NASA-TM-105571] p 209 N92-23564
- VISCOPLASTICITY**
A viscoplastic model for single crystals p 217 A92-24717
A viscoplastic theory for anisotropic materials
[ONERA, TP NO. 1992-90] p 217 A92-24721
A viscoplastic theory with thermodynamic considerations
[ONERA, TP NO. 1991-220] p 217 A92-26372
Viscoplastic analysis of an experimental cylindrical thrust chamber liner p 218 A92-28052
A viscoplastic theory with thermodynamic considerations p 219 A92-33903
Application of a thermal fatigue life prediction model to high-temperature aerospace alloys B1900 + Hf and Haynes 188 p 121 A92-45232
On the thermodynamic framework of generalized coupled thermoelastic-viscoplastic-damage modeling
[NASA-TM-105349] p 225 N92-14434
Asymptotic integration algorithms for first-order ODEs with application to viscoplasticity
[NASA-TM-105587] p 250 N92-24974
- VISCOSITY**
Central difference TVD and TVB schemes for time dependent and steady state problems
[AIAA PAPER 92-0053] p 166 A92-22168
Central difference TVD and TVB schemes for time dependent and steady state problems
[NASA-TM-105357] p 249 N92-15663
- VISCOUS FLOW**
A viscous flow study of shock-boundary layer interaction, radial transport, and wake development in a transonic compressor
[ASME PAPER 91-GT-69] p 2 A92-15539
Deterministic blade row interactions in a centrifugal compressor stage p 3 A92-15670
[ASME PAPER 91-GT-273] p 3 A92-15670
Improved nonequilibrium viscous shock-layer scheme for hypersonic blunt-body flowfields p 4 A92-24653
A turbulence model for iced airfoils and its validation
[AIAA PAPER 92-0417] p 6 A92-26267
Three-dimensional viscous analysis of a Mach 5 inlet and comparison with experimental data p 8 A92-28526
Subharmonic route to boundary-layer transition - Critical layer nonlinearity p 172 A92-35994
Linear stability of compressible Taylor-Couette flow p 173 A92-36187
A least-squares finite element method for incompressible Navier-Stokes problems p 173 A92-37387
Grid quality improvement by a grid adaptation technique p 248 A92-47072
Development of an efficient analysis for high Reynolds number inviscid/viscid interactions in cascades
[AIAA PAPER 92-3073] p 10 A92-48723
A fast, uncoupled, compressible, two-dimensional, unsteady boundary layer algorithm with separation for engine inlets p 11 A92-48729
Numerical modeling of fluid and electromagnetic phenomena in an arcjet
[AIAA PAPER 92-3106] p 258 A92-48747
A time-accurate algorithm for chemical non-equilibrium viscous flows at all speeds p 182 A92-54112
[AIAA PAPER 92-3639] p 182 A92-54112
Multigrad calculation of three-dimensional viscous cascade flows p 249 N92-10345
[NASA-TM-105257] p 249 N92-10345
A turbulence model for iced airfoils and its validation
[NASA-TM-105373] p 16 N92-15052

- Viscous three-dimensional calculations of transonic fan performance
[NASA-TM-103800] p 1 N92-17346
An investigation of DTNS2D for use as an incompressible turbulence modelling test-bed p 249 N92-22230
[NASA-TM-105593] p 249 N92-22230
High-speed inlet research program and supporting analysis p 188 N92-22542
High-Order Polynomial Expansions (HOPE) for flux-vector splitting p 190 N92-23353
TIGGERC: Turbomachinery interactive grid generator energy distributor and restart code p 35 N92-25719
An efficient and robust algorithm for time dependent viscous incompressible Navier-Stokes equations p 193 N92-25819
Viscous three-dimensional calculations of transonic fan performance p 195 N92-27467
A fast, uncoupled, compressible, two-dimensional, unsteady boundary layer algorithm with separation for engine inlets p 195 N92-27653
[NASA-TM-105686] p 195 N92-27653
Analysis of iced wings
[NASA-TM-105773] p 20 N92-34144
- VOICE COMMUNICATION**
20/30 GHz satellite personal communications networks
[AIAA PAPER 92-1908] p 143 A92-29839
A personal communications network using a Ka-band satellite p 145 A92-31780
A personal communications network using a Ka-band satellite p 151 N92-30934
- VOIDS**
Relationship between voids and interlaminar shear strength of polymer matrix composites p 98 A92-10241
Void probability as a function of the void's shape and scale-invariant models --- in studies of spacial galactic distribution p 267 A92-24456
An initial study of void formation during solidification of aluminum in normal and reduced-gravity p 138 A92-29611
[AIAA PAPER 92-0845] p 138 A92-29611
Void effects on the interlaminar shear strength of unidirectional graphite-fiber-reinforced composites p 105 A92-50348
Experiments with phase change thermal energy storage canisters for Space Station Freedom p 179 A92-50564
Shrinkage void formation and its effect on freeze and thaw processes of lithium and lithium-fluoride for space applications p 180 A92-50596
Experiments with phase change thermal energy storage canisters for Space Station Freedom p 86 N92-21216
[NASA-TM-104427] p 86 N92-21216
- VOLATILITY**
Volatile species in halide-activated-diffusion coating packs p 122 A92-57028
- VOLTAGE AMPLIFIERS**
Force analysis of magnetic bearings with power-saving controls p 212 N92-27795
- VOLTAGE CONVERTERS (DC TO DC)**
A 1 MW, 100 kV, less than 100 kg space based dc-dc power converter p 157 A92-50537
Test and evaluation of load converter topologies used in the Space Station Freedom power management and distribution dc test bed p 158 A92-50662
Multi-megawatt inverter/converter technology for space power applications p 159 N92-14294
[NASA-TM-105307] p 159 N92-14294
Stability testing and analysis of a PMAD DC test bed for the Space Station Freedom p 162 N92-31282
[NASA-TM-105846] p 162 N92-31282
Load converter interactions with the secondary system in the Space Station Freedom power management and distribution DC test bed p 164 N92-34219
[NASA-TM-105844] p 164 N92-34219
- VORTEX BREAKDOWN**
Modern developments in shear flow control with swirl p 9 A92-41265
Wind tunnel investigation of vortex flows on F/A-18 configuration at subsonic through transonic speed
[NASA-TP-3111] p 16 N92-14968
Breakdown of the Karman vortex street due to forced convection and flow compressibility p 196 N92-32472
[NASA-TM-105853] p 196 N92-32472
- VORTEX GENERATORS**
A study on vortex flow control of inlet distortion in the re-engined 727-100 center inlet duct using computational fluid dynamics p 4 A92-23767
[AIAA PAPER 92-0152] p 4 A92-23767
Effect of tabs on the evolution of an axisymmetric jet p 26 A92-40151
Design and analysis of vortex generators on reengined Boeing 727-100QF center inlet S-duct by a reduced Navier-Stokes code p 10 A92-45542
[AIAA PAPER 92-2700] p 10 A92-45542

- Supersonic jet mixing enhancement by 'delta-tabs'
[AIAA PAPER 92-3548] p 12 A92-49063
Application of computational fluid dynamics to the study of vortex flow control for the management of inlet distortion p 13 A92-54013
[AIAA PAPER 92-3177] p 13 A92-54013
The structure and development of streamwise vortex arrays embedded in a turbulent boundary layer p 14 N92-10012
[NASA-TM-105211] p 14 N92-10012
Vortex generator design for aircraft inlet distortion as a numerical optimization problem p 23 N92-13959
A study on vortex flow control on inlet distortion in the re-engined 727-100 center inlet duct using computational fluid dynamics p 14 N92-13998
[NASA-TM-105321] p 14 N92-13998
Supersonic jet mixing enhancement by delta-tabs
[NASA-TM-105664] p 18 N92-24958
Application of computational fluid dynamics to the study of vortex flow control for the management of inlet distortion p 230 N92-34112
[NASA-TM-105672] p 230 N92-34112
- VORTEX RINGS**
Direct evaluation of aeroacoustic theory in a jet p 253 A92-50296
- VORTEX SHEDDING**
Comparison of the SMAC, PISO, and iterative time-advancing schemes for unsteady flows p 175 A92-47158
Breakdown of the Karman vortex street due to forced convection and flow compressibility
[NASA-TM-105853] p 196 N92-32472
- VORTICES**
Aerodynamics of loaded cascades in subsonic flows subject to unsteady three-dimensional vortical disturbances p 4 A92-23762
[AIAA PAPER 92-0146] p 4 A92-23762
A study on vortex flow control of inlet distortion in the re-engined 727-100 center inlet duct using computational fluid dynamics p 4 A92-23767
[AIAA PAPER 92-0152] p 4 A92-23767
Features of wavy vortices in a curved channel from experimental and numerical studies p 171 A92-31638
Flow visualization and motion analysis for a series of four sequential brush seals p 204 A92-36976
A study of three dimensional turbulent boundary layer separation and vortex flow control using the reduced Navier Stokes equations p 9 A92-40105
Effect of tabs on the evolution of an axisymmetric jet p 26 A92-40151
Second order modeling of boundary-free turbulent shear flows p 174 A92-41275
Experimental investigation of the flowfield of an oscillating airfoil p 9 A92-45494
[AIAA PAPER 92-2622] p 9 A92-45494
The influence of higher harmonics on vortex pairing in an axisymmetric mixing layer p 175 A92-46251
Supersonic jet mixing enhancement by 'delta-tabs'
[AIAA PAPER 92-3548] p 12 A92-49063
Time domain numerical calculations of unsteady vortical flows about a flat plate airfoil p 12 A92-50473
Surface heat transfer and flow properties of vortex arrays induced artificially and from centrifugal instabilities p 183 A92-56371
The structure and development of streamwise vortex arrays embedded in a turbulent boundary layer p 14 N92-10012
[NASA-TM-105211] p 14 N92-10012
A study on vortex flow control on inlet distortion in the re-engined 727-100 center inlet duct using computational fluid dynamics p 14 N92-13998
[NASA-TM-105321] p 14 N92-13998
Wind tunnel investigation of vortex flows on F/A-18 configuration at subsonic through transonic speed
[NASA-TP-3111] p 16 N92-14968
An iterative implicit diagonally-dominant factorization algorithm for solving the Navier-Stokes equations
[NASA-TM-105259] p 249 N92-16663
Kolmogorov behavior of near-wall turbulence and its application in turbulence modeling p 191 N92-24050
[NASA-TM-105663] p 191 N92-24050
Supersonic jet mixing enhancement by delta-tabs
[NASA-TM-105664] p 18 N92-24958
Breakdown of the Karman vortex street due to forced convection and flow compressibility p 196 N92-32472
[NASA-TM-105853] p 196 N92-32472
Application of computational fluid dynamics to the study of vortex flow control for the management of inlet distortion p 230 N92-34112
[NASA-TM-105672] p 230 N92-34112
- VORTICITY**
A study on vortex flow control of inlet distortion in the re-engined 727-100 center inlet duct using computational fluid dynamics p 4 A92-23767
[AIAA PAPER 92-0152] p 4 A92-23767
Vorticity dynamics of inviscid shear layers
[AIAA PAPER 92-0420] p 168 A92-26270

The structure and development of streamwise vortex arrays embedded in a turbulent boundary layer [AIAA PAPER 92-0551] p 7 A92-28204
 Distortion of a flat-plate boundary layer by free-stream vorticity normal to the plate p 173 A92-36343
 A study on vortex flow control on inlet distortion in the re-engineered 727-100 center inlet duct using computational fluid dynamics [NASA-TM-105321] p 14 N92-13998
 An iterative implicit DDADI algorithm for solving the Navier-Stokes equation --- upwind split flux technique p 192 N92-25810

VSAT (NETWORK)
 Operational uses of ACTS technology [AIAA PAPER 92-1964] p 144 A92-29887
 Technology requirements for mesh VSAT applications [AIAA PAPER 92-1982] p 144 A92-29902
 ACTS T1-VSAT - The intelligent earth station [AIAA PAPER 92-2037] p 145 A92-29952

W

WAFERS
 Photoluminescence lifetime measurements in InP wafers p 262 A92-48092
 National Aerospace Plane engine seals: High temperature seal performance evaluation p 207 N92-15103
 An overview of silicon carbide device technology [NASA-TM-105402] p 263 N92-15815

WAKES
 Navier-Stokes solution of transonic cascade flows using nonperiodic C-type grids p 8 A92-28523
 Airfoil wake and linear theory gust response including sub and superresonant flow conditions [AIAA PAPER 92-3074] p 11 A92-48724

WALL FLOW
 The three-dimensional turbulent boundary layer near a plane of symmetry p 167 A92-24757
 Near-wall response in turbulent shear flows subjected to imposed unsteadiness p 174 A92-41652
 Development of an algebraic turbulence model for analysis of propulsion flows [AIAA PAPER 92-3861] p 183 A92-54209
 Advancements in engineering turbulence modeling [PAPER-105] p 189 N92-23350
 Kolmogorov behavior of near-wall turbulence and its application in turbulence modeling [NASA-TM-105663] p 191 N92-24050
 Comment on two-equation models --- turbulence models p 191 N92-24520
 Advances in engineering turbulence modeling --- computational fluid dynamics p 193 N92-25820
 Development of an algebraic turbulence model for analysis of propulsion flows [NASA-TM-105701] p 250 N92-27517
 A new time scale based k-epsilon model for near wall turbulence [NASA-TM-105768] p 196 N92-32868

WALL TEMPERATURE
 Combined conjugated heat transfer from a scattering medium p 175 A92-44390
 Hydrogen no-vent fill testing in a 1.2 cubic foot (34 liter) tank [NASA-TM-105273] p 185 N92-13401
 Thermal stratification potential in rocket engine coolant channels [NASA-TM-4378] p 87 N92-25616
 Breakdown of the Karman vortex street due to forced convection and flow compressibility [NASA-TM-105853] p 196 N92-32472

WALLS
 Comparative study of turbulence models in predicting hypersonic inlet flows [AIAA PAPER 92-3098] p 11 A92-48740
 Engine panel seals for hypersonic engine applications: High temperature leakage assessments and flow modelling [NASA-TM-105260] p 208 N92-16336
 Turbulence modeling p 189 N92-23338
 Comparative study of turbulence models in predicting hypersonic inlet flows [NASA-TM-105720] p 19 N92-28102

WATER
 Modelling and experimental verification of a water alleviation system for the NASP --- National Aerospace Plane [NASA-TM-105661] p 189 N92-23224

WATER INJECTION
 Contingency power for a small turbohaft engine by using water injection into turbine cooling air [NASA-TM-105680] p 37 N92-29661

WATER VAPOR
 Arcing of negatively biased solar cells in low earth orbit [AIAA PAPER 92-0578] p 59 A92-26985
 Preliminary characterizations of a water vaporizer for resistojet applications [AIAA PAPER 92-3533] p 74 A92-54041

WAVE ATTENUATION
 An optical method for determining level in two-phase cryogenic fluids [NASA-TM-104524] p 200 N92-15366

WAVE DISPERSION
 Optical dispersion relations for 'diamondlike' carbon films p 262 A92-44533

WAVE EQUATIONS
 Long time behavior of unsteady flow computations [NASA-TM-105584] p 190 N92-23565

WAVE INTERACTION
 On the nonlinear development of three-dimensional instability waves in natural transition [AIAA PAPER 92-0741] p 170 A92-28222
 Nonlinear spatial equilibration of an externally excited instability wave in a free shear layer p 170 A92-31469

WAVE PROPAGATION
 Effect of surface deposits on electromagnetic propagation in uniform ducts p 142 A92-23964
 Pressure wave propagation studies for oscillating cascades [AIAA PAPER 92-0145] p 5 A92-25682
 Subharmonic route to boundary-layer transition - Critical layer nonlinearity p 172 A92-35994
 Pressure wave propagation studies for oscillating cascades [NASA-TM-105406] p 16 N92-15977

WAVEGUIDE ANTENNAS
 Electromagnetic coupling between coplanar waveguide and microstrip antennas p 154 A92-21292
 Coplanar waveguide aperture coupled patch antennas with ground plane/substrate of finite extent p 154 A92-24488
 Laser ablated YBa₂Cu₃O(7-x) high temperature superconductor coplanar waveguide resonator p 155 A92-31631
 Coplanar waveguide aperture-coupled microstrip patch antenna p 146 A92-37222
 New coplanar waveguide feed network for 2 x 2 linearly tapered slot antenna subarray p 156 A92-45619
 Analysis of shielded CPW discontinuities with air-bridges p 152 N92-32971

WAVEGUIDES
 New techniques for exciting linearly tapered slot antennas with coplanar waveguide p 155 A92-34844
 Conductor-backed coplanar waveguide resonators of YBa₂Cu₃O(7-delta) on LaAlO₃ p 158 A92-51042
 A flexible CPW package for a 30 GHz MMIC amplifier --- coplanar waveguide [NASA-TM-105630] p 161 N92-23193
 Solid State Technology Branch of NASA Lewis Research Center [NASA-TM-105159] p 151 N92-23412
 A 1-W, 30-GHz, CPW amplifier for ACTS small terminal uplink [NASA-TM-105671] p 161 N92-26096
 Coplanar waveguide feeds for phased array antennas p 152 N92-32970
 Analysis of shielded CPW discontinuities with air-bridges p 152 N92-32971
 A flexible CPW package for a 30 GHz MMIC amplifier p 152 N92-32972
 A 1-W, 30-GHz, CPW amplifier for ACTS small terminal uplink p 152 N92-32973

WEAK INTERACTIONS (FIELD THEORY)
 Fluctuation-driven electroweak phase transition --- in early universe p 269 A92-54464

WEAR
 Studies of mechanochemical interactions in the tribological behavior of materials p 124 A92-32410
 Relative sliding durability of two candidate high temperature oxide fiber seal materials [AIAA PAPER 92-3713] p 126 A92-49095
 Relative sliding durability of two candidate high temperature oxide fiber seal materials [NASA-TM-105199] p 95 N92-10064
 Tribological and mechanical comparison of sintered and hiped PM212: High temperature self-lubricating composites [NASA-TM-105379] p 96 N92-15128
 Tribology needs for future space and aeronautical systems [NASA-TM-104525] p 128 N92-15191
 Properties data for opening the Galileo's partially unfurled main antenna [NASA-TM-105355] p 130 N92-20660
 Sliding durability of two carbide-oxide candidate high temperature fiber seal materials in air to 900 C [NASA-TM-105554] p 97 N92-21175

WEAR RESISTANCE
 A bulk flow model of a brush seal system [ASME PAPER 91-GT-325] p 203 A92-15696
 Tribological properties of ceramic-(Ti3Al-Nb) sliding couples for use as candidate seal materials to 700 C p 124 A92-32407
 Lubrication of space systems: Challenges and potential solutions [NASA-TM-105560] p 130 N92-21579
 Self-lubricating coatings for high-temperature applications p 130 N92-22516
 Tribological and microstructural comparison of HIPed PM212 and PM212/Au self-lubricating composites [NASA-TM-105615] p 97 N92-26142

WEAR TESTS
 Extended testing of xenon ion thruster hollow cathodes [AIAA PAPER 92-3204] p 65 A92-48811
 A vacuum (10(exp -9) Torr) friction apparatus for determining friction and endurance life of MoSx films [NASA-TM-104478] p 129 N92-16129
 Environmental effects on friction and wear of diamond and diamondlike carbon coatings [NASA-TM-105634] p 131 N92-23192
 Deposition of adherent Ag-Ti duplex films on ceramics in a multiple-cathode sputter deposition system [NASA-TM-105586] p 34 N92-23225
 Derated ion thruster design issues [NASA-TM-105576] p 87 N92-23534
 Development of a full-scale transmission testing procedure to evaluate advanced lubricants [NASA-TP-3265] p 213 N92-30396

WEAVING
 Structural design methodologies for ceramic-based material systems p 103 A92-39866
 Computational simulation of surface waviness in graphite/epoxy woven composites due to initial curing [NASA-TM-105313] p 106 N92-14118

WEIBULL DENSITY FUNCTIONS
 Reliability analysis of a structural ceramic combustion chamber [ASME PAPER 91-GT-155] p 24 A92-15591
 Transmission overhaul and component replacement predictions using Weibull and renewal theory p 215 A92-17201
 Mechanical behaviour and failure phenomenon of an in situ toughened silicon nitride p 127 A92-54504
 Reliability analysis of structural ceramic components using a three-parameter Weibull distribution [NASA-TM-105370] p 129 N92-17060

WEIGHT REDUCTION
 Multiobjective shape and material optimization of composite structures including damping p 218 A92-28055
 Advanced tube-bundle rocket thrust chambers p 62 A92-44509
 Advanced Rotorcraft Transmission (ART) Program summary [AIAA PAPER 92-3365] p 205 A92-48938
 Effects of anisotropic conduction and heat pipe interaction on minimum mass space radiators [NASA-TM-105297] p 80 N92-11138
 Advanced Rotorcraft Transmission (ART) program summary [NASA-TM-105665] p 210 N92-24984

WEIGHTING FUNCTIONS
 Fatigue crack growth in unidirectional metal matrix composite p 99 A92-19734

WHISKER COMPOSITES
 Strength, toughness and R-curve behaviour of SiC whisker-reinforced composite Si3N4 with reference to monolithic Si3N4 p 101 A92-34202
 Analysis of whisker-toughened CMC structural components using an interactive reliability model [AIAA PAPER 92-2490] p 221 A92-34582
 Structural design methodologies for ceramic-based material systems p 103 A92-39866
 Elevated temperature mechanical behavior of monolithic and SiC whisker-reinforced silicon nitrides [NASA-TM-105245] p 128 N92-15192
 Plasma etching a ceramic composite --- evaluating microstructure [NASA-TM-105430] p 130 N92-22305
 Ceramics for engines p 131 N92-22517

WHISKERS (CRYSTALS)
 A simple test for thermomechanical evaluation of ceramic fibers p 123 A92-21096

WHITE NOISE
 Least reliable bits coding (LRBC) for high data rate satellite communications [AIAA PAPER 92-1868] p 142 A92-29807
 An IIR median hybrid filter p 246 A92-40375

WIDEBAND COMMUNICATION
 An overview of Space Communication Artificial Intelligence for Link Evaluation Terminal (SCAILET) Project p 148 N92-14212

WIND EFFECTS

WIND EFFECTS

Effects of windblown dust on photovoltaic surfaces on Mars p 45 A92-50573

WIND PROFILES

Effect of a simulated glaze ice shape on the aerodynamic performance of a rectangular wing [AIAA PAPER 92-4042] p 14 A92-56861

WIND TUNNEL APPARATUS

Flow quality studies of the NASA Lewis Research Center 8- by 6-foot supersonic/9- by 15-foot Low Speed Wind Tunnel [AIAA PAPER 92-3916] p 41 A92-56748
Flow quality studies of the NASA Lewis Research Center 8- by 6-foot supersonic/9- by 15-foot low speed wind tunnel [NASA-TM-105417] p 42 N92-28673

WIND TUNNEL CALIBRATION

Investigation of the diffuser flow quality in an icing research wind tunnel p 40 A92-24406

WIND TUNNEL MODELS

LDV measurements on a rectangular wing with a simulated glaze ice accretion [AIAA PAPER 92-2690] p 10 A92-45537
Laser-driven hypersonic air-breathing propulsion simulator [AIAA PAPER 92-3922] p 41 A92-56753

WIND TUNNEL TESTS

Investigation of the diffuser flow quality in an icing research wind tunnel p 40 A92-24406
Mechanisms resulting in accreted ice roughness [AIAA PAPER 92-0297] p 21 A92-25750
Far-field noise and internal modes from a ducted propeller at simulated aircraft takeoff conditions [AIAA PAPER 92-0371] p 252 A92-26230
Finite wing aerodynamics with simulated glaze ice [AIAA PAPER 92-0414] p 5 A92-26265
Experimental investigation of turbulent flow through a circular-to-rectangular transition duct p 168 A92-26412

Performance of the Phase Doppler Particle Analyzer icing cloud droplet sizing probe in the NASA Lewis Icing Research Tunnel [AIAA PAPER 92-0162] p 198 A92-26926

Results of an icing test on a NACA 0012 airfoil in the NASA Lewis Icing Research Tunnel [AIAA PAPER 92-0647] p 7 A92-27021

Tensile properties of impact ices [AIAA PAPER 92-0883] p 94 A92-29644
Full field flow visualization and computer-aided velocity measurements in a bank of cylinders in a wind tunnel p 199 A92-50040

Wind tunnel performance results of swirl recovery vanes as tested with an advanced high speed propeller [AIAA PAPER 92-3770] p 28 A92-54159

Laser-driven hypersonic air-breathing propulsion simulator [AIAA PAPER 92-3922] p 41 A92-56753

Effect of particle size of Martian dust on the degradation of photovoltaic cell performance [NASA-TM-105232] p 79 N92-11133

Wind tunnel investigation of vortex flows on F/A-18 configuration at subsonic through transonic speed [NASA-TP-3111] p 16 N92-14968

Results of an icing test on a NACA 0012 airfoil in the NASA Lewis Icing Research Tunnel [NASA-TM-105374] p 16 N92-15051

Far-field noise and internal modes from a ducted propeller at simulated aircraft takeoff conditions [NASA-TM-105369] p 254 N92-16702

Structural analysis of low-speed composite propfan blades for the LRCSW wind tunnel model [NASA-TM-105266] p 229 N92-25753

Turbulent heat flux measurements in a transitional boundary layer [NASA-TM-105623] p 19 N92-27377

Lewis icing research tunnel test of the aerodynamic effects of aircraft ground deicing/anti-icing fluids [NASA-TP-3238] p 22 N92-30395

WIND TUNNEL WALLS

Wind tunnel wall effects in a linear oscillating cascade [ASME PAPER 91-GT-133] p 2 A92-15576

WIND TUNNELS

Calibration of hemispherical-head flow angularity probes [AIAA PAPER 92-4005] p 200 A92-56828
Inflatable traversing probe seal p 209 N92-22692

WIND VELOCITY

Effects of windblown dust on photovoltaic surfaces on Mars p 45 A92-50573

WINDOWS (APERTURES)

Effect of InAlAs window layer on the efficiency of indium phosphide solar cells p 234 A92-53163

Effect of InAlAs window layer on efficiency of indium phosphide solar cells [NASA-TM-105354] p 161 N92-25176

WING FLAPS

Experimental ice shape and performance characteristics for a multi-element airfoil in the NASA Lewis Icing Research Tunnel [NASA-TM-105380] p 17 N92-17347

WING OSCILLATIONS

Euler flow predictions for an oscillating cascade using a high resolution wave-split scheme [ASME PAPER 91-GT-198] p 3 A92-15623

WING PROFILES

Finite wing aerodynamics with simulated glaze ice [AIAA PAPER 92-0414] p 5 A92-26265
Analysis of iced wings [AIAA PAPER 92-0416] p 8 A92-29972
Simulation of iced wing aerodynamics p 21 N92-21686

WING SPAN

Comparison of two-dimensional and three-dimensional droplet trajectory calculations in the vicinity of finite wings [AIAA PAPER 92-0645] p 8 A92-28215

WING TIP VORTICES

Unsteady wing surface pressures in the wake of a propeller [AIAA PAPER 92-0277] p 5 A92-25731
Spatial instability of a swirling jet - Theory and experiment p 174 A92-41274

WINGS

Wind tunnel investigation of vortex flows on F/A-18 configuration at subsonic through transonic speed [NASA-TP-3111] p 16 N92-14968
Comparison of two-dimensional and three-dimensional droplet trajectory calculations in the vicinity of finite wings [NASA-TM-105617] p 188 N92-23154

WIRE

Composites of low-density trialuminides: Particulate and long fiber reinforcements [NASA-TM-105628] p 109 N92-25346

WIRING

Wiring for aerospace applications [NASA-TM-105777] p 162 N92-30427

WORK FUNCTIONS

Preliminary test results of a hollow cathode MPD thruster [NASA-TM-105324] p 84 N92-18474

WORK HARDENING

Hardening mechanisms in a dynamic strain aging alloy, Hastelloy X, during isothermal and thermomechanical cyclic deformation p 116 A92-24832

WORKING FLUIDS

Frozen start-up behavior of low-temperature heat pipes p 179 A92-49847
Design considerations for space radiators based on the liquid sheet (LSR) concept p 181 A92-50821
Alkali metal compatibility testing of candidate heater head materials for a Stirling engine heat transport system p 71 A92-50829

WORKSTATIONS

Color image processing and object tracking workstation [NASA-TM-105561] p 139 N92-26611

WROUGHT ALLOYS

Thermomechanical and bithermal fatigue behavior of cast B1900 + Hf and wrought Haynes 188 p 122 A92-45233

X

X RAY ABSORPTION

Near-edge study of gold-substituted YBa₂Cu₃O_{7-δ} p 259 A92-14950

X RAY APPARATUS

X ray based displacement measurement for hostile environments [NASA-TM-105551] p 202 N92-23155

X RAY DIFFRACTION

Composition dependence of superconductivity in YBa₂(Cu_{3-x}Al_x)O_y [NASA-TM-105358] p 131 N92-24715

X RAY SOURCES

X ray based displacement measurement for hostile environments [NASA-TM-105551] p 202 N92-23155

X RAY SPECTROSCOPY

An XPS study of the stability of Fomblin Z25 on the native oxide of aluminum --- x ray photoelectron spectroscopy [NASA-TM-105594] p 131 N92-23185

X RAYS

Near-edge study of gold-substituted YBa₂Cu₃O_{7-δ} p 259 A92-14950

X ray attenuation measurements for high-temperature materials characterization and in-situ monitoring of damage accumulation [NASA-TM-105577] p 110 N92-25996

XENON

Extended testing of xenon ion thruster hollow cathodes [AIAA PAPER 92-3204] p 65 A92-48811
Neutralizer optimization [NASA-TM-105578] p 86 N92-21976
Low-Isp derated ion thruster operation [NASA-TM-105787] p 92 N92-32237

Y

YAW

Full Navier-Stokes calculations on the installed F/A-18 inlet at a high angle of attack [AIAA PAPER 92-3175] p 13 A92-54012
Calibration of hemispherical-head flow angularity probes [AIAA PAPER 92-4005] p 200 A92-56828

YIELD STRENGTH

The decrease in yield strength in NiAl due to hydrostatic pressure p 120 A92-38990
Tensile behavior of the L(1)2 compound Al₆Ti₂Cr₈ p 122 A92-49694

YTTRIUM

High-T sub c fluorine-doped YBa₂Cu₃O_y films on ceramic substrates by screen printing [NASA-TM-105296] p 127 N92-11188

YTTRIUM COMPOUNDS

Composite thermal barrier coating [NASA-CASE-LEW-14999-1] p 108 N92-21725

YTTRIUM OXIDES

Near-edge study of gold-substituted YBa₂Cu₃O_{7-δ} p 259 A92-14950
Coaxial line configuration for microwave power transmission study of YBa₂Cu₃O_{7-δ} thin films p 154 A92-18455
Melting of the Abrikosov flux lattice in anisotropic superconductors p 260 A92-28075
On improving the fracture toughness of a NiAl-based alloy by mechanical alloying p 118 A92-30794
Laser ablated YBa₂Cu₃O_{7-x} high temperature superconductor coplanar waveguide resonator p 155 A92-31631

Performance of a four-element Ka-band high-temperature superconducting microstrip antenna p 146 A92-37224

Conductor-backed coplanar waveguide resonators of YBa₂Cu₃O_{7-δ} on LaAlO₃ p 158 A92-51042

Glass formation, properties, and structure of soda-yttria-silicate glasses [NASA-TM-104488] p 128 N92-11202
Glass precursor approach to high-temperature superconductors [NASA-TM-105590] p 263 N92-20519

Z

ZINC COMPOUNDS

The effects of RF plasma ashing on zinc orthotitanate/potassium silicate thermal control coatings [AIAA PAPER 92-2171] p 124 A92-31299

ZIPPERS

Inflatable traversing probe seal p 209 N92-22692

ZIRCONIUM ALLOYS

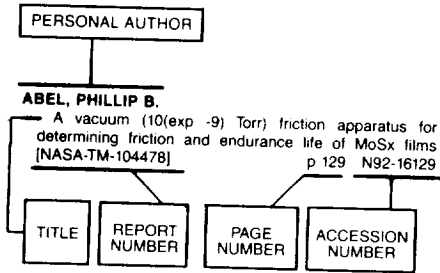
Correlation of deformation mechanisms with the tensile and compressive behavior of NiAl and NiAl(Zr) intermetallic alloys p 120 A92-38019

ZIRCONIUM OXIDES

Composite thermal barrier coating [NASA-CASE-LEW-14999-1] p 108 N92-21725
Guanidine based vehicle/binders for use with oxides, metals, and ceramics [NASA-CASE-LEW-15314-1] p 131 N92-23461

PERSONAL AUTHOR INDEX

Typical Personal Author Index Listing



Listings in this index are arranged alphabetically by personal author. The accession number denotes the number by which the citation is identified.

A

- ABBE, BRIAN**
ACTS aeronautical experiments
[AIAA PAPER 92-2042] p 50 A92-29956
- ABBOTT, JOHN M.**
Inlets, ducts, and nozzles p 188 N92-22523
- ABDUL-AZIZ, A.**
Effects of coolant parameters on steady state temperature distribution in phosphoric-acid fuel cell electrode p 233 A92-50737
- ABDUL-AZIZ, ALI**
Measurements of the effects of thermal contact resistance on steady state heat transfer in phosphoric-acid fuel cell stack p 180 A92-50738
- ABEL, PHILLIP B.**
A vacuum (10(exp -9) Torr) friction apparatus for determining friction and endurance life of MoSx films [NASA-TM-104478] p 129 N92-16129
- ABOUELKHEIR, M.**
Row-by-row off-design performance calculation method for turbines p 26 A92-44514
- ABRAMOVITZ, IRWIN**
Multichannel demultiplexer/demodulator technologies for future satellite communication systems [NASA-TM-105377] p 51 N92-18342
- ABUMERI, G. H.**
Analysis of aircraft engine blade subject to ice impact [NASA-TM-105336] p 226 N92-15402
- ABUMERI, GALIB H.**
Evaluation of MHOST analysis capabilities for a plate element [NASA-TM-105387] p 228 N92-23196
- ACKERMAN, EDWARD**
Interfaces for high-speed fiber-optic links - Analysis and experiment p 256 A92-24002
- ACOSTA, R. J.**
Microwave beam power transmission at an arbitrary range [NASA-TM-105424] p 150 N92-19992
- ACOSTA, ROBERTO J.**
Advanced Communication Technology Satellite (ACTS) multibeam antenna technology verification experiments [NASA-TM-105421] p 149 N92-16191
- Advanced Communication Technology Satellite (ACTS) multibeam antenna analysis and experiment**
[NASA-TM-105420] p 149 N92-17047
- Analysis of a generalized dual reflector antenna system using physical optics**
[NASA-TM-105425] p 149 N92-18281
- ADAMCZYK, J. J.**
The role of tip clearance in high-speed fan stall [ASME PAPER 91-GT-83] p 2 A92-15550
- A mathematical constraint placed upon inter-blade row boundary conditions used in the simulation of multistage turbomachinery flows**
p 195 N92-27458
- ADAMCZYK, JOHN J.**
The numerical simulation of a high-speed axial flow compressor [ASME PAPER 91-GT-272] p 3 A92-15669
- Unsteady aerodynamic interaction effects on turbomachinery blade life and performance**
[AIAA PAPER 92-0149] p 7 A92-28186
- Turbomachinery**
p 32 N92-22524
- ADAMOVSKY, GRIGORY**
RF modulated fiber optic sensing systems and their applications [NASA-TM-105801] p 257 N92-33896
- ADDY, HAROLD E., JR.**
Investigation of the diffuser flow quality in an icing research wind tunnel p 40 A92-24406
- Lewis icing research tunnel test of the aerodynamic effects of aircraft ground deicing/anti-icing fluids**
[NASA-TP-3238] p 22 N92-30395
- AESCHLIMAN, DANIEL P.**
Calibration of hemispherical-head flow angularity probes [AIAA PAPER 92-4005] p 200 A92-56828
- AFOLABI, D.**
Modal interaction in linear dynamic systems near degenerate modes [NASA-TM-105315] p 225 N92-12316
- AHEDO, E.**
Systems analysis of electrodynamic tethers p 62 A92-41550
- AHN, KYUNG H.**
A 2-D oscillating flow analysis in Stirling engine heat exchangers p 172 A92-36001
- AIELLO, ROBERT A.**
Improved accuracy for finite element structural analysis via a new integrated force method [NASA-TP-3204] p 227 N92-22227
- AIFER, E.**
Arcing of negatively biased solar cells in low earth orbit [AIAA PAPER 92-0578] p 59 A92-26985
- Arcing of negatively biased solar cells in a plasma environment. I - Experimental observations**
[AIAA PAPER 92-2990] p 63 A92-47000
- AINDOW, M.**
Compatibility of potential reinforcing ceramics with Ni and Fe aluminides p 105 A92-46874
- ALBRECHT, ANDREAS**
Perturbations from cosmic strings in cold dark matter p 268 A92-33353
- ALEXANDER, S.**
An accelerated development, reduced cost approach to lunar/Mars exploration using a modular NTR-based space transportation system [IAF PAPER 92-0574] p 43 A92-57053
- ALEXANDER, STEPHEN W.**
Mission and sizing analysis for the Beta II two-stage-to-orbit vehicle [AIAA PAPER 92-1264] p 47 A92-35868
- Minimum impulse trajectories for Mars round trip missions**
[AAS PAPER 91-500] p 44 A92-43339
- Mission and sizing analysis for the Beta 2 two-stage-to-orbit vehicle**
[NASA-TM-105559] p 48 N92-21547
- Fast track lunar NTR systems assessment for the First Lunar Outpost and its evolvability to Mars**
p 142 N92-33334

- ALEXOVICH, ROBERT E.**
Multiple-access phased array antenna simulator for a digital beam forming system investigation [NASA-TM-105422] p 149 N92-17062
- ALGER, DONALD**
Progress update of NASA's free-piston Stirling space power converter technology project [NASA-TM-105748] p 239 N92-33898
- ALKASAB, K. A.**
Effects of coolant parameters on steady state temperature distribution in phosphoric-acid fuel cell electrode p 233 A92-50737
- ALKASAB, KALIL A.**
Measurements of the effects of thermal contact resistance on steady state heat transfer in phosphoric-acid fuel cell stack p 180 A92-50738
- ALLAIRE, P. E.**
Optimal microgravity vibration isolation - An algebraic introduction p 54 A92-47495
- Microgravity vibration isolation: An optimal control law for the one-dimensional case**
[NASA-TM-105146] p 141 N92-11217
- Microgravity vibration isolation: Optimal preview and feedback control**
[NASA-TM-105673] p 142 N92-30692
- ALLEN, M. G.**
Doppler-shifted fluorescence imaging of velocity fields in supersonic reacting flows [AIAA PAPER 92-2964] p 199 A92-46979
- ALSTON, WILLIAM B.**
Substituted 1,1,1-triaryl-2,2,2-trifluoroethanes and processes for their synthesis [NASA-CASE-LEW-14345-6] p 96 N92-17882
- Structure-to-property relationships in addition cured polymers. 4: Correlations between thermo-oxidative weight losses of norbornenyl cured polyimide resins and their composites**
[NASA-TM-105553] p 108 N92-20039
- Cyclopentadiene evolution during pyrolysis-gas chromatography of PMR polyimides**
[NASA-TM-105629] p 132 N92-25348
- ALTENBURGER, GENE P.**
Simulating the arcjet thruster using a nonlinear active load [AIAA PAPER 92-3528] p 45 A92-49052
- ALTENKIRCH, ROBERT A.**
Opposed flow flame spread in normal, enhanced and reduced gravity p 111 A92-12898
- ALTEROVITZ, S. A.**
Temperature independent quantum well FET with delta channel doping p 157 A92-49596
- Enhancement of Shubnikov-de Haas oscillations by carrier modulation**
p 262 A92-50911
- A new technique for oil backstreaming contamination measurements**
[NASA-TM-105312] p 257 N92-13783
- Intermodulation in the oscillatory magnetoresistance of a two-dimensional electron gas**
p 163 N92-32975
- ALTEROVITZ, SAMUEL A.**
Optical dispersion relations for 'diamondlike' carbon films p 262 A92-44533
- Reduced mobility and PPC in In(20)Ga(80)As / Al(23)Ga(77)As HEMT structure**
p 265 N92-32976
- Study of InGaAs-based modulation doped field effect transistor structures using variable-angle spectroscopic ellipsometry**
p 265 N92-32977
- Microwave properties of peeled HEMT devices sapphire substrates**
p 265 N92-32978
- Magnetic flux relaxation in YBa2Cu3O(7-x) thin film. Thermal or athermal**
p 265 N92-32984
- AMADOR, C.**
'Wrong' bond interactions at inversion domain boundaries in GaAs p 260 A92-27297
- AMERI, A. A.**
Navier-Stokes analysis of turbomachinery blade external heat transfer p 170 A92-28518
- AMERI, ALI A.**
Navier-Stokes turbine heat transfer predictions using two-equation turbulence closures [AIAA PAPER 92-3067] p 177 A92-48721

AMIN, S.

AMIN, S.

Flow induction by pressure forces
[AIAA PAPER 92-3571] p 28 A92-54060

AMIROUCHE, F. M. L.

Minimization of vibration in elastic beams with time-variant boundary conditions p 224 A92-50511

AMUEDO, KURT C.

Hot gas ingestion characteristics and flow visualization of a vectored thrust STOVL concept p 26 A92-45316

ANDERSON, BERNHARD H.

A study on vortex flow control of inlet distortion in the re-engined 727-100 center inlet duct using computational fluid dynamics p 4 A92-23767

[AIAA PAPER 92-0152] p 4 A92-23767

Design and analysis of reengine Boeing 727-100 center inlet S duct by a reduced Navier-Stokes code p 8 A92-33320

[AIAA PAPER 92-1221] p 8 A92-33320

A study of three dimensional turbulent boundary layer separation and vortex flow control using the reduced Navier Stokes equations p 9 A92-40105

Design and analysis of vortex generators on reengine Boeing 727-100QF center inlet S-duct by a reduced Navier-Stokes code p 10 A92-45542

[AIAA PAPER 92-2700] p 10 A92-45542

Comparative study of turbulence models in predicting hypersonic inlet flows p 11 A92-48740

[AIAA PAPER 92-3098] p 11 A92-48740

Application of computational fluid dynamics to the study of vortex flow control for the management of inlet distortion p 13 A92-54013

[AIAA PAPER 92-3177] p 13 A92-54013

Vortex generator design for aircraft inlet distortion as a numerical optimization problem p 23 N92-13959

A study on vortex flow control on inlet distortion in the re-engined 727-100 center inlet duct using computational fluid dynamics p 14 N92-13998

[NASA-TM-105321] p 14 N92-13998

Inlets, ducts, and nozzles p 188 N92-22523

Comparative study of turbulence models in predicting hypersonic inlet flows p 19 N92-28102

[NASA-TM-105720] p 19 N92-28102

Application of computational fluid dynamics to the study of vortex flow control for the management of inlet distortion p 230 N92-34112

[NASA-TM-105672] p 230 N92-34112

ANDERSON, RONALD R.

An advanced intelligent control system framework p 65 A92-48785

[AIAA PAPER 92-3162] p 65 A92-48785

ANDERSON, W. G.

Alkali metal pool boiler life tests for a 25 kWe advanced Stirling conversion system p 206 A92-50797

Design of a pool boiler heat transport system for a 25 kWe advanced Stirling conversion system p 181 A92-50802

ANDERSON, WILLIAM J.

A 23.2:1 ratio, 300-watt, 26 N-m output torque, planetary roller-gear robotic transmission: Design and evaluation p 210 N92-25085

ANDERSON, WILLIAM P.

Fiber optic controls for aircraft engines - Issues and implications p 24 A92-46244

ANDREWS, J. C.

Electric propulsion - The future is now p 63 A92-48386

ANDRO, MONTY

Multiple-access phased array antenna simulator for a digital beam forming system investigation p 149 N92-17062

[NASA-TM-105422] p 149 N92-17062

ANGEL, PAUL W.

Glass formation, properties, and structure of soda-yttria-silicate glasses p 128 N92-11202

[NASA-TM-104488] p 128 N92-11202

ANGHAIE, SAMIM

Innovative nuclear thermal propulsion technology evaluation - Results of the NASA/DOE task team study p 58 A92-13160

[IAF PAPER 91-235] p 58 A92-13160

ANSARI, RAFAT R.

A fiber-optic probe for particle sizing in concentrated suspensions p 197 A92-21371

A fiber optic sensor for ophthalmic refractive diagnostics p 198 A92-34831

ANSPAUGH, BRUCE

Radiation performance of GaAs concentrator cells for 0.4 to 12 MeV electrons and 0.1 to 37 MeV protons p 159 A92-53193

ANTHAN, DONALD J.

Wavelength-multiplexed fiber-optic position encoder for aircraft control systems p 24 A92-42602

ANTON, D. L.

Intermetallic matrix composites; Proceedings of the MRS Symposium, San Francisco, CA, Apr. 18-20, 1990 p 104 A92-46826

[ISBN 1-55899-083-6] p 104 A92-46826

APPELBAUM, J.

Solar radiation on a catenary collector p 163 N92-32243

[NASA-TM-105751] p 163 N92-32243

Photovoltaic array for Martian surface power p 270 N92-33899

APPELBAUM, JOSEPH

Photovoltaic power options for Mars p 231 A92-20366

Solar radiation for Mars power systems p 81 N92-13259

APPLEBY, A. J.

Temperature dependence of the electrode kinetics of oxygen reduction at the platinum/Nafion interface - A microelectrode investigation p 115 A92-56950

ARIF, H.

COLD-SAT - A technology satellite for cryogenic experimentation p 52 A92-13425

Cryogenic fluid management investigations using the CONE flight experiment p 43 A92-23851

ARIF, HUGH

Evaluation of supercritical cryogen storage and transfer systems for future NASA missions p 47 A92-28512

ARMAND, SASAN

Modal test/analysis correlation of Space Station structures using nonlinear sensitivity p 230 N92-34221

ARMAND, SASAN C.

Design feasibility study of a Space Station Freedom truss p 214 N92-30571

[NASA-TM-105558] p 214 N92-30571

Influence of mass moment of inertia on normal modes of preloaded solar array mast p 230 N92-33476

ARNOLD, D.

A high temperature superconductivity communications flight experiment p 50 A92-55790

[IAF PAPER 92-0410] p 50 A92-55790

ARNETTE, S. A.

Filtered Rayleigh scattering based measurements in compressible mixing layers p 182 A92-54043

[AIAA PAPER 92-3543] p 182 A92-54043

ARNETTE, STEPHEN A.

Study of compressible mixing layers using filtered Rayleigh scattering based visualizations p 183 A92-54937

[NASA-TM-105213] p 226 N92-16371

Explicit robust schemes for implementation of a class of principal value-based constitutive models: Theoretical development p 227 N92-20212

[NASA-TM-105345] p 227 N92-20212

A differential CDM model for fatigue of unidirectional metal matrix composites p 230 N92-31505

[NASA-TM-105726] p 230 N92-31505

Viscoplastic analysis of an experimental cylindrical thrust chamber liner p 218 A92-28052

Influence of engineered interfaces on residual stresses and mechanical response in metal matrix composites p 109 N92-23195

[NASA-TM-105438] p 109 N92-23195

Effects of fiber and interfacial layer architectures on the thermoplastic response of metal matrix composites p 110 N92-32234

[NASA-TM-105802] p 110 N92-32234

ARNOLD, WILLIAM A.

Transport modes during crystal growth in a centrifuge p 138 A92-33835

Multigrad calculation of three-dimensional viscous cascade flows p 249 N92-10345

[NASA-TM-105257] p 249 N92-10345

Navier-Stokes solution of transonic cascade flows using nonperiodic C-type grids p 8 A92-28523

Navier-Stokes turbine heat transfer predictions using two-equation turbulence closures p 177 A92-48721

[AIAA PAPER 92-3067] p 177 A92-48721

Space applications of high temperature superconductivity technology p 259 A92-14724

[IAF PAPER 91-307] p 259 A92-14724

NASA Space applications of high-temperature superconductors p 271 N92-18455

[NASA-TM-105401] p 271 N92-18455

NASA space applications of high-temperature superconductors p 265 N92-32980

ARONOFF, IRENE

Applicability of Long Duration Exposure Facility environmental effects data to the design of Space Station Freedom electrical power system p 53 A92-29614

[AIAA PAPER 92-0848] p 53 A92-29614

Contamination effects on Space Station Freedom electric power system performance p 54 A92-50578

ARR, V. D.

Computer program for computing the properties of seventeen fluids p 241 A92-23849

ARRINGTON, E. A.

Flow quality studies of the NASA Lewis Research Center 8- by 6-foot supersonic/9- by 15-foot Low Speed Wind Tunnel p 41 A92-56748

[AIAA PAPER 92-3916] p 41 A92-56748

ARRINGTON, E. ALLEN

Flow quality studies of the NASA Lewis Research Center 8- by 6-foot supersonic/9- by 15-foot low speed wind tunnel p 42 N92-28673

[NASA-TM-105417] p 42 N92-28673

Performance comparison of axisymmetric and three-dimensional hydrogen film coolant injection in a 110 N hydrogen/oxygen rocket p 73 A92-54027

[AIAA PAPER 92-3390] p 73 A92-54027

ARYA, V.

Application of a thermal fatigue life prediction model to high-temperature aerospace alloys B1900 + Hf and Haynes 188 p 121 A92-45232

Reduction of thermal residual stresses in advanced metallic composites based upon a compensating/compliant layer concept p 105 A92-47106

Viscoplastic analysis of an experimental cylindrical thrust chamber liner p 218 A92-28052

1400 and 1500 K compressive creep properties of an NiAl-AIN composite p 103 A92-41575

Preliminary tests of annular ion optics p 64 A92-48776

[AIAA PAPER 92-3148] p 64 A92-48776

Preliminary tests of annular ion optics p 64 A92-48776

Aerodynamics of loaded cascades in subsonic flows subject to unsteady three-dimensional vortical disturbances p 4 A92-23762

[AIAA PAPER 92-0146] p 4 A92-23762

A finite-volume numerical method to calculate fluid forces and rotordynamic coefficients in seals p 183 A92-54132

[AIAA PAPER 92-3712] p 183 A92-54132

Comparison of analysis and experiment for gearbox noise p 210 N92-25396

[NASA-TM-105330] p 210 N92-25396

Effect of operating conditions on gearbox noise p 211 N92-26107

[NASA-TM-105331] p 211 N92-26107

LEDF spacecraft, ground laboratory, and computational modeling implications on Space Station Freedom's solar array materials and surfaces durability p 71 A92-53190

Plans for the development of cryogenic engines for space exploration p 79 N92-11135

[NASA-TM-105250] p 79 N92-11135

COSP - A computer model of cyclic oxidation p 114 A92-31849

Observations of soot during droplet combustion at low gravity - Heptane and heptane/monochloroalkane mixtures p 115 A92-50447

A high-performance photovoltaic concentrator array - The mini-dome Fresnel lens concentrator with 30 percent efficient GaAs/GaSb tandem cells p 72 A92-53199

Evaluation of supercritical cryogen storage and transfer systems for future NASA missions p 47 A92-28512

Development of an efficient analysis for high Reynolds number inviscid/viscid interactions in cascades p 10 A92-48723

[AIAA PAPER 92-3073] p 10 A92-48723

B

- BAKLINI, GEORGE Y.**
NDE of advanced turbine engine components and materials by computed tomography
[ASME PAPER 91-GT-287] p 215 A92-15681
X ray attenuation measurements for high-temperature materials characterization and in-situ monitoring of damage accumulation
[NASA-TM-105577] p 110 N92-25996
- BACHALO, E. J.**
Performance of the Phase Doppler Particle Analyzer icing cloud droplet sizing probe in the NASA Lewis Icing Research Tunnel
[AIAA PAPER 92-0162] p 198 A92-26926
- BACHALO, W. D.**
Performance of the Phase Doppler Particle Analyzer icing cloud droplet sizing probe in the NASA Lewis Icing Research Tunnel
[AIAA PAPER 92-0162] p 198 A92-26926
- BAEZ, ANASTACIO N.**
Description of the control system design for the SSF PMAD DC testbed p 45 A92-50654
- BAGWELL, JAMES W.**
Future communications satellite applications p 52 N92-22019
- BAHADORI, M. Y.**
Gravitational influences on the behavior of confined diffusion flames
[AIAA PAPER 92-0334] p 113 A92-25781
Effects of oxygen concentration on radiative loss from normal-gravity and microgravity methane diffusion flames
[AIAA PAPER 92-0243] p 113 A92-26928
- BAHCALL, J. N.**
Monte Carlo exploration of Mikheyev-Smirnov-Wolfenstein solutions to the solar neutrino problem p 270 A92-50927
- BAHIR, GAD**
A model for the trap-assisted tunneling mechanism in diffused n-p and implanted n(+)-p HgCdTe photodiodes p 156 A92-46007
- BAILEY, S. G.**
Advances in photovoltaic technology
[IAF PAPER 92-0599] p 235 A92-57055
- BAILEY, SHEILA**
Increased efficiency with surface texturing in ITO/InP solar cells p 232 A92-44548
High performance etchant for thinning p(+)-InP and its application to p(+)-InP solar cell fabrication p 263 A92-53155
Evaluation of the minority carrier diffusion length and surface-recombination velocity in GaAs p/n solar cells p 234 A92-53162
- BAILEY, SHEILA G.**
Advanced power systems for EOS p 70 A92-50640
Enhancing optical absorption in InP and GaAs utilizing profile etching p 263 A92-53154
Enhanced EOS photovoltaic power system capability with InP solar cells p 81 N92-13248
Enhancing optical absorption in InP and GaAs utilizing profile etching
[NASA-TM-105325] p 82 N92-14111
- BAILEY, W. J.**
Cryogenic fluid management investigations using the CONE flight experiment p 43 A92-23851
- BAIN, D. B.**
CFD mixing analysis of jets injected from straight and slanted slots into confined crossflow in rectangular ducts
[AIAA PAPER 92-3087] p 177 A92-48732
CFD mixing analysis of jets injected from straight and slanted slots into confined crossflow in rectangular ducts
[NASA-TM-105699] p 36 N92-26561
- BAKER, KARL W.**
Effects of anisotropic conduction and heat pipe interaction on minimum mass space radiators
[NASA-TM-105297] p 80 N92-11138
NASA Lewis steady-state heat pipe code users manual
[NASA-TM-105161] p 90 N92-28682
Solar thermal energy receiver
[NASA-CASE-LEW-14949-1] p 238 N92-29143
Design characteristics of a heat pipe test chamber
[NASA-TM-105737] p 238 N92-29662
- BAKHLE, M. A.**
Cascade flutter analysis with transient response aerodynamics p 217 A92-15972
- BAKHLE, MILIND A.**
Analysis of cascades using a two dimensional Euler aeroelastic solver
[AIAA PAPER 92-2370] p 26 A92-34598
- BALASUBRAMANIAM, R.**
Unsteady thermocapillary migration of isolated drops in creeping flow p 169 A92-27774
- BALDWIN, LARRY J.**
Addition curing thermosets endcapped with 4-amino (2,2) paracyclophane p 124 A92-33918
- BALDWIN, RICHARD S.**
The O₂ reduction at the IFC modified O₂ fuel cell electrode
[NASA-TM-105691] p 90 N92-29667
- BALL, CALVIN L.**
Supersonic throughflow fans for high-speed aircraft p 34 N92-22541
- BALLARINI, R.**
Near-tip dual-length scale mechanics of mode-I cracking in laminate brittle matrix composites
[AIAA PAPER 92-2491] p 221 A92-34583
- BALOMBIN, JOSEPH L.**
Operational uses of ACTS technology
[AIAA PAPER 92-1964] p 144 A92-29887
- BALOMBIN, JOSEPH R.**
ACTS system capability and performance
[AIAA PAPER 92-1961] p 143 A92-29884
- BANERJEA, AMITAVA**
Universal aspects of adhesion and atomic force microscopy p 260 A92-17979
- BANISH, MICHAEL**
Vapor crystal growth technology development: Application to cadmium telluride
[NASA-TM-103786] p 139 N92-16158
- BANKS, BRUCE A.**
SiO(X) coatings for atomic oxygen protection of polyimide Kapton in low earth orbit
[AIAA PAPER 92-2151] p 94 A92-31286
LDEF spacecraft, ground laboratory, and computational modeling implications on Space Station Freedom's solar array materials and surfaces durability p 71 A92-53190
Atomic oxygen undercutting of LDEF aluminized-Kapton multilayer insulation p 255 N92-24818
Atomic oxygen interactions with FEP Teflon and silicones on LDEF p 132 N92-24820
Monte Carlo modeling of atomic oxygen attack of polymers with protective coatings on LDEF p 132 N92-27281
Heat transfer device
[NASA-CASE-LEW-14162-3] p 111 N92-34208
- BANSAL, N. P.**
Low temperature synthesis of CaO-SiO₂ glasses having stable liquid-liquid immiscibility by the sol-gel process p 126 A92-44479
- BANSAL, NAROTTAM P.**
High-T sub c fluorine-doped YBa₂Cu₃O_(y) films on ceramic substrates by screen printing
[NASA-TM-105296] p 127 N92-11188
Chemical stability of high-temperature superconductors
[NASA-TM-105391] p 263 N92-19398
Glass precursor approach to high-temperature superconductors
[NASA-TM-105590] p 263 N92-20519
Phase transformations in SrAl₂Si₂O₈ glass
[NASA-TM-105657] p 264 N92-23890
Composition dependence of superconductivity in YBa₂(Cu_{3-x}Al_x)O_y
[NASA-TM-105358] p 131 N92-24715
- BARANKIEWICZ, WENDY**
Use of an approximate similarity principle for the thermal scaling of a full-scale thrust augmenting ejector
[AIAA PAPER 92-3792] p 28 A92-54171
- BARANKIEWICZ, WENDY S.**
Use of an approximate similarity principle for the thermal scaling of a full-scale thrust augmenting ejector
[NASA-TM-105724] p 36 N92-26613
- BARBER, FRANK J.**
Reliability training
[NASA-RP-1253] p 49 N92-32456
- BARINA, FRANK J.**
Reliability training
[NASA-RP-1253] p 49 N92-32456
- BARKHOUDARIAN, S.**
Advanced optical condition monitoring
[SAE PAPER 912164] p 199 A92-39994
Fiber optics in liquid propellant rocket engine environments p 62 A92-42610
- BARNES, SCOTT P.**
Real-time data compression of broadcast video signals
[NASA-CASE-LEW-14945-2] p 147 N92-10128
- BARNETT, M.**
Development of an efficient analysis for high Reynolds number inviscid/viscid interactions in cascades
[AIAA PAPER 92-3073] p 10 A92-48723
- BARRETT, C. A.**
The cyclic oxidation resistance at 1200 C of beta-NiAl, FeAl, and CoAl alloys with selected third element additions
[NASA-TM-105620] p 123 N92-24554
- BARRETT, CHARLES A.**
COSP - A computer model of cyclic oxidation p 114 A92-31849
- Cyclic oxidation resistance of a reaction milled NiAl-AlN composite p 105 A92-46871
- BARTOLOTTA, PAUL**
Thermomechanical testing of high-temperature composites - Thermomechanical fatigue (TMF) behavior of SiC(SCS-6)/Ti-15-3 p 104 A92-44606
- BARTOLOTTA, PAUL A.**
High-temperature fatigue behavior of a SiC/Ti-24Al-11Nb composite p 104 A92-44613
An evaluation of strain measuring devices for ceramic composites p 199 A92-46497
An evaluation of strain measuring devices for ceramic composites p 225 N92-14433
Post-test examination of a pool boiler receiver
[NASA-TM-105635] p 123 N92-27192
- BARTON, J. M.**
Renormalization group analysis of the Reynolds stress transport equation p 179 A92-49493
Renormalization group analysis of the Reynolds stress transport equation
[NASA-TM-105588] p 190 N92-23542
- BARTOS, KAREN F.**
A three-dimensional finite-element thermal/mechanical analytical technique for high-performance traveling wave tubes
[AIAA PAPER 92-1824] p 154 A92-29771
- BATHURST, RICHARD L.**
Wavelength-multiplexed fiber-optic position encoder for aircraft control systems p 24 A92-42602
- BATTERTON, PETER G.**
Supersonic STOV_L propulsion technology program: An overview p 33 N92-22539
- BATTLES, B. E.**
Quantitative fluorescence measurements of the OH radical in high pressure methane flames
[AIAA PAPER 92-2960] p 114 A92-46976
- BATUR, C.**
Adaptive temperature profile control of a multizone crystal growth furnace p 137 A92-29243
Identification and control of a multizone crystal growth furnace p 199 A92-39699
- BAUER, PETER H.**
An IIR median hybrid filter p 246 A92-40375
- BAUGHER, CHARLES R.**
Development of and flight results from the Space Acceleration Measurement System (SAMS)
[AIAA PAPER 92-0354] p 56 A92-28189
Development of and flight results from the Space Acceleration Measurement System (SAMS)
[NASA-TM-105652] p 57 N92-30301
- BAUM, H. R.**
Heat and mass transport from thermally degrading thin cellulosic materials in a microgravity environment p 174 A92-41810
- BAUMANN, E. D.**
Electrical properties of teflon and ceramic capacitors at high temperatures
[NASA-TM-105569] p 160 N92-20040
High temperature dielectric properties of Apical, Kapton, Peek, Teflon AF, and Uplex polymers
[NASA-TM-105753] p 162 N92-28675
- BAUMANN, ERIC D.**
Multi-megawatt inverter/converter technology for space power applications
[NASA-TM-105307] p 159 N92-14294
- BAUMBICK, R.**
Reconfigurable optical interconnection network for multimode optical fiber sensor arrays p 256 A92-37448
- BAUMBICK, ROBERT**
Multiple-mode reconfigurable electro-optic switching network for optical fiber sensor array p 256 A92-46245
Potential for integrated optical circuits in advanced aircraft with fiber optic control and monitoring systems p 24 A92-46246
- BAUMEISTER, KENNETH J.**
Effect of surface deposits on electromagnetic propagation in uniform ducts p 142 A92-23964
Modal element method for scattering of sound by absorbing bodies
[NASA-TM-105722] p 255 N92-28984
- BAUMGARTEN, WILLIAM J.**
Mission and sizing analysis for the Beta II two-stage-to-orbit vehicle
[AIAA PAPER 92-1264] p 47 A92-35868
Mission and sizing analysis for the Beta 2 two-stage-to-orbit vehicle
[NASA-TM-105559] p 48 N92-21547
- BAYGENTS, J. C.**
Electrophoresis of small particles and fluid globules in weak electrolytes p 114 A92-33924
- BAYLISS, ALVIN**
Mappings and accuracy for Chebyshev pseudo-spectral approximations p 248 A92-50469

BEACH, R. F.

- BEACH, R. F.**
Load flows and faults considering dc current injections
p 157 A92-50530
Description of the PMAD DC test bed architecture and integration sequence p 46 A92-50655
Description of the PMAD DC test bed architecture and integration sequence [NASA-TM-105284] p 77 N92-10055
- BEACH, T. A.**
Deterministic blade row interactions in a centrifugal compressor stage [ASME PAPER 91-GT-273] p 3 A92-15670
- BEAGLEY, N. R.**
Simulation of Space Station loads with active control systems p 56 N92-23824
- BEATTIE, J. R.**
Plasma erosion rate diagnostics using laser-induced fluorescence p 198 A92-36738
- BEATTLE, JOHN R.**
Electric propulsion - The future is now p 63 A92-48386
- BECK, R. G.**
Melting of the Abrikosov flux lattice in anisotropic superconductors p 260 A92-28075
- BEHEIM, GLENN**
Wavelength-multiplexed fiber-optic position encoder for aircraft control systems p 24 A92-42602
- BEHRENDT, DONALD R.**
Reaction-bonded Si₃N₄ and SiC matrix composites p 103 A92-39858
- BELCH, RICHARD A.**
High order parallel numerical schemes for solving incompressible flows p 193 N92-25818
- BELL, R. S.**
CONE - An STS-based cryogenic fluid management experiment p 43 A92-23850
- BELLOW, A. H.**
A versatile get away special furnace for materials processing in space [AIAA PAPER 92-0787] p 137 A92-27122
- BELTRAN, LUIS R.**
Advanced nozzle and engine components test facility [AIAA PAPER 92-3993] p 41 A92-56816
Advanced nozzle and engine components test facility [NASA-TM-103684] p 42 N92-17059
- BELYTSCHKO, T.**
A variationally coupled FE-BE method for elasticity and fracture mechanics p 222 A92-37510
- BELYTSCHKO, TED**
Fatigue crack growth reliability by probabilistic finite elements p 222 A92-37524
A stochastic damage model for the rupture prediction of a multi-phase solid. I - Parametric studies. II - Statistical approach p 224 A92-49784
- BENCIC, TIMOTHY J.**
Hot gas ingestion characteristics and flow visualization of a vectored thrust STOVL concept p 26 A92-45316
- BENDIKSEN, ODDVAR O.**
Unsteady transonic Euler solutions using finite elements [AIAA PAPER 92-2504] p 8 A92-34499
Finite element Euler calculations of unsteady transonic cascade flows [AIAA PAPER 92-2120] p 9 A92-35689
- BENJAMIN, M. A.**
Initial development of the axisymmetric ejector shear layer [AIAA PAPER 92-3567] p 178 A92-49068
- BENJAMIN, OWEN**
Development of a computer algorithm for the analysis of variable-frequency AC drives: Case studies included [NASA-TM-105327] p 29 N92-13070
- BENNETT, GARY L.**
NASA program planning on nuclear electric propulsion [AIAA PAPER 92-1557] p 61 A92-38651
An overview of the NASA Advanced Propulsion Concepts program [AIAA PAPER 92-3216] p 73 A92-54018
Nuclear propulsion for space exploration [IAF PAPER 92-0575] p 76 A92-57054
- BENSON, T. J.**
Fluid-flow of a row of jets in crossflow - A numerical study [AIAA PAPER 92-0534] p 169 A92-28198
Comparison of the SMAC, PISO, and iterative time-advancing schemes for unsteady flows p 175 A92-47158
- BENTS, D. J.**
Design of multihundred-watt dynamic isotope power system for robotic space missions p 69 A92-50633
SEI power source alternatives for rovers and other multi-kWe distributed surface applications p 80 N92-13206
Optimization of armored spherical tanks for storage on the lunar surface [NASA-TM-105700] p 91 N92-30187

- BENTS, DAVID J.**
Small Stirling dynamic isotope power system for multihundred-watt robotic missions p 62 A92-45448
[SAE PAPER 912066] p 62 A92-45448
SEI rover solar-electrochemical power system options p 45 A92-50574
Trade studies for nuclear space power systems [NASA-TM-105231] p 235 N92-10221
- BENTZ, M. D.**
Jet mixing in low gravity - Results of the Tank Pressure Control Experiment [AIAA PAPER 92-3060] p 182 A92-54001
- BERCAW, R. W.**
Wiring for aerospace applications [NASA-TM-105777] p 162 N92-30427
- BERCAW, ROBERT W.**
Electrical system options for space exploration [SAE PAPER 912065] p 62 A92-45447
Issues and status of power distribution options for space exploration p 80 N92-13207
- BERG, ROBERT F.**
NIST torsion oscillator viscometer response: Performance on the LeRC active vibration isolation platform [NASA-TM-105571] p 209 N92-23564
- BERKE, L.**
Neurobiological computational models in structural analysis and design p 245 A92-14509
Application of Newton modified barrier method (NMBM) to structural optimization [AIAA PAPER 92-2498] p 220 A92-34555
Neural network based decomposition in optimal structural synthesis p 247 A92-41895
Applications of artificial neural nets in structural mechanics p 223 A92-47283
Singularities in optimal structural design [NASA-TM-4365] p 228 N92-23527
- BERKE, LASZLO**
Improved accuracy for finite element structural analysis via a new integrated force method [NASA-TP-3204] p 227 N92-22227
Structural optimization of large structural systems by optimality criteria methods [NASA-TM-105423] p 229 N92-25446
Modal test/analysis correlation of Space Station structures using nonlinear sensitivity [NASA-TM-105850] p 230 N92-34221
- BERKOWITZ, BRIAN M.**
Experimental ice shape and performance characteristics for a multi-element airfoil in the NASA Lewis Icing Research Tunnel [NASA-TM-105380] p 17 N92-17347
- BERLAD, A. L.**
The structure of premixed particle-cloud flames p 114 A92-43779
- BESTERFIELD, GLEN H.**
Fatigue crack growth reliability by probabilistic finite elements p 222 A92-37524
- BETHEA, M.**
Determination of the critical parameters for remote microscope control [IAF PAPER 91-026] p 240 A92-12447
- BETHEA, MARK D.**
A full field, 3-D velocimeter for NASA's microgravity science program [AIAA PAPER 92-0784] p 56 A92-27119
- BHASIN, K.**
A high temperature superconductivity communications flight experiment [IAF PAPER 92-0410] p 50 A92-55790
- BHASIN, K. B.**
Microwave properties of YBa₂Cu₃O₇(δ) high-transition-temperature superconducting thin films measured by the power transmission method p 153 A92-14938
Coaxial line configuration for microwave power transmission study of YBa₂Cu₃O₇(δ) thin films p 154 A92-18455
Laser ablated YBa₂Cu₃O₇(δ) high temperature superconductor coplanar waveguide resonator p 155 A92-31631
Properties of large area ErBa₂Cu₃O₇(δ) thin films deposited by ionized cluster beams p 260 A92-33911
Performance of a K-band superconducting annular ring antenna p 146 A92-37067
Performance of a four-element Ka-band high-temperature superconducting microstrip antenna p 146 A92-37224
Performance of a wideband GaAs low-noise amplifier at cryogenic temperatures p 156 A92-37953
Electrical-transport properties and microwave device performance of sputtered TiCaBaCuO superconducting thin films p 263 A92-56599
Performance of a Y-Ba-Cu-O superconducting filter/GaAs low noise amplifier hybrid circuit [NASA-TM-105546] p 160 N92-21370

- Microwave conductivity of laser ablated YBa₂Cu₃O₇(δ) superconducting films and its relation to microstrip transmission line performance p 264 N92-21639
- C-band superconductor/semiconductor hybrid field-effect transistor amplifier on a LaAlO₃ substrate [NASA-TM-105828] p 163 N92-34204
- BHASIN, KUL B.**
Measurements of complex permittivity of microwave substrates in the 20 to 300 K temperature range from 26.5 to 40.0 GHz p 197 A92-13416
Conductor-backed coplanar waveguide resonators of YBa₂Cu₃O₇(δ) on LaAlO₃ p 158 A92-51042
NASA Space applications of high-temperature superconductors [NASA-TM-105401] p 271 N92-18455
Properties of large area ErBa₂Cu₃O₇(δ) thin films deposited by ionized cluster beams p 264 N92-23414
Dependence of the critical temperature of laser-ablated YBa₂Cu₃O₇(δ) thin films on LaAlO₃ substrate growth technique p 264 N92-23415
Monolithic mm-wave phase shifter using optically activated superconducting switches [NASA-CASE-LEW-14878-1] p 257 N92-28571
NASA space applications of high-temperature superconductors p 265 N92-32980
Measurement techniques for cryogenic Ka-band microstrip antennas p 153 N92-32981
Performance of a Y-Ba-Cu-O superconducting filter/GaAs low noise amplifier hybrid circuit p 163 N92-32982
Magnetic penetration depth of YBa₂Cu₃O₇(δ) thin films determined by the power transmission method p 265 N92-32983
- BHAT, R.**
High-field transport properties of InAs(x)P(1-x)/InP (x = 0.3-1.0) modulation doped heterostructures at 300 and 77 K p 262 A92-46331
- BHATT, H.**
Role of interfacial thermal barrier in the transverse thermal conductivity of uniaxial SiC fiber-reinforced reaction bonded silicon nitride p 102 A92-39605
- BHATT, HEMANSHU**
Role of interfacial carbon layer in the thermal diffusivity/conductivity of silicon carbide fiber-reinforced reaction-bonded silicon nitride matrix composites p 100 A92-25443
- BHATT, R. T.**
Role of interfacial thermal barrier in the transverse thermal conductivity of uniaxial SiC fiber-reinforced reaction bonded silicon nitride p 102 A92-39605
- BHATT, RAMAKRISHNA T.**
Influence of interfacial shear strength on the mechanical properties of SiC fiber reinforced reaction-bonded silicon nitride matrix composites p 99 A92-15145
Mechanical behavior of fiber reinforced SiC/RBSN ceramic matrix composites - Theory and experiment [ASME PAPER 91-GT-209] p 99 A92-15629
Role of interfacial carbon layer in the thermal diffusivity/conductivity of silicon carbide fiber-reinforced reaction-bonded silicon nitride matrix composites p 100 A92-25443
Oxidation effects on the mechanical properties of a SiC-fiber-reinforced reaction-bonded Si₃N₄ matrix composite p 100 A92-25445
Tension, compression, and bend properties for SiC/RBSN composites p 100 A92-32727
Reaction-bonded Si₃N₄ and SiC matrix composites p 103 A92-39858
- BHATTACHARJEE, SUBRATA**
Opposed flow flame spread in normal, enhanced and reduced gravity p 111 A92-12898
- BHATTACHARYYA, SAMIT K.**
NASA/DOE/DOD nuclear propulsion technology planning: Summary of FY 1991 interagency panel results [NASA-TM-105703] p 88 N92-26792
- BHATTACHARYA, P. K.**
High-field transport properties of InAs(x)P(1-x)/InP (x = 0.3-1.0) modulation doped heterostructures at 300 and 77 K p 262 A92-46331
Study of InGaAs-based modulation doped field effect transistor structures using variable-angle spectroscopic ellipsometry p 265 N92-32977
- BHATTACHARYA, PALLAB K.**
dc and microwave performance of a 0.1-micron gate InAs/In(0.52)Al(0.48)As MODFET p 156 A92-43891
- BHATTACHARYA, S. K.**
Fuels and materials development for space nuclear propulsion [NASA-TM-107806] p 85 N92-21187
- BHUTTA, BILAL A.**
Improved nonequilibrium viscous shock-layer scheme for hypersonic blunt-body flowfields p 4 A92-24653
New technique for low-to-high altitude predictions of ablative hypersonic flowfields p 166 A92-24654

- Low-to-high altitude predictions of three-dimensional ablative reentry flowfields
[AIAA PAPER 92-0366] p 168 A92-26227
An improved PNS scheme for predicting complex three-dimensional hypersonic flows
[AIAA PAPER 92-0753] p 8 A92-31679
- BIANCO, ROBERT**
Volatile species in halide-activated-diffusion coating packs p 122 A92-57028
- BICKFORD, R. L.**
An overview of in-flight plume diagnostics for rocket engines
[AIAA PAPER 92-3785] p 75 A92-54164
Demonstration of a flight capable system for plume spectroscopy
[AIAA PAPER 92-3786] p 57 A92-54165
Health management and controls for earth to orbit propulsion systems
[IAF PAPER 92-0646] p 77 A92-57089
An overview of in-flight plume diagnostics for rocket engines
[NASA-TM-105727] p 90 N92-28417
- BIDWELL, COLIN S.**
Comparison of two-dimensional and three-dimensional droplet trajectory calculations in the vicinity of finite wings
[AIAA PAPER 92-0645] p 8 A92-28215
Comparison of two-dimensional and three-dimensional droplet trajectory calculations in the vicinity of finite wings
[NASA-TM-105617] p 188 N92-23154
- BIERNACKI, JOHN**
Application of enhanced modern structured analysis techniques to Space Station Freedom electric power system requirements p 251 A92-50609
- BIESIADNY, THOMAS J.**
Contingency power for a small turboshaft engine by using water injection into turbine cooling air
[NASA-TM-105680] p 37 N92-29661
- BILANIN, ALAN J.**
Mechanisms resulting in accreted ice roughness
[AIAA PAPER 92-0297] p 21 A92-25750
- BILL, ROBERT C.**
Recent manufacturing advances for spiral bevel gears
[SAE PAPER 912229] p 204 A92-40024
Summary highlights of the Advanced Rotorcraft Transmission (ART) program
[AIAA PAPER 92-3362] p 23 A92-54026
- BINDER, MICHAEL**
Rocket engine diagnostics using qualitative modeling techniques
[AIAA PAPER 92-3164] p 65 A92-48787
Rocket engine diagnostics using qualitative modeling techniques
[NASA-TM-105714] p 88 N92-27033
- BINIENDA, W. K.**
Effect of contact stresses in four-point bend testing of graphite/epoxy and graphite/PMR-15 composite beams p 219 A92-33589
- BINIENDA, WIESLAW K.**
Mixed-mode fracture in unidirectional graphite epoxy composite laminates with central notch p 218 A92-29464
- BIRCHENOUGH, ARTHUR G.**
Development of a ninety string solar array simulator p 46 A92-50660
Large transient fault current test of an electrical roll ring
[NASA-TM-105278] p 55 A92-50661
Development of a ninety string solar array simulator
[NASA-TM-105278] p 55 N92-11086
Large transient fault current test of an electrical roll ring
[NASA-TM-105667] p 87 N92-24201
- BIRKNER, BJORN W.**
Effect of an arcjet plume on satellite reflector performance p 53 A92-16318
Arcjet nozzle area ratio effects
[NASA-TM-104477] p 83 N92-16022
- BIZON, THOMAS P.**
Real-time demonstration hardware for enhanced DPCM video compression algorithm
[NASA-TM-105616] p 150 N92-19700
- BLAHA, BERNARD J.**
Supersonic STOVL propulsion technology program: An overview p 33 N92-22539
- BLELLOCH, P. A.**
Simulation of Space Station loads with active control systems p 56 N92-23824
- BLEMKER, A. R.**
Laser ablated YBa₂Cu₃O_{7-x} high temperature superconductor coplanar waveguide resonator p 155 A92-31631
- BLISS, DONALD B.**
Eigenvalue calculation procedure for an Euler/Navier-Stokes solver with application to flows over airfoils p 3 A92-17429
- BLOOMFIELD, HARVEY S.**
Space reactor power system programs overview
[AIAA PAPER 92-1558] p 61 A92-38652
Trade studies for nuclear space power systems
[NASA-TM-105231] p 235 N92-10221
- BLUE, J. W.**
Fatigue damage accumulation in nickel prior to crack initiation p 120 A92-33947
- BOBER, LAWRENCE J.**
Advanced propeller research p 33 N92-22537
- BOBINSKY, E. A.**
Predictive onboard flow control in packet switching satellites
[AIAA PAPER 92-2004] p 144 A92-29923
Destination directed packet switch architecture for a geostationary communication satellite network
[IAF PAPER 92-0413] p 50 A92-55793
- BOBINSKY, ERIC A.**
Predictive onboard flow control for packet switching satellites
[NASA-TM-105566] p 150 N92-19379
- BOCK, LAWRENCE A.**
Far-field noise and internal modes from a ducted propeller at simulated aircraft takeoff conditions
[AIAA PAPER 92-0371] p 252 A92-26230
Far-field noise and internal modes from a ducted propeller at simulated aircraft takeoff conditions
[NASA-TM-105369] p 254 N92-16702
- BODI, ROBERT F.**
Test and evaluation of load converter topologies used in the Space Station Freedom power management and distribution dc test bed p 158 A92-50662
- BOEHME, D. R.**
Diffusion mechanisms in chemical vapor-deposited indium coated on chemical vapor-deposited rhenium p 117 A92-28017
- BOGDANSKI, MICHAEL S.**
Tribological and mechanical comparison of sintered and HIPped PM212: High temperature self-lubricating composites
[NASA-TM-105379] p 96 N92-15128
Tribological and microstructural comparison of HIPped PM212 and PM212/Au self-lubricating composites
[NASA-TM-105615] p 97 N92-26142
- BOGDONOFF, S. M.**
Crossing shock wave turbulent boundary layer interactions - Variable angle and shock generator length geometry effects at Mach 3
[AIAA PAPER 92-0636] p 6 A92-27014
- BOLDMAN, D. R.**
Qualitative investigation of cryogenic fluid injection into a supersonic flow field p 164 A92-13360
- BOLDMAN, DONALD R.**
Analysis of an advanced ducted propeller subsonic inlet
[AIAA PAPER 92-0274] p 5 A92-25728
Analysis of an advanced ducted propeller subsonic inlet
[NASA-TM-105393] p 15 N92-14002
- BOLERJACK, B.**
Description of the PMAD DC test bed architecture and integration sequence p 46 A92-50655
Description of the PMAD DC test bed architecture and integration sequence
[NASA-TM-105284] p 77 N92-10055
- BONACUSE, PETER J.**
Elevated temperature axial and torsional fatigue behavior of Haynes 188
[NASA-TM-105396] p 229 N92-28701
- BOND, THOMAS H.**
Advanced ice protection systems test in the NASA Lewis Icing Research Tunnel p 22 A92-14406
Results of an icing test on a NACA 0012 airfoil in the NASA Lewis Icing Research Tunnel
[AIAA PAPER 92-0647] p 7 A92-27021
Results of an icing test on a NACA 0012 airfoil in the NASA Lewis Icing Research Tunnel
[NASA-TM-105374] p 16 N92-15051
Model rotor icing tests in the NASA Lewis Icing Research Tunnel p 21 N92-21688
Experimental and computational ice shapes and resulting drag increase for a NACA 0012 airfoil
[NASA-TM-105743] p 20 N92-28674
Results of a low power ice protection system test and a new method of imaging data analysis
[NASA-TM-105745] p 20 N92-28696
- BONETTI, R. R.**
Performance of a Y-Ba-Cu-O superconducting filter/GaAs low noise amplifier hybrid circuit
[NASA-TM-105546] p 160 N92-21370
Performance of a Y-Ba-Cu-O superconducting filter/GaAs low noise amplifier hybrid circuit p 163 N92-32982
- BONHAM, CHARLES D.**
The application of a computer data acquisition system to a new high temperature tribometer p 93 A92-11823
- BOROWSKI, BRIAN A.**
Microgravity combustion of isolated n-decane and n-heptane droplets
[AIAA PAPER 92-0242] p 113 A92-26927
- BOROWSKI, S.**
An accelerated development, reduced cost approach to lunar/Mars exploration using a modular NTR-based space transportation system
[IAF PAPER 92-0574] p 43 A92-57053
- BOROWSKI, STANLEY**
Innovative nuclear thermal propulsion technology evaluation - Results of the NASA/DOE task team study
[IAF PAPER 91-235] p 58 A92-13160
- BOROWSKI, STANLEY K.**
Nuclear thermal rockets - Key to moon-Mars exploration p 63 A92-48385
Nuclear thermal rocket workshop reference system Rover/NERVA p 78 N92-11091
Fast track lunar NTR systems assessment for the First Lunar Outpost and its evolvability to Mars p 142 N92-33334
- BOSNYAK, C. P.**
An energy analysis of crack-initiation and arrest in epoxy p 224 A92-49777
- BOSSLER, R.**
Experimental testing of prototype face gears for helicopter transmissions
[NASA-TM-105434] p 214 N92-31349
- BOSSLER, R. B., JR.**
Application of face-gear drives in helicopter transmissions
[NASA-TM-105655] p 212 N92-28434
- BOSSLER, ROBERT B., JR.**
Advanced Rotorcraft Transmission program summary
[AIAA PAPER 92-3363] p 205 A92-48936
- BOWDITCH, DAVID N.**
Impact and promise of NASA aeropropulsion technology p 31 N92-22511
The future challenge for aeropropulsion
[NASA-TM-105613] p 35 N92-25164
- BOWLES, K. J.**
Effect of fiber reinforcement on thermo-oxidative stability and mechanical properties of polymer matrix composites p 101 A92-33587
- BOWLES, KENNETH J.**
Relationship between voids and interlaminar shear strength of polymer matrix composites p 98 A92-10241
Void effects on the interlaminar shear strength of unidirectional graphite-fiber-reinforced composites p 105 A92-50348
Isothermal aging effects on PMR-15 resin
[NASA-TM-105648] p 110 N92-30986
- BOWMAN, R. R.**
The effect of strain rate and temperature on the tensile properties of NiAl p 117 A92-28113
Flow and fracture behavior of NiAl in relation to the brittle-to-ductile transition temperature p 118 A92-30781
Microstructure and mechanical properties of a single crystal NiAl alloy with Zr or Hf rich G-phase precipitates p 119 A92-30841
Correlation of deformation mechanisms with the tensile and compressive behavior of NiAl and NiAl(Zr) intermetallic alloys p 120 A92-38019
Initial evaluation of continuous fiber reinforced NiAl composites p 104 A92-46867
Oxidation of Al₂O₃ continuous fiber-reinforced/NiAl composites p 106 A92-57029
- BOYCE, L.**
Probabilistic constitutive relationships for cyclic material strength models p 217 A92-21081
Probabilistic material degradation model for aerospace materials subjected to high temperature, mechanical and thermal fatigue, and creep
[AIAA PAPER 92-3419] p 224 A92-48978
- BOYD, I. D.**
Measurement and analysis of a small nozzle plume in vacuum
[AIAA PAPER 92-3108] p 64 A92-48748
- BOYD, IAIN D.**
Experimental and numerical investigations of low-density nozzle and plume flows of nitrogen p 183 A92-54917
- BOYD, JOSEPH T.**
Length minimization design considerations in photonic integrated circuits incorporating directional couplers p 256 A92-46240
- BOYLE, R. J.**
Three-dimensional Navier-Stokes heat transfer predictions for turbine blade rows
[AIAA PAPER 92-3068] p 12 A92-54003

BOZEK, JOHN

BOZEK, JOHN

Space transfer with ground-based laser/electric propulsion
[AIAA PAPER 92-3213] p 73 A92-54017

BOZZOLO, G. H.

Computational techniques in tribology and material science at the atomic level
[NASA-TM-105573] p 252 N92-26671

BOZZOLO, GUILLERMO

A new approximate sum rule for bulk alloy properties
p 117 A92-28240
Lattice parameters of fcc binary alloys using a new semiempirical method
p 120 A92-32898
Heats of formation of bcc binary alloys
[NASA-TM-105281] p 122 N92-16086
Lattice parameters of fcc binary alloys using a new semiempirical method
[NASA-TM-105304] p 123 N92-16111

BRACKBILL, J. U.

A continuum method for modeling surface tension
p 175 A92-45707

BRADY, R. A.

Mixing in the dome region of a staged gas turbine combustor
[AIAA PAPER 92-3089] p 177 A92-48734

BRAGG, M.

Helium bubble flow visualization of the spanwise separation on a NACA 0012 with simulated glaze ice
[AIAA PAPER 92-0413] p 7 A92-28192
Helium bubble flow visualization of the spanwise separation on a NACA 0012 with simulated glaze ice
[NASA-TM-105742] p 19 N92-26612

BRAGG, M. B.

Finite wing aerodynamics with simulated glaze ice
[AIAA PAPER 92-0414] p 5 A92-26265
Measurements in a leading-edge separation bubble due to a simulated airfoil ice accretion
p 21 A92-41262
LDV measurements on a rectangular wing with a simulated glaze ice accretion
[AIAA PAPER 92-2690] p 10 A92-45537
Simulation of iced wing aerodynamics
p 21 N92-21686

BRAND, HELMUT R.

Propagating confined states in phase dynamics
p 181 A92-50968
The Eckhaus and the Benjamin-Feir instability near a weakly inverted bifurcation
[NASA-TM-105334] p 185 N92-15336

BRAND, J. A.

Extrapolation procedures in Mott electron polarimetry
p 197 A92-21241

BRANDHORST, HENRY W., JR.

Energy requirements for the space frontier
[SAE PAPER 91-2064] p 62 A92-45446

BRAUN, M. J.

A bulk flow model of a brush seal system
[ASME PAPER 91-GT-325] p 203 A92-15696
Flow visualization and motion analysis for a series of four sequential brush seals
p 204 A92-36976
Full field flow visualization and computer-aided velocity measurements in a bank of cylinders in a wind tunnel
p 199 A92-50040

BREGE, MARK A.

Critical technology experiment results for lightweight space heat receiver
p 180 A92-50568

BREISACHER, KEVIN J.

3D rocket combustor acoustics model
[AIAA PAPER 92-3228] p 66 A92-48829
The 3D rocket combustor acoustics model
[NASA-TM-105734] p 88 N92-27035

BRENNAN, J. A.

Computer program for computing the properties of seventeen fluids
p 241 A92-23849

BREWE, D. E.

Frequency effects on the stability of a journal bearing for periodic loading
p 203 A92-22665
Two reference time scales for studying the dynamic cavitation of liquid films
p 204 A92-47173
Frequency effects on the stability of a journal bearing for periodic loading
[NASA-TM-105226] p 186 N92-18809
Effect of out-of-roundness on the performance of a diesel engine connecting-rod bearing
[NASA-TM-105600] p 215 N92-31536

BREWE, DAVID E.

A system-approach to the elastohydrodynamic lubrication point-contact problem
p 204 A92-35421
Numerical experiments with flows of elongated granules
[NASA-TM-105567] p 209 N92-23226

BREWER, DAVID N.

Controlled crack growth specimen for brittle systems
p 123 A92-21099

BRIDGES, JAMES

Direct evaluation of aeroacoustic theory in a jet
p 253 A92-50296

BRIGHT, MICHELLE M.

Piloted evaluation of an integrated propulsion and flight control simulator
[AIAA PAPER 92-4178] p 23 A92-52459
Piloted evaluation of an integrated propulsion and flight control simulator
[NASA-TM-105797] p 40 N92-34107

BRINDLEY, P. K.

Effect of fiber strength on the room temperature tensile properties of SiC/Ti-24Al-11Nb
p 102 A92-36389
The effect of temperature on the deformation and fracture of SiC/Ti-24Al-11Nb
p 106 A92-55143
Development of a new generation of high-temperature composite materials
p 109 N92-22515

BRINDLEY, PAMELA K.

Tribological properties of ceramic-(Ti3Al-Nb) sliding couples for use as candidate seal materials to 700 C
p 124 A92-32407
High-temperature fatigue behavior of a SiC/Ti-24Al-11Nb composite
p 104 A92-44613

BRINDLEY, W. J.

Thermal barrier coating life and isothermal oxidation of low-pressure plasma-sprayed bond coat alloys
p 119 A92-32398

BRINDLEY, WILLIAM J.

Oxidation resistant coating for titanium alloys and titanium alloy matrix composites
[NASA-CASE-LEW-15155-1] p 133 N92-29090

BRINKER, D. J.

Recent progress in InP solar cell research
p 158 A92-50653
High voltage thermally diffused p(+)-In solar cells
p 235 A92-53172
Radiation and temperature effects in heteroepitaxial and homoepitaxial InP cells
p 159 A92-53192
A high-performance photovoltaic concentrator array - The mini-dome Fresnel lens concentrator with 30 percent efficient GaAs/GaSb tandem cells
p 72 A92-53199

BRINKER, DAVID

High performance etchant for thinning p(+)-InP and its application to p(+)-InP solar cell fabrication
p 263 A92-53155

BRINKER, DAVID J.

Advanced photovoltaic experiment, S0014: Preliminary flight results and post-flight findings
p 237 N92-27101
The effect of the low Earth orbit environment on space solar cells: Results of the advanced photovoltaic experiment (S0014)
p 237 N92-27320

BRITTON, DORIS L.

Electrochemical impregnation and cycle life of lightweight nickel electrodes for nickel-hydrogen cells
p 113 A92-30978
Progress in the development of lightweight nickel electrode for aerospace applications
[NASA-TM-105591] p 236 N92-20493
Progress in the development of lightweight nickel electrode
[NASA-TM-105638] p 116 N92-26670

BRITTON, RANDALL K.

Ongoing development of a computer jobstream to predict helicopter main rotor performance in icing conditions
p 2 A92-14407
Model rotor icing tests in the NASA Lewis Icing Research Tunnel
p 21 N92-21688

BROCK, J. S.

The Baldwin-Lomax model for separated and wake flows using the entropy envelope concept
[AIAA PAPER 92-0148] p 4 A92-23764

BROCK, T.

dc and microwave performance of a 0.1-micron gate InAs/In(0.52)Al(0.48)As MODFET
p 156 A92-43891

BROKOPP, RICHARD A.

Small engine components test facility compressor testing cell at NASA Lewis Research Center
[AIAA PAPER 92-3980] p 41 A92-56806
Small engine components test facility compressor testing cell at NASA Lewis Research Center
[NASA-TM-105685] p 42 N92-30508

BROWN, GERALD

Determining structural performance
p 32 N92-22519

BROWN, GERALD V.

Performance tests of a cryogenic hybrid magnetic bearing for turbopumps
[NASA-TM-105627] p 30 N92-20523
Force analysis of magnetic bearings with power-saving controls
p 212 N92-27795

BROWN, HELEN C.

Evaluation of MHOST analysis capabilities for a plate element
[NASA-TM-105387] p 228 N92-23196

BROWN, LARRY

Advanced Communication Technology Satellite (ACTS) baseband processor development
p 50 A92-53693

BROWN, LAWRENCE E.

Possible sources of the Population I lithium abundance and light-element evolution
p 268 A92-33069

BROWN, S.

Mechanical properties of monolithic and particulate composites of L12 forms of Al3Ti
p 101 A92-36273

BROWN, S. A.

Compression, bend, and tension studies on forged Al67Ti25Cr8 and Al66Ti25Mn(g) L1(2) compounds
p 118 A92-30766
Tensile behavior of the L(1)2 compound Al67Ti25Cr8
p 122 A92-49694

Composites of low-density trialuminides: Particulate and long fiber reinforcements
[NASA-TM-105628] p 109 N92-25346

BRUCKNER, ERIC J.

Synergistic effects of ultraviolet radiation, thermal cycling and atomic oxygen on altered and coated Kapton surfaces
[AIAA PAPER 92-0794] p 93 A92-27125
The effects of RF plasma ashing on zinc orthotitanate/potassium silicate thermal control coatings
[AIAA PAPER 92-2171] p 124 A92-31299
Synergistic effects of ultraviolet radiation, thermal cycling, and atomic oxygen on altered and coated Kapton surfaces
[NASA-TM-105363] p 96 N92-14114

BRUCKNER, ROBERT J.

Engine component instrumentation development facility at NASA Lewis Research Center
[AIAA PAPER 92-3995] p 41 A92-56818
Engine component instrumentation development facility at NASA Lewis Research Center
[NASA-TM-105644] p 42 N92-25449

BRUNS, JAMES E.

Full Navier-Stokes calculations on the installed F/A-18 inlet at a high angle of attack
[AIAA PAPER 92-3175] p 13 A92-54012

BRUSH, A. S.

Development and testing of a 180-volt dc electronic circuit breaker with a 335-ampere carry and 1200-ampere interrupt rating
p 158 A92-50658

BRUSH, ANDREW S.

Stability testing and analysis of a PMAD DC test bed for the Space Station Freedom
[NASA-TM-105846] p 162 N92-31282

BRYDEN, TIMOTHY M.

An IIR median hybrid filter
p 246 A92-40375

BUCKMANN, P. S.

Design and test of an oxygen turbopump for a dual expander cycle rocket engine
p 59 A92-21062

BUDINGER, JAMES

Least reliable bits coding (LRBC) for high data rate satellite communications
[AIAA PAPER 92-1868] p 142 A92-29807
Flexible digital modulation and coding synthesis for satellite communications
p 148 N92-14235
Least Reliable Bits Coding (LRBC) for high data rate satellite communications
[NASA-TM-105431] p 150 N92-18921

BUDINGER, JAMES M.

Multichannel demultiplexer/demodulator technologies for future satellite communication systems
[NASA-TM-105377] p 51 N92-18342
NASA Lewis Research Center Advanced Modulation and Coding Project: Introduction and overview
p 51 N92-22002

BUDINGERS, J.

Multicarrier demodulator architecture for onboard processing satellites
p 49 A92-10465

BUFFUM, D. H.

Wind tunnel wall effects in a linear oscillating cascade
[ASME PAPER 91-GT-133] p 2 A92-15576

BUGGELE, ALVIN E.

Engine component instrumentation development facility at NASA Lewis Research Center
[AIAA PAPER 92-3995] p 41 A92-56818
Engine component instrumentation development facility at NASA Lewis Research Center
[NASA-TM-105644] p 42 N92-25449

BUI, TRONG T.

Implementation/validation of a low Reynolds number two-equation turbulence model in the Proteus Navier-Stokes code: Two-dimensional/axisymmetric
[NASA-TM-105619] p 187 N92-20520

BULLOCK, S. R.

Medium power hydrogen arcjet performance
[AIAA PAPER 91-2227] p 58 A92-15355

BULZAN, DANIEL L.

Particle-laden weakly swirling free jets: Measurements and predictions
[NASA-TM-100881] p 29 N92-14061

BURKARDT, LEO A.

Beta 2: A near term, fully reusable, horizontal takeoff and landing two-stage-to-orbit launch vehicle concept
p 86 N92-21536

- BURKE, CHRISTOPHER A.**
Low earth orbit durability evaluation of Haynes 188 solar receiver material
[AIAA PAPER 92-0850] p 117 A92-29616
- BURROWS, ADAM**
Massive Dirac neutrinos and SN 1987A
p 268 A92-45808
- BURROWS, LINDA M.**
Electromechanical systems with transient high power response operating from a resonant AC link
[NASA-TM-105716] p 37 N92-28985
An electromechanical actuation system for an expendable launch vehicle
[NASA-TM-105774] p 48 N92-30310
- BURTON, RODNEY L.**
Preliminary investigation of a low power pulsed arcjet thruster
[AIAA PAPER 92-3113] p 64 A92-48752
- BUTTON, ROBERT M.**
Development and testing of a source subsystem for the supporting development PMAD DC test bed
p 46 A92-50659
Stability testing and analysis of a PMAD DC test bed for the Space Station Freedom
[NASA-TM-105846] p 162 N92-31282
- C**
- CAIRELLI, JAMES E.**
Update on results of SPRE testing at NASA Lewis
p 71 A92-50780
NASA Lewis Stirling SPRE testing and analysis with reduced number of cooler tubes
[NASA-TM-105767] p 238 N92-28837
- CALCO, FRANK S.**
Three point lead screw positioning apparatus
[NASA-CASE-LEW-15216-1] p 208 N92-17678
- CALEDONIA, G. E.**
Fast oxygen atom facility for studies related to low earth orbit activities
[AIAA PAPER 92-3974] p 47 A92-56800
- CALOGERAS, JAMES E.**
Solar dynamic power for earth orbital and lunar applications
p 68 A92-50567
- CALOMINO, ANTHONY M.**
Controlled crack growth specimen for brittle systems
p 123 A92-21099
- CAMCI, C.**
Investigation of three-dimensional flow field in a turbine including rotor/stator interaction. I - Design development and performance of the research facility
[AIAA PAPER 92-3325] p 40 A92-48908
- CAMPBELL, MELANIE C. W.**
A fiber optic sensor for ophthalmic refractive diagnostics
p 198 A92-34831
- CAMPERCHOLI, WILLIAM P.**
Transonic turbine blade cascade testing facility
[AIAA PAPER 92-4034] p 42 A92-56856
Transonic turbine blade cascade testing facility
[NASA-TM-105646] p 47 N92-26129
- CANACCI, V. A.**
Flow visualization and motion analysis for a series of four sequential brush seals
p 204 A92-36976
Full field flow visualization and computer-aided velocity measurements in a bank of cylinders in a wind tunnel
p 199 A92-50040
- CANGIANE, P.**
A multi-channel demultiplexer/demodulator architecture, simulation and implementation
[AIAA PAPER 92-1972] p 144 A92-29895
- CANISTRARO, HOWARD A.**
X ray based displacement measurement for hostile environments
[NASA-TM-105551] p 202 N92-23155
- CAPPELLI, MARK A.**
Laser-induced fluorescence of atomic hydrogen in an arcjet thruster
[AIAA PAPER 92-0678] p 60 A92-27045
Modeling of the near-electrode regions of arcjets. I - Coupling of the flowfield to the non-equilibrium boundary layers
[AIAA PAPER 92-3109] p 258 A92-48749
Flow diagnostics of an arcjet using laser-induced fluorescence
[AIAA PAPER 92-3243] p 199 A92-48843
Vacuum ultraviolet absorption in a hydrogen arcjet
[AIAA PAPER 92-3564] p 259 A92-54055
- CARD, JOHN M.**
Microgravity combustion of isolated n-decane and n-heptane droplets
[AIAA PAPER 92-0242] p 113 A92-26927
- CARLETON, K. L.**
Arcing of negatively biased solar cells in a plasma environment. I - Experimental observations
[AIAA PAPER 92-2990] p 63 A92-47000
- CARLILE, JULIE A.**
An experimental investigation of high-aspect-ratio cooling passages
[AIAA PAPER 92-3154] p 64 A92-48780
Brush seal leakage performance with gaseous working fluids at static and low rotor speed conditions
[NASA-TM-105400] p 186 N92-16265
An experimental investigation of high-aspect-ratio cooling passages
[NASA-TM-105679] p 48 N92-25958
- CARLSON, FREDERICK**
Transport modes during crystal growth in a centrifuge
p 138 A92-33835
- CARPENTER, M. S.**
Significant long-term reduction in n-channel MESFET subthreshold leakage using ammonium-sulfide surface treated gates
p 153 A92-12272
- CARPINO, M.**
Life extending control for rocket engines
[NASA-TM-105789] p 142 N92-31263
- CARTER, CAMPBELL D.**
Saturated fluorescence measurements of the hydroxyl radical in laminar high-pressure C₂H₆/O₂/N₂ flames
p 198 A92-33987
- CARUSO, STEVEN C.**
Automatic grid generation for iced airfoil flowfield predictions
[AIAA PAPER 92-0415] p 6 A92-26266
- CASHMAN, WILLIAM F.**
Operational uses of ACTS technology
[AIAA PAPER 92-1964] p 144 A92-29887
- CASIELLO, FRANCISCO A.**
Discrete-time entropy formulation of optimal and adaptive control problems
p 247 A92-55930
- CASTELLI, M. G.**
Hardening mechanisms in a dynamic strain aging alloy, Hastelloy X, during isothermal and thermomechanical cyclic deformation
p 116 A92-24832
- CASTELLI, MICHAEL G.**
Thermomechanical testing of high-temperature composites - Thermomechanical fatigue (TMF) behavior of SiC(SCS-6)/Ti-15-3
p 104 A92-44606
Thermomechanical deformation behavior of a dynamic strain aging alloy, Hastelloy X
[NASA-TM-105316] p 228 N92-25179
- CATALDO, ROBERT**
A dynamic isotope power system for Space Exploration Initiative surface transport systems
[AIAA PAPER 92-1489] p 61 A92-38605
- CAVANO, PAUL**
New addition curing polyimides
[NASA-TM-105335] p 95 N92-13281
- CAVATORTA, ENRICO**
A study on vortex flow control of inlet distortion in the re-engineered 727-100 center inlet duct using computational fluid dynamics
[AIAA PAPER 92-0152] p 4 A92-23767
A study on vortex flow control on inlet distortion in the re-engineered 727-100 center inlet duct using computational fluid dynamics
[NASA-TM-105321] p 14 N92-13998
- CAWLEY, JAMES D.**
Fractal dimension of alumina aggregates grown in two dimensions
p 126 A92-49814
- CEBECI, T.**
Analysis of iced wings
[NASA-TM-105773] p 20 N92-34144
- CEBECI, TUNCER**
A turbulence model for iced airfoils and its validation
[AIAA PAPER 92-0417] p 6 A92-26267
Analysis of iced wings
[AIAA PAPER 92-0416] p 8 A92-29972
A turbulence model for iced airfoils and its validation
[NASA-TM-105373] p 16 N92-15052
- CELESTINA, M. L.**
The role of tip clearance in high-speed fan stall
[ASME PAPER 91-GT-83] p 2 A92-15550
- CH'EN, D. R.**
Advanced large scale GaAs monolithic IF switch matrix subsystem
[AIAA PAPER 92-1861] p 155 A92-29801
- CHABOCHE, J.-L.**
A viscoplastic theory with thermodynamic considerations
[ONERA, TP NO. 1991-220] p 217 A92-26372
A viscoplastic theory with thermodynamic considerations
p 219 A92-33903
- CHADWICK, M.**
Repair-level analysis for Space Station Freedom
[AIAA PAPER 92-1537] p 43 A92-38634
- CHAI, A. T.**
Convective flows in enclosures with vertical temperature or concentration gradients
p 171 A92-32277
- CHAIT, A.**
Numerical simulations of space processing - The reality, the myth, and the future
p 136 A92-12863
- Steady-state thermal-solutal convection and diffusion in a simulated float zone
p 137 A92-17056
- CHAIT, ARNON**
Transport modes during crystal growth in a centrifuge
p 138 A92-33835
- CHAMIS, C. C.**
Interphase layer optimization for metal matrix composites with fabrication considerations
p 98 A92-10262
METCAN updates for high temperature composite behavior - Simulation/verification
p 98 A92-10264
Micromechanics for ceramic matrix composites
p 98 A92-10282
Probabilistic constitutive relationships for cyclic material strength models
p 217 A92-21081
LDEXPT, an intelligent database system for the Composite Load Spectra project
p 59 A92-23695
Multiojective shape and material optimization of composite structures including damping
p 218 A92-28055
Computational simulation of high temperature metal matrix composite behavior
p 101 A92-32753
Computational simulation of concurrent engineering for aerospace propulsion systems
[AIAA PAPER 92-1144] p 241 A92-33285
HITCAN for actively cooled hot-composite thermostructural analysis
[ASME PAPER 91-GT-116] p 222 A92-36896
Towards the development of micromechanics equations for ceramic matrix composites via fiber substructuring
[NASA-TM-105246] p 108 N92-19595
Progressive fracture of polymer matrix composite structures: A new approach
[NASA-TM-105574] p 109 N92-23194
Computational simulation of matrix micro-slip bands in SiC/Ti-15 composite
[NASA-TM-105762] p 111 N92-32466
Computational simulation of structural fracture in fiber composites
p 111 N92-32531
- CHAMIS, CHRISTOS C.**
Computational simulation of microfracture in high temperature metal matrix composites
p 98 A92-10263
Mapping methods for computationally efficient and accurate structural reliability
[AIAA PAPER 92-2347] p 219 A92-34321
Nonuniform thermal environmental effects on space truss structural reliability
[AIAA PAPER 92-2352] p 54 A92-34325
Structural tailoring/analysis for hypersonic components - Executive system development
[AIAA PAPER 92-2471] p 219 A92-34360
Material nonlinear analysis via mixed-iterative finite element method
[AIAA PAPER 92-2479] p 220 A92-34368
Multidisciplinary tailoring of hot composite structures
[AIAA PAPER 92-2563] p 220 A92-34564
Structural durability of stiffened composite shells
[AIAA PAPER 92-2244] p 220 A92-34569
Probabilistic progressive buckling of trusses
[AIAA PAPER 91-0916] p 223 A92-38142
Combined bending and thermal fatigue of high-temperature metal-matrix composites - Computational simulation
p 223 A92-43494
Damage and fracture in composite thin shells
p 224 A92-51550
First-passage problems: A probabilistic dynamic analysis for degraded structures
[NASA-TM-103755] p 225 N92-11373
Damage and fracture in composite thin shells
[NASA-TM-105289] p 106 N92-13284
Computational simulation of surface waviness in graphite/epoxy woven composites due to initial curing
[NASA-TM-105313] p 106 N92-14118
Microfracture in high temperature metal matrix laminates
[NASA-TM-105189] p 106 N92-14122
Thermally-driven microfracture in high temperature metal matrix composites
[NASA-TM-105305] p 107 N92-15136
Analysis of aircraft engine blade subject to ice impact
[NASA-TM-105336] p 226 N92-15402
Probabilistic progressive buckling of trusses
[NASA-TM-105162] p 226 N92-15403
Probabilistic structural analysis of adaptive/smart/intelligent space structures
[NASA-TM-105408] p 227 N92-22267
Coupled multi-disciplinary simulation of composite engine structures in propulsion environment
[NASA-TM-105575] p 228 N92-23267
Computer codes developed and under development at Lewis
p 244 N92-25913
Structural durability of stiffened composite shells
[NASA-CR-190588] p 229 N92-29342
Computational simulation of intermingled-fiber hybrid composite behavior
[NASA-TM-105666] p 110 N92-31506

CHANG, C. T.

Probabilistic assessment of space trusses subjected to combined mechanical and thermal loads
[NASA-TM-105429] p 230 N92-33935

CHANG, C. T.

Simulations of free shear layers using a compressible kappa-epsilon model p 190 N92-23355

CHANG, CHING L.

An error analysis of least-squares finite element method of velocity-pressure-vorticity formulation for Stokes problem p 173 A92-37506

CHANG, K.-T.

Linear-stability theory of thermocapillary convection in a model of float-zone crystal growth
[AIAA PAPER 92-0604] p 169 A92-28211

CHANG, T. Y. P.

On the development of explicit robust schemes for implementation of a class of hyperelastic models in large-strain analysis of rubbers p 221 A92-36245

CHANG, Y. W.

Oxidation-chlorination of binary Ni-Cr alloys in flowing Ar-O₂-Cl₂ gas mixtures at 1200 K p 112 A92-17296

CHAO, LUEN-YUAN

Extreme value statistics analysis of fracture strengths of a sintered silicon nitride failing from pores p 127 A92-50191

CHARALAMIDES, P. G.

Near-tip dual-length scale mechanics of mode-I cracking in laminate brittle matrix composites
[AIAA PAPER 92-2491] p 221 A92-34583

CHATO, D. J.

On-orbit cryogenic fluid transfer research at NASA Lewis Research Center p 45 A92-23847

CHATO, DAVID J.

Modeling of impulsive propellant reorientation
p 59 A92-17187
Evaluation of supercritical cryogen storage and transfer systems for future NASA missions p 47 A92-28512
Pulsed thrust propellant reorientation - Concept and modeling p 62 A92-44507

Comparing the results of an analytical model of the no-vent fill process with no-vent fill test results for a 4.96 cu m (175 cu ft) tank
[AIAA PAPER 92-3078] p 72 A92-54007
Improved thermodynamic modeling of the no-vent fill process and correlation with experimental data
[NASA-TM-104492] p 79 N92-11129

CHEBOLU, SIVA R.

Mutual coupling between rectangular microstrip patch antennas p 159 A92-52423

CHEN, C. F.

Convection in superposed fluid and porous layers
p 166 A92-24752
Effects of g-jitter and cross-diffusion on the onset of convection in doubly diffusive systems
[AIAA PAPER 92-0246] p 167 A92-25705
Stability analysis of surface tension effects on a double-diffusive layer
[AIAA PAPER 92-0605] p 137 A92-27002

CHEN, FALIN

Convection in superposed fluid and porous layers
p 166 A92-24752

CHEN, G. C.

A versatile get away special furnace for materials processing in space
[AIAA PAPER 92-0787] p 137 A92-27122

CHEN, H. H.

Analysis of iced wings
[AIAA PAPER 92-0416] p 8 A92-29972
Analysis of iced wings
[NASA-TM-105773] p 20 N92-34144

CHEN, HSUN H.

A turbulence model for iced airfoils and its validation
[AIAA PAPER 92-0417] p 6 A92-26267
A turbulence model for iced airfoils and its validation
[NASA-TM-105373] p 16 N92-15052

CHEN, J.-Y.

A new unsteady mixing model to predict NO(x) production during rapid mixing in a dual-stage combustor
[AIAA PAPER 92-0233] p 25 A92-25696
A continuous mixing model for pdf simulations and its applications to combustor shear flows
p 174 A92-40139
Second order modeling of boundary-free turbulent shear flows
p 174 A92-41275

CHEN, JUANN-LIANG

Pointing and tracking control for freedom's Solar Dynamic modules and vibration control of freedom
[AAS PAPER 91-459] p 54 A92-43284

CHEN, K.-H.

A time-accurate algorithm for chemical non-equilibrium viscous flows at all speeds
[AIAA PAPER 92-3639] p 182 A92-54112

CHEN, KUO-HUEY

A numerical and experimental study of three-dimensional liquid sloshing in a rotating spherical container
[AIAA PAPER 92-0829] p 170 A92-29597

CHEN, R. T.

Reconfigurable optical interconnection network for multimode optical fiber sensor arrays p 256 A92-37448

CHEN, RAY T.

Multiple-mode reconfigurable electro-optic switching network for optical fiber sensor array p 256 A92-46245

CHEN, S. C.

An iterative implicit DDADI algorithm for solving the Navier-Stokes equation p 192 N92-25810

CHEN, S. K.

Factors influencing the effective spray cone angle of pressure-swirl atomizers p 166 A92-23300

CHEN, SHU-CHENG

An iterative implicit diagonally-dominant factorization algorithm for solving the Navier-Stokes equations
[NASA-TM-105259] p 249 N92-16663
Breakdown of the Karman vortex street due to forced convection and flow compressibility
[NASA-TM-105853] p 196 N92-32472

CHEN, T. K.

Performance of a wideband GaAs low-noise amplifier at cryogenic temperatures p 156 A92-37953

CHEN, Y. C.

dc and microwave performance of a 0.1-micron gate InAs/In(0.52)Al(0.48)As MODFET p 156 A92-43891

CHEN, Y.-J. D.

Application of face-gear drives in helicopter transmissions
[NASA-TM-105655] p 212 N92-28434

CHENG, G. C.

On turbulent flows dominated by curvature effects p 171 A92-32940

CHIARAMONTE, FRANCIS P.

An initial study of void formation during solidification of aluminum in normal and reduced-gravity
[AIAA PAPER 92-0845] p 138 A92-29611

CHILDS, D. W.

Development of advanced seals for space propulsion turbomachinery
[NASA-TM-105659] p 87 N92-24957

CHIMA, RODRICK V.

Viscous three-dimensional calculations of transonic fan performance
[NASA-TM-103800] p 1 N92-17346
TCGRID: A three dimensional C-grid generator for turbomachinery p 35 N92-25716
Viscous three-dimensional calculations of transonic fan performance p 195 N92-27467

CHITRE, D. M.

Satellite delivery of B-ISDN services
[AIAA PAPER 92-1831] p 142 A92-29777
Network architectures and protocols for the integration of ACTS and ISDN
[AIAA PAPER 92-2039] p 145 A92-29953

CHITSOMBOON, T.

Comment on two-equation models p 191 N92-24520

CHITSOMBOON, TAWIT

Implementation of a kappa-epsilon turbulence model to RPLUS3D code p 194 N92-25822

CHIZECK, HOWARD J.

Stochastic stability properties of jump linear systems p 246 A92-25878

CHO, MENGU

The arcing rate for a High Voltage Solar Array - Theory, experiment and predictions
[AIAA PAPER 92-0576] p 53 A92-26983

CHO, S. Y.

A computer model for one-dimensional mass and energy transport in and around chemically reacting particles, including complex gas-phase chemistry, multicomponent molecular diffusion, surface evaporation, and heterogeneous reaction p 181 A92-52406

CHO, SEOG Y.

Some further observations on droplet combustion characteristics - NASA LeRC-Princeton results p 111 A92-12897

CHOCK, RICAURTE

NASCAP/LEO simulations of Shuttle Orbiter charging during the SAMPIE experiment p 55 N92-22361

CHOI, MUN Y.

Some further observations on droplet combustion characteristics - NASA LeRC-Princeton results p 111 A92-12897

Observations on a slow burning regime for hydrocarbon droplets - n-heptane/air results p 112 A92-16602
Microgravity combustion of isolated n-decane and n-heptane droplets
[AIAA PAPER 92-0242] p 113 A92-26927

CHOI, S. R.

Crack healing behavior of hot pressed silicon nitride due to oxidation p 124 A92-32896

Strength, toughness and R-curve behaviour of SiC whisker-reinforced composite Si3N4 with reference to monolithic Si3N4 p 101 A92-34202

Mechanical behaviour and failure phenomenon of an in situ toughened silicon nitride p 127 A92-54504

CHOI, SUNG R.

Estimation of crack closure stresses for in situ toughened silicon nitride with 8 wt pct scandia p 126 A92-43478
Elevated temperature mechanical behavior of monolithic and SiC whisker-reinforced silicon nitrides
[NASA-TM-105245] p 128 N92-15192

CHOI, Y.

A time-accurate algorithm for chemical non-equilibrium viscous flows at all speeds
[AIAA PAPER 92-3639] p 182 A92-54112

CHOI, Y.-H.

Propulsion-related flowfields using the preconditioned Navier-Stokes equations
[AIAA PAPER 92-3437] p 178 A92-48994

CHOO, Y. K.

Grid quality improvement by a grid adaptation technique
MAG3D and its application to internal flowfield analysis p 243 N92-24421

CHOO, YUNG K.

Implementation of control point form of algebraic grid-generation technique p 248 A92-47058
Interactive solution-adaptive grid generation procedure
[NASA-TM-105432] p 18 N92-23563
Interactive solution-adaptive grid generation p 243 N92-24420

Interactive solution-adaptive grid generation procedure p 244 N92-25724

NASA Surface-Modeling and Grid-Generation (SM/GG) activities p 267 N92-25725

Techniques for grid manipulation and adaptation p 194 N92-25627

CHOPRA, M. A.

Growth-speed dependence of primary arm spacings in directionally solidified Pb-10 wt pct Sn p 117 A92-26526

Effect of thermal convection on the shape of a solid-liquid interface p 171 A92-35978

CHOREY, C. M.

Coaxial line configuration for microwave power transmission study of YBa₂Cu₃O(7-delta) thin films p 154 A92-18455

Electrical-transport properties and microwave device performance of sputtered TiCaBaCuO superconducting thin films p 263 A92-56598

Performance of a Y-Ba-Cu-O superconducting filter/GaAs low noise amplifier hybrid circuit
[NASA-TM-105546] p 180 N92-21370

Microwave conductivity of laser ablated YBa₂Cu₃O(7-delta) superconducting films and its relation to microstrip transmission line performance p 264 N92-21639

Performance of a Y-Ba-Cu-O superconducting filter/GaAs low noise amplifier hybrid circuit p 183 N92-32982

CHOU, TSU-WEI

Mechanical behaviors of ceramic matrix composites with matrix cracking and fiber debonding p 100 A92-23104

Predictions of the critical strain for matrix cracking of ceramic matrix composites p 218 A92-33127

Modeling of the flexural behavior of ceramic-matrix composites p 225 A92-52005

CHOW, CHUEN-YEN

Linear stability of compressible Taylor-Couette flow p 173 A92-36187

CHOY, F.

A bulk flow model of a brush seal system
[ASME PAPER 91-GT-325] p 203 A92-15696

CHOY, FRED K.

Modal simulation of gearbox vibration with experimental correlation
[AIAA PAPER 92-3494] p 207 A92-54036

Modal simulation of gearbox vibration with experimental correlation
[NASA-TM-105702] p 215 N92-31485

CHRISTIAN, J. L., JR.

Microwave beam power transmission at an arbitrary range
[NASA-TM-105424] p 150 N92-19992

Wiring for aerospace applications
[NASA-TM-105777] p 162 N92-30427

CHRISTIE, ROBERT J.

Applicability of Long Duration Exposure Facility environmental effects data to the design of Space Station Freedom electrical power system
[AIAA PAPER 92-0848] p 53 A92-29614

CHU, JUNE-LIANG

Diffusive crack growth at a bimaterial interface
[AIAA PAPER 92-2432] p 220 A92-34580

Asymmetric tip morphology of creep microcracks growing along bimaterial interfaces p 127 A92-56585

- CHU, M. L.**
A combined analytical-experimental tensile test technique for brittle materials p 123 A92-23225
Tensile properties of impact ices [AIAA PAPER 92-0883] p 94 A92-29644
- CHU, PONG P.**
On-board congestion control for satellite packet switching networks p 148 N92-14228
- CHUA, KIAT**
Mechanisms resulting in accreted ice roughness [AIAA PAPER 92-0297] p 21 A92-25750
- CHUANG, KATHY C.**
Effects of a noncoplanar biphenyldiamine on the processing and properties of addition polyimides [NASA-TM-105383] p 107 N92-15137
- CHUANG, TZE-JER**
Diffusive crack growth at a bimaterial interface [AIAA PAPER 92-2432] p 220 A92-34580
Asymmetric tip morphology of creep microcracks growing along bimaterial interfaces p 127 A92-56585
- CHUBB, DONALD L.**
Study of a cesium plasma as a selective emitter for thermophotovoltaic applications p 258 A92-33667
Design considerations for space radiators based on the liquid sheet (LSR) concept p 181 A92-50821
Selective emitters [NASA-CASE-LEW-14731-1] p 236 N92-22037
High efficiency thermal to electric energy conversion using selective emitters and spectrally tuned solar cells [NASA-TM-105755] p 238 N92-30426
- CHUDNOVSKY, A.**
An energy analysis of crack-initiation and arrest in epoxy p 224 A92-49777
- CHULYA, ABHISAK**
Mechanical behavior of fiber reinforced SiC/RBSN ceramic matrix composites - Theory and experiment [ASME PAPER 91-GT-209] p 99 A92-15629
Damage mechanisms in three-dimensional woven reinforced ceramic matrix composites under tensile and flexural loading at room and elevated temperatures [AIAA PAPER 92-2492] p 101 A92-34584
Failure mechanisms of 3-D woven SiC/SiC composites under tensile and flexural loading at room and elevated temperatures p 103 A92-39642
Structural design methodologies for ceramic-based material systems p 103 A92-39866
- CHUNG, B. T. F.**
Combined conjugated heat transfer from a scattering medium p 175 A92-44390
- CHUNG, CHAN-HONG**
Internal structure of shock waves in disparate mass mixtures [AIAA PAPER 92-0496] p 169 A92-28195
FDDO and DSMC analyses of rarefied gas flow through 2D nozzles [AIAA PAPER 92-2858] p 176 A92-47841
DSMC analysis of species separation in rarefied nozzle flows [AIAA PAPER 92-2859] p 176 A92-47842
- CLARK, BRUCE J.**
Computer program for Bessel and Hankel functions [NASA-TM-105154] p 243 N92-11691
- CLARK, EDWARD L.**
Calibration of hemispherical-head flow angularity probes [AIAA PAPER 92-4005] p 200 A92-56828
- CLARK, J.**
An accelerated development, reduced cost approach to lunar/Mars exploration using a modular NTR-based space transportation system [IAF PAPER 92-0574] p 43 A92-57053
- CLARK, JOHN S.**
Nuclear rocket propulsion technology - A joint NASA/DOE project [IAF PAPER 91-236] p 58 A92-13159
Nuclear thermal rockets - Key to moon-Mars exploration p 63 A92-48385
Nuclear rocket propulsion: NASA plans and progress - FY 1991 p 69 A92-50584
An improved heat transfer configuration for a solid-core nuclear thermal rocket engine [AIAA PAPER 92-3583] p 75 A92-54063
Nuclear Thermal Propulsion: A Joint NASA/DOE/DOD Workshop [NASA-CP-10079] p 78 N92-11088
Nuclear thermal propulsion workshop overview p 78 N92-11090
NASA/DOE/DOD nuclear propulsion technology planning: Summary of FY 1991 interagency panel results [NASA-TM-105703] p 88 N92-26792
- CLARK, W. A. T.**
Compatibility of potential reinforcing ceramics with Ni and Fe aluminides p 105 A92-46874
- CLASPY, P. C.**
Performance of a K-band superconducting annular ring antenna p 146 A92-37067
- Performance of a four-element Ka-band high-temperature superconducting microstrip antenna p 146 A92-37224
- Performance of a wideband GaAs low-noise amplifier at cryogenic temperatures p 156 A92-37953
- Measurement techniques for cryogenic Ka-band microstrip antennas p 153 N92-32981
- CLAUS, R. W.**
Numerical propulsion system simulation p 59 A92-20194
Multigrad calculations of a jet in crossflow p 170 A92-28525
- CLAUS, RUSSELL W.**
The NASA Computational Aerosciences Program - Toward teraFLOPS computing [AIAA PAPER 92-0558] p 240 A92-26968
- CLIFT, W. M.**
Diffusion mechanisms in chemical vapor-deposited iridium coated on chemical vapor-deposited rhenium p 117 A92-28017
- CLOUGH, R. C.**
The influence of higher harmonics on vortex pairing in an axisymmetric mixing layer p 175 A92-46251
- COE, H. H.**
Maximum life spiral bevel reduction design [AIAA PAPER 92-3493] p 205 A92-49030
Optimal design of compact spur gear reductions [NASA-TM-105676] p 213 N92-29351
- COIRIER, WILLIAM J.**
Cartesian based grid generation/adaptive mesh refinement p 192 N92-25722
- COLE, GARY L.**
Supersonic propulsion simulation by incorporating component models in the large perturbation inlet (LAPIN) computer code [NASA-TM-105193] p 30 N92-15993
- COLE, K. D.**
Solutions of the heat conduction equation in multilayers for photothermal deflection experiments p 141 A92-52205
- COLEMAN, ANTHONY S.**
Power management and distribution considerations for a lunar base [NASA-TM-105342] p 269 N92-13910
- COLLINS, J.**
Engine system assessment study using Martian propellants [AIAA PAPER 92-3446] p 73 A92-54030
- COLOZZA, A.**
SEI power source alternatives for rovers and other multi-kWe distributed surface applications p 80 N92-13206
- COLOZZA, ANTHONY J.**
SEI rover solar-electrochemical power system options p 45 A92-50574
Design and optimization of a self-deploying PV tent array p 233 A92-50642
Self-deploying photovoltaic power system [NASA-CASE-LEW-15308-1] p 237 N92-24057
- COLTRIN, ROBERT E.**
High-speed inlet research program and supporting analysis p 188 N92-22542
- COLVIN, JAMES E.**
Effect of inert propellant injection on Mars ascent vehicle performance [AIAA PAPER 92-3447] p 73 A92-54031
- CONCUS, PAUL**
Drop-tower experiments for capillary surfaces in an exotic container p 166 A92-20743
- CONNOLLY, D. J.**
Space applications of high temperature superconductivity technology [IAF PAPER 91-307] p 259 A92-14724
- CONNOLLY, DENIS J.**
NASA Space applications of high-temperature superconductors [NASA-TM-105401] p 271 N92-18455
- CONWAY, BRUCE A.**
Discrete approximations to optimal trajectories using direct transcription and nonlinear programming p 44 A92-46753
- COOK, JERRY D.**
The introduction of spurious models in a hole-coupled Fabry-Perot open resonator p 197 A92-21244
- COOPER, J. R.**
A 1 MW, 100 kV, less than 100 kg space based dc-dc power converter p 157 A92-50537
- COOPER, JAMES A., JR.**
Significant long-term reduction in n-channel MESFET subthreshold leakage using ammonium-sulfide surface treated gates p 153 A92-12272
- COOPER, JILL M.**
Atomic oxygen effects on SiO(x) coated Kapton for photovoltaic arrays in low earth orbit p 72 A92-53211
- CORBAN, R.**
An accelerated development, reduced cost approach to lunar/Mars exploration using a modular NTR-based space transportation system [IAF PAPER 92-0574] p 43 A92-57053
- CORDA, S.**
The F/A-18 external burning flight test [AIAA PAPER 91-5050] p 23 A92-44547
- CORRIELL, S. R.**
Growth and characterization of lead bromide crystals p 138 A92-56956
Effect of growth conditions on the quality of lead bromide crystals p 138 A92-56957
- CORNER, RALPH E.**
A preliminary characterization of the tensile and fatigue behavior of tungsten-fiber/Waspaloy-matrix composite [NASA-TM-105346] p 187 N92-22487
- CORRIGAN, ROBERT D.**
Removable hand hold [NASA-CASE-LEW-15196-1] p 213 N92-29092
- COURTOIS, H. A.**
A multi-channel demultiplexer/demodulator architecture, simulation and implementation [AIAA PAPER 92-1972] p 144 A92-29895
- COURTOIS, HECTOR A.**
Multichannel demultiplexer/demodulator technologies for future satellite communication systems [NASA-TM-105377] p 51 N92-18342
- COUTTS, T. J.**
Modeled performance of monolithic, 3-terminal InP/Ga(0.47)In(0.53)As concentrator solar cells as a function of temperature and concentration ratio p 234 A92-53153
InP concentrator solar cells p 234 A92-53166
Pilot production of 4 sq cm ITO/InP photovoltaic solar cells p 71 A92-53197
- COWLEY, S. J.**
Distortion of a flat-plate boundary layer by free-stream vorticity normal to the plate p 173 A92-36343
- COY, JOHN J.**
Rotorcraft transmissions p 33 N92-22533
Minimization of the vibration energy of thin-plate structure [NASA-TM-105654] p 211 N92-25448
Optimum design of a gearbox for low vibration [NASA-TM-105653] p 212 N92-28476
- CRAPO, J. A.**
SCAILET - An intelligent assistant for satellite ground terminal operations [IAF PAPER 92-0552] p 245 A92-55855
- CRAWFORD, ROBERT D.**
Maintenance and resupply in the unpressurized environment - Design and operational concepts for the Space Station Freedom logistics carriers [AIAA PAPER 91-4116] p 53 A92-24369
- CREPS, GARY M.**
Maintenance and resupply in the unpressurized environment - Design and operational concepts for the Space Station Freedom logistics carriers [AIAA PAPER 91-4116] p 53 A92-24369
- CROSS, G.**
Advanced optical condition monitoring [SAE PAPER 912164] p 199 A92-39994
- CRUTCHIK, M.**
Solar radiation on a catenary collector [NASA-TM-105751] p 163 N92-32243
- CULL, R. C.**
Integrated solar power satellites - An approach to low-mass space power p 231 A92-40427
Beam power options for the moon p 61 A92-40429
- CULL, RONALD C.**
Electrical system options for space exploration [SAE PAPER 912065] p 62 A92-45447
A mass sensitivity analysis of lunar orbiting beam power systems p 232 A92-50619
Issues and status of power distribution options for space exploration p 80 N92-13207
- CULLERS, C. L.**
The effect of strain rate and temperature on the tensile properties of NiAl p 117 A92-28113
Flow and fracture behavior of NiAl in relation to the brittle-to-ductile transition temperature p 118 A92-30781
- CURLETT, BRIAN P.**
The aerodynamic effect of fillet radius in a low speed compressor cascade [NASA-TM-105347] p 29 N92-14063
A graphical user-interface for propulsion system analysis [NASA-TM-105696] p 244 N92-33894
- CURRAN, FRANCIS M.**
Electric propulsion - An evolutionary technology [IAF PAPER 91-241] p 58 A92-13158
Medium power hydrogen arcjet performance [AIAA PAPER 91-2227] p 58 A92-15355

CURREN, A. N.

- Electric propulsion - The future is now p 63 A92-48386
- An overview of the NASA Advanced Propulsion Concepts program [AIAA PAPER 92-3216] p 73 A92-54018
- Development of arcjet and ion propulsion for spacecraft stationkeeping [IAF PAPER 92-0607] p 77 A92-57058
- High-power hydrogen arcjet performance [NASA-TM-105143] p 82 N92-14109
- Hydrogen arcjet technology [NASA-TM-105340] p 82 N92-15119
- Arcjet nozzle area ratio effects [NASA-TM-104477] p 83 N92-16022
- CURREN, A. N.**
A low-power, high-efficiency Ka-band TWTA p 156 A92-38163
- CURREN, ARTHUR**
Ion beam treatment of potential space materials at the NASA Lewis Research Center [NASA-TM-105398] p 97 N92-21548
- CURREN, ARTHUR N.**
A low-power, high-efficiency Ka-band TWTA [AIAA PAPER 92-1822] p 154 A92-29769
- CURTIS, H. B.**
Radiation and temperature effects in heteroepitaxial and homoepitaxial InP cells p 159 A92-53192
- CURTIS, HENRY B.**
Radiation performance of GaAs concentrator cells for 0.4 to 12 MeV electrons and 0.1 to 37 MeV protons p 159 A92-53193
- CURWEN, P. W.**
Magnetic bearings for free-piston Stirling engines [NASA-TM-105730] p 214 N92-30734
- CUTSHAW, C.**
Surface morphologies and photoluminescence of diamond films deposited in a hot filament reactor p 261 A92-42858

D

- DANIEL, I. M.**
Thermal stress analysis of a silicon carbide/aluminum composite p 222 A92-38097
- DARLING, DOUGLAS**
A fast, uncoupled, compressible, two-dimensional, unsteady boundary layer algorithm with separation for engine inlets [AIAA PAPER 92-3082] p 11 A92-48729
- Interface of an uncoupled boundary layer algorithm with an inviscid core flow algorithm for unsteady supersonic engine inlets [AIAA PAPER 92-3083] p 11 A92-48730
- Interface of an uncoupled boundary layer algorithm with an inviscid core flow algorithm for unsteady supersonic engine inlets [NASA-TM-105684] p 36 N92-27037
- A fast, uncoupled, compressible, two-dimensional, unsteady boundary layer algorithm with separation for engine inlets [NASA-TM-105686] p 195 N92-27653
- DAROLIA, R.**
Microstructure and mechanical properties of a single crystal NiAl alloy with Zr or Hf rich G-phase precipitates p 119 A92-30841
- DARYOUSH, AFSHIN S.**
Interfaces for high-speed fiber-optic links - Analysis and experiment p 256 A92-24002
- A theoretical and experimental study of the noise behavior of subharmonically injection locked local oscillators p 157 A92-46080
- DASGUPTA, SAMHITA**
Fiber optic controls for aircraft engines - Issues and implications p 24 A92-46244
- DAUGHERTY, ELAINE S.**
A software control system for the ACTS high-burst-rate link evaluation terminal [NASA-TM-105207] p 243 N92-16628
- DAVIDIAN, KENNETH O.**
Developments in REDES: The Rocket Engine Design Expert System p 78 N92-11120
- Analytical study of nozzle performance for nuclear thermal rockets [NASA-TM-105251] p 78 N92-11126
- DAVIS, D. O.**
Experimental investigation of turbulent flow through a circular-to-rectangular transition duct p 168 A92-26412
- Surface and flow field measurements in a symmetric crossing shock wave/turbulent boundary layer flow [AIAA PAPER 92-2634] p 10 A92-45574
- DAVIS, GARY A.**
Unsteady transonic Euler solutions using finite elements [AIAA PAPER 92-2504] p 8 A92-34499
- DAVIS, S. J.**
Doppler-shifted fluorescence imaging of velocity fields in supersonic reacting flows [AIAA PAPER 92-2964] p 199 A92-46979
- DAWSON, F.**
The F/A-18 external burning flight test [AIAA PAPER 91-5050] p 23 A92-44547
- DAWSON, VIRGINIA P.**
Rocket propulsion research at Lewis Research Center [NASA-CR-189187] p 266 N92-30908
- DAY, G. W.**
Fiber-optic sensors for aerospace electrical measurements - An update p 200 A92-50630
- DAYTON, J. A., JR.**
Submillimeter backward-wave oscillators p 155 A92-35054
- A low-power, high-efficiency Ka-band TWTA p 156 A92-38163
- DAYTON, JAMES A., JR.**
A low-power, high-efficiency Ka-band TWTA [AIAA PAPER 92-1822] p 154 A92-29769
- DE ABREU-GARCIA, J. A.**
A fundamental theorem for the model reduction of nonlinear systems p 246 A92-41165
- DE GROH, H. C., III**
Effect of radiation on convection at moderate temperatures p 168 A92-27058 [AIAA PAPER 92-0691]
- Effect of thermal convection on the shape of a solid-liquid interface p 171 A92-35978
- On the drag of model dendrite fragments at low Reynolds number p 95 A92-50868
- DE GROH, KIM K.**
Low earth orbit durability evaluation of Haynes 188 solar receiver material [AIAA PAPER 92-0850] p 117 A92-29616
- LDEF spacecraft, ground laboratory, and computational modeling implications on Space Station Freedom's solar array materials and surfaces durability p 71 A92-53190
- DE GROOT, WIM A.**
Species and temperature measurement in H₂/O₂ rocket flow fields by means of Raman scattering diagnostics [AIAA PAPER 92-3353] p 178 A92-48930
- DE WITT, KENNETH J.**
Heat transfer measurements from a smooth NACA 0012 airfoil p 165 A92-20215
- Roughness effects on heat transfer from a NACA 0012 airfoil p 166 A92-20217
- Internal structure of shock waves in disparate mass mixtures [AIAA PAPER 92-0496] p 169 A92-28195
- An initial study of void formation during solidification of aluminum in normal and reduced-gravity [AIAA PAPER 92-0845] p 138 A92-29611
- An efficient finite element method for aircraft de-icing problems [AIAA PAPER 92-0532] p 22 A92-31670
- FD00 and DSMC analyses of rarefied gas flow through 2D nozzles [AIAA PAPER 92-2858] p 176 A92-47841
- DSMC analysis of species separation in rarefied nozzle flows [AIAA PAPER 92-2859] p 176 A92-47842
- Measurement and analysis of a small nozzle plume in vacuum [AIAA PAPER 92-3108] p 64 A92-48748
- DE, BHOLA N.**
Study of temperature-dependent ultrathin oxide growth on Si(111) using variable-angle spectroscopic ellipsometry p 260 A92-32414
- DEADMORE, DANIEL L.**
Screen Cage Ion Plating (SCIP) and scratch testing of polycrystalline aluminum oxide [NASA-TM-105404] p 130 N92-22278
- DEBONIS, JAMES R.**
Full Navier-Stokes analysis of a two-dimensional mixer/ejector nozzle for noise suppression [AIAA PAPER 92-3570] p 27 A92-54059
- Full Navier-Stokes analysis of a two-dimensional mixer/ejector nozzle for noise suppression [NASA-TM-105715] p 37 N92-28419
- DECKER, ARTHUR J.**
Self-aligning optical measurement systems p 247 A92-50387
- DECKER, D. K.**
Multikilowatt power electronics development for spacecraft p 68 A92-50541
- DECKER, HARRY J.**
Full-scale transmission testing to evaluate advanced lubricants [NASA-TM-105668] p 212 N92-26560
- Analysis and modification of a single-mesh gear fatigue rig for use in diagnostic studies [NASA-TM-105416] p 212 N92-27879
- Development of a full-scale transmission testing procedure to evaluate advanced lubricants [NASA-TP-3265] p 213 N92-30396
- DEGANI, A. T.**
The three-dimensional turbulent boundary layer near a plane of symmetry p 167 A92-24757
- DEGROH, HENRY C., III**
Effect of radiation on convection at moderate temperatures [NASA-TM-105632] p 192 N92-25296
- DEGROH, KIM K.**
Atomic oxygen durability of solar concentrator materials for Space Station Freedom [NASA-TM-105378] p 85 N92-20065
- Atomic oxygen undercutting of LDEF aluminized-Kapton multilayer insulation p 255 N92-24818
- Monte Carlo modeling of atomic oxygen attack of polymers with protective coatings on LDEF p 132 N92-27281
- DEQUIRE, M. R.**
Review and statistical analysis of the use of ultrasonic velocity for estimating the porosity fraction in polycrystalline materials p 215 A92-28722
- DEQUIRE, MARK R.**
Ultrasonic evaluation of oxygen content, modulus, and microstructure changes in YBa₂Cu₃O_{7-x} occurring during oxidation and reduction p 261 A92-38418
- DESSLER, ROBERT G.**
Effect of spatial resolution on apparent sensitivity to initial conditions of a decaying flow as it becomes turbulent p 175 A92-45716
- On the most general tensor B(sub ij) which is zero for i does not equal j, and the most general isotropic tensor l(sub ij) [NASA-TM-105236] p 240 N92-10289
- Turbulent fluid motion 3: Basic continuum equations [NASA-TM-104386] p 184 N92-11317
- Turbulence and deterministic chaos p 194 N92-25823
- DESSLER, ROBERT J.**
Stable localized patterns in thin liquid films p 173 A92-37489
- Propagating confined states in phase dynamics p 181 A92-50968
- Stable localized patterns in thin liquid films [NASA-TM-105352] p 185 N92-14322
- The Eckhaus and the Benjamin-Feir instability near a weakly inverted bifurcation [NASA-TM-105334] p 185 N92-15336
- DEL ROSARIO, RUBEN**
Advanced nozzle and engine components test facility [AIAA PAPER 92-3993] p 41 A92-56816
- DEL ROSO, RICHARD L.**
Advanced nozzle and engine components test facility [AIAA PAPER 92-3993] p 41 A92-56816
- DELAAT, JOHN C.**
Real-time fault diagnosis for propulsion systems [NASA-TM-105303] p 29 N92-11017
- DELCHER, R.**
Fiber optics in liquid propellant rocket engine environments p 62 A92-42610
- DELLACORTE, CHRISTOPHER**
Tribological properties of ceramic-(Ti₃Al-Nb) sliding couples for use as candidate seal materials to 700 C p 124 A92-32407
- DELLACORTE, CHRISTOPHER**
The application of a computer data acquisition system to a new high temperature tribometer p 93 A92-11823
- Relative sliding durability of two candidate high temperature oxide fiber seal materials [AIAA PAPER 92-3713] p 126 A92-49095
- Relative sliding durability of two candidate high temperature oxide fiber seal materials [NASA-TM-105199] p 95 N92-10064
- Tribological and mechanical comparison of sintered and HIPped PM212: High temperature self-lubricating composites [NASA-TM-105379] p 96 N92-15128
- Sliding durability of two carbide-oxide candidate high temperature fiber seal materials in air to 900 C [NASA-TM-105554] p 97 N92-21175
- Tribological evaluation of an Al₂O₃-SiO₂ ceramic fiber candidate for high temperature sliding seals [NASA-TM-105611] p 97 N92-23190
- High temperature dynamic engine seal technology development [NASA-TM-105641] p 209 N92-23435
- Tribological and microstructural comparison of HIPped PM212 and PM212/Au self-lubricating composites [NASA-TM-105615] p 97 N92-26142
- DELLAVECCHIA, MICHAEL A.**
A fiber optic sensor for ophthalmic refractive diagnostics p 198 A92-34831

- DELOMBARD, RICHARD**
Development of and flight results from the Space Acceleration Measurement System (SAMS) [AIAA PAPER 92-0354] p 56 A92-28189
Space acceleration measurement system description and operations on the First Spacelab Life Sciences Mission [NASA-TM-105301] p 57 N92-13151
Early mission science support: Space Acceleration Measurement System (SAMS) p 57 N92-28451
Development of and flight results from the Space Acceleration Measurement System (SAMS) [NASA-TM-105652] p 57 N92-30301
- DELROSARIO, RUBEN**
Advanced nozzle and engine components test facility [NASA-TM-103684] p 42 N92-17059
- DELROSO, RICHARD L.**
Advanced nozzle and engine components test facility [NASA-TM-103684] p 42 N92-17059
- DELVIGS, PETER**
Vinyl capped addition polyimides [NASA-CASE-LEW-15027-2] p 131 N92-24053
- DEMERDASH, N. A.**
A combined vector potential-scalar potential method for FE computation of 3D magnetic fields in electrical devices with iron cores p 154 A92-23959
- DEMPSEY, PAULA J.**
Using silicon diodes for detecting the liquid-vapor interface in hydrogen [NASA-TM-105541] p 201 N92-18456
- DEMUREN, A. O.**
Multigrad acceleration and turbulence models for computations of 3D turbulent jets in crossflow [NASA-TM-105306] p 186 N92-18775
- DESAI, HEMANT D.**
Synthesis and characterization of fine grain diamond films p 262 A92-46330
- DETERMAN, W. R.**
Heat transfer and core neutronics considerations of the heat pipe cooled thermionic reactor p 180 A92-50591
- DEUR, J. M.**
A simplified reaction mechanism for prediction of NO(x) emissions in the combustion of hydrocarbons [AIAA PAPER 92-3340] p 114 A92-48919
Applied analytical combustion/emissions research at the NASA Lewis Research Center - A progress report [AIAA PAPER 92-3338] p 27 A92-54025
Applied analytical combustion/emissions research at the NASA Lewis Research Center [NASA-TM-105731] p 90 N92-29343
- DEVER, JOYCE A.**
Synergistic effects of ultraviolet radiation, thermal cycling and atomic oxygen on altered and coated Kapton surfaces [AIAA PAPER 92-0794] p 93 A92-27125
The effects of RF plasma ashing on zinc orthoitanate/potassium silicate thermal control coatings [AIAA PAPER 92-2171] p 124 A92-31299
Synergistic effects of ultraviolet radiation, thermal cycling, and atomic oxygen on altered and coated Kapton surfaces [NASA-TM-105363] p 96 N92-14114
Atomic oxygen interactions with FEP Teflon and silicones on LDEF p 132 N92-24820
- DEVER, THERESA M.**
Low earth orbit durability evaluation of Haynes 188 solar receiver material [AIAA PAPER 92-0850] p 117 A92-29616
Atomic oxygen durability of solar concentrator materials for Space Station Freedom [NASA-TM-105378] p 85 N92-20065
- DEWITT, K. J.**
Numerical analysis of a thermal deicer [AIAA PAPER 92-0527] p 22 A92-26950
- DEWITT, KENNETH J.**
Numerical modeling of fluid and electromagnetic phenomena in an arcjet [AIAA PAPER 92-3106] p 258 A92-48747
Experimental and numerical investigations of low-density nozzle and plume flows of nitrogen p 183 A92-54917
- DEWITT, RICHARD L.**
Slush hydrogen (SLH2) technology development for application to the National Aerospace Plane (NASP) p 140 A92-13432
- DHADWAL, HARBANS S.**
A fiber-optic probe for particle sizing in concentrated suspensions p 197 A92-21371
A fiber optic sensor for ophthalmic refractive diagnostics p 198 A92-34831
- DHAR, MANMOHAN**
Free-piston Stirling component test power converter p 206 A92-50784
- DI BLASI, C.**
Heat and mass transport from thermally degrading thin cellulosic materials in a microgravity environment p 174 A92-41810
- DIAZ, NILS**
Innovative nuclear thermal propulsion technology evaluation - Results of the NASA/DOE task team study [IAF PAPER 91-235] p 58 A92-13160
- DIB, N. I.**
Analysis of shielded CPW discontinuities with air-bridges p 152 N92-32971
- DICARLO, JAMES A.**
A simple test for thermomechanical evaluation of ceramic fibers p 123 A92-21096
High temperature structural fibers: Status and needs [NASA-TM-105174] p 107 N92-16037
Ceramics for engines p 131 N92-22517
- DICICCO, L. D.**
Description of a pressure measurement technique for obtaining surface static pressures of a radial turbine [AIAA PAPER 92-4006] p 200 A92-56829
- DICICCO, L. DANIELLE**
Description of a pressure measurement technique for obtaining surface static pressures of a radial turbine [NASA-TM-105643] p 202 N92-24959
- DICKMAN, J. E.**
Wiring for aerospace applications [NASA-TM-105777] p 162 N92-30427
- DIFILIPPO, FRANK**
Thermochemical energy storage for a lunar base [NASA-TM-105333] p 236 N92-14485
- DILL, LOREN H.**
Unsteady thermocapillary migration of isolated drops in creeping flow p 169 A92-27774
- DILLARD, RICHARD B.**
Reliability training [NASA-RP-1253] p 49 N92-32456
- DIMOFFE, FLORIN**
Fast methods to numerically integrate the Reynolds equation for gas fluid films [NASA-TM-105415] p 214 N92-30722
- DINNSEN, D.**
Fiber optics in liquid propellant rocket engine environments p 62 A92-42610
- DIPIETRO, M. S.**
Compression studies on particulate composites of ternary Al-Ti-Fe, and quaternary Al-Ti-Fe-Nb and Al-Ti-Fe-Mn L1(2) compounds p 119 A92-30845
Mechanical properties of monolithic and particulate composites of L12 forms of Al3Ti p 101 A92-36273
Composites of low-density trialuminides: Particulate and long fiber reinforcements [NASA-TM-105628] p 109 N92-25346
- DIRUSSO, ELISEO**
Design of a hydraulic actuator for active control of rotating machinery [ASME PAPER 91-GT-246] p 203 A92-15651
Performance tests of a cryogenic hybrid magnetic bearing for turbopumps [NASA-TM-105627] p 30 N92-20523
Determining structural performance p 32 N92-22519
- DITTMAR, JAMES H.**
Detailed noise measurements on the SR-7A propeller: Tone behavior with helical tip Mach number [NASA-TM-105206] p 255 N92-16705
An evaluation of some alternative approaches for reducing fan tone noise [NASA-TM-105356] p 255 N92-18282
- DOBYNS, ALAN**
Turning up the heat on aircraft structures p 23 A92-55131
- DOCHAT, GEORGE**
Free-piston Stirling component test power converter p 206 A92-50784
- DODELSON, SCOTT**
Constraints to the decays of Dirac neutrinos from SN 1987A p 255 A92-36249
- DOEBERLING, THOMAS J.**
Update on results of SPRE testing at NASA Lewis p 71 A92-50780
NASA Lewis Stirling SPRE testing and analysis with reduced number of cooler tubes [NASA-TM-105767] p 238 N92-28837
- DOHERTY, MICHAEL P.**
Nuclear Electric Propulsion Technology Panel findings and recommendations [NASA-TM-105547] p 85 N92-20355
Blazing the trailway: Nuclear electric propulsion and its technology program plans [NASA-TM-105605] p 86 N92-23252
NASA/DOE/DOD nuclear propulsion technology planning: Summary of FY 1991 interagency panel results [NASA-TM-105703] p 88 N92-26792
NEP systems engineering efforts in FY-92: Plans and status [NASA-TM-105775] p 91 N92-30308
- DOHOGNE, CAROLINE A.**
Design feasibility study of a Space Station Freedom truss [NASA-TM-105558] p 214 N92-30571
- DOLCE, JAMES L.**
Automated power management and control p 84 N92-17773
- DOLHERT, LEONARD E.**
Ultrasonic evaluation of oxygen content, modulus, and microstructure changes in YBa2Cu3O(7-x) occurring during oxidation and reduction p 261 A92-38418
- DOMBRO, L.**
A low-power, high-efficiency Ka-band TWTA p 156 A92-38163
- DOMBRO, LOUIS**
A low-power, high-efficiency Ka-band TWTA [AIAA PAPER 92-1822] p 154 A92-29769
- DOMINICK, SAM**
Space Station Freedom/lunar transfer vehicle propellant operation hazard analysis p 55 N92-17416
- DOMITZ, STANLEY**
Experimental breakdown of selected anodized aluminum samples in dilute plasmas p 259 N92-22369
- DONALDSON, K. Y.**
Role of interfacial thermal barrier in the transverse thermal conductivity of uniaxial SiC fiber-reinforced reaction bonded silicon nitride p 102 A92-39605
- DONALDSON, KIMBERLY Y.**
Role of interfacial carbon layer in the thermal diffusivity/conductivity of silicon carbide fiber-reinforced reaction-bonded silicon nitride matrix composites p 100 A92-25443
- DOWELL, EARL H.**
Eigenvalue calculation procedure for an Euler/Navier-Stokes solver with application to flows over airfoils p 3 A92-17429
- DOWNEY, A. N.**
A vertically integrated Ka-band phased array antenna [AIAA PAPER 92-1976] p 156 A92-38140
- DOWNEY, ALAN N.**
V-band pseudomorphic HEMT MMIC phased array components for space communications p 151 N92-32966
An optically controlled Ka-band phased array antenna p 152 N92-32968
- DOYCHAK, J.**
Oxidation-chlorination of binary Ni-Cr alloys in flowing Ar-O2-Cl2 gas mixtures at 1200 K p 112 A92-17296
Protective Al2O3 scale formation on NbAl3-base alloys p 119 A92-31850
Metal- and intermetallic-matrix composites for aerospace propulsion and power systems p 104 A92-43682
Oxidation of Al2O3 continuous fiber-reinforced/NiAl composites p 106 A92-57029
- DRAPER, S.**
Compatibility of potential reinforcing ceramics with Ni and Fe aluminides p 105 A92-46874
- DRAPER, S. L.**
Effect of fiber strength on the room temperature tensile properties of SiC/Ti-24Al-11Nb p 102 A92-36389
The effect of temperature on the deformation and fracture of SiC/Ti-24Al-11Nb p 106 A92-55143
- DRAVID, NARAYAN**
Functional models of power electronic components for system studies p 157 A92-50558
Modeling of Space Station power system components and their interactions p 68 A92-50559
- DRAVID, NARAYAN V.**
An EMTP system level model of the PMAD DC test bed p 46 A92-50657
- DRESHFIELD, R. L.**
The effect of porosity and gamma-gamma-prime eutectic content on the fatigue behavior of hydrogen charged PWA 1480 p 116 A92-12046
- DRESHFIELD, ROBERT L.**
Post-test examination of a pool boiler receiver [NASA-TM-105635] p 123 N92-27192
- DREVINSKY, P. J.**
Defect behavior, carrier removal and predicted in-space injection annealing of InP solar cells [NASA-TM-105624] p 161 N92-23562
- DRISCOLL, SUSAN L.**
Hydrogen no-vent fill testing in a 1.2 cubic foot (34 liter) tank [NASA-TM-105273] p 185 N92-13401
- DROTOS, M. N.**
A new technique for oil backstreaming contamination measurements [NASA-TM-105312] p 257 N92-13783
- DRUMMOND, CHARLES H., III**
Phase transformations in SrAl2Si2O8 glass [NASA-TM-105657] p 264 N92-23890
- DRUMMOND, COLIN K.**
Preliminary dynamic tests of a flight-type ejector [AIAA PAPER 92-3261] p 27 A92-54020

DRUMMOND, J. E.

- Preliminary dynamic tests of a flight-type ejector
[NASA-TM-105814] p 38 N92-30998
- DRUMMOND, J. E.**
Development of an algebraic turbulence model for analysis of propulsion flows
[AIAA PAPER 92-3861] p 183 A92-54209
Development of an algebraic turbulence model for analysis of propulsion flows
[NASA-TM-105701] p 250 N92-27517
- DRYER, F. L.**
A computer model for one-dimensional mass and energy transport in and around chemically reacting particles, including complex gas-phase chemistry, multicomponent molecular diffusion, surface evaporation, and heterogeneous reaction p 181 A92-52406
- DRYER, FREDERICK L.**
Some further observations on droplet combustion characteristics - NASA LeRC-Princeton results p 111 A92-12897
Observations on a slow burning regime for hydrocarbon droplets - n-heptane/air results p 112 A92-16602
Microgravity combustion of isolated n-decane and n-heptane droplets
[AIAA PAPER 92-0242] p 113 A92-26927
- DU, GUANG-WU**
Engine panel seals for hypersonic engine applications: High temperature leakage assessments and flow modelling
[NASA-TM-105260] p 208 N92-16336
High temperature dynamic engine seal technology development
[NASA-TM-105641] p 209 N92-23435
- DUBOIS-PELERIN, YVES**
An unconditionally stable staggered algorithm for transient finite element analysis of coupled thermoelastic problems p 222 A92-37517
- DUCHENE, G. A.**
A versatile get away special furnace for materials processing in space
[AIAA PAPER 92-0787] p 137 A92-27122
- DUCKERT, R. E.**
Thermomechanical and bithermal fatigue behavior of cast B1900 + Hf and wrought Haynes 188 p 122 A92-45233
- DUDEHOFER, JAMES E.**
Status of NASA's Stirling space power converter program p 69 A92-50608
Stirling machine operating experience p 206 A92-50788
Instantaneous heat transfer coefficient based upon two-dimensional analyses of Stirling space engine components p 181 A92-50827
Heat transfer in oscillating flows with sudden change in cross section p 88 N92-26654
[NASA-TM-105692]
Progress update of NASA's free-piston Stirling space power converter technology project
[NASA-TM-105748] p 239 N92-33898
- DUFFLOCCQ, M.**
Initial development of the axisymmetric ejector shear layer
[AIAA PAPER 92-3567] p 178 A92-49068
- DUFFY, S. F.**
Reliability analysis of laminated CMC components through shell subelement techniques
[AIAA PAPER 92-2348] p 219 A92-34322
- DUFFY, STEPHEN F.**
Structural reliability analysis of laminated CMC components
[ASME PAPER 91-GT-210] p 99 A92-15630
Analysis of whisker-toughened CMC structural components using an interactive reliability model
[AIAA PAPER 92-2490] p 221 A92-34582
Structural design methodologies for ceramic-based material systems p 103 A92-39866
Reliability analysis of structural ceramic components using a three-parameter Weibull distribution
[NASA-TM-105370] p 129 N92-17060
Reliability analysis of laminated CMC components through shell subelement techniques
[NASA-TM-105413] p 129 N92-20380
- DUGAN, EDWARD T.**
Thermal analysis of a conceptual design for a 250 We GPHS/FPSE space power system p 69 A92-50637
- DUH, J. C.**
Numerical investigation on Benard instability in a finite liquid layer p 164 A92-12865
- DUNCAN, BEVERLY**
Computational analysis of ramjet engine inlet interaction
[AIAA PAPER 92-3102] p 11 A92-48744
- DUNCAN, D. B.**
An overview of in-flight plume diagnostics for rocket engines
[AIAA PAPER 92-3785] p 75 A92-54164

- Demonstration of a flight capable system for plume spectroscopy
[AIAA PAPER 92-3786] p 57 A92-54165
An overview of in-flight plume diagnostics for rocket engines
[NASA-TM-105727] p 90 N92-28417
- DUNNING, F. B.**
Extrapolation procedures in Mott electron polarimetry p 197 A92-21241
- DUNNING, J. E.**
A new technique for oil backstreaming contamination measurements
[NASA-TM-105312] p 257 N92-13783
- DURKIN, JOHN**
GTEX: An expert system for diagnosing faults in satellite ground stations p 148 N92-14215
FIDEX: An expert system for satellite diagnostics p 148 N92-14218
Intelligent fault isolation and diagnosis for communication satellite systems p 248 N92-23365
- DUSTIN, MILES O.**
Solar dynamic power for earth orbital and lunar applications p 68 A92-50567
Solar thermal energy receiver
[NASA-CASE-LEW-14949-1] p 238 N92-29143
- DUTT, D. S.**
Nuclear electric propulsion development and qualification facilities
[NASA-TM-105521] p 91 N92-30818
- DUVAL, W. M. B.**
Adaptive temperature profile control of a multizone crystal growth furnace p 137 A92-29243
Identification and control of a multizone crystal growth furnace p 199 A92-39699
Growth and characterization of lead bromide crystals p 138 A92-56956
Effect of growth conditions on the quality of lead bromide crystals p 138 A92-56957
- DUVAL, WALTER M. B.**
Flight experiment on acousto-optic crystal growth p 136 A92-12880
Thermal and solutal convection with conduction effects inside a rectangular enclosure
[NASA-TM-105371] p 186 N92-15358
Vapor crystal growth technology development: Application to cadmium telluride p 139 N92-16158
[NASA-TM-103786]
- DUYAR, A.**
Identification of the Space Shuttle Main Engine dynamic models from firing data
[AIAA PAPER 92-3317] p 73 A92-54022
- DUYAR, AHMET**
A failure diagnosis system based on a neural network classifier for the Space Shuttle Main Engine p 58 A92-11474
State space representation of the open-loop dynamics of the Space Shuttle Main Engine p 59 A92-19607
Fault diagnosis for the Space Shuttle main engine p 60 A92-28137
A simplified dynamic model of Space Shuttle Main Engine p 60 A92-29289
Real-time fault diagnosis for propulsion systems
[NASA-TM-105303] p 29 N92-11017
A simplified dynamic model of the T700 turboshaft engine
[NASA-TM-105805] p 251 N92-30898

E

- EAGLESON, L. A.**
A review of computational/experimental methodology developments in aeroacoustics p 253 A92-39241
- EBIHARA, B. T.**
Microwave conductivity of laser ablated YBa₂Cu₃O_{7-δ} superconducting films and its relation to microstrip transmission line performance p 264 N92-21639
- EBIHARA, BEN T.**
Measurements of complex permittivity of microwave substrates in the 20 to 300 K temperature range from 26.5 to 40.0 GHz p 197 A92-13416
- ECCLES, J. V.**
Reactive collision terms for fluid transport theory p 257 A92-22693
- EDELMAN, RAYMOND B.**
Effects of oxygen concentration on radiative loss from normal-gravity and microgravity methane diffusion flames
[AIAA PAPER 92-0243] p 113 A92-26928
- EISEMAN, PETER R.**
A conformal block structured grid for turbomachinery cascades in two dimensions p 248 A92-47059
- EISEMANN, PETER R.**
Techniques for grid manipulation and adaptation p 194 N92-25827
- EL-GENK, MOHAMED S.**
Shrinkage void formation and its effect on freeze and thaw processes of lithium and lithium-fluoride for space applications p 180 A92-50596
- ELDEM, VASFI**
State space representation of the open-loop dynamics of the Space Shuttle Main Engine p 59 A92-19607
A simplified dynamic model of Space Shuttle Main Engine p 60 A92-29289
- ELDER, M. G.**
Analytical and experimental studies of heat pipe radiation cooling of hypersonic propulsion systems
[AIAA PAPER 92-3809] p 26 A92-49128
- ELDRIDGE, J. I.**
Initial evaluation of continuous fiber reinforced NiAl composites p 104 A92-46867
The effect of temperature on the deformation and fracture of SiC/Ti-24Al-11Nb p 106 A92-55143
- ELDRIDGE, JEFFREY I.**
Desktop fiber push-out apparatus
[NASA-TM-105341] p 107 N92-16036
- ELGHOBASHI, S.**
Effects of g-jitter on a thermally buoyant flow p 171 A92-32258
- ELIZALDE, E.**
Void probability as a function of the void's shape and scale-invariant models p 267 A92-24456
- ELLIOTT, G. S.**
Compressibility effects on large structures in free shear flows p 173 A92-39337
Filtered Rayleigh scattering based measurements in compressible mixing layers
[AIAA PAPER 92-3543] p 182 A92-54043
- ELLIOTT, GREGORY S.**
Study of compressible mixing layers using filtered Rayleigh scattering based visualizations p 183 A92-54937
- ELLIS, DAVID L.**
Thermal conductivity and thermal expansion of graphite fiber/copper matrix composites
[NASA-TM-105233] p 106 N92-14120
- ELLIS, JOHN R.**
Thermomechanical testing of high-temperature composites - Thermomechanical fatigue (TMF) behavior of SiC(SCS-6)/Ti-15-3 p 104 A92-44606
- ELROD, HAROLD G.**
Numerical experiments with flows of elongated granules
[NASA-TM-105567] p 209 N92-23226
- EMERY, K. A.**
Modeled performance of monolithic, 3-terminal InP/Ga(0.47)In(0.53)As concentrator solar cells as a function of temperature and concentration ratio p 234 A92-53153
InP concentrator solar cells p 234 A92-53166
- EMIGH, S. G.**
Final design of a free-piston hydraulic advanced Stirling conversion system p 206 A92-50798
- ENGLUND, DAVID R.**
Research sensors p 202 N92-22526
- ENRIGHT, PAUL J.**
Discrete approximations to optimal trajectories using direct transcription and nonlinear programming p 44 A92-46753
- ERICKSON, GARY E.**
Wind tunnel investigation of vortex flows on F/A-18 configuration at subsonic through transonic speed
[NASA-TP-3111] p 16 N92-14968
- ERNST, MICHAEL A.**
Determining structural performance p 32 N92-22519
Structural analysis of low-speed composite propfan blades for the LRCSW wind tunnel model
[NASA-TM-105266] p 229 N92-25753
- ERNST, STEVEN A.**
Maintenance and resupply in the unpressurized environment - Design and operational concepts for the Space Station Freedom logistics carriers
[AIAA PAPER 91-4116] p 53 A92-24369
- ERVIN, J. S.**
Transient pool boiling in microgravity p 170 A92-30494
- ERWIN, DANIEL**
Experimental unsteady pressures on an oscillating cascade with supersonic leading edge locus
[AIAA PAPER 92-4035] p 14 A92-56857
- ESCHER, W. J. D.**
Status of NASA's Earth-to-Orbit Propulsion Technology program
[IAF PAPER 91-258] p 58 A92-13154
The NASA-OAST earth-to-orbit propulsion technology program - The action plan
[AIAA PAPER 92-1478] p 61 A92-38597

- ESKER, BARBARA S.**
Experimental performance of three design factors for ventral nozzles for SSTOVL aircraft
[AIAA PAPER 92-3789] p 28 A92-54168
Internal reversing flow in a tailpipe offtake configuration for SSTOVL aircraft
[AIAA PAPER 92-3790] p 28 A92-54169
Computational and experimental investigation of subsonic internal reversing flows
[AIAA PAPER 92-3791] p 183 A92-54170
Experimental performance of three design factors for ventral nozzles for SSTOVL aircraft
[NASA-TM-105697] p 37 N92-27669
Internal reversing flow in a tailpipe offtake configuration for SSTOVL aircraft
[NASA-TM-105698] p 37 N92-28418
- ESTABROOK, POLLY**
ACTS aeronautical experiments
[AIAA PAPER 92-2042] p 50 A92-29956
- EUGENE, L. P.**
Multicarrier demodulator architecture for onboard processing satellites p 49 A92-10465
- EUSTACE, JOHN G.**
Wavelength-multiplexed fiber-optic position encoder for aircraft control systems p 24 A92-42602
RF modulated fiber optic sensing systems and their applications
[NASA-TM-105801] p 257 N92-33896
- EVANS, A. L.**
Numerical propulsion system simulation p 59 A92-20194
- EVANS, AUSTIN L.**
Activities for numerical propulsion systems simulation program p 244 N92-25726
- EVANS, J.**
Wiring for aerospace applications
[NASA-TM-105777] p 162 N92-30427
- F**
- FABIK, RICHARD H.**
Using silicon diodes for detecting the liquid-vapor interface in hydrogen
[NASA-TM-105541] p 201 N92-18456
- FACCA, ANTHONY A.**
Distributed visualization for computational fluid dynamics p 194 N92-25826
- FAGHRI, AMIR**
Frozen start-up behavior of low-temperature heat pipes p 179 A92-49847
- FAIRBANKS, E. S.**
A high-performance photovoltaic concentrator array - The mini-dome Fresnel lens concentrator with 30 percent efficient GaAs/GaSb tandem cells p 72 A92-53199
- FANG, J.**
Aerodynamics of loaded cascades in subsonic flows subject to unsteady three-dimensional vortical disturbances
[AIAA PAPER 92-0146] p 4 A92-23762
- FARDIS, F.**
Technology requirements for mesh VSAT applications
[AIAA PAPER 92-1982] p 144 A92-29902
- FARHAT, CHARBEL**
An unconditionally stable staggered algorithm for transient finite element analysis of coupled thermoelastic problems p 222 A92-37517
- FARMER, S. C.**
Mechanical properties of monolithic and particulate composites of L12 forms of Al₃Ti p 101 A92-36273
- FAROKHI, S.**
On turbulent flows dominated by curvature effects p 171 A92-32940
Modern developments in shear flow control with swirl p 9 A92-41265
Spatial instability of a swirling jet - Theory and experiment p 174 A92-41274
A computational study of advanced exhaust system transition ducts with experimental validation
[AIAA PAPER 92-3794] p 179 A92-49126
- FAROKHI, SAIED**
A study of three dimensional turbulent boundary layer separation and vortex flow control using the reduced Navier Stokes equations p 9 A92-40105
- FARRELL, D. E.**
Melting of the Abrikosov flux lattice in anisotropic superconductors p 260 A92-28075
- FARSHCHI, MOHAMMAD**
Automatic grid generation for iced airfoil flowfield predictions
[AIAA PAPER 92-0415] p 6 A92-26266
- FATEMI, N.**
High voltage thermally diffused p(+)-n solar cells p 235 A92-53172
- FATEMI, N. S.**
Sinterless contacts to shallow junction InP solar cells
[NASA-TM-105670] p 237 N92-24802
- FATEMI, NAVID**
Increased efficiency with surface texturing in ITO/InP solar cells p 232 A92-44548
High performance etchant for thinning p(+)-InP and its application to p(+)-n InP solar cell fabrication p 263 A92-53155
- FATEMI, NAVID S.**
A very low resistance, non-sintered contact system for use on indium phosphide concentrator/shallow junction solar cells p 233 A92-53146
Enhancing optical absorption in InP and GaAs utilizing profile etching p 263 A92-53154
A very low resistance, non-sintered contact system for use on indium phosphide concentrator/shallow junction solar cells
[NASA-TM-105279] p 235 N92-13482
Enhancing optical absorption in InP and GaAs utilizing profile etching
[NASA-TM-105325] p 82 N92-14111
The achievement of low contact resistance to indium phosphide: The roles of Ni, Au, Ge, and combinations thereof
[NASA-TM-105770] p 238 N92-33895
- FAUR, M.**
High voltage thermally diffused p(+)-n solar cells p 235 A92-53172
High voltage thermally diffused p(+)-n solar cells p 235 A92-53172
Radiation and temperature effects in heteroepitaxial and homoepitaxial InP cells p 159 A92-53192
- FAUR, MARIA**
High performance etchant for thinning p(+)-InP and its application to p(+)-n InP solar cell fabrication p 263 A92-53155
- FAUR, MIRCEA**
High performance etchant for thinning p(+)-InP and its application to p(+)-n InP solar cell fabrication p 263 A92-53155
- FAY, E. H.**
Beam power options for the moon p 61 A92-40429
- FEILER, CHARLES E.**
Institute for Computational Mechanics in Propulsion (ICOMP)
[NASA-TM-105612] p 250 N92-27196
- FEINGOLD, HARVEY**
Space Station Freedom/lunar transfer vehicle propellant operation hazard analysis p 55 N92-17416
- FEKADE, K.**
Anodic etching of p-type cubic silicon carbide p 127 A92-57027
- FELICELLI, S.**
Vertical solidification of dendritic binary alloys p 261 A92-37562
- FENG, H. J.**
Combustion synthesis of TiB₂-Al₂O₃-Al composite materials p 102 A92-36391
Combustion synthesis of ceramic-metal composite materials - The TiC-Al₂O₃-Al system p 115 A92-55139
- FENG, XIANGBO**
Stochastic stability properties of jump linear systems p 246 A92-25878
- FERBER, M. K.**
Determination of the stress distributions in a ceramic, tensile specimen using numerical techniques p 216 A92-14546
- FERGUSON, DALE C.**
Solar Array Module Plasma Interaction Experiment (SAMPIE): Technical requirements document
[NASA-TM-105660] p 56 N92-28683
- FERNANDES, P. J.**
Multicarrier demodulator architecture for onboard processing satellites p 49 A92-10465
- FERRANTE, J.**
Computational techniques in tribology and material science at the atomic level
[NASA-TM-105573] p 252 N92-26671
- FERRANTE, JOHN**
The analysis of high pressure experimental data p 266 A92-16101
Universal aspects of adhesion and atomic force microscopy p 260 A92-17979
A new approximate sum rule for bulk alloy properties p 117 A92-28240
Lattice parameters of fcc binary alloys using a new semiempirical method p 120 A92-32898
Pressure dependence of the melting temperature of solids - Rare-gas solids p 171 A92-33912
Heats of formation of bcc binary alloys
[NASA-TM-105281] p 122 N92-16086
Lattice parameters of fcc binary alloys using a new semiempirical method
[NASA-TM-105304] p 123 N92-16111
- FERRELL, RICHARD A.**
Hall voltage sign reversal in thin superconducting films p 261 A92-35349
- FESQ, LORRAINE M.**
Model-based diagnostics for Space Station Freedom p 245 A92-50535
- FIELDER, WILLIAM L.**
A study of Na(x)Pt₃O₄ as an O₂ electrode bifunctional electrocatalyst
[NASA-TM-105311] p 85 N92-20585
The O₂ reduction at the IFC modified O₂ fuel cell electrode
[NASA-TM-105691] p 90 N92-29667
- FIELDS, W. A.**
Features of wavy vortices in a curved channel from experimental and numerical studies p 171 A92-31638
- FINLAY, W. H.**
Features of wavy vortices in a curved channel from experimental and numerical studies p 171 A92-31638
- FINLEY, BRIAN D.**
Development of and flight results from the Space Acceleration Measurement System (SAMS)
[AIAA PAPER 92-0354] p 56 A92-28189
Space acceleration measurement system description and operations on the First Spacelab Life Sciences Mission
[NASA-TM-105301] p 57 N92-13151
Space acceleration measurement system triaxial sensor head error budget
[NASA-TM-105300] p 57 N92-25134
Development of and flight results from the Space Acceleration Measurement System (SAMS)
[NASA-TM-105652] p 57 N92-30301
- FINN, ROBERT**
Drop-tower experiments for capillary surfaces in an exotic container p 166 A92-20743
- FITE, E. B.**
A three-dimensional finite-element thermal/mechanical analytical technique for high-performance traveling wave tubes
[AIAA PAPER 92-1824] p 154 A92-29771
- FLANAGAN, PATRICK M.**
Design of a self-diagnostic beam-mode piezoelectric accelerometer
[AIAA PAPER 92-3656] p 200 A92-54106
- FLATICO, JOSEPH M.**
Wavelength-multiplexed fiber-optic position encoder for aircraft control systems p 24 A92-42602
- FLEETER, S.**
Wind tunnel wall effects in a linear oscillating cascade
[ASME PAPER 91-GT-133] p 2 A92-15576
- FLEETER, SANFORD**
Airfoil wake and linear theory gust response including sub and superresonant flow conditions
[AIAA PAPER 92-3074] p 11 A92-48724
- FLEMING, D. P.**
Magnetic bearings for free-piston Stirling engines
[NASA-TM-105730] p 214 N92-426734
- FLEMING, DAVID**
Determining structural performance p 32 N92-22519
- FLEMMING, ROBERT J.**
Model rotor icing tests in the NASA, Lewis Icing Research Tunnel p 21 N92-21688
- FLOOD, D. J.**
Influence of the dislocation density on the performance of heteroepitaxial indium phosphide solar cells p 234 A92-53156
High voltage thermally diffused p(+)-n solar cells p 235 A92-53172
A high-performance photovoltaic concentrator array - The mini-dome Fresnel lens concentrator with 30 percent efficient GaAs/GaSb tandem cells p 72 A92-53199
- FLOOD, DENNIS J.**
Advanced power systems for EOS p 70 A92-50640
Thin film, concentrator, and multijunction space solar cells: Status and potential p 81 N92-13230
Enhanced EOS photovoltaic power system capability with InP solar cells p 81 N92-13248
NASA programs in space photovoltaics
[NASA-TM-105428] p 87 N92-25343
High efficiency thermal to electric energy conversion using selective emitters and spectrally tuned solar cells
[NASA-TM-105755] p 236 N92-30426
Monolithic and mechanical multijunction space solar cells
[NASA-TM-105832] p 163 N92-32233
- FLOOD, JOSEPH D.**
Hot gas ingestion characteristics and flow visualization of a vectored thrust STOVL concept p 26 A92-45316
- FLOWE, ANITA C.**
Numerical modeling of fluid and electromagnetic phenomena in an arcjet
[AIAA PAPER 92-3106] p 258 A92-48747

FOERSTER, GEORGE

FOERSTER, GEORGE

An initial study of void formation during solidification of aluminum in normal and reduced-gravity
[AIAA PAPER 92-0845] p 138 A92-29611

FONG, D.

Description of the PMAD DC test bed architecture and integration sequence p 46 A92-50655
Description of the PMAD DC test bed architecture and integration sequence
[NASA-TM-105284] p 77 N92-10055

FONTANA, MARIO

Nuclear electric propulsion development and qualification facilities
[NASA-TM-105521] p 91 N92-30818

FORCE, D. A.

A low-power, high-efficiency Ka-band TWTA
p 156 A92-38163

FORCE, DALE A.

A low-power, high-efficiency Ka-band TWTA
[AIAA PAPER 92-1822] p 154 A92-29769

FORKEY, JOSEPH N.

Filtered Rayleigh scattering measurements in supersonic/hypersonic facilities
[AIAA PAPER 92-3894] p 200 A92-56733

FORRESTER, B. DAVID

A comparison between theoretical prediction and experimental measurement of the dynamic behavior of spur gears
[NASA-TM-105362] p 210 N92-25347

FORSQREN, ROGER C.

Adjustable depth gage
[NASA-CASE-LEW-14880-1] p 201 N92-21723

FORT, JAMES A.

Conical detonation waves - A comparison of theoretical and numerical results
[AIAA PAPER 92-0348] p 167 A92-25792

FOSTER, WILLIAM M., II

Thermal verification testing of commercial printed-circuit boards for spaceflight p 216 A92-56217
Thermal verification testing of commercial printed-circuit boards for spaceflight
[NASA-TM-105261] p 141 N92-11221

FOX, DENNIS S.

Oxidation kinetics of CVD silicon carbide and silicon nitride p 125 A92-39674
Environmental durability of ceramics and ceramic composites p 95 A92-39862
Reactions of silicon carbide and silicon(IV) oxide at elevated temperatures p 126 A92-43483
Elevated temperature mechanical behavior of monolithic and SiC whisker-reinforced silicon nitrides
[NASA-TM-105245] p 128 N92-15192

FRAAS, L. M.

A high-performance photovoltaic concentrator array - The mini-dome Fresnel lens concentrator with 30 percent efficient GaAs/GaSb tandem cells p 72 A92-53199

FRAAS, LEWIS

The mini-dome Fresnel lens photovoltaic concentrator array - Current program status p 70 A92-50648

FRALICK, GUSTAVE C.

X ray based displacement measurement for hostile environments
[NASA-TM-105551] p 202 N92-23155

FRANKLIN, J. E.

Diffusion mechanisms in chemical vapor-deposited iridium coated on chemical vapor-deposited rhenium
p 117 A92-28017

FRANKLIN, JAMES A.

Integrated flight/propulsion control for supersonic STOVL aircraft p 39 A92-45320

FRASCA, A. J.

Neutron, gamma ray, and temperature effects on the electrical characteristics of thyristors
[NASA-TM-105728] p 162 N92-28432

FRASER, H. L.

Compatibility of potential reinforcing ceramics with Ni and Fe aluminides p 105 A92-46874

FRATE, DAVID T.

Nickel-hydrogen cell low-earth-orbit life test update
p 70 A92-50700

FREED, A. D.

Stress versus temperature dependence of activation energies for creep p 217 A92-24719
A viscoplastic theory for anisotropic materials
[ONERA, TP NO. 1992-90] p 217 A92-24721
A viscoplastic theory with thermodynamic considerations
[ONERA, TP NO. 1991-220] p 217 A92-26372
A viscoplastic theory with thermodynamic considerations p 219 A92-33903

FREED, ALAN D.

Microstress analysis of periodic composites p 218 A92-30673
Three-dimensional deformation analysis of two-phase dislocation substructures p 121 A92-44218

Asymptotic integration algorithms for first-order ODEs with application to viscoplasticity
[NASA-TM-105587] p 250 N92-24974

Effects of fiber and interfacial layer architectures on the thermoplastic response of metal matrix composites
[NASA-TM-105802] p 110 N92-32234

FREEDMAN, M. R.

Mechanical behaviour and failure phenomenon of an in situ toughened silicon nitride p 127 A92-54504

FREEDMAN, MARC R.

Reliability analysis of a structural ceramic combustion chamber
[ASME PAPER 91-GT-155] p 24 A92-15591

FRENKLACH, MICHAEL

Optimization and analysis of large chemical kinetic mechanisms using the solution mapping method - Combustion of methane p 113 A92-19300

FRICKER, D. M.

Calculations of hot gas ingestion for a STOVL aircraft model
[AIAA PAPER 92-0385] p 25 A92-28191

FRICKER, DAVID M.

Calculations of hot gas ingestion for a STOVL aircraft model
[NASA-TM-105437] p 17 N92-19993

FRIEDLANDER, ALAN

Benefits of slush hydrogen for space missions
[NASA-TM-104503] p 134 N92-11214

FRIEDMAN, ROBERT

Risks, designs, and research for fire safety in spacecraft
[NASA-TM-105317] p 240 N92-13581

FRIEMAN, JOSHUA A.

Dark matter and the equivalence principle p 267 A92-14477
Constraints to the decays of Dirac neutrinos from SN 1987A p 255 A92-36249

FRIEND, D. G.

Computer program for computing the properties of seventeen fluids p 241 A92-23849

FRIMER, ARYEH A.

New addition curing polyimides
[NASA-TM-105335] p 95 N92-13281

FRIMPONG, STEPHEN

Relationship between voids and interlaminar shear strength of polymer matrix composites p 98 A92-10241

Void effects on the interlaminar shear strength of unidirectional graphite-fiber-reinforced composites p 105 A92-50348

FRISBEE, ROBERT H.

An overview of the NASA Advanced Propulsion Concepts program
[AIAA PAPER 92-3216] p 73 A92-54018

FRITSCH, KLAUS

Wavelength-multiplexed fiber-optic position encoder for aircraft control systems p 24 A92-42602

FRYE, ROBERT J.

The development of test beds to support the definition and evolution of the Space Station Freedom power system p 46 A92-50656

Overview and evolution of the LeRC PMAD DC Testbed
[NASA-TM-105842] p 163 N92-32867

FU, B.

Minimizing distortion in truss structures - A Hopfield network solution
[AIAA PAPER 92-2302] p 220 A92-34523

FUJIKAWA, GENE

Interference susceptibility measurements for an MSK satellite communication link
[AIAA PAPER 92-2018] p 144 A92-29936

Interference susceptibility measurements for an MSK satellite communication link
[NASA-TM-105395] p 149 N92-15306

FULMER, CHRISTOPHER

Preliminary design of a mobile lunar power supply p 233 A92-50635

FUQUA, S. J.

Features of wavy vortices in a curved channel from experimental and numerical studies p 171 A92-31638

FURST, J. E.

Extrapolation procedures in Mott electron polarimetry p 197 A92-21241

FUSARO, ROBERT L.

Solid lubricants on pretreated surfaces
[NASA-CASE-LEW-14474-2] p 127 N92-11186

Tribology needs for future space and aeronautical systems
[NASA-TM-104525] p 128 N92-15191

Lubrication of space systems: Challenges and potential solutions
[NASA-TM-105560] p 130 N92-21579

Liquid lubrication for space applications
[NASA-TM-105198] p 133 N92-31840

Liquid lubricants for advanced aircraft engines
[NASA-TM-104531] p 133 N92-32863

G

GABB, T. P.

The effect of porosity and gamma-gamma-prime eutectic content on the fatigue behavior of hydrogen charged PWA 1480 p 116 A92-12046

The effect of matrix mechanical properties on (0)B unidirectional SiC/Ti composite fatigue resistance p 99 A92-16220

Isothermal fatigue behaviour of a (90 deg)8 SiC/Ti-15-3 composite at 426 C p 100 A92-23313

GAETA, C. J.

Plasma erosion rate diagnostics using laser-induced fluorescence p 198 A92-36738

GAHN, RANDALL F.

The evaluation of layered separators for nickel-hydrogen cells p 89 A92-27161

GAIER, JAMES R.

Sensible heat receiver for solar dynamic space power system p 180 A92-50570

Effects of windblown dust on photovoltaic surfaces on Mars p 45 A92-50573

Effect of particle size of Martian dust on the degradation of photovoltaic cell performance
[NASA-TM-105232] p 79 N92-11133

Properties of novel CVD graphite fibers and their bromine intercalation compounds p 128 N92-14170

Method of intercalating large quantities of fibrous structures
[NASA-CASE-LEW-15077-1] p 107 N92-16025

Intercalated hybrid graphite fiber composite
[NASA-CASE-LEW-15241-1] p 107 N92-17861

Heat transfer device
[NASA-CASE-LEW-14162-3] p 111 N92-34208

GALINAITIS, W. S.

Algorithms for real-time fault detection of the Space Shuttle Main Engine
[AIAA PAPER 92-3167] p 215 A92-48789

GANDHI, RAJ

Massive Dirac neutrinos and SN 1987A p 268 A92-45808

GARCIA, R.

Three-dimensional flow fields inside a shrouded inducer at design and off-design conditions (CFD study)
p 196 N92-32291

GARG, S.

Design and evaluation of a robust dynamic neurocontroller for a multivariable aircraft control problem
[NASA-TM-105579] p 40 N92-20586

GARG, SANJAY

Integrated flight/propulsion control design for a STOVL aircraft using H-infinity control design techniques p 39 A92-29093

IMPAC - An integrated methodology for propulsion and airframe control p 39 A92-29118

Decentralized hierarchical partitioning of centralized integrated controllers p 39 A92-29119

Propulsion system performance resulting from an Integrated Flight/Propulsion Control design
[AIAA PAPER 92-4602] p 28 A92-55281

A parameter optimization approach to controller partitioning for integrated flight/propulsion control application
[NASA-TM-105826] p 40 N92-32241

GARG, VIJAY K.

Natural convection between concentric spheres p 179 A92-50445

GARLOW, R. K.

Technical and economic feasibility of integrated video service by satellite
[AIAA PAPER 92-2054] p 145 A92-29966

GARRIS, C. A.

Flow induction by pressure forces
[AIAA PAPER 92-3571] p 28 A92-54060

GARSCADDEN, ALAN

Synthesis and characterization of fine grain diamond films p 262 A92-46330

Environmental effects on friction and wear of diamond and diamondlike carbon coatings
[NASA-TM-105634] p 131 N92-23192

GAY, T. J.

Extrapolation procedures in Mott electron polarimetry p 197 A92-21241

GAYDA, J.

The effect of porosity and gamma-gamma-prime eutectic content on the fatigue behavior of hydrogen charged PWA 1480 p 116 A92-12046

The effect of matrix mechanical properties on (0)B unidirectional SiC/Ti composite fatigue resistance p 99 A92-16220

- isothermal fatigue behaviour of a (90 deg)8 SiC/Ti-15-3 composite at 426 C p 100 A92-23313
- GAYDA, JOHN**
Creep and fatigue research efforts on advanced materials p 227 N92-22514
- GAZTANAGA, E.**
Void probability as a function of the void's shape and scale-invariant models p 267 A92-24456
- GAZZANIGA, JOHN A.**
Wind tunnel performance results of swirl recovery vanes as tested with an advanced high speed propeller [AIAA PAPER 92-3770] p 28 A92-54159
- GDOUTOS, E. E.**
Thermal stress analysis of a silicon carbide/aluminum composite, p 222 A92-38097
- GEBAUER, LINDA**
SiO(X) coatings for atomic oxygen protection of polyimide Kapton in low earth orbit [AIAA PAPER 92-2151] p 94 A92-31286
LDEF spacecraft, ground laboratory, and computational modeling implications on Space Station Freedom's solar array materials and surfaces durability p 71 A92-53190
Atomic oxygen interactions with FEP Teflon and silicones on LDEF p 132 N92-24820
- GEDNEY, RICHARD T.**
Operational uses of ACTS technology [AIAA PAPER 92-1964] p 144 A92-29887
Advanced Communications Technology Satellite (ACTS) p 50 A92-38164
Advanced Communications Technology Satellite (ACTS) [IAF PAPER 92-0407] p 50 A92-55788
- GELDER, THOMAS F.**
Design and performance of controlled-diffusion stator compared with original double-circular-arc stator [NASA-TP-2852] p 34 N92-22863
- GENERAZIO, EDWARD R.**
Interfacing laboratory instruments to multiuser, virtual memory computers p 245 A92-13595
- GENG, S. M.**
Design of multihundred-watt dynamic isotope power system for robotic space missions p 69 A92-50633
- GENG, STEVEN M.**
Comparison of GLIMPS and HFAST Stirling engine code predictions with experimental data [NASA-TM-105549] p 267 N92-25395
Overview of NASA supported Stirling thermodynamic loss research [NASA-TM-105690] p 88 N92-27034
- GEORGE, J. A.**
Early Track NEP system options for SEI missions [AIAA PAPER 92-3200] p 65 A92-48808
- GEORGE, JEFFREY A.**
Multi-reactor power system configurations for multimewatt nuclear electric propulsion [NASA-TM-105212] p 77 N92-10057
- GEORGIADIS, N. J.**
Development of an algebraic turbulence model for analysis of propulsion flows p 183 A92-54209 [AIAA PAPER 92-3861]
Development of an algebraic turbulence model for analysis of propulsion flows [NASA-TM-105701] p 250 N92-27517
- GERWIN, RICHARD A.**
Preliminary investigation of power flow and electrode phenomena in a multi-megawatt coaxial plasma thruster [AIAA PAPER 92-3741] p 75 A92-54144
- GESSERT, T. A.**
Pilot production of 4 sq cm ITO/InP photovoltaic solar cells p 71 A92-53197
- GESSNER, F. B.**
Experimental investigation of turbulent flow through a circular-to-rectangular transition duct p 168 A92-26412
- GHOSN, L. J.**
Fatigue crack growth in unidirectional metal matrix composite p 99 A92-19734
- GHOSN, LOUIS**
Fatigue crack growth in a unidirectional SCS-6/Ti-15-3 composite p 102 A92-39036
- GHOSN, LOUIS J.**
Modeling of crack bridging in a unidirectional metal matrix composite p 104 A92-43085
Stochastic modeling of crack initiation and short-crack growth under creep and creep-fatigue conditions [ASME PAPER 92-APM-5] p 223 A92-44681
- GIBALA, R.**
Ductility enhancement from interface dislocation sources in a directionally solidified beta + gamma + gamma-prime Ni-Fe-Al composite alloy p 122 A92-46850
- GIBB, JAMES**
Application of computational fluid dynamics to the study of vortex flow control for the management of inlet distortion [AIAA PAPER 92-3177] p 13 A92-54013
Application of computational fluid dynamics to the study of vortex flow control for the management of inlet distortion [NASA-TM-105672] p 230 N92-34112
- GIEL, P. W.**
Three-dimensional Navier-Stokes heat transfer predictions for turbine blade rows [AIAA PAPER 92-3068] p 12 A92-54003
- GILBERT, C.**
Performance of a four-element Ka-band high-temperature superconducting microstrip antenna p 146 A92-37224
Measurement techniques for cryogenic Ka-band microstrip antennas p 153 N92-32981
- GILLAND, J. H.**
Early Track NEP system options for SEI missions [AIAA PAPER 92-3200] p 65 A92-48808
- GILLAND, JAMES**
Electric propulsion - The future is now p 63 A92-48386
- GILLAND, JAMES H.**
NEP systems engineering efforts in FY-92. Plans and status [NASA-TM-105775] p 91 N92-30308
- GINSBERG, D. M.**
Melting of the Abrikosov flux lattice in anisotropic superconductors p 260 A92-28075
- GINTY, CAROL A.**
NASA's high-temperature engine materials program for civil aeronautics p 95 A92-41117
- GIULIANI, JAMES E.**
Effect of model selection on combustor performance and stability using ROCCID [AIAA PAPER 92-3226] p 65 A92-48827
Effect of model selection on combustor performance and stability predictions using ROCCID [NASA-TM-105750] p 89 N92-27036
- GLASSMAN, ARTHUR J.**
Trends in aer propulsion research and their impact on engineering education [NASA-TM-105682] p 38 N92-31172
- GLEISER, MARCELO**
Fluctuation-driven electroweak phase transition p 269 A92-54464
- GLICKSMAN, M. E.**
The isothermal dendritic growth experiment - A USMP-2 space flight experiment [AIAA PAPER 92-0350] p 137 A92-28188
Growth and characterization of lead bromide crystals p 138 A92-56956
Effect of growth conditions on the quality of lead bromide crystals p 138 A92-56957
- GLIEBE, PHILLIP R.**
Turbomachinery noise p 253 N92-10601
- GLOVER, D.**
Subband coding for image data archiving [NASA-TM-105407] p 151 N92-20032
- GLUYAS, RICHARD E.**
Cyclopentadiene evolution during pyrolysis-gas chromatography of PMR polyimides [NASA-TM-105629] p 132 N92-25348
- GOEKOGLU, SULEYMAN**
Chemical vapor deposition modeling for high temperature materials [NASA-TM-105386] p 96 N92-18457
- GOKOGLU, SULEYMAN A.**
CVD of silicon carbide on structural fibers: Microstructure and composition [NASA-TM-105385] p 107 N92-18439
- GOLDBERG, ROBERT K.**
COMGEN-BEM: Boundary element model generation for composite materials micromechanical analysis [NASA-TM-105548] p 226 N92-19779
- GOLDIE, JAMES H.**
Flywheel energy storage for electromechanical actuation systems p 233 A92-50758
- GOLDING, LEN**
Operational uses of ACTS technology [AIAA PAPER 92-1964] p 144 A92-29887
- GOLDMAN, LOUIS J.**
Laser anemometer measurements and computations in an annular cascade of high turning core turbine vanes [NASA-TP-3252] p 20 N92-28980
- GOLDMEER, J.**
Determination of the natural convection coefficient in low-gravity [AIAA PAPER 92-0712] p 168 A92-27072
- GOLDSTEIN, M. E.**
Distortion of a flat-plate boundary layer by free-stream vorticity normal to the plate p 173 A92-36343
Noise from turbulent shear flows p 254 N92-10603
- GOMIDE, FERNANDO A. C.**
Design of multi-layer neural networks for accurate identification of nonlinear mappings p 246 A92-29030
- GOOD, BRIAN S.**
Molecular dynamics investigation of radiation damage in semiconductors p 159 A92-53157
- GOODRICH, JOHN W.**
An efficient and robust algorithm for two dimensional time dependent incompressible Navier-Stokes equations: High Reynolds number flows [NASA-TM-104424] p 184 N92-11320
An efficient and robust algorithm for time dependent viscous incompressible Navier-Stokes equations p 193 N92-25819
- GORADIA, C.**
Study of a cesium plasma as a selective emitter for thermophotovoltaic applications p 258 A92-33667
High voltage thermally diffused p(+)-n solar cells p 235 A92-53172
- GORADIA, CHANDRA**
Theoretical modeling, near-optimum design and predicted performance of n(+)-pp(+) and p(+)-nn(+)-indium phosphide homojunction solar cells p 234 A92-53152
- GORADIA, M.**
Study of a cesium plasma as a selective emitter for thermophotovoltaic applications p 258 A92-33667
High voltage thermally diffused p(+)-n solar cells p 235 A92-53172
- GORADIA, MANJU**
High performance etchant for thinning p(+)-InP and its application to p(+)-n InP solar cell fabrication p 263 A92-53155
- GORDON, W. L.**
Microwave properties of YBa2Cu3O(7-delta) high-temperature superconducting thin films measured by the power transmission method p 153 A92-14938
Microwave conductivity of laser ablated YBa2Cu3O(7-delta) superconducting films and its relation to microstrip transmission line performance p 264 N92-21639
- GORDON, WILLIAM L.**
Measurements of complex permittivity of microwave substrates in the 20 to 300 K temperature range from 26.5 to 40.0 GHz p 197 A92-13416
- GORLA, R. S. R.**
Navier-Stokes analysis of turbomachinery blade external heat transfer p 170 A92-28518
- GORLAND, S. H.**
Status of NASA's Earth-to-Orbit Propulsion Technology program [IAF PAPER 91-258] p 58 A92-13154
- GOTSIS, P. K.**
Metal matrix composite analyzer (METCAN) user's manual, version 4.0 [NASA-TM-105244] p 110 N92-30779
- GOTSIS, PASCAL K.**
Combined bending and thermal fatigue of high-temperature metal-matrix composites - Computational simulation p 223 A92-43494
Microfracture in high temperature metal matrix laminates [NASA-TM-105189] p 106 N92-14122
- GOTTI, DANIEL J.**
An initial study of void formation during solidification of aluminum in normal and reduced-gravity [AIAA PAPER 92-0845] p 138 A92-29611
- GOTTLIEB, M.**
Growth and characterization of lead bromide crystals p 138 A92-56956
Effect of growth conditions on the quality of lead bromide crystals p 138 A92-56957
- GRABER, EDWIN J.**
Overview of NASA PTA propan flight test program p 33 N92-22536
- GRADWOHL, BEN-AMI**
Dark matter and the equivalence principle p 267 A92-14477
- GRADY, J. E.**
Free vibrations of delaminated beams p 222 A92-36853
Free vibrations of delaminated beams [NASA-TM-105582] p 109 N92-25754
- GRADY, JOSEPH E.**
Effect of heat treatment on stiffness and damping of SiC/Ti-15-3 p 100 A92-25627
Effect of heat treatment on stiffness and damping of SiC/Ti-15-3 [NASA-TM-105564] p 108 N92-20841
- GRAHAM, RONALD E.**
Dynamics and control of the Space Station Freedom docking/array feathering maneuver [IAF PAPER 91-321] p 52 A92-14734

GRATZ, ROY F.

- GRATZ, ROY F.**
Substituted 1,1,1-triaryl-2,2,2-trifluoroethanes and processes for their synthesis
[NASA-CASE-LEW-14345-6] p 96 N92-17882
- GRAY, HUGH R.**
NASA's high-temperature engine materials program for civil aeronautics p 95 A92-41117
- GRAZIANI, R. A.**
Heat transfer in rotating serpentine passages with trips normal to the flow
[ASME PAPER 91-GT-265] p 165 A92-15663
- GREBER, ISAAC**
The structure and development of streamwise vortex arrays embedded in a turbulent boundary layer
[AIAA PAPER 92-0551] p 7 A92-28204
The structure and development of streamwise vortex arrays embedded in a turbulent boundary layer
[NASA-TM-105211] p 14 N92-10012
- GREENWALD, D. A.**
Three-dimensional flow fields inside a shrouded inducer at design and off-design conditions (CFD study)
p 196 N92-32291
- GREGOREK, G. M.**
Experimental unsteady pressures on an oscillating cascade with supersonic leading edge locus
[AIAA PAPER 92-4035] p 14 A92-56857
- GREITZER, E. M.**
The role of tip clearance in high-speed fan stall
[ASME PAPER 91-GT-83] p 2 A92-15550
- GRIER, NORMAN T.**
Experimental breakdown of selected anodized aluminum samples in dilute plasmas p 259 N92-22369
- GRISAFFE, SALVATORE J.**
NASA Lewis Research Center materials research and technology: An overview p 31 N92-22512
- GRISNIK, STANLEY P.**
Test facilities for high power electric propulsion
[NASA-TM-105247] p 80 N92-11136
- GROBSTEIN, T. L.**
Fatigue damage accumulation in nickel prior to crack initiation p 120 A92-33947
- GROBSTEIN, TONI**
Alkali metal compatibility testing of candidate heater head materials for a Stirling engine heat transport system p 71 A92-50829
- GRODSINSKY, C. M.**
Optimal microgravity vibration isolation - An algebraic introduction p 54 A92-47495
Controller design for microgravity vibration isolation systems
[IAF PAPER 92-0969] p 247 A92-57327
Microgravity vibration isolation: An optimal control law for the one-dimensional case
[NASA-TM-105146] p 141 N92-11217
Microgravity vibration isolation: Optimal preview and feedback control
[NASA-TM-105673] p 142 N92-30692
- GRODSINSKY, CARLOS**
Vibration isolation technology development to demonstration p 140 N92-28442
- GRODSINSKY, CARLOS M.**
NIST torsion oscillator viscometer response: Performance on the LeRC active vibration isolation platform
[NASA-TM-105571] p 209 N92-23564
- GROENEWEG, J. F.**
Unsteady blade-surface pressures on a large-scale advanced propeller - Prediction and data p 3 A92-17178
Unsteady Euler analysis of the flowfield of a propfan at an angle of attack p 3 A92-21070
- GROENEWEG, JOHN F.**
Turbomachinery noise p 253 N92-10601
Advanced propeller research p 33 N92-22537
- GRONSKI, ROBERT S.**
Small engine components test facility compressor testing cell at NASA Lewis Research Center
[AIAA PAPER 92-3980] p 41 A92-56806
Small engine components test facility compressor testing cell at NASA Lewis Research Center
[NASA-TM-105685] p 42 N92-30508
- GU, ZHEN**
A simplified dynamic model of the T700 turboshaft engine
[NASA-TM-105805] p 251 N92-30898
- GUO, T. H.**
Integrated health monitoring and controls for rocket engines
[NASA-TM-105763] p 90 N92-28693
- GUO, T.-H.**
Identification of the Space Shuttle Main Engine dynamic models from firing data
[AIAA PAPER 92-3317] p 73 A92-54022
- GUO, TEN-HUEI**
State space representation of the open-loop dynamics of the Space Shuttle Main Engine p 59 A92-19607

- A simplified dynamic model of Space Shuttle Main Engine p 60 A92-29289
Real-time fault diagnosis for propulsion systems
[NASA-TM-105303] p 29 N92-11017
An SSME high pressure oxidizer turbopump diagnostic system using G2(TM) real-time expert system
[NASA-TM-105328] p 247 N92-13717
- GUPTA, VINEY K.**
Modal test/analysis correlation of Space Station structures using nonlinear sensitivity
[NASA-TM-105850] p 230 N92-34221
- GUPTILL, J. D.**
Singularities in optimal structural design
[NASA-TM-4365] p 228 N92-23527
- GURU PRASAD, K.**
Boundary formulations for sensitivities of three-dimensional stress invariants p 224 A92-50883
- GYEKENYESI, J. P.**
Reliability analysis of laminated CMC components through shell subelement techniques
[AIAA PAPER 92-2348] p 219 A92-34322
- GYEKENYESI, JOHN P.**
Reliability analysis of a structural ceramic combustion chamber
[ASME PAPER 91-GT-155] p 24 A92-15591
Mechanical behavior of fiber reinforced SiC/RBSN ceramic matrix composites - Theory and experiment
[ASME PAPER 91-GT-209] p 99 A92-15629
Structural reliability analysis of laminated CMC components
[ASME PAPER 91-GT-210] p 99 A92-15630
Damage mechanisms in three-dimensional woven reinforced ceramic matrix composites under tensile and flexural loading at room and elevated temperatures
[AIAA PAPER 92-2492] p 101 A92-34584
Failure mechanisms of 3-D woven SiC/SiC composites under tensile and flexural loading at room and elevated temperatures p 103 A92-39642
Structural design methodologies for ceramic-based material systems p 103 A92-39866
Reliability analysis of laminated CMC components through shell subelement techniques
[NASA-TM-105413] p 129 N92-20380
- GYEKENYESI, JOHN Z.**
Damage mechanisms in three-dimensional woven reinforced ceramic matrix composites under tensile and flexural loading at room and elevated temperatures
[AIAA PAPER 92-2492] p 101 A92-34584
Failure mechanisms of 3-D woven SiC/SiC composites under tensile and flexural loading at room and elevated temperatures p 103 A92-39642
An evaluation of strain measuring devices for ceramic composites p 199 A92-46497
An evaluation of strain measuring devices for ceramic composites p 225 N92-14433

H

- HAAG, THOMAS W.**
Medium power hydrogen arcjet performance
[AIAA PAPER 91-2227] p 58 A92-15355
Development of arcjet and ion propulsion for spacecraft stationkeeping
[IAF PAPER 92-0607] p 77 A92-57058
High-power hydrogen arcjet performance
[NASA-TM-105143] p 82 N92-14109
Hydrogen arcjet technology
[NASA-TM-105340] p 82 N92-15119
- HAGEDORN, NORMAN H.**
Alkali metal carbon dioxide electrochemical system for energy storage and/or conversion of carbon dioxide to oxygen
[NASA-CASE-LEW-14973-1] p 235 N92-10222
- HAGGARD, JOHN B.**
Microgravity combustion of isolated n-decane and n-heptane droplets
[AIAA PAPER 92-0242] p 113 A92-26927
- HAGGARD, JOHN B., JR.**
Some further observations on droplet combustion characteristics - NASA LeRC-Princeton results p 111 A92-12897
Observations on a slow burning regime for hydrocarbon droplets - n-heptane/air results p 112 A92-16602
- HAGGERTY, JOHN S.**
Relationships between toughness and microstructure of reaction bonded Si3N4 p 125 A92-39687
- HAGHDoust, M.**
Determination of the natural convection coefficient in low-gravity
[AIAA PAPER 92-0712] p 168 A92-27072
- HAH, C.**
Navier-Stokes analysis of flow and heat transfer inside high-pressure-ratio transonic turbine blade rows p 165 A92-17193
- Navier-Stokes analysis of three-dimensional unsteady flows inside turbine stages
[AIAA PAPER 92-3211] p 13 A92-54016
A critical evaluation of a three-dimensional Navier-Stokes CFD as a tool to design supersonic turbine stages p 196 N92-32268
Three-dimensional flow fields inside a shrouded inducer at design and off-design conditions (CFD study)
p 196 N92-32291
- HAH, CHUNILL**
A viscous flow study of shock-boundary layer interaction, radial transport, and wake development in a transonic compressor
[ASME PAPER 91-GT-69] p 2 A92-15539
A critical evaluation of a three-dimensional Navier-Stokes method as a tool to calculate transonic flows inside a low-aspect-ratio compressor p 195 N92-27459
- HAHN, R. C.**
Determination of the critical parameters for remote microscope control
[IAF PAPER 91-026] p 240 A92-12447
The isothermal dendritic growth experiment - A USMP-2 space flight experiment
[AIAA PAPER 92-0350] p 137 A92-28188
- HAILYE, MICHAEL**
The flip flop nozzle extended to supersonic flows
[AIAA PAPER 92-2724] p 10 A92-45561
The flip-flop nozzle extended to supersonic flows
[NASA-TM-105570] p 18 N92-23269
- HAISSIG, CHRISTINE M.**
Canonical transformations for space trajectory optimization
[AIAA PAPER 92-4509] p 44 A92-52079
- HAJELA, P.**
Neurobiological computational models in structural analysis and design p 245 A92-14509
Minimizing distortion in truss structures - A Hopfield network solution
[AIAA PAPER 92-2302] p 220 A92-34523
Neural network based decomposition in optimal structural synthesis p 247 A92-41895
Applications of artificial neural nets in structural mechanics p 223 A92-47283
- HAKIMZADEH, ROSHANAK**
Evaluation of the minority carrier diffusion length and surface-recombination velocity in GaAs p/n solar cells p 234 A92-53162
- HALE, JEFFREY S.**
Atomic oxygen effects on thin film space coatings studied by spectroscopic ellipsometry, atomic force microscopy, and laser light scattering
[AIAA PAPER 92-2172] p 94 A92-31300
- HALFORD, G. R.**
The effect of matrix mechanical properties on (0)8 unidirectional SiC/Ti composite fatigue resistance p 99 A92-16220
Application of a thermal fatigue life prediction model to high-temperature aerospace alloys B1900 + Hf and Haynes 188 p 121 A92-45232
Thermomechanical and bithermal fatigue behavior of cast B1900 + Hf and wrought Haynes 188 p 122 A92-45233
- HALFORD, GARY R.**
Damage mechanisms in bithermal and thermomechanical fatigue of Haynes 188
[NASA-TM-105381] p 228 N92-24985
- HALL, DAVID G.**
Far-field noise and internal modes from a ducted propeller at simulated aircraft takeoff conditions
[AIAA PAPER 92-0371] p 252 A92-26230
Far-field noise and internal modes from a ducted propeller at simulated aircraft takeoff conditions
[NASA-TM-105369] p 254 N92-16702
Detailed noise measurements on the SR-7A propeller: Tone behavior with helical tip Mach number
[NASA-TM-105206] p 255 N92-16705
- HALL, STEPHEN W.**
Effect of KOH concentration on LEO cycle life of IPV nickel-hydrogen flight cell - Update II p 232 A92-48212
Effect of KOH concentration on LEO cycle life of IPV nickel-hydrogen flight cells - An update p 70 A92-50702
Destructive physical analysis results of Ni/H2 cells cycled in LEO regime p 70 A92-50707
Effect of LEO cycling on 125 Ah advanced design IPV nickel-hydrogen flight cells - An update p 71 A92-50708
Effect of KOH concentration on LEO cycle life of IPV nickel-hydrogen flight cells-update 2
[NASA-TM-105314] p 235 N92-13483
Validation test of advanced technology for IPV nickel-hydrogen flight cells: Update
[NASA-TM-105689] p 89 N92-27878

- HALLIWELL, I.**
Investigation of three-dimensional flow field in a turbine including rotor/stator interaction. I - Design development and performance of the research facility
[AIAA PAPER 92-3325] p 40 A92-48908
- HALLOCK, GARY A.**
Effect of an arcjet plume on satellite reflector performance
p 53 A92-16318
- HAMED, A.**
An investigation of shock/turbulent boundary layer bleed interactions
[AIAA PAPER 92-3085] p 182 A92-54008
- HAMILTON, J. C.**
Diffusion mechanisms in chemical vapor-deposited indium coated on chemical vapor-deposited rhenium
p 117 A92-28017
- HAMLEY, JOHN A.**
The evolutionary development of high specific impulse electric thruster technology
[AIAA PAPER 92-1556] p 61 A92-38650
Dependence of hydrogen arcjet operation on electrode geometry
[AIAA PAPER 92-3530] p 74 A92-54039
Hydrogen arcjet technology
[NASA-TM-105340] p 82 N92-15119
The evolutionary development of high specific impulse electric thruster technology
[NASA-TM-105712] p 92 N92-31342
The evolutionary development of high specific impulse electric thruster technology
[NASA-TM-105758] p 93 N92-33064
Dependence of hydrogen arcjet operation on electrode geometry
[NASA-TM-105855] p 93 N92-34113
- HAMMOUD, A. N.**
Electrical properties of teflon and ceramic capacitors at high temperatures
[NASA-TM-105569] p 160 N92-20040
High temperature dielectric properties of Apical, Kapton, Peek, Teflon AF, and Upilex polymers
[NASA-TM-105753] p 162 N92-28675
Wiring for aerospace applications
[NASA-TM-105777] p 162 N92-30427
- HAMMOUD, AHMAD N.**
Multi-megawatt inverter/converter technology for space power applications
[NASA-TM-105307] p 159 N92-14294
Evaluation of high temperature capacitor dielectrics
[NASA-TM-105622] p 161 N92-23561
- HAMPTON, R. D.**
Optimal microgravity vibration isolation - An algebraic introduction
p 54 A92-47495
Controller design for microgravity vibration isolation systems
[IAF PAPER 92-0969] p 247 A92-57327
Microgravity vibration isolation: An optimal control law for the one-dimensional case
[NASA-TM-105146] p 141 N92-11217
Microgravity vibration isolation: Optimal preview and feedback control
[NASA-TM-105673] p 142 N92-30692
- HANDSCHUH, R.**
Experimental testing of prototype face gears for helicopter transmissions
[NASA-TM-105434] p 214 N92-31349
- HANDSCHUH, R. F.**
Minimization of deviations of gear real tooth surfaces determined by coordinate measurements
[NASA-TM-105718] p 214 N92-30948
- HANDSCHUH, ROBERT F.**
Recent manufacturing advances for spiral bevel gears
[SAE PAPER 912229] p 204 A92-40024
A method for determining spiral-bevel gear tooth geometry for finite element analysis
[NASA-TP-3096] p 207 N92-10195
Effect of lubricant jet location on spiral bevel gear operating temperatures
[NASA-TM-105656] p 211 N92-26106
- HANLON, J. C.**
SEI power source alternatives for rovers and other multi-kWe distributed surface applications
p 80 N92-13206
- HANLON, JAMES C.**
SP-100 reactor with Brayton conversion for lunar surface applications
[NASA-TM-105637] p 92 N92-32108
- HANN, RAIFORD E.**
Glass formation, properties, and structure of soda-yttria-silicate glasses
[NASA-TM-104488] p 128 N92-11202
- HANNA, G. J.**
CONE - An STS-based cryogenic fluid management experiment
p 43 A92-23850
- HANSEN, IRVING G.**
Electromechanical systems with transient high power response operating from a resonant AC link
[NASA-TM-105716] p 37 N92-28985
- HANSMAN, R. J., JR.**
Heat transfer on accreting ice surfaces
p 166 A92-24415
Analysis of surface roughness generation in aircraft ice accretion
[AIAA PAPER 92-0298] p 169 A92-28187
- HANSON, D. B.**
Unsteady airloading panel method for proptans
p 253 A92-44512
- HANSON, JEFFERY C.**
Techniques for animation of CFD results
p 194 N92-25825
- HANSON, R. K.**
Quantitative fluorescence measurements of the OH radical in high pressure methane flames
[AIAA PAPER 92-2960] p 114 A92-46976
- HANSON, RONALD K.**
Laser-induced fluorescence of atomic hydrogen in an arcjet thruster
[AIAA PAPER 92-0678] p 60 A92-27045
Flow diagnostics of an arcjet using laser-induced fluorescence
[AIAA PAPER 92-3243] p 199 A92-48843
- HARABURDA, SCOTT S.**
Theoretical nozzle performance of a microwave electrothermal thruster using experimental data
[AIAA PAPER 92-3110] p 64 A92-48750
- HARDY, TERRY L.**
Slush hydrogen (SLH2) technology development for application to the National Aerospace Plane (NASP)
p 140 A92-13432
Technology issues associated with using densified hydrogen for space vehicles
[AIAA PAPER 92-3079] p 134 A92-48727
Slush hydrogen pressurized expulsion studies at the NASA K-Site Facility
[AIAA PAPER 92-3385] p 141 A92-48951
Benefits of slush hydrogen for space missions
[NASA-TM-104503] p 134 N92-11214
Technology issues associated with using densified hydrogen for space vehicles
[NASA-TM-105642] p 135 N92-25277
Slush hydrogen transfer studies at the NASA K-Site Test Facility
[NASA-TM-105596] p 135 N92-25957
Slush hydrogen pressurized expulsion studies at the NASA K-Site Facility
[NASA-TM-105597] p 135 N92-26131
- HARIHARAN, S. I.**
Time domain numerical calculations of unsteady vortical flows about a flat plate airfoil
p 12 A92-50473
Long time behavior of unsteady flow computations
[NASA-TM-105584] p 190 N92-23565
- HARLOFF, G. J.**
Navier-Stokes analysis and experimental data comparison of compressible flow within ducts
[NASA-TM-105796] p 38 N92-30972
- HARLOFF, GARY J.**
Navier-Stokes analysis and experimental data comparison of compressible flow in a diffusing S-duct
[AIAA PAPER 92-2699] p 10 A92-45541
Navier-Stokes analysis and experimental data comparison of compressible flow in a diffusing S-duct
[NASA-TM-105683] p 38 N92-33746
- HARRIS, G. L.**
Anodic etching of p-type cubic silicon carbide
p 127 A92-57027
- HARROD, CHARLES E.**
Metalized gelled monopropellants
[NASA-TM-105418] p 87 N92-24557
- HARTFIELD-WUNSCH, S.**
Ductility enhancement from interface dislocation sources in a directionally solidified beta + gamma + gamma-prime Ni-Fe-Al composite alloy
p 122 A92-46850
- HARTLEY, TOM T.**
Temperature control in continuous furnace by structural diagram method
p 246 A92-29162
A fundamental theorem for the model reduction of nonlinear systems
p 246 A92-41165
- HARTY, RICHARD B.**
A dynamic isotope power system for Space Exploration Initiative surface transport systems
[AIAA PAPER 92-1489] p 61 A92-38605
- HARVEY, W. L.**
A low-power, high-efficiency Ka-band TWTA
p 156 A92-38163
- HARVEY, WAYNE L.**
A low-power, high-efficiency Ka-band TWTA
[AIAA PAPER 92-1822] p 154 A92-29769
- HASAN, M. M.**
Vapor condensation on liquid surface due to laminar jet-induced mixing
p 164 A92-10446
Self-pressurization of a spherical liquid hydrogen storage tank in a microgravity environment
[AIAA PAPER 92-0363] p 168 A92-25798
Self-pressurization of a lightweight liquid hydrogen tank - Effects of fill level at low wall heat flux
[AIAA PAPER 92-0818] p 60 A92-29591
Self-pressurization of a spherical liquid hydrogen storage tank in a microgravity environment
[NASA-TM-105372] p 185 N92-14323
Self-pressurization of a lightweight liquid hydrogen tank. Effects of fill level at low wall heat flux
[NASA-TM-105411] p 135 N92-18442
Effect of liquid surface turbulent motion on the vapor condensation in a mixing tank
[NASA-TM-105555] p 187 N92-21498
- HASHIM, WAQAR**
Heat transfer in oscillating flows with sudden change in cross section
[NASA-TM-105692] p 88 N92-26654
- HASSELMAN, D. P. H.**
Role of interfacial carbon layer in the thermal diffusivity/conductivity of silicon carbide fiber-reinforced reaction-bonded silicon nitride matrix composites
p 100 A92-25443
Role of interfacial thermal barrier in the transverse thermal conductivity of uniaxial SiC fiber-reinforced reaction bonded silicon nitride
p 102 A92-39605
- HASTINGS, D.**
Arcing of negatively biased solar cells in low earth orbit
[AIAA PAPER 92-0578] p 59 A92-26985
- HASTINGS, D. E.**
Ionospheric plasma flow over large high-voltage space platforms. I - Ion-plasma-time scale interactions of a plate at zero angle of attack. II - The formation and structure of plasma wake
p 258 A92-41359
Theory of plasma contactor neutral gas emissions for electrodynamic tethers
p 258 A92-41549
Systems analysis of electrodynamic tethers
p 62 A92-41550
- HASTINGS, DANIEL E.**
The arcing rate for a High Voltage Solar Array - Theory, experiment and predictions
[AIAA PAPER 92-0576] p 53 A92-26983
The formation and structure of plasma wakes behind large high-voltage space platforms in ionosphere
[AIAA PAPER 92-0577] p 239 A92-26984
- HATCH, M. S.**
Jet mixing into a heated cross flow in a cylindrical duct - Influence of geometry and flow variations
[AIAA PAPER 92-0773] p 168 A92-27110
Jet mixing into a heated cross flow in a cylindrical duct. Influence of geometry and flow variations
[NASA-TM-105390] p 30 N92-15994
- HATHAWAY, M. D.**
NASA low-speed centrifugal compressor for 3-D viscous code assessment and fundamental flow physics research
[ASME PAPER 91-GT-140] p 3 A92-15580
- HATHAWAY, MICHAEL D.**
Design and performance of controlled-diffusion stator compared with original double-circular-arc stator
[NASA-TP-2852] p 34 N92-22863
- HAUER, ROBERT L.**
Removable hand hold
[NASA-CASE-LEW-15196-1] p 213 N92-29092
- HAUGLAND, E. J.**
Temperature independent quantum well FET with delta channel doping
p 157 A92-49596
Enhancement of Shubnikov-de Haas oscillations by carrier modulation
p 262 A92-50911
Intermodulation in the oscillatory magnetoresistance of a two-dimensional electron gas
p 163 N92-32975
- HAUGLAND, EDWARD J.**
Reduced mobility and PPC in In₂₀Ga₈₀As / Al₂₃Ga₇₇As HEMT structure
p 265 N92-32976
- HAWLEY, MARTIN C.**
Theoretical nozzle performance of a microwave electrothermal thruster using experimental data
[AIAA PAPER 92-3110] p 64 A92-48750
- HAWMAN, M. W.**
Algorithms for real-time fault detection of the Space Shuttle Main Engine
[AIAA PAPER 92-3167] p 215 A92-48789
- HAYES, J. R.**
High-field transport properties of InAs(x)P(1-x)/InP (x = 0.3-1.0) modulation doped heterostructures at 300 and 77 K
p 262 A92-46331
- HAYNES, DAVY A.**
Report of the Nuclear Propulsion Mission Analysis. Figures of Merit Subpanel: Quantifiable figures of merit for nuclear thermal propulsion
[NASA-TM-104179] p 43 N92-20925

HEAPS, WILLIAM S.

HEAPS, WILLIAM S.

Measurement of trace stratospheric constituents with a balloon borne laser radar p 239 N92-14500

HEATH, G.

Application of face-gear drives in helicopter transmissions [NASA-TM-105655] p 212 N92-28434

HEATH, GREGORY F.

Advanced Rotorcraft Transmission program summary [AIAA PAPER 92-3363] p 205 A92-48936

HEBSUR, M. G.

Protective Al₂O₃ scale formation on NbAl₃-base alloys p 119 A92-31850

HEBSUR, MOHAN G.

Influence of processing on the microstructure and mechanical properties of a NbAl₃-base alloy p 122 A92-48152

HEGDE, U.

Gravitational influences on the behavior of confined diffusion flames [AIAA PAPER 92-0334] p 113 A92-25781

HEIDELBERG, LAURENCE J.

Far-field noise and internal modes from a ducted propeller at simulated aircraft takeoff conditions [AIAA PAPER 92-0371] p 252 A92-26230

Far-field noise and internal modes from a ducted propeller at simulated aircraft takeoff conditions [NASA-TM-105369] p 254 N92-16702

HEIDENREICH, GARY R.

Critical technology experiment results for lightweight space heat receiver p 180 A92-53568

HEINEN, V. O.

Microwave properties of YBa₂Cu₃O₇(δ) high-transition-temperature superconducting thin films measured by the power transmission method p 153 A92-14938

Microwave conductivity of laser ablated YBa₂Cu₃O₇(δ) superconducting films and its relation to microstrip transmission line performance p 264 N92-21639

HEINEN, VERNON O.

Measurements of complex permittivity of microwave substrates in the 20 to 300 K temperature range from 26.5 to 40.0 GHz p 197 A92-13416

The introduction of spurious modes in a hole-coupled Fabry-Perot open resonator p 197 A92-21244

NASA Space applications of high-temperature superconductors [NASA-TM-105401] p 271 N92-18455

NASA space applications of high-temperature superconductors p 265 N92-32980

Magnetic penetration depth of YBa₂Cu₃O₇(δ) thin films determined by the power transmission method p 265 N92-32983

HEINRICH, J. C.

Vertical solidification of dendritic binary alloys p 261 A92-37562

HELMS, IRA

Innovative nuclear thermal propulsion technology evaluation - Results of the NASA/DOE task team study [IAF PAPER 91-235] p 58 A92-13160

HENDERSON, GREGORY H.

Airfoil wake and linear theory gust response including sub and superresonant flow conditions [AIAA PAPER 92-3074] p 11 A92-48724

HENDERSON, T. L.

Grid quality improvement by a grid adaptation technique p 248 A92-47072

MAG3D and its application to internal flowfield analysis p 243 N92-24421

HENDERSON, T. R.

Satellite delivery of B-ISDN services [AIAA PAPER 92-1831] p 142 A92-29777

Technical and economic feasibility of integrated video service by satellite [AIAA PAPER 92-2054] p 145 A92-29966

HENDERSON, TODD

Interactive solution-adaptive grid generation procedure p 244 N92-25724

HENDERSON, TODD L.

Interactive solution-adaptive grid generation procedure [NASA-TM-105432] p 18 N92-23563

Interactive solution-adaptive grid generation p 243 N92-24420

HENDRICKS, R. C.

Qualitative investigation of cryogenic fluid injection into a supersonic flow field p 164 A92-13360

A bulk flow model of a brush seal system [ASME PAPER 91-GT-325] p 203 A92-15696

Flow visualization and motion analysis for a series of four sequential brush seals p 204 A92-36976

Bonded ceramic foams reinforced with fibers for high temperature use p 125 A92-39628

A finite-volume numerical method to calculate fluid forces and rotordynamic coefficients in seals [AIAA PAPER 92-3712] p 183 A92-54132

Development of advanced seals for space propulsion turbomachinery [NASA-TM-105659] p 87 N92-24957

HENDRICKS, ROBERT C.

Investigation of two and three parameter equations of state for cryogenic fluids p 140 A92-13413

Seals related research at NASA. Lewis Research Center p 207 N92-15087

Brush seal leakage performance with gaseous working fluids at static and low rotor speed conditions [NASA-TM-105400] p 186 N92-16265

HENFLING, JOHN F.

Calibration of hemispherical-head flow angularity probes [AIAA PAPER 92-4005] p 200 A92-56828

HENINS, IVARS

Preliminary investigation of power flow and electrode phenomena in a multi-megawatt coaxial plasma thruster [AIAA PAPER 92-3741] p 75 A92-54144

HENNINGSEN, T.

Growth and characterization of lead bromide crystals p 138 A92-56956

Effect of growth conditions on the quality of lead bromide crystals p 138 A92-56957

HENRY, Z. S.

Advanced Rotorcraft Transmission (ART) - Component test results [AIAA PAPER 92-3366] p 205 A92-48939

HEPP, ALOYSIUS F.

Near-edge study of gold-substituted YBa₂Cu₃O₇(δ) p 259 A92-14950

Material processing with hydrogen and carbon monoxide on Mars p 231 A92-17769

In-situ carbon dioxide fixation on Mars p 134 A92-50613

Applications of thin-film photovoltaics for space p 70 A92-50641

Thin-film photovoltaics: Status and applications to space power p 81 N92-13228

HERBACH, B. A.

Determination of the critical parameters for remote microscope control [IAF PAPER 91-026] p 240 A92-12447

HERBELL, THOMAS P.

Monolithic ceramics p 125 A92-39854

HERR, JOEL L.

Ion collection from a plasma by a pinhole p 259 N92-22368

HERRERA-FIERRO, PILAR

An XPS study of the stability of Fomblin Z25 on the native oxide of aluminum [NASA-TM-105594] p 131 N92-23185

HEYWARD, ANN O.

Achieving spectrum conservation for the minimum span and minimum-order frequency assignment problems [AIAA PAPER 92-1960] p 143 A92-29883

Achieving spectrum conservation for the minimum-span and minimum-order frequency assignment problems [NASA-TM-105649] p 52 N92-23187

HICKEY, JOHN R.

Advanced photovoltaic experiment, S0014: Preliminary flight results and post-flight findings p 237 N92-27101

The effect of the low Earth orbit environment on space solar cells: Results of the advanced photovoltaic experiment (S0014) p 237 N92-27320

HICKMAN, GARY L.

Alkali metal compatibility testing of candidate heater head materials for a Stirling engine heat transport system p 71 A92-50829

HICKMAN, J. M.

Structural design concepts for a multimegawatt solar electric propulsion (SEP) spacecraft [AIAA PAPER 92-2536] p 54 A92-34380

HILL, CAROL M.

LDEF spacecraft, ground laboratory, and computational modeling implications on Space Station Freedom's solar array materials and surfaces durability p 71 A92-53190

Atomic oxygen interactions with FEP Teflon and silicones on LDEF p 132 N92-24820

HILL, EUGENE G.

Lewis icing research tunnel test of the aerodynamic effects of aircraft ground deicing/anti-icing fluids [NASA-TP-3238] p 22 N92-30395

HILLARD, G. B.

The Solar Array Module Plasma Interactions Experiment (SAMPPIE) - A Shuttle-based plasma interactions experiment p 69 A92-50583

HILLARD, G. BARRY

Environmental interactions in Space Exploration: Announcement of the formation of an Environmental Interactions Working Group [NASA-TM-105294] p 270 N92-17069

The Solar Array Module Plasma Interactions Experiment (SAMPPIE): Science and technology objectives p 86 N92-22360

Environmental interactions in space exploration: Environmental interactions working group p 239 N92-22382

Solar Array Module Plasma Interaction Experiment (SAMPPIE): Technical requirements document [NASA-TM-105660] p 56 N92-28683

HINGST, W. R.

Surface and flow field measurements in a symmetric crossing shock wave/turbulent boundary layer flow [AIAA PAPER 92-2634] p 10 A92-45574

A laser-induced heat flux technique for convective heat transfer measurements in high speed flows p 200 A92-54318

HINGST, WARREN R.

The structure and development of streamwise vortex arrays embedded in a turbulent boundary layer [AIAA PAPER 92-0551] p 7 A92-28204

The structure and development of streamwise vortex arrays embedded in a turbulent boundary layer [NASA-TM-105211] p 14 N92-10012

HIRSCHBERG, MARVIN H.

Aircraft engine hot section technology: An overview of the HOST Project p 33 N92-22535

HO, H.

LDEXPT, an intelligent database system for the Composite Load Spectra project p 59 A92-23695

A probabilistic approach to the evaluation of fatigue damage in a space propulsion system injector element [AIAA PAPER 92-2413] p 60 A92-34343

HOCHSTEIN, JOHN I.

Modeling of impulsive propellant reorientation p 59 A92-17187

Pulsed thrust propellant reorientation - Concept and modeling p 62 A92-44507

HOCKNEY, RICHARD L.

Flywheel energy storage for electromechanical actuation systems p 233 A92-50758

HOERIG, CRAIG

Flexible digital modulation and coding synthesis for satellite communications p 148 N92-14235

HOLDEMAN, J. D.

CFD analysis of jet mixing in low NO(x) flametube combustors [ASME PAPER 91-GT-217] p 24 A92-15634

Jet mixing into a heated cross flow in a cylindrical duct - Influence of geometry and flow variations [AIAA PAPER 92-0773] p 168 A92-27110

Calculations of hot gas ingestion for a STOVFL aircraft model [AIAA PAPER 92-0385] p 25 A92-28191

CFD mixing analysis of jets injected from straight and slanted slots into confined crossflow in rectangular ducts [AIAA PAPER 92-3087] p 177 A92-48732

Experimental study of cross-stream mixing in a rectangular duct [AIAA PAPER 92-3090] p 178 A92-48735

Jet mixing into a heated cross flow in a cylindrical duct: Influence of geometry and flow variations [NASA-TM-105390] p 30 N92-15994

A parametric numerical study of mixing in a cylindrical duct [NASA-TM-105695] p 35 N92-26553

CFD mixing analysis of jets injected from straight and slanted slots into confined crossflow in rectangular ducts [NASA-TM-105699] p 36 N92-26561

Experimental study of cross-stream mixing in a rectangular duct [NASA-TM-105694] p 36 N92-27652

HOLDEMAN, JAMES D.

Studies of the effects of curvature on dilution jet mixing p 166 A92-21079

Calculations of hot gas ingestion for a STOVFL aircraft model [NASA-TM-105437] p 17 N92-19993

HOLDERMAN, J. D.

A parametric numerical study of mixing in a cylindrical duct [AIAA PAPER 92-3088] p 177 A92-48733

Thermomechanical and bithermal fatigue behavior of cast B1900 + Hf and wrought Haynes 188 p 122 A92-45233

HOLLOWECKY, BRIAN

A parameter optimization approach to controller partitioning for integrated flight/propulsion control application [NASA-TM-105826] p 40 N92-32241

HOLST, TERRY L.

The NASA Computational Aerosciences Program - Toward teraFLOPS computing [AIAA PAPER 92-0558] p 240 A92-26968

Fast oxygen atom facility for studies related to low earth orbit activities [AIAA PAPER 92-3974] p 47 A92-56800

- HONEY, FRANK S.**
A vacuum (10(exp -9) Torr) friction apparatus for determining friction and endurance life of MoSx films [NASA-TM-104478] p 129 N92-16129
Deposition of adherent Ag-Ti duplex films on ceramics in a multiple-cathode sputter deposition system [NASA-TM-105586] p 34 N92-23225
- HONG, W. P.**
High-field transport properties of InAs(x)P(1-x)/InP (x = 0.3-1.0) modulation doped heterostructures at 300 and 77 K p 262 A92-46331
- HOPKINS, D.**
LDEXPT, an intelligent database system for the Composite Load Spectra project p 59 A92-23695
- HOPKINS, D. A.**
Metal matrix composite analyzer (METCAN) user's manual, version 4.0 [NASA-TM-105244] p 110 N92-30779
- HOPKINS, DALE A.**
Structural tailoring/analysis for hypersonic components - Executive system development [AIAA PAPER 92-2471] p 219 A92-34360
Improved accuracy for finite element structural analysis via a new integrated force method [NASA-TP-3204] p 227 N92-22227
Integrated analysis and applications p 32 N92-22521
A brief overview of computational structures technology related activities at NASA Lewis Research Center p 229 N92-25915
- HOPKINS, R. H.**
Growth and characterization of lead bromide crystals p 138 A92-56956
Effect of growth conditions on the quality of lead bromide crystals p 138 A92-56957
- HOROWITZ, JAY**
Techniques for animation of CFD results p 194 N92-25825
- HORSHAM, GARY A. P.**
MisTec - A software application for supporting space exploration scenario options and technology development analysis and planning [AIAA PAPER 92-1293] p 242 A92-38490
MisTec: A software application for supporting space exploration scenario options and technology development analysis and planning [NASA-TM-105214] p 243 N92-14649
- HORSTMAN, HOWARD Z.**
Unsteady flowfield simulation of ducted prop-fan configurations [AIAA PAPER 92-0521] p 6 A92-26946
- HORVAT, GLEN M.**
Minimum impulse trajectories for Mars round trip missions [AAS PAPER 91-500] p 44 A92-43339
- HOUCK, S.**
The F/A-18 external burning flight test [AIAA PAPER 91-5050] p 23 A92-44547
- HOVENAC, EDWARD A.**
Calculation of far-field scattering from nonspherical particles using a geometrical optics approach p 256 A92-20288
- HOWE, STEVEN D.**
Innovative nuclear thermal propulsion technology evaluation - Results of the NASA/DOE task team study [IAF PAPER 91-235] p 58 A92-13160
- HOYNIK, DANIEL**
Development of a steady potential solver for use with linearized, unsteady aerodynamic analyses [NASA-TM-105288] p 31 N92-20525
- HRACH, FRANK**
Method of reducing drag in aerodynamic systems [NASA-CASE-LEW-14791-1] p 21 N92-34243
- HSAIO, C. C.**
Combustion of liquid-fuel droplets in supercritical conditions p 114 A92-43778
- HSAIO, CHINGTENG**
Finite element Euler calculations of unsteady transonic cascade flows [AIAA PAPER 92-2120] p 9 A92-35689
- HSIEH, CHIH-MING**
Contact stresses in meshing spur gear teeth: Use of an incremental finite element procedure [NASA-TM-105388] p 209 N92-23536
- HSIEH, K. C.**
Runge-Kutta methods combined with compact difference schemes for the unsteady Euler equations [AIAA PAPER 92-3210] p 182 A92-54015
- HSU, A. T.**
A continuous mixing model for pdf simulations and its applications to combustor shear flows p 174 A92-40139
- HU, M.**
V-band pseudomorphic HEMT MMIC phased array components for space communications p 151 N92-32966
- HUANG, J. R.**
An efficient finite element method for aircraft de-icing problems [AIAA PAPER 92-0532] p 22 A92-31670
- HUANG, PAO S.**
A study on vortex flow control of inlet distortion in the re-engined 727-100 center inlet duct using computational fluid dynamics [AIAA PAPER 92-0152] p 4 A92-23767
Design and analysis of reengine Boeing 727-100 center inlet S duct by a reduced Navier-Stokes code [AIAA PAPER 92-1221] p 8 A92-33320
Design and analysis of vortex generators on reengined Boeing 727-100CF center inlet S-duct by a reduced Navier-Stokes code [AIAA PAPER 92-2700] p 10 A92-45542
A study on vortex flow control on inlet distortion in the re-engined 727-100 center inlet duct using computational fluid dynamics [NASA-TM-105321] p 14 N92-13998
- HUFF, DENNIS L.**
Euler flow predictions for an oscillating cascade using a high resolution wave-split scheme [ASME PAPER 91-GT-198] p 3 A92-15623
Pressure wave propagation studies for oscillating cascades [AIAA PAPER 92-0145] p 5 A92-25682
Analysis of cascades using a two dimensional Euler aeroelastic solver [AIAA PAPER 92-2370] p 26 A92-34598
Numerical analysis of flow through oscillating cascade sections p 9 A92-44513
Pressure wave propagation studies for oscillating cascades [NASA-TM-105406] p 16 N92-15977
Unsteady-flow-field predictions for oscillating cascades [NASA-TM-105283] p 17 N92-19437
- HULL, DAVID R.**
Plasma etching a ceramic composite [NASA-TM-105430] p 130 N92-22305
- HULLIGAN, DAVID D.**
Safety considerations in testing a fuel-rich aeropropulsion gas generator [NASA-TM-105258] p 30 N92-17061
- HULTGREN, LENNAERT S.**
Nonlinear spatial equilibration of an externally excited instability wave in a free shear layer p 170 A92-31469
- HUMPHREY, D. L.**
Oxidation kinetics of cast TiAl3 p 121 A92-38993
- HUNG, CHING-CHEH**
Brominated graphitized carbon fibers [NASA-CASE-LEW-14698-2] p 127 N92-10090
Graphite intercalation compound with iodine as the major intercalant [NASA-TM-105375] p 97 N92-25203
Graphite fluoride from iodine intercalated graphitized carbon [NASA-CASE-LEW-15360-1] p 116 N92-34206
- HUNT, MARIBETH E.**
A dynamic isotope power system for Space Exploration Initiative surface transport systems [AIAA PAPER 92-1489] p 61 A92-38605
A dynamic isotope power system portable generator for the moon or Mars p 232 A92-50634
- HURWITZ, FRANCES I.**
Polymeric precursors for fibers and matrices p 125 A92-39856
Approaches to polymer-derived CMC matrices [NASA-TM-105754] p 110 N92-29660
- HUSSAIN, FAZLE**
Direct evaluation of aeroacoustic theory in a jet p 253 A92-50296
- HUSTON, RONALD L.**
Contact stresses in meshing spur gear teeth: Use of an incremental finite element procedure [NASA-TM-105388] p 209 N92-23536
A basis for solid modeling of gear teeth with application in design and manufacture [NASA-TM-105392] p 209 N92-24202
- HUYNH, HUNG T.**
Numerical experiments on a new class of nonoscillatory schemes [AIAA PAPER 92-0421] p 7 A92-28193
Accurate upwind-monotone (nonoscillatory) methods for conservation laws p 193 N92-25812
- HUYNH, TAN**
Mutual coupling between rectangular microstrip patch antennas p 159 A92-52423
- HWANG, DANNY**
Grid management p 19 N92-25713
- HWANG, DANNY P.**
Numerical solution of a three-dimensional cubic cavity flow by using the Boltzmann equation [NASA-TM-105693] p 195 N92-30297
- HWANG, L.-T.**
Comparative evaluation of optical waveguides as alternative interconnections for high performance packaging p 153 N92-32974
- IANCULESCU, G. D.**
Classical and adaptive control algorithms for the solar array pointing system of the Space Station Freedom [AIAA PAPER 92-4484] p 57 A92-55314
- IANNELLI, G. S.**
Conservative-variable average states for equilibrium gas multi-dimensional fluxes [NASA-TM-105585] p 191 N92-25196
- IBRAHIM, MOUNIR**
Analysis of an advanced ducted propeller subsonic inlet [AIAA PAPER 92-0274] p 5 A92-25728
Instantaneous heat transfer coefficient based upon two-dimensional analyses of Stirling space engine components p 181 A92-50827
Use of an approximate similarity principle for the thermal scaling of a full-scale thrust augmenting ejector [AIAA PAPER 92-3792] p 28 A92-54171
Analysis of an advanced ducted propeller subsonic inlet [NASA-TM-105393] p 15 N92-14002
Heat transfer in oscillating flows with sudden change in cross section [NASA-TM-105692] p 88 N92-26654
- IBRAHIM, MOUNIR B.**
A 2-D oscillating flow analysis in Stirling engine heat exchangers p 172 A92-36001
Use of an approximate similarity principle for the thermal scaling of a full-scale thrust augmenting ejector [NASA-TM-105724] p 36 N92-26613
- IEK, CHANTHY**
Analysis of an advanced ducted propeller subsonic inlet [AIAA PAPER 92-0274] p 5 A92-25728
Analysis of an advanced ducted propeller subsonic inlet [NASA-TM-105393] p 15 N92-14002
- IGNACZAK, LOUIS R.**
Development and flight history of SERT 2 spacecraft [AIAA PAPER 92-3516] p 74 A92-54038
Development and flight history of SERT 2 spacecraft [NASA-TM-105636] p 90 N92-28983
- INGEBO, R. D.**
Effect of gas mass flux on cryogenic liquid jet breakup p 140 A92-23845
- INMAN, DANIEL J.**
Force analysis of magnetic bearings with power-saving controls p 212 N92-27795
- INOUE, KATSUMI**
Minimization of the vibration energy of thin-plate structure [NASA-TM-105654] p 211 N92-25448
Optimum design of a gearbox for low vibration [NASA-TM-105653] p 212 N92-28476
- INOUE, L. Y.**
Multikilowatt power electronics development for spacecraft p 68 A92-50541
- INUKAI, T.**
Technology requirements for mesh VSAT applications [AIAA PAPER 92-1982] p 144 A92-29902
- ISLAM, S.**
Near-tip dual-length scale mechanics of mode-I cracking in laminate brittle matrix composites [AIAA PAPER 92-2491] p 221 A92-34583
- ITOH, TATSUO**
Conductor-backed coplanar waveguide resonators of YBa2Cu3O(7-delta) on LaAlO3 p 158 A92-51042
- IVANCIC, W. D.**
Destination directed packet switch architecture for a geostationary communication satellite network [IAF PAPER 92-0413] p 50 A92-55793
- IVANCIC, WILLIAM D.**
Circuit-switch architecture for a 30/20-GHz FDMA/TDM geostationary satellite communications network [AIAA PAPER 92-2005] p 49 A92-29924
Evaluation of components, subsystems, and networks for high rate, high frequency space communications [NASA-TM-105274] p 147 N92-12151
Destination directed packet switch architecture for a 30/20 GHz FDMA/TDM geostationary communication satellite network p 148 N92-14204
Circuit-switch architecture for a 30/20-GHz FDMA/TDM geostationary satellite communications network [NASA-TM-105302] p 51 N92-15109
Multichannel demultiplexer/demodulator technologies for future satellite communication systems [NASA-TM-105377] p 51 N92-18342

JACKSON, G. S.

Destination-directed, packet-switching architecture for 30/20-GHz FDMA/TDM geostationary communications satellite network [NASA-TP-3201] p 51 N92-19762

J

JACKSON, G. S.

Observations of soot during droplet combustion at low gravity - Heptane and heptane/monochloroalkane mixtures p 115 A92-50447

JACOBS, M.

Engine system assessment study using Martian propellants [AIAA PAPER 92-3446] p 73 A92-54030

JACOBS, R. E.

Description of liquid nitrogen experimental test facility p 44 A92-23842

JACOBS, RICHARD E.

Description of Liquid Nitrogen Experimental Test Facility [NASA-TM-105215] p 134 N92-11208

JACOBSON, N. S.

Oxidation-chlorination of binary Ni-Cr alloys in flowing Ar-O₂-Cl₂ gas mixtures at 1200 K p 112 A92-17296
Fiber coating/matrix reactions in silicon-base ceramic matrix composites p 102 A92-39604

JACOBSON, NATHAN S.

Reactions of silicon carbide and silicon(IV) oxide at elevated temperatures p 126 A92-43483
Volatile species in halide-activated-diffusion coating packs p 122 A92-57028

High-temperature durability considerations for HSC combustor [NASA-TP-3162] p 129 N92-17070

JACOBY, BARRY A.

Plasma flow processes within magnetic nozzle configurations p 67 A92-50266

JAIN, L. K.

Effect of fiber orientation on the fracture toughness of brittle matrix composites p 103 A92-41841

JAIN, R. K.

Calculated performance of p(+)/n InP solar cells with In(0.52)Al(0.48)As window layers p 153 A92-13266
Recent progress in InP solar cell research p 158 A92-50653

Influence of the dislocation density on the performance of heteroepitaxial indium phosphide solar cells p 234 A92-53156

Effect of InAlAs window layer on the efficiency of indium phosphide solar cells p 234 A92-53163
Status and future directions of InP solar cell research [NASA-TM-105426] p 160 N92-18920

JAIN, RAJ K.

Effect of InAlAs window layer on efficiency of indium phosphide solar cells [NASA-TM-105354] p 161 N92-25176
Monolithic and mechanical multijunction space solar cells [NASA-TM-105832] p 163 N92-32233

JAMALI, M. M.

Multicarrier demodulator architecture for onboard processing satellites p 49 A92-10465

JAMES, ERIC

Gelled liquid oxygen/metal powder monopropellants [AIAA PAPER 92-3450] p 134 A92-49004

JANETZKE, D. C.

Parallel computation of aerodynamic influence coefficients for aeroelastic analysis on a transputer network p 241 A92-12367

JANETZKE, DAVID

Determining structural performance p 32 N92-22519

JANG, J. HOON

Design characteristics of a heat pipe test chamber [NASA-TM-105737] p 238 N92-29662

JANKOVSKY, ROBERT S.

Cyclic hot firing results of tungsten-wire-reinforced, copper-lined thrust chambers [NASA-TM-4214] p 91 N92-31249

JANKOWSKI, D. F.

Linear-stability theory of thermocapillary convection in a model of float-zone crystal growth [AIAA PAPER 92-0604] p 169 A92-28211

JANNSON, T.

Reconfigurable optical interconnection network for multimode optical fiber sensor arrays p 256 A92-37448

JANNSON, TOMASZ

Multiple-mode reconfigurable electro-optic switching network for optical fiber sensor array p 256 A92-46245

JANSSON, S.

Reduction of thermal stresses in continuous fiber reinforced metal matrix composites with interface layers p 105 A92-50347

JANUS, J. M.

Unsteady flowfield simulation of ducted prop-fan configurations [AIAA PAPER 92-0521] p 6 A92-26946

JASKOWIAK, MARTHA H.

Guanidine based vehicle/binders for use with oxides, metals, and ceramics [NASA-CASE-LEW-15314-1] p 131 N92-23461

JASSOWSKI, D. M.

Test experience, 490 N high performance (321 sec lsp) engine [AIAA PAPER 92-3800] p 67 A92-49127

JAWORSKE, D. A.

Observations of the freeze/thaw performance of lithium fluoride by motion picture photography p 180 A92-50751

JAYNE, DOUGLAS

Isothermal aging effects on PMR-15 resin [NASA-TM-105648] p 110 N92-30986

JEFFERIES, KENT S.

Concentrator testing using projected images p 69 A92-50615

JENDOUBI, SLAH

Radiative transfer solutions for cylindrical coordinates with emitting, absorbing, and anisotropic scattering medium [AIAA PAPER 92-0123] p 266 A92-28185
Comparisons of cylindrical and rectangular media radiative transfer solutions using the S-N discrete ordinates method [AIAA PAPER 92-2894] p 266 A92-54287

JENG, DUEN-REN

Internal structure of shock waves in disparate mass mixtures [AIAA PAPER 92-0496] p 169 A92-28195
FDDO and DSMC analyses of rarefied gas flow through 2D nozzles [AIAA PAPER 92-2858] p 176 A92-47841
DSMC analysis of species separation in rarefied nozzle flows [AIAA PAPER 92-2859] p 176 A92-47842

JENKINS, M. E.

Determination of the stress distributions in a ceramic, tensile specimen using numerical techniques p 216 A92-14546

JENKINS, M. G.

Mechanical behaviour and failure phenomenon of an in situ toughened silicon nitride p 127 A92-54504

JENKINS, P. P.

Radiation and temperature effects in heteroepitaxial and homoepitaxial InP cells p 159 A92-53192

JENKINS, PHILLIP

Increased efficiency with surface texturing in ITO/InP solar cells p 232 A92-44548
Surface etching for light trapping in encapsulated InP solar cells p 232 A92-48091
Photoluminescence lifetime measurements in InP wafers p 262 A92-48092
Minority carrier lifetime in indium phosphide p 262 A92-53148

JENKINS, SUSAN L.

Investigation of two and three parameter equations of state for cryogenic fluids p 140 A92-13413

JHA, SUNIL C.

Does a threshold stress for creep exist in HiC-dispersed NiAl? p 118 A92-30780

JI, YUANDONG

Stochastic stability properties of jump linear systems p 246 A92-25878

JIANG, BO-NAN

A least-squares finite element method for incompressible Navier-Stokes problems p 173 A92-37387

An error analysis of least-squares finite element method of velocity-pressure-vorticity formulation for Stokes problem p 173 A92-37506

Optimal least-squares finite element method for elliptic problems [NASA-TM-105382] p 249 N92-15662

JOHN, W. T.

Rayleigh-Brillouin scattering to determine one-dimensional temperature and number density profiles of a gas flow field p 198 A92-38067

JOHNS, ALBERT L.

Acoustic characteristics and dynamic structural loading of an ASTOVL aircraft in hover [AIAA PAPER 92-0370] p 253 A92-28190
Hot gas ingestion characteristics and flow visualization of a vectored thrust STOVL concept p 26 A92-45316

JOHNS, ROBERT

Turning up the heat on aircraft structures p 23 A92-55131

JOHNSON, B. V.

Heat transfer in rotating serpentine passages with trips normal to the flow [ASME PAPER 91-GT-265] p 165 A92-15663

Heat transfer in rotating serpentine passages with trips skewed to the flow [NASA-TM-105581] p 186 N92-20235

JOHNSON, DEXTER

Force analysis of magnetic bearings with power-saving controls p 212 N92-27795

JOHNSON, M. C.

Experimental verification of a secondary recirculation zone in a labyrinth seal p 205 A92-50271

JOHNSON, RICHARD A.

A dynamic isotope power system portable generator for the moon or Mars p 232 A92-50634

JOHNSON, RICHARD E.

The O₂ reduction at the IFC modified O₂ fuel cell electrode [NASA-TM-105691] p 90 N92-29667

JOHNSTON, J. C.

Determination of the critical parameters for remote microscope control [IAF PAPER 91-026] p 240 A92-12447

An initial study of void formation during solidification of aluminum in normal and reduced-gravity [AIAA PAPER 92-0845] p 138 A92-29611

JOHNSTON, R. T.

Unsteady wing surface pressures in the wake of a propeller [AIAA PAPER 92-0277] p 5 A92-25731

JONES, R. E.

SCAILET - An intelligent assistant for satellite ground terminal operations [IAF PAPER 92-0552] p 245 A92-55855

JONES, WILLIAM R.

An XPS study of the stability of Fomblin Z25 on the native oxide of aluminum [NASA-TM-105594] p 131 N92-23185

JONGEWARD, GARY A.

Using EPSAT to analyze high power systems in the space environment p 158 A92-50580

JORASCH, RONALD E.

Distribution of space-gathered data [AIAA PAPER 92-1888] p 143 A92-29821

JORDAN, E. H.

A viscoplastic model for single crystals p 217 A92-24717

JORDAN, ERIC H.

Microstress analysis of periodic composites p 218 A92-30673

JORDON, ERIC H.

X ray based displacement measurement for hostile environments [NASA-TM-105551] p 202 N92-23155

JORGENSEN, P.

Central difference TVD and TVB schemes for time dependent and steady state problems [AIAA PAPER 92-0053] p 166 A92-22168

Central difference TVD and TVB schemes for time dependent and steady state problems [NASA-TM-105357] p 249 N92-15663

JORGENSEN, PHILIP C. E.

Two-dimensional unstructured triangular grid generation p 192 N92-25721

JOSEPH, A. J.

Surface morphologies and photoluminescence of diamond films deposited in a hot filament reactor p 261 A92-42858

JOSHI, PRAKASH B.

Laser-driven hypersonic air-breathing propulsion simulator [AIAA PAPER 92-3922] p 41 A92-56753

JUHASZ, ALBERT J.

Design considerations for space radiators based on the liquid sheet (LSR) concept p 181 A92-50821

An overview of the Lewis Research Center CSTI thermal management program [NASA-TM-105310] p 92 N92-31916

JUHASZ, JOHN

Application of enhanced modern structured analysis techniques to Space Station Freedom electric power system requirements p 251 A92-50609

JUMPER, G.

Determination of the natural convection coefficient in low-gravity [AIAA PAPER 92-0712] p 168 A92-27072

JURNS, J. M.

Description of liquid nitrogen experimental test facility p 44 A92-23842

JURNS, JOHN M.

Description of Liquid Nitrogen Experimental Test Facility [NASA-TM-105215] p 134 N92-11208

K

- KACKLEY, N.**
Bifunctional alkaline oxygen electrodes
p 115 A92-50729
- KACPURA, THOMAS J.**
An EMTP system level model of the PMAD DC test bed
p 46 A92-50657
- KACZYNSKI, KENNETH J.**
Analytical study of nozzle performance for nuclear thermal rockets
[NASA-TM-105251] p 78 N92-11126
Thermal stratification potential in rocket engine coolant channels
[NASA-TM-4378] p 87 N92-25616
- KADAMBI, JAIKRISHNAN R.**
The effect of steady aerodynamic loading on the flutter stability of turbomachinery blading
[ASME PAPER 91-GT-130] p 2 A92-15574
- KALLURI, S.**
Thermomechanical and bithermal fatigue behavior of cast B1900 + Hf and wrought Haynes 188
p 122 A92-45233
- KALLURI, SREERAMESH**
Damage mechanisms in bithermal and thermomechanical fatigue of Haynes 188
[NASA-TM-105381] p 228 N92-24985
Elevated temperature axial and torsional fatigue behavior of Haynes 188
[NASA-TM-105396] p 229 N92-28701
- KAMAT, MANOHAR P.**
A study of equation solvers for linear and non-linear finite element analysis on parallel processing computers
[AIAA PAPER 92-2478] p 242 A92-34367
- KAMOTANI, Y.**
An experimental study of oscillatory thermocapillary convection in cylindrical containers
p 172 A92-36184
- KANE, J. H.**
Three-dimensional boundary element thermal shape sensitivity analysis
p 176 A92-47269
Boundary formulations for sensitivities of three-dimensional stress invariants
p 224 A92-50883
- KANE, JAMES H.**
Boundary formulations for shape sensitivity of temperature dependent conductivity problems
p 217 A92-25403
- KANKAM, M. D.**
Development of an analytical tool to study power quality of ac power systems for large spacecraft
p 67 A92-50529
Comparative survey of dynamic analyses of free-piston Stirling engines
p 206 A92-50793
- KANKAM, M. DAVID**
Development of a computer algorithm for the analysis of variable-frequency AC drives: Case studies included
[NASA-TM-105327] p 29 N92-13070
Development of a single-phase harmonic power flow program to study the 20 kHz AC power system for large spacecraft
[NASA-TM-105326] p 81 N92-13275
A free-piston Stirling engine/linear alternator controls and load interaction test facility
[NASA-TM-105825] p 238 N92-31262
- KANNAPAREDDY, MOHAN**
Instantaneous heat transfer coefficient based upon two-dimensional analyses of Stirling space engine components
p 181 A92-50827
- KANTZOS, P.**
Fatigue crack growth in unidirectional metal matrix composite
p 99 A92-19734
- KANTZOS, PETE**
Modeling of crack bridging in a unidirectional metal matrix composite
p 104 A92-43085
- KANTZOS, PETER**
Fatigue crack growth in a unidirectional SCS-6/Ti-15-3 composite
p 102 A92-39036
- KAO, KAI-HSIUNG**
Linear stability of compressible Taylor-Couette flow
p 173 A92-36187
- KAPOOR, KAMLESH**
Comparative study of turbulence models in predicting hypersonic inlet flows
[AIAA PAPER 92-3098] p 11 A92-48740
Comparative study of turbulence models in predicting hypersonic inlet flows
[NASA-TM-105720] p 19 N92-28102
- KAPOOR, V. J.**
Electrical-transport properties and microwave device performance of sputtered TiCaBaCuO superconducting thin films
p 263 A92-56599
C-band superconductor/semiconductor hybrid field-effect transistor amplifier on a LaAlO₃ substrate
[NASA-TM-105828] p 163 N92-34204
- KARALEKAS, D.**
Thermal stress analysis of a silicon carbide/aluminum composite
p 222 A92-38097
- KARASACK, V.**
A high temperature superconductivity communications flight experiment
[IAF PAPER 92-0410] p 50 A92-55790
- KARCHBER, ALLEN**
Combustion and core noise
p 254 N92-10607
- KASCAK, A. F.**
Electromechanical simulation and testing of actively controlled rotordynamic systems with piezoelectric actuators
[ASME PAPER 91-GT-245] p 203 A92-15650
Electromechanical simulation and testing of actively controlled rotordynamic systems with piezoelectric actuators
p 204 A92-39258
- KASCAK, ALBERT**
Determining structural performance
p 32 N92-22519
- KASEMSET, DUMRONG**
Interfaces for high-speed fiber-optic links - Analysis and experiment
p 256 A92-24002
- KASHIWAGI, T.**
Heat and mass transport from thermally degrading thin cellulosic materials in a microgravity environment
p 174 A92-41810
- KASHIWAGI, TAKASHI**
Global kinetic constants for thermal oxidative degradation of a cellulosic paper
p 113 A92-29488
- KASPER, HAROLD J.**
Graphite/epoxy composite adapters for the Space Shuttle/Centaur vehicle
[NASA-TP-3014] p 49 N92-31251
- KASSEMI, M.**
Effect of radiation on convection at moderate temperatures
[AIAA PAPER 92-0691] p 168 A92-27058
Combined conjugated heat transfer from a scattering medium
p 175 A92-44390
- KASSEMI, MOHAMMAD**
Effect of radiation on convection at moderate temperatures
[NASA-TM-105632] p 192 N92-25296
- KASSEMI, SIYASH A.**
Nature of buoyancy-driven flows in a reduced-gravity environment
p 175 A92-45844
- KATEHI, P. B.**
Analysis of shielded CPW discontinuities with air-bridges
p 152 N92-32971
- KAUFFMAN, MICHAEL T.**
Length minimization design considerations in photonic integrated circuits incorporating directional couplers
p 256 A92-46240
- KAUFMANN, K. J.**
Full-size solar dynamic heat receiver thermal-vacuum tests
p 68 A92-50565
Ground test program for a full-size solar dynamic heat receiver
p 68 A92-50566
- KAUPS, K.**
Analysis of iced wings
[AIAA PAPER 92-0416] p 8 A92-29972
Analysis of iced wings
[NASA-TM-105773] p 20 N92-34144
- KAUTZ, HAROLD E.**
Detecting Lamb waves with broad-band acousto-ultrasonic signals in composite structures
[NASA-TM-105557] p 216 N92-23189
- KAWAKAMI, YOSHIFUMI**
Predicted pressure distribution on a prop-fan blade through Euler analysis
p 10 A92-46791
- KAZA, KRISHNA**
Determining structural performance
p 32 N92-22519
- KAZA, KRISHNA RAO V.**
Semi-empirical model for prediction of unsteady forces on an airfoil with application to flutter
[NASA-TM-105414] p 17 N92-18760
- KAZAROFF, JOHN M.**
Advanced tube-bundle rocket thrust chambers
p 62 A92-44509
Cyclic hot firing results of tungsten-wire-reinforced, copper-lined thrust chambers
[NASA-TM-4214] p 91 N92-31249
- KEDDY, E. S.**
Analytical and experimental studies of heat pipe radiation cooling of hypersonic propulsion systems
[AIAA PAPER 92-3809] p 26 A92-49128
- KEE, PATRICK**
Synthesis and characterization of fine grain diamond films
p 262 A92-46330
- KEEFER, DENNIS**
Further study of the effect of the downstream plasma condition on accelerator grid erosion in an ion thruster
[AIAA PAPER 92-3829] p 76 A92-54192
- KEITH, T. G.**
Results from computational analysis of a mixed compression supersonic inlet
[NASA-TM-104475] p 14 N92-10976
- KEITH, T. G., JR.**
Cascade flutter analysis with transient response aerodynamics
p 217 A92-15972
Effect of type and location of oil groove on the performance of journal bearings
p 203 A92-21333
Numerical analysis of a thermal deicer
[AIAA PAPER 92-0527] p 22 A92-26950
A laser-induced heat flux technique for convective heat transfer measurements in high speed flows
p 200 A92-54318
Effect of out-of-roundness on the performance of a diesel engine connecting-rod bearing
[NASA-TM-105600] p 215 N92-31536
- KEITH, THEO G., JR.**
Investigation of the diffuser flow quality in an icing research wind tunnel
p 40 A92-24406
An efficient finite element method for aircraft de-icing problems
[AIAA PAPER 92-0532] p 22 A92-31670
Numerical modeling of fluid and electromagnetic phenomena in an arcjet
[AIAA PAPER 92-3106] p 258 A92-48747
- KELECY, FRANKLYN J.**
A numerical and experimental study of three-dimensional liquid sloshing in a rotating spherical container
[AIAA PAPER 92-0829] p 170 A92-29597
- KELLACKEY, C. J.**
Tensile properties of impact ices
[AIAA PAPER 92-0883] p 94 A92-29644
- KELLER, R. B.**
Transient pool boiling in microgravity
p 170 A92-30494
- KENNY, BARBARA H.**
Preliminary design of a mobile lunar power supply
p 233 A92-50635
Issues and status of power distribution options for space exploration
p 80 N92-13207
Power management and distribution considerations for a lunar base
[NASA-TM-105342] p 269 N92-13910
- KENT, RENEE M.**
Tensile strain measurements of ceramic fibers using scanning laser acoustic microscopy
p 198 A92-39629
Tensile strain measurements of ceramic fibers using scanning laser acoustic microscopy
[NASA-TM-105589] p 216 N92-24986
- KERCZEWSKI, ROBERT J.**
Interference susceptibility measurements for an MSK satellite communication link
[AIAA PAPER 92-2018] p 144 A92-29936
Evaluation of components, subsystems, and networks for high rate, high frequency space communications
[NASA-TM-105274] p 147 N92-12151
Interference susceptibility measurements for an MSK satellite communication link
[NASA-TM-105395] p 149 N92-15306
Multiple-access phased array antenna simulator for a digital beam forming system investigation
[NASA-TM-105422] p 149 N92-17062
- KEREMES, J.**
A probabilistic approach to the evaluation of fatigue damage in a space propulsion system injector element
[AIAA PAPER 92-2413] p 60 A92-34343
- KERHO, M.**
Finite wing aerodynamics with simulated glaze ice
[AIAA PAPER 92-0414] p 5 A92-26265
Helium bubble flow visualization of the spanwise separation on a NACA 0012 with simulated glaze ice
[AIAA PAPER 92-0413] p 7 A92-28192
LDV measurements on a rectangular wing with a simulated glaze ice accretion
[AIAA PAPER 92-2690] p 10 A92-45537
Helium bubble flow visualization of the spanwise separation on a NACA 0012 with simulated glaze ice
[NASA-TM-105742] p 19 N92-26612
- KERSLAKE, T. W.**
Full-size solar dynamic heat receiver thermal-vacuum tests
p 68 A92-50565
Ground test program for a full-size solar dynamic heat receiver
p 68 A92-50566
- KERSLAKE, THOMAS W.**
Experiments with phase change thermal energy storage canisters for Space Station Freedom
p 179 A92-50564
Parametric studies of phase change thermal energy storage canisters for Space Station Freedom
[NASA-TM-105350] p 55 N92-13143
Solar dynamic modules for Space Station Freedom: The relationship between fine-pointing control and thermal loading of the aperture plate
[NASA-TM-104498] p 84 N92-19780
Experiments with phase change thermal energy storage canisters for Space Station Freedom
[NASA-TM-104427] p 86 N92-21216

KERSLAKE, WILLIAM R.

KERSLAKE, WILLIAM R.

- Development and flight history of SERT 2 spacecraft
[AIAA PAPER 92-3516] p 74 A92-54038
- Development and flight history of SERT 2 spacecraft
[NASA-TM-105636] p 90 N92-28983

KERSTEIN, ALAN R.

- A new unsteady mixing model to predict NO(x) production during rapid mixing in a dual-stage combustor
[AIAA PAPER 92-0233] p 25 A92-25696

KESSELI, J.

- Design of a pool boiler heat transport system for a 25 kW advanced Stirling conversion system
p 181 A92-50802

KESSLER, W. J.

- Doppler-shifted fluorescence imaging of velocity fields in supersonic reacting flows
[AIAA PAPER 92-2964] p 199 A92-46979

KEYES, B. M.

- Modeled performance of monolithic, 3-terminal InP/Ga(0.47)In(0.53)As concentrator solar cells as a function of temperature and concentration ratio
p 234 A92-53153

KHACHEN, W.

- High temperature dielectric properties of Apical, Kapton, Peek, Teflon AF, and Uplex polymers
[NASA-TM-105753] p 162 N92-28675

KHAKOO, M. A.

- Extrapolation procedures in Mott electron polarimetry
p 197 A92-21241

KHAVARAN, A.

- Computation of supersonic jet mixing noise for an axisymmetric CD nozzle using k-epsilon turbulence model
[AIAA PAPER 92-0500] p 252 A92-26328

KHAVARAN, ABBAS

- A survey of the broadband shock associated noise prediction methods
[AIAA PAPER 92-0501] p 252 A92-26930
- Computation of supersonic jet mixing noise for an axisymmetric CD nozzle using k-epsilon turbulence model
[NASA-TM-105338] p 254 N92-14795

- A survey of the broadband shock associated noise prediction methods
[NASA-TM-105365] p 254 N92-14797

KHODADOUST, A.

- Finite wing aerodynamics with simulated glaze ice
[AIAA PAPER 92-0414] p 5 A92-26265
- Measurements in a leading-edge separation bubble due to a simulated airfoil ice accretion
p 21 A92-41262
- LDV measurements on a rectangular wing with a simulated glaze ice accretion
[AIAA PAPER 92-2690] p 10 A92-45537

KHODADOUST, ABDI

- Effect of a simulated glaze ice shape on the aerodynamic performance of a rectangular wing
[AIAA PAPER 92-4042] p 14 A92-56861

KHONSARI, MICHAEL M.

- Liquid lubrication for space applications
[NASA-TM-105198] p 133 N92-31840

KHOO, BOO-CHEONG

- Scalar rate correlation at a turbulent liquid free surface - A two-regime correlation for high Schmidt numbers
p 184 A92-56941

KHOSLA, P. K.

- Transient behavior of supersonic flow through inlets
p 7 A92-28043

KHOT, N. S.

- Application of Newton modified barrier method (NMBM) to structural optimization
[AIAA PAPER 92-2498] p 220 A92-34555

KIBA, W. M.

- Advanced large scale GaAs monolithic IF switch matrix subsystem
[AIAA PAPER 92-1861] p 155 A92-29801

KIELB, ROBERT

- Determining structural performance
p 32 N92-22519

KIM, A.

- An energy analysis of crack-initiation and arrest in epoxy
p 224 A92-49777

KIM, C. M.

- Computation of supersonic jet mixing noise for an axisymmetric CD nozzle using k-epsilon turbulence model
[AIAA PAPER 92-0500] p 252 A92-26328

KIM, CHAN M.

- A survey of the broadband shock associated noise prediction methods
[AIAA PAPER 92-0501] p 252 A92-26930
- Computation of supersonic jet mixing noise for an axisymmetric CD nozzle using k-epsilon turbulence model
[NASA-TM-105338] p 254 N92-14795

- A survey of the broadband shock associated noise prediction methods
[NASA-TM-105365] p 254 N92-14797

KIM, H.

- Destination directed packet switch architecture for a geostationary communication satellite network
[IAF PAPER 92-0413] p 50 A92-55793

KIM, H. D.

- An iterative implicit DDADI algorithm for solving the Navier-Stokes equation
p 192 N92-25810

KIM, HYEONGDONG

- Effect of an arcjet plume on satellite reflector performance
p 53 A92-16318
- Electromagnetic scattering from an inhomogeneous object by ray tracing
p 146 A92-51092

KIM, HYUN DAE

- An iterative implicit diagonally-dominant factorization algorithm for solving the Navier-Stokes equations
[NASA-TM-105259] p 249 N92-16663

KIM, J.

- Rotative quadrature phase-shift keying
p 146 A92-44233

KIM, JUNGHWAN

- Comparative study on the performance of power and bandwidth efficient modulations in LMSS under fading and interference
p 147 A92-54763

KIM, S. C.

- Numerical study of low-current steady arcs
p 67 A92-50264

KIM, S.-W.

- Fluid-flow of a row of jets in crossflow - A numerical study
[AIAA PAPER 92-0534] p 169 A92-28198
- Comparison of the SMAC, PISO, and iterative time-advancing schemes for unsteady flows
p 175 A92-47158

KIM, SUK C.

- Numerical study of low pressure nuclear thermal rockets
[AIAA PAPER 92-3815] p 75 A92-54182

KIM, T. K.

- Nongray radiative gas analyses using the S-N discrete ordinates method
p 266 A92-15443

KIM, TAE-KUK

- Radiative transfer solutions for cylindrical coordinates with emitting, absorbing, and anisotropic scattering medium
[AIAA PAPER 92-0123] p 266 A92-28185

KIMMEL, J. A.

- Optimal design of compact spur gear reductions
[NASA-TM-105676] p 213 N92-29351

KIMNACH, GREG L.

- Description of the control system design for the SSF PMAD DC testbed
p 45 A92-50654

KING, GALEN B.

- Saturated fluorescence measurements of the hydroxyl radical in laminar high-pressure C₂H₆/O₂/N₂ flames
p 198 A92-33987

KING, K. L.

- Microstructure and mechanical properties of near eutectic beta-NiAl plus alpha-Re alloys produced by rapid solidification and extrusion
p 119 A92-30844

KING, ROGER J.

- Simulating the arcjet thruster using a nonlinear active load
[AIAA PAPER 92-3528] p 45 A92-49052

KIRALY, LOUIS J.

- Determining structural performance
p 32 N92-22519

KIRK, K.

- Transient pool boiling in microgravity
p 170 A92-30494

KIRTLEY, JAMES L.

- Flywheel energy storage for electromechanical actuation systems
p 233 A92-50758

KIRTLEY, K. R.

- Deterministic blade row interactions in a centrifugal compressor stage
[ASME PAPER 91-GT-273] p 3 A92-15670

- Renormalization group based algebraic turbulence model for three-dimensional turbomachinery flows
p 9 A92-41268

KISER, JAMES D.

- Ceramics for engines
p 131 N92-22517

KISH, J. G.

- Advanced Rotorcraft Transmission (ART) Program summary
[AIAA PAPER 92-3365] p 205 A92-48938

- Advanced Rotorcraft Transmission (ART) program summary
[NASA-TM-105665] p 210 N92-24984

KITAMURA, TAKAYUKI

- Stochastic modeling of crack initiation and short-crack growth under creep and creep-fatigue conditions
[ASME PAPER 92-APM-5] p 223 A92-44681

KLANN, GARY A.

- Contingency power for a small turboshaft engine by using water injection into turbine cooling air
[NASA-TM-105680] p 37 N92-29661

KLEM, MARK D.

- Effect of model selection on combustor performance and stability using ROCCID
[AIAA PAPER 92-3226] p 65 A92-48827
- JANNAF Liquid Rocket Combustion Instability Panel research recommendations
p 115 N92-11124
- Coaxial injector spray characterization using water/air as simulants
[NASA-TM-105322] p 82 N92-14112

- Effect of model selection on combustor performance and stability predictions using ROCCID
[NASA-TM-105750] p 89 N92-27036

KLIMA, STANLEY J.

- NDE of advanced turbine engine components and materials by computed tomography
[ASME PAPER 91-GT-287] p 215 A92-15681

KLIMEK, ROBERT B.

- Color image processing and object tracking workstation
[NASA-TM-105561] p 139 N92-26611

KLOP, J. J.

- Classical and adaptive control algorithms for the solar array pointing system of the Space Station Freedom
[AIAA PAPER 92-4484] p 57 A92-55314

KNEISEL, KEITH

- Minority carrier lifetime in indium phosphide
p 262 A92-53148

KNIGHT, D. A.

- Optimization of armored spherical tanks for storage on the lunar surface
[NASA-TM-105700] p 91 N92-30187

KNOLL, R. H.

- Jet mixing in low gravity - Results of the Tank Pressure Control Experiment
[AIAA PAPER 92-3060] p 182 A92-54001

KNOLL, RICHARD H.

- A review of candidate multilayer insulation systems for potential use on wet-launched LH₂ tankage for the space exploration initiative lunar missions
[NASA-TM-104493] p 134 N92-13336

KNOSPE, C. R.

- Optimal microgravity vibration isolation - An algebraic introduction
p 54 A92-47495
- Controller design for microgravity vibration isolation systems
[IAF PAPER 92-0969] p 247 A92-57327

- Microgravity vibration isolation: An optimal control law for the one-dimensional case
[NASA-TM-105146] p 141 N92-11217

- Microgravity vibration isolation: Optimal preview and feedback control
[NASA-TM-105673] p 142 N92-30692

KO, FRANK

- Engine panel seals for hypersonic engine applications: High temperature leakage assessments and flow modelling
[NASA-TM-105260] p 208 N92-16336

- High temperature dynamic engine seal technology development
[NASA-TM-105641] p 209 N92-23435

KOBAYAKAWA, MAKOTO

- Predicted pressure distribution on a prop-fan blade through Euler analysis
p 10 A92-46791

KOCH, JOHN JR.

- Method of producing a plug-type heat flux gauge
[NASA-CASE-LEW-14967-2] p 201 N92-22038

KOEPEL, G.

- Performance of a four-element Ka-band high-temperature superconducting microstrip antenna
p 146 A92-37224

KOGAN, V. G.

- Melting of the Abrikosov flux lattice in anisotropic superconductors
p 260 A92-28075

KOHOUT, LISA L.

- SEI rover solar-electrochemical power system options
p 45 A92-50574

- Power supply for a manned international asteroid mission
p 80 N92-13205

- SEI power source alternatives for rovers and other multi-kWe distributed surface applications
p 80 N92-13206

KOLB, EDWARD W.

- Fluctuation-driven electroweak phase transition
p 269 A92-54464

KOLECKI, JOSEPH C.

- Environmental interactions in Space Exploration: Announcement of the formation of an Environmental Interactions Working Group
[NASA-TM-105294] p 270 N92-17069

- Environmental interactions in space exploration: Environmental interactions working group
p 239 N92-22382

- KOLTS, JAMES B.**
Preliminary tests of annular ion optics
[AIAA PAPER 92-3148] p 64 A92-48776
- KONG, KEON-SHIK**
Conductor-backed coplanar waveguide resonators of YBa₂Cu₃O₇(δ) on LaAlO₃ p 158 A92-51042
- KOO, K.-K.**
The isothermal dendritic growth experiment - A USMP-2 space flight experiment
[AIAA PAPER 92-0350] p 137 A92-28188
- KORAKIANITIS, T. P.**
Modeling of impulsive propellant reorientation
Pulsed thrust propellant reorientation - Concept and modeling p 59 A92-17187
p 62 A92-44507
- KORENYI-BOTH, A. L.**
Sinterless contacts to shallow junction InP solar cells
[NASA-TM-105670] p 237 N92-24802
- KOSS, D. A.**
On improving the fracture toughness of a NiAl-based alloy by mechanical alloying p 118 A92-30794
- KOSS, M. B.**
The isothermal dendritic growth experiment - A USMP-2 space flight experiment
[AIAA PAPER 92-0350] p 137 A92-28188
- KOSTER, J. N.**
Interfacial and gravitational convection in immiscible liquid layers
[IAF PAPER 92-0907] p 184 A92-57286
- KOSTRUBANIC, J.**
On improving the fracture toughness of a NiAl-based alloy by mechanical alloying p 118 A92-30794
- KOTHE, D. B.**
A continuum method for modeling surface tension p 175 A92-45707
- KRAFT, L. A.**
Development of an analytical tool to study power quality of ac power systems for large spacecraft p 67 A92-50529
- KRAFT, L. ALAN**
Development of a single-phase harmonic power flow program to study the 20 kHz AC power system for large spacecraft
[NASA-TM-105326] p 81 N92-13275
- KRAMER, JANE R.**
Structural tailoring/analysis for hypersonic components - Executive system development
[AIAA PAPER 92-2471] p 219 A92-34360
- KRANTZ, T. L.**
Advanced Rotorcraft Transmission (ART) Program summary
[AIAA PAPER 92-3365] p 205 A92-48938
Advanced Rotorcraft Transmission (ART) program summary
[NASA-TM-105665] p 210 N92-24984
- KRANTZ, TIMOTHY**
Dynamics of a split torque helicopter transmission
[NASA-TM-105681] p 213 N92-29136
- KRANTZ, TIMOTHY L.**
Gear tooth stress measurements of two helicopter planetary stages
[NASA-TM-105651] p 211 N92-26555
- KRASOWSKI, MICHAEL J.**
Wavelength-multiplexed fiber-optic position encoder for aircraft control systems p 24 A92-42602
- KRAUS, ROBERT**
Multi-megawatt inverter/converter technology for space power applications
[NASA-TM-105307] p 159 N92-14294
- KRECH, R. H.**
Fast oxygen atom facility for studies related to low earth orbit activities
[AIAA PAPER 92-3974] p 47 A92-56800
- KREIDER, KEVIN L.**
Computer program for Bessel and Hankel functions
[NASA-TM-105154] p 243 N92-11691
Modal element method for scattering of sound by absorbing bodies
[NASA-TM-105722] p 255 N92-28984
- KREIN, MARK A.**
QX MAN: Q and X file manipulation p 244 N92-25715
- KREJSA, E. A.**
Computation of supersonic jet mixing noise for an axisymmetric CD nozzle using k-epsilon turbulence model
[AIAA PAPER 92-0500] p 252 A92-26328
- KREJSA, EUGENE A.**
A survey of the broadband shock associated noise prediction methods
[AIAA PAPER 92-0501] p 252 A92-26930
Computation of supersonic jet mixing noise for an axisymmetric CD nozzle using k-epsilon turbulence model
[NASA-TM-105338] p 254 N92-14795
- A survey of the broadband shock associated noise prediction methods
[NASA-TM-105365] p 254 N92-14797
- KRISHEN, K.**
A high temperature superconductivity communications flight experiment
[IAF PAPER 92-0410] p 50 A92-55790
- KROEGER, E. W.**
COLD-SAT - A technology satellite for cryogenic experimentation p 52 A92-13425
- KRUCH, S.**
Differential continuum damage mechanics models for creep and fatigue of unidirectional metal matrix composites
[NASA-TM-105213] p 226 N92-16371
A differential CDM model for fatigue of unidirectional metal matrix composites
[NASA-TM-105726] p 230 N92-31505
- KUAN, C.**
Minimization of deviations of gear real tooth surfaces determined by coordinate measurements
[NASA-TM-105718] p 214 N92-30948
- KUBIAK, CLIFFORD P.**
In-situ carbon dioxide fixation on Mars p 134 A92-50613
- KUCERA, DONALD**
Graphite intercalation compound with iodine as the major intercalant
[NASA-TM-105375] p 97 N92-25203
- KUHARSKI, ROBERT A.**
Using EPSAT to analyze high power systems in the space environment p 158 A92-50580
- KUMAR, K. S.**
Compression, bend, and tension studies on forged Al67Ti25Cr8 and Al66Ti25Mn(g) L1(2) compounds p 118 A92-30766
Compression studies on particulate composites of ternary Al-Ti-Fe, and quaternary Al-Ti-Fe-Nb and Al-Ti-Fe-Mn L1(2) compounds p 119 A92-30845
Mechanical properties of monolithic and particulate composites of L12 forms of Al3Ti p 101 A92-36273
Interdiffusion between the L1(2) trialuminides Al66Ti25Mn9 and Al67Ti25Cr8 p 120 A92-37088
1200 and 1300 K slow plastic compression properties of Ni-50Al composites p 102 A92-38125
Discontinuously reinforced intermetallic matrix composites via XD synthesis p 103 A92-41867
Tensile behavior of the L1(2) compound Al67Ti25Cr8 p 122 A92-49694
Composites of low-density trialuminides: Particulate and long fiber reinforcements
[NASA-TM-105628] p 109 N92-25346
- KUNATH, R. R.**
A vertically integrated Ka-band phased array antenna
[AIAA PAPER 92-1976] p 156 A92-38140
An optically controlled Ka-band phased array antenna p 152 N92-32968
- KUNDU, K. P.**
A simplified reaction mechanism for prediction of NO(x) emissions in the combustion of hydrocarbons
[AIAA PAPER 92-3340] p 114 A92-48919
Applied analytical combustion/emissions research at the NASA Lewis Research Center - A progress report
[AIAA PAPER 92-3338] p 27 A92-54025
Applied analytical combustion/emissions research at the NASA Lewis Research Center
[NASA-TM-105731] p 90 N92-29343
- KUNINAKA, HITOSHI**
The arcing rate for a High Voltage Solar Array - Theory, experiment and predictions
[AIAA PAPER 92-0576] p 53 A92-26983
- KUO, WEN-SHYONG**
Mechanical behaviors of ceramic matrix composites with matrix cracking and fiber debonding p 100 A92-23104
Predictions of the critical strain for matrix cracking of ceramic matrix composites p 218 A92-33127
Modeling of the flexural behavior of ceramic-matrix composites p 225 A92-52005
- KURKOV, ANATOLE P.**
Optical measurements of unducted fan flutter
[ASME PAPER 91-GT-19] p 197 A92-15510
- KUSHIDA, G.**
Heat and mass transport from thermally degrading thin cellulosic materials in a microgravity environment p 174 A92-41810
- KUSIC, G. L.**
Load flows and faults considering dc current injections p 157 A92-50530
- KUSSMAUL, MICHAEL**
Ion beam treatment of potential space materials at the NASA Lewis Research Center
[NASA-TM-105398] p 97 N92-21548
- KWAN, R. K.**
Satellite delivery of B-ISDN services
[AIAA PAPER 92-1831] p 142 A92-29777
- Technology requirements for mesh VSAT applications
[AIAA PAPER 92-1982] p 144 A92-29902
Technical and economic feasibility of integrated video service by satellite
[AIAA PAPER 92-2054] p 145 A92-29966
- KWAN, ROBERT K.**
Satcom systems and technologies into the 21st century
[IAF PAPER 92-0412] p 147 A92-55792
- KWASNY, JAMES**
Arcjet nozzle area ratio effects
[NASA-TM-104477] p 83 N92-16022
- KWATRA, S. C.**
Multicarrier demodulator architecture for onboard processing satellites p 49 A92-10465
Rotative quadrature phase-shift keying p 146 A92-44233
Comparative study on the performance of power and bandwidth efficient modulations in LMSS under fading and interference p 147 A92-54763
Subband coding for image data archiving
[NASA-TM-105407] p 151 N92-20032
- KWON, O.**
A critical evaluation of a three-dimensional Navier-Stokes CFD as a tool to design supersonic turbine stages p 196 N92-32268
Three-dimensional flow fields inside a shrouded inducer at design and off-design conditions (CFD study) p 196 N92-32291
- KWON, O. J.**
Simulation of iced wing aerodynamics p 21 N92-21686
- KWON, OH J.**
Numerical investigation of performance degradation of wings and rotors due to icing
[AIAA PAPER 92-0412] p 5 A92-26264

L

LABORDE, ENRIQUE

A personal communications network using a Ka-band satellite p 145 A92-31780

LACKNEY, J. J.

HITCAN for actively cooled hot-composite thermostructural analysis
[ASME PAPER 91-GT-116] p 222 A92-36896

LAGHARI, J. R.

Dielectric breakdown studies of Teflon perfluoroalkoxy at high temperature p 125 A92-36287
Evaluation of high temperature dielectric films for high voltage power electronic applications p 261 A92-44273

High temperature dielectric properties of Apical, Kapton, Peek, Teflon AF, and Uplex polymers
[NASA-TM-105753] p 162 N92-28675

LAGIN, ALAN R.

Advanced Communication Technology Satellite (ACTS) multibeam antenna technology verification experiments
[NASA-TM-105421] p 149 N92-16191

Advanced Communication Technology Satellite (ACTS) multibeam antenna analysis and experiment
[NASA-TM-105420] p 149 N92-17047

Analysis of a generalized dual reflector antenna system using physical optics
[NASA-TM-105425] p 149 N92-18281

LAI, H. T.

Computation of H₂/air reacting flowfields in drag-reduction external combustion
[AIAA PAPER 92-3672] p 182 A92-54115

LAI, M. C.

CFD analysis of jet mixing in low NO(x) flametube combustors
[ASME PAPER 91-GT-217] p 24 A92-15634

LAKATOS, THOMAS F.

NASA Lewis Stirling SPRE testing and analysis with reduced number of cooler tubes
[NASA-TM-105767] p 238 N92-28837

LAKE, MAX L.

Properties of novel CVD graphite fibers and their bromine intercalation compounds
[NASA-TM-105295] p 128 N92-14170

LAKSHMINARAYANA, B.

Investigation of three-dimensional flow field in a turbine including rotor/stator interaction. I - Design development and performance of the research facility
[AIAA PAPER 92-3325] p 40 A92-48908

Investigation of three-dimensional flow field in a turbine including rotor/stator interaction. II - Three-dimensional flow field at the exit of the nozzle
[AIAA PAPER 92-3326] p 12 A92-48909

LALLI, VINCENT R.

Reliability training
[NASA-RP-1253] p 49 N92-32456

LAMBRECHT, W. R. L.

- LAMBRECHT, W. R. L.**
 'Wrong' bond interactions at inversion domain boundaries in GaAs p 260 A92-27297
- LAMOREAUX, CINDY**
 SiO(X) coatings for atomic oxygen protection of polyimide Kapton in low earth orbit [AIAA PAPER 92-2151] p 94 A92-31286
- LAN, G. L.**
 V-band pseudomorphic HEMT MMIC phased array components for space communications p 151 N92-32966
- LANDIS, G. A.**
 Calculated performance of p(+)-n InP solar cells with In(0.52)Al(0.48)As window layers p 153 A92-13266
 Integrated solar power satellites - An approach to low-mass space power p 231 A92-40427
 Effect of InAlAs window layer on the efficiency of indium phosphide solar cells p 234 A92-53163
 Advances in photovoltaic technology [IAF PAPER 92-0599] p 235 A92-57055
 Photovoltaic array for Martian surface power [NASA-TM-105827] p 270 N92-33899
- LANDIS, GEOFFREY A.**
 Material processing with hydrogen and carbon monoxide on Mars p 231 A92-17769
 Magnetic radiation shielding - An idea whose time has returned? p 53 A92-17796
 Tether methods for reactionless orbital propulsion p 44 A92-17797
 Space power by ground-based laser illumination p 59 A92-18401
 Photovoltaic power options for Mars p 231 A92-20366
 Moonbase night power by laser illumination p 44 A92-21086
 Acetylene fuel from atmospheric CO₂ on Mars p 133 A92-32199
 Structural scaling approximations for solar arrays p 231 A92-40935
 Increased efficiency with surface texturing in ITO/InP solar cells p 232 A92-44548
 Space power by ground-based laser transmission [AIAA PAPER 92-3024] p 63 A92-47027
 Surface etching for light trapping in encapsulated InP solar cells p 232 A92-48091
 Photoluminescence lifetime measurements in InP wafers p 262 A92-48092
 In-situ carbon dioxide fixation on Mars p 134 A92-50613
 Applications of thin-film photovoltaics for space p 70 A92-50641
 Minority carrier lifetime in indium phosphide p 262 A92-53148
 Enhancing optical absorption in InP and GaAs utilizing profile etching p 263 A92-53154
 Photovoltaic receivers for laser beamed power in space p 72 A92-53201
 Space transfer with ground-based laser/electric propulsion [AIAA PAPER 92-3213] p 73 A92-54017
 Effect of inert propellant injection on Mars ascent vehicle performance [AIAA PAPER 92-3447] p 73 A92-54031
 Laser beamed power - Satellite demonstration applications [IAF PAPER 92-0600] p 76 A92-57056
 Thin-film photovoltaics: Status and applications to space power p 81 N92-13228
 Solar radiation for Mars power systems p 81 N92-13259
 Enhancing optical absorption in InP and GaAs utilizing profile etching [NASA-TM-105325] p 82 N92-14111
 Effect of InAlAs window layer on efficiency of indium phosphide solar cells [NASA-TM-105354] p 161 N92-25176
- LANG, N.**
 Comment on two-equation models p 191 N92-24520
- LANGHALS, TAMMY J.**
 Experimental ice shape and performance characteristics for a multi-element airfoil in the NASA Lewis Icing Research Tunnel [NASA-TM-105380] p 17 N92-17347
- LAPOINTE, M.**
 Numerical simulation of geometric scale effects in cylindrical self-field MPD thrusters [AIAA PAPER 92-3297] p 258 A92-48885
- LAPOINTE, MICHAEL R.**
 An overview of the NASA Advanced Propulsion Concepts program [AIAA PAPER 92-3216] p 73 A92-54018
- LARIN, MAX**
 Power supply for a manned international asteroid mission p 80 N92-13205

- LARKO, JEFFREY M.**
 Advanced Communication Technology Satellite (ACTS) multibeam antenna technology verification experiments [NASA-TM-105421] p 149 N92-16191
 Advanced Communication Technology Satellite (ACTS) multibeam antenna analysis and experiment [NASA-TM-105420] p 149 N92-17047
- LAROSA, JUDITH L.**
 Fractal dimension of alumina aggregates grown in two dimensions p 126 A92-49814
- LARSEN, M.**
 Ductility enhancement from interface dislocation sources in a directionally solidified beta + gamma + gamma-prime Ni-Fe-Al composite alloy p 122 A92-46850
- LATHAM, THOMAS**
 Innovative nuclear thermal propulsion technology evaluation - Results of the NASA/DOE task team study [IAF PAPER 91-235] p 58 A92-13160
- LATTIME, S. B.**
 Optimal design of compact spur gear reductions [NASA-TM-105676] p 213 N92-29351
- LAURENDEAU, NORMAND M.**
 Saturated fluorescence measurements of the hydroxyl radical in laminar high-pressure C₂H₆/O₂/N₂ flames p 196 A92-33987
- LAWRENCE, CHARLES**
 Reaction-compensation technology for microgravity laboratory robots p 203 A92-23719
 Structural design concepts for a multimewatt solar electric propulsion (SEP) spacecraft [AIAA PAPER 92-2536] p 54 A92-34380
 Space Station Freedom solar dynamic modules structural modelling and analysis [NASA-TM-104506] p 226 N92-15405
 Determining structural performance p 32 N92-22519
- LAWRENCE, MARK A.**
 Fatigue crack growth reliability by probabilistic finite elements p 222 A92-37524
- LEAR, W. E.**
 Initial development of the axisymmetric ejector shear layer [AIAA PAPER 92-3567] p 178 A92-49068
- LEBED, RICHARD F.**
 LDEF spacecraft, ground laboratory, and computational modeling implications on Space Station Freedom's solar array materials and surfaces durability p 71 A92-53190
- LEBRON, RAMON C.**
 Test and evaluation of load converter topologies used in the Space Station Freedom power management and distribution dc test bed p 158 A92-50662
 Load converter interactions with the secondary system in the Space Station Freedom power management and distribution DC test bed [NASA-TM-105844] p 164 N92-34219
- LECKIE, F. A.**
 Reduction of thermal stresses in continuous fiber reinforced metal matrix composites with interface layers p 105 A92-50347
- LEE, D. D.**
 A multi-channel demultiplexer/demodulator architecture, simulation and implementation [AIAA PAPER 92-1972] p 144 A92-29895
- LEE, H. S.**
 Nongray radiative gas analyses using the S-N discrete ordinates method p 266 A92-15443
- LEE, H.-J.**
 METCAN updates for high temperature composite behavior - Simulation/verification p 98 A92-10264
 Metal matrix composite analyzer (METCAN) user's manual, version 4.0 [NASA-TM-105244] p 110 N92-30779
 Computational simulation of matrix micro-slip bands in SiC/Ti-15 composite [NASA-TM-105762] p 111 N92-32466
- LEE, HAEOK S.**
 Comparisons of cylindrical and rectangular media radiative transfer solutions using the S-N discrete ordinates method [AIAA PAPER 92-2894] p 266 A92-54287
- LEE, HAEOK, S.**
 Radiative transfer solutions for cylindrical coordinates with emitting, absorbing, and anisotropic scattering medium [AIAA PAPER 92-0123] p 266 A92-28185
- LEE, HO-JUN**
 Evaluation of MHOST analysis capabilities for a plate element [NASA-TM-105387] p 228 N92-23196
- LEE, J. H.**
 An experimental study of oscillatory thermocapillary convection in cylindrical containers p 172 A92-36184

- LEE, K. D.**
 Grid quality improvement by a grid adaptation technique p 248 A92-47072
 MAG3D and its application to internal flowfield analysis p 243 N92-24421
- LEE, K. N.**
 Fiber coating/matrix reactions in silicon-base ceramic matrix composites p 102 A92-39604
- LEE, KAI-FONG**
 Mutual coupling between rectangular microstrip patch antennas p 159 A92-52423
- LEE, KANG N.**
 Reactions of silicon carbide and silicon(IV) oxide at elevated temperatures p 126 A92-43483
- LEE, KI D.**
 Interactive solution-adaptive grid generation procedure [NASA-TM-105432] p 18 N92-23563
 Techniques for grid manipulation and adaptation p 194 N92-25827
- LEE, KIMYEONG**
 A classical instability of Reissner-Nordstrom solutions and the fate of magnetically charged black holes p 267 A92-26397
- LEE, R.**
 Ka-band MMIC arrays for ACTS Aero Terminal Experiment [IAF PAPER 92-0398] p 159 A92-55785
- LEE, R. O.**
 Coplanar waveguide aperture coupled patch antennas with ground plane/substrate of finite extent p 154 A92-24488
 New techniques for exciting linearly tapered slot antennas with coplanar waveguide p 155 A92-34844
 Performance of a K-band superconducting annular ring antenna p 146 A92-37067
 A vertically integrated Ka-band phased array antenna [AIAA PAPER 92-1976] p 156 A92-38140
 Mutual coupling between rectangular microstrip patch antennas p 159 A92-52423
- LEE, RICHARD**
 Ka-band active MMIC subarray development [AIAA PAPER 92-1863] p 155 A92-29803
- LEE, RICHARD Q.**
 Electromagnetic coupling between coplanar waveguide and microstrip antennas p 154 A92-21292
 Ka-band dual frequency array feed for a low cost ACTS ground terminal p 143 A92-29833
 Coplanar waveguide aperture-coupled microstrip patch antenna p 146 A92-37222
 New coplanar waveguide feed network for 2 x 2 linearly tapered slot antenna subarray p 156 A92-45619
 Planar dielectric resonator stabilized HEMT oscillator integrated with CPW/aperture coupled patch antenna [NASA-TM-105544] p 180 N92-18473
 Nonplanar linearly tapered slot antenna with balanced microstrip feed p 161 N92-23535
 Planar dielectric resonator stabilized HEMT oscillator integrated with CPW/aperture coupled patch antenna p 152 N92-32967
 An optically controlled Ka-band phased array antenna p 152 N92-32968
 Ka-band dual frequency array feed for a low cost ACTS ground terminal p 152 N92-32969
 Coplanar waveguide feeds for phased array antennas p 152 N92-32970
- LEE, SANBON**
 Diffusive crack growth at a bimaterial interface [AIAA PAPER 92-2432] p 220 A92-34580
 Asymmetric tip morphology of creep microcracks growing along bimaterial interfaces p 127 A92-56585
- LEE, Y. Y.**
 Oxidation-chlorination of binary Ni-Cr alloys in flowing Ar-O₂-Cl₂ gas mixtures at 1200 K p 112 A92-17296
- LEFEBVRE, A. H.**
 Factors influencing the effective spray cone angle of pressure-swirl atomizers p 166 A92-23300
- LEHMANN, G. A.**
 Final design of a free-piston hydraulic advanced Stirling conversion system p 206 A92-50798
- LEIB, S. J.**
 Distortion of a flat-plate boundary layer by free-stream vorticity normal to the plate p 173 A92-36343
- LEIBOVICH, S.**
 Nonlinear dynamics near the stability margin in rotating pipe flow p 165 A92-19959
- LEMPERT, WALTER R.**
 Filtered Rayleigh scattering measurements in supersonic/hypersonic facilities [AIAA PAPER 92-3894] p 200 A92-56733
- LENSKI, JOSEPH W., JR.**
 Boeing Helicopters Advanced Rotorcraft Transmission (ART) Program summary of component tests [AIAA PAPER 92-3364] p 205 A92-48937

- LEONARD, B. P.**
Development of an algebraic turbulence model for analysis of propulsion flows [AIAA PAPER 92-3861] p 183 A92-54209
ULTRA-SHARP solution of the Smith-Hutton problem [NASA-TM-105435] p 187 N92-22226
Development of an algebraic turbulence model for analysis of propulsion flows [NASA-TM-105701] p 250 N92-27517
- LEONARD, R.**
A high temperature superconductivity communications flight experiment [IAF PAPER 92-0410] p 50 A92-55790
- LEONARD, R. F.**
Space applications of high temperature superconductivity technology [IAF PAPER 91-307] p 259 A92-14724
- LEONARD, REGIS F.**
Advances in MMIC technology for communications satellites [AIAA PAPER 92-1899] p 155 A92-29830
- LEONHARDT, TODD A.**
Fluorescence microscopy for the characterization of structural integrity [NASA-TM-105253] p 96 N92-18970
Plasma etching a ceramic composite [NASA-TM-105430] p 130 N92-22305
Isothermal aging effects on PMR-15 resin [NASA-TM-105648] p 110 N92-30986
- LEPICOVSKY, JAN**
Engine component instrumentation development facility at NASA Lewis Research Center [AIAA PAPER 92-3995] p 41 A92-56818
Engine component instrumentation development facility at NASA Lewis Research Center [NASA-TM-105644] p 42 N92-25449
- LERCH, B. A.**
The effect of matrix mechanical properties on (0)B unidirectional SiC/Ti composite fatigue resistance p 99 A92-16220
- LERCH, BRAD A.**
A preliminary characterization of the tensile and fatigue behavior of tungsten-fiber/Waspaloy-matrix composite [NASA-TM-105346] p 187 N92-22487
- LERCH, BRADLEY A.**
Effect of heat treatment on stiffness and damping of SiC/Ti-15-3 p 100 A92-25627
Effect of heat treatment on stiffness and damping of SiC/Ti-15-3 [NASA-TM-105564] p 108 N92-20841
- LERUTTE, MARCEL G.**
Model-based diagnostics for Space Station Freedom p 245 A92-50535
- LESCO, DANIEL J.**
Optical measurement systems p 202 N92-22527
- LEUNG, C. P.**
Recent developments of the NESSUS probabilistic structural analysis computer program [AIAA PAPER 92-2411] p 242 A92-34342
- LEVENSON, L. L.**
Properties of large area ErBa₂Cu₃O_{7-x} thin films deposited by ionized cluster beams p 260 A92-33911
Properties of large area ErBa₂Cu₃O_{7-x} thin films deposited by ionized cluster beams p 264 N92-23414
- LEVINE, S. R.**
Ceramic composites: Enabling aerospace materials [NASA-TM-105599] p 133 N92-27378
- LEVINE, STANLEY R.**
Ceramics and ceramic matrix composites - Aerospace potential and status [AIAA PAPER 92-2445] p 94 A92-34474
Flight-vehicle materials, structures, and dynamics - Assessment and future directions. Vol. 3 - Ceramics and ceramic-matrix composites [ISBN 0-7918-0661-8] p 94 A92-39852
Ceramics and ceramic composites in future aeronautical and space systems p 95 A92-39853
Ceramics for engines p 131 N92-22517
- LEVY, RALPH**
Vortex generator design for aircraft inlet distortion as a numerical optimization problem p 23 N92-13959
- LEWANDOWSKI, J. J.**
The decrease in yield strength in NiAl due to hydrostatic pressure p 120 A92-38990
- LEWANDOWSKI, JOHN J.**
Fracture toughness and the effects of stress state on fracture of nickel aluminides p 117 A92-27422
- LEWICKI, D.**
Experimental testing of prototype face gears for helicopter transmissions [NASA-TM-105434] p 214 N92-31349
- LEWICKI, D. G.**
Transmission overhaul and component replacement predictions using Weibull and renewal theory p 215 A92-17201
- Application of face-gear drives in helicopter transmissions [NASA-TM-105655] p 212 N92-28434
- LEWICKI, DAVID G.**
Full-scale transmission testing to evaluate advanced lubricants [NASA-TM-105668] p 212 N92-26560
Development of a full-scale transmission testing procedure to evaluate advanced lubricants [NASA-TP-3265] p 213 N92-30396
- LEWIS, BRIAN**
Heat transfer and core neutronics considerations of the heat pipe cooled thermionic reactor p 180 A92-50591
- LEWIS, CLARK H.**
Improved nonequilibrium viscous shock-layer scheme for hypersonic blunt-body flowfields p 4 A92-24653
New technique for low-to-high altitude predictions of ablative hypersonic flowfields p 166 A92-24654
Low-to-high altitude predictions of three-dimensional ablative reentry flowfields [AIAA PAPER 92-0366] p 168 A92-26227
An improved PNS scheme for predicting complex three-dimensional hypersonic flows [AIAA PAPER 92-0753] p 8 A92-31679
- LEWIS, D. W.**
Optimal microgravity vibration isolation - An algebraic introduction p 54 A92-47495
Microgravity vibration isolation: An optimal control law for the one-dimensional case [NASA-TM-105146] p 141 N92-11217
Microgravity vibration isolation: Optimal preview and feedback control [NASA-TM-105673] p 142 N92-30692
- LEWIS, JOE**
Composite overwrapped nickel-hydrogen pressure vessels p 109 N92-22762
- LI, K.**
High-performance packaging for monolithic microwave and millimeter-wave integrated circuits [AIAA PAPER 92-1935] p 155 A92-31706
High-performance packaging for monolithic microwave and millimeter-wave integrated circuits [NASA-TM-105744] p 151 N92-31855
- LI, X.**
Pilot production of 4 sq cm ITO/InP photovoltaic solar cells p 71 A92-53197
- LI, XIAONAN**
Increased efficiency with surface texturing in ITO/InP solar cells p 232 A92-44548
- LIANG, A. D.**
The NASA-OAST earth-to-orbit propulsion technology program - The action plan [AIAA PAPER 92-1478] p 61 A92-38597
Development of advanced seals for space propulsion turbomachinery [NASA-TM-105659] p 87 N92-24957
- LICHON, PAUL J.**
Low-power arcjet test facility impacts [AIAA PAPER 92-3532] p 74 A92-54040
Low power arcjet test facility impacts [NASA-TM-105876] p 47 N92-34114
- LIEBERT, CURT H.**
Miniature high temperature plug-type heat flux gauges [NASA-TM-105403] p 201 N92-18759
Method of producing a plug-type heat flux gauge [NASA-CASE-LEW-14967-2] p 201 N92-22038
- LIEBESKIND, JOHN G.**
Laser-induced fluorescence of atomic hydrogen in an arcjet thruster [AIAA PAPER 92-0678] p 60 A92-27045
Flow diagnostics of an arcjet using laser-induced fluorescence [AIAA PAPER 92-3243] p 199 A92-48843
- LIGHTFOOT, ANNAMARIE**
Relationships between toughness and microstructure of reaction bonded Si₃N₄ p 125 A92-39687
- LIGRANI, P. M.**
Features of wavy vortices in a curved channel from experimental and numerical studies p 171 A92-31638
Surface heat transfer and flow properties of vortex arrays induced artificially and from centrifugal instabilities p 183 A92-56371
- LIM, HONG S.**
Destructive physical analysis results of Ni/H₂ cells cycled in LEO regime p 70 A92-50707
- LIM, SANG G.**
A system-approach to the elasto-hydrodynamic lubrication point-contact problem p 204 A92-35421
- LIM, T. C.**
Vibration transmission through rolling element bearings. IV - Statistical energy analysis p 218 A92-28756
- LIM, TEIK C.**
Statistical energy analysis of a geared rotor system p 204 A92-39227
- LIN, AVI**
High order parallel numerical schemes for solving incompressible flows p 193 N92-25818
- LIN, C. S.**
Vapor condensation on liquid surface due to laminar jet-induced mixing p 164 A92-10446
Self-pressurization of a spherical liquid hydrogen storage tank in a microgravity environment [AIAA PAPER 92-0363] p 168 A92-25798
Self-pressurization of a lightweight liquid hydrogen tank - Effects of fill level at low wall heat flux [AIAA PAPER 92-0818] p 60 A92-29591
Self-pressurization of a spherical liquid hydrogen storage tank in a microgravity environment [NASA-TM-105372] p 185 N92-14323
Effect of liquid surface turbulent motion on the vapor condensation in a mixing tank [NASA-TM-105555] p 187 N92-21498
- LIN, C.-S.**
Self-pressurization of a lightweight liquid hydrogen tank: Effects of fill level at low wall heat flux [NASA-TM-105411] p 135 N92-18442
- LIN, HSIANG H.**
Separation distance and static transmission error of involute spur gears [AIAA PAPER 92-3490] p 205 A92-49027
- LIN, HSIANG HSI**
Effect of contact ratio on spur gear dynamic load [NASA-TM-105606] p 210 N92-25447
Effect of operating conditions on gearbox noise [NASA-TM-105331] p 211 N92-26107
- LIN, PAUL**
Influence of mass moment of inertia on normal modes of preloaded solar array mast [NASA-TP-3273] p 230 N92-33476
- LIN, RENG R.**
Electromechanical simulation and testing of actively controlled rotordynamic systems with piezoelectric actuators p 204 A92-39258
- LIN, RENG RONG**
Electromechanical simulation and testing of actively controlled rotordynamic systems with piezoelectric actuators [ASME PAPER 91-GT-245] p 203 A92-15650
- LINDAMOOD, GLENN R.**
Electromagnetic coupling between coplanar waveguide and microstrip antennas p 154 A92-21292
- LING, HAO**
Effect of an arcjet plume on satellite reflector performance p 53 A92-16318
Electromagnetic scattering from an inhomogeneous object by ray tracing p 146 A92-51092
- LINNE, DIANE L.**
Material processing with hydrogen and carbon monoxide on Mars p 231 A92-17769
Technical prospects for utilizing extraterrestrial propellants for space exploration [IAF PAPER 91-669] p 133 A92-20612
Acetylene fuel from atmospheric CO₂ on Mars p 133 A92-32199
A compilation of lunar and Mars exploration strategies utilizing indigenous propellants [NASA-TM-105262] p 135 N92-19837
- LIOU, CHUEN-HUEI**
Effect of contact ratio on spur gear dynamic load [NASA-TM-105606] p 210 N92-25447
- LIOU, LARRY C.**
Combustion-wave ignition for rocket engines [NASA-TM-105545] p 84 N92-20043
- LIOU, M.-S.**
Multigrid calculation of three-dimensional viscous cascade flows [NASA-TM-105257] p 249 N92-10345
- LIOU, MAY-FUN**
High order parallel numerical schemes for solving incompressible flows p 193 N92-25818
- LIOU, MENG-S.**
Development of new flux splitting schemes p 189 N92-23343
- LIOU, MENG-SING**
Navier-Stokes solution of transonic cascade flows using nonperiodic C-type grids p 8 A92-28523
The Osher scheme for non-equilibrium reacting flows p 176 A92-48149
Center for Modeling of Turbulence and Transition (CMOTT). Research briefs: 1990 [NASA-TM-105243] p 1 N92-23336
Development of a new flux splitting scheme p 190 N92-23352
High-Order Polynomial Expansions (HOPE) for flux-vector splitting p 190 N92-23353
Development of new flux splitting schemes p 192 N92-25809
A new Lagrangian method for real gases at supersonic speed p 19 N92-25814

LIU, S. H.

- Upwind schemes and bifurcating solutions in real gas computations p 193 N92-25817
- LIU, S. H.**
Crystalline orientations of $Ti_2Ba_2Ca_2Cu_3O(x)$ grains on MgO , $SrTiO_3$, and $LaAlO_3$ substrates p 261 A92-41637
- LIU, W. W.**
On the basic equations for the second-order modeling of compressible turbulence [NASA-TM-105277] p 184 N92-11302
Workshop on Engineering Turbulence Modeling [NASA-CP-10088] p 191 N92-24514
- LIU, WILLIAM W.**
Modeling of compressible turbulent shear flows p 189 N92-23340
On the basic equations for the second-order modeling of compressible turbulence p 190 N92-23351
- LISCINSKY, D. S.**
Experimental study of cross-stream mixing in a rectangular duct [AIAA PAPER 92-3090] p 178 A92-48735
Experimental study of cross-stream mixing in a rectangular duct [NASA-TM-105694] p 36 N92-27652
- LITT, JONATHAN S.**
A simplified dynamic model of the T700 turboshaft engine [NASA-TM-105805] p 251 N92-30898
A demonstration of an intelligent control system for a reusable rocket engine [NASA-TM-105794] p 92 N92-31507
- LITVIN, F. L.**
Application of face-gear drives in helicopter transmissions [NASA-TM-105655] p 212 N92-28434
Minimization of deviations of gear real tooth surfaces determined by coordinate measurements [NASA-TM-105718] p 214 N92-30948
- LITVIN, FAYDOR L.**
A method for determining spiral-bevel gear tooth geometry for finite element analysis [NASA-TP-3096] p 207 N92-10195
- LIU, J.**
Rotative quadrature phase-shift keying p 146 A92-44233
- LIU, JIACHING**
Thermophysical properties of lysozyme (protein) solutions p 240 A92-44385
- LIU, JIAN**
Comparative study on the performance of power and bandwidth efficient modulations in LMSS under fading and interference p 147 A92-54763
- LIU, JOSEPH T. C.**
Near-wall response in turbulent shear flows subjected to imposed unsteadiness p 174 A92-41652
- LIU, N. S.**
An iterative implicit DDADI algorithm for solving the Navier-Stokes equation p 192 N92-25810
- LIU, NAN-SUEY**
An iterative implicit diagonally-dominant factorization algorithm for solving the Navier-Stokes equations [NASA-TM-105259] p 249 N92-16663
- LIU, W. K.**
A variationally coupled FE-BE method for elasticity and fracture mechanics p 222 A92-37510
- LIU, WING K.**
Fatigue crack growth reliability by probabilistic finite elements p 222 A92-37524
A stochastic damage model for the rupture prediction of a multi-phase solid. I - Parametric studies. II - Statistical approach p 224 A92-49784
- LIU, YUNG SHENG**
A basis for solid modeling of gear teeth with application in design and manufacture [NASA-TM-105392] p 209 N92-24202
- LO, EDMOND Y.**
Laser-driven hypersonic air-breathing propulsion simulator [AIAA PAPER 92-3922] p 41 A92-56753
- LOCCI, I.**
The decrease in yield strength in NiAl due to hydrostatic pressure p 120 A92-38990
- LOCCI, I. E.**
The mechanical properties of a Ni-30Al-20Fe-0.05Zr intermetallic alloy in the temperature range 300-1200 K p 118 A92-30793
On improving the fracture toughness of a NiAl-based alloy by mechanical alloying p 118 A92-30794
Microstructure and mechanical properties of a single crystal NiAl alloy with Zr or Hf rich G-phase precipitates p 119 A92-30841
Microstructure and mechanical properties of near eutectic beta-NiAl plus alpha-Fe alloys produced by rapid solidification and extrusion p 119 A92-30844

- Correlation of deformation mechanisms with the tensile and compressive behavior of NiAl and NiAl(Zr) intermetallic alloys p 120 A92-38019
- Deformation behavior of a Ni-30Al-20Fe-0.05Zr intermetallic alloy in the temperature range 300 to 1300 K p 121 A92-41668
- LOCCI, IVAN**
Fracture toughness and the effects of stress state on fracture of nickel aluminides p 117 A92-27422
- LOCCI, IVAN E.**
Influence of processing on the microstructure and mechanical properties of a NbAl₃-base alloy p 122 A92-48152
- LOCK, JAMES A.**
Rayleigh-Brillouin scattering to determine one-dimensional temperature and number density profiles of a gas flow field p 198 A92-38067
- LOFTIN, TIMOTHY A.**
Applications of high thermal conductivity composites to electronics and spacecraft thermal design [NASA-TM-102434] p 56 N92-24349
- LOH, C. Y.**
A new Lagrangian method for real gases at supersonic speed p 19 N92-25814
- LONG, KENWYN J.**
The introduction of spurious models in a hole-coupled Fabry-Perot open resonator p 197 A92-21244
- LONG, MARY J.**
Experimental investigation of an ejector-powered free-jet facility [AIAA PAPER 92-3569] p 41 A92-54058
- LOOMIS, WILLIAM R.**
Liquid lubricants for advanced aircraft engines [NASA-TM-104531] p 133 N92-32863
- LOPARO, KENNETH**
Design of multi-layer neural networks for accurate identification of nonlinear mappings p 246 A92-29030
- LOPARO, KENNETH A.**
Stochastic stability properties of jump linear systems p 246 A92-25878
Discrete-time entropy formulation of optimal and adaptive control problems p 247 A92-55930
- LOPEZ, ISAAC**
Transonic turbine blade cascade testing facility [AIAA PAPER 92-4034] p 42 A92-56856
Transonic turbine blade cascade testing facility [NASA-TM-105646] p 47 N92-26129
- LORENZO, C. F.**
Life extending control for rocket engines [NASA-TM-105789] p 142 N92-31263
- LORENZO, CARL F.**
IMPAC - An integrated methodology for propulsion and airframe control p 39 A92-29118
Life Extending Control p 246 A92-29166
Overview of rocket engine control [NASA-TM-105318] p 81 N92-13274
Directions in propulsion control p 32 N92-22530
- LOWE, R.**
Study of a cesium plasma as a selective emitter for thermophotovoltaic applications p 258 A92-33667
- LOWE, ROLAND A.**
High efficiency thermal to electric energy conversion using selective emitters and spectrally tuned solar cells [NASA-TM-105755] p 238 N92-30426
- LOWELL, CARL E.**
COSP - A computer model of cyclic oxidation p 114 A92-31849
Cyclic oxidation resistance of a reaction milled NiAl-AIN composite p 105 A92-46871
- LOWELL, T. A.**
Analysis of airframe/engine interactions for a STOVL aircraft with integrated flight/propulsion control [AIAA PAPER 92-4623] p 23 A92-55300
- LOWRY, P. A.**
Network architectures and protocols for the integration of ACTS and ISDN [AIAA PAPER 92-2039] p 145 A92-29953
- LOWRY, PETER A.**
ACTS T1-VSAT - The intelligent earth station [AIAA PAPER 92-2037] p 145 A92-29952
- LU, C. Y.**
Environmental interactions of the Space Station Freedom electric power system p 81 N92-13255
- LU, CHENG-YI**
Applicability of Long Duration Exposure Facility environmental effects data to the design of Space Station Freedom electrical power system [AIAA PAPER 92-0848] p 53 A92-29614
Contamination effects on Space Station Freedom electric power system performance p 54 A92-50578
Assessment of environmental effects on Space Station Freedom Electrical Power System p 55 A92-50581
- LU, H.**
Reconfigurable optical interconnection network for multimode optical fiber sensor arrays p 256 A92-37448

LU, Y. Y.

- A variationally coupled FE-BE method for elasticity and fracture mechanics p 222 A92-37510
- LUA, YUAN J.**
A stochastic damage model for the rupture prediction of a multi-phase solid. I - Parametric studies. II - Statistical approach p 224 A92-49784
- LUBOMSKI, JOSEPH F.**
International Workshop on Vibration Isolation Technology for Microgravity Science Applications [NASA-CP-10094] p 141 N92-28436
- LUCERO, JOHN M.**
Aeroelastic stability analyses of two counter rotating propfan designs for a cruise missile model [AIAA PAPER 92-2218] p 25 A92-34408
Aeroelastic stability analyses of two counter rotating propfan designs for a cruise missile model [NASA-TM-105268] p 227 N92-23191
- LUDWICZAK, D. R.**
Simulation of Space Station loads with active control systems p 56 N92-23824
- LUDWIG, KIMBERLY**
Description of real-time Ada software implementation of a power system monitor for the Space Station Freedom PMAD DC testbed p 242 A92-50533
- LUMLEY, J. L.**
Second order modeling of boundary-free turbulent shear flows p 174 A92-41275
- LUMLEY, JOHN L.**
A critical comparison of second order closures with direct numerical simulation of homogeneous turbulence [NASA-TM-105351] p 185 N92-15357
Kolmogorov behavior of near-wall turbulence and its application in turbulence modeling [NASA-TM-105663] p 191 N92-24050
- LUND, KURT O.**
Effects of anisotropic conduction and heat pipe interaction on minimum mass space radiators [NASA-TM-105297] p 80 N92-11138
- LUO, XIAOCHUN**
Fractals and cosmological large-scale structure p 268 A92-37413
Thick strings, the liquid crystal blue phase, and cosmological large-scale structure p 268 A92-48103
- LURIO, CHARLES A.**
Magnesium fluoride as energy storage medium for spacecraft solar thermal power systems p 67 A92-50274
- LUTON, MICHAEL J.**
1400 and 1500 K compressive creep properties of an NiAl-AIN composite p 103 A92-41575
- LYLTE, J. K.**
Numerical propulsion system simulation p 59 A92-20194
- M**
- MA, T.-Z.**
High voltage spheres in an unmagnetized plasma - Fluid and PIC simulations p 258 A92-47936
- MACHINCHICK, MICHAEL**
High temperature dynamic engine seal technology development [NASA-TM-105641] p 209 N92-23435
- MACKIN, MICHAEL**
Description of real-time Ada software implementation of a power system monitor for the Space Station Freedom PMAD DC testbed p 242 A92-50533
- MADI, FRANK J.**
Update on results of SPRE testing at NASA Lewis p 71 A92-50780
NASA Lewis Stirling SPRE testing and analysis with reduced number of cooler tubes [NASA-TM-105767] p 238 N92-28837
A free-piston Stirling engine/linear alternator controls and load interaction test facility [NASA-TM-105825] p 238 N92-31262
- MADZSAR, G.**
Demonstration of a flight capable system for plume spectroscopy [AIAA PAPER 92-3786] p 57 A92-54165
- MADZSAR, G. C.**
An overview of in-flight plume diagnostics for rocket engines [AIAA PAPER 92-3785] p 75 A92-54164
An overview of in-flight plume diagnostics for rocket engines [NASA-TM-105727] p 90 N92-28417
- MAHAJAN, A. J.**
Cascade flutter analysis with transient response aerodynamics p 217 A92-15972
- MAHAJAN, APARAJIT J.**
Eigenvalue calculation procedure for an Euler/Navier-Stokes solver with application to flows over airfoils p 3 A92-17429

- Aeroelastic stability analyses of two counter rotating propfan designs for a cruise missile model
[AIAA PAPER 92-2218] p 25 A92-34408
- Semi-empirical model for prediction of unsteady forces on an airfoil with application to flutter
[NASA-TM-105414] p 17 N92-18760
- Aeroelastic stability analyses of two counter rotating propfan designs for a cruise missile model
[NASA-TM-105268] p 227 N92-23191
- MAHAN, J. ROBERT**
Combustion and core noise p 254 N92-10607
- MAJUMDAR, ALOK K.**
Investigation of two and three parameter equations of state for cryogenic fluids p 140 A92-13413
- MALARIK, D. C.**
High molecular weight first generation PMR polyimides for 343 C applications p 105 A92-49819
- MALARIK, DIANE C.**
Viscoelastic properties of addition-cured polyimides used in high temperature polymer matrix composites p 124 A92-32632
- High molecular weight first generation PMR polyimides for 343 C applications
[NASA-TM-105364] p 129 N92-19498
- Vinyl capped addition polyimides
[NASA-CASE-LEW-15027-2] p 131 N92-24053
- MALDONADO, JAIME J.**
The design and performance estimates for the propulsion module for the booster of a TSTO vehicle
[NASA-TM-105299] p 29 N92-11995
- MALEC, HENRY A.**
Reliability training
[NASA-RP-1253] p 49 N92-32456
- MANDERSCHIED, JANE M.**
Reliability analysis of a structural ceramic combustion chamber
[ASME PAPER 91-GT-155] p 24 A92-15591
- MANKBADI, REDA R.**
On the nonlinear development of three-dimensional instability waves in natural transition
[AIAA PAPER 92-0741] p 170 A92-28222
- Subharmonic route to boundary-layer transition - Critical layer nonlinearity p 172 A92-35994
- Near-wall response in turbulent shear flows subjected to imposed unsteadiness p 174 A92-41652
- Quasi-steady turbulence modeling of unsteady flows p 177 A92-48204
- The present state of using RDT in turbulence modelling of unsteady flows p 191 N92-24535
- MANNAN, S. K.**
1200 and 1300 K slow plastic compression properties of Ni-50Al composites p 102 A92-38125
- MANNING, JOHN R.**
ACTS T1-VSAT - The intelligent earth station
[AIAA PAPER 92-2037] p 145 A92-29952
- MANNING, ROBERT M.**
Dynamic rain fade compensation techniques for the advanced communications technology satellite
[AIAA PAPER 92-2038] p 145 A92-31711
- MANSFIELD, BRIAN C.**
SP-100 reactor with Brayton conversion for lunar surface applications
[NASA-TM-105637] p 92 N92-32108
- MANTENIEKS, MARIS A.**
Multimegawatt MPD thruster design considerations
[NASA-TM-105405] p 83 N92-16024
- Preliminary test results of a hollow cathode MPD thruster
[NASA-TM-105324] p 84 N92-18474
- MANZELLA, DAVID H.**
Vacuum ultraviolet absorption in a hydrogen arcjet
[AIAA PAPER 92-3564] p 259 A92-54055
- MANZO, MICHELLE A.**
NASA Aerospace Flight Battery Systems Program: An update p 237 N92-22741
- Results of a technical analysis of the Hubble Space Telescope nickel-cadmium and nickel-hydrogen batteries p 89 N92-27167
- MARABITO, MARK**
Properties of novel CVD graphite fibers and their bromine intercalation compounds
[NASA-TM-105295] p 128 N92-14170
- MARAM, JON**
An advanced intelligent control system framework
[AIAA PAPER 92-3162] p 65 A92-48785
- MARCOPOLI, VINCENT R.**
Real-time demonstration hardware for enhanced DPCM video compression algorithm
[NASA-TM-105616] p 150 N92-19700
- MAREK, C. J.**
Simulations of free shear layers using a compressible kappa-epsilon model p 190 N92-23355
- MARGEVICIUS, R. W.**
The decrease in yield strength in NiAl due to hydrostatic pressure p 120 A92-38990
- MARINELLI, W. J.**
Arcing of negatively biased solar cells in low earth orbit
[AIAA PAPER 92-0578] p 59 A92-26985
- Arcing of negatively biased solar cells in a plasma environment. I - Experimental observations
[AIAA PAPER 92-2990] p 63 A92-47000
- MARKS, TIMOTHY S.**
NASA Lewis steady-state heat pipe code users manual
[NASA-TM-105161] p 90 N92-28682
- MARSHALL, ALBERT**
NASA/DOE/DOD nuclear propulsion technology planning: Summary of FY 1991 interagency panel results
[NASA-TM-105703] p 88 N92-26792
- MARTIN, CHARLES R.**
Temperature dependence of the electrode kinetics of oxygen reduction at the platinum/Nafion interface - A microelectrode investigation p 115 A92-56950
- MARTIN, ERIC R.**
Model-based diagnostics for Space Station Freedom p 245 A92-50535
- MARTIN, P. L.**
Intermetallic matrix composites; Proceedings of the MRS Symposium, San Francisco, CA, Apr. 18-20, 1990
[ISBN 1-55899-083-6] p 104 A92-46826
- MARTIN, R. A.**
Analytical and experimental studies of heat pipe radiation cooling of hypersonic propulsion systems
[AIAA PAPER 92-3809] p 26 A92-49128
- MARTZAKLIS, K. S.**
A vertically integrated Ka-band phased array antenna
[AIAA PAPER 92-1976] p 156 A92-38140
- An optically controlled Ka-band phased array antenna p 152 N92-32968
- MARUYAMA, N.**
Minimization of deviations of gear real tooth surfaces determined by coordinate measurements
[NASA-TM-105718] p 214 N92-30948
- MASON, D. P.**
Microstructure and mechanical properties of near eutectic beta-NiAl plus alpha-Re alloys produced by rapid solidification and extrusion p 119 A92-30844
- MASON, LEE S.**
A dynamic isotope power system portable generator for the moon or Mars p 232 A92-50634
- SP-100 reactor with Brayton conversion for lunar surface applications
[NASA-TM-105637] p 92 N92-32108
- MASSETH, J.**
Minimization of deviations of gear real tooth surfaces determined by coordinate measurements
[NASA-TM-105718] p 214 N92-30948
- MATOSSIAN, J. N.**
Plasma erosion rate diagnostics using laser-induced fluorescence p 198 A92-36738
- MATTERN, DUANE**
Propulsion system performance resulting from an Integrated Flight/Propulsion Control design
[AIAA PAPER 92-4602] p 28 A92-55281
- MATTERN, DUANE L.**
IMPAC - An integrated methodology for propulsion and airframe control p 39 A92-29118
- MATTHEWS, R. B.**
Fuels and materials development for space nuclear propulsion
[NASA-TM-107806] p 85 N92-21187
- MATTHIESEN, D. H.**
A versatile get away special furnace for materials processing in space
[AIAA PAPER 92-0787] p 137 A92-27122
- MATUS, LAWRENCE G.**
Mechanical properties of 3C silicon carbide p 126 A92-43761
- An overview of silicon carbide device technology
[NASA-TM-105402] p 263 N92-15815
- High-temperature electronics p 160 N92-22528
- MAUL, WILLIAM**
Rocket engine diagnostics using qualitative modeling techniques
[AIAA PAPER 92-3164] p 65 A92-48787
- Rocket engine diagnostics using qualitative modeling techniques
[NASA-TM-105714] p 88 N92-27033
- MAVRILIS, DIMITRIOS**
A basis for solid modeling of gear teeth with application in design and manufacture
[NASA-TM-105392] p 209 N92-24202
- MAY, BRIAN D.**
The Link Evaluation Terminal for the Advanced Communications Technology Satellite Experiments Program
[AIAA PAPER 92-2040] p 49 A92-29954
- The link evaluation terminal for the advanced communications technology satellite experiments program
[NASA-TM-105367] p 51 N92-16008
- MAYO, ROBERT**
Preliminary investigation of power flow and electrode phenomena in a multi-megawatt coaxial plasma thruster
[AIAA PAPER 92-3741] p 75 A92-54144
- MAZELSKY, R.**
Growth and characterization of lead bromide crystals p 138 A92-56956
- Effect of growth conditions on the quality of lead bromide crystals p 138 A92-56957
- MCCARDLE, JACK G.**
Flow in a ventral nozzle for short takeoff and vertical landing aircraft p 25 A92-28538
- Experimental and analytical study of close-coupled ventral nozzles for ASTOVL aircraft p 26 A92-45325
- Internal reversing flow in a tailpipe offtake configuration for SSTOVL aircraft
[AIAA PAPER 92-3790] p 28 A92-54169
- Flow studies in close-coupled ventral nozzles for STOVL aircraft
[NASA-TM-102554] p 17 N92-20934
- Internal reversing flow in a tailpipe offtake configuration for SSTOVL aircraft
[NASA-TM-105698] p 37 N92-28418
- MCCARTY, K. F.**
Diffusion mechanisms in chemical vapor-deposited iridium coated on chemical vapor-deposited rhenium p 117 A92-28017
- MCCARTY, R. D.**
Computer program for computing the properties of seventeen fluids p 241 A92-23849
- MCCATTY, S. A.**
Bifunctional alkaline oxygen electrodes p 115 A92-50729
- MCCOMAS, T. J.**
Design of multihundred-watt dynamic isotope power system for robotic space missions p 69 A92-50633
- MCCOMAS, THOMAS J.**
Thermal analysis of a conceptual design for a 250 We GPHS/FPSE space power system p 69 A92-50637
- MCCREDIE, BRADLEY D.**
Comparative evaluation of optical waveguides as alternative interconnections for high performance packaging p 153 N92-32974
- MCDANELS, DAVID L.**
Thermal conductivity and thermal expansion of graphite fiber/copper matrix composites
[NASA-TM-105233] p 106 N92-14120
- MCDONALD, G.**
Bonded ceramic foams reinforced with fibers for high temperature use p 125 A92-39628
- MCFADDEN, JOHN J.**
NASA's rotary engine technology enablement program: 1983-1991
[NASA-TM-105562] p 30 N92-20033
- MCFARLAND, ERIC**
Aerodynamics and heat transfer investigations on a high Reynolds number turbine cascade
[ASME PAPER 91-GT-157] p 164 A92-15593
- MCGAHAN, WILLIAM A.**
Solutions of the heat conduction equation in multilayers for photothermal deflection experiments p 141 A92-52205
- MCGAW, MICHAEL A.**
Cumulative creep-fatigue damage evolution in an austenitic stainless steel p 121 A92-45231
- Life prediction technologies for aeronautical propulsion systems p 32 N92-22520
- MCGEE, THOMAS J.**
Measurement of trace stratospheric constituents with a balloon borne laser radar p 239 N92-14500
- MCKERVEY, J. D.**
Fatigue damage accumulation in nickel prior to crack initiation p 120 A92-33947
- MCGUIRE, MELISSA L.**
An improved heat transfer configuration for a solid-core nuclear thermal rocket engine
[AIAA PAPER 92-3583] p 75 A92-54063
- MCILWAIN, MELVIN C.**
Nuclear thermal rockets - Key to moon-Mars exploration p 63 A92-48385
- MCKISSOCK, B. I.**
SEI power source alternatives for rovers and other multi-kWe distributed surface applications p 80 N92-13206
- MCKISSOCK, BARBARA I.**
Thermochemical energy storage for a lunar base
[NASA-TM-105333] p 236 N92-14485
- SP-100 reactor with Brayton conversion for lunar surface applications
[NASA-TM-105637] p 92 N92-32108

MCLALLIN, K. L.

- MCLALLIN, K. L.**
Full-size solar dynamic heat receiver thermal-vacuum tests p 68 A92-50565
Ground test program for a full-size solar dynamic heat receiver p 68 A92-50566
- MCMEEKING, R.**
Intermetallic matrix composites; Proceedings of the MRS Symposium, San Francisco, CA, Apr. 18-20, 1990 [ISBN 1-55899-083-6] p 104 A92-46826
- MCMURTRY, PATRICK A.**
A new unsteady mixing model to predict NO(x) production during rapid mixing in a dual-stage combustor [AIAA PAPER 92-0233] p 25 A92-25696
- MCNALLAN, M. J.**
Oxidation-chlorination of binary Ni-Cr alloys in flowing Ar-O₂-Cl₂ gas mixtures at 1200 K p 112 A92-17296
- MEADOR, MARY A. B.**
Addition curing thermosets endcapped with 4-amino (2,2) paracyclophane p 124 A92-33918
- MEADOR, MICHAEL A.**
Addition curing thermosets endcapped with 4-amino (2,2) paracyclophane p 124 A92-33918
High-temperature polymer matrix composites p 108 N92-22513
- MEADOWS, DAVID N.**
The ACTS NASA Ground Station/Master Control Station [AIAA PAPER 92-1965] p 45 A92-29888
- MEASE, KENNETH D.**
Canonical transformations for space trajectory optimization [AIAA PAPER 92-4509] p 44 A92-52079
- MEHMED, O.**
Aeroelastic analysis of advanced propellers using an efficient Euler solver [AIAA PAPER 92-0488] p 7 A92-28194
A numerical classical flutter analysis of advanced propellers [AIAA PAPER 92-2118] p 26 A92-35687
- MEHMED, ORAL**
Optical measurements of unducted fan flutter [ASME PAPER 91-GT-19] p 197 A92-15510
Aeroelastic stability analyses of two counter rotating propfan designs for a cruise missile model [AIAA PAPER 92-2218] p 25 A92-34408
Aeroelastic stability analyses of two counter rotating propfan designs for a cruise missile model [NASA-TM-105268] p 227 N92-23191
- MEHREGANY, MEHRAN**
Mechanical properties of 3C silicon carbide p 126 A92-43761
- MEISSNER, D. L.**
Measurement and analysis of a small nozzle plume in vacuum [AIAA PAPER 92-3108] p 64 A92-48748
- MEISSNER, DANA L.**
Experimental and numerical investigations of low-density nozzle and plume flows of nitrogen p 183 A92-54917
- MELCONIAN, JERRY O.**
The VRT gas turbine combustor - Phase II [AIAA PAPER 92-3471] p 27 A92-54035
- MELIS, M. E.**
Reduction of thermal residual stresses in advanced metallic composites based upon a compensating/compliant layer concept p 105 A92-47106
- MELLOCH, MICHAEL R.**
Significant long-term reduction in n-channel MESFET subthreshold leakage using ammonium-sulfide surface treated gates p 153 A92-12272
- MENA, R. A.**
Temperature independent quantum well FET with delta channel doping p 157 A92-49596
- MENA, RAFAEL A.**
Reduced mobility and PPC in In₂₀Ga₈₀As / Al₂₃Ga₇₇As HEMT structure p 265 N92-32976
Microwave properties of peeled HEMT devices sapphire substrates p 265 N92-32978
- MENART, J. A.**
Nongray radiative gas analyses using the S-N discrete ordinates method p 266 A92-15443
- MENNTRIETRIER, C.**
Effect of thermal convection on the shape of a solid-liquid interface p 171 A92-35978
- MENNTRIETRIER, CHRISTOPHE**
Thermal and solutal convection with conduction effects inside a rectangular enclosure [NASA-TM-105371] p 186 N92-15358
- MENON, SURESH**
A new unsteady mixing model to predict NO(x) production during rapid mixing in a dual-stage combustor [AIAA PAPER 92-0233] p 25 A92-25696
- MERKELO, HENRI**
Comparative evaluation of optical waveguides as alternative interconnections for high performance packaging p 153 N92-32974

- MERKLE, C. L.**
Propulsion-related flowfields using the preconditioned Navier-Stokes equations [AIAA PAPER 92-3437] p 178 A92-48994
- MEROLLA, ANTHONY**
Autonomous Power System intelligent diagnosis and control p 247 A92-50532
- MERRIGAN, M. A.**
Analytical and experimental studies of heat pipe radiation cooling of hypersonic propulsion systems [AIAA PAPER 92-3809] p 26 A92-49128
- MERRILL, W.**
A real time neural net estimator of fatigue life p 245 A92-21694
Design and evaluation of a robust dynamic neurocontroller for a multivariable aircraft control problem [NASA-TM-105579] p 40 N92-20586
- MERRILL, W. C.**
Identification of the Space Shuttle Main Engine dynamic models from firing data [AIAA PAPER 92-3317] p 73 A92-54022
Integrated health monitoring and controls for rocket engines [NASA-TM-105763] p 90 N92-28693
- MERRILL, WALT**
An advanced intelligent control system framework [AIAA PAPER 92-3162] p 65 A92-48785
- MERRILL, WALTER**
A failure diagnosis system based on a neural network classifier for the Space Shuttle Main Engine p 58 A92-11474
Fault diagnosis for the Space Shuttle main engine p 60 A92-28137
A simplified dynamic model of Space Shuttle Main Engine p 60 A92-29289
- MERRILL, WALTER C.**
State space representation of the open-loop dynamics of the Space Shuttle Main Engine p 59 A92-19607
Life Extending Control p 246 A92-29166
Real-time fault diagnosis for propulsion systems [NASA-TM-105303] p 29 N92-11017
A demonstration of an intelligent control system for a reusable rocket engine [NASA-TM-105794] p 92 N92-31507
- MERROW, JAMES**
Ion Beam Textured and Coated Surfaces Experiment (IBEX) p 132 N92-24832
- MERROW, JAMES E.**
Characteristics of hypervelocity impact craters on LDEF experiment S1003 and implications of small particle impacts on reflective surfaces p 269 N92-27252
- MERTE, H. JR.**
Transient pool boiling in microgravity p 170 A92-30494
- MESANDER, GEERT A.**
Advanced ice protection systems test in the NASA Lewis Icing Research Tunnel p 22 A92-14406
Results of a low power ice protection system test and a new method of imaging data analysis [NASA-TM-105745] p 20 N92-28696
- MESEROLE, J. S.**
Jet mixing in low gravity - Results of the Tank Pressure Control Experiment [AIAA PAPER 92-3060] p 182 A92-54001
- METZGER, FREDERICK B.**
Predicted pressure distribution on a prop-fan blade through Euler analysis p 10 A92-46791
- METZLER, S.**
Performance of a four-element Ka-band high-temperature superconducting microstrip antenna p 146 A92-37224
Measurement techniques for cryogenic Ka-band microstrip antennas p 153 N92-32981
- MEYER, CLAUDIA**
Rocket engine diagnostics using qualitative modeling techniques [AIAA PAPER 92-3164] p 65 A92-48787
Rocket engine diagnostics using qualitative modeling techniques [NASA-TM-105714] p 88 N92-27033
- MEYER, M.**
Engine system assessment study using Martian propellants [AIAA PAPER 92-3446] p 73 A92-54030
- MEYER, MARYUO B.**
A full field, 3-D velocimeter for NASA's microgravity science program [AIAA PAPER 92-0784] p 56 A92-27119
- MEYER, MICHAEL L.**
Technical prospects for utilizing extraterrestrial propellants for space exploration [IAF PAPER 91-669] p 133 A92-20612
Design issues for lunar in situ aluminum/oxygen propellant rocket engines [AIAA PAPER 92-1185] p 60 A92-33299

- Design issues for lunar in situ aluminum/oxygen propellant rocket engines [NASA-TM-105433] p 83 N92-16023
A compilation of lunar and Mars exploration strategies utilizing indigenous propellants [NASA-TM-105262] p 135 N92-19837
- MEYER, W. V.**
Extrapolation procedures in Mott electron polarimetry p 197 A92-21241
- MEYER, WILLIAM V.**
A fiber-optic probe for particle sizing in concentrated suspensions p 197 A92-21371
- MEYERS, ROGER M.**
The evolutionary development of high specific impulse electric thruster technology [NASA-TM-105758] p 93 N92-33064
- MICHAL, GARY M.**
Fracture toughness and the effects of stress state on fracture of nickel aluminides p 117 A92-27422
- MIHALOEW, JAMES R.**
Integrated flight/propulsion control for supersonic STOVL aircraft p 39 A92-45320
- MIKELIDIS, PAVLOS**
Plasma flow processes within magnetic nozzle configurations p 67 A92-50266
- MILES, RICHARD B.**
Filtered Rayleigh scattering measurements in supersonic/hypersonic facilities [AIAA PAPER 92-3894] p 200 A92-56733
- MILLER, BRENT A.**
Introduction to the internal fluid mechanics research session p 188 N92-22522
- MILLER, DAVID P.**
Implementation of control point form of algebraic grid-generation technique p 248 A92-47058
TIGGERC: Turbomachinery interactive grid generator energy distributor and restart code p 35 N92-25719
- MILLER, EDWARD F.**
Overview of Ka-band communications technology requirements for the space exploration initiative [NASA-TM-105308] p 269 N92-14953
- MILLER, JEFFREY H.**
Reaction-compensation technology for microgravity laboratory robots p 203 A92-23719
Engine panel seals for hypersonic engine applications: High temperature leakage assessments and flow modelling [NASA-TM-105260] p 208 N92-16336
High temperature dynamic engine seal technology development [NASA-TM-105641] p 209 N92-23435
- MILLER, R. A.**
Thermal barrier coating life and isothermal oxidation of low-pressure plasma-sprayed bond coat alloys p 119 A92-32398
- MILLER, THOMAS J.**
NASA program planning on nuclear electric propulsion [AIAA PAPER 92-1557] p 61 A92-38651
Nuclear rocket propulsion: NASA plans and progress - FY 1991 p 69 A92-50584
Nuclear propulsion for space exploration [IAF PAPER 92-0575] p 76 A92-57054
- MILLIS, MARC G.**
Technology readiness assessment of advanced space engine integrated controls and health monitoring [NASA-TM-105255] p 79 N92-11130
- MILLWATER, H.**
Recent developments of the NESSUS probabilistic structural analysis computer program [AIAA PAPER 92-2411] p 242 A92-34342
Structural reliability assessment capability in NESSUS [AIAA PAPER 92-3417] p 223 A92-48976
- MILLWATER, H. R.**
Structural system reliability calculation using a probabilistic fault tree analysis method [AIAA PAPER 92-2410] p 251 A92-34341
- MILNER, EDWARD J.**
High order parallel numerical schemes for solving incompressible flows p 193 N92-25818
- MINER, R. V.**
Hardening mechanisms in a dynamic strain aging alloy, Hastelloy X, during isothermal and thermomechanical cyclic deformation p 116 A92-24832
Microstructure and mechanical properties of a single crystal NiAl alloy with Zr or Hf rich G-phase precipitates p 119 A92-30841
- MINER, ROBERT V.**
Thermomechanical deformation behavior of a dynamic strain aging alloy, Hastelloy X [NASA-TM-105316] p 228 N92-25179
- MINNETYAN, L.**
Progressive fracture of polymer matrix composite structures: A new approach [NASA-TM-105574] p 109 N92-23194

- MINNETYAN, LEVON**
Structural durability of stiffened composite shells
[AIAA PAPER 92-2244] p 220 A92-34569
Damage and fracture in composite thin shells
p 224 A92-51550
Damage and fracture in composite thin shells
[NASA-TM-105289] p 106 N92-13284
Structural durability of stiffened composite shells
[NASA-CR-190588] p 229 N92-29342
- MIRACLE, D. B.**
Intermetallic matrix composites; Proceedings of the MRS
Symposium, San Francisco, CA, Apr. 18-20, 1990
[ISBN 1-55899-083-6] p 104 A92-46826
- MIRANDA, F. A.**
Microwave properties of YBa₂Cu₃O₇(δ)
high-transition-temperature superconducting thin films
measured by the power transmission method
p 153 A92-14938
Coaxial line configuration for microwave power
transmission study of YBa₂Cu₃O₇(δ) thin films
p 154 A92-18455
Microwave conductivity of laser ablated
YBa₂Cu₃O₇(δ) superconducting films and its relation
to microstrip transmission line performance
p 264 N92-21639
- MIRANDA, FELIX A.**
Measurements of complex permittivity of microwave
substrates in the 20 to 300 K temperature range from
26.5 to 40.0 GHz p 197 A92-13416
Conductor-backed coplanar waveguide resonators of
YBa₂Cu₃O₇(δ) on LaAlO₃ p 158 A92-51042
Dependence of the critical temperature of laser-ablated
YBa₂Cu₃O₇(δ) thin films on LaAlO₃ substrate growth
technique p 264 N92-23415
Magnetic penetration depth of YBa₂Cu₃O₇(δ) thin
films determined by the power transmission method
p 265 N92-32983
- MIRANDA, FELIX ANTONIO**
Microwave response of high transition temperature
superconducting thin films p 264 N92-23413
- MIRTIKH, MICHAEL J.**
LDEF spacecraft, ground laboratory, and computational
modeling implications on Space Station Freedom's solar
array materials and surfaces durability
p 71 A92-53190
Ion beam treatment of potential space materials at the
NASA Lewis Research Center
[NASA-TM-105398] p 97 N92-21548
Ion Beam Textured and Coated Surfaces Experiment
(IBEX) p 132 N92-24832
Characteristics of hypervelocity impact craters on LDEF
experiment S1003 and implications of small particle
impacts on reflective surfaces p 269 N92-27252
- MISRA, A.**
Ductility enhancement from interface dislocation
sources in a directionally solidified beta + gamma +
gamma-prime Ni-Fe-Al composite alloy
p 122 A92-46850
- MITAL, S. K.**
Computational simulation of matrix micro-slip bands in
SiC/Ti-15 composite
[NASA-TM-105762] p 111 N92-32466
- MITAL, SUBODH K.**
Computational simulation of microfracture in high
temperature metal matrix composites p 98 A92-10263
Microfracture in high temperature metal matrix
laminates
[NASA-TM-105189] p 106 N92-14122
Thermally-driven microfracture in high temperature
metal matrix composites
[NASA-TM-105305] p 107 N92-15136
Computational simulation of intermingled-fiber hybrid
composite behavior
[NASA-TM-105666] p 110 N92-31506
- MITCHELL, L. K.**
Acoustic characteristics and dynamic structural loading
of an ASTOVL aircraft in hover
[AIAA PAPER 92-0370] p 253 A92-28190
- MITTELMANN, H. D.**
Linear-stability theory of thermocapillary convection in
a model of float-zone crystal growth
[AIAA PAPER 92-0604] p 169 A92-28211
- MIYOSHI, KAZUHISA**
Studies of mechanochemical interactions in the
tribological behavior of materials p 124 A92-32410
Synthesis and characterization of fine grain diamond
films p 262 A92-46330
A vacuum (10(exp -9) Torr) friction apparatus for
determining friction and endurance life of MoS_x films
[NASA-TM-104478] p 129 N92-16129
Properties data for opening the Galileo's partially
unfurled main antenna
[NASA-TM-105355] p 130 N92-20660
Environmental effects on friction and wear of diamond
and diamondlike carbon coatings
[NASA-TM-105634] p 131 N92-23192
- MOAT, DICK**
Advanced Communication Technology Satellite (ACTS)
baseband processor development p 50 A92-53693
- MOBARK, AMIN**
Quasi-steady turbulence modeling of unsteady flows
p 177 A92-48204
- MOELLER, HANS J.**
Evaluation of the minority carrier diffusion length and
surface-recombination velocity in GaAs p/n solar cells
p 234 A92-53162
- MOHAJERI, KAYHAN**
Neutralizer optimization
[NASA-TM-105578] p 86 N92-21976
- MOHLER, STANLEY R., JR.**
Comparison of two-dimensional and three-dimensional
droplet trajectory calculations in the vicinity of finite
wings
[AIAA PAPER 92-0645] p 8 A92-28215
Comparison of two-dimensional and three-dimensional
droplet trajectory calculations in the vicinity of finite
wings
[NASA-TM-105617] p 188 N92-23154
- MOINUDDIN, ALIA**
Properties of novel CVD graphite fibers and their bromine
intercalation compounds
[NASA-TM-105295] p 128 N92-14170
- MOINUDDIN, ALIA M.**
Effects of windblown dust on photovoltaic surfaces on
Mars p 45 A92-50573
- MOKHTARI, SIMIN**
ULTRA-SHARP solution of the Smith-Hutton problem
[NASA-TM-105435] p 187 N92-22226
- MOLLS, FRANK B.**
Effect of spatial resolution on apparent sensitivity to
initial conditions of a decaying flow as it becomes
turbulent p 175 A92-45716
- MONASA, FRANK F.**
Collapse analysis of a waffle plate strongback for Space
Station Freedom
[NASA-TM-105412] p 227 N92-20045
- MONGIA, H. C.**
A parametric numerical study of mixing in a cylindrical
duct
[AIAA PAPER 92-3088] p 177 A92-48733
A parametric numerical study of mixing in a cylindrical
duct
[NASA-TM-105695] p 35 N92-26553
- MONGIA, HUKAM C.**
The VRT gas turbine combustor - Phase II
[AIAA PAPER 92-3471] p 27 A92-54035
- MONHEISER, JEFF M.**
An experimental study of impingement-ion-production
mechanisms
[AIAA PAPER 92-3826] p 76 A92-54190
- MONTAGUE, G. T.**
Electromechanical simulation and testing of actively
controlled rotordynamic systems with piezoelectric
actuators
[ASME PAPER 91-GT-245] p 203 A92-15650
Electromechanical simulation and testing of actively
controlled rotordynamic systems with piezoelectric
actuators p 204 A92-39258
- MOORE, BRAD W.**
Effects of a noncoplanar biphenyldiamine on the
processing and properties of addition polyimides
[NASA-TM-105383] p 107 N92-15137
- MOORE, J. J.**
Combustion synthesis of TiB₂-Al₂O₃-Al composite
materials p 102 A92-36391
- MOORE, JOHN J.**
Combustion synthesis of ceramic-metal composite
materials - The TiC-Al₂O₃-Al system
p 115 A92-55139
- MOORE, ROYCE D.**
Supersonic throughflow fans for high-speed aircraft
p 34 N92-22541
- MOORE, THOMAS J.**
Post-test examination of a pool boiler receiver
[NASA-TM-105635] p 123 N92-27192
- MORAN, M. M.**
On-orbit cryogenic fluid transfer research at NASA Lewis
Research Center p 45 A92-23847
- MORAN, MATTHEW E.**
Hydrogen no-vent testing in a 5 cubic foot (142 liter)
tank using spray nozzle and spray bar liquid injection
[AIAA PAPER 92-3063] p 63 A92-48719
Hydrogen no-vent fill testing in a 1.2 cubic foot (34 liter)
tank
[NASA-TM-105273] p 185 N92-13401
Hydrogen no-vent fill testing in a 5 cubic foot (142 liter)
tank using spray nozzle and spray bar liquid injection
[NASA-TM-105759] p 136 N92-28433
- MOREL, MICHAEL**
Interphase layer optimization for metal matrix
composites with fabrication considerations
p 98 A92-10262
- MORREN, W. E.**
Low-power arcjet test facility impacts
[AIAA PAPER 92-3532] p 74 A92-54040
Preliminary characterizations of a water vaporizer for
resistojet applications
[AIAA PAPER 92-3533] p 74 A92-54041
- MORREN, W. EARL**
Low power arcjet test facility impacts
[NASA-TM-105876] p 47 N92-34114
- MORRIS, RON**
Space Station Freedom solar dynamic modules
structural modelling and analysis
[NASA-TM-104506] p 226 N92-15405
- MORRISON, G. L.**
Experimental verification of a secondary recirculation
zone in a labyrinth seal p 205 A92-50271
- MORSCHER, GREGORY N.**
A simple test for thermomechanical evaluation of
ceramic fibers p 123 A92-21096
- MOSEER, J. A.**
Compatibility of potential reinforcing ceramics with Ni
and Fe aluminides p 105 A92-46874
- MOSES, J. L.**
Status of NASA's Earth-to-Orbit Propulsion Technology
program
[IAF PAPER 91-258] p 58 A92-13154
The NASA-OAST earth-to-orbit propulsion technology
program - The action plan
[AIAA PAPER 92-1478] p 61 A92-38597
- MOSSAYEBI, FARAMARZ**
A fundamental theorem for the model reduction of
nonlinear systems p 246 A92-41165
- MOTEVALLI, V.**
Determination of the natural convection coefficient in
low-gravity
[AIAA PAPER 92-0712] p 168 A92-27072
- MOTLOCH, CHET**
Innovative nuclear thermal propulsion technology
evaluation - Results of the NASA/DOE task team study
[IAF PAPER 91-235] p 58 A92-13160
- MULAC, RICHARD A.**
The numerical simulation of a high-speed axial flow
compressor
[ASME PAPER 91-GT-272] p 3 A92-15669
- MULARZ, EDWARD J.**
Chemical reacting flows p 188 N92-22525
- MULLEN, R. L.**
A bulk flow model of a brush seal system
[ASME PAPER 91-GT-325] p 203 A92-15696
Bonded ceramic foams reinforced with fibers for high
temperature use p 125 A92-39628
- MURTHY, D. V.**
Parallel computation of aerodynamic influence
coefficients for aeroelastic analysis on a transputer
network p 241 A92-12367
- MURTHY, DURBHA V.**
FREPS - A forced response prediction system for
turbomachinery blade rows
[AIAA PAPER 92-3072] p 242 A92-54006
Aeroelastic modal characteristics of mistuned blade
assemblies - Mode localization and loss of
eigenstructure p 225 A92-54921
- MURTHY, P. L. N.**
METCAN updates for high temperature composite
behavior - Simulation/verification p 98 A92-10264
Micromechanics for ceramic matrix composites
p 98 A92-10282
Computational simulation of high temperature metal
matrix composite behavior p 101 A92-32753
HITCAN for actively cooled hot-composite
thermostructural analysis
[ASME PAPER 91-GT-116] p 222 A92-36896
Analysis of aircraft engine blade subject to ice impact
[NASA-TM-105336] p 226 N92-15402
Towards the development of micromechanics equations
for ceramic matrix composites via fiber substructuring
[NASA-TM-105246] p 108 N92-19595
Progressive fracture of polymer matrix composite
structures: A new approach
[NASA-TM-105574] p 109 N92-23194
Metal matrix composite analyzer (METCAN) user's
manual, version 4.0
[NASA-TM-105244] p 110 N92-30779
Computational simulation of matrix micro-slip bands in
SiC/Ti-15 composite
[NASA-TM-105762] p 111 N92-32466
Computational simulation of structural fracture in fiber
composites p 111 N92-32531
- MURTHY, PAPPU L. N.**
Structural durability of stiffened composite shells
[AIAA PAPER 92-2244] p 220 A92-34569
Damage and fracture in composite thin shells
p 224 A92-51550
Damage and fracture in composite thin shells
[NASA-TM-105289] p 106 N92-13284

MUSGRAVE, J. L.

- Computational simulation of surface waviness in graphite/epoxy woven composites due to initial curing [NASA-TM-105313] p 106 N92-14118
Structural durability of stiffened composite shells [NASA-CR-190588] p 229 N92-29342

MUSGRAVE, J. L.

- Integrated health monitoring and controls for rocket engines [NASA-TM-105763] p 90 N92-28693
Implementation of an intelligent control system [NASA-TM-105795] p 241 N92-33897

MUSGRAVE, JEFFREY L.

- Linear quadratic servo control of a reusable rocket engine p 67 A92-50495
Linear quadratic servo control of a reusable rocket engine [NASA-TM-105291] p 79 N92-11128
Overview of rocket engine control [NASA-TM-105318] p 81 N92-13274
A demonstration of an intelligent control system for a reusable rocket engine [NASA-TM-105794] p 92 N92-31507

MUTHARASAN, RAJAKKANNU

- Engine panel seals for hypersonic engine applications: High temperature leakage assessments and flow modelling [NASA-TM-105260] p 208 N92-16336
High temperature dynamic engine seal technology development [NASA-TM-105641] p 209 N92-23435

MYERS, I. T.

- Electrical properties of teflon and ceramic capacitors at high temperatures [NASA-TM-105569] p 160 N92-20040
High temperature dielectric properties of Apical, Kapton, Peak, Teflon AF, and Uplex polymers [NASA-TM-105753] p 162 N92-28675
Wiring for aerospace applications [NASA-TM-105777] p 162 N92-30427

MYERS, IRA T.

- Multi-megawatt inverter/ converter technology for space power applications [NASA-TM-105307] p 159 N92-14294
Evaluation of high temperature capacitor dielectrics [NASA-TM-105622] p 161 N92-23561

MYERS, ROGER M.

- Electric propulsion - An evolutionary technology [IAF PAPER 91-241] p 58 A92-13158
Techniques for spectroscopic measurements in an arcjet nozzle p 59 A92-21087
The evolutionary development of high specific impulse electric thruster technology [AIAA PAPER 92-1556] p 61 A92-38650
Scaling of 100 kW class applied-field MPD thrusters [AIAA PAPER 92-3462] p 74 A92-54033
Anode power deposition in applied-field MPD thrusters [AIAA PAPER 92-3463] p 74 A92-54034
Test facilities for high power electric propulsion [NASA-TM-105247] p 80 N92-11136
Multimegawatt MPD thruster design considerations [NASA-TM-105405] p 83 N92-16024
Preliminary test results of a hollow cathode MPD thruster [NASA-TM-105324] p 84 N92-18474
The evolutionary development of high specific impulse electric thruster technology [NASA-TM-105712] p 92 N92-31342

N

NADELL, SHARI-BETH

- Mission and sizing analysis for the Beta II two-stage-to-orbit vehicle [AIAA PAPER 92-1264] p 47 A92-35868
Mission and sizing analysis for the Beta II two-stage-to-orbit vehicle [NASA-TM-105559] p 48 N92-21547

NAGAMATSU, H. T.

- Numerical study of low-current steady arcs p 67 A92-50264

NAHRA, HENRY K.

- Assessment of environmental effects on Space Station Freedom Electrical Power System p 55 A92-50581
Power supply for a manned international asteroid mission p 80 N92-13205
Environmental interactions of the Space Station Freedom electric power system p 81 N92-13255

NAHRA, J. J.

- C-band superconductor/semiconductor hybrid field-effect transistor amplifier on a LaAlO₃ substrate [NASA-TM-105828] p 163 N92-34204

NAIR, V. P.

- A classical instability of Reissner-Nordstrom solutions and the fate of magnetically charged black holes p 267 A92-26397

NALL, MARK E.

- Advanced Communications Technology Satellite (ACTS) p 53 A92-17780

NALLASAMY, M.

- Unsteady blade-surface pressures on a large-scale advanced propeller - Prediction and data p 3 A92-17178
Unsteady Euler analysis of the flowfield of a propfan at an angle of attack p 3 A92-21070
Unsteady blade pressures on a propfan at takeoff - Euler analysis and flight data [AIAA PAPER 92-0376] p 25 A92-26234
Unsteady blade pressures on a propfan - Predicted and measured compressibility effects [AIAA PAPER 92-3774] p 14 A92-54161

NAMBU, HIDESABURO

- Global kinetic constants for thermal oxidative degradation of a cellulose paper p 113 A92-29488

NAMDAR, BAHMAN S.

- Experimental ice shape and performance characteristics for a multi-element airfoil in the NASA Lewis Icing Research Tunnel [NASA-TM-105380] p 17 N92-17347

NARAYANAN, G. V.

- Structural tailoring/analysis for hypersonic components - Executive system development [AIAA PAPER 92-2471] p 219 A92-34360

NARVAEZ, ADABELLE

- Advanced Communication Technology Satellite (ACTS) multibeam antenna analysis and experiment [NASA-TM-105420] p 149 N92-17047

NATHAL, M.

- On improving the fracture toughness of a NiAl-based alloy by mechanical alloying p 118 A92-30794

NATHAL, M. V.

- Slow strain rate 1200-1400 K compressive properties of NiAl-1Hf p 116 A92-17977
Microstructure and mechanical properties of a single crystal NiAl alloy with Zr or Hf rich G-phase precipitates p 119 A92-30841

- Effect of fiber strength on the room temperature tensile properties of SiC/Ti-24Al-11Nb p 102 A92-36389
The effect of temperature on the deformation and fracture of SiC/Ti-24Al-11Nb p 106 A92-55143

NATHAL, MICHAEL V.

- Influence of processing on the microstructure and mechanical properties of a NbAl₃-base alloy p 122 A92-48152

NEINER, GEORGE H.

- Hot gas ingestion characteristics and flow visualization of a vectored thrust STOVL concept p 26 A92-45316

NEITZEL, G. P.

- Linear-stability theory of thermocapillary convection in a model of float-zone crystal growth [AIAA PAPER 92-0604] p 169 A92-28211

NELSON, CHRIS

- A fast, uncoupled, compressible, two-dimensional, unsteady boundary layer algorithm with separation for engine inlets [AIAA PAPER 92-3082] p 11 A92-48729
A fast, uncoupled, compressible, two-dimensional, unsteady boundary layer algorithm with separation for engine inlets [NASA-TM-105686] p 195 N92-27653

NELSON, EMILY

- An examination of anticipated g-jitter on Space Station and its effects on materials processes p 140 N92-28438

NEMETH, ED

- An advanced intelligent control system framework [AIAA PAPER 92-3162] p 65 A92-48785

NESBITT, J. A.

- Thermal response of various thermal barrier coatings in a high heat flux rocket engine p 119 A92-32399
Oxidation of Al₂O₃ continuous fiber-reinforced/NiAl composites p 106 A92-57029

NEUDECK, P. G.

- Significant long-term reduction in n-channel MESFET subthreshold leakage using ammonium-sulfide surface treated gates p 153 A92-12272

NEUDECK, PHILIP G.

- An overview of silicon carbide device technology [NASA-TM-105402] p 263 N92-15815

NEUMANN, ERIC S.

- An initial study of void formation during solidification of aluminum in normal and reduced-gravity [AIAA PAPER 92-0845] p 138 A92-29611

NEUMANN, H. E.

- Qualitative investigation of cryogenic fluid injection into a supersonic flow field p 164 A92-13360

NEWELL, J. F.

- LDEXPT, an intelligent database system for the Composite Load Spectra project p 59 A92-23695

NEWELL, JAMES F.

- Modal test/analysis correlation of Space Station structures using nonlinear sensitivity [NASA-TM-105850] p 230 N92-34221

NEWMAN, WYATT S.

- A 23.2:1 ratio, 300-watt, 26 N-m output torque, planetary roller-gear robotic transmission: Design and evaluation p 210 N92-25085

NEWTON, JAMES E.

- Heat transfer measurements from a smooth NACA 0012 airfoil p 165 A92-20215

NG, DANIEL

- Multiwavelength pyrometry for nongray surfaces in the presence of interfering radiation [NASA-TM-105286] p 201 N92-19107
Temperature-dependent reflectivity of silicon carbide [NASA-TM-105287] p 201 N92-19263
Multiwavelength pyrometry for nongray bodies [NASA-TM-105285] p 202 N92-24881

NG, W. F.

- The Baldwin-Lomax model for separated and wake flows using the entropy envelope concept [AIAA PAPER 92-0148] p 4 A92-23764

NG, WING-FAI

- Upwind relaxation methods for the Navier-Stokes equations using inner iterations p 170 A92-29553

NGO, P.

- A high temperature superconductivity communications flight experiment [IAF PAPER 92-0410] p 50 A92-55790

NGUYEN, H. L.

- Applied analytical combustion/emissions research at the NASA Lewis Research Center - A progress report [AIAA PAPER 92-3338] p 27 A92-54025

- Applied analytical combustion/emissions research at the NASA Lewis Research Center [NASA-TM-105731] p 90 N92-29343

NGUYEN, HUNG L.

- The VRT gas turbine combustor - Phase II [AIAA PAPER 92-3471] p 27 A92-54035

NGUYEN, TIEN M.

- ACTS aeronautical experiments [AIAA PAPER 92-2042] p 50 A92-29956

NICHOLS, L. D.

- Numerical propulsion system simulation p 59 A92-20194

NICHOLS, LESTER D.

- Aeropropulsion structures p 31 N92-22518

NIEDER, ERIN G.

- Metallized gelled monopropellants [NASA-TM-105418] p 87 N92-24557

NIEDRA, J. M.

- Comparison of high temperature, high frequency core loss and dynamic B-H loops of two 50 Ni-Fe crystalline alloys and an iron-based amorphous alloy p 157 A92-50551

- Comparison of high temperature, high frequency core loss and dynamic B-H loops of a 2V-49Fe-49Co and a grain oriented 3Si-Fe alloy [NASA-TM-105791] p 162 N92-30397

NIEDRA, JAMIS M.

- Analog synthesized fast-variable linear load p 157 A92-50539

- The 23 to 300 C demagnetization resistance of samarium-cobalt permanent magnets [NASA-TP-3119] p 159 N92-11252

NIEDZWECKI, RICHARD W.

- Small engine technology programs p 32 N92-22532

NOBLE, J.

- Alkali metal pool boiler life tests for a 25 kW advanced Stirling conversion system p 206 A92-50797
Design of a pool boiler heat transport system for a 25 kW advanced Stirling conversion system p 181 A92-50802

NOBLE, J. E.

- Final design of a free-piston hydraulic advanced Stirling conversion system p 206 A92-50798

NOBLE, JACK E.

- Alkali metal compatibility testing of candidate heater head materials for a Stirling engine heat transport system p 71 A92-50829

NOEBE, R.

- Ductility enhancement from interface dislocation sources in a directionally solidified beta + gamma + gamma-prime Ni-Fe-Al composite alloy p 122 A92-46850

NOEBE, R. D.

- The effect of strain rate and temperature on the tensile properties of NiAl p 117 A92-28113
Compressive strength of directionally solidified NiAl-NiAlNb intermetallics at 1200 and 1300 K p 117 A92-28248
Flow and fracture behavior of NiAl in relation to the brittle-to-ductile transition temperature p 118 A92-30781

- The mechanical properties of a Ni-30Al-20Fe-0.05Zr intermetallic alloy in the temperature range 300-1200 K p 118 A92-30793
- Microstructure and mechanical properties of a single crystal NiAl alloy with Zr or Hf rich G-phase precipitates p 119 A92-30841
- Microstructure and mechanical properties of near eutectic beta-NiAl plus alpha-Re alloys produced by rapid solidification and extrusion p 119 A92-30844
- Correlation of deformation mechanisms with the tensile and compressive behavior of NiAl and NiAl(Zr) intermetallic alloys p 120 A92-38019
- Deformation behavior of a Ni-30Al-20Fe-0.05Zr intermetallic alloy in the temperature range 300 to 1300 K p 121 A92-41668
- Initial evaluation of continuous fiber reinforced NiAl composites p 104 A92-46867
- Oxidation of Al₂O₃ continuous fiber-reinforced/NiAl composites p 106 A92-57029
- NOEBE, RONALD D.**
Solidification processing of intermetallic Nb-Al alloys p 120 A92-33866
- NORMAN, ARNIE**
An advanced intelligent control system framework [AIAA PAPER 92-3162] p 65 A92-48785
- NORUM, THOMAS D.**
Acoustic characteristics and dynamic structural loading of an ASTOVL aircraft in hover [AIAA PAPER 92-0370] p 253 A92-28190
- NOUAILHAS, D.**
A viscoplastic theory for anisotropic materials [ONERA, TP NO. 1992-90] p 217 A92-24721
- NOWLIN, BRENT C.**
Description of a pressure measurement technique for obtaining surface static pressures of a radial turbine [AIAA PAPER 92-4006] p 200 A92-56829
Description of a pressure measurement technique for obtaining surface static pressures of a radial turbine [NASA-TM-105643] p 202 N92-24959
- NYLAND, T. W.**
On-orbit cryogenic fluid transfer research at NASA Lewis Research Center p 45 A92-23847
- NYLAND, TED W.**
Liquid hydrogen mass flow through a multiple orifice Joule-Thomson device [AIAA PAPER 92-2881] p 176 A92-47862
Hydrogen no-vent testing in a 5 cubic foot (142 liter) tank using spray nozzle and spray bar liquid injection [AIAA PAPER 92-3063] p 63 A92-48719
Hydrogen no-vent fill testing in a 1.2 cubic foot (34 liter) tank [NASA-TM-105273] p 185 N92-13401
Liquid hydrogen mass flow through a multiple orifice Joule-Thomson device [NASA-TM-105583] p 189 N92-23268
Hydrogen no-vent fill testing in a 5 cubic foot (142 liter) tank using spray nozzle and spray bar liquid injection [NASA-TM-105759] p 136 N92-28433
- O**
- O'DONNELL, PATRICIA M.**
Space batteries for mobile battlefield power applications p 231 A92-29679
- O'HARA, K. J.**
Rocket engine propulsion system reliability [AIAA PAPER 92-3421] p 66 A92-48980
- O'MALLEY, TERENCE F.**
Early use of Space Station Freedom for NASA's Microgravity Science and Applications Program [IAF PAPER 92-0702] p 138 A92-57131
- O'NEILL, M. J.**
A high-performance photovoltaic concentrator array - The mini-dome Fresnel lens concentrator with 30 percent efficient GaAs/GaSb tandem cells p 72 A92-53199
- O'NEILL, MARK J.**
The mini-dome Fresnel lens photovoltaic concentrator array - Current program status p 70 A92-50648
- OKES, D.**
Fast oxygen atom facility for studies related to low earth orbit activities [AIAA PAPER 92-3974] p 47 A92-56800
- OBERLE, LAWRENCE G.**
An optical method for determining level in two-phase cryogenic fluids [NASA-TM-104524] p 200 N92-15366
- OCHSLE, V. L.**
A parametric numerical study of mixing in a cylindrical duct [AIAA PAPER 92-3088] p 177 A92-48733
A parametric numerical study of mixing in a cylindrical duct [NASA-TM-105695] p 35 N92-26553
- OGBUJI, LINUS U. J. T.**
Precautions toward XTEM of Si₃N₄/SiO₂ p 125 A92-33930
- OHTANI, RYUICHI**
Stochastic modeling of crack initiation and short-crack growth under creep and creep-fatigue conditions [ASME PAPER 92-APM-5] p 223 A92-44681
- OKIISHI, T. H.**
An experimental investigation of the flow in a diffusing S-duct [AIAA PAPER 92-3622] p 13 A92-54090
- OLDENBURG, J. R.**
Performance of the Phase Doppler Particle Analyzer icing cloud droplet sizing probe in the NASA Lewis Icing Research Tunnel [AIAA PAPER 92-0162] p 198 A92-26926
- OLESON, STEVE**
Space transfer with ground-based laser/electric propulsion [AIAA PAPER 92-3213] p 73 A92-54017
- OLIVER, ANGELA C.**
Test and evaluation of load converter topologies used in the Space Station Freedom power management and distribution dc test bed p 158 A92-50662
- OLIVER, B. F.**
Compressive strength of directionally solidified NiAl-NiAlNb intermetallics at 1200 and 1300 K p 117 A92-28248
- OLIVER, BEN F.**
Solidification processing of intermetallic Nb-Al alloys p 120 A92-33866
- OLLE, RAYMOND**
Ion Beam Textured and Coated Surfaces Experiment (IBEX) p 132 N92-24832
- OLLE, RAYMOND M.**
Low earth orbit durability evaluation of Haynes 188 solar receiver material [AIAA PAPER 92-0850] p 117 A92-29616
Atomic oxygen effects on SiO(x) coated Kapton for photovoltaic arrays in low earth orbit p 72 A92-53211
Durability evaluation of photovoltaic blanket materials exposed on LDEF tray S1003 p 132 N92-27100
- OLMSTEAD, DEAN A.**
Advanced Communications Technology Satellite (ACTS) Experiments Program - A market-driven approach to government/industry cooperation [AIAA PAPER 92-2036] p 145 A92-29951
- OLSON, SANDRA L.**
Opposed flow flame spread in normal, enhanced and reduced gravity p 111 A92-12898
- ORIENT, G.**
A probabilistic approach to the evaluation of fatigue damage in a space propulsion system injector element [AIAA PAPER 92-2413] p 60 A92-34343
- ORON, ALEXANDER**
Stable localized patterns in thin liquid films p 173 A92-37489
Stable localized patterns in thin liquid films [NASA-TM-105352] p 185 N92-14322
- OSTERWALD, C. R.**
Modeled performance of monolithic, 3-terminal InP/Ga(0.47)In(0.53)As concentrator solar cells as a function of temperature and concentration ratio p 234 A92-53153
InP concentrator solar cells p 234 A92-53166
- OSTRACH, S.**
An experimental study of oscillatory thermocapillary convection in cylindrical containers p 172 A92-36184
- OSTRACH, SIMON**
Nature of buoyancy-driven flows in a reduced-gravity environment p 175 A92-45844
Scaling of low-Prandtl-number thermocapillary flows p 176 A92-47271
- OSWALD, FRED B.**
Modal simulation of gearbox vibration with experimental correlation [AIAA PAPER 92-3494] p 207 A92-54036
Contact stresses in meshing spur gear teeth: Use of an incremental finite element procedure [NASA-TM-105388] p 209 N92-23536
A basis for solid modeling of gear teeth with application in design and manufacture [NASA-TM-105392] p 209 N92-24202
A comparison between theoretical prediction and experimental measurement of the dynamic behavior of spur gears [NASA-TM-105362] p 210 N92-25347
Comparison of analysis and experiment for gearbox noise [NASA-TM-105330] p 210 N92-25396
Effect of contact ratio on spur gear dynamic load [NASA-TM-105606] p 210 N92-25447
Effect of operating conditions on gearbox noise [NASA-TM-105331] p 211 N92-26107
- Analysis and modification of a single-mesh gear fatigue rig for use in diagnostic studies [NASA-TM-105416] p 212 N92-27879
Validation of finite element and boundary element methods for predicting structural vibration and radiated noise [NASA-TM-105359] p 213 N92-29697
Modal simulation of gearbox vibration with experimental correlation [NASA-TM-105702] p 215 N92-31485
- OTHMER, P.**
Delonation duct gas generator demonstration program [AIAA PAPER 92-3174] p 27 A92-54011
- OUZTS, PETER J.**
Integrated flight/propulsion control design for a STOVL aircraft using H-infinity control design techniques p 39 A92-29093
IMPAC - An integrated methodology for propulsion and airframe control p 39 A92-29118
- OVERTON, E.**
Electrical properties of teflon and ceramic capacitors at high temperatures [NASA-TM-105569] p 160 N92-20040
High temperature dielectric properties of Apical, Kapton, Peek, Teflon AF, and Uplex polymers [NASA-TM-105753] p 162 N92-28675
- OVERTON, ERIC**
The 23 to 300 C demagnetization resistance of samarium-cobalt permanent magnets [NASA-TP-3119] p 159 N92-11252
- OWEN, ALBERT K.**
A comparison of predicted and measured inlet distortion flows in a subsonic axial inlet flow compressor rotor [NASA-TM-105427] p 19 N92-26104
- P**
- PAI, SHANTARAM S.**
Nonuniform thermal environmental effects on space truss structural reliability [AIAA PAPER 92-2352] p 54 A92-34325
Probabilistic progressive buckling of trusses [AIAA PAPER 91-0916] p 223 A92-38142
Probabilistic progressive buckling of trusses [NASA-TM-105162] p 226 N92-15403
Probabilistic structural analysis of adaptive/smart/intelligent space structures [NASA-TM-105408] p 227 N92-22267
Probabilistic assessment of space trusses subjected to combined mechanical and thermal loads [NASA-TM-105429] p 230 N92-33935
- PALASZEWSKI, BRYAN A.**
Upper stages using liquid propulsion and metallized propellants [NASA-TP-3191] p 83 N92-17151
Metallized gelled monopropellants [NASA-TM-105418] p 87 N92-24557
- PALAZZOLO, A. B.**
Electromechanical simulation and testing of actively controlled rotordynamic systems with piezoelectric actuators [ASME PAPER 91-GT-245] p 203 A92-15650
Electromechanical simulation and testing of actively controlled rotordynamic systems with piezoelectric actuators p 204 A92-39258
- PALKO, JOSEPH L.**
Structural reliability analysis of laminated CMC components [ASME PAPER 91-GT-210] p 99 A92-15630
Analysis of whisker-toughened CMC structural components using an interactive reliability model [AIAA PAPER 92-2490] p 221 A92-34582
- PALMER, L. C.**
20/30 GHz satellite personal communications networks [AIAA PAPER 92-1908] p 143 A92-29839
A personal communications network using a Ka-band satellite p 151 N92-30934
- PALMER, LARRY**
Operational uses of ACTS technology [AIAA PAPER 92-1964] p 144 A92-29887
- PALMER, LARRY C.**
A personal communications network using a Ka-band satellite p 145 A92-31780
- PALMER, R. W.**
A low-power, high-efficiency Ka-band TWTA p 156 A92-38163
- PALMER, RAYMOND W.**
A low-power, high-efficiency Ka-band TWTA [AIAA PAPER 92-1822] p 154 A92-29769
COSP - A computer model of cyclic oxidation p 114 A92-31849

PAMULAPATI, J.

PAMULAPATI, J.

Study of InGaAs-based modulation doped field effect transistor structures using variable-angle spectroscopic ellipsometry p 265 N92-32977

PANDA, J.

Experimental investigation of the flowfield of an oscillating airfoil [AIAA PAPER 92-2622] p 9 A92-45494

Experimental investigation of the flowfield of an oscillating airfoil [NASA-TM-105675] p 20 N92-30182

PANIGRAHI, N.

Fatigue damage accumulation in nickel prior to crack initiation p 120 A92-33947

PAO, C. K.

V-band pseudomorphic HEMT MMIC phased array components for space communications p 151 N92-32966

PAPADOPOULOS, D. S.

Effect of contact stresses in four-point bend testing of graphite/epoxy and graphite/PMR-15 composite beams p 219 A92-33589

PAPELL, S. S.

Liquid hydrogen mass flow through a multiple orifice Joule-Thomson device [AIAA PAPER 92-2881] p 176 A92-47862

PAPELL, S. STEPHEN

Liquid hydrogen mass flow through a multiple orifice Joule-Thomson device [NASA-TM-105583] p 189 N92-23268

PARK, K. C.

An unconditionally stable staggered algorithm for transient finite element analysis of coupled thermoelastic problems p 222 A92-37517

PARKES, JAMES E.

Test facilities for high power electric propulsion [NASA-TM-105247] p 80 N92-11136

Multimegawatt MPD thruster design considerations [NASA-TM-105405] p 83 N92-16024

PARTHASARATHY, ARVIND

Temperature dependence of the electrode kinetics of oxygen reduction at the platinum/Nafion interface - A microelectrode investigation p 115 A92-56950

PASCHAL, WILLIAM

Design and analysis of reengine Boeing 727-100 center inlet S duct by a reduced Navier-Stokes code [AIAA PAPER 92-1221] p 8 A92-33320

PASCHAL, WILLIAM A.

A study on vortex flow control of inlet distortion in the re-engine 727-100 center inlet duct using computational fluid dynamics [AIAA PAPER 92-0152] p 4 A92-23767

A study on vortex flow control on inlet distortion in the re-engine 727-100 center inlet duct using computational fluid dynamics [NASA-TM-105321] p 14 N92-13998

PATAG, ALFREDO E.

Modeling of impulsive propellant reorientation p 59 A92-17187

Pulsed thrust propellant reorientation - Concept and modeling p 62 A92-44507

PATHARE, V. M.

Slow strain rate 1200-1400 K compressive properties of NiAl-1Hf p 116 A92-17977

PATNAIK, S. N.

Singularities in optimal structural design [NASA-TM-4365] p 228 N92-23527

PATNAIK, SURYA N.

Improved accuracy for finite element structural analysis via a new integrated force method [NASA-TP-3204] p 227 N92-22227

PATTERSON, MICHAEL J.

The evolutionary development of high specific impulse electric thruster technology [AIAA PAPER 92-1556] p 61 A92-38650

Krypton ion thruster performance [AIAA PAPER 92-3144] p 64 A92-48772

Development of arcjet and ion propulsion for spacecraft stationkeeping [IAF PAPER 92-0607] p 77 A92-57058

Neutralizer optimization [NASA-TM-105578] p 86 N92-21976

Deraled ion thruster design issues [NASA-TM-105576] p 87 N92-23534

The evolutionary development of high specific impulse electric thruster technology [NASA-TM-105712] p 92 N92-31342

Krypton ion thruster performance [NASA-TM-105818] p 92 N92-31901

Low-lsp deraled ion thruster operation [NASA-TM-105787] p 92 N92-32237

The evolutionary development of high specific impulse electric thruster technology [NASA-TM-105758] p 93 N92-33064

PATTERSON, RICHARD L.

Balancing reliability and cost to choose the best power subsystem p 216 A92-50625

Fiber-optic sensors for aerospace electrical measurements - An update p 200 A92-50630

PAULICK, MICHAEL J.

Color image processing and object tracking workstation [NASA-TM-105561] p 139 N92-26611

PAVLI, ALBERT J.

Advanced tube-bundle rocket thrust chambers p 62 A92-44509

PAWLAS, GARY E.

Numerical modeling of fluid and electromagnetic phenomena in an arcjet [AIAA PAPER 92-3106] p 258 A92-48747

PAXSON, DANIEL E.

A demonstration of an intelligent control system for a reusable rocket engine [NASA-TM-105794] p 92 N92-31507

PAXSON, DANIEL W.

A general numerical model for wave rotor analysis [NASA-TM-105740] p 196 N92-31484

PEASE, DOUGLAS M.

X ray based displacement measurement for hostile environments [NASA-TM-105551] p 202 N92-23155

PEECOOK, KEITH M.

NASA's nuclear thermal propulsion technology project [AIAA PAPER 92-3581] p 75 A92-54062

PELACCIO, D.

Engine system assessment study using Martian propellants [AIAA PAPER 92-3446] p 73 A92-54030

PELACCIO, DENNIS G.

Nuclear thermal rockets - Key to moon-Mars exploration p 63 A92-48385

PENCIL, ERIC J.

Dependence of hydrogen arcjet operation on electrode geometry [AIAA PAPER 92-3530] p 74 A92-54039

Development of arcjet and ion propulsion for spacecraft stationkeeping [IAF PAPER 92-0607] p 77 A92-57058

Dependence of hydrogen arcjet operation on electrode geometry [NASA-TM-105855] p 93 N92-34113

PENG, XIAOHANG

Further study of the effect of the downstream plasma condition on accelerator grid erosion in an ion thruster [AIAA PAPER 92-3829] p 76 A92-54192

PENKO, PAUL F.

Internal structure of shock waves in disparate mass mixtures [AIAA PAPER 92-0496] p 169 A92-28195

FDDO and DSMC analyses of rarefied gas flow through 2D nozzles [AIAA PAPER 92-2858] p 176 A92-47841

DSMC analysis of species separation in rarefied nozzle flows [AIAA PAPER 92-2859] p 176 A92-47842

Numerical modeling of fluid and electromagnetic phenomena in an arcjet [AIAA PAPER 92-3106] p 258 A92-48747

Measurement and analysis of a small nozzle plume in vacuum [AIAA PAPER 92-3108] p 64 A92-48748

Experimental and numerical investigations of low-density nozzle and plume flows of nitrogen p 183 A92-54917

PEPPER, STEPHEN V.

A vacuum (10(exp -9) Torr) friction apparatus for determining friction and endurance life of MoSx films [NASA-TM-104478] p 129 N92-16129

Properties data for opening the Galileo's partially unfurled main antenna [NASA-TM-105355] p 130 N92-20660

An XPS study of the stability of Fomblin Z25 on the native oxide of aluminum [NASA-TM-105594] p 131 N92-23185

PEPPING, RICHARD E.

A dynamic isotope power system portable generator for the moon or Mars p 232 A92-50634

PEREZ-DAVIS, MARLA E.

Sensible heat receiver for solar dynamic space power system p 180 A92-50570

Effects of windblown dust on photovoltaic surfaces on Mars p 45 A92-50573

Effect of particle size of Martian dust on the degradation of photovoltaic cell performance [NASA-TM-105232] p 79 N92-11133

Thermochemical energy storage for a lunar base [NASA-TM-105333] p 236 N92-14485

PERL, T. D.

New techniques for exciting linearly tapered slot antennas with coplanar waveguide p 155 A92-34844

PERL, THOMAS D.

New coplanar waveguide feed network for 2 x 2 linearly tapered slot antenna subarray p 156 A92-45619

Multiple-access phased array antenna simulator for a digital beam forming system investigation [NASA-TM-105422] p 149 N92-17062

Nonplanar linearly tapered slot antenna with balanced microstrip feed [NASA-TM-105647] p 161 N92-23535

PERRY, W. D.

Observations of the freeze/thaw performance of lithium fluoride by motion picture photography p 180 A92-50751

PERUSEK, GAIL P.

Experimental performance of three design factors for ventral nozzles for SSTOVL aircraft [AIAA PAPER 92-3789] p 28 A92-54168

Use of an approximate similarity principle for the thermal scaling of a full-scale thrust augmenting ejector [AIAA PAPER 92-3792] p 28 A92-54171

Use of an approximate similarity principle for the thermal scaling of a full-scale thrust augmenting ejector [NASA-TM-105724] p 36 N92-26613

Experimental performance of three design factors for ventral nozzles for SSTOVL aircraft [NASA-TM-105697] p 37 N92-27669

PETERS, REX B.

Space acceleration measurement system triaxial sensor head error budget [NASA-TM-105300] p 57 N92-25134

PETERSEN, R. A.

The influence of higher harmonics on vortex pairing in an axisymmetric mixing layer p 175 A92-46251

PETERSEN, W. C.

Advanced large scale GaAs monolithic IF switch matrix subsystem [AIAA PAPER 92-1861] p 155 A92-29801

PETREFSKI, CHRIS

Sensible heat receiver for solar dynamic space power system p 180 A92-50570

PETRIK, E. J.

SCAILET - An intelligent assistant for satellite ground terminal operations [IAF PAPER 92-0552] p 245 A92-55855

PETRIK, EDWARD J.

An overview of Space Communication Artificial Intelligence for Link Evaluation Terminal (SCAILET) Project p 148 N92-14212

GTEX: An expert system for diagnosing faults in satellite ground stations p 148 N92-14215

FIDEX: An expert system for satellite diagnostics p 148 N92-14218

Intelligent fault isolation and diagnosis for communication satellite systems p 248 N92-23365

PHARR, G. M.

Comments on the paper 'Does the subgrain size influence the rate of creep?' p 260 A92-33946

PHARR, GEORGE M.

Effect of temperature on the formation of creep substructure in sodium chloride single crystals p 260 A92-25444

PHILIPP, WARREN H.

Method of making contamination-free ceramic bodies [NASA-CASE-LEW-14984-1] p 128 N92-16122

Guanidine based vehicle/binders for use with oxides, metals, and ceramics [NASA-CASE-LEW-15314-1] p 131 N92-23461

PHILLIPS, R.

Surface morphologies and photoluminescence of diamond films deposited in a hot filament reactor p 261 A92-42858

PHILLIPS, R. L.

Development and testing of a 180-volt dc electronic circuit breaker with a 335-ampere carry and 1200-ampere interrupt rating p 158 A92-50658

PHILLIPS, RUDY L.

The development of test beds to support the definition and evolution of the Space Station Freedom power system p 46 A92-50656

PICCOLO, ANTONIO

Design and analysis of reengine Boeing 727-100 center inlet S duct by a reduced Navier-Stokes code [AIAA PAPER 92-1221] p 8 A92-33320

Design and analysis of vortex generators on reengine Boeing 727-100QF center inlet S-duct by a reduced Navier-Stokes code [AIAA PAPER 92-2700] p 10 A92-45542

PICKETT, MARK T.

Flow quality studies of the NASA Lewis Research Center 8- by 6-foot supersonic/9- by 15-foot Low Speed Wind Tunnel [AIAA PAPER 92-3916] p 41 A92-56748

Flow quality studies of the NASA Lewis Research Center 8- by 6-foot supersonic/9- by 15-foot low speed wind tunnel [NASA-TM-105417] p 42 N92-28673

- PIERRE, CHRISTOPHE**
Aeroelastic modal characteristics of mistuned blade assemblies - Mode localization and loss of eigenstructure p 225 A92-54921
- PINDERA, MAREK-JERZY**
Effects of fiber and interfacial layer architectures on the thermoplastic response of metal matrix composites [NASA-TM-105802] p 110 N92-32234
- PINERO, L. R.**
Microwave beam power transmission at an arbitrary range [NASA-TM-105424] p 150 N92-19992
- PING, YU**
Time domain numerical calculations of unsteady vortical flows about a flat plate airfoil p 12 A92-50473
- PISZCZOR, M. F.**
A high-performance photovoltaic concentrator array - The mini-dome Fresnel lens concentrator with 30 percent efficient GaAs/GaSb tandem cells p 72 A92-53199
- PISZCZOR, MICHAEL F.**
The mini-dome Fresnel lens photovoltaic concentrator array - Current program status p 70 A92-50648
- PLACHTA, DAVID W.**
Benefits and technology readiness for using cryogenic instead of storable propellants for return mission from Moon p 136 N92-33343
- PLECITY, MARK S.**
Advanced Communications Technology Satellite (ACTS) p 53 A92-17780
- PLENCHNER, ROBERT M.**
Overview of the Beta II Two-Stage-To-Orbit vehicle design [NASA-TM-105298] p 48 N92-11034
- PLETCHER, RICHARD H.**
A numerical and experimental study of three-dimensional liquid sloshing in a rotating spherical container [AIAA PAPER 92-0829] p 170 A92-29597
- PLINE, A.**
An experimental study of oscillatory thermocapillary convection in cylindrical containers p 172 A92-36184
- POHLCHUCK, BOBBY**
Preliminary evaluation of adhesion strength measurement devices for ceramic/titanium matrix composite bonds [NASA-TM-105803] p 1 N92-31267
- POINSATTE, PHILIP E.**
Heat transfer measurements from a smooth NACA 0012 airfoil p 165 A92-20215
Roughness effects on heat transfer from a NACA 0012 airfoil p 166 A92-20217
- POIRIER, D. R.**
Vertical solidification of dendritic binary alloys p 261 A92-37562
- POLYAK, R.**
Application of Newton modified barrier method (NMBM) to structural optimization [AIAA PAPER 92-2498] p 220 A92-34555
- PONCHAK, GEORGE E.**
Analysis of shielded CPW discontinuities with air-bridges p 152 N92-32971
- POPPEL, GARY L.**
Fiber optic controls for aircraft engines - Issues and implications p 24 A92-46244
- PORDAL, H. S.**
Transient behavior of supersonic flow through inlets p 7 A92-28043
- PORRO, A. R.**
A laser-induced heat flux technique for convective heat transfer measurements in high speed flows p 200 A92-54318
- POTAPCZUK, M. G.**
Icing simulation: A survey of computer models and experimental facilities p 21 N92-21684
Simulation of iced wing aerodynamics p 21 N92-21686
- POTAPCZUK, MARK G.**
LEWICE/E - An Euler based ice accretion code [AIAA PAPER 92-0037] p 4 A92-25676
LEWICE/E: An Euler based ice accretion code [NASA-TM-105389] p 15 N92-14001
Experimental ice shape and performance characteristics for a multi-element airfoil in the NASA Lewis Icing Research Tunnel [NASA-TM-105380] p 17 N92-17347
- POUCH, JOHN J.**
Optical dispersion relations for 'diamondlike' carbon films p 262 A92-44533
- POVINELLI, L. A.**
Multigrad calculation of three-dimensional viscous cascade flows [NASA-TM-105257] p 249 N92-10345
- POVINELLI, LOUIS A.**
Navier-Stokes solution of transonic cascade flows using nonperiodic C-type grids p 8 A92-28523
- Optimal least-squares finite element method for elliptic problems [NASA-TM-105382] p 249 N92-15662
Introduction to the internal fluid mechanics research session p 188 N92-22522
Center for Modeling of Turbulence and Transition (CMOTT). Research briefs: 1990 [NASA-TM-105243] p 1 N92-23336
Workshop on Engineering Turbulence Modeling [NASA-CP-10088] p 191 N92-24514
Trends in aer propulsion research and their impact on engineering education p 38 N92-31172
- POWER, JOHN L.**
Microwave electrothermal propulsion for space p 63 A92-46049
- POWERS, LYNN M.**
Reliability analysis of structural ceramic components using a three-parameter Weibull distribution [NASA-TM-105370] p 129 N92-17060
- PRAKASH, A.**
Interfacial and gravitational convection in immiscible liquid layers [IAF PAPER 92-0907] p 184 A92-57286
- PRASAD, K. G.**
Three-dimensional boundary element thermal shape sensitivity analysis p 176 A92-47269
- PRASANNA, M. G.**
Maximum life spiral bevel reduction design [AIAA PAPER 92-3493] p 205 A92-49030
- PRAATT, DAVID T.**
Conical detonation waves - A comparison of theoretical and numerical results [AIAA PAPER 92-0348] p 167 A92-25792
- PRICE, K. M.**
Satellite delivery of B-ISDN services [AIAA PAPER 92-1831] p 142 A92-29777
Technology requirements for mesh VSAT applications [AIAA PAPER 92-1982] p 144 A92-29902
Technical and economic feasibility of integrated video service by satellite [AIAA PAPER 92-2054] p 145 A92-29966
- PRICE, KENT M.**
Distribution of space-gathered data [AIAA PAPER 92-1888] p 143 A92-29821
- PRIEM, RICHARD J.**
3D rocket combustor acoustics model [AIAA PAPER 92-3226] p 66 A92-48829
The 3D rocket combustor acoustics model [NASA-TM-105734] p 88 N92-27035
- PROBST, HUBERT B.**
COSF - A computer model of cyclic oxidation p 114 A92-31849
- PROCTOR, M.**
Design and test of an oxygen turbopump for a dual expander cycle rocket engine p 59 A92-21062
- PROCTOR, M. P.**
Development of advanced seals for space propulsion turbomachinery [NASA-TM-105659] p 87 N92-24957
- PRUSSING, JOHN E.**
Simple proof of the global optimality of the Hohmann transfer p 44 A92-46760
- PRZEKWAS, A. J.**
A finite-volume numerical method to calculate fluid forces and rotodynamic coefficients in seals [AIAA PAPER 92-3712] p 183 A92-54132
- PUGH, EVAN R.**
Laser-driven hypersonic air-breathing propulsion simulator [AIAA PAPER 92-3922] p 41 A92-56753
- PUTERBAUGH, STEVEN L.**
A critical evaluation of a three-dimensional Navier-Stokes method as a tool to calculate transonic flows inside a low-aspect-ratio compressor p 195 N92-27459
- QUENTMEYER, RICHARD J.**
An experimental investigation of high-aspect-ratio cooling passages [AIAA PAPER 92-3154] p 64 A92-48780
An experimental investigation of high-aspect-ratio cooling passages [NASA-TM-105679] p 48 N92-25958
- QUINN, ROGER D.**
Pointing and tracking control for Freedom's Solar Dynamic modules and vibration control of Freedom [AAS PAPER 91-459] p 54 A92-43284
Solar dynamic modules for Space Station Freedom: The relationship between fine-pointing control and thermal loading of the aperture plate [NASA-TM-104498] p 84 N92-19780
- QUINN, TODD M.**
Autonomous Power System intelligent diagnosis and control p 247 A92-50532
- QUINTANA, J. A.**
Destination directed packet switch architecture for a geostationary communication satellite network [IAF PAPER 92-0413] p 50 A92-55793

R

- RABINOWITZ, MARTIN J.**
Optimization and analysis of large chemical kinetic mechanisms using the solution mapping method - Combustion of methane p 113 A92-19300
- RADENS, CARL J.**
Length minimization design considerations in photonic integrated circuits incorporating directional couplers p 256 A92-46240
- RADHAKRISHNAN, K.**
Combustion kinetics and sensitivity analysis computations p 112 A92-16981
- RAFFOUL, G.**
A high temperature superconductivity communications flight experiment [IAF PAPER 92-0410] p 50 A92-55790
- RAHMAT-SAMII, Y.**
Experimental code verification results for reflector antenna distortion compensation by array feeds [AIAA PAPER 92-2014] p 49 A92-29933
- RAI, A. K.**
Synthesis and characterization of fine grain diamond films p 262 A92-46330
- RAITT, W. J.**
Reactive collision terms for fluid transport theory p 257 A92-22693
- RAJ, S. V.**
Slow strain rate 1200-1400 K compressive properties of NiAl-1Hf p 116 A92-17977
Stress versus temperature dependence of activation energies for creep p 217 A92-24719
Flow and fracture behavior of NiAl in relation to the brittle-to-ductile transition temperature p 118 A92-30781
The mechanical properties of a Ni-30Al-20Fe-0.05Zr intermetallic alloy in the temperature range 300-1200 K p 118 A92-30793
Comments on the paper 'Does the subgrain size influence the rate of creep?' p 260 A92-33946
Correlation of deformation mechanisms with the tensile and compressive behavior of NiAl and NiAl(Zr) intermetallic alloys p 120 A92-38019
Fracture behavior of a B2 Ni-30Al-20Fe-0.05Zr intermetallic alloy in the temperature range 300 to 1300 K p 121 A92-41667
Deformation behavior of a Ni-30Al-20Fe-0.05Zr intermetallic alloy in the temperature range 300 to 1300 K p 121 A92-41668
Three-dimensional deformation analysis of two-phase dislocation substructures p 121 A92-44218
Influence of processing on the microstructure and mechanical properties of a NbAl3-base alloy p 122 A92-48152
- RAJ, SAI V.**
Effect of temperature on the formation of creep substructure in sodium chloride single crystals p 260 A92-25444
- RAJAGOPAL, K. R.**
A probabilistic approach to the evaluation of fatigue damage in a space propulsion system injector element [AIAA PAPER 92-2413] p 60 A92-34343
- RAMAN, GANESH**
Naturally occurring and forced azimuthal modes in a turbulent jet p 172 A92-35998
Control of an axisymmetric turbulent jet by multi-modal excitation p 174 A92-40071
The flip flop nozzle extended to supersonic flows [AIAA PAPER 92-2724] p 10 A92-45561
The flip-flop nozzle extended to supersonic flows [NASA-TM-105570] p 18 N92-23269
- RAMSEY, JOHN**
Experimental unsteady pressures on an oscillating cascade with supersonic leading edge locus [AIAA PAPER 92-4035] p 14 A92-56857
- RANDALL, LAURA A.**
Advanced Communications Technology Satellite (ACTS) Experiments Program - A market-driven approach to government/industry cooperation [AIAA PAPER 92-2036] p 145 A92-29951
- RANKIN, TOM R.**
Using EPSAT to analyze high power systems in the space environment p 158 A92-50580
- RAO, D. K.**
Magnetic bearings for free-piston Stirling engines [NASA-TM-105730] p 214 N92-30734

RAPP, DOUGLAS C.

- RAPP, DOUGLAS C.**
Metalized gelled monopropellants
[NASA-TM-105418] p 87 N92-24557
- RAPP, ROBERT A.**
Volatile species in halide-activated-diffusion coating packs p 122 A92-57028
- RAQUET, C.**
Ka-band MMIC arrays for ACTS Aero Terminal Experiment
[IAF PAPER 92-0398] p 159 A92-55785
- RAQUET, CHARLES**
Ka-band active MMIC subarray development
[AIAA PAPER 92-1863] p 155 A92-29803
- RAQUET, CHARLES A.**
ACTS aeronautical experiments
[AIAA PAPER 92-2042] p 50 A92-29956
- RASHIDI, MAJID**
Design of a hydraulic actuator for active control of rotating machinery
[ASME PAPER 91-GT-246] p 203 A92-15651
Dynamics of a split torque helicopter transmission
[NASA-TM-105681] p 213 N92-29136
- RAUCH, J. S.**
Comparative survey of dynamic analyses of free-piston Stirling engines p 206 A92-50793
- RAUCH, JEFFREY S.**
A free-piston Stirling engine/linear alternator controls and load interaction test facility
[NASA-TM-105825] p 238 N92-31262
- RAWLIN, VINCENT K.**
The evolutionary development of high specific impulse electric thruster technology
[AIAA PAPER 92-1556] p 61 A92-38650
Characterization of ion accelerating systems on NASA LeRC's ion thrusters
[AIAA PAPER 92-3827] p 76 A92-54191
Development of arcjet and ion propulsion for spacecraft stationkeeping
[IAF PAPER 92-0607] p 77 A92-57058
Derated ion thruster design issues
[NASA-TM-105576] p 87 N92-23534
The evolutionary development of high specific impulse electric thruster technology
[NASA-TM-105712] p 92 N92-31342
The evolutionary development of high specific impulse electric thruster technology
[NASA-TM-105758] p 93 N92-33064
- RAY, A.**
Life extending control for rocket engines
[NASA-TM-105789] p 142 N92-31263
- RAY, RANJAN**
Does a threshold stress for creep exist in HfC-dispersed NiAl? p 118 A92-30780
- REAGAN, JOHN**
Composite overwrapped nickel-hydrogen pressure vessels p 109 N92-22762
- REBBECCHI, BRIAN**
A comparison between theoretical prediction and experimental measurement of the dynamic behavior of spur gears
[NASA-TM-105362] p 210 N92-25347
- REDDY, D. R.**
Three-dimensional viscous analysis of a Mach 5 inlet and comparison with experimental data p 8 A92-28526
- REDDY, E. S.**
Mixed-mode fracture in unidirectional graphite epoxy composite laminates with central notch p 218 A92-29464
Analysis of aircraft engine blade subject to ice impact
[NASA-TM-105336] p 226 N92-15402
- REDDY, T. S. R.**
Euler flow predictions for an oscillating cascade using a high resolution wave-split scheme p 3 A92-15623
[ASME PAPER 91-GT-198]
Aeroelastic analysis of advanced propellers using an efficient Euler solver p 7 A92-28194
[AIAA PAPER 92-0488]
Analysis of cascades using a two dimensional Euler aeroelastic solver p 26 A92-34598
[AIAA PAPER 92-2370]
A numerical classical flutter analysis of advanced propellers p 26 A92-35687
[AIAA PAPER 92-2118]
- REDINBO, ROBERT**
Fault tolerance in onboard processors - Protecting efficient FDM demultiplexers
[AIAA PAPER 92-1969] p 144 A92-29892
- REED, BRIAN D.**
Performance comparison of axisymmetric and three-dimensional hydrogen film coolant injection in a 110 N hydrogen/oxygen rocket p 73 A92-54027
[AIAA PAPER 92-3390]
Hydrogen/oxygen auxiliary propulsion technology
[NASA-TM-105249] p 85 N92-20522

- REEDER, M. F.**
Compressibility effects on large structures in free shear flows p 173 A92-39337
Effect of tabs on the evolution of an axisymmetric jet p 26 A92-40151
[AIAA PAPER 92-3548] p 12 A92-49063
Supersonic jet mixing enhancement by 'delta-tabs'
[NASA-TM-105664] p 18 N92-24958
- REEHORST, ANDREW**
Analysis of surface roughness generation in aircraft ice accretion
[AIAA PAPER 92-0298] p 169 A92-28187
- REEHORST, ANDREW L.**
Prediction of ice accretion on a swept NACA 0012 airfoil and comparisons to flight test results p 4 A92-25677
[AIAA PAPER 92-0043]
Prediction of ice accretion on a swept NACA 0012 airfoil and comparisons to flight test results
[NASA-TM-105368] p 16 N92-15968
- REGEL', LIIA L.**
Transport modes during crystal growth in a centrifuge p 138 A92-33835
- REGIER, FRANK A.**
The ACTS multibeam antenna p 146 A92-46046
The ACTS multibeam antenna
[NASA-TM-105645] p 52 N92-30383
- REICHERT, B. A.**
An experimental investigation of the flow in a diffusing S-duct p 13 A92-54090
[AIAA PAPER 92-3622]
Navier-Stokes analysis and experimental data comparison of compressible flow within ducts
[NASA-TM-105796] p 38 N92-30972
- REICHERT, BRUCE A.**
Navier-Stokes analysis and experimental data comparison of compressible flow in a diffusing S-duct
[AIAA PAPER 92-2699] p 10 A92-45541
Trends in aeropropulsion research and their impact on engineering education p 38 N92-31172
[NASA-TM-105682]
Navier-Stokes analysis and experimental data comparison of compressible flow in a diffusing S-duct
[NASA-TM-105683] p 38 N92-33746
- REID, LONNIE**
A viscous flow study of shock-boundary layer interaction, radial transport, and wake development in a transonic compressor p 2 A92-15539
[ASME PAPER 91-GT-69]
Turbomachinery p 32 N92-22524
- REID, MARGARET A.**
Impedances of Li/SO₂ cells retrieved from the Long Duration Exposure Facility (LDEF satellite) and comparison with cells stored terrestrially p 236 N92-13484
[NASA-TM-104526]
- REINHART, EDWARD E.**
Frequency allocations for a new satellite service - Digital audio broadcasting p 143 A92-29881
[AIAA PAPER 92-1957]
- REINHART, R. C.**
SCAILET - An intelligent assistant for satellite ground terminal operations p 245 A92-55855
[IAF PAPER 92-0552]
- REINHART, RICHARD C.**
A software control system for the ACTS high-burst-rate link evaluation terminal p 243 N92-16628
[NASA-TM-105207]
- REINMANN, J. J.**
Technical evaluation report, AGARD Fluid Dynamics Panel Symposium on Effects of Adverse Weather on Aerodynamics p 1 N92-10002
[NASA-TM-105192]
Icing simulation: A survey of computer models and experimental facilities p 21 N92-21684
- REINMANN, JOHN J.**
The NASA aircraft icing research program p 23 N92-22534
[AIAA PAPER 92-0488]
NASA's aircraft icing technology program
[NASA-TM-104518] p 17 N92-23105
- RENO, CHARLES J.**
Implementation of control point form of algebraic grid-generation technique p 248 A92-47058
- RESHOTKO, E.**
Experimental study of boundary layer transition on a heated flat plate p 172 A92-36022
Turbulent heat flux measurements in a transitional boundary layer
[NASA-TM-105623] p 19 N92-27377
- RESHOTKO, ELI**
Naturally occurring and forced azimuthal modes in a turbulent jet p 172 A92-35998
Control of an axisymmetric turbulent jet by multi-modal excitation p 174 A92-40071

- REVIERE, R.**
Compressive strength of directionally solidified NiAl-NiAlNb intermetallics at 1200 and 1300 K p 117 A92-28248
- REYNOLDS, ROBERT S.**
Studies of the effects of curvature on dilution jet mixing p 166 A92-21079
- RHODES, JAMES A.**
Internal reversing flow in a tailpipe offtake configuration for SSTOVL aircraft p 28 A92-54169
[AIAA PAPER 92-3790]
Computational and experimental investigation of subsonic internal reversing flows p 183 A92-54170
[AIAA PAPER 92-3791]
Internal reversing flow in a tailpipe offtake configuration for SSTOVL aircraft p 37 N92-28418
[NASA-TM-105698]
- RHOMÉ, ROBERT C.**
Early use of Space Station Freedom for NASA's Microgravity Science and Applications Program
[IAF PAPER 92-0702] p 138 A92-57131
- RICE, E. J.**
On the mechanism of turbulence suppression in free shear flows under acoustic excitation p 252 A92-25678
[AIAA PAPER 92-0065]
Screesh noise source structure of a supersonic rectangular jet p 6 A92-26932
[AIAA PAPER 92-0503]
Modern developments in shear flow control with swirl p 9 A92-41265
Screesh noise source structure of a supersonic rectangular jet p 15 N92-14000
[NASA-TM-105384]
On the mechanism of turbulence suppression in free shear flows under acoustic excitation p 15 N92-14003
[NASA-TM-105360]
- RICE, EDWARD J.**
Naturally occurring and forced azimuthal modes in a turbulent jet p 172 A92-35998
Control of an axisymmetric turbulent jet by multi-modal excitation p 174 A92-40071
The flip flop nozzle extended to supersonic flows
[AIAA PAPER 92-2724] p 10 A92-45561
Turbomachinery noise p 253 N92-10601
Computer program for Bessel and Hankel functions
[NASA-TM-105154] p 243 N92-11691
Inlets, ducts, and nozzles p 188 N92-22523
The flip-flop nozzle extended to supersonic flows
[NASA-TM-105570] p 18 N92-23269
- RICE, J. P.**
Melting of the Abrikosov flux lattice in anisotropic superconductors p 260 A92-28075
- RICHARD, JACQUES C.**
Supersonic propulsion simulation by incorporating component models in the large perturbation inlet (LAPIN) computer code p 30 N92-15993
[NASA-TM-105193]
- RICHARD, M. A.**
Performance of a K-band superconducting annular ring antenna p 146 A92-37067
Performance of a four-element Ka-band high-temperature superconducting microstrip antenna p 146 A92-37224
Measurement techniques for cryogenic Ka-band microstrip antennas p 153 N92-32981
- RICHTER, G. P.**
Slush hydrogen (SLH2) technology development for application to the National Aerospace Plane (NASP) p 140 A92-13432
- RICHTER, SCOTT W.**
Technology development of fabrication techniques for advanced solar dynamic concentrators p 232 A92-50571
- RIDDLEBAUGH, STEPHEN M.**
Novel applications for TAZ-8A p 123 N92-22444
- RIGBY, D. L.**
Increased heat transfer to elliptical leading edges due to spanwise variations in the freestream momentum - Numerical and experimental results p 13 A92-54005
[AIAA PAPER 92-3070]
- RIGNEY, JOSEPH D.**
Fracture toughness and the effects of stress state on fracture of nickel aluminides p 117 A92-27422
- RIHA, D.**
Recent developments of the NESSUS probabilistic structural analysis computer program p 242 A92-34342
[AIAA PAPER 92-2411]
- RILEY, B. R.**
Kinetic theory model for the flow of a simple gas from a three-dimensional axisymmetric nozzle p 12 A92-52730
- RING, DARRYL S.**
Graphite/epoxy composite adapters for the Space Shuttle/Centaur vehicle p 49 N92-31251
[NASA-TP-3014]

- RINGER, MARK J.**
Autonomous Power System intelligent diagnosis and control p 247 A92-50532
- RITZERT, F. J.**
Thermomechanical and bithermal fatigue behavior of cast B1900 + Hf and wrought Haynes 188 p 122 A92-45233
- RIVAS, DAMIAN**
Scaling of low-Prandtl-number thermocapillary flows p 176 A92-47271
- RIVERA, JAMES M.**
Structural durability of stiffened composite shells [AIAA PAPER 92-2244] p 220 A92-34569
- RIVERS, JAMES M.**
Structural durability of stiffened composite shells [NASA-CR-190588] p 229 N92-29342
- ROACH, ROBERT L.**
A fast, uncoupled, compressible, two-dimensional, unsteady boundary layer algorithm with separation for engine inlets [AIAA PAPER 92-3082] p 11 A92-48729
A fast, uncoupled, compressible, two-dimensional, unsteady boundary layer algorithm with separation for engine inlets [NASA-TM-105686] p 195 N92-27653
- ROAN, V. P.**
Initial development of the axisymmetric ejector shear layer [AIAA PAPER 92-3567] p 178 A92-49068
- ROBAIDEK, JERROLD O.**
Viscoelastic properties of addition-cured polyimides used in high temperature polymer matrix composites p 124 A92-32632
- ROBERTS, G. D.**
Effect of contact stresses in four-point bend testing of graphite/epoxy and graphite/PMR-15 composite beams p 219 A92-33589
- ROBERTS, GARY D.**
Viscoelastic properties of addition-cured polyimides used in high temperature polymer matrix composites p 124 A92-32632
- ROBINSON, D.**
Reconfigurable optical interconnection network for multimode optical fiber sensor arrays p 256 A92-37448
- ROBINSON, DAVID N.**
Thermomechanical deformation behavior of a dynamic strain aging alloy, Hastelloy X [NASA-TM-105316] p 228 N92-25179
- ROCHE, JAMES C.**
Using EPSAT to analyze high power systems in the space environment p 158 A92-50580
- ROCHE, JOSEPH M.**
Collapse analysis of a waffle plate strongback for Space Station Freedom [NASA-TM-105412] p 227 N92-20045
- ROCK, STEPHEN M.**
Integrated flight/propulsion control specifications for systems with two-way coupling p 39 A92-29117
- RODGERS, FREDERICK C.**
Metallized gelled monopropellants [NASA-TM-105418] p 87 N92-24557
- RODRIGUEZ, C. D.**
SEI power source alternatives for rovers and other multi-kWe distributed surface applications p 80 N92-13206
- RODRIGUEZ, CARLOS D.**
SP-100 reactor with Brayton conversion for lunar surface applications [NASA-TM-105637] p 92 N92-32108
- RODRIGUEZ, ELVIN**
Synergistic effects of ultraviolet radiation, thermal cycling and atomic oxygen on altered and coated Kapton surfaces [AIAA PAPER 92-0794] p 93 A92-27125
Synergistic effects of ultraviolet radiation, thermal cycling, and atomic oxygen on altered and coated Kapton surfaces [NASA-TM-105363] p 96 N92-14114
- ROELKE, R. J.**
Enhancing control of grid distribution in algebraic grid generation p 248 A92-52552
- ROHAL, R.**
Safety issues p 78 N92-11115
- ROHDE, JOHN**
Airbreathing combined cycle engine systems p 31 N92-21523
- ROHN, DOUGLAS**
A 23.2:1 ratio, 300-watt, 26 N-m output torque, planetary roller-gear robotic transmission: Design and evaluation p 210 N92-25085
- ROHN, DOUGLAS A.**
Reaction-compensation technology for microgravity laboratory robots p 203 A92-23719
- ROJAS, A.**
The isothermal dendritic growth experiment - A USMP-2 space flight experiment [AIAA PAPER 92-0350] p 137 A92-28188
- ROLANDELLI, D. L.**
Multikilowatt power electronics development for spacecraft p 68 A92-50541
- ROLLBUHLER, J.**
Factors influencing the effective spray cone angle of pressure-swirl atomizers p 166 A92-23300
- ROLLBUHLER, R. JAMES**
Safety considerations in testing a fuel-rich aeropropulsion gas generator [NASA-TM-105258] p 30 N92-17061
- ROMANOVSKY, R. R.**
Microwave conductivity of laser ablated YBa₂Cu₃O(7- δ) superconducting films and its relation to microstrip transmission line performance p 264 N92-21639
- ROMANOVSKY, ROBERT R.**
Monolithic mm-wave phase shifter using optically activated superconducting switches [NASA-CASE-LEW-14878-1] p 257 N92-28571
- RONCACE, ELIZABETH A.**
Propulsion systems using in situ propellants for a Mars Ascent Vehicle [AIAA PAPER 92-3445] p 66 A92-49001
Propulsion systems using in situ propellants for a Mars ascent vehicle [NASA-TM-105741] p 89 N92-27654
- ROSE, A. H.**
Fiber-optic sensors for aerospace electrical measurements - An update p 200 A92-50630
- ROSE, GAYLE E.**
Wind tunnel performance results of swirl recovery vanes as tested with an advanced high speed propeller [AIAA PAPER 92-3770] p 28 A92-54159
- ROSEN, ROBERT**
The future challenge for aeropropulsion [NASA-TM-105613] p 35 N92-25164
- ROSENBERG, S. D.**
Test experience, 490 N high performance (321 sec Isp) engine [AIAA PAPER 92-3800] p 67 A92-49127
- ROSENBERGER, FRANZ**
Vapor crystal growth technology development: Application to cadmium telluride [NASA-TM-103786] p 139 N92-16158
- ROSENFELD, DAVID**
A model for the trap-assisted tunneling mechanism in diffused n-p and implanted n(+)-p HgCdTe photodiodes p 156 A92-46007
- ROSENFELD, J. H.**
Alkali metal pool boiler life tests for a 25 kWe advanced Stirling conversion system p 206 A92-50797
Design of a pool boiler heat transport system for a 25 kWe advanced Stirling conversion system p 181 A92-50802
- ROSENTHAL, B. N.**
Adaptive temperature profile control of a multizone crystal growth furnace p 137 A92-29243
Identification and control of a multizone crystal growth furnace p 199 A92-39699
- ROSS, B. A.**
Final design of a free-piston hydraulic advanced Stirling conversion system p 206 A92-50798
- ROSS, BRAD A.**
Stirling machine operating experience p 206 A92-50788
- ROSS, HOWARD D.**
An investigation of flame spread over shallow liquid pools in microgravity and nonair environments p 112 A92-16609
- ROSTAFINSKI, W.**
Detonation duct gas generator demonstration program [AIAA PAPER 92-3174] p 27 A92-54011
- ROTH, D. J.**
Review and statistical analysis of the use of ultrasonic velocity for estimating the porosity fraction in polycrystalline materials p 215 A92-28722
- ROTH, DON J.**
Interfacing laboratory instruments to multiuser, virtual memory computers p 245 A92-13595
Ultrasonic evaluation of oxygen content, modulus, and microstructure changes in YBa₂Cu₃O(7-x) occurring during oxidation and reduction p 261 A92-38418
- ROTH, MARY ELLEN**
Resonant mode controllers for launch vehicle applications [NASA-TM-105563] p 48 N92-25092
An electromechanical actuation system for an expendable launch vehicle [NASA-TM-105774] p 48 N92-30310
- ROUGE, CARL J.**
Oxidation resistant coating for titanium alloys and titanium alloy matrix composites [NASA-CASE-LEW-15155-1] p 133 N92-29090
- RUAN, YEEFENG F.**
Modal simulation of gearbox vibration with experimental correlation [AIAA PAPER 92-3494] p 207 A92-54036
Modal simulation of gearbox vibration with experimental correlation [NASA-TM-105702] p 215 N92-31485
- RUBIN, S. G.**
Transient behavior of supersonic flow through inlets p 7 A92-28043
- RUBINSTEIN, ASHER A.**
Fracture resistance development in ceramic composites with nonlinear fiber pullout relationship [AIAA PAPER 92-2493] p 221 A92-34585
Micromechanical model of crack growth in fiber reinforced brittle materials p 223 A92-46829
- RUBINSTEIN, R.**
Renormalization group analysis of the Reynolds stress transport equation p 179 A92-49493
Renormalization group analysis of the Reynolds stress transport equation [NASA-TM-105588] p 190 N92-23542
- RUCKMAN, MARK W.**
Near-edge study of gold-substituted YBa₂Cu₃O(7- δ) p 259 A92-14950
- RUDOFF, R. C.**
Performance of the Phase Doppler Particle Analyzer icing cloud droplet sizing probe in the NASA Lewis Icing Research Tunnel [AIAA PAPER 92-0162] p 198 A92-26926
- RUIZ, C. A.**
Algorithms for real-time fault detection of the Space Shuttle Main Engine [AIAA PAPER 92-3167] p 215 A92-48789
- RUNYAN, L. JAMES**
Lewis icing research tunnel test of the aerodynamic effects of aircraft ground deicing/anti-icing fluids [NASA-TP-3238] p 22 N92-30395
- RUSSELL, L. M.**
Full field flow visualization and computer-aided velocity measurements in a bank of cylinders in a wind tunnel p 199 A92-50040
- RUTLEDGE, SHARON K.**
Low earth orbit durability evaluation of Haynes 188 solar receiver material [AIAA PAPER 92-0850] p 117 A92-29616
SiO(X) coatings for atomic oxygen protection of polyimide Kapton in low earth orbit [AIAA PAPER 92-2151] p 94 A92-31286
LDEF spacecraft, ground laboratory, and computational modeling implications on Space Station Freedom's solar array materials and surfaces durability p 71 A92-53190
Atomic oxygen effects on SiO(x) coated Kapton for photovoltaic arrays in low earth orbit p 72 A92-53211
Ion Beam Textured and Coated Surfaces Experiment (IBEX) p 132 N92-24832
Durability evaluation of photovoltaic blanket materials exposed on LDEF tray S1003 p 132 N92-27100
- RUYTEN, WILHELMUS M.**
Further study of the effect of the downstream plasma condition on accelerator grid erosion in an ion thruster [AIAA PAPER 92-3829] p 76 A92-54192
- RYALL, KATHLEEN**
A graphical user-interface for propulsion system analysis [NASA-TM-105696] p 244 N92-33894

S

SACKSTEDER, KURT

The NASA microgravity combustion space experiment program [IAF PAPER 91-398] p 112 A92-18484

SACKSTEDER, KURT R.

The implications of experimentally controlled gravitational accelerations for combustion science p 112 A92-16601

Risks, designs, and research for fire safety in spacecraft [NASA-TM-105317] p 240 N92-13581

SADLER, GERALD

Application of enhanced modern structured analysis techniques to Space Station Freedom electric power system requirements p 251 A92-50609

SAFF, CHARLES

Turning up the heat on aircraft structures p 23 A92-55131

SAGER, PAUL H.

- SAGER, PAUL H.**
Design considerations in clustering nuclear rocket engines
[AIAA PAPER 92-3587] p 66 A92-49069
- SAIYED, N. H.**
Description of liquid nitrogen experimental test facility
p 44 A92-23842
- SAIYED, NASEEM H.**
Liquid hydrogen mass flow through a multiple orifice Joule-Thomson device
[AIAA PAPER 92-2881] p 176 A92-47862
Description of Liquid Nitrogen Experimental Test Facility
[NASA-TM-105215] p 134 N92-11208
Liquid hydrogen mass flow through a multiple orifice Joule-Thomson device
[NASA-TM-105583] p 189 N92-23268
- SAKOWSKI, BARBARA**
A fast, uncoupled, compressible, two-dimensional, unsteady boundary layer algorithm with separation for engine inlets
[AIAA PAPER 92-3082] p 11 A92-48729
Interface of an uncoupled boundary layer algorithm with an inviscid core flow algorithm for unsteady supersonic engine inlets
[AIAA PAPER 92-3083] p 11 A92-48730
Interface of an uncoupled boundary layer algorithm with an inviscid core flow algorithm for unsteady supersonic engine inlets
[NASA-TM-105684] p 36 N92-27037
A fast, uncoupled, compressible, two-dimensional, unsteady boundary layer algorithm with separation for engine inlets
[NASA-TM-105686] p 195 N92-27653
- SALAS, MANUEL D.**
The NASA Computational Aerosciences Program - Toward teraFLOPS computing
[AIAA PAPER 92-0558] p 240 A92-26968
- SALEEB, A. F.**
On the development of explicit robust schemes for implementation of a class of hyperelastic models in large-strain analysis of rubbers p 221 A92-36245
On the thermodynamic framework of generalized coupled thermoelastic-viscoplastic-damage modeling
[NASA-TM-105349] p 225 N92-14434
Explicit robust schemes for implementation of a class of principal value-based constitutive models: Theoretical development
[NASA-TM-105345] p 227 N92-20212
- SALEM, J. A.**
Determination of the stress distributions in a ceramic, tensile specimen using numerical techniques p 216 A92-14546
Strength, toughness and R-curve behaviour of SiC whisker-reinforced composite Si3N4 with reference to monolithic Si3N4 p 101 A92-34202
Mechanical behaviour and failure phenomenon of an in situ toughened silicon nitride p 127 A92-54504
- SALEM, JONATHAN A.**
Reliability analysis of a structural ceramic combustion chamber
[ASME PAPER 91-GT-155] p 24 A92-15591
Estimation of crack closure stresses for in situ toughened silicon nitride with 8 wt pct scandia p 126 A92-43478
Elevated temperature mechanical behavior of monolithic and SiC whisker-reinforced silicon nitrides
[NASA-TM-105245] p 128 N92-15192
- SALHI, A.**
A first-principles model for orificed hollow cathode operation
[AIAA PAPER 92-3742] p 259 A92-54145
- SALISMAN, J. F.**
Application of a thermal fatigue life prediction model to high-temperature aerospace alloys B1900 + Hf and Haynes 188 p 121 A92-45232
- SAMANT, NIRANJAN R.**
Interfaces for high-speed fiber-optic links - Analysis and experiment p 256 A92-24002
- SAMANTA ROY, R. I.**
Theory of plasma contactor neutral gas emissions for electrodynamic tethers p 258 A92-41549
- SAMANTHA ROY, R. I.**
Systems analysis of electrodynamic tethers p 62 A92-41550
- SAMIMY, M.**
Compressibility effects on large structures in free shear flows p 173 A92-39337
Effect of tabs on the evolution of an axisymmetric jet p 26 A92-40151
Supersonic jet mixing enhancement by 'delta-tabs'
[AIAA PAPER 92-3548] p 12 A92-49063
Filtered Rayleigh scattering based measurements in compressible mixing layers p 182 A92-54043
Supersonic jet mixing enhancement by delta-tabs
[NASA-TM-105664] p 18 N92-24958

- SAMIMY, MO**
Study of compressible mixing layers using filtered Rayleigh scattering based visualizations p 183 A92-54937
- SAMUELSEN, G. S.**
Mixing in the dome region of a staged gas turbine combustor
[AIAA PAPER 92-3089] p 177 A92-48734
Jet mixing into a heated cross flow in a cylindrical duct: Influence of geometry and flow variations
[NASA-TM-105390] p 30 N92-15994
- SAMUELSON, G. S.**
Jet mixing into a heated cross flow in a cylindrical duct - Influence of geometry and flow variations
[AIAA PAPER 92-0773] p 168 A92-27110
- SANABRIA, RAFAEL**
A review of candidate multilayer insulation systems for potential use on wet-launched LH2 tankage for the space exploration initiative lunar missions
[NASA-TM-104493] p 134 N92-13336
- SANDERS, WILLIAM A.**
Monolithic ceramics p 125 A92-39854
Estimation of crack closure stresses for in situ toughened silicon nitride with 8 wt pct scandia p 126 A92-43478
Elevated temperature mechanical behavior of monolithic and SiC whisker-reinforced silicon nitrides
[NASA-TM-105245] p 128 N92-15192
Plasma etching a ceramic composite
[NASA-TM-105430] p 130 N92-22305
- SANFELIZ, JOSE G.**
Computational simulation of surface waviness in graphite/epoxy woven composites due to initial curing
[NASA-TM-105313] p 106 N92-14118
- SANKAR, L. N.**
Simulation of iced wing aerodynamics p 21 N92-21686
- SANKAR, LAKSHMI N.**
Numerical investigation of performance degradation of wings and rotors due to icing
[AIAA PAPER 92-0412] p 5 A92-26264
- SANKOVIC, JOHN M.**
Medium power hydrogen arcjet performance
[AIAA PAPER 91-2227] p 58 A92-15355
Dependence of hydrogen arcjet operation on electrode geometry
[AIAA PAPER 92-3530] p 74 A92-54039
Development of arcjet and ion propulsion for spacecraft stationkeeping
[IAF PAPER 92-0607] p 77 A92-57058
Hydrogen arcjet technology
[NASA-TM-105340] p 82 N92-15119
Dependence of hydrogen arcjet operation on electrode geometry
[NASA-TM-105855] p 93 N92-34113
- SANTIAGO, WALTER**
A free-piston Stirling engine/linear alternator controls and load interaction test facility
[NASA-TM-105825] p 238 N92-31262
- SANTORO, G. J.**
Growth and characterization of lead bromide crystals p 138 A92-56956
Effect of growth conditions on the quality of lead bromide crystals p 138 A92-56957
- SARAVANAN, N.**
Identification of the Space Shuttle Main Engine dynamic models from firing data
[AIAA PAPER 92-3317] p 73 A92-54022
- SARAVANOS, D. A.**
Multiobjective shape and material optimization of composite structures including damping p 218 A92-28055
- SARAVANOS, DIMITRIS A.**
Interphase layer optimization for metal matrix composites with fabrication considerations p 98 A92-10262
- SARMIENTO, CHARLES J.**
Medium power hydrogen arcjet performance
[AIAA PAPER 91-2227] p 58 A92-15355
Dependence of hydrogen arcjet operation on electrode geometry
[AIAA PAPER 92-3530] p 74 A92-54039
Hydrogen arcjet technology
[NASA-TM-105340] p 82 N92-15119
Arcjet nozzle area ratio effects
[NASA-TM-104477] p 83 N92-16022
Dependence of hydrogen arcjet operation on electrode geometry
[NASA-TM-105855] p 93 N92-34113
- SARTORI, MICHAEL A.**
An IIR medium hybrid filter p 246 A92-40375
- SARVER-VERHEY, TIMOTHY R.**
Extended testing of xenon ion thruster hollow cathodes
[AIAA PAPER 92-3204] p 65 A92-48811

- SAULE, ARTHUR V.**
Computer program for Bessel and Hankel functions
[NASA-TM-105154] p 243 N92-11691
- SAUNDERS, J. D.**
Results from computational analysis of a mixed compression supersonic inlet
[NASA-TM-104475] p 14 N92-10976
- SAUNDERS, NEAL T.**
Impact and promise of NASA aer propulsion technology p 31 N92-22511
- SAUS, J. R.**
Life extending control for rocket engines
[NASA-TM-105789] p 142 N92-31263
- SAVAGE, M.**
Transmission overhaul and component replacement predictions using Weibull and renewal theory p 215 A92-17201
Maximum life spiral bevel reduction design
[AIAA PAPER 92-3493] p 205 A92-49030
Optimal design of compact spur gear reductions
[NASA-TM-105676] p 213 N92-29351
- SAVILLE, D. A.**
Electrophoresis of small particles and fluid globules in weak electrolytes p 114 A92-33924
- SCAVUZZO, R. J.**
A combined analytical-experimental tensile test technique for brittle materials p 123 A92-23225
Tensile properties of impact ices
[AIAA PAPER 92-0883] p 94 A92-29644
- SCHACHAM, S. E.**
Temperature independent quantum well FET with delta channel doping p 157 A92-49596
Enhancement of Shubnikov-de Haas oscillations by carrier modulation p 262 A92-50911
Comparative evaluation of optical waveguides as alternative interconnections for high performance packaging p 153 N92-32974
Intermodulation in the oscillatory magnetoresistance of a two-dimensional electron gas p 163 N92-32975
Reduced mobility and PPC in In₂₀Ga₈₀As / Al₂₃Ga₇₇As HEMT structure p 265 N92-32976
- SCHIEL, C.**
Engine system assessment study using Martian propellants
[AIAA PAPER 92-3446] p 73 A92-54030
- SCHIEIMAN, DAVID**
Increased efficiency with surface texturing in ITO/InP solar cells p 232 A92-44548
- SCHIEIMAN, DAVID A.**
Advanced photovoltaic experiment, S0014: Preliminary flight results and post-flight findings p 237 N92-27101
- SCHERTLER, RONALD J.**
Advanced Communications Technology Satellite (ACTS) Experiments Program - A market-driven approach to government/industry cooperation
[AIAA PAPER 92-2036] p 145 A92-29951
Advanced Communications Technology Satellite (ACTS) p 50 A92-38164
Advanced Communications Technology Satellite (ACTS) p 50 A92-55788
[IAF PAPER 92-0407] p 50 A92-55788
- SCHUEER, JAY**
Preliminary investigation of power flow and electrode phenomena in a multi-megawatt coaxial plasma thruster
[AIAA PAPER 92-3741] p 75 A92-54144
- SCHIERMAN, JOHN D.**
A framework for the analysis of airframe/engine interactions and integrated flight/propulsion control p 39 A92-29120
Analysis of airframe/engine interactions for a STOVL aircraft with integrated flight/propulsion control
[AIAA PAPER 92-4623] p 23 A92-55300
- SCHIMKE, S.**
Analysis of iced wings
[AIAA PAPER 92-0416] p 8 A92-29972
Analysis of iced wings
[NASA-TM-105773] p 20 N92-34144
- SCHLEGELMILCH, R. F.**
SCAILET - An intelligent assistant for satellite ground terminal operations
[IAF PAPER 92-0552] p 245 A92-55855
- SCHLEGELMILCH, RICHARD F.**
An overview of Space Communication Official Intelligence for Link Evaluation Terminal (SCAILET) Project p 148 N92-14212
GTEX: An expert system for diagnosing faults in satellite ground stations p 148 N92-14215
- SCHLOSSER, HERBERT**
The analysis of high pressure experimental data p 266 A92-16101
Pressure dependence of the melting temperature of solids - Rare-gas solids p 171 A92-33912
- SCHLUMBERGER, S.**
A bulk flow model of a brush seal system
[ASME PAPER 91-GT-325] p 203 A92-15696

- SCHMIDT, DAVID K.**
A framework for the analysis of airframe/engine interactions and integrated flight/propulsion control
p 39 A92-29120
- SCHMIDT, FRED**
Characteristics of a future aeronautical satellite communications system
[AIAA PAPER 92-2058] p 22 A92-29889
Characteristics of a future aeronautical satellite communications system
p 151 N92-30932
- SCHMIDT, JAMES F.**
Design and performance of controlled-diffusion stator compared with original double-circular-arc stator
[NASA-TP-2852] p 34 A92-22863
- SCHMIDT, PHILLIP**
Decentralized hierarchical partitioning of centralized integrated controllers
p 39 A92-29119
A parameter optimization approach to controller partitioning for integrated flight/propulsion control application
[NASA-TM-105826] p 40 N92-32241
- SCHMITZ, P. C.**
Design of multihundred-watt dynamic isotope power system for robotic space missions
p 69 A92-50633
SEI power source alternatives for rovers and other multi-kWe distributed surface applications
p 80 N92-13206
- SCHMITZ, PAUL C.**
Preliminary design of a mobile lunar power supply
p 233 A92-50635
- SCHNEIDER, MICHAEL G.**
Critical technology experiment results for lightweight space heat receiver
p 180 A92-50568
- SCHNEIDER, S. J.**
Spectrally resolved Rayleigh scattering diagnostic for hydrogen-oxygen rocket plume studies
p 67 A92-50253
- SCHNEIDER, STEVEN J.**
High temperature thruster technology for spacecraft propulsion
[IAF PAPER 91-254] p 58 A92-13155
Low thrust chemical rocket technology
[IAF PAPER 92-0669] p 77 A92-57105
Extended temperature range rocket injector
[NASA-CASE-LEW-14846-1] p 77 N92-10054
High temperature thruster technology for spacecraft propulsion
[NASA-TM-105348] p 82 N92-15125
Hydrogen/oxygen auxiliary propulsion technology
[NASA-TM-105249] p 85 N92-20522
Advanced liquid rockets
[NASA-TM-105633] p 87 N92-24560
- SCHNEUR, R.**
Application of Newton modified barrier method (NMBM) to structural optimization
[AIAA PAPER 92-2498] p 220 A92-34555
- SCHOBEIRI, TAHER**
Aerodynamics and heat transfer investigations on a high Reynolds number turbine cascade
[ASME PAPER 91-GT-157] p 164 A92-15593
- SCHOBIERI, T.**
Row-by-row off-design performance calculation method for turbines
p 26 A92-44514
- SCHOENBERG, KURT F.**
Preliminary investigation of power flow and electrode phenomena in a multi-megawatt coaxial plasma thruster
[AIAA PAPER 92-3741] p 75 A92-54144
- SCHOENMAN, L.**
Test experience, 490 N high performance (321 sec lsp) engine
[AIAA PAPER 92-3800] p 67 A92-49127
- SCHRAGE, DEAN S.**
Thermal modeling of nickel-hydrogen battery cells operating under transient orbital conditions
p 71 A92-50712
- SCHRAMM, D. N.**
Monte Carlo exploration of Mikheyev-Smirnov-Wolfenstein solutions to the solar neutrino problem
p 270 A92-50927
- SCHRAMM, DAVID N.**
Fractals and cosmological large-scale structure
p 268 A92-37413
The diffuse gamma-ray background, light element abundances, and signatures of early massive star formation
p 268 A92-43837
Thick strings, the liquid crystal blue phase, and cosmological large-scale structure
p 268 A92-48103
- SCHREIBER, J. G.**
Design of multihundred-watt dynamic isotope power system for robotic space missions
p 69 A92-50633
- SCHREIBER, JEFFREY G.**
Status of the advanced Stirling conversion system project for 25 kW dish Stirling applications
p 207 A92-50804
- SCHREINER, KEN E.**
Resonant mode controllers for launch vehicle applications
[NASA-TM-105563] p 48 N92-25092
- SCHUNK, R. W.**
High voltage spheres in an unmagnetized plasma - Fluid and PIC simulations
p 258 A92-47936
- SCHWAB, JOHN R.**
The Proteus Navier-Stokes code
p 192 N92-25811
- SCHWARZE, G. E.**
Comparison of high temperature, high frequency core loss and dynamic B-H loops of two 50 Ni-Fe crystalline alloys and an iron-based amorphous alloy
p 157 A92-50551
Neutron, gamma ray, and temperature effects on the electrical characteristics of thyristors
[NASA-TM-105728] p 162 N92-28432
Comparison of high temperature, high frequency core loss and dynamic B-H loops of a 2V-49Fe-49Co and a grain oriented 3Si-Fe alloy
[NASA-TM-105791] p 162 N92-30397
- SCOTT, J. R.**
Time domain numerical calculations of unsteady vortical flows about a flat plate airfoil
p 12 A92-50473
- SCOTT, JAMES N.**
Acoustic analysis using numerical solutions of the Navier-Stokes equations
[AIAA PAPER 92-0506] p 253 A92-26934
- SEASHOLTZ, R. G.**
Spectrally resolved Rayleigh scattering diagnostic for hydrogen-oxygen rocket plume studies
p 67 A92-50253
- SEASHOLTZ, RICHARD G.**
Rayleigh-Brillouin scattering to determine one-dimensional temperature and number density profiles of a gas flow field
p 198 A92-38067
Laser anemometer measurements and computations in an annular cascade of high turning core turbine vanes
[NASA-TP-3252] p 20 N92-28980
- SECHKAR, EDWARD A.**
Monte Carlo modeling of atomic oxygen attack of polymers with protective coatings on LDEF
p 132 N92-27281
- SECUNDE, RICHARD R.**
Solar dynamic power for earth orbital and lunar applications
p 68 A92-50567
- SEDGWICK, L. M.**
Full-size solar dynamic heat receiver thermal-vacuum tests
p 68 A92-50565
Ground test program for a full-size solar dynamic heat receiver
p 68 A92-50566
- SEFCIK, R.**
An accelerated development, reduced cost approach to lunar/Mars exploration using a modular NTR-based space transportation system
[IAF PAPER 92-0574] p 43 A92-57053
- SEGALL, B.**
"Wrong" bond interactions at inversion domain boundaries in GaAs
p 260 A92-27297
- SEGALLIS, G. P.**
Flexible high speed CODEC (FHSC)
[AIAA PAPER 92-1919] p 143 A92-29848
- SEKERKA, ROBERT F.**
Effective diffusion equation in a random velocity field
[AIAA PAPER 92-0245] p 167 A92-25704
- SEKULA-MOISE, P. A.**
Study of InGaAs-based modulation doped field effect transistor structures using variable-angle spectroscopic ellipsometry
p 265 N92-32977
- SELVA, R. J.**
Navier-Stokes analysis of flow and heat transfer inside high-pressure-ratio transonic turbine blade rows
p 165 A92-17193
- SENA, J. T.**
Analytical and experimental studies of heat pipe radiation cooling of hypersonic propulsion systems
[AIAA PAPER 92-3809] p 26 A92-49128
- SENG, GARY T.**
High-temperature electronics
p 160 N92-22528
Fiber optics for controls
p 40 N92-22529
- SENICK, PAUL F.**
Effects of turbine cooling assumptions on performance and sizing of high-speed civil transport
[NASA-TM-105610] p 34 N92-23537
- SERCEL, JOEL C.**
An overview of the NASA Advanced Propulsion Concepts program
[AIAA PAPER 92-3216] p 73 A92-54018
- SESHADRI, K.**
The structure of premixed particle-cloud flames
p 114 A92-43779
- SEYBERT, A. F.**
Comparison of analysis and experiment for gearbox noise
[NASA-TM-105330] p 210 N92-25396
- Validation of finite element and boundary element methods for predicting structural vibration and radiated noise
[NASA-TM-105359] p 213 N92-29697
- SHABBI, A.**
Workshop on Engineering Turbulence Modeling
[NASA-CP-10088] p 191 N92-24514
- SHABBI, AAMIR**
Experimental balances for the second moments for a buoyant plume and their implication on turbulence modeling
p 174 A92-40153
- SHAHIDI, A. K.**
SCAILET - An intelligent assistant for satellite ground terminal operations
[IAF PAPER 92-0552] p 245 A92-55855
- SHAHIDI, ANOOSH K.**
An overview of Space Communication Artificial Intelligence for Link Evaluation Terminal (SCAILET) Project
p 148 N92-14212
- SHALKHAUSER, MARY JO W.**
Real-time data compression of broadcast video signals
[NASA-CASE-LEW-14945-2] p 147 N92-10128
- SHALKHAUSER, K. A.**
High-performance packaging for monolithic microwave and millimeter-wave integrated circuits
[AIAA PAPER 92-1935] p 155 A92-31706
A vertically integrated Ka-band phased array antenna
[AIAA PAPER 92-1976] p 156 A92-38140
High-performance packaging for monolithic microwave and millimeter-wave integrated circuits
[NASA-TM-105744] p 151 N92-31855
An optically controlled Ka-band phased array antenna
p 152 N92-32968
- SHALKHAUSER, KURT A.**
A three-dimensional finite-element thermal/mechanical analytical technique for high-performance traveling wave tubes
[AIAA PAPER 92-1824] p 154 A92-29771
- SHALKHAUSER, M. J.**
Destination directed packet switch architecture for a geostationary communication satellite network
[IAF PAPER 92-0413] p 50 A92-55793
- SHALKHAUSER, MARY JO**
Destination directed packet switch architecture for a 30/20 GHz FDMA/TDM geostationary communication satellite network
p 148 N92-14204
Destination-directed, packet-switching architecture for 30/20-GHz FDMA/TDM geostationary communications satellite network
[NASA-TP-3201] p 51 N92-19762
- SHALTENS, RICHARD K.**
Status of the advanced Stirling conversion system project for 25 kW dish Stirling applications
p 207 A92-50804
- SHAPIRA, YAIR**
Upper bounds for convergence rates of vector extrapolation methods on linear systems with initial iterations
[NASA-TM-105608] p 250 N92-33742
- SHARP, G. R.**
A three-dimensional finite-element thermal/mechanical analytical technique for high-performance traveling wave tubes
[AIAA PAPER 92-1824] p 154 A92-29771
- SHARP, G. RICHARD**
Applications of high thermal conductivity composites to electronics and spacecraft thermal design
[NASA-TM-102434] p 56 N92-24349
- SHARPLESS, R. B.**
Adaptive temperature profile control of a multizone crystal growth furnace
p 137 A92-29243
Identification and control of a multizone crystal growth furnace
p 199 A92-39699
- SHAW, LORETTA M.**
Plans for the development of cryogenic engines for space exploration
[NASA-TM-105250] p 79 N92-11135
- SHAW, ROBERT J.**
Comparative study of turbulence models in predicting hypersonic inlet flows
[AIAA PAPER 92-3098] p 11 A92-48740
The NASA aircraft icing research program
p 23 N92-22534
Comparative study of turbulence models in predicting hypersonic inlet flows
[NASA-TM-105720] p 19 N92-28102
- SHEN, M.-H. H.**
Free vibrations of delaminated beams
p 222 A92-36853
Free vibrations of delaminated beams
[NASA-TM-105582] p 109 N92-25754
- SHERRY, M. A.**
A multi-channel demultiplexer/demodulator architecture, simulation and implementation
[AIAA PAPER 92-1972] p 144 A92-29895

SHETTY, DINESH K.

SHETTY, DINESH K.

Extreme value statistics analysis of fracture strengths of a sintered silicon nitride failing from pores p 127 A92-50191

SHI, X.

Monte Carlo exploration of Mikheyev-Smirnov-Wolfenstein solutions to the solar neutrino problem p 270 A92-50927

SHIAO, MICHAEL C.

Mapping methods for computationally efficient and accurate structural reliability [AIAA PAPER 92-2347] p 219 A92-34321

First-passage problems: A probabilistic dynamic analysis for degraded structures [NASA-TM-103755] p 225 N92-11373

SHIH, MING-HSIN

Grid generation for 3D turbomachinery configurations [AIAA PAPER 92-3671] p 243 A92-54114

SHIH, S. H.

An investigation of shock/turbulent boundary layer bleed interactions [AIAA PAPER 92-3085] p 182 A92-54008

SHIH, T. H.

A kappa-epsilon calculation of transitional boundary layers [NASA-TM-105604] p 187 N92-22398

A new time scale based k-epsilon model for near wall turbulence [NASA-TM-105768] p 196 N92-32868

SHIH, T. I.-P.

Enhancing control of grid distribution in algebraic grid generation p 248 A92-52552

SHIH, T.-H.

Second order modeling of boundary-free turbulent shear flows p 174 A92-41275

On the basic equations for the second-order modeling of compressible turbulence [NASA-TM-105277] p 184 N92-11302

Advancements in engineering turbulence modeling [PAPER-105] p 189 N92-23350

On the basic equations for the second-order modeling of compressible turbulence p 190 N92-23351

Workshop on Engineering Turbulence Modeling [NASA-CP-10088] p 191 N92-24514

The present status and the future direction of second order closure models for incompressible flows p 191 N92-24523

Advances in engineering turbulence modeling p 193 N92-25820

SHIH, TSAN-HSING

A critical comparison of second order closures with direct numerical simulation of homogeneous turbulence [NASA-TM-105351] p 185 N92-15357

Center for Modeling of Turbulence and Transition (CMOTT). Research briefs: 1990 [NASA-TM-105243] p 1 N92-23336

Turbulence modeling p 189 N92-23338

Kolmogorov behavior of near-wall turbulence and its application in turbulence modeling [NASA-TM-105683] p 191 N92-24050

SHIH, Y. C.

High-performance packaging for monolithic microwave and millimeter-wave integrated circuits [AIAA PAPER 92-1935] p 155 A92-31706

High-performance packaging for monolithic microwave and millimeter-wave integrated circuits [NASA-TM-105744] p 151 N92-31855

SHIMSKI, JOHN T.

Full-scale transmission testing to evaluate advanced lubricants [NASA-TM-105668] p 212 N92-26560

Development of a full-scale transmission testing procedure to evaluate advanced lubricants [NASA-TP-3265] p 213 N92-30396

SHIN, J.

Helium bubble flow visualization of the spanwise separation on a NACA 0012 with simulated glaze ice [AIAA PAPER 92-0413] p 7 A92-28192

Helium bubble flow visualization of the spanwise separation on a NACA 0012 with simulated glaze ice [NASA-TM-105742] p 19 N92-26612

Analysis of iced wings [NASA-TM-105773] p 20 N92-34144

SHIN, JAIWAN

Advanced ice protection systems test in the NASA Lewis Icing Research Tunnel p 22 A92-14406

SHIN, JAIWON

A turbulence model for iced airfoils and its validation [AIAA PAPER 92-0417] p 6 A92-26267

Results of an icing test on a NACA 0012 airfoil in the NASA Lewis Icing Research Tunnel [AIAA PAPER 92-0647] p 7 A92-27021

Analysis of iced wings [AIAA PAPER 92-0416] p 8 A92-29972

Results of an icing test on a NACA 0012 airfoil in the NASA Lewis Icing Research Tunnel [NASA-TM-105374] p 16 N92-15051

A turbulence model for iced airfoils and its validation [NASA-TM-105373] p 16 N92-15052

Experimental and computational ice shapes and resulting drag increase for a NACA 0012 airfoil [NASA-TM-105743] p 20 N92-28674

Results of a low power ice protection system test and a new method of imaging data analysis [NASA-TM-105745] p 20 N92-28696

SHIPITALO, WILLIAM

A 23:2:1 ratio, 300-watt, 26 N-m output torque, planetary roller-gear robotic transmission: Design and evaluation p 210 N92-25085

SHOEMAKER, M.

A critical evaluation of a three-dimensional Navier-Stokes CFD as a tool to design supersonic turbine stages p 196 N92-32268

SHOEMAKER, NEIL S.

Optical dispersion relations for 'diamondlike' carbon films p 262 A92-44533

SHRIMP, N. R.

Design and test of an oxygen turbopump for a dual expander cycle rocket engine p 59 A92-21062

SHUEN, J. S.

Combustion of liquid-fuel droplets in supercritical conditions p 114 A92-43778

SHUEN, J.-S.

A time-accurate algorithm for chemical non-equilibrium viscous flows at all speeds [AIAA PAPER 92-3639] p 182 A92-54112

SHUEN, JIAN-SHUN

Upwind differencing and LU factorization for chemical non-equilibrium Navier-Stokes equations p 171 A92-33829

Three-dimensional calculations of supersonic reacting flows using an LU scheme p 179 A92-50465

SIDI, AVRAM

Application of vector-valued rational approximations to the matrix eigenvalue problem and connections with Krylov subspace methods [NASA-TM-105858] p 250 N92-33571

Upper bounds for convergence rates of vector extrapolation methods on linear systems with initial iterations [NASA-TM-105608] p 250 N92-33742

Rational approximations from power series of vector-valued meromorphic functions [NASA-TM-105859] p 251 N92-33942

SIEG, R. M.

A new technique for oil backstreaming contamination measurements [NASA-TM-105312] p 257 N92-13783

Study of InGaAs-based modulation doped field effect transistor structures using variable-angle spectroscopic ellipsometry p 265 N92-32977

SIEG, ROBERT M.

Optical dispersion relations for 'diamondlike' carbon films p 262 A92-44533

SIEGEL, R.

Effect of index of refraction on radiation characteristics in a heated absorbing, emitting, and scattering layer p 181 A92-53031

SIEGEL, ROBERT

Transient cooling of a square region of radiating medium p 164 A92-10432

Finite difference solution for transient cooling of a radiating-conducting semitransparent layer p 166 A92-20310

Boundary heat fluxes for spectral radiation from a uniform temperature rectangular medium p 175 A92-44388

SIEGWARTH, J. D.

Liquid-vapour surface sensors for liquid nitrogen and hydrogen p 197 A92-23852

SIEVERS, G. KEITH

Overview of the subsonic propulsion technology session p 32 N92-22531

SIGALOVSKY, JULIA

Relationships between toughness and microstructure of reaction bonded Si3N4 p 125 A92-39687

SIL, AJIT K.

Ka-band dual frequency array feed for a low cost ACTS ground terminal [AIAA PAPER 92-1902] p 143 A92-29833

Ka-band dual frequency array feed for a low cost ACTS ground terminal p 152 N92-32969

SILK, JOSEPH

The diffuse gamma-ray background, light element abundances, and signatures of early massive star formation p 268 A92-43837

SILVERSTEIN, C. C.

Analytical and experimental studies of heat pipe radiation cooling of hypersonic propulsion systems [AIAA PAPER 92-3809] p 26 A92-49128

SIMON, D. L.

Implementation of an intelligent control system [NASA-TM-105795] p 241 N92-33897

SIMON, DONALD L.

Piloted evaluation of an integrated propulsion and flight control simulator [AIAA PAPER 92-4178] p 23 A92-52459

Piloted evaluation of an integrated propulsion and flight control simulator [NASA-TM-105797] p 40 N92-34107

SIMON, FREDERICK F.

Modeling of the heat transfer in bypass transitional boundary-layer flows [NASA-TP-3170] p 184 N92-11299

Progress towards understanding and predicting convection heat transfer in the turbine gas path [NASA-TM-105674] p 194 N92-26690

SIMON, J. S.

A Lyapunov based nonlinear control scheme for stabilizing a basic compression system using a close-coupled control valve p 246 A92-29316

SIMONEAU, ROBERT J.

Turbomachinery p 32 N92-22524

Progress towards understanding and predicting convection heat transfer in the turbine gas path [NASA-TM-105674] p 194 N92-26690

SIMONS, R.

A vertically integrated Ka-band phased array antenna [AIAA PAPER 92-1976] p 156 A92-38140

SIMONS, R. N.

Coplanar waveguide aperture coupled patch antennas with ground plane/substrate of finite extent p 154 A92-24488

New techniques for exciting linearly tapered slot antennas with coplanar waveguide p 155 A92-34844

New coplanar waveguide to rectangular waveguide end launcher p 156 A92-44243

SIMONS, RAINEE M.

Electromagnetic coupling between coplanar waveguide and microstrip antennas p 154 A92-21292

Ka-band dual frequency array feed for a low cost ACTS ground terminal [AIAA PAPER 92-1902] p 143 A92-29833

Coplanar waveguide aperture-coupled microstrip patch antenna p 146 A92-37222

New coplanar waveguide feed network for 2 x 2 linearly tapered slot antenna subarray p 156 A92-45619

Planar dielectric resonator stabilized HEMT oscillator integrated with CPW/aperture coupled patch antenna [NASA-TM-105544] p 160 N92-18473

A flexible CPW package for a 30 GHz MMIC amplifier [NASA-TM-105630] p 161 N92-23193

Nonplanar linearly tapered slot antenna with balanced microstrip feed [NASA-TM-105647] p 161 N92-23535

A 1-W, 30-GHz, CPW amplifier for ACTS small terminal uplink [NASA-TM-105671] p 161 N92-26096

Planar dielectric resonator stabilized HEMT oscillator integrated with CPW/aperture coupled patch antenna p 152 N92-32967

An optically controlled Ka-band phased array antenna p 152 N92-32968

Ka-band dual frequency array feed for a low cost ACTS ground terminal p 152 N92-32969

Coplanar waveguide feeds for phased array antennas p 152 N92-32970

A flexible CPW package for a 30 GHz MMIC amplifier p 152 N92-32972

A 1-W, 30-GHz, CPW amplifier for ACTS small terminal uplink p 152 N92-32973

SIMS, JAMES

Analysis of surface roughness generation in aircraft ice accretion [AIAA PAPER 92-0298] p 169 A92-28187

SIN, CHUNG-CHANG

Numerical simulation of conservation laws p 193 N92-25813

SINGER, JOSEPH

A study of Na(x)Pt3O4 as an O2 electrode bifunctional electrocatalyst [NASA-TM-105311] p 85 N92-20585

The O2 reduction at the IFC modified O2 fuel cell electrode [NASA-TM-105691] p 90 N92-29667

SINGH, N. B.

Flight experiment on acousto-optic crystal growth p 136 A92-12880

Identification and control of a multizone crystal growth furnace p 199 A92-39699

Growth and characterization of lead bromide crystals p 138 A92-56956

Effect of growth conditions on the quality of lead bromide crystals p 138 A92-56957

PERSONAL AUTHOR INDEX

- SINGH, R.**
Vibration transmission through rolling element bearings. IV - Statistical energy analysis p 218 A92-28756
- SINGH, RAJENDRA**
Statistical energy analysis of a geared rotor system p 204 A92-39227
- SINGHAL, S. N.**
Computational simulation of concurrent engineering for aerospace propulsion systems [AIAA PAPER 92-1144] p 241 A92-33285
HITCAN for actively cooled hot-composite thermostructural analysis [ASME PAPER 91-GT-116] p 222 A92-36896
- SINGHAL, SURENDRA N.**
Multidisciplinary tailoring of hot composite structures [AIAA PAPER 92-2563] p 220 A92-34564
Coupled multi-disciplinary simulation of composite engine structures in propulsion environment [NASA-TM-105575] p 228 N92-23267
- SIRBAUGH, J. R.**
Navier-Stokes analysis and experimental data comparison of compressible flow within ducts [NASA-TM-105796] p 38 N92-30972
- SIRIGNANO, W. A.**
Effects of g-jitter on a thermally buoyant flow p 171 A92-32258
- SIROCKY, PAUL J.**
High temperature, flexible pressure-actuated, brush seal [NASA-CASE-LEW-15086-1] p 208 N92-16318
High temperature dynamic engine seal technology development [NASA-TM-105641] p 209 N92-23435
- SIVASHANKARAN, S.**
Fatigue damage accumulation in nickel prior to crack initiation p 120 A92-33947
- SKARDA, J. RAYMOND LEE**
Thermal modeling with solid/liquid phase change of the thermal energy storage experiment [NASA-TM-103770] p 185 N92-13402
- SKOCH, GARY J.**
A 4-spot time-of-flight anemometer for small centrifugal compressor velocity measurements [NASA-TM-105717] p 202 N92-29105
- SLATER, ANDY**
Design and analysis of vortex generators on reengined Boeing 727-100QF center inlet S-duct by a reduced Navier-Stokes code [AIAA PAPER 92-2700] p 10 A92-45542
- SLINEY, HAROLD E.**
Tribological and mechanical comparison of sintered and HIPped PM212: High temperature self-lubricating composites [NASA-TM-105379] p 96 N92-15128
The effect of ion plated silver and sliding friction on tensile stress-induced cracking in aluminum oxide [NASA-TM-105366] p 129 N92-19450
Screen Cage Ion Plating (SCIP) and scratch testing of polycrystalline aluminum oxide [NASA-TM-105404] p 130 N92-22278
Self-lubricating coatings for high-temperature applications p 130 N92-22516
Tribological and microstructural comparison of HIPped PM212 and PM212/Au self-lubricating composites [NASA-TM-105615] p 97 N92-26142
- SMIALEK, J. L.**
Oxidation kinetics of cast TiAl3 p 121 A92-38993
- SMIALEK, JAMES L.**
The chemistry of Saudi Arabian sand: A deposition problem on helicopter turbine airfoils [NASA-TM-105234] p 128 N92-14179
Oxidation resistant coating for titanium alloys and titanium alloy matrix composites [NASA-CASE-LEW-15155-1] p 133 N92-29090
- SMITH, C. E.**
CFD analysis of jet mixing in low NO(x) flametube combustors [ASME PAPER 91-GT-217] p 24 A92-15634
CFD mixing analysis of jets injected from straight and slanted slots into confined crossflow in rectangular ducts [AIAA PAPER 92-3087] p 177 A92-48732
CFD mixing analysis of jets injected from straight and slanted slots into confined crossflow in rectangular ducts [NASA-TM-105699] p 36 N92-26561
- SMITH, C. F.**
Experimental and analytical study of close-coupled ventral nozzles for ASTOVL aircraft p 26 A92-45325
Full Navier-Stokes calculations on the installed F/A-18 inlet at a high angle of attack [AIAA PAPER 92-3175] p 13 A92-54012
Computational and experimental investigation of subsonic internal reversing flows [AIAA PAPER 92-3791] p 183 A92-54170
- SMITH, C. FREDERIC**
Flow studies in close-coupled ventral nozzles for STOVL aircraft [NASA-TM-102554] p 17 N92-20934
- SMITH, CRAWFORD F.**
Flow in a ventral nozzle for short takeoff and vertical landing aircraft p 25 A92-28538
- SMITH, EDWYN D.**
Microwave properties of peeled HEMT devices sapphire substrates p 265 N92-32978
- SMITH, F. T.**
The three-dimensional turbulent boundary layer near a plane of symmetry p 167 A92-24757
- SMITH, JOHN M.**
Trade studies for nuclear space power systems [NASA-TM-105231] p 235 N92-10221
- SMITH, JOHN R.**
Universal aspects of adhesion and atomic force microscopy p 260 A92-17979
Heats of formation of bcc binary alloys [NASA-TM-105281] p 122 N92-16086
- SMITH, PRESTON P.**
Solidification processing of intermetallic Nb-Al alloys p 120 A92-33866
- SMITH, TODD E.**
The effect of steady aerodynamic loading on the flutter stability of turbomachinery blading [ASME PAPER 91-GT-130] p 2 A92-15574
- SMITHRICK, JOHN J.**
Effect of KOH concentration on LEO cycle life of IPV nickel-hydrogen flight cell - Update II p 232 A92-48212
Effect of KOH concentration on LEO cycle life of IPV nickel-hydrogen flight cells - An update p 70 A92-50702
Destructive physical analysis results of Ni/H2 cells cycled in LEO regime p 70 A92-50707
Effect of LEO cycling on 125 Ah advanced design IPV nickel-hydrogen flight cells - An update p 71 A92-50708
Effect of KOH concentration on LEO cycle life of IPV nickel-hydrogen flight cells-update 2 [NASA-TM-105314] p 235 N92-13483
Validation test of advanced technology for IPV nickel-hydrogen flight cells: Update [NASA-TM-105689] p 89 N92-27878
- SMOLINSKI, PATRICK**
A variable multi-step method for transient heat conduction p 173 A92-37518
- SNYDER, CHRISTOPHER A.**
The design and performance estimates for the propulsion module for the booster of a TSTO vehicle [NASA-TM-105299] p 29 N92-11995
Effects of chemical equilibrium on turbine engine performance for various fuels and combustor temperatures [NASA-TM-105399] p 34 N92-23254
- SNYDER, DAVID B.**
Ion collection from a plasma by a pinhole p 259 N92-22368
- SNYDER, P. G.**
Study of InGaAs-based modulation doped field effect transistor structures using variable-angle spectroscopic ellipsometry p 265 N92-32977
- SNYDER, S. M.**
Liquid-vapour surface sensors for liquid nitrogen and hydrogen p 197 A92-23852
- SNYDER, WILLIAM J.**
Cyclopentadiene evolution during pyrolysis-gas chromatography of PMR polyimides [NASA-TM-105629] p 132 N92-25348
- SOCKOL, P. M.**
Navier-Stokes analysis of turbomachinery blade external heat transfer p 170 A92-28518
- SOCKOL, PETER M.**
Turbomachinery p 32 N92-22524
Chemical reacting flows p 188 N92-22525
- SOEDER, JAMES F.**
The development of test beds to support the definition and evolution of the Space Station Freedom power system p 46 A92-50656
Overview and evolution of the LeRC PMAD DC Testbed [NASA-TM-105842] p 163 N92-32867
- SOPRIN, THOMAS G.**
Turbomachinery noise p 253 N92-10601
- SOHN, K. H.**
Experimental study of boundary layer transition on a heated flat plate p 172 A92-36022
Turbulent heat flux measurements in a transitional boundary layer [NASA-TM-105623] p 19 N92-27377
- SOHN, P. Y.**
20/30 GHz satellite personal communications networks [AIAA PAPER 92-1908] p 143 A92-29839
- SOVIE, AMY L.**
A personal communications network using a Ka-band satellite p 151 N92-30934
- SOHN, PHILIP Y.**
Operational uses of ACTS technology [AIAA PAPER 92-1964] p 144 A92-29887
Characteristics of a future aeronautical satellite communications system [AIAA PAPER 92-2058] p 22 A92-29889
A personal communications network using a Ka-band satellite p 145 A92-31780
Characteristics of a future aeronautical satellite communications system p 151 N92-30932
- SOKOLOSKI, MARTIN M.**
NASA Space applications of high-temperature superconductors [NASA-TM-105401] p 271 N92-18455
NASA space applications of high-temperature superconductors p 265 N92-32980
- SOKOLOWSKI, DANIEL E.**
Aircraft engine hot section technology: An overview of the HOST Project p 33 N92-22535
- SOLTANI, M. R.**
Finite wing aerodynamics with simulated glaze ice [AIAA PAPER 92-0414] p 5 A92-26265
- SONI, BHARAT K.**
Grid generation for 3D turbomachinery configurations [AIAA PAPER 92-3671] p 243 A92-54114
- SONI, N. J.**
Destination directed packet switch architecture for a geostationary communication satellite network [IAF PAPER 92-0413] p 50 A92-55793
- SONIN, AIN A.**
Scalar rate correlation at a turbulent liquid free surface - A two-regime correlation for high Schmidt numbers p 184 A92-56941
- SONNENFROH, D. M.**
Doppler-shifted fluorescence imaging of velocity fields in supersonic reacting flows [AIAA PAPER 92-2964] p 199 A92-46979
Fast oxygen atom facility for studies related to low earth orbit activities [AIAA PAPER 92-3974] p 47 A92-56800
- SOSOKA, DON J.**
Distributed visualization for computational fluid dynamics p 194 N92-25826
- SOTOMAYOR, JORGE L.**
Wavelength-multiplexed fiber-optic position encoder for aircraft control systems p 24 A92-42602
- SOTOS, RAYMOND G.**
An investigation of flame spread over shallow liquid pools in microgravity and nonair environments p 112 A92-16609
Effects of oxygen concentration on radiative loss from normal-gravity and microgravity methane diffusion flames [AIAA PAPER 92-0243] p 113 A92-26928
- SOULAS, GEORGE C.**
Anode power deposition in applied-field MPD thrusters [AIAA PAPER 92-3463] p 74 A92-54034
- SOVEY, J.**
Nuclear electric propulsion development and qualification facilities [NASA-TM-105521] p 91 N92-30818
- SOVEY, JAMES S.**
Electric propulsion - An evolutionary technology [IAF PAPER 91-241] p 58 A92-13158
The evolutionary development of high specific impulse electric thruster technology [AIAA PAPER 92-1556] p 61 A92-38650
NASA's nuclear electric propulsion technology project [AIAA PAPER 92-3705] p 76 A92-57033
Development of arcjet and ion propulsion for spacecraft stationkeeping [IAF PAPER 92-0607] p 77 A92-57058
Test facilities for high power electric propulsion [NASA-TM-105247] p 80 N92-11136
The evolutionary development of high specific impulse electric thruster technology [NASA-TM-105712] p 92 N92-31342
NASA's nuclear electric propulsion technology project [NASA-TM-105811] p 93 N92-32463
The evolutionary development of high specific impulse electric thruster technology [NASA-TM-105758] p 93 N92-33064
- SOVIE, AMY**
Rocket engine diagnostics using qualitative modeling techniques [AIAA PAPER 92-3164] p 65 A92-48787
Rocket engine diagnostics using qualitative modeling techniques [NASA-TM-105714] p 88 N92-27033
- SOVIE, AMY L.**
Demonstrated survivability of a high temperature optical fiber cable on a 1500 pound thrust rocket chamber [NASA-TM-105835] p 136 N92-32230

SOWA, W. A.

SOWA, W. A.

- Jet mixing into a heated cross flow in a cylindrical duct
- Influence of geometry and flow variations
[AIAA PAPER 92-0773] p 168 A92-27110
- Mixing in the dome region of a staged gas turbine combustor
[AIAA PAPER 92-3089] p 177 A92-48734
- Jet mixing into a heated cross flow in a cylindrical duct:
Influence of geometry and flow variations
[NASA-TM-105390] p 30 N92-15994
- SPALVINS, TALIVALDIS**
A vacuum (10(exp -9) Torr) friction apparatus for determining friction and endurance life of MoSx films
[NASA-TM-104478] p 129 N92-16129
- The effect of ion plated silver and sliding friction on tensile stress-induced cracking in aluminum oxide
[NASA-TM-105366] p 129 N92-19450
- Screen Cage Ion Plating (SCIP) and scratch testing of polycrystalline aluminum oxide
[NASA-TM-105404] p 130 N92-22278
- SPEIER, H. J.**
A new technique for oil backstreaming contamination measurements
[NASA-TM-105312] p 257 N92-13783
- SPENCER, M. E.**
A multi-channel demultiplexer/demodulator architecture, simulation and implementation
[AIAA PAPER 92-1972] p 144 A92-29895
- SPIEGLER, JEFFREY D.**
ACTS T1-VSAT - The intelligent earth station
[AIAA PAPER 92-2037] p 145 A92-29952
- SPRING, S. A.**
Measurements in a leading-edge separation bubble due to a simulated airfoil ice accretion p 21 A92-41262
- SPUCKLER, C. M.**
Effect of index of refraction on radiation characteristics in a heated absorbing, emitting, and scattering layer p 181 A92-53031
- SRINIVASAN, RAM**
Studies of the effects of curvature on dilution jet mixing p 166 A92-21079
- SRINIVASAN, SUPRAMANIAN**
Temperature dependence of the electrode kinetics of oxygen reduction at the platinum/Nafion interface - A microelectrode investigation p 115 A92-56950
- SRIVASTAVA, R.**
An unsteady Euler scheme for the analysis of ducted propellers p 6 A92-26947
[AIAA PAPER 92-0522]
- Aeroelastic analysis of advanced propellers using an efficient Euler solver p 7 A92-28194
[AIAA PAPER 92-0488]
- A numerical classical flutter analysis of advanced propellers p 26 A92-35687
[AIAA PAPER 92-2118]
- SRIVATSAN, T. S.**
A combined analytical-experimental tensile test technique for brittle materials p 123 A92-23225
- SRIVINYUNON, T.**
Surface morphologies and photoluminescence of diamond films deposited in a hot filament reactor p 261 A92-42658
- STAN, M.**
Properties of large area ErBa₂Cu₃O(7-x) thin films deposited by ionized cluster beams p 260 A92-33911
- STAN, M. A.**
Magnetic flux relaxation in YBa₂Cu₃O(7-x) thin film: Thermal or athermal p 265 N92-32984
- STAN, MARK A.**
Conductor-backed coplanar waveguide resonators of YBa₂Cu₃O(7-delta) on LaAlO₃ p 158 A92-51042
- Properties of large area ErBa₂Cu₃O(7-x) thin films deposited by ionized cluster beams p 264 N92-23414
- STANG, D. B.**
Review and statistical analysis of the use of ultrasonic velocity for estimating the porosity fraction in polycrystalline materials p 215 A92-28722
- STANG, DAVID B.**
Interfacing laboratory instruments to multiuser, virtual memory computers p 245 A92-13595
- STANKIEWICZ, N.**
Submillimeter backward-wave oscillators p 155 A92-35054
- STANKIEWICZ, NORBERT**
The introduction of spurious models in a hole-coupled Fabry-Perot open resonator p 197 A92-21244
- STAPLES, EDWARD J.**
Multichannel demultiplexer/demodulator technologies for future satellite communication systems
[NASA-TM-105377] p 51 N92-18342
- STARLINGER, A.**
Reliability analysis of laminated CMC components through shell subelement techniques
[AIAA PAPER 92-2348] p 219 A92-34322

STARLINGER, ALOIS

- Reliability analysis of structural ceramic components using a three-parameter Weibull distribution
[NASA-TM-105370] p 129 N92-17060
- Reliability analysis of laminated CMC components through shell subelement techniques
[NASA-TM-105413] p 129 N92-20380
- STAVNES, M.**
Beam power options for the moon p 61 A92-40429
- Wiring for aerospace applications
[NASA-TM-105777] p 162 N92-30427
- STAVNES, MARK**
Space transfer with ground-based laser/electric propulsion
[AIAA PAPER 92-3213] p 73 A92-54017
- STAVNES, MARK W.**
A mass sensitivity analysis of lunar orbiting beam power systems p 232 A92-50619
- STEBBINS, ALBERT**
Perturbations from cosmic strings in cold dark matter p 268 A92-33353
- Large-scale microwave anisotropy from gravitating seeds p 269 A92-56914
- STEFFEN, CHRIS J., JR.**
High-Order Polynomial Expansions (HOPE) for flux-vector splitting p 190 N92-23353
- STEFFEN, CHRISTOPHER J., JR.**
An investigation of DTNS2D for use as an incompressible turbulence modelling test-bed
[NASA-TM-105593] p 249 N92-22230
- Development of new flux splitting schemes p 189 N92-23343
- Development of a new flux splitting scheme p 190 N92-23352
- Development of new flux splitting schemes p 192 N92-25809
- STEFKO, G. L.**
Cascade flutter analysis with transient response aerodynamics p 217 A92-15972
- STEFKO, GEORGE L.**
Aeroelastic stability analyses of two counter rotating propfan designs for a cruise missile model
[AIAA PAPER 92-2218] p 25 A92-34408
- FREPS - A forced response prediction system for turbomachinery blade rows p 242 A92-54006
[AIAA PAPER 92-3072]
- Aeroelastic stability analyses of two counter rotating propfan designs for a cruise missile model
[NASA-TM-105268] p 227 N92-23191
- STEINBERGER, CRAIG J.**
Model free simulations of a high speed reacting mixing layer p 167 A92-25715
[AIAA PAPER 92-0257]
- STEINETZ, BRUCE**
Tribological evaluation of an Al₂O₃-SiO₂ ceramic fiber candidate for high temperature sliding seals
[NASA-TM-105611] p 97 N92-23190
- STEINETZ, BRUCE M.**
Tribological properties of ceramic-(TiAl-Nb) sliding couples for use as candidate seal materials p 124 A92-32407
- Relative sliding durability of two candidate high temperature oxide fiber seal materials
[AIAA PAPER 92-3713] p 126 A92-49095
- Relative sliding durability of two candidate high temperature oxide fiber seal materials p 95 N92-10064
[NASA-TM-105199]
- National Aerospace Plane engine seals: High temperature seal performance evaluation p 207 N92-15103
- High temperature, flexible pressure-actuated, brush seal
[NASA-CASE-LEW-15086-1] p 208 N92-16318
- Engine panel seals for hypersonic engine applications: High temperature leakage assessments and flow modelling p 208 N92-16336
[NASA-TM-105260]
- Evaluation of an innovative high temperature ceramic water seal for hypersonic engine applications
[NASA-TM-105556] p 208 N92-20815
- Sliding durability of two carbide-oxide candidate high temperature fiber seal materials in air to 900 C
[NASA-TM-105554] p 97 N92-21175
- High temperature, flexible, fiber-preform seal
[NASA-CASE-LEW-15085-1] p 208 N92-22043
- High temperature dynamic engine seal technology development
[NASA-TM-105641] p 209 N92-23435
- STEINTHORSSON, E.**
Enhancing control of grid distribution in algebraic grid generation p 248 A92-52552
- STEPHAN, AMY**
Model-based diagnostics for Space Station Freedom p 245 A92-50533

STEPHENS, CRAIG A.

- Modeling of the heat transfer in bypass transitional boundary-layer flows
[NASA-TP-3170] p 184 N92-11299
- STEPHENS, JOSEPH R.**
Intermetallic and ceramic matrix composites for 815 to 1370 C (1500 to 2500 F) gas turbine engine applications p 99 A92-15128
- STEPHENSON, F. W.**
Status of NASA's Earth-to-Orbit Propulsion Technology program
[IAF PAPER 91-258] p 58 A92-13154
- The NASA-OAST earth-to-orbit propulsion technology program - The action plan
[AIAA PAPER 92-1478] p 61 A92-38597
- STERN, A.**
20/30 GHz satellite personal communications networks p 143 A92-29639
[AIAA PAPER 92-1908]
- A personal communications network using a Ka-band satellite p 151 N92-30934
- STERN, ALAN**
Characteristics of a future aeronautical satellite communications system
[AIAA PAPER 92-2058] p 22 A92-29889
- A personal communications network using a Ka-band satellite p 145 A92-31780
- Characteristics of a future aeronautical satellite communications system p 151 N92-30932
- STERN, ALAN L.**
Operational uses of ACTS technology
[AIAA PAPER 92-1964] p 144 A92-29887
- STEUER, G. D.**
Heat transfer in rotating serpentine passages with trips skewed to the flow
[NASA-TM-105581] p 186 N92-20235
- STEVENS, G. H.**
Rotative quadrature phase-shift keying p 146 A92-44233
- STEVENS, GRADY**
Satcom systems and technologies into the 21st century
[IAF PAPER 92-0412] p 147 A92-55792
- STEVENS, GRADY H.**
Data Distribution Satellite p 146 A92-48224
- Comparative study on the performance of power and bandwidth efficient modulations in LMSS under fading and interference p 147 A92-54763
- STEVENS, NICHOLAS**
Ion Beam Textured and Coated Surfaces Experiment (IBEX) p 132 N92-24832
- STEVENSON, STEVEN M.**
Space Station Freedom/lunar transfer vehicle propellant operation hazard analysis p 55 N92-17416
- STEWART, MARK E. M.**
Euler solutions for an unbladed jet engine configuration
[AIAA PAPER 92-0544] p 169 A92-28201
- Domain-decomposition algorithm applied to multielement airfoil grids p 9 A92-41261
- Euler solutions for an unbladed jet engine configuration
[NASA-TM-105332] p 184 N92-11328
- A two-dimensional Euler solution for an unbladed jet engine configuration p 190 N92-23560
[NASA-TM-105329]
- A multiblock grid generation technique applied to a jet engine configuration p 244 N92-24428
- A two-dimensional Euler solution for an unbladed jet engine configuration p 18 N92-24861
- Multiblock grid generation for jet engine configurations p 35 N92-25720
- STOCHL, ROBERT J.**
A review of candidate multilayer insulation systems for potential use on wet-launched LH₂ tankage for the space exploration initiative lunar missions
[NASA-TM-104493] p 134 N92-13336
- STOCKER, DENNIS P.**
Effects of oxygen concentration on radiative loss from normal-gravity and microgravity methane diffusion flames
[AIAA PAPER 92-0243] p 113 A92-26928
- STOKES, W. L.**
Crossing shock wave turbulent boundary layer interactions - Variable angle and shock generator length geometry effects at Mach 3
[AIAA PAPER 92-0636] p 6 A92-27014
- STONE, JAMES R.**
NASA's nuclear thermal propulsion technology project
[AIAA PAPER 92-3581] p 75 A92-54062
- NASA's nuclear electric propulsion technology project
[AIAA PAPER 92-3705] p 76 A92-57033
- Plans for the development of cryogenic engines for space exploration
[NASA-TM-105250] p 79 N92-11135

- Nuclear electric propulsion: An integral part of NASA's nuclear propulsion project
[NASA-TM-105309] p 83 N92-16019
NASA's nuclear electric propulsion technology project
[NASA-TM-105811] p 93 N92-32463
- STORTZ, MICHAEL W.**
Integrated flight/propulsion control for supersonic STOVL aircraft p 39 A92-45320
- STRACK, WILLIAM C.**
Propulsion challenges and opportunities for high-speed transport aircraft p 34 N92-22540
- STRAZISAR, ANTHONY J.**
Turbomachinery p 32 N92-22524
- STREET, KENNETH W.**
Fluorescence microscopy for the characterization of structural integrity
[NASA-TM-105253] p 96 N92-18970
- STROCK, THOMAS W.**
Hot gas ingestion characteristics and flow visualization of a vectored thrust STOVL concept p 26 A92-45316
- STROCKY, PAUL J.**
High temperature, flexible, fiber-preform seal
[NASA-CASE-LEW-15085-1] p 208 N92-22043
- STUBBS, ROBERT M.**
Numerical study of low pressure nuclear thermal rockets
[AIAA PAPER 92-3815] p 75 A92-54182
- STUEBER, THOMAS J.**
Evaluation of Kapton pyrolysis, arc tracking, and arc propagation on the Space Station Freedom (SSF) solar array flexible current carrier (FCC) p 72 A92-53209
- SU, T. F.**
Stability analysis of surface tension effects on a double-diffusive layer
[AIAA PAPER 92-0605] p 137 A92-27002
- SUBRAMANIAN, C. S.**
Features of wavy vortices in a curved channel from experimental and numerical studies p 171 A92-31638
Surface heat transfer and flow properties of vortex arrays induced artificially and from centrifugal instabilities p 183 A92-56371
- SUBRAMANYAM, G.**
Electrical-transport properties and microwave device performance of sputtered TiCaBaCuO superconducting thin films p 263 A92-56599
C-band superconductor/semiconductor hybrid field-effect transistor amplifier on a LaAlO₃ substrate
[NASA-TM-105828] p 163 N92-34204
- SUDER, KENNETH L.**
Design and performance of controlled-diffusion stator compared with original double-circular-arc stator
[NASA-TP-2852] p 34 N92-22863
- SUE, MILES K.**
ACTS aeronautical experiments
[AIAA PAPER 92-2042] p 50 A92-29956
- SUICH, RONALD C.**
Balancing reliability and cost to choose the best power subsystem p 216 A92-50625
- SULLIVAN, J. P.**
Unsteady wing surface pressures in the wake of a propeller
[AIAA PAPER 92-0277] p 5 A92-25731
- SUN, D. C.**
Two reference time scales for studying the dynamic cavitation of liquid films p 204 A92-47173
- SUN, D. J.**
Convective flows in enclosures with vertical temperature or concentration gradients p 171 A92-32277
- SURESH, AMBADI**
Numerical experiments on a new class of nonoscillatory schemes
[AIAA PAPER 92-0421] p 7 A92-28193
The Osher scheme for non-equilibrium reacting flows p 176 A92-48149
Perturbation of a normal shock - A test case for unsteady Euler codes
[AIAA PAPER 92-3180] p 178 A92-48795
Upwind schemes and bifurcating solutions in real gas computations p 193 N92-25817
- SUTHAR, J. L.**
Dielectric breakdown studies of Teflon perfluoroalkoxy at high temperature p 125 A92-36287
Evaluation of high temperature dielectric films for high voltage power electronic applications p 261 A92-44273
High temperature dielectric properties of Apical, Kapton, Peek, Teflon AF, and Upilex polymers
[NASA-TM-105753] p 162 N92-28675
- SUTJAHJO, EDHI**
Material nonlinear analysis via mixed-iterative finite element method
[AIAA PAPER 92-2479] p 220 A92-34368
- SUTTER, JAMES K.**
Addition curing thermosets endcapped with 4-amino (2,2) paracyclophane p 124 A92-33918
- SWAFFORD, TIMOTHY W.**
Euler flow predictions for an oscillating cascade using a high resolution wave-split scheme
[ASME PAPER 91-GT-198] p 3 A92-15623
Analysis of cascades using a two dimensional Euler aeroelastic solver
[AIAA PAPER 92-2370] p 26 A92-34598
- SWARTZ, C. K.**
Recent progress in InP solar cell research p 158 A92-50653
Radiation and temperature effects in heteroepitaxial and homoepitaxial InP cells p 159 A92-53192
Defect behavior, carrier removal and predicted in-space injection annealing of InP solar cells
[NASA-TM-105624] p 161 N92-23562
- SWEC, DIANE M.**
Update on results of SPRE testing at NASA Lewis p 71 A92-50780
NASA Lewis Stirling SPRE testing and analysis with reduced number of cooler tubes
[NASA-TM-105767] p 238 N92-28837
- SWETTE, L.**
Bifunctional alkaline oxygen electrodes p 115 A92-50729
- SWICKARD, S. M.**
Review and statistical analysis of the use of ultrasonic velocity for estimating the porosity fraction in polycrystalline materials p 215 A92-7272
- SYNOWICKI, R. A.**
Atomic oxygen effects on thin film space coatings studied by spectroscopic ellipsometry, atomic force microscopy, and laser light scattering
[AIAA PAPER 92-2172] p 94 A92-31300
- T**
- TAFTI, D. K.**
Hot gas environment around STOVL aircraft in ground proximity. II - Numerical study p 25 A92-24403
- TAGHAVI, R.**
Screech noise source structure of a supersonic rectangular jet
[AIAA PAPER 92-0503] p 6 A92-26932
Modern developments in shear flow control with swirl p 9 A92-41265
Spatial instability of a swirling jet - Theory and experiment p 174 A92-41274
A computational study of advanced exhaust system transition ducts with experimental validation
[AIAA PAPER 92-3794] p 179 A92-49126
Screech noise source structure of a supersonic rectangular jet
[NASA-TM-105384] p 15 N92-14000
- TAGUE, JOHN**
Flexible digital modulation and coding synthesis for satellite communications p 148 N92-14235
- TAKAKI, RYOJI**
Predicted pressure distribution on a prop-fan blade through Euler analysis p 10 A92-46791
- TALLO, DONALD**
FIDEX: An expert system for satellite diagnostics p 148 N92-14218
- TALLO, DONALD P.**
Intelligent fault isolation and diagnosis for communication satellite systems p 248 N92-23365
- TALPALLIKAR, M. V.**
CFD analysis of jet mixing in low NO(x) flamel tube combustors
[ASME PAPER 91-GT-217] p 24 A92-15634
- TAM, KWA-SUR**
Functional models of power electronic components for system studies p 157 A92-50558
Modeling of Space Station power system components and their interactions p 68 A92-50559
An EMTF system level model of the PMAD DC test bed p 46 A92-50657
- TAMASHIRO, R. N.**
A low-power, high-efficiency Ka-band TWTA p 156 A92-38163
- TAMASHIRO, RODNEY N.**
A low-power, high-efficiency Ka-band TWTA
[AIAA PAPER 92-1822] p 154 A92-29769
- TANG, D.**
Fiber-optic sensors for aerospace electrical measurements - An update p 200 A92-50630
- TANGIRALA, V.**
The structure of premixed particle-cloud flames p 114 A92-43779
- TATTERSON, G. B.**
Experimental verification of a secondary recirculation zone in a labyrinth seal p 205 A92-50271
- TAUB, S. R.**
New coplanar waveguide to rectangular waveguide end launcher p 156 A92-44243
- TAUB, SUSAN R.**
A flexible CPW package for a 30 GHz MMIC amplifier
[NASA-TM-105630] p 161 N92-23193
A 1-W, 30-GHz, CPW amplifier for ACTS small terminal uplink
[NASA-TM-105671] p 161 N92-26096
A flexible CPW package for a 30 GHz MMIC amplifier uplink p 152 N92-32972
A 1-W, 30-GHz, CPW amplifier for ACTS small terminal uplink p 152 N92-32973
- TAULBEE, DALE B.**
Prediction of unsteady rotor surface pressure and heat transfer from wake passages
[ASME PAPER 91-GT-267] p 165 A92-15665
- TAYLOR, ARTHUR C., III**
Upwind relaxation methods for the Navier-Stokes equations using inner iteration p 170 A92-29553
- TAYLOR, RUSSELL D.**
Preliminary investigation of a low power pulsed arcjet thruster
[AIAA PAPER 92-3113] p 64 A92-48752
- TAYLOR, W. J.**
On-orbit cryogenic fluid transfer research at NASA Lewis Research Center p 45 A92-23847
- TAYLOR, WILLIAM J.**
Comparing the results of an analytical model of the no-vent fill process with no-vent fill test results for a 4.96 cu m (175 cu ft) tank
[AIAA PAPER 92-3078] p 72 A92-54007
Improved thermodynamic modeling of the no-vent fill process and correlation with experimental data
[NASA-TM-104492] p 79 N92-11129
- TEIXEIRA, EDILBERTO**
Design of multi-layer neural networks for accurate identification of nonlinear mappings p 246 A92-29030
- TELESMAN, J.**
Fatigue crack growth in unidirectional metal matrix composite p 99 A92-19734
- TELESMAN, JACK**
Fatigue crack growth in a unidirectional SCS-6/Ti-15-3 composite p 102 A92-39036
Modeling of crack bridging in a unidirectional metal matrix composite p 104 A92-43085
- TEREPKA, FRANCIS M.**
CVD of silicon carbide on structural fibers: Microstructure and composition
[NASA-TM-105385] p 107 N92-18439
- TERLEP, JUDITH A.**
Low earth orbit durability evaluation of Haynes 188 solar receiver material
[AIAA PAPER 92-0850] p 117 A92-29616
Atomic oxygen durability of solar concentrator materials for Space Station Freedom
[NASA-TM-105378] p 85 N92-20065
- TERRONES, GUILLERMO**
Effects of g-jitter and cross-diffusion on the onset of convection in doubly diffusive systems
[AIAA PAPER 92-0246] p 167 A92-25705
- TERRY, JOHN D.**
Operating and service manual for the NASA Lewis automated far-field antenna range
[NASA-TM-105343] p 52 N92-22319
- TEW, ROY C.**
Instantaneous heat transfer coefficient based upon two-dimensional analyses of Stirling space engine components p 181 A92-50827
Comparison of GLIMPS and HFAST Stirling engine code predictions with experimental data
[NASA-TM-105549] p 267 N92-25395
Heat transfer in oscillating flows with sudden change in cross section
[NASA-TM-105692] p 88 N92-26654
Overview of NASA supported Stirling thermodynamic loss research
[NASA-TM-105690] p 88 N92-27034
- TEWARI, S. N.**
Growth-speed dependence of primary arm spacings in directionally solidified Pb-10 wt pct Sn p 117 A92-26526
- THACKER, B.**
Recent developments in the NESSUS probabilistic structural analysis computer program
[AIAA PAPER 92-2411] p 242 A92-34342
- THACKER, B. H.**
A new response surface approach for structural reliability analysis
[AIAA PAPER 92-2408] p 219 A92-34339
- THESLING, W.**
High voltage thermally diffused p (+) n solar cells p 235 A92-53172
- THESLING, WILLIAM**
Theoretical modeling, air optimum design and predicted performance of p (+) n pp (+) and p (+) nn (+) indium phosphide homojunction solar cells p 234 A92-53152

THIEMANN, H.

THIEMANN, H.

High voltage spheres in an unmagnetized plasma - Fluid and PIC simulations p 258 A92-47936

THIEME, LANNY G.

Component technology for Stirling power converters p 206 A92-50781

THOMAS, DAVID J.

Load redistribution considerations in the fracture of ceramic matrix composites [AIAA PAPER 92-2494] p 221 A92-34586

THOMAS, JOHN E.

Space acceleration measurement system triaxial sensor head error budget [NASA-TM-105300] p 57 N92-25134

THOMAS, SCOTT

Computational analysis of ramjet engine inlet interaction [AIAA PAPER 92-3102] p 11 A92-48744

THOMASSEN, K.

Nuclear electric propulsion development and qualification facilities [NASA-TM-105521] p 91 N92-30818

THORP, SCOTT A.

Integrating aerodynamic surface modeling for computational fluid dynamics with computer aided structural analysis, design, and manufacturing p 192 N92-25727

TIKARE, V.

Crack healing behavior of hot pressed silicon nitride due to oxidation p 124 A92-32896

TIRRES, LIZET

A comparison of the calculated and experimental off-design performance of a radial flow turbine [AIAA PAPER 92-3069] p 13 A92-54004

Description of a pressure measurement technique for obtaining surface static pressures of a radial turbine [AIAA PAPER 92-4006] p 200 A92-56829

Description of a pressure measurement technique for obtaining surface static pressures of a radial turbine [NASA-TM-105643] p 202 N92-24959

TITRAN, R. H.

Fuels and materials development for space nuclear propulsion [NASA-TM-107806] p 85 N92-21187

The cyclic oxidation resistance at 1200 C of beta-NiAl, FeAl, and CoAl alloys with selected third element additions [NASA-TM-105620] p 123 N92-24554

TOH, K. H.

Flow induction by pressure forces [AIAA PAPER 92-3571] p 28 A92-54060

TONCICH, S. S.

Performance of a wideband GaAs low-noise amplifier at cryogenic temperatures p 156 A92-37953

Performance of a Y-Ba-Cu-O superconducting filter/GaAs low noise amplifier hybrid circuit [NASA-TM-105546] p 160 N92-21370

Performance of a Y-Ba-Cu-O superconducting filter/GaAs low noise amplifier hybrid circuit p 163 N92-32982

C-band superconductor/semiconductor hybrid field-effect transistor amplifier on a LaAlO₃ substrate [NASA-TM-105828] p 163 N92-34204

TONG, LIJUN

Mechanical properties of 3C silicon carbide p 126 A92-43761

TORNG, T.

Recent developments of the NESSUS probabilistic structural analysis computer program [AIAA PAPER 92-2411] p 242 A92-34342

TORNG, T. Y.

Structural system reliability calculation using a probabilistic fault tree analysis method [AIAA PAPER 92-2410] p 251 A92-34341

TOWER, LEONARD K.

NASA Lewis steady-state heat pipe code users manual [NASA-TM-105161] p 90 N92-28682

TOWNE, CHARLES E.

The Proteus Navier-Stokes code p 192 N92-25811

TOWNSEND, DENNIS P.

A comparison between theoretical prediction and experimental measurement of the dynamic behavior of spur gears [NASA-TM-105362] p 210 N92-25347

Effect of contact ratio on spur gear dynamic load [NASA-TM-105606] p 210 N92-25447

Minimization of the vibration energy of thin-plate structure [NASA-TM-105654] p 211 N92-25448

Effect of operating conditions on gearbox noise [NASA-TM-105331] p 211 N92-26107

Improvement in surface fatigue life of hardened gears by high-intensity shot peening [NASA-TM-105678] p 211 N92-26108

Analysis and modification of a single-mesh gear fatigue rig for use in diagnostic studies [NASA-TM-105416] p 212 N92-27879

Optimum design of a gearbox for low vibration [NASA-TM-105653] p 212 N92-28476

TRAN, DONALD H.

Effects of chemical equilibrium on turbine engine performance for various fuels and combustor temperatures [NASA-TM-105399] p 34 N92-23254

TRAN, LE T.

Prediction of unsteady rotor-surface pressure and heat transfer from wake passages [ASME PAPER 91-GT-267] p 165 A92-15665

TRASH, L.

Description of the PMAD DC test bed architecture and integration sequence p 46 A92-50655

Description of the PMAD DC test bed architecture and integration sequence [NASA-TM-105284] p 77 N92-10055

TREFNY, C.

The F/A-18 external burning flight test [AIAA PAPER 91-5050] p 23 A92-44547

TREFNY, CHARLES J.

Experiments and analysis concerning the use of external burning to reduce aerospace vehicle transonic drag [NASA-TM-105397] p 30 N92-17546

TRIMARCHI, PAUL A.

Inflatable traversing probe seal p 209 N92-22692

TROUDET, T.

A real time neural net estimator of fatigue life p 245 A92-21694

Design and evaluation of a robust dynamic neurocontroller for a multivariable aircraft control problem [NASA-TM-105579] p 40 N92-20586

TRUE, B.

Experimental study of cross-stream mixing in a rectangular duct [AIAA PAPER 92-3090] p 178 A92-48735

Experimental study of cross-stream mixing in a rectangular duct [NASA-TM-105694] p 36 N92-27652

TRUONG, LONG V.

PC graphics generation and management tool for real-time applications [NASA-TM-105749] p 244 N92-28684

TSAI, Y.-L. P.

Three-dimensional calculations of supersonic reacting flows using an LU scheme p 179 A92-50465

Runge-Kutta methods combined with compact difference schemes for the unsteady Euler equations [AIAA PAPER 92-3210] p 182 A92-54015

TSAI, WYETING A.

Discrete-time entropy formulation of optimal and adaptive control problems p 247 A92-55930

TSAU, F.

Effects of g-jitter on a thermally buoyant flow p 171 A92-32258

TSE, DAVID K.

Separation distance and static transmission error of involute spur gears [AIAA PAPER 92-3490] p 205 A92-49027

TURCHI, P. J.

Qualitative spectroscopic study of magnetic nozzle flow [AIAA PAPER 92-3161] p 65 A92-48784

A first-principles model for orificed hollow cathode operation [AIAA PAPER 92-3742] p 259 A92-54145

TURCHI, PETER J.

Electric propulsion - The future is now p 63 A92-48386

TURKEL, E.

Central difference TVD and TVB schemes for time dependent and steady state problems [AIAA PAPER 92-0053] p 166 A92-22168

Central difference TVD and TVB schemes for time dependent and steady state problems [NASA-TM-105357] p 249 N92-15663

TURKEL, ELI

Mappings and accuracy for Chebyshev pseudo-spectral approximations p 248 A92-50469

TURLEY, R. S.

Plasma erosion rate diagnostics using laser-induced fluorescence p 198 A92-36738

TURLIK, I.

Comparative evaluation of optical waveguides as alternative interconnections for high performance packaging p 153 N92-32974

TURNER, MICHAEL S.

Constraints to the decays of Dirac neutrinos from SN 1987A p 255 A92-36249

Massive Dirac neutrinos and SN 1987A p 268 A92-45808

TURTLE, J.

Ka-band MMIC arrays for ACTS Aero Terminal Experiment [IAF PAPER 92-0398] p 159 A92-55785

TUZZOLO, M. F.

Surface heat transfer and flow properties of vortex arrays induced artificially and from centrifugal instabilities p 183 A92-56371

TZAFARAS, N.

Pilot production of 4 sq cm ITO/InP photovoltaic solar cells p 71 A92-53197

TZENG, Y.

Surface morphologies and photoluminescence of diamond films deposited in a hot filament reactor p 261 A92-42858

U

UMEKI, T.

Qualitative spectroscopic study of magnetic nozzle flow [AIAA PAPER 92-3161] p 65 A92-48784

UPSCHULTE, B. L.

Arcing of negatively biased solar cells in low earth orbit [AIAA PAPER 92-0578] p 59 A92-26985

Arcing of negatively biased solar cells in a plasma environment. I - Experimental observations [AIAA PAPER 92-2990] p 63 A92-47000

Fast oxygen atom facility for studies related to low earth orbit activities [AIAA PAPER 92-3974] p 47 A92-56800

URBAN, DAVID

Risks, designs, and research for fire safety in spacecraft [NASA-TM-105317] p 240 N92-13581

V

VALAVANI, L.

A Lyapunov based nonlinear control scheme for stabilizing a basic compression system using a close-coupled control valve p 246 A92-29316

VALCO, G. J.

Laser ablated YBa₂Cu₃O_{7-x} high temperature superconductor coplanar waveguide resonator p 155 A92-31631

VALCO, MARK J.

Boeing Helicopters Advanced Rotorcraft Transmission (ART) Program summary of component tests [AIAA PAPER 92-3364] p 205 A92-48937

VAN AKEN, D. C.

Microstructure and mechanical properties of near eutectic beta-NiAl plus alpha-Re alloys produced by rapid solidification and extrusion p 119 A92-30844

VAN DE WALL, ALLAN G.

A fast, uncoupled, compressible, two-dimensional, unsteady boundary layer algorithm with separation for engine inlets [AIAA PAPER 92-3082] p 11 A92-48729

VAN DRESAR, N. T.

Self-pressurization of a lightweight liquid hydrogen tank - Effects of fill level at low wall heat flux [AIAA PAPER 92-0818] p 60 A92-29591

Pressurization of cryogenics - A review of current technology and its applicability to low-gravity conditions [AIAA PAPER 92-3061] p 72 A92-54002

VAN FOSSEN, G. J.

Heat transfer measurements from a smooth NACA 0012 airfoil p 165 A92-20215

Roughness effects on heat transfer from a NACA 0012 airfoil p 166 A92-20217

Increased heat transfer to elliptical leading edges due to spanwise variations in the freestream momentum - Numerical and experimental results [AIAA PAPER 92-3070] p 13 A92-54005

VANDERAAR, M.

Destination directed packet switch architecture for a geostationary communication satellite network [IAF PAPER 92-0413] p 50 A92-55793

VANDERAAR, MARK

Least reliable bits coding (LRBC) for high data rate satellite communications [AIAA PAPER 92-1868] p 142 A92-29807

Flexible digital modulation and coding synthesis for satellite communications p 148 N92-14235

Least Reliable Bits Coding (LRBC) for high data rate satellite communications [NASA-TM-105431] p 150 N92-18921

VANDEWALL, ALLAN G.

A fast, uncoupled, compressible, two-dimensional, unsteady boundary layer algorithm with separation for engine inlets [NASA-TM-105686] p 195 N92-27653

- VANDRESAR, N. T.**
Self-pressurization of a lightweight liquid hydrogen tank: Effects of fill level at low wall heat flux [NASA-TM-105411] p 135 N92-18442
Pressurization of cryogenics: A review of current technology and its applicability to low-gravity conditions [NASA-TM-105746] p 136 N92-29669
- VANFOSSEN, G. JAMES**
Modelling and experimental verification of a water alleviation system for the NASP [NASA-TM-105661] p 189 N92-23224
- VANKA, S. P.**
Hot gas environment around STOVL aircraft in ground proximity. II - Numerical study p 25 A92-24403
Calculations of hot gas ingestion for a STOVL aircraft model [AIAA PAPER 92-0385] p 25 A92-28191
Multigrad calculations of a jet in crossflow p 170 A92-28525
- VANKA, SURYA P.**
Calculations of hot gas ingestion for a STOVL aircraft model [NASA-TM-105437] p 17 N92-19993
- VANNUCCI, R. D.**
High molecular weight first generation PMR polyimides for 343 C applications p 105 A92-49819
- VANNUCCI, RAYMOND D.**
Effects of a noncoplanar biphenyldiamine on the processing and properties of addition polyimides [NASA-TM-105383] p 107 N92-15137
High molecular weight first generation PMR polyimides for 343 C applications [NASA-TM-105364] p 129 N92-19498
Vinyl capped addition polyimides [NASA-CASE-LEW-15027-2] p 131 N92-24053
- VARY, ALEX**
Tensile strain measurements of ceramic fibers using scanning laser acoustic microscopy p 198 A92-39629
Tensile strain measurements of ceramic fibers using scanning laser acoustic microscopy [NASA-TM-105589] p 216 N92-24986
- VASEK, THOMAS E.**
Development of a ninety string solar array simulator p 46 A92-50660
Development of a ninety string solar array simulator [NASA-TM-105278] p 55 N92-11086
- VAUGHAN, DAVID F.**
Effects of oxygen concentration on radiative loss from normal-gravity and microgravity methane diffusion flames [AIAA PAPER 92-0243] p 113 A92-26928
- VEATCH, MARK S.**
Comparative evaluation of optical waveguides as alternative interconnections for high performance packaging p 153 N92-32974
- VEERARAGHAVAN, SHOBA**
Large-scale microwave anisotropy from gravitating seeds p 269 A92-56914
- VEITCH, LISA C.**
CVD of silicon carbide on structural fibers: Microstructure and composition [NASA-TM-105385] p 107 N92-18439
Guanidine based vehicle/binders for use with oxides, metals, and ceramics [NASA-CASE-LEW-15314-1] p 131 N92-23461
- VENKATESWARAN, S.**
Propulsion-related flowfields using the preconditioned Navier-Stokes equations [AIAA PAPER 92-3437] p 178 A92-48994
- VENTO, D. M.**
CONE - An STS-based cryogenic fluid management experiment p 43 A92-23850
- VERDON, J. M.**
Development of an efficient analysis for high Reynolds number inviscid/viscid interactions in cascades [AIAA PAPER 92-3073] p 10 A92-48723
- VERDON, JOSEPH M.**
Development of a steady potential solver for use with linearized, unsteady aerodynamic analyses [NASA-TM-105288] p 31 N92-20525
- VERES, JOSEPH P.**
A survey of instabilities within centrifugal pumps and concepts for improving the flow range of pumps in rocket engines [NASA-TM-105439] p 84 N92-18280
- VERHOFF, VINCENT G.**
Transonic turbine blade cascade testing facility [AIAA PAPER 92-4034] p 42 A92-56856
Transonic turbine blade cascade testing facility [NASA-TM-105646] p 47 N92-26129
Three-dimensional laser window formation [NASA-RP-1280] p 47 N92-30307
- VERRILLI, M. J.**
Application of a thermal fatigue life prediction model to high-temperature aerospace alloys B1900 + Hf and Haynes 188 p 121 A92-45232
- Thermomechanical and bithermal fatigue behavior of cast B1900 + Hf and wrought Haynes 188 p 122 A92-45233
- VETRONE, ROBERT H.**
Test facilities for high power electric propulsion [NASA-TM-105247] p 80 N92-11136
- VIJAYARAGHAVAN, D.**
Effect of type and location of oil groove on the performance of journal bearings p 203 A92-21333
Frequency effects on the stability of a journal bearing for periodic loading p 203 A92-22665
Frequency effects on the stability of a journal bearing for periodic loading [NASA-TM-105226] p 186 N92-18809
Effect of out-of-roundness on the performance of a diesel engine connecting-rod bearing [NASA-TM-105600] p 215 N92-31536
- VINALS, JORGE**
Effective diffusion equation in a random velocity field [AIAA PAPER 92-0245] p 167 A92-25704
- VINH, NGUYEN X.**
Canonical transformations for space trajectory optimization [AIAA PAPER 92-4509] p 44 A92-52079
- VITERI, F.**
Design and test of an oxygen turbopump for a dual expander cycle rocket engine p 59 A92-21062
- VITTA, SATISH**
Magnetic flux relaxation in YBa₂Cu₃O(7-x) thin film: Thermal or athermal p 265 N92-32984
- VLCEK, B. L.**
Qualitative investigation of cryogenic fluid injection into a supersonic flow field p 164 A92-13360
- VOTH, R. O.**
Liquid-vapour surface sensors for liquid nitrogen and hydrogen p 197 A92-23852
- Vranos, A.**
Experimental study of cross-stream mixing in a rectangular duct [AIAA PAPER 92-3090] p 178 A92-48735
Experimental study of cross-stream mixing in a rectangular duct [NASA-TM-105694] p 36 N92-27652
- W**
- WADEL, MARY F.**
Propulsion systems using in situ propellants for a Mars Ascent Vehicle [AIAA PAPER 92-3445] p 66 A92-49001
Propulsion systems using in situ propellants for a Mars ascent vehicle [NASA-TM-105741] p 89 N92-27654
- WAGNER, J. H.**
Heat transfer in rotating serpentine passages with trips normal to the flow [ASME PAPER 91-GT-265] p 165 A92-15663
Heat transfer in rotating serpentine passages with trips skewed to the flow [NASA-TM-105581] p 186 N92-20235
- WAGNER, P.**
Destination directed packet switch architecture for a geostationary communication satellite network [IAF PAPER 92-0413] p 50 A92-55793
- WAGNER, PAUL**
Least reliable bits coding (LRBC) for high data rate satellite communications [AIAA PAPER 92-1868] p 142 A92-29807
Least Reliable Bits Coding (LRBC) for high data rate satellite communications [NASA-TM-105431] p 150 N92-18921
- WAI, MING TO**
Numerical simulation of conservation laws p 193 N92-25813
- WALD, LAWRENCE W.**
The Solar Array Module Plasma Interactions Experiment (SAMPIE) - A Shuttle-based plasma interactions experiment p 69 A92-50583
- WALKER, J. D. A.**
The three-dimensional turbulent boundary layer near a plane of symmetry p 167 A92-24757
- WALKER, K. P.**
A viscoplastic model for single crystals p 217 A92-24717
Stress versus temperature dependence of activation energies for creep p 217 A92-24719
A viscoplastic theory with thermodynamic considerations [ONERA, TP NO. 1991-220] p 217 A92-26372
A viscoplastic theory with thermodynamic considerations p 219 A92-33903
- WALKER, KEVIN P.**
Microstress analysis of periodic composites p 218 A92-30673
- Three-dimensional deformation analysis of two-phase dislocation substructures p 121 A92-44218
Asymptotic integration algorithms for first-order ODEs with application to viscoplasticity [NASA-TM-105587] p 250 N92-24974
- WALLACE, D. A.**
Final design of a free-piston hydraulic advanced Stirling conversion system p 206 A92-50798
- WALTERS, J. L.**
SCAILET - An intelligent assistant for satellite ground terminal operations [IAF PAPER 92-0552] p 245 A92-55855
- WALTERS, JERRY L.**
An overview of Space Communication Artificial Intelligence for Link Evaluation Terminal (SCAILET) Project p 148 N92-14212
- WALTERS, ROBERT W.**
Upwind relaxation methods for the Navier-Stokes equations using inner iterations p 170 A92-29553
- WALTON, JAMES T.**
An improved heat transfer configuration for a solid-core nuclear thermal rocket engine [AIAA PAPER 92-3583] p 75 A92-54063
An overview of tested and analyzed NTP concepts [NASA-TM-105252] p 80 N92-11137
- WALTON, JOANNE C.**
Multiple-access phased array antenna simulator for a digital beam forming system investigation [NASA-TM-105422] p 149 N92-17062
- WANG, HAI**
Optimization and analysis of large chemical kinetic mechanisms using the solution mapping method - Combustion of methane p 113 A92-19300
- WANG, HUA**
Boundary formulations for shape sensitivity of temperature dependent conductivity problems p 217 A92-25403
- WANG, J.**
The formation and structure of plasma wakes behind large high-voltage space platforms in ionosphere [AIAA PAPER 92-0577] p 239 A92-26984
Ionospheric plasma flow over large high-voltage space platforms. I - Ion-plasma-time scale interactions of a plate at zero angle of attack. II - The formation and structure of plasma wake p 258 A92-41359
- WANG, J.-C.**
Application of face-gear drives in helicopter transmissions [NASA-TM-105655] p 212 N92-28434
Minimization of deviations of gear real tooth surfaces determined by coordinate measurements [NASA-TM-105718] p 214 N92-30948
- WANG, L. W.**
Convective flows in enclosures with vertical temperature or concentration gradients p 171 A92-32277
- WANG, M. R.**
Reconfigurable optical interconnection network for multimode optical fiber sensor arrays p 256 A92-37448
- WANG, MICHAEL R.**
Multiple-mode reconfigurable electro-optic switching network for optical fiber sensor array p 256 A92-46245
- WANG, R.**
A combined vector potential-scalar potential method for FE computation of 3D magnetic fields in electrical devices with iron cores p 154 A92-23959
- WANG, ZHU**
A conformal block structured grid for turbomachinery cascades in two dimensions p 248 A92-47059
- WANLASS, M. W.**
Modeled performance of monolithic, 3-terminal InP/Ga(0.47)In(0.53)As concentrator solar cells as a function of temperature and concentration ratio p 234 A92-53153
InP concentrator solar cells p 234 A92-53166
- WANUGA, STEPHEN**
Interfaces for high-speed fiber-optic links - Analysis and experiment p 256 A92-24002
- WARD, J. S.**
Modeled performance of monolithic, 3-terminal InP/Ga(0.47)In(0.53)As concentrator solar cells as a function of temperature and concentration ratio p 234 A92-53153
InP concentrator solar cells p 234 A92-53166
- WARNER, J. D.**
Microwave properties of YBa₂Cu₃O(7-delta) high-transition-temperature superconducting thin films measured by the power transmission method p 153 A92-14938
Microwave conductivity of laser ablated YBa₂Cu₃O(7-delta) superconducting films and its relation to microstrip transmission line performance p 264 N92-21639

WARNER, JOSEPH D.

WARNER, JOSEPH D.

Dependence of the critical temperature of laser-ablated $\text{YBa}_2\text{Cu}_3\text{O}_{7-\delta}$ thin films on LaAlO_3 substrate growth technique p 264 N92-23415
Magnetic flux relaxation in $\text{YBa}_2\text{Cu}_3\text{O}_{7-x}$ thin film: Thermal or athermal p 265 N92-32984

WARREN, JOHN

NASA/DOE/DOD nuclear propulsion technology planning: Summary of FY 1991 interagency panel results [NASA-TM-105703] p 88 N92-26792

WARSHAY, MARVIN

Space Electrochemical Research and Technology Conference, 3rd, NASA Lewis Research Center, Cleveland, OH, Apr. 9, 10, 1991, Proceedings p 231 A92-18936

WASSERBAUER, C. A.

NASA low-speed centrifugal compressor for 3-D viscous code assessment and fundamental flow physics research [ASME PAPER 91-GT-140] p 3 A92-15580

WATANABE, YOICHI

Radiation enhanced dissociation of hydrogen in nuclear rockets [AIAA PAPER 92-3817] p 67 A92-49129

WATERS, JOHN F.

Addition curing thermosets endcapped with 4-amino (2,2) paracyclophane p 124 A92-33918

WATERS, WILLIAM J.

Novel applications for TAZ-8A p 123 N92-22444

WATSON, BRIAN C.

A study of equation solvers for linear and non-linear finite element analysis on parallel processing computers [AIAA PAPER 92-2478] p 242 A92-34367

WEIDMAN, P. D.

On the drag of model dendrite fragments at low Reynolds number p 95 A92-50868

WEIKLE, DONALD H.

An optical method for determining level in two-phase cryogenic fluids [NASA-TM-104524] p 200 N92-15366

WEILAND, KAREN J.

Intensified array camera imaging of solid surface combustion aboard the NASA Learjet [AIAA PAPER 92-0240] p 137 A92-25702
Intensified array camera imaging of solid surface combustion aboard the NASA Learjet [NASA-TM-105361] p 138 N92-16156

WEINBERG, ERICK J.

A classical instability of Reissner-Nordstrom solutions and the fate of magnetically charged black holes p 267 A92-26397

WEINBERG, I.

Recent progress in InP solar cell research p 158 A92-50653
High voltage thermally diffused p(+)-In solar cells p 235 A92-53172
Radiation and temperature effects in heteroepitaxial and homoepitaxial InP cells p 159 A92-53192
Status and future directions of InP solar cell research [NASA-TM-105426] p 160 N92-18920
Defect behavior, carrier removal and predicted in-space injection annealing of InP solar cells [NASA-TM-105624] p 161 N92-23562

WEINBERG, IRVING

Photoluminescence lifetime measurements in InP wafers p 262 A92-48092
Advanced power systems for EOS p 70 A92-50640
Minority carrier lifetime in indium phosphide p 262 A92-53148
Theoretical modeling, near-optimum design and predicted performance of n(+)-pp(+) and p(+)-nn(+) indium phosphide homojunction solar cells p 234 A92-53152
High performance etchant for thinning p(+)-InP and its application to p(+)-In solar cell fabrication p 263 A92-53155
Enhanced EOS photovoltaic power system capability with InP solar cells p 81 N92-13248

WEINGARTNER, STEFAN

Power supply for a manned international asteroid mission p 80 N92-13205

WEIR, L. J.

Three-dimensional viscous analysis of a Mach 5 inlet and comparison with experimental data p 8 A92-28526

WEISLOGEL, MARK

Drop-tower experiments for capillary surfaces in an exotic container p 166 A92-20743
Stability of capillary surfaces p 172 A92-35979

WEISLOGEL, MARK W.

Pulse thermal energy transport/storage system [NASA-CASE-LEW-15235-1] p 195 N92-29125

WEISS, J. M.

Propulsion-related flowfields using the preconditioned Navier-Stokes equations [AIAA PAPER 92-3437] p 178 A92-48994

WEISS, JONATHAN M.

Rocket plume flowfield characterization using laser Rayleigh scattering [AIAA PAPER 92-3351] p 66 A92-48928
Species and temperature measurement in H_2/O_2 rocket flow fields by means of Raman scattering diagnostics [AIAA PAPER 92-3353] p 178 A92-48930
Rocket plume flowfield characterization using laser Rayleigh scattering [NASA-TM-105739] p 257 N92-28475

WEIZER, V. G.

Sinterless contacts to shallow junction InP solar cells [NASA-TM-105670] p 237 N92-24802

WEIZER, VICTOR G.

A very low resistance, non-sintered contact system for use on indium phosphide concentrator/shallow junction solar cells p 233 A92-53146
A very low resistance, non-sintered contact system for use on indium phosphide concentrator/shallow junction solar cells [NASA-TM-105279] p 235 N92-13482
The achievement of low contact resistance to indium phosphide: The roles of Ni, Au, Ge, and combinations thereof [NASA-TM-105770] p 238 N92-33895

WELLBORN, S. R.

An experimental investigation of the flow in a diffusing S-duct [AIAA PAPER 92-3622] p 13 A92-54090
Navier-Stokes analysis and experimental data comparison of compressible flow within ducts [NASA-TM-105796] p 38 N92-30972

WELLBORN, STEVEN R.

Navier-Stokes analysis and experimental data comparison of compressible flow in a diffusing S-duct [AIAA PAPER 92-2699] p 10 A92-45541
Navier-Stokes analysis and experimental data comparison of compressible flow in a diffusing S-duct [NASA-TM-105683] p 38 N92-33746

WELLS, S.

Finite wing aerodynamics with simulated glaze ice [AIAA PAPER 92-0414] p 5 A92-26265

WELSCH, G.

Fatigue damage accumulation in nickel prior to crack initiation p 120 A92-33947

WENDT, BRUCE J.

The structure and development of streamwise vortex arrays embedded in a turbulent boundary layer [AIAA PAPER 92-0551] p 7 A92-28204
The structure and development of streamwise vortex arrays embedded in a turbulent boundary layer [NASA-TM-105211] p 14 N92-10012

WERNET, MARK P.

A 4-spot time-of-flight anemometer for small centrifugal compressor velocity measurements [NASA-TM-105717] p 202 N92-29105

WERNLUND, J. V.

Flexible high speed CODEC (FHSC) [AIAA PAPER 92-1919] p 143 A92-29848

WEST, JEFF

Opposed flow flame spread in normal, enhanced and reduced gravity p 111 A92-12898

WESTERLUND, LARRY H.

Laser beamed power - Satellite demonstration applications [IAF PAPER 92-0600] p 76 A92-57056

WETHERHOLD, R. C.

Effect of fiber orientation on the fracture toughness of brittle matrix composites p 103 A92-41841

WETHERHOLD, ROBERT C.

Load redistribution considerations in the fracture of ceramic matrix composites [AIAA PAPER 92-2494] p 221 A92-34586

WETZEL, KYLE K.

Preliminary investigation of a low power pulsed arcjet thruster [AIAA PAPER 92-3113] p 64 A92-48752

WEYL, G.

Arcing of negatively biased solar cells in a plasma environment. I - Experimental observations [AIAA PAPER 92-2990] p 63 A92-47000

WEYL, G. M.

Arcing of negatively biased solar cells in low earth orbit [AIAA PAPER 92-0578] p 59 A92-26985

WHALEN, MARGARET V.

Slush hydrogen (SLH2) technology development for application to the National Aerospace Plane (NASP) p 140 A92-13432

Technology issues associated with using densified hydrogen for space vehicles [AIAA PAPER 92-3079] p 134 A92-48727

Slush hydrogen pressurized expulsion studies at the NASA K-Site Facility [AIAA PAPER 92-3385] p 141 A92-48951

Technology issues associated with using densified hydrogen for space vehicles p 135 N92-25277

[NASA-TM-105642] p 135 N92-25277
Slush hydrogen transfer studies at the NASA K-Site Test Facility p 135 N92-25957

[NASA-TM-105596] p 135 N92-25957
Slush hydrogen pressurized expulsion studies at the NASA K-Site Facility [NASA-TM-105597] p 135 N92-26131

WHEELER, DONALD R.

A vacuum (10(exp -9) Torr) friction apparatus for determining friction and endurance life of MoSx films [NASA-TM-104478] p 129 N92-16129

WHITE, C. W.

A 1 MW, 100 kV, less than 100 kg space based dc-dc power converter p 157 A92-50537

WHITE, CRAIG D.

Studies of the effects of curvature on dilution jet mixing p 166 A92-21079

WHITE, L. W.

Satellite delivery of B-ISDN services [AIAA PAPER 92-1831] p 142 A92-29777

Technical and economic feasibility of integrated video service by satellite [AIAA PAPER 92-2054] p 145 A92-29966

WHITFIELD, DAVID L.

Unsteady flowfield simulation of ducted prop-fan configurations [AIAA PAPER 92-0521] p 6 A92-26946

WHITTENBERGER, J. D.

Slow strain rate 1200-1400 K compressive properties of NiAl-1Hf p 116 A92-17977

Compressive strength of directionally solidified NiAl-NiAlNb intermetallics at 1200 and 1300 K p 117 A92-28248

Compression, bend, and tension studies on forged Al67Ti25Cr8 and Al66Ti25Mn(g) L1(2) compounds p 118 A92-30766

Does a threshold stress for creep exist in HfC-dispersed NiAl? p 118 A92-30780

Compression studies on particulate composites of ternary Al-Ti-Fe, and quaternary Al-Ti-Fe-Nb and Al-Ti-Fe-Mn L1(2) compounds p 119 A92-30845

Comments on the paper 'Does the subgrain size influence the rate of creep?' p 260 A92-33946
Mechanical properties of monolithic and particulate composites of L12 forms of Al3Ti p 101 A92-36273

Interdiffusion between the L1(2) trialuminides Al66Ti25Mn9 and Al67Ti25Cr8 p 120 A92-37088

1200 and 1300 K slow plastic compression properties of Ni-50Al composites p 102 A92-38125

1400 and 1500 K compressive creep properties of an NiAl-AIN composite p 103 A92-41575

Discontinuously reinforced intermetallic matrix composites via XD synthesis p 103 A92-41867

Cyclic oxidation resistance of a reaction milled NiAl-AIN composite p 105 A92-46871

Composites of low-density trialuminides: Particulate and long fiber reinforcements p 109 N92-25346

WHYTE, WAYNE A., JR.

Real-time data compression of broadcast video signals [NASA-CASE-LEW-14945-2] p 147 N92-10128

Real-time demonstration hardware for enhanced DPCM video compression algorithm [NASA-TM-105616] p 150 N92-19700

WICKENHEISER, TIMOTHY J.

NASA/DOE/DOD nuclear propulsion technology planning: Summary of FY 1991 interagency panel results [NASA-TM-105703] p 88 N92-26792

WICKMAN, JOHN H.

Gelled liquid oxygen/metal powder monopropellants [AIAA PAPER 92-3450] p 134 A92-49004

WIESERMAN, W. R.

Comparison of high temperature, high frequency core loss and dynamic B-H loops of two 50 Ni-Fe crystalline alloys and an iron-based amorphous alloy p 157 A92-50551

Comparison of high temperature, high frequency core loss and dynamic B-H loops of a 2V-49Fe-49Co and a grain oriented 3Si-Fe alloy [NASA-TM-105791] p 162 N92-30397

WIJAYARATNA, W. M. K. P.

Extrapolation procedures in Mott electron polarimetry p 197 A92-21241

WILBUR, PAUL J.

An experimental study of impingement-ion-production mechanisms [AIAA PAPER 92-3826] p 76 A92-54190

WILCOX, KATHERINE G.

Using EPSAT to analyze high power systems in the space environment p 158 A92-50580

WILCOX, WILLIAM R.

Transport modes during crystal growth in a centrifuge p 138 A92-33835

- WILKINSON, R. ALLEN**
Critical fluid thermal equilibration experiment (19-IML-1) p 139 N92-23640
- WILLIAMS, A. E.**
Performance of a Y-Ba-Cu-O superconducting filter/GaAs low noise amplifier hybrid circuit [NASA-TM-105546] p 160 N92-21370
Performance of a Y-Ba-Cu-O superconducting filter/GaAs low noise amplifier hybrid circuit p 163 N92-32982
- WILLIAMS, BEN R.**
Hot gas ingestion characteristics and flow visualization of a vectored thrust STOVL concept p 26 A92-45316
- WILLIAMS, FORMAN A.**
Microgravity combustion of isolated n-decane and n-heptane droplets [AIAA PAPER 92-0242] p 113 A92-26927
- WILLIAMS, GEORGE J.**
Krypton ion thruster performance [NASA-TM-105818] p 92 N92-31901
- WILLIAMS, GEORGE J., JR.**
Krypton ion thruster performance [AIAA PAPER 92-3144] p 64 A92-48772
- WILLIAMS, GLENN L.**
A video event trigger for high frame rate, high resolution video technology p 160 N92-22453
- WILLIAMSON, W. S.**
Plasma erosion rate diagnostics using laser-induced fluorescence p 198 A92-36738
- WILLIS, EDWARD A.**
NASA's rotary engine technology enablement program: 1983-1991 [NASA-TM-105562] p 30 N92-20033
- WILSON, D. S.**
Magnetic bearings for free-piston Stirling engines [NASA-TM-105730] p 214 N92-30734
- WILSON, J. F.**
A low-power, high-efficiency Ka-band TWTA p 156 A92-38163
- WILSON, JACK**
Perturbation of a normal shock - A test case for unsteady Euler codes [AIAA PAPER 92-3180] p 178 A92-48795
- WILSON, JOHN F.**
A low-power, high-efficiency Ka-band TWTA [AIAA PAPER 92-1822] p 154 A92-29769
- WILT, THOMAS E.**
Influence of engineered interfaces on residual stresses and mechanical response in metal matrix composites [NASA-TM-105438] p 109 N92-23195
- WINSA, E.**
The isothermal dendritic growth experiment - A USMP-2 space flight experiment [AIAA PAPER 92-0350] p 137 A92-28188
- WINTER, JERRY M.**
Status of NASA's Stirling space power converter program p 69 A92-50608
The NASA CSTI High Capacity Power Program [NASA-TM-105240] p 236 N92-16481
Progress update of NASA's free-piston Stirling space power converter technology project [NASA-TM-105748] p 239 N92-33898
- WINTUCKY, E. G.**
Space applications of high temperature superconductivity technology [IAF PAPER 91-307] p 259 A92-14724
- WINTUCKY, EDWIN G.**
NASA Space applications of high-temperature superconductors [NASA-TM-105401] p 271 N92-18455
- WIRTH, D. G.**
Combustion synthesis of TiB₂-Al₂O₃-Al composite materials p 102 A92-36391
Combustion synthesis of ceramic-metal composite materials - The TiC-Al₂O₃-Al system p 115 A92-55139
- WITROW, C. A.**
Design of multihundred-watt dynamic isotope power system for robotic space missions p 69 A92-50633
SEI power source alternatives for rovers and other multi-kWe distributed surface applications p 80 N92-13206
- WITROW, COLLEEN A.**
SEI rover solar-electrochemical power system options p 45 A92-50574
- WONG, E.**
Implementation of an intelligent control system [NASA-TM-105795] p 241 N92-33897
- WONG, KAM L.**
Reliability training [NASA-RP-1253] p 49 N92-32456
- WONG, WAYNE A.**
Update on results of SPRE testing at NASA Lewis p 71 A92-50780
- NASA Lewis Stirling SPRE testing and analysis with reduced number of cooler tubes [NASA-TM-105767] p 238 N92-28837
- WONGCHOTIGUL, K.**
Anodic etching of p-type cubic silicon carbide p 127 A92-57027
- WOO, K.**
Experimental code verification results for reflector antenna distortion compensation by array feeds [AIAA PAPER 92-2014] p 49 A92-29933
- WOOD, J. R.**
NASA low-speed centrifugal compressor for 3-D viscous code assessment and fundamental flow physics research [ASME PAPER 91-GT-140] p 3 A92-15580
- WOODWARD, RICHARD P.**
Far-field noise and internal modes from a ducted propeller at simulated aircraft takeoff conditions [AIAA PAPER 92-0371] p 252 A92-26230
Noise of two high-speed model counter-rotation propellers at takeoff/approach conditions p 253 A92-46799
Far-field noise and internal modes from a ducted propeller at simulated aircraft takeoff conditions [NASA-TM-105369] p 254 N92-16702
An evaluation of some alternative approaches for reducing fan tone noise [NASA-TM-105356] p 255 N92-18282
- WOOLLAM, J. A.**
Study of InGaAs-based modulation doped field effect transistor structures using variable-angle spectroscopic ellipsometry p 265 N92-32977
- WOOLLAM, JOHN A.**
Atomic oxygen effects on thin film space coatings studied by spectroscopic ellipsometry, atomic force microscopy, and laser light scattering [AIAA PAPER 92-2172] p 94 A92-31300
Study of temperature-dependent ultrathin oxide growth on Si(111) using variable-angle spectroscopic ellipsometry p 260 A92-32414
- WORTMAN, A.**
Detonation duct gas generator demonstration program [AIAA PAPER 92-3174] p 27 A92-54011
- WRIGHT, DAVID L.**
ACTS system capability and performance [AIAA PAPER 92-1961] p 143 A92-29884
Operational uses of ACTS technology [AIAA PAPER 92-1964] p 144 A92-29887
- WRIGHT, THEODORE**
Description of real-time Ada software implementation of a power system monitor for the Space Station Freedom PMAD DC testbed p 242 A92-50533
- WRIGHT, W. B.**
Numerical analysis of a thermal deicer [AIAA PAPER 92-0527] p 22 A92-26950
- WU, C.**
Spatial instability of a swirling jet - Theory and experiment p 174 A92-41274
A computational study of advanced exhaust system transition ducts with experimental validation [AIAA PAPER 92-3794] p 179 A92-49126
- WU, C. S.**
V-band pseudomorphic HEMT MMIC phased array components for space communications p 151 N92-32966
- WU, C. Y.**
Crystalline orientations of Ti₂Ba₂Ca₂Cu₃O(x) grains on MgO, SrTiO₃, and LaAlO₃ substrates p 261 A92-41637
- WU, M.-K.**
Life extending control for rocket engines [NASA-TM-105789] p 142 N92-31263
- WU, RICHARD L. C.**
Synthesis and characterization of fine grain diamond films p 262 A92-46330
Environmental effects on friction and wear of diamond and diamondlike carbon coatings [NASA-TM-105634] p 131 N92-23192
- WU, T. W.**
Comparison of analysis and experiment for gearbox noise [NASA-TM-105330] p 210 N92-25396
- WU, X. F.**
Validation of finite element and boundary element methods for predicting structural vibration and radiated noise [NASA-TM-105359] p 213 N92-29697
- WU, X.-T.**
A new response surface approach for structural reliability analysis [AIAA PAPER 92-2408] p 219 A92-34339
- WU, Y.-T.**
Structural system reliability calculation using a probabilistic fault tree analysis method [AIAA PAPER 92-2410] p 251 A92-34341
- Recent developments of the NESSUS probabilistic structural analysis computer program [AIAA PAPER 92-2411] p 242 A92-34342
Structural reliability assessment capability in NESSUS [AIAA PAPER 92-3417] p 223 A92-48976
- WURDEN, GLEN**
Preliminary investigation of power flow and electrode phenomena in a multi-megawatt coaxial plasma thruster [AIAA PAPER 92-3741] p 75 A92-54144

X

- XIA, LEI**
Temperature control in continuous furnace by structural diagram method p 246 A92-29162
- XIE, MINGJUN**
Minimization of vibration in elastic beams with time-variant boundary conditions p 224 A92-50511
- XU, KANG**
Micromechanical model of crack growth in fiber reinforced brittle materials p 223 A92-46829

Y

- YAMAGUCHI, KEIKO**
Heat transfer on accreting ice surfaces p 166 A92-24415
- YANCEY, R. N.**
NDE of advanced turbine engine components and materials by computed tomography [ASME PAPER 91-GT-287] p 215 A92-15681
- YANG, D.**
dc and microwave performance of a 0.1-micron gate InAs/In(0.52)Al(0.48)As MODFET p 156 A92-43891
High-field transport properties of InAs(x)P(1-x)/InP (x = 0.3-1.0) modulation doped heterostructures at 300 and 77 K p 262 A92-46331
- YANG, J. C.**
Observations of soot during droplet combustion at low gravity - Heptane and heptane/monochloroalkane mixtures p 115 A92-50447
- YANG, JAE Y.**
Shrinkage void formation and its effect on freeze and thaw processes of lithium and lithium-fluoride for space applications p 180 A92-50596
- YANG, LIFENG**
Functional models of power electronic components for system studies p 157 A92-50558
Modeling of Space Station power system components and their interactions p 68 A92-50559
- YANG, N. Y. C.**
Diffusion mechanisms in chemical vapor-deposited indium coated on chemical vapor-deposited rhenium p 117 A92-28017
- YANG, VIGOR**
Combustion of liquid-fuel droplets in supercritical conditions p 114 A92-43778
- YANG, WEN-JEI**
Thermophysical properties of lysozyme (protein) solutions p 240 A92-44385
- YANG, Z.**
Nonlinear dynamics near the stability margin in rotating pipe flow p 165 A92-19959
A kappa-epsilon calculation of transitional boundary layers [NASA-TM-105604] p 187 N92-22398
A new time scale based k-epsilon model for near wall turbulence [NASA-TM-105768] p 196 N92-32868
- YANIEC, J.**
Repair-level analysis for Space Station Freedom [AIAA PAPER 92-1537] p 43 A92-38634
- YAO, H. D.**
Study of InGaAs-based modulation doped field effect transistor structures using variable-angle spectroscopic ellipsometry p 265 N92-32977
- YAO, MINWU**
Asymptotic integration algorithms for first-order ODEs with application to viscoplasticity [NASA-TM-105587] p 250 N92-24974
- YEH, F. C.**
Heat transfer in rotating serpentine passages with trips normal to the flow [ASME PAPER 91-GT-265] p 165 A92-15663
Heat transfer in rotating serpentine passages with trips skewed to the flow [NASA-TM-105581] p 186 N92-20235
- YEH, FREDERICK**
Aerodynamics and heat transfer investigations on a high Reynolds number turbine cascade [ASME PAPER 91-GT-157] p 164 A92-15593
- YENNI, EDWARD J.**
Large transient fault current test of an electrical roll ring p 55 A92-50661

YERKES, J. W.

Large transient fault current test of an electrical roll ring
[NASA-TM-105667] p 87 N92-24201

YERKES, J. W.

A high-performance photovoltaic concentrator array - The mini-dome Fresnel lens concentrator with 30 percent efficient GaAs/GaSb tandem cells p 72 A92-53199

YETTER, R. A.

A computer model for one-dimensional mass and energy transport in and around chemically reacting particles, including complex gas-phase chemistry, multicomponent molecular diffusion, surface evaporation, and heterogeneous reaction p 181 A92-52406

YEUN, J. J.

An investigation of shock/turbulent boundary layer bleed interactions [AIAA PAPER 92-3085] p 182 A92-54008

YODER, DENNIS A.

Brush seal leakage performance with gaseous working fluids at static and low rotor speed conditions [NASA-TM-105400] p 186 N92-16265

YOKOTA, JEFFREY W.

Vorticity dynamics of inviscid shear layers [AIAA PAPER 92-0420] p 168 A92-26270

YORK, THOMAS M.

Plasma flow processes within magnetic nozzle configurations p 67 A92-50266

YOUNG, G. W.

Steady-state thermal-solutal convection and diffusion in a simulated float zone p 137 A92-17056

YOUNG, P. G.

Temperature independent quantum well FET with delta channel doping p 157 A92-49596

YOUNG, PAUL G.

Microwave properties of peeled HEMT devices sapphire substrates p 265 N92-32978

YU, JOHN

Multiple-access phased array antenna simulator for a digital beam forming system investigation [NASA-TM-105422] p 149 N92-17062

YU, JUN S.

Design characteristics of a heat pipe test chamber [NASA-TM-105737] p 238 N92-29662

YU, S. T.

Runge-Kutta methods combined with compact difference schemes for the unsteady Euler equations [AIAA PAPER 92-3210] p 182 A92-54015
Simulations of free shear layers using a compressible kappa-epsilon model p 190 N92-23355

YU, SHENG-TAO

Three-dimensional calculations of supersonic reacting flows using an LU scheme p 179 A92-50465

YUNGKURTH, C.

The F/A-18 external burning flight test [AIAA PAPER 91-5050] p 23 A92-44547

YUNGSTER, SHAYE

Numerical study of shock-wave/boundary-layer interactions in premixed combustible gases p 183 A92-54907

YUNGSTER, SHAYNE

Study of shock-induced combustion using an implicit TVD scheme p 116 N92-25816

YUNIS, I.

Simulation of Space Station loads with active control systems p 56 N92-23824

Z

ZACCARIA, M.

Investigation of three-dimensional flow field in a turbine including rotor/stator interaction. I - Design development and performance of the research facility [AIAA PAPER 92-3325] p 40 A92-48908

Investigation of three-dimensional flow field in a turbine including rotor/stator interaction. II - Three-dimensional flow field at the exit of the nozzle [AIAA PAPER 92-3326] p 12 A92-48909

ZAKHEM, R.

On the drag of model dendrite fragments at low Reynolds number p 95 A92-50868

ZAKRAJSEK, JAMES J.

Modal simulation of gearbox vibration with experimental correlation [AIAA PAPER 92-3494] p 207 A92-54036

Effect of operating conditions on gearbox noise [NASA-TM-105331] p 211 N92-26107

Analysis and modification of a single-mesh gear fatigue rig for use in diagnostic studies [NASA-TM-105416] p 212 N92-27879

Modal simulation of gearbox vibration with experimental correlation [NASA-TM-105702] p 215 N92-31485

ZAKRAJSEK, R.

Ka-band MMIC arrays for ACTS Aero Terminal Experiment [IAF PAPER 92-0398] p 159 A92-55785

ZALLER, MICHELLE M.

Coaxial injector spray characterization using water/air as simulants [NASA-TM-105322] p 82 N92-14112

ZAMAN, A. J.

Experimental code verification results for reflector antenna distortion compensation by array feeds [AIAA PAPER 92-2014] p 49 A92-29933

ZAMAN, AFROZ J. M.

Effect of an arcjet plume on satellite reflector performance p 53 A92-16318

ZAMAN, K. B. M. Q.

On the mechanism of turbulence suppression in free shear flows under acoustic excitation [AIAA PAPER 92-0065] p 252 A92-25678

Experimental study of boundary layer transition on a heated flat plate p 172 A92-36022

Effect of tabs on the evolution of an axisymmetric jet p 26 A92-40151

Effect of acoustic excitation on stalled flows over an airfoil p 9 A92-41267

Experimental investigation of the flowfield of an oscillating airfoil [AIAA PAPER 92-2622] p 9 A92-45494

Supersonic jet mixing enhancement by 'delta-tabs' [AIAA PAPER 92-3548] p 12 A92-49063

On the mechanism of turbulence suppression in free shear flows under acoustic excitation

[NASA-TM-105360] p 15 N92-14003

Supersonic jet mixing enhancement by delta-tabs [NASA-TM-105664] p 18 N92-24958

Turbulent heat flux measurements in a transitional boundary layer [NASA-TM-105623] p 19 N92-27377

Experimental investigation of the flowfield of an oscillating airfoil [NASA-TM-105675] p 20 N92-30182

ZAPLATYNSKY, ISIDOR

Composite thermal barrier coating [NASA-CASE-LEW-14999-1] p 108 N92-21725

ZELLER, MARY V.

Preliminary evaluation of adhesion strength measurement devices for ceramic/titanium matrix composite bonds [NASA-TM-105803] p 1 N92-31267

ZELTER, GABRIELA R.

Destructive physical analysis results of Ni/H₂ cells cycled in LEO regime p 70 A92-50707

ZEMACH, C.

A continuum method for modeling surface tension p 175 A92-45707

ZERNIC, MICHAEL J.

Solar dynamic technology status for Space Station Freedom application p 83 N92-17770

Space Station Freedom electric power system evolution analysis status p 84 N92-17771

ZHANG, XIANGDONG

A theoretical and experimental study of the noise behavior of subharmonically injection locked local oscillators p 157 A92-46080

ZHOU, XUESONG

A theoretical and experimental study of the noise behavior of subharmonically injection locked local oscillators p 157 A92-46080

ZIEMIANSKI, JOSEPH A.

NASA thrusts in high-speed aeropropulsion research and development: An overview p 33 N92-22538

ZIERTEN, THOMAS A.

Lewis icing research tunnel test of the aerodynamic effects of aircraft ground deicing/anti-icing fluids [NASA-TP-3238] p 22 N92-30395

ZUBE, DIETER M.

Techniques for spectroscopic measurements in an arcjet nozzle p 59 A92-21087

ZUBRIN, ROBERT

Benefits of slush hydrogen for space missions [NASA-TM-104503] p 134 N92-11214

ZUPANC, F. J.

Spectrally resolved Rayleigh scattering diagnostic for hydrogen-oxygen rocket plume studies p 67 A92-50253

ZUPANC, FRANK J.

Rocket plume flowfield characterization using laser Rayleigh scattering [AIAA PAPER 92-3351] p 66 A92-48928

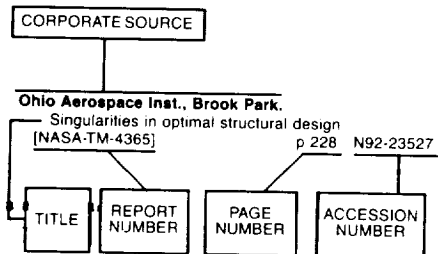
Rocket plume flowfield characterization using laser Rayleigh scattering [NASA-TM-105739] p 257 N92-28475

ZUZEK, JOHN E.

Evaluation of components, subsystems, and networks for high rate, high frequency space communications [NASA-TM-105274] p 147 N92-12151

CORPORATE SOURCE INDEX

Typical Corporate Source Index Listing



Listings in this index are arranged alphabetically by corporate source. The title of the document provides the user with a brief description of the subject matter. The report number helps to indicate the type of document cited (e.g., NASA report, translation, NASA contractor report). The accession number denotes the number by which the citation is identified. The titles are arranged under each corporate source in ascending accession number order.

A

- Aerjet TechSystems Co., Sacramento, CA.**
Design and test of an oxygen turbopump for a dual expander cycle rocket engine p 59 A92-21062
- Air Force Logistics Command, Tinker AFB, OK.**
Advanced ice protection systems test in the NASA Lewis Icing Research Tunnel p 22 A92-14406
- Akron Univ., OH.**
A bulk flow model of a brush seal system [ASME PAPER 91-GT-325] p 203 A92-15696
Steady-state thermal-solutal convection and diffusion in a simulated float zone p 137 A92-17056
Transmission overhaul and component replacement predictions using Weibull and renewal theory p 215 A92-17201
- Allied-Signal Aerospace Co., Phoenix, AZ.**
Studies of the effects of curvature on dilution jet mixing p 166 A92-21079
- Analex Corp., Cleveland, OH.**
Vapor condensation on liquid surface due to laminar jet-induced mixing p 164 A92-10446
- Army Aviation Systems Command, Cleveland, OH.**
NASA low-speed centrifugal compressor for 3-D viscous code assessment and fundamental flow physics research [ASME PAPER 91-GT-140] p 3 A92-15580
Mechanical behavior of fiber reinforced SiC/RBSN ceramic matrix composites - Theory and experiment [ASME PAPER 91-GT-209] p 99 A92-15629
Controlled crack growth specimen for brittle systems p 123 A92-21099
- A comparison of predicted and measured inlet distortion flows in a subsonic axial inlet flow compressor rotor [NASA-TM-105427] p 19 A92-26104
Experimental testing of prototype face gears for helicopter transmissions [NASA-TM-105434] p 214 A92-31349
A demonstration of an intelligent control system for a reusable rocket engine [NASA-TM-105794] p 92 A92-31507

Army Propulsion Lab., Cleveland, OH.
Influence of interfacial shear strength on the mechanical properties of SiC fiber reinforced reaction-bonded silicon nitride matrix composites p 99 A92-15145

B

Brookhaven National Lab., Upton, NY.
Near-edge study of gold-substituted YBa₂Cu₃O(7-delta) p 259 A92-14950

C

- California Univ., Berkeley.**
Drop-tower experiments for capillary surfaces in an exotic container p 166 A92-20743
- Case Western Reserve Univ., Cleveland, OH.**
Measurements of complex permittivity of microwave substrates in the 20 to 300 K temperature range from 26.5 to 40.0 GHz p 197 A92-13416
Microwave properties of YBa₂Cu₃O(7-delta) high-transition-temperature superconducting thin films measured by the power transmission method p 153 A92-14938
The effect of steady aerodynamic loading on the flutter stability of turbomachinery blading [ASME PAPER 91-GT-130] p 2 A92-15574
A bulk flow model of a brush seal system [ASME PAPER 91-GT-209] p 203 A92-15696
- CFD Research Corp., Huntsville, AL.**
CFD analysis of jet mixing in low NO(x) flamentube combustors [ASME PAPER 91-GT-217] p 24 A92-15634
- Cleveland State Univ., OH.**
Mechanical behavior of fiber reinforced SiC/RBSN ceramic matrix composites - Theory and experiment [ASME PAPER 91-GT-209] p 99 A92-15629
Structural reliability analysis of laminated CMC components [ASME PAPER 91-GT-210] p 99 A92-15630
Design of a hydraulic actuator for active control of rotating machinery [ASME PAPER 91-GT-246] p 203 A92-15651
The analysis of high pressure experimental data p 266 A92-16101
- Cornell Univ., Ithaca, NY.**
Nonlinear dynamics near the stability margin in rotating pipe flow p 165 A92-19959
- CPS Superconductors, Inc., Milford, MA.**
Slow strain rate 1200-1400 K compressive properties of NiAl-1Hf p 116 A92-17977
- Cray Research, Inc., Mendota Heights, MN.**
Navier-Stokes analysis of flow and heat transfer inside high-pressure-ratio transonic turbine blade rows p 165 A92-17193

D

Duke Univ., Durham, NC.
Eigenvalue calculation procedure for an Euler/Navier-Stokes solver with application to flows over airfoils p 3 A92-17429

F

- Fermi National Accelerator Lab., Batavia, IL.**
Dark matter and the equivalence principle p 267 A92-14477
- Florida Atlantic Univ., Boca Raton.**
A failure diagnosis system based on a neural network classifier for the Space Shuttle Main Engine p 58 A92-11474
State space representation of the open-loop dynamics of the Space Shuttle Main Engine p 59 A92-19607
- Florida Univ., Gainesville.**
Innovative nuclear thermal propulsion technology evaluation - Results of the NASA/DOE task team study [IAF PAPER 91-235] p 58 A92-13160

G

General Motors Research Labs., Warren, MI.
Universal aspects of adhesion and atomic force microscopy p 260 A92-17979

I

- Idaho National Engineering Lab., Idaho Falls.**
Innovative nuclear thermal propulsion technology evaluation - Results of the NASA/DOE task team study [IAF PAPER 91-235] p 58 A92-13160
Report of the Nuclear Propulsion Mission Analysis, Figures of Merit Subpanel: Quantifiable figures of merit for nuclear thermal propulsion [NASA-TM-104179] p 43 N92-20925
- Illinois Univ., Chicago.**
Oxidation-chlorination of binary Ni-Cr alloys in flowing Ar-O₂-Cl₂ gas mixtures at 1200 K p 112 A92-17296

J

- Jet Propulsion Lab., California Inst. of Tech., Pasadena.**
The formation and structure of plasma wakes behind large high-voltage space platforms in ionosphere [AIAA PAPER 92-0577] p 239 A92-26984
A low-power, high-efficiency Ka-band TWTA [AIAA PAPER 92-1822] p 154 A92-29769
Experimental code verification results for reflector antenna distortion compensation by array feeds [AIAA PAPER 92-2014] p 49 A92-29933
ACTS aeronautical experiments [AIAA PAPER 92-2042] p 50 A92-29956
A low-power, high-efficiency Ka-band TWTA p 156 A92-38163
Ionospheric plasma flow over large high-voltage space platforms. I - Ion-plasma-time scale interactions of a plate at zero angle of attack. II - The formation and structure of plasma wake p 258 A92-41359
The influence of higher harmonics on vortex pairing in an axisymmetric mixing layer p 175 A92-46251
Test experience, 490 N high performance (321 sec lsp) engine [AIAA PAPER 92-3800] p 67 A92-49127
Radiation performance of GaAs concentrator cells for 0.4 to 12 MeV electrons and 0.1 to 37 MeV protons p 159 A92-53193
An overview of the NASA Advanced Propulsion Concepts program [AIAA PAPER 92-3216] p 73 A92-54018

K

Kent State Univ., OH.
Universal aspects of adhesion and atomic force microscopy p 260 A92-17979

L

- Lockheed Missiles and Space Co., Huntsville, AL.**
Investigation of two and three parameter equations of state for cryogenic fluids p 140 A92-13413
- Los Alamos National Lab., NM.**
Innovative nuclear thermal propulsion technology evaluation - Results of the NASA/DOE task team study [IAF PAPER 91-235] p 58 A92-13160

M

- Massachusetts Inst. of Tech., Cambridge.**
The role of tip clearance in high-speed fan stall [ASME PAPER 91-GT-83] p 2 A92-15550
- Minnesota Univ., Minneapolis.**
Nongray radiative gas analyses using the S-N discrete ordinates method p 266 A92-15443
- Mississippi State Univ., Mississippi State.**
Opposed flow flame spread in normal, enhanced and reduced gravity p 111 A92-12898

Missouri Univ.

- Euler flow predictions for an oscillating cascade using a high resolution wave-split scheme
[ASME PAPER 91-GT-198] p 3 A92-15623
- Missouri Univ., Rolla.**
Extrapolation procedures in Mott electron polarimetry p 197 A92-21241

N

National Aeronautics and Space Administration, Washington, DC.

- Status of NASA's Earth-to-Orbit Propulsion Technology program p 58 A92-13154
[IAF PAPER 91-258]
- Space applications of high temperature superconductivity technology p 259 A92-14724
[IAF PAPER 91-307]
- Advanced Communications Technology Satellite (ACTS) p 53 A92-17780
- Reactive collision terms for fluid transport theory p 257 A92-22693
- Heat transfer on accreting ice surfaces p 166 A92-24415
- Void probability as a function of the void's shape and scale-invariant models p 267 A92-24456
- A classical instability of Reissner-Nordstrom solutions and the fate of magnetically charged black holes p 267 A92-26397
- Analysis of surface roughness generation in aircraft ice accretion p 169 A92-28187
[AIAA PAPER 92-0298]
- Advanced Communications Technology Satellite (ACTS) Experiments Program - A market-driven approach to government/industry cooperation p 145 A92-29951
[AIAA PAPER 92-2036]
- Possible sources of the Population I lithium abundance and light-element evolution p 268 A92-33069
- Perturbations from cosmic strings in cold dark matter p 268 A92-33353
- Transport modes during crystal growth in a centrifuge p 138 A92-33835
- Solidification processing of intermetallic Nb-Al alloys p 120 A92-33866
- Constraints to the decays of Dirac neutrinos from SN 1987A p 255 A92-36249
- Fractals and cosmological large-scale structure p 268 A92-37413
- Reconfigurable optical interconnection network for multimode optical fiber sensor arrays p 256 A92-37448
- An unconditionally stable staggered algorithm for transient finite element analysis of coupled thermoelastic problems p 222 A92-37517
- The NASA-OAST earth-to-orbit propulsion technology program - The action plan p 61 A92-38597
[IAF PAPER 92-1478]
- A dynamic isotope power system for Space Exploration Initiative surface transport systems p 61 A92-38605
[AIAA PAPER 92-1489]
- NASA program planning on nuclear electric propulsion p 61 A92-38651
[AIAA PAPER 92-1557]
- The diffuse gamma-ray background, light element abundances, and signatures of early massive star formation p 268 A92-43837
- Massive Dirac neutrinos and SN 1987A p 268 A92-45808
- Length minimization design considerations in photonic integrated circuits incorporating directional couplers p 256 A92-46240
- Comparison of the SMAC, PISO, and iterative time-advancing schemes for unsteady flows p 175 A92-47158
- Thick strings, the liquid crystal blue phase, and cosmological large-scale structure p 268 A92-48103
- Electric propulsion - The future is now p 63 A92-48386
- Comparative study of turbulence models in predicting hypersonic inlet flows p 11 A92-48740
[AIAA PAPER 92-3098]
- Advanced Rotorcraft Transmission (ART) Program summary p 205 A92-48938
[AIAA PAPER 92-3365]
- Slush hydrogen pressurized expulsion studies at the NASA K-Site Facility p 141 A92-48951
[AIAA PAPER 92-3385]
- Propulsion-related flowfields using the preconditioned Navier-Stokes equations p 178 A92-48994
[AIAA PAPER 92-3437]
- Observations of soot during droplet combustion at low gravity - Heptane and heptane/monochloroalkane mixtures p 115 A92-50447
- Time domain numerical calculations of unsteady vortical flows about a flat plate airfoil p 12 A92-50473
- Concentrator testing using projected images p 69 A92-50615

- Fiber-optic sensors for aerospace electrical measurements - An update p 200 A92-50630
- Preliminary design of a mobile lunar power supply p 233 A92-50635
- Advanced power systems for EOS p 70 A92-50640
- Recent progress in InP solar cell research p 158 A92-50653
- Description of the control system design for the SSF PMAD DC testbed p 45 A92-50654
- Description of the PMAD DC test bed architecture and integration sequence p 46 A92-50655
- The development of test beds to support the definition and evolution of the Space Station Freedom power system p 46 A92-50656
- An EMTP system level model of the PMAD DC test bed p 46 A92-50657
- Development and testing of a source subsystem for the supporting development PMAD DC test bed p 46 A92-50659
- Development of a ninety string solar array simulator p 46 A92-50660
- Large transient fault current test of an electrical roll ring p 55 A92-50661
- Test and evaluation of load converter topologies used in the Space Station Freedom power management and distribution dc test bed p 158 A92-50662
- Nickel-hydrogen cell low-earth-orbit life test update p 70 A92-50700
- Destructive physical analysis results of Ni/H₂ cells cycled in LEO regime p 70 A92-50707
- Effect of LEO cycling on 125 Ah advanced design IPV nickel-hydrogen flight cells - An update p 71 A92-50708
- Stirling machine operating experience p 206 A92-50788
- Comparative survey of dynamic analyses of free-piston Stirling engines p 206 A92-50793
- An overview of the NASA Advanced Propulsion Concepts program p 73 A92-54018
[AIAA PAPER 92-3216]
- Fluctuation-driven electroweak phase transition p 269 A92-54464
- Small engine components test facility compressor testing cell at NASA Lewis Research Center p 41 A92-56806
[AIAA PAPER 92-3980]
- Advanced nozzle and engine components test facility p 41 A92-56816
[AIAA PAPER 92-3993]
- Engine component instrumentation development facility at NASA Lewis Research Center p 41 A92-56818
[AIAA PAPER 92-3995]
- Description of a pressure measurement technique for obtaining surface static pressures of a radial turbine p 200 A92-56829
[AIAA PAPER 92-4006]
- Large-scale microwave anisotropy from gravitating seeds p 269 A92-56914
- Growth and characterization of lead bromide crystals p 138 A92-56956
- Effect of growth conditions on the quality of lead bromide crystals p 138 A92-56957
- Nuclear propulsion for space exploration p 76 A92-57054
[IAF PAPER 92-0575]
- Early use of Space Station Freedom for NASA's Microgravity Science and Applications Program p 138 A92-57131
[IAF PAPER 92-0702]
- Report of the Nuclear Propulsion Mission Analysis, Figures of Merit Subpanel: Quantifiable figures of merit for nuclear thermal propulsion p 43 N92-20925
[NASA-TM-104179]
- National Aeronautics and Space Administration, Ames Research Center, Moffett Field, CA.**
- The NASA Computational Aerosciences Program - Toward teraFLOPS computing p 240 A92-26968
[AIAA PAPER 92-0558]
- Crossing shock wave turbulent boundary layer interactions - Variable angle and shock generator length geometry effects at Mach 3 p 6 A92-27014
[AIAA PAPER 92-0636]
- Unsteady transonic Euler solutions using finite elements p 8 A92-34499
[AIAA PAPER 92-2504]
- Integrated flight/propulsion control for supersonic STOVL aircraft p 39 A92-45320
- Measurement and analysis of a small nozzle plume in vacuum p 64 A92-48748
[AIAA PAPER 92-3108]
- Experimental and numerical investigations of low-density nozzle and plume flows of nitrogen p 183 A92-54917
- National Aeronautics and Space Administration, Goddard Space Flight Center, Greenbelt, MD.**
- High voltage spheres in an unmagnetized plasma - Fluid and PIC simulations p 258 A92-47936
- National Aeronautics and Space Administration, Hugh L. Dryden Flight Research Facility, Edwards, CA.**
- The F/A-18 external burning flight test p 23 A92-44547
[AIAA PAPER 91-5050]

National Aeronautics and Space Administration, John C. Stennis Space Center, Bay Saint Louis, MS.

- Health management and controls for earth to orbit propulsion systems p 77 A92-57089
[IAF PAPER 92-0646]
- National Aeronautics and Space Administration, Lyndon B. Johnson Space Center, Houston, TX.**
- A high temperature superconductivity communications flight experiment p 50 A92-55790
[IAF PAPER 92-0410]
- Fast oxygen atom facility for studies related to low earth orbit activities p 47 A92-56800
[AIAA PAPER 92-3974]
- Temperature dependence of the electrode kinetics of oxygen reduction at the platinum/Nafion interface - A microelectrode investigation p 115 A92-56950
- Report of the Nuclear Propulsion Mission Analysis, Figures of Merit Subpanel: Quantifiable figures of merit for nuclear thermal propulsion p 43 N92-20925
[NASA-TM-104179]
- National Aeronautics and Space Administration, Langley Research Center, Hampton, VA.**
- Model free simulations of a high speed reacting mixing layer p 167 A92-25715
[AIAA PAPER 92-0257]
- The NASA Computational Aerosciences Program - Toward teraFLOPS computing p 240 A92-26968
[AIAA PAPER 92-0558]
- Acoustic characteristics and dynamic structural loading of an ASTOVL aircraft in hover p 253 A92-28190
[AIAA PAPER 92-0370]
- Second order modeling of boundary-free turbulent shear flows p 174 A92-41275
- Filtered Rayleigh scattering measurements in supersonic/hypersonic facilities p 200 A92-56733
[AIAA PAPER 92-3894]
- Report of the Nuclear Propulsion Mission Analysis, Figures of Merit Subpanel: Quantifiable figures of merit for nuclear thermal propulsion p 43 N92-20925
[NASA-TM-104179]
- National Aeronautics and Space Administration, Marshall Space Flight Center, Huntsville, AL.**
- Status of NASA's Earth-to-Orbit Propulsion Technology program p 58 A92-13154
[IAF PAPER 91-258]
- Development of and flight results from the Space Acceleration Measurement System (SAMS) p 56 A92-28189
[AIAA PAPER 92-0354]
- Electrophoresis of small particles and fluid globules in weak electrolytes p 114 A92-33924
- The NASA-OAST earth-to-orbit propulsion technology program - The action plan p 61 A92-38597
[IAF PAPER 92-1478]
- Advanced optical condition monitoring p 199 A92-39994
[SAE PAPER 912164]
- Combustion of liquid-fuel droplets in supercritical conditions p 114 A92-43778
- Propulsion-related flowfields using the preconditioned Navier-Stokes equations p 178 A92-48994
[AIAA PAPER 92-3437]
- Fast oxygen atom facility for studies related to low earth orbit activities p 47 A92-56800
[AIAA PAPER 92-3974]
- Health management and controls for earth to orbit propulsion systems p 77 A92-57089
[IAF PAPER 92-0646]
- Nuclear Utility Services, Inc., Gaithersburg, MD.**
- Innovative nuclear thermal propulsion technology evaluation - Results of the NASA/DOE task team study p 58 A92-13160
[IAF PAPER 91-235]

O

Oak Ridge National Lab., TN.

- Determination of the stress distributions in a ceramic, tensile specimen using numerical techniques p 216 A92-14546

Ohio Aerospace Inst., Brook Park.

- Singularities in optimal structural design p 228 N92-23527
[NASA-TM-4365]

P

Pacific Northwest Lab., Richland, WA.

- Report of the Nuclear Propulsion Mission Analysis, Figures of Merit Subpanel: Quantifiable figures of merit for nuclear thermal propulsion p 43 N92-20925
[NASA-TM-104179]

Pennsylvania State Univ., University Park.

- Optimization and analysis of large chemical kinetic mechanisms using the solution mapping method - Combustion of methane p 113 A92-19300

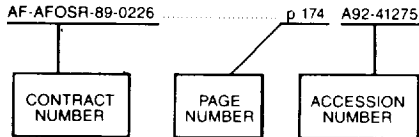
W

- Phillips Lab., Edwards AFB, CA.**
Report of the Nuclear Propulsion Mission Analysis, Figures of Merit Subpanel: Quantifiable figures of merit for nuclear thermal propulsion
[NASA-TM-104179] p 43 A92-20925
- Pratt and Whitney Aircraft Group, East Hartford, CT.**
Heat transfer in rotating serpentine passages with trips normal to the flow
[ASME PAPER 91-GT-265] p 165 A92-15663
- Princeton Univ., N.J.**
Some further observations on droplet combustion characteristics - NASA LeRC-Princeton results
p 111 A92-12897
Observations on a slow burning regime for hydrocarbon droplets - n-heptane/air results
p 112 A92-16602
- Purdue Univ., West Lafayette, IN.**
Significant long-term reduction in n-channel MESFET subthreshold leakage using ammonium-sulfide surface treated gates
p 153 A92-12272
Wind tunnel wall effects in a linear oscillating cascade
[ASME PAPER 91-GT-133] p 2 A92-15576
- R**
- Rensselaer Polytechnic Inst., Troy, NY.**
Determination of the critical parameters for remote microscope control
[IAF PAPER 91-026] p 240 A92-12447
Neurobiological computational models in structural analysis and design
p 245 A92-14509
- Rice Univ., Houston, TX.**
Extrapolation procedures in Mott electron polarimetry
p 197 A92-21241
- S**
- Sandia National Labs., Albuquerque, NM.**
Report of the Nuclear Propulsion Mission Analysis, Figures of Merit Subpanel: Quantifiable figures of merit for nuclear thermal propulsion
[NASA-TM-104179] p 43 A92-20925
- Schafer (W. J.) Associates, Inc., Chelmsford, MA.**
Status of NASA's Earth-to-Orbit Propulsion Technology program
[IAF PAPER 91-258] p 58 A92-13154
- Stanford Univ., CA.**
Drop-tower experiments for capillary surfaces in an exotic container
p 166 A92-20743
Turbulence modeling
p 189 A92-23338
- State Univ. of New York, Buffalo.**
Prediction of unsteady rotor-surface pressure and heat transfer from wake passings
[ASME PAPER 91-GT-267] p 165 A92-15665
- State Univ. of New York, Stony Brook.**
A fiber-optic probe for particle sizing in concentrated suspensions
p 197 A92-21371
- Sverdrup Technology, Inc., Brook Park, OH.**
Electric propulsion - An evolutionary technology
[IAF PAPER 91-241] p 58 A92-13158
Calculated performance of p(+)n InP solar cells with ln(0.52)Al(0.48)As window layers
p 153 A92-13266
Ongoing development of a computer jobstream to predict helicopter main rotor performance in icing conditions
p 2 A92-14407
The effect of steady aerodynamic loading on the flutter stability of turbomachinery blading
[ASME PAPER 91-GT-130] p 2 A92-15574
Deterministic blade row interactions in a centrifugal compressor stage
[ASME PAPER 91-GT-273] p 3 A92-15670
Unsteady blade-surface pressures on a large-scale advanced propeller - Prediction and data
p 3 A92-17178
Coaxial line configuration for microwave power transmission study of YBa₂Cu₃O_{7-δ} thin films
p 154 A92-18455
Photovoltaic power options for Mars
p 231 A92-20366
Unsteady Euler analysis of the flowfield of a propfan at an angle of attack
p 3 A92-21070
Moonbase night power by laser illumination
p 44 A92-21086
- Sverdrup Technology, Inc., Cleveland, OH.**
The application of a computer data acquisition system to a new high temperature tribometer
p 93 A92-11823
Numerical investigation on Benard instability in a finite liquid layer
p 164 A92-12865
Interfacing laboratory instruments to multiuser, virtual memory computers
p 245 A92-13595
The role of tip clearance in high-speed fan stall
[ASME PAPER 91-GT-83] p 2 A92-15550
- NASA low-speed centrifugal compressor for 3-D viscous code assessment and fundamental flow physics research
[ASME PAPER 91-GT-140] p 3 A92-15580
Electromechanical simulation and testing of actively controlled rotordynamic systems with piezoelectric actuators
[ASME PAPER 91-GT-245] p 203 A92-15650
Prediction of unsteady rotor-surface pressure and heat transfer from wake passings
[ASME PAPER 91-GT-267] p 165 A92-15665
The numerical simulation of a high-speed axial flow compressor
[ASME PAPER 91-GT-272] p 3 A92-15669
Material processing with hydrogen and carbon monoxide on Mars
p 231 A92-17769
Magnetic radiation shielding - An idea whose time has returned?
p 53 A92-17796
Tether methods for reactionless orbital propulsion
p 44 A92-17797
Space power by ground-based laser illumination
p 59 A92-18401
Fatigue crack growth in unidirectional metal matrix composite
p 99 A92-19734
Calculation of far-field scattering from nonspherical particles using a geometrical optics approach
p 256 A92-20288
A real time neural net estimator of fatigue life
p 245 A92-21694
Computers in aeronautics and space research at the Lewis Research Center
[NASA-TM-105096] p 241 A92-11642
- Sverdrup Technology, Inc., Huntsville, AL.**
Investigation of two and three parameter equations of state for cryogenic fluids
p 140 A92-13413
- T**
- Tel-Aviv Univ. (Israel).**
Photovoltaic power options for Mars
p 231 A92-20366
Central difference TVD and TVB schemes for time dependent and steady state problems
[AIAA PAPER 92-0053] p 166 A92-22168
- Texas A&M Univ., College Station.**
Aerodynamics and heat transfer investigations on a high Reynolds number turbine cascade
[ASME PAPER 91-GT-157] p 164 A92-15593
Electromechanical simulation and testing of actively controlled rotordynamic systems with piezoelectric actuators
[ASME PAPER 91-GT-245] p 203 A92-15650
- Texas Univ., Austin.**
Effect of an arcjet plume on satellite reflector performance
p 53 A92-16318
- Texas Univ., San Antonio.**
Probabilistic constitutive relationships for cyclic material strength models
p 217 A92-21081
- Toledo Univ., OH.**
Multicarrier demodulator architecture for onboard processing satellites
p 49 A92-10465
Parallel computation of aerodynamic influence coefficients for aeroelastic analysis on a transputer network
p 241 A92-12367
Euler flow predictions for an oscillating cascade using a high resolution wave-split scheme
[ASME PAPER 91-GT-198] p 3 A92-15623
Cascade flutter analysis with transient response aerodynamics
p 217 A92-15972
Eigenvalue calculation procedure for an Euler/Navier-Stokes solver with application to flows over airfoils
p 3 A92-17429
Heat transfer measurements from a smooth NACA 0012 airfoil
p 165 A92-20215
Roughness effects on heat transfer from a NACA 0012 airfoil
p 166 A92-20217
Effect of type and location of oil groove on the performance of journal bearings
p 203 A92-21333
- U**
- United Technologies Research Center, East Hartford, CT.**
Innovative nuclear thermal propulsion technology evaluation - Results of the NASA/DOE task team study
[IAF PAPER 91-235] p 58 A92-13160
Heat transfer in rotating serpentine passages with trips normal to the flow
[ASME PAPER 91-GT-265] p 165 A92-15663
- Washington Univ., Saint Louis, MO.**
Modeling of impulsive propellant reorientation
p 59 A92-17187
- Wayne State Univ., Detroit, MI.**
CFD analysis of jet mixing in low NO(x) flame tube combustors
[ASME PAPER 91-GT-217] p 24 A92-15634
- Westinghouse Electric Corp., Pittsburgh, PA.**
Flight experiment on acousto-optic crystal growth
p 136 A92-12880
- Winthrop Group, Inc., Cambridge, MA.**
Rocket propulsion research at Lewis Research Center
[NASA-CR-189187] p 266 A92-30908



CONTRACT NUMBER INDEX

Typical Contract Number Index Listing



Listings in this index are arranged alphanumerically by contract number. Under each contract number the accession numbers denoting documents that have been produced as a result of research done under that contract are arranged in ascending order. The accession number denotes the number by which the citation is identified.

AC-90-695	p 151	N92-30934	DE-AC03-76SF-00098	p 166	A92-20743	NAG3-1137	p 21	A92-41262
AF-AFOISR-89-0226	p 174	A92-41275	DE-AC04-76DP-00789	p 200	A92-56828	NAG3-1138	p 26	A92-34598
AF-AFOISR-89-0346	p 165	A92-19959	DE-AC05-80ER-10742	p 259	A92-14950		p 44	A92-46753
AF-AFOISR-89-0403	p 170	A92-29597	DE-AC06-87RL-10930	p 91	N92-30818		p 44	A92-46760
AF-AFOISR-89-0487	p 167	A92-24757	DE-AI01-91CR-50306	p 97	N92-26142	NAG3-1143	p 166	A92-20743
AF-AFOISR-90-0026	p 258	A92-47936	DE-AI04-85AL-33408	p 123	N92-27192	NAG3-1151	p 200	A92-54106
AF-AFOISR-90-0080	p 169	A92-28211	DE-AI05-87DR-21749	p 124	A92-32896	NAG3-1163	p 225	A92-54921
AF-AFOISR-90-0096	p 7	A92-28043	DE-FC05-85ER-25000	p 127	A92-54504	NAG3-1166	p 144	A92-29892
AF-AFOISR-91-0101	p 182	A92-54008	DE-FG02-85ER-45178	p 167	A92-25704	NAG3-1177	p 39	A92-29117
CNPQ-300729/86-3	p 246	A92-29030	DE-FG02-90ER-45427	p 112	A92-17296	NAG3-1178	p 7	A92-28043
DA PROJ. 1L1-61102-AH-45	p 186	N92-18809	DE-FG02-92ER-14247	p 260	A92-28075	NAG3-1180	p 261	A92-35349
	p 108	N92-20039	DEN3-377	p 121	A92-44218	NAG3-1183	p 148	N92-14235
	p 34	N92-22863		p 206	A92-50797	NAG3-1186	p 246	A92-40375
	p 209	N92-23226		p 206	A92-50798	NAG3-1187	p 178	A92-49068
	p 132	N92-25348		p 181	A92-50802	NAG3-1196	p 220	A92-34523
	p 19	N92-26104		p 71	A92-50829		p 247	A92-41895
	p 47	N92-26129	F33615-88-C-2823	p 215	A92-15681	NAG3-1198	p 251	N92-30898
	p 251	N92-30898	F33615-89-C-2950	p 262	A92-46330	NAG3-1206	p 76	A92-54190
DA PROJ. 1L1-62211-A-47-A	p 207	N92-10195	F33615-89-C-5618	p 215	A92-15681	NAG3-1213	p 182	A92-54008
	p 209	N92-24202	F49670-86-C-0087	p 181	A92-52406	NAG3-1221	p 169	A92-28211
	p 210	N92-24984	JPL-957882	p 67	A92-49127	NAG3-1230	p 26	A92-35687
	p 210	N92-25447	MDA972-88-C-0047	p 103	A92-41867	NAG3-1231	p 113	A92-26927
	p 211	N92-25448	NAGW-1321	p 268	A92-33069	NAG3-1255	p 115	A92-56950
	p 211	N92-26106		p 268	A92-37413	NAG3-1264	p 106	N92-14122
	p 211	N92-26107	NAGW-1340	p 268	A92-48103	NAG3-1268	p 167	A92-25705
	p 211	N92-26108		p 267	A92-14477		p 137	A92-27002
	p 211	N92-26555		p 267	A92-24456	NAG3-1275	p 13	A92-54090
	p 212	N92-26560	NAGW-1356	p 268	A92-33069	NAG3-1284	p 167	A92-25704
	p 212	N92-28434	NAGW-1388	p 268	A92-48103	NAG3-1315	p 76	A92-54192
	p 212	N92-28476	NAGW-1407	p 178	A92-48994	NAG3-147	p 112	A92-16981
	p 202	N92-29105	NAGW-2022	p 222	A92-37517	NAG3-154	p 141	A92-52205
	p 213	N92-29136		p 256	A92-46240	NAG3-157	p 146	A92-44233
	p 213	N92-29351		p 231	A92-20366		p 147	A92-54763
	p 213	N92-30396	NAGW-2145	p 81	N92-13259	NAG3-171	p 176	A92-47841
	p 214	N92-31349	NAGW-235	p 163	N92-32243		p 176	A92-47842
	p 215	N92-31485	NAGW-2381	p 270	N92-33899	NAG3-181	p 205	A92-50271
DA PROJ. 1L1-62211-A-47A	p 209	N92-23536		p 268	A92-45808	NAG3-259	p 114	A92-33924
	p 212	N92-27879	NAGW-976	p 257	A92-22693	NAG3-25	p 260	A92-27297
DAAL03-86-G-0013	p 40	A92-48908	NAG1-1122	p 267	A92-26397	NAG3-28	p 21	A92-41262
DAAL03-87-K-0007	p 156	A92-43891	NAG1-954	p 268	A92-33353	NAG3-294	p 112	A92-16981
DAAL03-87-K-0035	p 222	A92-37510	NAG2-718	p 255	A92-36249	NAG3-3139	p 26	A92-34598
DAAL03-88-K-0099	p 125	A92-39687	NAG3-1004	p 268	A92-37413		p 26	A92-35687
DASG60-88-C-0115	p 261	A92-42858	NAG3-1006	p 268	A92-45808	NAG3-354	p 253	A92-39241
DE-AC02-76CH-00016	p 259	A92-14950	NAG3-1011	p 269	A92-54464	NAG3-376	p 168	A92-26412
DE-AC02-76ET-53018	p 67	A92-50266	NAG3-1016	p 269	A92-56914	NAG3-431	p 127	A92-57027
DE-AC02-83CH-10093	p 71	A92-53197	NAG3-1020	p 138	A92-33835	NAG3-440751	p 265	N92-32984
DE-AC02-83HC-10093	p 234	A92-53153	NAG3-1026	p 167	A92-25715	NAG3-460	p 175	A92-46251
	p 234	A92-53166	NAG3-1034	p 174	A92-41652	NAG3-479	p 123	A92-23225
DE-AC02-88ER-13895	p 217	A92-24717	NAG3-1039	p 178	A92-48994	NAG3-512	p 217	A92-24717
	p 218	A92-30673	NAG3-1045	p 25	A92-24403	NAG3-520	p 7	A92-28204
			NAG3-1047	p 224	A92-49777		p 14	N92-10012
			NAG3-1058	p 261	A92-44273	NAG3-548	p 170	A92-28518
			NAG3-1060	p 180	A92-50596		p 177	A92-48721
			NAG3-1065	p 213	N92-29351	NAG3-570	p 172	A92-36184
			NAG3-1081	p 253	A92-26934		p 176	A92-47271
			NAG3-1086	p 261	A92-37562	NAG3-578	p 62	A92-44507
			NAG3-1089	p 240	A92-12447	NAG3-581	p 165	A92-15665
				p 113	A92-26927	NAG3-627	p 171	A92-32258
				p 245	A92-14509	NAG3-639	p 253	A92-50296
				p 217	A92-25403	NAG3-658	p 232	A92-48091
				p 176	A92-47269		p 262	A92-53148
				p 224	A92-50883	NAG3-663	p 170	A92-30494
				p 224	A92-50511	NAG3-666	p 166	A92-24415
				p 184	A92-57286		p 169	A92-28187
				p 174	A92-41274	NAG3-681	p 258	A92-41549
				p 54	A92-43284		p 62	A92-41550
				p 216	A92-50625	NAG3-695	p 239	A92-26984
				p 220	A92-34569		p 258	A92-41359
				p 224	A92-51550	NAG3-698	p 260	A92-27297
				p 229	N92-29342	NAG3-723	p 166	A92-24752
				p 45	A92-49052		p 261	A92-37562
				p 168	A92-27110	NAG3-724	p 3	A92-17429
				p 30	N92-15994	NAG3-72	p 165	A92-20215
				p 157	A92-50558		p 166	A92-20217
				p 68	A92-50559	NAG3-730	p 6	A92-26947
				p 69	A92-50637		p 7	A92-28194
				p 177	A92-48734	NAG3-731	p 184	A92-56941
				p 7	A92-28192	NAG3-732	p 4	A92-23762
						NAG3-746	p 12	A92-52730
						NAG3-755	p 126	A92-49814
						NAG3-764	p 182	A92-54043
							p 183	A92-54937
						NAG3-767	p 6	A92-26946

CONTRACT NUMBER INDEX

RTOP 506-41-11

NCC3-95	p 117	A92-26526	RTOP 474-74-10	p 46	A92-50660	RTOP 505-63-1A	p 95	N92-10064
NGL-22-009-640	p 166	A92-24415		p 55	N92-11086		p 96	N92-15128
NGL-22-069-640	p 169	A92-28187	RTOP 505-01-11	p 91	N92-31249		p 97	N92-21175
NSF ASC-87-19573	p 248	A92-50469	RTOP 505-12-21	p 191	N92-25196	RTOP 505-63-1B	p 226	N92-15405
NSF AST-88-22595	p 268	A92-48103	RTOP 505-33-13	p 131	N92-23185	RTOP 505-63-1M	p 128	N92-15192
NSF AST-89-14346	p 268	A92-45808	RTOP 505-52-62	p 18	N92-24958	RTOP 505-63-20	p 129	N92-17070
NSF CBT-84-51075	p 115	A92-50447	RTOP 505-62-OK	p 209	N92-23226	RTOP 505-63-36	p 205	A92-48938
NSF CBT-84-51076	p 266	A92-15443		p 19	N92-26104		p 210	N92-24984
	p 266	A92-28185	RTOP 505-62-OK	p 128	N92-14179		p 210	N92-25347
NSF CTS-84-51076	p 266	A92-54287	RTOP 505-62-00	p 128	N92-11202		p 210	N92-25396
NSF CTS-90-06879	p 182	A92-54043		p 35	N92-25164		p 210	N92-25447
	p 183	A92-54937	RTOP 505-62-10	p 31	N92-20525		p 211	N92-25448
NSF DDM-89-96171	p 217	A92-25403		p 196	N92-31484		p 211	N92-26106
	p 176	A92-47269	RTOP 505-62-12	p 30	N92-20033		p 211	N92-26107
	p 224	A92-50883	RTOP 505-62-20	p 1	N92-17346		p 211	N92-26108
NSF DMR-88-10058	p 122	A92-46850		p 36	N92-27037		p 211	N92-26555
NSF DMR-89-01723	p 261	A92-35349		p 195	N92-27653		p 212	N92-26560
NSF DMR-89-13651	p 260	A92-28075		p 195	N92-30297		p 212	N92-27879
NSF DMR-89-18889	p 141	A92-52205	RTOP 505-62-21	p 12	A92-50473		p 212	N92-28434
NSF DMR-90-17371	p 260	A92-28075		p 249	N92-10345		p 212	N92-28476
NSF DMS-88-14553	p 174	A92-41275		p 184	N92-11302		p 213	N92-29136
NSF DMS-89-02831	p 166	A92-20743		p 184	N92-11320		p 213	N92-29351
NSF DMS-89-21189	p 190	N92-23565		p 184	N92-11328		p 213	N92-30396
NSF ECS-86-57524	p 53	A92-16318		p 243	N92-11691		p 214	N92-30948
	p 146	A92-51092		p 225	N92-12316		p 214	N92-31349
NSF ECS-86-57951	p 152	N92-32971		p 15	N92-14000		p 215	N92-31485
NSF ECS-88-16733	p 246	A92-25878		p 29	N92-14061	RTOP 505-63-39	p 213	N92-29697
NSF EET-87-14628	p 221	A92-36245		p 185	N92-14322	RTOP 505-63-40	p 228	N92-25179
NSF MIP-90-02664	p 144	A92-29892		p 185	N92-15336		p 110	N92-29660
NSF MSM-86-11164	p 174	A92-41275		p 185	N92-15357	RTOP 505-63-5A	p 186	N92-18809
NSF MSM-87-02732	p 166	A92-24752		p 249	N92-15662		p 96	N92-18970
NSF MSM-88-00086	p 175	A92-46251		p 249	N92-15663		p 129	N92-19450
NSF MSS-91-02981	p 248	A92-50469		p 186	N92-18775		p 130	N92-22278
NSF MSS-91-57090	p 221	A92-34583		p 187	N92-22226		p 130	N92-22278
NSF PHY-87-0036P	p 260	A92-27297		p 249	N92-22230		p 130	N92-22305
NSF PHY-89-04035	p 261	A92-35349		p 187	N92-22398		p 97	N92-23190
NSF PHY-90-0772	p 197	A92-21241		p 1	N92-23336		p 250	N92-24974
NSF RII-84-13805	p 127	A92-57027		p 190	N92-23542		p 97	N92-26142
NSF RII-87-14676	p 127	A92-57027		p 190	N92-23560		p 133	N92-27378
NSG-3188	p 209	N92-23536		p 190	N92-23560		p 215	N92-31536
	p 209	N92-24202		p 190	N92-23565		p 133	N92-32863
NSG-3208	p 2	A92-15550		p 191	N92-24050	RTOP 505-63-5B	p 106	N92-13284
NSG-3299	p 64	A92-48750		p 191	N92-24514		p 106	N92-14118
NSG-3555	p 40	A92-48908		p 250	N92-27196		p 106	N92-14122
	p 12	A92-48909		p 196	N92-32868		p 128	N92-15191
N00013-86-K-0773	p 260	A92-27297		p 250	N92-33571		p 226	N92-15406
N00014-85-C-0639	p 103	A92-41867		p 250	N92-33742		p 208	N92-16336
N00014-86-C-2277	p 103	A92-41867	RTOP 505-62-3B	p 251	N92-33942		p 129	N92-20380
N00014-87-K-0030	p 122	A92-57028	RTOP 505-62-30	p 31	N92-22510		p 208	N92-20815
N00014-88-K-0527	p 153	A92-12272	RTOP 505-62-36	p 38	N92-30998		p 227	N92-22227
N00014-89-J-1361	p 253	A92-50296	RTOP 505-62-36	p 209	N92-24202		p 133	N92-31840
N00014-89-J-1864	p 153	A92-12272	RTOP 505-62-40	p 11	A92-48740		p 111	N92-32466
N00014-90-J-1672	p 104	A92-46826		p 19	N92-28102	RTOP 505-63-51	p 207	N92-10195
N00014-90-J-1730	p 183	A92-54937	RTOP 505-62-50	p 81	N92-13274	RTOP 505-63-53	p 109	N92-23194
N00014-90-J-1765	p 122	A92-57028		p 263	N92-15815		p 228	N92-23267
N00014-90-J-1921	p 261	A92-42858		p 40	N92-20586	RTOP 505-68-1C	p 226	N92-15402
N00014-91-J-1370	p 120	A92-38990		p 202	N92-29105	RTOP 505-68-10	p 1	N92-10002
N00019-89-J-1519	p 156	A92-43891		p 40	N92-32241		p 15	N92-14001
N60921-86-C-A226	p 261	A92-42858		p 257	N92-33896		p 16	N92-15051
RTOP 144-10-10	p 150	N92-19700	RTOP 505-62-51	p 40	N92-34107		p 16	N92-15052
	p 151	N92-20032	RTOP 505-62-52	p 34	N92-22863		p 16	N92-15968
RTOP 307-50-00	p 228	N92-23527		p 175	A92-47158		p 17	N92-17347
	p 229	N92-25446		p 14	N92-10012		p 188	N92-23154
RTOP 307-51-00	p 127	N92-11188		p 184	N92-11299		p 19	N92-26612
	p 263	N92-19398		p 14	N92-13998		p 20	N92-28674
	p 263	N92-20519		p 15	N92-14003		p 20	N92-28696
	p 131	N92-24715		p 249	N92-16663		p 20	N92-34144
RTOP 316-30-19	p 147	N92-12151		p 186	N92-20235	RTOP 505-68-11	p 17	N92-23105
	p 269	N92-14953		p 187	N92-20520		p 22	N92-30395
RTOP 323-53-62	p 240	N92-13581		p 18	N92-23269	RTOP 505-68-30-03	p 16	N92-14968
RTOP 323-57-4A	p 162	N92-30427		p 18	N92-23563	RTOP 505-68-32	p 37	N92-27669
RTOP 324-02-00	p 56	N92-24349		p 35	N92-25712		p 37	N92-28418
RTOP 326-81-10	p 91	N92-30187		p 35	N92-25808		p 37	N92-29661
RTOP 474-12-10	p 69	A92-50615		p 194	N92-26690	RTOP 505-68-71	p 17	N92-19993
RTOP 474-42-10	p 45	A92-50654		p 19	N92-27377	RTOP 505-69-10	p 29	N92-14063
	p 46	A92-50655		p 20	N92-28980	RTOP 505-69-40	p 48	N92-11034
	p 46	A92-50656		p 255	N92-28984		p 29	N92-11995
	p 46	A92-50657		p 20	N92-30182		p 48	N92-21547
	p 46	A92-50659		p 38	N92-30972		p 34	N92-23254
	p 55	A92-50661		p 38	N92-31172	RTOP 505-69-50	p 244	N92-33894
	p 158	A92-50662		p 38	N92-32472	RTOP 505-90-01	p 184	N92-11317
	p 77	N92-10055		p 38	N92-33746		p 202	N92-23155
	p 87	N92-24201		p 230	N92-34112	RTOP 505-90-52	p 240	N92-10289
	p 162	N92-31282	RTOP 505-62-71	p 17	N92-20934		p 122	N92-16086
	p 163	N92-32867		p 36	N92-26613	RTOP 505-90-53	p 252	N92-26671
	p 164	N92-34219	RTOP 505-62-84	p 41	A92-56806	RTOP 505-90-54	p 123	N92-16111
RTOP 474-46-10	p 70	A92-50700		p 41	A92-56816	RTOP 506-21-11	p 84	N92-20043
	p 96	N92-14114		p 41	A92-56818	RTOP 506-41-11	p 70	A92-50640
	p 227	N92-20045		p 42	N92-17059		p 158	A92-50653
	p 214	N92-30571		p 42	N92-25449		p 235	N92-13482
	p 230	N92-33476		p 47	N92-26129		p 82	N92-14111
	p 230	N92-34221		p 42	N92-28673		p 160	N92-18920
RTOP 474-52-10	p 55	N92-13143		p 47	N92-30307		p 161	N92-23562
	p 84	N92-19780	RTOP 505-63-00	p 42	N92-30508		p 237	N92-24802
	p 85	N92-20065		p 108	N92-20841		p 161	N92-25176
	p 86	N92-21216	RTOP 505-63-01	p 109	N92-25754		p 87	N92-25343
				p 123	N92-24554		p 238	N92-30426

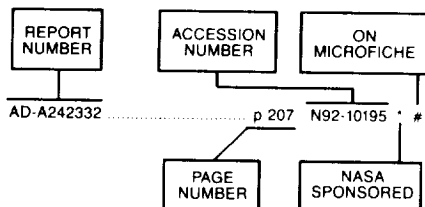
RTOP 506-41-21

CONTRACT NUMBER INDEX

	p 163	N92-32233		p 225	N92-14434	RTOP 591-41-41	p 79	N92-11135
	p 163	N92-32243		p 107	N92-15137	RTOP 593-12-11	p 79	N92-11130
	p 238	N92-33895		p 107	N92-16037	RTOP 593-12-21	p 88	N92-27033
	p 270	N92-33899		p 226	N92-16371	RTOP 593-21-00	p 185	N92-14323
RTOP 506-41-21	p 70	A92-50707		p 96	N92-18457		p 135	N92-18442
	p 71	A92-50708		p 201	N92-19107	RTOP 593-21-41	p 201	N92-18456
	p 235	N92-13483		p 201	N92-19263	RTOP 593-71-00	p 185	N92-13401
	p 236	N92-13484		p 129	N92-19498		p 78	N92-11088
	p 236	N92-20493		p 226	N92-19779	RTOP 593-71-11	p 88	N92-26792
	p 116	N92-26670		p 108	N92-20039		p 80	N92-11137
	p 89	N92-27878		p 227	N92-20212	RTOP 593-72-00	p 83	N92-16019
	p 90	N92-29667		p 187	N92-22487		p 85	N92-20355
RTOP 506-41-31	p 185	N92-13402		p 216	N92-23189		p 86	N92-23252
RTOP 506-41-41	p 79	N92-11133		p 109	N92-23195	RTOP 593-72-41	p 91	N92-30308
	p 81	N92-13275		p 264	N92-23890	RTOP 594-81-12-11	p 93	N92-32463
	p 269	N92-13910		p 202	N92-24881	RTOP 594-81-21	p 43	N92-20925
	p 128	N92-14170		p 216	N92-24986	RTOP 643-10-01	p 243	N92-14649
	p 159	N92-14294		p 109	N92-25346	RTOP 649-40-00	p 52	N92-23187
	p 236	N92-14485		p 132	N92-25348	RTOP 650-60-21	p 51	N92-16008
	p 270	N92-17069		p 110	N92-25996		p 147	N92-14202
	p 160	N92-20040		p 110	N92-30779		p 51	N92-15109
	p 97	N92-21548		p 110	N92-30986		p 51	N92-19762
	p 161	N92-23561		p 230	N92-31505	RTOP 650-60-23	p 51	N92-22001
	p 97	N92-25203	RTOP 510-10-50	p 110	N92-31506		p 149	N92-15306
	p 162	N92-28675		p 108	N92-19595		p 243	N92-16628
	p 244	N92-28684	RTOP 519-01-50	p 228	N92-23196	RTOP 674-21-05	p 149	N92-17062
	p 270	N92-30302		p 110	N92-32234		p 186	N92-15358
	p 48	N92-30310	RTOP 533-13-00	p 227	N92-22267		p 139	N92-16158
RTOP 506-41-51	p 238	N92-29662	RTOP 535-03-0B	p 227	N92-23191	RTOP 674-22-05	p 192	N92-25296
RTOP 506-42-00	p 83	N92-16023		p 229	N92-25753	RTOP 679-40-00	p 139	N92-27197
	p 266	N92-30908	RTOP 535-03-10	p 15	N92-14002		p 149	N92-16191
	p 85	N92-20585		p 16	N92-15977		p 149	N92-17047
RTOP 506-42-21	p 77	N92-10044		p 254	N92-16702		p 149	N92-18281
RTOP 506-42-31	p 80	N92-11136		p 255	N92-16705		p 150	N92-19992
	p 82	N92-14109		p 255	N92-18282	RTOP 694-03-OH	p 52	N92-30383
	p 82	N92-15119		p 17	N92-18760		p 141	N92-11221
	p 82	N92-15125		p 17	N92-19437		p 57	N92-13151
	p 83	N92-16022	RTOP 535-05-10	p 200	A92-56829		p 57	N92-25134
	p 83	N92-16024		p 202	N92-24959	RTOP 694-03-0C	p 57	N92-30301
	p 84	N92-18474	RTOP 537-01-22	p 34	N92-23537		p 141	N92-11217
	p 85	N92-20522	RTOP 537-02-02	p 35	N92-26553		p 138	N92-16156
	p 86	N92-21976	RTOP 537-02-20	p 30	N92-15994		p 141	N92-28436
	p 87	N92-23534		p 30	N92-17061	RTOP 694-03-0K	p 209	N92-23564
	p 87	N92-24560		p 36	N92-26561	RTOP 694-03-00	p 139	N92-26611
	p 257	N92-28475		p 36	N92-27652	RTOP 763-01-21	p 134	N92-11214
	p 90	N92-28983		p 90	N92-29343	RTOP 763-22-00	p 30	N92-17546
	p 92	N92-31342	RTOP 537-02-23	p 14	N92-10976		p 189	N92-23224
	p 92	N92-31901		p 254	N92-14795	RTOP 763-22-21	p 141	A92-48951
	p 92	N92-32237		p 254	N92-14797		p 135	N92-25277
	p 93	N92-33064		p 250	N92-27517		p 135	N92-25957
	p 93	N92-34113		p 37	N92-28419	RTOP 763-22-41	p 135	N92-26131
	p 47	N92-34114	RTOP 553-13-00	p 225	N92-11373	RTOP 763-22-51	p 209	N92-23435
RTOP 506-42-41	p 87	N92-25616		p 207	N92-14346	RTOP 778-32-11	p 1	N92-31267
RTOP 506-42-72	p 78	N92-11126		p 226	N92-15403	RTOP 906-11-03	p 129	N92-17060
	p 82	N92-14112		p 201	N92-18759	RTOP 920-00-00	p 37	N92-26985
	p 49	N92-15082		p 228	N92-24985	RTOP 946-02-2E	p 77	N92-10057
	p 186	N92-16265		p 229	N92-28701		p 29	N92-13070
	p 83	N92-17151		p 230	N92-33935		p 48	N92-25092
	p 84	N92-18280	RTOP 572-10-00	p 49	N92-32456	W-31-109-ENG-38	p 85	N92-21187
	p 135	N92-19837	RTOP 582-01-11	p 29	N92-11017	W-7405-ENG-36	p 175	A92-45707
	p 87	N92-24557		p 79	N92-11128	505-62-21	p 249	N92-10345
	p 89	N92-27654		p 92	N92-31507		p 184	N92-11302
	p 90	N92-28693	RTOP 582-01-41	p 247	N92-13717		p 184	N92-11320
RTOP 506-42-73	p 189	N92-23268	RTOP 589-01-1B	p 56	N92-28683		p 184	N92-11328
	p 136	N92-28433	RTOP 590-13-00	p 235	N92-10221		p 243	N92-11691
	p 136	N92-29669	RTOP 590-13-11	p 233	A92-50635		p 225	N92-12316
RTOP 506-43-11	p 129	N92-16129		p 206	A92-50788		p 15	N92-14000
	p 130	N92-20660		p 206	A92-50793		p 29	N92-14061
	p 131	N92-23192		p 159	N92-11252		p 185	N92-14322
	p 34	N92-23225		p 106	N92-14120		p 185	N92-15336
RTOP 506-43-41	p 130	N92-21579		p 236	N92-16481		p 185	N92-15357
RTOP 506-44-2C	p 160	N92-18473		p 267	N92-25395		p 249	N92-15662
	p 161	N92-23193		p 88	N92-26654		p 249	N92-15663
	p 161	N92-23535		p 88	N92-27034		p 186	N92-18775
RTOP 506-44-21	p 257	N92-13783		p 123	N92-27192		p 187	N92-22226
RTOP 506-48-00	p 79	N92-11129		p 238	N92-28837		p 249	N92-22230
	p 134	N92-13336		p 214	N92-30734		p 187	N92-22398
	p 187	N92-21498		p 238	N92-31262		p 1	N92-23336
RTOP 506-49-11	p 92	N92-32108	RTOP 590-13-21	p 239	N92-33898		p 190	N92-23542
RTOP 506-59-4C	p 151	N92-23412		p 80	N92-11138		p 190	N92-23560
RTOP 506-59-40	p 271	N92-18455		p 90	N92-28682		p 190	N92-23565
RTOP 506-72-00	p 150	N92-18921		p 92	N92-31916		p 191	N92-24050
RTOP 506-72-1B	p 160	N92-21370	RTOP 590-13-31	p 162	N92-28432		p 191	N92-24514
	p 151	N92-32965		p 162	N92-30397			
	p 163	N92-34204	RTOP 590-21-11	p 200	N92-15366			
RTOP 506-72-1C	p 52	N92-22319		p 86	N92-21517			
	p 151	N92-31855		p 87	N92-24957			
RTOP 506-72-1E	p 161	N92-26096		p 48	N92-25958			
RTOP 506-72-21	p 51	N92-18342		p 214	N92-30722			
	p 150	N92-19379	RTOP 590-21-21	p 142	N92-31263			
RTOP 509-10-03	p 30	N92-15993		p 88	N92-27035			
RTOP 510-01-0A	p 107	N92-15136		p 89	N92-27036			
RTOP 510-01-01	p 107	N92-18439	RTOP 590-21-31	p 30	N92-20523			
RTOP 510-01-04	p 107	N92-16036	RTOP 590-21-41	p 90	N92-28417			
RTOP 510-01-50	p 95	N92-13281		p 136	N92-32230			
	p 225	N92-14433	RTOP 591-23-00	p 134	N92-11208			

REPORT/ACCESSION NUMBER INDEX

Typical Report Number Index Listing



Listings in this index are arranged alphanumerically by report number. The accession number denotes the number by which the citation is identified. An asterisk (*) indicates that the item is a NASA report. A pound sign (#) indicates that the item is available on microfiche.

AAS PAPER 91-459	p 54	A92-43284 *
AAS PAPER 91-500	p 44	A92-43339 *
AD-A242332	p 207	N92-10195 * #
AD-A247566	p 186	N92-18809 * #
AD-A250302	p 209	N92-24202 * #
AD-A252378	p 211	N92-26555 * #
AD-A252379	p 210	N92-24984 * #
AD-A252380	p 212	N92-28476 * #
AD-A252381	p 212	N92-27879 * #
AD-A252382	p 212	N92-26560 * #
AD-A253050	p 108	N92-20039 * #
AD-A253127	p 47	N92-26129 * #
AD-A254358	p 213	N92-29351 * #
AD-A254804	p 251	N92-30898 * #
AD-A254805	p 40	N92-34107 * #
AD-A255413	p 241	N92-33897 * #
AD-A255720	p 92	N92-31507 * #
AD-A257175	p 214	N92-31349 * #
AD-A257176	p 214	N92-30948 * #
AD-A257204	p 213	N92-30396 * #
AD-A257220	p 215	N92-31536 * #
AD-A257375	p 213	N92-29136 * #
AIAA PAPER 90-0783	p 56	N92-24349 * #
AIAA PAPER 91-0916	p 223	A92-38142 * #
AIAA PAPER 91-1379	p 79	N92-11129 * #
AIAA PAPER 91-1999	p 79	N92-11128 * #
AIAA PAPER 91-2176	p 134	N92-13336 * #
AIAA PAPER 91-2226	p 82	N92-14109 * #
AIAA PAPER 91-2227	p 58	A92-15355 * #
AIAA PAPER 91-2581	p 14	N92-10976 * #
AIAA PAPER 91-3136	p 29	N92-11995 * #
AIAA PAPER 91-3175	p 48	N92-11034 * #
AIAA PAPER 91-3423	p 147	N92-12151 * #
AIAA PAPER 91-3424	p 269	N92-14953 * #
AIAA PAPER 91-3438	p 79	N92-11135 * #
AIAA PAPER 91-3440	p 85	N92-20522 * #
AIAA PAPER 91-3441	p 86	N92-23252 * #
AIAA PAPER 91-3499	p 80	N92-11136 * #
AIAA PAPER 91-3503	p 80	N92-11137 * #
AIAA PAPER 91-3518	p 235	N92-10221 * #
AIAA PAPER 91-3528	p 92	N92-31916 * #
AIAA PAPER 91-3578	p 78	N92-11126 * #
AIAA PAPER 91-3601	p 79	N92-11130 * #
AIAA PAPER 91-3629	p 236	N92-16481 * #
AIAA PAPER 91-4116	p 53	A92-24369 * #
AIAA PAPER 91-5050	p 23	A92-44547 * #
AIAA PAPER 92-0037	p 4	A92-25676 * #
AIAA PAPER 92-0037	p 15	N92-14001 * #
AIAA PAPER 92-0043	p 4	A92-25677 * #
AIAA PAPER 92-0043	p 16	N92-15968 * #
AIAA PAPER 92-0053	p 166	A92-22168 * #
AIAA PAPER 92-0053	p 249	N92-15663 * #
AIAA PAPER 92-0065	p 252	A92-25678 * #

AIAA PAPER 92-0065	p 15	N92-14003 * #
AIAA PAPER 92-0123	p 266	A92-28185 * #
AIAA PAPER 92-0145	p 5	A92-25682 * #
AIAA PAPER 92-0145	p 16	N92-15977 * #
AIAA PAPER 92-0146	p 4	A92-23762 * #
AIAA PAPER 92-0148	p 4	A92-23764 * #
AIAA PAPER 92-0149	p 7	A92-28186 * #
AIAA PAPER 92-0152	p 4	A92-23767 * #
AIAA PAPER 92-0152	p 14	N92-13998 * #
AIAA PAPER 92-0162	p 198	A92-26926 * #
AIAA PAPER 92-0233	p 25	A92-25696 * #
AIAA PAPER 92-0240	p 137	A92-25702 * #
AIAA PAPER 92-0240	p 138	N92-16156 * #
AIAA PAPER 92-0242	p 113	A92-26927 * #
AIAA PAPER 92-0243	p 113	A92-26928 * #
AIAA PAPER 92-0245	p 167	A92-25704 * #
AIAA PAPER 92-0246	p 167	A92-25705 * #
AIAA PAPER 92-0257	p 167	A92-25715 * #
AIAA PAPER 92-0274	p 5	A92-25728 * #
AIAA PAPER 92-0274	p 15	N92-14002 * #
AIAA PAPER 92-0277	p 5	A92-25731 * #
AIAA PAPER 92-0297	p 21	A92-25750 * #
AIAA PAPER 92-0298	p 169	A92-28187 * #
AIAA PAPER 92-0334	p 113	A92-25781 * #
AIAA PAPER 92-0348	p 167	A92-25792 * #
AIAA PAPER 92-0350	p 137	A92-28188 * #
AIAA PAPER 92-0354	p 56	A92-28189 * #
AIAA PAPER 92-0354	p 57	N92-30301 * #
AIAA PAPER 92-0363	p 168	A92-25798 * #
AIAA PAPER 92-0363	p 185	N92-14323 * #
AIAA PAPER 92-0366	p 168	A92-26227 * #
AIAA PAPER 92-0370	p 253	A92-28190 * #
AIAA PAPER 92-0371	p 252	A92-26230 * #
AIAA PAPER 92-0371	p 254	N92-16702 * #
AIAA PAPER 92-0376	p 25	A92-26234 * #
AIAA PAPER 92-0385	p 25	A92-28191 * #
AIAA PAPER 92-0385	p 17	N92-19993 * #
AIAA PAPER 92-0412	p 5	A92-26264 * #
AIAA PAPER 92-0413	p 7	A92-28192 * #
AIAA PAPER 92-0413	p 19	N92-26612 * #
AIAA PAPER 92-0414	p 5	A92-26265 * #
AIAA PAPER 92-0415	p 6	A92-26266 * #
AIAA PAPER 92-0416	p 8	A92-29972 * #
AIAA PAPER 92-0417	p 6	A92-26267 * #
AIAA PAPER 92-0417	p 16	N92-15052 * #
AIAA PAPER 92-0420	p 168	A92-26270 * #
AIAA PAPER 92-0421	p 7	A92-28193 * #
AIAA PAPER 92-0488	p 7	A92-28194 * #
AIAA PAPER 92-0496	p 169	A92-28195 * #
AIAA PAPER 92-0500	p 252	A92-26328 * #
AIAA PAPER 92-0500	p 254	N92-14795 * #
AIAA PAPER 92-0501	p 252	A92-26930 * #
AIAA PAPER 92-0501	p 254	N92-14797 * #
AIAA PAPER 92-0503	p 6	A92-26932 * #
AIAA PAPER 92-0503	p 15	N92-14000 * #
AIAA PAPER 92-0506	p 253	A92-26934 * #
AIAA PAPER 92-0521	p 6	A92-26946 * #
AIAA PAPER 92-0522	p 6	A92-26947 * #
AIAA PAPER 92-0527	p 22	A92-26950 * #
AIAA PAPER 92-0532	p 22	A92-31670 * #
AIAA PAPER 92-0534	p 169	A92-28198 * #
AIAA PAPER 92-0544	p 169	A92-28201 * #
AIAA PAPER 92-0551	p 7	A92-28204 * #
AIAA PAPER 92-0558	p 240	A92-26968 * #
AIAA PAPER 92-0576	p 53	A92-26983 * #
AIAA PAPER 92-0577	p 239	A92-26984 * #
AIAA PAPER 92-0578	p 59	A92-26985 * #
AIAA PAPER 92-0604	p 169	A92-28211 * #
AIAA PAPER 92-0605	p 137	A92-27002 * #
AIAA PAPER 92-0636	p 6	A92-27014 * #
AIAA PAPER 92-0645	p 8	A92-28215 * #
AIAA PAPER 92-0645	p 188	N92-23154 * #
AIAA PAPER 92-0647	p 7	A92-27021 * #
AIAA PAPER 92-0647	p 16	N92-15051 * #
AIAA PAPER 92-0678	p 60	A92-27045 * #
AIAA PAPER 92-0691	p 168	A92-27058 * #
AIAA PAPER 92-0691	p 192	N92-25296 * #
AIAA PAPER 92-0712	p 168	A92-27072 * #
AIAA PAPER 92-0741	p 170	A92-28222 * #
AIAA PAPER 92-0753	p 8	A92-31679 * #
AIAA PAPER 92-0773	p 168	A92-27110 * #
AIAA PAPER 92-0773	p 30	N92-15994 * #
AIAA PAPER 92-0784	p 56	A92-27119 * #

AIAA PAPER 92-0787	p 137	A92-27122 * #
AIAA PAPER 92-0794	p 93	A92-27125 * #
AIAA PAPER 92-0794	p 96	N92-14114 * #
AIAA PAPER 92-0818	p 60	A92-29591 * #
AIAA PAPER 92-0818	p 135	N92-18442 * #
AIAA PAPER 92-0829	p 170	A92-29597 * #
AIAA PAPER 92-0845	p 138	A92-29611 * #
AIAA PAPER 92-0848	p 53	A92-29614 * #
AIAA PAPER 92-0850	p 117	A92-29616 * #
AIAA PAPER 92-0883	p 94	A92-29644 * #
AIAA PAPER 92-1144	p 241	A92-33285 * #
AIAA PAPER 92-1185	p 60	A92-33299 * #
AIAA PAPER 92-1185	p 83	N92-16023 * #
AIAA PAPER 92-1221	p 8	A92-33320 * #
AIAA PAPER 92-122	p 51	N92-15109 * #
AIAA PAPER 92-1264	p 47	A92-35868 * #
AIAA PAPER 92-1264	p 48	N92-21547 * #
AIAA PAPER 92-1293	p 242	A92-38490 * #
AIAA PAPER 92-1293	p 243	N92-14649 * #
AIAA PAPER 92-1478	p 61	A92-38597 * #
AIAA PAPER 92-1489	p 61	A92-38605 * #
AIAA PAPER 92-1537	p 43	A92-38634 * #
AIAA PAPER 92-1556	p 61	A92-38650 * #
AIAA PAPER 92-1556	p 92	N92-31342 * #
AIAA PAPER 92-1557	p 61	A92-38651 * #
AIAA PAPER 92-1558	p 6	A92-38652 * #
AIAA PAPER 92-1822	p 154	A92-29769 * #
AIAA PAPER 92-1824	p 154	A92-29771 * #
AIAA PAPER 92-1831	p 142	A92-29777 * #
AIAA PAPER 92-1861	p 155	A92-29801 * #
AIAA PAPER 92-1863	p 155	A92-29803 * #
AIAA PAPER 92-1868	p 142	A92-29807 * #
AIAA PAPER 92-1888	p 143	A92-29821 * #
AIAA PAPER 92-1899	p 155	A92-29830 * #
AIAA PAPER 92-1902	p 143	A92-29833 * #
AIAA PAPER 92-1908	p 143	A92-29839 * #
AIAA PAPER 92-1919	p 143	A92-29848 * #
AIAA PAPER 92-1935	p 155	A92-31706 * #
AIAA PAPER 92-1957	p 143	A92-29881 * #
AIAA PAPER 92-1960	p 143	A92-29883 * #
AIAA PAPER 92-1960	p 52	N92-23187 * #
AIAA PAPER 92-1961	p 143	A92-29884 * #
AIAA PAPER 92-1964	p 144	A92-29887 * #
AIAA PAPER 92-1965	p 45	A92-29888 * #
AIAA PAPER 92-1969	p 144	A92-29892 * #
AIAA PAPER 92-1972	p 144	A92-29895 * #
AIAA PAPER 92-1976	p 156	A92-38140 * #
AIAA PAPER 92-1982	p 144	A92-29902 * #
AIAA PAPER 92-2004	p 144	A92-29923 * #
AIAA PAPER 92-2005	p 49	A92-29924 * #
AIAA PAPER 92-2014	p 49	A92-29933 * #
AIAA PAPER 92-2018	p 144	A92-29936 * #
AIAA PAPER 92-2018	p 149	N92-15306 * #
AIAA PAPER 92-2036	p 145	A92-29951 * #
AIAA PAPER 92-2037	p 145	A92-29952 * #
AIAA PAPER 92-2038	p 145	A92-31711 * #
AIAA PAPER 92-2039	p 145	A92-29953 * #
AIAA PAPER 92-2040	p 49	A92-29954 * #
AIAA PAPER 92-2040	p 51	N92-16008 * #
AIAA PAPER 92-2042	p 50	A92-29956 * #
AIAA PAPER 92-2054	p 145	A92-29966 * #
AIAA PAPER 92-2058	p 22	A92-29889 * #
AIAA PAPER 92-2118	p 26	A92-35687 * #
AIAA PAPER 92-2120	p 9	A92-35689 * #
AIAA PAPER 92-2151	p 94	A92-31286 * #
AIAA PAPER 92-2171	p 124	A92-31299 * #
AIAA PAPER 92-2172	p 94	A92-31300 * #
AIAA PAPER 92-2218	p 25	A92-34408 * #
AIAA PAPER 92-2244	p 220	A92-34569 * #
AIAA PAPER 92-2302	p 220	A92-34523 * #
AIAA PAPER 92-2347	p 219	A92-34321 * #
AIAA PAPER 92-2348	p 219	A92-34322 * #
AIAA PAPER 92-2348	p 129	N92-20380 * #
AIAA PAPER 92-2352	p 54	A92-34325 * #
AIAA PAPER 92-2352	p 230	N92-33935 * #
AIAA PAPER 92-2370	p 26	A92-34598 * #
AIAA PAPER 92-2408	p 219	A92-34339 * #
AIAA PAPER 92-2410	p 251	A92-34341 * #
AIAA PAPER 92-2411	p 242	A92-34342 * #
AIAA PAPER 92-2413	p 60	A92-34343 * #
AIAA PAPER 92-2432	p 220	A92-34580 * #
AIAA PAPER 92-2445	p 94	A92-34474 * #
AIAA PAPER 92-2471	p 219	A92-34360 * #

REPORT

AIAA PAPER 92-2478

AIAA PAPER 92-2478	p 242	A92-34367 * #	AIAA PAPER 92-3351	p 66	A92-48928 * #	AIAA PAPER 92-4035	p 14	A92-56857 * #
AIAA PAPER 92-2479	p 220	A92-34368 * #	AIAA PAPER 92-3351	p 257	N92-28475 * #	AIAA PAPER 92-4042	p 14	A92-56861 * #
AIAA PAPER 92-2490	p 221	A92-34582 * #	AIAA PAPER 92-3353	p 178	A92-48930 * #	AIAA PAPER 92-4178	p 23	A92-52459 * #
AIAA PAPER 92-2491	p 221	A92-34583 * #	AIAA PAPER 92-3362	p 23	A92-54026 * #	AIAA PAPER 92-4484	p 57	A92-55314 * #
AIAA PAPER 92-2492	p 101	A92-34584 * #	AIAA PAPER 92-3363	p 205	A92-48936 * #	AIAA PAPER 92-4509	p 44	A92-52079 * #
AIAA PAPER 92-2493	p 221	A92-34585 * #	AIAA PAPER 92-3364	p 205	A92-48937 * #	AIAA PAPER 92-4623	p 28	A92-55281 * #
AIAA PAPER 92-2494	p 221	A92-34586 * #	AIAA PAPER 92-3365	p 205	A92-48938 * #		p 23	A92-55300 * #
AIAA PAPER 92-2498	p 220	A92-34555 * #	AIAA PAPER 92-3365	p 210	N92-24984 * #			
AIAA PAPER 92-2504	p 8	A92-34499 * #	AIAA PAPER 92-3366	p 205	A92-48939 * #	ANL/CP-75370	p 85	N92-21187 * #
AIAA PAPER 92-2536	p 54	A92-34380 * #	AIAA PAPER 92-3384	p 135	N92-25957 * #			
AIAA PAPER 92-2563	p 220	A92-34564 * #	AIAA PAPER 92-3385	p 141	A92-48951 * #	ASME PAPER 91-GT-116	p 222	A92-36896 * #
AIAA PAPER 92-2622-CP	p 20	N92-30182 * #	AIAA PAPER 92-3385	p 135	N92-26131 * #	ASME PAPER 91-GT-130	p 2	A92-15574 * #
AIAA PAPER 92-2622	p 9	A92-45494 * #	AIAA PAPER 92-3390	p 73	A92-54027 * #	ASME PAPER 91-GT-133	p 2	A92-15576 * #
AIAA PAPER 92-2634	p 10	A92-45574 * #	AIAA PAPER 92-3417	p 223	A92-48976 * #	ASME PAPER 91-GT-140	p 3	A92-15580 * #
AIAA PAPER 92-2690	p 10	A92-45537 * #	AIAA PAPER 92-3419	p 224	A92-48978 * #	ASME PAPER 91-GT-155	p 24	A92-15591 * #
AIAA PAPER 92-2699	p 10	A92-45541 * #	AIAA PAPER 92-3421	p 66	A92-48980 * #	ASME PAPER 91-GT-157	p 164	A92-15593 * #
AIAA PAPER 92-2699	p 38	N92-33746 * #	AIAA PAPER 92-3421	p 178	A92-48994 * #	ASME PAPER 91-GT-198	p 3	A92-15623 * #
AIAA PAPER 92-2700	p 10	A92-45542 * #	AIAA PAPER 92-3437	p 66	A92-49001 * #	ASME PAPER 91-GT-199	p 197	A92-15610 * #
AIAA PAPER 92-2724	p 10	A92-45561 * #	AIAA PAPER 92-3445	p 89	N92-27654 * #	ASME PAPER 91-GT-209	p 99	A92-15629 * #
AIAA PAPER 92-2858	p 176	A92-47841 * #	AIAA PAPER 92-3445	p 73	A92-54030 * #	ASME PAPER 91-GT-210	p 99	A92-15630 * #
AIAA PAPER 92-2859	p 176	A92-47842 * #	AIAA PAPER 92-3446	p 73	A92-54031 * #	ASME PAPER 91-GT-217	p 24	A92-15634 * #
AIAA PAPER 92-2881	p 176	A92-47862 * #	AIAA PAPER 92-3447	p 134	A92-49004 * #	ASME PAPER 91-GT-245	p 203	A92-15650 * #
AIAA PAPER 92-2881	p 189	N92-23268 * #	AIAA PAPER 92-3450	p 74	A92-54033 * #	ASME PAPER 91-GT-246	p 203	A92-15651 * #
AIAA PAPER 92-2881	p 266	A92-54287 * #	AIAA PAPER 92-3462	p 74	A92-54034 * #	ASME PAPER 91-GT-265	p 165	A92-15663 * #
AIAA PAPER 92-2894	p 114	A92-46976 * #	AIAA PAPER 92-3463	p 27	A92-54035 * #	ASME PAPER 91-GT-267	p 165	A92-15665 * #
AIAA PAPER 92-2960	p 199	A92-46979 * #	AIAA PAPER 92-3471	p 205	A92-49027 * #	ASME PAPER 91-GT-272	p 3	A92-15669 * #
AIAA PAPER 92-2964	p 63	A92-47000 * #	AIAA PAPER 92-3490	p 205	A92-49027 * #	ASME PAPER 91-GT-273	p 3	A92-15670 * #
AIAA PAPER 92-2990	p 63	A92-47027 * #	AIAA PAPER 92-3493	p 207	A92-54036 * #	ASME PAPER 91-GT-287	p 215	A92-15681 * #
AIAA PAPER 92-3024	p 182	A92-54001 * #	AIAA PAPER 92-3494	p 215	N92-31485 * #	ASME PAPER 91-GT-325	p 203	A92-15696 * #
AIAA PAPER 92-3060	p 72	A92-54002 * #	AIAA PAPER 92-3494	p 74	A92-54038 * #	ASME PAPER 91-GT-329	p 2	A92-15539 * #
AIAA PAPER 92-3061	p 136	N92-29669 * #	AIAA PAPER 92-3516	p 90	N92-28983 * #	ASME PAPER 91-GT-83	p 2	A92-15550 * #
AIAA PAPER 92-3061	p 63	A92-48719 * #	AIAA PAPER 92-3528	p 45	A92-49052 * #	ASME PAPER 92-APM-5	p 223	A92-44681 * #
AIAA PAPER 92-3063	p 136	N92-28433 * #	AIAA PAPER 92-3530	p 74	A92-54039 * #			
AIAA PAPER 92-3063	p 177	A92-48721 * #	AIAA PAPER 92-3530	p 93	N92-34113 * #	AVSCOM-TR-C-016	p 47	N92-26129 * #
AIAA PAPER 92-3067	p 12	A92-54003 * #	AIAA PAPER 92-3532	p 74	A92-54040 * #			
AIAA PAPER 92-3068	p 13	A92-54004 * #	AIAA PAPER 92-3532	p 47	N92-34114 * #	AVSCOM-TR-88-C-013	p 34	N92-22863 * #
AIAA PAPER 92-3069	p 13	A92-54005 * #	AIAA PAPER 92-3533	p 74	A92-54041 * #	AVSCOM-TR-90-C-029	p 209	N92-23536 * #
AIAA PAPER 92-3070	p 242	A92-54006 * #	AIAA PAPER 92-3543	p 182	A92-54043 * #	AVSCOM-TR-91-C-006	p 209	N92-23226 * #
AIAA PAPER 92-3072	p 10	A92-48723 * #	AIAA PAPER 92-3548	p 12	A92-49063 * #	AVSCOM-TR-91-C-009	p 210	N92-25347 * #
AIAA PAPER 92-3073	p 11	A92-48724 * #	AIAA PAPER 92-3548	p 18	N92-24958 * #	AVSCOM-TR-91-C-020	p 207	N92-10195 * #
AIAA PAPER 92-3074	p 72	A92-54007 * #	AIAA PAPER 92-3564	p 259	A92-54055 * #	AVSCOM-TR-91-C-023	p 132	N92-25348 * #
AIAA PAPER 92-3078	p 134	A92-48727 * #	AIAA PAPER 92-3567	p 178	A92-49068 * #	AVSCOM-TR-91-C-025	p 210	N92-25447 * #
AIAA PAPER 92-3079	p 135	N92-25277 * #	AIAA PAPER 92-3569	p 41	A92-54058 * #	AVSCOM-TR-91-C-026	p 213	N92-30396 * #
AIAA PAPER 92-3079	p 11	A92-48729 * #	AIAA PAPER 92-3570	p 27	A92-54059 * #	AVSCOM-TR-91-C-027	p 212	N92-28476 * #
AIAA PAPER 92-3082	p 195	N92-27653 * #	AIAA PAPER 92-3570	p 37	N92-28419 * #	AVSCOM-TR-91-C-028	p 211	N92-25448 * #
AIAA PAPER 92-3082	p 11	A92-48730 * #	AIAA PAPER 92-3571	p 28	A92-54060 * #	AVSCOM-TR-91-C-030	p 210	N92-25396 * #
AIAA PAPER 92-3083	p 36	N92-27037 * #	AIAA PAPER 92-3581	p 75	A92-54062 * #	AVSCOM-TR-91-C-031	p 211	N92-26107 * #
AIAA PAPER 92-3083	p 182	A92-54008 * #	AIAA PAPER 92-3583	p 75	A92-54063 * #	AVSCOM-TR-91-C-033	p 211	N92-26106 * #
AIAA PAPER 92-3087	p 177	A92-48732 * #	AIAA PAPER 92-3587	p 66	A92-49069 * #	AVSCOM-TR-91-C-035	p 212	N92-26560 * #
AIAA PAPER 92-3087	p 36	N92-26561 * #	AIAA PAPER 92-3622	p 13	A92-54090 * #	AVSCOM-TR-91-C-036	p 212	N92-26555 * #
AIAA PAPER 92-3088	p 177	A92-48733 * #	AIAA PAPER 92-3639	p 182	A92-54112 * #	AVSCOM-TR-91-C-038	p 211	N92-28434 * #
AIAA PAPER 92-3089	p 177	A92-48734 * #	AIAA PAPER 92-3656	p 200	A92-54106 * #	AVSCOM-TR-91-C-040	p 186	N92-18809 * #
AIAA PAPER 92-3090	p 178	A92-48735 * #	AIAA PAPER 92-3671	p 243	A92-54114 * #	AVSCOM-TR-91-C-041	p 213	N92-29351 * #
AIAA PAPER 92-3090	p 36	N92-27652 * #	AIAA PAPER 92-3672	p 182	A92-54115 * #	AVSCOM-TR-91-C-042	p 211	N92-26108 * #
AIAA PAPER 92-3098	p 11	A92-48744 * #	AIAA PAPER 92-3705	p 76	A92-57033 * #	AVSCOM-TR-91-C-043	p 213	N92-29136 * #
AIAA PAPER 92-3102	p 19	N92-28102 * #	AIAA PAPER 92-3712	p 183	A92-54132 * #	AVSCOM-TR-91-C-044	p 209	N92-24202 * #
AIAA PAPER 92-3106	p 258	A92-48747 * #	AIAA PAPER 92-3713	p 126	A92-49095 * #	AVSCOM-TR-91-C-045	p 229	N92-28701 * #
AIAA PAPER 92-3108	p 64	A92-48748 * #	AIAA PAPER 92-3713	p 75	A92-54144 * #	AVSCOM-TR-91-C-049	p 212	N92-27879 * #
AIAA PAPER 92-3109	p 258	A92-48749 * #	AIAA PAPER 92-3741	p 259	A92-54145 * #	AVSCOM-TR-91-C-053	p 17	N92-19993 * #
AIAA PAPER 92-3110	p 64	A92-48750 * #	AIAA PAPER 92-3742	p 28	A92-54159 * #	AVSCOM-TR-92-C-001	p 19	N92-26104 * #
AIAA PAPER 92-3113	p 64	A92-48752 * #	AIAA PAPER 92-3770	p 14	A92-54161 * #	AVSCOM-TR-92-C-002	p 108	N92-20039 * #
AIAA PAPER 92-3123	p 266	N92-30908 * #	AIAA PAPER 92-3774	p 75	A92-54164 * #	AVSCOM-TR-92-C-003	p 214	N92-30948 * #
AIAA PAPER 92-3144	p 64	A92-48772 * #	AIAA PAPER 92-3785	p 90	N92-28417 * #	AVSCOM-TR-92-C-008	p 214	N92-31349 * #
AIAA PAPER 92-3148	p 64	A92-48776 * #	AIAA PAPER 92-3785	p 57	A92-54165 * #	AVSCOM-TR-92-C-011	p 210	N92-24984 * #
AIAA PAPER 92-3154	p 64	A92-48780 * #	AIAA PAPER 92-3786	p 28	A92-54168 * #	AVSCOM-TR-92-C-014	p 241	N92-33897 * #
AIAA PAPER 92-3154	p 48	N92-25958 * #	AIAA PAPER 92-3789	p 37	N92-27669 * #	AVSCOM-TR-92-C-018	p 215	N92-31485 * #
AIAA PAPER 92-3161	p 65	A92-48784 * #	AIAA PAPER 92-3790	p 28	A92-54169 * #	AVSCOM-TR-92-C-019	p 37	N92-29661 * #
AIAA PAPER 92-3162	p 65	A92-48785 * #	AIAA PAPER 92-3791	p 37	N92-28418 * #	AVSCOM-TR-92-C-024	p 251	N92-30898 * #
AIAA PAPER 92-3164	p 65	A92-48787 * #	AIAA PAPER 92-3792	p 183	A92-54170 * #	AVSCOM-TR-92-C-026	p 202	N92-29105 * #
AIAA PAPER 92-3164	p 88	N92-27033 * #	AIAA PAPER 92-3794	p 28	A92-54171 * #	AVSCOM-TR-92-C-028	p 40	N92-34107 * #
AIAA PAPER 92-3167	p 215	A92-48789 * #	AIAA PAPER 92-3800	p 36	N92-26613 * #	AVSCOM-TR-92-C-029	p 215	N92-31536 * #
AIAA PAPER 92-3174	p 27	A92-54011 * #	AIAA PAPER 92-3809	p 179	A92-49126 * #	AVSCOM-TR-92-C-050	p 213	N92-29697 * #
AIAA PAPER 92-3175	p 13	A92-54012 * #	AIAA PAPER 92-3815	p 67	A92-49127 * #			
AIAA PAPER 92-3177	p 13	A92-54013 * #	AIAA PAPER 92-3817	p 26	A92-49128 * #	CMOTT-91-07	p 1	N92-23336 * #
AIAA PAPER 92-3180	p 230	N92-34112 * #	AIAA PAPER 92-3826	p 75	A92-54182 * #	CMOTT-91-08	p 184	N92-11302 * #
AIAA PAPER 92-3200	p 178	A92-48795 * #	AIAA PAPER 92-3827	p 67	A92-49129 * #	CMOTT-91-09	p 186	N92-18775 * #
AIAA PAPER 92-3204	p 65	A92-48808 * #	AIAA PAPER 92-3829	p 76	A92-54190 * #	CMOTT-91-10	p 185	N92-15357 * #
AIAA PAPER 92-3204	p 65	A92-48811 * #	AIAA PAPER 92-3861	p 76	A92-54191 * #	CMOTT-92-02	p 191	N92-24514 * #
AIAA PAPER 92-3210	p 182	A92-54015 * #	AIAA PAPER 92-3861	p 76	A92-54192 * #	CMOTT-92-03	p 190	N92-23542 * #
AIAA PAPER 92-3211	p 13	A92-54016 * #	AIAA PAPER 92-3894	p 76	A92-54193 * #	CMOTT-92-04	p 249	N92-22230 * #
AIAA PAPER 92-3213	p 73	A92-54017 * #	AIAA PAPER 92-3916	p 183	A92-54209 * #	CMOTT-92-05	p 187	N92-22398 * #
AIAA PAPER 92-3216	p 73	A92-54018 * #	AIAA PAPER 92-3916	p 250	N92-27517 * #	CMOTT-92-06	p 191	N92-24050 * #
AIAA PAPER 92-3226	p 65	A92-48827 * #	AIAA PAPER 92-3922	p 200	A92-56733 * #	CMOTT-92-07	p 196	N92-32868 * #
AIAA PAPER 92-3226	p 89	N92-27036 * #	AIAA PAPER 92-3927	p 41	A92-56748 * #			
AIAA PAPER 92-3228	p 66	A92-48829 * #	AIAA PAPER 92-3974	p 42	N92-28673 * #	CONF-920104-23	p 91	N92-30818 * #
AIAA PAPER 92-3228	p 88	N92-27035 * #	AIAA PAPER 92-3980	p 41	A92-56753 * #	CONF-920104-31	p 85	N92-21187 * #
AIAA PAPER 92-3243	p 199	A92-48843 * #	AIAA PAPER 92-3993	p 47	A92-56806 * #			
AIAA PAPER 92-3261	p 27	A92-54020 * #	AIAA PAPER 92-3995	p 42	N92-30508 * #	DE92-004262	p 91	N92-30818 * #
AIAA PAPER 92-3297	p 258	A92-48885 * #	AIAA PAPER 92-3995	p 41	A92-56816 * #	DE92-007378	p 85	N92-21187 * #
AIAA PAPER 92-3317	p 73	A92-54022 * #	AIAA PAPER 92-4005	p 41	A92-56818 * #			
AIAA PAPER 92-3325	p 40	A92-48908 * #	AIAA PAPER 92-4006	p 42	N92-25449 * #	DOE/NASA/33408-6	p 123	N92-27192 * #

E-4969	p 49	N92-31251 * #	E-6588	p 122	N92-16086 * #	E-6754	p 161	N92-23535 * #
E-5175	p 56	N92-24349 * #	E-6589	p 249	N92-16663 * #	E-6759	p 185	N92-14323 * #
E-5326	p 123	N92-24554 * #	E-6592	p 96	N92-15128 * #	E-6760	p 16	N92-15052 * #
E-5337	p 91	N92-31249 * #	E-6593	p 141	N92-11221 * #	E-6761	p 16	N92-15051 * #
E-5369	p 17	N92-20934 * #	E-6595	p 128	N92-14170 * #	E-6762	p 97	N92-25203 * #
E-5456	p 49	N92-32456 * #	E-6596	p 185	N92-13401 * #	E-6765	p 51	N92-18342 * #
E-5506	p 229	N92-25446 * #	E-6597	p 147	N92-12151 * #	E-6767	p 17	N92-17347 * #
E-5521	p 186	N92-15358 * #	E-6600	p 184	N92-11302 * #	E-6768	p 228	N92-24985 * #
E-5535	p 51	N92-22001 * #	E-6601	p 55	N92-11086 * #	E-6769	p 249	N92-15662 * #
E-5628	p 207	N92-14346 * #	E-6604	p 235	N92-13482 * #	E-6770	p 107	N92-18439 * #
E-5638	p 227	N92-22227 * #	E-6607	p 77	N92-10057 * #	E-6772	p 96	N92-18457 * #
E-5808	p 22	N92-30395 * #	E-6608	p 84	N92-18474 * #	E-6773	p 228	N92-23196 * #
E-5837	p 207	N92-10195 * #	E-6613	p 17	N92-19437 * #	E-6775	p 30	N92-20523 * #
E-5902	p 42	N92-17059 * #	E-6614	p 77	N92-10055 * #	E-6776	p 209	N92-23536 * #
E-5976	p 30	N92-17061 * #	E-6616	p 202	N92-24881 * #	E-6777	p 252	N92-26671 * #
E-5993	p 226	N92-15406 * #	E-6617	p 201	N92-19107 * #	E-6778	p 15	N92-14001 * #
E-6007	p 267	N92-12786 * #	E-6618	p 201	N92-19263 * #	E-6780	p 30	N92-15994 * #
E-6011	p 225	N92-11373 * #	E-6620	p 31	N92-20525 * #	E-6781	p 263	N92-19398 * #
E-6032	p 185	N92-13402 * #	E-6622	p 212	N92-28476 * #	E-6782	p 209	N92-24202 * #
E-6046	p 184	N92-11299 * #	E-6623	p 211	N92-25448 * #	E-6784	p 15	N92-14002 * #
E-6048	p 208	N92-20815 * #	E-6624	p 106	N92-13284 * #	E-6786	p 149	N92-15306 * #
E-6062	p 139	N92-16158 * #	E-6628	p 79	N92-11128 * #	E-6788	p 229	N92-28701 * #
E-6088	p 1	N92-17346 * #	E-6629	p 226	N92-16371 * #	E-6789	p 30	N92-17546 * #
E-6096	p 47	N92-30307 * #	E-6633	p 270	N92-17069 * #	E-6790	p 135	N92-19837 * #
E-6102	p 86	N92-21216 * #	E-6635	p 127	N92-11188 * #	E-6794	p 97	N92-21548 * #
E-6105	p 83	N92-17151 * #	E-6636	p 80	N92-11138 * #	E-6795	p 34	N92-23254 * #
E-6109	p 84	N92-19780 * #	E-6637	p 227	N92-22267 * #	E-6796	p 186	N92-16265 * #
E-6123	p 159	N92-11252 * #	E-6641	p 48	N92-11034 * #	E-6801	p 271	N92-18455 * #
E-6135	p 87	N92-25616 * #	E-6642	p 29	N92-11995 * #	E-6803	p 263	N92-15815 * #
E-6152	p 187	N92-21498 * #	E-6647	p 57	N92-25134 * #	E-6805	p 201	N92-18759 * #
E-6196	p 184	N92-11317 * #	E-6648	p 57	N92-13151 * #	E-6806	p 188	N92-23154 * #
E-6219	p 49	N92-15082 * #	E-6649	p 51	N92-15109 * #	E-6807	p 83	N92-16024 * #
E-6242	p 186	N92-18809 * #	E-6650	p 29	N92-11017 * #	E-6808	p 17	N92-19993 * #
E-6257	p 184	N92-11320 * #	E-6651	p 129	N92-19450 * #	E-6809	p 84	N92-20043 * #
E-6291	p 229	N92-25753 * #	E-6652	p 110	N92-25996 * #	E-6811	p 16	N92-15977 * #
E-6322	p 14	N92-10976 * #	E-6653	p 123	N92-16111 * #	E-6813	p 135	N92-18442 * #
E-6324	p 129	N92-16129 * #	E-6657	p 107	N92-15136 * #	E-6816	p 139	N92-21797 * #
E-6336	p 128	N92-11202 * #	E-6658	p 186	N92-18775 * #	E-6817	p 227	N92-20045 * #
E-6343	p 129	N92-17070 * #	E-6661	p 269	N92-14953 * #	E-6819	p 129	N92-20380 * #
E-6350	p 79	N92-11129 * #	E-6662	p 83	N92-16019 * #	E-6820	p 17	N92-18760 * #
E-6351	p 134	N92-13336 * #	E-6664	p 85	N92-20585 * #	E-6823	p 35	N92-25712 * #
E-6354	p 20	N92-28980 * #	E-6665	p 257	N92-13783 * #	E-6824	p 214	N92-30722 * #
E-6364	p 134	N92-11214 * #	E-6666	p 106	N92-14118 * #	E-6826	p 212	N92-27879 * #
E-6367	p 226	N92-15405 * #	E-6667	p 235	N92-13483 * #	E-6827	p 42	N92-28673 * #
E-6374	p 35	N92-25808 * #	E-6668	p 225	N92-12316 * #	E-6829	p 87	N92-24557 * #
E-6388	p 17	N92-23105 * #	E-6672	p 240	N92-13581 * #	E-6830	p 191	N92-24514 * #
E-6391	p 130	N92-22278 * #	E-6673	p 81	N92-13274 * #	E-6835	p 149	N92-17047 * #
E-6393	p 187	N92-22226 * #	E-6677	p 1	N92-22659 * #	E-6836	p 149	N92-16191 * #
E-6397	p 83	N92-16022 * #	E-6679	p 14	N92-13998 * #	E-6838	p 149	N92-17062 * #
E-6398	p 200	N92-15366 * #	E-6681	p 82	N92-14112 * #	E-6839	p 90	N92-28983 * #
E-6399	p 128	N92-15191 * #	E-6683	p 82	N92-14111 * #	E-6841	p 150	N92-19992 * #
E-6400	p 236	N92-13484 * #	E-6686	p 228	N92-23527 * #	E-6842	p 149	N92-18281 * #
E-6407	p 133	N92-32863 * #	E-6687	p 81	N92-13275 * #	E-6843	p 19	N92-26104 * #
E-6418	p 82	N92-14109 * #	E-6688	p 29	N92-13070 * #	E-6844	p 87	N92-25343 * #
E-6422	p 141	N92-11217 * #	E-6689	p 247	N92-13717 * #	E-6845	p 230	N92-33935 * #
E-6439	p 243	N92-11691 * #	E-6691	p 190	N92-23560 * #	E-6846	p 130	N92-22305 * #
E-6447	p 151	N92-23412 * #	E-6695	p 184	N92-11328 * #	E-6847	p 230	N92-33476 * #
E-6450	p 90	N92-28682 * #	E-6696	p 210	N92-25396 * #	E-6848	p 150	N92-18921 * #
E-6451	p 226	N92-15403 * #	E-6700	p 236	N92-14485 * #	E-6851	p 201	N92-18456 * #
E-6456	p 78	N92-11088 * #	E-6701	p 185	N92-15336 * #	E-6852	p 263	N92-20519 * #
E-6460	p 1	N92-10002 * #	E-6702	p 95	N92-13281 * #	E-6853	p 18	N92-23563 * #
E-6491	p 106	N92-14122 * #	E-6703	p 226	N92-15402 * #	E-6855	p 83	N92-16023 * #
E-6494	p 30	N92-15993 * #	E-6704	p 225	N92-14433 * #	E-6859	p 84	N92-18280 * #
E-6500	p 133	N92-31840 * #	E-6705	p 254	N92-14795 * #	E-6860	p 160	N92-18473 * #
E-6502	p 95	N92-10064 * #	E-6707	p 82	N92-15119 * #	E-6863	p 215	N92-31536 * #
E-6511	p 107	N92-16037 * #	E-6709	p 107	N92-16036 * #	E-6864	p 130	N92-21579 * #
E-6518	p 77	N92-10044 * #	E-6710	p 269	N92-13910 * #	E-6866	p 109	N92-23195 * #
E-6519	p 255	N92-16705 * #	E-6712	p 52	N92-22319 * #	E-6868	p 30	N92-20033 * #
E-6520	p 243	N92-16628 * #	E-6714	p 227	N92-20212 * #	E-6869	p 160	N92-21370 * #
E-6523	p 14	N92-10012 * #	E-6716	p 187	N92-22487 * #	E-6870	p 85	N92-20355 * #
E-6529	p 243	N92-14649 * #	E-6717	p 29	N92-14063 * #	E-6871	p 226	N92-19779 * #
E-6530	p 134	N92-11208 * #	E-6718	p 82	N92-15125 * #	E-6872	p 202	N92-23155 * #
E-6531	p 213	N92-30396 * #	E-6720	p 107	N92-15137 * #	E-6876	p 108	N92-20039 * #
E-6539	p 51	N92-19762 * #	E-6722	p 151	N92-20032 * #	E-6877	p 97	N92-21175 * #
E-6542	p 92	N92-31916 * #	E-6723	p 225	N92-14434 * #	E-6881	p 216	N92-23189 * #
E-6543	p 159	N92-14294 * #	E-6724	p 55	N92-13143 * #	E-6882	p 214	N92-30571 * #
E-6545	p 208	N92-16336 * #	E-6725	p 185	N92-15357 * #	E-6883	p 48	N92-21547 * #
E-6548	p 147	N92-14202 * #	E-6726	p 185	N92-14322 * #	E-6885	p 139	N92-26611 * #
E-6554	p 235	N92-10221 * #	E-6728	p 161	N92-25176 * #	E-6887	p 48	N92-25092 * #
E-6556	p 79	N92-11133 * #	E-6729	p 130	N92-20660 * #	E-6888	p 108	N92-20841 * #
E-6557	p 106	N92-14120 * #	E-6730	p 255	N92-18282 * #	E-6890	p 150	N92-19379 * #
E-6559	p 128	N92-14179 * #	E-6732	p 211	N92-26107 * #	E-6891	p 209	N92-23226 * #
E-6561	p 240	N92-10289 * #	E-6734	p 249	N92-15663 * #	E-6894	p 160	N92-20040 * #
E-6567	p 236	N92-16481 * #	E-6735	p 51	N92-16008 * #	E-6895	p 18	N92-23269 * #
E-6570	p 1	N92-23336 * #	E-6737	p 131	N92-24715 * #	E-6896	p 209	N92-23564 * #
E-6571	p 110	N92-30779 * #	E-6738	p 160	N92-18920 * #	E-6899	p 228	N92-25179 * #
E-6572	p 128	N92-15192 * #	E-6739	p 15	N92-14003 * #	E-6900	p 109	N92-23194 * #
E-6574	p 108	N92-19595 * #	E-6740	p 138	N92-16156 * #	E-6901	p 228	N92-23267 * #
E-6576	p 80	N92-11136 * #	E-6741	p 96	N92-14114 * #	E-6902	p 87	N92-23534 * #
E-6578	p 85	N92-20522 * #	E-6742	p 129	N92-19498 * #	E-6903	p 86	N92-21976 * #
E-6579	p 79	N92-11135 * #	E-6743	p 254	N92-14797 * #	E-6905	p 40	N92-20586 * #
E-6580	p 78	N92-11126 * #	E-6744	p 15	N92-14000 * #	E-6908	p 186	N92-20235 * #
E-6581	p 80	N92-11137 * #	E-6745	p 85	N92-20065 * #	E-6909	p 109	N92-25754 * #
E-6582	p 96	N92-18970 * #	E-6746	p 16	N92-15968 * #	E-6910	p 189	N92-23268 * #
E-6584	p 79	N92-11130 * #	E-6747	p 254	N92-16702 * #	E-6912	p 190	N92-23565 * #
E-6587	p 249	N92-10345 * #	E-6749	p 129	N92-17060 * #	E-6913	p 191	N92-25196 * #

E-6914

E-6914	p 34	N92-23225 * #	E-7108	p 88	N92-27033 * #	IAF PAPER 92-0969	p 247	A92-57327 *
E-6916	p 250	N92-24974 * #	E-7109	p 37	N92-28419 * #	IAF-91-254	p 82	N92-15125 * #
E-6917	p 190	N92-23542 * #	E-7112	p 202	N92-29105 * #	ICOMP-91-17	p 1	N92-23336 * #
E-6919	p 216	N92-24986 * #	E-7113	p 37	N92-28985 * #	ICOMP-91-18	p 249	N92-10345 * #
E-6922	p 236	N92-20493 * #	E-7115	p 214	N92-30948 * #	ICOMP-91-19	p 184	N92-11302 * #
E-6924	p 249	N92-22230 * #	E-7116	p 19	N92-28102 * #	ICOMP-91-20	p 186	N92-18775 * #
E-6926	p 131	N92-23185 * #	E-7119	p 266	N92-30908 * #	ICOMP-91-21	p 225	N92-12316 * #
E-6929	p 86	N92-21517 * #	E-7124	p 36	N92-26613 * #	ICOMP-91-22	p 190	N92-23560 * #
E-6930	p 20	N92-28696 * #	E-7126	p 255	N92-28984 * #	ICOMP-91-23	p 184	N92-11328 * #
E-6932	p 135	N92-25957 * #	E-7127	p 213	N92-29697 * #	ICOMP-91-24	p 185	N92-15336 * #
E-6933	p 135	N92-26131 * #	E-7128	p 230	N92-31505 * #	ICOMP-91-25	p 185	N92-15357 * #
E-6935	p 133	N92-27378 * #	E-7130	p 90	N92-28417 * #	ICOMP-91-26	p 185	N92-14322 * #
E-6939	p 187	N92-22398 * #	E-7131	p 162	N92-28432 * #	ICOMP-91-27	p 249	N92-15663 * #
E-6941	p 86	N92-23252 * #	E-7135	p 90	N92-29343 * #	ICOMP-91-29	p 250	N92-27196 * #
E-6942	p 210	N92-25447 * #	E-7137	p 88	N92-27035 * #	ICOMP-92-01	p 191	N92-24514 * #
E-6943	p 35	N92-25164 * #	E-7141	p 196	N92-31484 * #	ICOMP-92-02	p 187	N92-22226 * #
E-6945	p 209	N92-23435 * #	E-7142	p 238	N92-29662 * #	ICOMP-92-03	p 190	N92-23565 * #
E-6946	p 250	N92-33742 * #	E-7145	p 257	N92-28475 * #	ICOMP-92-05	p 190	N92-23542 * #
E-6948	p 34	N92-23537 * #	E-7146	p 89	N92-27654 * #	ICOMP-92-06	p 249	N92-22230 * #
E-6949	p 97	N92-23190 * #	E-7147	p 19	N92-26612 * #	ICOMP-92-07	p 187	N92-22398 * #
E-6950	p 250	N92-27196 * #	E-7148	p 20	N92-28674 * #	ICOMP-92-08	p 250	N92-33742 * #
E-6952	p 97	N92-26142 * #	E-7149	p 151	N92-31855 * #	ICOMP-92-09	p 191	N92-24050 * #
E-6953	p 210	N92-25347 * #	E-7150	p 136	N92-29669 * #	ICOMP-92-10	p 196	N92-32868 * #
E-6954	p 150	N92-19700 * #	E-7153	p 239	N92-33898 * #	ICOMP-92-11	p 251	N92-33942 * #
E-6955	p 187	N92-20520 * #	E-7154	p 89	N92-27036 * #	ICOMP-92-12	p 250	N92-33571 * #
E-6960	p 161	N92-23561 * #	E-7156	p 163	N92-32243 * #	IEPC-91-018	p 82	N92-15119 * #
E-6962	p 19	N92-27377 * #	E-7158	p 244	N92-33894 * #	IEPC-91-076	p 84	N92-18474 * #
E-6963	p 161	N92-23562 * #	E-7160	p 151	N92-32965 * #	INT-PATENT-CLASS-A47H-1/144	p 213	N92-29092 *
E-6970	p 109	N92-25346 * #	E-7161	p 162	N92-28675 * #	INT-PATENT-CLASS-B23B-39/00	p 201	N92-21723 *
E-6971	p 132	N92-25348 * #	E-7165	p 110	N92-29660 * #	INT-PATENT-CLASS-B23H-9/00	p 201	N92-22038 *
E-6973	p 161	N92-23193 * #	E-7166	p 238	N92-30426 * #	INT-PATENT-CLASS-B32B-15/01	p 133	N92-29090 *
E-6975	p 192	N92-25296 * #	E-7170	p 93	N92-33064 * #	INT-PATENT-CLASS-B32B-15/20	p 133	N92-29090 *
E-6976	p 87	N92-24560 * #	E-7173	p 136	N92-28433 * #	INT-PATENT-CLASS-C01B-31/04	p 127	N92-10090 *
E-6977	p 131	N92-23192 * #	E-7179	p 111	N92-32466 * #	INT-PATENT-CLASS-C04B-35/10	p 128	N92-16122 *
E-6978	p 123	N92-27192 * #	E-7180	p 90	N92-28693 * #	INT-PATENT-CLASS-F02R-9/52	p 77	N92-10054 *
E-6983	p 92	N92-32108 * #	E-7184	p 238	N92-28837 * #	INT-PATENT-CLASS-F03G-6/00	p 238	N92-29143 *
E-6984	p 116	N92-26670 * #	E-7194	p 196	N92-32868 * #	INT-PATENT-CLASS-F16J-15/32	p 208	N92-16318 *
E-6986	p 211	N92-26108 * #	E-7195	p 238	N92-33895 * #	INT-PATENT-CLASS-F16J-15/46	p 208	N92-22043 *
E-6988	p 135	N92-25277 * #	E-7201	p 20	N92-34144 * #	INT-PATENT-CLASS-F28D-15/02	p 195	N92-29125 *
E-6989	p 202	N92-24959 * #	E-7202	p 48	N92-30310 * #	INT-PATENT-CLASS-H01C-31/58	p 236	N92-22037 *
E-6991	p 48	N92-25958 * #	E-7203	p 91	N92-30308 * #	INT-PATENT-CLASS-H01P-1/18	p 257	N92-28571 *
E-6993	p 18	N92-24958 * #	E-7204	p 162	N92-30427 * #	INT-PATENT-CLASS-H04N-7/13	p 147	N92-10128 *
E-6999	p 42	N92-25449 * #	E-7212	p 196	N92-32472 * #	ISBN 0-7918-0661-8	p 94	A92-39852 *
E-7000	p 52	N92-30383 * #	E-7217	p 92	N92-32237 * #	ISBN 1-55899-083-6	p 104	A92-46826 *
E-7001	p 227	N92-23191 * #	E-7219	p 142	N92-31263 * #	JPC-92-3144	p 92	N92-31901 * #
E-7002	p 47	N92-26129 * #	E-7221	p 162	N92-30397 * #	JPC-92-3203	p 92	N92-32237 * #
E-7007	p 110	N92-30986 * #	E-7222	p 92	N92-31507 * #	L-16799	p 16	N92-14968 * #
E-7009-1	p 163	N92-32233 * #	E-7225	p 241	N92-33897 * #	NAS 1.15:100881	p 29	N92-14061 * #
E-7010	p 52	N92-23187 * #	E-7226	p 38	N92-30972 * #	NAS 1.15:102434	p 56	N92-24349 * #
E-7015	p 211	N92-26555 * #	E-7227	p 40	N92-34107 * #	NAS 1.15:102554	p 17	N92-20934 * #
E-7016-1	p 270	N92-30302 * #	E-7231	p 257	N92-33896 * #	NAS 1.15:103747	p 226	N92-15406 * #
E-7018	p 57	N92-30301 * #	E-7232	p 110	N92-32234 * #	NAS 1.15:103753	p 267	N92-12786 * #
E-7019	p 212	N92-28434 * #	E-7233	p 1	N92-31267 * #	NAS 1.15:103755	p 225	N92-11373 * #
E-7020	p 211	N92-26106 * #	E-7235	p 251	N92-30898 * #	NAS 1.15:103770	p 185	N92-13402 * #
E-7021	p 264	N92-23890 * #	E-7242	p 93	N92-32463 * #	NAS 1.15:103786	p 139	N92-16158 * #
E-7024	p 87	N92-24957 * #	E-7245	p 38	N92-30998 * #	NAS 1.15:103800	p 1	N92-17346 * #
E-7026	p 189	N92-23224 * #	E-7249	p 92	N92-31901 * #	NAS 1.15:104179	p 43	N92-20925 * #
E-7027	p 210	N92-24984 * #	E-7259	p 238	N92-31262 * #	NAS 1.15:104386	p 184	N92-11317 * #
E-7028	p 110	N92-31506 * #	E-7260	p 40	N92-32241 * #	NAS 1.15:104424	p 184	N92-11320 * #
E-7029	p 87	N92-24201 * #	E-7262	p 270	N92-33899 * #	NAS 1.15:104427	p 86	N92-21216 * #
E-7032	p 212	N92-26560 * #	E-7263	p 163	N92-34204 * #	NAS 1.15:104475	p 14	N92-10976 * #
E-7033	p 56	N92-28683 * #	E-7270	p 136	N92-32230 * #	NAS 1.15:104477	p 83	N92-16022 * #
E-7035	p 141	N92-28436 * #	E-7285	p 163	N92-32867 * #	NAS 1.15:104478	p 129	N92-16129 * #
E-7036	p 237	N92-24802 * #	E-7287	p 164	N92-34219 * #	NAS 1.15:104488	p 128	N92-11202 * #
E-7037	p 161	N92-26096 * #	E-7289	p 162	N92-31282 * #	NAS 1.15:104492	p 79	N92-11129 * #
E-7039	p 230	N92-34112 * #	E-7297	p 230	N92-34221 * #	NAS 1.15:104493	p 134	N92-13336 * #
E-7042	p 142	N92-30692 * #	E-7311	p 93	N92-34113 * #	NAS 1.15:104498	p 84	N92-18780 * #
E-7043	p 194	N92-26690 * #	E-7317	p 250	N92-33571 * #	NAS 1.15:104503	p 134	N92-11214 * #
E-7046	p 20	N92-30182 * #	E-7318	p 251	N92-33942 * #	NAS 1.15:104506	p 226	N92-15405 * #
E-7048	p 213	N92-29351 * #	E-7341	p 47	N92-34114 * #	NAS 1.15:104518	p 17	N92-23105 * #
E-7053	p 244	N92-28684 * #	IAF PAPER 91-026	p 240	A92-12447 *	NAS 1.15:104524	p 200	N92-15366 * #
E-7058	p 37	N92-29661 * #	IAF PAPER 91-235	p 58	A92-13160 *	NAS 1.15:104525	p 128	N92-15191 * #
E-7060	p 213	N92-29136 * #	IAF PAPER 91-236	p 58	A92-13159 *	NAS 1.15:104526	p 236	N92-13484 * #
E-7061	p 38	N92-31172 * #	IAF PAPER 91-241	p 58	A92-13158 *	NAS 1.15:104531	p 133	N92-32863 * #
E-7062	p 38	N92-33746 * #	IAF PAPER 91-254	p 58	A92-13155 *	NAS 1.15:104536	p 241	N92-11642 * #
E-7063	p 36	N92-27037 * #	IAF PAPER 91-258	p 58	A92-13154 *	NAS 1.15:105096	p 82	N92-14109 * #
E-7064	p 42	N92-30508 * #	IAF PAPER 91-307	p 259	A92-14724 *	NAS 1.15:105143	p 82	N92-14109 * #
E-7065	p 195	N92-27653 * #	IAF PAPER 91-321	p 52	A92-14734 *	NAS 1.15:105144	p 141	N92-11217 * #
E-7069	p 89	N92-27878 * #	IAF PAPER 91-398	p 112	A92-18484 *	NAS 1.15:105154	p 243	N92-11691 * #
E-7071	p 88	N92-27034 * #	IAF PAPER 91-669	p 133	A92-20612 *	NAS 1.15:105159	p 151	N92-23412 * #
E-7073	p 90	N92-29667 * #	IAF PAPER 92-0398	p 159	A92-55785 *	NAS 1.15:105161	p 90	N92-28682 * #
E-7077	p 88	N92-26654 * #	IAF PAPER 92-0407	p 50	A92-55788 *			
E-7078	p 267	N92-25395 * #	IAF PAPER 92-0410	p 50	A92-55790 *			
E-7080	p 195	N92-30297 * #	IAF PAPER 92-0412	p 147	A92-55792 *			
E-7082	p 36	N92-27652 * #	IAF PAPER 92-0413	p 50	A92-55793 *			
E-7083	p 35	N92-26553 * #	IAF PAPER 92-0552	p 245	A92-55855 *			
E-7084	p 214	N92-31349 * #	IAF PAPER 92-0574	p 43	A92-57053 *			
E-7085	p 37	N92-27669 * #	IAF PAPER 92-0575	p 76	A92-57054 *			
E-7086	p 37	N92-28418 * #	IAF PAPER 92-0599	p 235	A92-57055 *			
E-7087	p 36	N92-26561 * #	IAF PAPER 92-0600	p 76	A92-57056 *			
E-7088	p 91	N92-30187 * #	IAF PAPER 92-0607	p 77	A92-57058 *			
E-7089	p 250	N92-27517 * #	IAF PAPER 92-0646	p 77	A92-57089 *			
E-7090	p 215	N92-31485 * #	IAF PAPER 92-0669	p 77	A92-57105 *			
E-7091	p 214	N92-30734 * #	IAF PAPER 92-0702	p 138	A92-57131 *			
E-7092	p 88	N92-26792 * #	IAF PAPER 92-0907	p 184	A92-57286 *			
E-7104	p 92	N92-31342 * #						

REPORT NUMBER INDEX

NAS 1.15:105666

NAS 1.15:105162	p 226	N92-15403 * #	NAS 1.15:105338	p 254	N92-14795 * #	NAS 1.15:105545	p 84	N92-20043 * #
NAS 1.15:105174	p 107	N92-16037 * #	NAS 1.15:105340	p 82	N92-15119 * #	NAS 1.15:105547	p 85	N92-20355 * #
NAS 1.15:105189	p 106	N92-14122 * #	NAS 1.15:105341	p 107	N92-16036 * #	NAS 1.15:105548	p 226	N92-19779 * #
NAS 1.15:105192	p 1	N92-10002 * #	NAS 1.15:105342	p 269	N92-13910 * #	NAS 1.15:105549	p 267	N92-25395 * #
NAS 1.15:105193	p 30	N92-15993 * #	NAS 1.15:105343	p 52	N92-22319 * #	NAS 1.15:105551	p 202	N92-23155 * #
NAS 1.15:105198	p 133	N92-31840 * #	NAS 1.15:105344	p 227	N92-20212 * #	NAS 1.15:105553	p 108	N92-20039 * #
NAS 1.15:105199	p 95	N92-10064 * #	NAS 1.15:105345	p 187	N92-22487 * #	NAS 1.15:105554	p 97	N92-21175 * #
NAS 1.15:105206	p 255	N92-16705 * #	NAS 1.15:105346	p 29	N92-14063 * #	NAS 1.15:105555	p 187	N92-21498 * #
NAS 1.15:105207	p 243	N92-16628 * #	NAS 1.15:105347	p 82	N92-15125 * #	NAS 1.15:105556	p 208	N92-20815 * #
NAS 1.15:105211	p 14	N92-10012 * #	NAS 1.15:105348	p 225	N92-14434 * #	NAS 1.15:105557	p 216	N92-23189 * #
NAS 1.15:105212	p 77	N92-10057 * #	NAS 1.15:105349	p 55	N92-13143 * #	NAS 1.15:105558	p 214	N92-30571 * #
NAS 1.15:105213	p 226	N92-16371 * #	NAS 1.15:105350	p 185	N92-15357 * #	NAS 1.15:105559	p 48	N92-21547 * #
NAS 1.15:105214	p 243	N92-14649 * #	NAS 1.15:105351	p 185	N92-14322 * #	NAS 1.15:105560	p 130	N92-21579 * #
NAS 1.15:105215	p 134	N92-11208 * #	NAS 1.15:105352	p 161	N92-25176 * #	NAS 1.15:105561	p 139	N92-26611 * #
NAS 1.15:105226	p 186	N92-18809 * #	NAS 1.15:105353	p 255	N92-18282 * #	NAS 1.15:105562	p 30	N92-20033 * #
NAS 1.15:105231	p 235	N92-10221 * #	NAS 1.15:105354	p 131	N92-24715 * #	NAS 1.15:105563	p 48	N92-25092 * #
NAS 1.15:105232	p 79	N92-11133 * #	NAS 1.15:105355	p 249	N92-15663 * #	NAS 1.15:105564	p 108	N92-20841 * #
NAS 1.15:105233	p 106	N92-14120 * #	NAS 1.15:105356	p 131	N92-24715 * #	NAS 1.15:105565	p 150	N92-19379 * #
NAS 1.15:105234	p 128	N92-14179 * #	NAS 1.15:105357	p 213	N92-29697 * #	NAS 1.15:105566	p 209	N92-23226 * #
NAS 1.15:105236	p 240	N92-10289 * #	NAS 1.15:105358	p 138	N92-16156 * #	NAS 1.15:105567	p 160	N92-20040 * #
NAS 1.15:105240	p 236	N92-16481 * #	NAS 1.15:105359	p 210	N92-25347 * #	NAS 1.15:105568	p 18	N92-23269 * #
NAS 1.15:105243	p 1	N92-23336 * #	NAS 1.15:105360	p 96	N92-14114 * #	NAS 1.15:105569	p 209	N92-23564 * #
NAS 1.15:105244	p 110	N92-30779 * #	NAS 1.15:105361	p 129	N92-19498 * #	NAS 1.15:105570	p 252	N92-26671 * #
NAS 1.15:105245	p 128	N92-15192 * #	NAS 1.15:105362	p 254	N92-14797 * #	NAS 1.15:105571	p 109	N92-23267 * #
NAS 1.15:105246	p 108	N92-19595 * #	NAS 1.15:105363	p 129	N92-19450 * #	NAS 1.15:105572	p 109	N92-23194 * #
NAS 1.15:105247	p 80	N92-11136 * #	NAS 1.15:105364	p 51	N92-16008 * #	NAS 1.15:105573	p 228	N92-23267 * #
NAS 1.15:105249	p 85	N92-20522 * #	NAS 1.15:105365	p 16	N92-15968 * #	NAS 1.15:105574	p 87	N92-23534 * #
NAS 1.15:105250	p 79	N92-11135 * #	NAS 1.15:105366	p 254	N92-16702 * #	NAS 1.15:105575	p 110	N92-25996 * #
NAS 1.15:105251	p 78	N92-11126 * #	NAS 1.15:105367	p 129	N92-17060 * #	NAS 1.15:105576	p 86	N92-21976 * #
NAS 1.15:105252	p 80	N92-11137 * #	NAS 1.15:105368	p 186	N92-15358 * #	NAS 1.15:105577	p 250	N92-26671 * #
NAS 1.15:105253	p 96	N92-18970 * #	NAS 1.15:105369	p 185	N92-14323 * #	NAS 1.15:105578	p 186	N92-20235 * #
NAS 1.15:105255	p 79	N92-11130 * #	NAS 1.15:105370	p 16	N92-15052 * #	NAS 1.15:105579	p 109	N92-25754 * #
NAS 1.15:105257	p 249	N92-10345 * #	NAS 1.15:105371	p 16	N92-15051 * #	NAS 1.15:105580	p 189	N92-23268 * #
NAS 1.15:105258	p 30	N92-17061 * #	NAS 1.15:105372	p 97	N92-25203 * #	NAS 1.15:105581	p 190	N92-23565 * #
NAS 1.15:105259	p 249	N92-16663 * #	NAS 1.15:105373	p 51	N92-18342 * #	NAS 1.15:105582	p 191	N92-25196 * #
NAS 1.15:105260	p 208	N92-16336 * #	NAS 1.15:105374	p 85	N92-20065 * #	NAS 1.15:105583	p 34	N92-23225 * #
NAS 1.15:105261	p 141	N92-11221 * #	NAS 1.15:105375	p 96	N92-15128 * #	NAS 1.15:105584	p 250	N92-24974 * #
NAS 1.15:105262	p 135	N92-19837 * #	NAS 1.15:105376	p 97	N92-17347 * #	NAS 1.15:105585	p 190	N92-23542 * #
NAS 1.15:105266	p 229	N92-25753 * #	NAS 1.15:105377	p 228	N92-24985 * #	NAS 1.15:105586	p 216	N92-24986 * #
NAS 1.15:105268	p 227	N92-23191 * #	NAS 1.15:105378	p 249	N92-15662 * #	NAS 1.15:105587	p 263	N92-20519 * #
NAS 1.15:105273	p 185	N92-13401 * #	NAS 1.15:105379	p 107	N92-15137 * #	NAS 1.15:105588	p 236	N92-20493 * #
NAS 1.15:105274	p 147	N92-12151 * #	NAS 1.15:105380	p 15	N92-14000 * #	NAS 1.15:105589	p 249	N92-22230 * #
NAS 1.15:105277	p 184	N92-11302 * #	NAS 1.15:105381	p 107	N92-18439 * #	NAS 1.15:105590	p 131	N92-23185 * #
NAS 1.15:105278	p 55	N92-11086 * #	NAS 1.15:105382	p 96	N92-18457 * #	NAS 1.15:105591	p 135	N92-25957 * #
NAS 1.15:105279	p 235	N92-13482 * #	NAS 1.15:105383	p 228	N92-23196 * #	NAS 1.15:105592	p 135	N92-26131 * #
NAS 1.15:105281	p 122	N92-16086 * #	NAS 1.15:105384	p 209	N92-23536 * #	NAS 1.15:105593	p 133	N92-27378 * #
NAS 1.15:105283	p 17	N92-19437 * #	NAS 1.15:105385	p 15	N92-14001 * #	NAS 1.15:105594	p 215	N92-31536 * #
NAS 1.15:105284	p 77	N92-10055 * #	NAS 1.15:105386	p 30	N92-15994 * #	NAS 1.15:105600	p 187	N92-22398 * #
NAS 1.15:105285	p 202	N92-24881 * #	NAS 1.15:105387	p 263	N92-19398 * #	NAS 1.15:105601	p 86	N92-23252 * #
NAS 1.15:105286	p 201	N92-19107 * #	NAS 1.15:105388	p 209	N92-24202 * #	NAS 1.15:105602	p 210	N92-25447 * #
NAS 1.15:105287	p 201	N92-19263 * #	NAS 1.15:105389	p 15	N92-14002 * #	NAS 1.15:105603	p 250	N92-33742 * #
NAS 1.15:105288	p 31	N92-20525 * #	NAS 1.15:105390	p 149	N92-15306 * #	NAS 1.15:105604	p 34	N92-23537 * #
NAS 1.15:105289	p 106	N92-13284 * #	NAS 1.15:105391	p 229	N92-28701 * #	NAS 1.15:105605	p 97	N92-23190 * #
NAS 1.15:105291	p 79	N92-11128 * #	NAS 1.15:105392	p 30	N92-17546 * #	NAS 1.15:105606	p 250	N92-27196 * #
NAS 1.15:105294	p 270	N92-17069 * #	NAS 1.15:105393	p 97	N92-21548 * #	NAS 1.15:105607	p 35	N92-25164 * #
NAS 1.15:105295	p 128	N92-14170 * #	NAS 1.15:105394	p 34	N92-23254 * #	NAS 1.15:105608	p 97	N92-26142 * #
NAS 1.15:105296	p 127	N92-11188 * #	NAS 1.15:105395	p 186	N92-16265 * #	NAS 1.15:105609	p 150	N92-19700 * #
NAS 1.15:105297	p 80	N92-11138 * #	NAS 1.15:105396	p 271	N92-18455 * #	NAS 1.15:105610	p 188	N92-23154 * #
NAS 1.15:105298	p 48	N92-11034 * #	NAS 1.15:105397	p 263	N92-15815 * #	NAS 1.15:105611	p 187	N92-20520 * #
NAS 1.15:105299	p 29	N92-11995 * #	NAS 1.15:105398	p 201	N92-18759 * #	NAS 1.15:105612	p 123	N92-24554 * #
NAS 1.15:105300	p 57	N92-25134 * #	NAS 1.15:105399	p 130	N92-22278 * #	NAS 1.15:105613	p 161	N92-23561 * #
NAS 1.15:105301	p 57	N92-13151 * #	NAS 1.15:105400	p 83	N92-16024 * #	NAS 1.15:105614	p 19	N92-27377 * #
NAS 1.15:105302	p 51	N92-15109 * #	NAS 1.15:105401	p 16	N92-15977 * #	NAS 1.15:105615	p 161	N92-23562 * #
NAS 1.15:105303	p 29	N92-11017 * #	NAS 1.15:105402	p 151	N92-20032 * #	NAS 1.15:105616	p 30	N92-20523 * #
NAS 1.15:105304	p 123	N92-16111 * #	NAS 1.15:105403	p 16	N92-15977 * #	NAS 1.15:105617	p 109	N92-25346 * #
NAS 1.15:105305	p 107	N92-15136 * #	NAS 1.15:105404	p 227	N92-22267 * #	NAS 1.15:105618	p 132	N92-25348 * #
NAS 1.15:105306	p 186	N92-18775 * #	NAS 1.15:105405	p 129	N92-27197 * #	NAS 1.15:105619	p 161	N92-23193 * #
NAS 1.15:105307	p 159	N92-14294 * #	NAS 1.15:105406	p 135	N92-18442 * #	NAS 1.15:105620	p 192	N92-25296 * #
NAS 1.15:105308	p 269	N92-14953 * #	NAS 1.15:105407	p 227	N92-20045 * #	NAS 1.15:105621	p 87	N92-24560 * #
NAS 1.15:105309	p 83	N92-16019 * #	NAS 1.15:105408	p 129	N92-20380 * #	NAS 1.15:105622	p 131	N92-23192 * #
NAS 1.15:105310	p 92	N92-31916 * #	NAS 1.15:105409	p 17	N92-18760 * #	NAS 1.15:105623	p 123	N92-27192 * #
NAS 1.15:105311	p 85	N92-20585 * #	NAS 1.15:105410	p 214	N92-30722 * #	NAS 1.15:105624	p 90	N92-28983 * #
NAS 1.15:105312	p 257	N92-13783 * #	NAS 1.15:105411	p 212	N92-27879 * #	NAS 1.15:105625	p 92	N92-32108 * #
NAS 1.15:105313	p 106	N92-14118 * #	NAS 1.15:105412	p 42	N92-28673 * #	NAS 1.15:105626	p 116	N92-26670 * #
NAS 1.15:105314	p 235	N92-13483 * #	NAS 1.15:105413	p 87	N92-24557 * #	NAS 1.15:105627	p 209	N92-23435 * #
NAS 1.15:105315	p 225	N92-12316 * #	NAS 1.15:105414	p 149	N92-17047 * #	NAS 1.15:105628	p 135	N92-25277 * #
NAS 1.15:105316	p 228	N92-25179 * #	NAS 1.15:105415	p 149	N92-16191 * #	NAS 1.15:105629	p 202	N92-24959 * #
NAS 1.15:105317	p 240	N92-13581 * #	NAS 1.15:105416	p 149	N92-17062 * #	NAS 1.15:105630	p 42	N92-25449 * #
NAS 1.15:105318	p 81	N92-13274 * #	NAS 1.15:105417	p 229	N92-25446 * #	NAS 1.15:105631	p 52	N92-30383 * #
NAS 1.15:105320	p 1	N92-22659 * #	NAS 1.15:105418	p 150	N92-19992 * #	NAS 1.15:105632	p 47	N92-26129 * #
NAS 1.15:105321	p 14	N92-13998 * #	NAS 1.15:105419	p 149	N92-18281 * #	NAS 1.15:105633	p 161	N92-23535 * #
NAS 1.15:105322	p 82	N92-14112 * #	NAS 1.15:105420	p 160	N92-18920 * #	NAS 1.15:105634	p 110	N92-30986 * #
NAS 1.15:105324	p 84	N92-18474 * #	NAS 1.15:105421	p 19	N92-26104 * #	NAS 1.15:105635	p 52	N92-23187 * #
NAS 1.15:105325	p 82	N92-14111 * #	NAS 1.15:105422	p 87	N92-25343 * #	NAS 1.15:105636	p 211	N92-26555 * #
NAS 1.15:105326	p 81	N92-13275 * #	NAS 1.15:105423	p 230	N92-33935 * #	NAS 1.15:105637	p 57	N92-30301 * #
NAS 1.15:105327	p 29	N92-13070 * #	NAS 1.15:105424	p 130	N92-22305 * #	NAS 1.15:105638	p 212	N92-28476 * #
NAS 1.15:105328	p 247	N92-13717 * #	NAS 1.15:105425	p 150	N92-18921 * #	NAS 1.15:105639	p 211	N92-25448 * #

NAS 1.15:105667

NAS 1.15:105667	p 87	N92-24201 * #	NAS 1.15:105842	p 163	N92-32867 * #	NASA-CP-3122	p 207	N92-14346 * #
NAS 1.15:105668	p 212	N92-26560 * #	NAS 1.15:105844	p 164	N92-34219 * #	NASA-CP-3132	p 147	N92-14202 * #
NAS 1.15:105670	p 237	N92-24802 * #	NAS 1.15:105846	p 162	N92-31282 * #	NASA-CR-189187	p 266	N92-30908 * #
NAS 1.15:105671	p 161	N92-26096 * #	NAS 1.15:105850	p 230	N92-34221 * #	NASA-CR-190588	p 229	N92-29342 * #
NAS 1.15:105672	p 140	N92-34112 * #	NAS 1.15:105853	p 196	N92-32472 * #	NASA-RP-1253	p 49	N92-32456 * #
NAS 1.15:105673	p 232	N92-30692 * #	NAS 1.15:105855	p 93	N92-34113 * #	NASA-RP-1280	p 47	N92-30307 * #
NAS 1.15:105674	p 142	N92-30692 * #	NAS 1.15:105858	p 250	N92-33571 * #	NASA-TM-100881	p 29	N92-14061 * #
NAS 1.15:105675	p 194	N92-26690 * #	NAS 1.15:105859	p 251	N92-33942 * #	NASA-TM-102434	p 56	N92-24349 * #
NAS 1.15:105676	p 20	N92-30182 * #	NAS 1.15:105876	p 47	N92-34114 * #	NASA-TM-102554	p 17	N92-20934 * #
NAS 1.15:105677	p 213	N92-29351 * #	NAS 1.15:105876	p 85	N92-21187 * #	NASA-TM-103684	p 42	N92-15406 * #
NAS 1.15:105678	p 211	N92-26108 * #	NAS 1.15:105876	p 22	N92-30395 * #	NASA-TM-103747	p 26	N92-12786 * #
NAS 1.15:105679	p 48	N92-25958 * #	NAS 1.15:105876	p 91	N92-31249 * #	NASA-TM-103755	p 225	N92-11373 * #
NAS 1.15:105680	p 37	N92-29661 * #	NAS 1.15:105876	p 228	N92-23527 * #	NASA-TM-103755	p 185	N92-13402 * #
NAS 1.15:105681	p 213	N92-29136 * #	NAS 1.15:105876	p 87	N92-25616 * #	NASA-TM-103786	p 139	N92-16158 * #
NAS 1.15:105682	p 38	N92-31172 * #	NAS 1.15:105876	p 160	N92-21370 * #	NASA-TM-103800	p 1	N92-17346 * #
NAS 1.15:105683	p 38	N92-33746 * #	NAS 1.15:105876	p 266	N92-30908 * #	NASA-TM-104179	p 43	N92-20925 * #
NAS 1.15:105684	p 36	N92-27037 * #	NAS 1.15:105876	p 229	N92-29342 * #	NASA-TM-104386	p 184	N92-11317 * #
NAS 1.15:105685	p 42	N92-30508 * #	NAS 1.15:105876	p 51	N92-22001 * #	NASA-TM-104424	p 184	N92-11320 * #
NAS 1.15:105686	p 195	N92-27653 * #	NAS 1.15:105876	p 49	N92-15082 * #	NASA-TM-104427	p 86	N92-21216 * #
NAS 1.15:105689	p 89	N92-27878 * #	NAS 1.15:105876	p 35	N92-25808 * #	NASA-TM-104475	p 14	N92-10978 * #
NAS 1.15:105690	p 88	N92-27034 * #	NAS 1.15:105876	p 78	N92-11088 * #	NASA-TM-104477	p 83	N92-16022 * #
NAS 1.15:105691	p 90	N92-29667 * #	NAS 1.15:105876	p 77	N92-10044 * #	NASA-TM-104478	p 129	N92-16129 * #
NAS 1.15:105692	p 88	N92-26654 * #	NAS 1.15:105876	p 191	N92-24514 * #	NASA-TM-104488	p 128	N92-11202 * #
NAS 1.15:105693	p 195	N92-30297 * #	NAS 1.15:105876	p 35	N92-25712 * #	NASA-TM-104492	p 79	N92-11129 * #
NAS 1.15:105694	p 36	N92-27652 * #	NAS 1.15:105876	p 86	N92-21517 * #	NASA-TM-104493	p 134	N92-13336 * #
NAS 1.15:105695	p 35	N92-26553 * #	NAS 1.15:105876	p 270	N92-30302 * #	NASA-TM-104498	p 84	N92-19780 * #
NAS 1.15:105696	p 244	N92-33894 * #	NAS 1.15:105876	p 141	N92-28436 * #	NASA-TM-104503	p 134	N92-11214 * #
NAS 1.15:105697	p 37	N92-27669 * #	NAS 1.15:105876	p 31	N92-22510 * #	NASA-TM-104506	p 226	N92-15405 * #
NAS 1.15:105698	p 37	N92-28418 * #	NAS 1.15:105876	p 207	N92-14346 * #	NASA-TM-104518	p 17	N92-23105 * #
NAS 1.15:105699	p 36	N92-26561 * #	NAS 1.15:105876	p 147	N92-14202 * #	NASA-TM-104524	p 200	N92-15366 * #
NAS 1.15:105700	p 91	N92-30187 * #	NAS 1.15:105876	p 34	N92-22863 * #	NASA-TM-104525	p 128	N92-15191 * #
NAS 1.15:105701	p 250	N92-27517 * #	NAS 1.15:105876	p 49	N92-31251 * #	NASA-TM-104526	p 236	N92-13484 * #
NAS 1.15:105702	p 215	N92-31485 * #	NAS 1.15:105876	p 207	N92-10195 * #	NASA-TM-104531	p 133	N92-32863 * #
NAS 1.15:105703	p 88	N92-26792 * #	NAS 1.15:105876	p 16	N92-14968 * #	NASA-TM-105096	p 241	N92-11642 * #
NAS 1.15:105712	p 92	N92-31342 * #	NAS 1.15:105876	p 159	N92-11252 * #	NASA-TM-105143	p 82	N92-14109 * #
NAS 1.15:105714	p 88	N92-27033 * #	NAS 1.15:105876	p 129	N92-17070 * #	NASA-TM-105146	p 141	N92-11217 * #
NAS 1.15:105715	p 37	N92-28419 * #	NAS 1.15:105876	p 184	N92-11299 * #	NASA-TM-105154	p 243	N92-11691 * #
NAS 1.15:105716	p 37	N92-28985 * #	NAS 1.15:105876	p 83	N92-17151 * #	NASA-TM-105159	p 151	N92-23412 * #
NAS 1.15:105717	p 202	N92-29105 * #	NAS 1.15:105876	p 51	N92-19762 * #	NASA-TM-105161	p 90	N92-28682 * #
NAS 1.15:105718	p 214	N92-30948 * #	NAS 1.15:105876	p 227	N92-22227 * #	NASA-TM-105162	p 226	N92-15403 * #
NAS 1.15:105720	p 19	N92-28102 * #	NAS 1.15:105876	p 20	N92-28880 * #	NASA-TM-105174	p 107	N92-16037 * #
NAS 1.15:105722	p 255	N92-28984 * #	NAS 1.15:105876	p 213	N92-30396 * #	NASA-TM-105189	p 106	N92-14122 * #
NAS 1.15:105724	p 36	N92-26613 * #	NAS 1.15:105876	p 230	N92-33476 * #	NASA-TM-105192	p 1	N92-10002 * #
NAS 1.15:105726	p 230	N92-31505 * #	NAS 1.15:105876	p 49	N92-32456 * #	NASA-TM-105193	p 30	N92-15993 * #
NAS 1.15:105727	p 90	N92-28417 * #	NAS 1.15:105876	p 47	N92-30307 * #	NASA-TM-105198	p 133	N92-31840 * #
NAS 1.15:105728	p 162	N92-28432 * #	NAS 1.15:105876	p 111	N92-34208 * #	NASA-TM-105199	p 95	N92-10064 * #
NAS 1.15:105730	p 214	N92-30734 * #	NAS 1.15:105876	p 96	N92-17882 * #	NASA-TM-105206	p 25	N92-16705 * #
NAS 1.15:105731	p 90	N92-29343 * #	NAS 1.15:105876	p 127	N92-11186 * #	NASA-TM-105207	p 243	N92-16628 * #
NAS 1.15:105734	p 88	N92-27035 * #	NAS 1.15:105876	p 21	N92-34243 * #	NASA-TM-105211	p 14	N92-10012 * #
NAS 1.15:105737	p 238	N92-29662 * #	NAS 1.15:105876	p 235	N92-10222 * #	NASA-TM-105212	p 77	N92-10057 * #
NAS 1.15:105739	p 257	N92-28475 * #	NAS 1.15:105876	p 131	N92-24053 * #	NASA-TM-105213	p 226	N92-16371 * #
NAS 1.15:105740	p 196	N92-31484 * #	NAS 1.15:105876	p 208	N92-17678 * #	NASA-TM-105214	p 243	N92-14649 * #
NAS 1.15:105741	p 89	N92-27654 * #	NAS 1.15:105876	p 131	N92-24057 * #	NASA-TM-105215	p 134	N92-11208 * #
NAS 1.15:105742	p 19	N92-26612 * #	NAS 1.15:105876	p 107	N92-17861 * #	NASA-TM-105226	p 186	N92-18809 * #
NAS 1.15:105743	p 20	N92-28674 * #	NAS 1.15:105876	p 237	N92-24057 * #	NASA-TM-105231	p 235	N92-10221 * #
NAS 1.15:105744	p 151	N92-31855 * #	NAS 1.15:105876	p 131	N92-23461 * #	NASA-TM-105232	p 79	N92-11133 * #
NAS 1.15:105745	p 20	N92-28696 * #	NAS 1.15:105876	p 116	N92-34206 * #	NASA-TM-105233	p 106	N92-14120 * #
NAS 1.15:105746	p 136	N92-29669 * #	NASA-CASE-LEW-14162-3	p 111	N92-34208 * #	NASA-TM-105234	p 128	N92-14179 * #
NAS 1.15:105748	p 239	N92-33898 * #	NASA-CASE-LEW-14345-6	p 96	N92-17882 * #	NASA-TM-105236	p 240	N92-10289 * #
NAS 1.15:105749	p 244	N92-28684 * #	NASA-CASE-LEW-14474-2	p 127	N92-11186 * #	NASA-TM-105240	p 236	N92-16481 * #
NAS 1.15:105750	p 89	N92-27036 * #	NASA-CASE-LEW-14791-1	p 21	N92-34243 * #	NASA-TM-105242	p 1	N92-23336 * #
NAS 1.15:105751	p 163	N92-32243 * #	NASA-CASE-LEW-14973-1	p 235	N92-10222 * #	NASA-TM-105243	p 110	N92-30779 * #
NAS 1.15:105752	p 151	N92-32965 * #	NASA-CASE-LEW-15027-2	p 131	N92-24053 * #	NASA-TM-105244	p 128	N92-15192 * #
NAS 1.15:105753	p 162	N92-28675 * #	NASA-CASE-LEW-15216-1	p 208	N92-17678 * #	NASA-TM-105245	p 108	N92-19595 * #
NAS 1.15:105754	p 110	N92-29660 * #	NASA-CASE-LEW-15241-1	p 107	N92-17861 * #	NASA-TM-105246	p 80	N92-11136 * #
NAS 1.15:105755	p 238	N92-30426 * #	NASA-CASE-LEW-15308-1	p 237	N92-24057 * #	NASA-TM-105249	p 85	N92-20522 * #
NAS 1.15:105758	p 93	N92-33064 * #	NASA-CASE-LEW-15314-1	p 131	N92-23461 * #	NASA-TM-105250	p 79	N92-11135 * #
NAS 1.15:105759	p 136	N92-28433 * #	NASA-CASE-LEW-15360-1	p 116	N92-34206 * #	NASA-TM-105251	p 78	N92-11126 * #
NAS 1.15:105762	p 111	N92-32466 * #	NASA-CP-10053	p 51	N92-22001 * #	NASA-TM-105252	p 80	N92-11137 * #
NAS 1.15:105763	p 90	N92-28693 * #	NASA-CP-10070	p 49	N92-15082 * #	NASA-TM-105253	p 96	N92-18970 * #
NAS 1.15:105765	p 238	N92-28837 * #	NASA-CP-10078	p 35	N92-25808 * #	NASA-TM-105255	p 79	N92-11130 * #
NAS 1.15:105767	p 196	N92-32868 * #	NASA-CP-10079	p 78	N92-11088 * #	NASA-TM-105257	p 249	N92-10345 * #
NAS 1.15:105768	p 238	N92-33895 * #	NASA-CP-10084	p 77	N92-10044 * #	NASA-TM-105258	p 30	N92-17061 * #
NAS 1.15:105770	p 20	N92-34144 * #	NASA-CP-10088	p 191	N92-24514 * #	NASA-TM-105259	p 249	N92-16663 * #
NAS 1.15:105774	p 48	N92-30310 * #	NASA-CP-10089	p 35	N92-25712 * #	NASA-TM-105260	p 208	N92-16336 * #
NAS 1.15:105775	p 91	N92-30308 * #	NASA-CP-10090	p 86	N92-21517 * #	NASA-TM-105261	p 141	N92-11221 * #
NAS 1.15:105777	p 162	N92-30427 * #	NASA-CP-10093	p 270	N92-33899 * #	NASA-TM-105262	p 135	N92-19837 * #
NAS 1.15:105787	p 92	N92-32237 * #	NASA-CP-10094	p 163	N92-34204 * #	NASA-TM-105266	p 229	N92-25753 * #
NAS 1.15:105789	p 142	N92-31263 * #	NASA-CP-10099	p 163	N92-32233 * #	NASA-TM-105273	p 227	N92-23191 * #
NAS 1.15:105791	p 162	N92-30397 * #	NASA-CP-3049	p 31	N92-22510 * #	NASA-TM-105277	p 185	N92-13401 * #
NAS 1.15:105794	p 92	N92-31507 * #				NASA-TM-105278	p 147	N92-12151 * #
NAS 1.15:105795	p 241	N92-33897 * #				NASA-TM-105279	p 184	N92-11302 * #
NAS 1.15:105796	p 38	N92-30972 * #				NASA-TM-105281	p 55	N92-11086 * #
NAS 1.15:105797	p 40	N92-34107 * #				NASA-TM-105282	p 235	N92-13482 * #
NAS 1.15:105801	p 257	N92-33896 * #				NASA-TM-105283	p 122	N92-16086 * #
NAS 1.15:105802	p 110	N92-32234 * #				NASA-TM-105284	p 17	N92-19437 * #
NAS 1.15:105803	p 1	N92-31267 * #				NASA-TM-105285	p 77	N92-10055 * #
NAS 1.15:105805	p 251	N92-30898 * #				NASA-TM-105286	p 202	N92-24881 * #
NAS 1.15:105811	p 93	N92-32463 * #				NASA-TM-105287	p 201	N92-19107 * #
NAS 1.15:105814	p 38	N92-30998 * #				NASA-TM-105288	p 31	N92-20525 * #
NAS 1.15:105818	p 92	N92-31901 * #				NASA-TM-105289	p 106	N92-13284 * #
NAS 1.15:105825	p 238	N92-31262 * #						
NAS 1.15:105826								

REPORT NUMBER INDEX

NASA-TM-105740

NASA-TM-105291	p 79	N92-11128 * #	NASA-TM-105396	p 229	N92-28701 * #	NASA-TM-105611	p 97	N92-23190 * #
NASA-TM-105294	p 270	N92-17069 * #	NASA-TM-105397	p 30	N92-17546 * #	NASA-TM-105612	p 250	N92-27196 * #
NASA-TM-105295	p 128	N92-14170 * #	NASA-TM-105398	p 97	N92-21548 * #	NASA-TM-105613	p 35	N92-25164 * #
NASA-TM-105296	p 127	N92-11188 * #	NASA-TM-105399	p 34	N92-23254 * #	NASA-TM-105615	p 97	N92-26142 * #
NASA-TM-105297	p 80	N92-11138 * #	NASA-TM-105400	p 186	N92-16265 * #	NASA-TM-105616	p 150	N92-19700 * #
NASA-TM-105298	p 48	N92-11034 * #	NASA-TM-105401	p 271	N92-18455 * #	NASA-TM-105617	p 188	N92-23154 * #
NASA-TM-105299	p 29	N92-11995 * #	NASA-TM-105402	p 263	N92-15815 * #	NASA-TM-105619	p 187	N92-20520 * #
NASA-TM-105300	p 57	N92-25134 * #	NASA-TM-105403	p 201	N92-18759 * #	NASA-TM-105620	p 123	N92-24554 * #
NASA-TM-105301	p 57	N92-13151 * #	NASA-TM-105404	p 130	N92-22278 * #	NASA-TM-105622	p 161	N92-23561 * #
NASA-TM-105302	p 51	N92-15109 * #	NASA-TM-105405	p 83	N92-16024 * #	NASA-TM-105623	p 19	N92-27377 * #
NASA-TM-105303	p 29	N92-11017 * #	NASA-TM-105406	p 16	N92-15977 * #	NASA-TM-105624	p 161	N92-23562 * #
NASA-TM-105304	p 123	N92-16111 * #	NASA-TM-105407	p 151	N92-20032 * #	NASA-TM-105627	p 30	N92-20523 * #
NASA-TM-105305	p 107	N92-15136 * #	NASA-TM-105408	p 227	N92-22267 * #	NASA-TM-105628	p 109	N92-25346 * #
NASA-TM-105306	p 186	N92-18775 * #	NASA-TM-105410	p 139	N92-27197 * #	NASA-TM-105629	p 132	N92-25348 * #
NASA-TM-105307	p 159	N92-14294 * #	NASA-TM-105411	p 135	N92-18442 * #	NASA-TM-105630	p 161	N92-23193 * #
NASA-TM-105308	p 269	N92-14953 * #	NASA-TM-105412	p 227	N92-20045 * #	NASA-TM-105632	p 192	N92-25296 * #
NASA-TM-105309	p 83	N92-16019 * #	NASA-TM-105413	p 129	N92-20380 * #	NASA-TM-105633	p 87	N92-24560 * #
NASA-TM-105310	p 92	N92-31916 * #	NASA-TM-105414	p 17	N92-18760 * #	NASA-TM-105634	p 131	N92-23192 * #
NASA-TM-105311	p 85	N92-20585 * #	NASA-TM-105415	p 214	N92-30722 * #	NASA-TM-105635	p 123	N92-27192 * #
NASA-TM-105312	p 257	N92-13783 * #	NASA-TM-105416	p 212	N92-27879 * #	NASA-TM-105636	p 90	N92-28983 * #
NASA-TM-105313	p 106	N92-14118 * #	NASA-TM-105417	p 42	N92-28673 * #	NASA-TM-105637	p 92	N92-32108 * #
NASA-TM-105314	p 235	N92-13483 * #	NASA-TM-105418	p 87	N92-24557 * #	NASA-TM-105638	p 116	N92-26670 * #
NASA-TM-105315	p 225	N92-12316 * #	NASA-TM-105420	p 149	N92-17047 * #	NASA-TM-105641	p 209	N92-23435 * #
NASA-TM-105316	p 228	N92-25179 * #	NASA-TM-105421	p 149	N92-16191 * #	NASA-TM-105642	p 135	N92-25277 * #
NASA-TM-105317	p 240	N92-13581 * #	NASA-TM-105422	p 149	N92-17062 * #	NASA-TM-105643	p 202	N92-24959 * #
NASA-TM-105318	p 81	N92-13274 * #	NASA-TM-105423	p 229	N92-25446 * #	NASA-TM-105644	p 42	N92-25449 * #
NASA-TM-105320	p 1	N92-22659 * #	NASA-TM-105424	p 150	N92-19992 * #	NASA-TM-105645	p 52	N92-30383 * #
NASA-TM-105321	p 14	N92-13998 * #	NASA-TM-105425	p 149	N92-18281 * #	NASA-TM-105646	p 47	N92-26129 * #
NASA-TM-105322	p 82	N92-14112 * #	NASA-TM-105426	p 160	N92-18920 * #	NASA-TM-105647	p 161	N92-23535 * #
NASA-TM-105324	p 84	N92-18474 * #	NASA-TM-105427	p 19	N92-26104 * #	NASA-TM-105648	p 110	N92-30986 * #
NASA-TM-105325	p 82	N92-14111 * #	NASA-TM-105428	p 87	N92-25343 * #	NASA-TM-105649	p 52	N92-23187 * #
NASA-TM-105326	p 81	N92-13275 * #	NASA-TM-105429	p 230	N92-33935 * #	NASA-TM-105651	p 211	N92-26555 * #
NASA-TM-105327	p 29	N92-13070 * #	NASA-TM-105430	p 130	N92-22305 * #	NASA-TM-105652	p 57	N92-30301 * #
NASA-TM-105328	p 247	N92-13717 * #	NASA-TM-105431	p 150	N92-18921 * #	NASA-TM-105653	p 212	N92-28476 * #
NASA-TM-105329	p 190	N92-23560 * #	NASA-TM-105432	p 18	N92-23563 * #	NASA-TM-105654	p 211	N92-25448 * #
NASA-TM-105330	p 210	N92-25396 * #	NASA-TM-105433	p 83	N92-16023 * #	NASA-TM-105655	p 211	N92-26106 * #
NASA-TM-105331	p 211	N92-26107 * #	NASA-TM-105434	p 214	N92-31349 * #	NASA-TM-105657	p 264	N92-23890 * #
NASA-TM-105332	p 184	N92-11328 * #	NASA-TM-105435	p 187	N92-22226 * #	NASA-TM-105659	p 87	N92-24957 * #
NASA-TM-105333	p 236	N92-14485 * #	NASA-TM-105437	p 109	N92-23195 * #	NASA-TM-105660	p 56	N92-28683 * #
NASA-TM-105334	p 185	N92-15336 * #	NASA-TM-105438	p 84	N92-18280 * #	NASA-TM-105661	p 189	N92-23224 * #
NASA-TM-105335	p 95	N92-13281 * #	NASA-TM-105439	p 91	N92-30818 * #	NASA-TM-105662	p 191	N92-24050 * #
NASA-TM-105336	p 226	N92-15402 * #	NASA-TM-105521	p 201	N92-18456 * #	NASA-TM-105663	p 18	N92-24958 * #
NASA-TM-105337	p 225	N92-14433 * #	NASA-TM-105541	p 160	N92-18473 * #	NASA-TM-105664	p 210	N92-24984 * #
NASA-TM-105338	p 254	N92-14795 * #	NASA-TM-105544	p 84	N92-20043 * #	NASA-TM-105666	p 110	N92-31506 * #
NASA-TM-105340	p 82	N92-15119 * #	NASA-TM-105545	p 160	N92-21370 * #	NASA-TM-105667	p 87	N92-24201 * #
NASA-TM-105341	p 107	N92-16036 * #	NASA-TM-105546	p 85	N92-20355 * #	NASA-TM-105668	p 212	N92-26560 * #
NASA-TM-105342	p 269	N92-13910 * #	NASA-TM-105547	p 226	N92-19779 * #	NASA-TM-105670	p 237	N92-24802 * #
NASA-TM-105343	p 52	N92-22319 * #	NASA-TM-105548	p 86	N92-20355 * #	NASA-TM-105671	p 161	N92-26096 * #
NASA-TM-105345	p 227	N92-20212 * #	NASA-TM-105549	p 267	N92-25395 * #	NASA-TM-105672	p 230	N92-34112 * #
NASA-TM-105346	p 187	N92-22487 * #	NASA-TM-105551	p 202	N92-23155 * #	NASA-TM-105673	p 142	N92-30692 * #
NASA-TM-105347	p 29	N92-14063 * #	NASA-TM-105553	p 108	N92-20039 * #	NASA-TM-105674	p 194	N92-26690 * #
NASA-TM-105348	p 82	N92-15125 * #	NASA-TM-105554	p 97	N92-21175 * #	NASA-TM-105675	p 20	N92-30182 * #
NASA-TM-105349	p 225	N92-14434 * #	NASA-TM-105555	p 187	N92-21498 * #	NASA-TM-105676	p 213	N92-29351 * #
NASA-TM-105350	p 55	N92-13143 * #	NASA-TM-105556	p 208	N92-20815 * #	NASA-TM-105678	p 211	N92-26108 * #
NASA-TM-105351	p 185	N92-15357 * #	NASA-TM-105557	p 216	N92-23189 * #	NASA-TM-105679	p 48	N92-25958 * #
NASA-TM-105352	p 185	N92-14322 * #	NASA-TM-105558	p 214	N92-30571 * #	NASA-TM-105680	p 37	N92-29661 * #
NASA-TM-105354	p 161	N92-25176 * #	NASA-TM-105559	p 48	N92-21547 * #	NASA-TM-105681	p 213	N92-29136 * #
NASA-TM-105355	p 130	N92-20660 * #	NASA-TM-105560	p 130	N92-21579 * #	NASA-TM-105682	p 38	N92-31172 * #
NASA-TM-105356	p 255	N92-18282 * #	NASA-TM-105561	p 139	N92-26611 * #	NASA-TM-105683	p 38	N92-33746 * #
NASA-TM-105357	p 249	N92-15663 * #	NASA-TM-105562	p 30	N92-20033 * #	NASA-TM-105684	p 36	N92-27037 * #
NASA-TM-105358	p 131	N92-24715 * #	NASA-TM-105563	p 48	N92-25092 * #	NASA-TM-105685	p 42	N92-30508 * #
NASA-TM-105359	p 213	N92-29697 * #	NASA-TM-105564	p 108	N92-20841 * #	NASA-TM-105686	p 195	N92-27653 * #
NASA-TM-105360	p 15	N92-14003 * #	NASA-TM-105566	p 150	N92-19379 * #	NASA-TM-105689	p 89	N92-27878 * #
NASA-TM-105361	p 138	N92-16156 * #	NASA-TM-105567	p 209	N92-23226 * #	NASA-TM-105690	p 88	N92-27034 * #
NASA-TM-105362	p 210	N92-25347 * #	NASA-TM-105569	p 160	N92-20040 * #	NASA-TM-105691	p 90	N92-29667 * #
NASA-TM-105363	p 96	N92-14114 * #	NASA-TM-105570	p 18	N92-23269 * #	NASA-TM-105692	p 88	N92-26654 * #
NASA-TM-105364	p 129	N92-19498 * #	NASA-TM-105571	p 209	N92-23564 * #	NASA-TM-105693	p 195	N92-30297 * #
NASA-TM-105365	p 254	N92-14797 * #	NASA-TM-105573	p 252	N92-26671 * #	NASA-TM-105694	p 36	N92-27652 * #
NASA-TM-105366	p 129	N92-19450 * #	NASA-TM-105574	p 109	N92-23194 * #	NASA-TM-105695	p 35	N92-26553 * #
NASA-TM-105367	p 51	N92-16008 * #	NASA-TM-105575	p 228	N92-23267 * #	NASA-TM-105696	p 244	N92-33894 * #
NASA-TM-105368	p 16	N92-15968 * #	NASA-TM-105576	p 87	N92-23534 * #	NASA-TM-105697	p 37	N92-27669 * #
NASA-TM-105369	p 254	N92-16702 * #	NASA-TM-105577	p 110	N92-25996 * #	NASA-TM-105698	p 37	N92-28418 * #
NASA-TM-105370	p 129	N92-17060 * #	NASA-TM-105578	p 86	N92-21976 * #	NASA-TM-105699	p 36	N92-26561 * #
NASA-TM-105371	p 186	N92-15358 * #	NASA-TM-105579	p 40	N92-20586 * #	NASA-TM-105700	p 91	N92-30187 * #
NASA-TM-105372	p 185	N92-14323 * #	NASA-TM-105581	p 186	N92-20235 * #	NASA-TM-105701	p 250	N92-27517 * #
NASA-TM-105373	p 16	N92-15052 * #	NASA-TM-105582	p 109	N92-25754 * #	NASA-TM-105702	p 215	N92-31485 * #
NASA-TM-105374	p 16	N92-15051 * #	NASA-TM-105583	p 189	N92-23268 * #	NASA-TM-105703	p 88	N92-26792 * #
NASA-TM-105375	p 97	N92-25203 * #	NASA-TM-105584	p 190	N92-23565 * #	NASA-TM-105712	p 92	N92-31342 * #
NASA-TM-105377	p 51	N92-18342 * #	NASA-TM-105585	p 191	N92-25196 * #	NASA-TM-105714	p 88	N92-27033 * #
NASA-TM-105378	p 85	N92-20065 * #	NASA-TM-105586	p 34	N92-23225 * #	NASA-TM-105715	p 37	N92-28419 * #
NASA-TM-105379	p 96	N92-15128 * #	NASA-TM-105587	p 250	N92-24974 * #	NASA-TM-105716	p 37	N92-28985 * #
NASA-TM-105380	p 17	N92-17347 * #	NASA-TM-105588	p 190	N92-23542 * #	NASA-TM-105717	p 202	N92-29105 * #
NASA-TM-105381	p 228	N92-24985 * #	NASA-TM-105589	p 216	N92-24986 * #	NASA-TM-105718	p 214	N92-30948 * #
NASA-TM-105382	p 249	N92-15662 * #	NASA-TM-105590	p 263	N92-20519 * #	NASA-TM-105720	p 19	N92-28102 * #
NASA-TM-105383	p 107	N92-15137 * #	NASA-TM-105591	p 236	N92-20493 * #	NASA-TM-105722	p 255	N92-28984 * #
NASA-TM-105384	p 15	N92-14000 * #	NASA-TM-105593	p 249	N92-22230 * #	NASA-TM-105724	p 36	N92-26613 * #
NASA-TM-105385	p 107	N92-18439 * #	NASA-TM-105594	p 131	N92-23185 * #	NASA-TM-105726	p 230	N92-31505 * #
NASA-TM-105386	p 96	N92-18457 * #	NASA-TM-105596	p 135	N92-25957 * #	NASA-TM-105727	p 90	N92-28417 * #
NASA-TM-105387	p 228	N92-23196 * #	NASA-TM-105597	p 135	N92-26131 * #	NASA-TM-105728	p 162	N92-28432 * #
NASA-TM-105388	p 209	N92-23536 * #	NASA-TM-105599	p 133	N92-27378 * #	NASA-TM-105730	p 214	N92-30734 * #
NASA-TM-105389	p 15	N92-14001 * #	NASA-TM-105600	p 215	N92-31536 * #	NASA-TM-105731	p 90	N92-29343 * #
NASA-TM-105390	p 30	N92-15984 * #	NASA-TM-105604	p 187	N92-22398 * #	NASA-TM-105734	p 88	N92-27035 * #
NASA-TM-105391	p 263	N92-19398 * #	NASA-TM-105605	p 86	N92-23252 * #	NASA-TM-105737	p 238	N92-29662 * #

REPORT DOCUMENTATION PAGE

Form Approved
OMB No. 0704-0188

Public reporting burden for this collection of information is estimated to average 1 hour per response, including the time for reviewing instructions, searching existing data sources, gathering and maintaining the data needed, and completing and reviewing the collection of information. Send comments regarding this burden estimate or any other aspect of this collection of information, including suggestions for reducing this burden, to Washington Headquarters Services, Directorate for Information Operations and Reports, 1215 Jefferson Davis Highway, Suite 1204, Arlington, VA 22202-4302, and to the Office of Management and Budget, Paperwork Reduction Project (0704-0188), Washington, DC 20503.

1. AGENCY USE ONLY (Leave blank)		2. REPORT DATE November 1993	3. REPORT TYPE AND DATES COVERED Technical Memorandum	
4. TITLE AND SUBTITLE Bibliography of Lewis Research Center Technical Publications Announced in 1992			5. FUNDING NUMBERS	
6. AUTHOR(S)			8. PERFORMING ORGANIZATION REPORT NUMBER E-7602	
7. PERFORMING ORGANIZATION NAME(S) AND ADDRESS(ES) National Aeronautics and Space Administration Lewis Research Center Cleveland, Ohio 44135-3191			10. SPONSORING/MONITORING AGENCY REPORT NUMBER NASA TM-106035	
9. SPONSORING/MONITORING AGENCY NAME(S) AND ADDRESS(ES) National Aeronautics and Space Administration Washington, D.C. 20546-0001			11. SUPPLEMENTARY NOTES Compiled by Technical Information Services Division, Lewis Research Center.	
12a. DISTRIBUTION/AVAILABILITY STATEMENT Unclassified - Unlimited Subject Category 82			12b. DISTRIBUTION CODE	
13. ABSTRACT (Maximum 200 words) This compilation of abstracts describes and indexes the technical reporting that resulted from the scientific and engineering work performed and managed by the Lewis Research Center in 1992. All the publications were announced in the 1992 issues of STAR (Scientific and Technical Aerospace Reports) and/or IAA (International Aerospace Abstracts). Included are research reports, journal articles, conference presentations, patents and patent applications, and theses.				
14. SUBJECT TERMS Bibliographies; Abstracts; Documentation; Indexes (Documentation)			15. NUMBER OF PAGES 440	
			16. PRICE CODE A19	
17. SECURITY CLASSIFICATION OF REPORT Unclassified	18. SECURITY CLASSIFICATION OF THIS PAGE Unclassified	19. SECURITY CLASSIFICATION OF ABSTRACT Unclassified	20. LIMITATION OF ABSTRACT	

**National Aeronautics and
Space Administration**

Lewis Research Center
21000 Brookpark Rd.
Cleveland, OH 44135-3191

**Official Business
Penalty for Private Use \$300**

